CONTENTS

NUMBER 1

NUMBER 2

NUMBER 3

NUMBER 5

NUMBER 8

NUMBER 9

HISTORICAL SKETCHES

NUMBER 12

HISTORICAL SKETCHES—A NEW FEATURE

UNFORTUNATELY, few chemists seem to have more than a passing interest in the history of chemistry. In contrast to the situation in the humanities, where the average student is expected to steep himself in the classics, the average chemistry graduate has little knowledge of the history of his chosen discipline. We take this situation for granted today, yet this has not always been the case.

The German poet and dramatist, Johann Wolfgang von Goethe, himself an amateur scientist, declared "Die Geschichte der Wissenschaft ist die Wissenschaft selbst" (This history of science is science itself). Many of the founders of chemistry were well acquainted with its history. The first history of chemistry in the English language was written in 1830–1831 by the Scottish chemist, Thomas Thomson, an active practicing scientist, and August Kekulé spent much time reading the classics of chemistry before making any original discoveries of his own.

Such a lack of historical perspective can result in a distorted view of chemistry. Science is more than its usual dictionary definition as "organised or classified knowledge". In addition to its cognitive, factual aspects, science is a process—the search for knowledge carried out by struggling and committed practitioners, both successful and unsuccessful, working in the context of their scientific, social, and political milieu, i.e. an exciting human activity. In the words of Professor John C. Bailar, Jr., "One cannot really understand or appreciate the present position of science unless he knows something of the slow and tortuous steps through which it developed. The scientist's ability to help it move forward will be greatly enhanced by an understanding of the thinking of the chemists who built the theories which we use today".[1]

Yet a knowledge and appreciation of history is not limited to its cultural and inspirational value. It can also be directly applicable to contemporary research efforts. As a case in point, when Lord Rayleigh encountered discrepancies between the density of atmospheric nitrogen and that of nitrogen prepared from compounds, he sought suggestions from the readers of the journal *Nature*.[2] William Ramsay[3] suggested that Rayleigh read Henry Cavendish's paper[4] of 1785 on nitrogen, which more than a century earlier had predicted the presence of an unknown gas in the atmosphere. Together Ramsay and Rayleigh went on to discover the first of the inert gases, argon, in 1894 and thereby to uncover the existence of a completely unsuspected periodic group of elements.

"**Historical Sketches**" is a new feature that will consist of occasional articles concerned with historical aspects of inorganic and organometallic chemistry, including biographies, developments of concepts and theories, and the role of inorganic and organometallic chemistry in human affairs.

Persons wishing to contribute an article to "**Historical Sketches**" should contact: Professor George B. Kauffman, Department of Chemistry, California State University at Fresno, Fresno, CA 82740, U.S.A.

D. C. BRADLEY
G. WILKINSON

REFERENCES

1. J. C. Bailar, Jr., in G. B. Kauffman, *Alfred Werner: Founder of Coordination Chemistry*, p. VII. Springer–Verlag, Berlin (1966).
2. Lord Rayleigh, *Nature* 1892, **46**, 512.
3. W. A. Tilden, *Sir William Ramsay, K.C.B., F.R.S., Memorials of His Life and Work*, p. 125. Macmillan, London (1918).
4. H. Cavendish, *Phil. Trans. Roy. Soc. London* 1785, **75**, 372.

ANNOUNCEMENT

Executive Editor, North America

The publisher, Robert Maxwell, and the Editors, are delighted to announce that Professor Malcolm Chisholm has agreed to become Executive Editor with responsibility for the United States and Canada. Contributions for *POLYHEDRON* from North American authors should be sent to:

<div align="center">

Professor Malcolm Chisholm
Department of Chemistry
Indiana University
Bloomington
IN 47405
U.S.A.

</div>

We trust that this new arrangement will reduce delays in mailing of manuscripts and proofs and so assist in more rapid publishing.

AUTHOR INDEX

THE ORIGIN AND DISSEMINATION OF THE TERM "LIGAND" IN CHEMISTRY†

WILLIAM H. BROCK

Victorian Studies Centre, The University, Leicester, LE1 7RH, England

K. A. JENSEN

Department of General and Organic Chemistry, University of Copenhagen, The H.C. Ørsted Institute,
DK-2100 Copenhagen, Denmark

CHRISTIAN KLIXBÜLL JØRGENSEN

Département de Chimie Minérale Analytique et Appliquée de l'Université,
Section Chimie-Sciences II, 1211 Genève 4, Switzerland

and

GEORGE B. KAUFFMAN

Department of Chemistry, California State University, Fresno, CA 93740, U.S.A.

Language has always been a central feature of chemical development. As Lavoisier noted in the *Méthode de Nomenclature Chimique* (1787):

> There are . . . three things to distinguish in all physical science: the series of facts which form the science; the ideas which recall the facts; and the words which express them. The word must suggest the idea; the idea must depict the fact: these are three marks of the same stamp.[1]

Savory has discussed the fortunate way in which scientists can invent words merely by defining them so that others may know how and when to use them, the only criterion being that of intelligibility.[2] However, it need not necessarily follow that a neologism will be automatically adopted by the scientific community, even if it does satisfy Lavoisier's criterion that it should suggest the idea of a definite chemical phenomenon. Force of habit alone will insure that a system of revolutionary character will not be accepted. The reformation of a nomenclature has to proceed step by step. For example, Auguste Laurent was responsible for a large chemical vocabulary, little of which was subsequently adopted; similarly, Charles Mansfield's strange language in his *Theory of Salts* was completely ignored.[3] Are there, therefore, perhaps criteria for the adoption and acceptance of scientific words? What makes a successful neologism?

An examination of the origins, dissemination, and eventual adoption of the term *ligand*, which is used by chemists to refer to atoms or groups attached to a central atom in the formation of coordination compounds or organometallic compounds,[4] throws some light on these questions. It will be suggested that it is essential that a successful conceptual term should possess an international form, i.e. that it is derived from Latin or Greek (with Roman transliteration).[5] Furthermore, in the twentieth century it has become necessary for a new term to be used in influential papers (i.e. ones which attract

multiple citation), and for the term to be endorsed by *Chemical Abstracts* and leading journals. Since the Second World War this process has been assisted by the nomenclature commissions of the International Union of Pure and Applied Chemistry (IUPAC). In principle, a term can be introduced in an English, German, French, Scandinavian, or any other language, but the acceptance of a new chemical term may be seriously delayed until it is adopted in English-language publications.

While engaged in pioneering experimental work on the hydrides of boron during his First World War sojourn at the Kaiser-Wilhelm-Institut für Chemie in Berlin, Alfred Stock (1876–1946) directed his attention to the analogous hydrides of silicon. Their highly reactive and volatile character, it was thought, might have military applications. At a meeting of the Kaiser–Wilhelm-Institut on 27 November 1916 Stock discussed the similarities between carbon and silicon chemistry first noticed by Wöhler.[6] For Stock, these analogies were made more evident and interesting by the deeper knowledge of atomic structure that was then becoming available to chemists:

> The surprisingly rapid development of our knowledge of the nature of atoms promises that in the not too distant future, it will be possible to develop an atomic-structural chemistry in which fundamental chemical properties of atoms, such as their affinities and valencies, will be explicable from their atomic structure.[7]

In the published version of the paper in 1917, the phrase "affinities and valencies" was accompanied by a footnote:

> To prevent misunderstandings the meaning of several words used here must be explained. Affinity is the expression for the firmness with which one element binds other elements or radicals (generally: "Ligands" (*ligare*[Latin], to bind); the introduction of a word hitherto lacking simplifies the manner of expression for this immediately clear concept).— Valence (*Valenz*) means the unit of force which can bind a univalent ligand; positive valencies bind nega-

tive ligands, negative valencies bind positive ligands.—Atomicity (*Wertigkeit*) is the number of valencies which an atom manifests; the highest atomicity is the highest number of valencies observed for an element.[8]

Thus Stock first coined "ligand" (Latin gerundive *ligandum*, "that should be bound") to fill the gap caused by the absence of a general term for the immediately clear concept of elements and radicals bound to another element.

Having made this clarification in the context of silicon chemistry—not, it should be stressed, in the context of Werner's coordination theory or in a discussion of inorganic complexes, Stock made no further use of the term ligand in the paper. Nor did he use it frequently in later experimental papers.[9] Although Stock's paper of 1917 was reviewed for the British Chemical Society in 1919,[10] the reviewer, E. C. C. Baly, drew no attention to the footnote; perhaps rightly, he was far more interested in Stock's preparation of, and proposed nomenclature for, the silanes.

Indeed, the word ligand seems to have been totally ignored by English-language chemists until the 1940s. It does not occur, for example, in either the first (1917) or second (1924) editions of the *German-English Dictionary for Chemists* by the American chemist and abstractor, Austin M. Patterson.[11] Furthermore, its adoption by coordination chemists in the 1950s evidently suggested to some of them that it was a term of recent vintage. In a monograph on chelating agents published in 1964, the Australian chemist D. P. Mellor dated "its introduction about 20 years ago," i.e. to about 1944.[12] As we shall see, Mellor was partly right. Similarly, although it does not purport to refer to the first recorded use of words, the *Oxford English Dictionary* cites a paper by Leslie E. Orgel published in 1952 as containing the word ligand.[13] Recent textbook writers are either content to define ligands as molecules coordinated to a central metal atom[14] or to use the term without any explanation.

How then did the word ligand come to be introduced into the English language? And how did it become a term particularly associated with Werner's chemistry of coordination compounds?

The classical textbooks of coordination chemistry by Werner, Urbain and Sénéchal, and Weinland[15] had no term corresponding to ligand (although Werner occasionally used "Addend"), probably because Werner's distinction between primary and secondary valencies made it difficult to consider all coordinated atoms or groups as equivalent. The widespread dissatisfaction with Werner's *Hauptvalenz* and *Nebenvalenz* acted as a strong deterrent to his entire theory for a number of years. A clear distinction between the two types of valence was not always possible, and a number of chemists considered the notion of primary and secondary valence bonds vague and unfounded.[16] Stock's proposal was not followed in the second edition of Weinland's book (1924) or in the fifth and final edition of Werner's *Neuere Anschauungen* edited by Paul Pfeiffer (1923).

However, during the 1920s the distinction between primary and secondary valencies disappeared—in Germany, through the elaboration of Walther Kossel's theory of electronic shells[17] by A. Magnus,[18] and in America and England through the atomic theories of G. N. Lewis[19] and N. V. Sidgwick.[20] In Germany a commission of the Deutsche Chemische Gesellschaft composed of R. Lorenz, R. J. Meyer, S. Meyer, P. Pfeiffer, A. Rosenheim and A. Stock was appointed to deal with the nomenclature of inorganic chemistry which had become confusing and troublesome. Its published rules[21] recommended that use of a Roman numeral (the Stock number[22]) to designate the "valence" (oxidation state) of an element. The complete German proposal, which was not published in German but is known from a French translation,[23] probably contained the term ligand to designate atoms, groups or molecules attached to a central atom—although it is absent in the preliminary version.[24] The proposal was submitted by Stock at the Hauptversammlung des Vereins deutscher Chemiker at Nürnberg in 1925, and one can deduce from the appearance of ligand in German literature since 1927 that the term was included in his report. The fourth edition of Ephraim's distinguished textbook, *Anorganische Chemie* (1929), adopted the word when introducing the elements of Periodic Group IV and referred to Stock explicitly as its originator.[25] According to Ephraim, echoing Stock, "Organic chemistry owes its diversity principally to the equal binding forces of the carbon atom towards the most dissimilar ligands". By 1930, therefore, the word ligand had become widely used in German publications,[26] including the monographs on stereochemistry by Stefan Goldschmidt and Freudenberg,[27] and was even adopted by the Japanese coordination chemist, Ryūtarō Tsuchida, when writing in English on spectrochemical series in a Japanese journal.[28] Due to the demonstration by Werner's former student and colleague, Paul Pfeiffer (1875–1951), that there was a close relationship between Werner's coordination theory and the structure of crystals as revealed by the then new experimental technique of X-ray diffraction,[29] one might have expected that geochemists and crystallographers would have used ligand at an early date. However, to take one example, the crystallographer, V. M. Goldschmidt, used instead the phrase "nächste Nachbarn" (nearest neighbours).[30]

Meanwhile, however, the international chemical community had moved along a different path. After the First World War the Union Internationale de Chimie Pure et Appliquée (UIC) was established, without Germany as a member, and with French as its official language. In 1921 the UIC appointed a Commission (with the Dutch chemist, W. P. Jorissen, as chairman) to deal with the nomenclature of inorganic chemistry.[31] At a meeting in 1926 the Commission discussed Werner's proposal[32] to use the endings -a, -o, -i, -e, -an, -on, -in, -en, to designate eight different valencies. Although this proposal had already been adopted officially by the previous international union (Association Internationale des Sociétés Chimiques) at a congress in 1913, it was rejected because grammatical and phonetic difficulties made it unacceptable in several languages, including English. Instead the Commission adopted the use of Stock numbers.[33] Following a further conference at Washington in 1926, a definite proposal was drawn up by Marcel Delépine and published by Jorissen in a Dutch journal.[34] The proposal contained detailed rules for naming coordination compounds by the use of Stock numbers; the term ligand was, however, not used.

After 1930, when Germany had been re-admitted to the UIC, a collaboration between the International and German Commissions on nomenclature was initiated, and a French translation (by Delépine) of the German proposal was published by R. J. Meyer.[35] In this there occurs the expression "ordre des constituants liés à

l'atome central"[36] as a rendering of the original "Reihenfolge der Liganden". Clearly, ligand was not acceptable as a French term.

At a further meeting in 1936, the International Commission, which now comprised H. Remy from Hamburg as the German representative, Jorissen, Delépine and Fichter (the English member, Clarence Smith, was absent), drafted a proposal which was finalised at a meeting in Berlin in 1938 and adopted at the Tenth Congress of the UIC at Rome in the same year. (Here A. Damiens and H. Bassett had replaced Delépine and Smith.) The German version was published in 1940 by Remy, who mentioned that Stock had been active in the German chemists' deliberations.[37] However, in translating this German report, Bassett, of the University of Reading, who perhaps showed a lack of linguistic instinct, rendered ligands as "attached atoms or groups",[38] just as the French had done in 1937. Although Bassett was not a coordination chemist, it is astonishing that he did not adopt ligand, the derivation of which from Latin ligare seems obvious.[39] No doubt he was affected by the outbreak of the Second World War, and the absence of the word in English textbooks,[40] Patterson's German–English Dictionary for Chemists,[41] and Chemical Abstracts.[42] Since Bassett's translation was used in the American version[43] with only minor amendments of spelling and footnotes, not surprisingly the word was omitted in Janet Scott's review of inorganic nomenclature published in 1943.[44] Similarly, the French version of the 1938 Rules avoided the term by rendering ligands as "radicaux".[45] The reluctance of English chemists to employ ligand is underlined by the use of the word groups in the English translation of Walter Hückel's important text, *Anorganische Strukturchemie*.[46]

On the other hand, there seems to have been less reluctance to take ligand into other languages either directly from German usage or from the German version of the 1938 Rules. For example, around 1935 K. A. Jensen introduced ligand into Danish, having learned the term from Pfeiffer's chapter on coordination chemistry in Freudenberg's *Stereochemie*.[47] After first using it in a paper on platinum complexes,[48] which he published in German, Jensen subsequently used it in Danish papers.[49] On Jensen's suggestion, Jannik Bjerrum (who became Jensen's colleague at the University of Copenhagen in 1936) adopted the word in 1941 in the context of discussions of stepwise equilibria, e.g. a "step system consisting of a central group M and n ligands A" and "ligand effect".[50] Although the two chemists used ligand freely in Danish and German conversations on coordination chemistry, Bjerrum was initially in doubt whether he could use ligand in English. However, Jensen assured him that because Stock's term was of Latin origin it could be used in any language. In this way, together with Tsuchida, Bjerrum became the first to use ligand in an English publication. His use of the term was also immediately accepted by some Swedish chemists[51] who were working in the same field.

Although in Brazil the German chemist Heinrich Rheinboldt, who was a Professor of Chemistry in São Paulo, introduced *ligante* into Portugese as a translation of ligand,[52] there seems to be no other language into which ligand has been taken from the German. The German version of the 1938 Rules was not translated into Russian. The word *addend*, which was in use in Russian chemistry around 1950, was obviously derived from Werner's *Neuere Anschauungen*. A little later the expression "addends or ligands" was used, for example in a book on coordination chemistry by Golovnya and Fedorov.[53] The Russian term "teoriya polya ligandov" has been used for "ligand field theory" since at least 1962.[54] Similarly, ligand did not appear in the huge Czech and Polish 6-language dictionaries published in the 1950s.[55] The former cites the German version of the 1938 Rules but uses the term "koordinované molekuly" for ligands. However, after 1960 ligand is used in Czech, Polish and Croatian. Clearly, its introduction into Slavic languages was due to the impact of the huge quantity of papers on coordination chemistry which were published in English during the early post-war years.

How then did *ligand* suddenly become so widespread in English? A decisive factor was undoubtedly the first post-war meeting in London in 1947 of the revived International Union, which was retitled the International Union of Pure and Applied Chemistry (IUPAC). Once again, nomenclature discussions were reopened by a Commission on the Nomenclature of Inorganic Chemistry, using the 1938 Rules as a starting point.[56] Although Bassett (who had replaced Jorissen as chairman) was not very happy with the proposal to adopt the continental nomenclature for coordination compounds, Niels Bjerrum[57] and K. A. Jensen, seconded by Bassett's secretary, R. V. G. Ewens, argued vigorously that the primary work of the Commission had to be an expansion of, and a more precise formulation of, the 1938 Rules. It followed that ligand should be used instead of expressions such as "attached groups and molecules". On the basis of this discussion Bassett and Ewens published a review paper[58] in 1949 in which ligand was used and which also contained the proposal (due to Ewens) to use the charge of the entire ion (later known as the Ewens–Bassett number) in cases where the central atom had no well-defined oxidation state.

Following further meetings of the Commission, a considerably extended set of rules for the nomenclature of inorganic chemistry was prepared and presented as "Tentative Rules" at a conference in Stockholm[59] in 1953. The contents of the new Rules were therefore known four years before they were finally adopted by the Council of the IUPAC at the conference in Paris in 1957 and published as "Nomenclature of Inorganic Chemistry 1957".[60]

The adoption of ligand into English by the IUPAC commission became immediately known to many chemists from the review paper by Ewens and Bassett[61] and by verbal information. However, the word ligand was already familiar to some English chemists—to those who worked with equilibria in solution from Bjerrum's thesis[62] and to those who worked with the preparation of coordination compounds of platinum and other transition metals from the German literature.[63] The effect of the IUPAC decision was primarily to reassure chemists that ligand would be an acceptable word in an English text. This is clearly demonstrated by the following fact: Bjerrum's English thesis exerted a great influence on coordination chemists working with the determination of stability constants. As has already been mentioned, the thesis induced Swedish chemists to use ligand, but chemists using English as their mother tongue accepted it only around 1949.[64]

The explosive dissemination of ligand during the 1950s can be explained as the result of a sort of branched chain reaction, the traces of which it is impossible to map out. It is reasonable to assume that the initiators were those

to whom the term was already familiar and who used ligand in their lectures and discussions. The foci for the dissemination of ligand in English were apparently University College, London, The Butterwick Research Laboratories, Welwyn, and the laboratory for inorganic chemistry at the University of Oxford. By communication between supervisor and student and between authors, referees and editors, the term became employed in a great number of English and American papers, in what Nyholm described as "The Renaissance of Inorganic Chemistry",[65] and from these it spread into other languages. The first two coordination chemistry conferences, at Welwyn in September 1950[66] and Copenhagen in August 1953,[67] undoubtedly did much to make the term familiar. In a lecture for the American Chemical Society in 1951 Fernelius stated "The coordinated ions or molecules have been referred to as ligands or ligates, addenda, and adducts", but his preference is evident from the text that follows where he employs ligand (together with "coordinated group").[68] Thus the term ligand was in widespread use even before the Stockholm conference in 1953.

At this time, too, ligand became frequently used in the context of "ligand field theory"—an expression first appearing in print in 1954 in the published version of the paper delivered by L. E. Orgel and L. E. Sutton at the Copenhagen meeting.[69] At the Solvay meeting in Brussels in May 1956, J. Bjerrum, C. K. Jørgensen, R. S. Nyholm and L. E. Orgel discussed the advantages of using "ligand field theory", and under what conditions.[70]

After Jannik Bjerrum had been appointed a full Professor in Copenhagen in 1948, he had a great number of American and Danish chemists working very intensely on· coordination chemistry, and several important publications in English[71] combined to make the term ligand known, and his American students brought it to the U.S.A. R. S. Nyholm, who attended the Welwyn Conference as an ICI Fellow, probably brought the term ligand to Australia on his return there the same year. At a meeting on coordination chemistry in Sydney[72] in 1953, Nyholm read a paper entitled "Nature of the Metal-Ligand Bond in Complex Compounds", leading his countryman, D. P. Mellor, to comment that "The use of the anything but euphonious term 'ligand' to designate the atom, group of atoms, or molecule attached to the central metal atom has now become so widespread that it is not likely to be abandoned."

CONCLUSIONS

As Crosland has noted in connection with organic nomenclature, "The establishment of any system of nomenclature presupposes the authority of an individual or group to impose such a system."[73] Partly because the phenomenon of isomerism forced attention on the problems of indexing compounds very early, organic chemists seem to have found international co-operation comparatively straightforward. (The Geneva Rules of 1892 were revised at Liège in 1930.) Conversely, as Fernelius has noted, since inorganic chemistry lacked "the barrier to mutual understanding" which the large numbers of compounds raised for organic chemistry, the inorganic nomenclature commission set up in 1919 "had to pioneer for such co-operative effort",[74] its communications and authority being hampered by the aftermath of the First World War and the disruption caused by the Second World War, when agreement might otherwise have been reached.[75]

By expressing in a non-committal way that something is "bound" to a central atom, ligand could be used in abstract papers without implying adherence to misleading metaphorical images. Its strength lay in its ready extension into combinations such as "ligand field", "ligand effect", or transformations such as "ligancy". Moreover, as we have seen, the term's Latin origin meant that it could be used in most Indo-European languages with no, or only minor, changes (see Appendix). Hence its adoption in influential post-war papers and its acceptance by the IUPAC Nomenclature Commission in 1947 were probably momentous for its acceptance by languages other than German.

REFERENCES

[1] Translation by W.H.B., *Méthode de Nomenclature Chimique*, p. 13. Paris (1787).
[2] T. H. Savory, *The Language of Science*, p. 46. London (1953).
[3] A. Laurent, *Chemical Method, Notation, Classification and Nomenclature*, transl. by W. Odling. London (1855); C. B. Mansfield (posth.), *A Theory of Salts: A Treatise on the Constitution of Bipolar (Two-Membered) Chemical Compounds*. London (1865). Other examples are the organic nomenclature systems of C. I. Istrati, G. Siboni and T. Sherlock Wheeler discussed by P. E. Verkade, Etudes historiques sur la nomenclature de chimie organique. *Bull. Soc. Chim. Fr.* 1966, 1807; 1968, 1358; 1969, 4297.
[4] In inorganic compounds it is generally possible in a polyatomic group to indicate a *characteristic atom* (as in ClO^-) or a *central atom* (as in ICl_4^-). Such a polyatomic group is designated as a *complex*, and the atoms, radicals, or molecules bound to the characteristic or central atom are termed *ligands*. Rule 2.24, International Union of Pure and Applied Chemistry, *Nomenclature of Inorganic Chemistry*, p. 18. London (1959), 2nd Edn 1971, p. 15. See also *Handbook for Chemical Society Authors*, p. 21. Chemical Society, London (1960). For an example of organic usage, see L. F. Fieser, *Advanced Organic Chemistry*, p. 484. London (1961) ("a central phosphorus atom surrounded by complexing phenyl groups as ligands").
[5] K. A. Jensen, Problems of an international chemical nomenclature. *Advances in Chemistry Series*, No. 8, pp. 38–48. American Chemical Society, Washington, D.C.. (1953). By adopting metaphorical English terms such as "charm" and "strangeness", theoretical physicists have broken this rule and consequently caused difficulties for non-English languages. For an amusing example, see N. D. Mermin, E Pluribus Boojum: the Physicist as Neologist. *Physics Today*, 1981, **34**, 46–53. See also W. Conrad Fernelius, The Nomenclature of coordination compounds from pre-Werner times to the 1966 IUPAC Report. In George B. Kauffman (ed.), *Werner Centennial*, pp. 147–160. American Chemical Society, Washington, D.C. (1967).
[6] F. Wöhler and H. Buff, Ueber eine Verbindung von Silicium mit Wasserstoff. *Ann. Chem.* 1857, **103**, 218–229. See also *ibid.*, 1857, **104**, 94–109.
[7] Alfred Stock, Siliciumchemie und Kohlenstoffchemie. *Ber. dtsch. chem. Ges.* 1917, **50**, 170–182. For an obituary of Stock, see Egon Wiberg, *Chem. Ber.* 1950, **83**, XIX–LXVIII.

[8]Stock, op. cit. (7), p. 170, footnote. Translations by W.H.B.

[9]For a later example, see A. Stock, Borwasserstoffe, XI. Strukturformeln der Borhydride. Ber. dtsch. chem. Ges. 1926, 59, 2226–2229, esp. p. 2228: Augenscheinlich kann es auch dreiwertig sein, so wie es negativen Liganden gegenüber (B_2O_3, BF_3, $B_2(NH)_3$ u.s.w.) und auch in den B-Alkylen ($B(CH_3)_3$) dreiwertig ist. Stock did not use the word in Alfred Stock, Ultra-Strukturchemie, Berlin, 1920 (The structure of Atoms, trans. by S. Sugden, London, 1923).

[10]Annual Reports of the Chemical Society (for 1918), pp. 36–37. London (1919).

[11]A. M. Patterson, A German–English Dictionary for Chemists, New York (1917); 2nd Edn. New York (1924). The word is entered and defined in the 3rd Edn. New York (1950). However, since there were innumerable printings during the 1930s and 1940s, each containing small amendments, there is a possibility of an earlier definition. We thank Dr. Leslie E. Sutton and Prof. J. Chatt for this reference.

[12]D. P. Mellor, Historical background and fundamental concepts. In F. P. Dwyer and D. P. Mellor (Eds), Chelating Agents and Metal Chelates, p. 2. New York and London (1964). Dwyer died prior to publication. Curiously the term "chelate" (Greek, chela, a crab's or lobster's claw) for complex compounds in which the central metal atom is attached to a single organic molecule by two (later, more) bonds, which was introduced by Morgan and Drew in 1920, was quickly adopted internationally. See G. T. Morgan and H. D. K. Drew, J. Chem. Soc. 1920, 117, 1456.

[13]Oxford English Dictionary. Supplement, Vol. 2, p. 669 (Oxford), referring to L. E. Orgel, The effect of crystal fields on the properties of transition metal ions. J. Chem. Soc. 1952, 4756–4761, 4757.

[14]E.g. F. Basolo and R. Johnson, Coordination Chemistry, p. 9. New York and Amsterdam (1964); B. E. Douglas and D. H. McDaniel, Concepts and Models of Inorganic Chemistry. New York and London (1965); C. S. G. Phillips and R. J. P. Williams, Inorganic Chemistry, Oxford (1965); F. A. Cotton and G. Wilkinson, Advanced Inorganic Chemistry. New York (1962); K. M. MacKay and R. Ann MacKay, Modern Inorganic Chemistry. London (1968); L. E. Orgel, An Introduction to Transition Metal Chemistry. Ligand Field Theory. New York (1960).

[15]A. Werner, Neuere Anschauungen auf dem Gebiete der anorganischen Chemie. Braunschweig (1905) (Werner often uses the verb "addieren" and the noun "Addition", and occasionally the term "Addenden", e.g. p. 45); G. Urbain and A. Sénéchal, Introduction à la Chimie des Complexes. Paris (1913); R. Weinland, Einführung in die Chemie der Komplex-Verbindungen (Werner Koordinationslehre) in elementarer Darstellung. Stuttgart (1919), 2nd Edn. Stuttgart (1924). Note also the absence in P. Pfeiffer, Organische Molekülverbindungen, 2nd Edn. Stuttgart (1927); G. Urbain, La Coordination des Atomes dans la Molécule et la Symbolique Chimique. Paris (1933).

[16]Werner was never satisfied with his artificial valence dichotomy, which he always regarded as tentative (vorläufig) and purely formal, and he sometimes wrote formulae without distinguishing the two types of valence. In an address before the British Association for the Advancement of Science at Leicester, he stated:

> If . . . the distinction between principal and auxiliary bonds and principal and auxiliary valencies is kept up, it is because it seems necessary, in view of the present transitional state of the doctrine of valency, to construct sharply defined partial conceptions which can afterwards serve as the foundation stones of a more comprehensive conception of valency ("Valency", Chemical News 1907, 96, 128–131).

See G. Schwarzenbach, Die Entwicklung der Valenzlehre und Alfred Werner, Experientia 1966, 22, 633–646 and Alfred Werner and his accomplishments. In Fasciculus Extraordinarius Alfred Werner 1866–1919, pp. 38–63. Basel (1967).

[17]W. Kossel, Ann. d. Phys. 1916, 49, 229–362.

[18]A. Magnus, Z. Anorg. Allg. Chem. 1927, 124, 289–321.

[19]G. N. Lewis, Valence and tautomerism. J. Am. Chem. Soc. 1913, 35, 1448–1455; The atom and the molecule. ibid. 1916, 33, 762–785; Valence and the Structure of Atoms and Molecules. New York (1923); reprinted 1966.

[20]N. V. Sidgwick, Co-ordination compounds and the Bohr atom. J. Chem. Soc. 1923, 123, 725–730. For an annotated version of this article see G. B. Kauffman, Classics in Coordination Chemistry, Part 3: Twentieth-Century Papers (1904–1935), pp. 132–142. New York (1968). See also Sidgwick's The Electronic Theory of Valency. London (1927). Sidgwick's systematic application of Lewis' "dative bond" to coordination compounds made chemists realize its widespread importance. Sidgwick never used ligand either at this time or later (but see note 66 below), referring instead to "groups" and "co-ordinate links", the term "link" meaning "bond" and having no linguistic connection with ligand through the Latin. We thank Dr. L. E. Sutton for confirming that Sidgwick did not use ligand. See Sutton's notice of Sidgwick in C. C. Gillispie (Ed.), Dictionary of Scientific Biography, Vol. 12, pp. 418–420. New York (1975).

[21]R. J. Meyer and A. Rosenheim, Z. Angew. Chem. 1925, 38, 713–715; R. J. Meyer, ibid. 1929, 42, 1059–1062.

[22]A. Stock, Z. Angew. Chem. 1919, 32, 373–374; ibid. 1934, 47, 568.

[23]See note 35 below.

[24]See note 21.

[25]F. Ephraim, Anorganische Chemie, 4th Edn, p. 651. Dresden and Leipzig (1929).

[26]Notably through the frequently-cited paper by W. Biltz, ". . . Natur des Lutepkomplexes," Z. Anorg. Allg. Chem. 1927, 164, 245–255, 251. In this paper Biltz distinguished between normal and penetration complexes. See also W. Klemm, H. Jacobi and W. Tilk, Über den magnetismus eininger carbonyle und anderer komplexverbindungen der eisengruppe. Z. Anorg. Allg. Chem. 1931, 201, 1–23, p. 2. We thank Professor Jannik Bjerrum for these references.

[27]S. Goldschmidt, Stereochemie, Leipzig, 1933 (chapter headings: "Elemente mit zwei und drei Liganden", etc.); P. Pfeiffer, Komplexverbindungen. In K. Freudenberg (Ed.), Stereochemie: Eine Zusammenfassung der Ergebnisse, Grundlagen und Probleme, pp. 1200–1377. Leipzig and Wien (1933).

[28]R. Tsuchida, Absorption spectra of co-ordination compounds. Bull. Chem. Soc. Japan 1938, 13, 388–401. See also note 90 below. In a footnote (p. 388) Tsuchida stated: "the word ligand will be used in its original German sense, i.e. an ion or a molecule co-ordinated in a complex radical".

[29]P. Pfeiffer, Die Kristalle als Molekülverbindungen. Z. Anorg. Allg. Chem. 1915, 92, 376–380; annotated and translated by George B. Kauffman, J. Chem. Educ. 1973, 50, 279–280. See G. B. Kauffman, Crystals as molecular compounds: Paul Pfeiffer's application of coordination chemistry to crystallography. J. Chem. Educ. 1973, 50, 277–278.

[30]V. M. Goldschmidt, Kristallographie und Stereochemie anorganischer Verbindungen. Chap. II of Freudenberg, op. cit. (27), 17–82; V. M. Goldschmidt, Kristallbau und chemische Zusammensetzung. Ber. dtsch. chem. Ges. 1927, 60, 1263–1296.

[31]Comptes Rendus de la Deuxième Conférence Internationale de la Chimie. Bruxelles (1921).

[32]A. Werner, Neuere Anschauungen (note 15), 5th posthumous ed. (Edited by Paul Pfeiffer), p. 83. Braunschweig (1923).

[33]Rapport du Comité de travail de réforme de la nomenclature de chimie minérale, Paris (1926). English translation in Chem. Weekbl. 1926, 23, 86–93.

[34]Commission de réforme de la nomenclature de chimie minérale. Rapport de M. Marcel Delépine, Recl. Trav. Chim. Pays-Bas 1929, 48, 652–663.

[35]R. J. Meyer, Rapport sur la nomenclature des combinations inorganiques. Helv. Chim. Acta 1937, 20, 159–175; English version Chem. Weekbl. 1936, 33, 722–729.

[36]Helv. Chim. Acta, 1937, 20, 171. "Reihenfolge der Liganden" is added in parenthesis after "ordre des constituants liés à l'atome central".

[37]I.U.C. Kommission für die Reform der Nomenclature der anorganischen Chemie: Richtsätze für die Benennung anorganischer Verbindungen. Ber. dtsch. Chem. Ges. 1940, 73A,

53–70. Remy also published an historical account of the 1938 Rules in 1942. See his "Die Richtsätze für die Benennung anorganischer Verbindungen. *Die Chemie* 1942, **55**, 267.

[38]W. P. Jorissen, H. Bassett, A. Damiens, F. Fichter and H. Remy, Rules for naming inorganic compounds: report of the committee for the reform of inorganic chemical nomenclature, 1940. *J. Chem. Soc.* 1940, 1404–1415. Because of the publication date, these are often called the 1940 Rules.

[39]Other, later, derivations were ligancy (see Linus Pauling, *The Nature of the Chemical Bond*, 3rd Edn, p. 2. Cornell University Press (1960) and R. S. Cahn, Sir Christopher K. Ingold and V. Prelog, Specification of molecular *chirality*. *Angew. Chem. Intern. Ed.* 1966, **5**, 386); and *ligate* (Cahn, Ingolb and Prelog, p. 386).

[40]In H. J. Eméleus and J. S. Anderson, *Modern Aspects of Inorganic Chemistry*, which was first published in 1938 and which in its several later unrevised impressions exerted a tremendous influence on post-World War II British chemistry students, the term ligand was not used until the 1960 edition. This refers (p. 115) to "so-called ligands". We owe this information to Professor J. Chatt, who adds: It seems that the name ligand was not familiar to main group chemists even then". Ligand was also notably absent in the work of American coordination chemists, e.g. John C. Bailar, Jr., The stereochemistry of complex inorganic compounds. *Chem. Rev.* 1936, **19**, 67–87, and Symposium on complex inorganic compounds: introduction to the symposium, *Ibid.* 1937, **21**, 1–2; M. J. Copley, L. S. Foster and J. C. Bailar, Jr., The stabilization of valences by coordination. *ibid.* 1942, **30**, 227–238; N. F. Hall, The acid-base properties of complex ions. *ibid.* 1936, **19**, 89–99; H. Diehl, The chelate rings. *ibid.* 1937, **21**, 39–111. Diehl writes only of "unidentate" and "bidentate groups" (dentate from Latin *dens* = tooth).

Finally, despite the fact that directions for the preparation of coordination compounds occur fairly frequently in the first five volumes of the journal of procedures, *Inorganic Syntheses* (Vol. 1, Ed., H. S. Booth, 1939; Vol. 2, Ed., W. C. Fernelius, 1946; Vol. 3, Ed., L. F. Audrieth, 1950; Vol. 4, Ed., J. C. Bailar, Jr., 1953; Vol. 5, Ed., T. Moeller, 1957), the term ligand does not appear until Vol. 6, 1960 (see pp. 67, 74, 176, 198).

[41]See note 11.

[42]That the term was still not used in the Fifth Decennial Index (1947–56) is perhaps more an indication that abstracts are better for locating compounds than concepts. The word finally appeared in the Sixth Collective Index (1957–61). See, however, note 62 below.

[43]*J. Am. Chem. Soc.* 1941, **63**, 889–897.

[44]J. D. Scott, Notes on the nomenclature of inorganic compounds, *Inorganic Syntheses* 1946, **2**, 257–267 ("Attached groups", p. 262). Her earlier, lengthier report, The need for reform in inorganic chemical nomenclature. *Chem. Rev.* 1943, **32**, 73–97 also avoids the term ("coordinating groups", p. 88), though she hailed the 1940 Report as a "giant stride towards improved and internationally standized nomenclature". Both reports arose from an interest in nomenclature at Ohio State University where *Chemical Abstracts* were produced and where Fernelius was editing *Inorganic Syntheses*, Vol. 2 (letter W. Conrad Fernelius, 9 February 1981). See W. C. Fernelius *et al.*, *Chem. Eng. News* 1948, **26**, 520–523.

[45]*Bull. Soc. Chim. Fr.*, 1941, 814–830.

[46]W. Hückel, *Anorganische Strukturchemie*, Stuttgart, 1948; Hückel's English translator, L. H. Long of Exeter University College, used the terminology of groups in *Structural Chemistry of Inorganic Compounds*, I–II, New York, Amsterdam, London and Brussels, 2 Vols., 1950, Vol. 1, pp. 54–55. Note also F. Hein, *Chemische Koordinationslehre*, Zürich, 1950, p. 11. The latter was known to R. G. Wilkins (see note 66).

[47]Pfeiffer (note 27).

[48]K. A. Jensen, Dipolmessungen an isomeren platokomplexen. *Z. Anorg. Allg. Chem.* 1935, **225**, 97–141 (p. 97).

[49]E.g. K. A. Jensen, *Om de Koordinativt firegyldige Metallers Stereokemi* (Stereochemistry of coordinatively 4-valent metals), Copenhagen (1937).

[50]J. Bjerrum, *Metal Ammine Formation in Aqueous Solution:*

Theory of Reversible Step Reactions, Copenhagen (1941); 2nd Edn. appeared in 1957.

[51]L. G. Sillén and B. Liljequist, *Sven. Kem. Tidskr.* 1944, **56**, 85–95 (p. 85); I. Leden, *ibid.* 1946, **58**, 129–144 (p. 132).

[52]H. Rheinboldt and H. Vieira de Campos, *Nomenclatura e Notacão de Química Inorganica*, São Paulo, 1954. However, in the translation of the IUPAC Rules of 1957 into European Portuguese, ligand was rendered as *ligando*. See *Rev. Port. Quim.* 1965, **7**, 32–63.

[53]V. A. Golovnya and I. A. Fedorov, *Osnovnye Ponyatiya Khimii Kompleksnykh Soedinenii*. Moscow (1961).

[54]I. B. Bersuker and A. V. Ablov, *Khimicheskaya Svyaz v Kompleksnykh Soedineniyakh*, Kishinev (1962). (Teoriya polya ligandov, pp. 58–85.)

[55]E. Votoček, *Chemický Slovník*. Prague (1952); Z. Sobecka, W. Choinski and P. Majorek, *Dictionary of Chemistry and Chemical Technology*. Oxford (1966). However, in an English–Polish Chemical Dictionary, edited by D. Kryt (Warsaw, 1964), the Polish word for ligand is given as "ligand, addent".

[56]At the meeting in 1947 the only member present from the old commission was Bassett. Some new members had been appointed by national delegations, but only A. Silverman and A. Ölander continued as members. The young British chemist, R. V. G. Ewens (who was killed in a railway accident in 1948), served as secretary. Niels Bjerrum and K. A. Jensen, who were present only as observers, were elected titular members at the following meeting (Amsterdam, 1949), together with J. Bénard, E. H. Buchner and G. H. Cheesman. At subsequent meetings between 1951 and 1955, W. Feitknecht, L. Malatesta and H. Remy became members of the commission which was finally responsible for the 1957 Rules.

[57]G. B. Kauffman, Niels Bjerrum (1879–1958): a centennial evaluation. *J. Chem. Educ.* 1980, **57**, 779–782, 863–867.

[58]R. V. G. Ewens and H. Bassett, Inorganic chemical nomenclature. *Chemistry and Industry* 1949, 131–139.

[59]*Comptes Rendus de la Dix-Septième Conférence*, Stockholm, 1953 (English text, pp. 98–119, with ligand, pp. 108–109). The Dutch member, E. H. Buchner, published a Dutch translation in *Chem. Weekbl.* 1955, **51**, 295–310. *Ligand* also appears in the "Editorial Report on Nomenclature, 1953", *J. Chem. Soc.* 1953, Part IV, p. 4201–4205, without comment, although it had not been used in earlier reports.

[60]This is often called "The Red Book". International Union of Pure and Applied Chemistry. *Nomenclature of Inorganic Chemistry*, 1957, London (1959); 2nd ed. (1970 Rules), 1971.

[61]Ewens and Bassett, *op. cit.* (58).

[62]Bjerrum's thesis was abstracted for *Chemical Abstracts* 1941, **35**, 6527–6534, by J. P. McReynolds at Ohio State University, where it attracted much interest (letter from W. Conrad Fernelius, 9 February 1981). The term ligand is used repeatedly in the abstract.

[63]E.g. R. S. Nyholm, Studies in coordination chemistry, Parts I–IV, *J. Chem. Soc.* 1950, 843–859.

[64]E.g. from the Inorganic Chemistry Laboratory at Oxford, H. Irving and R. J. P. Williams, On the order of stability of metal complexes. *Nature* 1948, **162**, 746, which is the first use of ligand in a British paper known to us. According to Prof. R. J. P. Williams, Prof. Irving adopted the term from Bjerrum's thesis.

[65]R. S. Nyholm, *The Renaissance of Inorganic Chemistry*, an inaugural lecture, University College, London (1956). Reprinted in Aaron J. Ihde and W. F. Kieffer (Eds.), *Selected Readings in the History of Chemistry*, pp. 181–184, Easton, Pa. (1965), from *J. Chem. Educ.* 1957, **34**, 166–169.

[66]Imperial Chemical Industries, *A Discussion on Coordination Chemistry*. Butterwick Research Laboratories Report No. BRL/146, The Frythe, Welwyn, Herts., 1951 (typescript prepared by J. Chatt and R. G. Wilkins). Ligand was used in six of the eleven lectures as well as in discussion. The participants included N. V. Sidgwick, H. Irving, G. Schwarzenbach, A. F. Wells, R. S. Nyholm, J. Chatt, R. G. Wilkins, K. A. Jensen, L. E. Orgel and L. E. Sutton. Sidgwick's remarks in discussion, in which *ligand* is used, were probably the subject of editing. See note 20.

[67]*Proceedings of the Symposium on Co-ordination Chemistry*,

Copenhagen, 1953. Danish Chemical Society, 1954. The word ligand was used in 17 of the 34 papers presented at this meeting: Danish: J. Bjerrum (pp. 35 and 51), J. Koefoed (p. 41), and K. A. Jensen (p. 119); German: O. Schmitz-Du Mont (p. 55), W. Klemm (p. 97), and K. Gleu (p. 126); Swedish: Sture Fronaeus (p. 63), I. Leden (p. 79), and D. Dyrssen (p. 133); Dutch: van Panthaleon van Eck (p. 67); Austrian: Nelly Konopik (p. 108); English: L. E. Orgel and L. E. Sutton (p. 21), P. George (p. 56), R. J. P. Williams (p. 68), N. N. Greenwood (p. 101), and J. Chatt (p. 115); American: A. W. Adamson (p. 49).

[68]W. Conrad Fernelius, Nomenclature of coordination compounds and its relation to general inorganic nomenclature. *Chemical Nomenclature*, p. 9. Advances in Chemistry Series, American Chemical Society (1953). The term "aducts" was Werner's. Despite Fernelius's support for *ligand* in his review it was not adopted in the influential college text, T. Moeller, *Inorganic Chemistry*. New York and London (1952). Pauling did not use the terms ligand or ligancy in print before 1945. J. C. Bailar, Jr. used terms like "donor molecule" (e.g. *J. Am. Chem. Soc.* 1953, **75**, 4574–4575) and "coordinating agent" (e.g. *ibid.* 1952, **74**, 3131–3134, 3535–3538), adopting ligand only in 1954 (*ibid.* 1954, **76**, 4051–4052).

[69]L. E. Orgel and L. E. Sutton, Factors determining the stability of complexes. *Proceedings* (note 67), pp. 17–24. As the report of the "Discussion" (p. 24) makes clear, the paper was revised for publication by Sutton, and papers published by Orgel during 1955 continued to use the term "crystal field". (See Spectra of transition-metal complexes. *J. Chem. Phys.* (June 1955), **23**, 1004–1014 which was submitted 11 October 1954; and Electronic structures of transition-metal complexes. *ibid.* (Oct. 1955), **23**, 819–823 which was submitted 28 December 1954). In an important paper entitled Ligand field theory, J. S. Griffith and L. E. Orgel stated: "We regard them both [i.e. crystal field and molecular orbital theory] as expressing certain aspects of a more complete theory which we call ligand field theory. *Quart. Rev.* 1957, **11**, 381–393.

[70]*Quelque Problèmes de Chimie Minérale*, 10. Conseil de Chimie Solvay, Bruxelles, 1956, p. 233, Nyholm's recommendation citing Orgel and Sutton's Copenhagen paper (note 67). Approval of the term came from Orgel himself (p. 314), J. Bjerrum (p. 339) and C. K. Jørgensen (p. 348). According to C. K. Jørgensen, Comparative ligand field studies. *Acta Chem. Scand* 1957, **11**, 53–72 submitted August 1956, "Orgel, Nyholm, J. Bjerrum and the present author proposed at the Xth Solvay Conference, Bruxelles, May 1956, to use the word 'ligand field theory' to denote the crystal field theory extended with the molecular orbital theory for partly intermixing with the orbitals of the ligands, when applied especially to the action of the first coordination sphere on the partly filled *d*-shell in a transition group complex" (p. 53, note). Hence it was at the Solvay meeting that the use of the term was defined.

[71]J. Bjerrum, Tendency of the metal ions towards complex formation. *Chem. Rev.* 1950, **46**, 381–401; J. Bjerrum and C. G. Lamm, Metal ammine formation in solution. VIII. Cupric pentammine formation with *n*-butylamine. *Acta Chem. Scand.* 1950, **4**, 997–1004; C. K. Jørgensen, Comparative crystal field studies of some ligands and the lowest singlet state of paramagnetic nickel (II) complexes. *Acta Chem. Scand* 1955, **9**, 1362–1377. Bjerrum's American visitors included F. A. Cotton, G. Wilkinson, A. W. Adamson and F. Basolo.

[72]A Conference on coordination chemistry, Sydney, May 1953. *Rev. Pure Appl. Chem.* 1954, **4**, 1–110. (R. S. Nyholm, pp. 15–40; D. P. Mellor, p. 47). For Nyholm (1917–71), see *Chem. Brit.*, August 1972, p. 341.

[73]M. P. Crosland, *Historical Studies in the Language of Chemistry*. London, Melbourne, Toronto (1962), p. 338; reprinted, Dover Books (1978).

[74]Fernelius (ref. 5), pp. 150–151.
[75]Jensen (ref. 5), p. 38.
[76]*Chem. Listý*, 1972, **66**, 1049–1089; 1973, **67**, 44–85, 197–208.
[77]*Dansk Kemi*, 1966, **47**, 97–109.
[78]*Mededel. Vlaam. Chem. Ver.* 1962, **24**, 107–166.
[79]*Bull. Soc. Chim. Fr.*, February 1975, numéro spécial.
[80]*Richtsätze für die Nomenklatur der anorganischen Chemie.* Verlag Chemie, Weinheim (1970).
[81]*A Magyar kémiai elnevesés és helyesirds szabályai*, Budapest, 1972, Vol. 1, pp. 17–109.
[82]*Annali di Chimica* 1959, **49**, 663–701; *Gazz. chim. ital.* 1959, **89**, 1243.
[83]Title, with Japanese Ideographs (read: *Muki Kagaku Meineiho*). 1957 Rules (1961), 1970 Rules (1977).
[84]Norwegian Chemical Society, *Retningslinjer for norganiskk-jemisk nomenklatur* (1966).
[85]See Ref. 52.
[86]*Nomenclatura chimiei anorganice după regulite elaborate de Uniane Internationalĕ de Chimie Purӑ si Aplicatӑ*, Bucharest (1977).
[87]*Rev. Soc. Quim. Mex.* 1967, **11**, 42–48; 1968, **12**, 265A–270A; 1969, **13**, 139B–143B, 277B–279B. J. Rodriguez Fernandez *et al.*, *Nomenclature de Compuestos Inorganicos*, Oviedo, 1972.
[88]*Svem. Kem. Tidskr.* 1960, **72**, 419–486.
[89]*Nomenklaturnye Pravila IYuPAK po Khimii*, Tom. 1, Polutom 1, *Neorganicheskaya khimiya, Fizicheskaya khimiya, Analiticheskaya khimiya*, Moscow, 1979.
[90]Personal communication from Professor Kazuo Yamasaki. See Ryütarö Tsuchida, *Nippon Kagaku Kaishi* 1938, **59**, 586.
[91]*Terminológia anorganickej a fyzikálnej chémie*, Slovenská Adakémia Vied, Bratislava (1956).
[92]J. Hanzlik and J. Klikorka, *Chem. Listý* 1972, **66**, 1045–1048.

APPENDIX

The adoption of ligand in other languages

The 1957 Nomenclature Rules and/or the revised 1970 Rules were translated into several languages: Czech,[76] Danish,[77] Dutch,[78] French,[79] German,[80] Hungarian,[81] Italian,[82] Japanese,[83] Norwegian,[84] Portugese,[85] Romanian,[86] Spanish,[87] Swedish,[83] and Russian.[89] The respective national committes had, therefore, to make a decision which word they would use for ligand in their languages. In most cases ligand was used with only small changes (often only of the plural form). In Japanese the word "hai-i shi" (coordinating entity or body) was retained for ligand. Yuji Shibata (1882–1980), who had studied under Werner at Zürich in 1911–1912, introduced the term "hai-i ki" (coordinating radical) in 1929. This was altered to "hai-i shi" by Shibata's student, Tsuchida, in 1938.[90] Examples are:

ligand (ligands)	English, French
ligand (liganden)	Dutch, German
ligand (ligander)	Danish, Norwegian, Swedish
ligand (ligandy)	Czech, Polish, Russian
ligando (ligandos)	Portuguese, Spanish
ligandum (ligandumok)	Hungarian
ligante (ligantes)	Spanish, Brazilian Portuguese
legante (leganti)	Italian
ligand (liganzi)	Romanian

Most languages (including Japanese) have also adopted Stock numbers, the only exceptions being Czech and Slovak,[91] where a very old system devised by J. S. Presl in 1828 has been retained.[92] In this system various valences are expressed by suffixes (manganity, manganisty, manganovy, etc.).

EFFECT OF ADDED SALTS ON THE RATES OF DISSOCIATION AND RACEMIZATION OF TRIS(1,10-PHENANTHROLINE)IRON(II) ION IN AQUEOUS METHANOL SOLUTIONS

SATOSHI TACHIYASHIKI*

Laboratory of Chemistry, Kagawa Nutrition College, Sakado, Saitama, 350-02, Japan

and

HIDEO YAMATERA

Department of Chemistry, Faculty of Science, Nagoya University, Chikusa-ku, Nagoya, 464, Japan

Abstract—The kinetics of dissociation and racemization of $[Fe(phen)_3]^{2+}$ have been studied in aqueous methanol solutions containing perchlorate, chloride, and thiocyanate ions. The racemization rate was decreased by ClO_4^- and increased by SCN^-, while the dissociation rate was decreased by ClO_4^- and increased slightly by Cl^- and remarkably by SCN^-. The effect of anions on the reaction rates became remarkable with the increase in methanol content of the solutions. The results were reasonably explained in terms of ion association. The dissociation rate of the complex ion in the ion-pair increased in the order, $ClO_4^- < Cl^- < SCN^-$, of associated anions, suggesting the ion-pair interchange mechanism for the dissociation. The ion-association constants were determined to be 11 ± 4, 18 ± 4, and 25 ± 15 ($I = 0.1$, 25°C) for ClO_4^-, Cl^-, and SCN^-, respectively, in 0.64 mole-fraction (0.8 volume-fraction) aqueous methanol.

INTRODUCTION

The kinetics of dissociation of $[Fe(phen)_3]^{2+}$ and $[Fe(bpy)_3]^{2+}$ have been studied extensively, and the effect of added salts on the reaction rates has been discussed in terms of ion-pair formation in aqueous[1] and non-aqueous[2,3] solutions. Blandamer *et al.*[4] studied the kinetics of the reactions of $[Fe(bpy)_3]^{2+}$ with cyanide and hydroxide ions in binary aqueous solvent mixtures. On the standpoint of associative mechanism they have concluded that the chemical potential changes of anions with the change in solvent composition were dominant in determining reactivities in their reaction with $[Fe(bpy)_3]^{2+}$.

We previously studied the effect of various inorganic anions on the rates of dissociation and racemization of $[Fe(phen)_3]^{2+}$ in aqueous solutions.[1] We analyzed the experimental results considering the ion-pair formation of the complex ion with an anion, and found the following trends. (1) The dissociation rate constant of the complex existing in the ion-pair increases with the increase in proton affinity (basicity) of the anion: $I^- < Br^- < Cl^- < NO_2^- < OCN^- < N_3^- < F^- < OH^- \simeq CN^-$. (2) The intramolecular racemization rate constant, given by apparent racemization rate constant minus dissociation rate constant, increases with the increase in polarizability (softness) of the anion: $OH^- \simeq CN^- \simeq F^- \simeq Cl^- < Br^- \simeq NO_2^- < OCN^- < I^- < N_3^-$. We thought it desirable to extend the study to include the systems containing perchlorate, which is one of the hardest, least basic anions, and thiocyanate, which is a very soft anion. However, the effects of these anions were difficult to measure in aqueous solution because of the low solubility of $[Fe(phen)_3]^{2+}$ in the presence of these anions;

only the effect of the thiocyanate ions on the racemization rate were measured in supersaturated solutions.

In the present study, the effects of perchlorate and thiocyanate ions on the dissociation and racemization of $[Fe(phen)_3]^{2+}$ were investigated in aqueous methanol solutions. It was also our object to study the solvent effect on the rates of dissociation and to see whether or not the reactions in aqueous methanol solutions can be explained by the same mechanism as in aqueous solutions.

EXPERIMENTAL

The dissociation and racemization rates were obtained respectively from the changes in absorbance (510 nm) and optical rotation (546 nm) of the solution containing 5×10^{-5} mol dm^{-3} $[Fe(phen)_3]$ $(ClO_4)_2$ in a thermostated (± 0.1°C) quartz cell. In measuring the dissociation rate of the complex, 3.1×10^{-4} mol dm^{-3} nickel(II) perchlorate was added to the sample solution except for the cases where the concentration of the nickel(II) salt or perchloric acid is explicitly described; nickel(II) and hydrogen ions are effective as scavengers of liberated phenanthroline molecules.[1] The absorbances at 510 nm of the complex-salt solutions containing nickel(II) or hydrogen ions became negligible after a sufficient time, indicating that the complex ions completely dissociated to give solvated iron(II) ions. All the reactions were followed for four half-lives, and were found to be first order in the metal complex concentration in the time range studied. The dissociation and racemization rates obtained were reproducible within ± 2 and $\pm 5\%$, respectively. Methanol, a guaranteed reagent of Wako Pure Chemical Indistries, Ltd., was purified by fractional distillation. Mixed solvents were prepared by mixing appropriate volumes of the methanol and water; 0.6 and 0.8 volume fractions of methanol corresponds to 0.40 and 0.64 mole fractions (m.f.), respectively. The racemization and dissociation experiments were carried out mainly in 0.40 and 0.64 m.f. aqueous methanol solutions, respectively. Solutions of higher methanol concentrations are not suited for investigating the effect of SCN^- ions on the rates because the reactions

---

proceed too fast. Other reagents and techniques were the same as those described in our previous paper.[1]

RESULTS AND DISCUSSION

As shown in Table 1, both the dissociation and intramolecular racemization rates increased in the presence of SCN^-, and they are decreased by ClO_4^- in 0.40 m.f. aqueous methanol solutions. The results extend the previous findings in aqueous solutions that the intramolecular racemization rate increased with the increase in the polarizability of the anion, while the dissociation rate increased with increasing basicity of the anion.[1] The same order of the effect of the added anions was also observed in 0.64 m.f. aqueous methanol and in pure methanol (Tables 2 and 3). The retarding effect of ClO_4^- on the racemization rate were also reported in several solvent systems by Van Meter and Neumann.[5]

For the analysis of the experimental results, the following reaction processes were assumed:

$$[Fe(phen)_3]^{2+} + X^- \underset{}{\overset{K_{(x)}^{IP}}{\rightleftharpoons}} [Fe(phen)_3]^{2+} \cdot X^- \qquad (1)$$

$$[Fe(phen)_3]^{2+} \overset{k_d}{\rightarrow} [Fe(phen)_2]^{2+} + phen$$

$$\overset{fast}{\rightarrow} Fe^{2+} + 3phen \qquad (2)$$

$$[Fe(phen)_3]^{2+} \cdot X^- \overset{k_{d(X)}^{IP}}{\rightarrow} [Fe(phen)_2]^{2+} \cdot X^- + phen$$

$$\overset{fast}{\rightarrow} Fe^{2+} + 3phen + X^-. \qquad (3)$$
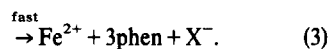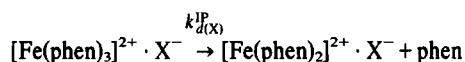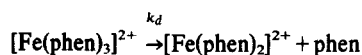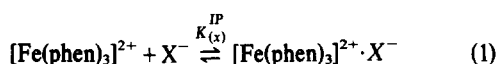
Then the thermodynamic ion-association constant for reaction (1), $K_{(X)}^{IP}$, and the dissociation rate constant, k_d^{obsd}, are given by:

$$K_{(X)}^{IP} = \frac{[Fe(phen)_3^{2+} \cdot X^-]}{[Fe(phen)_3^{2+}][X^-]} \frac{1}{f_2}. \qquad (4)$$

$$k_d^{obsd} = \frac{k_d + k_{d(X)}^{IP} K_{(X)}^{IP} f_2 [X^-]}{1 + K_{(X)}^{IP} f_2 [X^-]} \qquad (5)$$

Table 1. Dissociation and racemization rate constants of $[Fe(phen)_3]^{2+}$ in 0.40 m.f. aqueous methanol at 20.0°C

Added Salts		k_d^{obsd}	k_r^{obsd}	k_r^{i} *
mol dm^{-3}		10^{-3} s^{-1}	10^{-3} s^{-1}	10^{-3} s^{-1}
None		0.0797	2.75	2.67
NaClO$_4$	0.51	0.0482	1.95	1.90
KSCN	0.51	0.608	5.32	4.71

* Intramolecular racemization rate constant $(k_r^{obsd} - k_d^{obsd})$.

Table 2. Dissociation rate constants of $[Fe(phen)_3]^{2+}$ in 0.64 m.f. aqueous methanol at 25.0°C

Added Salts/mol dm^{-3}		$k_d^{obsd}/10^{-3}$ s^{-1}	$k_d^{calcd*}/10^{-3}$ s^{-1}
Ni(ClO$_4$)$_2$	0.00019	0.243	0.246
	0.00032	0.243	0.245
	0.00039	0.243	0.244
	0.00075	0.245	0.242
	0.00226	0.236	0.235
	0.00298	0.236	0.232
	0.00353	0.232	0.231
	0.0119	0.214	0.214
HClO$_4$	0.0160	0.212	0.214
	0.160	0.166	0.166
NiCl$_2$	0.00075	0.263	0.261
	0.0050	0.288	0.292
	0.101	0.385	0.380
	0.496	0.428	0.431
KSCN	0.0005	0.335	0.393
	0.0042	1.30	1.04
	0.0693	2.82	2.79
	0.804	3.98	4.06

* Calculated with the values given in Table 4.

Table 3. Dissociation rate constants of $[Fe(phen)_3]^{2+}$ in absolute methanol at 25.0°C.

Added Salts/mol dm^{-3}		$k_d^{obsd}/10^{-3}$ s^{-1}
Ni(ClO₄)₂	0.0005	0.036
	0.0021	0.036
	0.0111	0.038
KSCN	0.0081	8.00
	0.072	13.0

where k_d and $k_{d(X)}^{IP}$ are the rate constants for reactions (2) and (3), respectively. The activity coefficient, f_z, of an ion with a charge of $\pm z$ was estimated by using the extended Debye–Hückel equation:

$$\log f_z = -\frac{Az^2\sqrt{I}}{1 + Ba\sqrt{I}} + bI \qquad (6)$$

where $A = 0.2174$ $(e^2/\epsilon kT)\sqrt{(8\pi N\ e^2/1000\epsilon kT)}$ and $B = \sqrt{(8\pi N\ e^2/1000\epsilon kT)}$ with usual meanings of the notations.[6] The values of $a = (7-10)\times 10^{-8}$ cm and $b = 0.1z^2$ were assumed in the calculation, together with $\epsilon = 78.5$ for water and $\epsilon = 44.0$ for 0.64 m.f. aqueous methanol.

We first examine the effect of ion association on the concentration of free anion([X⁻]) and the ionic strength (I). The concentration of the complex salt was much lower than those of the added salt, and therefore it suffice to consider the effect of ion association only between added ions:

$$M^{n+} + X^- \rightleftharpoons M^{n+} \cdot X^- \qquad (7)$$
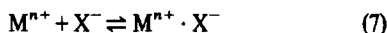
where M^{n+} ($n = 1$ or 2) and X^- represent the cation and anion of the added salt. The association constant, K, is given by:

$$K = \frac{[M^{n+}\cdot X^-]}{[M^{n+}][X^-]}\frac{f_{n-1}}{f_n f_1} = \frac{x}{(c-x)(nc-x)}\frac{f_{n-1}}{f_n f_1} \qquad (8)$$

where c is the total concentration of the added salt, and x the concentration of the ion-pair at equilibrium. With the knowledge of the values of K and f_z, the net concentration of the free anion, $nc - x$, can be obtained from eqn (8). In the absence of the experimental ion-association constants for such systems, K values for dipositive and mononegative ions and for monopositive and mononegative ions were calculated theoretically[7] using various values $((3-6)\times 10^{-8}$ cm$)$ of the closest distance of approach between ions. The approximate f_z values were obtained from eqn (6) by assuming the value of a to be $(3-6)\times 10^{-8}$ cm, and with the first approximation of $I = n(n+1)c/2$. Then, the value of x was calculated from eqn (8). The f_z were recalculated with $I = n(n+1)c/2 - nx$ to give a better x value as the second step of approximation. Further repetition of the procedure reproduced the x value within the limits of experimental error. The net concentration of the free anion and the ionic strength of the medium were calculated by the use of the x value thus obtained.

With the [X⁻] and I values obtained, the $K_{(X)}^{IP}$ and $k_{d(X)}^{IP}$ values were determined to give the best fit between the observed kinetic data and the calculated curve according to eqn (5). In obtaining the $K_{(X)}^{IP}$ and $k_{d(X)}^{IP}$ values for X = Cl⁻ and SCN⁻, we disregarded the effect of

perchlorate ions, contained in a low concentration $(7.2\times 10^{-4}\ \text{mol dm}^{-3})$ as counter ions of the complex cations and the added nickel(II) ions. The $K_{(X)}^{IP}$ values were transformed to the concentration ion-association constant, $K_{C(X)}^{IP}$, at $I = 0.1$ by means of eqn (6).

The rate constant for the dissociation of the complex ion in the ion-pair (eqn (3)) increased in the order, ClO₄⁻ < Cl⁻ < SCN⁻, of the associated anion in 0.64 m.f. aqueous methanol (Table 4). The sequence is consistent with those obtained in aqueous solutions;[1] i.e. the rate constant for the ion-pair increased with the increase in the pKa of the conjugate acid of the anion. This suggests that the mechanism of dissociation in this case is the same as that in aqueous solutions (ion-pair interchange mechanism[1]).

The dissociation rate constants of the complex in the presence of SCN⁻ and of Cl⁻ increased with the increase in methanol content, as can be seen from a comparison of the results given in Tables 1–3. Similar results were obtained for the dissociation of [Fe(bpy)₃]²⁺ by Seiden et al.[2] The increase in rate with the increase in methanol content is caused by the increase in the reactivity of the ion-pair as well as the increase in the association constant (see Table 4). The larger reactivity of the ion-pair in the solution of higher methanol content can be well understood by considering the influence of the dielectric constant of the medium. The free-energy difference between the polar ion-pair and the less polar activated complex is larger in a medium with a higher dielectric constant.[8] Thus, the activation energy becomes smaller with the decrease in the dielectric constant of a medium, or with the increase in methanol content. In this connection, it is interesting to note the fact that [Fe(phen)₃]Cl₂ and [Fe(pbm)₃](SCN)₂ are converted to [Fe(phen)₂Cl₂][9] and [Fe(pbm)₂(SCN)₂][10] in dichloromethane and chloroform, respectively, at rates much faster than the dissociation rates of the tris-complexes in aqueous solutions.

The dissociation rate of the free complex cation in 0.64 m.f. aqueous methanol was found to be considerably smaller than that in dimethyl sulfoxide (Table 4) reported by Farrington et al.,[3] in spite of the fact that the dielectric constants of the two solvents are almost the same. Similar but more pronounced tendencies were observed, when the complex cation was ion-paired with ClO₄⁻ and with Cl⁻. This shows that the coordinating ability, in addition to the dielectric constant, of solvent molecules makes a significant contribution to the dissociation rate of the complex ion.

As shown in Table 4, the ion-association constants increased in the order of ClO₄⁻ < Cl⁻ < SCN⁻ in 0.64 m.f. aqueous methanol; a consistent order was previously found in aqueous solution.[1] The $K_{C(X)}^{IP}$ values for Cl⁻ and SCN⁻ were greater in 0.64 m.f. aqueous methanol than in water. This trend is consistent with the theoretical prediction (Table 4). Table 4 also lists the $K_{C(X)}^{IP}$ values reported for ClO₄⁻ and Cl⁻ in dimethyl sulfoxide;[3] the values are much greater than those obtained in 0.64 m.f. aqueous methanol in the present study. However, the literature values cannot directly be compared with the present results, since the former were derived without allowance for the ion association of the added salt and for the change in ionic strength.

The effect of added salts on the rate of dissociation of [Fe(phen)₃]²⁺ in aqueous methanol solutions can reasonably be understood in terms of ion association of the complex with anions.

Table 4. Ion-association constants of $[Fe(phen)_3]^{2+}$ with anions and dissociation rate constants of the complex in ion-pairs at 25.0°C and $I = 0.1$

Counter Ion	$k_{d(X)}^{IP}/10^{-3}$ s^{-1}			$K_{C(X)}^{IP}/$mol dm^{-3}		
	water[a]	0.61 m.f. MeOH	dmso[b]	water	0.61 m.f. MeOH	dmso[b]
free ion	0.073	0.249±0.002	0.77	—	—	—
ClO_4^-	—	0.086±0.033	1.5	—	10.6± 3.6	39±10
Cl^-	—	0.452±0.022	580.	1.5±0.8[c]	18.4± 4.1	53±27
SCN^-	—	4.69 ±1.34	—	2.6±1.1[c]	25.1±14.9	—
Theory[d]						
a= 5 Å	—	—	—	2.6	13.0	13.0
a=10 Å	—	—	—	1.3	5.2	5.2

a) Data in 0.1 mol dm^{-3} HCl.

b) Ref. 3. The K values were obtained without considering the effect of ionic strength.

c) Ref. 1. The K values at 32.0°C.

d) Ref. 6a. The symbol a (Å=10^{-10}m) represents the closest distance of approach between ions.

REFERENCES

[1] S. Tachiyashiki and H. Yamatera, *Bull. Chem. Soc. Jpn.*, 1982, **55**, 1014.

[2] L. Seiden, F. Basolo and H. M. Neumann, *J. Am. Chem. Soc.* 1959, **81**, 3809.

[3] D. J. Farrington, J. G. Jones and M. V. Twigg, *J. Chem. Soc. (Dalton Trans.)* 1979, 221.

[4a] M. J. Blandamer, J. Burgess, J. G. Chambers, R. I. Haines and H. E. Marshall, *J. Chem. Soc. (Dalton Trans.)* 1977, 165; [b] M. J. Blandamer, J. Burgess and J. G. Chambers, *J. Chem. Soc. (Dalton Trans.)* 1976, 606.

[5] F. M. Van Meter and H. M. Neumann, *J. Am. Chem. Soc.* 1976, **98**, 1388.

[6] See, for example, R. A. Robinson and R. H. Stokes, *Electrolyte Solutions*, 2nd Edn., p. 230. Butterworths, London (1959).

[7a] H. Yokoyama and H. Yamatera, *Bull. Chem. Soc. Jpn.* 1975, **48**, 1770; [b] R. M. Fuoss, *J. Am. Chem. Soc.* 1959, **80**, 5059.

[8] A. A. Frost and R. G. Pearson, *Kinetics and Mechanism*, 2nd Edn, pp. 137–142. Wiley, New York (1961).

[9] T. Fujiwara, K. Matsuda and Y. Yamamoto, *Inorg. Nucl. Chem. Lett.* 1980, **16**, 301.

[10] S. Tachiyashiki and H. Yamatera, unpublished result. pbm = 2(2'-pyridyl)benzylidene methylamine.

NMR STUDY OF INTRAMOLECULAR PROCESSES IN EDTA METAL COMPLEXES

MARIA CARLA GENNARO*, PIERO MIRTI and CLAUDIO CASALINO
Istituto di Chimica Analitica, Università di Torino, via Giuria 5, I 10125, Torino, Italy

Abstract—The kinetics of the intramolecular acetate scramblings occurring in thirteen ethylenediaminetetraacetate (EDTA) complexes has been studied by analyzing the modification observed in the NMR spectra of their D_2O solutions, when temperature is changed. The experimental results indicate that the Δ, Λ conversion is a fast process on the NMR time scale for each of the complexes considered, whereas the nitrogen inversion occurs at an observable rate in the case of the Cd(II), In(III), Sc(III), Y(III) and Lu(III) chelates and is too rapid in the other complexes. Computer analysis of the experimental NMR spectra has been performed in order to obtain enthalpy, entropy and free energy of activation concerning the N inversion of the cited chelates. Twist and bond breaking mechanisms are discussed with reference to both scrambling processes.

INTRODUCTION

Proton magnetic resonance has proved to be a powerful technique in studying the intramolecular processes occurring in organic molecules.[1] Among the various fields of application of this technique, a particular interest can be found in the study of the labilities of the coordination bonds in metal complexes, because of the wide use of such compounds in many branches of modern chemistry. Particularly, polyaminepolycarboxylic acids are widely used as chelating agents, and among them, ethylenediaminetetraacetic acid (EDTA) is by far the most employed. The study of the intramolecular rearrangements occurring in EDTA complexes may therefore be considered worth being done. However, such an investigation should require a detailed knowledge of the structure of the solution forms of the metal chelates; unfortunately, literature data do not agree when dealing with the number of the coordination sites actually utilized by the ligand.[2–9] In this paper the generally accepted octahedral hexacoordinate structure will be referred to; the possible presence of differently coordinated species in solution would not affect the sense of the considerations given, because a rapid averaging among the various forms is very likely to occur in the working experimental conditions.

An hexacoordinate complex in solution can be present in two different configurations, which are normally referred to as Δ or Λ, respectively.[10] The two configurations show the same NMR spectrum, which is mainly characterized by the presence in the molecule of eight methylene protons in the four acetate groups. These protons can experience different magnetic environments owing to their different steric arrangement in the complex. Particularly, an acetate group can be referred to as in plane or out of plane, depending on its position in relation to the plane formed by the metal ion and the two nitrogen atoms. If the complex has a symmetrical structure, as in the case of EDTA chelates, the two out of plane positions are equivalent and so are the two in plane ones. Besides, each methylene proton in an acetate group can occupy an axial or equatorial position, in relation to the fact that the hydrogen to carbon bond is parallel or not to the symmetry axis passing through the centre of

the corresponding five-membered ring. In conclusion, the NMR spectrum of the methylene protons of a Δ or Λ configuration of an EDTA complex will show, in the absence of any intramolecular exchange, resonances corresponding to four magnetically non-equivalent protons, which can be named as out-of-plane axial and equatorial, and in-plane axial and equatorial, and will be referred to in this paper as H_a^0, H_e^0, H_a^i and H_e^i, respectively. Particularly, these protons give rise to two AB quartets in the NMR spectrum, because of the geminal coupling between the hydrogen nuclei belonging to the same acetate group.

A sufficient lability of the coordination bonds can cause, if not prevented by an excessive rigidity of the ligand backbone, an interchange between the Δ and Λ configurations (Δ, Λ conversion), or provoke the lone pair inversion of the nitrogen atoms (nitrogen inversion). The two processes are not necessarily interdependent, and give rise to different patterns in the NMR resonances of the methylene protons. In fact, both cause the two AB quartets to coalesce into only one AB pattern, but the spectral parameters are different in the two cases, because of the different exchange mechanism. Particularly, the Δ, Λ conversion makes the H_e^0 and H_a^0 protons average their magnetic environments with the H_a^i and H_e^i nuclei, respectively, whereas the nitrogen inversion causes an exchange of the type $H_e^0 \leftrightarrows H_e^i$ and $H_a^0 \leftrightarrows H_a^i$[11] (Fig. 1). When the processes occur simultaneously, a single methylene proton is bound to experience and average all the magnetic environments related to the axial and equatorial protons, in-plane and out-of-plane, and the NMR spectrum shows the collapse of the AB quartet into a single peak.

The possibility of observing the described modifications in the NMR spectrum of an EDTA chelate, depends on the fact that the considered intramolecular scramblings occur at a rate of the order of the extent of the NMR spectrum itself; therefore, only in this case is it possible to study the kinetics of these exchange processes.

The situations which may be encountered when dealing with an octahedral complex are summarized in Table 1. It must be noted that in the given scheme the possibility of a breaking of the metal-to-nitrogen bonds without previous rupture of the metal-to-oxygen bonds

---

*Author to whom correspondence should be addressed.
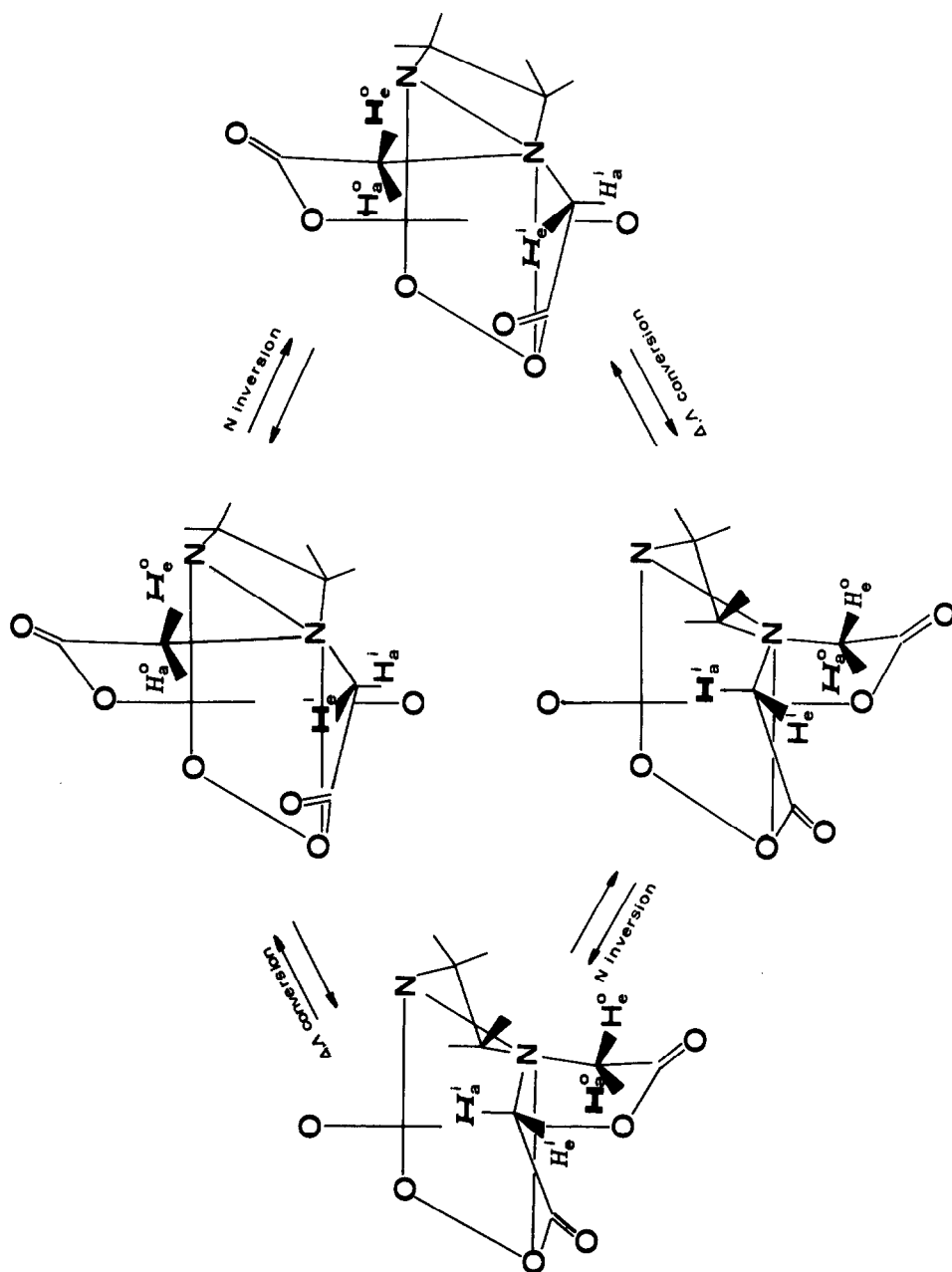
Fig. 1. General scheme of the intramolecular acetate scrambling processes in an octahedral symmetric complex.

Table 1. Summary of situations arising in the NMR spectrum of an octahedral symmetric complex, depending on the labilities, on the NMR time scale, of the metal to ligand bonds

Bonds' lability on the NMR time scale		Acetate scrambling occurring by		Number of methylenic protons with different magnetic environments	shape of the NMR spectrum
M − O	M − N	Δ,Λ conversion	nitrogen inversion		
not labile	not labile	no	no	4 (H_e^o , H_a^o , H_e^i , H_a^i)	two AB patterns
labile	not labile	no	no	4 (H_e^o , H_a^o , H_e^i , H_a^i)	two AB patterns
		yes	no	2 ($H_e^o \rightleftharpoons H_a^i$, $H_a^o \rightleftharpoons H_e^i$)	one AB pattern
labile	labile	no	yes	2 ($H_e^o \rightleftharpoons H_e^i$, $H_a^o \rightleftharpoons H_a^i$)	one AB pattern
		yes	yes	1 ($H_e^o \rightleftharpoons H_a^o \rightleftharpoons H_e^i \rightleftharpoons H_a^i$)	one single peak

has not been taken into account, because it is inconsistent with the considered structure of the complexes. On the same grounds, it follows that the nitrogen inversion (which requires the rupture of the M–N link to occur) can only take place in conditions in which also the Δ, Λ conversion occurs, unless this is hindered by steric factors. Because the EDTA backbone is flexible enough to allow the configurational exchange, it follows that the resonances of the methylene protons in the NMR spectrum of an EDTA chelate can be expected to change with the labilities of the coordination bonds by giving the coalescence of the two AB quartets into one AB pattern and then into a single peak.

EXPERIMENTAL

Weighed amounts of dried ethylenediaminetetraacetic acid and metal nitrates (C. Erba, Merck, K and K reagents) were dissolved in deuterium oxide in order to prepare solutions with concentrations of the metal complex ranging from 0.05 to 0.10 M Potassium deuteroxide was used to adjust the pD of the solutions to a value ensuring the complete formation of the complex in the investigated range of temperature, excluding any hydroxo- or protonated form.[12]

NMR spectra were recorded by means of a Varian T-60 spectrometer, equipped with a T-6057 lock-decoupler and a T-6080 temperature controller. The calibration of the probe temperature meter was obtained by measuring the chemical shift of the hydroxyl protons of both methanol and ethylene glycol.[13] The homogeneity of the magnetic field was checked before each run with the magnetic field locked on the HOD line.

Intramolecular rate constants (k) were obtained by complete line shape analysis of the experimental spectra; a slightly modified version of the DNMR program[14] was used, which performed calculation and plots of theoretical spectra by the input data of chemical shifts, coupling constants and transverse relaxation times of the exchanging sites; these were obtained from the spectra recorded in absence of the studied exchange process. The most reliable value of k was chosen for each spectrum by searching for the best fitting with the theoretical ones, computed by progressive adjustments of the imposed rate constant.

RESULTS AND DISCUSSION

Mg(II), Ca(II), Sr(II), Ba(II), Zn(II), Cd(II), Pb(II), Sc(III), Y(III), La(III), Lu(III), Al(III) and In(III) complexes of EDTA have been studied. In all cases the NMR spectra recorded at the lowest working temperature (the solutions' freezing points) revealed that the configurational exchange between the Δ and Λ forms was fast on the NMR time scale. Particularly, all spectra, except those recorded on Cd-, In-, Sc-, Y- and Lu-EDTA solutions, consisted of a single peak in all the investigated range of temperature (273–373 K), denoting the magnetic equivalence of all the methylene protons. This allows us to state that in these cases also the nitrogen inversion is a fast process on the NMR time scale. As a consequence, it was not possible to give a quantitative treatment of the kinetics of the intramolecular processes occurring in the corresponding complexes.

Things were different when examining the spectra recorded on Cd-, In-, Sc-, Y- and Lu-EDTA solutions. In these cases the resonances of the methylene protons consist of an AB pattern at the lowest working temperature; this means that two sets of protons interchanging their magnetic environments are present in the complexes in these conditions and supports the hypothesis of a rapid configurational exchange, but a slow nitrogen inversion on the NMR time scale. The failure to obtain the splitting of the AB quartet into two patterns prevented the possibility of studying the Δ, Λ conversion, but the N inversion was successfully investigated by analyzing the progressive collapse of the AB quartet with the increase of temperature. At such purpose the AB pattern was dealt with as the "frozen" spectrum with respect to the studied process and provided the spectral parameters required as input data in the computer program. It must be noted that only in the case of the indium complex was the complete collapse of the quartet into a single line observed, whereas this was not achieved for the other chelates up to their solutions' boiling point. However, the spectral modifications observed were sufficient to allow a reliable treatment of the exchange process also in these

cases. Furthermore, as regards the Cd-EDTA spectra, satellite peaks were observed, arising from the coupling of the proton with the ^{111}Cd and ^{113}Cd nuclei; these peaks were not taken into account in the computer analysis of the spectra owing to their relatively low intensity.

Figures 2 and 3 show the NMR spectra recorded at different temperatures on In- and Sc-EDTA solutions, together with their best fitting computed ones; for simplicity reasons, only the most characteristic inner peaks of the AB quartets are reported. The spectra of Cd-, Y- and Lu-EDTA complexes showed a behaviour rather similar to that of ScEDTA.

The intramolecular rate constants (k) obtained by the computer analysis of the spectra were plotted as ln k vs
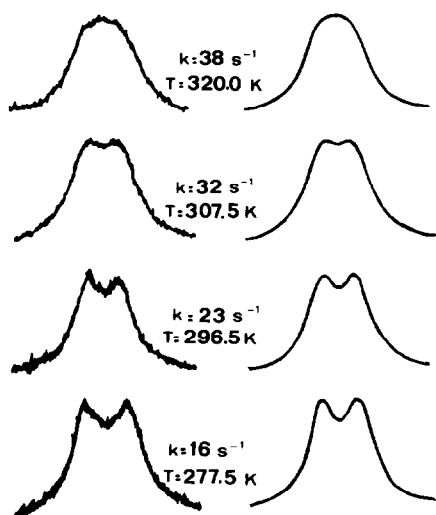
the reciprocal of the absolute temperature (T) (Fig. 4) and allowed to obtain frequency factors and activation energies of the studied processes, and therefore enthalpies, entropies and free energies of activation (see Table 2). By doing that, a transmission coefficient has to be taken into account, which gives the probability of the exchange process to occur actually after having reached the activated state; in the present case, its value has been set equal to 1/2 because of the identity of the energy levels of the exchanging sites and the consequent equal probability of reforming the nitrogen coordination having or not undergone the lone pair inversion.

The search for a likely pathway of intramolecular rearrangements in metal complexes is a much discussed problem and has been the object of several studies.[15-31] These include both dissociative and twist mechanisms, requiring or not the rupture of the coordination bonds, respectively. In the particular case of the processes studied in the present work, it must be noted that the twist mechanism, which may be suitable to account for the rapid Δ, Λ conversion of the investigated complexes, cannot explain a nitrogen inversion. In fact, this process can only occur if the metal to nitrogen bond is broken. However, the negative values obtained for the entropies of activation are more easily associated with twist rather than dissociative pathways[27] and are consistent with the increased state of order intrinsic in the trigonal prism representing the activated state of the twist process.[29] All that could be accounted for if a "twist with rupture" sequence is accepted, as proposed by Eaton et al.,[27] who supposed the possibility of a bond breaking in the intermediate state of the twist pathway.

Examination of literature data allows a comparison between the results of the present work with several others concerning EDTA complexes, even though these are mostly limited to qualitative deductions drawn from the presence or not of multiplet patterns in the NMR spectra. So Kula et al.[19] have shown the labilities of the metal-to-oxygen bonds in alkaline earth, Zn, Pb, Hg and

Fig. 2. NMR spectra of In-EDTA solutions at different temperatures (T) and corresponding best fitting computed ones. Only the inner peaks of the AB quartet are shown.
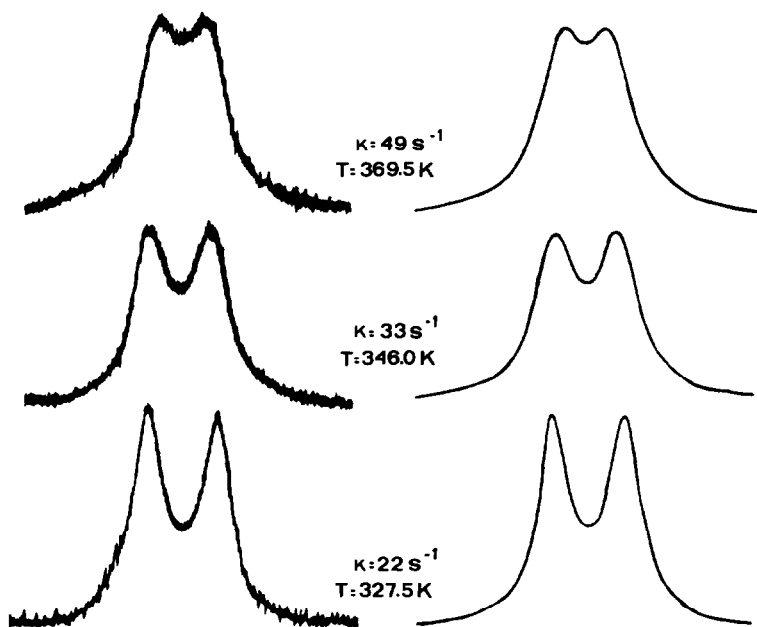
Fig. 3. NMR spectra of Sc-EDTA solutions at different temperatures (T) and corresponding best fitting computed ones. Only the inner peaks of the AB quartet are shown.
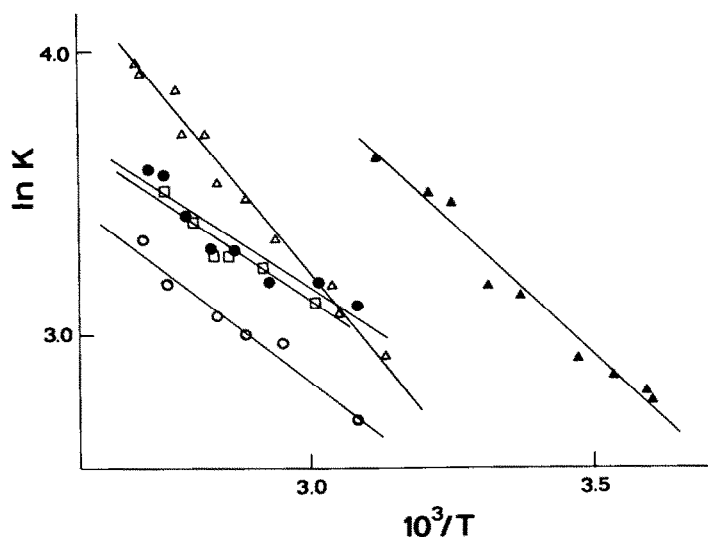
Fig. 4. Arrhenius plot referring to the nitrogen inversion of the Cd- (●), In- (▲), Sc- (△), Y- (○) and Lu-EDTA (□) complexes.

Table 2. Summary of activation parameters

metal ion	activation enthalpy (Kcal/mol) at 298 K	activation entropy (e. u.) at 298 K	free energy of activation (Kcal/mol) at 298 K
Sc(III)	4.1 ± 0.2	− 38.5 ± 0.7	15.6 ± 0.4
In(III)	3.1 ± 0.2	− 40.4 ± 0.8	15.1 ± 0.5
Y(III)	2.4 ± 0.3	− 44.4 ± 0.8	15.7 ± 0.5
Lu(III)	2.1 ± 0.4	− 45 ± 1	15.5 ± 0.8
Cd(II)	2.0 ± 0.4	− 45 ± 1	15.4 ± 0.7

Al complexes and Day and Reilley[10] have given evidence of the lifetimes of both oxygen and nitrogen coordination in the Pb, Cd and Co(III) complexes. Chan et al.[32] have studied the Mo(VI) binuclear complex, Ryhl[33] the lanthanum and lutetium complexes and Baisden and coworkers[34] the alkaline earth, Bi, Y, La, Lu and In chelates. Everhart and Evilia,[31] at last, have investigated the Ni and Co(II) systems. The results given in these papers are in agreement with those of this work, when referring to comparable situations. Particularly, Baisden and coworkers have put forward the hypothesis of a correlation between the z^2/r ratio (where z is the charge and r the radius of the cation) and lifetime of the intramolecular bonds, and proposed the value $z^2/r = 9$ as the limit beyond which an AB quartet is to be expected in the NMR spectrum of an EDTA chelate. This is in agreement with the whole of the data available on EDTA chelates, with the exceptions of the Cd (slow nitrogen inversion with $z^2/r = 4$) and Al complexes (fast interconversion despite its $z^2/r = 18$).

Another attempt to interpret the results obtained can be made by admitting that the lifetime of a coordination bond is mainly due to steric effects rather than to changes in the bond character itself;[5] this leads to considering the size of the metal ion as an important factor in determining the lability of the metal-to-ligand links.

The results concerning ten out of the thirteen complexes investigated are consistent with the hypothesis of setting a radius of 1 Å as the value over which the metal-to-nitrogen bond is labile enough to give a fast N inversion on the NMR time scale. The disagreement is given, in this case, by the fast N inversion observed for the complexes formed with the small Mg, Zn and Al ions.

REFERENCES

[1] J. A. Pople, W. G. Schneider and H. J. Bernstein, High-Resolution Nuclear Magnetic Resonance, McGraw-Hill, New York (1959).
[2] S. Kirschner, J. Am. Chem. Soc. 1956, 78, 2372.
[3] A. P. Brunetti, G. H. Nancollas and P. N. Smith, J. Am. Chem. Soc. 1969, 91, 4680.
[4] W. C. E. Higginson, J. Am. Chem. Soc. 1962, 84, 2761.
[5] D. W. Margerum and H. M. Rosen, Inorg. Chem. 1968, 7, 299.
[6] J. D. Carr and C. N. Reilley, Anal. Chem. 1970, 42, 51.
[7] R. G. Wilkins and R. Yelin, J. Am. Chem. Soc. 1967, 89, 5496.
[8] W. C. E. Higginson and B. Samuel, J. Chem. Soc. A 1970, 1579.
[9] R. G. Wilkins and R. Yelin, J. Am. Chem. Soc. 1970, 92, 1191.
[10] Inorg. Chem. 1970, 9, 1.
[11] L. E. Erickson, D. C. Young, F. F.-L. Ho, S. R. Watkins, J. B. Terrill and C. N. Reilley, Inorg. Chem. 1971, 10, 441.
[12] L. G. Sillen and A. Martell, Stability Constants of Metal-Ion Complexes, The Chemical Society, London, Spec. Publ. 17. 1964; 25, 1971.

[13]A. L. Van Geet, *Anal. Chem.* 1968, **40**, 2227.

[14]G. Binsch and D. A. Kleier, *QCPE Program* 140, Chemistry Department, Indiana University.

[15]R. C. Fay and T. S. Piper, *Inorg. Chem.* 1964, **3**, 348.

[16]C. S. Springer Jr. and R. H. Shaers, *Inorg. Chem.* 1967, **6**, 852.

[17]R. C. Fay and R. N. Lowry, *Inorg. Chem.* 1967, **6**, 1512.

[18]N. Serpone and R. C. Fay, *Inorg. Chem.* 1967, **6**, 1835.

[19]J. J. Fortman and R. E. Sievers, *Inorg. Chem.* 1967, **6**, 2022.

[20]M. L. Tobe, *Inorg. Chem.* 1968, **7**, 1260.

[21]J. E. Brady, *Inorg. Chem.* 1969, **8**, 1208.

[22]D. C. Bradley and C. E. Holloway, *J. Chem. Soc. A* 1969, 282.

[23]M. D. Alexander and H. G. Hamilton Jr., *Inorg. Chem.* 1969, **8**, 2131.

[24]J. C. Gordon II and R. H. Holm, *J. Am. Chem. Soc.* 1970, **92**, 5319.

[25]A. Y Girgis and R. C. Fay, *J. Am. Chem. Soc.* 1970, **92**, 7061.

[26]J. R. Hutchison, J. C. Gordon II and R. H. Holm, *Inorg. Chem.* 1971, **10**, 1004.

[27]S. S. Eaton, J. R. Hutchison, R. H. Holm and E. L. Muetterties, *J. Am. Chem. Soc.* 1972, **94**, 6411.

[28]D. J. Darensbourg, *Inorg. Chem.* 1979, **18**, 14.

[29]J. C. Bailar Jr., *J. Inorg. Nucl. Chem.* 1958, **8**, 165.

[30]N. Serpone and D. G. Bickley, *Prog. Inorg. Chem.* 1972, **17**, 391.

[31]D. S. Everhart and R. F. Evilia, *Inorg. Chem.* 1975, **14**, 2755.

[32]S. I. Chan, R. J. Kula and D. T. Sawyer, *J. Am. Chem. Soc.* 1964, **86**, 377.

[33]T. Ryhl, *Acta Chem. Scand.* 1972, **26**, 4001.

[34]P. A. Baisden, G. R. Choppin and B. B. Garrett, *Inorg. Chem.* 1977, **16**, 1367.

POTASSIUM FLUORIDE AND PHOSPHOROUS ACID: AB INITIO CALCULATIONS AND SPECTROSCOPIC INVESTIGATIONS

JOHN EMSLEY,* JEREMY LUCAS and ROBERT J. PARKER

Department of Chemistry, King's College, Strand, London WC2R 2LS, England

and

RICHARD E. OVERILL

Computer Centre, King's College, Strand, London WC2R 2LS, England

Abstract—Ab initio calculations including the effects of solvation on the hydrogen bonding interactions between F^- and phosphorous acid, HPO_3H_2, have been performed, resulting in a value of 61 kJ mol^{-1} for the hydrogen bond energy of $[HPO_3H_2F]^-$. Attempts to show that this species exists in aqueous solution have been made using ^{17}O, ^{19}F and ^{31}P NMR spectroscopy and pH and conductance studies, but these indicate that the principal reaction is an acid-base neutralization. Crystals of $KF.HPO_3H_2$ grow from aqueous solution but these are not the same as those from methanol solution which are known to be strongly hydrogen bonded.

INTRODUCTION

The bifluoride ion still ranks as the species which possesses the strongest hydrogen bond[1] but several other examples of strong or short bonds involving the fluoride ion are known.[2] In $KF.(CH_2CO_2H)_2$ and $KF.(CH_2CO_2D)_2$ the F^- acts as the acceptor to two hydrogen bonds formed with the carboxylic acid groups of different succinic acid molecules and $r(O\cdot\cdot F)$ is 244 pm.[3]

In crystals of $Te(OH)_6.2KF$ the fluoride ions each form three OHF hydrogen bonds and $r(O\cdot\cdot F)$ is 258.[4] A similar situation is present in $Te(OH)_6.NaF$.[5] The shortest OHF bonds are those in crystals of $(KHPO_3.HF)_2$ whose structure is based on cyclic dimers of the anion. The value of $r(O\cdot\cdot F)$ is 238 pm with the proton lying nearer the fluoride so that the hydrogen bond is essentially between a hydrogen phosphite group and HF, (I).[6] The OHO bonds holding the dimers together are also quite short, $r(O\cdot\cdot O) = 256$ pm.
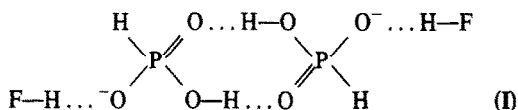
Somewhat surprisingly there has been no further investigation of $(KHPO_3.H.HF)_2$ since its discovery[7] and structural detetermination.[6,8] In view of the rarity of the OHF hydrogen bonds we have calculated the hydrogen bond energy of this bond and studied mixed solutions of KF and HPO_3H_2 with a view to observing (I) in an aqueous environment, following our discovery that crystals of the same empirical composition $KF.HPO_3H_2$ will grow from a saturated aqueous solution of KF and HPO_3H_2. The original method for producing the adduct used methanol as the solvent or alternatively an aqueous solution of HF and $KHPO_3H$.[8]

THEORETICAL PROCEDURE

Ab initio LCAO–MO–SCF calculations were performed on HPO_3H_2, HPO_3H^-, $HPO_3H_2F_2^{2-}$, HPO_3^{2-}, $HPO_3H_2F^-$ and HPO_3HF^{2-} using a version of the program GAUSSIAN 76.[9] This program has been modified to perform level-shifting of the Hartree–Fock Hamiltonian[10] directly in the atomic orbital basis to guarantee the convergence of the iterative SCF calculations.[11] Geometry optimizations (bond lengths to within ±1 pm, bond angles to within ±0.1°) were performed with the split-valence 4–31G and 44–31G basis sets,[12] using standard univariate quadratic interpolation procedures.

(a) *Phosphite ion*, HPO_3^{2-}

Starting with a tetrahedral geometry about phosphorus the following optimized parameters were obtained: $r(PH) = 150.8$ pm, $r(PO) = 159.8$ pm, HPO = 102.9°.

(b) *Hydrogen phosphite ion*, HPO_3H^-

To the optimized HPO_3^{2-} arrangement a proton was added with $r(OH) = 90.0$ pm and POH = 109.5°, and the structure was reoptimized to produce the values of (II). The dihedral angle HOPH was assumed to be zero.

(II)
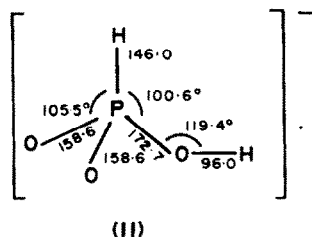
(c) *Phosphorous acid*, HPO_3H_2

The addition of another proton to (II) followed by reoptimization produced only marginal changes: $r(OH) = 96.2$ pm; POH = 119.6°.

---

*Author to whom correspondence should be addressed.

(d) *Hydrogen phosphite fluoride*, [HPO₃HF]²⁻

Adding a fluoride ion to (II) with $r(HF) = 120.0$ pm, the structure of the ion was optimized at the hydrogen bond centre to give $r(OH) = 105.1$ pm, $r(HF) = 137.4$ pm OHF = 180° (assumed) and POH = 121.6°, assuming the hydrogen bond to be linear.

(e) *Phosphorous acid fluoride*, [HPO₃H₂F]⁻

Starting from the optimized structure of (c), structure (III) was calculated by optimizing the parameters shown under the assumptions of a linear hydrogen bond and zero HOPH dihedral angles.
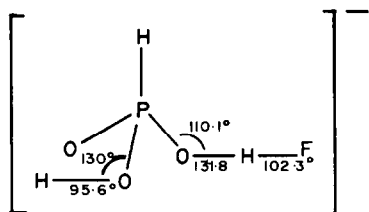
(III)

(f) *Phosphorous acid difluoride*, [HPO₃H₂F₂]²⁻

Starting with the optimized structure of (III) a second fluoride was added to the remaining acidic hydrogen such that $r(OH)$, $r(HF)$ and POH are equal to those in (III).

The hydrogen bond energy of [HPO₃H₂F]⁻ was then computed using the extended [6s4p/4s2p/2s1p] concentrated Gaussian basis set of Dunning[13] with an s-orbital scaling factor of √(2) and a p-orbital exponent of 0.7 for the protons. The effect of the addition of a set of single 3d Gaussian polarization functions $(\alpha_d = 0.43)$[14] on phosphorus was studied. This basis set has been shown to be sufficiently complete to yield hydrogen bond energies which are stable against further basis extensions and against "ghost orbital" corrections.[15] Single determinant SCF wavefunctions are generally adequate for the calculations of the energies of strong hydrogen bonds between closed shell molecules since the molecular extra correlation energy and the zero-point vibrational corrections are both small (*ca.* 5%).[16] Finally, the effect of solvation on the hydrogen bonding interaction was studied using the non-specific solvation method.[17] The results of the calculations are presented in Table 1.

EXPERIMENTAL

Instruments

Perkin Elmer 457 IR spectrometer (KBr discs, nujol mulls); Beckman pH electrode; Bruker HFX90 NMR spectrometer (¹⁹F, 84.66 MHz, referenced to CFCl₃; ³¹P, 36.43 MHz, referenced to 85% H₃PO₄) and Bruker WM250 NMR spectrometer (¹⁷O, 39.909 MHz, referenced to H₂O). *Materials*: KF, KHF₂, KHPO₃H and HPO₃H₂ were analytical grade, HF was a 40% solution in water.

Table 1. Total energies (hartrees)[a] and solvation energies (kJ mol⁻¹) of the molecules and ions studied

Molecular species	E_0 4-31G	E_0 [6s4p/4s2p/2s1p]	ΔE_{sol}[b]	r_0[c]
HPO₃²⁻	-564.95787	-565.62599 -565.80755[d]	-899	3.0
HPO₃H⁻	-565.70723	-566.39816 -566.54487[d]	-283	3.0
HPO₃H₂	-566.23910	-566.93035 -567.06267[d]	-54	3.1
[HPO₃HF]²⁻	-664.92480	-665.74233 -665.92279[d]	-870	3.1
[HPO₃H₂F]⁻	-665.62467	-666.46169 -666.60155[d]	-331	3.2
F⁻	-99.24782[e]	-99.41406[f]	-481	1.4
HF	-99.88729[e]	-100.03847[f]	-35	1.7
[HPO₃H₂F₂]²⁻	-764.98384	-765.83338 -765.98370[d]	-748	3.6
HF₂⁻	-199.23504	-199.53533	-269	2.5

[a] 1 hartree = 4.35981 x 10⁻¹⁸ J; [b] calculated with a dielectric constant ε = 33.0 (methanol); [c] cavity radius (Å) derived from the van der Waals radii of A. Bondi, *J. Phys. Chem.*, 1964, **68**, 441; [d] with 3d orbitals on phosphorus; [e] W. J. Bouma & L. Radom, *Chem. Phys. Letts.* 1979, **64**, 216; [f] see ref. 17.

Preparation of KF.HPO₃H₂

HPO₃H₂ (5 g, 0.06 mol) and KF (3.5 g, 0.06 mol) were dissolved in water (10 cm³). Evaporation under vacuum at room temperature produced crystals of the adduct KF.HPO₃H₂ m.p. 170°. Found: P, 22.0; H, 2.1; F, 13.6; K, 27.4%. Calculated for H₃FKO₃P: P, 22.1; H, 2.1; F, 13.5; K, 27.8%. The same compound was also grown from a solution of KHPO₃H in aqueous HF. The crystals are stable in air and can be recrystallized from water. Their solubility is ⩾4000 gkg⁻¹, the actual solubility being difficult to determine exactly because of the high viscosity of such solutions; the solubility of HPO₃H₂ in water at 0°C is 3090 gkg⁻¹.[18] When saturated solutions of KF and HPO₃H₂ were mixed a temperature rise of 12°C was recorded.

Crystals grown from an aqueous solution containing a 1:2 mole ratio of HPO₃H₂:KF were identified as KHF₂ by their IR spectrum and analysis. Found: P, <1; H, 1.4; F, 48.0; K, 49.2%. Calculated for F₂HK: H, 1.3; F, 48.7; K, 50.1%. Crystals grown from an aqueous solution of HPO₃H₂ and KHF₂ were also identified as KHF₂.

DISCUSSION

The original discoverers of (KHPO₃H.HF)₂ prepared it by anhydrous methods such as grinding together KF and phosphorous acid and extracting the syrup which formed with hot methanol.[6,8] Crystals of adduct were also obtained by complete dehydration of an aqueous solution of KHPO₃H in 40% HF followed by methanol extraction.[7]

Crystals of composition KF.HPO₃H₂ grow from a saturated solution of KF and HPO₃H₂. The melting point of these is 170°, compared to the 96° reported for (KHPO₃H.HF)₂. Alternative hydrogen bonded structures for the higher melting crystals can still involve OHF bonds, such as (IV), which is a polymeric rather than a dimeric form of (I), or (V), which has the HF molecules participating in two strong hydrogen bonds.

(IV)

(V)
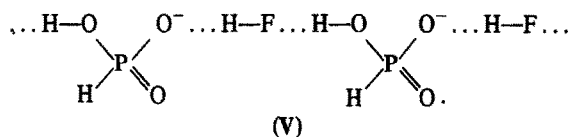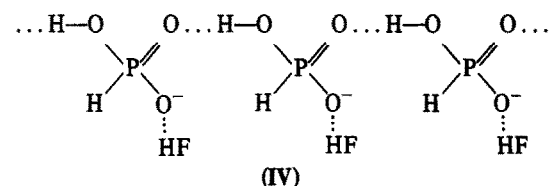
A structure similar to (V) has been discovered in the adduct of KF and malonic acid, KF.CH₂(CO₂H)₂.[19] Yet a third possibility is a polymeric anion involving F⁻ ions forming two hydrogen bonds to acidic groups as is found in KF.(CH₂CO₂H)₂.[20] In this last example the pK₁ of succinic acid at 4.16[21] is sufficiently less than that of HF (3.45) to prevent proton transfer to form HF as occurs with malonic acid (2.83) and HPO₃H₂ (2.00).

So far crystals of the new KF.HPO₃H₂ have not been produced which can be investigated by X-ray diffraction methods. It is even possible for them to be a mixed salt. The crystal structure of (KHPO₃H.HF)₂, however, shows short hydrogen bonds[6] and we now report on the calculated energies of such bonds between HPO₃H₂ and F⁻, this being the first time that the hydrogen bonding of an acid of a second row element has been computed.

Structure optimization of the hydrogen bonded com-

plex between F⁻ and HPO₃H₂ gave the parameters of (III) and showed the hydrogen bonding proton to reside near the fluorine nucleus at about the bond distance of hydrogen fluoride. In this respect the system is like the arrangement in the crystal dimers, (I). Using the double-zeta basis set the energy of the hydrogen bond of [HPO₃H₂F]⁻ is calculated to be 66 kJ mol⁻¹ relative to the lower energy isolated pair HPO₃H⁻ + HF.

Defined with respect to the components used in our synthesis of the complex, i.e. HPO₃H₂ + F⁻, the interaction energy is 308 kJ mol⁻¹. Again this is in accord with the exothermicity observed when solutions of HPO₃H₂ and KF are mixed.

Taking phosphorus 3d orbitals into account in our calculations changed these energies to 48 kJ mol⁻¹ (with respect to HPO₃H⁻ + HF) and 328 kJ mol⁻¹ (HPO₃H₂ + F⁻). Taking solvation effects of methanol into account altered these values to 61 and 124 kJ mol⁻¹ respectively. The former is thus the hydrogen bond energy of the complex, according to the agreed definition for systems of this kind.[22] Solvation effects in water are found to be virtually identical. This value is rather smaller than might have been predicted from the shortness of the hydrogen bond, r(O··F) = 238 pm (observed), 234 pm (calculated).

As a result of a referee's comments about the ion [HPO₃H₂F₂]²⁻ and its relative stability with respect to other species, including HF₂⁻, we have computed the relative energies of all possible combinations of HPO₃H₂ + 2F⁻ in both the free and solvated states. These are shown in Fig. 5. The double OHF hydrogen bond of [HPO₃H₂F₂]²⁻ is stable with respect to HPO₃H₂ + 2F⁻ by 244 kJ mol⁻¹ (122 kJ mol⁻¹ per hydrogen bond) in the free state, but unstable by 24 kJ mol⁻¹ (12 kJ mol⁻¹ per bond) in the solvated state. These are the *defined* hydrogen bond energies.[22] It does not mean that the hydrogen bonds in this complex ion are stronger than that of [HPO₂H₂F]⁻, in the free state; it is merely a consequence of changing the base from which the hydrogen bond energy is defined.

Figure 5 also shows that in the free state HF₂⁻ is the favoured hydrogen bonded species, but in solution [HPO₃H₂F]⁻ should be the preferred species.

How do the hydrogen bond energies of phosphorous acid—fluoride bonds compare with other strong hydrogen bonds' energies? The calculated hydrogen bond energy of HF₂⁻ (free state) is 214 kJ mol⁻¹ and r(F··F) = 226 pm.[1] The calculated energy of each of the hydrogen bonds between a single fluoride ion and two formic acid molecules, [HCO₂H··F··HO₂CH]⁻, is 179 kJ mol⁻¹ and the measured distance r(O··F) is 244 pm.[20] Other O··H··F strong hydrogen bond energies are 149 kJ mol⁻¹ for [H₃BO₃F]⁻,[23] 149 kJ mol⁻¹ for [RCONH₂F]⁻,[24] 127 kJ mol⁻¹ for [RCO₂HF]⁻,[20] and 101 kJ mol⁻¹ for [H₂O.F]⁻.[25] Other evidence and especially IR data supports these as being strong hydrogen bonds. Thus the value of 48 kJ mol⁻¹ for [HPO₃H₂F]⁻ (gas phase) appears rather too low. The calculated values for [HPO₃H₂F₂]⁻, on the other hand, appear to be of comparable strength, and are probably more representative of the energy of the PO··H··F⁻ bond in these ions.

The calculated Mulliken populations lend no support to the hypothesis of pπ–dπ back-donation on to the phosphorus atom; most of the negative charge is localized within the hydrogen bond itself.

Calculations have also been carried out on the species [HPO₃HF]²⁻, which show it to be unstable with respect

to HPO_3H^- and F^- by $184\,kJ\,mol^{-1}$ ($95\,kJ\,mol^{-1}$ if $3d$ orbitals are included) but is stable with respect to HPO_3^{2-} and HF by $204\,kJ\,mol^{-1}$ ($202\,kJ\,mol^{-1}$ if $3d$ orbitals are included). Again by the agreed definition of strong hydrogen bonds this doubly charged ion is thus unstable by $95\,kJ\,mol^{-1}$. However the $[HPO_3HF]^{2-}$ complex may be postulated as a hydrogen bonded intermediate in the reaction sequence:

$$HPO_3^{2-} + HF \rightarrow [HPO_3HF]^{2-} \rightarrow HPO_3H^- + F^-.$$

In solution the $[HPO_3HF]^{2-}$ complex is calculated to be stable with respect to both $HPO_3H^- + F^-$ (by $201\,kJ\,mol^{-1}$) and $HPO_3^{2-} + HF$ (by $138\,kJ\,mol^{-1}$).

The addition of KF to a solution of HPO_3H_2 should result in an acid-base neutralization reaction which is conventionally expressed as (1)

$$HPO_3H_2 + KF \rightarrow HF + KHPO_3H \qquad (1)$$
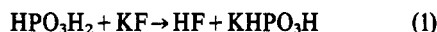
but is better expressed as (2), bearing in mind the nature of the species involved in solution. That a strongly

$$H_3O^+ + F^- \rightarrow [H_2\overset{+}{O}H\overset{-}{F}] \qquad (2)$$
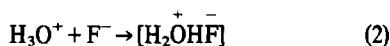
hydrogen bonded complex $[H_2\overset{+}{O}-H-\overset{-}{F}]$, is present as the chief species in hydrofluoric acid has recently been determined by Giguère.[26]

The resulting solution from the reaction of KF and HPO_3H_2 can however be seen as involving an equilibrium between the two possible acceptors and the donor HF (3).

$$[H_2O\cdot\cdot HF] + HPO_3H^- \rightleftharpoons H_2O + [HPO_3H\cdot\cdot HF]^-. \qquad (3)$$
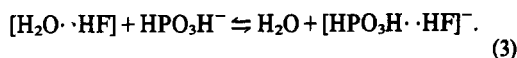
Only in concentrated solutions will $[HPO_3H_2F]^-$ be favoured but it may be possible to detect the presence of this ion under normal conditions, thus showing its relative hydrogen bond strength.

Excess fluoride over that required to neutralize HPO_3H_2 will not lead to the neutralization of HPO_3H^-. Instead the excess F^- would also compete as an acceptor for HF (4) in an equilibrium that lies very much to the

$$H_2O\cdot\cdot HF + F^- \rightleftharpoons H_2O + HF_2^- \qquad (4)$$
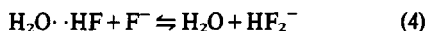
bifluoride side.

Evidence for the ion $[HPO_3H_2F]^-$ existing in aqueous solution was sought with the aid of ^{17}O, ^{19}F, and ^{31}P NMR spectroscopy. No unambiguous confirmation of its presence under these conditions was found. The spectra did nevertheless reveal some information.

The ^{17}O chemical shift of the phosphite oxygens is shown in Fig. 1 which reveals a sharp discontinuity at $112.5\,ppm$ corresponding to the end-point of (1). The value of $\delta(^{17}O, HPO_3H^-)$ is the same as that reported by Christ *et al.*[27] For HPO_3H_2 and HPO_2H^- the half-height line-width was $205\,Hz$, much less than the $600\,Hz$ reported,[27] and the doublet structure easily observed as $J_{OP} = 91.6\,Hz$, which is of the same order as the $98\,Hz$ of $J_{OP}[HPO(OMe)_2]$ and similar compounds.[28]

In this system the change in $\delta(^{17}O, HPO_3H_2)$ can be explained as simply due to the neutralization of the strongest acid proton by the base F^-. There is no in-
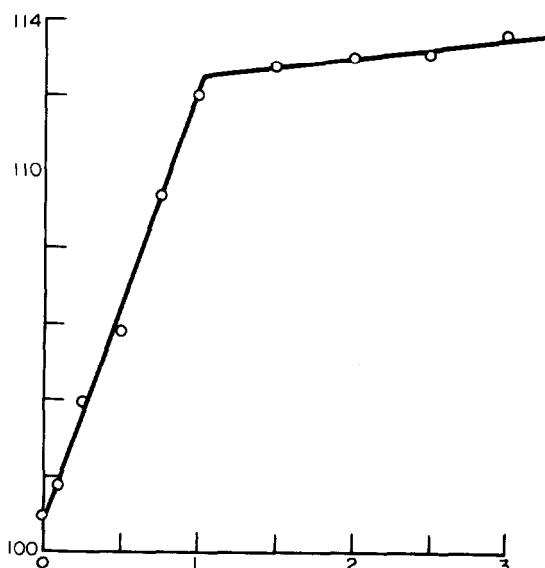
Fig. 1. $\delta(^{17}O, HPO_3H_2)$ vs mole ratio of added KF; $[HPO_3H_2 = 1.0\,m]$.

dication of any very strong hydrogen bonding between the conjugate base HPO_3H^- and HF or F^- even when the latter is in an excess beyond that necessary for the formation of HF_2^-.

The ^{19}F NMR signal from these solutions varies during the addition of KF to HPO_3H_2 solution in the manner shown in Fig. 2. The changes in $\delta(^{19}F)$ can be explained in terms of (1) and (4). In solutions of composition up to half neutralization there is an upfield shift from $\delta(F^-) = 118\,ppm$ towards $\delta(HF\,aq) = -196\,ppm$ as expected. No indication exists as to whether the HF is hydrogen bonding to HPO_3H^- or H_2O.

At half neutralization the signal begins to move downfield and almost linearly; back extrapolation to the
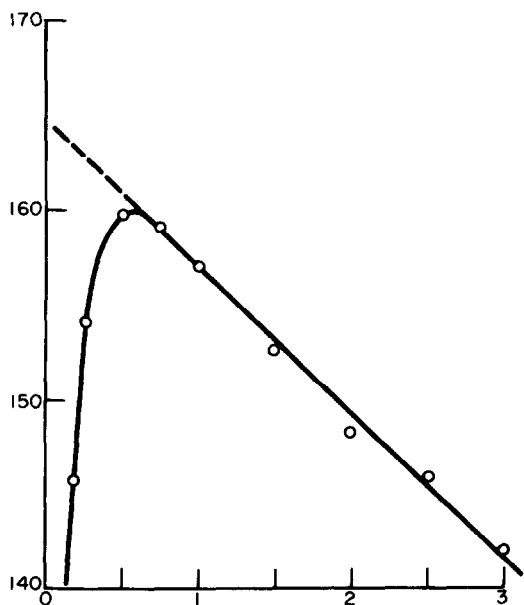
Fig. 2. $\delta(^{19}F, KF\,aq)$ vs mole ratio of added HPO_3H_2; $[HPO_3H_2 = 1.0\,M]$.

vertical axis gives a $\delta(^{19}F)$ of -165 ppm, exactly the value quoted for aqueous HF_2^-.[29] Thus above a ratio of $0.5:1$ of $KF:HPO_3H_2$ the predominant fluoride environment would appear to be HF_2^-, which exchanges with F^- as the ratio of $F^-:HF_2^-$ increases, thus causing the further downfield shift.

In methanol solution $KF.HPO_3H_2$ has moderate solubility and $\delta(^{19}F) = -184.8$ ppm, which is about that of HF and in the region expected for a strong hydrogen bond as in (I). Extra KF can be dissolved in such solutions up to a maximum ratio of $1.75\ KF:1\ HPO_3H_2$ (at 0.1 M concentration), and the signal moves downfield to -174.8 ppm. This is not likely to be due to the formation of HF_2^-, which is insoluble in this solvent but rather to the hydrogen bonded complex $[HPO_3H_2F_2]^{2-}$ with both protons of the acid engaged in such bonds.

The effect on $\delta(^{31}P, HPO_3H_2)$ of adding KF to its solution is shown in Fig. 3. There is also a sharp discontinuity at equimolar concentrations. Excess fluoride has little effect on $\delta(^{31}P, HPO_3H^-)$ showing that no strong hydrogen bonding is occurring between them.

The addition of KF to HPO_3H_2 however results in a broadening of the ^{31}P signal which reaches a maximum of 20 Hz $(W_{1/2})$ at half neutralization, and then disappears at the equimolar concentrations of the end point. This broadening would seem to support the formation of $HPO_3H_2F^-$.

The effect of hydrogen bonding on J_{PH} of hypophosphorous acid has been noted.[30] The principal influences on J_{PH} was the immediate acid proton environment of the molecule: thus $J_{PH}(H_2PO_2H_2^+) > J_{PH}(H_2PO_2H) > J_{PH}(H_2PO_2^-)$. The effect on $J_{PH}(HPO_3H_2)$ of added F^- is to change it from 674 Hz to 668 Hz (0.25 $KF:HPO_3H_2$), to 659 Hz (0.5:1), to 651 Hz (0.75:1) to 643 Hz (1:1), to 630 Hz (2:1), to 621 Hz (3:1) to 612 Hz (4:1). The value for $K^+HPO_3H^-$ in solution is 563 Hz. These values suggest that the acid protons of phosphorous acid are not being effectively removed by F^- to give HPO_3H^-, even when the base F^- is in excess. A close association of the

conjugate base with the HF in the formation of $[HPO_3H.HF]^-$ would explain the J_{PH} values observed. Equilibrium (3) may not be entirely upset in favour of (4) under these conditions.

Conductance and pH changes as a solution of 0.1 M HPO_3H_2 is titrated with 0.7 M KF are shown in Fig. 4. The results are consistent with (2) followed by (4). In the original study of $KF.HPO_3H_2$, crystals were first obtained by dehydrating $KHPO_3H$ solution in aqueous HF and these were then extracted with methanol to obtain the desired product. We were interested to see if the original crystals from aqueous solution contained KHF_2, as might be expected. When a solution of KF in glacial acetic acid is evaporated to dryness the resulting crystals are a mixture of the various strongly hydrogen bonded salts KHF_2, $KH(CH_3CO_2)_2$ and $KF.CH_3CO_2H$.[17] KHF_2 is particularly easily characterized by a strong sharp peak at *ca* 1200 cm^{-1}.

The i.r. spectrum of our crystals consists of very broad bands as expected for a strongly hydrogen bonded complex. The region 3500–1500 cm^{-1} shows a continuum with three broad maxima at *ca* 2750, 2250 and 1700 cm^{-1}. Below this there are sharper bands at 1255s, 1195 (sh), 1155s, 1078s, 1050s, 1015s, 910m, 835mw, 540s, 480s, and 445w cm^{-1} (KBr disc). The shoulder at 1195 cm^{-1} could arise from KHF_2 but in any event this cannot be a major component of these crystals.

In conclusion it can be said that an aqueous solution of HPO_3H_2 and KF behaves as if it were HPO_3H^- and HF, and that there is some evidence for an association between them in terms of a hydrogen bond. Addition of excess KF produces HF_2^-. *Ab initio* calculations suggest that the hydrogen bond in $[HPO_3H_2F]^-$ is not as strong as other hydrogen bonds formed between the fluoride ion and molecules containing first row atoms, yet the structure of (I) shows short, and therefore strong, hydrogen
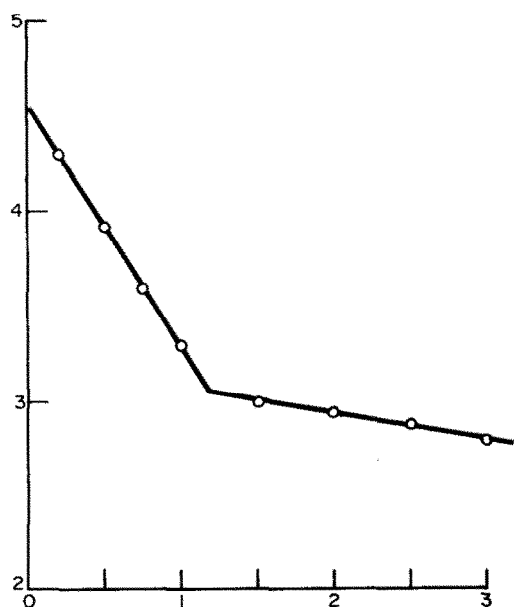
Fig. 3. $\delta(^{31}P, HPO_3H_2)$ vs mole ratio of added KF; $[HPO_3H_2 = 1.0\ M]$.
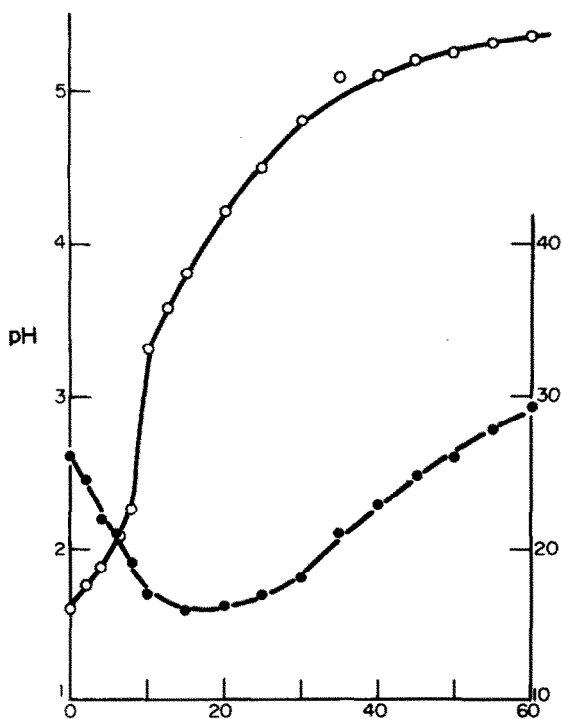
Fig. 4. pH and conductance (mmhos) plots for HPO_3H_2 (0.1 M) titrated with KF (0.7 M).
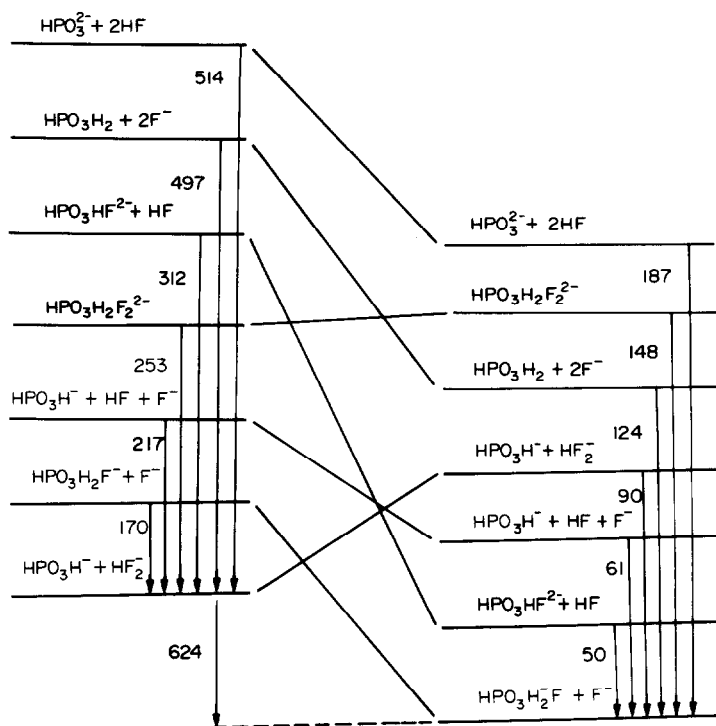
Fig. 5. Relative energy diagram for all combinations of $HPO_3H_2 + 2F^-$, not to scale. ($[6s4p1d/4s2p/2s1p]$ basis set.)

bonds. Crystals of composition $KF.HPO_3H_2$ grown from aqueous solutions are not the same as those from methanol i.e. (I), and they may even be a mixed phosphite bifluoride salt reflecting the species that are present in solution.

REFERENCES

[1] J. H. Clark, J. Emsley, D. J. Jones and R. E. Overill, *J. Chem. Soc. Dalton* 1981, 1219.
[2] J. Emsley, *Chem. Soc. Revs.* 1980, **9**, 93.
[3] J. Emsley, D. J. Jones and R. S. Osborn, *J. Chem. Soc. Chem. Comm.* 1980, 703; D-form: J. Emsley, D. J. Jones and R. Kuroda, *J. Chem. Soc. Dalton* 1981, 2141.
[4] R. Allman and W. Haase, *Inorg. Chem.* 1976, **15**, 804.
[5] R. Allman, *Acta Cryst.* 1976, **32B**, 1025.
[6] H. Altenburg and D. Mootz, *Acta Cryst.* 1971, **27B**, 1982.
[7] D. Heinz and M. Röhner, *Z. Chem.* 1969, **9**, 113.
[8] H. Falius, D. Mootz and H. Altenburg, *Angew. Chem. Int. Edn.* 1970, **9**, 459.
[9] J. A. Pople *et al. QCPE*, University of Indiana, 1978, **10**, 368.
[10] I. H. Hillier and V.R. Saunders, *Int. J. Quantum Chem.* 1973, **7**, 699.
[11] R. E. Overill, King's College Computing Bulletin, K5.10/1, 1980.
[12] R. Ditchfield, W. J. Hehre and J. A. Pole, *J. Chem. Phys.* 1971, **54**, 724; W. J. Hehre and W. A. Lathan, *J. Chem. Phys.* 1972, **56** 5255.
[13] T. H. Dunning, *J. Chem. Phys.* 1970, **53**, 2823; *Modern Theoretical Chemistry*, (Edited by H. F. Schaefer), vol. 3, p. 240 New York (1977).
[14] B. Roos and P. Siegbahn, *Theoret. Chim. Acta* 1970, **17**, 199.
[15] J. Emsley, O.P.A. Hoyte and R. E. Overill, *J. Am. Chem. Soc.* 1978, **100**, 3303.
[16] G. Diercksen, W. Kraemer and B. Roos, *Theor. Chim. Acta* 1974, **36**, 249; A. Støgard, A. Strich, B. Roos and J. Almlöf, *Chem. Phys.* 1975, **8**, 405; E. Clementi, H. Kistenmacher and H. Popkie, *J. Chem. Phys.* 1973, **59**, 5842.
[17] J. Emsley, J. Lucas and R. E. Overill, *Chem. Phys. Letts.* 1981, **84**, 593.
[18] R. C. Weast ed., *CRC Handbook of Chemistry and Physics*, 60/Edn, B106. CRC Press, Boca Raton, Florida (1980).
[19] J. Emsley, D. J. Jones and R. Kuroda, *J. Chem. Soc. Dalton* 1982, 1179.
[20] J. Emsley, D. J. Jones, R. S. Osborn and R. E. Overill, *J. Chem. Soc. Dalton* 1982, 809.
[21] Ref. 18 D165.
[22] W. J. Bouma and L. Random, *Chem. Phys. Lett.* 1979, **64**, 216; J. Emsley and R. E. Overill, *ibid.* 1979, **65**, 616.
[23] J. Emsley, V. Gold, J. Lucas and R. E. Overill, *J. Chem. Soc. Dalton* 1981, 783.
[24] J. Emsley, D. J. Jones, J. M. Miller, R. E. Overill and R. A. Waddilove, *J. Am. Chem. Soc.* 1981, **103**, 24.
[25] G. H. F. Diercksen and W. P. Kramer, *Chem. Phys. Lett.* 1970, **5**, 570.
[26] P. A. Giguère and S. Turrell, *J. Am. Chem. Soc.* 1980, **102**, 5473.
[27] H. A. Christ, P. Diehl, H. R. Schneider and H. Dahn, *Helv. Chim. Acta* 1961, **44**, 866.
[28] C. Rodger, N. Sheppard, H. C. E. McFarlane and W. McFarlane in *NMR and the Periodic Table* (Edited by R. K. Harris and B. E. Mann). Chap. 12, p. 399. Academic Press, London (1978).
[29] R. Hague and L. W. Reeves, *J. Am. Chem. Soc.* 1967, **89**, 250.
[30] J. H. Clark, J. Emsley and T. B. Middleton, *J. Chem. Soc. Dalton* 1979, 1963.

RESONANCE INDUCED PROPERTIES IN MONOTHIOCARBAMATES DERIVED FROM AROMATIC AMINES: COMPARISON OF THE COORDINATION CHEMISTRY OF INDOLE AND INDOLINE MONOTHIOCARBAMATES[1]

ROBERT D. BEREMAN,* DONALD M. BAIRD, JON BORDNER and JAY R. DORFMAN
Department of Chemistry, North Carolina State University, Raleigh, NC 27650, U.S.A.

Abstract—The syntheses of two new monothiocarbamate ligands and selected transition element complexes of each are reported. The complexes of indoline-N-carbothioate (*intc*) prepared are: $NiL_2 \cdot 1.5H_2O$, ZnL_2, $NiL_2 \cdot 2py$, $ZnL_2 \cdot 2py$. The complexes of indole-N-carbothioate (*iltc*) are: NiL'_2, ZnL'_2, CuI'. IR spectral results support a bidentate ligand behavior for both new monothiocarbamates except in $ZnL_2 \cdot 2py$. Comparison of the IR spectral features of *bis*(indolylcarbamoyl)-disulfide with that of coordinated indole-N-carbothioate allowed an assignment of the C–S and C–O vibrational frequencies. Evidence for differences in major resonance contributions to the electronic structures of each new ligand are presented. The crystal structure of the *bis*(indolylcarbamoyl)disulphide is also presented and a comparison is made to pyrrole-N-carbothioate, another aromatic amine monothiocarbamate. The disulphide crystallizes in the centrosymmetric monoclinic space group $P2_1/c$ with $a = 15.645(4)$Å, $b = 5.228(1)$Å, $c = 19.271(7)$Å, $\beta = 97.20(2)°$, $V = 1564(1)$Å^3, d(obsd)(calcd) = (1.50)(1.52) for a molecular weight = 356.1 and $Z = 4$. Diffraction data were collected with a Syntex P1 diffractometer with Cu$K\alpha$ radiation. Least squares refinement resulted in $R_f = 7.0\%$ for all 1213 non zero reflections have (I) $> 3\sigma$(I).

INTRODUCTION

In contrast to the large amount of work which has centered on the coordination chemistry of dithiocarbamate (dtc) complexes in recent years,[2] much less attention has been drawn to possibly more interesting monothiocarbamate ligands (mtc).[3] A comparison of potential resonance contributions to the ground state electronic structures of dithiocarbamates (Scheme I) with that of monothiocarbamates (Scheme II) suggests that a wider variety of chemistry might be expected to result from these latter systems. These *seem* to be supported from the limited structural results available for monothiocarbamate complexes.[4] It is also apparent that the sulphur atom in dialkyl-monothiocarbamates has considerable "mercaptide" character and polymeric complexes often result.[4c,5,6] To date, the primary

concern in monothiocarbamate chemistry has been to determine if differences between similar monothio- and dithiocarbamates exist. In an effort to alter the reactivity *within* the monothiocarbamate class, we have attempted to affect the bonding properties of the –COS moiety by altering the peripheral ligand structure. We have shown that the coordination chemistry of dithiocarbamate and dithiolate ligands can be dramatically altered by choosing R groups which favour one of the various possible resonance structures.[7,8] In particular, we have employed aromatic amines in dithiocarbamate complexes which virtually eliminate resonance form IB (Scheme I) and new coordination complexes and structures resulted.[7] In addition, we have recently shown that pyrrole-N-carbothioate(ptc) does yield coordination compounds of different stoichiometry ($Ni_2(ptc)_4 \cdot THF$)[9] or electronic structure ($Ni(ptc)_2py_2$)[4f] than dialkylmonothiocarbamates.

*Author to whom correspondence should be addressed.

Scheme 1.

Scheme 2.

iltc

intc

iltc–iltc
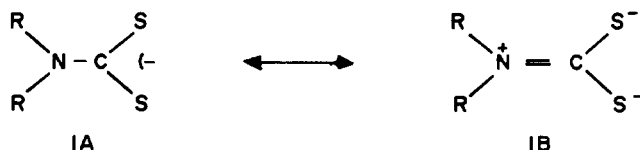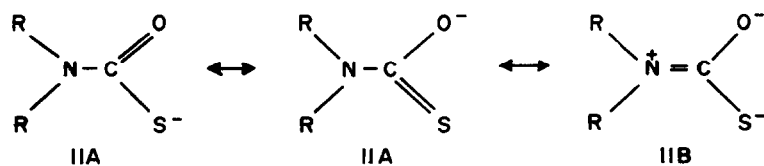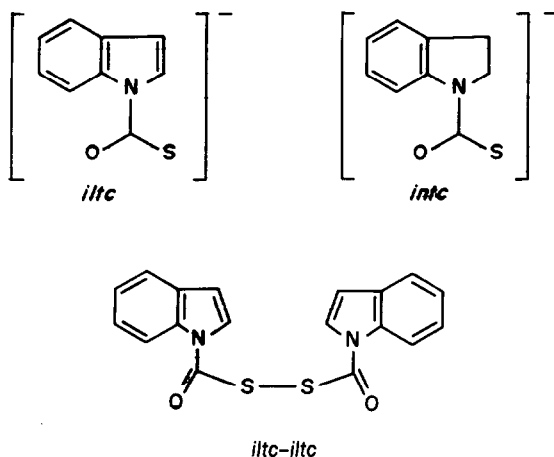
To establish more firmly the chemistry observed to date, we have prepared the aromatic amine monothiocarbamate derived from indole and the nonaromatic analogue derived from indoline. These ligands, *iltc* and *intc*, respectively, and representative transition element complexes have been prepared. Particular attention has been given to the assignment of the IR vibrational features due to the ligands and the interpretation of differences observed. In order to facilitate this IR study, the disulphide (*iltc–iltc*) derived from the indole ligand was prepared. The crystal and molecular structure of this molecule is also reported and a comparison of the significant bond distances is made with those reported[4j] in Ni(ptc)$_2$py$_2$ in order to further establish the nature of the resonance contributions in these new monothiocarbamates.

EXPERIMENTAL

Syntheses

Potassium indole-N-carbothioate (Kiltc). Indole (0.05 mole) was dissolved in 100 ml of dry THF (distilled from Na/benzophenone) under Ar. Potassium metal (0.05 mole) was added to the stirred solution and H$_2$ evolution began immediately. This reaction was allowed to continue for 24 hr during which a fine white precipitate formed. The reaction mixture was cooled to 0° and COS was bubbled into the solution until the solid dissolved (5 min.). This was followed by passing Ar into the solution to remove excess COS. Dry, chilled pentane was then added until a slightly turbid solution was produced. Refrigeration of this mixture for several hours produced a white, extremely air sensitive powder. The product was collected by filtration and used without further purification (yield ~ 80%).

Potassium indoline-N-carbothiolate (Kintc). Kintc was prepared as with *Kiltc* above. However, once formed, *Kintc* is air and moisture stable and can be handled in the atmosphere (yield ~ 95%).

Ni(*intc*)$_2$·1.5 H$_2$O. Kintc (1.0 g) was dissolved in 50 ml of 95% ethanol to which was added a solution of 0.71 g of NiBr$_2$·6H$_2$O in 50 ml of 95% ethanol. A green precipitate formed immediately and the reaction mixture was stirred for 1 hr. The product was collected by filtration, washed with ethanol and ether, and dried under vacuum (yield ~ 70%). IR data indicated that H$_2$O was present in the product. Found: C, 48.87; H, 4.36; S, 14.49; N, 6.34; Calc. for C$_{36}$H$_{30}$N$_4$O$_7$S$_4$Ni$_2$: C, 48.88; H, 4.56; S, 14.50; N, 6.33%.

Zn(*intc*)$_2$. This white compound was prepared in an identical manner to Ni(*intc*)$_2$·1.5 H$_2$O using ZnBr$_2$ (yield ~ 85%). Found: C, 51.00; H, 3.90; S, 15.60; N, 6.60. Calc. for C$_{18}$H$_{12}$N$_2$O$_2$S$_2$Zn: H, 3.82; S, 15.20, N, 6.64%.

Ni(*intc*)$_2$·2py. This compound was prepared by the recrystallization of Ni(*intc*)$_2$·1.5 H$_2$O from pyridine. Found: C, 58.57; H, 4.63; S, 11.09. Calc. for C$_{28}$H$_{22}$N$_4$O$_2$S$_2$Ni: C, 58.65; H, 4.57; S, 11.19%.

Zn(*intc*)$_2$·2py. This compound was prepared by recrystallization of Zn(*intc*)$_2$ from pyridine. Spectroscopic analysis for pyridine confirmed the stoichiometry.

Cu(*iltc*). Two equivalents of *Kiltc* in anhydrous THF were added to a solution of one equivalent of CuBr$_2$ in anhydrous THF. The intense colour characteristic of Cu(II) disappeared rapidly and an orange precipitate formed (yield ~ 70%). Found: C, 45.30; H, 3.25. Calc. for C$_9$H$_6$NOSCu: C, 45.58; H, 3.40%.

Ni(*iltc*)$_2$. K(*iltc*)$_2$ (1.0 g) in 50 ml of anhydrous THF was added very slowly to 0.50 g of NiBr$_2$ in 50 ml of anhydrous THF. A yellow solution and a white precipitate formed. The solid KBr was removed by filtration, the volume of the solution was reduced and anhydrous hexane was added. Refrigeration of this solution resulted in the formation of an air sensitive yellow powder. The product was collected by filtration and dried under vacuum for several hours. An IR spectrum showed that no THF was present in the dry product (yield ~ 80%).

Zn(*iltc*)$_2$. This white product was prepared employing the same procedure as that for Ni(*iltc*)$_2$ (yield ~ 70%).

Bis(indolylcarbamoyl)disulphide (iltc–iltc). The solution obtained after the isolation of Cu(*iltc*) above, when cooled yielded the disulphide of indole-N-carbothioate. Found: C, 61.23; H, 3.50: S, 18.32. Calc. for C$_{18}$H$_{12}$N$_2$O$_2$S$_2$: C, 61.34; H, 3.43; S, 18.20%.

Analyses. Elemental analyses were carried out at Atlantic Microlabs, Atlanta, Georgia.

Spectroscopic methods. IR spectra were recorded on a Perkin–Elmer 512 spectrophotometer using mull prepared in an inert atmosphere. Electronic spectra were recorded either on a Cary 14 or Hitachi 110 spectrophotometer.

CRYSTAL DATA COLLECTION AND STRUCTURE DETERMINATION

A nearly cubic crystal (0.14 mm × 0.16 mm × 0.20 mm) of *bis*(indolylcarbamoyl)disulphide was obtained from a slow evaporation of a saturated THF solution.

The crystal survey, unit cell dimension determination and data collection were accomplished on a Syntex P1̄ diffractometer using copper radiation ($\lambda = 1.5418$ Å) at room temperature employing procedures common to these laboratories.[10] Details of the crystal survey and data collection parameters are summarized in Table 1.

The diffractometer output and all subsequent crystallographic calculations were processed using subprograms of the CRYM crystallographic computer system.[11] Data processing procedures were as before.[10]

The refined coordinates were plotted using the ORTEP computer program of Johnson[12] (Fig. 1). Thermal parameters are available as part of the supplementary materials. Tables 2 and 3 contain final significant bond distances and angles. All other data pertaining to the structure have been deposited.†

RESULTS AND DISCUSSION

Potassium indole-N-carbothioate is a white, extremely air and moisture sensitive solid. All manipulations involving this ligand were done under inert atmosphere conditions. We were primarily interested in neutral complexes of divalent metals and Ni(II) and Zn(II) complexes were studied in detail. However, Cr(III) and Fe(III) complexes were also prepared as well as [Mo(II)]$_2$ compounds and these will be reported later.

---

†*Supplementary material available.* A listing of observed and calculated structure factor amplitudes (8 pages), atom coordinates (2 pages), and nonhydrogen anisotropic temperature factors (1 page) have been deposited with the Editor from whom copies are available on request. Atomic coordinates have also been deposited with the Cambridge Crystallographic Data Base.

Table 1. Physical data and data collection parameters

Molecular Formula	$C_{18}H_{12}N_2O_2S_2$
Molecular Weight	356.1
Crystal size, mm	0.14 x 0.16 x 0.20
Cell Dimensions	
$\underline{a}$, Å	15.645(4)
$\underline{b}$, Å	5.228(1)
$\underline{c}$, Å	19.271(7)
β, deg.	97.20(2)
V, Å^3	1564(1)
Space Group	$P2_1/c$
Molecules/unit cell	4
d calcd, g/cm^3	1.52
d obsd[a], g/cm^3	1.50
Scan Technique	θ/2θ
Scan Speed	$2°/min$ in 2θ
Scan Width	$1.2°$ below $K\alpha_1$, to $1.2°$ above $K\alpha_2$
Background Count Time	0.6 x scan time on each side of peak
No. of reflections	1613
No. of nonzero reflections[b]	1213

[a]Density was measured by the flotation technique using Hexane/1,3 Dibromo-ethane

[b]All intensities with values less than 3 x standard deviation were set equal to zero with zero weight.
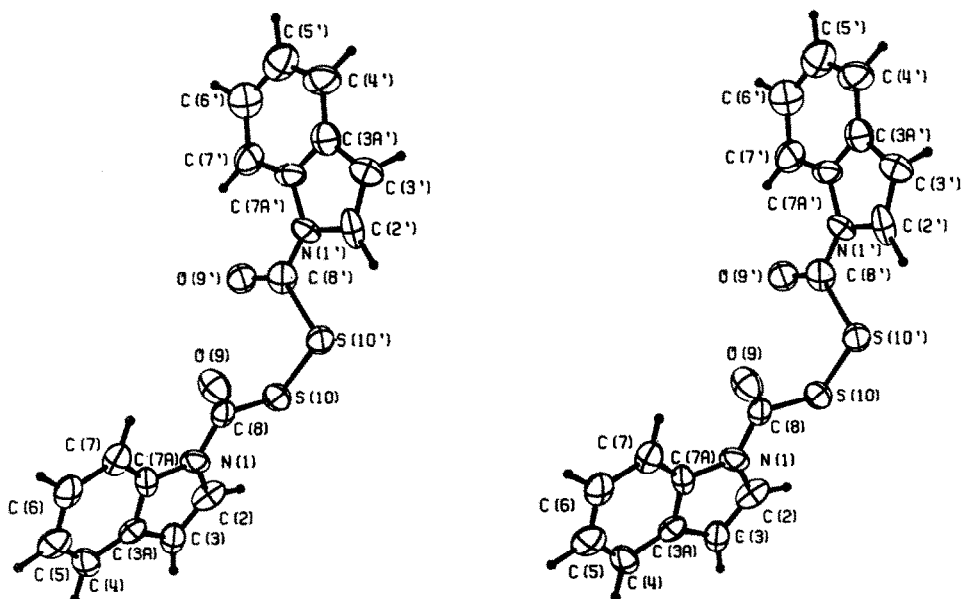
Fig. 1. Sterescopic ORTEP drawing 50% probability ellipsoids.

Table 2. Bond distances (Angstroms) in *Iltc–Iltc*

N(1)-C(2)	1.391(10)	N(1')-C(2')	1.409(10)
N(1)-C(7A)	1.425(10)	N(1')-C(7A')	1.400(11)
N(1)-C(8)	1.397(10)	N(1')-C(8')	1.391(11)
C(2)-C(3)	1.352(12)	N(2')-C(3')	1.336(13)
C(3)-C(3A)	1.452(11)	N(3')-C(3A')	1.430(12)
C(3A)-C(4)	1.397(12)	C(3A')-C(4')	1.381(12)
C(3A)-C(7A)	1.402(12)	C(3A')-C(7A')	1.382(12)
C(4)-C(5)	1.369(12)	C(4')-C(5')	1.368(14)
C(5)-C(6)	1.403(12)	C(5')-C(6')	1.381(13)
C(6)-C(7)	1.388(12)	C(6')-C(6')	1.390(13)
C(7)-C(7A)	1.372(11)	C(7')-C(7A')	1.384(12)
C(8)-O(9)	1.183(10)	C(8')-O(9')	1.204(10)
C(8)-S(10)	1.826(3)	C(8')-S(10')	1.801(9)
S(10)-S(10')	2.014(3)		

Table 3. Bond angles (degrees) in *Iltc–Iltc*

C(7A)-N(1)-C(2)	108.9(6)	C(7A')-N(1')-C(2')	107.4(7)
C(8)-N(1)-C(2)	127.8(7)	C(8')-N(1')-C(2')	126.4(7)
C(8)-N(1)-C(7A)	123.2(6)	C(7')-N(1')-C(7A')	126.1(7)
C(3)-C(2)-N(1)	109.5(7)	C(3')-C(2')-N(1')	109.4(7)
C(3A)-C(3)-C(2)	107.8(7)	C(3A')-C(3')-C(2')	107.9(8)
C(4)-C(3A)-C(3)	132.7(7)	C(4')-C(3A')-C(3')	132.2(8)
C(7A)-C(3A)-C(3)	107.7(7)	C(7A')-C(3A')-C(3')	107.7(8)
C(7A)-C(3A)-C(4)	119.6(7)	C(7A')-C(3A')-C(4')	119.9(8)
C(5)-C(4)-C(3A)	117.8(7)	C(5')-C(4')-C(3A')	119.2(8)
C(6)-C(5)-C(4)	121.6(8)	C(6')-C(5')-C(4')	120.2(8)
C(7)-C(6)-C(5)	121.3(7)	C(7')-C(6')-C(5')	122.1(8)
C(7A)-C(7)-C(6)	116.4(7)	C(7A')-C(7')-C(6')	116.3(8)
C(3A)-C(7A)-C(1)	106.1(6)	C(3A')-C(7A')-C(1')	107.5(7)
C(7)-C(7A)-N(1)	130.7(7)	C(7')-C(7A')-N(1')	130.3(8)
C(7)-C(7A)-C(3A)	123.2(7)	C(7')-C(7A')-C(3A')	122.1(8)
O(9)-C(8)-N(1)	125.8(7)	O(9')-C(8')-N(3')	123.2(8)
S(10)-C(8)-N(1)	111.0(6)	S(10')-C(8')-N(1')	112.4(6)
S(10)-C(8)-O(9)	123.2(6)	S(10')-C(8')-O(9')	124.4(6)
S(10')-S(10)-C(8)	99.4(3)	C(8')-S(10')-C(10)	101.5(3)

Indoline, unlike indole is not an aromatic amine and we expected that *intc* would behave as a normal dialkyl monothiocarbamate. If *intc* does indeed behave as a normal monothiocarbamate, then any difference between the properties of *intc* and the aromatic analogue *iltc* could be attributed to a decrease in the importance of the resonance form which concentrates charge on the amine nitrogen. (Clearly, both of these ligand systems have very similar steric properties, and the ligand "bite" should be nearly the same for each.) *Intc* was synthesized using the same procedure used to produce *iltc*. However, *Kintc* is air and moisture stable. Once isolated it can be stored under ambient conditions for long periods. The transition metal complexes of *intc* could be formed in aqueous ethanolic solution in open vessels. The Ni(II) and Zn(II) complexes were synthesized as well as *bis*-pyridine adducts of the Ni(II) and Zn(II) compounds. The reaction between *intc* and $Mo_2(Ac)_4$ was studied but will be reported later.

We were interested in two aspects of these ligands. First, what were the resonance properties of *intc* and *iltc* relative to those of dialkyl monothiocarbamates? Second, if the aromatic amine ligand does have peculiar resonance properties, how would the reactivity patterns of the ligand be affected?

With respect to the first point, an IR analyses of a series of metal complexes of these ligands could provide the information on the resonance properties. A great deal of work has centred on the positions of the ν(C⚊O) and ν(C⚊N) as well as ν(C—S) frequencies in the IR spectra of dialkyl monothiocarbamate complexes. It has been generally felt that dialkyl monothiocarbamates favoured resonance form IIB with some contribution from form IIA (Scheme II). Thus, IR spectra of R_2mtc should have resonances corresponding to a partial carbon-to-nitrogen double bond as well as a partial carbon-to-oxygen bond. The carbon-to-sulphur bond vibration, on the other hand, should be found in a region corresponding to a single bond. Early reports by Krankovits *et al.*[13] and

McCormick *et al.*[14] assigned a broad, strong band between $1500\,cm^{-1}$ and $1600\,cm^{-1}$ to ν(C⚊O) and ν(C⚊N). The position of this band will be indicative of the electronic properties of the various monothiocarbamates and therefore a study of the position of this band in the aromatic monothiocarbamate complexes should prove useful.

ν(C⚊S) bands have been reported in most cases to occur in the $650-700\,cm^{-1}$ region. This corresponds to the single carbon to sulphur bond region. Fay, on the other hand, reported ν(C–S) in the $950-1000\,cm^{-1}$ region for dithiocarbamates.[15]

The ν(C⚊O) band in the potassium salt *iltc* appears at $1525\,cm^{-1}$. The same band for Me_2mtc is reported at $1519\,cm^{-1}$ while Et_2mtc is at $1520\,cm^{-1}$.[15] The higher frequency found in the new ligand reported here is taken as indicative of increased multiple band character in the carbon to oxygen bond. The equivalent band in the Ni(II) complex appears at $1560\,cm^{-1}$. The question of bonding mode in these complexes arises here since previously values of ν(C⚊O) above $1550\,cm^{-1}$ have been assumed to indicate monodentate coordination through sulfur only. However, since the frequency ν(C⚊S) and ν(C⚊N), ν(C⚊O) in the ligand itself is higher than previously found, it is likely that the ligand is bonded in a bidentate fashion.[16]

A very strong broad band at around $1250-1300\,cm^{-1}$ appeared in all the complexes *iltc*. We suggest that this band is ν(C–N) since it is well within the region normally associated with carbon-to-nitrogen single bond vibrations $(1250-1350\,cm^{-1})$.[17] We suggest this assignment with some confidence, based on three observations. First, the ν(C⚊O) bands in all the *iltc* complexes are fairly sharp as opposed to the often very broad bands exhibited in this region in the dialkyl compound. The broadness of the band in R_2mtc complexes is apparently due to the presence of both the ν(C⚊O) and ν(C⚊N) bands in a highly coupled vibrational state.[18,19] The sharpness of this band in the spectra of our complexes suggests that ν(C⚊O) and ν(C⚊N) vibrations are not highly coupled in *iltc* complexes. Therefore, we might expect to find ν(C⚊N) at some other frequency. Secondly, a band corresponding to ν(C–N) single bond vibration was detected as a strong band at $1250-1300\,cm^{-1}$ in the aromatic dithiocarbamates.[20] The results of an X-ray diffraction study on $Fe(pdtc)_3$ showed a C–N bond distance which approximated a single bond distance of $[1.364(\text{Å})]$.[21]

Finally, we felt that if we could move the ν(C⚊O) band out of the $1500-1600\,cm^{-1}$ region which the strong band at $1250\,cm^{-1}$ remained we could conclude that the ν(C–N) band was not coincident with (C–O). Toward this end bis(indolylcarbamoyl)disulphide was synthesized. Since ν(C⚊O) had been assigned at $1680\,cm^{-1}$ in previous carbamoyldisulphides we felt that *iltc–iltc* would behave similarly.[22,23] The IR spectrum of this molecule does exhibit a band at $1680\,cm^{-1}$, which no bands appear between $1500\,cm^{-1}$ and $1600\,cm^{-1}$. The strong band at $1250\,cm^{-1}$ remains, however. Thus, based on these three pieces of evidence, it seems clear that we could assign this band to the carbon to nitrogen single bond vibration.

The IR band corresponding to the ν(C⚊S) vibration proved difficult to assign. ν(C⚊S) band positions in dithiocarbamates have been reported to occur in the $960-1000\,cm^{-1}$ region. These bonds have been shown crystallographically to possess considerable double bond

character.[24,25] If the resonance properties of the aromatic monothiocarbamate were predominated by a form which imparted some multiple bond character to the C–S bond, we would expect to find a band in the 950–1000 cm^{-1} region. Indeed this was the case. However, most previous reports concerning the IR-spectra of monothiocarbamates assigned a medium intensity band in the 650–700 cm^{-1} region to ν(C–S). A band of this sort also appeared in the spectra of our complexes. It was not until the results of a three dimensional X-ray diffraction study on Ni(ptc)$_2$·2py were obtained that we could make the assignment.[4j] This compound has by far the shortest C–S bond distance reported for a monothiocarbamate. Therefore we assign the band in the 950–1000 cm^{-1} region to ν(C⟶S).

It seems clear then that the aromatic nature of the indole ring does predominate the resonance properties of the monothiocarbamates derived from this amine. Since forms IIA and IIA′, but not IIB (Scheme II) completely describe the electronic structure of these ligands, we might expect the structural properties of *iltc* to mimic those of thiobenzoate rather than other monothiocarbamates.

An IR analysis was also carried out on *Kintc* and the complexes of this ligand. These spectra had two important features. First, the ν(C⟶O), ν(C⟶N) band in the 1500–1600 cm^{-1} region is very strong and very broad. This band in the spectra of *intc* complexes appears to be identical with the analogous band in the spectra of the dialkyl monothiocarbamate complexes. Second, no band assignable to ν(C⟶S) could be found in the 950–1000 cm^{-1} region. However, as is true for dialkyl species, a weak to medium band assignable to ν(C–S) is observed in the 650–700 cm^{-1} region. The broadness of the 1500–1600 cm^{-1} band is apparently due to the presence of both the ν(C⟶O) and ν(C⟶N) bands, as has been proposed by previous workers for dialkyl monothiocarbamate complexes.[13,14] As suggested above, the difference in the ν(C⟶N) resonance frequency is due to a shift in resonance properties brought on by the aromatic nature of indole as compared to indoline. IR spectra of the *intc* complexes indicate a predominance of IIB in Scheme II. The low ν(C–S) frequency along with the rather high ν(C⟶N) frequency are indicative of a C–S bond of essentially single bond character and a C–N bond with considerable multiple bond character. Comparison of the ν(C⟶O) frequency of *Kintc* (1520 cm^{-1}) with that of *Kiltc* (1535 cm^{-1}) show much less multiple bond character in the C–O bond of the non-aromatic *intc* system.

Since resonance form IIB (Scheme II) is much more important in the description of the properties of *intc*, we

would expect the sulphur atom to have considerable "mercaptide" character. This mercaptide character has been implicated as the predominant feature in the structural properties of the dialkyl monothiocarbamates.[4b] The complexes formed in our studies with *intc* are, in every case, identical to the analogous compounds formed with dialkyl monothiocarbamates as ligands (R = Me, Et, Pr, pip, pyr).[4b,18] Ni(*intc*)$_2$ is a green, insoluble solid. This insolubility precluded any molecular weight measurements. However, this same property indicates some degree of polymerization. The electronic spectrum of this compound indicates octahedral coordination for the Ni(II) atom. This fact also indicates some type of polymerization, undoubtedly involving sulphur atoms bridging adjacent Ni atoms, since elemental analysis shows no solvent molecules which might complete the octahedral coordination. In each of these properties Ni(*intc*)$_2$ mimics Ni(R$_2$mtc)$_2$ (R = Me, Et, etc.).[14] On the other hand, Ni(*iltc*)$_2$ is a red, soluble compound which appears to have a structure identical to Ni$_2$(ptc)$_4$·3THF.[9]
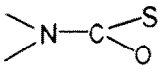
Zn(*intc*)$_2$ is also polymeric in nature as are the dialkyl complexes of Zn.[18] ν(C⟶O) for Zn(*intc*)$_2$ is located at 1530 cm^{-1} while the same band in Zn(pipmtc)$_2$ appears at 1525 cm^{-1}. It is known that reaction of Zn(pipmtc)$_2$ with amine bases such as pyridine or piperidine result in tetrahedral *bis*-amine adducts in which the monothiocarbamate is not coordinated. The X-ray structure of Zn(pipmtc)$_2$·2pip[4f] has been reported. The ν(C⟶O) band in this compound appears at a much higher frequency since the oxygen of the ligand is not bound to Zn. Zn(intc)$_2$ also reacts with pyridine to form Zn(intc)$_2$·2py. ν(C⟶O) is shifted to a frequency of 1590 cm^{-1} and therefore likely has a structure identical to that of the piperidine derivative.

Molecular structure of iltc–iltc

The crystal structure of *bis*(indolylcarbamoyl)disulphide was obtained to investigate the structural characteristics associated with resonance contributions of coordinated aromatic monothiocarbamates to non-delocalized systems. Table 4 summarizes the important bond lengths for this disulphide and also lists those same values found in Ni(ptc)$_2$·2py for comparison.[4j] These data are remarkable in that clearly, little C–N double bond character exists in the coordinated *ptc*. The elongated C–O bond and shortened C–S bond in the coordinated *ptc* are as expected from the IR analyses.

Table 4.

	Ni(ptc)$_2$·2py		iltc-iltc	
N–C	1.409 (12)	1.392 (14)	1.397 (10)	1.391 (11)
C–O	1.254 (12)	1.231 (11)	1.183 (10)	1.204 (10)
C–S	1.675 (10)	1.713 (10)	1.826 (8)	1.801 (9)

REFERENCES

[1]This paper is number 23 in the series, Coordination Chemistry of New Sulphur Containing Ligands, Paper Number 22. R. D. Bereman, D. M. Baird, J. R. Dorfman and J. Bordner, *Inorg. Chem.* 1982, **21**, 2365.

[2a]D. Coucouvanis, *Prog. Inorg. Chem.* 1970, **11**, 294; [b]D. Coucouvanis, *Prog. Inorg. Chem.* 1979, **26**, 301; [c]R. P. Burns, F. P. McCullough and G. A. McAuliffe, *Adv. Inorg. Radiochem.* 1980, **23**, 211.

[3]J. B. McCormick, R. D. Bereman and D. M. Baird, *Coor. Chem. Rev.* submitted.

[4a]J. Ahmed and J. A. Ibers, *Inorg. Chem.* 1977, **16**, 935; [b]C. G. Pierport, P. C. Dickinson and B. J. McCormick, *Inorg. Chem.* 1974, **13**, 1674; [c]B. F. Hoskins and C. D. Pannan, *Inorg. Nucl. Chem. Letters* 1974, **10**, 229; [d]R. Hesse and U. Aava, *Acta Chem. Scand.* 1970, **24**, 1355; [e]P. Janniche and R. Hesse, *Acta Chem. Scand.* 1971, **25**, 423; [f]D. L. Greene, B. J. McCormick and C. T. Pierpont, *Inorg. Chem.* 1973, **12**, 2148; [g]W. L. Steffen and R. C. Fay, *Inorg. Chem.* 1978, **17**, 2120; [h]S. L. Hawthorne and R. C. Fay, *J. Am. Chem. Soc.* 1979, **101**, 5270; [i]D. L. Perry, D. H. Templeton and A. Zalkin, *Inorg. Chem.* 1978, **17**, 3699; [j]R. D. Bereman, D. M. Baird, J. R. Dorfman and J. Bordner, *Inorg. Chem.* 1982, **21**, 2365.

[5]J. Willemse, *Inorg. Nucl. Chem. Letters* 1972, **8**, 45.

[6]K. Tanaka, Y. Miya-Uchi and T. Tanaka, *Inorg. Chem.* 1975, **14**, 1545.

[7]R. D. Bereman and D. J. Naleqajek, *Inorg. Nucl. Chem.* 1981, **43**, 423 and references therein.

[8]R. D. Bereman, M. R. Churchill and D. J. Nalewajek, *Inorg. Chem.* 1979, **18**, 3112 and reference therein.

[9]R. D. Bereman, W. Hatfield and D. M. Baird, *Inorg. Nucl. Chem.* 1982, **43**, 2729.

[10]R. D. Bereman, G. D. Shields, J. Bordner and J. Dorfman, *Inorg. Chem.* 1981, **20**, 2165.

[11]J. D. Duchamp, American Crystallographic Association Meeting, Bozeman, Montana, 1964, Paper B-14, p. 29.

[12]C. K. Johnson, "ORTEP" Report ORNL-3794, Oak Ridge National Laboratory, Oak Ridge, Tenn. (1965).

[13]E. M. Krankovits, R. J. Magee and M. J. O'Conner, *Inorg. Nucl. chem. Letters* 1971, **1**, 941.

[14]B. J. McCormick and B. P. Stormer, *Inorg. Chem.* 1972, **11**, 729.

[15]S. L. Hawthorne, A. H. Bruder and R. C. Fay, *Inorg. Chem.* 1978, **17**, 2114.

[16]The IR spectrum of Ni(ptc)$_2$(Ph$_3$P)$_2$ does exhibit ν(C$\because$O), at 1620 cm^{-1}. This high frequency is taken to indicate monodentate bonding through sulfur by those monothiocarbamate ligands.

[17]B. J. McCormick, *Inorg. Chem.* 1968, **7**, 1965.

[18]B. J. McCormick and D. L. Green, *Inorg. Nucl. Letters* 1972, **8**, 599.

[19]C. G. Pierpont, D. L. Green and B. J. McCormick, *J. Chem. Soc., Chem. Commun.* 1972, 960.

[20]R. D. Bereman and D. Nalewajek, *Inorg. Chem.* 1977, **16**, 2687.

[21]R. D. Bereman and D. Nalewajek, *Inorg. Chem.* 1979, **18**, 3112.

[22]S. Araki, K. Matsummoto, K. Tanaka and T. Tanaka, *J. Inorg. Nucl. Chem.* 1976, **38**, 727.

[23]E. L. Gregg, *J. Amer. Chem. Soc.* 1952, **74**, 3691.

[24]H. B. Gray, R. Williams, I. Bernal and E. Billig. *J. Amer. Chem. Soc.* 1962, **82**, 3596.

[25]R. Eisenberg and J. A. Ibers, *Inorg. Chem.* 1965, **4**, 605.

THE STEPWISE FORMATION OF COMPLEXES IN THE URANYL/AZIDE SYSTEM IN AQUEOUS MEDIUM

GILBERTO ORIVALDO CHIERICE*

Instituto de Física e Química de São Carlos, Depto. de Química e Física Molecular, USP, Brasil

and

EDUARDO ALMEIDA NEVES

Instituto de Química da USP, Sao Paulo, Brazil

Abstract—The use of an indirect potentiometric method with the glass electrode in a $N_3^-/HN_3/UO_2^{2+}$ solution leads to ligand number $\bar{n}$, at several azide concentrations, at 2.0 M ionic strength (NaClO₄), aqueous medium and $25.0 \pm 0.1°C$. The analysis of data under conditions where hydrolysis is avoided leads to the six overall stepwise constants: $\beta_1 = 1.39 \times 10^2 \, M^{-1}$; $\beta_2 = 8.26 \times 10^3 \, M^{-2}$; $\beta_3 = 4.9 \times 10^5 \, M^{-3}$; $\beta_4 = 7.1 \times 10^5 \, M^{-4}$; $\beta_5 = 2.3 \times 10^6 \, M^{-5}$; $\beta_6 = 1.2 \times 10^7 \, M^{-6}$.

INTRODUCTION

The reaction of uranyl cations with azide ion gives rise to strongly yellow coloured complexes as has been deduced by Feinstein[1] from spectrophotometric data, and who suggested analytical applications. Equilibrium studies have followed concerning the formation of the monoazide species with the resulting evidence of the existence of three species.[2–5] No mention of azide complexes was found in a review.[6]

Although those studies were not complete, the analytical potentialities alone of the reaction suggest a more detailed study of the complex formation equilibria. These are presented in this paper from measurements in aqueous solutions of ionic strength 2.0 M held with NaClO₄ and at 25°C. This has been conveniently performed by an indirect potentiometric method, by analogy to the one succesfully applied to a similar cobalt II/azide system.[7]

EXPERIMENTAL

Reagents and solutions

All reagents were chemically pure or of analytical grade (Merck, Fisher, K and Lab., Eastman, Carlo Erba). Sodium perchlorate and sodium azide were recrystallized twice from ethanol. Standardization of sodium perchlorate was performed gravimetrically by drying an aliquot of 5 M stock solution (for ionic strength adjustments) to constant weight at 110°C. Recrystallized sodium azide was washed with ethanol, dried in a desiccator over calcium chloride for several hours, followed by one hour in an oven at 110°C. This treatment produces a non-hygroscopic salt which can be used as a primary standard.[7] Uranyl perchlorate was prepared from uranyl acetate by treatment with a controlled excess of diluted perchloric acid and concentrated in a water bath. The uranyl content of the stock solution (1 M, with 0.1 M free perchloric acid), was gravimetrically determined as U_3O_8.[8] The excess of free strong acid (0.1 M) was calculated by pH measurements of 0.1 M uranyl solution at ionic strength 2.0 M held with NaClO₄ (see below).

Apparatus and procedures

A digital potentiometer, Orion 801A, was used in all pH measurements with a glass electrode combined with a calomel

reference electrode filled with saturated sodium chloride solution. All measurements were carried out at $25.0 \pm 0.1°C$. The conditional pH data measured at 2.0 M ionic strength (referring to hydrogen ion concentration instead of activity) require the use of a 2.00 standard pH solution, which is a 0.0100 M perchloric acid solution in 1.99 M NaClO₄. A 5 ml, Methrom piston burette Model EA. 734-5 was used for the reagents.

To 20.00 ml of a working azide solution of ionic strength 2.0 M a volume (0.5–1.5 ml) of 2.000 M perchloric acid was added, to obtain an azide/hydrazoic acid buffer of conditional pH_1. Then one small volume of standard uranyl 1 M solution was added (up to 1.5 ml) and a pH_2 was measured in a few seconds, due to "normal" complex equilibria, readily attained. After that a slow hydrolytic process takes places and a lower pH_3, is measured after its stabilization within ten minutes. The treatments of data with mass balances and all corrections due to dilution by reagent additions, was performed with a program for the Hewlet Packard HP-97 calculator, as described.[7] The pH_1 plus pH_2 data lead to conventional $\bar{n}$ data vs free ligand concentration. The pH_3 data lead to false conventional $\bar{n}$ data in average ligand numbers referred to hydrolyzed complexes if the adequate correction in the program is not introduced (see Results and Discussion). Program for HP-97 (Hewlet Packard Calculator) were used in the integration of $\bar{n}$ vs log (N_3^-) data and in other steps of the whole calculation process.'

RESULTS AND DISCUSSION

(1) *General pattern of the uranyl azide reaction*

The procedure adopted to obtain the equilibrium constants, is a competitive method based on measurement of the change of the conditional pH (referring to hydrogen ion concentration instead of its activity) of an azide/hydrazoic acid buffer, by the presence of uranyl cation. The mass balance applied to the system based on its pH change leads to final values of the ligand and average ligand number ($\bar{n}$) as has been fully discussed.[7]

It should be pointed out that the merit of this approach is to use a conditional pK of the weak acid (HN_3) of each particular working solution, instead of an average value, in order to compensate for some factors which could be a source of error, such as drifts in junction potential or reference electrode potential.

Figure 1 presents a series of selected $\bar{n}$ vs (N_3^-) data

---

*Author to whom correspondance should be addressed.
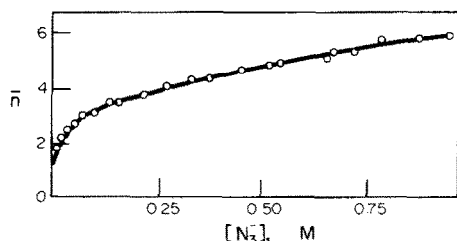
Fig. 1. Experimental data vs ligand concentration for uranyl/azide system, at 25.0°C and ionic strength 2.0 M.

Fig. 2. Tentative $\bar{n}$ data calculation on basis of monohydrolysis of uranyl cation, UO_2OH^+, vs free ligand concention.

referring to uranyl concentrations from 10^{-3} M to 10^{-1} M. The pH changed from 3.3 to 5.1 from the lower to the maximum azide concentration and an average pK of 4.46 ± 0.06 was calculated for hydrazoic acid from the set of the working solutions. No evidence of polynuclear species was found as $\bar{n}$ does not seem too dependent on the uranyl concentration. However, special care was taken in order to avoid hydrolysis of uranyl cation or its complexes, which has been found possible at higher pH and lower azide concentration. The data of Fig. 1 are confidently free from hydrolysis phenomenon (see also Experimental).

The $\bar{n}$ data arrived at for higher ligand concentrations are surprisingly high, evidencing a system with six sucessive complexes. This is not usually found in such a system, possibly because of difficulties inherent in the use of the indirect method, instead of the direct potentiometric one, which is widely accepted as being the most reliable. The uranyl cation is bulky enough to coordinate six monocoordinative ligands especially if the affinity is high enough to exchange some of the several coordinated water molecules and if the ligand is not abnormally large. In fact, recent measurements[9] confirm the existence of more than four thiocyanate ligands in uranyl complexes.

Another series of measurements was taken in conditions which favours hydrolysis, which is a slow process. The first initial equilibrium position is reached a few seconds after uranyl addition. Then a second equilibrium position is achieved after some minutes of pH drift toward lower values. Under such conditions a huge positive error in $\bar{n}$ data results because a false mass balance is considered in the normal calculation program[7] which does not distinguish between the causes of the pH lowering, whether due to complexation of the ligand, or due to hydrogen ions released by hydrolysis. The hydrolysis of uranyl cation was considered in the classical work of Ahrland[10] and that of Sutton.[11] A number of hydrolysis products are formed between the monohydrolysis, species $U_2O(OH)^+$ (actually $U_2O_5^{2+}$), and the fully hydrolysed $UO_2(OH)_2$.

Figure 2 shows an attempt to calculate $\bar{n}$ values from the hydrolyzed solutions based on a quantative formation of complexes with $UO_2(OH)^+$. This was done by including in the mass balances a release of (H^+) from hydrolysis, equivalent to the uranyl concentration. The results in Fig. 2 are highly dispersive and do not fit entirely the model of monohydrolysis. This could be acceptable for ligand concentrations lower than 0.5 M but not for higher ones, because a decreasing $\bar{n}$ is obtained which reveals a high hydrogen ion correction due to hydrolysis. It was inferred that at azide ion concentration higher than 0.50 M and hydrazoic acid
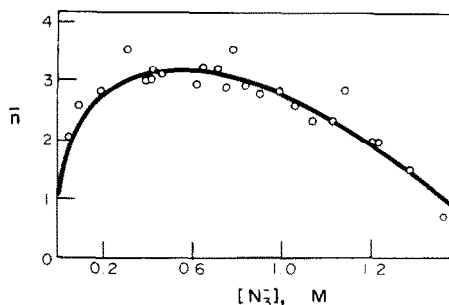
0.1 M the hydrolysis is progressively smaller and can be neglected at 1.0 M azide.

(2) *Calculation of the equilibrium constants*

This system is complicated by the presence of several stepwise complexes. Direct treatment of the $\bar{n}$ function data to obtain formation constants is well known to be inadequate in such cases. The Froneaus function F_0 is a commendable means if it can be obtained by integration from $\bar{n}$ vs $\log(L)$ data as fully discussed formerly.[12,13]

The integration should start from a lower value of $\bar{n}$ than 0.5 and its corresponding ligand concentration. In order to provide short increments in (N_3^-) and $\bar{n}$, conveniently distributed, we have normalized the available data by an appropriate procedure in short ranges by enlarged plot adjustment. In some ranges the $\bar{n}$ and (N_3^-) data were fitted to power, logaritmic or linear curves with the help of a calculator. The normalized data are presented in Table 1 as well as F_0 which is a well known polynomial.[12,13]

$$F_0 = 1 + \sum_1^n \beta_n(L)^n \qquad (1)$$

being β_n the overall formation constant of the species $VO_2(L)_n$ of ligand (L). All those normalized data are in Table 1.

The equilibrium constants were determined through a combination of strategies by using the classical graphic method[13] with some refinements, as will be described below.

The F_1 subsidiary function[13]

$$F_1 = \frac{F_0 - 1}{(L)} = \beta_1 + \beta_2(L) + \cdots \beta_j(L)^{(j-1)} \qquad (2)$$

was plotted vs (N_3^-) and presented a virtually linear relationship at low ligand concentration. A linear regression with the first five point of F_0 vs $((N_3^-)$, by a least squares fit, provided β_1 on intersection and β_2 as a slope. These preliminary data are 139 M^{-1} for β_1 and 9300 M^{-2} for β_2. The F_2 and F_3 subsidiary functions were then calculated[13] and the plot F_3 vs (N_3^-) was found to be a non-linear curve easily extrapolable to obtain β_3, as usual.

The F_4 function was calculated and provided data reliable only for azide concentrations higher than 0.2 M. This has been found to provide a steep non-linear curve when plotted vs (N_3^-), which is

$$F_4 = \beta_4 + \beta_5(N_3^-) + \beta_6(N_3^-)^2. \qquad (2)$$

Table 1. Experimental normalised data

$[N_3]_1 M$	$\bar{n}$	F_0	F_1	F_2	F_3
$6,250.10^{-4}$	0,08	1,0903	$1,4448.10^2$		
$1,250.10^{-3}$	0,16	1,1883	$1,5067.10^2$		
$1,953.10^{-3}$	0,26	1,3064	$1,5687.10^2$		
$2,500.10^{-3}$	0,33	1,4051	$1,6204.10^2$		
$3,906.10^{-3}$	0,52	1,6981	$1,7872.10^2$		
$5,000.10^{-3}$	0,66	1,9644	$1,9288.10^2$		
$6,250.10^{-3}$	0,83	2,3199	$2,1118.10^2$		
$7,813.10^{-3}$	1,03	2,8561	$2,3757.10^2$		
$8,500.10^{-3}$	1,13	3,1284	$2,5040.10^2$		
$1,000.10^{-2}$	1,28	3,8051	$2,8051.10^2$	$1,4151.10^4$	
$1,250.10^{-2}$	1,48	5,1825	$3,3460.10^2$	$1,5648.10^4$	
$1,563.10^{-2}$	1,69	7,3868	$4,0863.10^2$	$1,7250.10^4$	
$1,700.10^{-2}$	1,76	8,5366	$4,4333.10^2$	$1,7901.10^4$	
$2,000.10^{-2}$	1,90	$1,1486.10^1$	$5,2432.10^2$	$1,9206.10^4$	
$2,500.10^{-2}$	2,09	$1,7922.10^1$	$6,7688.10^2$	$2,1515.10^4$	
$3,150.10^{-2}$	2,20	$2,8935.10^1$	$8,9392.10^2$	$2,4157.10^4$	
$4,000.10^{-2}$	2,39	$5,1014.10^1$	$1,2503.10^3$	$2,7782.10^4$	$4,8806.10^5$
$5,000.10^{-2}$	2,53	$8,8810.10^1$	$1,7562.10^3$	$3,2344.10^4$	$4,8168.10^5$
$6,250.10^{-2}$	2,85	$1,6264.10^2$	$2,5863.10^3$	$3,9157.10^4$	$4,9435.10^5$
$8,000.10^{-2}$	2,90	$3,3462.10^2$	$4,1703.10^3$	$5,0391.10^4$	$5,2266.10^5$
$1,000.10^{-1}$	3,14	$6,6407.10^2$	$6,6307.10^3$	$6,4917.10^4$	$5,6657.10^5$
$1,250.10^{-1}$	3,30	$1,3624.10^3$	$1,0891.10^4$	$8,6016.10^4$	$6,2204.10^5$
$1,600.10^{-1}$	3,51	$3,1557.10^3$	$1,9716.10^4$	$1,2236.10^5$	$7,1310.10^5$
$2,000.10^{-1}$	3,76	$7,0985.10^3$	$3,5487.10^4$	$1,7674.10^5$	$8,4240.10^5$
$2,500.10^{-1}$	4,04	$1,6936.10^4$	$6,7741.10^4$	$2,7041.10^5$	$1,0486.10^6$
$3,200.10^{-1}$	4,37	$4,7793.10^4$	$1,4935.10^5$	$4,6628.10^5$	$1,4313.10^6$
$4,000.10^{-1}$	4,70	$1,3146.10^5$	$3,2866.10^5$	$8,2130.10^5$	$2,0326.10^6$
$5,000.10^{-1}$	4,99	$3,8773.10^5$	$7,7546.10^5$	$1,5506.10^6$	$3,0847.10^6$
$6,500.10^{-1}$	5,24	$1,4851.10^6$	$2,2847.10^6$	$3,5147.10^6$	$5,3945.10^6$
$8,000.10^{-1}$	5,60	$4,5762.10^6$	$5,7203.10^6$	$7,1502.10^6$	$8,9274.10^6$
$9,000.10^{-1}$	5,76	$8,9357.10^6$	$9,9286.10^6$	$1,1032.10^7$	$1,2166.10^7$
$9,600.10^{-1}$	5,86	$1,3004.10^7$	$1,3557.10^7$	$1,4121.10^7$	$1,4701.10^7$
$1,000$	5,92	$1,6539.10^7$	$1,6539.10^7$	$1,6538.10^7$	$1,6531.10^7$

The usual extrapolation procedure does not provide a reliable result for this β_4, not only because the curve is steep, but because the extrapolation is performed from high ligand concentration. This is a problem very common in systems with more than four ligands. In order to obtain more reliable data a matrix solution for the three unknown β_4, β_5 and β_6 constants was done based on a weighting factor previously proposed[14] for the F_0 data

$$W'_i = \frac{F_0 \max}{F_i} \qquad (3)$$

On this basis the F_0 data from 0.2 M to 1.0 M [azide] were used to build a system of three equations with six unknowns. As β_2, β_2 and β_3 were known, then a system of three unknowns was obtained, as shown in Table 2.

A refining of the constants started with the use of another auxiliary function, F'_i, where the formation constant terms with higher than two ligands were subtracted out from the F_0 data

$$F'_i =$$
$$\frac{F_0 - (1 + 4.88 \times 10^5 (N_3)^3 + 7.59 \times 10^5 (N_3)^4 + 2.70 \times 10^6 (N_3)^5)}{(N_3^-)}$$
$$\qquad (4a)$$

$$F'_i = \beta_i + \beta_2(L). \qquad (4b)$$

These F'_i data are now much closer to a linear equation than F_1 vs (N_3^-) data. Thus more reliable β_1 and β_2 data were now obtained from linear regression of F'_i vs (N_3^-). Figure 3 shows this typical plot.

The β_3 values were reestructured from these F_3 data in Table 1.

With these new β_1, β_2 and β_3 data a 6×6 system of linear equations was converted in a 3×3 one as shown in Table 2.

The solution of this matrix lead to new values of β_4, β_5, β_6, which were considered final.

An attempt to solve the entire system by a 6×6 matrix did not provide a real value for β_5: It shows that the solution of this system in parts is sometimes more reliable because there is a lack of F_0 data at higher ligand concentration, where the $\bar{n}$ data becomes less and less accurate. The final values are:

$$\beta_1 = \frac{[UO_2(N_3)]^+}{[UO_2^{2+}](N_3^-)} = 1.39 \times 10^{-2} \qquad K_1 = 139$$

Table 2. Conversion of a 6×6 matrix to 3×3 by introducing $\beta_1 = 1.39 \times 10^2\,M^{-1}$, $\beta_1 = 8.26 \times 10^3\,M^{-2}$; $\beta_3 = 5.1 \times 10^5\,M^{-3}$; of the 3×3 matrix: $\beta_4 = 6.1 \times 10^5\,M^{-4}$; $\beta_5 = 3.1 \times 10^6\,M^{-5}$; $\beta_6 = 1.2 \times 10^7\,M^{-6}$

$4.9615 \times 10^7 = 820.89$	$\beta_1 + 189.67$	$\beta_2 + 45.239$	$\beta_3 + 11.172$	$\beta_4 + 2.8605$	$\beta_5 + 0.75912 \quad \beta_6$
$4.9618 \times 10^7 = 78.892$	$\beta_1 + 35.499$	$\beta_2 + 16.443$	$\beta_3 + 7.8749$	$\beta_4 + 3.9136$	$\beta_5 + 2.0218 \quad \beta_6$
$6.6158 \times 10^7 = 6.7783$	$\beta_1 + 5.3251$	$\beta_2 + 5.3251$	$\beta_3 + 4.7751$	$\beta_4 + 4.3143$	$\beta_5 + 3.9267 \quad \beta_6$
$2.5660 \times 10^7 = 11.172$	$\beta_4 + 2.8605$	$\beta_5 + 0.75912$	β_6		
$4.1253 \times 10^7 = 7.8749$	$\beta_4 + 3.9136$	$\beta_5 + 2.0218$	β_6		
$6.3503 \times 10^7 = 4.7741$	$\beta_4 + 4.3143$	$\beta_5 + 3.9267$	β_6		
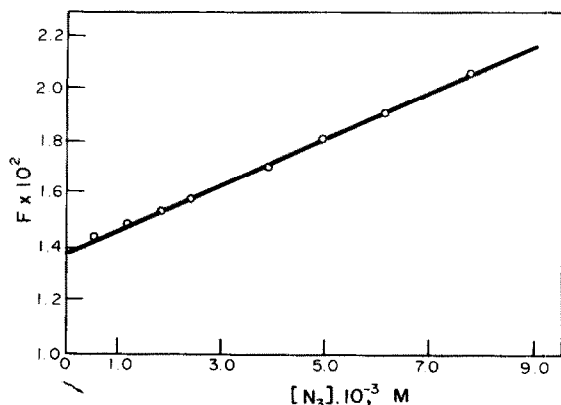
Fig. 3. Plot of F_1^1 data vs (N_3^-) in order to obtain a more reliable β_1 and β_2 (eqn 4).

Fig. 5. The average free energy change per ligand in the uranyl/azide system.

The uncertainty of the constants is not easily estimated. However the calculated F_0 data by eqn (1) differ by $\pm 0.14\%$ from the integrated value. This gives good support for the calculation procedure. The calculated $\bar{n}$ is consistent with the experimental $\bar{n}$ within $\pm 2.8\%$ which is a final test for both experimental data aquisition and calculation procedure. The β_1 and β_2 constants can be expresed in three significant figures and the others β_n by two.

Figure 4 shows the tendency of ligand attachment to uranyl cations. A marked decrease is observed at the entrance of the fourth ligand which could well be related to a change in configuration of the coordination centre.

Figure 5 shows that the average free energy changes non-linearly with the ligand and also presents a break at the third ligand. The literature does not refer to the attachment of six ligands to one uranyl cation. However in a review[16] the existence of several uranyl complexes with three bicoordinative ligands such as carbonate and oxalate was mentioned. The distribution of the ligands was in a hexagonal bipyramid (symmetry D_{6h}) with the two oxo ions placed in the vertical axis.[16,17] The same structure as for these octacoordinated complexes can be similarly attributed to the present system, where up to six small linear ligands can be attached to uranyl cations.

Fig. 4. The tendency toward stepwise attachment of azide ligands to uranyl cation.

$$\beta_2 = \frac{[UO_2(N_3)_2]}{(UO_2^{2+})(N_3^-)^2} = 8.26 \times 10^3\,M^{-2}\,K_2 = \frac{\beta_2}{\beta_1} = 59.4$$

$$\beta_3 = \frac{[UO_2(N_3)_3]^-}{[UO_2^{2+}](N_3^-)^3} = 5.1 \times 10^5\,M^{-3} \quad K_3 = \frac{\beta_3}{\beta_2} = 61$$

$$\beta_4 = \frac{[UO_2(N_3)_4]^{2-}}{[UO_2^{2+}](N_2^-)^4} = 6.1 \times 10^5\,M^{-4} \quad K_4 = \frac{\beta_4}{\beta_3} = 1.2$$

$$\beta_5 = \frac{[UO_2(N_3)_5]^{3-}}{[UO_2^{2+}](N_3^-)^5} = 3.1 \times 10^6\,M^{-5} \quad K_5 = \frac{\beta_5}{\beta_4} = 5.0$$

$$\beta_6 = \frac{[UO_2(N_3)_6]^{4-}}{(UO_2^{2+})(N_3^-)^6} = 1.2 \times 10^7\,M^{-6} \quad K_6 = \frac{\beta_6}{\beta_5} = 3.8.$$

REFERENCES

[1] H. I. Flinstein, Anal. Chim. Acta 1966, 15, 288.
[2] F. G. Sheriff and A. M. Awad, J. Inorg. Nucl. Chem. 1961, 19.
[3] F. G. Sheriff and A. M. Awad, Inorg. Chem. 1962, 24, 179.
[4] F. G. Sheriff and A. M. Awad, Anal. Chim. Acta 1962, 26, 235.

[5]B. K. S. Nair, L. H. Prabhv and D. E. Vartan, *J. Sci. Ind. Res. (Indian)* 1961, **20B**, 489. C.A., 1962, **56**, 15147.

[6]A. E. Comyns, *Chem. Rev.* 1960, **60**, 115.

[7]E. A. Neves, R. Tokoro and M. E. Suarez, *J. Chem. Res.* 1979 (9) 374; 4401 M.

[8]A. I. Vogel, *Química Analítica Qualitativa* (Edited by S. A. Kapelucz) 5 Edn, (1974).

[9]E. A. Neves, G. O. Chierice and L. Agnes, Unpublished results.

[10]S. Ahrland, *Acta Chem. Scand.* 1979 **3**, 374; 783; 1067.

[11]J. Sutton, *J. Chem. Soc., Suppl. Issue* 1949, 5273.

[12]F. J. C. Rossotti and H. Rossotti, *The Determination of Stability Constants.* McGraw-Hill,ew York (1961).

[13]K. B. Yatsimirsky and V. P. Vasilev, *Stability Constants of Complex Compounds*, p. 8. Pergamon Press, London (1960).

[14]E. A. Neves, D. W. Franco and N. Milken, *J. Inorg. Nucl. Chem.* 1981, **43**, 2081.

[15]D. Zvi, and F. R. Ziolo, *Chem. Rev.* 1973, **73**, 247.

[16]M. G. B. Drew, *Coord. Chem. Revs.* 1977, **24** 1976.

[17]F. A. Cotton and G. Wilkinson, *Advanced Inorganic Chemistry*, p. 28. Insterscience, New York (1972).

THE STUDY OF ENANTIOSELECTIVITY IN COPPER COMPLEXES WITH SOME 1,3-DICARBONYL LIGANDS BY CIRCULAR DICHROISM SPECTROSCOPY

A. A. KURGANOV,* L. YA. ZHUCHKOVA and V. A. DAVANKOV
Nesmeyanov Institute of Organo-Element Compounds, U.S.S.R. Academy of Sciences, 117813 Moscow, U.S.S.R.

Abstract—The circular dichroism spectra of copper(II) complexes with hydroxymethylene camphor, hydroxymethylene menthone, and trifluoroacetyl camphor as well as of mixed-ligand complexes with acetylacetone have been studied in different solvents at different temperatures. The changes observed in the spectra are attributed to a strong coordination of the solvent molecules in axial positions of square-planar complexes. It has been shown that the contributions of two ligands to the net spectrum of circular dichroism are additive and that the absorption spectra of the complexes do not depend on the optical configuration of the ligands. The conclusion has been drawn that no noticeable inter-ligand interactions exist in the complexes and no enantioselective effects are exhibited.

INTRODUCTION

Enantioselective effects in labile coordination compounds attract attention of many researchers due to an important role which they play in a number of biological systems[1] and in connection with the development of the method of ligand-exchange chromatographic resolution of racemic compounds.[2,3] The most part of investigations in this field involves amino acid ligands[1,2] whereas information on ligands of other types is much more limited. In previous papers we have considered the reasons for enantioselectivity in copper(II) complexes with N - alkyl - α - amino acids[4] and 1,2-diamines.[5] In this report we present the results of studying enantioselectivity in copper(II) complexes with 3-hydroxymethylene camphor (HMC), 3-trifluoroacetyl camphor (TFC), and 2-hydroxymethyl menthone (HMM).

1R – HMC   1R – TFC   1R – HMM
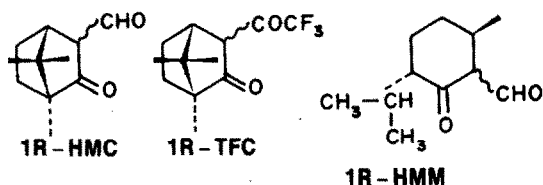
Complexes of transition metals with 1,3-dicarbonyl ligands were the object of numerous studies and are covered in several reviews.[6,7] These papers, however, give only minimum attention to chiroptical properties of Cu(II) complexes with HMC, TFC and HMM which, in our opinion, deserve thorough investigation.

RESULTS AND DISCUSSION

1. CD spectra of complexes

As is seen from Fig. 1, the spectra of circular dichroism (CD) of copper complexes with HMC, TFC, and HMM are characterized by 1–2 bands in the region of d–d transitions of Cu(II) atom and by a number of bands in a shorter wavelength region. Such a shape of the CD

spectrum, as is now well known, is related to the formation of a pseudoaromatic chelate ring in the complexes of 1,3-diketones and is caused by considerable delocalization of π-electron system of ligands.

We considered it interesting to study the effect of solvent and temperature on the shape of the CD spectrum. In aprotic non-polar solvents (hexane, toluene) the bands at ~560 and ~700 nm have a maximum intensity. The intensity decreases in solvents capable of coordination in axial positions of square-planar complexes (methanol, acetone, dioxane, acetonitrile). In the UV region the solvent effects weakly the shape of the CD spectra of Cu(HMC)$_2$ and Cu(TFC)$_2$ whereas in the case of Cu(HMM)$_2$ this effect is strongly pronounced and the transition from acetonitrile to hexane results in an almost complete disappearance of the band at ~340 nm and in a sign change of the band at ~400 nm. It should be, however, noted that correlation with the type of the solvent for Cu(HMM)$_2$ is less pronounced than for Cu(HMC)$_2$ and Cu(TFC)$_2$. Temperature practically does not affect the shape of the CD spectra: the most sensitive to a temperature change proves to be the band at ~400 nm whose intensity (in the case of Cu(HMC)$_2$) decreases by about 20% with a temperature rise from 25 to 55° (in methanol). The intensity of other bands changes by only 5–10%.

The fact that there is no correlation between the dependence of the CD spectra on the type of the solvent and temperature in a readily coordinating solvent may be explained if the equilibrium between a square-planar complex and its adduct with the solvent is almost completely shifted towards adduct and does not depend on temperature. This conclusion is supported by data in the literature,[8,9] showing that the formation constant of such adducts with a composition 1:1† is ~10^2 for Cu(HMC)$_2$ and Cu(HMM)$_2$ and ~10^3 l/mol for Cu(TFC)$_2$. Since the solvent concentration is high, these values correspond to almost quantitative formation of the adduct in solution.

Thus, the changes observed in CD spectra of Cu(HMC)$_2$ and Cu(TFC)$_2$, when passing from non-coordinating solvents to coordinating ones, are probably due to the formation of adducts with the solvents and refer, mainly, to the region of d–d transitions. As regards

---

*Author to whom correspondence should be addressed.
†The data obtained mainly, for different nitrogen-containing axial ligands.
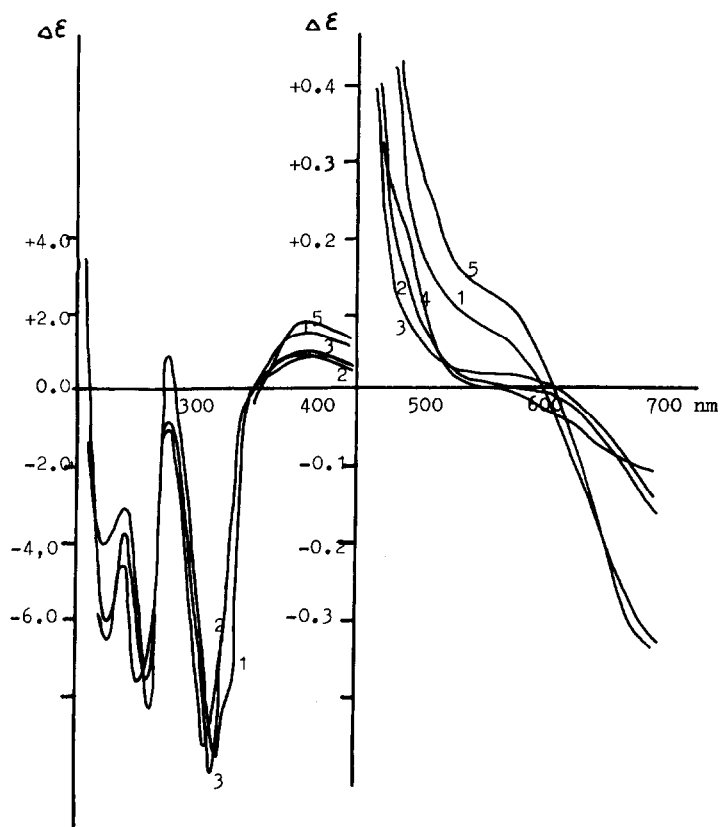
Fig. 1(a).
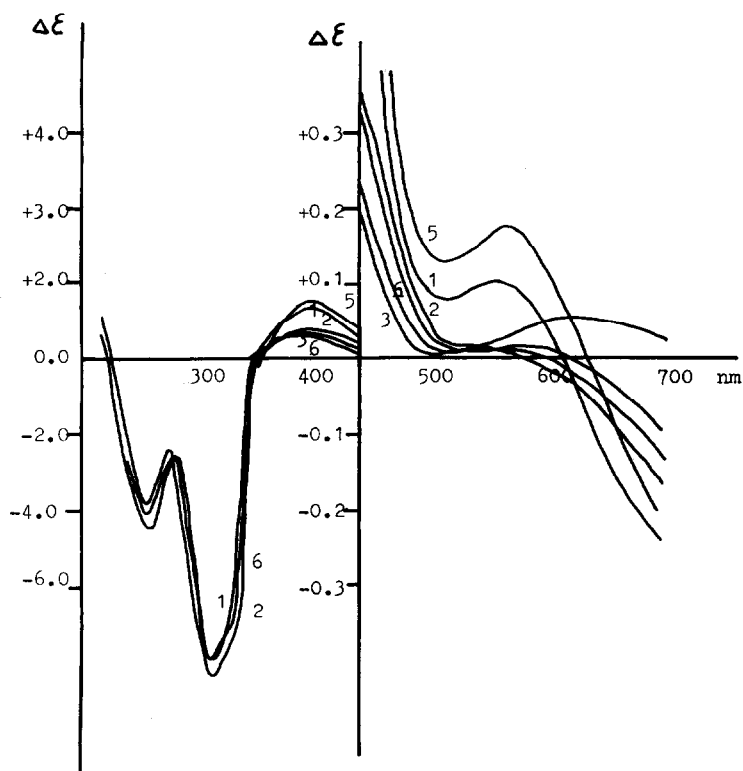
Fig. 1(b).
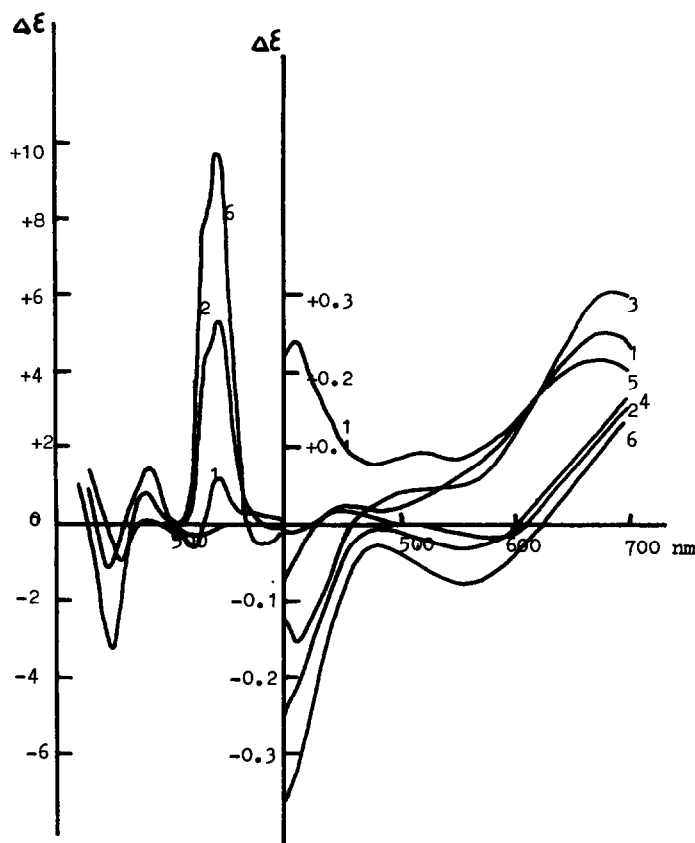
Fig. 1(c).

Fig. 1. CD spectra of the complexes Cu[(1S)-HMC]₂ (A), Cu[(1S)-TFC]₂ (B), Cu[(1R)-HMM]₂ (C) in different solvents: 1, hexane; 2, methanol; 3, dioxane; 4, acetone; 5, toluene; 6, acetonitrile.

Cu(HMM)₂ whose ligands are conformationally more labile than the ligands of camphor derivatives, the formation of adducts, is most likely accompanied by conformational changes and the effect of the solvent manifests itself in the whole region of wave lengths from 200 to 700 nm.

2. Enantioselectivity in complexes Cu(HMC)₂, Cu(TFC)₂ and Cu(HMM)₂

Enantioselectivity in complexes of the ML₂ type arises when there is a mutual effect between two ligands entering into the complex. This mutual effect appears in different forms. Thus, for instance, in the case of complexes of N - alkyl - α - amino acids[10] it manifests itself in the different ability of the complexes containing two ligands of identical or opposite configuration, to the addition of a solvent molecule in the axial position of Cu²⁺. In the CD spectra the mutual effect of the ligands appears as a deviation from additivity of the contributions of both ligands into the net CD spectrum.

To detect the deviations from the additivity of contributions, we have studied CD spectra of mixed complexes in which HMC, HMM, or TFC was one of the ligands and the acetylacetone (AA) molecule was the second ligand. Acetylacetone is one of the smallest ligands of the 1,3-dicarbonyl type and one may expect that no noticeable steric interactions with the second ligand will take place. Only in the case of Cu(HMC)₂ small deviations in the region ~ 620 nm were detected
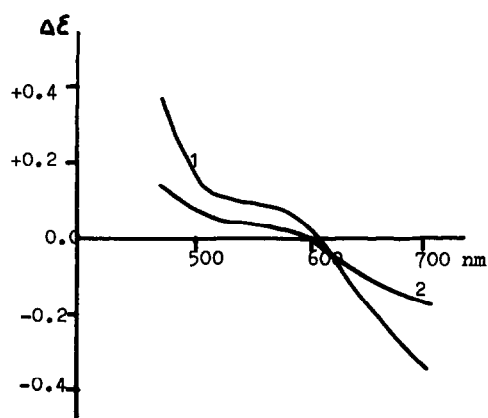
Fig. 2. CD spectra of mixed complexes Cu{[(1S)-HMC](AA)}, 1,3-initial complexes, 2-mixed complex. Chloroform as a solvent.

(Fig. 2). The formation constant of mixed complex is also close to 4 which means that distribution of the ligands in the system Cu(HMC)₂-Cu(AA)₂-Cu(HMC)(AA) is almost statistical in nature.

The absorption spectra of Cu[(1R)-(HMC)]₂, Cu[(1S)-(HMC)]₂ and Cu[(1R,1S)-(HMC)]₂ as well as of Cu[(1R)-TFC]₂, Cu[(1S)-TFC]₂ and Cu[(1R,1S)-(TFC)]₂ are completely identical; the differences between them are within the limits of accuracy of the measurements.

All the results obtained indicate that in complexes
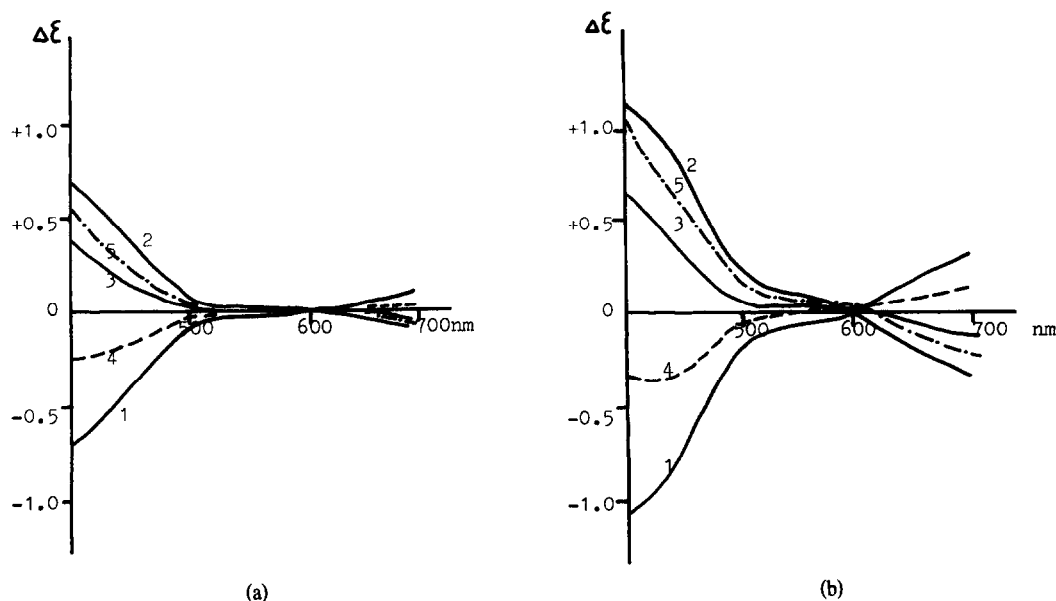
Fig. 3. CD spectra of mixed complexes HMC and TFC in methanol (A) and hexane (B). (1) Cu[(1R)–HMC]₂, (2) Cu[(1S)–HMC]₂, (3) Cu[(1S)–TFC]₂, (4) Cu{[(1R)–HMC][(1S)–TFC]}, (5) Cu{[(1S)–HMC][(1S)–TFC]}.

Cu(HMC)₂, Cu(TFC)₂ and Cu(HMM)₂ there are no noticeable inter-ligand interactions which could have caused great enantioselective effects. Axial positions of these complexes are easily accessible for the solvent molecules and the strength of the adducts formed does not depend on the optical configuration of the ligands comprising the complex. This situation is similar to that observed for the complexes of unsubstituted α-amino α acids and contrasts with the properties of the complexes of N - alkyl - α - amino acids.[4]

No enantioselectivity was observed in studying the majority of the systems containing complexes Cu(HMC)₂–Cu(TFC)₂ (Fig. 3) or Cu(HMC)₂–Cu(HMM)₂ (Fig. 4). In these cases a complete additivity of contributions of two ligands was observed, as a rule, which enter into the complex composition and the CD spectrum of the mixed complex is almost an average of the CD

spectra of the initial compounds. The noticeable deviations are observed only in the system Cu(1S)–(HMC)₂–Cu(1S)–(TFC)₂ in hexane (Fig. 4b). The constant of formation of the mixed complex (log k = 1.1) points that the mixed structure is more preferred than the initial ones. At the same time the CD spectrum of the corresponding diastereoisomeric structure Cu(1R)–HMC(1S)–(TFC) is intermediate between the CD spectra of the initial complexes and therefore, we cannot find the constnat of its formation. Thus, no quantitative information can be obtained about the possible difference in stability of these mixed-ligand diastereoisomeric structures.

EXPERIMENTAL

(1) Preparation of (1R); (1S) and (1R,1S)-hydroxy-methylene camphor, (1S)-trifluoroacetyl camphor and
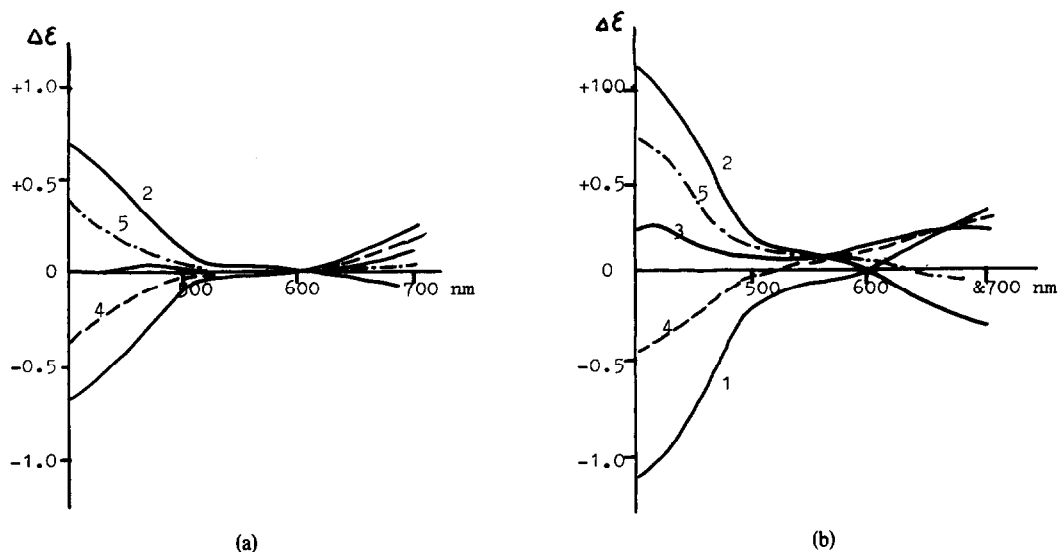
Fig. 4. CD spectra of mixed complexes of HMC and HMM in methanol (A) and hexane (B). (1) Cu[(1R)–HMC]₂, (2) Cu[(1S)–HMC]₂, (3) Cu[(1R)HMM]₂, (4) Cu{[(1R)–HMC][(1R)–HMM]}, (5) Cu{[(1S)–HMC][(1R)–HMM]}.

Table 1. Elemental analyses of synthesized complexes found (calculated)

Complex	C	H	Cu	F
1. Cu[(1R)–HMC]$_2$	62.5 (62.6)	7.0 (7.1)	15.5 (15.1)	—
2. Cu[(1S)–HMC]$_2$	62.4 (62.6)	6.9 (7.1)	15.3 (15.1)	—
3. Cu[(1R,1S)–HMC]$_2$	62.1 (62.6)	6.9 (7.1)	14.5 (15.1)	—
4. Cu[(1R)–TFC]$_2$	51.5 (51.7)	4.9 (5.0)	11.2 (11.3)	20.2 (20.4)
5. Cu[(1S)–TFC]$_2$	51.2 (51.7)	4.8 (5.0)	11.5 (11.3)	20.0 (20.4)
6. Cu[(1R,1S)–TFC]$_2$	51.4 (51.7)	5.2 (5.0)	11.7 (11.3)	20.7 (20.4)
7. Cu[(1R)–HMM]$_2$	62.0 (62.0)	8.2 (7.9)	15.2 (14.9)	—
8. Cu[(AA)]$_2$	46.0 (45.5)	5.5 (5.3)	24.4 (24.3)	—

(1R)-hydroxymethylene menthone was performed as described in Refs. 10–12. The products obtained were purified by either steam distillation (hydroxymethylene camphor) or vacuum distillation.

(2) Copper complexes with the synthesized ligands were prepared as described in Ref. 13 and purified by recrystallization from dioxane (for HMC) or by sublimation *in vacuo* (for HMM and TFC). The data of the elemental analyses are given in Table 1.

Acetylacetonate complex of copper was synthesized as described in Ref. 14 and purified by recrystallization from a mixture of methanol with chloroform. The data of the elemental analyses are given in Table 1.

(3) CD spectra of the complexes were recorded on the automatic spectropolarimeter "J-20 JASCO" (Japan) at a concentration of 5×10^{-3} mol/l (in the visible region) or 5×10^{-4} mol/l (in the UV region). The absorption spectra were recorded on the automatic spectrophotometer (GDR) at the same concentrations.

(4) Mixed complexes were prepared in solution by mixing the solutions of two different individual complexes. The constants of the formation of mixed complexes and their spectra were calculated by following the procedure described in Ref. 4.

REFERENCES

[1] L. D. Pettit and R. J. W. Wofford. In *Metal Ions in Biological Systems* (Edited by H. Sigel), Vol. 9. Marcel Dekker, New York (1979).

[2] V. A. Davankov, S. V. Rogozhin and A. A. Kurganov, *Russ. Chem. Rev.* 1974 **43**, 764.

[3] V. A. Davankov, *Adv. in Chromatography* (Edited by J. C. Giddings, E. Grushka, J. Cazes and P. R. Brown), Vol. 18, p. 139. Marcel Dekker, New York, 1890.

[4] V. A. Davankov, S. V. Rogozhin, A. A. Kurganov and L. Ya. Zhuchkova, *J. Inorg. Nucl. Chem.* 1975, **37**, 369.

[5] A. A. Kurganov, T. M. Ponomaryova, V. A. Davankov, *Inorg. Chim. Acta* 1980 **45**, L23.

[6] J. J. Fortman and R. E. Sievers, *Coord. Chem. Rev.* 1971 **6**, 331.

[7] K. C. Koshi, V. V. Pathoik, *Coord. Chem. Rev.* 1977 **22**, 371.

[8] J. Sasaki, M. Seikurada, M. Matsui and T. Shiymoitsu, *Bul. Chem. Soc. Japan* 1974 **52**, 245.

[9] D. P. Graddon and E. C. Wotton, *J. Inorg. Nucl. Chem.* 1961 **21**, 49.

[10] *Beilsteins Handbuch der Organishen Chemie*, VII, 592 (1925).

[11] *Beilsteins Handbuch der Organischen Chemie*, VII, 568 (1925).

[12] A. L. Henne, M. S. Newman, L. L. Quill and R. A. Staniforth, *J. Am. Chem. Soc.* 1947, **69**, 1819.

[13] *Beilsteins Handbuch der Organischen Chemie* 1, 781 (1928).

[14] A. A. Kurganov, L. Ya. Zhuchkova and V. A. Davankov, *J. Inorg. Nucl. Chem.* 1978, **40**, 1081.

UV PHOTOELECTRON SPECTRA OF SOME TRANSITION METAL(II) ACETYLACETONATES

SUSUMU KITAGAWA*

Department of Chemistry, Kinki University, Higashi-Osaka 577, Japan

ISAO MORISHIMA

Department of Hydrocarbon Chemistry, Kyoto University, Kyoto 606, Japan

and

KENICHI YOSHIKAWA

College of General Education, Tokushima University, Tokushima 770, Japan

Abstract—The He(I) photoelectron spectra of acetylacetone (HAA) and its metallo complexes, $M(II)(AA)_2$ (M(II) = Mn, Co, Ni, Cu and Zn), have been measured. These spectra show characteristic metal-dependence, from which the assignment is made. The order of the orbital energy level, $d \gtrsim \pi_3 > n_- > n_+$, holds for all the complexes reported here. The splitting of these orbitals is found to depend on the central metal ion specifically.

INTRODUCTION

Considerable efforts have been made to understand the electronic structure of metal complexes. Although the UV-VIS absorption spectroscopy has been the most useful experimental method for this purpose, it is available only for the energy differences between a ground and an excited state, and therefore, the energies of the occupied orbitals (i.e. ionization potential, IP) cannot be obtained. In the case decades, photoelectron (PE) spectroscopy has been proved to be useful to study the electronic structure of various organic compounds. However, PE study concerning the metallo complexes is quite limited due to the difficulty of the measurement of the IP in the vapour phase. In this manuscript, we succeeded in obtaining the PE spectra of a series of divalent metallo complexes with acetylacetone. Despite numerous reports on the electronic structure of the transition metallo complexes, $M(III)(AA)_3$, little attention has been paid to those of the divalent ones, $M(II)(AA)_2$. In order to gain an insight into the electronic structure of the divalent metallo acetylacetonates, especially partly filled d-shell, of which theoretical investigation is still lacking, we discuss here the electronic structure on the basis of UV PE spectra of acetylacetone and its divalent metal complexes such as Mn, Co, Ni, Cu and $Zn(AA)_2$.

EXPERIMENTAL

Acetylacetone and its metallo derivatives were all commercially available. These complexes for PES measurements were purified by a vacuum sublimation.

Photoelectron spectra, with He(I) resonance line at 21.21 eV, were recorded on a Perkin-Elmer PS 18 spectrometer using a heated inlet probe. The spectra were calibrated by the simultaneous admission of Xe and Ar gases mixture into the heated target chamber containing the sample vapour. The sample was heated gradually until the desired temperature was reached: the setting temperature was 91°C for $Zn(AA)_2$, 115°C for $Co(AA)_2$, 142°C for $Cu(AA)_2$, 174°C for $Ni(AA)_2$ and 200°C for $Mn(AA)_2$. The instrumental resolution was 20–30 mV for Ar $^2P_{1/2,3/2}$ peaks.

RESULTS AND DISCUSSION

He(I) PE spectra of the acetylacetonate complexes of divalent metals are illustrated in Figs. 1 and 2. The IPs for these complexes are listed in Table 1 together with some literature data.[1] As Figs. 1 and 2 show, the PE bands between 7 and 12 eV for the compounds are well resolved, while the bands at the higher ionization energy (IE) region which arise from ionization of C–H and C–C σ-bonding electrons, are overlapped and have no fine structure. Thus, we are concerned with the bands between 7 and 12 eV.

The PE spectrum of HAA shows two well resolved bands at 9.0 and 9.6 eV, which have been assigned[1,2] to the ionization due to the π_3 electron of the enol ring and the n_- electron of the oxygen lone pair, respectively. The third band has been assigned to the ionization from the symmetric combination (n_+) of the two oxygen lone pair orbitals by use of trifluoroacetylacetone.[1]

Figure 1 reveals that $Zn(AA)_2$ provides two intense bands at 8.34(A) and 9.29(B) eV. The low IE bands[1] of $Be(AA)_2$ has been assigned to π_3 and n_- electron ionization, respectively. The C and C' bands in Fig. 1 are well resolved and the gap of these two bands is 0.83 eV, which is in strong contrast to the overlapping of the corresponding bands of $Be(AA)_2$ (0.27 eV gap). These bands are attributable to the ionization of n_+ orbitals. The splitting of the n_+ orbital can be accounted for by a simple molecular orbital interaction model. In the gas phase, the divalent metal compounds is expected to exist as a monomer.[3] The electron diffraction studies[4,5] have shown that the structure of Ni and $Cu(AA)_2$ are almost square planar. Planar symmetry $(D_{2h}$ point group) allows the n_+ orbitals to show B_{2u} and A_g transformation. The interaction of the metal $ns(a_g)$ and $np(b_{2u})$ valence AOs provides two n_+ orbitals having energy gap, which depends on the extent of mixing of these two AOs. On the basis of PE spectra of $Zn(AA)_2$ and $Be(AA)_2$, this orbital mixing of $Zn(AA)_2$ is more enhanced than that of $Be(AA)_2$.

As Fig. 2 shows, $Ni(AA)_2$ gives well-resolved bands at low IE region. The d-electron ionizations appear as the

*Author to whom correspondence should be addressed.
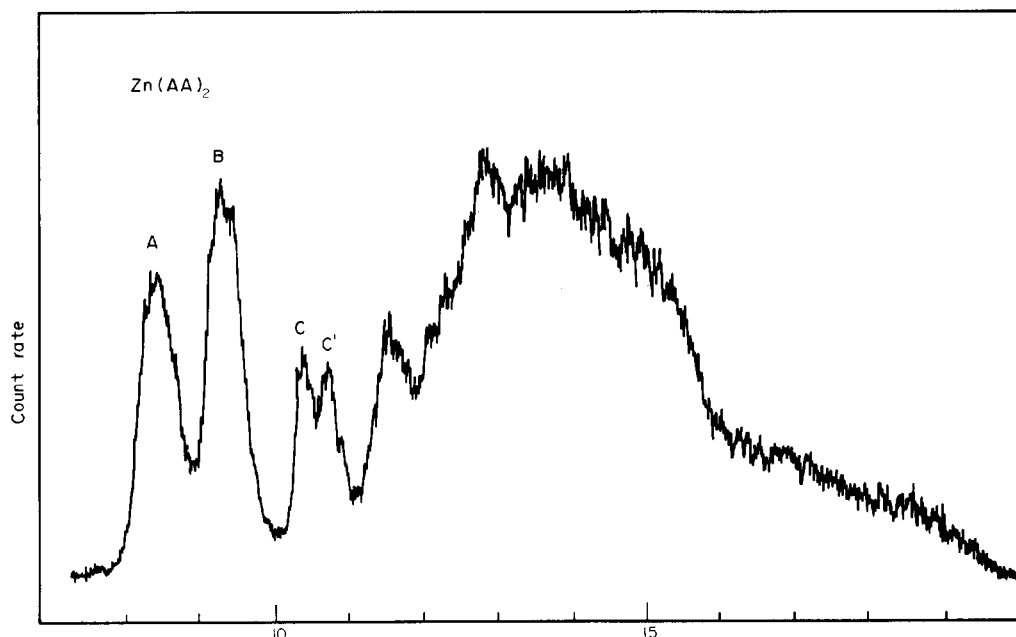
Fig. 1. He(I) photoelectron spectrum of $Zn(AA)_2$.

first three bands, which has been confirmed by use of mono and dithio analogues of $Ni(AA)_2$.[6] In contrast to this, d ionization peaks were not separately observed for Mn, Co and $Cu(AA)_2$, because these bands are masked under the broad envelope of the bands between 8 and 9 eV. It is to be noted in Fig. 2 that $Cu(AA)_2$ shows the first band (d) as a shoulder of the second broad and intense band (A) at 8.18 eV, and $Co(AA)_2$ also exhibits a shoulder peak at 7.93 eV. The corresponding bands were not observed in the spectrum of $Zn(AA)_2$ (Fig. 1). This finding makes us assign these shoulder bands to metal d orbitals. It is emphasized that the band ascribed to the ionization of the metal d orbital has lower intensity than that of oxygen and carbon p orbitals due to its small cross section.[7,8] In Fig. 2, the bands denoted as d have relatively small intensity, indicative of the validity of the above assignment. Under D_{2h} symmetry, the crystal field theory provides us with the order in the d orbital energy $d_{xy} > d_{xz} \sim d_{yz} > d_{z2} > d_{x2-y2}$. On the basis, the first band of $Ni(AA)_2$ has been assigned to the ionization from nearly degenerate $d_{xz,yz}$ orbitals,[6] since the upper d_{xy} orbital is empty. In the case of nearly quadratic

chromophere of $Cu(AA)_2$[4] with d^9 configuration, the first band at 7.66 eV is analogously considered as the electron-ejection from the singly occupied d_{xy} orbital. According to the above energy order of d orbitals in the case of quadratic chromophere and on the basis of the observed PE spectra of $Cu(AA)_2$ and $Ni(AA)_2$, it is worth noting that the d-orbital level of $Ni(AA)_2$ is higher than that of $Cu(AA)_2$. This trend about d orbital energy has also been found in the case of diethyldithiocarbamate[9] and difluorodithiophosphate[10] complexes of Ni and Cu. In the AA complexes of Cu and Ni, the Ni–O bond distance is shorter than the Cu–O distance.[4,5] This fact leads to the expectation that Ni ion interacts with the ligand more strongly than Cu ion, eventually indicative of the destabilization of the d orbitals of the Ni complex. The experimental observation on the relative d-orbital levels for Ni and $Cu(AA)_2$ should be theoretically reproduced. For our SCF UHF calculation, we used two Slater-type functions of different effective nuclear charges for $3d$ atomic orbitals.[11] The MO energies show that d levels of Ni complex lie higher by *ca.* 0.5 eV than those of the Cu complex.

Table 1. Vertical ionization potentials (peak maxima) from the photoelectron spectra of acetylacetone (HAA) and $M(II)(AA)_2$

Compound	Bands												eV
	d			A		B			C				
HAA[a]				9.00		9.60							
Mn(AA)$_2$	-[b]			-[b]		9.20			9.98	10.32	11.29		
Co(AA)$_2$	7.93			8.11	8.36	8.62	8.78		9.70	10.35	10.80	11.58	
Ni(AA)$_2$	7.62	8.05	8.21	8.59	8.78	9.02	9.39		10:24		11.02	11.59	
Cu(AA)$_2$	7.66			8.18	8.43	9.02			9.70	10.18	11.42	11.85	
Zn(AA)$_2$				8.34		9.29			10.38	10.72	11.55		

a) Ref.1   b) The overlapping bands between 7 and 8 eV are too complicated to separate each band, corresponding to the ionization of d and π_3 orbitals.
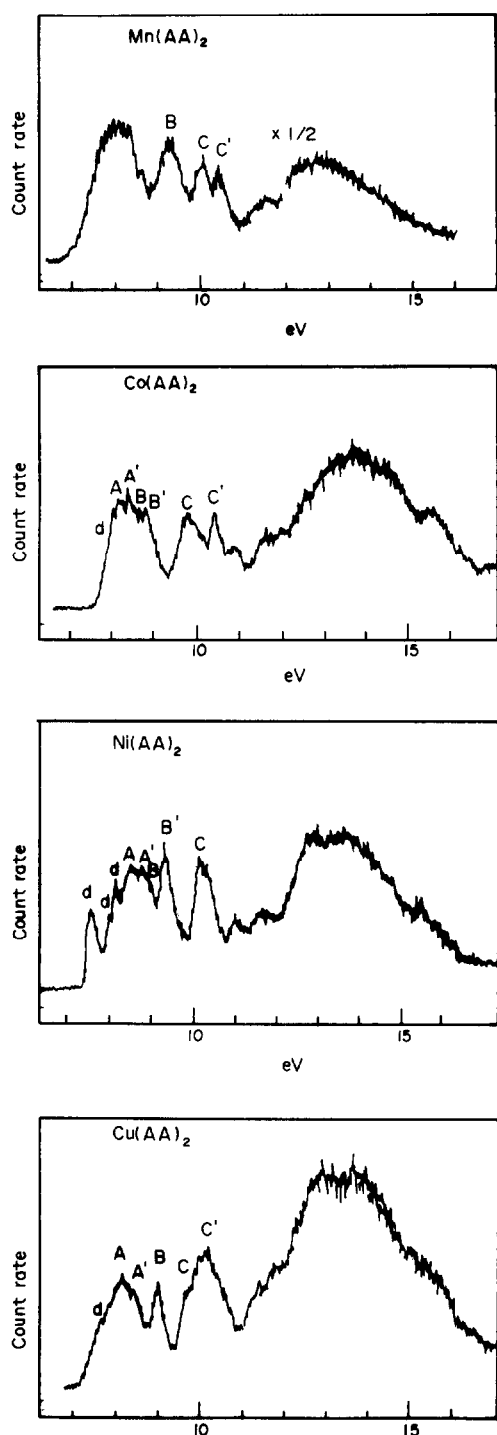
Fig. 2. He(I) photoelectron spectra of Mn(II)(AA)$_2$, Co(II)(AA)$_2$, Ni(II)(AA)$_2$ and Cu(II)(AA)$_2$.

Fig. 3. Correlation diagram of ionization energy in the PE spectra of M(II)(AA)$_2$. All the ionization energies except for Be(AA)$_2$[1] were obtained in the present experiment. The shaded portion shows a region with possible ionization energies obtained from the broad PE band.

The higher IE bands

As shown in Figs. 1 and 2, the PE bands (A) in the next higher IE region of Co, Ni and Cu(AA)$_2$ reveal the similarity close to the band A of Zn(AA)$_2$, characteristic of π_3 ionization. The unresolved broad band between 7.5 and 8.3 eV, however, appears in the spectrum of Mn(AA)$_2$. This band results from d and π_3 ionization which lie close in energy to those of Ni, Co and Cu(AA)$_2$. Figure 3 shows the energy level diagram of photoionized states constructed from the present results of PE measurements. It is emphasized in Fig. 3 that the π_3 level of Ni(AA)$_2$ is lower than those of other complexes. A simple analysis of the valence orbital interaction explains as follows: the stabilization of the π_3 orbital energy for Ni(AA)$_2$ results from an increase of the mixing among metal $3d(b_{3g})$, $4p(b_{1u})$, and $\pi_3(B_{3g}$ and $B_{1u})$ orbitals due to the relatively shorter Ni-O bond length in the square planar structure (D_{2h}).

The B-labeled bands at 8.5 eV are significantly associated with ionization from oxygen lone pair combination (n). The splitting (B and B') shows the metal-dependence, which is ascribed to the extent of the mixing between $n_-(B_{3u}$ and $B_{1g})$, metal $3d(b_{1g})$ and $4p(b_{3u})$ orbitals. Figure 3 also shows that the n_+ band splitting (C and C') of Co(AA)$_2$ is greater than that for other metal complexes. This implies an unusual structure of Co(AA)$_2$ in the vapour phase. It has been found[12] that unlike Ni(AA)$_2$, Co(AA)$_2$ encounters a tetrahedral form in the highly diluted solution. Hence, the greater splitting is associated with the structure such as tetrahedral form. PE spectra are, thus, available for the structural analysis, which should be developed together with the analysis of the electronic structure of metallo complexes.

The C-labeled peaks around 10 eV are assigned to ionizations of the n_+ electrons, which correspond to the peaks at 10.38 and 10.72 eV in the spectrum of Zn(AA)$_2$. The positions of these bands are not sensitive to the metal ions, while the splitting of bands C show the metal-dependence. By analogy with the splitting of n_-, this is explained in terms of the interaction between n_+, $4s$ and $4p$ orbitals. The former interaction is less sensitive to the structural deviation from the planarity of the complex than the latter, because of the spherical symmetry of the $4s$ orbital.

The weak bands about 11 eV in Fig. 2 are associated with the ionization from π_2 orbital, an anti-symmetric combination of the localized C-O π-bonding orbitals. As the electronegativity of the metal ion increases from Mn to Cu, these bands appear to shift to higher IE region except for the Co complex (Fig. 3). This unusual feature for Co(AA)$_2$ is also due to the structural deformation from the square planar to tetrahedral form.

REFERENCES

[1]S. Evans, A. Hamnet, A. F. Orchard and D. R. Lloyd, *Discuss. Faraday Soc.* 1972, **54**, 227.

[2]A. Schweig, H. Vermeer and U. Weinder, *Chem. Phys. Lett.* 1974, **26**, 229.

[3]S. R. Prescott, J. E. Campana, P. C. Jurs, T. H. Risby and A. L. Yergey, *Anal. Chem.* 1976, **48**, 829.

[4]S. Shibata and K. Sone, *Bull. Chem. Soc. Japan,* 1956, **29**, 852.

[5]S. Shibata, *Bull. Chem. Soc. Japan* 1957, **30**, 753.

[6]C. Cauletti and C. Furlani, *J. Elec. Spectr. Relat. Phenom.* 1975, **6**, 465.

[7]W. Thiel and A. Schweig, *Chem. Phys. Lett.* 1971, **12**, 49.

[8]F. L. Battye, A. Goldmann and L. Kasper, *Phys. Status Solidi* 1977, **(B)80**, 425.

[9]C. Cauletti and C. Furlani, *J. Chem. Soc. Dalton.* 1977, 1068.

[10]M. V. Andreocci, P. Dragoni, A. Flamini and C. Furlani, *Inorg. Chem.* 1978, **17**, 291.

[11]J. W. Richardson, W. C. Nieuwpoort, R. P. Powell and W. F. Edgell, *J. Chem. Phys.* 1962, **36**, 1957.

[12]F. A. Cotton and R. H. Soderberg, *Inorg. Chem.* 1964, **3**, 1.

METAL COMPLEXES OF PYRIMIDINE-DERIVED LIGANDS—III†

TRIS-COMPLEXES OF Co(II), Ni(II) AND Cu(II) FLUOROBORATES, PERCHLORATES AND IODIDES WITH 3,5-DIMETHYL-1-(4',6'-DIMETHYL-2'-PYRIMIDYL) PYRAZOLE, A POTENTIAL ANTI-TUMOUR AGENT

NITYANANDA SAHA* and DURGADAS MUKHERJEE
Department of Chemistry, University College of Science, Calcutta-700009, India

(Received 5 July 1982)

Abstract—Tris-complexes of Co(II), Ni(II), Cu(II) fluoroborates, perchlorates and iodides with the title ligand conform to the composition $M(DPymPz)_3X_2$, nH_2O [M = Co(II), Ni(II), Cu(II); X = ClO_4, BF_4 and I, n = 0, 2]. Physico-chemical characterisations of the complex species have been made from electronic and vibrational spectra, magnetic susceptibility measurements in the solid state and conductivity measurements in solution. Electronic spectral features together with the corresponding ligand field parameters suggest an overall octahedral environment for all the metallic complexes. For $[CuN_6]$ environment a D_3 symmetry is thought to be highly probable. Ir data point out the pyrazolyl nitrogen (tertiary) and one of the pyrimidyl nitrogens as bonding sites in forming these complexes while the anion (X) retains its identity (as in free form) in the said species.

INTRODUCTION

The significant role played by the pyrimidine derivatives (the ring system being an integral part of several nucleic acids, vitamins etc.) in many biological systems, has currently stimulated research into the coordination modes of pyrimidine-based ligands in order to gain detailed knowledge of the role of metal ions in such systems. Moreover, certain pyrimidino–pyrazoles are recently being studied in the fight against cancer.[1] As a part of our programme[2,3] to investigate the interaction of a variety of biologically active pyrimidine-derived ligands with metal ions, the present communication intends to report the coordination aspect of a pyrimidyl-pyrazole viz. the title ligand (hereinafter abbreviated as DPymPz) with isolation and physico-chemical characterisation of a few tris-complexes with $[MN_6]$ environment.

EXPERIMENTAL

Preparation of the ligand. The ligand was prepared by a condensation reaction of one mole 2 - hydrazino - 4,6 - dimethyl pyrimidine[4a,4b] (prepared in our laboratory) with 1.1 moles of freshly distilled acetylacetone following the method of Giuliano *et al.*[4c] The product yielded white flakes on recrystallisation from water. It melted with decomposition at 65°C (lit. m.p. 65°C) (Found: C, 65.07; H, 6.69; N, 27.98. Calc. for $C_{11}H_{14}N_4$: C, 65.34; H, 6.69; N, 27.98%). The ligand has been further characterised by its PMR spectral data recorded in DMSO-d_6 (not reported in the literature). The 80 MHz PMR spectrum of DPymPz shows two sharp one proton singlets at $\delta 7,18$ and $\delta 6.12$ which correspond to C-5' proton of the pyrimidine ring and C-4 proton of the pyrazole ring respectively; one 6-proton singlet at $\delta 2.47$ may be ascribed to the methyl groups at the C-6' and C-4' of the pyrimidine ring.[5] On the other hand two 3-proton singlets appearing at $\delta 2.45$ and $\delta 2.21$ in all probability correspond to two methyl groups at the C-3 and C-5 positions of the pyrazole ring;[5] the difference of these δ values is attributed to the greater shielding experienced by the C-5 methyl group of the pyrazole ring as these protons lie in approximate to the shielding region of the pyrimidine ring which is disposed in a perpendicular fashion with the pyrazole ring.

Preparation of the metal complexes. All the tris-complexes excluding the iodide one of Cu(II) were prepared by addition of hot ethanolic solution of the ligand (0.015 mole) to a solution of the hydrated metal(II) salt (0.005 mole) in the same solvent. The resultant solution, so formed, was heated at water-bath temperature for 5–10 min and then left at room temperature in a desiccator over concentrated H_2SO_4. The desired compound, in each case, separated within 24 hr. The compound was filtered, washed with ethanol and dried over silica gel. The compound of the composition $Cu(DPymPz)_3I_2$, $2H_2O$ was prepared by digesting the corresponding perchlorate complex (Table 1) with a saturated aqueous solution of KI at water-bath temperature for 15 min. The compound was filtered, washed repeatedly with ice-cold water and then with ethanol and collected as before.

Elemental analysis. Metal contents (*viz.* cobalt, nickel and copper) in the respective metal complexes were determined gravimetrically as anhydrous $CoSO_4$, nickel dimethyl glyoxime and $[Cu(en)_2HgI_4]$ (en = ethylene diamine) respectively. Nitrogen and carbon were estimated by micro-analytical laboratory of the Department. Chlorine and iodide were estimated gravimetrically as silver halides.

Physico-chemical measurements like molar conductance and magnetic susceptibility, electronic (both reflectance and solution) and vibrational spectral measurements were done as described earlier.[3]

RESULTS AND DISCUSSION

The analytical data for the complexes along with their colours, effective magnetic moment values and molar conductances are given in Table 1. The complexes are

---
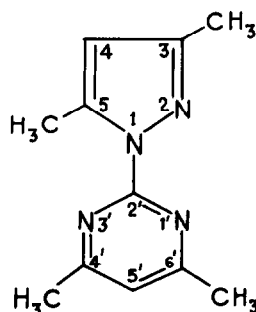
*Author to whom correspondence should be addressed.

†For Part II: N. Saha and S. K. Kar, *J. Inorg. Nucl. Chem.* 1979, **41**, 1233.

Fig. 1.

Table 1. Analytical, conductance and magnetic data for the complexes

Complexes	Colour	M(%)		Found (%)			Calc. (%)			Magnetic moment μ_B in B.M. at 301·K	Molar conductance conc. 1.0×10^{-3} M acetonitrile at 30°C ($ohm^{-1} cm^2 mole^{-1}$)
		Found	Calc.	C	N	X	C	N	X		
$Co(L)_3(ClO_4)_2$	Pink	6.80	6.92	45.68	19.98	8.27	45.80	20.07	8.21	4.68	230.46
$Co(L)_3(BF_4)_2$	Pink	7.12	7.03	47.01	19.92	-	47.20	20.06	-	4.70	232.02
$Co(L)_3I_2 \cdot 2H_2O$	Pale pink	5.99	6.07	41.28	17.64	26.47	41.46	17.59	26.59	4.72	206.48
$Ni(L)_3(ClO_4)_2 \cdot 2H_2O$	Blue violet	6.57	6.79	44.21	19.68	7.80	43.98	19.44	7.99	2.98	223.82
$Ni(L)_3(BF_4)_2$	Blue violet	7.01	7.04	47.01	20.01	-	47.24	20.07	-	2.93	223.56
$Ni(L)_3I_2 \cdot 2H_2O$	Pale blue	6.02	6.09	41.26	17.03	26.67	41.49	16.96	26.61	2.37	205.15
$Cu(L)_3(ClO_4)_2$	Bright green	7.34	7.31	45.39	19.46	8.24	45.56	19.34	8.17	1.82	237.63
$Cu(L)_3(BF_4)_2$	Bright green	7.49	7.53	46.74	20.21	-	46.90	20.09	-	1.78	229.12
$Cu(L)_3I_2 \cdot 2H_2O$	Reddish yellow	6.58	6.61	41.17	17.54	26.52	41.30	17.50	26.47	1.77	203.56

L = DPymPz = One molecule of 3,5-dimethyl-1-(4',6'-dimethyl-2'-pyrimidyl)-pyrazole

Table 2. Electronic spectral data for the complexes

Complexes	State	Absorption maxima in kK ε	ν_2/ν_1	Dq(cm^{-1})	B(cm^{-1})	β = B/B$_0$
Co(L)$_3$(ClO$_4$)$_2$	Reflectance / Methanol (Pink)	9.8; 20.7; 23.0sh / 9.09(5.69); 20.33(29.83)	-	1102	803	0.83
Co(L)$_3$(BF$_4$)$_2$	Reflectance / Methanol(Pink)	9.75; 20.6; 22.8sh / 9.00(3.23); 20.00(17.54)	-	1096	804	0.82
Co(L)$_3$I$_2$·2H$_2$O	Reflectance / Methanol(Pink)	9.80; 22.42 br.s / 9.60(4.54), 22.08(19.54)				
Ni(L)$_3$(ClO$_4$)$_2$2H$_2$O	Reflectance / Methanol(Pale blue)	10.40; 17.00 / 9.30(5.73); 16.39(7.31)	1.63	1040	973	0.94
Ni(L)$_3$(BF$_4$)$_2$	Reflectance / Methanol(Pale blue)	10.30; 17.00 / 9.30(8.83); 15.66(16.40)	1.65	1030	1043	1.01
Ni(L)$_3$I$_2$·2H$_2$O	Reflectance / Methanol (Pale blue)	10.4; 16.93 / 10.00(11.15); 16.66(9.45); 25.97(152.3)	1.63	1040	972	0.93
Cu(L)$_3$(ClO$_4$)$_2$	Reflectance / Nitromethane (Green)	10.40 br.s.; 6.00sh / 10.41(53.5); 14.28(110.4)				
Cu(L)$_3$(BF$_4$)$_2$	Reflectance / Nitromethane (Green)	10.20 br.s; 6.02sh / 10.15(51.5); 14.08(111.2)				
Cu(L)$_3$I$_2$·2H$_2$O	Reflectance / Nitromethane (Reddish yellow)	10.12; 27.27sh / 10.30(32.5); 27.02(167.0)				

L = DPymPz

soluble in water and common non-donor organic solvents. The aqueous solutions of complex species suffer appreciable change in colour with time indicating extensive solvolysis.

All the tris-complexes are magnetically normal high-spin 6-coordinate complexes (Table 1). The magnetic moments of the cobalt(II) complexes are above the spin only value of 3.89 B.M. for high spin octahedral complexes due to high orbital contribution.[6] Molar conductance data (in ohm^{-1} cm^2 mole^{-1}) in acetonitrile solution of the complexes indicate their ionic nature (1:2) at least in the said solvent.[7]

Co(II) *complexes.* The diffuse reflectance spectra of the Co(II) complexes are characterised by two main bands appearing around ~9.8 kK and ~20.7 kK which may be ascribed to $\nu_1[4T_{1g}(F) \rightarrow {}^4T_{2g}]$ and $\nu_3[{}^4T_{1g}(F) \rightarrow {}^4T_{1g}(P)]$ transitions respectively in an idealised octahedral environment.[8] The position of ν_3 band in the d.r.s. of the corresponding iodide complex could not be located in the expected position; alternatively, a broad band appeared at 22.42 kK which is believed to be mixed up with intense charge transfer absorption. The relevant ligand field parameters[9] viz. Dq (1096 and 1120 cm^{-1}), B (804 and 808 cm^{-1}) and β (0.82 and 0.83) for the fluoroborate and perchlorate complexes confirm the proposed pseudo-octahedral configuration. Electronic spectra (Table 2) of these complexes in methanol are characterised by a main band around 20.00 kK which indicate that there is no remarkable change in stereochemistry on dissolution in the said solvent.

Ni(II) *complexes.* The complexes have mostly identical spectral bands both in solid and in solution. Each is characterised by two main bands around ~10.4 and ~17.0 kK which may be attributed to $\nu_1[{}^3A_{2g} \rightarrow {}^3T_{2g}(F)]$ and $\nu_2[{}^3A_{2g} \rightarrow {}^3T_{1g}(F)]$ transitions respectively in an O_h symmetry. The calculated[10,11] ligand field parameters viz. Dq (1030 and 1040 cm^{-1}), B (972 and 1048 cm^{-1}) and β (0.93–1.01) closely correspond to those having (NiN$_6$) environment.[12] The ν_2/ν_1 ratio of 1.63–1.65 (Table 2) characterises all the Ni(II) complexes as essentially pseudo-octahedral species suggesting strong T_{1g} term interactions.[13] In the present study absence of ν_3 band $[{}^3A_{2g} \rightarrow {}^3T_{1g}(P)]$ may be either due to intense internal $\pi-\pi^*$ transitions of the ligand or due to intense CT absorption, arising from metal to ligand via the π antibonding level of the heterocyclic ligand.[14] The strong band at 25.97 kK with high molar extinction coefficient ($\epsilon \sim 1.52$ cm^{-1} mole^{-1}) in the spectrum of Ni(DPymPz)$_3$I$_2$, 2H$_2$O in methanol may be of charge-transfer origin.

Cu(II) *complexes.* The tris-pyrimidyl–pyrazole Cu(II) ions as perchlorate, fluoroborate and iodide salts furnish interesting spectral features having well-defined absorption bands near 10.12 kK which persist more or less in the same region both in the solid state and in nitromethane solution; additional bands around 6.00 kK (d.r.s.) and near 14.28 kK (in solution of nitromethane) are also discernible. The spectral data remind us of the well known Cu(bipy)$_3^{2+}$ and Cu(o-phen)$_3^{2+}$ [15] and our earlier reported Cu(DPyPz)$_3^{2+}$ [15a] [where DPyPz represents a molecule of 3,5 - dimethyl - 1 - (2' - pyridyl)pyrazole, having structural resemblance to our present ligand]. The point symmetry in these tris-Cu(II) species may, therefore, be regarded as essentially D$_3$ in which the $^2T_{2g}$ level (in O_h) is split into $^2E + {}^2A_1$ while the ^2E_g level is unaffected. The two transitions corresponding to $^2A_1 \leftarrow {}^2E$ and $^2E \leftarrow {}^2E$ are expected in order of increasing energy.[16] The main spectral bands in the present Cu(II) complexes are con-

sistent with this expectation. Although in absence of polarised data it is a conjecture, but it seems reasonable to consider Cu(DPymPz)$_3^{2+}$ as being essentially a trigonally distorted octahedral complex both in the solid state and in solution.

IR spectra

The i.r. spectrum of the uncomplexed ligand furnishes recognisable bands in the region 1600–1400 and at 1000 and 750 cm^{-1} which may be assigned to the $\nu_{C\dots C} + \nu_{C\dots N}$ and out-of-plane deformation vibrations respectively of both (1,2)-diazole (pyrazole) and (1,3)-diazine (pyrimidine) systems. On complexation these bands are found to experience shifts in the higher energy side ($\Delta\nu \sim 15$–30 cm^{-1}) indicating, thereby, the expected participation of both pyrazolyl and pyrimidyl ring nitrogens (one of the pyrimidyl nitrogens at a time as verified through construction of molecular model); contemplation of forming a stable 5-membered ring with the metal ion is thus supported. In the far i.r. spectra of a few compounds, the appearance of bands at 300–315 cm^{-1}(w) and around 245 cm^{-1}(ms) attributable to M–N (pyrazole ring)[17a,17b] and M–N (pyrimidine ring)[18] respectively further support the proposition.

Mode of linkage of the counterion (X)

Perchlorate complexes. The appearance of broad strong band at *ca.* 1110–1070 cm^{-1} (ν_1) along with another strong one at 625 cm^{-1} (ν_4) indicate the presence of ionic perchlorate species (T_d) in the compounds.[19]

Fluoroborate complexes. The strong broad bands at *ca.* 1120–1040 cm^{-1} (ν_3) indicate the presence of ionic fluoroborate species in the compounds.[20,21]

Therefore, the ligand (DPymPz) exhibits a neutral bidentate (N–N) function through the tertiary nitrogen atom of the pyrazole and one of the pyrimidine ring nitrogen atoms in complexation with a metal ion giving tris-complexes of [MN$_6$] environment with a relatively heavy counterion.

Further studies with the title ligand using different metal ions [like Fe(II), Pd(II), Pt(II)] are in progress and will be published in due course.

REFERENCES

[1] A. N. Cost and I. I. Grandberg, *Progress in Pyrazole Chemistry in Advances in Heterocyclic Chemistry* (Edited by A. R. Katritzky and A. J. Boulton) Vol. 6, pp. 348–349. Academic Press, New York, (1966).
[2] N. Saha and S. K. Kar, *J. Inorg. Nucl. Chem.* 1977, **39**, 195.
[3] N. Saha and S. K. Kar, *J. Inorg. Nucl. Chem.* 1979, **41**, 1233.
[4] aGennady M. Kosolapoff and Clarence H. Roy, *J. Org. Chem.* 1961, **26**, 1895; bMiss M. P. V. Boarland, J. F. Mcomie and R. N. Timms, *J. Chem. Soc.* 1952, 4693; cR. Giulino and G. Leanardi, *Farmaco (Pavia), Ed. Sci.* 1957, **12**, 394.
[5] *High resolution NMR Catalog,* compiled by N. S. Bhacca, D. P. Hollis, L. F. Jonson and E. A. Pier of the Instrument Division of Varian Associates, 1, spectrum No. 126, 2, spectrum No. 442.
[6] J. Lewis and R. J. Wilkins, *Modern coordination chemistry,* pp. 400–454. Interscience, New York (1960).
[7] W. J. Geary, *Coord. Chem. Rev.* 1971, **7**, 81.
[8] K. C. Patel and D. E. Gouldberg, *J. Inorg. Nucl. Chem.* 1972, **34**, 637.
[9] C. J. Ballhausen, *Introduction to Ligand Field Theory,* p. 265. McGraw-Hill, New York (1962).

[10]O. Bostoup and C. K. Jorgensen, *Acta. Chem. Scand.*, 1957, **11**, 1223.

[11]Y. Tanabe and S. Sugano, *J. Phys. Soc. Japan*, 1954, **9**, 753; 766.

[12]L. E. Orgel, *An Introduction to Transition Metal Chemistry, Ligand Field Theory*, p. 46. Metheun, London (1960).

[13]A. B. P. Lever, *Coord. Chem. Rev.* 1968, **3**, 119.

[14]A. B. P. Lever, *J. Chem. Educ.* 1974, **51**, 612.

[15]C. K. Jorgensen, *Acta. Chem., Scand*, 1955, **9**, 1362.

[15a]N. Saha and S. K. Kar, *J. Inorg. Nucl. Chem.* 1977, **39**, 1236.

[16]A. B. P. Lever, *Inorganic Electronic Spectroscopy*, p. 323. A. P., New York (1963).

[17a]. F. Mani and G. Scapacci, *Inorg. Chim. Acta* 1976, **16**, 163; [b]J. G. Vos and W. L. Groeneveld, *Inorg. Chim. Acta* 1977, **24**, 123; and refs therein.

[18]I. A. Dorrity and K. G. Orgel, *J. Inorg. Nucl. Chem.* 1974, **36**, 230.

[19]B. J. Hathway and A. E. Underhill, *J. Chem. Soc.* 1961, 3091.

[20]S. Buffagni, L. M. Vallarino and J. V. Quaglino, *Inorg. Chem.* 1964, 480; 671.

[21]N. N. Greenwood, *J. Chem. Soc.* 1959, 3811.

ALKOXY, AMIDO AND THIOLATO COMPLEXES OF TRIS (3, 5-DIMETHYLPYRAZOLYL)BORATO(NITROSYL) MOLYBDENUM FLUORIDE, CHLORIDE AND BROMIDE

A. STEPHEN DRANE and JON A. McCLEVERTY*†

Department of Chemistry, The University, Sheffield S3 7HF, England

Abstract—The complexes Mo{HB(Me₂pyz)₃}(NO)XY {HB(Me₂pyz)₃ ≡ HB(3, 5-Me₂C₃HN₂)₃; X=Y=F, Cl or Br; X=F, Y=OEt, NHMe or SBuⁿ; X=Cl, Y=NHR (R=Me Et, Buⁿ, Ph, p-MeC₆H₄), NMe₂ and SR (R=Buⁿ, C₆H₁₁, CH₂Ph, Ph); X=Br, Y=NHMe, NMe₂ and SBuⁿ} have been prepared and characterised spectroscopically. Their properties are generally similar to those of their iodo-analogues.

In a series of papers we have described the reactions of Mo{HB(Me₂pyz)₃}(NO)I₂, (1; X=Y=I) [HB(Me₂pyz)₃ =HB(3, 5-Me₂C₃HN₂)₃≡tris(3, 5-dimethyl-pyrazolyl)borate] with alcohols,[1,2] amines[3,4] and thiols,[5] affording alkoxy, amido and thiolato complexes of the type (1; X = I, Y=OR, NHR or SR). Our use of the diiodide precursor (1, X=Y=I) was dictated partly by its ease of preparation from (1, X=Y=CO),[1,6] and partly because the iodide ligand is bulky and therefore likely to be a good leaving group in potential substitution reactions. However, we felt that the preparation of the other halide derivatives should be attempted in order to explore the effects of the changes in electronegativity and ligand size in the properties of this unusual series of complexes.

SYNTHETIC STUDIES

In earlier attempts to prepare chloro- and bromo-complexes of the type (1; X=Y=CO) with chlorine and bromine we noted that partial halogenation of the pyrazolyl rings, especially at C-4, occurred very readily.[1] This caused great difficulties, and we were frequently unable to reproduce our results. Thus alternative routes to (1; X=Y=Cl and Br) were sought.

We have employed two methods for making the chloride and bromide precursors. Trofimenko had shown[7] that (1; X=Y=CO) reacted with NOCl to give (1; X=Y=Cl), and we found this the easiest and quickest way to prepare the chloride. The product so obtained was not usually very pure, but was entirely satisfactory for further reactions. The bromide was obtained similarly, using NOBr, and was isolated as a pure orange powder. The other method of synthesis involved reaction of (1; X=Y=OR; R usually Et) with HCl or HBr. The chloride was obtained as a yellow solid and this method is the best way of isolating the pure material. While the conversion of bis-alkoxide to dichloride is 70%, however, the overall yield from (1; X=Y=CO) is only 30%, requiring conversion of the dicarbonyl to (1; X=I; Y=OEt) and of this to (1, X=Y=OEt). The bromide obtained from HBr addition to (1; X=Y=OR) was not obtained sufficiently pure to justify exploration of this route, traces of water frequently interfering with the purification of the compound.

The difluoride, (1; X=Y=F) has not been previously described but was made by reaction of (1; X=Y=OEt) with aqueous HF. It was isolated as a virtually insoluble pale green solid (it is very slightly soluble in CHCl₃) which was substantially less stable towards air and moisture than its chloro-, bromo- and iodo-analogues.

The alkoxides (1; X=Cl, Br or I, Y=OR) have been previously described,[1] and are prepared by refluxing the appropriate dihalide in an alcohol. However, the fluoro ethoxide, (1, X=F, Y=OEt), despite the insolubility of the parent difluoride, is formed rapidly in ethanol without heating. The mono-amido species (1, X=F, Y=NHMe), (1; X=Cl, Y=NHMe, NHPh and NHC₆H₄Me-p) and (1; X=Br, Y=NHMe) were prepared in the same way as their iodo analogues,[3] namely by reaction of the dihalide with two mole equivalents of the amine in solution at room temperature. Similarly, the thiolato species (1, X=F, Y=SBuⁿ), 1, X=Cl, Y=SBuⁿ, SC₆H₁₁, SCH₂Ph and SPh) and (1, X=Br, Y=SBuⁿ) were obtained by refluxing the dihalide in hydrocarbon solvents containing the appropriate thiol.[5]

Of some interest was our ability to synthesise relatively stable dimethylamido complexes, (1; X=Cl or Br, Y=NMe₂). These compounds were obtained in the same way as their mono-alkylamido analogues, and are significantly more stable towards air, moisture and other hydroxylic solvents than the corresponding iodo complex (1; X=I, Y=NMe₂).[3] Indeed, the iodo species has been used as a convenient precursor for making alkoxides and monoalkylamides under mild conditions. We presume the lower chemical reactivity of the related chloro- and bromo-complexes is related to the relief of steric strain following the replacement of the iodide group by the less bulky Cl and Br.

Spectral studies

The IR spectra of the new complexes (Table 2) exhibit bands typical of the HB(Me₂pyz)₃ ligand, and a strong absorption due to ν(NO). The dichloride and dibromide exhibit ν(NO) at values very similar to those of the diiodide, whereas the frequency in the difluoride was lower. On electronegativity grounds alone, we would have expected an *increase* in ν(NO) in the difluoride if any change occurred. It is possible, however, that (1; X=Y=F) is di- or poly-meric, with Mo–F–Mo bridges, which would be consistent with its insolubility. The coordination sphere of the metal would then increase from 6 to 7 by virtue of F atom bridging, leading to more electron donation to Mo, and hence a lowering of ν(NO) relative to the other dihalides. There is very little evidence for a

---

Table 1. Analytical and molecular weight data obtained from [Mo{HB(Me₂pyz)₃}(NO)XY]

X	Complex Y	Elemental Analyses Found (Calcd)%				Mol wt.[a] Found(Calcd)
		C	H	N	Hal[b]	
F	F	39.3(39.1)	4.9(4.8)	20.8(21.3)	8.2(8.3)	
Cl	Cl	36.6(36.5)	4.5(4.5)	19.4(19.9)	14.0(14.4)	524(494)
Br	Br	30.7(30.9)	3.9(3.8)	16.5(16.8)	27.0(27.4)	620(583)
F	OEt	42.4(41.9)	5.97(5.61)	19.8(20.1)	3.6(3.9)	
F	NHMe	40.4(40.7)	5.81(5.51)	23.9(23.7)	4.2(4.0)	
Cl	NHMe	39.5(39.3)	5.5(5.4)	23.3(22.9)	7.6(7.3)	
Cl	NHEt	40.3(40.6)	5.9(5.6)	22.0(22.3)	7.3(7.1)	521(503)
Cl	NHBu^n	43.4(43.0)	6.0(6.1)	21.3(21.1)	6.4(6.7)	
Cl	NHPh	46.0(45.8)	5.2(5.1)	20.4(20.4)	6.3(6.4)	
Cl	NHC$_6$H$_4$Me	46.4(46.8)	5.2(5.4)	19.7(19.8)	6.5(6.3)	540(565)
Cl	NMe$_2$	40.2(40.5)	5.6(5.8)	22.5(22.3)	7.1(7.0)	
Br	NHMe	36.4(36.1)	4.7(4.9)	21.2(21.0)	15.2(15.0)	562(533)
Br	NMe$_2$	37.0(37.3)	4.9(5.2)	20.2(20.5)	14.3(14.6)	
F	SBu^n [c]	42.7(43.0)	5.7(5.8)	18.1(18.5)	3.9(3.6)	
Cl	SBu^n [d]	41.4(41.7)	5.7(5.7)	17.6(17.9)	6.4(6.5)	575(548)
Cl	SPh [e]	44.7(44.4)	4.6(4.8)	17.5(17.3)	6.1(6.2)	591(568)
Cl	SC$_6$H$_{11}$ [f]	43.6(44.0)	5.5(5.8)	16.8(17.1)	5.8(6.2)	
Cl	SCH$_2$Ph [g]	45.3(45.4)	5.3(5.0)	16.7(16.9)	5.8(6.1)	
Br	SBu^n [h]	38.8(38.5)	5.0(5.3)	16.8(16.6)	13.3(13.5)	

[a] Determined osmometrically in CHCl₃;   [b] F, Cl or Br;   [c] S: 5.8(6.1)%;
[d] S: 6.0(5.9)%;   [e] S: 5.84(5.7)%;   [f] S: 5.2(5.6)%;   [g] S: 5.6(5.5)%;
[h] S: 5.0(5.4)%.

Table 2. IR and NMR spectral data from Mo{HB(Me₂pyz)₃}(NO)XY

X	Y	ν(NO)(cm⁻¹) KBr	CHCl₃	δ(RA)[a]		Assignments
F	F	1688	[b]	6.03(2)[c] 5.31(1)	s s	C₃HMe₂N₂
				2.56 2.41 2.30 (18) 2.28	s s s s	C₃H(CH₃)₂N₂
Cl	Cl	1702	1720	5.98(2) 5.80(1)	s s	C₃HMe₂N₂
				2.40(18)	s;	C₃H(CH₃)₂N₂
Br	Br	1702	1720	6.00(2) 5.95(1)	s s	C₃HMe₂N₂
				2.60 2.51 2.46 (18) 2.41	s s s s	C₃H(CH₃)₂N₂
F	OEt	1666	[b]	[b]		
F	NHMe	1640	[b]	[b]		
F	SBu^n	1655	[b]	[b]		
Cl	NHMe	1643	1664	12.32(1)	s;	NHMe
				5.83(1) 5.82(1) 5.80(1)	s s s	C₃HMe₂N₂
				4.45(3)	d;	NHCH₃, ³J(HH)8.0Hz
				2.58 2.44 2.38 (18) 2.36 2.33 2.31	s s s s s s	C₃H(CH₃)₂N₂

Table 2 (*Contd.*)

X	Y	$\nu(NO)(cm^{-1})$ KBr	CHCl$_3$	$\delta(RA)^{\underline{a}}$		Assignments
Cl	NHEt	1649	1662	12.29(1)	s;	NHEt
				5.86(1)	s⎤	
				5.82(1)	s⎬	$C_3HMe_2N_2$
				5.80(1)	s⎦	
				4.89(2)		AB pair, δ(A)5.21, δ(B)4.57; J(AB)5.0Hz, ^{3}J(HH)8Hz; NHC$\underline{H}_2$Me
				2.58⎤	s⎤	
				2.48⎱	s⎮	
				2.37⎬ (18)	s⎬	$C_3H(C\underline{H}_3)_2N_2$
				2.35⎮	s⎮	
				2.33⎦	s⎦	
				1.36(3)	t;	NHCH$_2$C$\underline{H}_3$ ^{3}J(HH)7.0Hz.
Cl	NMe$_2$	1645	1672	5.89(1)$^{\underline{d}}$	s⎤	
				5.88(1)	s⎬	$C_3\underline{H}Me_2N_2$.
				5.83(1)	s⎦	
				4.35(3)	s⎱	N(C$\underline{H}_3$)$_2$
				3.26(3)	s⎰	
				ca.2.4(18)	m;	$C_3H(C\underline{H}_3)_2N_2$
Cl	NHPh	1654	1664	12.63(1)	s;	NHPh
				ca.7.25(5)	m;	NHC$_6$H$_5$
				5.87(1)	s⎤	
				5.85(1)	s⎬	$C_3\underline{H}Me_2N_2$
				5.78(1)	s⎦	
				2.68⎤	s⎤	
				2.40⎮	s⎮	
				2.34⎬ (18)	s⎬	$C_3H(C\underline{H}_3)_2N_2$
				2.33⎮	s⎮	
				1.98⎦	s⎦	
Cl	NHC$_6$H$_4$Me	1653	1662	12.72(1)	s;	NHC$_6$H$_4$Me
				7.30(4)		A$_2$B$_2$ mult; δ(A)7.39, δ(B)7.21, J(AB)8.0Hz; NHC$_6$H$_4$Me
				5.89(1)	s⎤	
				5.87(1)	s⎬	$C_3\underline{H}Me_2N_2$
				5.79(1)	s⎦	
				2.67(3)	s⎤	
				2.38(12)	s⎬	$C_3H(C\underline{H}_3)_2N_2$
				2.01(3)	s⎦	
				2.36(3)	s;	NHC$_6$H$_4$C$\underline{H}_3$
Br	NHMe	1654	1667	12.57(1)	s;	NHMe
				5.88(1)	s⎱	$C_3\underline{H}Me_2N_2$
				5.83(2)	s⎰	
				4.32(3)	d;	NH(C$\underline{H}_3$) ^{3}J(HH)8.0Hz
				2.61⎤	s⎤	
				2.50⎮	s⎮	
				2.40⎮	s⎮	
				2.37⎬ (18)	s⎬	$C_3H(C\underline{H}_3)_2N_2$
				2.36⎮	s⎮	
				2.35⎦	s⎦	
Br	NMe$_2$	1650	1659	5.92(1)	s⎤	
				5.86(1)	s⎬	$C_3\underline{H}Me_2N_2$
				5.80(1)	s⎦	
				4.32(3)	s⎱	N(C$\underline{H}_3$)$_2$
				3.22(3)	s⎰	
				ca.2.4(18)	m;	$C_3H(C\underline{H}_3)_2N_2$
Cl	SBu^n	1662	1680	5.91(1)	s⎱	$C_3\underline{H}(CH_3)_2N_2$
				5.80(2)	s⎰	
				5.18(2)	m;	SC$\underline{H}_2$Pr^n, ^{3}J(HH)7.0Hz
				2.54(3)⎤	s⎤	
				2.45(3)⎮	s⎮	
				2.42(3)⎬	s⎬	$C_3H(C\underline{H}_3)_2N_2$
				2.33(6)⎮	s⎮	
				2.22(3)⎦	s⎦	
				2.06(2)	quint;	SCH$_2$C$\underline{H}_2$Et, ^{3}J(HH)7.0Hz
				1.57(2)	sext;	SCH$_2$CH$_2$C$\underline{H}_2$Me, ^{3}J(HH)7.0Hz
				1.01(3)	t;	S(CH$_2$)$_3$C$\underline{H}_3$ ^{3}J(HH)8.0Hz.
Cl	SC$_6$H$_{11}$	1671	1678	5.90(1)	s⎱	$C_3\underline{H}Me_2N_2$
				5.80(2)	s⎰	
				2.55⎤	s⎤	
				2.46⎮	s⎮	
				2.42⎬ (18)	s⎬	$C_3H(C\underline{H}_3)_2N_2$
				2.33⎮	s⎮	
				2.22⎦	s⎦	
				1.75 (10)	m;	SC$_6$H$_{11}$; SC$\underline{H}$(CH$_2$)$_5$ not observed

Table 2 (Contd.)

X	Y	$\nu(NO)(cm^{-1})$ KBr	CHCl$_3$	$\delta(RA)^{\underline{a}}$	Assignments
Cl	SCH$_2$Ph	1671	1684	ca.7.4(5)	m; SCH$_2$C$_6$H$_5$
				6.32(2)	AB pair; δ(A)6.48, δ(B)6.15, J(AB)13.2Hz; SCH$_2$Ph
				5.90(1) s 5.86(1) s 5.84(1) s	C$_3$HMe$_2$N$_2$
				2.50 s 2.45 s 2.42 (18) s 2.37 s 2.30 s	C$_3$H(CH$_3$)$_2$N$_2$
Cl	SPh	1684	1691	7.89(2)	d; o-H, SC$_6$H$_5$, ^{3}J(HH)7.0Hz
				7.55(2)	t; m-H, SC$_6$H$_5$, ^{3}J(HH)7.0Hz
				7.37(1)	t; p-H, SC$_6$H$_5$, ^{3}J(HH)7.0Hz
				5.92(1) s 5.83(1) s 5.78(1) s	C$_3$HMe$_2$N$_2$
				2.53 s 2.50 s 2.45 (18) s 2.36 s 2.02 s	C$_3$H(CH$_3$)$_2$N$_2$
Br	SBu^n	1665	1682	5.96(1) s 5.82(1) s 5.80(1) s	C$_3$HMe$_2$N$_2$
				5.07(2)	m; SCH$_2$Pr^n; ^{3}J(HH)7.0Hz
				2.60(3) s 2.47(6) s 2.36(6) s 2.20(3) s	C$_3$H(CH$_3$)$_2$N$_2$
				2.15(2)	quint; SCH$_2$CH$_2$Et; ^{3}J(HH)8.0Hz
				1.57(2)	sext; SCH$_2$CH$_2$CH$_2$Me; ^{3}J(HH)8.0Hz
				1.03(3)	t; S(CH$_2$)$_3$CH$_3$ ^{3}J(HH)8.0Hz

$\underline{a}$ Recorded in CDCl$_3$ at 220 MHz, 37° using SiMe$_4$ as internal standard (rel. area);

$\underline{b}$ not recorded because of insolubility;

$\underline{c}$ Recorded in CDCl$_3$ at 400 MHz (Brucker FT instrument);

$\underline{d}$ Recorded in CD$_2$Cl$_2$ at 220 MHz.

halide or N- or S- ligand substituent effect on $\nu(NO)$ of the other monohalide complexes. In general $\nu(NO)$ in the amido and thiolato species averages 1664 and 1683 cm^{-1}, which is consistent with our observations elsewhere.[5]

The ^{1}H NMR spectra (Table 2) of the new complexes are generally unremarkable, and are consistent with the formulation of the new species. A group of signals in the region δ 2.7-1.9 is associated with the methyl groups of the pyrazolyl ring. The shape of these signals varies from compound to compound but in one complex (1; X=Y=Cl) it appears as a singlet. We have no explanation for this effect, but it is very useful for characterisation purposes. The group of signals occurring in the region δ 6.1-5.3 is due to the protons attached to C-4. In those complexes of the type (1; X=Y), the signals appear as a doublet of relative intensity 2:1. In the species where X ≠ Y, we would expect three singlets, since there is no plane of symmetry in the complexes, and this is usually observed. In two cases viz. (1; X=Cl, Y=SBu^n or SC$_6$H$_{11}$) only two resonances, of relative intensity 1:2, are observed and we assume this is due to accidental degeneracy; this effect has been noted before. In these complexes, as in all others reported previously, protons attached to the C

atom α to the donor atom at Mo resonate at lower fields than expected, and we reiterate that this is probably due to the strong electron-withdrawing properties of the metal. The NH signals in the mono-alkyl and aryl-amides also resonate at low fields (δ 12.7-12.3) for the same reason. The signals due to the dimethylamido group in (1; X=Cl or Br, Y=NMe$_2$) appear as two singlets, because of the asymmetry of the complexes, and the lack of facile inversion at the amido N atom in these complexes.

Conclusion

The properties of the new complexes are generally very similar to those of their iodo-analogues. We have noted in a qualitative way that the apparent rates at which the monosubstituted fluoro-, chloro- and bromo-complexes were generally faster than those of the related iodo-complexes. While we believe that the mechanism of formation of the species (1; X=I, Y=OR, Y=OR, NHR or SR) from (1; X=Y=I)[8] involves prior one-electron transfer, we are not yet in a position to determine whether this occurs with the other dihalides. This possibility is being studied.

EXPERIMENTAL

The complex Mo{HB(Me$_2$pyz)$_3$}(NO)(CO)$_2$ was prepared as described elsewhere.[1,6] All reactions were carried out under nitrogen and in N$_2$-degassed solvents. All yields are quoted relative to the molybdenum-containing precursor. IR and ^{1}H NMR spectral data were obtained using PE 297 and PE 180 spectrophotometers, and PE R34 instruments, respectively. Molecular weights were determined osmometrically in chloroform.

Mo{HB(Me$_2$pyz)$_3$}(NO)Cl$_2$ (1; X=Y=Cl)—*Method* 1. Nitrosyl chloride was generated *in situ*, and was bubbled through a dichloromethane solution of Mo{HB(Me$_2$pyz)$_3$}(NO)(CO)$_2$. The yellow-brown solution which formed was then evaporated to dryness *in vacuo*, and ethanol added in the cold. The slurry which formed was filtered, the *complex* being collected as a yellow powder. This could be recrystallised from toluene to give orange-red crystals (containing variable amounts of toluene of crystallisation) which, after repeated washing with n-pentane, changed to a yellow powder.

Method 2. Mo{HB(Me$_2$pyz)$_3$}(NO)(OEt)$_2$ was prepared as previously described, and dissolved in toluene. HCl gas was then bubbled through the stirred solution for 30 min during which time the colour of the solution became orange-red and some orange solid precipitated. The mixture was then refluxed for 30–45 min, filtered and allowed to cool slowly to room temperature. During this time, orange crystals separated which were collected by filtration, thoroughly washed with n-pentane, to afford the *complex* as a yellow powder (yield quantitative).

Mo{HB(Me$_2$pyz)$_3$}(NO)Br$_2$ (1; X=Y=Br). Nitrosyl bromide was generated in the same way as NOCl.[7] The red-brown gas was purified by passing through CaCl$_2$ and KCl, and was bubbled through a solution of Mo{HB(Me$_2$pyz)$_3$}(NO)(CO)$_2$ in dichloromethane. An orange solution quickly formed, and this was reduced in volume *in vacuo*. Ethanol was then added in the cold, causing precipitation of an orange powder. This was collected by filtration, recrystallised from toluene affording orange-red crystals of the toluene-solvated species. On repeated washing with n-pentane, the *complex* was obtained as an orange powder.

Mo{HB(Me$_2$pyz)$_3$}(NO)F$_2$, (1; X=Y=F). Mo{HB(Me$_2$pyz)$_3$}(NO)(OEt)$_2$ (0.3 g) was dissolved in dichloromethane (25 cm^3) and conc. HF (40% in water, 0.2 cm^3, PTFE beaker) was added. The mixture was stirred for 1 hr, and the solvent then removed *in vacuo* leaving the *complex* as a pale green powder (0.26 g, 90%).

Mo{HB(Me$_2$pyz)$_3$}(NO)F(OEt); (1; X=Y, Y=OEt). Mo{HB(Me$_2$pyz)$_3$}(NO)F$_2$ was suspended in ethanol and stirred at room temperature for 1 hr. The solvent was reduced in volume *in vacuo*, and the purple *complex* filtered off and dried *in vacuo*.

Mo{HB(Me$_2$pyz)$_3$}(NO)F(NHMe); (1; X=F, Y=NHMe). Mo{HB(Me$_2$pyz)$_3$}(NO)F$_2$ was suspended in methylamine and stirred at −10°C for 2 hr. The amine was then allowed to evaporate at room temperature, leaving the *complex* as a pale orange powder.

Mo{HB(Me$_2$pyz)$_3$}(NO)F(SBu^n); (1; X=F, Y=SBu^n). Mo{HB(Me$_2$pyz)$_3$}(NO)F$_2$ was suspended in n-heptane, and n-butanethiol (slight excess) added. The mixture was refluxed overnight and cooled, the brown *complex* being collected by filtration and dried *in vacuo*.

Mo{HB(Me$_2$pyz)$_3$}(NO)NHMe; (1; X=Cl, Y=NHMe). Mo{HB(Me$_2$pyz)$_3$}(NO)Cl$_2$ (0.3 g), dissolved in dichloromethane (30 cm^3), was treated with methylamine (33% ethanolic solution, 0.2 cm^3). The mixture was stirred at room temperature for 30 min during which time the solution became orange. The volume of solvent was reduced *in vacuo* to ca. 5 cm^3 and, after addition of diethylether, the precipitated [NH$_3$Me]Cl filtered off. The filtrate was reduced *in vacuo* to ca. 5 cm^3 whereupon the *complex* formed orange crystals (0.25 g, 83%).

The corresponding *ethyl-* and *n-butyl-amides* were obtained similarly as orange crystals (85 and 76% yields, respectively).

Mo{HB(Me$_2$pyz)$_3$}(NO)Cl(NMe$_2$) (1; X=Cl, Y=NMe$_2$). To Mo{HB(Me$_2$pyz)$_3$}(NO)Cl$_2$ (0.3 g) dissolved in dichloromethane (20 cm^3) was added dimethylamine (0.1 cm^3). The colour of the solution immediately became orange and the mixture was stirred for 30 min. The volume of the solution was reduced *in vacuo* to ca. 5 cm^3, treated with diethylether which caused precipitation of [NH$_2$Me$_2$]Cl which was filtered off. The filtrate was slowly

evaporated, effecting crystallisation of the orange *complex* (0.19 g, 61%).

Mo{HB(Me$_2$pyz)$_3$}(NO)Cl(NHPh); (1; X=Cl, Y=NHPh). A mixture of Mo{HB(Me$_2$pyz)$_3$}(NO)Cl$_2$ (0.3 g) and freshly redistilled aniline (0.1 ml) in dichloromethane (30 cm^3) was stirred overnight at room temperature. The solution had became yellow-brown, and the solvent was removed *in vacuo*. The residue was extracted with diethylether, the extract being filtered and allowed to cool at −5° until the *complex* had precipitated as a brown powder (0.26 g, 78%).

The related *p-toluidide*, Mo{HB(Me$_2$pyz)$_3$}(NO)Cl-(NHC$_6$H$_4$Me), (1; X=Cl, Y=p-MeC$_6$H$_4$NH), was prepared similarly using *p*-toluidine (0.1 g) and was isolated as a brown powder (0.27 g, 79%).

Mo{HB(Me$_2$pyz)$_3$}(NO)Cl(SBu^n); (1; X=Cl, Y=SBu^n). A mixture of Mo{HB(Me$_2$pyz)$_3$}(NO)Cl$_2$ (0.3 g) and n-butanethiol (0.2 cm^3) in n-heptane (20 cm^3) was refluxed overnight. The yellow-black solution which had formed was reduced *in vacuo* to ca. 10 cm^3 and the *complex* allowed to form as black crystals which were collected by filtration (0.23 g, 74%).

The related complexes Mo{HB(Me$_2$pyz)$_3$}(NO)Cl(SR) R=C$_6$H$_{11}$, CH$_2$Ph *and* Ph) were prepared similarly, using C$_6$H$_{11}$SH (0.2 cm^3), PhCH$_2$SH (0.1 g) and PhSH (0.2 cm^3) and were isolated as black (R=Ph) or dark green (R=C$_6$H$_{11}$, CH$_2$Ph) crystals. The yields were 0.26 g (75%), 0.25 g (72%) and 0.27 g (80%) respectively, and the toluene-α-thiolate could be recrystallised from dichloromethane/*n*-hexane mixtures; giving black microcrystals.

Mo{HB(Me$_2$pyz)$_3$}(NO)Br(NHMe); (1; X=Br, Y=NHMe). To Mo{HB(Me$_2$pyz)$_3$}(NO)-Br$_2$ (0.3 g) dissolved in dichloromethane (20 cm^3) was added methylamine (33% solution in ethanol, 0.2 cm^3). The solution immediately became orange, and was stirred at room temperature for 30 min. The volume of the solvent was then reduced to ca. 5 cm^3, and diethylether was added causing precipitation of [NH$_3$Me]Br which was filtered off. The volume of the filtrate was slowly reduced *in vacuo* until crystallisation began, and the *complex* formed as orange crystals at −5° (0.20 g, 73%).

Mo{HB(Me$_2$pyz)$_3$}(NO)Br(NMe$_2$); (1; X=Br, Y=NMe$_2$). A mixture of Mo{HB(Me$_2$pyz)$_3$}(NO)Br$_2$ (0.3 g) and dimethylamine (0.2 cm^5) in dichloromethane (20 cm^3) was stirred for 10 min, during which time an orange solution rapidly formed. The volume of the solvent was reduced *in vacuo* to ca. 5 cm^3, and diethylether added causing precipitation of [NH$_2$Me$_2$]Br, which was filtered off. The filtrate was partially evaporated *in vacuo* and allowed to stand at −5° until the *complex* had formed as orange crystals (0.16 g, 57%).

Mo{HB(Me$_2$pyz)$_3$}(NO)Br(SBu^n); (1; X=Br, Y=SBu^n). A mixture of Mo{HB(Me$_2$pyz)$_3$}(NO)Br$_2$ (0.25 g) and n-butanethiol (0.2 cm^3) in n-heptane (20 cm^3) was refluxed overnight during which time a yellow-black solution had formed. The solvent was evaporated *in vacuo* to ca. 10 cm^3, and the complex precipitated as an olive-green powder (0.22 g, 71%).

REFERENCES

[1] J. A. McCleverty, D. Seddon, N. A. Bailey and N. W. Walker, *J. Chem. Soc. Dalton* 1976, 898.
[2] J. A. McCleverty, A. E. Rae, I. Wolochowicz, N. A. Bailey and J. M. A. Smith, *J. Chem. Soc. Dalton* 1982, 951.
[3] J. A. McCleverty, A. E. Rae, I. Wolochowicz, N. A. Bailey and J. M. A. Smith, *J. Chem. Soc. Dalton* 1982, 429.
[4] J. A. McCleverty, G. Denti, A. S. Drane, N. El Murr, A. E. Rae, S. J. Reynolds, N. A. Bailey, H. Adams and J. M. A. Smith, *J. Chem. Soc. Dalton* 1982, in press (2/529).
[5] J. A. McCleverty, A. S. Drane, N. A. Bailey and J. M. A. Smith, *J. Chem. Soc. Dalton* 1982, in press (2/530).
[6] C. J. Jones, J. A. McCleverty, S. J. Reynolds and C. Smith, *Inorg. Synth.*, in press.
[7] S. Trofimenko, *Inorg. Chem.* 1969, **8**, 2675.
[8] J. A. McCleverty and N. El. Murr, *J. Chem. Soc. Chem. Commun.* 1981, 960.

NEW CHEMICAL REACTIVITY IN AROMATIC DITHIOCARBAMATE AND MONOTHIOCARBAMATE LIGANDS: SYNTHESES OF Mo₂L₄·2THF (L = PYRROLE OR INDOLE MONOTHIOCARBAMATE OR PYRROLE DITHIOCARBAMATE) AND Mo₂L₄ (L = INDOLINE MONOTHIOCARBAMATE)[1]

ROBERT D. BEREMAN,* DONALD M. BAIRD and CHARLES G. MORELAND
The Department of Chemistry, North Carolina State University, Raleigh, NC 27650, U.S.A.

Abstract—The reactions between $Mo_2(C_2H_3O_2)_4$ and several new dithio- and monothiocarbamates have been studied. The first example of a dimolybdenum compound of a dithiocarbamate with the "molybdenum acetate" structure is reported (Mo_2L_4·2THF; L = pyrrole dithiocarbamate). In addition, the synthesis of $Mo_2L'_4$·2THF (L' = pyrrole monothiocarbamate, indole monothiocarbamate, indole dithiocarbamate) and $Mo_2L''_4$ (L" = indoline monothiocarbamate) are reported. A discussion of the unique stabalization of the dithiocarbamate bridge by "aromatic" dithio- and monothiocarbamates is presented.

INTRODUCTION

The chemistry of compounds containing metal–metal bonds constitutes one of the major topics of inorganic chemistry currently attracting vigorous and diverse research efforts.[2] This realm of metal–metal bonds was largely unknown prior to 1970 and is an exciting area of study. A large array of ligands have been coordinated to the dimolybdenum unit (Mo_2^{4+}) including halides, amines and carboxylates.[3–5] Perhaps the most well studied of these systems are the carboxylates which have the structural features indicated below as shown by an X-ray diffraction study performed by Cotton.[6]
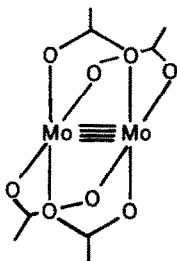
One of the most glaring absences in this array of ligands is the lack of dithiocarbamate (dtc) and mono-thiocarbamate (mtc) complexes of the dimolybdenum unit. The paucity of dithiocarbamate compounds is because of the unusual metal insertion into the C–S bond

of the dithiocarbamate, resulting in a thiocarbene linkage and a Mo=Mo double bond (Scheme 1).[7]

We choose to view this reaction as a "nucleophilic" attack of one of the Mo–Mo bonds on the CS_2 carbon (Scheme 2). If indeed this model were valid, we felt that
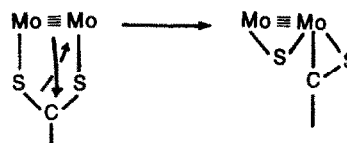
Scheme II

we could exploit the unique resonance properties of new aromatic mono- and dithiocarbamates recently prepared in these laboratories to synthesize the first examples of mono- or dithiocarbamate dimolybdenum complexes that adopted the dimolybdenum acetate structure. That is, we have recently show that "aromatic" dithiocarbamates such as those derived from pyrrole have only a minor contribution from the resonance form IIIB often used to describe dithiocarbamates[8] and it is this resonance form which would favor the "nucleophilic" attack for one of the Mo–Mo bonds on the CS_2 carbon.

EXPERIMENTAL

Syntheses of ligands

Potassium salts of pyrrole-N-carbodithioate (pdc), pyrrole-N-carbothioate (ptc),[9] indole-N-carbodithioate (ildc),[9] indole-N-

Mo₂(Ac)₄ + 4(Et₂dtc)Na ⟶
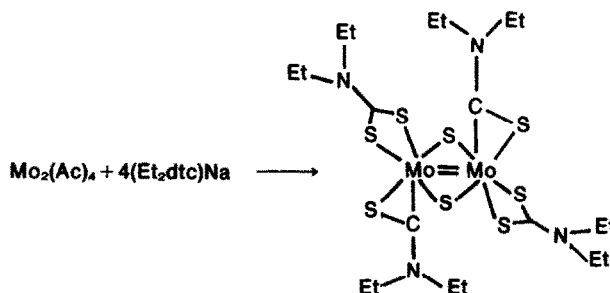
Scheme I

*Author to whom correspondence should be addressed.

carbothioate (iltc),[1] and indoline-N-carbothioate (intc)[1] were prepared as reported previously.

Mo₂(pdc)₄·2THF

Excess (1.7 eq.) of potassium pyrrole-N-carbodithioate dissolved in 50 ml dry THF was added slowly to a mixture of 1 g Mo₂ (OAc)₄ (OAc = acetate) in dry THF. The yellow color of the Mo₂(OAc)₄ was immediately replaced by a deep purple color. After all the Kpdc was added, the solution was filtered to remove any insoluble materials. The volume of the solution was reduced to about 50 ml, and 10 ml hexane was added. Refrigeration for several days produced purple crystals of Mo₂(pdc)₄·2THF. This compound was recrystallized by dissolution in THF and addition of an equal volume of hexane. Several elemental analyses were attempted; however, in each case some THF was lost so that analyses usually indicated somewhere between one and two THF molecules per Mo₂ unit. NMR spectra of freshly prepared samples integrated in such a way as to indicate two THF molecules per four pyrrole groups. NMR(d_6-DMSO) δ 2.0 (4H, m), 3.82 (4H, m), 6.57 (4H, m), 8.03 (4H, m). Found: C, 35.67; H, 3.31; S, 28.75; Calc. for $C_{28}H_{32}N_4O_2S_8Mo_2$: C, 37.14; H, 3.56; S, 28.35. This corresponds to the loss of approx. 20% of the THF.

Mo₂(iltc)₄·2THF

This compound was prepared by the same method as that above used for Mo₂(ptc)₄·2THF. This compound is dark purple and can be recrystallized from THF and hexane. Elemental analyses corresponded to approx. Mo₂(ildc)₄·1.6 THF. NMR again however integrated to give 2THF/4 indole groups.

Mo₂(ptc)₄·2THF and Mo₂(ptc)₄

A solution of 1.5 g Kptc in 50 ml THF was added slowly through a Schlenk frit to a mixture of 0.97 g Mo₂(OAc)₄ in 100 ml dry THF. During this period an orange solution formed and KOAc precipitated from solution. After an additional 1 hr of stirring the solution was filtered. The volume of solution was reduced by half by vacuum evaporation and an equal volume of hexane was added. Refrigeration for several days afforded an orange powder which was shown to be Mo₂(ptc)₄·2THF by NMR. However, when recrystallized from CH₂Cl₂, the THF molecules were lost. Found: C, 34.35; H, 2.39; S, 18.33; Calc. for $C_{20}H_{16}N_4O_4S_4Mo_2$: C, 34.50; H, 2.32; S, 18.41.

Mo₂(iltc)₄·2THF

A solution of 2 g Kiltc in 100 ml dry THF was added through a Schlenk frit to mixture of 0.98 g Mo₂(Ac)₄ in 50 ml dry THF. During this period an orange solution and a colorless precipitate formed (KAc). The solution was filtered to remove KAc. The volume of the solution was reduced to half and an equal volume of hexane was added. Refrigeration produced an orange powder which was collected by filtration.

Mo₂(Intc)₄

Since Kintc shows only very limited solubility in dry THF, this reaction was attempted in very dry ethanol. 1 g Kintc was added directly to 0.5 g Mo₂(Ac)₄ in 100 ml ethanol. After stirring for 2 hr an orange-red precipitate formed. This precipitate was collected on a Schlenk frit and dried under vacuum. This compound is *extremely* air sensitive. Exposure to air for even the briefest period transforms the compound to a brown and then black powder.

Spectral data collection

IR spectra were determined as before.[1] Optical data were obtained on either a Cary 14 or a Hitachi 110 spectrophotometer.

NMR

The ¹H and ¹³C NMR spectra were obtained on a Bruker WM-250 spectrometer operating in the pulsed-FT mode. The ¹H NMR spectra were run at 250 MHz and the ¹³C NMR spectra at 62.5 MHz.

RESULTS AND DISCUSSION

The reaction of the aromatic dithiocarbamates, pyrrole-N-carbodithioate and indole-N-carbodithioate, with Mo₂(OAc)₄ in dry THF, leads to dark purple compounds which we formulate as Mo₂L₄·2THF based on spectral analyses. IR and electronic spectra and ¹H and ¹³C spectral results suggest that a slow decomposition occurs wherein THF is lost with the *possible* concomitant formation of a thiocarbene linkage. All aromatic dithio- and monothio- ligands behaved in an identical fashion. Therefore, only data for Mo₂(pdc)₄·2THF and Mo₂(ptc)₄·2THF are presented.

IR studies

A report by Steele and Stephenson[10] of the attempted synthesis of a diethyldithiocarbamate complex of dimolybdenum suggested that in the presence of air the green reaction product immediately formed the violet Mo₂O₃(Et₂dtc)₄ compound. These Mo(V) dimers have been studied extensively by Newton[11] and the ν(Mo=O) vibration frequencies for Mo₂O₃(R₂dtc)₄ occur close to 938 cm⁻¹ as a strong band in the IR spectra. Since the molybdenum pyrroledithiocarbamate compound was also violet, the IR spectrum was recorded in order to rule out the presence of the Mo₂O₃ core. The spectrum of this compound exhibited bands at 1250 cm⁻¹, ν(C⎯⎯N), as well as bands at 1100 and 850 cm⁻¹ that are characteristic of the presence of pdc. However, no bands appeared between 900 and 1000 cm⁻¹ that were strong enough to be assigned to ν(Mo=O). The only band in this region was a medium intensity band at 980 cm⁻¹ which also appears in the IR spectra of all pdc complexes as well as in the spectrum of the ligand itself.[8,9] Therefore, this band is assumed to arise from the ligand, not from a Mo–O bond.

The IR spectrum of the analogous monothiocarbamate complex was also recorded. No Mo=O bands occured in this spectrum either. The ν(C⎯⎯O) frequency was located near 1580 cm⁻¹ in Mo₂(ptc)₄ which is fairly high; however, we feel that the oxygen is indeed coordinated to Mo in this orange compound.[1]

ELECTRONIC SPECTRA

The electronic spectra of both the dithiocarbamate and monothiocarbamate were recorded in CH₂Cl₂ solution between 900 and 350 nm. The lowest energy band was found at 510 nm for the dithiocarbamate and at 405 nm for the monothiocarbamate. This band is believed to correspond to the $\delta \rightarrow \delta^*$ transition, if indeed, the molybdenum acetate structure is preserved in these compounds. While the $\delta \rightarrow \delta^*$ band occurs between 500 and 700 nm ($\epsilon = 200$–3000) for most Mo₂⁴⁺ species,[12] it occurs at a much higher energy (340 nm) for tetrakiscarboxylates.[13] However, San Filippo and Sniadoch[14] have found that values for the $\delta \rightarrow \delta^*$ transition in aryl-carboxylates appear as a broad intense band centered between 350 and 480 nm. If our argument which eliminates resonance form IIIB (Scheme 3) were correct, we could then describe the aromatic mono- and dithio-carbamate as a COS or CS₂ group attached to an aromatic ring similar to monothio- or dithiobenzoate. As a result we can suggest that the position of the band in the spectra of our complexes agrees nicely with position and

III A   III B
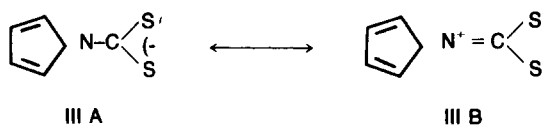
Scheme III

shape of the same band in arylcarboxylates of dimolybdenum. In other words, the spectra can be interpreted as indicating the presence of a Mo–Mo quadruple bond in these compounds. The spectra of both the monothio- and dithio-derivatives are very similar. Thus we believe, on the basis of this and the NMR data (see below), that the structures of the compounds are similar. Finally, the shift of the $\delta \rightarrow \delta^*$ band in the monothiocarbamate to higher energy is as expected for replacing a sulfur donor with an oxygen donor.

^1H NMR

The proton NMR spectrum of both the pdc complex and the ptc complex of Mo_2^{4+} exhibit resonance lines characteristic of the pyrrole ring; a pair of multiplets suggestive of an A A'B B' system. The pyrrole resonances are centered about δ 8.03 and δ 6.56 for the dithiocarbamate complex and δ 7.57 and δ 6.56 for the monothiocarbamate. Both spectra also exhibit resonances characteristic of THF. Integration of the spectra give pyrrole/THF as 2:1 as would be expected for a molybdenum acetate structure with two axially coordinated THF molecules. It is very important to note that THF molecules would not be expected to be associated with the thiocarbene complexes as the reported examples do not have solvent molecules associated.[15,16] On the other hand, Mo_2^{4+} does not have a strong affinity to bond donor molecules on the axial position except when the ligand is a dithio ligand.[17,18]

In order to be sure that the THF was coordinated, additional THF was added to the NMR sample of the monothiocarbamate complex. Exchange between coordinated and uncoordinated THF molecules is apparently slow on the NMR time scale since two sets of resonances were observed. Resonances at δ 3.72 and δ 1.86 associated with uncoordinated THF and resonances at δ 3.12 and δ 1.24 associated with coordinated THF were observed. The assignments were made based on the integration for ptc/THF using the upfield resonances, while the positions of the downfield resonances correlate closely with the reported value for uncoordinated THF (δ 1.79 and δ 3.60).[19]

^{13}C NMR

A recent study by van der Linden et al. reported the position of the CS_2 carbon in the ^{13}C spectra of 71 dithiocarbamates.[20] The carbon of the CS_2 group was found between 185 and 220 p.p.m. for every example. We felt that the ^{13}C spectrum of the dithiocarbamate complex here could help distinguish whether the molybdenum acetate structure of the thiocarbene structure was present in this compound. The spectrum of a dithiocarbamate with the acetate structure should exhibit only a single resonance line in the CS_2 region, while a dithiocarbamate with the thiocarbene structure should exhibit a pair of resonances in this region corresponding to the thiocarbene carbon and the normal dithiocarbamate carbon respectively. Unfortunately, the intensity of this resonance is very weak since there are no hydrogens

attached to the carbon. The lack of hydrogens coupled with limited solubility of the complex in available NMR solvents made detection of the desired signal very difficult. However, a spectrum of the complex (dissolved in d_8-THF) obtained by scanning 32000 times at 63.5 MHz did display resonance lines in the CS_2 carbon region. Unfortunately, there were three lines which were barely detectable and might correspond to the CS_2 carbon. The time frame of the experiment was sufficiently long that it appeared that a decomposition was occurring during the experiment. The most intense resonance line was at 209.8 p.p.m. and is suggested to result from $Mo_2(pdc)_4 \cdot 2THF$ which has the molybdenum acetate structure. This suggested assignment is made based on the proximity of this line to the CS_2 resonance in Kpdc which was found at 217 p.p.m.

In summary, it appears that the products of the reaction between $Mo_2(Ac)_4$ and Kpdc or Kptc have the molybdenum acetate structure, based on ^1H NMR and electronic spectra, at least for the length of time it takes to perform those measurements. However, the ^{13}C spectra as well as the loss of THF during mailing time for elemental analysis point to slow decomposition to thiocarbene or a dithiocarbamate-thiocarbene equilibrium.

REFERENCES

[1] This paper is number 24 in the series, Coordination Chemistry of New Sulfur Containing Ligands. Paper number 23: R.D. Bereman, D. M. Baird, J. Bordner and J. R. Dorfman, *Polyhedron*, in press.
[2] J. L. Templeton, *Prog. Inorg. Chem.* 1970, **26**, 211.
[3] J. V. Brencic and F. A. Cotton, *Inorg. Chem.* 1970, **9**, 351.
[4] A. R. Bowen and H. Taube, *Inorg. Chem.* 1974, **13**, 2245.
[5] A. B. Brignole and F. A. Cotton, *Inorg. Synth.* 1973, **13**, 81.
[6] F. A. Cotton, Z. C. Mester and T. R. Webb, *Acta Crystallogr.* 1974, **B30**, 5698.
[7] L. Ricard, J. Estienne and R. Weiss, *Inorg. Chem.* 1973, **9**, 2182.
[8] R. D. Bereman, M. R. Churchill and D. Nalewajek, *Inorg. Chem.* 1979, **18**, 3112.
[9] R. D. Bereman and D. Nalewajek, *Inorg. Chem.* 1978, **17**, 1085.
[10] D. F. Steele and T. A. Stephenson, *Inorg. Nucl. Chem. Lett.* 1973, **9**, 777.
[11] W. E. Newton, J. L. Corbin, D. C. Bravard, J. E. Searles and J. W. McDonald, *Inorg. Chem.* 1974, **13**, 1100.
[12] F. A. Cotton, *Chem. Soc. Rev.* 1975, **4**, 27.
[13] L. Dubicki and R. L. Martin, *Aust. J. Chem.* 1969, **22**, 1571.
[14] J. San Fillipo and H. J. Sniadoch, *Inorg. Chem.* 1975, **15**, 2209.
[15] L. R. Ricard, J. Estienn and R. Weiss, *Inorg. Chem.* 1973, **12**, 2182.
[16] D. F. Steele and T. A. Stephenson, *Inorg. Nucl. Chem. Lett.* 1973, **9**, 777.
[17] F. A. Cotton, P. E. Fanwick, R. H. Niswander and J. L. Sekutowski, *Acta Chem. Scand., Ser A.* 1978, **A32**, 663.
[18] L. R. Ricard, K. Karagiannidis and R. Weiss, *Inorg. Chem.* 1973, **12**, 2179.
[19] "N.M.R. of Common Solvents", Sadler Research Laboratories, In. p. 10.
[20] H. L. M. Van Goal, J. W. Diesveld, F. W. Pijpers and J. G. W. van der Linden, *Inorg. Chem.* 1979, **18**, 3251.

ESR STUDY ON PHOTOREACTION OF FORMATO COMPLEX OF EUROPIUM(III) IN HCOOH–HCOONa BUFFER SOLUTION

NAGAO AZUMA* and AKIRA MATSUMOTO

Laboratory of Chemistry, Faculty of General Education, Ehime University, Matsuyama 790, Japan

and

JIRO SHIOKAWA

Department of Applied Chemistry, Faculty of Engineering, Osaka University, Suita 565, Japan

Abstract—Matrix isolation ESR study showed that the ligated $HCOO^-$ ion was decomposed into H^+ and $\cdot COO^-$ radical anion through CTTM process at $\lambda = 254$ nm, by contrast, $\cdot CH_3$ radical and CO_2 were produced from CH_3COO^- ligand. In order to explain the photo- and related reactions in the liquid solution, a proposal is made for a cyclic scheme conjugated with the photo-decomposition of the complex. The cycle consists of three steps; photo-reduction of H^+ by Eu^{2+}, radical alternation from $\cdot H$ to $\cdot COO^-$, and oxidation of $\cdot COO^-$ by Eu^{3+}.

INTRODUCTION

Photochemistry of aqueous solutions of Eu^{3+} was studied extensively by Stein *et al.*[1] They observed the evolution of molecular hydrogen from the solutions containing H-atom scavengers, which was due to the following reactions:

$$Eu^{3+} - H_2O \xrightarrow{h\nu} \cdot OH + H^+ + Eu^{2+}, \qquad (1)$$

$$H^+ + Eu^{2+} \xrightarrow{h\nu} \cdot H + Eu^{3+} \qquad (2)$$

and

$$\cdot H + HR \longrightarrow \cdot R + H_2. \qquad (3)$$
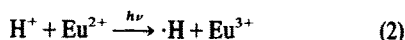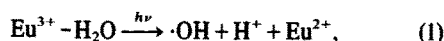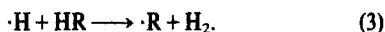
The reduction of Eu^{3+} by $\cdot R$ radical was proposed by them and was supported by means of pulse radiolysis of Eu^{3+} aqueous solution in the presence of formic acid, $HR = HCOOH$.[2] Previously we have studied the photo-reaction of $Eu(CH_3COO)_3$ in $CH_3COOH–CH_3COONa$ buffer solutions in which the organic species were used as H-atom scavenger and as ligand.[3] The acetato complexes were subjected to CTTM breakdown at $\lambda = 254$ nm, giving both CO_2 and $\cdot CH_3$ radical.

On the other hand, the two types of the breakdown are possible for $M^{n+}–HCOO^-$ complexes, that is,

$$U^{6+}–HCOO^- \xrightarrow{h\nu} \cdot COO^- + H^+ + U^{5+} \qquad (4)^4$$

and

$$Ce^{4+}–HCOO^- \xrightarrow{h\nu} \cdot H + CO_2 + Ce^{3+}. \qquad (5)^5$$
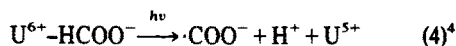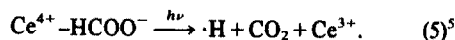
In order to clarify the primary step of the photoreaction of europium(III) formate system, an ESR study has been carried out for UV-irradiated $Eu(HCOO)_3$ in frozen HCOOH–HCOONa buffer solutions by means of the matrix isolation method. Based on the ESR study and result from room-temperature experiment,[6] a model of the reaction scheme will be proposed for the liquid solution of this system.

EXPERIMENTAL

$Eu(HCOO)_3$ was prepared by the method in literature.[7] The compositions of the samples were as follows:

Sample A; 0.01N-$Eu(HCOO)_3$ + 0.1N–HCOOH,
B; 0.01N-$Eu(HCOO)_3$ + 0.05N–HCOOH
+ 0.05N–HCOONa,
C; 0.01N-$Eu(HCOO)_3$ + 0.1N–HCOONa.

Samples F (0.1N–HCOOH) and S (0.1N–HCOONa) were employed in order to be compared with the above samples.

The samples filled in quartz tubes for ESR measurement were deaerated and irradiated at 77 K with $\lambda = 254$ nm from a 120W low-pressure mercury lamp. The first derivative ESR spectra were recorded on an X-band spectrometer at 77 K and elevated temperatures.

RESULTS AND DISCUSSION

The ESR spectra recorded at 77 K are presented in Fig. 1. Each sample showed a singlet and two kinds of doublet absorptions. The singlet can be assigned to carboxyl radical anion, $\cdot COO^-$, or its conjugate acid, $\cdot COOH$, with an anisotropic g-factor; $g_x = 2.003$, $g_y = 1.997$, and $g_z = 2.001$ which are very close to the values published.[8] One of the doublets is due to atomic hydrogen with a splitting of 50.4 mT (not being shown in Fig. 1). The anisotropic ESR parameters of the other are approximated as axial symmetry; $g_\parallel = 1.997$, $g_\perp = 2.003$, $A_\parallel = 14.5$, $A_\perp = 12.7$, and $A_{iso} = 13.3$ mT. This doublet is assigned to formyl radical, $\cdot CHO$, by comparing these parameters with those for that radical in CO matrix.[9]

Unresolved structure on the low-field portion of the central singlet appeared more evidently with increasing acidity of the sample. On warming to 100 K, the H-resonances were not observed any longer. The signals from $\cdot CHO$ survived till 150–170 K. In this temperature region, the line shapes of the central singlets were deformed strongly and, ultimately, anisotropic doublet

---

*Author to whom correspondence should be addressed.
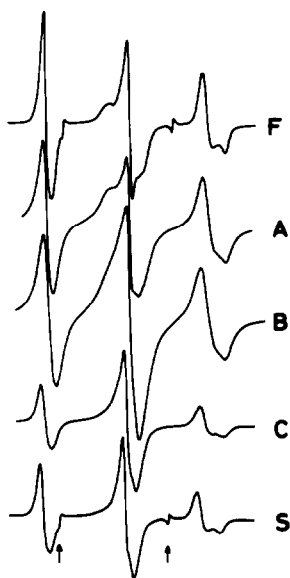
Fig. 1. ESR spectra of samples F, A, B, C and S recorded at 77 K with increasing field from left to right. The samples were UV-irradiated at 77 K for 150–180 min. The arrows show signal from Mn^{2+} in MgO ($a = 8.65$ mT).

spectra emerged at 200–230 K. These doublets were too weak to be characterized completely and disappeared at almost the same temperature region as just above. Although we cannot conclude at present whether these doublets are identical with the unresolved structures observed at 77 K, radical(s) of X–ĊH–Y type, such as HO–ĊH–O⁻(H),[10] ⁻OOC–O–ĊH–O⁻(H),[11] and O = CH–O–ĊH–O⁻(H), may be responsible in view of the presumptive ESR parameters. These radicals are regarded as the spin adducts of ·H, ·COO⁻ and ·CHO with HCOO⁻ or HCOOH.

Ratios for the peak-to-peak height of the CHO-signals to those of the COO⁻(H)-ones vs the irradiation time examined at 77 K are shown in Fig. 2, where the arrow indicates the time for the first detection of the H-resonance from each sample. All the ratios increase rapidly until the H-atoms are trapped in the matrices and, thereafter, do so gradually with increasing irradiation time. The value of the ratio and its slope are dependent on the acidity, and so is the ratio, R_0, extrapolated to zero time.

At the outset let us consider samples F and S. Taking
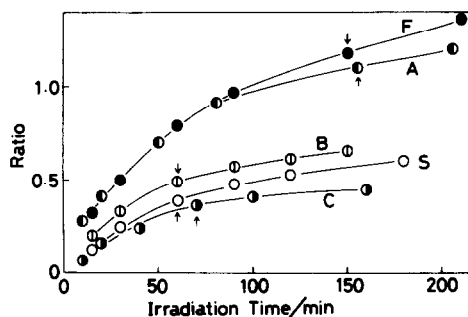
Fig. 2. The ratio of peak-to-peak height of the low-field component of the CHO-signal to that of the COO⁻(H)-signal vs the irradiation time examined at 77 K. The meaning of the arrows is presented in the text.

into account the direct proportion between the peak-height and radical-concentration ratios, the acidity dependent R_0 suggests a greater v_F/v_C ratio for F than for S. Here v_F and v_C are the rates for the CHO- and COO⁻(H)-formations, respectively. The positive slope would be expected if the rate for the decay of ·COO⁻(H) were faster than that of ·CHO or if there were some process, such as

$$\cdot COO^-(H) + X \rightarrow \cdot CHO + Y. \tag{6}$$

Formic acid in frozen 4M–HClO₄ aqueous solution containing Ce^{4+} was decomposed into ·H, ·CHO and ·COOH upon irradiation with $\lambda = 300$–360 nm.[5] These processes must take place also in the present case. It should be noted that $HCOOH + h\nu \rightarrow \cdot CHO + \cdot OH$ was more difficult than $HCOOH + h\nu \rightarrow \cdot H + \cdot COOH$ in view of the bond dissociation energies.[12] The mobile radicals, ·H and ·OH, are scavenged by the solutes and the radicals. Some of the scavenging modes give ·COO⁻(H) and ·CHO as follows;

$$\cdot H + HCOO^-(H) \rightarrow \cdot COO^-(H) + H_2, \tag{7a}$$

$$\cdot OH + HCOO^-(H) \rightarrow \cdot COO^-(H) + H_2O, \tag{7b}$$

and

$$\cdot H + HCOO^-(H) \rightarrow \cdot CHO + OH^-(H_2O). \tag{8}$$

The long induction period for the H-atom trapping supports the presence of the scavenging processes. On the other hand, both ·COO⁻(H) and ·CHO radicals exhibit UV-absorption around 254 nm with $\epsilon_{250} \simeq 1800$[13] and $\epsilon_{250} = 800$,[14] respectively. The UV-photo-decomposition of formyl radical has been noted by Adrian *et al.*[9]

$$\cdot CHO \xrightarrow{h\nu} \cdot H + CO. \tag{9}$$
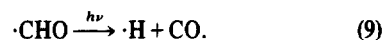
The following decays of ·COO⁻(H) in matrix are proposed;

$$\cdot COOH \xrightarrow{h\nu} \cdot H + CO_2 \tag{10}$$

and

$$\cdot COO^- + H^+ \xrightarrow{h\nu} \cdot H + CO_2. \tag{11}$$
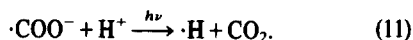
The value $\Delta H = 1$ kcal[15] for (10) and the photobleaching of ·COO⁻ in a matrix with $\lambda \leq 425$ nm[16] likely support this proposal. A certain fraction of these H-atoms gives ·CHO via (8), which is equivalent to the process (6).

The concentration ratio [·CHO]/[·COO⁻(H)] for sample C is significantly lower than that for the parent sample, i.e. sample S, as can be seen from Fig. 2. This decrease can be attributed to the increase in [·COO⁻] in view of the same [HCOO⁻] in both the samples. Therefore, the primary step of the photoreaction of the complexes is likely as follows;

$$Eu^{3+}-HCOO^- \xrightarrow{h\nu} \cdot COO^- + H^+ + Eu^{2+}. \tag{12}$$

The quantum yield for (2) has been measured at 77 K.[17] Some of Eu^{2+} ions with $\epsilon_{250} \simeq 2000$[1a] will reduce H^+ ions also in the present case.

It may be expected from the stability constants[18] that about 95 and 1% of Eu^{3+} ions are complexed in samples C and A, respectively. An apparent ϵ_{250} of the formato complexes in C was estimated as to 50–150. Then, the complexes in C absorb the light effectively but those in A do little. In the early stage of the irradiation, the behaviour of A will consequently be similar to that of sample F. After the exclusive decrease in [HCOOH], sample A finds itself in the situation

$$\epsilon(HCOOH) \cdot [HCOOH] \simeq$$
$$\epsilon(Eu^{3+}-HCOO^-) \cdot [Eu^{3+}-HCOO^-],$$

so the complexes in A become the light absorber in the later stage of the irradiation. Here the ϵ's denote the absorption coefficients of the indicated species. Thus, the downward deviation of the peak-height ratio of A from that of F in the later stage can be explained also based on the reaction (12).

On the other hand, we have proposed the following reaction for acetate system;[3]

$$Eu^{3+}-CH_3COO^- \xrightarrow{h\nu} \cdot CH_3 + CO_2 + Eu^{2+}. \quad (13)$$

In order to conclude whether $\cdot COO^-(H)$ radicals are present in the acetate system or not, the similar examination has been carried out by using ^{13}C-enriched samples. There has not appeared the $^{13}\cdot COO^-(H)$ radical featured by an anisotropic ^{13}C-doublet splitting of about 15 mT.[8b,16,19] Therefore, Eu^{2+} and H-atom reduced from H^+ by Eu^{2+} do not or scarcely reduce CO_2 into $\cdot COO^-$ and $\cdot COOH$, respectively, in the frozen acetate system and, accordingly, also in the frozen formate system. The process (12) is thus supported.

The results of the room-temperature experiment for samples F and A are summarized as follows.[6] (i) There appeared Eu^{2+} ions in A upon irradiation. (ii) The yields of CO_2, CO, and H_2 from HCOOH were respectively: F; 0.47, 0.21, 0.32, and A; 0.95, 0.04, 0.74. (iii) The material balance for F was approximately matched by assuming the yield 0.32 of HCHO which was detected qualitatively, (iv) and so was the balance for A by employing the decomposition ratio, $HCOOH : HCOO^- = 0.76 : 0.24$. (v) There was detected no acid other than formic acid in both F and A after the irradiation. In order to realize these results, the qualitative model for the reaction scheme is proposed in Schemes 1 and 2.

The Scheme 1 for the decomposition of the aqueous formic acid solution consists of three sub-cycles, I–III.

The cycles I and II hold the hydrogen atom in common and the steps in them have been discussed in the preceding sections. Owing to the mobility of $\cdot COO^-(H)$, $\cdot CHO$, and $HCOO^-(H)$ in the liquid phase, our photosteps to evolve CO_2 and CO probably include certain dark-reactions.[20,21] Smithies and Hart[21] have shown the following propagation steps in the chain reaction for γ-irradiated aqueous formic acid solution:

$$\cdot COOH + HCOOH \longrightarrow CO_2 + \cdot CHO + H_2O \quad (14)$$

and

$$\cdot CHO + HCOOH \longrightarrow HCHO + \cdot COOH. \quad (15)$$

These steps also connect the two sub-cycles and form cycle III. The evolution of CO_2, CO, H_2 and HCHO can be qualitatively realized by means of this scheme.

Scheme 2 shows how the europium redox couple prevents the cycle III in sample A. Because of $pK_a = 1.4 - 3.8$[22] for $\cdot COOH$ vs $pH = 2.6$ for A, $\cdot COO^-$ is exclusively used for simplicity in the same scheme. The
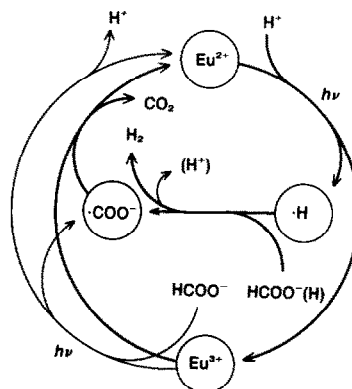
Scheme 2. Catalized decomposition of HCOOH.

rate for the following step (16) is so greater than that for the step (14) that $\cdot CHO$ is scarcely produced via cycle III:

$$\cdot COO^-(H) + Eu^{3+} \longrightarrow CO_2 (+H^+) + Eu^{2+}. \quad (16)$$

The ESR result indicates the faster rate for the production of the $\cdot COO^-(H)$ radical than for the formation of the $\cdot CHO$ radical. Therefore, the rates for the steps (7's)

Scheme 1. Decomposition of HCOOH. $^*\cdot COOH \rightleftharpoons \cdot COO^- + H^+$ should be noted. $^{**}\cdot OH$ radical will be reduced to H_2O via (7b), although the ESR evidence for this reaction could not be given.

are faster than that for (8), and the CO gas is hence scarcely evolved no longer. The ratio for the presumptive yield of HCHO to the observed yield of CO in sample A is much smaller than that in F, which may suggest the oxidation of the ·CHO radical:

$$\cdot CHO + Eu^{3+} \longrightarrow CO + H^+ + Eu^{2+}. \tag{17}$$
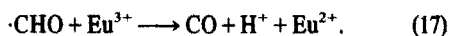
The material balance shown in (iv) indicates that $HCOO^-$ is decomposed faster than HCOOH, at least, by 30 times in consideration of their initial concentrations. This minimum ratio estimated roughly for the rate constants is about 1/10 of the $k_{H+HCOO^-}/k_{H+HCOOH}$ ratio estimated in solutions containing ferricyanide.[23] Here k's are the rate constants for the indicated H-abstraction reactions. This result is also consistent with the proposed scheme which includes the radical alternation step from ·H to ·COO⁻(H) via H-abstraction. The easily detectable amount of Eu^{2+} in the irradiated solution indicates the greater rate for the step (16) than for the step (2).

REFERENCES

[1a] Y. Haas, G. Stein and M. Tomkiewicz, *J. Phys. Chem.* 1970, **74**, 2558; [b] Y. Haas, G. Stein and R. Tenne, *Isr. J. Chem.* 1972, **10**, 529; M. Brandys and G. Stein, *J. Phys. Chem.* 1978, **82**, 852.

[2] J. D. Ellis, M. Green, A. G. Sykes, G. V. Buxton and R. M. Sellers, *J. Chem. Soc. Dalton Trans.* 1973, 1724.

[3] A. Matsumoto, N. Azuma and J. Shiokawa, *Radiochem. Radioanal. Lett.* 1981, **48**, 235.

[4] D. Greatorex, R. J. Hill, T. J. Kemp and T. J. Stone, *J. Chem. Soc. Faraday Trans.* 1, 1972, **68**, 2059.

[5] D. Greatorex and T. J. Kemp, *Trans. Faraday Soc.* 1971, **67**, 1576.

[6] A. Matsumoto *et al.*, unpublished data which will be presented in a separate paper together with those of the acetate system.

[7] F. D. Leipziger, W. J. Croft and J. E. Robert, *Anal. Chem.* 1964, **36**, 314.

[8a] G. W. Chantry, A. Horsfield, J. R. Morton and D. H. Whiffen, *Mol. Phys.* 1962, **5**, 589; [b] D. W. Ovenall and D. H. Whiffen, *Mol. Phys.* 1961, **4**, 135.

[9] F. J. Adrian, E. L. Cochran and V. A. Bowers, *J. Chem. Phys.* 1962, **36**, 1661.

[10] M. D. Sevilla, S. Swarts, R. Bearden, K. M. Morehouse and T. Vartanlan, *J. Phys. Chem.* 1981, **85**, 918 and references therein.

[11] R. E. Bellis and S. Clough, *Mol. Phys.* 1965, **10**, 33; N. Getoff, *Photochem. Photobiol.* 1965, **4**, 433 and references therein.

[12] H. Okabe, *Photochemistry of Small Molecules*, p. 314. Wiley, New York, 1978.

[13] G. V. Buxton and R. M. Sellers, *J. Chem. Soc. Faraday Trans.* 1, 1973, **69**, 555.

[14] M. Ya. Mel'nikov, *Chem. Phys. Lett.* 1982, **86**, 105.

[15] R. Gorden Jr. and P. Ausloos, *J. Phys. Chem.* 1961, **65**, 1033.

[16] P. M. Johnson and A. C. Albrecht, *J. Chem. Phys.* 1966, **44**, 1845.

[17] V. V. Korolev, N. M. Bazhin and S. F. Chentsov, *Russ. J. Phys. Chem.* 1981, **55**, 72.

[18] D. J. Macero, L. B. Anderson and P. Malachesky, *J. Electroanal. Chem.* 1965, **10**, 76.

[19] M. V. V. S. Reddy, K. V. Lingam and T. K. G. Rao, *Mol. Phys.* 1980, **41**, 1493; M. C. R. Symons and D. N. Zimmerman, *Int. J. Radiat. Phys. Chem.* 1976, **8**, 595.

[20] A. Fojtik, G. Czapski and A. Henglein, *J. Phys. Chem.* 1970, **74**, 3204.

[21] D. Smithies and E. J. Hart, *J. Am. Chem. Soc.* 1960, **82**, 4775.

[22] E. Papaconstantinou, *Anal. Chem.* 1975, **47**, 1592; G. V. Buxton and R. M. Sellers, *J. Chem. Soc. Faraday Trans.* 1, 1973, **69**, 555 and references therein.

[23] G. Czapski, J. Rabani and G. Stein, *Trans. Faraday Soc.* 1962, **58**, 2160.

ANNOUNCEMENT

10th International Symposium on the Reactivity of Solids, Dijon, 27 August–1 September 1984

The organizing Committee of the 10th International Symposium on the Reactivity of Solids has the pleasure to inform you that the Symposium will be held at the University of Dijon, France, from 27 August to 1 September 1984.

The closing dates for contributions are 1 March 1983 for titles (50 words), 30 November 1983 for abstracts (2 pages), and 31 May 1984 for registration.

Further details and registration forms may be obtained from the Executive Secretary of the Organizing Committee.

J. C. Colson
Laboratoire de Recherche sur la Réactivité des Solides
Faculté des Sciences Mirande, BP 138
21004 Dijon Cedex, France
Telex: Dijuniv 350 188 F

SYNTHESIS AND CHARACTERIZATION OF COBALT(II), NICKEL(II) AND COPPER(II) PERCHLORATE COMPLEXES WITH BIS [(DIPHENYLPHOSPHINYL)METHYL] PHENYLPHOSPHINE OXIDE, BIS [(DIPHENYLPHOSPHINYL)METHYL]ETHYL PHOSPHINATE, AND BIS [(DIPHENYLPHOSPHINYL)METHYL] PHOSPHINIC ACID

P. BRONZAN-PLANINIĆ and H. MEIDER*
Department of Physical Chemistry, Rudjer Bošković Institute, Zagreb, Yugoslavia

Abstract—The synthesis and characterization of cobalt(II), nickel(II) and copper(II) perchlorate complexes containing *bis* [(diphenylphosphinyl)methyl] phenylphosphine oxide (RPPh), *bis* [(diphenylphosphinyl)methyl] ethyl phosphinate (RPOEt), and *bis* [(diphenylphosphinyl)methyl] phosphinic acid (RPOH) have been studied. The substituent at the central phosphorus atom of the ligand is responsible for the types of complexes formed. The new complexes $[M(RPPh)_2](ClO_4)_2.nH_2O$, $[M(RPPh)_3](ClO_4)_2.4H_2O$, $[M(RPOEt)_2](ClO_4)_2.2H_2O$, and $[M(RPOH)_3]$ $(ClO_4)_2.nH_2O$ are characterized as high spin and most of them have an octahedral or distorted octahedral geometry [M = Co(II), Ni(II), or Cu(II); n = 2−5]. The coordination of two P = O groups from one ligand to the metal has been proposed for most of the complexes formed. The coordination of all three P = O groups has been assumed for complexes $[M(RPPh)_2](ClO_4)_2.nH_2O$ and $[M(RPOEt)_2](ClO_4)_2.2H_2O$.

INTRODUCTION

Many diphosphine oxides have been extensively studied as ligands in the formation of complexes with transition metals.[1–4] However, trisphosphine oxides and related compounds have received little attention. In fact, only a few data have been reported on the formation of complexes with the tridentate organophosphorus compound *bis*-methylimido-triphosphoric-acid-*pentakis*-dimethylamide (TRIPA). In this ligand, three phosphoryl groups are bridged by nitrogen atoms. The coordination of all P = O groups to the metal has been proposed.[5]

Organophosphorus compounds with three phosphoryl groups bridged by methylene groups, although already known for ten years,[6,7] have not been used in complex formation studies. These ligands were probably considered to be unsuitable for the preparation of complexes regarding the fact that the three P = O groups, bridged only by methylene groups, could sterically hinder the formation of stable chelate rings with metal ions.

Therefore, we have decided to study the formation of metal complexes with a group of ligands corresponding to the general formula $[(C_6H_5)_2P(O)CH_2]_2P(O)R$. We have chosen ligands which differ only by the substituent (R) at the central phosphorus atom. The substituent is either a phenyl, an ethoxy, or a hydroxy group. Depending on the nature of the substituent R, the ligands: *bis*[(diphenylphosphinyl)methyl] phenylphosphine oxide (RPPh), *bis*[(diphenyl-phosphinyl)methyl]ethyl phosphinate (RPOEt), and *bis*[(diphenyl-phosphinyl)methyl]-phosphinic acid (RPOH) are characterized as a phosphine oxide (R = C₆H₅), a phosphinate (R = OC₂H₅), and a phosphinic acid (R = OH), respectively.

The aim of this investigation was to establish the coordination properties of these ligands and define the influence of the substituent at the central phosphorus atom (R) on their capability for complex formation. It was also important to establish the conditions under which the ligands act as bidentate or tridentate complexing agents. Another question is the ability of the ligands to form binuclear complexes. The ligands RPPh, RPOEt, and RPOH have a structure similar to that of triketonates which are known for their ability to form binuclear copper(II), nickel(II) and cobalt(II) complexes.[8] Therefore, the formation of binuclear complexes by these organophosphorus compounds cannot be excluded.

Our previous investigations of the formation of zirconium(IV) and hafnium(IV) complexes with RPPh, RPOEt, and RPOH in solution and in the solid state[9] showed that the coordination of all phosphoryl groups might be proposed. However, the formation of polymeric species could not be excluded and, therefore, the coordination of all three P = O groups to the same metal ion in the above complexes is still an open question.

This paper describes the preparation and properties of cobalt (II), nickel(II), and copper(II) perchlorate complexes with the ligands RPPh, RPOEt, and RPOH. The results obtained show clearly the influence of the substituent (R) on the ability of the ligands to form complexes. Physico-chemical measurements indicate that the coordination of all three P = O groups to one metal ion is possible only in a few complexes formed.

RESULTS AND DISCUSSION

Complex formation

Perchlorate complexes isolated had different composition depending on the ligand-to-metal ratios in the reaction mixtures. The reaction of cobalt(II), nickel(II), and copper(II) perchlorates with solutions of the ligands yielded crystalline complexes listed in Table 1.

Complexes formed with RPPh. Two types of metal(II) perchlorate complexes were formed with this ligand. Compounds corresponding to the formula $[M(RPPh)_2]$ $(ClO_4)_2.nH_2O$ (M = Co(II), Ni(II) or Cu(II); *n* varies from

---

*Author to whom correspondence should be addressed.

Table 1. Summary of analytical data for the complexes

Compound	Colour	Analyses % [a]			
		Metal	P	Cl	H_2O
$[Co(RPPh)_2](ClO_4)_2 \cdot 3H_2O$	pink	4.47 (4.15)	12.73 (13.10)	5.18 (4.99)	3.65 (3.80)
$[Ni(RPPh)_2](ClO_4)_2 \cdot 5H_2O$	greenish	4.31 (4.05)	12.81 (12.78)	5.23 (4.87)	6.28 (6.18)
$[Cu(RPPh)_2](ClO_4)_2 \cdot 2H_2O$	bluish	4.31 (4.52)	13.09 (13.22)	5.38 (5.04)	2.33 (2.56)
$[Co(RPPh)_3](ClO_4)_2 \cdot 4H_2O$	pink	3.15 (2.96)	14.10 (13.99)	3.88 (3.56)	3.87 (3.62)
$[Ni(RPPh)_3](ClO_4)_2 \cdot 4H_2O$	greenish--yellow	2.88 (2.94)	13.63 (13.99)	3.72 (3.56)	3.35 (3.62)
$[Cu(RPPh)_3](ClO_4)_2 \cdot 4H_2O$	white	2.97 (3.18)	13.84 (13.97)	3.84 (3.55)	3.34 (3.67)
$[Co(RPOEt)_2](ClO_4)_2 \cdot 2H_2O$	pink	4.45 (4.40)	13.75 (13.88)	5.32 (5.30)	2.41 (2.69)
$[Ni(RPOEt)_2](ClO_4)_2 \cdot 2H_2O$	greenish	4.13 (4.39)	14.05 (13.88)	5.49 (5.30)	2.49 (2.69)
$[Cu(RPOEt)_2](ClO_4)_2 \cdot 2H_2O$	bluish	4.59 (4.73)	14.04 (13.83)	5.61 (5.28)	2.31 (2.68)
$[Co(RPOH)_3](ClO_4)_2 \cdot 3H_2O$	pink	3.52 (3.29)	15.53 (15.54)	4.13 (3.95)	2.85 (3.01)
$[Ni(RPOH)_3](ClO_4)_2 \cdot 2H_2O$	yellow	3.41 (3.31)	15.98 (15.70)	4.17 (3.99)	2.27 (2.03)

a) Calculated values are given in parentheses.

2 to 5) were isolated by dissolving metal(II) salts and ligands in absolute ethanol in the ratio of 1:2. Complexes having the composition [M(RPPh)$_3$](ClO$_4$)$_2$.4H$_2$O were obtained by mixing metal(II) perchlorates in ethanol solutions with a large excess of the ligand (ligand/metal ⩾ 3).

Complexes formed with RPOEt. Regardless of the reaction ratio used, only one type of metal complex was formed with this ligand. Unstable complexes containing coordinated ethanol were precipitated. After all the amount of ethanol had been released, complexes corresponding to the formula [M(RPOEt)$_2$] (ClO$_4$)$_2$.2H$_2$O(M = Co(II), Ni(II) or Cu(II)) were formed.

Complexes formed with RPOH. Nickel(II) and cobalt(II) complexes formed with RPOH contained quantities of the reagents in a stoichiometric ratio of 1:3. The isolated cobalt(II) and nickel(II) complexes corresponded to the formulae [Co(RPOH)$_3$](ClO$_4$)$_2$.3H$_2$O and [Ni(RPOH)$_3$](ClO$_4$)$_2$.2H$_2$O, respectively. No copper(II) complexes could be isolated.

Infrared spectral studies

The most significant absorption bands in the spectra of the ligands and their complexes are those of P = O stretching vibrations. The spectra of the ligands exhibit three strong bands in the range from 1250 to 1150 cm^{-1} which correspond to the P = O stretching vibration. In the spectra of the complexes these bands are shifted by 20–80 cm^{-1} towards lower wave numbers, thus indicating that the ligands are coordinated to the metals through oxygen atoms (Table 2 and Fig. 1).

The spectra of the complexes with RPPh exhibit only one absorption band corresponding to the P = O stretching vibration, with a maximum at 1170 cm^{-1}. The shape of this band is different for complexes with different ligand-to-metal ratios. The band appearing in the spectra of [M(RPPh)$_2$](ClO$_4$)$_2$.nH$_2$O (M = Co(II), Ni(II) or Cu(II), n = 2–5) is narrow, while the band in the spectra of [M(RPPh)$_3$](ClO$_4$)$_2$.4H$_2$O is rather broad.

The RPOEt spectrum exhibits a maximum at 1245 cm^{-1} which can be assigned to the P = O vibration of the central phosphoryl group.[10] As the spectra of the complexes do not show this maximum, this indicates that the central P = O group from the ligand is coordinated. Bands assigned to P–OC$_2$H$_5$ vibrations appear in both the RPOEt spectrum and the spectra of the complexes at 1035 and 965 cm^{-1}. However, the bands in the latter spectra are of much lower intensity.

The RPOH spectrum is characterized by three broad bands at 2600 cm^{-1}, 2200 cm^{-1}, and 1620 cm^{-1}, which can be assigned to P(O)OH vibrations perturbed by strong hydrogen bonding. These bands are absent in the spectra
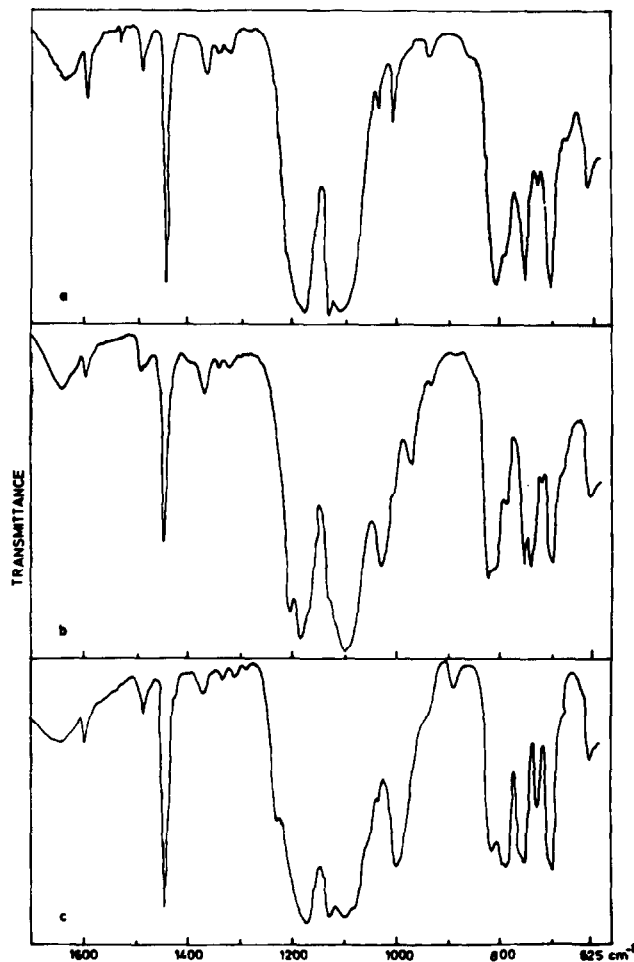
Fig. 1. IR spectra of (a) [Co(RPPh)$_3$] (ClO$_4$)$_2$.4H$_2$O; (b) [Co(RPOEt)$_2$](ClO$_4$)$_2$.2H$_2$O; (c) [Co(RPOH)$_3$](ClO$_4$)$_2$.3H$_2$O in the region of 1700–625 cm^{-1}.

Table 2. IR spectra, conductivity data and magnetic properties of the ligands and complexes

Compound	ν(P=O) (cm^{-1})	δ(P-C-P) (cm^{-1})	ν(O-H) (cm^{-1})	Λ_M (cm^2 ohm^{-1} mol^{-1})	μ_{eff} (B.M.)
RPPh	1215 s, 1192 vs, 1163 s	805 s, 790 sh			
[Co(RPPh)$_2$](ClO$_4$)$_2$·3H$_2$O	1170 vs, sp	785 m	3600 sh, 3400 m, br	43.85	4.86
[Ni(RPPh)$_2$](ClO$_4$)$_2$·5H$_2$O	1175 vs, sp	785 m	3600 sh, 3400 s, br	43.85	3.30
[Cu(RPPh)$_2$](ClO$_4$)$_2$·2H$_2$O	1165 vs, sp	785 m	3470 w	41.95	2.03
[Co(RPPh)$_3$](ClO$_4$)$_2$·4H$_2$O	1170 vs	800 s, 785 sh	3550 sh, 3420 s, br, 3250 sh	43.60	5.10
[Ni(RPPh)$_3$](ClO$_4$)$_2$·4H$_2$O	1170 vs	800 s, 785 sh	3580 sh, 3410 s, br, 3250 sh	43.50	3.18
[Cu(RPPh)$_3$](ClO$_4$)$_2$·4H$_2$O	1170 vs	800 s, 785 sh	3550 sh, 3410 s, br	41.60	2.07
RPOEt	1245 s, 1220 m, 1190 m	815 s, 785 sh			
[Co(RPOEt)$_2$](ClO$_4$)$_2$·2H$_2$O	1195 s, 1175 vs	815 m, 805 sh, 785 w	3380 m, 3240 sh	44.76	4.74
[Ni(RPOEt)$_2$](ClO$_4$)$_2$·2H$_2$O	1195 sh, 1180 vs	815 m, 805 sh, 780 w	3380 m, 3240 sh	44.34	3.29
[Cu(RPOEt)$_2$](ClO$_4$)$_2$·2H$_2$O	1175 s, 1165 s	815 m, 785 sh,	3520 m, 3410 m, 3250 sh	44.36	1.92
RPOH	1250 s, 1180 s, 1155 s	815 sh, 800 s	2600 br, 2200 br		
[Co(RPOH)$_3$](ClO$_4$)$_2$·3H$_2$O	1225 sh, 1168 vs	810 s, 790 sh, 780 s	3500 s, 3400 s, br	42.55	5.15
[Ni(RPOH)$_3$](ClO$_4$)$_2$·2H$_2$O	1220 sh, 1163 vs	805 sh 790 s	3400 s, br	44.50	3.25

of the complexes [M(RPOH)$_3$](ClO$_4$)$_2$.nH$_2$O. OH vibrations of the monomer[10,11] coordinated to the metal, which appear at 3500–3600 cm^{-1}, are overlapped by the absorption of OH vibrations of water molecules present in the complexes. A sharp band appears at 980 cm^{-1}. The intensity of the band decreases from cobalt(II) through nickel(II) to copper(II) complexes. This absorption band probably corresponds to the P–O(H) vibration[10] appearing in the spectrum of the ligand at 955 cm^{-1}.

Absorption bands appearing in the spectra of the ligands in the range 785–815 cm^{-1} are assigned to the P–C–P linkage vibrations;[12] in some of the spectra of the complexes these bands are shifted towards lower wave numbers.

As can be seen from the spectral data, the perchlorate ion does not seem to be coordinated to the metal ion. The perchlorate ion retains its Td symmetry as shown by its unsplit bands at 1090 cm^{-1} (ν_3), 935 cm^{-1} (ν_1) and 625 cm^{-1} (ν_4).

All the spectra exhibit two bands with maxima at ~ 3400 cm^{-1} and ~ 1630 cm^{-1}. The first maximum is assigned to O–H stretching and the second one to H–O–H bending modes from lattice or coordinated water molecules. In the region 785–805 cm^{-1}, in which absorption bands corresponding to coordinated water molecules are expected[13], the P–C–P vibrational bands are always present and they can overlap the wagging and rocking mode of the coordinated water. Band assignments for the ligands and complexes are listed in Table 2.

Conductivity measurements

Conductivity measurements of metal perchlorate complexes were carried out at room temperature from 10^{-3}M nitrobenzene solutions. All complexes which were isolated had molar conductance values close to those expected for 2 : 1 electrolytes[14] (Table 2).

Magnetic properties

All perchlorate complexes prepared are high-spin paramagnetic substances. The effective magnetic moments (μ_{eff}) for the cobalt(II) complexes isolated were estimated to be between 4.74 and 5.15 B.M. The magnetic moments of the [Co(RPPh)$_3$](ClO$_4$)$_2$.4H$_2$O and [Co(RPOH)$_3$](ClO$_4$)$_2$.3H$_2$O complexes were estimated to be 5.10 and 5.15 B.M., respectively. These values are due to the regular octahedral surrounding. The magnetic moments of the [Co(RPPh)$_2$](ClO$_4$)$_2$.3H$_2$O and [Co(RPOEt)$_2$](ClO$_4$)$_2$.2H$_2$O complexes were evaluated to be 4.86 and 4.74 B.M., respectively. These values indicate a loss in orbital degeneracy of the ground state, caused by any lower symmetry component. Hence, a departure from the regular octahedral surrounding of the cobalt(II) ion may be assumed in these complexes. The effective magnetic moments of nickel(II) perchlorate complexes range from 3.18 to 3.30 B.M. and are indicative of spin-free octahedral complexes with a significant orbital contribution. The copper(II) perchlorate complexes have effective magnetic moments in the range from 1.92 to 2.07 B.M. These values are characteristic of one unpaired d^9 electron and are more or less independent of the stereochemistry of the complexes. Table 2, shows the effective magnetic moments obtained for the complexes studied.

Electronic spectral data

For most of the perchlorate complexes studied there were recorded both, solid-state and solution electronic

spectra (Table 3). The solution spectra were sufficiently similar to the solid-state mull spectra to preclude any significant solvent interaction. All the complexes are very poorly coloured, and the visible absorption bands are of low intensity. The intensity, position and shape of the bands are typical of octahedral cobalt(II) and nickel(II) complexes.[15]

Whilst cobalt and nickel are expected to form more or less regular six coordinate complexes copper rarely does. The complexes [Cu(RPPh)$_2$](ClO$_4$)$_2$.2H$_2$O and [Cu(RPOEt)$_2$](ClO$_4$)$_2$.2H$_2$O are characterized by a broad, asymmetric band in the near IR region with maxima at 11700 and 11400 cm^{-1}, respectively. The bands can be compared with the spectra of known tetragonal distored copper(II) complexes. This distorsion is characteristic of Cu(II) compounds, and it appears as a consequence of the Jahn–Teller effect.[16] The complex [Cu(RPPh)$_3$](ClO$_4$)$_2$.4H$_2$O is white in colour and gives a single peak with maximum shifted to 10400 cm^{-1}. According to the low intensity of this band the possibility that this complex might be trigonal or tetrahedral has to be excluded.[16]

Spectral data of the nickel(II) complexes were used to calculate ligand field parameters, D$_q$ and B (Table 3). In the spectra of these complexes only two bands (ν_2 and ν_3) were assigned, and therefore the method given by Underhill and Billing was used.[17] Values of the parameters obtained for the ligands RPPh, RPOEt and RPOH are of the same order of magnitude as values of parameters for similar ligands having a weak ligand field.[18]

EXPERIMENTAL

Materials

Analytical-grade solvents and cobalt(II) perchlorate (Fluka) were used throughout the preparation. Nickel(II) perchlorate and copper(II) perchlorate were prepared by fuming their nitrates with perchloric acid.[19,20] Bis[(diphenylphosphinyl)methyl]-phenylphosphine oxide (RPPh), bis[(diphenylphosphinyl)methyl]ethyl phosphinate (RPOEt), and bis[(diphenylphosphinyl)methyl] phosphinic acid (RPOH) were prepared using the method of Kabachnik et al.[6]

For conductivity measurements, nitrobenzene was purified using the method of Taylor and Kraus.[21]

Physical measurements

IR spectra were recorded on KBr pellets and nujol mulls in the region 4000–625 cm^{-1} using a Perkin–Elmer Model 257 spectrophotometer. Electronic spectra were recorded by means of a Carry Model 17 spectrophotometer. Magnetic susceptibilities were determined at 295 K using the Gouy method with CuSO$_4$.5H$_2$O as calibrant.

Electrolytic-conductance measurements were performed at 295 K on a Tacussel conductivity bridge, type Cd7.

Elemental analyses were performed in the Microanalytical Laboratory of the Rudjer Bošković Institute.

The amount of water was determined using the Karl–Fischer method.

Preparation of complexes

General method of preparation. Metal(II) perchlorates as well as ligands were dissolved in hot absolute ethanol. Adequate amounts of these solutions were mixed together. After a few days (1–5) the crystalline precipitates were filtered off and washed with absolute ethanol and diethylether. The complexes isolated were dried at room temperature.

[M(RPPh)$_3$](ClO$_4$)$_2$.nH$_2$O. 0.75 mmol of the metal(II) perchlorate (0.274 g Co(ClO$_4$)$_2$.6H$_2$O or Ni(ClO$_4$)$_2$.6H$_2$O; 0.224 g Cu(ClO$_4$)$_2$.2H$_2$O) dissolved in 3 ml of hot absolute ethanol was mixed with 1.5 mmol (0.831 g) of RPPh dissolved in 7 ml of ethanol. After 5 days the crystalline precipitates were filtered off

P. BRONZAN-PLANINIĆ and H. MEIDER

Table 3. Electronic spectral data and ligand-field parameters of the complexes

Compound	$\bar{\nu}_{max}, (\varepsilon)$ $(cm^{-1} \times 10^3)$	Dq (cm^{-1})	B (cm^{-1})	Medium
$[Co(RPPh)_2](ClO_4)_2 \cdot 3H_2O$	20.8 sh, 18.7 (14.5)			acetone
	21.3 sh, 18.9			nujol[*]
$[Co(RPPh)_3](ClO_4)_2 \cdot 4H_2O$	20.6 sh, 18.5 (23)			acetone
$[Co(RPOEt)_2](ClO_4)_2 \cdot 2H_2O$	20.8 sh, 18.6 (17)			abs. ethanol
$[Co(RPOH)_3](ClO_4)_2 \cdot 3H_2O$	20.4 sh, 18.4 (27)			abs. ethanol
$[Ni(RPPh)_2](ClO_4)_2 \cdot 5H_2O$	24.2 (12.5), 14.7 sh, 13.0 (5)	773	929	abs. ethanol
$[Ni(RPPh)_3](ClO_4)_2 \cdot 4H_2O$	24.0 (11.5), 12.9 (5.6)	766	924	abs. ethanol
	23.8, 12.5, 8.3, 6.9			nujol[*]
$[Ni(RPOEt)_2](ClO_4)_2 \cdot 2H_2O$	24.0 (12), 14.7 sh, 12.9 (5), 7.1 (7.5)	772	918	acetone
	24.2 (23.5), 12.9 (7.5)			dichloro-ethane
	24.2, 13.2 sh, 12.8, 8.2, 7.0	758	950	nujol[*]
$[Ni(RPOH)_3](ClO_4)_2 \cdot 2H_2O$	24.2 (32), 14.7 sh, 12.8 (6.5)	760	943	acetone
	23.9, 14.6 sh, 12.8, 8.3, 7.0	758	928	nujol[*]
$[Cu(RPPh)_2](ClO_4)_2 \cdot 2H_2O$	11.7 (19)			acetone
$[Cu(RPPh)_3](ClO_4)_2 \cdot 4H_2O$	10.4 (21)			acetone
$[Cu(RPOEt)_2](ClO_4)_2 \cdot 2H_2O$	11.4 (17.5)			acetone

* = nujol mull.

and washed. Yields of 89.9%, 83.1% and 78.8% were obtained for Co(II), Ni(II), and Cu(II) complexes, respectively.

$[M(RPPh)_3](ClO_4)_2 \cdot 4H_2O$. 0.5 mmol of metal(II) perchlorate (0.183 g Co(ClO$_4$)$_2$.6H$_2$O or Ni(ClO$_4$)$_2$.6H$_2$O; 0.149 g Cu(ClO$_4$)$_2$.2H$_2$O) dissolved in 2 ml of hot absolute ethanol was added dropwise to a solution of 1.5 mmol of RPPh (0.831 g in 7 ml of absolute ethanol). An immediate precipitate was formed. After the mixture was allowed to stand for a short time, the crystalline precipitates were filtered off and washed. Yields of 44.7%, 40.3% and 46.3% were obtained for Co(II), Ni(II), and Cu(II) complexes, respectively.

$[M(RPOEt)_2](ClO_4)_2.2H_2O$. 0.75 mmol of the metal(II) perchlorate (0.274 g Co(ClO$_4$)$_2$.6H$_2$O or Ni(ClO$_4$)$_2$.6H$_2$O; 0.224 g Cu(ClO$_4$)$_2$.2H$_2$O) dissolved in 3 ml of hot absolute ethanol was added to a warm solution of 1.5 mmol (0.784 g) of RPOEt in 10 ml of absolute ethanol. The crystalline precipitates were filtered off, washed, and allowed to stand for a few weeks to stabilize

(replacement of ethanol by water molecules). Yields of 84.7%, 78.1% and 86.5% were obtained for Co(II), Ni(II), and Cu(II) complexes, respectively.

$[Co(RPOH)_3](ClO_4)_2.3H_2O$ and $[Ni(RPOH)_3]$ $(ClO_4)_2.2H_2O$. 0.5 mmol (0.183 g) of metal(II) perchlorate dissolved in 2 ml of hot absolute ethanol was added to a solution of 1.5 mmol (0.741 g) of RPOH dissolved in 30 ml of hot absolute ethanol. After 5 days the crystalline precipitates were filtered off and washed. Yields of 36.5 and 63.2% were obtained for Co(II) and Ni(II) complexes, respectively.

REFERENCES

[1] B. J. Brisdon, *J. Chem. Soc., Dalton Trans.* 1972, 2247.
[2] W. E. Slinkard and D. W. Meek, *J. Chem. Soc., Dalton Trans.* 1973, 1024.
[3] F. Mani and M. Bacci, *Inorg. Chim. Acta* 1972, **6**, 487.

[4]S. S. Sandhu and R. S. Sandhu, *J. Inorg. Nucl. Chem.* 1972, **34**, 2295.

[5]M. W. G. De Bolster, J. Den Heijer and W. L. Groeneveld, *Zeitschrift für Naturforsch.* 1972, **27b**, 1324.

[6]T. Ya. Medved, Yu. M. Polikarpov, S. A. Pisareva, E. I. Matrosov and M. I. Kabachnik, *Izv. Akad. Nauk SSSR, Ser. Khim.* 1968, 2062.

[7]L. Maier, *Helv. Chim. Acta* 1969, **52**, 827.

[8]J. M. Kuszaj, B. Tomlonovic, D. P. Murtha, R. L. Lintvedt and M. D. Glick, *Inorg. Chem.* 1973, **12**, 1297.

[9]P. Bronzan and H. Meider, *J. Less Common Metals* 1978, **59**, 101.

[10]L. C. Thomas, *Interpretation of the Infrared Spectra of Organosphosphorus Compounds.* Heyden, London (1974).

[11]S. M. Chackalackal and F. E. Stafford, *J. Am. Chem. Soc.* 1966, **88**, 4823.

[12]J. J. Richard, K. E. Burke, J. W. O'Laughlin and C. V. Banks, *J. Am. Chem. Soc.* 1961, **83**, 1722.

[13]K. Nakamoto, *Infrared and Raman Spectra of Inorganic and Coordination Compounds.* Wiley, New York (1978).

[14]C. M. Harris and R. S. Nyholm, *J. Chem. Soc.* 1956, 4375.

[15]R. L. Carlin, *Transition Metal Chemistry,* Vol. 4, 1968; Vol. 5. 1969. Vol. 1, 1965, Marcel Dekker, New York.

[16]A. B. P. Lever, *Inorganic Electronic Spectroscopy.* Elsevier, Amsterdam (1968).

[17]A. E. Underhill and D. E. Billing, *Nature* 1966, **210**, 834.

[18]S. S. Sandhu and R. S. Sandhu, *Inorg. Chim. Acta* 1972, **6**, 383.

[19]S. D. Ross, *Spectrochim. Acta* 1962, **18**, 225.

[20]H. Freund and C. R. Schneider, *J. Am. Chem. Soc.* 1959, **81**, 4780.

[21]E. G. Taylor and C. A. Kraus, *J. Am. Chem. Soc.* 1947, **69**, 1731.

SYNTHESIS AND SPECTROSCOPIC CHARACTERIZATION OF HETEROBIMETALLIC (α-ALKYNYL)IRON–COBALT HEXACARBONYL COMPLEXES, [μ-(1-σ, 2–3, η^2-R_2C–C≡CR')] [$(CO)_3$Fe–Co$(CO)_3$] AND [μ-(1-σ, 2–3, η^2-H_2C–C≡CCH₂OH)] [$(CO)_3$Fe–Co$(CO)_2$(PPh₃)]

SILVIO AIME and DOMENICO OSELLA*

Istituto di Chimica Generale ed Inorganica Dell'Università Corso Massimo d'Azeglio 48, 10125 Torino, Italy

LUCIANO MILONE

Istituto di Chimica Generale ed Inorganica dell'Università Viale Taramelli 12, 27100 Pavia, Italy

and

ANTONIO TIRIPICCHIO

Istituto di Chimica Generale ed Inorganica dell'Università, Centro di Studio per la Strutturistica Diffrattometrica del C.N.R., Via Massimo d'Azeglio 85, 43100 Parma, Italy

Abstract—The title compounds have been prepared from reactions of $Co_2(CO)_6$(μ-HOR₂CC₂R') or $Co_2(CO)_6$(μ-HOR₂CC₂R₂OH) complexes with Fe(CO)₅ in acetone. In the latter set of reactions the homobimetallic butatriene compounds, $Fe_2(CO)_6$-(μ-R₂C=C=CR₂), are also obtained. The striking feature of these reactions is the ability of Fe(CO)₅ to dehydroxylate the organic moiety and to replace a Co(CO)₃ unit forming mixed iron–cobalt derivatives. A direct interaction between the iron and the carbon atom, originally bearing the lost –OH group, is evident from the bulk of the spectroscopic data; thus the organic chain acts as an overall 5 electron donor, according to the E.A.N. formalism. The heterobimetallic compounds have been characterized by elemental analysis, mass spectrometry, IR spectroscopy and NMR studies. For the phosphine derivative FeCo(CO)₅(PPh₃)(H₂CC₂CH₂OH) a crudely refined X-ray analysis has been performed.

INTRODUCTION

Mixed metal compounds containing metal–metal bonds are receiving increasing attention since it has been suggested that the presence of different metallic centres on the same molecule can be important in the activation of organic substrates in stoichiometric and catalytic reactions.[1] Furthermore, they might represent a source for the preparation of highly dispersed metals on inorganic supports.[2] The development of new syntheses designed to produce stable heterometallic compounds is therefore worthwhile.

Actually, in the case of the synthesis of heterobimetallic complexes, all the possible combinations of metallic fragments bearing carbonyl and/or cyclopentadienyl ligands have been explored. Consequentely, a plethora of 34 electron heterobimetallic compounds has been obtained, mainly by Vahrenkamp[3] in the case of neutral complexes and by Ruff[4] in the case of ionic ones. Considering only first row Group VIII metals the following heterobimetallic complexes have been characterized: FeCo(CO)₆(η-C₅H₅),[5] FeNi(CO)₃(η-C₅H₅)₂,[6] CoNi(CO)₅-(η-C₅H₅)[5] and [FeCo(CO)₈⁻].[4]

So far, however, there have been few reports which have dealt with their reactivity toward unsaturated hydrocarbons. In principle an acetylenic moiety should be able to replace two CO groups in each of these complexes leading to the tetrahedral M₂C₂ structural framework, schematically represented below, already found in the corresponding

homobimetallic compounds: $Fe_2(CO)_6$(μ-C₂Bu₂') (which formally has an Fe–Fe double bond)[7], $Co_2(CO)_6$(μ-C₂R₂)[8] and Ni₂(η-C₅H₅)₂(μ-C₂R₂).[9]
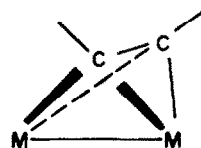
The heterobimetallic acetylenic complex [(CO₃Co–Ni(η-C₅H₅)](μ-C₂R₂) has been recently isolated from both the reaction of Ni(η-C₅H₅)₂(μ-C₂R₂) with $Co_2(CO)_8$ and the reaction of $Co_2(CO)_6$(μ-C₂R₂) with [Ni(CO)(η-C₅H₅)]₂.[10,11] Its solid state structure confirmed the expected pseudo-tetrahedral M₂C₂ framework.[10] On the contrary in 1963 Bassett,[12] in an attempt to prepare an acetylenic iron–nickel complex, observed only disproportionation:

2 FeNi(CO)₃(η-C₅H₅)₂ + RC≡CR→[Fe(CO)₂(η-C₅H₅)]₂ Ni₂(η-C₅H₅)₂(μ-C₂R₂).
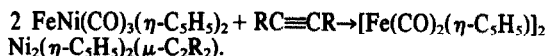
A quite different synthetic route was employed by Yasufuku et al.[13] who carried out the reaction of an ethynyltriphenylphosphonium salt with (η-C₅H₅)₂Ni and Fe₂(CO)₉ obtaining the complex [(CO)₃Fe–Ni(η-C₅H₅)]-(μ-Ph₃PC₂H), formulated as an internal salt, in which the functionalized alkyne formally acts as a 5e-donor.

During our previous studies of the reactions of alkynes

---

*Author to whom correspondence should be addressed.

with cobalt and iron carbonyls,[14] we found that the homobimetallic complex, $Co_2(CO)_6(EtC_2CHOHMe)$ (Ia) (formed *in situ* by oxygen incorporation from water present in the solvent) reacted further with excess $Fe(CO)_5$ to give the heterobimetallic compound $FeCo(CO)_6(MeHCC_2Et)$ (IIa). This reaction offers further evidence of the dehydroxylation ability of iron carbonyls toward unsaturated alcohols. With the aim of testing the validity of this method in synthesizing novel mixed iron-cobalt derivatives, we have carried out the reactions of $Fe(CO)_5$ with $Co_2(CO)_6(\mu$-acetylene) complexes, bearing one or two hydroxyl group α to the triple bond. In this way several $FeCo(CO)_6(\mu$-alkynyl) complexes have been obtained and spectroscopic analysis has unambiguously established their structure.

EXPERIMENTAL

Reactants and physical measurements

All reactions were carried out under nitrogen. $Co_2(CO)_8$ and $Fe(CO)_5$ were purchased from Fluorochem Ltd., 2-butyn-1-ol, 2-butyn-1, 4-diol and 2, 5-dimethyl-3-hexyn-2, 5-diol were from Farchan Division. $Co_2(CO)_6(MeC_2CH_2OH)$ (Ib), $Co_2(CO)_6(HOCH_2C_2CH_2OH)$ (Ic) and $Co_2(CO)_6$-$(HOMe_2CC_2CMe_2OH)$ (Id) complexes were synthesized using $Co_2(CO)_8$ and the corresponding alkyne according to previously reported procedures.[16] The purity of these compounds was checked by IR and MS spectroscopy, ^{13}CO (94.3%) was obtained from Monsanto Res. Corp. The heterobimetallic complexes were analyzed by use of a F & M 185 C, H, N analyzer and a Perkin–Elmer 303 Atomic Absorption Spectrophotometer. The IR spectra were recorded on a Perkin–Elmer 580 B instrument using 0.5 mm NaCl cells. The mass spectra were measured on a Hitachi Perkin–Elmer RMU-6H spectrometer. ^1H and ^{13}C NMR spectra were recorded on a Jeol C60-HL and a Jeol-PS-100-FT instruments respectively. Chemical shifts were reported downfield positive with respect to SiMe₄. $Cr(acac)_3 (\simeq 10^{-3} M)$ was added as a shiftless relaxation agent for the ^{13}C NMR measurements. The temperature was monitored by a Jeol-JNM-BT-P-5-H-100E temperature control unit. The physical properties, analytical data, IR spectra for the complexes are listed in Table 1; ^1H and ^{13}C NMR data in Table 2.

Preparation of $FeCo(CO)_6(H_2CC_2CH_3)$ (IIb)

In a typical run 1.0 g (2.7 mmol) of $Co_2(CO)_6(HOH_2CC_2CH_3)$ (Ib) and 2.0 ml (14.4 mmol) of $Fe(CO)_5$ were refluxed in 200 cm³ of acetone for 10 hr. After cooling and filtration the excess of $Fe(CO)_5$ and the solvent were removed *in vacuo* and the residue dissolved in dichloromethane and chromatographed on tlc preparative plates (Kieselgel P. F. Merck, eluant light petroleum and 10% diethyl ether). Besides unreacted Ia ($\simeq 20\%$) and a small amount of $Fe_3(CO)_{12}$, $FeCo(CO)_6(H_2CC_2CH_3)$ (IIb), ($\simeq 40\%$) was eluted. Mass spectrum m/e 336 [M⁺], followed by loss of six carbonyl groups.

Preparation of $FeCo(CO)_6(H_2CC_2CH_2OH)$ (IIc)

Ic and $Fe(CO)_5$ in the above ratio were refluxed in acetone for 10 hr. The same separation procedure afforded unreacted Ic ($\simeq 25\%$), small amount of $Fe_3(CO)_{12}$, $Fe_2(CO)_6(H_2CC_2CH_2)$ (IIIc) ($\simeq 5\%$) and $FeCo(CO)_6(H_2CC_2CH_2OH)$ (IIc), ($\simeq 25\%$). Mass spectrum m/e 352 [M⁺] followed by loss of six carbonyl groups and concomitant loss of H_2O.

Preparation of $FeCo(CO)_6(HMeCC_2CMe_2OH)$ (IId)

Id and $Fe(CO)_5$ reacted in the same conditions to afford unreacted Id ($\simeq 15\%$), small amount of $Fe_3(CO)_{12}$, $Fe_2(CO)_6(Me_2CC_2CMe_2)$ (IIId) ($\simeq 35\%$) and $FeCo(CO)_6(Me_2CC_2CMe_2OH)$ (IId) ($\simeq 25\%$). Mass spectrum m/e 408 [M⁺] followed by loss of six carbonyl groups and concomitant loss of H_2O.

Isotopic enrichment of IIc *and* IId

0.2 g of complex (IIc or IId) were dissolved in 100 cm³ of

cyclohexane and stirred for 4 days at $+40°C$ in the presence of <1 Atmosphere of ^{13}CO. Further purification on a SiO_2 column using light petroleum with 20% $CHCl_3$ as eluant was carried out before running the spectra.

Preparation of $FeCo(CO)_5(PPh_3)(H_2CC_2CH_2OH)$ (IVc)

1.0 g (2.8 mmol) of IIc was dissolved in 100 cm³ of acetone and added with 0.73 g (2.8 mmol) of PPh_3. The mixture was refluxed for 20 hr. After cooling and filtration, the solvent was removed under vacuum and the residue dissolved in CH_2Cl_2 and chromatographed on tlc (eluant light petroleum and 20% $CHCl_3$). Unreacted IIc ($\simeq 25\%$) and $FeCo(CO)_5(PPh_3)(H_2CC_2CH_2OH)$ (IVc) ($\simeq 40\%$) have been eluted.

Crystallographic data collection of IVc

Red-orange crystals of IVc were grown by slow cooling of a saturated solution of IVc in n-heptane, chloroform 2:1 mixture under N_2 atmosphere. A very thin crystal was used for the X-ray analysis. Crystal data are as follows: $C_{27}H_{20}FeCoO_6P$, M = 586.21, $a = 10.505(8)$, $b = 12.787(12)$, $c = 10.477(9)$ Å, $\alpha = 111.13(6)$, $\beta = 105.25(6)$, $\gamma = 84.60(7)°$, $U = 1266$ Å³, $Z = 2$, $D_c = 1.54$ g/cm³, space group $P\bar{1}$.

The intensities of 1949 reflections with θ in the range 3–22° were measured on a Siemens AED diffractometer (using the Nb-filtered Mo-K α radiation), but only 519, having $I \ge 2$ $\sigma(I)$ were considered observed and used in the analysis. The structure was solved by Patterson and Fourier methods, but the limited number of the observed reflections and the poor quality of them prevented a satisfactory refinement of the structure.

RESULTS AND DISCUSSION

Although all the reactions were performed in identical conditions, higher yields of the heterobimetallic complexes (II) were obtained from the alkyneol reactants (Ia, Ib) than from the alkynediols (Ic, Id). This is due to successive dehydroxylation and ligand transfer to Fe, which lead to the well known butatriene derivatives (IIIc, IIId) as shown in the following scheme:

$Co_2(CO)_6(HOR_2C-C\equiv C-R')$ [Ia, Ib]

$+ Fe(CO)_5$ $\Big\downarrow$ $-OH$

$FeCo(CO)_6(R_2C-C\equiv C-R')$ [IIa, IIb]

$Co_2(CO)_6(HOR_2C-C\equiv C-CR_2OH)$ [Ic, Id]

$+ Fe(CO)_5$ $\Big\downarrow$ $-OH$

$FeCo(CO)_6(R_2C-C\equiv C-CR_2OH)$ [IIc, IId]

$+ Fe(CO)_5$ $\Big\downarrow$ $-OH$

$Fe_2(CO)_6(R_2C=C=C=CR_2)$ [IIIc, IIId]
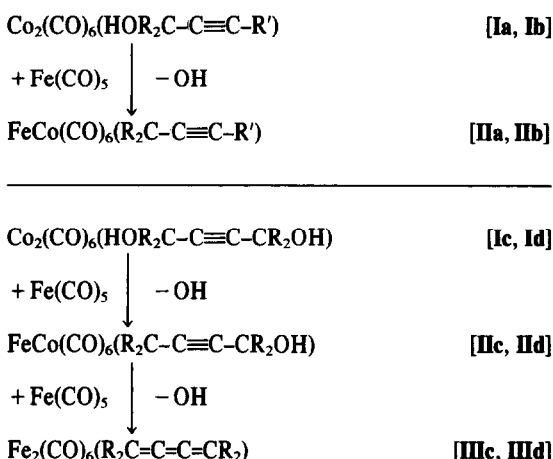
The heterobimetallic compounds are quite stable in the solid state under N_2 atmosphere, but they smoothly decompose in solution. They all have similar IR spectra (see Table 1), the slight shifts observed for the CO stretching frequencies can be related to the different electronic properties of the sustituents (H, Me, Et, OH). In the complexes IIc and IId the presence of the –OH group is confirmed by weak absorptions near 3600 cm⁻¹, which can be observed in concentrated CCl_4 solution.

Also their MS characteristics are very similar and strongly resemble those of the $Co_2(CO)_6(\mu$-alkyne)

Table 1. Analysis and IR spectra of the heterobimetallic complexes

Compd.	Physical state	Elemental analysis Found (calc.)%				IR,[a] ν(CO), cm^{-1}
		C	H	Fe	Co	
FeCo(CO)$_6$(MeHCC$_2$Et) **IIa***	orange oil					2083m, 2039vs, 2022s, 2013cm, 1991w, 1982m,
FeCo(CO)$_6$(H$_2$CC$_2$Me) **IIb**	orange oil	34.69 (35.71)	1.30 (1.49)	16.41 (16.67)	17.83 (17.56)	2084m, 2041vs, 2022s, 2014m, 1993w, 1981m.
FeCo(CO)$_6$(H$_2$CC$_2$CH$_2$OH) **IIc**	orange powder	33.60 (34.13)	1.22 (1.43)	16.03 (15.87)	16.97 (16.75)	3628w,[b] 2087m, 2044vs, 2026s, 2019m, 1995w, 1989m.
FeCo(CO)$_6$(Me$_2$CC$_2$CMe$_2$OH) **IId**	red powder	40.78 (41.21)	3.55 (3.21)	13.95 (13.69)	15.03 (14.44)	3609w,[b] 2080m, 2036vs, 2020s, 2012m, 1985w, 1976m.
FeCo(CO)$_5$(PPh$_3$)(H$_2$CC$_2$CH$_2$OH) **IVc**	red-orange crystals	54.60 (55.29)	3.80 (3.41)	10.02 (9.56)	10.43 (10.07)	2055vs, 2009s, 1993vs, 1973m.

[a]n-hexane, [b]γ(OH) measured in concentrated CCl$_4$ solution, *two enantiomers ref. 14.

Table 2. ^{1}H and ^{13}C NMR data and tentative assignments of the heterobimetallic complexes

Compd.	^{1}H NMR,[s,b] δ/ppm	^{13}C NMR,[a] δ/ppm
FeCo(CO)$_6$(MeHCC$_2$Et) **IIa***	C$_2$H$_5$: 2.83(m, 4), 1.69(t, 6); CH: 5.04(q, 1), 4.78(q, 1); CH$_3$: 1.27(d, 3), 1.20(d, 3).	FeCO: 210.3; CoCO: 203.1; C$_2$: 123.7, 118.4, 97.5, 94.8; CH: 89.3, 87.0; C$_2$H$_5$: 29.3, 27.2, 16.3, 15.9; CH$_3$: 25.2, 19.4.
FeCo(CO)$_6$(H$_2$CC$_2$CH$_3$) **IIb**	CH$_2$: 3.98 and 3.92 (each s, 1); CH$_2$: 2.69(s, 3)	FeCO: 209.0; CoCO: 202.2; C$_2$: 121.0, 87.4; CH$_2$: 66.1; CH$_3$: 18.5.
FeCo(CO)$_6$(H$_2$CC$_2$CH$_2$OH) **IIc**	FeCH$_2$: 4.86 and 4.80 (each s, 1); OHCH$_2$: 4.10(s, 2), OH: 2.10(s, br, 1)[c]	FeCo: 209.5; CoCO: 201.0; C$_2$: 122.4, 92.1; FeCH$_2$: 69.2(J_{CH} = 161 Hz); OHCH$_2$: 62.8 (J_{CH} = 142 Hz).
FeCo(CO)$_6$(Me$_2$CC$_2$CMe$_2$OH) **IId**	OHCH$_3$: 1.95 and 1.92 (each s, 3); FeCH$_3$: 1.69 and 1.65 (each s, 3); OH: 1.72(s, br,1)[c]	FeCO: 209.9; CoCO: 201.4; C$_4$: 117.6, I 13.2, 101.2, 73.7; FeCH$_3$: 32.7; OHCH$_3$: 26.9.
FeCo(CO)$_5$(PPh$_3$)(H$_2$CC$_2$CH$_2$OH) **IVc**	Ph: 7.27(m,15); OHCH$_2$: 4.11 (s, 2); FeCH$_2$: 3.94 and 3.91 (each s, 1); OH: 1.48(s, br, 1)	FeCO: 211.5; CoCO: 207.6, 205.5; Ph:135.1, 133.2, 130.4, 128.7; C$_2$: 122.0, 90.4; FeCH$_2$: 67.2(J_{CH} = 166 Hz); OHCH$_2$: 61.6(J_{CH} = 148 Hz).

[a]CDCl$_3$ at +25°C, [b]multiplicity and integrated intensities in parenthesis, [c]these chemical shifts were temperature- and concentration-dependent, *two enantiomers ref. 14.

Fig. 1. Structures of the homometallic complexes (I) and (III) and proposed structure of the heterobimetallic complex (II).

FeCo(CO)$_6$(MeCC$_2$CMe$_2$OH) (**IId**) shows four methyl resonances (see Table 2); as the temperature is increased the two lowfield signals broaden and merge into a new resonance at +45°C ($\Delta G^{\ddagger}$ = 74.4 kJ/mol) and on this basis we assign the two lowfield peaks to the –CMe$_2$OH group. This dynamic process has to be related to a partially hindered rotation around the ≡C–CMe$_2$OH bond. Similar arguments were used to assign the resonances in the other compounds prepared here. The ^{13}C NMR spectra of the title compounds are quite similar: of the two quaternary acetylenic carbon resonances one is found in the spectral region typical of the Co$_2$(CO)$_6$(μ-alkyne) complexes[18] and one in a lower field region (117.6–123.7 ppm) of the spectrum, which is assigned to the acetylenic carbon bonded to the carbon σ interacting with the iron atom. This low field shift is indicative of a change from sp to sp^2 hybridisation and suggests a delocalized bonding framework for the $\mu_2 - \eta^3$ system. In Fig. 1 are shown the structures of Co$_2$(CO)$_6$(μ-alkyne)[8] (**I**) and Fe$_2$(CO)$_6$(μ-butatriene)[19] (**III**) co-plexes together with the proposed structure of the title compounds (**II**). Complexes I, II and III are isoelectronic: two, three and four carbon atoms are engaged in the bonding scheme with the bimetallic fragment and the organic chain acts as a four-, five- and six-electron donor.

Although the chemical and spectroscopic evidence strongly support the proposed structure (**II**), several attempts were made to confirm it by X-ray analyses. However all were unsuccessful. In order to overcome crystallization problems the FeCo(CO)$_5$(PPh)-(R$_2$CC$_2$CR') derivatives were synthesized. The best result was achieved for R=H, R'=CH$_2$OH (**IVc**), though also in this case the quality of the crystals was poor and the crystals were twinned. An accurate structure determination was thus impossible, but the most significant features of the molecular structure could be extracted. The proposed structure, shown in Fig. 2, is in agreement with that proposed on the basis of the spectroscopic data (**II**). The organic ligand is σ-bonded to the Fe atom through the terminal C(6) carbon and η^2-interacts with both the metal atoms (Fe–Co distance: 2.55 Å) via the C(7)–C(8) bond. The triphenylphosphine group has substituted one carbonyl in an apical position on the cobalt atom. Similar regiospecific substitution of the phosphine for CO group in Co$_2$(CO)$_5$(PR$_3$)(μ-alkyne)

compounds.[1] It is interesting to note the relatively high abundance of the fragment corresponding to the [FeCoC$_3$H$_3$]$^+$ ion. Analogous [Co$_2$C$_3$H$_n$]$^+$ fragments have not been observed in the MS spectra of the Co$_2$(CO)$_6$(μ-C$_2$R$_2$) complexes. This supports the view that the heterobimetallic moiety is bonded to three carbon atoms of the organic chain. The high stability of the Fe–Co bond is suggested from the presence of 50–80% [FeCo]$^+$ ions in all the spectra. For **IIc** and **IId** the presence of the -OH group is further corroborated by the observation of a fragment ion which constitutes loss of H$_2$O from [M$^+$].

The assignment of the ^{1}H NMR signals of FeCo(CO)$_6$(H$_2$CC$_2$CH$_3$) (**IIb**) is straightforward: the methylene group appears as two broad singlets of relative intensity 1 at δ 3.98 and 3.93 respectively, the methyl group as a singlet of intensity 3 at δ 2.69. This pattern remains unchanged as the temperature is increased up to +80°C; above this temperature decomposition of sample is observed. The room temperature ^{1}H NMR spectrum of

Fig. 2. Proposed molecular shape of the compound FeCo(CO)$_5$(PPh$_3$) (H$_2$CC$_2$CH$_2$OH) (IVc).

derivatives has been reported on the basis of IR[20] and ^{13}C NMR[18] data. The poor accuracy of the structural parameters hampers a detailed discussion of the molecular structure. The J_{CH} values in the ^{13}C NMR spectrum of $FeCo(CO)_6(H_2CC_2CH_2OH)$ (IIc) also supports this picture. In the proton-coupled spectrum two triplets are observed at δ 62.8 and 69.2. The first shows J_{CH} = 142 Hz consistent with an sp^3 carbon bearing an electron withdrawing substituent ($HO-CH_2$), while the second shows J_{CH} = 161 Hz, suggesting a partial rehybridation towards an sp^2 character ($Fe-CH_2$). Similar features are observed for the corresponding monophosphine derivative (IVc) (see Table 2).

In conclusion, we feel that the structure of the title compounds (II) can be envisaged as the result of building up two halves obtained by dividing along the organic chain and the metal–metal bond the two homometallic compounds (I) and (III).

Dynamic behaviour

All the ^{13}C NMR spectra of the title complexes show two sets of CO absorptions at room temperature: the sharp Fe–CO resonances lie in the range 211.5–209.0 ppm, the very broad Co–CO resonances in the 207.6–201.0 ppm region. This assignment is consistent with previous observations of mixed iron-cobalt clusters, showing that the COs bonded to Fe resonate at lower field than the Co bonded ones.[21] In the VT ^{13}C NMR studies of [13]CO enriched samples of IIc and IId, lowering of temperature to −80°C results in a progressive sharpening of the Co–CO resonances. It then follows that the broadening observed in room temperature spectra is only due to the moderately rapid quadrupolar relaxation induced by the Co nuclei (I = 7/2). On the other hand, in the same temperature range the Fe–CO resonance splits into three peaks of relative intensity ratio 1 : 1 : 1, whose weighted average chemical shifts are in good accord with the room temperature value (IIc, −50°C, FeCO: 212.4, 210.3, 205.6; IId, −60°C, FeCO: 211.9, 209.4, 206.7).

At room temperature the carbonyls are locally exchanging at each "M(CO)₃" unit, but only the scrambling at Fe(CO)₃ can be frozen in the low temperature limiting spectrum. On the contrary the room temperature ^{13}C NMR spectrum of IVc shows three CO absorptions, one sharp at δ = 211.5 and two very broad at δ = 207.6 and 205.5 of relative intensity ratio 3 : 1 : 1. It follows that the presence of the bulky triphenylphosphine group

quenches, even at room temperature, the localized exchanged process at the Co(CO)₂ unit. Owing to the broadening of these two resonances, no J_{CP} could be extracted.

REFERENCES

[1] D. A. Roberts and G. L. Geoffroy, *Comprehensive Organometallic Chemistry* (Edited by G. Wilkinson, F. G. A. Stone and E. W. Abel), Chap. 40. Pergamon Press, Oxford (1982).
[2] M. Ichikawa, *J. Catal.* 1979, **56**, 127.
[3] T. Madach and H. Vahrenkamp, *Chem. Ber.* 1980, **113**, 2675.
[4] J. K. Ruff, *Inorg. Chem.* 1968, **7**, 1818.
[5] K. K. Joshi and P. L. Pauson, *Z. Naturforsch.* 1962, **17**, 565.
[6] J. F. Tilney-Bassett, *Proc. Chem. Soc. London* 1960, 419.
[7] F. A. Cotton, J. D. Jamerson and B. R. Stults, *J. Am. Chem. Soc.* 1976, **98**, 1774.
[8] W. G. Sly, *J. Am. Chem. Soc.* 1959, **81**, 18.
[9] Y. Wang and P. Coppens, *Inorg. Chem.* 1976, **15**, 1123.
[10] B. H. Freeland, J. E. Hux, N. C. Payne and K. G. Kyers, *Inorg. Chem.* 1980, **19**, 693.
[11] E. L. Muetterties, W. R. Pretzer, M. G. Thomas, B. F. Beier, D. L. Thorn, V. W. Day and A. B. Anderson, *J. Am. Chem. Soc.* 1978, **100**, 2090.
[12] J. F. Tilney-Bassett, *J. Chem. Soc.* 1963, 4748.
[13] K. Tasufuku, K. Aoki and H. Yamazaki, *J. Organomet. Chem.* 1975, **84**, C28.
[14] S. Aime, L. Milone, D. Osella, A. Tiripicchio, A. M. Manotti-Lanfredi, *Inorg. Chem.* 1982, **21**, 501.
[15] R. Victor, *J. Organomet. Chem.* 1977, **127**, C25.
[16] R. S. Dickson and P. J. Fraser, *Adv. Organomet. Chem.* 1975, 323.
[17] O. Gambino, G. A. Vaglio, R. P. Ferrari, M. Valle and G. Cetini, *Org. Mass Spectrom.* 1972, **6**, 723.
[18] S. Aime, L. Milone, R. Rossetti and P. L. Stanghellini, *Inorg. Chim. Acta*, 1977, **22**, 135.
[19a] D. Bright and O. S. Mills, *J. Chem. Soc. Dalton* 1972, 2465; [b] J. N. Gerlach, R. M. Wing and P. C. Ellgen, *Inorg. Chem.* 1976, **15**, 2959.
[20] G. Varadi, A. Vizi-Oroz, S. Vastag and G. Pàlyi, *J. Organomet. Chem.* 1976, **108**, 255.
[21] S. Aime and L. Milone, *Progress in NMR Spectroscopy*, 1977 **11**, 149.

SYNTHESIS OF TWO DIBENZO-3, 2, 3-TETRAMINES AND THEIR Ni(II), Zn(II) and Cd(II) COMPLEXES. THE X-RAY STRUCTURE OF DIIODO-[2, 3:10, 11-DIBENZO-1, 5, 8, 12-TETRAAZADODECANE]CADMIUM(II)

CHRISTOPHER W. G. ANSELL,* MARY McPARTLIN, PETER A. TASKER
and ANTOINETTE THAMBYTHURAI

School of Chemistry, The Polytechnic of North London, Holloway Road, London N7 8DB, England

Abstract—Convenient syntheses of the tetramines 2, 3:10, 11-dibenzo-1, 5, 8, 12-tetraazadodecane, (L1), and 3, 4:9, 10-dibenzo-1, 5, 8, 12-tetraazadodecane, (L2), are described. Both ligands form complexes with Ni(II), Zn(II) and Cd(II). The X-ray structure of [Cd(L1)I$_2$], confirms a five coordinate geometry for the Cd atom, where the two iodines are bonded to the metal and (L1) acts as a tridentate ligand. The complex crystallises in the monoclinic space group P2$_1$/c with $a = 19.741(4)$ Å, $b = 8.726(3)$ Å, $c = 12.221(4)$ Å, and $\beta = 104.55(3)°$. The structure was refined to R = 0.062 for 1051 reflections.

INTRODUCTION

Recently[1], macrocyclic species of the type (1) below have been extensively studied in this laboratory with a view to establishing the electrochemical properties of their divalent metal complexes and the coordinative selectivity of the ligand system towards a range of metal ions.

(1)

$R = -(CH_2)_2-, -(CH_2)_3-, -(CH_2)_4-$
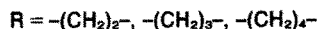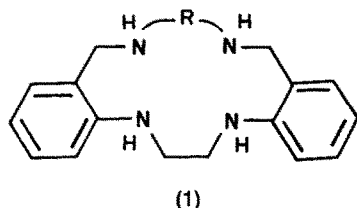
As an extension to this work, we here report convenient synthetic routes to the known[2] tetramine 2, 3:10, 11-dibenzo-1, 5, 8, 12-tetraazadodecane, (L1), and to the related ligand 3, 4:9, 10-dibenzo-1, 5, 8, 12-tetraazadodecane, (L2). Both species may be regarded as open chain analogues of the systems (1). The preliminary results of complexation reactions of the ligands are also presented, together with the X-ray structure of [Cd(L1)I$_2$].

RESULTS AND DISCUSSION

Scheme 1 outlines the synthetic route to the tetramines (L1) and (L2). Refluxing methyl anthranilate and ethylenediamine together for 3 days yields the diamide (2) as white plates after recrystallisation. Reduction with LiAlH$_4$ in diethyl ether gives (L1) in 75% yield. Mixing 2:1 quantities of anthranilonitrile with oxalyl chloride in diethyl ether gives an immediate white precipitate of (3) in 93% yield. Reduction of all four func-

tional groups by LiAlH$_4$ to give (L2) is accomplished readily and in 85% yield. Both (L1) and (L2) are pale yellow oils which, as has been observed in their aliphatic analogues[3], from solid hydrated species in moist air. Both readily form crystalline salts of stoichiometry L.2HX and L.4HX, where X = Cl$^-$ or ClO$_4^-$. In confirmation of the reported[2] instability of L1.4HX in aqueous media, it was found that both L1.2HX and L2.2HX could be readily isolated from aqueous solutions of the tetra-acid salt.

(L1) and (L2) both from complexes with Ni(II), Zn(II) and Cd(II), (see Table 1). Reaction of a 1:1 mixture of Ni(ClO$_4$)$_2$.6H$_2$O and either (L1) or (L2) in methanol gives a blue-green solution which, upon treatment with excess NH$_4$NCS deposits mauve precipitates of [Ni(L1 or L2)NCS$_2$]. νNCS occurs as a single sharp band at 2100 cm^{-1} in their infrared spectra, which is consistent[4] with N-bonded thiocyanate in a single environment. This observation, taken with the magnetic moments of 3.22 and 3.23 BM for the Ni(II) complexes of (L1) and (L2) respectively, the similarity of the ligands and the analy-

Table 1. Analytical data

	Found			Required		
	C	H	N	C	H	N
Diamide (2)	64.4	6.3	18.6	64.4	6.1	18.8
(L1).4HCl	56.1	6.8	16.0	56.0	7.0	16.3
(L1).4HClO$_4$	28.3	4.0	8.0	28.6	3.9	8.3
(L1).2HClO$_4$	40.8	5.0	12.0	40.8	5.1	11.9
Dinitrile (3)	66.1	3.3	19.0	66.2	3.4	19.3
(L2).4HCl	56.4	7.1	16.7	56.0	7.0	16.3
(L2).4HClO$_4$	28.7	4.1	8.7	28.6	3.9	8.3
(L2).2HClO$_4$	40.9	5.0	12.2	40.8	5.1	11.9
[Ni(L1)(NCS)$_2$]	48.8	5.2	19.0	48.9	5.0	19.0
[Ni(L2)(NCS)$_2$].H$_2$O	47.2	5.2	18.3	47.0	5.2	18.3
[Cd(L1)I$_2$]	30.1	3.6	8.7	30.2	3.5	8.8
[Cd(L2)I$_2$]	30.6	3.6	8.6	30.2	3.5	8.8
[Zn(L1)I$_2$]	32.9	3.8	9.9	32.6	3.7	9.5
[Zn(L2)I$_2$]	32.6	3.8	9.5	32.6	3.7	9.5

---

*Author to whom correspondence should be addressed.
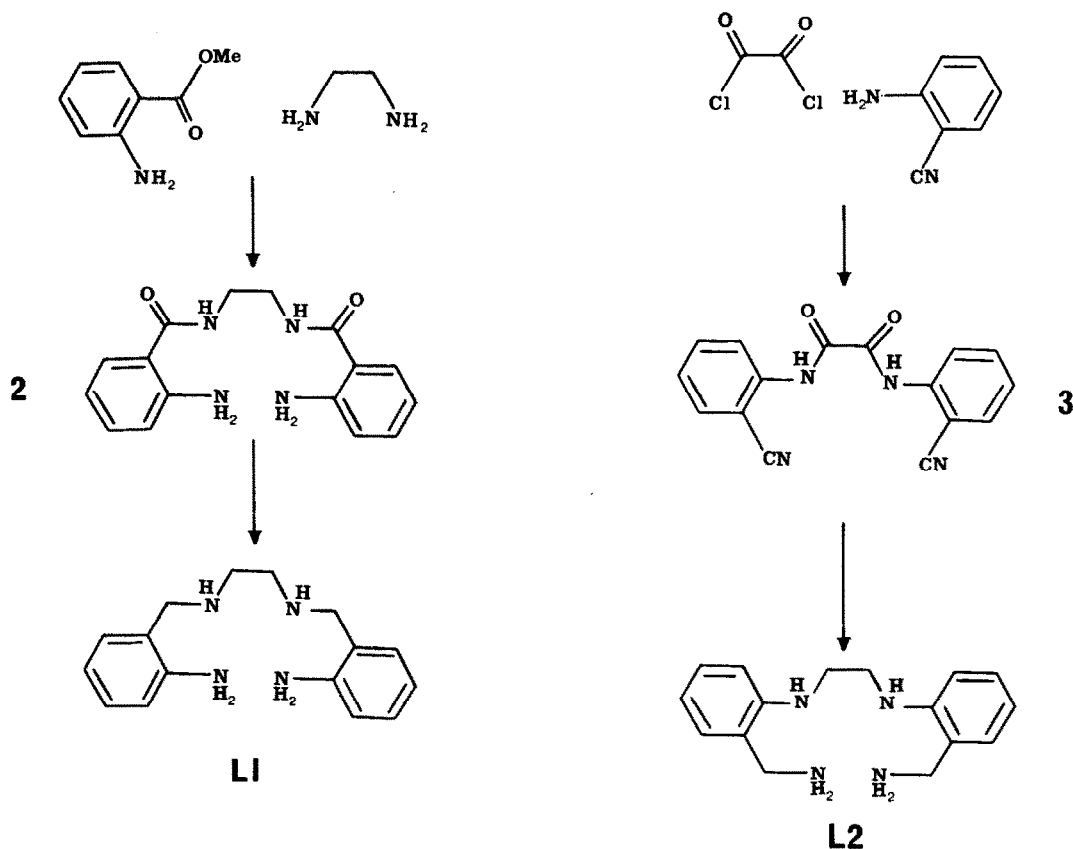
Scheme 1. The preparative routes to (L1) and (L2).

tically confirmed stiochiometries points to a *trans*-octa-hedral geometry for the nickel atom in both complexes, with the tetramine occupying the equatorial donor sites.

Reaction of ZnI₂ and CdI₂ in methanol with (L1) and (L2) gave good yields of the corresponding metal complexes [M(L1 or L2)I₂]. Crystals of the complex [Cd(L1)I₂] could be obtained from methanol and the X-ray structure of this species was undertaken. Figure 1 is a diagram of the complex, showing the numbering scheme. Hydrogen atoms have been omitted for clarity. The five coordinate geometry of the cadmium atom is immediately apparent. (L1) acts as a tridentate ligand via the anilino–nitrogen donor N(2a) and both aliphatic nitrogens N(1a) and N(1b). The two bonded iodines occupy the remaining sites. Severe disorder was apparent for the phenyl ring incorporating the uncomplexed –NH₂ group, but the essentials of the stereochemistry around the metal ion are nonetheless established. The geometry of the donors around the cadmium is best described as a distorted square based pyramid, with N(1a), N(2a), N(1b) and I(1) defining the base and I(2) in the apical position. The constituent atoms of the base are coplanar to within 0.24 Å, and the Cd atom is located 0.68 Å above their least squares plane towards the iodine I(2). The bond lengths between the Cd atom and the nitrogen donors are all close to 2.4 Å and are similar to those reported[5] in other five coordinate cadmium diiodide species containing tridentate polyamines. The bond lengths between Cd and I(1), and Cd and I(2) (2.795(3) Å and 2.791(3) Å) are in the range previously reported[6] for Cd–I bonds. More details of the environment of the metal ion are given in the caption to Fig. 1.

EXPERIMENTAL

2, 3 : 10, 11-*Dibenzo*-1, 5, 8, 12-*tetraazadodecane*-4, 9-*dione*, (2)

Ethylenediamine (7 cm³, 105 mmol) and methyl anthranilate (50 cm³, 387 mmol) were refluxed together for three days. The mixture solidified on cooling and was washed with portions of ethanol. The white residue was recrystallised from a 1 : 1 mixture of methanol and chloroform (500 cm³) to give the title diamide (2) (8.0 g, 25%) as white plates, m.p. 246–8°. Mass spectrum: 298 (M+) expected: 298. Principal IR bands (KBr disc) 3480(s), 3375(s), 3300(s, b), 1630(s, b), 1582(s).

2, 3 : 10, 11-*dibenzo*-1, 5, 8, 12-*tetraazadodecane*, (L1)

Lithium aluminium hydride (2.9 g, 77 mmol) was added to dry ether contained in a 2 dm³ 3-necked flask fitted with a sealed mechanical stirrer and a Soxhlet extractor and condenser. (2) (3.7 g, 12.4 mmol) was placed in a thimble in the Soxhlet extractor. The ether was refluxed gently in a heating mantle, and after 16 hr. all the solid had been introduced to the flask. The mixture was treated sequentially with water (3 cm³), 15% sodium hydroxide solution (3 cm³), and water (8.5 cm³). The mixture was filtered and the residue washed with ether. The combined filtrates were dried over magnesium sulphate and evaporated to give the product as a pale yellow oil (2.5 g, 75%). NMR(CDCl₃):2.68 σ (methylene, singlet) 3.0–3.7 σ (NH, broad, complex) 3.28 σ (NH, singlet) 3.71 δ (benzyl methylene, singlet) 6.4–7.3 δ (aromatics, complex). Addition of D₂O causes collapse of the signals at 3.28 and 3.0–3.7 δ. Mass spectrum: 270(M+); expected:270.

2, 2'-(oxalyldiimino)bis(o-benzonitrile), (3)

Anthranilonitrile (12.5 g, 0.1 mol) was dissolved in dry ether (150 cm³). Oxalyl chloride (6.2 g, 0.05 mol) was added slowly
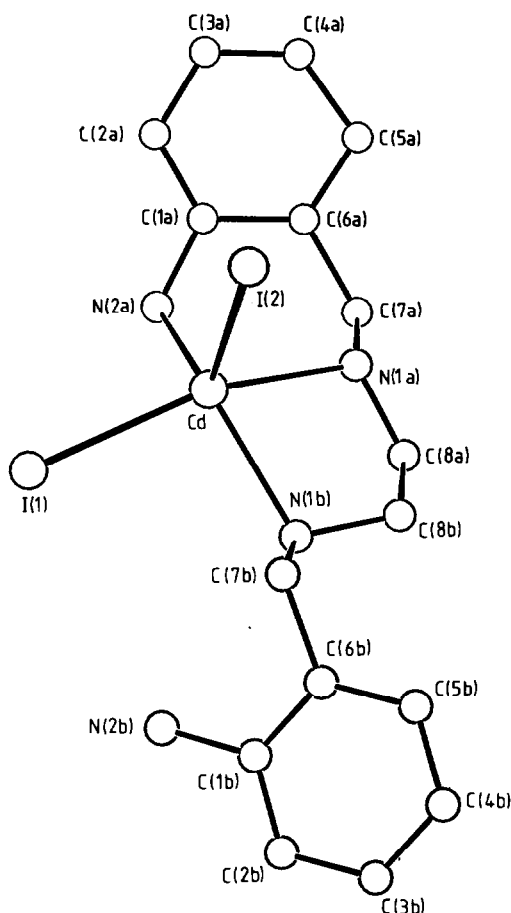
Fig. 1. The molecular structure of [Cd(L1)I₂]. Principal bond lengths and angles are: Cd–I(1) 2.795(3), Cd–I(2) 2.791(3), Cd–N(2a) 2.398(21), Cd–N(1a) 2.366(21), Cd–N(1b) 2.384(23)Å. I(2)–Cd–I(1) 106.5(1), N(2a)–Cd–I(1) 94.8(6), N(2a)–Cd–I(2) 112.6(6), N(1a)–Cd–I(1) 158.1(6), N(1a)–Cd–I(2) 95.2(6), N(1a)–Cd–N(2a) 79.1(8), N(1b)–Cd–I(1) 95.1(6). N(1b)–Cd–I(2) 108.3(6), N(1b)–Cd–N(2a) 132.9(8), N(1b)–Cd–N(1a) 74.8(8).

dropwise with vigorous stirring. The white precipitate of (3) was filtered, washed copiously with methanol and ether and dried *in vacuo*. Yield 14.3 g, 93%. The nmr spectrum of this compound could not be obtained due to its extreme insolubility. Principal IR bands(Nujol): 3320(s), 2250(s), 1700(s), 1620(m), 1600(m). Mass spectrum: 266(M+). Expected 266.

3, 4:9, 10-*dibenzo*-1, 5, 8, 12-*tetraazadodecane* (L2)

To a suspension of LiAlH₄ (5.2 g) in dry ether (500 cm³) in a 1 dm³ flask fitted with a reflux condenser was added in portions over twenty minutes (3) (10.0 g, 0.035 mol). The reaction mixture became yellow/green. After 12 hr under reflux the colour had faded, and the mixture was treated carefully and sequentially with water (5 cm³), 15% sodium hydroxide solution (5 cm³) and water (15 cm³). The basic hydroxides left after filtration were extracted three times with dichloromethane (200 cm³) and the combined extracts and filtrate evaporated after drying over MgSO₄ to give (L2) (8.9 g, 85%) as a pale yellow oil. Principal IR(Nujol): 3350(m), 3250(m), 1620(s), 1600(s). NMR: (CDCl₃): 3.43 δ (methylene, singlet) 3.84 δ (methylene, singlet) 2.0–3.0 δ (broad, NH) 6.4–7.3 δ (aromatics, complex). Addition of D₂O

†Atomic coordinates have also been deposited with the Cambridge Crystallographic Data Centre.

causes collapse of the signal 2.0–3.0 δ. Mass spectrum: 270(M+) expected: 270.

Salts of the tetramines

To a solution of the ligand (L1 or L2) in 1:1 dichloromethane: methanol was added an excess of either conc; HCl or HClO₄. The tetraacid salts precipitated on standing. The corresponding diacid salt could be obtained by treatment of an aqueous solution of the tetraacid salt with NEt₃ until precipitation was complete. The yields for both procedures are quantitative.

[Ni(*L1 or L2*) (*NCS*)₂]

Nickel(II) perchlorate hexahydrate (1.11 g, 3 mmol) was added to a hot solution of (L1) or (L2) (0.81 g, 3 mmol) in methanol and the blue–green solution stirred for 5 min. Ammonium thiocyanate (1.0 g, excess) was then added to precipitate the di(thiocyanato) complexes as mauve microcrystalline powders, yield 1.09 g, 82%.

[*M(L1 or L2)I₂*]*M* = Zn, Cd

0.15 Millimolar quantities of Metal(II) iodide and tetramine were mixed in warm methanol (30 cm³). On standing and cooling, analytically pure samples of the complexes were deposited. For the complexes of (L1), crystals of X-ray quality could be grown from methanol. The yields in the syntheses were greater than 65% in each case.

X-ray crystal structure

Crystal data: [C₁₆H₂₂N₄CdI₂]. M = 636.2, monoclinic, space group P2₁/c, a = 19.741(4) Å, b = 8.726(3) Å, c = 12.221(4) Å, β = 104.55(3)°, U = 2037.7 Å³, Z = 4. F(000) = 1200, μ(mo–Kα) = 38.23 cm⁻¹. Cc = 2.07 gcm⁻³. R = 0.062, Rw = 0.065 for 1051 unique intensity data, F > 6(σ)F.

The X-ray data were collected as previously described.[7] The cadmium and both iodine atoms were located from a Patterson map and all remaining non-hydrogen atoms from subsequent difference maps. Anisotropic thermal parameters were assigned to the cadmium and both iodines. Hydrogen atoms were not located directly but constrained to lie 0.95 Å from the parent carbon atom. A severe disorder was apparent for the phenyl ring containing the uncoordinated amino group. This disorder could not be satisfactorily resolved. N(2b) and C(7b) were fixed at the positions found in the difference map and the disordered phenyl ring refined as a regular hexagon of C–C bond distance 1.395 Å. Hydrogen atoms were not included on the disordered ring, N(2b) or C(7b). Neutral atom scattering factors were taken from reference 8. All crystallographic calculations were performed using SHELX.[9] Final atomic coordinates, bond lengths and angles together with tables of Fo/Fc have been deposited as supplementary material with the editor, from whom copies are available on request.†

REFERENCES

[1] C. W. G. Ansell, B. Seghi, L. F. Lindoy and P. A. Tasker, Unpublished results.
[2] D. W. Gruenwedel, *Inorg. Chem.* 1968 **7**, 495.
[3] E. K. Barefield, F. Wagner, A. W. Helinger and A. R. Dahl, *Inorg. Syn.* **16**, 20.
[4] K. Nakamoto, *Infrared Spectra of Inorganic and Coordination Compounds*, 2nd Edn. Interscience, New York (1970).
[5] M. G. B. Drew and S. Hollis, *Acta Cryst.* 1978, **B34**, 2853.
[6] P. L. Orioli and M. Ciampolini, *J. Chem. Soc. Chem. Comm.* 1972, 1280.
[7] M. K. Cooper, P. A. Duckworth, K. Henrick and M. McPartlin, *J. Chem. Soc. Dalton Trans.* 1981, 2357.
[8] *International Tables for X-ray Crystallography*, Vol. 4. Kynoch Press, Birmingham (1972).
[9] G. M. Sheldrick, *SHELX-76 program system*. University of Cambridge (1976).

ELECTROCHEMICAL REDUCTION OF DIALKYLAMIDE AND BIS-TRIMETHYLSILYLAMIDO COMPLEXES OF CHROMIUM(III) AND YTTERBIUM IN NON-AQUEOUS SOLVENTS

D. C. BRADLEY* and MUSHTAQ AHMED

Department of Chemistry, Queen Mary College, Mile End Road, London E1 4NS, England

Abstract—The electrochemical reductions of (a) $Cr[N(SiMe_3)_2]_3$, $Cr(NPr_2^i)_3$, $Cr(NO)[N(SiMe_3)_2]_3$, $Cr(NO)(NPr_2^i)_3$ and $Cr(NO)(OBu^t)_2(NPr_2^i)$ in acetonitrile, and (b) $Yb[N(SiMe_3)_2]_3$ in dimethylsulphoxide, have been studied using cyclic voltammetry (platinum bead electrode) and controlled potential coulometry (mercury pool electrode). The results are interpreted in terms of quasi-reversible or irreversible one-electron reduction and possible side-reactions. A number of similar complexes of titanium, vanadium, manganese, iron and cobalt were investigated but electrochemical studies were precluded due to reactions with solvent and/or supporting electrolyte.

INTRODUCTION

The synthesis of the metal dialkylamides $M(NR_2)_x$ and *bis*-trimethylsilyamides ($R = Me_3Si$) and their characterization by spectroscopic and X-ray crystallographic studies have revealed considerable details concerning their structure and chemical reactivity[1,2]. In particular it has been shown that by using particularly bulky ligands, the transition metals, lanthanides and actinides may be constrained to abnormally low coordination numbers and some unusual chemical reactivity. To gain further insight into the chemical behaviour of some of these compounds, we have explored their electrochemical behaviour in non-aqueous solvents. It was hoped that these studies would reveal reversible electrochemical processes from which useful data on the relative stability of different oxidation states could be deduced. It was further hoped that the results might point the way to novel methods of synthesis of new complexes which are not amenable to isolation using conventional procedures.

Since derivatives of titanium(IV and III), chromium(III and II) and cobalt(II and I) were known exhibiting two consecutive valence states, some of their compounds were selected for study. In addition it was considered worthwhile to investigate the *tris*-silylamides of iron and ytterbium.

RESULTS AND DISCUSSION

Although extensive studies were carried out in various non-aqueous solvents on a large number of compounds, meaningful results were obtained only on some chromium compounds in acetonitrile and ytterbium *tris*-silylamide in dimethylsulphoxide. Attempts were made to establish the electrochemical behaviour of these metal dialkylamides by studying Cyclic Voltammetry at a platinum bead electrode and by Controlled Potential Electrolysis at a mercury pool electrode.

(a) Cyclic voltammetry

The experiments were carried out at various voltage scan rates on dilute solutions of the metal dialkylamide

(0.2–1.0 millimolar) in acetonitrile with tetraethylammonium tetrafluoroborate (0.1 M) as supporting electrolyte. In Fig. 1 are shown the cyclic voltammograms of $Cr[N(SiMe_3)_2]_3$ and $Cr(NPr_2^i)_3$ with the behaviour of the supporting electrolyte alone for comparison. The chromium compounds each showed a main reduction wave which was quasi-reversible or irreversible. At very slow scan rates a small peak at $+0.10$ V appeared after the anodic peak of the main reduction wave and this suggested that a product of the quasi-reversible or irreversible electron transfer processes was being oxidized. Bearing in mind the chemical reactivity of these metal complexes it was considered necessary to demonstrate their stability under these electrochemical conditions. Thus the peak current for $Cr[N(SiMe_3)_2]_3$ was found to be unchanged over a five day period giving confidence to the reliability of the results. Some comparative data on peak potentials (Ep) at the same voltage scan rate are listed in Table 1 for $Cr[N(SiMe_3)_2]_3$, $Cr(NO)[N(SiMe_3)_2]_3$, $Cr(NPr_2^i)_3$, $Cr(NO)(NPr_2^i)_3$ and $Cr(NO)(OBu^t)_2(NPr_2^i)$. Unfortunately the lack of true reversibility limits the scope for discussion of these data, but it is clear that the di-isopropylamido-complexes have slightly lower reduction potentials than the *bis*-trimethylsilylamido-complexes whilst the addition of nitric oxide appears to make only a small change in the peak potentials.

Data obtained for each compound over a 40-fold range in voltage scan rate (0.0125–0.5 V/sec) are presented in Tables 2–6 and give some indication of the electrochemical behaviour of each complex. Thus it appears that the peak current (ip_c) was approximately proportional to the square root of the voltage scan rate. The "best-behaved" compounds were $Cr(NPr_2^i)_3$, and $Cr(NO)(NPr_2^i)_3$ which showed peak potentials almost invariant with voltage scan rate in contrast with the behaviour of the chromium silylamide complexes.

The ytterbium *tris*-silylamide $Yb[N(SiMe_3)_2]_3$ gave reproducible and reliable cyclic voltammograms in dimethylsulphoxide solution (Fig. 2) using sodium perchlorate as supporting electrolyte. One main reduction peak was obtained and the peak potentials were almost independent of voltage scan rate (Table 7). The stability of the ytterbium complex in dimethylsulphoxide solution was

---

*Author to whom correspondence should be addressed.
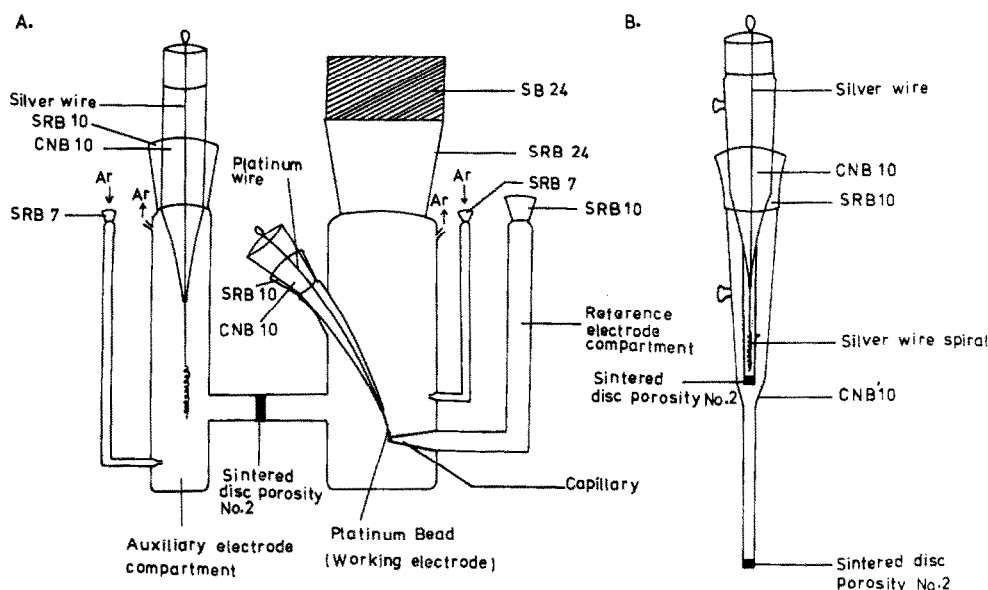
Fig. 1. Electrochemical cell. (A) Electrode configuration. (B) Reference electrode.

Table 1. Cyclic voltammetry of chromium dialkylamides

Compound	Concentration (mM)	Ep_c (Volts)	Ep_a (Volts)	ΔEp^a (Volts)
$Cr[N(SiMe_3)_2]_3$	0.4	-0.816	-0.570	0.246
$Cr(NO)[N(SiMe_3)_2]_3$	0.2	-0.770	-0.440	0.330
$Cr(NPr^i_2)_3$	1.0	-0.520	-0.430	0.090
$Cr(NO)(NPr^i_2)_3$	0.4	-0.560	-0.430	0.130
$Cr(NO)(OBu^t)_2(NPr^i_2)$	0.4	-0.820	-0.560	0.260

a
  In acetonitrile at 25°C with 0.1M $(NEt_4)BF_4$ supporting electrolyte at a
  voltage scan rate of 0.1 volts/sec., vs. $Ag/AgClO_4$. Potentials ± 0.004 v.

confirmed by finding that the peak current remained constant over a 5-day period.

(b) *Controlled potential electrolysis*

Using a mercury-pool electrode, constant potential coulometry was carried out at -1.00 V (vs $Ag/AgClO_4$ electrode) on solutions of $Cr[N(SiMe_3)_2]_3$, $Cr(NPr^i_2)_3$, and $Cr(NO)(OBu^t)_2(NPr^i_2)$ in acetonitrile. The results (Table 8) showed that only $Cr(NPr^i_2)_3$ gave quantitative reduction whilst the electrolysis of the other compounds was accompanied by other reactions. Moreover it was noted in the electrolysis of $Cr(NPr^i_2)_3$ under controlled potential that the current rapidly declined to zero and the colour of the solution was discharged. Similarly the controlled potential electrolysis of $Yb[N(SiMe_3)_2]_3$ in dimethylsulphoxide at -1.20 V (vs $Ag/AgClO_4$ electrode) gave quantitative reduction (Table 8) with the current rapidly declining to zero with rapid discharge of the colour of the solution.

The above results suggest that one-electron reductions

have occurred but that only in $Cr(NPr^i_2)_3$, $Yb[N(SiMe_3)_2]_3$ and probably $Cr(NO)(NPr^i_2)_3$ is there quasi-reversibility.

Before discussing this interesting electrochemical behaviour of these low coordination complexes of chromium it is useful to review some of their chemistry. Both $Cr[N(SiMe_3)_2]_3$ and $Cr(NPr^i_2)_3$ were shown to be monomeric 3-coordinated paramagnetic Cr(III) complexes with interesting X-ray structures[3-5] and electronic configurations as deduced from spectroscopic studies.[6-8] They do not form addition compounds with neutral ligands such as THF but react more or less readily with water, oxygen, nitric oxide, carbon dioxide and carbon–disulphide. The *tris*-di-isopropylamide is extremely sensitive to dioxygen and it is difficult to prepare a dilute solution free from the blue coloured initial product of oxygenation which gives an intense characteristic ESR signal.[9] The reaction with nitric oxide gave the considerably more stable diamagnetic mono-nitrosyls $Cr(NO)(NR_2)_3$ (R = $SiMe_3$ or Pr^i) in which the chromium is tetrahedrally coordinated.[10] The linear CrNO systems and diamag-

Table 2. Cyclic voltammetry of $Cr[N(SiMe_3)_2]_3^a$

Voltage Scan Rate (R) (Volts/sec.)	$ip_c/R^{\frac{1}{2}}$ ($\mu Av.^{-\frac{1}{2}}sec.^{\frac{1}{2}}$)	ip_a/ip_c	Ep_c (Volts)	Ep_a (Volts)	ΔEp (Volts)
0.0125	26.8	0.80	−0.730	−0.579	0.160
0.025	26.6	1.19	−0.750	−0.570	0.180
0.05	27.7	1.16	−0.780	−0.560	0.220
0.10	36.0	1.00	−0.816	−0.570	0.246
0.15	34.5	0.94	−0.845	−0.540	0.305
0.20	33.5	0.93	−0.850	−0.580	0.270
0.25	28.0	0.79	−0.860	−0.540	0.320
0.30	26.5	0.80	−0.890	−0.520	0.370
0.35	28.5	0.80	−0.910	−0.510	0.400
0.40	31.0	0.71	−0.920	−0.520	0.400
0.50	31.1	0.64	−1.000	−0.520	0.480

[a] 0.4 mM in CH_3CN at 25°C using 0.1M $(NEt_4)BF_4$ supporting electrolyte and Pt bead electrode.

Table 3. Cyclic voltammetry of $Cr(NO)[N(SiMe_3)_2]_3^a$

Voltage Scan Rate (R) (Volts/sec.)	$ip_c/R^{\frac{1}{2}}$ ($\mu Av.^{-\frac{1}{2}}sec.^{\frac{1}{2}}$)	ip_a/ip_c	Ep_c (Volts)	Ep_a (Volts)	ΔEp (Volts)
0.0125	107	0.875	−0.725	−0.460	0.265
0.025	109	0.780	−0.745	−0.460	0.285
0.05	77	0.694	−0.800	−0.540	0.260
0.10	101	0.640	−0.770	−0.440	0.330
0.15	110	0.741	−0.860	−0.510	0.350
0.20	112	0.720	−0.890	−0.507	0.383
0.25	132	0.697	−0.920	−0.500	0.420
0.30	117	0.641	−0.940	−0.500	0.440
0,35	122	0.555	−0.960	−0.520	0.440
0.40	120	0.579	−0.960	−0.500	0.460
0.50	133	0.489	−0.980	−0.520	0.460

[a] 0.2 mM in CH_3CN at 25°C using 0.1M $(NEt_4)BF_4$ supporting electrolyte and Pt bead electrode.

<div align="center">D. C. BRADLEY and M. AHMED</div>

Table 4. Cyclic voltammetry of $Cr(NPr^i_2)_3$[a]

Voltage Scan Rate(R) (Volts/sec.)	$ip_c/R^{\frac{1}{2}}$ (μAv.$^{-\frac{1}{2}}$sec.$^{\frac{1}{2}}$)	ip_a/ip_c	Ep_c (Volts)	Ep_a (Volts)	ΔEp (Volts)
0.0125	268	0.867	−0.51	−0.43	0.08
0.025	285	0.889	−0.51	−0.43	0.08
0.05	295	0.909	−0.51	−0.43	0.08
0.10	304	0.948	−0.52	−0.43	0.09
0.15	315	0.951	−0.52	−0.43	0.09
0.20	331	0.960	−0.52	−0.42	0.10
0.25	338	0.976	−0.52	−0.42	0.10
0.30	338	0.962	−0.52	−0.41	0.11
0.35	326	0.959	−0.52	−0.41	0.11
0.40	311	0.964	−0.52	−0.41	0.11
0.45	298	0.950	−0.53	−0.40	0.13
0.50	283	0.950	−0.53	−0.41	0.12

[a] 1.0 mM in CH_3CN at 25°C using 0.1M $(NEt_4)BF_4$ supporting electrolyte and Pt bead electrode.

Table 5. Cyclic voltammetry of $Cr(NO)(NPr^i_2)_3$[a]

Voltage Scan Rate(R) (Volts/sec.)	$ip_c/R^{\frac{1}{2}}$ (μAv.$^{-\frac{1}{2}}$sec.$^{\frac{1}{2}}$)	ip_a/ip_c	Ep_c (Volts)	Ep_a (Volts)	ΔEp (Volts)
0.0125	107	1.042	−0.55	−0.42	0.13
0.025	88	1.036	−0.55	−0.42	0.13
0.05	87	1.026	−0.56	−0.45	0.11
0.10	82	1.077	−0.56	−0.43	0.13
0.15	90	0.971	−0.56	−0.43	0.13
0.20	94	1.024	−0.55	−0.42	0.13
0.25	104	1.039	−0.56	−0.43	0.13
0.30	99	1.241	−0.56	−0.43	0.13
0.35	122	1.028	−0.57	−0.42	0.15
0.40	130	1.024	−0.56	−0.42	0.14
0.50	164	1.164	−0.57	−0.42	0.15

[a] 0.4 mM in CH_3CN at 25°C using 0.1M $(NEt_4)BF_4$ supporting electrolyte and Pt bead electrode.

Table 6. Cyclic voltammetry of $Cr(NO)(OBu^t)_2(NPr^i_2)$[a]

Voltage Scan Rate (R) (Volts/sec.)	$ip_c/R^{\frac{1}{2}}$ ($\mu Av.^{-1} sec.^{\frac{1}{2}}$)	ip_a/ip_c	Ep_c (Volts)	Ep_a (Volts)	ΔEp (Volts)
0.0125	125	0.536	-0.73	-0.58	0.15
0.025	92	0.345	-0.78	-0.60	0.18
0.05	98	0.340	-0.80	-0.57	0.23
0.10	114	0.333	-0.82	-0.56	0.26
0.15	73	0.643	-0.86	-0.54	0.32
0.20	107	0.417	-0.88	-0.58	0.30
0.25	104	0.385	-0.88	-0.54	0.34

[a] 0.4 mM in CH_3CN at $25^\circ C$ using 0.1M $(NEt_4)BF_4$ supporting electrolyte and Pt bead electrode.
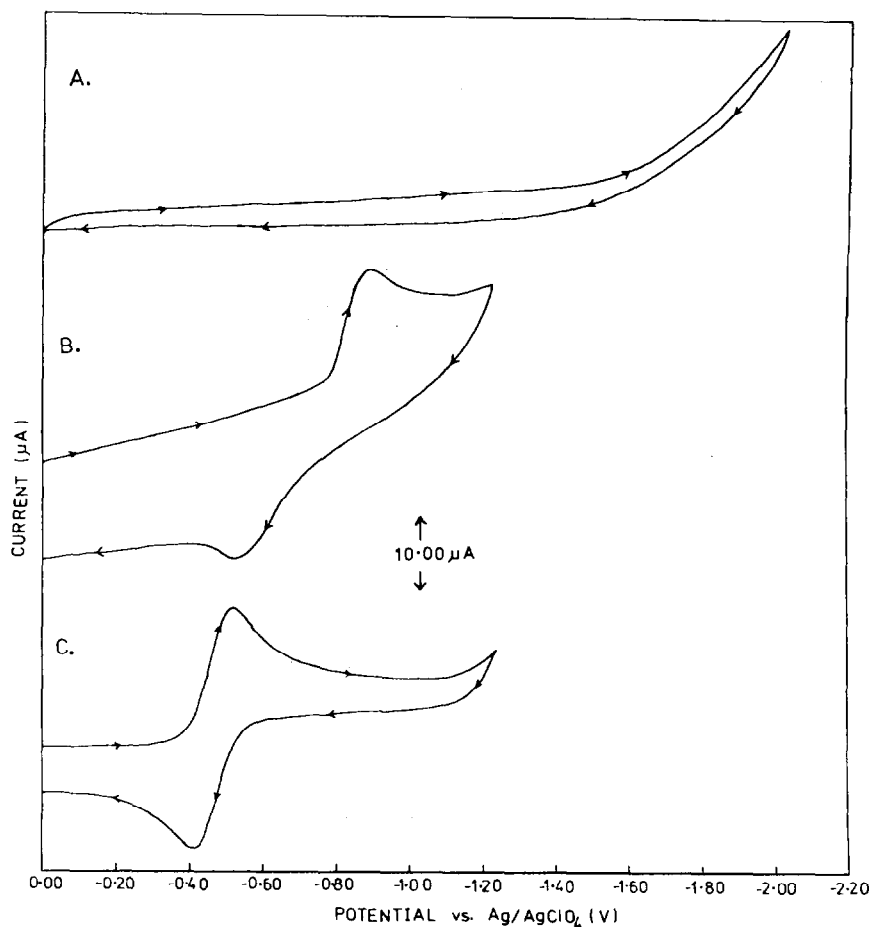
Fig. 2. Cyclic voltammograms in acetonitrile (25°C). (A) $(NEt_4)BF_4$ (0.1 M), voltage scan rate 0.3 V sec.$^{-1}$ (B) $Cr[N(SiMe_3)_2]_3$ (0.4 mM), $(NEt_4)BF_4$ (0.1 M), voltage scan rate 0.3 V sec^{-1}. (C) $Cr(NPr^i_2)_3$(0.4 M), $(NEt_4)BF_4$ (0.1 M), voltage scan rate 0.3 V sec.$^{-1}$.

Table 7. Cyclic voltammetry of $Yb[N(SiMe_3)_2]_3^a$

Voltage Scan Rate (R) (Volts/sec.)	$\dfrac{ip_c/R^{\frac{1}{2}}}{(\mu Av.^{-1}sec.^{\frac{1}{2}})}$	ip_a/ip_c	Ep_c (Volts)	Ep_a (Volts)	ΔEp (Volts)
0.01	20.6	0.523	-1.04	-0.80	0.24
0.02	14.7	0.519	-1.04	-0.80	0.24
0.03	17.5	0.362	-1.05	-0.80	0.25
0.04	15.3	0.663	-1.06	-0.80	0.26
0.05	17.9	0.512	-1.04	-0.76	0.28
0.06	16.7	0.735	-1.04	-0.78	0.26
0.07	21.2	0.571	-1.08	-0.76	0.32
0.08	21.9	0.645	-1.08	-0.76	0.32
0.10	21.5	0.603	-1.10	-0.74	0.36

[a] 0.4 mM in DMSO at 25°C using 0.4M $NaClO_4$ supporting electrolyte and Pt bead electrode.

Table 8. Coulometric results

Compound	Mol. Electrolysed $(\times 10^5)$	Charge (Coulombs)	$\dfrac{a}{n}$
$Cr[N(SiMe_3)_2]_3$ [b]	2.19	0.410	0.19
	2.44	0.155	0.49
	3.41	0.810	0.25
	2.44	1.045	0.44
$Cr(NPr^i_2)_3$ [b]	4.31	4.595	1.10
	3.97	3.805	0.99
	5.16	5.450	1.09
	4.85	5.045	1.08
$Cr(NO)(OBu^t)_2(NPr^i_2)$ [b]	4.63	1.550	0.35
	4.32	1.400	0.33
	4.87	2.250	0.48
$Yb[N(SiMe_3)_2]_3$ [c]	4.28	3.940	0.95
	2.90	2.840	1.01
	2.75	2.750	1.04
	3.82	3.540	0.96
	3.44	3.250	0.98

[a] n = Ratio of Faradays per Mol electrolysed.

[b] Electrolysis at -1.00 volts $(Ag/AgClO_4)$ in CH_3CN at 25°C using 0.1M $(NEt_4)(BF_4)$ supporting electrolyte.

[c] Electrolysis at -1.20 volts $(Ag/AgClO_4)$ in Me_2SO at 25°C using 0.4M $NaClO_4$ supporting electrolyte.

netism suggested that the low-spin electronic structure corresponded to a pseudo-Cr(II) $3d^4$ complex due to the NO acting as a 3-electron donor. By contrast the truly bivalent complex $Cr[N(SiMe_3)_2]_2(THF)_2$ was isolated as an extraordinarily oxygen-sensitive paramagnetic square planar (trans) compound with the high spin $3d^4$ configuration.[11]

It seemed reasonable to expect that the electrochemical reduction of $Cr(NR_2)_3$ ($R = SiMe_3$ or Pr^i) might give rise to a reversible 1-electron transfer involving the formation of an unstable 3-coordinate Cr(II) anion $[Cr(NR_2)_3]^-$.

$$Cr(NR_2)_3 + e \rightleftharpoons [Cr(NR_2)_3]^-. \qquad (1)$$

Since the solvent CH_3CN is potentially a donor ligand the unstable anion might then react by forming either a neutral high spin square planar complex $Cr(NR_2)_2(CH_3CN)_2$ or a diamagnetic tetrahedral anion $[Cr(NR_2)_3(CH_3CN)]^-$.

$$[Cr(NR_2)_3]^- + 2CH_3CN \rightleftharpoons Cr(NR_2)_2(CH_3CN)_2 + NR_2^- \qquad (2)$$

$$[Cr(NR_2)_3]^- + CH_3CN \rightleftharpoons [Cr(NR_2)_3(CH_3CN)]^-. \qquad (3)$$
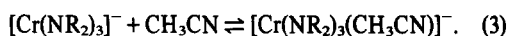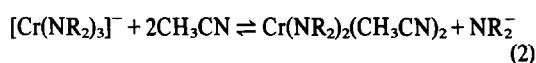
In the first case, the dialkylamide anion NR_2^- released (eq. 2) might react with the solvent leading to irreversible reactions. Metal dialkylamides are known to react with acetonitrile.[12] Additional experiments confirmed that lithium dialkylamides did react with solutions of the supporting electrolyte in acetonitrile. In the anodic phase of the cyclic voltammetry the dialkylamide anion could be oxidized to the radical which could also lead to irreversible reactions.

$$NR_2^- - e \rightarrow NR_2 \qquad (4)$$

$$2NR_2 \rightarrow R_2NNR_2 \qquad (5)$$

$$2NR_2 \rightarrow R_2NH + \text{imine}. \qquad (6)$$

The feasibility of the alternative reaction of $[Cr(NR_2)_3]^-$ with one molecule of CH_3CN (eqn 3) should depend on the ability of one acetonitrile ligand and three dialkylamido groups to promote sufficient splitting of the d-orbital energy levels to produce a stable tetrahedral diamagnetic Cr(II) species.

Dealing first with the electrochemistry of $Cr[N(SiMe_3)_2]_3$ the data in Tables 2 and 8 suggest that the electron-transfer reduction is not wholly reversible but it is not clear what chemical reactions are subsequently involved. The formation of $Cr[N(SiMe_3)_2]_2(CH_3CN)_2$ (eqn 2) analogous to the THF complex would be accompanied by the release of $[N(SiMe_3)_2]^-$ which in the form of its lithium derivative reacts rapidly with the supporting electrolyte in acetonitrile. In assessing the possibility of forming a stable diamagnetic tetrahedral species $Cr[N(SiMe_3)_2]_3(CH_3CN)$ it must be noted that the $3d^5$ complex $Fe[N(SiMe_3)_2]_3$ is high-spin.[8,13] Unfortunately we found that $Fe[N(SiMe_3)_2]_3$ reacted immediately with acetonitrile with decomposition and we could not determine whether it would form a low-spin complex with one molecule of CH_3CN of addition. Although the strong π-acceptor NO^+ does cause spin pairing by coordination with $Cr[N(SiMe_3)_2]_3^-$, it seems that CH_3CN (which is not a good π-acceptor is not capable of producing a stable diamagnetic adduct and thus eqn (2) appears to be favoured relative to (3) for the silylamide complex.

The data in Tables 4 and 8 show that the electrochemical reduction of $Cr(NPr_2^i)_3$ is quasi-reversible and its cyclic voltammogram (C) in Fig. 1 looks much more reversible than that of $Cr[N(SiMe_3)_2]_3$ (B). It also appears that $Cr(NP_2^i)_3$ has a less negative reduction potential than the silylamide. Therefore the reduced species from the di-isopropylamide is more readily formed and is more stable than the corresponding disilylamide complex. Thus if $[Cr(NPr_2^i)_3(CH_3CN)]^-$ (eqn 3) is relatively stable, a more reversible system is expected to occur. It is relevant to note here that in $Cr(NO)(NPr_2^i)_3$ the NO stretching frequency (1643 cm^{-1}) is lower than that in $Cr(NO)[N(SiMe_3)_2]_3$ $(1698 \text{ cm}^{-1})^{[10]}$, which implies greater delocalisation of the two pairs of d-electrons into the π^* antibonding (NO^+) orbitals in the di-isopropylamide complex and presumably greater stability. Therefore it is reasonable to suggest that although CH_3CN is not a strong π-acceptor it would in fact form a more stable adduct with $[Cr(NPr_2^i)_3]^-$ than with $Cr[N(SiMe_3)_2]_3^-$.

Turning now to the electrochemical behaviour of the nitrosyl complexes $Cr(NO)[N(SiMe_3)_2]_3$, $Cr(NO)(NPr_2^i)_3$ and $Cr(NO)(OBu^t)_2(NPr_2^i)$, the data in Tables 3, 5 and 6 show that the peak potential of the silylamido complex varied most with the voltage scan rate whereas the potentials for the tris-di-isopropylamido complex were practically independent of the scan rate. Somewhat surprisingly the data for $Cr(NO)(NR_2)_3 (R = SiMe_3$ and $Pr^i)$ are very close to the values for the parent 3-coordinated species $Cr(NR_2)_3$. Assuming that a one-electron reduction gives the anionic species $[Cr(NO)(NR_2)_3]^-$ the additional electron must be accommodated in a higher energy $3d$-orbital unless there is an electronic rearrangement.

$$Cr(NO)(NR_2)_3 + e \rightleftharpoons [Cr(NO)(NR_2)_3]^-. \qquad (7)$$
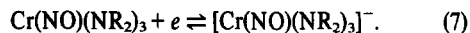
The NO could change into a 2-electron donor or it might dissociate or be replaced by acetonitrile (viz. eqns 8 and 9) depending on whether $R = SiMe_3$ or Pr^t.

$$2CH_3CN + [Cr(NO)(NR_2)_3]^- \rightarrow Cr(NR_2)_2(CH_3CN)_2 + NR_2^- + NO \qquad (8)$$

$$CH_3CN + [Cr(NO)(NR_2)_3]^- \rightleftharpoons [Cr(NR_2)_3(CH_3CN)]^- + NO. \qquad (9)$$
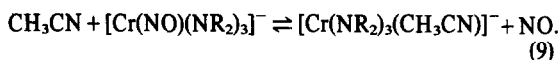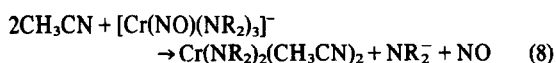
Thus the dissociation (eqn 8) might be expected for the silylamide but the di-isopropylamide derivative may retain its nitric oxide as a 2-electron donor in preference to acetonitrile (eqn 9). The electrochemical behaviour of the mixed ligand complex $Cr(NO)(OBu^t)_2(NPr^i)$ is interesting in view of the value of its ν_{NO} 1684 cm^{-1} which is nearer to that of $Cr(NO)[N(SiMe_3)_2]_3$ than to $Cr(NO)(NPr_2^i)_3$.[10] In fact its cyclic voltammetric (Table 6) behaviour was indeed more akin to that of the tris-silylamido complex and its coulometric behaviour (Table 8) showed that the electron transfer reduction process was accompanied by other reactions.

Finally we note that the electrochemical behaviour of $Yb[N(SiMe_3)_2]_3$ in DMSO showed a quasi-reversible 1-electron reduction. A cyclic voltammogram is shown in Fig. 2 and the data in Table 7 show that the peak potentials are almost independent of voltage scan rate. The coulometric data in Table 8 also show that a simple reduction takes place implying considerable stability for the Yb(II) species formed. This is not surprising since the anion $Yb[N(SiMe_3)_2]_3^-$ (eqn 1) would be isoelectronic with the stable neutral lutecium complex $Lu[N(SiMe_3)_2]_3$.[14,15] In

fact the solvent would probably coordinate to give {Yb[N(SiMe₃)₂]₃(DMSO)}⁻ since it has been shown that the lanthanide *tris*-silylamides form stable complexes with phosphine oxides Ln[N(SiMe₃)₂]₃(R₃PO).[16,17]

EXPERIMENTAL

All of the compounds studied, especially the 3-coordinated complexes, are air-sensitive and it was found to be essential to take extremely rigorous precautions in manipulating the dilute solutions used in the electrochemical measurements.

Preparations

The compounds were prepared by using essentially the original methods reported[1,2] and purity was checked by an appropriate physical measurement (i.e. m.p., IR-, NMR- or mass-spectra) and elemental analyses. The following compounds were prepared: $Ti(NEt_2)_4$, $TiCl[N(SiMe_3)_2]_3$, $Ti[N(SiMe_3)_2]_3$, $V[N(SiMe_3)_2]_3$, $Cr[N(SiMe_3)_2]_3$, $Cr(NPr_2^i)_3$, $Cr(NO)[N(SiMe_3)_2]_3$, $Cr(NO)(NPr_2^i)_3$, $Cr(NO)(OBu^t)_2(NPr_2^i)$, $Mn[N(SiMe_3)_2]_2$, $Fe[N(SiMe_3)_2]_3$, $Co[N(SiMe_3)_2]_2$, and $Yb[N(SiMe_3)_2]_3$.

Careful preliminary work was carried out to determine whether stable solutions in a suitable non-aqueous solvent could be made in the presence of an excess of a supporting electrolyte. Unfortunately some of the above compounds proved to be too reactive towards either the solvent or the electrolyte. Solvents tried were acetonitrile, dimethyl-sulphoxide, dimethylformamide, methylene chloride and propylene carbonate and the electrolytes were tetraalkyl-ammonium salts of chloride, iodide, perchlorate, tetrafluoroborate and tetraphenylborate.

ELECTROCHEMICAL STUDIES

Acetonitrile was very rigorously purified by the method of Walter and Ramaley[18] and finally collected by fractional distillation. Dimethylsulphoxide was purified as described by Mann[19] and stored over molecular sieve (type 5A).

For Cyclic Voltammetry a standard three-electrode, IR-compensated system was used (Fig. 3) with an Electrochemical Instrument. Calibration was made using aqueous $[Fe(oxalate)_3]^{3-}$ solution and also *bis*-cyclopentadienyliron(II) in acetonitrile with 0.2 M NaClO₄ as supporting electrolyte.

Platinum wire was used for both the auxiliary and the working electrodes. The reference electrode was $Ag/AgClO_4(0.02 M)\{(NEt_4)BF_4, (0.2 M)\}$ in acetonitrile[20] and was separated from the test solution by a salt-bridge containing the same solution of supporting electrolyte in acetonitrile as used in the test solution. The platinum bead working electrode was cleaned in nitric acid (1 M), washed with water and rinsed with the acetonitrile/supporting electrolyte solution. The current–voltage data were displayed on a Tektronix D13 storage-oscilloscope and/or an X–Y recorder. Measurements were performed using positive feedback circuitry to minimize the IR drop in potential.

All measurements were made at $25.0 \pm 0.2°C$ under an atmosphere of purified argon.

Coulometric measurements were made on 50 ml solutions using a mercury-pool electrode (dia. 4.6 cm) at a constant potential on the plateau of the reduction wave. The very small contribution from the background current due to the supporting electrolyte was subtracted.
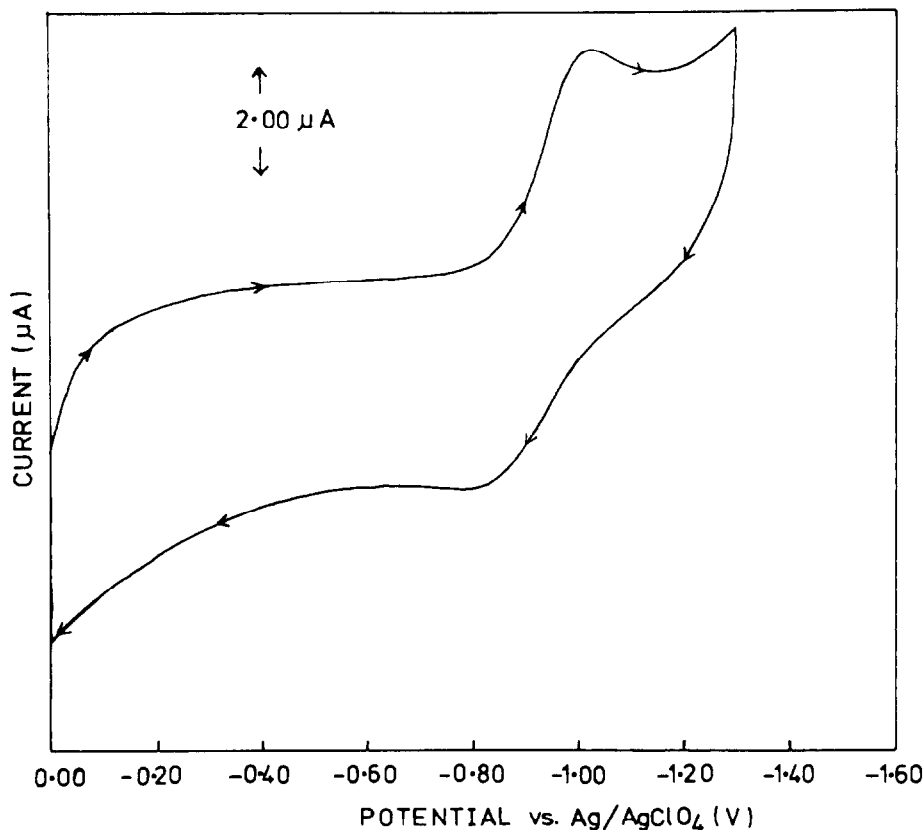
Fig. 3. Cyclic voltammograms in dimethylsulphoxide (25°). Yb[N(SiMe₃)₂]₃ (0.4 mM), NaClO₄ (0.4 M) voltage scan rate 0.05 V sec.⁻¹.

REFERENCES

[1] D. C. Bradley, *Coordination Chemistry (IUPAC)* 1980, **20**, 249.
[2] D. C. Bradley and M. H. Chisholm, *Acc. Chem. Res.* 1976, **9**, 273.
[3] E. C. Alyea, J. S. Basi, D. C. Bradley and M. H. Chisholm, *J. C. S. Chem. Commun.* 1968, 495.
[4] D. C. Bradley, M. B. Hursthouse and P. F. Rodesiler, *J. C. S. Chem. Commun.* 1969, 14.
[5] D. C. Bradley, M. B. Hursthouse and C. W. Newing, *J. C. S. Chem. Commun.* 1971, 411.
[6] E. C. Alyea, D. C. Bradley and R. G. Copperthwaite, *J. C. S. Dalton* 1972, 1580.
[7] E. C. Alyea, D. C. Bradley, R. G. Copperthwaite and K. D. Sales, *J. C. S. Dalton* 1973, 185.
[8] D. C. Bradley, R. G. Copperthwaite, S. A. Cotton, J. Gibson and K. D. Sales, *J. C. S. Dalton* 1973, 191.
[9] D. C. Bradley, J. C. W. Chien, W. Kruse and C. W. Newing, *J. C. S. Chem. Commun.* 1970, 1177.
[10] D. C. Bradley and C. W. Newing, *J. C. S. Chem. Commun.* 1970, 219.
[11] D. C. Bradley, M. B. Hursthouse, C. W. Newing and A. J. Welch, *J. C. S. Chem. Commun.* 1972, 567.
[12] D. C. Bradley and M. C. Ganorkar, *Chem. Ind.* 1968, 1521.
[13] E. C. Alyea, D. C. Bradley, M. G. Copperthwaite, B. W. Fitzsimmons, C. E. Johnson and K. W. Sales, *J. C. S. Chem. Commun.* 1970, 1715.
[14] D. C. Bradley, J. S. Ghotra and F. A. Hart, *J. C. S. Chem. Commun.* 1972, 349.
[15] D. C. Bradley, J. S. Ghotra and F. A. Hart, *J. C. S. Dalton*, 1973, 1021.
[16] D. C. Bradley, J. S. Ghotra, F. A. Hart, M. B. Hursthouse and P. R. Raithby, *J.C.S. Dalton* 1977, 1166.
[17] D. C. Bradley and Y. C. Gao, *Polyhedron* 1982, **1**, 307.
[18] M. Walter and L. Ramaley, *Anal. Chem.* 1973, **45**, 165.
[19] C. K. Mann, *Electroanalyt. Chem.* 1969, **3**, 57.
[20] E. Kirowa-Eisner and E. Gileadi, *J. Electroanalyt. Chem. Interfac. Electrochem.* 1970, **25**, 481.

PHOTOREDUCTION OF CHLOROHEMIN IN
PURE PYRIDINE

CARLO BARTOCCI,* ANDREA MALDOTTI, ORAZIO TRAVERSO,
CARLO A. BIGNOZZI and VITTORIO CARASSITI

Centro di Studio sulla Fotochimica e Reattività degli Stati Eccitati dei Composti di Coordinazione del C.N.R.,
Istituto Chimico dell'Università di Ferrara, Via L. Borsari, 46, Ferrara, Italy

Abstract—Chlorohemin (Fe(III)PPCl) undergoes photoreduction when irradiated in pure pyridine solution with 400–450 nm light. A thermal reduction is observed to occur simultaneously with the photochemical one, but after a one hour irradiation about 75% of the reduction product is formed in a photochemical way. Both five- and six-coordinated species are observed to be present in solution; however, only the Fe(III)PPpy$^+$ five coordinated complex is photoreducible. A mechanism is proposed whereby the primary photochemical act is an axial pyridine → iron electron transfer process yielding Fe(II)PP and py$^+$ species. The Fe(II)PP moiety gives rise to the formation of the spectrophotometrically detectable Fe(II)PP(py)$_2$ complex. ESR spin trapping results are consistent with the formation of 2-pyridyl radicals from py$^+$ cation by fast transfer of a proton to a pyridine molecule.

INTRODUCTION

The study of porphyrin iron complexes under conditions approaching the physiological state appears very useful for a thorough understanding of the vital functions these compounds play in biological systems. Thus, redox processes involving the central iron as well as the porphyrin ring are a matter of particular interest due to the role that the cytochromes, heme-containing proteins, play in the transfer of electrons in the respiratory chain.

The use of photochemical methods appears quite well suited to the study of electron transfer processes in complex molecular systems such as iron porphyrins, since irradiation, at suitably selected wavelengths, allows one to avoid the difficulties arising from simultaneous reactions that often occur when more usual chemical methods are used. Recently, Bartocci *et al.*[1] reported a study on the photochemical reduction of Fe(III) protoporphyrin IX chloride (chlorohemin) in pyridine-containing aqueous alcoholic solutions. In that paper it was observed that, under irradiation, Fe(III) was reduced to Fe(II) and that a bis-pyridine Fe(II) protoporphyrin complex was formed. However, the use of aqueous mixed solvents presented some problems in establishing the photoreduction mechanism since, under those conditions, complex coordination equilibria impeded a clear identification of the photoreactive species.[2] For this reason, although an alcoholate → iron electron transfer was indicated as the most likely means of photoreduction, other mechanisms involving pyridine or OH$^-$ could not be ruled out.

In a recent paper[3] on the photoreduction of ferrideuteroporphyrin in benzene, water, or micelle solutions containing primary or secondary alcohols, Bizet *et al.* indicated that an alcoholate → Fe(III) intramolecular electron transfer was responsible for the primary photoreduction.

However, the results reported in this paper cannot be correlated with those obtained by Bartocci *et al.*[1] due to the different natures of both the solvents and the substrate used. Therefore, in order to provide a clearer

understanding of the possible mechanism in the photoreduction of hemin, the photochemical behavior of chlorohemin in pure pyridine is reported here. The use of pure pyridine produces two advantages with respect to mixed aqueous solvents: (i) it allows one to study the photochemical behavior of chlorochemin under conditions which approach the aprotic environment of the heme-containing protein sheath. (ii) a better understanding of the nature of the axial ligands can be obtained.

EXPERIMENTAL

Materials

Commercial chlorohemin (Fluka) was recrystallized following the reported[4] glacial acetic acid method.

Spectroscopic grade pyridine (Merck) was dried with calcium hydride, twice distilled and used within 24 hr after the purification. Phenyl-*tert*-butylnitrone (PBN) (Aldrich) was used without further purification. All the other chemicals were reagent grade commercial products.

Apparatus and methods

UV–VIS spectra were recorded in the 350–700-nm range with a Varian Cary 219 Spectrophotometer. X-band electron spin resonance spectra were recorded with a Bruker 220 SE spectrometer and calibrated using α,α'-diphenylpicrylhydrazyl (DPPH). Irradiations were carried out with a 150 W xenon lamp, equipped with a glass filter which cut off light with wavelengths shorter than 400 nm. The irradiation light was focussed on the reaction vessel through quartz lenses. In order to identify radical intermediates, solutions contained in 2-mm tubes were irradiated in the presence of PBN as spin trap[5] in the ESR cavity.

All other experiments were carried out using spectrophotometric cells as reaction vessels. The solutions were degassed before irradiation to less than 10^{-5} Torr by means of at least three vacuum line freeze/thaw pump cycles. Before running the experiments in oxygenated solutions, oxygen was allowed to flow into the previously degassed solutions until a pressure of 1 atmosphere was reached.

RESULTS

Irradiation of 1 × 10^{-4} M deaerated pyridine solutions of Fe(III)PPCl by light with λ > 400 nm resulted in the spectral variations shown in Fig. 1. The new bands at 480, 524 and 556 nm are typical of Fe(II)PP(py)$_2$ (bis-pyridine hemochrome) formed in the photoreduction

---

*Author to whom correspondence should be addressed.
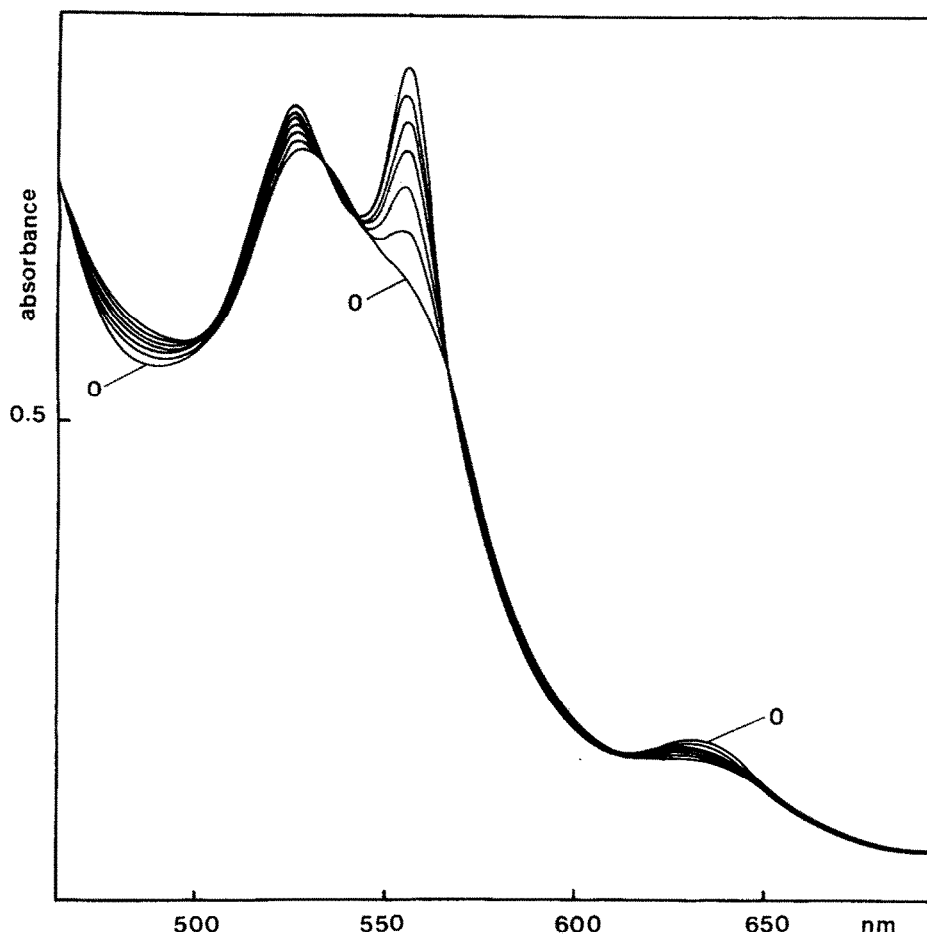
Fig. 1. Spectral variations observed upon $\lambda > 400$ nm irradiation of a 1×10^{-4} M deaerated solution of Fe(III)PPCl in
pure pyridine at 25°C, O, initial spectrum; irradiation periods, 10 min.

process.[1] The net isosbestic points observed at 535, 544 and 578 nm indicate that the photoreaction did not involve the porphyrin ring.[1]

In Fig. 2 the spectral variations observed when an identical solution was kept in the dark during the above photochemical run are reported. It can be observed that spectral variations are qualitatively the same as those observed under irradiation (Fig. 1). This suggests that both thermal and photochemical reduction of Fe(III)PPCl occur simultaneously to yield Fe(II)PP(py)$_2$. Polarographic measurements[6] showed that the Fe(II) concentration immediately after the dissolution of the chlorohemin in pyridine was quite negligible. This permits the calculation of the Fe(II)PP(py)$_2$ fraction formed by the thermal reaction. Using absorbance variations reported in Figs. 1 and 2, it was seen that 24% of the reduction product was thermally formed after 1 hr.

No appreciable photoreduction was observed to occur under the following conditions:

(1) By irradiation with light of $\lambda > 450$ nm.

(2) In an oxygen atmosphere (see Experimental). When oxygen was allowed to bubble into the previously irradiated solutions, spectral variations were observed indicating that the expected re-oxidation of the Fe(II) complex was occurring very slowly.

(3) In the presence of an excess of chloride (i.e. the pyridinium salt). In this case there is a wide difference between the absorption spectra of chlorohemin in pyri-

dine solutions with or without an excess of chloride (Fig. 3).

At 100 K, 2×10^{-3} M pyridine solutions of chlorohemin exhibit a typical[7] high-spin ESR spectrum with $g_\perp = 6$ and $g_\parallel = 2$ (Fig. 4). The addition of excess Cl$^-$ or oxygenation did not modify the ESR spectrum.

ESR experiments were carried out at room temperature during the irradiation of carefully deaerated pyridine solutions of chlorohemin containing 5×10^{-2} M phenyl-*tert*-butylnitrone (PBN) as a spin trap. An intense spectrum increasing with irradiation time was revealed (Fig. 4), suggesting the involvement of radical intermediates in the photoreduction process. It consists of 1:1:1 doublets with $a_N = 14.5$ G and $a_H = 2.2$ G. An identical solution kept in the dark did not exhibit any ESR signals. Since the use of a nitroso spin trap yields direct information on radical species structure,[8] it is often utilized. However, when irradiated with $\lambda > 400$ nm light the pyridine solutions of nitroso compounds usually used as spin traps (e.g. 2,4,6-tri-*tert*-butylnitrosobenzene, TBN), exhibit ESR signals which clearly indicate the photoinstability of these compounds.

DISCUSSION

The apparent thermal reduction of Fe(III)PPCl in pure pyridine is a very striking phenomenon. In fact, some noticeable reduction of this compound in pyridine was observed several years ago,[9] although the presence of
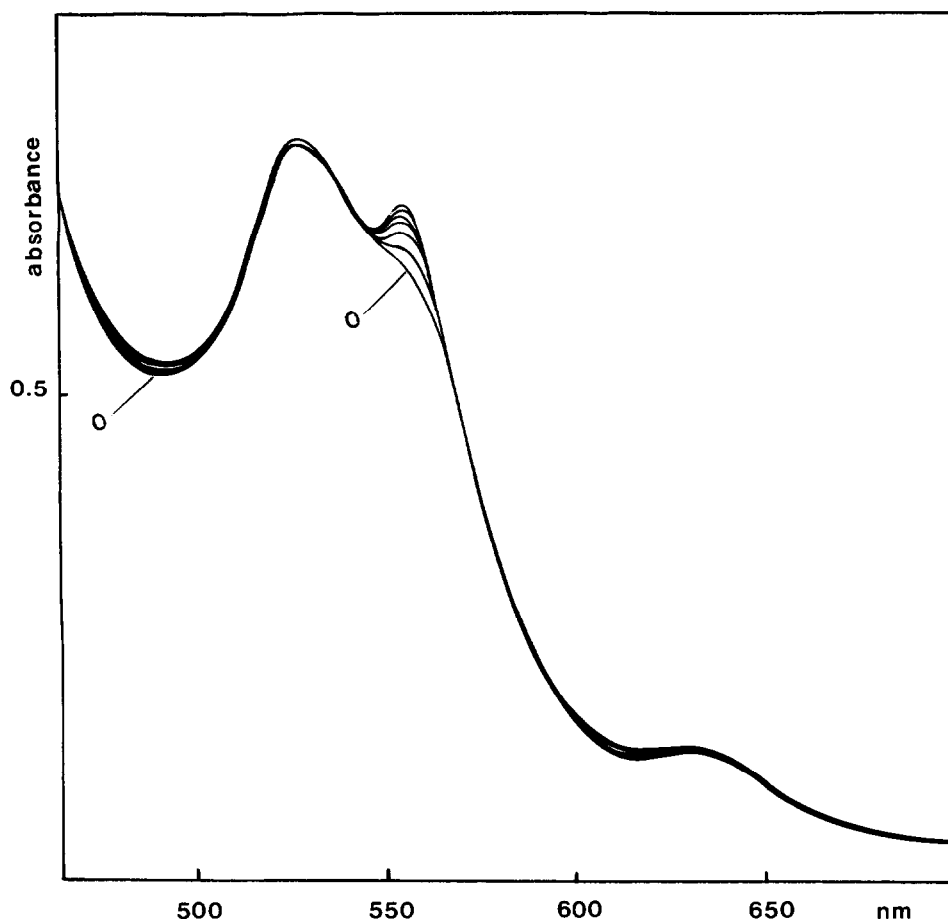
Fig. 2. Spectral variations observed when a 1×10^{-4} M pyridine solution of Fe(III)PPCl was kept 1 hr in the dark. O; initial spectrum.

Fe(II) under these conditions was afterwards ruled out by other authors.[10,11] To date, the nature of this self-reduction is not clear. One cannot rule out the possibility that, even after a careful purification of all chemicals used, some impurities remain in solution, and are responsible for the observed reduction.

Comparison of the spectral variations reported in Figs. 1 and 2 indicates that formation of the reduced species Fe(II)PP(py)$_2$ is strongly accelerated under irradiation and that more than 75% of the reduction products are formed by photochemical means.

When chlorohemin is dissolved in pure pyridine, axial complexes are formed.[10,12] Several structures consisting of bis-pyridine and chloro-pyridine six-coordinated as well as chloro and pyridine five-coordinated complexes could be proposed. Our ESR results, however, indicate that only high-spin species are present, ruling out the presence of appreciable amounts of Fe(III)PP(py)$_2$ which is known[13] to exhibit an ESR spectrum typical of low spin or, at most, mixed high-spin/low-spin species. Thus the only possible Fe(III) protoporphyrin complexes present in pyridine solutions of chlorohemin are Fe(III)PPCl, Fe(III)PPpy$^+$ and Fe(III)PPpyCl. The presence of iron porphyrin complexes containing undissociated chloride ligand in pure pyridine is not unexpected. In fact, the replacement of Cl$^-$ by pyridine is not likely due to the low coordinating ability of pyridine on Fe(III) porphirin axial positions as well as its low

solvating power with respect to Cl$^-$ ions. On the other hand, the clear change in the absorption spectrum observed when an excess of pyridinium chloride is present (Fig. 3) suggests that appreciable amounts of pyridine-containing complexes are in equilibrium with chloro-containing complexes. Therefore, the situation in a pyridine solution of chlorohemin can be accurately described by Scheme 1.
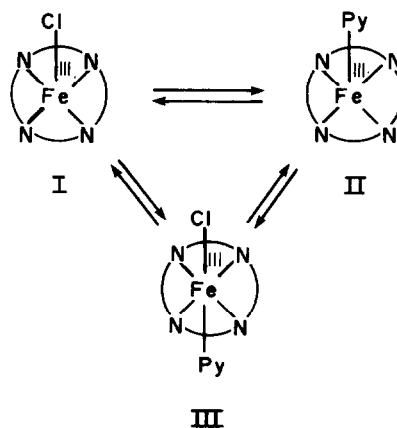
Scheme 1.
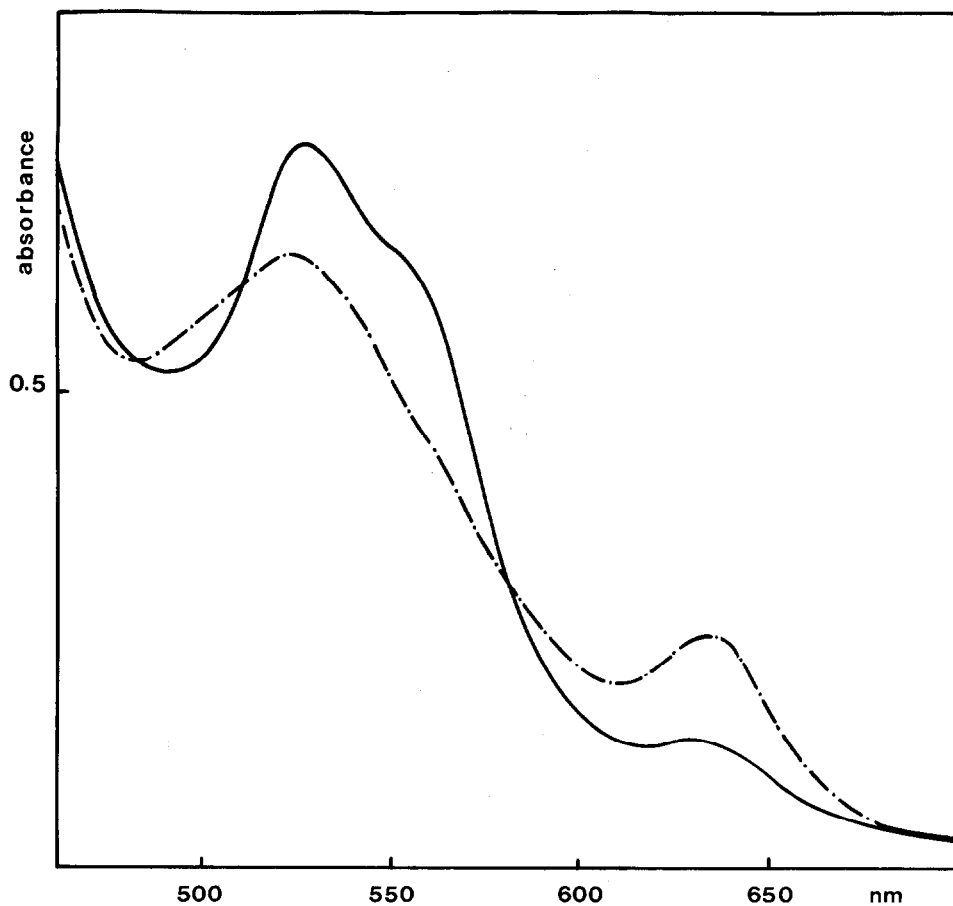
Fig. 3. Absorption spectra of Fe(III)PPCl in pure pyridine: ---- immediately after the dissolution, —— after the addition of an excess of pyridinium chloride.
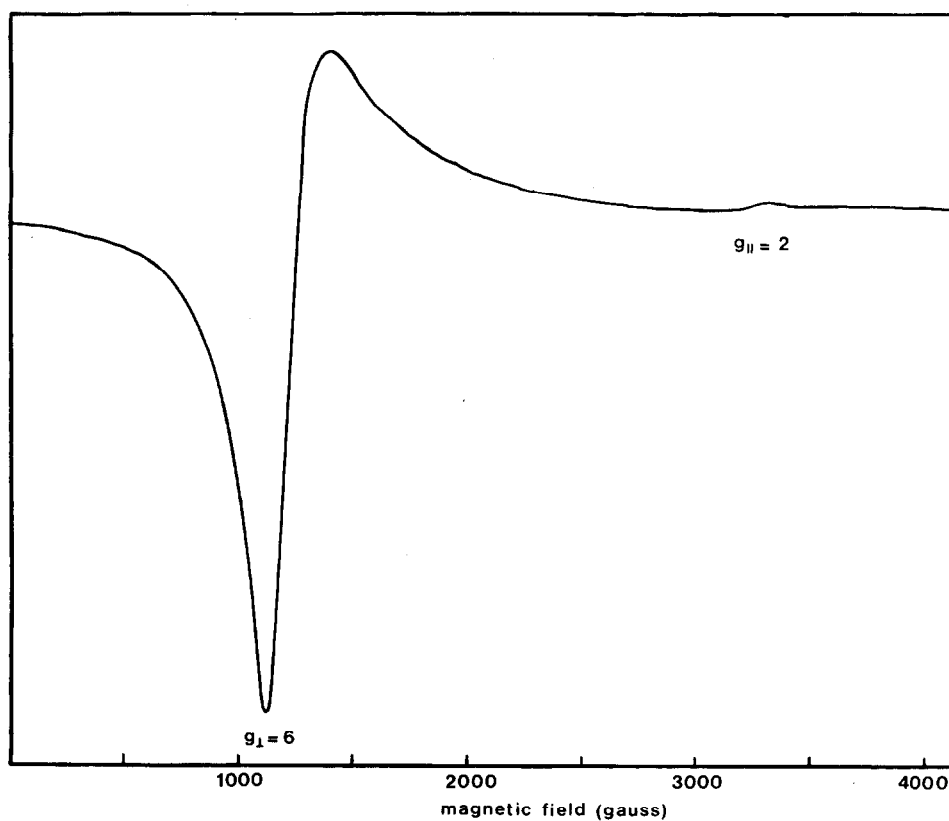
Fig. 4. ESR spectrum of a 2×10^{-3} M pyridine solution of Fe(III)PPCl at 100 K.

$$Fe(III)PPpy^+ \rightarrow {}^*Fe(III)PPpy^+ \quad (1)$$

$$Fe(III)PPpy^+ \rightarrow Fe(II)PP\ldots py^+ \quad (2)$$

$$Fe(II)PP\ldots py^+ \rightarrow Fe(III)PPpy^+ \quad (3)$$

$$Fe(II)PP\ldots py^+ \rightarrow Fe(II)PP + py^+ \quad (4)$$

$$Fe(II)PP + 2py \rightarrow Fe(II)PP(py)_2 \quad (5)$$

$$py^+ \rightarrow products \quad (6)$$
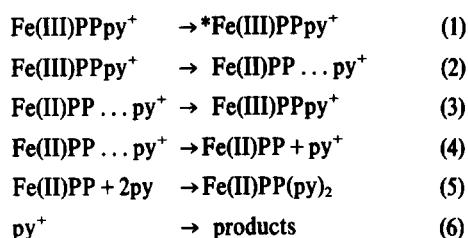
Scheme 2.

In the presence of excess Cl⁻, the equilibria reported in Scheme 1 predominantly favour species I and/or III. The absence of appreciable photoreduction in these conditions clearly indicates that $Fe(III)PPpy^+$ is the only photoreducible species. On these grounds three mechanisms can be proposed for the photoreduction process.

(1) Intermolecular electron transfer from the pyridine solvent to the excited $Fe(III)PPpy^+$ complex.

(2) Intramolecular electron transfer from coordinated pyridine to central Fe(III).

(3) Intramolecular electron transfer from the porphyrin ring to central Fe(III).

Due to the short lifetime of the excited species,[14] bimolecular processes involving excited states are known to be quite unusual and hence mechanism 1 can be ruled out. Mechanism 3 implies that a porphyrin→Fe(III) charge transfer transition is responsible for the photoreduction. However, unless pyridine leads to a drastic change in the excited state energy of the complex it is very likely that a fast deactivation to low-energy $d–d$ states occurs before any photoreduction can occur. Therefore, an electron transfer from the coordinated pyridine to central Fe(III) (Mechanism 2) appears to be the most probable process. On this bases, Scheme 2 summarizes the photoreduction mechanism.

Due to the probable dissociative character of the pyridine→Fe(III) charge transfer excited state, the excitation (eqn 1) is followed by an instantaneous charge separation (eqn 2). The diffusion away of Fe(II)PP and py^+ moieties (eqn 4) occurs in competition with the solvent-cage back electron transfer (eqn 3). The coordination of two pyridine molecules in the axial positions of Fe(II)PP (eqn 5) gives the spectrophotometrically-detected $Fe(II)PP(py)_2$ complex.

The ESR trapping results (Fig. 5) show that radical species are formed as photoredox products. The signal observed, consisting of a triplet of doublets, and the

hyperfine splitting values are consistent with the 2-pyridyl radical[15] trapped by PBN:
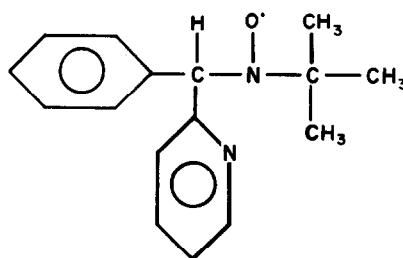
This suggests that the pyridine radical cation formed in the primary photoreduction (eqn 4) gives rise to very fast proton transfer to a pyridine molecule yielding a 2-pyridyl radical (eqn 7).

$$(7)$$
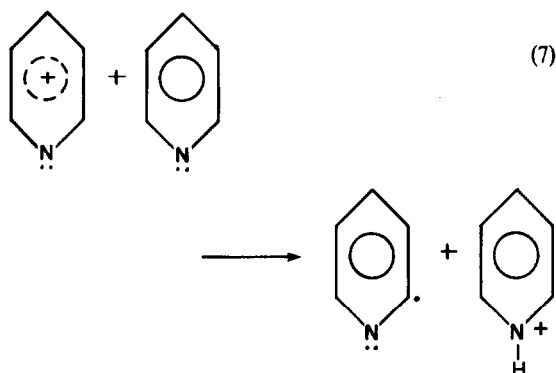
There seems to be a discrepancy between the observed photoinactivity of the Fe(III)PPpyCl complex and the primary photoreduction which occurs through an electron transfer from coordinated pyridine to Fe(III). However, this discrepancy can be justified by taking the electron donor character of the chlorine ligand into consideration. In fact, coordination of Cl⁻ in the axial position *trans* to pyridine increases the central metal electron density, making inner-sphere Fe(III) reduction more difficult in the pyridine chloro complex than in the pyridine complex. As a consequence, the pyridine→Fe(III) CT absorption band is expected to be shifted towards wavelengths lower than those of the irradiating light.

The re-oxidation of $Fe(II)PP(py)_2$, observed when previously-irradiated hemin solutions are kept in an oxygen atmosphere, is very slow in accordance with the known[16] stability of this complex towards oxidation by

5 G
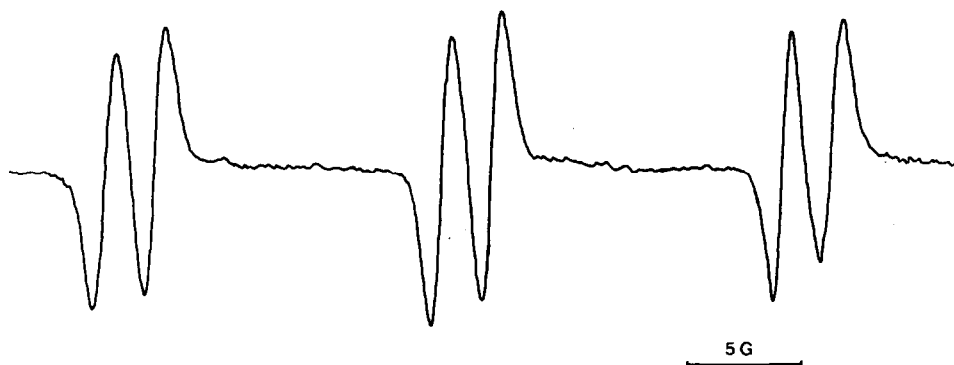
Fig. 5. ESR spectrum obtained at 298 K after 1 hr irradiation with $\lambda > 400$ nm light of Fe(III)PCl in pyridine solution containing 5×10^{-2} M PBN.

oxygen. For this reason, when irradiation is carried out in an oxygen atmosphere the absence of any appreciable photoreduction can be ascribed to fast re-oxidation of intermediate Fe(II)PP before pyridine axial coordination (eqn 5), rather than to oxidation of the final product.

The irradiation wavelength range (see results) within which the photoredox process has been observed, suggests that a charge transfer pyridine → Fe(III) absorption band should be present in this spectral region, although the very intense π–π^* band centered at 400 nm (Soret Band) hides it completely.

These results point to the strong possibility that a mechanism involving an electron transfer from pyridine to Fe(III) is involved in hemin photoreduction in pyridine-containing mixed solvents, although other mechanisms, e.g. alcoholate → Fe(III) electron transfer, may be more likely in these cases.

REFERENCES

[1] C. Bartocci, F. Scandola, A. Ferri and V. Carassiti, *J. Am. Chem. Soc.* 1980, **102**, 7067.

[2] C. Bartocci, F. Scandola, A. Ferri and V. Carassiti, *Inorg. Chim. Acta* 1979, **37**, L473.

[3] C. Bizet, P. Morliere, D. Brault, O. Delgado, M. Bazin and R. Santus, *Photochem. Photobiol.* 1981, **34**, 315.

[4] J. H. Furhop and K. M. Smith, In *Porphyrins and Metalloporphyrins* (Edited by K. M. Smith), p. 809. Elsevier, Amsterdam, 1975.

[5] E. G. Janzen, *Acc. Chem. Res.* 1971, **4**, 31.

[6] C. Bartocci and P. Zanello, work in progress.

[7] J. S. Griffith, *Proc. Roy. Soc.* 1956, **A235**, 23.

[8] T. W. Bentley, J. A. John, R. A. W. Johnstone, P. J. Russel and L. H. Sutcliffe, *J. Chem. Soc. Perkin II* 1973, 1040.

[9] L. M. Epstein, D. K. Straub and C. Maricondi, *Inorg. Chem.* 1967, **6**, 1720.

[10] T. H. Moss, A. J. Bearden and W. S. Caughey, *J. Chem. Phys.* 1969, **51**, 2624.

[11] L. A. Constant and D. G. Davis, *Anal. Chem.* 1975, **47**, 2253.

[12] W. S. Caughey, In *Inorganic Biochemistry* (Edited by G. L. Eichhorn), p. 797. Elsevier, Amsterdam, 1973.

[13] G. N. La Mar and F. A. Walker (Jensen), In *The Porphyrins* (Edited by D. Dolphin), Vol. IV, p. 93. Academic Press, New York, 1979.

[14] F. R. Hopf and D. G. Whitten, Ref. 4, p. 667.

[15] A. Ledwith and P. J. Russel, *J. Chem. Soc. Perkin II* 1974, 582.

[16] W. S. Caughey, Ref. 12, p. 827.

NOTES

Metal template synthesis of chromium(III) complexes

Abstract—Chromium(III) complexes of Schiff bases resulting from the condensation of one mole of diacetyl with two moles of ethylene-diamine or 1,3 diaminopropane has been isolated by metal template reaction. The isolated complexes have been assigned *cis* configurations.

A large number of metal template reactions, particularly for the synthesis of macrocyclic complexes, have been reported. But all these reactions have been carried out in the presence of divalent metal ions like Cu(II), Ni(II), Co(II), Zn(II) and Mn(II).[1-3] A trivalent metal ion due to its higher nuclear charge should be equally efficient in polarising the $\ce{>C=O}$ bond and hence should be efficient for metal template reactions. Unfortunately there are not many reports on the metal template reactions of trivalent metal ions.[4] Hence we attempted the metal template reactions of chromium(III) for the condensation of diacetyl and ethylenediamine or 1,3-diaminopropane and we were able to isolate complexes of the ligands A and B in appreciable yield.

A   **B**
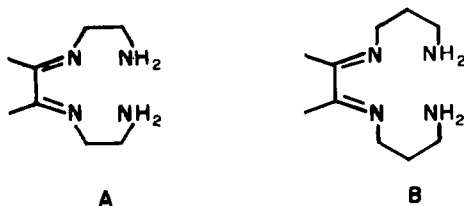
EXPERIMENTAL

Elemental analysis. Carbon and hydrogen was analysed by the courtesy of the microanalyst of the University of Madras. Nitrogen content was evaluated using micro-Kjeldahl technique and chromium was analysed as chromate after oxidising an aqueous solution of the complex with alkaline peroxide.

Conductivity measurements. Conductivity measurements were performed using a Mullard conductivity bridge. Molar conductance were determined at 25°C in acetonitrile solution (10^{-3} M).

Spectral measurements. The electronic spectrum of the aqueous solution of the complexes were measured using a Pye–Unicam SP 1800 spectrophotometer. IR spectra of the complexes were obtained with a Perkin–Elmer 337 model grating spectrophotometer and KBr mull sampling technique.

Preparation of [Cr A(H$_2$O)$_2$](ClO$_4$)$_3$. Chromium(III) acetate hexahydrate (3.4 g) in 50 ml of acetonitrile was refluxed with diacetyl (0.86 g) for 15 min. Then ethylenediamine (1.2 g) was added to the reaction mixture and again refluxed for another 4 hr. Volume of the solution was reduced to 25 ml by rotary evaporation. To this solution NaClO$_4$ (3.4 g) was added, filtered and cooled. The red orange crystals which formed were removed by filtration, washed with cold methanol and ether. Found: C, 17.41; H, 3.81; N, 9.92; Cr, 9.12. Calc. for Cr(C$_8$H$_{22}$N$_4$O$_2$)(ClO$_4$)$_3$: C, 17.25; H, 3.95; N, 10.06; Cr, 9.34%.

Preparation of [Cr B(H$_2$O)$_2$](ClO$_4$)$_3$. This complex was prepared in a similar way as the above one by taking 1,3 diaminopropane in the place of ethylenediamine (1.2 g) was added. Found: C, 20.32; H, 4.49; N, 9.44; Cr, 8.81. Calc. for Cr(C$_{10}$H$_{26}$N$_4$O$_2$)(ClO$_4$)$_3$: C, 20.53; H, 4.45; N, 9.58; Cr, 8.89%.

Preparation of [Cr A(H$_2$O)(NCS)](NCS)$_2$. The diaquo complex

[Cr A(H$_2$O)$_2$](ClO$_4$)$_3$ (1.1 g) was refluxed with KSCN (0.58 g) in 30 ml of acetonitrile for 30 min. The precipitated KClO$_4$ was filtered off. On cooling the solution the desired product was obtained. Found: C, 31.72; H, 4.89; N, 23.52; Cr, 12.48. Calc. for Cr(C$_8$H$_{20}$N$_4$O)(NCS)$_3$: C, 31.88; H, 4.83; N, 23.67; Cr, 12.56%.

Preparation of [Cr B(H$_2$O)(NCS)](NCS)$_2$. It was prepared in a similar way as the above complex by treating the diaquo complex [Cr B(H$_2$O)$_2$](ClO$_4$)$_3$ with KSCN. Found: C, 35.12; H, 5.48; N, 22.03; Cr, 11.62. Calc. for Cr(C$_{10}$H$_{24}$N$_4$O)(NCS)$_3$: C, 35.29; H, 5.42; N, 22.17; Cr, 11.76%.

RESULTS AND DISCUSSION

The elemental analyses show that 2 molecules of diamine have condensed with 1 molecule of diacetyl. Even when the reaction was carried out with the molar ratio of diamine and diketone as 1:1, the same products were obtained, showing that the Schiff's base formed does not react further with another molecule of diketone to form a macrocycle. The charge characteristics of the complexes have been determined by conductivity measurements. Molar conductance of the complexes [Cr A(H$_2$O)$_2$](ClO$_4$)$_3$, [Cr B(H$_2$O$_2$)$_2$](ClO$_4$)$_3$, [Cr A(H$_2$O)(NCS)](NCS)$_2$ and [Cr B(H$_2$O) (NCS)](NCS)$_2$ were found to be 399, 372, 224 and 219 Ω^{-1} cm^2 respectively. It is evident therefore, that in the absence of added thiocyanate, the compounds crystallize as diaquo complexes and in the presence of added thiocyanate as aquothiocyanato complexes.

The electronic spectral data for the complexes are shown in Table 1. All the complexes show two absorption bands in the visible region due to the $^4A_{2g}(F) \rightarrow {}^4T_{2g}(F)$ and $^4A_{2g}(F) \rightarrow {}^4T_{1g}(F)$ transitions. The thiocyanato derivatives show the high energy charge-transfer bands in addition to the d–d transitions. If the complexes were to have *trans* configuration, one would expect splitting of the d–d bands,[5] but in the present case no splitting has been observed. The spectra are typical of *cis* configuration.

The IR spectra of all the complexes show bands in the region of 1630–1600 cm^{-1} (C=N stretch) and no band which could be assigned to carbonyl stretching frequency is observed. All the complexes show strong bands in the region of 3300–3200 cm^{-1} (N—H stretch). The wagging mode of coordinated water shows up in the region 820–790 cm^{-1}. The thiocyanato complexes show an additional band at 2060 cm^{-1} whereas the diaquo complexes have additional bands in the region of 1150–1100 cm^{-1} for perchlorate. Absorptions in the CH$_2$ rocking region (940–860 cm^{-1}) have been used by previous workers for assigning configuration of cobalt and chromium complexes.[6] The complexes isolated show three medium intensity bands in this region, which is typical of the *cis*-configuration. *Trans*-complexes are known to show 4–5 bands in this region.

The fact that ring closure to give a macrocycle does not take place, is again indicative of a *cis*-configuration for the isolated complexes. In a folded *cis*-configuration the macrocycle with four imine linkages will be highly strained. In a planar *trans*-configuration ring closure would have been much easier. The template synthesis of macrocyclic complexes of chromium(III) would also have been possible if the precursor complexes were in a *trans*-configuration.

Table 1. Electronic spectral data

Compound	λ_{max}/nm	ϵ_{max}/M^{-1} cm^{-1}	λ_{max}/nm	ϵ_{max}/M^{-1} cm^{-1}	λ_{max}/nm	ϵ_{max}/M^{-1} cm^{-1}
[Cr A(H$_2$O)$_2$]$^{3+}$	521	56	398	52	–	–
[Cr B(H$_2$O)$_2$]$^{3+}$	519	54	398	51	–	–
[Cr A(H$_2$O)(NCS)]$^{2+}$	511	52	397	72	294	364
[Cr B(H$_2$O)(NCS)]$^{2+}$	509	49	396	76	295	372

BALACHANDRAN UNNI NAIR*†
T. RAMASAMI
D. RAMASWAMY

Central Leather Research Institute
Adyar
Madras 600020
India

*Author to whom correspondence should be addressed.
†Present address: Department of Chemistry, Princeton University, Princeton, NJ 08544, U.S.A.

REFERENCES

[1] N. F. Curtis, *Coord. Chem. Rev.* 1968, **3**, 3.
[2] L. F. Lindoy and D. H. Busch, *Prep. Inorg. Reactions* 1971, **6**, 1.
[3] W. M. Coleman, R. K. Boggess, J. W. Hughes and L. T. Taylor, *Inorg. Chem.* 1981, **20**, 1253.
[4] D. R. Prasad, T. Ramasami, D. Ramaswamy and M. Santappa, *Synth. React. Inorg. Met-Org. Chem.* 1981, **11**, 431.
[5] W. A. Baker, Jr. and M. G. Phillips, *Inorg. Chem.* 1965, **4**, 915.
[6] D. A. House and C. S. Garner, *J. Am. Chem. Soc.* 1966, **88**, 2156.

Hexahalogenotin(IV) complexes in aqueous mixed hydrogen halide solutions in the glassy state

(Received 27 July 1982)

Abstract—The configurations of hexahalogenotin(IV) complex ions in glassy aqueous mixed hydrogen halide solutions were determined by Mössbauer and Raman spectroscopies. *Trans*-(SnF$_4$Cl$_2$)$^{2-}$, (SnCl$_5$Br)$^{2-}$ and *trans*-(SnF$_4$Br$_2$)$^{2-}$ ions are the main tin complex ions in the aqueous Sn(IV)–HF–HCl, Sn(IV)–HCl–HBr and Sn(IV)–HF–HBr solutions in the glassy state, respectively.

INTRODUCTION

It is well known that Sn(IV) ions in aqueous solution containing excess HX (X = F, Cl and Br) exist as hexahalogenotin(IV) complex ions (SnX$_6^{2-}$).[1-3] In considering the differences of the complex formation abilities and sizes of halide ions (F$^-$, Cl$^-$ and Br$^-$), it seemed interesting to investigate what configurations among various mixed-halide tin(IV) complex ions are stabilized in a binary mixture of aqueous HX solutions at low temperatures.

As Mössbauer and Raman spectroscopies are both powerful tools for elucidating a local configuration around a complex ion in the solid, we used both methods in this study to characterize the mixed-halide tin(IV) complex ions in binary hydrogen halide solutions in the glassy state. It is shown that employment of both spectroscopic methods enabled us to determine the configurations of mixed-halide tin(IV) complex ions more easily than the case where only one method would have been employed.

EXPERIMENTAL

Aqueous sample solutions were prepared from anhydrous SnF$_4$, SnCl$_4$ and SnBr$_4$ by dissolving them in aqueous HX solutions and subsequent diluting and mixing resultant aqueous solutions: 3SnF$_4$ · 100HF · 300H$_2$O, 6SnCl$_4$ · 100HCl · 600H$_2$O, 6SnBr$_4$·100HBr·600H$_2$O, and three solutions of the composition 3SnX$_4$·3SnY$_4$·50HX·50HY·600H$_2$O (X and Y denote different halide ions: F$^-$Cl$^-$ and Br$^-$). Glass formation was attained by quenching each solution in liquid nitrogen.

The Mössbauer spectra of the glassy solutions (0.6 cm^3, corresponding to the absorber thickness of 6 mgSn/cm^2) were measured at 77 K against a Ca ^{119m}SnO$_3$ source with a constant acceleration type spectrometer. All isomer shift data are reported with respect to BaSnO$_3$ resonance at room temperature. The Raman spectra were taken with a JASCO R-800 spectrometer using 500–600 mW of the 514.5 nm line of a CR-8 argon-ion laser as an exciting source. The details of the Mössbauer and Raman measurements were essentially the same as those previously reported.[3,4]

RESULTS AND DISCUSSION

The Mössbauer spectra for all the glassy solutions are shown in Fig. 1 together with the obtained Mössbauer parameters (isomer shift: δ and line width: Γ) for each spectrum. The Mössbauer parameters obtained for the monohalide solutions are in good agreement with the reported values[5,6] for the [SnX$_6$]$^{2-}$ complex ions, confirming that Sn(IV) ions exist as [SnX$_6$]$^{2-}$ in these mono-halide solutions in the glassy state. From the results for the mono-halide solutions, it is expected that Sn(IV) ions in the mixed-halide solutions also have the six coordination as the total concentration of halide ions is the same as that in the mono-halide solutions.

As compared with the mono-halide complexes, line broadening was observed in all mixed-halide solutions. There are two possible causes for the observed line broadening: one is due to the result of unresolved quadrupole splitting and the other the existence of several different mixed-halide tin complexes in the mixed-halide solutions. However, the line broadening is almost the same magnitude as that for the mixed-halide complexes of the type [(C$_2$H$_5$)$_4$N]$_2$·[SnX$_4$Y$_2$],[7] indicating that one or two com-

Table 1. Electronic spectral data

Compound	λ_{max}/nm	ϵ_{max}/M^{-1} cm^{-1}	λ_{max}/nm	ϵ_{max}/M^{-1} cm^{-1}	λ_{max}/nm	ϵ_{max}/M^{-1} cm^{-1}
[Cr A(H$_2$O)$_2$]$^{3+}$	521	56	398	52	–	–
[Cr B(H$_2$O)$_2$]$^{3+}$	519	54	398	51	–	–
[Cr A(H$_2$O)(NCS)]$^{2+}$	511	52	397	72	294	364
[Cr B(H$_2$O)(NCS)]$^{2+}$	509	49	396	76	295	372

BALACHANDRAN UNNI NAIR*†
T. RAMASAMI
D. RAMASWAMY

Central Leather Research Institute
Adyar
Madras 600020
India

*Author to whom correspondence should be addressed.
†Present address: Department of Chemistry, Princeton University, Princeton, NJ 08544, U.S.A.

REFERENCES

[1] N. F. Curtis, *Coord. Chem. Rev.* 1968, **3**, 3.
[2] L. F. Lindoy and D. H. Busch, *Prep. Inorg. Reactions* 1971, **6**, 1.
[3] W. M. Coleman, R. K. Boggess, J. W. Hughes and L. T. Taylor, *Inorg. Chem.* 1981, **20**, 1253.
[4] D. R. Prasad, T. Ramasami, D. Ramaswamy and M. Santappa, *Synth. React. Inorg. Met-Org. Chem.* 1981, **11**, 431.
[5] W. A. Baker, Jr. and M. G. Phillips, *Inorg. Chem.* 1965, **4**, 915.
[6] D. A. House and C. S. Garner, *J. Am. Chem. Soc.* 1966, **88**, 2156.

Hexahalogenotin(IV) complexes in aqueous mixed hydrogen halide solutions in the glassy state

(Received 27 July 1982)

Abstract—The configurations of hexahalogenotin(IV) complex ions in glassy aqueous mixed hydrogen halide solutions were determined by Mössbauer and Raman spectroscopies. *Trans*-(SnF$_4$Cl$_2$)$^{2-}$, (SnCl$_5$Br)$^{2-}$ and *trans*-(SnF$_4$Br$_2$)$^{2-}$ ions are the main tin complex ions in the aqueous Sn(IV)–HF–HCl, Sn(IV)–HCl–HBr and Sn(IV)–HF–HBr solutions in the glassy state, respectively.

INTRODUCTION

It is well known that Sn(IV) ions in aqueous solution containing excess HX (X = F, Cl and Br) exist as hexahalogenotin(IV) complex ions (SnX$_6$$^{2-}$).[1–3] In considering the differences of the complex formation abilities and sizes of halide ions (F$^-$, Cl$^-$ and Br$^-$), it seemed interesting to investigate what configurations among various mixed-halide tin(IV) complex ions are stabilized in a binary mixture of aqueous HX solutions at low temperatures.

As Mössbauer and Raman spectroscopies are both powerful tools for elucidating a local configuration around a complex ion in the solid, we used both methods in this study to characterize the mixed-halide tin(IV) complex ions in binary hydrogen halide solutions in the glassy state. It is shown that employment of both spectroscopic methods enabled us to determine the configurations of mixed-halide tin(IV) complex ions more easily than the case where only one method would have been employed.

EXPERIMENTAL

Aqueous sample solutions were prepared from anhydrous SnF$_4$, SnCl$_4$ and SnBr$_4$ by dissolving them in aqueous HX solutions and subsequent diluting and mixing resultant aqueous solutions: 3SnF$_4$ · 100HF · 300H$_2$O, 6SnCl$_4$ · 100HCl · 600H$_2$O, 6SnBr$_4$·100HBr·600H$_2$O, and three solutions of the composition 3SnX$_4$·3SnY$_4$·50HX·50HY·600H$_2$O (X and Y denote different halide ions: F$^-$Cl$^-$ and Br$^-$). Glass formation was attained by quenching each solution in liquid nitrogen.

The Mössbauer spectra of the glassy solutions (0.6 cm^3, corresponding to the absorber thickness of 6 mgSn/cm^2) were measured at 77 K against a Ca ^{119m}SnO$_3$ source with a constant acceleration type spectrometer. All isomer shift data are reported with respect to BaSnO$_3$ resonance at room temperature. The Raman spectra were taken with a JASCO R-800 spectrometer using 500–600 mW of the 514.5 nm line of a CR-8 argon-ion laser as an exciting source. The details of the Mössbauer and Raman measurements were essentially the same as those previously reported.[3,4]

RESULTS AND DISCUSSION

The Mössbauer spectra for all the glassy solutions are shown in Fig. 1 together with the obtained Mössbauer parameters (isomer shift: δ and line width: Γ) for each spectrum. The Mössbauer parameters obtained for the monohalide solutions are in good agreement with the reported values[5,6] for the [SnX$_6$]$^{2-}$ complex ions, confirming that Sn(IV) ions exist as [SnX$_6$]$^{2-}$ in these mono-halide solutions in the glassy state. From the results for the mono-halide solutions, it is expected that Sn(IV) ions in the mixed-halide solutions also have the six coordination as the total concentration of halide ions is the same as that in the mono-halide solutions.

As compared with the mono-halide complexes, line broadening was observed in all mixed-halide solutions. There are two possible causes for the observed line broadening: one is due to the result of unresolved quadrupole splitting and the other the existence of several different mixed-halide tin complexes in the mixed-halide solutions. However, the line broadening is almost the same magnitude as that for the mixed-halide complexes of the type [(C$_2$H$_5$)$_4$N]$_2$·[SnX$_4$Y$_2$],[7] indicating that one or two com-

Fig. 1. Mössbauer spectra of the Sn(IV)–HX or Sn(IV)–HX–HY solutions in the glassy state. The unit for both isomer shift (δ) and line width (Γ) is in mm/s.

plexes predominate in the mixed-halide solutions in the glassy state. We conclude, therefore, that the line broadening in the mixed-halide solution is mainly the result of unresolved quadrupole splitting.

It is difficult to determine what type of the $[SnX_pY_q]^{2-}$ ion $(p+q=6)$ is stabilized in the glassy mixed-halide solution only from the Mössbauer parameters. In these solutions, the equilibrium reactions among various tin(IV) complex ions must be displaced to one side in the glassy state, resulting in the trapping of most stable tin complex ions.

It is well established[6,7] that there is a linear relation between isomer shift and the average electronegativity of the halides in the coordination sphere of the tin atom for the complexes of the types $(SnX_6)^{2-}$ and $(SnX_4Y_2)^{2-}$ ions. Our results for the $(SnF_6)^{2-}$, $(SnCl_6)^{2-}$ and $(SnBr_6)^{2-}$ ions, shown in Fig. 2, also fall on a straight line with a slope of -0.40, which is very close to the value of -0.41 for the complexes of the $(SnX_6)^{2-}$ ions $(X = F, Cl, Br$ and $I)$ reported by Clausen and Good.[7] Assuming that the isomer shifts of these mixed-halide solutions are also on the same straight line, we can get the possible halide configurations for the stabilized tin complex ions: $[SnF_3Cl_3]^{2-}$ and $[SnF_4Cl_2]^{2-}$ ions for the Sn(IV)–HF–HCl solution, $[SnF_3Br_3]^{2-}$ and $[SnF_4Br_2]^{2-}$ ions for the Sn(IV)–HF–HBr solution, and $[SnCl_3Br_3]^{2-}$, $[SnCl_4Br_2]^{2-}$ and $[SnCl_5Br]^{2-}$ ions for the Sn(IV)–HCl–HBr solution. We cannot at the moment preclude the possibility that two or more tin complex ions are equally stabilized at low temperatures. However, as noted before, the line width broadening validates to a first approximation the assumption that a single tin complex species predominates in the mixed-halide solutions in the glassy state.

From Raman spectra shown in Fig. 3, we can immediately confirm that $[SnX_6]^{2-}$ ion is the predominant tin complex ions in the mono-halide solutions. In the glassy Sn(IV)–HCl–HBr solution, the Sn–Cl stretching Raman band is observed at 310 cm^{-1}, only a few wavenumbers away from the value (314 cm^{-1}) for the $[SnCl_6]^{2-}$ ions, while the Sn–Br stretching band at 204 cm^{-1} is distant from the value (186 cm^{-1}) for the $[SnBr_6]^{2-}$ ions. This suggests that the number of chloride ions coordinating to a Sn(IV) ion is close to six. Therefore, we conclude that $[SnCl_5Br]^{2-}$ ions are the predominant species in the glassy Sn(IV)–HCl–HBr solution. This conclusion is supported by the observation that there are four polarized Raman bands because the MX$_5$Y configuration (M is a central atom) is expected to give four polarized Raman bands.[8] The δ value ($+0.57$ mm/s) is a
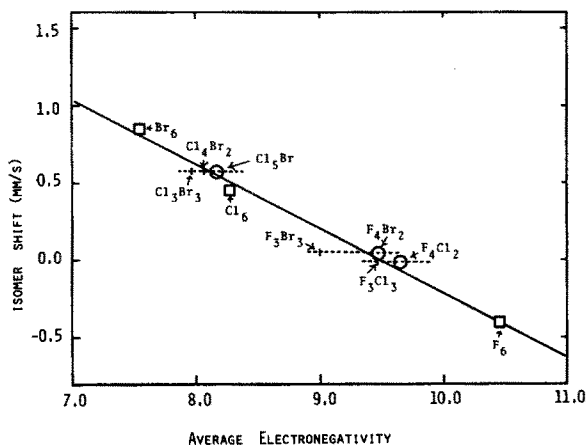
Fig. 2. Relation between isomer shift and the average electronegativity. $[SnF_3Br_3]^{2-}$ is represented by F_3Br_3 in the figure. The straight line is based on the data of the SnX_6^{2-} ions ($\square$). The open circle ($\bigcirc$) indicates the most probable configuration stabilized in each mixed halide solution.

little smaller than that ($+0.67$ mm/s) for the $[SnCl_4Br_2]^{2-}$ ions[7] is also consistent with our conclusion. The half-band width for the Sn–Cl stretching Raman band is almost the same as that for the $[SnCl_6]^{2-}$ ions, indicating that a single tin complex ion, i.e. $[SnCl_5Br]^{2-}$, predominates in the glassy solution.

The Raman spectra for the glassy Sn(IV)–HF–HCl and Sn(IV)–HF–HBr solutions are shown in Fig. 4. In these solutions, there are only two (one is a Sn–F stretching and the other a Sn–Cl or Sn–Br stretching Raman band) polarized Raman bands ascribable to the tin complex ions. Accordingly among the possible configurations expected from the Mössbauer data, we consider that trans-$[SnF_4Cl_2]^{2-}$ and trans-$[SnF_4Br_2]^{2-}$ ions are the dominant tin complex ions in these solutions, respectively. In the case of the latter solution, the Sn–Br stretching band at 225 cm^{-1} is a little diffuse toward a lower frequency region, suggesting that there exist a small amount of other complex ions such as $[SnF_3Br_3]^{2-}$ ions.

Fig. 3. Raman spectra of the Sn(IV)-(HCl, Sn(IV)-HBr and Sn(IV)-HCl-HBr solutions in the glassy state.

Fig. 4. Raman spectra of the Sn(IV)-HF-HCl and Sn(IV)-HF- HBr solutions in the glassy state.

REFERENCES

[1] S. L. Ruby, P. K. Tseng, H. Cheng and N. C. Li, *Chem. Phys. Lett.* 1968, **2**, 39.
[2] F. A. Cotton and G. Wilkinson, *Advances Inorganic Chemistry*, Chap. 11. Interscience, London (1973).
[3] M. Takeda, H. Kanno and T. Tominaga, *J. de Phys.* 1979, **40**, 345.

[4] H. Kanno and J. Hiraishi, *Chem. Phys. Lett.* 1979, **68**, 46.
[5] N. N. Greenwood and J. N. R. Ruddick, *J. Chem. Soc. A*, 1967, 1679.
[6] R. H. Herber and H. S. Cheng, *Inorg. Chem.* 1969, **8**, 2145.
[7] C. A. Clausen and M. L. Good, *Inorg. Chem.* 1970, **9**, 817.
[8] K. Nakamoto, *Infrared and Raman Spectra of Inorganic and Coordination Compounds*, 3rd Edn, Chap. 1. Wiley, New York (1978).

M. KATADA
H. KANNO*
H. SANO

Department of Chemistry
Faculty of Science
Tokyo Metropolitan University
Fukasawa, Setagaya
Tokyo 158, Japan

*Author to whom correspondence should be addressed at Department of Chemistry, Meisei University, Hodokubo, Hino, Tokyo 191, Japan.

Complexes of bivalent cations with a hydroxamic acid from maize extracts

(*Received* 11 *August* 1982)

Cyclic hydroxamic acids may constitute up to 2% of the dry weight of Gramineae such as wheat, maize and rye.[1] The chelating properties of hydroxamic acids[2] suggest that those present in Gramineae may play a role in the plant mineral nitrition.[3] We report here the stability constants of complexes between bivalent cations and 2,4-dihydroxy-7-methoxy-1,4-benzoxazin-3-one

Fig. 3. Raman spectra of the Sn(IV)-(HCl, Sn(IV)-HBr and Sn(IV)-HCl-HBr solutions in the glassy state.

Fig. 4. Raman spectra of the Sn(IV)-HF-HCl and Sn(IV)-HF- HBr solutions in the glassy state.

REFERENCES

[1] S. L. Ruby, P. K. Tseng, H. Cheng and N. C. Li, *Chem. Phys. Lett.* 1968, **2**, 39.
[2] F. A. Cotton and G. Wilkinson, *Advances Inorganic Chemistry*, Chap. 11. Interscience, London (1973).
[3] M. Takeda, H. Kanno and T. Tominaga, *J. de Phys.* 1979, **40**, 345.

[4] H. Kanno and J. Hiraishi, *Chem. Phys. Lett.* 1979, **68**, 46.
[5] N. N. Greenwood and J. N. R. Ruddick, *J. Chem. Soc. A*, 1967, 1679.
[6] R. H. Herber and H. S. Cheng, *Inorg. Chem.* 1969, **8**, 2145.
[7] C. A. Clausen and M. L. Good, *Inorg. Chem.* 1970, **9**, 817.
[8] K. Nakamoto, *Infrared and Raman Spectra of Inorganic and Coordination Compounds*, 3rd Edn, Chap. 1. Wiley, New York (1978).

M. KATADA
H. KANNO*
H. SANO

*Department of Chemistry
Faculty of Science
Tokyo Metropolitan University
Fukasawa, Setagaya
Tokyo 158, Japan*

*Author to whom correspondence should be addressed at Department of Chemistry, Meisei University, Hodokubo, Hino, Tokyo 191, Japan.

Complexes of bivalent cations with a hydroxamic acid from maize extracts

Cyclic hydroxamic acids may constitute up to 2% of the dry weight of Gramineae such as wheat, maize and rye.[1] The chelating properties of hydroxamic acids[2] suggest that those present in Gramineae may play a role in the plant mineral nitrition.[3] We report here the stability constants of complexes between bivalent cations and 2,4-dihydroxy-7-methoxy-1,4-benzoxazin-3-one

(DIMBOA), the main hydroxamic acid isolated from maize extracts.[4]

EXPERIMENTAL

Stability constants of the complexes were determined by potentiometric titration of a 3.4 mM solution of the cation (as chloride) in 0.66 mM $HClO_4$ with a 10 mM solution of the anion of DIMBOA (pH 8.5), under constant ionic strength (0.1 M with $NaClO_4$). Titrations were carried out at $3 \pm 0.5°$. Under these conditions the decomposition of DIMBOA[5] was negligible (half-life = 32.7 hr) compared with the time needed for titration (20 min). The pK_a of DIMBOA at this temperature and ionic strength was 6.96. The data obtained was analyzed by the method of Bjerrum.[6] Distribution diagrams were calculated with a modified version of the program COMICS.[7]

RESULTS AND DISCUSSION

The formation curves (Fig. 1) allow the estimation of the logarithms of the stability constants of the 1 : 1 complexes of Cu (5.4), Ni (4.5), Zn (4.2), Mn (3.4) and Ca (3.0) and of the 2 : 1 complexes of Ni (3.6) and Zn (3.5). The low stability of the Mg complex and the insolubility of the Fe complex precluded the estimation of their stability constants. A precipitate appeared during the titration of the Cu when an $\bar{n}$ value of 0.5 was reached.
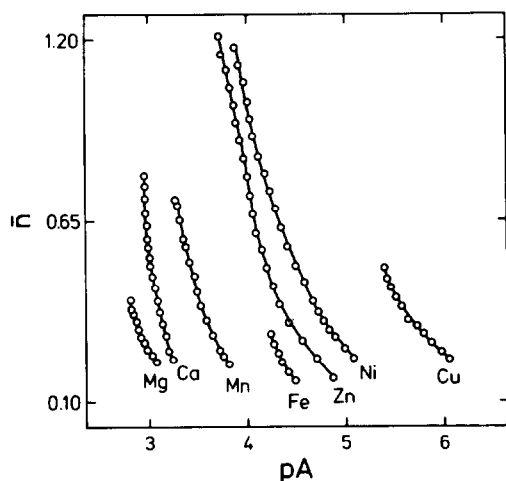
Fig. 1. Formation curves for complexes between DIMBOA and bivalent cations. pA = − log [DIMBOA].

*Author to whom correspondence should be addressed.

The formation constant of the 1 : 1 complex between DIMBOA and Cu has been determined by the method of Irving–Rosotti at 10, 20 and 30°.[8] Extrapolation of these data to 3° gives a value of log $K_1 = 5.7$, comparable to that reported in this paper. The formation constants of the 1 : 1 complexes follow the Irving–Williams order, i.e. Mn(Ni(Cu)Zn, as shown for other ligands.[9] The complexes of DIMBOA were less stable than those of hydroxamic acids of the type Ar–NOH–CO–Ar,[10] probably a reflection of the greater pK_a values of these latter acids.

The distribution of species in a solution containing DIMBOA, citric acid and malic acid, and Cu(II), Zn(II), Ca(II), Mn(II) and Fe(III) cations was calculated at pH 5.5, the pH of the plant extract. Citric and malic acids are two of the most abundant complexing agents found in maize exudates. The concentrations used in the calculations were those determined in whole plants.[4,11,12] Formation constants were obtained from the literature.[3,13] Under these conditions, 57% of the DIMBOA remained uncomplexed, while the complexes CaL, FeL₂ + FeL₃, CuL, ZnL + ZnL₂ and MnL with L = DIMBOA anion were 35, 7, 0.1, 0.5 and 0.3% of the total DIMBOA, respectively. In all cases, these complexes accounted for a substantial proportion of the total cation (Table 1). More of each cation was complexed by DIMBOA than by citric and malic acids together. Thus, it is possible that DIMBOA and other related hydroxamic acids in Gramineae may participate in the plant mineral nutrition as chelating agents. To further establish the participation of hydroxamic acids in mineral nutrition it would be necessary to determine their concentration as well as that of organic acids, cations and hydrogen ions in the different plant compartments at the tissular and cellular levels.

REBECA G. DABED
MARIA INES TORAL
LUIS J. CORCUERA
HERMANN M. NIEMEYER*

Facultad de Ciencias Básicas y Farmacéuticas
Universidad de Chile
Casilla 653
Santiago, Chile

REFERENCES

[1] J. I. Willard and D. Penner, *Residue Rev.* 1976, **64**, 67.
[2] B. Chatterjee, *Coord. Chem. Rev.* 1978, **26**, 281.
[3] C. L. Tipton and E. L. Buell, *Phytochemistry* 1970, **9**, 1215.

Table 1. Complexation of cations by DIMBOA, citric acid and malic acid at pH 5.5

Cation	% of total metal complexed by			% of free ion
	DIMBOA	Citric acid	Malic acid	
Fe(III)	74.6	25.3	0.1	0.0
Zn(II)	70.3	4.2	2.8	22.7
Cu(II)	55.1	37.6	5.7	1.6
Mn(II)	22.8	0.8	10.1	66.3
Ca(II)	11.8	0.6	1.1	86.5

Concentrations used (mM): DIMBOA (7), citric acid (1.9), malic acid (1.3), Fe (0.21), Zn (0.04), Cu (0.02), Mn (0.075) and Ca (21).

[4]M. D. Woodward, L. J. Corcuera, J. P. Helgeson, A. Kelman and C. D. Upper, *Plant Physiol.* 1979, **63**, 14.

[5]H. M. Niemeyer, H. R. Bravo, G. F. Peña and L. J. Corcuera in: *Biology and Chemistry of Hydroxamic Acids* (Edited by H. Kehl), pp. 22–28. Karger, New York (1982).

[6]R. J. Angelici, *Synthesis and Technique in Inorganic Chemistry*, pp. 105–116. W. B. Saunders, Philadelphia (1969).

[7]D. Perrin and I. Sayce, *Talanta* 1967, **14**, 833.

[8]V. Hiriart, L. Corcuera, I. Crivelli and C. Andrade, *XIII Congreso Latinoamericano de Química*, pp. 87–88. Lima, Perú (1978).

[9]R. J. Angelici and G. L. Eichhorn, (Editors). *Inorganic Bio-chemistry*, pp. 63–101. Elsevier, Amsterdam (1973).

[10]Y. K. Agrawal and V. P. Khare, *J. Inorg. Nucl. Chem.* 1976, **38**, 1663.

[11]R. B. Clark, *Crop Sci.* 1968, **8**, 165.

[12]R. B. Clark, *Crop Sci.* 1969, **9**, 341.

[13]L. E. Sillén and A. E. Martell, *Stability Constants of Metal-ion Complexes*, 2nd edn., Special Publication No. 17, The Chemical Society, London (1964); L. E. Sillén and A. E. Martell, *Stability Constants of Metal-Ion Complexes*, Special Publication No. 25, The Chemical Society, London (1971); A. E. Martell and R. M. Smith, *Critical Stability Constants*. Plenum Press, New York (1977).

Isolation of dithiocarbamate anions as salts of biscyclopentadienyl titanium(IV) chelates

Abstract—A series of $[Cp_2TiL]^+[RR'NCS_2]^-$ complexes, where L is the conjugate base of acetylacetone, benzoylacetone or 8-hydroxyquinoline and $R = CH_3$, $R' = C_6H_5CH_2$; $R = C_2H_5$, $R' = C_6H_4CH_3$; $R = H$, $R' = C_5H_9$; $RR' = C_6H_{12}$, have been synthesised in aqueous medium by the reaction of $[Cp_2TiL]^+Cl^-$ with $RR'NCS_2^-Na^+$. Conductivity measurements in nitrobenzene solution indicate that these complexes are electrolytes. Both the IR and NMR studies demonstrate that the ligand L is chelating in all these complexes. Consequently, tetrahedral coordination about the titanium atom is proposed. In addition to these studies, elemental analyses and magnetic susceptibility have been carried out for these complexes.

INTRODUCTION

During the course of our recent investigations,[1-3] we elucidated that coordination of four oxygen or two oxygen and two nitrogen atoms by strong covalent bonds to the $RR'M^{2+}(IV)$ moiety ($R = R' = C_5H_5$; $R = C_5H_5$, $R' = C_4H_4N$; $R = C_5H_5$, $R' = C_9H_7$ and $M = Ti$ or Zr) would lead to weakening of the metal-ring bonds. In this communication we report an extension of these studies to the dithiocarbamate derivatives of biscyclopentadienyl titanium(IV) chelates, with the aim that behaviour of free dithiocarbamate anion would provide additional information on the nature of bonding. A number of complexes of the type $[Cp_2TiL]^+[RR'NCS_2]^-$, where L is the conjugate base of acetylacetone, benzoylacetone or 8-hydroxyquinoline and $R = CH_3$, $R' = C_6H_5CH_2$; $R = C_2H_5$, $R' = C_6H_4CH_3$; $R = H$, $R' = C_5H_9$; $RR' = C_6H_{12}$ have been synthesised. These compounds possess a low solvation energy, as evident from the ease of their preparation.

EXPERIMENTAL

Reagents and general techniques

All the chemicals and reagents used were of analytical grade. Biscyclopentadienyl titanium(IV) dichloride was obtained from Fluka AG Switzerland and used as such without further purification. Nitrobenzene for conductance measurements was purified by the method described by Fay *et al.*[4] Sodium dithiocarbamates were prepared by the method of Gilman and Blatt.[5]

Microanalyses of carbon and hydrogen contents were carried out in our Departmental Microanalytical laboratory. Titanium, nitrogen and sulphur were estimated by the standard methods as described by Vogel.[6]

Conductance measurements were made in nitrobenzene at $30.00 \pm 0.05°C$ using an Elico Conductivity Bridge Model CM82. Solid state IR spectra were recorded in "KBr pellets" in the region $4000-200 \text{ cm}^{-1}$ with a Perkin–Elmer 621 grating spectrophotometer. Magnetic measurements were carried out by Gouy's method using mercury tetrathiocyanatocobaltate(II) as calibrant. Proton NMR spectra were recorded in $CDCl_3$ on a Perkin–Elmer R-32 spectrophotometer at a sweep width of 900 Hz. The magnetic field was calibrated with a standard sample of $CHCl_3$ and TMS (1% by volume).

Preparation of complexes

An aqueous solution of $[Cp_2TiL]^+Cl^-$ where L is the conjugate base of acetylacetone, benzoylacetone or 8-hydroxyquinoline was obtained by stirring an aqueous solution of Cp_2TiCl_2 with slight excess of acetylacetone, benzoylacetone or 8-hydroxyquinoline for 2 hr. Any resulting precipitate was removed by filtration. The filtrate was then added slowly with shaking, to a concentrated hot aqueous solution of appropriate sodium dithiocarbamate. The precipitate so obtained was digested on water bath at 60–70° for 1 hr. It was then filtered, washed with hot water, diethyl ether (40–60°) and finally dried under vacuum. In order to remove any acetylacetone impurity, the precipitates were dissolved in dichloromethane and reprecipitated by adding petroleum ether (60–80°).

RESULTS AND DISCUSSION

Table 1 lists the analytical data and physical characteristics of the complexes. The complexes are quite stable in the solid state and in solution. They are moderately soluble in dichloromethane, chloroform, carbon tetrachloride and nitrobenzene. All the complexes are thermally stable but decompose slowly at higher temperatures without melting. Conductivity measurements reveal that the chelates are 1:1 electrolytes in nitrobenzene. Magnetic susceptibility values at room temperature indicate that all these complexes are diamagnetic in nature.

The assignments of IR bands have been made on the basis of published work. The IR spectra of the compounds show usual peaks for C_5H_5 group,[7] *viz.*, the C–H stretching frequency at $\sim 3000 \text{ cm}^{-1}$, the perpendicular hydrogen wagging mode at $\sim 860 \text{ cm}^{-1}$, the parallel hydrogen wagging vibration at $\sim 1030 \text{ cm}^{-1}$. The band owing to C–C stretching mode and ring breathing mode of π-bond occur at ~ 1430 and $\sim 1170 \text{ cm}^{-1}$ respectively. Apart from this, an additional band near 440 cm^{-1} can be assigned to $Ti-C_5H_5$ vibrations.[8]

[4]M. D. Woodward, L. J. Corcuera, J. P. Helgeson, A. Kelman and C. D. Upper, *Plant Physiol.* 1979, **63**, 14.

[5]H. M. Niemeyer, H. R. Bravo, G. F. Peña and L. J. Corcuera in: *Biology and Chemistry of Hydroxamic Acids* (Edited by H. Kehl), pp. 22–28. Karger, New York (1982).

[6]R. J. Angelici, *Synthesis and Technique in Inorganic Chemistry*, pp. 105–116. W. B. Saunders, Philadelphia (1969).

[7]D. Perrin and I. Sayce, *Talanta* 1967, **14**, 833.

[8]V. Hiriart, L. Corcuera, I. Crivelli and C. Andrade, *XIII Congreso Latinoamericano de Química*, pp. 87–88. Lima, Perú (1978).

[9]R. J. Angelici and G. L. Eichhorn, (Editors). *Inorganic Bio-chemistry*, pp. 63–101. Elsevier, Amsterdam (1973).

[10]Y. K. Agrawal and V. P. Khare, *J. Inorg. Nucl. Chem.* 1976, **38**, 1663.

[11]R. B. Clark, *Crop Sci.* 1968, **8**, 165.

[12]R. B. Clark, *Crop Sci.* 1969, **9**, 341.

[13]L. E. Sillén and A. E. Martell, *Stability Constants of Metal-ion Complexes*, 2nd edn., Special Publication No. 17, The Chemical Society, London (1964); L. E. Sillén and A. E. Martell, *Stability Constants of Metal–Ion Complexes*, Special Publication No. 25, The Chemical Society, London (1971); A. E. Martell and R. M. Smith, *Critical Stability Constants*. Plenum Press, New York (1977).

Isolation of dithiocarbamate anions as salts of biscyclopentadienyl titanium(IV) chelates

Abstract—A series of $[Cp_2TiL]^+[RR'NCS_2]^-$ complexes, where L is the conjugate base of acetylacetone, benzoyl-acetone or 8-hydroxyquinoline and $R = CH_3$, $R' = C_6H_5CH_2$; $R = C_2H_5$, $R' = C_6H_4CH_3$; $R = H$, $R' = C_5H_9$; $RR' = C_6H_{12}$, have been synthesised in aqueous medium by the reaction of $[Cp_2TiL]^+Cl^-$ with $RR'NCS_2^-Na^+$. Conductivity measurements in nitrobenzene solution indicate that these complexes are electrolytes. Both the IR and NMR studies demonstrate that the ligand L is chelating in all these complexes. Consequently, tetrahedral coordination about the titanium atom is proposed. In addition to these studies, elemental analyses and magnetic susceptibility have been carried out for these complexes.

INTRODUCTION

During the course of our recent investigations,[1–3] we elucidated that coordination of four oxygen or two oxygen and two nitrogen atoms by strong covalent bonds to the $RR'M^{2+}(IV)$ moiety ($R = R' = C_5H_5$; $R = C_5H_5$, $R' = C_4H_4N$; $R = C_5H_5$, $R' = C_9H_7$ and $M = Ti$ or Zr) would lead to weakening of the metal-ring bonds. In this communication we report an extension of these studies to the dithiocarbamate derivatives of biscyclopentadienyl titanium(IV) chelates, with the aim that behaviour of free dithiocarbamate anion would provide additional information on the nature of bonding. A number of complexes of the type $[Cp_2TiL]^+[RR'NCS_2]^-$, where L is the conjugate base of acetyl-acetone, benzoylacetone or 8-hydroxyquinoline and $R = CH_3$, $R' = C_6H_5CH_2$; $R = C_2H_5$, $R' = C_6H_4CH_3$; $R = H$, $R' = C_5H_9$; $RR' = C_6H_{12}$ have been synthesised. These compounds possess a low solvation energy, as evident from the ease of their preparation.

EXPERIMENTAL

Reagents and general techniques

All the chemicals and reagents used were of analytical grade. Biscyclopentadienyl titanium(IV) dichloride was obtained from Fluka AG Switzerland and used as such without further purification. Nitrobenzene for conductance measurements was purified by the method described by Fay *et al.*[4] Sodium dithio-carbamates were prepared by the method of Gilman and Blatt.[5]

Microanalyses of carbon and hydrogen contents were carried out in our Departmental Microanalytical laboratory. Titanium, nitrogen and sulphur were estimated by the standard methods as described by Vogel.[6]

Conductance measurements were made in nitrobenzene at $30.00 \pm 0.05°C$ using an Elico Conductivity Bridge Model CM82. Solid state IR spectra were recorded in "KBr pellets" in the region $4000-200 \, cm^{-1}$ with a Perkin-Elmer 621 grating spec-trophotometer. Magnetic measurements were carried out by Gouy's method using mercury tetrathiocyanatocobaltate(II) as calibrant. Proton NMR spectra were recorded in $CDCl_3$ on a Perkin-Elmer R-32 spectrophotometer at a sweep width of 900 Hz. The magnetic field was calibrated with a standard sample of $CHCl_3$ and TMS (1% by volume).

Preparation of complexes

An aqueous solution of $[Cp_2TiL]^+Cl^-$ where L is the conjugate base of acetylacetone, benzoylacetone or 8-hydroxyquinoline was obtained by stirring an aqueous solution of Cp_2TiCl_2 with slight excess of acetylacetone, benzoylacetone or 8-hydroxyquinoline for 2 hr. Any resulting precipitate was removed by filtration. The filtrate was then added slowly with shaking, to a concentrated hot aqueous solution of appropriate sodium dithio-carbamate. The precipitate so obtained was digested on water bath at $60-70°$ for 1 hr. It was then filtered, washed with hot water, diethyl ether $(40-60°)$ and finally dried under vacuum. In order to remove any acetylacetone impurity, the precipitates were dissolved in dichloromethane and reprecipitated by adding petroleum ether $(60-80°)$.

RESULTS AND DISCUSSION

Table 1 lists the analytical data and physical characteristics of the complexes. The complexes are quite stable in the solid state and in solution. They are moderately soluble in dichloromethane, chloroform, carbon tetrachloride and nitrobenzene. All the complexes are thermally stable but decompose slowly at higher temperatures without melting. Conductivity measurements reveal that the chelates are 1:1 electrolytes in nitrobenzene. Magnetic susceptibility values at room temperature indicate that all these complexes are diamagnetic in nature.

The assignments of IR bands have been made on the basis of published work. The IR spectra of the compounds show usual peaks for C_5H_5 group,[7] viz., the C–H stretching frequency at $\sim 3000 \, cm^{-1}$, the perpendicular hydrogen wagging mode at $\sim 860 \, cm^{-1}$, the parallel hydrogen wagging vibration at $\sim 1030 \, cm^{-1}$. The band owing to C–C stretching mode and ring breathing mode of π-bond occur at ~ 1430 and $\sim 1170 \, cm^{-1}$ respectively. Apart from this, an additional band near $440 \, cm^{-1}$ can be assigned to $Ti–C_5H_5$ vibrations.[8]

Table 1. Analytical data and physical characteristics

Compound	Yield (%)	Colour	Decomp. Temp. (°C)	% Found (Calc.)				
				C	H	Ti	S	N
1	2	3	4	5	6	7	8	9
$[Cp_2Tiacac]^+[RR'NCS_2]^-$ a	72	Light green	142	60.63 (60.88)	5.76 (5.70)	10.08 (10.14)	13.66 (13.53)	3.04 (2.95)
$[Cp_2Tiacac]^+[RR'NCS_2]^-$ b	69	Green	160	61.72 (61.60)	5.87 (5.95)	9.93 (9.85)	13.22 (13.14)	2.96 (2.87)
$[Cp_2Tiacac]^+[RR'NCS_2]^-$ c	66	Dark green	167	57.69 (57.66)	6.30 (6.17)	10.78 (10.98)	14.83 (14.64)	3.31 (3.20)
$[Cp_2Tiacac]^+[RR'NCS_2]^-$ d	70	Dark green	132	58.61 (58.53)	6.52 (6.43)	10.50 (10.64)	14.08 (14.19)	3.01 (3.10)
$[Cp_2Tibzac]^+[RR'NCS_2]^-$ a	71	Yellowish green	146	65.17 (65.04)	5.56 (5.42)	8.83 (8.97)	11.78 (11.96)	2.68 (2.61)
$[Cp_2Tibzac]^+[RR'NCS_2]^-$ b	74	Light yellow	162	65.45 (65.87)	5.60 (5.64)	8.86 (8.74)	11.68 (11.65)	2.75 (2.55)
$[Cp_2Tibzac]^+[RR'NCS_2]^-$ c	62	Dark yellow	165	62.71 (62.52)	5.73 (5.81)	9.69 (9.61)	12.89 (12.82)	2.92 (2.80)
$[Cp_2Tibzac]^+[RR'NCS_2]^-$ d	68	Dark green	142–144	63.26 (63.15)	6.00 (6.04)	9.40 (9.35)	12.51 (12.47)	2.77 (2.72)
$[Cp_2Tiox]^+[RR'NCS_2]^-$ a	59	Light green	175	64.98 (64.86)	4.87 (5.01)	9.36 (9.26)	12.32 (12.35)	5.48 (5.40)
$[Cp_2Tiox]^+[RR'NCS_2]^-$ b	55	Yellow	190	65.62 (65.41)	5.32 (5.26)	9.14 (9.02)	11.94 (12.03)	5.32 (5.26)
$[Cp_2Tiox]^+[RR'NCS_2]^-$ c	63	Orange	196	62.16 (62.24)	5.28 (5.39)	9.83 (9.95)	13.18 (13.27)	5.96 (5.80)
$[Cp_2Tiox]^+[RR'NCS_2]^-$ d	60	Yellowish	203	63.08 (62.90)	5.52 (5.64)	9.76 (9.67)	12.84 (12.90)	5.71 (5.64)

a where R = CH_3, R' = $C_6H_5CH_2$; b where R = C_2H_5, R' = $C_6H_4CH_3$; c where R = H, R' = C_5H_9 and d where RR' = C_6H_{12}

The bands occurring around $1560 \, cm^{-1}$, $1520 \, cm^{-1}$ and $475 \, cm^{-1}$ in the $[Cp_2Tiacac]^+[RR'NCS_2]^-$ and $[Cp_2Tibzac]^-[RR'NCS_2]^-$ complexes may be assigned to $\nu(C \cdots O)$, $\nu(C \cdots C)$ and $\nu(Ti-O)$ vibrations.[9] Further, the phenyl group of benzoylacetonato group is indicated by additional peaks at $\sim 1640 \, cm^{-1}$ (C–C stretching), $\sim 1340 \, cm^{-1}$ (C–H stretching), $\sim 760 \, cm^{-1}$ (C–H out of plane bending) and $\sim 700 \, cm^{-1}$ (methylene rocking vibration).[10]

The IR spectra of $[Cp_2Tiox]^+[RR'NCS_2]^-$ complexes show an intense absorption at $\sim 1340 \, cm^{-1}$ due to the vibration of the $C \cdots N$ bond in the 8-hydroxyquinolinato group. The free 8-hydroxyquinoline shows this absorption in the $1450–1500 \, cm^{-1}$ range. This indicates considerably less double bond character of the (C–N) bond in the 8-hydroxyquinolinate group. It may be assumed that the lone pair on nitrogen is involved in the formation of a coordinate bond with the titanium(IV) ion, thus reducing double bond formation of the $C \cdots N$ bond as compared to free 8-hydroxyquinoline and indicating that the 8-hydroxyquinolinato group is chelating in all the 8-hydroxyquinoline complexes.[41] Apart from this, the bands occurring around 750, 1100, 530 and $505 \, cm^{-1}$ may be assigned to in plane ring deformation, C–O stretching, $\nu(M-O)$ and $\nu(C-O)$ in plane bending frequencies.[12,13]

The ^1H NMR spectra of these complexes have been recorded in deuterated chloroform. The resonance signal due to cyclopentadienyl groups were observed as a singlet near δ 6.60 ppm. The existence of a single sharp C_5H_5 resonance is attributed to rapid rotation of the ring about the metal ring axis.

The γ-protons (–CH=) resonance of the acetylacetonato and benzoylacetonato group in the chelates occur at a lower field (δ 6.1–6.0 ppm). This is probably due to at least, in part to the net positive charge on the complex ion. The δ values of methyl protons (δ 2.5 ppm) in acetylacetonato and benzoylacetonato moiety in the complexes is also lower than the values reported for other acetylacetonato and benzoylacetonato complexes. It may also be due to the cationic charge on the complex ion.[14] The

^1H NMR spectra of 8-hydroxyquinolinato chelates show that the protons at C_2 absorb at a lower field (δ 9.05, q, J = 4.0 Hz, 1.8 Hz) than observed for free 8-hydroxyquinoline (δ 8.78). This supports the conclusion that 8-hydroxyquinolinato ligand is chelating.

The resonance signals of different alkyl, cyclopentyl and hexamethylene groups in the dithiocarbamate moiety occur at almost the same frequency as for the free dithiocarbamate ligand. The intensities of all the resonance lines were determined by planimetric integration. The integrated proton ratios correspond to the formula assigned for these complexes.

Both the IR and ^1H NMR studies carried out for the present complexes indicate that ligand L is chelating and Cp_2Ti^{2+} moiety possess a wedge like sandwich structure with essentially tetrahedral coordination about the metal atom similar to that of dichlorides.[15] Typical vibrational frequencies assigned to the dithiocarbamate moiety in all the chelates fully support the view that dithiocarbamate anion is free anion.

The possibility of ligand L bonding by simple hardsphere coulombic interactions to Cp_2Ti^{2+} moiety is ruled out because in such cases a bischelate complex in contrast with the present observations, with four oxygen or two oxygen and two nitrogen atoms in the xy plane and parallel cyclopentadienyl rings could be isolated. Such a structure would maximise the coordination number of the metal ion and simultaneously maximise the total metal ring overlap. Since, the π-clouds are used in the formation of metal-ring bonds and would exert a less steric effect on the equatorial ligands, this configuration cannot be described as unstable on the basis of steric grounds.

Department of Chemistry
University of Delhi
Delhi-110 007
India

B. KHERA
A. K. SHARMA
N. K. KAUSHIK*

*Author to whom correspondence should be addressed.

REFERENCES

[1]G. S. Sodhi, A. K. Sharma and N. K. Kaushik, *J. Organometal. Chem.* 1982, **238**, 117. *Synth. React. Inorg. Met.-Org. Chem.* 1982, **12**.

[2]G. S. Sodhi and N. K. Kaushik, *Inorg. Nucl. Chem. Lett.* 1981, **17**, 211; *Bull. Soc. Chim. France* 1981, 45.

[3]A. K. Sharma and N. K. Kaushik, *Bull. Soc. Chim. France* 1982 in press; *Ind. J. Chem.* 1982 in press.

[4]R. C. Fay and R. N. Lowry, *Inorg. Chem.* 1967, **6**, 1512.

[5]H. Gilman and A. H. Blatt, *Organic Synthesis, Collective* Vol. 1, John Wiley, New York, 448 (1958).

[6]A. I. Vogel, *A Text Book of Quantitative Inorganic Analysis*, 4th Edn. Longmans, London (1978).

[7]H. P. Fritz, *Advances in Organometallic Chemistry*, Vol. 1, p. 279. Academic Press, New York (1964).

[8]R. S. P. Coutts and P. C. Wailes, *J. Organometal. Chem.* 1975, **84**, 47.

[9]J. J. Salzmann, *Helv. Chim. Acta* 1968, **51**, 601.

[10]G. W. H. Scherf and R. K. Brown, *Can. J. Chem.* 1960, **38**, 697.

[11]G. S. Sodhi and N. K. Kaushik, *Synth. React. Inorg. Met.-Org. Chem.* 1981, **11**, 641.

[12]J. E. Tackett and O. T. Sawyer, *Inorg. Chem.* 1964, **3**, 692.

[13]R. J. Magee and L. Gordan, *Talanta* 1963, **10**, 851.

[14]J. P. Fackler, Jr., *Progress in Inorg. Chem.* 1966, **7**, 361.

[15]N. V. Alekseev and I. A. Ronova, *Zh. Strukt. Khim.* 1966, **7**, 103.

MIXED ALDEHYDE CONDENSATIONS ON COPPER GLYCINATE

Patrick Sharrock, Département de chimie
Université de Sherbrooke, SHERBROOKE, Québec Canada J1K 2R1

Abstract. Glycine coordinated to cupric ions reacts in basic solution with a stoichiometric quantity of aldehydes to give β-hydroxyaminoacids. When the reaction contains a mixture of aldehydes, one of them being acetaldehyde, threonine is produced in the solution together with a variable amount of the bulkier substituted serine. An intermediate complex may be isolated which affords a larger proportion of substituted serines with predominance of the *threo* isomers. Acetaldehyde and benzaldehyde give a 66% yield of *threo* β-phenylserine.

Introduction. Condensation of aldehydes on amino acids complexed to metal ions[1] leads to various products. Such reactions provide a route for the synthesis of β-hydroxyaminoacids[2], but even under mild reaction conditions, serine for example undergoes a complex degradation pattern[3]. Schiff base formation has been used to protect amino groups, but yields are only fair[4]. This prompts us to report that mixed aldehyde condensation reactions can give specific β-hydroxyaminoacids in good yields.

Results. When 20 mmoles of acetaldehyde or acetone are added together with 20 mmoles of an aliphatic or aromatic aldehyde to 10 mmoles of *cis bis*-glycinato copper (II) monohydrate (I), a variety of condensation products is observed. Concentrated solutions precipitate blue to green complexes at room temperature after a few hours. The solids and the mother liquors treated as previously described[5] give different aminoacids in total recovery yields of 60 to 84% after recrystallisation from water/EtOH. The final products, analysed by ^{1}H NMR, are listed in the table. The yields are not statistically distributed and reflect stereoelectronic effects.

Acetaldehyde is the most reactive aldehyde and threonine in the *threo* to *erythro* ratio of 6/4 can be produced (run 8) in 96% yield. When acetaldehyde is mixed with other aldehydes, as in runs 9, 15, 17 and 18, threonine is the major product isolated from the mother liquors. However, these same reactions also give solid precipitates which rarely contain unreacted glycine, and yield less threonine than the other possible β-hydroxyamino acid. Comparing runs 10 and 11, the proportion of threonine increases when the stoichiometric ratio acetaldehyde/(I) is greater than 2. Strongly basic conditions or long reaction periods often result in the partial decomposition of the amino acids. The runs with acetone typically develop a gray color and brown to black copper precipitate. Operating under a nitrogen atmosphere (run 2) only slightly increases the recovery of amino acids.

Of special interest is the high *threo* to *erythro* ratio of substituted serines (IV) obtained from the solid intermediate complexes (III), as evidenced in runs, 9, 12, 13 and 15 to 18. We improved the results of run 13 with a larger scale reaction and obtained a 66% yield of the pure *threo* isomer (see experimental part). This clearly makes a mixed aldehyde method as attractive as the Schiff base one. Indeed, we only obtained a 21.5% yield of phenylserine as a mixture of isomers from a modification of the previously used procedure on N-pyruvilideneglycinatoaquo copper[6].

Discussion. Erlenmeyer synthesized phenylserine in 1893 by condensing two moles of benzaldehyde on one mole of glycine, with no other metal than sodium. Aliphatic aldehydes, however, require cupric ions to promote the reactions, the only reported exception to our knowledge being isobutyraldehyde[7]. The small yields of *threo* and *erythro* phenylserines obtained (run 14) and reported[8] when benzaldehyde is used alone could reflect condensation on uncomplexed glycine (copper hydroxide precipitates quantitatively from (I) at pH 12). Phenolic aldehydes do not react to give the desired products. Salicylaldehyde for example prefers to chelate the cupric ions in a Schiff base type complex. 4-methyl-benzaldehyde, on the other hand, mixed with equimolar acetaldehyde produces tolylserine[9] in 39% yield.

Table .   Results of the reaction of (I) with aldehydes and ketones.

run number	mmoles of Cu(gly)$_2$·H$_2$O	reaction conditions[a]	reaction time (hr)	reagent[b] A(mmoles)	aldehyde B(mmoles)	observations	Amino acids[c] recovered (mmoles, %)
1	10	1, 2	5	c (40)	–	–	gly (25), dimeser (19)
2	10	1, 2, 8	6	c (40)	–	–	gly (32), dimeser (23)
3	10	1, 2	70	c (60)	–	–	gly (29), dimeser (21)
4	10	1, 2	5	c (20)	acetaldehyde (20)	–	thr (67)
5	5	2, 3	28	c (10)	acetaldehyde (10)	decomposes	gly (10), thr (29)
6	10	1, 2	5.5	c (20)	benzaldehyde (20)	–	gly (30), φser (30)
7	10	1, 2	5.5	a (40)	–	–	gly (17), thr (72)
8	100	6, 1	22	a (600)	–	–	threo-thr (58), erythro-thr (38)
9	25	5, 7	7	a (50)	benzaldehyde (50)	solids	thr (0.8), threo-φser (39)
						solution	gly (6), thr (23), φser (7)
10	5	4, 5	70	a (10)	benzaldehyde (10)	decomposes	gly (6), thr (5), φser (19)
11	5	4, 5	70	a (20)	benzaldehyde (20)	decomposes	gly (4), thr (10), φser (15)
12	10	5, 9	90	a (20)	benzaldehyde (20)	solids	gly (5), thr (5), threo-φser (10)
						solution	gly (5), thr (5), φser (15)
13	10	3, 10	90	a (20)	benzaldehyde (20)	solids	threo-φser (16)
						solution	gly (15), thr (5), φser (15)
14	5	2, 3	48	b (20)	–	decomposes	gly (9), φser (10)
15	10	1, 2	27	a (20)	benzaldehyde (20)	solids	gly (2), thr (0.5), φser (3)
						solution	gly (5), thr (52), φser (12)
16	10	1, 2	27	a (20)	n-butyraldehyde (20)	solids	gly (1.5), thr (3), n-butser (13)
						solution	gly (6), thr (33), n-butser (46)
17	10	1, 2	27	a (20)	isobutyraldehyde (20)	solids	gly (0.5), thr (1), isobutser (13)
						solution	gly (3), thr (44), isobutser (8)
18	10	1, 2	27	a (20)	pivalaldehyde (20)	solids	thr (2), t-butser (8)
						solution	gly (4), thr (54), t-butser (2)

a
The reaction contains:1: NaOH = 1.5 $\underline{M}$, 2: 10 ml H$_2$O, 3: NaOH = 0.75 M, 4: NaOH = 0.50 M, 5: 15 ml H$_2$O, 6: 100 ml H$_2$O, 7: 1.5 g Na$_2$CO$_3$, 8: N$_2$ atmosphere, 9: NaOH = 0.33 $\underline{M}$, 10: NaOH = 0.05 $\underline{M}$.

b
The compound used is: a: acetaldehyde, b: benzaldehyde, c: acetone.

c
Abreviations for amino acids are: gly = glycine, dimeser = 3, 3'-dimethyl-serine, thr = threonine, φser = 3-phenylserine, isobutser = 3-isobutylserine, t-butser = 3-t-butylserine, n-butser = 3n-butylserine.

Another feature of the mixed aldehyde method is that excess aldehydes are not needed. We also note that a stoichiometric quantity of 4 moles acetaldehyde for one mole (I), run in D_2O and NaOD, gives a 94% yield of threonine after 5 hours, with no indication of deuterium incorporation at the α-carbon. Acetaldehyde reacts rapidly at the coordinated nitrogen to form a N-hydroxyethyl derivative (II), as evidenced by the rapid colour change from blue to violet. Subsequently or simultaneously, the seond aldehyde reacts with the α-carbanion formed under basic conditions and cyclises to give the *bis*-oxazolidine copper (II) complex (III)[10].
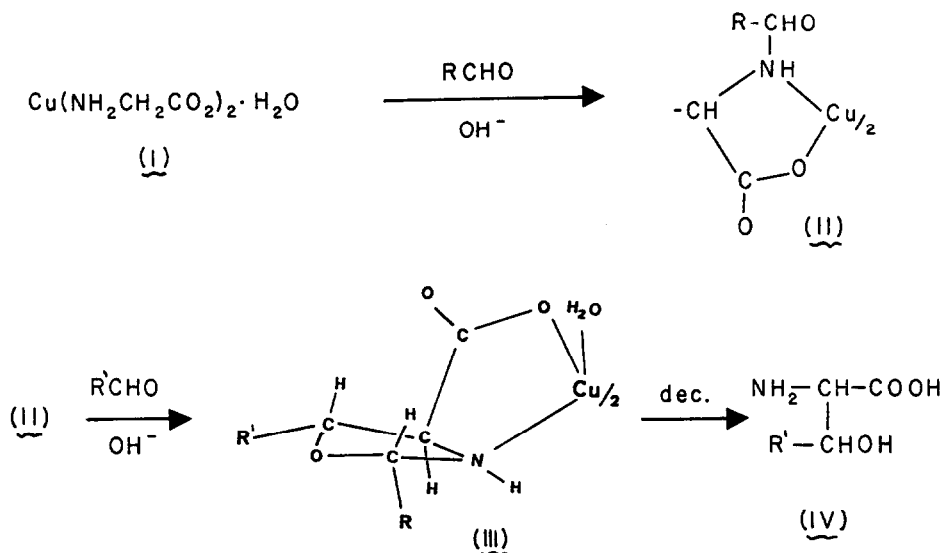
It has been suggested that steric interactions in intermediate complexes are responsible for the enantioselectivity in related aldol condensations[11] and reactions on similar amino acid[12] and peptide[13] Schiff base complexes. A recent report states stereoselectivity may be ascribed to steric inter-cycle interactions[8] in analogy with conclusions drawn from reactions on octahedral cobalt (III) complexes[14]. This is unlikely to hold true for labile square-planar copper (II) complexes. The exclusive formation of *threo* phenylserine from (III) and of the *threo* isomer of threonine by electrodecomposition[5] arises from intra-cycle steric interactions between substituents on the oxazolidine ring. Analysis of the solids in runs 15 to 18 shows threonine is present in *threo/ertho* ratios of 75/25 and the other substituted serines in corresponding ratios near 90/10, except for *t*-butylserine with a 40/60 ratio[15]. When the bulky substituents R and R'in (III) occupy pseudo equatorial positions in the oxazolidine ring then the *threo* isomer results. An *erythro* product requires R' in a pseudo axial position. A *threo/erythro* ratio near unity is observed for all amino acids isolated from the mother liquors, reflecting epimerisation at the α-carbon in basic solutions. Oxazolidines are known to be formed with very high stereoretention[16].

Conclusion. In previous work formaldehyde coupled with acetaldehyde gave inconclusive results[17]. Our findings show mixed aldehyde condensation without formaldehyde give β-hydroxyaminoacids readily and provide insight into the mechanism of this reaction.

Experimental. *Cis-bis* glycinato-copper (II) monohydrate was prepared by mixing aqueous solutions of two moles of glycine with one mole of copper sulphate and adjusting the pH to 7. The precipitate was recyrstallized once from water. The aldehydes used were of commercial origin. n-Butyraldehyde, isobutyraldehyde and pivalaldehyde were of technical grade.

The condensation reactions were carried out with magnetic stirring in tightly closed Erlenmeyer flasks, to avoid loss of acetaldehyde by evaporation. Because the reactions are exothermic, a Stirr-Kool model SK-12 from Thermoelectrics was used to maintain the temperature below 28° in the initial stages. In several runs, the solid precipitates were separated from the mother liquors by filtration. Both fractions were decomposed with concentrated ammonia and the aminoacids were recovered from a Dowex 50W-8X resin by elution with 1 M NH₄OH, followed by evaporation to dryness *in vacuo*. The products were recrystallized by slowly adding ethanol to concentrated aqueous solutions. The weight of the fractions was determined and the mole % of amino-acids determined by integration of the corresponding NMR peaks in D_2O solution. In some cases, the *threo* to *erythro* isomers gave distinct absorptions. Paper chromatography was used for semi-quantitative separation of *threo* and *erythro* isomers with a solvent composed of 40 ml n-butanol, 5 ml acetone, 30 ml H_2O and 5 ml concentrated NH₄OH, followed by revelation with ninhydrin.

Threo phenylserine in 66% yields was obtained by condensing 5.7 ml acetaldehyde and 10.2 ml benzaldehyde on 11 g of (I) in 10 ml H_2O + 20 ml NaOH 1 M in a 50 ml closed Schlenk Tube. An 85 hours reaction period gave a blue complex (III) which was washed with cold ethanol (yield 16.5 g). This compound was insoluble in water (with or without acetic acid) and could not be electrolysed. It was decomposed with concentrated ammonia and gave 11.96 g of phenylserine.

References and notes

1. L. Casella, A. Pasini, R. Ugo and M. Visca. J. Chem. Soc. Dalton 1980, 1655; R.D. Gillard and D.A. Phipps, J. Chem. Soc. Chem. Comm.; 1976, 285.

2. S.M. Hecht, K.M. Rupprecht and P.M. Jacobs, J. Am. Chem. Soc., 1979, 101, 3982.

3. L. Casella, Inorg. Chim.-Acta, 1981, 55, L9.

4. K. Harada and J.I. Oh-Hashi, J. Org. Chem., 1967, 32, 1103.

5. P. Sharrock and C. Eon, J. Inorg. Nucl. Chem., 1979, 41, 1087.

6. T. Ichikawa, S. Maeda, Y. Araki and Y. Ishido, J. Am. Chem. Soc., 1970, 92, 5514.

7. T. Wieland, H. Cords and E. Keck, Chem. Ber., 1954, 87, 1312.

8. M. Girnth-Weller and W. Beck, Inorg. Chim. Acta, 1982, 57, 107.

9. A. Hajos, Acta Chim. Acad. Scien. Hung. 1973, 471.

10. G. Larchères and M. Pierrot, Acta Cryst. 1971, B27, 442; P. Maldonado, C. Richaud, J.P. Aune and J. Metzger, Bull. Soc. Chim. Fr., 1971, 2933.

11. D.A. Evans and L.R. McGee, J. Am. Chem. Soc., 1981, 103, 2876.

12. Yu N. Belokon', A.S. Melikyan, V.I. Bakhmutow, S.V. Vitt and V.M. Belikov, Inorg. Chim. Acta, 1981, 55, 117.

13. S. Suzuki, H. Marita and K. Harada, J. Chem. Soc. Chem. Comm., 1979, 29.

14. J. Dabrowiak and D.W. Cooke, Inorg. Chem. 1975, 14, 1305; R.D. Gillard, S.H. Laurie, D.C. Price, D.A. Phipps and C.F. Weick, J. Chem. Soc., Dalton, 1974, 1385.

15. To determine these ratios by paper chromatography, the more mobile compound was assigned the *threo* geometry, which may be false for t-butylserine.

16. H. Abdallah, R. Grée and R. Carrié, Tetrahedron Letters, 1982, 503; E.E. George and J. B. Polya, Aust. J. Chem., 1979, 32, 2701.

17. T. Ishikawa, S. Maeda, T. Okamoto, Y. Araki and Y. Ishido, Bull. Chem. Soc. Jap., 1971, 44, 2779.

Evaluation of the interaction energy by clathration in Hofmann's benzene clathrate using the INDO method.

Isamu Uemasu

(Received 27 September 1982)

Department of Chemistry, College of General Education,

The University of Tokyo, Komaba, Meguro, Tokyo 153

Abstract – The INDO method was applied to estimate the interaction energy attributable to clathration in Hofmann's benzene clathrate using a model. Host–guest and guest–guest interactions were clarified and a stabilization energy fairly consistent with that obtained by differential scanning calorimetry was calculated.

INTRODUCTION

In previous work,[1] the enthalpy changes associated with guest liberation of the Hofmann's clathrates $Ni(NH_3)_2Ni(CN)_4 \cdot 2G$ (G= C_6H_6, C_4H_4S, C_4H_5N, and C_6H_5OH) were determined by differential scanning calorimetry(DSC). The enthalpy changes for the pyrrole and phenol clathrates were greater than those for the benzene and thiophene clathrates by ca.10 kJ mol^{-1} respectively. The difference seemed too great to be explained in terms of dipole–dipole interaction among the guests and it was mainly ascribed to the π hydrogen bond between the CN group of the host lattice and the hydrogen atom (–NH or –OH) of the guest molecule. The presence of such bonding in the aniline clathrate and its contribution to the stability were pointed out earlier in connection with its study by infrared spectroscopy.[2] In that paper, the presence of a hydrogen bond between ammine ligand and aromatic guest was also suggested. It stimulated the author to evaluate the host–guest interaction by the molecular orbital method and relate it to the enthalpy change. Methods ranging from the extended Hückel MO to *ab initio* SCF MO have been used to investigate the π hydrogen bond for various systems.[3] To the author's knowledge, such an estimate of the stabilization energy by MO calculations has not been made for Hofmann's clathrate. However, a single crystal of Hofmann's pyrrole or phenol clathrate has not yet been obtained[4] and only data from powder X-ray diffractometry are available. Therefore the author first carried out MO calculations for the benzene clathrate, whose crystal structure was analyzed first by Rayner and Powell.[5]

METHOD

Since the d orbital cannot be treated in the version of the CNDO/2 and INDO programs used here,[6] the calculations were performed on the model illustrated in Figures 1 and 2. In the model, both the octahedral and the square planar nickel atoms were ignored and HCN was used instead of the CN group. The carbon and nitrogen atoms of HCN were located at the same positions as those in the original crystal structure.[5] The interatomic distance and bond angle of NH_3 were assumed to be identical with those of the equilibrium structure in the gas phase. The intermolecular energy was calculated as the difference between the total energy of the

coupled molecule and the sum of the total energy of the separate molecules. Although the calculations were performed using both CNDO/2 and INDO, the author describes here only the result by the latter method, noting that no significant difference was found between the results using both methods.

<div align="center">RESULTS AND DISCUSSION</div>

The results of the MO calculations proved that NH_3-C_6H_6, CN-C_6H_6 and C_6H_6-C_6H_6 interactions contribute to the stabilization arising from clathration.

The interaction between NH_3 and C_6H_6 was calculated by rotating NH_3 about its C_3 axis : the rotation of the ammine ligand with little hindrance was known from proton magnetic resonance spectra.[7] The dependence of the intermolecular energy(ΔE) on the rotation angle(Θ) of NH_3 is shown in Figure 3. From least-squares fitting using the program of SALS,[8] equation(1) was obtained.

$$\Delta E = -0.001410 - 0.000788 \sin(3(\Theta + 18.40)) \tag{1}$$

It indicates that the mean value of the energy for interaction between NH_3 and C_6H_6 is 0.001410 a.u.. There being four NH_3 molecules around a C_6H_6 molecule, the mean value of the total interaction energy is 0.005640 a.u., which was ascertained by performing the MO calculation on the combination of a C_6H_6 molecule and four NH_3 molecules. In this case, the intermolecular energy is due to the π hydrogen bond forming between NH_3 as the proton donor and C_6H_6 as the π electron donor. The variation of the energy with the rotaion angle corresponded to that of the charge transfer from C_6H_6 to NH_3.

As to the interaction between CN and C_6H_6, the bond order matrix indicated that the interaction between 1s orbitals of the hydrogen atoms of C_6H_6 and 2p orbitals of the carbon

<div align="center">Table 1. Intermolecular energy(ΔE) calculated by INDO for the model.</div>

M	ΔE(a.u.)	n
NH_3	−0.001410	4
HCN(1)	−0.000580	4
HCN(2)	−0.000267	4
C_6H_6	−0.001174	2

M : Molecule interacting with a C_6H_6 molecule.

n : Number of M.

See text as to HCN(1) and (2).
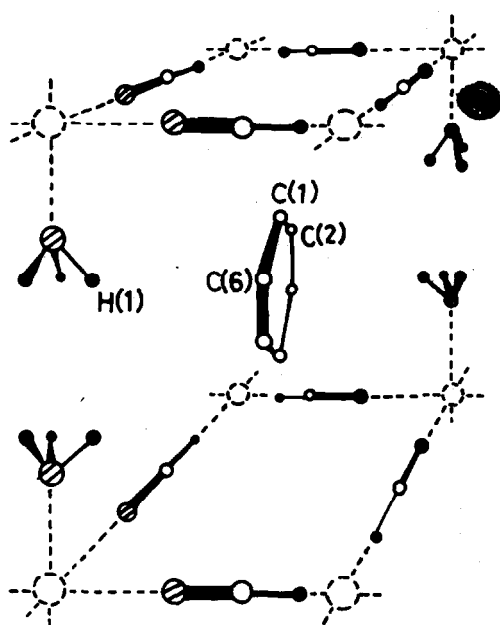
●:H, O:C, ⊘:N, ○:Ni

Fig. 1. Model of the Hofmann's benzene clathrate for the MO calculation. The hydrogen atoms of C_6H_6 were omitted in this illustration.

●:H, O:C, ⊘:N
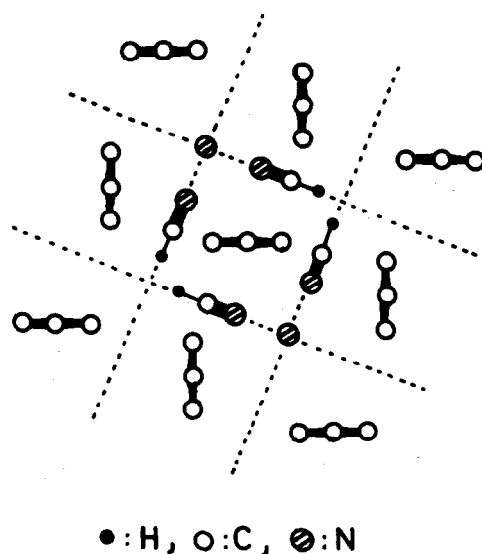
Fig. 2. Arrangement in horizontal section of the model. The hydrogen atoms of C_6H_6 and NH_3 were omitted.
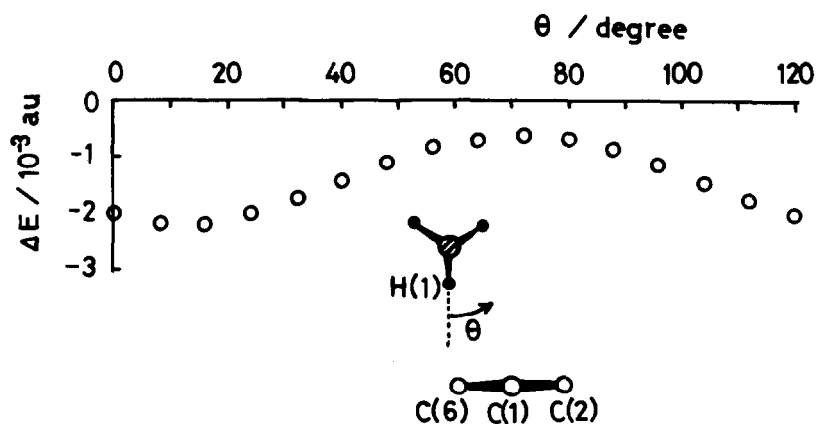
Fig. 3. Dependence of the intermolecular energy (ΔE) on the rotation angle (θ) of NH_3. The numbering of atoms is consistent with that in Figure 1.

atom of HCN contributed to the stabilization. The effect was greater for HCN almost perpendicular to the ring of C_6H_6 (HCN(1) in Table 1) than for HCN almost parallel to the ring of C_6H_6 (HCN(2) in Table 1. See Figure 2.). In this case, it may as well be distinguished from the π hydrogen bond because the hydrogen atoms of C_6H_6 are unlike those of NH_3, which are partially positively charged. When C_6H_6 rotated about the C_2 axis perpendicular to the nickel cyanide network, the minimum point of the interaction energy was found in the vicinity of the angle actually found in the crystal structure.[5] Therefore the orientation of C_6H_6 seemed to be determined by the interaction between the guest molecule and the CN group of the host lattice.

The guest-guest interaction energy was calculated between a C_6H_6 molecule and others lying vertical to it, while no appreciable interaction was found between a guest and others lying parallel to it(See Figure 2). The bond order matrix showed that the interaction between 2p orbitals of the carbon atoms of a C_6H_6 molecule and 1s orbitals of the hydrogen atoms of another C_6H_6 molecule contributed to the stabilization just as in the case of C_6H_6 and HCN.

The results of the INDO calculations are listed in Table 1. The stabilization energy from clathration amounted to ca.30 kJ mol^{-1}, consistent with the result obtained by DSC.[1]

It is impossible to perform a similar calculation on Hofmann's phenol clathrate because single crystal structure data have not yet been obtained. However, the interaction energy for the π hydrogen bond between the hydrogen atom of the OH group and the CN group of the host lattice was calculated, assuming (a) that C_6H_5OH was situated in the middle of the adjacent nickel cyanide networks whose separation was known from X-ray powder data and (b) that the orientation of the guest molecule was identical with that of the benzene clathrate. The intermolecular energy was ca.21 kJ mol^{-1}. It is greater by ca.20 kJ mol^{-1} than that of the benzene clathrate. The value is thought to correspond to the difference between the enthalpy changes of the respective clathrates.[1]

The model for Hofmann's clathrate adopted here poses considerable problems in some respects. For example, the electron density of each atom in the model is not identical with that in the original clathrate. The structure of NH_3 assumed here must be a little different from that in the actual clathrate. The interaction between the guest molecule and the hydrogen atom of HCN was not negligible in the MO calculation. However, the result obtained here seems to be reasonable and may well hold also for the actual clathrate.

                                    REFERENCES

[1] I. Uemasu and T. Iwamoto, Chem. Lett., 1982, 973.

[2] S. Akyüz, A. B. Dempster, and R. L. Morehouse, Spectrochim. Acta, 1974, 30A, 1989.

[3] K. Morokuma, H. Kato, T. Yonezawa, and K. Fukui, Bull. Chem. Soc. Jpn., 1965, 38, 1263;
K. Morokuma, J. Chem. Phys., 1971, 55, 1236; K. Morokuma and G. Wiff, Chem. Phys. Lett.,
1980, 74, 400; J. E. Del Bene and F. T. Marchese, J. Chem. Phys., 1973, 58, 926; J. E. Del
Bene, Chem. Phys. Lett., 1974, 24, 203; P. Kollman, J. McKeley, A. Johansson, and S.
Rothenberg, J. Amer. Chem. Soc., 1975, 97, 955.

[4] T. Iwamoto, Isr. J. Chem., 1979, 18, 240.

[5] J. H. Rayner and H. M. Powell, J. Chem. Soc., 1952, 319.

[6] H. Kihara, Program Code:Y4/TC/CBO4NN, Program Library, The Computer Centre, The University
of Tokyo, 1977. The program was based on that by Quantum Chemistry Program Exchange.

[7] T. Miyamoto, Inorg. Chim. Acta, 1969, 3, 511.

[8] T. Nakagawa and Y. Oyanagi, SALS, Program Library, The Computer Centre, The University of
Tokyo, 1979.

COMMUNICATIONS

The characterization and thermal stability of a cluster $HRu_3(CO)_{10}(O–Si{\diagdown}^{\diagup})$ grafted on silica surface

Abstract—$Ru_3(CO)_{12}$, supported on silica in the absence of oxygen, reacts with silanol groups of the surface to produce a grafted cluster $HRu_3(CO)_{10}(OSi{\diagdown}^{\diagup})$, which has been characterized by IR and Raman spectroscopy; the molecular formula of this cluster is in agreement with the stoichiometric balance of CO evolved during its formation from $Ru_3(CO)_{12}$. The grafted cluster is an intermediate step to produce by thermal decomposition small metallic ruthenium particles of 14 Å together with some Ru(II) carbonyl species encapsulated in the silica surface.

Recent interest has been devoted to the chemical behaviour and the catalytic activity of mononuclear or cluster carbonyl complexes supported on inorganic oxides.[1]

Some attention has been paid to the chemistry of $Ru_3(CO)_{12}$ on silica[2–4] since it was reported that $Ru_3(CO)_{12}$ on silica is active in various catalytic reactions, such as α-olefin hydrogenation or isomeration[5,6] or CO reduction to hydrocarbons.[7]

However, in the previous works,[2–4] which were mainly supported by surface IR studies, it was difficult to understand the real surface chemistry, because the experiments were not carried out in the absence of surface adsorbed water and of dioxygen, since the samples were always prepared in the air. On the contrary under our standard experimental conditions,[8] we could investigate the adsorption of $Ru_3(CO)_{12}$ on silica surfaces, treated under high vacuum at 500°C for 16–20 hr, and follow the transformation of the supported cluster under different experimental conditions, including progressive heating in high vacuum.

In this way, we have found that the first "species" obtained by thermal decomposition of $Ru_3(CO)_{12}$ physisorbed on partially dehydrated silica is a grafted molecular cluster $HRu_3(CO)_{10}(OSi{\diagdown}^{\diagup})$ resulting from the oxidative addition of a surface silanol group into the metal–metal bond of the original cluster. Such grafted cluster thermally decomposes only above *ca.* 373 K to produce, upon aggregation, ruthenium metal particles covered with CO and some oxidized Ru(II) carbonyl surface species.

When $Ru_3(CO)_{12}$, dissolved in pentane solution, is adsorbed under vacuum onto a silica disc which was previously treated at 773 K under vacuum (10^{-5} torr) for 16 hr, the resulting IR spectrum exhibits bands at 2063 (s), 2032 (m), 2018 (m, sh) which are identical in frequency and intensity to those of $Ru_3(CO)_{12}$. By treatment under vacuum at *ca.* 353 K for a few hours a progressive modification of the spectrum is observed with new carbonyl bands appearing at 2111 (w), 2077 (m), 2066 (m), 2033 (s, br) and 1995 (sh) cm^{-1}.

The new IR spectrum is quite similar in intensity and frequencies to that of the well characterized osmium cluster $(H)Os_3(CO)_{10}(OSi{\diagdown}^{\diagup})$ grafted on a silica Surface[8]; in addition similar IR spectra are reported for molecular clusters of the type $(H)Ru_3(CO)_{10}X$ ($X = SC_2H_5$)[9] (Table 1).

The Raman spectrum of the supported cluster after decarbonylation at 318 K has been recorded using low power (< 30 mW) of the 647.1 nm laser line and sample spinning cell techniques in order to avoid any decomposition. In the low frequency region this spectrum exhibits several bands of the starting $Ru_3(CO)_{12}$ cluster[10] and two additional new bands at 201 and 162 cm^{-1} which can be tentatively assigned to metal–metal

stretching vibrations of a grafted cluster. The stoichiometry of the surface reaction:

$$Ru_3(CO)_{12} + HOSi{\diagdown}^{\diagup} \rightarrow (H)Ru_3(CO)_{10}(OSi{\diagdown}^{\diagup}) + 2CO$$
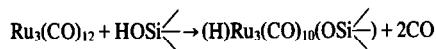
is confirmed by the following experiment. A pentane solution of $Ru_3(CO)_{12}$ (30 mg; 0.05 m.mole) was adsorbed onto a silica sample (about 1 g) previously treated at 773 K under vacuum for 16 hr. After removal of the solvent under vacuum at room temperature, thermal decomposition of the supported cluster at increasing temperature, resulted in the evolution of 1.7 ± 0.2 moles of CO/mole of cluster in the temperature range of 343–393 K. No significant evolution of H_2 nor CO_2 was observed in this temperature range which is in agreement with the proposed structure
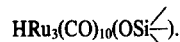
$$HRu_3(CO)_{10}(OSi{\diagdown}^{\diagup}).$$

The thermal stability of the grafted ruthenium cluster has been followed by analysis of the gas phase during thermal decomposition by infrared spectroscopy and electron microscopy Upon heating the grafted cluster $(H)Ru_3(CO)_{10}(OSi{\diagdown}^{\diagup})$ above 393 K, a progressive evolution of about 10 moles of CO per mole of cluster was observed when the temperature was increased up to 523 K. Meanwhile a certain amount of H_2 was evolved, which may be ascribed to a partial oxidation of zerovalent ruthenium by surface OH groups with formation of surface oxidised Ru(II) $(CO)_n$ species.[2] After thermal decarbonylation of $HRu_3(CO)_{10}(O–Si{\diagdown}^{\diagup})$ above 393 K or at 393 K for 16 h under high vacuum (10^{-5} mm Hg), the IR spectrum presented a broad peak centered at 2037 cm^{-1}, typical of CO coordinated to metallic ruthenium, and some peaks of smaller intensity at 2122, 2081 and 1957 cm^{-1} probably corresponding to Ru(II) $(CO)_n$ ($n = 2, 3$) species formed in low concentration.

As it is well known for CO coordinated to metallic ruthenium[11] a progressive decarbonylation occurs with increasing temperature, corresponding to a shift of $\nu(CO)$ frequency from 2037 cm^{-1} at $\theta \approx 1$ to 1985 cm^{-1} at $\theta \approx 0.1$. Such decarbonylation is reversible as determined by the frequency and intensity of the $\nu(CO)$ band obtained after recarbonylation at 25°C. The presence of small particles of ruthenium metal was confirmed by electron microscopy. Such particles exhibit a very narrow distribution of particle size around 14 Å. Similar sizes have been obtained in another laboratory.[17]

The assignment of the other IR bands to a mixture of Ru(II) carbonyl species is substantiated by the easy formation of surface species characterised by similar IR absorptions, by thermal encapsulation of $Ru(II)CO_3Cl_2$ into silica (Table 1). These oxi-

Table 1.

Compound	$\nu(CO)$ cm.$^{-1}$	(M – M) cm.$^{-1}$	Ref.
$Ru_3(CO)_{12}$	2060 vs, 2030 s, 2011 m^a		This work
	2059 s, 2054 sh, 2039 m, 2025 s,		This work
	2016 s, 1998 s, 1986m^{b}4		
	2063 vs, 2032 m, 2018 sh^c		This work
$HOs_3(CO)_{10}(OSi\langle)$	2114 w, 2079 s, 2068 s, 2032 vs,	159, 118	8, 10
	2012 sh, 1995 m		
$HRu_3(CO)_{10}(SC_2H_5)$	2105 m, 2064 s, 2056 s, 2025 vs,		9
	2012 m, 2008 s, 1994 m^a		
$HRu_3(CO)_{10}(OSi\langle)$	2111 w, 2077 s, 2066 s, 2033 s, br.	200, 155	This work
	1995 sh		
$Ru(CO)_4Cl_2$	2182 w, 2132 s, 2113 ms, 2080 s^d		15
$Ru(CO)_3Cl_2Py$	2136 s, 2075 s, 2051 s^e		15
$Ru(CO)_2Cl_2Py_2$	2070 s, 2006 s^e		15 ·
$[Ru(CO)_3Cl_2]_2$	2143 s, 2082 s^e		15
	2140 s, 2092 s, 2066 s, 2045 w,		15
	2026 w^b		
$[Ru(CO)_2Cl_2]_m$	2076 vs, 2018 vs^b		16
$[Ru(CO)_2(OSiPh_3)_2]_x$	2062 s, 1995 s^f		This work
$[Ru(CO)_3(OSi\langle)_2]_n$	2138 m, 2073 s, 2014 s^g		This work
	2150 s, 2092 vs, 2035 m^h		This work
$[Ru(CO)_2(OSi\langle)_2]_n$	2072 s, 2002 s^g		This work
	2085 s, 2027 s^h		This work
CO/Ru_{metal} $\theta \simeq 1$	2037 br		This work
$\theta \simeq 0.1$	1985 br		This work

^{a}hexane; ^{b}nujol mull; ^{c}on silica heated in vacuum at 500°C; ^{d}CH$_2$Br$_2$; ^{e}CH$_2$Cl$_2$; ^{f}CH$_2$Cl$_3$; ^{g}from Ru$_3$(CO)$_{12}$ on silica heated in vacuum at 500°C; ^{h}from [Ru(CO)$_3$Cl$_2$]$_2$ on silica heated in vacuum at 500°C.
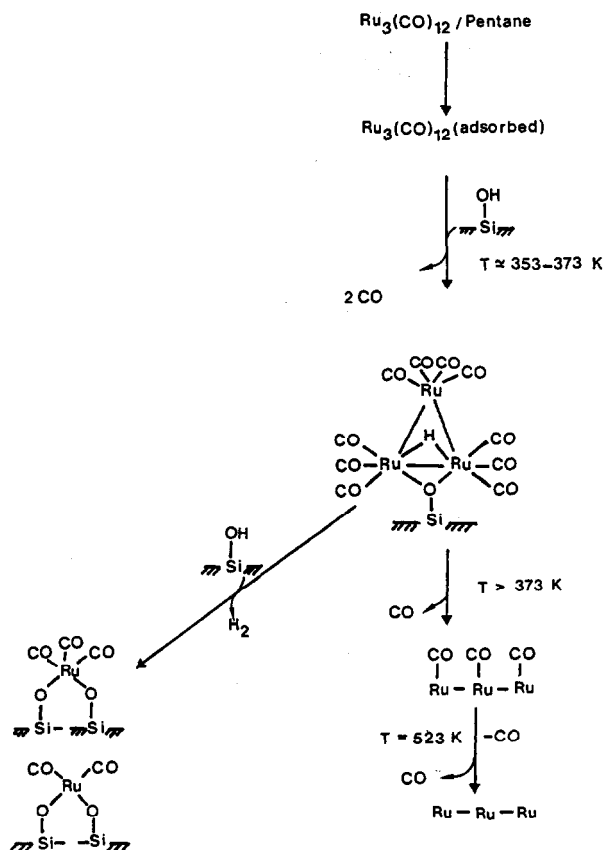
dised species are in thermal equilibrium of decarbonylation (and carbonylation) (Table 1):

$$[Ru(CO)_3(OSi{\small\diagdown})_2]_n \underset{CO}{\rightleftharpoons} [Ru(CO)_2(OSi{\small\diagdown})_2]_n + n\ CO.$$
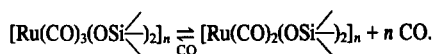
Similar species are obtained by treatment of $Ru_3(CO)_{12}$ adsorbed on silica or the grafted cluster $(H)Ru_3(CO)_{10}(OSi{\small\diagdown})$ with oxygen, confirming that an oxidation of the ruthenium atoms occurs. Finally a molecular species with similar IR absorption bands at 2062 (s), 1995 (s) cm^{-1} is obtained by treatment of $[Ru(CO)_3Cl_2]_2$ with TlOSiPh$_3$ (Table 1).

The various steps leading to surface grafting and then to the formation of metallic particles and Ru(II) carbonyl species (see Scheme) require well defined and narrow conditions, so that all these species may coexist if the experiments are not carried out under the appropriate conditions, which explains some of the previous results.[5] It is worth mentioning that $Ru_3(CO)_{12}$ reacts much like $Os_3(CO)_{12}$ with the silanol groups of silica, whereas $Fe_3(CO)_{12}$ exhibits a different behaviour.[12]

However in contrast with the corresponding osmium species, the ruthenium grafted cluster is not stable at room temperature in the presence of oxygen or adsorbed water.

It is probably for this reason that this particular surface species was not detected by previous workers,[2,3] whilst the corresponding surface osmium species $(H)Os_3(CO)_{10}X$ $(X = OSi{\small\diagdown}, OAl{\small\diagdown}, OZn, OTi{\small\diagdown})$, were observed even if the original samples were prepared in the air.[13]

In addition, in contrast to osmium, the ruthenium grafted cluster decomposes above *ca* 393 K to metal particles covered with CO and to oxidised Ru(II) surface carbonyl species, whilst with osmium the metallic state is reached under more drastic conditions.[8]

ALBERT THEOLIER,
AGNÈS CHOPLIN,
LINDORA D'ORNELAS,
JEAN-MARIE BASSET*

*Institut de Recherche sur la Catalyse 2,
avenue Albert Einstein-69626 Villeurbanne Cédex-France*

GIANMARIA ZANDERIGHI
*Renato UGO,
Rinaldo PSARO Istituto di Chimica Generale ed Inorganica,
Centro CNR Università di Milano-21,
via Venezian-20133 Milano-Italia*

C. SOURISSEAU
*LASIR-CNRS 2,
2, rue H. Dunant*-94320 *Thiais France*

REFERENCES

[1] D. C. Bailey and S. H. Langer, *Chem. Rev.* 1981, **81**, 110 and references therein.

[2] V. L. Kutznetsov, A. T. Bell and Y. Yermakov, *J. Cat.* 1980, **65**, 374.

[3] J. Goodwin and C. Naccache, *J. Mol. Cat.* 1981, **14**, 259.

[4] A. Zecchina, E. Guglielminotti, A. Bossi and M. Camia, *J. Cat.* 1982, **74**, 225.

[5] J. Robertson and G. Webb, *Proc. Roy. Soc. A* 1974, **341**, 383.

[6] R. A. Sanchez-Delgado, I. Duran, J. Montfort and E. Rodriguez, *J. Mol. Cat.* 1981, **11**, 193.

[7] A. K. Smith, A. Theolier, J. M. Basset, R. Ugo, D. Commereuc and Y. Chauvin, *J. Am. Chem. Soc.* 1978, **100**, 2550.

[8] R. Psaro, R. Ugo, G. M. Zanderighi, B. Besson, A. K. Smith and J. M. Basset. *J. Organomet. Chem.* 1981, **213**, 215.

[9] G. R. Crooks, B. F. G. Johnson, J. Lewis and I. G. Williams, *J. Chem. Soc (A)* 1969, 797.

[10] C. O. Quiksall and T. G. Spiro, *Inorg. Chem.* 1968, **7**, 2365; S. Kishner, P. J. Fitzpatrick, F. R. Plowman and I. S. Butler, *J. Mol. Struct.* 1981, **74**, 29.

[11] A. Bradshaw, *J.C.S. Chem. Comm.* 1980, 366.

[12] F. Hugues, A. K. Smith, Y. Ben Taarit, J. M. Basset, D. Commereuc and Y. Chauvin, *J.C.S. Chem. Comm.* 1980, 68.

[13] M. Deeba and B. C. Gates, *J. Cat.* 1981, **67**, 303.

[14] J. L. Bilhou, V. Bougnol, W. F. Graydon, A. K. Smith, G. M. Zanderighi, J. M. Basset and R. Ugo, *J. Organomet. Chem.* 1978, **153**, 73.

[15] E. Benedetti, G. Braca, G. Sbrana, F. Salvetti and B. Grassi, *J. Organomet. Chem.* 1972, **37**, 361.

[16] M.J. Cleare and W.P. Griffith, *J. Chem. Soc. (A)* 1969, 372.

[17] A. F. Simpson and R. Whyman, *J. Organomet. Chem.* 1981, **213**, 157.

REACTIONS OF METAL COMPLEXES WITH CARBOHYDRATES. 3.[1,2]

THE CRYSTAL STRUCTURE OF (ETHYLENEDIAMINE)(2-[(2-AMINOETHYL)AMINO]-

2-DEOXY-L-SORBOSE)NICKEL(II) DICHLORIDE HEMI METHANOL –

[Ni(en)(L-sor-en)]Cl$_2 \cdot \frac{1}{2}$CH$_3$OH

TARO TSUBOMURA, SHIGENOBU YANO*, SADAO YOSHIKAWA*

Department of Synthetic Chemistry, Faculty of Engineering,

The University of Tokyo, Hongo, Bunkyo-ku, Tokyo 113, Japan

KOSHIRO TORIUMI, TASUKU ITO

National Institute for Molecular Science, Okazaki-city 444, Japan

We have previously reported the synthesis and characterization of new nickel(II) complexes containing N-glycoside which were derived from the reaction of tris(ethylenediamine)nickel(II) dichloride dihydrate with D-glucose, D-mannose, or D-fructose, including the X-ray structure determination of the complex derived from D-fructose (Figure 1).[1]

The bindings of carbohydrates to metal ions are interesting matters as coordination phenomena,[3] and as bioinorganic systems. As a part of study to elucidate interactions between metals and carbohydrates, we present both the synthesis and the crystal structure of a nickel complex containing an N-glycoside (L-sor-en) formed by the reaction between ethylenediamine and L-sorbose, where L-sor-en is 2-[(2-aminoethyl)amino]-2-deoxy-L-sorbose (Figure 2). L-sorbose, which is C5 epimer of D-fructose, is considerably important as an intermediate in the chemical synthesis of L-ascorbic acid.

Figure 1. A perspective drawing of [Ni(en)(D-fru-en)]$^{2+}$.
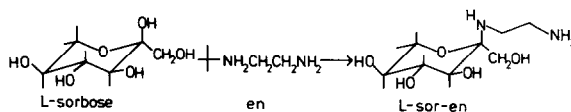
Figure 2. Reaction scheme.

The complex was synthesized as follows. L-Sorbose (17.6 mmol) was added to the solution containing [Ni(en)$_3$]Cl$_2$ 2H$_2$O (8.8 mmol) in 80 mL of methanol. As a catalyst NH$_4$Cl (8.8 mmol) was added.[4] The violet solution was refluxed for 1h., then it became blue. It was evapolated to 40 mL and loaded on a Sephadex LH-20 gel permeation column, and eluted with methanol. The reaction materials seperated into violet, blue, yellow, and orange bands. The blue fractions were collected and concentrated to about 15 mL, then it was kept at 5°C. Blue crystals were obtained and were recrystallized from a minimum amount of hot methanol.

Elemental analysis indicates that this complex has one ethylenediamine ligand (en), and one N-glycoside ligand (L-sor-en). Calculated for [Ni(en)(L-sor-en)]Cl$_2 \cdot \frac{1}{2}$CH$_3$OH (C$_{10.5}$H$_{28}$N$_4$O$_{5.5}$Cl$_2$Ni): C, 29.46; H, 6.61; N, 13.09; Cl, 16.56 Found: C, 29.19; H, 6.86; N, 13.36; Cl, 16.50. The near infrared and visible spectrum of methanolic solution shows three bands with comparatively low intensities, which are characteristic of octahedral Ni(II) complex (Figure 4). The magnetic moment at room temperature is 3.16μ_B, which falls within the range of reported octahedral nickel(II) complexes. The structure of this complex was determined by as X-ray crystallographic study. This compound crystallizes in the monoclinic space group C2 with a = 17.862 (2) Å, b = 8.212 (1) Å,

c = 12.644 (2) Å, β = 90.89°, and z = 4. After absorption correction, the structure was solved by heavy atom methods, and structure parameters including almost all hydrogen atoms were refined by least-square methods to R = 0.032 (Rw = 0.042)[5] for 2680 independent reflections with Fo>3σ(Fo). All calculations were performed with universal program system UNICS III.[6]

A perspective drawing of the complex cation showing thermal motion is given in Figure 3. It reveals that nickel is octahedrally coordinated with a bidentate ethylenediamine ligand and a tetradentate N-glycoside ligand of L-sor-en. The pyranose ring is in the usual α-$^2C_5$ chair form.[7] The conformation of bidentate ligand en is δ. The absolute configuration of the secondary nitrogen atom is S. The nickel-nitrogen bond distances fall within the expected range (Table 1). Each of the interior angles of five-membered chelate rings subtended at nickel atom is smaller than ninety degrees. They are normal for five-membered chelate rings.

Figure 3.   A perspective drawing of [Ni(en)(L-sor-en)]$^{2+}$.

The CD spectra of [Ni(en)(L-sor-en)]$^{2+}$ and [Ni(en)(D-fru-en)]$^{2+}$ in methanol are shown in Figure 4. They have opposite sign of CD curves in the first absorption region.

Table 1.   Selected bond length and angles.

bond length (Å)		angles (degree)	
Ni-O(1)	2.137(3)	O(1)-Ni-N(1)	76.1(1)
Ni-O(3)	2.118(2)	O(3)-Ni-N(1)	78.2(1)
Ni-N(1)	2.109(3)	O(3)-Ni-N(2)	162.8(1)
Ni-N(2)	2.068(3)	N(1)-Ni-N(2)	84.6(1)
Ni-N(3)	2.059(3)	N(3)-Ni-N(4)	83.9(1)
Ni-N(4)	2.078(3)		

It is generally accepted that the contribution of vicinal effect to optical activity, which is the effect of asymmetric groups on the ligand, is small. The structure of [Ni(en)(L-sor-en)]$^{2+}$ ion is similar to that of [Ni(en)(D-fru-en)]$^{2+}$ ion except for the absolute configurations around the C(5) atom and the gauche conformation of bidentate ethylenediamine chelate, which usually makes a rapid interconversion between δ and λ in solution. Therefore, it is a very interesting fact that the CD spectra of both complexes are quite different from each other as stated above.

The result of two crystal structures suggest the usual coordination patterns of the N-glycoside ligands derived from ketoses.

Figure 4.   Absorption and CD spectra of [Ni(en)(L-sor-en)]$^{2+}$ and [Ni(en)(D-fru-en)]$^{2+}$.

References

1. Part 1, Takizawa, S.; Sugita, H.; Yano, S.; Yoshikawa, S.; J.Am.Chem.Soc., 1980, 102, 7969.

2. Part 2, Yano, S.; Sakai, Y.; Yoshikawa, S.; submitted for publication.

3. Adam, M.J.; Hall, L.D.; J.Chem.Soc.Chem.Comm., 1979, 234.

4. Barry, C.P.; Honeyman, J.; J.Chem.Soc., 1952, 4157.

5. R=Σ||Fo|-|Fc||/Σ|Fo|, Rw=[Σw(|Fo|-|Fc|)²/Σw|Fo|²]$^{1/2}$, where $\frac{1}{w}$ = σc²+(0.015|Fo|)²

6. Sakurai, T.; Kobayashi, K.; Rigaku Kenkyusho Hokoku, 1979, 55, 69.

7. Kim, S.H.; Resenstein, R.D.; Acta.cryst., 1967, 22, 648.

THERMAL INTRAMOLECULAR ELECTRON TRANSFER REACTIONS OF [N,N'-ETHYLENE-
BIS(SALICYLIDENEAMINATO)](2,4-PENTANEDIONATO)COBALT(III) COMPLEXES
IN THE SOLID STATE

Setsuko KINOSHITA*, Kikuo MIYOKAWA, Hisanobu WAKITA, and Isao MASUDA

Department of Chemistry, Faculty of Science, Fukuoka University,
Nanakuma, Jonan-ku, Fukuoka 814-01, Japan

ABSTRACT——The title complexes with the formula Co(salen)L where L is a series
of 2,4-pentanedionates underwent thermally induced one-electron transfer
reactions from L to Co(III). The reaction left behind a stoichiometric amount
of the crystalline Co^{II}(salen) complex which took up oxygen in a molar ratio
of $Co:O_2$ = 2:1. The kinetic analyses showed that the electron transfer
reaction rate was apparently dominated by activation entropy rather than by
activation enthalpy.

Thermally induced intramolecular electron transfer reactions occurring in solid
transition metal complexes are of significance in connection with the catalytic behavior
of metal complexes. However, there have so far been only a few investigations on such
redox reactions.[1,2] Present paper communicates that upon heating, the solid Co^{III}(salen)L[3]
undergo one-electron transfer reaction from the L to the Co(III) ion and leave behind a
stoichiometric amount of Co^{II}(salen) in the crystalline form which is active toward oxygen
uptake in the solid phase.

TG and DTA curves recorded in a flowing nitrogen atmosphere showed that Co(salen)L
were endothermally decomposed in the 440-490K temperature range. The weight-loss in the
TG curves corresponded to the following decomposition scheme: Co^{III}(salen)L $\longrightarrow Co^{II}$(salen).
The analytical data and μ_{eff} = 2.51 μ_B(300K) of the solid pyrolysis product also supported
the above scheme. Moreover, the IR spectra and X-ray powder diffraction patterns of the
pyrolysis products were in fair agreement with those of the authentic Co^{II}(salen) complex
prepared by the literature method.[4] The pyrolysis gas chromatographic measurements[1]
carried out under the conditions: Column packing, DEGA; pyrolysis temperature, 490K,
confirmed that the gaseous products evolved by the pyrolysis included 1/2 mol of the
corresponding free HL per mole of the pyrolyzed Co(salen)L complex. For Co(salen)(acac),
gaseous products were found to include, besides HL, non-stoichiometric amount of acetone,
methanol, and ethanol.

Under non-isothermal conditions,[5] the reactions were found to proceed following the
contracting-disc equation: $1-(1-\alpha)^{1/2}$ = kt, where α is the molar fraction of the Co(II)
complex produced from the Co(III) complex; k, the rate constant; and t, the reaction time.
The kinetic results are given in Table 1. As Table 1 shows, the rate constants at
460K increase in the following order of the mixed ligand L: acetylacetonato < propionyl-
acetonato < n-butyrylacetonato < n-caproylacetonato. Therefore, from the increase in the
rate constants the activation enthalpy $\Delta H^{\ddagger}$ may generally be expected to decrease in the
above order. However, contrary to this expectation the $\Delta H^{\ddagger}$ values actually increase in

Table 1. Kinetic data of the thermal electron transfer reactions of $Co^{III}(salen)L$

L	$\Delta H^{\ddagger}(460K)/kJ\ mol^{-1}$	$\log(A/s^{-1})$	$\Delta S^{\ddagger}(460K)/JK^{-1}mol^{-1}$	$k(460K)/s^{-1}$
acetylacetonato	193±3	18.7±0.5	101±9	$(2.00\pm0.72)\times10^{-4}$
propionylacetonato	227±6	23.4±0.6	190±11	$(1.38\pm0.27)\times10^{-3}$
n-butyrylacetonato	252±9	26.6±0.9	252±17	$(3.09\pm0.92)\times10^{-3}$
n-caproylacetonato	298±11	32.2±1.4	359±26	$(7.75\pm2.45)\times10^{-3}$

$\Delta H^{\ddagger}$, Activation enthalpy; A, pre-exponential factor; k, rate constant. The values of
activation entropy $\Delta S^{\ddagger}$, were calculated from the relation, $\Delta S^{\ddagger}= R(\ln\frac{Ah}{kT} - 1)$, where R is
gas constant, k Boltzman constant, h Plank constant, and T absolute temperature.
The kinetic analysis was carried out on the basis of the fact that all reactions followed
the contracting-disc equation.

this order. This fact led us to take the entropy term into consideration. The $\Delta S^{\ddagger}$ values,
activation entropy, calculated by assuming κ(transmission coefficient) = 1 are shown in
Table 1. It is seen from Table 1 that the $\Delta S^{\ddagger}$ value for L = n-caproylacetonato complex is
$ca.$ 3.5 times larger than that for L = acetylacetonato complex. Thus, it is clear that
the activation entropy plays an important role in the present solid state reactions. The
positive and rather large $\Delta S^{\ddagger}$ values are considered to suggest that the reaction rate is
determined by the dissociation process of L^6, which occurs with the concomitant electron
transfer process.

It is noticed that the pyrolysis of the complexes gave rise to the $Co^{II}(salen)$ complex
in a crystalline form. On standing this $Co^{II}(salen)$ complex in dry air or oxygen atmos-
phere at room temperature, it took up oxygen in a few hours and turned the color from
brown to black. The O_2-adduct liberated oxygen endothermally at $ca.$ 340K with a weight-
loss 4.8%, corresponding to the composition of the O_2-adduct, $[Co(salen)]_2O_2$. The O_2-
adduct showed μ_{eff} = 1.06 μ_B at 300K.

REFERENCES

1. K. Miyokawa, H. Masuda, and I. Masuda, Bull. Chem. Soc. Jpn., 1980, 53, 3573.
2. W. W. Wendlandt, J. Inorg. Nucl. Chem., 1963, 25, 1267; ibid, 1963, 25, 545;
    N. Tanaka and M. Nanjo, Bull. Chem. Soc. Jpn., 1964, 37, 1330; G. W. Watt, Inorg.
    Chem., 1964, 3, 325; Y. Ihara, A. Uehara, R. Tsuchiya, and E. Kyuno, Bull. Chem.
    Soc. Jpn., 1978, 51, 2578.
3. S. N. Poddar and K. Biswas, J. Inorg. Nucl. Chem., 1969, 31, 565.
4. T. Tsumaki, Bull. Chem. Soc. Jpn., 1938, 13, 252.
5. A. W. Coats and J. P. Redfern, Nature, 1964, 201, 68.
6. A Ohyoshi, S. Kohata, M. Nishimori, Y. Shimura, and N. Iwasaki, Bull. Chem. Soc.
    Jpn., 1976, 49, 1284.

Preparation and Chelation Properties of the Polystyrene Resins Containing Pendant Multidentate Ligands

TOSHISHIGE M. SUZUKI* and TOSHIRO YOKOYAMA

Government Industrial Research Institute, Tohoku

Haranomachi, Sendai, Japan 983

Chelating polymer resins have been widely applied to metal ion collector in the fields of environmental chemistry and chemical industry.[1] Since the stability of a metal complex increases with the number of chelate rings, it is desirable to immobilize multidentate ligand into polymer matrix. Blasius prepared chelating resins by the reaction of alkylpolyamines with chloromethylated styrene-divinylbenzene copolymer.[2] But the intra- and interstrand bridging reactions are inevitable by the N-alkylation of the primary and the secondary amino groups of polyamine. These bridging reactions bring about the decrease in ligand content introduced in the polymer and steric restrictions for the chelate formation. Improved methods have been reported to avoid such bridging reactions,[3,4] but they require relatively long reaction steps.

In this communication we report a simple method to introduce multidentate ligands based on diethylenetriamine into polystyrene beads without causing the undesirable bridging reactions. The preparative scheme is given in Fig. 1.
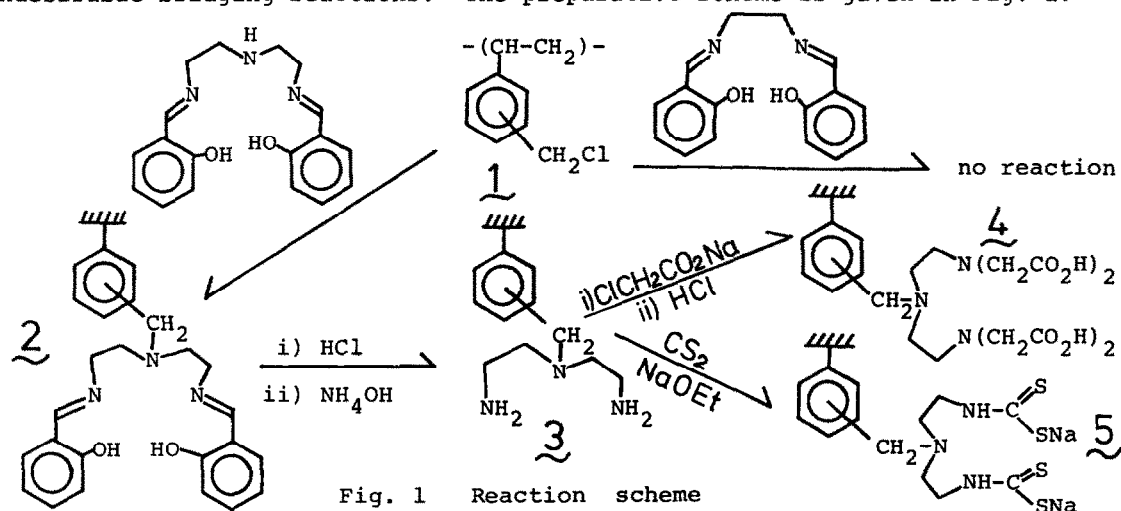
Fig. 1   Reaction   scheme

Preparation of the chelating resins.   Reaction of bis(salicylidene-iminate)diethylenetriamine (93.3 g) with resin **1**[5] (26.0 g) in refluxed dioxane (400 cm^3) for 48 h gave yellow resin **2**. Yield: 50.4 g. Hydrolysis of **2** (49.1 g) with 6M HCl (600 cm^3) at 60 °C for 12 h yielded **3** in hydrochloride form. The resin in the free amine form was obtained by treatment with 2 M aqueous ammonia. Yield: 30.5 g. A mixture of sodium monochloroacetate (117.5 g in 200 cm^3 of water) and **3** (30.0 g) was heated at 70 °C for 12 h. Aqueous sodium carbonate solution was added to maintain the reaction solution basic (pH 9–10). The resin was washed with 2M HCl, water and acetone and vacuum dried. Yield: 49.9 g. Resin **5** was obtained by stirring resin **3** (5 g) with carbon disulfide (15.2 g) and sodium ethoxide (13.4 g) in ethanol (100 cm^3) at 50 °C for 12 h. Yield: 7.9 g. The analytical data of the resins are summerized in Table 1 along with the concentration of ligating groups and the reaction conversion.

Table 1. Analytical data and concentration of ligating groups of the resins

Resin	Analytical data (%)		Concentration of ligating group [a] (mmole/g-resin)	Conversion (%)[b]
	Cl	N		
1	20.5	–	5.78	–
2	1.09	8.81	2.10	94
3	0	12.70	3.02	72
4	0	7.74	1.84	87
5	0	7.58	1.80	78

a) Calculated from actual chlorine content (1), and nitrogen content (2, 3, 4 and 5).[6] Concentration of ligating group $= \dfrac{\% \; N}{14 \; n}$ X 10, where n=number of nitrogen atom.

b) Based on the ratio of the actual ligand content to the theoretical value calculated from total displacement of chlorine by ligand.[6]

Characterization and evaluation of the resins. The Schiff base bound resin 2 is presumed to have a structure as depicted in Fig. 1 in which direct N-alkylation has occurred. It is noted that bis(salicylideneiminate)ethylene-diamine did not react with 1, indicating that O-alkylation of the hydroxide groups in the ligand did not take place. Hence 2 does not contain bridging structures in the ligand moiety. Resin 2 gave IR band at around 1630 cm^{-1} due to (C=N) stretching vibration of the pendant ligand. Acid hydrolysis of 2 gave 3, where ν(C=N) band disappeared. Strong band of ν(C=O) was observed at around 1730 cm^{-1} for the resin 4 indicating that the desired reaction had took place.
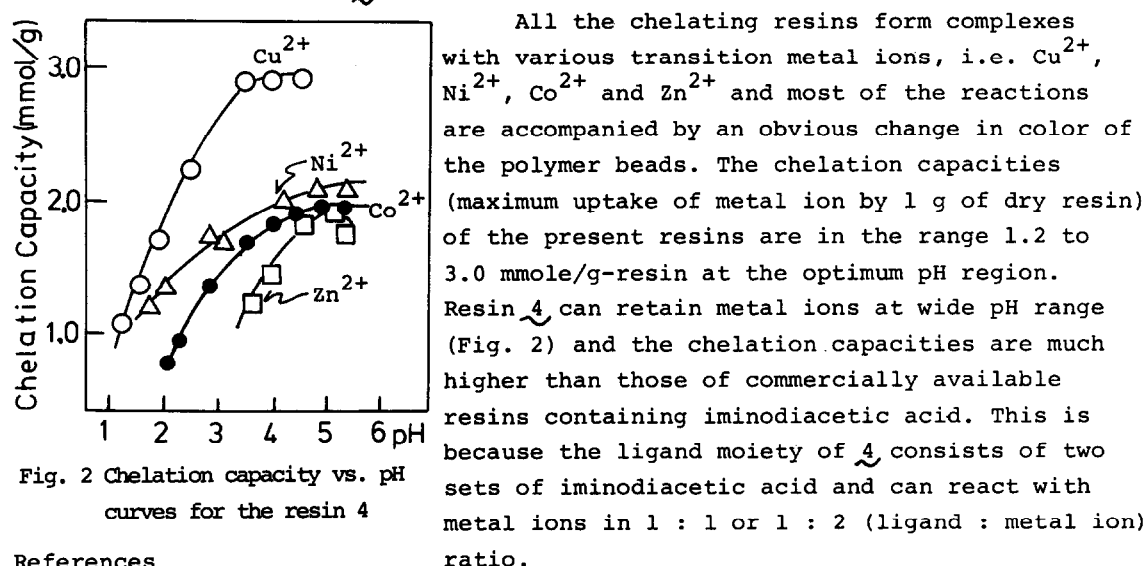
Fig. 2 Chelation capacity vs. pH curves for the resin 4

All the chelating resins form complexes with various transition metal ions, i.e. Cu^{2+}, Ni^{2+}, Co^{2+} and Zn^{2+} and most of the reactions are accompanied by an obvious change in color of the polymer beads. The chelation capacities (maximum uptake of metal ion by 1 g of dry resin) of the present resins are in the range 1.2 to 3.0 mmole/g-resin at the optimum pH region. Resin 4 can retain metal ions at wide pH range (Fig. 2) and the chelation capacities are much higher than those of commercially available resins containing iminodiacetic acid. This is because the ligand moiety of 4 consists of two sets of iminodiacetic acid and can react with metal ions in 1 : 1 or 1 : 2 (ligand : metal ion) ratio.

References

1. A. K. Coleman, *Chem. Ind. (London)*, 1975, 534.
2. E. Blasius, and I. Bock, *J. Chromatogr.*, 1964, 14, 244.
3. R. S. Drago, J. Gaul, A. Zombeck, and D. K. Straub, *J. Am. Chem. Soc.*, 1980, 102, 1033.
4. E. M. Moyers and J. S. Fritz, *Anal. Chem.*, 1977, 49, 418.
5. The chlorine content of the beads (100 200 mesh) was 20.50 %, which corresponds to chloromethylation 86 % of the available benzene rings.
6. L. R. Melby, *J. Am. Chem. Soc.*, 1975, 97, 4044.

SYNTHESIS AND SPECTRAL STUDIES ON PLATINUM COMPLEXES WITH MONO- AND BIDENTATE N-DONOR ORGANIC LIGANDS†

P. UMAPATHY* and RASHIDA A. HARNESSWALA

National Chemical Laboratory, Poona 411008, India

Abstract—Platinum(II) complexes of types $PtLX_2$, PtL_2X_2, $PtLX'$ and the Pt(IV) complexes PtLXY (where L = mono- or bidentate organic ligand containing nitrogen donor atoms; X = Cl or Br; X' = oxalate or malonate and Y = Br) have been synthesized and characterized from their elemental analysis, IR and X-ray photoelectron spectral data. The Pt $4f_{7/2}$ binding energies indicate that 1,8-naphthalene-diamine ligand is a better donor of electron density to the metal than other ligands studied here. The Cl $2p_{3/2}$ binding energies in the square planar Pt(II) complexes are observed in the range 198.8 ± 0.8 eV. The ν (Pt–Cl) vibrations (ca 335 and 320 cm^{-1}) corresponding to two cis-Cl ligands were observed in the IR spectra.

The extent of the interaction between cis-dichloro-bis-(theophylline)platinum(II) with calf thymus DNA has been studied. The UV difference spectra resulting from aquated Pt^{II}(theoph)$_2$-DNA interaction exhibit bands at 282 and 292 nm attributable to the change in the electron distribution of the base moieties induced by binding with platinum and due to the loss of base stacking. Melting profiles for the DNA samples treated with Pt-complex showed decrease in the melting temperature. Binding of the guanine residues of the DNA, involving probably (N7)–O(6) positions to the metal is implied.

INTRODUCTION

The encouraging and rapid progress in clinical development of anti-tumour platinum drugs has been the main impetus behind studies of the mechanism of action. Currently[1] the most convincing mechanism for the cytotoxic action of these agents on cells in culture is that reactions with DNA impair its function as a template for further DNA replication. The anti-cancer action of cis-dichlorodiammine platinum(II) cis-PtCl$_2$(NH$_3$)$_2$ (cis-platin), which is currently used in many hospitals in the treatment of ovarian, testicular and other forms of cancer, is thought to involve coordination to a guanosine residue in DNA. Little is presently known about the specific covalent attachment sites of cis-PtCl$_2$(NH$_3$)$_2$ and platinum uracil blues on DNA. However, various studies have implicated N-7 and possibly O–6 of guanine.[2–5] Although high overall response rates for cis-platin in the treatment, particularly ovarian and testicular forms of cancer, were reported[6,7] when the drug was used in combination with vinblastine and bleomycin or doxorubicin, efforts increasingly are being made to synthesize new platinum compounds with decreased toxicity and greater therapeutic properties. We have, in continuation of our work[8] on Pt(II) and Pd(II) chelates, synthesised several new Pt(II) complexes of the type, $PtLX_2$, PtL_2X_2, $PtLX'$ and Pt(IV) complexes PtLXY where L = mono- or bidentate ligand, such as, 8-aminoquinoline, 1,8-naphthalenediamine or a derivative of 1,10-phenanthroline, theophylline, 5-nitro-2-aminopyridine, etc. X = Cl or Br; X' = oxalate or malonate; Y = Br.

Some of these compounds were screened for their activity at Imperial Cancer Research Fund Laboratories, London, and the preliminary in vitro tests indicate appreciable antitumour activity, especially for the compounds dichloro(8-aminoquinoline)Pt(II) and oxalato(8-aminoquinoline)-Pt(II). Furthermore, we have also studied in solution the reaction of dichloro-bis-(theophylline)Pt(II) with calf thymus DNA by recording the UV difference spectra at various pH's and temperatures. Solubility problems precluded the study of other Pt-complexes.

EXPERIMENTAL

K$_2$PtCl$_4$ and K$_2$PtBr$_4$ were prepared by the reported methods.[9,10] The ligands, 5-notro- and 5,7 - dibromo - 1,10 - phenanthroline, 5 - nitro - 2 - aminopyridine, 1 - isonicotinyl - 2D - glucosylhydrazine, theophylline, 7 - methyltheophylline, 6 - amino - 5 - nitroso - 1,3 - dimethyl uracil were synthesized by the known procedures.[11–15] Their purity was checked by elemental analysis, m.ps and spectral data. Calf thymus DNA (Type I), thymine hydrochloride, 8 - amino - quinoline and 1,8-naphthalenediamine were purchased. (Sigma Chemical Co., Fluka AG, Buchs SG, Switzerland and Aldrich Chemical Company, Inc., U.S.A.) All other chemicals used were of reagent grade. Solvents were purified and dried prior to use. IR spectra were recorded on a Perkin–Elmer model 599B infrared spectrophotometer.

X-ray photoelectron spectra were recorded using a VG Scientific ESCA–3MK–2 electron spectrometer. Powered samples were mounted on a nickel sample holder. Magnesium K$_\alpha$ radiation (1253 · 6) was used as a source. Nitrogen 1s, Pt 4f, Cl 2p, Br 3p binding energies were referred to C 1s line of impurity carbon at 283 eV. An attempt was also made to reference the spectra to the Au $4f_{7/2}$ line at 83 eV by vacuum deposition of gold onto the sample. The final values of the binding energies for each sample were determined from measurements in triplicate on several sample preparations and their accuracy is within ±0.20 eV. Visual examination of the samples after measurement revealed no evidence of radiation damage.

DNA stock solutions were prepared by dissolving DNA in 0.01 M phosphate buffers pHs 6.8, 8.04 and 9.95 containing 0.01 M NaCl by gentle stirring in a refrigerator. The concentration of DNA was estimated by absorbance measurement at 260 nm using the coefficient ϵ (P) = 6650.[16] The platinum complexes were dissolved before use in 0.01 M phosphate buffer, pH 6.8 containing 0.01 M NaCl. The aquated cis-Pt(theoph)$_2^{2+}$ was prepared by stirring solutions of stoichiometric amounts of AgNO$_3$ and cis-Pt(theoph)$_2$Cl$_2$ overnight at room temperature in dark. The AgCl that precipitated was removed by filtration and the clear filtrate was diluted with buffer to the final stock concentration [1.0×10^{-14}M aq cis(theoph)$_2$Pt^{++}]. The pH adjust-

---

†NCL Communication No. 2841.
*Author to whom correspondence should be addressed.

ment of all solutions to 6.8 was made by the addition of standard NaOH solution. All the pH measurements were made on a digital pH meter, model PHN63 (Radiometer, Copenhagen).

Reactions were carried out at different concentrations of DNA, concentration of aq. cis-(theoph)₂Pt⁺⁺, temperature and pH. The difference spectra were obtained using four 1 cm path length cells. The sample compartment contained two cells, one containing the reaction solution (cis-(theophy)₂Pt⁺⁺/DNA) and the other containing the buffer solution, whereas the reference compartment contained individual cells of DNA and the aquated cis-(theoph)₂Pt⁺⁺ solutions respectively at the same conditions (0.01 M phosphate buffer, pH, temperature and initial concentration). The difference spectra reported at 30°C were obtained on a 0.500 expanded absorbance scale on a Pye Unicam Model SP8-100 spectrophotometer. The melting temperature, Tm, is defined as the temperature at half denaturation.[17] Melting profiles were recorded manually (rate of heating 5°/min. initially and 1°/min. in the steep part of the curve at 260 nm.

Pt(II) complexes of the type Pt(II)LX₂, Pt(II)L₂X₂ were synthesized by following the general procedure given below:

Clear (filtered if necessary) solutions of K₂PtCl₄ or K₂PtBr₄ in water (10 ml) and the appropriate organic ligand in excess of hot water (80 ml) in 1:1 or 1:2 mole ratios were mixed together and heated on a water-bath for about 8–12 hr. (In case of 5 - nitro - and 5,7 - dibromo - 1,10 - phenthroline solvent DMF was used and the mixture was refluxed; in the preparation of 1-isonicotinyl - 2D - glucosyl hydrazine complex, the reaction mixture was stirred at room temperature for 24 hr.) The solid products that separated out were collected on a filtered under suction, washed with hot water repeatedly (5 ml portions) and dried under vacuum. Yield ~ 80%.

(1) *Dichloro(8-aminoquinoline)platinum(II)*, Pt(8–NH₂Q)Cl₂: m.p. decomp 335°C (330°C).[18] Found: C, 27.2; H, 2.10; N, 7.2; Cl, 16.9; Pt, 47.41. Calc. for C₉H₈N₂Cl₂Pt: C, 26.35; H, 1.96; N, 6.83; Cl, 17.28; Pt, 47.56%.

(2) *Dibromo(8 - aminoquinoline)platinum(II)*, Pt(8–NH₂Q)Br₂: decomp. ~ 190°C. Found: C, 22.71; H, 1.93; N, 6.19; Br, 31.4; Pt, 39.44. Calc. for C₉H₈N₂Br₂Pt: C, 21.63; H, 1.6; N, 5.61; Br, 32.00; Pt, 39.09%.

(3) *Dichloro(1,10 - phenanthroline)platinum(II)*, Pt(1,10 - phen)Cl₂: was prepared by the reported method[19] and also by the general procedure using DMF solvent. Found: C, 31.9; H, 1.95; Pt, 43.2. Calc. for C₁₂H₈N₂Cl₂Pt: C, 32.29; H, 1.81; Pt, 43.73%.

(4) *Dichloro(5 - nitro - 1,10 - phenanthroline)platinum(II)*, Pt(5 - NO₂ - 1,10 - phen)Cl₂: decomp. 315°C. Found: C, 30.4; H, 1.94; N, 7.9; Cl, 14.61; Pt, 39.52. Calc. for C₁₂H₇N₃O₂Cl₂Pt: C, 29.3; H, 1.44; N, 8.56; Cl, 14.43; Pt, 39.71%.

(5) *Dichloro(5,7 - dibromo - 1,10 - phenanthroline) platinum(II)*, Pt(5,7 - Br₂ - 1,10 - phen)Cl₂: decomp. ~ 295°C. Found: C, 24.07; H, 1.36; N, 4.60; Pt, 31.82. Calc. for C₁₂H₆N₂Br₂Cl₂Pt: C, 23.84; H, 1.0; N, 4.64; Pt, 32.33%.

(6) *Dichloro(1,8 - naphthalenediamine)platinum(II)*, Pt(1,8 - NH₂ - Naphth)Cl₂: decomp. > 250°C. Found: C, 28.90; H, 2.6; N, 6.0; Cl, 16.74; Pt, 45.52. Calc. for C₁₀H₁₀N₂Cl₂Pt: C, 28.29; H, 2.36; N, 6.6; Cl, 16.71; Pt, 45.99%.

(7) *Dichloro(1 - isonicotinyl - 2D - glucosylhydrazine) platinum(II)*: dihydrate, Pt(ISNGH)Cl₂.2H₂O: decomp. ~240°C. Found: C, 23.84; H, 3.27; Cl, 12.01; Pt, 33.46. Calc. for C₁₂H₂₁N₃O₈Cl₂Pt: C, 23.95; H, 3.52; Cl, 11.79, Pt, 32.44%.

(8) *Dichlorobis(methyltheophylline)platinum(II)*, Pt(7-CH₃-theoph)₂Cl₂ decomp. 310°C, found: C, 29.80; H, 3.3; N, 16.87; Cl, 10.2; Pt, 29.35. Calc. for C₁₆H₂₀N₈O₄Cl₂Pt: C, 29.35; H, 3.08; N, 17.12; Cl, 10.83; Pt, 29.82%.

(9) *Dichlorobis(theophylline)platinum(II)*, Pt(theoph)₂Cl₂: decomp. ~340°C. Found: C, 27.54; H, 3.4; N, 16.36; Cl, 11.78; Pt, 30.93. Calc. for C₁₄H₁₆N₈O₄Cl₂Pt: C, 26.84; H, 2.57; N, 17.89; Cl, 11.31; Pt, 31.11%.

(10) *Dichlorobis(2-aminopyridine)platinum(II)*, Pt(2-NH₂py)₂Cl₂: decomp. 280°C (285°C).[20] Found: C, 26.28; H, 3.2; Pt, 43.05. Calc. for C₁₀H₁₂N₄Cl₂Pt: C, 26.42; H, 2.64; Pt, 42.96%.

(11) *Dichlorobis(5 - nitro - 2 - aminopyridine)platinum(II)*: Pt(5 - NO₂ - 2 - NH₂ - py)₂Cl₂: decomp. >300°C. Found: C, 21.11; H, 2.5; N, 14.83; Pt, 36.18. Calc. for C₁₀H₁₀N₆O₄Cl₂Pt: C, 22.05; H, 1.84; N, 15.44; Pt, 35.86%.

(12) *Dichloro bis(6 - amino - 5 - nitroso - 1,3 - dimethyl uracil)-*: platinum(II), Pt(6 - NH₂ - 5 - NO, 1,3-CH₃ Urac)₂Cl₂: decomp. ~216°C Found: C, 22.63; H, 2.92; N, 16.82; Cl, 11.0; Pt, 30.38. Calc. for C₁₂H₁₆N₈O₆Cl₂Pt: C, 22.72; H, 2.53; N, 17.67; Cl, 11.18; Pt, 30.76%.

(13) *Dichloro bis(thymine)platinum(II)*, Pt(thy)₂Cl₂: decomp. 280°C. Found: C, 22.20; H, 2.6; N, 9.48; Cl, 12.84; Pt, 38.03. Calc. for C₁₀H₁₂N₄Cl₂Pt. C, 23.17; H, 2.33; N, 10.81; Cl, 13.68; Pt, 37.65%.

(14) *Tetrachloro(8 - aminoquinoline)platinum(IV)*; Pt(8–NH₂Q)Cl₄: Chlorine was bubbled into a well stirred suspension of Pt(8–NH₂Q)Cl₂ (0.41 g; 0.001 mole) in dry chloroform (~120 ml) for 20–25 min. After an additional 20 min. of stirring, the yellow product was filtered out, washed twice with CHCl₃ (5 ml portions) and vacuum dried. Yield of the greenish yellow product 0.32 g (66%). decomp 300°C. Found: C, 21.36; H, 1.87; N, 6.24; Pt, 39.71. Calc. for C₉H₈N₂Cl₄Pt: C, 22.51; H, 1.68; N, 5.83; Pt, 40.64%.

(15) *Dibromodichloro(8 - aminoquinoline)platinum(IV)*: Pt(8–NH₂Q)Cl₂Br₂: To a suspension of Pt(8–NH₂Q)Cl₂ (0.41 g; 0.001 mole) in chloroform (~ 50 ml) bromine (2 g) in chloform (50 ml) was added dropwise with stirring at room temperature. The stirring was continued for 4 hr. The greenish brown solid obtained was collected on a filter, washed with chloroform (20–25 ml) and dried in vacuum. Yield, 0.4 g (71%), decomp. ~260°C. Found: C, 19.94; H, 2.02; N, 4.76; Pt, 33.6. Calc. for C₉H₈N₂Cl₂Br₂Pt: C, 19.09; H, 1.41; N, 4.92; Pt, 34.23%.

(16) *Oxalato(8 - aminoquinoline)platinum(II)*, Pt(8–NH₂Q) (Oxal): Clear (filtered if necessary) solutions of potassium *bis*-oxalatoplatinate(II) dihydrate[21] in water (10 ml) (0.39 g; 0.001 mole) and 8-aminoquinoline in hot water (25 ml) (0.14 g; 0.001 mole) were mixed together and heated on a water bath for 4 hr. The deeply coloured violetish-black solid that separated was collected on a filter, washed with hot water and dried under vacuum. Yield 0.3 g (69%); decomp ~290°C. Found: C, 30.52; H, 2.49; N, 5.96; Pt, 44.78. Calc. for C₁₁H₈N₂O₄Pt: C, 30.82; H, 1.89; N, 6.56; Pt, 45.66%.

(17) *Malonato(8-aminoquinoline)platinum(II)*, Pt(8-NH₂.Q) (Malon): was prepared by following the above procedure starting with potassium *bis*-malonatoplatinate(II) dihydrate and 8-aminoquinoline: Yield ~65%. decomp. ~310°C. Found: C, 31.64; H, 2.66; N, 6.72; Pt, 43.78. Calc. for C₁₂H₁₀N₂O₄Pt: C, 32.64; H, 2.28; N, 6.35; Pt, 44.21%.

RESULTS AND DISCUSSION

The interaction of platinum complex, dichloro-*bis*-(theophylline)platinum(II) with calf thymus DNA in buffer solutions was followed by UV difference spectral and melting techniques. The UV difference spectrum for the DNA solution mixed with cis-Pt-(theoph)₂Cl₂ did not change indicating no reaction with DNA bases. However when the aquated Pt-complex was mixed with DNA, the spectrum exhibited large hyperchromism with a wavelength shift of the peak absorption from 259 to 282–290 nm (Figs. 1 and 2). It was postulated[22,23] that reactions of compounds such as cis-PtCl₂(NH₃)₂ with the DNA bases and even DNA itself *in vivo* go through an aquation product, supposedly [Pt(NH₃)₂(H₂O)₂]²⁺. Rosenberg *et al.*[24-27] recently have shown that aqueous solutions of the aquation product are very complex and, in addition to such species as the above contain substantial amounts of hydroxide-bridged species containing two, three and four platinum atoms. The aquated cis-Pt(theoph)₂Cl₂ solution may contain presumably cis-[(theoph)₂Pt(H₂O)₂]²⁺, cis-[(theoph)₂Pt(H₂O)(OH)]⁺ species along with hydroxide bridged species containing two or three platinum atoms. The extent of the reaction depends on pH, time, temperature and the mole ratio of Pt/DNA system. The time required to reach the end of the reaction under optimum conditions (pH 8–9, time 24 hr; mole ratio 1:2) is of the order of 24–30 hr at 30°C.
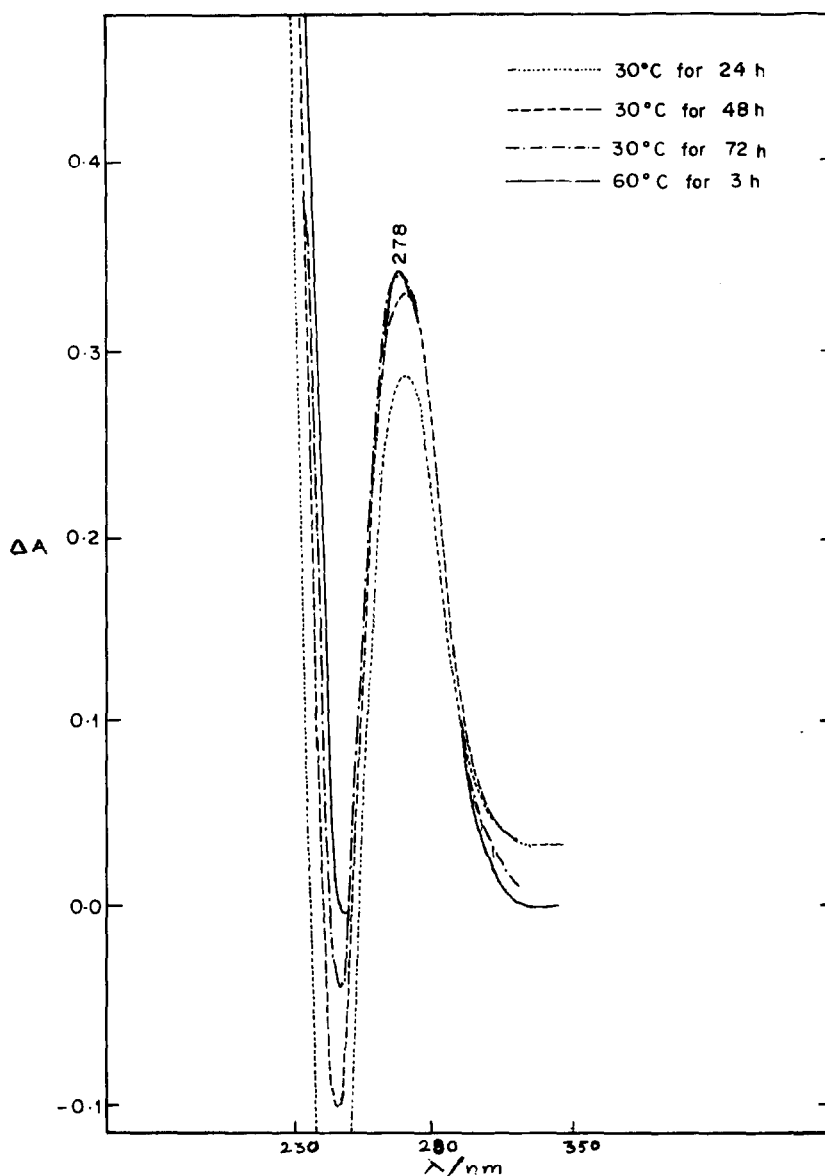
Fig. 1. UV difference spectra resulting from aquated cis-(theoph)$_2$ Pt^{II}-DNA interaction pH, 6.8; T 30 and 60°C
[DNA] 0.5 mg/ml of buffer, [Pt^{II}] $= 1 \times 10^{-4}$ M.

It seems well established[4,28] now that the interaction between Pt compounds and DNA takes place through the complex aquated charged species of platinum and that a high concentration of chloride ions (> 0.01 M) inhibits the reaction to an appreciable extent. The aquo complexes bind more readily to cellular targets such as DNA since water is relatively a good leaving group. Furthermore, the formation of charge aquo complexes equally may raise the affinity of the complexes to phosphates.[29] The UV difference spectrum in the reactions with aquated species of the Pt-complex with DNA at pH 6.8 and at pH 8.04 exhibit λ_{max} at 282 nm and at 292 nm respectively while λ_{min} was observed in both at 250 nm. ΔA at 282 nm and at 292 nm increased with increasing concentration of DNA as well as Pt-concentration. Similar changes were noticed when DNA was treated with another Pt-complex namely potassium bis-malonatoplatinum(II)dihydrate. The reaction with DNA was however, rapid compared with [(theoph)$_2$Pt(OH)(H$_2$O)]$^+$.

Melting profiles of DNA samples treated with platinum complexes were examined and the results show increase in melting temperatures, Tm. (Tm for (theoph)$_2$Pt(II), 65° and for K$_2$PtC$_3$H$_2$O$_4$, 61°C). Binding of the Pt-complex to DNA distorts the secondary structure of neighbouring base pairs in DNA and helps to destroy the secondary structure of DNA on heating.[17] The results suggest that the increment of ΔA at 282 nm may be attributed to the loss of base stacking. The increment of ΔA at 292 nm may be due to the change in electron distribution of base moieties induced by binding with platinum.

The interaction of the aquated species cis-[(theo)$_2$Pt(OH)-(H$_2$O)]$^+$ conceivably liberates a hydroxide from the coordination sphere on complexation which would yield a net increase in pH. It was in fact, observed that at pH ~ 9.00 the shift of the 259 nm band (of DNA) was quite large. It is also possible that the aquated species binds to guanine residue at N-7 position with the resulting liberation of proton at N-1 position as
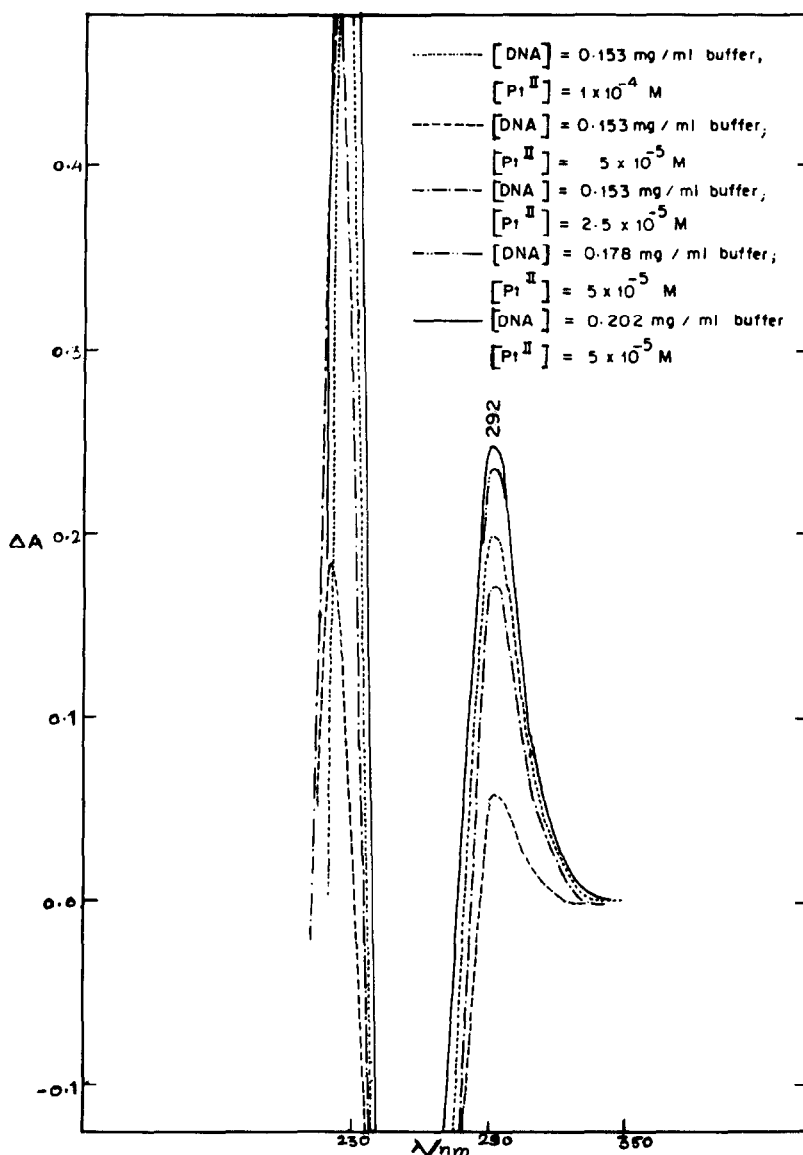
Fig. 2. UV difference spectra resulting from aq cis-(theoph)$_2$ Pt^{II}-DNA interaction pH 9·95 T 30°C; 68 hr.

has been postulated[30] in the cis-(NH$_3$)$_2$Pt(II)-inosine reaction. Scobell and O'Connor[31] observed in their studies of aquated cis-(NH$_3$)$_2$Pt(II) with nucleic acid constituents that deprotonation of the guanosine does not occur and that in the complexation reaction monodentate coordination occurs with displacement of water. The interaction of the aquated species [(cis-(theoph)$_2$Pt(H$_2$O)$_2$]$^{2+}$ with DNA may be predominant at pH 6.8. Millard et al.[32] have suggested that in the cis-(NH$_3$)$_2$Pt^{II} interaction with DNA, guanosine acts as a chelate, binding through the N-7 and O-6 positions. The binding mode of cis-(NH$_3$)$_2$Pt(II) to DNA as an interbase crosslink which corresponds to the intrastrand crosslink has also been suggested.[33–35] The large shift of the 259 nm band of DNA to 292 nm at pH ~9.00 observed in the UV difference spectrum of aquated cis-(theop)$_2$Pt(II)-DNA interaction, is indicative of chelation possible involving N-7-O-6 positions of the guanine residues, rather than Pt-intrastrand crosslinking. In the UV difference spectra resulting from aquated cis-

(NH$_3$)$_2$Pt(II)-guanosine interaction the peak was observed[30] at ~290 nm.

The XPS data for the platinum complexes investigated are given in Table 1. The Pt 4f$_{7/2}$ binding energies of compounds Nos. 1–5 imply a marked decrease of electron density on the metal relative to 1,8-naphthalenediamine complex. All the complexes are formally square planar Pt(II) compounds presumably containing cis-PtCl$_2$ fragment. Variations in relaxation effect should be minimized in this series and the differences in metal binding energies should primarily be due to differences in the electron donating ability of the coordinated ligands.[36] The data indicate that 1,8-naphthalenediamine is a better complexing agent, i.e. better donors of electron density compared to 5,6 - dibro - 1,10 - phenanthroline or 7-methyl theophylline. The substantial shift in the binding energy of N(1s) clearly confirms a net electron transfer from nitrogen to platinum in these complexes. The N(1s) photoelectron spectra of these complexes consist of doublets or broad bands indicative of unresolved peaks.
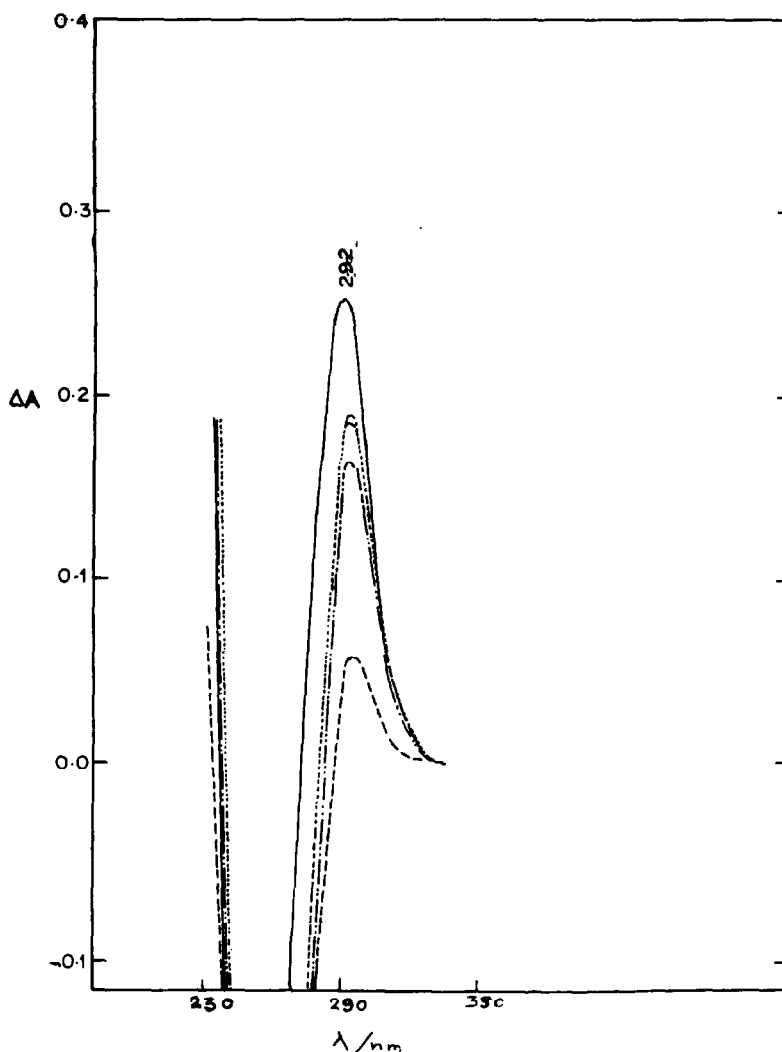
Fig. 2(a). Concentrations same as Fig. 2 after 140 hr.

The directly coordinated nitrogen has presumably the greater positive charge.

The change in the Pt $4f_{7/2}$ binding energies shows both the effect of oxidation state and of ligand character. The higher the formal oxidation state of platinum the higher the binding energy. All the platinum(II) complexes of the general formula $Pt^{II}X_2L_2$ or PtX_2L investigated here have $4f_{7/2}$ binding energies ranging from 74.4 to 73.4 eV, which is in agreement with the range reported by Riggs[37] for Pt(II) complexes.

The $Cl(2p_{3/2,1/2})$ binding energies for all the complexes studied studied are in the range 198.8 ± 0.8 eV. In general, within the closely related series of complexes, the chlorine binding energy gives a good indication of the effect of changes in overall electron density on the Pt–Cl bond. The Cl(2p) binding energies of these complexes of the type PtL_2Cl_2 or $PtLCl_2$ are lower than that of $K_2(PtCl_4)$ indicating partial ionic character of the Pt–Cl bond. In complexes, where L = a bidentate ligand, the square planar geometry presumably implies cis-Cl configuration. The IR spectral date confirm this. The other complexes may also have cis-chlorines in view of the observed narrow range of Cl(2p) binding energies. X-ray crystallographic data show quite clearly that there is a considerable increase in metal-halogen bond length in going from trans- to cis-isomer in square planar Pt(II) and Pd(II) complexes of the type $(PR_3)_2MX_2$. For X = Cl, n.q.r. data[38] suggest that the bond lengthening is accompanied by a considerable electron drift to chlorine. Clark and Adams[39] observed that in a given cis-trans pair, the binding energy of the metal is the same but that of the halogen is considerably lower in the cis-isomer. The ^{35}Cl resonance signals in the three trans-L_2PtCl_2 complexes are found at higher frequencies than in the corresponding cis-complex and this difference is related to the charges on the ligands. The tentative conclusion is that the trans- influence in the ^{35}Cl quadrupole resonance of the complexes of the type L_2MCl_2 [M = Pt(II) or Pd(II), Ni(II)] manifests itself in a general lowering of the frequencies on going from trans- to the cis-complex and the difference Δ being related to the position of the ligand L in the trans-series. There is evidence,[40] however, that relative to $PtCl_4^{2-}$, the binding energy of the cis-chlorines is raised (decrease in negative charge) and that of the trans-chlorine is lowered. This is in agreement with the other ground state phenomena which relate to the trans- effect; increase in Pt–Cl bond length is accompanied by electron drift to chlorine.
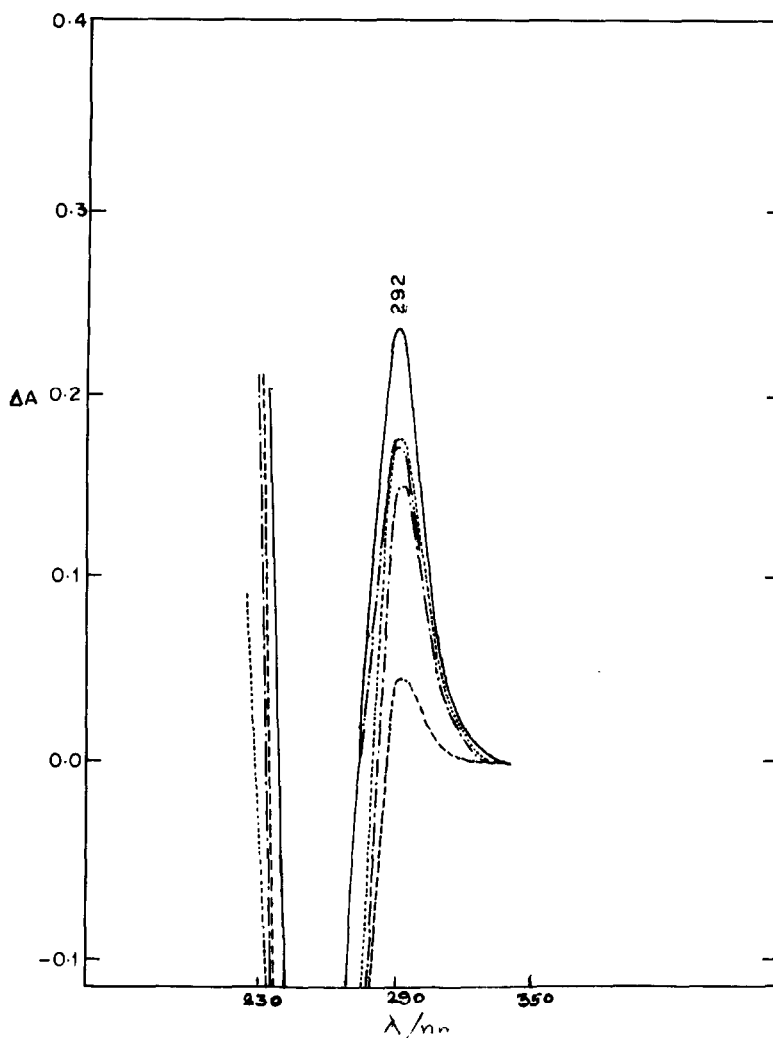
Fig. 2(b). Concentrations same as Fig. 2 after 4 hr, T 55°C.

The infrared spectra of Pt(II) complexes with organic ligands, 8-aminoquinoline, 5-nitro- or 5,7-dibromo-1,10-phenanthroline, 1-isonicotinyl-2D-glucosyl hydrazine, theophylline and its methyl derivative, etc. show absorptions in the region 600–200 cm^{-1}, assignable to Pt-halogen stretching vibrations which are absent in the spectra of the corresponding ligands. The spectrum of the complex Pt(8-NH$_2$Q)Cl$_2$ shows two medium intense absorption at ca. 335 and at ca. 320 cm^{-1} ascribable to ν(Pt-Cl) vibrations corresponding to two Cl ligands in cis-arrangement. The ν(Pt-Cl) absorptions in the spectra of the complexes, Pt(5-NO$_2$-1,10 phen)Cl$_2$, Pt(5,7-Br$_2$-1,10-phen)Cl$_2$ and Pt(ISNGH)Cl$_2$ are observed at 340 and 335 cm^{-1}; 345 and 335, 330 and 300 cm^{-1} respectively. In the IR spectra of Pt(II) complexes with nitrogen donor ligands (mono- or bidentate) bands observed at ca. 330 and 320 cm^{-1} have been assigned to asymmetric and symmetric ν(Pt-Cl) vibrations corresponding to two Cl ligands in cis-arrangement.[18,20] The medium intense band observed at ca. 270 cm^{-1} with a shoulder at ca. 275 cm^{-1} in the spectrum of Pt(8-aminoQ)Br$_2$ may arise due to (Pt-Br)-vibrations. In view of the bidentate nature of the ligand and the square planar geometry presumed for these complexes, these bands may tentatively be assig-

ned to cis-ν(Pt-Br) vibrations. ν(Pt-Br) vibrations in Pt(II) complexes with N-methyl imidazole[41] and in Pt(II) complex anions[42] were reported to occur at ca. 220 cm^{-1} and at ca. 205 cm^{-1} respectively.

In the spectra of Pt(IV) complexes, Pt(8-NH$_2$Q)Cl$_4$ and Pt(8-NH$_2$Q)Cl$_2$Br$_2$ (isolated by the reactions of Pt(8-NH$_2$Q)Cl$_2$ with halogens), absorption bands at 350(sh), 345 and 320 cm^{-1} were observed. It is, however, difficult to locate precisely the trans- ν(Pt-Cl) vibrations since this region is obscured by the strong absorptions caused by the equatorial chlorides. However, the absorption observed at ca. 255 cm^{-1} in (Pt(8-NH$_2$Q)Cl$_2$Br$_2$ may arise due to trans-ν(Pt-Br) vibrations. In Pt(II) complexes with 1,10-phenanthroline and its derivatives, axial bromides are reported[19] to absorb at 251–253 cm^{-1}. All platinum complexes containing the bidentate ligand, 8-aminoquinoline show ν(N-H) at ca. 3120 cm^{-1} in their IR spectra indicating a coordinated NH$_2$[18,43].

The Pt(II) complex with methyl theophylline shows bands at 350(s), 345(s) assignable to asymmetric and symmetric cis-ν(Pt-Cl) vibrations. The Pt(II) complex with theophylline shows medium to strong intense band at 330 cm^{-1} with a shoulder at 325 cm^{-1}. The shoulder could be due to symmetric Pt-Cl vibration and indicates

Table 1. N(1s), Pt(4f), Cl(2p) and Br(3p) X-p.e. binding energies (eV) for platinum complexes

Compound	$Pt4f_{7/2}$	$N1s_{1/2}$	$Cl2p_{3/2}$	$Br3p_{1/2,3/2}$
1. K_2PtCl_4	73.4^b		199.4^b	
			198.0	
	(73.9), 74.46		(200.3)	
			(200.7)	
2. K_2PtBr_4	73.9^c			183.8
3. Pt(ISNHG)Cl$_2$	74.44	397.8, 401.88	199.08	
4. Pt(7–CH$_3$–theoph)$_2$Cl$_2$	74.44	398.88, 402.52	199.84	
5. Pt(theoph)$_2$Cl$_2$	74.4	398.2, 402.4	200.0	
			200.08	
6. Pt(5,6–Br$_2$-1,10-phen)Cl$_2$	74.32	397.8, 402.0	200.08	
7. Pt(8–NH$_2$–Q)Cl$_2$	74.32	397.68, 401.4	199.9	
			200.9	
8. Pt(phen)Cl$_2$	74.2	398.4, 401.64	199.6	
9. Pt(5-NO$_2$-2-NH$_2$-py)$_2$Cl$_2$	74.08	400.04	198.88	
		397.92	200.92	
10. Pt(thym)$_2$Cl$_2$	74.08	397.68, 400.92	199.84	
11. Pt(2-NH$_2$py)$_2$Cl$_2$	74.08	400.8	199.24	
12. Pt(5-NO$_2$-1,10-phen)Cl$_2$	73.72	398.28, 402.4	199.6	
13. Pt(8-NH$_2$Q)oxal)	73.72	397.67, 400.2	–	
14. Pt(8-NH$_2$Q)Br$_2$	73.5	397.2, 400.68	–	189.2
				182.8
15. Pt(1,8-NH$_2$Naph)Cl$_2$	73.44	398.76, 402.24	199.2	

^{a}Binding energies are in electron volts.

^{b,c}Data from electron spectroscopy, D. A. Shirley (Editor), pp. 713, 725 and from reference, *Anal. Chem.*, 1972, 44, 830.

the *cis*-complex. The IR spectrum of Pt(II)-theophylline complex shows strong bands at 1500–1700 cm^{-1} and 1200–1250 cm^{-1} attributed to theophylline coordination.[44] Theophylline anion is bound to metal through N-7 in most of the reported metal–ion theophylline complexes,[45,46] and various other ligands are attached to the central metal. In fact the anion does not seem to act as a chelate in many complexes whose structures have been determined.[47] Recently a new mode of theophylline anion metal bonding—a trimeric complex with trimethyl platinum(IV) which contains Pt-N(7)-N(9)-Pt bridges and a weak direct (C-6) O-Pt bond has been however, reported by Hall *et al.*[48] In methyl theophylline (caffeine) anion formation through loss of a proton on nitrogen (N-7) is not possible and N-9 lone pair is the only nitrogen site available for bonding. The crystal and molecular structure of aquadichloro caffeine copper(II), [CuCl$_2$(C$_8$H$_{10}$N$_4$O$_2$)H$_2$O], has been determined.[49] The caffeine ligand acts as a unidentate and N-9 is involved in bonding with copper.

REFERENCES

[1] J. J. Roberts and A. J. Thomson, The mechanism of reaction of antitumor platinum compounds. *Progress in Nucleic Acid Research and Molecular Biology* (Edited by W. E. Cohn), Vol. 22, p. 71. Academic Press, New York (1979).

[2] S. Mansy, R. Rosenberg and A. J. Thomson, *J. Am. Chem. Soc.* 1973, **95**, 1633.

[3] A. B. Robins, *Chem. Biol. Interactions* 1973, **6**, 35.

[4] S. J. Lippard, *Acc. Chem. Res.* 1978, **11**, 211.

[5] L. G. Marzilli, *Prog. Inorg. Chem.* 1977, **23**, 255.

[6] H. W. Bruckner, C. C. Cohen, G. Deppe, B. Kabakow, R. C. Wallach, E. M. Greensfan, S. B. Gusberg and I. F. Holland, *J. Clin. Hematol. Oncol.* 1977, **7**, 619.

[7] L. H. Einhorn, B. E. Furnas and N. Powell, *Proc. Am. Soc. Clin., Oncol.* 1976, **17**, 240.

[8] P. Umapathy, S. Chandrasekar and K. D. Ghuge, *J. Indian Chem. Soc.* 1981, **58**, 220.

[9] G. Brauer, *Handbook of Preparative Inorganic Chemistry*, 2nd Edn, Vol. 2, p. 1572. Academic Press, New York (1965).

[10] G. A. Shagisultanova, *Russ. J. Inorg. Chem.* 1961, **6**, 904.

[11] J. Mlochowski and Z. Skrowaczewska, *Roczniki. Chem.* 1973, **47**, 2255.

[12] J. Mlochowski, *Roczniki. Chem.* 1974, **48**, 2145.

[13] L. N. Pino and W. S. Zehrung III, *J. Am. Chem. Soc.* 1955, **77**, 3154.

[14] BIOS report, 1404.

[15] H. H. Fox, *J. Org. Chem.* 1953, **18**, 990.

[16] H. J. Lin and E. Chargaff, *Biochem. Biphys. Acta.* 1966, **123**, 66.

[17] K. Inagaki and V. Kidani, *Inorg. Chim. Acta* 1980, **46**, 35.

[18] H. A. Hudali, J. V. Kingston and H. A. Tayim, *Inorg. Chem.* 1979, **18**, 1391.

[19] K. D. Hodges and J. V. Rund, *Inorg. Chem.* 1975, **14**, 525.

[20] S. Haghighi and C. A. McAuliffe, *Inorg. Chim. Acta* 1980, **43**, 113.

[21] P. Pascal, *Traite de Chemie Minerale*, p. 672. Masson et Cie, Paris (1928).

[22] H. J. S. King, *J. Chem. Soc.* 1938, 1338.

[23] M. J. Cleare, *Coord. Chem. Rev.* 1974, **12**, 349.

[24] R. Faggiani, B. Lippert, C. J. L. Lock and B. Rosenberg, *J. Am. Chem. Soc.* 1977, **99**, 777.

[25] R. Faggiani, B. Lippert, C. J. L. Lock and B. Rosenberg, *Inorg. Chem.* 1977, **16**, 1192.

[26] R. Faggiani, B. Lippert, C. J. L. Lock and B. Rosenberg, *Inorg. Chem.* 1978, **17**, 1941.

[27] B. Lippert, C. J. L. Lock, B. Rosenberg and M. Zvagulis, *Inorg. Chem.* 1978, **17**, 2971.

[28] M. C. P. Gillet, C. Houssier and E. Fredericq, *Chem. Biol. Interactions* 1979, **25**, 87.

[29] P. Horáček and J. Drobník, *Biochim. Biophys. Acta.* 1971, **254**, 341.

[30]G. Y. H. Chu and R. S. Robias, *J. Am. Chem. Soc.* 1976, **98**, 2641.

[31]W. M. Scovell and T. O'Conner, *J. Am. Chem. Soc.* 1977, **99**, 120.

[32]M. M. Millard, J. P. Macquet and T. Theophanides, *Biochim. Biophys. Acta.* 1975, **402**, 166.

[33]I. A. G. Ross, *Chem. Biol. Interact.* 1977, **16**, 39.

[34]I. A. G. Ross, A. J. Thomson and S. Mansy, *J. Am. Chem. Soc.* 1974, **96**, 6484.

[35]P. J. Stone, A. D. Kelman, F. M. Sinex, M. M. Bhargava and H. D. Halvorson, *J. Mol. Biol.* 1976, **104**, 793.

[36]P. Brant and J. H. Enemark, *J. Organometal Chem.* 1976, **114**, 99.

[37]W. M. Riggs, *Anal. Chem.* 1972, **44**, 830.

[38]C. W. Fryer and J. A. S. Smith, *J. Chem. Soc., A* 1970, 1029.

[39]D. T. Clark and D. B. Adams, *J. C. S. Chem. Commm.* 1971, 602.

[40]D. T. Clark, D. Briggs and D. B. Adams, *J. C. S. Dalton* 1973, 169.

[41]C. G. Vankralingen and J. Reedijk, *Inorg. Chim. Acta* 1978, **30**, 171.

[42]P. J. Hendra, *J. Chem. Soc. A.* 1967, 1298.

[43]D. Brodzki and G. Pannetier, *J. Organometal Chem.* 1976, **104**, 241.

[44]M. S. Zitzman, R. R. Krebs and W. J. Birdsall, *J. Inorg. Nucl. Chem.* 1978, **40**, 571.

[45]W. J. Birdsall and M. S. Zitzman, *J. Inorg. Nucl. Chem.* 1979, **41**, 116.

[46]T. Sorrell, L. G. Marzilli and T. J. Kistenmacher, *J. Am. Chem. Soc.* 1976, **98**, 2181.

[47]L. G. Marzilli and T. J. Kistenmacher, *Acc. Chem. Res.* 1977, **10**, 146.

[48]N. H. Angew, T. G. Appleton, J. R. Hall, G. F. Kilmister and I. J. McMohon, *J. C. S. Chem. Comm.* 1979, 324.

[49]G. Bandoli, M. C. Biagini, D. A. Clemente and G. Rizzardi, *Inorg. Chim. Acta* 1970, **20**, 71.

CRYSTAL AND MOLECULAR STRUCTURE OF
[N N'-(3,3'-DIPROPYLAMINE)-
BIS(SALICYLIDENEAMINATO)MONOACETATE]COBALT(III)
COMPLEX

NAOHIDE MATSUMOTO*, MASAHIKO IMAIZUMI and AKIRA OHYOSHI

Department of Industrial Chemistry, Faculty of Engineering, Kumamoto University, Kurokami 2-39-1, Kumamoto
860, Japan

Abstract—The crystal and molecular structure of [N,N'-(3,3'-dipropylamine)*bis*(salicyclideneaminato)-monoacetate]cobalt(III) complex has been determined by a three-dimensional X-ray diffraction study. In the complex, the cobalt ion has an octahedral coordination environment with *cis*-geometry for the two salicyclideneaminato moieties. An oxygen atom of the acetate ion is coordinated to cobalt ion and another oxygen atom is hydrogen-bonded to the secondary amine nitrogen atom.

INTRODUCTION

It is well known that the complex [N,N'-(3,3'-dipropyl-amine)*bis*(salicyclideneaminato)]cobalt(II) (1) reacts reversibly with molecular oxygen to form the 1:1 O_2 adduct complex.[1] Recently, a single-crystal X-ray diffraction study has confirmed that the coordination geometries of the precursor complex (1) and its 1:1 O_2 adduct complex (2) are a trigonal bipyramid and an octahedron, respectively, with *trans*-geometry for the two salicyclideneaminato moieties as shown in Fig. 1.[2] This result implies that the conformational rearrangement of the ligand has occurred during the formation of the O_2 adduct.

In this study, the crystal structure of the title compound containing the same ligand, has been determined by the single-crystal X-ray diffraction technique. Since the electronic structure of the 1:1 O_2 adduct was assumed to be $Co^{III}-O_2^-$ based on the ESR spectral investigation,[3] it is of interest to compare the coordination geometry of the present complex with that of the 1:1 O_2 adduct. In addition, this structural result can be expected to propose a clearer idea for the conformational rearrangement during the formation of the O_2 adduct (2) from the precursor complex (1).

---

*Copies are available, on request, from the Editor at Queen Mary College.

RESULTS AND DISCUSSION

The structure of the title compound with the atom numbering scheme is shown in Fig. 2. As shown in Fig. 2, the cobalt atom assumes an octahedral coordination array with *cis*-geometry for the two salicyclideneaminato moieties and the dihedral angle between the two benzene rings is 82.8°. The average Co–O(phenolic) bond length of 1.888(7) Å is shorter than the Co–O(3)(acetate) bond length of 1.924(7) Å. The average Co–N(imine) bond length of 1.933(8) Å is shorter than the Co–N(secondary amine) bond length of 1.983(9) Å. An oxygen atom of the acetate is coordinated to the cobalt atom. It is noteworthy that another oxygen atom is hydrogen-bonded to the secondary amine nitrogen atom and the distance (O(4) $\cdots$ N(4)) is 2.825 Å.

The saturated six-membered chelate ring defined by Co, N(1), C(8), C(9), C(10) and N(2) takes a boat conformation and the other six-membered chelate ring defined by Co, N(2), C(11), C(12), C(13) and N(3) takes a chair conformation.

The coordination geometry of the present complex is apparently different from both the trigonal bipyramid of the precursor (1) and the octahedron with *trans*-geometry of the O_2 adduct (2). The coordination geometry containing this type of ligand system seems to be affected by both the sixth ligand, i.e. O_2 and CH_3COO^-, and the hydrogen bond. In the present complex, a

1   **2**
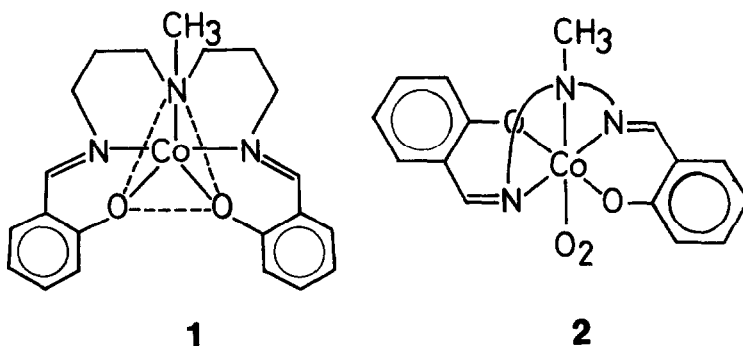
Fig. 1. Structures of the precursor complex and the 1:1 O_2 adduct.
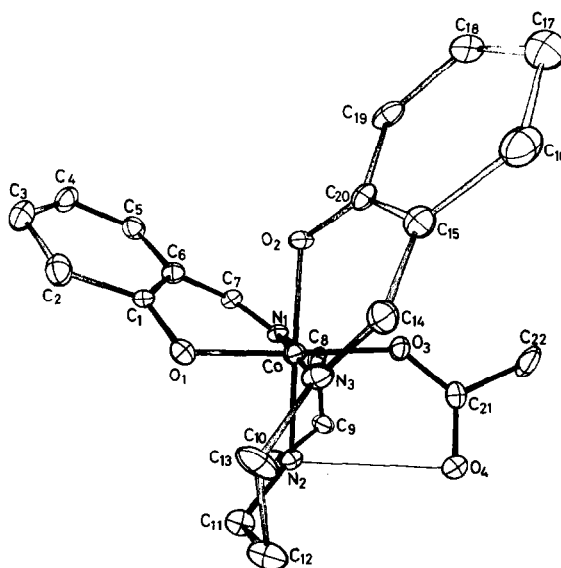
Fig. 2. Perspective drawing of the molecule. The thermal ellipsoids are drawn at 20% probability level and hydrogen atoms are omitted for clarity.

hydrogen bond between an oxygen atom of the acetate and the secondary amine nitrogen atom might be one of the important factors in the adoption of a *cis*-geometry. The observed *cis*-geometry of the Schiff base ligand is similar to those of the binuclear μ-peroxo-cobalt(III) complex [4] and the 1:1:1 peroxyquinolato-cobalt(III) complex obtained from 2,4,6-tri-t-butylphenol, molecular oxygen and the cobalt(II) complex.[5] However, the conformation of the two saturated six-membered chelate rings assumes chair-envelope and skew-chair forms for the former and the latter complexes, respectively. These structural results indicate that the ligand system is flexible.

EXPERIMENTAL

The title complex was prepared according to the literature.[1] Brown rhombic crystals suitable for the X-ray diffraction work were obtained from the ethylether solution. A crystal was examined with a Rigaku Denki AFC-5 four-circle automated diffractometer. The unit cell dimensions and their estimated standard deviations were obtained from a least-squares fit to setting angles of 15 reflections using Mo Kα graphite monochromatized radiation at room temperature. The crystal data are as follows: $CoO_4N_3C_{22}H_{26}$, F.W. = 455.4; Found; C, 57.79; H, 5.84: N, 9.18. Calc. C, 58.02; H, 5.75; N, 9.23%. Monoclinic, space group = $P2_1/n$, a = 16.846(4), b = 9.417(2), c = 14.032(4) Å, β = 111.29(1)°, V = 2074.1(9) Å^3, D_m = 1.44 (by flotation method in aqueous KI solution), D_x = 1.458 g · cm^{-3}, Z = 4, μ(Mo Kα) = 10.3 cm^{-1}.

Intensity data were collected by the $\theta - 2\theta$ scan technique with a scan rate 8° min^{-1}. For the weak reflections the peak scan was repeated up to four times depending on their intensities. The intensities of three standard reflections were monitored every 100 reflections and showed a good stability. A total of 3628 reflections with 2.5° < 2θ < 48° were collected and of which 2381 independent reflections with $|F_o| > \sigma(|F_o|)$ were used for the structure determination. The intensity data were corrected for Lorentz and polarization effects, but not for absorption.

The structure was solved by the conventional heavy-atom

Table 1(a). Bond distance (Å) with their estimated standard deviations

(a)	Coordination Sphere		
Co-O(1)	1.885(7)	Co-N(1)	1.918(8)
Co-O(2)	1.891(7)	Co-N(2)	1.983(9)
Co-O(3)	1.924(7)	Co-N(3)	1.947(8)
(b)	Ligand		
O(1)-C(1)	1.312(13)	C(12)-C(13)	1.538(18)
C(1)-C(2)	1.407(16)	C(13)-N(3)	1.462(15)
C(2)-C(3)	1.378(16)	N(3)-C(14)	1.288(13)
C(3)-C(4)	1.377(18)	C(14)-C(15)	1.444(14)
C(4)-C(5)	1.352(18)	C(15)-C(16)	1.409(15)
C(5)-C(6)	1.428(16)	C(16)-C(17)	1.345(17)
C(6)-C(1)	1.393(15)	C(17)-C(18)	1.388(17)
C(6)-C(7)	1.417(16)	C(18)-C(19)	1.361(16)
C(7)-N(1)	1.298(14)	C(19)-C(20)	1.414(15)
N(1)-C(8)	1.463(15)	C(20)-C(15)	1.426(14)
C(8)-C(9)	1.526(18)	C(20)-O(2)	1.300(12)
C(9)-C(10)	1.532(19)	O(3)-C(21)	1.274(12)
C(10)-N(2)	1.478(16)	C(21)-C(22)	1.508(18)
N(2)-C(11)	1.494(15)	C(21)-O(4)	1.256(14)
C(11)-C(12)	1.498(18)		

Table 1(b). Bond angles (°) with their estimated standard deviations

(a)	Metal Coordination Sphere		
O(1)-Co-O(2)	90.8(2)	O(2)-Co-N(3)	89.7(3)
O(1)-Co-O(3)	176.6(3)	O(3)-Co-N(1)	89.4(3)
O(1)-Co-N(1)	90.3(3)	O(3)-Co-N(2)	92.0(3)
O(1)-Co-N(2)	91.3(3)	O(3)-Co-N(3)	92.1(3)
O(1)-Co-N(3)	87.8(3)	N(1)-Co-N(2)	90.4(3)
O(2)-Co-O(3)	85.7(2)	N(1)-Co-N(3)	176.4(3)
O(2)-Co-N(1)	87.1(3)	N(2)-Co-N(3)	92.7(3)
O(2)-Co-N(2)	176.7(3)		
(b)	Ligand		
Co-O(1)-C(1)	121.2(6)	C(6)-C(7)-N(1)	125.2(10)
Co-O(2)-C(20)	120.9(6)	N(1)-C(8)-C(9)	110.3(9)
Co-O(3)-C(21)	132.1(6)	C(8)-C(9)-C(10)	114.0(10)
Co-N(1)-C(7)	121.8(7)	C(9)-C(10)-N(2)	112.3(10)
Co-N(1)-C(8)	120.3(6)	N(2)-C(11)-C(12)	112.1(9)
C(7)-N(1)-C(18)	117.8(9)	C(11)-C(12)-C(13)	114.1(10)
Co-N(2)-C(10)	114.4(7)	C(12)-C(13)-N(3)	113.2(9)
Co-N(2)-C(11)	115.1(6)	N(3)-C(14)-C(15)	124.3(9)
C(10)-N(2)-C(11)	111.3(8)	C(14)-C(15)-C(16)	120.9(9)
Co-N(3)-C(13)	120.1(6)	C(14)-C(15)-C(20)	119.7(8)
Co-N(3)-C(14)	122.6(6)	C(16)-C(15)-C(20)	118.7(9)
C(13)-N(3)-C(14)	116.9(8)	C(15)-C(16)-C(17)	123.5(10)
O(1)-C(1)-C(2)	118.6(9)	C(16)-C(17)-C(18)	117.8(11)
O(1)-C(1)-C(6)	123.5(9)	C(17)-C(18)-C(19)	121.3(10)
C(2)-C(1)-C(6)	118.3(9)	C(18)-C(19)-C(20)	122.2(10)
C(1)-C(2)-C(3)	120.5(10)	C(19)-C(20)-C(15)	116.1(9)
C(2)-C(3)-C(4)	121.7(11)	C(19)-C(20)-O(2)	119.4(8)
C(3)-C(4)-C(5)	118.5(11)	C(15)-C(20)-O(2)	124.1(8)
C(4)-C(5)-C(6)	122.0(11)	O(3)-C(21)-C(22)	113.2(9)
C(5)-C(6)-C(1)	118.7(10)	O'(3)-C(21)-O(4)	126.4(10)
C(5)-C(6)-C(7)	120.0(10)	C(22)-C(21)-O(4)	120.3(10)
C(1)-C(6)-C(7)	120.8(10)		

method, and refined by block-diagonal least-squares, in which the function minimized was $\Sigma w(|Fo| - k|Fc|)^2$, where k is scale factor and $w = 1$ is adopted. The atomic scattering factors were taken from the International Tables for X-ray Crystallography Vol. IV.[6] Anomalous dispersion corrections for Co were also taken from the literature.[6] All the calculations were carried out on a FACOM M-200 computer at the Computer Center of Kyushu University by the use of a local version of the UNICS II system.[7,8]

Final refinement including hydrogen atoms which were experimentally determined yielded the final values of 8.69 and 9.60% for $R_1 = \Sigma||Fo| - |Fc||/\Sigma|Fo|$ and $R_2 = [\Sigma w(|Fo| - |Fc|)^2/\Sigma w|Fo|^2]^{1/2}$, respectively. The final shifts in the atomic parameters of the nonhydrogen atoms were less than 0.25σ. A final difference Fourier synthesis showed no peaks higher than 0.7 eÅ^{-3}.

Final positional and thermal parameters with their estimated standard deviations and a list of observed and calculated struc-

ture factors have been deposited as supplementary data.* Bond lengths and angles are given in Table 1(a, b), respectively.

REFERENCES

[1] R. H. Bailes and M. Calvin, J. Am. Chem. Soc. 1947, 69, 1886.
[2] R. Cini and P. Orioli, J. Chem. Soc., Chem. Commun. 1981, 196.
[3] S. Koda, A. Misono and Y. Uchida, Bull. Chem. Soc. Jpn 1970, 43, 3143.
[4] L. A. Lindflom, W. P. Schaefer and R. E. March, Acta Crystallogr. 1971, B27, 1461.
[5] A. Nishinaga, H. Tomita, K. Nishizawa, T. Matsuura, S. Ooi and K. Hirotsu, J. Chem. Soc., Dalton Trans. 1981, 1504.
[6] International Tables for X-ray Crystallography, Vol. IV. Kynoch Press, Birmingham (1974).
[7] S. Kawano, Rep. Comp. Cent. Kyushu Univ. 1980, 13, 39.
[8] T. Sakurai, H. Iwasaki, Y. Watanabe, K. Kobayashi, Y. Bando and Y. Nakamichi, Rep. Inst. Phys. Chem. 1972, 50, 75.

*Values of atomic positional parameters have also been deposited with the Cambridge Crystallographic Data Centre.

SYNTHESIS AND STRUCTURE OF THE NEW HETERONUCLEAR PALLADIUM–MERCURY CLUSTER

E. G. MEDNIKOV, V. V. BASHILOV, V. I. SOKOLOV, Yu. L. SLOVOKHOTOV* and Yu. T. STRUCHKOV
A. N. Nesmeyanov Institute of Organoelement Compounds, USSR Academy of Sciences, Moscow V-334, 28 Vavilov St., U.S.S.R.

Abstract—Interaction of the tetra-nuclear phosphinecarbonyl complex of zero-valent palladium, $Pd_4(CO)_5(PEt_3)_4$ (I), with a four-fold excess of 8-(α-bromomercuryethyl)quinoline gives a new neutral heteronuclear cluster $Pd_4Hg_2Br_2(CO)_4(PEt_3)_4$ (IV). The structure of (IV) was determined by an X-ray analysis. The molecule of (IV) contains a "butterfly" $Pd_4(\mu_2\text{-}CO)_4(PEt_3)_4$ moiety, whose triangular "wings" are capped by Hg atoms bonded also to bromo-ligands. The metal Hg_2Pd_4 polyhedron consists of two heteroatomic Pd_3Hg tetrahedra with a common Pd–Pd edge. The IR- and ^{31}P-NMR spectra of (IV) were also studied.

INTRODUCTION

As has been found recently, the mononuclear carbonyl derivatives of zero-valent palladium tend to form polyhedral cluster complexes under mild conditions.[1,2] A high reactivity of the compounds thus obtained, their diversity and interconversions of clusters with differently sized and shaped Pd_n polyhedra, observed in organic media, give rise to a growing interest to this area of coordination chemistry.[3–7] To date structural studies have been made of a number of cluster complexes of Pd with carbonyl ligands, including tetra-nuclear derivatives wherein the Pd_4 moiety has a configuration of a planar tetragon,[3] "butterfly",[4] distorted[5] and symmetrical[6] tetrahedron. The recently synthesized complex $Pd_4(CO)_5(PR_3)_4$ (I, R = Et, Bu^n), probably having a "butterfly" structure, by analogy with the earlier studied cluster $Pd_4(CO)_5(PMe_2Ph)_4$ (II),[4] may serve as a starting compound in the synthesis of more complex homo- and heternuclear Pd clusters. The transformation of (I) into the symmetrical tetrahedral complex $Pd_4(CO)_6(PR_3)_4$ (III), found in solution, and the ability of (I) to further condensation with coordination of phosphine to give decanuclear Pd clusters[6] suggested rich synthetic potentialities of reactions involving (I). Until recently, however, the only chemical interactions of homo- and heteronuclear Pd clusters studied have been limited by their interconversions under variation of ligand concentration,[6,7] whereas the action of "modifying" reagents on complexes of the $Pd_n(CO)_x(PR_3)_y$ type has resulted in the complete decomposition of the polynuclear structure.

In the present study we have found a method of modifying (I) by treatment with the organomercury compound, 8-(α-bromomercuryethyl)quinoline,* and determined the structure of the resulting heteronuclear cluster. A peculiarity of this reaction, in contrast to the earlier cases studied,[6,7] consists in retaining a metalloligand framework existing in the starting complex and in its "enlargement" by two HgBr fragments to form a heteroatomic Hg_2Pd_4 metallopolyhedron, wherein the Hg atom increases its coordination from a linear one in the starting compound to tetrahedral in the reaction product.

EXPERIMENTAL

All the operations involved in the synthesis, isolation and investigation of $Pd_4Hg_2Br_2(CO)_4(PEt_3)_4$ (IV) were carried out under CO. The IR spectrum was measured with an IR-10 instrument in KBr pellets. The ^{31}P-NMR spectrum was studied at $-70°C$ in toluene with a Bruker–HX–90 spectrometer. Chemical shifts were measured relative to H_3PO_4 (85% concentration).

Synthesis of (IV)

To a suspension of 8-(bromomercuryethyl)quinoline[8] (1.22 g) in benzene (28 ml) was added $Pd_4(CO)_5(PEt_3)_4$ (0.73 g), obtained as described elsewhere,[2] and the mixture was stirred under CO at 20°C for 30 min. CO was evolved and a black precipitate (Pd, Hg) formed. The reaction mixture was left for 15 hr at 5°C, then the solution was filtered off from the precipitate, and pentane (200 ml) was added to the orange filtrate. The orange–red crystalline precipitate of (IV) was filtered off, washed with pentane and dried in vacuo. 0.26 g (23.5%) of (IV) was obtained; dec. temp. 86°C. Found: C, 21.81; H, 3.91; Br, 10.45; Hg, 25.79; Pd, 26.90. Calcd. for $C_{28}H_{66}O_4P_4Br_2Hg_2Pd_4$, C, 21.41; H, 3.85; Br, 10.18; Hg, 25.55; Pd, 27.09%. IR (ν, cm^{-1}): CO 1855 (s), 1897 (m); C–H 2880 (s), 2908 (s), 2930 (s). ^{31}P–{^1H}–NMR, δ (ppm): 8.7 triplet, 2P; 20.9 triplet, 2P; ^3J (^{31}P, ^{31}P) 23.1 Hz.

For an X-ray structural analysis the ruby-coloured crystals of (IV) were obtained in a similar manner with the only difference that the filtrate, after separation of the black metal precipitate, was diluted with pentane (100 ml).

X-Ray structural study of (IV)

The crystals of (IV) are monoclinic, $a = 20.205(5)$, $b = 16.815(6)$, $c = 13.183(4)$ Å, $\beta = 97.17(2)°$, space group C2/c, Z = 4. Unit cell parameters and intensities of 4273 independent reflections (of which 3933 with $I > 2\sigma$ were used in calculations) were measured at $-120°C$ with an automatic four-circle Syntex P2$_1$ diffractometer (λMoK$_\alpha$, graphite monochromator, $\theta/2\theta$ scan, $2\theta \leqslant 50°$). Absorption corrections were made according to the method described in Ref. [9]. The structure was solved by direct methods using the MULTAN program and refined by full-matrix least-squares in an anisotropic approximation. Finally $R = 0.050$, $R_w = 0.066$ for 3426 reflections with $I > 5\sigma(I)$ and sin $\theta/\lambda > 0.10$. Atomic coordinates of the independent part of the molecule of (IV), which occupies a special position on the two-fold axis, and their anisotropic thermal parameters have been deposited as supplementary material with the Editor, from whom copies are available.‡ All the calculations were performed with an Eclipse S/200 computer by the modified EXTL programs.§

---

*Author to whom correspondence should be addressed.

†Reactions of phosphine-carbonyl Pd clusters with other organomercury compounds will be described elsewhere.

‡Atomic co-ordinates have also been deposited with the Cambridge Crystallographic Data Centre.

§Program modification was carried out in our laboratory by A. I. Yanovsky and R. G. Gerr.

RESULTS AND DISCUSSION

Initially we expected to attain modification of the zero-valent Pd cluster derivatives by treatment with organo-mercury compounds with insertion of an organic or organo-mercury fragment. 8-(α-Bromomercuryethyl)quinoline was chosen as a potential source of a chelating N,C-ligand due to the presence of two active centres (N and Hg atoms) in its molecule. In fact, however, the reaction proceeded along an unexpected route with elimination of the organic part R of the RHgBr molecule and insertion of the HgBr residue into the polyhedron of the new heteroatomic cluster:

$$Pd_4(CO)_5(PEt_3)_4 + C_9H_8NCH(Me)HgBr \xrightarrow[-CO]{}$$

$$Pd_4Hg_2Br_2(CO)_4(PEt_3)_4. \quad (1)$$
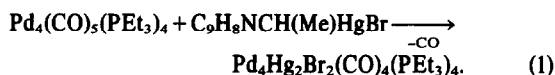
The formation of a neutral cluster molecule implies a homolytical cleavage of the C–Hg bond. Formally reaction (1) represents a substitution of the CO ligand for two HgBr residues. However the Hg atoms are coordinated with the $Pd_4(CO)_4(PEt_3)_4$ moiety of the resulting cluster (IV) in a most unusual fashion.

A similar reaction of phenylmercury(II) bromide with a trinuclear carbonyl hydride ruthenium complex has been studied recently:[10]

$$(C_6H_9)Ru_3(CO)_9H + C_6H_5HgBr \xrightarrow{THF}$$

$$(C_6H_9)Ru_3(CO)_9HgBr. \quad (2)$$
$$(V)$$
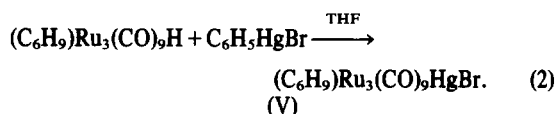
This interaction proceeding essentially as replacement of the hydride ligand in the starting complex resulted in the formation of the heteronuclear cluster (V) with a "butterfly" configuration, which underwent dimerization due to the formation of halide bridges. In the molecule of (V) the Hg atom is bonded to two Ru atoms (2.733 and 2.739 Å), the dihedral angle between the Ru_2Hg and Ru_3 planes in the butterfly-shaped (V) being 127°.

Bond lengths in (IV) are given in Table 1, and bond angles in Table 2. In the crystal the molecule of (IV) (see Fig. 1) occupies a special position on the two-fold symmetry axis and involves the butterfly-shaped

$Pd_4(CO)_4(PEt_3)_4$ fragment whose triangular wings are capped asymmetrically by the Hg atoms [the Hg–Pd(1) distance, 2.993(1) Å, is substantially greater than two others, Hg–Pd(2), 2.717(1) Å, and Hg–Pd(2'), 2.704(1) Å]. Tetrahedral coordination of the Hg atom is completed by the Br ligand (Hg–Br 2.544(1) Å). A dihedral angle of 100.2° between the Pd_3 planes in the $Pd_4(CO)_4(PEt_3)_4$ fragment exceeds the corresponding value in the butterfly (II) (93°),[4] being accompanied by increasing the nonbonded Pd(1)...Pd(1') distance (3.365 Å in (II) and 3.428(1) Å in (IV)). However both the last two values are close to the lengths of the "elongated" edges, 3.3–3.4 Å, in the Pd_{10} polyhedron of the cluster $Pd_{10}(CO)_{12}(PBu_3^n)_6$ (VI).[1,6] The peripheral Pd–Pd bonds of the Pd_4 butterfly in (IV) are tightened by the bridging CO ligands. The lengths of these bonds, 2.687(1) and 2.702(1) Å, are close to those of the "short" Pd–Pd edges in (V), also reinforced by μ_2-CO bridges (av. 2.056 Å[6]). The absence of a bridging CO ligand at the Pd(2)–Pd(2') bond is accompanied by its lengthening to 3.015(1) Å. In the molecule of (IV) only an average Pd–Pd bond length of 2.750(2) Å is reported.[4] Coordination of the μ_2-CO ligands in (IV) reveals a small, but distinct asymmetry (Tables 1 and 2), viz., though a difference in the lengths of the C–Pd bonds to the "peripheral", Pd(1), and "central", Pd(2), metal atoms, 2.01(1) and 2.09(1) for C(1), and 2.03(1) and 2.08(1) for C(2), respectively, is close to the experimental error, the corresponding bond angles Pd(1)CO and Pd(2)CO, 144.3(9) and 133.2(9)° for C(1), 143.7(9) and 134.5(9)° for C(2), are, in fact, significantly unequal, suggesting a stronger bonding of the bridging CO to the "peripheral" Pd atoms. Both C and O atoms of the μ_2-CO ligands are close to the plane of the corresponding Pd(1)Pd(2)Pd(2') triangle, the out-of-plane deviations in the direction from the Hg atom being 0.10(1) for C(1), 0.23(2) Å for O(1), 0.05(1) for C(2), and 0.11(1) Å for O(2). The P(1) atom bonded to the Pd(1) atom is displaced from this plane by only 0.081(3) Å, and thus, despite involvement of the peripheral Pd(1) and Pd(1') in the metallopolyhedron, they retain a predominantly planar trigonal ligand environment, the sum of the bond angles P(1)Pd(1)C(1), P(1)Pd(1)C(2) and C(1)Pd(1)C(2') being 359.1°. On the contrary, coordination of the Hg atom is close to sym-

Table 1. Bond lengths d (Å) for compound (IV)

Bond	d	Bond	d
Hg–Pd(1)	2.993(1)	C(1)–O(1)	1.16(1)
Hg–Pd(2)	2.717(1)	C(2)–O(2)	1.14(1)
Hg–Pd(2')	2.704(1)	P(1)–C(3)	1.81(1)
Hg...Hg'	3.251(1)	P(1)–C(5)	1.80(1)
Hg–Br	2.544(1)	P(1)–C(7)	1.82(1)
Pd(1)–Pd(2)	2.687(1)	P(2)–C(9)	1.82(1)
Pd(1)–Pd(2')	2.702(1)	P(2)–C(11)	1.82(1)
Pd(2)–Pd(2')	3.015(1)	P(2)–C(13)	1.83(1)
Pd(1)...Pd(1')	3.428(1)	C(3)–C(4)	1.53(2)
Pd(1)–P(1)	2.295(3)	C(5)–C(6)	1.55(2)
Pd(2)–P(2)	2.333(3)	C(7)–C(8)	1.49(2)
Pd(1)–C(1)	2.01(1)	C(9)–C(10)	1.52(2)
Pd(1)–C(2)	2.03(1)	C(11)–C(12)	1.50(2)
Pd(2)–C(1')	2.09(1)	C(13)–C(14)	1.51(2)
Pd(2)–C(2)	2.08(1)		

Table 2. Bond angles ω ($^\circ$) for compound (IV)

Angle	ω	Angle	ω
Pd(1)HgBr	141.76(3)	Pd(1)C(1)O(1)	144.3(9)
Pd(2)HgBr	150.62(3)	Pd(2)C(1)O(1)	133.2(9)
Pd(2')HgBr	139.19(3)	Pd(1)C(1)Pd(2')	82.4(4)
Pd(1)HgPd(2)	55.90(2)	Pd(1)C(2)O(2)	143.7(9)
Pd(1)HgPd(2')	56.35(2)	Pd(2)C(2)O(2)	134.5(9)
Pd(2)HgPd(2)	67.58(2)	Pd(1)C(2)P (2)	81.8(4)
Pd(2)Pd(1)Hg	56.85(2)	Pd(1)P(1)C(3)	115.5(4)
Pd(2')Pd(1)Hg	56.42(2)	Pd(1)P(1)C(5)	117.1(4)
Pd(2)Pd(1)Pd(2')	68.04(3)	Pd(1)P(1)C(7)	111.7(4)
Pd(2)Pd(1)P(1)	143.48(7)	C(3)P(1)C(5)	106.0(6)
Pd(2')Pd(1)P(1)	148.37(7)	C(3)P(1)C(7)	102.5(5)
P(1)Pd(1)C(1)	98.3(3)	C(5)P(1)C(7)	102.4(6)
P(1)Pd(1)C(2)	93.6(3)	Pd(2)P(2)C(9)	110.9(4)
C(1)Pd(1)C(2)	167.2(4)	Pd(2)P(2)C(11)	116.3(4)
HgPd(2)Pd(1)	67.26(2)	Pd(2)P(2)C(13)	117.4(4)
HgPd(2)Hg	73.69(2)	C(9)P(2)C(11)	105.1(6)
Pd(1)Pd(2)Pd(1')	78.99(3)	C(9)P(2)C(13)	104.2(5)
Pd(1)Pd(2)Pd(2')	56.21(2)	C(11)P(2)C(13)	101.5(5)
HgPd(2)Pd(2')	56.41(2)	P(1)C(3)C(4)	115.8(8)
HgPd(2)P(2)	98.35(7)	P(1)C(5)C(6)	114.9(9)
Pd(1)Pd(2)P(2)	141.65(7)	P(1)C(7)C(8)	114.6)9)
Pd(2')Pd(2)P(2)	144.59(7)	P(2)C(9)C(10)	115.7(8)
P(2)Pd(2)C(1')	99.8(3)	P(2)C(11)C(12)	114.7(9)
P(2)Pd(2)C(2)	100.9(3)	P(2)C(13)C(14)	113.3(8)
C(1)Pd(2)C(2)	92.4(4)		
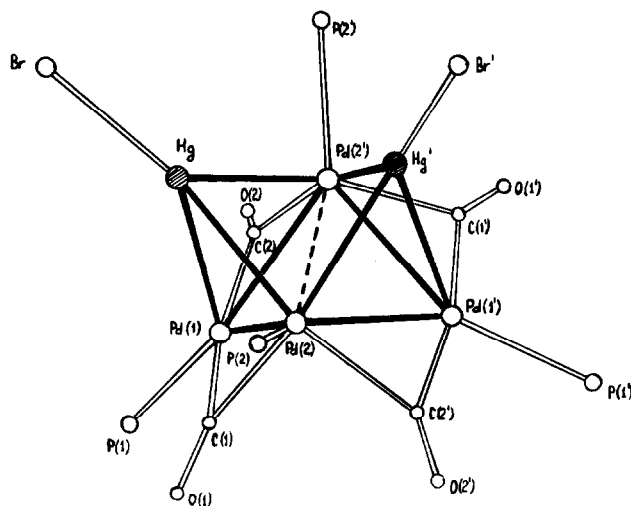
Fig. 1. Molecule (IV) (ethyl substituents of the phosphine ligands omitted for clarity).

metrical tetrahedral, and the Br atom deviates from the HgPd(2)Pd(2') plane by 0.438(1) Å. The Hg–Hg distance, 3.251(1) Å, is close to the values found in various polynuclear mercury compounds, both in the tetramercurated methane derivatives, $C(HgX)_4$ where, probably, there is no Hg...Hg bonding interaction (X = CN, 3.280–3.398 Å;[11] X = OAc, 3.251–3.436 Å,[12]) and in the heteronuclear cluster $RH_4Hg_6(PMe_3)_{12}$ with a Hg_6 octahedron (3.131–3.149 Å) wherein four noncontiguous faces have μ_3-Rh(PMe$_3$)$_3$ bridges.[13] To conclude unequivocally

if there is any Hg...Hg bonding in (IV), one has to compare the geometrical parameters of the Pd_4 "butterfly" in (IV) and (I), a structural study of the latter being our immediate purpose.

REFERENCES

1 E. G. Mednikov, N. K. Eremenko, V. A. Mikhailov, S. P. Gubin, Yu. L. Slovokhotov and Yu. T. Struchkov, J. Chem. Soc. Chem. Comm. 1981, 989.
2 E. G. Mednikov and N. K. Eremenko, Izv. AN SSSR, ser. Khim. 1981, 2400 (Russ.).

[3]I. I. Moiseev, T. A. Stromnova, M. N. Vargaftic, G. Ja. Maso, L. G. Kuzmina and Yu. T. Struchkov, *J. Chem. Soc. Chem. Comm.* 1978, 27.

[4]J. Dubrawski, J. C. Krieg-Simondsen and R. D. Feltman, *J. Amer. Chem. Soc.* 1980, 102, 2089.

[5]M. N. Vargaftic, T. A. Stromnova, T. S. Khodashova, M. A. Porai-Koshits and I. I. Moiseev, *Koord. Khim.* 1981, 7, 132 (Russ.).

[6]E. G. Mednikov, N. K. Eremenko, S. P. Gubin, Yu. L. Slovokhotov and Yu. T. Struchkov, *J. Organometal. Chem.* in press.

[7]G. Longoni, M. Manassero and M. Sansoni, *J. Amer. Chem. Soc.* 1980, 102, 3242.

[8]O. A. Reutov, V. V. Bashilov, V. I. Sokolov, *Izv. AN SSSR, Ser. Khim.* 1981, 1169 (Russ.).

[9]R. G. Gerr, M. Yu. Antipin, N. G. Furmanova and Yu. T. Struchkov, *Kristallografiya* 1979, 24, 951 (Russ.).

[10]R. Falmry, K. King, E. Rosenberg, A. Tiripiccio and M. Tiripiccio-Camelfini, *J. Amer. Chem. Soc.* 1980, 102, 3626.

[11]D. Grdenič, M. Sikirica and B. Korpar-Čolig, *J. Organometal. Chem.* 1978, 153, 1.

[12]D. Grdenič and M. Skirica, *Z. Kristallografic.* 1979, 150, 107.

[13]R. A. Jones, F. M. Real, G. Wilkinson, A. M. R. Galas and M. B. Hursthouse, *J. Chem. Soc., Dalton Trans.* 1981, 126.

SYNTHESIS AND CHARACTERIZATION BY IR SPECTROSCOPY AND X-RAY DIFFRACTION OF A QUINAZOLINE-COMPLEX OF DIBUTYLDICHLOROTIN(IV)

C. PELIZZI, G. PELIZZI* and P. TARASCONI

Istituto di Chimica Generale ed Inorganica, Università degli Studi, Centro di Studio per la Strutturistica Diffrattometrica del C.N.R., Via M. D'Azeglio 85, 43100 Parma, Italy

Abstract—The synthesis, the X-ray analysis and the IR spectrum of the complex $SnBu_2Cl_2(AIP)$ [AIP = 2-(2'-pyridyl)-3-(N-2-picolylimino)-4-oxo-1,2,3,4 - tetrahydroquinazoline] are reported. The coordination polyhedron can be described as a distorted pentagonal bipyramid. The AIP molecule behaves as a terdentate ONN donor ligand, with the N atoms involved in two equational weaker interactions with respect to the O atom.

INTRODUCTION

We have shown previously the structural flexibility of N,O-containing ligands in metal complexes, in connection with the nature of the metal and of the inorganic anion.[1,2] Among these ligands, 2 - (2' - pyridyl) - 3 - (N - 2 - picolylimino) - 4 - oxo - 1,2,3,4 - tetrahydroquinazoline (AIP), obtained by condensation of 2-aminobenzoylhydrazine and pyridine-2-carbaldehyde, is able to act as a ONN[3] or NNN[4] terdentate ligand when coordinating to metals.

As part of a continuing interest in the organotin(IV) complexes with ligands obtained by condensation of acylhydrazines with aldehydes or ketones,[5–7] we now report the synthesis, the X-ray analysis and the infrared spectrum of $SnBu_2Cl_2(AIP)$.

EXPERIMENTAL

Synthesis. Bu_2SnCl_2 was commercially available (Merck) and used as received. AIP was prepared as described previously.[8] The complex $SnBu_2Cl_2(AIP)$ was obtained by adding a chloroform solution of Bu_2SnCl_2 to an acetone solution of the organic ligand. After refluxing for *ca.* $\frac{1}{2}$ hr the solution was allowed to crystallize. Analytical (C, H, N, Sn) data agree with the formula $C_{27}H_{33}Cl_2$ and N_5OSn.

X-ray data collection. All X-ray measurements were performed using a computer-controlled Siemens AED three-circle diffractometer employing CuK_α radiation ($\lambda = 1.54178$ Å). The compound crystallizes in the monoclinic space group $C2/c$ with a unit-cell of dimensions: $a = 14.701(5)$, $b = 16.727(4)$, $c = 22.963(6)$ Å, $\beta = 100.38(4)°$, and $Z = 8$. Intensity data were collected with a small ($0.13 \times 0.16 \times 0.24$ mm) prismatic crystal to a maximum 2θ of $128°$ for hkl with $l = 0$–3, and of $110°$ for hkl with $l = 4$–23, a total of 3012 reflections being measured from profile analysis following the method of Lehmann and Larsen.[9] After symmetry-equivalent reflections were averaged and reflections which had $I < 2\sigma(I)$ were excluded, 1801 unique data were obtained and used in the refinement. No crystal decomposition occurred during data collection. Corrections were applied for Lorentz and polarization effects, but not for absorption ($\mu \bar{r} = 0.69$).

---

*Author to whom correspondence should be addressed.

†Atomic coordinates have also been deposited with the Cambridge Crystallographic Data Centre for inclusion in their Data Base.

Structure solution and refinement. The structure was solved by heavy-atom method except for hydrogen atom locations. Refinement was by full-matrix least-squares calculations with anisotropic thermal parameters for the Sn, Cl, O, N and for all C atoms except those of the butyl groups, since for these last anisotropic refinement resulted in physically meaningless parameters. The hydrogen atoms from the AIP molecule were inserted at calculated positions, even though some were visible on the Fourier difference map, and they were isotropically refined as "riding" atoms. The hydrogen atoms from the butyl chains were neglected. A final conventional residual index of 0.0538 resulted. The function minimized was $\Sigma w(F_o - F_c)^2$, where the weight for each reflection was unity at first, while in the last cycles the weighting scheme $w = 0.34/[\sigma^2(F_o) + 0.0082 F_o^2]$ was employed. A final difference map had peaks of up to 0.8 $e\text{Å}^{-3}$ in the region of the butyl groups. A total of 309 parameters, including one scale factor, was refined yielding a data: parameter ratio of 5.8:1.

Scattering factors used in the structure factor calculations were taken from Ref. 10 and allowance was made for anomalous dispersion.[11] All computations were performed, using the SHELX-76 system of computer programs,[12] on the Cyber 76 Computer of CINECA (Casalecchio, Bologna), with the financial support from the University of Parma.

Selected bond distances and angles are given in Table 1. Atomic positional coordinates, thermal parameters, additional bond distances and angles, and a list of observed and calculated structure factors have been deposited with the Editor as supplementary material.†

Infrared spectra. The infrared spectra were recorded on a Perkin–Elmer mod. 283 B instrument in KBr discs. Main vibrational bands (cm^{-1}) with relative assignments of AIP, $SnBu_2Cl_2$ (AIP), $Mn(AIP)Cl_2$, $Cd(AIP)Cl_2$, $Cu(AIP)Cl_2$ are listed in Table 2.

RESULTS AND DISCUSSION

The molecular structure is shown in Fig. 1, along with the numbering scheme used for the atoms. There is some difficulty in defining the geometry of the coordination polyhedron, which is quite irregular. In fact, if we consider only the immediate bonding about tin, the coordination could be described in terms of a highly distorted tetragonal pyramid, having two butyl carbon atoms, a chlorine atom (*Cl*1), and the oxygen atom of the AIP ligand at the basal corners, and the second chlorine at the apex, at a Sn–Cl distance unexpectedly shorter (0.14 Å) than the equatorial one. The atoms at the base of the
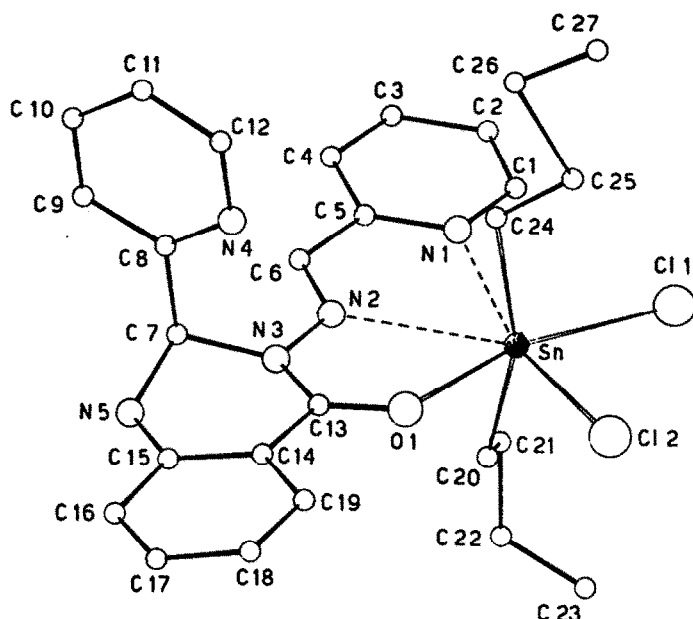
Fig. 1. A perspective view of the molecule.

Table 1. Selected bond distances (Å) and angles (°)

Sn-Cl1	2.610(4)	Sn-C24	2.18(2)	N5-C7	1.46(3)
Sn-Cl2	2.470(4)	O-C13	1.22(2)	N5-C15	1.36(3)
Sn-O	2.42(1)	N2-N3	1.34(2)	C5-C6	1.48(3)
Sn-N1	2.73(1)	N2-C6	1.22(3)	C7-C8	1.53(2)
Sn-N2	2.73(1)	N3-C7	1.49(2)	C13-C14	1.48(3)
Sn-C20	2.13(1)	N3-C13	1.38(2)	C14-C15	1.41(2)
C20-Sn-C24	158.3(7)	N1-Sn-Cl1	78.8(5)	N5-C7-C8	116(2)
Cl1-Sn-O	161.8(3)	N2-Sn-O	59.1(6)	N3-C7-C8	112(1)
O-Sn-C24	83.6(6)	Sn-O-C13	129(1)	O-C13-N3	121(2)
O-Sn-C20	88.5(5)	N3-N2-C6	121(2)	N3-C13-C14	117(2)
Cl2-Sn-C24	101.8(6)	N2-N3-C13	113(1)	O-C13-C14	122(2)
Cl2-Sn-C20	95.7(4)	N2-N3-C7	122(1)	C13-C14-C15	118(2)
Cl2-Sn-O	75.3(3)	C7-N3-C13	120(1)	N5-C15-C14	118(2)
Cl1-Sn-C24	100.1(6)	C7-N5-C15	121(2)	N5-C15-C16	125(2)
Cl1-Sn-C20	93.7(4)	N2-C6-C5	121(2)	Sn-C20-C21	118(1)
Cl1-Sn-Cl2	86.5(1)	N3-C7-N5	106(1)	Sn-C24-C25	115(2)

pyramid show a strong tetrahedral deformation as indicated by the deviations form the weighted least-squares plane running through them: Cl1 −0.02, O −0.25, C20 0.38, C24 0.82 Å. Alternatively, if also two more loosely bonded atoms, N1 and N2, both at 2.73(1) Å from tin, are regarded as being part of the coordination sphere, the tin environment is consistent with a geometry based on a distorted pentagonal bipyramid, whose apical sites are occupied by the two carbon atoms. The pentagonal girdle is almost planar, none of the five atoms being displaced more than 0.11 Å out of the mean plane, the sum of the angles in the girdle being 360.1°. In our opinion, the seven coordination model is to be preferred, in view of a more regularity in the coordination polyhedron. Moreover, there is also further evidence to support this conclusion. In fact, a similar mode of coordination for AIP has been found in the previously determined structures of Mn[3] and Cd[1] complexes, in which the ligand acts too as a ONN terdentate agent giving rise to two planar five-membered rings. By contrast, in the Cu[4] and Co[13] complexes a NNN terdentate ligand behaviour has been found. The two conformations AIP shown in the coordination differ by

Table 2. Selected vibrational bands (cm^{-1}) of AIP in its free state and in Sn, Cd, Mn and Cu complexes

AIP	SnBu$_2$Cl$_2$(AIP)	Cd(AIP)Cl$_2$	Mn(AIP)Cl$_2$	Cu(AIP)Cl$_2$	Assignments
3240m	3280ms	3280ms	3290s	3160m	ν(NH)
3100w	3100w	–	–	–	
3040w	3060w	3060w	3050w	3060m	ν(CH)$_{aryl}$
3010w	3030w	3020w	3020w	–	
2950w	2960ms	2960w	2950w	2915m	ν(CH)$_{alkyl}$
–	2940ms	–	–	2845w	
–	2870m	–	–	–	
1650vs	1635vs	1630vs	1615vs	1675vs	ν(CO), δ(NH)
1622s	1615vs	1610vs	1610sh	1610vs	
1590m	1590s	1588m	1590m	1590sh	rings
1565m	1570sh	1570sh	1570sh	–	
1513m	1510s	1512m	1510s	1520m	ν(CN)
–	1490m	–	–	–	
1483m	1480mw	1485m	1483w	1483w	
1470sh	1450m	1470w	1470m	1467w	rings
1448m	1435sh	1448m	1455s	1443s	
1430m	1405s	1430sh	1430sh	1428sh	

rotation about the N–N bond and are also evident by comparing the main vibrational bands of Sn and Mn (or Cd) compounds with those of the Cu complex (Table 2). In despite of bond distances and angles in the O–C–N–N system, which are poorly influenced by the different coordinating behaviour of the ligand, significant differences occur in the CO and CN stretching mode. In fact, a positive shift of the ν(CO) value in the Cu complex (1675 cm^{-1}) and a negative shift in the Mn (1615 cm^{-1}), Cd (1630 cm^{-1}) and Sn (1635 cm^{-1}) complexes are observed with respect to the value (1650 cm^{-1}) observed for the free ligand; moreover, the ν(CO) band values in the Sn compound have stronger similarities to that of the Cd compound than to that of the Mn derivative. It can be noted also that the infrared spectrum of the Sn complex, as a whole, is very similar to that of SnPh$_2$Cl$_2$(AIP), for which a seven-membered coordination has been suggested previously.[5]

The three aromatic rings are rigorously planar within experimental errors; bond lengths and angles show no significant deviation from the standard values. The two pyridine rings are mutually inclined at 89.4°. The six-membered heterocyclic ring is slightly puckered into a *sofa* conformation with five atoms practically coplanar, the sixth atom, C7, being 0.57 Å out of this plane. The Cremer and Pople ring puckering parameters[14] are: $q_2 = 0.355$, $q_3 = 0.198$, $Q = 0.407$ Å: $\phi_2 = 236.1$ and $\theta_2 = 60.9°$.

The two butyl chains are shown to adopt different conformations, synclinal and antiperiplanar respectively, as indicated by the torsion angles: Sn–C20–C21–C22 = 166(1), C20–C21–C22–C23 = −80(2); Sn–C24–C25–C26 = −180(1), and C24–C25–C26–C27 = −168(2)°. Due to large thermal motion, some distances and angles in these chains depart from the expected values.

The crystal packing is mainly determined by the following interactions, the first of which has to be considered as hydrogen bond:

N5 ... Cl1($x - \frac{1}{2}, \frac{1}{2} + y, z$)   3.30(2) Å
N5 ... C6($\bar{x}, y, \frac{1}{2} - z$)   3.52(3) Å
C4 ... Cl2($\frac{1}{2} - x, \frac{1}{2} + y, \frac{1}{2} - z$)   3.56(2) Å
C12 ... Cl2($\frac{1}{2} - x, \frac{3}{2} - y, 1 - z$)   3.51(3) Å.
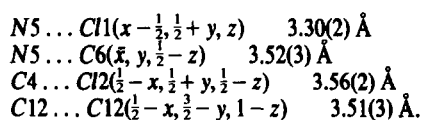
REFERENCES

[1]M. Nardelli, C. Pelizzi and G. Pelizzi, *Transition Met. Chem.* 1977, **2**, 174.
[2]P. Domiano, A. Musatti, M. Nardelli, C. Pelizzi and G. Predieri, *Transition Met. Chem.* 1980, **5**, 172.
[3]C. Pelizzi and G. Pelizzi, *Acta Cryst.* 1974, **B30**, 2421.
[4]A. Mangia, M. Nardelli, C. Pelizzi and G. Pelizzi, *Acta Cryst.* 1974, **B30**, 17.
[5]C. Pelizzi and G. Pelizzi, *Inorg. Chim. Acta* 1976, **18**, 139.
[6]C. Pelizzi and G. Pelizzi, *J. C. S. Dalton* 1980, 1970.
[7]P. Domiano, A. Musatti, M. Nardelli, C. Pelizzi and G. Predieri, *Inorg. Chim. Acta* 1980, **38**, 9.
[8]C. Pelizzi and G. Pelizzi, *Gazz. Chim. Ital.* 1975, **105**, 7.
[9]M. S. Lehmann and F. K. Larsen, *Acta Cryst.* 1974, **A30**, 580.
[10]*International Tables for X-Ray Crystallography*, Vol. IV, pp. 99–101. Kynoch Press, Birmingham, England, 1974.
[11]*International Tables for X-Ray Crystallography*, Vol. IV, pp. 149–150. Kynoch Press, Birmingham, England, 1974.
[12]G. M. Sheldrick, SHELX76, *A Program for Crystal Structure Determination*. University of Cambridge, Cambridge, England, 1976.
[13]A. Mangia, M. Nardelli and G. Pelizzi, *Acta Cryst.* 1974, **B30**, 487.
[14]D. Cremer and J. A. Pople, *J. Am. Chem. Soc.* 1975, **97**, 1354.

RING GEOMETRY AND SECONDARY INTERACTIONS IN A SALT OF S₃N₂Cl⁺; THE CRYSTAL STRUCTURE OF 1-CHLORO-1,2,4-TRITHIA-3,5-DIAZOLIUM TETRACHLOROFERRATE(III)

HARRISON M. M. SHEARER†, ARTHUR J. BANISTER, JOAN HALFPENNY* AND GRAHAM WHITEHEAD

Department of Chemistry, University of Durham, South Road, Durham DH1 3LE, England

Abstract—The structure of the title compound has been determined using single crystal X-ray methods. The tetrachloroferrate(III) ion is approximately tetrahedral, with three Fe–Cl bonds at 2.178(2), 2.182(2) and 2.183(2) Å, and one, Fe–Cl(2), at 2.215(2) Å, which is weakened by interactions between Cl(2) and two sulphurs of the cation. The four sulphur-nitrogen distances [1.546(6)–1.604(6) Å, mean 1.578 Å] are typical of a delocalised SN system; the two-coordinate atoms (only) are coplanar within experimental error. The S(2)–S(3) bond [2.181(2) Å] and exocyclic S(2)–Cl(1) bond [2.086(2) Å] are respectively 0.045 Å longer and 0.08 Å shorter than in S₃N₂Cl⁺Cl⁻; this is interpreted as being due to weaker cation-anion interaction in the tetrachloroferrate (III) salt. Ring angles at S(1) [105.8(3)°], N(2) [121.5(4)°], S(3) [95.6(2)°] S(2) [95.9(2)°] and N(1) [119.6(4)°] are under compression due to constraint within the small ring.

INTRODUCTION

Abnormally short intermolecular contacts between species containing a disulphur group, and one or more external atoms, have been shown to give rise to compounds of novel structural types. These interactions usually involve sulphur and atoms of similar or higher electronegativity; for instance, several three-centre examples have been described[1-3] where an organic or inorganic dithiolium cation interacts with a halide ion (e.g. I)[2] or with oxygen of an oxo-anion[3]. More recently compounds of a new structural class have been discovered, in which a pair of delocalised five-membered rings interact via their disulphur groups. For instance, in (PhCN₂S₂)₂ (II)[4] and (S₃N₂)₂²⁺ (III)[5] two five-membered rings interact respectively in *cis*(eclipsed) and *trans* configurations:
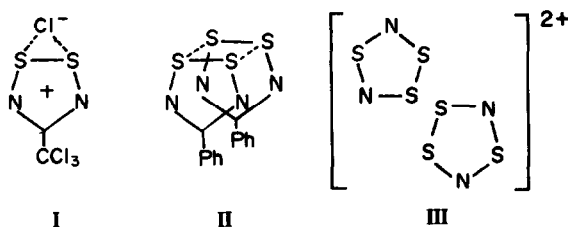
In all these compounds, the secondary interactions tend to perturb the geometry of the component rings and so, for comparison, it is of increasing importance to determine the structures of relatively unperturbed systems. In this paper we describe the crystal structure of the title compound [S₃N₂Cl]⁺[FeCl₄]⁻ and compare cation parameters with those for [S₃N₂Cl]⁺Cl⁻ where cation-anion interactions are quite strong.

EXPERIMENTAL

The title product crystalised as brown needles from a 1 : 1 molar mixture of iron(III) chloride (suspension) and tetrasulphur tetranitride in thionyl chloride solution; it was separated from other products by recrystallisation from thionyl chloride[5]. An alternative and more convenient preparation is from the reaction between iron(III) chloride and S₃N₂Cl₂ suspended in thionyl chloride[5].

Crystal data. Cl₅FeN₂S₃, [S₃N₂Cl]⁺[FeCl₄]⁻, monoclinic, *a* = 9.264(1), *b* = 10.610(1), *c* = 11.259(1) Å, *β* = 92.1(1)°, space group P2₁/n, *D*c = 2.15 Mg m⁻³ with Z = 4, *μ* = 3.07 cm⁻¹ for MoKα radiation, *λ* = 0.71069 Å.

Intensity data for 1952 unique reflections were measured with a ω − 2θ scan on a Hilger and Watts Y-290 four-circle diffractometer, using MoKα radiation. No corrections were made for absorption. The structure determination (heavy atom method) and refinement were performed with the programs of F.R. Ahmed *et al.*[6], only 1412 reflections for which I ≥ 3σ(I) being included. Least squares refinements of the atomic parameters (all atoms with anisotropic temperature factors) were terminated when the shifts on all parameters were less than 0.06 of the e.s.d. and R = 0.048. Final atomic positions, observed and calculated structure factors and anisotropic thermal parameters have been deposited as supplementary material with the Editor from whom copies are available on request. Atomic co-ordinates have also been deposited with the Cambridge Crystallographic Data Centre. Bond distances and angles are listed in Table 1.

DISCUSSION

Each tetrachloroferrate anion is loosely associated with one cation as shown in Fig. 1. The convention of atom numbering for the cation is the same as that used by Zalkin *et al.*[7] for S₃N₂Cl₂. The S–N distances in the cation (average *d*SN = 1.578 Å, 1.589 Å in S₃N₂Cl₂) alternate shorter/longer round the ring as in S₃N₂Cl₂[7] and are close to those in other thiazenium cations (see the average values of 1.563 Å and 1.562 Å in [S₄N₃]₂SbCl₅[8] and [S₅N₅][S₃N₃O₄][9]). The bond angles all betray some compression due to constraint within a small ring. Correlations[10,11] between bond distances (pm) and bond angles (°) for unstrained and largely unstrained sulphur-nitrogen compounds (viz. *d*NS = 177.47−0.1421 N̂ and *d*SN = 213.14−0.4816 Ŝ) indicate compressions of the order of 10° at N(1), 25° at N(2) and 10° at S(1). These values are very approximate, because the calculation ignores the effects of the secondary interactions with the

---

*Author to whom correspondence should be addressed.
†Deceased.

Table 1. Bond distances (Å) and bond angles (°)

Fe - Cl(2)	2.215(2)	S(1) - N(1)	1.604(6)	S(3) - N(2)	1.586(6)
Fe - Cl(3)	2.178(2)	N(1) - S(2)	1.576(6)	N(2) - S(1)	1.546(6)
Fe - Cl(4)	2.182(2)	S(2) - S(3)	2.181(2)	S(2) - Cl(1)	2.086(2)
Fe - Cl(5)	2.183(2)				

Cl(2) - Fe - Cl(3)	110.3(1)	Cl(1) - S(2) - S(3)	101.1(1)
Cl(2) - Fe - Cl(4)	108.3(1)	Cl(1) - S(2) - N(1)	107.3(2)
Cl(2) - Fe - Cl(5)	108.7(1)	S(2) - S(3) - N(2)	95.6(2)
Cl(3) - Fe - Cl(4)	112.3(1)	S(3) - N(2) - S(1)	121.5(4)
Cl(3) - Fe - Cl(5)	108.6(1)	N(2) - S(1) - N(1)	105.8(3)
Cl(4) - Fe - Cl(5)	108.5(1)	S(1) - N(1) - S(2)	119.6(4)
		N(1) - S(2) - S(3)	95.9(2)
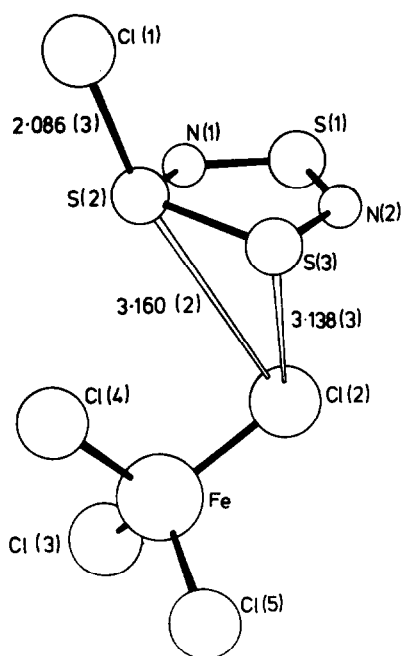
Fig. 1. 'View of one unit of structure of 1-chloro-1,2,4-trithia-3,5-diazolium tetrachloroferrate.'

anion, and assumes that constraint compresses angles without affecting distances. (The calculated values are also quite sensitive to errors in bond distance.) The ring angle N(1)Ŝ(2)S(3) [95.9(2)°] at the three-coordinate sulphur atom also appears to be under compression; by analogy with other trigonal–pyramidal tricoordinate sulphur compounds, the preferred ring angle at tricoordinate S(2) is likely to be 100–110°[10,12] (i.e. OŜCl = 106.3° in SOCl$_2$, and NŜN = 105.2° in CF$_3$SO$_2$N–S(Me)–N(SO$_2$CF$_3$)SnMe$_3$[13]).

Van der Waals radii for sulphur and for the chloride ion are approximately 1.8 Å[14]; non-bonded S . . . Cl distances shorter than 3.6 Å are given as Table 2. Only two [Cl(2)–(S(2) = 3.160(2) and Cl(2)–S(3) = 3.138(3) Å] are below 3.2 Å; both interactions involve Cl(2) and this would account for the long Fe–Cl(2) distance of 2.215(2) Å. The three remaining iron-chlorine distances are shorter (average 2.181 Å). The largest Cl–F̂e–Cl bond angle [112.3(1)°] in the approximately tetrahedral anion, is between the two atoms, Cl(3) and Cl(4), which are least involved in secondary interactions (Fe–Cl bond pair repulsions will tend to be highest for bond pairs closest to the iron atom).

For S$_3$N$_2$Cl$_2$, Zalkin, Hopkins and Templeton[7] reported a "polar dispersion shift" (a relative shift of light and heavy atoms along a polar direction during least squares refinement) which introduced some doubt concerning the

Table 2. Non-bonded S · · · Cl distances less than 3.6 Å

Cl(1) - S(3)	3.296(3)	Cl(2) - S(3)	3.138(3)	Cl(4) - S(1)[II]	3.529(3)
Cl(2) - S(1)	3.455(2)	Cl(3) ÷ S(1)[I]	3.267(2)	Cl(4) - S(3)[III]	3.408(2)
Cl(2) - S(2)	3.160(2)	Cl(4) - S(2)	3.502(2)	Cl(5) - S(2)[IV]	3.219(2)

Roman numeral superscripts refer to the following equivalent positions with respect to the molecule at x, y, z:

I: -1 + x   y   z   II: -½ + x   ½ + y   ½ - z

III: -½ + x   ½ - y   -½ + z   IV: -½ + x   ½ - y   ½ + z
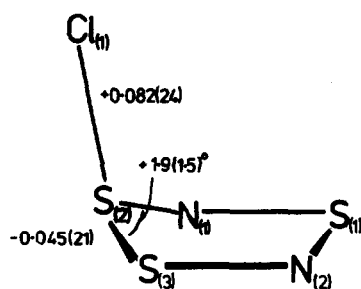
Fig. 2. Comparison of bond parameters in $[S_3N_2Cl]^+Cl^-$(I) and $[S_3N_2Cl]^+[FeCl_4]^-$(II). Where the difference is positive, the distance (Å) or angle (°) is larger in I than in II. Three times the sum of e.s.d.'s for the two structures are given in brackets; differences in parameters less than this are not shown.

geometry of the cation, especially the distances $S(1)$–$N(1)$ and $S(1)$–$N(2)$. (Their estimated standard deviations were about 0.005 Å on the distances and about 0.3° on the angles). Consequently the significant differences between the two structures are the angle $N(1)S(2)S(3)$ and bond distances d_{SS} and d_{SCl} (see Fig. 2).

In $S_3N_2Cl_2$, the chloride ion $Cl(2)$ makes a close approach [2.90 Å at $S(1)$, 3.04 Å at $S(2)$] to all three sulphur atoms and so this is most likely to affect the cation where there are two adjacent interaction sites (e.g. at the $S(2)$–$S(3)$ bond; this is found to be the case. Compared with $[S_3N_2Cl]^+[FeCl_4]^-$, the increased charge transfer from the anion strengthens the disulphur link (by 0.045 Å) and weakens the $S(2)$–$Cl(1)$ bond (by 0.082 Å). In a survey of the directional preferences of non-bonded atomic contacts with divalent sulphur, (XSY), Dunitz et al.[15] showed that donor atoms such as oxygen and fluorine tend to form bonds in the XSY plane. They interpreted this as being due to an interaction of the donor atoms with the LUMO's on sulphur which they identify as the antibonding orbitals associated with the SX and SY bonds. Our results, and also the observations by Gillespie et al.[16] for $(S_3N_2)^+$ and $(S_3N_2)_2^{2+}$, are in accord with this generalization. A similar situation has been found[17] for $(S_4N_3)^+$ and $(CCl_3 . CN_2S_2)^+$ where the lowest unoccupied orbital (LUMO), apart from one or two of π character, is bonding with respect to S–S and antibonding with respect to the neighbouring bonds (disulphur S to N). Consequently, electron drift into this unoccupied orbital

strengthens the disulphur link[17]. The ordering of molecular orbitals is different for some other dithiolium cations, for example in the case of 4-phenyl-1,2-dithiolium iodide and bromide increasing partial S-halogen bonding causes a very small lengthening (0.001–0.002 Å) of the S–S bond[1].

A further interesting feature of the structure of $[S_3N_2Cl]^+[FeCl_4]^-$ (and $[S_3N_2Cl]^+Cl^-$) is the shape of the S_3N_2 ring.

Deviations of atoms from least squares planes are given as Table 3. The four atoms $S(3)N(2)S(1)N(1)$ are planar within the limits of error. The three-coordinate sulphur atom $S(2)$ and the attached chlorine atom $Cl(1)$ lie 0.243 and 2.296 Å respectively above the plane through these four atoms, the $S(2)$–$Cl(1)$ bond making an angle of 112.8° with this plane. Since all ring angles are under compression (loc. cit), and any movement of $S(2)$ out of the $S(3)N(2)S(1)N(1)$ plane causes more reduction of ring angles, further bonding or repulsion forces must be operating, e.g. (i) a bonding interaction between $S(2)$ and the upper lobes of π molecular orbitals at $S(3)$ and $N(1)$, and (ii) lattice forces; secondary interactions between the chlorine atoms of the anion and the cation positions $S(2)$ and $S(3)$ have already been noted, and the fairly short $Cl(1)\ldots S(3)$ distance of 3.296(3) Å may indicate that some interaction is occurring here also.

There are four intermolecular contacts shorter than 3.6 Å (see Table 2). These very weak interactions link ions of opposite charge together throughout the structure.

This structural study shows that in $(S_3N_2Cl)^+$ salts, the geometry of the cation at the disulphur position is sensitive to secondary cation-anion interactions. Since S_3N_2 is a small and hence rather inflexible ring, we anticipate that when large-ring S/N dithiolium salts are prepared, cation-anion interactions will have a much more marked distorting effect.

REFERENCES

[1] A. Hordvik, *Quart. Rep. Sulfur Chem.* 1970, **5**, 21.
[2] T. N. Guru Row and P. Coppens, *Inorg. Chem.* 1978, **17**, 1670.
[3] A. Vegas, A. Pérez-Salazar, A. J. Banister and R. G. Hey, *J. C. S. Dalton* 1980, 1812.
[4] A. J. Banister, H. G. Clarke, I. Rayment and H. M. M. Shearer, *Inorg. Nucl. Chem. Lett.* 1974, **10**, 647.
[5] A. J. Banister and P. J. Dainty, *J. C. S. Dalton* 1972, 2658.
[6] F. R. Ahmed, S. R. Hall, M. E. Pippy and C. P. Huber, *NRC*

Table 3. Deviations of atoms from least squares planes (Å)

(a) **Plane through S(1)S(3)N(1)N(2)**

$$0.9510x + 0.2889y - 0.1100z - 4.2886 = 0*$$

S(1)	0.001	S(3)	0.000	N(1)	-0.004
N(2)	-0.008	S(2)	0.243	Cl(1)	2.296

(b) **Plane through S(1)S(2)S(3)N(1)N(2)**

$$0.9723x + 0.2332y - 0.0165z - 4.5665 = 0*$$

S(1)	0.007	S(3)	-0.013	N(1)	-0.173
N(2)	0.073	S(2)	0.014	Cl(1)	2.021

* x, y, and z are in Å with respect to the orthogonal axes a, b and c.

Crystallographic Programs for the IBM 360 System, World List of Crystallographic Computer Programs, 2nd Edn, Appendix, p. 52.

[7] A. Zalkin, T. E. Hopkins and D. H. Templeton, *Inorg. Chem.* 1966, **5**, 1767.

[8] B. Kruss and M. L. Zeigler, *Z. Anorg. Chem.* 1972, **388**, 158.

[9] H. W. Roesky, W. Grosse-Böwing, I. Rayment and H. M. M. Shearer, *J. C. S. Chem. Comm* 1975, 735.

[10] A. J. Banister and J. A. Durrant, *J. Chem. Res (S)*, 1978, 150 and 152.

[11] M. T. Averbuch-Pouchot, A. Durif, A. J. Banister, J. A. Durrant and J. Halfpenny, *J. C. S. Dalton* 1982, 221.

[12] P. H. Laur, *Sulfur in Organic and Inorganic Chemistry* (Edited by A. Senning), Vol. 3 Chap. 24. Marcel Dekker, New York (1977).

[13] J. W. Bats, H. Fuess, M. Diehl and H. W. Roesky, *Inorg. Chem.* 1978, **17**, 3031.

[14] A. Bondi, *J. Phys. Chem.* 1964, **68**, 441; O. Andreasen, A. C. Hazell and R. G. Hazell, *Acta Cryst.* 1977, **B33**, 1109.

[15] R. E. Rosenfield, R. Parthasarathy and J. D. Dunitz, *J. Am. Chem. Soc.* 1977, **99**, 4860.

[16] R. J. Gillespie, J. P. Kent and J. F. Sawyer, *Inorg. Chem.* 1981, **20**, 3784.

[17] B. E. Svenningsen and R. G. Hazell, in preparation.

STUDIES IN METAL SULPHITE CHEMISTRY—III

W. D. HARRISON, J. B. GILL and D. C. GOODALL*
Department of Inorganic and Structural Chemistry, The University, Leeds LS2 9JT, England

Abstract—Manganese(II) iodide, iron(II) iodide and copper(I) iodide each react with tetramethylammonium disulphite to form anhydrous manganese(II) sulphite, iron(II) sulphite and copper(I) disulphite respectively. Iron(II) sulphite and copper(I) disulphite react with dimethylsulphoxide–sulphur dioxide to form iron(II) disulphate and copper(II) disulphate respectively. Hydrated sulphites of manganese(II), iron(II), magnesium(II) and calcium(II) were also prepared. The properties of the sulphites were investigated using thermogravimetric and IR measurements.

INTRODUCTION

In recent years considerable study has been devoted to the preparation of anhydrous inorganic oxyanion compounds, many of which exhibit remarkable differences when comparison is made with the hydrated compounds. It is not clear how, and to what extent, the absence or presence of water of hydration affects the nature of the oxyanion in such compounds. Our studies relate to the preparation of anhydrous transition metal sulphites, few of which have been prepared and characterised,[1] and to some hydrated transition and non-transition metal sulphites, in order to ascertain the influence of metal ion and water of hydration upon the characteristics of the oxyanion.

RESULTS AND DISCUSSION

Earlier studies[1] on anhydrous transition metal sulphites have shown that it is generally not possible to prepare them by thermal dehydration of the hydrates since water and sulphur dioxide are simultaneously lost. It is necessary to make use of metathetical reactions in non-aqueous media. The metal under study, in the form of its iodide salt, was treated with tetramethylammonium disulphite in acetone. Samples of manganese(II) sulphite, iron(II) sulphite and copper(I) disulphite were prepared. These compounds are all extremely sensitive to air and water. As experienced in our earlier work,[1] it proved impossible to remove all traces of occluded tetramethylammonium salts. This difficulty arises on account of the extreme insolubility of the sulphites, which cannot thus be recrystallised or reprecipitated, and of the lack of a solvent which is suitable for the complete solution of the reactants. Anhydrous manganese(II) sulphite may also be prepared by thermal decomposition of the hydrate, but it exists only within a small temperature range (310–370°), according to thermogravimetric studies referred to later; it is very unstable, and surface decomposition commences very soon after the compound is formed, as a result of spontaneous loss of sulphur dioxide.

However, for each of the anhydrous transition metal sulphites, the metal:sulphur dioxide ratio is in accord with the formula, and two of them were converted to pure disulphates on treatment with the mixed system dimethylsulphoxide–sulphur dioxide.[2] It may be inferred from this that the original materials are essentially anhydrous metal sulphite (disulphite in the case of copper). Iron(II) sulphite gave rise to the formation of $FeS_2O_7 \cdot 6dmso$[3] and copper(I) disulphite to the formation of $CuS_2O_7 \cdot 6dmso$[3]. In the case of manganese(II) sulphite, an oily yellow product formed, which could not be characterised.

The IR bands, shown in Table 1, indicate that, in the anhydrous manganese(II) and iron(II) sulphites, the sulphite group coordinates through oxygen to the metal, very likely in the form of bridging sulphite groups, especially in view of the extreme insolubility of the compounds, which indicates some high molecular weight structure which is likely to arise from such a bridging arrangement. Copper(I) disulphite is considered to contain disulphite covalently bonded to the metal. Its IR spectrum is similar in many ways to those of $K_2S_2O_5$ and $(NMe_4)_2S_2O_5$, but it shows a complex series of bands in the region 700–400 cm^{-1}. Two bands of medium intensity, at 380 cm^{-1} and 330 cm^{-1}, in the copper compound, which are not present in the spectra of $K_2S_2O_5$ or $(NMe_4)_2S_2O_5$, probably arise from Cu–S or Cu–O bonds. It is clear that the sulphite groups in these anhydrous transition metal sulphites are not present as free ions.[1]

Four hydrated sulphites were prepared, two containing main group metals and two containing transition metals, in order to ascertain what effects both metal ion and water of hydration have on the mode of attachment of the sulphite group, and to see whether the anhydrous sulphites in these cases could be prepared by thermal decomposition of the hydrated compounds.

Much of the earlier work associated with the preparation of hydrated metal sulphites has been shown to be unreliable. Preparative methods[4,5] yielded several samples for which reproducible analytical data could not be obtained; perhaps this is in part accounted for by the fact that hydrated sulphites are extremely sensitive to oxidation, particularly the iron(II) compound. We have characterised compounds using methods of preparation developed by us which give products for which reliable analytical data were consistently obtained.

$MnSO_3 \cdot H_2O$, $CaSO_3 \cdot 0 \cdot 5H_2O$ and $MgSO_3 \cdot 3H_2O$ were all made by treating an aqueous suspension of the metal carbonate with sulphur dioxide until all the carbonate had dissolved. Excess sulphur dioxide was removed by warming the solution, and the hydrated sulphite was obtained as a crystalline solid. $FeSO_3 \cdot 3H_2O$ was prepared by treating iron(II) sulphate solution with amalgamated zinc, sodium sulphite and sulphur dioxide. If

---

*Author to whom correspondence should be addressed.

Table 1. IR bands of metal sulphites (cm^{-1})

	ν_1(sym.str.)ν_3(asym.str.)		ν_2(sym.bend)		ν_4(asym.bend)	
$MnSO_3$	1015m	960s	645s		470w	
	890s					
$FeSO_3$	980sh	942s	620s		470m	
	900s					
$MgSO_3$	942m		625m		480w	
$CaSO_3$	970s	950s	665m	650m	520w	480w
						458w
$MnSO_3 \cdot H_2O$	1040sh	975m	635s		470w	
	880s					
$FeSO_3 \cdot 3H_2O$	1020sh	950s	630s		480s	
	880s					
$MgSO_3 \cdot 3H_2O$	940s		620m		480w	
$CaSO_3 \cdot 0.5H_2O$	975s	950s	668m	650m	520w	485w
						455w

s = strong; m = medium; w = weak; sh = shoulder. All bands are broad.

precautions are not taken to exclude air strictly from all the operations and to work in reducing conditions, basic sulphates and thiosulphates form readily, and iron(II) easily reduces aqueous sulphur dioxide to dithionite.

Thermograms were obtained for all the hydrated sulphites prepared, and are shown in Fig. 1. $MnSO_3 \cdot H_2O$ is quite stable and only begins to lose H_2O at 255°. Anhydrous $MnSO_3$ is present from 310–370°, but some surface decomposition occurs within this range. Above 370°, loss of SO_2 occurs at an irregular rate. MnO exists beyond 750°. $FeSO_3 \cdot 3H_2O$ begins to lose H_2O at 135°. A point of inflection is observed in the thermogram at 400°, when

loss of H_2O is almost complete, and rapid irregular loss of SO_2 commences. FeO exists above 830°. No intermediate decomposition products are observed.

$CaSO_3 \cdot O \cdot 5H_2O$ is remarkably stable. It begins to lose H_2O at 400°. Anhydrous $CaSO_3$ is present from 450–710°. SO_2 is lost beyond 710°, and at this temperature, slow disproportionation of sulphite to sulphate and sulphide occurs. At 920° isothermal decomposition of sulphate to oxide and SO_3 occurs. $MgSO_3 \cdot 3H_2O$ begins to lose H_2O at 100°. Anhydrous $MgSO_3$ is evident at 310°, but very soon afterwards, a slow irregular decomposition begins, which is not complete at 1000°. Final decomposition
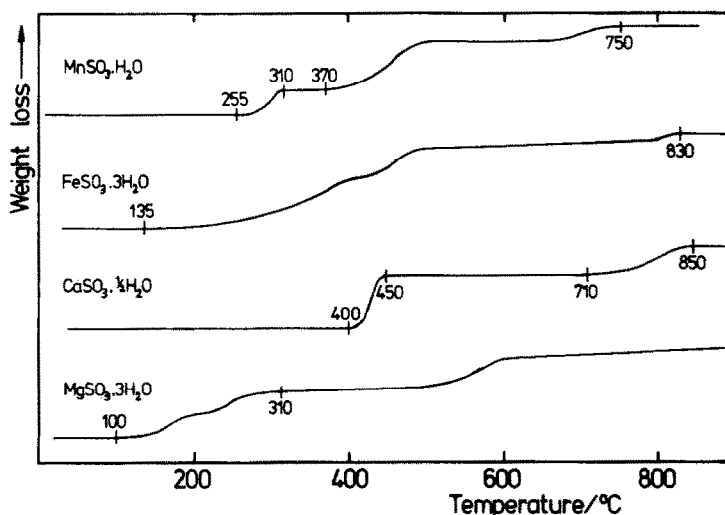
Fig. 1. Thermograms of hydrated metal sulphites.

products include MgO and MgS, and these probably arise from reactions similar to those occurring for the calcium compound.

Infrared bands are recorded in Table 1.

Nyberg and Larsson[6] made a detailed study of the IR spectra of a range of solid metal sulphites. Interpretation is not easy, as many of the bands are broad, and the stretching vibrations ν_1 and ν_3 in sulphite are often superimposed. However, it is usually possible to distinguish between ionic sulphite and covalently bonded sulphite.

The spectra of $MgSO_3 \cdot 3H_2O$ and $MgSO_3$ indicate that sulphite is present as the free ion, which may be loosely attached to the metal ion and hydrogen-bonded to water in the case of the hydrate.

The spectra of $CaSO_3 \cdot 0 \cdot 5H_2O$ and $CaSO_3$ are more complex than those of the magnesium compounds, and suggest some degree of interaction between the metal ion and sulphite, as well as hydrogen-bonding between sulphite and water in the hydrate. The water molecules are very strongly attached and the compound exhibits high thermal stability.

$MnSO_3 \cdot H_2O$ (pale pink) and $FeSO_3 \cdot 3H_2O$ (pale green) have colours in accord with octahedrally coordinated metal ions. The central metal ion is probably surrounded by oxygen-bonded sulphite groups and by water molecules. This is borne out by the complexity of peaks. ν_3 is most likely split and responsible for the complexity in the region $1020-880 \text{ cm}^{-1}$. If sulphite were sulphur-bonded, a simpler spectrum would be expected in this region, as ν_3 would remain a singlet and absorption would be most intense above 975 cm^{-1}.[6]

The support which IR studies give to the type of bonding in these compounds is enhanced by the thermogravimetric studies.

Both $MnSO_3 \cdot H_2O$ and $FeSO_3 \cdot 3H_2O$ decompose with loss of SO_2 at very much lower temperatures than the hydrated sulphites of calcium and magnesium, indicating some fundamental differences in structure. They decompose to give pure oxides (MnO, FeO), whereas the sulphites of magnesium and calcium decompose rather reluctantly to give mixtures of sulphides and oxides and sulphates.

The sulphites of manganese and iron should be compared with those of cobalt and nickel, which yield pure oxides CoO and NiO on heating.[1,2] The relative ease with which transition metal sulphites decompose, and the fact that they give an oxide only, favours a fairly strong metal–oxygen bond in these sulphites. The metal sulphite is easily decomposed on heating, with loss of SO_2, through fission of the oxygen–sulphur bond, which is weaker than in the free sulphite ion.

Thermogravimetric studies on transition metal sulphites also indicate that, whilst most of the SO_2 is evolved between 250° and 600°, in the cases of the hydrated sulphites $FeSO_3 \cdot 3H_2O$, $CoSO_3 \cdot 2 \cdot 5H_2O$ and $NiSO_3 \cdot 6H_2O$ further loss of SO_2 occurs at rather higher temperatures. This is probably due to the presence in these compounds of some sulphite ion as well as to covalently bonded sulphite.

Compounds containing free sulphite do not decompose substantially until higher temperatures are reached (710° in the case of $CaSO_3$ and 600° in the case of $MgSO_3$, neither being completely decomposed at 1000°). The decomposition of anhydrous $CoSO_3$ to CoO and of $NiSO_3$ to NiO is complete at 570° and no secondary loss of SO_2 is observed at higher temperatures. This, together with IR data,[1] suggests that these sulphites contain exclusively covalently bonded sulphite groups and no free sulphite ions.

EXPERIMENTAL

All operations were carried out in a closed system under dry nitrogen. Manganese(II) iodide was prepared by heating manganese(II) iodide tetrahydrate *in vacuo* over phosphorus(V) oxide at 140°C. Iron(II) iodide was prepared as described by Winter.[7] Copper(I) iodide was freshly prepared by adding sodium iodide (7.5 g) in water (150 ml) to copper(II) nitrate trihydrate (12.0 g) in water (100 ml) and passing sulphur dioxide. The white precipitate was filtered, washing with sulphurous acid, ethanol and dry ether. The product was dried *in vacuo* over phosphorus(V) oxide for 12 hr.

Manganese(II) sulphite. Manganese(II) iodide (11.0 g) was refluxed with tetramethylammonium disulphite (10.5 g), added in four aliquots, in dry acetone (250 ml) for 40 hr. The white product was filtered, dried, washing with liquid sulphur dioxide (8 × 20 ml), and finally dried at $125°/10^{-4}$ mm. (Found: Mn, 39.2; SO_2, 46.1. Calc. for MnO_3S: Mn, 40.7; SO_2, 47.5.)

Iron(II) sulphite. The method described for the corresponding manganese compound was followed. A green product was obtained. (Found: Fe, 39.7; SO_2, 45.8. Calc. for FeO_3S: Fe, 41.1; SO_2, 47.1.)

Copper(I) disulphite. Copper(I) iodide (9.1 g) and sodium iodide (5.5 g) were refluxed with tetramethylammonium disulphite (9.0 g) in dry acetone (200 ml) and the method described for the corresponding manganese compound was followed. A white product was obtained. (Found: Cu, 45.0; SO_2, 45.8. Calc. for $Cu_2O_5S_2$: Cu, 46.9; SO_2, 47.25.)

Manganese(II) sulphite monohydrate. Sulphur dioxide was passed into a suspension of manganese(II) carbonate (3.0 g) in distilled water (20 ml) until a clear solution was obtained. The solution was heated on a steam bath under a stream of nitrogen. Crystalline manganese(II) sulphite monohydrate formed. When no more sulphur dioxide was evolved, the solution was allowed to cool under nitrogen. The product was filtered under nitrogen, washed with ethanol previously boiled and saturated with sulphur dioxide, dried with ether under nitrogen, and finally dried at 10^{-4} mm for 12 hr. The product was stored in a sealed tube under pure nitrogen. (Found: Mn, 35.8; SO_2, 41.5. Calc. for H_2MnO_4S: Mn, 35.65; SO_2, 41.85.)

Iron(II) sulphite trihydrate. All solutions were prepared and stored in a stream of pure nitrogen (previously deoxygenated by passing through chromium(II) chloride solution). Iron(II) sulphate pentahydrate (3.0 g) was dissolved in distilled water (20 ml) previously boiled and cooled under nitrogen. Concentrated hydrochloric acid (0.2 ml) and a piece of zinc were added. In another portion of water (20 ml), sodium sulphite (5.0 g) was dissolved and the solution saturated with sulphur dioxide. The two solutions were mixed, the zinc removed, and sulphur dioxide passed into the solution for 15 min. The stream of sulphur dioxide was replaced with nitrogen, and the solution heated to 100°C. When no more sulphur dioxide was evolved, the solution was allowed to cool. The pale green crystals were filtered, washed with ethanol previously boiled and saturated with sulphur dioxide, dried with ether, and finally dried at 10^{-4} mm for 12 hr. The product was stored in a sealed tube under pure nitrogen. (Found: Fe, 29.2; SO_2, 33.45. Calc. for H_6FeO_6S: Fe, 29.4; SO_2, 33.7.)

Calcium(II) sulphite hemihydrate. The method described for the corresponding manganese(II) sulphite monohydrate was followed. A white crystalline product was obtained. (Found: Ca, 31.4; SO_2, 48.9. Calc. for $HCaO_{3.5}S$: Ca, 31.45; SO_2, 49.6.)

Magnesium(II) sulphite trihydrate. The method described for the corresponding manganese(II) sulphite monohydrate was followed. A white crystalline product was obtained. (Found: Mg, 15.25; SO_2, 40.2. Calc. for H_6MgO_6S: Mg, 15.35; SO_2, 40.4.)

Physical measurements. Infrared spectra were recorded on a Perkin-Elmer 457 grating spectrophotometer as Nujol mulls. Thermogravimetric curves were obtained using a Stanton thermobalance. Metals were determined gravimetrically: manganese as ammonium manganese(II) phosphate monohydrate, iron as

iron(III) oxide, copper as dipyridinedithiocyanato copper(II), and magnesium as ammonium magnesium phosphate hexahydrate.

Sulphur dioxide was determined iodometrically and gravimetrically as barium sulphate, after oxidation of sulphite with hydrogen peroxide. Calcium was determined by Mr. A. Hedley of this department.

REFERENCES

[1] R. Maylor, J. B. Gill and D. C. Goodall, Part I, *J. Inorg. Nuclear Chem.* 1971, **33**, 1975.

[2] R. Maylor, J. B. Gill and D. C. Goodall, Part II, *J.C.S. Dalton* 1973, 534.

[3] W. D. Harrison, J. B. Gill and D. C. Goodall, *J.C.S. Dalton* 1979, 847.

[4] Mellow, *Comprehensive Treatise of Inorganic and Theoretical Chemistry.* Longmans (1930), London, and references therein.

[5] Gmelin, "Handbuch der anorg. Chem."C6 1976, **56**.

[6] B. Nyberg and R. Larsson, *Acta Chem. Scand.* 1973, **27**, 63.

[7] Winter, *Inorganic Synthesis* 1973, **14**, 102.

CRYSTALLINE PHASE EFFECTS ON ESCA VALENCE BANDS OF Zr(IV) AND Ti(IV) ACID PHOSPHATES

GIOVANNI MARLETTA,* ORAZIO PUGLISI and SALVATORE PIGNATARO
Istituto Dipartimentale di Chimica, Università di Catania, Viale A. Doria, 95100 Catania, Italy

and

GIULIO ALBERTI and UMBERTO COSTANTINO
Dipartimento di Chimica, Università di Perugia, Via Elce di Sotto, 06100 Perugia, Italy

Abstract—The valence bands (V.B.) of ESCA spectra of Zr(IV) and Ti(IV) acid phosphates in different crystalline phases are reported. The various bands are assigned by comparison with Li_3PO_4. Variations on changing the crystalline phase for compounds having the same M(IV) ion are found. Two types of molecular orbitals are mainly involved. One related to P–O bonds is affected by the crystalline phase. The other, related to M(IV)–O bonds and confined into the layers of the compounds, are less sensitive to crystalline environment. Variation in the symmetry of the tetrahedral type PO_4^{3-} anion are proposed to be mainly responsible of the observed effects.

INTRODUCTION

Several attempts have been made in order to characterize the electronic effects of structural variations, due to changes in the crystalline phase, by means of the ESCA technique.[1-5] The study of the binding energy shifts of core levels on going from one to another crystalline phase does not give any conclusive answer to the problem of the detectability of structural changes. This is because the variation in crystalline phase influences primarily the Madelung potential that is expected to shift all the binding energies (B.E.) of the core levels in the same sense.[6,7] The Valence Band (V.B.) region of the ESCA spectrum seems to be more appropriate to detect structural changes. Large efforts have been made in the characterization of V.B. patterns for amorphous and crystalline phases in semiconducting compounds.[8,9] In addition, changes in the V.B. pattern for metal/dielectric and semiconductor/metal phase transitions and in general for a compound before and after a temperature induced phase transition have been reported.[10-13] Changes in the V.B. pattern of samples epitaxially grown in two different crystalline structures have been described also; however this last study deals with quite simple systems such as cubic (s.c.) and face centred cubic (f.c.c.) thallous halides.[14]

No dependence of V.B. structure on the crystalline phase has been reported for complex inorganic salts having polyatomic anions.

In connection with a general program of ESCA characterization of inorganic ion-exchangers and/or solid electrolytes we are carrying out[1,15] a systematic investigation on the acid phosphates of tetravalent metals and their salt forms. It was thought that these materials could be suitable compounds to study the eventual effect of the crystalline phase variation on the ESCA spectra of V.B. In fact, the acid salts of tetravalent metals, M(IV)·(HPO₄)₂, can be obtained, other than as amorphous materials, also in two different layered structures named as α- and γ-phases.[16-18] Thus, the V.B. spectra of the phosphate group can be examined and compared in three different materials of same chemical composition, while

the effect of the tetravalent metal can be investigated by comparing the results obtained with analogous crystalline phases of different M(IV) phosphates.

In this paper the results obtained with α-, γ- and amorphous acid phosphates of Zr(IV) and Ti(IV) are reported and discussed.

EXPERIMENTAL

Amorphous zirconium phosphate was prepared by slowly mixing 1 M $ZrOCl_2$ solution with 2 M H_3PO_4 solution. Microcrystalline α-$|Zr(PO_4)_2|H_2 \cdot H_2O$ and γ-$|Zr(PO_4)_2|H_2 \cdot 2H_2O$ were obtained with the slow precipitation[19] and refluxing[20] procedures respectively. The α-$|Ti(PO_4)_2|H_2 \cdot H_2O$ and γ-$|Ti(PO_4)_2|H_2 \cdot 2H_2O$ were obtained as described in Refs. 21 and 22 respectively. The amorphous and α-phases were stored over phosphorus pentoxide while the γ-phase were conditioned in vacuum desiccator over a NaCl saturated solution at room temperature ($P/P_0 = 0.7$).

The ESCA spectra were obtained with a KRATOS ES-300 electron spectrometer. The samples were introduced in the spectrometer chamber as powder pellets, obtained under rotary vacuum pump and attached to a Ni–Cr wire with a silver glue. The measurements were performed with Al_{K_α} radiation under a vacuum of 10^{-9} Torr.

It is always very difficult to assess the behaviour of water containing materials in the high vacuum of an X-ray Photoelectron Spectrometer.[23] In our case one can think that water of crystallization may or may not be pumped away. In both cases we should not have interference with the anion spectrum. If it is pumped away the crystalline structures remain unchanged.[22] If it has not been pumped away, the water O $2p$ cross section is so low with respect to metal–oxygen bonding orbitals to ensure little contribution to the valence band.

Carbonaceous contamination, previously discussed,[1] might also influence the V.B. spectra. However the good reproducibility of the spectra taken in different experimental conditions ensures that this disturbing factor should play a negligible role.

No attempt was made to remove the residual carbon contamination by Argon sputtering since this procedure causes strong damage in the examined samples.[15,24]

RESULTS AND DISCUSSION

Figure 1 shows the V.B. region of the ESCA spectrum of the amorphous $Zr(HPO_4)_2$. In the same figure the spectrum of Li_3PO_4 is also reported for comparison. The high K.E. part of the V.B. spectra of α, γ and amorphous

---

*Author to whom correspondence should be addressed.
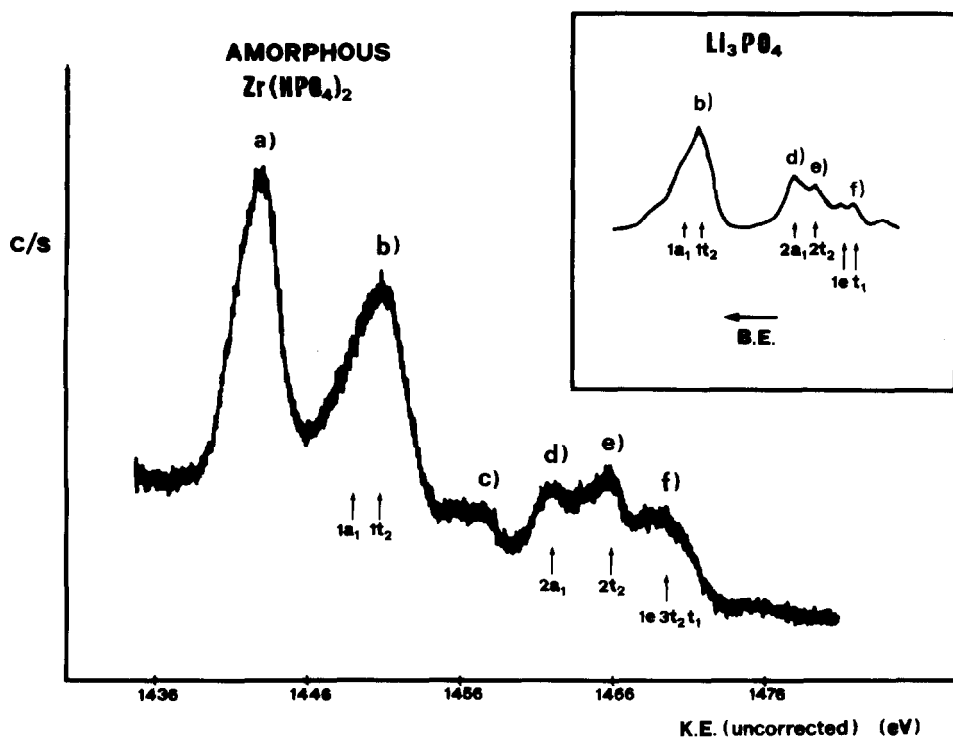
Fig. 1. Valence Band region (Al_{K_α}) of ESCA spectrum of amorphous $Zr(HPO_4)_2$. The Li_3PO_4 spectrum reported for comparison is from Ref. 25.

$Zr(HPO_4)_2$ are compared in Fig. 2. Figure 3 shows the same spectra for α and γ $Ti(HPO_4)_2$.

The assignment of the various bands in Figs. 1–3 is made by comparing the amorphous $Zr(HPO_4)_2$ and Li_3PO_4 spectra.

The structure (a) in the spectrum of the amorphous zirconium phosphate (Fig. 1) is due to the photoionization of 4p electrons of Zr(IV) ions; the rather sharp shape of this band suggests that the 4p orbitals are not strongly involved in the bonding. The weak structure (c) may be due to shake-up transitions involving the bands at higher K.E.

The structures (b), (d), (e) and (f) resemble those found in Li_3PO_4. This is not surprising, since, this part of the spectrum is free from metal Zr(IV) orbitals. Thus, it must be correlated to the PO_4^{3-} moiety and can be assigned to the same type of orbitals attributed to the corresponding bands in the Li_3PO_4 spectrum.[25-30] This because also the V.B. of this last compound is free from metal orbitals.

On this basis, the band (b) is assigned to four strongly bonding O-2s orbitals which are split by tetrahedral field in $1a_1$ and $1t_2$ orbitals having some P-3s and P-3p contribution respectively.

The bands (d) and (e) are assigned to $2a_1$ and $2t_2$-like orbitals. These orbitals arise from the mixing of four orbitals P-3s and P-3p with four $O-2p_\sigma$ orbitals. These two bands correspond to the two types of P-O σ-bonding, with $2a_1$ linked to the s-symmetry and with the $2t_2$ band linked to the p-symmetry.[25,26] The $2a_1$ band is mainly due to a P-3s/O-2p bonding orbital in which the little contribution of O-2s is of opposite sign of the P-3s. The $2t_2$ band arises from O-2p with P-3p strong contribution.

The band (f) is attributed to the convolution of three structures $1t_1$, $3t_2$ and $1e_1$ that arise from the splitting in

tetrahedral field of the eight 2p π orbitals of oxygen atoms. Strong contribution of Zr 4d orbitals to $2t_2$ and to $1t_1$, $3t_2$ and $1e$ is expected.

A closer comparison of the V.B. patterns of the Li_3PO_4 and of the amorphous $Zr(HPO_4)_2$ shows some differences (Fig. 1) in the relative intensities, shapes and relative B.E.'s of the various bands. Differences are also noted in the spectra of the Zr(IV) vs Ti(IV) compounds and for the same cation comparing the different crystalline structures (Figs. 2 and 3). These differences can be interpreted considering that the Valence Band features should be influenced by the following structural factors:

(1) Bond lengths between the central atom and the oxygens of oxoanions,

(2) Symmetry of the oxoanions in the crystalline lattice,

(3) Madelung potential effect arising on the peculiar crystal packing,

(4) Nature of the cations which in turn influence bonding features as polarity, covalency percentage, lengths and orientation of the bonds.

On the basis of the above considerations the differences between Li_3PO_4 and Zr(IV) or Ti(IV) phosphates, should be due to:

(a) the higher covalent nature of M(IV)-O bonding with respect to the more ionic nature of Li-O bonds,

(b) the different P-O length in $M(IV)(HPO_4)_2$ compound compared to that in Li_3PO_4 (1.53 Å in α-$Zr(HPO_4)_2$ against 1.56 Å in Li_3PO_4[16]),

(c) the distortion from tetrahedral symmetry mainly due to the P-OH bond which is longer for example, in α-$Zr(HPO_4)_2 \cdot H_2O$, than the other P-O bonds of about 0.06 Å.[31,32]

In particular, the first factor should account for the higher intensity of the (f) band in M(IV) phosphates. This
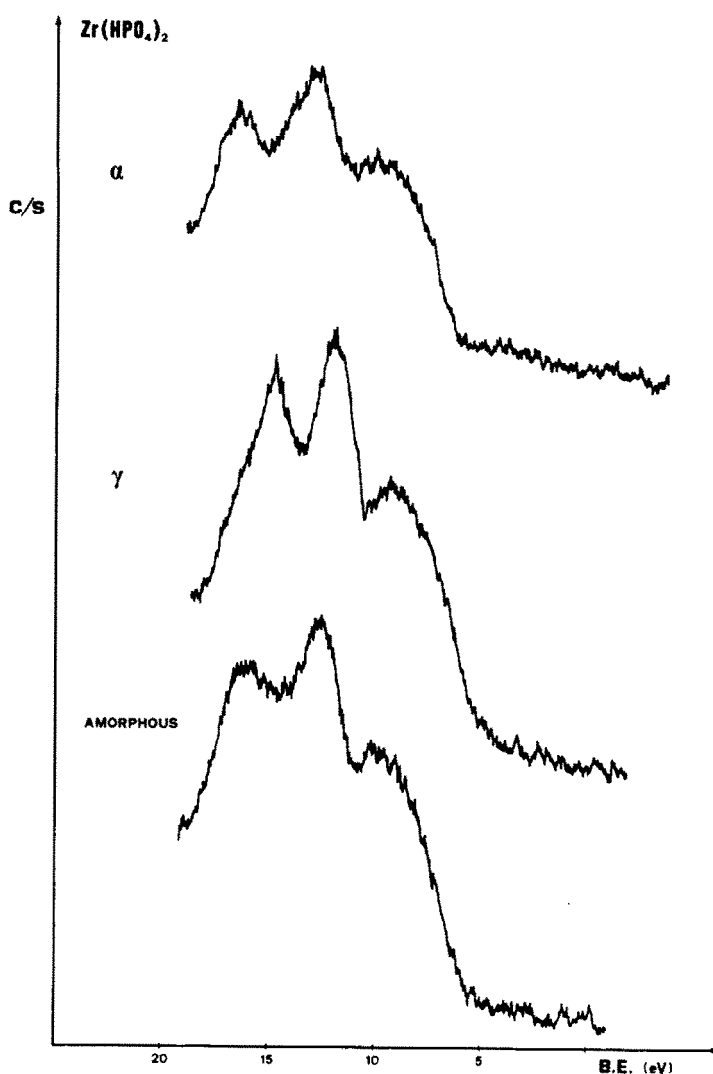
Fig. 2. Valence Band region in expanded scale of ESCA spectra of amorphous, α- and γ-Zr(HPO$_4$)$_2$.

Table 1. Binding energies (eV) of amorphous, α and γ Zr(HPO$_4$)$_2$

	O$_{1s}$	P$_{2s}$	Zr 3d 5/2	Zr 4s	Zr 4p	(b)	(d)	(e)	(f)
					(a)				
Amorphous	533.4	193.8	185.9	56.7	34.4	26.6	15.9	12.6	9.8
α	533.3	193.4	185.5	56.8	34.2	26.4	15.8	12.4	9.4
γ	532.7	193.0	185.0	56.2	33.7	25.9	14.6	11.9	9.1
Li$_3$PO$_4$	536.6	195.5	-	-	-	29.3	17.6	15.0	11.5 - 9.0

The figures for the Zr compounds are referred to the B.E. of the Zr 3 d5/2 core level (1)

The Li$_3$PO$_4$ values are taken from ref. 25.

because the covalent nature of the bonding should give a strong contribution of Zr 4d and 5s orbitals (or Ti 3d and 4s) to the oxoanion's molecular orbitals 1e$_1$, 1t$_1$ and 3t$_2$. An increased photoionization cross-section is indeed to be expected[33] for Zr 4d (or Ti 3d) orbital contribution to the low photoionization cross section of the O-2p like orbitals.

The B.E. lowering of the (f) band (distance O 2s-(f)

band centroid: Zr(HPO$_4$)$_2$ = 16.8 eV, Ti(HPO$_4$)$_2$ = 17.7 eV; Li$_3$PO$_4$ = 19.05 eV) should be mainly due to the increase of positive charge density of the oxygen atoms covalently bonded to M(IV) ions, with respect to the PO$_4^{3-}$ moiety in the Li$^+$ salts. The trend seems to be unaltered by eventual final state effects. The increased splitting of 2a$_1$.and 2t$_2$ like components from 2.5 eV for Li$_3$PO$_4$ to 3.3 eV for α-Zr(HPO$_4$)$_2$ or 3.6 eV for α-
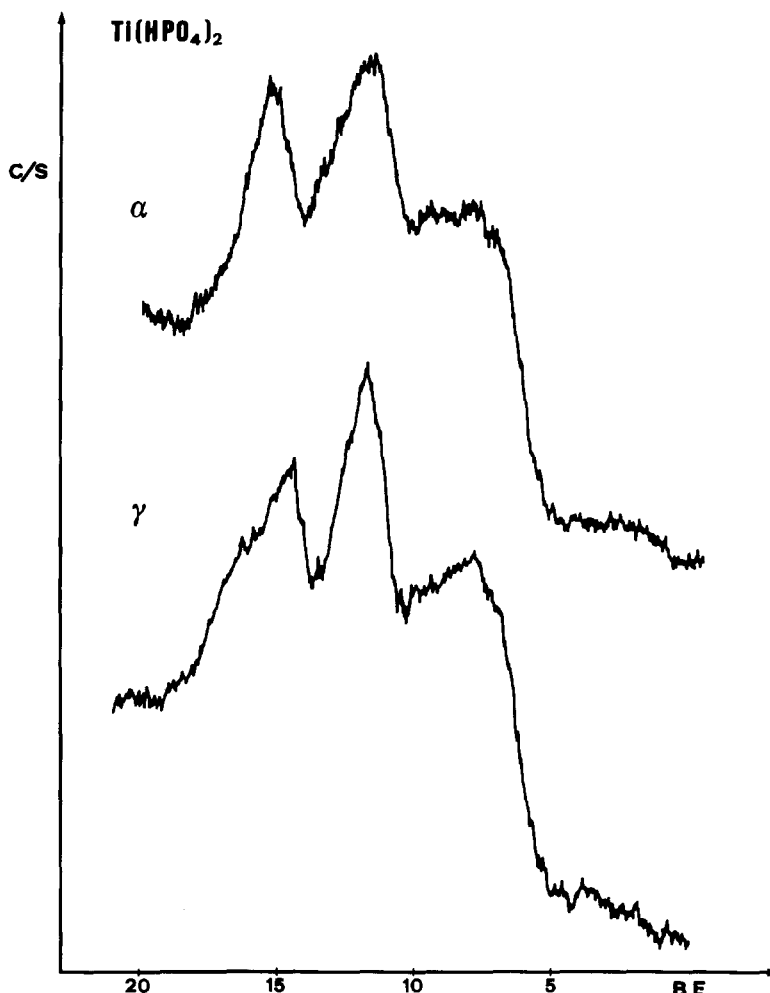
TI(HPO₄)₂

Fig. 3. Valence Band region of ESCA spectra of α- and γ-Ti(HPO$_4$)$_2$.

$Ti(HPO_4)_2$ should be due to the concurrent influence of the decrease of the P–O distances and distortion of the tetrahedral symmetry of PO_4^{3-} group. The shorter bonds imply a stronger crystalline field effect on the energy levels in the anionic group, which should increase the separation of the levels. On the other hand the distortion of the tetrahedral symmetry is expected to remove band degeneracies, by splitting the $2a_1$ and $2t_2$ orbitals in different components convoluted in the broad (d) and (e) bands.

Several factors may contribute to the intensity inversion of the two $2a_1$ and $2t_2$ like bands. Due to the short P–O bond in M(IV) phosphates the interactions between the P 3s–O 2s orbitals are expected to be stronger than in Li_3PO_4. As a consequence, due to the opposite sign in the molecular combination, the intensity of $2a_1$ like band is reduced with respect to that of $2t_2$. To this effect concurs the above mentioned distortion of the tetrahedral symmetry on going from the Li to the M(IV) compounds. Because of the lower symmetry, the splitting of the (d) band takes place with a consequent lowering of its intensity. On the other hand the $2t_2$ like band should have some Zr 4d or Ti 3d contribution which should increase the intensity of the (e) band for the same reasons invoked for the (f) band.

A comparison of the V.B. region of ESCA spectra of

$Zr(HPO_4)_2$ and $Ti(HPO_4)_2$ with different crystalline arrangements shows the strong importance of the phase effects versus the "chemical" effect of the substitution of Li with Zr(IV) or Ti(IV) ions. The previous hypothesis allow to interpretate these effects.

Let us first compare the V.B. region of amorphous, α- and γ-zirconium phosphates. Figure 2 shows the (d), (e) and (f) bands in expanded scale. Remarkable differences both in B.E. and in shape for the three samples can be observed. The (a) and (b) bands are instead not reported being very similar.

The distance between the maxima of (d) and (e) bands is greater in α- and amorphous than in γ-phases. The γ-phase figure is closer to that of the model compound (see Fig. 2 and Table 1). The previously hypothesized correlation of this parameter to the symmetry of the PO_4^{3-} group would suggest in this case a more regular symmetry of the anionic groups in the γ-phase.

However the (d) band of the γ-phase shows a definite component at the low K.E. side and the energy difference of the centroid of the whole band with respect to the (e) band is 3.3 eV, very close to that found for the α-phase.

The α- and amorphous phases are characterized by a distorted tetrahedral symmetry of the anionic group with the P–OH bond significantly longer than the other P–O

bonds.[31,32] Unfortunately the structure of the γ-phase is yet unknown but some indirect evidences[34-36] lead to assume that there are two kinds of $PO_3(OH)$ groups, crystallographically different. This hypothesis seems to be supported by the observation of a low K.E. component of the (d) band, the deconvolution of this band giving an approximate 2:1 ratio between the more and less intense component. These two components might then be attributed to two different types of $PO_3(OH)$ groups. The low K.E. component should be due to a distorted tetrahedral situation. The more populated high K.E. band should be due to the presence of $PO_3(OH)$ groups with a more regular tetrahedral symmetry, since its energy difference from the sharp (e) band is closer to that of the tetrahedral model compound.

The (e) band seems very sharp in shape for the γ- and amorphous phases while it is broader in the α-one. This sharpening is probably to be connected again to symmetry factors.

In particular, in a previous work,[22] it was found that the structure of the γ-macroanions is more dense than that of the α-ones. It was supposed that the dense structure of the γ-layer could arise from a linking of $PO_3(OH)$ tetrahedra to the $M(IV)O_6$ octahedra different from that observed for the α-layer. In this latter macroanion the tetravalent metal atom is coordinated to six oxygens of six different $PO_3(OH)$ groups; in the γ-one the 6-coordination may be obtained with a lower number of $PO_3(OH)$ tetrahedra, probably four.

On the other hand, one has to take into account that angular variations in a given anion structure leads to modification in the V.B. pattern,[37] so that the modification observed in the (e) band may be connected to different packing, which involves angular variations in $PO_3(OH)$ tetrahedra on changing phase. The (f) band appears to be more similar in the case of the γ and amorphous phases with respect to the α-one. In particular the (f) band seems to be broader and less close to the (e) band in the series, $\alpha > \gamma >$ amorphous.

The sharpening of the (f) band seems reasonably connected to the poor band overlap in the amorphous phase, due to the lack of any regularity in the lattice. In the γ-phase, because of the same feature of the (f) band, the presence of some distortion in the crystal lattice should be considered. Indeed, the high density of the γ-sheets, that implies the distortion of the regular octahedral symmetry of the ZrO_6^{8-} clusters could cause the missing of part of the symmetry pattern found in the α-phase. This decrease of symmetry (from general solid state band considerations) could account of the observed band sharpening.

Similar conclusion can be drawn by examinating the V.B. spectra of α- and γ-titanium phosphates (see Fig. 3). In particular, the splitting of the (d) band in two components on going from α to γ phase is much stronger. This effect gives supports to the hypothesis made for the zirconium phosphates since it is just the effect expected on the base of the differences in the molecular internal distances. It is known that the distance between the M(IV) ions, lying nearly in a plane, is 5.3 Å (Zr) and 5.0 Å (Ti) for the α-compounds[16] and 4.6 Å (Zr) and 4.4 Å (Ti) for the γ-ones.[34,38]

Also the behaviour of the (e) and (f) bands resembles that observed for Zr(IV) phosphates on going from the α- to the γ-phase. The asymmetric shape of (e) band in α-Ti(HPO$_4$)$_2$ is removed in γ-Ti(HPO$_4$)$_2$, and the (f) band has a more flat shape in the α and a well peaked shape in

the γ-phase. Furthermore, the distance between the maxima of (d) and (e) bands is very similar to that found for the α and γ-Zr(IV) compounds: i.e. 3.6 eV in the α-phase and 2.7 eV in the γ-phase.

All of this suggests that the described differences in the V.B. patterns are peculiar to the various structures and that each phase is characterized by rather well defined features. The replacement of Zr(IV) with Ti(IV) leads only to small differences.

CONCLUSION

The comparative study of the V.B. region of the ESCA spectra of acid salts of tetravalent metals, having different structures, has shown that the V.B. patterns are affected by variation in the crystalline structure.

The structural variations influence in different extent the different parts of the V.B. pattern. In particular the (d) and the (e) bands (a$_1$ and t$_2$ orbitals) are those which seems to be mainly affected by the crystalline environment. This is connected to the fact that these bands refer to orbitals, (P–O) which are external to the macroanionic layers.

On the other hand the (f) band (e, t$_2$ and t$_1$ orbitals) is less affected by crystalline environment and the consequent symmetry variations. This is connected to the fact that these bands refer to orbitals, (mainly M(IV)–O), which are inside of the macroanionic layers.

Work is in progress in our laboratories on the alkali forms of these layered ion exchangers in order to study the effect of the intercalation of the cations on their V.B. patterns.

REFERENCES

[1] G. Alberti, U. Costantino, G. Marletta, O. Puglisi and S. Pignataro, *J. Inorg. Nucl. Chem.* 1981, **43**, 3329.
[2] T. Dickinson, A. F. Povey and P. M. A. Sherwood, *J. Solid-St. Chem.* 1975, **13**, 237.
[3] D. S. Urch and S. Murphy, *J. Electron Spectrosc. Relat. Phenom.* 1974, **5**, 167.
[4] G. K. Wertheim, L. F. Mattheiss, M. Campagna and T. P. Pearsall, *Phys. Rev. Lett.* 1974, **32**, 997.
[5] R. M. Friedman, R. E. Watson, J. Hudis and M. L. Perlman, *Phys. Rev. B* 1973, 3569.
[6] R. T. Poole, *Chem. Phys. Lett.* 1976, **42**, 151.
[7] P. H. Citrin and T. D. Thomas, *J. Chem. Phys.* 1972, **57**, 4446.
[8] N. E. Erickson, *Phys. Scripta* 1977, **16**, 462.
[9] V. V. Nemoshkalenko and V. G. Aleshin, *Phys. Scripta* 1977, **16**, 457.
[10] C. Blaauw, F. Zeenhouts, F. Van Der Wonde and G. A. Sawatzky, *J. Phys. C* 1975, **8**, 459.
[11] S. Vasudevan, M. S. Hegde and C. N. R. Rao, *Solid-St. Comm.*, 1978, **27**, 131.
[12] L. I. Johansson, C. W. B. Martinsson, P. E. Nilsson-Jatko, S. E. Karlsson and S. B. M. Hagström, *Phys. Scripta* 1975, **14**, 105.
[13] G. K. Wertheim, *J. Franklin Inst. (USA)* 1974, **298**, 289.
[14] L. Porte, *J. Chem. Phys.* 1980, **73**, 1104.
[15] S. Pignataro, G. Marletta, O. Puglisi, U. Costantino and G. Alberti, *J. Electron Spectrosc. and Relat. Phenom.* 1982, **25**, 49.
[16] A. Clearfield, G. H. Nancollas and R. Blessing, In *Ion Exchange and Solvent Extraction* (Edited by J. A. Marinsky and Y. Marcus), Vol. 5, Chap. 1. M. Dekker, New York (1973).
[17] G. Alberti, *Acc. Chem. Res.* 1978, **11**, 163.
[18] A. Clearfield (Ed.), *Inorganic Ion Exchange Materials.* CRC Press, Baca Roton, chap. 1-2 (1982).
[19] G. Alberti and E. Torracca, *J. Inorg. Nucl. Chem.* 1968, **30**, 317.

[20] A. Clearfield and J. A. Stynes, *J. Inorg. Nucl. Chem.* 1964, **26**, 117.

[21] G. Alberti, P. Cardini-Galli, U. Costantino and E. Torracca, *J. Inorg. Nucl. Chem.* 1967, **29**, 571.

[22] G. Alberti, U. Costantino, M. L. Luciani Giovagnotti, *J. Inorg. Nucl. Chem.* 1979, **41**, 643.

[23] K. Hirokawa and Y. Danzaki, *SIA Surf. Interf. Anal.* 1982, **4**, 63.

[24] S. Pignataro, G. Marletta, O. Puglisi, U. Costantino and G. Alberti, *J. Electron Spectrosc. and Relat. Phenom.* 1982, **25**, 49; Idem, to be published.

[25] V. I. Nefedov, Y. A. Buslaev, N. P. Sergushin, Y. V. Kojunov, V. V. Kovalev and L. Bayer, *J. Electron Spectrosc. and Relat. Phenom.* 1975, **6**, 221.

[26] R. Prins, *J. Chem. Phys.* 1974, **61**, 2580.

[27] A. Calabrese and R. G. Hayes, *J. Am. Chem. Soc.* 1973, **95**, 2819.

[28] T. Sasaki and H. Adachi, *J. Electron Spectrosc. and Relat. Phenom.*, 1980, **19**, 261.

[29] J. Weber, *Chem. Phys. Lett.* 1976, **40**, 275.

[30] G. Höjer, S. Meza-Höjer and G. Hernandez de Pedrero, *Chem. Phys. Lett.* 1976, **37**, 301.

[31] A. Clearfield and G. D. Smith, *Inorg. Chem.* 1969, **8**, 431.

[32] J. M. Troup and A. Clearfield, *Inorg. Chem.* 1977, **16**, 3311.

[33] S. Hüfner, In *Photoemission in Solids* (Edited by L. Ley and M. Cardona), Vol. II. Springer-Verlag, Berlin-Heidelberg (1979).

[34] S. Yamanaka and M. Tanaka, *J. Inorg. Nucl. Chem.* 1979, **41**, 45.

[35] A. Clearfield and J. M. Garces, *J. Inorg. Nucl. Chem.* 1979, **41**, 879.

[36] S. Yamanaka and M. Hattori, *Inorg. Chem.* 1981, **20**, 1269.

[37] W. R. Salaneck, C. F. Brucker, J. E. Fischer and A. Metrot, *Phys. Rev. B.* 1981, **24**, 5037.

[38] G. Alberti, U. Costantino and M. L. Luciani Giovagnotti, *J. Chromatogr.* 1980, **201**, 175.

NEW BIIMIDAZOLE AND BIBENZIMIDAZOLE DERIVATIVES: MONO AND BINUCLEAR PALLADIUM(II) OR PLATINUM(II) COMPLEXES AND HETEROBINUCLEAR PALLADIUM(II)-RHODIUM(I) OR PLATINUM(II)-RHODIUM(I) COMPLEXES

RAFAEL USÓN,* JOSÉ GIMENO, LUIS A. ORO, MIGUEL A. AZNAR
and JAVIER A. CABEZA
Departamento de Química Inorgánica, Universidad de Zaragoza, Zaragoza, Spain

Abstract—Novel neutral biimidazolate or bibenzimidazolate palladium(II) and platinum(II) complexes of the type $M(N-N)_2(dpe)$ [M = Pd, Pt; $(N-N)_2^{2-}$ = BiIm^{2-}, BiBzIm^{2-}. dpe = 1,2-*bis*(diphenylphosphino) ethane] have been obtained by reacting $MCl_2(dpe)$ with $Tl_2(N-N)_2$. Complexes $M(N-N)_2(dpe)$ which are Lewis bases react with $HClO_4$ or $[M(dpe)(Me_2CO)_2](ClO_4)_2$ to yield, respectively, mononuclear cationic complexes of general formula $[M\{H_2(N-N)_2\}(dpe)](ClO_4)_2$ (M = Pd, Pt; $H_2(N-N)_2$ = H$_2$BiIm, H$_2$BiBzIm) and homobinuclear palladium(II) or platinum(II) cationic complexes of the type $[M_2\{\mu-(N-N)_2\}(dpe)_2](ClO_4)_2$. Reactions of M(BiBzIm)(dpe) with $[Rh(COD)(Me_2CO)_x](ClO_4)$ render similar heterobinuclear palladium(II)-rhodium(I) and platinum(II)-rhodium(I) cationic complexes, of general formula $[(dpe)M(\mu-BiBzIm)Rh(COD)](ClO_4)$ (M = Pd, Pt; COD = 1,5-cyclooctadiene). Di- and mono-carbonyl derivatives $[(dpe)M(\mu-BiBzIm)Rh(CO)L](ClO_4)$ (M = Pd, Pt; L = CO, PPh$_3$) have also been prepared. The structures of the resulting complexes have been elucidated by conductance studies and IR spectroscopy.

INTRODUCTION

Our recent contributions to the coordination chemistry of biimidazolate (BiIm^{2-}) and bibenzimidazolate (BiBzIm^{2-}) anions have shown the ability of these ligands to form bi-,[1–4] tri-[3,4] and tetra-nuclear[3,5] complexes. Particularly, we have described[3,4] several homonuclear gold(I) or heterotrinuclear gold(I)–palladium(II) and gold(I)–rhodium(I) complexes which have been prepared starting from $Au_2(\mu-BiBzIm)L_2$ (L = phosphine) (A) as precursors, where BiBzIm^{2-} is acting as bidentate bridging ligand. These binuclear gold(I) complexes are Lewis bases, since they contain two nitrogen atoms as potential donors.

In the present paper we report the synthesis and properties of neutral mononuclear palladium(II) or platinum(II) complexes (B, C) of the type $[M(N-N)_2(dpe)]$ (M = Pd, Pt; $(N-N)_2^{2-}$ = BiIm^{2-}, BiBzIm^{2-}; dpe = 1,2-

bis(diphenylphosphino) ethane) which, similarly to the aforementioned gold(I) complexes, behave as a potential bidentate ligands. This allows the preparation of mono- and bi-nuclear palladium(II) and platinum(II) cationic complexes of the type $[M\{H_2(N-N)_2\}(dpe)](ClO_4)_2$, $[M_2\{\mu-(N-N)_2\}(dpe)_2](ClO_4)_2$ (M = Pd, Pt) as well as heteronuclear palladium(II)–rhodium(I) and platinum(II)–rhodium(I) cationic complexes of general formula $[(dpe)M(\mu-BiBzIm)RhL_2](ClO_4)$ (M = Pd, Pt; L_2 = 1,5-cyclooctadiene; L = CO), along with the monocarbonyl derivatives $[(dpe)M(\mu-BiBzIm)Rh(CO)L](ClO_4)$ (M = Pd, Pt; L = PPh$_3$).

RESULTS AND DISCUSSION

Reaction between dichloromethane solutions of $MCl_2(dpe)$ (M = Pd, Pt; dpe = 1,2-*bis*(diphenyl-phosphino) ethane) and thallium salts of BiIm^{2-} or BiB-
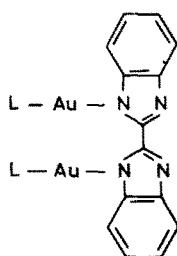
---

*Author to whom correspondence should be addressed.
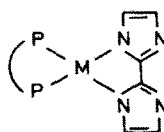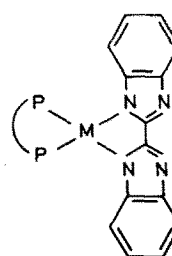
(A)   (B)   (C)

zIm^{2-} according to eqn (1):

$$MCl_2(dpe) + Tl_2(N-N)_2 \rightarrow M(N-N)_2(dpe) + 2TlCl \quad (1)$$

$$M = Pd; (N-N)_2{}^{2-} = BiIm^{2-}(I), \; BiBzIm^{2-}(II)$$

$$M = Pt; (N-N)_2{}^{2-} = BiIm^{2-}(III), \; BiBzIm^{2-}(IV)$$

lead to the precipitation of TlCl and solutions from which the mononuclear biimidazolate and bibenzimidazolate palladium(II) or platinum(II) complexes I–IV (Table 1), where the anions are acting as bidentate chelate ligands, can be obtained.

These complexes (B, C) havè two uncoordinated nitrogen donor atoms and are therefore Lewis bases. Thus, the addition of a stoichiometric amount of perchloric acid to dichloromethane solutions of I–IV (eqn 2)

$$M(N-N)_2(dpe) + 2HClO_4 \; ac. \rightarrow [M\{H_2(N-N)_2\}(dpe)](ClO_4)_2$$

$$M = Pd; H_2(N-N)_2 = H_2BiIm(V), \; H_2BiBzIm(VI) \quad (2)$$

$$M = Pt; H_2(N-N)_2 = H_2BiIm(VII), \; H_2BiBzIm(VIII)$$
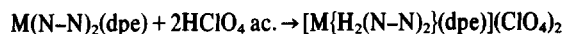
produces the protonation of the basic nitrogen atoms leading to the formation of cationic complexes V–VIII, in form of the perchlorate salts. Alternatively, these complexes can also be obtained from the cationic precursors[6] $[M(dpe)(Me_2CO)_2](ClO_4)_2$ by displacement with H_2BiIm or, respectively, $H_2BiBzIm$ of the poorly coordinated Me_2CO (eqn 3)

$$[M(dpe)(Me_2CO)_2](ClO_4)_2 + H_2(N-N)_2 \rightarrow$$

$$[M\{H_2(N-N)_2\}(dpe)](ClO_4)_2 + 2Me_2Co \quad (3)$$
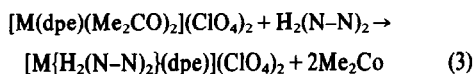
Since complexes (I–IV) are stronger Lewis bases than acetone, they react with the cationic complexes $[M(dpe)(Me_2CO)_2](ClO_4)_2$ (M = Pd, Pt) affording solutions of homobinuclear cationic complexes (eqn 4)

$$[M(dpe)(Me_2CO)_2](ClO_4)_2 + M(N-N)_2(dpe) \rightarrow$$

$$[M_2\{\mu-(N-N)_2\}(dpe)_2](ClO_4)_2 + 2Me_2CO \quad (4)$$

$$M = Pd; (N-N)_2{}^{2-} = BiIm^{2-}(IX), \; BiBzIm^{2-}(X)$$

$$M = Pt; (N-N)_2{}^{2-} = BiIm^{2-}(XI); \; BiBzIm^{2-}(XII)$$
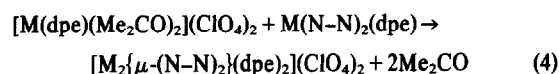
from which, after partial evaporation of the solvent, complexes (IX–XII) are obtained.

The process of eqn (4) is a general one and can be extended to the synthesis of heterobinuclear complexes.

Thus, palladium(II)–rhodium(I) and platinum(II)–rhodium(I) complexes (XIII–XIV) can be prepared, according to eqn (5)

$$[Rh(COD)(Me_2CO)_x](ClO_4) + M(BiBzIm)(dpe) \rightarrow$$

$$[(dpe)M(\mu-BiBzIm)Rh(COD)](ClO_4) + xMe_2CO \quad (5)$$

$$M = Pd(XIII), Pt(XIV) \quad COD = 1,5\text{-cyclooctadiene.}$$
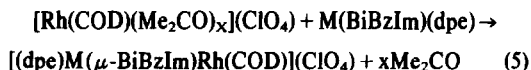
All the reactions take place smoothly at room temperature.

Bubbling of carbon monoxide through dichloromethane solutions of the heterobinuclear complexes XIII and XIV leads to the displacement of the diolefin and to the formation of the dicarbonyl derivatives $[(dpe)M(\mu-BiBzIm)Rh(CO)_2](ClO_4)$ (M = Pd(XV), Pt(XVI)). Addition of an equimolecular amount of triphenylphosphine to dichloromethane solutions of XV and XVI causes the substitution of one mole of carbon monoxide by the phosphine and leads to the formation of the monocarbonyl complexes $[(dpe)M(\mu-BiBzIm)Rh(CO)(PPh_3)](ClO_4)$ [M = Pd(XVII), Pt(XVIII)].

All the complexes described herein are air-stable. Table 1 lists their analytical data, decomposition points, molecular weights of the neutral complexes along with the conductivity data of the cationic complexes. The values of the slope A in Onsager's equation (nitromethane solutions) for the cationic complexes V–XVIII (see experimental) confirm that they are 1:2 (A = 427–477) or 1:1 (A = 230, 249) electrolytes supporting the proposed formulation and ruling out other possible structures (D, E) for which higher values of A should be expected.[7]

The IR spectra of the complexes (Nujol mulls) show absorption bands due to the anions BiIm^{2-} or BiBzIm^{2-} which are basically identical with those described for these ligands in other related complexes.[1,3] Nevertheless, some differences are observed in the 1300–1100 cm^{-1} region (in plane C–H bending) where the spectra of mononuclear and homobinuclear complexes I–IX and XI exhibit two absorption bands. The spectra of the cationic complexes VI–XVIII show the two absorption bands which are characteristic of the perchlorate anion[8] (Td) at *ca.* 1095(s, br) and 623(s) cm^{-1}. For the complexes $[M\{H_2(N-N)_2\}(dpe)](ClO_4)_2$ (V–VIII) these results contrast with the IR spectra of the related rhodium (I) cationic complexes $[Rh\{H_2(N-N)_2\}(diolefin)](ClO_4)$ where the corresponding absorptions of the perchlorate group (C$_{3v}$) point to a bonding via N–H ... OClO$_3$.[4,9] The stretching ν(N–H) in the complexes V–VIII appears as a strong and broad band in the 3500–3000 cm^{-1} region.

(D)

M = Pd, Pt
H$_2$(N–N)$_2$ = H$_2$BiIm, H$_2$BiBzIm

(E)

M = M' = Pd, Pt. n = 4
M = Pd, Pt. M' = Rh. n = 2
(N–N)$_2{}^{2-}$ = BiIm^{2-}, BiBzIm^{2-}
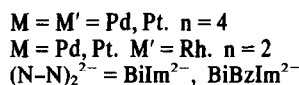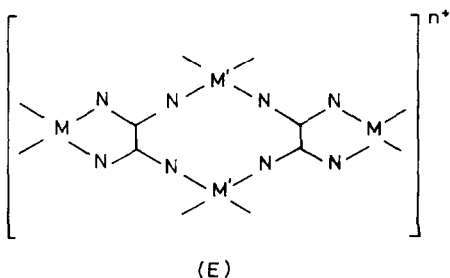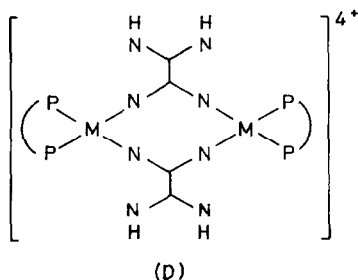
Table 1. Analytical data, conductivity measurements and other physical data of the novel complexes

Compound	Found (calc.) (%)			Colour	$\Lambda_M{}^{c,d}$ (ohm^{-1} cm^2 mol^{-1})	M.P.(°C)[b]
	C	H	N			
(I) Pd(BiIm)(dpe)[a]	59.70(60.34)	4.57(4.43)	8.85(8.79)	orange	–	203
(II) Pd(BiBzIm)(dpe)[a]	65.38(65.18)	4.51(4.37)	7.66(7.60)	yellow	–	262
(III) Pt(BiIm)(dpe)[a]	52.10(52.96)	4.05(3.88)	7.38(7.72)	yellow	–	>300
(IV) Pt(BiBzIm)(dpe)[a]	58.08(58.18)	3.91(3.90)	6.57(6.78)	pale-yellow	–	>300
(V) [Pd(H$_2$BiIm)(dpe)](ClO$_4$)$_2$	46.69(45.87)	3.44(3.60)	6.72(6.68)	white	146^{c,e}	214
(VI) [Pd(H$_2$BiBzIm)(dpe)](ClO$_4$)$_2$	51.40(51.22)	3.77(3.65)	5.81(5.97)	yellow	150^{c,e}	202
(VII) [Pt(H$_2$BiIm)(dpe)](ClO$_4$)$_2$	41.68(41.48)	3.34(3.26)	6.02(6.04)	white	148^{c,e}	178
(VIII) [Pt(H$_2$BiBzIm)(dpe)](ClO$_4$)$_2$	46.96(46.79)	3.30(3.33)	5.44(5.45)	yellow	146^{c,e}	243
(IX) [Pd$_2$(μ–BiIm)(dpe)$_2$](ClO$_4$)$_2$	51.24(51.96)	3.78(3.90)	4.09(4.17)	yellow	148^{c,e}	230
(X) [Pd$_2$(μ–BiBzIm)(dpe)$_2$](ClO$_4$)$_2$	54.73(55.02)	3.98(3.91)	3.85(3.88)	yellow	142^{c,e}	>300
(XI) [Pt$_2$(μ–BiIm)(dpe)$_2$](ClO$_4$)$_2$	44.82(45.89)	3.41(3.45)	4.24(3.69)	white	156^{c,e}	206
(XII) [Pt$_2$(μ–BiBzIm)(dpe)$_2$](ClO$_4$)$_2$	48.24(48.98)	3.95(3.48)	3.58(3.46)	yellow	152^{c,e}	>300
(XIII) [(dpe)Pd(μ–BiBzIm)Rh(COD)](ClO$_4$)	54.79(54.83)	4.41(4.22)	5.21(5.33)	yellow	82^{c,e}	>250
(XIV) [(dpe)Pt(μ–BiBzIm)Rh(COD)](ClO$_4$)	50.89(50.74)	4.13(3.90)	4.73(4.93)	yellow	83^{c,e}	>250
(XV) [(dpe)Pd(μ–BiBzIm)Rh(CO)$_2$](ClO$_4$)^f	50.74(50.48)	3.54(3.23)	5.36(5.61)	orange	132^d	>250
(XVI) [(dpe)Pt(μ–BiBzIm)Rh(CO)$_2$](ClO$_4$)^f	46.72(46.45)	3.48(2.97)	4.85(5.16)	orange	134^d	>250
(XVII) [(dpe)Pd(μ–BiBzIm)Rh(CO)(PPh$_3$)](ClO$_4$)^f	58.36(57.63)	4.31(3.85)	3.89(4.56)	pale-yellow	129^d	>250
(XVIII) [(dpe)Pt(μ–BiBzIm)Rh(CO)(PPh$_3$)](ClO$_4$)^f	54.06(53.75)	3.74(3.59)	4.08(4.25)	pale-yellow	122^d	>250

[a] Molecular weights. Found(Calc.): (I) 690(636.9), (II) 787(737), (III) 744(725.6), (IV) 843(825.7). [b] Decomposition point.
[c] In nitromethane. [d] In acetone. [e] Values of A in Onsager's equation: see experimental. [f] ν(CO)(cm^{-1}, CH$_2$Cl$_2$) 2085, 2020;
(XVI) 2087, 2020; (XVII) 1980; (XVIII) 1980.

The dicarbonyl complexes **XV** and **XVI** exhibit two strong absorptions (CH_2Cl_2 solutions) due to $\nu(CO)$, as expected for *cis*-dicarbonyl derivatives whilst the spectra of monocarbonyl complexes **XVII** and **XVIII** show a single absorption band (Table 1).

EXPERIMENTAL

C, H, N analyses were carried out with a Perkin–Elmer 240 microanalyzer. The IR spectra were recorded over the 4000–200 cm^{-1} range on a Perkin–Elmer 577 spectrophotometer using Nujol mulls or CH_2Cl_2 solutions. Conductivities were generally measured in *ca.* 5×10^{-4} M acetone or nitromethane solutions with a Philips 9501/01 conductimeter. Values of A were calculated in Onsager's equation $\Lambda_e = \Lambda_0 - A\sqrt{c}$ using several concentrations in the 5×10^{-3}–5×10^{-4} M range. The molecular weights were determined in chloroform solutions with a Hitachi-Perkin Elmer 115 osmometer. Decomposition points were determined under air in a Buchi apparatus.

PREPARATION OF COMPLEXES

Mononuclear palladium(II) or platinum(II) neutral complexes: M(BiIm)(dpe) *and* M(BiBzIm)(dpe) (*I-IV*)

An equimolecular mixture of Tl_2BiIm or $Tl_2BiBzIm^1$ and $MCl_2(dpe)^{10}$ (M = Pd, Pt) (0.5 mmol) in 50 ml of CH_2Cl_2 was stirred at room temperature for 2 hr. After filtering off the TlCl, partial evaporation of the solvent and addition of ether led to the precipitation of complexes I–IV. Yield %: (I) 64, (II) 79, (III) 83, (IV) 75.

Mononuclear palladium(II) or platinum(II) cationic complexes: $[M_2(\mu\text{-BiIm})(dpe)_2](ClO_4)_2$ (*V, VII*) *and* $[M(H_2BiBzIm)(dpe)](ClO_4)_2$ (*VI, VIII*)

Method (a). To a solution of 0.173 mmol of $[M(dpe)(Me_2CO)_2](ClO_4)_2$ (M = Pd, Pt)^6 in 50 ml of acetone (obtained *in situ* by reacting 0.173 mmol of $MCl_2(dpe)$ with 0.347 mmol of $AgClO_4$ and subsequent removal of AgCl) was added 0.173 mmol of H_2BiIm or $H_2BiBzIm$.^{11} After stirring at room temperature for 3 hr solutions were filtered off yielding the respective complexes by: partial evaporation of the filtrate and addition of ether (V, VII) or evaporation to dryness and stirring the oily residue in ether (VI, VIII). Yield %: (V) 84, (VI) 82, (VII) 87, (VIII) 90, A = (V) 435, (VI) 434, (VII) 460, (VIII) 477.

Method (b). A solution of 0.1 mmol of I–IV in 60 ml of CH_2Cl_2 was treated with 0.022 ml of $HClO_4$ 60% and stirred at room temperature for 1 hr. Complexes V–VIII were isolated after partial evaporation of the solution and addition of ether. Yields %: (V) 87, (VI) 80, (VII) 88, (VIII) 82.

Homobinuclear palladium(II) or platinum(II) cationic complexes: $[M_2(\mu\text{-BiIm})(dpe)_2](ClO_4)_2$ (*IX, XI*) *and* $[M_2(\mu\text{-BiBzIm})(dpe)_2](ClO_4)_2$ (*X, XII*)

An equimolecular mixture of $[Pd(dpe)(Me_2CO)_2](ClO_4)_2$ (obtained *in situ* as described above) and Pd(BiIm)(dpe) (I) or Pd(BiBzIm)(dpe) (II) (0.157 mmol) in 50 ml of acetone was stirred at room temperature for 3 hr. Complexes IX and X were precipitated by addition of ether to the partially evaporated solution. Platinum complexes XI and XII were similarly prepared. Yields %:

(IX), 80, (X) 88, (XI) 87, (XII) 93. A = (IX) 430, (X) 424, (XI) 427, (XII) 448.

Heterobinuclear palladium(II)–rhodium(I) or platinum(II)–rhodium(I) cationic complexes $[(dpe)M(\mu\text{-BiBzIm})Rh(COD)](ClO_4)$. M = Pd, (*XIII*), Pt (*XIV*)

A mixture of $[Rh(\mu\text{-Cl})(COD)]_2^{12}$ (0.033 g; 0.068 mmol), $AgClO_4$ (0.028 gr, 0.138 mmol) and 0.136 mmol of M(BiBzIm)(dpe) [M = Pd(II), Pt(IV)] in 30 ml of $H_2CCl_2Me_2CO$ (1 : 1) was stirred at room temperature for 20 min. AgCl was filtered off and the filtrate evaporated until *ca.* 1 ml. Yellow complexes **XIII** and **XIV** were precipitated by addition of ether. Yields %: (XIII) 79, (XIV) 94. A = (XIII) 230, (XIV) 249.

$[(dpe)M(\mu\text{-BiBzIm})Rh(CO)_2](ClO_4)$ M = Pd (*XV*), Pt (*XVI*)

Carbon monoxide was bubbled through a dichloromethane solution (20 ml) of **XIII** and **XIV** at atmospheric pressure for 20 min. The resulting solutions were partially evaporated and the required orange complexes **XV**, **XVI** precipitated by addition of ether. Yields %: (XV) 92, (XVI) 91.

$[(dpe)M(\mu\text{-BiBzIm})Rh(CO)(PPh_3)](ClO_4)$ M = Pd (*XVII*), Pt (*XVIII*)

An equimolecular mixture of **XV** (0.013 g; 0.013 mmol) or of **XVI** (0.039 g; 0.036 mmol) and PPh_3 in 20 ml of CH_2Cl_2 was stirred at room temperature until CO evolution is not observed (in *ca.* 2 hr). Pale yellow complexes **XVII** and **XVIII** were isolated after partial evaporation of solutions and addition of hexane. Yields %: (XVII) 91, (XVIII) 96.

REFERENCES

^{1}R. Usón, J. Gimeno, J. Forniés and F. Martínez, *Inorg. Chim. Acta* 1981, **50**, 173.
^{2}R. Usón and J. Gimeno, *J. Organometal. Chem.* 1981, **220**, 173.
^{3}R. Usón, J. Gimeno, J. Forniés, F. Martínez and C. Fernandez, *Inorg. Chim. Acta* 1981, **54**, L95; *Ibid.* 1982, **63**, 91.
^{4}R. Usón, L. A. Oro, J. Gimeno, M. A. Ciriano, J. A. Cabeza, A. Tiripicchio and M. Tiripicchio Camellini, *J. Chem. Soc., Dalton* in press.
^{5}R. Usón, J. Gimeno, L. A. Oro, J. M. Martínez de Ilarduya, J. A. Cabeza, A. Tiripicchio and M. Tiripicchio Camellini, submitted for publication.
^{6}J. A. Davies, F. R. Hartley and S. G. Murray, *J. Chem. Soc., Dalton* 1980, 2246.
^{7}R. O. Feltham and R. G. Hayter, *J. Chem. Soc.* 1964, 4587; K. W. Bagnall, D. Brown, P. J. Jones and J. G. H. Du Preez, *J. Chem. Soc.* 1965, 3594; W. J. Geary, *Coord. Chem. Rev.* 1971, **7**, 81.
^{8}B. J. Hathaway and A. E. Underhill, *J. Chem. Soc.* 1961, 3091; J. Peone Jr, and L. Vaska, *Angew. Chem. Int. Ed.* 1971, **10**, 511.
^{9}R. Usón, J. Gimeno, L. A. Oro, M. Valderrama, R. Sariego and E. Martínez, *Transition Met. Chem.* 1981, **6**, 103.
^{10}A. R. Sanger, *J. Chem. Soc.* (A) 1977, 1971; G. Booth and J. Chatt, *J. Chem. Soc.* (A) 1966, 634.
^{11}B. J. Fieselmann, D. N. Hendrickson and G. A. Stucky, *Inorg. Chem.* 1978, **19**, 2078.
^{12}J. Chatt and L. M. Venanzi, *J. Chem. Soc.* 1957, 4735.

STUDIES OF THE REACTIONS OF LITHIUM ATOMS WITH METHYL CYANIDE AND METHYL ISOCYANIDE IN INERT GAS MATRICES

ZAKYA A. KAFAFI, ROBERT H. HAUGE and JOHN L. MARGRAVE†
Rice University, Department of Chemistry, Houston, TX 77251, U.S.A.

Abstract—Linear LiNC is known to be the more stable isomer when isolated in inert gas matrices at low temperatures (4–15K).[1] In an attempt to form the other geometrical isomer, LiCN, studies of the reaction of lithium atoms with CH_3CN and CH_3NC were undertaken. A new absorption in the CN stretching region was observed when lithium atoms were co-condensed with CH_3NC in solid argon and xenon matrices. Photolysis of the matrices with a medium pressure Hg lamp during deposition of Li/CH_3NC seemed to favour the formation of the more stable isomer, LiNC. Reactions of lithium atoms with CH_3CN only led to the formation of LiNC, with or without photolysis.

INTRODUCTION

Early *ab initio* Hartree–Fock calculations on the structures and stabilities of gaseous LiCN and LiNC indicated that linear LiNC should be more stable by ~9 kcal/mole than linear LiCN.[2] From the different measured isotopic shifts for the three fundamental modes of carbon-13, nitrogen-15 and lithium-6 enriched samples, IR matrix isolation studies carried out on this molecule confirmed the greater stability of LiNC. Shortly after the experimental studies, Clementi *et al.*[3] reinvestigated the LiCN and LiNC molecules in the linear configuration making use of a larger basis set in their calculations. The resulting atomization energies were found to be 310.71 and 317.63 kcal/mole for LiCN and LiNC, respectively, again demonstrating the stability of LiNC over LiCN. However the emphasis in this work was on the study of the energy surface for a lithium atom reacting with a CN radical which represents the isomerization reaction surface for conversion from LiCN to LiNC. Particular interest was paid to the height of the energy barrier between the two configurations. No energy barriers were found to exist in the conversion of LiCN to LiNC, or between the linear and non-linear configurations.

Recently it was shown[6] that if correlation effects are included in the calculations of the isomerization energy for LiNC ↔ LiCN, the molecule shows almost no energy change for rearrangement in support of the idea of the "polytopic" bond.

Lunichev and Rambidi[5] derived equations that describe nuclei distributions of LiNC molecules for lower states of deformation vibrations. It was found that on increasing the vibrational energy, the average distance of the Li nucleus from the center of mass of the NC group increases and the average arrangement of LiNC nuclei changes from near linear to triangular. The same authors[6] studied the motion of the Li atom in a LiNC molecule and these calculations showed that the LiNC nuclear framework is highly non-rigid at low vapour temperatures as reflected from the high population of excited states. However the fraction of states where pseudo-rotation of the Li atom is possible, was not large

even at rather high vapour pressures because of the low vaporization temperature (~ 800 K).

The atomization energies of gaseous alkali metal monocyanides were recently experimentally measured[7] using an atomic absorption spectrometric method. The measured atomization energy of 317.17 kcal/mole for the lithium compound compares very well with that calculated (317.63 kcal/mole) for LiNC.[3]

This paper deals with the study of the nature of reactions of lithium atoms with CH_3CN and CH_3NC in solid inert gas matrices. An end-on attack of a lithium atom on CH_3CN and CH_3NC is expected to form LiNC and LiCN, respectively, while an approach from the side should produce a mixture of the isomers.

EXPERIMENTAL

The matrix isolation apparatus used in this study has been previously described in detail.[9,10] Lithium was heated in a stainless steel crucible in the temperature range 350–400°C. The temperature of the furnace was measured with alumel–chromel thermocouple wires placed at the back of the cell. In a typical experiment, an atomic beam of the metal was co-condensed with the reactant gas, CH_3CN or CH_3NC, with excess inert gas for a period of 1 hr. The matrix surface, a polished copper mirror, was then rotated 180° and the infrared reflection spectra of the trapped species were measured with a Beckman IR-9 spectrophotometer. Absolute frequencies were usually read to an accuracy of ±0.5 cm⁻¹ and were calibrated against the standard water spectrum. A closed cycle helium refrigerator was used for cooling the copper block to the desired temperature. Photolysis of the matrix with a medium pressure short-arc mercury lamp and a water/pyrex filter was sometimes carried out during deposition.

The lithium metal, obtained from Alfa Inorganics, was of high purity (99%). An isotopically-enriched sample of metal (96% ⁶Li) was furnished by the Oak Ridge National Laboratory. Methyl cyanide (99+%) was purchased from Aldrich Chemical Company. Methyl isocyanide was prepared according to the method described in Ref. 11. Both the cyanide and isocyanide compounds were frozen at liquid N_2 temperature and pumped on for a short period of time. These freeze-thaw cycles were repeated several times until the liquids were completely degassed. Matheson argon (99.99%) was purified by passing it through hot titanium (900°C) prior to deposition. Xenon (99.99%) was obtained from Cryogenic Rare Gas Laboratories and was used without further purification. The flow rates of the reactant gases

---

†Author to whom correspondence should be addressed.

and the inert gases were separately controlled through two different needle values connected to thermocouple gauges.

DISCUSSIONS OF RESULTS

When lithium atoms were co-condensed with methyl isocyanide in excess argon, a new absorption appeared in the CN stretching region at $2230.5 \, cm^{-1}$ as shown in Figs. 1(B) and 1(B'). The frequency of this band was not altered upon substitution of lithium-6. A weak absorption was also detected at $617.4 \, cm^{-1}$ which has been assigned to the out-of-plane bending mode of the methyl radical. When photolysis of the matrix was carried out during deposition using a short arc Hg lamp, two bands appeared at 646.5 and $2080.5 \, cm^{-1}$. The frequencies of these bands are very close to the LiN ($646.4 \, cm^{-1}$) and NC ($2084.5 \, cm^{-1}$) stretching frequencies of lithium isocyanide.[1] The peak at $646.5 \, cm^{-1}$ shifts by $40 \, cm^{-1}$ when an enriched sample of the metal (96% ^6Li) is used. Again the measured frequency is very close to that of the ^6LiN ($696.5 \, cm^{-1}$) stretching frequency of ^6LiNC. These absorptions can be assigned to the molecule, LiNC.

Reactions of lithium atoms with methyl cyanide in the presence or absence of light led only to the formation of LiNC as evidenced from the absorption band due to the NC stretching mode as shown in Fig. 2. It is obvious from these spectra that photolysis of the matrix during deposition enhanced the yield of the lithium isocyanide produced. Similar results were obtained for the reactions of lithium atoms with CH_3NC or CH_3CN in xenon matrices.

The spectra measured after simultaneous co-condensation of lithium with methyl isocyanide in inert gas matrices suggest the formation of a new compound containing a CN functional group. Lithium cyanide and methyl lithium cyanide are two possible products that can be formed. If the complex CH_3LiCN were produced, one would expect to observe a large shift in the out-of-plane mode of the methyl radical by analogy to that
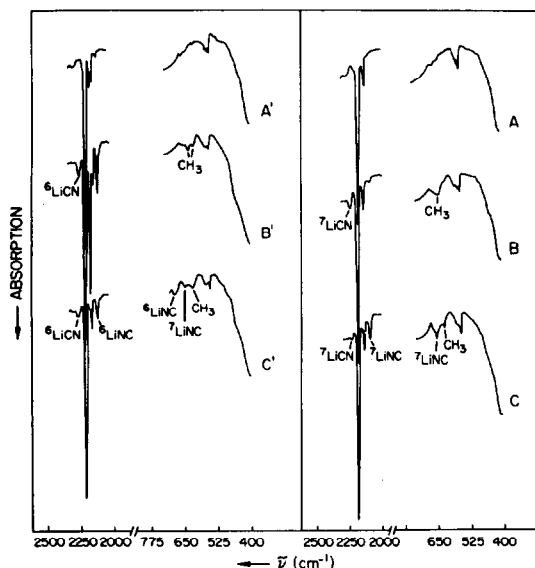
Fig. 1. IR spectra of the products of the reactions of ^7Li or ^6Li with CH_3NC in solid argon × A and A' Pure CH_3NC, B and B' $CH_3NC/^7Li$ and $CH_3NC/^6Li$ and C and C' $CH_3NC/^7Li$ and $CH_3NC/^6Li$ after photolysis with a medium pressure Hg lamp ($\lambda \geq 3000$ Å) for a period of 1 hr.
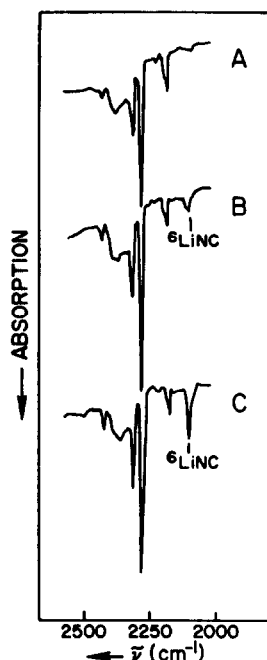
Fig. 2. IR spectra of the products of the reactions of ^6Li with CH_3CN in solid argon × A Pure CH_3CN, B $CH_3CN/^6Li$ and C $CH_3CN/^6Li$ after photolysis with a medium pressure Hg lamp ($\lambda \geq 3000$ Å) for a period of 1 hr.

observed in case of the methyl alkali halide complexes where the perturbed CH_3 frequency is shifted to the region between 730 and $680 \, cm^{-1}$.[12,13] This blue shift would be indicative of a methyl radical strongly interacting with a lithium cyanide molecule. A broad absorption near the peak assigned to unperturbed methyl suggested that some of the methyl groups may be undergoing weak interactions with neighbouring groups; however, the shifts were much smaller than those reported for methyl in a complex such as CH_3LiX. Thus, one concludes that an appreciable amount of essentially free methyl radical was produced which suggests that the following reaction has occurred

$$Li + CH_3NC \rightarrow LiCN + CH_3$$
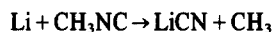
where lithium has attacked the methyl isocyanide end-on from the side opposite the methyl leading to the formation of only lithium cyanide. Photolysis during deposition causes the formation of some LiNC in addition to LiCN. This result is not surprising since it is known that lithium isocyanide is more stable than lithium cyanide.[1-6]

Table 1 compares the CN stretching frequencies for the molecules HCN[14] vs HNC[15], LiCN vs LiNC[1] and CH_3CN[16] vs CH_3NC[16]. It is clear from these data that the CN frequencies for the cyanides are higher than those for the respective isocyanides. This result is not surprising since one expects the CN bond in the MCN species to have more triple-bond character and resemble closely that of CN^-.

CONCLUSIONS

This study of the reactions of lithium atoms with CH_3CN and CH_3NC supports a mechanism in which the met attacks the CN or NC groups end at the end

Table 1. Comparison between the CN and NC stretching frequencies for MCN and MNC

M	$\tilde{v}_{NC}(cm^{-1})$	$\tilde{v}_{CN}(cm^{-1})$
H	2029.2	2093.4
Li	2084.5	2230.5
CH_3	2160.6	2258.4

opposite the methyl group. The following reactions take place when lithium atoms are co-condensed with CH_3NC and CH_3CN in excess argon or xenon.
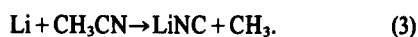
$$Li + CH_3NC \rightarrow LiCN + CH_3 \quad (1)$$

$$Li + CH_3NC \xrightarrow{uv\text{-}vis} LiCN \text{ and } LiNC + CH_3 \quad (2)$$

$$Li + CH_3CN \rightarrow LiNC + CH_3. \quad (3)$$

REFERENCES

[1] Z. K. Ismail, R. H. Hauge and J. L. Margrave, *J. Chem. Phys.* 1972 **57**, 5137.
[2] B. Bak, E. Clementi and R. N. Kotzeborn, *J. Chem. Phys.* 1970 **52**, 764.
[3] E. Clementi, H. Kistenmacher and H. Popkie, *J. Chem. Phys.* 1973 **58**, 2460.
[4] L. T. Redmons, G. D. Purvis, III and R. J. Bartlett, *J. Chem. Phys.* 1980 **72**, 986.
[5] V. N. Lunichev and N. G. Rambidi, *Zh. Strukt. Kim.* 1977 **18**, 377.
[6] N. G. Rambidi and V. N. Lunichev, *J. Mol. Struc.* 1978 **48**, 293.
[7] B. V. L'vov and L. A. Pelieva, *Zh. Prikl. Spectrosk.* 1979 **31**, 395; *J. Appl. Spec.* 1979 **31**, 1078.
[8] P. Politzer and A. Politzer, *J. Amer. Chem. Soc.* 1973 **95**, 5450.
[9] Z. H. K. Ismail, Ph.D. Thesis, Rice University, 1972.
[10] J. W. Kauffman, Ph. D. Thesis, Rice University, 1981.
[11] E. J. Corey (Ed), *Organic Syntheses* 1966 **46**, 75.
[12] L. Andrews and G. C. Pimentel, *J. Chem. Phys.* 1967 **47**, 3637.
[13] L. Y. Tan and G. C. Pimentel, *J. Chem. Phys.* 1968 **48**, 5202.
[14] C. M. King and E. R. Nixon, *J. Chem. Phys.* 1968 **48**, 1685.
[15] D. E. Milligan and M. E. Jacox, *J. Chem. Phys.* 1967 **47**, 278.
[16] T. B. Freedman and E. R. Nixon, *Spectr. Chim. Acta* 1972 **28A**, 1375.

A SYNTHETIC ROUTE TO HETERONUCLEAR CLUSTERS CONTAINING IRIDIUM AND RHODIUM: X-RAY CRYSTAL STRUCTURES OF [IrOs$_3$(μ-H)$_2$(μ-Cl)(CO)$_{12}$] AND [Ir$_2$Rh$_2$(μ-CO)(μ_3-CO)$_2$(CO)$_4$(η-C$_5$Me$_5$)$_2$]

LOUIS J. FARRUGIA, A. GUY ORPEN and F. GORDON A. STONE

Department of Inorganic Chemistry, The University of Bristol, Bristol BS8 1TS, England

Abstract—The iridium and rhodium complexes [MCl(CO)$_2$(NH$_2$C$_6$H$_4$Me-4)] (M = Ir or Rh) react with [Os$_3$(μ-H)$_2$(CO)$_{10}$] to give the tetranuclear clusters [MOs$_3$(μ-H)$_2$(μ-Cl)(CO)$_{12}$]; the iridium compound being structurally identified by X-ray diffraction. Similarly, [IrCl(CO)$_2$(NH$_2$C$_6$H$_4$Me-4)] and [Rh$_2$(μ-CO)$_2$(η-C$_5$Me$_5$)$_2$] afford the tetranuclear cluster [Ir$_2$Rh$_2$(μ-CO)(μ_3-CO)$_2$(CO)$_4$(η-C$_5$Me$_5$)$_2$], also characterised by single-crystal X-ray crystallography.

The isolobal relationship existing between carbenes CR$_2$ on the one hand and the "carbene-like" metal fragments W(CO)$_5$, Fe(CO)$_4$, Rh(CO)(η-C$_5$Me$_5$) and PtL$_2$ (L$_2$ = cod = cyclo-octa-1,5-diene, or L = PR$_3$ or CO) on the other[1] has enabled us to prepare a variety of complexes containing heteronuclear metal–metal bonds.[2–4] Useful conceptual relationships result. Thus the PtL$_2$, Fe(CO)$_4$ and W(CO)$_5$ groups all readily added to the dirhodium compound [Rh$_2$(μ-CO)$_2$(η-C$_5$Me$_5$)$_2$], as does CR$_2$. Isolobal with the dirhodium compound is [(OC)$_4$Fe=Fe(CO)$_4$], which although unstable[5] can be complexed by Pt(cod) in the stable species [Fe$_2$Pt(CO)$_8$(cod)].[6] However, although the analogy between inorganic and organic fragments with similar electronic structures allows synthetic strategies to be developed, it does not necessarily follow that the nature of the final products are those predicted by a simple consideration of isolobal relationships. This is because an initially formed species can transform into another to gain greater kinetic or thermodynamic stability. Herein we report some examples of the apparent limitation of the isolobal analogy, but which nevertheless provide a new and useful route to heteronuclear clusters of iridium and rhodium.

The similarity of the frontier orbitals of the metal ligand fragments ML$_5$(d^n, C_{4v}) and ML$_3$(d^{n+2}, C_{2v} or T-shaped), e.g. W(CO)$_5$ vs MCl(CO)$_2$ (M = Rh or Ir), as well as the relationship between W(CO)$_5$ and PtL$_2$ or CH$_2$ allows the isolobal mapping.[1]

$$W(CO)_5 \longleftrightarrow IrCl(CO)_2 \longleftrightarrow PtL_2 \longleftrightarrow CH_2.$$
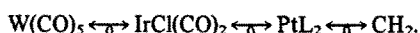
Hence, since PtL$_2$[3,7] or CR$_2$[3,8–10] fragments readily add to [Os$_3$(μ-H)$_2$(CO)$_{10}$] and [Rh$_2$(μ-CO)$_2$(η-C$_5$Me$_5$)$_2$] to give products in which PtL$_2$ or CR$_2$ groups can be identified, it was reasonable to suppose that MCl(CO)$_2$ (M = Rh or Ir) fragments, derived from [MCl-(CO)$_2$(NH$_2$C$_6$H$_4$Me-4)], would also react with these electrophilic triosmium and dirhodium compounds. Reactions readily occur, but the end products do not contain MCl(CO)$_2$ fragments.

Treatment of [Os$_3$(μ-H)$_2$(CO)$_{10}$] in dichloromethane

with one equivalent of [IrCl(CO)$_2$(NH$_2$C$_6$H$_4$Me-4)] at room temperature gave the yellow crystalline compound (1) in 70–80% yield [ν_{CO} (cyclohexane), 2087s, 2080m, 2049s, 2028m, 2014m, and 1988w cm^{-1}]. The ^{1}H NMR spectrum (CDCl$_3$) of (1) showed a characteristic resonance for the μ-HOs$_2$ hydrido ligands at $\delta -14.66$ ppm, an interesting feature of which was the observation of ^{187}Os satellite peaks [J(OsH)$_{av}$ 32 Hz]. The rhodiumtriosmium compound (2) [ν_{CO} 2078s, 2052m, 2029m, 2012m, and 2004s(sh) cm^{-1}] was similarly prepared, but in lower yield, due to concomitant formation of the complexes [Os$_3$(μ-H)(μ-Cl)(CO)$_{10}$] and [Rh$_2$(μ-Cl)$_2$(CO)$_4$]. In the ^{1}H NMR, the two hydrido ligands gave a resonance at $\delta -19.73$ ppm; failing to observe ^{103}Rh coupling establishing the absence of Rh–H bonds. A single-crystal X-ray diffraction study was carried out on (1) to establish the molecular structure.

Crystal data. C$_{12}$H$_2$ClIrO$_{12}$Os$_3$, $M = 1136.4$, Monoclinic, space group $P2_1/m$, $a = 7.364(4)$, $b = 16.157(6)$, $c = 8.659(3)$Å, $\beta = 111.39(3)°$, $U = 959.5(7)$Å^3, $Z = 2$, $F(000)$ 984, $D_c = 3.93$ g cm^{-3}, μ(Mo-K$_\alpha$) 269.2 cm^{-1}, Mo-K$_\alpha$ X-radiation, $\bar{\lambda} = 0.71069$ Å.

The structure was solved by heavy atom Fourier methods and refined using blocked cascade full-matrix least squares. For 2163 unique, absorption corrected, observed data [$I > 2.5\sigma(I)$], measured at 200 K on a Nicolet *P3m* diffractometer in the range $4 \leq 2\theta \leq 60°$, the current residual R is 0.084.

The molecule (Fig. 1) contains a "butterfly" arrangement of four metal atoms, with the non-bonded Os(1)–Os(1′) vector being bridged by a chlorine atom. As such the structure is related to that[11] of [Os$_4$(μ-H)$_3$(μ-I)-(CO$_{12}$)], with an Os(μ-I)Os bridge. Both molecules have 62 cluster valence electrons.

[MOs$_3$(μ-H)$_2$(μ-Cl)(CO)$_{12}$]
(1) M = Ir
(2) M = Rh
[Ir$_2$Rh$_2$(μ-CO)(μ_3-CO)$_2$(CO)$_4$(η-C$_5$Me$_5$)$_2$]
(3)
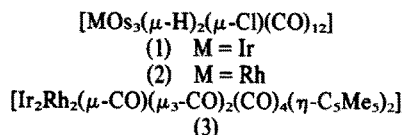
Because the molecule has crystallographic mirror sym-

metry, although not located directly, the two hydrido ligands in (1) must bridge the Os(1)–Os(2) and Os(1')–Os(2) edges of the butterfly. Thus Os(1)–Os(2) and Os(1')–Os(2) [2.994(1)Å] are appreciably longer than the other metal–metal bonds, and may be compared with corresponding Os(μ-H)Os separations in the butterfly clusters [Os$_3$Rh(μ-H)$_2$(acac)(CO)$_{10}$] [2.968(1)Å][7] and [Os$_4$(μ-H)$_3$(μ-I)(CO)$_{12}$] [3.055(1)Å].[11] Potential energy calculations[12] also suggest location of the hydrido ligands in (1) as bridging Os(2)–Os(1) and Os(2)–Os(1'), as do Os–Os–CO bond angle considerations. In contrast with the C_s symmetry of (1), the neutron diffraction study[11] of [Os$_4$(μ-H)$_3$(μ-I)(CO)$_{12}$] revealed that the two equivalent hydrido ligands bridge Os–Os bonds such that the molecule has C_2 symmetry.

Treatment of Rh$_2$(μ-CO)$_2$(η-C$_5$Me$_5$)$_2$] with one equivalent of [IrCl(CO)$_2$(NH$_2$C$_6$H$_4$Me-4)] in toluene (12 hr, 60 °C) gave a dark purple solution and red crystals; the latter as yet unidentified. Removal of solvent from the solution and chromatography (alumina, with dichloromethane—light petroleum as eluant) gave a purple band which afforded black crystals (20%, based on [Rh$_2$(μ-CO)$_2$(η-C$_5$Me$_5$)$_2$]), from light petroleum, of the compound (3); structurally identified by X-ray crystallography.

---

*ν_{max}(CO), 2 040s, 2 021vs, 2 007s, 1 847m, 1 704m, and 1 682m (cm^{-1}). NMR: ^{1}H (CDCl$_3$, 25°C), δ 1.76 (s, C$_5$Me$_5$); ^{13}C (CDCl$_3$, -80°C), δ 235.6 [t, μ_3-CO, J(RhC) 32 Hz], 180.9 (s, IrCO and Ir(μ-CO)Ir), 104.4 (C$_5$Me$_5$) and 9.3 ppm (Me).

Crystal data. C$_{27}$H$_{30}$Ir$_2$O$_7$Rh$_2$, M = 1 056.4, Monoclinic, space group $P2_1/n$, a = 11.458(2), b = 15.318(2), c = 16.837(3)Å, β = 94.75(2)°, U = 2 945.1(9)Å^3, Z = 4, $F(000)$ = 1 968, D_c = 2.35 g cm^{-3}, μ(Mo-K$_\alpha$) = 101.0 cm^{-1}, Mo-K$_\alpha$ X-radiation, $\bar{\lambda}$ = 0.710 69 Å.

The structure was solved by direct methods and refined using blocked cascade full-matrix least squares. An empirical absorption correction was applied to the 3 904 independent observed reflections [I > 2.0σ(I)] measured at 293 K on a Nicolet $P3m$ diffractometer in the range $3 \le 2\theta \le 50°$. The current residual R is 0.037 (R' 0.037).

The molecule (Fig. 2) contains a tetrahedron of two rhodium and two iridium atoms. The arrangement of ligands is very similar to the analogous 60 electron homonuclear tetracobalt cluster [Co$_4$(μ-CO)(μ_3-CO)$_2$(CO)$_4$(η-C$_5$Me$_5$)$_2$].[13] The molecule has a near perfect mirror symmetry, though not crystallographically defined. There is evidently dynamic behaviour of the terminally bound and μ_2-bridging CO ligands, as shown by the appearance of only one CO resonance for these five ligands in the ^{13}C NMR spectrum measured at -80 °C. However, in the IR spectrum* the band at 1 847 cm^{-1} may be assigned to the Ir(μ-CO)Ir group. The presence of the latter fragment is unusual, this mode of bridge bonding being uncommon for a third row transition element. The compound [Ir$_2$W$_2$(CO)$_{10}$(η-C$_5$H$_5$)$_2$], synthesised by the conventional route of treating [IrCl(CO)$_2$(NH$_2$C$_6$H$_4$Me-4)] with the anion [W(CO)$_3$(η-C$_5$H$_5$)]$^-$, has only terminal CO ligands.[14]

It is reasonable to propose that [IrCl-
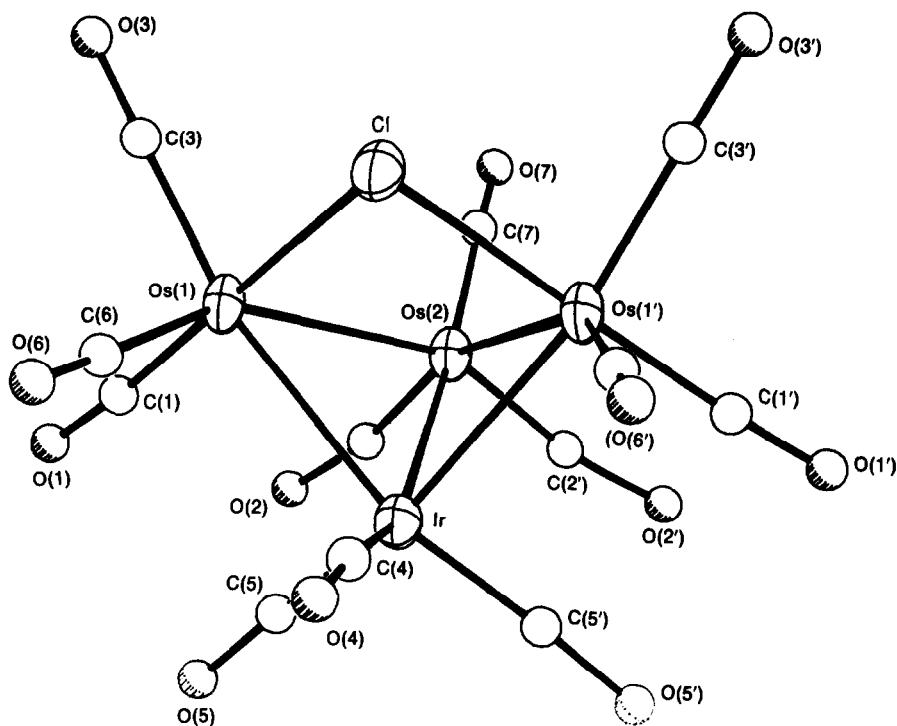
Fig. 1. Molecular structure of [IrOs$_3$(μ-H)$_2$(μ-Cl)(CO)$_{10}$]. Important geometrical parameters are: Ir–Os(1) 2.803(1), Ir–Os(2) 2.749(2), Os(1)–Os(2) 2.994(1), Os(1)....Os(1') 3.636(1), Os(1)–Cl 2.435(6)Å; Os(2)–Os(1)–C(3) 114.6(7), Os(1)–Os(2)–C(7) 113(1)°; other M–M–C angles range from 87(1) to 97.2(8)°. Dihedral angle Os(1)–Os(2)–Ir–Os(1') 91.0(1)°.
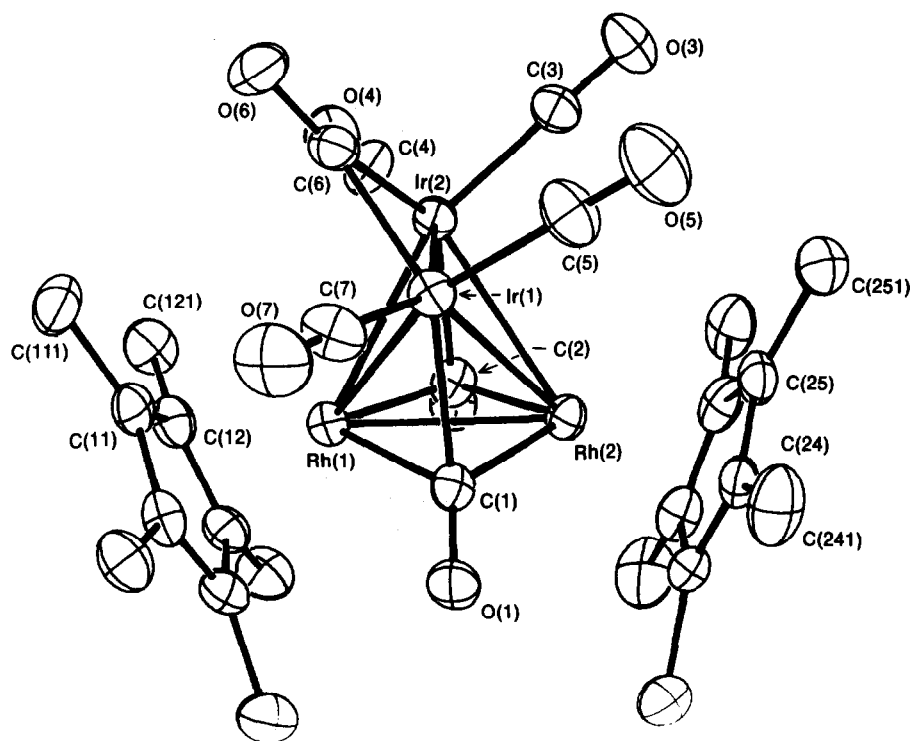
Fig. 2. Molecular structure of [Ir₂Rh₂(μ-CO)(μ₃-CO)₂(CO)₄(η-C₅Me₅)₂]. Important geometrical parameters are: Ir(1)–Ir(2) 2.645(1), Ir(1)–Rh(1) 2.716(1), Ir(1)–Rh(2) 2.787(1), Ir(2)–Rh(1) 2.731(1), Ir(2)–Rh(2) 2.786(1), Rh(1)–Rh(2) 2.704(1)Å. Dihedral angle Ir(1)–Rh(1)–Rh(2)–Ir(2) 66.9(1)°.

(CO)₂(NH₂C₆H₄Me-4)] acts as a source of the fragment IrCl(CO)₂ which initially adds to the electrophilic LUMO's of [Os₃(μ-H)₂(CO)₁₀] and [Rh₂(μ-CO)₂(η-C₅Me₅)₂].[15] The reactions are complex, however, and in both cases proceed with cleavage of the Ir–Cl bond, indicating that the chloride ligand is not chemically innocent. Nevertheless, [IrCl(CO)₂(NH₂C₆H₄Me-4)] is a useful reactant for generating heteronuclear metal–metal bonds.

REFERENCES

[1] R. Hoffmann, *Les Prix Nobel* 1981. Almqvist and Wiksell, Stockholm 1982; *Angew. Chem., Int. Ed. Engl.* in press.

[2] T. V. Ashworth, M. Berry, J. A. K. Howard, M. Laguna and F. G. A. Stone, *J. Chem. Soc., Chem. Commun.* 1979, 43; T. V. Ashworth, J. A. K. Howard, M. Laguna and F. G. A. Stone, *J. Chem. Soc., Dalton Trans.* 1980, 1593; J. A. K. Howard, K. A. Mead, J. R. Moss, R. Navarro, F. G. A. Stone and P. Woodward, *ibid* 1981, 743.

[3] N. M. Boag, M. Green, R. M. Mills, G. N. Pain, F. G. A. Stone and P. Woodward, *J. Chem. Soc., Chem. Commun.* 1980, 1171; M. Green, J. A. K. Howard, R. M. Mills, G. N. Pain, F. G. A. Stone and P. Woodward, *ibid* 1981, 869; M. Green, R. M. Mills, G. N. Pain, F. G. A. Stone and P. Woodward, *J. Chem. Soc., Dalton Trans.* 1982, 1309.

[4] M. L. Aldridge, M. Green, J. A. K. Howard, G. N. Pain, S. J. Porter, F. G. A. Stone and P. Woodward, *J. Chem. Soc., Dalton Trans.* 1982. 1333./M. Green, R. Barr and F. G. A. Stone, *J. Chem. Soc., Dalton Trans.* in press.

[5] M. Poliakoff and J. J. Turner, *J. Chem. Soc. (A)* 1971, 2403.

[6] L. J. Farrugia, J. A. K. Howard, P. Mitrprachachon, F. G. A. Stone and P. Woodward, *J. Chem. Soc., Dalton Trans.* 1981, 1134.

[7] L. J. Farrugia, J. A. K. Howard, P. Mitrprachachon, F. G. A. Stone and P. Woodward, *J. Chem. Soc., Dalton Trans.* 1981, 162, 171.

[8] R. B. Calvert, J. R. Shapley, A. J. Schultz, J. M. Williams, S. L. Suib and G. D. Stucky, *J. Am. Chem. Soc.* 1978, 100, 6240; R. B. Calvert and J. R. Shapley, *ibid,* 1977, 99, 5225; 1978, 100, 7726.

[9] W. A. Herrmann, C. Bauer, J. Plank, W. Kalcher, D. Speth and M. L. Ziegler, *Angew. Chem., Int. Ed. Engl.* 1981, 20, 193.

[10] A. D. Clauss, P. A. Dimas and J. R. Shapley, *J. Organomet. Chem.* 1980, 201, C31.

[11] B. F. G. Johnson, J. Lewis, P. R. Raithby, K. Wong and K. D. Rouse, *J. Chem. Soc., Dalton Trans.* 1980, 1248.

[12] A. G. Orpen, *J. Chem. Soc., Dalton Trans.* 1980, 2509.

[13] L. M. Cirjak, R. E. Ginsburg and L. F. Dahl, *J. Chem. Soc., Chem. Commun.* 1979, 470.

[14] J. R. Shapley, S. J. Hardwick, D. S. Foose and G. D. Stucky, *J. Am. Chem. Soc.* 1981, 103, 7383; M. R. Churchill, C. Bueno and J. P. Hutchinson, *Inorg. Chem.* 1982, 21, 1359.

[15] A. R. Pinhas, T. A. Albright, P. Hofmann and R. Hoffmann, *Helv. Chim. Acta* 1980, 63, 29.

THE DETECTION OF TRACE AMOUNTS OF
trans-Pt(NH₃)₂Cl₂ IN THE PRESENCE OF
cis-Pt(NH₃)₂Cl₂. A HIGH PERFORMANCE
LIQUID CHROMATOGRAPHIC APPLICATION
OF KURNAKOW'S TEST

J. DEREK WOOLLINS,* ANN WOOLLINS and BARNETT ROSENBERG

Department of Biophysics, Michigan State University, East Lansing, MI 48824, U.S.A.

Abstract—Treatment of mixtures of *cis* and *trans* Pt(NH₃)₂Cl₂ with thiourea (thu) gave Pt(thu)₄Cl₂ and *trans* [Pt(NH₃)₂(thu)₂]Cl₂ which were separated and quantified by high-performance liquid chromatography using a strong cation exchange column. Several platinum–thiourea compounds have been studied by NMR (^{1}H, ^{13}C, ^{195}Pt), an increase in the coalescence temperature of the NH₂ resonances being observed as a result of co-ordination. The NMR data has also been used to show the presence of interactions between the Pt(thu)₄²⁺ and PtCl₆²⁻ ions of [Pt(thu)₄][PtCl₆] in dimethylsulphoxide solution.

INTRODUCTION

Since the discovery[1] of the anti-tumour activity of *cis*-Pt(NH₃)₂Cl₂, **1**, there has been great interest in the chemistry of simple platinum compounds. As part of our studies we have developed a high-performance liquid chromatography (HPLC) method for the detection of *trans*-Pt(NH₃)₂Cl₂, **2**, in **1**. The *trans*-isomer, **2**, which is inactive against tumours[2], is normally observed as a by-product in the preparation of **1** with tedious recrystallisations being required to purify **1** completely. The simple procedure described here allows the purity of preparations to be checked quite easily and should enable studies on *cis–trans* isomerisation in dilute solution to be undertaken. The separation we have employed makes use of derivatisation of the platinum complexes with thiourea (the classic Kurnokow test[3]) before injection into the HPLC. As part of the general characterisation of the thiourea complexes we have measured their NMR spectra (^{1}H, ^{13}C, ^{195}Pt) and note that upon co-ordination the barrier to rotation in thiourea increases significantly.

It is the twofold purpose of this paper to report an HPLC method for the trace detection of **2** in **1** and the results of a multinuclear NMR study on several thiourea complexes.

EXPERIMENTAL

All reactants and solvents were of at least reagant grade. Thiourea was purchased from Mallindrockt, *cis* and *trans*-Pt(NH₃)₂Cl₂, K₂PtCl₄ and Na₂PtCl₆ were supplied by Johnson Matthey and Engelhard Industries.

The high performance liquid chromatograph (Waters Assoc.) consisted of a 6000A pump, U6K injector and model 440 dual wavelength absorbance detector (operating at 254nm with the second electronics module being used for expanded scale recordings), together with a 4.6 × 250 mm Whatman Partisil PXS 10/25 SCX strong cation exchange column. The eluent (0.25 M NH₄H₂PO₄) was filtered through 0.47 μm filters (Millipore) and thoroughly degassed prior to use. Sample solutions were filtered through 0.22 μm filters before injection.

NMR measurements were made using a Bruker WM 250 (^{1}H and ^{13}C) and a Bruker WH 180 (^{195}Pt). Infrared spectra were obtained with a Perkin Elmer 457 spectrometer with samples prepared as pressed KBr discs.

Microanalyses were performed by Canadian Microanalytical Services, Vancouver, B.C.

Pt(thu)₄Cl₂, **3**, *trans*-[Pt(NH₃)₂(thu)₂]Cl₂, **4**, and *trans*-PtCl₂(thu)₂ (thu = thiourea) were prepared by well-known procedures.[3] The reaction of K₂PtCl₄ ·or **1** with thiourea in dimethylformamide (dmf) was also found to be a convenient route to **3** in the following manner.

Pt(thu)₄Cl₂.dmf. Thiourea (3.42 g, 45 mMol) and K₂PtCl₄ or *cis*-Pt(NH₃)₂Cl₂ (10 mMol) were stirred together in dmf (100 ml) for 16 hr. The resulting light yellow precipitate was filtered off, washed with dmf, ethanol and diethyl ether and air dried, yield 6.3 g, 98%. Conversion to Pt(thu)₄Cl₂ could be accomplished by recrystallisation from hot water (70% yield) or by dissolution of the Pt(thu)₄Cl₂.dmf in hot water and precipitation using HCl (yield 97%).

[Pt(thu)₄][PtCl₄]. Filtered aqueous solutions of K₂PtCl₄ (0.83 g, 2 mMol) and Pt(thu)₄Cl₂dmf (1.2 g, 2 mMol) were combined. The resulting light red precipitate was filtered off, washed with water, ethanol and diethyl ether and dried *in vacuo*, yield 1.25 g, 75%.

[Pt(thu)₄][PtCl₆]. Filtered aqueous solutions of Na₂PtCl₆ (0.9 g, 2 mMol) and Pt(thu)₄Cl₂dmf (1.2 g, 2 mMol) were combined. The resulting brick red precipitate was filtered off, washed with water, ethanol and diethyl ether and dried in vacuo, yield 1.4 g, 77%.

HPLC Analysis. The Pt(NH₃)₂Cl₂ mixture to be analysed was dissolved in water at a concentration of approx. 1 mg/ml acidified (50 μl of 1 M HNO₃ per ml of Pt(NH₃)₂Cl₂ solution) and then treated with thiourea (100 μl of a 20 mg/ml solution per ml of Pt(NH₃)₂Cl₂ solution), and heated at 60°C for 30 minutes. After this time the solution was filtered and injected (20 μl) into the HPLC.

Standards for calibration were prepared using pure samples of Pt(thu)₄Cl₂ and *trans*-[Pt(NH₃)₂(thu)₂]Cl₂ dissolved in water at known concentrations.

RESULTS AND DISCUSSION

HPLC analysis

A number of chemical tests[4] for distinguishing **1** and **2** are known but there does not seem to be a good method for the trace detection of **2** in **1**, although the reaction[5] with oxydiphenylenetellurium hydrogen sulphate does permit detection of minute amounts of **1** in **2**. Cleare[6] has discussed the application of spectroscopic techniques to the problem and also shown that separation of **1** from **2**

---

*Author to whom correspondence should be addressed.

may be achieved by HPLC but has not reported any details of the procedure or the detection limits.

In order to take full advantage of the HPLC technique it is preferable to have easily detected species which are well separated. Platinum diammine dichlorides are poorly soluble in water, have very low absorbances in the operating range of most HPLC detectors (i.e. 254 nm) and represent a "difficult" separation. However, treatment of the platinum compounds with thiourea using the classic Kurnakow test[3] alleviates these problems. As a result of the *trans* directing ability of thiourea 1 is converted to Pt(thu)$_4$Cl$_2$, **3**, and **2** yields *trans*-[Pt(NH$_3$)$_2$(thu)$_2$Cl$_2$, **4**, when treated with thiourea. These complexes are easily separated by HPLC and have strong absorbances in the UV.

Figure 1 shows the results of derivatisation and chromatography upon known mixtures of **1** and **2**. The chromatographic conditions employed here achieve a good separation of thiourea, **3** and **4**. The use of different concentrations of ammonium phosphate as the eluent has a marked effect upon the retention times of the platinum containing species. For example, the retention times of **3** and **4** go from 5.3 and 7.3 min. respectively when using 0.25 M NH$_4$H$_2$PO$_4$ as the eluent to 3.4 and 4.6 min. respectively when using 0.5 M NH$_4$H$_2$PO$_4$. The concentration of ammonium phosphate chosen is thus a compromise between better separation and loss of sensitivity as a result of peak broadening.

Calibrations were carried out using pure samples of **3** and **4** which had been separately prepared and analysed (Table 1). Agreement between the standards and the samples prepared *in situ* was found to be good, the chromatograms from the analysis being very clean with only bands due to thiourea, **3** and **4** being observed. Injection of an equimolar mixture of **3** and **4** showed, as expected, that **3** gave peak areas of very close to twice those of **4**. However, this is not a problem, because of the large dynamic range of the detector, detection limits of 0.01% *trans* in *cis* were obtained. We did not make
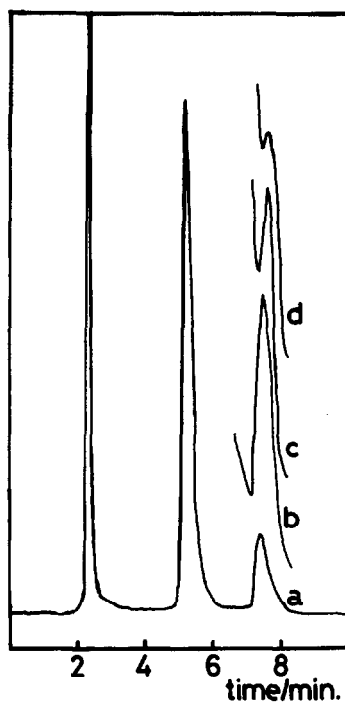
Fig. 1. HPLC of various mixtures of **1** and **2** after treatment with thiourea. Column: Partisil PXS 10/25 SCX (4.6×250 mm). Eluent: 0.25 M NH$_4$H$_2$PO$_4$. Flow rate 2 ml/min. Detector 254 nm, using the following sensitivities for expansions (a) 2.0 absorbance units full scale, (AUFS) mixture containing 25% *trans*-Pt(NH$_3$)$_2$Cl$_2$, **2**, in *cis*-Pt(NH$_3$)$_2$Cl$_2$, **1**, (b) 0.02 AUFS, 1% **2** in **1**, (c) 0.005 AUFS, 0.1% **2** in **1**, (d) 0.005 AUFS, 0.01% **2** in **1**.

any efforts to obtain detection limits for *cis* in *trans* but it should be at least as good as the above.

The results obtained here reveal the high sensitivity that the HPLC technique can achieve with the absolute

Table 1. Analytical and spectroscopic data

	%C	%H	%N	%S	%Cl	^{1}Hδ/ppm[a] (T_c/°C)	^{13}Cδ/ppm	^{195}Ptδ/ppm[b]	ν(C=S)/cm^{-1}
trans-Pt(thu)$_2$Cl$_2$	5.71 (5.77)	1.52 (1.92)	13.00 (13.46)	15.19 (14.90)	17.67 (17.07)	8.17(26)	175.48	[c]	710
Pt(thu)$_4$Cl$_2$·dmf	13.11 (13.06)	3.46 (3.58)	19.30 (19.59)	19.36 (19.91)	11.51 (11.04)	–	–		–
Pt(thu)$_4$Cl$_2$	8.58 (8.42)	2.35 (2.83)	19.46 (19.64)	22.64 (22.48)	12.69 (12.43)	8.30(35)	175.61	3912 (dmso) 4035 (H$_2$O)	708
[Pt(NH$_3$)$_2$(thu)$_2$]Cl$_2$	5.50 (5.31)	2.92 (3.12)	18.35 (18.58)	14.62 (14.18)	16.25 (15.58)	8.25(25)	175.52	3239 (H$_2$O)	709
[Pt(thu)$_4$][PtCl$_4$]	5.50 (5.71)	1.35 (1.92)	13.30 (13.46)	15.08 (14.90)	18.11 (17.01)	8.23(35)	175.50	3915 [d]	710
[Pt(thu)$_4$][PtCl$_6$]	5.38 (5.32)	1.31 (0.89)	11.91 (12.40)	15.60 (14.17)	24.22 (23.92)	8.06(27)	175.34	3979 [d]	706

Theoretical analyses are in parentheses, all NMR spectra were measured in d^6-dmso solution unless otherwise indicated.

a   Chemical shift is taken as centre of absorption at 25°C.

b   to high field of Na$_2$PtCl$_6$ in D$_2$O (external), ± 0.5 ppm.

c   this signal showed a very rapid (< 5 min.) time dependence.

d   the halide containing ions are not listed.

detection limit of 1 or 2 being better than 20 ng. It should also be possible using platinum atomic absorption or electrochemical detection to measure quite low levels of 1 in physiological fluids.

NMR Studies

The effect of co-ordination upon the barrier to rotation in substituted thioureas[7] has been studied by ^{1}H NMR but no reports are available for simple thiourea complexes.

The solvent used here (d^6-dimethylsulphoxide) did not allow the "no exchange" limit to be reached, and together with the linewidth of the signals (Fig. 2), this makes the data obtained unsuitable for simple thermodynamic analysis, thus only coalescence temperature (T_c) and chemical shifts are reported (Table 1).

As expected, co-ordination of the thiourea through sulphur results in a downfield shift of the proton resonances together with an increase in T_c, thiourea itself having[8] a chemical shift of 7.08 and $T_c = -40°C$ (in ethyl acetate). The rise in coalescence temperature is due to the increasing importance of resonance form B upon complexation and thus agrees well with

$$S = C \begin{matrix} \diagup NH_2 \\ \diagdown NH_2 \end{matrix} \qquad S^- - C \begin{matrix} \diagup\mkern-10mu/ {}^+NH_2 \\ \diagdown NH_2 \end{matrix}$$

$$\text{A} \qquad\qquad\qquad \text{B}$$

the sulphur co-ordination[9] of thiourea.

Platinum stacking compounds such as Magnus Green salt [Pt(NH₃)₄] [PtCl₄] and [Pt(NH₃)₄][PtCl₆] are currently widely studied and it is of interest to establish techniques for assessing solution interactions in these types of compounds. We prepared [Pt(thu)₄][PtCl₄] and [Pt(thu)₄] [PtCl₆] and note that for the mixed valence compound quite a substantial shift (relative to 3) in the NH resonance is observed. This may arise from hydrogen-bonding interactions between the chloroligands of PtCl₆²⁻ and the hydrogens on the thiourea, thus indicating some organised interaction between the PtCl₆²⁻ and the Pt(thu)₄²⁺ ions in dmso solution.

The ^{13}C spectra of the complexes all show a high field shift relative to thiourea (which has $\delta = 183.49$) and are all singlets with no Pt–C couplings being observed. The absence of Pt–C coupling is not surprising[10] at the high fields used here, whilst the lack of any other splittings indicates that the doublets in the proton spectra are correctly assigned as being due to restricted rotation about the C–N bond in thiourea and cannot be assigned as being due to isomerisations to N-co-ordinated species.

The ^{195}Pt NMR chemical shifts all fall within the range one would predict from current literature[11–13] values and show for the first time the chemical shift for a platinum atom surrounded by four donor sulphur ligands. Once again, of interest is the difference in chemical shift between 3 and [Pt(thu)₄][PtCl₆]. The observation that no such difference is seen between 3 and [Pt(thu)₄][PtCl₄] indicates the relative insensitivity of ^{195}Pt NMR to the counter-ion in simple systems and lends support to the argument that some interactions are occuring in solution for [Pt(thu)₄][PtCl₆].

The time dependence in the spectrum of *trans*-PtCl₂(thu)₂ is probably coming about as a result of replacement of the chloro ligands by dmso followed by isomerisation; similar effects have been observed for 1 in dmso by Kerrison and Sadler.[14]
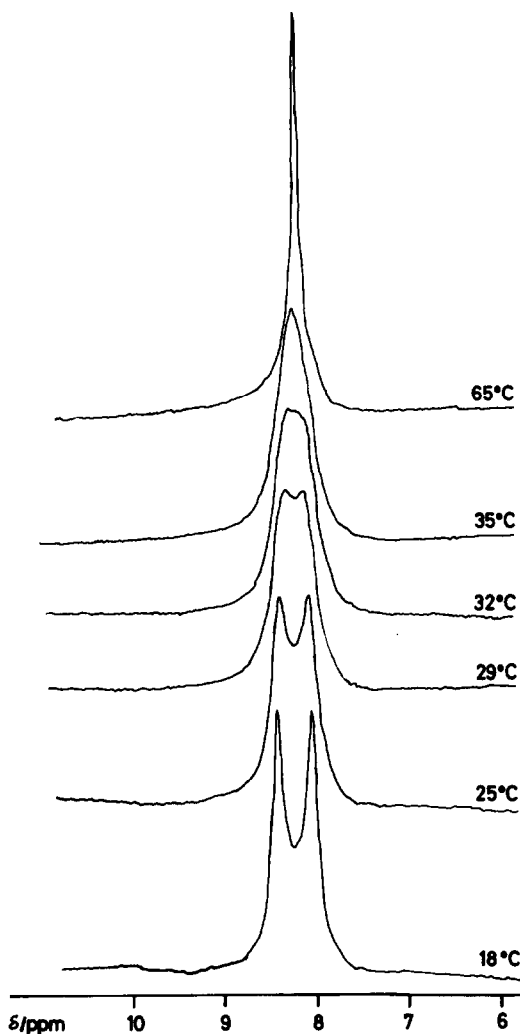
Fig. 2. Temperature dependence of NH₂ resonances in the ^{1}H NMR of Pt(thu)₄Cl₂ in d^6-dmso solution.

REFERENCES

[1] B. Rosenberg, L. Van Camp, J. E. Trosko and V. H. Mansour, *Nature* 1969, **222**, 385.
[2] M. J. Cleare and J. D. Hoeschele, *Bioinorg. Chem.* 1973, **2**, 187.
[3] N. Kurnakow, *J. prakt. Chem.* 1894, **50**, 481.
[4] G. B. Kauffman and D. O. Cowan, *Inorg. Synth.* 1963, VII, 239, and references therein.
[5] H. D. K. Drew, F. W. Pinkard, W. Wardlaw and E. G. Cox, *J. Chem. Soc.* 1932, 988.
[6] M. J. Cleare, Mead Johnson advances in therapeutics, Vol. 1. Neoplatin and cancer therapy. *Proc. of an Int. Symp.* London, March 1979.
[7] D. A. Gattegno, A. M. Giuliani, M. Bossa and G. Ramunni, *J. C. S. Dalton* 1973, 1399.
[8] G. N. Boiko, E. N. Loginova and K. V. Titova, *Russ J. Inorg. Chem.* 1979, **24**, 1313.
[9] D. M. Adams and J. B. Cornell, *J. Chem. Soc.* (A) 1967, 884.
[10] I. M. Ismail, S. J. Kerrison and P. J. Sadler, *Polyhedron* 1982, **1**, 57.

[11]A. Pidcock, R. E. Richards and L. M. Venanzi, *J. Chem. Soc(A)* 1968, 1970.

[12]J. D. Kennedy, W. McFarlane, R. J. Puddephatt and P. J. Thompson, *J. C. S. Dalton* 1976, 874.

[13]P. L. Goggin, R. J. Goodfellow, S. R. Haddock, B. F. Taylor and I. R. H. Marshall, *J. C. S. Dalton* 1976, 459.

[14]S. J. Kerrison and P. J. Sadler, *J. C. S. Chem. Comm.* 1977, 861.

RAMAN STUDY OF GALLIUM CHLOROSULPHIDES
IN CHLORIDE MELTS

ROLF W. BERG* and NIELS J. BJERRUM

Chemistry Department A, The Technical University of Denmark, DK-2800 Lyngby, Denmark

Abstract—The reaction between sulphur and gallium in chlorobasic melts at *ca.* 500°C was studied by visual observation and by Raman spectroscopy. The results suggest the formation of charged long chains (–GaCl₂–S–GaCl₂–S–) in these melts and the presence of the radical anion S_3^- under certain conditions.

In a continued effort[1-3] to understand the chemical behavior of the sulphide ion in molten salts, the reaction between sulphur and metallic gallium in chloride melts was studied. Previously, it has been found[1] that aluminium and sulphur in molten CsCl–AlCl₃ mixtures (with an excess of CsCl, i.e. chlorobasic melts) reacted according to $2Al + 3S + CsAlCl_4 + 2CsCl \rightarrow 3/n\ Cs_n$-$(AlSCl_2)_n$ (large n). The $[AlSCl_2^-]_n$ polymer was characterised by its polarized Raman band at ~325 cm⁻¹, and this band was assigned to the occurrence of AlCl₂–S–AlCl₂ units in chain-like ions of the type $[Al_nS_{n-1}Cl_{2n+2}]^{n-}$, or simply $[AlSCl_2^-]_n$ for large n.

The objective of this investigation was to study what happens if gallium substitutes aluminium. The qualitative similarities between the chemistry of Al(III) and Ga(III) in alkali chloride melts are well-known[4-6], but the chemistry of gallium sulphide chlorides is very little known. The formation of polymeric ions $[GaSCl_2^-]_n$ was to be expected, giving rise to a strong polarised Raman-band in the neighbourhood of 325 cm⁻¹.

EXPERIMENTAL

Anhydrous, high purity (>99.9% by weight) chemicals were used in evacuated Pyrex or quartz cells, which were equilibrated in rocking furnaces (as in Ref. 1–3). The evaporation of weighed GaCl₃ was avoided by cooling the cells to be sealed in liquid nitrogen. The Raman spectra were measured using argon-ion laser radiation and a Jeol-JRS–400D spectrometer equipped with cooled extended S–20 PM-detector and a photon counting system.

Two kinds of chlorobasic molten salts were used as solvents: (i) Cs[GaCl₄] and CsCl at compositions near a molar ratio of CsCl/GaCl₃ = 60/40, with melting points below *ca.* 400 °C. (Cs[GaCl₄], which melts congruently at 400 ± 20 °C[7,8] was obtained from equimolar amounts of CsCl and GaCl₃). (ii) Mixtures of NaCl and CsCl with a molar ratio NaCl/CsCl of *ca.* 35/65 and a melting point around 500°C[9,10]

RESULTS AND DISCUSSION

CsCl–GaCl₃ *melts as solvent*

With a molar excess of CsCl relative to GaCl₃, the pure solvent melt has been shown[4-6] to contain Ga(III) as tetrahedral $[GaCl_4]^-$ complex ions, in accordance also with the crystal structure of CsGaCl₄.[11] As for other tetrahedral ions, four Raman bands can be observed from molten CsGaCl₄: $\nu_1(a_1) \cong 343$; $\nu_2(e) \cong 120$; $\nu_3(t_2) \cong 370$ and $\nu_4(t_2) \cong 153$ cm⁻¹; ν_1 being polarised and ν_2–ν_4

depolarised.[4-6] The addition of sulphur alone to the melt did not produce any strong new Raman band; the dissolved sulphur molecules scattered negligibly relative to $[GaCl_4]^-$, see Fig. 1(C).

In melts to which small amounts of gallium metal and sulphur have been added (in near equimolar amounts), a reaction consuming these materials quickly proceeded. After approximately one hour at 400 °C no more unreacted Ga or S was left. The main reaction products were colourless when the molar ratio Ga/S was 2/3 and easily soluble in the melts. The more gallium and sulphur added, the more viscous seemed the melts and the more pronounced the tendency to foam formation. In experiments with an excess of sulphur, yellow-brown sulphur or polysulphide colours were always observed. In addition to this, sometimes a deep blue colour (similar to the one found for S_3^- in other melts[2]) was seen. In combination with the yellow colour this blue produced greenish to black colours when much excess sulphur was present. The stability of the blue species depended on a number of circumstances: The presence of excessive sulphur and sufficient free chloride, the temperature and probably also the sulphide formality. A permanent blue-green colour seems to exist only:

(1) If excessive sulphur (according to the reaction $2Ga + 3S \rightarrow$ "Ga_2S_3") is present. Even in the first stages of experiments having excessive but yet undissolved metallic gallium the blue colour has been seen.

(2) If the chlorobasicity is sufficiently large. Probably the molar ratio of CsCl/GaCl₃ needs to be at least of the order of 60/40 or larger.

(3) If the temperature is sufficiently high. When the ratio CsCl/GaCl₃ was around 66/34, the temperature should be around 500 °C or higher, otherwise only yellow–brown colours were seen.

(4) It seemed as if the total concentration of sulphide (S(-II)) had an influence on the stability of the blue species. A small sulphide concentration (e.g. in the first stages of reaction) were favourable for blue colours. The exact conditions necessary for the formation of the blue coloured solutions are very complicated and not presently understood.

The addition of GaCl₃ to a blue melt in amounts necessary to consume all free chloride, (CsCl/GaCl₃ ≅ 45/55), destroyed the colour and produced a yellow–white precipitate, which probably was "GaSCl".[12-13] The
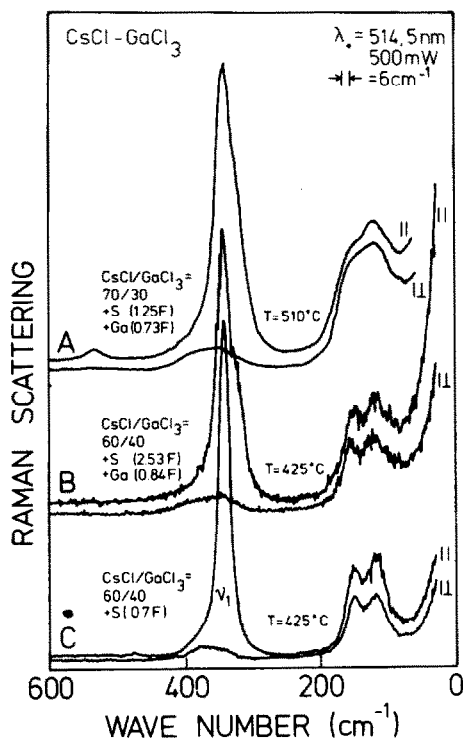
Fig. 1. Raman spectra of basic CsCl–GaCl₃ melts with addition of gallium and excess of sulphur according to the reaction $2Ga + 3S \rightarrow 2Ga^{3+} + 3S^{2-}$: A: blue, B and C: brown. Formalities are based on an estimated density of 2.5 g/cm³. In A and B: S(O)/S(–II) = 0.2 and 1.0, respectively.

Raman spectrum of the melt over the precipitate only showed the bands at ~343 and ~366 cm⁻¹ characteristic of simultaneous presence of $[GaCl_4]^-$ and $[Ga_2Cl_7]^-$.[4-5]

The Raman spectra of the basic clear, colourless or yellow melts obtained after Ga and S had reacted, always showed in addition to the $[GaCl_4]^-$ bands a new polarized Raman band at 315–320 cm⁻¹. This is analogous to what was seen in the case of Al, which had a similar band at ~325 cm⁻¹.[1] The fact that this band appears also in the gallium case indicates that most probably –GaCl₂–S–GaCl₂– chain polymers (of formula $[Ga_nS_{n-1}Cl_{2n+2}]^{n-}$) are formed from $[GaCl_4]^-$ and S^{2-} in the same way as the polymers –AlCl₂–S–AlCl₂– of formula $[Al_nS_{n-1}Cl_{2n+2}]^{n-}$ are formed from $[AlCl_4]^-$ and S^{2-}.[1] The formation of precipitates of "AlSCl" or "GaSCl" by addition of sufficient AlCl₃ or GaCl₃, respectively, is in accordance with this opinion of analogy between the chlorosulphides of aluminium (III) and gallium (III). Probably "GaSCl" is really $[Ga_nS_{n-1}Cl_{2n+2-m}]^{(n-m)-}$ with n large and m < n.[1]

The melts with excess sulphur did not produce any new Raman bands when brown; when blue, a band at 525 cm⁻¹ was observed in addition to the bands already mentioned. This band is a clear indication that the blue color is indeed due to the radical ion S_3^-, which is known to have its resonance enhanced symmetric stretching Raman band ν_1 at ~530 cm⁻¹.[2-3] No bands due to sulphur or polysulphides were observed, which probably means that these species which are believed to be present just scatter too weakly to be seen (similar results were found in the CsCl–AlCl₃ experiments³).

NaCl–CsCl melts as solvent

The pure NaCl–CsCl solvent, like other completely dissociated, monatomic ionic liquids showed no definite Raman band. When GaCl₃ was added, Raman bands appeared due to the formation of $[GaCl_4]^-$ ions (Fig. 2A). When either GaCl₃ and Na₂S or gallium metal, GaCl₃ and sulphur were added to the solvent, the new band assigned to -GaCl₂–S–GaCl₂- appeared (like in Fig. 1 but now at ~318 cm⁻¹). As the sulphide concentration was increased (see Fig. 2), the strong $[GaCl_4]^-$ ν_1 Raman band at ~343 cm⁻¹ gradually disappeared and at the same time the 318 cm⁻¹ band increased. When the molar ratio S:Ga exceeded ~1, the ν_1 band of $[GaCl_4]^-$ was completely lost. This is analogous to the behavior in the case of aluminium,[1] showing that the reaction between the metal and the sulphur is essentially a 1:1 reaction. The observed formation of foam when shaking the melts, finds a reasonable explanation by formation of polymers.
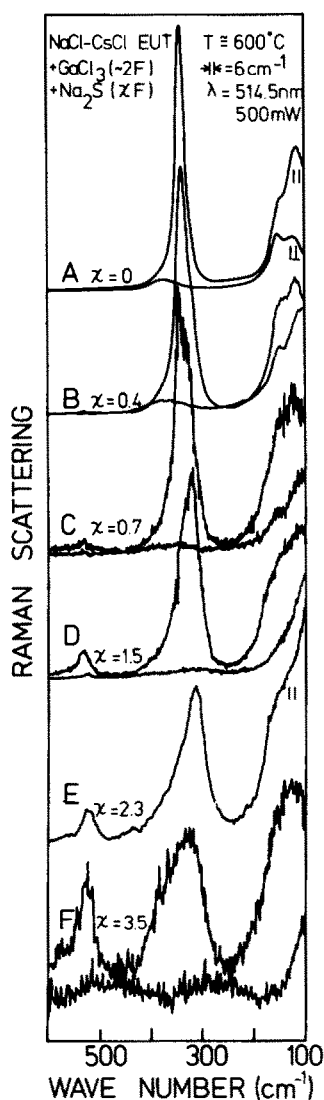
Fig. 2. Raman spectra of NaCl–CsCl melts (NaCl/CsCl molar ratio = 34.5/65.5) with ~2F GaCl₃ and increasing formality of Na₂S. A: waterclear. B–F: increasingly bluish. Na₂S in NaCl–CsCl with no GaCl₃ added gave a yellow melt with no Raman band.

It is of interest to note that also the blue colour and the S_3^- Raman band (at 527 cm^{-1}) could be seen in the more concentrated solutions of $GaCl_3$ and Na_2S, even without addition of sulphur. Na_2S alone did not produce any blue color in the NaCl–CsCl melt. Probably the partial oxidation of S^{2-} to S_3^- is coupled to a reduction of Ga^{3+} to Ga^+. Also in experiments with gallium metal and excessive sulphur in the NaCl–CsCl melt a blue solution was obtained with a S_3^- Raman band at 526 cm^{-1}.

"Cs GaSCl₂"-glass

When gallium, sulphur, CsCl and $GaCl_3$ in the molar ratios 2/3/3/1 (i.e. as in the formula $CsGaSCl_2$) were reacted for 5 days at 600 °C, a colourless, clear and viscous melt remained, with no reactant left over. Again the Raman spectrum of the melt was dominated by a strong polarized band at ~315 cm^{-1}, which again is assigned to the $-GaCl_2-S-GaCl_2-$ skeleton. The melt formed a stable fully transparent glass when cooled to room temperature. This formation of the $[Ga_nS_{n-1}Cl_{2n+2}]^{n-}$ polymer is analogous to the behavior in the case of aluminium.[1]

CONCLUSION

In chloride melts sulphur and gallium seem to react forming $[Ga_nS_{n-1}Cl_{2n+2}]^{n-}$, i.e. long charged $-GaCl_2-S-GaCl_2-$ chains. The degree of polymerisation is unknown and the chemistry is very complicated, as the existence of crystals of $Ga_9S_8Cl_{11}$ also proved some years ago.[13] In acidic melts (with an excess of $GaCl_3$) a precipitate is formed, probably consisting of "GaSCl" or $[Ga_nS_{n-1}Cl_{2n+2-m}]^{(n-m)-}$ salts with $n \gtrsim m$.

Under certain conditions (such as presence of excessive sulphur in highly chlorobasic melts and temperatures around 500–600 °C) the S_3^--radical ion with ν_1 Raman bands at 525–527 cm^{-1} is stable in these environments, as it is in analogous aluminium substituted melts. It should be of interest to investigate if the radical is free or bound to Ga(III), (like for Al(III)[3]) in which case the ESR spectrum should show a hyperfine splitting into 4 lines due to the $I = 3/2$ state of the two natural Ga isotopes.

Our present experimental setup for measuring ESR-spectra[3] is unfortunately not well suited for operating at temperatures much higher than ca. 400 °C, but we hope soon to be able to perform such investigations.

REFERENCES

[1] R. W. Berg, S. v. Winbush and N. J. Bjerrum, Inorg. Chem. 1980, 19, 2688.
[2] R. W. Berg, N. J. Bjerrum, G. N. Papatheodorou and S. v. Winbush, Inorg. Nucl. Chem. Lett 1980, 16, 201.
[3] R. Fehrmann, S. v. Winbush, G. N. Papatheodorou, R.\W. Berg and N. J. Bjerrum, Inorg. Chem. 1982, 21, 3396.
[4] H. A. Øye and W. Bues, Inorg. Nucl. Chem. Lett 1972, 8, 31.
[5] H. A. Øye and W. Bues, Acta Chem. Scand. 1975, A29, 489.
[6] D. Mascherpa-Corral and A. Potier, J. Chim. Phys. 1977, 74, 1077.
[7] P. I. Fedorov and V. V. Tsimbalist, Russ. J. Inorg. Chem. 1964, 9, 908.
[8] V. A. Sryvtsev, V. N. Arbekov and E. S. Petrov, see Chem. Abstr. 1968, 69, 99931.
[9] R. G. Samuseva and V. E. Plyushchev, Russ. J. Inorg. Chem. 1961, 6, 1092.
[10] S. Zemczuzny and F. Rambach, Z. Anorg. Allgem. Chem. 1910, 65, 403.
[11] R. C. Gearhart, J. D. Beck and R. H. Wood, Inorg. Chem. 1975, 14, 2413. See also G. Meyer and E. Schwan, Z. Naturf. 1980, B35, 117.
[12] H. Hahn and H. Katscher, Z. Anorg. Allgem. Chem. 1963, 321, 85.
[13] A. Hardy and D. Cottreau, Compt. Rend. Acad. Sci. Paris 1966, 262C, 739.

NUCLEOPHILIC ADDITION OF THE THIOCYANATE ION TO FERROCENYL-STABILISED CARBOCATIONS

ALBERTO CECCON*, ALESSANDRO GAMBARO, DANIELE PAOLUCCI and ALFONSO VENZO

Istituto di Chimica Fisica, Università di Padova, 2, Via Loredan, 35100 Padova, Italy

Abstract— The reaction of ferrocenylmethylcarbocations with the ambident thiocyanate ion produces only the isothiocyanate isomer.

Some years ago, the reaction of secondary and tertiary ferrocenylmethyl tetrafluoborates with a variety of nucleophilic reagents was described as a convenient high-yield operation for the synthesis of ferrocenyl derivatives of great potential interest.[1] We report here the results obtained from the reaction of some ferrocenylmethyl tetrafluoborates with the ambident nucleophile, [SCN]⁻. Ferrocenylmethylisothiocyanate, which was used as a "tag" in metabolic polypeptide studies,[2] is obtained from ferrocenylmethylamine and thiophosgene;[3] moreover, a yellow product which the authors claimed to be ferrocenylmethylthiocyanate is formed on refluxing N, N - dimethylaminomethylferrocene methiodide with an aqueous solution of KSCN.[4]

The tetrafluoborates of the ions $Fc-\overset{+}{C}R_1R_2(Fc = C_5H_5FeC_5H_4; R_1=R_2=H, C_6H_5; R_1=H, R_2=C_6H_5)$ were prepared from solutions of the corresponding carbinols in Et_2O by adding fluoboric acid; the primary cation prepared by this procedure has been shown to be strongly solvated by ether molecules so that it can be considered an oxonium rather than a carbenium ion.[5] The addition of the thiocyanate ion to the salts has been made either by shaking a water solution of KSCN with a CH_2Cl_2 solution of the ferrocenylmethyl ions or by adding the nucleophile dissolved in CH_3CN to a solution of the cation in the same solvent. The results of the homogeneous and heterogeneous processes did not differ substantially, though higher yields were obtained from the heterogeneous experiments. The details of the "quenching" experiments carried out on the secondary ferrocenyl(phenyl)methyl carbenium ion will be described.

The IR analysis of the organic phase of the heterogeneous quenching and of the acetonitrile solution in the homogeneous one showed a band centered at 2079 cm⁻¹ whose position, intensity and shape are characteristic of organic isothiocyanates and not of thiocyanates which show a weaker (by a factor of 10) sharp absorption band at *ca.* 2150 cm⁻¹. Portions of this solution were sealed in vials under nitrogen and heated at 60°C for various periods of time. The IR spectrum of the solution after 20 min. heating did not show any appreciable variation with respect to the initial one, but longer heating times (1 hr) caused a definite change in the shape and frequency (2065 cm⁻¹) of the absorption band. This was attributed to the stretching of the inorganic SCN⁻ ion, by comparison with a standard solution of KSCN. Very prolonged heating (*ca.* 20 hr) afforded shining dark-brown crystals, m.p. 140°C (dec.) which were identified as thiocyanato complexes of Fe(III).

After removal of the solvent from the initial unheated solution, one obtains a yellow–brown viscous oil; its ¹H NMR spectrum contains sharp signals (s) at δ 7.30 (5 phenyl protons) at 4.26 and 4.17 (5 and 4 cyclopentadienyl protons) and at 5.64 (1 methine proton). Treatment of the oil with *n*-heptylamine in cyclohexane gave, on cooling, a yellow precipitate which after recrystallization from cyclohexane was identified as *N*-(*n*-heptyl)*N*'-(ferrocenyl(phenyl)methyl)thiourea, from elemental analysis and ¹H NMR spectrum (see Experimental). The IR spectrum of the mother solution showed the total disappearance of the band of the isothiocyanates and the absence of any other band in the region characteristic of the SCN stretching (2050–2160 cm⁻¹). Attempts to crystallise the viscous and pungent oil were unsuccessful; on the other hand, purification by column chromatography on SiO_2 gave the ferrocenyl(phenyl)methyl alcohol as the only product. The above findings allow the following conclusions: (a) the only product of the quenching of the ferrocenyl(phenyl)methyl carbenium ion and SCN⁻ is the ferrocenyl(phenyl)methyl isothiocyanate, as confirmed by IR and NMR spectra and by the formation of the corresponding thiourea; (b) the absence of the thio-isomer in the reaction mixture is proved by the lack of the band characteristic of organic thiocyanates after reaction of the crude product with the amine and by the unchanged intensity of the isothiocyanate band after short heating. On the other hand, on the basis of the data obtained for the triphenylmethyl- structure for which only the isothio isomer could be synthetised,[6] one would expect that, even if formed, the ferrocenyl thiocyanate isomerises instantaneously. In fact, since the isomerization proceeds through an electron-deficient transition state[7] this should be extraordinary stabilised by the ferrocenyl-methyl residue if one takes into account that the ferrocenyl (phenyl)methyl carbenium ion ($pK_{R^+} = +0.4$)[8] is several powers of ten more stable than the triphenylmethyl ion ($pK_{R^+} = -6.6$); (c) the thermal instability and the facile hydrolysis to the corresponding alcohol make the compound obtained an isothiocyanate of a particular nature. In fact the stability of the ferrocenyl-(phenyl)methyl carbenium ion allows, contrary to most organic isothiocyanates, the easy rupture of the carbon-to-nitrogen bond. The subsequent thermal decomposition of the organometallic cation to give thiocyanic complexes of Fe(III) probably · occurs by a mechanism very similar to that proposed for other ferrocenylmethyl salts;[9] however, an intermediate in which the iron atom interacts directly with the S-end of the SCN group (see Fig. 1) cannot be excluded.

The reactions of tertiary diphenyl and the primary
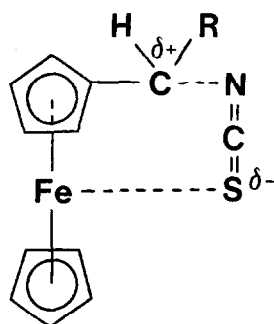
Fig. 1.

ferrocenylmethyl cations with SCN⁻ were not investigated in detail, but the conclusions which can be drawn from the IR spectra of the quenching solutions are that only the isothiocyanate isomer could be identified. A great amount of decomposition products occurred in the case of the primary ferrocenylmethyl cation probably due to the lower thermal stability[5] of this species.

EXPERIMENTAL

IR and ^{1}H NMR spectra were recorded on a Beckman IR-9 spectrophotometer and a Bruker HFX-90 spectrometer, respectively. The ferrocenylmethylfluoborates were prepared as described[5] and investigated under nitrogen.

Reaction of ferrocenyl(phenyl)methyl fluoborate with SCN⁻
The dried title salt (2 mmol) was dissolved in 20 ml of dry, cold CH₂Cl₂ and added at 0° with vigorous stirring to an oxygen-free aqueous 1.3 M solution of KSCN (20 ml). During the addition the colour of the solution changed from brown to dark yellow. The organic phase was then separated, dried with Na₂SO₄, filtered and the solvent pumped off until a brown–yellow oil was obtained. The oil was dissolved in cyclohexane and 4 mmol of *n*-heptyl amine were added slowly. The solution becomes yellow and was kept overnight at 0°C. The precipitate was filtered off, washed with petroleum ether and crystallzed from cyclohexane. (Yield 0.425 g., 47%) m.p. 105–107°C. Found: C, 66.7; H, 7.8; N = 6.1. C₂₅H₃₂FeN₂S requires: C, 66.9; H, 7.2; N, 6.2%.

NMR (in CDCl₃, δ from internal TMS): 7.38 (*s*, 5H: C₆H₅); 6.87 and 5.50 (two broad singlets, 1 H each: N–H); 4.16 (*s*, 5H: C₅H₅); 4.16 (*m*, 4H: C₅H₄); 3.96 (*s*, 1H: methine CH); 3.44, 1.16 and 0.87 (three multiplets, 15H overall: *n*-C₇H₁₅-protons).

REFERENCES

[1] S. Allenmark, *Tetrahedron Lett.* 1974, **4**, 371.
[2] L. T. Mann, Jr., *J. Label. Compounds* 1967, **3**, 87; T. J. Gill and L. T. Mann, Jr., *J. Immunol.* 1966, **96**, 906.
[3] M. Uber and S. Toma, *Zh. Pr. Chemickotechnol Fak. SVST* 1971, 49.
[4] A. N. Nesmeyanov, E. G. Perevalova, L. S. Shilvovtseva and Yu. A. Ustynyuk, *Doklady Akad. Nauk SSSR* 1959, **124**, 331.
[5] A. Ceccon, G. Giacometti, A. Venzo, D. Paolucci and D. Benozzi, *J. Organometal. Chem.* 1980, **185**, 231.
[6] A. Iliceto, A. Fava and U. Mazzucato, *J. Org. Chem.* 1960, **25**, 1445; U. Miotti and A. Ceccon, *Ann. Chim. (Rome)* 1964, **54**, 851.
[7] A. Iliceto, A. Fava, U. Mazzucato and O. Rossetto, *J. Am. Chem. Soc.* 1961, **83**, 2729.
[8] G. Cerichelli, B. Floris and G. Ortaggi, *J. Organometall. Chem.* 1974, **78**, 241.
[9] N. Cully, W. D. Quail, W. E. Watts, *J. Organometal. Chem.* 1978, **152**, C9.

PREPARATION AND PROPERTIES OF DINITROGEN TRIMETHYLPHOSPHINE COMPLEXES OF MOLYBDENUM AND TUNGSTEN—II†

SYNTHESIS AND CRYSTAL STRUCTURES OF [MCl(N₂)(PMe₃)₄] (M = Mo, W) AND *TRANS*-[MoCl₂(PMe₃)₄]

ERNESTO CARMONA,* JOSÉ M. MARÍN and MANUEL L. POVEDA
Departamento de Química Inorgánica, Facultad de Química, Universidad de Sevilla, Sevilla, Spain

and

JERRY L. ATWOOD* and ROBIN D. ROGERS
Department of Chemistry, University of Alabama, University, AL 35486, U.S.A.

Abstract—Sodium amalgam reduction of the complexes [MCl₃(PMe₃)₃] (M = Mo, W) in tetrahydrofuran, under dinitrogen, yields dark red–brown suspensions from which red–orange crystals of composition *trans*-[MCl(N₂)·(PMe₃)₄] can be collected. Spectroscopic and chemical evidence indicate the compounds are best formulated as mixtures of *trans*-[M(N₂)₂(PMe₃)₄] and *trans*-[MCl₂(PMe₃)₄] species, but attempts to isolate the pure *bis*(dinitrogen) derivatives have proved unsuccessful. Single crystals of analytical composition [MCl(N₂)(PMe₃)₄] have been studied by X-ray crystallography, and the structure of *trans*-[MoCl₂(PMe₃)₄] has been determined for comparison. *trans*-[MCl(N₂)(PMe₃)₄] (M = Mo, W) and *trans*-[MoCl₂(PMe₃)₄] are all isostructural, crystallizing in the tetragonal space group I4̄2 *trans*-[MoCl(N₂)(PMe₃)₄] has $a = 9.597(5)$, $b = 12.294(6)$ Å, $D_c = 1.36$ g cm⁻³ for $Z = 2$ and was refined to a final R value of 0.021 based on 319 independent observed reflections. The tungsten analogue has $a = 9.573(4)$, $b = 12.278(5)$ Å, $D_c = 1.63$ g cm⁻³ for $Z = 2$ and was refined to R = 0.19 with 322 independent observed reflections. *trans*-[MoCl₂(PMe₃)₄] has cell parameters $a = 9.675(5)$, $b = 12.311(6)$ Å $D_c = 1.36$ g cm⁻³ for $Z = 2$ and was refined to R = 0.043 with 316 independent observed reflections. In each case the metal atom resides on a crystallographic 4̄2m position. For *trans*-[MoCl(N₂)(PMe₃)₄] (M = Mo, W) the chlorine and dinitrogen ligands are disordered. M–N distances of 2.08(1) Å (M = Mo) and 2.04(2) Å (M = W) and M–Cl bond lengths of 2.415(8) Å (M = Mo) and 2.46(1) Å (M = W) are observed. In *trans*-[MoCl₂(PMe₃)₄], where there is no disorder, the Mo–Cl distance is 2.420(6) Å.

A number of dinitrogen complexes of Group VI metals, containing tertiary phosphine ligands have been isolated, and some of them have been structurally characterized.[1,2] The range of complexes prepared is however limited, and for monodentate tri-alkyl phosphines, apparently only *cis*-[Cr(N₂)₂(PMe₃)₄] is known.[3] We have recently reported[4] that the reduction of [MoCl₃(PMe₃)₃] with dispersed sodium gives *cis*-[Mo(N₂)₂(PMe₃)₄] in good yields. Using sodium amalgam, under similar conditions, red–orange crystals of a compound we first formulated as *trans*-[Mo(N₂)₂(PMe₃)₄] on the basis of analytical and spectroscopic data (see below) were obtained. In this paper, we present evidence that indicates the proposed formulation to be incorrect, and that this compound, of composition [MoCl(N₂)(PMe₃)₄], behaves in fact as a mixture of *trans*-[Mo(N₂)₂(PMe₃)₄] and *trans*-[MoCl₂(PMe₃)₄]. We have also prepared the tungsten analogue and determined the X-ray structures of both compounds. For comparative purposes, the structure of *trans*-[MoCl₂(PMe₃)₄] is also reported.

RESULTS AND DISCUSSION

The addition of a tetrahydrofuran (thf) solution of [MoCl₃(PMe₃)₃],[5] to a suspension of sodium amalgam in thf, produces a change in colour from yellow to deep green and finally to very dark red–brown. The formation of a green solution is also observed at the early stages of the preparation of *cis*-[Mo(N₂)₂(PMe₃)₄],[4] but attempts to isolate this intermediate species from either system have been unsuccessful. The final, dark red–brown, light sensitive solution yields, after several purification operations, a red–orange crystalline material as the only isolable pure product. The workup of this solution is considerably facilitated if it is previously stirred, in daylight for 24–48 hr.

The formation of the red–orange crystals of the molybdenum dinitrogen complex from the sodium amalgam reduction of [MoCl₃(PMe₃)₃], clearly shows the complexities involved in the synthesis of transition metal dinitrogen complexes, by reduction of suitable precursors under a nitrogen atmosphere. The difficulties found in isolating the orange crystals of [MoCl(N₂)·(PMe₃)₄], are probably similar to those encountered in the preparation of other related complexes using magnesium metal as reducing agent, where isolation of the dinitrogen complex requires the use of methanol to hydrolyze some magnesium adduct.[6] On the other hand, as in other related systems,[1] the choice of precursor is also of the greatest importance, no dinitrogen species being detected from the reduction of either [MoCl₃(thf)₃] or [MoCl₃(PMe₃)₃] in the presence of an excess of phosphine, or from [MoCl₂(PMe₃)₄]. [WCl₂(PMe₃)₄] has similarly been found to be unreactive towards sodium

†For part 1 see Ref. 4.
*Authors to whom correspondence should be addressed.

amalgam.[7] Furthermore, the use of *in situ* solutions of [MoCl$_3$(PMe)$_3$], prepared from [MoCl$_3$(thf)$_3$] and PMe$_3$ in tetrahydrofuran,[5] and subsequent removal of the excess of PMe$_3$ yields mainly [MoCl$_2$(PMe$_3$)$_4$], together with some decomposition products, and only small amounts of the dinitrogen complex. Attempts to improve the yield of the final product in a manner similar to that used for the synthesis of *cis*-[Mo(N$_2$)$_2$(PMe$_3$)$_4$], (addition of *ca.* 80% of the required amount of phosphine a few minutes after the appearance of the green color[4]) were unsuccessful. The only observable effect was an increase in the amounts of [MoCl$_2$(PMe$_3$)$_4$] formed in the reaction. Finally, the selection of the reducing agent is also of much importance since, while the use of sodium amalgam produces mainly [MoCl(N$_2$)(PMe$_3$)$_4$] and small amounts of *cis*-[Mo(N$_2$)$_2$(PMe$_3$)$_4$], the sodium dispersion reduction yields the *cis* complex in *ca.* 60% yields, with very small amounts of the [MoCl(N$_2$)(PMe$_3$)$_4$].

The first sets of analytical data obtained for the red-orange crystals of the molybdenum complex, together with the results of molecular weight determinations (cryoscopically in benzene) closely fitted the composition [Mo(N$_2$)$_2$(PMe$_3$)$_4$]; this formulation was also substantiated by spectroscopic data. Thus the IR spectrum shows a strong absorption at 1930 cm^{-1}, assignable to the antisymmetric N–N stretch (A_{2u} in the assumed D_{4h} geometry for the *trans*-[Mo(N$_2$)$_2$(PMe$_3$)$_4$] species) and a very weak band at 2005 cm^{-1} assignable to the symmetric stretch (A_{1g} in D_{4h}), in agreement with data reported for other similar complexes.[8] On the other hand, the ^{1}H NMR spectrum (C$_6$D$_6$, 35°C) shows a slightly broad singlet, centred at $\delta = 1.5$, with some fine structure on both sides, and the ^{31}P NMR is a singlet at $\delta = -0.8$ ppm.† The IR spectrum of the C$_6$D$_6$ solution used for the NMR studies displays a unique strong absorption at 1930 cm^{-1}, due to the N–N stretch. Since structural data on Mo and W dinitrogen complexes are rather scarce, and since comparison with the structure of *cis*-[Mo(N$_2$)$_2$(PMe$_3$)$_4$][4] would be of interest, a structural analysis of the supposed *trans*-[Mo(N$_2$)$_2$(PMe$_3$)$_4$] complex was undertaken. X-Ray studies on two different crystals (from different crops) seemed to indicate (see below) the presence of the molecule *trans*-[MoCl(N$_2$)PMe$_3$)$_4$], with the *trans*-chloro and dinitrogen ligands completely disordered. Since this situation cannot be immediately differentiated from one in which *trans*-[Mo(N$_2$)$_2$(PMe$_3$)$_4$] and *trans*-[MoCl$_2$(PMe$_3$)$_4$] have co-crystallized, approximately in a 1:1 ratio, we attempted to solve this problem with the aid of spectroscopic and chemical studies.

Molybdenum(I) complexes are uncommon, and those containing coordinated dinitrogen are of interest since species of the type [MX(N$_2$)(dppe)$_2$] (M = Mo, W; X = Cl, Br, I; dppe = Ph$_2$PCH$_2$CH$_2$PPh$_2$) are thought to be intermediates in the alkylation reactions of co-ordinated dinitrogen in *trans*-[M(N$_2$)$_2$(dppe)$_2$] complexes.[9] In addition to the cationic Mo(I) complex, [Mo(N$_2$)$_2$(dppe)$_2$]$^+$, that can be generated by chemical or electrochemical oxidation[1] of [Mo(N$_2$)$_2$(dppe)$_2$], species of composition [MoX(N$_2$)(dppe)$_2$] (X = Cl, Br) have been claimed, although Chatt *et al.* later demonstrated[10] that a product with spectroscopic properties identical to those of [MoCl(N$_2$)(dppe)$_2$] could be obtained by mixing equimolar amounts of [MoCl$_2$(dppe)$_2$] and [Mo(N$_2$)$_2$(dppe)$_2$];

they concluded that the complexes [MoX(N$_2$)(dppe)$_2$] (X = Cl, Br) do not exist as stable species at room temperature. Other similar Mo(I) species, particularly [Mo(N$_2$)(SCN)(dppe)$_2$], were later prepared[11] and seem to be stable at room temperature. For our [MCl(N$_2$)· (PMe$_3$)$_4$] (M = Mo, W) complexes the situation is analogous to that encountered for [MoCl(N$_2$)(dppe)$_2$], and analytical, spectroscopic and chemical data, indicate that the compounds should be considered as mixtures of *trans*-[Mo(N$_2$)$_2$(PMe$_3$)$_4$] and *trans*-[MoCl$_2$(PMe$_3$)$_4$]. This proposal is based on the following grounds.

Although the first two sets of analytical data obtained for the molybdenum complex were consistent with the initial formulation,[4] *trans*-[Mo(N$_2$)$_2$(PMe$_3$)$_4$], as discussed above, further analytical data from different laboratories, on samples of identical properties to the initial ones, consistently gave nitrogen contents lower than the expected values for the above formulation. Furthermore, although in some cases analytical figures agree well with the formulation [MCl(N$_2$)(PMe$_3$)$_4$], they are often inconsistent, even in samples that have been recrystallized four or five times. Crystals of [MoCl(N$_2$)· (PMe$_3$)$_4$] look different from [MoCl$_2$(PMe$_3$)$_4$]. Addition of solid [MoCl$_2$(PMe$_3$)$_4$] to [MoCl(N$_2$)(PMe$_3$)$_4$] (*ca.* 5–10% in weight), followed by recrystallization from toluene, yields red–orange crystals which can hardly be distinguished from those of [MoCl(N$_2$)(PMe$_3$)$_4$]. If, on the other hand, free PMe$_3$ is added during the reduction of [MoCl$_3$(PMe$_3$)$_3$] a few minutes after the solution turns deep-green in colour (see above), red–orange crystals can be collected after workup. These are again very similar to those obtained when the reaction is carried out in the absence of free phosphine, but have a lower nitrogen content. We therefore conclude that [Mo(N$_2$)$_2$(PMe$_3$)$_4$] and [MoCl$_2$(PMe$_3$)$_4$] co-crystallize together, not only when they are present in equimolar amounts but over a wide range of composition. We also believe that the initial analytical determinations that led us to formulate the complex as *trans*-[Mo(N$_2$)$_2$(PMe$_3$)$_4$], were incorrect.

The evidence for the existence in solution of the *trans*-dichloro and dinitrogen species is as follows: (i) the ^{1}H NMR spectrum shows, in addition to the broad singlet centred at $\delta = 1.5$, that we assign to the phosphine methyl protons in *trans*-[Mo(N$_2$)$_2$(PMe$_3$)$_4$], a very broad hump centred at $\delta = -8.8$ which is characteristic for *trans*-[MoCl$_2$(PMe$_3$)$_4$]. At 60 MHz, this signal was observed only with difficulty but it is easily detected in the 200 MHz spectrum. Interestingly, the presence of paramagnetic *trans*-[MoCl$_2$(PMe$_3$)$_4$] does not cause significant broadening of the phosphine methyl protons resonance at $\delta = 1.5$, nor of the phosphine resonance in the ^{31}P NMR spectrum. The above indicate that it is either a mixture or it disproportionates very rapidly in solution,[10] but since the compound can be recrystallized a number of times, the latter would require the disproportionation to be reversible, which is highly unlikely. (ii) when a tetrahydrofuran solution of [MoCl(N$_2$)· (PMe$_3$)$_4$] is heated at 40–50°C for *ca.* 24 hr. in the presence of an excess of PMe$_3$, the strong IR absorption at 1930 cm^{-1} gradually disappears, and a new band arises at 1945 cm^{-1}. From the resulting solution (see Experimental) [Mo(N$_2$)(PMe$_3$)$_5$][4] and [MoCl$_2$(PMe$_3$)$_4$] can be crystallized. Since *cis*-[Mo(N$_2$)$_2$(PMe$_3$)$_4$] readily transforms[4] into [Mo(N$_2$)(PMe$_3$)$_5$], it seems likely that under the above conditions *trans*-[Mo(N$_2$)$_2$(PMe$_3$)$_4$] isomerizes to the *cis* isomer. This process is very slow at room temperature but is accelerated by heating at 40–50°C,

---

† ^{31}P chemical shifts are to high frequency of external 85% H$_3$PO$_4$.

although, as indicated below, partial decomposition occurs. (iii) a tetrahydrofuran solution of [MoCl(N₂)·(PMe₃)₄] was stirred at 45°C, for 20 hr in the presence of an excess of KI. The resulting solution was shown to contain [MoI₂(PMe₃)₄],[12] cis-[Mo(N₂)₂(PMe₃)₄] and [Mo(N₂)(PMe₃)₅], the latter being formed at the expense of the phosphine produced in the decomposition of some of the cis complex. (iv) carbon monoxide was bubbled through a tetrahydrofuran solution of [MoCl(N₂)·(PMe₃)₄], at 50°C for 6–8 hr. A mixture of [Mo(CO)$_x$(PMe₃)$_{6-x}$] (x = 2, 3) complexes, identical to that resulting from the interaction of cis-[Mo(N₂)₂(PMe₃)₄] and CO, and pure [MoCl₂(CO)₂(PMe₃)₃][12] were obtained.

The above evidence together with the low value found for μ_{eff} (1.40 μ_B) and the absence of any ESR signals in X-band for Mo^I complexes, indicate that the products of composition [MCl(N₂)(PMe₃)₄] (M = Mo, W) should be considered as mixtures of trans-[MoCl₂(PMe₃)₄] and trans-[M(N₂)₂(PMe₃)₄]. It is possible that the trans-[MCl(N₂)(PMe₃)₄] complexes are formed at some stage during the reduction of the trichloro derivatives [MCl₃(PMe₃)₃] (M = Mo, W), but they are probably unstable under the reaction conditions, and if they form they must readily and irreversibly disproportionate to give a mixture of the M(O) and M(II) species. It is not clear why we have been unable to isolate the pure trans-[M(N₂)₂(PMe₃)₄] derivatives. Also it is difficult to rationalize that while the complexes [MoX(N₂)(dppe)₂] (X = Cl, Br) and [MCl(N₂)(PMe₃)₄] (M = Mo, W) are too unstable to be isolated at room temperature, other similar derivatives such as [Mo(SCN)(N₂)(dppe)₂] seem to be surprisingly stable[11] under the same conditions.

The molecular structures and atom numbering schemes for trans-[MCl(N₂)(PMe₃)₄] (M = Mo, W) and trans-[MoCl₂(PMe₃)₄] are presented in Figs. 1–3, respectively. Bond lengths and angles are given in Tables 1 and 2. In each the metal atom resides on a $\bar{4}2m$ crystallographic site. For trans-[MCl(N₂)(PMe₃)₄] (M = Mo, W) the Cl and N₂ ligands are disordered and in these cases it is not possible to distinguish crystallographically between trans-[MCl(N₂)(PMe₃)₄] (Fig. 1a) and a mixture of co-crystallized (Fig. 1b) trans-[MCl₂(PMe₃)₄] and trans-[M(N₂)₂(PMe₃)₄]. In both cases refinement of the Cl and N occupancy factors (see Experimental) produced no change in the R value and both occupancy factors refined to within experimental error of a 50–50% disorder.

Disorder in dinitrogen complexes is quite common,[2] e.g. in [ReCl(N₂)(PMe₂Ph)₄][13] and a related simulation has recently been reported for trans-[W(Me)(CMe)(PMe₃)₄] which is isostructural with the title compounds.[14] An unfortunate result of the crystallographic problem is a decrease in the accuracy of the bond lengths and angles. In trans-[MoCl(N₂)(PMe₃)₄] the Mo–N bond distance is 2.08(1) Å and the N–N length, 1.14(2) Å. Both of these are slightly larger than values found for similar Mo-dinitrogen complexes, 2.014 and 1.118 Å in trans-[Mo(N₂)₂(dppe)₂][2] and 2.068 and 1.087 Å in trans-[Mo(CO)(N₂)(dppe)₂]·1/2C₆H₆.[2] The Mo–N–N bond angle is symmetry constrained to be 180°. In cis-[Mo(N₂)₂(PMe₃)₄] the Mo–N lengths average 1.97(1) Å but an identical N–N average of 1.14(1) Å has been observed.[15]

In trans-[WCl(N₂)(PMe₃)₄] the W–N distance of 2.04(2) Å is shorter than found for the Mo analogue
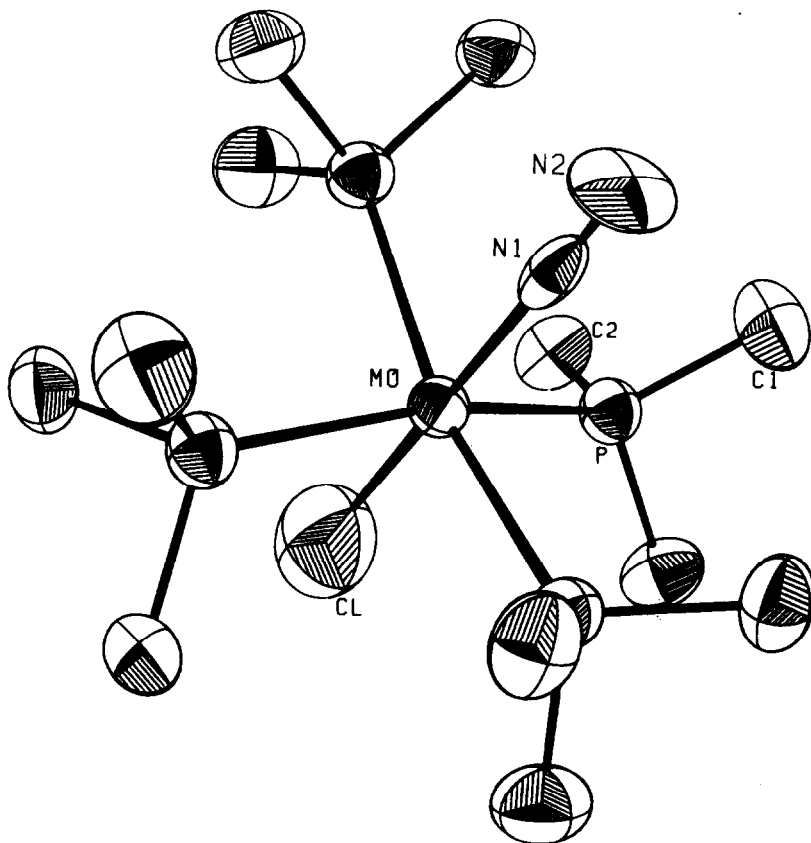
Fig. 1(a).
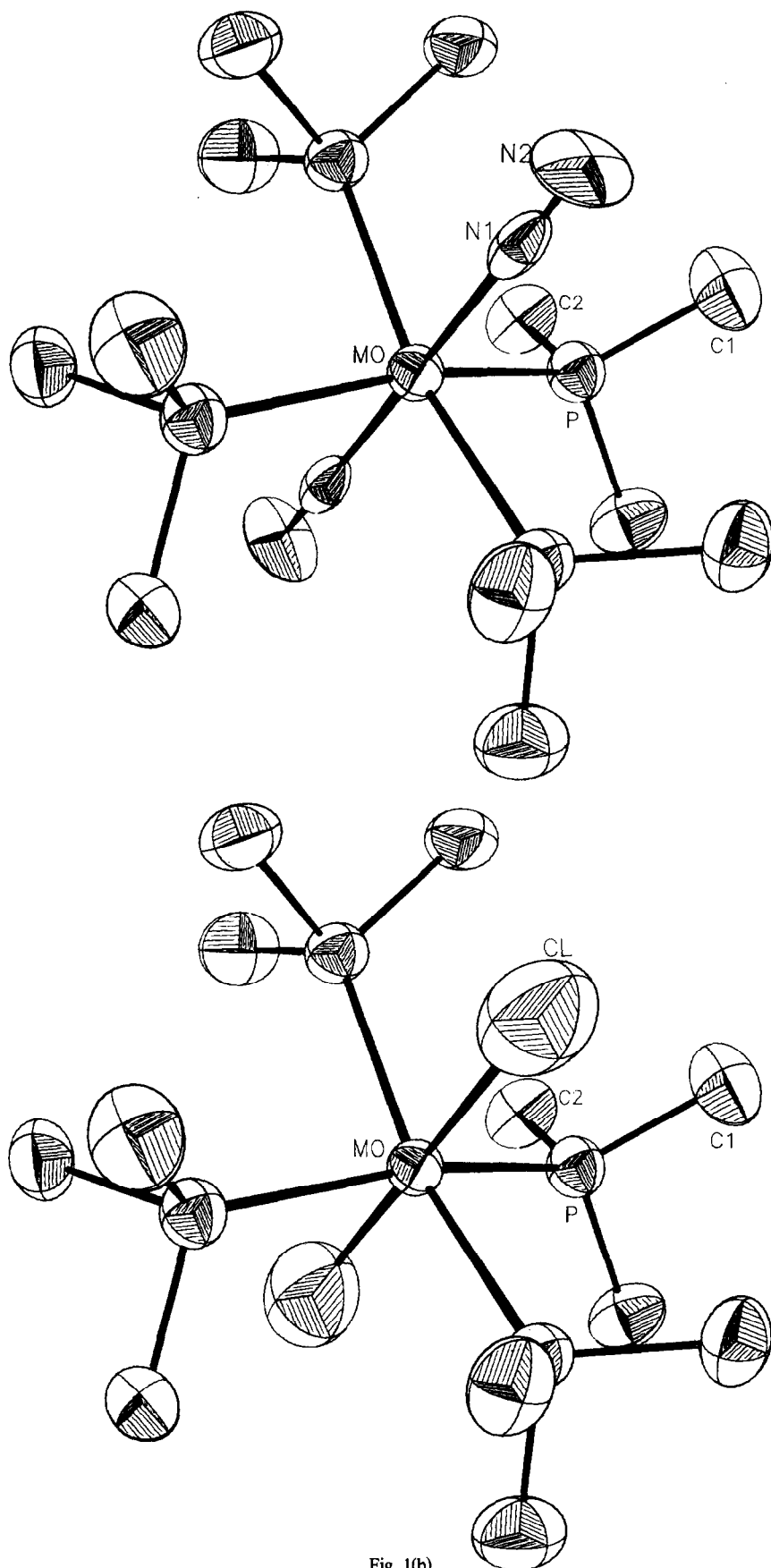
Fig. 1(b).

Fig. 1. (a) The molecular structure of one orientation of the disorder model *trans*-[MoCl(N₂)(PMe₃)₄]. The atoms are represented by their 50% probability ellipsoids for thermal motion. (b) The molecular structures of the second crystallographically equivalent disorder model, a co-crystallization of a mixture of *trans*-[Mo(N₂)₂(PMe₃)₄] and *trans*-[MoCl₂(PMe₃)₄].
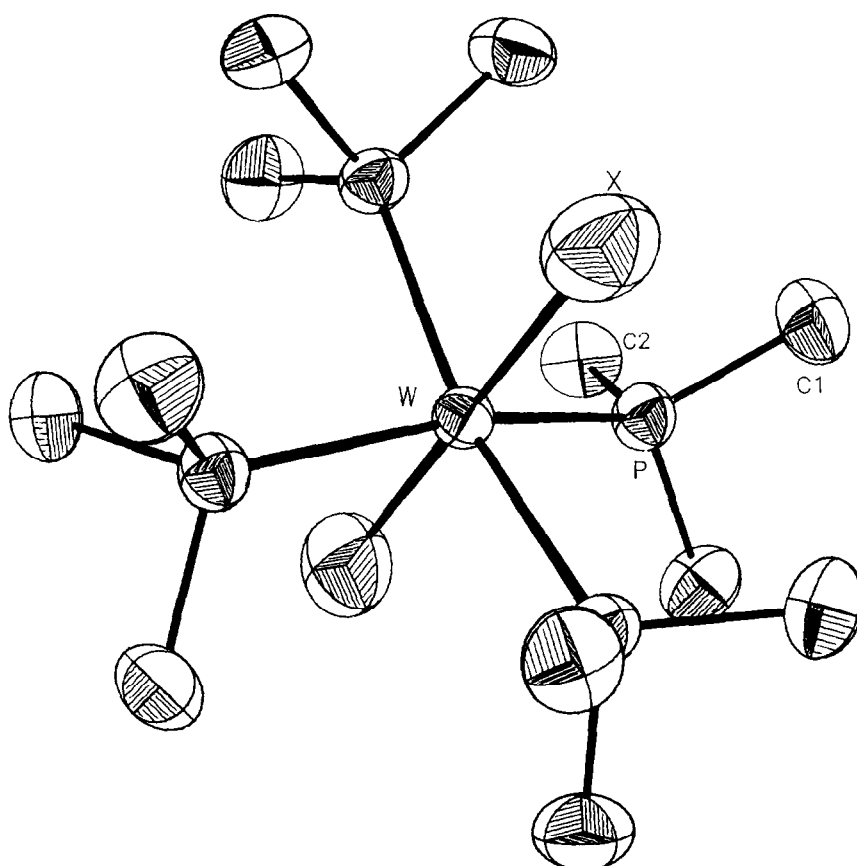
Fig. 2. The molecular structure of one of the possible disorder models for *trans*-[WCl(N$_2$)(PMe$_3$)$_4$].
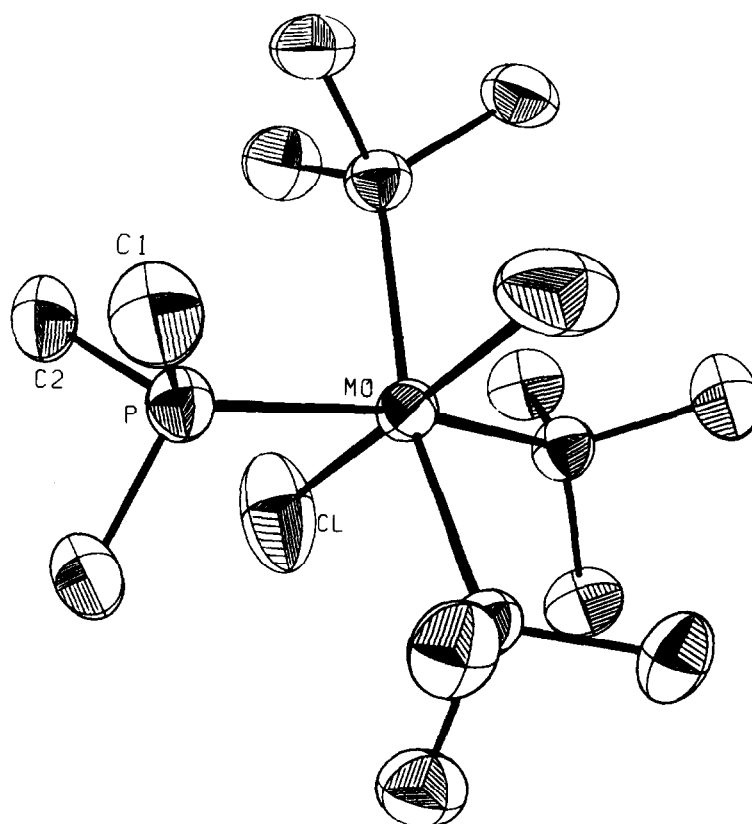
Fig. 3. The molecular structure of *trans*-[MoCl$_2$(PMe$_3$)$_4$].

Table 1. Bond distances (Å) and angles (°) for *trans*-[MCl(N₂)(PMe₃)₄] (M = Mo, W)

Atoms			Distance (M = Mo)	Distance (M = W)
M	--	P	2.461(1)	2.458(2)
M	--	Cl	2.415(8)	2.46(1)
M	--	N(1)	2.08(1)	2.04(2)
P	--	C(1)	1.826(6)	1.86(1)
P	--	C(2)	1.846(5)	1.839(8)
N(1)	--	N(2)	1.14(2)	1.19(3)

Atoms					Angle (M = Mo)	Angle (M = W)
P	--	M	--	Cl	98.81(3)	99.04(5)
Pᵃ	--	M	--	Cl	81.19(3)	80.96(5)
P	--	M	--	N(1)	98.81(3)	99.04(5)
Pᵃ	--	M	--	N(1)ᵇ	81.19(3)	80.96(5)
Cl	--	M	--	N(1)	180.000	180.000
P	--	M	--	Pᵃ	91.34(5)	91.41(8)
P	--	M	--	Pᶜ	162.39(6)	161.9(1)
M	--	P	--	C(1)	122.1(2)	121.6(3)
M	--	P	--	C(2)	116.3(1)	116.0(3)
C(1)	--	P	--	C(2)ᵈ	100.2(2)	101.3(4)
C(2)	--	P	--	C(2)	97.3(3)	96.5(5)
M	--	N(1)	--	N(2)	180.000	180.000

ᵃAtoms are related to those in Tables 3 and 4 by (x, -1-y, -1-z).

ᵇ(-1-x, y, -1-z).

ᶜ(-1-x, -1-y, z).

ᵈ(y, x, z).

Table 2. Bond distances (Å) and angles (°) for *trans*-[MoCl₂(PMe₃)₄]

Atoms			Distance	Atoms			Distance
Mo	--	P	2.496(3)	Mo	--	Cl(2)	2.420(6)
P	--	C(1)	1.84(2)	P	--	C(2)	1.82(1)

Atoms				Angle	Atoms				Angle
Cl	--	Mo	--	Clᵃ	180.000	P	--	Mo	--	Clᵇ	81.07(7)
Pᵇ	--	Mo	--	Cl	98.93(7)	P	--	Mo	--	Pᵇ	91.38(2)
P	--	Mo	--	Pᶜ	162.1(1)	Mo	--	P	--	C(1)	118.6(5)
Mo	--	P	--	C(2)	117.6(4)	C(1)	--	P	--	C(2)	101.5(5)
C(2)	--	P	--	C(2)ᵈ	96.5(6)					

ᵃAtoms related to those in Table 5 by (x, 1-y, 1-z).

ᵇ(1-x, y, 1-z).

ᶜ(1-x, 1-y, z).

ᵈ(y, x, z)

(considering a difference in metallic radii of $\Delta_{W-Mo} = 0.008$ Å),[16] but is identical to the average value found in [WH(N₂)₂(dppe)₂]HCl₂·2thf.[2] All of these, however, and the N–N distance in *trans*-[WCl(N₂(PMe₃)₄] probably agree within expectations at the 3σ level.

trans-[MoCl₂(PMe₃)₄] exhibits a Mo–Cl and a Mo–P bond distance of 2.420(6) and 2.496(3) Å, respectively. Differences in the observed M–Cl and M–P bond lengths for *trans*-[MoCl(N₂)(PMe₃)₄] (2.415(8), 2.461(1) Å), *trans*-[WCl(N₂)(PMe₃)₄] (2.46(1), 2.458(2) Å and thus for *trans*-[MoCl₂(PMe₃)₄] are not significant in view of the high ESD's (which in turn have their origin in the disorder problem).

EXPERIMENTAL

Microanalyses were by Butterworth Microanalytical Consultancy Ltd., Middlesex, Pascher Microanalytical Laboratory Bonn, and Schwarzkopf Microanalytical Laboratory, Woodside, New York. Molecular weights were measured cryoscopically, in benzene, under nitrogen. The spectroscopic instruments used were a Perkin-Elmer model 577 for IR spectra, a Perkin-Elmer R12A(¹H), a Varian XL-100-12 (³¹P, F. T) and a Nicolet NT-200 (¹H, F. T) for NMR spectra. Magnetic susceptibilities were measured in solution by the Evans' method.[17]

All preparations and other operations were carried out under oxygen-free nitrogen following conventional Schlenk techniques. Solvents were dried and degassed before use.

The light petroleum used had b.p. 40–60°C. PMe₃,[18] [MoCl₃(thf)₃][19] and [WCl₃(PMe₃)₃][20] were prepared according to literature methods.

Dichlorotetrakis(trimethylphosphine)molybdenum (II)

This complex was prepared by the Zn powder reduction of [MoCl₃(PMe₃)₃].[21] Details for its preparations were as follows: [MoCl₃(thf)₃] (1.68 g. *ca.* 4 mmol) was placed in a 250 ml three-necked flask, provided with a gas-inlet and a side-arm containing 1.3 g (20 mmol) of Zn powder, activated by heating at 150°C for 4–6 hr. 80 cm³ of dry thf were added and the resulting suspension reacted with PMe₃ (1.8 cm³ *ca.* 18 mmol) for 8–10 hr. The Zn powder was then poured into the flask, the mixture stirred overnight, then centrifuged. The solvent was removed *in vacuo* and the residue extracted with toluene (80 cm³) and filtered or centrifuged, if necessary. Evaporation of the solvent to *ca.* 20 cm³ and cooling at −20°C afforded [MoCl₂(PMe₃)₄] as yellow-orange crystals. Yield 1.3 g 70%. The compound can be recrystallized from toluene, diethyl ether, acetone or tetrahydrofuran. [Found C, 31.1; H, 7.7; Cl, 14.5%; M 452. C₁₂Cl₂H₃₆MoP₄ requires C, 30.6; H, 7.6; Cl, 15.1%; M 471].

IR (KBr disc) bands at: 2980, 2965, 2900, 1435, 1425, 1420, 930, 850, 725, 705, 660 cm⁻¹. ¹H NMR data: δ = −8.8 (very broad); $\mu_{eff} = 2.75$ μ_B.

Dinitrogen complexes. The complexes of composition [MCl(N₂)(PMe₃)₄] (M = Mo, W) were prepared by reduction of the trichloro derivatives [MCl₃(PMe₃)₃] with sodium amalgam. The procedures are similar and therefore only the synthesis of the molybdenum complex is described in detail. To a suspension of [MoCl₃(thf)₃] (1.68 g, *ca.* 4 mmol) in 40 cm³ of THF, were added 1.4 cm³ (*ca.* 14 mmol) of PMe₃, and the mixture stirred at room temperature for 8–10 hr. The solvent was evaporated almost to dryness and precipitation of the yellow [MoCl₃(PMe₃)₃] achieved by the successive addition of 20 cm³ of Et₂O and 20 cm³ of petroleum, while cooling at 0°C. The solid was filtered off, washed with 20 cm³ of a 1:1 mixture of Et₂O:petroleum and dissolved in 40 cm³ of thf. The resulting solution was filtered into a 250 cm³ flask, containing 1% sodium amalgam (0.9 g Na) and 10 cm³ of thf. After stirring at room temperature for a few minutes a deep green colour developed which changed to almost black and then to very dark red–brown. This suspension was stirred for 5 hr at room temperature and then centrifuged. The solvent was evaporated to dryness and the black, tacky residue, extracted with 60 ml of toluene and centrifuged. The solvent was removed *in vacuo* until the final volume was *ca.* 5 cm³, 40 cm³ of petroleum ether were added and the flask was cooled at −20°C for 24–48 hr. The resulting solid was filtered off, washed with 2 × 5 cm³ of petroleum at −20°C, and twice recrystallized from diethyl ether. Red–orange crystals were collected in *ca.* 25% yields (referred to PMe₃). The yields vary from one preparation to another, the best results being obtained when the reduction of [MoCl₃(PMe₃)₃] is carried out in relatively small scale (1 mmol). Work up of the dark suspension, after the reaction is over, often requires a number of filtrations and/or centrifugations before a pure crystalline solid can be isolated. Five different crops of crystals were analytically determined. The following figures correspond to the crystalline material used for the X-ray studies [Found C, 31.0; H, 7.9; N, 6.2%; *M* 464. C₁₂ClH₃₆MoN₂P₄ requires C, 31.1; H, 7.8; N, 6.0%, *M* 456].

Infrared (Nujol mull) bands at: 2005 (vw), 1930, 1430, 1425, 1375, 1290, 1275, 1265, 930, 850, 840, 725, 710, 690, 650 cm⁻¹. NMR data: ¹H(C₆D₆) δ = 1.5 and −8.8 (*trans*-[Mo(N₂)₂(PMe₃)₄] and *trans*-[MoCl₂(PMe₃)₄] respectively). ³¹P(C₆D₆-toluene) δ = −0.8 ppm. μ_eff = 1.40 μ_B.

Yields for the tungsten complex were consistently lower (10–15%) [Found C, 26.6; H, 6.6; N, 6.5. C₁₂ClH₃₆N₂P₄W requires C, 26.1; H, 6.5; N, 5.1%]. These figures correspond to the material used for the X-ray studies. A second determination on an apparently identical sample gave N, 3.2%].

Infrared (Nujol mull) bands at: 1980 (vw), 1900, 1430, 1425, 1415, 1285, 1270, 1260, 920, 845, 715, 695, 680, 640, cm⁻¹. ¹H NMR data: δ = 3.8 (very broad, *trans*-[WCl₂(PMe₃)₄][20]), and 1.5 (broad singlet with fine structure, resembling a triplet, *trans*-[W(N₂)₂(PMe₃)₄]).

Reactions of [MoCl(N₂)(PMe₃)₄]

(a) *with* PMe₃ *under* He. [MoCl(N₂)(PMe₃)₄] (0.225 g, *ca.* 0.5 mmol) was dissolved in thf (20 cm³) and reacted with a large excess of PMe₃ (0.3 cm³, *ca.* 3 mmol) at 50°C, under helium or argon, for 24 hr. The solvent was removed *in vacuo* and the residue extracted with petroleum. The undissolved solid gave yellow–orange crystals upon recrystallization from ether, that were identified as *trans*-[MoCl₂(PMe₃)₄] by comparison of their IR and NMR spectra with those of an authentic sample. Additional, although small amounts of this complex, were separated from the petroleum solution by cooling at −20°C overnight. Concentration of the mother-liquor to *ca.* 2–3 cm³ and cooling at −20°C gave yellow crystals of [Mo(N₂)₂(PMe₃)₅][4] (identified by IR, ¹H and ³¹P NMR spectroscopy).

(b) *with* KI. [MoCl(N₂)(PMe₃)₄] (0.135 g, *ca.* 0.3 mmol) was dissolved in thf (15 ml) and reacted with an excess of KI (0.83 g, *ca.* 5 mmol) at 45°C for 20 hr, under nitrogen. Some decomposition took place as evidenced by the presence of small amounts of a black, finely divided solid. The mixture was allowed to cool at room temperature, the solution filtered and the solvent evaporated, precipitation of a red crystalline solid being observed when the volume of the solution was *ca.* 1–2 cm³. The residue was extracted with petroleum ether and the solution shown by IR

to be a mixture of *cis*-[Mo(N₂)₂(PMe₃)₄] and [Mo(N₂)(PMe₃)₅]. Since the *cis*-complex is very soluble in most common organic solvents and it is difficult to crystallize from dilute solutions, the petroleum solution was reacted with PMe₃ (0.2 cm³, *ca.* 2 mmol) at room temperature for 6–8 hr, whereby complete conversion to [Mo(N₂)(PMe₃)₅] took place. This latter complex was crystallized from petroleum anf characterized as in (a). The petroleum insoluble solid was dissolved in 5 cm³ of thf, the solution centrifuged and the volume reduced to *ca.* 1–2 cm³. Upon cooling at −20°C overnight, red crystals of [MoI₂(PMe₃)₄][12] were obtained.

(c) *with* CO. Carbon monoxide was bubbled through a tetrahydrofuran (40 cm³) solution of [MoCl(N₂)(PMe₃)₄] (0.45 g, *ca.* 1 mmol), at 50°C, for 6–8 hr. The solution was then cooled at room temperature and the solvent evaporated. The resulting yellow residue was treated with 2 × 20 cm³ of petroleum. The petroleum solution was filtered and shown (IR) to be identical to the mixture of carbonyls [Mo(CO)ₓ(PMe₃)₆₋ₓ (x = 2, 3) obtained from *cis*-[Mo(N₂)₂(PMe₃)₄] and CO at room temperature,[4] and it was not investigated any further. The yellow solid was dissolved in a 2:1 mixture of petroleum:dichloromethane, and the resulting suspension centrifuged. Partial removal of the solvent *in vacuo* and cooling at −20°C gave yellow-crystals of [MoCl₂(CO)₂(PMe₃)₃].[12]

X-ray data collection, structure determination and refinement for trans-[MCl(N₂)(PMe₃)₄] (M = Mo, W)—*Crystal data*

C₁₂H₃₆ClMoN₂P₄, (C₁₂H₃₆ClWN₂P₄), M = 463.7 (551.6), tetragonal, *a* = 9.597(5) (*a* = 9.573(4)), *b* = 12.294(6) (12.279(5) Å), U = 1132.3 (1125.2 Å³), Z = 2(2), Dc = 1.36 (1.63 gcm⁻³) μ(MoKα) = 9.61 (58.31 cm⁻¹), space group *I* 4̄2m. The lattice parameters were determined from a least-squares refinement of the angular setting of 15 reflections (2θ > 40°) accurately centered on an Enraf-Nonius CAD-4 diffractometer.

A crystal of dimensions 0.88 × 1.00 × 1.13 (0.38 × 0.50 × 0.45 mm) was sealed in a thin-walled capillary under a nitrogen atmosphere. Data were collected on the diffractometer with graphite crystal monochromated molybdenum radiation. The diffracted intensities were measured by the ω-2θ scan technique in a manner similar to that described previously.[22] All independent reflections in one octant out to 2θ ≤ 50°(50°) were measured; 319 (322) were considered observed [I ≥ 3σ(I)]. The intensities were corrected for Lorentz and polarization effects. The intensities for *trans*-[WCl(N₂)(PMe₃)₄] were corrected for absorption.

Calculations were carried out with the SHELX system of computer programs.[23] The function w(|Fo|-|Fc|)² was minimized. No corrections were made for extinction. Atomic scattering factors for Mo(W), Cl, P, N and C were taken from Cromer and Waber;[24] those for H were taken from Ref. 25. The scattering for molybdenum (tungsten) was corrected for the real and imaginary components of anomalous dispersion using the values of Cromer and Liberman.[26]

The existence of 2 molecules in the unit cell required that the molybdenum atom reside or a 4̄2m site. A difference Fourier map phased on the molybdenum atom readily revealed the positions of the non-hydrogen atoms and the disorder of the Cl and N₂ ligands. The Cl and 2N atoms were given half weight occupancy factors of 0.125 each initially. In a attempt to deduce the nature of the disorder, the occupancy factors were refined in the following manner: one cycle of refinement of the Cl positional and thermal parameters, one cycle of refinement of the N positional and thermal parameters and one cycle of refinement of the occupancy factors (constrained so that the sum was 0.5). No significant changes in the R factor or the bond distances and angles was noted. The occupancy factors refined to within experimental error of 0.125, 0.125 even when starting values of 0.05 and 0.45 (and vice versa) were used. A second data set was collected on a crystal of *trans*-[MoCl(N₂)(PMe₃)₄] from a different preparation with similar results. For all final refinements reported here the occupancy factors were fixed at 0.125 for Cl and 0.125 for the N atoms and were not refined.

The positional parameters for *trans*-[MoCl(N₂)(PMe₃)₄] were used as the starting point in the refinement of the tungsten analogue. Least-squares refinement with isotropic thermal

Table 3. Final fractional coordinates for trans-[MoCl(N$_2$)(PMe$_3$)$_4$].

Atom	x/a	y/b	z/c
Mo	-0.5000	-0.5000	-0.5000
P	-0.3208(1)	-0.3208(1)	-0.4694(1)
Cl	-0.5000	-0.5000	-0.6965(7)
N(1)	-0.5000	-0.5000	-0.670(1)
N(2)	-0.5000	-0.5000	-0.7621(9)
C(1)	-0.2327(6)	-0.2327(6)	-0.5816(6)
C(2)	-0.1693(5)	-0.3735(5)	-0.3865(4)
H(1)[C(1)]	-0.1884	-0.1884	-0.5463
H(2)[C(1)]	-0.2963	-0.2034	-0.6303
H(3)[C(2)]	-0.2027	-0.4241	-0.3188
H(4)[C(2)]	-0.1192	-0.2989	-0.3662
H(5)[C(2)]	-0.1320	-0.4930	-0.4181

Table 4. Final fractional coordinates for trans-[WCl(N$_2$)(PMe$_3$)].

Atom	x/a	y/b	z/c
W	-0.5000	-0.5000	-0.5000
P	-0.3207(2)	-0.3207(2)	-0.4686(2)
Cl	-0.5000	-0.5000	-0.7004(8)
N(1)	-0.5000	-0.5000	-0.666(2)
N(2)	-0.5000	-0.5000	-0.763(2)
C(1)	-0.231(1)	-0.231(1)	-0.583(1)
C(2)	-0.1711(8)	-0.3738(9)	-0.3842(6)
H(1)[C(1)]	-0.1472	-0.1472	-0.5767
H(2)[C(1)]	-0.2989	-0.1823	-0.6162
H(3)[C(2)]	-0.1140	-0.3102	-0.3530
H(4)[C(2)]	-0.2011	-0.4225	-0.3203
H(5)[C(2)]	-0.1177	-0.4246	-0.4421

Table 5. Final fractional coordinates for trans-[MoCl$_2$(PMe$_3$)$_4$].

Atom	x/a	y/b	z/c
Mo	0.5000	0.5000	0.5000
P	0.3198(3)	0.3198(3)	0.4685(2)
Cl	0.5000	0.5000	0.3035(5)
C(1)	0.238(1)	0.238(1)	0.587(1)
C(2)	0.169(1)	0.368(1)	0.3878(8)
H(1)[C(1)]	0.1884	0.1884	0.5336
H(2)[C(1)]	0.2884	0.1720	0.6434
H(3)[C(2)]	0.2146	0.4033	0.3223
H(4)[C(2)]	0.1260	0.4528	0.4231
H(5)[C(2)]	0.1006	0.3119	0.3527

parameters led to $R = \Sigma\|F_0|-|F_c\|/\Sigma|F_0| = 0.058$ (M = Mo) and 0.068 (M = W). The methyl hydrogen atoms were located with the aid of a difference Fourier map; their positional and thermal parameters were not refined. Refinement of the nonhydrogen atoms with anisotropic temperature factors led to final R values of $R = 0.021$ for trans-[MoCl(N$_2$)(PMe$_3$)$_4$] (0.019, M = W) and Rw = 0.024 (0.023). The two nitrogen atom of trans-[WCl(N$_2$)(PMe$_3$)$_4$] could not be refined with anisotropic thermal parameters and were therefore isotropic in the final refinement. Refinement of the inverse configurations resulted in the final R values shown. Refinement prior to the conversion to the inverse configurations gave R = 0.032 (M = Mo) and 0.038 (M = W). A final difference Fourier showed no feature greater than 0.3 e-/Å^3.

The weighting scheme was based on unit weights; no systematic variation of $w(|F_0|-|F_c|)$ vs $|F_0|$ or $(\sin\theta)/\lambda$ was noted. The final values of the positional parameters are given in Tables 3 (M = Mo) and 4(M = W).[27] The thermal parameters and the observed and calculated structure factor amplitudes are given in supplementary Publications No. SUP 00000(00 pp).

X-Ray data collection, structure determination, and refinement for trans-[MoCl$_2$(PMe$_3$)$_4$].

Crystal data. C$_{12}$H$_{36}$Cl$_2$MoP$_4$, M = 471.2, tetragonal, $a = 9.675(5)$, $b = 12.311(6)$ Å, U = 1152.4 Å^3, Z = 2, D$_c$ = 1.36 gcm^{-3}, μ(MoKα) = 10.55 cm^{-1}, space group $I\bar{4}2$. The lattice parameters were determined from a least-squares refinement of the angular settings of 15 reflections ($2\theta > 40°$) accurately centred on the diffractometer. The data were obtained and treated as above.

The positional parameters for trans-[MoCl(N$_2$)(PMe$_3$)$_4$] were used as a starting point in the refinement of this compound. No evidence of any N$_2$ was located. Least-squares refinement with isotropic thermal parameters led to R = 0.065. The hydrogen atoms were located with the aid of a difference Fourier map and their parameters were not refined. Refinement of the nonhydrogen atoms with anisotropic thermal parameters led to R = 0.044. Refinement of the inverse configuration led to final values of R = 0.043 and R$_w$ = 0.051. The weighting scheme was based on unit weights; no systematic variation of $w(|F_0|-|F_0|)$ vs $|F_0|$ or $(\sin\theta)/\lambda$ was noted. The final positional parameters are given in Table 5. The thermal parameters and the observed and calculated structure factor amplitudes are given in Supplementary Publications No. SUP 00000 (00 pp).

REFERENCES

[1] See J. Chatt, J. R. Dilworth and R. L. Richards, *Chem. Rev.* 1978, **78**, 589 and references therein.
[2] A. J. L. Pombeiro, In *New Trends in the Chemistry of Nitrogen Fixation* (Edited by J. Chatt, L. M. da Camara Pina and R. L. Richards), Chap. 6, Academic Press, New York (1980).
[3] H. H. Karsch, *Angew. Chem.*, 1977, **89**, 57; *Angew. Chem. Int. Ed. Engl.* 1977, **16**, 56.
[4] E. Carmona, J. M. Marín, M. L. Poveda, J. L. Atwood, R. D. Rogers and G. Wilkinson, *Angew. Chem. Int. Ed. Engl.* 1982, **21**, 441; *Angew Chem. Suppl.* 1982, 1116–1120; E. Carmona, J. M. Marín, M. L. Poveda, J. L. Atwood and R. D. Rogers, accepted for publication in *J. Am. Chem. Soc.*

[5]J. L. Atwood, W. E. Hunter, E. Carmona and G. Wilkinson, *J. Chem. Soc., Dalton Trans.* 1980, 467.

[6]J. Chatt, *Chem. Tech.* 1981, 162.

[7]P. R. Sharp, personal communication and R. C. Chiu and G. Wilkinson, unpublished results.

[8]E. I. Stiefel, *Progr. Inorg. Chem.* 1977, **22**, 1, and references therein.

[9]G. J. Leigh, Chapter 8 of Ref. 2, and references therein.

[10]J. Chatt, R. A. Head, G. J. Leigh and C. J. Pickett, *J. Chem. Soc., Dalton Trans.* 1978, 1638.

[11]J. Chatt, G. J. Leigh, H. Neukomm, C. J. Pickett and D. R. Stanley, *J. Chem. Soc., Dalton Trans.* 1980, 121.

[12]E. Carmona and J. M. Marín, unpublished results.

[13]B. R. Davis and J. A. Ibers, *Inorg. Chem.* 1971, **10**, 578.

[14]K. W. Chiu, R. A. Jones, G. Wilkinson, A. M. R. Galas, M. B. Hursthouse and K. M. A. Malik, *J. Chem. Soc., Dalton Trans.* 1981, 1204.

[15]R. D. Rogers, J. L. Atwood and E. Carmona, unpublished results, and ref. 4 of this paper.

[16]L. Pauling, *The Nature of the Chemical Bond*, 3rd Edn., p. 256. Cornell University Press (1960).

[17]D. F. Evans, *J. Chem. Soc.* 1959, 2003.

[18]W. Wolfsberger and H. Schmidbaur, *Synth. React. Inorg. Metal Org. Chem.* 1974, **4**, 149.

[19]M. W. Anker, J. Chatt, G. J. Leigh and A. G. Wedd, *J. Chem. Soc., Dalton Trans.* 1975, 2639.

[20]P. R. Sharp and R. R. Schrock, *J. Am. Chem. Soc.* 1980, **102**, 1430.

[21]A. Nielson and G. Wilkinson, unpublished work.

[22]J. Holton, M. F. Lappert, D. G. H. Ballard, R. Pearce, J. L. Atwood and W. E. Hunter, *J. Chem. Soc., Dalton Trans.* 1979, 46.

[23]SHELX, a system of computer programs for X-ray structure determination by G. M. Sheldrick (1976).

[24]D. T. Cromer and J. T. Waber, *Acta Crystallogr.* 1965, **18**, 104.

[25]*International Tables for X-ray Crystallography*, Vol. IV, p. 72. Kynoch Press, Birmingham, England (1974).

[26]D. T. Cromer and D. Liberman, *J. Chem. Phys.* 1970, **53**, 1891.

[27]See paragraph at the end of paper regarding supplementary material.

TRANSITION METAL THIOCYANATES OF 5,7-DIMETHYL[1, 2, 4] TRIAZOLO [1,5-*a*]-PYRIMIDINE STUDIED BY SPECTROSCOPIC METHODS. THE CRYSTAL STRUCTURES OF DIAQUABIS (DIMETHYLTRIAZOLOPYRIMIDINE-*N*³) BIS (THIOCYANATO-*N*) CADMIUM(II) AND BIS (DIMETHYLTRIAZOLOPYRIMIDINE-*N*³) BIS (THIOCYANATO-*S*)-MERCURY(II)

J. DILLEN and A. T. H. LENSTRA
Departement Scheikunde, Universiteit Antwerpen (U.I.A.), Universiteitsplein 1, B-2610 Wilrijk, Belgium

and

J. G. HAASNOOT* and J. REEDIJK
Department of Chemistry, Gorlaeus Laboratories, State University Leiden, P.O. Box 9502, 2300 RA Leiden, The Netherlands

(Received 5 August 1982)

Abstract—5,7-Dimethyl[1,2,4]triazolo[1,5-*a*]pyrimidine (dmtp) is used as a ligand for divalent metal thiocyanates. Compounds of formula $M(NCS)_2(dmtp)_2(H_2O)_x$ are formed, with $x = 2$ for M = Mn, Fe, Co, Ni and Cd and $x = 0$ for M = Zn and Hg. Infrared and ligand field spectra are discussed. The crystal structures of compounds $Cd(NCS)_2(dmtp)_2(H_2O)_2$ and $Hg(SCN)_2(dmtp)_2$ are described. $Cd(NCS)_2(dmtp)_2(H_2O)_2$ is monoclinic, C2/c, $a = 15.823(8)$ Å, $b = 8.358(7)$ Å, $c = 17.650$ Å, $\beta = 102.82(5)°$, $Z = 4$, $d_c = 1.634$ Mg · m⁻³, $R = 4.8\%$ based on 2437 reflections. Cd^{2+} is (distorted) octahedrally coordinated by two N(3)-bonded ligands (*trans*-oriented) with Cd–N = 2.366(2) Å, two water molecules (*cis*) with Cd–O = 2.344(4) Å and two N-bonded NCS ions with Cd–N = 2.259(4) Å. The molecules are held together by Van der Waals forces and OH ... S hydrogen bonds (O ... S = 3.263(2) Å).

$Hg(SCN)_2(dmtp)_2$ is triclinic, P$\bar{1}$, $a = 10.343(7)$ Å, $b = 13.225(8)$ Å, $c = 8.060(6)$ Å, $\alpha = 97.15(4)°$, $\beta = 103.43(3)°$, $\gamma = 79.01(4)$, Z = 2, $d_c = 1.941$ Mg · m⁻³, R = 7.8% based on 3218 reflections. The (distorted) tetrahedral coordination around Hg^{2+} consists of two N(3)-bonded ligands with Hg–N = 2.386(8) and 2.427(8) Å and two S-bonded tiocyanate ions with Hg–S = 2.414(4) and 2.441(4) Å; the valence angles S–Hg–S and N–Hg–N are 134.9(1)° and 98.0(3)° respectively. The crystal packing is determined solely by Van der Waals forces. The ligand geometry appears to be the same for both compounds, within experimental error.

INTRODUCTION

The coordination chemistry of heterocyclic ligands is a field of increasing interest. The study of the imidazole-type ligands and that of the purines and pyrimidines is especially rapidly expanding, due to the realisation that the interaction between such ligands and metal ions plays an important rôle in a variety of biological systems.[1,2] Examples are the imidazole ligands in many copper, zinc and iron proteins, and the interaction between "essential" ions like Mg^{2+}, Zn^{2+} and "toxic" ions as Cd^{2+} and Hg^{2+} with nucleic acids.

Usually such heterocyclic bases have more than one donor atom available for coordination, so that no straightforward prediction of their coordination mode can be made. Previous studies[3–5] on 1,2,4-triazoles have shown that either one or two of the *N*-atoms coordinate to many metal ions.

Comparative binding studies on the naturally-occurring bases in DNA have shown that the purine ligands frequently use the (imidazole-type) N(7) atom, but that also coordination can occur at N(9) (the proton residing on N(7)), N(3) or N(1).[6,7] With adenine a bidentate bridge (coordination through N(3) and N(9)) has been found for several copper(II) compounds.[8,9] Pyrimidine bases are known to use N(3) for coordination to a large variety of metal ions.[6] In addition to the naturally-occurring nucleic acid bases pyrimidine, purine and derivatives, a number

of modified bases have been studied. For instance the 8-azapurines containing the 1,2,3-triazole nucleus are of interest because of their anti-neoplastic activity.[10]

5-Azapurines contain the 1,2,4-triazole nucleus, and have no substitutions at N(9) or N(7). Therefore, additional types of coordination may be expected To study the influence of steric effects upon the coordination of this type of ligands we have developed a synthetic program towards the coordination chemistry of (modified) 5-azapurines.

The numbering of these ring systems has often caused confusion, because of the special numbering in use for the purine derivatives. In this paper we will use the IUPAC[11] numbering as depicted in Fig. 1.

Because of our earlier experience with thiocyanate salts[3–5] and because of their ambidentate character (both N and S coordination can occur) and the easy crystallisation of their coordination compounds, this first study
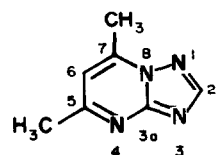
Fig. 1. 5,7-Dimethyl[1,2,4]triazolo[1,5-*a*]pyrimidine following IUPAC ring numbering. In purine ring numbering the sequence 1–8 becomes: 7, 8, 9, 4, 3, 2, 1, 6, 5.

---

*Author to whom correspondence should be addressed.

Table 1. Crystal data of dmtp compounds

Compound	$Cd(NCS)_2(dmtp)_2(H_2O)_2$ (1)	$Hg(SCN)_2(dmtp)_2$ (7)
Empirical formula	$CdC_{16}H_{20}N_{10}O_2S_2$	$HgC_{16}H_{16}N_{10}S_2$
Molecular weight	560.9	613.1
Space group	C2/c, monoclinic	$P\bar{1}$ triclinic
Cell constants	a=15.823(8) Å	a=10.343(7) Å
	b= 8.358(7) Å	b=13.225(8) Å
	c=17.650(8) Å	c=8.060(6) Å
	α= 90°	α= 97.15(4)°
	β=102.82(5)°	β=103.43(3)°
	γ= 90°	γ= 79.01(4)°
Packing	Z = 4	Z = 2
Density	d_{calc}=1.634 Mg.m^{-3}	d_{calc}=1.941 Mg.m^{-3}
	d_{obs}=1.63 Mg.m^{-3}	d_{obs}=1.94 Mg.m^{-3}
Data collection	θ < 28°	θ < 25°
No of reflections measured	2921	3668
No of reflections used	2437	3218
Residual (R)	0.048	0.073

deals with the transition-metal(II) thiocyanates of the new ligand 5,7-dimethyl[1,2,4]triazolo[1,5-a]pyrimidine (abbreviated dmtp) (Fig. 1). In the case of monodentate coordination, bonding through N(3) would be expected for steric reasons, but bidentate coordination through N(3) and N(4) (chelating), or through N(1) and N(3) thereby polynucleating, cannot be excluded.

In the present paper both the synthesis and characterisation of the new compounds are described. Two crystal structure determinations were performed to obtain unambiguous evidence about the coordination of dmtp.

EXPERIMENTAL

The ligand dmtp was prepared according to the method of Bülow and Haas[12] from pentanedion-2,5 and 3-amino-1,2,4-triazole.

Metal thiocyanates were prepared *in situ* by metathesis from hydrated metal nitrates and two equivalents of ammonium thiocyanate in water. The hydrated dmtp compounds were prepared by mixing the metal thiocyanate solutions (2 mmol in 20 ml of water) with a dmtp solution (4 mmol in 20 ml of water). All compounds crystallise within several hours. The anhydrous zinc and mercury compounds are rather insoluble in water. Therefore, they were prepared from commercial metal thiocyanate and dmtp in acetone solutions. Yields were generally better than 95%.

Doping of Cu^{2+} compound and of Co^{2+} in the Zn^{2+} compound was effected by the addition of 3–5% of Cu^{2+} or Co^{2+} in the form of their thiocyanates to the solutions of Cd^{2+} and Zn^{2+} respectively prior to crystallisation.

X-Ray powder diffractograms, taken on a Philips diffractometer, showed all hydrates to be mutually isomorphous.

Ligand field spectra were recorded at room temperature on a Beckman DK2-A UV-VIS-NIR spectrophotometer, in the solid state, by means of the diffuse reflectance technique.

Infrared spectra were taken on a Perkin–Elmer model 580 IR spectrophotometer as nujol mulls between KRS-5 and polythene (below 400 cm^{-1}) windows and as CsCl discs (concentration about 1%).

The cadmium and mercury compounds were recrystallised respectively from water and acetone. Monocrystals were grown easily from the solutions by cooling slowly to room temperature. For both compounds a monocrystal suitable for X-ray analysis was found.

Reflections for crystals were measured on an Enraf Nonius CAD4 diffractometer, using Mo-K$_\alpha$ radiation and a graphite monochromator. The data were corrected for Lorentz and polarisation effects, but absorption nor extinction corrections were applied. Table 1 shows the relevant crystallographic data.

The structure of compound 1 was partly solved using MUL-TAN.[13] The remainder of the atoms were found using conventional (difference) Fourier techniques. Some hydrogen atoms were placed on calculated positions.

To determine the structure of 7, only Patterson and (difference) Fourier techniques were applied.

For both molecules reflections with $I > 2\sigma(I)$ were used in the refinement, employing the Gauss–Seidel block method.[4] Counting statistics served as a basis for the weighting scheme.

During the refinement, the temperature factors of all hydrogen atoms were held fixed.

For 1 the space coordinates of the hydrogen atoms of one methyl group were fixed. No coordinates of hydrogen atoms were refined for 7. All bond distances and valence angles containing hydrogen atoms appeared to have physically realistic values.

The final residuals, defined as $R = [\Sigma w(|F_o| - |F_c|)^2/\Sigma w|F_o|^2]^{1/2}$ are shown in Table 1. Lists of structure factors, fractional coordinates and anisotropic thermal parameters have been deposited as Supplementary Material with the Editor, from whom copies are available on request. Atomic coordinates have also been deposited with the Cambridge Crystallographic Data Centre.[15] The atoms are numbered as given in Figs. 2 and 3.
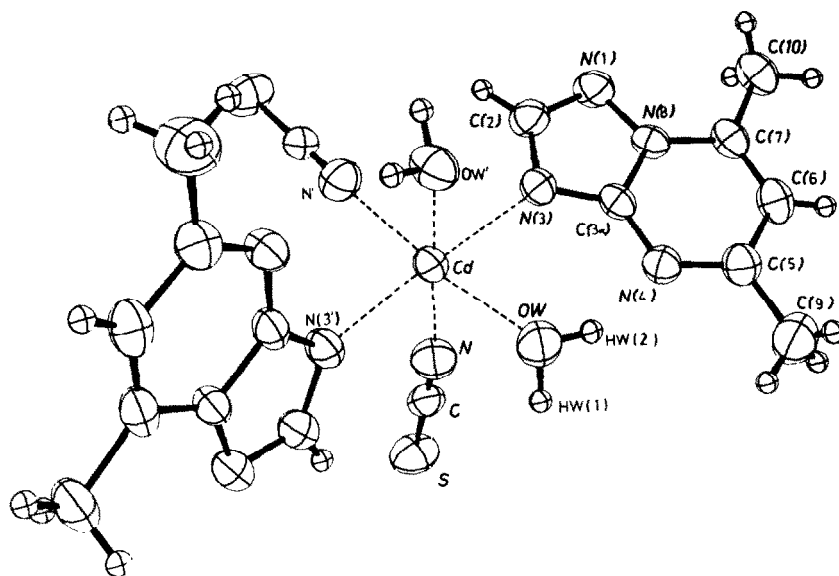
Fig. 2. ORTEP-drawing and numbering of atoms for $Cd(NCS)_2(dmtp)_2(H_2O)_2$.
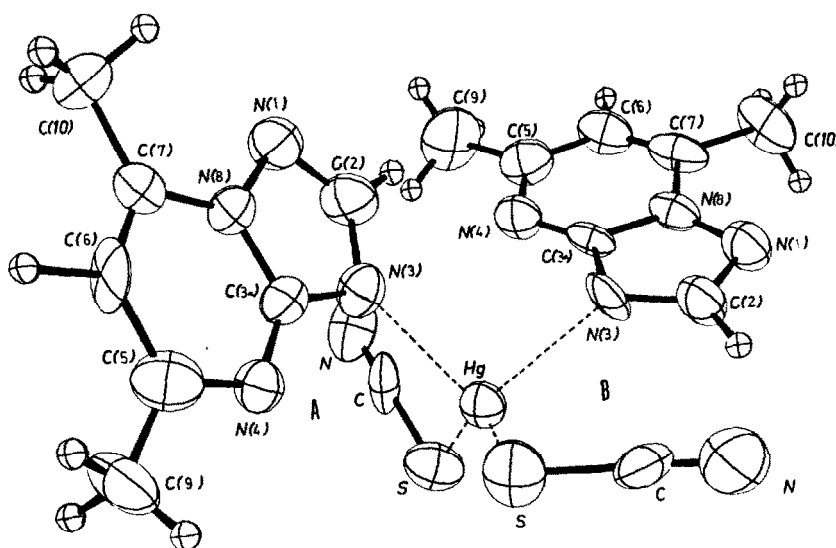
Fig. 3. Perspective view and atom numbering for $Hg(SCN)_2(dmtp)_2$.

RESULTS AND DISCUSSION

General

Table 2 lists the compounds prepared together with their colours, relevant elemental analysis and powder diffraction types. Because of the mutual isomorphism, C, H and N analyses were determined only in one case. All compounds appear to be stable in air upon standing. With copper(II) thiocyanate several types of crystals were found, which will be the subject of future investigations.

For the characterisation several spectroscopic techniques were used, which will be described below.

Ligand field spectra

The ligand field spectra of the hydrated compounds could be interpreted on the basis of an averaged octa-hedral environment for the central metal ion. No clear splittings of the bands were observed, so that deviations from octahedral symmetry must be small. On the other hand low-symmetry splittings in distorted octahedral complexes are known to be small in case of a *cis* geometry of the weakest ligands[16] (in this case H_2O). Because of the presence of three different kinds of ligands, the symmetry must be C_{2v} or lower.

In Table 3 the experimental values of the band maxima of these compounds are listed, including the copper-doped cadmium compound (8) and the cobalt-doped zinc compound (9). The spectrum of (9) was interpreted on the basis of a distorted tetrahedral symmetry for the central metal ion.

Dq and B parameter values were calculated in accordance with the assignment given.[16-18] The Dq values

Table 2. Compounds of formula $M(NCS)(dmtp)_2(H_2O)_x$, colours, analyses and X-ray diffraction types

			metal analyses		
nr.	compound	colour	found	calc.	X-ray type
1	$Cd(NCS)_2(dmtp)_2(H_2O)_2$	white	20.1	20.0	A
2	$Mn(NCS)_2(dmtp)_2(H_2O)_2$	white	11.2	10.9	A
3	$Fe(NCS)_2(dmtp)_2(H_2O)_2$	yellow	11.4	11.1	A
4	$Co(NCS)_2(dmtp)_2(H_2O)_2$	red	11.8	11.6	A *
5	$Ni(NCS)_2(dmtp)_2(H_2O)_2$	blue	11.4	11.6	A
6	$Zn(NCS)_2(dmtp)_2$	white	13.9	13.7	B
7	$Hg(SCN)_2(dmtp)_2$	white	31.8	32.7	C
8	3% Cu-dope in <u>1</u>	yellow	–	–	A
9	3% Co-dope in <u>6</u>	blue	–	–	B

*C, H and N analyses for this compound: found (calc.) 37.5 (37.9),

4.1 (4.0) and 27.3 (27.6) %, respectively.

Table 3. Ligand field spectra of $M(NCS)_2(dmtp)_2(H_2O)_x$ (x = 2, 0). Band maxima in 10^3 cm^{-1}, Dq and B values in cm^{-1}

	Compound	Band maxima	Assignment†	Dq*	B*
(2)	$Mn(NCS)_2(dmtp)_2(H_2O)_2$	17.4	$^4T_{1g} \leftarrow {}^6A_{1g}$		
		20.6	$^4T_{2g} \leftarrow {}^6A_{1g}$		
		24.4	$^4A_{1g}, {}^4E_g \leftarrow {}^6A_{1g}$		
(3)	$Fe(NCS)_2(dmtp)_2(H_2O)_2$	10.2 sh			
		10.9	$^5E_g \leftarrow {}^5T_{2g}$		
(4)	$Co(NCS)_2(dmtp)_2(H_2O)_2$	9.05	$^4T_{2g}(F) \leftarrow {}^4T_{1g}$		
		20.0	$^4T_{1g}(P) \leftarrow {}^4T_{1g}$	990	810
(5)	$Ni(NCS)_2(dmtp)_2(H_2O)_2$	9.7	$^3T_{2g}(F) \leftarrow {}^3A_{2g}$		
		16.4	$^3T_{1g}(F) \leftarrow {}^3A_{2g}$		
		26.5	$^3T_{1g}(P) \leftarrow {}^3A_{2g}$	970	920
(8)	$(Cu, Cd)(NCS)_2(dmtp)_2(H_2O)_2$	12.6	$^2T_{2g} \leftarrow {}^2E_g$		
(9)	$(Co, Zn)(NCS)_2(dmtp)_2$	8.9	$^4T_1(F) \leftarrow {}^4A_2$		
		16.9	$^4T_1(P) \leftarrow {}^4A_2$	530	670

*Calculated for (4) according Ref. 17; for (5) and (9) according Ref. 18.
†Assignment according to octahedral geometry for (2–8), according to T_d symmetry for (9).

show that dmtp can be placed near imidazole in the spectrochemical series. For instance, using 960 cm^{-1} for Dq of $[Ni(NCS)_6]^{4-}$[19], 860 cm^{-1} for $[Ni(H_2O)_6]^{2+}$[20] and the 1080 cm^{-1} value of $[Ni(imidazole)_6]^{2+}$[21], the rule of average environment calculates Dq for 5 to be 965 cm^{-1}, in accordance with the experimental value of 970 cm^{-1}.

The Dq and B values of 9 are consistent with N coordination of the thiocyanate anion in the zinc compound.

IR *spectra*

Anion vibrations. The anion parts of the IR spectra reflect the different coordination modes of the thiocyanate ion. Especially the positions of ν_{CN} and ν_{CS} in the mercury compound are clear indications for the S-bonding mode of the thiocyanate in this compound. The absorptions relevant to the thiocyanate ion are tabulated in Table 4. The $\nu_{CN} + \nu_{CS}$ combination bands have also been listed because they are helpful in assigning the often very weak ν_{CS} absorption.

The pseudo-tetrahedral zinc and mercury compounds

show split ν_{CN} absorptions in accordance with the C_{2v} symmetry. The other compounds in which the thiocyanate ions are *cis*-oriented show only one absorption. This indicates that only small electronic coupling occurs between the CN bonds in these compounds.[22]

Water vibrations. The absorptions associated with the

vibrations of the M–O⟨H H⟩ parts of the compounds 1–5

can be assigned easily and are given in Table 5. They are rather broad as is expected because all hydrogen atoms are involved in hydrogen-bond formation with non-coordinating nitrogen atoms of the dmtp ligands and sulphur atoms of the thiocyanates, as will be demonstrated in the section about the structure determination.

There is a distinct metal dependency, especially for ρ_{MOH_2} and $\rho^w_{MOH_2}$, which parallels the Irving and Williams sequence.[23] The highly coupled $\delta^{sym}_{OH_2}$ and ν_{MO} vibrations show, however, a much less pronounced metal dependency and moreover do not follow the Irving and

Table 4. Thiocyanate IR bands (cm^{-1}) of transition metal dmtp compounds

	Compound	$\nu_{CN} + \nu_{CS}$	$\nu_{CN}{}^{*}$	$2\delta_{NCS}$	ν_{CS}	δ_{NCS}
(1)	$Cd(NCS)_2(dmtp)_2(H_2O)_2$	2880	2082	942	789	468
(2)	$Mn(NCS)_2(dmtp)_2(H_2O)_2$	2886	2090	955	795	476
(3)	$Fe(NCS)_2(dmtp)_2(H_2O)_2$	2885	2092	957	792	476
(4)	$Co(NCS)_2(dmtp)_2(H_2O)_2$	2900	2102	954	796	475
(5)	$Ni(NCS)_2(dmtp)_2(H_2O)_2$	2905	2110	955, 950	791	474
(6)	$Zn(NCS)_2(dmtp)_2$	2925	2108, 2083	950	846	483
(7)	$Hg(SCN)_2(dmtp)_2$	2922	2132, 2120	914, 879, 859	706, 699	456, 429

**C^{13}-isotopic satellites are not listed.

Table 5. IR bands (in cm^{-1}) of M–O⟨^H_H⟩ groups

	Compound	$\nu^{as}_{OH_2}$	$\nu^{sym}_{OH_2}$	$\delta^{sym}_{OH_2}$	$\rho^{rock}_{MOH_2}$	$\rho^{wag}_{MOH_2}$	ν_{MO}
(1)	$Cd(NCS)_2(dmtp)_2(H_2O)_2$	3355	3240	1685	685	650	463
(2)	$Mn(NCS)_2(dmtp)_2(H_2O)_2$	3370	3245	1688	695	645	464
(3)	$Fe(NCS)_2(dmtp)_2(H_2O)_2$	3370	3250	1690	723	660	466
(4)	$Co(NCS)_2(dmtp)_2(H_2O)_2$	3375	3255	1657	740	665	456
(5)	$Ni(NCS)_2(dmtp)_2(H_2O)_2$	3375	3258	1666	755	692	458

Williams sequence, but in fact show a decrease from iron to cobalt. This decreased metal dependency is attributed to lack of deformation in the structure on going from cadmium to nickel, which opposes the decrease of the radius of the metal ion. The relatively rigid structure held together by hydrogen bonds, tends to maintain the metal-ligand distances. This effect appears to be strongest for cobalt and nickel. The smaller force constants associated with this effect lower the wavenumbers of the metal-ligand vibrations.

This same effect is observed for the metal-nitrogen vibrations, (*vide infra*).

Metal–nitrogen vibrations. The metal–nitrogen vibrations, which are expected in the far-IR region below 350 cm^{-1}, show a clear metal dependency. An assignment is not given because the absorptions of metal-thiocyanate and metal-dmtp are expected to be rather close to each other and coupled. Moreover, three vibrations of the free ligand (at 312, 280 and 230 cm^{-1}) interfere and hamper an adequate discernment. It was found, however, that the order of the metal-dependent absorptions parallels the order of the metal–oxygen absorptions.

Description of molecular and crystal structures

In compound **1** the ligands form a pseudo-octahedral configuration around the central Cd^{2+} ion. The dmtp molecules are in *trans*-position to each other apparently as a result of steric effects. They form two parallel crossing layers with a plane-to-plane distance of 3.54 Å, which is about twice the Van der Waals radius of an aromatic π-system.[24] The thiocyanate ions are mutually *cis*-coordinated *via* their nitrogen atoms to the central ion.

The compound shows relatively strong hydrogen bonding between HW(1)[x, y, z]...S[$x+\frac{1}{2}$, $y-\frac{1}{2}$, z] with HW(1)...S = 2.41(4) Å, OW...S = 3.263(4) Å, OW...HW(1)...S = 161(4)° and HW(2)[x, y, z]...

N(4)[$\bar{x}$, y, $\frac{1}{2}-z$] with HW(2)...N(4) = 2.12(4) Å, OW...N(4) = 2.879 Å and OW...HW(2)...N(4) = 147(4)°.

The ligands of **7** form a very distorted tetrahedral configuration around the metal ion. As in **1** the rings form parallel layers with a distance of twice the Van der Waals radius of the π-system. There are no hydrogen bonding interactions in this compound. The most important bond distances and valence angles for **1** are listed in Table 6. Those for **7** are presented in Table 7.

As can be seen from Tables 6 and 7 and Figs. 2 and 3 the dmtp molecules coordinate in the same way for both

Table 6. Bond distances (Å) and valence angles (degrees) for $Cd(NCS)_2\text{-}(dmtp)_2(H_2O)_2$. Estimated standard deviations (2x) in parentheses

Cd–N(3)	2.366(2)	N(3)–Cd–(OW)	87.4(1)
Cd–OW	2.344(4)	N(3)–Cd–N	95.4(1)
Cd–N	2.259(4)	OW–Cd–N	172.4(1)
N(1)–N(8)	1.368(4)	N(8)–N(1)–C(2)	101.5(3)
N(1)–C(2)	1.318(4)	N(1)–C(2)–N(3)	116.2(4)
C(2)–N(3)	1.358(4)	C(2)–N(3)–C(3a)	103.6(3)
N(3)–C(3a)	1.333(4)	N(3)–C(3a)–N(4)	128.8(4)
C(3a)–N(4)	1.334(4)	N(3)–C(3a)–N(8)	108.1(3)
C(3a)–N(8)	1.376(4)	N(4)–C(3a)–N(8)	123.1(3)
N(4)–C(5)	1.322(4)	C(3a)–N(4)–C(5)	116.6(3)
C(5)–C(6)	1.421(6)	N(4)–C(5)–C(6)	121.7(4)
C(5)–C(9)	1.480(6)	N(4)–C(5)–C(9)	117.3(4)
C(6)–C(7)	1.350(6)	C(6)–C(5)–C(9)	121.1(4)
C(7)–N(8)	1.371(4)	C(5)–C(6)–C(7)	121.9(4)
C(7)–C(10)	1.482(4)	C(6)–C(7)–N(8)	114.8(3)
		C(6)–C(7)–C(10)	127.1(4)
N–C	1.146(6)	N(8)–C(7)–C(10)	118.1(4)
C–S	1.629(4)	N(1)–N(8)–C(3a)	110.6(3)
		N(1)–N(8)–C(7)	127.5(3)
		C(3a)–N(8)–C(7)	121.9(3)
		HW(1)–OW–HW(2)	98(4)
		S–C–N	173.5(4)

Table 7. Bond distances (Å) and valence angles (degrees) for Hg(SCN)$_2$(dmtp)$_2$. Estimated standard deviations (2x) in parentheses

Distances			Angles		
Hg–S(A)	2.447(4)		S(A)–Hg–S(B)	134.9(1)	
Hg–S(B)	2.421(4)		S(A)–Hg–N(3A)	98.6(2)	
Hg–N(3A)	2.38 (1)		S(A)–Hg–N(3B)	105.8(2)	
Hg–N(3B)	2.418(8)		S(B)–Hg–N(3A)	103.6(2)	
			S(B)–Hg–N(3B)	109.2(2)	
			N(3A)–Hg–N(3B)	98.2(3)	
	A	B		A	B
N(1)–N(8)	1.37(1)	1.37(1)	N(8)–N(1)–C(2)	111.7(9)	113.3(8)
N(1)–C(2)	1.32(1)	1.33(1)	N(1)–C(2)–N(3)	117(7)	115(7)
C(2)–N(3)	1.35(1)	1.35(1)	C(2)–N(3)–C(3a)	103.1(9)	106.2(9)
N(3)–C(3a)	1.37(1)	1.34(1)	N(3)–C(3a)–N(4)	127(1)	129(1)
C(3a)–N(4)	1.32(1)	1.29(1)	N(3)–C(3a)–N(8)	107(1)	104.7(9)
C(3a)–N(8)	1.36(1)	1.38(1)	N(4)–C(3a)–N(8)	126(1)	126.0(9)
N(4)–C(5)	1.32(1)	1.35(1)	C(3a)–N(4)–C(5)	116(1)	116(1)
C(5)–C(6)	1.45(1)	1.42(1)	N(4)–C(5)–C(6)	118(1)	122(1)
C(5)–C(9)	1.48(1)	1.49(1)	N(4)–C(5)–C(9)	121(1)	116(1)
C(6)–C(7)	1.30(1)	1.33(1)	C(6)–C(5)–C(9)	121(1)	122(1)
C(7)–N(8)	1.36(1)	1.40(1)	C(5)–C(6)–C(7)	128(1)	122(1)
C(7)–C(10)	1.45(1)	1.48(1)	C(6)–C(7)–N(8)	111(1)	116(1)
			C(6)–C(7)–C(10)	129(1)	129(1)
N–C	1.15(1)	1.16(1)	N(8)–C(7)–C(10)	120(1)	115(1)
C–S	1.65(1)	1.65(1)	N(1)–N(8)–C(3a)	111.7(9)	113.3(8)
			N(1)–N(8)–C(7)	125.7(9)	127.7(9)
			C(3a)–N(8)–C(7)	123(1)	119(1)
			S–C–N	117(1)	117(1)

compounds, i.e. through their N(3) atoms. The ligand geometry is the same for both compounds and there are no significant differences in bond lengths and angles within the ligands.

Comparing the coordination polyhedron around cadmium in 1 with those of other cadmium compounds with nucleic acid fragments it is seen that the Cd–N (ligand) distance of 2.366 Å is in the usually-observed range (2.32[25], 2.37[26] and 2.35 Å[27]) and quite normal for a Cd–N(sp^2) bondlength. The Cd–N(sp) distance to the thiocyanates is shorter, but lies in the range for other Cd–thiocyanates.[28–30] The Cd–O bond lengths of 2.344 Å too fall in the range found for related cadmium compounds: 2.24–2.34 Å.[26,28,31]

As is usually observed for mercury compounds, the SCN groups in 7 bind to the metal via the sulphur atom. The S–C and C–N bondlengths are normal. The Hg–S distances (2.447 and 2.421 Å) are well below the sum of the covalent radii of sulphur (1.04 Å) and tetrahedrally coordinated mercury(II) (1.48 Å).[32] They are among the shortest found so far for mercury(II) thiocyanates. Typical distances reported for Hg–SCN in tetrahedral units are between 2.48 and 2.58 Å.[33,34] The N–Hg–N angle (98°) is significantly below the tetrahedral angle value, while the S–Hg–S angle of 135° is much higher, tending to become linear. This again demonstrates a relatively strong covalent interaction between mercury and sulphur. As a consequence of this, the Hg–N bondlengths (2.38 and 2.42 Å) are relatively long when compared with other Hg–N bonds in mercury nucleic-base compounds.[35,36] The structure can best be compared with that of the compound 3Hg(SCN)$_2$2PyNO[37] in which mercury has a very distorted tetrahedral coordination. Here again a large S–Hg–S angle (156°) occurs

in combination with very short Hg–S bond distances (2.38 Å).

CONCLUDING REMARKS

The ligand dmtp has a clear preference for coordination through its N(3) atom in reactions with transition-metal thiocyanates. Its spectrochemical strength is comparable to that of imidazole. The thiocyanate ions coordinate via their N atom in compounds 1–6 and via S in 7 (the mercury compound).

The coordination polyhedra in 1–5 are distorted octahedra of two ligand N (trans), two thiocyanate N (cis) and two water O atoms. The zinc compound is tetrahedral, with two ligands and two thiocyanates. The coordination around mercury in 7 is distorted tetrahedral, composed of two ligands and two strongly covalent Hg–S bonds.

REFERENCES

[1] P. M. Colman, H. C. Freeman, J. M. Guss, M. Murata, V. A. Norris, J. A. M. Ramshaw and M. P. Venkatappa, Nature (London) 1978, 272, 319.

[2] E. T. Adman, R. E. Stenkamp, L. C. Sieker and L. H. Jensen, J. Mol. Biol. 1978, 123, 35.

[3] D. W. Engelfriet, W. den Brinker, G. C. Verschoor and S. Gorter, Acta Cryst. B 1979, 35, 2922.

[4] D. W. Engelfriet, G. C. Verschoor and W. den Brinker, Acta Cryst. B 1980, 36, 1554.

[5] G. Vos, J. G. Haasnoot and W. L. Groeneveld, Z. Naturforsch. 1981, 36b, 802.

[6] D. J. Hodgson, Prog. in Inorg. Chem. 1977, 23, 211.

[7] R. W. Gellert and R. Bau, *Metal Ions in Biological Systems* 1978, **8**, 1.

[8] M. A. Guichelaar and J. Reedijk, *Rec. Trav. Chim. Pays-Bas* 1978, **97**, 295.

[9] P. de Meester and A. Skapski, *J. Chem. Soc., Dalton*, 1972, 2400.

[10] L. L. Bennet, Jr. and J. A. Montgomery, *Methods in Cancer Research.* 1967.

[11] IUPAC, *Nomenclature of Organic Chemistry.* 1979 Edition, Section B, Rule B-3, 1979.

[12] C. Bülow and K. Haas, *Ber.* 1909, **42**, 4638.

[13] G. Germain, P. Main and M. M. Woolfson, *Acta Cryst. A* 1971, **27**, 368.

[14] R. A. Sparks, Least-squares tutorial. *Am. Crystallogr. Assoc. Meet.* Berkeley, CA. 1974.

[15] Cambridge Crystallographic Data Centre, University Chemical Laboratory, Cambridge, U.K.

[16] A. B. P. Lever, *Inorganic Electronic Spectroscopy*, p. 193. Amsterdam (1968).

[17] J. Reedijk, W. L. Driessen and W. L. Groeneveld, *Rec. Trav. Chim. Pays-Bas* 1969, **88**, 1095.

[18] E. König, *Structure and Bonding* 1971, **9**, 175.

[19] D. Foster and D. M. L. Goodgame, *Inorg. Chem.* 1965, **4**, 823.

[20] J. Reedijk, P. W. N. M. van Leeuwen and W. L. Groeneveld, *Rec. Trav. Chim. Pays-Bas* 1968, **87**, 129.

[21] J. Reedijk, *Rec. Trav. Chim. Pays-Bas* 1969, **88**, 1451.

[22] P. Gans, *Vibrating Molecules*, Chap. 9. London (1971).

[23] H. Irving and R. J. P. Williams, *J. Chem. Soc.* 1953, 3192.

[24] *CRC Handbook of Chemistry and Physics*, 60th Edn, D 194. Boca Raton, Florida (1980).

[25] E. A. H. Griffith and E. L. Amma, *J. Chem. Soc., Chem. Comm.* 1979, 1013.

[26] K. Aoki, *Acta Cryst. B*, 1976, **32**, 1454.

[27] L. G. Purnell, E. D. Estes and D. J. Hodgson, *J. Am. Chem. Soc.* 1976, **98**, 740.

[28] F. Bigoli, A. Braibanti, M. A. Pellinghelli and A. Tiripicchio, *Acta Cryst. B*, 1972, **28**, 962.

[29] M. Cannas, G. Carta, A. Cristini and G. Marongiu, *Inorg. Chem.* 1977, **16**, 228.

[30] L. Cavalca, M. Nardelli and G. Fava, *Acta Cryst.* 1960, **13**, 125.

[31] D. M. L. Goodgame, I. Jeeves, C. D. Reynolds and A. C. Skapski, *Nucl. Acids Res.* 1975, **2**, 375.

[32] D. Grdenic, *Quart. Rev.* 1965, **19**, 303.

[33] A. L. Beauchamp, L. Pazdernik and R. Rivest, *Acta Cryst. B*, 1976, **32**, 650.

[34] E. C. Aleya, G. Ferguson and R. J. Restivo, *J. Chem. Soc., Dalton*, 1977, 1845.

[35] N. B. Behrens, B. A. Cartwright, D. M. L. Goodgame and A. C. Skapski, *Inorg. Chim. Acta* 1978, **31**, L471.

[36] M. Authier-Martin, J. Hubert, R. Rivest and A. L. Beauchamp, *Acta Cryst.* 1978, **34**, 273.

[37] D. Grdenic, B. Kamenar, M. Sikirica and J. Vernic, *Cryst. Struct. Comm.* 1976, **5**, 833.

SYNTHESIS AND CHARACTERISATION OF NIOBIUM(V) AND NIOBIUM(IV) POLY(1-PYRAZOLYL)BORATES

LILIANE G. HUBERT-PFALZGRAF* and MITSUKIMI TSUNODA

Laboratoire de Chimie de Coordination, Université de Nice, Parc Valrose, 06034 Nice, France

Abstract—Reactions between Nb_2Cl_{10} or $NbCl_4$ and hydridotris and hydridobis(1-pyrazolyl)borate potassium salts were investigated in different ligand to metal molar ratios (R). Room or low temperature reactions between Nb_2Cl_{10} and the poly(1-pyrazolyl)borates in a $R = 1$ stoichiometry lead to niobium(V) ionic species such as $\{NbCl_5[HB(pz)_3]\}K$ and $\{NbCl_5[H_2B(pz)_2]\}K$. Reduction to niobium(IV) was observed if the preceding reactions were conducted at higher temperature or if R increased, and molecular species, which could generally also be obtained directly from $NbCl_4$, were then isolated. All the niobium(IV) molecular species: $Nb_2Cl_6[H_2B(pz)_3]_2$, $Nb_2Cl_6[H_2B(pz)_3]_2(pzH)_2$, $Nb_2Cl_4[HB(pz)_3]_4$, $Nb_2Cl_6[H_2B(pz)_2]_2(MeCN)_2$, $Nb_2Cl_5[H_2B(pz)_2]_3$, $Nb_2Cl_4[H_2B(pz)_2]_4$ and $Nb_2Cl_2[H_2B(pz)_2]_6$, were found to be diamagnetic in the solid as in solution. Their characterisation was achieved by microanalysis, molecular weight data, IR and ^1H spectroscopy.

INTRODUCTION

By virtue of their steric and electronic properties, poly(1-pyrazolyl)borates stabilize unusual coordination geometries and oxidation states.[1] The transition metal chemistry of the hydridotris(1-pyrazolyl)borate anion $[HB(pz)_3]^-$ ($pzH = C_3H_3N_2H$) is to some degree reminiscent of that of the cyclopentadienyl ion, while the hydridobis(1-pyrazolyl)borate anion $[H_2B(pz)_2]^-$ is more closely related to the β-diketonato ligands. The stabilizing effect of the $[HB(pz)_3]^-$ anion, which behaves as a η^3 or η^2 ligand, has for instance been exploited in making stable copper carbonyl[2] or molybdenum–nitrosyl[3] derivatives, as well as a variety of five-coordinated platinum compounds.[4] On the other hand, $M[H_2B(pz)_2]_2$ (M = Co, Ni, Cd, Zn...) derivatives appear as reducing agents in organic chemistry.[5] As part of a general project concerning the synthesis of molecular low-valent niobium derivatives, and because the polypyrazolylborate derivatives of group V metals were limited to $NbO(OMe)_2[HB(pz)_3]$[6] and $[H_2B(pz)_2]TaMe_3$,[7] we have investigated the reactions between niobium(V) and niobium(IV) chlorides and hydridotris and hydridobis potassium pyrazolylborate salts. Indeed, polypyrazolylborate ligands are known to be reducing agents towards early transition metal derivatives in high oxidation states.[8]

We now wish to report the synthesis and characterization in the solid and in solution of niobium(V) and niobium(IV) polypyrazolylborate derivatives $\{NbCl_5[HB(pz)_3]\}K$, $\{NbCl_4[HB(pz)_3]\}K$, $[Nb_2Cl_6[HB(pz)_3]_2$, $Nb_2Cl_6[HB(pz)_3]_2(pzH)_2$, $Nb_2Cl_4[HB(pz)_3]_4$, $\{NbCl_5[H_2B(pz)_2]\}K$, $Nb_2Cl_6[H_2B(pz)_2]_2$, $Me(N)_1$, $Nb_2Cl_5[H_2B(pz)_2]_3$, $Nb_2Cl_4[H_2B(pz)_2]_4$ and $Nb_2Cl_2[H_2B(pz)_2]_6$.

RESULTS AND DISCUSSION

Synthesis of niobium poly(1-pyrazolyl)borates

The formation of the products obtained by reacting Nb_2Cl_{10} or $NbCl_4$ with the potassium poly(1-pyrazolyl)borate salts $KHB(pz)_3$ or $KH_2B(pz)_2$ was of course influenced by the ligand to metal molar ratio R (varying from 1 to 4), but also, very drastically, by the course of

the reaction: solvent composition, reaction time, temperature, concentration. Schemes 1 and 2 summarize the various routes that allowed the isolation, despite complicated reactions, of hydridotrispyrazolylborate and hydridobispyrazolylborate niobium derivatives. Among the various solvents investigated (toluene, tetrahydrofuran, dichloromethane or acetonitrile) the two last-named, in pure form or as their mixtures, appear the most useful, as they generally allow an easy separation from the KCl precipitate, and avoid the formation of oxo derivatives, which was observed when THF was used. Acetonitrile behaves as an additional ligand when the coordination sphere is less crowded, and $Nb_2Cl_6[H_2B(pz)_2]_2(MeCN)_2$ was thus isolated.

As expected, the bulky poly(1-pyrazolyl)borate anions generally act as reducing agents towards $NbCl_5$, leading to niobium(IV) derivatives. In fact, niobium(V) compounds could only be isolated if the reaction between $NbCl_5$ and hydridotris or hydridobispyrazolylborate salts was conducted in a $R = 1$ *stoichiometry* and at low or room temperature. However, the niobium(V) derivatives obtained as major product in these conditions correspond to ionic species of formula $K\{NbCl_5[H_xB(pz)_{4-x}]\}$ (x = 1 or 2), insoluble in common organic solvents. For instance, the reaction between $NbCl_5$ and $KBH(pz)_3$ (R = 1) in MeCN at $-30°C$ leads to a precipitate of $K\{NbCl_5[HB(pz)_3]\}$ (58%), while a reduced molecular species, $Nb_2Cl_6[HB(pz)_3]_2$, was obtained from the mother liquor, but only in a low yield (17%). Evidence for the formation of ionic poly(1-pyrazolyl)borate derivatives has also been reported for uranium(IV)[9] or molybdenum(III).[10] The formation of niobium(IV) molecular complexes was favoured by proceeding at higher temperature, thus giving a KCl precipitate instead of a niobium potassium one. Finally, no molecular niobium(V) polypyrazolylborate complex could be obtained directly from $NbCl_5$, but we were able to isolate $NbCl_4[HB(pz)_3]$ by a smooth reoxidation of $Nb_2Cl_6[HB(pz)_3]_2$ formed *in situ*, using carbon tetrachloride for precipitation. It is noticeable that the hydridotrispyrazolylborate anion displays a stronger tendency to form ionic species with niobium, as compared to the hydridobis(1-pyrazolyl)borate ligand, and $\{NbCl_4[HB(pz)_3]\}K$ was also obtained from a 1:1 molar reaction between $NbCl_4(MeCN)_3$ and $KHB(pz)_3$ in

---

*Author to whom correspondence should be addressed.
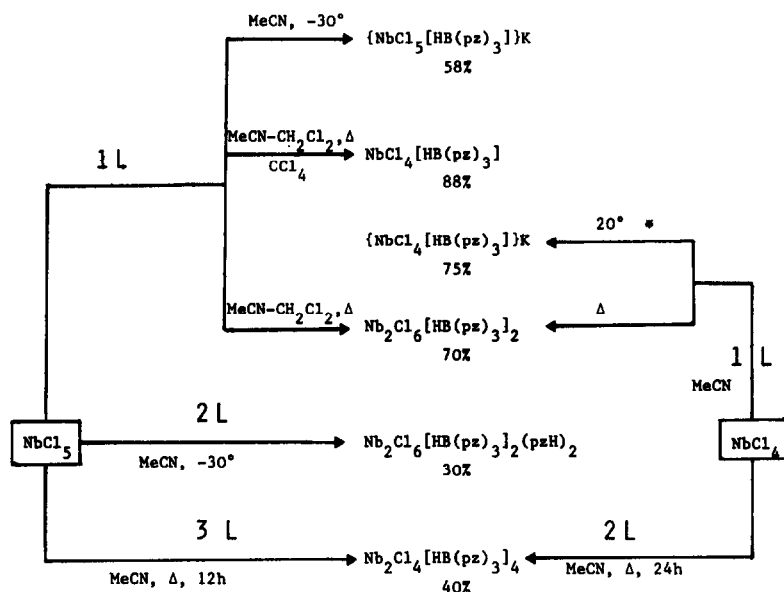
Scheme 1. Synthesis of niobium(V) and niobium(IV) hydridotris(1-pyrazoly)borates. (L = HB(pz)$_3^-$). *From NbCl$_4$(MeCN)$_3$ instead NbCl$_4$.
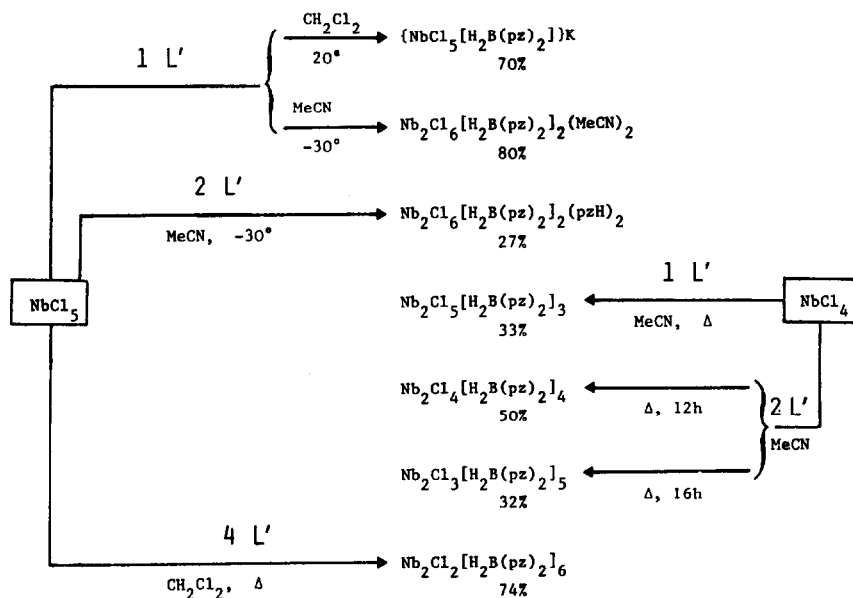
Scheme 2. Synthesis of niobium(V) and niobium(IV) hydridobis(1-pyrazolyl)borates. (L' = H$_2$B(pz)$_2^-$).

acetonitrile at room temperature. No ionic niobium(IV) product was obtained in the case of the hydridobis(1-pyrazolyl)borate salt. The conductivity measurements obtained for the ionic species on dimethylformamide solutions are as expected for 1:1 electrolytes.[11]

If more than one equivalent of polypyrazolylborate per metal (R > 1) was used, only molecular niobium(IV) derivatives were obtained. Another general observation is the fact that, by contrast to TiCl$_4$[8] for instance, and with regard to the behaviour of ZrCl$_4$[12] or UCl$_4$,[9] one can replace more than one chlorine per metallic center by a poly(1-pyrazolyl)borate ligand. As a result highly substituted products could be obtained. However, the yields

were often reduced by disproportionation reactions, which are favoured by the fact that the niobium(IV) species obtained are all dimeric, and small changes in the experimental procedures can lead to the isolation of several different products. For instance, the reaction between NbCl$_4$ and H$_2$B(pz)$_2$K (R = 2) in acetonitrile leads to Nb$_2$Cl$_4$[H$_2$B(pz)$_2$]$_4$ or Nb$_2$Cl$_3$[H$_2$B(pz)$_2$]$_5$ if the heating is maintained for a longer time.

Side reactions, involving the cleavage of the B–N bond, were observed, and products having pyrazole in the coordination sphere of the metal were then obtained. The pyrazole seems to interact strongly with the niobium moiety, and no displacement by a ligand such as

phenyldimethylphosphane could be achieved. Similar side reactions have already been reported in the case of the hydridotrispyrazolylborate ligand[13] as well as for the hydridobispyrazolylborate ligand.[14] Apparently these side reactions were favoured for the hydridotrispyrazolylborate anion, by the acidity of the pentahalides, and by low or room temperature reactions (a complete B–N cleavage of $HB(pz)_3^-$ was, for instance, observed in its 1:1 reaction with $TaCl_5$ at room temperature[15]). As a consequence, although highly substituted products analyzing for instance as $Nb_2Cl_2[HB(pz)_3]_6$ could be isolated, these highly crowded products are unstable in the solid and in solution, and appear (IR, NMR) as structurally different.

Characterization

The various products were characterized by elemental analysis (Table 1), magnetic susceptibility measurements, molecular weight data, IR (Table 2), mass and ^1H NMR spectroscopy (Table 3).

The IR spectra in the solid state of the isolated product show numerous absorptions due to the pyrazolyl groups. Three absorption regions corresponding respectively to the νBH, νNH and νNb–Cl stretching frequencies, are more useful for proposing a formula. First of all, the presence of νBH absorptions ranging from 2500 to 2300 cm^{-1} confirms that of poly(1-pyrazolyl)borate ligands in the coordination sphere and negates the occurrence of extensive B–N bond cleavage as well as the possibility of B–H–M interactions (which would strongly decrease the BH frequency, for instance to 2039 cm^{-1} in $[H_2B(pz)_2]PtMe_3$[16]). As generally observed, the νB–H stretching absorptions are always shifted to higher frequencies by coordination. The presence of additional absorptions in this region for $Nb_2Cl_6[H_2B(pz)_2]_2(MeCN)_2$ was attributed to acetonitrile (νC≡N 2318 and 2292 cm^{-1}). The presence of νNH absorptions around 3160 cm^{-1} for $Nb_2Cl_6[HB(pz)_3]_2(pzH)_2$ implies a neutral pyrazole ligand in the coordination sphere (νNH of the free ligand = 3540 cm^{-1}) and supports the occurrence of B–N cleavage reactions. It is noteworthy that no absorptions which could be attributed to νC–Cl vibrations, and thus to chlorination of the pyrazolyl ring, were observed (the absence of such products was also confirmed by the non-existence in the NMR spectra of singlets located around 7.5 ppm). The niobium–chlorine vibrations were found as expected below 400 cm^{-1}.[18]

Magnetic susceptibility measurements on the solid state show that all niobium(IV) derivatives are essentially diamagnetic. This suggests spin–spin interactions directly between the metallic centers or superexchange phenomena through bridging ligands in at least dinuclear units. For the most stable complexes such as $Nb_2Cl_6[H_2B(pz)_2]_2(MeCN)_2$, we were able to establish a dimeric character by vapour pressure osmometry on acetonitrile solutions ($M_{obs.}$ = 710; $M_{calc.}$ = 387.5). The good volatility of the niobium(IV) derivatives also allowed their characterization by mass spectrometry. The Nb$_2$ unit is generally retained in the gas phase. The formation of diamagnetic niobium(IV) poly(1-pyrazolyl)borate derivatives is surprising, since no counterparts have hitherto been found for niobium(IV) cyclopentadienyls or β-diketonates.[19] Bridging through chlorine is common for niobium chemistry, but polypyrazolylborates are also able to act as bridging ligands and should constitute an alternative. For instance, $[(pz)_2B(pz)_2]^-$ was assumed to ligate two Cp$_2$Ti moieties[8] and RX studies

Table 1. Analytical data

Compound	Colour	Microanalysis (%) Found (Calc)				
		C	H	N	B	Cl
{NbCl$_5$[HB(pz)$_3$]}K	pale yellow	21.15 (20.64)	2.00 (1.93)	15.68 (16.05)	2.21 (2.10)	33.08 (33.92)
{NbCl$_4$[HB(pz)$_3$]}K	light salmon	21.90 (22.18)	1.99 (2.07)	16.49 (17.22)	2.42 (2.26)	28.65 (29.16)
NbCl$_4$[HB(pz)$_3$]	dark red	23.32 (24.13)	2.17 (2.25)	17.68 (18.77)	2.25 (2.41)	33.05 (31.66)
Nb$_2$Cl$_6$[HB(pz)$_3$]$_2$(pzH)$_2$	fuschia red	29.09 (29.91)	2.75 (2.93)	22.62 (23.27)	2.51 (2.28)	21.79 (22.12)
Nb$_2$Cl$_6$[HB(pz)$_3$]$_2$	red brown	25.65 (26.21)	2.51 (2.44)	19.35 (20.39)	2.61 (2.62)	24.26 (25.79)
Nb$_2$Cl$_4$[HB(pz)$_3$]$_4$	red brown	36.74 (36.65)	3.42 (3.42)	28.25 (28.50)	3.37 (3.66)	11.73 (12.00)
{NbCl$_5$[H$_2$B(pz)$_2$]}K	yellow grey	13.64 (14.63)	1.82 (1.64)	11.07 (11.39)	2.35 (2.23)	35.30 (36.07)
Nb$_2$Cl$_6$[H$_2$B(pz)$_2$]$_2$(MeCN)$_2$	grey violet	25.38 (26.46)	2.94 (2.86)	17.66 (18.87)	2.69 (2.83)	28.33 (27.48)
Nb$_2$Cl$_6$[H$_2$B(pz)$_2$]$_2$(pzH)$_2$	buff color	25.00 (26.05)	2.82 (2.91)	19.66 (20.26)	2.41 (2.61)	25.08 (25.69)
Nb$_2$Cl$_5$[H$_2$B(pz)$_2$]$_3$	yellow brown	26.62 (26.90)	3.09 (3.01)	19.36 (20.92)	3.35 (3.79)	22.80 (22.10)
NB$_2$Cl$_4$[H$_2$B(pz)$_2$]$_4$	brown	32.86 (31.44)	3.58 (3.42)	24.02 (24.54)	4.53 (4.80)	14.72 (15.50)
Nb$_2$Cl$_2$[H$_2$B(pz)$_2$]$_6$	black	39.23 (37.94)	4.38 (4.25)	29.49 (29.51)	5.56 (5.68)	6.45 (6.23)

Table 2. IR spectroscopic data

Compound	IR (Nujol mulls)(cm^{-1})		Miscellaneous
	ν B-H	ν Nb-Cl	(ν NH or ν C≡N)
K BH(pz)$_3$	2435s, 2400w		
{NbCl$_5$[HB(pz)$_3$]}K	2518m, 2500sh	360sh, 350vs, 330s	
{NbCl$_4$[HB(pz)$_3$]}K	2520m	325s, 280m, 240m	
NbCl$_4$[HB(pz)$_3$]	2520w	340s, 305sh, 280sh	
Nb$_2$Cl$_6$[HB(pz)$_3$]$_2$(pzH)$_2$	2525s, 2500m, 2470sh	365sh, 340vs, 330sh, 310s	3160m, 3150m
Nb$_2$Cl$_6$[HB(pz)$_3$]$_2$	2510m, 2508m	300m, 290m, 250m, 225w	
Nb$_2$Cl$_4$[HB(pz)$_3$]$_4$	2480m	360s, 348vs, 340sh, 330m	
K BH$_2$(pz)$_2$	2440s, 2400s, 2375sh, 2275m		
{NbCl$_5$[H$_2$B(pz)$_2$]}K	2520w, 2500sh	380sh, 360s, 330vs, 290w	
Nb$_2$Cl$_6$[H$_2$B(pz)$_2$]$_2$(MeCN)$_2$	2510m, 2430m, 2400m, 2360sh	365sh, 330vs	2318w, 2292m
Nb$_2$Cl$_6$[H$_2$B(pz)$_2$]$_2$(pzH)$_2$	2510m, 2500m	360sh, 350vs, 340sh, 310vs	3140w
Nb$_2$Cl$_5$[H$_2$B(pz)$_2$]$_3$	2480s, 2440vs, 2420vs, 2360m	335vs, 310sh	
Nb$_2$Cl$_4$[H$_2$B(pz)$_2$]$_4$	2520sh, 2500sh, 2480m, 2420sh	365sh, 340vs, 335vs, 310sh	
Nb$_2$Cl$_2$[H$_2$B(pz)$_2$]$_6$	2480sh, 2420s, 2372m	360sh, 320vs, 310sh, 270s	

s : strong ; sh : shoulder ; m : medium ; w : weak.

on [HB(pz)$_3$]$_2$Cu have established that [HB(pz)$_3$]$^-$ presents two terminal pyrazolyl ligands (one to each copper) and one cross-wise bridging pyrazolyl.[20] Indeed, the value of the dihedral angle between pz groups in various polypyrazolylborate compounds varies greatly; it reflects the very flexible nature of the polypyrazolylborate ligands and their adjustable bite, which allows the adoption of a wide range of conformations for the B(pz)$_2$M ring.

The diamagnetic character of all niobium(IV) derivatives, like the convenient solubility of the molecular products (which increases with the degree of chlorine substitution), allowed us to gain structural information by using ^{1}NMR integration techniques (Table 3). The spectra were generally measured at room temperature on fresh solutions in deuterioacetonitrile (slow disproportionation reactions were sometimes observed). It should be mentioned that the nature and the quality of the solvent are very important for the NMR study of this class of complexes. Although all products are soluble in dichloromethane, its acidity favoured B–N cleavage as well as disproportionation reactions; on the other hand small amounts of water in acetonitrile again induced B–N cleavage (appearance of a NH peak while no νNH was detected by IR on the solid) as well as possible formation of B–OH bonds.[21] Therefore the ^{1}H NMR spectra were first used as a probe to confirm that the pyrazolylborate

anions are unchanged (presence of sets of two doublets and one triplet, in a 1:1:1 intensity ratio, which are always shifted to lower field with respect to the potassium salt). The spectra often display numerous resonances (Fig. 1), especially when the metal is highly substituted by poly(1-pyrazolyl)borate groups.

The spectra of the monomeric NbCl$_4$[HB(pz)$_3$] account for the presence in solution of one molecular species displaying equivalent pyrazolyl groups, as only one set of a couple of doublets (at 8.27 and 8.12 ppm) and one triplet (at 6.81 ppm; J = 2.6 Hz) are observed. The hydridotrispyrazolylborate ligand appears to behave as tridentate, the niobium atom therefore being heptacoordinated.. For all other hydridotrispyrazolylborate derivatives, which are dinuclear, niobium(IV) species, [HB(pz)$_3$]$^-$ acts as a bidentate, but exchange between coordinated and uncoordinated pyrazolyl was never observed. As also noted for instance for UCl$_2$[HB(pz)$_3$]$_2$,[9] the resonances of the uncoordinated pyrazolyl are generally more shielded, and slightly broader, than those of the coordinated one.

Thus the spectra of the solutions Nb$_2$Cl$_6$[HB(pz)$_3$]$_2$(pzH)$_2$ and Nb$_2$Cl$_6$[HB(pz)$_3$]$_2$ show only two sets of pyrazolyl resonances each in a constant 2:1 ratio. The main difference is due, for Nb$_2$Cl$_6$[HB(pz)$_3$]$_2$(pzH)$_2$, to the additional resonances of the coordinated pyrazole, which appears equivalent

Table 3. ^{1}H NMR (in CD$_3$CN at room temperature)

Compound	Concentration (10^{-3} molar)	δ in ppm ; J (in Hz) Pyrazolyl groups		Other ligands (pzH or MeCN)	Relative area of the various species
		doublets	triplets		
KHB(pz)$_3$	3	7.67, 7.57	6.17(2)		—
NbCl$_4$[HB(pz)$_3$]	0.5	8.27, 8.12	6.81(2.6)		a
Nb$_2$Cl$_6$[HB(pz)$_3$]$_2$	0.35	8.26, 8.06 / 8.15, 8.13	6.72(2) / 6.42(2) } 2:1*		a
Nb$_2$Cl$_6$[HB(pz)$_3$]$_2$(pzH)$_2$	0.25	8.13, 7.92 / 8.05, 8.07	6.38(2.1) / 6.40(2.2) } 2:1*	7.85(d), 7.83(d), 6.60(t) (2.2); 14.4 (NH)	(95% of the total area)
Nb$_2$Cl$_4$[HB(pz)$_3$]$_4$	0.4	8.08, 7.57 / 7.90, 7.51	6.35(2.1) / 6.36(2.1) } 2:1*		
KH$_2$B(pz)$_2$	2	7.62, 7.50	6.17(2)		—
Nb$_2$Cl$_6$[H$_2$B(pz)$_2$]$_2$	0.3	9.26, 8.07	6.81(2.6)	2.52	a
Nb$_2$Cl$_6$[H$_2$B(pz)$_2$]$_2$(pzH)$_2$	0.08	8.16, 8.00	6.41(2.2)	8.06(d), 8.04(d), 6.62(t) (2.7); 14.1(NH)	a
Nb$_2$Cl$_5$[H$_2$B(pz)$_2$]$_3$	0.03	7.88, 7.78 / 8.03, 7.92	6.39(2.2) / 6.32(2.2) } 2:1*		a
Nb$_2$Cl$_4$[H$_2$B(pz)$_2$]$_4$	0.3	8.14, 7.92 / 7.81, 7.57 / 8.09, 8.00 / 7.83, 7.63 / 8.14, 7.72	6.73(2.1) / 6.25(2.1) } 1:1* / 6.61(2.2) / 6.50(2.2) } 1:1 / 6.40(2.2)		(60% of the total area) **
Nb$_2$Cl$_2$[H$_2$B(pz)$_2$]$_6$	0.04	7.74, 7.56 / 7.66, 7.51	6.42(2) / 6.38(2.1) } 2:1		(80% of the total area)

* relative area ; ** see figure ; d : doublet ; t : triplet ; a : only one molecular species.
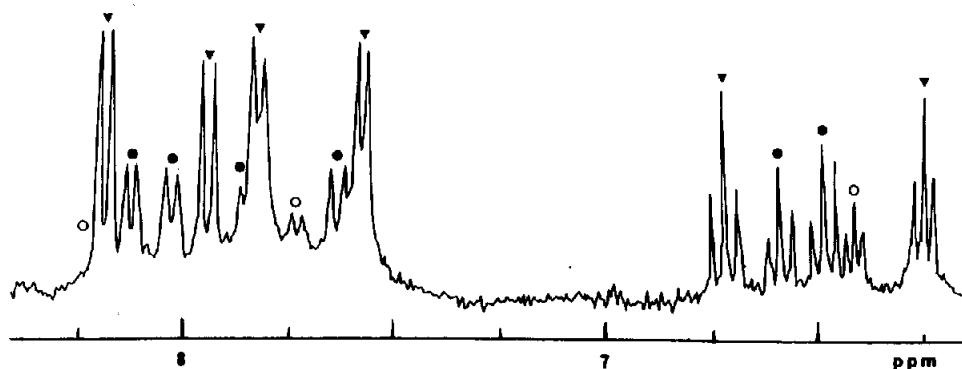
Fig. 1. ^{1}H NMR spectra of Nb$_2$Cl$_4$[H$_2$B(pz)$_2$]$_4$ in CD$_3$CN (0.03·10^{-3} M) at room temperature (peaks marked with the same symbol belong to the same species).

(δNH = 14.4 ppm; 7.85(d), 7.83(d), 6.60(t); J = 2.2 Hz). These data are in agreement with the presence of a single molecular species in each solution. The pattern of the pyrazole resonances indicates that the heterocycle functions as a monohapto neutral ligand, via the 2-N atom, as previously observed.[1,22] The most probable structure would be isomer A—the metal center being hexacoordinated—for Nb$_2$Cl$_6$[HB(pz)$_3$]$_2$. For Nb$_2$Cl$_6$[HB(pz)$_3$]$_2$-(pzH)$_2$, species having bridging or chelating η^2-hydridotrispyrazolylborates (four isomers for each one) are possible, but only one isomer is detected in its solution.

A
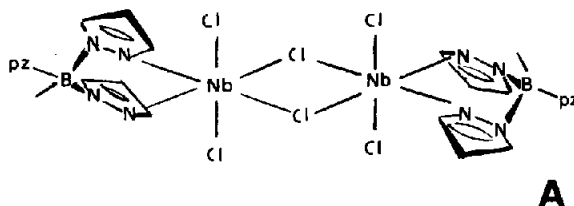
One molecular species mainly (95% of the total peaks area) is found for the solutions of freshly prepared Nb$_2$Cl$_4$[HB(pz)$_3$]$_4$. That species displays only two types of pyrazolyl groups, in a 2:1 area ratio, thus suggesting equivalent but η^2-hydridotrispyrazolylborate ligands, and isomer B appears as the most probable. Other species in dynamic equilibrium, but not yet determined, were found for the solutions prepared from Nb$_2$Cl$_4$[HB(pz)$_3$]$_4$ more than two months old.

B
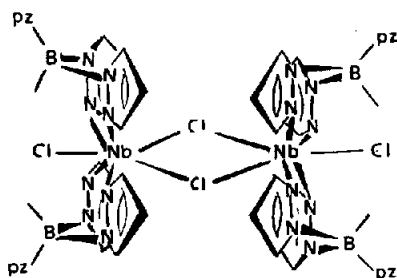
The spectra of Nb$_2$Cl$_6$[H$_2$B(pz)$_2$]Y$_2$ (Y = MeCN or pzH) display only one type of signal for the polypyrazolylborate [doublets at 9.26, 8.07 and 8.17, 8.00 ppm; triplets at 6.81 and 6.41 ppm (J = 2.6 and 2.2 Hz) respectively]. The presence of MeCN in the coordination sphere of Nb$_2$Cl$_6$[H$_2$B(pz)$_2$]$_2$(MeCN)$_2$ was confirmed by a singlet at 2.53 ppm. The pyrazole ligand of

Nb$_2$Cl$_6$[H$_2$B(pz)$_2$]$_2$(pzH)$_2$ is characterized by a deshielded NH signal (δ = 14.1 ppm), as two doublets at 8.06 and 8.04 ppm and one triplet at 6.62 ppm (J = 2.7 Hz) in a 1:2 intensity ratio (by comparison with the pyrazolyl signals). NMR monitoring shows that Nb$_2$Cl$_6$[H$_2$B(pz)$_2$]$_2$(pzH)$_2$ could not be obtained by ligand exchange from Nb$_2$Cl$_6$[H$_2$B(pz)$_2$](MeCN)$_2$ at room temperature. The spectra of Nb$_2$Cl$_6$[H$_2$B(pz)$_2$]$_2$Y$_2$ account for the presence in solution of a single molecular species in which the pyrazolyl groups appear equivalent, as are the neutral ligands acetonitrile or pyrazole. These data are similar to those for Nb$_2$Cl$_6$[HB(pz)$_3$]$_2$(pzH)$_2$, and the geometry of the Nb$_2$Cl$_6$[H$_2$B(pz)$_2$]$_2$Y$_2$ adducts is probably closely related to that of the former compound, in which the [HB(pz)$_3$]$^-$ ligand functions as a bidentate like [H$_2$B(pz)$_2$]$^-$.

Only one molecular species is also detected in the solutions of Nb$_2$Cl$_5$[H$_2$B(pz)$_2$]$_3$, the polypyrazolylborate groups being inequivalent in a 2:1 intensity ratio (Table 3). Only one isomer C fits these spectroscopic data:

C
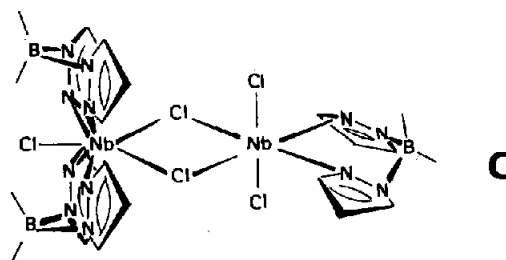
Contrary to the preceding compounds, the spectra of Nb$_2$Cl$_4$[H$_2$B(pz)$_2$]$_4$ and Nb$_2$Cl$_2$[H$_2$B(pz)$_2$]$_6$ depend on the dilution, thus suggesting the presence of different molecular species, but no indications of disproportionation reactions were found, and we therefore favour the presence of geometrical isomers in equilibrium. The spectra are often complicated as a result of resonances overlapping. For instance, the spectra of Nb$_2$Cl$_4$[H$_2$B(pz)$_2$]$_4$ (Fig. 1) consist of 5 sets of pyrazolyl signals, which can be attributed (on the basis of their constant relative area for various concentrations) to three molecular species. Two species (one being always predominant—60% for a 0.3 10^{-3} molar solution) display non-equivalent hydridobispyrazolylborate ligands in a 1:1 intensity ratio. Three isomers (D, E, F) are compatible with these data, but molecular models show that the coordination sphere is less crowded for isomer D than for E or F.
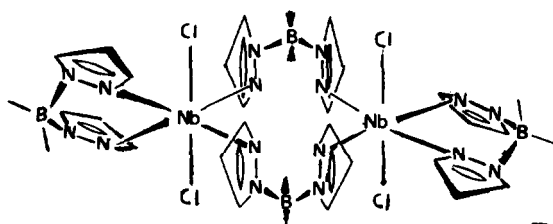
D
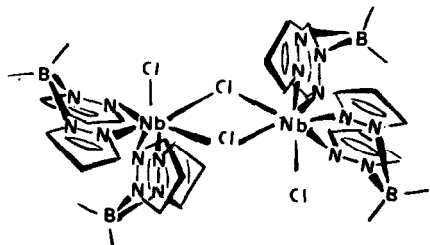
E
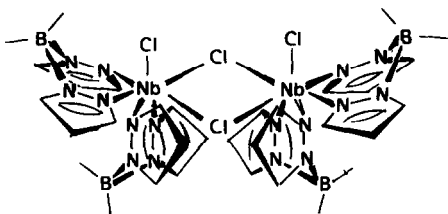
F

Two molecular species are detected for the solutions of Nb$_2$Cl$_2$[H$_2$B(pz)$_2$]$_6$. The main species (80% for a 0.4 10^{-3} molar solution) presents two types of [H$_2$B(pz)$_2$]$^-$ ligand (2:1 intensity ratio). Isomer G in which the metal is heptacoordinated should be the most favoured for steric considerations, but other isomers having only chelating [H$_2$B(pz)$_2$]$^-$ groups, and for which the metal is octacoordinated, may be possible. Note that high coordination numbers are also common for niobium(IV) β-diketonates.[19]
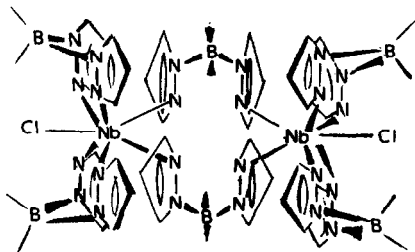
G

EXPERIMENTAL

All manipulations were conducted under dry de-oxygenated argon, using Schlenk tubes and vacuum-line techniques. The solvents were carefully distilled over the standard drying reagents and de-oxygenated. NbCl$_4$,[23] NbCl$_4$(MeCN)$_3$[24] and the polypyrazolylborate potassium salts[25] were synthesised as described in the literature. IR spectra were recorded as nujol mulls on a Perkin–Elmer 577 spectrometer. The NMR spectra were obtained on a WH-90 Bruker spectrometer operating in the Fourier transform mode. Molecular weight data were measured on a Knauer pressure osmometer. The mass spectra (VG Micromass 70-70 spectrometer) and the microanalysis data were effected by the Service Central de Microanalyses du CNRS.

Synthesis of {NbCl$_5$[HB(pz)$_3$]}K

A solution of KBH(pz)$_3$ (1.55 g, 6.13 mmol) in 15 ml MeCN was added to a solution of NbCl$_5$ (1.66 g, 6.14 mmol) in 60 ml of MeCN maintained at −30°C. Precipitation started immediately. Stirring was continued for about one hour and the temperature raised slowly to room temperature. The reaction mixture was filtered off. After washing with CH$_2$Cl$_2$ and vacuum drying, 1.58 g (58%) of a pale yellow powder of {NbCl$_5$[HB(pz)$_3$]}K was obtained. (10^{-3} M in DMF; Λ = 75 ohm^{-1}·cm^2·mole^{-1}).

Synthesis of {NbCl$_4$[HB(pz)$_3$]}K

A solution of KBh(pz)$_3$ (0.85 g, 3.36 mmol) in 20 ml MeCN was added to a solution of NbCl$_4$(MeCN)$_3$ (1.21 g, 3.38 mmol) in 15 ml MeCN at room temperature. A slightly exothermic reaction occurred immediately, with formation of a precipitate. After 16 h stirring, 1.22 g (75%) of {NbCl$_4$[HB(pz)$_3$]}K in the form of a powder was isolated by filtration. (1.5 10^{-3} M in DMF; Λ = 72 ohm^{-1}·cm^2·mole^{-1}).

Synthesis of NbCl$_4$[HB(pz)$_3$]

A suspension of KBH(pz)$_3$ (0.71 g, 2.83 mmol) in 10 ml CH$_2$Cl$_2$ was slowly added to a solution of NbCl$_5$ (0.73 g, 2.69 mmol) in 24 ml of a mixture of CH$_2$Cl$_2$ and MeCN (4:1) at room temperature. The yellow solution rapidly became cloudy and dark orange. The reaction was completed by refluxing for 18 h. The reaction mixture was filtered at room temperature, the filtrate evaporated to dryness and extracted with CH$_2$Cl$_2$. Precipitation was obtained by adding CCl$_4$; 0.98 g (88%) of red crystals of NbCl$_4$[HB(pz)$_3$] were obtained.

Synthesis of Nb$_2$Cl$_6$[HB(pz)$_3$]$_2$(pzH)$_2$

A solution of KBH(pz)$_3$ (1.88 g, 7.34 mmol) in 15 ml MeCN was slowly added to a solution of NbCl$_5$ (1 g, 3.74 mmol) in 50 ml MeCN at −30°C. Stirring was maintained for 12 h at −30°C, and the insoluble product was then removed by filtration. During the concentration of the filtrate, crystallisation started and was completed by storing at −30°C for 2 days. Finally 0.91 g (30%) of red crystals of Nb$_2$Cl$_6$[HB(pz)$_3$]$_2$(pzH)$_2$ were collected. Mass spectrometry (120°C, chemical ionisation) M = NbCl$_3$[HB(pz)$_3$](pzH) (M$_2$–pzH) (1%), M$_2$–2pzH (2%), Nb$_2$Cl[HB(pz)$_3$][H$_2$B(pz)$_2$] (10%), Nb$_2$[HB(pz)$_3$][H$_2$B(pz)$_2$] (23%), Nb[H$_2$B(pz)$_2$]$_2$ (5%), NbClN$_2$[HB(pz)$_3$] (15%), pzH (100%).

Synthesis of Nb$_2$Cl$_6$[HB(pz)$_3$]$_2$

A suspension of KHB(pz)$_3$ (1.51 g, 5.97 mmol) in 20 ml CH$_2$Cl$_2$ was slowly added to a solution of NbCl$_5$ (1.63 g, 6.05 mmol) in 60 ml of a CH$_2$Cl$_2$:MeCN (4:1) mixture, and the reaction medium was allowed to reflux for 12 h, giving a brown suspension; KCl was separated by filtration. The filtrate was concentrated to about 6 ml, and 1.789 (72%) of a reddish brown solid, Nb$_2$Cl$_6$[HB(pz)$_3$]$_2$ crystallised out and was separated by filtration. Mass spectrometry (70 eV, 150°C): [M = NbCl$_3$[BH(pz)$_3$]M (4%), M–Cl (46%), (M–Cl–$\frac{1}{2}$N$_2$) (32%), M–pzH (46%), M–pzH–N$_2$ (46%), NbCl$_2$(pz)$_2$ (72%), pzH (100%).

Synthesis of Nb$_2$Cl$_4$[HB(pz)$_3$]$_4$

A suspension of KBH(pz)$_3$ (1.75 g, 6.9 mmol) in 18 ml MeCN was slowly added to a stirred suspension of NbCl$_4$ (0.514 g, 2.19 mmol) in 34 ml MeCN at room temperature. The suspension became violet and then grey–green. The reaction was completed by refluxing 24 h and a dark red suspension was obtained. After cooling, the precipitate of KCl was separated by filtration and the filtrate evaporated to dryness. The residue was redissolved in CH$_3$CN and crystallisation was induced by adding CCl$_4$, and completed by leaving in the cold (−30°C). Finally, 0.45 g (35%) of dark red crystals of Nb$_2$Cl$_4$[HB(pz)$_3$]$_4$ were obtained.

Synthesis of {NbCl$_5$[H$_2$B(pz)$_2$]}K

Potassium hydridobispyrazolylborate (1.36 g, 7.25 mmol) in solution in 20 ml MeCN was added to a suspension of NbCl$_5$ (1.90 g, 7.04 mmol) in 40 ml CH$_2$Cl$_2$. An insoluble product formed immediately. The reaction was completed by stirring at room temperature for 12 h and refluxing for 1 h more. Filtration left 2.7 g (70%) of a grey–yellow powder. (0.8·10^{-1} M in DMF; Λ = 81 ohm^{-1}·cm^2·mole^{-1}).

A solution of KBH$_2$(pz)$_2$ (0.91 g, 4.89 mmol) in 15 ml MeCN was added to a solution of NbCl$_5$ (1.30 g, 4.81 mmol) in 50 ml MeCN at −30°C. The solution became brown–yellow, and then brown–green, and a precipitate appeared. Stirring was maintained at −30°C for 1 h and the reaction mixture was allowed to reach and stay at room temperature for 14 h. The precipitate was eliminated by filtration and washed with MeCN. The filtrate was concentrated to about 10 ml, a red–brown precipitate appeared and the crystallization was improved by storing alternately at −30° and −5°C. After 5 days, the mother liquor was separated by syringe. After washing with toluene and vacuum drying, 1.26 g (80%) of a grey–violet product were collected. Mass spectrometry (70 eV, 120°C) M = NbCl$_3$[H$_2$B(pz)$_2$](MeCN); M$_2$-MeCN (4%); M$_2$-2MeCN (8%), Nb$_2$Cl$_2$[H$_2$B(pz)$_2$]$_2$ (21%); Nb$_2$[H$_2$B(pz)$_2$]$_2$ (10%); NbClN$_2$[H$_2$B(pz)$_2$] (20%), pzH (100%).

Synthesis of Nb$_2$Cl$_6$[H$_2$B(pz)$_2$]$_2$(pzH)$_2$

KBH$_2$(pz)$_2$ (1.34 g, 7.20 mmol) in 15 ml MeCN was added to NbCl$_5$ (0.98 g, 3.6 mmol) in 50 ml MeCN at −30°C. Stirring was maintained for 2 h at −30°C and for 12 h at room temperature, giving a reddish brown suspension. The insoluble products were removed by filtration. Concentration of the filtrate to about 10 ml induced crystallisation which was improved by leaving at 0°C for 24 h. Filtration left 0.4 g (27%) of a buff colored solid, Nb$_2$Cl$_6$[H$_2$B(pz)$_2$]$_2$(pzH)$_2$. Mass spectrometry (70 eV, 150°C): M = NbCl$_3$[H$_2$B(pz)$_2$](pzH); M$_2$-pzH (1%); M$_2$-2pzH (4%), Nb$_2$Cl$_3$[H$_2$B(pz)$_2$]$_2$(pzH) 18%, Nb$_2$Cl$_2$[H$_2$B(pz)$_2$]$_2$ 15%, Nb$_2$[H$_2$B(pz)$_2$]$_2$(pzH) (11%), NbCl[H$_2$B(pz)$_2$](pzH) 12%, pzH (100%).

Synthesis of Nb$_2$Cl$_5$[H$_2$B(pz)$_2$]$_3$

A solution of KBH$_2$(pz)$_2$ (1.07 g, 5.74 mmol) in 30 ml MeCN was added to a suspension of NbCl$_4$ (1.35 g, 5.74 mmol) in 40 ml MeCN. After 2 h stirring at room temperature, the reaction mixture was refluxed for about 12 h. The KCl precipitate was separated by filtration and the yellow–brown filtrate concentrated to about 7 ml. A yellow solid started to precipitate, and the precipitation was imporved by adding a small amount of diethyl-ether. 0.76 g (33%) of yellow crystals of Nb$_2$Cl$_5$[H$_2$B(pz)$_2$]$_3$ were obtained.

Synthesis of Nb$_2$Cl$_4$[H$_2$B(pz)$_2$]$_4$

KBH$_2$(pz)$_2$ (1.72 g, 9.24 mmol) in 30 ml MeCN was added to a stirred suspension of NbCl$_4$ (1.08 g, 4.6 mmol) in 40 ml MeCN. The mixture was refluxed for about 12 h. The brown solution was separated from KCl by filtration and was concentrated to about 4 ml. Addition of diethyl-ether led to the crystallization of a brown solid, Nb$_2$Cl$_4$[H$_2$B(pz)$_2$]$_4$ (1.05 g, 50%). Mass spectrometry (70 eV, 150°C): Nb$_2$[H$_2$B(pz)$_2$]$_3$ (1%) Nb$_2$[H$_2$B(pz)$_2$]$_3$-½N$_2$ (2%), Nb$_2$[H$_2$B(pz)$_2$]$_2$(pz)Cl (3%), Nb$_2$[H$_2$B(pz)$_2$]$_2$H (2%), Nb$_2$(pzH)$_3$H (40%), NbClBN$_5$C$_6$H$_8$ (7%), pzH (100%).

A longer reaction time (16 h instead of 12 h) led to the isolation of Nb$_2$Cl$_3$[H$_2$B(pz)$_2$]$_5$.

Synthesis of Nb$_2$Cl$_2$[H$_2$B(pz)$_2$]$_6$

A solution of KBH$_2$(pz)$_2$ (2.22 g, 11.9 mmol) in 35 ml CH$_2$Cl$_2$ was added at room temperature to a suspension of NbCl$_5$ (0.77 g, 2.85 mmol) in 35 ml CH$_2$Cl$_2$. A brown suspension was obtained and the reaction was completed at reflux for 24 h. The KCl precipitate was eliminated by filtration. The filtrate was concentrated to about 5 ml; addition of pentane resulted in the formation of an oily precipitate; the mother liquor was eliminated by syringe. 1.2 g (74%) of a brown–black powder was obtained after drying under high vacuum.

The ionic products are air-stable in the solid state. Most of the

neutral products can be handled in the air for short periods, and their stability generally increases with the number of poly(1-pyrazolyl)borate groups per niobium, but the dinuclear species having an odd number of chlorine atoms remain highly air-sensitive. In solutions, all products are unstable in air.

The molecular products are insoluble in toluene, CCl$_4$, Et$_2$O, soluble but often unstable in CH$_2$Cl$_2$, more stable in MeCN. The ionic products were found to be insoluble in most organic solvents such as MeCN or acetone but slightly soluble in pyridine and in dimethylformamide.

REFERENCES

[1a] S. Trofimenko, *Chem. Rev.* 1972, **72**, 497; [b] S. Trofimenko, *Inorganic Compounds with Unusual Properties* (Edited by R. B. King), p. 289. Chemical Society, Washington (1976).

[2] C. S. Arcus, J. L. Wilkinson, C. Mealli, T. J. Marks and J. A. Ibers, *J. Am. Chem. Soc.* 1974, **96**, 7564.

[3a] J. A. McCleverty, A. E. Rae, I. Wolochowicz, N. E. Bailey and J. M. A. Smith, *J. Organometal. Chem.* 1979, **168**, C1; [b] J. A. McCleverty, D. Seddon, N. A. Bailey and N. W. Walker, *J.C.S. Dalton* 1976, 898.

[4] H. C. Clark and L. E. Manzer, *Inorg. Chem.* 1974, **13**, 1291, 1996.

[5] G. Paolucci, S. Cacchi and L. Cagliati, *J.C.S. Perkin* 1979, 1129.

[6] L. G. Hubert-Pfalzgraf and J. G. Riess, *Inorg. Chim. Acta* 1981, **47**, 7.

[7] D. H. Williamson, C. Santini-Scampucci and G. Wilkinson, *J. Organometal. Chem.* 1974, **77**, C25.

[8a] L. E. Manzer, *J. Organometal. Chem.* 1975, **102**, 167; [b] P. Burchill and M. G. H. Wallbridge, *Inorg. Nucl. Chem. Let.* 1976, **12**, 93.

[9] K. W. Bagnall, J. Edwards, J. G. H. du Preez and R. F. Warren, *J.C.S. Dalton* 1975, 140.

[10] M. Millar, S. Lincoln and S. A. Koch, *J. Am. Chem. Soc.* 1982, **104**, 288.

[11] W. J. Geary, *Coord. Chem. Rev.* 1971, **7**, 81.

[12] S. Asslani, R. Rahbarnoohi and B. L. Wilson, *Inorg. Nucl. Chem. Let.* 1979, **15**, 59.

[13a] J. K. Kouba and S. S. Wreford, *Inorg. Chem.* 1976, **15**, 2313; [b] N. F. Borkett and M. I. Bruce, *J. Organometal. Chem.* 1974, **65**, C51; [c] R. B. King and A. Bond, *J. Organometal. Chem.* 1972, **46**, C53.

[14] A. Bond and M. Green, *J. Chem. Soc.* (A), 1971, 682.

[15] L. G. Hubert-Pfalzgraf, unpublished results.

[16] R. B. King and A. Bond, *J. Am. Chem. Soc.* 1974, **96**, 1338.

[17] J. G. Vos and W. L. Groeneveld, *Inorg. Chim. Acta*, 1978, **26**, 71.

[18] I. R. Beattie, T. R. Gilson and G. A. Ozin, *J. Chem. Soc.* (A), 1968, 2765.

[19] D. L. Kepert, *The Early Transition Metals*. Academic Press, London (1972).

[20a] C. Mealli, C. S. Arcus, J. L. Wilkinson, T. J. Marks and J. A. Ibers, *J. Am. Chem. Soc.* 1976, **98**, 711; [b] H. C. Clark and L. E. Manzer, *Inorg. Chem.* 1974, 13, 1996.

[21] F. A. Cotton, B. W. S. Kolthammer and G. N. Mott, *Inorg. Chem.* 1981, **20**, 3980.

[22] D. A. Johnson, W. C. Deese and M. L. Howe, *Inorg. Nucl. Chem. Let.* 1980, **16**, 53.

[23] E. E. Manzer, *Inorg. Chem.* 1977, **16**, 525.

[24] R. Gut and W. Perron, *J. Less Common Metals* 1972, **26**, 369.

[25] S. Trofimenko, *J. Am. Chem. Soc.* 1967, **89**, 3170, 6288.

CRYSTAL AND MOLECULAR STRUCTURE OF TETRACHLOROPHOSPHORUS(V)

HEXACHLOROURANATE(V)

J.C. Taylor* and A.B. Waugh

Division of Energy Chemistry, CSIRO
Lucas Heights Research Laboratories, Private Mail Bag 7,
Sutherland, NSW, 2232, Australia.

ABSTRACT

The crystal structure of tetrachlorophosphorus(V) hexachlorouranate(V), $PCl_4^+ \cdot UCl_6^-$, has been solved with 2492 independent $F(hkl)$ collected by necessity from one component of a bicrystal; all crystals prepared were twinned. The structure is triclinic, space group $P\bar{1}$, with a = 7.038(4), b = 7.373(4), c = 13.706(8) Å, α = 89.38(3), β = 88.80(3), γ = 105.20(3)°, with Z = 2. The two components of the bicrystal, in the volume ratio of 2.5 to 1, had their reciprocal lattice spots sufficiently separated to allow collection of the data set from component 1 with AgKα radiation (λ = 0.5608 Å). A model was derived from the Patterson synthesis and refined by least squares to $R = \Sigma(|Fo|-|F_c|)/\Sigma|Fo| = 0.146$. The structure was confirmed by a final $(\rho_o - \rho_c)$ synthesis.

The structure is an assembly of octahedral $U(1)Cl_6^-$, $U(2)Cl_6^-$ and tetrahedral PCl_4^+ groups. The chlorine atom array is hexagonal close-packed, while the polyhedra are regular within the experimental errors. The structure is isomorphous with the transition metal analogues $PCl_5 \cdot NbCl_5$ and $PCl_5 \cdot TaCl_5$.

INTRODUCTION

Several addition compounds of UCl_5 have been reported, e.g. $UCl_5 \cdot SOCl_2$, $UCl_5 \cdot R_3PO$ (R = NMe_2, Ph or $PhCH_2$), $5UCl_5 \cdot CCl_2 = CClCOCl$, and $UCl_5 \cdot PCl_5$[1]. The latter, the subject of the present study, was first prepared by Cronander[2] in 1873. Its properties were further studied by Panzer and Suttle[3] whose optical measurements showed that the bright orange-red crystals were triclinic, and highly twinned (the twinning precluded further structural studies.) Panzer and Suttle found that $UCl_5 \cdot PCl_5$ formed the ions PCl_4^+ and UCl_6^- in non-aqueous ionising solvents, but were uncertain whether these existed in the solid. $UCl_5 \cdot SOCl_2$ is considered[4] to be $SOCl^+ UCl_6^-$. Some $UCl_5 \cdot PCl_5$ was prepared, in connection with studies in this laboratory on the volatilities of uranium complexes. As found earlier[3], all crystals showed twinning, and structural analysis was commenced, by necessity, on a fragment that was not single. The structure was solved, and is compared, in the Discussion, with analogous transition metal structures[5,6,7].

EXPERIMENTAL

The air-sensitive crystals were prepared in accordance with the method of Panzer and Suttle[3]. Preparation and manipulation were done under drybox conditions,

and crystals were sealed for study in glass capillaries. Of ten crystals mounted,
only three were unhydrolysed after several days and one of these kept for long
enough for the present data collection. Weissenberg photographs could not be
interpreted because the crystal was multiple and the irregular morphology was not
helpful in determining axial directions. All the definitive work was done on a
4-circle diffractometer with AgKα radiation (to minimise absorption, λ = 0.5608 Å),
the counter being an Si/Li solid state detector.

A scan of reciprocal lattice spots showed the crystal was essentially a bicrystal.
Two identical reciprocal lattices were observed, the volume ratio of
crystal 1:crystal 2 being approximately 2.5:1. At χ=0, the b* axis of crystal 1 at
ϕ = 139.0° was nearly coincident with the a* axis of crystal 2 (ϕ = 137.4°) while
at χ - -26°, the a* axis of crystal 1 (ϕ = 65.8°) was nearly coincident with the b*
axis of crystal 2 (ϕ = 63.4°). The c* axes of crystals 1 and 2 ran in opposite
directions. Thus the two orientations could be described as an interchange of the
a* and b* axes in the basal plane with the c* axes in opposite senses. As the
superposition was not exact, this crystal was called a bicrystal rather than a twin.
Unit cell dimensions measured for crystals 1 and 2 agreed within the experimental
errors. (hkl) intensities for crystals 1 and 2 showed general agreement, but there
were irregularities which were thought to be due to the obscuring of one crystal
component by the other. Superposition of reciprocal lattice spots was uncommon.

A set of (hkl) intensity data were collected for crystal 1. 2860 intensities gave,
on averaging equivalents, 2492 independent I(hkl). The intensities were normalised
to a standard reflexion, corrected for absorption (μ = 109 cm^{-1}) and Lorentz and
polarisation factors[8], and reduced to F(hkl) values. The crystal shape was
described by eight (hkl) planes, and transmission factors lay between 0.03 and 0.08.
The irregular shape and the uncertainty as to which parts of the crystal belonged to
crystal 1 and which to crystal 2 produced systematic errors in the absorption
corrections. Crystal data are summarised in Table 1.

TABLE 1.   CRYSTAL DATA FOR TETRACHLOROPHOSPHORUS (V)

HEXACHLOROURANATE (V)

$PCl_4^+ \cdot UCl_6^-$:   Formula weight = 1247.1, density = 3.02 g cm^{-3}(calc) = 3.02 g cm^{-3}
(obs[3]), melting point = 154°C, triclinic, P1 or P$\bar{1}$. P1 confirmed by structure analysis,
unit cell volume = 686 Å, molecules/cell = 2, volume/Cl$^-$ ion = 34.3 Å^3 (36.0 in
α-and β-UCl$_5$ and 31.6 in PCl$_5$), linear absorption coefficient = 109 cm^{-1} (AgKα)

Unit Cell Dimensions (Å and deg)

Crystal Component of Bicrystal	a	b	c	α	β	γ
Crystal 1	7.038(4)	7.373(4)	13.706(8)	89.38(3)	88.80(3)	105.20(3)
Crystal 2	7.042(14)	7.375(15)	13.736(30)	89.17(12)	88.71(7)	104.90(5)

ANALYSIS AND REFINEMENT

The space group was either P1 or P$\bar{1}$ while the unit cell volume was consistent with two formula units per cell. The reflexions with L = 2n+1 were generally weak while all others were strong. This showed the uranium atoms formed a subcell of half the c-dimension, with uranium atoms at (000) and (00$\frac{1}{2}$). A Patterson synthesis confirmed this, and showed 24 peaks, each of about one tenth the height of the U-U vectors. The latter were U-Cl and U-P vectors. The U-Cl vectors indicated octahedra about U(1) and U(2), differing in orientation. One orientation was arbitrarily fitted around U(1) and the other around U(2). Four more Cl locations were found from the map which completed a hexagonal close-packed Cl lattice. A further vector appeared to be a U-P vector to a P atom in a tetrahedral hole in this lattice. The arrangement derived was a packing of U(1)Cl$_6^-$ octahedra, and PCl$_4^+$ tetrahedra, the polyhedra being discrete (i.e. no chlorine bridging of uranium, such as that found in UCl$_5^9$). The space group was P$\bar{1}$ by the structure analysis.

The model was refined with the least-squares program LINUS[10], with neutral scattering factors for U,P and Cl and $\Delta f' = -6.7$ and $\Delta f'' = 10.6$ e for uranium. During the refinement, a trend was noticed for some reflexions to have Fo > Fc. These 33 reflexions were given reduced weights in the refinement. The 'unobserved' reflexions were given values of F = $\bar{F}$ where $\bar{F}$ is the mean calculated F_{hkl} over the unobserved reflexions. The model refined smoothly until all shifts were < 0.002 e.s.d. The final value of R = $\Sigma(|Fo|-|Fc|)/\Sigma|Fo|$ was 0.146. Although this was higher than usual, due to systematic errors caused by the bicrystal, the structure was well-determined because of the large ratio of observed reflexions to variable parameters, and a final difference synthesis confirmed its correctness. In this synthesis, there was a peak 0.8 Å from uranium of $\frac{1}{25}$ the height of the uranium peak, while elsewhere the average value of the points in the map was $\sim\pm\frac{1}{30}$ the height of a Cl atom, except for a few points where it became $\sim\pm\frac{1}{6}$ the height of a chlorine atom. Thus the final difference synthesis showed systematic errors only.

A table of positional and thermal parameters is given in Table 2 and interatomic distances and angles in Table 3. A table of Fo and Fc may be obtained from the authors on request.

TABLE 2   POSITIONAL AND THERMAL* PARAMETERS IN TETRACHLOROPHOSPHORUS (V)
          HEXACHLOROURANATE (V)

Atom	10^3 x	10^3 y	10^3 z	10^3 $\beta 11$	10^3 $\beta 22$	10^3 $\beta 33$	10^3 $\beta 12$	10^3 $\beta 13$	10^3 $\beta 23$
U(1)	000	000	000	14.6(7)	13.5(6)	2.1(1)	3.1(5)	-1.4(2)	2.0(2)
U(2)	000	000	500	13.8(6)	17.2(7)	3.6(2)	3.1(5)	-1.6(2)	2.4(2)
Cl(1)	-241(3)	172(3)	-52(2)	34(6)	33(5)	8(1)	21(5)	-4(2)	1(2)
Cl(2)	241(3)	315(3)	24(2)	35(5)	23(4)	6(1)	-1(4)	-6(2)	3(2)
Cl(3)	115(3)	5(3)	-172(1)	37(6)	33(5)	4(1)	11(4)	3(2)	3(2)
Cl(4)	143(3)	-183(3)	380(1)	23(4)	23(4)	7(1)	9(3)	4(2)	2(2)
Cl(5)	-324(2)	-82(2)	417(1)	13(3)	24(4)	7(1)	3(3)	-5(1)	2(2)
Cl(6)	114(2)	288(2)	394(1)	19(3)	24(4)	6(1)	6(3)	1(1)	7(2)

Atom	$10^3 x$	$10^3 y$	$10^3 z$	$10^3 \beta_{11}$	$10^3 \beta_{22}$	$10^3 \beta_{33}$	$10^3 \beta_{12}$	$10^3 \beta_{13}$	$10^3 \beta_{23}$
Cl(7)	868(3)	478(3)	195(1)	22(4)	31(5)	6(1)	6(4)	2(2)	6(2)
Cl(8)	472(3)	170(2)	225(1)	24(4)	21(4)	7(1)	2(3)	−5(2)	1(2)
Cl(9)	470(3)	588(2)	228(1)	23(4)	23(4)	6(1)	10(3)	−3(2)	4(2)
Cl(10)	657(3)	420(3)	401(1)	26(4)	33(5)	4(1)	7(4)	0(1)	2(2)
P	616(2)	412(2)	262(1)	15(3)	19(3)	4(1)	4(3)	−2(1)	2(1)

*T.F. = exp-($\beta_{11} h^2 + 2\beta_{12} hk + \ldots$)

TABLE 3   INTERATOMIC DISTANCES AND ANGLES IN TETRACHLOROPHOSPHORUS(V)
         HEXACHLOROURANATE(V) (A° AND DEG)

U(1)-Cl(1)	2.474(13) Å	Cl(2)-U(1)-Cl(3)	90.3(5)
U(1)-Cl(2)	2.517(14)	Cl(1)-U(1)-Cl(3)	91.2(5)
U(1)-Cl(3)	2.475(13)	Cl(1)-U(1)-Cl(3)	88.8(6)
U(2)-Cl(4)	2.495(13)	Cl(1)-U(1)-Cl(2)	92.1(6)
U(2)-Cl(5)	2.501(10)	Cl(4)-U(2)-Cl(5)	91.4(5)
U(2)-Cl(6)	2.500(11)	Cl(4)-U(2)-Cl(5)	88.6(5)
		Cl(4)-U(2)-Cl(6)	90.2(4)
P-Cl(7)	1.925(18)	Cl(4)-U(2)-Cl(6)	89.8(4)
P-Cl(8)	1.886(18)	Cl(5)-U(2)-Cl(6)	89.7(4)
P-Cl(9)	1.910(16)	Cl(5)-U(2)-Cl(6)	90.3(4)
P-Cl(10)	1.930(16)	Cl(7)-P-Cl(8)	109.6(9)
		Cl(7)-P-Cl(9)	109.7(8)
Cl(1)-U(1)-Cl(2)	87.9(6)°	Cl(7)-P-Cl(10)	109.0(8)
Cl(2)-U(1)-Cl(3)	89.7(5)	Cl(8)-P-Cl(10)	111.0(8)
		Cl(9)-P-Cl(10)	109.1(9)

DISCUSSION

The crystal structure of $UCl_5 \cdot PCl_5$ is shown in Figure 1. This analysis has shown that $UCl_5 \cdot PCl_5$ is in fact $PCl_4^+ \cdot UCl_6^-$, i.e. tetrachlorophosphorus(V) hexachlorouranate(V); thus these ions occur in the solid as well as in solution. The compound may alternatively be thought of as an arrangement of hexagonal close-packed chloride ions, with P^{5+} and U^{5+} ions in tetrahedral and octahedral holes. As the bond lengths, Table 3, are shorter than the ionic contact distances[11] (2.57 Å for U^{6+}-Cl^- and 2.12 Å for P^{5+} - Cl^-), the former description in terms of an assemblage of discrete UCl_6^- and PCl_4^+ ions is preferable. The UCl_6^- and PCl_4^+ polyhedra are regular within the experimental errors. The U-Cl distances are comparable with the U-Cl distance (average) in α- and β-UCl_5[9,12] of 2.52 Å and the P-Cl distance of 1.97 Å in the tetrahedra of PCl_5[13]. (PCl_5 consists of PCl_4^+ tetrahedra and PCl_6^- octahedra).
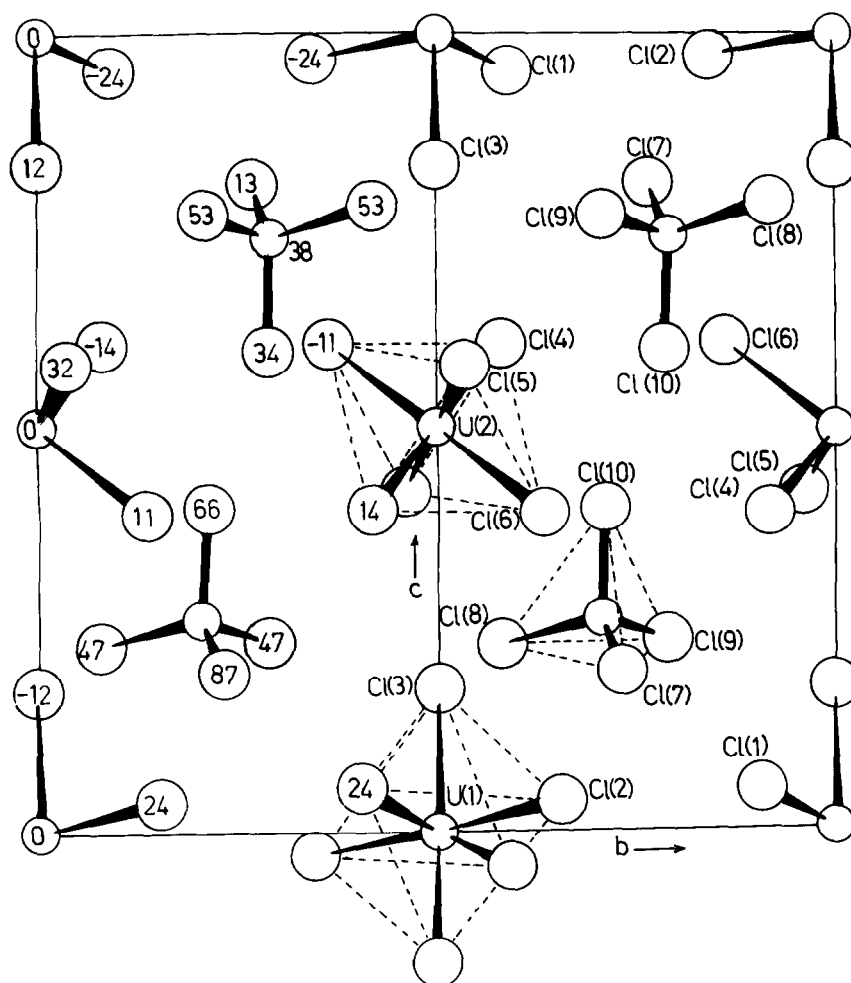
Figure 1. Crystal structure of UCl$_5$.PCl$_5$ as viewed
down the a-axis. Numbers shown are x-coordinates
in hundredths of a.

Kistenmacher and Stucky[6] solved the structures of the interesting compounds $[PCl_4]_2[Ti_2Cl_{10}]$ and $[PCl_4][Ti_2Cl_9]$. The first is based on PCl_4^+ tetrahedra and Ti_2Cl_{10} dimers of the type found in α- and β-UCl_5. The second is built of PCl_4^+ tetrahedra and triply-bridged Ti_2Cl_9 dimers. The structure of $PCl_4 \cdot VCl_5$[7] consists of PCl_4^+ tetrahedra and VCl_5^- bipyramids.

Structural studies by Preiss[5] of the transition metal analogues $PCl_5 \cdot NbCl_5$ and $PCl_5 \cdot TaCl_5$ were brought to our notice after the present work was complete. An examination of his data showed that these compounds were isostructural with $UCl_5 \cdot PCl_5$ but that the coordinates differed from ours as his origin was selected at $(0,0,\frac{1}{2})$ instead of $(0,0,0)$ and his long axis ran in the opposite direction. The α and γ angles of Preiss were indistinguishable from 90°, as his unit cell angles were ± 1.1°; in the present study, the errors in the angles are ± 0.03° or 37 times less. It was of interest that the actinide and transition metal analogues belonged to the same structural type, as this is not always the case[14].

Twinning was also occasionally seen in $PCl_5 \cdot NbCl_5$ and $PCl_5 \cdot TaCl_5$[5], but here the twinning there was an exact superposition, quite different to the bicrystal formation in the $UCl_5 \cdot PCl_5$ crystal. Preiss also redetermined the PCl_5 structure[15] and found a P-Cl distance of 1.90(1) Å in the tetrahedra in PCl_5. This is the same as the average P-Cl distance in $UCl_5 \cdot PCl_5$.

REFERENCES

1. D. Brown, Halides of the Lanthanides and Actinides, p.129. Wiley and Sons, London, (1968).

2. A.W. Cronander, Bull. Soc. Chim. Paris, 19, 500 (1873).

3. R.E. Panzer and J.F. Suttle, J. Inorg. Nucl. Chem., 20, 229 (1961).

4. A.E. Comyns, The Coordination Chemistry of Uranium, a Critical Review, AERE 2320 (1957).

5. H. Preiss, Zeit. fur. anorg. und allg. Chemie, 380, 56 (1971).

6. T.J. Kistenmacher and G.D. Stucky, Inorg. Chem., 10, 122 (1971).

7. M.L. Zeigler, B. Nuber, K. Weidenhammer and G. Hoch, Z. Naturforsch., 32, 18 (1977).

8. M.M. Elcombe, G.W. Cox, A.W. Pryor and F.H. Moore, AAEC/TM578 (1971).

9. G.S. Smith, Q. Johnson and R.E. Elson, Acta Cryst., 22, 300 (1967).

10. P. Coppens and W.C. Hamilton, Acta Cryst., A26, 71 (1970).

11. R.D. Shannon and C.T. Prewitt, Acta Cryst., B25, 925, (1969).

12. U. Muller and W. Kolitsch, Z. Anorg. Chem., 410, 32 (1974).

13. D. Clark, H.M. Powell and A.F. Wells, J. Chem. Soc. (Lond.), 1942, 642.

14. J.C. Taylor, Coord. Chem. Reviews, 20, 197(1976).

15. H. Preiss, Zeit. fur anorg. und allg. Chemie, 380, 51 (1971).

THE CRYSTAL AND MOLECULAR STRUCTURE OF

DIOXO BIS (2,2,6,6 - TETRAMETHYLHEPTANE

-3,5 DIONATO)METHANOL URANIUM (VI)

P.I. Mackinnon[†] and J.C. Taylor[*]

† Chemistry Department
   Monash University
   Wellington Rd, Clayton, Victoria, 3168
   Australia

* CSIRO Division of Energy Chemistry
   Lucas Heights Research Laboratories
   Private Mail Bag 7, Sutherland, NSW, 2232,
   Australia

ABSTRACT

$UO_2(thd)_2$ CH_3OH (thd = tetramethylheptane-3,5-dione) is monoclinic, with a = 10.602(11),
b = 22.883(20), c = 12.054(11) Å and β = 105.90(3)°, Z = 4 and space group $P2_1/c$.
The structure, which is molecular, was solved by conventional Patterson and Fourier
techniques with 3173 independent (hkl) reflexions collected with MoKα radiation
(λ = 0.7107 Å), and refined to R = $\Sigma(|Fo|-|Fc|)/\Sigma|Fo|$ = 0.093. The uranium
coordination polyhedron is a pentagonal bipyramid, with U-O (carbonyl) distances
between 2.25 and 2.37 Å and a longer U-O (methanol) distance of 2.50 Å. The uranyl
group is linear (uranyl angle 179.3(8)°). The pentagon oxygen atoms and uranium do
not form a planar system, as there are deviations of up to 0.17 Å from the mean plane.
If the methanol oxygen atom O(7) is excluded from the plane calculation, the remaining
atoms are more nearly planar. The four carbonyl oxygens are coplanar, with uranium
0.08 Å from their plane. The methanol oxygen is 0.28(4) Å from this second plane.

The two (thd) molecules, excluding methyl carbons, are planar and are inclined
at 43.6° to each other in a boat form and at 29.1 and 14.5° to the pentagonal plane.
The methanol C-O bond is inclined at 133° to the U-O bond, confirming the ligand is
the neutral CH_3OH molecule, and not CH_3O^-.

INTRODUCTION

At the Lucas Heights laboratories, we have studied the crystal structures of various
uranyl chelate compounds including α- and β-$UO_2(hfa)_2$tmp (I,II)[1,2] $UO_2(hfa)_2$ (III)[3],
$UO_2(hfa)_2$ NH_3 (IV)[4], $UO_2(acac)_2$ tppo C_6H_6 (V)[5] and UO_2(3-Cl acac)$_2$tppo (VI)[5], where
hfa = hexafluoroacetylacetonate, tmp = trimethyl phosphate, acac = acetylacetonate
and tppo = triphenylphosphine oxide. Interesting structural features have emerged,
e.g. the different molecular conformations in I and II, the trimeric molecule in
III, and the hydrogen-bonded NH_3 complex in IV. A similar compound, $UO_2(hfa)_2$thf,
where thf = tetrahydrofuran, has been the subject of a structural study[6]. Another
ligand of interest is thd = tetramethylheptane-3,5-dione, a somewhat bulkier ligand
than acac or hfa. The neutral ligand used here was CH_3OH, the complex being

$UO_2(thd)_2CH_3OH$ (VII); the crystal structure of this complex is reported.

EXPERIMENTAL AND ANALYSIS

Several large crystals (3 mm x 1 mm x 1 mm) of $UO_2(thd)_2CH_3OH$ were grown from solution. As the compound was moisture sensitive, a fragment $\sim$ 600 µm thick was mounted in a glass capillary and Weissenberg photographs gave the monoclinic space group $P2_1/c$. Approximately 5000 (hkl) reflexions were measured on a 4-circle X-ray diffractometer with a Si/Li solid-state detector and MoKα radiation (λ = 0.7107 Å). The intensities were normalised to a standard reflexion and corrected for Lorentz, polarisation and absorption factors[7]. On averaging equivalents, 3173 independent (hkl) were available for analysis. The crystal was irregular in shape, but, for absorption correction, its shape was approximated by 6 (hkl) planes (Table 1). As the linear absorption coefficient was large (55.4 cm^{-1}), the absorption was difficult to calculate accurately. Crystal data for $UO_2(thd)_2CH_3OH$ are given in Table 1.

TABLE 1.   CRYSTAL DATA FOR $UO_2(thd)_2CH_3OH$

$UO_7C_{23}H_{44}$, M = 670.63, monoclinic, a = 10.602(11), b = 22.883(20), c = 12.054(11) Å, β = 105.90(3)°, U = 2812 $Å^3$, Z = 4, D_c = 1.584 g cm^{-3}, F(ooo) = 1292, space group $P2_1/c$. MoKα radiation (λ = 0.7107 Å), µ(MoKα) = 55.4 cm^{-1}. Crystal bounding planes :

hkl	dist.(cm) from centre
059	0.019
0$\bar{1}1\bar{5}$	0.019
05$\bar{1}$	0.033
0$\bar{5}$1	0.035
81$\bar{2}$	0.036
$\bar{8}\bar{1}2$	0.036

A Patterson synthesis gave the uranium location in the unit cell, and the remaining atoms were located in successive $(\rho_o-\rho_c)$, structure factor cycles. The complete model was refined with the program LINUS[8], using neutral atomic scattering factors, and $\Delta f'$ = -4.9, $\Delta f''$ = 11.3 for uranium. The final value of R = $\Sigma(|Fo|-|Fc|)/\Sigma|Fo|$ was 0.093. No peaks of structural significance were observed on the final $(\rho_o-\rho_c)$ map. Positional and thermal parameters are given in Table 2 and interatomic distances and angles in Table 3. The observed and calculated structure factors may be obtained from the authors on request.

TABLE 2. POSITIONAL AND THERMAL PARAMETERS* IN $UO_2(thd)_2CH_3OH$

Atom	$10^3\,x$	$10^3\,y$	$10^3\,z$	$10^3\,\beta_{11}$ or B	$10^3\,\beta_{22}$	$10^3\,\beta_{33}$	$10^3\,\beta_{12}$	$10^3\,\beta_{13}$	$10^3\,\beta_{23}$
U	370.9(2)	103.9(1)	24.9(1)	8.8(2)	3.0(1)	6.9(2)	0.2(1)	0.4(1)	0.7(1)
Uranyl Oxygens									
O(1)	378(3)	36(1)	69(3)	5(3)	3(1)	11(3)	0(1)	1(2)	-2(1)
O(2)	366(3)	170(2)	-19(3)	5(3)	3(1)	15(4)	1(1)	1(3)	-1(2)
Carbonyl Oxygens									
O(3)	510(3)	140(2)	195(3)	5(3)	4(1)	10(3)	1(1)	1(3)	0(2)
O(4)	244(3)	137(2)	140(3)	8(3)	4(1)	9(3)	0(1)	1(3)	-2(2)
O(5)	167(4)	87(2)	-87(3)	15(5)	6(1)	4(3)	1(2)	0(3)	-1(2)
O(6)	386(3)	71(2)	-157(3)	7(4)	6(2)	6(3)	0(2)	2(3)	0(2)
Methanol Oxygen									
O(7)	599(3)	81(2)	16(3)	11(4)	4(1)	10(4)	1(2)	1(3)	-3(2)
thd (1)									
C(1)	41(10)	145(4)	244(8)	12.0(26)					
C(2)	55(11)	230(5)	120(10)	14.3(32)					
C(3)	132(8)	237(3)	327(7)	9.5(20)					
C(4)	127(5)	202(3)	219(4)	11(6)	5(2)	7(5)	2(3)	0(4)	-2(2)
C(5)	253(5)	179(2)	205(4)	11(6)	3(1)	7(4)	0(2)	5(4)	-2(2)
C(6)	372(5)	203(2)	269(4)	10(6)	3(1)	8(4)	0(2)	2(4)	-1(2)
C(7)	495(4)	181(2)	263(4)	5(5)	3(1)	8(4)	0(2)	-1(4)	-2(2)
C(8)	620(5)	209(2)	341(5)	9(6)	3(1)	10(5)	0(2)	2(4)	-1(2)
C(8)	613(15)	270(7)	344(13)	12.5(41)					
C(9)	604(12)	207(5)	464(10)	16.6(36)					
C(10)	723(12)	160(5)	373(10)	16.5(36)					
C(11)	700(10)	235(5)	261(9)	13.9(29)					
thd (2)									
C(12)	-111(12)	80(5)	-360(11)	16.0(38)					
C(13)	-102(12)	111(5)	-168(11)	15.2(36)					
C(14)	-64(13)	14(6)	-203(11)	16.2(39)					
C(15)	-42(5)	71(3)	-227(4)	14(7)	3(1)	6(4)	-1(3)	0(4)	-1(2)
C(16)	106(5)	76(2)	-192(5)	10(6)	3(1)	13(7)	1(2)	3(5)	1(2)
C(17)	176(5)	72(3)	-277(4)	9(7)	6(2)	3(4)	1(3)	-2(4)	0(2)
C(18)	306(5)	69(2)	-258(4)	14(8)	3(1)	4(4)	-1(3)	1(5)	-1(2)
C(19)	376(5)	61(3)	-355(4)	20(7)	8(3)	14(5)	2(3)	3(5)	1(3)
C(20)	372(10)	-8(5)	-384(9)	12.8(29)					
C(21)	516(9)	74(4)	-317(7)	10.3(22)					
C(22)	300(10)	89(4)	-465(9)	12.6(28)					
Methanol Carbon									
C(23)	721(5)	79(3)	99(5)	10(7)	5(2)	10(6)	1(3)	-3(5)	-2(3)

* T.F. = $\exp-(\beta_{11}\,h^2 + 2\,\beta_{12}\,hk +...)$

TABLE 3   INTERATOMIC DISTANCES AND ANGLES IN $UO_2(thd)_2CH_3OH$

			thd(1)		thd(2)	
U–O(1)	1.63(2)Å	(uranyl)	C(4)–C(1)	1.67(5)	C(15)–C(12)	1.58(6)
U–O(2)	1.60(2)	(uranyl)	C(4)–C(2)	1.38(5)	C(15)–C(13)	1.42(6)
U–O(3)	2.33(2)	(carbonyl)	C(4)–C(3)	1.51(4)	C(15)–C(14)	1.36(6)
U–O(4)	2.31(2)	(")	C(4)–C(5)	1.49(3)	C(15)–C(16)	1.52(3)
U–O(5)	2.25(2)	(")	C(5)=O(4)	1.23(2)	C(16)=O(5)	1.28(3)
U–O(6)	2.37(2)	(")	C(5)–C(6)	1.40(3)	C(16)–C(17)	1.41(3)
U–O(7)	2.50(2)	(Methanol)	C(6)–C(7)	1.42(3)	C(17)–C(18)	1.34(3)
			C(7)=O(3)	1.28(2)	C(18)=O(6)	1.27(3)

Methanol Molecule

	thd(1)		thd(2)	
C(23)–O(7) 1.41(3)	C(7)=C(8)	1.53(3)	C(18)–C(19)	1.55(3)
	C(8)–C(9)	1.54(5)	C(19)–C(20)	1.61(5)

Methanol Angle

	C(8)–C(10)	1.54(5)	C(19)–C(21)	1.47(4)
U–O(7)–C(23) 133.2(14)	C(8)–C(11)	1.57(5)	C(19)–C(22)	1.50(5)
	C(8)–C(8)'	1.40(7)		

Angles about Uranium

Pentagon Angles

O(1)–U–O(2)	179.3(8)°	O(2)–U–O(3)	84.9(7)	O(3)–U–O(4)	71.6(5)
O(1)–U–O(3)	95.2(6)	O(2)–U–O(4)	85.4(7)	O(4)–U–O(5)	78.2(5)
O(1)–U–O(4)	95.3(6)	O(2)–U–O(5)	91.5(7)	O(5)–U–O(6)	71.6(5)
O(1)–U–O(5)	88.8(7)	O(2)–U–O(6)	89.7(6)	O(6)–U–O(7)	65.3(5)
O(1)–U–O(6)	89.7(6)	O(2)–U–O(7)	97.4(7)	O(7)–U–O(3)	74.3(5)
O(1)–U–O(7)	81.9(7)				

thd(1)

C(1)–C(4)–C(2)	108(3)	C(6)–C(7)–O(3)	124(2)		
C(2)–C(4)–C(3)	113(3)	C(6)–C(7)–C(8)	119(2)		
C(1)–C(4)–C(3)	98(2)	O(3)–C(7)–C(8)	117(2)		
C(1)–C(4)–C(5)	107(3)	C(7)–C(8)–C(9)	106(3)		
C(2)–C(4)–C(5)	111(3)	C(7)–C(8)–C(10)	107(3)		
C(3)–C(4)–C(5)	118(2)	C(7)–C(8)–C(11)	108(2)		
C(4)–C(5)–C(6)	120(2)	C(7)–C(8)–C(8')	113(3)		
C(4)–C(5)–O(4)	116(2)	C(9)–C(8)–C(10)	90(3)		
O(4)–C(5)–C(6)	124(2)	C(10)–C(8)–C(11)	88(3)		
C(5)–C(6)–C(7)	123(2)	C(11)–C(8)–C(8')	71(3)		
		C(8')–C(8)–C(9)	89(4)		

thd(2)

C(13)–C(15)–C(12)	106(3)	C(15)–C(16)–O(5)	119(2)		
C(12)–C(15)–C(14)	107(3)	C(15)–C(16)–C(17)	120(2)		
C(14)–C(15)–C(13)	112(4)	O(5)–C(16)–C(17)	120(2)		
C(14)–C(15)–C(16)	104(3)	C(16)–C(17)–C(18)	127(2)		
C(12)–C(15)–C(16)	115(3)	C(17)–C(18)–C(19)	124(2)		
C(13)–C(15)–C(16)	112(3)				

C(17)–C(18)–O(6)	123(2)
O(6)–C(18)–C(19)	113(2)
C(18)–C(19)–C(22)	112(3)
C(18)–C(19)–C(20)	106(3)
C(18)–C(19)–C(21)	114(3)
C(18)–C(19)–C(22)	112(3)
C(20)–C(19)–C(21)	103(3)
C(21)–C(19)–C(22)	116(3)
C(20)–C(19)–C(22)	104(3)

Angle between (thd)(1) and thd(2) planes
= 43.6(15)°

DISCUSSION

The molecular structure is illustrated in the ORTEP diagram of Figure 1, and the packing of molecules in the unit cell is shown in Figure 2. The main structural features are described below.
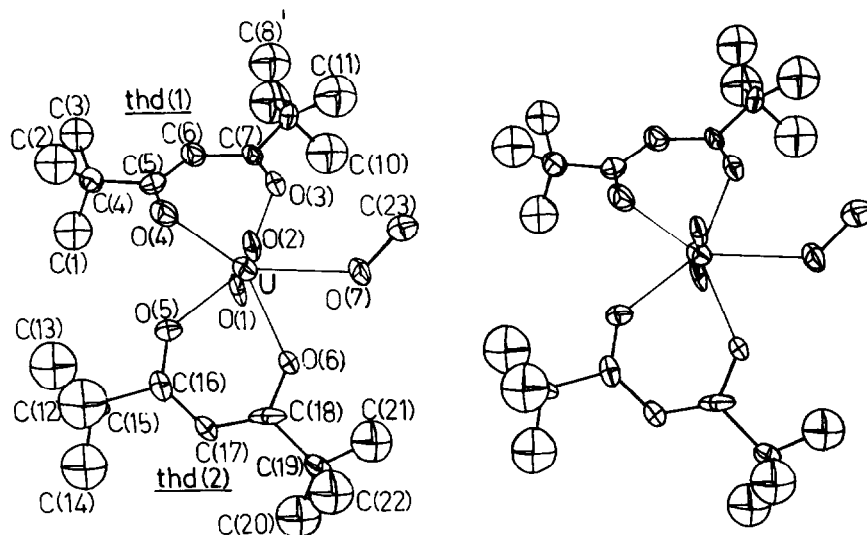
Figure 1.   Stereo diagram of the $UO_2(thd)_2CH_3OH$ molecule.
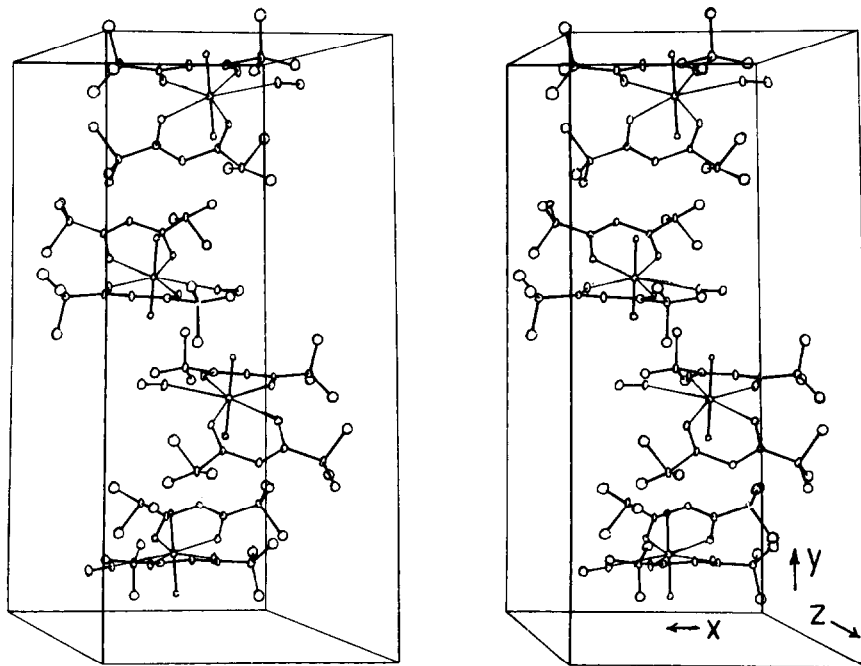
Figure 2.   Stereo diagram showing the packing of four
$UO_2(thd)_2CH_3OH$ molecules in the unit cell.

The U pentagonal bipyramid

The uranium coordination polyhedron is a pentagonal bipyramid formed by the uranyl
group, four carboxyl oxygens and the hydroxyl oxygen. The O(1)-U-O(2) angle is
essentially linear, 179.3(8)°. The U-O(uranyl) distances, 1.63(2) and 1.60(2) Å
are slightly shorter than the usual distance, 1.71 Å. The U-O(carbonyl) distances
lie between 2.25(2) and 2.37(2)Å, whereas the U-O bond to the methanol oxygen O(7)
is longer, 2.50(2)Å. Table 4 summarises interatomic distances of interest in the
series of uranyl chelates we have so far studied. Table 4 shows the U-O(7) bond is
weaker then the U-O bonds to the other neutral ligands in the series. This is because
the (thd) group is a weaker Lewis acid than the (hfa) group. The O-U-O angles in the
pentagon are between 65 and 78°, close to the theoretical value of 72° for a regular
pentagon.

TABLE 4   COMPARISON OF INTERATOMIC DISTANCES IN THE
PRESENT SERIES OF URANYL CHELATES

Bond	α-UO$_2$(hfa)$_2$tmp	β-UO$_2$(hfa)$_2$tmp	UO$_2$(hfa)$_2$thf	UO$_2$(hfa)$_2$NH$_3$	UO$_2$(thd)$_2$MeOH	UO$_2$(hfa)$_2$
U-O (uranyl)	1.73	1.69	1.66	1.69	1.62	1.74
U-O (carbonyl)	2.40	2.40	2.38	2.40	2.31	2.32
U-O (neutral ligand)	2.31(3)	2.26(3)	2.35(2)	2.48(6) (N)	2.50(2)	-
C=O	1.25	1.27	1.30	1.24	1.26	1.32
C-C(ring)	1.49	1.46	1.35	1.50	1.46	1.50
Ref.	1	2	6	4	this work	3

The angles O(1)-U-O(7) (81.9(7)°) and O(2)-U-O(7) (97.4(7)°) suggest that the methanol
oxygen atom O(7) is out of the plane formed by the other pentagon oxygen atoms and
uranium. The least squares plane through uranium and O(3) to O(7) is given in Table 5.
The system is not planar, with O(3), O(6) and O(7) deviating by 0.13(4), 0.17(4) and
-0.17(4)Å from the plane. The plane through uranium and O(3) to O(6) is shown in
Table 5. When O(7) is excluded from the plane calculation it is seen that the four
carbonyl oxygen atoms O(3) to O(6) lie in a plane with uranium slightly out of this
plane by 0.08 Å and the methanol oxygen 0.28(4)Å from this plane. The uranyl group,
however, is normal to the pentagon plane, as the O(1)-U-O and O(2)-U-O angles in
Table 3 both average to 90°.

TABLE 5   LEAST-SQUARES PLANES IN $UO_2(thd)_2CH_3OH$

The equation is in the form $Aax+Bb(\frac{1}{2}+y)+Ccz = D$ where x,y and z are in fractional coordinates.

Plane	Atom	Distance to Plane (Å)	A	B	C	D
Pentagonal Plane Atoms	U	-0.019(2)	0.119	0.921	-0.390	13.10
	O(3)	0.13(4)				
	O(4)	-0.03(4)				
	O(5)	-0.07(4)				
	O(6)	-0.17(4)				
	O(7)	0.17(4)				
Pentagonal Plane, minus O(7)	U	-0.078(2)	0.050	0.928	-0.370	12.98
	O(3)	0.01(4)				
	O(4)	0.04(4)				
	O(5)	-0.01(4)				
	O(6)	0.04(4)				
	O(7)*	-0.28(4)				
thd(1) ring atoms	O(3)	-0.03(4)	0.186	0.659	-0.753	8.86
	O(4)	0.05(4)				
	C(4)	0.00(6)				
	C(5)	-0.02(5)				
	C(6)	-0.03(5)				
	C(7)	-0.00(5)				
	C(8)	0.04(6)				
thd(2) ring atoms	O(5)	-0.08(5)	0.022	0.990	-0.141	13.39
	O(6)	-0.10(5)				
	C(15)	-0.09(6)				
	C(16)	0.02(6)				
	C(17)	0.08(7)				
	C(18)	0.00(5)				
	C(19)	0.01(7)				

* not included in plane calculation.

The (thd) ligands

The bond distances and angles for the (thd) molecules in Table 3 are normal. The C-C bonds average 1.50 Å for thd(1) and 1.48 Å for thd(2), and the carbonyl distances lie between 1.23 and 1.28 Å. The least-squares planes in Table 5 show that thd(1) and thd(2) are (excluding methyl carbons) planar to within the experimental error. However the thd(1) and thd(2) molecular planes are tilted at 43.6(15)° to each other in the form of a boat. This is not unusual to these compounds, e.g. the interplanar

angle of 45° in α-UO$_2$(hfa)$_2$tmp[1] (boat), and the tilt of 31° in UO$_2$ (3-Cl acac)$_2$tppo[5]. The thd(1) and thd(2) groups are inclined to the pentagonal plane calculated without O(7), by 29.1 and 14.5° respectively. Tilt angles of diketonate planes in the present series of uranyl chelates are collected in Table 6.

TABLE 6   TILTS OF DIKETONATE PLANES 1 AND 2 WITH RESPECT
          TO THE UO$_5$ PENTAGONAL PLANE, AND THE TOTAL
          CONFIGURATION

Compound	θ_1°	θ_2°	Configuration	Ref
α-UO$_2$(hfa)$_2$tmp	22.5	22.5	boat	1
β-UO$_2$(hfa)$_2$tmp	3.7	13.9	boat	2
UO$_2$(hfa)$_2$thf	13.2	18.9	boat	6
UO$_2$(hfa)$_2$NH$_3$	7.7	7.7	boat	4
UO$_2$(3-Clacac)$_2$tppo	2	23	L-shape	5
UO$_2$(acac)$_2$tppo.C$_6$H$_6$	10	11	chair	5
UO$_2$(thd)$_2$CH$_3$OH	29.1	14.5	boat	this work

Disorder was observed in the methyl groups of thd(1) but not in thd(2); four electron density maxima were observed about C(8). The extra methyl carbon location is labelled C(8)' in Table 2 and can be observed in Figure 1. In this complex, the thermal factors on the peripheral methyl carbons are large. Disorder was also observed in the CF$_3$ groups of the uranyl (hfa) complexes studied previously.[1,3,4]

(c)   The Neutral Ligand CH$_3$OH

The only atoms observed directly in this molecule are the carbon and oxygen atoms, C(23) and O(7). The C(23)-O(7) distance is 1.41 (3) Å, and the hydroxyl oxygen is weakly bonded to uranium (U-O(7) = 2.50(2) Å). Although the hydrogens were not directly observed, this analysis has established that, on the basis of bond angles, the ligand is CH$_3$OH rather than CH$_3$O$^-$. Figure 1 shows clearly the C-O bond is inclined to the U-O bond. The angle U-O(7)-C(23) is 133.2(14)°; an angle of 180° would be expected if there were no hydroxyl hydrogen attached to O(7).

REFERENCES

1.   J.C. Taylor and A.B. Waugh, J. Chem. Soc. (Dalton Trans.), 1977, 1630.

2.   J.C. Taylor and A.B. Waugh, J. Chem. Soc. (Dalton Trans.), 1977, 1636.

3.   J.C. Taylor, A. Ekstrom and C.H. Randall, Inorg. Chem., 17, 3285 (1978).

4.   D.A. Johnson, J.C. Taylor and A.B. Waugh, J. Inorg. Nucl. Chem., 41, 827 (1979).

5.   J.C. Taylor and A.B. McLaren, J. Chem. Soc. (Dalton Trans.), 1979, 460.

6.   G.M. Kramer, M.B. Dines, R.B. Hall, A.J. Jacobson and J.C. Scanlon, Inorg. Chem., 19, 1340 (1980).

7.   M.M. Elcombe, G.W. Cox, A.W. Pryor and F.H. Moore, AAEC/TM578 (1971).

8.   P. Coppens and W.C. Hamilton, Acta Cryst., A26, 71 (1970).

RECOIL TRITIUM REACTIONS ON MONOGERMANE

M. Castiglioni[*] and P. Volpe

Institute of General and Inorganic Chemistry, University of Torino
Corso Massimo d'Azeglio 48, 10125 Torino, Italy

Abstract – The reactions of recoil tritium with germane have been studied. Excited GeH_3T molecules decompose mainly to HT. Both scavengers and moderator fail to affect the HT and GeH_3T yields. This has been attributed both to the low energy of Ge–H bonds and to the high reaction rate of H atoms with germane. Apparently there is no lack of continuity on the reactivity of T atoms with GeH_4 from hot to thermal energies.

Introduction

Gas-phase high energy tritium reactions greatly contributed to the knowledge of the "recoil chemistry"[1].

A great deal of work has been done during the last two decades and the best approach to the fundamental knowledge of the hot reactions has been obtained from very simple systems such $T + H_2$, $T + D_2$[2,3] and $T + CH_4$[4].

We already studied recoil T reactions with hydrides such SiH_4[5], Si_2H_6[6], methylsilanes[7,8,9,10] and NH_3[11] to get information on the influence of the chemical properties of the reactant on the hot reaction.

In this paper we report on the reactions of recoil T atoms with an other simple hydride of the IVth group: GeH_4, which exhibit the same molecular geometry as CH_4 and SiH_4, but longer bond distance and lower bond energy.

Experimental.

GeH_4 was prepared by reduction of GeO_2 with KBH_4, accordingly to W.L. Jolly and J.E. Drake[12], and purified by gas-chromatography. NO was prepared by reduction of diluted HNO_3 with copper wires and purified by gas-chromatography. ^3He used as target for the $^3He(n,p)T$ reaction was purchased from The Radiochemical Centre-Amersham (England). Details on samples preparation and neutrons bombardment are reported in previous papers[5,13]. Neutrons bombardment was performed in the TRIGA Mark II reactor of the University of Pavia.

Analysis was carried on by radio-gas-chromatography using Chromosorb 102 and Silicone oil 702 columns in the -10 to +150°C temperature range.

Isotopic exchange and ^{71}Ge activity. No isotopic exchange was observed on heating for 15 days at 330°K mixtures of HT and GeH_4 or H_2 and GeH_3T.

The natural abundance of ^{70}Ge is 20.55% and its nuclear cross section for the $^{70}Ge(n,\gamma)^{71}$Ge reaction is 3.9 x 10^{-24} cm^2. ^{71}Ge decays for E.C. with an half life of 11.6 d. The soft X-rays associated with the E.C. are detectable by the flow ionization chamber used as radioactivity detector. Under our experimental conditions at the end of the neutrons bombardment the calculated activity of ^{71}Ge was about of the same order of magnitude of that of tritium. This activity could seriously interfere with the measurement of any GeH_3T and Ge_2H_5T. Experiments performed bombarding $GeH_4 + {}^3He$ mixtures and pure GeH_4 showed that 25 days after bombardment the contribution of ^{71}Ge to the total activity of the sample was negligible. Each sample was then stored in the dark for thirty days at 253°K before the analysis.

Total activity and recoil loss.: The total activity of each sample was both calculated from ^3He content and measured from a butane sample filled and bombarded at the same time of GeH_4 samples.

In low pressure samples the detected activity was corrected for recoil loss using a range of 0.126 cm for tritons in GeH_4 at STP; 1.128 cm, 0.287 cm, 0.271 cm and 1.592 cm have been used as tritons ranges in Ne, O_2, NO and He respectively[14].

Results.

Decomposition of T for H substituted species often occurs in hot atom chemistry due to the energy released to the molecule by the hot reaction. The aim of the pressure dependence study is to know to what extent the decomposition of excited species could affect the primary products distribution.

Table 1 shows that at reactant pressure higher than 106 KPa the unimolecular decomposition of excited GeH_3T^* molecules becomes negligible.

The yields of GeH_3T and Ge_2H_5T are about the same as for other simple hydrides of the IV group no other Germanium-hydrides have been detected in measurable amounts. HT yield is high, more close to that from SiH_4[5] than to that from CH_4[15].

The activity detected in gas phase was always very close to the total calculated activity suggesting that the decomposition of hot products leads mainly to volatile substances.

Table 1. Yields of HT, GeH$_3$T and Ge$_2$H$_5$T in the 13-200 KPa pressure range.[a]

GeH$_4$	HT	GeH$_3$T	Ge$_2$H$_5$T	Tot. experim. Activity / Tot. calcul. Activity
200 KPa	71,2 + 3,7	25,3 + 2,2	2,1 + 0,7	1.02 + 0.03
160 KPa	72,4 + 4,0	24,1 + 1,6	1,9 + 0,6	0.97 + 0.06
106 KPa	71,7 + 4,1	24,6 + 1,8	1,8 + 1,0	0.99 + 0.02
80 KPa	74,3 + 3,2	21,5 + 0,9	2,4 + 0,9	0.95 + 0.06
40 KPa	77,0 + 2,6	17,3 + 0,8	2,9 + 1,1	1.01 + 0.09
13 KPa	81,1 + 5,2	13,6 + 1,2	3,3 + 0,9	0.98 + 0.02

[a] Yields are percentage of total activity experimentally determined from butane samples bombarded at the same time. The total calculated activity was obtained taking into account: ^{3}He content, neutron fluxes and recoil losses for each sample.

The total hot yield may be obtained using radical scavengers to clean the system from interfering reactions such reaction /1/.

$$GeH_4 + T \ (thermal) \longrightarrow GeH_3 + HT \qquad\qquad /1/$$
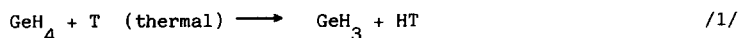
O_2 and NO were used because I_2 and Br_2 easily react with GeH$_4$.

Table 2 shows the effect of both O_2 and NO as scavergers on the yields of HT, GeH$_3$T and Ge$_2$H$_5$T.

Table 2. Effect of scavengers on the T* + GeH$_4$ system.[a]

GeH$_4$	Scavenger	HT	GeH$_3$T	Ge$_2$H$_5$T	Tot. experim. Activity / Tot. calcul. Activity
106 KPa	NO 1 KPa	70,6 + 5,1	23,4 + 3,0	1,8 + 0,9	0.97 + 0.02
106 KPa	O$_2$ 1 KPa	71,3 + 4,6	22,8 + 2,2	1,9 + 0,3	0.99 + 0.03
13 KPa	NO 2 KPa	79,2 + 6,1	13,2 + 0,8	2,2 + 0,3	1.04 + 0.04
13 KPa	NO 4 KPa	77,2 + 3,7	11,5 + 1,1	1,5 + 0,4	0.96 + 0.08

[a] See note on Table 1.

The effect of Ne added to the system as inert moderator for the recoiling T atoms is reported on Figure 1. In spite of its very low efficiency, NO was added in increasing amounts (from 10 to 30%) as the mole fraction of Ne increased[16].

Substitution reaction appears to be affected by the decrease of the energy of the tritium atoms (i.e. by moderation), whereas HT yield increases of about 5% in highly moderated samples.

Discussion

The possible reactions of hot T on GeH_4 give rise to HT by hydrogen abstraction /2/ and, by hydrogen substitution /3/, to GeH_3T which can be found in an excited state (GeH_3T^*):

$$T^* + GeH_4 \longrightarrow GeH_3 + HT \qquad\qquad /2/$$

$$T^* + GeH_4 \longrightarrow GeH_3T + H \qquad\qquad /3/$$
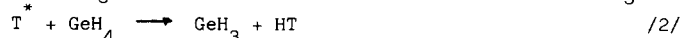
Some highly excited substituted molecules, GeH_3T^*, may decompose before collisional deactivation to GeHT (T-germylene) or HT. The decomposition to germyl radicals (GeH_2T or GeH_3) is energetically unfavourite as shown by RRKM calculations[17], Fig. 2. Further reaction of germylene-T radicals with the substrate is responsible for the formation of digermane /4/[18]

$$GeHT + GeH_4 \longrightarrow Ge_2H_5T \qquad\qquad /4/$$

Decreasing the pressure of the system from 200 to 13 KPa the yield of GeH_3T decreases of about 11% whereas HT increases of 10% and Ge_2H_5T of about 1%.

From the calculated decomposition rates (Fig. 2) it also appears that the decomposition of GeH_3T^* to HT should be less favourite than the decomposition to GeHT and hence the yield of Ge_2H_5T should increase more than HT as the pressure decreases.

The small increase of Ge_2H_5T and the 10% increase of HT suggest that only a small fraction of GeHT species survive long enougth to undergo reactive collision with GeH_4 /4/ while the larger fraction further decomposes accordingly reaction /5/

$$GeHT \longrightarrow Ge + HT \qquad\qquad /5/$$

Reaction /5/ is thermodinamically feasible, fast and probably with a low activation energy[19].

As reported on Table 2 neither O_2 nor NO show a significant effect on both HT and Ge_2H_5T. There is some uncertainty on the efficiency of the above scavengers on GeH_3 and GeH_2 radicals[18] but they are known to be good scavengers for thermal T atoms[20]. It could then be supposed that reaction /1/, which is known to be very fast[21,22], may compete with the scavenger for the reaction of thermal T atoms. On the other hand it appears from moderator experiments that the HT yield does not decreases as expected (also with high percentage of NO). The failure of moderation suggests that a different mechanism may contribute to the HT yield and that such mechanism should be insensitive to thermal radical scavengers and favoured by the decrease of the energy of the recoiling T atoms. Moreover, the increase of HT at very high moderation suggests that, besides a possible decomposition to HT of excited GeH_3T^* molecules by collision with Ne, the abstraction reaction /2/ could

occur also at very low energies consuming the T atoms which being moderated are no more able to react as in /3/ [**].

To sum up, the question arises if either the substrate molecules compete with the scavenger for thermal T atoms or monogermane exhibit a kind of shadowing effect on NO, i.e. GeH_4 reacts with both thermal and quasi-thermal(epithermal) T atoms, sharply decreasing the number at T atoms that, once thermal, could be scavenged by NO or O_2.

Although the literature data on the rate of reaction /1/ are discordant and could indicate a considerable energy dependence (different rate constants have been observed using different hydrogen atom generation methods)[21,22] it seems unlikely that the rate constant for reaction /1/ could be higher than that of scavenging reaction. Hence we suggest that the lack of scavenging effect is due to shadowing effect.

The above suggestion is upported by: a) the cross section for the abstraction reaction increases as the energy of the involved bond decreases, because the low energy threshold for the reaction decreases with the bond energy[24]. b) RRKM calculations show that the mean energy released to the GeH_3T molecule by the substitution reaction is low (only 4×10^{19} J). This implies that the mean energy of the T for H substitution is low, ·it could than be inferred that also the abstraction reaction occurs at low energy.

Conclusions.

It has been already pointed out[25] that in hot T chemistry the hot HT yield is correlated with the dissociation energy of the bond involved in the reaction. Ge-H bonds are relatively weak and therefore the HT yield should be high, however the inefficiency of scavengers towards the HT yield in GeH_4, in addition to the high reaction rate for thermal hydrogen abstraction, suggests that tritium atoms abstract hydrogen from germane without lack of continuity from hot to thermal energies. On the contrary the T for H substitution yield is apparently unaffected by bond energy: in fact the simple hydrides CH_4, SiH_4 and GeH_4, having the same molecular geometry but different bond energies and lengths, exhibit the same T for H substitution yield, i.e. about 25%.

[**]   The scavenger inefficiency prevented us to perform a complete kinetic analysis. However the second kind plot of the Estrup-Wolfgang theory[23] (obtained using: $\sigma_{T+GeH_4} = 0.44$ nm^2, $\sigma_{T+Ne} = 0.22$ nm^2, $\sigma_{T+NO} = 0.30$ nm^2 and $\alpha_{GeH_4} = 0.263 = 0.96 \alpha_{Ne}$) shows a non-linear trend with an intercept $\simeq 0.5$ α_{Ne} (other values of α_{GeH_4} have been tested with the same result). The curvature of the plot confirms that the values at higher moderation are lowered by the unimoleculaar decomposition; the extrapolation using only the values from low moderation experiments gives: $I_{GeH_3} = 0.65 \alpha_{Ne}$.
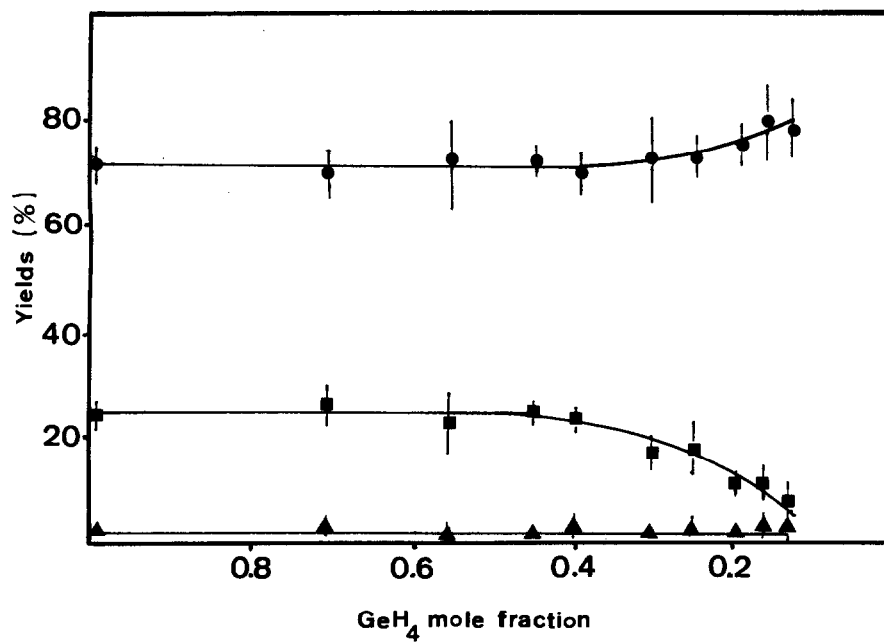
Fig. 1. Effect of Ne moderation on the products yields for the T^* + GeH$_4$ reaction. Yields as percentage of total activity. HT = ● ; GeH$_3$T = ■ ; Ge$_2$H$_5$T = ▲
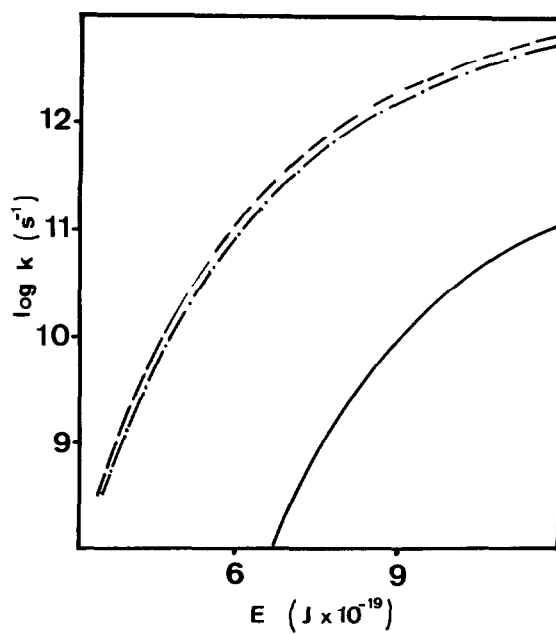
Fig. 2. RRKM calculated specific rate constants for decomposition reactions: $GeH_3T \longrightarrow$ GeH_2T + H $=$———; $GeH_3T \longrightarrow GeHT$ + H_2 $=-\cdot-\cdot-$ and $GeH_3T \longrightarrow GeH_2$ + HT $=----$. The i.r. frequencies used for the calculations where taken from L.P. Lindeman and M.K. Wilson, Z. Physik. Chem. 9, 29 (1956). Activation energies from ref. 26 and 19 respectively.

References

[1] G. Stocklin, Chimie des Atomes Chauds, Masson e Cie Paris, 1972.

[2] M. Karplus, R.N. Porter and R.D. Sharma, J. Chem. Phys., 45, 3871 (1966).

[3] D. Seewald and R. Wolfgang, J. Chem. Phys., 47, 143 (1967).

[4] R. Wolfgang, J. Chem. Phys., 39, 2983 (1963).

[5] G. Cetini, O. Gambino, M. Castiglioni and P. Volpe, J. Chem. Phys., 46, 89 (1967).

[6] G. Cetini, O. Gambino, M. Castiglioni e P. Volpe, Atti Accad. Sci. Torino, 99, 1093 (1965).

[7] P. Volpe e M. Castiglioni, Atti Accad. Sci. Torino, 105, 293 (1970-71).

[8] M. Castiglioni and P. Volpe, Gazz. Chim. Ital., 102, 709 (1972).

[9] M. Castiglioni and P. Volpe, Gazz. Chim. Ital., 106, 699 (1976).

[10] P. Volpe and M. Castiglioni, J. Chem. Soc., Faraday Trans I., 74, 818 (1978).

[11] M. Castiglioni and P. Volpe, Gazz. Chim. Ital., 105, 247 (1975).

[12] W.L. Jolly and J.E. Drake, Inorg. Syntheses, vol. 7 pag. 36.

[13] G. Cetini, O. Gambino e B. Minasso, Atti Accad. Sci. Torino, 99, 1137 (1962-63).

[14] J.W. Root and F.S. Rowland, Radiochim. Acta, 10, 104 (1968).

[15] P.J. Estrup and R. Wolfgang, J. Am. Chem. Soc., 82, 2665 (1960).

[16] D.J. Malcolme-Lawes, Radiochim. Acta, 16, 57 (1971).

[17] W. Frost, Theory of Unimolecular Reactions. Academic Press, N.Y. 1973, pag. 28.

[18] P.P. Gaspar and J.J. Frost, J. Am. Chem. Soc., 95, 6567 (1973).

[19] C.G. Newman, J. Dzarnoski, M.A. Ring and H.E. O'Neal, Int. J. Chem. Kinet., 12, 661 (1980).

J. Dzarnoski, H.E. O'Neal and M.A. Ring, J. Am. Chem. Soc., 103, 5740 (1981).

[20] D.C. Fee, S.S. Markowittz and J.K. Garland, Radiochim. Acta, 17, 135 (1972).

[21] K.J. Choo, P.P. Gaspar and A.P. Wolf, J. Phys. Chem., 79, 1752 (1975).

[22] E.R.Austin and F.W. Lampe, J. Phys. Chem., 81, 1134 (1977).

[23] R. Wolfgang, J. Chem. Phys., 39, 2983 (1963).

[24] G. Stocklin, Chimie des Atomes Chaudes, Masson e Cie, Paris 1972, pag. 84.

[25] F.S. Rowland, M.T.P. International Rev. of Science, Phys. Chem. Series One, 9, 109 (1972).

[26] M.J. Almoud, A.M. Doncaster, P.N. Noble and R. Walsh, J. Am. Chem. Soc., 104, 4717 (1982).

POLYHEDRON REPORT NUMBER 3

MECHANISMS IN THE RACEMIZATION OF OPTICALLY ACTIVE CO-ORDINATION COMPLEXES IN THE SOLID STATE. A REVIEW

P. O'BRIEN

Department of Chemistry, Chelsea College, Manresa Road, London SW3 6LX, England

CONTENTS

1. INTRODUCTION

Although reactions of coordination compounds in the solid state have been known since the time of Werner[1] detailed studies of the kinetics and mechanism of such reactions remain (relative to solution studies) rare. Racemization (1) is a particularly simple reaction, no new chemical species need necessarily be transported to or from the reaction site for its occurrence:

$$2L \rightarrow D + L. \tag{1}$$

Various kinetic studies of the racemization of coordination compounds in the solid state have appeared, and a collection of many of these references is available.[2] The purpose of this article is to reconsider the validity of such kinetic work in relation to the complicated but well documented theory of rate processes in the solid state.

The vast majority of studies to date have modelled racemization with a simple unimolecular rate law. It is shown here that a more accurate model of the kinetics of these reactions is available in well known equations for the kinetics of solid state processes; subsequently the correlation of activation parameters with elementary chemical steps is fraught with difficulties.

The first observation of solid state racemization is usually attributed to Johnson and Mead,[3] strictly they studied the mutarotation of strychninium salts of [Co(ox)₃]. Later, a study of the racemization of $K_3[Cr(ox)_3]$ was reported.[4] There were few studies of such systems until the 1960s, when Bailar's school investigated the solid state racemization of $[Cr(en)_2X_2]$[5] and $[Co(en)_3]X$.[6] An isolated and thorough study of $K_3[Cr(ox)_3]$ appeared in 1969.[7] More recently, Yamamoto *et al.* have studied the racemization of tris(chelate) complexes of Ni(II) and Fe(II) with 2,2-bipyridyl and 1,10-phenanthroline.[8,9] In parallel to the above studies of thermal racemization a number of studies of pressure induced racemization have appeared; this work will be considered separately.

Consideration will now be given to the more relevant aspects of the theory of rate processes in the solid state and the implications of this for studies limited to formal kinetics. This will be followed by a detailed examination of reported studies of solid state racemisations.

2. STUDIES ON THE FORMAL KINETICS OF SOLID STATE SYSTEMS

Excellent reviews of the mechanisms possible for solid state processes are available.[10–13] The majority of coordination chemists studying racemization in the solid state choose a unimolecular rate

law; there seem to be two main reasons for this:

(a) analogy with solution studies (nearly always performed under first order or pseudo-first order conditions).

(b) assumptions, regarding the process occurring in the lattice based on the Scheme 2 shown below:

$$2L \xrightarrow{k_{rac}} L + D \quad \text{racemization}$$

$$L \xrightarrow{k_{inv}} D \quad \text{inversion} \quad k_{inv} = \frac{k_{rac}}{2} \tag{2}$$
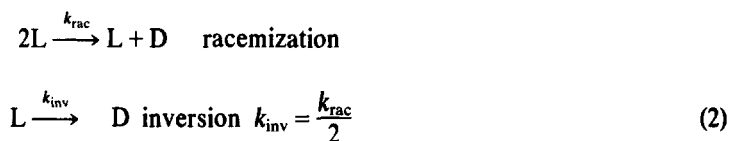
(L and D are enantiomorphs, k_{inv} and k_{rac} are the rate constants for inversion and racemization, respectively). In dilute solutions prepared with achiral solvents, the above scheme is usual and correct. In the solid state the complexes racemize within an asymmetric lattice. Optically pure and racemic compounds are not isomorphous; hence simple correlations of inversion and racemization rate constants are not valid.

Alternatively, an individual optically active molecule undergoing inversion in the solid state (by whatever mechanism) is necessarily in intimate contact with its nearest neighbour. Its neighbour being chiral leads to a diastereomeric situation which might be represented as in[3]:

$$nL \rightarrow (n-1)L + D. \tag{3}$$

All molecules within the lattice do not have an equal probability of undergoing inversion, it is thus extremely unlikely that when racemization is complete, asymmetric centres will continue to invert at the same rate. The formal kinetics of a solid state process deals with exactly this kind of problem. The kinetics of solid state processes are difficult to interpret, two main approaches are available.

(a) A careful consideration of the formal kinetics of the process, observed under varying conditions should be made, (the subject of this section).

(b) Other crucial experiments, microscopic examination, morphology, texture, etc. should all be considered (the subject of the next section).

Some commonly used rate equations for solid state processes are summarized below (Table 1). These equations fall into three main classes, those based on diffusion control of reaction rate D_1, D_2 and D_4, those based on the concept of an order of reaction R_2, R_3 and F_1 and those describing nucleation and growth kinetics A_2 and A_3.[14] There are various methods of assigning rate law, a number of these are mainly of value in deciding on the type of mechanism, viz. D, R or A. Reduced time plots (plots of α (fractional reaction) vs $t/t_{0.5}$) fall into this category. Such plots have the same shape irrespective of the magnitude of the rate constant, using a master curve it is easy to compare quantities of data. The curves for $R_2 R_3$ are quite similar making delineation within this group difficult. Figure 1 shows some data for the racemization of $[K_3Cr(ox)_3]$ (anhydrous sample D[14]) compared with the theoretical curves for rate laws R_3 and A_3. The fit to R_3 is excellent; however the main conclusion from such a graph should only be that the concept of an order is appropriate.

An alternative to this method has been introduced by Sharp and Hancock.[15] Plots of $\ln-\ln(1-\alpha)$ vs $\ln$ time are used, the gradient (m) of such plots in the region $0.1 < \alpha < 0.5$ is characteristic of the type of

Table 1. Some commonly used rate equations for solid state reactions

Mechanism	Integrated form[a]	Notation[a]	m^{ab}
Diffusion control 1 dimension	$\alpha^2 = (k/x^2)t$	$D_1(\alpha)$	0.62
Diffusion control 2 dimensions	$(1-\alpha)\ln(1-\alpha) + \alpha = (k/r^2)t$	$D_2(\alpha)$	0.57
Diffusion control 3 dimensions	$(1-2\alpha/3) - (1-\alpha)^{2/3} = (k/r^2)t$	$D_4(\alpha)$	0.57
Phase boundary control 2 dimensions	$1 - (1-\alpha)^{1/2} = (u/r)t$	$R_2(\alpha)$	1.11
Phase boundary control 3 dimensions	$1 - (1-\alpha)^{1/2} = (u/r)t$	$R_3(\alpha)$	1.07
First order (random nucleation)	$\ln(1-\alpha) = -kt$	F_1	1.00
Nucleation and growth 2 dimensions	$[-\ln(1-\alpha)]^{1/2} = kt$	$A_2(\alpha)$	2.00
Nucleation and growth 3 dimensions	$[-\ln(1-\alpha)]^{1/3} = kt$	$A_3(\alpha)$	3.00

[a]Notation of Sharp et al. Ref. 14 is used.
[b]Slope of plot of $\ln-\ln(1-\alpha)$ vs $\ln t$ after Sharp and Hancock. Ref. 15.
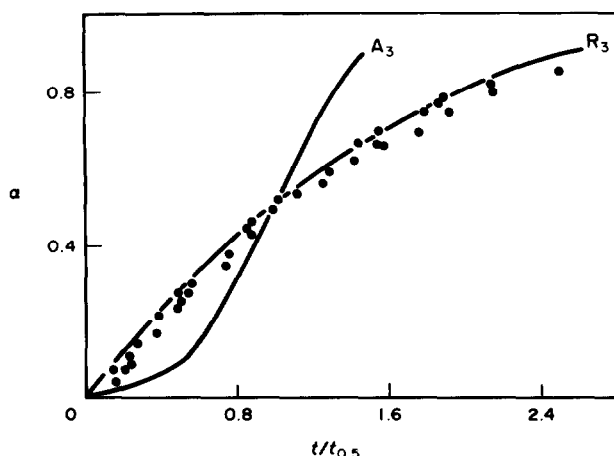
Fig. 1. The use of a reduced time plot. Solid lines are theoretical curves for mechanisms A_3 and R_3, points are α
vs $t/t_{0.5}$ for anhydrous sample D of d-$K_3[Cr(ox_4)_3]^{37}$ (data at 242, 246 and 251°C).

mechanism. Briefly for the gradient $m \sim 1$ the concept of an order of reaction (R_2, R_3 or F_1) is valid, for $m \sim 0.5$ diffusion control (D_1, D_2 or D_4) is appropriate and $m \sim 2$ is consistent with nucleation and growth (A_2 or A_3 Avrami/Erofeyer) kinetics. The straight lines obtained in this way are only approximate, but the method seems reliable.

These two techniques help us to decide to which class a solid state process belongs. A simple inspection of the data plotted as α vs time is also worthwhile.[16] The presence or absence of an induction period should always be investigated, as this may help to rule out certain of the above mechanisms.

The problem of deciding which particular-rate law to use within a type is more difficult. If the concept of an order of reaction is valid (R_2, R_3 or F_1) we have recently advocated a differential method,[17,18] based on equation (4) as being extremely useful:

$$\frac{-(1-\alpha)}{d(1-\alpha)/dt} = (n-1)t + \frac{1}{k}. \tag{4}$$

Accurate and reliable values for the order (n), and (in the absence of a zero time error) rate constant (k) may be determined by an approximation procedure.[18]

Another possibility is simply to consider the statistical fit of the various possible integrated rate equations (care is needed with the range of values considered). When no serious zero time error is involved a comparison of theoretically predicted and observed values for the intercept on the $f(1-\alpha)$ axis is also extremely useful. Dolimore et al.[19] have suggested that the linearization of reduced time plots may be a worthwhile procedure.

A combination of the above procedures provides a useful method of screening kinetic data for solid state rate processes. In closing some brief mention must be made of the possible marked effect of particle size distribution. There have been several studies of the effect of particle size distribution,[20-23], and it should always be borne in mind that change in particle size assembly can produce as marked a change in formal kinetics as a change of mechanism.[23]

3. OTHER METHODS RELEVANT TO KINETIC STUDIES OF SOLID STATE SYSTEMS

It has been variously suggested[24-26] that a full study of the mechanism of a solid state reaction should not be limited to formal kinetics alone. The following have been itemized as being particularly informative methods.[23].

(a) Structure: the lattice (crystal structure) of both product and reactant should be known.

(b) Texture: studies of the actual crystals; grain aggregation, crystallite sizes, orientation or crystallites surface area and lattice defects.

(c) Morphology: direct observation of nucleation, subsequent reaction and behaviour of particles.

Much of this can be difficult, and racemizations have on occasions proved singularly intractable, e.g. Bailar and Kutal could observe no interface during the reaction of (+)-$[Co(en)_3]X_3$.[6]

The molecular nature of the racemization of coordination compounds in the solid state should also be
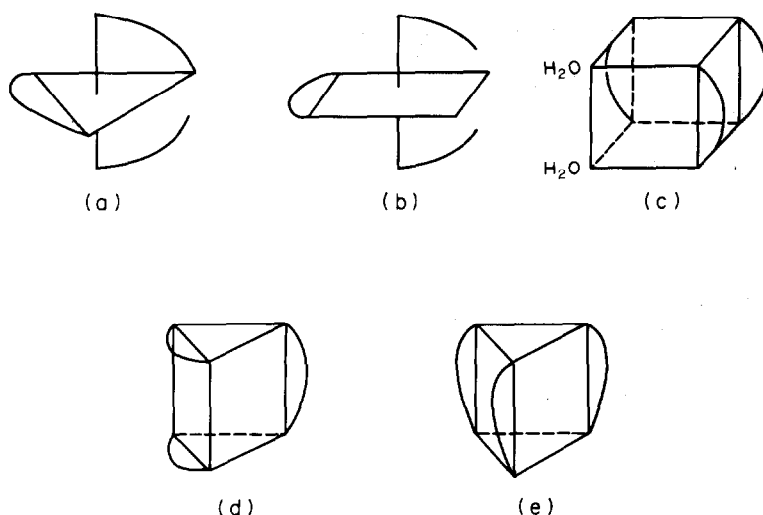
Fig. 2. Commonly proposed transition state for the racemization of tris-chelated coordination complexes.

considered. In Fig. 2 we collate some commonly suggested transition states for the racemization of tris-chelated coordination complexes. In the solid state formal kinetics does not on the whole provide a method of determining which of these mechanisms is operating; although studies of pressure induced racemization may be helpful *vide infra*. In certain cases mechanisms may be eliminated on the basis of chemical considerations, e.g. Fig. 2c is impossible for an anhydrous complex *in vacuo*.

Symmetry considerations have proved to be extremely useful in chemistry.[27-29] The reactions of coordination compounds have been considered by Eaton[30] and later more thoroughly by Whitesides.[31] Notably the racemization of tris-chelate d^3 systems by a twist mechanism, was found to be thermally allowed for weak field cases.[32-34] This lends some support to the frequent suggestions that such mechanisms operate in the solid state.

4. OXALATO COMPLEXES

Johnson and Mead first reported[4] the solid state "racemization" of [Co(ox)₃] in 1932, however as strychninium salts were used this is really not a racemization. In fact the diastereomeric strychninium salts of d and l [Co(ox)₃] showed different rates and final percentages of inversion. The majority of work reported by Johnson *et al.*[4,5,35] in the 1930s concerned such diastereoisomers, but a brief study of K₃[d-Cr(ox)₃] was carried out.

Historically these were the first solid state thermal racemizations to be studied. A number of interesting observations were made: diastereoisomers showed markedly different behaviour in the solid state, a first order model of the kinetics was found to be unsatisfactory, the racemization of anhydrous complexes was demonstrated (although in general at a rate slower than for the corresponding hydrate) and the effect of crystal size on reaction rate was investigated. This work was thorough and made the best use of the then available experimental methods.[36] Brief mention of the slow rate of solid state racemization of [Cr(ox)₃] was made by Billardon[36] but no detailed studies were carried out.

Perhaps the most thorough study of the kinetics of the thermal racemization of a co-ordination complex in the solid state was carried out by Chowdry and Harris.[7,37] Both hydrated and anhydrous forms of K₃[Cr(ox)₃] were studied, rapid racemization was observed during dehydration of the complex, in line with the earlier findings of Johnson *et al.* No real effort was made to investigate the mechanism of this rapid reaction but the possibility of expansion of the complex with lattice water (Fig. 2c) was noted. Anhydrous samples were found to racemise at a faily reproducible rate; racemization rate constants were determined from plots of $(1 - \alpha)$ vs time on logarithmic paper. A first order model with an induction period was considered appropriate. Apart from observations on dehydration, and a study of the effect of neutron irradiation this work was limited to formal kinetics interpreted as outlined above.

We have reinvestigated the data of Chowdry and Harris[7,37] in some detail. A typical set of data, (anhydrous sample D Ref. 37)† will be considered using the scheme outlined in Section 2. Plots of α vs time (or $t/t_{0.5}$) Fig. 2 are deceleratory throughout, the reduced time plot lying closest to the theoretical

Table 2. Kinetic data for the racemization of anhydrous sample D of
K₃[Cr(ox₄)₃]

Temperature (°C)	$10^3 \, k/hr^{-1a}$	intercept[b]	m[c]	E_a
242	2.64(± 0.13)	1.00(± 0.01)	0.80	
242	2.86(±0.09)	1.02(±0.01)	1.2	
246	4.27(±0.24)	0.999(± 0.01)	0.8	228 kJ mole⁻¹
246	3.96(±0.13)	1.01(±0.01)	1.1	
251	7.11(±0.39)	0.999(±0.001)	1.3	
251	6.73(±0.27)	0.999(±0.01)	1.3	

[a]Rate constant obtained from plots of $(1 - \alpha)^{1/3}$ vs t in min⁻¹.
[b]Intercept of plot of $(1 - \alpha)^{1/3}$ vs t on $(1 - \alpha)^{1/3}$ axis.
[c]Slope of plot of ln–ln$(1 - \alpha)$ vs ln t $(0.1 < \alpha < 0.5)$.

line for R_3. The slope of plots of ln–ln $(1 - \alpha)$ vs ln t $(0.1 < \alpha < 0.5)$ are all close to unity (Table 2); the above suggest that the concept of an order of reaction $(R_2R_3F_1)$ is appropriate.

Delineation between these order based mechanisms is achieved in a number of ways. Plots of integrated rate equations [Fig. 3, Table 2] show R_3 to provide the best fit to the data at all temperatures. Plots of $(1 - \alpha)^{1/3}$ are colinear with the expected 0, 1 origin [Table 2, Fig. 4], not the case for R_2 or F_1.
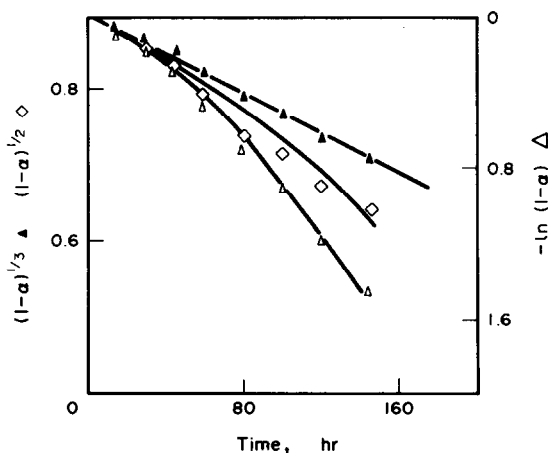
Fig. 3. Comparison of order based rate equations for anhydrous d-K₃[Cr(ox₄)₃]. Anhydrous sample D of
d-K₃[Cr(ox₄)₃] at 242°C:[37] ▲ $(1 - \alpha)^{1/3}$, ◇ $(1 - \alpha)^{1/2}$, △ ln$(1 - \alpha)$.
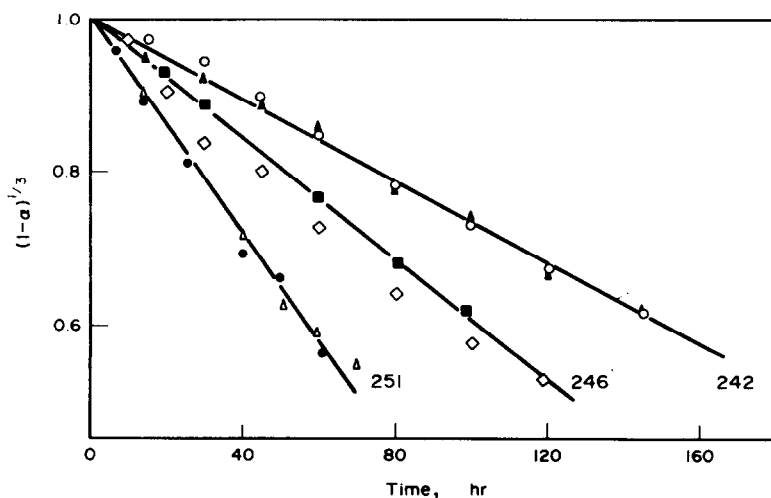
Fig. 4. Plots of $(1 - \alpha)^{1/3}$ vs time for d-K₃[Cr(ox₄)₃] at various temperatures. ▲, ○ duplicate runs at 242°C,
◇, ■ duplicate runs at 246°C, ●, △ duplicate runs at 251°C.

There are unfortunately insufficient data for a proper application of our differential method;[18] orders between 0.6 and 0.8 are obtained in cases where enough data[37] for a preliminary analysis are available.

The two third order rate constants determined by these methods may be used to obtain an activation energy of 227 kJ mole^{-1} (for anhydrous sample D). This may be contrasted with the two values 570 kJ mole^{-1} (for the induction period) and 159 kJ mole^{-1} (for racemization) reported for the same sample by Chowdry.[37] Support for our interpretation of the formal kinetics of this system may be obtained by the method by Ng;[12] plots of log $t_{0.5}$ vs $1/T$ K^{-1} lead to an activation energy of 235 kJ mole^{-1}, comparing very favourably with the activation energy from our single step mechanism.

There are insufficient data on the activation energy of solid state racemization of this kind for a detailed comment on our value of $\sim$227 kJ mole^{-1}. However it is similar to others reported for phase boundary controlled reactions in the solid state. The activation energy of $\sim$500 kJ mole^{-1} reported by Harris and Chowdry,[7,37] seems unreasonably high even for nucleation in the solid state.

It seems clear that in this case there are at least two mechanisms for the solid state racemization. The first, appropriate for hydrated samples, may well involve expansion of the first co-ordination sphere with lattice water and has been little studied. The second, that of anhydrous samples, is most accurately described by phase boundary control in 3 dimensions (R_3), and possibly proceeds at the molecular level by a twist mechanism.[31] More work is needed to elucidate fully the mechanisms operating for this system.

5. COMPLEXES OF 2,2-BIPYRIDYL AND 1,10-PHENANTHROLINE

Yamamoto *et al.*[8,9] have reported on the racemization of various anhydrous salts of Ni(II) and Fe(II) with 2,2-bipyridyl and 1,10-phenanthroline. Throughout unimolecular rate laws were applied; we have again carefully recalculated fully reported data.[8] Considering each complex in turn, for [Fe(phen)$_3$] (ClO$_4$)$_2$ we find m (the slope of plots of ln–ln (1 − α)vs ln time $\sim$1 at all temperatures, suggesting that the concept of an order of reaction is valid. A statistical and graphical analysis of the results Fig. 5 and Table 3 leads to the conclusion that a phase boundary controlled process in two dimensions (R$_2$) best describes the kinetics. The results of our calculations are similar for [Ni(phen)$_3$] (ClO$_4$)$_2$, however the delineation of the mechanism between those based on order (F$_1$R$_2$ or.R$_3$) is not quite so clear as for the corresponding iron complex.

For the bipyridyl complexes the gradients of ln time vs ln–ln (1 − α) plots are much steeper (Table 3), suggesting nucleation and growth kinetics are appropriate. Yamamoto's plots of ln(1 − α) vs time are not colinear with the origin for any of these complexes, and many graphs show marked curvature. The slopes of the ln–ln(1 − α) plots lead to the conclusion that nucleation and growth in two dimensions occur for the nickel complex and in three for the iron complex. For all four complexes reduced time plots indicate that the reactions belong to the types postulated above. The quantity of data available is·
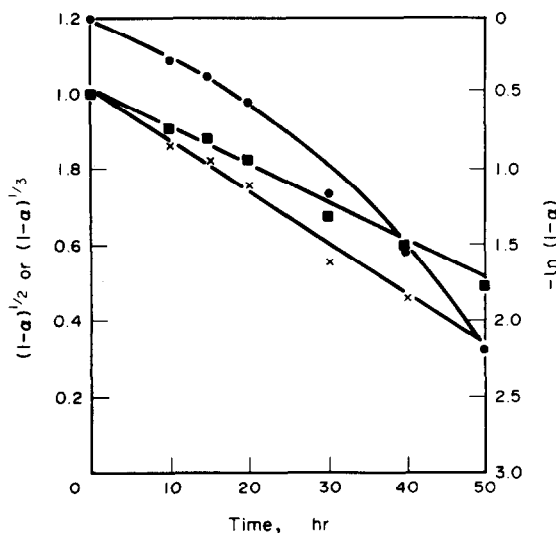
Fig. 5. Comparison of rate laws for the racemization of Fe(phen)$_3$(ClO$_4$)$_2$. Graphical representation of various rate laws: ● ln (1 − α), ■ (1 − α)$^{1/3}$, × (1 − α)$^{1/2}$.

Table 3. Summary of rate constant calculations

Compound	T K	10^6 k/s	r^a	m^b	Rate law	$E_a{}^c$	10^6 k/s	$E_a{}^{cd}$
[Fe(phen)$_3$](ClO$_4$)$_2$	413	0.486	0.936	~1.3	$(1-\alpha)^{1/2}$	173	0.777	179
	421	1.36	0.942	~1.2			1.81	
	428	3.76	0.996	~2.0			6.38	
	435	5.71	0.984	~1.0	$R_2(\alpha)$		9.72	
[Ni(phen)$_3$](ClO$_4$)$_2$	460	7.86	0.994	~1.2	$(1-\alpha)^{1/2}$	214	0.944	272
	463	11.4	0.976	~1.1			2.13	
	470	33.0	0.992	~1.2			5.83	
	475	41.2	0.919	~1.1	$R_2(\alpha)$		13.6	
[Fe(bipy)$_3$](ClO$_4$)$_2$	398	4.99	0.861	~3.0	$^3\sqrt{-\ln(1-\alpha)}$	140	0.306	188
	405	8.38	0.968	~5.0			0.917	
	413	15.4	0.984	~3.0			2.31	
	421	5.34	0.961	—	$A_3(\alpha)$		6.67	
[Ni(bipy)$_3$](ClO$_4$)$_2$	456	7.47	0.992	~1.7	$^2\sqrt{-\ln(1-\alpha)}$	141	0.333	209
	463	16.01	0.993	~1.9	$A_2(\alpha)$		1.25	
	468	22.9	0.951	~1.7			1.83	
	476	36.2	0.991	~2.2			3.89	

^{a}Correlation coefficient.
^{b}m, slope of plot of ln time vs ln–ln $(1-\alpha)$.
^{c}Activation energy in kJ mole^{-1}.
^{d}Results of Yamamoto. Ref. 9.

unfortunately rather limited both in terms of α vs time and temperature range, however it seems clear that there is little theoretical justification for the use of a first order rate law.

Yamamoto[9] also correlated variations in activation parameters, most notably for the racemization of (–)[Ni(bipy)$_3$] with the donicity of the lattice counter ions. Unfortunately in this paper full data were not reported, however activation parameters are often relatively insensitive to the rate law chosen.[13] As a first approximation published values of $\Delta H^{\ddagger}$ for the racemization of [Ni(bipy)$_3$] as the perchlorate, iodide bromide and chloride are considered. An alternative explanation for this marked variation in enthalpies of activation with counter ion could be changes in lattice energy. Lattice energies may be approximated by the Kapustinski equation[38,39] shown in its simplest form below (5):

$$U = \frac{287.2\gamma Z_+ Z_-}{d_0}\left[1 - \frac{0.345}{d_0}\right]$$

or

$$U \approx \frac{287.2\gamma Z_+ Z_-}{d_0} \tag{5}$$

(where $d_0 = r_a + r_c$ the sum of ionic radii of anion and cation).

The lattice energy with a constant cation is thus approximately inversely proportional to the radius of the anion. Figure 6 shows a plot of $(\Delta H^{\ddagger})^{-1}$ against r_a for the perchlorate, iodide, bromide, chloride of optically active [Ni(bipy)$_3$]. A clear correlation exists and although at present tentative, such ideas are probably worthy of more attention.

6. ETHYLENE DIAMINE COMPLEXES

(a) l cis-[Cr(en)$_2$Cl$_2$]Cl·H$_2$O

This complex was found[5] to racemize only during dehydration; no evidence was found for the racemization of the anhydrous complex. Bailar and Le May concluded that a scheme of the kind shown below explained their observations:

$$l\text{-}cis\text{-}[Cr(en)_2Cl_2)Cl_2]Cl \cdot H_2O \rightarrow l\text{-}cis\text{-}[Cr(en)_2Cl_2]Cl + H_2O$$

$$l\text{-}cis\text{-}[Cr(en)_2Cl_2]Cl + H_2O \rightarrow l\text{-}cis\text{-}[Cr(en)_2Cl(H_2O)]Cl_2$$

$$l\text{-}cis\text{-}[Cr(en)_2Cl(H_2O)]Cl_2 \rightarrow rac\text{-}cis\text{-}[Cr(en)_2Cl_2]Cl + H_2O.$$
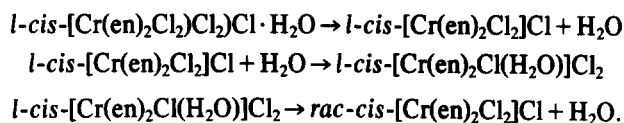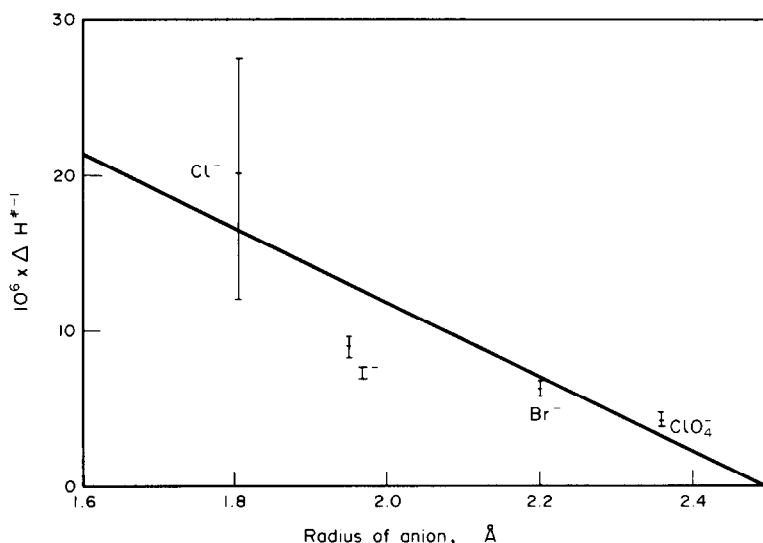
Fig. 6. Correlation of activation energy and radius of anion for [Ni(bipy)$_3$]X$_2$. A plot of $\Delta H^{\ddagger-1}$ vs r_a, correlation coefficient = 0.851; the point corresponding to Cl$^-$ is well off the line and carries a large error bar (based on Yamamoto's data), excluding this point the correlation is excellent viz. correlation coefficient = 0.994. It is interesting to note that the higher values of $\Delta H^{\ddagger}$ are associated with the lower lattice energies (when calculated by Kapustinski's method). This is the opposite of our intuitive expectations. Little is known of the processes involved in racemization and at present the correlation presented is purely empirical.

Racemization occurring in the second or third steps. Interestingly X-ray powder pictures showed $d \cdot l$-cis-[Cr(en)$_2$Cl$_2$]Cl obtained by dehydrating the racemic compound to have a markedly different structure from rac-cis-[Cr(en)$_2$Cl$_2$]Cl obtained by the simultaneous dehydration and racemization of the l complex. This is the only detailed study of an optically active cis-bis-chelated complex, and in contrast to tris-chelated complexes the anhydrous complex has not been shown to racemize.

Some analogy may be drawn with solution studies of similar complexes, the rate of racemization has been found to be similar to the rate of chloride exchange, again suggesting an "aquation–anation" pathway. The solid state racemization of this complex is worthy of more attention, chloride exchange during racemization/dehydration could provide firmer evidence for the above mechanism. Isothermal studies of the dehydration of the optically active complex would be expected to show more than one mechanism of dehydration to occur. Finally, an interesting and unassigned exotherm was noticed in the DTA of l-cis-[Cr(en$_2$Cl$_2$]Cl H$_2$O, the origin of which may be significant.

(b) (+)-[Co(en)$_3$]X$_3$·nH$_2$O

The racemization of optically active [Co(en)$_3$]I$_3$ in the solid state was first reported by Dwyer et al.[40] A detailed study of this system was undertaken by Kutal and Bailar.[6] The mechanism was attributed to a twist process; the marked acceleration of racemization during dehydration at higher temperatures being attributed to disruption of the lattice. Electron microscopy revealed marked modification to the crystal after dehydration, but no interface could be detected for the racemization process.

Samples dehydrated at relatively low temperature, when heated to high temperature underwent thermal racemization. Quantitative kinetic studies for such samples were not reported, and for no samples was the reaction followed to completion. However qualitatively the rate of racemization was reproducibly found to be I$^-$ > Br$^-$ > Cl$^-$ (Fig. 7); this is exactly the order expected if lattice energy were controlling the reaction vide supra. Although no formal kinetics were studied by Kutal and Bailar this singularly thorough study used many of the techniques listed in Section 3 and as such remains unique. It is reasonable to suggest that such reactions could and should be followed to completion if possible, and that a more detailed kinetic study might reveal much new information.

(c) Other ethylene diamine complexes

d-cis-[Co(en)$_2$[H$_2$O)Cl]Cl$_2$. was shown[41] to undergo simultaneous, racemization, anation and dehydration at 100°C.
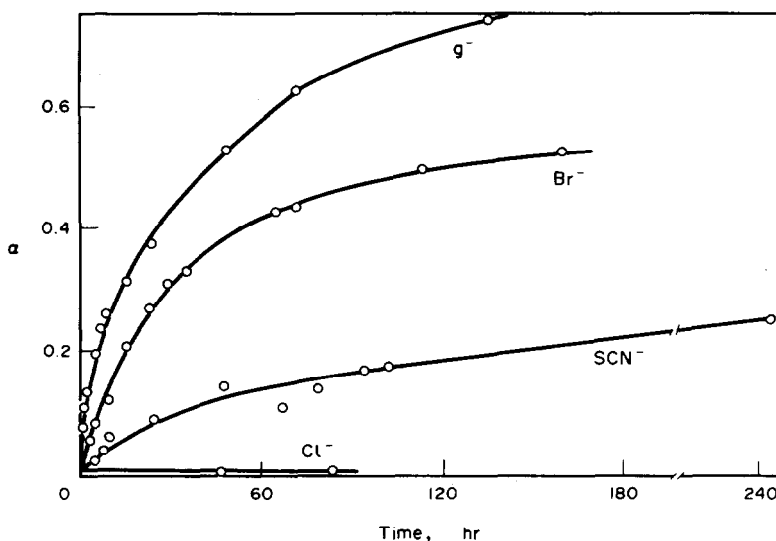
Fig. 7. Effect of counter ion on the racemization of (+)-[Co(en)₃]X₃ at 127°C.

d-cis-[Co(en)₂Cl₂]Cl·H₂O. Racemized largely after dehydration[5] (24 hr at 160°C), no conversion to the *trans* isomer was observed. Insufficient is known of these racemizations for any serious speculation regarding mechanism to be made.

7. COBALOXIME COMPLEXES

A series of papers have appeared[48-50] reporting the racemization of complexes of the kind R-α-cyanoethyl (s-α-methylbenzylamine) cobaloxime. The cyano ethyl group in this complex racemizes during X-ray exposure at ambient temperatures. The mechanism suggested for this unusual reaction is that a planar cyanoethyl radical produced by Co–C band cleavage, rotated about the CoC=N axis to face the opposite side of the plane to the cobalt atom; then recombines to give the racemic complex.

8. PRESSURE INDUCED RACEMIZATION

High pressure of the order of 10,000 atm promotes the racemization of (−) K₃[Co(C₂O₄)₃],[42,44] (+) [Ni(phen)₃] (ClO₄)₂[43,45] and (−)[Fe(phen)₃] (ClO₄)₂.[43] A first order model was used as the basis of the kinetic analysis in each of these studies; for (−)K₃[Co(C₂O₄)₃][44] the fit obtained to a first order rate law is excellent (although some unspecified correction for decomposition was made). The limited quantities of data available from such studies make verification of the rate law difficult.

In all the above cited studies negative volumes of activation [$\Delta V^{\ddagger}$] were found. It seems likely that the sign of the volume of activation will be unaffected by the choice of rate law and that these negative values are reliable. Negative values of $\Delta V^{\ddagger}$ are usually correlated with a twist type of mechanism for racemization, and this was concluded to be the case in all the above studies.[42-45] However it is difficult to make a very strong case based on negative values of $\Delta V^{\ddagger}$ alone. As pointed out by Brady *et al*.[44] lattice distortions over large distances, which may accompany local volume changes in the complex ion, make it difficult to interpret volumes of activation in terms of volume changes of the complex ion alone. Also the extrapolation of high pressure results[42] for Ni(II) and F(II) tris phenanthroline complexes to atmospheric pressure suggests a fairly high rate of racemization for these complexes in the solid state under ambient conditions; this is known not to be the case. A mechanism change at high pressures provides a possible explanation for this observation.

Perhaps analogy with solution chemistry is useful here; it has recently been shown [46,47] that negative values of $\Delta V^{\ddagger}$ may be consistent with dissociatively activated mechanisms. Thus causing earlier ideas[46] based on a simple interpretation of $\Delta V^{\ddagger}$ alone to be revised. The interpretation of the solution kinetics experiments is generally much less ambiguous than that of corresponding ones in the solid state but much caution is obviously needed in equating the magnitude and sign of volumes of activation with molecular mechanisms.

9. CONCLUSIONS

There are a number of general and specific conclusions to be drawn from this article. Firstly, well documented rate laws for solid state processes may well describe the kinetics of racemization of coordination compounds in the solid state better than the generally applied unimolecular rate law. Some methods of screening kinetic data have been briefly outlined. As the rate determining step may be rearrangements within the lattice itself, the correlation of activation parameters, etc. with molecular changes responsible for the reaction may not in many cases be possible. The kinetics of solid state reactions is a complicated and often contentious matter, studies limited to formal kinetics are not recommended, and the comment of Gomes on the application of rate laws should always be borne in mind.[51]

On a more specific level the role of lattice water in solid state racemization needs careful consideration. Frequently anhydrous and hydrated samples of a complex have been compared with no regard to the fact that during dehydration the crystal structure is much disrupted. The anhydrous sample may well contain many new defects, providing one explanation of the frequent observation,[9,44] that anhydrous complexes racemize more rapidly than hydrated ones.

In marked contrast the absence of solid state racemization when water is not present e.g. $[Cr(en)_2Cl_2]Cl^5$ may implicate water in the mechanisms. In the case of optically active $K_3[Cr(ox)_3]$ two mechanisms operate. The hydrated form racemizes rapidly, possibly by expansion of the co-ordination sphere with lattice water, the anhydrous complex more slowly by a phase boundary controlled process.

Crystallography has not yet provided the necessary structures of racemate and optically active complex needed for a better understanding of solid state racemizations. Indeed the frequent observation,[5,7] that the thermally racemized solid complex has a different crystal structure from dehydrated racemic complex needs further investigation. The crystal structures of some of these apparently simple complexes are not trivial and a recent extensive investigation[52] of d-l-$K_3[Cr(ox)_3]$ highlights this problem.

The kinetics and mechanism of solid state racemizations are as yet relatively poorly understood. Only with a proper appreciation of the complexity of solid state processes can real progress be made. In many ways the ideas expressed in this article are in line with recent suggestions (of a general nature) made by House,[53] and have been briefly outlined earlier by the author.[54]

REFERENCES

[1] A. Werner and A. Frohlich, *Chem. Ber.* 1907, **40**, 2228.
[2] N. Serpone and D. G. Bickley, *Prog. Inorg. Chem.* 1972, **17**, 391.
[3] C. H. Johnson and A. Mead, *Trans. Farad. Soc.* 1933, **29**, 626.
[4] C. H. Johnson, *Trans. Farad. Soc.* 1935, **31**, 1612.
[5] H. E. LeMay Jr. and J. C. Bailar Jr., *J. Amer. Chem. Soc.* 1968, **90**, 1729.
[6] C. Kutal and J. C. Bailar Jr., *J. Phys. Chem.* 1972, **76**, 119.
[7] D. M. Chowdry and G. M. Harris, *J. Phys. Chem.* 1969, **73**, 3366.
[8] A. Tatehata, T. Kumamaru and Y. Yamamoto, *J. Inorg. Nucl. Chem.*, 1971, **33**, 3427.
[9] T. Fujiwara and Y. Yamamoto, *Inorg. Chem.* 1980, **19**, 1904.
[10] D. A. Young, *Decomposition of Solids.* Pergamon Press, Oxford (1966).
[11] W. E. Garner, *Chemistry of the Solid State.* Butterworths, London (1955).
[12] W. L. Ng, *Austral. J. Chem.*, 1975, **28**, 1169.
[13] S. F. Hulbert, *J. Brit. Ceram. Soc.* 1969, 11.
[14] J. H. Sharp, G. W. Brindley and B. N. Narahari Achar, *J. Amer. Ceram. Soc.*, 1966, **49**, 379.
[15] J. D. Hancock and J. H. Sharp, *J. Amer. Ceram. Soc.*, 1972, **55**, 74.
[16] P. W. M. Jacobs and F. C. Tompkins, p. 184, in Ref. 11.
[17] S. D. Ross, *Int. J. Chem. Kinetics*, 1982, **14**, 535.
[18] P. O'Brien and S. D. Ross, *Thermochimica Acta.* 1981 **46**, 327.
[19] L. F. Jones and D. Dollimore, T. Nicklin, *Thermochimica Acta.* 1975, **13**, 240.
[20] K. J. Gallagher, In *Reactivity of Solids. Proc. 5th I.S.R.S.* (Edited by G. M. Schwab), p. 192. Munich, 1964, Amsterdam 1965.
[21] J. H. Taplin, *J. Am. Ceram Soc.* 1974, **57**, 140.
[22] P. C. Kapur, *J. Am. Ceram Soc.* 1973, **56**, 79.
[23] R. Giovanoli and R. Brutsch, *Thermochimica Acta.* 1975, **13**, 15.
[24] K. J. Gallagher, W. Feitknecht and A. Mannweiler, *Nature*, 1968, **217**, 1118.
[25] W. Feitknecht, *Pure Appl. Chem.* 1964, **9**, 423.
[26] R. Grovanoil and R. Brütsch, *Chimia* 1974, **28**, 188.
[27] F. A. Cotton, *Chemical Applications of Group Theory*, 2nd Edn. Wiley-Interscience, New York (1971).
[28] R. G. Pearson. *J. Amer. Chem. Soc.*, 1972, **94**, 8287.

[29]R. G. Pearson, *Acc. Chem. Res.* 1971, **4**, 152.

[30]D. R. Eaton, *J. Am. Chem. Soc.*, 1968, **90**, 4272.

[31]T. H. Whitesides, *J. Am. Chem. Soc.* 1969, **91**, 2395.

[32]J. C. Bailar Jr., *J. Inorg. Nucl. Chem.* 1958, **8**, 165.

[33]P. Ray and K. Z. Datt, *J. Indian Chem. Soc.* 1943, **20**, 81.

[34]C. S. Springer and R. E. Sievers, *Inorg. Chem.* 1967, **6**, 852.

[35]C. H. Johnson and A. Mead, *Trans. Farad. Soc.* 1939, **31**, 1621.

[36]M. Billardon, *J. Chim. Phys.* 1965, **62**, 273.

[37]D. M. Chowdry, Thermal and radiation effects on the solid state racemization of d-potassium tris oxalato chromium(III) complex. Ph.D. Thesis 1967. State University of New York at Buffalo.

[38]A. F. Kapustinski, *Quart Revs. Chem. Soc.* 1956, 238.

[39]The notation is used of J. Lagowski, *Modern Inorganic Chemistry*. Marcel Dekker, New York (1973).

[40]J. A. Brromhead, F. P. Dwyer and J. W. Hogart, *Inorg. Synth.* 1960, **6**, 183.

[41]J. P. Mathieu, *Bull. Soc. Chim. France.* 1937, **4**, 687.

[42]J. Brady, F. Dachille and C. D. Schmulbach, *Inorg. Chem.* 1963, **2**, 803.

[43]C. D. Schmulbach, F. Dachille and M. E. Bunch, *Inorg. Chem.* 1964, **3**, 808.

[44]C. D. Schmulbach, J. Brady and F. Dachille, *Inorg. Chem.* 1968, **7**, 287.

[45]G. E. Humiston and J. E. Brady, *Inorg. Chem.* 1969, **8**, 1773.

[46]F. K. Meyer, K. E. Newman and A. E. Merbach, *J. Am. Chem. Soc.* 1979, **101**, 5588.

[47]C. H. Langford, *Inorg. Chem.* 1979, **18**, 3288.

[48]Y. Ohashi and Y. Sasada, *Nature* 1977, **267**, 142.

[49]Y. Ohashi, Y. Sasada and Y. Ohgo, *Chem. Lett.* 1978 457.

[50]Y. Ohashi, Y. Sasada and Y. Ohgo, *Chem. Lett.* 1978, 743.

[51]W. E. Gomes, *Nature* 1961, **192**, 865.

[52]D. Taylor, *Austral. J. Chem.*, 1978, **31**, 1455.

[53]J. E. House Jr., *Thermoc. Act*, 1980, **38**, 59.

[54]P. O'Brien, *J. Chem. Soc. Dalton* 1982, 1173.

BINARY, TERNARY AND QUATERNARY COMPLEXES INVOLVED IN THE SYSTEMS PYRIDOXAMINE-GLYCINE-IMIDAZOLE WITH SOME BIVALENT METAL IONS

MOHAMED S. EL-EZABY*†, MOUSTAFA RASHAD† and NAGIB M. MOUSSA‡
Faculty of Science, Kuwait University, Kuwait

Abstract—Equilibrium-based computer models using MINIQUAD-75 program were utilized to determine the stoichiometry and formation constants involved in the systems pyridoxamine(Pm)-glycine (Gly)-imidazole (Imd) with CO(II), Ni(II), Cu(II), Zn(II) and Cd(II) metal ions. The data were obtained from potentiometric pH titration of the various binary, ternary and quaternary systems under physiological-like conditions (0.15 M NaNO₃–37°C). Various composition ratios of metal and ligands were used. The ligand concentrations did not exceed 4 times the concentration of metal ion in the binary systems and 4 times of the metal ions in ternary systems. In case of the quaternary systems only imidazole concentrations were two or four times the concentrations of metal ions keeping those of other ligands equal to that of metal ions. The stability constants of the quaternary species are discussed in terms of binary and ternary constants as are the effect of ring size on the stability of mixed ligand species. In addition, electrostatic as well as statistical effects also are mentioned and the biological implications of these model equilibria are described.

INTRODUCTION

Considerable progress has been made in the last two decades in the treatment of many diseases by the introduction of long-term feeding regimens and/or drug treatment. For instance gastrointestinal diseases may be treated by the introduction of long-term supplementation of solutions with protidic, lipidic and glucidic compositions that have been found to be suitable for maintaining healthy tissue metabolism in patients.[1] A major concern lies in the adequate supply of essential trace metals which should be included in the regimens to avoid impairment in some biochemical processes. Supplementation of trace metal concentrations in nutritive mixtures have been made.[2] The doses appear to have been chosen somewhat randomly and very little correlation between the administered levels, plasma concentrations and overall metal ion balance was observed.[3] This may lead to the toxicity by the unknown greater concentration of an essential metal ion and the loss of the relationship between the nutritive requirement for a metal ion and its rate of excretion. A better understanding of the interactions between ligands and metal ions is essential prior to any chemotherapeutic medical treatment. Many attempts to correlate physiological responses with the 1:1 metal-ligand binary formation constants have appeared in the literature.[4] These fail to take into account a large number of other important reactions that determine the overall degree of complexation such as protonation, ternary and quaternary complex equilibria.

In this study we have investigated the equilibria which may be involved in the interaction of pyridoxamine (a vitamin B₆ compound), glycine and imidazole with some divalent metal ions. This may serve as an example of the presence of not only binary complexes but also ternary as well as quaternary complexes in biological fluids.

Moreover, glycine in combination with imidazole may serve as a model for histidine interaction with metal ions.

EXPERIMENTAL

The ligands glycine (Gly) (>99%; BDH), (99%; BDH) and pyridoxamine dihydrochloride (Pm) (>99%; Merck) were used without further purification. Imidazole (Imd) (Aldrich) was crystallized from benzene and dried under reduced pressure. The stock solutions of the ligands were kept at 5°C in dark.

Cobalt(II), nickel(II), copper(II), zinc(II) and cadmium(II) nitrates (>99%; BDH) were used as provided. The concentrations of the stock solutions were checked by potentiometric methods. The method is essentially EDTA titration of metal ions using Radiometer pH meter model pH M62 provided with Radiometer cupric selectrode type 1112 Cu as indicator electrode and Radiometer calomel electrode type K401 as a reference electrode[5].

The titrimetric data were acquired using Orion Research microprocessor ionalyzer type 901, using Radiometer combined glass electrode type GK 2301 C. The ionalyzer in the pH mode was calibrated using two Radiometer buffers at pH's 6.98 and 4.03 at 37°C. All pH-metric titrations were carried out as previously described[6]. The ionic strength of all titration solutions was adjusted to 0.15 M NaNO₃. The temperature of the titration cell was kept constant at 37°C. The titrant in most cases was a solution of 0.1 M carbonate-free NaOH which was 0.15 M in NaNO₃ and in few cases was 0.1 M HNO₃. In all titrations, purified nitrogen was passed into the solution before and during the titration time. The metal ion concentration was in the range (0.6–2.0)10⁻³ M. The ligand concentrations did not exceed 4 times the concentration of metal ions in the binary systems. In ternary systems, the concentrations of each ligands were not more than twice the concentration of metal ions except in case of imidazole where its concentration did not exceed 4 times that of metal ions. In the quaternary systems, the concentrations of each ligand was identical to that of metal ions except imidazole where its concentration was not more than 4 times that of metal ions. Multiple titrations were carried out for each system. The hydrogen-ion concentration was taken as 10⁻ᵖᴴ.

Methods

Titration data were analysed by using MINIQUAD-75 program[7]. Different equilibrium models have been tested. The results were assessed by observing the values of chi square (Xi^2),

---
*Author to whom correspondence should be addressed.
†Department of Chemistry.
‡Department of Biochemistry.

Table 1. Protonation constants of Pm, Gly, and Imd at $1.0 = 0.15$ M and T = 37°C, n = number of titration points, and σ = standard deviation

System	l p q r s*	log β (σ)⁺	n	pH range	literature values	Ref., I,T
Pm	1 0 0 0 1	10.407(.012)	388	6.7-10.5	10.40	6, 0.5,30°
	1 0 0 0 2	18.562(.019)			18.45	
	1 0 0 0 3	22.063(.010)	96	3.2-4.4	21.95	
Gly	·0 1 0 0 1	9.335(.001)	158	7.6-10.3	9.38	8, 0.15, 37°
	0 1 0 0 2	11.868(.002)	159	4.3-2.4	11.76	
Imd	0 0 1 0 1	7.090(.003)	51	6.1-9.3	7.12	9, 0.2, 25°

* l, p, q, r, s are the stoichiometric coefficients corresponding to Pm⁻, Gly⁻, Imd, M^{2+}, and H^+, respectively.

⁺ The ranges of S, Xi^2 and R are $((4.37-60.0)10^{-8})$, (38-88) and (.002-.036), respectively.

crystallographic factor (R) and sum of squared residuals (S). The model which gave the lowest R values, Xi^2 value (or both) and S value has been adopted taking in consideration the errors in experimental quantities and rules for propagation of errors.

The protonation constants of Pm, and Gly were determined by titrating 25 ml of the aqueous solution of the ligands in the concentration range $(1-3)10^{-3}$ M with CO_3^{2-} free NaOH of 0.1 M. In addition, 25 ml of the aqueous solutions of Gly and Imd in the concentration range of $(0.5-1.0)10^{-2}$ M were titrated with 0.1 M HNO_3. Table 1 depicts the values of protonation constants obtained at I = 0.15 M and T = 37°C.

The conditions of measurements for the determination of the

Table 2(a). Formation constants of the binary metal complexes of Pm at I = 0.15 M, T = 37°C, n = number of titration points and σ-standard deviation

M^{2+}	l p q r s	log β (σ)⁺	n	pH range	literature values	Ref.,I,T
Co	1 0 0 1 0	5.591(.037)	144	7.1-9.1	5.09	15,0.1,25°
	2 0 0 1 0	10.255(.054)			9.60	
	2 0 0 1 2	27.435(.055)				
Ni	1 0 0 1 0	6.464(.017)	136	6.8-9.7	6.00	
	1 0 0 1 1	14.203(.055)				
	2 0 0 1 0	10.521(.036)			10.92	
	2 0 0 1 2	28.137(.072)				
Cu	1 0 0 1 1	17.225(.023)	328	3.1-4.7		
	1 0 0 1 2	21.337(.034)				
	2 0 0 1 3	38.914(.021)				
	1 0 0 1 0	10.805(.033)	174	6.7-8.4	10.20	
	2 0 0 1 0	17.471(.018)			15.97	
	2 0 0 1 1	25.458(.017)				
	2 0 0 1 2	32.535(.044)				
Zn	1 0 0 1 0	6.411(.034)	276	7.0-8.9	5.68	
	2 0 0 1 0	11.874(.050)				
Cd	1 0 0 1 0	5.379(.011)	426	6.5-9.2	4.59	
	2 0 0 1 0	8.214(.295)				
	1 0 0 1 1	13.231(.032)				

⁺ The ranges of S, Xi^2 and R are $((1.21-401.0)10^{-8})$, (7-171) and (.003-.034), respectively.

Table 2(b). Formation constants of binary metal complexes of Gly at I = 0.15 M and 37°

M^{2+}	l p q r s	log β (σ)[+]	n	pH range	literature values	Ref., I, T
Co	0 1 0 1 0	4.651(.068)	158	7.4-9.1	4.64	17
	0 2 0 1 0	8.490*			7.98	.2, 40°
	0 3 0 1 0	12.377(.054)			10.76	19, .15,26°
Ni	0 1 0 1 0	5.554(.014)	180	6.3-9.9	5.70	8
	0 2 0 1 0	9.978(.015)			10.47	.1, 30°
Cu	0 1 0 1 0	7.832(.005)	126	3.8-6.4	8.17	8
	0 2 0 1 0	13.870(.010)			15.06	.1, 30°
Zn	0 1 0 1-2*	-11.681(.046)	162	7.0-9.0		
	0 1 0 1-1†	-3.214(.096)				
	0 1 0 1 0	5.205(.033)			4.90	21
	0 2 0 1 0	9.019(.142)			9.01	
	0 3 0 1 0	12.687(.123)			11.31	
Cd	0 1 0 1 0	4.618(.082)	244	7.7-9.9	4.60	22, .2, 40°
	0 1 0 1 1	12.560(.119)				
	0 2 0 1 0	6.585(.105)			8.20	

* The -ve sign indicates dissociation of proton from the ligand or the formation of hydroxy species or both.

+ Ranges of values of S, Xi² and R did not exceed 1.0x10⁻⁶, 150 (except in few cases) and 0.040, respectively.

† Estimated value .

Table 2(c). Formation constants of the binary metal complexes of Imd at I = 0.15 and T = 37°C

M^{2+}	l p q r s	log β (σ)	n	pH range	literature values	Ref. I,T
Co	0 0 1 1 0	3.027(.039)	98	6.1-7.9	2.47	24
	0 0 2 1 0	5.601(.035)			4.40	.16,25°
Ni	0 0 1 1 0	3.198(.031)	274	5.6-8.6	3.09	24
	0 0 2 1 0	5.250(.178)			5.56	.16,25°
	0 0 4 1 0	10.113(.300)			9.10	
Cu	0 0 1 1 0	4.015(.019)			4.31	24
	0 0 2 1 0	7.550(.023)			7.84	.16,25°
	0 0 2 1-2	-8.487(.018)	294	4.6-8.1		
	0 0 3 1 0	10.079(.101)			10.76	
	0 0 8 2 0	29.666(.053)				
Zn	0 0 1 1 0	2.982(.056)	122	6.1-7.5	2.57	25
	0 0 2 1 0	5.632(.070)			4.93	
Cd	0 0 1 1 0	2.737(.080)	154	6.3-7.9	2.620	8
	0 0 2 1 0				4.650	.15,35°
	0 0 3 1 0				6.200	
	0 0 4 1 0				7.160	

* The values of S, Xi² and R did not exceed 1.0E-6, 261 (depending on the number of titration data) and .013, respectively.

stability constants of the binary, ternary and quaternary complex species were the same as for the protonation constants of ligands. The composition ratios of ligands to metal ions (M^{2+}) were always 1:1, 2:1, and 3:1 in case of Gly:M^{2+} and Pm:M^{2+} and 2:1 and 4:1 in case of Imd:M^{2+} binary systems. Table 2 lists the values of stability constants of the binary systems. In the ternary systems, the ratios of Pm:Gly:M^{2+} were 1:1:1, 1:2:1, 2:1:1, while the ratios of Pm:Imd:M^{2+} and Gly:Imd:M^{2+} were 1:2:1 and 1:4:1. Table 3 depicts the values of the ternary stability constants obtained in this work. In the quaternary systems, the ratios of Pm:Gly:Imd:M^{2+} were 1:1:2:1 and 1:1:4:1. The values of the stability constants are listed in Table 4.

In calculating the stability constants of the binary complexes using MINIQUAD-75 program, the protonation constants were kept constant while varying the values of the binary species. In case of ternary systems, the values of protonation constants of ligands and the stability constants of binary complex species were kept constant while varying those of ternary complex species. In case of the quaternary system the values of protonation constants of ligands, the stability constants of 1:1 binary complex species and those of 1:1:1 ternary complex were kept constant while varying those of the quaternary complex species.

The ionization of water (pK_w) was taken to be 13.38 at $I = 0.15$ and 37°C.[10]

RESULTS AND DISCUSSION

Binary metal complexes

Interactions of the bivalent metal ions Co(II), Ni(II), Cu(II), Zn(II) and Cd(II) with the ligands Pm, Gly and Imd have been the subject of many reports.[11-25] The formation constants have been re-evaluated at the ionic strength, $I = 0.15$ M and temperature of 37°C (this being isotonic with blood plasma). If allowance is made for the effect of

different reported solution media, some of the formation constants reported in this work are more or less in accord with those reported by other authors, Table 2 (a, b and c).

Although, pyridoxamine complexes of various metal ions have been studied by different investigators[6,11,15] variation in their results are mostly due to variation in experimental conditions and methods of calculation. Upon using wider pH range and different initial metal ion and Pm concentrations, revealed that Cu(II)–Pm system may exhibit somewhat different set of equilibria from what have been previously reported, Table 2(a). In the Cu(II)–Pm system, the titration data were divided into two parts at two pH ranges, 3.1–4.7 and 6.5–8.4. Upon analyzing the data at lower pH range by using MINIQUAD-75 program, protonated binary Cu(II)–Pm complexes were obtained, Table 2(a). In the 1:1:1 (Pm:Cu(II):H) species, it is believed that the proton is located on the hetero-nitrogen atom of Pm rather than on the amino group if a 6-membered chelate is assumed to be formed. In such case, the protonation constant of the hetero-nitrogen atom should be greater than that of the amino group, opposite to what one expects for the free ligand. Other protonated species may indicate that Pm can also act as monodentate ligand species. The formation constants of the non-protonated species were obtained at the higher pH range when the titration data were analysed by the same program keeping those obtained at lower pH range constant.

The other bivalent metal ions-Pm equilibrium reactions are more or less in agreement with those previously reported, Table 2(a). Moreover, it has been proved that Pm cannot form *tris*-metal complex species under the experimental conditions used.

Table 3(a). Formation constants of the ternary metal ion complexes at $I = 0.15$ and $T = 37$°C for Pm–Gly systems

M^{2+}	l p q r s	$\log \beta$ (σ)	S	XI^2	R	n	pH range	Reported values	Ref.,I,T
Co	1 1 0 1 0	9.309(.281)	1.01E-6	128	.021	193	6.8–9.7	10.49	,.5,30
	1 1 0 1 1	17.746(.299)						18.38	
	1 2 0 1 0	13.787(.087)						13.79	
Ni	1 1 0 1 0	11.538(.060)	1.34E-6	288	.023	248	6.3–10.0	11.54	" "
	1 1 0 1 1	19.170(.291)						19.57	
	1 2 0 1 1	23.669(.149)							
Cu	1 1 0 1 0	16.605(.165)	2.20E-7	80	.010	192	3.2–10.1	16.99	
	1 1 0 1 1	25.394(.119)						24.61	
	1 1 0 1 2	31.515(.124)							
	1 1 0 1 3	35.930(.133)							
	1 2 0 1 1	30.078(.136)							
	1 2 0 1 2	37.946(.210)							
	2 1 0 1 2	39.490(.127)							
Zn	1 2 0 1 1	23.301(.119)	7.64E-8	101	.010	86	6.8–9.3		
	2 1 0 1 4	47.910(.174)							
Cd	1 1 0 1 0	8.625(.069)	4.00E-7	109	.012	278	7.0–9.7		
	1 2 0 1 1	21.372(.104)							
	1 2 0 1 2	30.586(.089)							
	2 1 0 1 4	48.717(.081)							

Table 3(b). Formation constants of the ternary metal ion complexes at I = 0.15 and T = 37°C for Pm–Imd systems

M^{2+}	l p q r s	log β (σ)	S	xi^2	R	n	pH range
Co	1 0 1 1 1	16.947(.071)	2.46E-7	118	.007	204	6.7-9.2
	1 0 3 1 0	14.502(.026)					
	2 0 2 1 0	16.517(.042)					
	2 0 2 1 2	33.925(.042)					
Ni	1 0 1 1 1	17.984(.035)	1.16E-7	112	.008	186	6.7-9.7
	1 0 3 1 0	15.697(.033)					
	2 0 2 1 0	17.649(.044)					
	2 0 2 1 2	34.873(.072)					
Cu	1 0 1 1 1	21.049(.044)	2.29E-7	39	.006	242	4.0-8.3
	1 0 2 1 0	16.788(.033)					
	1 0 2 1 1	24.060(.040)					
	2 0 2 1 1	31.388(.045)					
Zn	1 0 2 1 2	28.125(.180)	6.07E-7	486	.016	232	6.7-8.1
	1 0 3 1 0	16.203(.083)					
	1 0 4 1 2	34.307(.084)					
	2 0 1 1 0	16.150(.093)					
Cd	1 0 1 1 0	8.494(.037)	1.06E-7	218	.008	204	6.7-9.4
	1 0 1 1 1	17.500(.028)					
	1 0 2 1 2	27.818(.060)					

Table 3(c): Formation constants of the ternary complexes at I = 0.15 and T = 37°C for Cly-Imd systems

M^{2+}	l p q r s	log β (σ)	S	xi^2	R	n	pH range
Co	0 1 1 1 0	7.889(.031)	2.75E-7	116	.010	180	7.3-9.2
	0 1 4 1 0	15.514(.058)					
Ni	0 1 1 1 0	8.849(.032)	6.23E-8	118	.007	184	7.0-9.5
	0 1 4 1 0	16.846(.101)					
	0 2 2 1 0	16.247(.020)					
Cu*	0 1 1 1 0	11.86(.064)	7.11E-8	135	.006	164	6.3-9.4
	0 1 3 1 0	18.080(.046)					
	0 2 1 1 0	16.856(.070)					
Zn	0 1 1 1 0	7.911(.138)	1.40E-6	256	.027	234	6.7-8.8
	0 1 4 1 0	16.693(.117)					
Cd	0 1 1 1-1	-0.341(.023)	5.16E-7	107	.020	184	7.4-9.2
	0 1 1 1 0	8.030(.038)					

* M. Mohan et al. (19) obtained log β values for the complex species

   o 1 1 1 0 and 0 1 2 1 0 equal to 12.16 and 15.14, respectively.

Table 4. Formation constants of metal ions complexes involved in the quaternary systems under consideration at I = 0.15 and 37°C, S = sum of squared residuals, Xi^2 = Chi square and R = crystallographic factor

M^{2+}	l p q r s	log β (σ)	S	XI^2	R	n	pH range
Co^{2+}	1 1 1 1 0	13.174(.049)	1.24E-7	17	.007	140	6.7-9.2
	1 1 1 1 1	21.958(.112)					
	1 1 1 1 2	29.321(.368)					
	1 1 2 1 1	24.644(.155)					
	1 1 2 1 2	32.589(.123)					
Ni^{2+}	1 1 1 1 1	23.080(.030)	7.23E-8	157	.005	180	6.4-9,6
	1 1 1 1 2	29.543(.625)					
	1 1 1 1 3	36.416(.344)					
	1 1 2 1 2	33.426(.067)					
Cu^{2+}	1 1 1 1 0	21.575(.044)	1.71E-8	101	.003	138	5.1-8.7
	1 1 1 1 3	42.510(.044)					
	1 1 2 1 1	32.861(.053)					
	1 1 2 1 2	39.966(.068)					
	1 1 2 1 3	46.341(.088)					
Zn^{2+}	1 1 1 1 3	37.902(.055)	9.43E-8	91	.005	160	6.6-8.5
	1 1 2 1 1	26.354(.042)					
	1 1 2 1 2	33.533(.070)					
Cd^{2+}	1 1 1 1 3	38.519(.046)	8.40E-8	67	.007	178	6.7-9.8
	1 1 2 1 1	25.384(.073)					
	1 1 2 1 2	33.847(.041)					
	1 1 1 1-1	3.490(.053)					

Glycine binary metal complexes were extensively studied in the last two decades.[16] Various equilibria and their formation constants were reported. At least two unprotonated complexes were detected in the present work. Table 2(b) depicts their formation constants. Of course, 5-membered metal chelates are assumed to be formed. It has been proved that other species may also be formed. Cd(II) may form protonated complex species with glycine and Zn(II) forms soluble hydroxy glycinate complex species in solution, Table 2(b). The presence of triglycinate complexes were not confirmed under the experimental conditions used in this work, except in the Zn(II) system.

Complexes of imidazole of various metal ions were studied by several investigators.[8,24-26] It has been observed that precipitation was fast at slightly alkaline medium under the experimental conditions used in this work. This behaviour precluded our obtaining enough titration data for the determination of the formation constants of the binary complexes. However, it has been confirmed that polymerization of complexes is not the trend among the metal complexes studied except in the Cu(II) system, Table 2(c). In the latter system several polymeric complexes were detected. It has been reported that these types of Cu(II) complexes with imidazole are dependent on the ionic strength of the medium and the salt type used in its adjustment.[26] Actually there was no correlation between our work and that reported by previous other authors in case of the Cu(II) system except in the possibility of the formation mononuclear species.

Ternary and quaternary metal ion complexes.

The stability constants of the ternary metal ion complexes reported in Tables 3 and 4 are for the following equilibrium reaction.

$$1 \, Pm^- + p \, Gly^- + q \, Imd + r \, M^{2+} + s \, H^+$$
$$\rightleftharpoons M_r Pm_l \, Gly_p \, Imd_q \, H_s. \quad (1)$$
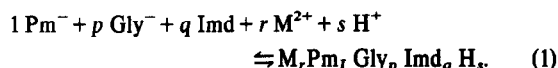
At least 20 sets of complexes for each system were examined using MINIQUAD-75 programme. Many were rejected when chi square (XI^2), crystalographic factor (R) and sum of squared residuals (S) are large or when constants had large standard deviations. Furthermore, the effect of variations in the values of protonation and binary constants on the constants of the chosen ternary model (and also ternary constants in case of the chosen quaternary model) were examined and was concluded that the choices were correct with errors in the values of the stability constants within the standard deviation shown in Tables 3 and 4.

(i) Ternary metal ion complexes

The ternary complexes involving Pm as one of the ligands are mostly protonated. Since Gly and Imd ligate metal ions when they are not protonated it may be expected to stay this way in their ternary complexes. One should expect that the protons may be located on the Pm moiety in their ternary complexes such as 1:1:0:1:1, 2:1:0:1:2, 1:2:0:1:1 and 2:0:2:1:1 species. The presence of other protonated ternary species may indicate that Pm and Gly can act as monodentate ligands. It is noted that some of the intermediate species in the Pm–Imd–M^{2+} system are absent (e.g. 1:0:2:1:sH) except in Cu(II) and Cd(II) systems. There is likely a preference to particular structures; penta-coordinated and hexa-coordinated structures in case of Co(II), Ni(II) and Zn(II) systems (e.g. 1:0:3:1:0 and 2:0:2:1:0 species) and tetra-coordinated and hexa-coordinated structures in Cu(II) and tetra-coordinated and hexa-coordinated structures in Cu(II) and Cd(II) systems (e.g. 1:0:2:1:0 and 2:0:2:1:1 species). In such complexes two or more Imd molecules are involved.

The ternary complexes not involving Pm are entirely unprotonated, (i.e. Gly–Imd–M^{2+} system), Table 3(c). Similar to the system Pm–Imd–M^{2+}, stepwise species are absent and preference to penta-coordinated structures is more obvious. In these complexes more than one Imd moiety and, in rare cases, more than one Gly moiety are involved. The presence of species containing more than one Gly molecule (in the Gly–Imd–M^{2+} system) is less than those containing more than 2 Pm molecules in the Pm–Imd–M^{2+} system. This may be explained as due to the better π-acceptor character of Pm over that of Gly. However, six-membered chelate of Pm should be expected to exert more hindrance than the five-membered chelate of Gly. This may explain why more than one molecule of Imd prefer Gly containing complexes rather than those containing Pm where steric factor is greater. In the ternary systems studied, the aquated 1:1:1 species (for Pm or Gly:Imd:M^{2+}) are stable at a certain pH range (which is usually below pH 7.0), where Imd, in particular, is not completely deprotonated.

The formation of 1:1:0:1:s or 1:0:1:1:s (Pm^-:Gly^-:Imd:sH$^+$:M:sH) ternary complex species from binary species may result from either one of the following reactions or both:

$$MLH_m + ML'H_n \rightleftharpoons M + MLL'H_s\,;$$
$$K^I = \beta_{ITH_s}/\beta_{IMLH_m}\beta_{IML'H_n} \tag{2a}$$

$$M(LH_m)_2 + M(L'H_n)_2 \rightleftharpoons 2MLL'H_s\,;$$
$$K^{II} = \beta_{ITH_s}^2/\beta_{2MLH_m}\beta_{2ML'H_n} \tag{2b}$$
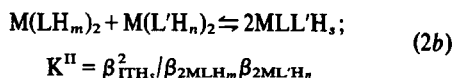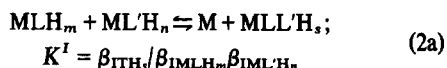
where β_{ITH_s}, β_{IMLH_m}, β_{2MLH_m}, $\beta_{IML'H_n}$, and $\beta_{2ML'H_n}$ are the formation constants of the ternary complex, first and second complex species of LH$_m$ and first and second complex species of L'H$_n$, and $s = n + m$.

Table 5 lists the values of log K^I and log K^{II} (log K and log X used by Sigel[27]) for 1:1:1:0:s, 1:0:1:1:s and 0:1:1:1:0 complex species whenever the binary constants data were available. It is generally found that the formations of most ternary complexes under consideration, are favored over the formations of the bi-binary metal complexes as well as most mono-binary species. It should be kept firmly in mind that the magnitudes of log K^I and log K^{II} are strongly influenced by statistical differences in the formation of each complex as well as differences in bonding. The statistical values of log K^I and log K^{II} depend on the coordination number of the metal ion and denticity of the ligands,[28,29] e.g. for the tetragonal complex of Cu(II) with bidentate ligands the statistical value is -0.6 log units. For other situations, the statistical values may be less but is always negative. Values of log K^I and log K^{II} greater than -0.6 log units indicate that ternary metal complex formation is more favored than that of binary metal complexes. Table 5 shows that the values of log K^I and log K^{II} are mostly greater than -0.6. The log K^I values of M–Pm–Gly systems are more negative than those of M–Pm–Imd and M–Gly–Imd systems. This is not surprising since the latter systems exhibit less steric hindrance than the former.

The formation of 1:1:1:s (Pm:Gly or Imd:M:sH) ternary complex species involving Pm may also be discussed in the light of the following equations;

$$MPmH_s + L \rightleftharpoons MPmLH_s\,; \quad K^{III} = \beta_{ITH_s}/\beta_{IMPmH_s} \tag{3a}$$

$$M + PmH_s \rightleftharpoons MPmLH_s\,; \quad K^{IV} = \beta_{ITH_s}/\beta_{ITH_s}/\beta_{IML} \tag{3b}$$

(L may stand for either Gly or Imd). Table 6 lists the values of log K^{III} and log^{IV} for 1:1:1:0 and 1:1:1:1 complex species. It is obvious that the values of log K^{IV} are greater than those of log K^{III} for most metal ion complexes. This may reflect the type of bonding of Pm to these metal ions. Pm may increase the electron density in the vicinity of the metal ions rendering them less electrophilic towards the other ligands, Gly and Imd. Furthermore, upon inspecting Table 6, one may also find that the size of chelate rings affect the stability of the ternary complex species. Six (Pm), five (Gly)-membered chelates are more stable than five (Gly), five (Gly)-membered chelates. However, six (Pm), Six (Pm)-membered chlates are more stable than five (Gly), six (Pm)-membered chelates except in Ni(II) and Cd(II) systems.

Table 5. The values of log K^I and log K^{II} defined by the eqns (2a and 2b) for all ternary systems studied in this work

System	l p q r s	log K^I					log K^{II}				
		Co(II)	Ni(II)	Cu(II)	Zn(II)	Cd(II)	Co(II)	Ni(II)	Cu(II)	Zn(II)	Cd(II)
Pm-Gly	1 1 0 1 0	-0.93	-0.48	-2.03	--	-1.37	-0.13	+2.58	+1.87	--	+2.45
	1 1 0 1 1	---	-0.58	+0.34	--	--	-0.42	+0.63	+0.48	--	--
Pm-Imd	1 0 1 1 1	---	+0.58	-0.19	--	+1.53	--	+2.57	+2.01	--	--
Gly-Imd	0 1 1 1 0	+0.21	+0.10	+0.01*	-0.28	+0.68	+1.69	+2.47	+2.30	+1.17	+4.83

* M. Mohan et al. (19) obtained a value of -0.28

Table 6. The values of K^{III} and K^{IV} expressed by eqns 3(a) and (b)

L, Stoichiometry	log K^{III}					log K^{IV}				
	Co	Ni	Cu	Zn	Cd	Co	Ni	Cu	Zn	Cd
Pm	Six (Pm), six-membered (Pm) chelates									
1 1 0 1 0	(4.66)	(4.06)	(6.66)	(5.46)	(2.83)					
1 1 0 1 1	–	–	(14.65)	–	–					
Gly	Five, six-membered (Pm) chelates					Six(Pm), Five-membered (Gly)chelates				
1 1 0 1 0	3.72	5.08	5.80	3.51	3.24	4.66	6.00	8.78	4.71	4.00
	–	(4.43)	(6.04)	(3.82)	(1.96)	–	(4.43)	(6.04)	(3.82)	(1.96)
1 1 0 1 1	4.42	4.97	8.17	–	–	13.10*	13.62*	17.56*	–	–
Imd	Monodentate ligand(Imd), six-membered(Pm) chelates					Six(Pm), monodentate (Imd) complexes				
1 0 1 1 1	3.62	3.78	3.83	–	4.27	13.92	14.78	17.03	–	14.98
	Monodentate ligand (Imd), five-membered (Gly) chelates									
0 1 1 1 0	3.24	3.30	4.03	2.70	3.41					

( )   Correspond to the equilibria: $M\,LH_n + LH_m \rightleftharpoons M\,L_2H_{n+m}$

*   Correspond to the equilibria: $ML + PmH \rightleftharpoons M\,Pm\,LH$

The stability enhancement of imidazole ligation in ternary complex formation may be revealed when the values of log K^{III}, Table 6, are compared with the 1:1 binary species, Table 2(c). The presence of Gly or Pm H usually enhance the nucleophilic attack of Imd to metal ions. Although, PmH has slight higher electron releasing power than Gly, yet Imd seems to prefer ligation to the mono-binary species containing PmH rather than that containing Gly. This finding may indicate that interaction between Pm and Imd is less than that between Gly and Imd.

MINIQUAD distribution diagrams for Cu(II) ternary systems, as representative example, are shown in Fig. 1(a–c). The figures compare the complex distributions of Cu(II) with Pm–Gly, Pm–Imd and Gly–Imd systems. It should be borne in mind that these distribution curves are dependent on the initial concentrations of the reactants. In selecting these diagrams for representation, we have made the choice for those showing the distribution of the greatest number of the species mentioned in Table 3.

(ii) Quaternary metal ion complexes

Table 4 lists the formation constants of the quaternary complexes represented by eqn (1). It is clear from this table that most of the complexes are protonated in solutions of the same pH range used before in case of the binary and ternary systems. Again one may expect that the protons are preferably located on the Pm moiety specially in mono and di-protonated species. In the triprotonated species, Gly may also be protonated. This protonation is an indication of a decrease in the positive character of metal ions as many ligands clustered around them. It may also indicate that ligands of multidentate nature may behave as mono-dentate is presence of other ligands. Table 4 also shows that there are no unique stoichiometry for various quaternary species among the metal ions studied. However, three species are present in

common, 1:1:1:1:3, 1:1:1:2:1:1 and 1:1:2:1:2 species. The persistence of the latter two species emphasize the preference of hexa- and penta-coordinated structure among these metal ions complexes. The chelation of the metal ions with Pm and Gly facilitate their ligation with imidazole. This may be verified by comparing the formation constants of the following

$T_{Pm} = T_{Gly} = 2\,T_{Cu} = 3.2 \times 10^{-3}M$

	PN	Gly	Cu	H
A	2	1	1	2
B	1	1	1	2
C	1	1	1	3
D	1	2	1	1
E	1	2	1	2
G	2	0	1	0

(a)

$$T_{Gly} = \frac{1}{2} T_{Imd} = 2 \, T_{Cu} = 1.6 \times 10^{-3} M$$

(b)

(c)
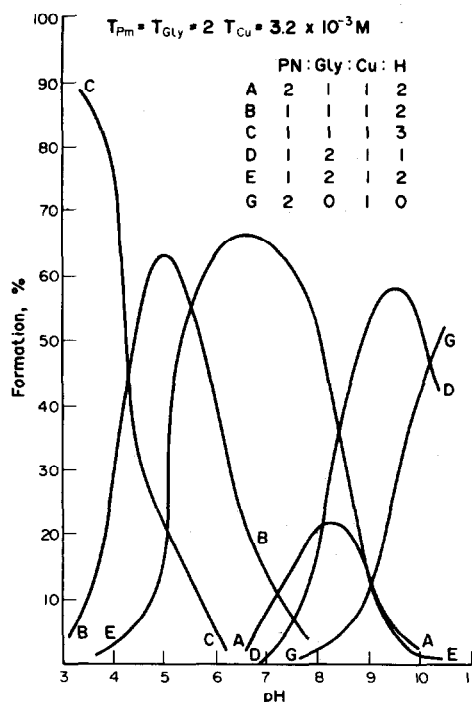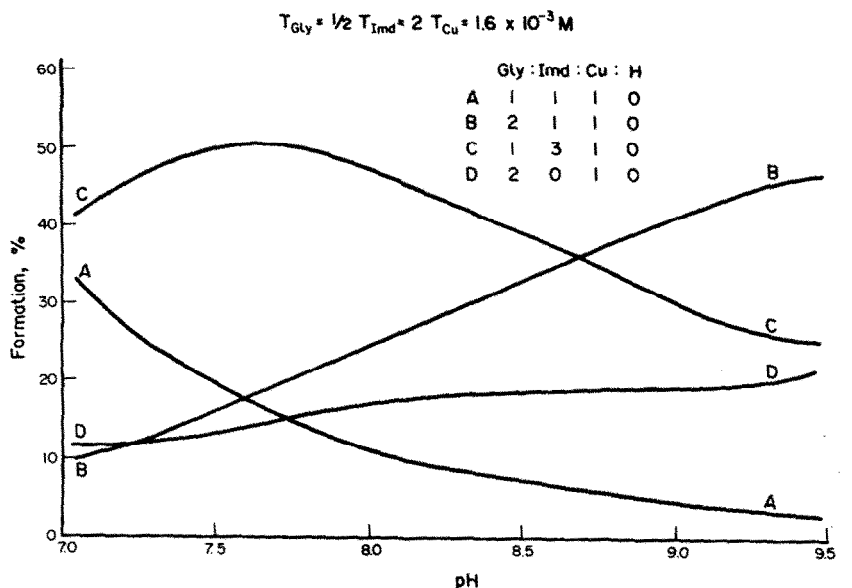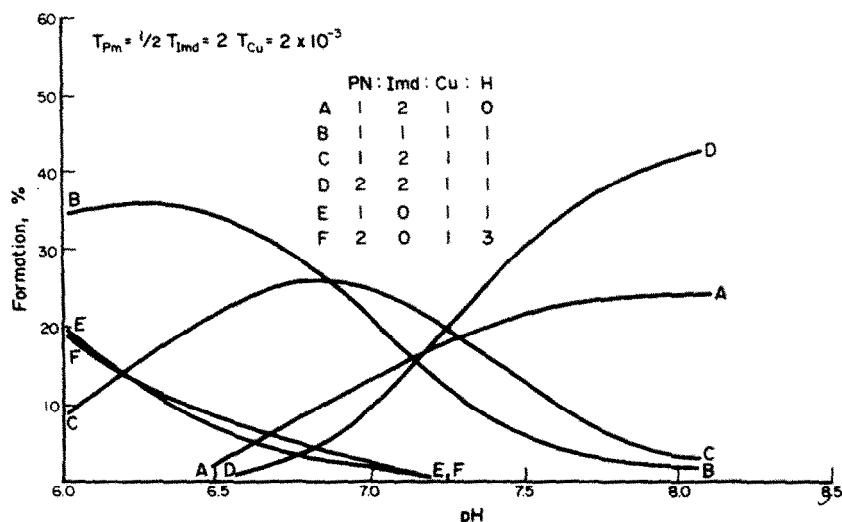
Fig. 1. MINIQUAD computed distribution of complex species with pH of Cu(II) ternary systems. (a) Pm–Gly–Cu(II) system. (b) Pm–Imd–Cu(II) system. (c) Gly–Imd–Cu(II) system.

equilibrium reactions;

$$M \, Pm \, Gly \, H_s + Imd \rightleftharpoons M \, Pm \, Gly \, Imd \, H_s;$$
$$K^V = \beta_{IQH_s}/\beta_{ITH_s} \tag{4a}$$

$$M \, Pm \, Gly \, H_s + 2 \, Imd \rightleftharpoons M \, Pm \, Gly \, Imd_2 H_s;$$
$$K^{VI} = \beta_{2QH_s}/\beta_{ITH_s} \tag{4b}$$
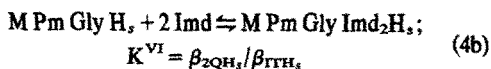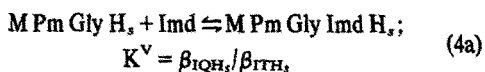
(where β_{IQH_s} and β_{2QH_s} are the formation constants of the quaternary cvomplex species $1:1:1:1:s$ and $1:1:2:1:s$ respectively) with those of the binary complexes of these metal ions with imidazole, Table 2(c). The log K^V values for $1:1:1:1:0$ species of Co(II) and Cu(II) systems are 3.86 and 4.97 which are greater than

that for $0:0:1:1:0$ species by approximately one log unit. Moreover, the log K^V values for $1:1:1:1:1$ species involving Co(II) and Ni(II) are 4.21 and 3.91 which are still greater than that of the mono-binary species of Imd by more than one log unit. The nucleophilic attack of Imd seems not to depend primarily on the diminished positive character of the central metal ions but also on the electron density of other ligands in the complex. Furthermore, the log K^{VI} values are still greater than that corresponding to the bi-binary species of Imd by more than one log unit, e.g. the log K^{VI} for $1:1:2:1:1$ of the Co(II) and Cu(II) systems are 6.99 and 7.47, respectively.

There is a tremendous number of equilibrium reactions involved in the formation of the $1:1:1:1:s$ quaternary complex. It may be formed from the combination of

three different binary species or one binary and one ternary species or from two ternary species. It has been shown, Table 5 that mono-binary species are mainly in equilibrium with the ternary species, in most cases. One should expect that the most important species in the quaternary system are the mono-binary as well as the ternary species. The formation of the quaternary species may be examined if the following equilibria are considered,

$$ML + ML'L''H_s \rightleftharpoons MLL'L''H_s + M;$$
$$K^{VII} = \beta_{IQH_s}/\beta_{IML}\beta_{IML'L''H_s} \tag{5}$$

$$ML' + MLL''H_s \rightleftharpoons MLL'L''H_s + M;$$
$$K^{VIII} = \beta_{IQH_s}/\beta_{IML'}\beta_{IMLL''H_s} \tag{6}$$

$$ML''H_s + MLL' \rightleftharpoons MLL'L''H_s + M;$$
$$K^{IX} = \beta_{IQH_s}/\beta_{IML''H_s}\beta_{IMLL'} \tag{7}$$
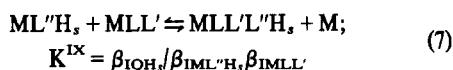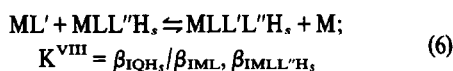
(L, L' and L''H$_s$ stand for Gly, Imd and Pm, respectively). Due to the lack of the formation constants of the necessary species to calculate the log K^{VII}, log K^{VIII} and log K^{IX}, only the values for few species may be obtained. It has been found that the log K^{VII}, log K^{VIII} and log K^{IX} are 0.36, 1.18 and 0.74 for the 1:1:1:1:1 species of the Co(II) system. This finding indicates that quaternary complex formation is moderately enhanced with the equilibrium reaction six more than that of 5 and 7, confirming the great affinity of Imd to ternary complexes containing Gly and Pm. Ni(II) quaternary system behaves similarly but with lower values of the log K's (−0.45, +0.71 and +0.03, respectively). For the 1:1:1:1:0 species of Cu(II) system, the values for the log K's are −1.75, −0.55 and −1.36, respectively. The negative values show that quaternary complex formation is diminished but still equilibrium reaction 6 is the least which confirm the favorable tendency of Imd to attack the ternary species involving Gly and Pm.

The formation of the 1:1:1:1:s quaternary complex species may also arise from the combination of two different ternary complex species;

$$MLL' + MLL'H_s \rightleftharpoons MLL'L''H_s + ML;$$
$$K^X = \beta_{IQH_s}\beta_{IML}/\beta_{IMLL'}\beta_{IMLL''H_s} \tag{8}$$

$$MLL' + ML'L''H_s \rightleftharpoons MLL'L''H_s + ML'$$
$$K^{XI} = \beta_{IQH_s}\beta_{IML'}/\beta_{IMLL'}\beta_{IML'L''H_s} \tag{9}$$

$$MLL''H_s + ML'L''H_s \rightleftharpoons MLL'L''H_s + ML''H_s$$
$$K^{XII} = \beta_{IQH_s}\beta_{IML''H_s}/\beta_{IMLL''H_s}\beta_{IML'L''H_s}. \tag{10}$$
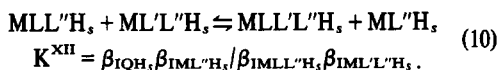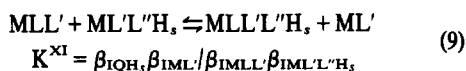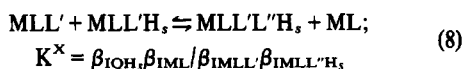
It has been found that log K^X, log K^{XI} and log X^{XII} are 0.99, 0.15 and 0.59 for the 1:1:1:1:1 species of Co(II) system. The same trend was obtained for Ni(II) system except the log values are less in magnitude than that in Co(II) system, i.e. 0.61, −0.65 and 0.13, respectively. These results showed that the equilibrium reaction (9) is not favored in comparison with the reactions (8) and (10) and they reflect the high stability of the monobinary species of Gly and Pm with respect to that of Imd. The log values for K^X, K^{XI} and K^{XII} for 1:1:1:1:0 for Co(II) quaternary species are greater (0.26, 0.21 and 1.32, respectively) than that of Cu(II) system (−0.56, −1.76 and 0.28, respectively). One may conclude that the formation of quaternary species from ternary species are more

favored in Co(II) system than in that of Cu(II) system. The rationale is probably of structural origin.

The stabilization enhancement of the formation of 1:1:2:1:s complex species may be analyzed in a way similar to that discussed for the 1:1:1:1:s species. In such case lots of equilibrium reactions may be considered. However, the most important reacting species are the mono-binary and ternary species. One may consider only the following equilibria;

$$ML + 2ML' + ML''H_s \rightleftharpoons MLL'_2L''H_s + 3M;$$
$$K^{XIII} = \beta_{2QH_s}/\beta_{IML}\beta^2_{IML'}\beta_{IML''H_s} \tag{11}$$

$$ML + ML'_2L''H_3 \rightleftharpoons MLL'_2L''H_s + M;$$
$$K^{XIV} = \beta_{2QH_s}/\beta_{IML}\beta_{IML_2L''H_s} \tag{12}$$

$$2ML' + MLL''H_s \rightleftharpoons MLL'_2L''H_s + 2M;$$
$$K^{XV} = \beta_{2QH_s}/\beta^2_{IML'}\beta_{MLL''H_s} \tag{13}$$

$$ML''H_s + MLL'_2 \rightleftharpoons MLL'_2L''H_s + M;$$
$$K^{XVI} = \beta_{2QH_s}/\beta_{IML''H_s}\beta_{MLL'_2} \tag{14}$$

$$MLL' + ML'L''H_s \rightleftharpoons MLL'_2L''H_s + M;$$
$$K^{XVII} = \beta_{2QH_s}/\beta_{MLL'}\beta_{ML'L''H_s} \tag{15}$$
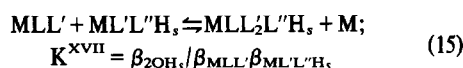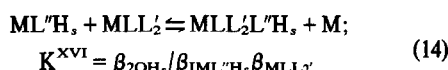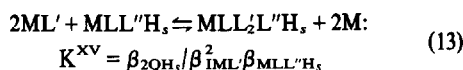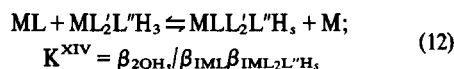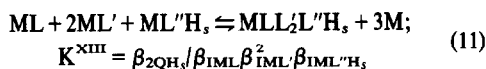
where β_{2QH_s} is the formation constants of the species 1:1:2:1:s. Unfortunately, not all the formation constants in eqns (11)–(15) can be evaluated due to the lack of binary as well as ternary formation constants. The formation constants K^{XIV} and K^{XVI} for the species 1:1:2:1:1 cannot be determined since we have not obtained the ternary species $ML'_2L''H_s$ and MLL'_2 except in one Cu(II) system, Table 3(b). The log values for K^{XVII} for the same quaternary species are negative for the most metal ions (−0.20, −1.35, −1.53, −0.15 for Co(II), Ni(II) Cu(II) and Cd(II), respectively). It may be noticeable that Ni(II) and Cu(II) exhibit the largest negative values for the log K^{XVII}. This finding reflects the great stability of the ternary species of both Ni(II) and Cu(II) shown in the equilibrium reaction (15). The log values for K^{XIII} and K^{XV} for the species 1:1:2:1:1 follow the same trends for all metal ions (log K^{XIII} = 0.60, −0.67, −1.71, 1.03, 2.13 and log K^{XV} = 0.83, −0.09, −2.05, 2.03, 2.92 for Co(II), Ni(II), Cu(II), Zn(II) and Cd(II). The negative values for the log K's are restricted to Ni(II) and Cu(II). The forementioned results indicated that the formation of quaternary species 1:1:2:1:1 cannot arise from just the iteraction of mono-binary species among each other or the interaction of mono-binary species with ternary species or the interaction of ternary species with each other except in Co(II), Zn(II) and Cd(II). This may lead to the conclusion that structural reasons are playing a role in such complex formation. Cu(II) and Ni(II) binary and ternary species are less apt to form the oactahedral structural quaternary species, easily allowed for other metal ions.

It is worth to mention that the values of log K's evaluated for the eqns (4)–(15) are not corrected statistically since the structures of the complexes and the magnitude of the thermodynamic *trans*-effect were unknown. However, under the assumption that these metal ions can have octahedral structures and that the thermodynamic *trans* effect is negligible, there is a statistical correction of −log 6 (−0.78) for all log K's. The log values which are greater than −0.78 will imply enhancement of quaternary complex formation.
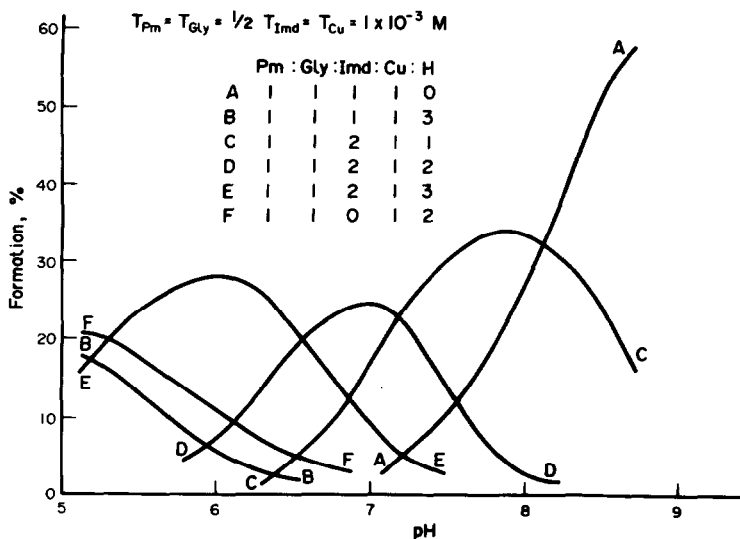
Fig. 2. MINIQUAD computed distribution of complex species with pH of Cu(II) quaternary systems, Pm–Gly–Imd–Cu(II).

A representative complex distributions of the Cu(II) quaternary systems are shown in Fig. 2. It is clear that binary complexes are unable to compete successfully with quaternary and ternary complexes at pH's lower than 8.5 in both systems. In addition, quaternary complexes are more predominant than ternary complexes. The ternary complexes which were found to co-exist with quaternary complexes are mainly 1:1:0:1:2 species (Pm:Gly:Imd:M:sH) system. Due to the early precipitation (at pH ~ 9) in the glycine quaternary systems, one cannot predict the type of complex species which may exist at pH's higher than 9.0.

CONCLUSION

In the mammalian body, the variation in the ligand types and their concentrations exceed the various metal concentrations in such a way that a wide range of complexing species compete actively for different metal ions. In this work we have proved that not only binary and/or ternary complexes could be formed but quaternary complexes may also be formed. Clearly, mixed-ligand formation has important biological implications due to the enhanced probability of bringing of different ligands together or of facilitating enzyme-substrates interaction through a metal ion link. This was found to be true in the ternary and quaternary systems studied in this work. Generally, the presence of Pm (specially the protonated forms) in the vicinity of metal ions facilitate the further attack of other nucleophilic ligands which leads to the formation of the quaternary complex species. It also seems that the electrostatic interactions between different ligands are diminished as Pm becomes protonated. These complexes are positively charged in most cases which effectively facilitate their transport in biological fluids. However, transfer of these complexes through cell membranes requires them to be neutral, a criterion not in their favor. This is only fulfilled in case of some of the ternary complexes of Pm–Gly system.

It has been shown in this work that free metal ions cannot exist in a wide pH range (>6–9), and are mostly found in the form of mixture of ternary and quaternary complex species and hence they may be found as such in most mammalian biological fluids. However, at pH's higher than 9 or less than 6, they may exist in the form of a mixture of binary, ternary and quaternary species and are probably found as free ions at pH's lower than 4.0 (specially in Cu(II) systems).

REFERENCES

[1] K. N. Jeejeebhoy, W. Zohrab, B. Langer, M J. Phillips, A. Kuksis and G. H. Anderson, *Gastroenterology* 1973, **65**, 811.
[2] N. W. Solomons, T. S. Layden, I. H. Rosenberg, K. Vokhatcw and H. H. Sandstead, *Gastroenterology* 1976, **70**, 1022.
[3] S. Jacobson and P. O. Wester, *Brit. J. Nutr.* 1977, **37**, 107.
[4] P. M. May, D. R. Williams and P. W. Linder, *Metal Ions in Biological Systems* (Edited by H. Sigel), Vol. 7, p. 29 Marcel Dekker, New York (1978).
[5] Instruction Manual for Cupric Selectrode Type FIII 2Cu, Radiometer A/S, Copenhagen, 1972.
[6] M. S. El-Ezaby, H. Maarafie and S. Farid, *J. Inorg. Biochem.* 1979, **11** 317.
[7] P. Gans, A. Sabatini and A. Vacca, *Inorg. Chim. Acta* 1976, **18**, 237.
[8] C. W. Childs and D. D. Perrin, *J. Chem. Soc.* (A) 1969, 1039.
[9] A. Chakravorty and F. A. Cotton, *J. Phys. Chem.* 1963, **67**, 2878.
[10] G. Berthon, P. M. May and D. R. Williams, *J. Chem. Soc. Dalton* 1978, 1433.
[11] M. S. El-Ezaby and F. R. El-Eziri, *J. Inorg. Nucl. Chem.* 1976, **38**, 1901.
[12] M. S. El-Ezaby, M. Rashad and N. Moussa, *J. Inorg. Nucl. Chem.* 1977, **37**, 175.
[13] B. Abd El-Nabey and M. S. El-Ezaby, *J. Inorg. Nucl. Chem.* 1978, **40**, 739.
[14] M. S. El-Ezaby and N. El-Shatti, *J. Inorg. Biochem.* 1979, **10**, 169.
[15] R. I. Gustafson and A. E. Martell, *Arch. Biochem. Biophys.* 1957, **68**, 485.
[16] V. S. Sharma, H. B. Mathur and P. S. Kulkarni, *Indian J. Chem.* 1963, **3**, 146, 475.
[17] A. Gergely, I. Nagypal and J. Mojzes, *Acta. Chim. Acad. Sci. Hung.* 1967, **51**, 381.

[18]J. B. Gilbert, M. C. Otev and J. Z. Hearon, *J. Amer. Chem. Soc.* 1955, **77**, 2599.

[19]M. S. Mohan, D. Bancroft and E. H. Abbott, *Inorg. Chem.* 1979, **18**, 6, 1527.

[20]M. S. Nair, M. Satappa and P. Natarajan, *Inorg. Chim. Acta.* 1980, **41**, 7.

[21]R. M. Izatt, H. D. Johnson and J. J. Christensen, *J. Chem. Soc. Dalton* 1952, 1152.

[22]N. C. Li, E. Doody and J. M. White, *J. Amer. Chem. Soc.* 1957, **79**, 5859.

[23]M. K. Kim and A. E. Martell, *J. Amer. Chem. Soc* 1967, **89**, 5138.

[24]Y. Nozaki, F. R. N. Gurd, R. F. Chen and J. T. Edsall, *J. Amer. Chem. Soc.* 1957, **79**, 2123.

[25]G. Tanford and M. L. Wagner, *J. Amer. Chem. Soc.* 1953, **75**, 434.

[26]S. Sjoberg, *Acta Chem. Scand.* 1973, **27**, 3721.

[27]H. Sigel, *J. Inorg. Nucl. Chem.* 1975, **37**, 507.

[28]B. Sen, *Anal. Chim. Acta* 1962, **27**, 515.

[29]V. S. Sharma, T. J. Schubert, *J. Chem. Ed.* 1969, **46**, 506.

SYNTHESIS AND THERMAL DECOMPOSITION OF METHYLSILOXANE OLIGOMERS CONTAINING TWO LINKED CYCLOSILOXANE UNITS

N. N. MAKAROVA

Institute of Organo-element Compounds, Academy of Sciences of the U.S.S.R., Moscow, U.S.S.R.

and

M. BLAZSÓ* and E. JAKAB

Research Laboratory for Inorganic Chemistry, Hungarian Academy of Sciences, Budapest (Hungary) H-1112, Budapest, Budaörsi ut 45, Hungary

Abstract—Ten separated oligomeric methylsiloxanes, with cyclic and linear segments of different size, have been prepared and studied. The thermal decomposition of these compounds has been investigated in the temperature range from 400–600°C. The pentasiloxy cycle proved to be more stable than the tetrasiloxy in the investigated compounds. Compounds containing the strained cyclotrisiloxy group have the lowest stability. On the basis of the pyrolysis product distributions, a general mechanism of dimethylsiloxane elimination and addition is proposed.

INTRODUCTION

The works dealing with the thermal decomposition of siloxanes were concentrated for long on siloxane polymers. Very important conclusions have been drawn concerning the decomposition of the polydimethylsiloxane to cyclic oligomers under heat treatment.[1-3] In a previous paper[4] we studied some cyclolinear methylsiloxane polymers and reported how the thermal decomposition of the macromolecular chain is influenced by the branching points regularly built in. In order to get more information about the thermally induced processes in the siloxanes at the linear and branched molecular segments, we turned to the study of volatile oligomeric siloxane compounds.

The investigated compounds are composed of two metylsilsesquioxy $(CH_3SiO_{1.5})$ and six to twelve dimethylsiloxy $[(CH_3)_2SiO]$ groups arranged so that two cyclotrisiloxanyl, cyclotetrasiloxanyl, or cyclopentasiloxanyl rings are linked by a dimethylsiloxane chain.

EXPERIMENTAL

The following examples are given to illustrate the general procedures used in the synthesis of methylbicyclosiloxanes.[5,6] The physical constants of the compounds synthetized are given in Table 1.

Bis(pentamethylcyclotrisiloxy) tetramethyldisiloxane

In a three-neck flask equipped with stirrer and thermometer 10 cm^3 of dry benzene was placed. 16.0 g (0.0958 mol) of 1,3-dihydroxytetramethyldisiloxane, 19.5 g (0.193 mol) of triethylamine in 100 cm^3 dry benzene and 9.6 g (0.0638 mol) of methyltrichlorosilane in 100 cm^3 dry benzene were added dropwise over two hours at 5°C. The mixture was kept at 20–22°C for 6 hr. The triethylamine hydrochloride was filtered off, the solution was washed with water, then distilled at 13 mbar to yield 9.6 g (51.9%) of bis(pentamethylcyclotrisiloxy)tetramethyldisiloxane at 120–122°C. Found: C, 29.25; H, 7.39; Si, 38.20; Calc. for $C_{14}H_{42}Si_8O_9$: C, 29.03; H, 7.31; Si, 38.80%.

1-(Heptamethylcyclotetrasiloxy) - 3 - (nonamethylcyclopentasiloxy) - tetramethyldisiloxane

In a three-necked flask equipped with stirrer and thermometer 9.13 g (0.045 mol) of 1,3-dichlorotetramethyldisiloxane in 50 cm^3 of dry diethyl ether was placed. 11.19 g (0.030 mol) of hydroxynonamethylcyclopentasiloxane and 3.1 g (0.030 mol) of aniline in 50 cm^3 dry diethyl ether were added dropwise over 2 hr while the mixture was kept at 20–22°C. Two hours later an additional 8.94 g (0.030 mol) of hydroxyheptamethylcyclotetrasiloxane and 3.15 g (0.030 mol) of aniline in 50 cm^3 dry diethyl ether were added. The mixture was stirred for several hours then the aniline hydrochloride was filtered off. The distillation at 0.3 mbar yielded 2.7 g of bis(heptamethylcyclotetrasiloxy)tetramethyldisiloxane (b.p. 105°C), 3.6 g of 1-(heptamethylcyclotetrasiloxy) - 3 - (nonamethylcyclopentasiloxy)tetramethyldisiloxane (b.p. 115–116°C) and 2.0 g of bis(nonamethylcyclopentasiloxy) tetramethyldisiloxane (b.p. 126–128°C).

Hydroxyheptamethylcyclopentasiloxane

In a two-necked flask equipped with stirrer and thermometer 0.9 g (0.05 mol) of water, 4.29 g (0.046 mol) of aniline and 1 g acetone in 100 cm^3 of diethyl ether were placed. 17.3 g (0.044 mol) of chlorononamethylcyclopentasiloxane in 10 cm^3 of diethyl ether was added dropwise over 1 hr, while the temperature of the mixture was kept at 5–8°C. The mixture was stirred for 2 hr, the aniline hydrochloride was filtered off. The solution was washed with water, then distilled at 20 mbar to yield 12.8 g (78.0%) of hydroxyheptamethylcyclopentasiloxane.

Chlorononamethylcyclopentasiloxane

In a three-necked flask, equipped with stirrer and thermometer 75 cm³ dry diethyl ether was placed. 30.0 g (0.0955 mol) of 1, 7-dihidroxyoctamethyltetrasiloxane and 18.1 g (0.194 mol) of aniline in 150 cm^3 of dry diethyl ether and 19.7 g (0.130 mol) of trichloromethylsilane in 150 cm^3 of dry diethyl ether were added dropwise simultaneously over 2 hr while the temperature was kept at 4–6°C. The reaction mixture was stirred for 8 hr then the aniline hydrochloride was filtered off. The mixture was distilled at 20 mbar to yield 20.9 g (56.2%) chlorononamethylcyclopentasiloxane (b.p. 65–67°C).

Pyrolysis

Pyrolysis experiments were performed at 400–600°C in evacuated and sealed Pyrex glass tubes. The sample weight was 5 mg,

---

*Author to whom correspondence should be addressed.

Table 1. Physical constants of the investigated separated methysiloxanes

Molecular structure[*]	Relative molecular mass	Boiling point, °C	Density g/cm³ (d_4^{20})	Index of refraction (n_D^{20})
$\overset{D}{\underset{D}{>}}T\!-\!D_2\!-\!T\!\overset{D}{\underset{D}{<}}$	579.2	120–122[a]	1.0196	1.3992
$D\!\overset{D}{\underset{D}{<}}T\!-\!T\!\overset{D}{\underset{D}{>}}D$	579.2	110–112[a]	1.0354	1.4059
$\overset{D}{\underset{D}{>}}T\!-\!D_3\!-\!T\!\overset{D}{\underset{D}{<}}$	653.4	90–91[b]	1.022	1.4026
$D\!\overset{D}{\underset{D}{<}}T\!-\!D_2\!-\!T\!\overset{D}{\underset{D}{>}}D$	727.6	105–107[c]	1.0240	1.4062
$\overset{D}{\underset{D}{>}}T\!-\!D_3\!-\!T\!\overset{D-D}{\underset{D-D}{<}}$	801.6	117–119[b]	1.0135	1.4038
$D\!\overset{D}{\underset{D}{<}}T\!-\!D_3\!-\!T\!\overset{D}{\underset{D}{>}}D$	801.6	190–195[d]	1.0197	1.4058
$D\!\overset{D}{\underset{D}{<}}T\!-\!D_2\!-\!T\!\overset{D-D}{\underset{D-D}{<}}$	801.6	115–116[c]	1.0199	1.4058
$\overset{D-D}{\underset{D-D}{>}}T\!-\!D_2\!-\!T\!\overset{D-D}{\underset{D-D}{<}}$	875.8	·126–127[c]	1.0126	1.4062
$\overset{D-D}{\underset{D-D}{>}}T\!-\!D_3\!-\!T\!\overset{D-D}{\underset{D-D}{<}}$	949.9	150–154[b]	1.0103	1.4065
$D\!\overset{D}{\underset{D}{<}}T\!-\!D_6\!-\!T\!\overset{D}{\underset{D}{>}}D$	1024.1	138–142[e]	1.0133	1.4059

[*]$D = (CH_3)_2SiO$ $\qquad T = CH_3SiO_{1.5}$

a: 13 mbar;   b: 1 mbar;   c: 0.3 mbar;   d: 133 mbar
e: 0.1 mbar.

the volume of the tube was about 0.17 cm³. In fused silica tubes the same degradation products were found as in pyrex glass, but the decomposition was slightly slower.

Analysis of the pyrolysis products

The analysis of the pyrolysates was performed on a Perkin–Elmer-900 gas chromatograph equipped with Flame Ionization Detector and electronic integrator PE D-26. The peak area values were converted into molar amounts with response factors measured for cyclic and bicyclic methylsiloxane standards. Identification of the pyrolysis products was based on the retention time coincidence with pure authentic materials on three gas chromatographic columns. The following columns were used:

—3.5 m, 2 mm i.d. packed column; support: 80–100 mesh Chromosorb G; phase: 5% OV-17; temperature program from 40–280°C at 6.5°/min.

—3 m, 2 mm i.d. packed column: support: 80–100 mesh Chromosorb G; phase: 3% OF-1; temperature program: from 40–220°C at 6.5°/min.

—20 m, 0.2 mm i.d. Fused silica capillary column, coated with OV-101 phase; temperature program: from 50–200°C at 6°/min.

RESULTS AND DISCUSSION

The thermal stability of the ten compounds has been compared on the basis of the amounts that remained unchanged after pyrolysis performed under similar conditions. These values, determined after pyrolysis at 500°C for 20 min, are given in Fig. 1. The following tendencies of the relation of thermal stabilities are observed in this figure:

(1) The strained cyclotrisiloxy group containing compounds have the poorest stability among the isomeric bicycles (see T_2D_6 and T_2D_9 isomers).

(2) The stability increases with ring size, if compounds composed of 3, 4, and 5 siloxane membered rings (see the full lines in Fig. 1) are considered.

(3) The more siloxane groups separate the two rings the less stable is the compound (see the dashed lines in Fig. 1).

The thermal decomposition of methylsiloxanes leads to a series of products, most of them identical for all samples. Figure 2 shows the pyrolysis product distribution of 1,3-bis(pentamethylcyclotrisiloxy)tetramethyldisiloxane at 500°C. The methylcyclosiloxane oligomers (mainly D_3 and D_4) are the more important products. Their amount increases as the pyrolysis temperature is raised. The variation of the quantity of dimethylsiloxane in cyclic pyrolysis products with the molecular composition of the pyrolysed siloxane is shown in Fig. 3 for two different pyrolysis temperatures. There is a linear relationship between the molar amount of D units, forming cyclic pyrolysis products, and the D content of the pyrolysed molecule, at both temperatures examined.

The pyrolysis products range from T_2D_3 to T_2D_{n+2} when T_2D_n separated molecules are pyrolysed. The process taking place under pyrolysis may be described by the following general formulae:

$$T_2D_n \underset{450\text{–}500^\circ C}{\overset{450\text{–}600^\circ C}{\rightleftharpoons}} T_2D_{n-x} + x[D] \quad \begin{matrix}(n = 6, 7, \ldots 12)\\(x = 1, 2, \ldots n-5)\end{matrix} \quad (1)$$

$$T_2D_n + y[D] \overset{450\text{–}500^\circ C}{\rightleftharpoons} T_2D_{n+y} \quad (y = 1, 2) \quad (2)$$
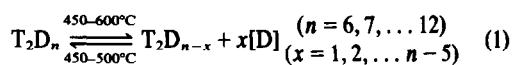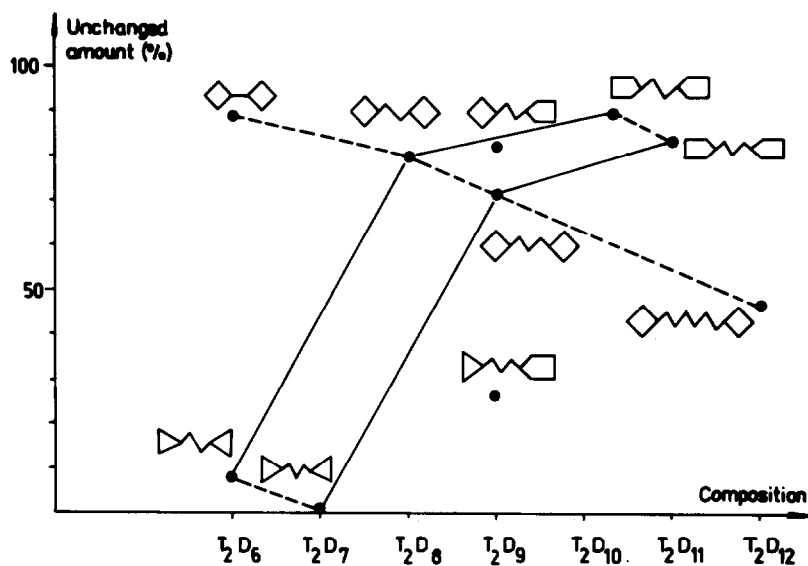
Fig. 1. The amounts remained unchanged after pyrolysis at 500°C for 20 min, characterizing the relative thermal stabilities, plotted against molecular composition. Symbols: > = D, i.e. $(CH_3)_2SiO$ >— = T, i.e. $CH_3SiO_{1.5}$.
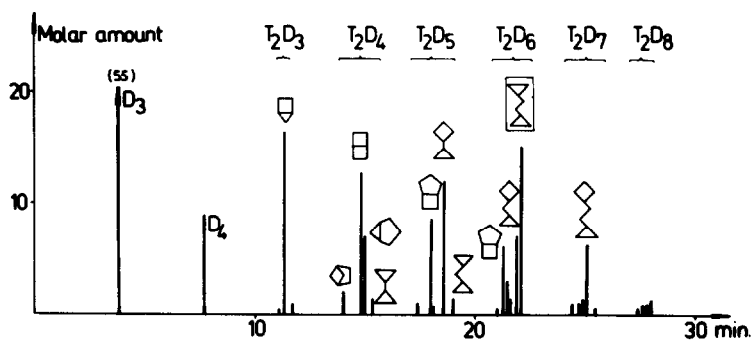
Fig. 2. Pyrolysis products of 1,3-bis(pentamethylcyclotrisiloxy)tetramethyldisiloxane (T_2D_6, structure in frame), separated on OV-101 capillary gas chromatographic column. Pyrolysis: 500°C, 20 min. For structural symbols see Fig. 1.
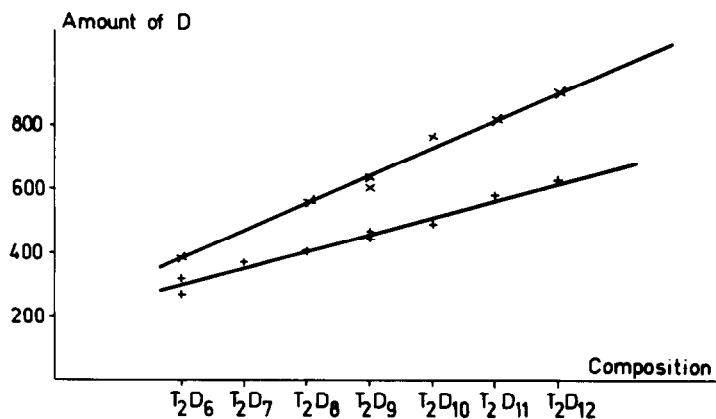
Fig. 3. The number of D units produced from 100 molecules of bicyclic siloxane, forming cyclosiloxanes under pyrolysis at 500°C(+) and 580°C(x) resp., plotted against the molecular composition of the pyrolysed compounds.

$$T_2D_z \underset{500-600°C}{\overset{}{\rightleftharpoons}} T_2D_{z-1} + [D] \quad (z = 3,4,5,6) \qquad (3)$$

$$3[D] \underset{450-600°C}{\overset{}{\rightleftharpoons}} D_3 \qquad (4)$$

$$D_3 + [D] \underset{450-600°C}{\overset{}{\rightleftharpoons}} D_4 \qquad (5)$$
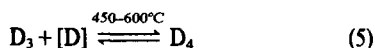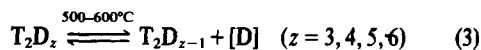
Reactions (4) and (5) proposed by Davidson and Thompson,[7] involving dimethylsilanone intermediate [D], explain the formation of cyclic oligomers. On the basis of the quantitative and structural analysis of the siloxanes occurring in the reactions (1)–(3), the following conclusions can be drawn:

(1) The elimination of dimethylsilanone from the separated siloxanes—reaction (1)–takes place equally from the linear separating segment and from the tetrasiloxy or pentasiloxy cycle. The reaction leads to new separated compounds containing two linked rings in which the size of the cyclic groups becomes gradually smaller and the separating chain gradually shorter. In Fig. 4. these processes are illustrated in a scheme of decomposition of the siloxane given as an example in Fig. 2.
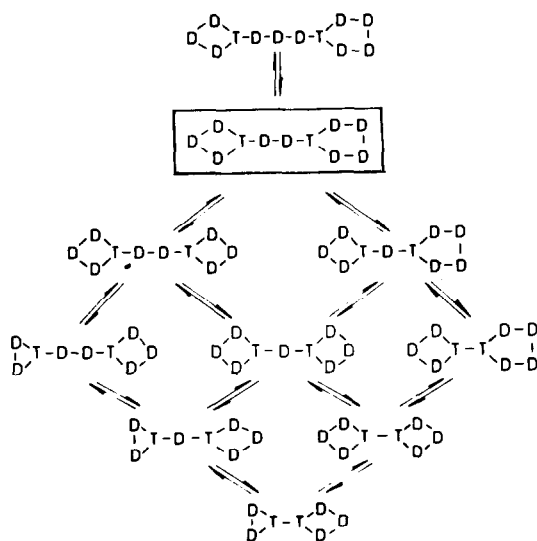
Fig. 4. Scheme of [D] elimination and addition reactions under pyrolysis of a T_2D_9 bicyclic siloxane.

(2) The backward reaction, the readdition of dimethylsilanone happens preferably to the cyclotrisiloxy group. The same preference can be observed in the case of the addition of the dimethylsilanone to the original compound, resulting products of higher molecular mass than the parent molecule (reaction 2). Note that these reactions are important only in the lower pyrolysis temperature range.

(3) The elimination and addition from and to the bicyclic products of lower molecular mass (T_2D_{3-6}, most of them can be of cumulated structure only) seem to reach an equilibrium soon (reaction 3). We have to point out that the relative amounts of the fused-ring bicyclic products are roughly the same for all kind of methylsiloxanes examined at a given temperature. Two out of the four most important fused-ring bicyclic pyrolysis products contain a trisiloxane cycle known as a strained ring.[8] In this way the relative amounts do not reflect the relative thermal stabilities. The distribution of these products (see Fig. 2) may be interpreted as being produced by the equilibrium between elimination and addition reactions.

The above discussion of the thermally induced reactions involves only the products formed in quantities larger than 0.5% of the pyrolysate.

Smaller amounts of different tricycles (T_4D_n) have been also found in the pyrolysates above 550°C.

REFERENCES

[1] T. H. Thomas and T. C. Kendrick, *J. Polym. Sci.* 1969, **A2**, 7, 537.
[2] K. A. Andrianov, V. S. Papkov, G. L. Slonimskii, A. A. Zhdanov and S. Ye. Yakushkina, *Visokomolek. Soedin.* 1969, **A11**, 2030.
[3] N. Grassie and I. G. Macfarlane, *Eur. Polym. J.* 1978, **14**, 875.
[4] M. Blazsó, G. Garzó, K. A. Andrianov, N. N. Makarova, A. I. Cheravski and I. M. Petrov, *J. Organometal. Chem.* 1979, **165**, 273.
[5] K. A. Andrianov, N. N. Makarova, T. V. Popova, *Bull. Izobr.* 1977, **28**, 74.
[6] K. A. Andrianov, A. I. Chernavski and N. N. Makarova, *Izv. AN USSR Ser. Chem.* 1979, **8**, 1835.
[7] I. M. T. Davidson and J. F. Thompson, *J. Chem. Soc. Chem. Commun.* 1971, 251.
[8] H. Oberhammer, H. Zeil and G. Fogarasi, *J. Mol. Struct.* 1973, **18**, 309.

STEREOSELECTIVITY IN THE ADDUCT FORMATION BETWEEN CHIRAL Eu(III) β-DIKETONE COMPLEXES AND SULPHOXIDES, SULPHONES AND PHOSPHATE ESTERS

HARRY G. BRITTAIN[1]
Chemistry Department, Seton Hall University, South Orange, NJ 07079, U.S.A.

Abstract—The adduct formation which takes place when Eu(III) chelates of trifluoroacetyl-*d*-camphor and heptafluorobutyryl-*d*-camphor bind substrates has been studied. Enhancement of Eu(III) luminescence as a function of substrate concentration has been used to obtain information on the nature of the chelate/substrate adducts, and the stereochemistry of the complexes was studied by means of circularly polarized luminescence (CPL) spectroscopy. While no optical activity can be measured for, the free chelates, formation of the adduct complexes usually led to the observation of very strong chirality even though the substrates were themselves achiral. It was concluded that adduct formation causes the bulky camphorato ligands to interact and adopt a configuration of lowest energy. This process perturbs the diastereomer ratios and yields a partial resolution of these very labile complexes.

INTRODUCTION

The existence of stereoselectivity in transition metal complexes containing chiral β-diketone ligands has become well established, and studies of this effect provide interesting information regarding interligand interactions in metal chelate systems. Most of these works have involved complexes in which the β-diketone contains the camphorato moiety:
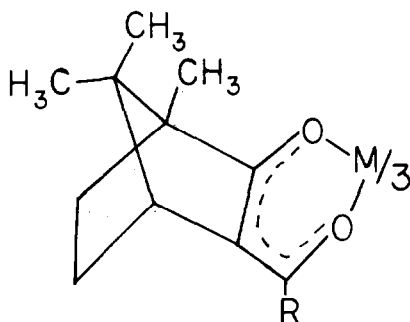
The most commonly studied systems are those of (+)-hydroxymethylenecamphor (where R = H, and abbreviated as HMC) and (+)-acetylcamphor (R = CH₃, and abbreviated as ATC). A racemic mixture of a *tris*-octahedral complex would contain four diastereomers: Δ-*cis* and Λ-*cis* (the facial isomers), as well as Δ-*trans* and Λ-*trans* (the meridional isomers).

Early work established that with kinetically inert Co(III) complexes, if (+)-R,R-HMC or (+)-R,R-ATC was used to prepare the chelates then the Λ-*trans*-diastereomer was present in the greatest excess.[2,3] It was subsequently shown through x-ray diffraction studies that the absolute configuration of Cr(+ATC)₃ was indeed Λ-*trans*.[4] Later studies determined the relative abundances of the four diastereomers in the racemic preparations of Co(+ATC)₃[5,6], Cr(+ATC)₃[5] and Ru(+ATC)₃,[7] and found that while the Λ-isomer was present in the largest excess, considerable amounts of the Δ-isomer was also produced. One general conclusion associated with all the studies was that the existence of

the two *trans*-isomers was greatly favored over the two *cis*-isomers.

In our laboratory, we have been investigating the stereoselectivity associated with the lanthanide complexes of chiral β-diketones. Recently, it was demonstrated that the optical activity of labile Tb(+ATC)₃ was profoundly affected by the solvent the material was dissolved in.[8] The lanthanide chelates differ from the transition metal analogues somewhat in that the lanthanide complexes can expand their coordination number through adduct formation, and it was found that the steric nature of the substrate in the Tb(+ATC)₃ adduct determined the particular diastereomer which dominated *even though the substrates were not themselves chiral.*[8] This behavior is quite analogous to work carried out on labile V(+ATC)₃ complexes in which the Δ-*trans*/Λ-*trans* ratio (as determined by NMR methods) could be varied from 0.31 to 0.97 depending on the nature of the solvent used.[9]

Eu(III) chelates of fluorinated camphorato β-diketones have been used in the NMR determination of enantiomeric purity,[10,11] but no attention has been paid to the effects which stereoselectivity might have on such measurements. Such effects have been shown to exist; Eu(TFAC)₃ (TFAC = (+)-3-trifluoroacetylcamphor, and has R = CF₃) shows no optical activity in noncoordinating solvents, but shows extremely intense optical activity when dissolved in dimethyl sulphoxide solvent.[12] Similar results were reported for Eu(HFBC)₃ (HFBC = (+)-3-heptafluorobutyrylcamphor, with R = C₃F₇), but the sign of the optical activity was found to be opposite to that of Eu(TFAC)₃ even though the absolute configuration of both ligands was the same.[13] Synthesis of mixed-ligand Eu(III) chelates subsequently showed that the stereoselectivity arose from the adduct formation with the substrate molecules.[14]

In the current work, we present the results of studies involving the adduct formation of Eu(TFAC)₃ and Eu(HFBC)₃ with phosphate esters, sulphoxides and sulphones. In many cases, adduct formation with these substrates leads to strong optical activity with this chirality clearly being a stereoselective effect. The optical activity was measured via circularly polarized luminescence (CPL) spectroscopy rather than the more

conventional method of circular dichroism, since the f-f absorptions of the lanthanide complexes are too weak to permit CD work except at high concentrations. Recent correlations relating the absolute configuration of trigonal Eu(III) complexes with the signs of CD and CPL peaks permitted the prediction of which particular isomer predominated in the Eu(TFAC)₃ and Eu(HFBC)₃ adduct systems.

EXPERIMENTAL

Eu(TFAC)₃ and Eu(HFBC)₃ were purchased from Aldrich, and dried for a prolonged period in a vacuum desiccator. Spectrograde CHCl₃ (dried over molecular sieves) was used as the solvent for all studies. Trimethyl phosphate, triethyl phosphate, tributyl phosphate, dimethyl sulphoxide, di-n-butyl sulphoxide, diphenyl sulphoxide, dimethyl sulphone, di-n-butyl sulphone and diphenyl sulphone were all obtained from Aldrich and used as received.

Luminescence titrations were carried out for each of the Eu(III) chelates with each of the substrates. Stock solutions of Eu(TFAC)₃ and Eu(HFPC)₃ were prepared to be 5 mM, and titrated with microlitre amounts of substrate solutions (whose concentrations ranged from 0.1 M to 0.5 M, depending on the desired ratio of substrate/chelate) which were added to 3 ml of the Eu(III) solution in the fluorescence cuvette. The total luminescence (TL) and CPL spectra of the $^5D_0 \rightarrow {}^7F_0$ (580 nm), $^5D_0 \rightarrow {}^7F_1$ (595 nm), and $^5D_0 \rightarrow {}^7F_2$ (615 nm) was followed after each addition. Reproducibility in the Eu(III) TL intensities was monitored by periodically recording the emission intensity of a piece of uranium glass.

All luminescence measurements were obtained on a medium-resolution CPL spectrometer constructed in our laboratory, and whose basic operation has been described.[15] An excitation wavelength of 365 nm was used to excite the compounds (obtained by passing the output of a 200-W Hg-Xe arc lamp through a 0.1-m grating monochromator and suitable glass filters), with a bandpass of 16-nm being used. As before, the emission was collected at 180° to the exciting light (to eliminate any possible linear polarization effects) and passed through a concentration solution of NaNO₂ to remove any unabsorbed exciting light. The emission was analyzed by a 0.5-m grating monochromator at 1-nm bandpass, and detected by an EMI 9798B photomultiplier tube (S-20 response). No attempt was made to correct the spectra for system response since the wavelength regions scanned were quite narrow and any correction would be minor at best. The TL and CPL signals were recorded simultaneously to insure that the ratio of these quantities would account for any instrumental fluctuations.

RESULTS

Irradiation of the Eu(III) chelates in the near-UV region of the spectrum results in efficient population of the excited $^5D_0$ state, and to luminescence occurring in red spectral regions. Unlike most other Eu(III) β-diketone complexes, the luminescence of free Eu(FTAC)₃ and Eu(HFBC)₃ is exceedingly weak and difficult to measure. However, on our equipment the TL is large enough to demonstrate that no CPL is present in the luminescence spectrum. This result is not surprising when one considers that in a racemic mixture of a highly labile chelate, all four diastereomers would be present and the CPL of these would approximately cancel. This has been shown for the analogous transition metal complexes, where the CD of the two cis-isomers is essentially equal in magnitude but opposite in sign to that of the two trans-isomers.[5] While for the transition metal complexes, one finds an excess of the Λ-isomers (when starting with (+)-TFAC or (+)-HFBC) in the free chelates,[5-7] the larger ionic radius of the lanthanide ions apparently allows the three β-diketone ligands to coexist without significant interaction.

Sulphoxides

The addition of dimethyl sulphoxide to a CHCl₃ solution of either Eu(TFAC)₃ or Eu(HFBC)₃ results in a modest increase in the TL intensity within the $^5D_0 \rightarrow {}^7F_J$ transitions of the Eu(III) ion. Such increases have been attributed in the past to protection of the metal ion from solvent quenching via formation of an insulating sheath,[16] and is a feature characteristic of adduct formation.[17-20] In these earlier works,[19,20] we have outlined the basic methods whereby one may use these TL intensity enhancements to obtain the association constants for the 1:1 and 1:2 adducts:

$$Eu(DK)_3 \;\; + S \rightleftharpoons Eu(DK)_3(S)$$
$$Eu(DK)_3(S) + S \rightleftharpoons Eu(DK)_3(S)_2.$$
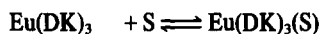
In Fig. 1, the enhancement of Eu(TFAC)₃ and Eu(HFBC)₃ luminescence by dimethyl sulphoxide is shown for the initial portions of the titration. One may easily see that the luminescence intensity does not reach a limiting value even after the addition of 15 equivalents of substrate per mole of Eu(III) chelate, although the amount of increase tapers off substantially. Continued addition of substrate results in further increases in TL intensity, although limiting values can be eventually reached. The titration curves up to 150 equivalents of substrate may be found in Fig. 2, and the final limiting intensity was obtained by dissolving an equivalent amounts of chelate in neat dimethyl sulphoxide solvent. The tendency of the titration curves not to reach a limiting value except at very high concentrations of
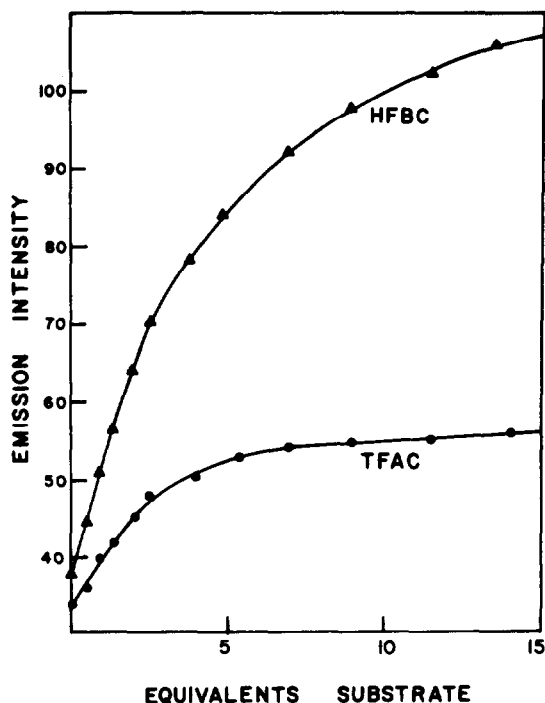
Fig. 1. Luminescence titration of Eu(HFBC)₃ (upper trace) and Eu(TFAC)₃ (lower trace) with dimethyl sulphoxide. Only the initial portion of the titration is shown, and the emission intensities are given in arbitrary units.
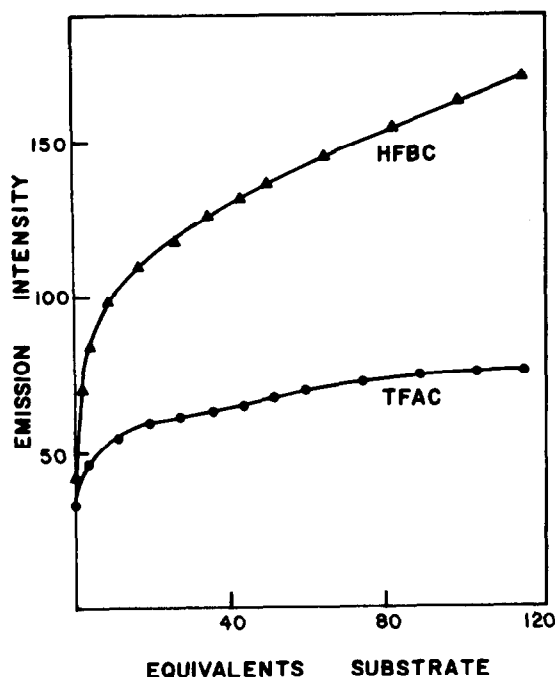
Fig. 2. Full luminescence titration of Eu(HFBC)₃ (upper) and Eu(TFAC)₃ (lower with dimethyl sulphoxide. The intensity scale is in arbitrary units.

substrate prevented a calculation of the association constant in the usual manner.[19,20] However, examination of Fig. 2 reveals that the initial portion of the curves provides evidence for the efficient formation of the 1:1 chelate/substrate complex. The remaining portion of the titration curve probably represents formation of the 1:2 adduct, as well as geometrical rearrangements of the β-diketone ligands in the manner as has been reported previously.[19] Application of Job's method of continuous variations led to somewhat ambiguous results, but did indicate the existence of 1:1 and higher stoichiometries. Dibutyl sulphoxide was found to yield much smaller degrees of TL enhancement with Eu(TFAC)₃ and no enhancement with Eu(HFBC)₃. No sharp increases in TL intensity was noted, and the Job's plots only indicated the presence of 1:1 complexes. In fact, it was found that addition of solid dibutyl sulphoxide in large quantities never led to peaking of the TL spectra. We conclude that the 1:1 dibutyl sulphoxide adduct only forms partially, even at huge ratios of substrate to chelate. Such behavior is consistent with the existence of very weak complexation (and possibly no complexation in the case of Eu(HFBC)₃).

No data could be obtained when diphenyl sulphoxide was added to CHCl₃ solutions of either Eu(TFAC)₃ or Eu(HFBC)₃, as no TL enhancements could be measured at any concentration of this substrate. One may conclude that either this substrate does not enhance the luminescence intensity upon binding, or the degree of complexation is so small that no enhancement is seen. Given the bulkiness of the camphorato ligands, the latter possibility is quite likely.

Accompanying the TL increases associated with the dimethyl sulphoxide adduct formation is the appearance of optical activity within the Eu(III) emission bands. However, this optical activity is not observed until a

considerable amoung of substrate is added to the chelate solutions (at least 50 equivalents of dimethyl sulphoxide per mole of Eu(III) chelate is required). The CPL spectra obtained for the $^5D_0 \rightarrow {}^7F_1$ band system at high concentrations of dimethyl sulphoxide are shown in Fig. 3 for Eu(TFAC)₃ and Eu(HFBC)₃, while the spectra associated with the $^5D_0 \rightarrow {}^7F_2$ transitions are found in Fig. 4. These spectra are essentially the same as we have presented earlier for Eu(TFAC)₃[12] and Eu(HFBC)₃[13] in neat DMSO solvent. It is highly significant to note that while both β-diketone ligands are derived from the same isomer of d-camphor, the chirality experienced by the Eu(III) ion is the opposite in these two cases. This observation immediately suggests that a stereoselective mechanism is responsible for the observed optical activity, and that opposite diastereomers have been selected in the two systems.

The CPL data may be placed on a quantitative basis by computing the luminescence dissymmetry factor, a quantity which is related to the rotational strength.[21] If the emitted intensities of left- and right-circularly polarized light are represented by I_L and I_R, respectively, then the TL intensity is defined as:

$$I = 1/2(I_L + I_R)$$

and the CPL intensity is given by:

$$\Delta I = I_L - I_R.$$

The luminescence dissymetry factor is defined as:

$$g_{lum} = \Delta I/I$$

and is analogous to the Kuhn dissymmetry factor used in
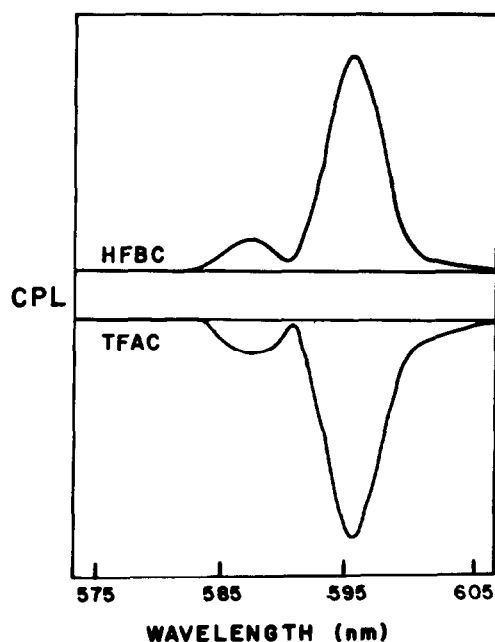
Fig. 3. Circularly polarized luminescence spectra obtained for the Eu(TFAC)₃/dimethyl sulphoxide (lower trace) and Eu(HFBC)₃/dimethyl sulphoxide (upper trace) adducts in CHCl₃ solution. The spectra correspond to emission within the $^5D_0 \rightarrow {}^7F_1$ transition.
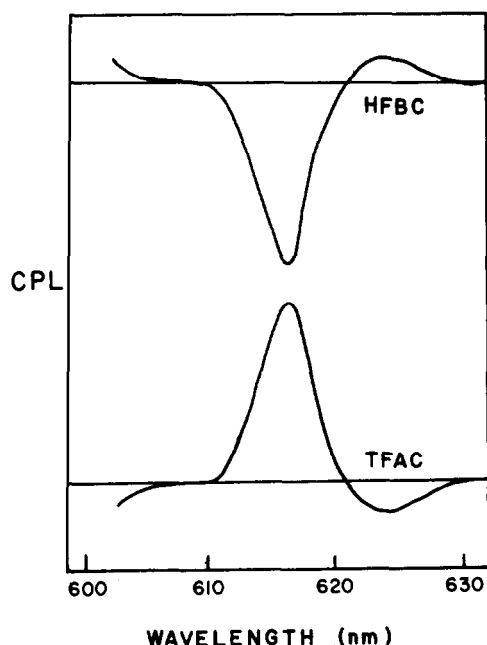
Fig. 4. Circularly polarized luminescence spectra obtained within the $^5D_0 \rightarrow {}^7F_2$ (Eu(III) transition for Eu(TFAC)$_3$/ dimethyl sulphoxide (lower trace) and Eu(HFBC)$_3$/dimethyl sulphoxide (upper trace).

circular dichroism spectroscopy. Values for the dissymmetry factors have been collected in Table 1 for the Eu(TFAC)$_3$ and Eu(HFBC)$_3$ complexes with dimethyl sulphoxide, and these results are essentially the same as those we have previously presented for studies carried out on completely different equipment.[12,13]

No CPL was found when complexing Eu(HFBC)$_3$ with either dibutyl sulphoxide or diphenyl sulphoxide. Such observations are consistent with the earlier TL enhancement results. However, very weak optical activity was found in the case of Eu(TFAC)$_3$/dibutyl sulphoxide. The CPL spectrum was identical to that obtained for Eu(TFAC)$_3$/dimethyl sulphoxide, although the dissymmetry factors (as shown in Table 1) were

significantly smaller in magnitude. All the data indicate that while dimethyl sulphoxide reacts fairly strongly with the chelates to form 1:1 and 1:2 adducts, the other sulphoxides react only weakly or not at all. In addition, adduct formation with Eu(HFBC)$_3$ is seen to be much weaker than with the adduct formation of Eu(TFAC)$_3$ in spite of the extra fluorination (and predicted increased Lewis acidity) associated with the HFBC chelate.

Sulphones

It has been established that sulphones are capable of binding to Eu(III) chelates composed of achiral[22] and chiral[11] β-diketone ligands. We find that addition of dimethyl sulphone or dibutyl sulphone to a CHCl$_3$ solution of Eu(TFAC)$_3$ or Eu(HFBC)$_3$ yields no more than a 5% increase in TL intensity, and that the addition of diphenyl sulphone yields no TL enhancement that we can measure. These very low degrees of luminescence enhancement prevented the calculation of association constants for the sulphone adducts. It is quite clear that while these substrates are capable of bonding to the Eu(III) chelates,[11,22] the mode of attachment is such that the emission intensity of the Eu(III) ion is not enhanced. These observations would imply that the sulphones form poor shields which do not adequately protect the Eu(III) ion from solvent quenching. Application of Job's method of continuous variations to the sulphone adducts yielded poor quality results due to the low TL enhancements, but apparently only 1:1 adducts form in the CHCl$_3$ solution for both the dimethyl and dibutyl sulphone substrates. This behaviour is quite different from what was observed with the sulphoxide adducts; in that situation the dimethyl sulphoxide substrate could form 1:1 and 1:2 adducts with Eu(TFAC)$_3$ and Eu(HFBC)$_3$, while dibutyl sulphoxide formed a 1:1 complex with Eu(TFAC)$_3$ and no complex with Eu(HFBC)$_3$.

However, while the TL enhancement with the sulphones is minor at best with dimethyl and dibutyl sulphone, it was found that CPL spectra could be obtained in some cases. Unlike dimethyl sulphoxide (where strong CPL and TL signals were found), with dimethyl sulphone no CPL was observed. On the other hand, CPL was obtained in the dibutyl sulphone adducts with both Eu(TFAC)$_3$ and Eu(HFBC)$_3$ (which is somewhat different from the analogous sulphoxide results). No

Table 1. Luminescence dissymmetry factors for the Eu(TFAC)$_3$ and Eu(HFBC)$_3$ adducts with sulphoxides

Adduct	$^5D_0 \rightarrow {}^7F_1$	$^5D_0 \rightarrow {}^7F_2$
Eu(TFAC)$_3$/DMSO	-0.75 (a) -1.80 (b)	+0.35
Eu(HFBC)$_3$/DMSO	+0.15 (a) +0.29 (b)	-0.040
Eu(TFAC)$_3$/DBSO	- (a) -0.081 (b)	+0.0074

Notes: (1) DMSO = dimethyl sulfoxide, and DBSO = dibutyl sulfoxide.

(2) Within the $^5D_0 \rightarrow {}^7F_1$ band, two CPL peaks are noted: peak (a) is at 587 nm and peak (b) is found at 596 nm. With the DBSO adduct, peak (a) could not be measured due to its extremely low intensity.

optical activity was noted with the diphenyl sulphone systems. Values for the luminescence dissymmetry factors of the dibutyl sulphone adducts may be found in Table 2. The CPL spectra were essentially identical in lineshape to those shown in Figs. 3 and 4, and only differed in the observed magnitudes.

Phosphate esters

Addition of either trimethyl, triethyl or tributyl phosphate to a $CHCl_3$ solution of $Eu(TFAC)_3$ or $Eu(HFBC)_3$ results in a sizable increase in TL intensity. We have used these TL increases previously to obtain association constants for the chelate/substrate adducts, and noted at that time that only 1:1 complexes were produced.[30] Addition of triphenyl phosphate resulted in very little TL enhancement, which we took to imply that adduct formation was quite weak with this substrate. Typically the TL intensity was observed to reach an apparent maximum by the time two equivalents of phosphate ester substrate had been added per mole of Eu(III) chelate, and approximately 75% of the limiting value was attained after the addition of one equivalent.[20] The data obtained at this time indicated that only 1:1 chelate/substrate complexes formed.

During the course of the present studies, it was found that the titration curves presented earlier[20] were incomplete. While the data we had presented did indeed appear to level off, addition of large excesses of neat substrate led to further increases in TL intensity. These observations parallel those just made for the dimethyl sulphoxide titrations, and also indicate that 1:2 chelate/substrate complexes form as well as the 1:1 complexes. However, it was found that the limiting TL intensity could only be reached in the neat solvent, indicating that the possible formation of the 1:2 complex is only a weak process. This observation regarding the titration curves indicated that formation constants calculated from such results would be of dubious value. As a result, they have not been obtained from the spectroscopic results.

Accompanying this rise in TL intensity was the appearance of CPL within the Eu(III) emission bands. The CPL lineshapes were absolutely identical to those already shown for the sulphoxide and sulphone adducts (which we have shown in Figs. 3 and 4). However, no CPL is observed until a considerable excess of substrate has been added, and the CPL does not reach a limiting intensity unless the chelate is dissolved in neat solvent. Values for the luminescence dissymmetry factors asso-

ciated with all Eu(III) emission bands of the chelates dissolved in neat solvents may be found in Table 3.

One very striking difference between the sulphoxide and phosphate ester results is that with the latter substrates the sign of the CPL for the $Eu(TFAC)_3$ and $Eu(HFBC)_3$ chelates is the same in every case (opposite signs were found with sulphoxide and sulphone adducts). These trends indicate that with the phosphate esters, the nature of the stereoselectivity is such that the steric nature of the ligand sidechain does not play an important role in determining the predominant diastereomer (as it does with the sulphoxide substrates).

DISCUSSION

The data presented in the earlier sections clearly show that the nature of the bonding existing between the Eu(III) chelates and the substrates used in the present work appears to be different in every case. Given the general bonding trends of lanthanide β-diketone complexes, it is quite likely that the substrate bonds directly to the metal ion via a terminal oxygen. All substrates form a 1:1 adduct:

$$Eu(DK)_3 + S \rightleftharpoons Eu(DK)_3(S)$$

while 1:2 adducts form when the substrate (S) is dimethyl sulfoxide or a phosphate ester:

$$Eu(DK)_3(S) + S \rightleftharpoons Eu(DK)_3(S)_2.$$

This behaviour is possible since it is also well known that lanthanide ions are capable of expanding their coordination number beyond six.

In a previous work, it had been found that in the titration curves of $Eu(TFAC)_3$ and $Eu(HFBC)_3$ with simple amines, 1:2 complexes formed with the substrate molecules being added in a cooperative manner.[19] It has been shown that if $K_1 = 4 K_2$, then the two substrate molecules bind with equal efficiency.[23] Non-equivalent bonding of substrates has been noted for the $Eu(FOD)_3$ (FOD = 6,6,7,7,8,8,8 - heptafluoro - 2,2 - dimethyloctane - 3,5 - dione) adducts of dimethyl sulphoxide,[24] although the cooperativity demonstrated here was opposite to that illustrated earlier.[19] The existence of positive and negative cooperativities in substrate bonding provides evidence that rearrangement of the β-diketone ligands accompanies the adduct formation.

Prior to the adduct formation, the $Eu(TFAC)_3$ and $Eu(HFBC)_3$ chelates undergo rapid diastereomer

Table 2. Luminescence dissymmetry factors for the adducts formed between dibutyl sulphone and $Eu(TFAC)_3$ and $Eu(HFBC)_3$

Chelate	$^5D_0 \rightarrow {}^7F_1$	$^5D_0 \rightarrow {}^7F_2$
$Eu(TFAC)_3$	-0.61 (a) -1.46 (b)	+0.089
$Eu(HFBC)_3$	+0.12 (a) +0.23 (b)	-0.011

Note: The two peaks within the $^5D_0 \rightarrow {}^7F_1$ band system are located at

(a) 587 nm and (b) 596 nm.

Table 3. Luminescence dissymmetry factors for the Eu(TFAC)$_3$ and Eu(HFBC)$_3$ adducts with phosphate esters

Adduct	$^5D_0 \rightarrow {}^7F_1$	$^5D_0 \rightarrow {}^7F_2$
Eu(TFAC)$_3$/TMP	-0.17 (a) -0.60 (b)	+0.040
Eu(HFBC)$_3$/TMP	-0.062 (a) -0.15 (b)	+0.011
Eu(TFAC)$_3$/TEP	-0.10 (a) -0.48 (b)	+0.051
Eu(HFBC)$_3$/TEP	-0.043 (a) -0.18 (b)	+0.013
Eu(TFAC)$_3$/TBP	-0.056 (a) -0.11 (b)	+0.026
Eu(HFBC)$_3$/TBP	-0.041 (a) -0.093 (b)	+0.015

Notes: (1) TMP = trimethyl phosphate, TEP = triethyl phosphate, and

TBP = tributyl phosphate.

(2) Within the $^5D_0 \rightarrow {}^7F_1$ band, two CPL peaks are noted: peak

(a) is found at 587 nm and peak (b) is found at 596 nm.

interconversion, and the lack of observable CPL in noncoordinating solvents indicates an approximately equal ratio of Λ (cis and trans) and Δ (cis and trans) isomers. The cooperative nature of the substrate binding is undoubtedly related to the geometrical rearrangements required to fit these substrates in the inner coordination sphere of the Eu(III) ion, and these rearrangements are seen to be critically dependent on the nature (both chemical and steric) of the substrate donor atoms. The acidity of the chelate and basicity of the substrate must also play an important role in the adduct formation process. It is clear, however, that any perturbation of the Λ/Δ isomer ratio will yield optical activity in the complex mixture, as such a process may be viewed as a partial resolution of the very labile metal complexes. The observation that addition of an achiral substrate to a solution of either Eu(TFAC)$_3$ or Eu(HFBC)$_3$ often leads to the observation of optical activity indicates that the aforementioned ligand rearrangement can be accompanied by stereoselectivity. It is equally clear that the signs of the optical activities within the CPL bands contain information regarding the absolute configuration of the Eu(III) ion, but the source of the chirality experienced by the metal must first be established. It is well established that a metal ion interacts with a dissymmetric environment through three major mechanisms: (a) the vicinal effect (chirality induced at the metal by the simple presence of an asymmetric atom on the ligand), (b) the conformational effect (additional chirality arising when the asymmetric atom is part of a chelate ring), and (c) the configurational effect (chirality due to an asymmetric disposition of chelate rings about the metal).[25]

For the Eu(III) β-diketone complexes studied here, only the vicinal and configurational effects can contribute

to the Eu(III) ion chirality, as the chelate ring is quite planar and does not contain an asymmetric atom. We have examined the nature of the vicinal effect in detail for (Eu(III) complexes containing camphorato ligands by synthesizing and studying chelates whose general formulae are Eu(DK)$_2$(CDK) and Eu(DK)(CDK)$_2$ (where DK = any achiral β-diketone and CDK = chiral β-diketone derived from d-camphor).[14] In this earlier work, it was shown that optical activity arising from the vicinal effect was at least two orders of magnitude smaller than the effects found in the present work with dimethyl sulphoxide and phosphate ester substrates. It therefore appears quite safe to conclude that the chirality experienced by the Eu(III) ion (and manifested through the CPL spectra) in the adduct complexes is configurational in nature. We believe that the adduct formation causes crowding of the bulky camphorato ligands, and these adopt the configuration which minimizes these interactions. Since the ligands are themselves chiral, the isomer which forms in largest excess must be chiral and thus the adduct formation is accompanied by a spontaneous resolution of the very labile chelate.

The mirror images of dissymmetric six-coordinate trigonal metal complexes are denoted Λ and Δ.[25] This nomenclature is not really applicable to the Eu(III) chelate adducts as these certainly are not trigonal, and do not even possess axial symmetry.[26] Nevertheless, it is possible to speak of the free Eu(III) β-diketone complexes as being six-coordinate and trigonal, and we suggest that the Λ and Δ labels might be used to identify and approximate stereochemistry for the adduct complexes.

Complicating the picture is the fact that no correlation has yet been made between the absolute configuration of a chiral Eu(III) β-diketone complex and its chiroptical spectra. However, such a correlation has been made for

Eu(oxydiacetate)$_3$ (which happens to crystallize in an optically active space group), and it has been determined that the circular dichroism associated with the $^7F_0 \rightarrow ^5D_1$ Eu(III) absorption[27,28] and the circularly polarized luminescence of the $^5D_0 \rightarrow ^7F_1$ Eu(III) emission[29] is negative in sign if the absolute configuration of the Eu(III) ion is Δ. We have used this information to correlate observed chirality with Eu(III) and Tb(III) absolute configurations in a variety of solution-phase studies where the optical activity was induced in a trigonal complex through outer-sphere association (Pfeiffer effects).[30-32]

That the optical activity associated with the Eu(III) β-diketone chelate adducts of the present study may be approximately described by the Λ and Δ nomenclature comes from examination of the CPL spectra. The CPL spectra of partially resolved Eu(DPA)$_3^{3-}$ (DPA =pyridine - 2,6 - dicarboxylate) are very distinctive and different from CPL spectra taken in a variety of studies we have made where conformational effects dominate. Since with Eu(DPA)$_3^{3-}$ we have shown that inner-sphere complexation is negligible,[31] we believe that the CPL spectra shown in Figs. 3 and 4 are indicative of trigonal, configurational optical activity (the magnitudes of the dissymmetry factors further support this assignment). Since the CPL spectra of the Eu(III) chelate adducts are absolutely identical in lineshape and of approximately the same order of magnitude as the earlier work, we conclude that the presence of negative CPL in the $^5D_0 \rightarrow ^7F_1$ luminescence band indicates that the diastereomer present in largest excess is that of the Δ-configuration.

For transition metal complexes of camphorato β-diketones, it has been generally found that if one begins with R,R-ligand then the Λ-isomer of the metal complex is formed to the greatest extent. The degree of stereoselectivity is solvent dependent for labile complexes; the Λ/Δ ratio runs from 3.2 to 1.03 for V(+ATC)$_3$.[9] In most of the Eu(III) complexes, the opposite situation is found to hold: if the chelates are prepared from R,R-TFAC or R,R-HFBC then the Δ-isomer is present in the largest amount. Only for the sulphone and sulphoxide adducts of Eu(HFBC)$_3$ does the

Λ-isomer form to the greatest extent. One also notes that the entire series of phosphate esters all stabilize the Δ-isomers, while dimethyl sulphoxide and dibutyl sulphone lead to the predominance of different isomers in the case of Eu(TFAC)$_3$ and Eu(HFBC)$_3$.

It had been noted earlier that the 596 nm component of the $^5D_0 \rightarrow ^7F_1$ Eu(III) transition of Eu(TFAC)$_3$ dissolved in neat dimethyl sulphoxide was totally circularly polarized.[12] We have now proposed that the Δ-isomers of this chelate give rise to this optical activity, and this information enables a calculation of the diastereomer abundance for this chelate. Since this band cannot contain any further optical activity, one may assume that complete conversion of the initial racemic mixture into the Δ-isomer is achieved in neat DMSO. All other solvents yield an excess of this Δ-isomer, but the observed dissymmetry factors are much lower in magnitude. This may be interpreted to imply that the complex is only partially resolved, and that the degree of resolution may be calculated from the g_{lum} factors listed in Tables 1-3. We have presented these values in Table 4, and it may be noted that increasing the steric nature of the substrate invariably results in a lower Δ/Λ ratio. No such calculations were calculated for Eu(HFBC)$_3$, as the limiting dissymmetry factors for this band is not yet established.

It has been noted that the plots of induced differential shifts, $\Delta\Delta\delta$, (obtained during the course of nmr experiments) ought to increase to a maximum as one titrates a substrate with a Eu(III) shift reagent. However, this situation is not usually observed.[11] It has been suggested that differing magnetic environments[33] or varying stoichiometries[11] produced during the experiment can account for these effects. The present study confirms that both effects may be important, as we have shown that the stoichiometry can vary with chelate/substrate ratios and that the existence of ligand rearrangements indicates varying magnetic environments. It has proven difficult in the past to obtain absolute configurations of unknown materials by nmr methods, as the proton resonances to not always appear to shift in a rational manner. The work presented in this latest investigation has provided an insight into this behaviour; if the adduct formation is

Table 4. Diastereomeric abundances obtained for Eu(TFAC)$_3$ as a function of solvent

Substrate	Mole Fraction		
	Δ-Isomer	Λ-Isomer	Δ/Λ Ratio
Dimethyl sulfoxide	0.95	0.05	19.0
Dibutyl sulfoxide	0.52	0.48	1.08
Dibutyl sulfone	0.87	0.13	6.41
Trimethyl phosphate	0.65	0.35	1.86
Triethyl phosphate	0.62	0.38	1.63
Tributyl phosphate	0.53	0.47	1.13
Chloroform	0.50	0.50	1.00

Note: The results were obtained using the 596 nm component of the $^5D_0 \rightarrow ^7F_1$ Eu(III) emission band.

accompanied by ligand rearrangements (which are in turn dictated by steric requirements), the chirality of the resulting predominant diastereomer does not necessarily have to correlate with the absolute configuration of any asymmetric atom. Further studies are under way to clarify the nature of these processes.

REFERENCES

[1] Teacher–Scholar of the Camille and Henry Dreyfus Foundation, 1980–85.
[2] J. H. Dunlop, R. D. Gillard and R. Ugo, *J. Chem. Soc. A.* 1966, 1540.
[3] Y. T. Chen and G. W. Everett, *J. Am. Chem. Soc.* 1968, **90**, 6660.
[4] W. D. Horrocks, D. L. Johnston and D. MacInnes, *J. Am. Chem. Soc.* 1970, **92**, 7620.
[5] R. M. King and G. W. Everett, *Inorg. Chem.* 1971, **10**, 1237.
[6] C. S. Springer, R. E. Sievers and B. Feibush, *Inorg. Chem.* 1971, **10**, 1242.
[7] G. W. Everett and R. M. King, *Inorg. Chem.* 1972, **11**, 2041.
[8] H. G. Brittain, *Inorg. Chem.* 1980, **19**, 2233.
[9] R. M. King and G. W. Everett, *Inorg. Chim. Acta* 1973, **7**, 43.
[10] M. D. McCreary, D. W. Lewis, D. L. Wernick and G. M. Whitesides, *J. Am. Chem. Soc.* 1974, **96**, 1038.
[11] H. L. Goering, J. N. Eikenberry, G. S. Koermer and C. J. Lattimer, *J. Am. Chem. Soc.* 1974, **96**, 1493.
[12] H. G. Brittain and F. S. Richardson, *J. Am. Chem. Soc.* 1976, **98**, 5858.
[13] H. G. Brittain and F. S. Richardson, *J. Am. Chem. Soc.* 1977, **99**, 65.
[14] C. K. Chan and H. G. Brittain, *J. Inorg. Nucl. Chem.* 1981, **43**, 2399.
[15] H. G. Brittain, *J. Am. Chem. Soc.* 1980, **102**, 3693.
[16] F. Halverson, J. S. Brinen and J. R. Leto, *J. Chem. Phys.* 1964, **41**, 157.
[17] H. G. Brittain and F. S. Richardson, *J. Chem. Soc. Dalton Trans.* 1976, 2253.
[18] H. G. Brittain, *J. Chem. Soc. Dalton Trans.* 1979, 1187.
[19] H. G. Brittain, *J. Am. Chem. Soc.* 1979, **101**, 1733.
[20] H. G. Brittain, *Inorg. Chem.* 1980, **19**, 640.
[21] F. S. Richardson and J. P. Riehl, *Chem. Rev.* 1977, **77**, 773.
[22] W. D. Anderson and J. J. Uebel, *Tetrahedron Lett.* 1970, 5253.
[23] D. A. Deranleau, *J. Am. Chem. Soc.* 1969, **91**, 4044; 4050.
[24] J. Reuben, *J. Am. Chem. Soc.* 1973, **95**, 3534.
[25] F. S. Richardson, *Chem. Rev.* 1979, **79**, 17.
[26] F. S. Richardson and H. G. Brittain, *J. Am. Chem. Soc.* 1981, **103**, 18.
[27] F. R. Fronczek, A. K. Benerjee, S. F. Watkins and R. W. Schwartz, *Inorg. Chem.* 1981, **20**, 2745.
[28] A. C. Sen, M. Chowdhury and R. W. Schwartz, *J. Chem. Soc. Far. Trans. II* 1981, **77**, 1293.
[29] J. P. Morley, J. D. Saxe and F. S. Richardson, *Mol. Phys.*, in press.
[30] F. Yan, R. A. Copeland and H. G. Brittain, *Inorg. Chem.* 1982, **21**, 1180.
[31] F. Yan and H. G. Brittain, *Polyhedron*, 1982, 1, 195.
[32] H. G. Brittain, *Inorg. Chem.*, 1982, 21, 2955.
[33] H. L. Goering, J. N. Eikenberry and G. S. Koermer, *J. Am. Chem. Soc.* 1971, **93**, 5913.

DISTORTED TETRAHEDRAL COPPER(I) COMPLEXES OF 2,2'-BI-4,5-DIHYDROTHIAZINE AND 2,2'-BI-2-THIAZOLINE

MICHAEL G. B. DREW* and TIMOTHY R. PEARSON
Department of Chemistry, University of Reading, Whiteknights, Reading RG6 2AD, England

and

BRIAN P. MURPHY and S. MARTIN NELSON*
Department of Chemistry, Queens University, Belfast BT9 5AG, Northern Ireland

Abstract—The copper(I) complexes [Cu(btz)$_2$](BPh)$_4$ (I) and [Cu$_2$(bt)$_4$][ClO$_4$]$_2$ (II) have been prepared (btz = 2,2'-bi-4,5-dihydrothiazine and bt = 2,2'-bi-2-thiazoline). Crystals of (I) are orthorhombic with a = 10.927(8), b = 11.743(8), c = 15.000(6) A, Z = 2, spacegroup P2$_1$2$_1$2. Crystals of (II) are monoclinic with a = 21.928(11), b = 11.925(8), c = 14.716(11) A, β = 103.6(1), Z = 8, spacegroup C2/c. 2121 and 2204 independent reflections have been measured on a diffractometer and the structures refined to R 0.061 and 0.063 respectively. In the cation of (I) the two btz ligands are coordinated via the α-di-imine groups (Cu–N 2.010(6), 2.024(6) Å). The resulting CuN$_4$ coordination geometry is a flattened tetrahedron with a dihedral angle of 68.9° between the two "CuN$_2$" planes. It is suggested that this distortion is an intrinsic property of the molecule associated with metal-to-ligand d_π–p_π* charge transfer rather than a consequence of lattice packing effects. In the dimeric cation (II), each copper(I) ion is bonded to the α-di-imine group of one bt molecule (A) but with appreciably different Cu–N bond lengths (2.277(6), 1.999(5) Å), to one nitrogen atom of a second ligand molecule (B) in the *trans* configuration (Cu–N 1.961(5) Å) and to one sulphur atom (Cu–S 2.428(2)Å) of a third ligand molecule (C). The coordination geometry is a very distorted tetrahedron if a very weak interaction (Cu … S 3.039(2) Å) with a sulphur atom of ligand B is discounted. It is suggested that the different structures arise from the different "bites" of the two ligands.

INTRODUCTION

It is generally assumed that in the absence of ligand constraints the preferred geometry of four-coordinate copper(I) is regular tetrahedral.[1]

For the copper(II) on the other hand, which prefers higher coordination numbers, configurations based on the square plane, i.e. the square pyramid and the tetragonally elongated octahedron, are particularly common.[2] Interest in copper coordination environments intermediate between tetrahedral and "square" has been stimulated recently by the discovery of distorted tetrahedral active sites in the "blue" copper proteins plastocyanin[3] and azurin[4] and in the recognition of the dependence of copper(I)/copper(II) redox potentials[5] and, possibly also, rates of electron transfer[6] on the degree of such distortion of the reduced and oxidised species from regular tetrahedral and square respectively.

Copper(II) complexes containing the Cu(bp)$_2$ or Cu(phen)$_2$ groupings do not adopt a square planar configuration because of interligand steric interactions between hydrogen atoms α to the nitrogens.[7] Structural studies have shown that in such complexes the Cu(ligand)$_2$ moiety is tetrahedrally distorted or that the metal ion adopts an approximate trigonal bipyramidal configuration.[8–11] With copper(I) having a filled d-shell, on the other hand, there is no obvious steric or electronic reason why the two "CuN$_2$" planes should be disposed at other than an angle of 90°, but this is not always observed. Recent structural studies[12–16] of several copper(I) complexes of substituted 2,2'-bipyridine and 1,10-phenanthroline ligands of the type [Cu(ligand)$_2$]$^+$ have revealed significant flattening of the "CuN$_4$" coordination sphere (see Discussion).

In this paper we report the crystal and molecular

structures of the copper(I) complexes [Cu(btz)$_2$] (BPh$_4$) (I) and [Cu$_2$(bt)$_4$] (ClO$_4$)$_2$ (II) where btz and bt are 2,2' - bi - 4,5 - dihydrothiazine and 2,2' - bi - 2 - thiazoline respectively. These ligands have obvious similarities to

btz   bt
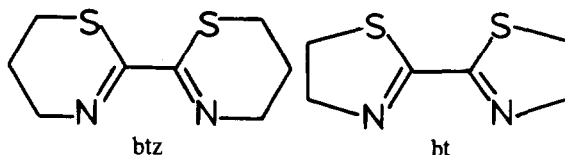
2,2'bipyridine but differ in that the α-di-amine group is not part of a conjugated system. Previous studies[17] on complexes with iron(II) and other divalent first row transition metal ions have shown that both ligands chelate via the α-di-imine group. In this paper we show that this also is the case for [Cu(btz)$_2$]$^+$ which also exhibits severe tetrahedral distortion. In (II) the structure is more complex involving both α-di-imine and sulphur coordination.

RESULTS AND DISCUSSION

Physical properties of the complexes

Both complexes (I) and (II) are diamagnetic. (I) is readily soluble in a range of organic solvents (acetonitrile, dimethylformamide, acetone, 1,2-dichloroethane) while (II) has much more limited solubility in the more polar solvents only. Both complexes are stable to air in the solid state but solutions slowly turn green on exposure to air. The IR spectra of both ligands show a strong ν(C=N) absorption at 1614 cm^{-1} in btz and at 1590 cm^{-1} in bt, and strong bands in the 800–1200 cm^{-1} region corresponding to skeletal vibrations of the heterocyclic rings.[17] A weak-to-medium intensity band at 650–660 cm^{-1} in both ligands may be due to the ν(C–S) vibration. There are marked changes in the IR spectra on

---

*Authors to whom correspondence should be addressed.

coordination to copper(I). In (I), the strong band at 1614 cm^{-1} has virtually disappeared being replaced by a medium intensity band at 1530 cm^{-1} while the vibration at 660 cm^{-1} tentatively assigned to ν(C–S) is relatively unchanged, now occurring more weakly at 670 cm^{-1}. These observations are fairly consistent with coordination *via* the α-di-imine group subsequently proved by the X-ray structure determination (see below). The large coordination shift (84 cm^{-1}) of ν(C=N) to lower energies together with the alteration in intensity is indicative of strong coupling between vibration modes within the Cu(N=C–C=N) chelate ring.[21,22] This could arise from metal d_π-to-ligand p_π^* back coordination. Similar effects have been observed in low-spin iron(II) complexes of α-di-imine ligands.[17,22] Significantly in the copper(II) complex [Cu(btz)$_3$] (ClO$_4$)$_2$ where little metal-to-ligand charge transfer is expected, ν(C=N) is shifted to lower frequencies only by 46 cm^{-1} and without appreciable loss in intensity.

In the case of the bt complex (II), a more complex pattern is apparent in the 1500–1600 cm^{-1} region of the IR spectrum. The single strong ν(C=N) vibration occurring at 1590 cm^{-1} in the free ligand is replaced by three medium intensity bands at 1600, 1572 and 1552 cm^{-1}. The 652 cm^{-1} vibration in the free ligand is apparent also in the spectrum of the complex though with much reduced intensity and there are also a number of other weak bands in this region. While assignment of these bands to particular vibrations is difficult and beyond the scope of this paper there is the clear indication that the coordination mode of bt in (II) is different from that of btz in (I) as confirmed by the X-ray structure determinations.

There are also notable differences in the electronic spectra of the two complexes. In the solid state (I) displays a strong broad absorption consisting of a maximum at 20,200 cm^{-1} with a pronounced shoulder at 16,900 cm^{-1} and another weaker one at *ca.* 26,000 cm^{-1}. The solid state spectrum of (II) consists of a broad unresolved absorption band centred at 25,200 cm^{-1} (Fig. 1).

The different energies of the two (presumably) Cu(I) to ligand charge transfer systems reflect the different coordination environments of the metal ion in the two com-

plexes. The much lower energy of the charge transfer in (I) may be taken as an indication of the good π-accepting capacity of the α-di-imine group. Similar low energy metal-to-ligand d_π–p_π^* charge transfer has been noted[17] in the low spin iron(II) complex [Fe(btz)$_3$]$^{2+}$. Good correspondence between the spectra of (I) obtained in the solid state and in 1,2-dichloroethane solution was obtained an apparent extinction coefficient of 1640 dm^{3}mol^{-1}cm^{-1} being observed for the absorption maximum at 20,500 cm^{-1} in this solvent. In more polar solvents such as dimethyl formamide and particularly acetonitrile marked deviations from Beer's law were found indicating extensive dissociation in dilute solution. The effect of added btz ligand was to partially restore the spectrum. Complex (II) is insoluble in 1,2-dichloroethane while in polar solvents such as acetonitrile even more extensive dissociation occurred, preventing measurement of the spectrum of the complex in solution even in the presence of a large excess of free bt ligand.

EXPERIMENTAL

Preparation of the complexes: The ligands were synthesised according to the methods described by Tomalia and Page.[18] Purification was by extraction of the crude products with hexane followed by recrystallisation from carbon tetrachloride or acetone. Complexes were prepared by addition of [Cu(MeCN)$_4$] (ClO$_4$) to an excess of the ligand in warm de-oxygenated acetonitrile under N$_2$. Orange crystals of [Cu$_2$(bt)$_4$] (ClO$_4$)$_2$ separated on cooling. Found C, 28.3, H, 3.1, N, 11.1%. [Cu$_2$(bt)$_4$] (ClO$_4$)$_2$ requires C, 28.4, H, 3.2; N, 11.0%. No perchlorate salt of [Cu(btz)$_2$]$^+$ could be isolated but the tetraphenylborate was obtained as dark brown cubes on addition of Na(BPh$_4$) to the reaction mixture. Found C 61.3, H 5.7, N 7.2% [Cu(btz)$_2$] (BPh$_4$) requires C 61.2, H, 5.7; N, 7.1%

STRUCTURE DETERMINATION

Crystal data are given in Table 1. The two crystals were mounted in turn on a Stoe STADI2 diffractometer and data was collected via variable width *w* scan. Background counts were 20 s and the scan rate of 0.033°/s was applied to a width of $(1.5 + \sin \mu/\tan \theta)$. Absorption and extinction corrections were not applied.

Both structures were solved by the Patterson method and the positions of non-hydrogen atoms found from the Fourier syntheses. The hydrogen atoms were generated in trigonal or tetrahedral positions and an overall isotropic thermal parameter was refined. Structures were refined by full-matrix least squares with a weighting scheme $w = 1/(\sigma^2(I) + 0.003 F^2)$. Final R values were 0.061 and 0.063 respectively. Calculations were carried out using Shelx76[19] at the University of Manchester Computing Centre. Atomic scattering factors and dispersion corrections were taken from Ref. 20. Important dimensions are given in Table 2. Atomic parameters, some dimensions, thermal parameters and a list of structure factors have been deposited with the editor as supplementary material; copies are available on request.

Atomic coordinates have also been deposited with the Cambridge Crystallographic Data Centre.

The structure of [(Cu(btz)$_2$)(BPh$_4$) (I)

This compound contains discrete [Cu(btz)$_2$]$^+$ cations and [BPh$_4$]$^-$ anions. Both ions have crystallographic C$_2$ symmetry with the Cu and B atoms positioned on two fold axes. In the cation (Fig. 2) the copper atom is bonded to two btz ligands via Cu–N bonds (2.010(6), 2.024(6) Å). The two "CuN$_2$" planes intersect at an angle of 68.9° so that the coordination geometry is a distorted (flattened) tetra-
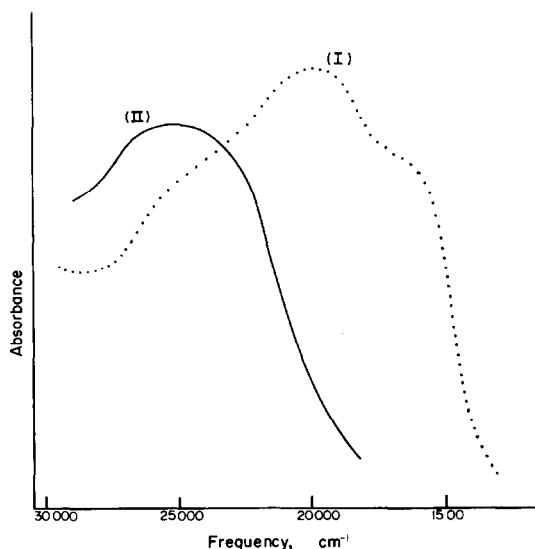
Fig. 1. The electronic absorption spectra of [Cu(btz)$_2$] (BPh$_4$) (I) and [Cu$_2$(bt)$_4$] (ClO$_4$)$_2$ (II) in the solid state.

Table 1. Crystal Data and Refinement Details

	(I)	(II)
Formula	[Cu(btz)$_2$] (BPh$_4$)	[Cu$_2$(bt)$_4$] (ClO$_4$)$_2$
	CuC$_{40}$H$_{44}$S$_4$N$_4$B	Cu$_2$C$_{24}$H$_{32}$S$_8$N$_8$Cl$_2$O$_8$
M	734.9	1014.7
Crystal Class	Orthorhombic	Monoclinic
Spacegroup	P2$_1$2$_1$2	C2/c
Absences	0k0,k=2n+1	h+k,h+k=2n+1
	h00,h=2n+1	h0l,l=2n+1
a(A)	10.927(8)	21.928(11)
b(A)	11.743(8)	11.925(8)
c(A)	15.000(6)	14.716(11)
β(deg)	(90)	103.6(1)
U(A^3)	1924.7	3739.9
Z	2	4
F(000)	820	2064
dm(g.cm^{-3})	1.33	1.78
dc(g.cm^{-3})	1.35	1.80
λ(A)	0.7107	0.7107
μ(cm^{-1})	8.73	18.09
Crystal Size(mm^3)	0.5*0.5*0.55	0.8*0.2*0.6
Rotation Axis	c	b
2*theta max	50	45
No of data	3206	3225
Criteria for data inclusion	I > 2 σ (I)	I > 3 σ (I)
No of data used in refinement	2121	2204
No of parameters	225	244
R	0.061	0.063
R$_w$	0.065	0.071

hedron. As noted in the introduction several other copper(I) complexes, of α-di-imine ligands also show this kind of distortion. In (Cu(dmbp)$_2$)(BF$_4$),[12] (Cu(tmbp)$_2$)(ClO$_4$),[13] (Cu(dmp)$_2$)(ClO$_4$),[14] (Cu(dmbp)$_2$)(NO$_3$)[15] and (Cu(dmp)$_2$)(NO$_3$)·2H$_2$O,[16] where dmbp = 6,6' - dimethyl - 2,2' - bipyridine, tmbp = 4,4',6,6' - tetramethyl - 2,2' - bipyridine, tmp = 2,9 - dimethyl - 1,10 phenanthroline, the dihedral angles between the two planar bidentate ligands are respectively 80.9, 67.6, 81.8, 80 and 85.4°. In all these structures the Cu–N bond lengths fall within the range 2.01–2.08 Å.

In (I) five of the atoms of the six-membered heterocyclic rings are planar within experimental error. However C(3) and C(10) lie 0.66 and 0.70 Å from their respective planes. Bond distances within the rings are as expected, though it is noticeable that S(5)–C(6) and S(8)–C(7) at 1.747(6) and 1.738(6) are significantly shorter than S(5)–C(4) and S(8)–C(9) at 1.823(10), and 1.809(10) Å. There is a small twist around the C(6)–C(7) bond connecting the

two six-membered rings. Thus, the N(1)–C(6)–C(7)–N(12) torsion angle is −13.9, i.e. slightly larger than the twist angles (4.4, 5.0 and 12.3°) observed for the copper(I)-substituted bipyridine complexes referred to above.[12,13]

The only intramolecular contacts between non-hydrogen atoms of less than 3.5 Å are N(1)...N(1*) 3.46, N(12)...N(12*) 3.34 Å. There are no contacts between cation and anion less than 3.5 Å. The only intermolecular contact of note is S(8)...S(8) $(1 - x, -y, -z)$ of 3.28 Å.

It is difficult to identify the reason for the large deviation of the dihedral angle between the two "CuN$_2$" planes in (I) from 90°. Intermolecular packing effects could, of course, account for small distortions but the deviation (21°) seems large for a purely packing effect. Moreover the observation of dihedral angles ranging from 68 to 85° in all the Cu(I)-α-di-imine structures so far solved seems to suggest that there may be an intrinsic electronic origin. The assignment of the intense visible absorption in (I) to a metal-to-ligand charge transfer has been discussed above. Possibly there is some mixing of the excited state, formally a complex of Cu(II) with a ligand radical anion with the ground state. Alternatively the flattening of the tetrahedral configuration may lead to an improved d_π-p_π^* overlap.

The structure of [Cu$_2$(bt)$_4$] (ClO$_4$)$_2$ (II)

The structure consists of discrete ClO$_4^-$ anions and dimeric [Cu$_2$(bt$_4$)]$^{2+}$ cations. Each copper atom is bonded to two nitrogen atoms of one ligand molecule (A) (Cu–N 2.277(6), 1.995(5) Å). By comparison with the chelating α-di-imine groups in (I) the first Cu–N bond is lengthened by ca. 0.26 Å. The metal atom is also strongly bonded to one nitrogen N(1B) of a second ligand molecule (B) at 1.961(5) Å. This ligand molecule is in the trans configuration and the sulphur atoms S(10B) cis to N(1B) is 3.039(2) Å distant from the metal (Fig. 3). The copper atom is also strongly bonded (2.428(2) Å) to S(10B*) of a centrosymmetrically related "Cu(bt)" unit. The two nitrogen atoms of ligand A together with N(1) and S(10) of ligand B constitute an approximate square planar environment about the copper atom. Least squares plane calculations show that the metal atom is 0.49 Å out of plane in the direction of S(10B*). If S(10B) is considered to be coordinated to the metal (Cu...S 3.039 (2) Å) then the coordination geometry is a distorted square pyramid with the angles involving the axial Cu–S (10B*) bond being 102.8(2), 102.6(2), 108.7(2) and 97.0(2)°. However it is probably not realistic to consider the Cu...S contact as a conventional bond, particularly as the Cu–S (10B)–C (9B) angle is 168.1(3)°, so that the coordination geometry is better viewed as a very distorted tetrahedron the angles subtended at the metal by the four donor atoms N(1A), N(7A), N(1B) and S(10B*) ranging from 78 to 145°.

The five-membered rings of the bt ligands are nearly planar. Deviations from the plane are irregular in the four examples and we presume that there is no favoured conformation.

As in (I) the S(4)–C(5) and S(10)–C(9) bonds are somewhat shorter at 1.752(7), 1.771(8) Å, 1.747(7), 1.752(6) Å than S(4)–C(3), S(10)–C(9) at 1.813(8), 1.809(9), 1.792(11), 1.826(9) Å. The N(1A)–C(5A)–C(6A)–N(7A) torsion angle is 0.2 while that of N(1B)–C(5B)–C(6B)–S(10B) is 7.4°. The Cu...Cu distance is 3.65 Å. There are no close contacts between the two halves of the dimer nor are there any cation...anion interactions of note. There

Table 2. Molecular dimensions in the cations distances, A and angles, degrees

METAL COORDINATION SPHERE IN (I)

CU	—	N(1)	2.010(6)		N(1A)	—	CU(1)	—	N(1B)	110.39(21)
CU	—	N(12)	2.024(6)		N(7A)	—	CU(1)	—	N(1B)	144.64(22)
N(1)	—	CU	—	N(12)	91.48(23)		N(1A)	—	CU(1)	—	S(10B**)	102.82(22)
N(1)	—	CU	—	N(1*)	118.73(24)		N(1B)	—	CU(1)	—	S(10B**)	102.60(21)
N(1)	—	CU	—	N(12*)	136.41(24)		N(7A)	—	CU(1)	—	S(10B**)	108.77(22)

LIGAND DIMENSIONS   **OTHER DIMENSIONS IN THE CATION**

S(5)	—	C(4)	1.823(10)	N(1A)	—	C(2A)	1.476(9)
S(5)	—	C(6)	1.747(7)	N(1A)	—	C(5A)	1.264(9)
S(8)	—	C(7)	1.738(6)	C(2A)	—	C(3A)	1.540(12)
S(8)	—	C(9)	1.810(10)	C(3A)	—	S(4A)	1.792(11)
N(1)	—	C(6)	1.275(9)	S(4A)	—	C(5A)	1.746(7)
N(1)	—	C(2)	1.477(10)	C(5A)	—	C(6A)	1.477(10)
N(12)	—	C(7)	1.285(8)	C(6A)	—	N(7A)	1.289(8)
N(12)	—	C(11)	1.472(9)	C(6A)	—	S(10A)	1.738(7)
C(4)	—	C(3)	1.497(16)	N(7A)	—	C(8A)	1.469(8)
C(6)	—	C(7)	1.528(10)	C(8A)	—	C(9A)	1.541(9)
C(9)	—	C(10)	1.512(13)	C(9A)	—	S(10A)	1.813(8)
C(11)	—	C(10)	1.537(11)	N(1B)	—	C(2B)	1.473(9)
C(2)	—	C(3)	1.518(14)	N(1B)	—	C(5B)	1.292(8)

C(4)	—	S(5)	—	C(6)	101.3(4)	C(2B)	—	C(3B)	1.526(11)
C(7)	—	S(8)	—	C(9)	100.9(3)	C(3B)	—	S(4B)	1.809(9)
CU	—	N(1)	—	C(6)	113.9(4)	S(4B)	—	C(5B)	1.752(6)
CU	—	N(1)	—	C(2)	123.9(4)	C(5B)	—	C(6B)	1.475(9)
C(6)	—	N(1)	—	C(2)	121.4(6)	C(6B)	—	N(7B)	1.260(9)
CU	—	N(12)	—	C(7)	112.8(4)	C(6B)	—	S(10B)	1.771(6)
CU	—	N(12)	—	C(11)	124.5(4)	N(7B)	—	C(8B)	1.472(10)
C(7)	—	N(12)	—	C(11)	121.5(5)	C(8B)	—	C(9B)	1.499(10)
S(5)	—	C(4)	—	C(3)	110.9(6)	C(9B)	—	S(10B)	1.826(7)
S(5)	—	C(6)	—	N(1)	130.0(5)	CU(1)	—	N(1A)	—	C(2A)	140.3(5)
S(5)	—	C(6)	—	C(7)	114.7(4)	CU(1)	—	N(1A)	—	C(5A)	107.4(4)
N(1)	—	C(6)	—	C(7)	115.1(5)	C(2A)	—	N(1A)	—	C(5A)	112.3(6)
S(8)	—	C(7)	—	N(12)	129.6(5)	N(1A)	—	C(2A)	—	C(3A)	109.0(7)
S(8)	—	C(7)	—	C(6)	115.1(4)	C(2A)	—	C(3A)	—	S(4A)	107.9(6)
N(12)	—	C(7)	—	C(6)	115.2(5)	C(3A)	—	S(4A)	—	C(5A)	89.1(3)
S(8)	—	C(9)	—	C(10)	111.0(6)	N(1A)	—	C(5A)	—	S(4A)	119.9(5)
N(12)	—	C(11)	—	C(10)	115.0(6)	N(1A)	—	C(5A)	—	C(6A)	119.6(6)
C(9)	—	C(10)	—	C(11)	110.5(6)	S(4A)	—	C(5A)	—	C(6A)	120.4(5)

DIMENSIONS IN (II)

					C(5A)	—	C(6A)	—	N(7A)	118.1(6)

METAL CO-ORDINATION SPHERE

					C(5A)	—	C(6A)	—	S(10A)	122.9(5)
CU(1)	—	N(1A)	2.277(6)		N(7A)	—	C(6A)	—	S(10A)	119.0(5)
CU(1)	—	N(7A)	1.999(5)		CU(1)	—	N(7A)	—	C(6A)	116.4(4)
CU(1)	—	N(1B)	1.961(5)		CU(1)	—	N(7A)	—	C(8A)	132.6(4)
CU(1)	—	S(10B**)	2.428(2)		C(6A)	—	N(7A)	—	C(8A)	110.9(5)
N(1A)	—	CU(1)	—	N(7A)	78.36(22)		N(7A)	—	C(8A)	—	C(9A)	109.5(5)

Table 2 (Contd.)

C(8A)	–	C(9A)	–	S(10A)	104.8(4)	S(4B) – C(5B) – C(6B)	117.1(4)
C(6A)	–	S(10A)	–	C(9A)	89.6(3)	C(5B) – C(6B) – N(7B)	120.4(5)
CU(1)	–	N(1B)	–	C(2B)	115.1(4)	C(5B) – C(6B) – S(10B)	120.3(4)
CU(1)	–	N(1B)	–	C(5B)	132.6(4)	N(7B) – C(6B) – S(10B)	119.3(5)
C(2B)	–	N(1B)	–	C(5B)	112.1(5)	C(6B) – N(7B) – C(8B)	111.5(5)
N(1B)	–	C(2B)	–	C(3B)	111.7(6)	N(7B) – C(8B) – C(9B)	110.9(5)
C(2B)	–	C(3B)	–	S(4B)	107.0(5)	C(8B) – C(9B) – S(10B)	106.5(4)
C(3B)	–	S(4B)	–	C(5B)	90.7(3)	C(6B) – S(10B) – C(9B)	88.2(3)
N(1B)	–	C(5B)	–	S(4B)	118.5(4)	CU(1**)– S(10B) – C(9B)	101.8(3)
N(1B)	–	C(5B)	–	C(6B)	124.5(5)	CU(1**)– S(10B) – C(9B)	108.8(3)

*,** REFER TO SYMMETRY ELEMENTS 1-X,1-Y,Z AND
    -X,1-Y,-Z RESPECTIVELY
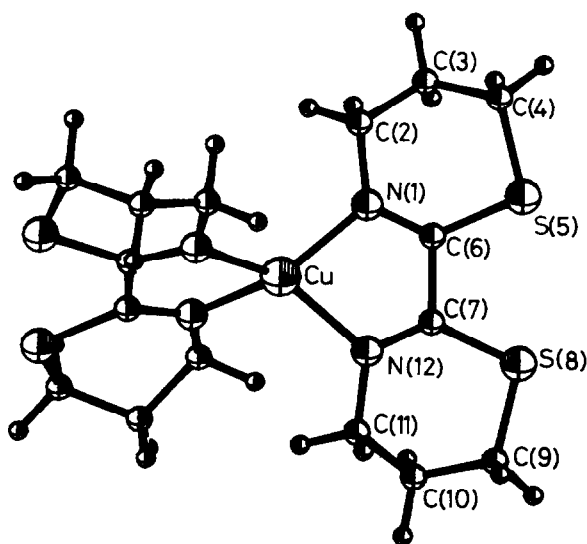
Fig. 2. The structure of (I), [Cu(btz)₂]⁺.
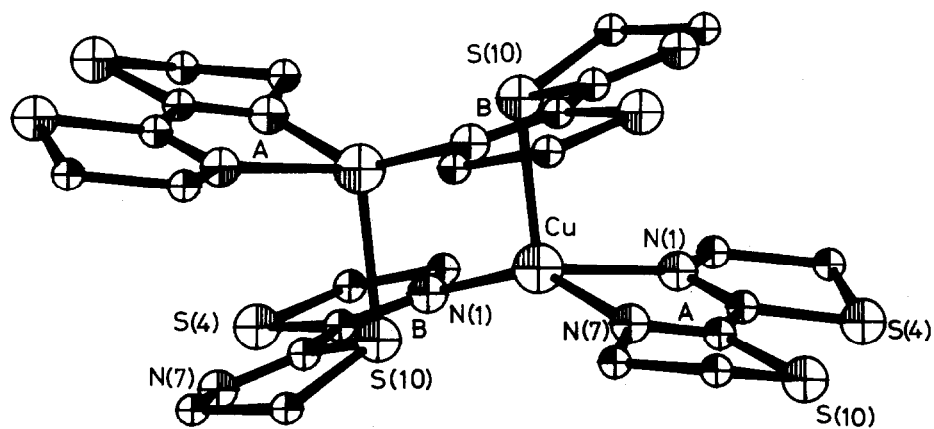
Fig. 3. The structure of (II), [Cu₂(bt)₄]²⁺.

are no Cu . . . O contacts less that 3.75 Å although there are some O . . . S and O . . . C distances of *ca.* 3.2 Å.

The widely different structures of the two complexes is unexpected. Earlier studies[17] have established that in iron(II) complexes of the type [Fe(ligand)$_3$]$^{2+}$, both btz and bt coordinate via the α-di-imine group. Copper(I) is known, of course, to have an affinity for sulphur but it is far from obvious why the two ligands should behave differently towards this metal ion. A possible answer may be found from the different sizes of the heterocyclic rings. The btz ligand chelates efficiently with the MN$_2$C$_2$ ring approximately planar. The N . . . N separation is 2.63 Å and both atoms are strongly bonded subtending an angle of 81.5° at the metal.

On the other hand, there are several indications that the N . . . N chelation of the bt ligand A in (II) is less stable. First the two bond lengths are unequal, the Cu(1)–N(1A) bond at 2.277(6) Å being particularly long. Concomitant with this is an Cu–N(1)–C(2) angle of 140.3(5)°. Even the Cu–N(7)–C(8) angle is 132.6(4)° compared to similar angles of *ca.* 124° in (I). This may be a consequence of strain in the five-membered rings. An indication of this is the C–S–C angles which range from 88.2 to 90.7°. (They are *ca.* 100 in btz in (I)). The CuN$_2$C$_2$ ring in (II) is still planar despite these distortions. The N . . . N separation in ligand A is 2.71 Å and the angle subtended at the metal is 78.3°. It would appear then that the α-di-imine group of (I) is better suited for chelation though it is not clear to what extent the Cu–N(1A) bond in (II) might be lengthened because of steric effects concomitant with the square planar arrangement of N(1A), N(7A), N(1B) and S(10B) around the copper atom.

Whatever the disadvantage in the "bite" of bt compared to btz the effect must be small enough not to influence critically the coordinating properties of the α-di-imine group towards iron(II) both ligands generating ligand fields strong enough to cause spin pairing.[17] It may be that in the case of copper(I) with its known affinity for sulphur there is a delicate balance between α-di-imine chelation and sulphur coordination so that both coordination modes occur in the same molecule.

The chelating capacity of bt in the *trans* configuration, i.e. using one nitrogen and one sulphur atom, might well be expected to be inferior since the sulphur lone pairs will not lie in the same plane as the nitrogen lone pair, in the planar ligand molecule. Thus the copper atom prefers to bond strongly with the sulphur atom of another ligand molecule in an adjacent "Cu(bt)$_2$" unit. The angles subtended at the sulphur S(10B*) by the Cu and C atoms are 88.2(3), 101.8(3), 108.8(3)°.

There are no intramolecular contacts of note in the two structures. It therefore seems unlikely that packing effects could account for the different coordination spheres in the two structures.

REFERENCES

[1] For a review of copper(I) chemistry, see F. H. Jardine, *Adv. Inorg. Chem. Radiochem.* 1975, **17**, 115.

[2] F. A. Cotton and G. Wilkinson, *Advanced Inorganic Chemistry*, 4th Edn. Wiley-Interscience, New York (1980).

[3] P. M. Colman, H. C. Freeman, J. M. Guss, M. Nurata, V. A. Norris, J. A. M. Ramshaw and P. M. Venkatappa, *Nature* 1978 **272**, 319.

[4] E. Adman, R. E. Stenkamp, L. C. Sieker and L. H. Jenson, *J. Mol. Biol.* 1978, **123**, 35.

[5] H. Yokoi and A. W. Addison, *Inorg. Chem.* 1977, **16**, 1341; G. S. Patterson and R. H. Holm *Bioinorg. Chem.* 1975, **4**, 257.

[6] M. A. Augustin and J. K. Yandell, *Inorg. Chem.* 1979, **18**, 577.

[7] E. D. McKenzie, *Coord. Chem. Rev.* 1971, **6**, 187.

[8] H. Nakai, *Bull. Chem. Soc. Japan* 1971, **44**, 2412.

[9] J. Kaiser, G. Brauer, F. A. Schroder, I. F. Taylor and S. E. Rasmussen, *J. Chem. Soc. Dalton Trans.* 1974, 1490.

[10] M. B. Farrar, G. G. Fava and C. Pelizzi, *J. Chem. Soc. Chem. Comm* 1977, 8.

[11] G. Druhan and B. J. Hathaway, *Acta Cryst.* 1979, **B35** 344; W. D. Harrison, B. J. Hathaway and D. Kennedy, *ibid*, 1979, **B35** 2301.; W. D. Harrison and B. J. Hathaway, *ibid*, 1979, **B35**, 2910.

[12] P. J. Burke, D. R. McMillan and W. R. Robinson, *Inorg. Chem.* 1980, **19**, 1211.

[13] P. J. Burke, K. Hendrik and D. R. McMillan *Inorg. Chem.* 1982, **21**, 1881.

[14] G. Dessy and V. Fares, *Cryst. Struct. Commun.* 1979, **8**, 507.

[15] R. Hamalainen, M. Ahlgren, U. Tupeinen and T. Raikes, *Cryst. Struct. Commun.* 1979, **8**, 75; see also footnote in Ref. 12.

[16] R. Hamalainen, U. Turpeinen, M. Ahlgren and T. Raikes, *Finn. Chem. Lett.* 1978, **199**, 274.

[17] J. Nelson, S. M. Nelson and W. D. Perry *J. Chem. Soc. Dalton* 1976, 1282.

[18] D. A. Tomalia and J. N. Paige, *J. Org. Chem.* 1973, **38**, 3949.

[19] G. M. Sheldrick, *Shelx76 Program for Crystal Structure Determination*, Cambridge (1976).

[20] *International Tables for X-ray Crystallography*, Vol. IV. Kynoch Press, Birmangham (1974).

[21] K. Nakamoto, *Advances in the Chemistry of the Coordination Compounds* (Edited by S. Kirschner) p. 437. Macmillan, New York (1961).

[22] W. Stratton and D. H. Busch, *J. Am. Chem. Soc.* 1960, **82**, 4834.

ENTHALPIES OF REACTION OF TRIFLUOROMETHANESULPHONIC ACID WITH VARIOUS BASES

KEITH J. FISHER

Department of Chemistry, Faculty of Education, University of Khartoum, Republic of Sudan

Abstract—The enthalpies of reaction of CF_3SO_3H with a series of bases have been measured calorimetrically in nitrobenzene. Conductivity studies have been carried out and these have indicated the complexity of the acid-base products in solution. The failure of attempts to fit the enthalpy data to the Drago E and C equation reinforce the need for caution in its use.

INTRODUCTION

The E and C equation has been reported by Drago *et al.*[1] for the correlation of a very large number of neutral acids and bases which form un-ionized adducts.

$$-\Delta H = E_A E_B + C_A C_B.$$

Non-polar solvents have been used in an attempt to reduce the possibilities of complex or ionic products, for example:

$$n B_{(sol)} + n HX_{(sol)} \rightleftharpoons (BHX)_{n(sol)} \rightleftharpoons (BHX)_{n-m(sol)}^{m-} + mH_{(sol)}^+.$$

The above system involves many energetic contributions leading to the net enthalpy, which is quite different from the gas phase enthalpy useful in Drago's equation.

Acid-base reactions which result in ionic products have often been studied in polar solvents. Drago has warned against the attempted use of these data and also the potential complexity of pK_a and pK_b data.[2] Various studies have been carried out using a strong acid such as FSO_3H as both solvent and acid.[3–5] The studies of the enthalpy of ionization of various acid-base adducts yield large variable solvation enthalpies and cannot be used in the E and C approach, and would not seem to have any understandable meaning. It seems possible that reactions in non-polar solvents could provide more meaningful results which might correlate with Drago's equation.

In order to test these ideas and the Drago equation, calorimetric measurements of the heats of reaction of trifluoromethylsulphonic acid with various bases were carried out. Trifluoromethylsulphonic acid has been shown by conductivity studies to be a stronger acid than perchloric acid.[6] It reacts with a large number of bases to give 1:1 acid-base adducts and seems likely to give ionic products, making it an ideal acid to test whether the Drago equation might be simply number fitting.

Trifluoromethylsulphonic acid, besides being extremely hygroscopic, is not soluble in non-polar solvents such as cyclohexane or carbon tetrachloride. Thus nitrobenzene, a weakly basic solvent, was chosen, as this solvent has been used in previous studies[7] and a solvent correction has enabled the data to fit the Drago equation. Drago[8] has also shown that the G value approach gives poor correlations especially with this solvent.

EXPERIMENTAL

All operations were carried out under dry nitrogen.

Baker Analysed nitrobenzene was initially dried with phos-

phorus pentoxide and then distilled at ~1 mm Hg. The middle fraction of the distillation, 50–51°, was collected and used within a few hours. Methylene chloride was dried with phosphorus pentoxide and distilled immediately before use. Trifluoromethylsulphonic acid was distilled before use and stored in a sealed flask under dry nitrogen. The bases were dried as previously described.[9]

The calorimeter used was an all-glass type used in a previous study.[10] The calorimeter was evacuated and flushed with dry nitrogen before use. The solvent (generally 100 ml) was added to the nitrogen-filled calorimeter via a syringe. Weighed amounts of the base were added to the acid solution using a calibrated Hamilton gas tight syringe which had been allowed to reach thermal equilibrium within the calorimeter. This method was found to give inconsistent results; more consistent results were obtained by the reverse addition of known amounts of acid to a solution containing excess base. The first addition of acid generally gave high results possibly due to a trace of water in the system. Subsequent additions of acid were found to give consistent results. In most cases the base concentration was about 0.5 molar and the acid additions were not greater than 0.12 molar.

In all systems the values of H' (heat evolved per increment of acid added, corrected for the heat of solution of the acid in nitrobenzene) suggested that the acid was a limiting reagent and that complete reaction had occurred ($K \geq 10^4$).

Conductivity studies were carried out in an all-glass, previously evacuated, conductivity cell. An Industrial Instrument Conductivity Bridge Model R1682 was used and the cell calibrated with potassium chloride solutions. The problem of traces of moisture reluctantly caused us to use higher solution concentrations than those considered ideal.[11] Concentrations of solutions of approximately 5×10^{-3} and 1×10^{-2} molar were used.

RESULTS

The enthalpies of reaction of various bases with trifluoromethylsulphonic acid are shown in Table 1. The values are given in kcal mol^{-1} to conform with other data in the literature.

DISCUSSION

The calorimetric data reported in Table 1 will have a contribution from the displacement of the acid from the base nitrobenzene.

$$AB' + B'' \rightarrow AB'' + B'.$$
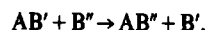
This contribution should have a constant value and so we should employ the modified eqn[9] in the E and C fit.

$$-\Delta H + \omega = E_A E_B + C_A C_B.$$

Fitting seven enthalpies (from Table 1) with the known E_B and C_B values gives more flexibility than for the

Table 1. Enthalpies of reaction of various bases with CF_3SO_3H

Nitrobenzene solvent	
Base	**Measured** $-\Delta H$ (kcal mol^{-1})
Ether	8.95 ± 0.15
Acetonitrile	3.10 ± 0.10
Tetrahydrofuran	9.99 ± 0.25
Dimethylsulphide	5.37 ± 0.13
Dimethylsulphoxide	23.46 ± 0.30
Tetrahydrothiophene	5.54 ± 0.15
Hexamethylphosphoramide	25.20 ± 0.30
Methylene chloride solvent	
Nitrobenzene	3.99 ± 0.10
Ether	14.43 ± 0.20
Dimethylsulphoxide	25.79 ± 0.30

The conductivity studies in nitrobenzene are shown in Table 2.

normal E and C equation. Even with this extra flexibility no reasonable fit of the data could be obtained. As examples the best fit value for ω was -25.2 kcal mol^{-1}, but when the enthalpy for tetrahydrofuran was calculated using the best fit E_A and C_A values, a heat of 13.2 kcal mol^{-1} was obtained, which compares very

poorly with the measured value of 9.99 kcal mol^{-1}. Similarly, the calculated value for dimethylsulphoxide was 19.5 compared with the measured value of 23.46. These kinds of deviations are not acceptable and indicate that the E and C equation is not so heavily parameterized as to fit almost any batch of data.

The reason for this failure may be seen in the conductivity data. Several of the conductivities obtained are large enough to indicate predominantly ionic species in solution. The rather erratic nature of the results in some cases and the higher values in high base concentrations suggests a large degree of complexity of the species in solution. The problem of traces of water cannot be ruled out, but as every possible precaution was taken in this work to exclude moisture we think that water would have only a minimal effect on the data.

The conductivity studies indicate that only the interactions of the acid with diethyl ether, acetonitrile and tetrahydrofuran may be considered to give essentially non-ionic products. Using these heats would give a meaningless fit to the extended E and C equation ($-\Delta H + \omega = E_A E_B + C_A C_B$). The adducts of the acid with hexamethylphosphoramide and triphenylphosphine seem to be completely ionic but the other adducts probably contain ionic and covalent species.

In several other enthalpy studies, particularly those of Arnett,[3-5] a strong acid, FSO_3H, has been used as both acid and solvent. These studies have not been accompanied by conductivity data and one would expect significant ionic contributions to the measured data. Fluorosulphonic acid as a solvent should be a better solvating medium than nitrobenzene and it is therefore

Table 2. Conductivity studies in nitrobenzene of CF_3SO_3H adducts

	Concentration of acid ×10³ M	Concentration of base ×10³ M	Λ_m
Acid only	5.66	—	2.04
	5.66	—	2.07
	11.3	—	2.02
	11.3	—	1.92
Diethylether adduct	13.6	19.0	2.15
Acetonitrile adduct	11.3	1.20	2.09
	11.3	38.3	2.11
Tetrahydrofuran adduct	11.3	12.3	2.08
	11.3	36.9	2.83
Diethylsulphide adduct	11.3	7.4	5.45
	11.3	9.8	5.90
	11.3	17.3	6.44
Dimethylsulphoxide adduct	13.6	17.1	15.6
	13.6	24.0	15.9
Tetrahydrothiophene adduct	11.3	17.0	7.95
	11.3	22.8	7.95
Hexamethylphosphoramide adduct	5.66	5.7	6.3
	5.66	14.3	32.8
	11.3	14.3	10.0
	11.3	20.0	25.6
Triphenylphosphine adduct	5.66	13.0	25.7
	11.3	13.0	29.8
	13.6	12.6	20.4

expected that complete ionization for many, but not all, of the systems will occur.

We recommend that all acid-base enthalpy studies with solvents and acids which might produce ionic products should include conductivity data, especially if the data are to be fitted into, or used to disprove, the Drago equation.

REFERENCES

[1] R. S. Drago, G. C. Vogel and T. E. Needham, *J. Am. Chem. Soc.* 1971, **93**, 6014.

[2] R. S. Drago, K. F. Purcell, *Progress in Inorganic Chemistry* 1964. Vol. 6, 271–322. Interscience.

[3] E. M. Arnett, R. P. Quirk and J. J. Burke, *J. Am. Chem. Soc.* 1970, **92**, 1260.

[4] E. M. Arnett, R. P. Quirk and J. W. Larsen, *J. Am. Chem. Soc.* 1970, **92**, 3977.

[5] E. M. Arnett, J. J. Burke, J. V. Carter and C. F. Douty, *J. Am. Chem. Soc.* 1972, **94**, 7837.

[6] G. Gramstad, *Tisskr. Kjemi Bergvesen Met.* 1959, **62**; *Chem. Abst.* 1960, **54**, 12739.

[7] R. S. Drago and R. M. Guidry, *J. Phys. Chem.* 1974, **78**, 454.

[8] R. S. Drago, L. S. Parr and C. S. Chamberlain, *J. Am. Chem. Soc.* 1977, **99**, 3203.

[9] R. S. Drago and R. M. Guidry, *J. Am. Chem. Soc.* 1973, **95**, 759.

[10] R. S. Drago and K. J. Fisher, *Inorg. Chem.* 1975, **14**, 2804.

[11] W. J. Geary, *Coord. Chem. Rev.* 1971, **7**, 81.

SYNTHESIS, CHARACTERIZATION AND PHOTOCHEMISTRY OF SOME MONOMETALLIC AND BIMETALLIC 2,2'-BIPYRIMIDINE COMPLEXES OF CHROMIUM AND TUNGSTEN CARBONYLS

KATHY J. MOORE and JOHN D. PETERSEN*
Department of Chemistry, Clemson University, Clemson, SC 29631, U.S.A.

Abstract—Synthesis, electronic absorption spectra, ^{13}C NMR and photochemistry are reported for the complexes $M(CO)_4$bpym (M = Cr or W) and $[W(CO)_4]_2$bpym. The electronic absorption spectra indicate, for these complexes, that the lowest lying metal-to-ligand (L) charge transfer (MLCT) excited state is lower in energy than the ligand field (LF) excited states. The ^{13}C NMR spectra showed that the chemical shifts of C(5) and C(6) for the M-bpym complexes move downfield with respect to that of the free ligand, bpym, while C(4) moves upfield upon complexation. Small, wavelength-dependent quantum yields for loss of CO were obtained upon irradiation. These quantum yields were an order of magnitude larger for the Cr-bpym complex than for the W complexes ($\Phi = 2.4 \times 10^{-2}$ quanta/min for Cr-bpym, 2.5×10^{-3} quanta/min for W-bpym and 1.1×10^{-3} quanta/min for W-bpym-W, $\lambda_{irr} = 366$ nm).

INTRODUCTION

Numerous photochemical studies have been performed for the low spin d^6 octahedral complexes $Ru(NH_3)_5L^{2+}$ [1,2] $Fe(CN)_5L^{3-}$,[3] and $W(CO)_5L^4$ (L = aromatic nitrogen heterocycle). Each of these complexes exhibit an intense metal-to-ligand (L) charge-transfer (MLCT) absorption band in the visible region of the spectrum which shifts to a lower energy as the electron withdrawing ability of L increases. Previous studies indicate that the photosubstitution behaviour of these complexes is dependent upon the nature of the lowest lying excited state.[1–4] For complexes in which the lowest, triplet, ligand-field (^{3}LF) excited state is lower in energy than the MLCT manifold initially populated, the predominant photosubstitution reaction which occurs upon irradiation is efficient dissociative loss of L owing to an increase in σ^* electron density. However, when the MLCT excited state is tuned to an energy lower than the ^{3}LF excited state by changing the substituents on L, a dramatic decrease in the photosubstitution of L results. The same behaviour was observed for a series of $W(CO)_4L_2$ complexes.[5]

Studies of complexes of the type $M(CO)_4L$ (M = Cr, Mo, or W, and L = bidentate unsaturated nitrogen donor) have been reported previously.[6,7] For each of these complexes the MLCT excited state is presumed to be lower in energy than the ^{3}LF excited state and no photosubstitution of L occurs. However, photosubstitution of *cis*-CO does occur with small wavelength dependent quantum yields.[6,7]

Complexes of the type $M(CO)_4L$, in which L = 2,2'-bipyrimidine (bpym), are of special interest to our group. By analogy to the complexes of this type previously studied and described above, this system should exhibit a visibly absorbing MLCT band and be photosubstitutionally stable with respect to loss of L. Also, for L = bpym, the possibility exists for bimetallic complex formation where bpym allows efficient communication between the two metal centers as shown for the systems $[Ru(bpy)_2]_2L^{4+}$(L = 2,2'-bpym or 4,4'-dimethyl-2,2'-bpym

and bpy = 2,2'-bipyridine)[8,9] and $[Ru(NH_3)_4]_2L^{4+}$(L = 2,2'-bpym).[10]

The stability of the bridge with respect to photosubstitution, along with the efficient communication experienced between the metal centers, are desirable characteristics which should enable us to study energy transfer reactions of various mixed-metal bimetallic systems. Upon absorption of visible light, one end of the system serves as the visibly absorbing fragment while the other end serves as the reactive fragment. In this report, the synthesis, electronic spectra, ^{13}C NMR and photochemistry of the monometallic complexes $M(CO)_4$bpym (M = Cr or W) and the bimetallic complex $[W(CO)_4]_2$bpym are presented.

EXPERIMENTAL

Materials. Analytical reagent grade compounds and solvents were used for all preparations described in this work. $W(CO)_6$, $Cr(CO)_6$ and 2,2'-bipyrimidine (bpym) were obtained from Alfa. Solvents used for ^{13}C NMR were spectro grade. Elemental analyses were performed by Atlantic Microlab, Atlanta, Georgia.

Syntheses. The complexes $M(CO)_4$bpy (M = Cr or W) were prepared by the method of Stiddard.[11] (Care was taken to shield all reaction mixtures from light.)

Cr(CO)$_4$bpym. A mixture of 0.55 g (2.50 mmol) $Cr(CO)_6$ and 0.42 g (2.66 mmol) bpym in 25 ml toluene was heated at reflux for 3 hr under nitrogen. The dark brown crystals which formed upon cooling to room temperature were collected by filtration. The product was washed thoroughly with light petroleum ether and dried under vacuum. Yield 0.72 g (89%). Anal. Calcd for $C_{12}H_6CrN_4O_4$: C, 44.74; H, 1.88; N, 17.39. Found: C, 43.51; H, 2.14; N, 16.84.

W(CO)$_4$bpym. A mixture of 0.87 g (2.47 mmol) $W(CO)_6$ and 0.41 g (2.59 mmol) bpym in 40 ml xylene was heated at reflux for 2 hr under nitrogen. The dark brown crystals which formed upon cooling to room temperature were collected by filtration. The product was washed and dried as above. Yield 0.93 g (83%). Anal. Calcd for $C_{12}H_6N_4O_4W$: C, 31.75; H, 1.33; N, 12.34. Found: C, 31.65; H, 1.25; N, 12.30.

[W(CO)$_4$]$_2$bpym. A mixture of 1.73 g (4.92 mmol) $W(CO)_6$ and 0.42 g (2.66 mmol) bpym in 50 ml xylene was heated at reflux for 4 hr under nitrogen. The dark green–black crystals which formed upon cooling to room temperature were collected by filtration. The product was washed with acetonitrile and petroleum ether and dried as above. Yield 1.84 g (100%). Anal. Calcd for

---

*Author to whom correspondence should be addressed.

$C_{16}H_6N_4O_8W_2$: C, 25.63; H, 0.81; N, 7.47. Found: C, 26.73; H, 0.99; N, 7.38.

Spectroscopy. All absorption spectra and absorbance measurements used for the quantum yield determinations were recorded on a Bausch & Lomb Spectronic 2000 spectrophotometer. Proton-decoupled ^{13}C NMR spectra were obtained on a JEOL FX-90Q operating at 22.5 MHz using chloroform-d as a solvent and as an internal reference. Chemical shifts are reported versus external TMS using the following equation:

$$\delta_{ext\ TMS} = \delta_{int\ CDCl_3} - 77.0\ ppm.$$

Photochemistry. Photosubstitution quantum yields were determined using a continuous beam photolysis apparatus described elsewhere.[3] The incident intensity, I_0^i, of the irradiation beam was determined by ferrioxalate[12] ($\lambda_{irr} \leq 436\ nm$) or Reineckate[13] ($\lambda_{irr} > 436\ nm$) actinometry. The values of I_0^i obtained for each wavelength used were approximately 3.2×10^{17} quanta/min ($\lambda_{irr} = 366\ nm$), 2.4×10^{17} quanta/min ($\lambda_{irr} = 405\ nm$), 2.2×10^{17} quanta/min ($\lambda_{irr} = 436\ nm$), and 1.7×10^{18} quanta/min ($\lambda_{irr} = 546\ nm$).

All photolyses were carried out at 25°C in 2- or 5-cm cylindrical quartz cells in acetonitrile solutions ($\approx 10^{-4}\ M$). The solutions were thoroughly deoxygenated and transferred into the cells under nitrogen as previously described.[14] Disappearance quantum yields were calculated from absorbance changes in the electronic spectra as a function of irradiation time. All spectroscopic measurements were corrected for thermal reactions. The photolysis products formed were identified spectroscopically.

RESULTS AND DISCUSSION

Electronic spectra

The visible and near-UV electronic absorption spectral data for the complexes $M(CO)_4L$ (M = Cr or W; L = bpy or bpym) and $[W(CO)_4]_2$bpym are presented in Table 1. The spectra are shown in Fig. 1. Each complex exhibits an intense, low-energy, absorption maximum which is sensitive to the nature of L and also to the polarity of the solvent. For the monometallic complexes, as the electron withdrawing ability of L increases and the molecular orbitals of L are stabilized going from bpy to bpym, this low energy absorption maximum shifts to a longer wavelength by approx. 40 nm when CH_2Cl_2 is the solvent. For the W-bpym-W bimetallic complex, this absorption maximum is shifted to an even longer wavelength (225 nm for W-bpy in CH_2Cl_2). This dramatic shift to a longer wavelength for the bimetallic complex not only indicates that the remote metal center increases the electron withdrawing ability of bpym by acting as a Lewis acid, but also, as explained previously for bimetallic complexes,[10,15,16] the HOMO of the bimetallic complex is destabilized with respect to the HOMO of the monometallic complex and thus a lower energy transition results. The shift to a longer wavelength as L increases in electron withdrawing ability indicates, as shown previously for similar systems,[4-6,17] that the low energy absorption band has charge transfer character and is

Table 1. Electronic absorption spectra of the $M(CO)_4L$ Complexes (M = Cr or W and L = bpy or bpym) and $[W(CO)_4]_2$bpym[a]

Complex	Solvent	λ_{max}, nm(ε, $M^{-1}cm^{-1}$)	
		LF	MLCT
Cr-bpy	C_6H_6	380(sh)	525
	CH_2Cl_2	400(sh)	503[b]
	CH_3CN	410(sh)	473
Cr-bpym	C_6H_6	404	553
	CH_2Cl_2	402(6748)	547(2718)
	CH_3CN	389(5630)	499(2401)
W-bpy	C_6H_6	362	511
	CH_2Cl_2	385(sh) 352	485[b]
	CH_3CN	390(sh) 340(sh)	453
W-bpym	C_6H_6	410(sh) 382	535
	CH_2Cl_2	410(sh) 378(7470)	525(4151)
	CH_3CN	371(6940)	478(3973)
W-bpym-W	CH_2Cl_2	384 455	710
	CH_3CN	385(12506) 421(13200)	610(6076)

[a] 298 K.

[b] Ref. 6 reports 497(3715) for $Cr(CO)_4$bpy and 487(5130) for $W(CO)_4$bpy.

therefore assigned as being a MLCT transition ($d_\pi \to p_{\pi^*}$).

The solvent dependence of the MLCT band for similar systems of the type $M(CO)_4L$ (M = Cr, Mo or W; L = aromatic nitrogen heterocycle) has also been investigated.[6,18] The MLCT absorption maximum shifts to a shorter wavelength as the polarity of the solvent is increased. This trend is shown in Fig. 1 for the complexes listed in Table 1 as the solvent polarity is increased from CH_2Cl_2 to CH_3CN. The bpym and the W-bpy complexes exhibit a higher energy absorption maximum in the 340–455 nm region which was also found to be slightly sensitive to the polarity of the solvent and to the nature of L. Therefore, this band is also assigned as being a MLCT transition.

The energy of the MLCT absorption maximum is dependent upon the ease of oxidation of the central metal. The general trend is an increase of oxidation potential as the energy of the MLCT transition increases

which implies a stabilization of metal molecular orbitals. From Table 1, it appears as though the energetic ordering for the metal molecular orbitals is Cr > W. A qualitative assessment of the electrochemistry corresponding to the compounds listed in Table 1 agrees with this energetic ordering. Cyclic voltammetry experiments[19] indicated that a reversible redox process occurs for Cr-bpym with an oxidation potential of 0.822 V (NHE). The anodic peak position for Cr-bpym is 0.879 V. An irreversible redox process was observed for W-bpym with an anodic peak position at 1.070 V. Two reversible redox processes were observed for W-bpym-W with oxidation potentials at 0.984 and 0.713 V and anodic peak positions at 1.040 and 0.746 V, respectively. The anodic peak positions of the W complexes occur at higher potentials than the anodic peak position of Cr-bpym. This qualitative electrochemical comparison implies that the metal molecular orbitals of the W complexes are stabilized with respect to the metal molecular orbitals of Cr-bpym, in accord with the electronic spectra.

Wrighton et al.[5,6] have determined for a series of $M(CO)_4L$ (L = bidentate ligand) and cis-$M(CO)_4L_2$ (L = monodentate ligand) complexes that the lowest lying excited states are LF in character when L is an aliphatic amine. The energies of these LF excited states are relatively invariant to the nature of L and to the polarity of the solvent. Thus, the absorption maxima which occur at approximately 450 and 402 nm for each complex of this series are assigned as ^3LF ($^3A_1$, $^3B_2 \leftarrow {}^1A_1$) and ^1LF ($^1A_1$, $^1B_2 \leftarrow {}^1A_1$) transitions, respectively. For the $M(CO)_4L$ (L = aromatic nitrogen heterocycle) complexes which have lowest lying MLCT excited states, the spin-allowed LF transition is still present at approx. 400 nm. The less intense spin-forbidden transition is covered by the MLCT absorption band. Also, Stufkens et al.[20] found the LF band between 370 and 400 nm for a series of $Mo(CO)_4L$ complexes (L = unsaturated nitrogen donor chelate). From these results, we would expect to find the LF band in the 400 nm region for the complexes in this study. The shoulder which occurs at approx. 400 nm for the complexes listed in Table 1 is shown in Fig. 1 to be relatively insensitive to the polarity of the solvent and to the nature of L. We assign this shoulder as a LF ($^1A_1$, $^1B_2 \leftarrow {}^1A_1$) transition. The large extinction coefficients corresponding to these LF bands have been attributed to having some MLCT character in the transition.[6] The spin-allowed LF transition of the Cr-bpym complex is obscured by the intense MLCT band at approx. 400 nm. Also, an interesting point to note is that the higher energy MLCT absorption maximum of the monometallic complexes lies above the spin-allowed LF transition; however, for the bimetallic W-bpym-W complex this MLCT maximum is shifted below the LF transition. The lowest lying absorption band for all of the bpym complexes is lower in energy than 450 nm, thus the energetic ordering of the excited states is determined to be LF > MLCT. The significance of this ordering will be discussed below.
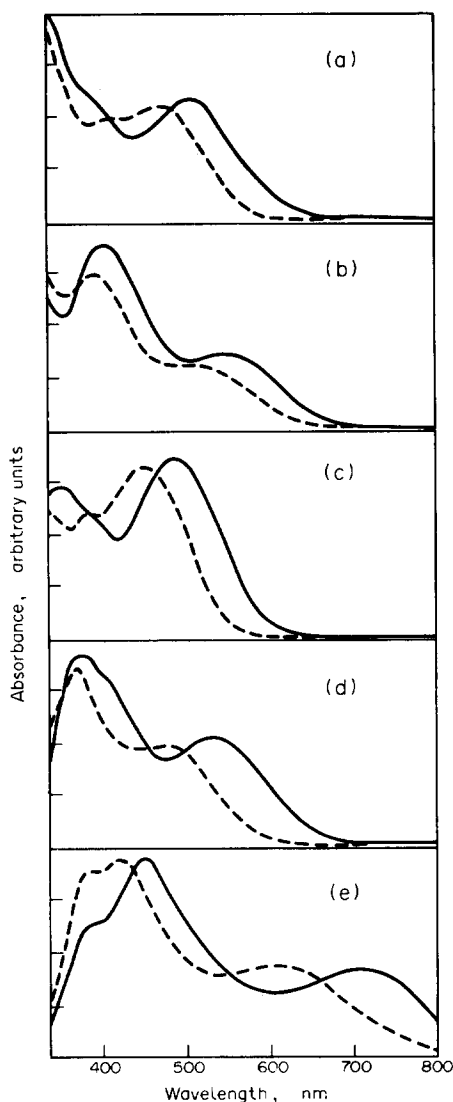
Fig. 1. Electronic absorption spectra of the $M(CO)_4L$ and $(CO)_4WbpymW(CO)_4$ complexes at 289 K in CH_3CN (----) and CH_2Cl_2(——). A = Cr$(CO)_4$bpy, B = Cr$(CO)_4$bpym, C = W$(CO)_4$bpy, D = W$(CO)_4$bpym and E = $(CO)_4$WbpymW$(CO)_4$.

^{13}C NMR

^{13}C NMR studies for the complexes $Ru(NH_3)_5L^{2+}$ [21] and $Fe(CN)_5L^{3-}$ [22,23] (L = aromatic nitrogen heterocycle) have been previously reported in the literature. The general trend found for these systems when compared to the ^{13}C NMR spectra of the free ligand, L, is a downfield chemical shift of the carbons ortho (C(6)) to the bonded nitrogen while the remaining carbons (C(3),

C(4) or C(5)) of the ring shift upfield. This upfield shift was related to the amount of $d\pi \to p\pi^*$ back-bonding to the ring system.[21-23] As the π-back-bonding to L increases, the shielding of these carbons (C(3), C(4) or C(5)) increases, and hence the chemical shift moves upfield. The downfield shift of the ortho carbons (C(6)) was more difficult to interpret. In a recent study of the complex $Ru(NH_3)_4bpym^{2+}$,[24] the upfield shift was attributed to a through-bond polarization toward the coordinated nitrogen or changes in electron density from changes in the σ-donating and π-accepting characteristics of L.

Table 2 lists the ^{13}C NMR data for the free ligands and the Cr and W complexes studied here. Due to compound solubility, the ^{13}C NMR of the bimetallic complex was unattainable within reasonable instrument time.[25] For each of the bpy and bpym complexes, the chemical shift of C(6) is shifted downfield with respect to the free ligand. Also, the chemical shift of C(6) for the Cr complexes occurs downfield with respect to that of the W complexes. This trend strenghtens the assumption of a through-bond polarization interaction between the coordinated nitrogen and the ortho carbon, C(6). Since Cr is more electronegative than W, Cr should inductively withdraw electrons in the σ sense through the M-N-C(6) bond system to a greater extent than W. Therefore it would be expected that C(6) of the Cr systems is more deshielded than that of the W systems. The expected trend, increasing downfield shift of C(6) with increasing electronegativity of the remote atom bonded to nitrogen, free space < W < Cr, thus corresponds with the experimental results.
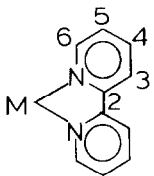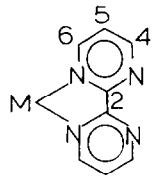
The general downfield shift of C(3), C(4) and C(5) for the bpy complexes is in contrast to the upfield shift occurring for the pyridine systems previously studied.[21-23]

The bonding interaction between L and the metal center is a complex combination of σ bonding from L to M and π bonding from M back into L. For carbonyl complexes, π-back-bonding into CO also occurs and is competitive with the backbonding into L. This competitive back-bonding into CO could decrease the π electron density delocalized over the ring system with respect to the other systems studied.[21-23] Thus, for C(3), C(4) and C(5) of the bpy complexes and C(5) of the bpym complexes the inductive σ electron withdrawal upon coordination to the metal appears to be predominant although the π affects are still apparent. These shifts are slightly downfield for the W complexes in relation to the Cr complexes. This indicates that the π back-bonding into L is less for the W complexes than for the Cr complexes which is in accord with the electronic spectra. For the bpym complexes, C(4) shifts upfield relative to that of the free ligand. This is in accord with the π back-bonding model of other systems[21-23] and indicates that bpym is a better π acceptor than bpy which is in agreement with the electronic spectra. ^{13}C NMR studies of similar Mo-bpy and -bpym systems showed downfield shifts of C(3), C(4) and C(5) relative to the free ligand in all cases.[25] It appears as though the shift of C(6) is governed by an inductive σ-withdrawing interaction of M while the shift of C(3), C(4) and C(5) depends upon a combination of the σ and π interactions between M and L.

Photochemistry

The photochemistry corresponding to systems of the type $M(CO)_4L$ or $M(CO)_4L_2$ (M = Cr, Mo or W and L = unsaturated nitrogen donor) has been studied by Wrighton *et al.*[5,6] and by others.[7] Wrighton and co-workers found from their work that irradiation at 436 nm

Table 2. ^{13}C NMR spectra of the complexes $M(CO)_4L$ (M = Cr or W and L = bpy or bpym) and the free ligands

Compound	$\delta(^{13}C)$, ppm[a]				
	C(6)	C(5)	C(4)	C(3)	C(2)
bpy	148.94	120.83	136.59	123.43	155.93
Cr-bpy	153.28	121.26	136.43	124.78	b
W-bpy	152.89	122.24	136.92	125.87	b
bpym	157.83	121.31	157.83	_____	b
Cr-bpym	160.32	121.80	157.45	_____	b
W-bpym	159.67	122.83	157.45	_____	b

[a]Chemical shift in $CDCl_3$ reported vs. external TMS.

[b]Signal too small to be extracted from noise.

of $W(CO)_4L_2$ (L = monodentate) resulted in loss of only L and not CO. The quantum yields for loss of L dramatically decreased as the MLCT excited state was tuned below the LF excited state. However, for complexes of the type $W(CO)_4L$ (L = bidentate) in which the MLCT excited state is the lowest lying excited state, no photosubstitution of L occurs upon irradiation from 313 to 436 nm. Dissociative loss of CO, however, does occur, with very small, wavelength-dependent quantum yields. The quantum yield for CO substitution was found to increase with the energy of irradiation. Therefore, it was concluded for the complexes having lowest lying MLCT excited states that the excited states responsible for the CO loss are the higher energy LF excited states, and the MLCT excited state is unreactive with respect to to loss of CO or L.

The photochemistry corresponding to the Cr and W carbonyls studied here is presented in Table 3. Figure 2 represents the electronic absorption changes as a function of time for the monometallic complex, $W(CO)_4$ bpym, using deoxygenated acetonitrile as a solvent. Air-saturated solutions of this complex were found to be very stable at room temperature if left in the dark; however, the photolysis solutions undergo degradation if not deoxygenated. As photolysis of the deoxygenated solution proceeds, the MLCT absorption bands are shifted to longer wavelengths with an isosbestic point at 412 nm. In analogy to the $W(CO)_4L$ systems previously studied[6], the phoreaction which occurs is suggested to be loss of CO as shown in reaction (1).

$$W(CO)_4bpym \xrightarrow[CH_3CN]{h\nu} W(CO)_3(CH_3CN)bpym + CO.$$
$$(1)$$
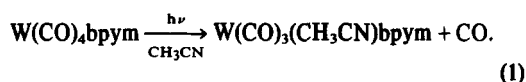
The quantum yields for CO substitution were found to be very small and wavelength dependent (λ_{irr} 366 nm, $\Phi = 2.5 \times 10^{-3}$ quanta/min; λ_{irr} 405 nm, $\Phi = 6.0 \times 10^{-4}$ quanta/min).

Photolysis of the bimetallic complex $[W(CO_4]_2$bpym is shown in Fig. 2. As for W-bpym the MLCT absorption bands are also shifted to longer wavelengths upon irradiation, with isosbestic points at 476, 574 and 688 nm. By analogy with the monometallic W complex, the reaction which occurs upon irradiation is suggested to be that of equation 2.

$$(CO)_4WbpymW(CO)_4 \xrightarrow[CH_3CN]{h\nu} (CO)_3(CH_3CN)Wbpym$$
$$W(CO)_4 + CO. \qquad (2)$$
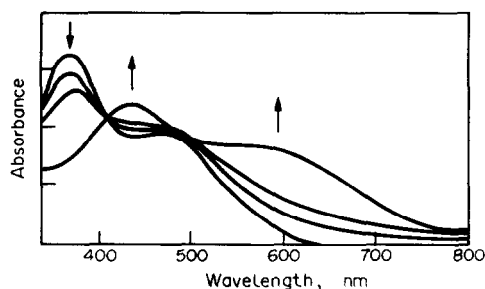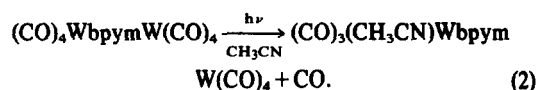
Fig. 2. Absorption spectral changes upon 366 nm irradiation of $W(CO)_4$bpym in deoxygenated CH_3CN ($\approx 10^{-4}$ M) at 298 K.

The photosubstitution quantum yield for CO loss from W-bpym-W was also found to be small (λ_{irr} 366 nm, $\Phi = 1.1 \times 10^{-3}$ quanta/min).

The photochemistry of the monometallic complex $Cr(CO)_4$bpym differed slightly from that of the W complexes. During the initial irradiation times a well defined isosbestic point was obtained at 444 nm. However, after approx. 1 hr of irradiation, degradation took place resulting merely in a decrease in absorbance of the MLCT bands. The absorbance of the dark control solutions decreased in the same manner. As a result of this degradation, the extinction coefficient at the monitored wavelength of the photoproduct could not be calculated. Therefore, the quantum yields for CO loss corresponding to the initial irradiation times are approximated by comparing the absorption spectra of Cr-bpym to that of W-bpym and the W photo-product. Also, the quantum yields for substitution of CO upon irradiation at 366 nm are an order of magnitude larger for Cr-bpym than for the W complexes. The same reaction occured for Cr-bpym upon irradiation into the low energy MLCT band at 546 nm whereas irradiation at 436 nm of the W complex gave no reaction. Larger quantum yields for loss of CO from Cr complexes vs W complexes of the type $M(CO)_5L$ have been reported previously.[26,27]

To explain the photochemical behavior for the bpym complexes, first of all consider that only CO is substituted whereas for the complexes $W(CO)_5L$ and $W(CO)_4L_2$, loss of L predominates owing to a more labile ground state M-N bond. This difference probably results from the chelate effect of bpym.[6] Also, the quantum yields were found to increase as the wavelength of irradiation increased. Therefore, in analogy to the systems investigated by Wrighton and co-workers[5,6], the

Table 3. Photosubstitution of $M(CO)_4L(M = Cr$ or W) to yield $M(CO)_4(CH_3CN)L^a$

M	L	Φ_{546nm}	Φ_{436nm}	Φ_{405nm}	Φ_{366nm}
Cr	bpym	1.1×10^{-3}		2.0×10^{-2}	2.4×10^{-2}
W	bpym		0	6.0×10^{-4}	2.5×10^{-3}
W	$W(CO)_4$bpym				1.1×10^{-3}

^{a}Quantum yields were determined using deoxygenated solutions of CH_3CN at 298 K.

states responsible for CO substitution are suggested to be the upper electronic LF excited states.

Stufkens and co-workers[7] have investigated the relationship between the resonance Raman spectra and the photo-substitution quantum yields corresponding to *cis*-CO loss for a series of $M(CO)_4L$ complexes. They found that irradiation into the MLCT band of these complexes resulted in an enhancement of Raman intensity of the symmetrical stretch corresponding to the carbonyls *cis* to L, $\nu_s(CO_{cis})$, whereas $\nu_s(CO_{trans})$ was not observed in the spectra. In addition, they found the photosubstitution quantum yield for *cis*-CO loss as well as the intensity of $\nu_s(CO_{cis})$ to increase as the electron density about the nitrogen which is coordinated to the metal increased. They concluded from these observations that *cis*-CO loss upon MLCT irradiation results from a delocalization of the MLCT excited state over the *cis*-carbonyls. This delocalization involves an overlap of orbitals which are localized at L and at the *cis*-carbonyls. The negative charge thus acquired by the *cis*-carbonyls reduces metal-to-CO π-back-bonding and hence weakens the M–C bond.

As can be seen from Fig. 1, the MLCT and LF excited states overlap to a large extent, so the LF excited states have a deal of MLCT character. We therefore suggest that the CO dissociation, which is assumed to occur from the LF excited state, is enhanced by the delocalization of the MLCT excited states over the *cis*-carbonyls. Good evidence for this is the difference in magnitude between the quantum yields of CO loss for the W-bpym and Cr-bpym complexes. Since Cr is smaller in size than W, the overlap of orbitals localized at L and at the *cis*-carbonyls of the Cr complex should be greater than that of the W complexes which corresponds to larger quantum yields for loss of CO from the Cr complex. Also, as shown from the ^{13}C NMR and the electronic spectra, the π-back-bonding into L is greater for the Cr complexes than for the W complexes which would result in a larger overlap of L and *cis*-carbonyl orbitals for the Cr complexes.
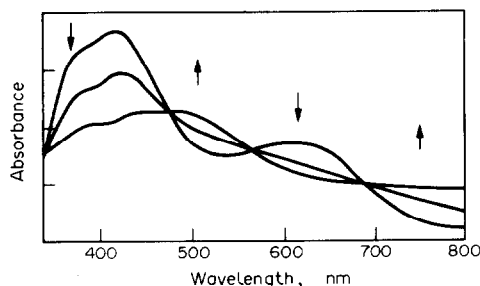
Fig. 3. Absorption spectral changes upon 366 nm irradiation of $(CO)_4WbpymW(CO)_4$ in deoxygenated CH_3CN ($\approx 10^{-4}\underline{M}$) at 298 K.

CONCLUSIONS

The bpym complexes were found to be stable with respect to bpym loss upon irradiation and therefore should be useful for studying energy transfer reactions in mixed metal bimetallic systems. Irradiation of these complexes did result in *cis*-CO substitution with very small, wavelength-dependent quantum yields. It was suggested that CO loss occurs from the LF excited states and is enhanced by the large degree of MLCT character of these states.

REFERENCES

[1] G. Malouf and P. C. Ford, *J. Am. Chem. Soc.* 1977, **99**, 7213; *ibid.* 1974, **96**, 601

[2] R. E. Hintze and P. C. Ford, *Inorg. Chem.* 1975, **14**, 1211; D. A. Chaisson, R. E. Hintze, D. H. Stuermer, J. D. Peterson, D. P. McDonald and P. C. Ford, *J. Am. Chem. Soc.* 1972, **94**, 6665.

[3] J. E. Figard and J. D. Petersen, *Inorg. Chem.* 1978, **17**, 1059.

[4] M. S. Wrighton, H. B. Abrahamson and D. L. Morse, *J. Am. Chem. Soc.* 1976, **98**, 4105.

[5] M. S. Wrighton and H. B. Abrahamson, *Inorg. Chem.* 1978, **17**, 3385.

[6] M. S. Wrighton and D. L. Morse, *J. Organomet. Chem.* 1975, **97**, 405.

[7] R. W. Balk, T. Snoeck, D. J. Stufkens and A. Oskam, *Inorg. Chem.* 1980, **19**, 3015.

[8] E. V. Dose and L. J. Wilson, *Inorg. Chem.* 1978, **17**, 2660.

[9] M. Hunziker and A. Ludi, *J. Am. Chem. Soc.* 1977, **99**, 7370.

[10] R. R. Ruminski and J. D. Petersen, *Inorg. Chem.* 1982, **21**, 3706.

[11] M. H. B. Stiddard, *J. Chem. Soc.* 1962, 4712.

[12] C. G. Hatchard and C. A. Parker, *Proc. R. Soc. London, Ser. A* 1956, **235**, 578.

[13] E. E. Wegner and A. W. Adamson, *J. Am. Chem. Soc.* 1966, **88**, 394.

[14] P. C. Ford, J. R. Kuempel and H. Taube, *Inorg. Chem.* 1968, **7**, 1976.

[15] A. M. Zwickel and C. Creutz, *Inorg. Chem.* 1971, **10**, 2395.

[16] C. Creutz and H. Taube, *J. Am. Chem. Soc.* 1973, **95**, 1086.

[17] P. L. Gaus, J. M. Boncella, K. S. Rosengren and M. O. Funk, *Inorg. Chem.* 1982, **21**, 2174.

[18] H. Saito, J. Fumita and K. Saito, *Bull. Chem. Soc. Jpn.* 1968, **41**, 863.

[19] K. J. Moore and J. D. Petersen, Unpublished observations.

[20] R. W. Balk, D. J. Stufkens and A. Oskam, *Inorg. Chim. Acta* 1978, **28**, 133.

[21] D. K. Lavalee, M. D. Baughman and M. P. Phillips, *J. Am. Chem. Soc.* 1977, **99**, 718.

[22] J. E. Figard, J. V. Paukstelis, E. F. Byrne and J. D. Petersen, *J. Am. Chem. Soc.* 1977, **99**, 8417.

[23] J. M. Malin, C. F. Schmidt and H. E. Toma, *Inorg. Chem.* 1975, **14**, 2924.

[24] R. R. Ruminski and J. D. Petersen, *Inorg. Chim. Acta* 1982, **65**, L177.

[25] C. Overton and J. A. Connor, *Polyhedron* 1982, **1**, 53.

[26] G. Boxhoorn, D. J. Stufkens and A. Oskam, *Inorg. Chim. Acta* 1979, **33**, 215.

[27] D. J. Darensbourg and M. A. Murphy, *Inorg. Chem.* 1978, **17**, 884.

CHELATE COMPOUND STABILITY CONSTANT CALCULATIONS ON METAL DIKETONATE COMPLEXES

L. G. VAN UITERT

Bell Laboratories, Murray Hill, NJ 07974, U.S.A.

Abstract—Acetylacetone ($CH_3COCH_2COCH_3$ or Hacac) may give up a proton and chelate with a metal ion through the two oxygen atoms. The stability constant for the neutral complex (given as log β_Σ) in aqueous solution can be calculated using the electrostatic relation log $\beta_\Sigma = N_A V_c^2 e^2/(2.3RT\epsilon/d)$ when cations in $\bar{S}$ states are involved. Larger values that reflect exchange related electron correlation as well as electrostatic contributions to cohesive energy are obtained using transition metal ions. Separate values for the two energies are determined (see the text for definitions of the symbols).

INTRODUCTION

Chemical bonding is a subject of continuing interest. Understanding the nature of the interactions between chelate complexing agents and metal ions is particularly germane as this relates to life processes. The problem may be approached using molecular orbital and other complex treatments, but not without some loss of understanding of the physics involved. Indeed, considering the complexity of life related processes in general, it is well to use the simplest of analytical measures and foster an intuitive feel for the interactions of concern. Graphical analysis, though somewhat unpopular in the computer era, is one of the better ways to meet these goals. This approach, combined with easily understood principles of electrostatics, provide valuable insight if the data is resolved so as to reflect relations consistent with accepted concepts of bonding.

In this paper, it is shown that a simple ion–ion electrostatic relation can be used to calculate the (electrostatic) solution chelation energy (E_1) of complexes involving the anion (acac) of acetylacetone (Hacac, $CH_3COCH_2COCH_3$) and metal ions, particularly those that have empty valence shells in the uncomplexed state (i.e. in $\bar{S}$ states). Further, for transition metal ions, one can obtain a separate estimate of the electrodynamic contribution to cohesion (E_2). As will be shown (E_2) is dependent upon the polarization of the oxygen atoms of the anion and upon the presence of electrons in d states of the valence shell, and therefore is due to correlative interactions between the valence shell electrons of the abutting atoms. Of course, the total chelation energy in solution (E_0) equals E_1 plus E_2. Separate determination of these two energies is facilitated by the fact that E_1 is dependent on the dielectric constant (ϵ) of the medium while (as shown herein) E_2 is not.[1]

DATA

Although numerous determinations of stability constants of chelate complexes have been made over the past half century, most of the data are not suitable for the present purposes.[2–4] For example, chelate formation using neutral complexing agents, such as ethylenediamine, involves complicated ion–dipole rather than simple ion–ion interactions.[5] Also the data for most chelate complexes involving oxyanions is relatively incomplete and much of the data in the more complete sets is questionable due to hydrolysis competing with chelation in the solutions used for measurement. Further, for many

otherwise applicable data sets, large quantities of NaCl or KCl were added to the solution to be measured. ostensibly to maintain a fixed ionic strength. However, even in aqueous solutions Cl^- can complex with multivalent cations to an appreciable extent. This can lower measured values for stability constants by an order of magnitude (one log unit) or more. In addition, data measured in mixed solvents (water–dioxane, water–alcohol, etc.) cannot be employed unless corrections to obtain thermodynamic values have been made.[6,7]

To minimize such uncertainties, the data employed herein have been restricted to thermodynamic values obtained potentiometrically using the glass electrode to measure dilute perchlorate soluions that are free of extraneous salt additions, as far as practicable. Four sets of stability constants are considered. These are given as log β_Σ values (log β_Σ being the logarithm of the constant for the neutral species). The first set is for acetylacetonates using water as the solvent (see Table 1).[2–4,8,9] The second set is for dibenzoylmethanates using 25–75 water-dioxane as the solvent (see Table 2).[3,10,11] The third set is composed of Ba, Ni and Cu diacetylacetonates and ditrifluoroacetylacetonates in the same mixed solvent (divalent metal chlorides were used in obtaining this data (see Table 3)).[12] And the fourth set is for ethylacetoacetate measured using water and using ethanol as the solvent (relevant data are given in the text).[7] Ethanol is used as the second unmixed solvent (the first being water) simply because it fits the Born relation for expected changes in the primary medium effect (or the relative activity of H^+ for infinite dilution).[13] Hence, the effect of changing the medium on the stability of the chelate can be investigated without introducing new complications.

For acetylacetone (Hacac), the negative logarithm of the acid dissociation constant (pK_a) equals 9.0 in water. This value is too low to permit accurate measurements to be made for a broad range of chelates. Dibenzoylmethane (Hdbm, $PhCOCH_2COPh$) would have a greater pK_a (13.75 compared to 12.7 for Hacac in 25–75 v/o water–dioxane) but it is not soluble in water. Hence, ethylacetoacetate (Haa, $CH_3COCH_2COOC_2H_5$) for which $pK_a = 10.7$ in water and 15.8 in ethanol is used for comparing results measured using these two solvents.

COMMENTS

A number of things should be made clear:
(a) The M–O bondlength (between the metal ion and the oxygens of the ligand) in these betadiketones is

Table 1. Stability constants for neutral acetylacetonate complexes in water

M²⁺	r(VI)	d	log β_Σ	d log β_Σ	Σp2
Be	0.27(IV)	1.62	14.6	22.2	
Mg	0.72	2.07	6.2	12.9	15.03
Mn	0.83	2.18	7.3	15.9	15.64
Fe	0.78	2.13	8.7	18.5	16.18
Co	0.75	2.10	9.5	20.0	17.05
Ni	0.69	2.04	10.6	21.6	18.15
Zn	0.74	2.09	9.0	18.8	17.96
Cd	0.95	2.30	6.7	15.3	16.90
Pb	1.19	2.54	6.3	16.0	15.03
Cu	0.56(IV)	1.92	14.7	28.2	20.29
M³⁺					
Al	0.54	1.89	22.3	42.1	
Ti	0.67	2.02	24.9	50.3	
Fe	0.65	2.00	26.2	52.4	
Ga	0.62	1.97	23.7	46.7	
Y	0.90	2.25	13.9	31.3	
La	1.03	2.38	11.9	28.3	
Lu	0.86	2.21	14.6	32.3	
Ce	1.01	2.36	12.7	30.0	
M⁴⁺					
Th	1.05(VIII)	2.40	26.7	64.1	
U	1.00(VIII)	2.35	29.5	69.3	
Np	0.98(VIII)	2.33	30.2	70.4	

Table 2. Dibenzoylmethanates in 25–75 v/o water–dioxane

M⁺	r(VI)	d	log β_Σ	d log β_Σ
Li	0.68	2.03	5.95	12.1
Na	0.98	2.33	4.18	9.7
K	1.34	2.69	3.67	9.9
Rb	1.49	2.84	3.52	10.0
Cs	1.67	3.02	3.42	10.3
Ag	1.15	2.50	6.17	15.4
Tl	1.50	2.85	5.92	16.9
M²⁺				
Mg	0.72	2.07	16.7	34.6
Ca	1.00	2.35	14.2	33.4
Sr	1.18	2.53	12.4	33.4
Ba	1.35	2.70	11.9	32.1
Mn	0.83	2.18	18.2	39.7
Co	0.75	2.10	20.5	43.0
Ni	0.69	2.04	21.0	42.8
Zn	0.74	2.09	20.0	41.8
Cd	0.95	2.30	17.1	39.3
Pb	1.19	2.54	20.2	51.3
Cu	0.57(IV)	1.92	26.5	50.9
Ce³⁺	1.01	2.36	30.4	71.7
Th⁴⁺	1.05(VIII)	2.40	53.3	127.9

approximately equal to $r + 1.35$ angstroms, where r is the cation radius as given by Shannon.[14] The ligand oxygen radius of 1.35 Å is deduced in Refs. 15 and 16.

(b) The ion–ion electrostatic energy of association of the complex (E_1) in solution is not the energy required to separate the ions to an infinite distance from each other, but is the residual electrostatic energy of the complex. In water, the latter value is only 1.3% of the former. Further, the change with dielectric constant is in the opposite direction.

(c) The solvation state of the free ions is not of concern for the present purposes as the constants employed were derived taking the concentration of the cations or anions to be the sum of the solvated and nonsolvated species present. Indeed, the actual concentration of the unsolvated ion is exceedingly small (i.e. less by many orders of magnitude).

(d) The ionization of the M–O bond in these oxychelates is essentially 100% when $\bar{S}$ state cations are involved. This appears to favor negative charge localization on the betadiketone oxygens in such complexes and thereby facilitate the use of simple ion–ion electrostatic interactions.

(e) In addition, as H_2O molecules may orient themselves about charged particles almost as readily in mixed solvents as in water, and the activity of H_2O increases (rather than decreases) upon mixing in considerable amounts of paradioxane, one need not be surprised that the "effective" dielectric constant for much of the mixed medium is greater than the normally measured values.[13,17]

EQUATIONS

The electrostatic energy (E_1) of one mole of a 100% ionized chelate complex is:[1,5,8]

$$E_1 = N_A e^2 V_c V_a Z/(\epsilon d) \qquad (1)$$

where N_A is Avogadro's number (6.02×10^{23}), e is the charge on the electron $(4.8 \times 10^{-10}$ esu), V_c is the valence of the cation, V_a is the valence of the anion, Z is the

Table 3. Stability constants for acetylacetonates and trifluoroacetylacetonates in 25–75 v/o water–dioxane

Salt	Betadiketone	pK_a	d	log β_2	d log β_2
BaCl₂	Hacac	12.7	2.70	9.0	24.3
BaCl₂	F₃-Hacac	8.7	2.70	8.8	23.8
NiCl₂	Hacac	12.7	2.04	17.4	35.5
NiCl₂	F₃-Hacac	8.7	2.04	14.2	29.0
CuCl₂	Hacac	12.7	2.08	22.6	47.0
CuCl₂	F₃-Hacac	8.7	2.08	17.2	35.8

number of anions per cation and may be viewed as a Madelung constant derived from the location and charge of the anion oxygens surrounding the cation in each complex and $\underline{d}$ is the M–O bond length in angstroms. The electrostatic energy is reduced by changing from $\epsilon = 1.00$ for air to a medium with $\epsilon > 1.00$, while the difference in energy for $\epsilon = 1.00$ and $\epsilon > 1.00$ (e.g. the heat of solvation) increases.[1] Since $ZV_a = V_c$ for the chelates of interest and $N_A e^2 = 1387$ kilojoules/mole, for one mole of a betadiketonate chelate complex dispersed in a solvent the electrostatic contribution to cohesive energy is:

$$E_1 = 1387 V_c^2/(\epsilon \underline{d}) \text{ kJ/mole}. \tag{2}$$

In its equilibrium constant form, relation (2) becomes:

$$\log \beta_\Sigma = \frac{E_1}{2.3RT} = \frac{1387 \times 10^3 V_c^2}{5.7 \times 10^3 \epsilon \underline{d}} = \frac{243 V_c^2}{\epsilon \underline{d}}. \tag{3}$$

Here, $R = 8.31$ J/mole and temperature $T = 298$ K. Further, the difference in $\log \beta_\Sigma$ values for a complex in a medium ϵ_3 and in a medium ϵ_2 is:

$$\Delta \log \beta_\Sigma = 243 V_c^2 (1/\epsilon_3 - 1/\epsilon_2)/\underline{d}. \tag{4}$$

In addition, other things being equal, the logarithm of the stepwise stability constants for a given cation and chelating agent should be in the ratio: $1:3:5:7:9$, etc. proceeding as far as required from the last to the first. Deviations from this pattern can be related to solvation differences and/or salt anion–cation association.

FIGURES

Figures 1 and 2 depict $\underline{d} \log \beta_\Sigma$ vs the index number of the period in the periodic table in which the cation occurs for (1) acetylacetonate data taken using an aqueous medium and (2) essentially thermodynamic data for dibenzoylmethanate complexes taken using 25–75 v/o water–dioxane as the medium.[2–4,6,8–11] The horizontal guidelines fit relation (4) with $\epsilon = 78.5$ for the first figure and with $\epsilon = 30$ for the second. The vertical lines indicate displacement from the relevant horizontal line. In Fig. 1, only the points for Mg and La fit the calculated guideline. These ions are in $\bar{S}$ states and, obviously, the acac ions provide little steric hinderence. If similar data were
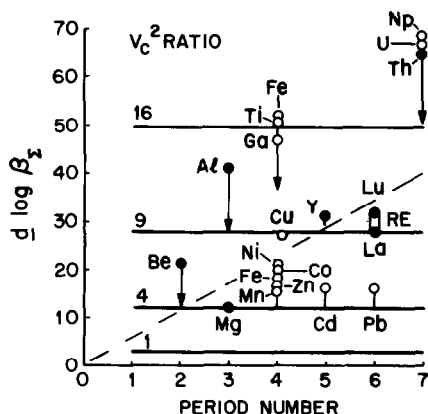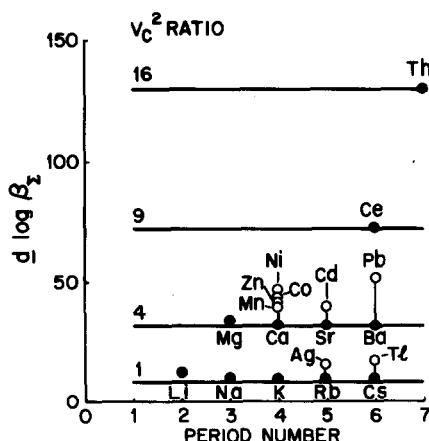
Fig. 2. $\underline{d} \log \beta_\Sigma$ vs period number for metal ion dibenzoylmethanates measures using 25–75 v/o water–dioxane as the solvent. The horizontal lines represent values calculated using relation (3), $\epsilon = 30$ and $V_c^2 = 1, 4, 9$ and 16 in ascending order.

available for the Na–Cs and Ca–Ba acetylacetonates, it is expected that their data points would also fit these lines. However, due to the low value of $\log \beta_\Sigma$ constants that apply when water is used as the solvent, they have not been measured.[2,3] Most of the remaining data points that fall below the dashed line that passes through the origin in Fig. 1 are for complexes that have cations with partially filled valence shells. Most of the data for the points that fall above the dashed line in Fig. 1 are of questionable value as they represent attempts to estimate constants from pH data measured in the presence of relatively large quantities of acid added to suppress hydrolysis.[2,3,9] For example, the correct positions for trivalent Fe, Ti and Ga probably lie about half way to the guideline as indicated by the arrow.

The stability constants measured using Hdbm and 25–75 v/o water–dioxane as the solvent (as shown in Fig. 2) are much larger than those measured using Hacac and water. This can be attributed to a smaller "effective" dielectric constant for the solvent; including some increase due to steric effects and (for transition metal ions) to enhanced polarization of the oxygens of the betadiketone. The increased stability of these complexes makes it possible to measure $\log \beta_\Sigma$ for all of the alkali metal and alkaline earth cations in this medium. As can be seen in Fig. 2, these data points and those for trivalent Ce and tetravalent Th as well fall on or very close to their respective guidelines. In comparison, data points for complexes in which the valence shell of the cation is partially filled fall above the relevant guideline for $\bar{S}$ state ions.

Figure 3(a) depicts $\underline{d} \log \beta_2$ for the acetylacetonates (indicated by the end groups, CH_3—CH_3) and trifluoroacetylacetonates (CF_3–CH_3) of divalent Ba, Ni and Cu vs pK_a values for the chelating agents (as measured in 25–75 v/o water–dioxane).[12] It is evident that $\underline{d} \log \beta_2$ is little affected by the change in pK_a for the $\bar{S}$ state cation (Ba^{2+}). Further, it is evident that the trifluoroacetylacetonate ions as well as the acetylacetonate ions themselves offer little steric hinderence.

Figure 3(b) depicts $\underline{d} \log \beta_2$ and $\underline{d} E_0$ for the indicated $M(acac)_2$ complexes vs $ip2$ (the second ionization potential of the metal) for data measured in water.[2] Points for V^{2+} or Cr^{3+} are not included as these ions oxidize during

Fig. 1. $\underline{d} \log \beta_\Sigma$ vs period number for metal ion acetylacetonates measured using water as the solvent. The horizontal lines represent values calculated using relation (3), $\epsilon = 78.5$ and $V_c^2 = 1, 4, 9$ and 16 in ascending order.

L. G. VAN UITERT
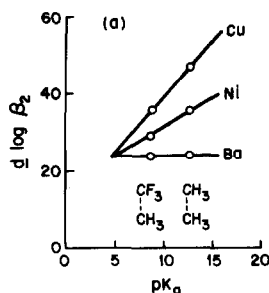
Fig. 3(a) $\underline{d}$ log β_2 vs pK$_a$ for Ba, Ni and Cu diacetylacetonates (CH—CH$_3$) and ditrifluoroacetylacetonates (CF$_3$—CH$_3$) measured using 25–75 v/o water–dioxane as the solvent and divalent chlorides as the salts.
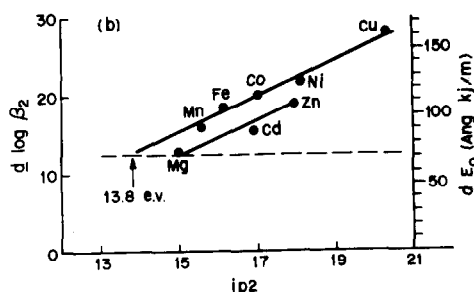
Fig. 3(b). $\underline{d}$ log β_2 vs ip2 for the M(acac)$_2$ complexes of the indicated cations measured using water as the solvent. The horizontal line fits relation (3).
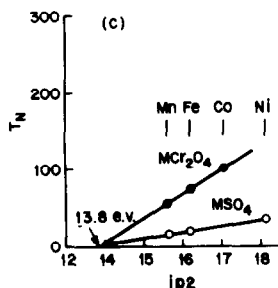
Fig. 3(c). T$_N$ vs ip2 for the indicated chromates and sulfates.

measurement and therefore tend to greater values than they would have if stable.[19] The horizontal line roughly separates cohesive contributions E$_1$ (below) and E$_2$ (above).

Figure 3(c) represents Néel temperature (T$_N$) for divalent metal chromates (MCr$_2$O$_4$) and sulfates (MSO$_4$) vs ip2.[20] This figure is included to show the common dependence of E$_2$ and T$_N$ on ip2 for the Mn, Fe, Co, and Ni series. Point displaced by spin-orbital coupling are not presented in this figure.

DISCUSSION

Most expressions of cohesive energy between charged particles are in terms of the electrostatic energy given up upon consolidation.[5] Such relations predict a reduction in E$_1$ or log β_Σ values with a reduction in ϵ for the medium. However, comparison of log β_Σ values measured in ethanol ($\epsilon = 24.3$) to those obtained using water ($\epsilon = 78.5$) show the opposite to be the case.[7,8] For example. log $\beta_\Sigma = 26$ for Ni(acac)$_2$ in ethanol and $= 10.4$ in water.[7] This is in agreement with relations (3) and (4). By inserting $\underline{d} = 2.04$ (for the nickel complex), $\epsilon_3 = 24.3$ (for ethanol and $\epsilon_2 = 78.5$ (for water) into relation (4) one calculates Δ log $\beta_\Sigma = 13.5$. In comparison, the experimental difference is 13.2. Similar results can be deduced for Mg, Zn and Ca.[7,8] In general, the change in log β_Σ found employing these ions agrees with that expected using relation (4) and either $\bar{S}$ state or transition metal ions. This demonstrates that E$_2$ is little affected by changes in ϵ.

Even through relation (3) should apply, it is evident from Fig. 1 that it would be difficult to fit it to the existing data for acetylacetonates measured using water as the solvent. Much of the needed data for $\bar{S}$ state ions has not been obtained, or involves hydroxide formation, and most of the remaining cations have d states occupied in the valence shell. However, a suitable correlation is possible employing the extended data for monovalent and divalent cations in $\bar{S}$ states and the values for Ce and Th shown in Fig. 2. It is evident from this figure that the points for the indicated cations essentially fit the (V^2) position lines expected from relation (3). This strongly supports the view that bonding for these chelates is close to 100% electrostatic.

Actual values for E$_1$ and E$_2$ can be estimated for divalent transition metal cations using data measured employing water as the solvent and acetylacetone as the chelating agent as this minimizes any effects related to mixed solvents and steric factors. But first it is well to establish the nature of the electrodynamic interactions involved.

As represented in Fig. 3(a), the stability constant changes little upon going from the acetylacetonate to the trifluoroacetylacetonate of Ba^{2+} even though pK$_a$ changes by 4. This is as expected for electrostatic interactions provided steric effects are minimal for both betadiketones used. However, for Ni^{2+} and Cu^{2+}, the slope of the connecting lines increase with ip2. The relation of the three lines indicates that electrodynamic correlation effects between electrons about the oxygen atoms of the chelating agent anion and the cation depend upon the presence of electrons (principally in d states) in the valence shell of the latter as well as the ability of the cation to polarize the anion. Further, the convergence of the slopes (meeting at pK$_a = 5.0$) indicates that electrodynamic exchange also is a function of the polarization of the anion. This increases with pK$_a$.

Values of E$_1$ and E$_2$ for M(acac)$_2$ transition metal ion complexes in water can be deduced using Fig. 3(b). The horizontal (dashed) line passing close by the point for Mg(acac)$_2$ represents the $\underline{d}$E$_1$ or $\underline{d}$ log β_Σ value for all divalent S state cation complexes. As can be seen, the $\underline{d}$ log β_2 values for Mn–Cu lie above this line and tend to increase linearly with ip2. The second half of the 3d subshell is being filled in the course of this transit. Points for Zn and Cd, which have filled d^{10} sets fall at lower values as it is somewhat more difficult for d^{10} electrons to enter into spin correlation interactions with electrons in the valence shell of the anion. The line through the Mn–Cu points intercepts the electrostatic (horizontal) guideline at 13.8 eV. As shown in Fig. 3(c) the onset of

magnetic exchange in the oxides (MCr_2O_4 and MSO_4) also occurs at 13.8 eV. This indicates a common dependence on the electron affinity of the cation to foster interatomic correlative interactions. Electrodynamic interactions may occur for a lower (first) ionization potential (e.g. Ag 7.57 and Tl 6.11 eV) for non $\bar{S}$ state cations provided they are in asymmetric sites where they can polarize extensively (e.g. in monochelates). Related binding effects are expected to increase exponentially as mutual polarization overlap increases linearly. Hence, it is not surprising that $\not{d} \log \beta_1$ values for Ag^+ and Tl^+ dibenzoylmethanates are considerably larger than those for the comparable $\bar{S}$ state cations (see Fig. 2).

One ordinarily tends to think of electrostatic and electrodynamic cohesive interactions as having comparable dependences on bondlength and therefore to be difficult to separate quantitatively. Since the latter tend to decrease ionization, E_1 may be expected to decrease as E_2 increases. However, upon going from air to water E_1 decreases as the inverse ratio of the dielectric constant of the medium (to $1 \times 100/78.5 = 1.27\%$ of the former value) while E_2 is essentially unaffected. This is supported by the measurements reported above for ethylacetoacetates in ethanol and in water. Consider a complex for which E_1 is 98% and E_2 is 2% of E_0 in air. Upon dissolving the complex into water, E_1 decreases to $98/78.5 = 1.25\%$ of the air value of E_0 while E_2 remains at 2%. Clearly the value of E_1 in water is only decreased 2% by the electrodynamic interactions present, even though the ratio of E_2/E_1 may be greater than unity in the solvent. In as much as this example applies reasonably well to the data in Fig. 3(b), the horizontal line in that figure can be taken to divide $\not{d}E_0$ into $\not{d}E_1$ and $\not{d}E_2$ contributions for interactions in water.

CONCLUSIONS

Thermodynamic $\log \beta_\Sigma$ values for betadiketonates of cations that are in $\bar{S}$ states essentially fit the simple ion–ion electrostatic interaction model indicated by relation (3). In particular, the correct values for the acetylacetonates of this group should provide an excellent fit as shown by the data points for $Mg(acac)_2$ and $La(acac)_3$ in Fig. 1. Using relation (3) and a known value of $\log \beta_2$ for $Mg(acac)_2$ measured by other means (see Refs. 6 and 7), one can deduce an "effective" dielectric constant for

mixed solvents that may be employed. Using this constant and the appropriate bondlengths, one may then calculate $\log \beta_\Sigma$ values for the acetylacetonates of the remaining $\bar{S}$ state cations. When more complex betadiketones are employed, steric hinderence should be considered as well. The effects can be estimated as the difference in $\log \beta_\Sigma$ values for the new complex and the acetylacetonate of the same ion, particularly for $\bar{S}$ state cations. Further, some adjustment for anion and/or cation polarizability may also be needed when considering complexes of transition and post transition metal ions.

REFERENCES

[1] M. Born, Z. Physik 1920, 1, 45.
[2] R. M. Smith and A. E. Martell, Critical Stability Constants. Plenum Press, New York 1977.
[3] L. G. Sillen and A. E. Martell, Stability Constants of Metal-Ion Complexes. The Chemical Society, Burlington House, London 1964.
[4] J. J. Christensen, D. J. Eatough and R. M. Izatt, Handbook of Metal-Ligand Heats and Related Thermodynamic Quantities. Marcell Dekker, New York 1975.
[5] F. Basolo and R. G. Pearson, Mechanisms of Inorganic Reactions. Wiley, New York 1967.
[7] L. G. Van Uitert and C. G. Haas, J. Am. Chem. Soc. 1953, 75, 451.
[7] C. E. Van Uitert, L. D. Spicer and L. G. Van Uitert, J. Phys. Chem. 1977, 81, 40.
[8] L. G. Van Uitert, W. C. Fernelius and B. E. Douglas, J. Am. Chem. Soc. 1953, 75, 2739.
[9] R. M. Izatt, W. C. Fernelius, and B. P. Block, J. Phys. Chem. 1955, 59, 80.
[10] L. G. Van Uitert, Doctorial Thesis. The Pennsylvania State University, University Park, PA (1952).
[11] L. G. Van Uitert, Mat. Res. Bull. 1982 17, 223.
[12] L. G. Van Uitert, W. C. Fernelius and B. E. Douglas, J. Am. Chem. Soc. 1953 75, 457.
[13] H. S. Harned and B. B. Owen, The Physical Chemistry of Electrolytic Solutions, 2nd Edn. Reinhold, New York (1950).
[14] R. D. Shannon, Acta Cryst. 1976, A32, 751.
[15] B. Morosin and H. Mortgomery, Acta Cryst. 1969 B25, 1354.
[16] A. F. Wells, Structural Inorganic Chemistry, 4th Edn. Clarendon Press, Oxford (1975).
[17] F. Hovorka, R. A. Schafer and D. Dreisbach J. Am. Chem. Soc. 1936, 58, 2264.
[18] C. S. G. Phillips and R. S. Williams, Inorganic Chemistry. Vol. 1. Oxford University Press, New York (1965).
[19] W. P. Schaefer, Inorganic Chem. 1965, 4, 642.
[20] L. G. Van Uitert, J. Phys. Chem. Solids 1965, 26, 423.

BIS- AND TRIS-(TRIMETHYLSILYL)METHYL
DERIVATIVES OF ANTIMONY

HANS JOACHIM BREUNIG* WALTER KANIG and ALI SOLTANI-NESHAN
University of Bremen, P.O. Box 330 440, D-2800 Bremen, Federal Republic of Germany

Abstract—Reaction of RMgCl [R = (Me$_3$Si)$_2$CH] with SbCl$_3$ affords RSbCl$_2$. Also R$_2$SbCl reacts with RLi to yield R$_3$Sb, while R'SbCl$_2$ [R' = (Me$_3$Si)$_3$C] is synthesized from R'Li and SbCl$_3$. Mass spectra of RSbCl$_2$ and R'SbCl$_2$ show that fragmentations proceed with elimination of Me$_3$SiCl. The chlorides RSbCl$_2$, R$_2$SbCl and R'SbCl$_2$ are thermally very stable.

INTRODUCTION

Silylmethyl groups like (Me$_3$Si)$_2$CH- or (Me$_3$Si)$_3$C- combine bulkiness with the capability to form strong metal- or element-carbon bonds. Therefore they have been used for the syntheses of organometallic compounds with unusual coordination numbers and chemical properties.[1] In the course of our investigations on steric effects in organoantimony synthesis,[2] we were interested in the preparation and chemistry of alkylantimony chlorides with these substituents. We hoped that a part of their chemistry might be the thermal 1,2-elimination of Me$_3$SiCl, yielding stiba-alkenes. Analogous reactions are known in phosphorus chemistry.[3]

SYNTHESES AND PROPERTIES OF (Me$_3$Si)$_3$CSbCl$_2$ (1), [(Me$_3$Si)$_2$CH]SbCl$_2$ (2), [(Me$_3$Si)$_2$CH]$_2$SbCl (3), and [(Me$_3$Si)$_2$CH]$_3$Sb (4)

Reaction of (Me$_3$Si)$_3$CLi with SbCl$_3$ in tetrahydrofuran (THF) results in the substitution of one chlorine atom (eqn 1) and formation of colourless crystals of compound 1, which are stable towards water and air but become dark brown in the sunlight. 1 is soluble in common organic solvents. It can be sublimed at reduced pressure and recrystallized from methanol.

$$(\text{Me}_3\text{Si})_3\text{CLi} + \text{SbCl}_3 \rightarrow (\text{Me}_3\text{Si})_3\text{CSbCl}_2 + \text{LiCl}. \quad (1)$$
$$1$$
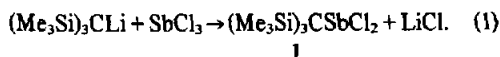
Its mass spectrum shows intense signals for the ions (M$^+$-Me) and (M$^+$-Me-Me$_3$SiCl). The latter ion corresponds to a (M$^+$-Me) fragment ion of a stiba-alkene (Me$_3$Si)$_2$C=SbCl. Attempts to eliminate Me$_3$SiCl from 1 under preparative conditions have however not been successful, but proved the remarkable thermal stability of 1. Under the conditions of the synthesis of 1 used here, it was not possible to substitute a second chlorine atom in 1.

The considerably reduced steric demand of a (Me$_3$Si)$_2$CH group is shown by the substitution of one to three chlorine atoms in SbCl$_3$, which yields the complete series R$_{(3-n)}$SbCl$_n$

$$[R = (\text{Me}_3\text{Si})_2\text{CH}; 2: n = 2, 3: n = 1, 4: n = 0].$$
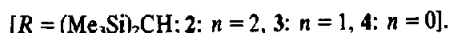
The dichloride 2 is prepared by the Grignard reaction (2)

$$(\text{Me}_3\text{Si})_2\text{CHMgCl} + \text{SbCl}_3 \rightarrow (\text{Me}_3\text{Si})_2\text{CHSbCl}_2 + \text{MgCl}_2$$
$$2$$
$$(2)$$
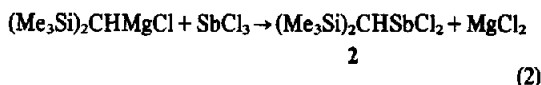
and obtained as a colourless liquid, which is thermally

very stable but sensitive to oxygen. Fragmentations of 2 in the mass spectra resemble those of compound 1. Again we observe the formation of an ion corresponding to the (M$^+$-Me) fragment of a stiba-alkene. Heating 2 to 280°C did not, however, result in elimination of Me$_3$SiCl, but caused the decomposition of the whole molecule.

The substitution of two or three chlorine atoms in SbCl$_3$ was accomplished by reactions of (Me$_3$Si)$_2$CHLi with this substrate. The chloride 3 is synthesized by reaction (3)[1b] using appropriate molar amounts of the reagents.

$$2(\text{Me}_3\text{Si})_2\text{CHLi} + \text{SbCl}_3 \rightarrow [(\text{Me}_3\text{Si})_2\text{CH}]_2\text{SbCl} + 2\text{LiCl}.$$
$$3 \quad (3)$$
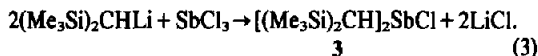
3 reacts in tetrahydrofuran with one more molar equivalent of (Me$_3$Si)$_2$CHLi yielding the tertiary stibine 4.

$$[(\text{Me}_3\text{Si})_2\text{CH}]_2\text{SbCl} + (\text{Me}_3\text{Si})_2\text{CHLi}$$
$$3 \qquad \rightarrow [(\text{Me}_3\text{Si})_2\text{CH}]_3\text{Sb} + \text{LiCl}. \quad (4)$$
$$4$$
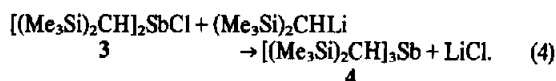
3 and 4 were isolated as liquids with considerable stability in air. They are soluble in common organic solvents. 3 is thermally stable up to 290°C whereas 4 decomposes at 180°C and cannot be distilled under reduced pressure. Attempts to eliminate Me$_3$SiCl by thermal cracking of 3 have not been successful. Mass spectra of 3 and 4 show intense molecular ions and the expected fragments. There is no elimination of a Me$_3$SiCl unit in the fragmentation of 3.

The ^{1}H-NMR spectra of 1, 2 and 4 show singlets for the Me$_3$Si groups whereas in the spectrum of 3 the Me$_3$Si signal is more complicated. This corresponds to a diastereotopic situation, which indicates configurational stability in 3. It must be noticed however, that we observe more signals than the expected two singlets. The relative positions of the signals of the tertiary stibine 4 and the dichloride 2 show the expected trend: substitution of two alkyl groups in 4 by chlorine atoms causes a downfield shift for the Me$_3$Si protons.

Preliminary results show that all these alkyl-antimonychlorides (1, 2, 3) react with Mg in THF with abstraction of chlorine atoms. There is evidence for the formation of cyclo(polystibanes) of the composition (RSb)$_n$ [R = (Me$_3$Si)$_2$CH] by dehalogenation of 2 [(18 eV, 100°C): m/z = 840 (5%) R$_5$Sb$_5$$^{+\cdot}$, 68$_1$ (5%) R$_2$Sb$_3$$^+$]. The reaction of 3 with Mg/THF yields a distibane R$_4$Sb$_2$ [R = (Me$_3$Si)$_2$CH; (25 eV, 100°C): m/z = 719 (5%) R$_3$Sb$_2$$^+$].

---

*Author to whom correspondence should be addressed.

DISCUSSION

Because of the high steric requirements of both the $(Me_3Si)_3C$ and the $(Me_3Si)_2CH$ substituents, we observe the expected decrease of reactivity on the antimony (III) centers. This prevents the introduction of more than one $(Me_3Si)_3C$ group under the conditions of the preparation fo **1** and allows selective syntheses of the alkyl(chloro)stibines **2–4**. Similar reactions with alkyl reagents which have no steric hindrance always afford peralkylated stibines. Partial alkylation has been achieved, however, with tertiary-butyl substituents. A decrease in reactivity is also observed towards oxygen: **1, 3** and **4** are stable in air. Another unusual feature of **1–3** is their termal stability.

EXPERIMENTAL

All preparations of air sensitive compounds were carried out in an atmosphere of purified Ar and in dry solvents. The following spectrometers were used: NMR, EM 360 Varian; IR, PE 577 Perkin Elmer; MS, CH7 A, Varian MAT; mass spectral data are given for ^{121}Sb and ^{35}Cl. The peak patterns correspond to theoretical values based on the natural abundance of isotopes. Elemental analyses were carried out by Fa. Beller, Göttingen.

Tris(trimethylsilyl)methylantimonydichloride (1)

22·8 g (0·1 mol) $SbCl_3$ were added at 0°C to a solution of $(Me_3Si)_3CLi$,[4] which had been prepared by reaction of 14·4 g (0·062 mol) $(Me_3Si)_3CH^5$ with MeLi in THF. Distillation of the solvent afforded a brown oily residue, which contained unreacted $(Me_3Si)_3CH$ (b.p.$_{0·01}$ 50°C) and 8·7 g (33%) of white crystalline **1** (m.p. 196°C) which sublimed at 140°C 0.01 mm Hg and could be recrystallized from methanol.

Heating of **1** for 5 hr did not yield Me_3SiCl, but black solids were produced when the temperature reached 280°C. **1**: ^1H-NMR (C_6H_6) $\delta = 0.30$ ppm S; IR (nujol) 1250 s, 840 s, 670 m, 600 m, 330 s $\nu SbCl$; MS (35 eV, 90°C) m/z (rel. int. %): 407 (100) $(M^+ - Me)$, 299 (30) $(M^+ - Me - Me_3SiCl)$, 223 (20), 221 (100), 201 (10), 73 (100). $C_{10}H_{27}Cl_2SbSi_3$ (424·2); found: C 28·2 (28·3); H 6·2 (6·3); Cl 16·9 (16·7); Sb 28·4 (28·7)%.

Bis (trimethylsilyl)methylantimonydichloride (2)

A THF solution of $(Me_3Si)_2CHMgCl$ was prepared from 3.0 g (0.125 mol) Mg and 19·5 g (0·1 mol) $(Me_3Si)_2CHCl^7$ and added slowly to 22·8 g (0.1 mol) $SbCl_3$ in 50 ml THF at 0°C then stirred 12 hr at 0°C and 2 hr at 25°C. After removal of the solvent at reduced pressure, the residue was hydrolysed and extracted with ether. **2** was obtained by distillation at 75°C/0·01 mm Hg as a yellow liquid [yield 18·5 g (53%)]. **2**: ^1H-NMR $(CDCl_3)$ $\delta = 0.18$ ppm S (18 H), $\delta = 0.86$ ppm S (1 H). IR (film) 1255 s, 845 s, 765 w, 665 w, 330 $(\nu SbCl)$; MS (30 eV, 20°C) m/z (rel. int. %): 335 (100) $(M^+ - Me)$, 227 (40) $(M^+ - Me - Me_3SiCl)$, 129 (80), 73 (60).

$C_7H_{19}Cl_2SbSi_2$ (352·1); found: C 23·4 (23.9); H 5·2 (5·4); Cl 20·5 (20.2)%.

Bis[bis(trimethylsilyl)methyl]antimonychloride (3)[1b]

$(Me_3Si)_2CHLi^6$ was prepared from 1·4 g (0.2 mol) Li sand and 16 g (0·08 mol) $(Me_3Si)_2CHCl$,' analysed (80% conversion) and added to 6·8 g (0·03 mol) $SbCl_3$. Work up as described [1b] yielded 11·5 g (81%), Lit.[1b] 65%, of **3** as a colourless oil. b.p.$_{0·01}$ 103–105°C, Lit.[1b] b.p.$_2$ 147–149°C.

3: ^1H-NMR $(CDCl_3)$ sharp signals at $\delta = 0.15$; 0·20; 0·25 ppm 18 H; $\delta = 0.95$ ppm (1 H) *S*. IR (film): 1255 s, 840 s, 535 m, 330 m $(\nu SbCl)$ cm^{-1}. MS (30 eV, 25°C) m/z (rel. int. %): 474 (30) (M^+), 459 (80) $(M^+ - Me)$, 443 (85), 389 (30), 369 (70), 355 (10), 315 (90), 221 (30), 207 (100), 147 (80), 73 (100). $C_{14}H_{38}ClSbSi_4$ (476·0); found: C 35·7 (35·3); H 8·1 (8·1)%.

Tris[bis(trimethylsilyl)methyl]antimony (4)

A solution of 6 g (0·012 mol) **3** in 20 ml THF was added to a solution of $(Me_3Si)_2CHLi$ in THF prepared from 3·3 g (0·017 mol) $(Me_3Si)_2CHCl$ and 0·25 g (0·036 mol) Li. The solution was stirred under reflux for 12 hr, the solvent was then stripped off *in vacuo* and the residue extracted with pentane. After distillation of this solvent **4** remained as a yellow oil (3 g, 42%). Attempts to distil **4** caused decomposition. **4**: ^1H-NMR $(CDCl_3)$ $\delta = 0.15$ ppm *S* (18 H); $\delta = 0.7$ ppm *S* (1 H), IR (film: 1255 s, 840 s, 530 m. MS (20 eV, 70°C) m/z (rel. int.%): 598 (30) (M^+), 439 (100) (R_2Sb^+), 369 (10), 269 (2). $C_{21}H_{57}SbSi_6$ (600·0); found: C 42·1 (42·0); H 9·31 (9·58); Sb 19·3 (20·3).

REFERENCES

[1a] P. J. Davidson, D. H. Harris and M. F. Lapport, *J. Chem. Soc. Dalton Trans.* 1976, 2268.

[1b] M. J. S. Gynane, A. Hudson, M. F. Lappert, P. P. Power and H. Goldwhite, *J. Chem. Soc. Dalton Trans.* 1980, 2428.

[1c] F. Glockling, P. Harriot and W.-K. Ng, *J. Chem. Res. (M)* 1979, 275 and references cited in this paper.

[2a] H. J. Breunig, *Z. Naturforsch.* 1979, **33b**, 242.

[2b] H. J. Breunig and W. W. Kanig, *Chemiker Ztg.* 1978, **102**, 263.

[2c] H. J. Breunig and H. Kischkel, *Z. Naturforsch.* 1981, **36b**, 1105.

[3] K. Issleib, H. Schmidt and C. Wirkner, *Z. Anorg. Allg. Chem.* 1981, **473**, 85.

[4] M. A. Cook, C. Eaborn, A. E. Jukes and D. R. M. Walton, *J. Organomet. Chem.* 1970, **24**, 529.

[5] R. L. Merker and M. J. Scott, *J. Org. Chem.* 1964, **29**, 953.

[6] P. J. Davidson, D. H. Harris and M. F. Lappert, *J. Chem. Soc. Dalton Trans.* 1976, 2269.

[7] M. A. Cook, C. Eaborn and D. R. M. Walton, *J. Organomet. Chem.* 1971, **29**, 389.

THERMAL, SPECTRAL AND MAGNETIC STUDIES ON SOME
TRANSITION METAL COMPLEXES OF EMBELIN

K.K.ABDUL RASHEED, JACOB CHACKO AND P.N.K. NAMBISAN*
Department of Marine Sciences, University of Cochin,
Cochin - 682 016, India

Abstract - Complexes of embelin with Mn(II), Ni(II), Cu(II)
and Zn(II) have been prepared and characterised for the first
time. Spectral, thermal and magnetic studies suggest an
octahedral coordination for Mn(II), Ni(II) and Zn(II) ions
while a tetrahedrally distorted planar configuration is
proposed for the Cu(II) complex.

INTRODUCTION

Embelin (2,5 dihydroxy-3-undecyl-2,5-cyclohexadiene-1,4-dione),
an orange pigment isolated from the berries of Indian shrub Embelia
ribes, is of great medicinal importance, because of its anthelmintic
properties[1]. However, only very scant information is available on
metal chelates of embelin[2,3], which could function as possible basis
for anthelmintic drugs. We have, therefore, undertaken a systematic
study on the synthesis and structure of transition metal complexes of
embelin and here in report the results of our investigation. Complexes
of Mn(II), Ni(II), Cu(II) and Zn(II) with embelin have been synthesised
and characterised by elemental analysis, IR spectra, reflectance spectra,
thermal and magnetic studies.

EXPERIMENTAL

Preparation of the ligand

Pure natural embelin was prepared by the method of Fieser and
Chamberlin[1]. The crushed embelia ribes were extracted with solvent
ether in a soxhlet apparatus. The crude embelin thus isolated was
purified by defatting twice with petroleum ether (60-80°C) and
recrystallizing twice from absolute alcohol. Pure embelin (mp 142°C)
was obtained in ∼ 2% yield.

Preparation of the complexes

Aqueous ethanolic solutions of the corresponding metal acetates
and ethanolic solutions of the ligand in 1:1 molar ratio (with the metal
salt in slight excess) were mixed together and refluxed on a water bath

---

*for correspondence

for 20-30 minutes. The metal complexes precipitated out and were washed repeatedly with aqueous ethanol to remove excess metal ions. The complexes were dried in vacuum over P_2O_5.

Elemental analysis and physical measurements

The complexes were decomposed with a mixture of HCl and HNO_3 and manganese, copper and zinc were analysed complexometrically and nickel gravimetrically[4]. IR spectra (4000-600 cm^{-1}) were recorded as KBr pellets on a Beckman Acculab 7 IR spectrophotometer. Simultaneous TGA-DTA of the samples were carried out on a Stanton Redcroft TR-01 Thermobalance with a DTA attachment. Magnetic susceptibilities were measured by the Gouy method using mercury tetra-thiocyanato cobaltate (II) as the calibrant[5]. As the complexes were found to be insoluble in most of the common organic solvents, conductance measurements and molecular weight determinations could not be carried out. The electronic spectra were recorded in the solid state using a Schimadzu SP 200 spectrophotometer with a reflectance attachment using magnesium oxide as the reference.

RESULTS AND DISCUSSION

The insolubility of the complexes in most of the common organic solvents indicates a polymeric nature. All the complexes are mildly hygroscopic and hence experimentally determined values of the metal content (Table I) are slightly lower than those theoretically expected for a 1:1 polymer. Such variations in analytical data were observed by earlier workers too[6,7].

IR spectra

The important IR frequencies of the ligand and of the metal complexes are presented in Table I. The O-H stretching frequency is observed as a strong band at 3300 cm^{-1} for embelin. The disappearance of this band in the spectra of the complexes indicates that the phenolic hydrogens present on the ligand molecule are lost on chelation. The broad, medium intense peak occurring between 3300 and 3450 cm^{-1} in the spectra of Mn(II), Ni(II) and Zn(II) complexes may be attributed to the O-H stretching frequency of the coordinated water molecules. The O-H bending frequency is observed as a weak band at 1650 cm^{-1} for Mn(II), Ni(II) and Zn(II) complexes.
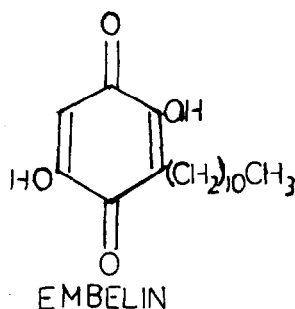
EMBELIN

Table I

Analytical, magnetic and spectral data of Embelin and its complexes

Compound	Colour	% metal found	% metal calcd	μ_{eff} (BM)	Reflect-ance spectra λ_{max} (cm^{-1})	Assignments of important i r spectral bands ν_{O-H} Phenolic (cm^{-1})	ν_{O-H} Coord water (cm^{-1})	δ_{O-H} Phenolic (cm^{-1})	δ_{O-H} Coord water (cm^{-1})	$\nu_{C=O}$ (cm^{-1})
Embelin $C_{17}H_{26}O_4$	Orange-yellow				17800 28570 33330	3300		1640		1610
Mn(Em)2H$_2$O	Grey	14.30	14.35	5.84	19230 23800 28570 33330		3400		1650	1520
Ni(Em)2H$_2$O	Green	14.90	15.20	3.20	17240 25000 33330		3400		1650	1520
Cu(Em)	Brownish black	17.10	17.86	2.12	11460 14700 20000 22720 33330					1460
Zn(Em)2H$_2$O	Bluish violet	15.70	16.60	-	16660 28570 33330		3400		1650	1520

Em = $C_{17}H_{24}O_4^=$

Both these bands are absent in the spectra of the Cu(II) complex indicating the absence of any water molecules. Vibrational bands, in the 880–650 cm^{-1} region, characteristic of coordinated water molecules[8] could not be located owing to strong ligand absorptions in this region. The carbonyl stretching frequency, observed as a strong peak at 1610 cm^{-1}, is found shifted to 1520 cm^{-1} in the spectra of Mn(II), Ni(II) and Zn(II) complexes and to 1460 cm^{-1} in the case of the copper complex. The Cu(II) complex of 2,5-dihydroxy-2,5-cyclohexadiene-1,4-dione is also known to exhibit a similar enhanced shift for the carbonyl stretching frequency[6,7]. Thus the assignments of the spectral bands indicate that embelin acts as a tetra dentate ligand coordinating through its phenolic and carbonyl oxygens.

Electronic spectra

      Reflectance spectra of the complexes in the region (900–200 nm) were studied (Table I). Ligand absorptions and charge transfer transitions complicate the assignment of bands observed in the UV region.

      Being spin and multiplicity forbidden, the d-d transitions of the Mn(II) complex have very low intensities. The band at 19230 cm^{-1} could be assigned to the $6A_1 \longrightarrow 4T_2(G)$ transition and that at 23800 cm^{-1} to the $6A_1 \longrightarrow 4E(G)$, $6A_1 \longrightarrow 4A_1(G)$ doublet. The $6A_1 \longrightarrow 4T_1(G)$ transition, expected around 17000 cm^{-1}, is probably obscured by the fairly strong ligand absorption at $\sim$ 17800 cm^{-1}. The observed spectral bands of the Mn(II) complex thus suggest an octahedral symmetry[9,10].

      The absorption bands observed for the Ni(II) complex at 17240 cm^{-1} and at 25000 cm^{-1} may be assigned to the spin allowed transitions from the ground state $3A_{2g}(F)$ to $3T_{1g}(F)$ and $3T_{1g}(P)$ levels respectively. This is in conformity with the expected d-d transitions for octahedrally coordinated Ni(II) complexes[11].

      In the case of Cu(II) complex, the d-d transition bands are seen to undergo a red shift and are located at 11460 cm^{-1} and 14700 cm^{-1} and an asymmetric and weak LF band is observed at $\sim$ 20000 cm^{-1}. This suggests a tetrahedrally distorted planar configuration[12], especially in view of the steric hindrance caused by the bulky embelin molecules. Copper complexes with other bulky ligands too have been known to exhibit similar spectral and magnetic behaviour[13]. The observed band at 22720 cm^{-1} may be ascribed to a charge transfer transition[14].

      Since no ligand field transition is expected for a d^{10} configuration, the observed bands in the spectrum of the zinc complex are due to ligand absorptions and/or charge transfer transitions.

Magnetic properties

      The room temperature magnetic moment of 5.84 BM (Table I) for the Mn(II) complex indicates an octahedral environment for the metal ion[15].

Table II

Thermo-analytical data of the metal complexes of Embelin

Complex	Stability range in TG from ambient upto (°C)	pdt+ (°C)	Peak temp. (°C)		Dehydration and decomposition temp. ranges (°C)		% mass loss from TG curve		% mass loss from indepedent pyrolysis**
			DTG	DTA	DTG	DTA	After dehydr- ation*	After final stage	
Mn(Em)2H2O	170	260	210 395	220 endo 400 exo	170-250 260-500	160-250 endo 260-500 exo	8.85 (9.39)	79.40	79.39 (79.38)
Ni(Em)2H2O	180	270	210 385	220 endo 400 exo	190-270 270-560	180-280 endo 280-550 exo	9.40 (9.30)	81.11	81.36 (80.68)
Cu(Em)	250	250	350	360 exo	250-500	260-500 exo	-	76.91	77.90 (77.64)
Zn(Em)2H2O	120	300	160 390	170 endo 400 exo	120-290 300-480	120-270 endo 290-500 exo	9.20 (9.15)	75.10	79.88 (79.30)

+   Procedural decomposition temperature

*   Theoretical value in brackets

**   Theoretical value, based on metal oxide composition, in brackets.

The Ni(II) complex has a μ_{eff} value of 3.2 BM and is quite expected for an octahedrally coordinated Ni(II) ion with an orbital contribution arising from a second order process[11]. Cu(II) complexes, in general, have μ_{eff} values between 1.75-2.2 BM and magnetic moments, strictly, cannot be used to distinguish between the stereochemistries of the complexes. Nevertheless, lower magnetic moments (<1.93 BM) are frequently attributed to square planar configurations[16]. Since tetrahedral distortions are expected to lead to increased magnetic moments[13], a μ_{eff} value of 2.12 BM further supports the stereochemistry proposed on the basis of the electronic spectral behaviour. The Zn(II) complex is diamagnetic as expected.

Thermal behaviour

Thermal studies on the metal complexes of embelin were carried out under static air conditions. Thermo-analytical data obtained from TG, DTG and DTA curves and independent pyrolysis are presented in Table II. The thermograms for the Mn(II) and the Zn(II) complexes indicate two clear cut stages: the first corresponding to the dehydration of the coordinated water molecules and the second to the decomposition process. In the case of the Ni(II) complex, the dehydration step is seen to merge with the decomposition process resulting in a single extended stage. The temperature ranges for the dehydration step, in this case has, therefore, been deduced from the DTG curve and the percentage mass loss corresponding to this range has been attributed to the loss of water molecules. The Cu(II) complex shows only a single stage, being devoid of any water molecules. Dehydration peaks in the DTG for Mn(II), Ni(II) and Zn(II) complexes are parallelled by corresponding endothermic DTA peaks. Exothermicity of the decomposition peaks may be attributed to the concomitant oxidation reactions of the ligand. Final residues of independent pyrolysis (upto 700°C) of the complexes were subjected to chemical analysis[4] and were found to have metal contents corresponding to the compositions of Mn_2O_3, NiO, CuO and ZnO. On the basis of the procedural decomposition temperatures, the complexes are seen to follow the stability sequence Zn > Ni > Mn > Cu which is in good agreement with the order of thermal stabilities observed for the coordination polymers[6]. However, the increased shift in the carbonyl frequency of the Cu(II) complex suggests an extra stability which is portrayed in terms of the initial stability range of the complex in the TG curve.

REFERENCES

1. L.F.Fieser and E.M. Chamberlin, *J. Am. Chem. Soc.* 1948, <u>70</u>, 71.
2. Ch.Bheema Sankara Rao and V. Venkiteswaralu, *Curr. Sci.* 1960, <u>29</u>, 136.
3. Ch.Bheema Sankara Rao and V. Venkiteswaralu, *Z. Anal. Chem.* 1961, <u>178</u>, 277.

4. Vogel's Text Book of Quantitative Inorganic Analysis, Fourth Edn.
     ELBS, London, (1978).

5. B.N. Figgis and R.S. Nyholm, J. Chem. Soc. 1958, 4190.

6. R.S. Bottei and J.T. Fangman, J. Inorg. Nucl. Chem. 1966, 28, 1259.

7. H.D. Coble and H.F. Holtzclaw Jr., J. Inorg. Nucl. Chem. 1974, 36, 1049.

8. J. Fijitha, K. Nakamoto and M. Kobayashi, J. Am. Chem. Soc. 1956, 78,
     3963.

9. A.B.P. Lever, 'Inorganic Electronic Spectroscopy', Elsevier, Amsterdam,
     (1968).

10. L.F. Larkworthy and D. Sattari, J. Inorg. Nucl. Chem. 1980, 42, 551.

11. F.A. Cotton and G. Wilkinson, 'Advanced Inorganic Chemistry', Third Edn.,
      Wiley Eastern, New Delhi (1979).

12. S.J.Gruber, C.M.Harris and E. Sinn, J. Inorg. Nucl. Chem. 1968, 30, 1805.

13. L.Sacconi and M. Ciampolini, J. Chem. Soc. 1964, 276.

14. L.E. Orgel, Quart. Revs. 1954, 8, 422.

15. A. Earnshaw, 'Introduction to Magnetochemistry', Academic Press, London,
      (1968).

16. B.N.Figgis and J. Lewis, 'Progress in Inorganic Chemistry', Vol. VI,
      Inter Science Publishers, New York, (1964).

NOTES

Synthesis, molecular structure and electrochemistry of pentagonal bipyramidal nickel(II) complexes of quinquedentate macrocyclic ligand incorporating a 2,2':6',2"-terpyridyl moiety

Abstract—The synthesis and single crystal X-ray structure of the pentagonal bipyramidal nickel(II) complex [Ni(L)(EtOH)$_2$](BF$_4$)$_2$ involving the quinquedentate terpyridyl macrocyclic ligand L is reported; the electrochemical reduction of such complexes yields, in solution, d^9 nickel(I) species.

INTRODUCTION

We have recently reported structural[1] and electrochemical[2] studies on transition metal complexes of pentadentate macrocycles incorporating 2,2'-bipyridyl or 1,10-phenanthroline units. The stabilisation of low valent metal species in these systems has been correlated with the π-acceptor properties and stereochemical requirements of the diimine macrocyclic ligand. It has been demonstrated that similar π-acceptor properties are shown by higher diimine chelates such as terpyridyl[3] and quinquepyridyl[4] derivatives. We have therefore undertaken to incorporate such higher diimine units into macrocyclic arrangements and to study their subsequent stereochemical and redox behaviour.

In this communication we report the synthesis and single crystal X-ray structure of the pentagonal bipyramidal nickel(II) complex [Ni(L)(EtOH)$_2$](BF$_4$)$_2$, the first macrocyclic complex incorporating a 2,2':6',2"-terpyridyl moiety, and the electrochemical reduction of such complexes to the corresponding d^9 nickel(I) species.

EXPERIMENTAL

The template condensation of 6,6"-bis(methylhydrazino)-4'-phenyl-2,2':6',2"-terpyridine[5] with glyoxal in the presence of Ni(OAc)$_2$·4H$_2$O in refluxing methanol yielded, on addition of [n-Bu$_4$N]$^+$[BF$_4$]$^-$, yellow micro crystals of [Ni(L)(MeOH)$_2$](BF$_4$)$_2$. Recrystallisation of this product from ethanol gave single crystals of [Ni(L)(EtOH)$_2$](BF$_4$)$_2$ a single crystal X-ray structural determination of which was undertaken to confirm its stereochemistry.

Electrochemical measurements were recorded on a Princeton Applied Research Electrochemistry System Model 170. Cyclic voltammetric studies were carried out using a three-electrode potentiostatic system with platinum wire as auxiliary and working electrodes and an Ag–AgNO$_3$ reference electrode at a scan rate of 1 V sec^{-1}. All readings were taken in acetonitrile with 0.1 mol l^{-1} [n-Bu$_4$N]$^+$[BF$_4$]$^-$ present as base electrolyte. Controlled potential electrolysis experiments were carried out using platinum gauze as the working electrode, a salt bridge being incorporated to separate oxidised and reduced species. ESR spectra were measured as glasses in acetonitrile at 77 K. All solvents were distilled, dried and degassed before use.

RESULTS AND DISCUSSION

Crystal data: [C$_{29}$H$_{33}$N$_7$NiO$_2$]$^{2+}$ (BF$_4^-$)$_2$, M = 743.93, monoclinic, a = 14.271(3), b = 17.365(5), c = 12.364(4) Å, β = 98.03(3) Å, U = 3033.95 Å^3, D$_c$ = 1.628 g cm^{-3}, Z = 4, Cu-K$_\alpha$ radiation, λ = 1.5418 Å, μ(Cu-K$_\alpha$) = 8.09 cm^{-1}, F(000) = 764,

†Copies of atomic co-ordinates, thermal parameters and F$_o$/F$_c$ values have been deposited as Supplementary material with the Editor, from whom copies are available on request. Atomic co-ordinates have also been deposited with the Cambridge Crystallographic Data Centre.

space group C2/c. 2773 intensities were recorded on a Syntex P2$_1$ diffractometer (2θ$_{max}$ = 125°) using graphite monochromated Cu-K$_\alpha$ radiation and a ω/2θ scan technique. The data were not corrected for absorption, but were averaged to give 1944 unique observed reflections [F > 3σ(F)]. The structure was solved by a combination of direct method and Fourier difference techniques and refined by blocked-cascade least squares to R = 0.068 and R$_w$ = 0.067 [w = {σ^2(F) + 0.0008|F|^2}$^{-1}$]. Anisotropic temperature factors were introduced for all the non-hydrogen atoms except for the carbon atoms of the coordinated ethanol molecules. The hydrogen atoms, with the exception of the unique hydrogen atom lying on the two-fold axis, were constrained to refine in geometrically idealised positions 1.08 Å from the relevant carbon atoms. The methyl groups were treated as rigid bodies. Common isotropic temperature factors were introduced for each type of hydrogen atom; the hydrogen atoms of the ethanol ligands were not located.†

The structure of the cation is shown in Fig. 1, together with some important bond parameters, the hydrogen atoms and the tetrafluoroborate anions having been omitted for clarity. The cation lies on a crystallographic two-fold axis which passes through the atoms C(14), C(10), N(4) and Ni(1).

The X-ray analysis confirms the presence of the seven co-ordinate pentagonal bipyramidal nickel(II) centre. The five nitrogen donor atoms of the macrocyclic ligand occupy the equatorial plane (deviations from planarity N(3): +0.0064 Å, N(4): −0.0101 Å) with two axial ethanol molecules. The non-coordinated nitrogen atoms N(2) and N(2') are planar sp^2 hybridised, the sum of the bond angles around these atoms being 359.6°. The phenyl group subtends an angle of 14.9° to the terpyridyl unit, the separation between the two hydrogen atoms H(9) and H(12) of 1.958 Å is significantly shorter than the sum of the Van der Waals radii. This indicates a significant π-interaction between the phenyl ring and the terpyridyl unit, and is consistent with the unusually short bond length of 2.015 Å for Ni(1)–N(4). The molecule shows no tendency to octahedral coordination as observed for nickel(II) complexes of more flexible pentadentate macrocyclic ligands,[6] and represents one of the few d^8 complexes with pentagonal bipyramidal stereochemistry.[7]

Cyclic voltammetry of the bis-acetonitrile adduct [Ni(L)(CH$_3$CN)$_2$](BF$_4$)$_2$ in acetonitrile at platinum electrodes shows two reversible one electron reduction waves at $^1E_{1/2}$ = −1.07 V and $^2E_{1/2}$ = −1.49 V. Controlled potential electrolysis of [Ni(L)(CH$_3$CN)$_2$](BF$_4$)$_2$ at a platinum gauze in acetonitrile at −1.1 V led to the reduction of the nickel(II) complex to give a dark green solution, the e.s.r. spectrum of which as an acetonitrile glass at 77 K, shows the features of a d^9 nickel(I) product; g$_\parallel$ = 2.4390, g$_\perp$ = 2.1184. Addition of CO or P(OMe)$_3$ to the nickel(I) product gives axially substituted univalent complexes; g$_\parallel$ = 2.5008, g$_\perp$ = 2.0491 (for CO), g$_\parallel$ = 2.4177, g$_\perp$ = 2.0684 (for P(OMe)$_3$). We propose the formation of six coordinate pentagonal pyramidal or seven coordinate pentagonal bipyramidal nickel(I) complexes.
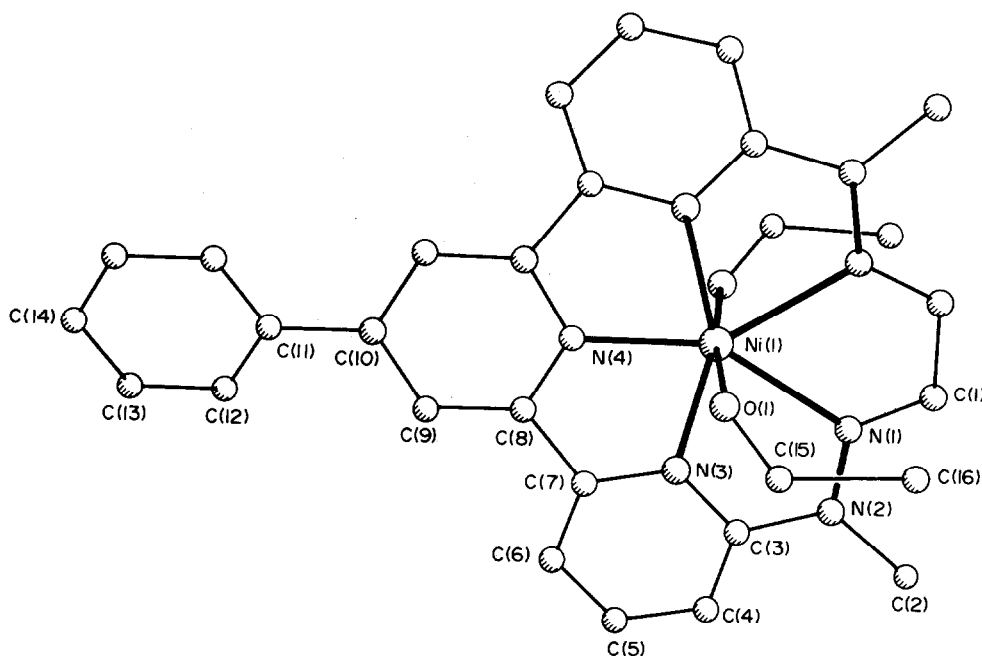
Fig. 1. The molecular structure of the $[Ni(L)(EtOH)_2]^{2+}$ cation. Bond lengths: N(1)–Ni(1) 2.234; N(3)–Ni(1) 2.104; N(4)–Ni(1) 2.015; O(1)–Ni(1) 2.084 Å.

(L)
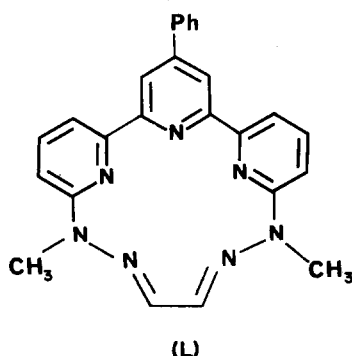
Electrochemical reduction of $[Ni(L)(CH_3CN)_2](BF_4)_2$ at the secondary reduction potential -1.6 V yields a mauve reduction solution, the e.s.r. spectrum of which at 77 K, shows the formation of nickel(I) stabilised ligand radical species with two essentially discrete paramagnetic centres, the second electron residing on the macrocyclic ligand; $g_{||} = 2.3103$, $g_{\perp} = 2.1928$ (for d^9 nickel(I) centre), $g_{iso} = 2.0245$ (for ligand radical). The stabilisation of the nickel(I) oxidation state by L parallels the redox behaviour of related 1,10-phenanthroline based macrocyclic systems,[2] although the presence of a secondary reduction process in the terpyridyl macrocycle reflects a tendency of this diimine system to form radical species.[4,5] At present the role of the 4′-phenyl group in the bonding in both the nickel(I) and nickel(II) complexes is not clear, although we believe it plays an important part in determining the π-acceptor properties of the ligand.[3]

*Author to whom correspondence should be addressed.

REFERENCES

[1] M. M. Bishop, J. Lewis, T. D. O'Donoghue and P. R. Raithby, J. Chem. Soc., Chem. Commun. 1978, 476; M. M. Bishop, J. Lewis, T. D. O'Donoghue, P. R. Raithby and J. N. Ramsden, J. Chem. Soc., Chem. Commun. 1978, 828; J. Lewis, T. D. O'Donoghue and P. R. Riathby, J. Chem. Soc., Dalton Trans. 1980, 1383; J. Lewis and T. D. O'Donoghue, J. Chem. Soc., Dalton Trans. 1980, 743; J. Lewis, T. D. O'Donoghue, Z. P. Haque and P. A. Tasker, J. Chem. Soc., Dalton Trans. 1980, 1664; M. M. Bishop, J. Lewis, T. D. O'Donoghue, P. R. Raithby and J. N. Ramsden, J. Chem. Soc., Dalton Trans. 1980, 1390.
[2] C. W. G. Ansell, J. Lewis, P. R. Raithby, J. N. Ramsden and M. Schröder, J. Chem. Soc. Chem. Commun. 1982, 546; C. W. G. Ansell, J. Lewis, M. C. Liptrot, P. R. Raithby and M. Schröder, J. Chem. Soc., Dalton Trans. 1982, 1593.
[3] M. C. Hughes, D. J. Macero and J. M. Rao, Inorg. Chim. Acta 1981, 49, 241 and references therein; J. M. Rao, M. C. Hughes and D. J. Macero, Inorg. Chim. Acta 1976, 16, 231; M. C. Hughes and D. J. Macero, Inorg. Chem. 1976, 15, 2040.
[4] E. C. Constable, J. Lewis and M. Schröder, Polyhedron. In press.
[5] E. C. Constable and J. Lewis, Polyhedron. In press.
[6] Coordination Chemistry of Macrocyclic Compounds (Edited by G. A. Melson). Plenum Press, New York, 1980; M. C. Rakowski, M. Rycheck and D. H. Busch, Inorg. Chem. 1975, 14, 1194; C. Cairns, S. G. McFall, S. M. Nelson and M. G. B. Drew, J. Chem. Soc., Dalton Trans. 1979, 446; M. G. B. Drew, J. Nelson and S. M. Nelson, J. Chem. Soc., Dalton Trans. 1981, 1691.
[7] M. G. B. Drew, J. Nelson and S. M. Nelson, J. Chem. Soc., Dalton Trans. 1981, 1685; D. Webster and G. J. Palenik, J. Am. Chem. Soc. 1974, 96, 7565; T. J. Giordano, G. J. Palenik, R. C. Palernik and D. A. Sullivan, Inorg. Chem. 1979, 18, 2445.
[8] E. C. Constable, J. Lewis and M. Schröder, Unpublished results.

University Chemical Laboratory   EDWIN C. CONSTABLE
Lensfield Road   JACK LEWIS*
Cambridge CB2 1EW   MICHAEL C. LIPTROT
England   PAUL R. RAITHBY
                                         MARTIN SCHRÖDER

NOTES

A CONVENIENT ONE-POT SYNTHESIS OF o-PHENYLENE BIS(DIPHENYLPHOSPHINE)

by H.C.E. McFarlane and W. McFarlane

Chemistry Department, City of London Polytechnic,

Jewry Street, London, EC3N 2EY.

Summary. The reaction between o-difluorobenzene and sodium diphenylphosphide in liquid ammonia provides a convenient synthesis of the title compound.

The ligand o-phenylene bis(diphenylphosphine) (I) has considerable potential in transition metal chemistry[1-3], but has been used less frequently than might have been expected because its published syntheses are low yielding and/or multi-stage[3]. Thus the direct reaction[4] between lithium- or sodium-diphenylphosphide and o-dichloro- or o-dibromobenzene gives yields of less than 1%, whilst for the reportedly "optimum" synthesis[2] using the sequence (1) the overall yield is only 18% and it is necessary to isolate and purify the intermediate o-chlorodiphenylphosphinobenzene.

(1)
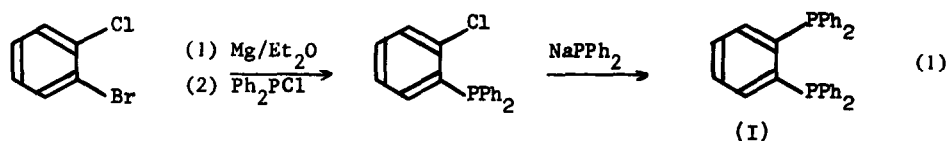
Other reported routes involve more stages and are similarly low yielding[3,5].

In this note we describe a simple one-step synthesis based on the reaction in liquid ammonia between sodium diphenylphosphide and o-difluorobenzene which produces (I) in yields of 35% in a straightforward way. A typical procedure is as follows, all operations being conducted with exclusion of atmospheric dioxygen. A deaerated solution of triphenyl phosphine (131 g, 0.5 mole) in dry tetrahydrofuran (250 ml) is added over a period of 1 hr to a stirred solution of sodium (23 g, 1 mole) in liquid ammonia (2 l). Solid dry ammonium chloride (26.7 g, 0.5 mole) is added in small portions over 1 hr to destroy phenyl sodium, followed by dropwise addition of a deaerated solution of o-difluorobenzene (28.5 g, 0.25 mole) in tetrahydrofuran (100 ml). The ammonia is allowed to evaporate overnight. After addition of toluene (600 ml) and refluxing for 1 hr, methanol (5 ml) is added to destroy any residual sodium and the mixture is filtered hot and the solvents are stripped. Recrystallization from EtOH/toluene then yields (I) (46.5 g, 35%) as white crystals m.p. 183-185°. (Lit. 186°).

Although the yield obtained by this route is only moderate, it is superior to that hitherto achieved and is based upon readily available and cheap starting materials. In addition, the procedure is very convenient and is easily adapted to different scales of operation; we are currently investigating other applications of fluoroaromatic compounds to the preparation of polyphosphorus ligands.

References

1.   W.A. Fordyce and G.A. Crosby, Inorg. Chem., 1982, 21, 1455; C.W. Jung and
      P.E. Garrou, Organometallics, 1982, 1, 658; W. Levason, C.A. McAuliffe and
      R.D. Sedgwick, J. Organometall. Chem., 1975, 84, 239; C. Ihmels and D. Rehder,
      J. Organometall. Chem., 1981, 218, (54)

2.   R. Talay and D. Rehder, Z. Naturforsch., 1981, 36b, 451.

3.   C.A. McAuliffe and W. Levason, Phosphine, Arsine and Stibine Complexes of the
      Transition Elements, Elsevier, Amsterdam, 1979.

4.   F.A. Hart, J.C.S., 1960, 3324.

5.   B. Chiswell and L.M. Venanzi, J. Chem. Soc.(A), 1966, 417.

COMMUNICATION

COORDINATIVELY UNSATURATED ALKYNE COMPLEXES: SYNTHESIS OF MONO AND BIS-ALKYNE COMPLEXES OF TUNGSTEN (II)

Jack L. Davidson[*] and Giuseppe Vasapollo[†]

Department of Chemistry, Heriot-Watt University, Riccarton,
Currie, Edinburgh EH14 4AS,UK.

Summary. $[WBr_2(CO)_4]_n$ reacts with alkynes to give complexes $[WBr_2CO(RC\equiv CR)_2]_2$ (1) (R = R' = Me, Et, Ph; R = Me, R' = Ph), which react with nucleophiles L{L = $CNBu^t$, PPh_3, or $P(OMe)_3$} to give monoalkyne derivatives $[WBr_2(CO)(RC\equiv CR')L_2]$ (2).   An intermediate bis-alkyne adduct $[WBr_2CO(MeC\equiv CMe)_2(CNBu^t)]$ (3) was isolated in the reaction of $[WBr_2(CO)(MeC\equiv CMe)_2]_2$ with $CNBu^t$ illustrating that cleavage of the dimer(1) is the first stage in these reactions.

In recent years it has become clear that alkyne ligands can involve both sets of filled π-orbitals in bonding with a transition metal and thus stabilise coordinative unsaturation[1,2].   This phenomenon is particularly pronounced in divalent molybdenum and tungsten, (d^4), complexes containing one or two coordinated alkyne ligands.   Following recent indications that 4-electron donation may lead to activation of a coordinated alkyne towards nucleophilic rather than electrophilic attack,[2a,b,3] we now report the synthesis of new alkyne complexes of W(II) and their reactions with nucleophiles.

Reactions of $[WBr_2(CO)_4]_n$ with alkynes RC≡CR' (R = R' = Me, Et, Ph: R = Me, R' = Ph) in hexane at 20°C give good yields of alkyne complexes $[WBr_2CO(RC\equiv CR)_2]_n$ which according to molecular weight studies in solution are dimeric i.e. n = 2.   However the mass spectra in each case only gives identifiable peaks due to mononuclear fragments $[P/2 = CO]^+$,$[P/2 - (CO + RC\equiv CR')]^+$,$[P/2 - (CO + Br)]^+$ although very weak dinuclear ions were observed in some cases.   Spectroscopic data : e.g. $[WBr_2(CO)(MeC\equiv CMe)_2]_2$; i.r., ($CCl_4$), 2098 cm^{-1}, wm, 2060 cm^{-1}, vs; ^1H nmr., δ2.96(s, 6H) 2.33(s, 6H).   The two ^1H nmr resonances suggest two sets of inequivalent alkynes or that all four alkynes are equivalent but the two substituents are magnetically non-equivalent and on this basis structures (1a) or (1b) are proposed.   However, since alkynes are able to function as 4-electron donors an alternative structure to (1) without a metal-metal double bond is equally plausible.   Interestingly $CF_3C\equiv CCF_3$ and $[WBr_2(CO)_4]_n$ give a mononuclear complex $[WBr_2CO(CF_3C\equiv CCF_3)_2]$ under similar reaction conditions[2b] while $[Mo(SBu^t)_2(CNBu^t)_4]$ reacts with alkynes to give $[Mo(SBu^t)_2(CNBu^t)_2 (RC\equiv CR)]$ (R = H, Ph)[3].

[†] Present address: Instituto di Chimica Generale,
                     Via Amendola 173,
                     Bari, Italy.
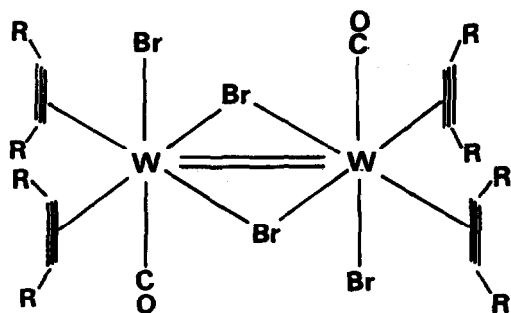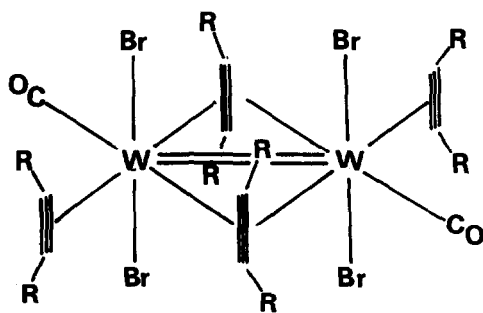
(1a)   (1b)

Mononuclear complexes $[WBr_2CO(RC\equiv CR)L_2]$, (2) were readily obtained from reactions of
(1) with nucleophiles L = PPh_3, $P(OMe)_3$ or $CNBu^t$ and in one case an intermediate bis alkyne
complex $[WBr_2CO(MeC\equiv CMe)_2(CNBu^t)]$ (3), was also isolated. Spectroscopic data:
$[WBr_2CO(MeC\equiv CMe)_2(CNBu^t)]$; i.r. ($CHCl_3$), $\nu C\equiv N$ 2218 cm^{-1}s. νCO 2092 cm^{-1}vs; ^1H nmr ($CDCl_3$),
$\delta 2.93$ (q, J = 0.79 Hz, 6H), 2.89 (q, J = 0.79 Hz, 6H), 1.80 (s 9H); mass spectrum-highest
peak $[WBr_2(MeC_2Me)_2]^+$. The presence of CH_3-CH_3 coupling in the ^1H nmr spectrum indicates
inequivalence of the CH_3 groups at either end of each acetylene rather than inequivalent
acetylene ligands and structure (3) is therefore proposed. Structures with *trans* alkynes
are also possible but six-coordinate bis alkyne d^4 metal complexes appear to prefer *cis*
alkyne ligands[2a].
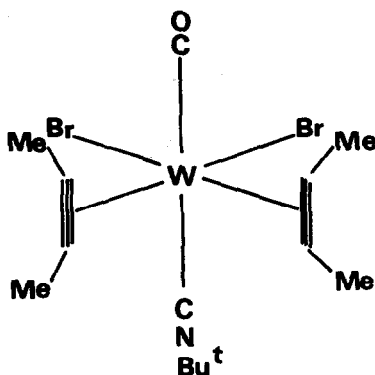
(3)

Spectroscopic data: $[WBr_2CO(MeC\equiv CMe)(CNBu^t)_2]$ i.r. ($CHCl_3$), $\nu C\equiv N$ 2194 s, 2160 cm^{-1}s;
νCO 2002 cm^{-1}vs, ^1H nmr $\delta 3.16$ (s, 6H), 1.74 (s, 9H), 1.36 (s, 9H) mass spectrum –
decomposition observed in the probe. The ^1H nmr spectrum of $[WBr_2CO(MeC\equiv CMe)(CNBu^t)_2]$
indicates two inequivalent isocyanide ligands and a single acetylenic CH_3 resonance in
accord with *cis* $CNBu^t$ groups. ^1H and ^{31}P nmr spectra of $[WBr_2CO(RC\equiv CR')\{P(OMe)_3\}_2]$
similarly suggest *cis* phosphite ligands with R = R' = Me. Spectroscopic data: ^1H nmr:

δ = 3.94 (d, J_{P-H} = 9.81 Hz, 9H)   3.47 (d, J_{P-H} = 10.46 Hz, 9H) 3.03 (d, J_{P-H} = 1.77, 6H); ^{31}P[^{1}H] 119.95 (AB quartet), but *trans* P(OMe)$_3$ ligands with R = R' = Ph ^{1}H nmr δ7.75 (m, 4H), 7.48 (m, 6H), 3.61 (t, J_{P-H} = 5.42 Hz, 18H); ^{31}P[^{1}H], δ117.96 (s).   However monitoring of the spectra of [WBr$_2$CO(MeC≡CMe){P(OMe)$_3$}$_2$]revealed that isomerisation of the kinetic *cis* isomer occurs to a more stable *trans* form: ^{1}H nmr δ3.66 (t, J_{P-H} = 5.38 Hz, 18H), 3.14 (t, J_{P-H} = 1.59 Hz, 6H); ^{31}P [^{1}H], δ120.03 (s).   Variable temperature ^{1}H nmr spectra also revealed that the CH$_3$C≡CCH$_3$ doublet δ3.03 of the *cis* isomer splits into two equal intensity multiplets at low temperatures (T. coalescence = 14°C) whereas no change is observed in the spectrum of the *trans* isomer down to -85°C.   This suggests propeller rotation of the alkyne ligand but with significantly higher barriers to rotation in the *cis* isomer.   Such a conclusion is based on the proposal that in both isomers the alkyne should be in an asymmetric environment as in the illustrated structures (2a,b,c).   This follows from simple bonding arguments[1,3] which dictate that for the alkyne to function as a four electron donor ligand in (2) the CO and RC≡CR ligands must be mutually *cis* while the most stable alkyne orientation will be that in which the C≡C bond lies parallel to the M-CO bond.

(2a)
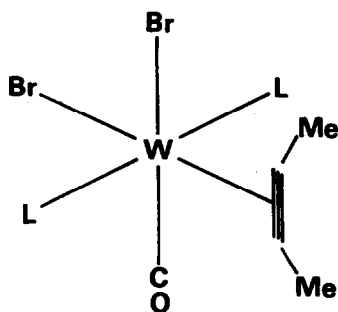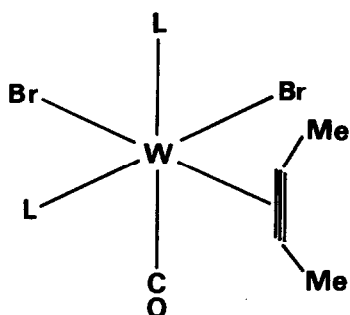
(2b)   (2c)
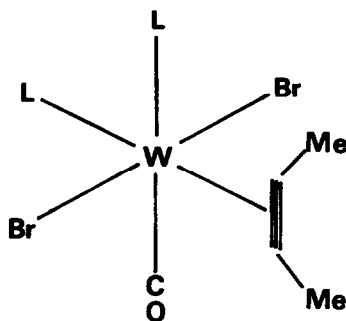
L = P(OMe)$_3$

    These structures are based on the premise that the phosphines are coordinated to the metal a fact confirmed by the presence of ^{31}P - ^{183}W coupling in the ^{31}P nmr spectra of the complexes.   In contrast P(OMe)$_3$ reacts with [WBr$_2$CO(CF$_3$C≡CCF$_3$)$_2$] to give a vinyl derivative as a result of addition to an acetylenic carbon[2b].   Thus, although nucleophilic attack at

an acetylenic carbon may be promoted by four-electron donation to a metal [2a,b,3] these results indicate that the presence of electron withdrawing groups (CF_3) also appears to be necessary in some circumstances.

Finally we note the increasing range of stoichiometries exhibited by d^4 Mo(II) and W(II) alkyne complexes.[1-5] Since coordinative unsaturation in d^4 complexes can also be stabilised by inorganic donor ligands[1a] it seems probable that the wide range of stoichiometries available to the alkyne complexes may be a consequence of π-donation by both the alkynes and the inorganic ligands. Thus differences in the π-donor abilities of SBu^t and Br could account for the preference for five coordination in $[Mo(SBu^t)_2(CNBu^t)_2(PhC\equiv CPh)]$[3] relative to six coordination found with $[WBr_2CO(CNBu^t)_2(PhC\equiv CPh)]$.

References

1. (a) J.L. Templeton, P.B. Winston and B.C. Ward, J.Amer.Chem.Soc., 1981,103,7713 and
        ref. therein.

    (b) P.S. Braterman, J.L. Davidson and D.W.A.Sharp, J.Chem.Soc. Dalton Trans., 1976,241.

    (c) K. Tatsumi, R. Hoffmann and J.L. Templeton, Inorg.Chem., 1982,21,466.

2. (a) J.L. Davidson, I.E.P. Murray, P.N. Preston, M.V. Russo, Lj. Manojlovic-Muir and
        K.W. Muir, J.Chem.Soc.Chem.Commun., 1981,1059.

    (b) J.L. Davidson, G. Vasapollo, Lj. Manojlovic-Muir and K.W. Muir, J.Chem.Soc.Chem.
        Commun., 1982,1025.

3. M. Kamata, T. Yoshida, S. Otsuka, K. Hirotsu, T. Higachi, M. Kido, K. Tatsumi and
    R. Hoffmann, Organometallics, 1982,1,227.

4. J.L. Davidson and D.W.A. Sharp, J.Chem.Soc., 1975,2531.

5. C.M. Giandomenico, C.T. Lam and S.J. Lippard, J.Amer.Chem.Soc.,1982,104,1263.

THE METAL COMPLEXES OF HETEROCYCLIC β-DIKETONES AND THEIR DERIVATIVES—II

LANTHANIDE CHELATES OF 1-PHENYL-3-METHYL-4-ACETYLPYRAZOLONE-5, (HPMAP)

EMMANUEL CHUKWUEMEKA OKAFOR

Coordination Chemistry Research Unit, Department of Chemistry, University of Nigeria, Nsukka, Anambra State, Nigeria

Abstract—Some lanthanide chelates of 1-phenyl-3-methyl-4-acetyl-pyrazolone-5, HPMAP, have been synthesized and investigated. Characterisation involved elemental analysis, conductivity measurements, IR and proton magnetic resonance spectra, melting points and Karl–Fischer titrations. The complexes are shown to be neutral chelates with the empirical formula $Ln(PMAP)_3 \cdot xH_2O \cdot yC_2H_5OH$ were for Ln = La, Ce and Nd, $x = 2$ and $y = 1$, and for Ln = Y, Eu, Gd, Dy, Er and Lu, $x = 2$ and $y = 0$. IR, PMR and electronic spectral data together with band assignments are presented. The Nd chelate was found to exhibit positive nephelauxetic effect and Sinha's parameters were calculated and discussed for Nd and Er.

In a previous communication[1] the synthesis and spectral properties of some anhydrous lanthanide chelates of 1-phenyl-3-methyl-4-benzoyl–pyrazolone-5, (HPMBP) were described. In continuation of this serial study, the investigation has been extended to the lanthanide complexes of 1-phenyl-3-methyl-4-acetyl-pyrazolone-5, (HPMAP).

EXPERIMENTAL

Reagents

The following Merck reagents of analytical quality were used: $YCl_3 \cdot 6H_2O$, $La(NO_3)_3 \cdot 6H_2O$, $Nd(NO_3)_3 \cdot 5H_2O$, $Eu(NO_3)_3 \cdot 5H_2O$, $Gd(NO_3)_3 \cdot 5H_2O$, $Dy(NO_3)_3 \cdot 5H_2O$, $Er(NO_3)_3 \cdot 5H_2O$, Lu_2O_3, CeO_2, H_2O_2, 1-phenyl-3-methyl-pyrazolone-5, acetyl chloride, dioxane, 95% and absolute ethanol.

1-Phenyl-3-methyl–pyrazolone-5 (17 g) was dissolved in dioxane (100 cm^3) by warming and $Ca(OH)_2$ (15 g) added. Acetyl chloride (7 cm^3) was next added, drop by drop, with stirring within 3 min. After refluxing gently for 1 hr, the orange mixture was cooled and poured with stirring into chilled 3M HCl (300 cm^3). A handful of ice–salt mixture was added and vigorous stirring continued for another 30 min, after which, the reaction mixture was kept in a refrigerator until crystallisation occurred. Filtration of the product gave 76% yield of light brown crystals, m.p. 64–65°C. Recrystallization of the product from *n*-hexane gave the yellowish enol tautomer, m.p. 66–67°C. IR (Nujol): ν_{max} (cm^{-1}), 1635 (C=O); 2200–3500, weak and broad, (O–H ... O). Anal. Calc. for $C_{12}H_{11}O_2N_2$: C, 66.65; H, 5.60; N, 12.96. Found: C, 66.58; H, 5.57; N, 12.91.

Preparation of rare earth complexes

The complexes of La, Nd, Eu, Gd, Dy, Er and Y were obtained by the following general procedure: A 0.5 M aqueous solution of sodium hydroxide (10 cm^3) was added to a solution of 1-phenyl-3-methyl-4-acetyl-pyrazolone-5, (5 mM) in 95% ethanol (45 cm^3). The reaction mixture was put aside for about 24 hr. The resulting solution of the monosodium salt of the ligand was added dropwise with constant stirring to a solution of 1.67 mM of lanthanon salt in 10 cm^3 of 95% ethanol. The reaction mixture containing precipitates was stirred magnetically for 2 hr and thereafter filtered under suction. The product was washed with aqueous ethanol (1/1), air-dried for 2 days, and stored in a desiccator over P_2O_5.

The above procedure was modified slightly in the case of Ce^{3+} and Lu^{3+} complexes. Hydrated chlorides of Ce(III) and Lu(III) (1.67 MM of each) were dissolved in 400 cm^3 and 300 cm^3 of 95% ethanol respectively. Into each filtered lanthanon salt solution, the solution of the monosodium salt of the ligand was added dropwise. The resulting reaction mixture was stirred magnetically for 2 hr and concentrated down to about 50 cm^3. The crystals which deposited on cooling were filtered and treated as described earlier.

The hydrated Ce(III) chloride was obtained from CeO_2 by treating CeO_2 first with H_2O_2, next with conc. HCl, and evaporating the resulting solution cautiously to dryness to obtain white crystals, while the hydrated Lu(III) chloride was obtained by treating Lu_2O_3 with conc. HCl and evaporating to dryness.

Physical measurements

IR spectra were recorded on a Perkin–Elmer 577 spectrophotometer. Other measurements are as described previously.[1]

Elemental analyses

Microanalyses for C, H and N were performed by the microanalytical unit of the Department of Pure and Applied Chemistry, University of Strathclyde, Glasgow, Scotland.

RESULTS AND DISCUSSION

Table 1 lists the complexes prepared together with some of their physical properties and microanalytical data.

The analytical data show that the complexes have the general formula $Ln(PMAP)_3 \cdot xH_2O \cdot yC_2H_5OH$ where for Ln = La, Ce and Nd, $x = 2$ and $y = 1$ and for Ln = Y, Eu, Gd, Dy, Er and Lu, $x = 2$ and $y = 0$. The amount of water associated with the complexes has been determined by Karl–Fischer titrations.[2] This technique was applied successfully to β-diketonate complexes of lanthanides by Wagner[3] and Springer *et al.*[4] The agreement between the Karl–Fischer determinations and the proton NMR spectral integration of the proton signals of the associated water in the case of diamagnetic complexes is excellent. The proton NMR spectra reveal the presence of ethanol molecules in the case of La, Ce and Nd (Table 3). Conductivity measurements in DMF reveal that all

Table 1. Physical and analytical data for 1-phenyl-3-methyl-4-acetyl-pyrazolone-5, HPMAP, and some of its lanthanide complexes

Compound	Colour	Yield (%)	Melting Point (°C)	Calc. (%)			Found (%)		
				C	H	N	C	H	N
HPMAP (enol)	Yellow	76	66–67	66.65	5.60	12.96	66.58	5.57	12.91
Y(PMAP)$_3$.2H$_2$O	yellow	79	169–170	56.10	4.84	10.91	56.20	4.90	10.87
La(PMAP)$_3$.2H$_2$O.EtOH	Light yellow	94	180–182	52.66	5.00	9.70	52.61	4.96	9.66
Ce(PMAP)$_3$.2H$_2$O.EtOH	light brown	43	101 dec.	52.59	4.99	9.69	52.49	4.98	9.63
Nd(PMAP)$_3$.2H$_2$O.EtOH	pink	74	167–168	52.35	4.97	9.64	52.32	4.95	9.70
Eu(PMAP)$_3$.2H$_2$O	yellow	63	176–178	51.87	4.47	10.08	51.82	4.43	10.00
Gd(PMAP)$_3$.2H$_2$O	yellow	76	188–189	51.53	4.44	10.02	51.48	4.39	9.98
Dy(PMAP)$_3$.2H$_2$O	yellow	81	180–181	51.22	4.42	9.86	51.17	4.37	9.92
Er(PMAP)$_3$.2H$_2$O	cream	75	156–157	50.93	4.39	9.90	50.86	4.33	9.85
Lu(PMAP)$_3$.2H$_2$O	cream	56	200–201	50.47	4.35	9.81	50.42	4.32	9.78

HPMAP, 1-phenyl-3-methyl-4-acetyl-pyrazolone-5; PMAP, anion of HPMAP; EtOH, C$_2$H$_5$OH.

Table 2. Observed vibrational frequencies of HPMAP and its lanthanum complex

Ligand (m.p. 66 – 67°C)	La	Tentative Assignment
	3600 sh	ν O–H of H_2O
	3400 (s,br)	
3080 w	3080 sh	Aryl ν C–H
2938 w	2930 sh	saturated ν C–H
1635 vs		ν C=O enol form of β –diketone
	1620 vs	ν_{as} C $\doteq$ O
1600 vs	1600 s	phenyl ring ν C $\doteq$ C
1575 w	–	pyrazole ring stretch
–	1540 sh	pyrazole ring stretch
1505 vs	1490 vs	ν_{as} C $\doteq$ C $\doteq$ C
1468 m	1460 w	phenyl ring ν C $\doteq$ C
1448 m	1450 w	pyrazole ring stretch
	1418 m	β_{as} CH_3
1400 w	1398 m	pyrazole ring stretch
	1380 w	β_s CH_3
1360 w	1360 s	ν_s C $\doteq$ O
1328 m	1310 w	β_s CH_3
1210 s	1242 m	ν_s C $\doteq$ C $\doteq$ C
1185 w	1172 vw	β C–H
1165 sh	1152 w	
1118 w		pyrazole ring breathing
1085 vs	1080 vs	C–H in-plane def. monosubst. phenyl ring
1070 w	1058 s	
1025 m	1015 s	
1005 w	995 vw	CH_3 rocking
960 s	955 vs	C–C_6H_5 stretch
905 m	908 m	C–CH_3 stretch
	873 m	

Table 2 (*Contd.*)

Ligand (m.p. 66 – 67°C)	La	Tentative Assignment
828 m	838 s	γ C–H
760 vs	753 vs	
685 s	688 s	chelate ring deformation
648 w	642 s	
591 m	608 s	chelate ring vibrations
525 s	524 m	
–	504 m	ν M–O
402 w	401 s	chelate ring vibrations
356 w	339 w	

Legend: w, weak; vw, very weak; m, medium; s, strong; vs, very strong;

ν, stretching; γ, out of plane bending; β, bending or deformation

the complexes are non-conducting and are therefore neutral non-ionic complexes. The complexes are very soluble in such polar solvents as acetone, DMF, and DMSO but slightly soluble in chloroform and insoluble in such non-polar solvents like benzene and *n*-hexane.

IR spectra

Previous work on 1,3-diketonates[1,5-11] have been taken into consideration in the assignment of frequencies. The IR spectrum of the enol tautomer of the ligand is considered as reference. Since these complexes have identical IR spectra, only the spectral data of the ligand and a representative complex—the lanthanum complex—are listed in Table 2, the vibrational frequencies (4000–200 cm^{-1}) with possible assignments being given. The following features of the IR spectra are of interest:

(1) The presence of coordinated water is indicated by the presence of a broad peak centred at 3400 cm^{-1} with a shoulder at 3600 cm^{-1} attributable to the OH stretching frequencies of water.

(2) The weak broad band in the 2200–3500 cm^{-1} region which has been attributed to ν_{as} (OH) of O–H...O in enols[12] is absent in the spectra of the complexes. This fact implicates deprotonated OH in bonding.

(3) The shift of the C=O stretching frequency from 1635 cm^{-1} in the ligand to ~1620 cm^{-1} (ν_{as}C $\leftrightarrows$ O) in the lanthanum complex suggests that C=O is involved in chelation.

(4) The presence of bands between 300 and 500 cm^{-1} typical of metal 1,3-diketonates (νM–O) suggests bonding through oxygen atoms.[13]

IR spectral evidence, therefore, suggest that the ligand bonds to the metal ion through the carbonyl and the deprotonated hydroxyl groups of an enol form of the ligand.

Proton magnetic resonance (PMR) spectra

Table 3 gives the PMR spectral data of the ligand and some of its lanthanide complexes together with assignment of the proton signals.

The PMR spectra of the complexes confirm IR evidence that the complexes are hydrated by revealing peaks due to water. The chemical shifts of these peaks are listed in Table 3. In the case of lanthanum, cerium and neodymium complexes, the proton NMR spectra demonstrate clearly the presence of ethanol molecule in each chelate molecule. The PMR spectra in DMF-d_7 of these C_2H_5OH adducts indicate that the C_2H_5OH molecule is not coordinated to the Ln ion since the C_2H_5OH signals are not shifted at all in the case of methyl resonances and only very slightly in the case of methylene and hydroxyl signals (Table 3) relative to the signals of the uncomplexed C_2H_5OH in DMF-d_7. These slight methylene and hydroxyl shifts could be attributed to solution (medium) effects. On the other hand, the proton signals of the associated water molecules exhibit significant shifts relative to the signal of uncomplexed H_2O in DMF-d_7 which occurs at δ 4.33 ppm indicating that the H_2O molecules are coordinated. In the case of the diamagnetic complexes, the signals of the water protons experience appreciable upfield (diamagnetic) shifts to δ (ppm): 3.13 (Y), 3.57 (La) and 3.00 (Lu) whereas in the case of the paramagnetic complexes the signals of the H_2O protons apart from experiencing some broadening suffer extensive downfield (paramagnetic) shifts to δ (ppm): 10.16 (Ce), 10.67 (Nd) and 10.73 (Eu). Our results are in agreement with the recent conclusions of Richardson and Wagner[14] that when water and an organic donor are both present, only the water is coordinated to the lanthanide ion, the organic donor molecules being hydrogen-bonded or held in the crystal by lattice forces. Careful integration of the proton signals reveals the number of H_2O and C_2H_5OH molecules associated with each complex molecule. Two water molecules are coordinated to the lanthanide in La, Nd, Ce, Eu, Lu and Y complexes whereas one C_2H_5OH molecule is associated with each molecule of La, Nd and Ce complexes.

In all the complexes, the methyl signals experience upfield (diamagnetic) shifts—δ (ppm): 2.33 (Y), 2.30 (La),

Table 3. Proton NMR spectral data of HPMAP and some of its rare earth complexes (chemical shifts in δ ppm relative to TMS)

Compound	Ligand Methyl Protons	Water Protons	Ethanol Protons			Ligand Phenyl Protons	Ligand Hydroxyl Proton	Solvent for NMR
			CH_3 Protons	-CH_2- Protons	OH Proton			
Ligand (HPMAP)	2.45(sp,s)	-	-	-	-	7.20-8.00(m)	12.27	$CDCl_3$
Y(PMAP)$_3$.2H$_2$O	2.33(sp,s)	3.13(sp,s)	-	-	-	7.10-8.20(m)	-	$CDCl_3$+DMSO-d$_6$
La(PMAP)$_3$.2H$_2$O. C$_2$H$_5$OH	2.30(sp,s)	3.57(sp,s)	1.00-1.23(tp)	3.57	4.25-4.45	7.00-8.30(m)	-	DMF-d$_7$
Ce(PMAP)$_3$.2H$_2$O. C$_2$H$_5$OH	1.73(br)	10.16(br)	1.00-1.23(tp)	3.20(br)	4.00-4.20	7.20-7.70(s,br)	-	DMF-d$_7$+CDCl$_3$
Nd(PMAP)$_3$.2H$_2$O. C$_2$H$_5$OH	2.18 (br)	10.67(br)	1.00-1.23(tp)	3.20(br)	4.10-4.30	7.25-7.80(br,s)	-	DMF-d$_7$
Eu(PMAP)$_3$.2H$_2$O	0.93, 2.23	10.73(br)				5.20-7.00	-	$CDCl_3$+DMSO-d$_6$
Lu(PMAP)$_3$.2H$_2$O	2.13, 2.33 (sp)	3.00(sp,s)				7.00-8.20(m)	-	$CDCl_3$+DMSO-d$_6$

Legend: sp, sharp; br, broad; s, singlet; tp, triplet; qt, quartet; m, multiplet; v, variable.

1.73 (Ce), 2.18 (Nd), 0.93 and 2.23 (Eu), and 2.13 and 2.33 (Lu) relative to that of the ligand (2.45 ppm). It is interesting to note that in the case of the europium complex the two methyl groups in the ligand with different environments have widely separated signals. In both the ligand and the diamagnetic complexes of La, Y, and Lu the methyl signals are sharp whereas these signals have been broadened in the case of the paramagnetic chelates of Ce and Nd. The phenyl multiplet experiences slight downfield (paramagnetic) shifts in the case of the diamagnetic complexes of Y, La and Lu (~7.00–8.30 ppm) relative to the multiplet of the ligand (7.20–8.00 ppm) whereas in the case of the paramagnetic complexes the shift is upfield—Ce (7.20–7.70 ppm), Nd (7.25–7.80 ppm) and Eu (5.20–7.00 ppm). The signal due to the hydroxyl proton in the ligand at δ 12.27 ppm is absent in the PMR spectra of all the complexes providing conclusive evidence that the hydroxyl proton is lost during complexation.

In the PMR spectra of the chelates of gadolinium, dysprosium and erbium, no proton signals were picked up at all even at very high spectral amplitudes. This might be due to huge shifts or extensive broadening of the signals or a combination of both.

Electronic spectra

The electronic spectra of the lanthanide chelates of HPMAP may be conveniently divided into three types of bands which are derived from intraligand, charge-transfer, and f–f transitions and are found at decreasing energy (and intensity). The absorption maxima together with their molar absorptivities are reported in Tables 4 and 5.

(a) *Intraligand transition.* The UV spectra of the lanthanide complexes are similar to that of the ligand and show virtually no shifts in the positions of the absorption maxima (Table 4) as was the case in the spectra of 1-phenyl-3-methyl-4-benzoyl-pyrazolone-5, HPMBP and its lanthanide chelates.[1] The absorption at 262 nm (~38,000 cm^{-1}) is ascribed to intraligand $\pi \to \pi^*$ transition.

(b) *The charge transfer transition.* HPMAP complexes are not sufficiently soluble in 95% ethanol. The visible spectra of the ligand and the complexes have therefore been recorded in DMF in which these complexes are very soluble. The complexes of yttrium, lanthanum, gadolinium, dysprosium, erbium and lutetium show L → M charge transfer bands around 23 kK (Table 4).

(c) *f–f Transitions.* Visible spectral data for the neodymium and erbium chelates are reported in Table 5 together with band (J level) assignments. The complexes of yttrium, lanthanum, cerium, europium, gadolinium, dysprosium and lutetium did not show any bands assignable to f–f transitions.

Generally, the f–f transitions are slightly affected by the immediate surrounding of the lanthanide cation and this is commonly attributed to the "buried" or shielded nature of the $4f$ orbitals by the overlying $5s^2$ and $5p^6$ shells; however, shifts, sometimes splitting and intensity enhancement of certain bands can be observed on complex formation. The nephelauxetic effect has been correlated with the covalency of the metal–ligand bonding[15,16] and Sinha's parameter[17] is usually supposed to be a measure of covalency.

The absorption spectrum of the neodymium(III) chelate shows the expected red shift, with respect to aquo-ion, of the "hypersensitive" transitions; the value of Sinha's parameter was found to be positive but smaller than unity ($\delta = 0.7$). If these shifts are effectively an accurate measure of covalent bonding the Nd(III) chelate shows weak covalent bonding. But in the case of the erbium(III) chelate, the absorption spectrum does not

Table 4. Electronic spectral data—intraligand and charge transfer transitions of rare earth complexes of HPMAP

	Intraligand transitions			Charge Transfer (C.T) transitions		
	λ_{max} (nm)	Wave Number (kK)	ε	λ_{max} (nm)	Wave Number (kK)	ε
Ligand (HPMAP)	262	38.17	40,625	–	–	–
Y(PMAP)$_3$·2H$_2$O	262	38.17	87,500	435	22.99	29.57
La(PMAP)$_3$·2H$_2$O· C$_2$H$_5$OH	262	38.17	48,750	440	22.73	21.67
Ce(PMAP)$_3$·2H$_2$O· C$_2$H$_5$OH	262	38.17	43,750	–	–	–
Nd(PMAP)$_3$·2H$_2$O· C$_2$H$_5$OH	262	38.17	73,750	–	–	–
Eu(PMAP)$_3$·2H$_2$O	262	38.17	67,500			
Gd(PMAP)$_3$·2H$_2$O	262	38.17	58,750	435	22.99	27.43
Dy(PMAP)$_3$·2H$_2$O	262	38.17	66,250	435	22.99	33.20
Er(PMAP)$_3$·2H$_2$O	261	38.31	100,000	430	23.26	19.07
Lu(PMAP)$_3$·2H$_2$O	262	38.17	72.500	435	22.99	24.50

Table 5. f-f transitions of rare earth complexes of HPMAP

Compound	$\lambda_{max}(nm)$	Wave Number (kK)	ϵ	Assignment
Nd(PMAP)$_3$·2H$_2$O· C$_2$H$_5$OH	428	23.36	9.15	$^4I_{9/2} \longrightarrow {}^2P_{1/2}$
	474	21.10	6.98	$\longrightarrow {}^4G_{9/2}$
	508	19.69	6.54	$\longrightarrow {}^2G_{9/2}$
	520	19.23	8.72	$\longrightarrow {}^4G_{7/2}$
	566 sh	17.67	14.82	$\longrightarrow {}^2G_{9/2}$
	574	17.42	25.28	$\longrightarrow {}^4G_{5/2}$
	620 sh	16.13	1.31	$\longrightarrow {}^2H_{11/2}$
	674 sh	14.84	0.87	$\longrightarrow {}^4F_{9/2}$
	732	13.66	6.10	$\longrightarrow {}^4F_{7/2}$
	784	12.76	6.98	$\longrightarrow {}^2H_{9/2}$
	835	11.98	2.18	$\longrightarrow {}^4F_{3/2}$
Er(PMAP)$_3$·2H$_2$O	378	26.46	53.75	$^4I_{15/2} \longrightarrow {}^4G_{11/2}$
	405	24.69	19.51	$\longrightarrow {}^2H_{9/2}$
	446 sh	22.42	19.51	$\longrightarrow {}^4F_{5/2}$
	480 sh	20.83	10.83	$\longrightarrow {}^4F_{7/2}$
	515	19.42	22.54	$\longrightarrow {}^2H_{11/2}$
	536	18.66	5.64	$\longrightarrow {}^4S_{3/2}$
	641	15.60	4.34	$\longrightarrow {}^4F_{9/2}$

sh, shoulder.

show any shift whatsoever with respect to aquo-ion, of the "hypersensitive" transitions; the value of Sinha's parameter was found to be zero. This would imply that the Er(III) chelate is on the border line between ionic and covalent bonding since according to Sinha[17] negative values of δ indicate ionic bonding. However, of all the synthesized lanthanon chelates of HPMAP, the Er(III) chelate has the lowest melting point, 156–157°C (Table 1) and besides, the M–O stretching frequency of ~504 cm^{-1} suggests much greater covalent bonding than in the sodium chelate with νM–O of 427 cm^{-1}. To what extent, Sinha's parameter is a good index for measuring covalency is a matter for future investigation.

Assignments of the f-f transitions of the Nd and Er chelates of HPMAP (Table 5) are based on the calculations and analysis of the electronic spectra of trivalent Nd and Er carried out by Wybourne[18] and on the term assignments recently made for the absorption

bands of Nd^{3+} and Er^{3+} in aqueous solution by Katzin and Barnett[19] and Ryan and Jorgensen.[20]

CONCLUSION

HPMAP bonds to lanthanide ions through the carbonyl and hydroxyl groups of an enol form, the hydroxyl proton being liberated during complexation. The resulting metal complex is a neutral tris chelate, each chelate molecule having two water molecules coordinated to its lanthanide atom which thereby exhibits a coordination number of eight.

REFERENCES

[1] E. C. Okafor, *J. Inorg. Nucl. Chem.* 1980, **42**, 1155.
[2] A. I. Vogel, *A Text-book of Quantitative Inorganic Analysis*, 3rd Edn, p. 948. Lowe and Brydon Ltd., London (1968).
[3] W. F. Wagner, *Record Chem. Prog.* (Kresge-Hooker Sci. Lib.) 1962, **23**, 155.
[4] C. S. Springer Jr., D. W. Meek and R. E. Sievers, *Inorg. Chem.* 1967, **6**, 1105.
[5] L. J. Bellamy and R. F. Branch, *J. Chem. Soc.* 1954, 4491.
[6] K. E. Lawson, *Spectrochim. Acta* 1961, **17**, 248.
[7] S. Pinchas, B. L. Silver and I. Laulicht, *J. Chem. Phys.* 1967, **46**, 1506.
[8] H. Junge and H. Musso, *Spectrochim. Acta* 1968, **24A**, 1219.
[9] S. Musumi and N. Iwasaki, *Bull. Chem. Soc. Jap.* 1967, **40**, 550.
[10] C. Y. Liang, E. J. Schimitschek and J. A. Trias, *J. Inorg. Nucl. Chem.* 1970, **32**, 811.
[11] K. C. Joshi and V. N. Pathak, *J. Inorg. Nucl. Chem.* 1973, **35**, 3161.
[12] S. F. Tayyari, TH. Zeegers-Huyskens and L. L. Wood, *Spectrochim. Acta* 1979, **35A**, 1267 and reference therein.
[13] J. R. Ferraro, *Low Frequency Vibrations of Inorganic and Coordination Compounds*, p. 93. Plenum Press, New York (1971).
[14] M. F. Richardson, W. F. Wagner and D. E. Sands, *J. Inorg. Nucl. Chem.* 1969, **31**, 1417.
[15] C. K. Jorgensen, *Progr. Inorg. Chem.* 1962, **4**, 73.
[16] J. L. Ryan and C. K. Jorgensen, *J. Phys. Chem.* 1966, **70**, 2845.
[17] S. P. Sinha, *Spectrochim. Acta* 1966, **22**, 57.
[18] R. G. Wybourne, *J. Chem. Phys.* 1960, **32**, 639.
[19] L. I. Katzin and M. L. Barnett, *J. Phys. Chem.* 1964, **68**, 3781.
[20] R. L. Ryan and C. K. Jorgensen, *J. Phys. Chem.* 1966, **70**, 2845.

MIXED LIGAND COMPLEXES OF RUTHENIUM(III), RHODIUM(III) AND IRIDIUM(III) WITH DIPICOLINIC ACID AND SOME MONOBASIC BIDENTATE NITROGEN, OXYGEN DONOR LIGANDS

S. K. SENGUPTA*, S. K. SAHNI and R. N. KAPOOR
Department of Chemistry, University of Delhi, Delhi-110007, India

Abstract—The trivalent ruthenium, rhodium and iridium complexes of dipicolinic acid and its mixed ligand complexes with several nitrogen, oxygen donor molecules, of types: $Na[M(dipic)_2] \cdot 2H_2O$ and $[M(dipic)(N-O)] \cdot nH_2O$ (where $M = Ru(III)$, $Rh(III)$ or $Ir(III)$; $dipicH_2$ = dipicolinic acid; N–OH represents different nitrogen, oxygen donor molecules, viz., picolinic acid, nicotinic acid, isonicotinic acid, glycine, aminophenol, o- or p-aminobenzoic acid), have been synthesized and characterised on the basis of elemental analyses, electrical conductance, magnetic susceptibility measurements and spectral (electronic and infrared) data. The parent dipicolinic acid complexes are found to have a six-coordinate pseudooctahedral structure, whereas for mixed ligand complexes, a polymeric six-coordinate structure has been assigned. Various ligand field and nephelauxetic parameters have also been evaluated.

Dipicolinic acid or pyridine 2,6-dicarboxylic acid is a versatile ligand and it can function as a neutral, monobasic or dibasic tridentate chelating agent. A large number of bivalent or trivalent transition metal and lanthanide(III) complexes of dipicolinic acid have been studied.[1–4] Recently, some cobalt(II) and cobalt(III) complexes of dipicolinic acid have been synthesized to explore the possibility of their use as models to explain some intricate reactions in biological systems.[5, 6] The reactions of acetylacetonates of cobalt(II), nickel(II), iron(III) and manganese(III) with dipicolinic acid have also been carried out to obtain complexes of unusual structure.[7, 8]

However, no systematic study of mixed ligand complexes of trivalent metal ions with dipicolinic acid as primary ligand together with bidentate ligands appears to have been carried out. It is, therefore, of interest to synthesize such complexes, with a view to obtaining five-coordinate ruthenium(III), rhodium(III) and iridium(III) complexes, which occur rarely. The various nitrogen, oxygen donor bidentate molecules selected for this work include picolinic acid (picH), nicotinic acid (nicH), isonicotinic acid (inicH), glycine (glyH), aminophenol (apH), o-aminobenzoic acid (oabH) and p-aminobenzoic acid (pabH). The complexes have been isolated in the solid state and structures have been assigned tentatively on the basis of their elemental analyses, and spectral and magnetic properties.

EXPERIMENTAL

The platinum metal salts used were obtained from Johnson Mathey Products, London. Commercial ruthenium trichloride, which contains some ruthenium(IV), was evaporated several times with concentrated hydrochloric acid to ensure conversion into ruthenium(III) chloride. The pyridine carboxylic acids, amino carboxylic acids and aminophenol used as ligands, were Analar grade (B.D.H. and E. Merck).

A common procedure has been adopted to prepare and isolate ruthenium(III), rhodium(III) and iridium(III) complexes.

Preparation of $Na[M(dipic)_2] \cdot 2H_2O(M = Ru(III)$ or $Ir(III)$; dipic H_2 = dipicolinic acid)

An ethanolic solution of the appropriate metal trichloride (0.01 mol) was added to a refluxing aqueous ethanolic solution of dipicolinic acid (0.02 mol) containing sodium hydroxide (0.01 mol). The refluxing was continued for ca. 2–4 hr. On concentrating the resulting solution, the coloured mass obtained was filtered, washed with water and dried in vacuo at room temperature.

Preparation of the mixed ligand complexes, $[M(dipic)(N-O)] \cdot nH_2O$ ($M = Ru(III)$, $Rh(III)$ or $Ir(III)$; N–OH represents secondary ligand)

All these complexes have been prepared by the following procedure. An aqueous ethanolic solution of the appropriate metal trichloride (0.01 mol) was added to an aqueous ethanolic solution of dipicolinic acid (0.01 mol). To this mixture was added the appropriate bidentate N,O donor compound (0.01 mol) and the solution was refluxed for ca. 4–8 hr; the coloured mass obtained was filtered, washed with ethanol and dried in vacuo at room temperature.

RESULTS AND DISCUSSION

The elemental analysis (Table 1) reveals 1:2 metal to ligand stoichiometry for the parent $M(III)$-dipicH_2 complexes, and it is 1:1:1 (metal:dipicH_2:N–O⁻) in the case of the mixed ligand complexes, where N–O⁻ represents a monobasic, bidentate nitrogen, oxygen donor molecule. The parent complexes are soluble in dimethylformamide, dimethylsulphoxide, nitrobenzene and partially soluble in ethanol and acetone, whereas mixed ligand complexes are partially soluble in dimethylformamide and dimethylsulphoxide. Thermogravimetric data indicate a loss of weight at 100–120°C corresponding to two water molecules for the parent complexes and one water molecule for the mixed ligand complexes of aminophenol, glycine, and o-and p-aminobenzoic acids, with all three metal ions. The mixed ligand complexes of ruthenium(III), rhodium(III) and iridium(III) with picolinic, nicotinic and isonicotinic acid do not show any weight loss up to 200°, indicating the absence of water molecules. The electrical conductance of the parent complexes, measured in dimethylformamide, show them to be essentially non-electrolytes. Accordingly, the parent and the mixed ligand complexes

Table 1. Analytical and magnetic data of the complexes

Complex	Colour	M.P. °C	Found(Calcd) % of C	H	N	M	μ_{eff} B.M. (300K)
1	2	3	4	5	6	7	8
Na[Ru(dipic)$_2$].2H$_2$O	Brown	140	34.2 (34.3)	1.8 (2.0)	5.1 (5.7)	20.2 (20.6)	1.72
[Ru(dipic)(pic)]	brown	220(d)	39.9 (40.2)	1.8 (1.8)	6.7 (7.2)	25.2 (26.0)	1.75
[Ru(dipic)(nic)]	brown	240(d)	40.2 (40.2)	1.7 (1.8)	7.0 (.7.2)	25.4 (26.0)	1.75
[Ru(dipic)(inic)]	brown	245(d)	40.1 (40.2)	1.7 (1.8)	7.0 (7.2)	25.3 (26.0)	1.75
[Ru(dipic)(gly)].H$_2$O	blackish brown	210(d)	30.0 (30.1)	2.2 (2.5)	7.2 (7.8)	27.5 (28.2)	1.80
[Ru(dipic)(ap)].H$_2$O	brown	170(d)	39.7 (39.8)	2.5 (2.8)	6.9 (7.1)	25.1 (25.8)	1.79
[Ru(dipic)(oab)].H$_2$O	black	250	39.7 (39.9)	2.4 (2.6)	6.2 (6.7).	23.4 (24.0)	1.76
[Ru(dipic)(pab)].H$_2$O	black	250	39.6 (39.9)	2.6 (2.6)	5.9 (6.7)	23.6 (24.0)	1.75
Na[Rh(dipic)$_2$].2H$_2$O	Orange	152	34.0 (34.1)	1.8 (2.0)	5.2 (5.7)	20.4 (20.9)	Diamag.
[Rh(dipic)(pic)]	Orange	245(d)	39.8 (40.0)	1.6 (1.8)	7.0 (7.2)	26.0 (26.4)	Diamag.
[Rh(dipic)(nic)]	Orange	248(d)	39.8 (40.0)	1.7 (1.8)	6.7 (7.2)	25.4 (26.4)	Diamag.
[Rh(dipic)(inic)]	Orange	240(d)	40.0 (40.0)	1.6 (1.8)	6.9 (7.2)	25.8 (26.4)	Diamag.
[Rh(dipic)(gly)].H$_2$O	Brown	170	29.9 (30.0)	2.4 (2.5)	7.1 (7.8)	28.0 (28.6)	Diamag.
[Rh(dipic)(ap)].H$_2$O	Brown	190(d)	39.4 (39.6)	2.5 (2.8)	6.7 (7.1)	25.7 (26.1)	Diamag.
[Rh(dipic)(oab)].H$_2$O	brownish orange	230(d)	39.6 (39.8)	2.6 (2.6)	6.4 (6.6)	24.2 (25.4)	Diamag.
[Rh(dipic)(pab)].H$_2$O	brownish orange	210(d)	39.5 (39.8)	2.6 (2.6)	6.1 (6.6)	23.7 (24.4)	Diamag.
Na[Ir(dipic)$_2$].2H$_2$O	red	130	29.7 (29.8)	1.2 (1.4)	4.7 (4.9)	33.5 (34.1)	Diamag.
[Ir(dipic)(pic)]	red	180(d)	32.5 (32.5)	1.4 (1.4)	5.6 (5.8)	39.5 (40.1)	Diamag.
[Ir(dipic)(nic)]	red	210(d)	32.5 (32.5)	1.3 (1.4)	5.2 (5.8)	39.8 (40.1)	Diamag.
[Ir(dipic)(inic)]	red	190(d)	32.4 (32.5)	1.2 (1.4)	5.4 (5.8)	39.6 (40.1)	Diamag.
[Ir(dipic)(gly)].H$_2$O	orange	160(d)	24.0 (24.0)	1.8 (2.0)	6.2 (6.2)	42.1 (42.1)	Diamag.
[Ir(dipic)(ap)].H$_2$O	red	187(d)	32.0 (32.2)	2.1 (2.2)	5.5 (5.7)	39.0 (39.7)	Diamag.
[Ir(dipic)(oab)].H$_2$O	orange	220(d)	32.8 (32.8)	2.0 (2.1)	5.0 (5.4)	36.8 (37.5)	Diamag.
[Ir(dipic)(pab)].H$_2$O	orange	232(d)	32.0 (32.8)	2.0 (2.1)	5.1 (5.4)	37.1 (37.5)	Diamag.

where dipicH$_2$ = dipicolinic acid or pyridine 2,6-dicarboxylic acid,
picH = picolinic acid, nicH = nicolinic acid,
inicH = isonicotinic acid, glyH = glycine, apH = aminophenol
oabH = o-aminobenzoic acid and pabH = p-amino benzoic acid

of ruthenium(III), rhodium(III) and iridium(III) can be formulated as $Na[M(dipic)_2] \cdot 2H_2O$ and $[M(dipic)(N-O)] \cdot nH_2O$, respectively. These formulations have been further corroborated on the basis of magnetic and spectral properties of these complexes.

Magnetic moments and electronic spectra

Ruthenium(III) complexes. The room temperature magnetic moments of the ruthenium(III) complex of dipicolinic acid and of the mixed ligand complexes lie in the range 1.75–1.80 B.M. (Table 1), which are lower than the predicted value[9] of 2.10 B.M. The lowering in μ_{eff} values may arise due to low symmetry ligand fields, metal–metal interactions or extensive electron delocalization.[10]

The electronic spectra of the ruthenium(III) complex of dipicolinic acid and its mixed ligand complexes show bands at *ca.* 13000–14000, 17000–18000 and 22000–23000 cm^{-1} which may be assigned[11-14] to $^2T_{2g} \rightarrow {}^4T_{1g}$, $^2T_{2g} \rightarrow {}^4T_{2g}$ and $^2T_{2g} \rightarrow {}^2A_{2g}, {}^2T_{1g}$ transitions, in increasing order of energy.

The electronic spectra of these complexes are further rationalised[12] in terms of ligand field parameters (10 Dq) and interelectronic repulsion parameters (B and C). The values of these parameters along with that of β given in Table 2, are comparable to those reported for other ruthenium(III) derivatives involving nitrogen, oxygen donor molecules.[11,14,15] The B values are about 74–86% of the free ion value in the ruthenium(III) complexes. The considerable decrease in the value of the Racah

Table 2. Electronic spectral data

Complex 1	Bands observed 2 cm^{-1}	Assignments 3	ν_2/ν_1 4	10 Dq cm^{-1} 5	B cm^{-1} 6	C cm^{-1} 7	β 8
$Na[Ru(dipic)_2] \cdot 2H_2O$	13500	$^2T_{2g} \rightarrow {}^4T_{1g}$					
	17200	$^2T_{2g} \rightarrow {}^4T_{2g}$	1.27	26362.5	462.5	2637.5	0.74
	22800	$^2T_{2g} \rightarrow {}^2A_{2g}, {}^2T_{1g}$					
$[Ru(dipic)(pic)]$	13700 17600 22600	–do–	1.28	26053.9	487.5	2479.1	0.78
$[Ru(dipic)(nic)]$	13650 17600 22700	–do–	1.29	26259.7	493.7	2522.8	0.78
$[Ru(dipic)(inic)]$	13600 17800 22600	–do–	1.30	26300	540	2500	0.86
$[Ru(dipic)(gly)] \cdot H_2O$	1300 17100 22000	–do–	1.32	23000	520	2500	0.83
$[Ru(dipic)(ap)] \cdot H_2O$	14000 18000 22800	–do–	1.28	26233.2	500	2433.3	0.80
$[Ru(dipic)(oab)] \cdot H_2O$	1300 17200 23000	–do–	1.32	26633.2	540	2733.3	0.86
$[Ru(dipic)(pab)] \cdot H_2O$	13100 17300 22800	–do–	1.32	26733.2	540	2733.2	0.86
$Na[Rh(dipic)_2] \cdot 2H_2O$	1800	$^1A_{1g} \rightarrow {}^3T_{1g}$					
	20200	$^1A_{1g} \rightarrow {}^1T_{1g}$	1.12	21300	256.2	1100	0.35
	24300	$^1A_{1g} \rightarrow {}^1T_{2g}$					
$[Rh(dipic)(pic)]$	17000 20000 25000	–do–	1.17	21500	312.5	1500	0.43
$[Rh(dipic)(nic)]$	17200 20100 24800	–do–	1.16	21550	293.7	1450	0.40
$[Rh(dipic)(inic)]$	17000 20000 25000	–do–	1.17	21500	312.5	1500	0.43

Table 2 (*Contd.*)

1	2	3	4	5	6	7	8
[Rh(dipic)(gly)].H$_2$O	18000 22000 26000	–do–	1.22	24000	250	2000	0.34
[Rh(dipic)(ap)].H$_2$O	17000 24000	–do–	–	–	–	–	–
[Rh(dipic)(oab)].H$_2$O	17800 20100 24800	–do–	1.39	21250	293.7	1150	0.40
[Rh(dipic)(pab)].H$_2$O	17500 20200 24800	–do–	1.15	21550	287.5	1350	0.39
Na[Ir(dipic)$_2$].2H$_2$O	23500	$^1A_{1g} \rightarrow {}^3T_{1g}$					
	30000	$^1A_{1g} \rightarrow {}^1T_{1g}(\nu_1)$	1.12	30873	219	876	0.33
	33500	$^1A_{1g} \rightarrow {}^1T_{2g}(\nu_2)$					
[Ir(dipic)(pic)]	30800 34000	–do–	1.10	31600	200	800	0.33
[Ir(dipic)(nic)]	30800 34200	–do–	1.08	30848	212	848	0.32
[Ir(dipic)(inic)]	31500 34000	–do–	1.08	32372	218	872	0.33
[Ir(dipic)(gly)].H$_2$O	24200 30200 33000	–do–	1.09	30900	175	700	0.27
[Ir(dipic)(oab)].H$_2$O	32000 33800	–do–	1.06	32448	112	448	0.19
[Ir(dipic)(pab)].H$_2$O	31700 33600	–do–	1.06	32176	119	476	0.18
[Ir(dipic)(m-ap)].H$_2$O	30000 33800	–do–	1.13	30948	237	948	0.35

interelectronic repulsion parameter B from that of the free ion suggests that strong covalent bonding occurs between the ligands and the metal atom.[12] The overall effect of some covalent bonding will be an increase in the observed value of Dq; high values of Dq are usually associated with considerable electron delocalization.[10]

Rhodium(III) complexes. Rhodium(III) complexes are diamagnetic as expected. This is consistent with an octahedral arrangement of the donor atoms around the metal ions, producing a strong field.[9]

The electronic spectra of rhodium(III) complexes show bands at *ca.* 17000–17800, 20000–21000 and 24000–25000 cm^{-1}. These spectra resemble those of other six-coordinate rhodium(III) complexes[12, 15–17] and may be assigned[18] to $^1A_{1g} \rightarrow {}^3T_{1g}$, $^1A_{1g} \rightarrow {}^1T_{1g}$ and $^1A_{1g} \rightarrow {}^1T_{2g}$ transitions, in increasing order of energy. The electronic spectra of these d^6 complexes can be used[19] to evaluate ligand field and nephelauxetic parameters: values of 10 Dq, B and β thus calculated are given in Table 2. The values are comparable to those observed for other complexes of this metal ion with nitrogen and oxygen donor ligands[15, 16, 18]. The B values are of the order of 34–43% of the free ion values, suggesting considerable orbital overlap with strong covalency in the metal-ligand σ-bond. The decreasing values of B are associated with a reduction in the effective positive charge of the metal ion and with an increasing tendency to be reduced to the next lower oxidation state.

Iridium(III) complexes. The iridium(III) complexes are diamagnetic, with donor atoms producing a strong octahedral field.[18]

The mull spectra of these complexes show bands in the 30000–32000 and 33000–34000 cm^{-1} regions (Table 2) which can be assigned[18] to $^1A_{1g} \rightarrow {}^1T_{1g}(\nu_1)$ and $^1A_{1g} \rightarrow {}^1T_{2g}(\nu_2)$ transitions in increasing order of energy. In some of the complexes, an additional band is also observed at *ca.* 23500–24200 cm^{-1} which can be assigned[12] to a $^1A_{1g} \rightarrow {}^3T_{1g}$ transition. The ratios of ν_2 and ν_1 in the iridium(III) complexes lie in the range 1.06–1.13. These values for the present complexes having the chromophore IrN$_2$O$_4$ are slightly lower than those observed[19, 20] for IrN$_3$X$_3$ and IrO$_3$X$_3$(X = Cl, Br, I) chromophores (1.10–1.20). This is expected in view of the different positions of these donor atoms in the spectrochemical series.[12] The two transitions ν_1 and ν_2 have been used[19] to evaluate the ligand field (10 Dq or Δ) and

nephelauxetic (B) parameters. The values of these parameters along with that of β (covalency parameters) are given in Table 2, and are comparable to those reported for other iridium(III) complexes involving similar donors.[18, 20] The B values are about 18–35% of the free ion value (660 cm^{-1}). This can be taken as an indication of considerable overlap with significant covalency in the metal–ligand σ-bond.

IR spectra. The IR spectrum of dipicolinic acid shows two bands at *ca.* 1700 and 1300 cm^{-1} due to $\nu_{asym}(COO)$ and $\nu_{sym}(COO)$ vibrations, respectively. In the mixed ligand complexes, these two bands appear at *ca.* 1600–1580 and 1460–1430 cm^{-1}, respectively, indicating the involvement of the carboxylic group in bond formation with metal.[21, 22] This is also supported by the appearance of new bands at 340–300 cm^{-1}, assignable to $\nu(M–O)$ vibrations.[23, 24] However, it is worth noting that the lowering (*ca.* 100 cm^{-1}) of $\nu_{asym}(COO)$ (which is mainly due to $\nu(C=O)$ of the COOH group) and also the difference $\Delta\nu = \nu_{asym}(COO) - \nu_{sym}(COO) \sim 150$ cm^{-1} are considerable, which clearly indicates that the $\diagdown$C=O moiety of the –COOH group is also coordinated to the metal atom, resulting from loss of electrons on coordination.[8] This situation (I) is similar to that observed by Nakamoto *et al.*[25] in $[Cu_2(OAc)_4] \cdot 2H_2O(II)$ and later explained by Lever *et al.*[26]
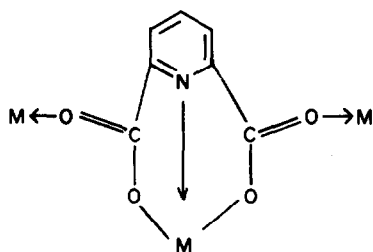
(I)
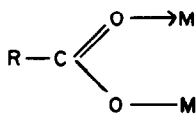
(II)

However, in the parent dipicolinic acid complexes, the shift of the $\nu_{asym}(COO)$ band is of the order of 40–30 cm^{-1}, excluding the possibility of coordination of the $\diagdown$C=O group to an other metal atom.[27] In different pyridine or aminocarboxylic acids, these two bands appear at *ca.* 1710–1690 and 1340–1320 cm^{-1}. On complexation these bands also show similar type of changes as in the parent dipicolinic acid complex, indicating that the carboxylic group coordinates to the metal atom.

The infrared spectrum of *m*-aminophenol shows one band at 3350 cm^{-1} which may be assigned to $\nu(OH)$. However, in its mixed ligand complexes, this band disappears completely, indicating the bond formation of phenolic oxygen to metal through deprotonation.[28] In the

mixed ligand complexes of amino acids and aminophenol the shift of the $\nu(NH)$ band, which occurs at *ca.* 3300–3100 cm^{-1} in the ligands to lower frequency (~ 100 cm^{-1}) indicates the amino group coordination to the metal atom.[28] This has been confirmed by the appearance of a new band in the far infrared region at 460–420 cm^{-1} which may be assigned to a $\nu(M–N)$ vibration.[24]

Ligands containing the pyridine ring show bands at *ca.* 1610–1570, 630–590 and 430–390 cm^{-1} which may be assigned to 8a or 8b (ring deformation), 6a (in-plane deformation) and 16b (out-of-plane deformation) vibrations,[29, 30] respectively. In the complexes, these bands show an upward shift (~ 20 cm^{-1}) and in some cases the splitting of the 6a band has also been observed. The upward shift and splitting of 6a and 16b bands are consistent with coordination of the pyridine nitrogen to a metal atom[30, 31]. The bands due to $\nu(M–Py)$ are located at 280–255 cm^{-1}. In addition to the above, the parent complex of dipicolinic acid and mixed ligand complexes of *m*-aminophenol, *o*- and *p*-aminobenzoic acids and amino acetic acid show one broad band at *ca.* 3450 cm^{-1} which may be assigned to $\nu(OH)$ of the water present in the lattice.[28]

Thus, on the basis of above discussion it appears that the mixed ligand complexes are polymeric in nature, as is also supported by their limited solubility in organic solvents, and each unit of polymeric structure possesses a pseudo-octahedral stereochemistry. The electronic spectra of these complexes which are typical of octahedral ruthenium(III), rhodium(III) and iridium(III) also corroborate a polymeric structure. The $\diagdown$C=O moiety of the COOH group appears to provide the sixth coordination sites, three being provided by dipicolinic acid $(N, O^-, \bar{O})$ and two $(N, \bar{O})$ being provided by the monobasic, bidentate ligands, making these complexes polymeric. Thus the tentative structure of these complexes can be depicted as follows:
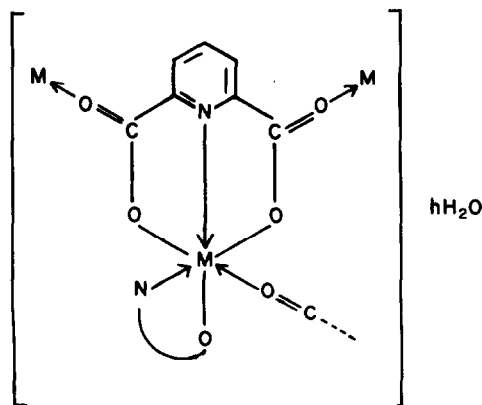
M = Ru (III), Rh(III) or Ir (III); n = 0 or 1

However, the parent complexes appear to be monomeric. If they are assigned a structure similar to that suggested for mixed ligand complexes, they would have seven-coordinate units; however this is ruled out by the electronic spectra, which support a six-coordinated structure. A polymeric structure for the parent complexes can also be ruled out on the basis of steric

arguments. Their structure can, therefore, be tentatively depicted as follows:
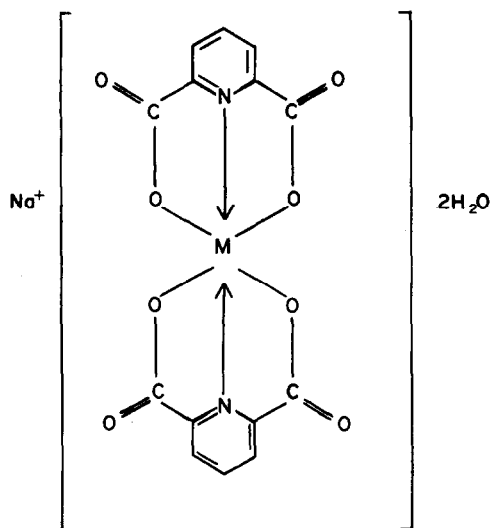
M = Ru(III), Rh(III) or Ir(III).

REFERENCES

[1] U. Casellato and P. A. Vigato, *Coord. Chem. Rev.* 1978, **26**, 85.
[2] G. D'Ascenzo, A. Marino, M. Sabbatini and T. Bica, *Thermochim. Acta* 1978, **25**, 325.
[3] S. Ghosh, T. K. Banerjee and P. K. Ray, *J. Indian Chem. Soc.* 1978, **55**, 610.
[4] W. Furst, P. Gouzenh and Y. Jeannin, *J. Coord. Chem.* 1978, **8**, 237.
[5] A. G. Mank, C. L. Coyle, E. Bordignon and H. B. Gray, *J. Am. Chem. Soc.* 1979, **101**, 5054.
[6] P. C. Harrington and R. G. Wilkins, *J. Inorg. Biochem.* 1980, **12**, 107.
[7] R. W. Matthews, A. D. Hamer, D. L. Hoof, D. G. Tisley and R. A. Walton, *J. Chem. Soc. Dalton Trans.* 1973, 1035.
[8] D. L. Hoof and R. A. Walton, *Inorg. Chim. Acta* 1975, **12**, 71.
[9] J. Lewis and B. N. Figgis, *Prog. Inorg. Chem.* 1964, **6**, 105.
[10] S. E. Livingstone, J. H. Mayfield, D. S. Moore, *Aust. J. Chem.* 1975, **28**, 2531.
[11] R. W. Olliff and A. L. Odell, *J. Chem. Soc.* 1964, 2467.
[12] A. B. P. Lever, *Inorganic Electronic Spectroscopy.* Elsevier, Amsterdam (1968).
[13] Y. Tanabe and S. Sagano, *J. Phys. Soc. Japan* 1954, **9**, 766.
[14] M. R. Gajendragad and U. Agarwala, *J. Inorg. Nucl. Chem.* 1975, **37**, 2429.
[15] J. S. Dwivedi and U. C. Agrawala, *Indian J. Chem.* 1972, **10**, 657.
[16] E. Bertelli, C. Preti and G. Tosi, *J. Inorg. Nucl. Chem.* 1975, **37**, 1421.
[17] B. N. Figgis, *Introduction to Ligand Fields.* Wiley Eastern Ltd., New Delhi (1976).
[18] C. Preti and G. Tosi, *Transition Met. Chem.* 1978, **3**, 17.
[19] C. K. Jørgensen, *Prog. Inorg. Chem.* 1962, **4**, 73.
[20] C. K. Kalia and A. Chakravarty, *Inorg. Chem.* 1969, **8**, 2586.
[21] J. Michel and R. A. Walton, *J. Inorg. Nucl. Chem.* 1975, **37**, 71.
[22] V. Kumari, S. K. Sahni, S. Kher and R. N. Kapoor, *Synth. React. Inorg. Met. Org. Chem.* 1979, **9**, 409.
[23] D. M. Adams, *Metal Ligand and Related Vibrations.* E. Arnold, London (1967).
[24] J. R. Ferraro, *Low-Frequency Vibrations of Inorganic and Coordiantion Compounds.* Plenum Press, New York (1971).
[25] K. Nakamoto, J. Fujita, S. Tanaka and M. Kobayashi, *J. Am. Chem. Soc.* 1957, **79**, 4904.
[26] A. B. P. Lever, J. Lewis and R. S. Nyholm, *J. Chem. Soc.* 1962, 5262.
[27] J. D. Donaldson, J. F. Knifton and S. D. Ross, *Spectrochim. Acta* 1965, **21**, 275.
[28] K. Nakamoto, *Infrared Spectra of Inorganic and Coordination Compounds.* Wiley, New York (1970).
[29] R. J. H. Clark and C. S. Williams, *Inorg. Chem.* 1965, **4**, 350.
[30] D. P. Madden, M. M. daMota and S. M. Nelson, *J. Chem. Soc.* (A), 1970, 790.
[31] S. Kher, S. K. Sahni, V. Kumari and R. N. Kapoor, *Inorg. Chim. Acta*, 1979, **37**, 121.

AN EXAMINATION OF THE RELATIONSHIP BETWEEN THE X-RAY DIFFRACTION-DERIVED MOLECULAR STRUCTURE OF CHLORO (1,11-DIAMINO-3,6,9-TRITHIAUNDECANE)COBALT(III) CATION AND ITS INNER SPHERE REDUCTION BY IRON(II)

JAMES D. KORP and IVAN BERNAL*
Chemistry Department, University of Houston, Houston, TX 77004, U.S.A.

and

JAY H. WORRELL*
Chemistry Department, University of South Florida, Tampa, FL 33620, U.S.A.

Abstract—The crystal structure of racemic $[Co(NSSSN)Cl](ClO_4)Cl$ was determined by X-ray diffraction methods. It crystallizes in the monoclinic system, space group $P2_1/c$, with cell constants of $a = 9.795(3)$, $b = 10.412(3)$ and $c = 16.323(8)$ Å and $\beta = 93.87(4)°$; $V = 1661$ Å^3 d (meas.; flotation) $= 1.85$ gm-cm^{-3}, d (calc.; $Z = 4$ molecules/unit cell) $= 1.88$ gm-cm^{-3}. The molecules, a racemic mixture, have the absolute configurations $\lambda\lambda\delta\lambda$ or $\delta\delta\lambda\delta$ at each of the four five-membered rings and resémble, in general, the so called $\alpha\alpha$ conformer already described by Snow[1] in his study of the Co(tetraen)Cl^{2+} cation. However, the torsional angles at C2, C3 and C8, C9 in the two terminal C–C–NH$_2$ fragments are quite different in the two systems. For Co(tetraen)Cl^{2+} they are 44.7° and −20.2° respectively, whereas for Co(NSSSN)Cl^{2+} the values −52.3° and −44.6° obtain. Also, the ring Co–S1–C3–C2–N1 does not have the classical, low energy conformation found in Co(tetraen)Cl^{2+}. The presence of the larger Co–S bonds causes the two terminal –NH$_2$ groups to be pushed toward each other, and to minimize steric hindrance between adjacent –NH$_2$ hydrogens and ligand twists C2 down and staggers the terminal hydrogens. We visualize the propagation of these distortion effects in solution as being transferred from one side to the other across the entire ligand chain with concomitant effects on the activation of the precursor complex in electron transfer reactions, resulting in ~10^7 rate enhancement over the Co(tetraen)Cl^{2+} system. Kinetic data for the reduction of Co(NSSSN)X^{2+} and Co(NSNSN)X^{2+} (X = Cl$^-$, Br$^-$) by Fe(II) is also presented and discussed.

From a crystallographic standpoint, it is challenging to study the geometrical details of substances which, though closely related in composition and even stereochemistry, are sufficiently different so that other physical properties, such as reactivity, rates of electron transfer and/or ligand exchange, etc... differ by significant orders of magnitude. The hope is, of course, that stereochemically significant changes in these substances can be assigned as the origin of the alteration of properties under consideration. Such is the case of previous work we have conducted in collaboration with Prof. Dobson in elucidating the stereochemical reasons for changes in the rates of ligand exchange in metal carbonyls.[2,3] The availability of data on the pair of related substances [Co(NSSSN)Cl](ClO$_4$)Cl and [Co(tetraen)Cl](ClO$_4$)Cl[1], where NSSSN = 1,11 - diamino - 3,6,9 - trithiaundecane and tetraen = 1,3,6,9,11 - pentaazaundecane, now permits their comparison as well. Based on all available chemical evidence[4,5] we inferred that the so-called $\alpha\alpha$ conformer is present in the NSSSN, as in Snow's[1] compound. One perplexing question related to Co(NSSSN)Cl^{2+} and Co(tetraen)Cl^{2+} was, why is Co(NSSSN)Cl^{2+} reduced by Fe(II) at a rate ~10^7 times faster than the amine analog if they both possess the same geometry? Is this rate enhancement due to a structural *trans* effect as being researched by Deutsch *et al.*[6,7] for Co(en)$_2$X$_2$$^{n+}$ type

complexes, or is it due to an electronic ground state effect due to the nature and presence of the thioether donors as suggested earlier,[8,9] or is there a structural driving force that promotes activation of the Co(NSSSN)Cl^{2+} complex?

In this work we report and discuss the results of an X-ray structural determination for [Co(NSSSN)Cl](ClO$_4$)Cl in conjunction with several kinetic studies involving the Fe(II) reduction of octahedral cobalt(III) complexes derived from both N–S–S–S–N and N–S–N–S–N type pentadentate ligands.

EXPERIMENTAL

X-Ray study

Crystals of [Co(C$_8$H$_{20}$N$_2$S$_3$)Cl](ClO$_4$)Cl were grown from an aqueous HClO$_4$ solution of recrystallized [Co(NSSSN)Cl] [ZnCl$_4$]. The crystal structure was determined from 3891 reflections collected by X-ray diffraction methods using a computer-controlled diffractometer equipped with a Mo-target tube whose radiation was monochromatized by a dense graphite crystal. Table 1 summarizes the experimental data collection and processing parameters. Tables of atomic positional and thermal parameters and F$_0$/F$_c$ values have been deposited as supplementary data with the Editor, from whom copies are available on request.†

Materials

All common laboratory chemicals were of reagent grade. Stock solutions of aqueous iron(II) perchlorate, perchloric acid and lithium perchlorate were prepared using triply distilled water and standardized using methodologies reported earlier.[10] The complexes [Co(NSNSN)Cl](ClO$_4$)$_2$, [Co(NSNSN)Br](ClO$_4$)$_2$, [Co(NSSSN)Cl](ClO$_4$)$_2$, and [Co(NSSSN)Br](ClO$_4$)$_2$ were pre-

---

*Authors to whom correspondence should be addressed.

†Atomic coordinates have also been deposited with Cambridge Crystallographic Data Centre.

Table 1. Summary of data collection and processing parameters

Space Group	$P2_1/c$, monoclinic
Cell Constants	$a = 9.795(3)$ Å
	$b = 10.412(3)$
	$c = 16.323(8)$
	$\beta = 93.87(4)°$
	$V = 1661$ Å^3
Molecular Formula	$CoCl_3S_3O_4N_2C_8H_{20}$
Molecular Weight	469.74
Molecules per Cell	$Z = 4$
Density (calc.)	$\rho_c = 1.88$ g-cm^{-3}
Density (meas.)	$\rho_m = 1.85$ g-cm^{-3}
Absorption Coefficient	$\mu = 18.0$ cm^{-1}
Radiation (MoKα)	$\lambda = 0.71073$ Å
Collection Range	$4° \leq 2\theta \leq 60°$
Scan Width	$\Delta\theta = (1.00+0.35 \tan \theta)°$
Maximum Scan Time	240s
Scan Speed Range	0.4 to 5.0° min^{-1}
Total Data Collected	5225
Independent Data with $I>3\sigma(I)$	3891
Total Variables	270
R $\quad$ $\Sigma \left\| \left\|F_o\right\| - \left\|F_c\right\| \right\| / \Sigma \left\|F_o\right\|$	0.030
R $\quad$ $[\Sigma_w (\left\|F_o\right\| - \left\|F_c\right\|)^2 / \Sigma_w \left\|F_o\right\|^2]^{\frac{1}{2}}$	0.031
Weights	$\sigma(F)^{-2}$

pared as reported in the literature.[4,11,12] All complexes ($\Delta_m = 190-225 \, \Omega^{-1} \, cm^2$) were recrystallized from dilute HClO$_4$–NaClO$_4$ and their C, H, N, and S analyses, as determined by Chemalytics Inc. of Tempe, Arizona, verify the above analytical formulations.

Kinetic procedures

Predetermined volumes of deoxygenated stock solutions were delivered into a 5.0 cm cell under argon and the cell allowed to equilibrate at the desired temperature. Thermostated iron(II) solution was then added to the cell by syringe. The cell was shaken and absorption measurements using a Cary-14 were begun. Temperature was maintained at ±0.1°C and monitored using the apparatus described previously.[10]

Pseudo-first-order conditions were maintained by having iron(II) consumption less than 10% of the total iron(II). Rate constants were obtained from computer calculated least-squares slopes of plots of ln $(D_t - D_x)$ vs time. Such plots were found to be linear over 95% reaction. Data were collected by having triplicate determinations for k_t at any given set of conditions. The error limits reported are standard deviations. Reactions were followed at λ_{max} for the low energy d–d envelope observed for each complex. Visible UV Spectral characteristics $\lambda_{max}(\epsilon)$ are as follows: Co(NSNSN)Cl^{2+}, 565(207), 505(159), 278(15,260); Co(NSNSN)Br^{2+}, 586(242), 505(148), 281(21,950); Co(NSSSN)Cl^{2+}, 548(351), 380(390), 288(15,440); Co(NSSSN)Br^{2+}, 566(364), 370(790), 299(14,960).

RESULTS AND DISCUSSION

Structure description of [Co(NSSSN)Cl]ClO$_4$)Cl

As can be seen in Fig. 1, the Co(NSSSN)Cl^{2+} cation closely resembles the $\alpha\alpha$ isomer of Co(tetraen)Cl^{2+} which was investigated by Snow,[1] in that the central

sulfur donor (S2) is the one *trans* to chlorine. The absolute configuration shown in Fig. 1 is designated $\lambda\lambda\delta\lambda$ (starting from N1) according to IUPAC convention,[13] although the $\delta\delta\lambda\delta$ racemate is also present in the lattice since the compound was unresolvable[4] and crystallizes in a centrosymmetric space group. A tabulation of bond distances is presented in Table 2, and intramolecular bond angles are given in Table 3. The averages of the essentially chemically equivalent bond distances in Table 2 are as follows: Co–S = 2.235(1), Co–N = 1.973(2), C–S = 1.820(3), C–N = 1.489(4), C–C = 1.499(4) Å. Two of the C–S bonds, namely S1–C4 and S3–C7, are markedly shorter than the other four, and since they are in similar positions in the ligand one is tempted to suggest and assign some electronic phenomenon to this observation. In this case however, there is no such ready explanation available. Excluding the bonds to sulphur, the remaining bond averages are insignificantly different from those reported by Snow,[1] and also from those found in other related compounds both with sulphur ligands[7,16] and without.[14,15] The Co–S distances are in good agreement with previous results,[7,16] and there is no indication of any *trans* effect in either the Co–S2 bond or the Co–N bonds. In compounds exhibiting a structural *trans* effect, the Co–N bond length increases to about 2.00 Å. Also, according to Deutsch *et al.*, only in those ligands where the sulfur atom carries a formal negative charge will a significant *trans* effect be observed upon chelation,[17] and this is not the case in the present compound. The Co–Cl

Fig. 1. Stereoscopic view of the cation showing the atom labelling scheme. Hydrogens are numbered the same as the atom to which each is attached. Non-hydrogens are shown as 50% equi-probability envelopes, and hydrogens as spheres of arbitrary diameter. Note the $\lambda\lambda\delta\lambda$ configuration of the ligand (starting from N1).

Table 2. Intramolecular bond distances (Å)

Co-S1	2.241(1)	C9-N10	1.495(4)
Co-S2	2.236(1)	N1-H1A	0.95(3)
Co-S3	2.229(1)	N1-H1B	0.92(3)
Co-Cℓ1	2.268(1)	C2-H2A	0.91(3)
Co-N1	1.968(2)	C2-H2B	0.99(3)
Co-N10	1.978(2)	C3-H3A	0.90(3)
Cℓ2-O1	1.414(2)	C3-H3B	0.85(3)
Cℓ2-O2	1.427(2)	C4-H4A	1.01(3)
Cℓ2-O3	1.422(2)	C4-H4B	0.98(3)
Cℓ2-O4	1.415(3)	C5-H5A	0.94(3)
N1-C2	1.483(3)	C5-H5B	1.01(3)
C2-C3	1.494(4)	C6-H6A	0.95(3)
C3-S1	1.823(3)	C6-H6B	1.10(3)
S1-C4	1.813(3)	C7-H7A	0.93(3)
C4-C5	1.497(4)	C7-H7B	0.98(3)
C5-S2	1.825(3)	C8-H8A	0.97(3)
S2-C6	1.826(3)	C8-H8B	0.97(3)
C6-C7	1.502(4)	C9-H9A	0.95(3)
C7-S3	1.808(3)	C9-H9B	1.07(3)
S3-C8	1.823(3)	N10-H10A	0.90(3)
C8-C9	1.503(4)	N10-H10B	0.91(3)

bond distances in $Co(NSSSN)Cl^{2+}$ and $Co(Tetraen)Cl^{2+}$ are 2.268(1) and 2.263(3) Å respectively, eliminating the idea of a sulfur induced structural *trans* effect influencing the reactivity of groups positioned across the octahedron from sulfur.

The crystal lattice structure $[Co(NSSSN)Cl](ClO_4)Cl$ is held together by an extensive system of hydrogen bonding which can be seen in Figs. 2 and 3. The close intermolecular contacts are listed in Table 4. Both the chloride and the perchlorate anions, separately, bridge adjacent cations through the amino hydrogens. The perchlorate anion links pairs of cations, and these pairs

are themselves linked by pairs of chlorides into infinite chains parallel to the *a* axis. The separate chains are segregated from one another by C–H/C–H repulsions, although there may be some weak electrostatic attractions between the perchlorate oxygen lone pairs and the empty *d* orbitals on the sulfurs. These contact distances are listed in Table 4, and the orientation of the S1 and S3 atoms to O4 can be seen in the two packing diagrams. The O1 type oxygens and the ligated chlorine atoms serve no role in the intricate hydrogen bonding scheme.

Since chemical reactivity studies have shown appreciable differences between $Co(NSSSN)Cl^{2+}$ and

Table 3. Intramolecular bond angles (°)

Cℓ1-Co-S1	89.7(1)	C2-C3-S1	107.9(2)
Cℓ1-Co-S2	176.0(1)	C3-S1-C4	101.0(1)
Cℓ1-Co-S3	85.1(1)	Co-S1-C3	98.7(1)
Cℓ1-Co-N1	90.3(1)	Co-S1-C4	104.9(1)
Cℓ1-Co-N10	88.7(1)	S1-C4-C5	111.8(2)
S1-Co-S2	90.0(1)	C4-C5-S2	113.2(2)
S1-Co-S3	94.3(1)	C5-S2-C6	103.3(1)
S1-Co-N1	87.3(1)	Co-S2-C5	104.3(1)
S1-Co-N10	176.3(1)	Co-S2-C6	104.9(1)
S2-Co-S3	90.9(1)	S2-C6-C7	114.2(2)
S2-Co-N1	93.6(1)	C6-C7-S3	114.3(2)
S2-Co-N10	91.8(1)	C7-S3-C8	103.7(2)
S3-Co-N1	175.2(1)	Co-S3-C7	104.9(1)
S3-Co-N10	88.9(1)	Co-S3-C8	97.9(1)
N1-Co-N10	89.4(1)	S3-C8-C9	112.4(2)
Co-N1-C2	111.8(2)	C8-C9-N10	109.4(2)
N1-C2-C3	109.3(2)	C9-N10-Co	114.6(2)

Fig. 2. Stereoscopic view of the molecular packing in the unit cell, as viewed along the *b*-axis. Only the amino hydrogens are shown, with thin lines indicating the hydrogen bonding contacts. Note how two chlorine atoms bridge the pair of cations in the right-rear portion of the unit cell.

Co(tetraen)Cl^{2+}, it is of interest to compare the major structural features of the two complexes for a possible explanation. To this end we employed a program written by Liu[18] to produce Fig. 4, which overlays the two cations by minimizing the Co, Cl, N1 and N10 distances. It is quickly seen that the basic framework involving the sulfurs of NSSSN and the -NH groups of tetraen are the same, given the longer Co–S bond length. The two terminal C–C–N fragments, however, are quite different in the two molecules. In the tetraen complex, the C2, C3 and C8, C9 torsion angles are 44.7° and −20.2°, respectively, while in the NSSSN compound the corresponding angles are −52.3° and −44.6°. A comparison of selected torsion angles for both molecules is presented in Table 5. The differences in both sign and magnitude of rotation are important, showing that Co(NSSSN)Cl^{2+} is somewhat more buckled, and with the opposite sense with regard to C2, C3. The configuration of Co(tetraen)Cl^{2+} is

Fig. 3. Stereoscopic view of the packing as viewed along the *a*-axis. Note how two perchlorates bridge the pair of cations in the right center portion of the cell.

Table 4. Hydrogen bonding parameters and close S ... O contacts

A1, B, A2	B-A1	B...A2	A1...A2	A1-B...A2
N1, H1A, Cℓ3	0.95(3)Å	2.31(3)Å	3.285(3)Å	168(2)°
N1, H1B, Cℓ3	0.92(3)	2.62(3)	3.452(3)	146(2)
N1, H1B, O2	0.92(3)	2.74(3)	3.245(4)	114(2)
N10, H10A, O3	0.90(3)	2.67(3)	3.375(4)	135(2)
N10, H10B, O2	0.91(3)	2.34(3)	3.211(4)	157(3)
N10, H10B, O3	0.91(3)	2.85(3)	3.375(4)	128(2)
Cℓ2, O4, S1	1.415(3)	3.518(3)	4.884(2)	165(1)
Cℓ2, O4, S3	1.415(3)	3.361(3)	4.495(2)	137(1)

Fig. 4. Stereoscopic comparison of Co(NSSSN)Cl^{2+} [larger circles] with Co(tetraen)Cl^{2+} [smaller circles]. The view and the labelling are the same as in Fig. 1. Note the difference in conformation between the two compounds at C2 and C3.

Table 5. Comparison of selected torsion angles (°)

Angle	This Work	Ref. 1*
Co-N1-C2-C3	53.3	-27.6
N1-C2-C3-S1	-52.3	44.7
C2-C3-S1-C4	135.2	80.3
C3-S1-C4-C5	-67.4	-91.8
S1-C4-C5-S2	-45.6	-39.8
C4-C5-S2-C6	-76.2	-86.8
C5-S2-C6-C7	83.4	87.4
S2-C6-C7-S3	37.9	43.1
C6-C7-S3-C8	71.4	89.5
C7-S3-C8-C9	-81.0	-93.0
S3-C8-C9-N10	-44.6	-20.2
C8-C9-N10-Co	42.2	-0.1

*The signs of the angles have all been reversed for purposes of comparison, since the two molecules are of opposite chirality.

$\delta\lambda\delta\lambda$ instead of $\lambda\lambda\delta\lambda$ as found in $Co(NSSSN)Cl^{2+}$. The main consequence of this divergence in configuration of the Co-S1-C3-C2-N1 ring is to effectively stagger the terminal amino hydrogen atoms of NSSSN, while they remain eclipsed in tetraen. The reason behind the divergence is most probably the longer Co-S bond distance, which forces the amino hydrogen atoms more toward each other. To relieve this interaction the ligand twists C2 down and staggers the terminal hydrogens. By manipulating an accurate scale model of aa-$Co(NSSSN)Cl^{2+}$ into the $\delta\lambda\delta\lambda$ configuration,[19] there appears to be an even more strained contact between H2A and H5A than between H1B and H10B, and this certainly accentuates the driving force toward the $\lambda\lambda\delta\lambda$ configuration.

This structure determination is in accord with our earlier aa geometric assignment for complexes of $Co(NSSSN)X^{2+}$ based then on indirect chemical evidences. Although we as yet have not been able to grow $[Co(NSNSN)Cl](ClO_4)_2$ crystals of suitable quality for a structure determination, we are confident that they also possess the aa configuration due to the stereochemical constraints required by the donor atoms in the NSNSN ligand[5] and the complexes' very close chemical and physical similarity to the $Co(NSSSN)X^{2+}$ series.[4]

Kinetic studies

The Fe(II) reduction of $Co(NSSSN)X^{2+}$ and $Co(NSNSN)X^{2+}$ (X = Cl⁻, Br⁻) was examined under a variety of complex concentrations, Fe(II) concentrations, acidities and temperatures. In all cases, the total $[ClO_4^-]$ was adjusted to 1.0 M using appropriate volumes of standardized $LiClO_4$-$HClO_4$. Table 6 summarizes the conditions and values of k_t obtained. Pseudo first-order conditions were employed in which consumption of Fe(II) was negligible, thus $k_t = k_{obs}/Fe(II)$. From this

Table 6. Derived second order rate constants and kinetic data for the Fe(II) reduction of $Co(NSNSN)X^{2+}$ and $Co(NSSSN)X^{2+}$ complexes[a]

# of individual determinations of k_t	Complex	$[Co(III) \times 10^4]$ M	$[Fe(II)]$ M	$[H_3O^+]$ M	Temp. °C	Ave. k_t[b] $M^{-1} s^{-1}$
27	$Co(NSNSN)Cl^{2+}$	5.92-11.8	0.02-0.05	0.20-0.80	25.0	0.226±.004
3		11.8	.03	0.20	15.0	0.117
4		11.8	.03	0.20	35.0	0.428
46	$Co(NSSSN)Cl^{2+}$	2.6-10.4	0.02-0.07	0.10-0.90	25.0	0.193±.006
3		5.2	0.04	0.50	18.1	0.118
3		5.2	0.04	0.50	32.6	0.309
25	$Co(NSNSN)Br^{2+}$	3.25-6.50	0.01-0.05	0.20-0.80	25.0	0.0304±.0007
3		6.5	0.05	0.20	18.7	0.0160
3		6.5	0.05	0.20	33.4	0.0613
36	$Co(NSSSN)Br^{2+}$	2.4-9.6	0.02-0.07	0.10-0.90	25.0	0.0154±.0006
3		4.8	0.04	0.50	17.7	0.786
3		4.8	0.04	0.50	33.0	2.67

[a]Total ClO_4^- was adjusted to 1.00 M using standardized $LiClO_4$-$HClO_4$

[b]Variations in k_t are given in standard deviations from the average

data we conclude that reduction of all four complexes is first order in Co(III) and Fe(II) and follows the common acid independent $(0.20\,M < H_3O^+ < 0.90\,M)$ rate law:

$$-d[\text{complex}]/dt = k_t[\text{Co(III)}][\text{Fe(II)}].$$

It has been established generally that similar Fe(II)–Co(III) systems undergo reaction via an inner-sphere electron transfer mechanism,[20] and we assume that basic mechanism in this work.

Activation parameters for the iron(II) reduction of the Co(NSSSN)X^{2+} and Co(NSNSN)X^{2+} complexes are presented in Table 7 along with the corresponding values for the analogous halopenta–aminecobalt(III) species.

Previous studies demonstrated that the placement of thioether donors *trans* to potential inner-sphere bridging groups enhanced the reduction rate by factors of $\sim 10^2$–10^3 as compared to nitrogen donors similarly placed in the coordination sphere.[3,9] The exact nitrogen analog to Co(NSSSN)Cl^{2+} and Co(NSNSN)Cl^{2+} is Co(tetraen)Cl^{2+}. Second order Fe(II) reduction rate constants at 25°C are $0.193\,M^{-1}\,s^{-1}$, $0.226\,M^{-1}\,s^{-1}$ and $\sim 1 \times 10^{-8}\,M^{-1}\,s^{-1}$ respectively. The latter value is an estimate because the Co(tetraen)Cl^{2+}–Fe(II) reaction was found to be extremely slow.[21] Reactivity trends in k_t have been attributed to the circumstance that the oxidant acceptor orbital (probably dz^2) is made more available by simultaneously removing the bridging ligand and the donor group *trans* to it. Experimentally one observes that k_t is significantly reduced as chelation is increased in a series of cobalt(III) complexes when NH$_3$'s are replaced by ethylenediamine, triethylenetetramine and tetraethylenepentaamine respectively.[8] Presumably increased chelation reduces the ability of a *trans* donor to stretch along the axis of inner-sphere interaction and thus we would expect any complex derived from a pentadentate ligand to exhibit the greatest reduction in k_t. In this work, with the presence of thioether donors, the above decrease in k_t is not observed; instead we have a $\sim 10^7$ fold rate enhancement.

From the structure data on Co(NSSSN)Cl^{2+} and Co(tetraen)Cl^{2+} we clearly must exclude any structural *trans* effect, the Co–Cl bond distances in both being almost identical (2.268(1) and 2.263(3) Å respectively). We believe a major factor contributing to the increased reduction rate begins with the fact that the Co–S1–C3–C2–N1 ring does not have the classical low energy conformation as found in the tetraen derivative. In Co(NSSSN)Cl^{2+} one of the two adjacent terminal – NH$_2$'s must be twisted to assume a position in which the

hydrogens on the two amino groups are staggered, minimizing hydrogen–hydrogen steric effects. Since the ligand is symmetrical, this phenomenon must alternate from one side to the other in solution, inasmuch as the mirror image molecule must have the distorted ring on the opposite side from that shown in Fig. 4, and the enantiomers are in equilibrium. Therefore, one can visualize this phenomenon as a propagation of the distortion from one side to the other across the entire chain with concomitant effects on the activation step associated with the precursor complex, and the observation of enhanced k_t.

Another feature to consider is the possibility of an Fe(II)–S–Co inner-sphere reduction path. Deutsch *et al.* have demonstrated that Cr(II)–Sulphur bridges to Co(III) centers are fairly common.[6,7] Several observations suggest that in our case Fe(II) does not favour such a bridge. In Table 6 we find that the reduction rate of Co(NSNSN)X^{2+} in several orders of magnitude greater than the corresponding Co(NSSSN)X^{2+} species, even though the latter has more sulphur atoms available for possible interaction with Fe(II). With Fe(II) as reductant the bridging efficiency of Cl$^-$ is greater than that of R–S–R and if both paths were operative to varying degrees one would observe nonlinear $\ln(D_t - D_\infty)$ vs time plots. Such is not the case as the graphs are exceptionally linear over 95% of reaction demonstrating reaction singularity. In previous work[9] complexes of the type Co(NSSN)-diamine were observed to be unreactive, even at high Fe(II) concentrations, demonstrating the Fe(II)–Thioether bridge is an unfavourable path for electron transfer. Preliminary experiments with Co(NSNSN)NCS^{2+} and Fe(II) gives $k_t \sim 6 \times 10^{-5}\,M^{-1}\,s^{-1}$, again demonstrating the disdain Fe(II) has for inner-sphere sulphur bridges. It has been noted elsewhere that a large ratio of k_{N_3}/k_{NCS} is suggestive of an inner-sphere Fe(II) reduction path and reflects the affinity of Fe(II) for nitrogen rather than sulphur bridges. The ratio of the azide rate constant[8] to the N-thiocyanato rate constant is $1.35\,M^{-1}\,sec^{-1}/6 \times 10^{-5}\,M^{-1}\,s^{-1}$ or $\sim 2 \times 10^5$, consistent with our assignment of a bridged inner-sphere mechanism not involving the thioether donor atoms.

Examination of Tables 6 and 7 shows that the Co(NSSSN)X^{2+} complexes are reduced slower than the Co(NSNSN)X^{2+} analogs in which the central thioether donor has been replaced by a CH$_3$–N moiety. The slight increase in k_t due to this structural modification may imply that the methyl group via solvation interactions is

Table 7. Activation parameters for the Fe(II) reduction of cobalt(III) complexes

Oxidant	$k_t\ M^{-1}s^{-1}$ $25°C$	$\Delta H^{\ddagger}$ kcal/mole	$\Delta S^{\ddagger}$ e.u.	$\Delta G^{\ddagger}$ kcal/mole
Co(NSNSN)Cl^{2+}	0.226	13.6	-16.0	18.3
Co(NSSSN)Cl^{2+}	0.193	11.1	-24.4	18.4
Co(NSNSN)Br^{2+}	0.0304	15.5	-13.0	19.4
Co(NSSSN)Br^{2+}	0.0154	13.5	-21.7	19.9
Co(NH$_3$)$_5$Cl^{2+}	1.35×10^{-3}	12.5[a]	-30	21.4
Co(NH$_3$)$_5$Br^{2+}	7.3×10^{-4}	15.5[b]	-20.1	21.5

[a] J. H. Espenson, *Inorg. Chem.*, **4**, 121 (1965);

[b] R. G. Linck, *ibid.*, **9**, 2529 (1970).

pulled into the bulk solvent, thus facilitating expansion of the cobalt radius along the critical axis as the reduction process proceeds with Co(III) becoming Co(II). The presence of CH_3-N physically causes a marked increase in solubility between the two series of complexes. In Table 6, a noticeable feature is the consistently more negative entropy of activation for $Co(NH_3)_5X^{2+}$ and $Co(NSSSN)X^{2+}$ species, again suggesting a less stringent structural ordering in the activated complex for reduction of $Co(NSNSN)X^{2+}$ complexes. In each case the bromo complex is reduced at a rate considerably slower than observed for the chloro derivative. This may be a manifestation of soft–hard (Br–Fe^{2+}) vs the favored hard–hard (Cl–Fe^{2+}) interaction in forming the precursor complex.

In this and previous studies we observed that placement of thioether donors *trans* to potential bridging groups greatly enhances the reduction rate compared to comparable complexes with amino donors. The exact reasons for such rate enhancement ($\sim 10^2$–10^7) are not easily isolated because of the difficulty in systematically controlling or varying only one of the numerous contributory features present in a molecule. Several emerging investigative routes include the synthesis of new molecules having specific stereochemistries and structural studies to examine the role of bond lengths, angle and ring conformations in conjunction with the reduction rate. The possible role of ground state electronic effects, especially in sulphur-containing ligands such as NSSN, NSNSN and NSSSN awaits theoretical and/or photochemical investigation.

REFERENCES

[1] M. R. Snow, *J. Am. Chem. Soc.* 1970, **92**, 3610.

[2] G. M. Reisner, I. Bernal and G. R. Dobson, *J. Organometal. Chem.* 1978, **157**, 23.

[3] G. M. Reisner, I. Bernal and G. R. Dobson, *Inorg. Chim. Acta*, in press.

[4] J. H. Worrell, P. Behnken and R. A. Goddard, *J. Coord. Chem.* 1979, **9**, 53.

[5] J. H. Worrell and T. A. Jackman, *Inorg. Chem.* 1978, **17**, 3360.

[6] J. N. Cooper, J. D. McCoy, M. G. Katz and E. Deutsch, *Ibid.* 1980, **19**, 2265 and references therein.

[7] M. H. Dickman, R. J. Doedens and E. Deutsch, *Ibid.* 1980, **19**, 945 and references therein.

[8] J. H. Worrell, R. Goddard and T. Jackman, *Inorg. Chim. Acta*, 1979, **32**, L71.

[9] J. H. Worrell and T. Jackman, *J. Am. Chem. Soc.* 1971, **93**, 1044.

[10] J. H. Worrell, R. Goddard and R. Blanco, *Inorg. Chem.* 1978, **17**, 3308.

[11] J. H. Worrell and T. Jackman, *Ibid.* 1978, **17**, 3358.

[12] The pentadentate ligand NSNSN = $NH_2CH_2CH_2$-S-CH_2-CH_2-N-CH_2CH_2-S-$CH_2CH_2NH_2$, 7 - methyl - 4,10 - diathia - 1,7,13 - triazatridecane.

[13] Commission on the Nomenclature of Inorganic Chemistry of the IUPAC, *Inorg. Chem.* 1970, **9**, 1.

[14] M. R. Snow, *J. C. S. Dalton Trans.* 1972, 1627.

[15] L. S. Magill, J. D. Korp and I. Bernal, *Inorg. Chem.* 1981, **20**, 1187.

[16] R. C. Elder, L. R. Florian, R. E. Lake and A. M. Yacynych, *Ibid.* 1973, **12**, 2690.

[17] R. C. Elder, G. J. Kennard, M. D. Payne and E. Deutsch, *Ibid.* 1978, **17**, 1296.

[18] L. K. Liu, Program BMFIT for Molecular Comparison, University of Texas, Austin, 1977. (As modified by Watkins, Creswick and Korp). The tetraen molecular coordinates were inverted in order to conform to the handedness of the NSSSN coordinates.

[19] Model courtesy of Houston Molecular Models, 6427 Hillcroft, Suite 230, Houston, TX 77081.

[20] A. Haim and N. Sutin, *J. Am. Chem. Soc.* 1966, **88**, 5343.

[21] Y. Kurimura and K. Ohashi, *Bull. Chem. Soc. Japan* 1971, **44**, 1797.

[22] J. H. Espenson, *Inorg. Chem.* 1965, **4**, 121.

THE DISTRIBUTION OF CERIUM (III) CATIONS BETWEEN AQUEOUS AND NITROBENZENE PHASES IN THE PRESENCE OF DICARBOLIDE ANIONS

I. PODZIMEK, M. KYRŠ,* J. RAIS and P. VAŇURA

Nuclear Research Institute, 250 68 Řež, Czechoslovakia

Abstract—Extraction of micro- and macroquantities of Ce^{3+} ($C^o_{Ce} = 10^{-6}$–10^{-1} mole/dm^3) with a nitrobenzene solution of dicarbolide ($C^o_{H^+B^-} = 0.04$–0.5 mole/dm^3) from a nitric acid solution ($C^o_{HNO_3} = 0.1$–0.3 mole/dm^3) was investigated. Coextraction of water and simultaneous extraction of Ce^{3+} and Ba^{2+} ($C_{Ce^+} + C_{Ba} = 0.3$ mole/dm^3) from 0.3 and 0.5 M HNO$_3$ was also studied. It was found that the reaction $Ce^{3+} + 3\bar{H} \rightleftharpoons \overline{Ce^{3+}} + 3H$ ($K_{Ce/3H}$) takes place in all cases. The dependence of the apparent exchange extraction constant $K_{Ce/3H}$ on the initial composition of both phases was determined and the effect of the composition of the aqueous phase on the values of $K_{Ce/3H}$ and $K_{Ba/2H}$ was discussed. The stability constant of the $CeNO_3^{2+}$ complex and the hydration number of the Ce^{3+} cation in the organic phase ($h_{Ce^{3+}} = 16.2 \pm 2$) was determined and a linear correlation between individual extraction constants of mono-, bi- and trivalent cations and the hydration numbers in the nitrobenzene phase was found using data from the present paper and values given in literature.

In the previous paper[1] the reasons were given for the investigation into solvent extraction of barium in the title system. In this work an analogical study has been performed on cerium III cations. This particular choice of cation is based upon the presence of cerium among nuclear fission products and because the system has been proposed for the isolation of radioactive cesium and strontium from radioactive wastes generated in Purex reprocessing of irradiated nuclear fuel.[2] Furthermore, cerium was selected as a suitable representative of trivalent cations which have almost been up to now ignored in investigations of similar solvent extraction systems based upon the presence of the bulky hydrophobic dicarbolide anion acting as the extractant.

The simultaneous extraction of barium and cerium in this system was studied also with the aim of investigating a possible mutual interaction of these two cations in the solvent extraction process.

EXPERIMENTAL

The experimental technique, e.g. the determination of water and proton concentrations in the organic phase, followed rather strictly the experimental pattern described previously.[1] For the determination of the distribution ratios of tracer amounts of cerium (D_{Ce}) tracing with ^{144}Ce was used and the ratioactivity of aliquots of the two phases was measured after reaching (in 2 hr) radioactive equilibrium between ^{144}Ce and the daughter element ^{144}Pr. In experiments where Ba and Ce were simultaneously present two parallel sets of experiments were performed in which the chemical composition of the extraction systems was exactly equal, but one set was labelled with ^{144}Ce in order to determine the D_{Ce} values, the other one with ^{133}Ba. Weighable amounts of Ce in the stock solution were determined using a complexometric method (pH 4.4, indication with xylenol orange).

RESULTS AND DISCUSSION

The dependence of D_{Ce} values for tracer amounts of Ce upon the concentration of HNO$_3$ in the aqueous phase and upon the concentration of the reagent in the organic phase is given in Fig. 1. Similarly to analogical

results[1] obtained with Ba, the values of log D_{Ce} depend linearly upon the initial acidity of the aqueous phase $c^o_{HNO_3}$ (at constant initial reagent concentration in the organic phase (c^o_{HB})), the slope being this time -3. For constant $c^o_{HNO_3}$ values in the aqueous phase log D_{Ce} values increase linearly with c^o_{HB} the slope being approximately $+3$. Accordingly, the prevailing equilibrium underlying the solvent extraction process can be formulated as follows: $Ce^{3+} + 3H^+_{org} \rightleftharpoons Ce^{3+}_{org} + 3H^+$ ($K_{CE/3H}$).

In order to investigate if the same simple reaction takes place also when weighable amounts of cerium are extracted systematic experiments were performed in which the initial concentrations of the threee components varied in the ranges: 0.1–0.3 mole/dm^3 HNO$_3$; 0.04–0.5 mole/dm^3 HB; 10^{-6}–10^{-1} mole/dm^3 Ce and distribution ratios of Ce and equilibrium concentrations of protons in both phases were determined. The total number of these distribution experiments was 124. The method of calculating the $K_{Ce/3H}$ values was analogical to that described previously.[1] The values $K_{Ce/3H}$ showed no dependence upon the concentration of the reagent in the whole range investigated and upon the concentration of Ce in the range 10^{-6}–10^{-2} M Ce. On the other hand, a slight decrease in $K_{Ce/3H}$ values was observed with increasing aqueous acidities. For low concentration of Ce (< 0.01 M) the empirical relationship is valid log $K^{Ce}_{3M} = 1.49 - 0.26c^o_{HNO_3}$.

In the whole concentration range a rather complicated empirical relationship has been derived:[3]

$$\log K^{Ce}_{3H} = 1.31 - 0.19\, c^o_{HNO_3} + 1.21\, c^o_{H^+B^-} - 3.63\, c^o_{Ce}$$
$$+ 0.34\, c^o_{H^+B^-}c^o_{HNO_3} - 0.77\, c^o_{H^+B^-}c^o_{Ce}$$
$$+ 1.35\, c^o_{HNO_3}c^o_{Ce} - 2.32(c^o_{H^+B^-})^2 - 0.059$$
$$\times (c^o_{HNO_3})^2 + 8.02(c^o_{Ce})^2.$$

The fact that the $K_{Ce/3H}$ values vary only slightly when the initial concentrations of the three components of the solvent extraction system change in wide ranges can be considered as a corroboration of the validity of the chemical model of the extraction proposed (no asso-

---

*Author to whom correspondence should be addressed.

Fig. 1. The logarithmic dependence of the distribution ratio of tracer amounts of Ce upon the initial concentration of nitric acid and dicarbolide. Curve 1—$c_{HB}^0 = 0.037$ mole/dm³; 2—0.092; 3—0.184; 4—0.276; 5—0.46; 6—$c_{HNO_3}^0 = 3.0$ mole/dm³; 7—2.5; 8—2.0; 9—1.5; 10—1.0; 11—0.7; 12—0.5; 13—0.3. Broken lines indicate slopes -3 and $+3$.

ciation of the extracted species and the extractant in the organic phase, no association of the ions Ce^{3+} and B^- in the aqueous phase, no extraction of HNO_3).

Another evidence in favour of the proposed main chemical reaction of the extraction process can be inferred from the data on the proton transfer from the organic phase into the aqueous phase during the solvent extraction of weighable amounts of cerium (Table 1). It can be seen that the coincidence of calculated and experimentally found values of the increase of H^+ concentration in the aqueous phase (Δ_{aq}) and its decrease in the organic phase ($-\Delta_{org}$) is fairly good. The average value from all data available is $\Delta_{aq}/[Ce^{3+}]_{org} = 3.12 \pm 0.15$ and $-\Delta_{org}/[Ce^{3+}]_{org} = 3.14 \pm 0.17$ which is very close to the theoretically expected value of 3 protons per cerium cation.

For the interpretation of the results obtained the behaviour of cerium (III) nitrate complexes might be of importance.[4,5] Therefore the effect upon Ce^{3+} extraction was investigated of the type of the anion of the mineral acid present. In these experiments tracer amounts of Ce^{3+} were used, three concentrations (0.1, 0.2, 0.3 M) of the extractant and the initial acidity in the aqueous phase was adjusted to 0.2–2 M H^+ using alternatively the following acids: HNO_3, $HClO_4$, HCl, and H_2SO_4. With all four acids the linear dependence of log D_{Ce} upon log C_{H^+} with the slope of -3 was observed. The values of D_{Ce} increased according to the sequence $HCl \leq HNO_3 < H_2SO_4 < HClO_4$. The values for HCl were about 95%, those for H_2SO_4 140% and for $HClO_4$ 175% of the value for HNO_3 taken as reference.

These results show that in the solutions of perchloric

acid, which is known to be in most cases a noncomplexing medium, the distribution ratios of Ce(III) exhibit the highest values observed which could be interpreted as a result of the absence of complex formation between Ce^{3+} and the anion as compared to some degree of masking in the other media tested. The differences between the D_{Ce} values for different acids are small compared to the strong scattering of published stability constants[6] of the complex 1:1. Therefore, on the basis of literature data available the question whether the order of the acids according to the degree of Ce complexing is identical to that of decreasing D_{Ce} values cannot be answered with reliability.

For this reason we investigated in more detail the dependence of D_{Ce} upon $c_{HNO_3}^0$ in a medium of constant ionic strength (replacing gradually $HClO_4$ by equivalent concentrations of HNO_3). The experimental curves are given in Fig. 2.

The theoretical curves calculated on the assumption that Ce^{3+} and $CeNO_3^{2+}$ are the only species of Ce(III) in the aqueous phase and $CeNO_3^{2+}$ is nonextractible coincide satisfactorily with experimental data if the values of the stability constant of $CeNO_3^{2+}$ are assumed to be 2.19 ($\mu = 0.3$) and 2.84 ($\mu = 0.5$). The comparison of these log K_1 values with available data from the literature given in Table 2 shows that the values found in our system do not contradict values found by other authors. Therefore we are prone to ascribe the lower values of D_{Ce} in nitric acid than in perchloric to the formation of inextractible $CeNO_3^{2+}$ species. Consequently the values of $K_{Ce/3H}$ given in this paper ignoring the formation of these species must be characterized as "conditional" concen-

Table 1. Verification of the equivalence of the exchange of Ce^{3+} for H^+_{org} in solvent extraction. Values Δ indicate changes in concentrations (mole/1) of H^+ in the respective phase during the solvent extraction process, theor. relates to theoretical values calculated using the cation exchange relationship from the D_{Ce} values measured; Δ pertains to experimentally found values; $c°$ denotes initial concentrations of the respective components in the particular phase

c^o_{HB}	$c^o_{HNO_3}$	c^o_{Ce}	$0.25M\ Ce^{3+}$	$0.1M\ Ce^{3+}$	$0.05M\ Ce^{3+}$	$0.01M\ Ce^{3+}$
0.15M	0.3M	theor.	0.101	0.074	0.052	0.017
		Δ_{aq}	0.090	0.075	0.039	0.012
		$\Delta_{org.}$	0.089	0.058	0.047	0.015
0.2 M	0.3M	theor.	0.102	0.081	0.066	0.023
		Δ_{aq}	0.106	0.081	0.064	0.024
		$\Delta_{org.}$	0.086	0.086	0.070	0.031
0.2 M	0.5 M	theor.	0.082	0.057	0.022	0.014
		Δ_{aq}	0.068	0.068	-	0.020
		$\Delta_{org.}$	0.086	0.056	0.022	0.014
0.2 M	0.7M	theor.	0.059	0.043	0.028	0.008
		Δ_{aq}	0.062	0.050	0.020	0.007
		$\Delta_{org.}$	0.050	0.059	0.027	0.012
0.2 M	1.0M	theor.	0.030	0.019	-	-
		Δ_{aq}	0.044	0.029	-	-
		$\Delta_{org.}$	0.035	0.023	-	-
0.3 M	0.3 M	theor.	0.143	0.142	0.108	0.027
		Δ_{aq}	0.156	0.129	0.106	0.021
		$\Delta_{org.}$	0.153	0.145	0.115	0.031
0.3 M	0.5 M	theor.	0.135	0.105	0.078	0.022
		Δ_{aq}	0.126	0.111	0.066	0.019
		$\Delta_{org.}$	0.139	0.112	0.070	0.016
0.3 M	0.7 M	theor.	0.118	0.065	0.055	0.016
		Δ_{aq}	0.128	0.076	0.040	0.027
		$\Delta_{org.}$	0.136	0.072	0.056	0.025
0.3 M	1.0 M	theor.	0.068	0.046	-	-
		Δ_{aq}	0.15	0.15	-	-
		$\Delta_{org.}$	0.060	0.036	-	-
0.3 M	1.5 M	theor.	0.030	0.016		
		Δ_{aq}	0.020	0.025		
		$\Delta_{org.}$	0.029	0.024		

Table 2. Stability constant of $CeNO_3^{2+}$ (298K)

Method of determination	Medium, ionic strength	log. K_1	Reference
distribution (extraction)	$1H^+(ClO_4^-)$	0.21	(6)
	$2H^+(ClO_4^-)$	1.04	(4)
	$0.5M\ (ClO_4^-)$	0.454	This work
cation exchange	$0.3M\ (ClO_4^-)$	0.340	This work
	HNO_3(various)	0.4	(6)

Fig. 2. The influence of nitric acid concentration upon the extraction of cerium. f = molar fraction $c^o_{HNO_3}/(c^o_{HNO_3} + c^o_{HClO_4})$ in the initial aqueous phase. Curve 1—c^o_{HB} = 0.1 mole/dm^3; $c^o_{HNO_3} + c^o_{HClO_4}$ = 0.3 mol/dm^3; 2—0.3; 0.5.

tration constants[7] which are valid only for the degree of the metal masking occurring in the presence of the ligand concentration, which was used in the determination of the $K_{Ce/3H}$ constant.

Thus the influence of HNO_3 concentration upon the $K_{Ce/3H}$ values found in this paper is due to two factors: changing degree of Ce^{3+} masking and changing activity coefficients of the species in the aqueous and to some extent—in the organic phase.

Since the exchange constants $K_{Ce/3H}$ and $K_{Ba/2H}$ have been found[1] to be reasonably constant in systems, where a pair of cations only was present, it seemed worthwhile to investigate the validity of this approach to systems

with the simultaneous presence of three types of cations (H^+, Ba^{2+}, Ce^{3+}).

In these types of experiments the $c^o_{HNO_3}$ and c^o_{HB} were held constant and the ration c^o_{Ba}/c^o_{Ce} was varied in a wide range maintaining the sum $c^o_{Ba} + c^o_{Ce}$ constant. In all cases the values D_{Ba}, D_{Ce} and $c^{tot}_{H_2O}$ were determined. The distribution of metals is shown in Fig. 3 for three concentrations of HB. The values of constants $K_{Ce/3H}$ and $K_{Ba/2H}$ were calculated

(a) for each $c_{H^+B^-}$ and $c^o_{HNO_3}$ separately

(b) for all $c^o_{H^+B^-}$ with constant $c^o_{HNO_3}$ together and

(c) for all $c^o_{H^+B^-}$ and $c^o_{HNO_3}$ together.

The special version of general least squares minimizing

Fig. 3. The concentration of water in extracts containing simultaneously Ba and Ce. Circles—$\bar{c}_{H_2O}$ vs f_{Ba} in individual distribution experiments; squares—average values $\bar{c}_{H_2O}$ over the whole f_{Ba} range vs c^o_{HB}. Curve 1—0.3 mol/dm^3 HB, 0.3 mole/dm^3 HNO$_3$; 2—0.3, 0.5; 3—variable, 0.3; 4—0.2, 0.3; 5—0.2, 0.5; 6—0.15, 0.3; 7—0.1, 0.3; 8—0.04, 0.3.

program LETAGROP (Ref. 8) was used for this calculation involving the function

$$U = \Sigma\{[(\log D_{Ba}(exp) - \log D_{Ba}(calc)]^2$$
$$+ [\log D_{Ce}(exp) - \log D_{Ce}(calc)]^2\} \qquad (2)$$

where $D_{Ba}(exp)$, $D_{Ba}(calc)$ resp. $D_{Ce}(exp)$, $D_{Ce}(calc)$ are experimental and calculated values of distribution ratios of Ba resp. Ce. Results are summarized in Table 3.

Values of both $K_{Ce/3H}$ and $K_{Ba/2H}$ show no dependence on acidities of both the aqueous and the organic phase. The scattering of these values is probably caused by experimental errors and neglecting the changes of activity with component concentration during constant calculation. Both $K_{Ce/3H}$ and $K_{Ba/2H}$ are approximately three times lower than these found in the systems containing Ba^{2+} resp. Ce^{3+} in microamounts. This difference may be caused by changing of activity coefficients in one or even both phases.

For the discussion of this difference in $K_{Ce/3H}$ values it is useful to start with the obvious relationship:

$$K_{Ce/3H} = K_{Ce/3H}^{th} \times \frac{\bar{\gamma}_H^3 \times \gamma_{Ce}}{\bar{\gamma}_{Ce} \times \gamma_H^3}.$$

The assumption can be made that the ratio $\bar{\gamma}_H^3/\bar{\gamma}_{Ce}$ does not depend significantly on the composition of the aqueous phase and on the ionic strength of the organic phase. This is indicated by the fact (see Table 3) that the dependence of $K_{Ce/3H}$ and $K_{Ba/2H}$ on the value of c_{HB}^o are very feeble.

As for the activity coefficient of the protons or acids, we assume that they are practically equal for both cases, i.e. 0.3–1.0 M HNO_3 or 0.3 M $HNO_3 + 0.3$ M ($Ce(NO_3)_3$–$Ba(NO_3)_2$). This assumption is based upon an analogy with the systems $BaCl_2 + HCl$ (Ref. 9) and $Nd(NO_3)_3 + HNO_3$ (Ref. 10). In the latter case values almost constant were found for the acidity range 0.1–1.0 mole/kg and practically independent of Nd concentration in the range 0–0.2 mole/kg. In the former similarly constant values of γ_{HCl} are reported.

Thus, the change of $K_{Ce/3H}$ would mainly be ascribed to the change in γ_{Ce}. In the case of microamounts of Ce the value of γ_{Ce} can be assumed to be close to unity in

extraction systems with nitrobenzene and dicarbolide anion. This statement is based on the observed independence of $K_{Ce/3H}$ constant on the acidity of aqueous phase (Fig. 1).

In the case of both multi-charge cations (Ba^{2+} a Ce^{3+}) present in weighable amounts in the aqueous phase rather low values of γ_{Ce} and γ_{Ba} should be anticipated (~ 0.2–0.35) based on the analogy with the systems containing $Ba(NO_3)_2$ or $La(NO_3)_3$ and $Pr(NO_3)_3$ (see Refs. 11, 12) which is in accordance with observed decrease of $K_{Ce/3H}$ and $K_{Ba/2H}$ for macroamounts of Ce and Ba.

In an attempt to ascertain the hydration of Ce^{3+} ions in the nitrobenzene extract the overall concentration of water in the extract was determined in dependence on the equilibrium concentration Ce^{3+} ions ($[Ce^{3+}]_{org}$) in the organic phase (Fig. 4). The calculation of the hydration number of Ce^{3+} in the organic phase ($h_{Ce^{3+}}$) was performed using the simplified procedure discussed previously,[1] based upon the balance:

$$c_{H_2O}^{tot} = c_{H_2O}^o + h_{H^+} \times [H^+]_{org} + h_{Ce^{3+}} \times [Ce^{3+}]_{org},$$

where $c_{H_2O}^o$ is the solubility of water in the pure solvent, h_{H^+} was determined previously and $[H^+]_{org}$ and $[Ce^{3+}]_{org}$ values were determined by the analytical methods mentioned.

From the fact that the curves in Fig. 4 run almost parallel to the lines of constant $c_{H_2O}^{tot}$ values it can be seen that the values of $h_{Ce^{3+}}$ should correspond to $3h_{H^+}$ since one Ce^{3+} replaces three H^+ cations during extraction.

In our previous paper the h_{H^+} values found amounted to 5.2–7.6 so that the expected range of $h_{Ce^{3+}}$ values is about 15.6–23. Unlike for h_{H^+} no correlation between the actual $h_{Ce^{3+}}$ value and the composition of the extraction system could be found and therefore the $h_{Ce^{3+}}$ values for the various points in Fig. 4 were included in the calculation of an average overall value $h_{Ce^{3+}}$, which was found to be 16.2 ± 2 mole of H_2O/mole Ce^{3+}. The limitations to the precision and accuracy of h values calculated in this way has been discussed previously in connection with the determination of $h_{Ba^{2+}}$.

Comparing the value 16.2 ± 2 for Ce with 11.5 ± 1 found[1] for Ba one can conclude that the exchange reac-

Table 3. Logarithmic values of constants $K_{Ce/3H}$ and $K_{Ba/2H}$ for systems with various ratios c_{Ba}^o/c_{Ce}^o
($c_{Ba}^o + c_{Ce}^o = 0.3$ mol l^{-1})

$c_{H^+B^-}^o$ (mol.l^{-1})	$c_{HNO_3}^o$ (mol.l^{-1})	$K_{Ce/3H}$	$K_{Ba/2H}$	$K_{2Ce/3Ba}$	n^d
0.04[a]	0.30	1.09(1.33)	0.45(0.68)	0.82	7
0.10[a]	0.30	0.95(1.16)	0.31±0.23	0.96	7
0.15[a]	0.30	1.19(1.43)	0.49±0.24	0.89	7
0.20[a]	0.30	0.57(0.83)	0.09±0.24	0.88	7
0.30[a]	0.30	1.31(1.61)	0.56(0.80)	0.94	7
0.04–0.30[b]	0.30	1.03±0.17	0.38±0.13	0.90	35
0.15[a]	0.5	0.98(1.22)	0.32±0.25	0.98	5
0.2[b]	0.5	1.19(1.46)	0.44(0.65)	1.07	5
0.15–0.2[b]	0.5	1.07±0.24	0.37±0.18	1.02	10
0.04–0.30[c]	0.3–0.5	1.04±0.14	0.38±0.11	0.93	45

[a,b,c]The constants calculated according to methods a, b, c, respectively, given in the text;
( ) maximum value;
Errors of the constants and their maximum values are calculated according to Sillén and Wirnqvist[8];
[d]Number of experimental points, n
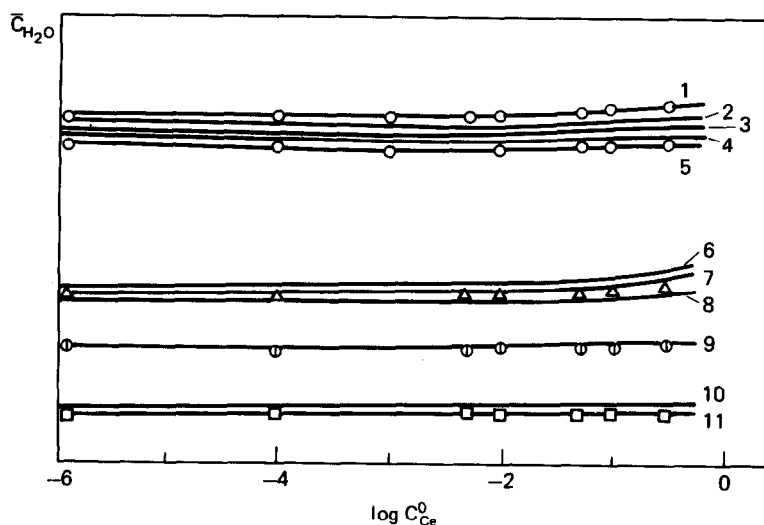
Fig. 4. The concentration of H_2O in extracts in dependence on equilibrium cerium concentration in the organic phase.
Curve 1—$c_{HB}^o = 0.3$ mole/dm^3, $C_{HNO_3}^o = 0.3$; 2—0.3, 0.5; 3—0.3, 0.7; 4—0.3, 1.0; 5—0.3, 1.5; 6—0.2, 0.3; 7—0.2, 0.5; 8—0.2, 0.7; 9—0.15, 0.3; 10—0.1, 0.3; 11—0.1, 0.5.
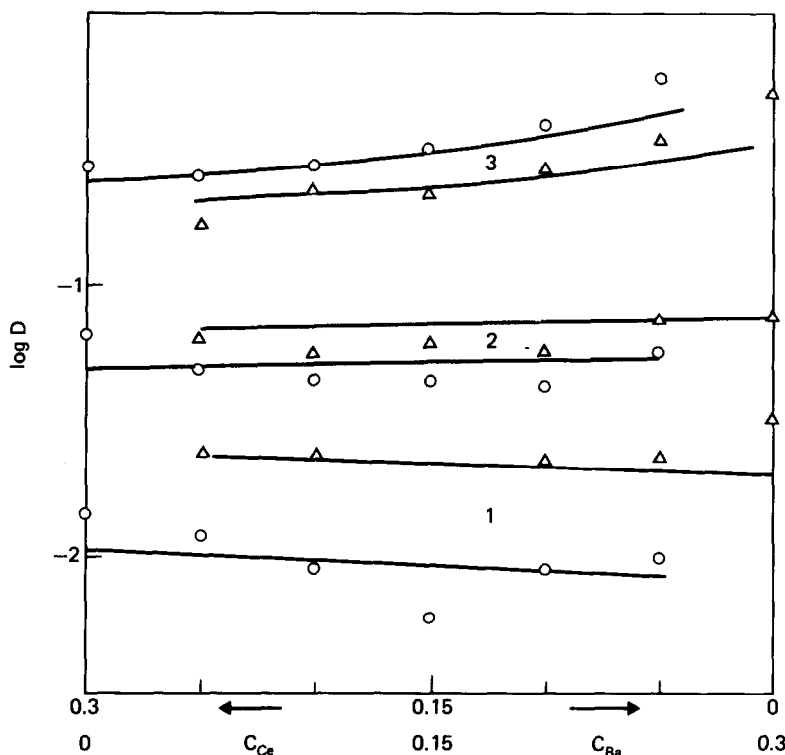
Fig. 5. Extraction of barium (triangles) and cerium (circles) by the nitrobenzene solution of dicarbolide from aqueous solution 0.3 M HNO_3–0.3 M[$Ce(NO_3)_3$ + $Ba(NO_3)_2$]. (1) 0.04 M dicarbolide, (2) 0.10 M dicarbolide, (3) 0.30 M dicarbolide. Full lines are calculated for log $K_{Ba/2H} = 0.38$ and log $K_{Ce/3H} = 1.03$.

tion 3 Ba^{2+} + 2 $Ce_{org}^{3+} \rightleftharpoons 3$ Ba_{org}^{2+} + 2 Ce^3 should be accompanied with a very little change in overall cation hydration in the extract ([(3 × 11.5–2 × 16.2)/2 × 16.2] × 100 = 6.5%) which is well within the uncertainty of the hydration numbers found. Since in all experiments also the concentration of water in the extract was determined, the anticipated independence of $c_{H_2O}^{tot}$ upon f_{Ba} in the whole range of f_{Ba} values could be checked. The results (Fig. 5) corroborate the above reasoning. The fact that a practically

linear dependence of c_{H_2O} upon c_{HB}^o values was found is in coincidence with the observation that for hydration numbers of both Ba^{2+} and Ce^{3+} no dependence on c_{HB}^o values could be found.

It is interesting to compare the hydration number value of Ce in the extract with the hydration numbers of the same cation in aqueous solution since some authors[13,14] came to the conclusion that the hydration numbers of anions in nitrobenzene extracts "should be considered
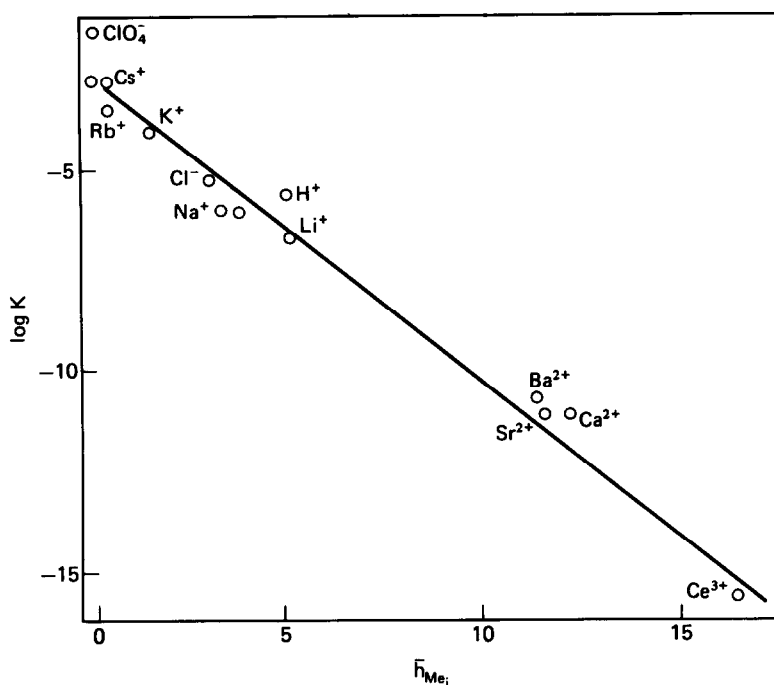
Fig. 6. Correlation between individual extraction constants of cations from water to nitrobenzene and their hydration numbers in nitrobenzene. Data for Ce from this work, other data see Ref. 1.

only lower limits to the first-shell coordination numbers as they represent average values for distributions that may well range from 0 (unhydrated anions) to 4 or even 6 water molecules (the first—shell coordination number)". As a matter of fact a remarkable similarity was found between the organic phase hydration numbers of Cl^- and Br^- to the values found in aqueous solutions by compressibility and ionic vibration methods.[14]

For Ce^{3+} the following hydration numbers in aqueous phases have been found: 6.7 by diffusion measurements and 7.5 by volume fraction statistics,[15] 8 in sulphate media from thermodynamic parameters,[16] 9 spectrophotometrically,[17] 9 from molar volumes and 13 by compressibility method.[18] Similarly to Ba^{2+} behavior[1] these are much lower than the above $h_{Ce^{3+}}$ value found in nitrobenzene which shows again that the assumption of the first-shell coordination number being a higher limit to organic phase hydration number cannot be considered to be of general validity. The reasons for the possibility of the organic phase hydration number exceeding markedly that in the aqueous phase have been discussed in connection with Ba^{2+} hydration.[1]

The determination of the hydration number of Ce^{3+} in nitrobenzene offers an opportunity of testing the validity of the correlation between hydration number values in nitrobenzene and individual solvent extraction constants. Combining data given in Fig. 8 in Škarda and coworkers paper,[19] (Fig. 5) from the previous work,[1] and the value of $h_{Ce^{3+}}$ found herein we obtain the presently most general correlation plot (Fig. 6) which shows that the correlation is valid both for investigated cations of charge $+1$, $+2$, and $+3$ and investigated anions with charge -1.

REFERENCES

[1]I. Podzimek, M. Kyrš and J. Rais, *J. Inorg. Nucl. Chem.* 1980, **42**, 1481.

[2]B. Ya. Galkin, L. N. Lazarev, R. I. Ljubcev *et al.*, Paper on the *5th Symp. Council of Mutual Economic Aid*. Research in reprocessing and radioactive waste management, held on 7th April 1981 in Mariánské Lázně, Czechoslovakia.

[3]M. Kyrš and J. Hálová, Report ÚJV 5144 CH (1979). Institute of Nuclear Research, Řež, Czechoslovakia.

[4]G. Choppin and W. F. Strazik, *Inorg. Chem.* 1965, **4**, 1250.

[5]J. Knoeck, *Anal. Chem.* 1969, **41**, 2063.

[6]L. G. Sillén and A. E. Martell, *Stability Constants of Metal-Ion Complexes*, p. 169. Chemical Soc. Spec. Pub. No. 17. London, 1964.

[7]A. Ringbom, *Complexation in Analytical Chemistry*. Interscience, New York, 1963.

[8]L. G. Sillén and B. Warnqvist, *Arkiv Kemi*, 1969, **31**, 315.

[9]M. H. Lietzke and R. W. Stoughton, *J. Phys. Chem.* 1966, **70**, 756.

[10]W. G. O'Brien and R. G. Bautista, *Adv. Chem. Ser* 1979, 177 (Thermodyn. Behav. Electrolytes Mixed Solvents, 2), 299.

[11]R. A. Robinson and R. H. Stokes, *Electrolyte Solutions*, p. 483. Butterworths, London, 1955.

[12]J. A. Rard and D. G. Miller, *J. Chem. Eng. Data* 1979, **24**, 348.

[13]J. J. Bucher, T. J. Conocchioli, E. R. Held, J. A. Labinger, B. A. Sudbury and R. M. Diamond, Rep. LBL-2351, 1974.

[14]T. Kenjo and R. M. Diamond, *J. Inorg. Nucl. Chem.* 1974, **36**, 183.

[15]E. Glueckauf, *Trans. Far. Soc.* 1955, **51**, 1235.

[16]M. C. F. Ladd and W. H. Lee, *J. Phys. Chem.* 1965, **69**, 1840.

[17]B. Jezowska-Trzebiatowska, *XIX Int. Conf. on Coordination Chem.*, Prague, 4. 9. 1978, Plenary Lecture.

[18]J. Čeleda and V. Jedináková, *ibid.*

[19]V. Škarda, J. Rais and M. Kyrš, *J. Inorg. Nucl. Chem.* 1979, **41**, 1443.

REACTIONS OF COORDINATED COMPOUNDS. CHELATE-INDUCED ACCELERATION OF METHYL-PROTON DISSOCIATION FROM ACETOPHENONES

TOSHIO KAWATO

Laboratory of Chemistry, College of General Education, Kyushu University, Ropponmatsu, Chuo-ku, Fukuoka 810, Japan

Abstract—Rate constants of acetyl-proton exchange of alkali acetylphenolates and related acetyl aromatics were measured and compared in D_2O and in CD_3OD. The results exhibited chelate-induced activation of acetyl C–H bonds. A palladium complex with N,N,N',N'-tetramethylethylenediamine turned out to catalyze the acetyl proton exchange of *o*-hydroxyacetophenone due to chelation.

Reactions of coordinated molecules have been investigated widely, while little has been studied about the reactivity of C–H bonds outside chelate rings. In a previous work, kinetics of proton dissociation from acetyl groups of β-dicarbonyl compounds were measured and discussed in connection with chelate effects.[1] In such a system, however, there was some uncertainty in measuring the kinetics because hydrolysis (C–C bond cleavage in the ligands) occurred during measurement. The chelate effect on the rate of acetyl-proton exchange was successfully observed by use of a series of hydroxy-acetophenones. This paper will expand the original communication[2] and describe the chelate-induced acceleration of proton dissociation from acetyl groups as well as a catalytic character of a palladium complex.

EXPERIMENTAL

General comments

UV absorption spectra were measured on a Hitachi EPS-3T spectrophotometer using H_2O and N,N-dimethylformamide (DMF) solutions. IR spectra were recorded on a Hitachi EPI-S2 spectrophotometer in nujol mulls or neat films. NMR spectra were determined at 60 MHz on a Hitachi R-24 spectrometer using $CDCl_3$, CD_3OD, or D_2O solutions with TMS or sodium 2,2-dimethyl-2-silapentane-5-sulfonate as the internal standard. Rate of proton dissociation was expressed by rate of disappearance of NMR peaks due to acetyl–methyl protons in D_2O or in CD_3OD. Kinetic measurement and calculation were performed by a general method described in the previous paper.[1]

Materials

o-, *m*-, and *p*-Hydroxyacetophenone(Hooa, Hmoa, and Hpoa, respectively) and other acetyl compounds were commercially available; the purity was confirmed by IR and NMR spectra. Sodium *o*-acetylphenolate, Na(ooa), has been prepared in the previous work.[1] Other alkali–metal salts were obtained similarly by mixing of solutions of hydroxyacetophenones in methanol and aqueous alkali hydroxides. The purity of the salts was confirmed by elemental analyses (Table 1); sets of small letters represent anions derived from corresponding hydroxyacetophenones.

Palladium complex with N,N,N',N'-tetramethylethylenediamine (tmen) and Hooa, [Pd(tmen)(ooa)]ClO₄

When an aqueous $K_2[PdCl_4]$ was treated with N,N,N',N'-tetramethylethylenediamine(tmen), a water-insoluble complex, $[Pd(tmen)Cl_2]$, was produced as orange–yellow crystals.[3] To a suspension of $[Pd(tmen)Cl_2]$ (0.3 g) in water (30 cm³) was added a solution of $AgClO_4$ (0.4 g) in water (10 cm³) with vigorous stirring. The mixture was stirred at 80°C for 10 min and filtered. To the cold filtrate was added a solution of Na(ooa) (0.15 g) in water (10 cm³). After stirring the mixture for 10 min, the resulting yellow crystalline powder was collected and recrystallized from water to yield (almost theoretical %) yellow needles of the desired complex, $[Pd(tmen)(ooa)]ClO_4$: NMR(CDCl₃) $\delta 2.66$(s, COCH₃, 3H), 2.81 and 2.83 (2s, NCH₃, 12H), 3.07(s, NCH₂, 4H); IR(nujol) 1607(m, C = C), 1573(s, C = O), 1525(m, C = C) cm⁻¹. Found: C, 36.80; H, 5.02; N, 6.11. Calc for $C_{14}H_{23}N_2O_6ClPd$: 36.78; H. 5.07; N, 6.13%.

RESULTS AND DISCUSSION

Rate constants, k_{H-D}, of acetyl-proton exchange of sodium salts of *o*-hydroxyacetophenone(Hooa), *m*-hydroxy–acetophenone(Hmoa), and *p*-hydroxy-acetophenone(Hpoa) in D_2O are shown in Table 2. By use of a mixture of the three salts in D_2O, the rate constants for the salts could be measured simultaneously under the same conditions: the rate constants obtained from the mixture are shown in parentheses in Table 2. The fact that each of the values measured in the mixture is larger than the corresponding rate constant obtained from the single solution is attributable to higher concentration of an OD^- ion in the mixture. The order of the rate constants, Na(ooa) > Na(moa) > Na(poa), in both series can be ascribed to the effect of conjugation in the *p*-isomer and neighbouring hydroxyl-group participation in the *o*-isomer similarly to the case of thallium(I) salts described before.[1] Carbonyl stretching vibrations in IR spectra: 1647 and 1637 cm⁻¹ for Hooa and Na(ooa), 1666 and 1687 cm⁻¹ for Hmoa and Na(moa), 1649 and 1652 cm⁻¹ for Hpoa and Na(poa), exhibit the considerable enhancement of the polarity of the carbonyl bonds resulting from the resonance in Hooa, Hpoa, and their salts.

Table 1. Analytical data of alkali acetylphenolates

Compound	Formula	Colour	Found(Calcd)	
			C	H
Li(ooa)	$C_8H_7O_2Li$	Yellow	67.60 (67.63)	4.98 (4.97)
Li(poa)	$C_8H_7O_2Li$ $1/6H_2O$	White	66.12 (66.22)	5.13 (5.10)
Na(moa)	$C_8H_7O_2Na$ $1/5H_2O$	Pale yellow	59.36 (59.41)	4.40 (4.61)
Na(poa)	$C_8H_7O_2Na$	White	60.53 (60.76)	4.44 (4.46)
K(ooa)	$C_8H_7O_2K$	Yellow	55.39 (55.15)	4.16 (4.05)
K(poa)	$C_8H_7O_2K$ $1/8H_2O$	White	54.68 (54.44)	4.44 (4.14)

Table 2. Exchange-rate constants (k_{H-D}, min^{-1})† at 36°C, concentration (M)†, chemical shifts(δ) of acetyl-proton resonances of alkali acetylphenolates in D_2O

Compound	Conc.(M)	$COCH_3(\delta)$	$k_{H-D}(min^{-1})$
Li(ooa)	0.14	2.60	4.0×10^{-2}
Li(poa)	0.13	2.45	1.6×10^{-4}
Na(ooa)	0.13 (0.11)	2.63	5.0×10^{-2} (9.3×10^{-2})
Na(moa)	0.12 (0.11)	2.58	1.2×10^{-2} (2.7×10^{-2})
Na(poa)	0.13 (0.13)	2.45	1.6×10^{-4} (1.7×10^{-3})
K(ooa)	0.13	2.63	5.4×10^{-2}
K(poa)	0.11	2.45	1.6×10^{-4}

†Values obtained from a mixture of the three sodium salts are designated in parentheses.

The presence of intramolecular bonding in alkali–metal salts of Hooa in solution can be confirmed by cation and solvent effects on UV absorptions according to the method of Zaugg and Schaefer.[4] Ultraviolet absorption spectra of the salts of Hooa and Hpoa were measured in dimethylformamide (DMF) and in water: $\pi - \pi^*$ transition energies of acetylphenolate anions were characterized by strong absorptions ($\epsilon_{max} \simeq 10^4$). In Fig. 1, the wave numbers ($\bar{\nu}$ in cm^{-1}) of the corresponding absorption maxima are plotted on the abscissa vs the inverse cation radii($1/r$ in A^{-1}). The cation effects observed in the salts of Hooa markedly in DMF and slightly in water are attributable to the association or the incomplete dissociation of the ooa salts in the solutions. The absence of such a cation effect for the salts of Hpoa shows clearly that the salts are ionized almost completely in solution. The linear correlations of the inverse cation radii with the transition energies show the absence of appreciable covalent interactions between the anions and the alkali metal ions. From Fig. 1, the absorption maxima

for the free solvated anions, ΔE_0, were obtained by extrapolation of the $\bar{\nu}$ values to infinite cation radius($1/r = 0$) followed by conversion of the resulting $\bar{\nu}_0$ to its energy equivalents (Kcal/mol). The hypsochromic shifts observed in going from DMF to water, $\Delta E_0^{H_2O} - \Delta E_0^{DMF}$, were 8.1 Kcal/mol for Hooa and 7.0 Kcal/mol for Hpoa, respectively. These values were then plotted against their respective aqueous pKa values, 10.82[5] for Hooa and 8.05[6] for Hpoa(Fig. 2). The plot for Hpoa fell close to the straight line which had been proposed by Zaugg et al.,[4] showing that the energy of the anionic ground-state-hydration was proportional to the anion

Fig. 1. Correlation of absorption maxima($\bar{\nu}$) with cation radii(r). O(●), Alkali(ooa) in DMF(in H₂O); □(■), Alkali(poa) in DMF(in H₂O).
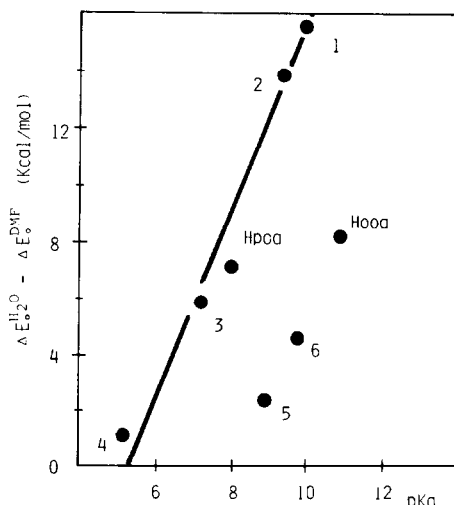
Fig. 2. Plots of anion basicities(pKa) vs ground-state hydration. 1, phenol; 2, p-chlorophenol; 3, p-nitrophenol, 4, dimedone; 5, acetylacetone; 6, dibenzoylmethane. For the values of 1−6, see Ref. 4.

basicity like many phenols and enols with no chelating ability. For Hooa, like β-diketones capable of forming chelate compounds, such a plot deviates from the line. Because of the association with cations in solution, the anionic ground state of Hooa is not stabilized by hydrogen bonded solvation to the extent that the basicity would indicate.

Figure 3 shows cation effects on the exchange-rate constants, k_{H-D}, of alkali–metal salts of Hooa and Hpoa. The presence of a marked cation effect in the salts of Hooa can be taken as a strong evidence of the partial association of Hooa anions with alkali–metal ions in water and, indirectly as an evidence of chelation of Hooa with the cations. The rate constants of the salts of Hooa were found to be inversely proportional to the cationic radii. It was thus suggested that the reactivity of the acetyl-methyl groups in the alkali–metal salts of Hooa was proportional to the magnitude of the ionic or electrostatic interaction between the o-acetylphenolate anion and the alkali–metal ions.

The other type of the cation effects on the exchange rate constant for Na(ooa) was exhibited by a mass action effect from the addition of sodium ion to a solution. Figure 4 shows the change of the exchange-rate constants when various equivalences of sodium iodide were added to 0.13 ± 0.01 M solutions of Na(ooa) in D_2O. The rate constant of Na(ooa) decreases with increasing sodium ion concentration: a limiting constant, 3.7×10^{-2} min^{-1}, is finally reached.

The cation effects on the exchange-rate in this study should be discussed by considering the relative amount of associated and dissociated species in the equilibrium of the salts in D_2O. The order of relative abilities of alkali–metal ions to form chelates, Li > Na > K, has been found for related systems.[7,8] From these results and the data in Figs. 3 and 4, the acetyl–methyl group in the dissociated o-acetylphenolate anion seems to be more active than that in the associated ion pair. However, this phenomenon should be accounted for by change in the amount of an OD$^-$ ion due to the solvation of the anion in the reaction mixture.

The limiting k_{H-D} value, 3.7×10^{-2} min^{-1}, can be taken as the H-D exchange rate constant for the chelated form of Na(ooa). On the other hand, the rate constant for the dissociated form of ooa-anion must be same as or a little larger than the k_{H-D} value of K(ooa), 5.4×10^{-2} min^{-1}. On the basis of these values and the observed rate constant, 5.0×10^{-2} min^{-1} for Na(ooa), the relative
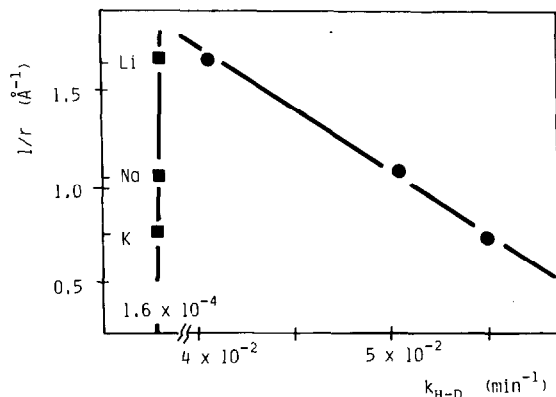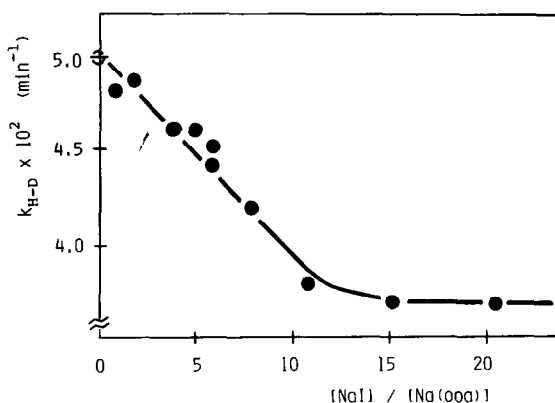
Fig. 4. Plots of exchange-rate constant (k_{H-D}) of Na(ooa) vs mole ratios [NaI]/[Na(ooa)].

amount of associated species in the equilibrium of the salt in D_2O can be estimated to be more than 24% under these conditions. However, the dissociation constant of the salt is not available because of a lack of ideality due to the high concentration and changing ionic strength. When a few equivalents of lithium chloride were added to a 0.13 M solution of Li(ooa) in D_2O, a pale yellow precipitate of Li(ooa) separated out because of its poor solubility in water. Therefore, the NMR spectra of the lithium salt were taken at 0.045 M in D_2O solution; the rate constant changed from about 4×10^{-2} to 3.5×10^{-2} min^{-1} when 10 equivalents of lithium chloride were added. Thus the relative amount of associated species for Li(ooa) could be estimated to be about 75%.

In order to determine the effects of coordinated metal ions other than alkali–metal ions, a mixed ligand complex of palladium(II) with N,N,N',N'-tetramethylethylenediamine (tmen) and Hooa, [Pd(tmen)(ooa)]ClO$_4$, was prepared. This complex was slightly soluble in water and soluble in methanol. The proton exchange of the acetyl group in the Pd(II) complex was complete in CD$_3$OD within 10 hr. The rate constants, k'_{H-D}, of Na(ooa) and Na(moa) in CD$_3$OD solutions (0.11 M) were measured to be 4.6×10^{-1} and 1.8×10^{-2} min^{-1}, respectively. The proton exchange is faster in CD$_3$OD than in D_2O.

By use of mixtures of two or more acetyl compounds in basic CD$_3$OD, the H-D exchange rate of their acetyl–methyl groups could be compared with each other. The decreasing order of the rate constants was observed as follows. The chemical shifts of the acetyl groups are designated in parentheses.

[Pd(tmen)(ooa)]ClO$_4$(δ 2.70) > 4-acetylpyridine (δ 2.64) > 3-acetylpyridine(δ 2.64), p-nitroacetophenone (δ 2.65), o-nitroacetophenone(δ 2.55) $\gtrsim$ m-nitroacetophenone(δ 2.66) > Hooa(δ 2.60) > 2-acetylpyridine(δ 2.68) > acetophenone(δ 2.58) $\gtrsim$ m-methoxyacetophenone(δ 2.57) $\gtrsim$ Hmoa(δ 2.55) > o-methoxyacetophenone(δ 2.57), p-methoxyacetophenone(δ 2.54) > Hpoa(δ 2.42).

Replacement of the hydroxyl group of Hooa by a methoxy group inhibits intramolecular bonding of the molecule, thus the chelate effect disappears. On the other hand, introduction of a nitro group on the benzene ring of acetophenone increases the rate constant of the methyl proton exchange due to decreasing electron density of the aromatic ring. The most important point is the largest rate constant for [Pd(tmen)(ooa)]ClO$_4$. This is

Fig. 3. Correlation of exchange-rate constants(k_{H-D}) with cation radii(r). ●, Alkali(ooa); ■, Alkali(poa).
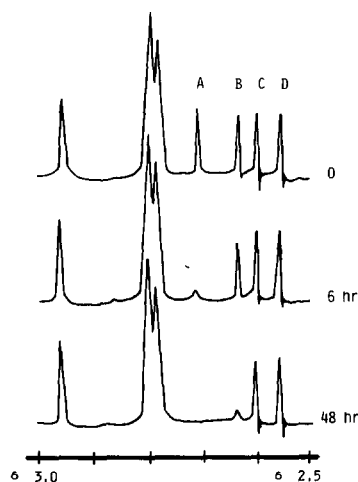
Fig. 5. NMR peaks of acetyl groups of [Pd(tmen)(ooa)]ClO$_4$ (A), Hooa (B), acetophenone (C), and Hmoa (D) measured at appropriate time intervals(hr) after being mixed in CD$_3$OD.

ethylene and methyl protons of "tmen" under a different situation appeared at δ 2.66 and δ 2.58 with time.

The rate constant of the methyl–proton exchange of the Schiff base of Hooa with methylamine, 2-(N-methylacetimidoyl)phenol (or N-methyl-2-hydroxy-acetophenimine), in CD$_3$OD was measured to be 6×10^{-1} min^{-1}, which is extremely large and cannot bear comparison with that of Hooa under the neutral conditions. This can be understood from analogy with ketimine intermediates in amine-catalyzed enolization of acetone.[9] However, it is worthwhile noting that the Schiff base in this study possesses an appreciable amount of a nonaromatic keto amine form in solutions.[10]

The simple application of NMR spectroscopy used in this study turned out to be very effective in revealing chelating ability of acetyl compounds and equilibrium problems of their salts. The chelation of o-hydroxy-acetophenone with alkali-metal ions in water was thus characterized.

attributable clearly to the electron-withdrawing effect of the coordinated metal ion.

Figure 5 shows the NMR peaks of a mixture of [Pd(tmen)(ooa)]ClO$_4$, Hooa, acetophenone, and Hmoa in CD$_3$OD. The singlet at δ 2.96 and two singlets at δ2.81 and δ2.79 were assigned to the ethylene protons and methyl protons of (tmen), respectively. The others are due to the acetyl methyl protons. Without the Pd(II) complex, the H–D exchange of the acetyl group of Hooa did not occur appreciably within a week. The activation of the acetyl protons of Hooa by the Pd(II) complex is ascribed to a slow exchange of the coordinated (ooa) anion. The ligand exchange seemed to be fast when the concentrations of Hooa and OD$^-$ ion in the reaction mixture were high; the acetyl-proton exchange of Na(ooa) in CD$_3$OD was accelerated by the addition of the Pd(II) complex. In a highly basic solution of [Pd(tmen)(ooa)]ClO$_4$ in CD$_3$OD, however, the Pd(II) complex decomposed and new NMR peaks due to the

REFERENCES

[1] T. Kawato, *J. Inorg. Nucl. Chem.* 1977, **39**, 1351.
[2] T. Kawato, *Chem. Lett.* 1976, 1165.
[3] M. Suzuki and Y. Nishida, *J. Inorg. Nucl. Chem.* 1977, **39**, 1459.
[4] H. E. Zaugg and A. D. Schaefer, *J. Am. Chem. Soc.* 1965, **87**, 1857.
[5] A. Agren, *Acta Chem. Scand.* 1955, **9**, 39.
[6] Z. L. Ernst and F. G. Herring, *Trans. Faraday Soc.* 1965, **61** 454.
[7] E. A. Noe and M. Raban, *Chem. Commun.* 1976, 165.
[8] O. Siiman, J. Fresco, and H. B. Gray, *J. Am. Chem Soc.* 1974, **96**, 2347.
[9] M. L. Bender and A. Williams, *J. Am. Chem. Soc.* 1966, **88**, 2502; W. Tagaki and F. H. Westheimer, *Biochemistry* 1968, **7**, 901; G. Hammons, F. H. Westheimer, K. Nakaoka, and R. Kluger, *J. Am. Chem. Soc.* 1975, **97**, 1568.
[10] G. O. Dudek and E. P. Dudek, *J. Am. Chem. Soc.* 1966, **88**, 2407.

STABILITY CONSTANTS OF DIAZA-CROWN-ETHER COMPLEXES OF UNIVALENT METAL IONS AND FREE ENERGIES OF TRANSFER OF LIGAND AND COMPLEXES FROM ACETONITRILE TO SEVERAL SOLVENTS

B. G. COX*
Department of Chemistry, University of Stirling, Stirling FKA 4LA, Scotland

and

P. FIRMAN, H. HORST and H. SCHNEIDER*
Max–Planck-Institut für biophysikalische Chemie, 3400 Göttingen, Germany

Abstract—1:1 complexes of 1,7,10,16-tetraoxa-4,13-diazacyclooctadecane (2,2) with Ag^+ and Tl^+ have been determined by potentiometric pAg measurements in several polar nonaqueous solvents at 25°C. A comparison of the results with those for the cryptand (2,2,2) including alkali metal ions shows that interactions for a given ion with the two ligands are similar but differ considerably for different ions. The free energies of transfer of ligand (2,2) and its complexes have been determined from distribution measurements and are around zero between acetonitrile and aprotic solvents.

The complexes of the monocyclic diaza-polyether ligand, 1,7,10,16-tetraoxa-4,13-diazacyclooctadecane (2,2) with alkali metal ions in water and in methanol[1–4] are less stable than the corresponding complexes of 18-crown-6 (18C6)[4–6] and the bicyclic cryptand (2,2,2)[2,7,8], whereas the stability constants of Ag^+ complexes with (2,2) and (2,2,2) are quite similar and several orders of magnitude larger than the stability constants of the Ag^+ complex with 18C6[2,5–7].

A comparison of the results for these three macrocyclic ligands is of some interest because of certain similarities between them. The monocyclic ligands (2,2) and 18C6 are very similar in structure and have ring cavities of almost equal size, which are formed by a nearly planar, centrosymmetrical arrangement of bonding groups around a cation of appropriate size. Thus a comparison of stability constants for these ligands should show the difference in bonding of ether oxygen and nitrogen. The cavities of (2,2) and (2,2,2) also have almost equal diameters, but (2,2,2) forms a three-dimensional, spherical cavity which is much less flexible in dynamic complexation and decomplexation processes with cations of a given size than the ring cavity of (2,2).

In previous investigations the stability constants, K_s, of (2,2) complexes with alkali metal ions, the silver ion and the thallous ion have been measured in nonaqueous solvents using mainly NMR and conductance measurements.[3,4] These methods are useful for the determination of stability constants for complexes with $K_s \leq 10^5 M^{-1}$, and to complement this work we have carried out potentiometric measurements with the silver electrode in order to obtain stability constants $> 10^5 M^{-1}$ for complexes of (2,2) with mainly Ag^+ and Tl^+. A comparison of the stability constants for metal ion complexes of (2,2) and (2,2,2) shows that interactions for a given ion with the two ligands are similar in nature, but differ considerably

for the different ions, including Ag^+, Tl^+ and alkali metal cations.

In this paper we also report the free energies of transfer of the ligand (2,2) between acetonitrile and various solvents. These values have been used, together with stability constants, to estimate free energies of transfer of $M(2,2)^+$. Among aprotic solvents both $\Delta G_{tr}(2,2)$ and $\Delta G_{tr}(M(2,2)^+)$ are around zero, but in water and methanol the ligand is more strongly solvated and the metal ion complexes less strongly solvated than in acetonitrile.

EXPERIMENTAL AND RESULTS

The macrocycle (2,2)-$HN(CH_2CH_2OCH_2CH_2OCH_2CH_2)_2NH$— was purchased from Merck. Potentiometric titrations showed that the purity of the samples was better than 99%.

Acetone (Baker) was dried over molecular sieves and distilled at atmospheric pressure.

Nitromethane (Baker, Gold Label), hexadecane (Merck) and glycerine (Fluka) were used without further purification. The origin and handling of all other solvents and electrolytes as well as the preparation of solutions has been described previously.[8,9]

The stability constant K_s, of $Ag(2,2)^+$, i.e. the equilibrium constant for the complexation reaction (1) was determined by

$$Ag^+ + (2,2) \rightleftharpoons Ag(2,2)^+ \qquad (1)$$
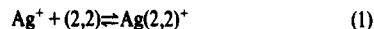
pAg–potentiometry in a direct titration of a silver perchlorate solution with (2,2) using a three compartment cell.[9,10] Total Ag^+ and (2,2) concentrations were around 1×10^{-3} M and 2×10^{-3} M respectively. The solvent used in the preparation of the bridge solution (0.1 M Et_4NClO_4) and the reference solution (1.0×10^{-3} M $AgClO_4$) was always the same as that in the reaction vessel. The ionic strength was varied using Et_4NClO_4 in order to study the effect of ionic strength and ion-pair formation, especially in solvents of low donor number,[11] such as acetone and nitromethane. It was found, however, that the stability constants differed by only 0.3 log K_s units when measured in solutions of low ionic strength ($\leq 10^{-3}$ M) containing only $AgClO_4$ and (2,2) and in solution of ionic strength I = 0.1 M. The stability constants of $Ag(2,2)^+$ are given in Table 1. The accuracy is ± 0.05 in log K_s for the solvents of better solvating ability.

The stability constants of $Ag(2,2)^+$ have been used in con-

---

*Authors to whom correspondence should be addressed.

Table 1. Stability constants (log K_s) of (2,2)-complexes in various solvents at 25°C

Solvent	Ag^+	Tl^+	Li^+	Na^+	K^+	Rb^+	Cs^+
Nitromethane (NM)	13.63; 13.30[a]	7.54; 7.71[a]	6.98	3.37[d]			2.79[d]
Acetonitrile (AN)	7.94	6.82	4.39[d]	4.45; 4.30[f]	4.32[f]	3.37[f]	2.26[d]; 2.48[f]
Propylenecarbonate (PC)	15.57	7.05	3.67[d]				1.95[d]
Acetone (AC)	13.39; 13.14[a]	6.81	2.13[d]	1.96[d]			1.89[d]
Dimethylformamide (DMF)	9.91	3.41; 3.22[d]	~0.0[d]				0.61[d]
Dimethyl sulphoxide (DMSO)	7.39	2.38; 2.13[d]	~0.0[d]	1.19[d]			0.0[d]
Methanol (MeOH)	9.99; 10.18[b]	3.54	1.07[e]	1.0[g]	2.04[h]	`1.2[g]	
Water (W)	7.8[c]; 8.08[f]	1.1[c]					

(a) Ionic strength, I = 0.1 M, adjusted with Et_4NClO_4.
(b) B. Spiess, F. Arnaud-Neu and M. J. Schwing-Weill, *Helv. Chim. Acta* 1980, **63**, 2287.
(c) G. Anderegg, *Helv. Chim. Acta* 1975, **58**, 1218.
(d) M. Shamsipur and A. I. Popov, *Inorg. Chim. Acta* 1980, **43**, 243.
(e) G. Anderegg, *Helv. Chim. Acta* 1981, **64**, 1790; log K_s in methanol/water = 95/5.
(f) S. Kulstadt and Å. Malmsten, *J. Inorg. Nucl. Chem.* 1980, **42**, 573.
(g) J. M. Lehn, *Struct. Bonding* 1973, **16**, 1.
(h) H. K. Frensdorff, *J. Am. Chem. Soc.* 1971, **93**, 600.

junction with equilibrium constants for the exchange reaction (2) to determine the stability constants of $M(2,2)^+$ for the

$$Ag(2,2)^+ + M^+ \rightleftharpoons M(2,2)^+ + Ag^+ \qquad (2)$$
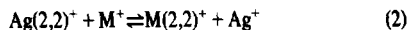
complexation equilibrium (3), where $M^+ = Tl^+$, Ag^+ and Na^+.

$$M^+ + (2,2) \rightleftharpoons M(2,2)^+. \qquad (3)$$
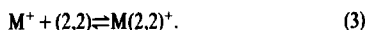
The results are also given in Table 1, and the accuracy in solvents of high donor number is ±0.1 in log K_s.

In order to study the contribution of ligand solvation to the thermodynamics of equilibria (1) and (3), the distribution of (2,2) between hexadecane and various polar solvents, S, has been measured. A solution of known concentration of (2,2) in S was brought into contact with hexadecane, the volume of which was five times larger than that of S, except in the case of S = propylenecarbonate when equal volumes were used. The initial concentration of (2,2) in S was in the range 1×10^{-3} M to 1.5×10^{-2} M. Equilibrium was obtained by vigorous stirring for at least 4 hr at 25.0 ± 0.1°C. The solutions were then allowed to stand for at least 2 hr before three samples from each phase were taken and analyzed by pH-metric titrations with aqueous 10^{-3} M HNO_3 in water using a Metrohm Dosimat E507. A centrifuge was used to separate the phases in distribution experiments with glycerine (see below) and with hexadecane when the densities of the polar solvent (methanol) and hexadecane were similar. In experiments with protic solvents, only the proportion of (2,2) in the hexadecane phase was determined directly. The titration of the hexadecane samples were carried out sufficiently slowly to allow the ligand to reach equilibrium at all stages.

The distribution of (2,2) between hexadecane and water has been analyzed by two different methods. The first method involved equilibration of the hexadecane phase with an aqueous solution of (2,2) containing sufficient tetraethylammonium hydroxide to prevent any significacant protonation of (2,2), followed by analysis of the hexadecane layer using pH-titrations as described above. Since the distribution strongly favoured the aqueous layer, an alternative method of analysis was also used in which the concentration of (2,2) in the hexadecane layer was determined spectrophotometrically as the $Tl(2,2)ClO_4$ complex ($\epsilon = 4950$ M^{-1} cm^{-1} at 237 nm). In this case the separated hexadecane samples were brought into contact with dry $TlClO_4$. This latter method was used for experiments in which the aqueous layer contained no tetraethylammonium hydroxide, and the concentration of unprotonated (2,2) in water was calculated using the known protonation constant (pK = 9.2).[12]

In all cases the partition coefficient, P, of (2,2) between hexadecane (hex) and polar solvent, S, (eqn 4) was determined

$$P = \frac{[2,2]_{hex}}{[2,2]_S} \qquad (4)$$

for at least three different total concentrations of (2,2) and P was found to be independent of concentration. The results are given in Table 2, together with the free energies of transfer of (2,2) from acetonitrile (AN) to the remaining solvents.

$$\Delta G_{tr}(2,2) = -RT \ln ([2,2]_S/[2,2]_{AN}). \qquad (5)$$

It was not possible to determine the free energy of transfer to acetone directly by this method because of the high solubility of acetone in hexadecane. To avoid this problem the partition coefficients of (2,2) between glycerine and (a) acetone (9.4 ± 1.2) and (b) nitromethane (1.31 ± 0.06) were determined and used with the ΔG_{tr} value of nitromethane in Table 2 to calculate the free energy of transfer of (2,2) from acetonitrile to acetone.

DISCUSSION

Inspection of the stability constants in Table 1 shows that they depend upon the properties of the solvents as reflected in the solvation energies of the metal ions (Table 3). In most cases they decrease in the order $Ag^+ > Tl^+ > Li^+ > Na^+ > Cs^+$ but there is an indication that in solvents which are good donors, complexes of Li^+ are less stable than those of the other alkali metals (e.g. in DMSO).

The stability constants of complexes between Ag^+ and (2,2) are almost 6 orders of magnitude larger than those of the corresponding Tl^+ complexes, because of the strong bonding between Ag^+ and the two nitrogen atoms of the ligand. The only exception is in acetonitrile where a competition between the nitrogen atoms of the ligand and solvent for Ag^+ results in the formation of a weaker complex with a stability constant which approaches that for $Tl(2,2)^+$. The stability constants of the Tl^+ complexes, however, are still larger than those of the alkali metal ion–(2,2) complexes. This suggests the presence of an effective covalent interaction in addition to the purely electrostatic interaction assumed to dominate in the formation of alkali metal complexes. The thallous ion does not show any pronounced preference for bonding to nitrogen as opposed to oxygen atom of (2,2), because the thallous ion complexes with (2,2) and 18C6 have stability constants of almost the same magnitude.

The stability constants of the (2,2) complexes in Table

Table 2. Partition coefficients P for the distribution of (2,2) between hexadecane and various polar solvents at 25°C and related free energies of transfer from acetonitrile to the other solvents

Solvent	$10^2 P$	$\Delta G_{tr}(2,2)\,kJ\,mol^{-1}$
Nitromethane	1.28 ± 0.08	-1.2 ± 0.4
Acetonitrile	2.05 ± 0.20	0.0
Propylenecarbonate	3.06 ± 0.22	$+1.0 \pm 0.4$
Acetone		$+3.7 \pm 0.7^a$
Dimethylformamide	2.26 ± 0.18	$+0.2 \pm 0.4$
Dimethyl sulphoxide	2.63 ± 0.05	$+0.6 \pm 0.3$
Methanol	0.72 ± 0.01	-2.6 ± 0.3
Water	0.168 ± 0.007^b; 0.13	-6.2 ± 0.4^b; -6.8

(a) Calculated from the distributions of (2,2) between glycerine and acetone, nitromethane.

(b) Determined spectrophotometrically.

1 may also be compared with those of the corresponding complexes of the macrobicyclic cryptand (2,2,2).[8] A sufficient number of data is available to allow quite reasonable comparison to be made for Ag^+, Tl^+, and Cs^+ cations. The presentation in Fig. 1 shows that the silver ion complexes with (2,2) and (2,2,2) have very similar magnitude, due to the dominant influence of bonding of Ag^+ with the nitrogen atoms of the ligands. The stability constants in all cases are greater than 10^6, and the correlation between them is good, tending to pass through the origin. Although there is some scatter, there is no indication that an increase in the number of oxygen atoms on going from (2,2) to (2,2,2) has a significant effect. A similar correlation exists for Tl^+ complexes, but in this case shifted by 4 to 5 orders of magnitude in K_s below the line for the Ag^+ complexes. This represents the difference in stability between (2,2) and (2,2,2) complexes with Tl^+. The correlations for Tl^+ and Ag^+ in Fig. 1 hold for both protic (filled symbols) and aprotic solvents (open symbols).

Data for the alkali metal complexes are more sparse. However, it may be seen (Fig. 1) that for Cs^+, although only weak complexes are formed, an excellent correlation exists between (2,2) and (2,2,2) complexes, shifted from the origin by 1.4 units. These results are more difficult to interpret because Cs^+ is too large to fit into

the ring and spherical cavities. In an exclusive complex[13] between Cs^+ and (2,2,2), the Cs^+ can presumably interact with only four oxygen atoms, as in the (2,2) complexes. However, the extra stability of Cs^+-(2,2,2) complexes suggests that the third ether bridge does play a role. Where comparison is possible for the smaller alkali metal cations, the results show a significant increase in stability on going from (2,2) to (2,2,2) ligands. In acetonitrile, for example, (2,2,2) complexes of Li^+, Na^+, K^+ and Rb^+ are between 3 (Li^+) and 7 (K^+) orders of magnitude more stable than those of (2,2). A smaller effect for Li^+ (also observed in comparisons between Li^+ and Na^+ complexes in other solvents) probably results from the fact that Li^+ is too small to interact effectively with all of the oxygen atoms in the ligand bridges.

Overall, the comparison between (2,2) and (2,2,2) complexes suggests that except where specific interactions such as between Ag^+ and nitrogen exist, the addition of an extra ether bridge to (2,2) has a strong influence on the stabilities of the complexes, but not on the variation of stability with solvent. The effects may be as large as 6-7 orders of magnitude for cations such as Na^+, K^+, and Tl^+ which are of an appropriate size for the ligand cavities.

The free energies of transfer of the uncomplexed ligand from acetonitrile to the various polar solvents (Table 2) are around zero for aprotic solvents and are negative for transfer to methanol ($-2.6\,kJ\,mol^{-1}$) and water ($-6.2\,kJ\,mol^{-1}$). The stronger solvation of (2,2) in water and methanol relative to the aprotic solvents is probably because of hydrogen bonding between (2,2) and the protic solvents. The ΔG_{tr} values of ligand and metal ions (Tables 2 and 3) have been combined with the stability constants in Table 1 to calculate the free energies of transfer of the complexes, ΔG_{tr} $[M(2,2)^+]$ between acetonitrile (AN) and solvent S as in equation (6).

$$\Delta G_{tr}[M(2,2)^+] = \Delta G_{tr}(2,2) + \Delta G_{tr}(M^+) - RT \ln\{K_s(S)/K_s(AN)\}. \quad (6)$$

The results in Table 3 demonstrate that ΔG_{tr} $[M(2,2)^+]$ values are around zero for transfer among acetonitrile, propylene carbonate, acetone and dimethylformamide. Dimethyl sulfoxide seems to be an exception to this behaviour with ΔG_{tr} values grouped around $-8.5\,kJ$ mol^{-1}, although only three results are available. The complexes $M(2,2)^+$ in methanol and particularly in water are in a higher free energy state than in acetonitrile
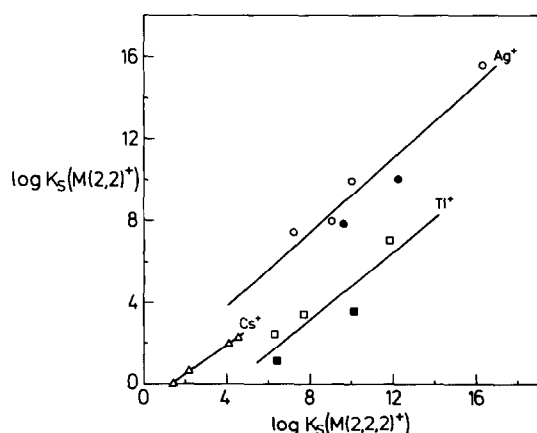
Fig. 1. Comparison between stability constants (log K_s) of (2,2) and (2,2,2) complexes with Ag^+, Tl^+ and Cs^+ in several solvents. (protic solvent: filled symbols; aprotic solvents: open symbols).

Table 3. Free energies of transfer (kJ mol⁻¹) for metal ions and their complexes[a] with (2,2) from acetonitrile to polar solvents at 25°C

Solvent[b]	$\Delta G_{tr}(\text{Ag}^+)$	$\Delta G_{tr}[\text{Ag}(2,2)^+]$	$\Delta G_{tr}(\text{Tl}^+)$	$\Delta G_{tr}[\text{Tl}(2,2)^+]$	$\Delta G_{tr}(\text{Li}^+)$	$\Delta G_{tr}[\text{Li}(2,2)^+]$	$\Delta G_{tr}(\text{Na}^+)$	$\Delta G_{tr}[\text{Na}(2,2)^+]$	$\Delta G_{tr}(\text{Cs}^+)$	$\Delta G_{tr}[\text{Cs}(2,2)^+]$
NM	46.2[c]	12.5	6.8[c]	1.5	20.7[g]	4.7	12.6[g]	17.6	-2.0[g]	-6.2
AN	0.0[d]	0.0	0.0	0.0	0.0	0.0	0.0	0.0	0.0	0.0
PC	42.3[d]	-0.3	-0.8[f]	-1.1	-1.1[d]	4.0	1.9[d]		-0.9[d]	1.9
AC	25.7[c]	-1.7	-6.7[c]	-2.9			-9.7[c]	8.2	-5.8[c]	0.0
DMF	6.4[d]	-4.6	-20.9[f]	-1.2						
DMSO	-11.9[d]	-8.2	-34.3[f]	-8.4	-18.7[d]	-2.3	-28.6[d]	-9.4	-12.0[d]	-2.4
MeOH	30.8[d]	16.5	-5.0[f]	11.1			-4.4[d]	12.7		
W	23.0[d]	17.6	-9.2[f]	17.3						

(a) The free energies of transfer of the complexes have been calculated (eqn 5) using always the first value of log K_s in Table 1.
(b) Abbreviations as in Table 1.
(c) R. Alexander, A. J. Parker, J. H. Sharp and W. E. Waghorne, *J. Am. Chem. Soc.* 1972, **94**, 1148; $\Delta G_{tr}(\text{Ph}_4\text{As}^+) = \Delta G_{tr}(\text{BPh}_4^-)$ assumption.
(d) Calculated from ΔG_{tr} (MI) values in B. G. Cox, J. Garcia-Rosas and H. Schneider, *J. Am. Chem. Soc.* (1981) **103**, 1384, using $\Delta G_{tr}(\text{I}^-)$ from water to non-aq. solvents: 6.7 kJ mol⁻¹ (MeOH); 14.3 kJ mol⁻¹ (PC) from M. H. Abraham and A. F. Danil de Namor, *J. C. S. Faraday I*, 2101 and 18.8 kJ mol⁻¹ (AN); 13.4 kJ mol⁻¹ (DMSO); 18.8 kJ mol⁻¹ (DMF) from ref. *f*.
(e) G. Gritzner, *Inorg. Chim. Acta* 1977, **24**, 5; $\Delta G_{tr}(\text{BBCr}^-) = \Delta G_{tr}(\text{BBCr}^+)$ assumption.
(f) B. G. Cox, *Ann. Rep. Prog. Chem., Sect. A, Phys. Inorg. Chem.* 1973, **70**, 249, $\Delta G_{tr}(\text{Ph}_4\text{As}^+) = \Delta G_{tr}(\text{BPh}_4^-)$ assumption.
(g) J. Badoz-Lambling and C. J. Bardin, *J. Electrochim. Acta* 1975, **19**, 725; $\Delta G_{tr}(\text{Fic}^+) = \Delta G_{tr}(\text{Foc})$ assumption with respect to water and combined with data from *f*.

and in this respect are solvated like large organic ions. The only exception to this is Li(2,2)$^+$ in methanol.

The data do not indicate any noticeable contribution to the free energies of transfer of the complexes from a direct interaction between that part of the metal ion in the M(2,2)$^+$ complexes which is not covered by the ligand. Taking the extremes of dimethyl sulphoxide as a very good cation solvator and nitromethane as a very poor solvent for cations, it is possible to see evidence of some dependence of ΔG_{tr} [M(2,2)$^+$] on the metal ions, but in general there is little correlation between ΔG_{tr} [M(2,2)$^+$] and ΔG_{tr}(M$^+$) values. Ion association involving the uncomplexed cations may provide an obvious explanation for the more positive ΔG_{tr}[M(2,2)$^+$] values observed for transfer to nitromethane, although the slight variation in log K_s with changes in ionic strength argues against this.

REFERENCES

[1] H. K. Frensdorff, *J. Am. Chem. Soc.* 1971, **93**, 600.

[2] G. Anderegg, *Helv. Chim. Acta* 1975, **58**, 1218.

[3] S. Kulstad and L. Å. Malmsten, *J. Inorg. Nucl. Chem.* 1980, **42**, 573.

[4] M. Shamsipur and A. I. Popov, *Inorg. Chim. Acta* 1980, **43**, 243.

[5] R. M. Izatt, R. E. Terry, B. L. Haymore, L. D. Hansen, N. K. Dalley, A. G. Avondet and J. J. Christensen, *J. Am. Chem. Soc.* 1976, **98**, 7620.

[6] J. D. Lamb, R. M. Izatt, C. S. Swain and J. J. Christensen, *J. Am. Chem. Soc.* 1980, **102**, 475.

[7] J. M. Lehn and J. P. Sauvage, *J. Am. Chem. Soc.* 1975, **97**, 6700.

[8] B. G. Cox, J. Garcia-Rosas and H. Schneider, *J. Am. Chem. Soc.* 1981, **103**, 1384.

[9] J. Gutknecht, H. Schneider and J. Stroka, *Inorg. Chem.* 1978, **17**, 3326.

[10] B. G. Cox, H. Schneider and J. Stroka, *J. Am. Chem. Soc.* 1978, **100**, 4746.

[11] V. Gutmann, *Coordination Chemistry in Nonaqueous Solvents.* Springer-Verlag, Vienna (1968).

[12] F. Arnand-Neu, B. Spiess and M.-J. Schwing-Weill, *Helv. Chim. Acta* 1977, **60**, 2633.

[13] E. Mei, A. I. Popov and J. L. Dye, *J. Am. Chem. Soc.* 1977, **99**, 6532.

ETHYLPHOSPHINEDIACETIC ACID: SYNTHESIS, CHARACTERIZATION AND COORDINATING BEHAVIOUR TOWARDS Ca(II), Ni(II) AND Hg(II) IONS IN SOLUTION†

D. NOSKOVÁ and J. PODLAHOVÁ*

Charles University, Department of Inorganic Chemistry, 12840 Prague, Czechoslovakia

Abstract—The new ligand, ethylphosphinediacetic acid, H_2Z, was synthesized and characterized by spectral methods. The Z^{2-} anion is protonated in three steps with the pK values of 6.10 (phosphorus atom), 2.75 and 0.9 (carboxyl groups). The ligand is highly selective for soft metal ions as demonstrated by the stability constants of the water-soluble complexes $CaHZ^-$ (log β_{CaHZ}^{HZ} 0.73), NiZ_2^{2-} (log β_2 9.06) and HgZ_4^{6-} (log β_4 40.9). The differences in behaviour compared to related phosphineacetic acids are mainly consequences of the high basicity of the phosphorus atom.

Tertiary phosphines bearing a second functional group of the hard donor type, which are frequently called "hybrid" ligands[1,2] possess interesting potential capabilities, e.g. in homogeneous catalysis.[3] With properly chosen hard donor groups, a further potential advantage of the designed ligands can be achieved, namely the solubility of the ligands and/or their complexes in polar solvents including water. Such a class of compounds is represented by two series of phosphineacetic acids synthesized and studied in this laboratory:[4] (C_6H_5)$_{3-n}$ P(CH$_2$COOH)$_n$ ($n = 1^{4a}$, 2^{4b}, 3^{4c}) and (C_6H_5)$_{2-m}$ (HOOCCH$_2$)$_m$PCH$_2$CH$_2$P(CH$_2$COOH)$_m$(C_6H_5)$_{2-m}$ ($m = 1^{4d}$, 2^{4e}). The presence of the phenyl groups in these ligands, which is advantageous in synthetic respects, however, considerably lowers both the σ-basicity of phosphorus and the solubility of the ligands in water. It was the aim of this work to investigate the influence of the ethyl group as a less sterically and electronically demanding substituent on the coordinating properties of the –P(CH$_2$COOH)$_2$ portion.

EXPERIMENTAL

All synthetic work and manipulation with solutions were carried out under inert gas (nitrogen or argon) with solvents dried and degassed before use.

The chemicals used were products of the firms Lachema, Merck and Pierce Inorganics and were purified by appropriate methods where necessary. Metal perchlorate solutions containing a slight excess of perchloric acid were prepared from CaCO$_3$, basic nickel carbonate or HgO by dissolving them in 30% perchloric acid and heating to expel CO$_2$. They were analyzed for the metals by EDTA titration and for excess acid by the Gran method. Sodium perchlorate was purified following the recommended procedure.[5] Triply distilled mercury was used for polarographic measurements.

Physical measurements and data treatment were described previously.[4e,6]

Ligand synthesis

A solution of ethyl bromzincacetate was prepared[7] from 66.0 g zinc (1.01 mol; 200 mesh, activated with iodine) and 167 g ethyl bromoacetate (1.00 mol; freshly distilled) in 250 cm³ ether. Ethyl-

dichlorophosphine[8] (58.9 g; 0.45 mol) in 100 cm³ ether was added dropwise at −35 to −40°C. After allowing the mixture to warm to room temperature, the excess organometallic was destroyed with 150 cm³ water and the ether layer was washed with water and dried over sodium sulphate. Distillation at 126–127°C/90 Pa gave ethylphosphinediacetic acid bis(ethyl ester) as a colourless liquid in 67% yield. The ester is slowly oxidized in air, $n_D^{25} = 1.4671$. For $C_{10}H_{19}O_4P$ found C, 50.54; H, 8.21; P, 12.95; calc. C, 51.28; H, 8.18; P, 13.22. IR (neat): 460w ν(PC), 580w, 662w, 855w, 953w, 1038m, 1120vs ν_s(COC), 1272vs ν_{as}(COC), 1370–1470w δ(CH$_2$, CH$_3$), 1743vs ν(C=O), 2880–2990m ν(CH$_2$, CH$_3$). ^{1}H-NMR (CDCl$_3$): 1.00 ppm, 3H, triplet, ^{3}J(H, H) 7 Hz, PCH$_2$C*H*$_3$; 1.25, 6H, triplet, ^{3}J(H, H) 7, OCH$_2$C*H*$_3$; 1.48, 2H, overlapping doublet of quartets, ^{2}J(P, H) 11, ^{3}J(H, H) 7, PC*H*$_2$CH$_3$; 2.57, 4H, doublet, ^{2}J(P, H) 6, PC*H*$_2$COO; 4.17, 4H, quartet, ^{3}J(H, H) 7, OC*H*$_2$. ^{31}P{^{1}H}-NMR (CDCl$_3$): −23.15 singlet.

The ester (70.0 g; 0.30 mol) was dissolved in 500 cm³ petroleum ether (40–60°C) and the solution of sodium hydroxide prepared from 20.7 g sodium metal (0.90 mol) and 500 cm³ 96% ethanol was added. After several hours at *ca.* 0°C, the crude disodium salt was filtered, washed with ethanol and dried *in vacuo* yielding 54.6 g of a white powder. According to TLC, IR and NMR, the salt contained small amounts of phosphine oxide and unhydrolyzed ester groups as impurities. The crude salt (54.0 g) was vacuum-evaporated at 40°C with 85 cm³ 48% HBr and the product was extracted into 600 cm³ hot acetonitrile. The filtrate was vacuum-evaporated to dryness and the resulting oil was crystallized from acetic acid to obtain 46.6 g ethylphosphinediacetic acid hydrobromide as colourless hygroscopic crystals of m.p. 74°C (sealed capillary). The compound is stable in dry air and fairly soluble in water. For $C_6H_{12}BrO_4P$ found C, 28.01; H, 4.83; P, 11.85; Br, 30.60; alcalim. equiv. 86.5; calc. C, 27.82; H, 4.67; P, 11.96; alcalim. equiv. 86.35. IR (nujol, hexachlorobutadiene): 455m ν(PC), 656s, 792m, 820m, 910s, 944s, 1028w, 1275s δ(COH), 1372w δ(CH$_3$), 1390w δ(COH), 1470w δ(CH$_2$), 1735vs ν(C=O), 2410m, ν(PH), 2910w ν(CH$_2$), 2950vs,b ν(OH), 2970w ν(CH$_3$), 3400s,b ν(OH). ^{1}H-NMR (H$_2$O): 1.29, 3H, doublet of triplets, ^{3}J(P, H) 19, ^{3}J(H, H) 8, CH$_3$; 2.50, 2H, overlapping doublet of quartets, ^{2}J(P, H) 13, ^{3}J(H, H) 8, PC*H*$_2$CH$_3$; 3.72, 4H, doublet, ^{2}J(P, H) 13, PCH$_2$COO. ^{31}P{^{1}H}-NMR (D$_2$O): 5.02 singlet.

The hydrobromide (21.0 g; 0.081 mol) was dissolved in a slight excess of 5M-NaOH and the pH was carefully adjusted to 8.0 with a HBr solution. The solution was added dropwise with stirring to a mixture of 250 cm³ methanol and 250 cm³ ether. The precipitated disodium salt was filtered off, washed thoroughly with methanol and dried *in vacuo*. Yield 17.6 g (98%) of a white powder, soluble in water, stable under inert gas, limitedly stable in air (oxidation to phosphine oxide with $\tau_{1/2}$ *ca.* 4 months). For $C_6H_9Na_2O_4P$ found C, 32.51; H, 4.20; Na, 20.55; P, 13.77; calc. C, 32.45; H, 4.08; Na, 20.67; P, 13.49. IR (nujol, hexachlorobutadiene): 449m ν(PC), 623w, 665w, 817w, 936m, 1132s, 1382s

---

†Part XXI in the series "Compounds structurally related to complexones—XX", *Coll. Czech. Chem. Commun.*, in press.
*Author to whom correspondence should be addressed.

ν_s(COO), 1390–1450w δ(CH$_2$, CH$_3$), 1590vs ν_{as}(COO), 2880–2970w ν(CH$_2$, CH$_3$). ^{1}H-NMR (D$_2$O): 1.06, 3H, overlapping doublet of triplets, ^{3}J(P, H) 16, ^{3}J(H, H) 7, CH$_3$; 1.51, 2H, overlapping doublet of quartets, ^{2}J(P, H) 7, ^{3}J(H, H) 7, CH$_2$CH$_3$; 2.47, 4H, doublet, ^{2}J(P, H) 2, PCH$_2$COO. ^{31}P{^{1}H}-NMR (D$_2$O): −24.68 singlet.

RESULTS AND DISCUSSION

The synthetic procedure followed a general method used before.[4b,c,e] The ligand was isolated with a total yield of 40% as the well-crystallizing hydrobromide and the disodium salt. Numerous attempts to obtain the free acid met with no success.

The protonation of the Z^{2-} anion is described by the constants given in Table 1. The constant K$_3$ = [H$_3$Z]/([H][H$_2$Z]) was determined by spectrophotometry with p-nitroaniline as indicator[9] at I = 1.0(H, K)Cl because of the high acidity required for the protonation. The mechanism of the proton uptake follows clearly from the IR and NMR spectra of the ligand in D$_2$O solutions of various acidity.

The ν_{as}(COO) region of the IR spectra is presented in Fig. 1. The four possible forms of the carboxyl group absorb in three separate regions[10]: R$_2$PCH$_2$COO$^-$ at ca. 1575 cm^{-1}, R$_2$P$^+$(H)CH$_2$COO$^-$ at 1615 cm^{-1} and R$_2$PCH$_2$COOH together with R$_2$P$^+$(H)CH$_2$COOH at ca. 1720 cm^{-1}. It is obvious from the spectra that the first proton added is bonded completely to the phosphorus atom and the second to the carboxyl. The ratios of the computer-separated areas under the peaks agree within experimental error with those calculated from the proton association constants (after an appropriate correction of the pH-readings in D$_2$O). The protonation of the second carboxyl group could not be followed by IR spectra because of poor transmittance of strong DCl solutions in the cells used.

The proposed mechanism is strongly supported by the
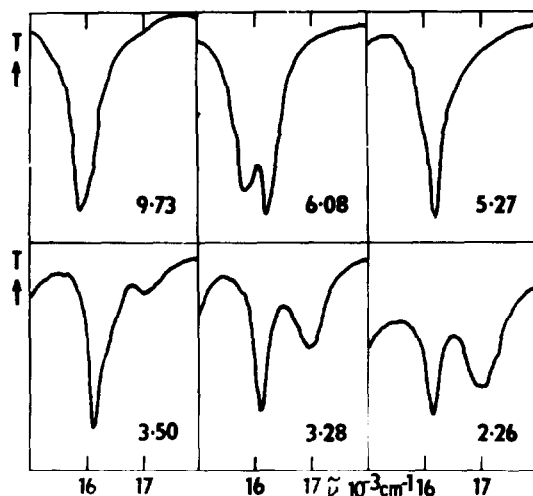
Fig. 1. The IR spectra of 0.2M solutions of Na$_2$Z in D$_2$O at various pD.

NMR spectra. Control ^{1}H spectra were always taken in H$_2$O because of the fast exchange[11] of the PCH$_2$COO protons with deuterium in acid solution. The exchange at pH 2 is essentially complete within 20 min at room temp. Fig. 2 summarizes the shifts of various hydrogen atoms and of the phosphorus atom with acidity. The results are in complete accordance with the conclusions following from the IR spectra and, in addition, confirm the bonding of the third proton to the second carboxyl group. Besides the chemical shifts, the P, H coupling constants are also acidity-dependent but, as usual,[12,13] with no readily interpretable trends. The extensive broadening of the phosphorus resonance during the uptake of the first proton indicate a relatively slow (in the NMR time scale)

Table 1. Cumulative stability constants of ethylphosphinediacetate complexes at 25°C and I = 0.1(NaClO$_4$). Charges are omitted for clarity. ^{a}gl—potentiometry with a glass electrode; sp—spectrophotometry. pol—polarography. ^{b}log [H$_3$Z]/([H][H$_2$Z]), I = 1.0(H, K)Cl. ^{c}log [CaHZ]/([Ca][HZ])

Complex	log β ($\sigma_{\log\beta}$)	Concn. range studied −log(mol dm^{-3})	Method ^{a}
HZ	6.10(4)	Z, 2.7–3.2	gl
H$_2$Z	8.86(7)	H, 2–12	
H$_3$Z	0.9(1)^b	Z, 1.8–2.2	sp
		H, 0.3–2.5	
CaHZ	0.73(9)^c	Ca, 2.0–3.0	gl
		Z, 1.8–3.5	
		H, 3.0–7.5	
NiZ$_2$	9.06(2)	Ni, 2.0–4.0	gl, sp
NiHZ$_2$	12.69(5)	Z, 2.2–3.0	
NiH$_2$Z$_2$	16.21(6)	H, 2–12	
HgZ$_4$	40.9(1)	Hg, 2.7–4.5	pol
HgHZ$_4$	44.8(1)	Z, 2.5–3.5	gl
HgH$_2$Z$_4$	47.9(1)		
HgH$_3$Z$_4$	50.7(1)		
HgH$_4$Z$_4$	53.2(2)		
HgH$_5$Z$_4$	55.3(2)		
HgH$_6$Z$_4$	57.2(2)		
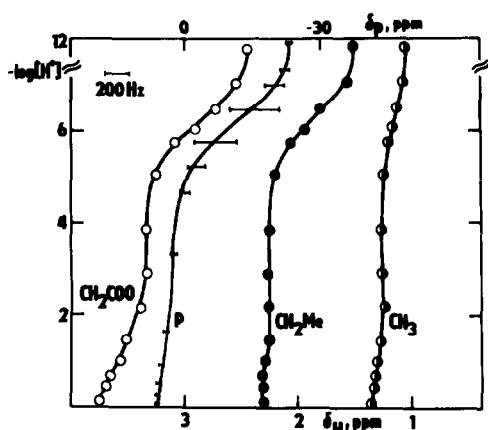
Fig. 2. The dependence of the chemical shifts of hydrogen atoms (lower scale) and phosphorus (upper scale) on acidity.

exchange of protons between the phosphine and the phosphonium structure of the ligand.

The mechanism of the proton uptake can be summarized as follows:

$$C_2H_5P(CH_2COO^-)_2 \overset{H}{\rightarrow} C_2H_5\overset{|}{P^+}(CH_2COO^-)_2 \rightarrow$$

$$\overset{H}{\underset{\rightarrow C_2H_5P^+}{|}}\diagup{CH_2COO^-}\diagdown{CH_2COOH}$$

$$\overset{H}{\rightarrow C_2H_5\overset{|}{P^+}(CH_2COOH)_2}.$$
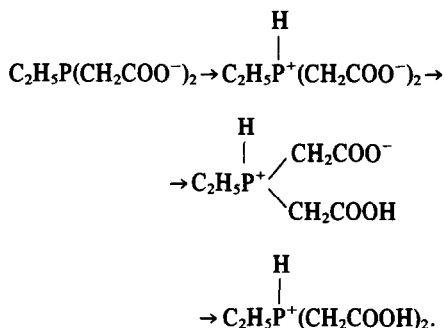
Hence, no tautomerization equilibria typical for the closely related ethylenediphosphinetetraacetate anion[10] take place for Z^{2-}.

For the investigation of the coordinating behaviour of the ligand, the Ca(II), Ni(II) and Hg(II) ions were selected as typical representatives of the hard, intermediate and soft type, respectively. Table 2 summarizes the stability constants of the complexes which describe best the experimental data accumulated in the regions given.

The stability of the complexes in solution clearly demonstrates the highly selective behaviour of the ligand towards metal ions, depending on their softness. In general, this behaviour is similar to that of the phosphineacetates studied previously but markedly different from the nitrogen analogue of the ligand.[14,15]

The hard Ca(II) ion is probably bonded only to the carboxyl group(s) with the phosphorus atom remaining uncoordinated and protonated. From this point of view, the lowering of pH on complex formation between Ca(II) and HZ^- must be only inductive in origin and does not reflect a direct competition of Ca^{2+} and H^+ ions for the phosphorus atom. This concept is supported by the similarity of the constant β_{CaHZ}^{HZ} to those of Ca complexes of α, ω-dicarboxylic acids.[16] For example, Ca(II) glutarate, which is structurally analogous but contains the CH_2 group instead of phosphorus, has the $\log \beta_1$ value of 0.55 to 1.06 depending on the experimental conditions.[17,18]

Nickel(II) as a typical representative of borderline ions forms complexes with Z^{2-} in which the coordination of phosphorus must be assumed as the factor mainly res-

ponsible for their stability. As can be seen from the disappearance of the yellow colour, the nickel-phosphorus bond remains intact in the region of the protonation of phosphorus in the free ligand (pH ca. 6) and of the first carboxyl group (pH ca. 4.5) but breaks down at pH < 3.5, where both carboxyl groups became protonated. Clearly, the ligand cannot coordinate to nickel in aqueous solution through phosphorus alone but can only chelate together with, most probably, one carboxyl group. This situation is markedly different from that of P,P-chelating bis(phosphine)acetates[6,19] but similar to monophosphineacetates.[4a,20,21] The most closely related ligand of this kind, phenylphosphinediacetic acid, yields also a 1:2 nickel complex[21] which is, however, considerably less stable ($\log \beta_2$ 6.49) despite the fact that it is octahedral with terdentate ligands. The stability, diamagnetism and the UV-visible spectrum of the NiZ_2^{2-} complex strongly support a square-planar structure with P,O-bidentate ligands. The uncoordinated carboxyl groups are readily protonated without noticeably changing the coordination environment of nickel. The obvious explanation for this specific behaviour of the Z^{2-} ligand is the higher basicity of phosphorus producing a stronger ligand field which forces spin-pairing in the complex.

The typically soft mercury(II) ion forms a highly stable 1:4 complex with the ligand studied. Its 1:4 analogues with other phosphineacetates are either of considerably lower stability or cannot be detected at all. Again, the evident reason is the higher basicity and lower steric requirements of the ethyl-substituted phosphorus atom. Most probably, the ligand is coordinated to mercury in a monodentate fashion through the phosphorus atom, and the carboxyl groups are protonated quite independently without any noticeable influence on the HgP_4 core.

REFERENCES

[1] W. Levason and C. A. McAuliffe, Advan. Inorg. Chem. Radiochem. 1972, 14, 173.

[2] C. J. Moulton and B. L. Shaw, J. Chem. Soc. Dalton Trans. 1980, 299 and references therein.

[3] R. G. Nuzzo, D. Feitler and G. M. Whitesides, J. Am. Chem. Soc. 1979, 101, 3683.

[4a] T. Jarolím and J. Podlahová, J. Inorg. Nucl. Chem. 1976, 38, 125; [b] J. Podlahová, Coll. Czech. Chem. Commun. 1978, 43, 57. [c] J. Podlahová, Ibid. 1978, 43, 3007. [d] J. Ludvík and J. Podlahová, J. Inorg. Nucl. Chem. 1978, 40, 967. [e] J. Podlahová and J. Podlaha, Coll. Czech. Chem. Commun. 1980, 45, 2049.

[5] G. Biederman and L. G. Sillén, Ark. Kemi 1953, 5, 425.

[6] J. Podlahová and J. Podlaha, Coll. Czech. Chem. Commun. 1982, 47, 1078.

[7] M. W. Rathke, Organic Reactions 1975, 22, 423.

[8] I. P. Komkov and K. V. Karavanov, Zh. Obshch. Khim. 1958, 28, 2963.

[9] K. N. Bascombe and R. P. Bell, J. Chem. Soc. 1959, 1096.

[10] J. Podlahová, B. Kratochvíl, V. Langer, J. Šilha and J. Podlaha, Coll. Czech. Chem. Commun. 1981, 46, 3063.

[11] M. T. Reetz and F. Eibach, Liebig's Ann. 1977, 242.

[12] L. I. Petrovskaya, M. V. Proskurnina, Z. S. Novikova and I. F. Lutsenko, Izv. Akad. Nauk USSR, Ser. Khim. 1968, 1277.

[13] M. J. Gallagher, Austr. J. Chem. 1968, 21, 1197.

[14] Z. Mighri and P. Rumpf, Bull. Soc. Chim. Fr. 1975, 689.

[15] M. B. Jones and L. Pratt, J. Chem. Soc. Dalton Trans. 1976, 1207.

[16] L. G. Sillén and A. E. Martell, Stability Constants, Chem. Soc. Spec. Publ. No. 17 (1964), No. 25 (1971).

[17] R. K. Cannan and A. Kirbrick, J. Am. Chem. Soc. 1938, 60, 2314.

[18] J. Schubert and A. Lindenbaum, J. Am. Chem. Soc. 1952, 74, 3529.

[19] J. Ludvík and J. Podlahová, J. Inorg. Nucl. Chem. 1978, 40, 1045.

[20] J. Podlahová, Coll. Czech. Chem. Commun. 1980, 45, 1477.

[21] J. Podlahová, Coll. Czech. Chem. Commun. 1978, 43, 64.

PRECIPITATION AND COMPLEX FORMATION IN THE SYSTEM Mn(ClO₄)₂–Na₄P₂O₇–pH (295 K, $I = 0.5$ AND $I \approx 0$ mol dm⁻³)*

HALKA BILINSKI

Department of Physical Chemistry, "Ruder Boškovic" Institute, Zagreb, Yugoslavia

Abstract—The precipitation of manganese from aqueous solution of manganese perchlorate and sodium pyrophosphate was investigated in a broad concentration range of both precipitation components and at various pH values, at 295 K and $I = 0.5$ mol dm⁻³. Tyndallometric technique was used. A soluble range has been observed in ten-fold excess of pyrophosphate and at $7 < pH < 10$, where manganese forms complex with pyrophosphate. In the precipitation range the following precipitates were identified: $Na_2MnP_2O_7$, $Mn_2P_2O_7$ and MnO_x. Quantitative solubility experiments have been performed at $I \approx 0$ mol dm⁻³.

From experimental data the following values for equilibrium constants have been obtained:

$$\log [Mn^{2+}]^2 \cdot [H_2P_2O_7^{2-}] \cdot [H^+]^{-2} = -1.39$$

$$\log [MnP_2O_7^{2-}]^2 \cdot [P_2O_7^{4-}]^{-1} = -4.22$$

$$\log [MnP_2O_7^{2-}][Mn^{2+}]^{-1} \cdot [P_2O_7^{4-}]^{-1} = 6.51.$$

A brief and the most complete survey of the work on complex formation between different metal ions and pyrophosphate ion is given in Tables of Stability constants by Sillén and Martell[1] and by Martell and Smith.[2] The chemistry of pyrophosphate was extensively investigated after 1964. Miller and Parris[3] have synthetized pyrophosphate at low temperature, using compounds with high free energies of hydrolysis that might have occurred on the primitive earth. They suggested that pyrophosphate may have played an important part in polymerisation and dehydration reactions of organic compounds leading to the origin of life. Baltscheffsky and Stendigk[4] have investigated inorganic pyrophosphate in connection with biological energy transformations. They suggested that inorganic pyrophosphate may serve as energy donor in phosphorylating electron transport system. Zell et al.[5] have found that degradation of DNA by H_2O_2 producing methylhydrazines was stopped by pyrophosphate. This effect was attributed to complex formation of manganese ions with pyrophosphate, which prevented the formation of the catalytically active ternary complex. Equilibrium constant of soluble complex has according to our knowledge not yet been determined.

Solid $Mn_2P_2O_7$ is applied in number of industries as on synthesis of high polymers,[6] in ceramic materials,[7] in textiles[8] and in plastic technology,[9] but its solubility constants has not been determined. The pyrophosphates of calcium[10] and zinc[11,12] whose atomic numbers are close to that of manganese have been more investigated.

The aim of this work was to find concentration and pH conditions where manganese forms precipitate or soluble complex with pyrophosphate ligand and to determine the stability constant of the complex formed.

EXPERIMENTAL

Chemicals. Solutions were prepared by dissolving the following reagent grade chemicals in twice distilled water: $Mn(ClO_4)_2 \cdot 6H_2O$, $NaClO_4$ anhydrous, $HClO_4$ (G. Frederick Smith Chemical Co., Columbus, Ohio); $Na_4P_2O_7 \cdot 10H_2O$ (J. T. Baker Chemical Co., Phillipsburg, New Jersey); NaOH (Reagent A. C. S. Code 2255 Gen. Chem. Div. Morristown, New Jersey). Stock solutions were standardized.

Qualitative precipitation experiments were performed using the method described earlier by Tezak et al.[13] in the following way: Samples were made up in glass tubes by mixing 5 cm³ of diluted manganese perchlorate of constant concentration in each series and 5 cm³ of sodium pyrophosphate of various concentrations. Both precipitation components varied in concentrations. In another series of qualitative experiments the influence of pH was studied at constant concentration of manganese perchlorate in all samples. Sodium hydroxide or perchloric acid were added to various concentrations of sodium pyrophosphate. Constant ionic strength $I = 0.5$ mol dm⁻³ was adjusted by adding sodium perchlorate. For determination of solubility of $Mn_2P_2O_7$(s) and for determination of stability constants of the formed complex, samples were prepared in 250 cm³ volumetric flasks, aged 10–12 days, centrifuged and analyzed for manganese and pH. Soluble pyrophosphate was calculated as $[P_2O_7]_{sol} = [P_2O_7]_{tot} - ([Mn]_{tot} - [Mn]_{sol})/2$

Instruments. "Precipitation bodies" have been determined by observing the Tyndall effect in the beam of strong light or by Zeiss tyndallometer attached to a Pulfrich photometer. Crystals were detected by naked eye. X-ray diffraction patterns of some characteristic precipitates were used to distinguish various manganese salts. Precipitates were separated from supernatants using Beckman Model L-2 ultracentrifuge with 28000 RPM for 30 min. Soluble manganese was determined by Beckman Model D U Quartz Spectrophotometer with quartz cells of 1, 2, 5 and 10 cm, using formaldoxime method.[14] The concentration of [H⁺] was determined by a Radiometer 25 pH-meter with a glass and calomel electrode.

RESULTS

Figure 1 presents one type of "precipitation body" of manganese pyrophosphate system, when both precipitation components varied in concentration. Ionic

---

*The work has been performed in part at Department of Environmental Health and Engineering, California Institute of Technology, Pasadena, CA, U.S.A.
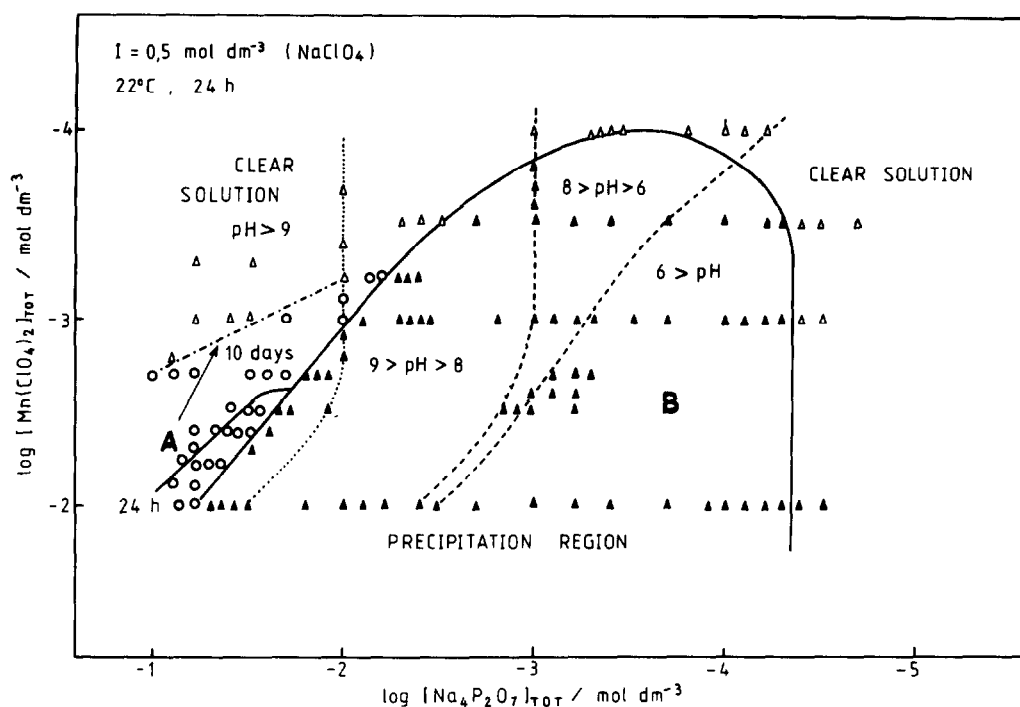
Fig. 1. The ground plan of a three-dimension concentration tyndallogram. The solubility limit after 24 hr of ageing is plotted vs the log. concn. of manganese perchlorate and sodium pyrophosphate. The metastable range of phase A became broader after 10 days. ($I = 0.5$ mol dm^{-3}, 295 K).

strength is 0.5 mol dm^{-3} (NaClO$_4$ was added). After 24 hr of ageing two types of precipitate have been observed and identified:

(a) Na$_2$MnP$_2$O$_7$ and   (b) Mn$_2$P$_2$O$_7$.

Upon standing 10–12 days, range A became much broader. It is evident from Fig. 1 that both salts of manganese pyrophosphate readily dissolve with increasing concentration of pyrophosphate. The effect can be attributed to the ability of pyrophosphates to form soluble complexes with a number of cations.

In Fig. 2 is presented the precipitation diagram observed after 24 hr, for constant manganese concentration $1 \cdot 10^{-3}$ mol dm^{-3}, for various pyrophosphate concentrations in the range from $2 \cdot 10^{-5}$ to $6 \cdot 10^{-2}$ mol dm^{-3} and for pH values from 1.5 to 11.5. The solid phase corresponds to Mn$_2$P$_2$O$_7$. Narrow range of soluble complexes exists at pH from 7 to 10 at pyrophosphate concentrations that are at least, ten times higher than that of manganese. It indicates that the most stable complex of manganese is with completely dissociated pyrophosphate ligand. Upon ageing the range of soluble complexes became narrower, due to the slow formation of Na$_2$MnP$_2$O$_7 \cdot 4$H$_2$O crystals, for pyrophosphate concentrations up to $2 \cdot 10^{-2}$ mol dm^{-3}. Curve 0 in Fig. 2 separates systems in which HClO$_4$ was added toward lower pH values, and NaOH toward higher pH values than in the pure systems. Curve 1 separates white precipitate of Mn$_2$P$_2$O$_7$ from the brown one, where oxidation of manganese took place in a visible amount.
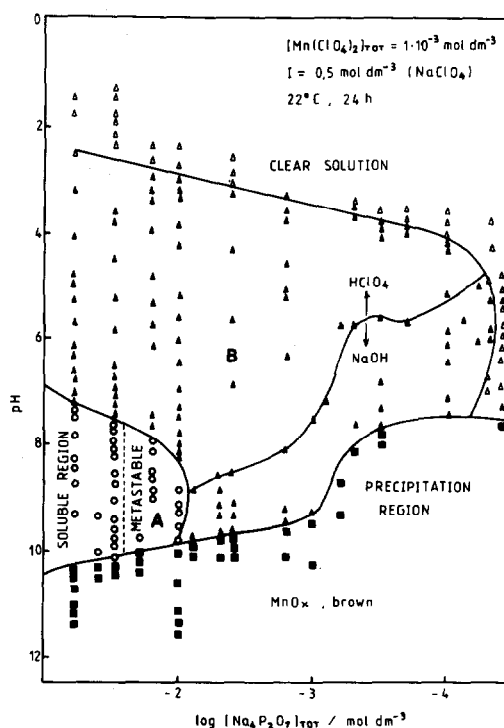
Fig. 2. The ground plan of a precipitation diagram formed in mixtures with Mn(ClO$_4$)$_2$ = 1 × 10^{-3} mol dm^{-3}, Na$_4$P$_2$O$_7$ = various, pH = various, after 24 hr.
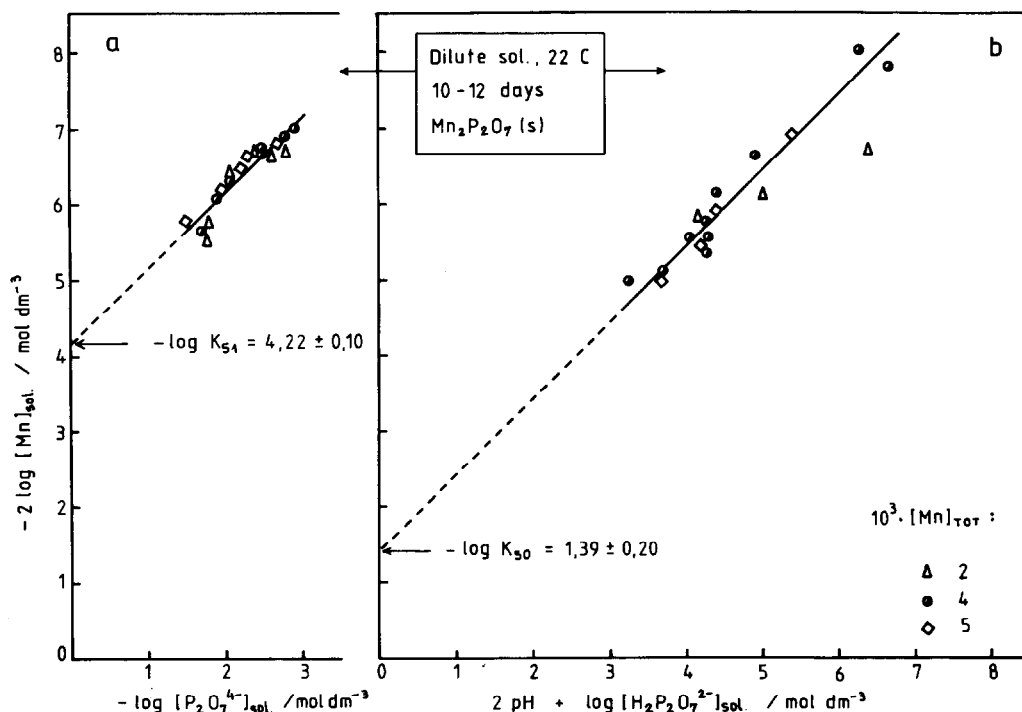
Fig. 3(a). Graphical determination of $\log K_{S1} = \log [MnP_2O_7^{2-}]^2 \cdot [P_2O_7^{4-}]^{-1}$ from experimental data in Table 1. $(I \approx 0$ mol dm^{-3}, 295 K). (b). Graphical determination of $\log K_{SO} = \log [Mn^{2+}]^2 \cdot [H_2P_2O_7^{2-}] \cdot [H^+]^{-2}$ from experimental data in Table 1. $(I \approx 0$ mol dm^{-3}, 295 K).

Quantitative experiments of solubility and complex formation constants in manganese pyrophosphate system were performed in distilled water to avoid the formation of sodium containing solid phase.

Table 1. shows results of quantitative determination of soluble manganese in equilibrium with $Mn_2P_2O_7(s)$ and corresponding pH values. Three series of samples have been prepared with constant concentration of total manganese. At the minimum of solubility curve very stable negatively charged colloids exist, which could be removed from solution only by ultracentrifuge.

At total concentrations of pyrophosphate higher than $3 \cdot 10^{-2}$ mol dm^{-3}, crystals of the composition $Na_2MnP_2O_7 \cdot 4H_2O$ are formed.

The dissolution of $Mn_2P_2O_7(s)$ in excess of manganese can be presented as

$$Mn_2P_2O_7(s) + 2H^+ = 2Mn^{2+} + H_2P_2O_7^{2-}$$
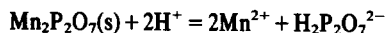
with solubility product

$$K_{SO} = [Mn^{2+}]^2 \, [H_2P_2O_7^{2-}] \, [H^+]^{-2}.$$

Dissolution in excess of pyrophosphate can be expressed as

$$Mn_2P_2O_7(s) + P_2O_7^{4-} = 2MnP_2O_7^{2-}$$
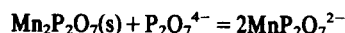
with solubility product

$$K_{SI} = [MnP_2O_7^{2-}]^2 \cdot [P_2O_7^{4-}]^{-1}.$$

In Fig. 3 is presented graphical determination of the

two solubility constants, using experimental data from Table 1. Concentration of $H_2P_2O_7^{2-}$ and $P_2O_7^{4-}$ ions are calculated from total soluble pyrophosphate, pH value and acidity constants for pyrophosphoric acid, determined by Davis[15] (log $\beta_1 = 9.25$, log $\beta_2 = 15.85$; and log $\beta_3 = 18.21$). The obtained values from the intercepts of the two straights lines are:

$$-\log K_{SO} = 1.39$$
$$-\log K_{SI} = 4.22.$$

From these two solubility constants and from log β_2 value it is possible to calculate equilibrium constant for complex formation:

$$K_1 = [MnP_2O_7^{2-}] \cdot [Mn^{2+}]^{-1} \cdot [P_2O_7^{4-}]^{-1}$$

$$\log K_1 = 6.51 \quad (I = 0 \text{ mol dm}^{-3}).$$

This value cannot be compared directly with the corresponding literature values as they are not to our knowledge available. However, it can be compared with the values for other elements.

In Fig. 4 are the values for log K_1 for various monovalent and bivalent ions[1,2] plotted vs, atomic number of these elements. Data fit two straight lines. The value for log K_1 determined for manganese is very close to the values for calcium and zinc and fits perfectly to the straight line obtained for bivalent ions. Therefore it might be concluded that the value obtained in this work for stability constant of manganese pyrophosphate is a realistic one.

Table 1. Dissolution of $Mn_2P_2O_7(s)$. Diluted solutions, $I \approx 0$ mol dm^{-3}, 10–12 days, 295 K

$10^3 \cdot [Mn(ClO_4)_2]_{TOT}$	$10^3 \cdot [Na_4P_2O_7]_{TOT}$	pH	$10^3 \cdot [Mn]_{sol}$
2	0.4	4.37	1.26
	0.6	4.70	0.88
	0.8	5.50	0.452
	1.0	6.60	0.070
	1.2	7.53	0.076
	1.4	7.91	0.209
	1.6	8.74	0.254
	1.8	9.20	0.338
	2.0	9.33	0.379
	3.0	9.70	0.455
	4.0	9.85	0.452
	6.0	9.92	0.488
	10.0	10.02	0.644
	20.0	10.04	1.315
	22.0	10.05	1.675
	28.0	10.05	2.0
4	0.4	3.92	3.250
	0.6	3.99	2.906
	1.0	4.25	2.123
	1.2	4.26	1.675
	1.2	4.33	1.680
	1.4	4.37	1.260
	1.6	4.48	0.860
	1.8	4.68	0.470
	2.0	5.31	0.098
	2.0	5.44	0.126
	2.4	7.14	0.077
	3.0	8.87	0.248
	3.0	8.46	0.196
	3.4	9.26	0.318
	4.0	9.51	0.372
	4.0	9.37	0.325
	6.0	9.78	0.455
	8.0	9.79	0.440
	12.0	9.93	0.670

Table 1. (Contd.)

$10^3 \cdot \left[Mn(ClO_4)_2\right]_{TOT}$	$10^3 \cdot \left[Na_4P_2O_7\right]_{TOT}$	pH	$10^3 \cdot \left[Mn\right]_{sol}$
4	16.0	9.96	0.920
	24.0	9.98	1.523
	32.0	10.15	2.313
5	1.0	3.95	3.125
	1.6	4.18	1.950
	2.0	4.35	1.095
	2.4	4.75	0.347
	3.0	6.90	0.176
	4.0	9.05	0.260
	5.0	9.49	0.358
	8.0	9.78	0.490
	10.0	9.88	0.600
	15.0	9.97	0.800
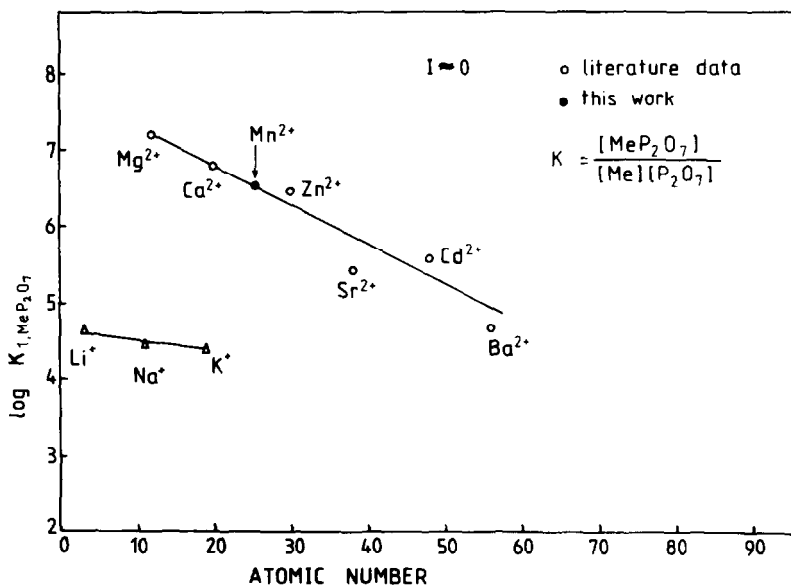
Fig. 4. The values of log K_{1,MeP_2O_7} from the literature[1,2] (circles) are plotted vs atomic number of corresponding elements. Two straight lines, for monovalent and for bivalent ions are presented. The experimental value for manganese (·) is inserted for comparison.

REFERENCES

[1] Stability constants of metal ion complexes L. G. Sillén and A. E. Martell compilers) Chem. Soc. Spec. Publ. No. 1964, 17, Supplement Spec. Publ. No. 1971, 25, London.
[2] Critical Stability Constants, (Edited by A. E. Martell and R. M. Smith), Vol. 3: Other Organic Ligands. Plenum Press, New York 1976.

[3]S. L. Miller and M. Parris, *Nature* 1964, **204**, 1248.

[4]H. Baltscheffsky and L. V. Stedingk, *Biochem. and Biophys. Res. Comm.* 1966, **22**, 722.

[5]R. Zell, Ḥ. Sigel and H. Erlenmayer, *Helv. Chim. Acta* 1966, **49**, 1275.

[6]I. Sobolev, *U.S. Patent* 3 215 674 (*Cl.* 260–67) (1965).

[7]R. A. Long, *U.S. Patent* 3 189 470 (Cl. 106–39) (1965).

[8]V. Hurt, M. Benicky and J. Pcolinsky, Czech Patent 114 769 (CL. DOlf) (1965).

[9]W. Heussler, East Germany Patent 46543 (Cl. CO8g) (1966).

[10]A. G. Zdukos and Z. Kamalov, *Zh. neorg. Khim.* 1975, **20**, 307.

[11]J. F. McCullough and J. D. Hatfield *J. Chem. Engng* Data 1972, **17**, 344.

[12]N. Ju. Morozova, N. M. Selivanova, *Zh. neorg. Khim.* 1976, **21**, 1606.

[13]B. Težak, E. Matijević and K. Shultz, *J. Phys Colloid Chem.* 1951, **55**, 1557.

[14]J. J. Morgan and W. Stumm, *Jour. A. W. W. A.* 1965, **57**, 107.

[15]J. A. Davis, Thesis, Indiana University (1955), quoted in Ref.1.

MIXED HALIDE DIALKYLDITHIOPHOSPHATE
DERIVATIVES OF ARSENIC(III) AND ANTIMONY(III)

H. P. S. CHAUHAN, G. SRIVASTAVA and R. C. MEHROTRA*

Department of Chemistry, University of Rajasthan, Jaipur-302004 India

Abstract—Mixed chloride dialkyldithiophosphates of arsenic(III) and antimony(III), $[(RO)_2PSS]_nMCl_{3-n}$ (M = As, Sb; n = 1, 2; R = C_2H_5, $n-C_3H_7$, $i-C_3H_7$ and $i-C_4H_9$) have been synthesized for the first time by the reactions of metal chlorides with sodium dialkyldithiophosphates or alternatively by co-disproportionation reactions of metal chlorides with metal tris(dialkyldithiophosphates) in different stoichiometric ratios. Mixed halide dialkyl-dithiophosphates of antimony(III) have also been prepared by the cleavage reactions of antimony tris(diisopropyl-dithiophosphate) with bromine or iodine. Hydrolysis reactions of a few of these compounds have also been studied.

The new compounds have been characterized by elemental analyses, molecular weight determinations (cryoscopic) as well as IR and NMR (^1H, ^{31}P) data; chelated structures with bidentate dialkyldithiophosphate groups are proposed.

Dialkyldithiophosphate ligands exhibit bidentate[1,2] as well as monodentate[3,4] behaviour and form stable complexes with transition as well as main group elements. In spite of an extensive literature on derivatives of arsenic(III) and antimony(III) with sulphur-containing ligands,[5–13] studies on the corresponding dialkyldithio-phosphate derivatives have been limited. A variety of tris-derivatives[14–18], $M[S_2P(OR)_2]_3$ (M = As, Sb) have been synthesized in a number of laboratories, and Raman spectra,[18] photometric properties[14] and analytical applications[14,19] of some of these have also been reported. The utility of these compounds as lubricant additives[17,20,21] and for regeneration of cracking catalysts[22,23] has also been pointed out. The X-ray electron spectrum[24] of $[(BuO)_2PSS]_3Sb$ has been studied and the crystal structure[25] of $[(EtO)_2PSS]_3Sb$ has been reported. We have recently reported the synthesis of 2-dialkyldithiophosphato-1,3,2-dioxarsolanes and arsenanes.[26] The corresponding halide dialkyl-dithiophosphate derivatives of arsenic(III) and anti-mony(III) are still unknown. In view of the exciting chemistry of mixed halide dithiocarbamates[9–11] of arsenic(III) and antimony(III) it was thought of interest to synthesize a number of mixed halide dialkyl-dithiophosphate derivatives of arsenic(III) and anti-mony(III) and characterize them by various physico-chemical techniques.

EXPERIMENTAL

Materials

Moisture was carefully excluded throughout experimental manipulations. Solvents (benzene, petroleum ether, chloroform) and alcohols (ethanol, n-propanol, i-propanol and i-butanol) were dried by standard methods. Arsenic trichloride (b.p., 130°) and antimony trichloride (b.p., 223°) were distilled before use. Arsenic and antimony isopropoxides,[27] dialkyldithiophosphoric acids[28–31] and their sodium[26] and ammonium[29] salts were prepared by previously reported methods.

Product analyses

Sulphur was estimated gravimetrically as barium sulphate.[3] Arsenic and antimony isopropoxides,[27] dialkyldithiophosphoric pound by sulphuric acid followed by oxidation of As(III) and

Sb(III) to As(V) and Sb(V) respectively by heating with $KMnO_4$; excess $KMnO_4$ was decolourized by H_2O_2 and excess H_2O_2 was removed by evaporation. The remaining solid mass was dissolved in HCl, KI was added and liberated iodine was titrated against standard sodium thiosulphate solution using starch as an internal indicator.

Measurements

Molecular weights were determined cryoscopically in benzene. IR spectra using CsI cells were recorded as neat liquids or in the form of Nujol mulls (in case of solid products) on a Perkin-Elmer 577 spectrometer in the range 4000–200 cm^{-1}. ^1H NMR spectra in CCl_4 or $CDCl_3$ were recorded on a Perkin-Elmer R 12 B spectrophotometer using tetramethylsilane as an external standard; ^{31}P NMR spectra in $CDCl_3$ solutions were recorded on a Varian XL-100A spectrophotometer using H_3PO_4 as an internal standard.

General methods of preparation of various dialkyl-dithiophosphates of arsenic(III) and antimony(III)

(a) *Reaction of metal oxide with dialkyldithiophosphoric acid in 1:6 molar ratio.* A mixture of metal oxide (As_2O_3 or Sb_2O_3) and dialkyldithiophosphoric acid in 1:6 molar ratio in benzene or alcohol was heated under reflux (~4h) until a clear solution was obtained. Solvent was removed under reduced pressure and the product so obtained was crystallized from aqueous alcohol.

(b) *Reaction of metal isopropoxide with dialkyl-dithiophosphoric acid in 1:3 molar ratio.* The reaction of metal (arsenic, antimony) isopropoxide with dialkyldithiophosphoric acid in 1:3 molar ratio in refluxing benzene for about 4 hr (completion of the reaction was checked by estimating the iso-propanol collected azeotropically with benzene) yielded a yellow crystalline solid on removing volatile solvent. The product was purified by crystallization from aqueous isopropanol.

(c) *Reaction of metal chloride with dialkyldithiophosphoric acid in 1:3 molar ratio.* Metal (arsenic, antimony) trichloride and dialkyldithiophosphoric acid in 1:3 molar ratio were mixed in benzene and heated under reflux for about 4 hr till the liberation of HCl ceased. On removing the solvent under reduced pressure, a yellow crystalline solid was obtained, which was crystallized from aqueous alcohol.

(d) *Reaction of metal chloride with sodium(ammonium) dialkyldithiophosphate in different (1:1, 1:2 and 1:3) molar ratios.* Metal (arsenic, antimony) trichloride and sodium(am-monium) dialkyldithiophosphate in different stoichiometric ratios (1:1, 1:2 or 1:3) were mixed and stirred with slight heating for about 2 hr. Precipitated sodium(ammonium) chloride was removed by filtration, followed by removal of the solvent, giving the desired product.

(e) *Co-disproportionation reaction of metal chloride or metal isopropoxide with metal tris(diisopropyldithiophosphate) in* 1:2 *or* 2:1 *molar ratio.* Metal (As, Sb) trichloride or antimony isopropoxide and metal *tris*(diisopropyldithiophosphate) in 1:2 or 2:1 molar ratio in benzene were stirred with heating for about 2 hr. Solvent was removed under reduced pressure to give the desired product.

(f) *Reaction of antimony tris(diisopropyldithiophosphate) with halogens in* 2:1 *molar ratio.* To the antimony *tris*(diisopropyldithiophosphate) in carbon tetrachloride or benzene was added halogen (bromine or iodine) in 2:1 molar ratio and stirred for about half an hour. Solvent was removed under reduced pressure and the products, *monohalo* antimony *bis*(diisopropyldithiophosphate) and *bis*(diisopropylphosphorothionyl) disulphide, were separated by fractional crystallization in light petroleum (b.p., 60–80°).

RESULTS AND DISCUSSION

Tris(diisopropyldithiophosphates) of arsenic(III) and antimony(III) have been prepared by the reactions of diisopropyldithiophosphoric acids with corresponding metal oxide, isopropoxide or chloride in refluxing benzene:

$$M_2O_3 + 6(i\text{-}C_3H_7O)_2PSSH \rightarrow$$
$$2[(i\text{-}C_3H_7O)_2PSS]_3M + 3H_2O \uparrow \quad (1)$$

$$MX_3 + 3(i\text{-}C_3H_7O)PSSH \rightarrow [(i\text{-}C_3H_7O)_2PSS]_3M + 3HX \uparrow$$
$$(2)$$
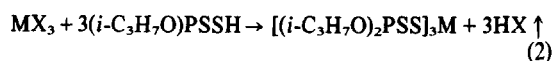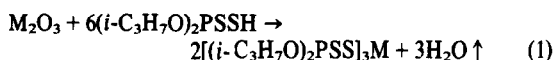
(M = As, Sb; X = Cl, i-C$_3$H$_7$O).

All these reactions are exothermic and quite facile in the initial stages. As the reactions tend to slow down towards the end, the reactants were refluxed to ensure the completion of the reactions which were further facilitated by simultaneous removal of water, isopropanol or hydrogen chloride.

In view of the difficulties of purifying dialkyldithiophosphoric acids (even freshly distilled samples are generally contaminated with disulphide to an extent of ~ 5%) further syntheses were carried out by the reactions of sodium or ammonium dialkyldithiophosphates with metal chlorides:

$$MCl_3 + 3(RO)_2PSSM' \rightarrow [(RO)_2PSS]_3M + 3M'Cl \downarrow$$
$$(3)$$
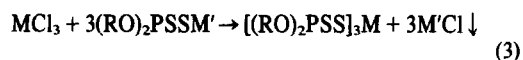
(M = As, Sb; M' = Na, NH$_4$; R = C$_2$H$_5$, n-C$_3$H$_7$, i-C$_3$H$_7$, i-C$_4$H$_9$ and C$_6$H$_5$).

Mixed chloride dialkyldithiophosphate derivatives were prepared by the reactions of metal chlorides with sodium dialkyldithiophosphates in stoichiometric ratios and also by co-disproportionation reactions of metal *tris*(dialkyldithiophosphates) with metal chlorides

$$MCl_3 + n(RO)_2PSSNa \rightarrow [(RO)_2PSS]_nMCl_{3-n} + nNaCl \downarrow$$
$$(4)$$

$$MCl_3 + 2[(RO)_2PSS]_3M \rightarrow 3[(RO)_2PSS]_2MCl \quad (5)$$

$$2MCl_3 + [(RO)_2PSS]_3M \rightarrow 3[(RO)_2PSS]MCl_2 \quad (6)$$
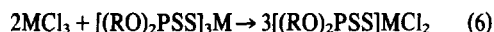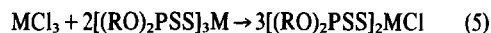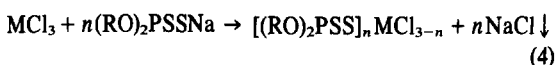
Table 1. Syntheses of dialkyldithiophosphate derivatives of arsenic(III)

S. No.	Compound	Method of preparation	Yield %	Physical state	Melting point °C	Mol.Wt. Found (Calcd)	Analyses As	Found (Calcd) S
1	2	3	4	5	6	7	8	9
1.	$[(C_2H_5O)_2PSS]_3As$	d	91	Yellow crystalline solid	52°	620 (631)	11.86 (11.88)	30.05 (30.51)
2.	$[(C_2H_5O)_2PSS]_2AsCl$	d	88	Colourless viscous liquid	-	-	16.04 (15.58)	26.20 (26.67)
3.	$[(C_2H_5O)_2PSS]AsCl_2$	d	88	,,	-	-	23.02 (22.63)	18.97 (19.37)
4.	$[(n\text{-}C_3H_7O)_2PSS]_3As$	d	96	Pale yellow viscous liquid	-	697 (715)	10.72 (10.48)	26.70 (26.91)
5.	$[(n\text{-}C_3H_7O)_2PSS]_2AsCl$	d,e	93	,,	-	524 (537)	14.44 (13.95)	24.62 (23.89)
6.	$[(n\text{-}C_3H_7O)_2PSS]AsCl_2$	d,e	92	,,.	-	-	21.35 (20.86)	18.56 (17.86)
7.	$[(i\text{-}C_3H_7O)_2PSS]_3As$	a,b,c,d	93	Yellow crystalline solid	100°	702 (715)	10.50 (10.48)	27.06 (26.91)
8.	$[(i\text{-}C_3H_7O)_2PSS]_2AsCl$	d,e	92	Pale yellow sticky solid	-	552 (537)	14.32 (13.95)	24.17 (23.89)
9.	$[(i\text{-}C_3H_7O)_2PSS]AsCl_2$	d,e	72	Pale yellow viscous liquid	-	372 (359)	21.13 (20.86)	18.76 (17.86)
10.	$[(i\text{-}C_4H_9O)_2PSS]_3As$	a,c,d	86	Yellow crystalline solid	114°	808 (799)	9.58 (9.38)	24.43 (24.08)
11.	$[(i\text{-}C_4H_9O)_2PSS]_2AsCl$	d,e	75	Yellow sticky solid	-	602 (593)	13.10 (12.64)	21.02 (21.64)
12.	$[(i\text{-}C_4H_9O)_2PSS]AsCl_2$	d,e	75	Pale yellow viscous liquid	-	-	20.50 (19.34)	17.17 (16.55)
13.	$[(C_6H_5O)_2PSS]_3As$	d	91	Yellow sticky solid	-	-	18.32 (18.18)	20.89 (21.00)

All the above reactions (3–6) are even more facile and appear to be completed at room temperature simply by stirring the reaction mixture in benzene for 2–3 hr.

Mixed alkoxide (isopropoxide) diisopropyl-dithiophosphates of antimony(III) were prepared by the co-disproportionation reaction of antimony isopropoxide with antimony $tris$(diisopropyldithiophosphate) in $1:2$ and $2:1$ molar ratios in benzene:

$$Sb(OC_3H_7-i)_3 + 2[(i-C_3H_7O)_2PSS]_3Sb \rightarrow$$
$$3[(i-C_3H_7O)_2PSS]_2Sb(OC_3H_7-i) \quad (7)$$

$$2Sb(OC_3H_7-i)_3 + [(i-C_3H_7O)_2PSS]_3Sb \rightarrow$$
$$3[(i-C_3H_7O)_2PSS]Sb(OC_3H_7-i)_2. \quad (8)$$
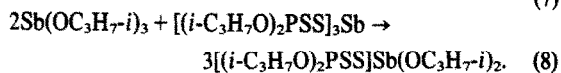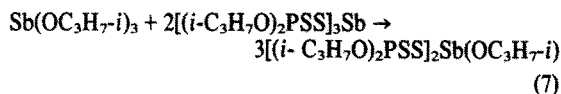
Antimony $tris$(diisopropyldithiophosphate), [$(i$-C_3H_7O)_2PSS]_3Sb, reacts with halogens (bromine and iodine) in $2:1$ molar ratio to give monohalo antimony bis(diisopropyldithiophosphate) and bis(diisopropyl-

phosphorothionyl) disulphide, which are separated by fractional crystallization in light petroleum (b.p., 60–80°).

$$2[(i-C_3H_7O)_2PSS]_3Sb + X_2 \rightarrow$$
$$2[(i-C_3H_7O)_2PSS]_2SbX + [(i-C_3H_7O)_2PSS]_2 \quad (9)$$
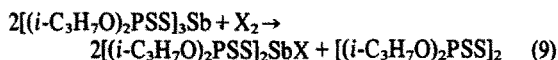
Arsenic $tris$(diisopropyldithiophosphate), [$(i$-C_3H_7O)_2PSS]_3As, also appears to react with halogens in a similar manner but only bis(diisopropyl-phosphorothionyl)disulphide is crystallized from light petroleum (b.p., 60–80°), and monohalo arsenic bis(diisopropyldithiophosphate) could not be obtained in a pure form.

Mixed chloride diisopropyldithiophosphate derivatives of arsenic and antimony in isopropanol on treatment with an excess of water give the corresponding metal (arsenic and antimony) $tris$(diisopropyldithiophosphates) and oxides:

$$6[(i-C_3H_7O)_2PSS]_2MCl + 3H_2O \rightarrow$$
$$4[(i-C_3H_7O)_2PSS]_3M + M_2O_3 + 6HCl \quad (10)$$
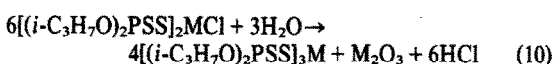
Table 2. Syntheses of dialkyldithiophosphate derivatives of antimony(III)

S. No.	Compound	Method of preparation	Yield %	Physical state	Melting point °C	Mol. Wt. Found (Calcd)	Analyses Sb	Found (Calcd) S
1	2	3	4	5	6	7	8	9
1.	[(C_2H_5O)_2PSS]_3Sb	d	93	Yellow crystalline solid	56°	692 (677)	17.63 (17.97)	27.28 (27.40)
2.	[(C_2H_5O)_2PSS]_2SbCl	d	97	,,	100^c	–	23.84 (23.08)	24.33 (24.31)
3.	[(C_2H_5O)_2PSS]SbCl_2	d	77	,,	105^c	–	32.10 (32.22)	16.84 (16.97)
4.	[(n-C_3H_7O)_2PSS]_3Sb	d	95	Pale yellow viscous liquid	–	746 (762)	16.04 (15.99)	25.13 (25.26)
5.	[(n-C_3H_7O)_2PSS]_2SbCl	d,e	98	,,	–	602 (584)	20.36 (20.86)	22.24 (21.97)
6.	[(n-C_3H_7O)_2PSS]SbCl_2	d,e	98	,,	–	–	30.77 (29.99)	15.74 (15.80)
7.	[(i-C_3H_7O)_2PSS]_3Sb	a,b,c,d	90	Yellow crystalline solid	78^c	758 (762)	15.75 (15.99)	25.42 (25.26)
8.	[(i-C_3H_7O)_2PSS]_2SbCl	d,e	86	,,	92^c	588 (584)	20.46 (20.86)	22.24 (21.97)
9.	[(i-C_3H_7O)_2PSS]SbCl_2	d,e	82	Pale yellow viscous liquid	–	416 (406)	30.60 (29.99)	15.87 (15.80)
10.	[(i-C_3H_7O)_2PSS]_2Sb(OC_3H_7-i)	e	87	Yellow crystalline solid	76°	–	19.04 (20.05)	21.97 (21.11)
11.	[(i-C_3H_7O)_2PSS]Sb(OC_3H_7-i)_2	e	92	Pale yellow viscous liquid	–	–	26.60 (26.86)	13.08 (14.15)
12.	[(i-C_3H_7O)_2PSS]_2SbBr	f	71	Yellow crystalline solid	105°	598 (628)	19.72 (19.39)	20.38 (20.74)
13.	[(i-C_3H_7O)_2PSS]_2SbI	f	70	Brown crystalline solid	85°	679 (675)	18.46 (18.04)	18.83 (18.96)
14.	[(i-C_4H_9O)_2PSS]_3Sb	a,c,d	88	Yellow crystalline solid	124^c	858 (846)	14.72 (14.40)	22.66 (22.75)
15.	[(i-C_4H_9O)_2PSS]_2SbCl	d,e	95	,,	80^c	655 (640)	19.58 (19.03)	19.65 (20.04)
16.	[(i-C_4H_9O)_2PSS]SbCl_2	d,e	97	Pale yellow viscous liquid	–	–	27.65 (28.06)	15.70 (14.78)
17.	[(C_6H_5O)_2PSS]_3Sb	d	90	Yellow sticky solid	–	–	13.04 (12.65)	20.42 (19.98)

$3[(i\text{-}C_3H_7O)_2PSS]MCl_2 + 3H_2O \rightarrow$

$\qquad [(i\text{-}C_3H_7O)_2PSS]_3M + M_2O_3 + 6HCl. \qquad (11)$
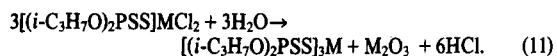
On treatment of diisopropyldithiophosphate derivatives of arsenic and antimony with an excess of ammonia in aqueous media, only insoluble metal oxides are obtained;

$2[(i\text{-}C_3H_7O)_2PSS]_3M + 6NH_4OH \rightarrow$

$\qquad M_2O_3 + 6(i\text{-}C_3H_7O)_2PSSNH_4 + 3H_2O. \qquad (12)$
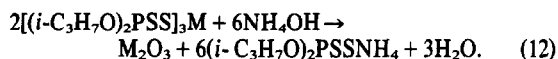
Compounds of the type $Cl_2Sb[SSP(OR)_2]$ on heating disproportionate into $SbCl_3$ and $[(RO)_2PSS]_2SbCl$; the latter appear to decompose further into products which could not be identified. This was confirmed by heating a sample of $[(RO)_2PSS]_2SbCl$, synthesized as mentioned earlier. The reaction can be represented by the following equation on the basis of the amount of $SbCl_3$ liberated:

$2[(RO)_2PSS]SbCl_2 \rightarrow SbCl_3 + [(RO)_2PSS]_2SbCl.$

$\qquad\qquad\qquad\qquad\qquad\qquad\qquad\qquad (13)$
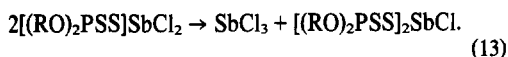
It is interesting to note that the compounds of the type $R_2SbS_2CNR_2$ have been reported[12] to disproportionate spontaneously into 1:1 mixtures of R_3Sb and $RSb(S_2CNR_2)_2$.

Dialkyldithiophosphate derivatives of arsenic and antimony are generally yellow crystalline solids or pale yellow oily viscous liquids soluble in common organic solvents like benzene, chloroform, carbon tetrachloride, acetone, hexane, ether, light petroleum, alcohols etc. The *tris* derivatives are insoluble in water and can be crystallized from aqueous alcohols. Mixed chloride derivatives are sensitive to moisture and solid compounds

amongst these can be crystallized from light petroleum (b.p., 60–80°). Molecular weight determinations in freezing benzene indicate the monomeric nature of these derivatives. All these compounds are non-volatile even under reduced pressure, and tend to decompose at ~120°C.

IR spectra of these new derivatives have been measured in the range $4000\text{--}200\ cm^{-1}$ and assignments have been made on the basis of earlier reports.[1,3,26] The bands in the regions, 1025–975 and 890–745 cm^{-1} are assigned to (P)–O–C and P–O–(C) stretching modes respectively. A strong band due to $\nu(P = S)$ observed in the region 680–620 cm^{-1} in the spectra of dialkyldithiophosphoric acids and their sodium and ammonium salts is shifted to lower frequencies by ~30 cm^{-1} in the corresponding antimony derivatives. This probably indicates a strong bidentate chelation of the ligand with antimony. In the case of arsenic derivatives the shift in the $\nu(P = S)$ peak appears to be small or negligible. Bands of medium intensity present in the region 580–500 cm^{-1} are due to P–S asymmetric and symmetric stretching vibrations. Bands of medium intensity present in the region 400–250 cm^{-1} are due to M–S[27] and M–Cl[32] stretching vibrations.

The PMR spectra (Tables 3 and 4) show the characteristic proton resonances of the corresponding alkoxy groups. The ^{31}P NMR spectral data (Table 5) for only a few representative compounds could be obtained. In proton-decoupled spectra, only one peak for each compound in the range of 89.0 to 91.8 ppm is obtained, which indicates[33] the bidentate behaviour of dialkyldithiophosphate ligands in all these derivatives.

For the sake of comparison, it may be recorded here that the X-ray crystallographic data show that

Table 3. ^1H NMR spectral data for a few arsenic(III) dialkyldithiophosphates*

S.No.	Compound	Chemical Shifts δ ppm
1.	$\left[(C_2H_5O)_2PSS\right]_3As$	1.64–1.87,t, CH_3(18H) 4.40–4.67,q, CH_2O(12H)
2.	$\left[(i\text{-}C_3H_7O)_2PSS\right]_3As$	1.54–1.64,d, CH_3(36H) 4.74–5.37,m, (7 peaks) CHO(6H)
3.	$\left[(i\text{-}C_3H_7O)_2PSS\right]_2AsCl$	1.78–1.88,d, CH_3(24H) 4.97–5.60,m, (7 peaks) CHO(4H)
4.	$\left[(i\text{-}C_3H_7O)_2PSS\right]AsCl_2$	1.75–1.85,d, CH_3(12H) 4.90–5.60,m, CHO(2H)
5.	$\left[(n\text{-}C_3H_7O)_2PSS\right]_3As$	1.20–1.42,t, CH_3(18H) 1.82–2.36,m, (6 peaks) (12H) 4.19–4.55,m, (6 peaks) CH_2O(12H)
6.	$\left[(n\text{-}C_3H_7O)_2PSS\right]_2AsCl$	0.91–1.15,t, CH_3(12H) 1.50–1.95,m, (6 peaks) CH_2(8H) 3.88–4.25,m, (6 peaks) CH_2O(8H)
7.	$\left[(i\text{-}C_4H_9O)_2PSS\right]_3As$	0.90–1.00,d, CH_3(36H) 1.80–2.10,m, (broad) CH(6H) 3.66–3.92,q, CH_2O(12H)
8.	$\left[(C_6H_5O)_2PSS\right]_3As$	7.47,s, C_6H_5O(30H)

d=doublet, m=multiplet, q=quartet, t=triplet, and s=singlet.

* In CCl_4 solution

Table 4. ^{1}H NMR spectral data for a few antimony(III) dialkyldithiophosphates*

S.No.	Compound	Chemical Shifts δ ppm
1.	$[(C_2H_5O)_2PSS]SbCl_2$	1.34-1.57,t,CH_3(6H)
		4.01-4.52,o,CH_2O(4H)
2.	$[(i-C_3H_7O)_2PSS]_3Sb$	1.65-1.75,d,CH_3(36H)
		4.80-5.45,m(7 peaks)CHO(6H)
3.	$[(i-C_3H_7O)_2PSS]_2SbCl$	1.67-1.77,d,CH_3(24H)
		4.85-5.47,m(7 peaks)CHO(4H)
4.	$[(i-C_3H_7O)_2PSS]SbCl_2$	1.74-1.84,d,CH_3(12H)
		4.94-5.57,m(7 peaks)CHO(2H)
5.	$[(i-C_3H_7O)_2PSS]_2(i-C_3H_7O)$	1.45-1.71,q,CH_3(30H)
		4.86-5.52,m,CH_3(5H)
6.	$[(i-C_3H_7O)_2PSS]Sb(i-C_3H_7O)_2$	1.47-1.74,q,CH_3(24H)
		4.47-5.43,m,CHO(4H)
7.	$[(n-C_3H_7O)_2PSS]_3Sb$	1.28-1.50,t,CH_3(18H)
		1.88-2.34,m,CH_2(12H)
		4.24-5.12,m(6 peaks)CH_2O(12H)
8.	$[(n-C_3H_7O)_2PSS]_2SbCl$	0.81-1.06,t,CH_3(12H)
		1.43-2.00,m,(6 peaks)CH_2(8H)
		3.35-3.88,m(6 peaks)CH_2O(8H)
9.	$[(n-C_3H_7O)_2PSS]SbCl_2$	0.89-1.13,t,CH_3(6H)
		1.53-2.10,m(6 peaks)CH_2(4H)
		3.98-4.35,m(6 peaks)CH_2O(4H)
10.	$[(i-C_4H_9O)_2PSS]_3Sb$	0.90-1.02,d,CH_3(36H)
		1.70-2.35,mCH(6H)
		3.76-4.01,q,CH_2(12H)
11.	$[(i-C_4H_9O)_2PSS]_2SbCl$	0.94-1.04,d,CH_3(24H)
		1.70-2.37,m,CH(4H)
		3.73-3.98,q,CH_2O(8H)

d=doublet, m=multiplet, o=octet, q=quartet and t=triplet.

* In CCl_4 solution except compounds 9 and 10 for which $CDCl_3$ was used as solvent.

Table 5. ^{31}P NMR spectral data for dialkyldithiophosphate derivatives of arsenic(III) and antimony(III)

S.No.	Compound	Chemical Shifts proton decoupled ppm	Chemical Shifts proton coupled		Coupling constant JPOCH
1.	$[(i-C_4H_9O)_2PSS]_3As$	90.2 ppm	3932.5-3968 Hz	5 peaks	8.87 Hz
2.	$[(i-C_4H_9O)_2PSS]_3Sb$	91.8 ppm	3995.6-4031 Hz	5 peaks	8.86 Hz
3.	$[(i-C_4H_9O)_2PSS]_2SbCl$	89.0 ppm	4609-4645 Hz	5 peaks	9.00 Hz

tris(dialkyldithiocarbamates)[7,8] of arsenic(III) and antimony(III) possess distorted octahedral geometry whereas the monobromo bis(diethydithiocarbamate) of arsenic(III)[9] possesses a distorted square pyramidal structure with Br$^-$ at the apex. $Br_2As(S_2CNEt_2)$[11] is reported to be monomeric in solution, while in the solid state it exists as a loosely held centrosymmetric dimer with bridging bromine ions: the geometry around 5-coordinate As(III) is intermediate between square pyramid and trigonal bipyramid with a stereochemically

active lone pair occupying one site in a distorted octahedral coordination.

The available X-ray crystallographic data of $[(EtO)_2PSS]_3Sb$[25] show a distorted capped octahedral environment around antimony with a stereochemically acitve lone pair at the capping position.

The spectroscopic data discussed earlier in this paper for the newly-synthesized halide dialkyldithiophosphates of arsenic(III) and antimony(III) indicate the chelating nature of the dithiophosphate moieties. Considering the

monomeric nature of all these derivatives, the mono-halide *bis*(dialkyldithiophosphates) should contain a 5-coordinate metal atom and possess a distorted octahedral geometry with the stereochemically active lone pair occupying one of the positions. The corresponding dihalide derivatives having a 4-coordinate metal atom may similarly possess a distorted trigonal bipyramidal geometry. Efforts are being made to obtain X-ray crystallographic data for some of these interesting compounds.

REFERENCES

[1] J. R. Wasson, G. M. Woltermann and H. J. Stoklosa, *Topics in Current Chemistry* 1973, **35**, 65.

[2] S. L. Lawton, C. J. Fuhrmeister, R. G. Haas, C. S. Jarman and F. G. Lothmeyer, *Inorg. Chem.* 1974, **13**, 135.

[3] B. P. Singh, G. Srivastava and R. C. Mehrotra, *J. Organometal. Chem.* 1979, **171**, 35.

[4] J. L. Lefferts, K. C. Molloy, J. J. Zuckerman, I. Haidue, C. Guta and D. Ruse, *Inorg. Chem.* 1980, **19**, 1662.

[5] G. Carrai and G. Gottardi, *Z. Krist.* 1960, **113**, 373.

[6] G. Gottardi, *Z. Krist.* 1961, **115**, 451.

[7] M. Colapietro, A. Domenicano, L. Scaramuzza and A. Vaciago, *Chem. Commun.* 1968, **6**, 302.

[8] G. E. Manoussakis and C. A. Tsipis, *J. Inorg. Nucl. Chem.* 1973, **35**, 743.

[9] R. Bally, *C.R. Acad. Sci.* 1970, **271**, 1436.

[10] G. E. Manoussakis, C. A. Tsipis and C. C. Hadjikostas, *Can. J. Chem.* 1975, **53**, 1530.

[11] J. A. Cras, P. J. H. A. M. Van de Leemput, J. Willemse and W. P. Bosman, *Recl. Trav. Chim.* 1977, **96**, 78.

[12] H. A. Meinema and J. G. Noltes, *J. Organometal. Chem.* 1970, **25**, 139.

[13] D. Coucouvanis, *Progress in Inorganic Chemistry* 1979, **26**, 801.

[14] A. I. Busev and M. I. Ivanyutin, *Anal. Khim.* 1960, **11**, 172.

[15] H. Bode and W. Arnswald, *Z. Anal. Chem.* 1962, **185**, 99.

[16] N. A. Chadaeva, G. Kamai and K. A. Mamakov, *Zh. Obshch. Khim.* 1966, **36** 1994; C. A. 1967, **66**, 95136.

[17] H. H. Farmer, B. W. Malone and H. F. Tompkis, *Lubric. Eng.* 1967, **23**, 57.

[18] T. P. Eremeeva and I. A. Vorsina, *Ser. Khim. Nauk.* 1976, **3**, 24; C. A. 1976, **85**, 101538.

[19] I. S. Levin, V. V. Sergeeva and I. A. Vorsina, *Ser. Khim. Nauk.* 1975, **2**, 107: C. A. 1975, **83**, 66255.

[20] *U.S. Patent*, 3,428,563; C. A. 1969, **70**, 69976.

[21] L. S. Kharchenko, G. G. Kupko, G. M. Rykhlevskii and Yu. T. Tordash, *Khim. Tekhnol. Topl. Mael.* 1974, **1**, 46; C.A. 1974, **81**, 123954.

[22] *Belg. Patent.* 845,345; C.A. 1978, **88**, 25448.

[23] *Fr. Demande Patent.* 2,362,207; C.A. 1979, **90**, 41172.

[24] E. K. Zhumadilov, E. I. Markova and V. I. Nefedov, *Koord. Khim.* 1978, **4**, 997; C. A. 1978, **89**, 138095.

[25] R. O. Day, M. M. Chauvin and W. E. McEwen, *Phosphorus Sulphur.* 1980, **8**, 121.

[26] H. P. S. Chauhan, G. Srivastava and R. C. Mehrotra, *Synth. React. Inorg. Met.-Org. Chem.* 1981, **11**, 565.

[27] T. B. Brill and N. C. Campbell, *Inorg. Chem.* 1973, **12**, 1884.

[28] J. H. Fletcher, J. C. Hamilton, I. Hechenbleikner, E. I. Hoegberg, B. J. Sertl and J. T. Cassaday, *J. Am. Chem. Soc.* 1950, **72**, 2461.

[29] R. F. Makens, H. H. Vaughan and R. R. Chelberg, *Anal. Chem.* 1955, **27**, 1062.

[30] V. P. Wystrach, E. O. Hook and G. L. M. Christopher, *J. Org. Chem.* 1956, **21**, 705.

[31] G. H. Sin and S. G. Ryom, *Hwahak Kwa Hwahak Knogop.* 1974, **17**, 334; C.A. 1975, **82**, 124652.

[32] E. Maslowsky, Jr., *J. Organometal. Chem.* 1974, **70**, 153.

[33] C. Glidewell, *Inorg. Chim. Acta* 1977, **25**, 159.

MAGNETIC AND EPR PROPERTIES OF Mn(II), Fe(III), Ni(II) and Cu(II) COMPLEXES OF THIOSEMICARBAZONE OF α-HYDROXY-β-NAPTHALDEHYDE

YUDHVIR K. BHOON

Sri Venkateswara College, Dhaula Kuan, New Delhi, 110021, India

Abstract—Mn(II), Fe(III), Ni(II) and Cu(II) complexes of the thiosemicarbazones of α-hydroxy-β-naphthaldehyde have been isolated. Ni(II) complex is diamagnetic, Cu(II) is planar involving metal–metal interactions, Mn(II) complex ($\mu_{\text{eff}} = 3.86$ B.M) has been assigned a planar structure with $S = 3/2$ while Fe(III) complex is five coordinated with $S = 3/2$.

Thiosemicarbazide ($NH_2 \cdot CS \cdot NH \cdot NH_2$) and thiosemicarbazones ($NH_2 \cdot CS \cdot NH \cdot N = CR_1R_2$) usually react as chelating ligands with transition metal ions by bonding through the sulphur and hydrazinic nitrogen atoms, although in a few cases, they behave as monodentate ligands and bond through the sulphur atom only. Since Domagk's original report[1] on the anti-tubercular activity of thiosemicarbazones, the number of papers on the pharmacology of these compounds has expanded dramatically. They have also been found to be active against influenza,[2] protozoa,[3] smallpox[4] and certain kinds of tumour[5] and have been suggested as pesticides[7] and fungicides.[6] Their activity has frequently been thought to be due to their ability to chelate trace metals. These findings have led recently to an increased interest in the chemistry of transition metal chelates of thiosemicarbazones. Thiosemicarbazone of α-hydroxy-β-napthaldehyde abbreviated as, HNATSC(I), is a newly synthesized compound. Mn(II), Fe(III), Ni(II) and Cu(II) complexes of HNATSC, have been prepared and characterized by magnetic susceptibility (from RT to 4 K) and ESR spectral measurements in the powdered state.

I
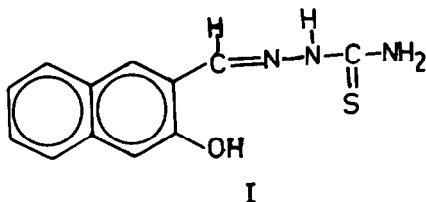
EXPERIMENTAL

Preparation of HNATSC, I

The thiosemicarbazone of α-hydroxy-β-baphthaldehyde was prepared by mixing the equimolar ethanolic solutions of thiosemicarbazide and α-hydroxy-β-naphthaldehyde.

The resulting solution was refluxed for about 1 hr and the thiosemicarbazone was separated out as grannular buff coloured compound which was filtered off and washed with cold alcohol and dried in a vacuum desiccator over silica gel. (Found: C, 58.43; N, 16.84; H, 4.01 and S, 12.83%. HNATSC requires: C, 58.77; N, 17.14; H, 4.49 and S, 13.06%).

Preparation of complexes

For preparing the complexes, equimolar solutions of metal halides and the thiosemicarbazone in DMF were mixed and the resulting solution was refluxed on a water bath for about 1 hr. Excess of the solvent was distilled off under reduced pressure and water was added to the concentrate. In each case, the complexes were precipitated, washed with hot water and acetone and finally dried in a vacuum desiccator over P_2O_5. The complexes are insoluble in water, ethanol, chloroform and acetone. The results of microanalysis on the complexes are presented in Table 1.

Physical measurements

The magnetic susceptibility measurements on powdered samples were carried out by Gouy's method using $Hg[Co(CNS)_4]$ as the calibrant. The results of measurements are presented in Table 1.

RESULTS AND DISCUSSION

(a) Copper(II)-HNATSC

The susceptibility measurements on the complex at room temperature yield magnetic value to be 1.54 B.M

Table 1. Micro-analytical and magnetic susceptibility data of complexes

Complex	% C Found (Calcd.)	% N Found (Calcd.)	% M Found (Calcd.)	% S Found (Calcd.)	% Cl Found (Calcd.)	μ_{eff} (B.M)
Cu(HNATSC)Cl	41.80 (41.97)	12.01 (12.24)	18.30 (18.52)	9.40 (9.33)	10.20 (10.35)	1.54
Ni(HNATSC)Cl	42.40 (42.57)	12.10 (12.47)	17.24 (17.35)	9.43 (9.46)	10.06 (10.49)	—
Mn(HNATSC)Cl	42.64 (43.05)	11.98 (12.55)	15.64 (16.42)	9.43 (9.56)	10.12 (10.61)	3.86
Fe(HNATSC)Cl$_2$	38.62 (38.83)	12.41 (12.67)	14.83 (15.06)	8.50 (8.63)	18.79 (19.14)	—

which is much below the spin only value of 1.73 B.M for mononuclear Cu(II) complexes. In view of the terdentate character of the thiosemicarbazone and chemical composition, planar stereochemistry may be proposed for the complex. Since the planar Copper(II) complexes are more prone to the metal–metal interaction along the axial positions, the lowering in magnetic moment could obviously be due to these interactions.

(b) Nickel(II)-HNATSC

The complex is diamagnetic and therefore, planar structure may be proposed for it. The planar structure for the complex also confirms the terdentate character of the thiosemicarbazone.

(c) Iron(III)-HNATSC

The results of magnetic susceptibility measurements on the powdered sample down to liq. helium temperature are presented in Table 3.

The magnetic behaviour of simple mononuclear high spin iron(III) complexes is generally uncomplicated. High spin iron(III) complexes ($S = 5/2$) with $^6A_1$ as the ground state have magnetic moment values around 5.92 B.M independent of temperature. Low-spin iron(III) complexes with strong ligands have magnetic moments corresponding to one unpaired electron. The ground state in such complexes is $^2T_2$ and the magnetic moment is temperature dependent.[8] It is interesting to note that if the geometry of the complexes is either octahedral or tetrahedral the possibility for the quartet state $^4T_1$ as the ground state with $S = 3/2$ is excluded by ligand field theory.[9] However, for d^5 configuration, this restriction does not necessarily apply to lower symmetry situations. Thus, an $S = 3/2$ ground state ($^4A_2$) has been established for a series of five coordinated iron(III) dithiocarbamates[10,11] and in the present studies, the iron(III) complex also seems to be a pentacoordinated with the square-pyramidal configuration and $S = 3/2$.

The detailed magnetic susceptibility measurements (Table 3) carried out on the powdered sample at different temperatures by SQUID susceptometer described earlier,[20] yield magnetic moments for the complex to be continuously rising from near 3.00 B.M at 4.2 K to 4.46 B.M at 143.4 K. This seems to be a slightly unusual behaviour if it is in fact a genuine $S = 3/2$ iron(III) compound because they have a moment of 3.9 B.M and independent of temperature.[8] Therefore, this compound

seems to be a 5 coordinate ($S = 3/2$) in which the excited states must be close enough to raise the moment to 4.47 B.M at room temperature which gets support from the EPR spectra recorded in the polycrystalline state both at room temperature and liquid nitrogen temperature. Very few compounds of iron(III), where the ground state has three unpaired electrons, have been subjected to EPR studies. Mono-chlorophthalocyaninato iron(III) is perhaps the first of this kind for which ESR studies were made by Gibson et al.[13] Among the series, $Fe(R_2 dtc)_2X$ polycrystalline ESR spectra are reported[14] for $Fe(Et_2 dtc)_2X$ where $X = Cl$, Br, I and NCS. Complete analysis of the EPR spectra in the present case has not been possible because of failure to obtain single crystals but it has definitely supported the 5 coordinated stereochemistry for the complex as the appearance of the signals at $g \simeq 4$ and $g \simeq 2$ could be explained by this geometry only. The ESR results for the systems with $^4A_2$ ground state can be described by the spin Hamiltonian,[14-17]

$$\mathscr{H} = D\left[\hat{S}_z^2 - \frac{1}{3}S(S+1)\right] + E(\hat{S}_x^2 - \hat{S}_y^2) + g\beta H \cdot S$$

with $S = 3/2$ and $g = 2.00$. When $E = 0$ and also when $D \gg h\nu$, there are two Kramers doublets $M_s = \pm 3/2$ and $\pm 1/2$, with effective g-tensor principal values $g_x = g_y = 0$; $g_z = 6$ and $g_x = g_y = 4$; $g_z = 2$ as shown below.

$D \gg h\nu$, $E = 0$

For the ($\pm 1/2$) doublet ignoring orbital contribution (since Fe(III) is $^6S_{5/2}$, $L = 0$)

$$g_{xx} = g_{yy} = 2\left\langle +\frac{1}{2}|S_\perp| - \frac{1}{2}\right\rangle$$

$$= 2\left\langle +\frac{1}{2}|(S_+ + S_-)2| - \frac{1}{2}\right\rangle$$

$$= 2\sqrt{\left(\frac{3}{2} + \frac{5}{2} - \left(\frac{1}{2} + \frac{1}{2}\right)\right)}$$

$$= 2\sqrt{(4)} = 4$$

$$g_\perp = 4$$

$$g_\parallel = 2\left\langle \frac{1}{2}|2S_z|\frac{1}{2}\right\rangle$$

$$= 2 \times 2 \times \frac{1}{2} = 2$$

Table 2. Selective IR spectral bands (cm^{-1})

Assignment	HNATSC	Cu(HNATSC)Cl	Ni(HNATSC)Cl	Mn(HNATSC)Cl	Fe(HNATSC)Cl$_2$
ν OH	3580 S	--	--	--	--
ν NH	↑ 3333 S	3440 S	3440 m	3420	3440
	↑ 3320 S	3300 S	3480 m	3300	3270
		3060 S	3340 m	3040	3180
			3180 m		
δ (NH) + CN	1525 m	1570 S	1560 S	1560 S	1565 S
	1500 m				
Amide III	1325 S	1390 S	1395 S	1375 S	1390 S
ν (CS)	820 S	750 S	740 S	740 S	745 S
ν M-O	--	380 S	380 S	385 S	386 S

Table 3: Variable temperature magnetic susceptibility data on Fe(III) HNATSC

Temp. (K)	χ_M^{Corr} (c.g.s)	μ_{eff} (B.M)
4.42	0.29167	3.21
5.26	0.15675	3.29
7.52	0.1939	3.42
10.43	0.15068	3.55
12.08	0.1333	3.54
15.75	0.1085	3.69
21.11	0.08400	3.76
31.3	0.05818	3.82
50.5	0.04019	4.03
89.57	0.0237	4.16
106.9	0.02100	4.24
143.4	0.01733	4.46

For the $(\pm 3/2)$ *doublet*

$$g_\perp = 2\left\langle +\frac{3}{2}|2S_\perp|-\frac{3}{2}\right\rangle$$

$$= 2\left\langle +\frac{3}{2}|S_+ + S_-|-\frac{3}{2}\right\rangle$$

$$= 2\times 0 = \underline{0}$$

$$g_{zz} = g_{||} = 2\left\langle +\frac{3}{2}|2S_z|+\frac{3}{2}\right\rangle$$

$$= 2\times 2\times\frac{3}{2} = \underline{6}.$$

The compound under investigation show identical ESR properties (Fig. 1) which may be described by the above

Hamiltonian for E = 0. Such a system should give rise to g value of 6, 4 and 2. For the compound under study, $g \approx 2$ signal is quite broad and $g \approx 4$ signal is comparatively strong while $g = 6$ signal is not observed, as it is not expected to be populated appreciably.

(d) *Manganese(II)-HNATSC*

As discussed above, crystal field theory specifically excludes the possibility of a quartet ground state (S = 3/2) for Mn(II) (d^5) configuration in octahedral geometry but not for the low symmetry. As S = 3/2 ground state has been established for a series of five coordinated iron(III) dithiocarbamates and manganese(II) phthalocyanin,[12] manganese(II)-HNATSC also appears to have a
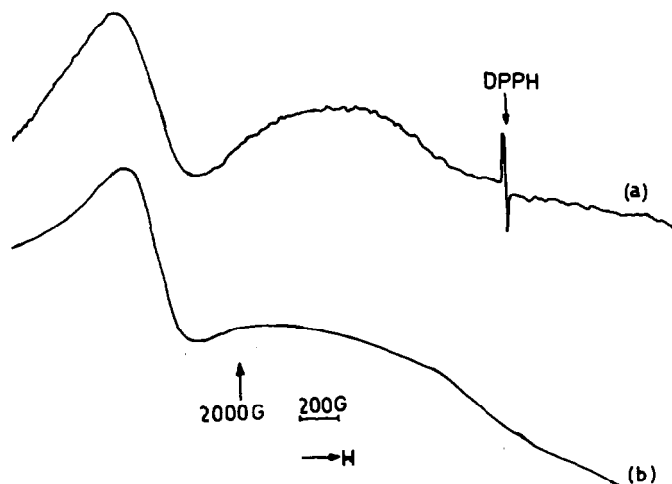
Fig. 1. ESR spectra of Fe^{III} (HNATSC) in polycrystalline state (a) RT (b) LNT.
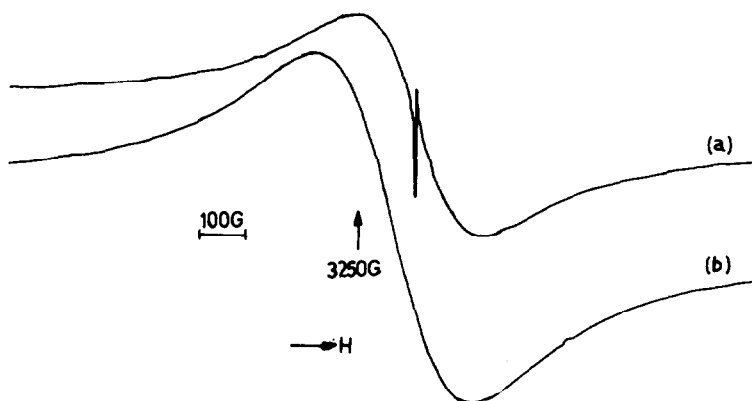
Fig. 2. ESR spectra of $Mn^{II}(HNATSC)Ci$ in polycrystalline state (a) RT. (b) LNT.

quartet ground state since the magnetic moment value is very close to the spin only value of 3.88 B.M in a square planar environment.

Infrared spectra

The selective IR spectral bands observed in the spectra of HNATSC and its corresponding complexes are presented in Table 2 along with the assignments. The IR spectra of Fe(III) (HNATSC) Cl_2 has provided additional information regarding the configuration of five coordinated complex.

Trigonal bipyramid(II) and square pyramid(III) are the 2 possible arrangements for the 5 coordinated molecule and they will differ in their IR spectral behaviour. In TBP, as the two chlorine atoms are trans to one another, one will expect only one ν_{Fe-Cl} band while in SP structure, the two Fe–Cl positions are different, the molecule is expected to give two ν_{Fe-Cl} bands as a result of splitting due to C_{2v} symmetry and the complex under study also shows two strong bands at 410 and 405 cm^{-1} which could be assigned to Fe–Cl. Thus on the basis of IR spectral data a square pyramidal structure could be assigned to the complex.

II

III
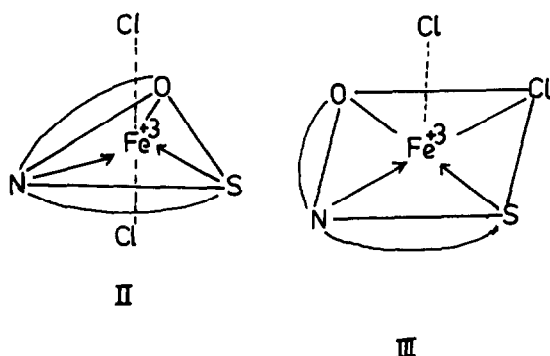
ESR spectral studies

High spin (S = 3/2) manganese complexes have been extensively studied by ESR technique but the reports on the complexes with S = 3/2 are not many.[18,19] Mn(II) phthalocyanine seems to be the first manganese(II) complex with a quartet ground state (S = 3/2) which was studied by ESR. The complex showed a very broad signal centered around g = 2.00. The manganese(II) complex under discussion also yields a similar ESR signal

(Fig. 2) in the polycrystalline state both at RT and LNT. The g value very close to that of DPPH (g = 2.0023) indicate that there is little orbital contribution which is in agreement with the results of magnetic susceptibility measurements which give the value of magnetic moment at RT to be 3.86 B.M, very close to the spin only value (3.88 B.M).

REFERENCES

[1] G. Domagk, R. Behnisch, F. Mietzsch and S. Schmidt, *Naturwissenchaften* 1946, 33, 315.
[2] N. N. Orlova, V. A. Aksenova, D. A. Selidovkin, N. S. Bogdanova and G. N. Pershin, *Russ. Pharm. Toxic* 1968, 348.
[3] K. Butler, U.S. Patent No. 3, 1968, 382, 266.
[4] D. J. Bauer, L. St. Vincent, C. H. Kempe and A. W. Downe, *Lancet* 1963, 2, 494.
[5] H. G. Petering, H. H. Buskirk and G. E. Underwood, *Cancer Res.* 1964, 64, 367.
[6] B. G. Benns, B. A. Gingers and C. H. Bayley, *Appl. Microbiol.* 1961, 8, 353.
[7] C. W. Johnson, J. W. Joyner and R. P. Perry, *Antibiotics and Chemotherapy* 1952, 2, 636.
[8] M. Kotani, *J. Phy. Soc. Japan* 1949, 4, 293.
[9] J. S. Griffith, *J. Inorg. Nucl. Chem.* 1956, 2, 1.
[10] H. H. Wickman, A. M. Trozzolo, H. J. Williams, G. W. Hull and F. R. Merritt, *Phys. Rev.* 1967, 155, 563.
[11] B. F. Hoskins, R. L. Martin and A. H. White, *Nature* 1966, 211, 627; *Inorg. Chem.* 1967, 611, 712.
[12] C. G. Barraclough, R. L. Martin and S. Mitra, *J. Chem. Phy.* 1970, 53, 1638.
[13] J. F. Gibson, D. T. E. Ingram and D. Schonland, *Discuss. Faraday Soc.* 1958, 26, 72.
[14] G. E. Chapps, S. W. McCann, H. H. Wickman and R. C. Sherwood, *J. Chem. Phys.* 1974, 60, 990.
[15] T. Castner, G. S. Newell, W. C. Holton and C. P. Slichter, *J. Chem. Phys.* 1960, 32, 668.
[16] H. H. Wickman, M. P. Klein and D. A. Shirly, *J. Chem. Phys.* 1965, 42, 2113.
[17] M. C. Chan and J. O. Arkman, *Phys. Rev.* 1969, 187, 723.
[18] D. J. E. Ingram and J. E. Bennett, *J. Chem. Phys.* 1954, 22, 1136.
[19] D. J. E. Ingram and J. E. Bennett, *J. Chem. Phys.* 1955, 23, 140.
[20] A. K. Gregson, P. C. Healy and D. M. Doddrell, *Inorg. Chem.* 1978, 17, 1216.

PREPARATION AND CHARACTERISATION OF COPPER, COBALT AND NICKEL COMPLEXES OF TETRADENTATE N₆ MACROCYCLIC LIGAND

WAHID U. MALIK,† R. BEMBI and RANDHIR SINGH*
Department of Chemistry, University of Roorkee, Roorkee-247672, U.P., India

Abstract—Macrocyclic complexes of copper, nickel and cobalt were synthesised via template reactions. These 14-membered N₆ tetradentate macrocyclic complexes were characterised by magnetic, conductance, electronic and IR spectral studies. The macrocyclic ligand coordinates through the four azomethine nitrogen atoms which are bridged by 2,3-butanedione moieties, but far IR spectra suggest that the pyridine nitrogens are not coordinated. These macrocyclic complexes are considered to have distorted octahedral configurations.

Considerable attention has been paid to the characterisation of macrocyclic complexes prepared by the condensation of ketones with transition-metal complexes of tetraamines.[1–3] The relationship of electronic properties and reactivities of these synthetic macrocyclic complexes to those of naturally occurring macrocycles, such as porphyrins and corrins, continues to promote great interest in their design and preparation. Much work in this field has resulted in substantial progress in the development of cyclisation reactions, usually involving metal ions, which has led to a variety of macrocyclic complexes.[4] The effect of varying the macrocyclic ring size has also received attention; 16-membered macrocyclic complexes have been reported.[5]

In the present paper the preparation and properties of a number of copper(II), nickel(II) and cobalt(II) complexes of 14-membered macrocycles and their derivatives are reported.

EXPERIMENTAL

Preparation of the complexes. All the chemicals employed were reagent grade and used without further purification. 2,6-Diamino-pyridine (0.02 mol) and 2, 3-butanedione (0.02 mol) were mixed in a minimum quantity of MeOH and a MeOH solution of the metal salt (0.01 mol) was added; the mixture was refluxed on a water bath. After refluxing for about 12 hr hydrochloric acid (1 cm³) was added and refluxing was maintained for a few more hours. The mixture was concentrated to half volume on a rotary evaporator and kept as such for 2 days. The greenish brown crystals were filtered off and washed with methanol and ether and dried in vacuum. The complexes so obtained are stable upto 200°C and are soluble in methanol, water, dimethyl sulphoxide and acetonitrile whereas copper complexes are partially soluble in these solvents. The derivatives of these complexes were prepared by metathesis by stirring and adding slowly NaBr and NH₄CNS solutions to an ethanolic solution of metal chloride, and the NaCl or NH₄Cl, formed during the exchange reaction, was filtered off. The nitrate complexes were prepared from metal nitrate salts. The metal contents were determined by spectrophotometric methods while halides were estimated by Volhard's method and nitrate as nitron salt.

Magnetic and spectral measurements: Magnetic measurements were carried out using a Princeton Applied Research Model 155

---

†Present address: Prof. W. U. Malik, Vice-Chancellor, University of Kashmir, Seinagar (J&K).
*Author to whom correspondence should be addressed.

vibrating sample magnetometer incorporating a digital readout. The electromagnet current was maintained using a Polytronic Constant Current Regulator Type CP-200. The instrument was calibrated using a standard pure nickel pallet and cross checked against Hg[Co(CNS)₄] as calibrant.

Absorbance measurements (DMF solutions) were carried out on a Carl Zeiss Specord UV.-VIS spectrophotometer using 10 mm glass cells. Conductance measurements of 1.0 mM solutions were made using the solvent acetonitrile which had been distilled from calcium hydride under nitrogen atmosphere and a Systronics Conductivity Meter Type 302 at 25 ± 1°C using a dip type conductivity cell. IR spectra were recorded on Beckmann IR-20 spectrophotometer in KBr pellets in 4000–600 cm⁻¹ range and in Nujol mulls in the 650–200 cm⁻¹ range on a Beckmann IR-12 spectrophotometer. The molecular weights of soluble complexes (MeOH solution) were determined cryoscopically.

RESULTS AND DISCUSSION

The analytical data (Table 1) show that the macrocyclic complexes can be represented as [M(C₁₈H₁₈N₆)X₂] where M = Ni(II), Co(II), Cu(II) and X = Cl, Br, NO₃ and NCS. The conductance measurements show their non-electrolytic nature and molecular weights of the nickel and cobalt complexes showed that they are monomeric (Table 2).

IR *spectral and magnetic studies.* The IR spectra of all compounds do not contain any band that could be assigned to C=O or NH groups.[6] The spectra of the condensation product of these compounds show various vibrations of the pyridine ring,[7–9] and azomethine[10] and 2,3-butanedione moiety.[7] By comparing the spectra with those of the amine, a strong band at *ca.* 1625 cm⁻¹ and a shoulder at *ca.* 1610 cm⁻¹ may be assigned to symmetric and asymmetric ν (C=N) vibrations, respectively. The absence of bands at *ca.* 3300–3200 cm⁻¹ indicates that all amino groups of 2,6-diaminopyridine have condensed with 2,3-butanedione. This contention is supported by the presence of bands at *ca.* 2925 cm⁻¹, *ca.* 1355 cm⁻¹, *ca.* 1270 cm⁻¹ and 680 cm⁻¹ characteristic of the 2,3-butanedione moiety and may be assigned to ν(CH₃), ν(C–CH₃), Sym(CH₃) and ring deformation modes.[6] However, some changes are observed in the spectra of these complexes. The spectra do not show any change in pyridine ring vibrations and it appears that in these complexes the nitrogen atom of pyridine does not participate in coordination.

Table 1. Analytical data of copper, cobalt, and nickel macrocyclic complexes

Complex	% of C		N		H		X		M	
	Calc.	Found	Calc.	Found	Calc.	Found	Calcd.	Found	Calc.	Found
[Cu(C$_{18}$H$_{18}$N$_6$)Cl$_2$]	47.8	47.0	18.6	18.4	3.9	4.0	15.7	15.0	13.9	13.2
[Cu(C$_{18}$H$_{18}$N$_6$)Br$_2$]	39.9	38.8	15.5	15.2	3.3	3.6	29.5	29.2	11.6	11.4
[Cu(C$_{18}$H$_{18}$N$_6$)(NO$_3$)$_2$]	42.7	42.2	16.6	16.3	3.6	3.2	24.6	24.1	12.5	12.0
[Cu(C$_{18}$H$_{18}$N$_6$)(NCS)$_2$]	43.5	43.2	16.9	16.5	3.6	3.8	23.4	23.0	12.7	12.1
[Co(C$_{18}$H$_{18}$N$_6$)Cl$_2$]	48.2	48.0	18.8	18.2	4.0	4.2	15.8	15.2	13.2	13.0
[Co(C$_{18}$H$_{18}$N$_6$)Br$_2$]	40.2	40.4	15.6	15.4	3.4	3.1	29.8	29.3	10.9	10.2
[Co(C$_{18}$H$_{18}$N$_6$)(NO$_3$)$_2$]	43.1	43.2	16.8	16.2	3.6	3.2	24.8	24.1	11.8	11.2
[Co(C$_{18}$H$_{18}$N$_6$)(NCS)$_2$]	44.7	43.5	17.4	17.0	3.7	3.1	24.0	23.8	12.2	12.6
[Ni(C$_{18}$H$_{18}$N$_6$)Cl$_2$]	48.3	47.4	18.8	18.1	4.0	4.3	15.9	15.3	12.9	13.0
[Ni(C$_{18}$H$_{18}$N$_6$)Br$_2$]	40.3	40.1	15.7	15.0	3.4	3.2	29.8	29.0	10.8	10.9
[Ni(C$_{18}$H$_{18}$N$_6$)(NO$_3$)$_2$]	43.2	42.6	16.8	16.2	3.6	3.4	24.8	24.1	11.6	12.0
[Ni(C$_{18}$H$_{18}$N$_6$)(NCS)$_2$]	43.9	43.0	17.1	17.0	3.7	3.5	23.6	23.0	11.8	11.2

Table 2. Electronic spectral and magnetic data of cobalt and nickel macrocyclic complexes. Calculated values of transition energies (cm^{-1})

Complex	Spectral data cm^{-1}	Molecular weight (Found)	Molar conductance (ohm^{-1})	μ_{eff} B.M. (300K)	Dq / DT	B / DS	β / DQ	γ_2/γ_1 / DQ^{xy}	DQ^z	DT/DQ	Dq^{xy}	Dq^z	Dt
[Co(C$_{18}$H$_{18}$N$_6$)Cl$_2$]	21560,18640, 15895,8650	440	10.28	4.92	1060	820	0.82	1.82					
[Co(C$_{16}$H$_{16}$N$_6$)Br$_2$]	21490,18470, 16260,8270	530	9.80	4.90	1030	810	0.86	1.91					
[Co(C$_{18}$H$_{18}$N$_6$)(NO$_3$)$_2$]	21480,18550, 15770,8560	495	5.24	5.12	1050	800	0.81	1.82					
[Co(C$_{18}$H$_{18}$N$_6$)(NCS)$_2$]	21520,18460, 16140,8740	480	10.00	4.81	1080	780	0.83	1.86					
[Ni(C$_{18}$H$_{18}$N$_6$)Cl$_2$]	34840,27840, 18190,11720, 10730	443	11.26	3.40	1540	11680	30350	32100	26670	0.05	1170	970	118
[Ni(C$_{18}$H$_{18}$N$_6$)Br$_2$]	35050,28210, 18230,11780, 10740	531	9.75	3.31	1610	11470	30422	32340	26610	0.05	1180	960	120
[Ni(C$_{18}$H$_{18}$N$_6$)(NO$_3$)$_2$]	35210,28330, 18270,11790, 10640	494	5.20	3.24	1630	11560	30460	32400	26570	0.06	1175	950	125
[Ni(C$_{18}$H$_{18}$N$_6$)(NCS)$_2$]	34770,28290, 18240,11680, 10580	488	9.84	3.35	1740	11490	30060	32150	25940	0.06	1165	940	130

It is apparent from the spectra that both the amino groups of 2,6-diaminopyridine react with oxygen atoms of 2,3-butanedione forming a two-carbon atom bridge between the two amino groups, similar to those reported in coordinated amines.[11] The absence of stretching and bending (C–O) group vibrations at ca. 1525 cm^{-1} and ca. 1280 cm^{-1} also indicate the absence of this group in these macrocyclic complexes. The frequencies of the ν(C=N) vibrations indicate coordination through this site.[13] Thus in the presence of metal salts, a quadridentate macrocyclic complex is formed which coordinates through azomethine nitrogens while pyridine nitrogen does not take part in coordination. These observations are in accordance with the idea that the formation of quadridentate macrocycles is easier than hexadentate or quinquedentate macrocycles.[12] It is also evident that azomethine nitrogen, being equally active, excludes coordination through pyridine nitrogen perhaps because this would involve the formation of unstable four-membered rings.

The far IR spectra of these complexes show some new bands at ca. 310 cm^{-1}, ca. 280 cm^{-1} and 275 cm^{-1} which can be assigned to ν(Co–Cl), ν(Ni–Cl) and ν(Cu–Cl) vibrations,[13] respectively. Similarly bands in bromocomplexes are observed at ca. 225 cm^{-1} and ca. 210 cm^{-1} for cobalt and nickel complexes and can be assigned to ν(Co–Br) and ν(Ni–Br) vibrational modes. The single bands observed and their regions are consistent with the octahedral nature of the complexes.

In nitrato complexes the spectra show some new bands at ca. 1265 cm^{-1}, ca. 1010 cm^{-1} and ca. 860 cm^{-1} which can be assigned to the monodentate nature of the nitrate group.[6] In thiocyanato complexes, some strong bands appear at ca. 2110 cm^{-1} (ν_1) ν(C=N), ca. 480 cm^{-1} (ν_2) NCS bending and ca. 830 cm^{-1} (ν_3), ν(C=S) of the NCS group, respectively in accord with the monodentate N-bonded thiocyanato group. The appearance of new bands at ca. 225–245 cm^{-1} support the coordination of nitrate and thiocyanate groups, which are assignable to ν(M–O) of the nitrate group and ca. 260–280 cm^{-1} assignable to ν(M–NCS), respectively. The appearance of bands in the region 430–495 cm^{-1} implies ν(M–N) (azomethine) vibrational modes and confirms the involvement of azomethine nitrogen. The data from the magnetic measurements of these complexes are given in Table 2. The magnetic moments of cobalt, nickel and copper complexes lie in the ranges 4.81–5.12, 3.24–3.35 and 1.75–1.86 B.M. respectively, at room temperature. The magnetic data are in accord with the high-spin nature of the nickel and cobalt complexes and indicate a pseudo-octahedral enviroment around the metal ions.[13] The distorted octahedral environment arises due to the steric interaction of the 2,6-diaminopyridine rings with methyl substituents on the macrocyclic ring. The resulting strain is relieved through a distortion of the ring to give a non-planar structure. The strain is relieved through the twisting of the torsional angles about the C–N bonds on the N$_6$-ring, which is the most readily deformable site. The extent of deviation from the dihedral angle in an ideally planar structure depends on the single and double bond characters of the various bonds in the macrocyclic ring. In this distorted structure, the four nitrogens lone pairs of the macrocyclic ring are directed[14] out of the N$_6$-plane, so that the metal "sits atop" and not inside the N$_6$-cavity. The macrocycle is distorted such that the metal ion is lying outside the nitrogens' plane on the side opposite the folding. Thus

the ligand field exerted by the nitrogen system is very weak, which results in high-spin complexes even with strong donor ligands.

Electronic spectral studies: The electronic spectra of complexes of copper show a maximum at ca. 17810–19315 cm^{-1} and a shoulder at ca. 14540–17110 cm^{-1}. This indicates that these macrocyclic complexes are distorted octahedral.[15] The shifting of bands is towards higher energy in the order NCS > NO$_3$ > Br > Cl, i.e. in order of weakening interaction of the metal ion with the anions. Assuming tetragonal distortion in the molecule, the energy level sequence for these complexes may be, $x^2 - y^2 > z^2 > xy > xz > yz$ and the shoulder can be assigned to $z^2 \rightarrow x^2 - y^2 (^2B_{1g} \rightarrow {}^2B_{2g})$ and the broad band contains both the $xy \rightarrow x^2 - y^2 (^2B_{1g} \rightarrow {}^2E_g)$ and $xz, yz \rightarrow x^2 - y^2 (^2B_{1g} \rightarrow {}^2A_{2g})$ transitions.[16] The separation of bands in the spectra of these complexes is of the order of 2520 cm^{-1} which is in accord with the proposed geometry of the complexes.[17]

The nickel complexes show three strong bands at ca. 10610–12355, 15000–17000 and 25000–28100 cm^{-1} with a shoulder at ca. 8500–9510 cm^{-1} towards the low energy side of the first band. The spectral bands are well within the range for hexacoordinate octahedral complexes of nickel reported earlier.[18] The first two bands result from the splitting of one band, ν_1, and can be assigned to $^3B_{1g} \rightarrow {}^3E_g(\nu_1)$ and $^3B_{1g} \rightarrow {}^3B_{2g}(\nu_2)$ assuming the effective symmetry[16] to be D_{4h} (components of $^3T_{2g}$ in O$_h$ symmetry) and the other two higher bands can be assigned to $^3B_{1g} \rightarrow {}^3A_{2g}$(F), $^3F_g(\nu_3)$ and $^3B_{1g} \rightarrow {}^3A_{2g}$(P). The intense higher energy band appeared at ca. 35060 cm^{-1} can be assigned to a $\pi \rightarrow \pi^*$ transition of the C = N group. A regular pattern is not followed by various bands and this seems to be anion independent. The spectral data are consistent with the distorted octahedral nature of these macrocyclic complexes. The values calculated for Dq^{xy} and Dq^z are given in Table 2. Thus, all the complexes studied herein show pseudooctahedral geometry conforming to D$_{4h}$ symmetry. On the basis of symmetry arguments, Lever[18] has given a theory applicable to D$_{4h}$ molecules. This newly-developed theory is called normalised spherical harmonic Hamiltonian theory (NSH). This theory correlates ligand field parameters to NSH absolute ligand field parameters, DQ, DS and DT. Dq is a measure of the in-plane ligand field while DQ is a measure of the average ligand field experienced by the metal ion. The DT/DQ ratio gives the information about the distortion of the molecule. The values given in the Table 2 indicate that these macrocyclic complexes are moderately distorted and the distortion increases in the order: NCS > NO$_3$ > Br > Cl.

The spectral bands at ca. 8255–8750 cm^{-1} (ν_1) and 15750–16260 cm^{-1} (ν_2), with a broad band at ca. 21050 cm^{-1} (ν_3) can be assigned to Co(II) complexes,[18] reported to be distorted octahedral with D$_{4h}$ symmetry. These macrocyclic complexes exhibit a band in the visible region which shows a structure and splitting due to low symmetry fields. The splitting causes band overlap and some broad bands are observed. Thus, assuming the effective symmetry to be D$_{4h}$, these bands observed can be assigned to $^4T_{1g} \rightarrow {}^4T_{2g1}$, $^4T_{1g} \rightarrow {}^4A_{2g}$ and $^4T_{1g} \rightarrow {}^4T_{1g}$(P) at ca. 8510, 1620 and 20060 cm^{-1}, respectively. The first band (ν_1) is in the visible region and the assignment of the visible band to $^4A_{2g}$ cannot be spin forbidden. The values of Dq, B, β and ν_2/ν_1 ratio are given in Table 2.

On the basis of above discussion the following structure (A) may be proposed for these macrocyclic complexes:
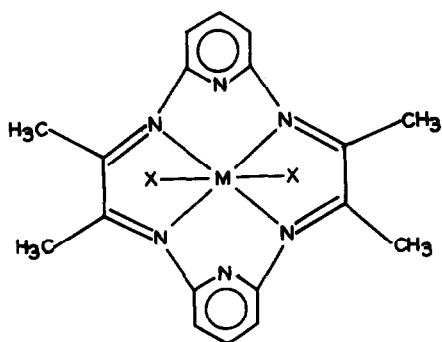
M = Cu(II),Co(II),Ni(II)

X = Cl,Br,NO₃,NCS

[A]

REFERENCES

1. N. F. Curtis, *Coord. Chem. Rev.* 1968, **3**, 3.
2. J. W. L. Martin, J. H. Johntan and N. F. Curtis, *J. Chem. Soc. Dalton Trans.* 1967, 68.
3. D. F. Cook and N. F. Curtis, *J. Chem. Soc. Dalton Trans.* 1973, 1076.
4. D. H. Busch, *Helv. Chim. Acta, Fasciculus extra ordinarius Alfred-werner* 1967, 174.
5. Vidya B. Rana, Dharma P. Singh, Prabha Singh and Mahendra P. Teotia, *Trans. Met. Chem.* 1981, **6**, 36.
6. K. Nakamoto, *Infrared Spectra of Inorganic and Coordination Compounds.* Wiley Interscience, New York (1970).
7. V. B. Rana, S. K. Sangal, S. P. Gupta and S. K. Sahni, *J. Ind. Chem. Soc.* 1977, **54**, 200.
8. S. K. Sahni, S. K. Sangal, S. P. Gupta and V. B. Rana, *J. Inorg. Nucl. Chem.* 1977, **39**, 1098.
9. V. B. Rana, J. N. Gurtu and M. P. Teotia, *Ind. J. Chem.* 1980, **19A**, 133.
10. C. N. R. Rao, *Chemical Applications of Infrared Spectroscopy.* Academic Press, New York (1963).
11. B. E. Douglas, *Inorg. Synthesis* 1978, **18**, 1.
12. L. F. Lindoy and D. H. Busch, In *Preparative Inorg. Reactions* (Edited by W. L. Jolly), Vol. 6, p. 1 (1971).
13. R. J. H. Clark and C. S. Williams, *Inorg. Chem.* 1965, **4**, 350.
14. M. C. Weiss and V. L. Goedken, *J. Chem. Soc. Chem. Commun.* 1976, 531.
15. M. J. M. Combell and R. Grezeskoviak, *Inorg. Nucl. Chem. Lett.* 1969, **5**, 27.
16. A. B. P. Lever and E. Mantovani, *Inorg. Chem.* 1971, **10**, 817.
17. M. L. Goodgame and L. I. B. Haines, *J. Chem. Soc.* 1966, 176.
18. A. B. P. Lever, *Inorganic Electronic Spectroscopy*, Elsevier, Amsterdam (1968).

RATE OF HYDROLYSIS OF Na₄P₂O₇ AND Na₅P₃O₁₀ AT 100°C AND THE EFFECT OF UREA

JOHN EMSLEY and SHAHIDA NIAZI

Department of Chemistry, King's College, Strand, London WC2R 2LS, England

Abstract—^{31}P NMR analysis has been used to measure the rates of hydrolysis of $Na_4P_2O_7$ and $Na_5P_3O_{10}$ at 100°; the rate constants are 6.07×10^{-3} and 2.24×10^{-1} hr^{-1} respectively. The presence of urea has a catalytic effect on the former but an inhibiting effect on the latter. These observations are explained by the hydrogen-bonding capabilities of urea.

Urea is known to have a profound effect when heated with phosphoric acid or ammonium hydrogen phosphates—it causes polymerization to cyclic or linear polyphosphates, P_n, depending upon the temperature.[1,2] In these reactions it behaves as a dehydrating agent and can cause condensation $nP_1 \rightarrow P_n$ at temperatures as low as 100°C. The products from such reactions are suggested as fertilizers, etc.[3] in which case their hydrolysis to monophosphate would be an essential prerequisite to absorption by plants. The urea in these products is also a source of nitrogen for plants. The effect of urea on the hydrolysis of P_n has not been investigated. As model systems for such an investigation tetrasodium diphosphate $Na_4P_2O_7(P_2)$ and pentasodium triphosphate $Na_5P_3O_{10}(P_3)$ have been chosen.

The hydrolysis of P_n has been studied over many years and the catalytic effect of various countercations has been noted.[4] Even sodium has a slight catalytic effect[5] compared to Et₄N$^+$ but is much weaker than most other cations especially those of divalent and transition metals.[6] Other factors also have a profound influence on the rate of hydrolysis especially the solvent[7] and pH.[5] In this paper we report on the effect of urea.

EXPERIMENTAL

Na₅P₃O₁₀ was reagent grade from Hopkin & Williams purified as in Ref. 5. Urea and Na₄P₂O₇ were analytical grade from Fisons and were used without further purification.

^{31}P NMR analysis

As a method of analysis this is not as accurate as conventional methods but it has the advantage of convenience and the technique has been successfully used in following the hydrolysis of diphosphate in the presence of a cobalt(III) complex.[8] Moreover the rate constant for the hydrolysis of Na₄P₂O₇ at 100°C reported here is 6.07×10^{-3} hr^{-1} which compares favourably with that reported in the literature for this temperature; 6.12×10^{-3} hr^{-1}.[9]

Broad band decoupled ^{31}P NMR spectra were recorded at 36.43 MHz on a Bruker HFX90 spectrometer at 300 ± 3k. Peak positions were measured from 85% H₃PO₄ as an external standard and P_1, P_2 and P_3 signals were integrated to determine the concentrations in solution. Machine settings were: filter band width 7500 Hz; sweep width 6000 Hz; sweep offset 4500 Hz with no systematic noise reduction; Fourier transform (pulse width 12.5 μsec, 8K data points, 30° flip angle, time constant—2 sec). The observation that ammonium polyphosphate solutions, prepared from urea-phosphate heated in excess urea,[1] were more stable than normal, prompted this investigation. Na₅P₃O₁₀ was chosen as a model system for the investigation because of its commercial importance and because both it and its hydrolysis products can be clearly distinguished by ^{31}P NMR analysis.

Samples were drawn from the reaction mixtures, cooled and their pH (Pye meter) and ^{31}P NMR spectra recorded; the latter after the addition of an equal volume of D₂O. The averaged results of two runs under various ratios of P_2: urea and P_3: urea are given in Table 1. The temperature of 100°C was chosen to give a relatively rapid rate of hydrolysis of P_2 and P_3 under the slightly alkaline conditions of their sodium salts. The solutions studied were 5% w/v solutions, and they were not buffered to show whether the effects were due to pH changes.

DISCUSSION

Adding urea to an aqueous solution of Na₄P₂O₇ at 100°C increases the rate of hydrolysis three-fold; the first order rate constants are 6.07×10^{-3} hr^{-1} and 21.5×10^{-3} hr^{-1} for the non-catalyzed and catalyzed reactions respectively. The factors which enhance polyphosphate hydrolysis have been identified as (i) lowered (acid) pH; (ii) complexation by metal cations, and (iii) ring formation.[10]

Change of pH does not explain the results reported here, nor does a change in complexation, so that the third factor, cyclization, seems the most appropriate. Can urea have this effect?

Urea and phosphoric acid form a strongly hydrogen-bonded complex $CO(NH_2)_2 \cdot H_3PO_4$ of structure (I).[11] In aqueous solution at pH 8.5 the anion of Na₄P₂O₇ will be $H_2P_2O_7{}^{2-}$ so that a cyclic hydrogen bonded system can be envisaged, e.g. (II).

(I)

(II)
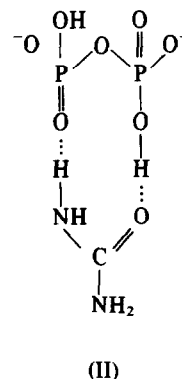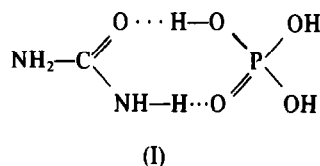
Table 1. Hydrolysis of $Na_4P_2O_7$ and $Na_5P_3O_{10}$ in the presence of urea at 100%

Compound	Urea, mole ratio $[P_n:U]$	Time (h)	pH	Composition (%, ± 0.5%)		
				P_3	P_2	P_1
$Na_4P_2O_7$	nil	2	8.65	–	98.8	1.2
		3	8.6	–	98.4	1.6
		4	8.6	–	97.5	2.5
		5	8.6	–	96.8	3.2
		10	8.6	–	94.1	5.9
$Na_4P_2O_7$	1: 0.5	2	8.45	–	96.2	3.8
		3	8.4	–	94.0	6.0
		4	8.4	–	91.6	8.4
		5	8.4	–	89.0	11.0
		10	8.5	–	81.4	18.6
$Na_5P_3O_{10}$	nil	1	8.2	82.4	16.0	1.6
		2	7.9	70.0	24.2	4.8
		3	7.7	52.2	35.7	12.1
		4	7.6	43.4	39.1	17.5
		5	7.5	31.2	42.6	26.2
$Na_5P_3O_{10}$	1: 0.25	1	8.5	91.4	7.4	1.2
		2	8.3	84.8	12.2	3.0
		3	8.2	80.7	15.5	3.8
		4	8.1	77.9	17.3	4.8
		5	8.0	72.6	20.9	6.5
$Na_5P_3O_{10}$	1: 0.5	1	8.5	87.6	9.9	2.5
		2	8.35	78.1	16.4	5.5
		3	8.25	68.9	21.5	9.6
		4	8.15	62.8	25.4	11.8
		5	8.1	54.9	29.0	16.1
$Na_5P_3O_{10}$	1: 1.25	1	8.6	91.9	6.7	1.4
		2	8.4	82.9	11.7	5.4
		3	8.35	73.7	19.0	7.8
		4	8.3	64.0	25.0	11.0
		5	8.2	52.4	31.2	16.4
$Na_5P_3O_{10}$	1:6	1	8.5	91.1	7.2	1.7
		2	8.5	78.0	17.0	5.0
		3	8.5	66.7	24.2	9.1
		4	8.7	59.1	29.5	11.4
		5	8.9	51.8	33.3	14.9

(III)
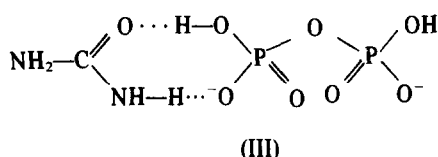
This might then serve to encourage nucleophilic attack at either phosphate centre by drawing away electron density towards the hydrogen bonds. Even a cyclic hydrogen bonded arrangement at only one phosphate as in (III) may serve the same purpose.

If this is the explanation of the enhanced rate of hydrolysis of diphosphate by urea it cannot serve to explain the behaviour of triphosphate, hydrolysis of which is *inhibited* by urea, see Table 1. The rate constants for this hydrolysis are 2.24×10^{-1} (no urea); 7.49×10^{-2} (1:0.25 ratio $Na_5P_3O_{10}$: urea); 1.30×10^{-1} (1:0.5); 1.17×10^{-1} (1:1.25); 1.36×10^{-1} (1:6) hr^{-1}. Thus a low ratio of urea decreases the rate by a factor of 3 but larger amounts of urea do not have a correspondingly larger effect. Again the changes in pH are not sufficient to cause this effect. The rate constant for the hydrolysis of P_3 at 100° agrees well with other values reported in the

literature for $60°C(0.45 \times 10^{-3})^5$, $70°(0.43 \times 10^{-3})^{12}$ and $90°(1.52 \times 10^{-1})^5$. A determination at 80° by us gave a value of 2.21×10^{-2}.

Displacing Na^+ from around the anion should reduce the rate of hydrolysis, but this explanation would apply also to diphosphate.† Cyclization may also occur as in (I) or (II) but again this should enhance the rate of hydrolysis. An explanation, also involving hydrogen bonding may be possible even though it involves cyclization. In aqueous solution the triphosphate ion will be chiefly $H_2P_3O_{10}^{3-}$ at pH 8 with the two protons attached to the terminal oxygens. These may then be involved in hydrogen bonds to urea, with each urea attracting several triphosphate ions. This has some basis of support since crystals of composition $CO(NH_2)_2 \cdot 2Na_5P_3O_{10}$ grow from these solutions. That the minimum rate was observed for the $1:0.25(P_3:$urea) ratio suggests that in such solutions several triphosphate ions can cluster around one urea molecule and that such clusters are less susceptible to nucleophilic attack by water by virtue of their macrostructure.

Unlike complexation to metal ions, when there is a marked chemical shift change of the phosphate signals,[13] the chemical shift changes in the presence of urea are small. Even with a P_3:urea ratio of 1:6, the end groups shift only from -5.39 to -5.55 ppm and the middle groups from -19.98 to -20.10 ppm, while J_{POP} remains the same. Hydrogen bonding does not have a profound effect on ^{31}P chemical shift of phosphates which are more susceptible to other effects such as pH.

The discovery reported here may have commercial implications. Already urea-ammonium polyphosphate

---

†Although many substances are known to enhance diphosphate hydrolysis few will retard the process. One such compound however is the polyelectrolyte polyethyleneimine ($-CH_2CH_2NH-$), which is thought to act via an electrostatic interaction with P_2: D. Turyn, E. Baumgertner and R. Fernandez-Prini, *Biophys. Chem.* 1974, **2**, 269.

mixtures are used in solution as liquid fertilizers and urea may have a two-fold effect—as a nitrogen fertilizer in its own right plus as a stabilizer for the soluble polyphosphates. Similarly the use of Na$_5$P$_3$O$_{10}$ as a detergent "builder" may be improved by the addition of urea which would preserve the triphosphate throughout more of the wash cycle especially in hot water laundering.

REFERENCES

[1] J. Emsley and S. Niazi, *J.C.S. Dalton*, 1982, 2527.
[2] J. F. McCullough, R. C. Sheridan and L. L. Frederick, *J. Agric. Food Chem.* 1978, **26**, 670.
[3] M. E. Walker, T. C. Keisling, W. H. Marchant and D. D. Morey, *Soil Sci. Soc. Am. J.* 1979, **43**, 606.
[4] E. J. Griffith and R. L. Buxton, *J. Am. Chem. Soc.* 1967, **89**, 2884 and references therein. More recently: F. D. Tudzharova, *Khim. Ind.*, 1974, **46**, 247 [C.A. **82**, 72116 h] and S. N. Graz, N. S. Tishkina and S. A. Aleshkevich, *Vopr. Khim. Khim. Tekhnol* 1979, **54**, 3 [C.A. **92**, 47897 n].
[5] J. R. Van Wazer, E. J. Griffith and J. F. McCullough, *J. Am. Chem. Soc.* 1955, **77**, 287.
[6] W. Wieker and E. Thilo, *Z. Anorg. Allgem. Chem.* 1960, **306**, 48.
[7] M. Wanatabe, *Bull Chem. Soc. Japan*, 1974, **47**, 2048.
[8] P. W. A. Hubner and R. M. Milburn, *Inorg. Chem.* 1980, **19**, 1267.
[9] *Tables of Chemical Kinetics of Homogeneous Reactions*, Vol. 1, p. 269, 1950. NBC-NRC, Washington.
[10] G. M. Woltermann, R. L. Belford and G. P. Haight Jr., *Inorg. Chem.* 1977, **16**, 2985.
[11] D. Mootz and K. R. Albrand, *Acta Cryst.* 1972, **28B**, 2459.
[12] C. Y. Shen and D. R. Dyroff, *Ind. Eng. Chem. Prod-Res. Dev.* 1966, **5**, 97.
[13] M. M. Crutchfield and R. R. Irani, *J. Am. Chem. Soc.* 1965, **87**, 2815.

IR SPECTROSCOPIC STUDIES ON SUBSTITUTED PYRIDINE N-OXIDE COMPLEXES OF TIN(IV) CHLORIDE IN ACETONITRILE

C. L. WILD†, M. SPAHIS†, R. D. BLANKENSHIP†, J. W. ROGERS and R. J. WILLIAMS*

Department of Chemistry, Midwestern State University, Wichita Falls, TX 76308, U.S.A.

Abstract—Complexes of eleven substituted pyridine N-oxide donors with stannic chloride in acetonitrile solution were investigated ultizing IR spectroscopy. Two distinct types of behaviour were noted: (1) Pyridine N-oxide donors containing electron releasing substituents generally form strong complexes with SnCl₄ and exhibit maxima in continuous variation plots at a 2:1 ligand-to-metal ratio. Little or no free ligand is detected in these solutions until this ratio is exceeded. Ligands exhibiting this behaviour include the 2-methyl-, 3-methyl-, 4-methyl-, 4-methoxy- and 4-phenylpyridine N-oxides.

(2) Pyridine N-oxide donors containing electron neutral to electron with-drawing substituents generally form weaker complexes with SnCl₄ and exhibit maxima in continuous variation plots at a 1:1 ligand-to-metal ratio. Free ligand is evident in these solutions even at ligand-to-metal ratios as low as 1:3. Formation plots for these complexes indicate the possibility that 1:2 and 1:1 ligand to metal complexes exist in the concentration ranges studied. Ligands exhibiting this behaviour include the 4-chloro-, 4-nitro-, 3 and 4-acetyl-pyridine N-oxides and 2-pyridine methanol N-oxide.

The complex of 2,6-lutidine N-oxide with SnCl₄ exhibits behaviour characteristic of the 1:1 complexes even though the substituents are electron releasing. This ligand contains the most sterically crowded N–O group in the series, however, and steric factors are invoked to explain this behavior.

These results are rationalized in terms of an equilibrium model which includes the postulated existence of oxygen bridged dimers comprising a dominant species in solutions containing the 1:1 complexes. Some supporting ¹H NMR and polarographic data are also presented and discussed.

A number of solid complexes of SnCl₄ with N, O, P and S donor atom ligands have been synthesized and characterized recently.[1–5] For the most part these complexes are reported to be monomeric and to exhibit octahedral geometries. When the ligands are unidentate, 2:1 complexes (all ratios given are ligand-to-metal) with SnCl₄ are the rule and a number of studies of the possible cis-trans isomerism in these complexes have been reported.[6–9] Some unidentate ligands have been reported to give 1:1 complexes,[10–12] presumably with trigonal bipyramidal geometries. Glutaronitrile is reported to form cis-2:1 octahedral complexes bridged through glutaronitrile to form a one dimensional polymer.[13] Attempts to predict the stoichiometry and geometry in these compounds based upon steric and bond strength arguments have thus far been largely unsuccessful.

Fewer studies of SnCl₄ complexes in solution have been reported. Stannic chloride has been shown to form a cis-2:1 complex with acetonitrile (ACN)[14,15] and a 1:1 complex with 2,2'-bipyridine with a log k > 7.[16] Complexes of SnCl₄ with substituted benzonitriles are reported to be 2:1 unless the substituent has a large electron withdrawing effect, whereupon the monoamide complex is favored over the diamide.[17]

Recent work in these laboratories has focused upon the electrolyte and complex formation behaviour of SnCl₄[18] and SnCl₂[19–22] in ACN solutions. These studies indicate SnCl₂ is only slightly dissociated in ACN and forms the stable SnCl₃⁻ species upon addition of

chloride ion and 1:1 complexes upon addition of a substituted pyridine N-oxide ligand. Stability constants of these complexes were determined utilizing an IR technique[22] and were found to range in value from 22 to 243 depending upon the nature of the substituent.

Polarographic studies show that SnCl₄ is also essentially a non-electrolyte in ACN solution but forms the stable SnCl₆²⁻ species upon addition of chloride ion. These studies also show that stable complexes of SnCl₄ form in ACN when a substituted pyridine N-oxide ligand is added. This present study was undertaken to further characterize these complexes.

EXPERIMENTAL

Chemicals. 2, 3 and 4-picoline N-oxides; 2,6-lutidine N-oxide; 4-methoxy-, 4-phenyl- and 4-nitropyridine N-oxides; and 2-pyridine methanol N-oxide were obtained from Aldrich Chemical Company. The 3 and 4-acetyl pyridine N-oxides were obtained from Ennox Chemical Company. These compounds were purified by sublimation or vacuum distillation before use. 4-chloro-pyridine N-oxide was synthesized and purified by standard methods[23] (m.p., 132–5°C).

SnCl₄.5H₂O was obtained from Pfaltz & Bauer and utilized without further purification. Found: Cl, 40.48; O, 22.44; H, 2.88; Calc.: Cl, 40.45; O, 22.82; H, 2.88%. Gold label acetonitrile was obtained from Aldrich Chemical Company and used without further purification.

Solutions. All solutions were prepared in class A volumetric flasks. Two sets of solutions were prepared for each study and IR spectra obtained from each solution. One set, containing ligand in ACN in the concentration range 0.003 to 0.012 M, was utilized to assign the N–O stretching frequency for each ligand. The absorbances from this set of solutions were also utilized in Beer's Law plots to determine the molar absorptivities at the frequency of the N–O stretching band for each free ligand.

The other set conisted of six to eight mixed solutions in ACN of SnCl₄·5H₂O and ligand in continuous variation concentration ratios of 0.002M metal + 0.010M ligand to 0.01M metal + 0.002M ligand. Two to five complete studies were utilized for each ligand.

Instrumentation. IR spectra were obtained in Wilks Scientific KBr precision sealed cells utilizing a Perkin–Elmer Model 283 grating IR spectrophotometer. In some cases matched cells were used to compensate for solvent absorption. Proton NMR spectra were obtained utilizing a Perkin–Elmer Model R32 spectrometer.

Method. ACN has a transmission window in the IR region between approx. 1300 and 1100 cm⁻¹. Fortunately this is the region, in which the very strong stretching absorption band of N-oxides appears. Coordination of N-oxides to metals causes a shift to lower frequencies of this absorption by 255–150 cm⁻¹.[21,22] Thus it is possible to determine free ligand concentrations and relative complexed ligand concentrations from measurements of absorbances of these bands. Details of these methods were given earlier.[22]

RESULTS

Table 1 contains a listing of the assigned N–O stretching frequencies of free and complexed ligands from this study. IR spectra of the ligand solutions were recorded and absorbances of the N–O stretching band, at the frequency for free ligand noted in Table 1, were determined utilizing the base line method.[23] Beer's Law plots of absorbance versus concentration were linear for all ligands.

IR spectra of the ACN solutions containing ligand and SnCl₄ were also recorded. The total concentration was limited to 0.012M due to the restricted solubility of the complexes. The concentration of free ligand in these solutions was determined from the measured absorbances of the free ν(N → O) band and the results of the Beer's Law plots. Relative concentrations of complexed ligand were determined from the absorbances of the complexed ν(N → O) band at the frequencies listed in the second column of Table 1. Continuous variation plots in the form absorbance at the frequency of the complexed band vs the mole fraction of ligand were then made for each complex.

Complex formation occurred in all cases but two distinct types of behaviour were observed. The 2, 3- and 4-picoline, 4-methoxy- and 4-phenylpyridine N-oxides were observed to form relatively strong complexes and exhibit maxima in continuous variation plots at a 2:1 ratio. Typical absorption spectra of these 2:1 type complexes in he 1100–1300 cm⁻¹ region are illustrated by those of the 2-picoline N-oxide complex shown in Fig. 1(a). The spectrum of the free ligand is shown in Fig. 1a(1). Two ligand bands appear superimposed upon the ACN spectrum in this region; an intense band at 1254 cm⁻¹, assigned to the predominantly N–O stretching mode, and a weaker band at 1222 cm⁻¹, assigned to C–H in-plane deformation.[24–27] Addition of SnCl₄·5H₂O causes a band at 1254 cm⁻¹ to appear as shown in Fig. 1a(2). Since solutions of SnCl₄·5H₂O are transparent in this region, this band is assigned to the N–O stretching mode of complexed ligand. As the ligand-to metal ratio is increased but the total concentration kept fixed, this band grows and reaches a maximum at a 2:1 ratio and diminishes thereafter as shown in Figs. 1a(2)–(4). Free ligand in these solutions is not detectable until a 2:1 ratio is exceeded.

Representative continuous variation plots for this series of complexes are shown in Fig. 2(a). Maxima occur close to a mole fraction of ligand corresponding to a 2:1 ratio. Some of these plots have rounded or irregular shapes possibly indicative of two or more absorbing species present in the solutions.

On the other hand, the 3 and 4-acetyl-, the 4-nitro- and the 4-chloropyridine N-oxides, the 2,6-lutidine N-oxide and the 2-pyridine methanol N-oxide ligands appear to form weaker complexes and exhibit maxima in continuous variation plots at a 1:1 ratio. Typical of complexes exhibiting this behaviour is the 4-acetylpyridine N-oxide complex. IR spectra in ACN for this ligand exhibit an assigned N–0 stretching band at 1262 cm⁻¹ and a C–H in-plane deformation band at 1170 cm⁻¹ as shown in Fig. 1(b)(1). Additions of SnCl₄·5H₂O to this ligand in ACN causes a relative decrease in the free N–O stretching absorbance and the appearance of an absorption band at 1212 cm⁻¹ attributable to the complexed N–O stretching band. Contrary to the former complexes, free ligand is detected in all complex mixtures studied. As the ligand-to-metal ratio is increased at constant total concentration, the absorbance of the band at 1212 cm⁻¹ increases, reaching a maximum at a 1:1 ratio and diminishing thereafter as shown in Figs. 1b(2)–(4).

Table 1. Assigned N–O stretching frequencies in cm⁻¹ of free ligand and ligand complexed to SnCl₄ in ACN solution

Ligand	(N→O) free	(N→O) complexed
2-picoline N-oxide	1254	1196
3-picoline N-oxide	1282	1255
4-picoline N-oxide	1259	1212
2,6-lutidine N-oxide	1250	1190
4-chloropyridine N-oxide	1258	1205
4-phenylpyridine N-oxide	1260	1215
4-methoxypyridine N-oxide	1230	1201
4-nitropyridine N-oxide	1287	1211
3-acetylpyridine N-oxide	1216	1184
4-acetylpyridine N-oxide	1262	1212
2-pyridine methanol N-oxide	1252	1210 & 1200

Some representative continuous variation plots of these complexes are shown in Fig. 2(b). All show maxima at 1:1 ratio and are less rounded than those from the complexes exhibiting 2:1 behaviour. There is some tailing of these plots at higher ligand mole fraction indicating the possible presence of small amounts of 2:1 or higher complexes in these solutions.

Table 2 gives the fraction of the total ligand that is uncomplexed, β, for various ligand-to-metal ratios for representative systems. For the 1:1 type complexes it can be seen that approximately 1/3 of the ligand remains uncomplexed at a 1:1 ratio while generally 1/2 and 2/3 remains uncomplexed at 2:1 and 3:1 ratios respectively. For the 2:1 type complexes no uncomplexed ligand is detected at a 1:1 ratio, and only approximately 15% and 40% remain uncomplexed at 2:1 and 3:1 ratios respec-
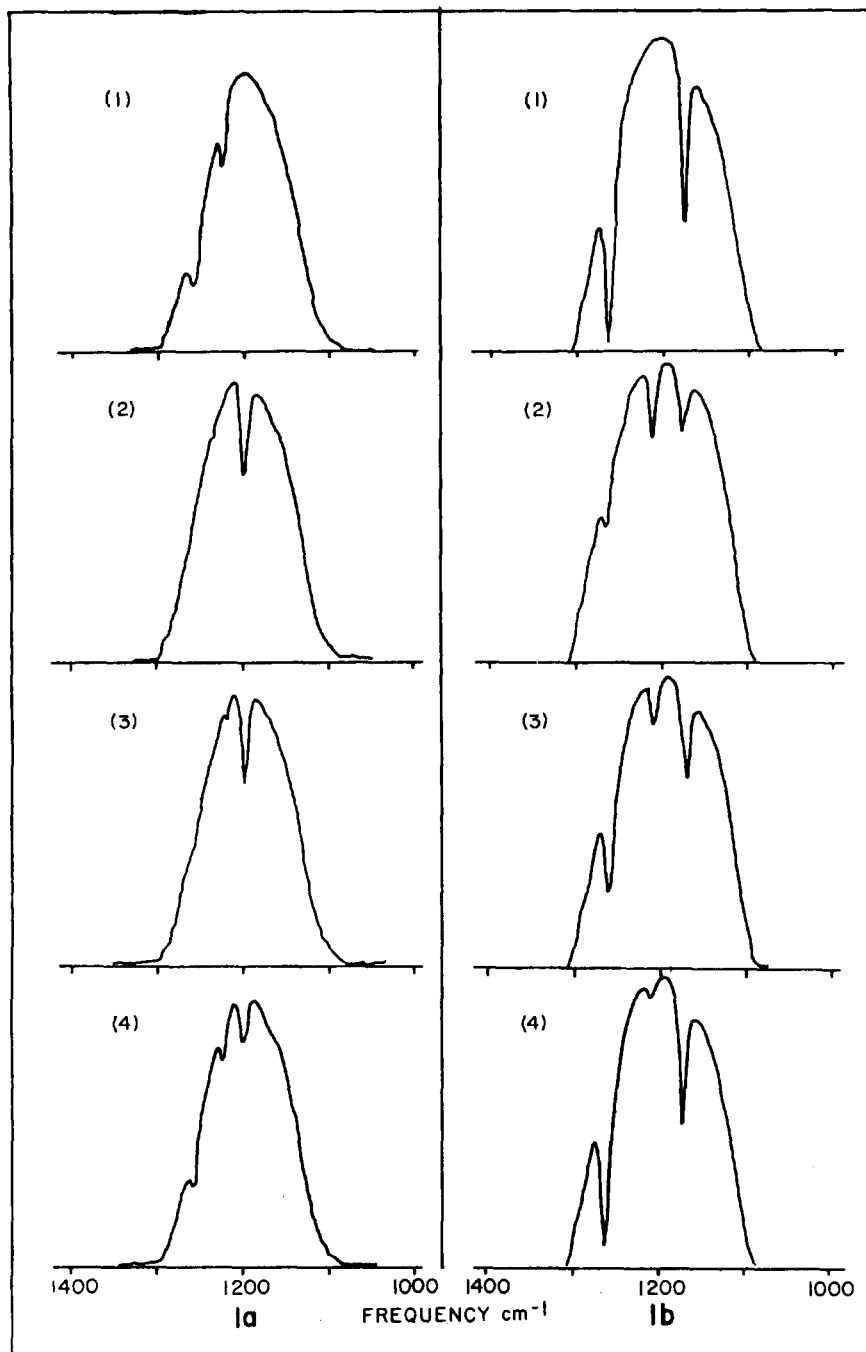
Fig. 1. IR spectra in the region 1100–1300 cm^{-1} for: 1a, 2-picoline N-oxide (2PNO)-SnCl$_4$·5H$_2$O mixtures and, 1b, 4-acetylpyridine N-oxide (4APNO)-SnCl$_4$·5H$_2$O mixtures in ACN solution. 1a(1): 0.012M 2PNO, 1a(2): 0.006M 2PNO + 0.006M SnCl$_4$·5H$_2$O, 1a(3): 0.008M 2PNO + 0.004M SnCl$_4$·5H$_2$O, 1a(4): 0.009M 2PNO + 0.003M SnCl$_4$·5H$_2$O. 1b(1): 0.012M 4APNO, 1b(2): 0.006M 4APNO + 0.006M SnCl$_4$·5H$_2$O, 1b(3): 0.008M 4APNO + 0.004M SnCl$_4$·5H$_2$O, 1b(4): 0.009M 4APNO + 0.003M SnCl$_4$·5H$_2$O.
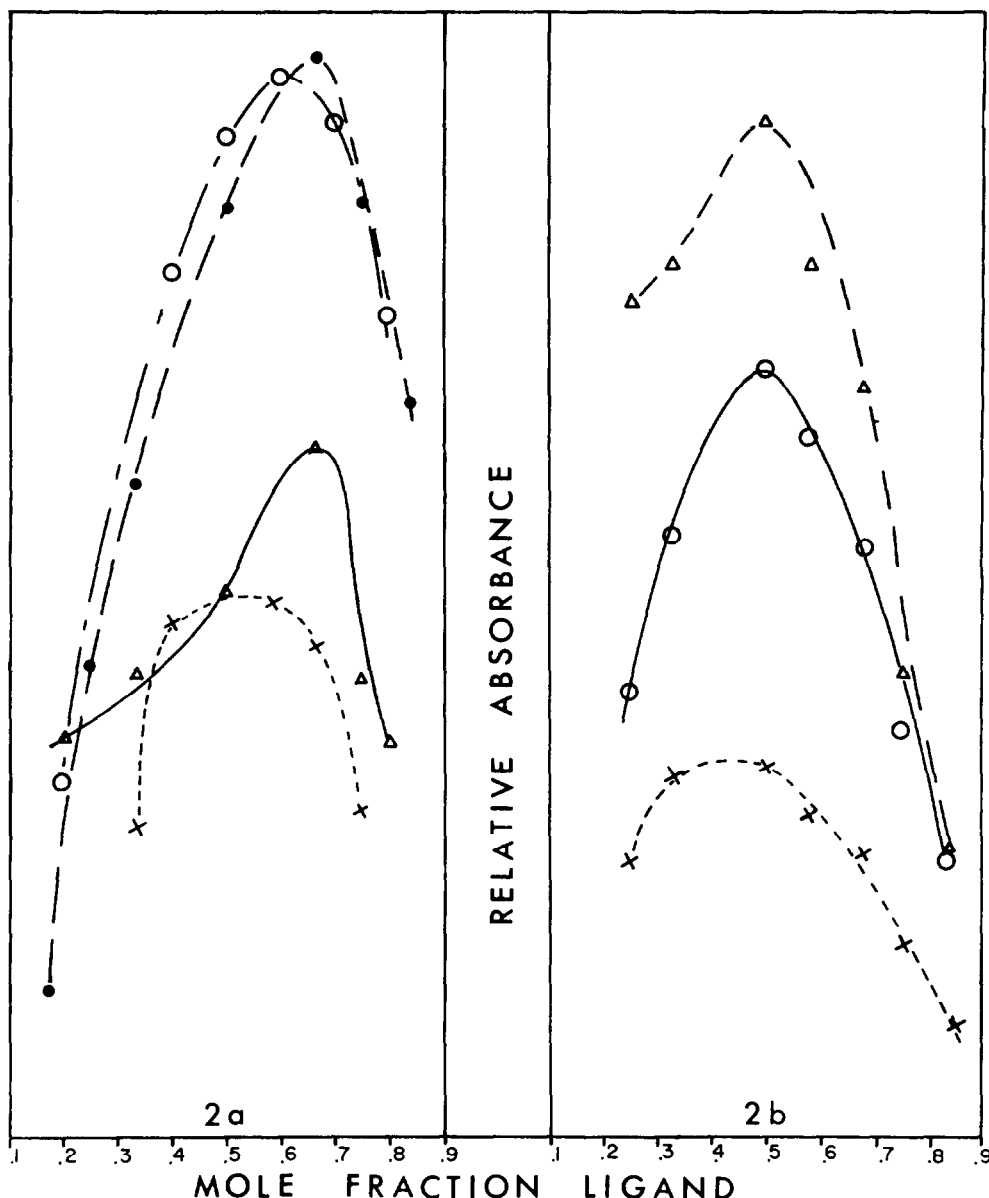
Fig. 2. Continuous variation plots for substituted pyridine 4-oxide complexes of $SnCl_4 \cdot 5H_2O$ in ACN solutions. 2a: representative complexes exhibiting 2:1 behavior: O, 4-picoline N-oxide complex; △, 2-picoline N-oxide complex; ×, 4-phenylpyridine N-oxide complex; ● data from integrated ^1H NMR spectra of 4-picoline N-oxide-$SnCl_4 \cdot 5H_2O$ complexes in 25% DMSO, 75% ACN. 2b: representative complexes exhibiting 1:1 behavior: O, 4-acetylpyridine N-oxide complex; △, 4-chloropyridine N-oxide complex; ×, 4-nitropyridine N-oxide complex.

tively. The distinction between the two types of complex behaviour is not always sharp. For example, 4-phenyl-pyridine N-oxide exhibits intermediate behaviour. It appears this ligand may form stronger 1:1 complexes than the typical 1:1 type complex but weaker 2:1 and higher complexes than the typical 2:1 type complexes.

Some independent investigations utilizing proton NMR and polarographic techniques provide some confirmation for the IR results and further insights into the behaviour of these systems. The solubility of these complexes in pure ACN is limited to approx. 0.02M but the concentration and, therefore, the sensitivity of the NMR probe may be enhanced ten-fold in a mixed solvent consisting of 25% dimethylsulphoxide (DMSO) and 75% ACN.

However, this solvent mixture does introduce high concentrations of DMSO, an excellent Lewis base.

These NMR studies were limited to 4-substituted pyridine N-oxide ligands due to the ease of interpretation of the spectra in the aromatic proton region. In all cases tetramethylsilane (TMS) was added as an internal standard and all chemical shifts are reported relative to TMS.

The NMR spectrum of 0.1 M 4-picoline N-oxide (4PNO) in ACN in the aromatic proton region exhibited the characteristic pair of doublets due to two pairs of equivalent ring protons with chemical shifts of 7.09, 7.16, 7.92 and 8.00 ppm. NMR spectra of solutions containing 0.01M $SnCl_4 \cdot 5H_2O$ and 0.02, 0.03, 0.04, 0.05 and 0.06M 4 PNO exhibited resonances characteristic of free ligand

Table 2. The fraction of the total ligand, β, that is uncomplexed in $SnCl_4 \cdot 5H_2O$-substituted pyridine N-oxide solutions in ACN for 1:1, 2:1 and 3:1 ratios

Ligand	Complex Type	$\beta 1:1$	$\beta 2:1$	$\beta 3:1$
2-picoline N-oxide	2:1	0.00	0.15	0.35
4-picoline N-oxide	2:1	0.00	0.09	0.38
4-phenylpyridine N-oxide	2:1	0.00	0.20	0.44
4-chloropyridine N-oxide	1:1	0.27	0.48	0.56
4-acetylpyridine N-oxide	1:1	0.26	0.56	0.64
4-nitropyridine N-oxide	1:1	0.32	0.62	0.76
2,6-Lutidine N-oxide	1:1	0.42	0.55	0.68

and an additional pair of doublets shifted downfield with chemical shifts of 7.55, 7.63, 8.48 and 8.56 ppm. The latter resonances were assigned to the aromatic protons of 4PNO complexed to $SnCl_4$. Chemical exchange processes are, therefore, relatively slow and aromatic proton environments on all complexed ligands appear either identical or very similar. Significant amounts of free ligand are detected only after the ligand to metal ratio exceeds 2:1. For example, a solution containing 0.03M 4PNO and 0.01M $SnCl_4$ exhibited a ratio of complexed to free ligand of approx. 1:1. The sensitivity of this technique was too low at these concentrations to obtain reliable quantitative data from integrated peak areas.

In the DMSO-ACN mixed solvent the solubility of the complexes is greatly enhanced and more reliable NMR data may be obtained. A series of solutions of 4PNO and $SnCl_4 \cdot 5H_2O$ in this solvent mixture were prepared with ligand and metal concentrations ranging from 0.04 to 0.20 M but with a total concentration of 0.24M as in a continuous variation study. Proton NMR spectra of these solutions in the aromatic proton region are shown in Fig. 3. Again a pair of doublets is observed for the free ligand in this region with chemical shifts close to those of 4PNO in pure ACN, 7.14, 7.21, 7.99 and 8.07 ppm. Addition of $SnCl_4 \cdot 5H_2O$ produces another pair of doublets due to complexed ligand with chemical shifts of 7.61, 7.69, 8.52 and 8.60 ppm respectively. Integration of each pair of doublets yields approximate concentrations of free and complexed ligand. These along with initial concentrations of metal and ligand and values of β are given for these solutions in Table 3.

A continuous variation plot of concentration of complex vs mole fraction ligand is superimposed on the plots from the IR results in Fig. 2(a), and is seen to be quite similar with a maximum at a 2:1 ratio. Similar results were obtained with 4-methoxypyridine N-oxide, which also exhibited behaviour characteristic of the 2:1 type complexes.

However, similar studies of solutions of $SnCl_4 \cdot 5H_2O$ and 4-nitro- or 4-acetylpyridine N-oxide in the mixed solvent indicated only free ligand was present, regardless of the ligand-to-metal ratio. The characteristic set of doublets in the aromatic proton region of the NMR spectrum due to free ligand showed no change in intensity and no change in chemical shift upon addition of $SnCl_4 \cdot 5H_2O$. Evidently these ligands, which exhibited behaviour characteristic of the 1:1 complexes in the IR study, form weaker complexes with $SnCl_4$ than do DMSO, 4PNO or 4-methoxypyridine N-oxide.

Polarographic studies of these systems in ACN at concentrations around one millimolar indicate the same two types of behaviour.[28] For those complexes exhibiting 2:1 behaviour, there is one reduction wave due to complexed ligand at approximately -0.33 V relative to a saturated calomel electrode (SCE) and significant free ligand is not detected until a 2:1 ratio is exceeded. For those complexes exhibiting 1:1 behaviour there is one reduction wave due to complexed ligand at approx. -0.29 V relative to the SCE and significant free ligand is

CHEMICAL SHIFT
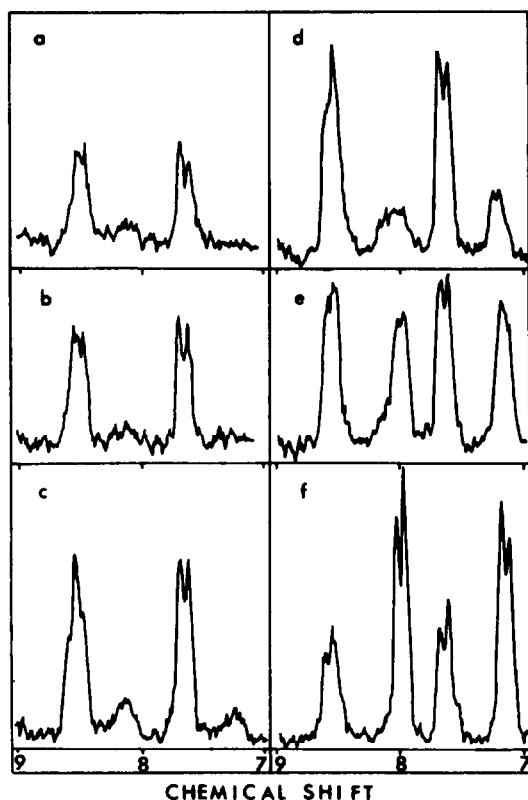
Fig. 3. ^1H NMR spectra of equilibrium mixtures of 4-picoline N-oxide (4PNO) and $SnCl_4 \cdot 5H_2O$ in 25% DMSO + 75% ACN solution. (a) 0.06M 4PNO + 0.18M $SnCl_4 \cdot 5H_2O$. (b) 0.08M 4PNO + 0.16M $SnCl_4 \cdot 5H_2O$. (c) 0.12M 4PNO + 0.12M $SnCl_4 \cdot 5H_2O$. (d) 0.16M 4PNO + 0.08M $SnCl_4 \cdot 5H_2O$. (e) 0.18M 4PNO + 0.06M $SnCl_4 \cdot 5H_2O$. (f) 0.20M 4PNO + 0.04M $SnCl_4 \cdot 5H_2O$.

Table 3. Initial $SnCl_4 \cdot 5H_2O$ and initial and equilibrium molar concentrations of free and complexed 4-picoline N-oxide in 25% DMSO, 75% ACN from proton NMR spectra. Values of β are given for each mixture

$[SnCl_4 \cdot 5H_2O]_0$	$[4PNO]_0$	$[4PNO]_{Free}$	$[4PNO]_{Complexed}$	$\underline{\beta}$
0.04	0.20	0.128	0.072	0.64
0.06	0.18	0.087	0.093	0.48
0.08	0.16	0.045	0.115	0.28
0.12	0.12	0.020	0.100	0.17
0.16	0.08	0.003	0.077	0.04
0.18	0.06	0.002	0.058	0.03
0.20	0.04	0.000	0.040	0.00

detected at a 1:1 ligand-to-metal ratio. All polarographic and NMR results are consistent with those from the IR studies.

DISCUSSION

It is somewhat surprising to find two fairly distinct types of behaviour for a series of complexes of a single metal species with ligands so similar to one another. Two generalizations may be drawn from the data collected and analyzed thus far: it appears that substituents on a pyridine N-oxide ring that are electron withdrawing to electron neutral induce the observed 1:1 behaviour while those that are electron releasing induce the 2:1 behaviour. Also the IR and NMR results indicate that ligands exhibiting 2:1 behaviour form stronger complexes with $SnCl_4$ than those exhibiting 1:1 behaviour. It is apparent that complexes containing 2:1 or higher ligand to metal ratios may exist for ligands exhibiting either type of behaviour. However, ligand molecules in these complexes appear to have identical or very similar environments as only one type of complexed species is detected by IR, NMR or polarographic techniques.

The application of standard methods[29] of determining stability constants assuming a simple model consisting of stepwise formation of 1:1 followed by 2:1 complexes was unsuccessful. Formation plots of $\bar{n}$ (total bound ligand/total metal)vs pL (negative logarithm of free ligand concentration) over the very limited concentration ranges studied revealed small plateaus for the 1:1 complexes at $\bar{n}$ values of 0.5 to 0.7 and at $\bar{n}$ values of 1.0–1.2. Formation plots for the 2:1 complexes could not be made for the concentrations utilized since free ligand was generally not detected until a 2:1 ratio was exceeded. Graphical elimination methods[30] assuming $N = 2$ gave scattered, inconsistent values of stability constants. It is apparent from these calculations that this simple model is invalid and the possibility of multi-nuclear complexes cannot be ruled out.

Recently a series of solid adducts of $SnCl_4 \cdot 5H_2O$ and various substituted pyridine N-oxides have been synthesized from tetrahydrofuran solution, purified and partially characterized in these laboratories.[31] The ligands studied include those exhibiting both 1:1 and 2:1 behavior in ACN solutions as described above. Elemental analyses indicate all complexes have a 2:1 ligand-to-metal ratio in the solid state. No water was observed in any of the adducts.

It is assumed that all 2:1 complexes exhibit an octahedral geometry and, therefore, consideration of *cis*-

trans isomerism is important. IR studies in the cesium bromide region may allow isomeric assignments for these complexes and the newly synthesized solid adducts and these studies are planned for the near future. However, a single crystal X-ray diffraction structure determination of the tetrachlorobis(4-picoline N-oxide) tin(IV) compound, presenttly in progress, has shed some light on this question. Density, space group and Patterson function determinations require the tin and oxygen atoms to occupy special positions which would require a *trans*-octahedral geometry. This complex in ACN solution exhibited the 2:1 type behaviour discussed above and it is assumed that it maintains the *trans*-octahedral geometry in solution.

It is felt that some elements of a model for this sytem may be gleaned from these results. The presence of two distinct types of behaviour suggests that consideration of *cis*–*trans* isomerism may be important. The evidence for multi-nuclear complexes suggests that bridging by chlorine atoms or the N-oxide oxygen atoms between two or more tin atoms may exist. Bridging by N-oxides to form dimers or polymers is known in some transition metal systems.[32-34]

The importance of $d\pi$–$p\pi$ bonding in tin complexes must also be considered. This bonding has been considered significant in some tin(II) and tin(IV) complexes but insignificant in others.[35] Evidence for multiple bonding in $SnCl_2$ complexes of substituted pyridine N-oxides includes very large red shifts in the N–O stretching frequencies upon coordination. These are attributed primarily to a weakening of the N–O bond due to donation of electron density from the d-orbitals of the Sn(II) species to a π^* orbital on the ligand.[21,22] $SnCl_4$ complexes of substituted pyridine N-oxides exhibit smaller shifts even though the d-electrons is $SnCl_4$ should be more stable than those in $SnCl_2$. This could be attributed to poorer orbital energy matching in $SnCl_4$ complexes between the d orbitals of tin and the lowest lying π^* orbital of the ligand, i.e. the π^* orbital is too high in energy for effective overlap. If this is the case electron withdrawing substituents on the pyridine N-oxide ring may destablilize the highest occupied bonding molecular orbital but stabilize the lowest unoccupied antibonding molecular orbital, enhancing $d\pi$–$p\pi$ bonding. If this bonding is an important component of the metal ligand bond, the *cis*-isomer would be favoured for octahedral complexes. This effect then could cause the ligands with electron withdrawing substituents to form *cis* 2:1 complexes while causing those with electron

neutral or donating substituents to form sterically less hindered *trans* 2:1 complexes.

The first step in the complex formation equilibrium scheme is undoubtedly replacement of an ACN molecule by the pyridine N-oxide ligand (L):

$$SnCl_4 \cdot 2ACN + L \rightarrow SnCl_4 \cdot L \cdot ACN + ACN. \quad (1)$$
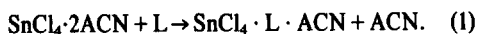
Complexes resulting from step (1) containing those ligands with electron neutral or withdrawing substituents could then either add another ligand *cis* to the first, (2), or add another $SnCl_4$ group to form a bridged 1:2 complex, (3):

$$SnCl_4 \cdot L \cdot ACN + L \rightarrow SnCl_4 \cdot 2L(Cis) + ACN \quad (2)$$

$$SnCl_4 \cdot L \cdot ACN + SnCl_4 \cdot 2ACN \rightarrow (SnCl_4 \cdot ACN)_2 \cdot L + ACN. \quad (3)$$
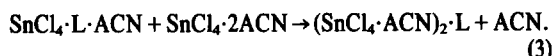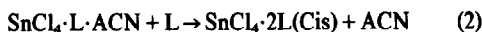
Either of the resulting species from steps (2) or (3) could then form a bridged dimer:

$$SnCl_4 \cdot 2L(Cis) + SnCl_4 \cdot 2ACN \quad (4)$$

$$(SnCl_4 \cdot ACN)_2 L + L \quad (5)$$
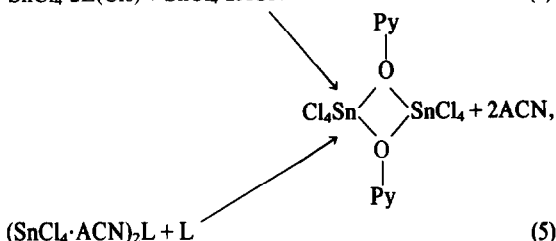
where Py stands for a substituted pyridine ring.

The dimer, could be stabilized by multiple $d\pi$-$p\pi$ bonding involving two d-orbitals on each tin atom. The dimer could be destroyed by addition of further ligand to form a *cis*-octahedral complex:

$$(SnCl_4 \cdot L)_2 + 2L \rightarrow 2SnCl_4 \cdot 2L \ (Cis). \quad (6)$$

There is evidence from the formation plots for species such as that produced in step (3) and if the dimer formed from steps (4) and (5) is stable, this may explain why these ligands exhibit maxima in continuous variation plots at a 1:1 ratio. This proposed model would also allow the tin atom to maintain its favoured octahedral coordination geometry in all complex formation steps.

Complexes from step (1) containing those ligands with electron donating substituents would not be significantly stabilized by $d\pi$-$p\pi$ back bonding and so would form the *trans*-complex upon addition of another ligand molecule:

$$SnCl_4 \cdot L \cdot ACN + L \rightarrow SnCl \cdot 2L(trans) + ACN. \quad (7)$$
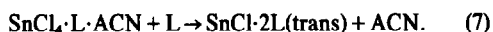
These complexes might also bridge to form multinuclear one-dimensional polymeric species

$$n(SnCl_4 \cdot L \cdot ACN) \rightarrow (SnCl_4 \cdot L)n + nACN. \quad (8)$$

However, if the *trans*-octahedral monomer is very stable, one would expect maxima in continuous variation plots at a 2:1 ratio as observed.

The 2,6-lutidine N-oxide molecule is the only ligand with severe steric crowding around the N-oxide oxygen atom. Examination of space filling models indicates it

would be very difficult for the N-0 bond in this ligand to maintain any double bond character while bonding to tin through sp^2 type orbitals. This would mean $d\pi$-$p\pi$ back bonding would be very unlikely in this complex. The fact that 2,6-lutidine forms 1:1 type complexes even though it contains electron releasing substituents may be due to the existence of a relatively stable 5-coordinate 1:1 complex which is favoured because it is sterically less hindered than the expected *trans*-2:1 complex.

The determination of the validity of this model awaits further experimental results. Experiments are presently planned to attempt to synthesize and characterize solid 1:1 adducts of these complexes and to determine the number of significant species in these solutions and the stability constants of these species utilizing more precise experimental techniques.

REFERENCES

[1] I. R. Beattie, *J. Chem. Soc.* 1963, 382–405.
[2] W. H. Nelson, *Inorg. Chem.* 1967, **6**, 1509.
[3] P. P. Singh, O. P. Agrawal and A. K. Gupta, *Inorg. Chim. Acta*, 1976, **18**, 19.
[4] N. Ohkaku and K. Nakamoto, *Inorg. Chem.*, 1973, **12**, 2440.
[5] P. G. Harrison, B. C. Lane and J. J. Zuckermann, *Inorg. Chem.* 1972, **11**, 1537.
[6] I. R. Beattie, G. P. McQuillan, L. Rule and M. Webster, *J. Chem. Soc.*, 1963, 1514.
[7] I. R. Beattie and L. Rule, *J. Chem. Soc.*, 1964, 3267.
[8] I. R. Beattie, M. Webster and G. W. Chantry, *J. Chem. Soc.*, 1964, 6172.
[9] I. Tanaka, *Organometal. Chem. Rev. Sect. A.*, 1970, **5**, 1.
[10] S. C. Jain and Roland Rivest, *Inorg. Chem.* 1967, **6**, 467.
[11] R. A. Slavinskaya, T. N. Sumarokova, M. Nurakhynova and N. A. Dolgova, *Zh. Obshch. Khim.* 1980, **50**, 406.
[12] Sh. Sh. Bashkirov, I. Ya, Kuramshin, A. S. Khromov and A. N. Pudovik, *Koord. Khim.* 1980, **6**, 386.
[13] D. M. Barnhart, C. N. Caughlan and M. Ul-Haque, *Inorg. Chem.* 1968, **7**, 1135.
[14] M. Webster and H. E. Blayden, *J. Chem. Soc. A.* 1969, 2443.
[15] I. R. Beattie and G. A. Ozin, *J. Chem. Soc. A*, 1970, 370.
[16] G. Matsubayashi, Y. Kawasaki, T. Tanaka and R. Okawara, *J. Inorg. Nucl. Chem.* 1966, **28**, 2937.
[17] R. A. Slavinskaya, T. N. Sumarokova, M. Nurakhynova and N. A. Dolgova, *Zh. Obshch. Khim.* 1980, **50**, 406.
[18] L. K. Young, M. E. Coles, J. W. Meux, S. D. Sorey, R. J. Williams, and J. W. Rogers, *J. Electrochem. Soc.* 1980, **127**, 1525.
[19] A. R. Brajer, T. E. Farley, J. W. Kauffman, L. K. Young, R. J. Williams, and J. W. Rogers, *Anal. Chim. Acta* 1977, **92**, 361.
[20] D. Pool, L. K. Young, R. J. Williams and J. W. Rogers, *Anal. Chim. Acta* 1977, **92**, 361.
[21] J. W. Kauffman, D. H. Moor and R. J. Williams, *J. Inorg. Nucl. Chem.* 1977, **39**, 1165.
[22] P. T. Scott, J. W. Kauffman, J. W Rogers and R. J. Williams, *J. Inorg. Nucl. Chem.* 1977, **39**, 2253.
[23] A. R. Katritzky, *J. Chem. Soc.* 1956, 2404.
[24] H. Shindo, *Chem. Pharm. Bull.* 1958, **6**, 117.
[25] H. Shindo, *Chem. Pharm. Bull.* 1956, **4**, 460.
[26] A. R. Katritzky and J. N. Gardner, *J. Chem. Soc.*, 1958, 2192.
[27] A. R. Katritzky, J. A. T. Beard and N. A. Coats, *J. Chem. Soc.* 1959, 3680.
[28] Jay Meux, Alex Drtil, R. J. Williams and J. W. Rogers, in preparation.
[29] F. R Hartley, C. Burgess and R. M. Alcock, *Solution Equilibria*. Wiley, New York (1980).
[30] F. J. C. Rossotti and H. Rossotti, *The Determination of Stability Constants*. McGraw-Hill, New York (1961).

[31]K. Wild, M. Spahis, R. Blankenship, J. W. Rogers and R. J. Williams, To be published.

[32]R. S. Sager, R. J. Williams and W. H. Watson, *Inorg. Chem.* 1967, **6**, 951.

[33]R. J. Williams, W. H. Watson and A. C. Larson, *Acta Cryst.*, 1975, **B31**, 2362.

[34]W. H. Watson, *Inorg. Chem.* 1969, **8**, 1879.

[35]D. R. Eaton and W. R. McClellan, *Inorg. Chem.* 1967, **6**, 2134.

KINETICS OF THE PHOTOAQUATION OF HEXACYANOFERRATE(II) ION

VILMOS GÁSPÁR and MIHÁLY T. BECK*

Institute of Physical Chemistry, Kossuth Lajos University, H-4010 Debrecen, Hungary

Abstract—Kinetics of the photoaquation of hexacyanoferrate(II) ion in aqueous solution were studied potentiometrically and spectrophotometrically. Supposing the simplest mechanism (see Fig. 3. in text), the photoaquation in alkaline medium can be well described. The value of the constants at pH = 11.0 are: $\phi = 0.8$–1.0, $k_6 = (3.0 \pm 0.5) \times 10^{-8} \text{ s}^{-1}$ and $k_{-6} = 1.5 \pm 0.2 \text{ mol}^{-1} \text{ dm}^3 \text{ s}^{-1}$. To describe the photoaquation in neutral medium the scheme was extended ($k' = 3.33 \times 10^2 \text{ mol}^{-1} \text{ dm}^3 \text{s}^{-1}$). The quantum yield in acidic medium can be calculated by combination of ϕ values of different protonated complexes. The reversibility of photoaquation in alkaline medium is also explained by the scheme.

The photosensitivity of different cyanocomplexes is well known. The kinetics and mechanism of these photochemical reactions have been intensively studied for a long time.[1] Nevertheless, the reversible photoaquation of hexacyanoferrate(II) ion is still an unsolved problem. The following primary photoprocess was established:

$$[Fe(CN)_6]^{4-} \xrightarrow[H_2O]{h\nu} [Fe(CN)_5H_2O]^{3-} + CN^-.$$
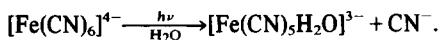
On illumination the concentration of aquapentacyanoferrate(II) ion reaches to a well-defined value, but after interrupting the illumination the concentration decreases.[2] Illuminating an alkaline or a neutral solution of the complex, the pH increases due to the hydrolysis of cyanide ion formed. In the next dark period the pH decreases. According to Asperger[3] the characteristic changes in the concentration of complex and in pH are totally reversible while MacDiarmid and Hall[4] found only partial reversibility.

Asperger followed the changes of pH and established some qualitative conclusions, namely:

—the initial rate of photoprocess and the maximum concentration of free cyanide ion increased with increasing initial concentration of complex,

—the initial rate of reversible dark (thermal) reaction decreased with increasing total concentration of complex.

Different quantum yields (ϕ) were determined with different methods (Table 1). Explanation of the dependence of ϕ on the pH has not yet been given.

The reasons for the contradictions are as follows:

(a) *The light was not monochromatic.* The authors should have taken into account the disturbing effect of photooxidation. On illumination with light of shorter wavelength than 330 nm, only the photooxidation occurs according to Stein.[5] The photoaquation takes place on illumination with longer wavelength light.

(b) *The atmosphere was not inert*, and the effect of thermal oxidation was not eliminated. Toma[7] found that trace amounts of iron(II) ion strongly catalysed the oxidation of aquapentacyanoferrate(II) ion even in the dark.

(c) *The reagents used* (sodium azide,[7] nitrosobenzene,[2] 2,2'-dipyridyl and 1,10-phenanthroline[8]) *considerably*

influenced the studied systems since they react with the components of them.

Under such experimental conditions the kinetic data calculated from the concentration versus time curves are contestable. One cannot separate the effects of different reactions such as thermal dissociation, thermal and photochemical oxidation, photoaquation, reversible thermal reaction between the products and the substitution reactions with reagents.

Sodium aquapentacyanoferrate(II) monohydrate (the so-called Hofmann salt) is the reference compound for spectrophotometric determination of the concentration of primary product. The preparation and purification of the complex are further problems since it is not very stable in the solid state.[7] In an inert atmosphere, sodium azide cannot be used as a reagent according to the results of Jaselkis[9] and Swinehart.[10] They indicated that the reaction between azide ion and aquapentacyanoferrate(II) ion does not occur in the absence of oxygen.

Nitrosobenzene is not a suitable reagent, either. In the standard procedure, mercuric chloride is used as a catalyst since the mercuric ion accelerates and reaction between the primary product and nitrosobenzene. The problem here is that the velocity of the catalysed reaction depends on pH and the negative effect of chloride ion must also be considered according to Hadjiioannou.[11] Moreover, some investigations[12] indicated that the uncatalysed reaction between the aquapentacyanoferrate(II) ion and the reagent strongly depends on pH and there is also a slow reaction between hexacyanoferrate(II) ion and nitrosobenzene.

By the use of monochromatic irradiation (365 nm), an inert atmosphere (argon) and potentiometric monitoring of pCN⁻ and pH, the reaction could be followed in alkaline medium without perturbing the system. In nearly neutral solutions the processes were followed by a pH potentiometric method since the cyanide ion-selective electrode shows anomalous behaviour at lower pH[13]. In acidic medium the reaction was followed by measuring the absorbance of primary product.

EXPERIMENTAL

The light source was a HANOVIA 6515–36–A type medium-pressure mercury lamp (preheated for 15 min). The light was filtered with a solution filter system containing two solutions such as 0.31 mol dm⁻³ copper sulphate and 3.1×10^{-4} mol dm⁻³ tris-phenanthrolineiron(II) ion in acetate buffer at pH = 4.0. The two solutions were divided by a glass wall as in the presence of

---

*Author to whom correspondence should be addressed.

387

Table 1. Different quantum yields (ϕ)determined by different methods for the photoaquation reaction of hexacyanoferrate(II) ion in aqueous solution. (a) V. Carassiti and V. Balzani, *Ann. Chim. Rome* 1960, **50**, 782. (b) G. Emschwiller and J. Legros, *Compt. rend.* 1965, **261**, 1533. (c) G. Emschwiller, *Compt. rend.* 1954, **239**, 1491. (d) S. Ohno, *Bull. Chem. Soc. Japan*, 1967, **40**, 1765

No.	Wavelength (nm)	pH-range	method	ϕ	Ref.
1.	365	7–10	pH-potentiometric	0.1	a.
2.	365	7–10	spectrophotometric determination of the concentration of aqua-pentacyanoferrate(II) ion using nitrosobenzene	0.4	b,c.
3.	365	below 7	spectrophotometric determination of the concentration of aqua-pentacyanoferrate(II) ion using sodium azide	0.5–0.9 (pH dependent)	d.
4.	313	10	the same method as in entry 2.	0.4	b.

copper(II) ion the iron(II) complex decomposes on illumination. The transmission of the filter system has a maximum at 365 nm. The intensity of light was measured by the ferrioxalate method.[14] Its value was 5.0×10^{-11} mole of photons (365 nm)/cm^{2}s^1.

The solutions were kept under argon atmosphere in a dark glass cuvette ($5 \times 3.7 \times 9.8$ cm) that was thermostatted (298 ± 0.1 K). A magnetic stirrer was used. The volume of irradiated solutions was constant (120 cm^3). The distance between the lamp and the cuvette was 13 cm.

Before following the photoaquation in alkaline medium, the pH values of the nearly neutral aqueous solutions were set to 10.5–11.0 by adding a few drops of 1.0 mol dm^{-3} carbonate-free sodium hydroxide solution. The free cyanide concentration was monitored potentiometrically by using an OP–711–D–I Radelkis ion-selective electrode and radiometer Type K 401 saturated calomel electrode with an OP–205 Radelkis mV-meter (reproducibility was ± 0.5 mV). The pH was measured by a combined glass electrode (GK 2301 B Radiometer) and PHM 51 Radiometer mV-meter (reproducibility was ± 0.1 pH).

The solutions were prepared in acetate buffer (pH = 4.0) for following the photoaquation in acidic medium. A Hitachi-Perkin-Elmer 139 single beam spectrophotometer was used for actinometry and determination of the concentration of primary product ($\epsilon_{440\,nm} = 640$ mol^{-1}dm^3). The optical length of the flow cell was 0.51 cm.

RESULTS AND DISCUSSION

In aqueous solution of hexacyanoferrate(II) at pH values from 10 to 12, there is a slow aquation reaction even in the dark. On illumination the rate of aquation increases. If the illumination period is short, the increase of cyanide ion concentration continues in the dark until the equilibrium state is attained. If the illumination period is long enough, the concentration of cyanide reaches a higher value than that which corresponds to the dark equilibrium (Fig. 1). The system returns to the equilibrium state when the illumination is interrupted. This alternating increase and decrease of cyanide concentration can be repeated several times.

The pH changes similarly in nearly neutral solution (pH = 7–7.5) of hexacyanoferrate(II) ion on illumination (Fig. 2). If the dark period is long enough, after illumination the pH decreases to the initial value. If the system was in thermal equilibrium before illumination, the change of pH is completely reversible.

The behaviour of this system can be quantitatively described by the following scheme (Fig. 3): where I_c is the average number of moles of photons (365 nm) absorbed by the complex per unit volume and unit time. In our experiments it amounts to 1.5×10^{-8},* as the excited complex ion, k_6, k_{-6} is the reaction rate constants (rrc) of thermal reactions, k_r is the rrc of the recombination reaction, k_f is the rrc of the products forming reaction, K_d is the dissociation constant of hydrogen cyanide at a certain ionic strength.[13]

Introducing the quantum yield as $\phi = k_f/(k_f + k_r)$ and applying the steady-state approximation for the concentration of the excited complex, the following rate equation is obtained:

$$-\frac{d[Fe(CN)_6]^{4-}}{dt} = \frac{d[Fe(CN)_5H_2O]^{3-}}{dt} = \phi I_c + k_6[Fe(CN)_6]^{4-} - k_{-6}[Fe(CN)_5H_2O]^{3-}[CN^-].$$

If the total concentration of cyanide (T_{CN}) is known at a certain time, the concentrations of hydrogen cyanide, cyanide ion, hydroxide ion and proton can be calculated as the components of an acid-base equilibrium system. T_{CN} is always equal to the concentration of aquapentacyanoferrate(II) ion.

On illumination, the system approaches the photostationary state when the following equation is valid:

$$\phi I_c + k_6[Fe(CN)_6]^{4-} = k_{-6}[Fe(CN)_5H_2O]^{3-}[CN^-].$$

In the dark, changes occur towards thermal equilibrium.

The exact values of the constants (ϕ, k_6, k_{-6}) were calculated by a least-squares method from the linear algebraic system of equations given for the parameters. The calculation of kinetic curves was based on the required combination of the fourth-order Runge–Kutta and the Newton–Raphson numberical methods.[15]

As shown in Fig. 4, there is excellent agreement between the experimental (full circles) and calculated (line) concentrations of cyanide ion, when ϕ, k_6 and k_{-6} are 0.8–1.0, 1.5 ± 0.2 mol^{-1}dm^{3}s^{-1} and $(3.0 \pm 0.5) \times 10^{-8}$ s^{-1}, respectively.

To characterize the conversion of the aquation process it is convenient to introduce the kinetic mean coor-
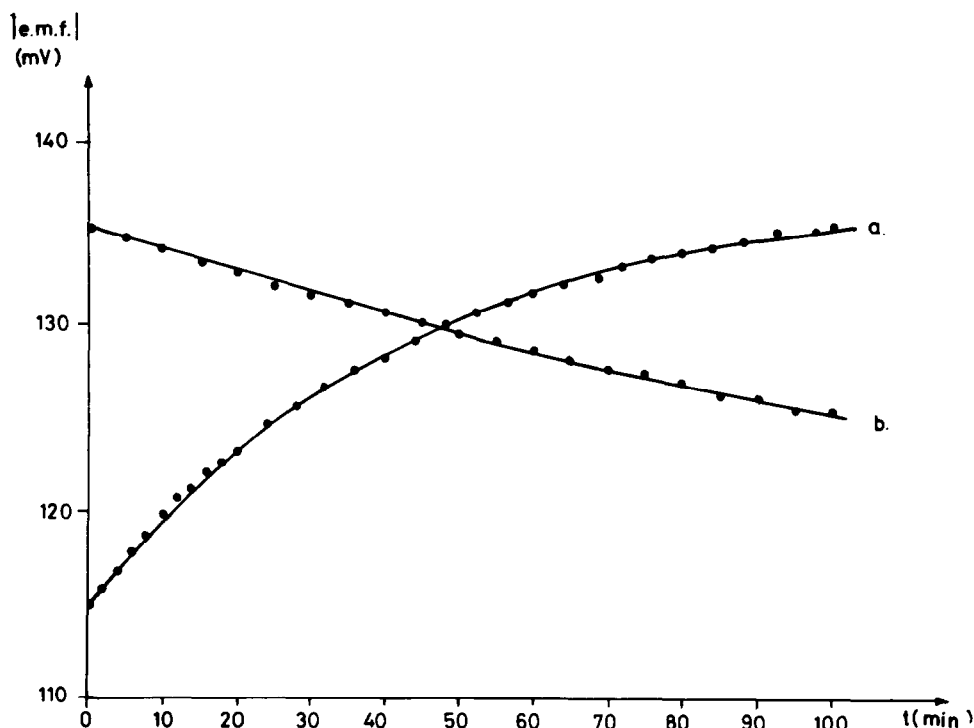
Fig. 1. The change of e.m.f. in hexacyanoferrate(II) solution C: 0.1 mol dm^{-3}, pH$_0$ = 10.75, (a) on irradiation (365 nm), (b) after interrupting the illumination.
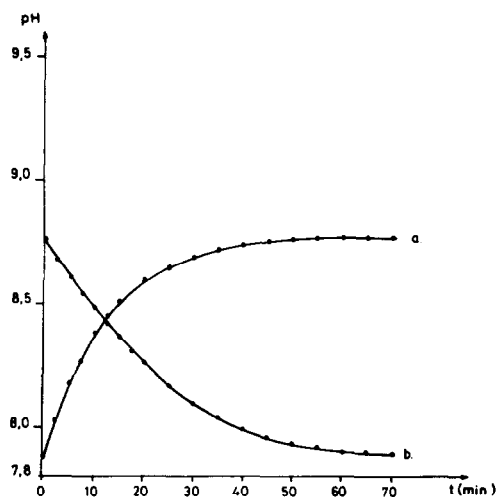
Fig. 2. The change of pH of hexacyanoferrate(II) solution. C: 0.1 mol dm^{-3}, pH$_0$ = 7.85, (a) on irradiation (365 nm), (b) in the dark reaction, after illumination.
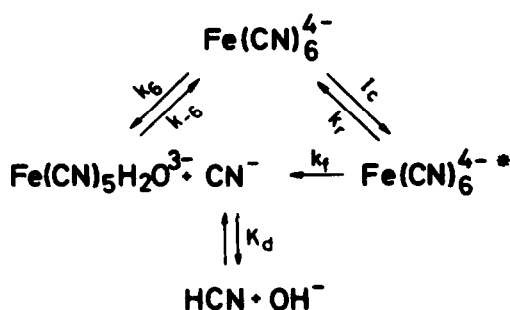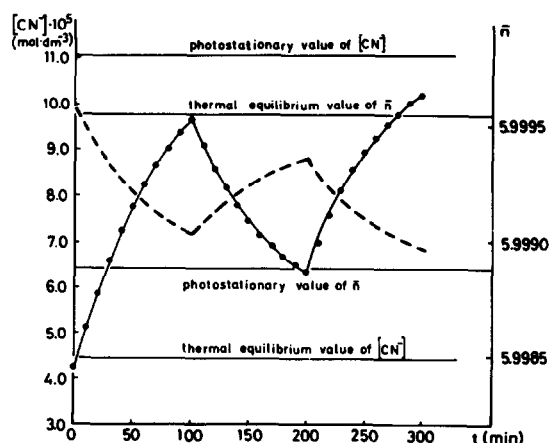
Fig. 4. Experimental (●) and calculated (line) cyanide ion concentrations in 0.1 mol dm^{-3} hexacyanoferrate(II) solution at pH$_0$ = 10.75 on illumination and in the next dark period. Dashed line: the change of the kinetic mean coordination number ($\bar{n}_t$). Values of ϕ, k_6 and k_{-6} are 1.0, 3.0×10^{-8} s^{-1} and 1.5 mol^{-1} dm^{3}s^{-1}, respectively.

Fig. 3. The scheme of photaquation reaction.

dination number ($\bar{n}_t$):

$$\bar{n}_t = \frac{T'_{CN} - CN_t^-}{T_{Fe}},$$

where T'_{CN} and T_{Fe} are analytical concentrations and CN_t^- is the free cyanide concentration at a certain moment.

The conversion both of the photo and the thermal (dark) reaction is extremely small (0.112 and 0.045%, respectively). Nevertheless, these very small changes of $\bar{n}_t$ can be quite exactly determined because of the high sensitivity of the cyanide ion-selective electrode and the
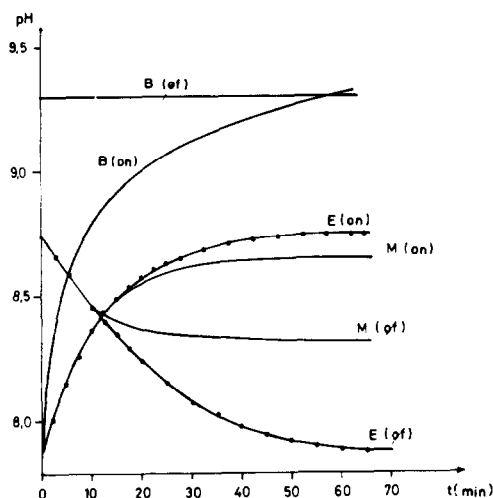
Fig. 5. The change of pH of hexacyanoferrate(II) solution. C: 0.1 mol dm^{-3}, pH$_0$ = 7.0 *on*: on illumination, *off*: after illumination E: experimental, B: calculated curve using the constants determined in alkaline medium (Fig. 4), M: calculated by the extended scheme.

large total concentration of the complex. The very small value of conversion is responsible for the fact that no satisfactory kinetic investigation was made earlier. It follows from the kinetic data that the stability constant of the sixth complex (K_6) is $(5.2 \pm 1.5) \times 10^7$ mol^{-1} dm^3. This value differs somewhat from that predicted theoretically (1.41×10^6)[16] or earlier determined experimentally (2×10^9).[18]

Because of the differences between the experimental and calculated (based on the constants determined in alkaline medium) curves in nearly neutral medium, the scheme should be extended by the following reaction:

$$[Fe(CN)_5H_2O]^{3-} + HCN \xrightarrow{k'} [Fe(CN)_6]^{4-} + H_2O + H^+,$$
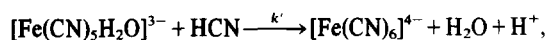
$k' = 3.33 \times 10^{-2}$ mol^{-1} dm^3 s^{-1}. The correlation between the experimental and calculated photostationary pH-values is good. The quantum yield of hydroxide production (0.17) agrees with the literature value.[1]

When illuminating an acidic solution (pH = 4.0) of the complex, a photostationary state was not reached. After interrupting the illumination, the absorbance of primary product did not decrease but slowly increased. The reason for this situation is the continuous formation of hydrogen cyanide that is continuously taken away by the bubbled argon gas.

Figure 6 shows a typical absorbance versus time curve at 0.01 mol dm^{-3} complex concentration. Assuming zero order photodecomposition, the calculated ϕ value is 0.85–0.95 at pH = 4.0 and, in the range of complex concentration 0.01–0.015 mol dm^{-3}, in good agreement with Ohno.[7]

From a comparison of the curve relating quantum yield in acidic medium (ϕ_a) to pH with the distribution curves of the different protonated hexacyanoferrate(II) complexes,[17] it seems possible that the decrease of ϕ_s with decreasing pH is connected with the occurence of differently protonated complexes.

Introducing the $\bar{n}_H/\bar{n}_{H,max}$ ratio to characterize the degree of protonation, the ϕ_a values can be calculated by the following expression:

$$\phi_a = \phi_b \left(1 - \frac{\bar{n}_H}{\bar{n}_{H,max}} \right)$$

where ϕ_b is the quantum yield determined in alkaline solution at the same concentration of complex, and $\bar{n}_{H,max}$ equals 4.

The calculated and determined values agree, considering the experimental error of measuring the protonation constants and ϕ (Fig. 7).

Comparing the ϕ_s vs pH curve with the distribution curves it follows that $\phi_{H_1} \sim 0.8$, $\phi_{H_2} \sim 0.6$, $\phi_{H_3} \sim 0.5$ and $\phi_{H_4} \sim 0$.

The ϕ_a value at a certain pH is the weighted average of the ϕ_{H_i} values ($i = 1,.., 4$).
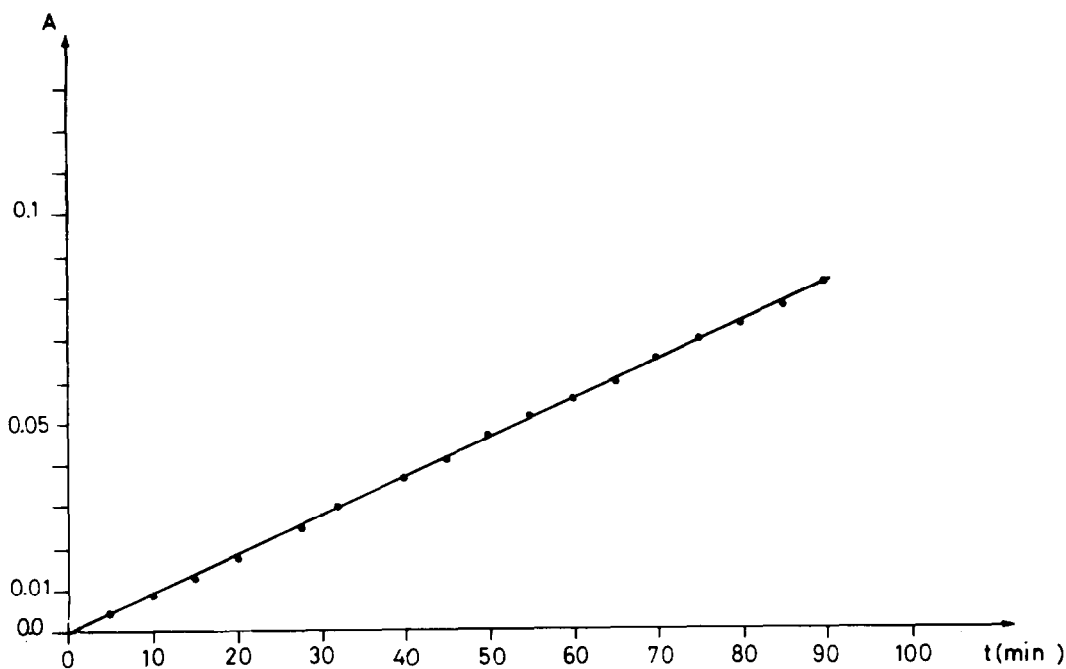
Fig. 6. The change of absorbance at 440 nm on illumination. C: 0.01 mol dm^{-3}, pH = 4.0 (acetate buffer).
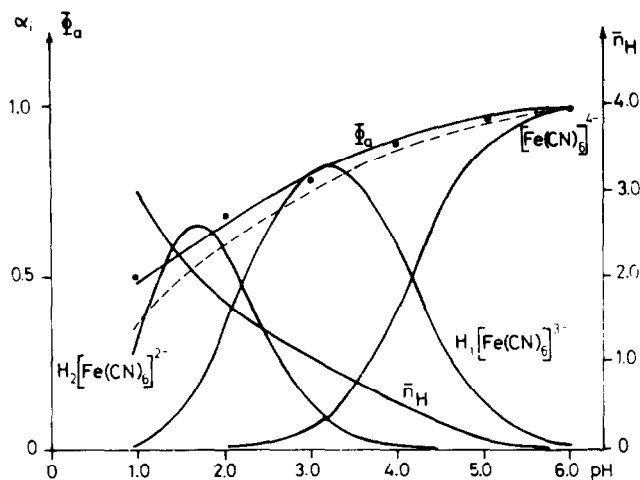
Fig. 7. Distribution curves of different protonated hexacyanoferrate(II) complexes[17] and ϕ_a vs pH curve: (●): experimental,[7] dashed line: calculated.

REFERENCES

[1]V. Balzani and V. Carassiti, *Photochemistry of Coordination Compounds.* Academic Press, New York, 1970.

[2]S. Asperger, I. Murati and D. Pavlovic, *J. Chem. Soc.* 1960, 730.

[3]S. Asperger, *J. Farad. Trans.* 1952, **48**, 617.

[4]A. G. MacDiarmid and N. F. Hall, *J. Am. Chem. Soc.* 1960, **75**, 5204.

[5]G. Stein, *Israel J. Chem.* 1970, **8**, 691.

[6]H. E. Toma, *Inorg. Chim. Acta* 1975, **15**, 205.

[7]S. Ohno, *Bull. Chem. Soc. Japan* 1967, **40**, 1765.

[8]V. Karas and T. Pinter, *Z. Phys. Chem. Leipzig* 1962, **220**, 327.

[9]B. Jaselkis, *J. Am. Chem. Soc.* 1961, **83**, 1082.

[10]S. K. Wolfe, C. Androde and J. Swinehart, *Inorg. Chem.* 1974, **13**, 2567.

[11]T. P. Hadjiioannou, *Anal. Chim. Acta* 1966, **35**, 351.

[12]I. Orosz, *M.Sc. Thesis.* Debrecen, 1970.

[13]V. Gáspár and M. T. Beck, *Magy. Kém. Foly.* 1980, **86**, 177.

[14]C. G. Hatchard and C. A. Parker, *Proc. Roy. Soc.* (London) 1956, **A235**, 518.

[15]V. Gáspár, *Ph.D. dissertation.* KLTE, Debrecen, 1980.

[16]M. T. Beck, *Critical Survey of Stability Constants of Cyano-Complexes, Pure Appl. Chem.* (in preparation).

[17]J. Jordan and J. G. Ewing, *Inorg. Chem.* 1962, **1**, 578.

[18]G. Emschwiller, *Compt. rend.* 1953, **236**, 72.

ACID-BASE STUDIES OF SOME
SILYLAMINES RNHSiMe₃

KEITH J. FISHER*
University of Khartoum, Sudan, Africa

and

CHIKE E. EZEANI[1]
University of Lagos, Nigeria, Africa

Abstract—The interactions of silylamines with phenol and iodine have been studied. Enthalpies of reaction have been determined and used to calculate E and C values for these bases. The calculated enthalpies with chloroform and trimethylaluminium indicate that the alkylsilylamines may not be weaker bases than corresponding aliphatic amines.

There have been several studies involving the acid-base interactions of organosilylamines (R_3SiNHR' and R_3SiNR_2') with Lewis acids.[2-6] The major acid studied has been chloroform; enthalpies of mixing, NMR shift data and C-D IR shift data have been produced.

The heat of mixing of the base using chloroform as both acid and solvent is not a simple property, and the results would differ markedly from those of a study of the chloroform base interaction in an inert solvent. Drago[7] has shown that C-D IR stretching frequencies cannot be used as a reliable estimate of the enthalpy of adduct formation with a wide variety of bases. Drago[7] has also shown that NMR data can also be an unreliable measure of enthalpy. In one NMR study[5] carbon tetrachloride was used as solvent. This solvent is known to have a specific interaction with amines and our study has shown that this is the case for silylamines.

Since many spectroscopic studies have been carried out with iodine and phenol, we set out to investigate these acids with silylamines. As the silylamines are sensitive to hydrolysis exceedingly dry conditions were used. The solvents chosen were hexane and cyclohexane which could be dried thoroughly and acted as non-interacting solvents. Iodine-silylamine studies indicated a 1:1 interaction but on standing over several hours secondary changes occurred. Freshly prepared and mixed solutions were used throughout this study. Similarly, IR studies with phenol indicated the initial formation of an adduct but on standing the adduct disappeared.

Enthalpy data were obtained for the interaction of several silylamines with these acids, and the Drago equation[7] was used to calculate E and C values for the bases.

EXPERIMENTAL

All operations were carried out under either dry nitrogen or under vacuum.

Hexane and cyclohexane were stored over sodium, distilled before use and further stored over Linde 4A molecular seives.

Phenol and iodine were sublimed under vacuum before use. Pyrrole was fractionally distilled and stored over Linde 4A molecular seives.

The secondary amines, RNHSiMe₃ were prepared by the reaction of chlorotrimethylsilane with primary amines and were distilled before use. Hexamethyldisilazane and N, N-diethyltrimethylsilylamine were purchased from Aldrich Chemical Company and distilled before use. All physical properties of the amines corresponded to literature values and gas chromatography was used as a further check on purity.

Phenoxytrimethylsilane was prepared by the reaction of phenol with trimethylchlorosilane.

Infrared studies were carried out using 1 cm pathlength solution cells with sodium chloride windows. Scale expansions were used when measurements of $\Delta\nu_{OH}$ were being made. As the O-H absorption band was generally weak and well removed from the free O-H absorption of phenol, no problem of overlap was experienced. Generally solutions of approximate concentrations of 1 to 5×10^{-3} molar were used. Similar measurements were made with pyrrole.

Visible studies of iodine with the bases were carried out on a PMQ3 spectrophotometer at 525 nm. Acid and base solutions of varying concentrations were used to determine equilibrium constants. Enthalpies were determined by carrying out the reactions at seven temperatures in the range 290–330°K. The results were treated by the least-squares method to obtain the slope of log K vs 1/T, and correlation coefficients were calculated.

RESULTS AND DISCUSSION

The values of $\Delta\nu_{OH}$ for the interaction of the amines with phenol and those for $-\Delta H$ (kcal mol⁻¹) determined from $\Delta\nu_{OH}$ are shown in Table 1. Also shown in Table 1 are the equilibrium constants for the interaction of iodine with the amines at 303°K in cyclohexane. The enthalpy values calculated from a Van't Hoff plot are also shown in Table 1.

The IR studies with phenol indicated the initial formation of an adduct but on standing the absorption for the adduct disappeared. This reaction was investigated and the final products of the reactions were shown to be a primary amine and $(CH_3)_3SiOC_6H_5$. $(CH_3)_3SiOC_6H_5$ was prepared by another method and gas chromatography was used to show that this was a product of the reaction. Cyclohexane was chosen as solvent after studies in carbon tetrachloride indicated lower equilibrium constants and lower heats of about 1.2 kcal per mole. This indicates that, as with pyridine,[7] there is an interaction of the silylamines with carbon tetrachloride (slightly greater than that with pyridine).

Using pyrrole as acid only two adducts were observed, with hexamethyldisilazane and with PhNHSiMe₃. The

---

*Author to whom correspondence should be addressed.

Table 1. Spectroscopic studies of silylamines with phenol and iodine using cyclohexane as solvent

Amine	Phenol		Iodine	
	$\Delta\nu_{OH}$	$-\Delta H$ kcal mol^{-1}	K	$-\Delta H$ kcal mol^{-1}
MeNHSiMe$_3$	420	7.70	125	7.36
EtNHSiMe$_3$	420	7.70	126	5.72
iPrNHSiMe$_3$	420	7.70	80.7	5.15
iBuNHSiMe$_3$	430	7.82	426	a
tBuNHSiMe$_3$	410	7.59	400	7.17
Et$_2$NSiMe$_3$	415	7.65	402	4.04
(Me$_3$Si)$_2$NH	240	5.69	11.8	b
C$_6$H$_5$NHSiMe$_3$	195	5.18	37.2	5.65

a) Erratic results giving a correlation coefficient of only 0.84.

b) Results with this base were inconsistent.

shifts of the N–H vibration of pyrrole, $\Delta\nu_{NH}$, were 130 and 97 cm^{-1} for hexamethylsilazane and PhNHSiMe$_3$ respectively. These lead to heats of interaction of 3.54 and 3.13 kcal mol^{-1}.

Some studies were carried out with p-chlorophenol and these gave similar results to phenol. As p-chlorophenol is not a significantly different acid from phenol, the data was not used quantitatively but used to indicate the reliability of the phenol data.

The visible spectra studies with iodine were also conducted in cyclohexane and selected results in hexane gave similar values. Studies with the amines and iodine indicated an isobestic point at approximately 485 nm. As with the phenol studies, fresh solutions were used in the measurements, as on standing a secondary reaction seemed to occur. Initial iodine concentrations of 1×10^{-3} molar and varying concentrations of base of approx. 3×10^{-3} molar were used in the studies. The data for change of equilibrium concentration with temperature were treated by a least-squares method and gave results shown in Table 1. With the exception of the isobutyl derivative and hexamethyldisilazane, they gave correlation coefficients of 0.99. With the isobutyl compound, there was a correlation coefficient of only 0.84. Hexamethyldisilazane gave inconsistent results and so $-\Delta H$ was not calculated for this base.

Early work in this area by Jarvie[2] examined the heats of mixing of various alkylamines and silylamines with chloroform using chloroform as both solvent and reference acid. The conclusion drawn was that "the alkylsilylamines are in general weaker bases than aliphatic amines". The problem is that the acid as solvent complicates the data as shown in the following Born–Haber cycle:

$$A_{(g)} + B_{(g)} \xrightarrow{\Delta H_{AB}} AB_{(g)}$$
$$\Delta H' \uparrow \qquad \uparrow \Delta H'' \qquad \downarrow \Delta H_{(solv)}$$
$$A_{(solv)} + B_{(solv)} \xrightarrow{\Delta H_0} AB_{(solv)}.$$
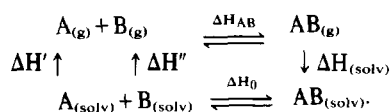
The observed enthalpy in solution ΔH_0 will be the sum of all the other terms.

$$\Delta H_0 = \Delta H_{AB} + \Delta H_{(solv)} + \Delta H' + \Delta H''.$$

Thus if ΔH_0 is approximately to equal the gas phase

enthalpy of adduct formation, ΔH_{AB}, the sum of $\Delta H_{(solv)}$, $\Delta H'$ and $\Delta H''$ must be approximately zero. $\Delta H''$ will differ markedly with the base used, but $\Delta H'$ will remain constant and $\Delta H_{(solv)}$ should not be a large term and remains fairly constant unless some specific interactions are occurring.

To highlight this problem, the enthalpy of triethylamine (one of the amines measured in Jarvie's study) with chloroform in an inert solvent has been measured.[8] Jarvie obtained a value of 0.87 kcal mol^{-1} whereas the later measurement gave a value of 4.8 kcal mol^{-1}. This discrepancy throws into doubt the work of Abel[4] where a correlation of the heat of mixing with the proton dilution shift gave a straight line.

Andrianov[5] et al. confirmed that NMR measurements of proton shifts of silylamines in chloroform do not correlate with estimated values of pKa; after assuming the heats of mixing correlated with proton shifts. Kelling[6] et al. have attempted a correlation of $\Delta\nu_{C-D}$ and $\Delta\nu_{N-H}$ values as a measure of the basicity of similar silylamines. Drago[7] has shown that C–D infra shifts do not correlate with other data such as the O–H shift with phenol and the N–H shift with pyrrole.

Thus all the previous studies have only been able to show the basic conclusion given by Jarvie, "the alkylsilylamines are weaker bases than aliphatic amines".

Using our data we may calculate E and C values (Table 2) and compare them with other aliphatic amines. We may also use these values to calculate possible enthalpies with acids not measured and compare those values with the enthalpies available for the interaction with aliphatic amines with those acids. Having only two sets of data for two different acids allows an easy solution of the E and C equation but these values must be regarded as only tentative until more data is available.

Our data produce only one test of the calculated E and C values and that is the heat of interaction of pyrrole with PhNHSiMe$_3$. The value obtained was 3.13 kcal mol^{-1} and that calculated from the E and C values was 3.27 kcal mol^{-1}. Although the difference is slightly greater than 0.1 kcal mol^{-1} it shows that the E and C values calculated are of the correct order of magnitude.

One observation from Table 2 is that Jarvie's statement is questionable. Two very different acids, CHCl$_3$

Table 2. E and C values for amines and calculated heats of interaction of the amines with chloroform and trimethylaluminium

Compound	$E_B{}^a$	$C_B{}^a$	$-\Delta H{}^b$ CHCl₃	$-\Delta H{}^b$ Al(CH₃)₃
MeNHSiMe₃	1.18	6.18	4.55	28.8
EtNHSiMe₃	1.35	4.37	4.77	29.1
iPrNHSiMe₃	1.41	3.74	4.85	29.2
tBuNHSiMe₃	1.17	6.00	4.49	28.4
PhNHSiMe₃	0.715	4.93	2.94	16.3
Et₂NSiMe₃	1.52	2.52	4.99	29.3
Me₂NH	1.09	8.73	4.68	30.8^c
Me₃N	0.808	11.54	4.28	30.0
Et₂NH	0.866	8.83	4.02	27.3
Et₃N	0.991	11.09	4.8^c	32.6

a) Values for the silylamines calculated from the interactions with phenol and iodine.

b) -ΔH calculated using the E and C values for chloroform and trimethyl-aluminium⁹.

c) Values taken from ref. 8.

and Al(CH₃)₃, give similar interactions with the aliphatic amines and the silylamines. The only silylamine that stands out as being markedly weaker is the phenyl derivative. The changes of E_B and C_B show no distinct pattern: the aliphatic amines show an increase in the C_B value on going from a secondary amine to a tertiary amine but the reverse seems to be the case for EtNHSiMe₃ and Et₂NSiMe₃. The silylamines show an increase in E_B and a decrease in C_B as the alkyl group changes from methyl to ethyl to isopropyl, but the t-butyl derivative shows a marked decrease in E_B with an increase in C_B.

REFERENCES

¹Abstracted in part from the M.Sc. thesis of C. E. Ezeani, University of Lagos, Nigeria, 1980.
²A. W. Jarvie and D. Lewis, *J. Chem. Soc.* 1963, 1073.
³S. W. Jarvie and D. Lewis, *J. Chem. Soc.* 1963, 4758.
⁴E. W. Abel, D. A. Armitage and S. P. Tyfield, *J. Chem. Soc.* (A), 1967, 554.
⁵K. A. Andrianov, V. M. Kopylov, V. V. Yastrebov. A. I. Chernyshev, Zh. S. Syrtsova and V. A. Nuikin. *Zh. Obschchei* 1973, **43**, 2445.
⁶H. Kelling, R. Rennau, R. Unglaube, E. Popowski, *Z. Chemie* 1981, **21**, 140.
⁷D. G. Brown, R. S. Drago and F. L. Slejko, *J. Am. Chem. Soc.* 1972, **94**, 9210.
⁸R. S. Drago, G. C. Vogel, T. E. Needham, *J. Am. Chem. Soc.* 1971, **93**, 6015.
⁹R. S. Drago, *Coord. Chem. Rev.* 1980, **33**, 251.

SYNTHESIS AND CHARACTERIZATION OF A NEW IRON (II)—DINITROGEN COMPOUND WITH PDTA AS LIGAND

M. CARMEN PUERTA,* M. F. GARGALLO and F. GONZALEZ-VILCHEZ

Departamento de Química Inorgánica, Facultad de Ciencias, Universidad de Cadiz, España

Abstract—A new dinitrogen complex of formula $Na_2[Fe(PDTA) (N_2)] (H_2O)_2$ has been synthesized in aqueous solution from [Fe(H-PDTA) (H_2O)], $3/2H_2O$ and NaN_3. The complex has been characterized by chemical analysis, IR and electronic spectra, and magnetic measurements. The thermal decomposition process has been studied by using DTA and TG techniques. The evolution of gases was followed by Gas Chromatography.

Since Allen and Senoff[1] isolated the first dinitrogen complex in 1965, a great interest has been awakened in the clear possibility of carrying out the "fixation" of this molecule by means of coordination compounds.[2-4]

It is a well-known fact that the enzymological fixation of nitrogen requires the presence of Fe and Mo and that the means of the reaction is water. For this reason in chemical nitrogen-fixing systems the synthesis of nitrogen complexes in an aqueous medium is of great interest at the present time.

Numerous works[5-8] have been published on dinitrogen compounds with ligands of a simple aminic type $[M(NH_3)_5(N_2)]^{2+}$, but there are no bibliographical antecedents on dinitrogen compounds which contain complexones as ligands. Only Diamantis[9] showed recently and during the course of our own investigations, the great avidity of the complexone EDTA to act as a pentadentate ligand in dinitrogen complexes, obtaining the species $[Ru(EDTA) (N_2)]^{2+}$ and $[(EDTA)Ru-N_2-Ru(EDTA)]^{4+}$ in an aqueous solution.

In our work a general method of synthesis has been used based on the conversion to coordinate N_2 of a ligand which has a nitrogen-nitrogen link,[10] and the compound $Na_2[Fe(PDTA) (N_2)]^2(H_2O)$ from [Fe(H-PDTA) (H_2O)] $3/2H_2O$ using sodium azide (NaN_3) in an aqueous solution has been synthesised.

EXPERIMENTAL

$Fe(NO_3)_3 \cdot 9H_2O$ and NaN_3 were obtained from Merck, and PDTA-H_4 from Fluka BDH Chem. Ltd. Both of them were used without further purification.

DTA was performed in a Stanton Redcroft 673-4 thermobalance, and TG in a Cahn RG electrobalance. The gases evolved were analysed in a Hewlett-Packard 5700 A chromatograph.

IR spectrum was recorded in the 4000–$400 \, cm^{-1}$ region using a Perkin–Elmer 577 double beam instrument. The sample was prepared as KBr pellet.

Electronic spectrum was recorded on a Perkin–Elmer 124 spectrophotometer using 2 cm quartz cells, and water as reference.

A Gouy balance was used for magnetic measurements at room temperature. The ESR spectrum at room temperature and 77 K were recorded at the Instituto de Catálisis y petroquímica Rocasolano (C.S.I.C.), Madrid.

C, H, and N analysis were performed at the Departamento de Microanálisis del Instituto de Química Orgánica General del C.S.I.C., Barcelona. Iron was determined by gravimetry and by

atomic absorption spectrometry. Sodium was determined by Flame spectrophotometry. The water content was determined in a Karl–Fischer titrator, and confirmed by TG.

Synthesis of $Na_2[Fe(PDTA) (N_2)] \cdot 2H_2O$

0.750 g. of [Fe(H-PDTA) (H_2O)], $3/2H_2O$,[11] were dissolved in 25 cm³ of water heated in double saucepan at 40°C. To the resulting green solution, 0.750 g. of solid NaN_3 were added, precipitating then a reddish compound that dissolved almost immediately. The mixture was heated in a double saucepan at 50°C for 3 min, cooled in the refrigerator and when the first microcrystals appeared, 25 cm³ of absolute ethanol were added. The orange-coloured microcrystalline product was filtered and washed with absolute ethanol, and dried on phosphorous pentoxide. Found: Fe, 11.8; Na, 9.6; C, 28.2; H, 3.2; N, 12.0; H_2O, 7.7. Calc.: Fe, 11.9; Na, 9.7; C, 28.2; H, 3.8; N, 12.0 H_2O, 7.7%.

RESULTS

Thermal behaviour

The DTA curve (Fig. 1) obtained in an atmosphere of He, shows the existence of several endothermic effects. The first of these, at 130°C, probably corresponds to the elimination of water of crystallization. The second effect is registered at 220°C and can be attributed to the loss of the coordinated dinitrogen molecule, since decarboxylation in these conditions takes place at higher temperatures, according to what can be remarked in the remaining endothermic effects in the diagram.

The thermogravimetric curve (Fig. 2), shows two not very pronounced jumps between 120 and 240°C to which there corresponds loss of weight of 7.7 and 5.9% respectively, so they can be associated with the elimination of hydration water and coordinated dinitrogen. From 300°C pyrolysis of the compound begins and continues up to 500°C.

These results were corroborated by means of gas chromatography and by volumetric determination of dinitrogen in the complex, following a similar method to that used by Allen,[8] and whose results are included in Table 1. The determinations performed with the recently prepared complex (A) and after three months in a desiccator (B), allow us to deduce that the compound decomposes slowly on contact with air, although long periods of time are necessary for the decomposition to be significant.

IR spectra

In Fig. 3 the IR spectrum of the compound $Na_2[Fe(PDTA) (N_2)] \cdot 2H_2O$ is represented, and in Table 2 the most significant data of the same are shown.

At $3400 \, cm^{-1}$ a wide band can be observed which

---

*Author to whom correspondence should be addressed.

TEMPERATURE, °C
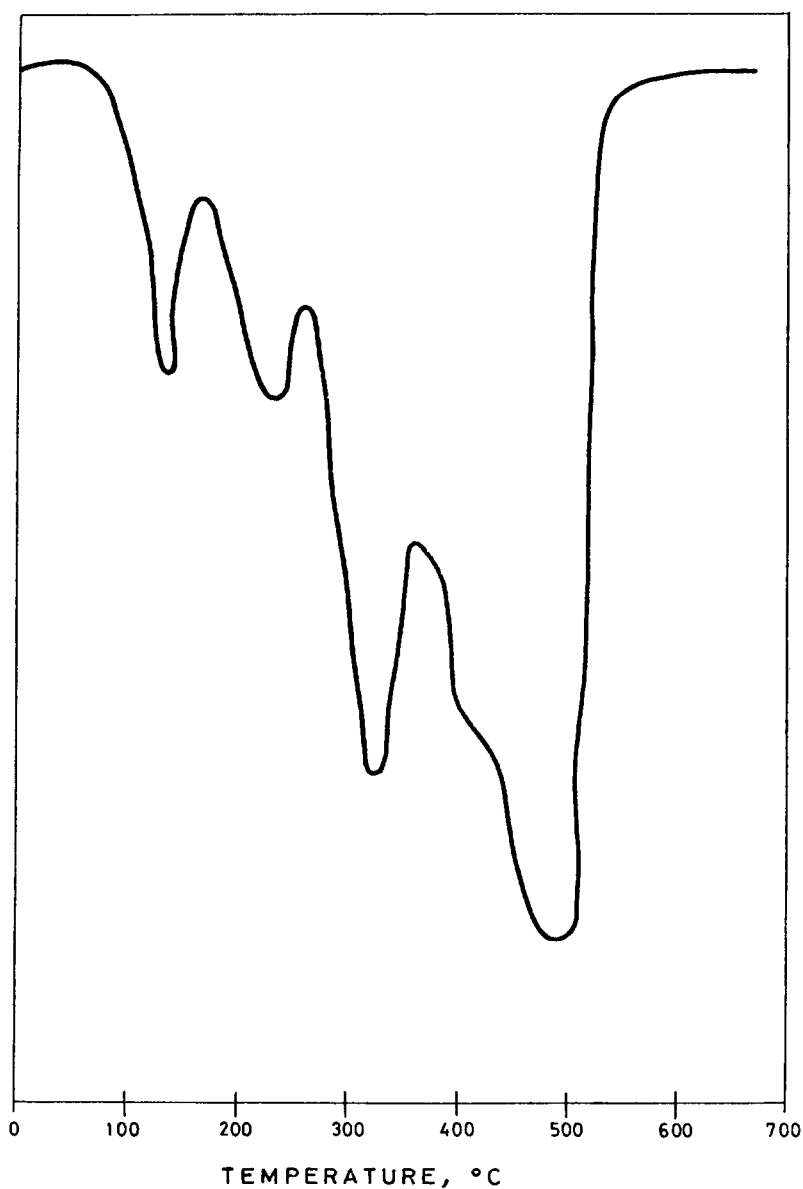
Fig. 1. DTA curve for $Na_2[Fe(PDTA) (N_2)] \cdot 2H_2O$, obtained under a dynamic helium atmosphere.

Table 1. N_2 contents determined for samples A and B in $Na_2[Fe(PDTA) (N_2)] \cdot 2H_2O$

	Initial weight of compound(mg)	Silicon oil pressure(mm)	(N_2) in compound	%(N_2) over the theoretical value
A)	20.5	160.5	4.23×10^{-5}	97.5
B)	24.0	29.0	0.76×10^{-5}	17.3

A) Sample recently synthesised.

B) Sample three months after its synthesis.
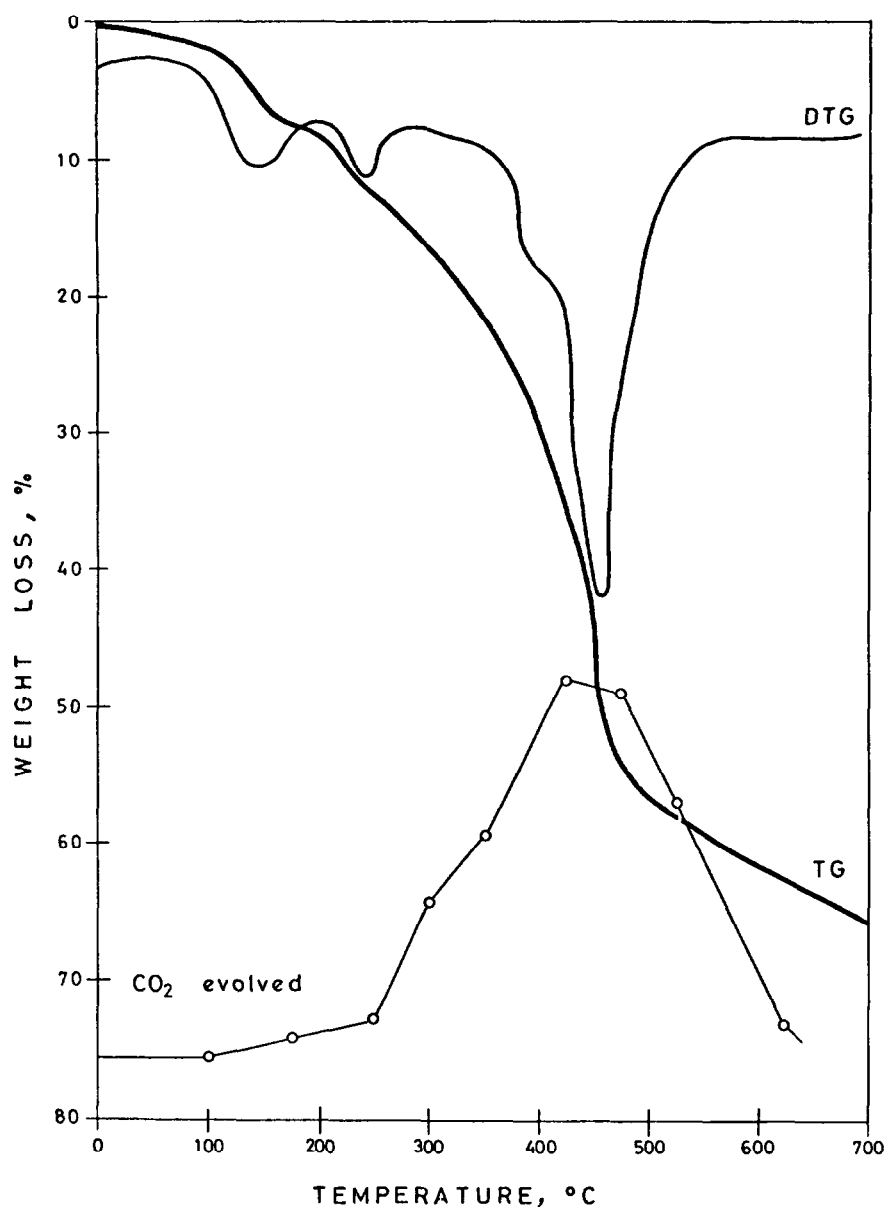
Fig. 2. TG and DTG curves for $Na_2[Fe(PDTA)(N_2)]\cdot 2H_2O$, obtained under a synamic helium atmosphere.

Table 2. Main IR absorption bands of $Na_2[Fe(PDTA)(N_2)]\cdot 2H_2O$ (cm^{-1})

ν_{O-H}	ν_{-CH_2}	$\nu_{(N\equiv N)}$	$\nu_{(COO^-_{assym})}$	$\nu_{(COO^-_{sym.})}$	$\nu_{(C-N)}$
3400	2960 2940	2030	1620	1390	1100

WAVENUMBER, cm^{-1}
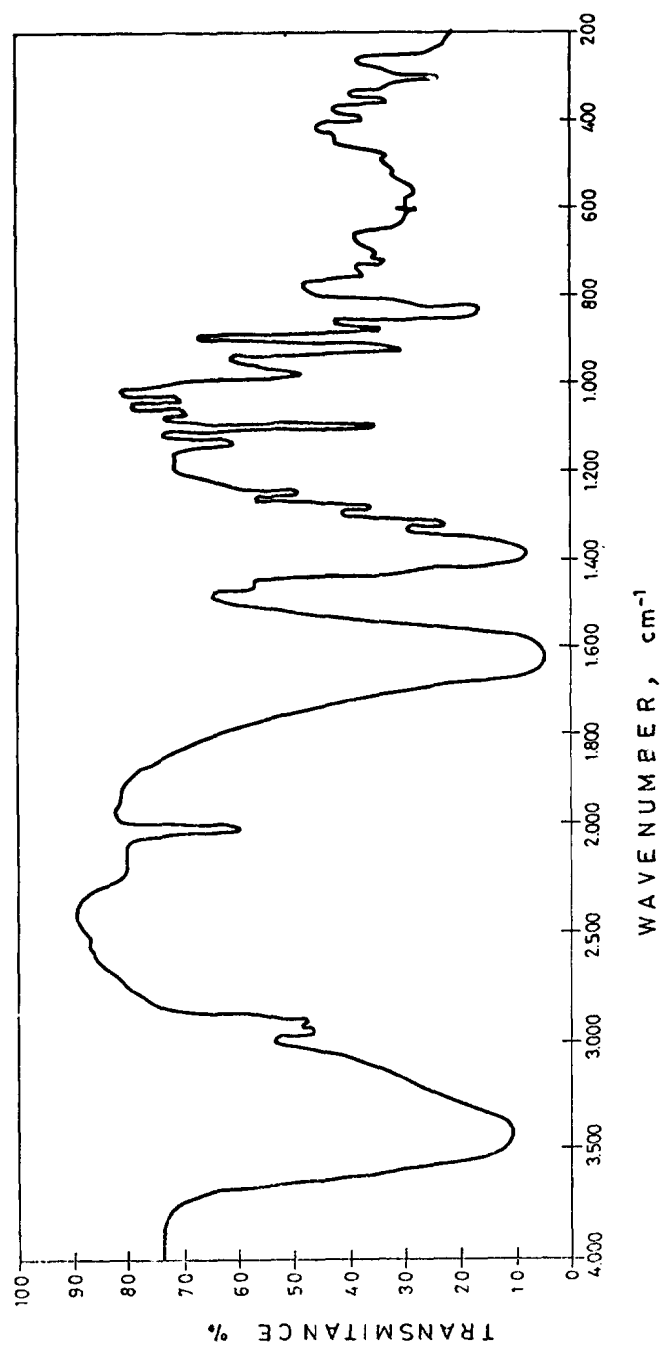
Fig. 3. IR spectrum of Na$_2$[Fe(PDTA)(N$_2$)]·2H$_2$O.

% TRANSMITTANCE
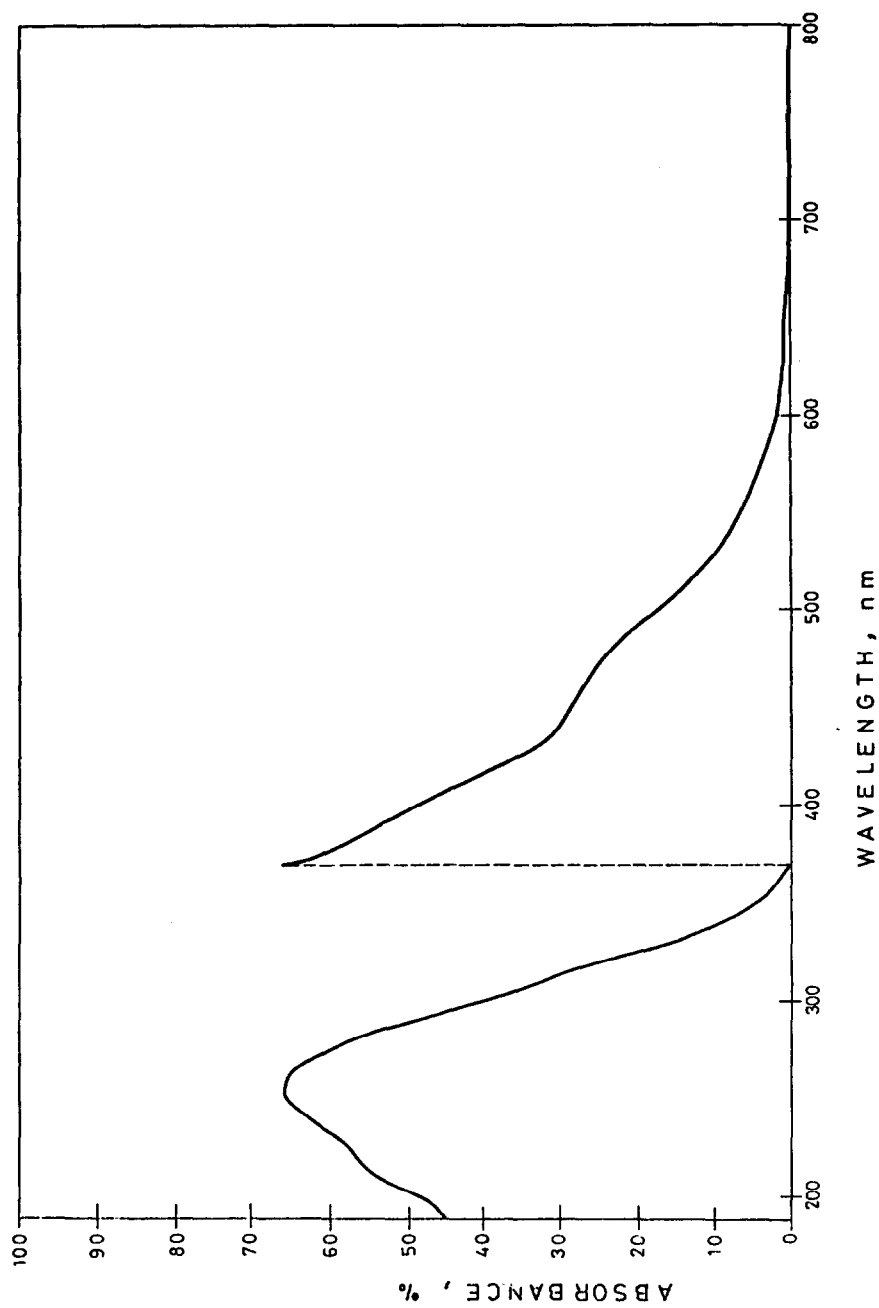
Fig. 4. Electronic spectrum of $Na_2[Fe(PDTA)(N_2)]\cdot 2H_2O$ in aqueous solution.

corresponds to the vibrations of symmetrical and asymmetrical stretching of the O–H link of the crystallization water.

The bands which correspond to the stretching vibrations of the methylene groups have a similar intensity, which suggests an analogous character among all the methylene groups of the ligand.

The characteristic absorption of the dinitrogen complexes which appears between 2100 and 1900 cm^{-1}, corresponds to the stretching vibration of N $\equiv$ N. The intensity and frequency of this band indicate the degree of covalency of the metal–nitrogen link.[12,13] The said band is registered in this compound at 2030 cm^{-1} with medium intensity, which seems to suggest a moderate overlapping of the metal "d" orbitals with the π^* of the N_2 and as a result of this a not very pronounced degree of covalency for the metal–dinitrogen link.

At 1620 cm^{-1} a band appears which can be attributed to the assymetrical stretching vibration of the carboxylate groups. The difference between the latter and the most intense peak which corresponds to the symmetrical vibration of the $-COO^-$ groups which is recorded at 1390 cm^{-1}, (225 cm^{-1}), suggests a moderately covalent link in the carboxylate–metal combinations.

UV and visible spectra

The Fe(II) in the $Na_2[Fe(PDTA)(N_2)] \cdot 2H_2O$ complex, is a d^6 system of low spin and fundamental term $^1A_{1g}$. The formation of this type of compound (t_{2g}) of low spin is favoured by ligands with an intense field, which facilitate besides the reduction of the electronic density on the metal, that is to say the electronic back-bonding from the "d" orbitals of the metal to the empty (π^*) orbitals of the ligand.

The absorption spectrum in an aqueous solution (Fig. 4) shows a not very intense band at 460 nm (21700 cm^{-1}), $\epsilon = 71$, due probably to the transition $^1A_{1g} \rightarrow {}^1T_{1g}$. In the UV region there appears a band at 38500 cm^{-1} and another in the form of a shoulder, at 221 nm (45400 cm^{-1}) which through their energy and intensity can be considered as charge-transfer bands.

Study of the magnetic properties

In the Fe(II) compound of low spin, there exists no Zeeman effect of the first order ($J = S = 0$) and the magnetic susceptibility is due therefore the Zeeman effect of the second order.

The corrected magnetic molar susceptibility of the diamagnetism of the ligand, of the ion Na^+ and of the water molecules, has a value of 78.3 X_M to which there corresponds an effective magnetic momentum of 0.38 B.M.

The diamagnetism of this compound has been checked in addition by spectroscopy of ESR, which only registers a very weak signal due perhaps to the impurities of Fe^{3+}.

REFERENCES

[1] A. D. Allen and C. V. Senoff, *J. Chem. Soc. Chem. Commun.* 1965, 621.
[2] J. Chatt, A. J. Pearman and R. L. Richards, *Nature* 1975 **253**, 39.
[3] J. Chatt and J. R. Dilworth, *J. Chem. Soc. Chem. Commun.* 1975, 983.
[4] J. Chatt, *J. Organomet. Chem.* 1975, **100**, 17.
[5] A. D. Allen, T. Eliades, R. O. Harris and P. Reinsahr, *Can. J. Chem.* 1969, **47**, 1605.
[6] L. A. P. Kane-Macquire, P. S. Sheridan, F. Basolo and R. G. Pearson, *J. Am. Chem. Soc.* 1968, **90**, 5295.
[7] R. O. Harris and B. A. Wright, *Can. J. Chem.* 1970, **48**, 1815.
[8] C. Creutz and H. Taube, *Inorg. Chem.* 1971, **10**, 2664.
[9] A. A. Diamantis and J. V. Dubrawsky, *Inorg. Chem.* 1981, **20**, 1142; Preliminary reports of this paper were presented by A. A. Diamantis and J. V. Dubrawsky at the 6th (Adelaide, May 1975) and 7th (La Trobe, Melbourne, Feb. 1977) Coordination and Metal Organic Conferences.
[10] A. D. Allen, F. Bottomley, R. O. Harris, P. Reinsalu and C. V. Senoff, *J. Am. Chem. Soc.* 1967, **89**, 5595.
[11] J. M. Suarez Cardeso, Doctoral Thesis, University of Salamanca, Spain (1968).
[12] B. Folkesson, *Acta Chem. Sand.* 1972, **26**, 4106.
[13] B. Folkesson, *Acta Chem. Scand.* 1972, **26**, 4008.

OPTICAL ABSORPTION SPECTRA OF PRASEODYMIUM ACETATE COMPLEXES IN SOLUTION

S. V. J. LAKSHMAN* and S. BUDDHUDU

Spectroscopic Laboratories, Department of Physics, S. V. University, Tirupati 517 502, India

Abstract—Results of analyses of the solution spectra of Pr^{3+} in the acetates of praseodymium, magnesium, calcium and cadmium complexes are presented. Slater–Condon (F_2, F_4 and F_6), configurational interaction (α, β), spin–orbit (ζ_{4f}), nephelauxetic ($\bar\beta$), bonding (δ) and Judd–Ofelt (T_2, T_4 and T_6) intensity parameters are evaluated. Judd–Ofelt intensity relationship has been used in the calculation of electric dipole line-strengths. Theoretical evaluation of predicted radiative lifetimes (τ_R) of the electronic excited states $^3P_1$, $^3P_0$ and $^1D_2$ of Pr^{3+} in four different hosts has been carried out.

Carnall et al.[1] correlated the experimental and theoretical (Judd–Ofelt) intensities of the solution absorption spectra of Pr^{3+} in ethyl acetate. Paramagnetic resonance studies on the mixed complexes of praseodymium acetate have been reported by Maiti et al.[2] Surana et al.[3] have studied the solution absorption spectrum of Pr^{3+} in haloacetates and reported the interacting, bonding and intensity parameters.

Since the optical absorption studies have not previously been reported in the literature for Pr^{3+} in $Mg(C_2H_3H_2)_2$, $Ca(C_2H_3O_2)_2$ and $Cd(C_2H_3O_2)_2$ complexes, the authors have carried out this investigation. For the first time, the second derivative spectra of these Pr^{3+} complexes have been studied.

EXPERIMENTAL

One mole% of praseodymium acetate (99.99% purity) was introduced into the saturated solutions of magnesium acetate, calcium acetate and cadmium acetate. One mole% praseodymium acetate was also separately prepared for the present investigation.

The UV-visible spectra from 3500 to 6500 Å were recorded on a Perkin–Elmer 551 recording spectrophotometer. Using a derivative accessory, second derivative spectra were also recorded in this wavelength region. The NIR spectra from 11,000 to 5000 cm^{-1} were recorded on a Carl–Zeiss Specord 61 recording spectrophotometer. Since there is no derivative accessory for this instrument, only normal spectra were recorded in this wavelength region.

The refractive indices of the solutions studied have been measured on a PZO Warszawava 3275 refractometer. The oscillator strengths of the bands were measured from their profiles.

RESULTS AND ANALYSIS

Energy levels

The observed spectrum of $Pr^{3+}:Pr(C_2H_3O_2)_3 3H_2O$ is shown in Figs. 1 and 1(a). The observed band maxima positions and their assignments are presented in Table 1 for all the four praseodymium acetate complexes.

The energy E_j of the jth level may be written in a Taylor series expansion as

$$E_j = E_{0j} + \sum_{K=2}^{6} \frac{dE_J}{dF_K}\Delta F_K + \frac{dE_J}{d\alpha}\Delta\alpha + \frac{dE_J}{d\beta}\Delta\beta + \frac{dE_J}{d\zeta_{4f}}\Delta\zeta_{4f}\ldots \quad (1)$$

where E_{0j} is the zero-order energy of the jth level and (dE_J/dF_K), $(dE_J/d\alpha)$, $(dE_J/d\beta)$ and $(dE_J/d\zeta_{4f})$ are the partial derivatives. Using the experimental energy levels for E_j and the numerical values of zero-order energy and partial derivatives,[4,5] a number of linear equations equal to the number of observed levels were formed. By employing the least-squares fit method, the values of the correction factors ΔF_K, $\Delta\alpha$, $\Delta\beta$ and $\Delta\zeta_{4f}$ were calculated. These were added to the zero-order parameter to obtain the parameters F_2, F_4, F_6, α, β and ζ_{4f} for the Pr^{3+} complexes studied. Thus

$$F_2 = F_2{}^0 + \Delta F_2; \quad \alpha = \alpha^0 + \Delta\alpha$$
$$F_4 = F_4{}^0 + \Delta F_4; \quad \beta = \beta^0 + \Delta\beta$$
$$F_6 = F_6{}^0 + \Delta F_6; \quad \zeta_{4f} = \zeta_{4f}{}^0 + \Delta\zeta_{4f}$$

where $F_2{}^0$, $F_4{}^0$, $F_6{}^0$, α^0, β^0 and $\zeta_{4f}{}^0$ are the zero-order parameters.[4,5] These zero-order parameters, zero-order energies and the partial derivatives are given in Table 1(a). The calculated values of Slater–Condon (F_2, F_4 and F_6), configurational interaction (α, β) and spin–orbit (ζ_{4f}) parameters for the Pr^{3+} complexes studied are presented in Table 2. The r.m.s. deviation is calculated from the formula

$$\sigma = \left(\sum \frac{\Delta_i{}^2}{N}\right)^{1/2} \quad (3)$$

where Δ_i is the deviation of the ith level and N is the number of levels fitted. The small r.m.s. deviations found suggests a good fitting of the energy levels.

Spectral intensities

The intensity of an absorption band is measured by its oscillator strength which is directly proportional to the area under the absorption curve. The oscillator strength (f) can be expressed in terms of the molar absorptivity ϵ and the energy of the transition in wavenumbers (ν) by the following relation.[6]

$$f = 4.32 \times 10^{-9} \int \epsilon(\nu)\,d\nu. \quad (4)$$

Here (f) is a dimensionless quantity. The molar absorptivity (ϵ) at a given energy is computed from the Beer–Lambert law[6]

$$\epsilon = \frac{1}{cl}\log\frac{I_0}{I} \quad (5)$$

---

*Author to whom correspondence should be addressed.
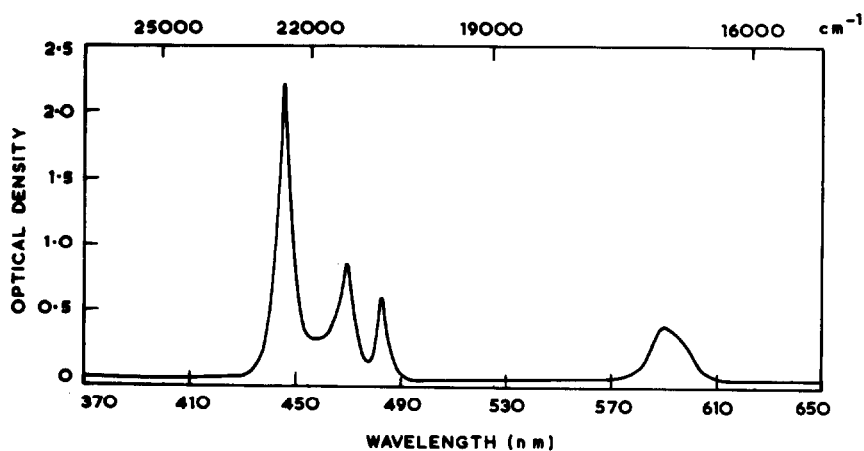
Fig. 1. Absorption spectrum of Pr^{3+}: $Pr(C_2H_3O_2)_3 3H_2O$.
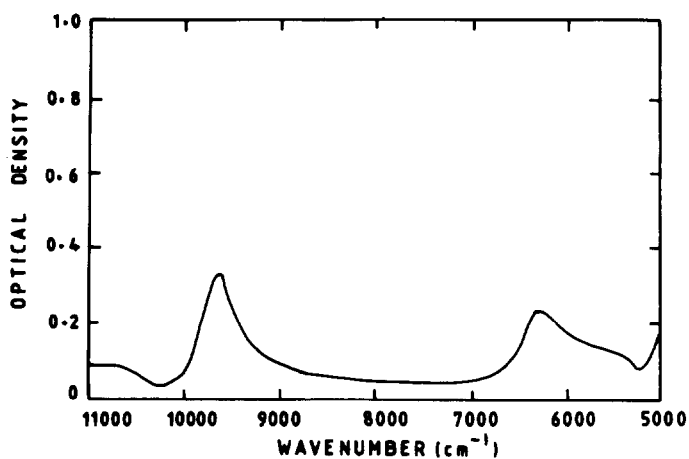
Fig. 1(a). Near IR absorption spectrum of Pr^{3+}: $Pr(C_2H_3O_2)_3 3H_2O$.

Table 1. Experimental and calculated energy levels for Pr^{3+} complexes in solution

Energy levels from the ground state. $^3H_4$	Pr^{3+} $Pr(C_2H_3O_2)_3 3H_2O$		Pr^{3+} $Mg(C_2H_3O_2)_2$		Pr^{3+} $Ca(C_2H_3O_2)_2$		Pr^{3+} $Cd(C_2H_3O_2)_2$	
	E_{expt} (cm^{-1})	E_{calc} (cm^{-1})	E_{expt} (cm^{-1})	E_{calc} (cm^{-1})	E_{expt} (cm^{-1})	E_{calc} (cm^{-1})	E_{expt} (cm^{-1})	E_{calc} (cm^{-1})
$^3P_2$	22388	22395	22365	22378	22415	22406	22440	22425
$^3P_1$	21219	21215	21136	21191	21225	21227	21180	21245
$^3P_0$	20600	20598	20613	20573	20612	20618	20655	20604
$^1D_2$	16821	16820	16847	16894	16830	16896	16810	16811
$^1G_4$	9619	9620	9640	9653	9600	9639	9680	9682
$^3F_4$	-	6713	6750	6622	-	6645	-	6710
$^3F_3$	6210	6210	6250	6117	6250	6141	6300	6221
r.m.s deviation	± 3.0		± 75.0		± 56.0		± 44.0	

Table 1(a). Zero-order energies and partial derivatives for Pr^{3+} ($4f^2$) configuration

Energy levels from $^3H_4$	E_{oj}	$\dfrac{dE_j}{dF_2}$	$\dfrac{dE_j}{dF_4}$	$\dfrac{dE_j}{dF_6}$	$\dfrac{dE_j}{d\zeta_{4f}}$	$\dfrac{dE_j}{d\alpha}$	$\dfrac{dE_j}{d\beta}$
$^3P_2$	21491	67.56	68.42	-1077	5.029	27.335	0.010
$^3P_1$	20261	70.07	80.66	-1278	3.934	27.741	-0.005
$^3P_0$	19683	70.17	81.81	-1253	1.905	27.759	-0.015
$^1D_2$	16559	45.97	-37.63	510	2.906	24.023	0.106
$^1G_4$	9760	0.04	112.10	4	5.792	11.348	-0.017
$^3F_4$	6607	10.24	43.97	188	3.146	15.885	-0.042
$^3F_3$	5925	15.00	14.65	274	2.983	17.744	-0.655

Free Ion Parameters

$F_2^\circ = 305.00$ $\zeta_{4f}^\circ = 730.5$

$F_4^\circ = 51.88$ $\alpha^\circ = 23.684$

$F_6^\circ = 5.321$ $\beta^\circ = -585.41$

where c is the concentration of the lanthanide ion in moles/litre, l is the light path in the solution (cm) and $\log(I_0/I)$ is the absorptivity or optical density. Some magnetic dipole mechanism though responsible for a few transitions (f_{md}), an induced electric dipole mechanism (f_{ed}) must be invoked to account for the intensities of most lanthanide absorption bands. The weak intra f^N transitions are accounted for by assuming that a small amount of the character of higher lying opposite parity configurations is mixed into the f^N states via the odd terms in the potential due to the ligand field.[7] Neglecting higher multipole mechanism such as electric quadrupole

Table 2. Slater–Condon (F_2, F_4, F_6), Racah (E^1, E^2, E^3), spin–orbit (ζ_{4f}) configuration interaction (α, β), nephelauxetic ratio ($\bar\beta$) bonding (δ), refractive index (n) and Judd–Ofelt intensity (T_2, T_4, T_6) parameters for Pr^{3+} complexes in solution

Parameters	Pr^{3+} : $Pr(C_2H_3O_2)_3 3H_2O$	Pr^{3+} : $Mg (C_2H_3O_2)_2$	Pr^{3+} : $Ca (C_2H_3O_2)_2$	Pr^{3+} : $Cd (C_2H_3O_2)_2$
F_2	313.34	319.70	320.29	314.75
F_4	49.95	51.07	51.31	50.32
F_6	4.93	5.15	5.13	4.95
E^1	4817.59	4944.01	4949.53	4845.75
E^2	21.97	22.51	22.47	21.99
E^3	473.27	478.63	480.78	476.28
ζ_{4f}	745.04	746.57	745.16	756.96
α	22.57	10.45	10.70	18.30
β	-672.42	-753.74	-783.72	-720.59
$\bar\beta$	-	1.0009	1.0011	1.0038
δ	-	-0.0976	-0.1178	-0.3874
n	1.3318	1.3407	1.3593	1.3473
$T_2 (\times 10^9)$	1.465	0.452	-0.040	-0.108
$T_4 (\times 10^9)$	0.321	0.103	0.210	0.195
$T_6 (\times 10^9)$	0.462	0.056	0.466	0.781

etc., we have

$$f = f_{ed} + f_{md} \qquad (6)$$

According to Judd–Ofelt[8,9] theory

$$f_{ed} = \sum_{\lambda=2}^{6} T_\lambda \nu (\psi J \| U^\lambda \| \psi' J')^2 \qquad (7)$$

where ν (cm^{-1}) is mean energy of the transition $\psi J \to \psi' J'$, U^λ is a unit tensor operator of rank λ, the sum running over the three values $\lambda = 2, 4$ and 6 and T_λ are the parameters which can be evaluated from the experimental data. The values of reduced matrix elements $\|U^\lambda\|^2$ have been evaluated for Pr^{3+} complexes[5] by using the following relation.

$$(f^N \alpha SLJ \| U^\lambda \| f^N \alpha' SL'J)$$
$$= (-1)^{S+J+L'+\lambda} [(2J+1)(2J'+1)]^{1/2}$$
$$\begin{Bmatrix} J & J' & \lambda \\ L' & L & S \end{Bmatrix} (f^N \alpha SL \| U^\lambda \| f^N \alpha SL').$$
$$(8)$$

The matrix elements on the right hand side of the above equation were taken from the tables of Nielson et al.[10] The values of 6j symbols were taken from the tables of Rotenberg et al.[11] From the above equation, it is found that the sign of the numerical value depends on the S, L', J' and λ values. The sign of the value does not play any significant role in the LS basis because we are always using squared values of $\|U^\lambda\|$. But in the intermediate coupling case the sign plays a dominant role because the states of f^N electronic configuration are taken as linear combinations.

$$|f^N \psi J\rangle = \sum_{\alpha, S, L} C(\alpha SL) |f^N \alpha SLJ\rangle \qquad (9)$$

where $C(\alpha SL)$ are the numerical coefficients resulting

from the diagonalization of the matrices. The eigenvalues and eigenvectors for Pr^{3+} complexes have been computed by diagonalizing complete energy matrices of $4f^2$ configuration on an IBM 370/155 computer using the parameters E^1, E^2, E^3, α, β and ζ_{4f}. The reduced matrix elements have been transformed from LS basis states to the physical coupling scheme prior to being squared and substituted in eqn (7). The squared values of U^2, U^4 and U^6 were substituted in eqn (7) and using f_{expt} for f_{ed} (neglecting for the moment f_{md} as it is very small compared to f_{ed}), the values of T_λ parameters were evaluated by the least squares fit method and presented in Table 2.

Theoretical estimation of the oscillator strength (f) has been carried out by the method of electric (s_{md}) and magnetic (s_{md}) dipole linestrengths[6]

$$f^{e \cdot m} = \frac{8\pi^2 mc\nu}{3he^2(2J+1)} \left[\frac{(n^2+2)^2}{9n} S_{ed} + n S_{md} \right] \qquad (10)$$

where n = refractive index of the medium, S_{ed} = electric dipole linestrength, S_{md} = magnetic dipole linestrength, m = mass of an electron, c = velocity of light, h = Planck's constant, e = energy of the electron in coloumbs, ν = energy of the band in (cm^{-1}), and J = value of the initial J level.

The values of electric (S_{ed}) dipole linestrengths were evaluated using the formula[6]

$$S_{ed} = e^2 \sum \Omega_\lambda (\psi J \| U^\lambda \| \psi' J')^2 \qquad (11)$$

where

$$\Omega_\lambda = [(1.085) \times (10^{11}) \times (n(n^2+2))/9]^{-1}(2J+1)T_\lambda \qquad (12)$$

and T_λ ($\lambda = 2, 4, 6$) are the Judd–Ofelt parameters. The values of the magnetic (S_{md}) dipole linestrength were obtained with the following relation[4]

$$S_{md} = \frac{e^2 h^2}{16\pi^2 m^2 c^2} (\psi J \| L + 2S \| \psi' J')^2. \qquad (13)$$

Table 3. Experimental and calculated oscillator strengths ($f \times 10^6$) for Pr^{3+} complexes in solution

Energy levels from the ground state $^3H_4$	Pr^{3+}:Pr(C$_2$H$_3$O$_2$)$_3$3H$_2$O			Pr^{3+}: Mg(C$_2$H$_3$O$_2$)$_2$			Pr^{3+}: Ca(C$_2$H$_3$O$_2$)$_2$			Pr^{3+}: Cd(C$_2$H$_3$O$_2$)$_2$		
$^3P_2$	2.28	1.68	1.68	1.28	1.46	1.25	1.51	1.11	1.58	1.72	2.60	2.60
$^3P_1$	1.28	1.17	1.17	0.78	0.37	0.37	0.97	0.75	0.77	1.01	0.72	0.72
$^3P_0$	1.04	1.14	1.14	0.31	0.36	0.36	0.71	0.74	0.74	0.90	0.70	0.69
$^1D_2$	0.85	0.54	0.54	0.49	0.42	0.39	0.69	0.32	0.45	0.78	0.71	0.71
$^1G_4$	0.14	0.14	0.14	0.02	0.03	0.04	0.14	0.09	0.13	0.17	0.26	0.26
$^3F_4$	-	-		0.43	0.28	0.28	-	-	-	-	-	-
$^3F_3$	3.28	3.28	3.20	0.48	0.44	0.43	2.42	1.82	2.48	3.67	3.84	3.84
r.m.s deviation	± 0.279			± 0.202			± 0.343			± 0.395		

Table 4. Electric ($S_{ed} \times 10^{22}$), and magnetic ($S_{md} \times 10^{22}$) dipole linestrengths for Pr^{3+} complexes in solution

Energy levels from $^3H_4$	Pr^{3+}: $Pr(C_2H_3O_2)_3 3H_2O$		Pr^{3+}: $Mg(C_2H_3O_2)_2$		Pr^{3+}: $Ca(C_2H_3O_2)_2$		Pr^{3+}: $Cd(C_2H_3O_2)_2$	
	S_{ed}	S_{md}	S_{ed}	S_{md}	S_{ed}	S_{md}	S_{ed}	S_{md}
$^3P_2$	52.55	0	7.89	0	48.25	0	80.03	0
$^3P_1$	38.35	0	12.20	0	24.81	0	23.42	0
$^3P_0$	38.57	0	12.22	0	24.67	0	23.03	0
$^1D_2$	22.40	0	3.84	0	18.14	0	29.20	0
$^1G_4$	10.19	0.182	2.51	0.122	8.87	0.063	18.40	0.084
$^3F_4$	-	-	28.29	0.289	-	-	-	-
$^3F_3$	370.33	0.023	48.09	0.022	272.32	0.020	42.20	0.018

The experimental spectral intensities (f) and theoretical estimates of spectral intensities obtained from Judd–Ofelt (f^{J-O}) and electric–magnetic dipole linestrength (f^{e-m}) methods for the Pr^{3+} complexes have been given in Table 3. The calculated values of the parameters S_{ed} and S_{md} for Pr^{3+} complexes are presented in Table 4.

Bonding

The nephelauxetic ratio β is given by[12]

$$\beta = \nu_c/\nu_a \qquad (14)$$

where ν_c and ν_a refer to the energies of the corresponding transition in the complex and aquo ions respectively. The β values for all the observed transitions were computed and their average value $\bar\beta$ was used to estimate the bonding parameter (δ). The bonding parameter (δ) is given by[12,13]

$$\delta = \frac{1-\bar\beta}{\bar\beta}. \qquad (15)$$

The bonding will be covalent or ionic depending upon the positive or negative nature of the δ value. In all the Pr^{3+} complexes reported here (Table 2) since the δ value is found negative, the nature of the bonding in these complexes is ionic.

From Table 2, it is found that the Judd–Ofelt parameter T_2 has negative values for Pr^{3+} in $Cd(C_2H_3O_2)_2$ and $Ca(C_2H_3O_2)_2$. A similar result has been found for Pr^{3+} in yttrium aluminate by Weber.[14] He has suggested that the reason for such behaviour in praseodymium complex may be due to the proximity of the $5d$ band of Pr^{3+} to $4f$ and of strong $f - d$ mixing.[15,16]

$^1D_2$ Term splittings

Second derivative spectrum of praseodymium acetate complexes have exhibited a splitting of the $^1D_2$ level into two components. The observed splittings of $^1D_2$ term in the second derivative spectrum of these complexes are presented in Table 5.

Since the crystal field splitting has been observed only in the $^1D_2$ level no calculation of crystal field parameters was attempted.

Radiative lifetimes (τ_R)

Theoretical radiative lifetimes of certain electronic excited states of praseodymium ion have been very extensively studied by several authors.[17–19] Carnall *et al.*[6,20] have evaluated radiative lifetimes for $^3P_1$, $^3P_0$ and

Table 5. The observed crystal field splitting of $^1D_2$ term in the second derivative spectrum of Pr^{3+} complexes in solution

Transition	Pr^{3+}: $Pr(C_2H_3O_2)_3 3H_2O$ E (cm^{-1})	Pr^{3+}: $Mg(C_2H_3O_2)_2$ E (cm^{-1})	Pr^{3+}: $Ca(C_2H_3O_2)_2$ E (cm^{-1})	Pr^{3+}: $Cd(C_2H_3O_2)_2$ E (cm^{-1})
$^3H_4 \rightarrow {}^1D_2$	16915	16928	16905	16920
	16710	16738	16725	16720

Table 6. Predicted lifetimes τ_R (μ sec) for the $^3P_1$, $^3P_0$ and $^1D_2$ states of Pr^{3+} complexes in solution

Complexes $\tau_R(\mu\,Sec)$	Pr^{3+}: $Pr(C_2H_3O_2)_3 3H_2O$	Pr^{3+}: $Mg(C_2H_3O_2)_2$	Pr^{3+}: $Ca(C_2H_3O_2)_2$	Pr^{3+}:$Cd(C_2H_3O_2)_2$
$^3P_1$	41	117	172	145
$^3P_0$	137	379	188	177
$^1D_2$	351	1020	2070	1700

$^1D_2$ states of Pr^{3+} in solutions. The calculation of radiative lifetimes for the above excited states of praseodymium acetate complexes have been carried out in the present work.

The squared reduced matrix elements $\|U^\lambda\|^2$ between $^3P_1$, $^3P_0$ and $^1D_2$ and all the next lower lying levels were calculated for praseodymium aquo ion.[5] Reisfeld[18] and also Riseberg[21] have pointed out that the resulting matrix elements exhibit only small differences and hence $\|U^\lambda\|^2$ values obtained for one host may generally be used for the other hosts. In view of this and in view of lack of computer facilities in the university, the calculation of matrix elements $\|U^\lambda\|^2$, were carried out only for praseodymium aquo ion.[5] The same reduced matrix elements were used for calculation of electric dipole linestrengths of lines of Pr^{3+} in $Mg(C_2H_3O_2)_2$, $Ca(C_2H_3O_2)_2$ and $Cd(C_2H_3O_2)_2$ complexes. Following Carnall et al.[22] the total radiative transition probability $A(\psi J; \psi'J')$ was calculated using the intensity parameters (T_2, T_4, T_6) evaluated in the absorption measurements.

$$A(\psi J; \psi'J') = \frac{64\pi^4\nu^3}{3h(2H+1)}\left[\frac{n(n^2+2)^2}{9}S_{ed} + n^3 S_{md}\right].$$
(16)

The total radiative relaxation (A_T) was evaluated using the expression

$$A_T(\psi J) = \sum_{\psi'J'} A(\psi J; \psi'J')$$
(17)

where the sum runs over all $\psi'J'$ lower in energy than ψJ. The radiative lifetime (τ_R) of a state is given as

$$\tau_R(\psi J) = [A_T(\psi J)]^{-1}.$$
(18)

Predicted radiative lifetime (τ_R) of $^3P_1$, $^3P_0$ and $^1D_2$ states for the Pr^{3+} acetate complexes studied, are given in Table 6. From this table it is found that the predicted lifetimes of the excited states $^3P_1$, $^3P_0$ and $^1D_2$ are in the increasing order in the following manner.
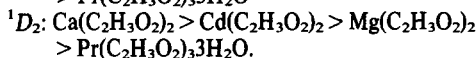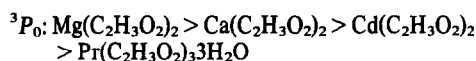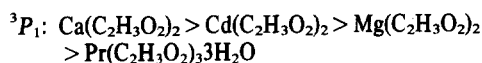
$^3P_1$: $Ca(C_2H_3O_2)_2 > Cd(C_2H_3O_2)_2 > Mg(C_2H_3O_2)_2$
$> Pr(C_2H_3O_2)_3 3H_2O$

$^3P_0$: $Mg(C_2H_3O_2)_2 > Ca(C_2H_3O_2)_2 > Cd(C_2H_3O_2)_2$
$> Pr(C_2H_3O_2)_3 3H_2O$
$^1D_2$: $Ca(C_2H_3O_2)_2 > Cd(C_2H_3O_2)_2 > Mg(C_2H_3O_2)_2$
$> Pr(C_2H_3O_2)_3 3H_2O$.

REFERENCES

[1] W. T. Carnall, P. R. Fields and B. G. Wybourne, *J. Chem. Phys.* 1965, **42**, 3797.
[2] B. Maiti and R. M. Sathe, *J. Inorg. Nucl. Chem.* 1980, **42**, 1064.
[3] S. S. L. Surana, M. Singh and S. N. Misra, *J. Inorg. Nucl. Chem.* 1980, **42**, 61.
[4] E. Y. Wong, *J. Chem. Phys.* 1963, **38**, 976.
[5] S. Buddhudu, Ph.D. Thesis, S.V. University, Tirupati, India, 1981.
[6] W. T. Carnall, H. Crosswhite and H. M. Crosswhite, Energy level structure and transition probabilities of trivalent lanthanides in LaF₃, Argonne National Laboratory, Argonne, Illinois, U.S.A., 1978.
[7] B. G. Wybourne, *Spectroscopic Properties of Rare Earths.* Interscience, New York (1965).
[8] B. R. Judd, *Phys. Rev.* 1962, **127**, 750.
[9] G. S. Ofelt, *J. Chem. Phys.* 1962, **37**, 511.
[10] C. W. Nielson and G. F. Koster, *Spectroscopic Coefficients for p^n, d^n and f^n Configurations.* MIT Press, Cambridge, Mass. (1964).
[11] M. Rotenberg, R. Bivins and W. Metropolis, *The 3j and 6j Symbols.* MIT Press, Cambridge, Mass. (1959).
[12] S. P. Tandon and R. C. Govil, *Z. Naturf.* 1971, **26**, 1357.
[13] S. P. Sinha, *Spectrochim. Acta* 1966, **22**, 57.
[14] M. J. Weber, *Phys. Rev.* 1967, **157**, 262.
[15] M. J. Weber, *J. Chem. Phys.* 1968, **49**, 4774.
[16] R. Reisfeld, *J. Non. Cryst. Solids* 1979, **30**, 337.
[17] M. J. Weber, T. E. Varitmos and B. H. Matsinger, *Phys. Rev. B* 1973, **8**, 47.
[18] R. Reisfeld, *Structure and Bonding* 1975, **22**, 123.
[19] F. J. Bartoli, *Appl. Opt.* 1979, **18**, 3365.
[20] W. T. Carnall, *Hand Book Phys. Chem. Rare Earths* 1979, **3**, 171.
[21] L. A. Riseberg and M. J. Weber, *Relaxation on Phenomenon in Rare Earth Luminescence.* North Holland Publishers, Amsterdam (1979).
[22] W. T. Carnall, J. P. Hessler and F. J. Wagner, *J. Chem. Phys.* 1978, **82**, 2152.

IMPROVED SYNTHESES OF Ru(CO)$_2$(O$_3$SCF$_3$)$_2$(BIDENTATE) COMPLEXES
AND THEIR CONVERSION INTO NEW [Ru(CO)$_2$(BIDENTATE)$_2$]$^{2+}$ COMPLEXES

DAVID ST.C. BLACK, GLEN B. DEACON* and NICHOLAS C. THOMAS

Chemistry Department, Monash University, Clayton, Victoria, Australia, 3168

Abstract – Reaction of the complexes Ru(CO)$_2$Cl$_2$L [L = 2,2'-bipyridyl (bpy) or 1,10-phenanthroline (phen)] with trifluoromethanesulphonic acid under carefully controlled conditions yields Ru[cis-(CO)$_2$][cis-(O$_3$SCF$_3$)$_2$](bidentate) complexes. From reactions of the trifluoromethanesulphonates with the appropriate bidentate ligands, the new complexes [cis-Ru(CO)$_2$-L(L')]$^{2+}$ (L as above; L' = 4,4'-dimethyl-2,2'-bipyridyl or 4,4'-diisopropyl-2,2'-bipyridyl) as well as the known [cis-Ru(CO)$_2$L$_2$]$^{2+}$ and [cis-Ru(CO)$_2$bpy(phen)]$^{2+}$ have been prepared.

INTRODUCTION

The complexes Ru(CO)$_2$(O$_3$SCF$_3$)$_2$phen (phen = 1,10-phenanthroline) and [Ru(CO)$_2$(MeCN)$_2$L]$^{2+}$ [L = phen or 2,2'-bipyridyl (bpy)] readily undergo substitution with uncharged bidentate ligands to give the novel dicarbonyls [Ru(CO)$_2$L$_2$]$^{2+}$ and [Ru(CO)$_2$L(L')]$^{2+}$ (L' ≠ L = phen, bpy or 3,4,7,8-tetramethyl-1,10-phenanthroline)[1,2] (subsequently, alternative syntheses of [Ru(CO)$_2$L$_2$]$^{2+}$ have also been reported[3,4]). The route to Ru(CO)$_2$(O$_3$SCF$_3$)$_2$phen and [Ru(CO)$_2$-(MeCN)$_2$L]$^{2+}$ complexes from the convenient reagents Ru(CO)$_2$Cl$_2$L involves conversion into Ru(CO)$_2$(O$_2$CMe)$_2$L derivatives and then reaction with trifluoromethanesulphonic acid either alone (giving the first complex, but unsuccessful for the bpy analogue) or in acetonitrile.[1,2] We now report a one-step synthesis of Ru(CO)$_2$(O$_3$SCF$_3$)$_2$L (L = phen *and* bpy) complexes and their conversion into new [Ru(CO)$_2$bidentate$_2$]$^{2+}$ derivatives.

RESULTS AND DISCUSSION

The complexes Ru(CO)$_2$(O$_3$SCF$_3$)$_2$L are conveniently prepared by heating the analogous chloro derivatives with trifluoromethanesulphonic acid.

$$Ru(CO)_2Cl_2L + 2CF_3SO_3H \rightarrow Ru(CO)_2(O_3SCF_3)_2L + 2HCl \qquad (1)$$
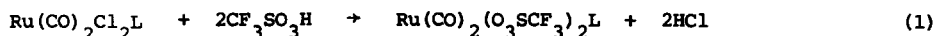
Careful control of the conditions is needed for L = bpy to prevent decomposition into (bpyH)$^+$[O$_3$SCF$_3$]$^-$. The chloro complexes are more labile than the corresponding acetato derivatives in reactions with trifluoromethanesulphonic acid, since conversion of RuCl$_2$(CO)$_2$bpy into Ru(CO)$_2$(O$_3$SCF$_3$)$_2$bpy occurs under conditions (Experimental Section) which permit only partial replacement of acetate by trifluoromethanesulphonate.[2]

The trifluoromethanesulphonato complexes are considered to have structure (1) on the basis of two ν(CO) frequencies and ^{1}H n.m.r. spectra (Experimental Section) indicative of unsymmetrical coordination of the bidentate ligands. Their formation by reaction (1) involves a stereochemical change since the chloro-complexes have structure (2a).

(1)

(2)
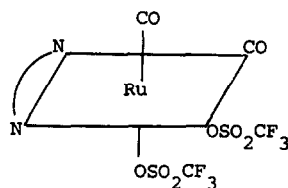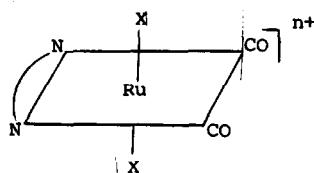
(1a)	N̑ N̑ = bpy	(2a)	N̑ N̑ = phen or bpy, X = Cl, n = 0
(1b)	N̑ N̑ = phen	(2b)	N̑ N̑ = phen, X = OSO_2CF_3, n = 0
		(2c)	N̑ N̑ = phen or bpy, X = OCOMe, n = 0
		(2d)	N̑ N̑ = phen or bpy, X = MeCN, n = 2
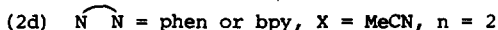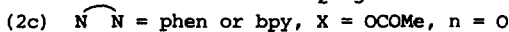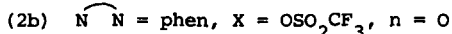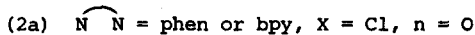
This contrasts with retention of stereochemistry in the formation of $Ru(CO)_2(O_3SCF_3)_2phen$ with structure (2b) [cf (1b) from reaction (1)] from $Ru(CO)_2(O_2CMe)_2phen$ [structure (2c)] and trifluoromethanesulphonic acid.[1,2] Although (1b) is obtained under milder conditions than (2b), it cannot be isomerized into the latter on being heated in CF_3SO_3H under conditions used to obtain (2b) from (2c).

Reactions of the new trifluoromethanesulphonates (1) with 2,2'-bipyridyl, 1,10-phen-anthroline, 4,4'-dimethyl-2,2'-bipyridyl (Me_2bpy), and 4,4'-diisopropyl-2,2'-bipyridyl (Pr_2bpy) give the known $[Ru(CO)_2L_2]^{2+}$ (L = phen or bpy)[1-4] and $[Ru(CO)_2bpy(phen)]^{2+}$ [1,2] as well as the new complexes $[Ru(CO)_2L(L')]^{2+}$ (L = phen or bpy; L' = Me_2bpy or Pr_2bpy),

e.g. $Ru(CO)_2(O_3SCF_3)_2L + L' \rightarrow [Ru(CO)_2L(L')]^{2+} + 2CF_3SO_3^-$.
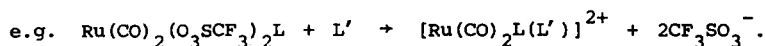
The infrared spectra of the new compounds, isolated as hexafluorophosphates, showed two $\nu(CO)$ frequencies and the [1]H n.m.r. spectra unsymmetrical coordination of the bidentate ligands, indicative of structure (3). Since the new $Ru(CO)_2(O_3SCF_3)_2L$ complexes (1) are as reactive towards bidentate ligands as (2b) or the acetonitrile derivatives (2d) and are more readily prepared, they should supersede them as a source of $[Ru(CO)_2L_2]^{2+}$ or $[Ru(CO)_2L(L')]^{2+}$ complexes.

(3) N̑ N̑ = phen or bpy, N̑' N̑' = phen or bpy Me_2bpy or Pr_2bpy
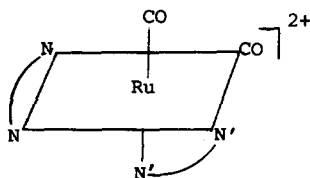
(3)
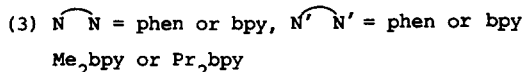
EXPERIMENTAL

(a) *General*

Microanalyses were by the Australian Microanalytical Service, Melbourne. Infrared spectra were recorded with a Perkin-Elmer 180 spectrophotometer. Compounds were examined as Nujol or hexachlorobutadiene mulls (4000 - 650 cm^{-1}). Silver chloride plates were used for trifluoromethanesulphonato complexes. Uncharged complexes were also examined in CH_2Cl_2 (2400 - 1800 cm^{-1}). [1]H n.m.r. spectra were recorded with a Bruker WH-90 spectrometer. Proton chemical shifts are in ppm downfield from internal tetramethylsilane. Uncharged and charged complexes were examined in $CDCl_3$ and $(CD_3)_2SO$ respectively. Integrations were satisfactory for the proposed compositions and are not listed. Mass spectra were obtained with a VG Micromass spectrometer. The m/e values correspond to the most intense peak (containing [102]Ru) of a cluster with the correct isotope pattern. Conductivities of solutions

(0.9 - 1.2 x 10^{-3} mol dm^{-3}) in nitromethane were measured at 20-25°C with a Wayne Kerr B221A bridge using a cell of standard design fitted with shiny platinum electrodes.

(b) Reagents

Ru(CO)$_2$Cl$_2$L (L = phen or bpy) complexes were prepared as previously reported.[2] 4,4'-Dimethyl-2,2'-bipyridyl and 4,4'-diisopropyl-2,2'-bipyridyl were supplied by Dr. W.H.F. Sasse, Division of Applied Organic Chemistry, CSIRO, Melbourne. Trifluoromethanesulphonic acid (3M) was distilled (0.1 mm, 26°C) before use.

(c) Trifluoromethanesulphonatoruthenium(II) Complexes

a,b-(2,2'-Bipyridyl)-c,d-dicarbonyl-e,f-bis(trifluoromethanesulphonato)ruthenium(II)   (1a)

2,2'-Bipyridyldicarbonyldichlororuthenium(II) (0.60g) was heated in trifluoromethane-sulphonic acid (2 cm^3) for 1h at 105°C under nitrogen. The mixture was cooled in ice and ether was slowly added. The white precipitated product was collected, washed with water to remove any 2,2'-bipyridinium trifluoromethanesulphonate, and recrystallized from methylene chloride/ether under nitrogen (0.40g, 40%), m.p. 202-204°C (Found: C,27.3; H,1.4; N,4.5). C$_{14}$H$_8$F$_6$N$_2$O$_8$RuS$_2$ requires C,27.5; H,1.3; N,4.6%). Mass spectrum: m/e 584[8%,(M-CO)$^+$], 556[38,(M-2CO)$^+$], 463[4,(M-CF$_3$SO$_3$)$^+$], 407[23,(M-2CO-CF$_3$SO$_3$)$^+$]. ^{1}H n.m.r. spectrum: 7.57-7.73, m,H5'; 7.84-8.00,m,H5; 8.12-8.42,m,H3,3',4,4'; 8.79,m,^{3}J5.6Hz,H6'; 9.04,m,^{3}J5.6Hz,H6. Infra-red absorption: 3020w, 2104s and 2024s[ν(CO)], 1603w, 1476m, 1455m, 1332s[ν(SO$_3$)], 1230s[ν(CF)], 1195s[ν(CF)], 1158vs(br)[ν(SO$_3$) + ν(CF)], 1009s[ν(SO$_3$)], 993s, 771s, 726m, 620s cm^{-1}. In CH$_2$Cl$_2$: 2082, 2020[ν(CO)]cm^{-1}. Mol. cond. (MeNO$_2$), 20.8 Scm^{2}mol^{-1} (134 after 48h owing to solvolysis).

a,b-Dicarbonyl-c,d-(1,10 phenanthroline)-e,f-bis(trifluoromethanesulphonato)ruthenium(II)   (1b)

Dicarbonyldichloro(1,10-phenanthroline)ruthenium(II) (1.10g) was heated with trifluoro-methanesulphonic acid (2 cm^3) under nitrogen for 2h at 110°C. The mixture was cooled and ether (50 cm^3) was slowly added and was allowed to stand until precipitation of the white product was complete. This was filtered off, washed with water and recrystallized under nitrogen from methylene chloride/ether (1.08g, 65%), m.p. 263-265°C (Found: C,30.4; H,1.6. C$_{16}$H$_8$F$_6$N$_2$O$_8$RuS$_2$ requires C,30.6; H,1.3%). Mass spectrum: m/e 636[2%,M$^+$], 608[16,(M-CO)$^+$], 580[100,(M-2CO)$^+$], 431[40,(M-2CO-CF$_3$SO$_3$)$^+$]. ^{1}H n.m.r. spectrum: 7.88-8.03,m,H8; 8.14-8.29, m,H3,5,6; 8.69-8.91,2d(overlapping),^{3}J8.4 and 8.7Hz,H4,7; 9.12,d,^{3}J5.3Hz,H9; 9.36,d,^{3}J5.0Hz, H2*. Infrared absorption: 3000w, 2098s and 2038s[ν(CO)], 1632w, 1603w, 1587w, 1521w, 1430s, 1372s, 1325s[ν(SO$_3$)], 1242s, 1228s[ν(CF)], 1180vs(br)[ν(SO$_3$) + ν(CF)], 1148s[ν(CF)], 1010s[ν(SO$_3$)], 991s(sh), 852s, 788w, 770w, 753w, 730w(sh), 722s cm^{-1}. In CH$_2$Cl$_2$: 2091, 2034[ν(CO)] cm^{-1}. Mol. cond. (MeNO$_2$), 15.5 Scm^{2}mol^{-1} (158 after 48h).

(d) Preparations of [Ru(CO)$_2$(bidentate)$_2$]$^{2+}$ Complexes

The complex Ru(CO)$_2$(O$_3$SCF$_3$)$_2$L (L = phen or bpy) (1a,b) (ca. 0.2g) and the bidentate ligand (bpy, phen, Me$_2$bpy or Pr$_2$bpy) (ca. 0.2g) were heated in ethanol (20-40 cm^3) under reflux for 1h in an atmosphere of nitrogen. The solvent was evaporated to dryness, and the residue was dissolved in hot water. After filtration, addition of aqueous ammonium hexafluorophosphate gave a yellow precipitate, which was recrystallized from acetone/ethanol and then acetone/ ether to give the required complex as white crystals. In assignments of ^{1}H n.m.r. spectra of [Ru(CO)$_2$L(L')]$^{2+}$ complexes, the nitrogen atoms *trans* to each other [see (3)] are designated N1.

---

*H2 (N1 *cis* to two CF$_3$SO$_3$ groups) and H9 are tentatively assigned on the basis that the environment of N1 rather than N10 is more similar to that of the nitrogens in the previously characterized[1,2] isomer [structure (2b)].

Dicarbonyl(4,4'-dimethyl-2,2'-bipyridyl)(1,10-phenanthroline)ruthenium(II) hexafluorophosphate

Yield 55% (Found: C,37.9; H,2.2; N,7.0. $C_{26}H_{20}F_{12}N_4O_2P_2Ru$ requires C,38.5; H,2.5; N,6.9%). ^1H n.m.r. spectrum: 2.46,s,4'-Me; 2.78,s,4-Me; 7.28,d,$^3J5.0Hz,H9$; 7.52,d,$^3J6.0Hz$, H6'; 7.93-8.08,m,H5',8; 8.22,m,$^3J5.0Hz,H5(Me_2bpy)$; 8.35-8.59,m,H3,5,6(phen); 8.69,m,H3'; 8.86,m,H3(Me_2bpy); 9.00,d,$^3J8.0Hz,H7$; 9.25,d,$^3J8.0Hz,H4$; 9.38,m,$^3J6.0Hz,H6(Me_2bpy)$; 9.91,d, $^3J5.0Hz,H2(phen)$. Infrared absorption: 3150w, 3100w, 2100vs and 2038vs[ν(CO)], 1620m, 1526w, 1456w(sh), 1435m, 1420w(sh), 1320w, 1230w, 1157w, 1038w, 916w, 845vs(br)[ν(PF) and phen], 806w, 779w, 770w, 747w, 724m cm^{-1}. Mol. cond. (MeNO$_2$), 158 Scm^{2}mol^{-1}.

Dicarbonyl(4,4'-diisopropyl-2,2'-bipyridyl(1,10-phenanthroline)ruthenium(II) hexafluorophosphate

Yield 60% (Found: C,41.6; H3.3; N,6.6. $C_{30}H_{28}F_{12}N_4O_2P_2Ru$ requires C,41.5; H,3.3; N,6.6%). ^1H n.m.r. spectrum:1.18,s,Me(4'-Pr); 1.48,s,Me(4-Pr); 3.00-3.29,m,CH(4,4'-Pr); 7.34,d,$^3J5.0Hz,H9$; 7.56,d,$^3J6.0Hz,H6'$; 7.91-8.06,m,H5',8; 8.22,m,$^3J5.0Hz,H5(Pr_2bpy)$; 8.37-8.52,m,H3,5,6(phen); 8.80,m,H3'; 8.97,m,H3(Pr_2bpy); 9.00,d,$^3J8.0Hz,H7$; 9.26,d,$^3J8.0Hz$, H4; 9.44,d,$^3J6.0Hz,H6(Pr_2bpy)$; 9.92,d,$^3J5.0Hz,H2(phen)$. Infrared absorption: 2995w, 2950w, 2885w, 2100vs and 2034vs[ν(CO)], 2020w(sh), 1618m, 1511w, 1436m, 1430m(sh), 1158w, 1036w, 916w, 840vs(br)[ν(PF) and phen], 768w, 746w, 723m cm^{-1}. Mol. cond. (MeNO$_2$), 189 Scm^{2}mol^{-1}.

2,2'-Bipyridyldicarbonyl(4,4'-dimethyl-2,2'-bipyridyl)ruthenium(II) hexafluorophosphate

Yield 60% (Found: C,36.3; H,2.5; F,28.5; N,6.9. $C_{24}H_{20}F_{12}N_4O_2P_2Ru$ requires C,36.6; H,2.6; F,28.9; N,7.1%). ^1H n.m.r. spectrum: 2.54,s,4-Me'; 2.75,s,4-Me; 7.47-7.98,m,H5', 6'(bpy) and H5,5',6'(Me_2bpy); 8.11,m,$^3J6.0Hz,H5(bpy)$; 8.38,m,$^3J8.0Hz,H4'$; 8.55-9.00,m, H3,3',4(bpy) and H3,3'(Me_2bpy); 9.29,d,$^3J6.1Hz,H6(Me_2bpy)$; 9.48,d,$^3J5.3Hz,H6(bpy)$. Infrared absorption: 3150w, 3105w, 2088vs and 2038vs[ν(CO)], 1627sh, 1623s, 1557w, 1485m, 1456s, 1320w, 1246m, 1222w, 1080w, 1035m, 928w, 900m, 830vs(br)[ν(PF)], 767w, 740w, 720w cm^{-1}. Mol. cond. (MeNO$_2$), 151 Scm^{2}mol^{-1}.

2,2'-Bipyridyldicarbonyl(4,4'-diisopropyl-2,2'-bipyridyl)ruthenium(II) hexafluorophosphate

Yield 65% (Found: C,39.6; H,3.4; N,6.6 $C_{28}H_{28}F_{12}N_4O_2P_2Ru$ requires C,39.9; H3.4; N,6.6%). ^1H n.m.r. spectrum: 1.25,s,Me(4'-Pr); 1.45,s,Me(4-Pr); 3.07-3.35,m,CH(4,4'-Pr); 7.59-7.80,m,H5',6'(bpy) and H5',6'(Pr_2bpy); 7.98-8.20,m,H5(bpy) and H5(Pr_2bpy); 8.35,m, $^3J8.0Hz,H4'$; 8.64,m,$^3J8.0Hz,H4$; 8.80-8.90,m,H3,3'(bpy) and H3,3'(Pr_2bpy); 9.35,d,$^3J6.0Hz$, H6(Pr_2bpy); 9.51,d,$^3J5.0Hz,H6(bpy)$. Infrared absorption: 2990w, 2950w, 2880w, 2098vs and 2032vs[ν(CO)], 1610s, 1554w, 1497w, 1480w, 1458w, 1430w, 1316w, 1244m, 1160w, 1110w, 1063m, 1030m, 926w, 830vs(br)[ν(PF)], 771m, 720w cm^{-1}. Mol. cond. (MeNO$_2$), 188 Scm^{2}mol^{-1}.

Known Complexes

Similar preparations gave [Ru(CO)$_2$(phen)$_2$](PF$_6$)$_2$ (65%), [Ru(CO)$_2$(bpy)$_2$](PF$_6$)$_2$ (50%) and [Ru(CO)$_2$bpy(phen)](PF$_6$)$_2$ (60%), which had infrared spectra in agreement with those of authentic samples[1,2].

REFERENCES

1. D.St.C. Black, G.B. Deacon and N.C. Thomas, *Transition Metal Chem.*, 1980, 5, 317.

2. D.St.C. Black, G.B. Deacon and N.C. Thomas, *Aust. J. Chem.*, 1982, 35, 2445.

3. J.M. Kelly, C.M. O'Connell and J.G. Vos, *Inorg. Chim. Acta*, 1982, 64, L75.

4. G. Choudhury, R.F. Jones, G. Smith and D.J. Cole-Hamilton, *J. Chem. Soc., Dalton Trans.*, 1982, 1143.

REACTION OF HEXABORANE(10) WITH EXCESS TRIMETHYLPHOSPHINE

Mitsuaki Kameda and Goji Kodama*

Department of Chemistry

University of Utah

Salt Lake City, Utah 84112, U.S.A.

Abstract—Bis(trimethylphosphine)-hexaborane(10), $B_6H_{10} \cdot 2P(CH_3)_3$, reacted with trimethylphosphine and gave a solid with the total composition "$B_6H_{10} \cdot 6P(CH_3)_3$" which consisted of twice the number of moles of the original $B_6H_{10} \cdot 2P(CH_3)_3$. The solid was inert to excess $P(CH_3)_3$. When treated with HCl, it gave a 1:2 mixture of $BH_3 \cdot P(CH_3)_3$ and $BH_2Cl \cdot P(CH_3)_3$. The framework of $B_6H_{10} \cdot 2P(CH_3)_3$ appeared to be cleaved and converted by $P(CH_3)_3$ into $B_2H_4 \cdot 2P(CH_3)_3$ and $B_4H_6 \cdot 4P(CH_3)_3$, and into two $B_3H_5 \cdot 3P(CH_3)_3$.

INTRODUCTION

Pentaborane(9) reacts with trimethylphosphine to give the bisphosphine adduct of the borane, $B_5H_9 \cdot 2P(CH_3)_3$[1]. This adduct of B_5H_9[2] further reacts with $P(CH_3)_3$, and the five-boron framework is cleaved into two fragments:
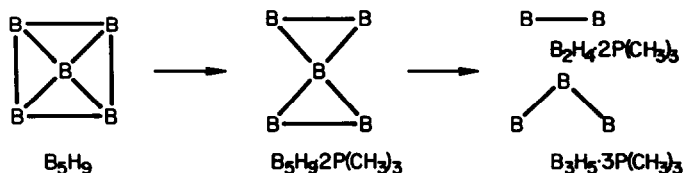
Hexaborane(10) also reacts with $P(CH_3)_3$ to give $B_6H_{10} \cdot P(CH_3)_3$[3] and $B_6H_{10} \cdot 2P(CH_3)_3$[4]. Thus, the pyramid-shaped structure of B_6H_{10}[5] undergoes a series of transformation and changes to a belt-shaped structure:
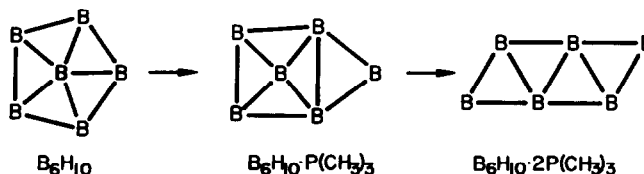
It was of interest to us to see how the bisphosphine adduct of B_6H_{10} would further react with $P(CH_3)_3$ and to compare the reaction with that of the B_5H_9 adduct.

RESULTS AND DISCUSSION

When B_6H_{10} was mixed with a large excess of $P(CH_3)_3$ at $-80 \sim -60^\circ C$, and the mixture was allowed to warm to room temperature, the formation of the mono- and bisphosphine adducts occurred in rapid succession. The bisphosphine adduct further reacted slowly with $P(CH_3)_3$. The same reaction occurred when dichloromethane or acetonitrile was used as the solvent. The
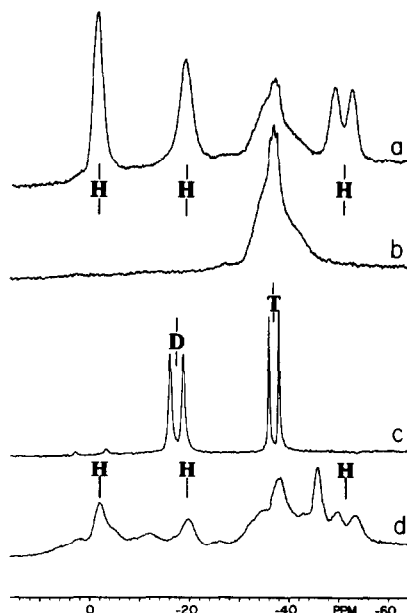
Figure 1. ^{11}B NMR spectra, ^{1}H-spin decoupled, at 25°C in dichloromethane. H, T and D denote the signals of $B_6H_{10}\cdot 2P(CH_3)_3$, $BH_3\cdot P(CH_3)_3$ and $BH_2Cl\cdot P(CH_3)_3$, respectively.

(a) Hexaborane(10) with excess $P(CH_3)_3$ in CH_2Cl_2, shortly after the temperature was raised to 25°C.

(b) The same solution as in (a), 4 hours later.

(c) The reaction solution "$B_6H_{10}\cdot 6P(CH_3)_3$" + 4HCl in CH_2Cl_2.

(d) The sublimation residue.

last phase of the change as observed on the ^{11}B NMR spectra is shown in Figures 1a and 1b. When the volatile components were removed from the resulting solution at $-23\sim0$°C by pumping, a white solid with the composition "$B_6H_{10}\cdot\underline{5.9\sim6.3}P(CH_3)_3$" was left behind. The solution of the solid in dichloromethane gave the ^{11}B NMR spectrum identical with that in Figure 1b. Its ^{31}P NMR spectrum indicated that free $P(CH_3)_3$ was present in only a small amount (less than 4% of the total P in the sample.) Other signals of ^{31}P were overlapped in the region of $0\sim3.6$ ppm [85% H_3PO_4 standard, low field shifts being taken as positive], indicating that the phosphines were attached to the boron atoms. When the solid residue was treated with anhydrous HCl in dichloromethane, $BH_3\cdot P(CH_3)_3$ and $BH_2Cl\cdot P(CH_3)_3$ were produced in a 1:2 molar ratio. Only insignificant amounts of side products were detected in the ^{11}B spectrum of the resulting solution. See Figure 1c.

Shown in Figure 2 is the vapor pressure depression data of trimethylphosphine solution of B_6H_{10}. The data points are compared with the curve calculated for the two-fragment formation in which six moles of $P(CH_3)_3$ are utilized per mole of B_6H_{10}. Two other lines are drawn for two hypothetical fragmentation patterns. See the caption of the figure. Thus, the curves for most of other patterns of fragmentation would appear outside of the shaded area. The $P(CH_3)_3$ solution stayed clear and colorless during the entire period of the measurements (3 days) at 18.5°C.
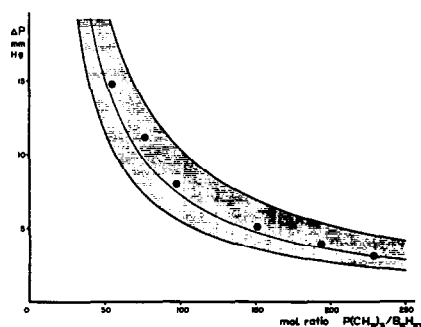
Figure 2. Vapor Pressure depression of trimethylphosphine solutions of Hexaborane(10). Middle curve; calculated for two-fragment formation with the use of six $P(CH_3)_3$. Upper curve; calculated for three-fragment formation with the use of two $P(CH_3)_3$. Lower curve; calculated for 1.5-fragment formation with the use of six $P(CH_3)_3$.

In Figure 3 the ^{11}B spectrum of the final products (Figure 1b) is expanded and compared with that of $B_2H_4 \cdot 2P(CH_3)_3$. The presence of $B_2H_4 \cdot 2P(CH_3)_3$ in the B_6H_{10} cleavage products is evident. When the above mentioned solid residue was subjected to sublimation under vacuum at room temperature, $B_2H_4 \cdot 2P(CH_3)_3$ was obtained as the sublimate in a yield of 0.55~0.78 mole per mole of the B_6H_{10} used. The residue of the sublimation was a complex mixture of boron compounds containing a significant amount of $B_6H_{10} \cdot 2P(CH_3)_3$. See Figure 1d. The intensity of the $B_6H_{10} \cdot 2P(CH_3)_3$ signal was estimated to be about 15% of the total ^{11}B signal intensity in the spectrum.

The reaction of B_5H_9 with excess $P(CH_3)_3$ gave a 1:1 mixture of $B_2H_4 \cdot 2P(CH_3)_3$ and $B_3H_5 \cdot 3P(CH_3)_3$. The spectrum of the mixture is shown in Figure 3b. A similarity between this spectrum and that of the B_6H_{10} cleavage product (Figure 3a) is noted. Subtraction of the $B_2H_4 \cdot 2P(CH_3)_3$ spectrum (in an intensity 2) from the spectrum in Figure 3b (in an intensity 5) gave the spectrum for $B_3H_5 \cdot 3P(CH_3)_3$. When a similar operation was performed on the spectrum in Figure 3a by adjusting the intensity ratio 2:6, an inverted image of the $B_2H_4 \cdot 2P(CH_3)_3$ signal was produced in the resulting difference spectrum. Apparently, the amount of the diborane(4) adduct in the products was less than that expected for a simple cleavage into $B_2H_4 \cdot 2P(CH_3)_3$ and $B_4H_6 \cdot 4P(CH_3)_3$. If it is assumed that the B_6-framework was cleaved into two fragments, and that any of the fragments did not undergo further reactions, except for combining with $P(CH_3)_3$, the cleavage into two units of $B_3H_5 \cdot 3P(CH_3)_3$ would be another possible reaction. The cleavage into $BH_3 \cdot P(CH_3)_3$ and $B_5H_7 \cdot 5P(CH_3)_3$ would have to be excluded from the consideration, since $BH_3 \cdot P(CH_3)_3$ was not found in the products. The presence of $B_6H_{10} \cdot 2P(CH_3)_3$ in the sublimation residue may be due to the recombination of the B_3 units, as such was observed when $B_2H_4 \cdot 2P(CH_3)_3$ was sublimed from the cleavage products of B_5H_9.

The molecules with the formula $B_nH_{n+2} \cdot nP(CH_3)_3$ are electron sufficent. The addition of n numbers of the phosphine to a B_nH_{n+2} unit removes the electron deficiency of the unit, and the valence bond structure of the molecule can be expressed without the use of two-electron three-center bonds. Thus, $B_2H_4 \cdot 2P(CH_3)_3$ and $B_3H_5 \cdot 3P(CH_3)_3$ are inert to $P(CH_3)_3$.

The $-\overset{|}{\underset{|}{B}}-\overset{|}{\underset{|}{B}}-$ bond, however, is reactive to hydrogen chloride, and is cleaved readily into $-\overset{|}{\underset{|}{B}}-H$ and $Cl-\overset{|}{\underset{|}{B}}-$ even at $-80^\circ C$. The ^{11}B chemical shifts for $B_2H_4 \cdot 2P(CH_3)_3$ and $B_3H_5 \cdot 3P(CH_3)_3$ appear within a range of ± 2.0 ppm from the shift of $BH_3 \cdot P(CH_3)_3$ which is another member of the series. Accordingly, $B_4H_6 \cdot 4P(CH_3)_3$, the next higher member, would also be reactive to HCl, and its ^{11}B shifts would appear also in the same range. So far, the separation of the products, except for $B_2H_4 \cdot 2P(CH_3)_3$, has been unsuccessful due to the instability of the compounds above $0^\circ C$ in the absence of excess $P(CH_3)_3$. However, the observations presented in this paper may suggest that the belt-shaped framework of $B_6H_{10} \cdot 2P(CH_3)_3$ was cleaved by $P(CH_3)_3$ into two fragments in two ways:

→ 600 Hz ←

$$B_6H_{10} \cdot 2P(CH_3)_3 \begin{cases} \overset{a}{\longrightarrow} B_2H_4 \cdot 2P(CH_3)_3 + B_4H_6 \cdot 4P(CH_3)_3 \\ \overset{b}{\longrightarrow} 2B_3H_5 \cdot 3P(CH_3)_3 \end{cases}$$

a

b

c

-37.5 PPM
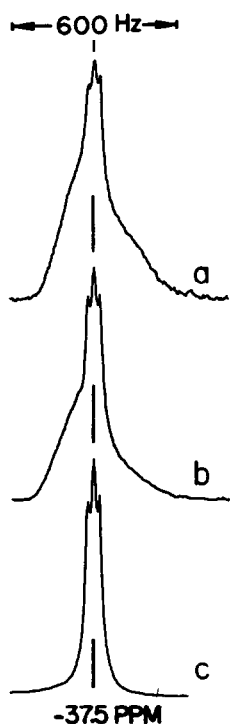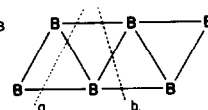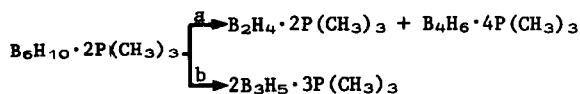
Figure 3. ^{11}B NMR spectra, ^{1}H-spin decoupled. (a) "$B_6H_{10} \cdot 6P(CH_3)_3$" in dichloromethane. (b) "$B_5H_9 \cdot 5P(CH_3)_3$" in acetonitrile. (c) $B_2H_4 \cdot 2P(CH_3)_3$ in acetonitrile.

EXPERIMENTAL

The sources of chemicals and the general methods of experimental procedures were de-
scribed elsewhere.[2,3]   Teflon valves and o-ring joints were used throughout. The NMR spectra
were recorded on a Varian XL-100-15 spectrometer, operating at 32.1 and 40.5 MHz for ^{11}B and
^{31}P nuclei, respectively.

The reaction of B_6H_{10} with $P(CH_3)_3$ proceeded uncontrollably fast unless a special care
was taken. Samples of B_6H_{10} and $P(CH_3)_3$ were measured out first. Then, a portion of the
B_6H_{10} sample was condensed near the botton of a reaction tube (10 mm o.d. Pyrex) as a thin
layer at $-197^{\circ}C$, and a portion of the $P(CH_3)_3$ sample was condensed above the layer. The
tube was allowed to warm slowly to about $-60^{\circ}C$ (slightly above the melting point of B_6H_{10})
and the mixture was shaken well at that temperature. Then the tube was cooled to $-197^{\circ}C$, and
next portions of B_6H_{10} and $P(CH_3)_3$ were condensed in and treated likewise. This procedure
was repeated until all of the B_6H_{10} sample was transfered into the tube. Finally the
remainder of the $P(CH_3)_3$ sample was condensed in the tube, and the tube was allowed to warm
slowly to room temperature while the mixture was agitated. A total of 0.3~0.5 mmole sample
of B_6H_{10} was used for the preparation of each reaction mixture.

REFERENCES AND NOTES

(1) Fratini, A.V.; Sullivan, G.W.; Denniston, M.L.; Hertz, R.K.; Shore, S.G. J. Am. Chem.
     Soc. 1974, 96, 3013.

(2) Kameda, M,; Kodama, G. Inorg. Chem. 1980, 19, 2288.

(3) Kameda, M,; Kodama, G. Inorg. Chem. 1981, 20, 1072.

(4) Mangion, M.; Hertz, R.K.; Denniston, M.L.; Long, J.R.; Clayton, W.R.; Shore, S.G.
     J. Am. Chem. Soc. 1976, 98, 449.

(5) Hirschfeld, F.L.; Eriks, K.; Dickerson, R.E.; Lippert, E.L.Jr.; Lipscomb, W.N. J.
     Chem. Phys. 1958, 28, 56.

(6) The ^{31}P shift values for $P(CH_3)_3$ adducts of several boranes are listed below for
     comparision. $BH_3 \cdot P(CH_3)_3$. -1.8; $B_3H_7 \cdot P(CH_3)_3$, -1.3 [Bishop, V.L.; Kodama,G. Inorg.
     Chem. 1981, 20, 2723]; $B_4H_8 \cdot 2P(CH_3)_3$, 1.8 [Kodama, G.; Kameda, M. Inorg. Chem. 1979,
     18, 3302]; $B_2H_4 \cdot 2P(CH_3)_3$, 2.8; "$B_5H_9 \cdot 5P(CH_3)_3$", broad signal centered at 2.0 [Refer-
     ence 2].

(7) It is noted that, if the spectrum in Figure 3a was
     assumed to be an overlap of the signals of $B_2H_4 \cdot 2P(CH_3)_3$,
     $B_3H_5 \cdot 3P(CH_3)_3$ and $B_4H_6 \cdot 4P(CH_3)_3$ in a 1:2:2 intensity
     ratio (or a 3:4:3 molar ratio), the difference spectrum
     shown in the figure could be obtained for $B_4H_6 \cdot 4P(CH_3)_3$.
     The peak positions are at -35.4 and -38.1 ppm.

-30   -40   PPM
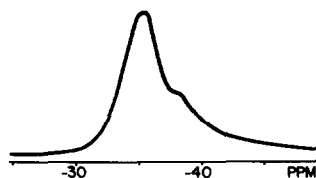
NOTES

VANADIUM (IV) PORPHYRINS : SYNTHESIS AND SPECTRO-
CHEMICAL CHARACTERIZATION OF THIOVANADYL PORPHYRINS.
EXAFS STRUCTURAL STUDY OF THIO (2, 3, 7, 8, 12, 13,
17, 18 - OCTAETHYLPORPHYRINATO) VANADIUM (IV).

JEAN-LUC PONCET and ROGER GUILARD*
Laboratoire de Synthèse et d'Electrosynthèse Organo-
métallique Associé au C.N.R.S. (LA 33), Faculté des
Sciences, "Gabriel", 6, Bd Gabriel, 21100 DIJON,
France.
        and
PASCALE FRIANT and JOSE GOULON*
Laboratoire de Chimie Théorique (ERA C.N.R.S. n° 22),
Université de Nancy I, B.P. 239, 54506 VANDOEUVRE-Lès-
NANCY cedex, France et LURE (Laboratoire pour l'Utili-
sation du Rayonnement Electromagnétique), Laboratoire
propre du C.N.R.S. Associé à l'Université de PARIS-
SUD, ORSAY, France.

(Received 13 *December* 1982)

Abstract – The action of elemental sulfur with
vanadium (II) porphyrins complexes $\left[V^{II}(por)(THF)_2\right]$
(por = porphyrinate) affords the thiovanadyl porphy-
rins $\left[V^{IV}(por)(S)\right]$. EXAFS spectroscopy at the V K-edge
of $\left[V^{IV}(oep)(S)\right]$ confirms the axial symmetry of these
complexes.

Although complexes containing the vanadyl ion,
$V=O^{2+}$, are well known, there are very few studies of
vanadium compounds in which the thiovanadyl ion is
present[1,2]. K.P. Callahan et al[1]. recently have deve-
loped a synthetic route to the previously unknown
thiovanadyl species, V=S Ln, which involves reaction
of V=O Ln with B_2S_3. As such thiovanadyl species are
of likely relevance to certain industrial catalysts in
petrochemistry[3], we report here a convenient procedure
for the isolation of thiovanadium (IV) porphyrins
$\left[V^{IV}(por)(S)\right]$ (por = oep, tpp, tmtp or tptp)[+] by reac-
tion of low-valent vanadium porphyrins with elemental
sulfur. EXAFS spectroscopy at the V K-edge provides
convincing evidence for the monomeric nature of the
complexes, as well as the multiple V=S bond.

Reduction[++] by zinc amalgam (1g) of a dry oxygen

[+]Abbreviations used : por = porphinato ; oep = octae-
thylporphinato ; tpp = meso-tetraphenylporphinato ;
tmtp = meso-tetra-m-tolylporphinato ; tptp = meso-
tetra-p-tolylporphinato.

[++]All operations were carried in Schlenk tubes under
purified argon and with dried oxygen free solvents.

[+++]THF = tetrahydrofuran.

free tetrahydrofuran[+++] solution (60 cm^3) containing
$\left[V^{IV}(tptp)(Cl_2)\right]$[4], (1d)(0.65g, 0.8 mmol) led to a
brown solution of $\left[V^{II}(tptp)(THF)_2\right]$[5] after 24 h of
vigourous stirring at room temperature. Excess of zinc
amalgam was filtered and elemental sulfur (0.1g,3 mmol)
was added to the filtrate. The mixture was then stir-
red for 5 h at room temperature and concentrated in
vacuum. The excess sulfur was then sublimated (0.1mm
Hg) at 110-120°C. The obtained residue was purified by
chromatography on an aluminium oxide column (eluent :
toluene) and recrystallized in a mixture of toluene-
heptane (1/2) $\Big(0.27$ g, 45% yield of $\left[V^{IV}(tptp)(S)\right]$,
(2d)$\Big)$[6].

The analytical results and the mass-spectral data
agree perfectly with the proposed molecular formula
$\left[V^{IV}(por)(S)\right]$. The parent peak corresponds either to
the molecular peak $\left[V^{IV}(por)(S)\right]^{+\cdot}$ or to the recombi-
nation ion $\left[V^{IV}(por)(S)+H\right]^+$. The IR spectra of these
complexes show a medium to strong intensity band in
the 550 – 565 cm^{-1} range ; this band corresponds to
the V=S stretching vibration[2]. The isotropic EPR
spectral parameters g_{av} and A_{av} as well as the prin-
cipal components of the <g> tensor and the hyperfine
interaction tensor <A> for the thiovanadyl complexes
(2) – are given in Table 1.

The complexes (2) exhibit eight-line isotropic
solution spectra, indicative of a d^1 V(IV) nucleus.
The tensor components calculated from spectra measured
on frozen solutions correspond to axially symmetric
compounds. EXAFS spectroscopy at the V K-edge confirms
this square – plane pyramidal molecular structure.

For the sake of comparison we have reproduced on
the same plots the FT-EXAFS spectra of both
$\left[V^{IV}(oep)(O)\right]$ and $\left[V^{IV}(oep)(S)\right]$: the power spectra
$\left|\tilde{x}_1(R)\right|$ and the imaginary part $Im\tilde{x}_1(R)$ being respec-
tively displayed in figures 1a and 1b. It is worth
mentioning here that according to a now standard
procedure detailed elsewhere[4,7,8], these FT – spectra
were corrected for both the amplitudes and phase-
shifts of the V ...N shell which we expected to be the
dominant signal of a typical porphyrinic pattern. As
illustrated by figures 1a/1b the contributions of the
carbons of the porphyrinic ring are fairly identical,
for both compounds, whereas a strong destructive
interference effect is clearly detected in the case
of $\left[V^{IV}(oep)(S)\right]$, as a direct consequence of the
scattering phase shift difference between S and N.
As the geometry of the porphyrinic ring remains iden-
tical, for both compounds a difference FT – spectrum
gives (Fig 2) the negative contribution of the V=O
shell ($R_1 \approx 1.6$Å) together with the unknown V=S signal
($R_2 = 2.06 \pm 0.02$Å) . The latter distance is in excellent
agreement with the V=S distance reported for another
compound[1].

Table I — E P R spectral parameters of thiovanadyl complexes

Complex	A_{av} (10^{-4} cm^{-1})	$A//$ (10^{-4} cm^{-1})	$A\perp$ (10^{-4} cm^{-1})	g_{av}	$g//$	$g\perp$
$[V^{IV}(oep)(S)]$	79.76	143.40	51.50	1.9691	1.9635	1.9717
$[V^{IV}(tpp)(S)]$	80.31	142.10	50.88	1.9712	1.9651	1.9711
$[V^{IV}(tmtp)(S)]$	80.52	144.10	50.93	1.9727	1.9655	1.9732
$[V^{IV}(tptp)(S)]$	80.71	141.50	51.83	1.9734	1.9656	1.9724
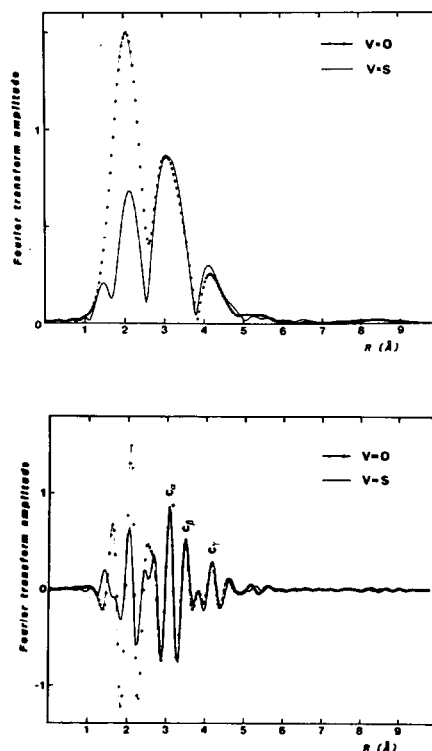
Fig. 1　a) comparison of the modulus of $\tilde{\chi}_1(R)$ for $[V^{IV}(oep)(O)]$ (dotted line) and $[V^{IV}(oep)(S)]$ (full line)

b) Imaginary parts $Im\tilde{\chi}_1(R)$ for $[V^{IV}(oep)(O)]$ (dotted line) and $[V^{IV}(oep)(S)]$ (full line)
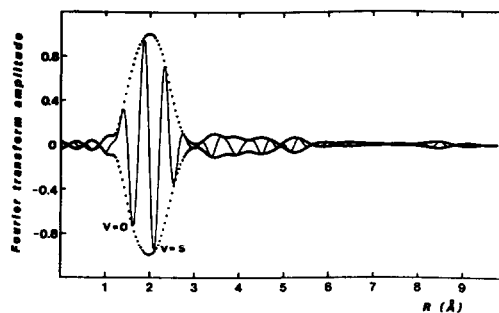
Fig 2　Difference spectra $[V^{IV}(oep)(S)] - [V^{IV}(oep)(O)]$ ($|\tilde{\chi}(R)|$ dotted line ; $Im\ \tilde{\chi}(R)$ full line)

The reaction of elemental sulfur with low-valent organometallic systems led normally to chair-like metal pentasulfide molecules ; in contrast, reaction of the low-valent vanadium (II) porphyrins with excess sulfur led to the thiovanadyl complexes. We plan to report further studies on the catalyst deactivating agents during petroleum hydrodesulfurization ; these agents contain sulfur and vanadium, also, thiovanadyl petroporphyrins are very interesting models for the catalyst poisons.

REFERENCES

[1] K.P. Callahan, P.J. Durand and P.H. Rieger, *J. Chem. Soc., Chem. Commun.* 1980, 75 ; M. Sato, K.M. Miller, J.H. Enenark, C.E. Strouse and K.P. Callahan, *Inorg. Chem.* 1981, 20, 3571.

[2] V.L. Goedhen and J.A. Ladd, *J. Chem. Soc., Chem. Commun.* 1981, 910.

[3] B.G. Silbernagel, *Journal of Catalysis* 1979, 56, 315

[4] P. Richard, J.L. Poncet, J.M. Barbe, R. Guilard, J. Goulon, D. Rinaldi, A. Cartier and P. Tola, *J. Chem. Soc., Dalton Trans.* 1982, 8, 1451.

[5] J.L. Poncet, J.M. Barbe, R. Guilard, H. Oumous, C. Lecomte and J. Protas, unpublished results.

[6] The other complexes $[V^{IV}(por)(S)]$ were prepared in a similar way (yield % ≈ 45) : $[V^{IV}(oep)(S)]$ (2a) ; $[V^{IV}(tpp)(S)]$ (2b) ; $[V^{IV}(tmtp)(S)]$ (2c).

[7] J. Goulon, C. Goulon, F. Niedercorn, C. Selve and B. Castro, *Tetrahedron* 1981, 37, 3707.

[8] J. Goulon, C. Goulon-Ginet, H. Chabanel, *J. Sol. Chem.* 1981, 10,9.

NOTES

Mössbauer studies of solid state photolysis of barium and strontium tris(oxalato) ferrates (III)

Abstract—Solid state photolysis of strontium and barium tris(oxalato) ferrate(III) was done under a medium pressure lamp and investigated with Mössbauer spectroscopy. The product $[Fe^{II}(C_2O_4) (H_2O)_2]^{2-}$ formed during photolysis is found to be quite stable and does not convert to ferric state on long standing in air.

The photolysis of potassium tris(oxalato) ferrate(III) in solid state and solutions[1–4] and recently the Mössbauer study of the solid state photolysis of alkali tris(oxalato) ferrate(III) have been reported[5] indicating the effect of cation on photoinduced decomposition. Mössbauer study of solid state photolysis of sodium pentacyanonitroferrate(II) monohydrate has been done.[6] Thermal decomposition of barium and strontium tris(oxalato) ferrate(III) has also been reported.[7] In the present study the solid state photolysis of barium and strontium tris(oxalato) ferrates(III) has been investigated with the help of Mössbauer spectrosopy.

EXPERIMENTAL

Barium and strontinum tris(oxalato) ferrates(III) were prepared by standard method and characterised by IR, chemical analysis and thermal analysis techniques.

Mössbauer spectrometer MBS-35 (ECIL, India) coupled with MCA-38B, constant acceleration drive was employed to record the spectrum. A 2.5-mi $^{57}Co(Rh)$ source was used. The values of isomer shift are reported with respect to natural iron. All the spectra were recorded at temp. (25 ± 2°C). A sample containing approx. 10 mg/cm^2 of the natural iron was taken for each measurement. All the spectra have been fitted to Lorentzian line shape using a programme and fitting procedures on computer ICL 2960, IIT Delhi. Mössbauer spectra were almost symmetrical. Slight deviation may be due to powdered random samples and due to spin lattice relaxation effect.[8] For photoirradiation, powdered samples spread over a glass plate were exposed to medium pressure 250 W mercury lamp for 50, 100, 200 and 300 hr.

RESULTS AND DISCUSSION

The Mössbauer spectrum of strontium tris(oxalato) ferrate(III) at room temperature (25 ± 2°C) exhibits a doublet having isomer shift 0.25 mm/sec and quadrupole splitting 0.40 mm/sec (Fig. 1a) while barium tris(oxalato) ferrate(III) gives a broad single absorption band (Fig. 2a) indicative of spin relaxation effect.[9] The isomer shift to barium tris(oxalato) ferrate(III) is 0.31 mm/sec^{-1}.

*Authors to whom correspondence should be addressed.

Barium and strontium tris(oxalato) ferrate(III) were exposed to radiations up to 300 hr. The Mössbauer spectrum of the sample irradiated for 50 hr is shown in Fig. 1(b). This shows a asymmetrical doublet, the first band is due to the overlapping of two bands, one due to parent complex and the other due to the new product formed during photolysis. The isomer shift and quadrupole splitting values are 1.28 and 2.61 mm sec^{-1} in case of barium tris(oxalato) ferrate(III) photolysis while 1.18 and 2.30 mm sec^{-1} in case of strontium tris(oxalato) ferrate(III) photolysis.

On irradiation for 200 hr the Mössbauer spectrum shown in Fig. 1(c) clearly indicates that the decomposition increases with the increase of the irradiation time. Mössbauer spectrum shows a quadrupole doublets with isomer shift and quadrupole splitting 1.07 and 2.57 mm sec^{-1} in case of barium tris(oxalato) ferrate(III) and 1.26 and 2.25 mm sec^{-1} in case of strontium tris(oxalato) ferrate(III):

On irradiation for 300 hr Mössbauer spectrum shown in Fig. 1(d) shows almost complete decomposition to a product having isomer shift and quadrupole splitting 1.28, 2.20 and 2.61 mm sec^{-1} in case of strontium tris(oxalato) ferrate(III). The value of isomer shift and quadrupole splittings show that the product formed contains Fe(II) in high spin state.

The value of isomer shift 1.22 mm sec^{-1} and quadrupole splitting 2.53 mm sec^{-1} for $Fe^{II}(C_2O_4)_2(H_2O)_2^{3-5}$ are very close to the products formed during photolysis of the barium and strontium tris(oxalato) ferrate(III), indicating that the products are $M[Fe^{II}(C_2O_4)_2(H_2O)_2]$ (M = Ba^{2+}, Sr^{2+}). The high value of quadrupole splitting in the case of barium tris(oxalato) ferrate(III) irradiated for 300 hr is indicative of more distortion in the product (II) than the product (I) formed in strontium tris(oxalato) ferrate(III). Values are given in Table 1. The rate of decomposition (Figs. 1(d)) is more in the case of strontium complex than in barium complex which may be due to the different nature of cation. Intermediate $K_6[Fe_2^{II}(OX)_5]$ formed during the photolysis of potassium tris(oxalato) ferrate(III) gets converted to $K[Fe^{III}(C_2O_4)_2(H_2O)_2]$ on long standing in air.[4,5] While in the case of other alkali tris(oxalato) ferrate(III) ferrous oxalate was formed which on long standing in air gets oxidised to ferric state. The product $[Fe^{II}(C_2O_4)_2(H_2O)_2]^{2-}$ formed during the photolysis of barium and strontium tris(oxalato) ferrate(III) is found to be quite stable and does not convert to ferric state. This clearly

Table 1. Mössbauer parameters of strontium and barium tris(oxalato) ferrates(III)

S.No. Name of the complex	Isomer shift (mm sec^{-1})	Quadrupole splitting (mm sec^{-1})	Tentative assignment
1. $Sr_3[Fe(C_2O_4)_3]_2 12H_2O$	0.25 ± 0.03	0.40 ± 0.03	Parent complex
2. $Ba_3[Fe(C_2O_4)_3]_2 10H_2O$	0.31 ± 0.03	—	Parent complex
3. Product (I)†	1.28 ± 0.03	2.21 ± 0.03	$[Fe^{II}(C_2O_4)_2(H_2O)_2]^{2-}$
4. Product (II)‡	1.28 ± 0.03	2.61 ± 0.03	$[Fe^{II}(C_2O_4)_2(H_2O)_2]^{2-}$

†Product from $Sr_3[Fe(C_2O_4)_3]_2$. 12H$_2$O irradiated for 300 hr.
‡Product from $Ba_3[Fe(C_2O_4)_3]_2$. 10H$_2$O irradiated for 300 hrs.
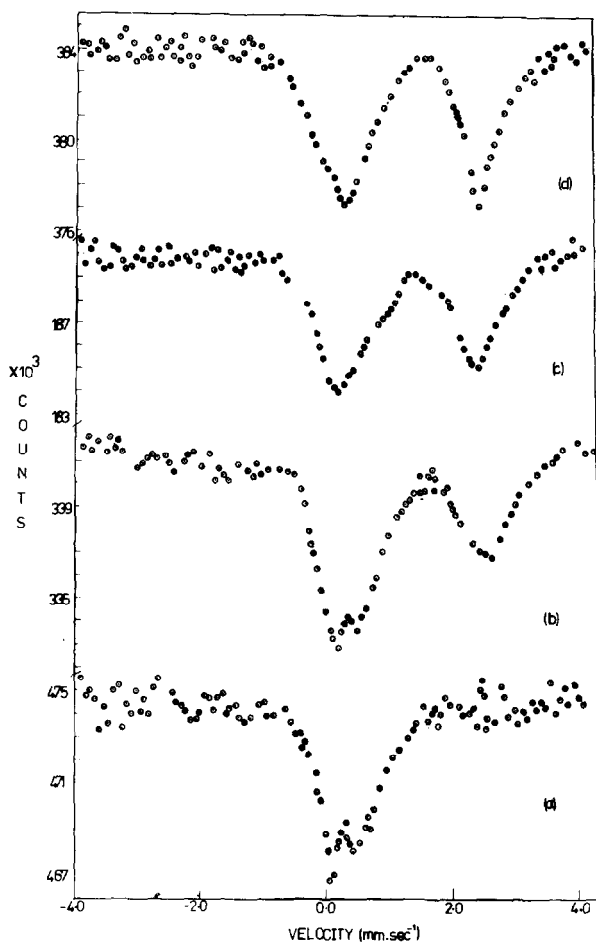
Fig. 1. (a) Mössbauer spectrum of strontium tris(oxalato) ferrate(III) at room temperzture (25°C). (b) Mössbauer spectrum of strontium tris(oxalato) ferrate(III) irradiated for 50 hr. (c) Mössbauer spectrum of strontium tris(oxalato) ferrate(III) irradiated for 200 hr. (d) Mössbauer spectrum of strontium tris(oxalato) ferrate(III) irradiated for 300 hr.

indicates the influence of barium and strontium on the solid state photo-induced decomposition of these complexes.

However, the solid state photoinduced decomposition may be complex but on the basis of the investigations of Mössbauer studies following mechanism have been proposed.

$$[Fe(C_2O_4)_3]^{3-} \cdot nH_2O \xrightarrow{h\nu} [Fe^{II}(C_2O_4)_2(H_2O)_2]^{2-} + C_2O_4^-$$

$$[Fe(C_2O_4)_3]^{3-} \cdot nH_2O + C_2O_4^- \longrightarrow [Fe^{II}(C_2O_4)_2(H_2O)_2]^{2-} + C_2O_4^{2-} + 2CO_2.$$
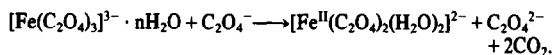
Chemistry Department   A. S. BRAR*†
Guru Nanak Dev University   S. BRAR
Amritsar–143005, *India*   S. S. SANDHU

*Author to whom correspondence should be addressed.
†Chemistry Department, Indian Institute of Technology, New Delhi–110016, India.

REFERENCES

[1]W. W. Wendlandt and E. L. Simmons, *J. Inorg. Nucl. Chem.* 1966, **28**, 2420.

[2]G. M. Bancroft, K. G. Dharmawardena and A. G. Maddock, *J. Chem. Soc.(A)* 1969, 2914.

[3]H. Sato and T. Tominaga. *Radiochem. Radioanal, Lett.* 1977, **30**, 165.

[4]H. Sato and T. Tominaga, *Bull. Chem. Soc. Japan* 1979, **52**, 1402.

[5]A. S. Brar and B. S. Randhawa, *Bull. Chem. Soc. Japan* 1981, **54**, 3166.

[6]A. S. Brar and S. K. Mazumdar, *Radiochem. Radioanal. Lett.* 1981, **47**, 267.

[7]P. K. Gallagher and C. R. Kurjian, *Inorg. Chem.* 1966, **5**, 214.

[8]P. Gutlich, R. Link and A. Trautwein, *Mössbauer Spectroscopy and Transition Metal Chemistry*, p. 53 Springer–Verlag, Berlin (1979).

On the Pauling electronegativity scales—I

Abstract—It is shown that the Pauling electronegativity scale χ is closely related to the electrostatic potential near the physical meaningful boundary between the core and valence regions in an atom, and is well reproduced by the relationship:

$$\chi = \frac{(N_v + 1)}{2} f(n),$$

where N_v is the valence electron number and the factor $f(n)$ is empirically given by

$$f(n) = \left[1 - \frac{2}{9}(n-1)^{1/2}\right]; \quad n \geqq 1,$$

n being the periodic number.

There have been many theoretical studies[1–9] of the electronegativity,[10] of which the recent proposal of Parr *et al.*[1–3] that equates the electronegativity to the negative of the chemical potential within the context of the density functional theory of Hohenberg and Kohn[11] is of special interest. In the present study, it is shown from a quite different point of view with the above that the Pauling electronegativity scale[10] is closely related to the electrostatic potential near the core-valence boundary in an atom.

It has been shown by Politzer and Parr[12] that the outermost minimum in the radial density defines a physically meaningful boundary between the core and valence regions of a ground state atom. In order to investigate in detail the electrostatic potential V near such a boundary, we expand that potential with a radial distance r from the nucleus;

$$V(r_m + \Delta r) = V(r_m) + \left(\frac{\partial V}{\partial r}\right)_{r_m}(\Delta r) + \frac{1}{2}\left(\frac{\partial^2 V}{\partial r^2}\right)_{r_m}(\Delta r)^2 + \cdots \quad (1)$$

where r_m is the radial distance at which the radial density function $4\pi r^2 \rho(r)$ has the outermost minimum, and the partial differentials with respect to r are evaluated at the position r_m. To a first approximation, we may take the first and second terms truncated after the higher order terms, i.e.

$$V(r_m + \Delta r) = V(r_m) + \left(\frac{\partial V}{\partial r}\right)_{r_m}(\Delta r). \quad (2)$$

Here, we note the elegant relationships derived by Politzer[13,14] who has studied the electrostatic potential-electronic density relationships in an atom;

$$\left(\frac{\partial V}{\partial r}\right)_{r_m} = -\frac{2V(r_m)}{r_m}, \quad (3)$$

and

$$V(r_m) = \int_{r_m}^{\infty} \frac{\rho(\mathbf{r}')}{|\mathbf{r}_m - \mathbf{r}'|} d\mathbf{r}' = \frac{N_m e}{2r_m}, \quad (4)$$

where ρ is the electron density, e is the electronic charge, and N_m is the electron number which is located beyond the radial distance r_m from the nucleus. Introducing equations (3) and (4) into eqn (2), we have

$$V(r_m + \Delta r) = \frac{N_m e}{2r_m}\left[1 - \frac{2(\Delta r)}{r_m}\right], \quad (5)$$

which is the approximate electrostatic potential produced at the near outermost minimum by the nucleus and the electrons N_m. There is no doubt that this potential is a good measure of the electronegativity in an atom.

We now define conveniently the electronegativity χ from eqn (5) as

$$\chi = \int \frac{r_m}{e} V(r_m + \Delta r)\, dr = \int_{-\Delta r_m}^{\Delta r_m} \frac{N_m}{2}\left[1 - \frac{2(\Delta r)}{r_m}\right] dr, \quad (6)$$

and, to obtain the Pauling electronegativity scale,[10] we take the following integration range:

$$\Delta r_m = \frac{N_m + 1}{2N_m}. \quad (7)$$

The integration result is simply given by

$$\chi = \int \frac{r_m}{e} V(r_m + \Delta r)\, dr = \frac{N_m + 1}{2}. \quad (8)$$

Since r_m and N_m may be replaced by the core radius r_c and the valence electron number N_v,[12,14] eqn (8) becomes

$$\chi = \int \frac{r_c}{e} V(r_c + \Delta r)\, dr = \frac{N_v + 1}{2}, \quad (9)$$

which means that the Pauling electronegativity .scale[10] can be expressed with the valence electron number or the valence electronic charge.

It will be simply verified that eqn (9) works completely as it is for atoms (Li, Be, B, C, N, O, F) in the first period. However, for atoms belonging to the other periods, eqn (9) needs a slight modification taking into accocunt the periodicity. Such a modification may be accomplished by slightly varying the integration range of eqn (7). Introducing a correction factor $f(n)$ into eqn (7),

$$\Delta r_m = \frac{(N_m + 1)}{2N_m} f(n), \quad (10)$$

and then integrating similarly eqn (6), we have

$$\chi = \int \frac{r_m}{e} V(r_m + \Delta r)\, dr = \frac{(N_m + 1)}{2} f(n)$$

$$= \frac{(N_v + 1)}{2} f(n), \quad (11)$$

which is the desired result. Here, $f(n)$ may be assumed empirically as

$$f(n) = \left[1 - \frac{2}{9}(n-1)^{1/2}\right]; \quad n \geq 1 \qquad (12)$$

n being the periodic number.

We can easily confirm by numerical calculations that eqn (11) combined with eqn (12) reproduces well the Pauling electronegativity scales[10] for most atoms except for the hydrogen atom. The results are shown in Table 1. It may therefore be concluded that the electrostatic potential near the physical meaningful boundary between the core and valence regions in an atom is closely related to the Pauling electronegativity scale.[10]

It is well known that the Pauling electronegativity scales[10] are proportional to Mulliken electronegativities[15] which can be calculated from ionization potentials (IP) and electron affinities (EA) using (IP + EA)/2. It is also of interest to investigate the relation between the Pauling electronegativity scale[10] and the negative of the chemical potential. This will be reported in the near future.

Acknowledgement—The referee's suggestions were very helpful.

Division of Chemistry   KEN OHWADA
Japan Atomic Energy Research Institute
Tokai-mura, Naka-gun, Ibaraki-ken
Japan

Table 1. Calculated Pauling electronegativity scales[a,b]

H 2.1							He 5.2
Li 1.0 (1.0)	Be 1.5 (1.5)	B 2.0 (2.0)	C 2.5 (2.5)	N 3.0 (3.0)	O 3.5 (3.5)	F 4.0 (4.0)	Ne 4.5 (4.5)
Na 0.9 (0.8)	Mg 1.2 (1.2)	Aℓ 1.5 (1.6)	Si 1.8 (1.9)	P 2.1 (2.3)	S 2.5 (2.7)	Cℓ 3.0 (3.1)	Ar 3.2 (3.5)
K 0.8 (0.7)	Ca 1.0 (1.0)	Sc 1.3 (1.4)	Ge 1.8 (1.7)	As 2.0 (2.1)	Se 2.4 (2.4)	Br 2.8 (2.7)	Kr 2.9 (3.0)
Rb 0.8 (0.6)	Sr 1.0 (0.9)	Y 1.2 (1.2)	Sn 1.8 (1.5)	Sb 1.9 (1.8)	Te 2.1 (2.2)	I 2.5 (2.5)	Xe 2.4 (2.8)
Cs 0.7 (0.6)	Ba 0.9 (0.8)	La-Lu 1.1-1.2 (1.1)	Pb 1.8 (1.4)	Bi 1.9 (1.7)	Po 2.0 (1.9)	At 2.2 (2.2)	Rn 2.1 (2.5)
Fr 0.7 (0.5)	Ra 0.9 (0.8)	Ac 1.1 (1.0)					

[a]Calculated values in parentheses.
[b]Electronegativity values for noble gas elements were taken from L. C. Allen and J. E. Huheey, *J. Inorg. Nucl. Chem.* 1980, 42, 1523.

REFERENCES

[1]R. G. Parr, R. A. Donnelly, M. Levy and W. E. Palke, *J. Chem. Phys.* 1978, **68**, 3801.
[2]N. K. Ray, L. Samuels and R. G. Parr, *J. Chem. Phys.* 1979, **70**, 3680.
[3]L. J. Bartolotti, S. R. Gadre and R. G. Parr, *J. Am. Chem. Soc.* 1980, **102**, 2945.
[4]J. Chelikowsky and J. C. Phillips, *Phys. Rev.* 1978, **B17**, 2453.
[5]R. E. Watson and L. H. Bennett, *J. Phys. Chem. Solids* 1978, **39**, 1235.

[6]R. E. Watson and L. H. Bennett, *Phys. Rev.* 1978, **B18**, 6439.
[7]J. A. Alonso and L. A. Girifalco, *Phys. Rev.* 1979, **B19**, 3889.
[8]N. H. March, *J. Chem. Phys.* 1979, **71**, 1004.
[9]J. A. Alonso and L. A. Girifalco, *J. Chem. Phys.* 1980, **73**, 1313.
[10]L. Pauling, *The Nature of the Chemical Bond*. Cornell University Press, Ithaca, New York (1960).
[11]P. Hohenberg and W. Kohn, *Phys. Rev.* 1964, **B136**, 864.
[12]P. Politzer and R. G. Parr, *J. Chem. Phys.* 1976, **64**, 4634.
[13]P. Politzer, *J. Chem. Phys.* 1980, **72**, 3027.
[14]P. Politzer, *J. Chem. Phys.* 1980, **73**, 3264.
[15]R. S. Mulliken, *J. Chem. Phys.* 1934, **2**, 782; 1935, **3**, 573.

Temperature dependence of the Mössbauer spectrum and magnetic susceptibility [Fe(uridine)Cl₂]∞: Novel magnetic ordering of transition metal complexes based on nucleoside ligands

Abstract—The zero-field Mössbauer spectra and magnetic susceptibility of a polycrystalline sample of the polymeric material [Fe(uridine)Cl₂]ₓ have been measured in the temperature range 1.7–300 K. The compound exhibits two magnetic transitions. The isomer shift and quadrupole splitting indicate a distorted pseudo-octahedral FeCl₄O₂ chromophore resulting from condensation to a network structure via chloro and uridine ligand bridging.

The title compound was synthesized by the method of Goodgame[1] who characterized a number of first transition series complexes based on the simple nucleosides, uridine (Fig. 1) and thymidine. The empirical formula suggests either coordinative unsaturation, e.g. pseudo-tetrahedral monomer or association to polymer or network structure via chloro and/or nucleoside ligand bridging. As part of our continuing program of detailed studies of the cooperative magnetic behavior of novel high spin ferrous systems, we now present some new results for [Fe(uridine)Cl₂]ₓ.

MAGNETIC SUSCEPTIBILITY

We find a maximum in χ'_M vs T at 22.6 K suggesting 3-D antiferromagnetic (AF) ordering and a sharp minimum in χ'_M vs T at 12.5 K suggesting a spin reorientation transition (probably canting of the AF sublattices). These are most clearly seen in the corresponding minimum and maximum observed in the reciprocal susceptibility (Fig. 2c). The overall decrease in magnetic moment (5.24 μ_B 298 K to 1.55 μ_B at 1.73 K Fig. 2b) and high critical temperature (~23 K) indicate surprisingly strong anti-ferro-

which is the desired result. Here, $f(n)$ may be assumed empirically as

$$f(n) = \left[1 - \frac{2}{9}(n-1)^{1/2}\right]; \quad n \geq 1 \qquad (12)$$

n being the periodic number.

We can easily confirm by numerical calculations that eqn (11) combined with eqn (12) reproduces well the Pauling electronegativity scales[10] for most atoms except for the hydrogen atom. The results are shown in Table 1. It may therefore be concluded that the electrostatic potential near the physical meaningful boundary between the core and valence regions in an atom is closely related to the Pauling electronegativity scale.[10]

It is well known that the Pauling electronegativity scales[10] are proportional to Mulliken electronegativities[15] which can be calculated from ionization potentials (IP) and electron affinities (EA) using $(IP + EA)/2$. It is also of interest to investigate the relation between the Pauling electronegativity scale[10] and the negative of the chemical potential. This will be reported in the near future.

Acknowledgement—The referee's suggestions were very helpful.

Division of Chemistry   KEN OHWADA
Japan Atomic Energy Research Institute
Tokai-mura, Naka-gun, Ibaraki-ken
Japan

Table 1. Calculated Pauling electronegativity scales[a,b]

H 2.1							He 5.2
Li 1.0 (1.0)	Be 1.5 (1.5)	B 2.0 (2.0)	C 2.5 (2.5)	N 3.0 (3.0)	O 3.5 (3.5)	F 4.0 (4.0)	Ne 4.5 (4.5)
Na 0.9 (0.8)	Mg 1.2 (1.2)	Al 1.5 (1.6)	Si 1.8 (1.9)	P 2.1 (2.3)	S 2.5 (2.7)	Cl 3.0 (3.1)	Ar 3.2 (3.5)
K 0.8 (0.7)	Ca 1.0 (1.0)	Sc 1.3 (1.4)	Ge 1.8 (1.7)	As 2.0 (2.1)	Se 2.4 (2.4)	Br 2.8 (2.7)	Kr 2.9 (3.0)
Rb 0.8 (0.6)	Sr 1.0 (0.9)	Y 1.2 (1.2)	Sn 1.8 (1.5)	Sb 1.9 (1.8)	Te 2.1 (2.2)	I 2.5 (2.5)	Xe 2.4 (2.8)
Cs 0.7 (0.6)	Ba 0.9 (0.8)	La-Lu 1.1-1.2 (1.1)	Pb 1.8 (1.4)	Bi 1.9 (1.7)	Po 2.0 (1.9)	At 2.2 (2.2)	Rn 2.1 (2.5)
Fr 0.7 (0.5)	Ra 0.9 (0.8)	Ac 1.1 (1.0)					

[a]Calculated values in parentheses.
[b]Electronegativity values for noble gas elements were taken from L. C. Allen and J. E. Huheey, *J. Inorg. Nucl. Chem.* 1980, **42**, 1523.

REFERENCES

[1]R. G. Parr, R. A. Donnelly, M. Levy and W. E. Palke, *J. Chem. Phys.* 1978, **68**, 3801.
[2]N. K. Ray, L. Samuels and R. G. Parr, *J. Chem. Phys.* 1979, **70**, 3680.
[3]L. J. Bartolotti, S. R. Gadre and R. G. Parr, *J. Am. Chem. Soc.* 1980, **102**, 2945.
[4]J. Chelikowsky and J. C. Phillips, *Phys. Rev.* 1978, **B17**, 2453.
[5]R. E. Watson and L. H. Bennett, *J. Phys. Chem. Solids* 1978, **39**, 1235.
[6]R. E. Watson and L. H. Bennett, *Phys. Rev.* 1978, **B18**, 6439.
[7]J. A. Alonso and L. A. Girifalco, *Phys. Rev.* 1979, **B19**, 3889.
[8]N. H. March, *J. Chem. Phys.* 1979, **71**, 1004.
[9]J. A. Alonso and L. A. Girifalco, *J. Chem. Phys.* 1980, **73**, 1313.
[10]L. Pauling, *The Nature of the Chemical Bond.* Cornell University Press, Ithaca, New York (1960).
[11]P. Hohenberg and W. Kohn, *Phys. Rev.* 1964, **B136**, 864.
[12]P. Politzer and R. G. Parr, *J. Chem. Phys.* 1976, **64**, 4634.
[13]P. Politzer, *J. Chem. Phys.* 1980, **72**, 3027.
[14]P. Politzer, *J. Chem. Phys.* 1980, **73**, 3264.
[15]R. S. Mulliken, *J. Chem. Phys.* 1934, **2**, 782; 1935, **3**, 573.

Temperature dependence of the Mössbauer spectrum and magnetic susceptibility [Fe(uridine)Cl₂]∞: Novel magnetic ordering of transition metal complexes based on nucleoside ligands

Abstract—The zero-field Mössbauer spectra and magnetic susceptibility of a polycrystalline sample of the polymeric material [Fe(uridine)Cl₂]ₓ have been measured in the temperature range 1.7–300 K. The compound exhibits two magnetic transitions. The isomer shift and quadrupole splitting indicate a distorted pseudo-octahedral FeCl₄O₂ chromophore resulting from condensation to a network structure via chloro and uridine ligand bridging.

The title compound was synthesized by the method of Goodgame[1] who characterized a number of first transition series complexes based on the simple nucleosides, uridine (Fig. 1) and thymidine. The empirical formula suggests either coordinative unsaturation, e.g. pseudo-tetrahedral monomer or association to polymer or network structure via chloro and/or nucleoside ligand bridging. As part of our continuing program of detailed studies of the cooperative magnetic behavior of novel high spin ferrous systems, we now present some new results for [Fe(uridine)Cl₂]ₓ.

MAGNETIC SUSCEPTIBILITY

We find a maximum in χ_M' vs T at 22.6 K suggesting 3-D antiferromagnetic (AF) ordering and a sharp minimum in χ_M' vs T at 12.5 K suggesting a spin reorientation transition (probably canting of the AF sublattices). These are most clearly seen in the corresponding minimum and maximum observed in the reciprocal susceptibility (Fig. 2c). The overall decrease in magnetic moment (5.24 μ_β 298 K to 1.55 μ_β at 1.73 K Fig. 2b) and high critical temperature (~ 23 K) indicate surprisingly strong anti-ferro-

$[Fe(uridine)Cl_2]_\infty$

Fig. 1. Proposed polymer structure for $[Fe(uridine)Cl_2]_\infty$.
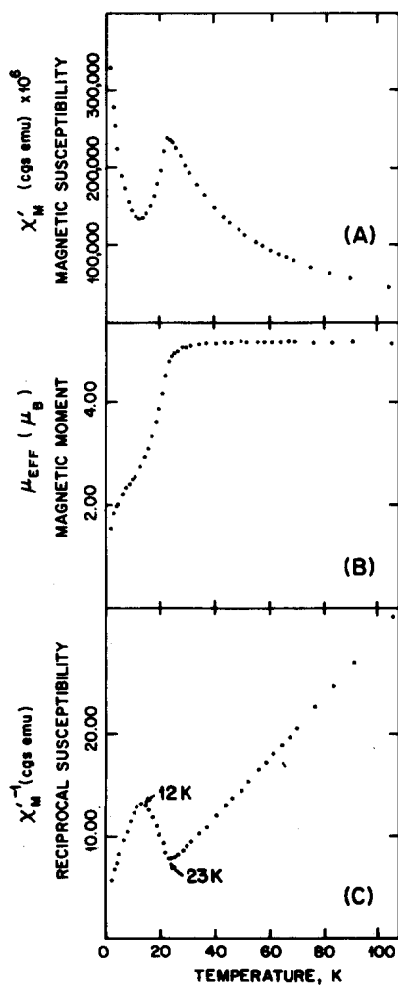
Fig. 2. Reciprocal susceptibility, magnetic moment and susceptibility vs temperature.
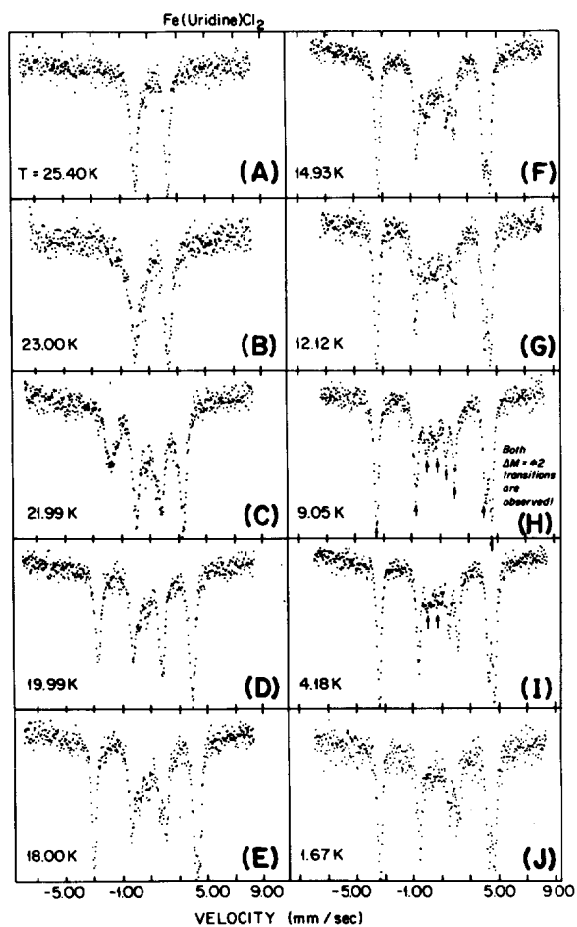
Fig. 3. Mössbauer spectra of $Fe(uridine)Cl_{2\infty}$ at some selected temperatures. Note the disappearance of the $\Delta M_I = \pm 2$ transitions ($\uparrow$).

magnetic exchange interactions ($\theta = -15.9$ K). As we do not know the details of molecular geometry, we cannot comment on the exact nature of these interactions at present. However, the foregoing magnetic transitions appear to be clearly mirrored in the temperature dependence of the zero-field Mössbauer spectra.

MÖSSBAUER SPECTRA

Between 2.2 and 23.0 K the Mössbauer spectrum shows fully resolved magnetic hyperfine splitting corresponding to one metal site and confirming cooperative 3D magnetic ordering, Fig. 3 (a–c). The magnetic splitting appears to reach saturation value at ~ 13 K, $H_n \approx 260$ kG, Fig. 3 (d–g). Below this temperature, what appear to be clearly resolved $\Delta m_I = \pm 2$ transitions steadily decrease in intensity and vanish. See Fig. 3(h–j). The combined effect of a quadrupole interaction and magnetic hyperfine splitting are obvious in the low temperature spectra. The fact that the normally forbidden $\Delta m_I = \pm 2$ transitions are observed at all implies substantial *lack of axial symmetry*, i.e. $\eta \neq 0$, for the electric field gradient at the ferrous sites.[2] This in turn suggests inequivalent metal halogen distances for the structure we have proposed in Fig. 1.

The isomer shift ($\delta_{Fe=0}$) and quadrupole splitting in the paramagnetic temperature range (T > 23.0 K) are 1.27 mms^{-1} (77 K) and 2.55 mms^{-1} respectively. These values are consistent with *six-coordinate* high-spin Fe^{2+} centers and a polymeric structure. In particular, the relatively large positive isomer shift is noteworthy. We believe that this indicates partial *oxygen* ligation in a chromophore such as $FeCl_4O_2$. In the absence of single crystal

X-ray diffractometry study, we can only speculate on the molecular structure of $Fe(uridine)Cl_2$. In their original spectroscopic characterization, Goodgame and Johns did not propose a specific structure. A plausible partial structure consistent with the results of this work and the previous characterization, i.e. six coordination of iron, a ligand to metal stoichiometry ratio of 1:1 and a condensed structure capable of sustaining cooperative, three dimensional magnetic order is proposed in Fig. 1. Primary coordination of the uridine via the carbonyl oxygen of C-4 (Fig. 1) is suggested by the IR studies of Goodgame.[1] Further *association* of chlorobridged "chains" might then occur by coordination of the ribose sugar hydroxyl groups of bridging uridine ligands. To test these ideas, we are initiating detailed studies of other members of the $M(uridine)\chi_2$ series.

CLAUDIO NICOLINI†
WILLIAM MICHAEL REIFF*

Department of Chemistry
Northeastern University
Boston
MA 02115
U.S.A.

---

†Present address: Center for Materials Research Mass. Institute of Technology, Cambridge, MA, U.S.A.
*Author to whom correspondence should be addressed.

REFERENCES

[1] M. Goodgame and K. W. Johns, *J.C.S. Dalton*, 1978, 1294.
[2] N. N. Greenwood and T. C. Gibb, *Mössbauer Spectroscopy*, pp. 56, 60 and 70. Chapman and Hall, London, 1971.

BROMINE NQR STUDY OF STRUCTURE AND MOLECULAR TORSIONAL MOTION IN $N_4P_4Br_8$ AND $N_3P_3Br_6$

K. R. SRIDHARAN and J. RAMAKRISHNA*

Department of Physics, Indian Institute of Science, Bangalore 12, India

Abstract—The bromine NQR spectrum of tetrameric bromocyclophosphazene, $N_4P_4Br_8$, has been studied in the temperature range from 77 to 300 K. The negative temperature coefficients of the resonance frequencies have been analysed using Bayer–Kushida–Brown equations. Torsional modes in the frequency range 10–15 cm^{-1} are shown to characterise the observed motional averaging and are only slightly temperature dependent. The multiplicity and relative intensities of resonances in the trimer, $N_3P_3Br_6$, have been correlated with the known electron density distribution. The results for the bromo-derivatives are compared with those reported for the corresponding chloro-derivatives.

The compounds under investigation belong to a family of inorganic ring systems called cyclophosphazenes and have the representative structures shown in Fig. 1. There have been several studies of chlorine NQR of cyclophosphazene derivatives which have demonstrated the potential of the quadrupole resonance technique in elucidating the structural features of these compounds in the solid state.

The first observation of Br NQR in cyclophosphazenes was reported by the authors[1] earlier wherein we obtained the resonance frequencies at 77 K and at room temperature for $N_4P_4Br_8$ and $N_3P_3Br_6$. In the present paper, we discuss (i) the temperature dependence of Br NQR in $N_4P_4Br_8$ in the temperature range from 77 to 300 K and (ii) the correlation of electron charge density values at the halogen sites with the Br NQR spectrum in $N_3P_3Br_6$.

The samples were prepared by the methods described in the literature. A home-made (push–pull, tuned transmission-line) SRO spectrometer (140–380 MHz) was used to make the measurements. A 2-turn sample coil (14 SWG/1 cm dia.) was found adequate. A liquid nitrogen cryostat facilitated low-temperature studies and the sample temperature was measured with a copper–constantan thermocouple to an accuracy of ±0.5 K.

2. RESULTS AND DISCUSSION

2.1 *Temperature dependence of* Br NQR *in* $N_4P_4Br_8$

The spectrum consists of two equally intense signals in the range 195–200 MHz and two more in the range 235–245 MHz. The two pairs belong to the two isotopes of Bromine, the high frequency pair belonging to ^{79}Br in view of its larger quadrupole moment. The presence of two, equally intense signals in this compound is consistent with the presence of two inequivalent but equally populated Br sites in the crystal unit cell.[2] The ^{79}Br signals have been studied as a function of temperature in the range 77–298 K. The frequencies decrease with increase in temperature and are plotted in Fig. 2. A small discontinuity in the slope, $(d\nu/dT)$, of the curves was noted at ~230 K for both the signals. No discontinuity in the frequency has been observed. This observation might represent a small structural transition of the II order type.

It is well known that the temperature dependence of the nuclear quadrupole interaction in molecular solids is mainly due to the averaging of the electric field gradient (EFG) by the molecular librational (torsional) modes. Bayer's equation[3] for the temperature dependence of NQR frequency as modified by Tatsuzaki *et al.*[4] is given below:

$$\nu_Q(T) = \nu_0 \left[1 - \frac{3h}{8\pi^2 c} \sum_i \frac{\sin^2 \alpha_i}{A_i f_i} \left(\frac{1}{2} + \frac{1}{e^{(hcf_i/kT)} - 1} \right) \right].$$

Here, ν_0 is the NQR frequency for the stationary molecule, f_i is the frequency (cm^{-1}) of the ith torsional mode, A_i is the corresponding moment of inertia, α_i is the angle between the axis of the ith torsional mode and the

(a)

(b)
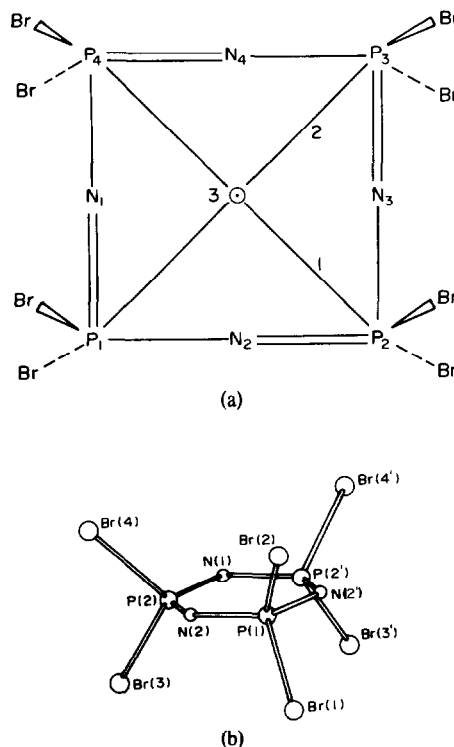
Fig. 1. Representative structure of (a) $N_4P_4Br_8$ and (b) $N_3P_3Br_6$.

*Author to whom correspondence should be addressed.
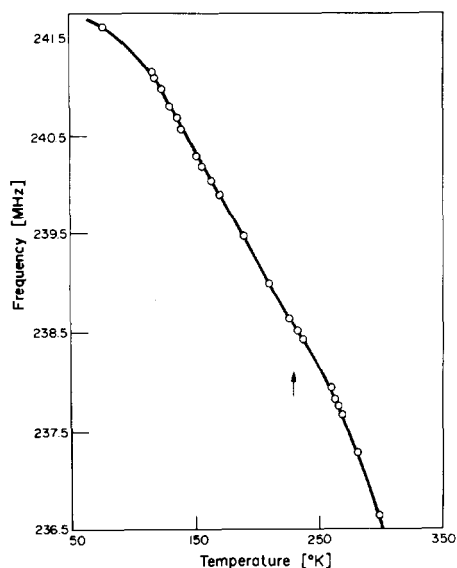
Fig. 2(a). Temperature dependence of ^{79}Br NQR frequency of
Line I in N$_4$P$_4$Br$_8$.
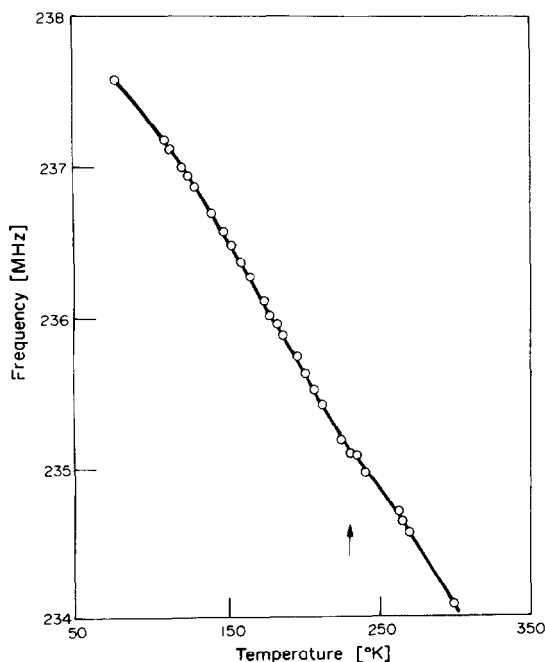
Fig. 2(b). Temperature dependence of ^{79}Br NQR frequency of
Line II in N$_4$P$_4$Br$_8$.

principal z axis of the EFG tensor, and T is the absolute
temperature.

The molecule is non-planar. The three axes that are
indicated in Fig. 1(a) could be considered as the principal
axes of the moment of inertia tensor. A three-mode
analysis would be ideal but the numerical solution
becomes complicated; a two-mode analysis has therefore
been carried out. The axes 1 and 2 have been considered
in view of the correspondingly larger values of the
weighting factor, $(\sin^2 \alpha_i)/A_i$. The P–Br bond direction

has been considered as the principal z-axis of the EFG at
the corresponding bromine.

The torsional frequencies, f_1 and f_2, have been evalu-
ated using a procedure similar to the one used by Vijaya
and Ramakrishna.[5] The frequencies are found to fall in
the very low range of 10–15 cm^{-1} and exhibit a rather
small temperature dependence (Table 1).

The temperature coefficients of NQR frequencies in
the bromo-compounds are smaller than those observed in
chloro-cyclophosphazene derivatives.[6] In this context,
the close Br...Br intermolecular contacts of less than
the sum of van der Waals' radii, and P–Br...Br linear
arrays observed in the unit cell packing, are relevant.
This closer packing implies smaller thermal amplitudes
and would explain the smaller temperature coefficient of
the Br NQR frequency.

Regarding the temperature dependence of torsional
frequencies (due to volume expansion), Brown's linear
equation

$$f_i = f_i^0(1 - g_i t)$$

is used.[7] Brown expressed the average temperature
coefficient $\langle g \rangle$ in terms of the first and second derivatives
of ν_Q vs t. In order to evaluate these derivatives and to
compare different descriptions of the functional depen-
dence of ν_Q vs T, the following equations were con-
sidered for least-squares fitting:

(i) $\nu_Q = A' + B'(T - T_0) + C'(T - T_0)^2$ Brown's
                                                   "parabolic"
                                                   equation

(ii) $\nu_Q = A + BT + CT^2 + DT^3 + ET^4$

                                                   a fourth-order
                                                   polynomial

(iii) $\nu_Q = a + bT + c/T$ Kushida's high
                                                   temperature
                                                   expression.

                                                            (8)

The parabolic and fourth-order equations are found to
provide equally good fits to the experimental curves as
shown by the mean square deviations given in Table 2.
The high temperature expression of Kushida provides a
poor fit. Since the quadritic equation can be obtained
from Kushida's equation[8] by assuming a linear tem-
perature dependence of the torsional frequencies, our
results show that the volume expansion effects are not

Table 1. Torsional frequencies about the axes 1 and
2 in N$_4$P$_4$Br$_8$ calculated from data of Line I†

Temperature (K)	Torsional frequency (cm^{-1})	
	f_1	f_2
77	13	13
109.5	12	13
128	12	12
158	11	12
199.5	11	11
205.5	11	11

†Similar values have been obtained from data of
Line II.

Table 2. Least-squares fit parameters and $\langle g \rangle$ from the data for Line I in $N_4P_4Br_8$†

Equation§	Parameters	
4th-order polynomial	ν_0	242.580
	$\langle g \rangle$	0.0008
	250 K	
	Δ	5874‡
KBB–Brown	$\langle g \rangle$	0.0005
	250 K	
	Δ	4633‡
HTE	Δ	163178‡

†Similar results have been obtained from data for Line II.

‡Note that the linewidths are themselves high, ~35 KHz.

§4th-order polynomial:

$$\nu_Q = A + BT + CT^2DT^3 + ET^4$$

KBB Brown equation:

$$\nu_Q = A' + B'(T - T_0) + C'(T - T_0)^2; \quad T_0 = 180 \text{ K}$$

HTE (Kushida's):

$$\nu_Q = a + bT + c/T; \quad \nu_0 = \nu_Q(T = 0 \text{ K}) \text{ MHz};$$

$$\langle g \rangle \text{ in units of } K^{-1};$$

$$\Delta = \text{mean square deviation in } (KHz)^2.$$

negligible, similar to our observations in other cyclophosphazenes.[9]

These results for $N_4P_4Br_8$ can be compared with the ^{35}Cl NQR results for $N_4P_4Cl_8$[10,11]. The spectrum of the bromo-compound is similar to that of the K-form of $N_4P_4Cl_8$. Secondly, X-ray investigations[2] of $N_4P_4Br_8$ at 120°C reveal that there is no phase transition to any other structure, unlike the chloro-derivative which undergoes a metastable-to-stable phase transition at 63°C[11]. Thirdly, we observe a divergence of the two ^{79}Br frequencies as temperature is lowered to 77 K unlike the behaviour of the isostructural K-form of $N_4P_4Cl_8$. This shows that the two Br sites are distinct even in the stationary molecule (in the absence of thermal motions).

2.2 Frequency assignment in $N_3P_3Br_6$

Br NQR signals in $N_3P_3Br_6$ could be observed only at 77 K using phase sensitive detection. Corresponding to the ^{81}Br isotope there are two signals, at 201.319 MHz and 202.415 MHz, with relative intensities 1:2 (respectively) and two more signals near 198 MHz. The frequencies of the latter two signals could not be fixed more accurately because of overlapping sets of sidebands of the SRO but are within 200 KHz of each other and they also differ in their intensities by 2:1 (as ν_Q increases). A similar pattern of two well-separated signals, at 241.035 and 242.290 MHz, and two other signals near 236.5 MHz, has been observed for ^{79}Br.

The crystal structure of this compound has been investigated by several groups.[12–14] The crystal is orthorhombic, of space group P_{cmn}, containing 4 molecules in the unit cell. The molecule is slightly non-planar and the asymmetric unit consists of two $NPBr_2$ groups (Fig. 1). Thus, there are four inequivalent Br sites. The occupancies of these four sites in the unit cell are as 4:4:8:8 from Br(1) to Br(4) in the crystal structure notation.

Table 3. Assignment of ^{81}Br NQR in $N_3P_3Br_6$

Site	Electron density e.Å^{-3}	Population in Unit cell	NQR frequency (MHz)	Observed relative intensity
Br(3)	28.71	8	202.415	2
Br(2)	29.91	4	201.319	1
Br(4)	32.57	8	~198.2	1
Br(1)	32.71	4	~198	2

The observation of four signals in the ^{81}Br (as well as ^{79}Br) spectrum is consistent with the number of inequivalent Br sites. Secondly, the result that the signals are not all of the same intensity is understandable since the site populations are different. However, as all the P–Br bond lengths are identical within experimental error,[14] no site assignment of frequencies is possible on the basis of bond lengths.

We have tried to make an assignment of NQR frequencies based on site electron density maxima available from the crystal structure (F_c differential synthesis) analysis of Giglio and Puliti.[12] It is known that in molecular solids the NQR frequency is directly related to the electron distribution in the vicinity of the quadrupolar nucleus.[15] From simple quantum mechanical treatments of halogen bonding and NQR frequencies, it is known that the electric field gradient (i.e. NQR frequency) is decided by the p-electron density. Furthermore, we ascribe the differences in the electron density at the four inequivalent Br sites to differing σ bond populations of the various halogens, since the bond lengths point to negligible π character of P–X bonds in cyclophosphazenes. As it is known that the lower the σ bond population the higher is the NQR frequency,[15] we arrive at an assignment of the spectrum as detailed in Table 3.

The observation of a well-separated pair of signals of intensity ratio 2:1 (as ν decreases) is in very good agreement with the expected result. The observation of a close-lying doublet at the lower frequency of 198 MHz is in conformity with the nearly *equal* and relatively *higher* electron densities of Br(4) and Br(1). However, individual site assignment of this doublet cannot be reliably made since the two electron densities differ by an amount much less than the standard deviation error ($\sigma(\rho_0) = 0.40 \text{ e A}^{-3}$) quated in the X-ray work.

REFERENCES

[1] K. R. Sridharan, J. Ramakrishna, S. S. Krishnamurthy and M. N. Sudheendra Rao, *Current Sci.* 1978, **47**, 938.
[2] H. Zoer and A. J. Wagner, *Acta Cryst.* 1972, **B28**, 252.
[3] H. Bayer, *Z. Physik* 1951, **130**, 227.
[4] I. Tatsuzaki and Y. Yokozawa, *J. Phys. Soc., Japan* 1957, **12**, 802.
[5] M. S. Vijaya and J. Ramakrishna, *Molec. Phys.* 1970, **19**, 131.
[6] K. R. Sridharan, Ph.D. Thesis. Indian Institute of Science, Bangalore (1979).
[7] R. J. C. Brown, *J. Chem. Phys.* 1960, **32**, 116.

[8]T. Kushida, G. Benedek and N. Bloembergen, *Phys. Rev.* 1956, **104**, 1364.

[9]K. R. Sridharan, J. Ramakrishna, K. Ramachandran and S. S. Krishnamurthy, *J. Molec. Structure* 1980, **69**, 105.

[10]M. A. Whitehead, *Can. J. Chem.* 1964, **42**, 1212.

[11]M. Dixon, H. D. B. Jenkins, J. A. S. Smith and D. A. Tong, *Trans. Faraday Soc.* 1967, **63**, 2852.

[12]E. Giglio and R. Puliti, *Acta Cryst.* 1967, **22**, 304.

[13]P. De Santis, E. Giglio and A. Pipamonti, *J. Inorg. Nucl. Chem.* 1962, **24**, 469.

[14]H. Zoer and A. J. Wagner, *Acta Cryst.* 1970, **B26**, 1812.

[15]C. H. Townes and B. P. Dailey, *J. Chem. Phys.* 1949, **17**, 782.

REACTIONS OF NICKEL IONS WITH NITROSO-NAPHTHOLS—IV FORMATION KINETICS OF NICKEL (1-NITROSO-2-NAPHTHOL-6-SULPHONATE)

S. A. BAJUE, T. P. DASGUPTA AND G. C. LALOR*

Department of Chemistry, University of the West Indies, Kingston 7, Jamacia

Abstract—The formation kinetics of Ni(1-nitroso-2-naphthol-6-sulphonate) are reported in the temperature range 20–30°C at an ionic strength of 0.1 M. Both the acidic (HL^-) and basic (L^{2-}) forms of the ligand react with nickel ions, the latter at a much higher rate. The rate constants are similar in magnitude to those observed with 1-nitroso-2-naphthol-3, 6-disulphonate and variation of rate constant with respect to temperature is reproduced by the equation

$$k_b = 4.01 \times 10^{13}(1\ mol^{-1}\ sec^{-1}) \exp(-12,900/RT).$$

Ortho-nitroso-naphthols are powerful complexing agents.[1] The parent compound 1-nitroso-2-naphthol and two sulphonated derivatives are well known[2] for their chelating properties.

These ligands react with Ni(II) ions in aqueous solution at rates which are convenient for stopped-flow spectrophotometry. In previous studies[3-5] it was found that the dissociation rates of certain nickel nitroso-naphthol complexes depend on the relative positions of the -NO and -OH groups and on the number and position of sulphonate group substituents. Also the formation rate of nickel (1-nitroso-2-naphthol-3, 6-disulphonate), (NiNRS), shows an unusual pH dependence in that the rate, instead of approaching a limiting value at low pH decreases as the pH is decreased.[8] In the dissociation of this complex there is also an expected and not fully explained lack of dependence of the rate constant on ionic strength. In order to gain further information about these reactions we studied the formation rate of Ni(1-nitroso-2-naphthol-6-sulphonate), (NiL), over the temperature range 20–30° over a range of acidities and at ionic strength 0.1 M.

EXPERIMENTAL

Reagents
Freshly prepared glass-distilled water was used throughout.

*Author to whom correspondence should be addressed.

The ligand was prepared by nitrosation of sodium 2-naphthol-6-sulphonate at 0°C. The yellow sodium salt which formed was recrystallized several times from water and air-dried. Solutions of nickel(II) nitrate were prepared and analysed as described previously.[5] Ionic strengths were maintained constant by use of
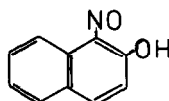
1-nitroso-2-naphthol
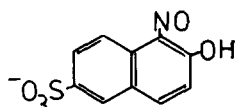
1-nitroso-2-naphthol-6-sulphonate

1-nitroso-2-naphthol-3,6-disulphonate

lithium nitrate and 2,6-lutidine/nitric acid mixtures were used for pH control.

Kinetics
Kinetic measurements were carried out as described previously.[3] After each run the pH of the reaction mixture was measured on an Orion 801A ion analyser fitted with a combination glass electrode. Temperature control was better than ±0.2°.

RESULTS AND DISCUSSION
The mechanism of the reaction can be written as

$$Ni^{2+} + HL^- \rightleftharpoons NiL + H^+ \qquad (1)$$

$$Ni^{2+} + L^{2-} \rightleftharpoons NiL \qquad (2)$$

where HL^- and L^{2-} represent the acidic and basic forms of the ligand respectively. The rate equation for the formation of NiL is then

$$\frac{1}{[Ni^{2+}]} \frac{d[NiL]}{dt} = k_{obs}[L_T] \qquad (3)$$

$$= k_a[HL^-] + k_b[L^{2-}] \qquad (3)$$

L_T is the total concentration of ligand and k_b and k_a are the formation rate constants for the reactions of L^{2-} and HL^- respectively. Equation (4) is equivalent to

$$\frac{k'}{[Ni^{2+}]}\left(1+\frac{K}{\{H^+\}}\right) = k_a + k_b \frac{D}{\{H^+\}} \quad (5)$$

where k' and K are the pseudo- first order rate constant and the dissociation constant respectively of the ligand. Hydrogen ion activities rather than concentration are used since K is a "mixed" constant.

The measured pK values at 0.1 M ionic strength are: 15°C, 6.79; 25°C, 7.06. These values were used to obtain values of K at 20 and 30° to match two of the temperatures used in the kinetics work by use of eqn (6):

$$K = 1.494 \times 10^{-15} \exp\frac{(10594)}{(RT)}. \quad (6)$$

The values of K which were used are shown in Table 1. Table 2 contains the kinetic data for the formation reaction at three temperatures.

The data in Table 2 were fitted by the linear least squares method to eqn (5) using the respective pKa values in Table 1. The results are shown in eqns (7)–(9):

At 20°C; $k_{obs}(1 + K/\{H^+\}) = 2.97(1.8) \times 10^2$
$$+ 9.95(0.18) \times 10^3 \frac{K}{\{H^+\}} \quad (7)$$

Table 1. pK$_a$ values of 1-nitroso-2-naphthol-6-sulphonate at various temperatures, I = 0.10 M

Temp. °C	pK	pK (kinetics)
20	6.93	7.0
25	7.06	7.16
30	7.19	7.43

Table 2. Kinetics of formation of Ni(1-nitroso-2-naphthol-6-sulphonate) as a function of pH. Ionic strength = 0.10 M. $[Ni^{2+}] = 5 \times 10^{-3}$ M

pH	k'/s^{-1}	$10^7\{H^+\}$	$\frac{K}{\{H^+\}}$	$\frac{k'}{[Ni^{2+}]}\left(1+\frac{k}{\{H^+\}}\right)\times 10^3$	Temp/°C
4.98	2.42	105	0.011	0.49	20
5.61	5.17	24.5	0.048	1.08	"
6.34	9.66	4.57	0.258	2.43	"
6.71	19.4	1.95	0.605	6.23	"
6.86	23.0	1.38	0.855	8.53	"
6.95	27.6	1.12	1.05	11.3	"
6.97	26.5	1.07	1.10	11.1	"
7.12	30.9	0.759	1.55	15.8	"
7.19	32.5	0.646	1.83	18.4	"
5.51	11.8	30.9	0.028	2.43	25
5.92	14.7	12.0	0.073	3.15	"
6.33	18.6	4.68	0.186	4.41	"
6.68	29.0	2.09	0.417	8.22	"
6.83	35.6	1.48	0.589	11.3	"
6.85	35.4	1.41	0.618	11.5	"
6.91	38.1	1.23	0.708	13.0	"
7.04	42.9	0.912	0.955	16.8	"
6.22	27.9	6.02	0.108	6.18	30
6.58	36.9	2.63	0.246	9.20	"
6.83	42.9	1.48	0.438	12.3	"
6.96	50.2	1.10	0.589	16.0	"
7.04	53.0	0.912	0.710	18.1	"
7.12	56.0	0.759	0.854	20.8	"
7.20	58.8	0.631	1.03	23.8	"
7.26	67.8	0.550	1.18	29.5	"

* The K values at different temperatures are calculated from the experimental pK values given in Table 1.

Table 3. Formatation rate constant (k_b) for Ni and NiNRS⁻

Temp/°C	NiL[a] $k_b/10^4$ M^{-1} s^{-1}	NiNRS⁻[b] $k_b/10^4$ M^{-1} s^{-1}
15	-	1.17
20	0.99	1.54
25	1.57	1.96
30	2.06	-

(a) I, 0.10 M   (b) I, 0.50 M (Ref.3)

At 20°C; $k_{obs}(1 + K/\{H^+\}) = 1.84(0.12) \times 10^3$

$$+ 1.57(0.023) \times 10^4 \left\{\frac{K}{\{H^+\}}\right\}. \quad (8)$$

At 30°C; $k_{obs}(1 + K/\{H^+\}) = 3.70(0.62) \times 10^3$

$$+ 2.06(0.08) \times 10^4 \left\{\frac{K}{\{H^+\}}\right\}. \quad (9)$$

The terms in brackets are standard deviations.

Because $k_a \ll k_b$ the intercepts cannot be regarded as accurate. The values are of the right order of magnitude however, since a combination of, for example, the value of k_a at 25° with the dissociation rate of 2240 l m^{-1} sec^{-1} obtained at the same ionic strength and temperature[4] gives an equilibrium constant for reaction (1) of 0.78 is reasonable agreement[6] with the measured value of 0.32.

The best fit to eqn (5) was also obtained by varying K to produce a minimum sum of squares of the deviations between k_{obs} and k_{calc}. This yielded the value of pK shown in the final column of Table 1 and provides some additional justification for the mechanism accepted.

The slopes of the least squares lines give reasonably accurate values at k_b. These values, which are summarized in Table 3, give, when fitted to an Arrhenius type equation, the following temperature variation:

$$k_b = 4.01 \times 10^{13} \exp -(12,900/RT) \quad (10)$$

Also shown in Table 3 are some formation rate constants for NiNRS⁻ and these are seen to be similar to those for NiL, although the conditions of measurement were somewhat different. The 3-sulphonate substituent therefore has no marked effect on the formation rates in the pH range available for experimental study. The k_b values reported here are also of the same order of magnitude observed for a variety of ligands, both monodentate and bidentate.[7]

The features indicate that the ring closure is not rate determining and that the removal of water from the coordinaton sphere of $Ni(H_2O)_6^{2+}$ is the controlling process.

REFERENCES

1. Spectrophotometric Data for Colorimetric Analysis IUPAC, 105 Butterworths, London (1963).
2. H. Saarinen, Ann. Acad. Sci. Fennical AII 1973, 173.
3. G. C. Lalor, Inorg. Chim. Acta 1975, 14, 179.
4. T. P. Dasgupta and G. C. Lalor, J. Ind. Chem. Soc. 1977, 54, 74.
5. S. A. Bajue, T. P. Dasgupta and G. C. Lalor, Rev. Latinoamer. Quim. 1979, 10, 40.
6. The values are considered to be in reasonable agreement since the value 0.78 has been calculated purely from kinetic data and hence, is subjected to a considerable error.
7. R. G. Wilkins, Acc. Chem. Res. 1970, 3, 408.
8. T. P. Dasgupta and G. C. Lalor, unpublished results.

BINUCLEAR TUNGSTEN(V) OXO-COMPLEXES
WITH 1,1-DITHIOLATE LIGANDS

R. LOZANO,* E. ALARCÓN, A. L. DOADRIO and A. DOADRIO

Departamento de Química Inorgánica, Facultad de Farmacia, Universidad Complutense de Madrid, Madrid (3),
Spain

Abstract—In this paper we report the synthesis of some new oxo and sulphido bridged tungsten(V) complexes with
N-ethylanilindithiocarbamate and N,N-methylcyclohexyldithiocarbamate as ligands. These complexes have been
characterised by analytical, magnetochemical and spectral methods. The results permit us to assign the formulae:
$W_2O_3(LL)_4$, $W_2O_4(LL)_2$, $W_2O_2S_2(LL)_2$ and $W_2O_3S(LL)_2$. The low magnetic moments observed in these complexes,
are due either to an interaction through the bridging atoms or to a direct spin-spin interaction. IR and
electronic absorption spectra of these complexes are sensitive to substitution of sulphur atoms into the bridge
system. The systematic changes upon bridge modification are useful in characterizing the compounds and in
clarifying assignments of W–O and W–S bridge stretching frequencies. The results are discussed on the basis of
structural information available for tungsten complexes.

In recent years, considerable interest has grown in sulphur-containing compounds of molybdenum with respect to the biochemical implications of their redox behaviour.[1] Synthesis and structure of mononuclear and binuclear molybdenum complexes were previously reported.[2–4]

Tungsten often presents very close properties to molybdenum, but such binuclear compounds are not so numerous in tungsten chemistry.

The object of the present study, has been to obtain binuclear complexes of tungsten(V) with N-ethyl-anilindithiocarbamate and N,N-methylcyclohexyl-dithiocarbamate as ligands

In this paper, we describe the isolation and characterization of four different dimeric complexes of tungsten(V).

(a) Tungsten(V) oxo-complexes with a monoxo bridge—$W_2O_3(LL)_4$.

(b) Tungsten(V) oxo-complexes with a dioxo bridge—$W_2O_2(LL)_2$.

(c) Tungsten(V) oxo-complexes with a disulphido bridge—$W_2O_2S_2(LL)_2$.

(d) Tungsten(V) oxo-complexes with oxo-sulphido bridge—$W_2O_3S(LL)_2$.

We have proved too that the 4 kinds of binuclear tungsten(V) complexes that have been obtained here, have the same structure and characteristics as the dimeric complexes of molybdenum(V) obtained by us, showing that tungsten and molybdenum present a very similar behaviour.

EXPERIMENTAL

(a) *Materials*

$Na_2WO_4 \cdot 2H_2O$ was Merck commercial product used as supplied. Sodium N-ethylanilindithiocarbamate and sodium N,N-methyl-cyclohexyldithiocarbamate, were prepared by the reaction of sodium hydroxide with carbon disulphide and N-ethylaniline in water or N,N-methylcyclohexylamine in alcohol respectively, and were recrystallized from alcohol. The solvents used to prepare the complexes were Carlo Erba or Merck; the solutions for absorption spectra were prepared with dimethylsulphoxide (DMSO) and CH_2Cl_2 spectral grade Merck–Uvasol.

(b) *Analytical procedures*

Elemental analyses were performed by "Instituto de Química Orgánica" C.S.I.C., Madrid, Spain. Tungsten was determined by atomic absorption spectrophotometry, with a Perkin–Elmer model 430 atomic absorption spectrophotometer after the complex had been decomposed by heating with concentrated sodium hydroxide.

Analytical data are given in Table 1.

(c) *Methods*

Magnetic susceptibility was determined by the Gouy method at room temperature in a Mettler H-51 A.R. balance and a type C Newport electromagnet. Molar susceptibilities given are corrected for the diamagnetism of the constituent atoms.

The magnetic moments were calculated according to the formula $\mu = 2.84(\chi_M \cdot T)^{0.5}$ B.M., where χ_M is the corrected molar susceptibility.[5]

Table 2 shows the results obtained.

The IR spectra have been registered on a Perkin–Elmer recording spectrophotometer model 283. The samples were run as KBr pellets. Important IR absorption peaks for the complexes prepared in this study are listed in Table 3.

The visible-near UV spectra of the compounds, were measured in the range 200–900 nm on a Perkin–Elmer recording spectrophotometer model 554, over dissolutions of the complexes in DMSO and CH_2Cl_2. We have registered the same peaks for both solvents, however we give in Table 4 the results obtained in DMSO as solvent, because all the complexes have a limited solubility in CH_2Cl_2.

(d) *Preparation of the complexes*

All the compounds prepared in this study were susceptible to air oxidation, therefore all manipulations and reactions were carried out in a nitrogen atmosphere dry box or on a vacuum line.

$W_2O_3(S_2CNC_8H_{10})_4$. $Na_2WO_4 \cdot 2H_2O$ (1.65 g) was dissolved in water (30 cm^3) and it was treated with concentrated sodium hydroxide to avoid the polymerization. This solution was added to a solution of sodium N-ethylanilindithiocarbamate (2.35 g) in water (35 cm^3) with vigorous stirring. The resulting yellow solution, was added to a solution (freshly prepared) of sodium dithionite (0.5 g) in water (20 cm^3). Lastly, drop by drop, glacial acetic acid was added till reaching pH = 5. There was an immediate dark-violet precipitate. The suspension was set aside for 1 hr and then filtered *in vacuo*. The residue was washed with a boiling water–ethanol mixture (50%) and dried over P_2O_5. Yield: 52%.

$W_2O_4(S_2CNC_8H_{10})_2$. A solution of $Na_2WO_4 \cdot 2H_2O$ (3.30 g) in water (40 cm^3) was treated with concentrated sodium hydroxide. The resulting solution was added to a solution of sodium N-ethylanilindithiocarbamate (2.35 g) in water (35 cm^3). A solution of sodium dithionite (1.0 g) in water (20 cm^3) was prepared and this

---

*Author to whom correspondence should be addressed.

Table 1. Elemental analyses, (%) of tungsten(V) oxo-complexes

	CALCULATED					FOUND				
	C	H	N	S	W	C	H	N	S	W
$W_2O_3(S_2CNC_8H_{10})_4$	36.00	3.33	4.66	21.33	30.66	36.09	3.25	4.55	21.43	30.74
$W_2O_3(S_2CNC_7H_{14})_4$	32.87	4.79	4.79	21.91	31.50	32.80	4.56	4.62	22.13	31.12
$W_2O_4(S_2CNC_8H_{10})_2$	26.21	2.42	3.39	15.53	44.66	26.10	2.41	3.42	15.59	44.56
$W_2O_4(S_2CNC_7H_{14})_2$	23.76	3.46	3.46	15.84	45.54	23.70	3.41	3.54	15.90	45.61
$W_2O_2S_2(S_2CNC_8H_{10})_2$	25.23	2.33	3.27	22.42	42.99	25.45	2.30	3.33	22.16	43.04
$W_2O_2S_2(S_2CNC_7H_{14})_2$	22.85	3.33	3.33	22.85	43.80	22.99	3.39	3.42	22.62	43.89
$W_2O_3S(S_2CNC_8H_{10})_2$	25.71	2.38	3.33	19.04	43.80	25.62	2.44	3.61	19.12	43.54
$W_2O_3S(S_2CNC_7H_{14})_2$	23.30	3.39	3.39	19.41	44.66	23.44	3.29	3.35	19.25	44.75

Table 2. Magnetic properties of tungsten(V) oxo-complexes

	$\chi\,(10^6\,cgs)$	$\chi_M\,(10^6\,cgs)$	$\chi_M'\,(10^6\,cgs)$ *	$\mu\,(B.M.)$
$W_2O_3(S_2CNC_8H_{10})_4$	-0.149166	-179	283	0.58
$W_2O_3(S_2CNC_7H_{14})_4$	-0.249144	-291	255	0.55
$W_2O_4(S_2CNC_8H_{10})_2$	-0.224514	-185	52	0.25
$W_2O_4(S_2CNC_7H_{14})_2$	-0.336634	-272	7	0.09
$W_2O_2S_2(S_2CNC_8H_{10})_2$	-0.296729	-254	3	0.06
$W_2O_2S_2(S_2CNC_7H_{14})_2$	-0.355952	-299	0.1	0.01
$W_2O_3S(S_2CNC_8H_{10})_2$	-0.290476	-244	3	0.06
$W_2O_3S(S_2CNC_7H_{14})_2$	-0.349514	-288	1	0.03

Temperature = 294°K

* The corrected χ_M' values of these dimers have been divided by two to give the χ_M' value/mole W.

solution was added to the previous one, and the resulting solution takes a brown color. Dilute hydrochloric acid was added dropwise until precipitation of the complex was complete. The precipitate was filtered by suction and the violet residue was washed with hot water and absolute ethanol, and dried *in vacuo* over P_2O_5. Yield: 70%.

$W_2O_2S_2(S_2CNC_8H_{10})_2$. 3.30 g of $Na_2WO_42H_2O$ was dissolved in water (40 cm³) and to this was added 10 ml of concentrated sodium hydroxide. The resulting solution, was treated with sodium N-ethylanilindithiocarbamate (2.35 g) in water (35 cm³). Hydrogen sulphide was passed through the resulting solution with simultaneous cooling in freezing mixture for 30 min. The solution gradually takes a brown color. Drop by drop, glacial acetic acid was added till reaching pH = 6, and a brown solid precipitates. The suspension was heated, cooled and filtered. The brown residue was washed with hot water and dried *in vacuo* over P_2O_5. Yield: 75%.

$W_2O_3S(S_2CNC_8H_{10})_2$. A solution of $Na_2WO_4 \cdot 2H_2O$ (3.30 g) in 2M sodium hydroxide (40 cm³), was treated with dilute hydrochloric acid till reaching pH = 6. Hydrogen sulphide was bubbled slowly through the resulting solution for 1 hr. The solution gradually takes a reddish brown color, and it was added to a solution of sodium N-ethylanilindithiocarbamate (2.35 g) in water (35 cm³). Lastly, glacial acetic acid was added dropwise until the precipitation of the complex was complete. The precipitate was filtered *in vacuo* and the brown residue was washed with hot water and dried over P_2O_5. Yield: 72%.

A similar preparation was carried out for the complexes with N,N-methylcyclohexyldithiocarbamate as ligand.

RESULTS AND DISCUSSION
Preparation of complexes
The analytical data shown in Table 1 and the spectroscopic data to be presented later, are consistent with the formation of four series of μ-oxo, di-μ-oxo, μ-oxo-

μ-sulphido and di-μ-sulphido tungsten(V) complexes. The preparative procedures described in the Experimental Section are simple.

If we start from $Na_2WO_4 \cdot 2H_2O$ solution and make it react with a solution of the ligand in water, and reduce W(VI) to W(V) with sodium dithionite, such reactions precipitate complexes of dimeric structure in an acid medium.

If we effect the precipitation at pH = 5, with acetic acid, the complexes obtained present a monoxo bridge, the thoichiometry is 2:1 and the tungsten is six-coordinated. The formula which most closely fits the analyses is $W_2O_3(LL)_4$. We suggest that the structure for these complexes should be as follows:

However, if we precipitate the complexes at pH = 2, the stoichiometry of the compounds is 1:1, the tungsten is five-coordinated and these complexes present a dioxo bridge. The formula which we assign to these complexes is $W_2O_4(LL)_2$ and we suggest that the compounds
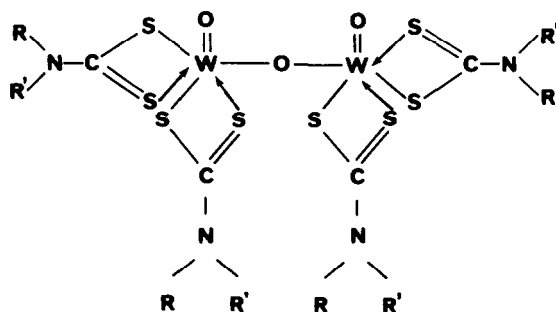
Table 3. IR absorption maxima, in cm^{-1}, of tungsten(V) oxo-complexes

Compound	ν C-N	ν C-S	ν_s W=O	ν_a W-O$_b$	ν_s W-O$_b$	ν_a W-S$_b$	ν_s W-S$_b$	ν W-S
W$_2$O$_3$(S$_2$CNC$_8$H$_{10}$)$_4$	1523	1119	946	810	440	---	---	337
W$_2$O$_3$(S$_2$CNC$_7$H$_{14}$)$_4$	1517	1138	938	821	450	---	---	342
W$_2$O$_4$(S$_2$CNC$_8$H$_{10}$)$_2$	1525	1120	950	805	430	---	---	340
W$_2$O$_4$(S$_2$CNC$_7$H$_{14}$)$_2$	1515	1134	940	819	447	---	---	339
W$_2$O$_2$S$_2$(S$_2$CNC$_8$H$_{10}$)$_2$	1530	1122	955	---	---	463	360	345
W$_2$O$_2$S$_2$(S$_2$CNC$_4$H$_{14}$)$_2$	1512	1135	945	---	---	474	370	337
W$_2$O$_3$S(S$_2$CNC$_8$H$_{10}$)$_2$	1527	1120	952	803	425	465	365	335
W$_2$O$_3$S(S$_2$CNC$_7$H$_{14}$)$_2$	1520	1137	943	815	445	476	372	341

Table 4. Electronic absorption spectra of tungsten(V) oxo-complexes

Compound	λ (nm)	$\tilde{\nu}$ (kk)	ε ($M^{-1}cm^{-1}$)	Transition
$W_2O_3(S_2CNC_8H_{10})_4$	712 (sh)	14.0	10	$^2B_2 \rightarrow {}^2E(I)$
	598 (sh)	16.8	21	$^2B_2 \rightarrow {}^2B_1$
	470	21.3	183	Charge-transfer
	425	23.5	6497	Charge-transfer
	347	28.8	8042	Intraligand
	296 (sh)	33.8	16760	Intraligand
	264	37.9	21924	Intraligand
$W_2O_3(S_2CNC_7H_{14})_4$	715 (sh)	13.9	12	$^2B_2 \rightarrow {}^2E(I)$
	582 (sh)	17.2	22	$^2B_2 \rightarrow {}^2B_1$
	470	21.3	197	Charge-transfer
	410	24.4	6320	Charge-transfer
	339	29.5	8121	Intraligand
	298 (sh)	33.6	16421	Intraligand
	266	37.6	20020	Intraligand
$W_2O_4(S_2CNC_8H_{10})_2$	637 (sh)	15.7	15	$^2B_2 \rightarrow {}^2E(I)$
	553 (sh)	18.1	34	$^2B_2 \rightarrow {}^2B_1$
	470	21.3	260	Charge-transfer
	425	23.5	6574	Charge-transfer
	348	28.7	8996	Intraligand
	300 (sh)	33.3	16807	Intraligand
	267	37.5	22349	Intraligand
$W_2O_4(S_2CNC_7H_{14})_2$	628 (sh)	15.9	18	$^2B_2 \rightarrow {}^2E(I)$
	560 (sh)	17.9	45	$^2B_2 \rightarrow {}^2B_1$
	482	20.7	296	Charge-transfer
	421	23.8	7644	Charge-transfer
	340	29.4	9916	Intraligand
	295 (sh)	33.9	18437	Intraligand
	265	37.7	24041	Intraligand
$W_2O_2S_2(S_2CNC_8H_{10})_2$	647 (sh)	15.5	19	$^2B_2 \rightarrow {}^2E(I)$
	566 (sh)	17.7	54	$^2B_2 \rightarrow {}^2B_1$
	475	21.1	412	Charge-transfer
	452 (sh)	22.1	4584	Charge-transfer
	421	23.8	8126	Charge-transfer
	345	29.0	11121	Intraligand
	301 (sh)	33.2	17650	Intraligand
	268	37.3	23174	Intraligand
$W_2O_2S_2(S_2CNC_7H_{14})_2$	655 (sh)	15.3	24	$^2B_2 \rightarrow {}^2E(I)$
	561 (sh)	17.8	64	$^2B_2 \rightarrow {}^2B_1$
	476	21.0	524	Charge-transfer
	449 (sh)	22.3	5067	Charge-transfer
	419	23.9	10724	Charge-transfer
	343	29.2	12961	Intraligand
	298 (sh)	33.6	19418	Intraligand
	264	37.9	25976	Intraligand
$W_2O_3S(S_2CNC_8H_{10})_2$	650 (sh)	15.4	17	$^2B_2 \rightarrow {}^2E(I)$
	563 (sh)	17.8	39	$^2B_2 \rightarrow {}^2B_1$
	470	21.3	370	Charge-transfer
	440 (sh)	22.7	4313	Charge-transfer
	420	23.8	7182	Charge-transfer
	342	29.2	10213	Intraligand
	295 (sh)	33.9	16342	Intraligand
	263	38.0	22640	Intraligand
$W_2O_3S(S_2CNC_7H_{14})_2$	650 (sh)	15.4	20	$^2B_2 \rightarrow {}^2E(I)$
	584 (sh)	17.1	48	$^2B_2 \rightarrow {}^2B_1$
	465	21.5	465	Charge-transfer
	438 (sh)	22.8	4812	Charge-transfer
	425	23.5	9243	Charge-transfer
	342	29.2	11418	Intraligand
	297 (sh)	33.7	18137	Intraligand
	270	37.0	24128	Intraligand

present the following structure:
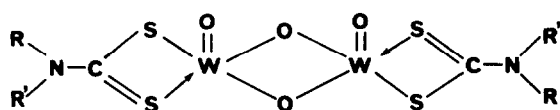
The complexes obtained when bubbling H_2S upon the solution of $Na_2WO_4 \cdot 2H_2O$ and the ligand in water, present a stoichiometry 1:1, the tungsten being 5-coor-

dinated. The union between two atoms of tungsten is made by means of a disulphido bridge. The formula which we assign to these complexes is $W_2O_2S_2(LL)_2$, and the structure should be as follows:
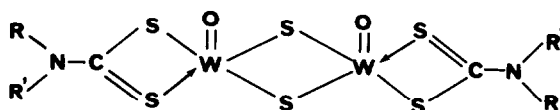
The complexes synthesized when bubbling H_2S into $Na_2WO_4 \cdot 2H_2O$ in dilute hydrochloric acid, followed by addition of the ligand, present a oxo-sulphido bridge, the stoichiometry is 1:1 and the tungsten is 5-coordinated. The formula which most closely fits the analyses is $W_2O_3S(LL)_2$ and we suggest that the structure for these complexes should be as follows:
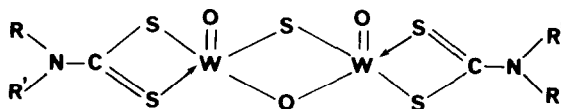
Magnetic properties

The low values of magnetic susceptibilities and magnetic moments, suggest the presence of dimeric species for these complexes.

The complexes of formula $W_2O_3(LL)_4$ gave values for the magnetic moments of 0.58 B.M. and 0.55 B.M. (see Table 2) respectively for the complexes with monoxo bridge and N-ethylanilindithiocarbamate and N,N-methylcyclohexyldithiocarbamate as ligands. These low magnetic moments then arise by interaction through the oxide bridge. Similar behaviour occurred in molybdenum(V) oxo-complexes with a monoxo bridge.[2-4]

The magnetic moments found for the complexes of formulas $W_2O_4(LL)_2$, $W_2O_2S_2(LL)_2$ and $W_2O_3S(LL)_2$, which present a dimeric structure with dioxo bridge, disulphido bridge and oxo-sulphido bridge respectively, 0.25 B.M.–0.01 B.M. (see Table 2), are lower than the magnetic moments of the dimeric complexes with a monoxo bridge. This is due to the possible formation of a direct metal–metal bond, which is more favorable to the dioxo, disulphido and oxo-sulphido bridge than to the monoxo bridge, due to the shorter bond length between the tungsten atoms, as it has been proved for molybdenum(V) oxo-complexes.[6]

IR *spectra*

The IR spectra of the four different kinds of complexes studied, exhibit a very strong band in the range 940–952 cm⁻¹, which we attribute to the vibration of the symmetric stretching mode of the terminal W=O bond. The antisymmetric stretching mode has not been detected. However, the appearance of the symmetric stretching mode, is sufficient to designate, in the dimeric complexes, a *cis* disposition of the two terminal W=O.[6]

Although the terminal oxygen–metal bonds are very sensitive to the variations produced in the metal donor atom, as it is habitual in all oxocation complexes of metal-oxo group, we have not observed any particular change for the frequency of the W=O terminal bonds. The IR spectra of the complexes with monoxo bridge, dioxo bridge and oxo-sulphido bridge, exhibit two bands between 815 and 440 cm⁻¹, which we attribute to the vibration of the antisymmetric and symmetric stretching mode, respectively, of the W–O bridge bond.

Upon comparing the IR spectra of the complexes with monoxo bridge and the IR spectra of the complexes with dioxo bridge, one observes no differences for the vibration frequency of the antisymmetric stretching mode in contrast to what was claimed by other workers,[7] who tried to solve the problem of differentiating the monoxo and dioxo bridge by means of the IR spectra.

The IR spectra of the complexes with disulphido and oxo-sulphido bridge, show two bands over 470 and 365 cm⁻¹, which we attribute to the vibration of the antisymmetric and symmetric stretching mode, respectively, of the W–S bridge bond.

If we compare the IR spectra of tungsten(V) dithiocarbamates complexes with the IR spectra of sodium dithiocarbamates, we observe that tungsten(V) complexes exhibit in the IR spectra the band of the stretching mode of the C–N bond displaced to higher frequencies than sodium dithiocarbamates. The IR spectra of tungsten(V) complexes exhibit this band in the range 1527–1512 cm⁻¹ (see Table 3), while the IR spectra of sodium N-ethylanilindithiocarbamate and sodium N,N-methylcyclohexyldithiocarbamate exhibit this band at 1460 and 1445 cm⁻¹ respectively. This difference may be attributed to a substantial contribution of resonance form:
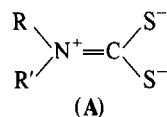
Fig. 1. Resonance form A.

in tungsten(V) dithiocarbamates complexes, while in sodium dithiocarbamates, the following resonance forms take place:[8]
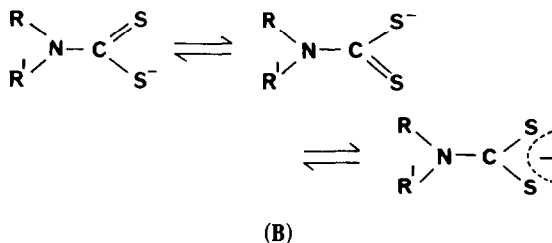
Fig. 2. Resonance forms B.

Consequently, the frequencies of the stretching mode of the C–S bond must be lower in tungsten(V) dithiocarbamates complexes than in sodium salts, because the C–S bond is not so strong in tungsten(V) complexes due to the stronger C–N bond. The IR spectra of tungsten(V) dithiocarbamates complexes exhibit the band of the C–S stretching mode in the range 1137–1119 cm⁻¹ while in the IR spectra of sodium N-ethylanilindithiocarbamate and sodium N,N-methylcyclohexyldithiocarbamate, this band appears at 1145 and 1170 cm⁻¹, respectively.

The IR spectra of all dithiocarbamate complexes show also other absorptions, over 335–345 cm⁻¹, attributed to tungsten–sulphur frequencies. The results of the present work are in good agreement with the assignments reported by Nieuwpoort and Steggerda[9] for eight-coordinated 1,1-dithio ligand complexes of W(IV).

Electronic spectra

The electronic spectra of the dimeric complexes with monoxo bridge and formula $W_2O_3(LL)_4$ exhibit two bands in the 715–590 nm region, which we attribute to d–d transitions $^2B^2 \rightarrow {}^2E(I)$ and $^2B_2 \rightarrow {}^2B_1$ respectively, according to the Balhausen–Gray scheme[10] for an octahedral structure. These complexes exhibit two other bands in the 470–420 nm region which we assign to a charge-transfer of the ligand-to-metal.

In the electronic spectra of the dimeric complexes with

dioxo bridge, oxo-sulphido bridge and disulphido bridge, we cannot observe appreciable differences between them, and that is why we propose the same structure for all these complexes. These complexes exhibit two bands over 640 and 560 nm that we attribute to $^2B_2 \rightarrow {}^2E(I)$ and $^2B_2 \rightarrow {}^2B_1$ transitions, respectively, for a possible square-pyramidal structure.[11]

In the visible region, we can detect two other bands over 470–420 nm, which we attribute to charge-transfer transitions.

The dimeric complexes with disulphido and oxo-sulphido bridges, present another transition over 450–440 nm which we assign to a charge-transfer as we have observed in similar complexes of molybdenum(V).[12,13]

On comparing the visible spectra of the dimeric complexes with monoxo-, dioxo, disulphido and oxo-sulphido bridges, one observes that the change produced in the d–d transitions on varying the coordination and passing from an octahedral structure for the six-coordinated complexes with monoxo bridge, to a square pyramidal structure for the complexes with 5-coordination and dioxo, disulphido and oxo-sulphido bridges.

The electronic spectra of tungsten(V) dithiocarbamate complexes, prepared in this study, show, in the ultraviolet region, three bands over 340, 300 and 260 nm. The electronic spectra of the sodium dithiocarbamates exhibit also three bands at the same wavelength. The differences are not significant. We attribute these bands to intraligand transitions. The first to a $n \rightarrow \pi^*$ transition, the second to a $\pi \rightarrow \pi^*$ transition and the last to a $n \rightarrow \sigma^*$ transition.

REFERENCES

[1] E. I. Stiefel, *Prog. Inorg. Chem.* 1977, **22**, 1.
[2] R. Lozano, A. Doadrio and A. L. Doadrio, *Polyhedron* (in press).
[3] A. Doadrio, A. L. Doadrio and R. Lozano, *An. Quim.* 1978, **74**, 566.
[4] A. Doadrio, R. Lozano and A. L. Doadrio, *An. Quim.* 1980, **76B**, 193.
[5] P. W. Selwood, *Magnetochemistry.* Interscience, New York (1956).
[6] F. A. Cotton, D. L. Hunter, L. Ricard and R. Weiss, *J. Coord. Chem.* 1974, **3**, 259.
[7] R. M. Wing and K. P. Callahan, *Inorg. Chem.* 1969, **8**, 871.
[8] D. Coucouvanis, *Prog. Inorg. Chem.* 1979, **26**, 301.
[9] A. Nieuwpoort and J. J. Stegerda, *Rec. J. Royal Neth. Chem. Soc.* 1976, **95**, 10,250.
[10] C. J. Bellhausen and H. B. Gray, *Molecular Orbital Theory.* W. A. Benjamin Inc., New York (1965).
[11] G. Bunzey and J. H. Enemark, *Inorg. Chem.* 1978, **17**, 682.
[12] A. Kay and P. C. H. Mitchell, *J. Chem. Soc. (A)* 1970, 2421.
[13] R. Lozano, A. L. Doadrio and A. Doadrio, *An. Quim.* 1981, **77B**, 56.

MULTINUCLEAR MAGNETIC RESONANCE AND RELATED STUDIES ON SOME ORGANOTIN(IV) COMPLEXES OF DITHIOCARBAZATES

ANIL SAXENA† and J. P. TANDON*

Department of Chemistry, University of Rajasthan, Jaipur 302004, India

Abstract—Synthesis, characterization and geometrical features of pentacoordinated dibutyltin(IV) dithiocarbazate complexes of the type n-Bu$_2$Sn L {(where L = dianion of S-methyl-B-N (2-hydroxy-phenyl) methylene and methyl dithiocarbazate} are described. These are obtained as viscous oils from the reactions of n-Bu$_2$SnO with equimolar proportions of the ligands in benzene. On the basis of UV, IR, NMR (^{1}H, ^{13}C, ^{119}Sn) spectra along with the mass spectral fragmentation pattern a trigonal bipyramidal geometry is proposed. The N atom probably occupies the axial site, while the remaining two donor atoms O and S and the dibutyl groups rest in an equatorial plane. These complexes are active against P.388 Lymphocyte leukaemia system.

The number and diversity of S N chelating agents used to prepare new coordination and organometallic compounds has increased rapidly during the past few years. The pronounced biological activity[1,2] of the metal complexes of ligands derived from dithiocarbazic acids has created considerable interest in their coordination chemistry. Complexes of dithiocarbazates with many different transition metal ions[3,4] have been studied extensively over the last years and only limited information on the bonding and structural features is available for the tin(IV) complexes.[5] Our continuing interest in chelated tin(IV) derivatives[6] has led us to describe the synthetic and stereochemical features of some dibutyltin(IV) dithiocarbazate complexes.

EXPERIMENTAL

Materials and methods. Chemicals and solvents used were dried and purified by standard methods, and moisture was excluded from the glass apparatus using CaCl$_2$ drying tubes. The ligands were prepared by the literature method.[7] The complexes were prepared, purified and analyzed by methods similar to those reported in our earlier publications.[5]

Spectral measurements. The electronic spectra were recorded in methanol on a Pye-Unicam-SP-8-100 spectrophtometer. Infrared spectra were obtained on a Perkin–Elmer 577 grating spectrophotometer an Nujol mulls or in benzene solution. ^{1}H NMR spectra were recorded on a Perkin–Elmer RB-12 spectrometer in CDCl$_3$ using TMS as an internal standard at 90 MHz. ^{13}C NMR spectra were recorded on Bruker HFX-90 spectrometer in CHCl$_3$ using TMS as internal standard at 25.15 MHz. Coupling constants were obtained from between 1000 and 12000 pulses and the assignments are based on off-resonance decoupling and satellite peaks. ^{119}Sn NMR spectra were recorded on a Bruker HFX-90 spectrometer in CHCl$_3$ using TMT as external standard at 22.7 MHz. Mass spectra were recorded on VG Micromass-7070 F spectrometer at 70 eV with ionization chamber at 220°C and calibrated using perfluorokerosene.

RESULTS AND DISCUSSION

The reactions of dibutyl tin oxide with the ligands proceed smoothly with the elimination of water, which

was removed azeotropically with benzene:

$$Bu_2SnO + H_2L \rightarrow Bu_2SnL + H_2O. \quad (1)$$

The derivatives so isolated are highly viscous oils, miscible with most organic solvents and hydrolyzable in nature.

In the electronic spectra of the ligands,[8] a band at ca. 216 nm is observed which may be assigned to ^{1}B band of the phenyl ring. This shifts to higher wave length on complexation and is observed at ca. 222 nm in the complexes. Also the ligand chromophore >C=N, which absorbs at ca. 290 nm, shifts to a higher wavelength and is observed at ca. 298 nm in the complexes. Three sharp bands are observed in the region, 250–270 nm and assigned as change transfer bands, suggesting the formation of σ-bonds[9] and (p → d) bonds[10] between p-orbitals of O and S and vacant 5d orbitals of tin.

The IR spectra of the ligands[11] show a broad and strong band in the region, 3300–2850 cm^{-1} attributable to ν(OH) and ν(NH) modes and no band is observed at ca. 2570 cm^{-1}, showing the absence of ν(SH). However, it does appear in the solution spectra with the disappearance of ν(NH) and ν(C=S) bands. This suggests the existence of a tautomeric equilibrium[12] between the two forms of ligand as shown below:

(thione)

(thiol) (2)
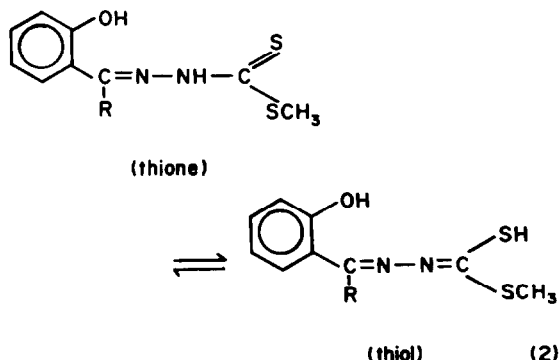
In the IR spectra of the complexes, all νOH or νSH bands are absent, showing the bonding of oxygen and

---

*Author to whom correspondence should be addressed.

†Present address: School of Molecular Sciences, University of Sussex, Brighton BN1 9QJ, England.

sulphur to the metal by the loss of thiolic and phenolic protons of the ligands. A band of medium intensity at *ca.* 1585 cm^{-1} in the complexes may be assigned to ν(C=N) vibration, and which originally appears in the ligand at *ca.* 1605 cm^{-1} in both the solution and solid states. The shift of this band to the lower energy indicates the coordination of the azomethine nitrogen to the tin atom[13] Two bands at *ca.* 600 and 510 cm^{-1} are also observed and which may be assigned to (Sn–C) asymmetric and symmetric modes respectively and thus indicating the presence of a bent C–Sn–C moiety.[14]

Besides this, several new bands observed at *ca.* 565, 425 and 325 cm^{-1} in the complexes may be assigned to ν(Sn–O), ν(Sn–O) and ν(Sn–S), respectively and thus lending support to the proposed coordination in the complexes.

In the ^{1}H NMR spectra, a broad signal at δ 7.15 ppm is observed in all the complexes owing to the phenyl protons of the salicylaldehyde and *o*-hydroxyacetophenone residues. A further sharp signal is observed at δ2.50 ppm attributable to the –CH$_3$ protons of dithiocarbazate moiety. In the complexes, the disappearance of the signals at *ca.* δ11.20, 4.35 and 10.05 ppm assigned to OH, SH and NH protons, respectively, in the spectra of the ligands clearly indicates their deprotonation. Signals at δ8.7 ppm in complex (I) and δ2.8 ppm in complex (II) occur owing to the –CH and –CH$_3$ protons, respectively. These are shifted downfield as compared to their positions in the ligands owing to the coordination of C=N group with the metal atom. The complexes show additional signals at δ 0.7–1.8 ppm owing to the protons of butyl group.

The mass spectral fragmentation scheme of the compound Bu$_2$Sn[OC$_6$H$_4$.C(CH$_3$):N.N.CS(SCH$_3$)] is shown in Fig. 1. The molecular ion peak due to ^{119}Sn isotope is observed at *m/e* 471. The peaks at *m* + 1 and *m* – 1 have also been observed due to the presence of ^{118}Sn and ^{120}Sn isotopes. The fragmentation starts with the simple cleavage of Sn–Bu bond eliminating Bu of 57 a.m.u. leading to the formation of a three coordinate Sn fragment ion[15]. The base peak is observed at *m/e* 352. However, the Sn–S bond is more readily cleaved than the Sn–O bond. Some low abundance ions containing Sn–S at *m/e* 151 are also obtained by the processes not involving cleavage of bonds[16]. The last step in the fragmentation is the removal of HCN molecule, which is characteristic of the Schiff base complexes.[17]

^{13}C NMR data have been recorded for both the ligands
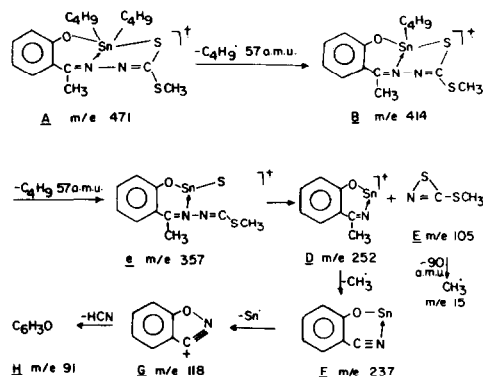
Fig. 1. Mass spectrum of C$_{18}$H$_{28}$S$_2$N$_2$OSn.
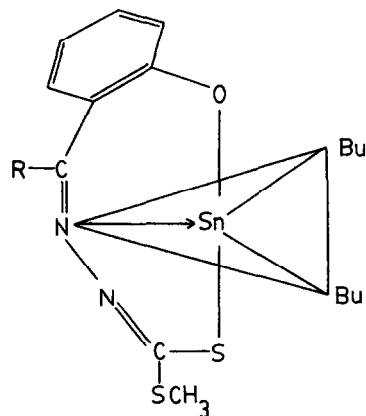
Fig. 2. Structure of organotin complex.

and the complexes. The shifts in carbons attached to O, S and N indicate the involvement of O, S and N atoms in coordination. The α(C) shifts and ^{1}J(^{119}Sn–^{13}C) values of 555 and 561 Hz indicates the five coordination around the tin atom in these complexes. Domazetis *et al.*[18] have reported a value of 560 Hz for Bu$_2$Sn complexes of thioamino acids and which are further supported by Mitchell *et al.*[19]

These complexes give sharp signals at δ-130.4 and – 156.7 ppm in ^{119}Sn NMR spectra and which strongly support the five coordination around tin in a trigonal

Table 1. Analysis and physical characteristics of complex
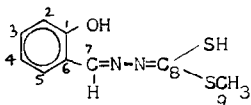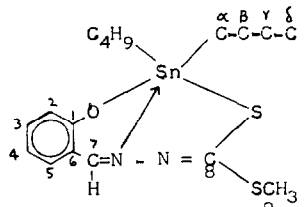
Compound	State	Yield %	Color	Mol. wt. Found (Calcd.)	Analysis %			
					Sn Found (Calc.)	S Found (Calc.)	C Found (Calc.)	H Found (Calc.)
(C$_4$H$_9$)$_2$Sn(C$_9$H$_8$N$_2$S$_2$O)	Oily liquid	95	Green	441.00 456.98	25.85 26.03	12.92 14.00	42.05 44.54	6.23 5.68
(C$_4$H$_9$)$_2$Sn(C$_{10}$H$_{10}$N$_2$S$_2$O)	Oily liquid	92	Yellow brown	453.00 470.98	24.92 25.26	12.23 13.58	43.92 45.86	5.13 5.94

Table 2. ^{1}H and ^{119}Sn NMR data (δ ppm) of ligands and complexes

Ligands and complexes	-OH	$-C_6H_4$*	-C-R R= -H $\approx$ -CH$_3$	-NH	-CH$_3$	n-C$_4$H$_9$	^{119}Sn
OH.C$_6$H$_4$.CH:N.NH.C:S.S.CH$_3$	11.20	7.20	8.52	9.95	2.45	-	-
(C$_4$H$_9$)$_2$Sn(O.C$_6$H$_4$.CH:N.N:C.S:SCH$_3$)	-	7.11	8.70	-	2.50	0.70-1.82	-130.4
OH.C$_6$H$_4$.C(CH$_3$):N.NH.C:S.SCH$_3$	12.52	7.10	2.65	10.05	2.48	-	-
(C$_4$H$_9$)$_2$Sn(O.C$_6$H$_4$.C(CH$_3$):N.N:C.S.SCH$_3$)	-	7.16	2.82	-	2.57	0.62-1.80	-156.7

* = Centre of multiplet.

Table 3. ^{13}C NMR data of ligands and their organotin complex

Structure	Chemical shift in ppm								
	1	2	3	4	5	6	7	8	9
	158.67	120.36	133.59	121.09	129.45	117.92	146.65	198.60	18.34
	168.6	117.1	136.1	122.0	134.6	116.3	165.6	174.8	15.00

^1J (^{119}Sn- ^{13}C) = 561 Hz

^2J (^{119}Sn- ^{13}C) = 32 Hz

^3J (^{119}Sn - ^{13}C) = 89 Hz

	α	β	γ	δ
Structure 1:	-	-	-	-
Structure 2:	26.3	27.5	26.5	13.5

bipyramidal geometry. Values[20] for similar five-coordinated Bu$_2$Sn(IV) complexes have been reported in the range of δ − 128 to − 165 ppm.

On the basis of the foregoing spectral evidences, the following geometry (Fig. 2) may be assigned to these complexes:

REFERENCES

[1] S. Kirschner, Y. K. Wei, D. Francis and J. G. Bergman, *J. Med. Chem.* 1966, 9, 369.

[2] S. E. Livingstone and M. Das, *Brit. J. Cancer* 1978, 37, 466.

[3] M. Das and S. E. Livingstone, *Inorg. Chim. Acta* 1976, 19, 5.

[4] M. A Ali, S. E. Livingstone and D. J. Philips, *Inorg. Chim. Acta* 1971, 5, 119.

[5] A. Saxena, J. K. Koacher and J. P. Tandon, *Inorg. Nucl. Chem. Lett.* 1981, 17, 229.

[6] A. Saxena, J. P. Tandon, K. C. Molloy and J. J. Zuckerman, *Inorg. Chim. Acta.* 1982, 63, 71.

[7] M. A. Ali, S. E. Livingstone and D. J. Philips, *Inorg. Chim. Acta* 1973, 7, 179.

[8] S. A. Pardley, S. Gopinathan and C. Gopinathan, *Ind. J. Chem., Sect. A*, 1980, 19, 130.

[9] M. A. Ali and S. E. Livingstone, *Coord. Chem. Rev.* 1974, 13, 101.

[10] A. Saxena, J. K. Koacher and J. P. Tandon, *J. Inorg. Nucl. Chem.* 1981, 43, 3091.

[11] M. A. Ali and R. Bose, *J. Inorg. Nucl. Chem.* 1977, 39, 265.

[12] M. A. Ali, S. E. Livingstone and D. J. Philips, *Inorg. Chim. Acta*, 1972, 6, 11.

[13]R. H. Holm, G. V. Everett, Jr. and A. Chakravorty, *Prog. Inorg. Chem.* 1966, **7**, 161.

[14]W. D. Honnick and J. J. Zuckerman, *J. Organomet. Chem.* 1979, **178**, 133.

[15]J. K. Terlouw, W. Heerma, P. C. M. Frintrop, G. Dijkstra and H. A. Meinema, *J. Organomet. Chem.* 1974, **64**, 205.

[16]D. B. Chambers and F. Glocking, *Inorg. Chimica, Acta.* 1970, **4**, 150.

[17]J. M. Fernandezg, E. Cortes and J. G. Larra, *J. Inorg. Nucl. Chim.* 1975, **37**, 1385.

[18]G. Domazetis, R. J. Magee and B. D. James, *J. Organomet. Chem.* 1978, **148**, 339.

[19]T. N. Mitchell, *J. Organomet. Chem.* 1974, **71**, 39.

[20]A. G. Davies, P. G. Harrison, J. D. Kennedy, R. J. Puddephatt, T. N. Mitchell and W. McFarlane, *J. Chem. Soc.* C, 1136 (1969).

CONDENSATION OF β,δ-TRIKETONE DERIVED FROM DEHYDROACETIC ACID WITH ALIPHATIC AMINES AND COPPER(II) COMPLEXES OF THE SCHIFF BASES

V. DREVENKAR, A. DELJAC and Z. ŠTEFANAC*
Department of Chemistry, Faculty of Science, University of Zagreb, Strossmayerov trg 14, YU-41000, Zagreb, Yugoslavia

and

J. SEIBL
Department of Organic Chemistry, Swiss Federal Institute of Technology, Zürich, Switzerland

Abstract—The condensation of ethyl-2-hydroxy-4-oxo-4-(4-hydroxy-6-methyl-2-pyrone-3-yl)-2-butenoate with primary aliphatic monoamines occurs at 4-hydroxy group of the pyrone ring according to ^{1}H NMR and mass spectrometric data. The ketamine tautomeric form of the prepared Schiff bases is predominantly present in chloroform solutions. Isolated crude copper(II) complexes of the condensation products are shown to be mononuclear with the 1:2 metal to ligand ratio.

Several possibilities of applying ethyl - 2 - hydroxy - 4 - oxo - 4 - (4 - hydroxy - 6 - methyl - 2 - pyrone - 3 - yl) - 2 - butenoate as an analytical reagent have been reported previously.[1-4] Chelate complexes with numerous cations are formed owing to the predominantly present bisenolic form of this β,δ-tricarbonyl compound.[4] Generally, the Schiff bases prepared by condensation of β-hydroxy-, β-di- and β-tri-ketones with mono- or diamines act as potentially di-, tri- or polydentate ligands, so that the preparation plays a distinctive role in the specific design of new complexing agents.[5] Considering such an approach for the oddly substituted tricarbonyl system of the reagent we performed the condensation with primary aliphatic monoamines and studied the structural characteristics as well as the complexation behaviour of the obtained Schiff bases using copper(II) complexes as a model system.

EXPERIMENTAL

Apparatus

The UV/VIS spectrophotometer Varian Techtron Series 635D was used throughout the experiments. The IR spectra were taken in KBr pellets with a Perkin–Elmer model 257 or 167 Grating spectrophotometer. The ^{1}H-NMR spectra were recorded on a Varian A-60 or EM-390 90 MHz spectrometer in CDCl₃ with TMS as internal standard. The mass spectra were taken on a Varian MAT CH7 or a CEC 21-110C instrument.

Materials

Dehydroacetic acid, purum 98%, cyclohexylamine p.a. and n-hexylamine, puriss. were purchased from FLUKA AG (Buchs, Switzerland) while dimethyloxalate, purum, was obtained from the same firm as a gift gratefully appreciated by the authors.

2,2 - Dimethylthio - 1 - amino - ethane was prepared following the procedure described previously.[6]

All other chemicals and solvents were p.a. products of Kemika (Zagreb, Yugoslavia).

Procedures

Preparation of dehydroacetic acid derivatives. Ethyl - 2 - hydroxy - 4 - oxo - 4 - (4 - hydroxy - 6 - methyl - 2 - pyrone - 3 - yl) - 2 - butenoate (I) was prepared elsewhere by condensation of

3-acetyl-4-hydroxy-6-methyl-2-pyrone (dehydroacetic acid) with diethyloxalate in the presence of sodium ethoxide as catalyst. The raw product kindly donated by the authors[7] was purified by recrystallisation from ethanol, dried at room temperature and checked by IR, ^{1}H NMR and mass spectra.[4]

Methyl - 2 - hydroxy - 4 - oxo - 4 - (4 - hydroxy - 6 - methyl - 2 - pyrone - 3 - yl) - 2 - butenoate (II) was obtained by the following procedure.

A suspension of 6.72 g (0.04 mole) of dehydroacetic acid in 15 cm³ of tetrahydrofuran followed by a solution of 4.72 g (0.04 mole) of dimethyl oxalate in 20 cm³ of tetrahydrofuran was slowly added from the separatory funnel to sodium methoxide prepared from 2 g of metallic sodium and 3.2 cm³ of absolute methanol in 25 cm³ of tetrahydrofuran.

The mixture was stirred over a period of 24 hr. The precipitated sodium salt was sucked off, dried in the air and then dissolved in deionized water. The water solution, mixed on a magnetic stirrer, was acidified by addition of Amberlite IR-120 ion exchanger until a yellow precipitate appeared. The solution was filtered and methyl - 2 - hydroxy - 4 - oxo - 4 - (4 - hydroxy - 6 - methyl - 2 - pyrone - 3 - yl) - 2 - butenoate was separated from ion exchanger beads by dissolution in hot ethanol.

For purification the crude product was recrystallized from ethanol.

Compound II, C₁₁H₁₀O₇, yellow powder, m.p. 137–139°C. Found (Calc.): C 51.93 (51.98); H 4.54 (3.97)%. IR-spectrum, $\bar{\nu}$ cm⁻¹ rel. intensity: 3440 b, 3140 w, 2960 w, 1740 vs, 1710 s, 1650 s, 1625 s, 1615 s, 1585 s, 1550 sh, 1540 s, 1455 m, 1430 m, 1250 s, 1230 s, 1120 s, 1000 m. ^{1}H NMR spectrum, δ ppm (multiplicity, comprised H): 2.30 (singl. 3H), 3.90 (singl. 3H), 5.90 (singl. 1H), 7.75 (singl. 1H), 13.00 (broad, 1H), 15.23 (singl. 1H). Mass spectrum, m/e (rel. intensity, %): 254 (9), 239 (4), 212 (15), 197 (6), 195 (39), 166 (5), 153 (100), 126 (4), 111 (11), 85 (23), 69 (38), 43 (50).

Preparation of Schiff bases. An equimolar quantity of the aliphatic amine was added to a solution of compound I (0.006 mole) in abs. ethanol (50 cm³), refluxed on a water-bath during 3 hr whereby the reaction course was pursued by thin-layer chromatography using chloroform/ether (1:1) as mobile phase.

The solvent was evaporated to 25 cm³, the precipitate formed by cooling down the solution was separated and recrystallized from ethanol. The following condensations were performed: compound I with n-hexylamine afforded a yellow woollen precipitate (III) (R_f 0.55, yield 44%) and with cyclohexylamine yellow crystals IV (R_f 0.53, yield 30%); according to thin-layer chromatograms (CHCl₃ as mobile phase) two products were

---

*Author to whom correspondence should be addressed.

formed in the course of the condensation of compound **I** with 2,2-dimethylthio-1-amino–ethane. However, after prolonged refluxing (4 hr) only brown needle-shaped crystals of compound **V** were obtained (R_f 0.45, yield 38%).

The condensation of compound **II** with *n*-hexylamine performed analogously yielded Schiff base **VI** as a yellow powder.

Characterization of Schiff bases. Compound **III**, $C_{18}H_{25}O_6N$, light yellow crystals, m.p. 105–106°C. Found (calc): C 61.05 (61.54); H 7.55 (7.12); N 4.54 (4.49)%. IR spectrum, $\bar{\nu}$ cm^{-1} rel. intensity: 3440 b, 2940 m, 2870 w, 1750 s, 1730 sh, 1655 m, 1595 m, 1530 vs, 1360 m, 1240 vs, 1130 w. ^{1}H NMR spectrum, δ ppm (multiplicity, comprised H): 0.90 (tripl, 3H), 1.05–1.90 (multipl. 8H), 1.38 (tripl. 3H), 2.18 (singl. 3H), 3.34 (quart. 2H), 4.35 (quart 2H), 6.53 (singl. 1H), 6.82 (singl. 1H), 10.73 (broad 1H), 19.10 (singl. 1H). Mass spectrum, *m/e* (rel. intensity %); 351 (100), 336 (15), 322 (19), 308 (14), 294 (10), 278 (16), 252 (43), 251 (22), 236 (9), 194 (30), 181 (10), 168 (91), 152 (30), 140 (100), 138 (30), 126 (76), 110 (11), 100 (30), 96 (20), 84 (65), 69 (28), 55 (28), 43 (57).

Compound **IV**, $C_{18}H_{23}O_6N$, yellow crystals, m.p. 145–147°C. Found (calc). C 61.38 (61.60); H 7.00 (6.58); N 4.32 (4.01)%. IR spectrum, $\bar{\nu}$ cm^{-1} rel. intensity: 3440 b, 2930 m, 2860 w, 1740 sh, 1725 vs, 1660 m, 1600 m, 1530 vs, 1350 m, 1230 vs, 1100 s, 1010 m.

^{1}H NMR spectrum, δ ppm (multiplicity, comprised H): 1.10–2.15 (multipl. 10H), 1.35 (tripl. 3H), 2.15 (singl. 3H), 3.52 (broad 1H), 4.38 (quart. 2H), 6.50 (singl. 1H), 6.80 (singl. 1H), 10.50 (broad 1H), 19.00 (singl. 1H). Mass spectrum, *m/e* (rel. intensity %): 349 (65), 268 (67), 251 (29), 234 (8), 194 (48), 166 (44), 152 (65), 138 (100), 124 (30), 110 (21), 98 (67), 84 (88), 69 (44), 58 (75), 55 (69), 41 (60).

Compound **V**, $C_{16}H_{21}O_6S_2N$, brown needles, m.p. 165–167°C. Found (calc): C49.53 (49.61); H 5.64 (5.43); N 3.56 (3.62)%.

IR spectrum, $\bar{\nu}$ cm^{-1} rel. intensity: 3440 b, 3240 w, 2920 w, 1740 sh, 1720 s, 1660 w, 1590 s, 1445 s, 1355 m, 1240 vs, 1100 m, 1020 m.

^{1}H NMR spectrum, δ ppm (multiplicity, comprised H): 1.38 (tripl. 3H), 2.17 (singl. 9H), 3.52–3.84 (multipl. 3H), 4.38 (quart. 2H), 6.58 (singl. 1H), 6.82 (singl. 1H), 9.97 (broad 1H), 18.2 (singl. 1H).

Mass spectrum, *m/e* (rel. intensity %): 387 (30), 340 (3), 280 (91), 251 (7), 224 (5), 211 (10), 197 (14), 194 (3), 183 (5), 156 (4), 153 (5), 138 (100), 120 (30), 107 (80), 96 (20), 84 (55), 69 (23), 55 (8), 41 (10), 68 (m*).

Compound **VI**, $C_{17}H_{23}NO_6$, yellow crystals, m.p. 95–97°C. Found (calc): C 60.27 (60.52); H 6.75 (6.87)%. IR spectrum, $\bar{\nu}$ cm^{-1} rel. intensity: 3260 w, 3130 vw, 2960 m, 2920 m, 2860 m, 1730 vs, 1715 s, 1660 m, 1595 vs, 1525 vs b, 1435 s, 1356 vs, 1325 s, 1315 s, 1305 s, 1268 vs, 1238 vs, 1194 m, 1205 vw, 1120 m, 1100 s, 1087 s, 1000 s, 918 m, 850 m, 830 w, 810 s, 770 m, 715 m, 632 m.

^{1}H NMR spectrum, δ ppm (multiplicity, comprised H): 0.90 (tripl. 3H), 1.10–1.90 (multipl. 8H), 2.17 (singl. 3H), 3.32 (quart. 2H), 3.90 (singl. 3H), 6.43 (singl. 1H), 6.73 (singl. 1H), 10.2 (broad 1H), 18.7 (singl. 1H).

Mass spectrum, m/e (rel. intensity %): 337 (58), 323 (12), 308 (11), 294 (12), 280 (7), 278 (9), 267 (11), 249 (9), 238 (31), 237 (17), 236 (7), 194 (20), 181 (12), 168 (100), 152 (23), 140 (84), 138 (27), 126 (63), 110 (11), 100 (24), 96 (18), 84 (54), 69 (29), 55 (19), 43 (51).

Preparation of crude Cu(II)-complexes was performed by precipitation from the aqueous solution of copper(II) sulphate or nitrate (1×10^{-2} M) with the equimolar ethanolic solution of the particular Schiff base at room temperature. The precipitates were purified by repeated recrystallization from ethanol.

Characterization of Cu(II)-complexes with Schiff bases. Crude complex with compound **III**, $(C_{18}H_{24}O_6N)_2Cu$, yellow green cryst. powder, m.p. 220–230°C (decomp.). Found (calc) C 56.80 (56.58); H 6.51 (6.32); N 3.85 (3.66); Cu 7.94 (8.31)%. IR spectrum, $\bar{\nu}$ cm^{-1} rel. intensity: 3440 b, 2930 m, 2860 w, 1730 m, 1700 m, 1600 s, 1500 vs, 1440 s, 1350 s, 1260 s, 1100 w, 1080 w.

Field desorption mass spectrum, *m/e* (rel. intensity %): 7.64 (3), 763 (12), 762 (8), 761 (17), 353 (5), 352 (23), 351 (100).

Complex with compound **IV**, $(C_{18}H_{22}O_6N)_2Cu$, yellow green cryst. powder, m.p. 250°C (decomp.). Found (calc): C56.19 (56.88); H 6.48 (5.82); N 3.87 (3.68); Cu 7.78 (8.35)%. IR spec-

trum, $\bar{\nu}$ cm^{-1} rel. intensity: 3440 b, 2925 m, 2850 w, 1730 s, 1700 s, 1595 s, 1500 vs, 1445 s, 1372 s, 1355 m, 1270 s, 1100 s, 1025 m. Field desorption mass spectrum, *m/e* (rel. intensity %): 760 (4). 759 (13), 758 (10), 757 (23), 351 (6), 350 (28), 349 (100).

Complex with compound **V**, $(C_{16}H_{20}O_6S_2N)_2Cu$, brown green cryst. powder, m.p. 210–215°C (decomp.). Found (calc): C 45.62 (45.95); H 5.34 (4.81), N 3.49 (3.34); Cu 8.11 (7.60)%. IR spectrum, $\bar{\nu}$ cm^{-1} rel. intensity: 3450 b, 2925 w, 1730 s, 1700 s, 1650 s, 1585 s, 1505 vs, 1435 s, 1350 s, 1300 s, 1250 s, 1110 m.

Field desorption mass spectrum, *m/e* (rel. intensity %): 836 (4), 835 (17), 834 (12), 833 (27), 389 (8), 388 (27), 387 (100).

DISCUSSION

Unsymmetrical β,δ-triketones can take triketo, two different monoenol and bisenol forms in their tautomeric equilibrium.[5] In the case of ethyl - 2 - hydroxy - 4 - oxo - 4 - (4 - hydroxy - 6 - methyl - 2 - pyrone - 3 - yl) - 2 - butenoate (compound **I**)[4] and the corresponding methyl ester (compound **II**) the prevalence of the bisenol form is in accordance with the recorded spectroscopic data. The IR absorption bands in the region 1800–1500 cm^{-1} correspond to lactone and chelate ring $\nu_{C=O}$ and α-pyrone nucleus $\nu_{C=C}$ vibrations of dehydroacetic acid[8] accompanied by ester and chelate ring carbonyl bands at frequencies analogous to those of ethyl and methyl-diacetoacetate[9] (Table 1). Similarly the ^{1}H NMR spectra might be compared with those of diacetoacetates supplemented with the signals of dehydroacetic acid protons. Instead of acetyl methyl protons $\delta = 2.6$ ppm the singlet $\delta = 7.8$ ppm appears corresponding to the proton of the methyne group that links both enolic moieties. The hydroxyl proton $\delta = 16.6$ of dehydroacetic acid[8] and $\delta = 18.55$ of ethyl diacetoacetate[9] shifted to $\delta = 13.08$ (13.00) and $\delta = 15.22$ (15.20) ppm respectively in compound **I** (**II**) confirm that the bisenol form is predominantly present: 80–90% based on the signal area (Table 2).

Congruence of the mass spectra confirms also analogous structures of compounds **I** and **II**: fragmentation of the ester group results in both cases in *m/e* 195 ion which is followed by an identical series of fragments.[4] The condensation of β,δ-triketones with amines takes place on the terminal carbonyl groups but not on the central group of heptane-2,4,6-trione[10] and in the case of benzoylacetylacetone, anisoylacetylacetone, p-toluylacetylacetone and p-bromobenzoylacetylacetone only on the carbonyl group with the methyl in the α-position.[11]

These regularities could not apply to our case because of the dissimilarity of the triketone. Therefore all carbonyl groups, except lactone and ester carbonyl, have been considered as possible condensation sites paying attention also to the predominantly present tautomeric form of the condensation product.[12]

Considering the central carbonyl group of triketones **I** and **II** as the condensation site, the spectroscopic characteristics of α-pyrone part in obtained Schiff bases are expected to be congruent with those of products of the reaction between dehydroacetic acid and alkyl-amines. Namely, the latter condensation takes place on acetyl carbonyl and the presence of the ketamine tautomeric form has been confirmed by ^{1}H NMR data.[13,14] Spectroscopic characteristics of condensation products as related to dehydroacetic acid can be assembled in the following way. The wavenumber of lactone carbonyl IR absorption bands is decreased for ~20 cm^{-1} and is accompanied by increase of $\nu_{C5=C6}$ value for ~ 30 cm^{-1}.[13,15] Chemical shift δ-values in ^{1}H NMR spectra of Schiff bases for C-5, C-6 methyl and hydrogen

Table 1. Characteristic IR absorption bands in 1800–1500 cm^{-1} region

Compound	ν C=O Lactone two bands	ν C=O Ester	Assignment ν C_3=C_4 $\tilde{\nu}$ cm^{-1}	ν C=C Chelate	ν C_5=C_6	Reference
Dehydroacetic acid	1730 ; 1715		1640	1610	1550	8
Ethyl diacetoacetate		1710		1560		9
Compound I	1740	1710	1655	1615; 1585	1550 sh;1525	4
Compound II	1740	1710	1650	1620; 1585	1540	

Table 2. ^{1}H NMR spectroscopic data

Compound	-CH$_2$C$\underline{H}_3$	Pyrone C-6-CH$_3$	-COCH$_3$	Assignment -COOCH$_3$ chemical shift δ ppm Multiplicity (included H)	-COOC$\underline{H}_2$-CH$_3$	Pyrone C-5 H	Chelate-CH=	$\overset{H}{\underset{O\ O}{\diagup}}$	Reference
Dehydroacetic acid		2.25 s(3H)	2.63 s(3H)			5.93 s(1H)		16.6 s(1H)	8
Ethyl diacetoacetate	1.57 t(3H)		2.63 s(6H)	4.57 q (2H)			.	18.55 s(1H)	9
Compound I	1.39 t(3H)	2.35 s(3H)		4.38 q (2H)		5.99 s(1H)	7.82 s(1H)	13.08;15.22 b(1H);s(1H)	4
Compound II		2.30 s(1H)	3.85 s(3H)			5.90 s(1H)	7.82 s(1H)	13.00;15.20 b(1H);s(1H)	

Table 3. ^{1}H NMR spectroscopic evidence for ketaminoform of compounds III, IV, V and VI

N-alkyl substituent (Compound)	Chemical shift, δ ppm Amino proton	(Multiplicity of signal;Included H) N-methylene (methyne) protons	Coupling constants J, Hz
n-Hexyl (III)	10.73 (broad)	3.34 (app. quartet ; 2H triplet split to doublets)	$J_{CH_2-CH_2N}$ J_{CH_2NH} 6Hz
Cyclohexyl (IV)	10.5 (doublet)	3.52 (broad 1H)	J_{CHNH} 6Hz
2,2-Dimethylthioethyl (V)	9.97	3.52-3.84 (multiplet ≥ 10 lines ; 1H)*	
n-Hexyl (VI)	10.2 (triplet)	3.32 (app. quartet ; 2H triplet split to doublets)	$J_{CH_2-CH_2N}$ J_{CH_2NH} 6Hz

* Obviously not AB$_2$ (8 lines) but AB$_2$X spin system incompletely resolved.

bounded enolic proton are reduced by 0.25, 0.20 and 2.82 ppm, respectively. The unambiguous evidence for the ketamine tautomeric form resulted from the presence of a bonded amino-proton signal (δ = 13.78 ppm) and from the observed coupling with alkyl substituents[13] as well as from the correlation of the associated coupling constant (J = 5.00 Hz) with that for the N-methyl group in N-methylacetamide.[14]

Analogously the predominant presence of the ketamine form can be deduced for the Schiff bases of triketones I and II (Table 3). As far as the central carbonyl group as condensation site is concerned the changes of spectroscopic data accompanying the conversion of triketones I and II are not in conformity with those occurring along with the condensation of dehydroacetic acid. Thus apart from incomplete splitting of the lower band (overlapping with ester carbonyl) there is no remarkable change in lactone carbonyl band position

and the wavenumber of $\nu_{C_5-C_6}$ vibrations is increased by not more than $10-15\,cm^{-1}$. Moreover, the increase of C-5 proton chemical shift amounts to $0.59 > \Delta\delta \geq 0.50\,ppm$, an increment suiting better the replacement of substituent in greater proximity.

Additional evidence excluding as the condensation site not only the central carbonyl but also the one next to the ester group has been derived from the mass spectroscopic fragmentation scheme. The base peak m/e 153 corresponding to 3-carbonyl-4-hydroxy-6-methyl-α-pyrone cation characteristic of the mass spectra of triketones I and II is reduced to a much smaller share in the case of Schiff bases and appears as attendant of the more pronounced m/e 152 fragment. This fact eliminates the condensation with amines at the ester terminus of the triketo system because in such a case the fragment m/e 153 should be abound and m/e 152 ion absent. The series of fragments m/e 194, 152 and 84 might come from the fragmentation of molecular ions if condensation at either

C-3 carbonyl or C-4 hydroxyl group on α-pyrone nucleus is proposed (Scheme I). However, fragment m/e 168 in the mass spectrum of compound III can be explained only by fragmentation of the species that arises from condensation at hydroxyl group on α-pyrone ring. The more so as the measured mass 168.1396 is congruent with elemental formula $C_{10}H_{18}ON$. Ethoxy rearrangement as another explanation for the origin of ion m/e 168 (Scheme II) has been eliminated by synthesizing the methyl ester (II) and its Schiff base (VI). The presence of m/e 168 in the mass spectrum of compound VI is a definite proof that condensation occurs at α-pyrone hydroxyl group. Correspondent fragment m/e 166 is present in the mass spectrum of condensation product IV (Scheme III).

Fragments with unbroken (unimpaired) pyrone ring still bearing a carbonyl group and an N-alkyl substituent are also recorded as ions m/e 236 for compounds III and VI and m/e 234 for compound IV. More aboundant ions
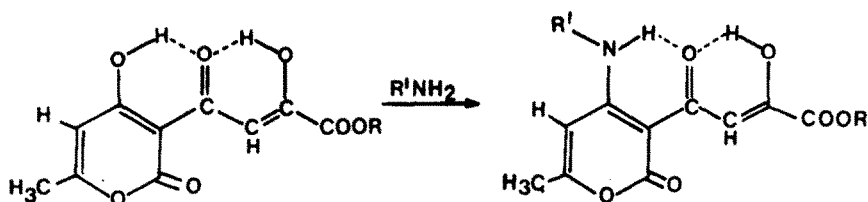
R : $-CH_2CH_3$ COMPOUND I

Ethyl 2-hydroxy-4-oxo-4-(4-hydroxy-6-methyl-2-pyrone-3-yl)-2-butenoate

R : $-CH_3$ COMPOUND II

Methyl 2-hydroxy-4-oxo-4-(4-hydroxy-6-methyl-2-pyrone-3-yl)-2-butenoate

COMPOUND III   R : $-CH_2CH_3$ R' : $-(CH_2)_5\,CH_3$

Ethyl 2-hydroxy-4-oxo-4-(4-hexylamino-6-methyl-2-pyrone-3-yl)-2-butenoate

COMPOUND IV   R : $-CH_2CH_3$ R' : $-CH(CH_2)_5$

Ethyl 2-hydroxy-4-oxo-4-(4-cyclohexylamino-6-methyl-2-pyrone-3-yl)-2-butenoate

COMPOUND V   R : $-CH_2CH_3$ R' : $-CH_2CH(SCH_3)_2$

Ethyl 2-hydroxy-4-oxo-4-[4-(2',2'-bismethylthio)ethylamino-6-methyl-2-pyrone-3-yl]--2-butenoate

COMPOUND VI   R : $-CH_3$ R' : $-(CH_2)_5CH_3$

Methyl 2-hydroxy-4-oxo-4-(4-hexylamino-6-methyl-2-pyrone-3-yl)-2-butenoate

Scheme I.

Scheme II.

COMPOUND III⎤
COMPOUND VI⎦ m/e 236

COMPOUND IV m/e 234

m/e 168
m/e 166
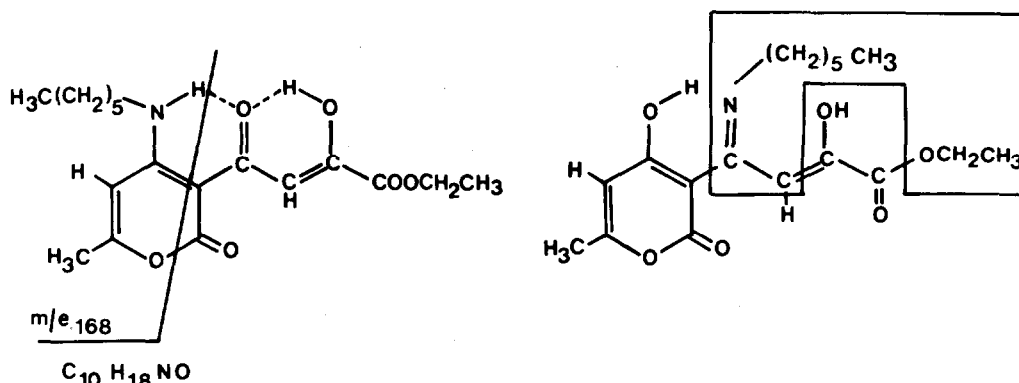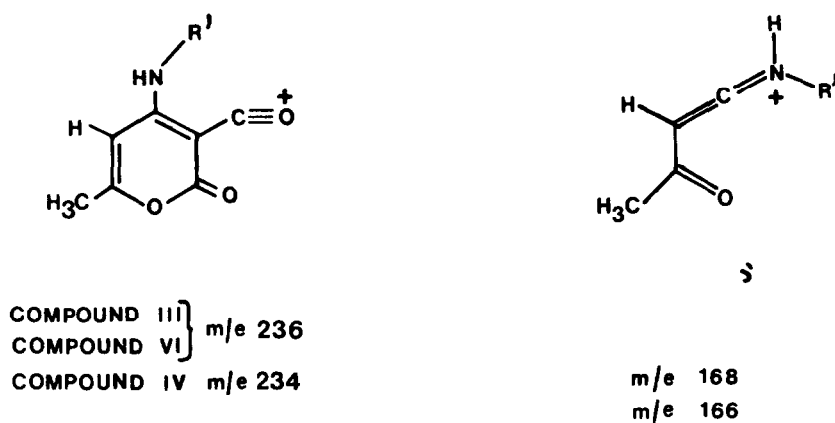
Scheme III.

m/e 238 and m/e 237 in the mass spectrum of Schiff base VI corresponding to m/e 252 and m/e 251 of Schiff base III very probably have origin in the N-alkyl residue cleavage from molecular ion.

Apart from the different ester groups, Schiff bases III and VI have the same structures affording a series of fragments exactly alike, with m/e values less than 200.

In the case of compound V primary fragmentation is predetermined by the –CH(SCH₃)₂ group mass 107), leading at first to fragments m/e 280 (M⁺ – 107) and m/e 107 (M⁺ – 280). From here the origin of the base peak m/e 138 can very well be documented by metastable ion

m* 68.0. The transition $280 \xrightarrow[m^*]{-142} 138$ can be interpreted as the cleavage of the whole ketoester residue accompanied by H-rearrangement to the pyrone ring substituted with N-methylene but not hydroxyl group.

The ligand-to-metal ratios of the species present in ethanolic solutions pursued by UV/VIS spectrophotometric measurements and continuous variation method with Schiff bases III, IV and V used as ligands did not afford regularly shaped curves thus indicating the simultaneous presence of more than one species.

Crude copper(II) complexes however, isolated from

Table 4. Characteristic absorption bands in 1500–1600 cm⁻¹ region of IR spectra recorded for mononuclear copper complexes and associated ligands

Compound	$\tilde{\nu}$ cm⁻¹				Reference
2-Acetoacetyl phenol	1580				17
(2-Acetoacetylphenol)₂Cu	1580	1570		1515	17
Compound I	1585 s		1525 vs		4
(Compound I)₂Cu	1580 sh	1550 vs		1510 vs	4
Compound III	1595 m		1530 vs		
(Compound III)₂Cu	1600 vs		1530 sh	1500 vvs	
Compound IV	1600 m		1530 vs		
(Compound IV)₂Cu	1595 s		1525 sh	1500 vvs	
Compound V	1590 s		1540 s		
(Compound V)₂Cu	1585 vs		1535 sh	1505 vvs	
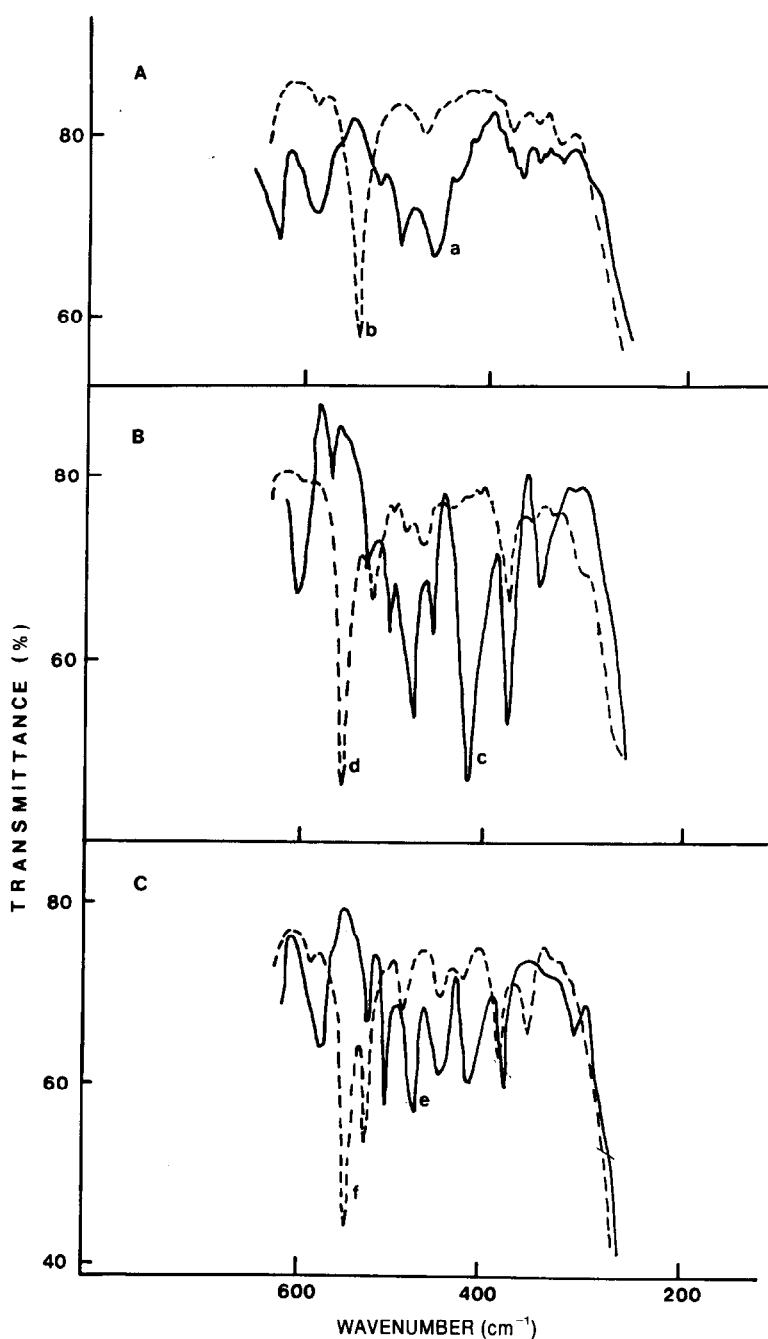
Fig. 1. Lower frequency region 600–200 cm^{-1} of IR spectra of crystalline species in KBr pellets recorded on a Perkin–Elmer Model 580B spectrometer: (A) compound III (curve a) and corresponding Cu(II) complex (curve b); (B) compound IV (curve c) and corresponding Cu(II) complex (curve d); (C) compound V (curve e) and corresponding Cu(II) complex (curve f).

the ethanolic medium at room temperature and at 40°C steadily have given identical elemental analyses and IR spectra.

Mononuclear complexes of compounds III, IV and V isolated from ethanolic solutions in crude form are conformable to the 2:1 ligand-to-metal ratio as confirmed by the presence in field desorption mass spectra of ions m/e 763, m/e 759 and m/e 835, respectively. The coordination site of copper in complexes with acyclic Schiff bases derived from triketones has been characterized by the presence or absence of definite absorption bands.[10,11]

The distinction of the pointed out bands from ester and α-pyrone $\nu_{C=O}$ or $\nu_{C=C}$ bands of the latter moiety is not possible in the IR spectra of copper complexes with Schiff bases III, IV and V.

More convincing is the comparison with copper complexes of triketones (Scheme IV) justified by the following facts. Copper is coordinated to oxygen in synthesized acyclic Schiff bases and to nitrogen and oxygen only if the acyclic complexes are obtained by hydrolysis of the initially cyclic ligands.[11] Electronic spectra of prepared complexes in chloroform solution show low intensity
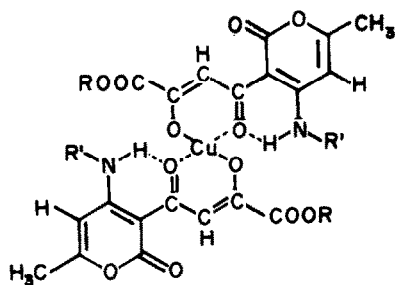
Scheme IV.

maxima at λ = 580–590 nm corresponding better to the value for bis(benzoylacetonato)copper(II) than for bis(acetylacetone)ethylenediimino copper(II).[11] Increased intensity of the band at about 1600 cm^{-1} and the appearance of a very strong band at 1500 cm^{-1} (Table 4) allow matching of coordination sites with those proposed for the mononuclear copper complex with 2-acetoacetylphenol to be at the acetoacetyl group and characterized by appearance of new bands at 1570 and 1515 cm^{-1}.[16]

Direct information about the structure of the complexes and the nature of the metal–ligand bonds is provided by the metal–ligand vibrations in the low-frequency region. However, as ligand and lattice vibrations appear in this region too (Fig. 1) the assignment is far from being simple and straightforward. The idea to undertake a thorough study by applying one or the other of the specific methods used to assign the metal–ligand vibrations[17,18] has been neglected because the realization in our circumstances would raise remarkable difficulties.

Thus reliable information on structural features of crude complexes is still lacking the more so as the attempts to prepare crystalline forms appropriate for X-ray analysis have been unsuccessful so far.

REFERENCES

[1] M. Laćan, S. Malazogu, H. Džanić and I. Sušnik-Rybarski, *Bull. Soc. Chem. Technol. Sarajevo (Yugoslavia)* 1973–1974, **21/32**, 35.

[2] V. Drevenkar, Z. Štefanac and A. Brbot, *Microchem. J.* 1976, **21**, 402.

[3] A. Gertner and D. Pavišić, *Microchem. J.* 1978, **23**, 336.

[4] V. Drevenkar, B. Štengl, M. J. Herak and Z. Štefanac, *Microchem. J.* 1979, **24**, 199.

[5] U. Casellato, P. A. Vigato and M. Vidali, *Coord. Chem. Rev.* 1977, **23**, 31.

[6] V. Drevenkar, A. Deljac, J. Kuftinec and Z. Štefanac, *J. Inorg. Nucl. Chem.* 1975, **37**, 1629.

[7] M. Laćan, I. Sušnik-Rybarski, A. Brbot, B. Katušin and V. Drenovački, submitted for publication.

[8] R. Gren, *Deut. Apoth. Ztg.* 1971, **111**, 219.

[9] S. Forsén and M. Nilsson, *Acta Chem. Scand.* 1960, **14**, 1333.

[10] T. Yano, T. Ushijima, M. Sasaki, H. Kobayashi and K. Ueno, *Bull. Chem. Soc. Jpn.* 1972, **45**, 2452.

[11] D. E. Fenton and S. E. Gayda, *Inorg. Chim. Acta* 1975, **14**, L11.

[12] G. O. Dudek and R. H. Holm, *J. Am. Chem. Soc.* 1962, **84**, 2691.

[13] J. D. Edwards, J. E. Page and M. Pianka, *J. Chem. Soc.* 1964, 5200.

[14] S. Garratt, *J. Org. Chem.* 1963, **28**, 1886.

[15] J. Moszew, J. Jamrozik and W. Solarski, *Zesz. Nauk. Univ. Jagiellon. Prace Chem.* 1970, **CCXXXVIII**, 151.

[16] Y. Taguchi, F. Sagara, H. Kobayashi and K. Ueno, *Bull. Chem. Soc. Jpn.* 1970, **43**, 2470.

[17] G. C. Percy and D. A. Thornton, *J. Inorg. Nucl. Chem.* 1972, **34**, 3357.

[18] N. Mohan, A. Müller and K. Nakamoto, *Advances in Infrared and Raman Spectroscopy* (Edited by R. J. H. Clark and R. E. Hester), Vol. 1, p. 173. Heyden & Son, London (1975).

THERMAL DECOMPOSITION AND REARRANGEMENT OF BRANCHED METHYLSILOXANE OLIGOMERS

M. BLAZSÓ* and E. GÁL
Research Laboratory for Inorganic Chemistry, Hungarian Academy of Sciences, Budapest/Hungary/ H–1112.
Budapest, Budaörsi ut 45, Hungary

and

N. N. MAKAROVA
Institute of Organo-element Compounds, Academy of Sciences of the U.S.S.R., Moscow, U.S.S.R.

Abstract—The pyrolysis products of bi-, tri- and poly-cyclic methylsiloxane oligomers were studied using gas chromatography; it was concluded that reversible elimination and addition of dimethylsilanone groups led to the observed product distribution. Polycyclic siloxane oligomers were pyrolysed together with cyclic dimethylsiloxanes in order to investigate the addition reactions. The splitting of the polycycles into bicycles containing only two branching points was observed as a consequence of dimethylsiloxane addition above 500°C.

Thermal decomposition of branched-chain methylsiloxane polymers results in a series of cyclic, bicyclic and polycyclic volatile products. For the better understanding of the processes taking place in polysiloxanes at high temperature we have studied the thermal decomposition of bicyclic and polycyclic methylsiloxane oligomers. In our previous work[1] a series of compounds with two cyclosiloxane units separated by a dimethylsiloxane chain were pyrolysed. The following general mechanism of elimination and addition of a dimethylsilanone intermediate was proposed to explain the distribution of the pyrolysis products:

$$T_2D_n \rightleftharpoons T_2D_{n-x} + x[D] \quad (n = 6, 7, \ldots x = 1, 2, \ldots) \quad (1)$$
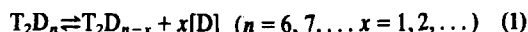
where $T = CH_3SiO_{1.5}$ (methylsilsesquioxy group) and $D = (CH_3)_2SiO$ (dimethylsiloxy group). Similar reactions were described by other authors dealing with the pyrolysis of cyclosiloxane oligomers,[2,3] such as:

$$D_n \rightleftharpoons D_{n-1} + [D] \equiv (n = 4, 5). \quad (2)$$
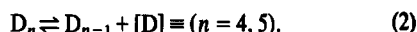
In the present work we have extended the investigations to fused-ring bicyclic derivatives and to tricyclosiloxanes and polycyclosiloxanes as well.

RESULTS AND DISCUSSION

Decomposition products of bicyclic siloxanes

According to the thermal decomposition mechanism of the cyclosiloxane units separated by a dimethylsiloxane chain (reaction 1), a series of new bicycles is formed under pyrolysis. At higher degradation conversions the cyclosiloxanes and fused-ring bicyclosiloxanes of lower molecular mass predominate in the pyrolysates. We observed[1] that the relative amounts of the cumulated bicyclic products are roughly the same when pyrolysing any kind of dimethylsiloxane chain linked cyclosiloxanes at a given temperature.

If the pyrolysis is carried out in the inert gas stream of a pyrolyser coupled to gas chromatograph, a low conversion of decomposition is observed only, because the largest portion of the investigated sample has evaporated from the heated boat prior to decomposition. Nevertheless, we can elucidate the primary decomposition products: they are T_2D_3 and T_2D_4 of structure (III) and (V), respectively, shown in Fig. 1. Both compounds contain cycles of four siloxane members only. Figure 1 illustrates all the reactions of elimination and addition of [D] dimethylsilanone intermediate leading from the primary products (in frame) to the quasi-equilibrium of product distribution found in the pyrolysates.

In the scheme of Fig. 1, the contribution of T_2D_2 molecule is assumed, although it could not be identified directly due its instability. If the pyrolysis is carried out on line with a gas chromatograph, a product appears with the retention expected for T_2D_2.

Thermal decomposition of fused-ring bicycles

The mechanism given in Fig. 1 is confirmed by pyrolysing the fused-ring bicyclosiloxanes of structure (III) and (V). The distribution of fused-ring bicyclic products is given in Table 1. The first and second columns refer to pyrolystates of compounds with two cyclosiloxane units separated by a dimethylsiloxane chain. The product dis-
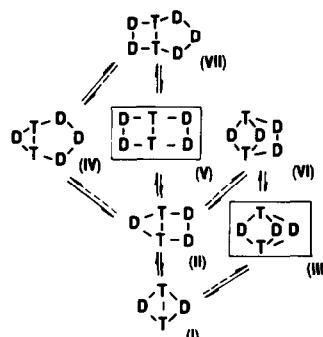
Fig. 1. Scheme of [D] elimination and addition reactions under pyrolysis of cumulated bicyclosiloxanes (starting compounds are in frame).

---

*Author to whom correspondence should be addressed.

tribution of T_2D_4 (structure V) is similar to these, although the amount of the pyrolysed compound remained yet higher than the other products after 10 min. pyrolysis at 560°C. Pyrolysing T_2D_3 (structure III) together with D_6 cyclosiloxane, the decay of the pyrolysed bicyclic compound takes place faster, the distribution of the resulting fused-ring bicycles becomes similar to the above (see Table 1).

Thermal decomposition of tricyclic methylsiloxanes

The molecule of the methylsiloxane oligomers containing four branching points (T groups), which form three separated cycles, splits into two bicyclic parts under pyrolysis above 500°C. Further decomposition follows according to the reactions of the bicyclosiloxanes. Thus the product distribution of T_4D_8 [1,5-bis(heptamethylcyclotetrasiloxy) hexamethylcyclotetrasiloxane:
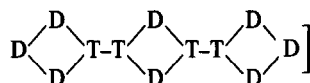
and T_4D_{14}(1,5-bis[(heptamethylcyclotetrasiloxy) hexamethyltrisiloxy] hexamethylcyclotetrasiloxane:
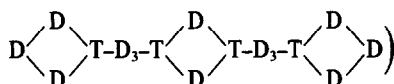
is similar to that of T_2D_6[(heptamethylcyclotetrasiloxy) heptamethylcyclotetrasiloxane] and T_2D_9 [1,5-bis(heptamethylcyclotetrasiloxy)hexamethyltrisiloxane], respectively.

When fused-ring tricyclic compounds containing fewer D groups are pyrolysed, new tricycles are formed according to the scheme given in Fig. 2, by elimination and addition of D groups. In the pyrolysate at 560°C of T_4D_3 (structure X), two isomers of T_4D_2, two additional isomers of T_4D_3 and a T_4D_4 compound were the main products. In addition small amounts of D_3, D_4 cyclosiloxanes and T_2D_{3-5} bicyclosiloxanes and T_8 polycyclosiloxane (octamethyloctasilsesquioxane) were also formed. The fused-ring bicyclosiloxanes were only byproducts, mainly T_2D_3 (structure II) was found (see Table 1).
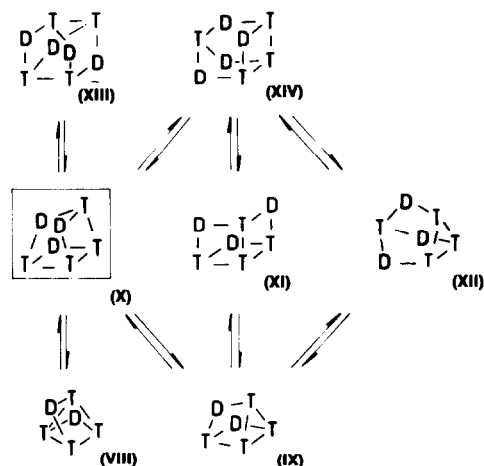
Fig. 2. Scheme of [D] elimination and addition reactions under pyrolysis of T_4D_3 (structure X, in frame).

In consequence of [D] addition, the fused-ring tricyclosiloxane molecules may reach a size that is able to split into two stable bicyclosiloxanes, as follows:
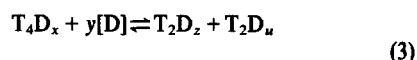
$$T_4D_x + y[D] \rightleftharpoons T_2D_z + T_2D_u$$
(3)
$$(x = 2, 3, \ldots; \quad y = 4, 5, \ldots; \quad z = 3, 4, \ldots; \quad u = 3, 4, \ldots;).$$

This reaction proved to be reversible; some tricyclosiloxanes appear in the pyrolysates of T_2D_3 and of T_2D_4 although they are minor products.

If the pyrolysis of T_4D_3 is carried out in the presence of D_6, the possibility for [D] addition—consequently for reaction (3)—increases. That is why the amount of tricyclosiloxane pyrolysis products decreases considerably and the distribution of the fused-ring bicyclosiloxanes produced becomes similar to that of T_2D_4, demonstrated in Fig. 3 (see also Table 1).

We pyrolysed T_8 as well, in the presence of D_6, in order to see whether [D] addition could occur onto a polycyclosiloxane built up of T groups only. A process similar to reaction (3) takes place after the addition of at least four D groups, i.e. then the molecule splits into two

Table 1. Relative amounts of fused-ring bicyclic products of pyrolysis at 560°C for 10 min

Pyrolysed compound(s)	T_2D_9	T_2D_6	T_2D_4	$T_2D_3+D_6$	T_4D_{14}	T_4D_8	T_4D_3	$T_4D_3+D_6$	T_8+D_6
Product N° Symbol									
I. T_2D_2	0	0	2	0.5	0	0	0	4	2
II. T_2D_3	22	27	21	22	22	21	55	21	16
III. T_2D_3	5	5	5	8	5	5	15	6	5
IV. T_2D_4	13	11	7	8	12	12	5	9	8
V. T_2D_4	24	21	35	27	23	21	15	27	30
VI. T_2D_4	10	8	11	15	11	11	8	14	16
VII. T_2D_5	26	28	18	20	27	29	2	19	23

T: $(CH_3) Si O_{1.5}$;   D: $(CH_3)_2 Si O$
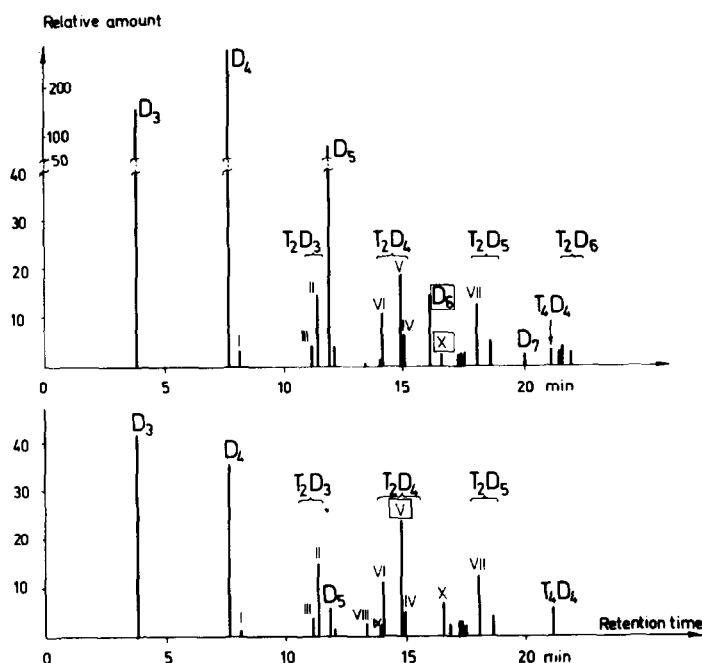
Fig. 3. Schematic chromatogram of pyrolysate of D_6–T_4D_3 (structure X), mixture of equal weights, and that of T_2D_4 (structure V) on OV–101 coated capillary column. Pyrolysis: 560°C, 20 min (numbers labeling the products refer to those given in Figs. 1 and 2).

parts. A possible scheme for this reaction is given in Fig. 4. Nevertheless, the thermal decomposition does not stop at D_4T_2, but in the presence of cyclosiloxanes, reaction (3) leads to the same fused-ring bicyclosiloxanes as found in the pyrolysates analysed so far and the distributions of which are given in Table 1.

CONCLUSION

Results of pyrolysis experiments on different methylsiloxane oligomers containing branching groups show that the decomposition process involves elimination and addition of dimethylsiloxane groups. The pyrolysed oligomer gradually releases its D content until the residue becomes a fused-ring compound. The eliminated [D] intermediates partly form cyclosiloxanes, and is partly incorporated into other molecules. The [D] addition to cumulated polycyclosiloxanes results in compounds of larger cycles. When the cycles become large enough, the polycyclosiloxane may split into two stable parts both containing branching points.

Summarizing the observed processes, the separation of D and T units takes place under pyrolysis of the branched methylsiloxane oligomers. The D content of the molecule is eliminated to form cyclosiloxanes while the fusion of T units results in polycyclosiloxanes. However, these processes may be reversed by introducing an excess of cyclosiloxanes into the system. In this case [D]

addition expands the fused-ring polycyclosiloxanes so much that they split into smaller products containing less T and more D in their molecules.

EXPERIMENTAL

Starting materials

1,5 - bis(heptamethylcyclotetrasiloxy)hexamethyltrisiloxane (T_2D_9) and (heptamethylcyclotetrasiloxy)heptamethylcyclotetrasiloxane (T_2D_6) were prepared and analysed according to published methods.[1,4]

Octamethylbicyclo [3.3.3]-pentasiloxane (T_2D_3, structure III.) and decamethylbicyclo [5.5.1]-hexasiloxane (T_2D_4, structure V) and decamethyltricyclo [5.5.1.3[3.9]]-hexasiloxane (T_4D_3, structure X) were isolated from the pyrolysate of a branched chain methylsiloxane polymer by preparative scale gas chromatography and analysed by mass spectrometry[5] and ^{29}Si NMR spectroscopy.[6] The structures of the first two compounds were confirmed by X-ray diffraction[7] and by electron diffraction[8] as well.

Synthesis of 1,5-bis(heptamethylcyclotetrasiloxy)hexamethylcyclotetrasiloxane (T_4D_8)

3.37 g (0.010 mol) of 1, 5-dichlorohexamethylcyclotetrasiloxane in 50 cm³ dry diethyl ether was added with stirring to 7.45 g (0.025 mol) of hydroxyheptamethylcyclotetrasiloxane and 2.02 g (0.020 mol) of triethylamine in 100 cm³ dry diethyl ether at 20–22°C. Stirring was continued for several hours, then the triethylamine hydrochloride filtered off. The solution was washed with water, distilled at 0.25 mbar to yield 5.3 g (61.6%) of an oily liquid at 137–138°C ($n_D^{20} = 1.4090$, $d_4^{20} = 1.0620$, MW = 861.7). Found: C, 28.41; H, 7.00; Si, 38.95; Calc. for $C_{20}H_{60}Si_{12}O_{14}$: C, 27.88; H, 7.01; Si, 39.12%.

Synthesis of 1,5-bis[(heptamethylcyclotetrasiloxy)hexamethyltrisiloxy]hexamethylcyclotetrasiloxane (T_4D_{14})

The synthesis was carried out according to the aboves, starting from 1-hydroxy-5-(heptamethylcyclotetrasiloxy) hexamethylcyclotrisiloxane. After filtration the solution was boiled for 5 hr, then washed with water and distilled. The b.p. of the yielding oil (53.5%) was 210–215°C at 0.1 mbar ($n_D^{20} = 1.4080$, $d_4^{20} = 1.0319$,
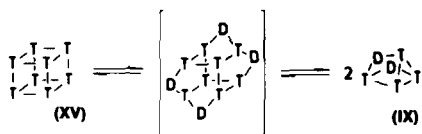
Fig. 4. An example of the splitting of T_8 polycyclosiloxane into two tricyclosiloxanes after [D] addition.

MW: 1306.6). Found: C, 29.72; H, 7.40; Si, 38.08; Calc. for $C_{32}H_{96}Si_{18}O_{20}$: C, 29, 29.41; H, 7.39; Si, 38.70%.

For 1 - hydroxy - 5 - (heptamethylcyclotetrasiloxy)hexamethyltrisiloxane synthesis 13.60 g (0.043 mol) of heptamethylchlorocyclotetrasiloxane[1] in 100 cm³ dry diethyl ether was added with stirring to 15.6 g (0.065 mol) of 1,5-dihydroxyhexamethyltrisiloxane and 6.05 g (0.065 mol) of aniline in 100 cm³ dry diethyl ether at 5–8°C. When the reaction was completed aniline hydrochloride was removed. The solution was washed with water and distilled at 13 mbar yielding 9.1 g (40.7%) of 1-hydroxy-5-(heptamethylcyclotetrasiloxy) hexamethyltrisiloxane at 90–100°C.

Synthesis of octamethyloctasilsesquioxane (T_8)

The method of Barry *et al.*[9] was used. Found: C, 18.04; H, 4.54; Si, 41.82; Calc. for $C_8H_{24}Si_8O_{12}$: C, 17.89; H, 4.50; Si, 41.85%, MW: 536.

Pyrolysis

The pyrolysis experiments were performed in the temperature range of 460–560°C for 5–60 min in evacuated and sealed quartz tubes. The sample weight was 1–5 mg, the volume of the tube 0.17 cm³. Additional pyrolyses were also carried out for 10–30 s in a tantalum boat and open quartz tube in a flowing inert atmosphere, on line with the gas chromatograph.

Analysis of the pyrolysis products

Product analysis was performed on a Perkin–Elmer gas chromatograph with Flame Ionization Detector and a PE D–26 Electronic Integrator. The products were identified by comparison of retention time on three different columns with authentic samples. The following columns were used:

—3.5 m, 2 mm i.d packed column; support: 80–100 mesh Chromosorb G; phase: 5% OV–17; temperature program from 40 to 280°C at 6.5/min.

—20 m, 0.2 mm i.d. fused silica capillary column, coated with OV–101 phase; temperature program from 50 to 300°C at 6°/min.

—20 m, 0.2 mm i.d. glass capillary column, coated with OV–225 phase; temperature program from 50 to 220°C at 6°/min.

REFERENCES

[1] N. N. Makarova, M. Blazsó and E. Jakab, *Polyhedron* 1983, 2, 257.
[2] I.M.T. Davidson and I. F. Thompson, *J. Chem. Soc., Chem. Commun.*, 1971, 251.
[3] L. E. Gusel'nikov, N. S. Nametkin, T. H. Islamov, A. A. Sobtsov and V. M. Vdovin, *Izv. Akad. Nauk. SSSR., Ser. Khim.* 1, 1971, 84.
[4] K. A. Andrianov, N. N. Makarova, T. V. Popova, *Bull. Izobr.* 1977, 28, 74.
[5] G. Garzó, J. Tamás, T. Székely and K. Ujszászi, *Acta Chim. Acad. Sci. Hung.* 1971, 69, 273.
[6] H. Jancke, G. Engelhardt, M. Mägi and E. Lippmaa, *Z. Chem.* 1973, 13, 392.
[7] G. Menzel and J. Kiss, *Acta Cryst.* 1975, B31, 1214.
[8] B. Rozsondai, I. Hargittai, G. Garzó, *Magy. Kém. Foly.* 1976, 82, 515.
[9] A. J. Barry, W. H. Dandt, J. J. Domicone and J. W. Gilkey, *J. Amer. Chem. Soc.* 1955, 77, 4248.

STABILITY, SPECTRA AND STRUCTURE OF THE COPPER(II) CHLORIDE COMPLEXES IN ACETIC ACID

M. A. KHAN, J. MEULLEMEESTRE, M. J. SCHWING and F. VIERLING*
E.N.S.C.S., Laboratoire de Chimie Physique ERA No. 166 1, rue Blaise Pascal, 67008 Strasbourg, France

Abstract—The stability constants and the electronic spectra of four molecular chlorocomplexes formed in acetic acid solutions have been calculated. The spectrophotometric measurements were performed at wavelengths ranging from 260 to 500 nm and, in the near IR from 600 to 1400 nm. The matrix rank treatment of more than 1000 spectrophotometric data demonstrates a minimum of five absorbing species: the solvated copper(II) acetate and four chlorocomplexes. The overall stability constants of $Cu(OAc)Cl$, $CuCl_2$, $LiCuCl_3$ and $LiCuCl_4$ are respectively: $\log \beta_1 = 3.38$; $\log \beta_2 = 5.57$; $\log \beta_3 = 7.36$; $\log \beta_4 = 7.83$. The structure of the monochlorocuprate with the Cu–OAc bonding in the primary coordination sphere is supported by near-IR evidence. The bathochromic shift of the absorption maxima of the d–d transition bands indicates structural changes of the complexes with a square planar configuration for $Cu(OAc)Cl$ promoted to a flattened tetrahedron for Li_2CuCl_4.

An exhaustive study of the copper(II) chloride complexes in aqueous solution was carried out by Schwing and Khan[1,2] who concluded the presence of four mononuclear successive complexes, calculated their equilibrium constants and discussed briefly the structure of the $CuCl_4^{2-}$ ion in aqueous solution. The emphasis now seems to have shifted to the study of these copper(II) chlorocomplexes in nonaqueous solutions. This is mainly because of very small values of the overall equilibrium constants, β_j, in water, in contrast to their very high values in nonaqueous solvents. Moreover in water there is an overlapping of the characteristic bands of the complexes, which are well separated in the latter solvents.

Furlani and Morpurgo[3] suggest a flattened tetrahedral (D_{2d} symmetry) structure for tetrachlorocuprates after studies in solid state and such organic solvents as acetonitrile, nitromethane, ethylalcohol, dimethylformamide (DMF) and dimethylsulphoxide (Me$_2$SO). Manahan and Iwamoto[4] have proposed very high values for the equilibrium constants of $CuCl^+$ and $CuCl_2$ in acetonitrile.

Gutman *et al.* have shown spectrophotometrically the existence of four chlorocomplexes in DMF[5] in acetonitrile and in trimethylphosphate[6] at the same time postulating a very small equilibrium constant for $CuCl_2$. On the other hand Courtot *et al.*[7] using potentiometric and spectrophotometric means propose three copper(II) chlorocomplexes, $CuCl^+$, $CuCl_2$, $CuCl_3^-$ in Me$_2$SO. Scharff as also proposed the existence of these complexes in propylene carbonate.[8]

Very recent work published from our laboratory confirms the presence of three complexes postulated by Gutman *et al.* in DMF but with $CuCl^+$, $CuCl_3^-$ and $CuCl_4^{2-}$.[9]. The absence of the dichlorocomplex in this model is due to similar solvent and ligand donor numbers, inducing dissociation of $CuCl_2$ and autocomplex formation of $CuCl^+$ and $CuCl_3^-$.[10] The same [1, 3, 4] model, i.e. $CuCl^+$, $CuCl_3^-$ and $CuCl_4^{2-}$ is found in

Me$_2$SO instead of [1–3], i.e. $CuCl^+$, $CuCl_2$ and $CuCl_3^-$ suggested in Ref.[7], but the [1–4] model, i.e. $CuCl^+$, $CuCl_2$, $CuCl_3^-$ $CuCl_4^{2-}$ is clearly established in propylene carbonate[11] against the unsatisfactory [1–3] proposed in the same medium by Scharff.[8]

Beside these dissociating solvents, the non-dissociating acetic acid has also been used for the study of the copper(II) chlorocomplexes. Eswein *et al.*[12] suggest an equilibrium between the D_{4h} (square planar) and D_{2d} symmetry species for the tetrachlorocomplex in acetic acid, assigning the peak at 450 nm to D_{2d} and that at 375 nm to D_{4h} configuration. They identify the absorption maximum at 670 nm as that of cupric acetate in acetic acid but it is surprising that they do not observe any isosbestic point.

Sawada *et al.* have studied in detail the equilibria of copper(II) acetate in acetic acid with perchloric acid and lithium acetate[13] and with hydrochloric acid and copper(II) chloride.[14] They suggest that the characteristic absorption maximum of copper acetate in acetic acid is at 685 nm and observe isosbestic points at 360 and 440 nm and postulate the presence of tri- and tetrachlorocomplexes. However their work is limited to the interpretation of data obtained only at two wavelengths.

This work pertains to the formation of copper(II) chlorocomplexes in acetic acid at 25°C. The number of complexes present in the solution and their equilibrium constants were determined after a spectrophotometric study in the UV and visible region, from 270 to 500 nm and in the near-IR from 600 to 1400 nm. A quantitative interpretation of the whole spectrum (UV, vis., IR) was undertaken. All data were taken into account to calculate the equilibrium constants and the variation of the extinction coefficients of the individual copper(II) chlorocomplexes. Tests for different models of complexes present in the solution were performed in accordance with the results of the matrix rank method, mentioned in our discussion.

EXPERIMENTAL

Anhydrous acetic acid, pro analysis (Merck) was used after adding calculated amount of acetic anhydride, p.a. (Merck), with the addition of three drops of 0.001 M perchloric acid, 70% p.a.

---

*Author to whom correspondence should be addressed.

(Merck) and letting the solution stand overnight.[15] Copper solutions were prepared from a stock solution of copper(II) acetate, p.a. (Merck). Lithium chloride p.a., (Merck) was used without any purification.

The final analytical concentration of copper was 5×10^{-4} M for measurements in UV-vis. and 3.75×10^{-3} M in IR region. In these spectrum regions chloride concentrations were varied from 5×10^{-4} to 1 M, with $l = 0.5$ cm, and from 2.5×10^{-3} to 1 M, with $l = 2$ cm, respectively.

Acetic acid was the spectrophotometric reference solution. The final solutions of copper and chloride were prepared just before the measurements. The optical densities were obtained with a CARY 17D instrument with digital interfacing and a Periferic Zip 30 rapid printer and puncher. The numerical analysis was performed on a UNIVAC 1110 computer.

RESULTS AND DISCUSSION

Acetic acid is a molecular solvent, its dielectric constant being 6.2, and therefore non-ionic in character. However two series of measurements were carried out. One with lithium perchlorate to keep the molecular environment constant and equal to 1 M and the other, without lithium perchlorate. The absorption spectra of the two series in UV, visible and IR being identical, the simpler of the two equilibria, i.e. the direct mixing of copper(II) acetate and lithium chloride solutions was retained for the study.

(a) Spectra of copper(II) chloride in acetic acid

When chloride is added to the copper(II) solution in acetic acid the colour changes from blue to greenish yellow, and eventually to bright yellow with the increase in chloride concentration. The absorption variations with respect to the chloride concentration in UV, visible and IR are presented in Fig. 1.

The free solvated copper(II) acetate has an absorption maximum at about 252 nm. The addition of chloride shows the formation of a peak at 300 nm which undergoes a hypsochromic effect as the chloride concentration increases with a shift to 280 nm. This maximum is not

Gaussian suggesting a superposition of two maxima. For chloride concentrations much higher than 0.02 M there appears a maximum at 445 nm and for concentrations higher than 0.05 M another at 380 nm. These two maxima coalesce at 385 nm at still higher concentrations. Three isobestic points are observed at 302, 357 and 437 nm. Sawada et al.[14] have reported only two isobestic points at 360 and 440 nm whereas the work of Eswein et al. is conspicuous by its statement that "no isobestic points are observed". It is to be remarked that this latter work was carried out by preparing chloride solutions by dissolving the chloride salt first in small quantity of water before adjusting the volume with acetic acid. In our case it was observed that the addition of small quantities of water has a profound effect on the complexation, a few drops being sufficient to render the solution colourless from greenish yellow or bright yellow. This aquation effect has also been noted by Sawada and Tanaka.[16]

In the IR region the characteristic maximum of copper(II) acetate in acetic acid is observed at 680 nm $(198 \, M^{-1} \, cm^{-1})$. This peak which has been variously reported at 650[15], 670[12] and 685 nm[14] disappears as the chloride concentration increases and shifts to 1060 nm. This shift of 380 nm of the solvated copper(II) ion in acetic acid, from 680 to 1060 nm, is remarkably similar to the bathochromic shift in DMF,[9] propylene carbonate and Me₂SO.[11]

(b) Equilibrium in solution

Copper(II) acetate in acetic acid has been reported to have a maximum at 365 nm which has been ascribed to copper–copper bond by Yamada et al.[17] and Martin and Whitley,[18] indicating that the salt is dimerised in solution. This is confirmed by Sawada[13] who has located this maximum at 370 nm. This maximum although not visible in our work because of low copper concentration in UV-visible, appears distinctly at 375 nm with copper concentration 3.75×10^{-3} M. In view of this and the fact that acetic acid being a non-dissociating solvent, molecular
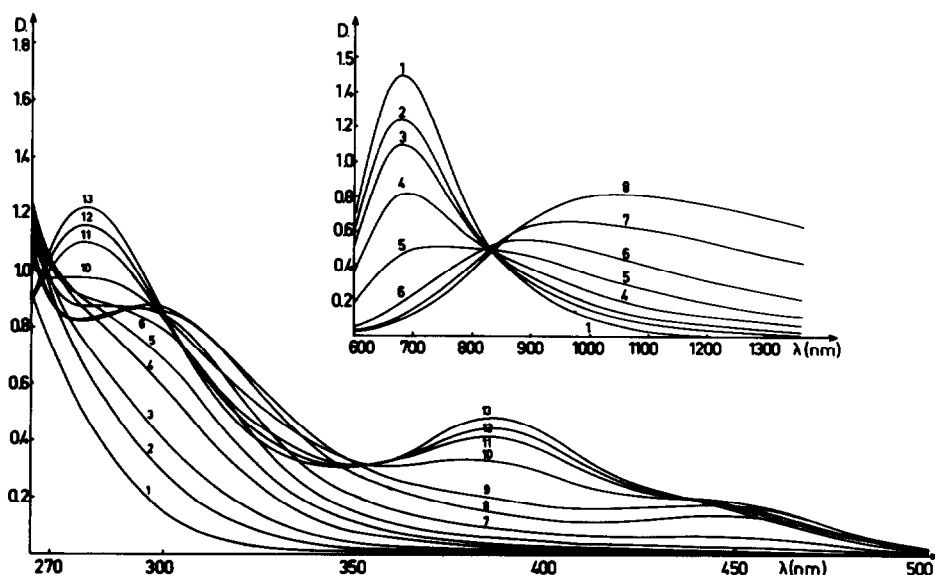
Fig. 1. Experimental spectra of copper(II) chloride solutions: spectrum/$10^3 \times$ [Cl⁻]$_{anal}$. UV-visible: [Cu(OAc)₂]$_{anal}$. = $5 = 10^{-4}$ M; $l = 0.5$ cm 1/0, 2/0.5, 3/1, 4/2, 5/3, 6/5, 7/10, 8/30, 9/70, 10/300, 11/700, 12/1000, 13/1300. near-IR: [Cu(OAc)₂]$_{anal}$. = 3.75×10^{-3} M; $l = 2$ cm 1/0, 2/2.5, 3/5, 4/10, 5/20, 6/40, 7/200, 8/1000.

association occurs and the following equilibria are proposed:

$$Cu_2(OAc)_4 + 2LiCl \rightleftharpoons 2CuCl(OAc), 2LiOAC$$
$$Cu_2(OAc)_4 + 4LiCl \rightleftharpoons 2CuCl_2, 4LiOAc$$
$$Cu_2(OAc)_4 + 6LiCl \rightleftharpoons 2CuCl_3Li, 4LiOAc$$
$$Cu_2(OAc)_4 + 8LiCl \rightleftharpoons 2CuCl_4Li_2, 4LiOAc.$$
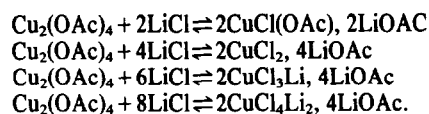
The copper(II) acetate has a dimeric structure in acetic acid but the copper(II) chlorocomplexes are monomeric.[14] The formulation of the monochlorocomplex as Cu(OAc)Cl is supported by the near-IR evidence and is discussed further on.

(c) Experimental data and numerical analysis

The optical density variations as a function of chloride concentration were plotted from 260 to 500 nm, at intervals of 10 nm. These plots were used to obtain N optical density values for each selected wavelength for computation. Eventually a set of 24 wavelengths in the UV-visible range with N = 28 for each wavelength were considered. In the near IR region 20 wavelengths, from 600 to 1400 nm, at intervals of 40 nm, with N = 24 for each wavelength, were taken into account.

A matrix rank treatment method was performed for determining the minimum number of absorbing species present in the solution[19] which requires a set of N × L data, where N is the number of solutions and L the number of wavelengths, with N imperatively greater than L. The interpretation of 1152 spectrophotometric data indicated a minimum of four species: the solvated copper(II) acetate and at least three copper(II) chlorocomplexis.

(d) Calculated models and equilibrium constants

The theoretical expressions and the mathematical treatment has been explained in our earlier publication.[9] The computation was performed at three different mononuclear complexes models: the [1–3], the [1, 3, 4] and the [1–4] model in accordance with the matrix rank analysis results. Table 1 summarises the results of the numerical analysis of the three different models:

The quadratic mean, σ, for the first two models has a value of 0.128 and 0.130 respectively. On the other hand a far better value of $\sigma = 0.054$ is obtained for the model [1–4]. Consequently the existence of four mononuclear successive complexes is proposed in acetic acid for copper(II) chloride solutions.

The stability of the complexes is much higher than in water but comparable to that found in other solvents such as DMF[9] or Me$_2$SO:[11] despite the different associative property of these solvents this is particularly true for the overall stability constant of the monochlorocom-

plex and the stepwise formation constant of the tetra-chlorocomplex. On the contrary, very higher β'_is were calculated in the propylene carbonate solutions for an identical [1–4] model: the associative solvent effect, predicted by the very low dielectric constant of acetic acid ($\epsilon = 6$) compared to that of propylene carbonate ($\epsilon = 69$) should be one of the factors which supports these stability differences.

Incomplete formation for each of the four species, represented in Fig. 3, is found in the acetic acid system, which render impossible the β_i determination of one separated species and explain the drastic higher value found by Sawada et al. for CuCl$_2$ (log β_2 = 15.2).[14] These authors used data at 300 nm where they do not observe any further shift of the absorption with ligand concentration increase: consequently they postulate the unique presence of Cu(OAc)Cl and CuCl$_2$. As a matter a fact, at 300 nm the absorption maximum does not change with higher chloride concentration as seen in our experimental spectra of Fig. 1. But other absorption maxima appear, particularly at 280 and 385 nm with chloride ligand increase, which is obviously consistent with the presence of one or two other complexes. The individual electronic spectra calculation shown next in Fig. 2 indicate clearly that the extinction coefficients of LiCuCl$_3$ and Li$_2$CuCl$_4$ cannot be neglected at 300 nm.

On the other hand, we found stepwise formation constants K$_3$ and K$_4$ very similar (1.78 and 0.45) to those calculated by Sawada et al.[14] (1.68 and −0.15) using data at 385 and 450 nm: at those wavelengths the absorption due to Cu(OAc)Cl and CuCl$_2$ are effectively neglegeable compared to those of LiCuCl$_4$ (Fig. 2). Another evidence for the unique presence of the latter complexes involves the presence of isobestic points at 302, 357 and 437 nm. But once again, the discussion shows the necessity to use absorption data over the whole wavelengths range for a precise determination of the best model and accurate stability constants values.

(e) Electronic spectra of the copper(II) chlorocomplexes in acetic acid

The electronic spectra of the individual chlorocomplexes for the [1–4] model in the UV, visible and the near IR are presented in Fig. 2.

Monochlorocomplex, CuCl(OAc). In the near IR there is a peak at 680 (1970 M^{-1} cm^{-1}) which is obviously due to the acetate ion associated with the complex. This transition is clearly characteristic of the copper–acetate bond as it is located at the same wavelength as that observed for the copper(II) acetate solution, with a comparable extinction coefficient (680 nm— 198 M^{-1} cm^{-1}; spectrum 1—Fig. 1). Therefore the formulation of the monochlorocomplex is proposed as

Table 1. Results of the numerical analysis of the theoretical models for the acetic acid–copper(II) chloride solutions

	[1,2,3]	[1,3,4]	[1,2,3,4]
log β_1	3.20	8.97	3.38
log β_2	5.66	–	5.57
log β_3	7.46	14.26	7.36
log β_4	–	15.93	7.83
σ(uv-vis)	0.128	0.130	0.054
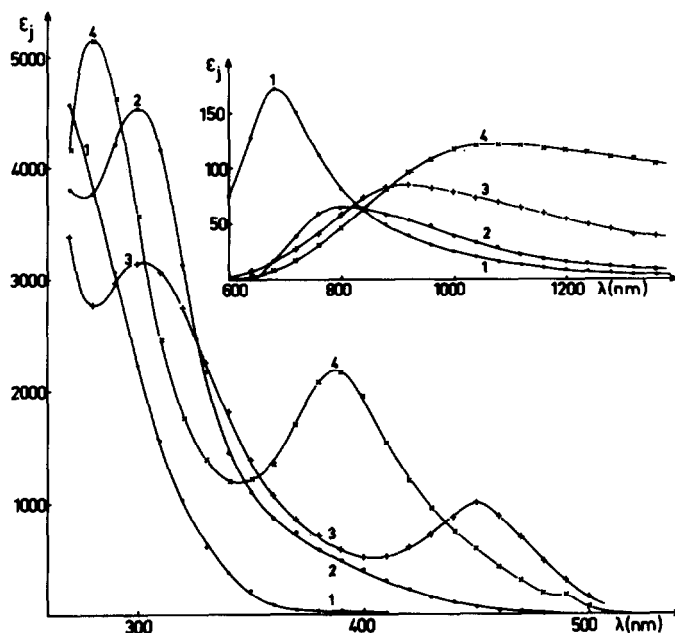
Fig. 2. Calculated electronic spectra of the copper(II) chlorocomplexes in acetic acid.

CuCl(OAc). This complex may also present a maximum at 260 nm as in water[2] and DMF.[9] Unfortunately this absorption maximum could not be ascertained because of absorption interference due to solvent below 270 nm.

It may be pointed out here that copper acetate was used instead of copper perchlorate because with the latter, at copper concentrations greater than 10^{-3} M precipitation occurs for higher chloride concentration, especially in the presence of lithium perchlorate. Had copper perchlorate been used it would have rendered difficult the exploration of the spectrum in the near IR region where, for copper concentration less than 10^{-3} M the absorption is very low.

Dichlorocomplex, $CuCl_2$. The absorption maximum of this complex is centred at 300 nm ($455 \, M^{-1} \, cm^{-1}$) in the UV region and can be compared to that at 315 nm in propylene carbonate. In the IR, $CuCl_2$ has a $\lambda_{max} = 800$ nm ($65 \, M^{-1} \, cm^{-1}$).

Trichlorocomplex, $CuCl_3Li$. It presents three maxima,

one each in UV, visible and IR, at 300 ($3150 \, M^{-1} \, cm^{-1}$), 450 ($900 \, M^{-1} \, cm^{-1}$) and 910 nm ($85 \, M^{-1} \, cm^{-1}$). The peaks in UV and visible are comparable to those in DMF and Me_2SO, but differ by 20 nm from those in propylene carbonate.

Tetrachlorocomplex, $CuCl_4Li_2$. The tetrachlorocomplex has an intense absorption maximum at 280 nm ($5160 \, M^{-1} \, cm^{-1}$) and another at 388 nm ($2170 \, M^{-1} \, cm^{-1}$). These two bands, with slight differences, have been widely reported in many previous works. It is probable that the differences in the position of these bands are due to different solvents used in each work. There seems to be another hidden band of feeble intensity at 490 nm ($180 \, M^{-1} \, cm^{-1}$). In the IR the tetrachlorocomplex peaks out at 1080 nm ($120 \, M^{-1} \, cm^{-1}$).

(f) Isosbestic points

A very good harmony is noted between experimental and calculated isosbestic points.
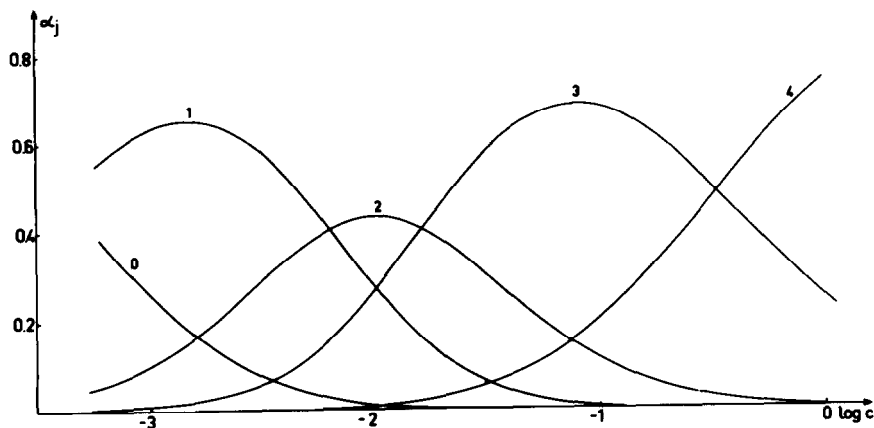
Fig. 3. Formation curves of the copper(II) chlorocomplexes in acetic acid.

Isosbestic points (λ in nm)	
Experimental	Calculated
302	303
357	354
437	437

(g) Formation and structure

Figure 3 represents the formation curves of the four copper(II) chlorocomplexes showing a very different pattern than either in water or in propylene carbonate. It is seen that for dilute solutions, chloride concentrations as low as 0.025 M, the fourth complex begins to form in appreciable quantities.

It is proposed that the tetrachlorocomplex has a D_{2d} symmetry in acetic acid. This can be inferred by the presence of a probable charge transfer band at 490 nm and the absence of any d-d transition band below 1000 nm. It is recalled that the ion of D_{4h} symmetry presents normally two bands in this region, one between 700 and 800 nm and the other between 900 and 950 nm whereas the configuration D_{2d} presents absorption maxima at 1100 nm and above.[20] The presence of a band at 1080 nm and the absence of any band between 700 and 950 nm are favorable arguments for a D_{2d} structure of the tetrachlorocomplex in acetic acid.

REFERENCES

[1] M. J. Schwing-Weill, *Bull. Soc. Chim. Fr.* 1973, **3**, 823.
[2] M. A. Khan and M. J. Schwing-Weill, *Inorg. Chem.* 1976, **15**, 2202.
[3] C. Furlani and G. Morpurgo, *Theor. Chim. Acta* 1963, **1**, 102.
[4] S. Manahan and R. T. Iwamoto, *Inorg. Chem.* 1965, **4**(10), 1409.
[5] H. Hubacek, B. Stancie and V. Gutmann, *Monatsh. Chem.* 1963, **94**, 1118.
[6] M. Baaz, V. Gutmann, G. Hampel and J. Masaguer, *Monatsh. Chem.* 1962, **93**, 1416.
[7] A. Foll, M. Ledemezet and J. Courtot-Coupez, *J. Electroanal. Chem.* 1972, **35**, 41.
[8] J. P. Scharff, *Bull. Soc. Chim. Fr.* 1972, **1**, 43.
[9] M. Elleb, J. Meullemeestre, M. J. Schwing and F. Vierling, *Inorg. Chem.*, 1980, **19**, 2699.
[10] V. Gutmann, *Coordination Chemistry in Non-Aqueous solvents*, p. 30. Springer-Verlag, New York (1968).
[11] M. Elleb, J. Meullemeestre, M. J. Schwing and F. Vierling, *Inorg. Chem.* 1982, **21**, 1477.
[12] R. P. Eswein, E. S. Howald, R. A. Howald and D. P. Keeton. *J. Inorg. Nucl. Chem.* 1967, **29**, 437.
[13] K. Sawada, H. Ohtaki and M. Tanaka, *J. Inorg. Nucl. Chem.* 1972, **34**, 625.
[14] K. Sawada, H. Ohtaki and M. Tanaka, *J. Inorg. Nucl. Chem.* 1972, **34**, 3455.
[15] A. I. Popov, *The Chemistry of Non-Aqueous Solvents* (Edited by J. J. Lagowski, III), p. 243. Academic Press, New York (1970).
[16] K. Sawada and M. Tanaka, *J. Inorg. Nucl. Chem.* 1973, **35**, 2455.
[17] S. Yamada, H. Nakamura and R. Tuschida, *Bull. Chem. Soc. Jap.* 1957, **30**, 953.
[18] R. L. Martin and A. Whitley, *J. Chem. Soc.* 1958, 1394.
[19] Z. Z. Hugus and A. A. El Awady, *J. Phys. Chem.* 1971, **75**, 2954.
[20] M. A. Khan, Thesis. Université Louis Pasteur, Strasbourg, France, 1975.

REACTIONS OF DIIODO(NITROSYL){TRIS(3,5-DIMETHYL-PYRAZOLYL)BORATO}MOLYBDENUM WITH o-DISUBSTITUTED BENZENES CONTAINING OH, SH AND/OR NH₂ GROUPS, THE FORMATION OF MONO-ARYLAMIDO AND MONO-THIOLATO COMPLEXES, AND THE STRUCTURE OF [Mo(NO)(3,5-Me₂C₃HN₂H)₃(O₂C₆H₄)]I₃, THE PRODUCT OF A DEBORONATION REACTION

HARRY ADAMS, NEIL A. BAILEY,* A. STEPHEN DRANE and JON A. McCLEVERTY*†
Department of Chemistry, The University, Sheffield S3 7HF, England

Abstract—Reactions of Mo{HB(Me₂pyz)₃}(NO)I₂ {HB(Me₂pyz)₃ = HB(3,5-Me₂C₃HN₂)₃} with o-C₆H₄(NH₂)₂, o-C₆H₄(NH₂)(OH), o-C₆H₄(NH₂)(SH) and 3,4-C₆H₃Me(SH)₂ afforded the non-substituted species Mo{HB(Me₂pyz)₃}(NO)IX where X = NHC₆H₄NH₂, NHC₆H₄OH, NHC₆H₄SH and SC₆H₃Me(SH). Reaction of the diiodo complex with o-C₆H₄(OH)₂ afforded [Mo(NO)(C₃HMe₂N₂H)₃(O₂C₆H₄)]I₃, whose structure was established by X-ray crystallography.

We have previously described the reactions of Mo{HB(Me₂pzy)₃}(NO)I₂ {HB(Me₂pyz)₃ = HB(3,5-Me₂-C₃H · N₂)₃; (1, X = Y = I)} with thiophenol[1] and with aniline and phenol derivatives[2] in which complexes of the type (1, X = I, Y = SPh), (1; X = I, Y = NHAr) and (1, X = I, Y = OAr) were formed. In some cases we were able to remove the second I atom, affording species such as (1, X = Y = SPh), and (1, X = OR, Y = NHAr; R = alkyl). It occurred to us that we might induce (1; X = Y = I) to react with o-disubstituted benzenes such as o-phenylenediamine, catechol or toluene-3,4-dithiol, forming complexes where the ligand was bidentate towards the metal, both I atoms having been displaced. Such reactions would parallel that of [Mo(η⁵-C₅H₅)(NO)I₂]₂ with toluene-3,4-dithiol, in which [Mo(η⁵-C₅H₅)(NO)(S₂C₆H₃Me)]₂ is formed.[3]

Synthetic studies

Reaction of o-phenylenediamine and o-aminophenol with (1; X = Y = I) afforded the brown or black mono-iodo complexes 1; X = I, Y = o-NHC₆H₄NH₂ or o-NHC₆H₄OH (analytical data, Table 1). NHC₆H₄SH and SC₆H₃MeSH complexes were prepared in

refluxing solutions, but in no case was there any evidence of removal of the second I atom, to afford chelated species e.g. Mo{HB(Me₂pyz)₃}(NO)NHC₆H₄S. Treatment of the reaction mixture containing (1; X = Y = I), C₆H₃Me(SH)₂ and Ag(OAc) afforded a green powder, but we were unable to characterise this compound satisfactorily. From the method of synthesis which we have used to make (1, X = Y = SR)[1], the colour of the compound and the value of ν(NO), we think that Mo{HB(Me₂pyz)₃}(NO)SC₆H₃MeS may have been produced, but in such an impure form that we could not characterise it effectively by elemental analyses.

The reaction with o-catechol followed a different course. In conditions under which we successfully prepared (1; X = I, Y = OPh) and (1; X = Y = OPh), and even in refluxing benzene, we observed no reaction between C₆H₄(OH)₂ and (1; X = Y = I). However, overnight in boiling toluene, a red–brown solution was formed from which we ultimately obtained [Mo(NO)(C₃HMe₂N₂H)₃(O₂C₆H₄)]I₃. This reaction had clearly resulted in the sequestration of the B atom, presumably as B₂(O₂C₆H₄)₃ or [B(O₂C₆H₄)₂]⁻, and, since the complex was obtained in good yields, we presume it was isolated as a mixture of mono- and tri-iodide salts. The complex was actually characterised first by crystallographic methods but finally reasonably good elemental analytical and spectroscopic data were obtained.

---

*Authors to whom correspondence should be addressed.
†Present address: Department of Chemistry, University of Birmingham, P.O. Box 363, Birmingham B15 2TT, England.

Table 1. Elemental analytical data obtained from the molybdenum complexes

Complex	Analytical data: Found(Calc.)%				
	C	H	N	S	I
Mo{HB(Me₂C₃HN₂)₃}(NO)I(NHC₆H₄NH₂)	38.4(38.2)	4.6(4.6)	19.5(19.2)	–	19.0(19.3)
Mo{HB(Me₂C₃HN₂)₃}(NO)I(NHC₆H₄OH)	37.5(38.4)	4.6(4.3)	16.1(17.0)	–	20.0(19.3)
Mo{HBMe₂C₃HN₂)₃}(NO)I(NHC₆H₄SH)	37.1(37.4)	4.5(4.2)	16.0(16.6)	4.5(4.8)	19.4(18.8)
Mo{HB(Me₂C₃HN₂)₃}(NO)I(SC₆H₃MeSH)	37.3(37.5)	4.1(4.1)	13.8(13.9)	9.5(9.1)	18.4(18.0)
Mo(NO)(Me₂C₃HN₂H)₃(O₂C₆H₄)]I₃	28.2(27.9)	2.9(3.1)	10.9(10.9)	–	29.1(42.2)†

†The inaccuracy of this determination may have been due to insufficient degradation of the I₃⁻ ion.

Spectroscopic studies

The IR spectra of the tris(pyrazolyl)borate complexes exhibited (Table 2) the expected absorptions due to the HB(Me$_2$pyz)$_3$ ligand [*ca.* 2500 cm^{-1} due to ν(BH) and *ca.* 1400 cm^{-1} associated with the pyrazolyl ring]. The complex (1; X = I, Y = *o*-NHC$_6$H$_4$NH$_2$) exhibited three ν(NH) bands, at 3280, 3390 and 3490 cm^{-1}, (due to NH and NH$_2$) while (1; X = I, Y = *o*-NHC$_6$H$_4$OH) contained two absorptions, at 3200 cm^{-1} [probably ν(NH)], and 3500 cm^{-1} (broad) [probably ν(OH)]. We were unable to detect ν(SH) in (1; X = I, Y = SC$_6$H$_3$MeSH).

The NO stretching frequencies of those complexes containing NHAr groups occurred in the range normally observed for this class of compound, i.e. 1655–1675 cm^{-1}, and that for (1; X = I, Y = SC$_6$H$_3$MeSH) in the range for mono-arylthiolato species, i.e. *ca.* 1690 cm^{-1} (Ref. 1).

The complex [Mo(NO)(C$_3$HMe$_2$NH)$_3$(O$_2$C$_6$H$_4$)]I$_3$ does not, of course, exhibit ν(BH), but the NO stretching frequency is not substantially different from that of (1; X = Y = OPh).[2]

The ^{1}H NMR spectra of (1; X = I, Y = *o*-

Table 2. IR and ^{1}H NMR spectral studies

Complex	ν(NO)(cm^{-1}) KBr	CHCl$_3$	^{1}H NMR Spectra δ(RA)[a]		assignment
Mo{HB(Me$_2$pyz)$_3$}(NO)I(NHC$_6$H$_4$NH$_2$)	1675	1675	13.24(1)	s;	NHC$_6$H$_4$NH$_2$
			7.25(4)	m;	NHC$_6$H$_4$NH$_2$
			5.88(1)	s	
			5.85(1)	s	C$_3$HMe$_2$N$_2$
			5.80(1)	s	
			3.38(2)	s;	NHC$_6$H$_4$NH$_2$
			2.69	s	
			2.53	s	
			2.47	(18) s	C$_3$H(CH$_3$)$_2$N$_2$
			2.35	s	
			2.0	s	
Mo{HB(Me$_2$pyz)$_3$}(NO)I(NHC$_6$H$_4$OH)	1670	1676	not measured		
Mo{HB(Me$_2$pyz)$_3$}(NO)I(NHC$_6$H$_4$SH)	1668	1664	12.90(1)	s;	NHC$_6$H$_4$SH
			6.70(4)	m;	NHC$_6$H$_4$SH
			5.79(2)	s	C$_3$HMe$_2$N$_2$
			5.69(1)	s	
			3.60(1)	br;	NHC$_6$H$_4$SH
			2.47	s	
			2.38	(18) s	C$_3$H(CH$_3$)$_2$N$_2$
			2.35	s	
			2.01	s	
Mo{HB(Me$_2$pyz)$_3$}(NO)I(SC$_6$H$_3$MeSH)	1684	1687	6.90(3)	brm;	SC$_6$H$_3$MeSH
			6.00(1)	s	
			5.92(1)	s	C$_3$HMe$_2$N$_2$
			5.81(1)	s	
			2.56	s	
			2.50	s	
			2.47	(18) s	C$_3$H(CH$_3$)$_2$N$_2$
			2.33	s	
			2.18(3)	s;	SC$_6$H$_3$CH$_3$SH
[Mo(MO)(C$_3$HMe$_2$N$_2$H)$_3$(O$_2$C$_6$H$_4$)]I$_3$	1671	1669	11.05(3)	br;	C$_3$HMe$_2$N$_2$H
			7.00(4)	m;	O$_2$C$_6$H$_4$
			6.11(1)	s	C$_3$HMe$_2$N$_2$H
			5.92(2)	s	
			2.63(3)	s	
			2.58(3)	s	
			2.52(3)	s	C$_3$H(CH$_3$)$_2$N$_2$H
			2.38(3)	s	
			2.27(6)	s	

[a] Spectrum measured in CDCl$_3$ (TMS internal standard); relative areas of peaks in parentheses.

NHC$_6$H$_4$NH$_2$), and (1; X = I, Y = SC$_6$H$_3$MeSH) contain the expected three signals due to the inequivalent C(4)-H protons of the pyrazolyl ring. The fact that these signals in the spectra of (1; X = I, Y = o-NHC$_6$H$_4$SH) appear as two lines of relative intensity 2:1 is probably due to accidental degeneracy. All complexes exhibit resonances due to the methyl groups of the pyrazolyl rings, and we were also able to observe signals due to NH$_2$ and SH in those complexes containing these groups, and in these complexes with NHAr groups. δ(NH) of the amido group appeared in the range 12.90–13.24 ppm, consistent with previous observations.

It is quite clear from the combined spectroscopic data, and from a comparison of complexes of the type (1; X = I, Y = NHAr), (1; X = OR, Y = NHAr) and (1; X = NHAr, Y = SR), that none of the foregoing species actually contains a chelated ligand, i.e. that species of the type [Mo{HB(Me$_2$pyz)$_3$}(NO)QC$_6$H$_4$EH]^z (Q = O, E = N; Q = E = S or N; $x = 0$, $z = 0$, $x = 1$, $z = +1$) are not formed, confirming our synthetic findings.

The ^{1}H NMR spectrum of [Mo(NO)(C$_3$HMe$_2$NH)$_3$(O$_2$C$_6$H$_4$)]$^+$ was consistent with the structure in the solid state. Thus, it is clear from the C(4)-H resonances that one pyrazolyl ring is magnetically inequivalent to the other two. The signals due to the NH protons appeared as a broad signal at $\delta = 11.05$.

Crystallographic studies

The structure of the cation is illustrated in the Fig. 1 with the atom labelling used in the corresponding tables. Important bond lengths and angles (together with estimated standard deviations) are given in Table 3. Tables comprising all bond lengths and angles with estimated standard deviations and details of planar fragments have been deposited.

The cation possesses a distorted octahedral geometry about the molybdenum with three unidentate dimethylpyrazole ligands in a meridional arrangement, the remaining sites being occupied by a nitrosyl and a biden-
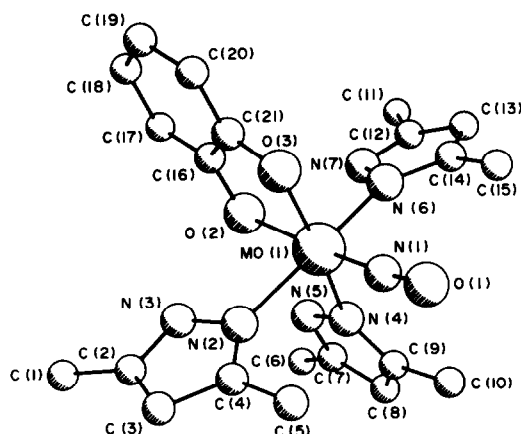
Fig. 1. Structure of the cation [Mo(NO)(3,5-Me$_2$C$_3$HN$_2$H)$_3$(O$_2$C$_6$H$_4$)]$^+$ showing the atom labelling.

tate catecholate ligand. The three dimethylpyrazole ligands have similar and conventional geometries, although it is perhaps worth noting that the external bond angles at the donor nitrogen atoms are very different, Mo-N-C being some 20° greater than Mo-N-N. The three molybdenum-nitrogen(pyrazole) bond lengths are similar, with those to the mutually trans ligands being marginally (2.5σ) shorter than that to the pyrazole which is trans to an oxygen of the catecholate ligand. The planes of two of the pyrazole rings are each approximately perpendicular to the meridional plane; the third pyrazole is inclined at 74°: thus, the three pyrazole planes each approximately eclipse the nitrosyl group. Each pyrazole ring is closely planar with coplanar methyl substituents; the molybdenum atom lying to varying extents (up to 0.2 Å) out of the mean planes. The catecholate ligand is also closely planar with the molybdenum atom lying in the mean plane. The two molybdenum-oxygen bonds differ greatly in length, that trans

Table 3. Bond lengths (Å) and bond angles (°) with estimated standard deviations in parentheses

I(1)–I(2)	2.843(2)	N(1)–O(1)	1.188(18)
I(2)–I(3)	3.017(2)	O(2)–C(16)	1.356(15)
Mo(1)–O(2)	2.093(8)	O(3)–C(21)	1.346(15)
Mo(1)–O(3)	1.933(9)	C(16)–C(17)	1.384(19)
Mo(1)–N(1)	1.771(13)	C(17)–C(18)	1.385(21)
Mo(1)–N(2)	2.140(12)	C(18)–C(19)	1.405(22)
Mo(1)–N(4)	2.169(11)	C(19)–C(20)	1.359(22)
Mo(1)–N(6)	2.143(11)	C(20)–C(21)	1.389(19)
		C(21)–C(16)	1.401(18)
O(2)–Mo(1)–O(3)	79.5(3)	I(1)–I(2)–I(3)	176.23(6)
O(2)–Mo(1)–N(1)	172.3(5)	Mo(1)–N(1)–O(1)	173.3(12)
O(2)–Mo(1)–N(2)	84.8(4)	Mo(1)–O(2)–C(16)	111.8(7)
O(2)–Mo(1)–N(4)	87.6(4)	Mo(1)–O(3)–C(21)	117.0(8)
O(2)–Mo(1)–N(6)	84.9(4)	O(2)–C(16)–C(17)	124.2(12)
O(3)–Mo(1)–N(1)	92.8(5)	O(2)–C(16)–C(21)	115.1(11)
O(3)–Mo(1)–N(2)	95.1(4)	C(21)–C(16)–C(17)	120.6(12)
O(3)–Mo(1)–N(4)	166.7(4)	C(16)–C(17)–C(18)	118.3(13)
O(3)–Mo(1)–N(6)	92.3(4)	C(17)–C(18)–C(19)	121.3(14)
N(1)–Mo(1)–N(2)	95.4(5)	C(18)–C(19)–C(20)	119.9(14)
N(1)–Mo(1)–N(4)	100.2(5)	C(19)–C(20)–C(21)	120.0(14)
N(1)–Mo(1)–N(6)	96.1(5)	C(20)–C(21)–C(16)	120.0(12)
N(2)–Mo(1)–N(4)	86.7(4)	O(3)–C(21)–C(16)	116.5(11)
N(2)–Mo(1)–N(6)	166.0(4)	O(3)–C(21)–C(20)	123.5(12)
N(4)–Mo(1)–N(6)	83.5(4)		

to the nitrosyl ligand being 0.16 Å longer than that *trans* to pyrazole, reflecting the much greater competitive π-accepting capacity of nitrosyl for the available π-electrons. The molybdenum–nitrosyl system is essentially linear. The triiodide anion is also linear but the bond lengths differ markedly (by 0.17 Å, approx. 100σ) although there are no particularly short interactions to the cation.

Conclusion

It appears that the diiodo complex, (1; X = Y = I), is unwilling to form chelated complexes of the type Mo–XC$_6$H$_4$Y. On the basis of our earlier inability to synthesise complexes of the type (1; X = Y = NHR), we were not wholly surprised at our failure to prepare *o*-phenylenediimine complexes. However, we have obtained mixed complexes of the type (1; X = OR, Y = NHR) and (1; X = SR, Y = NHR). It has to be said, however, that none of these mixed species contained NHAr substituents. These observations may be related to the overall mechanism of reaction for the formation of these complexes. We have proposed[4] that the first step in the formation of (1; X = Y, Y = NHR) from (1; X = Y = I) is the one-electron reduction of the latter, giving [(1; X = Y = I)]$^-$ (and of course, RNH$_2^+$). This paramagnetic species dissociates giving [1; X = I, Y = solvent] and I$^-$, and the solvated species is believed to react with NHR (from RNH$_2^+ \rightarrow$ RNH$^\cdot$ + H$^+$) or NHR$_2$, giving the amido complex. If this mechanism is generally applicable, then a second substitution involving a prior electron transfer will involve reduction of (1; X = I, Y = NHR). We know from other studies, that the one-electron reduction of (1; X = I, Y = NHAr) is much more difficult to achieve than that of (1; X = Y = I) (*ca.* −2.0V vs +0.11V),[5] and this probably cannot be achieved by ROH, RSH or RNH$_2$. Consequently, the inability to effect removal of both I atoms, without the assistance of Ag$^+$, is perhaps not so surprising.

The reaction with catechol took a different course, presumably because of the affinity of boron for catecholate ligands. Indeed, sequestration of the B atom in HB(Me$_2$pyz)$_3$ complexes of Mo has been noted by us before, in the reaction between (1; X = Y = I) and acetone or diacetone alcohol.[6] Fragments of this reaction, in particular the bicyclic salt which must be derived from pyrazole, can presumably only be produced after removal of the B atom, presumably by the bidentate O–O' ligand diacetone alcohol.

EXPERIMENTAL

The complex Mo{HB(Me$_2$pyz)$_3$}(NO)I$_2$ was prepared as described previously.[7] All reactions were carried out under N$_2$ in thoroughly degassed solvents. All yields are quoted relative to the metal-containing starting material. IR and ^{1}H NMR spectra were measured using PE 197, PE 180 and PE R34 instruments.

Mo[HB(Me$_2$pyz)$_3$](NO)I(NHC$_6$H$_4$NH$_2$). (1; X = I, Y = *o*-NHC$_6$H$_4$NH$_2$). To a solution of Mo{HB(Me$_2$pyz)$_3$}(NO)I$_2$ (0.5 g) in dichloromethane (20 cm^3) was added *o*-phenylenediamine (0.15 g). The mixture was stirred at room temperature for 2 h during which time a brown solution formed. The solvent was reduced *in vacuo* to *ca.* 5 cm^3, diethylether was added causing precipitation of a white solid (probably C$_6$H$_4$(NH$_2$)$_2$HI), and the filtrate partially evaporated *in vacuo*. On standing at −5°, the *complex* formed as black microcrystals (0.31 g, 63%).

Mo{HB(Me$_2$pyz)$_3$}(NO)I(SC$_6$H$_4$MeOH); (1; X = I, Y = *o*-NHC$_6$H$_4$OH). This complex was prepared in the same way as its *o*-phenylenediamido analogue above, affording a green–brown solution in dichloromethane, from which the *complex* was isolated as a brown powder (0.22 g, 45%).

Mo{HB(Me$_2$pyz)$_3$}(NO)I(NHC$_6$H$_4$OH); (1; X = I, Y = *o*-NHC$_6$H$_4$SH). A mixture of Mo{HB(Me$_2$pyz)$_3$}(NO)I$_2$ (0.3 g), *o*-aminothiophenol (10 drops) and silver acetate (0.1 g) was refluxed in *n*-heptane (40 cm^3) overnight. The purple solution which had formed was cooled and filtered, a black powder being collected. This was dissolved in chloroform, filtered, and to the filtrate *n*-hexane was added. The mixture was slowly evaporated *in vacuo* until crystallisation apparently began. The *complex* was obtained as a dark purple powder (0.15 g, 49%).

Mo{HB(Me$_2$pyz)$_3$}(NO)I(SC$_6$H$_3$MeSH); (1; X = I, Y = *o*-SC$_6$H$_3$MeSH). A mixture of Mo{HB(Me$_2$pyz)$_3$} (NO)I$_2$ (0.5 g) and toluene-3,4-dithiol (0.2 g) was refluxed overnight in *n*-heptane (30 cm^3). The purple solution which had formed was cooled, filtered and a black powder collected. This was washed with methanol and *n*-pentane, affording the complex (0.39 g, 74%).

[Mo(NO)(Me$_2$C$_3$HN$_2$H)$_3$(O$_2$C$_6$H$_4$)]I$_3$. A mixture of Mo{HB(Me$_2$pyz)$_3$}(NO)I$_2$(0.5 g) and *o*-catechol (0.1 g) was refluxed overnight in toluene (30 cm^3). The red–brown solution which formed was then evaporated *in vacuo*, the residual oil being dissolved in dichloromethane. Addition of *n*-hexane to the solution caused preciptation of a red–brown oil which slowly crystallised over three days, giving the *complex* as black needles (0.40 g, 62%).

Crystallographic studies

Crystal data. [Mo(NO)(C$_3$HMe$_2$N$_2$H)$_3$(O$_2$C$_6$H$_4$)$^+$[I$_3$]$^-$; C$_{21}$H$_{28}$I$_3$MoN$_7$O$_3$; M = 903.11, crystallises from dichloromethane/hexane as black, elongated plates; crystal dimensions 0.40 × 0.05 × 0.18 mm. Triclinic a = 10.276(2), b = 10.814(3), c = 15.948(4) Å, α = 106.14(2), β = 86.88(2), γ = 113.14(2)°, U = 1562.3(7) Å^3, D_m = 1.90, D_c = 1.920 g cm^{-3}, Z = 2, space group $P\bar{1}$ (assumed and confirmed by the analysis), Mo K_α radiation ($\bar{\lambda}$ = 0.71069 Å), μ(Mo K_α) = 33.74 cm^{-1}, F(000) = 856.

Three-dimensional X-ray diffraction data were collected in the range $3.5 < 2\theta < 50°$ on a Nicolet/Syntex R3 diffractometer by the omega-scan method. 2437 Independent reflections for which I/σ(I) > 3.0 were corrected for Lorentz and polarisation effects. The structure was solved by superposition, Patterson and Fourier methods and refined by block-diagonal least-squares. Hydrogen atoms were detected and were placed in calculated positions (C–H 0.97, N–H 0.92 Å, C–C–H(methyl) 112°); their contributions were included in structure factor calculations (B = 8.0 Å^2) but no refinement of positional parameters was permitted. Refinement converged at R=0.0443 with allowance for anisotropic thermal motion of all non-hydrogen atoms and for the anomalous scattering of iodine and molybdenum. Tables of atomic positional parameters and anisotropic thermal vibrational parameters each with estimated standard deviations, predicted hydrogen atom positional parameters and observed structure amplitudes and calculated structure factors have been deposited.† Scattering factors were taken from Ref. 8; unit weights were used throughout the refinement; computer programs formed part of the Sheffield X-ray system.

REFERENCES

[1] J. A. McCleverty, A. S. Drane, N. A. Bailey and J. M. A. Smith, *J. Chem. Soc. Dalton Trans.*, 1983, 91.

[2] J. A. McCleverty, G. Denti, A. S. Drane, N. El Murr, A. E. Rae, S. J. Reynolds, N. A. Bailey, H. Adams and J. M. A. Smith, *J. Chem. Soc. Dalton Trans.* 1983, 81.

[3] T. A. James and J. A. McCleverty, *J. Chem. Soc. A* 1971, 1068; J. A. McCleverty and D. Seddon, *J. Chem. Soc. Dalton Trans.* 1972, 2588.

[4] J. A. McCleverty and N. El Murr, *J. Chem. Soc. Chem. Commun.* 1981, 960.

†Copies are available on request from the Editor. Atomic co-ordinates have also been deposited at the Cambridge Crystallographic Data Centre.

[5]C. J. Jones, J. A. McCleverty, B. D. Neaves and S. J. Reynolds, to be published.

[6]H. Adams, N. A. Bailey, G. Denti, J. A. McCleverty, J. M. A. Smith and A. Wlodarczyk, *J. Chem. Soc. Chem. Commun.* 1981, 348.

[7]J. A. McCleverty, D. Seddon, N. A. Bailey and N. W. Walker, *J. Chem. Soc. Dalton Trans.* 1976, 898; C. J. Jones, J. A. McCleverty, S. J. Reynolds and C. Smith, *Inorg. Synthesis,* in press.

[8]*International Tables for X-ray Crystallography,* Vol. 4. Kynoch Press, Birmingham (1974).

ZINC(II), CADMIUM(II) AND MERCURY(II) COMPLEXES OF 4,6-DIMETHYL-PYRIMIDINE-2(1H)-ONE

RAFFAELE BATTISTUZZI* and GIORGIO PEYRONEL

Istituto di Chimica Generale e Inorganica, Università di Modena, 41100 Modena, Italy

Abstract—The following zinc(II), cadmium(II) and mercury(II) complexes of 4,6-dimethylpyrimidine-2(1H)-one (L) have been prepared and investigated by conductometric, IR and Raman methods: MX_2L_2 (M = Zn, X = Cl, Br(CHCl_3), I(CHCl_3), CF_3COO; M = Cd, X = Cl, Br, CF_3COO; M = Hg, X = Cl, CF_3COO), $Cd_2L_4L_3$, $Hg_3X_6L_2$ (X = Cl, Br), $Hg_3X_6L_4$ (X = Br, I), $MX_2L_4·6H_2O$ (M = Zn, Cd, X = ClO_4, BF_4; M = Hg, X = ClO_4). The ligand is principally bonded through the unprotonated nitrogen atom and in some complexes also through the carbonylic oxygen atom. The zinc halide complexes are tetrahedrally coordinated, the trifluoroacetate ion is coordinated as a monodentate ligand.

A problem relating to the binding of metal ions to nucleic acid components[1,2] is concerned with the coordination by exocyclic atoms of derivatives of the base pyrimidine. In previous work we have shown that in most of the zinc(II), cadmium(II) and mercury(II) complexes of neutral and deprotonated 4,6 - dimethylpyrimidine - 2(1H) - thione,[3] the ligand is strongly bonded through the unprotonated nitrogen atom and more weakly bonded through the exocyclic sulphur atom. In all the investigated copper(I) and copper(II) complexes of 4,6 - dimethylpyrimidine - 2(1H) - one[4] the ligand is bonded through the unprotonated nitrogen atom and the carboxylic oxygen atom. Only two zinc and two cadmium complexes of this last ligand have been previously described and partially investigated by IR spectroscopy.[5] We were interested in investigating more systematically, by IR and Raman spectroscopy and conductometric methods, the complexes of this ligand with zinc(II), cadmium(II) and mercury(II) ions.

EXPERIMENTAL

The ligand 4,6 - dimethylpyrimidine - 2(1H) - one (L) was prepared by the method previously reported.[4] The complexes were prepared as follows:

$ZnCl_2L_2$ and $ZnX_2L_2·CHCl_3$ (X = Br, I). A solution of the metal halide (4 mmol) in acetone (3 ml) was added with stirring to a suspension of 8 mmole of the ligand in 15 ml of $CHCl_3$ and 3 ml of acetone. The products precipitated on standing overnight and were washed with $CHCl_3$/acetone (3 : 1).

CdX_2L_2 (X = Cl, Br) and $Cd_2I_4L_3$. The solid metal halide (2.5 mmol) in 10 ml of H_2O (chloride) or EtOH (bromide) was added with stirring to a concentrated aqueous solution (10 ml) of L (5 mmol). The compounds precipitated immediately and, after standing for 2 hr, were washed with EtOH and ethyl ether.

$Hg_3X_6L_2$ (X = Cl, Br). A solution of the metal halide (2.5 mmol) in 10 ml of H_2O (chloride) or EtOH (bromide) was slowly added to a stirred aqueous solution (8 ml) of the ligand (5 mmol). The products precipitated after standing overnight and were washed with H_2O and EtOH.

$HgCl_2L_2$ and $Hg_3Br_6L_4$. An ethanolic solution (5 ml) of the metal halide (2.5 mmol) was added to a stirred solution of L (5 mmol) in 1:1 acetone + $CHCl_3$ (20 ml) and the products were washed with the same mixture.

$Hg_3I_6L_4$. The solid ligand (5 mmol) was dissolved in a solution of HgI_2 (2.5 mmol) in 30 ml of acetone. The resulting solution was concentrated to a small volume (10 ml) *in vacuo* and the light yellow product was washed with EtOH.

$MX_2L_4·6H_2O$ (M = Zn, Cd, X = ClO_4, BF_4; M = Hg, X = ClO_4) and $M(CF_3COO)_2L_2$ (M = Zn, Cd, Hg). An acetone solution (5 ml) of the metal salt (2 mmol) was added to a hot solution of 8 mmol of L (4 mmol for the trifluoroacetates) in 20 ml of 1:1 acetone + $CHCl_3$. Upon concentrating or cooling the solutions the products crystallized and were washed with 1:3 acetone + $CHCl_3$.

All the complexes are white or slightly yellow. They were dried *in vacuo* over KOH. The analyses of the metal ions were carried out by complexometric titration of EDTA[6] and for carbon, hydrogen and nitrogen by microanalysis. Conductivity measurements were performed on freshly prepared DMF solutions with a WTW conductivity bridge type L.B.B. (Table 1).

Infrared spectra were recorded on the solids as Nujol mulls or KBr disks (4000–250 cm⁻¹) and on polythene (600–60 cm⁻¹) with a Perkin–Elmer 180 spectrophotometer. Raman spectra (20–600 cm⁻¹) were recorded on the solids with a Jobin Yvon Ramanor HG2S spectrometer equipped with a Spectra-Physics 165 argon ion laser (514.5 nm line) using a rapidly rotating sample holder. The spectra were calibrated by means of the plasma lines of the laser. Satisfactory Raman spectra could not be obtained for the perchlorates, for all the mercury complexes, and for the zinc fluoroborate complex because these compounds were unstable or highly fluorescent under the laser beam. The spectra are reported in Table 2.

The molecular weights of the halide and trifluoroacetate complexes could not be determined because of their very low solubility or insolubility in all the solvents suitable for cryoscopic or osmometric measurements.

RESULTS AND DISCUSSION

The molar conductivities indicate that the halide complexes behave as non-electrolytes in DMF solution, excepting the zinc iodide complex which has a 1:1 electrolyte conductivity ($\Lambda_M = 65$–90),[7] probably due to solvolysis. The molar conductivity of the $Hg_3Br_6L_4$ complex ($\Lambda_M = 40$) excludes an ionic constitution such as [HgL_4][Hg_2Br_6] or [Hg_2Br_2L_4][HgBr_4]. The molar conductivities of $Cd_2I_4L_3$ ($\Lambda_M = 40$) and of the trifloroacetate complexes ($\Lambda_M = 54$–60), just under the lower limit of the 1:1 electrolyte conductivities, may indicate a partial solvolysis. The perchlorate and fluoroborate complexes have molar conductivities ($\Lambda_M = 133$–158) corresponding to those of 1:2 electrolytes ($\Lambda_M = 130$–170).[7]

In the IR spectra of the $ZnX_2L_2·CHCl_3$ (X = Br, I) complexes, two very strong bands at 758 and 750 cm⁻¹ may be assigned to the chloroform deformation mode (ν_5, E).[8]

---

*Author to whom correspondence should be addressed.

Table 1. Analytical data, found % (calcd.%) and molar conductivities $\Lambda_M(\Omega^{-1}\,mol^{-1}\,cm^2)$ in 10^{-3} M DMF solution at 25°C of the 4,6-dimethylpyrimidine-2(1H)-one (L) complexes

	M	C	H	N	Λ_M
$ZnCl_2L_2$	17.01(17.00)	37.23(37.44)	4.23(4.19)	14.44(14.56)	6
$ZnBr_2L_2\cdot CHCl_3$	11.01(11.03)	26.29(26.31)	2.89(2.89)	9.45(9.44)	11
$ZnI_2L_2\cdot CHCl_3$	9.50(9.52)	22.75(22.71)	2.51(2.50)	8.19(8.15)	92
$Zn(CF_3COO)_2L_2$	12.09(12.11)	35.58(35.58)	3.06(2.99)	10.31(10.37)	61
$Zn(BF_4)_2L_4\cdot 6H_2O$	7.75(7.75)	34.09(34.14)	5.30(5.26)	13.25(13.28)	135
$Zn(ClO_4)_2L_4\cdot 6H_2O$	7.51(7.52)	33.10(33.15)	5.08(5.10)	12.89(12.89)	144
$CdCl_2L_2$	25.98(26.04)	33.30(33.36)	3.71(3.73)	12.89(12.97)	17
$CdBr_2L_2$	21.60(21.59)	27.70(27.66)	3.10(3.09)	10.60(10.76)	18
$Cd_2I_4L_3$	20.36(20.36)	19.57(19.55)	2.19(2.19)	7.60(7.60)	40
$Cd(CF_3COO)_2L_2$	19.15(19.15)	32.71(32.72)	2.78(2.75)	9.56(9.54)	55
$Cd(BF_4)_2L_4\cdot 6H_2O$	12.62(12.62)	32.27(32.34)	4.90(4.98)	12.56(12.58)	154
$Cd(ClO_4)_2L_4\cdot 6H_2O$	12.15(12.27)	31.46(31.44)	4.76(4.84)	12.14(12.23)	158
$HgCl_2L_2$	38.34(38.59)	27.55(27.70)	3.09(3.10)	10.43(10.77)	6
$Hg_3Cl_6L_2$	56.49(56.62)	13.45(13.55)	1.47(1.52)	5.16(5.27)	15
$Hg_3Br_6L_2$	45.19(45.26)	10.89(10.83)	1.24(1.21)	4.17(4.21)	11
$Hg_3Br_6L_4$	37.98(38.14)	18.11(18.25)	2.02(2.04)	7.03(7.09)	40
$Hg_3I_6L_4$	32.29(32.33)	15.44(15.47)	1.74(1.73)	5.90(6.02)	14
$Hg(CF_3COO)_2L_2$	29.66(29.72)	28.27(28.45)	2.43(2.39)	8.18(8.29)	54
$Hg(ClO_4)_2L_4\cdot 6H_2O$	19.71(19.88)	28.64(28.68)	4.34(4.41)	11.08(11.16)	133

In the 1750–1600 cm^{-1} region the ligand and its L·HCl derivative show several bands which are more distinct for the spectra recorded in Nujol mulls and in CHCl₃ solution than those recorded in KBr disks. Only the frequencies recorded in Nujol mulls will be considered for the ligand and its complexes:

L (CHCl₃ solution)	1720 m,
L (Nujol mulls)	1738 m,
L. HCl (Nujol mulls)	1740 vvs.

In the ZnX_2L_2 complexes, which are tetrahedral, the ligand is certainly monodentate. These complexes clearly show a blue shift of the ligand band at 1667 cm^{-1} to 1685–1675 cm^{-1} and a red shift of the ligand band at 1628 cm^{-1} to 1620–1610 cm^{-1}. These frequency shifts agree well with an electronic shift such as that resulting from the following resonance forms:
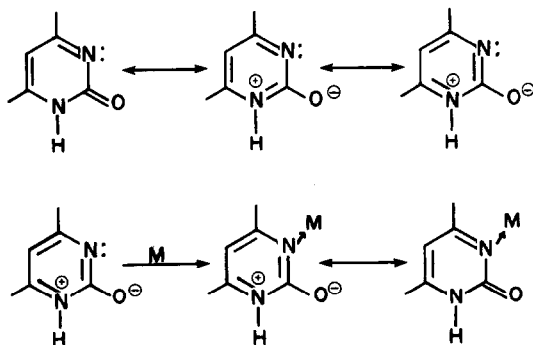
in which the coordination of the unprotonated nitrogen atom gives an increased C=O and a decreased C=N double bond character. In the pyrimidine - 2 - one

hydrochloride the protonation of the unprotonated ring-nitrogen atom gives rise to a shortening of the C=O and an elongation of both the C—N—C bonds.[9,10]

Consequently a predominantly ν(C=O) character may be assigned to the band at 1667 cm^{-1} and a predominantly ν(C=N) character to the band at 1628 cm^{-1},

1680 ms,	1655 vvs,	1625 vvs	cm^{-1}
1692 m,	1667 vvs,	1628 vvs	
1715 s,	1682 ms,	1625 vvs.	

even if this mode is coupled with other ring vibration modes.

A red shift is observed for the band at 1628 cm^{-1} for all the complexes of this series. A blue shift of the band at 1667 cm^{-1} is observed for all the zinc complexes, while for the cadmium complexes and the mercury perchlorate, fluoroborate, and trifluoroacetate complexes two very strong bands appear at 1687–1660 and 1670–1650 cm^{-1}.

In the far IR spectra of the complexes new mostly strong bands are observed in the 320–270 cm^{-1} region. Similar freqeuncies were observed for the ν(MN) bands of the 4,6 - dimethylpyrimidine - 2(1H) - thione complexes of zinc (II), cadmium(II) and mercury(II) ions[3] and other cations[11,12] and also for the Cu(I) and Cu(II) complexes of 4,6 - dimethylpyrimidine - 2(1H) - one.[4]

Halide complexes

The ZnX_2L_2 (X = Cl, Br, I) complexes show two ν(ZnN) and two ν(ZnX) bands, all IR and Raman active, supporting a (2N, 2X) tetrahedral coordination. The ν_{Br}/ν_{Cl} (0.83–078) and ν_I/ν_{Cl} (0.67–0.65) ratios are almost in the range accepted for complexes having similar coordination environments.[13] The ν(ZnBr) and ν(ZnI) frequencies are close to many other literature values

Table 2. Principal for IR and Raman (R) bands (cm^{-1}) of the 4,6-dimethylpyrimidine-2(1H)-one (L) complexes

	ν(ML)	ν(MX)
$ZnCl_2L_2$	326m,303s	272vs,258vs
	R 322vw,304vw	276vw,258mw
$ZnBr_2L_2 \cdot CHCl_3$	300m,280ms	225vs,201vs
	R 298vw,285wm	229w,205mw
$ZnI_2L_2 \cdot CHCl_3$	297mw,279sm	183vs,167vs
	R 287wm,282w	182vw,168vw
$Zn(ClO_4)_2L_4 \cdot 6H_2O$	302sh,295m,240ms,203m	
$Zn(BF_4)_2L_4 \cdot 6H_2O$	301sh,292mw,238ms,202ms	
$Zn(CF_3COO)_2L_2$	307vs,275vs	210vs,195vs
	R 307w,283wm	213vw,188mw
$CdCl_2L_2$	300s,245vs	245vs,238vs
	R 300w,249m	249m,238m
$CdBr_2L_2$	300s,249ms	200vs,182vs
	R 302w,252wm	194mw,183w
$Cd_2I_4L_3$	295ms,259ms	170s,155vs
	R 300w,258wm	179m,158s
$Cd(ClO_4)_2L_4 \cdot 6H_2O$	298ms,273sm,255mw,223m	
$Cd(BF_4)_2L_4 \cdot 6H_2O$	295ms,267ms,254mw,223ms	
	R 295wb,266wm	
$Cd(CF_3COO)_2L_2$	301vs,273vs,254mw	185sh,168vs
	R 303w,280w,258mw	188wm,158vw
$HgCl_2L_2$	302ms	239vs,221vs
$Hg_3Cl_6L_2$	305sh	320vs,224s,206s
$Hg_3Br_6L_2$	294m	248vs,227vs,174m
$Hg_3Br_6L_4$	295ms	250m,219vs
$Hg_3I_6L_4$	291m	193ms,101vs
$Hg(ClO_4)_2L_4 \cdot 6H_2O$	295m,274m,255mw,207mb	
$Hg(CF_3COO)_2L_2$	301ms,270vs	211sm,160s
L IR	264s,282mw,227wm,210m,197sh,96ms	
R	353mw,252w,220w,187mw,133wm,109s,96wm	
L.HCl IR	340vs,293w,213sm,145vs,124vs,98ms	

while the ν(ZnCl) frequencies are slightly lower than most of those reported in the literature, and this explains the rather high ν_X/ν_{Cl} ratios. However, ν(ZnCl) frequencies close to the present values are also reported in the literature: 270,266 cm^{-1} [14] and 276,264 cm^{-1} [15].

The CdX$_2$L$_2$ (X = Cl, Br) and Cd$_2$I$_4$L$_3$ complexes show two ν(CdN) and two ν(CdX) bands, all IR and Raman active, with ν(CdX) frequencies in agreement with many other literature values for terminal Cd–X bonds. The ν_{Br}/ν_{Cl} (0.82–0.76) and ν_I/ν_{Cl} (0.72–0.65) ratios are in an acceptable range for similar coordination environments. A substantially tetrahedral coordination may therefore be assigned to these complexes. However, because of the tendency of cadmium ion to adopt six coordination, a flattened 2N, 2X tetrahedron with axial interactions may also be possible for the CdX$_2$L$_2$ complexes. The dinuclear Cd$_2$I$_4$L$_3$ complex has terminal Cd–I bonds and probable (N, O)-bridging ligand molecules. The fact that in

these complexes the ligand ν (CO) band at 1667 cm^{-1} gives rise to two very strong bands, one of which is at a lower frequency, indicates that the carbonyl oxygen atom is involved in the coordination.

The HgCl$_2$L$_2$ complex shows one ν(HgN) band corresponding to trans-coordinated ligand molecules and two ν(HgCl) bands whose low frequency values correspond to bridging metal–chloride bonds. For the Hg$_3$X$_6$L$_2$ (X = Cl, Br) and Hg$_3$X$_6$L$_4$ (X = Br, I) complexes an ionic constitution may be excluded on the basis of their molar conductivities.

Perchlorate, fluoroborate and trifluoroacetate complexes

Some of the IR bands of the perchlorate, fluoroborate and trifluoroacetate ions, and particularly the ν_1 band of the perchlorate ion, are superimposed on ligand bands and may only tentatively be assigned:

ClO_4^-	Zn	1125 sh,	1110 vs,	1065 vs,	(927 ms),	623 vs	cm^{-1}
	Cd	1095 vs,	(910 mb),	623 vs			
	Hg	1095 vs,	(915 sh),	622 vs			
BF_4^-	Zn	1080 vs,	765 wm				
	Cd	1090 s,	1054 vs,	1025 s,	760 w,	518 m	

CF_3COO^-	Zn	1715 vs,	1700 vs,	1437 s,	1425 sm,	$\Delta(CO_2) = 278, 275$
	Cd	1745 sh,	1687 vs,	1444 s		301, 243
	Hg	1745 sm,	1430 sm			315

The slight distortion from T_d symmetry for the perchlorate and floroborate ions[16] may be attributed to hydrogen bonds. The $\Delta(CO_2)$ separations for the trifluoroacetate ions correspond to unidentate behaviour.[17]

The $MX_2L_4 \cdot 6H_2O$ (X = ClO_4, BF_4) complexes show at 3500–3400 cm^{-1} a medium strong broad band associated with $\nu(OH)$ modes of lattice water. No characteristic bands of coordinated water could be recognized in the 880–500 cm^{-1} region.[18] These complexes show four new bands attributable to $\nu(ML)$ modes, the anions and the water molecules being very likely not coordinated. Probably some of the ligand molecules are bonded through the ring nitrogen and the carbonylic oxygen atoms. This point of view is supported by the fact that in the cadmium and mercury complexes the $\nu(CO)$ band at 1667 cm^{-1} gives rise to two very strong bands instead of one.

In the $M(CF_3COO)_2L_2$ (M = Zn, Cd, Hg) complexes the anion is coordinated in a monodentate fashion. The very strong band at about 275 cm^{-1} may be superimposed in the zinc and cadmium complexes on the medium or weak band of the trifluoro-acetate anion appearing in the 270–280 cm^{-1} region[19] which is distinctly observed at 277 cm^{-1} in the mercury complex. Two $\nu(MN)$ and two $\nu(MO)$ bands, all IR and Raman active, indicate a tetrahedral (2N, 2O)-coordination for the zinc trifluoroacetate complex, for which bridging ligand molecules may be excluded because a single very strong $\nu(CO)$ band is observed at 1673 cm^{-1}. For the cadmium trifluoroacetate complex, three bands assignable to metal-ligand stretching modes, all IR and Raman active, indicate that the carbonyl oxygen atom is also involved in the coordination. This probably occurs also for the mercury trifluoroacetate complex. For both these complexes, indeed, the $\nu(CO)$ band at 1667 cm^{-1} gives rise to two very strong bands at 1687 and 1670 cm^{-1} for the cadmium and at 1680 and 1652 cm^{-1} for the mercury complex.

The ligand acts therefore preferably as N-monodentate for the zinc ion and more frequently as N,O-bidentate for the cadmium and mercury(II) ions.

REFERENCES

[1] D. J. Hodgson, *Progr. Inorg. Chem.* 1977, 23, 211.
[2] L. G. Marzilli, *Progr. Inorg. Chem.* 1977, 23, 255.
[3] R. Battistuzzi and G. Peyronel, *Spectrochim. Acta* 1980, 36A, 113.
[4] R. Battistuzzi and G. Peyronel, *Spectrochim. Acta* 1980, 36A, 511.
[5] M. Goodgame and K. W. Jones, *Inorg. Chim. Acta* 1981, 55, 15.
[6] H. A. Flaschka, *EDTA Titrations.* Pergamon Press, New York (1964).
[7] W. J. Geary, *Coord. Chem. Rev.* 1971, 7, 81.
[8] J. C. T. Rendell and L. K. Thompson, *Can. J. Chem.* 1979, 57, 1.
[9] S. Furberg and J. Solbakk, *Acta Chem. Scand.* 1970, 24, 3230.
[10] S. Furgerg and J. B. Aas, *Acta Chem. Scand.* 1975, A29, 713.
[11] R. Battistuzzi and G. Peyronel, *Transition Met. Chem.* 1978, 3, 345.
[12] R. Battistuzzi and G. Peyronel, *Can. J. Chem.* 1981, 59, 591.
[13] A. M. Brodie and C. J. Wilkins, *Inorg. Chim. Acta* 1974, 8, 13.
[14] G. B. Aitken, J. L. Duncan and G. P. McQuillan, *J. Chem. Soc. Dalton* 2103 (1972).
[15] G. P. Kennedy and A. B. P. Lever, *Can J. Chem.* 1972, 50, 3488.
[16] D. H. Brown, R. H. Nuttal, J. McAvoy and D. W. A. Sharp, *J. Chem. Soc. (A)* 892 (1966).
[17] G. B. Deacon and R. J. Phillips, *Coord. Chem. Rev.* 1980, 33, 227.
[18] K. Nakamoto, *Intrared Spectra of Inorganic and Coordination Compounds*, p. 167. Wiley, New York (1970).
[19] K. O. Christe and D. Naumann, *Spectrochim. Acta* 1973, 29A, 2017.

COPPER(I) AND SILVER(I) COMPLEXES OF
2-AMINO-1,3,4-THIADIAZOLE AND
2-ETHYLAMINO-1,3,4-THIADIAZOLE

ANTONIO C. FABRETTI, GIORGIO PEYRONEL*, ALEARDO GIUSTI and ALINE F. ZANOLI

Istituto di Chimica Generale e Inorganica, Università di Modena, 41100 Modena, Italy

Abstract—The following copper(I) and silver(I) complexes of 2-amino-1,3,4-thiadiazole (*atz*) and 2-ethylamino-1,3,4-thiadiazole (*eatz*) have been prepared and studied by conductometric, IR and Raman methods: CuXL(X = Cl, Br, I; L = *atz, eatz*), CuXL$_3$(X = ClO$_4$, NO$_3$; L = *atz, eatz*), AgClO$_4$·1.5*atz*·1/3 EtOH, AgNO$_3$·2.5*atz*, AgClO$_4$·3*eatz*, AgNO$_3$·*eatz*. The ligands are bonded through the amine nitrogen atoms with ν(MN) bands in the 520–410 cm^{-1} region. The CuXL complexes have a trigonal (N, 2X$_b$) coordination with a probable weaker axial interaction. The CuXL$_3$ and AgClO$_4$·3*eatz* complexes probably have a trigonal pyramidal (3N, O) coordination. In the *atz* complexes of silver perchlorate and nitrate some ligand molecules are bridging. The AgNO$_3$·2.5*atz* complex is likely to have a dimeric structure with tetrahedral coordination of the silver ion.

The copper(I) and silver(I) complexes of 2-amino-1,3,4-thiadiazole (*atz*) and 2-ethylamino-1,3,4-thiazole (*eatz*) have been prepared and studied in order to compare the coordination behaviour of these ligands which differ from each other only by the presence of an ethyl substituent in the amine group.

EXPERIMENTAL

The ligands *atz* (Fluka), *eatz* (Eastman Kodak) and the other reagents were of the best commercial grade. The compounds were prepared as follows.

CuXL(X = Cl, Br; L = atz, eatz)

A warm solution of CuCl$_2$·2H$_2$O (or CuBr$_2$) (0.5 mmol) in EtOH (2 cm^3) was slowly added to a warm solution of L (3 mmol) and hydroquinone (3 mmol) in EtOH (8 cm^3). The compounds precipitated instantaneously and were stirred in their mother solutin for about 1 hr. Then they were filtered and washed with EtOH and dried *in vacuo* on KOH.

CuIL and CuClO₄L₃(L = atz, eatz)

A solution of Cu(NO$_3$)$_2$·3H$_2$O (0.5 mmol) or Cu(ClO$_4$)$_2$·6H$_2$O (0.5 mmol) respectively, in H$_2$O (1 cm^3) was slowly added, with stirring, to a solution of L (3 mmol) and KI (0.5 mmol) (for the iodides) or NaClO$_4$ (0.5 mmol) (for the perchlorates) and hydroquinone (0.5 mmol) in EtOH (2 cm^3) and H$_2$O (8 cm^3). The instantaneous precipitates were stirred for some time in their mother solution, filtered and washed with a mixture of EtOH and H$_2$O (1:4) and EtOH.

CuNO₃L₃ (L = atz, eatz)

A solution of Cu(NO$_3$)$_2$·3H$_2$O (1 mmol) in EtOH (5 cm^3) was added, with stirring, to a solution of L (1 mmol) and hydroquinone (2 mmol) in EtOH (8 cm^3). The instantaneous precipitates were stirred for some time in their mother solution, filtered and washed with EtOH.

AgNO₃·2.5atz, AgClO₄·1.5atz, AgNO₃·eatz, AgClO₄·3eatz

A solution of the silver salt (0.5 mmol) in EtOH (3 cm^3) was added to a warm solution of L (1.5 mmol) in EtOH (3 cm^3). The instantaneous precipitates were stirred for some time in their mother solution, filtered and washed with EtOH. The compounds

could not be recrystallized but they appeared as homogeneous and pure crystals under the microscope.

The compounds are white excepting the cooper iodide and the silver perchlorate complexes which are light brown. Any attempt to prepare the solid silver halide complexes was unsuccessful. The silver halides dissolve in a DMF solution of the ligands, indicating that complexes are formed in solution, but are reprecipitated by other solvents such CHCl$_3$, C$_6$H$_{12}$, or C$_6$H$_6$.

The compounds were analysed by standard methods (Table 1). Molar conductivities were determined with a WTW conductivity bridge. IR spectra (Table 2) were recorded in KBr disks (4000–250 cm^{-1}) and as Nujol mulls on polythene (600–60 cm^{-1}) with a Perkin–Elmer 180 spectrophotometer. The IR spectra of the silver complexes were also recorded in the 4000–250 cm^{-1} region as Nujol mulls on KBr disks in order to avoid any reaction of the silver ion with potassium bromide. The Raman spectra were recorded with a Jobin–Yvon Ramanor HG 2S spectrometer equipped with a Spectrophysics 165 argon ion laser using the 514.5 nm line.

RESULTS AND DISCUSSION

The ν(NH) bands shown by the ligands in CHCl$_3$ solution in the 3440–3210 cm^{-1} region are shifted to lower frequencies for the *atz*-(3370–3150 cm^{-1}) and *eatz*-complexes (3240–3100 cm^{-1}).

The very strong band at 1507 cm^{-1} for *atz* and 1517 cm^{-1} for *eatz* is assignable to ring vibration modes with a high ν(C = N) contribution[1]. This band appears at 1510–1505 cm^{-1} for the *atz* copper halides and at 1527–1514 cm^{-1} for the other *atz* complexes and shifts to 1588–1550 cm^{-1} for the *eatz* complexes.

A ν(C–NHR) contribution may be assigned[2] to the *eatz* band at 1198 cm^{-1} which shifts to lower frequencies (1160–1148 cm^{-1}) in its complexes.

An important ν(C–S) contribution may be attributed[2] to the bands appearing at 680 and 610 cm^{-1} for *atz* and 610 cm^{-1} for *eatz*. They show increased frequencies in the *atz* (700–695 and 640–626 cm^{-1}) and *eatz* (640–622 cm^{-1}) complexes.

All these frequency shifts agree well with the electronic shifts:

---
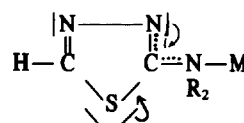
*Author to whom correspondence should be addressed.

Table 1. Analytical data, found % (calc. %) and molar conductivities $\Lambda_M(\Omega^{-1}\,mol^{-1}\,cm^2)$ at 24°C in 10^{-3} M DMF solution of the *atz* and *eatz* complexes

	N	C	H	Λ_M
CuCl·atz	20.58(20.99)	11.94(12.00)	1.39(1.51)	46
CuBr·atz	17.15(17.18)	9.85(9.82)	1.10(1.24)	ins.
CuI·atz	14.36(14.41)	8.60(8.24)	0.90(1.04)	29
CuNO$_3$·3 atz	32.12(32.65)	16.92(16.80)	2.10(2.11)	53
CuClO$_4$·3 atz	27.31(27.03)	15.76(15.45)	1.88(1.95)	94
AgNO$_3$·2.5 atz	27.86(28.17)	14.32(14.21)	1.72(1.79)	60
AgClO$_4$·1.5 atz·1/3 EtOH	16.82(16.84)	11.73(11.77)	1.68(1.75)	62
CuCl·eatz	18.42(18.42)	21.39(21.05)	3.05(3.09)	36
CuBr·eatz	15.23(15.41)	17.93(17.62)	2.56(2.59)	36
CuI·eatz	13.00(13.15)	15.12(15.03)	2.14(2.21)	ins.
CuNO$_3$·3 eatz	27.06(27.30)	27.97(28.09)	4.22(4.13)	63
CuClO$_4$·3 eatz	22.82(22.90)	26.26(26.18)	3.96(3.84)	70
AgNO$_3$·eatz	18.66(18.73)	16.08(16.07)	2.29(2.36)	62
AgClO$_4$·3eatz	21.44(21.19)	24.46(24.23)	3.60(3.56)	42

Table 2. Principal IR and Raman (R) bands (cm^{-1}) of the *atz* and *eatz* complexes

		ν (MN)	ν (MX)
CuCl·atz		426 vs	201 vs,186 wm
CuBr·atz		425 sh	145 s,133 w
CuI·atz		462 sm	132 m,103 mw
	R		138 sh,107 vs
CuClO$_4$·3 atz	(a)	466 vsb,418 vs	172 s
CuNO$_3$·3 atz	(b)	511 s,423 s	180 s
	R	420 ms	185 sh
AgClO$_4$·1.5 atz·1/3 EtOH	(c)	456 ms	166 s
AgNO$_3$·2.5 atz	(d)	506 s,406 vs	161 s
CuCl·eatz		447 s	224 ms,204 vs
	R	449 ms	225 wb,203 wm
CuBr·eatz		443 s	161 vs,158 s
	R	445 ms	169 s,158 s
CuI·eatz		441 s	149 vs,125 wm
	R	442 ms	141 s
CuClO$_4$·3 eatz	(e)	446 vs	183 ms
CuNO$_3$·3 eatz	(f)	446 vs	183 sm
	R	447 m	185 sh
AgClO$_4$·3 eatz	(g)	520 s,442 vs	(175 vs,169 vs)
AgNO$_3$·eatz	(h)	448 s	
	R	450 m	

ClO$_4^-$ bands: (a) 1140 vs, 1110 vs, 1082 vs, 940 w, 622 s, 466 vsb

(c) 1140 s, 1105 sh, 1085 vs, 940 w, 626 sm

(e) 1154 s, 1105 s, 1087 vs, 930 sm, 623 vs

(g) 1155 s, 1105 s, 1088 vs, 928 mw, 625 vs, 460 w

NO$_3^-$ bands: (b) 1290 sh, 828 w, 715 sh (d) 828 wm, 710 w

(f) 1495 wm, 1290 w, 850 mb, 715 sh

(h) 1290 vs, 1017 s, 840 m, 720 mw

Ligands bands < 500 cm^{-1} atz : 410 vs,279 w,266 mw,225 w,177 mb,130 vs

eatz : 401 s,339 w,278 wb, 243 wm,178 m,149 w,126 wb,117 wb

due to a R_2N-coordination of the ligand to the metal.

Some new bands appearing at 511–425 and 520–442 cm^{-1} for the *atz* and *eatz* complexes, respectively, may be assigned to $\nu(MN)$ modes in agreement with the frequency values reported for an amine nitrogen coordination[3] and for the complexes of similar ligands.[4-7]

Both ligands form $CuXL(X = Cl, Br, I; L = atz, eatz)$ complexes behaving as non-electrolytes in DMF solution.[8] Their $\nu(CuX)$ frequencies are in the range of values given for bridging CuX bonds[9-11] with ν_{Br}/ν_{Cl} (0.78–0.72) and ν_I/ν_{Cl} (0.67–0.56) ratios in the range given for complexes with similar coordination environments[12]. A single $\nu(CuN)$ and two $\nu(CuX)_b$ bands, IR and Raman active (when observed in the Raman spectrum) indicate for these complexes a trigonal $(N, 2X_b)$ coordination, with a probable longer axial interaction as frequently occurs in cuprous complexes.

The molar conductivities in DMF solution of the perchlorate and nitrate complexes are mostly at the lower limit or below the values given for 1 : 1 electrolytes $(\Lambda_M = 65–90\ \Omega^{-1}\ mol^{-1}\ cm^2)^8$. Some IR bands may be assigned (Table 2) to the perchlorate and nitrate ions even if with some difficulty for the nitrates because of the superposition of the ligand bands. For most of these complexes the anion bands indicate that they are coordinated in the solid state[3] even if the molar conductivities indicate a more or less pronounced solvolysis in solution. Some new far IR bands may be tentatively assigned to $\nu(MO)$ modes.

For the $CuXL_3(X = ClO_4, NO_3; L = atz, eatz)$ complexes a trigonal pyramidal coordination with three Cu–N bonds in the base and a weaker apical Cu–O bond seems to be likely.

The same trigonal pyramidal coordination may be proposed for the $AgClO_4 \cdot 3eatz$ complex which shows two $\nu(AgN)$ bands and a $\nu(AgO)$ band localizable either at 175 or 169 cm^{-1}.

For the $AgNO_3 \cdot eatz$ complex a single $\nu(AgN)$ band, IR and Raman active, corresponds to the bond of the silver ion with the aminic nitrogen atom. No bands could be identified corresponding to bonds of the silver ion either with a ring nitrogen atom of a bridging ligand molecule or with the nitrate ion which may act as mono- or bidentate.

The *atz* complexes of silver perchlorate and nitrate have a fractional number of ligand molecules per silver ion. The $AgNO_3 \cdot 2.5atz$ complex is likely to have a dimeric $(L_2AgNO_3)_2L$ structure with a bridging ligand molecule and tetrahedral coordination of the silver ion.

REFERENCES

[1] A. C. Fabretti, G. C. Franchini and G. Peyronel, *Transition Met. Chem.*, 1982, 7, 306.

[2] C. N. R. Rao, *Chemical Application of Infrared Spectroscopy*, pp. 251, 297. Academic Press, New York (1963).

[3] J. R. Ferraro, *Low-Frequency Vibrations of Inorganic and Coordination Compounds*. pp. 79, 219. Plenum Press, New York (1971).

[4] A. C. Fabretti, G. Peyronel and G. C. Franchini, *Inorg. Chim. Acta* 1979, 35, 49.

[5] M. R. Gajendragad and U. Agarwala, *J. Inorg. Nucl. Chem.* 1975, 37, 2429.

[6] M. R. Gajendragad and U. Agarwala, *Bull. Chem. Soc. Japan* 1975, 48, 1024.

[7] M. R. Gajendragad and U. Agarwala, *Indian J. Chem.* 1975, 13, 1331.

[8] W. J. Geary, *Coord. Chem. Rev.* 1971, 7, 81.

[9] B. K. Teo and D. M. Barnes, *Inorg. Nucl. Chem. Lett.* 1976, 12, 681.

[10] W. R. McWhinnie and V. Rattanaphani, *Inorg. Chim. Acta* 1974, 9 153.

[11] L. Volponi, B. Zarli and G. G. DePaoli, *Inorg. Nucl. Chem. Lett.* 1972, 8, 309.

[12] A. Brodie and C. J. Wilkins, *Inorg. Chim. Acta* 1974, 8, 13.

POLAROGRAPHIC STUDY OF Sn(IV) CHLORIDE-PYRIDINE N-OXIDE COMPLEXES IN ACETONITRILE

A. DRTIL,† JAY MEUX,† J. W. MEUX, R. J. WILLIAMS and J. W. ROGERS*

Department of Chemistry, Midwestern State University, Wichita Falls, TX 76308, U.S.A.

Abstract—Polarograms recorded of Sn(IV) chloride in acetonitrile in the presence of controlled quantities of each of nine substituted pyridine N-oxide ligands demonstrated the formation of stable and soluble complexes with a stoichiometry dependent upon the nature and position of the ring substituent. The polarographic data associated with each complex and the free ligands are used to substantiate a proposed bonding model which explains the dependency of the complex formula on the ligand structure.

The salt $SnCl_4 \cdot 5H_2O$ was employed as a source of Sn(IV) and the complete polarographic behaviour of this salt in acetonitrile is described as a basis for the interpretation of complex reduction behaviour.

Results of IR and proton magnetic resonance studies of complexes of substituted pyridine N-oxides with $SnCl_4$ in acetonitrile (ACN) solution have recently been reported.[1] Two types of behaviour were noted. Pyridine N-oxide donors containing electron releasing substituents were generally found to form strong complexes with $SnCl_4$ and exhibited maxima in continuous variation plots at a 2:1 ligand-to-metal ratio. Pyridine N-oxide donors containing electron neutral to electron withdrawing substituents were found to form generally weaker complexes with $SnCl_4$ and exhibited maxima in continuous variation plots at a 1:1 ligand-to-metal ratio. Evidence for multi-nuclear and 2:1 or higher complexes was discussed and the results were rationalized in terms of an equilibrium model for this system.

The essential elements of the model include the assumption of octahedral geometry for all complexes of sterically unhindered N-oxide ligands and a consideration of the contribution of $d\pi p\pi$ backbonding to the coordinate bond and the effect of this bonding on the possible *cis-trans* isomerism in these complexes. The importance of $d\pi p\pi$ backbonding in these complexes should be dependent upon the degree of orbital energy matching between the d-orbitals of tin and the lowest unoccupied π^* orbital of the ligand. Electron releasing substituents on a pyridine N-oxide ring are expected to raise the energy of this π^* orbital so that it is too high in energy for effective overlap and, therefore, diminish the importance of $d\pi p\pi$ bonding in $SnCl_4$ complexes of these ligands. Complexes containing pyridine N-oxide ligands with electron releasing substituents were then expected to form stable, *trans*-2:1 complexes resulting in maxima in continuous variation plots at a 2:1 ligand-to-metal ratio.

Electron withdrawing substituents on a pyridine N-oxide ring are expected to lower the energy of the lowest unoccupied π^* orbital and enhance $d\pi p\pi$ backbonding. Assuming this backbonding is an important component of the coordinate bond, these ligands would be expected to form *cis*-2:1 complexes which were postulated subsequently to form stable, oxygen bridged dimers in solu-

tion. This would result in the observed maxima in continuous variation plots at a 1:1 ligand-to-metal ratio for these complexes.

Previously published UV spectrophotometric and electrochemical data demonstrate that tin (IV) chloride, $SnCl_4$ is a nonelectrolyte in ACN and that in this solvent the neutral complex acts as the Lewis acceptor.[2] The electrochemical reduction of $SnCl_4$ occurs *via* irreversible steps, not allowing the application of standard methods to the determination of thermodynamic properties. However, the polarographic studies have previously been shown to provide a straightforward means of specifying the electrolyte properties and stoichiometry of Sn(II) and Sn(IV) complexes in the low basicity solvent ACN.[2-4]

In an attempt to confirm the results of the IR and proton magnetic studies and to further test the proposed bonding model extensive polarographic data have been taken on solutions of $SnCl_4$ in ACN containing controlled quantities of a series of substituted pyridine N-oxides. The polarographic behaviour of a metal complex is frequently dictated by properties of the metal moiety.[5] In contrast, the data leading to the previously postulated bonding model are derived from physical properties directly associated with the ligand in complexed and noncomplexed states.

Polarographic data presented herein support the previously presented IR and proton magnetic data and the resulting conclusions and bonding model. Various substituted pyridine N-oxides are found to form complexes with $SnCl_4$ in ACN in a ligand-to-metal coordination ratio dependent on the electronic nature of the ring substituent. The polarographic test solutions were prepared from the solid pentahydrate of $SnCl_4$ as opposed to the liquid anhydrous form. The polarographic characteristics of the pentahydrate salt in ACN, not previously reported, are discussed in detail as a basis for interpretation of polarographic data relating to the complexation chemistry of Sn(IV) chloride acting as a Lewis acceptor.

EXPERIMENTAL

Chemicals. All pyridine N-oxide ligands (Aldrich Chemical Co.) were purified by sublimation or vacuum distillation before use. $SnCl_4 \cdot 5H_2O$ (Pfaltz and Bauer) was utilized without purification following confirmatory quantitative analysis. Spec-

---

*Author to whom correspondence should be addressed.
†Robert A. Welch Foundation Undergraduate Scholars.

troquality acetonitrile containing less than 0.03% water (Aldrich Chemical Co.), polarographic-grade tetrapropylammonium perchlorate and tetramethylammonium chloride (Southwestern Analytical Chemicals) were employed throughout. The supporting electrolyte, tetrapropylammonium perchlorate, was recrystallized from acetonitrile-water solutions and vacuum dried before use. All solutions were prepared and transferred under a nitrogen atmosphere.

Apparatus. The polarographic cell was of conventional design and has been described previously.[6] The polarograms were recorded on a Houston Instruments Omnigraphic 2000 X-Y plotter using a Princeton Applied Research Model 173 potentiostat and Exact Model 7050 wave form generator for potential control.

RESULTS

Polarography of Sn(IV) chloride pentahydrate in ACN

Polarographic test solutions of ACN, containing 1.0 mM $SnCl_4$ prepared from the pentahydrate salt, $SnCl_4 \cdot 5H_2O$ and 1.0 M tetrapropylammonium perchlorate, exhibited two well-defined reduction current plateaus, Fig. 1(a). The lower potential plateau exhibiting a half-wave potential of -0.08 V vs saturated calomel (s.c.e.) does not exhibit the distortion or the maximum noted in the corresponding wave of similar test solutions prepared from anhydrous $SnCl_4$.[2] The higher potential wave is very broad and preceded by an adsorption maximum. The half-wave potential of the wave appears near 1 V vs s.c.e. The ratio of the total current of both waves to the square root of the corrected mercury column head height is constant signifying diffusion control. The current constants (Id) of the low and high potential waves measured at 25°C and at 1.0 mM con-

centration are 4.01 and 9.43 respectively (DME characteristics at open circuit and 50 cm Hg head: $m = 0.049$ mg/sec, $t = 6.50$ sec). Both currents are apparently the result of irreversible electrochemical processes (slope of $\log[(id - i)/i]$ vs EDME for wave appearing at -0.08 V is 120 mV).

Addition of measured quantities of noncomplexed chloride ion in the form of tetramethylammonium chloride (TMACl) to the polarographic test solution resulted in a behaviour analogous to that exhibited by $SnCl_2$ and $SnCl_4$ solutions prepared from the anhydrous form of each.[2,3] Increasing quantities of chloride up to 2.0 mM decreased the plateau current of the lower potential wave. The total polarographic current is unaltered. The lower potential wave is no longer detectable at concentrations of added chloride exceeding a ratio of 2:1 with respect to the metal. Only at concentrations of added chloride exceeding the 2:1 ratio is the characteristic oxidation of chloride observed at positive dropping mercury electrode potentials.

The observed behaviour of polarographic test solutions prepared from $SnCl_4 \cdot 5H_2O$ in the presence of added chloride is consistent with the behaviour demonstrated by solutions prepared from anhydrous $SnCl_4$ even though the half-wave potential at the lower potential wave is significantly more negative and is not distorted. These data are consistent with an electrode reduction mechanism in which a water complex of $SnCl_4$ is reduced at the first polarographic wave, releasing free chloride thereby controlling the wave current by displacement of water and subsequent production of the hexachloro complex $SnCl_6^{2-}$, a species reducible only at potentials of the second polarographic wave.[2-4] This sequence of events may be represented in the following manner:

Lower potential wave

$$SnCl_4(H_2O)_2 + Hg + 4e^- \rightarrow Sn(Hg) + 2H_2O + 4Cl^-$$
$$SnCl_4(H_2O)_2 + 2Cl^- \rightarrow SnCl_6^{2-} + 2H_2O.$$

Higher potential wave

$$SnCl_6^{2-} + Hg + 4e^- \rightarrow Sn(Hg) + 6Cl^-.$$
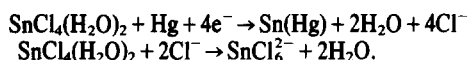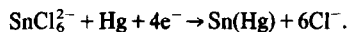
Polarography of Sn(IV) chloride pyridine N-oxide complexes

The stable physical properties of the pentahydrate form of Sn(IV) chloride and the lack of distortions in its polarograms in ACN made it a desirable source of the salt for polarographic studies dealing with the Lewis acceptor properties of $SnCl_4$ in a weakly coordinating solvent. Consistent with previous studies,[1] the effects of adding controlled quantities of substituted pyridine N-oxides to polarographic test solutions prepared from $SnCl_4 \cdot 5H_2O$ in ACN containing TRAP supporting electrolyte reveal the production of complexes with stoichiometries that are dependent upon the nature and position of ring substituents.

Addition of the ligands pyridine N-oxide (pno), 3-pyridine methanol N-oxide (3-pmno), 2-picoline N-oxide (2-picno), 4-phenylpyridine N-oxide (4-phenpno), 3-picoline N-oxide (3-picno) and 4-picoline N-oxide (4-picno) in sufficient quantities to bring test solutions of 1.0 mM $SnCl_4 \cdot 5H_2O$ to ligand-to-metal ratios of 1:2, 1:1, 2:1 and 2.5:1 bring about very similar changes in the structure of the resulting polarograms. Polarograms
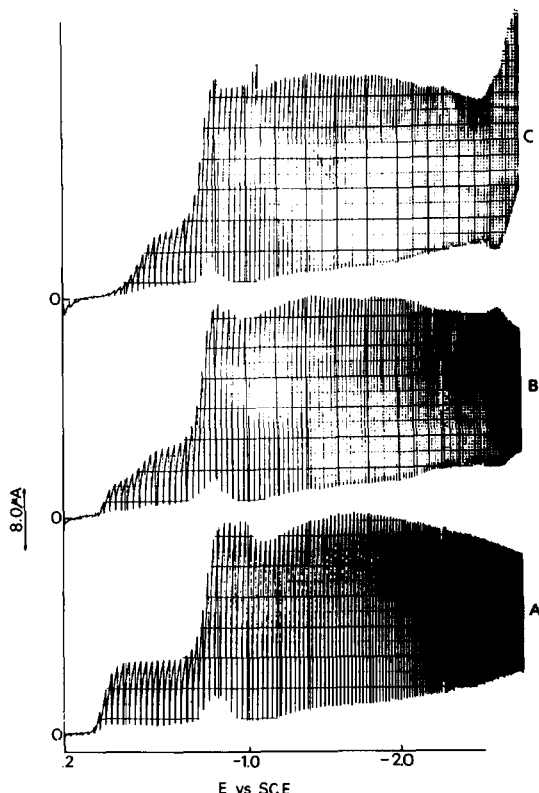
Fig. 1. Polarogram of (a) 1.0 mM $SnCl_4 \cdot 5H_2O$ in ACN (b) 1.0 mM $SnCl_4 \cdot 5H_2O$ in ACN containing 1.0 mM pno (c) 1.0 mM $SnCl_4 \cdot 5H_2O$ in ACN containing 2.0 mM pno.

recorded in solutions containing 0.5 mM ligand (1:2 ratio) exhibit pronounced splitting of the lower potential wave resulting in a new polarographic plateau appearing near −0.3 V vs s.c.e., Figs. 1 and 2. It is reasonable to assume that the appearance of this wave signifies the existence and subsequent reduction of a SnCl₄-pyridine N-oxide complex. Increasing ligand to metal ratios bring about an increase in this complex reduction plateau current at the direct expense of the plateau current attributable to the reduction of the substrate complex, SnCl₄·2H₂O, Fig. 2. The ratio of the complex wave current to the metal chloride substrate wave current is 1.0 at a ligand-to-metal ratio of 1.0, Fig. 2. The plateau current associated with the reduction of SnCl₄·2H₂O is not detectable at a organic ligand to metal ratio of 2:1 or greater, Fig. 2. These data obviously suggest the formation of a stable SnCl -pno adduct with the stoichiometry SnCl₄·2L.

The properties of the polarographic wave associated with the reduction of each SnCl₄·2L complex are equivalent but at variance with those of the reduction wave of SnCl₂·2H₂O. The polarographic $E_{1/2}$ of the reduction plateau of each complex is observed to be −0.33 V vs s.c.e. The complex wave deviates slightly from diffusion controlled behaviour and is significantly broadened relative to that of the Sn(IV) chloride reduction, Fig. 2. The current constant (Id) is found to be 3.64. The plateau current associated with the reduction of the $SnCl_6^{-2}$ complex is unperturbed by addition of organic ligands and subsequent complex formation, Fig. 1.
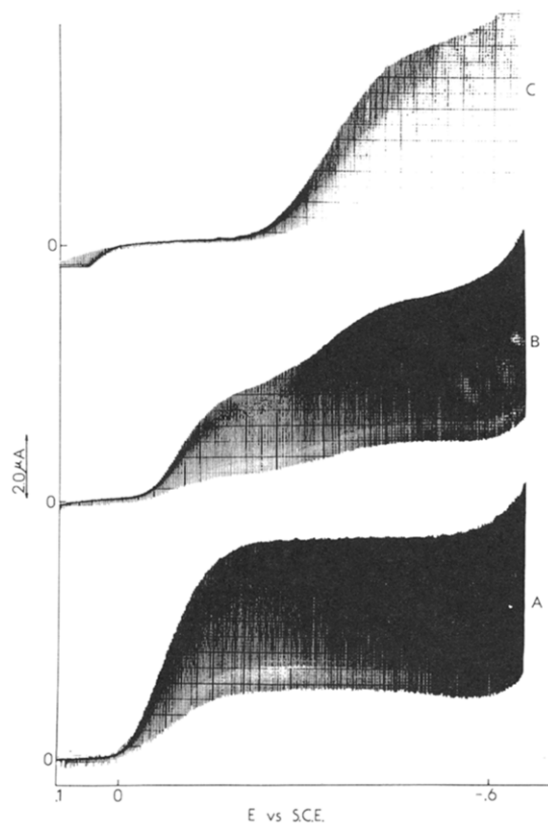
Addition of the ligands 2,6-lutidine N-oxide (lno), 2-pyridinemethanol N-oxide (2-pmno) and 4-chloropyridine N-oxide (4-Clpno) in sufficient quantities to bring test solutions of 1.0 mM SnCl₄·5H₂O to a ligand-to-metal ratio of 0.5:1 splits the lower potential polarographic plateau into two waves of equal current. Increasing the organic ligand-to-metal ratio to 1:1 brings about the complete replacement of the lower potential plateau by the complex reduction plateau suggesting the formation of a stable complex with the stoichiometry SnCl₄·L.

The characteristics of the plateau current associated with the reduction of each SnCl₄·L complex are equivalent. The polarographic $E_{1/2}$ is observed to be −0.29 V vs s.c.e. The wave is broadened relative to that of the reduction of SnCl₄·SH₂O and the observed current constant (Id) value of 3.26 is less than that of SnCl₄·2H₂O and the SnCl₄·2L complexes. The wave attributable to the reduction of $SnCl_6^{2-}$ is characteristically unaltered.

Addition of noncomplexed chloride in the form of tetramethylammonium chloride (TMACl) to test solutions containing ligand enhances the plateau current resulting from the reduction of $SnCl_6^{2-}$ at the direct expense of the wave attributable to the reduction of the complex. For example, see Fig. 3. The complex reduction current is not detectable in test solutions containing equal molar volumes of pyridine N-oxide ligand TMACl. The characteristic wave associated with the oxidation of chloride is observed only in test solutions containing TMACl in excess of the Sn(IV) chloride substrate.

Each of the nine substituted pyridine N-oxide ligands described herein exhibits a characteristic polarographic reduction plateau at potentials negative of the plateau

Fig. 2. Polarograms showing only lowest potential cathodic waves (expanded scale) of ACN solutions containing (a) 1.0 mM SnCl₄·5H₂O (b) 1.0 mM SnCl₄·5H₂O and 1.0 mM pno (c) 1.0 mM SnCl₄·5H₂O and 2.0 mM pno.
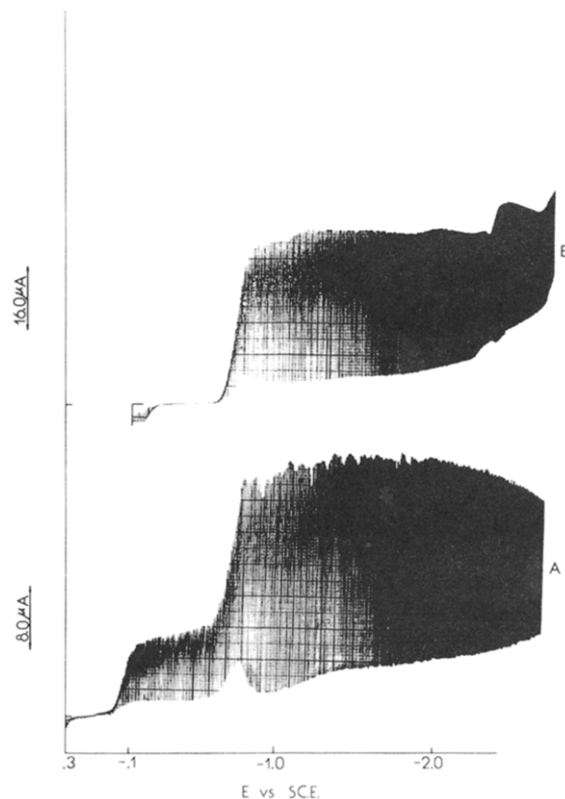
Fig. 3. Polarograms of (a) 1.0 mM SnCl₄·5H₂O in ACN and (b) 1.0 mM SnCl₄·5H₂O in ACN containing 2.0 mM pno and 2.0 mM TMACl (reduced scale).

currents associated with the reduction of all Sn(IV) species produced and described in ACN, Fig. 3. The compounds pno, 4-Clpno, 2-, 3- and 4-picno, lno and 4-phenpno each exhibit reversible one-electron reduction plateaus at -2.26, -1.88, -2.33, -2.30, -2.30, -2.43 and -2.00 V respectively. The compounds 2- and 3-methanolpyridine N-oxide exhibit a two-wave reduction process probably resulting from the reduction of the methanolic hydrogen and the subsequent reduction of the anion product.

The reduction plateau characteristic of each N-oxide is observed to be superimposed on the total current resulting from the reduction of all Sn(IV) species. The current associated with the reduction of the noncomplexed ligand varies in proportion to the concentration in the range 0.5–10 mM.

DISCUSSION

Data have been presented which demonstrate that in ACN the salt $SnCl_4 \cdot 5H_2O$ is reduced in two electrochemical steps resulting in well-defined polarographic current plateaus via a mechanism analogous to that previously reported for anhydrous $SnCl_4$.[2] This information has been used as a basis for a polarographic study of $SnCl_4$-pno complex formation in ACN. Addition of each of the six ligands pno, 3-pmno, 2-picno, 4-phenpno, 3-picno and 4-picno to test solutions containing $SnCl_4$ in a ligand to metal ratio of 2:1 brings about the replacement of the plateau associated with the reduction of the water complex of $SnCl_4$ with a current plateau that may be reasonably associated with the reduction of a pyridine N-oxide $SnCl_4$ adduct having the formula $SnCl_4 \cdot 2L$. Similarly conducted experiments employing the ligands lno, 2-pmno and 4-Clpno reveal analogous behaviour but with the formation of adducts apparently having the forlula $SnCl_4 \cdot L$. The polarographic reduction current associated with the reduction of the stable $SnCl_6^{2-}$ complex is unperturbed in all polarographic experiments conducted in this study.

The polarographic wave associated with the reduction of each 2:1 complex appears at an $E_{1/2}$ of -0.33 V and is irreversible. According to conventional criteria the wave current deviates slightly from diffusion control behaviour and the measured current constant value of 3.64 is small in comparison to most four-electron processes. Similar observations related to $SnCl_4$ electrochemistry have been discussed previously.[2,7,8]

The polarographic wave associated with the reduction of each of the three 1:1 complexes studied appears at an $E_{1/2}$ of -0.29 V and is irreversible. The measured current deviates slightly from diffusion controlled behaviour and the current constant value of 3.26 is suppressed relative to that of $SnCl_4 \cdot 2H_2O$ as well as that of the 2:1 complexes.

The destruction of the 2:1 and the 1:1 complex reduction wave as well as that of $SnCl_4 \cdot 2H_2O$ by the addition of TMACl and the concurrent enhancement of the wave associated with the reduction of the $SnCl_6^{2-}$ complex ion demonstrates the great stability of the hexachloro anion relative to each of the other complexes of Sn(IV). The unperturbable current wave and the predictably large current constant of the four-electron reduction of the $SnCl_6^{2-}$ anion also signifies its great stability and diffusion controlled reduction.

These observations may be summarized with the following set of reactions:

First Cathodic Wave (Lowest Cathodic Potential)

$$SnCl_4 \cdot 2H_2O(s) + Hg + 4e^- \rightarrow Sn(Hg) + 4Cl^-(s) + 2H_2O$$
$$SnCl_4 \cdot 2H_2O(s) + 2Cl^-(s) \rightleftarrows SnCl_6^{2-}(s) + 2H_2O.$$
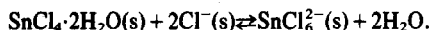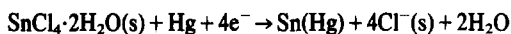
Second Cathodic Wave (Complex Reduction)

$$SnCl_4 \cdot nL(s) + Hg + 4e^- \rightarrow Sn(Hg) + 4Cl^-(s) + nL(s)$$
$$SnCl_4 \cdot nL(s) + 2Cl^-(s) \rightleftarrows SnCl_6^{2-}(s) + nL(s).$$
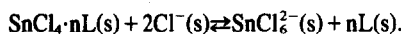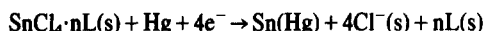
Third Cathodic Wave

$$SnCl_6^{2-}(s) + Hg + 4e^- \rightarrow Sn(Hg) + 6Cl^-(s).$$
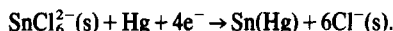
Fourth Cathodic Wave (Highest Cathodic Potential)

$$L + e^- \rightleftarrows L^{\cdot-}.$$
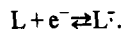
Where L is pno, 2, 3, and 4-picno, 4-phenpno and 4-Clpno.

In addition to these reactions describing the electrochemistry of $SnCl_4$ species in ACN and the current ratios which define the formulas of stable adducts, two other polarographic observations are central to the postulated bonding model[1] and its relationship to the nature of ring substituents. These are the polarographic $E_{1/2}$ values of the noncomplexed ligands and the diminished currents of the reduction waves of the 1:1 complexes relative to those of the 2:1 complexes and the $SnCl_4 \cdot 2H_2O$ complex.

It is postulated that the increased matching of metal d-orbitals with lowest π^* ligand orbitals through lowering of the π^* energy as a result of the electronic and mesomeric effects of electron withdrawing substituents enhances $d\pi p\pi$ backbonding promoting the formation of stable 1:1 complexes at the expense of the 2:1 form. The reported polarographic $E_{1/2}$ values of those ligands which undergo reversible one-electron reductions are, with the exception of lno[1], clearly consistent with the postulated substituent effect on the lowest π^* orbital. As an example, the $E_{1/2}$ values of 4-picno (2:1 complex) and 4-Clpno (1:1 complex) are -2.30 and -1.878 V respectively. It is well known that the value of the polarographic $E_{1/2}$ for a reversible electrochemical reaction is proportional to the Hückel (HMO) value of the lowest π^* energy.[9,10,11] Employing the calculations of Streitwieser[12] in which the $E_{1/2}$ values of fifty aromatic substances undergoing reversible one-electron additions in aqueous dioxane (the dielectric effects of the solvent are found to be small) are correlated with the HMO value of the lowest π^* orbital, the difference in the $E_{1/2}$ between 4-picno and 4-Clpno corresponds to a lowest π^* energy lowering by Cl-substitution of approx. 0.38 eV.

This observed sensitivity of the lowest π^* orbital of pyridine N-oxide to substituents in the 2- and 4-position is predicted by HMO calculations using generally accepted heteroatom parameters for nitrogen and oxygen exchange and Coulomb integrals.[12] Treating both 2- and 4-position substituents as Coulomb perturbations by varying the Coulomb parameter, h, of the 2- or 4-carbon in the conventional manner[12] over a range of 2.0 shifts the lowest π^* energy of 4-substituted pyridine N-oxides by 0.44 β_0 units and of 2-substituted pyridine N-oxides by 0.67 β_0 units. Treating a 3-position substituent per-

turbation in a similar manner does not alter the lowest π^* energy. The highest bonding π-orbital energy is unaltered by substitution in all calculations.

Empirical evidence presented in previous studies[1] in support of the proposed existence of 1:1 complexes in an oxygen-bridged dimeric form is indirect at best. Consequently the diminution of the 1:1 complex reduction current relative to that of the 2:1 complex reduction current appears to be quite significant but must be interpreted with caution owing to the complex nature of the electrochemical processes controlling the wave current. All polarographic wave currents are found to be proportional to the concentration of the reduced species in the range 1.0–10.0 mM and all wave currents are the result of four-electron processes. Additionally, the polarographic data suggests that the production of free chloride in the double layer and the concomitant production of $SnCl_6^{2-}$ from all $SnCl_4$ complexes diffusing to the electrode surface is rapid and irreversible. This results in a constant, current-limiting effect, on each of the current waves resulting from the reduction of a $SnCl_4$ complex. Consequently the diminished current of the 1:1 complex may be explained in terms of a diminished diffusion coefficient. This, in turn, supports the existence of a 1:1 species of larger physical dimension than the 2:1 species, i.e. a dimeric complex.

REFERENCES

[1] C. L. Wild, M. Spahis, R. D. Blankenship, J. W. Rogers and R. J. Williams, *Polyhedron*, to be published.

[2] L. K. Young, M. E. Coles, J. W. Meux, S. D. Sorey, R. J. Williams and J. W. Rogers, *J. Electrochem. Soc.* 1980, 127, 1525.

[3] A. R. Brajer, T. E. Farley, J. W. Kauffman, L. K. Young, R. J. Williams and J. W. Rogers, *Anal. Chim. Acta* 1977, 91, 165.

[4] D. Pool, L. K. Young, R. J. Williams and J. W. Rogers, *Anal. Chim. Acta* 1977, 92, 361.

[5] L. Meites, *Polarographic Techniques.* Interscience, New York (1965).

[6] W. N. Greig and J. W. Rogers, *J. Electrochem. Soc.* 1970, 117, 1141.

[7] F. G. Thomas and I. M. Kolthoff, *J. Electroanal. Chem. Interfacial Electrochem.* 1971, 31, 423.

[8] I. M. Kolthoff and J. J. Lingane, *Polarography*, Vol. 2, Chap. XXIII and XXXI. Interscience, New York (1952).

[9] H. A. Laitinen and S. Wawzouek, *J. Am. Chem. Soc.* 1942, 64, 1765.

[10] S. Wawzonek and H. A. Laitinen, *J. Am. Chem. Soc.* 1942, 64, 2365.

[11] G. J. Hoijtink and J. van Schooten, *Rec. Trav. Chim.* 1952, 71, 1089.

[12] A. Streitwieser Jr., *Molecular Orbital Theory for Organic Chemist.* Wiley, New York (1961).

PHOTOSUBSTITUTION IN SOME CYANIDE COMPLEXES OF CHROMIUM(III)[1]

ADAM MARCHAJ and ZOFIA STASICKA*

Institute of Chemistry, Jagiellonian University, Karasia 3, 30–060 Kraków, Poland

Abstract—Photosubstitution by OH⁻ ligand was concluded from a photochemical study of the $[Cr(CN)_6]^{3-}$ and $[Cr(CN)_5OH]^{3-}$ complexes in alkaline medium. Photoaccelerated aquation was found to proceed in the case of aquocyanochromates(III): $[Cr(CN)_5H_2O]^{2-}$ and $[Cr(CN)_3(H_2O)_3]$.

Ligand-field photochemistry of hexacyanochromate(III) has been studied repeatedly.[2-11] It was concluded that the only photochemical mode arising from continuous irradiation was photosolvation of one CN⁻ ligand

$$[Cr(CN)_6]^{3-} \xrightarrow[S]{h\nu} [Cr(CN)_5S]^{2-} + CN^- \qquad (1)$$
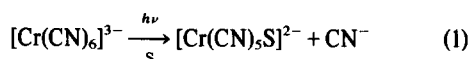
where $S = H_2O$,[4,5,9-11] DMF,[7,9] or DMSO.[6] Photochemical solvation was reported to be followed by secondary processes leading in aqueous solutions to aquation of further CN⁻ ions by thermal[5] or photochemical[4] routes.

The photochemical behavior of aquocyanochromates(III) was not studied in detail except for the $[Cr(CN)(H_2O)_5]^{2+}$ complex. In this case photoaquation of the CN⁻ ligand

$$[Cr(CN)(H_2O)_5]^{2+} \xrightarrow[H_2O]{h\nu} [Cr(H_2O)_6]^{3+} + CN^- \qquad (2)$$
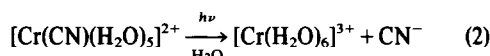
was reported to proceed with a relatively high quantum yield.[12]

In this paper the photochemical study of the $[Cr(CN)_6]^{3-}$ complex has been extended to strongly alkaline solution. To solve the problem of secondary processes, the photochemical behaviour of hexacyanochromate(III) and some relatively stable cyanochromates(III) substituted by H_2O or OH⁻ ligands, was followed using both continuous illumination and flash photolysis techniques.

RESULTS AND DISCUSSION

In all systems studied no transient species could be observed upon flashing at delay times longer than 10 μs.

The only product observed in flash photolyzed solutions of hexacyanochromate(III) was the aquopentacyanochromate(III) complex, except when pH was too high. Then, the $[Cr(CN)_5OH]^{3-}$ complex was recorded with delay times between microseconds and seconds The results obtained at lower pH values were consistent

with the reported earlier photoaquation (eqn 1) following the reactive decay of the quartet excited state.[7-9]

In strongly alkaline medium, the photosubstitution by OH⁻ ligand

$$[Cr(CN)_6]^{3-} \xrightarrow[OH^-]{h\nu} [Cr(CN)_5OH]^{3-} + CN^- \qquad (3)$$
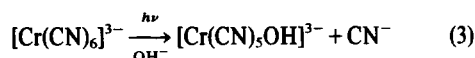
or rapid deprotonation of the aquopentacyanochromate(III) complex was considered. The latter path is supported by the value of the protonation constant of $[Cr(CN)_5OH]^{3-}$, reported[13] to be about 10^9. However, unlike the thermal aquation,[14] the photosubstitution was found to be accelerated by an increase in pH. The photosubstitution quantum yield values measured in this as well as in other studies (Table 1) increase nearly linearly with an increase in pH†. The correlation strongly suggests that the photosubstitution by OH⁻ ligand (eqn 3) is effectively competing with photoaquation in alkaline solutions of the hexacyanochromate(III) complex.

From the data presented in Table 1 the influence of spectral range on the photosubstitution quantum yield can also be followed. In accordance with the previous report[5] this seems to be insignificant although its importance seems greater at higher pH. Moreover, in alkaline solutions of hexacyanochromate(III) in the presence of oxygen, a quite new photochemical mode[15] was found to accompany the photosubstitution upon exposure to radiation with $\bar{\nu} > 33 \times 10^3$ cm⁻¹.

Prolonged irradiation of the $[Cr(CN)_6]^{3-}$ solution leads to a substitution of further CN⁻ ligands by H_2O molecules or OH⁻ ions, depending on pH. To solve the problem of secondary processes, thermal and photochemical behaviour of the $[Cr(CN)_5H_2O]^{2-}$ and $[Cr(CN)_5OH]^{3-}$ complexes has been compared. Thermal substitution of the latter complex was found to proceed slightly more slowly than that of the aquo-complex. For both complexes substitution was shown to be considerably photoaccelerated, as illustrated in Fig. 1. However, in both cases, the first possible substitution product, $[Cr(CN)_4(H_2O)_2]^-$ or $[Cr(CN)_4(OH)_2]^{3-}$, was never observed.‡ Instead, $[Cr(CN)_3(H_2O)_3]$ was the first product recorded both in thermal and photochemical aquation of aquopentacyanochromate(III), while a mixture of hydroxocyanochromates(III) was observed upon exposure of the $[Cr(CN)_5OH]^{3-}$ complex. Due to lack of any transient species even at 20 μs upon flashing, no suggestions about the detailed mechanism could be made. In alkaline medium, an additional difficulty arose

---

*Author to whom correspondence should be addressed.

†Only the first result[4] provides an exception, presumably due to inadequacies in the analytical method used.

‡These complexes were also never isolated by other authors. For a more detailed discussion concerning the $[Cr(CN)_4(H_2O)_2]^-$ species see Ref. 13.

Table 1. Photosubstitution quantum yields

Complex	pH	λ [nm] ($\bar{\nu} \times 10^{-3}$ [cm^{-1}])						References
		436 (22.9)	405 (24.5)	366 (27.4)	313 (31.9)	280 (35.7)	265 (37.7)	
$[Cr(CN)_6]^{3-}$	?			0.1	0.1	0.1		9
	3			0.10				10
	5.3			0.119[b] ±0.003	0.105[b] ±0.003		0.12[b] ±0.01	this work
	6.8			0.16	0.18			4
	8.9	0.14	0.118	0.125	0.111			5
	14			0.149[b] ±0.010	0.118[b] ±0.003			this work
$[Cr(CN)_5H_2O]^{2-}$	5.8	0.045[a] ±0.004						this work
$[Cr(CN)_5OH]^{3-}$	14	0.091[a,b] ±0.006		0.074[a,b] ±0.015	0.063[a,b] ±0.005			this work
$[Cr(CN)_3(H_2O)_3]$	5.3	0.07[a] ±0.01		0.02[a] ±0.007				this work

[a] from substrate analysis ;   [b] from product analysis
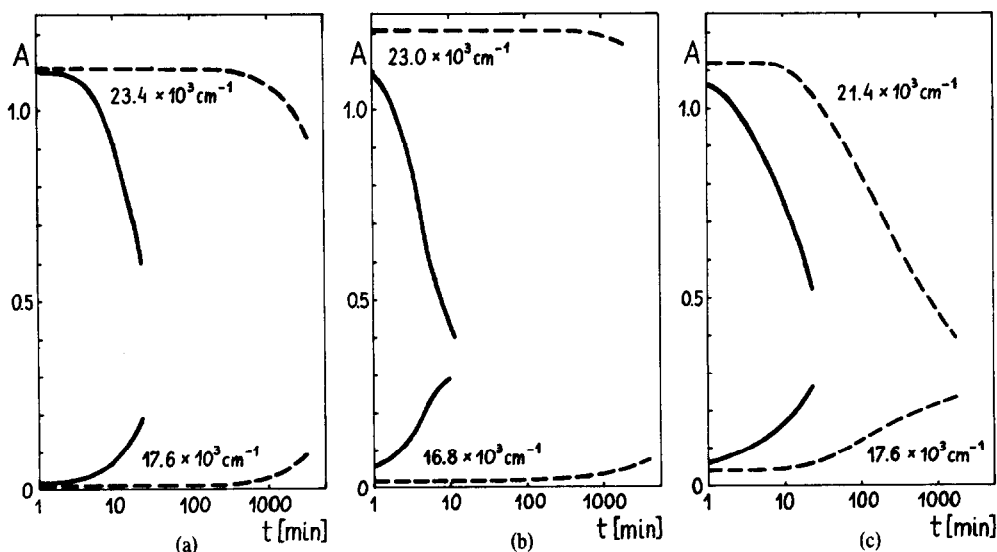
Fig. 1. Absorption changes recorded at $\bar{\nu}_{max}$ of substrates (upper curves) and products (lower curves) during photochemical (——) and thermal (---) reactions proceeding in 5×10^{-3} M solutions of: (a) $[Cr(CN)_5H_2O]^{2-}$ in acetate buffer at pH 5.8, (b) $[Cr(CN)_5OH]^{3-}$ in 1 M KOH, (c) $[Cr(CN)_3(H_2O)_3]$ in acetate buffer at pH 5.8.

from fast thermal reactions of the $[Cr(CN)_{6-x}(OH)_x]^{3-}$ complexes (where $x > 1$) leading within a few hours to the complete substitution of all the CN^- ligands.

The photosubstitution quantum yield (Table 1) was found to be relatively low in the case of the $[Cr(CN)_5H_2O]^{2-}$ complex, but considerably higher for the hydroxo-complex. This suggests again the direct photosubstitution by OH^- ligand proceeding in alkaline solutions. The influence of spectral range on the Φ values could be

followed only in the case of the $[Cr(CN)_5OH]^{3-}$ complex and appeared to be more significant than that for hexacyanochromate(III). Similarly to the alkaline solutions of $[Cr(CN)_6]^{3-}$, photosubstitution of the $[Cr(CN)_5OH]^{3-}$ complex was accompanied by another photochemical reaction upon exposure to radiation from CT bands in the presence of oxygen.[15]

Continuous irradiation with polychromatic light of the $[Cr(CN)_5H_2O]^{2-}$ complex led to the generation of a mix-

ture of the $[Cr(CN)_{6-x}(H_2O)_x]^{3-x}$ complexes (where $3 \leqslant x \leqslant 6$), with the aquo-complex of chromium(III) as major product.† The same products were found to be generated in thermal or photochemical aquation of the $[Cr(CN)_3(H_2O)_3]$ complex. In this case, the increased rate of thermal aquation made it difficult to determine accurate values of quantum yield. Nevertheless, the effect of photoacceleration was evidently observed [see Fig. 1(c) and Table 1]. Despite fast thermal substitution, the effect of photoacceleration was also noticed for the $[Cr(CN)_{6-x}(OH)_x]^{3-}$ complexes, where $x > 1$.

EXPERIMENTAL

Materials. Potassium hexacyanochromate(III), $K_3[Cr(CN)_6]$, was prepared according to the literature method[17] and recrystallized several times from aqueous solution. Its purity was checked by chemical analysis and infrared and ultraviolet spectroscopy. The aquocyanochromates(III), $[Cr(CN)_5H_2O]^{2-}$ and $[Cr(CN)_3(H_2O)_3]$, were obtained in aqueous solution following the procedure of Schapp *et al.*[14] For further experiments only those samples were used whose electronic spectra fitted those reported earlier.[14,18] The hydroxopentacyanochromate(III), $[Cr(CN)_5OH]^{3-}$, was obtained from its parent aquo-complex by deprotonation in 1 M KOH solution. Its purity was tested spectrally.[13] Other chemicals were best available commercial reagents used without further purification.

Apparatus and procedure. Flash photolysis apparatus was that described earlier.[19] Continuous irradiations were carried out using a high-pressure (HBO 200, Narva, DDR) or a medium-pressure (ASH 400) mercury lamp. For quantum yield measurements, glass filters (Schott, Jena, DDR) were used to isolate 436, 366 and 313 nm wavelengths, and an interference filter (KIF 265, C. Zeiss, Jena, DDR) for 265 nm radiation. Irradiations were performed in a thermostated rectangular quartz cell ($d = 1$ cm) at 295 ± 0.5 K with a continuous flow of nitrogen. The reaction progress was followed by means of a Specord UV–VIS or VSU 2P spectrophotometer (both C. Zeiss, Jena, DDR). Concentrations were chosen to assure a large excess over the minima required for $>99\%$ absorption of light at the desired wavelengths. Irradiations were limited to less than 10% conversion. Due to considerable contributions from thermal processes, the photoreaction progress was calculated from differences in optical density between the irradiated sample and one kept in the dark under precisely the same conditions. Moreover, quantum yield values were corrected for inner filter effect.[5,20] Actinometry was carried out with trisoxalatoferrate(III).[21]

---

†In acetate buffer solution, anation by the CH_3COO^- ligand[16] was also observed.

REFERENCES

[1] Taken in part from a thesis submitted by A. Marchaj to the Chemistry Department of the Jagiellonian University in partial fulfillment of the requirements for the Ph. D. degree in Chemistry, 1982. Presented in part at the 3rd Symposium on Photochemical and Thermal Reactions of Coordination Compounds, Mogilany—Kraków, Poland, May 1980 and at the 22nd International Conference on Coordination Chemistry, Budapest, Hungary, August 1982.
[2] L. Moggi, F. Bolletta, V. Balzani, and F. Scandola, *J. Inorg. Nuclear Chem.* 1966, **28**, 2589.
[3] A. W. Adamson, *J. Phys. Chem.* 1967, **71**, 798.
[4] A. Chiang and A. W. Adamson, *J. Phys. Chem.* 1968, **72**, 3827.
[5] H. F. Wasgestian, *Z. Phys. Chem.* (Frankfurt am Main), 1969, **67**, 39.
[6] D. C. McCain, *Inorg. Nucl. Chem. Lett.* 1969, **5**, 873.
[7] H. F. Wasgestian, *J. Phys. Chem.* 1972, **76**, 1947.
[8] N. Sabbatini and V. Balzani, *J. Am. Chem. Soc.* 1972, **94**, 7587.
[9] N. Sabbatini, M. A. Scandola, and V. Carassitti, *J. Phys. Chem.* 1973, **77**, 1307.
[10] V. Carassiti, N. Sabbatini, M. A. Scandola, and A. Maldotti, *Atti Acad. Sci. Ist. Bologna, Cl. Sci. Fis., Rend.* 1976, **13**, 103.
[11] V. Balzani and V. Carassiti, *Photochemistry of Coordination Compounds*, pp. 92–93. Academic Press, London, 1970.
[12] W. F. Coleman and W. Schaap. *J. Chem. Soc., Chem. Commun.* 1975, 226.
[13] L. Jeftić and S. Feldberg, *J. Am. Chem. Soc.* 1970, **92**, 5272; *J. Phys.Chem.* 1971, **75**, 2381.
[14] W. B. Schaap, R. Krishnamurthy, D. K. Wakefield, and W. F. Coleman, In *Coordination Chemistry* (Edited by S. Kirschner), pp. 177–206. Plenum Press, New York, 1969.
[15] A. Marchaj and Z. Stasicka, to be published.
[16] S. C. Tyagi and A. A. Khan, *J. Inorg. Nucl. Chem.* 1979, **41**, 1447.
[17] J. H. Bigelow, *Inorg. Synth.* 1946, **2**, 203.
[18] R. Krishnamurthy, W. B. Schaap, and J. R. Perumareddi, *Inorg. Chem.* 1967, **6**, 1338.
[19] T. Jarzynowski, T. Senkowski, and Z. Stasicka, *Polish J. Chem.* 1981, **55**, 3.
[20] H. F. Wasgestian and H. L. Schläfer, *Ber. Bunsenges. Phys. Chem.* 1967, **71**, 489.
[21] C. A. Parker, *Proc. Roy. Soc. A.* 1953, **220**, 104; C. G. Hatchard and C. A. Parker, *Proc. Roy. Soc. A.* 1956, **235**, 518.

THE PREPARATION AND ELECTROCHEMISTRY OF MANGANESE(II) COMPLEXES OF AN UNSATURATED PENTADENTATE MACROCYCLIC LIGAND

CHRISTOPHER W. G. ANSELL, JACK LEWIS*, JOHN N. RAMSDEN
and MARTIN SCHRÖDER
University Chemical Laboratory, Lensfield Road, Cambridge CB2 1EW, England

Abstract—The preparation of a series of six and seven coordinate manganese(II) complexes $[Mn^{(II)}(L)X]^+$, and $[Mn^{(II)}(L)X_2]^{2-}$ (X = halide, water, triphenylphosphine oxide, imidazole, 1-methyl imidazole and pyridine) incorporating the pentadentate planar macrocylic ligand L is described. Cyclic voltammetry of these complexes in acetonitrile each shows a reversible one-electron reduction wave near -1.4 V vs a Ag/AgNO₃ reference electrode. Quantitative reduction of these complexes by controlled potential electrolysis at a platinum gauze at -1.4 V yields the corresponding one-electron reduction products which have been shown by ESR spectroscopy to be manganese(II)–ligand radical species, the electron being thought to reside on the di-imino pyridine moiety of the macrocyclic ligand. No metal reduced species could be isolated even in the presence of π-acceptor ligands such as CO or phosphines.

We have recently reported work on the redox properties of nickel(II)[1] and cobalt(II)[2] complexes of the pentadentate unsaturated macrocyclic ligand L and in particular the electrochemical reduction of these complexes to give univalent metal species. We now wish to report, as a continuation or our previous studies on manganese(II) complexes of L,[3,4] the electrochemical redox behaviour of pentagonal pyramidal and pentagonal bipyramidal manganese(II) macrocyclic complexes of L.
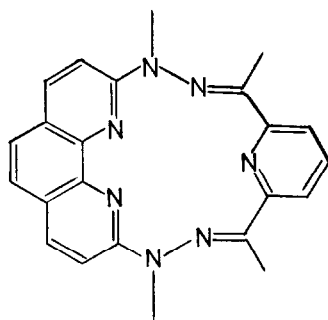
(L)

The reduction of transition metal complexes of potential π-acceptor macrocyclic ligands such as L is of interest because of the possibility of forming either metal reduced species, e.g. metal(I) or metal(O), or metal stabilised ligand radical species in which the electron resides mainly on the macrocyclic ligand. We and others[1,2,5–10] have previously shown that the redox properties of macrocyclic complexes may be highly dependent on the axial ligation, net π-acceptor axial ligands stabilising metal reduced species. We have therefore carried out studies on the redox chemistry of manganese(II) complexes of L in the presence of a series of

axial ligands to determine whether variations in redox properties might be observed.

RESULTS AND DISCUSSION

The manganese(II) macrocyclic complex $[Mn^{(II)}(L)Cl]^+$ was prepared by condensation of 2, 9-di(N-methyl)hydrazino-1,10-phenanthroline with 2,6-diacetyl pyridine in the presence of manganese(II) dichloride in refluxing water.[3,4] Halide coordination could be varied by changing the manganese halide starting material. Treatment of $[Mn^{(II)}(L)Cl]^+$ in refluxing water with AgBF₄, filtration and addition of NaBF₄ yielded the pentagonal pyramidal aquo complex $[Mn^{(II)}(L)H_2O]^{2+}$. The IR spectrum of this product showed a band near 3400 cm^{-1} assigned to the O–H stretching vibration, ν_{O-H}, of the coordinated water molecule. This complex was used as the starting material for the synthesis of a series of axially substituted adducts. Solutions of $[Mn^{(II)}(L)H_2O]^{2+}$ were treated with excess of axial ligand X in refluxing methanol to give products $[Mn^{(II)}(L)X_2]^{2+}$ (X = triphenylphosphine oxide, imidazole, 1-methyl imidazole and pyridine). The complexes are all high spin d⁵ species, conductivity measurements in dmso confirming that they are 2:1 electrolytes in that solvent. Table 1 lists analytical data for these complexes.

Cyclic voltammetric measurements on the above manganese(II) complexes in acetonitrile all show a reversible or quasi-reversible reduction wave near $E_{1/2} = -1.4$ V at a platinum electrode relative to a Ag/AgNO₃ reference. Coulometric measurements confirm that, in the absence of water, these reductions are one electron processes. The fact that the value of the half-wave potential $E_{1/2}$ remains essentially constant with variations in axial ligand suggest that the reduction occurs at the macrocyclic ligand; variation of axial ligand would be expected to have dramatic effect on the value of $E_{1/2}$ for a metal redox process.[1,2] To confirm that the reduction is indeed centred on the macrocyclic ligand, the complexes were quantitatively reduced by controlled potential electrolysis at -1.4 V in acetonitrile at a platinum gauze electrode and the reactions followed by

Table 1. Analytical data for manganese(II) macrocyclic complexes

Complex	Found			Calculated			Λ^a
	C	H	N	C	H	N	
$[Mn(L)(H_2O)](BF_4)_2$	41.7	3.8	14.8	41.7	3.8	14.8	
$[Mn(L)(H_2O)_2](BF_4)_2 \cdot H_2O$	40.9	3.8	14.9	40.7	4.0	14.5	62.4
$[Mn(L)(OPPh_3)_2](BF_4)_2$	60.4	4.4	8.4	60.6	4.3	8.3	63.2
$[Mn(L)(C_3H_4N_2)](PF_6)_2$	39.0	3.1	15.9	38.6	3.1	15.6	
$[Mn(L)Br]Br$	45.1	3.5	16.2	45.3	3.5	16.2	
$[Mn(L)Br](PF_6)$	41.4	3.3	14.5	40.9	3.1	14.5	
$[Mn(L)(C_4H_6N_2)_2](BF_4)_2 \cdot H_2O$	46.2	4.3	19.1	46.2	4.1	18.7	
$[Mn(L)(C_4H_6N_2)_2](PF_6)_2$	41.5	4.0	16.8	41.2	3.7	17.0	64.3
$[Mn(L)(C_5H_5N)_2](PF_6)_2 \cdot H_2O$	43.1	3.5	13.5	43.2	3.6	13.8	

^{a} Measured with 10^{-3} M solutions in DMSO at room temperature.

ESR spectroscopy. On reduction, the orange solution of the manganese(II) starting material darkened with concomitant development of an isotropic signal in the ESR spectrum at $g = 2.002$ (measured at 77 K as an acetonitrile glass) assigned to unpaired electron density on the macrocyclic ligand.

The broad manganese(II) ESR signal[11] at $g_{av} = 2.960$ remained essentially unchanged during the course of the reaction. The ESR data are consistent with the formation of manganese(II) stabilised ligand radical species. In the presence of water [for example in the reduction of $[Mn^{(II)}(L)(H_2O)]^{2+}$] more than one equivalent of electrons was consumed during the course of the reaction with no ligand radical species being detected in the ESR spectrum. The IR spectrum of the dark brown product obtained from this reduction showed bands near 3100 cm^{-1} assigned to N–H stretching vibration ν_{N-H} of a reduced macrocycle ligand. In addition a marked decrease in the intensity of the C=N stretching vibration of the imino functions at 1620 cm^{-1} was noted. We assign these spectral data to a product in which the diimine bonds of the macrocyclic ligand have been fully reduced. This suggests that in the manganese(II)–ligand radical species described above, the electron resides on the di-imino pyridine moiety; this is consistent with results obtained for other metal stabilised di-imino ligand radical species.[5-9]

The extreme rarity of manganese(I) complexes stabilised by nitrogen donor macrocyclic ligands led us to investigate the possibility of stabilising metal reduced species in the above electrochemical reductions. Addition of $P(OMe)_3$ or CO to solutions of $[Mn^{(II)}(L)(CH_3CN)_2]^{2+}$ in the electrochemical cell showed essentially no shifts in the value of $E_{1/2}$ for the above reduction process, although some loss of reversibility was observed. No manganese(I) species could be detected in the quantitative reductions of such solutions. This is in contrast to the redox properties of nickel(II) and cobalt(II) complexes of L in which the stabilisation of

metal(I) has been readily achieved in the presence of CO or phosphine ligands.[1,2]

The electrochemical results described above are analogous to the redox properties observed for d^{10} zinc(II) complexes of L in which reduction occurs also at the macrocyclic ligand centre.[13] Current work is directed to the investigation of the redox properties of manganese(II) complexes involving macrocycles derived from terpyridine and related open chain complexes.[14]

EXPERIMENTAL

Infrared spectra were measured as Nujol mulls between potassimum bromide discs using Perkin–Elmer 257 and 457 spectrometers over the range $400-4000 \text{ cm}^{-1}$. Conductance measurements were made with a Wayne–Kerr Universal bridge. Magnetic moments were recorded on a Newport–Gouy balance and the readings corrected for ligand and inner-core diamagnetism by using Pascal's constants.[17] Microanalyses were performed by the University Chemical Laboratory Microanalytical Department.

Electrochemical measurements were performed on a Princeton Applied Research Electrochemistry System Model 170. All readings were taken using a three electrode potentiostatic system in acetonitrile with 0.1 moles/l of $nBu_4N^+BF_4^-$ present as supporting electrolyte. Cyclic voltammetric studies were carried out using platinum wires as auxiliary and working electrodes and a $Ag/AgNO_3$ reference electrode. Controlled potential electrolysis experiments were carried out using a platinum gauze as the working electrode, a salt bridge being incorporated to separate oxidised and reduced species. ESR spectra were measured as glasses in acetonitrile or as solid samples at 77 K on a Varian E109E. For the reduction products described, all solvents were distilled, dried and degassed before use and air-sensitive compounds handled under a nitrogen or argon atmosphere using Schlenk tube techniques. 2, 6-Diacetyl pyridine was used without further purification (from Aldrich) and 2, 9-di(1-methyl hydrazino)-1, 10-phenanthroline was prepared by the published procedure.[15,16]

Preparation of $[Mn^{(II)}(L)Cl](BF_4)^4$

Manganese dichloride hexahydrate (0.087 g, 0.44 mM) was dissolved in refluxing water (50 cm^3) and solid 2, 9-di(1-methyl-

hydrazino)-1, 10-phenathroline (0.11 g, 0.44 mM) was added with vigorous stirring. When all the solid had dissolved, 2, 6-diacetyl pyridine (0.07 g, 0.44 mM) was added with a few drops of concentrated HCl. The reaction mixture was refluxed under nitrogen for 2 hr and allowed to cool to 60°C. Addition of excess of $NaBF_4$ with stirring and cooling gave the complex $[Mn^{(II)}(L)Cl]-$(BF_4) as an orange crystalline product which was recrystallised from water by the addition of $NaBF_4$, washed copiously with diethyl ether and dried in vacuo Yield:- 70%.

Preparation of $[Mn^{(II)}(L)(H_2O)](BF_4)_2$

The complex $[Mn^{(II)}(L)Cl](BF_4)$ (0.1 g, 0.17 mM) was dissolved in refluxing methanol (50 cm³) and $AgBF_4$ (0.049 g, 0.25 mM) added. The solution was refluxed under nitrogen for 2 hr and filtered hot to remove precipitated AgCl. On cooling the filtrate and addition of $NaBF_4$, the aquo adduct $[Mn^{(II)}(L)(H_2O)](BF_4)$ was obtained as a dark orange product which was recrystallised from water by the addition of $NaBF_4$. Yield:- 80%. This complex was used as the starting material for the formation of axially substituted adducts with pyridine, imidazole, 1-methyl imidazole and triphenyl phosphibe oxide. The preparation of the pyridine adduct $[Mn^{(II)}(L)(C_5H_5N)_2](PF_6)_2$ is typical.

Preparation of $[Mn^{(II)}(L)(C_5H_5N)_2](PF_6)_2$

The complex $[Mn^{(II)}(L)(H_2O)](PF_6)_2$ (0.05 g, 0.07 mM) was dissolved in refluxing methanol (20 cm³) and excess of pyridine (0.02 g, 0.3 mM) was added. The solution was refluxed under nitrogen for 2 hr. On cooling and addition of diethyl ether orange crystals of the pyridine adduct $[Mn^{(II)}(L)(C_5H_5N)_2](PF_6)_2$ were obtained. The product was recrystallised from methanol and diethyl ether containing pyridine. Yield: 70%.

REFERENCES

[1] C. W. G. Ansell, J. Lewis, P. R. Raithby, J. N. Ramsden and M. Schröder, *J. Chem. Soc. (Chem. Commun.)* 1982, 546.

[2] C. W. G. Ansell, J. Lewis, M. C. Liptrot, P. R. Raithby and M. Schröder, *J. Chem. Soc. (Dalton Trans.)* 1982, 1593.

[3] M. M. Bishop, J. Lewis, T. D. O'Donoghue and P. R. Raithby, *J. Chem. Soc. (Chem. Commun.)* 1978, 476.

[4] J. Lewis, T. D. O'Donoghue and P. R. Raithby, *J. Chem. Soc. (Dalton Trans.)* 1980, 1383.

[5] J. Lewis and M. Schröder, *J. Chem. Soc. (Dalton Trans.)* 1982, 1085.

[6] R. R. Gagné, J. L. Allison, R. S. Gall and C. A. Koval, *J. Am. Chem. Soc.* 1977, 99, 7170.

[7] A. W. Addison, M. Carpenter, L. K-M. Lau and M. Wicholas, *Inorg. Chem.* 1978, 17, 1545.

[8] R. R. Gagné, J. L. Allison and D. M. Ingle, *Inorg. Chem.* 1979, 18, 2767.

[9] R. R. Gagné and D. M. Ingle, *J. Am. Chem. Soc.* 1980, 102, 1444.

[10] V. L. Goedken and S-M. Peng, *J. Chem. Soc. (Chem. Commun.)* 1974, 914.

[11] B. A. Goodman and J. B. Raynor, *Advances in Inorg. Chem. and Radiochem.*, Vol. 13, p. 136. Academic Press, New York (1970).

[12] R. R. Gagné, D. M. Ingle and G. C. Lisensky, *Inorg. Chem.* 1981, 20, 1991.

[13] C. W. G. Ansell, J. Lewis, P. R. Raithby, J. N. Ramsden and M. Schröder, unpublished results.

[14] E. C. Constable, J. Lewis and M. Schröder, *Polyhedron* 1982, 1, 311.

[15] S. Ogawa, T. Yamaguchi and N. Gotoh, *J. Chem. Soc. (Perkin I)* 1974, 976.

[16] J. Lewis and T. D. O'Donoghue, *J. Chem. Soc. (Dalton Trans.)* 1980, 736.

[17] B. N. Figgis and J. Lewis, *Modern Coordination Chemistry* (Edited by J. Lewis and R. G. Wilkins). Interscience, New York (1960).

ORGANOMERCURY DERIVATIVES OF ARYLAZOBENZOIC ACIDS

K. K. SARKAR, T. K. CHATTOPADHYAY and B. MAJEE*
Department of Chemistry, North Bengal University, Darjeeling-734430, India

Abstract—A number of organomercury derivatives of arylazobenzoic acids have been prepared and characterised by analytical, IR, PMR and electronic absorption spectral data. In the 3-coordinated organomercury complexes the N→Hg bond appears to be weak. The 4-coordinated complexes obtained from the terdentate ligands *o*-(2-hydroxybenzene-azo) benzoic acids show a large bathochromic shift of the π–π* transition of the ligand indicating a much stronger N→Hg bond.

o-Arylazobenzoic acids and related compounds (I) have been widely used as ligands in transition metal chemistry.[1-6] Ease of synthesis, favourable steric arrangement and variability of the number of donor sites with suitable substituents make this group of compounds excellent ligands for synthesising many interesting complexes.[7]
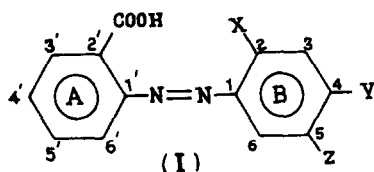
This prompted us to undertake the synthesis of organomercury complexes of these ligands and study

their spectral and structural characteristics. The organomercury derivatives of the *p*-carboxy compounds (II) were also prepared and their spectral characteristics compared with those of (I) to ascertain the effect of N→Hg coordination on the absorption spectra.

(I)

(II)
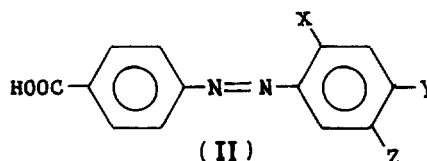
EXPERIMENTAL

(a) *Preparation of arylazobenzoic acids*
Ligands 1–4 (Table 1) were prepared according to the method described by Vogel.[21] ligands 5–7 and 13–15 were prepared according to the methods reported by Majee *et al.*[7] L^8H and L^9H were prepared by the standard acetylation procedure.[21] Ligands

*Author to whom correspondence should be addressed.

Table 1(a). Ligands (I) and their abbreviation

	Abbreviation used	X	Y	Z
1.	L^1H	H	$N(CH_3)_2$	H
2.	L^2H	H	$N(C_2H_5)_2$	H
3.	L^3H	H	NHC_2H_5	H
4.	L^4H	H	$NHCH_3$	H
5.	L^5H	OH	H	CH_3
6.	L^6H	H	OH	CH_3
7.	L^7H	CH_3	OH	H
8.	L^8H	H	$OCOCH_3$	CH_3
9.	L^9H	CH_3	$OCOCH_3$	H
10.	$L^{10}H$	H	OCH_3	CH_3
11.	$L^{11}H$	CH_3	OCH_3	H
12.	$L^{16}H$	OCH_3	H	CH_3

Table 1(b). Ligands (II) and their abbreviation

Abbreviation used	X	Y	Z
13. $L^{12}H$	H	$N(CH_3)_2$	H
14. $L^{13}H$	OH	H	CH_3
15. $L^{14}H$	H	OH	CH_3
16. $L^{15}H$	H	OCH_3	CH_3

10–12 and 16 were prepared from the corresponding hydroxy compounds by methylation with dimethyl sulphate followed by hydrolysis with 5% aqueous sodium hydroxide.

The purity of the compounds were checked by analytical data, m.p., IR spectra and mass spectra.

(b) *Preparation of organomercury derivatives of arylazo benzoic acids*

A few typical preparative details are given below:

(i) PhHgL[1]. A mixture of L[1]H (3 g) in 75.2 cm³ of ethanolic NaOH (0.148N) and phenylmercuric acetate (3.75 g) in 125 cm³ ethanol was refluxed for 6 hr. Ethanol was removed by evaporation, the product extracted with benzene and crystallized from benzene and petroleum ether (60–80); yield 95%.

(ii) PhHgL[2]. A mixture of equivalent amounts of L[2]H and phenylmercuric hydroxide was refluxed for 16 hr in dry benzene. The solution was concentrated and petroleum ether was added to separate out the crude product. Repeated crystallisation from benzene and petroleum ether (60–80) gave the pure product; yield 55%.

(iii) p-Tol·HgL[2]. A mixture of 0.5 g of p-tolylmercuric chloride and 0.9 g of the Ag-salt of L[2]H in 100 cm³ dry benzene was refluxed for 8 hr. The solution was filtered, the filtrate concentrated and hot petroleum ether added. On cooling, the crude product separated out as a gummy mass which was purified by repeated crystallisation from benzene and petroleum ether (60–80). p-Tol·HgL[2] was obtained as a red powder; yield 40%.

(iv) PhHgL[5]. A mixture of 3.4 g of phenylmercuric acetate and 2.8 g of Na-salt of L[5]H in 160 cm³ of methanol was refluxed for 8 hr. The solution was concentrated by distillation, then cooled, when red crystals separated. Recrystallisation from benzene and petroleum ether (60–80) afforded the pure product; yield 90%.

All solvents used for spectral studies were of Uvasol (E. Merck) grade. The absorption spectra were measured with a Beckman DU-2 spectrophotometer.

RESULTS AND DISCUSSION

The formulae of the ligands and their abbreviations are given in Table 1.

(a) *Method of preparation of the organomercury derivatives*

In principle, organomercury derivatives of o-aryl-azobenzoic acids may be prepared by any of the following reactions:

$$RHgCl + L \cdot Na \rightarrow RHgL + NaCl \qquad (1)$$

$$RHgCl + L \cdot Ag \rightarrow RHgL + AgCl \qquad (2)$$

$$RHgOAc + L \cdot Na \rightarrow RHgL + NaOAc \qquad (3)$$

$$RHgOH + L \cdot H \rightarrow RHgL + H_2O. \qquad (4)$$
(L·H = o-arylazobenzoic acid).
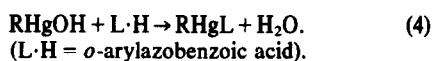
However, the yield and purity of the desired product depend to a great extent on the particular reaction employed. For example, reaction (1) does not occur even on prolonged refluxing. On the other hand, reaction (2) is quite general though the yield is usually low, thus making it unsuitable as a preparative method.

Reaction (3) is found to be the most satisfactory. The yields are 75–95%, depending on the ligand. The presence of an –OH group at the 4-position in the coupling moiety hinders this reaction, presumably due to the hydrazone form[2,8-11] (III) which destroys the planarity of the molecule in the azo form. This is expected to affect the stability of the chelated structure adversely.

(III)
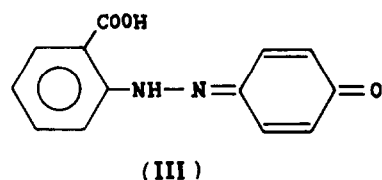
In such cases, reaction (4) has been used successfully, though the yields are low.

Another point which merits some comment is the facile hydrolysis of the acetyl group in L[8]H or L[9]H during reaction with phenylmercuric hydroxide. In both cases, complete hydrolysis of the 4-acetyl group occurred, resulting in 4-hydroxy compounds.

The products, m.p. and yields are summarised in Table 2. Analytical data are given in Table 3.

(b) *IR spectra*

The IR spectra of the organomercury arylazocarboxylates are very complex and a complete assignment of the absorption bands is not possible. The frequencies of the important vibrations that could be assigned are listed in Table 2.

Asymmetric OCO vibrations in the organomercury derivatives have been identified by comparison of the IR spectra with those of the free ligands. Due to overlapping of ν_{as}(OCO) with the ring vibrations[7] at ~ 1600 cm^{-1}, the exact position of this band is somewhat uncertain in some cases. In fact, the compounds are characterised by a rather broad and intense band around ~ 1600 cm^{-1} with distinct shoulders.

The lowering of the asymmetric carboxylate stretch in the organomercury derivatives may be ascribed to the canonical structure (IVB) because intermolecular polymerisation involving the –COO group may be ruled out

Table 2. IR, NMR and electron spectral data of the organomercury derivatives

Compound* (Mp.°C; Yield %)	IR bands (ν_{as} and ν_s OCO cm^{-1})	NMR** (δ ppm)	Electron Spectra in Methanol*** λ_{max} nm(logε)
1. PhHgL^1[b] (146, 95)	1580	3.02[d]	
2. p-Tol.HgL^1[b] (155, 95)	1565	2.36[e], 3.04[d]	
3. PhHgL^2[a,c] (86, 55-60)	1600, 1330		
4. p-Tol.HgL^2[a] (84, 40)	1598, 1330		
5. PhHgL^3[b] (90, 75)	1565, 1325	1.28(t)[f],3.25(q)[g]	
6. PhHgL^4[b] (126, 90-95)	1595	2.97[d]	
7. PhHgL^5[b,c] (174, 70-90)	1615, 1325	2.39[e]	250(4.16),325 (4.33),390(3.97)
8. p-Tol.HgL^5[a] (169, 95)	1600, 1330		325(4.25),390 (3.89)
9. p-Et$_2$NC$_6$H$_4$HgL^5[a] (156, 70)	1615, 1320		250,325,390
10. PhHgL^6[c] (180, 45)	1580, 1350		247,352, 475
11. PhHgL^7[c] (193, 42)	1590		248, 355, 470
12. PhHgL^8[c] (180, 20)			
13. PhHgL^9[c] (194, 30)			
14. PhHgL^{10}[c] (97, 90)	1590, 1340		245(4.20),350(4.37)
15. PhHgL^{11}[c] (153, 95-90)	1555, 1380	2.46[e],3.60[h]	245(4.11), 350(4.29)
16. PhHgL^{12}[c] (210, 80-85)	1615, 1328		270(4.12), 420(4.54)
17. PhHgL^{13}[c] (194, 90-95)	1630, 1333	2.40[e]	330(4.37), 395(4.02)

* Ph=C_6H_5, Tol=$CH_3.C_6H_4$, Ac = $-COCH_3$

    a, b and c refer to methods of preparation by reactions(2),

    (3) and (4) respectively.

** t = triplet, q = quartet.

    Protons responsible (underlined)for the signals are:

    N→C$\underline{H}_3$ (d), Aryl - C$\underline{H}_3$(e), N-CH$_2$-C$\underline{H}_3$(f),

    N -C$\underline{H}_2$-CH$_3$(g), Aryl-OC$\underline{H}_3$(h).

*** Absorption maxima in some nonpolar solvents:

    C_6H_6 - PhHgL^5 350(4.23), 407 (3.86); p-Tol.HgL^5 350(4.24),

        405(3.86); PhHgL^6 354, 448; PhHgL^7 390, 440;

        PhHgL^{10} 360(4.06); PhHgL^{11} 360(4.09); PhHgL^{12}

        428(4.33); PhHgL^{13} 335 (4.42), 410(4.04).

   CCl$_4$ - PhHgL^5 407; PhHgL^{12} 420.

   Cyclo - C_6H_{12} - PhHgL^5 405.

Table 3. Analytical data

Compound*	Found (Calc.) (%)		
	C	H	Hg
PhHgL[1]	46.22(46.19)	3.50(3.48)	36.69(36.77)
p-Tol.HgL[1]	47.07(47.18)	3.70(3.75)	35.73(35.85)
PhHgL[2]	48.31(48.12)	4.03(4.01)	34.89(34.97)
p-Tol.HgL[2]	49.08(49.01)	4.23(4.25)	34.09(34.14)
PhHgL[3]	46.21(46.19)	3.49(3.48)	36.70(36.77)
PhHgL[4]	45.16(45.15)	3.22(3.20)	37.70(37.74)
PhHgL[5]	45.08(45.06)	3.01(3.00)	37.59(37.66)
p-Tol.HgL[5]	46.12(46.10)	3.30(3.29)	36.68(36.70)
p-Et₂HC₆H₄HgL[5]	47.74(47.71)	4.15(4.14)	33.22(33.23)
PhHgL[6]	45.06(45.06)	3.03(3.00)	37.61(37.66)
PhHgL[10]	46.11(46.10)	3.28(3.29)	36.68(36.70)
PhHgL[7]	45.08(45.06)	3.01(3.00)	37.63(37.66)
PhHgL[11]	46.11(46.10)	3.27(3.29)	36.65(36.70)
PhHgL[12]	46.35(46.19)	3.43(3.48)	36.61(36.77)
PhHgL[13]	45.10(45.06)	3.01(3.00)	37.60(37.66)

* Ph = C_6H_5; Tol = $CH_3.C_6H_4$.

as ν_{as} (OCO) is found to be nearly the same in the solid and in solution.

(IVA)

(IVB)
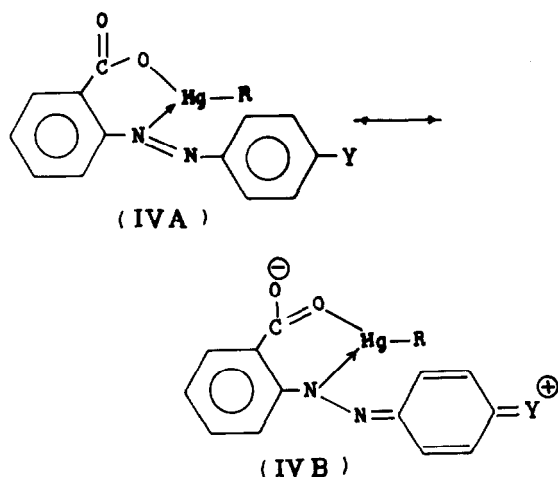
This is also consistent with ν_{as}(OCO) in PhHgL[1] being lower in frequency ($\sim$1580 cm^{-1}) than that in PhHgL[12] (1615 cm^{-1}) where such resonance is not possible.

The symmetric OCO stretch in the carboxylates reported here occurs as a medium to strong intensity band in the 1360–1320 cm^{-1}.

(c) *PMR spectra*

The low solubility of the azo compounds and their organomercury derivatives in common solvents made it difficult to obtain good PMR spectra except in a few cases. The chemical shifts of interest in these compounds are given in Table 2.

Of the two benzene rings present in the arylazobenzoates, the chemical shifts of the protons on ring B(I) and the substituents attached to it provide more useful information.

In general, the observed shift of the side chain protons, e.g. -NCH₃, -NCH₂CH₃, -OCH₃, Ar–CH₃ etc. present in the substituents X, Y and Z are readily identified by their position, multiplicity and relative intensities. The observed chemical shifts agree closely with the reported shifts in other azo dyes.[12,13]

The PMR spectrum of compounds with Y = – NR₁R₂ are characterised by two signals at $\delta \sim$ 6.50–6.7 and $\delta \sim$ 6.66–6.79 corresponding to one proton each. From a comparison with the available data,[12,13] these two signals can be assigned to protons at 3 and 5 positions respectively on ring B.

The signal at $\delta \sim$ 2.16 in compounds with Y = -NHR, -NHCH₃ or -NHC₂H₅ is absent in fully alkylated compounds (Y = NR₁R₂) and therefore, arises from the amino proton. The amino proton in the azo compounds is thus more shielded compared to other aromatic amines[14] ($\delta \sim$ 2.9–4.8). The data given in Table 2 show that the signals of the side chain protons undergo an upfield shift in the phenylmercury derivatives of bidentate ligands (X = H in I) compared to that in the free ligand. The signals of protons at 3 and 5 positions show a similar high field shift of about 0.06–0.1 ppm in the mercury derivatives. On the other hand, terdentate ligands (X = OH in I) and their organomercury derivatives have almost identical chemical shifts for the side chain and ring protons. The apparently anomalous results are readily
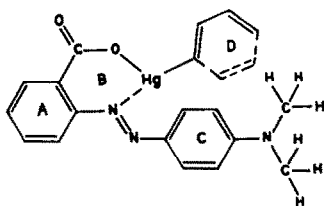
Fig. 1. Probable structure of 3-coordinate trigonal organomercury complex (the plane of the ring D is perpendicular to the plane containing the rings A, B and C).
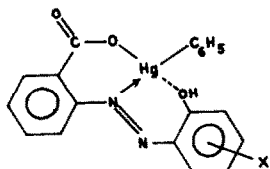
Fig. 2. Probable structure of 4-coordinate organomercury (sp^3) complexes.

explained in terms of 3- and 4- coordinated structures for the organomercury derivatives.

Bidentate ligands are expected to form 3-coordinated organomercury complexes having trigonal planar geometry. A model of a 3-coordinate complex using bond lengths for Hg–C, Hg–N and Hg–O observed in amino acid derivatives[15] and standard bond lengths for the bonds in the azo system[16] is shown in Fig. 1. Because of the planarity of the O, N, C and Hg atoms in the three-coordinate planar geometry, the benzene ring (D) attached to the mercury atom would orient itself preferably in a direction perpendicular to the plane of the ring B to avoid steric interaction. Because of this, the protons on ring B, particularly the side chain protons at the 4 position which lie above the plane of ring D, would be more shielded due to ring current effects.[17] The observed upfield shift in the organomercury derivatives, therefore, provides strong evidence in favour of a 3-coordinate structure. Absence of such upfield shift in the organomercury derivatives of the p-arylazobenzoic acids where similar coordination is not possible supports this interpretation.

The absence of a similar high field shift in the organomercury derivatives of terdentate ligands (X = – OH in I) which can form 4-coordinate complexes provides further support. The geometry of 4-coordinated mercury is known to be tetrahedral. In the tetrahedral 4-coordinate organomercury chelates (Fig. 2), the benzene ring attached to the mercury atom lies in a direction perpendicular to the plane of the azo system. The organomercury group is, thus, expected to have little effect on the protons on ring B in the 4-coordinate complexes. The experimental data confirm this.

(d) *Electronic absorption spectra*

The electronic absorption spectra of the organomercury (aryl azo) benzoates can be explained in terms of the π–π^* transition characteristic of the azo compounds.[16,18] The spectral data are given in Table 2.

The absorption spectra of the organomercury 4-hydroxybenzeneazobenzoates are characterised by two solvent-dependent overlapping absorption maxima in the

340–390 nm region. That the two bands arise from azo-hydrazone type equilibrium (eqn 5), well-known in many 0- and p-hydroxy azo compounds,[2,8–11] is shown by the electronic absorption spectra of the methylated derivatives and the corresponding organomercury derivatives.

Methylation of the 4-OH group which eliminates the possibility of azo-hydrazone tautomerism results in a single absorption maximum in the visible region. Thus, both $L^{10}Me$ and PhHgL[10] have a single absorption at ~360 nm while the corresponding hydroxy compounds have an additional band at longer wavelengths. Clearly, the ~360 nm band arises from the azo form while the ~450 nm band present in the hydroxy compounds L^6Me and PhHgL[6] must originate from the hydrazone form which generally absorbs at longer wavelength than the corresponding azo form.[19] Interestingly, the free acids L^6H and $L^{10}H$ have only a single absorption maximum which undergoes a considerable hypsochromic shift (~35 nm) on esterification of the –COOH group. The same behaviour is shown by the 2-methyl derivatives also. Esterification of the –COOH group is not expected to have a significant effect on the absorption spectra unless some intra- or inter-molecular interaction involving the –COOH group exists. For example, absorption maxima of the p-carboxy compounds, $L^{15}H$ and $L^{15}Me$ differ by only 5 nm.

In the o-carboxy compounds, intramolecular H-bonding as shown in (V) is possible. Esterification of the –COOH groups is then expected to result in a large hypsochromic shift of the absorption maximum because the π^*-level will certainly be lower in energy in the H-bonded form due to a shift of electron charge cloud from the N atom towards to H atom.[18] Thus the observed hypsochromic shifts are consistent with intramolecular H-bonding. Such bonding is not favoured in the corresponding hydrazone from which, consequently, is much less stable in the free acid. Because of this the free acids show only a single absorption peak corresponding to the azo form.
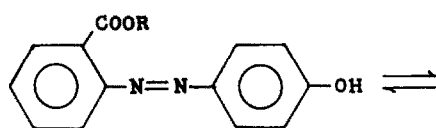
azo form
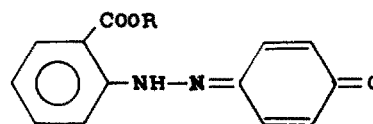
hydrazone form   ······(5)
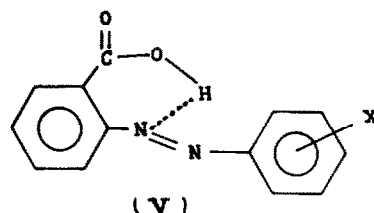
(V)

A bathochromic shift of the longest wavelength $\pi-\pi^*$ transition is expected due to $N \rightarrow Hg$ coordination and electron withdrawal from the N-atom[18,19] relative to the compound in which no such interaction is present, e.g. the methyl ester (comparison with the free acid is not possible due to the presence of intramolecular hydrogen bonding). The small bathochromic shift ($\sim 5-10$ nm) of the absorption maxima in the organomercury derivatives relative to those in the corresponding esters, therefore, indicates the formation of a weak $N \rightarrow Hg$ bond. Such weak $N \rightarrow Hg$ interaction is a common feature of 3-coordinated mercury complexes.[20]

The organomercury derivatives of the *o*-2-hydroxybenzeneazobenzoic acids show larger bathochromic shifts of the $\pi-\pi^*$ transition indicating stronger coordination in this case. Unlike the 4-hydroxybenzeneazobenzoates, the absorption spectra are not greatly affected by solvents showing the absence of azo-hydrazone tautomeric equilibria in such cases. This is presumably due to the formation of more stable 4-coordinate complexes (Fig. 2) with the 2-hydroxybenzeneazobenzoic acids which can act as terdentate ligands.

As expected, the organomercury derivatives of the *p*-arylazobenzoic acids (II) have absorption spectra closely similar to those of the free ligands, as the derivatives in such cases are comparable to the corresponding alkyl esters.

REFERENCES

[1] K. Venkataraman, *The Chemistry of Synthetic Dyes*, Vol. 1, Chap. 14. Academic Press, New York (1952).
[2] R. Price, *The Chemistry of Synthetic Dyes* (Edited by K. Venkataraman), Vol. 3, p. 303. Academic Press, New York (1970).
[3] M. Elkins and L. Hunter, *J. Chem. Soc.* 1958, 1598.
[4] H. D. K. Drew and J. K. Landquist, *J. Chem. Soc.* 1938, 292.
[5] H. B. Jonassen, M. M. Cook and J. S. Wilson, *J. Am. Chem. Soc.* 1951, **73**, 4683.
[6] W. F. Beech and H. D. K. Drew, *J. Chem. Soc.* 1940, 608.
[7] B. Majee and S. Banerjee, *J. Organometal. Chem.* 1977, **39**, 139.
[8] A. Burawoy, A. G. Salem and A. R. Thompson, *J. Chem. Soc.* 1952, 4793.
[9] A. Burawoy and A. R. Thompson, *J. Chem. Soc.* 1953, 1443.
[10] K. J. Morgan, *J. Chem. Soc.* 1961, 2151.
[11] A. Burawoy and J. T. Chamberlain, *J. Chem. Soc.* 1952, 2310; 3724.
[12] A. Foris, *The Analytical Chemistry of Synthetic Dyes* (Edited by K. Venkataraman), p. 217. Wiley, New York (1977).
[13] T. E. Beukelman, A. Foris and R. K. Miller, *The Analytical Chemistry of Synthetic Dyes* (Edited by K. Venkataraman), p. 317. Wiley, New York (1977).
[14] L. M. Jackman and S. Sternhell, *Applications of Nuclear Magnetic Resonance Spectroscopy in Organic Chemistry*, p. 216. Pergamon Press, New York (1969).
[15] N. W. Alcock, P. A. Lampe and P. Moore, *J. Chem. Soc.* 1978, 1324.
[16] H. Suzuki, *Electronic Absorption Spectra and Geometry of Organic Molecules*. Academic Press, New York (1967).
[17] J. A. Pople, W. G. Schneider and H. J. Bernstein, *High Resolution Nuclear Magnetic Resonance*. McGraw Hill, New York (1959).
[18] B. Majee and S. Banerjee, *J. Organometal. Chem.* 1977, **140**, 151.
[19] J. Griffiths, *Colour and Constitution of Organic Molecules*. Academic Press, New York (1976).
[20] D. P. Graddon and J. Mondal, *J. Organometal. Chem.* 1976, **107**, 1.
[21] A. I. Vogel, *A Textbook of Practical Organic Chemistry*. E.L.B.S., London (1971).

MÖSSBAUER STUDY OF THE AFTER-EFFECTS OF THE CONVERTED ISOMERIC TRANSITION IN ^{119m}Sn IN FROZEN SOLUTIONS OF SnCl$_2$ AND IN SOLID ADDUCTS OF SnCl$_2$· AND SnBr$_4$ WITH ORGANIC DONOR MOLECULES

SUMIO ICHIBA* and MASAAKI YAMADA

Department of Chemistry, Faculty of Science, Hiroshima University, Naka-ku, Hiroshima 730, Japan

Abstract—As an after-effect of the converted isomeric transition in ^{119m}Sn, about 30% yield of the oxidised aliovalent species Sn^{4+} was observed in Mössbauer spectra of frozen solutions of ^{119m}SnCl$_2$ in organic solvents such as dimethyl sulphoxide and methanol. On the other hand, the reduced aliovalent species Sn^{2+} was observed in the emission spectra of crystalline solid adducts of ^{119m}SnBr$_4$ with dimethyl sulphoxide and other donors. As a mechanism for the stabilization of the oxidized aliovalent species observed in the emission spectra of the frozen solutions, it is proposed that the electrons released by Auger processes are trapped in imperfections of the glassy matrices of the medium. On the other hand, a possible mechanism for the formation of reduced species from adducts of ^{119m}SnBr$_4$ is that reducing radicals are formed by dissociative electron capture in autoradiolysis of the closest ligands within the molecules. The large yields of the oxidized aliovalent species Sn^{4+} observed in the emission spectra of the crystalline solid adducts of ^{119m}SnCl$_2$ with dimethyl sulphoxide, pyridine N-oxide, and pycoline N-oxides are also to be understood in terms of dissociative electron capture in autoradiolysis of the ligand.

After-effects of nuclear transformations, mainly those of electron capture, EC, ^{57}Co and converted isomeric transition, CIT, in ^{119m}Sn have been studied by Mössbauer emission spectroscopy, or source experiments.[1-3] Both EC in ^{57}Co and CIT in ^{119m}Sn are followed by Auger processes in which vacancies in the outer atomic shells are developed by a vacancy cascade and the decayed atoms are left in highly charged states at the Mössbauer level. The fate of the hot atoms thus created in the solids is very interesting, and the lifetime of the highly charged atomic state and the stable charge state of the daughter atoms in various matrices have been studied by Mössbauer emission spectroscopy.

Friedt *et al.* have investigated complex ligand compounds by Mössbauer emission spectroscopy and proposed a model of autoradiolysis of the ligands for the stabilization of the aliovalent species in the host matrix.[4-6] On the other hand, Bondarrevskii *et al.* have proposed a model of competing acceptors for the electrons between hot atoms and surrounding medium to explain the aliovalent species observed in the emission spectra of the rapidly frozen solutions containing ^{119m}Sn.[7-9]

We have reported previously a large yield of the oxidized aliovalent species of Sn^{4+} in the adducts of SnCl$_2$ with some oxygen- and nitrogen-containing donor molecules as ligands.[10,11] In the present work, source experiments on frozen solutions of ^{119m}SnCl$_2$ in some organic solvents and on crystalline solid adducts of ^{119m}SnBr$_4$ with organic ligands were performed, to study the mechanisms for the stabilization of the aliovalent species observed in the emission spectra.

EXPERIMENTAL

Preparation of sources. The sources containing ^{119m}Sn were prepared from ^{119m}Sn metal purchased from New England

Nuclear. Radioactive tin metal was dissolved in hydrochloric acid, and anhydrous stannous chloride was obtained by heating the solution to dryness under a nitrogen gas flow. The anhydrous stannous chloride obtained was dissolved in the organic solvent to be examined at a concentration of 10^{-2} M. The adducts of SnBr$_4$ labelled with ^{119m}Sn were synthesized as follows. About 30 mg of tin powder which contained 0.2 mCi ^{119m}Sn was reacted with bromine in chloroform solution. SnBr$_4$ was isolated by evaporating the solvent. Making use of radioactive SnBr$_4$, the source adducts were prepared according to the method described by Philips *et al.*[12]

Measurements. The Mössbauer absorption spectra of the adduct sources were measured with a CaSnO$_3$ source to identify the sample compounds. The absorption spectra of the SnCl$_2$ solutions were measured for other samples prepared from natural tin because radioactive tin contains mainly ^{118}Sn. The emission spectra were measured against the ^{119}Sn-enriched CaSnO$_3$ absorber (2.0 mg ^{119}Sn/cm^2) at room temperature. Both the absorption and emission spectra were measured by cooling the sample in a liquid helium flow type cryostat. Mössbauer parameters were deduced from Lorentzian curves computer-fitted to the spectra by the least-squares method.

RESULTS AND DISCUSSION

Both the absorption and emission spectra of the frozen solutions of SnCl$_2$ in dimethyl sulfoxide (DMSO) and methanol are shown in Figs. 1 and 2 as examples. The Mössbauer parameters deduced from the absorption and emission spectra are shown in Tables 1 and 2, respectively. The parameters for the emission spectra were deduced by the least-squares method by constraining all the line widths to be equal in the spectrum and setting the isomer shift of Sn^{2+} to the value obtained from the absorption spectrum. The data for solid adducts with tetrahydrofuran, DMSO, and pyridine(Py) are also shown in the Tables.

In Table 1, the values of both the isomer shift and the quadrupole splitting were higher for the solutions
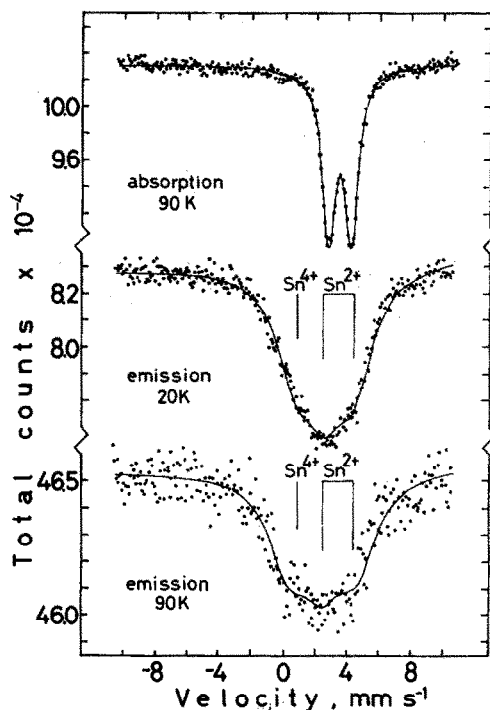
Fig. 1. Mössbauer absorption and emission spectra of a frozen solution of SnCl$_2$ in dimethyl sulfoxide.

than those for the solid adducts. In the solid adducts, tin has trigonal pyramidal coordination, with one tin–ligand and two Sn–Cl bonds.[13,14] In an aprotic solvent such as acetonitrile, however, electrochemical studies indicate that the predominant species in solution is the SnCl$_2$ molecule.[15] If discrete SnCl$_2$ molecules exist in these solutions without forming Sn–
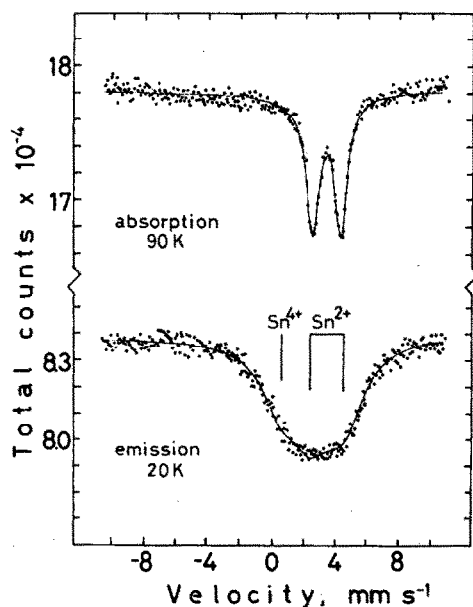
Fig. 2. Mössbauer absorption and emission spectra of a frozen solution of SnCl$_2$ in methanol.

Table 1. Mössbauer absorption parameters for frozen solutions of SnCl$_2$ in organic solvents

Solvent	δ (mm/)	Δ (mm/s)	Γ (mm/s)
C$_4$H$_8$O	3.63	1.95	1.11
SnCl$_2$·2C$_4$H$_8$O[a]	3.32	1.68	—
CH$_3$OH	3.51	1.93	1.07
C$_2$H$_5$OH	3.41	2.01	1.24
(CH$_3$)$_2$SO	3.61	1.56	1.12
SnCl$_2$·2(CH$_3$)$_2$SO[b]	3.48	1.50	1.05
C$_5$H$_5$N	3.44	1.65	1.17
SnCl$_2$·2C$_5$H$_5$N[c]	3.25	1.60	0.99

[a]Ref. 13, solid. adduct.
[b]Ref. 10, solid adduct.
[c]Ref. 11, solid adduct.

ligand bonds, the tin atoms will have more electrons than those in the solid adducts, because formally tin electrons are used for the covalent bond between tin and ligand and acquire some ligand character in the solid adducts. The observed increases of isomer shift and quadrupole splitting are compatible with those increases of electron density at tin in the discrete SnCl$_2$ molecules in the solutions.

In Table 2, about 30% of the yield of the oxidized aliovalent species Sn^{4+} was observed in the emission spectra of the ^{119m}SnCl$_2$ solutions examined, though the yield of Sn^{4+} in the solid adducts of SnCl$_2$ was 48% in ^{119m}SnCl$_2$·2DMSO and zero in ^{119m}SnCl$_2$·2Py, as shown in Table 2. Temperature dependence of the yield was not observed in experiments using dimethyl sulfoxide solutions. Bondarevskii et al. have studied the after-effects of CIT in ^{119m}Sn and EC in ^{57}Co in frozen solutions of some organic solvents and acids.[7-9] Perfiliev et al. have also studied the after-effects in glassy solutions of sulphuric, perchloric, and nitric acids.[16] They have explained the stabilization of the aliovalent species observed in the emission spectra of the frozen solution by the model of competition between hot atoms and other components of the solution to capture the Auger electrons. Our data are reasonably consistent with their results except in the case of the methanol solutions, for which their data showed reduced yields of the oxidized aliovalent species.[9] A mechanism for the stabilization of the aliovalent species observed in the frozen solutions will be proposed, based on the capture of the Auger electrons by the medium so that the charge relaxation does not proceed to the original valence state. It seems that in those organic solutions the Auger electrons are trapped in imperfections of the glassy matrices (as is well known in the radiolysis of glassy frozen alcohol, ether, and other polar organic solvents), because the capturing yield does not depend on the properties of the solvents, such as electron scavenging.

Both the absorption and emission spectra of ^{119m}SnBr$_4$·2DMSO and ^{119m}SnBr$_4$·2DPSO are shown in Figs. 3 and 4, respectively. Though the absorption spectra showed that the samples were purely tetravalent, the reduced aliovalent species of Sn^{2+} were observed in the emission spectra. The Mössbauer parameters for the adducts of ^{119m}SnBr$_4$ with the ligands of organic donor molecules are shown in Table 3 along with the area ratios of Sn^{2+} to total.

Table 2. Mössbauer emission parameters and area ratios of Sn^{4+} to total for frozen solutions of $^{119m}SnCl_2$ in organic solvents at 20 K

| Solvent | Sn^{2+} | | | Sn^{4+} | $\dfrac{A(Sn^{4+})}{A(Total)}$ |
	δ (mm/))	Δ (mm/s)	Γ (mm/s)	δ (mm/s)	
C_4H_8O	3.63	2.13	3.10	0.60	0.29
CH_3OH	3.51	2.10	3.15	0.59	0.26
C_2H_5OH	3.41	2.46	3.90	0.64	0.28
$(CH_3)_2SO$	3.61	1.95	2.93	0.82	0.30
$(CH_3)_2SO$ (90 K)	3.61	2.27	3.02	0.34	0.33
$SnCl_2 \cdot 2(CH_3)_2SO^a$	3.47	1.76	2.53	0.84	0.48
C_5H_5N	3.44	1.88	2.75	0.62	0.28
$SnCl_2 \cdot 2C_5H_5N^b$	3.21	2.04	3.42	—	—

^{a}Ref. 10, solid adduct.
^{b}Ref. 11, solid adduct.

The parameters were deduced from the spectra by the least-squares method as a superimposition of a Sn^{4+} singlet peak and a Sn^{2+} doublet peak without constraining the width.

Sanchez et al. have reported reduced aliovalent species of Sn^{2+} in the emission spectra of $^{119m}SnBr_4 \cdot 2Py$ and $^{119m}SnBr_4 \cdot Bipy$. They have discussed the results in terms of an autoradiolysis model. The radicals created by the autoradiolysis of the closest ligands of pyridine and bipyridine during Auger processes stabilize aliovalent charge states, depending on their reducing properties. Our result for the pyridine adduct is in good agreement with that of Sanchez et al. In the case of dimethyl sulphoxide, it

is well known that this compound decomposes to methyl radical-methanosulphenate anion pairs formed by dissociative electron capture in γ-irradiated crystalline solids according to:[17]

$$(CH_3)_2SO + e^- \rightarrow CH_3SO^- - - - - - \cdot CH_3.$$

The methyl radicals thus created reduce the tetravalent tin in $SnBr_4 \cdot 2DMSO$. However, it seems likely that in the case of the crystalline solid adducts the autoradiolysis by Auger electrons is effective only with the closest ligand molecules, because reduction by methyl radicals was not observed in solutions of dimethyl sulphoxide in which discrete molecules of
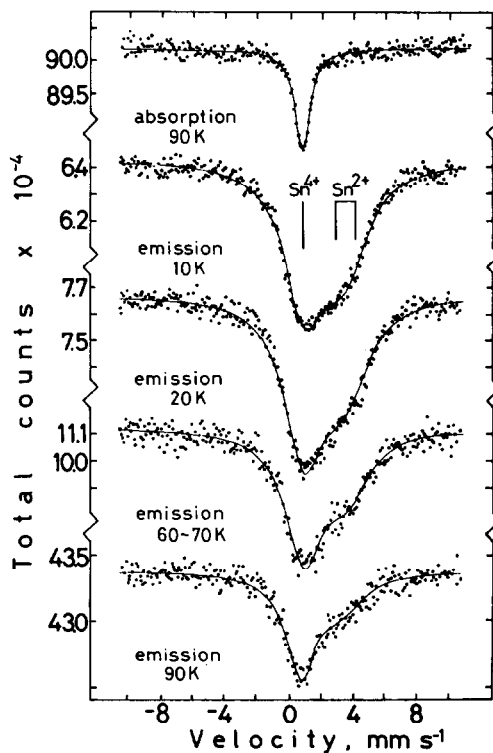
Fig. 3. Mössbauer absorption and emission spectra of $^{119m}SnBr_4 \cdot 2(CH_3)_2SO$.
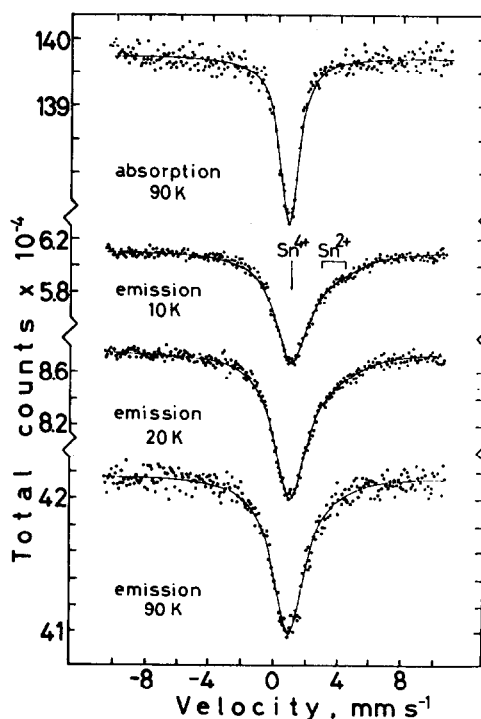
Fig. 4. Mössbauer absorption and emission spectra of $^{119m}SnBr_4 \cdot 2(C_6H_5)_2SO$.

Table 3. Mössbauer emission parameters and area ratios of Sn^{2+} to total for solid adducts of $^{119m}SnBr_4$ with organic donor molecules

Compound		Sn^{4+}		Sn^{2+}			$A(Sn^{2+})$
		δ (mm/s)	Γ (mm/s)	δ (mm/s)	Δ (mm/s)	Γ (mm/s)	A(Total)
$SnBr_4 \cdot 2(CH_3)_2SO$	(9.5 K)	0.98	3.05	3.47	0.82	3.17	0.43
$SnBr_4 \cdot 2(CH_3)_2SO$	(20 K)	0.99	3.07	3.54	0.99	3.21	0.40
$SnBr_4 \cdot 2(CH_3)_2SO$	(60 K)	0.90	2.93	3.64	0.66	3.02	0.33
$SnBr_4 \cdot 2(CH_3)_2SO$	(90 K)	0.78	2.47	3.44	0.95	2.65	0.28
$SnBr_4 \cdot 2(CH_3)_2SO$	(90 K)[a]	0.66	1.23	—	—	—	—
$SnBr_4 \cdot 2(C_6H_5)_2SO$	(9.5 K)	0.87	2.58	3.57	1.67	2.65	0.15
$SnBr_4 \cdot 2(C_6H_5)_2SO$	(20 K)	0.85	2.51	3.43	1.66	2.56	0.13
$SnBr_4 \cdot 2(C_6H_5)_2SO$	(90 K)	0.83	2.47	3.50	1.66	2.56	0.03
$SnBr_4 \cdot 2(C_6H_5)_2SO$	(90 K)[a]	0.48	1.68	—	—	—	—
$SnBr_4 \cdot 2C_5H_5NO$	(9.5 K)	0.95	2.73	3.75	1.21	2.98	0.24
$SnBr_4 \cdot 2C_5H_5NO$	(20 K)	0.90	2.78	3.55	1.32	3.01	0.22
$SnBr_4 \cdot 2C_5H_5NO$	(90 K)	0.77	2.20	3.54	1.35	2.45	0.17
$SnBr_4 \cdot 2C_5H_5NO$	(90 K)[a]	0.76	0.76	1.18	—	—	—
$SnBr_4 \cdot 2C_5H_5N$	(9.5 K)	0.49	2.74	3.42	1.21	2.81	0.26
$SnBr_4 \cdot 2C_5H_5N$	(20 K)	0.49	3.21	3.33	1.47	3.25	0.22
$SnBr_4 \cdot 2C_5H_5N$	(90 K)	0.37	2.51	3.70	1.48	2.54	0.11
$SnBr_4 \cdot 2C_5H_5N$	(90 K)[a]	0.70	1.37	—	—	—	—

[a]Mössbauer absorption parameters.

$SnCl_2$ exist. The small yield of Sn^{2+} from the adduct of $^{119m}SnBr_4$ with diphenyl sulphoxide (DPSO) must result from the high radiation stability of the phenyl group on the ligands. The temperature dependence of the area ratio of Sn^{2+} to total will also confirm the occurrence of the reducing reaction by radicals, which will change the environment of the tin atoms from the original one.

In our previous work, a large yield of the oxidized aliovalent species was observed in the emission spectra of the adducts of $^{119m}SnCl_2$ with oxygen- and nitrogen-containing donor molecules.[10,11] The mechanism for the stabilization of the oxidised aliovalent species in those compounds can also be described in the same way as the above discussion. The relevant data are reproduced in Table 4. The ligand molecules diphenyl sulphoxide, pyridine N-oxide, and picoline N-oxide would be equal to dimethylsulphoxide as good electron scavengers in autoradiolysis of the crystalline solids.

In the adduct with dimethyl sulphoxide the highly charged hot atoms, Sn^{n+}, created by Auger processes are rapidly relaxed to Sn^{4+} by recapturing electrons

from their surroundings. However, further electron capture by Sn^{4+} to give the original valence state of Sn^{2+} would not proceed as a result of the capturing of Auger electrons by the ligands. Methyl radicals generated by the dissociative electron capture of the ligands would reduce a portion of Sn^{4+} to Sn^{2+}. Thus the yield of the oxidized aliovalent species in $^{119m}SnCl_2 \cdot 2DMSO$ is lower than that in $^{119m}SnCl_2 \cdot 2DPSO$, because the phenyl groups involved in the ligand of DPSO are stable in radiolysis.

The results for adducts with pyridine N-oxide and the series of picoline N-oxides as ligands are also explained in the same way. In these adducts, the Auger electrons are also captured by the ligand molecules. Methyl radicals will be formed by processes of dissociative electron capture in the autoradiolysis of picoline N-oxides. The methyl radicals formed, in their order of closeness to the tin atom, i.e. in the order: α-, β-, and γ-positions, will reduce Sn^{4+} to Sn^{2+} in accordance with the order of decreasing yields of Sn^{4+}. The yield of Sn^{4+} in the adduct with γ-picoline N-oxide was almost the same as the value for the adduct with pyridine N-oxide, so that the radicals formed at the γ-position, i.e. at the longest distance, are not effective in reducing the tin atoms.

These autoradiolysis mechanisms for stabilization of aliovalent species observed in the Mössbauer emission spectra as the after-effects of CIT in ^{119m}Sn probably have a short life-time related to the Mössbauer time-scale $(10^{-8}–10^{-7}$ s) at low temperatures.

Table 4. Area ratios of Sn^{4+} to total in the Mössbauer emission spectra of solid adducts of $^{119m}SnCl_2$ with organic donor molecules at 20 K

Compound	$\dfrac{A(Sn^{4+})}{A(Total)}$	Ref.
$SnCl_2 \cdot 2(CH_3)_2SO$	0.40	(10)
$SnCl_2 \cdot 2(C_6H_5)_2SO$	0.68	(10)
$SnCl_2 \cdot 2C_6H_5)_2SO\,(90\,K)$	0.65	(10)
$SnCl_2 \cdot C_5H_5NO$	0.52	(10)
$SnCl_2 \cdot \alpha\text{-}CH_3C_5H_4NO$	0.35	(10)
$SnCl_2 \cdot \beta\text{-}CH_3C_5H_4NO$	0.45	(10)
$SnCl_2 \cdot \gamma\text{-}CH_3C_5H_4NO$	0.56	(10)

REFERENCES

[1] J. P. Adlof, In Chemical Effects of Nuclear Transformations in Inorganic Systems (Edited by G. Harbottle and A. G. Maddock), Chap. 24. North-Holland, Amsterdam (1979).

[2]P. P. Seregin, F. S. Nasredinov and L. N. Vasilev, *Phys. Status Solidi (a)* 1978, **45**, 11.

[3]J. M. Friedt and J. Danon, *Radioch. Acta* 1972, **17**, 173.

[4]J. M. Friedt and Y. Llabador, *Radiochem. Radioanal. Lett.* 1972, **9**, 237.

[5]Y. Llabador and J. M. Friedt, *J. Inorg. Nucl. Chem.* 1973, **35**, 2351.

[6]J. P. Sanchez, Y. Llabador and J. M. Friedt, *J. Inorg. Nucl. Chem.* 1973, **35**, 3557.

[7]S. I. Bondarevskii and V. A. Tarasov, *Soviet Radiochem.* 1972, **14**, 172.

[8]N. E. Ablesimov and S. I. Bondarevskii, *Soviet Radiochem.* 1973, **15**, 472.

[9]S. I. Bondarevskii, V. A. Tarasov and E. E. Shcherbakov, *Soviet Radiochem.* 1973, **15**, 913.

[10]S. Ichiba, M. Yamada and H. Negita, *Radiochem. Radioanal. Lett.* 1978, **35**, 31.

[11]S. Ichiba, M. Yamada and H. Negita, *Radiochem. Radioanal. Lett* 1978, **36**, 93.

[12]J. Philip, M. A. Mullins and C. Curran, *Inorg. Chem.* 1968, **7**, 1895.

[13]J. D. Donaldson and D. G. Nicholson, *J. Chem. Soc. (A)*, 1970, 145.

[14]J. W. Kauffman, D. H. Moor and R. J. Williams, *J. Inorg. Nucl. Chem.* 1977, **39**, 1165.

[15]A. R. Brajer, T. E. Farley, J. W. Kauffman, L. K. Young, R. J. Williams and J. W. Rogers, *Anal. Chim. Acta* 1977, **91**, 165.

[16]Yu. D. Perfiliev, L. A. Kulikov, L. T. Bugaenko, A. M. Babeshkin and M. I. Afanasov, *J. Inorg. Nucl. Chem.* 1976, **38**, 2145.

[17]Y. J. Chung, K. Nishikida and F. Williams, *J. Phys. Chem.* 1974, **78**, 1882.

INFLUENCE OF CATIONS ON ZINC(II) INCORPORATION INTO CROWN PORPHYRINS

V. THANABAL and V. KRISHNAN*

Department of Inorganic and Physical Chemistry, Indian Institute of Science, Bangalore-560012, India

Abstract—The decrease in rate constants of Zn(II) incorporation into fully and partially benzo-15-crown-5 meso substituted porphyrins in the presence of cations has been explained on the basis of cation complexation ability of the crown ether cavities rather than steric effects.

Recently we designed cavity-bearing porphyrins with crown ether units derived from benzo-15-crown-5, appended at the 5-, the 5- and 10-, the 5-, 10- and 15-, and the 5-, 10-, 15- and 20-positions of the porphyrin skeleton for studying their cation complexation behaviour.[1] It occured to us that these compounds can be used to study the effect of cations, bound in the ether voids, on the rates of metal insertion reactions into crown porphyrins. The factors that contribute to the rates of porphyrin metallation reactions are the basicity of the free-base porphyrins, the relative ease of deformation of the porphyrin skeleton and the ease of deprotonation as a consequence of desolvation;[2] however, the role played by cations in such reactions remain unclear. As this study will show, the presence of alkali and alkaline-earth cations in the ether voids decreases the rates of Zn(II) incorporation into the porphyrin moiety and the relative ease of access of metal ions in determining the geometric disposition of the ether voids in the crown porphyrins. The rate data obtained here are of significance in view of the structural resemblance between the cation-bound crown porphyrins and meso-tetrapyridyl porphyrin with four positively-charged $C_5H_5N^+$ groups or cation salts of meso-aryltetracarboxylato and tetrasulphonato-porphyrins where the cations are ionically bound with the peripheral groups.

Tetra(benzo-15-crown-5) porphyrin(TCP) (1) was synthesised by condensing a mixture of 4'-formyl benzo-15-crown-5 and pyrrole in 1:1 proportions in refluxing propionic acid. By changing the mole proportions, the tris (2), cis and trans-di (3), and mono (4) crown ether-substituted porphyrins have been prepared. The structural integrity of these cavity-bearing porphyrins (Fig. 1) is established using ^{1}HNMR, optical absorption and emission spectral methods.

The Zn(II) incorporation into the free base porphyrins in a $CHCl_3$:CH_3OH (1:1) mixture at 25°C was studied using an optical absorption spectral method. The decrease in absorption of the Q band at 515 nm of TCP as a function of time was monitored. A representative plot of $\ln(OD_t - OD_\infty)$ vs time (t), where OD_t and OD_∞ represent absorbance at time ($_t$) and at the completion of the reaction, respectively, for a given concentration of Zn(II), is given in Fig. 2. The values of k_{obsd} were calculated from the slopes of the plot. The metallation reaction follows a second-order rate law, first order with respect to porphyrin and to Zn^{2+} ion. The concentration of crown porphyrin was held constant (5.0×10^{-5}M) and the concentration of Zn(II) acetate was varied from 1.0×10^{-3} to 2.0×10^{-2} maintaining pseudo first-order conditions (see Fig. 2 inset). The experiments are carried out in the presence of various cations and the rate data

for Zn(II) incorporation into crown porphyrin are given in Table 1.

An inspection of Table 1 reveals that the rate of Zn(II) incorporation into crown porphyrin is about 2.5 times greater than that into tetraphenyl porphyrin (TPP) under the same experimental conditions. This enhanced rate can be ascribed to the possible deformation of the porphyrin ring as a result of attachment of the four macrocyclic crown ether moieties at the 5-, 10-, 15-, and 20-positions of the porphyrin core. Such a deformation can promote easy deprotonation of the H-H groups[2], thereby increasing the metal incorporation rates. Alternately, the substitution of crown ether moieties in the phenyl ring at meta and para positions can be viewed as meta, para-disubstituted TPP, in which case TCP will be
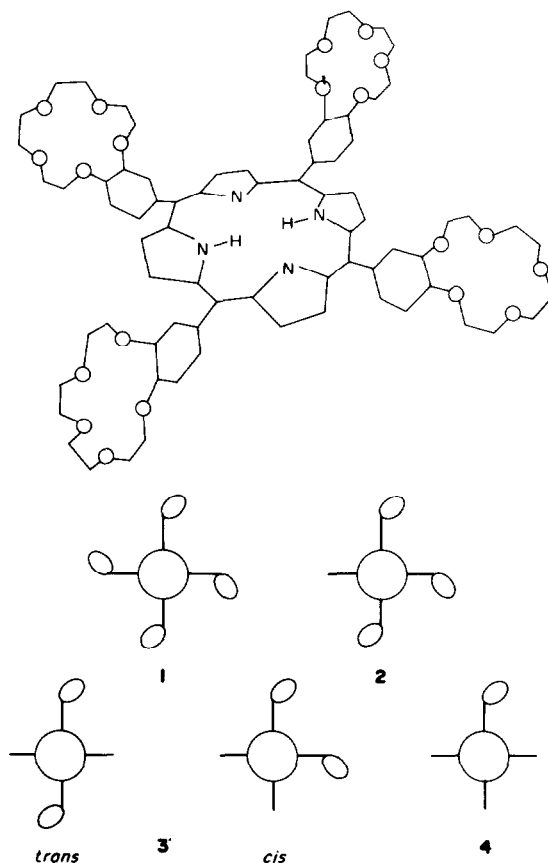
Fig. 1. Chemical structure of tetra(benzo-15-crown-5) porphyrin. The partially-substituted crown porphyrins are shown. The full circle represents the porphyrin, while the ellipse and the line denote the substitutents, benzo-15-crown-5 cavity and phenyl rings respectively, in the methine positions.

*Author to whom correspondence should be addressed.
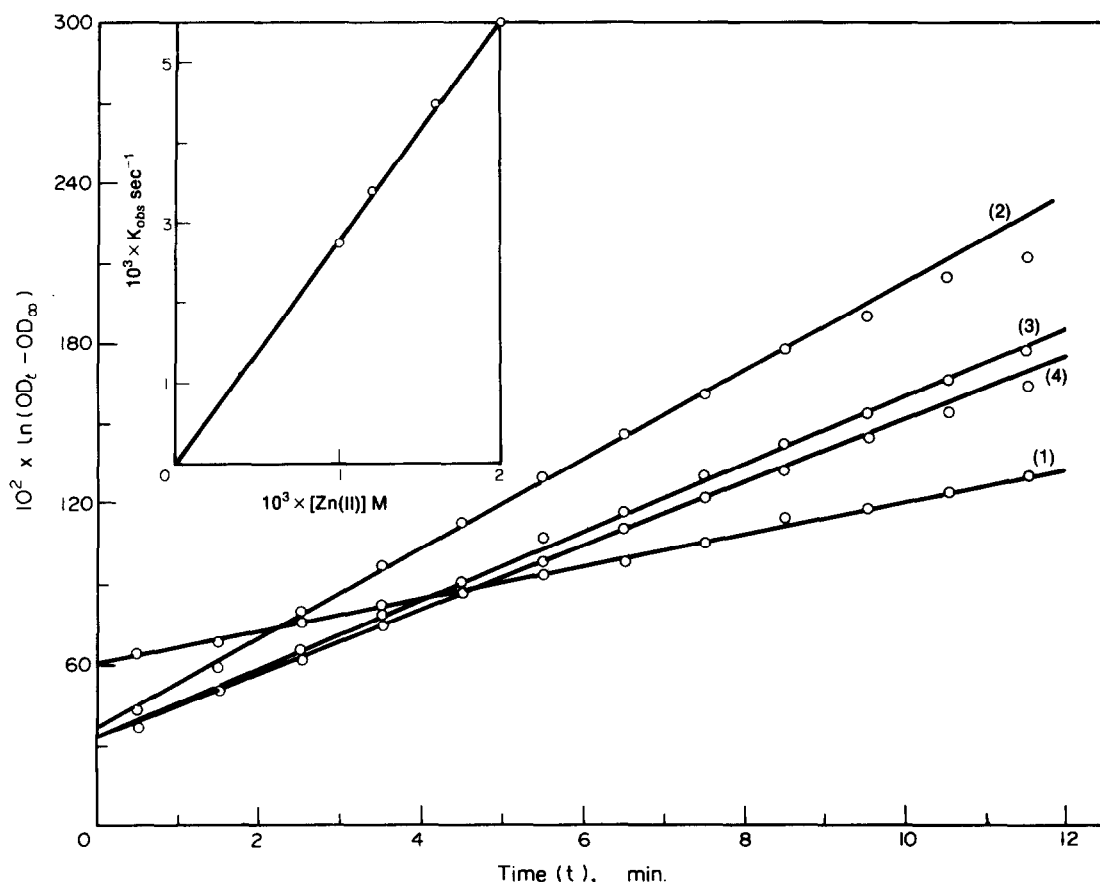
Fig. 2. Plot of $\ln(OD_t - OD_\infty)$ vs time(t)- (1) TPP containing 0.1M tBuAP, (2) TCP containing 0.1M tBuAP, (3) TCP containing 0.1M NaClO$_4$ and (4) TCP containing 0.1M tBuAP and 5.0×10^{-4} NaCO$_4$. The inset shows the plot of K_{obsd} vs the concentration of the added Zn(II) ion.

Table 1. Rate data for Zn(II) incorporation into TPP and crown porphyrins at 25°C in CHCl$_3$:CH$_3$OH (1:1) solvent mixture

Porphyrin	Cation[a]	$10^3 \times K_{obs}$sec^{-1}
TPP	tBuAP(0.1M)	1.0
TPP	NaClO$_4$(0.1M)	1.1
TPP	Mg(ClO$_4$)$_2$(0.1M)	1.1
TCP (1)	tBuAP(0.1M)	2.7
TCP	NaClO$_4$(0.1M)	1.9
TCP	tBuAP(0.1M) + NaClO$_4$(5.0 × 10^{-4}M)	2.1
TCP	Mg(ClO$_4$)$_2$(0.1M)	1.9
TCP	tBuAP(0.1M) + Mg(ClO$_4$)(5 × 10^{-4}M)	1.9
TrisCP (2)	tBuAP(0.1M)	2.8
TrisCP	NaClO$_4$(0.1M)	2.0
cisDCP (3)	tBuAP(0.1M)	2.7
cisDCP	NaClO$_4$(0.1M)	2.2
MCP (4)	tBuAP(0.1M)	2.7
MCP	NaClO$_4$(0.1M)	2.4

[a]tBuAP = Tetrabutylammonium perchlorate; the value in parenthesis denotes the concentration of the cation employed in the study.

more basic than TPP since -OR group is an electron-donating group. Cyclic voltammetry of the crown porphyrin shows a marginal increase in the first reduction potential compared to TPP and we believe the enhanced rates of Zn(II) incorporation arise from the electronic effects. Construction of CPK models of the crown porphyrins show that the deformation of the porphyrin ring is minimal.

Interestingly, the presence of Na$^+$, Ca^{2+} and Mg^{2+} ions reduces the rate of Zn(II) incorporation to about 30%. Normally the rate differences in porphyrin metallation reactions in the presence of cations are explained either in terms of the formation of SAT complexes[3] or by an introduction of an ususal anion term in the rate law.[4] In the present study we did not observe the characteristic SAT visible spectra of the free-base porphyrins in

presence of cations, and a change in the anions (counterparts of cations) does not significantly alter the rates of Zn(II) incorporation into crown porphyrins. We attribute the observed decrease in the Zn(II) incorporation rates to cation complexation effects by crown ether voids. An explanation for the present finding is traced to the encapsulation of cations by the ether oxygens which induces an electron-withdrawing effect in the phenyl rings, and a transmission of this effect results in the decreased bascity of the N-H protons thereby reducing the rates of Zn(II) incorporation into the porphyrin macrocycle. The cation complexation by the peripheral crown ether oxygen atoms[3] is evidenced by the downfield shifts (~ 0.40 δ) of the ether proton and aryl proton resonances.[1] The decrease in the basicity of the porphyrin ring on addition of cations is also demonstrated in the small changes of the redox potentials as observed in the cyclic voltagramms of the cation complexes of TCP. That these cation complexation effects on the rates of Zn(II) incorporation are real and of significance is further supported by the reduced rates of Zn(II) incorporation (to about 30%) in the systems containing TCP, tBuAP (0.1M) and cations ($\sim 10^{-4}$M). Despite the close resemblance the cation-bound freebase crown porphyrins bear with *meso* N-methyl-tetrapyridyl-porphyrins and cation complexes of *meso* tetraaryltetra-carboxylato or tetrasulphonato porphyrins, the observed rates for the Zn(II) insertion reactions in the present study are distinct and different. In the former the observed rates are predominantly dictated by the differential solvation term[2] and we tend to believe the influence of these may be negligible in the crown porphyrins.

The cations K^+, NH_4^+, Ba^{2+}, and Cs^+ induce dimer formation of the free base porphyrins[1] and the metal incorporation rates could not be followed using optical absorption spectral methods.

In crown porphyrins, the crown ether moieties are oriented perpendicular to the porphyrin plane and do not sterically hinder the access of metal ions into the porphyrin core. However, in the sterically crowded tetrapivalylamidophenyl porphyrin of Collman *et al.*,[5] it has been found that the rate of metal insertion is lowered compared to that of TPP.[6] The observation that the less substituted porphyrins (tris, *cis* and *trans* DCP) exhibit rates of Zn(II) incorporation not significantly different from that observed for TCP provides further support for the absence of steric effect.

The present results show the influence of bound cations (in the peripheral positions of porphyrin) on the rates of Zn(II) incorporation. The nature of the cations apparently has no percepitable effects on the rates, since the recognition of cations by the host ethers are primarily governed by the relative sizes of the ether cavity and the cations.

REFERENCES

[1] V. Thanabal and V. Krishnan, *J. Am. Chem. Soc.* 1982, **104**, 3643.
[2] W. Schneider, *Struct. Bonding* 1975, **23**, 123.
[3] E. S. Fleischer and J. H. Wang, *J. Am. Chem. Soc.* 1960, **82**, 3498.
[4] M. Bain-Ackerman and D. K. Lavallee, *Inorg. Chem.* 1979, **18**, 3358.
[5] J. P. Collman, R. Gagne, C. A. Reed, T. Halberg, G. Lang and W. T. Robinson, *J. Am. Chem. Soc.* 1975, **97**, 1427.
[6] J. Jurray and P. Hambright, *Inorg. Chem. Acta Lett.* 1981, **53**, L 147.

THE GENERATION OF THE GERMANIUM DIHALIDES

S. M. VAN DER KERK

Department of Physical Chemistry, Free University, De Boelelaan 1083, 1081 HV Amsterdam, The
Netherlands

Abstract—A method is described for the generation of GeX_2 ($X = F$, Cl, Br, I) as uncoordinated monomers in the gas phase, free from impurities. These species were identified by UV photoelectron spectroscopy and mass spectroscopy.

Being formal carbene analogues, the divalent compounds of the group IV A elements other than carbon have, during the past decades, elicited interest in quite different fields of chemistry. However, the more stable, and thus the more accessible the compounds MX_2 are, the less is their actual carbene-like character, whether the latter be considered from a synthetical or from a more theoretical point of view. For an unambiguous assessment of their carbene-like properties, the MX_2 molecules should be studied in a monomeric, uncoordinated state.

The methods used for the synthesis of germanium dihalides[1,2] can be roughly divided into two categories.

(a) Methods which yield the dihalides in the gas phase in an uncoordinated, monomeric form.

(b) Methods which yield the dihalides in a polymeric form (i.e. coordination polymers) or in a coordinated form (e.g. to a solvent).

From a PE spectroscopical point of view, the latter methods are not suitable. Heating of the polymeric dihalides generally does not produce the monomers without interference from oligomeric species.[3] For spectroscopic purposes, GeF_2, $GeCl_2$, and $GeBr_2$ are often synthesized by reaction between elemental germanium and the germanium tetrahalide:

$$Ge + GeX_4 \rightleftarrows 2GeX_2 \quad (X = F, Cl, Br).$$
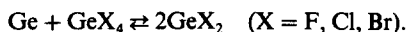
Further, $GeCl_2$ and $GeBr_2$ are formed in the thermal decomposition of the corresponding trihalogermane:

$$HGeX_3 \rightarrow GeX_2 + HX \quad (X = Cl, Br).$$

The obvious disadvantage of these methods is that the wanted product (made *in situ*) is invariably accompanied by other products which, in the case of PE spectroscopy, may obscure its spectrum.

In 1978, Feltz and Dresler[4] reported the isolation (by sublimation) of polymeric $GeCl_2$ upon reaction of a powdered Ge_2S_3 glass with eutectic mixtures of $KCl/AgCl$, $PbCl_2/AgCl$, or $KCl/CuCl$ at temperatures of 250–350°C *in vacuo*. They proposed the following reaction equation:

$$Ge_2S_3 + 2AgCl \rightarrow GeCl_2 + GeS_2 + Ag_2S.$$

In the same paper[4] it was briefly stated that crystalline germanium monosulphide also reacts with a eutectic $KCl/AgCl$ mixture at a temperature of 310° to form $GeCl_2$.

It was decided to study the latter reaction as, in our opinion, it offered the possibility of generating the germanium dihalides as uncoordinated, monomeric species in the gas phase, according to:

$$GeS + 2AgX \rightarrow GeX_2 + Ag_2S \quad (X = F, Cl, Br, I).$$

All experiments were performed in sealed tubes and in the PE spectrometer as well. It proved rather difficult to free germanium monosulphide, synthesized according to the Inorganic Synthesis method[5] (in this way, red, amorphous GeS is obtained) from all traces of water. Moreover, Schumb and Smyth[6] have established that GeS synthesized in this fashion may contain up to 20% of chloride. Therefore GeS was synthesized (in brown–black, crystalline form) by heating an equimolar mixture of GeS_2[5] and germanium powder to 550–600° under nitrogen and by subsequent sublimation of the GeS formed in vacuo at temperatures up to 650°.

In the first experiments, crystalline GeS was heated with a eutectic $KCl/AgCl$ mixture. However, only germanium tetrachloride was formed. Next, excess GeS, intimately mixed with AgCl, was heated. PE spectroscopy showed that a small amount of $GeCl_2$ was formed, together with $GeCl_4$ (at 280–310°). With a mixture of excess GeS and AgBr the same result was obtained (at temperatures of 230–270°): the tetrahalide was formed predominantly. Only a trace of $GeBr_2$ was observed. These phenomena suggested that the following redox reaction was occurring:

$$Ge^{II} + 2Ag^{I} \rightarrow Ge^{IV} + 2Ag^0.$$
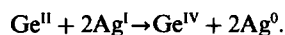
This idea was borne out by the fact that upon heating a mixture of GeS and AgF at 170°, a fiercely exothermic reaction took place, in which metallic silver was formed. In order to avoid the possibility of a redox reaction, but to retain the advantage of forming a stable, non-volatile sulphide, lead(II) halides were used instead. In this way, using excess crystalline GeS with the corresponding lead(II) halide, GeF_2, $GeCl_2$, $GeBr_2$ and GeI_2 could be generated in the gas phase as uncoordinated monomers, in the case of $X = F$, Cl, Br virtually free from impurities, as was proven by PE spectroscopy. The PE spectra of these species will be published separately.[7–9]

The mass spectra of the germanium dihalides were obtained by heating the GeS/PbX_2 mixtures in the direct insertion probe of the mass spectrometer. The resulting mass spectra of GeF_2, $GeCl_2$, $GeBr_2$ and

GeI_2 are shown in Figs. 1(a), 2(a), 3(a) and 4(a), respectively. For comparison, the mass spectra of GeF_4,[10] $GeCl_4$,[11] $GeBr_4$ and GeI_4 are given in Figs. 1(b), 2(b), 3(b) and 4(b), respectively. The strength of the germanium–fluorine bonds in GeF_2^+ is illustrated by the fact that in the mass spectrum of GeF_2 the parent peaks (naturally occurring germanium is composed of five isotopes) form the base peaks, while in the mass spectra of the other dihalides the base peaks are those of GeX^+. In the mass spectra of $GeCl_2$ and GeI_2 the peaks corresponding to GeX_3^+ and $GeX_4^+\cdot$ could be observed. It is improbable that the odd-electron ions $GeX_4^+\cdot$ are formed by a recombination reaction in the ionization source. In our opinion the ions $GeX_4^+\cdot$ and GeX_3^+ derive from the tetrahalides, which are formed in a redox reaction between GeS

and PbX_2, in quantities depending on the experimental conditions. This supposition is, in the case of the iodine compound, supported by the PE spectroscopic results.[9] In the mass spectra of the tetrahalides the $GeX_2^+\cdot$ ion peaks have a very low intensity. Further, in the mass spectra of GeF_2 and $GeBr_2$ no ions $GeX_4^+\cdot$ and GeX_3^+ are found. Therefore it can be stated that the germanium dihalides have been positively identified not only by means of PE spectroscopy[7-9] but by mass spectrometry as well.

GeF_2 (from $Ge + CaF_2$[12]), $GeCl_2$,[13-15] and $GeBr_2$[15] (the latter two from $Ge + GeX_4$) have been studied by mass spectrometry before.

It should be noted that both in the PE and in the mass spectroscopic experiments, contamination of the spectrometer was a serious problem.
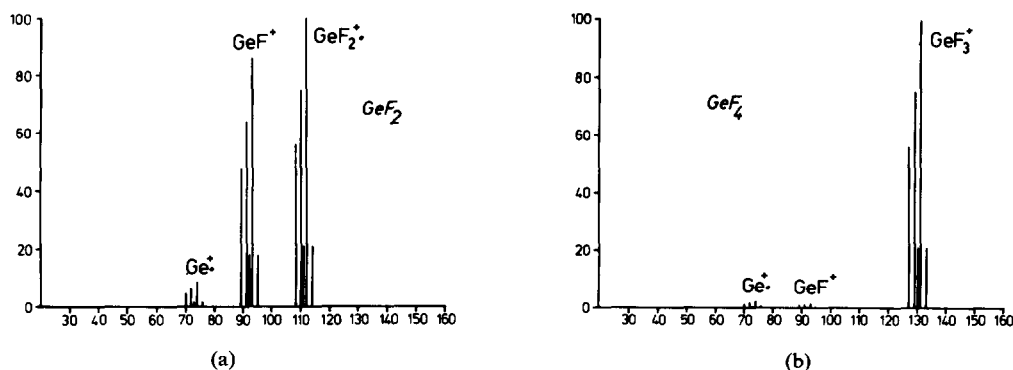
Fig. 1. (a) Mass spectrum of GeF_2. (b) Mass spectrum of GeF_4.[10]
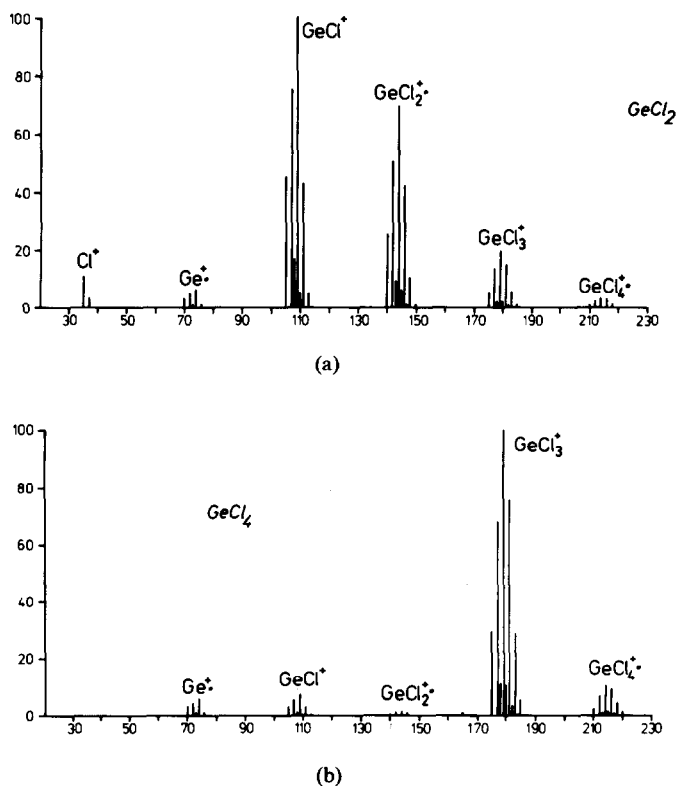
Fig. 2. (a) Mass spectrum of $GeCl_2$. (b) Mass spectrum of $GeCl_4$.[11]
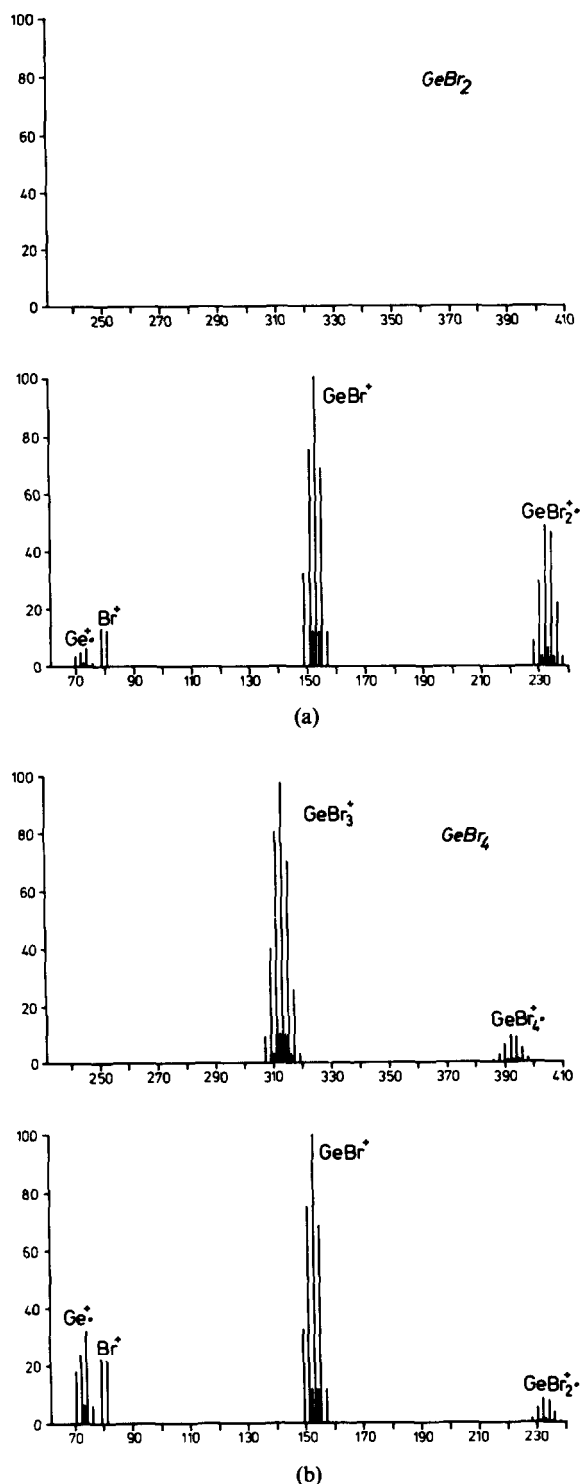
Fig. 3. (a) Mass spectrum of GeBr$_2$. (b) Mass spectrum of GeBr$_4$.

An attempt was made to generate germanium dicyanide by heating a mixture of crystalline GeS and CuCN. However, only formation of cyanogen was observed. This might be explained by the occurrence of the following redox reaction:

$$Ge^{II}S + 2CuCN \rightarrow Ge^0 + (CN)_2 + Cu_2S.$$

Preliminary experiments have indicated that the apparatus, used by Timms and others for the reaction of metal atoms with various substrates[16,17] is very well suited for the reactions of monomeric germanium dihalides, generated as described here, with suitable substrates. Only moderately high temperatures (250–350°) are needed and relatively large quantities of the pure dihalides can be produced.
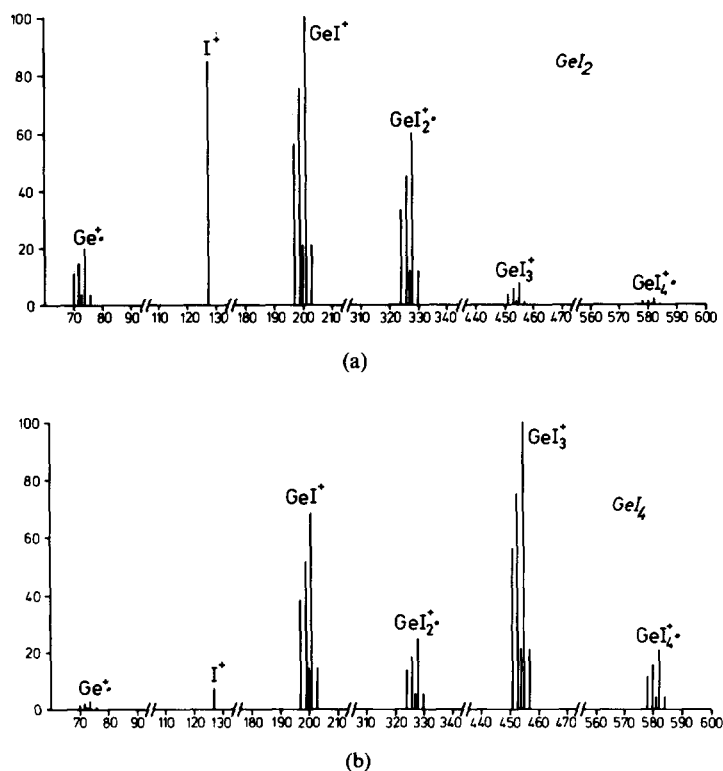
Fig. 4. (a) Mass spectrum of GeI_2. (b) Mass spectrum of GeI_4.

EXPERIMENTAL

He(I) PE spectra of GeF_2, $GeCl_2$, $GeBr_2$, and GeI_2 were recorded on a home-built PE spectrometer described previously.[18]

Mass spectra of GeF_2, $GeCl_2$, $GeBr_2$, GeI_2, $GeBr_4$, and GeI_4 were obtained using a Finnigan 3100 D Mass Spectrometer with 6110 Data System.

Experiments were carried out under an atmosphere of dry, oxygen-free nitrogen in Schlenk vessels equipped with an inserted, water-cooled cold finger. All solids were finely ground and were thoroughly dried (if necessary) prior to use by heating in vacuo. In the syntheses of the compounds GeX_2 (X = F, Cl, Br, I) GeS was always used in excess. Reaction temperatures were dependent on reaction conditions (particle size, degree of mixing). Reaction took place between 250 and 350° for all four halides, at pressures of ca. 0.1 Torr.

After formation, the germanium dihalides (eventually) polymerized to form solids. GeF_2 is slowest in polymerizing. $[GeF_2]_n$ condenses as colourless droplets which slowly turn into a waxy yellowish white solid. $[GeCl_2]_n$ condenses as a colourless viscous fluid which turns into a white solid considerably faster than the fluoride. $[GeBr_2]_n$ directly sublimes as a solid, in the form of white needles. $[GeI_2]_n$ sublimes as a yellow–brown solid, faster so than the bromide. All four solid germanium dihalides thus formed are hygroscopic, especially the fluoride.

REFERENCES

[1] J. Satgé, M. Massol and P. Rivière, J. Organometal. Chem. 1971, 56, 1, and references cited therein.
[2] J. L. Margrave, K. G. Sharp and P. Wilson, Fortschr. Chemie 1970 26, 1, and references cited therein.
[3] K. F. Zmbov, J. W. Hastie, R. Hauge and J. L. Margrave, Inorg. Chem. 1968, 7, 608.
[4] A. Feltz and G. Dresler, Zeitschr. Chemie 1978, 18, 420.
[5] L. S. Foster, Inorg. Synth. 1946, 2, 102.
[6] W. C. Schumb and D. M. Smyth, J. Am. Chem. Soc. 1955, 77, 3003.
[7] G. Jonkers, S. M. van der Kerk, R. Mooyman and C. A. de Lange, Chem. Phys. Lett. 1982, 90, 252.
[8] G. Jonkers, S. M. van der Kerk and C. A. de Lange, Chem. Phys. 1982, 70, 69.
[9] G. Jonkers, S. M. van der Kerk, R. Mooyman, C. A. de Lange and J. G. Snijders, Chem. Phys. Lett. in press.
[10] P. W. Harland, S. Cradock and J. C. J. Thynne, Int. J. Mass. Spectrom. Ion Phys. 1972, 10, 169.
[11] K. Matsumoto, N. Kiba and T. Takeuchi, Talanta 1975, 22, 321.
[12] T. C. Ehlert and J. L. Margrave, J. Chem. Phys. 1964, 41, 1066.
[13] E. Vajda, I. Hargittai, M. Kolonits, K. Ujszászy, J. Tamás, A. K. Maltsev, R. G. Mikaelian and O. M. Nefedov, J. Organometal. Chem. 1976, 105, 33.
[14] G. Y. Schultz, J. Tremmel, I. Hargittai, I. Berecz, S. Bohátka, N. D. Kagramanov, A. K. Maltsev and O. M. Nefedov, J. Molec. Struct. 1979, 55, 207.
[15] O. Manuel Uy, D. W. Muenow and J. L. Margrave, Trans. Faraday. Soc. 1969, 65, 1296.
[16] P. L. Timms, Adv. Inorg. Radiochem. 1972, 14, 121.
[17] P. L. Timms, Angew. Chem. 1975, 87, 295.
[18] G. Jonkers, C. A. de Lange and J. G. Snijders, Chem. Phys. 1980, 50, 11.

FORMATION OF PROTONATED SALICYLATE COMPLEXES OF Cd(II) AND Zn(II)

KYU SUN BAI

Department of Chemistry, Soong Jun University, Sang-Do Dong, Seoul, Korea

Abstract—The formation constants of the protonated complexes of Cd(II) and Zn(II) with salicylic acid (H_2Sal) and the equilibrium constants for the extraction of these complexes into cyclohexane containing tributyl phosphate (TBP) have been determined. For the complex formation:

$$M^{2+}_{aq} + HSal^-_{aq} \xrightleftharpoons{K_{11}} MHSal^+_{aq}$$
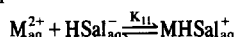
$\log K_{11}$ is 1.9 for Cd(II) and 1.4 for Zn(II) at 30°C and 0.1 M $NaClO_4$. For the extraction:

$$M^{2+}_{aq} + 2H_2Sal_{aq} + 2TBP_{org} \xrightleftharpoons{K_{ex}} M(HSal)_2TBP_{2org} + 2H^+_{aq}$$

$\log K_{ex}$ is -1.6 for Cd(II) and -2.2 for Zn(II).

In solvent extraction studies of metal ions, it is a standard procedure to plot the logarithm of the metal distribution coefficient against the pH of the aqueous phase or against the logarithm of the concentration of the extractant in one phase or the other. From analysis of slopes of such plots, the compositions of the extracting species and the extraction equilibrium constants of such reactions may be determined . Even if linear plots are obtained, the values of the slopes may or may not be integers. Many investigators commonly assume such fractional slopes to be the nearest integers in order to simplify the interpretations.[1–5]

In a recent paper,[6] a method for quantitatively interpreting such noninteger slopes has been presented. It is not only unnecessary to assume fractional slopes to be the nearest integer slopes, but also more accurate values of the constants are obtained by not making such assumptions.

In an extreme case,[3] even slopes closer to 1 than to 2 were considered to be 2 in order to explain the experimental results according to the proposed extraction model. In the present paper, the method[6] has been modified and applied to some published data[3] on the distribution of Cd(II) and Zn(II) between aqueous salicylates and cyclohexane containing tributyl phosphate.

As far as the author is aware, the present paper is the first report of the formation constants of the protonated complexes of Cd(II) and Zn(II) with salicylic acid.

DISTRIBUTION EQUILIBRIA

In systems of metal ion extraction with complexing agents, a series of complexes may be formed between the metal ion and the complexing extractant in the aqueous phase. In the case of salicylic acid as the extractant, both the "ordinary" complexes and the protonated complexes may be formed. The following reactions take place in such systems for Cd(II) and Zn(II) ions:

$$M^{2+}_{aq} + HSal^-_{aq} \xrightleftharpoons{K_{11}} MHSal^+_{aq}$$

$$M^{2+}_{aq} + 2HSal^-_{aq} \xrightleftharpoons{K_{22}} M(HSal)_{2aq}$$

$$M^{2+}_{aq} + Sal^{2-}_{aq} \xrightleftharpoons{K_1} MSal_{aq}.$$
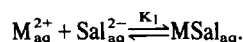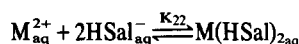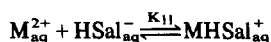
The species extracted in the presence of TBP in the organic phase (cyclohexane) have been identified as the $M(HSal)_2(TBP)_2$ type, where M is Zn(II) or Cd(II).[3] This type has also been identified for Zn(II)[7] and for some other divalent metal ions.[7,8] The equation for the extraction of these metal ions may then be represented as:

$$M^{2+}_{aq} + 2H_2Sal_{aq} + 2TBP_{org} \xrightleftharpoons{K_{ex}}$$
$$M(HSal)_2(TBP)_{2org} + 2H^+_{aq}. \quad (1)$$
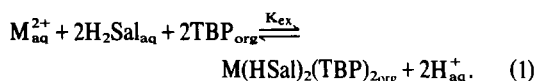
The equilibrium constant for this reaction is given by:

$$K_{ex} = \frac{[M(HSal)_2TBP_2]_{org}[H^+]^2_{aq}}{[M^{2+}]_{aq}[H_2Sal]^2_{aq}[TBP]^2_{org}}$$

$$= \frac{[M(HSal)_2TBP_2]_{org}K^2_{H2}}{[M^{2+}]_{aq}[HSal^-]^2_{aq}[TBP]^2_{org}}$$

where K_{H2} is the first acid dissociation constant of salicylic acid. The metal distribution coefficient is given by:

$$D = \frac{[M(HSal)_2TBP_2]_{org}}{[M^{2+}]_{aq} + [MHSal^+]_{aq} + [M(HSal)_2]_{aq} + [MSal]_{aq}}.$$

Using the various equilibrium constants shown above, this equation may be expressed as:

$$D = \frac{K_{ex}[HSal^-]^2_{aq}[TBP]^2_{org}}{(1 + K_{11}[HSal^-]_{aq} + K_{22}[HSal^-]^2_{aq} + K_1[Sal^{2-}]_{aq})K^2_{H2}}.$$

Hence

$$\log D + \log F_x = \log K_{ex} - 2\log K_{H2} + 2\log [HSal^-]_{aq}$$
$$+ 2\log [TBP]_{org} \quad (2)$$

where F_x may be called a formation function and is

defined by:

$$F_x = 1 + K_{11}[HSal^-]_{aq} + K_{22}[HSal^-]^2_{aq} + K_1[Sal^{2-}]_{aq}.$$

(3)

If the higher terms in F_x are neglected, eqn (2) becomes:

$$\log D = \log K_{ex} - 2 \log K_{H2} + 2 \log [TBP]_{org}$$
$$+ 2 \log [HSal^-]_{aq}.$$

This is the equation used by Singh and Tandon,[3] and was derived assuming that the complex formation of the metals with an excess of salicylic acid is negligible.

RESULTS AND DISCUSSION

Singh and Tandon[3] first carried out quantitative studies on the extraction of Zn(II) and Cd(II) with salicylic acid and TBP. Some of their results are shown in Figs. 1 and 2 (Graphs 1A and 2A). The slopes of these distribution curves indicate that aqueous complex formation in such systems is not negligible. In fact, complex formation between the metal ions and salicylic acid occurs in the aqueous phase to a large extent.

In order to explain the experimental data on the distribution of the metals, slopes even smaller than 1.5 were considered to be 2.[3] Actually, the difference between the number of charges on the metal ion and the experimental slope of such plots is a measure of the extent of complex formation in the aqueous phase.

In the case of uranyl ion extraction with anthranilic acid in the presence and in the absence of TBP, a similar situation was observed.[6] When log D was plotted against pH or against the logarithm of the acid concentration, linear relationships were obtained but the slopes were all between 1.6 and 1.8. It was found that uranyl ion formed binary complexes with anthranilic acid in the aqueous phase. Therefore, separate experiments were carried out to determine the binary complex formation constants. In
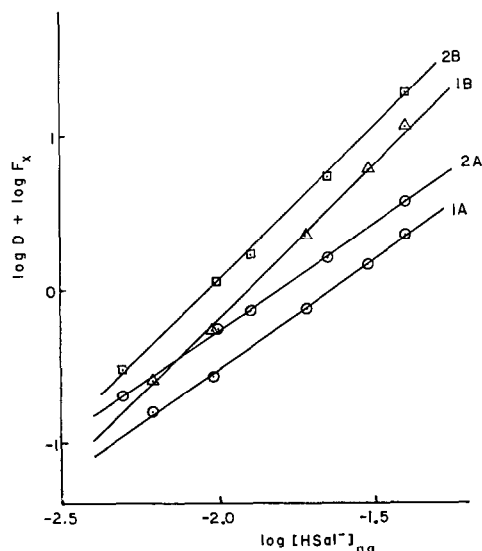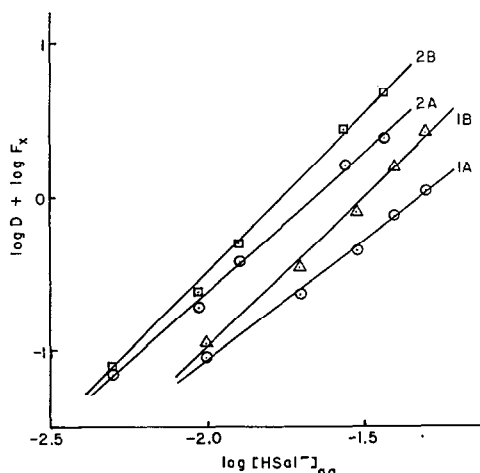
Fig. 2. Distribution of Zn(II) salicylate between aqueous 0.1 M NaClO$_4$ and TBP-cyclohexane at 30°C. Graph 1. 0.5 M TBP. Graph 2. 1.0 M TBP. Initially $1 \times 10^{-4} M$ Zn(II); Equilibrium pH 6.0. The ordinate is log D for Graphs 1A and 2A which are reproduced from Ref. 3. Slopes. 1A, 1.55; 1B, 1.94; 2A, 1.83; 2B, 2.05.

the extraction systems, allowances were then made for the presence of the aqueous complexes using the formation constants so determined. When this was done, slopes of 2 corresponding to the charge on the metal ion were obtained when log D plus log formation function was plotted against pH or against the logarithm of the acid concentration.

In the present paper, the formation constants of the protonated binary complexes are calculated from the distribution data. The extraction constants are also calculated from the same distribution data.

The extraction constants calculated assuming that the metals are present only as the aquo M^{2+} ion in the aqueous phase depend on the level of HSal$^-$ concentration. For the data in Table 2(a) of Ref. 3, the value of log K$_{ex}$ calculated for Cd(II) using eqn (1) of Ref. 3 regularly varies from −1.85 to −2.39 in going down the column. The value of pK$_{H2}$ = 2.88 for 30°C and 0.1 ionic strength[9] was used in these calculations. Had Singh and Tandom entered all the values of K$_{ex}$ in their table (Ref. 3, Table 2(a), column 4), the changing trend would have been obvious. The same changing trend may also be seen by entering all the values of K$_{ex}$ in column 4 of Table 2(b) of Ref. 3.

In the case of Zn(II), a similarly changing trend may be noticed by entering all the values of K$_{ex}$ in column 4 of Table 1 of Ref. 3. Only when the slopes of such plots are integers corresponding to the charge on the metal ion, are identical values of K$_{ex}$ obtained from all regions of the distribution curve.

In the extraction systems, salicylic acid is present in large excess of the metal ions, and the amount of salicylates combined with the metals may be neglected. The Sal^{2-} ion is also negligible under the experimental conditions employed. The mass balance for salicylates is then given by

$$[Sal]_t = [H_2Sal]_{aq} + [HSal^-]_{aq} + [H_2Sal]_{org}$$
$$+ 2[(H_2Sal)_2]_{org}.$$

By introducing the first acid dissociation constant (K$_{H2}$), the partition constant (P$_x$), and the dimerization constant

Fig. 1. Distribution of Cd(II) salicylate between aqueous 0.1 M NaClO$_4$ and TBP-cyclohexane at 30°C. Graph 1. 0.5 M TBP. Graph 2. 1.0 M TBP. Initially $1 \times 10^{-4} M$ Cd(II); Equilibrium pH 6.0. The ordinate is log D for Graphs 1A and 2A which are reproduced from Ref. 3. Slopes. 1A, 1.42; 1B, 2.00; 2A, 1.40; 2B, 2.00.

Table 1. Comparison of some protonated complexes of salicylic acid

Equilibrium quotient	salicylic acid (H_2L)		benzoic acid (HL)
	$\dfrac{[MHL]}{[M][HL]}$	$\dfrac{[ML]}{[M][L]}$	$\dfrac{[ML]}{[M][L]}$
Metal	log K	log K	log K
H^+	2.81	13.4	4.00
Ca^{2+}	0.36		0.2
Zn^{2+}	1.4*	6.85	0.9
Cd^{2+}	1.9*	5.55	1.4
UO_2^{2+}	2.2	12.08	
Fe^{3+}	4.4	16.3	
La^{3+}	2.08		
Th^{4+}	4.25		

*This work; all other values from Ref. 12 (mostly for 25°C and 0.1 ionic strength).

(K_{dim}) of salicylic acid in the organic phase, the following equation is obtained and may be solved for $[HSal^-]_{aq}$ for each experimental point.

$$\frac{2K_{dim}P_s^2}{K_{H2}^2}[H^+]_{aq}^2[HSal^-]_{aq}^2 + \left[1 + \frac{1+P_s}{K_{H2}}[H^+]_{aq}\right][HSal^-]_{aq}$$

$$= [Sal]_t.$$

The values of the constants used are $pK_{H2} = 2.88$, $P_s = 0.14$, and $K_{dim} = 580$ for cyclohexane. The values of the last two constants were obtained by interpolating the data of Banewicz et al.[10] Singh and Tandon[3] reported the value 0.585 as the partition constant of salicylic acid between cyclohexane and water. The difference between the two values of P_s for salicylic acid did not materially affect the calculation for $[HSal^-]_{aq}$, however. The calculations revealed that practically all the salicylate is present as $HSal_{aq}^-$.

The values of the protonated complex formation constants were determined using eqns (2) and (3) by systematically varying these parameters until slopes of 2 were obtained. Allowances for the presence of MSal alone as complex did not explain the experimental results. The values of K_1 used were $10^{5.55}$ for Cd(II) and $10^{6.85}$ for Zn(II).[11] Actually MSal was completely negligible for the Cd(II) systems. For Zn(II) it was only a minor species at high ends of the distribution curves. The best value of K_{11} is $10^{1.9}$ for Cd(II) and $10^{1.4}$ for Zn(II). These values were used in constructing Graphs 1B and 2B of Figs. 1 and 2. At any given concentration of $HSal_{aq}^-$, the difference between Graphs 1B and 1A or between 2B and 2A is the correction term, log F_x.

The values of K_{22} could not be determined accurately. Only the upper limits of these constants could be estimated. The distribution curves for Cd(II) (Fig. 1, Graphs 1B and 2B) were quite insensitive to variations in the value of K_{22} when log K_{22} is less than about 2.8. The curves for Zn(II) (Fig. 2, Graphs 1B and 2B) were also insensitive to variations in the value of K_{22} when log K_{22} is less than about 2.2. Above these values of K_{22}, the distribution curves seriously departed from linearity, bending upward in the high ends.

Since $HSal^-$ is a part of the extracting species, it is quite natural that binary complexes are formed between it and the metal ions in the aqueous phase. In Ref. 11, the experimental conditions were such that only the ordinary complexes exist in the aqueous solutions. In Ref. 3, on the other hand, $HSal^-$ exists in large excess of the metals and therefore the conditions are favorable for the formation of the protonated complexes.

Owing to the electroneutrality and the large size of the organic portion of $M(HSal)_2$, this species is not expected to be water-soluble to any appreciable extent. Hence the uncertainty in the values of K_{22}.

The values of the extraction constants were calculated from Graphs 1B and 2B of Figs. 1 and 2 using eqn (2). The values of log K_{ex} obtained for Cd(II) are -1.4 and -1.7 from Graphs 1B and 2B, respectively, of Fig. 1. The average, -1.6, is taken as the best. The value for Zn(II) is -2.2 from both Graphs 1B and 2B of Fig. 2. From eqn (1) involving 2 TBP molecules, the vertical spacing between Graphs 1A and 2A or between 1B and 2B should be 0.6 log unit. In Fig. 1, it is seen that the spacing is smaller than 0.6. This is reflected as the somewhat larger uncertainty in the value of K_{ex} for Cd(II).

The values of K_{11} are smaller than the corresponding values of K_1 by several orders of magnitude. This is consistent with the monodentate nature of the ligand in $M(HSal)^+$. For the protonated complexes, the Cd(II) complex is more stable than the Zn(II) complex while the opposite is the case for the ordinary complexes.[11] These results are in accord with the coordinating tendencies usually observed with these metals. Examination of the literature[12] revealed that with many monodentate ligands the Cd(II) complex is more stable than the Zn(II) complex, while the opposite is generally the case with chelating ligands. The larger stability constant of the protonated Cd(II) complex is reflected in its better extractability. Comparison of Figs. 1 and 2 indicates that Cd(II) is extracted better than Zn(II) is; the value of K_{ex} is larger for Cd(II) than for Zn(II).

Protonated complexes are quite common for salicylic acid. In Table 1 are given stability constant data for the protonated complexes of some metals with salicylic acid. Some data for benzoic acid are included for comparison.

The constants for the protonated complexes of Zn(II) and
Cd(II) are comparable to the stabilities of the benzoate
complexes. This is as expected from the similarity of the
ligands in the two cases. The relative stabilities of the
protonated salicylate complexes of Cd(II) and Zn(II) are
the same as for the benzoate complexes of these metals.

REFERENCES

[1] W. M. Davis, J. W. Holt and R. A. Tournier, In *Solvent
Extraction* (Edited by J. G. Gregory, B. Evans and P. C.
Weston), p. 984. Society of Chemical Industry, London (1971).
[2] J. M. Singh and S. N. Tandon, *Can. J. Chem.* 1978, **56**, 2922.
[3] J. M. Singh and S. N. Tandon, *J. Inorg. Nucl. Chem.* 1979, **41**,
1205.
[4] B. Jain, J. M. Singh, R. N. Goyal and S. N. Tandon, *Can. J.
Chem.* 1980, **58**, 1558.
[5] J. M. Singh, B. Gupta and S. N. Tandon, *J. Inorg. Nucl. Chem.*
1981, **43**, 1863.
[6] K. S. Bai, *J. Inorg. Nucl. Chem.* 1981, **43**, 2525.
[7] J. Aggett, D. J. Evans and R. Hancock, *J. Inorg. Nucl. Chem.*
1968, **30**, 2529.
[8] J. Aggett and P. Crossley, *J. Inorg. Nucl. Chem.* 1967, **29**, 1113.
[9] L. G. Sillen and A. E. Martell, *Stability Constants of Metal-Ion
Complexes*. The Chemical Society, London (1964).
[10] J. J. Banewicz, C. W. Reed and M. E. Levitch, *J. Am. Chem.
Soc.* 1957, **79**, 2693.
[11] D. D. Perrin, *Nature* 1958, **182**, 741.
[12] A. E. Martell and R. M. Smith, *Critical Stability Constants.*
Vol. 1. *Amino Acids* (1974). Vol. 2. *Amines* (1975) and Vol. 3.
Other Organic Ligands (1977). Plenum Press, New York.

COMPLEXES CONTAINING PHOSPHORUS LIGANDS—16[1]

NEW PHOSPHINITE, PHOSPHONITE AND PHOSPHITE DERIVATIVES OF RUTHENIUM, OSMIUM AND IRIDIUM

CLIFFORD J. CRESWELL†, STEPHEN D. ROBINSON* and ARVIND SAHAJPAL
Department of Chemistry, King's College, Strand, London WC2R 2LS, England

Abstract—The complexes [MHCl(CO)(PPh$_3$)$_3$] (M = Ru or Os) readily undergo substitution at the site *trans* to the hydride ligand to afford phosphinite-, phosphonite-, or phosphite-containing products [MHCl(CO)(PPh$_3$)$_2$L] [L = P(OR)Ph$_2$, P(OR)$_2$Ph or P(OR)$_3$ respectively; R = Me or Et]. The ruthenium complexes alone undergo further substitution to afford complex cations [RuH(CO)(PPh$_3$)$_n$L$_{4-n}$]$^+$ [n = 2, L = P(OMe)$_3$; n = 1, L = P(OR)$_3$; n = 0, L = P(OR)$_2$Ph or P(OR)Ph$_2$] which were isolated and characterised as their tetraphenylborate salts. Synthesis of the cationic complexes [IrHL$_3$][BPh$_4$]$_2$ [L = P(OR)$_3$, R = Me or Et] is also reported. Stereochemical assignments based on NMR data are given, and second order ^{31}P and high field ^{1}H NMR patterns are analysed.

In contrast to the tertiary phosphines, tertiary phosphite esters, P(OR)$_3$, and the closely related phosphonites, P(OR)$_2$Ph, and phosphinites P(OR)Ph$_2$(R = alkyl) have attracted relatively little attention as ligands in platinum metal chemistry.[2] This situation has been corrected to some degree in recent years by the incorporation of these less common phosphorus donor ligands in a series of cationic complexes which can be readily isolated as tetraphenylborate, tetrafluoroborate or hexafluorophosphate salts of relatively low solubility. Much of the early work in this area originated from our own laboratory.[3–5] We now report an extension of our studies and describe a new range of ruthenium, osmium, and iridium complexes containing phosphorus donor ligands of the type under discussion.

RESULTS AND DISCUSSION

The complexes MHCl(CO)(PPh$_3$)$_2$L (M = Ru, Os)

The hydrido complexes [MHCl(CO)(PPh$_3$)$_3$] (M = Ru or Os) react with phosphorus donor ligands [L = P(OR)$_x$Ph$_{3-x}$, R = Me or Et, x = 1 – 3] in boiling benzene or alcohol (ROH) solution to afford the uncharged monosubstituted products [MHCl(CO) (PPh$_3$)$_2$L] as air-stable, white crystalline solids, soluble in most common organic solvents. The high field proton NMR spectra of these products each comprise a doublet of triplets pattern [^{2}J(PH)$_{trans}$ = *ca.* 120–180 Hz(Ru) or *ca.* 90–140 Hz(Os); ^{2}J(PH)$_{cis}$ = *ca.* 20–22 Hz] indicative of stereochemistry (I). This assignment is similar to those made for other ruthenium complexes [RuHCl(CO)(PR$_3'$)$_2$L], prepared by analogous substitution processes, and is in accord with the known high *trans* labilizing influence of the hydride ligand.[6]

The osmium complexes do not undergo further substitution when subjected to prolonged and/or vigorous treatment in the presence of excess ligand.

However, their more labile ruthenium analogues, when similarly treated with a large excess of ligand, L, give solutions which upon addition of sodium tetraphenylborate deposit complex salts of the general stoichiometry [RuH(CO)(PPh$_3$)$_n$L$_{4-n}$] [BPh$_4$](n = 0 – 2).

The complex salt [RuH(CO)(PPh$_3$)$_2$L$_2$][BPh$_4$] [L = P(OMe)$_3$]. This product was obtained as an air-stable, white, crystalline solid, soluble in acetone, chloroform and dichloromethane, but sparingly soluble in alcohols. The proton NMR spectrum displays aryl, methyl and hydride protons in the required ratio 50:18:1. The methyl resonance, consisting of two doublets of equal intensity [^{3}J(PH) = *ca.* 10.25 Hz], establishes the presence of two non-equivalent P(OMe)$_3$ ligands. The absence of a large coupling ^{2}J(PP')$_{trans}$ from the ^{31}P NMR spectrum implies that the P(OMe)$_3$ ligands are not *trans* to triphenylphosphine. These data establish stereochemistry (IIa) for the complex. The high field proton resonance consists of a broad second order pattern which does not directly afford stereochemical information, except to confirm the location of a phosphorus donor ligand *trans* to the hydride. However, iterative analysis of the ^{31}P and high field ^{1}H NMR spectra gave the data shown below which are consistent with the proposed structure (IIa).

An isomeric product, present in small quantity (*ca.* 10%), displays a compact second order high field proton NMR pattern together with a virtual coupling triplet in the methyl region. The former implies the absence of a phosphorus donor ligand *trans* to the hydride and the latter indicates the presence of a *trans* pair of P(OMe)$_3$ ligands[7] thus establishing stereochemistry (IIb) for this minor product.

The complex salts [RuH(CO)(PPh$_3$)L$_3$][BPh$_4$] [L = P(OR)$_3$]. These products were obtained as airstable, white, crystalline solids soluble in acetone, chloroform and dichloromethane but sparingly soluble in alcohols. The proton resonance of the triethyl phosphite complex shows aryl, methylene, methyl

*Author to whom correspondence should be addressed.
†Hamline University, St. Paul, Minnesota, U.S.A.

$\delta(\text{RuH}) = -7.82 \ (\tau \ 17.82)$
$\delta P^1 = -40.77 \text{ ppm}$
$\delta P^2 = -133.3 \text{ ppm}$
$\delta P^3 = -133.6 \text{ ppm}$

$^2J(HP^1) = 17.75 \text{ Hz}, \ ^2J(HP^2) = 37.9 \text{ Hz}, \ ^2J(HP^3) = -124.5 \text{ Hz}.$
$^2J(P^1P^2) = 43.45 \text{ Hz}, \ ^2J(P^1P^3) = 36.45 \text{ Hz}, \ ^2J(P^2P^3) = 38.35 \text{ Hz}.$
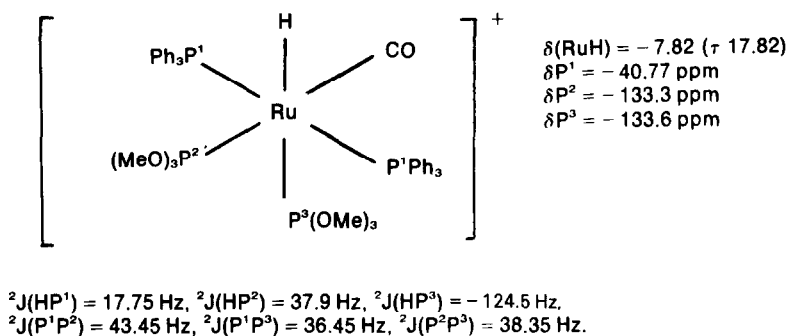
and hydride protons in the required ratio 35:18:27:1. The methyl resonance, comprising three triplet of equal intensity, establishes the presence of three non-equivalent P(OEt)$_3$ ligands, and the broad, second order, high field proton NMR pattern betrays the presence of a *trans* coupling $^2J(PH)$. On the basis of this evidence we assign stereochemistry (IIIa) to this product. In contrast, the proton NMR spectrum of the corresponding trimethyl phosphite complex establishes stereochemistry (IIIb). The methyl resonance comprises a doublet and a triplet (relative intensities 1:2) and the high field proton pattern consists of a complex pattern which when subjected to iterative analysis affords the following data

The complex salts [RuH(CO)L$_4$][BPh$_4$] [L = P(OR)$_x$Ph$_{3-x}$, R = Me or Et, n = 1 or 2]. These products were obtained as air-stable, white crystalline solids. Their high field proton NMR spectra each consist of a regular first order quintet pattern indicative of stereochemistry (IV). Virtual coupling patterns consistent with the presence of four equivalent P(OMe)$_x$Ph$_{3-x}$ ligands arranged in a square planar manner are observed for the methyl diphenylphosphinite and dimethyl phenylphosphonite derivatives.[8]

The complex salts [IrHL$_5$][BPh$_4$]$_2$ [L = P(OR)$_3$; R = Me or Et]. These air-stable, white crystalline solids are soluble in dichloromethane but only very sparingly soluble in chloroform and alcohols. Their proton NMR spectra show aryl, alkyl and hydride proton resonances with the correct intensity ratios, but do not distinguish between axial (*trans* to hydride) and equatorial P(OR)$_3$ ligands. The ^{31}P and high field ^{1}H NMR spectra are second order and therefore do not provide stereochemical information directly. However, iterative analysis of the ^{31}P and high field ^{1}H NMR spectra (mixed CDCl$_3$/d_6-DMSO solvent) gave the following data

High field proton NMR spectra recorded at 250 MHz were first order and yielded data for [IrH{P(OEt)$_3$}$_5$][BPh$_4$]$_2$ in good agreement with those presented above [$\delta(\text{IrH}) = -12.3 \ (\tau \ 22.3)$ $^2J(PH)_{trans} = 170 \text{ Hz}, \ ^2J(PH)_{cis} = 16 \text{ Hz}.$

Attempts to prepare the carbonyl species [IrH(CO){P(OEt)$_3$}$_4$][BPh$_4$]$_2$ by carbonylation of [IrH{P(OEt)$_3$}$_5$][BPh$_4$]$_2$ for 1½ hr in boiling ethylmethylketone gave only unchanged starting material.

The stereochemical assignments made for the ruthenium complexes (I)–(IV) establish that the ligand substitution reactions are accompanied by a carbonyl

$\delta(\text{RuH}) = -7.16 \ (\tau \ 17.16)$
$\delta P^1 = -141.7 \text{ ppm}$
$\delta P^2 = -139.7 \text{ ppm}$
$\delta P^3 = -41.4 \text{ ppm}$

$^2J(HP^1) = 21.3 \text{ Hz}, \ ^2J(HP^2) = 19.25 \text{ Hz}, \ ^2J(HP^3) = 15.65 \text{ Hz},$
$^2J(P^1P^2) = 64.2 \text{ Hz}, \ ^2J(P^1P^3) = 43.95 \text{ Hz}, \ ^2J(P^2P^3) = -330.3 \text{ Hz}$

R = Me, $\delta(\text{IrH}) = -12.35 \ (\tau \ 22.35)$
$\delta P^1 = -70.65 \text{ ppm}$
$\delta P^2 = -74.9 \text{ ppm},$
$^2J(HP^1) = 18.3 \text{ Hz},$
$^2J(HP^2) = -167 \text{ Hz},$
$^2J(P^1P^2) = 36.6 \text{ Hz}.$
R = Et, $\delta(\text{IrH}) = -12.36 \ (\tau \ 22.36)$
$\delta P^1 = -62.7 \text{ ppm}$
$\delta P^2 = -69.35 \text{ ppm},$
$^2J(HP^1) = 16.35 \text{ Hz},$
$^2J(HP^2) = -170.55 \text{ Hz},$
$^2J(P^1P^2) = 36.45 \text{ Hz}.$

Scheme I.
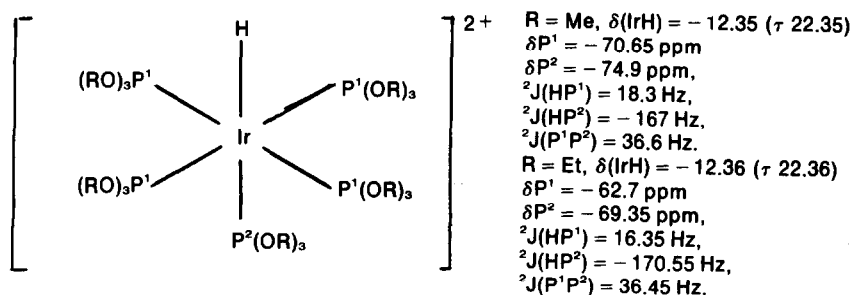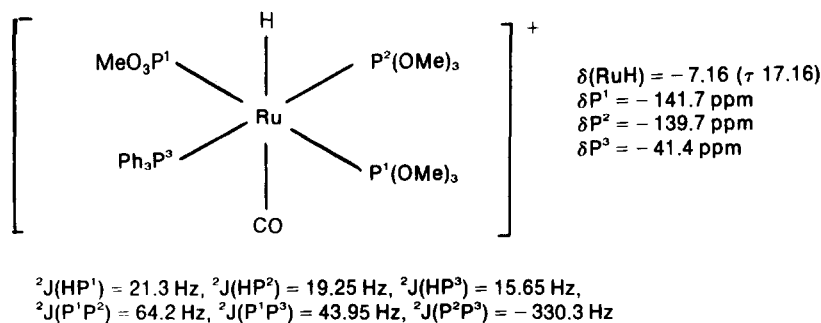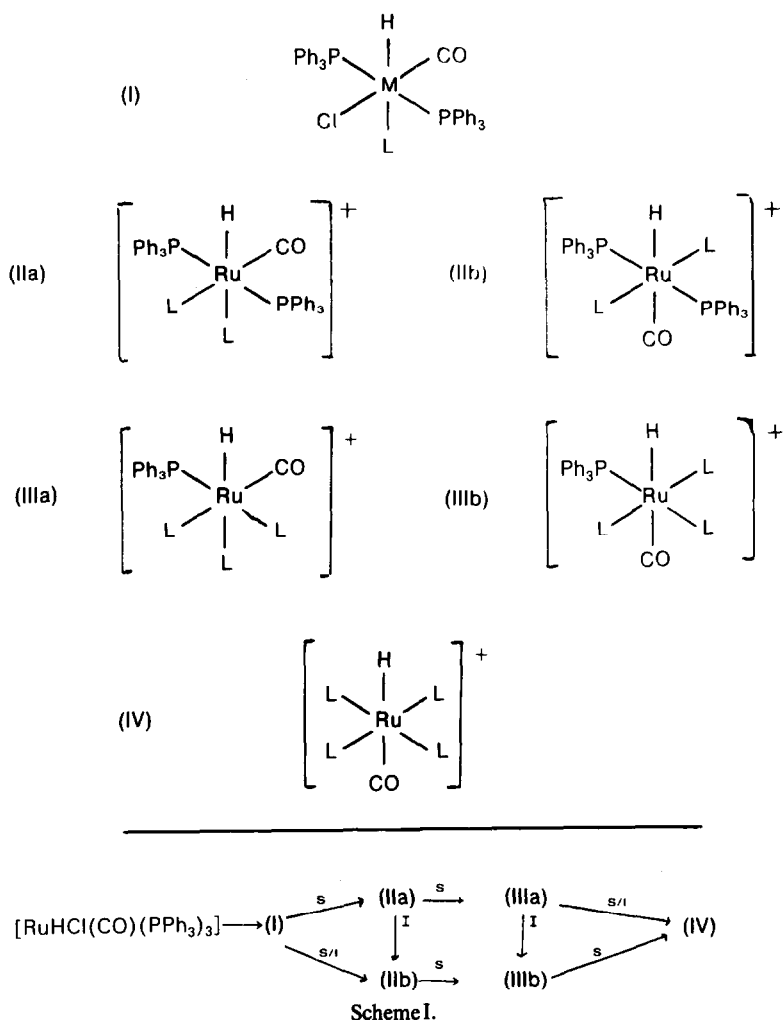
migration step. It appears that, in order to minimise the effect of the increasing number of strong π-acceptor phosphorus donor ligands, the carbonyl ligand migrates to the site *trans* to the strong σ-donor hydride ligand. The proposed substitution (S) and isomerisation (I) processes are collected in Scheme 1.

EXPERIMENTAL

Platinum metal salts and phosphorus donor ligands were obtained from Johnson Matthey and the Maybridge Chemical Co. Ltd., respectively. Platinum metal triphenylphosphine complexes were made as previously described.[9] Reagent grade organic solvents were used as purchased. All reactions were performed under nitrogen but the products were worked-up in air. Analyses, by the microanalytical laboratory, University College, London, and melting points, taken in sealed tubes under nitrogen, are given in Table 1. IR spectra were taken for nujol mulls using a Perkin-Elmer 457 grating spectrometer. Proton NMR spectra were obtained using a Perkin-Elmer R12B (60 MHz) and a Bruker HFX90 (90 MHz) spectrometer. ^{31}P NMR spectra were obtained using the Bruker HFX90 spectrometer operating at 36.43 MHz and are referenced to external H_3PO_4 in the sense that positive values are to low field. Spectroscopic data are recorded in Table 2. Iterative analyses of second order NMR data were performed using an ITRCAL programme.[10]

Carbonylchlorohydrido (*trimethylphosphite*)*bis*(*triphenylphosphine*)*ruthenium*(*II*). Carbonyl chlorohydridotris(triphenylphosphine)ruthenium (0.34 g) and trimethyl phosphite (0.12 g) in a mixture of methanol (30 cm^3) and benzene (5 cm^3) were heated under reflux for *ca*. 1 hr. The resultant clear solution was filtered while hot, concentrated under reduced pressure and set aside overnight. The crystals which separated were filtered off, washed successively with methanol and light petroleum (60–80), then recrystallised from dichloromethane-methanol to yield the required product as colourless microcrystals (0.175 g, 61%).

Similarly prepared using the appropriate ligand and alcoholic solvent were: *carbonylchlorohydrido*(*triethyl phosphite*)*bis*(*triphenylphosphine*) *ruthenium*(*II*) as colourless microcrystals (61%); *carbonylchlorohydrido*(*dimethyl phenylphosphonite*)*bis*(*triphenylphosphine*) *ruthenium*(*II*) as colourless crystals (66%); *carbonylchlorohydrido*(*diethyl phenylphosphonite*)*bis*(*triphenylphosphine*)*ruthenium*(*II*) as white crystals (63%); and *carbonylchlorohydrido*(*methyl diphenylphosphinite*)*bis*(*triphenylphosphine*)*ruthenium*(*II*) as colourless crystals (63%).

Similarly prepared from carbonylchlorohydridotris(triphenylphosphine)osmium were: *carbonylchlorohydrido*(*trimethyl phosphite*)*bis*(*triphenylphosphine*)*osmium*(*II*) as colourless crystals (83%); *carbonylchlorohydrido*(*triethyl phosphite*)*bis*(*triphenylphosphine*) *osmium*(*II*) as colourless crystals (86%); *carbonylchlorohydrido*(*dimethyl phenylphosphonite*)*bis*(*triphenylphosphine*)*osmium*(*II*) as colourless crystals (75%); *carbo-*

Table 1. Analysis and melting point data

COMPLEX	%C*	%H*	M.p./°C
{RuHCl(CO)(PPh$_3$)$_2$[P(OMe)$_3$]}	59.88(59.00)	4.99(4.95)	156–158
{RuHCl(CO)(PPh$_3$)$_2$[P(OEt)$_3$]}	60.47(60.33)	5.42(5.42)	154–157
{RuHCl(CO)(PPh$_3$)$_2$[P(OMe)$_2$Ph]}	62.64(62.8)	4.96(4.92)	157–158
{RuHCl(CO)(PPh$_3$)$_2$[P(OEt)$_2$Ph]}	62.98(63.54)	5.29(5.22)	159–162
{RuHCl(CO)(PPh$_3$)$_2$[P(OMe)Ph$_2$]}	65.40(66.26)	5.1 (4.89)	141–143
{RuH(CO)(PPh$_3$)$_2$[P(OMe$_3$)$_2$]}{BPh$_4$}	65.99(65.85)	5.86(5.69)	169–171
{RuH(CO)(PPh$_3$)[P(OMe)$_3$]$_3$}{BPh$_4$}	57.7 (57.62)	5.97(5.86)	124–126
{RuH(CO)(PPh$_3$)[P(OEt)$_3$]$_3$}{BPh$_4$}	60.81(60.59)	6.52(6.75)	174–176
{RuH(CO)[P(OEt)$_2$Ph]$_4$}{BPh$_4$}	63.75(62.89)	6.52(6.57)	164–165
{RuH(CO)[P(OMe)Ph$_2$]$_4$}{BPh$_4$}	70.88(70.36)	5.76(5.61)	188–190
{RuH(CO)[P(OEt)Ph$_2$]$_4$}{BPh$_4$}	71.16(70.99)	6.00(5.97)	204–205
{RuH(CO)[P(OMe)$_2$Ph]$_4$}{BPh$_4$}	60.63(60.87)	6.11(5.81)	192–193
{OsHCl(CO)(PPh$_3$)$_2$[P(OMe)$_3$]}	52.87(52.9)	4.41(4.76)	198–201
{OsHCl(CO)(PPh$_3$)$_2$[P(OEt)$_3$]}	54.93(54.4)	4.93(5.24)	207–209
{OsHCl(CO)(PPh$_3$)$_2$[P(OMe)$_2$Ph]}	57.52(57.36)	4.3 (4.56)	207–208
{OsHCl(CO)(PPh$_3$)$_2$[P(OEt)$_2$Ph]}	57.87(57.76)	4.74(4.71)	177–178
{OsHCl(CO)(PPh$_3$)$_2$[P(OMe)Ph$_2$]}	58.9 (58.44)	4.36(4.33)	185–188
{OsHCl(CO)(PPh$_3$)$_2$[P(OEt)Ph$_2$]}	62.41(62.6)	4.8 (4.74)	178–179
{IrH[P(OMe)$_3$]$_5$}{BPh$_4$}$_2$	52.02(52.17)	6.02(5.98)	202–204
{IrH[P(OEt)$_3$]$_5$}{BPh$_4$}$_2$	56.46(56.4)	7.00(7.04)	208–209

* Calculated figures in parentheses

nylchlorohydrido(diethyl phenylphosphonite)bis(triphenyl-phosphine)osmium(II) as colourless crystals (59%); carbonylchlorohydrido(methyl diphenylphosphinite)bis(triphenylphosphine)osmium(II) as colourless crystals (90%); and carbonylchlorohydrido(ethyl diphenylphosphinite)bis(triphenylphosphine)osmium(II) as colourless crystals (72%).

Carbonylhydridobis(trimethyl phosphite)bis(triphenylphosphine)ruthenium(II) tetraphenylborate—Carbonylchlorohydridotris(triphenylphosphine)ruthenium (0.34 g) and trimethyl phosphite (0.2 g) in a mixture of methanol (20 cm^3) and chloroform (10 cm^3) were heated under reflux for 30 min. The resultant clear solution was filtered while hot, then treated with sodium tetraphenylborate (0.2 g) in methanol (5 cm^3), and stirred until precipitation commenced. The white precipitate was allowed to stand overnight then filtered off, washed with methanol and light petroleum (60–80), recrystallised from dichloromethane–methanol and dried in vacuo to yield the required product as colourless crystals (0.25 g, 61%). NMR data (see Discussion) indicate the presence of a second isomer (ca. 10%).

Carbonylhydridotris(trimethyl phosphite)(triphenylphosphine)ruthenium(II) tetraphenylborate—Carbonylchlorohydridotris(triphenylphosphine)ruthenium (0.34 g) and trimethyl phosphite (0.2 g) in a mixture of methanol (30 cm^3) and benzene (5 cm^3) were heated together under reflux for ca. 3 hr. The resultant clear solution was filtered while hot, treated with sodium tetraphenylborate (0.2 g) in methanol (5 cm^3), then concentrated to a small volume on a water bath before being allowed to cool with gentle stirring. The white

precipitate was allowed to stand for a few hours, then filtered off, washed with methanol and light petroleum (60–80), recrystallised from dichloromethane–methanol and dried in vacuo to yield the required product as colourless microcrystals (0.23 g, 64%).

Carbonylhydridotris(triethyl phosphite)(triphenylphosphine)ruthenium(II)tetraphenylborate. Similarly obtained as colourless crystals (62%) using triethyl phosphite and ethanol in place of trimethyl phosphite and methanol. Carbonylhydridotetrakis(diethyl phenylphosphonite)ruthenium(II) tetraphenylborate — carbonylchlorohydridotris(triphenylphosphine)ruthenium (0.34 g) and diethyl phenylphosphonite (1.0 g) in a mixture of ethanol (20 cm^3) and benzene (10 cm^3) were heated under reflux for ca. 2 hr. The resultant clear solution was filtered while hot, treated with sodium tetraphenylborate (0.2 g) in ethanol (5 cm^3), then concentrated to a small volume under reduced pressure and stirred until precipitation occurred. The precipitate was allowed to stand overnight then filtered off, washed thoroughly with ethanol and light petroleum (60–80), recrystallised from dichloromethane–ethanol and dried in vacuo as white crystals (0.25 g, 61%).

Carbonylhydridotetrakis(methyl diphenylphosphinite) ruthenium(II) tetraphenylborate—Carbonylchlorohydridotris(triphenylphosphine)ruthenium (0.34 g) and methyl diphenylphosphinite (1.0 g) in a mixture of methanol (20 cm^3) and benzene (5 cm^3) were heated under reflux for 1 hr. The resultant clear solution was filtered, cooled to ambient temperature and treated with a solution of sodium tetraphenylborate (0.2 g) in methanol (5 cm^3). The white precip-

Table 2. IR[a] and proton NMR[b] data

COMPLEX	ν(CO)	νMH cm⁻¹	τ(CH₃)	τ(CH₂)	^3J(PH) Hz	^3J(HH') Hz	τ(MH)	^2J(PH)$_{trans}$ Hz	^2J(PH)$_{cis}$ Hz
{RuHCl(CO)(PPh₃)₂[P(OMe)₃]}	1938(s)	1815(w)	6.75(d)		10.3		15.52 (d of t)	179.43	20.5
{RuHCl(CO)(PPh₃)₂[P(OEt)₃]}	1955(s)	1818(w)	9.01(t)	6.39(qn)		7.05	15.64 (d of t)	174.28	21.3
{RuHCl(CO)(PPh₃)₂[P(OMe)₂Ph]}	1955(s)	1820(vw)	6.59(d)		10.7		15.6 (d of t)	150.76	20.7
{RuHCl(CO)(PPh₃)₂[P(OEt)₂Ph]}	1950(s)	1822(vw)	8.96(t)	(5.9–6.6) c p		7.05	15.7 (d of t)	147.9	21.2
{RuHCl(CO)(PPh₃)₂[P(OMe)Ph₂]}	1950(s)	1820(vw)	7.37(d)		10.6		16.3 (d of t)	122.8	21.3
{RuH(CO)(PPh₃)₂[P(OMe)₃]₂}{BPh₄}[e]	2000(s)	1820(w)	6.85(d) 7.14(d)		10.25 10.25		17.82 c.p.		
{RuH(CO)(PPh₃)[P(OMe)₃]₃}{BPh₄}	2018(s)	1820(w)	6.4(d) 6.78(t)		10.9 5.5		17.16 c.p.		
{RuH(CO)(PPh₃)[P(OEt)₃]₃}{BPh₄}	2018(s)	1818(w)	8.73(t) 8.81(t) 9.0(t)	(6.02–6.3) c p		7.05 7.05 7.05	18.28 c.p.		
{RuH(CO)[P(OEt)₂Ph]₄}{BPh₄}	2008(s)	1820(vw)	8.9(t)	(6.42–7.1) c p			16.2(qn)		21.3
{RuH(CO)[P(OMe)Ph₂]₄}{BPh₄}	2008(s)	1820(w)	7.39(vc)[f]				14.7(qn)		19.8
{RuH(CO)[P(OEt)Ph₂]₄}{BPh₄}	1995(s)	1820(w)	9.65(t)	(6.94–7.02) c p		6.75	14.87(qn)		19.8
{RuH(CO)[P(OMe)₂Ph]₄}{BPh₄}	1955(s)	1820(vw)	7.4(vc)[g]				16.37(qn)		20
{OsHCl(CO)(PPh₃)₂[P(OMe)₃]}	1938(s)	1820(w)	6.78(d)		10.5		15.41 (d of t)	138.25	21.3
{OsHCl(CO)(PPh₃)₂[P(OEt)₃]}	1935(s)	1820(w)	9.05(t)	6.45(qn)		7.05	15.56 (d of t)	134.57	22.1
{OsHCl(CO)(PPh₃)₂[P(OMe)₂Ph]}	1940(s)	1820(w)	6.63(d)		10.5		15.55 (d of t)	117	20.6
{OsHCl(CO)(PPh₃)₂[P(OEt)₂Ph]}	1934(s)	1820	8.98(t)	(5.85–6.77)		7.1	15.67 (d of t)	115	21.2
{OsHCl(CO)(PPh₃)₂[P(OMe)Ph₂]}	1935(s)	1820(w)	7.41(d)		10.6		16.14 (d of t)	97.3	21.2
{OsHCl(CO)(PPh₃)₂[P(OEt)Ph₂]}	1930(s)	1820(w)	9.33(t)	7.07(qn)		6.2	16.19 (d of t)	~98	21
{IrH[P(OMe)₃]₅}{BPh₄}₂[c]		2070(m)	3.75(vc)[h]				22.35 c p		
{IrH[P(OEt)₃]₅}{BPh₄}₂[d]		2082(m)	8.59(t)	5.7(q)		7.1	22.36 c p		

a) I.r. spectra taken in CHCl₃ solution; w = weak, s = strong.

b) N.m.r. spectra run in CDCl₃ (c) DMSO or (d) (CD₃)₂CO solution.

   d = doublet, t = triplet, q = quartet, qn = quintet, vc = virtual coupling pattern, cp = complex pattern.

(e) major isomer

(f) separation of outer satellite peaks, ca. 11.9 Hz.

(g) separation of outer satellite peaks, ca. 11 Hz.

(h) The methyl protons give rise to a complex asymmetrical signal, the shape of which is consistent with the presence

   of a doublet, due to the axial P(OMe)₃, partly submerged under a vc pattern due to the 4 equivalent P(OMe)₃ ligands.

itate which rapidly deposited was filtered off, washed with methanol and hexane then dried, *in vacuo* to yield the required product as white microcrystals (0.35 g, 76%).

Carbonylhydridotetrakis(ethyl diphenylphosphinite)ruthenium(II)tetraphenylborate. Similarly obtained as white microcrystals (0.41 g, 85%) using ethyl diphenylphosphinite and ethanol in place of methyl diphenylphosphinite and methanol.

Carbonylhydridotetrakis(dimethyl phenylphosphonite) ruthenium(II) tetraphenylborate—Carbon monoxide was bubbled through a refluxing solution of {RuH[P(OMe)₂Ph]₅}{BPh₄} (0.25 g) in ethylmethyl ketone (20 ml) for *ca.* 1½ hr. The solution was cooled to ambient temperature and concentrated to a small volume under reduced pressure, then diluted with methanol (10 cm³) to precipitate the product as a white solid. The precipitate was filtered off and washed with methanol and light petroleum (60–80). Recrystallisation from dichloromethane–methanol

gave the required product as colourless microcrystals (0.22 g, 59%).

Hydridopentakis(trimethylphosphite)iridium(III)tetraphenylborate — Carbonyldichlorohydridobis(triphenylphosphine)iridium (0.27 g), trimethylphosphite (0.25 g), and sodium tetraphenylborate (0.4 g) suspended in a mixture of ethylmethylketone (20 cm³) and methanol (10 cm³) were heated under reflux for *ca.* 3 hr. The mixture was filtered to remove a quantity of undissolved material, evaporated under reduced pressure until crystallisation commenced, then diluted with methanol and set aside until crystallisation was complete. The white precipitate was filtered off, washed with methanol and light petroleum (60–80) then recrystallised from dichloromethane–methanol and dried *in vacuo* as *white crystals* (0.25 g, 52%).

Hydridopentakis(triethyl phosphite)iridium(III) tetraphenylborate. Was similarly obtained as white crystals (51%), using triethyl phosphite and ethanol in place of trimethyl phosphite and methanol.

REFERENCES

[1]Part 15, M. Preece, S. D. Robinson and J. N. Wingfield, *J. C. S. Dalton* 1976, 613.

[2]For a review of work in this area see C. A. McAuliffe and W. Levason *Studies in Inorganic Chemistry*—1. *Phosphine, Arsine and Stibine Complexes of the Transition Elements*, Chaps. III and VI. Elsevier, Amsterdam 1979.

[3]D. A. Couch and S. D. Robinson, *Inorg. Chim. Acta* 1974, 9, 39.

[4]D. A. Couch and S. D. Robinson, *Inorg. Chem.* 1974, 13, 456.

[5]D. A. Couch, S. D. Robinson and J. N. Wingfield, *J. Chem. Soc. Dalton Trans.* 1974, 1309.

[6]P. G. Douglas and B. L. Shaw, *J. Chem. Soc. (A)* 1970, 1556.

[7]R. K. Harris, *Can. J. Chem.* 1964, 42, 2275.

[8]Reference 4 and references therein.

[9]N. Ahmad, J. J. Levison, S. D. Robinson and M. F. Uttley, *Inorg. Synth.* 1974, 15, 45.

[10]ITRCAL programme (1973). Iteration of calculated NMR spectra using least squares criteria; Instructions for use, Nicolet Instrument Corporation; Madison, Wisconsin 53711, U.S.A.

XPS of coordination compounds: additive ligand effect in some copper(I) and copper(II)

chelates with 1,2 phosphino (or phosphine/oxide)-sulfido ethane ligands

by M. Bressan, C. Furlani* and G. Polzonetti*

Institute of Analytical Chemistry and CNR Center, University of Padova, and

* Institute of General and Inorganic Chemistry, University of Rome.

Summary

XPS spectra of $Ph_2P-CH_2-CH_2-S-R$ ligands, of their P-oxides and of the corresponding 1:

2 complexes with Cu(I) and Cu(II) indicate a moderate donor shift on complexation of about

0.4 eV for S, and 0.3 eV for P on the 2p signals, and confirm complete chelation for both

ligands in their metal complexes. The chemical shifts of $Cu2p_{3/2}$ b.e. values can be quant-

itatively described by a model of additive ligand contribution, for which parameter values

of -0.2 eV for -S-, and -0.5÷-0.6 eV for -O⁻ donors are proposed.

Introduction

XPS (X-ray photoelectron spectroscopy) has proved a useful tool for the elucidation of

the electronic structure of coordination compounds by allowing determination of energy levels

of both valence and inner-core orbitals of atoms belonging to the coordination sphere, and

detection of chemical shifts on the latter quantity, reflecting intra-and intermolecular

atomic charge distributions. Emphasis is now being laid on attempts at more quantitative

evaluation of XPS data; one of the most recent proposals in this direction is the model of

additive ligand contributions by Feltham and Brant[1], according to which the ligand con-

tributions are regarded as a measure of the electron donor or acceptor ability of the ligands.

Although lacking rigorous theoretical background, and although formulated so as to be valid

only on a statistical basis, the model by Feltham and Brant is nevertheless attractive in

suggesting a quantitative representation of the chemical concept of electron donor/acceptor

properties of ligands, and may prove useful for an empirical classification of ligands, not

unlike other empirical series such as the spectrochemical, nephelauxetic and X_{opt} series.

We undertook a study of XPS characterization and structural confirmation of some

chelates of Cu(I) and Cu(II) with neutral chelating agents of $R_2P-CH_2-CH_2-S-R'$ and $R_2(O)P-$

CH_2-CH_2-SR' type[2], and tried to apply the model by Feltham and Brant to the rationalization

of the b.e. data. The investigated series of compounds proved particularly well suited to

this scope, both because of the good quality of the XP spectra and of their similarity of

structure, which allows significant comparisons to be drawn, while varying in a systematic

way the nature of donor atoms in the ligands. As a result we were able to conclude that the

investigated series of chelates of copper(I) and (II) can be adequately described in this

XPS behaviour by the Feltham and Brant model[1], and to propose values of additive ligand con-

tributions for sulfur and oxygen donors, which were not included in the original classifica-

tion by Feltham and Brant[1].

Experimental

We measured the solid state X-ray photoelectron spectra of the ligand molecules (di-phenylphosphino)-ethylthioethane $(C_6H_5)_2$ P-CH_2-CH_2- SC_2-H_5 (P-SEt), (diphenylphosphino)-phenyl-thioethane $(C_6H_5)_2$P-CH_2-CH_2-SC_6-H_5 (P-SPh), and the corresponding phosphine oxides (OP-SEt and OP-SPh), and of the complexes Cu^I(P-SEt)$_2$(ClO_4), Cu^I(P-SPh)$_2$(ClO_4), $Cu^I Cu^{II}$(P-SEt)$_2$ (OP-SEt)$_2$(ClO_4)$_3$, Cu^{II}(OP-SEt)$_2$(ClO_4)$_2$ and Cu^{II}(OP-SPh)$_2$(ClO_4)$_2$. The complexes were synthesized for the first time and characterized preliminarly by one of us in a previous investigation[2]. The purity of the compounds used in the present work was checked by elemental analysis and values of physical constants, and found to be satisfactory. The coordination geometry was proposed[2] to be of tetrahedral or pseudotetrahedral type for both Cu^I and Cu^{II} species, with chromophores [Cu^I P_2S_2], and [$Cu^{II}O_2S_2$] respectively, but the known tendency of Cu^I to 3- co-ordination, and of Cu^{II} to 5-coordination suggested the utility of a further structural con-firmation; actually as we shall discuss below, XPS data for the Cu^{II} species are better com-patible with a loose 5-coordination of one anion to an enlarged pseudotetrahedral coordina-tion around Cu^{II}.

XP spectra were run on a VG ESCA-3 spectrometer equipped with AlK$\alpha_{1,2}$ source (1486,6 eV). Powder specimens were dusted as thin films onto a gold bearing plate, whose Au4f$_{7/2}$ signal at 84.0 eV was used for check of the instrument scale. Reported data are averages of repeated runs on different samples (usually three runs for three different samples of each compound), the reproducibility being seldom worse than 0.1 eV. Surface charging effects (usually in the range 1-2 eV) were corrected by referring to the C1s b.e. value taken as 285.0 eV; C1s signals were narrow and well defined, hence suitable for dependable reference, and were due to superposition of practically coincident signals from ligand carbon atoms (mostly from the phenyl groups), and contamination carbon (Santovac 5 diffusion pump oil). No detectable radiation damage by X-ray was observed, so measurements could be performed at room tempera-ture.

For each element, more than one inner-core ionization line was measured whenever pos-sible, so for Cu and S besides the more common 2pj signals also Cu3p and S2s signals were measured, the former being particularly significant for check of the effective transmission function of the spectrometer, and therefore for quantitative intensity evaluation. Only the copper LVV Auger signals around 917 eV were of poor quality, being broader and less structur-ed than in simple copper species, and therefore unsuited for exact structural characteriza-tion. Intensity measurements of the XPS bands were performed in order to check the atomic composition of the XPS sampling layers; atomic ratios were computed by the simple formula $n_i/n_j = I_i\sigma_j\lambda_j$ $S_j$exp(-d/λ_j) / $I_j\sigma_i\lambda_i S_i$exp (-d/λ_i) (cross sections from the tabulation by Scofield[3], IMFP (λ) from[4], and S values approximately $\backsim E_K^{-\frac{1}{2}}$ according to[5] and found in satis-factory agreement with elemental composition, if proper account was taken of contamination overlayers, thus confirming that surface radiation damage was negligible, and that measured XPS data were truly representative of the structure of the investigated molecular solids.

Results and discussion

XP spectral data for the investigated ligands and complexes are listed in the table,

and the shape profiles of some representative spectra are reported in the figure. The results

will be discussed first in terms of structural assignements, and subsequently from the point

of view of quantitative data evaluation in the model by Feltham and Brant[1].

The general patterns of XP spectra reproduce with considerable accuracy the typical

features of copper complexes, thus yielding further support to their structural character-

ization. Cu2p signals have, as expected, higher b.e. for Cu(II) species (935.6 eV) than for

Cu(I) (934.0 eV); a quantitative discussion of the b.e. difference will be given below. FWHM

is larger for Cu(II) (Cu2p$_{3/2}$ ca. 2.8 eV) than for Cu(I) (2.0-2.1 eV under our experimental

conditions) because of unresolved multiplet splitting due to presence of a partly filled

valence shell in Cu(II) only. In Cu(II) species there is a well-defined satellite (ΔE_{av} $\sim$ 9.8

eV) on the high b.e. side of each 2p$_j$ signals, with moderate intensity (ca. 33% of the total

area of both satellite and the main line Cu2p$_j$; (compare relative intensities of 19-25% in

copper(II) dithiocarbamates[6] or up to 40% in Cu(II) oxide systems[7]), whereas Cu(I) spectra

are fully void of 2p satellites. This latter fact is significant with regard to the long

dispute in the literature whether diamagnetic (S=0) transition metal complexes do have true

although weak 2p satellites, or are exempt from satellites, and possible accompanying signals

are due to paramagnetic impurities. Our present results show, at least for the d^{10} configura-

tion of Cu(I), a case of unequivocal total absence of satellites from diamagnetic transition

metal complexes.

The mixed species Cu$_2$(P-SEt)$_2$(OP-SEt)$_2$(ClO$_4$)$_3$ behaves, on XPS evidence, as a double salt

without specific interactions between Cu(I) and Cu(II), its XP spectrum being just the super-

position of those of the separate Cu(P-SEt)$_2$(ClO$_4$) and Cu(OP-SEt)$_2$(ClO$_4$)$_2$ species in 1:1 ratio.

B.e. and FWHM values are intermediate between those of the simple Cu(I) and (II) species,

for Cu2p and P2p signals, the difference between the two species being too small to give rise

to separate signals. Also the intensity of the Cu2p$_{3/2}$ satellite (ΔE $\sim$ 10 eV) is almost exact-

ly the half (14% of the total area of both satellite and the main peak) of the Cu(II) value;

since position, shape and intensity of 2p satellites depend critically upon the structural

environment of central atoms in transition metal complexes[8], our observed satellite intensity

can be taken as evidence for absence of strong coupling interactions between Cu(I) and Cu(II)

in the present case.

Sulfur 2p$_{av}$ b.e. values are in the range 163.8-164.5 eV, as typical for neutral or near-

ly neutral sulfur atoms[9]. No significant difference is found between the S-ethyl and the S-

phenyl ligands, nor for their complexes. ΔE between complexes and uncomplexed ligand, a

measure for the S donor effect towards copper, is in the range 0.4($\pm$0.2) eV; this is somewhat

less than observed for complexes of thiol ligands (e.g. dithiocarbamates, ΔE $\sim$0.7-1.0 eV[6,10])

as expected on the ground of the negative sulfur charge, and larger availability of electron

for σ donation in the latter case. Among neutral sulfur ligands, only thioureas and related

ligands show a higher ΔE on complexation (e.g.$\sim$ 1 eV[11]), which can be however explained by

the occurrence of thioamide resonance forms of $\begin{smallmatrix} R \\ R \end{smallmatrix}\!\!>\!\!\overset{+}{N} = C\!\!<\!\!\overset{\textstyle\diagdown}{}S^-$ type[11,12]. Also P2p b.e. values

fall in the normal range (131.1$\pm$0.1 eV for free, and 131.4 eV for ligated phosphines), with

a more pronounced shift to higher b.e. occurring on donation to oxygen in the phosphine ox-

ides (132.8$\pm$0.1 eV).

Both sulfur and phosphorus XPS signals in the copper complexes are, within experimental error, as narrow as in the free ligands (except of course phosphorus in the double salt of Cu(I), Cu(II)), and therefore indicative of only one species of S and P in the complexes: for sulfur the situation is particularly clear-cut with 2s signals which are singlets and therefore more symmetric and possibly more sensitive to such effects than the 2p doublet. XPS evidence confirms therefore that both ligands are chelated in an essentially equivalent way to the central metal atom, with minimum chromophore configurations $[Cu^{I}S_2P_2]$ and $[Cu^{II}S_2O_2]$ respectively.

As for a possible quantitative interpretation of the chemical shifts on copper b.e. values in terms of addition ligand contributions, the original paper by Feltham and Brant[1] does not quote parameter values for S and O ligands, so we shall have to make a reasonable guess for the latter quantities on the ground of our experimental results. Thus, the $Cu2p_{3/2}$ b.e. value of 934.0 eV for $Cu^{I}(P-SR')_2$ (ClO_4) results from the bare metal value of 935.6 eV[1] by adding +1.0 eV (formal oxidation state of Cu +1[1]) and subtracting the ligand contributions (2.3 eV for two chelating phosphorus atoms[1]), leaving −0.3 eV as the contribution from two sulfur ligands −S− of thioether type. This suggests, rounding to the larger figure, a contributive parameter value of about −0.2 eV for neutral sulfur ligands in the Feltham-Brant scale[1].

Using the figure just derived for the sulfur ligands in the analysis of the Cu^{II} complexes, the $Cu2p_{3/2}$ b.e. value of 935.6 eV derives from the reference value of 937.6 eV for bare Cu^{2+} minus 0.3 eV for two S ligands in the chromophore, leaving us with a contribution of −1.7 eV to be assigned to the remaining ligands. This would imply an upper limit of about −0.8 eV contribution for each oxygen ligand in an isolated, purely 4-coordinated $[Cu^{II}O_2S_2]$ chromophore; since however apparently 4-coordinated Cu(II) chromophores often reach 5-coordination either by dimerization[13] or by loose interaction with a solvent molecule or an external anion (as could be the present case), we prefer to assume that the donor effect of 1.7 eV is to attributed to three rather than two oxygen donor, each of them contributing −0.5÷−0.6 eV to the total effect.

In conclusion, the XPS characterization of the Cu(I) and Cu(II) chelates investigated here allows on the one hand further elucidation of the proposed structures, and presents further cases of applicability of the model of additive ligand contributions by Feltham and Brant[1]. Parameter values of −0.2 eV for −S− and −0.5÷−0.6 eV for −O⁻ ligands are proposed; although their validity has to be tested in future through more extended statistics, such values appears reasonable and in keeping with the donor-acceptor concept of the Feltham-Brant series, since the smaller negative value for sulfur is consistent with a lower σ-donor ability (if compared to negative −O⁻ donors), and a larger π-acceptor tendence, possibly by use of empty S3d orbitals, with respect to oxygen ligands.

Rome and Padova, December 1982
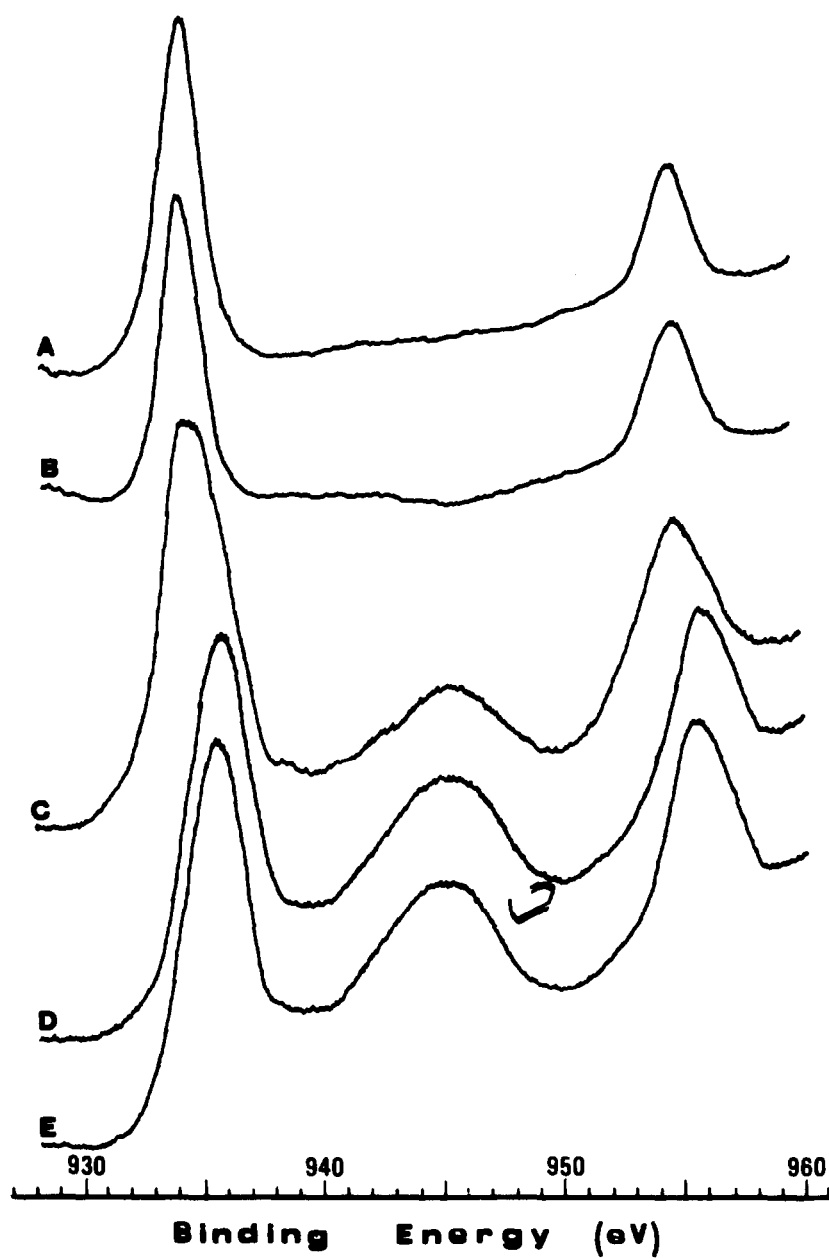
Fig.

Cu2p XP spectra of solid Cu(I) and Cu(II) chelates (for experimental conditions, see text).
A) $Cu^{I}(Ph_2P-SEt)_2ClO_4)$; B) $Cu^{I}(Ph_2P-SPh)_2(ClO_4)$; C) $Cu^{I}(Ph_2P-SEt)_2 \cdot Cu^{II}(Ph_2(O)P-SEt)_2(ClO_4)_3$;
D) $Cu^{II}(Ph_2(O)P-SEt)_2(ClO_4)_2$; E) $Cu^{II}(Ph_2(O)P-SPh)_2 (ClO_4)_2$.

M. BRESSAN *et al.*

TABLE

Relevant XPS data for solid Cu(I) and Cu(II) chelates, in eV [a]

Compound	$Cu2p_{3/2}$		Cu3p	S2p	S2s	P2p
A [b]				163.9 (2.5)	227.9 (2.8)	131.3 (2.7)
B				164.1 (2.4)	228.0 (2.7)	131.0 (2.2)
C				163.8 (2.4)	227.8 (2.8)	132.7 (2.1)
D				164.2 (2.4)	228.0 (2.7)	132.7 (2.1)
E	934.0[e](2.1)[c]		76.8 (4.5)	164.2 (2.5)	228.0 (2.8)	131.4 (2.2)
F	934.0 (2.0)		77.0 (4.5)	164.2 (2.4)	228.3 (3.0)	131.5 (2.4)
G	934.6 (2.6)	14.2[d]	76.7 (5.0)	164.2 (2.5)	228.3 (3.0)	132.4 (3.3)
H	935.6 (2.6)	33.7	78.3 (4.5)	164.5 (2.6)	228.6 (3.2)	132.9 (2.2)
I	935.4 (2.9)	34.9	78.6 (5.0	164.7 (2.6)	229.0 (3.0)	133.1 (2.3)

a) C1s = 285.0 eV

b) A) Ph_2P-SEt; B) Ph_2P-SPh; C) $Ph_2(O)P-SEt$; D) $Ph_2(O)P-SPh$; E) $Cu^I(Ph_2P-SEt)_2 ClO_4$;

   F) $Cu^I(Ph_2P-SPh)_2 ClO_4$; G) $Cu^I(Ph_2P-SEt)_2 \cdot Cu^{II}(Ph_2(O)P-SEt)_2 (ClO_4)_3$;

   H) $Cu^{II}(Ph_2(O)P-SEt)_2 (ClO_4)_2$; I) $Cu^{II}(Ph_2(O)P-SPh)_2 (ClO_4)_2$.

c) FWHM = Full width at half maximum, in parentheses.

d) % Intensity satellite.

e) B.e.

Literature references

1. R. Feltham and I. Brant, J.Am.chem.Soc., **104**, 641 (1982).

2. P. Rigo and M. Bressan, 1st IUPAC Symposium on Organometallic Chemistry, Ft. Collins, USA, 44 (1981).

3. J.H. Scofield, J. Electron Spectrosc. Relat. Phenom., **8**, 129 (1976).

4. M.P. Seah and W.A. Dench, Surf. Interf. Analysis, **1**, 1 (1979).

5. B. Wamberg, U. Gelius and K. Siegbahn, J. Phys. E, **7**, 149 (1974).

6. M.S. Ioffe and Yu.G. Borod'ko, J. Electron Spectrosc. Relat. Phenom., **11**, 235 (1977).

7. F.M. Capece, V. Di Castro, C. Furlani, G. Mattogno, C. Fragale, M. Gargano, M. Rossi, J. Electron Spectrosc. Relat. Phenom. **27**, 119 (1982).

8. G.A. Vernon, G. Stucky and T.A. Carlson, Inorg. Chem. **15**, 278 (1976)

9. R.A. Walton, Coord. Chem. rev., **31**, 183 (1980).

10. C. Furlani, G. Polzonetti, C. Preti and G. Tosi, Inorg. Chim. Acta (1982) in the press.

11. F.A. De Villanova, C. Furlani, G. Mattogno, G. Verani, R. Zanoni, Gazzetta Chim. Italiana, **110**, 19 (1980).

12. M.V. Andreocci, M. Bossa, F.A. De Villanova, C. Furlani, G. Mattogno, G. Verani and R. Zanoni, J. Mol. Structure, **71**, 227 (1981).

13. M. Bonamico, A. Vaciago, L. Zambonelli and G. Dessy, C. Mariani, G. Mazzone, A. Mignoli, Acta Cryst. **19**, 868 (1965).

Ni(II) COMPLEXES WITH 8-AMINOQUINOLINE DERIVATIVES

M. Izquierdo, J. Casabó [*].

Departament de Química Inorgànica, Universitat Autònoma de Barcelona

(Bellaterra), Barcelona, Spain.

C. Díaz, J. Ribas

Departamento de Química Inorgánica, Universidad de Barcelona

Barcelona, Spain.

Abstract.– Some Ni(II) complexes with 5,7-dicloro-8-aminoquinoline
(dcaq), 5,7-dibromo-8-aminoquinoline(dbaq) and 5,7-diiodo-8-amino-
quinoline(diaq) are described. The compounds are of stoichiometry
NiL_2X_2(L= dcaq, dbaq, diaq; X= NO_3^- and L= dbaq; X= Cl^-, Br^-, I^-,
NCS^-) and $NiLX_2 \cdot H_2O$(L= dcaq, diaq; X= Cl^-). The electronic spectra
and magnetic susceptibility data at room temperature, are consistent
with octahedral geometry for the Ni(II) in each compound. I.r. spectra
show the presence of ionic and bridging nitrate groups in the com-
pounds $NiL_2(NO_3)_2$(L= dcaq, dbaq, diaq) and we assign them polymeric
structures. Polymeric structures with bridging chloride are proposed
for the compounds $NiLCl_2 \cdot H_2O$(L= dcaq, diaq) and monomeric octahedral
structures for NiL_2X_2(L= dbaq; X= Cl, Br, I, NCS).

INTRODUCTION

The ligand properties of 8-aminoquinoline have been the object of considerable attention
in the last few years.[1,2] In a previous paper, the authors reported complexes of Cu(II)
with ligands derived from 8-aminoquinoline, namely 5,7-dichloro-8-aminoquinoline(dcaq);
5,7-dibromo-8-aminoquinoline(dbaq); 5,7-diiodo-8-aminoquinoline(diaq).[3] Polymeric structures
have been proposed for all of them and they closely resemble their ethylenediamine or bipy-.
ridyl analogues.

Here we describe complexes of Ni(II) with the same ligands. The objective was to define
the ligand behaviour of these substances and to compare them with 8-aminoquinoline and
with ethylenediamine and 2,2'-bipyridyl.

[*] Author to whom correspondence should be addressed.

RESULTS AND DISCUSSION

I.r. Spectra

Table 1 shows the frequencies of the bands assigned to vibrational modes of the NH_2 group of the ligands and their complexes. The stretching modes of the NH_2 group appear in the 3000–3500 cm^{-1} region. In all the complexes these bands appear at lower frequencies than in the free ligands. This effect is indicative of the coordination of the amine group of the ligands in all the complexes.[4]

In the 1550–1620 cm^{-1} region the free ligands exhibit a wide band with a pronounced fine structure due to the partially coupled stretching vibration $\nu(C=C)$, $\nu(C=N)$ of the aromatic rings and the deformation mode of NH_2 groups. This was shown in the case of 8–aminoquinoline by deuteration studies.[5] Coordination changes the coupling of these modes, and a clear splitting of this broad band into two components can be seen in all the complexes. The higher frequency component is assigned mainly to the $\delta(NH_2)$ mode and the other to the aromatic ring vibrations. In the 1350–1375 cm^{-1} region, there is a band corresponding to the $\nu(C-NH_2)$ stretching mode. In the 1020–1060 cm^{-1} region, there is a band corresponding to the wagging mode of the coordinate NH_2 group. This appears also in the free ligands as a weak band, due to the formation of intermolecular hydrogen bonds. This band is the most sensitive to the chemical environments of the Ni(II) ions, as observed for other complexes of 8–aminoquinoline.[2]

In the 600–800 cm^{-1} region appear the rocking and twisting bands of the NH_2 coordinated group, which are, in general, difficult to assign and have little interest. The metal–amine nitrogen stretching mode appears in the 500–600 cm^{-1} region.

Nitrate complexes

Table 2 shows the frequencies assigned to the NO_3^- group in the three complexes containing this ligand. There are bands that may be assigned to the ionic nitrate group, and others corresponding to the coordinated ligand.[4] The $\nu_3(E')$ mode of ionic nitrate can be seen to be split by coordination in two components at 1435–1440 cm^{-1} and 1300 cm^{-1}. At the same time there remains a very intense band at 1380–1370 cm^{-1} attributed to ionic nitrate. In this last region the ligands dcaq, dbaq, diaq show several bands, one of which coincides with that assigned to ionic nitrate. However, by observing the i.r. spectra with very dilute KBr pellets it is possible to detect this very intense and characteristic band corresponding to $\nu_3(E')$ mode of ionic nitrate.

In the 1000–1100 cm^{-1} region the compounds show two intense bands. One of them is due to the $\nu_1(A_1')$ mode of the coordinate group (1020–1030 cm^{-1})(Table 2). The second, of higher frequency, has been assigned to the wagging mode of the NH_2 group. This last band overlaps the one due to the ionic nitrate which also appears in this region (1050 cm^{-1}). The $\nu_2(A_2'')$

mode due to coordinated and free nitrate group is observed with medium intensity in the 820–830 cm^{-1} region. The $\nu_4(E')$ mode appears between 710–720 cm^{-1}, as a weak band and without splitting, because in this region there are several bands due to the amine-ligands.

The coordination mode of the nitrate group cannot be deduced unequivocally from these data, but the physicochemical characteristics of these nitrate complexes are compatible with polymeric linear structures with nitrate groups bridging between Ni(II) ions and with ionic nitrate groups in the lattice.

Complexes with thiocyanate

The only complex prepared with thiocyanate ligand is Ni(SCN)$_2$(dbaq)$_2$. In the ν(CN) stretching mode region there is one intense band at 1995 cm^{-1} which can be assigned to this mode. Two other bands corresponding to the ν(CS) and δ(SCN) modes can be seen at 795 cm^{-1} and 490 cm^{-1}, respectively. These spectral characteristics show a coordination via nitrogen atom of the thiocyanate group in the complex.[7] The previously reported compounds with ligands 8-aminoquinoline[2] and 6-metil-2-aminoethylpiridine[8] have a similar i.r. spectra.

Electronic Spectra

Table 3 summarises the electronic spectra of all the compounds and of the similar compounds with ethylenediamine and pyridine together with the proposed assignments. All the compounds of ML$_2$X$_2$ and also MLX$_2$ stoichiometry show the same spectral characteristics which are consistent with an octahedral environment[9,10] around the Ni(II) ion.

The first band which appears in the near infrared zone, is attributable to the transition $^3A_{2g} \rightarrow {}^3T_{2g}$ and gives the 10Dq value of the complex. The frequency of this band in the compounds: Ni(dbaq)$_2$Cl$_2$, Ni(dbaq)$_2$Br$_2$, Ni(dbaq)$_2$I$_2$, Ni(dbaq)$_2$(NO$_3$)$_2$ and Ni(dbaq)$_2$(NCS)$_2$ reflects the position of the ligands, Cl$^-$, Br$^-$, I$^-$ and NO$_3$ in the spectrochemical series. Also the 10Dq value of the compound: Ni(dbaq)$_2$(NCS)$_2$ confirms the NCS group coordination, via nitrogen atom, to the Ni(II) ion. On the other hand the low energy of this transition in the compound Ni(dcaq)Cl$_2$·H$_2$O similar to the Ni(dbaq)$_2$I$_2$, is consistent with the polymeric structure with bridging chloride proposed for it.

Generally the last band attributable to the transition $^3A_{2g} \rightarrow {}^3T_{1g}$(P) is overlapped with charge transfer bands due to the amine-ligands, except in the compounds in which the ligands are in the later part of the spectrochemical series, as I$^-$ and μ-Cl$^-$ in Ni(dbaq)$_2$I$_2$, Ni(dcaq)Cl$_2$·H$_2$O and Ni(diaq)Cl$_2$·H$_2$O, respectively.

Magnetic susceptibility measurements

At room temperature the magnetic moment is that expected for a d^8 ion in an octahedral environment and with little orbital contribution for all the compounds(Table 4). Only the

compound $Ni(dcaq)Cl_2$ was measured down to $-196°C$. It follows the Curie-Weiss law with good approximation over the investigated temperature range, with a positive Weiss constant[14,3,12] showing the existence of ferromagnetic interactions among the Ni(II) ions.[11] The non-zero value of the Weiss constant is consistent with the polymeric structure with bridging chloride proposed for it. Several others polymeric Ni(II) complexes with ferromagnetic interactions have been described in the literature.[16]

EXPERIMENTAL

The dcaq, dbaq and diaq ligands were prepared by literature methods.[13,14,15]

For the synthesis of the new complexes we used anhydrous solvents distilled twice from $CaCl_2$. The reactions were carried out in air, except in the preparation of the diaq complexes, for which, because of their ease of oxidation, a nitrogen atmosphere was employed. Analytical Data are consistent with formulae proposed for all of them.

I.r. spectra were obtained in a Beckman IR-20A spectrophotometer using KBr pellets. For the $600-250$ cm^{-1} region, the ratio of KBr to complex was c.a. 1:1 in order to assign metal-ligand bands of small intensity. Electronic spectra were measured in the solid state because of the low solubility of the complexes and the possibility of exchange of the ligand with solvent. They were obtained with a Beckman DU-2 (visible, u.v. and near i.r.) and Beckman 5230 UV (visible and u.v.) spectrophotometers. In some cases we also used diffuse reflectance measurements with a Cary 17 spectrophotometer, with an MgO reference.

The magnetic susceptibility measurements were carried out with a Cahn 2000 electrobalance sensitive to 0.001 mg, a Brucker N-177 electromagnet and an Oxford Instruments CF100 cryostat. Measurements were made for different values of magnetic field.

Complexes $Ni(ligand)X_2 \cdot H_2O$

$NiCl_2(dcaq) \cdot H_2O$.— Dcaq(1g) was dissolved in hot EtOH(40 cm^3); an ethanolic concentrated solution of $NiCl_2 \cdot 6H_2O(1.2g)$ and a drop of HCl 2M were added. The pale blue powder which precipitated was filtered and washed with EtOH and Et_2O, and let to dry in the air. Found: C, 29.9; N, 7.3; Cl, 39.4; H, 2.0; Ni, 16.2 ; Calc.: C, 29.9; N, 7.7; Cl, 39.4; H, 2.2; Ni, 16.3.

$NiCl_2(diaq) \cdot H_2O$.— To a solution of $NiCl_2 \cdot 6H_2O(0.6g)$ in the minimum quantity of hot EtOH, a hot concentrated solution of diaq(1.0g) in EtOH was slowly added. A pale green powder precipitated in the cold. Yield: 85%. Found: C, 20.5; N, 5.2; halogen, 48.2; H, 1.3; Ni, 11.0; Calc.: C, 20.5; N, 5.3; halogen, 48.3; H, 1.2; Ni, 11.2%.

Complexes $NiX_2(ligand)_2$

To a concentrated solution of ligand in hot Me_2CO, a solution of the corresponding Ni(II) salt in the minimum quantity of hot EtOH was added. The powder which precipitated in the cold was filtered and washed with EtOH and Me_2CO and allowed to dry in a desiccator.

$Ni(dcaq)_2(NO_3)_2$. Found: C, 35.5; N, 13.7; Cl, 22.9; H, 2.0; Ni, 9.6; Calc.: C, 35.5; N, 13.8; Cl, 23.3; H, 1.9; Ni, 9.6%.

$Ni(dbaq)_2(NO_3)_2$. Found: C, 27.6; N, 10.4; Br, 18.1; H, 1.6; Calc.: C, 27.5; N, 10.7; Br, 18.0; H, 1.5%.

$Ni(diaq)_2(NO_3)_2$. Found: C, 22.1; N, 8.5; I, 51.9; N, 6.0; Calc.: C, 22.2; N, 8.6; I, 52.1; Ni, 6.0%.

$Ni(dbaq)_2Cl_2$. Found: C, 29.3; N, 7.3; halogen, 29.0; H, 1.7; Calc.: C, 29.5; N, 7.6; halogen, 29.5; H, 1.7%.

$Ni(dbaq)_2Br_2$. Found: C, 26.2; N, 6.9; Br, 25.5; H, 1.5; Calc.: C, 26.3; N, 6.8; Br, 25.9; H, 1.5%.

$Ni(dbaq)_2I_2$. Found: C, 23.6; N, 5.9; halogen, 22.9; H, 1.3; Calc.: C, 23.6; N, 6.1; halogen, 23.2; H, 1.3%.

$Ni(dbaq)_2(NCS)_2$. Found: C, 30.8; N, 10.9; Br, 41.0; H, 1.4; Calc.: C, 30.8; N, 10.8; Br, 41.1; H, 1.6%.

REFERENCES

1. J.C.Fanning, L.T.Taylor; J.Inorg.Nucl.Chem., 1965, 27, 2217.

2. J.Casabó, J.Ribas, J.Bartrolí; Rev.Chim.Min., 1976, 13, 149.

3. J.Casabó, J.Ribas, C.Díaz, M.Izquierdo; Transition Metal Chemistry, in press.

4. K.Nakamoto, "Infrared Spectra of Inorganic and Coordination Compounds", J.Wiley, New York-1970.

5. K.A.Jensen, P.H.Nielsen; Acta Chem.Scand., 1964, 18, 1.

6. C.C.Adison, D.Sutton; Prog.Inorg.Chem., 1967, 8, 197.

7. R.A.Bailey, T.W.Michelsen; J.Inorg.Nucl.Chem., 1971, 33, 3206.

8. S.Utsuno; J.Inorg.Nucl.Chem., 1970, 32, 1631.

9. A.B.P.Lever, S.M.Nelson, T.M.Sepherd; Inorg.Chem., 1964, 4, 810.

10. M.R.Litzow, L.F.Power, A.M.Tort; J.Chem.Soc. A, 1970, 275.

11. F.E.Mabbs, D.J.Machin, "Magnetism and Transition Metal Complexes", Chapman and Hall, London-1973.

12. P.Ginsberg, R.L.Martin, R.W.Brookes, R.C.Sherwood; Inorg.Chem., 1972, 11, 2884.

13. F.C.Hurdis, J.Org.Chem., 1958, 23, 891.

14. K.Glen, W.Yagermann; J.Prak.Chem., 1936, 145, 258.

15. Rusell, Thompson; J.Chem.Soc., 1955, 483.

16. R.L.Carlin, A.J.van Duyneveldt, "Magnetic Properties of Transition Metal Compounds", Springer-Verlag, New York-1977.

Table 1. Selected i.r. frequencies (4000–250 cm^{-1}) assigned to the ligands.

dcaq	dbaq	diaq	Ni/dcaq/NO$_3$	Ni/dbaq/NO$_3$	Ni/diaq/NO$_3$	Ni/dcaq/Cl	Ni/dbaq/Cl	Ni/diaq/Cl	Ni/dbaq/Br	Ni/dbaq/I	Ni/dbaq/NSC	Assignm.
3420	3420	3460	3200	3235	3250	3200	3215	3200	3260	3270	3260	ν(NH)
3290	3290	3360	3100	3100	3100	3090	3160	3100	3180	3170	3205	ν(NH)
1610	1610		1610	1610	1610	1615	1600	1600	1605	1600	1600	δ(NH$_2$)
1590	1590	1595	1580	1580	1585	1590	1575	1570	1585	1575	1575	aromatic rings
1585	1585	1585										
1375	1365	1355	1360	1355	1350	1370	1355	1350	1365	1350	1355	ν(C–NH$_2$)
1060	1040	1050	1060	1055	1050	1035	1040	1040	1025	1020	1020	ρ(NH$_2$)
1050	1040											
			740	725	725	730	720	725	730	720	720	γ(NH$_2$)
			645	650	640	655	640	630	630	630	640	ρ$_t$(NH$_2$)
			570	575	555	540	520	535	530	525	535	ν(N–Co)

Table 3. Electronic spectra (cm^{-1})

	v_1 $^3A_{2g} \rightarrow {}^3T_{2g}$	$^3A_{2g} \rightarrow {}^1A_{1g}$	v_2 $^3A_{2g} \rightarrow {}^3T_{1g}(F)$	$^3A_{2g} \rightarrow {}^1E_g$	v_3 $^3A_{2g} \rightarrow {}^3T_{1g}(P)$
Ni(dcaq)$_2$(NO$_3$)$_2$	a	12903		18182	
Ni(dbaq)$_2$(NO$_3$)$_2$	a	13030		18812	
Ni(diaq)$_2$(NO$_3$)$_2$	11500	12903	14185	18182	
NidcaqCl$_2$·H$_2$O	8475		14815		25000
Ni(dbaq)$_2$Cl$_2$	9808		14706	18168	
Ni(diaq)Cl$_2$·H$_2$O	a				25000
Ni(dbaq)$_2$Br$_2$	9091	12903	14760	17637	
Ni(dbaq)$_2$I$_2$	8702		15748	17544	27397
Ni(dbaq)$_2$(NCS)$_2$	11495	12821			
Ni(en)$_2$(NO$_3$)$_2$	8703	14105			29155
Ni(py)$_2$Cl$_2$	8404	12210	19012	22223	24155
Ni(en)$_2$(NCS)$_2$	8700	12300	15600	17699	28012

[a] region not investigated.

Table 2. i.r. frequencies attributed to the NO_3 group.

NO_3^- [a]	$Ni(NO_3)(dcaq)_2\ NO_3$	$Ni(NO_3)(dbaq)_2\ NO_3$	$Ni(NO_3)(diaq)_2\ NO_3$	
	$1435\ cm^{-1}$	$1440\ cm^{-1}$	$1440\ cm^{-1}$	
$1390\ cm^{-1}$	$1380\ cm^{-1}$	$1380\ cm^{-1}$	$1370\ cm^{-1}$	$\nu_3(E')$
	$1300\ cm^{-1}$	$1300\ cm^{-1}$	$1300\ cm^{-1}$	
$1050\ cm^{-1}$	$1020\ cm^{-1}$	$1030\ cm^{-1}$	$1030\ cm^{-1}$	$\nu_1(A_1')$
	$835\ cm^{-1}$ (sh)	$835\ cm^{-1}$ (sh)	$840\ cm^{-1}$	
$831\ cm^{-1}$				$\nu_2(A_2'')$
	$820\ cm^{-1}$	$825\ cm^{-1}$	$820\ cm^{-1}$	
$720\ cm^{-1}$	$710\ cm^{-1}$	$710\ cm^{-1}$	$710\ cm^{-1}$	$\nu_4(E')$

[a] ref. 14.

Table 4. Magnetic moments (B.M.)

	T(K)	(B.M.)
$Ni(dbaq)_2Cl_2$	293.5	3.35
$Ni(dbaq)_2Br_2$	294.5	3.43
$Ni(SCN)_2(dbaq)_2$	295	3.12
$Ni(NO_3)(dbaq)_2\ NO_3$	294.5	3.36
$NidcaqCl_2 \cdot H_2O$	290.3	3.55

NOTES

The optical resolution of tris(pentane-2,4-dionato)metal(III) complexes

ALEX F. DRAKE, JOHN M. GOULD, STEPHEN F. MASON,* CARLO ROSINI† and FRANCIS J. WOODLEY

Chemistry Department, King's College, London WC2R 2LS, England

Abstract—A facile large-scale optical resolution of neutral [M(pd)₃] complexes, M = Cr(III), Co(III), Ru(III), Rh(III) and Ir(III), through enantioselective complex formation with (2R, 3R)-(−)-dibenzoyltartaric acid, is described.

Liquid column chromatography is the principal method available for the optical resolution of the neutral *tris*(pentane-2,4-dionato) complexes of metal(III) ions, [M(pd)₃].[1-10] With D-(+)-lactose columns 90–480 cm in length at ambient temperature, using gravity elution, the resolutions[1-4] are generally small-scale, partial, and time-consuming, although the efficiency is improved, and the scope of the method is extended to the more optically-labile [M(pd)₃] complexes, by the use of 30 cm columns at low temperature with an elevated pressure above the mobile phase.[5] More recently, short columns of the Δ-(−)-*tris*(1,10-phenanthrolline)nickel(II) complex ion supported on anionic SP-Sephadex.[6] (10 cm) or montmorillonite[7,8] (2.5 cm) are reported to partially resolve the enantiomers of [Co(pd)₃][6,7] and of [Ru(pd)₃],[8] and partial[9] or base-line[10] chromatographic resolutions of [Cr(pd)₃] on a column of chiral *cis*(NO₂)-*trans*(N)-[Co(III)-(amino acid)₂ (NO₂)₂] complex ion salts[9] or of (+)-poly(triphenylmethyl-methacrylate) coated on silica gel[10] have been described.

An alternative stationary phase, consisting of (2R, 3R)-(−)-dibenzoyltartaric acid, (−)-DBT, adsorbed on alumina has been investigated for the optical resolution of racemic [M(pd)₃] complexes using a cyclohexane-benzene (2:1) mobile phase. With a system[11] for the simultaneous monitoring at a given analytical wavelength of the absorbance (A) and the differential circularly-polarised absorbance ($\Delta A = A_L - A_R$) of a chiral solute in the eluate from a liquid chromatography column, it was found, in the attempted resolution of racemic [Rh(pd)₃], that the optical activity of the two enantiomers in the eluate from the (−)-DBT/Al₂O₃ column do not sum to zero over the chromatogram as a whole (Fig. 1). The chromatographic resolution is partial, and, while one enantiomer, the Λ-isomer, is wholly eluted, a substantial fraction of the other (∼40%) is retained by the stationary phase, from which it is stripped, together with much of the (−)-DBT, by ethanol.

The further investigation of the strongly enantioselective complex formed by (−)-DBT with the Δ-isomer of neutral [M(pd)₃] coordination compounds afforded a general method for the large-scale optical resolution of racemic [M(pd)₃] complexes (Table 1). A typical resolution procedure is as follows: Racemic [Co(pd)₃] (3.56 g, 10 mmol), (2R, 3R)-(−)-dibenzoyl-tartaric acid monohydrate (9.4 g, 25 mmol), benzene (60 cm³), and cyclohexane (120 cm³), were stirred at ambient temperature for two days. Over this period, approximately one-half of the total [Co(pd)₃] was taken up by the formation of a solid (−)-DBT-Δ-[Co(pd)₃] phase, leaving a supernatant fluid phase containing Λ-[Co(pd)₃] with an optical purity of ∼90%, indicated by absorption and CD spectroscopy. The same result is achieved -more expeditiously by employing anhydrous (−)-DBT, rather than the monohydrate. The solid crystalline complex, (−)-DBT-Δ-[Co(pd)₃], filtered and washed with a cyclohexane-benzene (2:1) mixture, is taken up into chloroform solution, from which the (−)-DBT is extracted with aqueous sodium bicarbonate. Following the removal of the

---

*Author to whom correspondence should be addressed.

†Permanent address: Centro di Studio del C.N.R. per le Macromolecole, Stereordinate ed Otticamenta Attive, The University, 56100 Pisa, Italy.
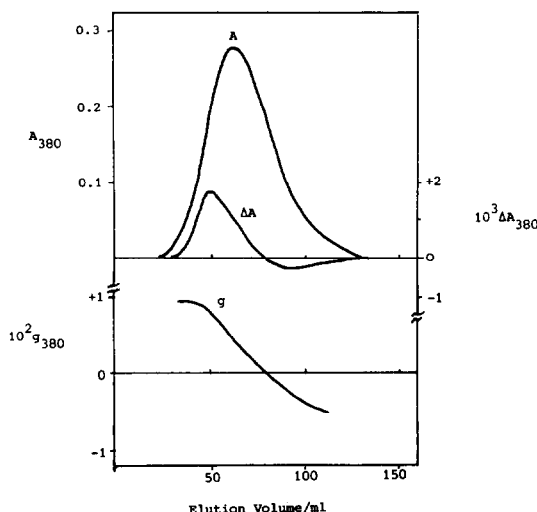
Fig. 1. The chromatographic optical resolution of racemic [Rh(pd)₃] (10 mg) on a column (25 cm long, 2 cm i.d.) of (2R, 3R)-(−)-dibenzoyltartaric acid adsorbed on alumina (Woelm basic activity, grade I) eluted with a cyclohexane-benzene mixture (2:1) at a rate of 5.5 ml min⁻¹. The chromatogram records, as a function of elution volume, the simultaneous monitoring at 380 nm of the absorbance, A (top curve), the circular dichroism, $\Delta A = A_L - A_R$ (middle curve), and the dissymmetry ratio, $g = \Delta A/A$ (bottom curve).

Table 1. The absorption and the cd spectra in ethanol of the [M(pd)₃] isomer forming enantioselectively a crystalline complex with (2R, 3R)-(−)-dibenzoyltartaric acid. The g-ratio ($g = \Delta\epsilon/\epsilon = \Delta A/A$) at the analytical wavelength, λ_{cd}, provides a measure of optical purity

Complex	λ_{abs}/nm	ϵ_{max}	λ_{cd}/nm	$\Delta\epsilon_{max}$	$10^3 g(\lambda_{cd})$
Δ-[Co(pd)₃]	592	132	647	+2.88	+42.5
	325	8130	574	−8.11	−67.5
Δ-[Cr(pd)₃]	560	70	608	+1.67	+42.4
	389	454	537	−5.00	−82.5
Δ-[Rh(pd)₃]	318	10,660	334	+64.0	+7.87
	255	9,190	295	+24.2	+3.62
Δ-[Ru(pd)₃]	504	1,590	480	+4.71	+3.63
	346	8,500	415	+11.84	+7.25
Δ-[Ir(pd)₃]	312	9,950	362	+36.8	+7.88
	260	24,000	306	−18.8	−1.93

solvent from the dried chloroform solution and recrystallisation of the residual solid, 1.3 g of optically pure Δ-(+)₅₄₆-[Co(pd)₃] is obtained with the cd characteristics listed (Table 1).

The original filtrate, containing the corresponding Λ-isomer, is washed with aqueous sodium bicarbonate and dried. The solid remaining after the removal of the solvent is ~90% optically pure and it is difficult to enhance that percentage purity further by standard fractional crystallisation, since the solubility of the enantiomer is approximately an order of magnitude larger than that of the racemate in paraffin and chloro-solvents. However, slow recrystallisation from a 2 : 1 mixture of petroleum (b.p. 80–100°) and dichloromethane affords two sets of large morphologically-distinct single crystals, which are readily separable by hand-sorting. Each crystal of the major set contains optically-pure Λ(−)₅₄₆-[Co(pd)₃], with an optical activity equal in magnitude and opposite in sign to that of the Δ-isomer isolated from the solid crystalline complex with (−)-DBT (Table 1).

The procedure provides in addition a simple optical resolution on a >1 g scale of the racemic complexes, [Cr(pd)₃], [Rh(pd)₃], [Ru(pd)₃], and [Ir(pd)₃] (Table 1). The determination of the absolute configuration of Λ-(−)₅₄₆-[Co(pd)₃][12] and Δ-(−)-[Cr(pd)₃][13] by X-ray diffraction methods, and the corresponding cd spectra, indicate that the enantiomer selectively forming a crystalline complex with (−)-DBT is the Δ-isomer in each case. The same conclusion follows for the cases of [Ru(pd)₃] and [Rh(pd)₃] from a comparison of the cd spectra of the resolved isomers with the corresponding spectra of each of the four diastereomers, with a known configuration, of the tris[(+)-3-acetylcamphorato] complexes of Ru(III)[14] and Rh(III)[15]. The consistency between these four cases suggests that the enantiomer of other [M(pd)₃] compounds selectively forming a complex with (−)-DBT is the Δ-isomer.

The fractional optical purity of a chiral compound is measured by the dissymmetry ratio ($g = \Delta\epsilon/\epsilon = \Delta A/A$) at an analytical wavelength, relative to the corresponding g-ratio of one of the pure enantiomers. The g-ratios of the [M(pd)₃] enantiomers listed (Table 1) refer in each case to a single-crystal sample, in order to ensure enantiomeric purity. In a chromatographic optical resolution, a finite g-ratio constant with respect to elution volume

indicates that the chiral solute in the eluate is optically pure.[11] On this criterion, the chromatographic resolution of [M(pd)₃] complexes on a (−)-DBT/Al₂O₃ column is not efficient (Fig. 1), although the investigation of the method provided the basis for the more efficient large-scale procedure described. An analogous enantioselective complex formation probably underlies the partial resolution of [Co(pd)₃] by the zone-melting of a frozen solution of the racemic complex and sodium (−)-dibenzoyl-tartrate in dioxan-water.[16]

REFERENCES

[1]T. Moeller and E. Gulyas, *J. Inorg. Nucl. Chem.* 1958, **5**, 245.
[2]J. P. Collman, R. P. Blair, R. L. Marshall and L. Slade, *Inorg. Chem.* 1963, **2**, 576.
[3]R. C. Fay and T. S. Piper, *Inorg. Chem.* 1964, **3**, 348.
[4]R. C. Fay, A. Y. Girgis and U. Klabunde, *J. Am. Chem. Soc.* 1970, **92**, 7056.
[5]B. Norden and I. Jonas, *Inorg. Nucl. Chem. Lett.* 1976, **12**, 33, 43.
[6]M. Yamamoto, R. Iwamoto, A. Kozasa, K. Takemoto, Y. Yamoto and A. Tatshata, *Inorg. Nucl. Chem. Lett.* 1980, **16**, 71.
[7]A. Yamagishi, R. Ohnishi and M. Soma, *Chem. Lett.* 1982, 85.
[8]A. Yamagishi, *J.C.S. Chem. Comm.* 1981, 1168.
[9]M.B. Célap, I. M. Hodzić and T. J. Janjić, *J. Chromatogr.* 1980, **198**, 172.
[10]Y. Okamoto, S. Honda, I. Okamoto, H. Yuki, S. Murata, R. Noyori and H. Tanaka, *J. Am. Chem. Soc.* 1981, **103**, 6971.
[11]A. F. Drake, J. M. Gould and S. F. Mason, *J. Chromatogr.* 1980, **202**, 239.
[12]R. B. von Dreele and R. C. Fay, *J. Am. Chem. Soc.* 1971, **93**, 4936.
[13]R. Kuroda and S. F. Mason, *J. C. S. Dalton Trans.* 1979, 273.
[14]G. W. Everett, Jr. and R. M. King, *Inorg. Chem.* 1972, **11**, 2041.
[15]G. W. Everett, Jr. and A. Johnson, *Inorg. Chem.* 1974, **13**, 489.
[16]V. F. Doran and S. Kirschner, *Inorg. Chem.* 1962, **1**, 539.

Catalytic asymmetric hydrogenation with the cluster Rh₆(CO)₁₀[(−)DIOP]₃†

R. MUTIN, W. ABBOUD, J. M. BASSET*

Institut de Recherches sur la Catalyse, 2, avenue Albert Einstein, 69626 Villeurbanne Cédex, France

and

D. SINOU

Laboratoire de Chimie Organique II, ERA CNRS 689, Universite de Lyon 1, 43, Boulevard du 11 Novembre 1918, 69621 Villeurbanne Cédex, France

Abstract—$Rh_6(CO)_{10}[(−)DIOP]_3$ has been isolated after ligand exchange between $Rh_6(CO)_{16}$ and DIOP. The molecular cluster is an efficient catalyst for asymmetric reduction of various prochiral olefins; optical yields up to 47% have been achieved; the results are compared with those obtained with mononuclear rhodium (I) complexes.

Although polynuclear complexes constitute now a new generation of organometallic complexes, their use in catalysis is still rare.[1] Moreover, within a few exceptions,[2] there are no reported cases of true cluster catalysed reaction, although molecular clusters are often used as precursor complexes.[3] One possibility to prove the reality of a cluster catalysed reaction is to use chiral clusters[4] the chirality being due to the cluster metallic framework. However, under catalytic condition, racemization may occur, which makes it difficult to induce an asymmetric catalytic reaction.[4a] Another possibility is to use chiral ligands with chiral metallic framework. But in this latter case, interpretation of the results is more difficult. In our general approach of cluster catalysis,[1] we have recently shown that rhodium clusters of the type $Rh_6(CO)_{(6−x)} L_x^{5−6}$ are catalysts for olefin hydrogenation and spectroscopic as well as kinetic data suggested that the cluster itself could act as a catalyst. It was therefore reasonable to undertake an asymmetric hydrogenation with the same family of complexes bearing chiral ligands. In the mean time Balavoine *et al.*[7] as well as Dang *et al.*[8] reported asymmetric hydrogenation of various olefins with an *in situ* mixture of $Rh_6(CO)_{16}$ and various chiral ligands. In our approach of such asymmetric reaction, we started from the cluster $Rh_6(CO)_{10}[(−)DIOP]_3$ and found effectively an asymmetric induction in the hydrogenation of various prochiral olefins.

There are already two reported cases of asymmetric hydrogenation with Ru clusters bearing DIOP ligands such as $H_4Ru_4(CO)_8[(−)DIOP]_2$ and $Ru_6(CO)_{18}[(−)DIOP]_3$. Infrared data indicate no significant change of the structure of the cluster during the catalytic reaction.[9]

RESULTS

$Rh_6(CO)_{10}[(−)DIOP]_3$ was prepared from $Rh_6(CO)_{16}$ and 3 equivalent of (−)DIOP in boiling benzene and purified by HPLC (column: styragel 500 Å; eluent: toluene) (yield = 33%). The elemental analysis and molecular weight were consistent with the formulation $Rh_6(CO)_{10}[(−)DIOP]_3(A)$. The IR spectrum of (A) exhibits $\nu(CO)$ bands at 2073 (w), 1972 (s, br) in the linear region and 1810 and 1780 (s, br) in the bridging region. Obviously the real structure of the cluster cannot be assumed with certitude unless X-ray structure is known.[11] However, considering the structure of the parent cluster $Rh_6(CO)_{10}(dppm)_3$,[10] it is likely

that in our case, probably due to steric crowding by the chiral ligands, the bridging CO ligands are hypothetically edge bridging.

This complex is stable in the solid state in the air, but less stable in solution.

Standard hydrogenation experiments were carried out with this cluster using amino-acid precursors and itaconic acid. The optical yields achieved in our experiments are listed in Table 1.

Generally speaking, in contrast with the results obtained with mononuclear complexes of $Rh(I)(DIOP)^{12}$ the acid substrates are reduced with lower asymmetric induction than the esters. Besides although the same enantiomer is obtained using (A) or Rh(I)(DIOP) complexes, the e.e. are lower in the first case. The value obtained for α-acetamido cinnamic acid, is identical to that obtained by Balavoine *et al.*[7] using a mixture of $Rh_6(CO)_{16}$ and 3 equivalents of (−)(DIOP). The temperature seems to have no influence on the enantioselectivity, but, in presence of UV-irradiation, there is an increase of the rate of hydrogenation (80% hydrogenation in 5 hr), but a drastic decrease in the enantioselectivity.

In conclusion these preliminary results constitute the first example of an asymmetric reduction using a rhodium cluster bearing chiral ligand. Although the catalytic behavior of $Rh_6(CO)_{10}[(−)DIOP]_3$ is different from the known mononuclear complexes of the type $Rh^I[(−)DIOP]$, (rate of hydrogenation, type of substrate which are hydrogenated, e.e.). The enantiomer obtained is the same in both cases. It is therefore difficult to make a clear cut distinction between a true cluster catalysed reaction and a catalysis by a mononuclear fragment. Studies are in progress to try to understand at a molecular level the mechanism of such reaction.
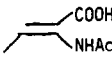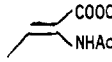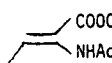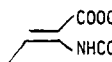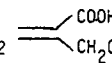
EXPERIMENTAL

¹H NMR spectra were recorded on a Brucker 80 spectrometer, IR spectra were taken with a Perkin–Elmer 225 spectrometer in various solvents. The cluster was purified by HPLC using a Watters M 6000 A. The column was a micro styragel (500 Å) of 50 cm, used in semi-preparative scale (solvent: toluene flow = 1 ml/min; temperature 25°C). The rotatory powers were measured on a Perkin–Elmer 241 polarimeter. Molecular weight determination of the cluster was carried out by vapor pressure osmometry. Catalytic hydrogenations were carried in a glass batch reactor equipped with a septum for kinetic measurements and connected with a hydrogen reservoir kept at constant atmospheric pressure.

---

*Author to whom correspondence should be addressed.

†DIOP = 0-isopropylidene 2,3-dihydroxy 2,3-bis(diphenylphosphinomethyl) 1,4-butane.

Table 1. Asymmetric hydrogenation in the presence of $Rh_6(CO)_{10}[(-)DIOP]_3$[a]

Substrate	T(°C)	$\frac{[substrate]}{[cat]}$	Conversion (%)	e.e. (%) (c)	Time(h)
Ph—CH, COOH, NHAc	25	220	100	20 (R)	28
Ph—, COOCH₃, NHAc	80 25 b) 25 b)	100 270 220	100 100 100	47 (R) 45 (R) 6 (R)	24 45 27
Ph—, COOC₂H₅, NHAc	25	230	100	34 (R)	50
Ph—, COOCH₃, NHCOPh	25	220	60	3 (R)	75
CH₂—, COOH, CH₂COOH	25	457	100	0	4

(a) Solvent : ethanol ; p_{H_2} = 1 atm.

(b) Hydrogenation in the presence of U.V. irradiation. $\rangle$(max) = 365 nm

(c) Enantiomeric excesses were calculated using the specific rotation of the pure enantiomers :

N - acetyl - (R) - Phenylalanine $[\alpha]_D^{25}$ = - 46.0 (c = 1 ; EtOH) (13).

N - acetyl - (R) - Phenylalanine methyl ester $[\alpha]_D^{25}$ = - 101.5 (c = 1 ; CHCl₃) (14)

N - acetyl - (R) - phenylalanine ethyl ester $[\alpha]_D^{25}$ = - 85.9 (c = 1 ; CHCl₃) (14)

N - benzoyl (S) - phenylalanine methyl ester $[\alpha]_D^{25}$ = - 45.3 (c = 1 ; EtOH) (13)

(R) Methyl - succinic acid $[\alpha]_D^{20}$ = + 16.88 (c = 2.1 ; EtOH) (15)

Preparation of $Rh_6(CO)_{10}[(-)DIOP]_3$

In a typical experiment 1.4 g (2.8 10⁻³ mole) of (−)DIOP dissolved in 100 cm³ of C_6H_6 is introduced dropwise under stirring in 70 cm³ of a refluxing solution of benzene containing 1 g of $Rh_6(CO)_{16}$ (9.4 10⁻⁴ mole).

After cooling to 25°C, the solution is concentrated under vacuum and the cluster is precipitated by addition of 30 cm³ of *n*-pentane. Purification by HPLC yields a black amorphous solid (33% yield). Found: C, 48.08; H. 3.97; P, 7.86; Rh, 25.9; mol. wt., 2475. $C_{103}H_{96}P_6Rh_6O_{16}$ calc.: C, 51.68; H, 4.04; P, 7.78; Rh, 25.8; md. wt., 2393. IR spectrum: $v(CO)$ bonds (chloroform solution) at 2073 (w), 1972 (s, br), 1810 (s, br), 1780 (s, br).

Hydrogenation procedure

In a typical experiment 13 mg of (A) (5.10⁻⁶ mole) and 10⁻³ mole of the olefinic substrate are vigorously stirred in 25 cm³ of ethanol under 1 atm. of H_2. The reaction is monitored by the absorption of H_2 with time and by quantitative analysis of the reactants by GLC. The hydrogenated products are treated as previously described.[12]

REFERENCES

[1] A. K. Smith and J. M. Basset, *J. Mol. Cat.* 1977, **2**, 229.

[2] A. J. Deeming and S. Hasso, *J. Organometal. Chem.* 1976, **114**, 313. B. Besson, A Choplin, L. D'ornelas and J. M. Basset, *J.C.S. Chem. Comm.* 842 (1982).

[3] R. Laine, *J. Mol. Cat.* 1982, **14**, 137.

[4a] A. Agapiou, S. E. Pedersen. L. A. Zyzyck and J. R. Norton, *J. Chem. Soc. Chem. Comm.* 1977, 393; [b] F. Richter and H. Vahrenkamp, Ang. Chem. Int. Ed. 1978, **17**, 864; [c] C. U. Pittmann and R. C. Ryan, *CHEMTECH* 1978, 170.

[5] W. Reimann, W. Abboud, J. M. Basset, R. Mutin, G. L. Rempel and A. K. Smith, *J. Mol. Cat.* **9**, 349 (1980); A. K. Smith, W. Abboud, J. M. Basset, W. Reimann, G. L. Rempel, J. L. Bilhou, V. Bougnol, W. F. Graydon, J. Dunogues, W. Ardoin and N. Duffaut, *Fundamental Research in Homogenous Catalysis*, Vol. 3, p. 621. Plenum, New York (1979).

[6] W. Abboud, Y. Ben Taarit, R. Mutin and J. M. Basset, *J. Organometal. Chem.* 1981, **220**, C15–C19.

[7] G. Balavoine, T. Dang, C. Eskenazi and H. B. Kagan, *J. Mol. Cat.* 1980, **7**, 531.

[8] T. P. Dang, P. Aviron-Violet, Y. Colleuille and J. Varagnat, *J. Mol. Cat.* 1982, **16**, 51.

[9] C. Botteghi, S. Gladiali, M. Bianchi, U. Matteoli, P. Frediani, P. G. Vergamini and E. Benedetti, *J. Organometal. Chem.* 1977, **140**, 221; M. Bianchi, F. Piacenti, P. Frediani, U. Matteoli, C. Botteghi, S. Gladiali and E. Bendetti, *I. Organometal. Chem.* 1977, **141**, 107.

[10] dppm = bis-1,2-diphenyl-phosphino-methane.
The X-ray structure of this cluster is derived from an octahedron of 6 RH atoms with 3 chelating dppm ligand coordinated to the 6 rhodium atoms 4 triply bridged CO ligands are observed along with 6 linear CO on the 6 rhodium atoms. A. Ceriotti, G. Ciani, L. Garlaschelli, V. Sartorelli and A. Sironi,

J. Organometal. Chem. 1982, 229, C9; D. F. Foster, B. S. Nicholls and A. K. Smith, J. Organometal. Chem. in press (1982).
[11]The cluster could not be crystallized in a form suitable for X-ray structure determination.

[12]H. B. Kagan and T. P. Dang, J. Am. Chem. Soc. 1972, 94, 6429.
[13]G. Gelbard, H. B. Kagan and R. Stern, Tetrahedron 1976, 32, 233.
[14]R. Glaser and B. Vainas, J. Organometal. Chem. 1976, 121, 249.
[15]E. Berner and R. Leonardsen, J. Liebig Ann. Chem. 1939, 538, 1.

Synthesis and structural characteristics of fac-ReCl₃[P(OEt)₃]₃ a route to the phosphite complexes

W. K. RYBAK* and J. J. ZIÓŁKOWSKI

Institute of Chemistry, Wrocław University, Joliot Curie 14, 50-383 Wrocław, Poland

Abstract—Reaction of the oxo-complex $ReOCl_3(PPh_3)_2$ with an excess of triethylphosphite yields a deoxygenated rhenium phosphite complex fac-$ReCl_3[P(OEt)_3]_3$; its structure was confirmed by ^1H NMR and IR spectroscopy.

The chemistry of rhenium phosphine complexes is well developed,[1] contrary to that of the phosphite complexes. Such complexes of rhenium and other metals have recently been given considerable attention.[2] In continuation of our studies on reactivities of rhenium phosphine complexes[3] we have been interested in synthesis of the respective phosphite complexes having in mind different properties of that ligand.

The present paper reports a convenient method for synthesis of phosphite complexes from their respective metal phosphine oxo derivatives taking the rhenium complexes as an example (reaction 1).

trans-ReOCl₃(PPh₃)₂ + 3 P(OEt)₃ → fac-

(I)

ReCl₃[P(OEt)₃]₃ + P(O)Ph₃ + PPh₃   (1)

(II)

The authors believe that this method can be used for other transition metal oxo-complexes (e.g. Tc, Mo, W), due to the strong deoxygenating properties of the phosphine ligand.[1b,4] Reaction (1) in which rhenium (V) is reduced to rhenium (III) with simultaneous substitution of the phosphine ligand is probably preceded by isomerization† of the yellow trans complex (I) to a green cis complex (I) in which the oxygen atom and phosphine ligand are in trans positions.[5]

The reaction of complex (I) (3.6 mmol) and a ten-fold excess of P(OEt)₃ carried out in boiling benzene solution (60 cm³) under nitrogen for 7 hr yields a light yellow solution containing the products of reaction (1) in about 100% yield. The excess of free P(OEt)₃ was removed by prolonged evaporation of the mixture to dryness in vacuo. P(O)Ph₃ was separated from other components of the reaction mixture as a hexane-insoluble residue. Free phosphine was separated from complex (II) by means of

column chromatography using activated silica gel (350°C for 4 hr in vacuo) as packing and hexane-benzene, benzene and finally, benzene – 10% methanol as eluents, under oxygen-free conditions. Complex (II) was recrystallized from hexane (– 15°C) [Found: C 27.1, H 5.58, P 11.7%; $C_{18}H_{45}O_9Cl_3P_3Re$ requires: C 27.22, H 5.73, P 11.74%].

The structure of the facial complex (II) is confirmed by both the IR and ^1H NMR spectra. Over the frequency range characteristic of the Re–Cl bonds, complex (II) exhibits two strong bands in the IR region at 269 and 314 cm⁻¹, which indicates C_{3v} symmetry. By comparison, we find that mer-ReCl₃(PMe₂Ph)₃, of C_{2v} symmetry, has a more complicated IR spectrum in that region. Like rhenium (III) complexes with phosphine ligands,[6a] complex (II) is paramagnetic; however, quite sharp lines are found in the ^1H NMR spectrum in deuterobenzene at 30°C. Predictably, marked isotropic shifts are also observed. The integrated spectrum contains two triplets (intensity ratio 2:1, CH₃, δ 2.25 ppm, 3H and δ 3.12 ppm, 6H) and two quartets (2:1, CH₂, δ 10.07 ppm, 2H and δ 11.15 ppm, 4H). The coupling constant for the protons of two groups ^3J (H–H) = 7 Hz. The coupling constant ^3J(P–H) of 7 Hz for free P(OEt)₃ is not observed for a coordinated ligand. This spectrum shows that all three phosphite ligands in complex (II) are equivalent, although the ethoxy groups are inequivalent to each other in a (2:1) ratio. From among three ethoxy groups for each phosphite ligand, two groups are on one side of the plane determined by the three phosphorus atoms coordinated to the rhenium atom, whereas the third ethoxy group is on the other side of that plane.

The facial geometry of complex (II) is most probably the effect of a smaller cone angle of the phosphite ligand and of its stronger π-acceptor properties as compared with the phosphine ligand which instead prefers meridional geometry in similar known ternary complexes.[6]

Complex (II) undergoes no exchange reaction of the phosphite ligand (on the NMR time scale at 80°C) but may, however, be reduced (NaBH₄/EtOH) to yield monomeric and dimeric hydride complexes.

---

*Author to whom correspondence should be addressed.

†Trans-cis isomerization of complex (I) was found to take place in boiling pure benzene.

J. Organometal. Chem. 1982, **229**, C9; D. F. Foster, B. S. Nicholls and A. K. Smith, *J. Organometal. Chem.* in press (1982).

[11]The cluster could not be crystallized in a form suitable for X-ray structure determination.

[12]H. B. Kagan and T. P. Dang, *J. Am. Chem. Soc.* 1972, **94**, 6429.

[13]G. Gelbard, H. B. Kagan and R. Stern, *Tetrahedron* 1976, **32**, 233.

[14]R. Glaser and B. Vainas, *J. Organometal. Chem.* 1976, **121**, 249.

[15]E. Berner and R. Leonardsen, *J. Liebig Ann. Chem.* 1939, **538**, 1.

Synthesis and structural characteristics of fac-ReCl₃[P(OEt)₃]₃ a route to the phosphite complexes

W. K. RYBAK* and J. J. ZIÓŁKOWSKI

Institute of Chemistry, Wrocław University, Joliot Curie 14, 50-383 Wrocław, Poland

Abstract—Reaction of the oxo-complex ReOCl₃(PPh₃)₂ with an excess of triethylphosphite yields a deoxygenated rhenium phosphite complex fac-ReCl₃[P(OEt)₃]₃; its structure was confirmed by ¹H NMR and IR spectroscopy.

The chemistry of rhenium phosphine complexes is well developed,[1] contrary to that of the phosphite complexes. Such complexes of rhenium and other metals have recently been given considerable attention.[2] In continuation of our studies on reactivities of rhenium phosphine complexes[3] we have been interested in synthesis of the respective phosphite complexes having in mind different properties of that ligand.

The present paper reports a convenient method for synthesis of phosphite complexes from their respective metal phosphine oxo derivatives taking the rhenium complexes as an example (reaction 1).

trans-ReOCl₃(PPh₃)₂ + 3 P(OEt)₃ → fac-

(I)

ReCl₃[P(OEt)₃]₃ + P(O)Ph₃ + PPh₃   (1)

(II)

The authors believe that this method can be used for other transition metal oxo-complexes (e.g. Tc, Mo, W), due to the strong deoxygenating properties of the phosphine ligand.[1b,4] Reaction (1) in which rhenium (V) is reduced to rhenium (III) with simultaneous substitution of the phosphine ligand is probably preceded by isomerization† of the yellow *trans* complex (I) to a green *cis* complex (I) in which the oxygen atom and phosphine ligand are in *trans* positions.[5]

The reaction of complex (I) (3.6 mmol) and a ten-fold excess of P(OEt)₃ carried out in boiling benzene solution (60 cm³) under nitrogen for 7 hr yields a light yellow solution containing the products of reaction (1) in about 100% yield. The excess of free P(OEt)₃ was removed by prolonged evaporation of the mixture to dryness *in vacuo*. P(O)Ph₃ was separated from other components of the reaction mixture as a hexane-insoluble residue. Free phosphine was separated from complex (II) by means of

column chromatography using activated silica gel (350°C for 4 hr *in vacuo*) as packing and hexane–benzene, benzene and finally, benzene − 10% methanol as eluents, under oxygen-free conditions. Complex (II) was recrystallized from hexane (− 15°C) [Found: C 27.1, H 5.58, P 11.7%; C₁₈H₄₅O₉Cl₃P₃Re requires: C 27.22, H 5.73, P 11.74%].

The structure of the facial complex (II) is confirmed by both the IR and ¹H NMR spectra. Over the frequency range characteristic of the Re–Cl bonds, complex (II) exhibits two strong bands in the IR region at 269 and 314 cm⁻¹, which indicates C_{3v} symmetry. By comparison, we find that *mer*-ReCl₃(PMe₂Ph)₃, of C_{2v} symmetry, has a more complicated IR spectrum in that region. Like rhenium (III) complexes with phosphine ligands,[6a] complex (II) is paramagnetic; however, quite sharp lines are found in the ¹H NMR spectrum in deuterobenzene at 30°C. Predictably, marked isotropic shifts are also observed. The integrated spectrum contains two triplets (intensity ratio 2:1, CH₃, δ 2.25 ppm, 3H and δ 3.12 ppm, 6H) and two quartets (2:1, CH₂, δ 10.07 ppm, 2H and δ 11.15 ppm, 4H). The coupling constant for the protons of two groups ³J (H–H) = 7 Hz. The coupling constant ³J(P–H) of 7 Hz for free P(OEt)₃ is not observed for a coordinated ligand. This spectrum shows that all three phosphite ligands in complex (II) are equivalent, although the ethoxy groups are inequivalent to each other in a (2:1) ratio. From among three ethoxy groups for each phosphite ligand, two groups are on one side of the plane determined by the three phosphorus atoms coordinated to the rhenium atom, whereas the third ethoxy group is on the other side of that plane.

The facial geometry of complex (II) is most probably the effect of a smaller cone angle of the phosphite ligand and of its stronger π-acceptor properties as compared with the phosphine ligand which instead prefers meridional geometry in similar known ternary complexes.[6]

Complex (II) undergoes no exchange reaction of the phosphite ligand (on the NMR time scale at 80°C) but may, however, be reduced (NaBH₄/EtOH) to yield monomeric and dimeric hydride complexes.

---

*Author to whom correspondence should be addressed.

†*Trans–cis* isomerization of complex (I) was found to take place in boiling pure benzene.

REFERENCES

[1a]J. Chatt and G. A. Rowe, *J. Chem. Soc.* 1962, 4019. [b]G. Rouschias and G. Wilkinson, *J. Chem. Soc. (A)*, 1967, 993. [c]J. Chatt and R. S. Coffey, *J. Chem. Soc. (A)*, 1969, 1963. [d]H. P. Gunz and G. J. Leigh, *J. Chem. Soc. (A)*, 1971, 2229.

[2]H. W. Choi and E. L. Muetterties, *J. Am. Chem. Soc.* 1982, **104**, 153 and references therein.
[3]M. A. Green, J. C. Huffman, K. G. Caulton, W. K. Rybak and J. J. Ziólkowski, *J. Organomet. Chem.* 1981, **218**, C39.
[4]J. Deli and G. Speier, *Trans. Met. Chem.* 1981, **6**, 227.
[5]N. K. Kobilov and K. V. Kotegov, Deposited Doc. 1977, VINITI, 3068 *Russ. Chem. Abs.* **90**, 179329x.
[6a]E. W. Randall and D. Shaw, *Mol. Phys.* 1965, **10**, 41. [b]J. Chatt, G. J. Leigh, D. M. P. Mingos, E. W. Randall and D. Shaw, *Chem. Commun.* 1968, 419.

Reductive Nitrosylation Of Tetraoxometallates. Part V[1]. Single Pot And A Virtually Single Step Synthesis Of Chromium(1) Cyanonitrosyl Derivatives Directly From Chromate(VI) In Aqueous-Aerobic Media.

R. G. Bhattacharyya,* G. P. Bhattacharjee and (Mrs.) N. Ghosh
Department of Chemistry, Jadavpur University,
Calcutta 700 032, India.

Abstract : Cyanonitrosyl complexes and their derivatives of the types $[Cr(NO)(CN)_4]^{2-}$, $[Cr(NO)(CN)_3H_2O]^-$ and $[Cr(NO)(CN)_2 LL]$ [LL = 2,2' bipyridine (bipy) or 1, 10-Phenanthroline (phen)] are synthesised directly from CrO_4^{2-} using $NH_2OH.HCl$, OH^- and CN^- and other appropriate ligands, virtually in a single step process in an aqueous aerobic medium. The compounds are characterised by IR, molar conductance, magnetic susceptibility, e.s.r, electronic spectra and thermoanalytical data.

INTRODUCTION : Single step conversion of tetraoxometallates to the cyanonitrosyl derivatives, (viz, [$M(NO)(CN)_2 LL$] where LL is a bidentate ligand or two unidentate ligands) is still unknown. Sarkar et al[2] have reported the synthesis of the cyanonitrosyl derivatives of Fe and V starting from $[Fe(NO)(CN)_5]^{2-}$ and $[V(NO)(CN)_6]^{4-}$ respectively in a boiling acetic acid medium followed by thermolysis of the anionic complexes. We have described single step synthesis of the thiocyanato nitrosyl derivatives of Cr (Ref. 3), Re (Ref. 1a) and Mo (Ref. 1b) directly from CrO_4^{2-} , ReO_4^- and MoO_4^{2-} respectively. Herein is described, for the first time, a single pot and a virtually single step synthesis of the hitherto unknown cyanonitrosyl derivatives of formally Cr(1) of the types $[Cr(NO)(CN)_2 LL]$ (LL = bipy or phen) and the anionic complexes of the types $[Cr(NO)(CN)_4]^{2-}$ and $[Cr(NO)(CN)_3H_2O]^-$ directly from CrO_4^{2-} in aqueous aerobic media.

EXPERIMENTAL :

Preparation of the complexes - In a solution of KOH (3 g in 20 ml of H_2O) were added K_2CrO_4 (0.5 g, 2.6 mmol) and KCN (2.5 g, 38.6 mmol) and the mixture was stirred for 5 min at ~ 80°. To this solution, $NH_2OH.HCl$ (2.7 g, 38.6 mmol) was added portionwise with constant stirring at ~80° and the stirring was continued for another 45 min to get a yellowish green solution. This was cooled to room temperature (pH = 10.5) (solution A) and then pH was adjusted to ~5 with 6 M HCl. (solution B).

1. $(Ph_4P)_2 [Cr(NO)(CN)_4].H_2O$ - An aqueous solution of $(C_6H_5)_4PCl$ (2.4 g, 6.4 mmol in 25 ml of water) was added to the solution B obtained above with constant stirring at room temperature to yield a bright yellow precipitate. The stirring was continued for 30 min , allowed to settle and filtered. The yellow residue was washed thoroughly with water, dried over

P_4O_{10} and then washed with ether and finally dried over fused $CaCl_2$ in vacuo. The compound was recrystallised twice from acetonitrile-ether mixture. Yield 1.65 g, 72 %. M. Pt 150°. Found : C, 71.1 ; H, 4.6 ; N, 8.3 ; P, 7.5 ; Cr, 5.2 ; H_2O (lost at 80°, exothermic), 2.2 . $C_{52}H_{40}P_2O$ $N_5Cr.H_2O$ requires C, 70.7 ; H, 4.5 ; N, 7.9 ; P, 7.0 ; Cr, 5.9 ; H_2O, 2.0 %. IR : ν_{CN} 2110 (s) , 2150 (sh) ; ν_{NO} 1670 (s) and $\nu_{Cr-N}(NO)$ 620 (w) cm^{-1}. λ_{max} 710 (sh), 448 (sh) and 340 (sh) nm. μ_{eff} = 1.9 B.M. Λ_m = 230 ohm^{-1} cm^2 mol^{-1} in acetonitrile.

2. (Me_4N) $[Cr(NO)(CN)_3$ $H_2O]$ – To a solution of $(CH_3)_4NCl$ (0.42 g, 3.8 mmol in 5 ml of water) was added the above solution (solution B) with constant stirring at room temperature for 30 min . A greenish yellow precipitate was obtained which was filtered off, washed with methanol and dried over fused $CaCl_2$ in vacuo. The dried product was further recrystallised from water-methanol mixture. Yield 0.54 g, 83 %. Found : C, 33.0 ; H, 5.1 ; N, 27.2 ; Cr, 20.1 ; H_2O (130°, exothermic), 7.0. $C_7H_{12}N_5O$ $Cr.H_2O$ requires C, 33.3 ; H, 4.8 ; N, 27.8 ; Cr, 20.6 ; H_2O, 7.1 %. IR : ν_{CN} 2120 (s) ; ν_{NO} 1665 (s) and ν_{Cr-N} (NO) 620 (w) cm^{-1}. λ_{max} 740 (30.0), 450 (105) and 344 (sh) nm . μ_{eff} = 1.7 B.M. Λ_m = 130 ohm^{-1} mol^{-1} cm^2 in water.

3. $(Me_4N)_2[Cr(NO)(CN)_4].H_2O$ – Instead of adjusting the pH of the solution A to ~5, the same was adjusted at 7.5 and this solution was added to an aqueous solution of $(CH_3)_4$ NCl (0.7 g, 6.4 mmol in 5 ml of water) with constant stirring at room temperature for 30 min. An yellowish green precipitate was obtained which was filtered, washed with methanol, ether and dried in vacuo. The dried product was recrystallised from water-methanol mixture. Yield 0.6 g, 65 %. Found : C, 41.3 ; H, 7.1 ; N, 27.4 ; Cr, 14.6 ; H_2O (85°, exothermic), 4.9 . $C_{12}H_{24}N_7O$ $Cr.H_2O$ requires C, 40.9 ; H, 6.8 ; N, 27.8 ;.Cr, 14.8 ; H_2O , 5.1 %. IR : ν_{CN} 2120 (s), 2140 (s) ; ν_{NO} 1670(s); ν_{Cr-N} (NO) 615 (w). λ_{max} 744 (30), 452 (110) and 340 (sh) nm. μ_{eff}=1.7 B.M. Λ_m= 246 ohm^{-1} cm^2 mol^{-1} in water.

4. $[Cr(NO)(CN)_2(bipy)].H_2O$ – To the solution B obtained above was added a hot aqueous solution of 2,2'-bipyridine (0.6 g, 3.8 mmol) with constant stirring for 30 min at ~80°. A brown precipitate was obtained which was filtered, washed with water, ethanol, ether and dried in vacuo. The dried product was recrystallised from dimethylformamide-ether mixture. Yield 0.46 g, 58 %. Found : C, 47.1 ; H, 2.9 ; N, 23.2 ; Cr, 16.3 ; H_2O (80°, exothermic), 5.7 . $C_{12}H_8N_5O$ $Cr.H_2O$ requires C, 46.8 ; H, 2.6 ; N, 22.7 ; Cr, 16.9 ; H_2O , 5.8 %. IR : ν_{CN} 2120 (w) and 2150 (w) ; ν_{NO} 1690 (s); $\nu_{Cr-N}(NO)$ 610(w) λ_{max} 716 (sh), 460 (sh) and 372 (sh) nm. μ_{eff} = 1.8 B.M.

5. $[Cr(NO)(CN)_2(phen)].H_2O$ – Same as described under bipy complex. Yield 0.55 g, 64 %. Found : C, 51.0 ; H, 2.5 ; N, 20.8 ; Cr, 15.4 ; H_2O (80° , exothermic), 5.2 . $C_{14}H_8N_5O$ $Cr.H_2O$ requires C, 50.6 ; H, 2.4 ; N, 21.1 ; Cr, 15.7 ; H_2O, 5.4 %. IR : ν_{CN} 2120 (w), 2150 (w) ; ν_{NO} 1690 (s); ν_{Cr-N} (NO) 620 (w). λ_{max} 716 (sh), 456 (sh); 380 (sh) nm. μ_{eff} = 1.8 B.M.

RESULTS AND DISCUSSION :

The cyano complexes very naturally undergo dissociation at a lower pH ($\sim$5) and lead to the isolation of [$Cr(NO)(CN)_3$ H_2O]$^-$ or [$Cr(NO)(CN)_2$ LL] but at a somewhat higher pH, [$Cr(NO)(CN)_4$]$^{2-}$ is formed when the cation is a tetramethyl ammonium ion. With the tetraphenyl phosphonium cation, however, [$Cr(NO)(CN)_4$]$^{2-}$ could be isolated even from a solution of pH$\sim$5, as well as at a neutral pH ($\sim$7), but not from the solution A. Also, while the potassium salt of the cyanonitrosyl complex is of the type K_3 [$Cr(NO)(CN)_5$] (Ref. 4), only the dianionic complex is formed in the case of the bulky and charge delocalised tetraphenyl phosphonium cation. Moreover, the thiocyanate analogue being a trianion, viz, [$Cr(NO)(NCS)_5$]$^{3-}$ with tetraphenyl phosphonium cation, the high π - trans effect of the NO^+ ligand prevents the formation of such a type of cyano complex with the same charge delocalised cation. These molecular formulae are also supported from the electrolytic conductance data of the complexes ; 4 and 5 being non electrolytes, 2 is a 1 : 1 and 1 and 3 are 2 : 1 electrolytes[5] in the respective solvents (see the experimental section). Only in the case of the complex 2, a single and sharp ν_{CN} band (as against two bands in all other cases) is observed and this may be due to its TBP structure containing equatorial cyano ligands. Considering the NO^+ formalism the formal oxidation state of chromium should be +1 which is evident from the magnetic moment and the e.s.r. ($g_{av} \approx 1.9$) data of all the complexes[3,6]. The $d_{(metal)} \longrightarrow \pi^*(NO)$ transition[7] in the electronic spectra of the isolated complexes are at a lower wave number region than those of the thiocyanate derivatives[3]. This may be due to larger crystal field splitting involving stronger CN^- ligand. Only the compound 2 loses water at a higher temperature (130°) compared to the other complexes (ca 80°) as revealed by their TGA, DTA and DTG curves, and so in the former complex, water is considered to be within the coordination sphere.

REFERENCES :

1.   (a) Part IV. R. G. Bhattacharyya and P. S. Roy, Indian J. Chem., (In Press) (b) Part III. R. G. Bhattacharyya and G. P. Bhattacharjee, J. Chem. Soc., Dalton Trans. (In Press).

2.   S. Sarkar, R. Singh and R. Mishra,   J. Inorg. Nucl. Chem., 1974,
      37, 578 ; S. Sarkar and R. Shrivastava ; Trans. met. Chem.,
      1980, 5, 122.

3.   R. G. Bhattacharyya, G. P. Bhattacharjee and P. S. Roy, Inorg.
      Chim. acta., 1981, 54, L263.

4.   W. P. Griffith, J. Lewis and G. Willkinson,   J. Chem. Soc.,
      1959, 872.

5.   W. J. Geary, Coord. Chem. Rev., 1971, 7, 81.

6.   B. A. Goodman and J. B. Rayner, 'Advances in Inorganic Chemistry
      and Radio Chemistry', A. J. Emeleus and A. G. Sharp (ed.), Vol. 13,
      Academic Press, New York, 1970, p. 135 and references cited therein.

7.   J. H. Enemark and R. D. Feltham, Coord. Chem. Rev., 1974, 13, 339.

COMMUNICATION

COMPLEXES OF COPPER AND SILVER WITH TETRACYANOBIIMIDAZOLE

Paul G. Rasmussen* and James E. Anderson
Department of Chemistry
The University of Michigan
Ann Arbor, Michigan 48109

We have recently reported the synthesis and properties of a remarkable new ligand 4,4',5,5'-tetracyano-2,2'-biimidazole (H_2Tcbiim).[1] This acidic ligand readily binds metal ions in its dianionic form and appears to act as a strong pi acceptor. Its use as a quadridentate bridging ligand allows study of metal-metal interactions through a planar conjugated system and extends earlier work by us[2] and by Hendrickson and coworkers[3] on 2,2'-biimidazole. In this communication we report on the reactions of H_2Tcbiim with Ag(I), Cu(I) and Cu(II) salts.

The silver(I) and copper(I) complexes have the general formulae $(M_{py})_2$Tcbiim and $[M(bpy)]_2$Tcbiim where py = pyridine and bpy 2,2'-bipyridine and M = Cu, Ag. The compound $[Cu(P\phi_3)_2]_2$ Tcbiim has also been prepared where $P\phi_3$ is triphenyl phosphine. The Cu(II) compounds are $Cu(py)_2$Tcbiim, Cu(bpy)Tcbiim and $[(Cu - diene)_2$Tcbiim]$(NO_3)_2$ where diene = diethylenetriamine. All of these compounds can be made in high yield; they have been characterized by analytical, spectroscopic and magnetic techniques.

The syntheses of these compounds are straightforward. To a solution of the metal nitrate salt in acetonitrile an excess of L is added, L = bpy, py for Cu and Ag and L = $P\phi_3$ for Cu only. A stoichiometric amount of H_2Tcbiim dissolved in acetonitrile is then added, the solution is stirred for 2 hours and the resulting complexes precipitate. The Cu(I) nitrate is

*Author for correspondence

formed <u>in situ</u> in acetonitrile by the reduction of $Cu(NO_3)_2$ with Cu metal. Attempts to synthesize Ag(II) complexes containing Tcbiim^{2-} resulted in the formation of the corresponding Ag(I) complex. In a typical reaction a silver(II) salt, such as $Ag(bpy)_2S_2O_8$ would react with H_2Tcbiim in a 1:1 mole ratio to form $Ag_2(bpy)_2$Tcbiim and unidentified oxidation products.

The copper(II) compounds are made in a similar way. Copper(II) nitrate was dissolved in methanol, a excess of L is added, where L = bpy, py and diene. A stoichiometric amount of H_2Tcbiim, dissolved in methanol, is then added and after two hours the green product is collected.

The structural evidence for the dimers is clearest in the case of the $[(P\phi_3)_4Cu_2]$Tcbiim (Figure 1). C^{13} NMR shows three
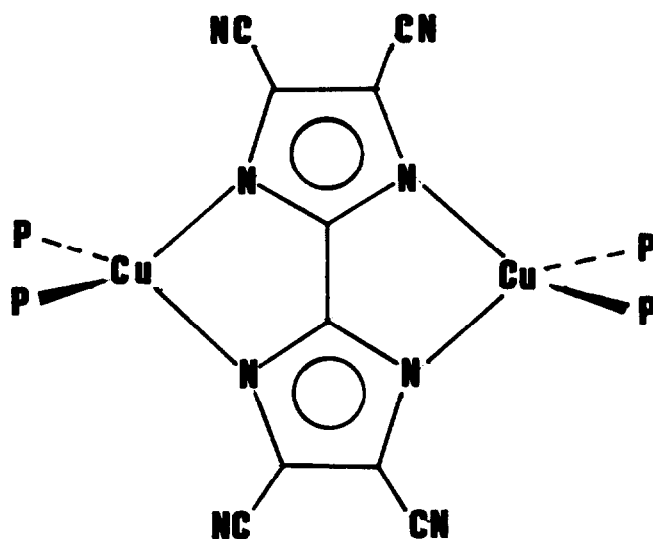
Figure 1.   Proposed structure of $[(P\phi_3)_4Cu_2]$Tcbiim, phenyl rings omitted for clarity.

signals at 151.2, 119.6, and 113.4 ppm relative to Me_4Si indicating a symmetrically bridged tetracyanobiimidazole. ^{31}P NMR gives only one signal showing equivalent phosphines. The IR spectrum shows a sharp singlet due to nitrile at 2220 cm^{-1}. The low solubility of the other Cu(I) compounds precludes good NMR.

<div align="center">

(py)Cu(Tcbiim)Cu(py)   (bpy)Cu(Tcbiim)Cu(bpy)

I   II

</div>

Compound I appears from stoichiometry to contain three coordinate copper. Furthermore, the nitrile stretch in the IR at 2220 cm^{-1} is unsplit. Compound II could be three coordinate in two ways, a) monodentate bpy and symmetrically bonded to $Tcbiim^{2-}$ or b) bidentate to bpy and coordinated to $Tcbiim^{2-}$ only once. We favor case b) since the nitrile peak at 2220 cm^{-1} shows a reasonable splitting (~ 10 cm^{-1}) suggesting inequivalent nitrile groups. It appears that univalent copper is satisfied with three coordination when the strongly pi accepting phosphines are absent but increases to four when they are present. We are pursuing this model of behavior by trying to effect further syntheses. Polymeric structures cannot be ruled out however at this time.

The Cu(II) dimer is directly analogous to those synthesized by Hendrickson.[3] Since biimidazole was found to give weak magnetic coupling between the copper ions, it was of interest to see if the tetracyanobiimidazole bridge enhances the interaction. Room temperature magnetic moment measurements were used to give a preliminary assay, and the value of $\mu = 1.58 \pm .05$ BM per mole of Cu, is indication of significant interaction. A more definitive study is underway.

The fact that Tcbiim^{2-} will act as a bridging group in both
Cu(I) and Cu(II) systems is noteworthy. It suggests the possi-
bility of preparing mixed valence dimers which, if the coordin-
ation geometry is properly contrived, can sustain substantial
interaction through the bridge. Pairs of Cu(II) ions bridged by
imidazoles have been extensively reported on as models for active
sites in enzymes.[4] The compounds described here offer further
examples of such model systems, which can be synthesized under
significantly less basic conditions than those previously ob-
served. Work on both these aspects is continuing.

1. P. G. Rasmussen, R. L. Hough, J. E. Anderson, O. H. Bailey,
    J. C. Bayon, J. Am. Chem. Soc. 1982, 104, 6155.

2. S. W. Kaiser, R. B. Saillant, P. G. Rasmussen, J. Am. Chem.
    Soc. 1975, 97, 425.

    S. W. Kaiser, R. B. Saillant, W. M. Butler, P. G. Rasmussen,
    Inorg. Chem. 1976, 15, 2681; 1976, 15, 2688.

3. M. S. Haddad, D. M. Hendrickson, Inorg. Chem. 1978, 17,
    2622.

4. G. Kolks, C. R. Frihart, P. K. Coughlin, S. J. Lippard,
    Inorg. Chem. 1981, 20, 2933 and references contained
    therein.

POLYHEDRON REPORT NUMBER 4

THE REACTIONS OF NUCLEOPHILES WITH COMPLEXES OF CHELATING HETEROCYCLIC IMINES; A CRITICAL SURVEY

EDWIN C. CONSTABLE

University Chemical Laboratory, Lensfield Road, Cambridge CB2 1EW, England

CONTENTS

INTRODUCTION

Coordination chemistry has traditionally been concerned with the effects that ligands may have upon the properties of metal ions, but it has become increasingly evident that coordination to a metal also results in a profound modification of the reactivity of a ligand. This review is concerned with the reactivity of α,α'-diimine complexes with nucleophiles, and endeavours to interpret the available data and mechanistic proposals in a unified manner.

It is well established that electron-deficient aza-heterocycles may react with water to form "covalent hydrates" in which the oxygen atom of the water molecule is covalently bonded to a ring carbon atom of the heterocycle (Fig. 1).[1-3]
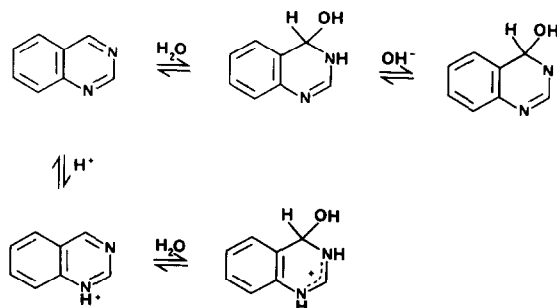
Fig. 1.

As shown in the figure, deprotonation of the covalent hydrate may occur, to give the conjugate base. Obviously, the position of equilibrium for the formation of the covalent hydrate will depend upon the particular heterocyclic system being studied, but, in general, protonation or quaternisation of a ring nitrogen atom increases the electron-deficiency, and results in a greater equilibrium concentration of the covalent hydrate. Other nucleophiles may also attack electron-deficient heterocycles, as, for example, in the formation of a neutral pseudobase in the reaction of hydroxide ion with the 1,5-naphthyridinium cation (Fig. 2).
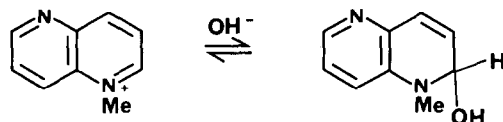
Fig. 2.

This is reminiscent of Meisenheimer complex formation between nucleophiles and other electron-deficient systems, such as aromatic nitro compounds (Fig. 3) and it is evident that covalent hydration, pseudobase formation and Meisenheimer complex formation are very closely related,[1-1/] although this close interrelation has only recently been explicitly stated.[10]
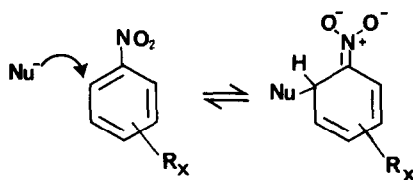
Fig. 3.

In recent years, Gillard and others have proposed that coordination of a heterocycle to a transition metal ion has an effect similar to quaternisation, and that such coordinated heterocycles are activated towards attack by nucleophiles.[11] These proposals have met with some criticism, and this review hopes to assess the evidence which has been presented for such activation. Much of the spectroscopic and structural evidence which has been reported relates to square-planar platinum complexes, and this review will accordingly discuss such systems in some detail. The current interest in α,α'-diimine complexes of transition metal ions as components of solar energy conversion systems has emphasised the need for an understanding of the reactions of such complexes, and the second part of the review will discuss the evidence presented for nucleophilic attack upon octahedral complexes of α,α'-diimines.

Throughout this review the following abbreviations will be used

bipy	2,2'-bipyridine
bipym	2,2'-bipyrimidine
Me$_2$bipy	dimethyl-2,2'-bipyridine
Me$_2$phen	dimethyl-1,10-phenanthroline
dmso	dimethyl sulphoxide
en	1,2-diaminoethane
5-nitrophen	5-nitro-1,10-phenanthroline
phen	1,10-phenanthroline
py	pyridine
pym	pyrimidine
terpy	2,2':6',2''-terpyridine
tpt	2,4,6-(2-pyridyl)-1,3,5-triazine

REACTIONS OF THE FREE LIGANDS

Aqueous or mixed aqueous solutions of bipy show a weak absorption band at 306 nm, which is associated with a strong fluorescence centred at 328 nm, and this has been interpreted in terms of covalent hydrate formation.[12] However, more recent studies by Kotlicka and Grabowski, have shown that this behaviour is due to the formation of an intensely fluorescent zinc complex, the metal ions being leached from the glassware.[13] No evidence has been presented for the covalent hydration of phen, and the suggestion that the well-known monohydrate might be a covalent hydrate, rather than a hydrogen-bonded system, appears to be unlikely.[11] 5-Nitrophen has been shown to undergo easy, complete reaction with nucleophiles to produce the corresponding Meisenheimer adducts, although it may be noted that these compounds are unstable, and undergo further, degradative, reactions.[14-16] It is of interest that bipy will reach with powerful nucleophiles, and treatment with alkyllithium reagents leads to the formation of 6- and 6,6'-alkyl substituted derivatives.[17-19]

A number of workers have investigated the reactions of cyclic diquaternary salts of bipy and phen with hydroxide, and the reported K_{eq} values are consistent with pseudobase formation.[16,20,21] It is perhaps relevant to note that the 1-methylphenanthrolinium cation shows no observable interaction with hydroxide ion at pH 14,[20] and that there is no evidence for the formation of pseudobases of the 1-methylpyridinium cation.[10]

Williams and his co-workers have reported the results of INDO molecular orbital calculations for a series of α,α'-diimines, and these confirm that the carbon atom adjacent to a ring-nitrogen is indeed electron-deficient, although they make no quantitative prediction of the ease of attack at this position.[22]

REACTIONS OF SQUARE-PLANAR COMPLEXES WITH NUCLEOPHILES

Substitution reactions of square-planar complexes

$$[ML_3X] + Y^- \longrightarrow [ML_3Y] + X^-.$$
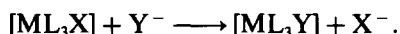
Reactions of this type have been widely investigated, and it is well established that the reaction proceeds via a five-coordinate species, which may be a true intermediate, or merely a transition state.[23,24] The rate expression for such a substitution reaction is of the form:

$$\rho = k_{obs}[ML_3X]$$

where

$$k_{obs} = k_s + k_y[Y].$$

This rate dependence indicates the operation of two parallel pathways, the pseudo first-order term arising from the formation of a five-coordinate solvo-complex:

$$[ML_3X] + S \xrightarrow{k_s} [ML_3XS] \xrightarrow{fast} products$$
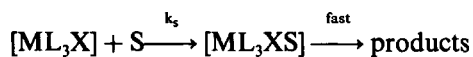
and the second order term from:

$$[ML_3X] + Y \xrightarrow{k_y} [ML_3XY] \xrightarrow{fast} products.$$

It is within this framework that any assessment of the addition of nucleophiles to square-planar complexes of platinum and palladium must be made, and we shall now discuss the evidence which has been presented for the reactions of such complexes.

Bis(2,2'-bipyridine)platinum(II)

Aqueous solutions of $[Pt(bipy)_2]^{2+}$ show rapid (initially) reversible changes in their electronic spectra upon the addition of hydroxide ions, changes which are associated with two isosbestic

points.[11,25-31] Similar changes in the electronic spectrum are observed on the addition of halide or pseudohalide ions to aqueous solutions or of methoxide to methanolic solutions of $[Pt(bipy)_2]^{2+}$,[30,31-33] and also upon the addition of hydroxide to aqueous solutions of $[PtL_2]^{2+}$ (L = 5,5'-Me$_2$bipy).[11,25,27,29-31] On treatment with nucleophiles, solutions of $(Pt(bipy)_2]^{2+}$ show a broadening of their ^{1}H NMR spectra, and a new feature is observed at $\sim 7 \delta$.[25,30] The early NMR studies leave a little to be desired, but more recent high-field investigations have produced spectra of excellent quality, and will be discussed shortly. Over longer periods of time, further, non-reversible changes in the electronic spectrum occur, with the formation of $[Pt(bipy)(Nu)_2]$.[26,30,31,34] Nord has investigated the kinetics of the reaction of $[Pt(bipy)_2]^{2+}$ with hydroxide, and quotes an equilibrium constant for the rapid reversible reaction with the nucleophile of $10^{4.8}$ M^{-1} at 298 K, and reports that the intermediate so produced has a half life of 480 hr.[26]

Gillard has interpreted all of these observations as evidence for the attack of the nucleophile on the coordinated ligand (Fig. 4).[25,27,28,33] In contrast, other workers have interpreted these results in terms of a five or six-coordinate intermediate (Figs. 5 and 6).[26,29-31]
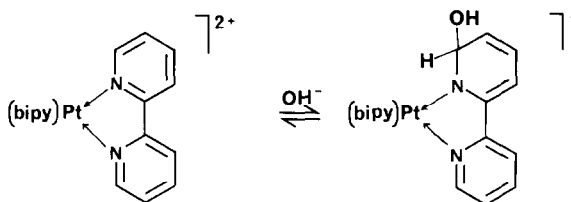
Fig. 4.
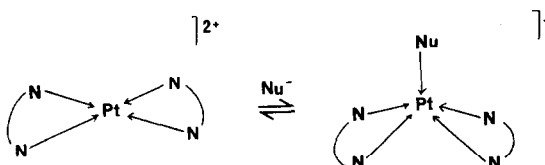
Fig. 5.
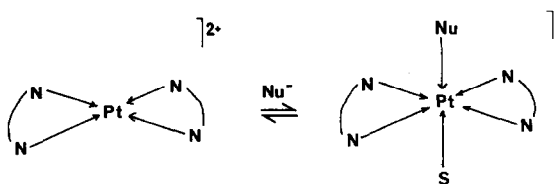
Fig. 6.

Gillard has dismissed the possibility of formation of a five-coordinate intermediate, and states that neither chloride nor cyanide ions produce changes in the electronic or ^{1}H NMR spectra similar to those produced by hydroxide. It is now clear that halide and pseudohalide ions do produce changes in the electronic spectrum,[30,32,35] and as early as 1964 Livingstone and Wheelahan had demonstrated the formation of 1:1 complexes of halide with $[Pt(bipy)_2]^{2+}$ in nitromethane or nitrobenzene solution, and had also isolated compounds which were throught to possess a five or six-coordinate structure.[32] Whilst it is possible that these 1:1 complexes with halide are of the type proposed by Gillard for nother nucleophiles, it is hard to envisage such a structure persisting in solution, and a five-coordinate structure appears to be the more likely. Neither $[Pt(bipy)(py)_2]^{2+}$ nor $[Pt(py)_4]^{2+}$ show similar changes in their electronic spectra upon the addition of hydroxide ion,

and Nord has proposed that it is distortion from square-planar geometry which is responsible for the tendency of the *bis*(bipy) complex to adopt a five-coordinate geometry.[26] Such distortions were predicted by McKenzie and others[36,37] and recent crystallographic studies have confirmed that the two ligands are distorted from coplanarity in the $[Pt(bipy)_2]^{2+}$ cations.[38,39] This distortion arises as a result of the Van der Waals interactions between H_6 of the ligands, which are brought into close proximity in the complex. Whilst the strain introduced in the complex satisfactorily explains a tendency to form five-coordinate species, it would, of course, also favour the attack of nucleophiles at C_6, with the concommittant release of strain in the formation of an sp^3 carbon.

The ^1H NMR and ^{13}C NMR spectra of aqueous solutions of $[Pt(bipy)_2]^{2+}$ show that the four pyridyl rings are all equivalent on the NMR time-scale, but that they become inequivalent on the addition of hydroxide.[29] The low-field spectra published by Gillard do not lend themselves to a detailed analysis of the spectral changes produced by nucleophiles. The later studies, however, show clearly that the intermediate is formed after the addition of only one hydroxide ion, and the ^1H and ^{13}C NMR spectra reveal that the symmetry of the cation alters so as to give two pairs of magnetically equivalent pyridyl rings. Unless the hydroxide group undergoes a fast exchange between two of the four pyridyl rings, these results appear to exclude the possibility of attack at the ligand. Such an exchange process appears to be very unlikely, and it is proposed that a fluxional six-coordinate system (Fig. 7) is formed. A trigonal bipyramidal structure may also be consistent
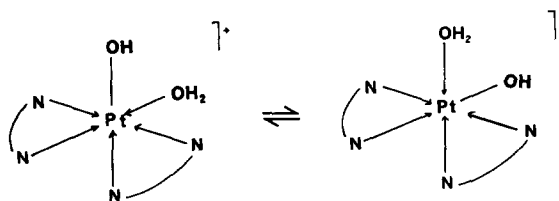
Fig. 7.

with the NMR studies, and no final conclusion as to the nature of the solution species may yet be drawn, although it is clear that attack is at the metal and not at the ligand. The high-field resonance at $\sim 7\,\delta$, which was assigned by Gillard to the tetrahedral C–H, is now seen to be due to $H_{5'}$, which is in the deshielding region above the plane of a pyridyl ring. Similar effects are observed in the ^1H NMR spectrum of $[Ru(bipy)_3]^{2+}$.[30]

Bis(1,10-*phenanthroline*)*platinum*(*II*)

Aqueous solutions of $[Pt(phen)_2]^{2+}$ show changes in their electronic and ^1H NMR spectra upon the addition of hydroxide similar to those described for $[Pt(bipy)_2]^{2+}$.[27] Gillard has demonstrated that these spectral changes parallel those observed for the bipy system, and also described the formation of dark-coloured solids in the reaction of $[Pt(phen)_2]^{2+}$ with hydroxide. These compounds were formulated as $[Pt(phen)(phen·OH)]X$ ($X = Cl$ or Br) on the basis of their electronic, vibrational and ^1H NMR spectra.[27] More recently, Wernberg and Hazell demonstrated the formation of a 1:1 complex between cyanide ion and $[Pt(phen)_2]^{2+}$ by conductiometric methods, and also showed that the spectroscopic changes in the $[Pt(phen)_2]^{2+}/[CN]^-$ system parallel those observed for the $[Pt(phen)_2]^{2+}/[OH]^-$ and $[Pt(phen)_2]^{2+}/[SH]^-$ systems. The ^{13}C NMR spectrum of the intermediate clearly shows that the cyanide ion is directly bonded to the metal, with satellites due to $^1J_{195_{Pt}-13_C}$ of 1516 Hz (*cf.* 1029 Hz in $[Pt(CN)_4]^{2-}$), and also by the absence of coupling between the ring carbon atoms and the cyanide carbon atom when ^{13}C enriched cyanide was used. On the basis of these observations it was proposed that the cyanide ion was not bonded to the ligand, but was directly bonded to the metal to give a five-coordinate species of the type $[Pt(phen)_2(CN)]^+$. A solid product, formulated as $[Pt(phen)_2(CN)][NO_3]$ was isolated, and aqueous solutions of this solid exhibited electronic spectra identical to those of 1:1 mixtures of $[Pt(phen)_2]^{2+}$ and cyanide, and it was thus concluded that the material truly represented the solid phase corresponding to the solution intermediate. A single crystal structural analysis of this compound has shown definitively that, in the solid state, the compound is a five-coordinate platinum(II)

complex in which the cyanide is coordinated to the metal, and is not bound to the ligand (Fig. 8).[40]
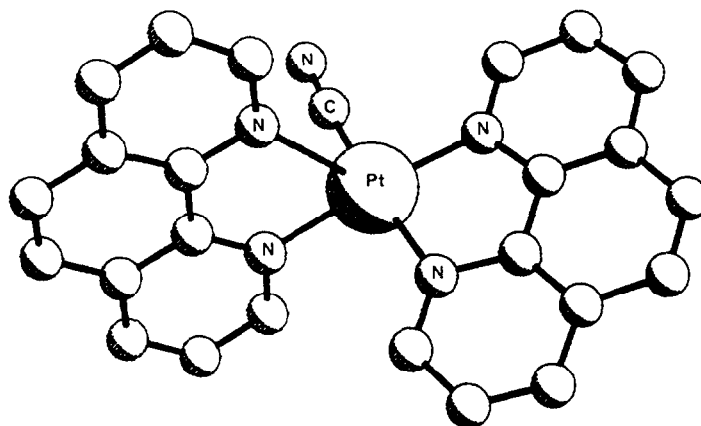
Fig. 8.

The results described above establish unequivocally the formation of a five-coordinate complex in the reaction of $[Pt(phen)_2]^{2+}$ with cyanide, a structure which persists both in the solid state and in solution. It is thought that the formation of the five-coordinate intermediate is favoured by the interactions between H_2 and H_9 of the ligands, and support for this comes from a recently reported crystal structure of $[Pt(phen)_2]Cl_2 \cdot 3H_2O$, which clearly demonstrates a tetrahedral distortion of the PtN_4 unit, and a marked distortion from planarity of the phen ligand.[41] The H_2–$H_{2'}$ distance was shown to be only 1.95 Å.

The similarity in the spectroscopic changes observed in the reactions of $[Pt(bipy)_2]^{2+}$ and $[Pt(phen)_2]^{2+}$ with cyanide and other nucleophiles very strongly suggests that similar reaction pathways are followed, and that attack occurs at the metal, and not at the ligand.

The reaction of hydroxide ion with $[PtL_2]^{2+}$ (L = 5-nitrophen) in dmso has been investigated, but the published NMR spectra are of low quality, and it is not possible to determine the site of attack.[33]

Other platinum(II) complexes

It has been reported that solutions of $[PtL(CN)_2]$ (L = bipy) exhibit temperature-dependent ^1H NMR spectra. At 100° the (red) solution exhibited the spectrum expected from a $[PtLX_2]$ system, but on cooling to 25° the (yellow) solution gave a spectrum with a new feature at 6.5 δ.[42] Attempts to repeat this work have been unsuccessful,[30,31,43] and it is now evident that the earlier reports relied upon a misinterpretation of the spectrum. Specifically, the spectrum reported by Gillard appears to have a narrow sweep width, and the resonances due to $H_{6,6'}$ are outside the spectrometer window, and hence missing from, or folded into, the spectrum. As a result of this the spectrum is totally misassigned.

It is well-known that the complexes $[PtLX_2]$ (L = bipy or phen; X = halide) may exist in dimorphic forms in the solid state,[28,4–48] but it has been demonstrated crystallographically that these only differ in the crystal packing, and do not possess significant halide–ligand interactions.[47,48] A number of groups have investigated the substitution reactions of $[Pt(bipy)Cl_2]$ and have shown that the kinetics follow those expected for a square-planar complex: there has been no suggestion of attack of the incoming nucleophile upon the bipy ligand.[49–52]

The complex $[PtCl(PEt_3)_2 \text{ (phen)}] [BF_4]$ is apparently five-coordinate, but a crystal structural analysis has demonstrated that, in the solid state, the phenanthroline is monodentate (Pt–N$_1$, 2.84 Å; Pt–N$_2$, 2.24 Å).[53] This is one of the few examples of a monodentate diimine ligand, and raises the question of such structures being responsible for some of the anomalous properties of diimine complexes. The complexes $[PtL(CN)_2] \cdot xH_2O$, $[PtLCl_2] \cdot yH_2O$ and $[PtLCl_2] \cdot dmf$ (L = bipym; x = 1 or 1.5; y = 0 or 0.5) have been described, but there is no change in the bipym frequencies in the vibrational spectra of the hydrated forms, and it is likely that these compounds have structures analogous to the corresponding bipy and phen complexes.[54]

The reaction of [Pt(terpy)Cl]$^+$ with nucleophiles has been investigated, and the rate equations shown to be of the form:

$$k_{obs} = k_1 + k_2[Y]$$

as expected for attack at either the metal or the ligand. The activation parameters are consistent with an associative mechanism, and the changes in the electronic spectrum of [Pt(terpy)Cl]$^+$ on the addition of hydroxide parallel those observed with [Pt(phen)$_2$]$^{2+}$.[55] These observations suggest that a five-coordinate intermediate is involved, although Mureinik has proposed that chloride ion attacks C$_6$ of the ligand, with concommittant degradation of a pyridyl ring.[56] In particular the reported reaction:

$$[Pt(terpy)Cl]^+ \xrightarrow[\text{(ii) [SCN]}^-]{\text{(i) Ag}^+} [Pt(bipy)(SCN)_2]$$
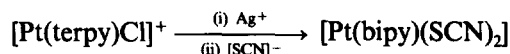
appears to be rather unlikely, and deserves reinvestigation.[56]

Palladium complexes

Gillard has investigated a number of palladium(II) complexes of 8-hydroxyquinoline and 2,9-Me$_2$phen, and concludes that there is no evidence for covalent hydration in complexes of these types.[57] Crystal structural analyses of the complexes [Pd(phen)$_2$][ClO$_4$]$_2$[58] and [Pd(bipy)$_2$](NO$_3$)$_2$·H$_2$O[59, 60] have confirmed that the diimine ligands are considerably distorted from the idealised square-planar geometry. Power et al. have produced a considerable amount of evidence for the formation of five-coordinate complexes of palladium with substituted phenanthrolines.[61–63] Livingstone and Wheelahan have proposed that five or six-coordinate complexes are formed in the reaction of [Pd(bipy)$_2$]$^{2+}$ have halide.[32]

The complex [Pd(terpy)Cl]Cl·2H$_2$O is a 1:1 electrolyte, and a crystal structural analysis has shown that the palladium atom is displaced from the N_3Cl plane towards a nitrogen atom of a neighbouring cation, to give a pseudo-pyramidal structure (Pd-N', 3.13 Å).[64]

REACTIONS OF OCTAHEDRAL COMPLEXES WITH NUCLEOPHILES

Substitution reactions of octahedral complexes

Octahedral tris(2,2'-bipyridine) complexes of transition metals may undergo substitution reactions via mechanisms which are basically associative or basically dissociative (Fig. 9).[23] It is commonly thought that a dissociative mechanism, involving a monodentate diimine, cannot apply to phen complexes, although the crystallographic results for [PtCl(PEt$_3$)$_2$(phen)][BF$_4$] suggest that this conclusion may be premature.[53] Gillard has proposed that covalent hydrates, and the related pseudo-bases, of the coordinated diimine play a critical role in the reactions of these complexes, and has presented a considerable amount of evidence to support this claim.[11,25,65,66] It is apparent that this proposal has not met with universal accpetance, and the present, unsatisfactory, situation is highlighted in a number of recent reviews.[67–73]

In the following sections we shall discuss the evidence which has been presented for the attack of nucleophiles on coordinated diimines in octahedral transition metal complexes.

Chromium

The photochemistry of chromium(III) diimine complexes has attracted considerable attention, and the enhanced reactivity of the photochemically excited states has led to a number of kinetic investigations of these systems. Much of the available data has been reviewed recently by Serpone,[74] who has a conducted intensive studies of the ground-state and photo-assisted aquation of [CrL$_3$]$^{3+}$ (L = phen or bipy). The reader is referred to this review for an in-depth discussion of these systems, and only the mechanistic conclusions are discussed in this section. A consideration of the lifetimes of the excited doublet states $^2T_1/^2E$ led Henry and Serpone to propose a model for octahedral tris diimine complexes in which solvent molecules are sited in "pockets" between the polypyridyl ligands.[75–77] This model is closely related to that proposed for the racemization and aquation of [Fe(phen)$_3$]$^{2+}$ (vide infra), and Serpone regards it as a useful general model for the behaviour of transition metal diimine complexes. Supportive evidence comes from an NMR
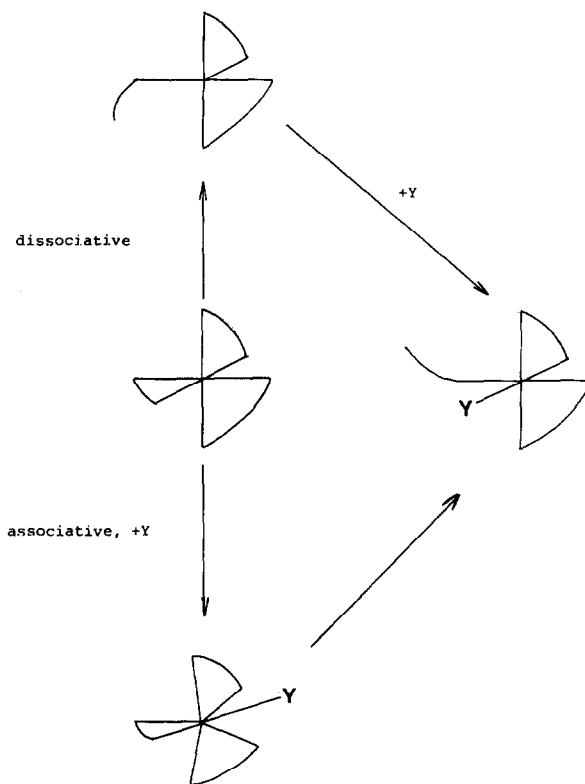
Fig. 9.

investigation of $[Cr(phen)_3]^{2+}$, which revealed that the water molecules were up to 2 Å within the inner-sphere,[78] and from the crystal structure of $[Cr(terpy)_2][ClO_4]_3 \cdot H_2O$, in which the perchlorate counter-ions are observed to be deep within the inter-ligand pockets (although it must be noted that the water molecule is *not* within such a site, but is hydrogen-bonded to two perchlorate oxygen atoms).[79] The kinetics observed in the ground-state and excited-state base hydrolysis of $[CrL_3]^{3+}$ are consistent with either a Gillard pseudo-base mechanism, or with the formation of a seven-coordinate intermediate. It is thought that the $^2E/^2T_1$ state is involved in the photo-aquation of $[CrL_3]^{2+}$, and this might be expected to favour attack at the metal, rather than at the ligand. It is known that the ^2E state of *trans*-$[Cr(en)_2(NCS)_2]^+$ reacts directly with hydroxide, but this does not necessarily involve the formation of a seven-coordinate intermediate. The important point about the Gillard mechanism is that the covalent hydrate is invoked as an intermediate, and thus studies of the stable crystal forms give little direct evidence as to the location of water molecules in the transition state. Indeed, in spatial terms the difference between a water molecule in an inter-ligand pocket and one involved in a bonding interaction with a ligand is minimal, although the potential energy terms will be very different indeed. In conclusion, the majority of the kinetic studies on chromium(III) diimine complexes are interpreted by Serpone in in terms of the formation of a seven-coordinate intermediate, and not of a covalent hydrate, although, in this reviewer's opinion, it is not yet possible definitively to preclude the Gillard mechanism.

Molybdenum

This section is concerned with the reactions of $[Mo(CO)_4L]$ (L = diimine) although the majority of the studies described have also considered the corresponding chromium and tungsten compounds, which are also discussed here. The complexes $[M(CO)_4L]$ (M = Cr, Mo or W; L = diimine) are readily prepared by the thermal or photochemical reaction of $[M(CO)_6]$ with L. The reduction of $[M(CO)_4L]$ by metallic sodium leads, initially, to the formation of $[M(CO)_4L]^-$, which has been shown by esr spectroscopy to have the electron localised on the diimine ligand radical.[80,81] This indicates that the ligand π^* orbitals are at lower energy than the metal d orbitals, but does not necessarily imply that the kinetic site of attack by a nucleophile is at the ligand. Wrighton and

Moore have investigated the photosubstitution reaction:

$$[W(CO)_4L] \xrightarrow[X]{h\nu} [W(CO)_3XL]$$
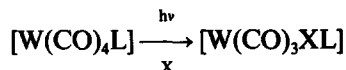
with irradiation at the lowest metal–ligand charge transfer (MLCT) frequency.[82] The reaction proceeds with the formation of a single isosbestic point, and the rates for bipy and phen complexes are similar, suggesting that the intermediacy of a monodentate diimine via the chelate ring-opening mechanism is not an important factor in W–C labilisation. A nucleophile may attack $[M(CO)_4L]$ at the metal, the diimine, or the carbonyl group, and Dobson has reviewed the reactions of nucleophiles with octahedral transition metal carbonyls.[83] Angelici has investigated the reactions of $[M(CO)_4L]$ with a wide range of phosphines nad phosphites,[84–88] and has shown that with M = Cr the rate expression is of the form:

$$\rho = k_1[\text{complex}]$$

whilst for the molybdenum and tungsten complexes a second-order term becomes important, and the expression becomes:

$$\rho = (k_1 + k_2[\text{nucleophile}])[\text{complex}].$$

although $\log k_1$ correlates well with the pK_a of the ligand, the correlation with $\log k_2$ is not good, and it is not clear whether the k_2 term corresponds to attack at the ligands or the metal. It is tempting to propose that attack at the metal will be more facile with the larger molybdenum and tungsten complexes, and this might explain the absence of the k_2 term for the chromium complex. The reaction:

$$[M(CO)_3(PR_3)L] + PR_3' \longrightarrow [M(CO)_2(PR_3)(PR_3')L] + CO$$
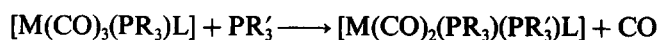
has also been investigated, and shown to obey the rate expression:

$$\rho = (k_1 + k_2[PR_3'])[\text{complex}]$$

for all three metals, although the k_2 term is only important for 5-nitrophen complexes,[88] and even here it is a very minor contribution to the overall rate. Burgess has shown that the lowest energy MLCT bands are markedly solvatochromic, and that a linear relationship exists between the frequency of the MLCT band and the solvent parameter E_T.[89,90] Connor has shown that the ^1H NMR spectra of $[Mo(CO)_4L]$ species are also solvent-dependent.[91]

Burgess has also investigated the reaction of $[Mo(CO)_4(5\text{-nitrophen})]$ with cyanide, and shown that a two-step reaction occurs, with the first step being a rapid addition of cyanide. This almost certainly corresponds to the formation of the Meisenheimer-type adduct, and it is proposed that the second step corresponds to the transfer of the cyanide group from the ligand to the metal. It is not clear, however, whether the product is $[Mo(CO)_3(CN)(5\text{-nitrophen})]$, or whether the second step is some further reaction at the ligand.[92] This complex also reacts rapidly with $[OH]^-[OMe]^-$, and sodium diethyldithiocarbamate in a similar reaction.[94] The reaction of $[Mo(CO)_4(bipy)]$ with cyanide obeys the rate law:

$$\rho = (k_1 + k_2[CN])[\text{complex}]$$

in dmso or methanol, and at room temperature the k_2 term is dominant. Similar kinetics are obeyed for the reaction of the phen complexes with cyanide, and for both types of complex with a range of other nucleophiles. Burgess believes that the desolvation of the cyanide ion is an important factor in reactions of this type, and has investigated the activation volumes for the reaction of $[Mo(CO)_4(bipy)]$ with cyanide in methanol and dmso:

$$\Delta V^{\neq}(\text{MeOH}) \simeq +4\,\text{cm}^3\,\text{mol}^{-1}$$

$$\Delta V^{\neq}(\text{dmso}) \simeq -9\,\text{cm}^3\,\text{mol}^{-1}.$$

The cyanide ion is less solvated in dmso than methanol, resulting in the positive contribution to $\Delta V^{\neq}$ in methanol.[93,94]

Iron

The reactions of iron diimine complexes have been the subject of an enormous amount of research over the past 30 years, and there seems to be little doubt that these complexes show specific interactions, of some type, with nucleophiles. The kinetic studies of Gillard and Burgess are notable, and have established the common occurrence of rate expressions of the type:

$$\rho = (k_1 + k_2[\text{nucleophile}])[\text{FeL}_3^{n+}]$$

although mechanistic studies cannot establish the nature of the transition state or intermediate involved in the second-order term. The reactions of the diimine complexes of iron are the subject of two forthcoming reviews, and it is not proposed to discuss the matter in any depth herein.[95,96] Suffice it to say that the lability of these complexes creates added complications in their investigation, and that there are a large number of apparently contradictory reports in the literature. The kinetic stability of the ruthenium(II) complexes renders them more suitable for investigation, and these are discussed in detail in the next section.

Ruthenium and osmium

There is little doubt that $[\text{Ru(5-nitrophen)}_3]^{2+}$ salts undergo a rapid, quantitative reaction with nucleophiles such as hydroxide, alkoxides and cyanide to produce 1:1 adducts, although there is some controversy over the initial site of attack.[14,15,97-101] A recent high-field NMR study indicates that the thermodynamic product of the reaction of $[\text{Ru(5-nitrophen)}_3]^{2+}$ with $[\text{OMe}]^-$ dmso-d_6 involves attack at C_6, although initial kinetically controlled attack at C_2 or C_9 is not precluded.[14] The reaction of the complex ions $[\text{Ru(5-nitrophen)}_x(\text{bipy})_{3-x}]^{2+}$ with $[\text{CD}_2\text{NO}_2]^-$ (generated *in situ* from CD_3NO_2 and $\text{C}_5\text{D}_5\text{N}$) has been investigated, and attack shown to occur at C_6 of the 5-nitrophen in each case.[102] It is notable that there is no evidence for attack at the coordinated bipy in the above systems, although this might be expected to be competitive with a kinetically controlled attack at C_2 and C_9 of the 5-nitrophen.

The complex ion $[\text{Ru(bipy)}_2(\text{py})_2]^{2+}$ shows reversible changes in its electronic and ^{1}H NMR spectra upon the addition of alkali, and Gillard has associated these changes with the attack of hydroxide upon the ligand.[103] Similar changes are observed in the spectra of a series of mixed complexes with substituted pyridines and 2,2'-bipyridines on treatment with a range of nucleophiles. A high-field (400 MHz) NMR study has confirmed that changes do occur in the spectrum of $[\text{Ru(bipy)}_2(\text{py})_2]^{2+}$ upon the addition of alkali, but these are not associated with the appearence of a new feature at $\sim 6.5\,\delta$.[104] It is possible that these changes are associated with a specific outer-sphere interaction between the nucleophile and the complex, rather than with covalent hydration, and it si attractive to postulate a mechanism in which the nucleophile enters a "cleft" between the two rings of a bipy, and is associated with $H_{3,3'}$. A 400 MHz ^{1}H NMR study of a series of $[\text{RuL}_3]^{2+}$ species has demonstrated that the T_1 relaxation time of $H_{3,3'}$ is abnormally fast, an observation in accord with the Van der Waals interactions between these two protons.[105] The ^{1}H NMR spectra of tris(diimine)ruthenium(II) complexes are solvatochromic,[104] and it is of interest to note that Connor has demonstrated similar behaviour in the electronic and NMR spectra of $[\text{Mo(CO)}_4\text{L}]$ (L = diimine) species.[91] Bosnich and Dwyer investigated the reaction of *cis*-$[\text{Ru(phen)}_2(\text{py})_2]^{2+}$ with a number of nucleophiles, and demonstrated that first-order kinetics were obeyed, depending only upon [complex].[106,107] These observations were interpreted in terms of an unimolecular dissociative mechanism, proceeding via a solventato or five-coordinate intermiediate. In the case of azide or nitrite nucleophiles, second-order terms were involved and a π-bonding interaction of the anion with the transition-state was postulated. For those nucleophiles exhibiting first-order kinetics (Br, Cl, I or SCN] nucleophilic attack at the ligand would appear to be precluded, although the kinetics might deserve reinvestigation.

The complexes $[\text{RuL}_3][\text{CN}]_2 \cdot 6\text{H}_2\text{O}$ (L = phen or bipy) show the expected CN stretching frequencies at $\sim 2080\,\text{cm}^{-1}$, but also a second frequency at $2170\,\text{cm}^{-1}$, characteristic of a nitrile.[108] Schilt also investigated these cyanide complexes and demonstrated the protonation of

the cyanide ligand in complexes of the type $[Ru(bipy)_2(CNH)_2][ClO_4]_2$.[109] This conclusion has been confirmed by Demas et al.[110,111] It is relevant to note that the IR spectrum of anhydrous $[Ru(bipy)_2(CN)_2]$ is dependent on the method of preparation, and that the material recrystallised from chloroform exhibits a band at $2070\ cm^{-1}$.[112] It is thus evident that these cyanide complexes do exhibit unusual properties, but it is not yet certain whether these are due to an unusual interaction with the water molecules, the presence of $[RuL_2(CN)_2]$ in samples of "$[RuL_3][CN]_2$" or of a further impurity not yet characterised.

The unusual pH dependence of the redox properties of $[Ru(terpy)_2]^{2+}$ and $[RuL_3]^{2+}$ (L = phen or bipy) were interpreted by Gillard in terms of covalent hydration, and this would appear to be a satisfactory explanation[11,113] although it is possible that a strong interaction between $H_{3,3'}$ and either hydroxide or water may be involved in these complexes. Creutz and Sutin suggested that the evolution of dioxygen from alkaline aqueous $[Ru(bipy)_3]^{3+}$ solutions involved nucleophilic attack upon C_4 of the ligand,[114] although this suggestion no longer appears to be likely.[115,116] The photochemistry of $[RuL_3]^{n+}$ has been widely investigated in the past few years, and this area has been recently reviewed.[116] It is apparent that photosubstitution reactions occur, but it is thought that these proceed through achiral five or six-coordinate intermediates, arising from a dissoviative process involving a monodentate diimine. The formation of ortho-metallated species in these photoreactions does not appear to have been considered.

The treatment of $[Ru(bipy)_3]Cl_2$ with $[CD_3O]^-$ in $CD_3OD/dmso$-d_6 results in a very specific deuterium exchange reaction of $H_{3,3'}$, and this was initially interpreted in terms of nucleophilic attack at C_4, followed by deprotonation of the 3,4-dihydropyridine.[117] It is now thought that the reaction proceeds via deprotonation at C_3 to give an anion which can rearrange to give an intermediate metallated species (Fig. 10). Gillard has reported a number of puzzling observations
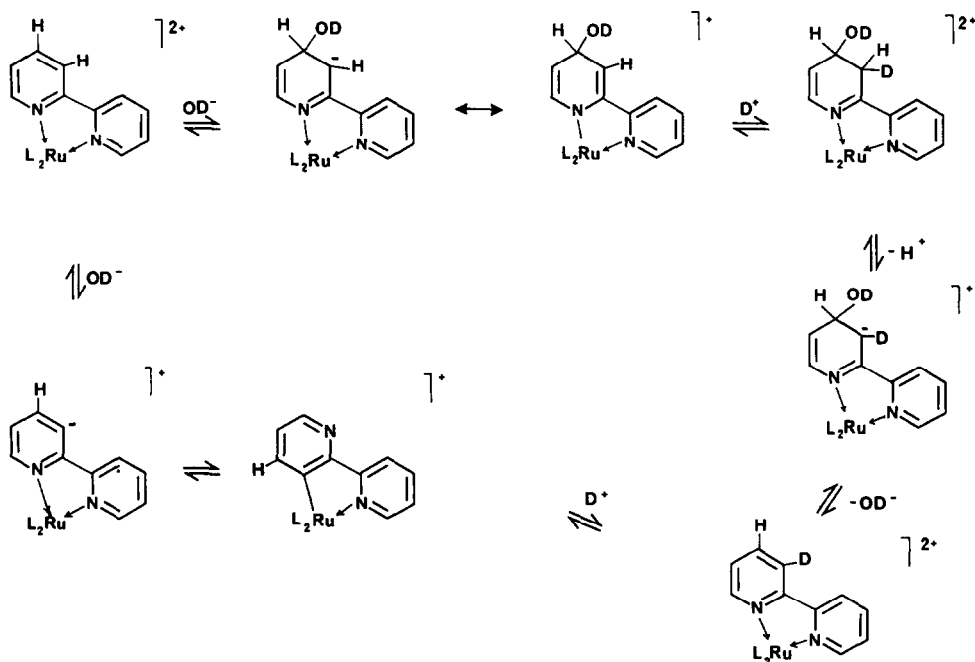
Fig. 10.

on the $[RuL_3]^{3+}$ system, which are consistent with the formation of covalently hydrated species,[118] but the recent results of Serpone, together with those discussed above raise the possibility that metallated species may also be involved.

$[Ru(bipym)_3]^{2+}$ reacts with hydroxide to give a product formulated as $[Ru(bipym)_2(pym)(OH)]^+$, with the concomitant formation of one mole of formate ion.[119] Similar results are obtained with azide or cyanide as the nucleophile, and it is proposed that the key step involves nucleophilic attack at C_2 of the coordinated ligand. The evidence presented for this transformation is very convincing, although the precise mechanistic details are not yet clear.

Although it is not known whether 2,2'-bipyrimidine is covalently hydrated in aqueous acidic solution, it is relevant to note that 1-methylpyrimidinium salts are converted to 1-methylpyrimidin-2(1H)-one on treatment with hydroxide,[120] and that a member of pyrimidines bearing electron-withdrawing substituents in the 5-position are 100% covalently hydrated in aqueous acidic conditions.[121]

[Ru(tpt)$_2$]$^{2+}$ reacts reversibly with hydroxide to produce a stable intermediate, in which it is proposed that the nucleophile has added to the triazine ring.[122,123] The ^{1}H NMR spectrum of the complex shows that the addition of hydroxide ion results in a loss of molecular symmetry, with the two coordinated pyridyl residues becoming non-equivalent, although no new signal at $\sim 6.5\ \delta$ was observed. This eliminates the possibility of attack at a pyridyl ligand rather than the triazine. In concentrated alkali, free tpt is precipitated from the solution. Although 1,3,5-triazine is very rapidly hydrolysed in water, the 2,4,6-triphenyl derivative requires vigorous conditions, and there is little evidence for the covalent hydration of free 2,4,6-triaryltriazines.[124,125] These observations are in marked contrast to those on the copper(II) complexes of tpt, in which reaction with hydroxide leads to hydrolysis of the triazine ring of the ligand.[126,127]

In general, osmium(II) diimine complexes resemble those of the corresponding ruthenium(II) species, and, where they have been investigated, show similar behaviour on treatment with nucleophiles. Nord has proposed a specific interaction of [Os(phen)$_3$]$^{2+}$ with water in its oxidation in aqueous conditions.[128] Although bipy is expected to metallate in the 3-position in mono-nuclear complexes, other possibilities occur in polynuclear species, and Deeming has reported the formation of the novel *triangulo* triosmium cluster [Os$_3$(CO)$_{10}$H(C$_{10}$H$_7$N$_2$)] (see Fig. 11) in the reaction of [Os$_3$(CO)$_{10}$(cycooctene)] with bipy.[129]
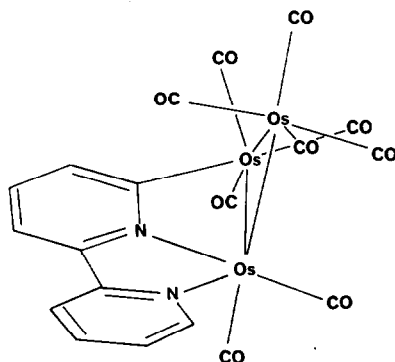
Fig. 11.

As a postscript, it may be added that Tobe has investigated the methoxydechlorination reaction of free and coordinated 5-chloro-1,10-phenanthroline in dmso/MeOH, and has demonstrated a considerable rate enhancement with the ruthenium(II), osmium(II) and nickel(II) complexes.[130,131] Although an S$_N$Ar intermediate of the type shown in Fig. 12 may be involved,
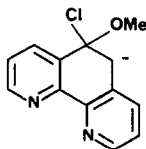
Fig. 12.

it is interesting to note that quaternisation of the 5-chloro-1,10-phenanthroline prevents the methoxydechlorination reaction from occurring. On the basis of NMR studies the authors concluded that pseudobase formation (at C$_2$ or C$_9$) is not involved in these reactions of the complexes, and that the pseudobases or covalent hydrates are present to an extent of less than 10% in the reaction mixture.

Cobalt and iridium

In this section we shall concentrate upon the reactions of the less labile iridium complexes, species for which a considerable amount of structural and kinetic data has been amassed. However, Gillard has shown that $[Co(5\text{-nitrophen})_3]^{2+}$ undergoes reversible reaction with hydroxide to form, presumably, the Meisenheimer adduct,[132] and that $[Co(tpy)(OH)_3]^-$ gives a pseudobase on treatment with hydroxide.[133] Aqueous solutions of $[Co(tpt)_2]^{2+}$ are stable for long periods of time,[134,135-137] but treatment with hydroxide leads to rapid pseudobase formation, followed by an irreversible loss of tpt to form $[Co(tpt)(OH)_3]^-$.[134] The crystal structure of the complex $[Co_2Cl_4(tpt)(H_2O)]\cdot H_2O$ has been reported (Fig. 13) and it is apparent that the uncoordinated water
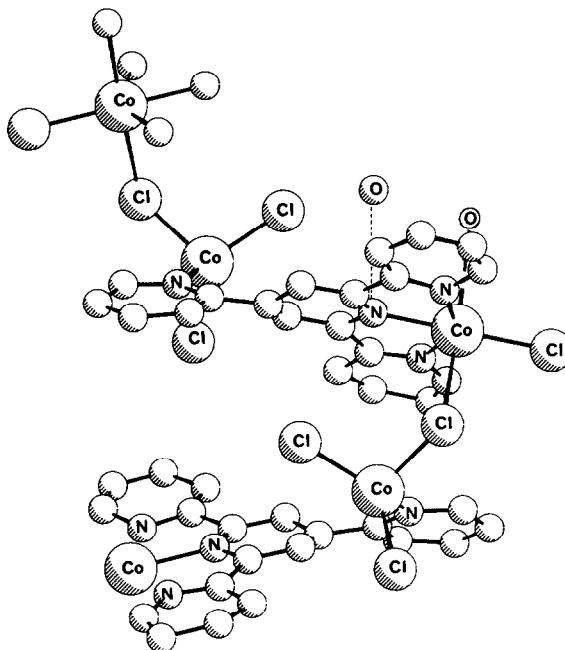
Fig. 13.

molecule is located above the C=N bond of the triazine ring, although it does not appear to be present as a covalent hydrate.[138] This molecule may be regarded as a model for the approach of water to a coordinate heterocycle, and provides strong evidence for interactions of the type proposed by Gillard. A number of cobalt (II) triazine complexes have been described in which a water molecule is strongly associated with the ligand, and it is likely that these compounds are covalently hydrated, although there are no structural data yet available.[139]

Tris(2,2'-bipyridine)iridium (III)

The $[Ir(bipy)_3]^{3+}$ cation has had a chequered and controversial history, and has been the subject of a number of novel structural proposals. As it is one of the few examples of a diimine complex for which a single crystal structural analysis of a proposed covalent hydrate is available, the system will be discussed in some detail. Martin and Waind first reported a complex analysing as $[Ir(bipy)_3][ClO_4]_3$ in 1958, as a product of the reaction of $K_2[IrCl_6]$ with bipy,[140] and later workers confirmed that a yellow solid of this apparent formulation was indeed formed.[141] DeSimone and Drago[142] and Gillard and Heaton[66] independently demonstrated that the products of this reaction were $[Ir(bipy)_2Cl_2]^+$ salts, and that the displacement of the two remaining chloride ligands by bipy could not be easily achieved. Gillard also suggested that the phen ligands in $[Ir(phen)_2Cl_2]^+$ might be covalently hydrated.[66] The ^1H NMR spectrum of the yellow complex showed conclusively that it was a *bis*-bipyridine system, and DeSimone and Drago proposed a *cis*-$[Ir(bipy)_2Cl_2]^+$ structure.[142] Throughout the early literature there are references to the formation of a less soluble orange compound in the preparation of $[Ir(bipy)_2Cl_2]^+$ salts, a species which has been variously formulated as a trace quantity of *tris*-complex or an aquated or photoaquated

derivative. An early report concerning the luminescence of solutions of "[Ir(bipy)$_3$]$^{3+}$" almost certainly refers to [Ir(bipy)$_2$Cl$_2$]Cl.[143] In 1974, Flynn and Demas reported the preparation of [Ir(bipy)$_3$]$^{3+}$ under halide-free conditions, and demonstrated that the ^{13}C and ^{1}H NMR spectra were fully consistent with a complex of D_3 symmetry.[144] The ^{13}C NMR spectrum showed five well-resolved resonances and the ^{1}H NMR spectrum resembled those of other [M(bipy)$_3$]$^{n+}$ complexes. It was later shown that a complex of the type {Ir(bipy)$_3$Cl$_3$(H$_2$O)$_4$} could be obtained from the reaction of IrCl$_3$ with bipy in glycerol at 180°, followed by treatment with methanolic sodium methoxide and ion-exchange chromatography.[145] These authors demonstrated that the absorption spectrum of this complex shows bands at 250, 305 and 315 nm, characteristic of a coordinated bipy ligand, and also weak absorption shoulders at 360, 448 and 470 nm, the feature at 470 nm disappearing on treatment with base. In the IR spectrum the complex exhibits an N–H stretching frequency at 2650 cm^{-1}, and, in addition to the bands expected from coordinated bipy ligands, shows absorptions at 1311, 1292, 1275 and 1246 cm^{-1}, unique in *tris*-bipyridine complexes.[145,146] Treatment with hydroxide leads to the formation of {Ir(bipy)$_3$(OH)Cl$_2$} (pK ~ 3.0 ± 0.1); no protonation to {Ir(bipy)$_3$(H$_2$O)Cl$_3$H}$^{4+}$ was observed. The analyses for total halide and ionic halide were identical, thus eliminating any formulations in which a chloride ion is coordinated to the metal. It was proposed that the complex should be formulated [Ir(bipy)$_2$(H$_2$O)(bipy′)]Cl$_3$·3H$_2$O, in which bipy′ represents a *monodentate* 2,2′-bipyridine.[145] A covalently hydrated structure was rejected on the grounds that acidic and alkaline solutions of authentic [Ir(bipy)$_3$]$^{3+}$ possessed identical electronic absorption spectra.[145] The deprotonated species was formulated as [Ir(bipy)$_2$(OH)(bipy′)]$^{2+}$, and it was suggested that equilibria of the type shown in Figs. 14 and 15, could occur.[145,147] The monodentate bipy′ was thought to be
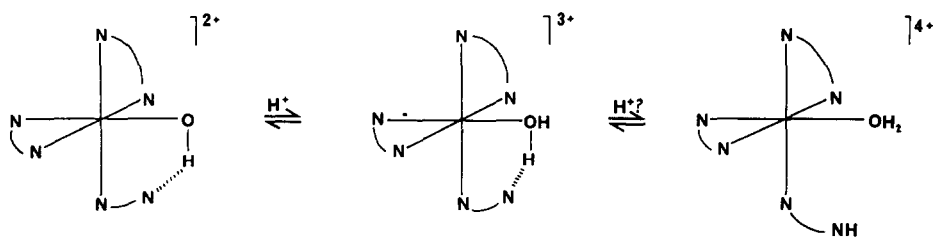
Fig. 14.
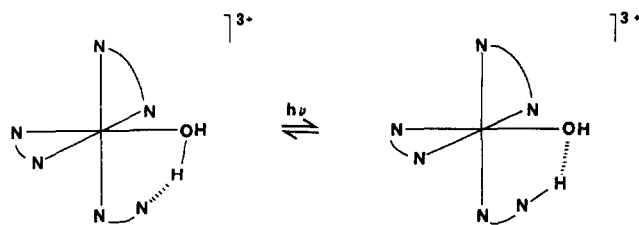
Fig. 15.

hydrogen-bonded to the coordinated water molecule, this possibly accounting for the N–H stretching frequency and the non-formation of [Ir(bipy)$_2$(H$_2$O)(bipy′H)]$^{4+}$ Gillard questioned these conclusions, and claimed that the observations were more in accord with a covalently hydrated structure [Ir(bipy)$_2$(bipy·OH$_2$)]$^{3+}$, and pointed out that the *kinetic* stability of [Ir(bipy)$_3$]$^{3+}$/H$_2$O and [Ir(bipy)$_2$(bipy·OH$_2$)]$^{3+}$ could differ.[146] This would mean that the similarity of the absorption spectrum of [Ir(bipy)$_3$]$^{3+}$ in 0.1 M acid and base need not necessarily preclude covalent hydrate formation. Gillard also reported the ^{1}H NMR spectrum of the complex, and considered that the complexity of the spectrum, combined with the observation of multiplets at ~ 6.65 and ~ 7.14 was in accord with a covalently hydrated structure. Later workers have confirmed the unexpected complexity of both the ^{1}H and ^{13}C NMR spectra,[148,149] although Spellane and Watts[149] interpret

these in terms of a structure containing a monodentate bipy ligand. In 1982, Serpone reported the crystal structure of the anomalous complex, and described it as a C-metallated species (Fig. 16). This structure is fully in accord with the basic conditions required for the formation of the complex,
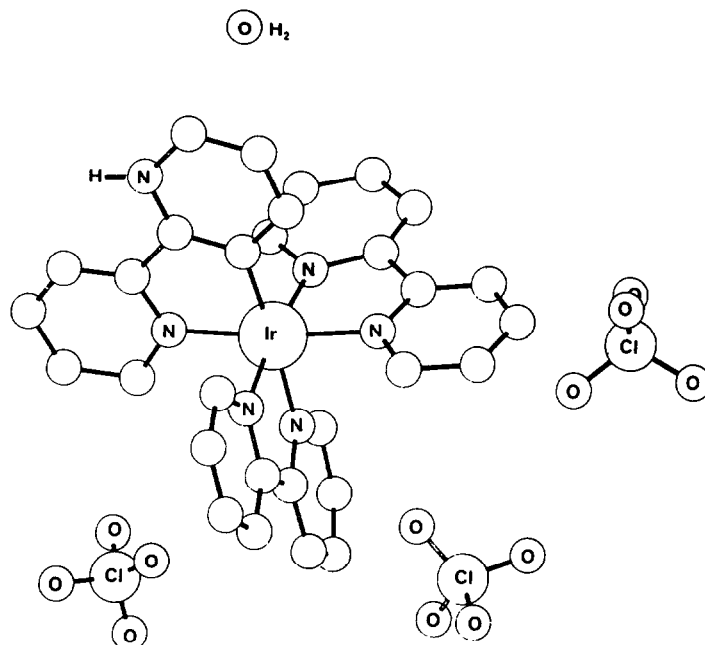
Fig. 16.

explains the complexity of the ^1H and ^{13}C NMR spectra, the acidity of the compound, the presence of an N–H stretching frequency in the IR spectrum, and the inability to undergo further protonation to form tetracationic species. It is difficult to distinguish carbon and nitrogen atoms crystallographically, and the structure described above is open to criticism on these grounds, although the application of Hamilton's test fully confirms the metallated structure.[150,151] If the complex is the metallated species proposed by Serpone, it should be possible to isolate the deprotonated compound formed in the reaction:[152,153]

$$[Ir(bipy)_2(bipy'H)]^{3+} \xrightarrow{OH'} [Ir(bipy)_2(bipy')]^{2+}.$$
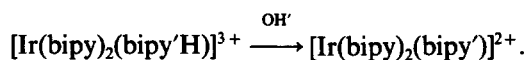
Serpone has now isolated such complexes, and has performed a crystallographic study, showing that the cation has an overall 2+ charge, and that there are no water molecules in the vicinity of the coordinated ligand.[151] These results indicate that metallated structures must be considered as possible intermediates or products in the reactions of tris-bipyridine complexes under forcing conditions. The reports of an anomalous $[Ir(phen)_2(phen')]^{3+}$ complex are not consistent with such a metallated structure and deserve reinvestigation.[148] Gillard has also investigated the structure of an iridium pyridine complex, and has shown that although the complex is hydrated, the water molecules form a hydrogen-bonded network rather than a covalent hydrate.[153]

Nickel and platinum

The majority of the discussion of nickel(II) diimine complexes has centred around the mechanisms for the racemisation and aquation reactions. The mechanism of racemisation of $[NiL_3]^{2+}$ (L = phen or bipy) has been the subject of intensive investigation and discussion for many years, and it is apparent that solvent effects are very important. It was initially proposed that these complexes racemised by an intramolecular mechanism, although it is now established that a dissociative mechanism is implicated.

The racemisation of $[Ni(phen)_3]^{2+}$ was first investigated by Dwyer and Davies, who demonstrated that the rate was independent of acid concentration and of added phen, although it increased in alkaline conditions.[154,155] Numerous workers have confirmed that the rate of racemisation is independent of acid concentration at moderate pH values.[156,157] Basalo showed that, in acidic solution, the rates of racemisation and dissociation were identical, and interpreted these results in terms of a dissociative mechanism.[158] Wilkins later demonstrated that the rates of racemisation and dissociation in both neutral and basic solution were also, within experimental error, identical, and proposed a dissociative mechanism under these conditions.[156] A number of groups have investigated the effect of mixed solvents upon the rate of racemisation of $[Ni(phen)_3]^{2+}$, and it is evident that solvent interactions have a dramatic effect upon ρ_{rac}.[159-162] Yamamoto has shown that the rate of racemisation may be correlated with the donor number of the solvent, and that in dichloromethane–water the rate drops to zero in the absence of water.[160-162] These results were interpreted in terms of an associative intermediate $[Ni(phen)_3(H_2O)]^{2+}$.[160,161] It was also shown that the rate of racemisation was increased by halide ions, but not by non-coordinating anions such as perchlorate.[155,161,163] In mixed CH_2Cl_2–tert–BuOH–H_2O systems it was shown that the increase in the rate of racemisation was in the order

$$ClO_4 < I < Br < Cl$$
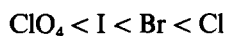
and it was proposed that a general mechanism of the type:

$$[Ni(phen)_3]^{2+} + D^{n-} \rightleftharpoons \{[Ni(phen)_3]^{2+}D^{n-}\}$$
$$\Updownarrow$$
$$products \longleftarrow [Ni(phen)_3D]^{(2-n)+}$$
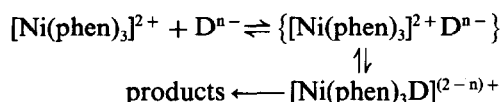
in which D^{n-} was a coordinating solvent or counter-ion, was operating. As iodide was expected to be a better nucleophile towards carbon than chloride, it was suggested that $[Ni(phen)_3D]^{(2-n)+}$ represented a seven-coordinate species, rather than a covalently hydrated structure. Gillard proposed that the role of solvent and nucleophile in the racemisation and dissociation of $[Ni(phen)_3]^{2+}$ were better accommodated in a model with nucleophilic attack at the coordinated ligand,[164] and presented evidence for the covalent hydrate being the predominant solution species over a large pH range in aqueous conditions. In alkaline solution the pseudo-base was thought to be formed.

Lawrance and Stranks have investigated the aquation and racemisation of $[Ni(phen)_3]^{2+}$ in acidic conditions, and have determined values of $\Delta H^{\neq}$, $\Delta S^{\neq}$ and $\Delta V^{\neq}$ for the reactions. It was found that $\Delta V^{\neq}$ was close to zero, which is consistent with an intramolecular trigonal twist mechanism for racemisation, but this does not provide a common mechanism for racemisation and aquation. It was thus proposed that the initial step in the reaction was an associative interaction with a water molecule, followed by the dissociation of a phen molecule later along the reaction coordinate.[165]

From the above discussion it is evident that an intimate complex-solvent or complex-nucleophile interaction is implicated in reactions of $[Ni(phen)_3]^{2+}$, which could be of the covalent hydrate type, a seven-coordinate species, or with the nucleophile in a "ligand-pocket". Nucleophilic attack of halide on a coordinated diimine seems to be unlikely, and the "ligand-pocket" model seems to be the most attractive. The intimate assocation of water with $[Ni(phen)_3]^{2+}$ seems to be more in accord with this structure than with a seven-coordinate ground state. Bosnich and Watts demonstrated Pfeiffer effects in the $[Ni(phen)_3]Cl_2$-$(-)$-2,3-butanediol system[166], and proposed a solvent complex interaction of the "ligand-pocket" type (Fig. 17), although it seems likely that the hydroxy groups would be buried deep within the cleft, rather than facing out into the bulk medium.

The importance of outer-sphere stacking interactions has been demonstrated by Cayley and Margerum, who have proposed interactions of the type shown in Fig. 18 in the reaction:

$$[Ni(phen)(H_2O)_4]^{2+} + phen \longrightarrow [Ni(phen)_2(H_2O)_2]^{2+}$$

Yamamoto and others have investigated the solid-state racemisation of $[Ni(phen)_3]^{2+}$ species,
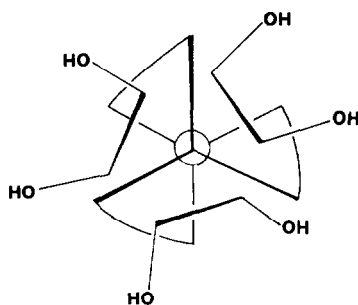
Fig. 17.
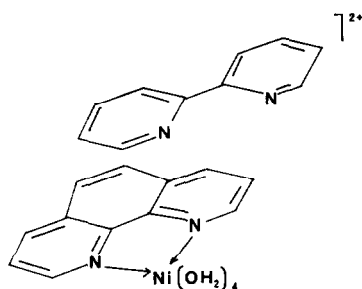
Fig. 18.

and it has been shown that lattice water hinders the racemisation of $[Ni(phen)_3][ClO_4]_2$, suggesting that covalent-hydrate formation is not implicated in the solid state.[168,172] It was also shown that the halide salts racemised more rapidly than the perchlorates, and that the complex [Ni·(phen)$_3$][ClO$_4$]$_2$·2H$_2$O dehydrates completely before any racemisation or decomposition occurs. It seems most probably that a Bailar twist mechanism is involved in the solid-state racemisation.

The racemisation of $[Ni(bipy)_3]^{2+}$ has also been investigated, and the rate shown to increase in either acidic or basic conditions,[156,158,173] and a dissociative mechanism is proposed for this reaction also. In the solid state the racemisation is thought to proceed in a similar manner to that of $[Ni(phen)_3]^{2+}$.[168,172] A number of $[NiL_3]^{2+}$ (L = substituted bipy) complexes have been studied by ^{1}H NMR methods, and the contact-shifted spectra analysed to yield electron spin densities on the ring protons.[174] Dwyer has investigated a number of mixed bipy and phen complexes of nickel(II), and has shown that the effects of solvent, pH and added ions resemble those described for the complexes discussed above.[157]

The complexes $[Ni(terpy)(H_2O)_3]^{2+}$[175] and $[Ni(terpy)_2]^{2+}$[176] have been investigated, and it is proposed that a strong outer-sphere interaction with the incoming ligand (possibly of the stacking type) is involved in the reaction:

$$[Ni(terpy)(H_2O)_3]^{2+} + terpy \longrightarrow [Ni(terpy)_2]^{2+}$$
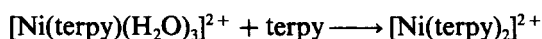
and also for the corresponding reaction of the manganese(II), iron(II), cobalt(II), copper(II), zinc(II) and cadmium(II) complexes.

Gillard has demonstrated the formation of an intermediate in the reaction of $[Ni(5\text{-nitrophen})_3]^{2+}$ with hydroxide, which is almost certainly the Meisenheimer adduct[132]. A crystal structure of the complex $[Ni(tptH)(H_2O)_3]Br_3·H_2O$ has been reported: the non-coordinated water molecule is part of a hydrogen bonding network incorporating the bromide ions, and is not involved in a covalent hydrate of the ligand.[177]

In recent months, there has been some controversy over the behaviour of the complex ion

$[Pt(py)_4Cl_2]^{2+}$ in aqueous solution. Gillard has reported that the complex ion forms strongly acidic aqueous solutions, and attributed this to the equilibrium:[178,179]

$$[Pt(py)_4Cl_2]^{2+} + H_2O \rightleftharpoons [Pt(py)_3(pyOH)Cl_2]^+ + H^+.$$

Nord queries these results, and suggested tha the complex was contaminated with an acidic impurity.[180] Gillard has replied to this in a convincing manner, and recent results suggest the highly purified complex gives acidic solutions, and that the pH falls before chloride ion is released from the complex.[179,181]

Uranium

A note has recently appeared in which the reaction depicted in Fig. 19 is described.[182] This might suggest that these uranium complexes activate the bipy towards attack by strong nucleophiles, but no further evidence for these systems is yet available.
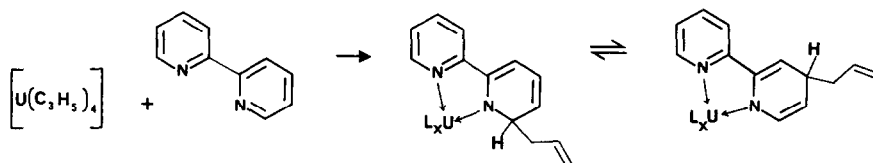
Fig. 19.

CONCLUSIONS

Complexes of the diimine ligands have been known since the discovery of 2,2'-bipyridine and 1,10-phenanthroline by Blau, and have played a formative role in the development of modern coordination chemistry. I hope to have shown in this review that the reactions of complexes of these and other α,α'-diimine ligands are not as simple as previously thought, and that a variety of hitherto unsuspected mechanistic pathways are open to them. The reactions of the complexes with nucleophiles cannot be described by one all-embracing mechanism, but it is possible to distinguish various classes which are expected to react by a particular pathway. At this point it is necessary to add a warning about the interpretation of the ^1H NMR spectra of these complexes. The presence of a resonance in the 6–7 δ region has frequently been interpreted as evidence for the formation of a covalent hydrate, but it is now apparent that a number of other structural features may result in the shielding of one or more aromatic protons (e.g. formation of an orthometallated structure, shielding by an adjacent aromatic ring, Meisenheimer adduct formation). The message must be *caveat emptor*.

Ligands which are know to undergo covalent hydration in the absence of a metal ion form a class in which the.metal complexes are also expected to form covalent hydrates. Ligands in this class include bipym, triazine and possibly tpt, and Gillard has produced numerous convincing examples of complexes in this class forming covalent hydrates. It seems likely that coordination of tpt to a transition metal ion greatly activates it towards nucleophilic attack, exactly as predicted from the analogy of a complex to quaternary salt.

Complexes of 5-nitrophen form a second class in which reaction with a nucleophile results in the formation of a coordinated Meisenheimer adduct. Once again, Gillard has produced convincing evidence that 5-nitrophen is activated towards nucleophilic attack on coordination to a transition metal ion.

The final class consists of complexes of ligands which do not react with weak nucleophiles (water or hydroxide) in the absence of a metal ion. The ligands of importance are bipy, phen and pyridine, and represent the major class of complexes in which we are interested. The results with ligands in the two classes described above indicate that coordination to a metal does activate the ligand towards nucleophilic attack, but it is not apparent how great this activation is. Thus although complexes of bipy and phen undoubtedly are activated towards nucleophilic attack, attack at the ligand does not necessarily provide the lowest energy reaction pathway. This is seen

in reactions of square-planar complexes of these ligands, in whcih five-coordinate species are formed in preference to attack at the ligand. In octahedral complexes the situation is nowhere near so clearly defined, and it is quite likely that a number of mechanisms may exist. There is no doubt that octahedral complexes of bipy and phen do show unique interactions with nucleophiles, but it is not certain whether this interaction is with the metal (seven-coordination), and ligand (covalent-hydration) or the outer sphere (ligand-pockets). The only crystal structural analysis of a supposed covalent hydrate has revealed that the complex contains an orthometallated bipy.

The ligand-pocket approach would be of importance in the ground state of the complexes, but covalent hydration represents an intermediate which is not necessarily structurally similar to the gound state, and may be important in the aquation of diimine complexes. However, there is no structural evidence for the formation of covalent hydrates of transition metal complexes of bipy or phen, and the kinetic results are not unambiguous. In conclusion, it is possible that covalent hydrates are of importance in the reactions of transition metal complexes of bipy and phen, but there is, as yet, no unambiguous evidence for their formation. It is, however, more likely that stronger nucleophiles do attack bipy and phen ligands coordinated to transition metals, and this provides an opening into a new, and very interesting area of chemistry. To quote Gillard "... the link between one major branch of inorganic chemistry and a major branch of organic chemistry seems likely to offer useful explanations for .... phenomena in the highly important systems involving an N-heterocycle, a metal ion, and a nucleophile ...".[178]

Note added in proof. There have been a number of recent results bearing on the subject matter of this review, and these are briefly discussed below.

Nord has re-investigated the $[Ir(bipy)_3]^{n+}$ system, and has structurally characterised the (red) deprotonated complex $[Ir(bipy-N,N')_2(bipy-C,N')][ClO_4]_2 \cdot \frac{1}{3}H_2O$.[183] It is now apparent that there are *two* yellow *tris* complexes, one of which contains an *ortho*-metallated bipy. Gillard has reported a number of complexes of the *N*-methylbipyridinium cation, which is a model for a monodentate bipy,[184] and has shown that the platinum and palladium complexes rearrange to give species thought to contain an *ortho*-metallated ligand.[185]

REFERENCES

1. A. Albert and W. L. F. Armarego, *Adv. Heterocycl. Chem.* 1965, **4**, 1.
2. D. D. Perrin, *Adv. Heterocycl. Chem.* 1965, **4**, 43.
3. A. Albert, *Adv. Heterocycl. Chem.* 1976, **20**, 117.
4. E. Buncel, A. R. Norris and K. E. Russell, *Q. Rev. Chem. Soc.* 1968, **22**, 123.
5. P. Buck, *Angew. Chem. Int. Ed., Engl.* 1969, **8**, 120.
6. M. R. Crampton, *Adv. Phys. Org. Chem.* 1969, **7**, 211.
7. M. J. Strauss, *Chem. Rev.* 1970, **70**, 667.
8. R. Foster and C. A. Fyfe, *Rev. Pure Appl. Chem.* 1966, **16**, 61.
9. C. F. Bernasconi, *Acc. Chem. Res.* 1978, **11**, 147.
10. J. W. Bunting, *Adv. Heterocycl. Chem.* 1979, **25**, 1.
11. R. D. Gillard, *Coord. Chem. Rev.* 1975, **16**, 67.
12. M. S. Henry and M. Z. Hoffman, *J. Am. Chem. Soc.* 1977, **99** 5201.
13. J. Kotlicaka and Z. R. Grabowski, *J. Photochem.* 1979, **11**, 413.
14. D. W. W. Anderson, P. Roberts, M. V. Twigg and M. B. Williams, *Inorg. Chim. Acta* 1979, **34**, L281.
15. R. D. Gillard, R. P. Houghton and J. N. Tucker, *J. Chem. Soc., Dalton Trans.* 1980, 2102.
16. R. D. Gillard, C. T. Hughes, W. S. Walters and P. A. Williams, *J. Chem. Soc., Dalton Trans.* 1979, 1769.
17. T. Kauffmann, J. König and A. Woltermann, *Chem. Ber.* 1976, **109**, 3864.
18. R. F. Knott and J. G. Breckenridge, *Can J. Chem.* 1954, **32**, 512.
19. T. Kauffmann, J. König, D. Korber, H. Lexy, H-J. Streitberger, A. Vahrenhorst and A. Woltermann, *Tetrahedron Letters* 1977, 389.
20. J. W. Bunting and W. G. Meathrel, *Can. J. Chem.* 1974, **52**, 975.
21. D. J. Norris, J. W. Bunting and W. G. Meathrel, *Can. J. Chem.* 1977, **55**, 2601.
22. D. W. Clack, L. A. P. Kane-Maguire, D. W. Knight and P. A. Williams, *Transition Met. Chem. (Weinheim, Ger.)*, 1980, **5**, 376.

23. F. Basolo and G. Pearson, *Mechanisms of Inorganic Reactions*, 2nd Edn. Wiley–Interscience, New York (1967).
24. R. J. Mureinik, *Coord. Chem. Rev.* 1978, **25**, 1.
25. R. D. Gillard and J. R. Lyons, *J. Chem. Soc., Chem. Commun.* 1973, 585.
26. G. Nord, *Acta Chem. Scand., Sect. A* 1975, **29**, 270.
27. E. Bielli, R. D. Gillard and D. W. James, *J. Chem. Soc., Dalton Trans.* 1976 1837.
28. E. Bielli, P. M. Gidney, R. D. Gillard and B. T. Heaton, *J. Chem. Soc., Dalton Trans.* 1974, 2133.
29. O. Farver, O. Mønsted and G. Nord, *J. Am. Chem. Soc.* 1979, **101**, 6118.
30. E. C. Constable, D. Phil Thesis, Oxford, (1980).
31. E. C. Constable, J. E. Day and K. R. Seddon, Manuscript in preparation.
32. S. E. Livingstone and B. Wheelahan, *Aust. J. Chem.* 1964, **17**, 219.
33. K. H. Al-Obaidi, R. D. Gillard, L. A. P. Kane-Maguire and P. A. Williams, *Transition Met. Chem. (Weinheim, Ger.)* 1977, **2**, 64.
34. G. T. Morgan and F. H. Burstall, *J. Chem. Soc.* 1934, 965.
35. G. Nord, Personal communication.
36. E. D. McKenzie, *Coord. Chem. Rev.* 1971, **6**, 187.
37. L. H. Berka, W. T. Edwards and P. A. Christian, *Inorg. Nucl. Chem. Lett.* 1971, **7**, 265.
38. V. Dong, H. Endres, H. J. Keller, W. Moroni and D. Nòthe and *Acta Crystallogr., Sect. B* 1977, **34B**, 2428.
39. H. Endres, H. J. Keller, W. Moroni, D. Nöthe and V. Dong, *Acta Crystallogr., Sect. B* 1978, **34B**, 1823.
40. O. Wernberg and A. Hazell, *J. Chem. Soc., Dalton Trans.* 1980, 973.
41. A. Hazell and A. Mukhopadhyay, *Acta Crystallogr., Sect. B* 1980, **36B**, 1647.
42. R. D. Gillard, L. A. P. Kane-Maguire and P. A. Williams, *Transition Met. Chem. (Weinheim, Ger.)* 1976, **1**, 247.
43. G. Nord and B. V. Agarwala, *Acta Chem. Scand., Sect. A* 1981, **35**, 231.
44. G. T. Morgan and F. H. Burstall, *J. Indian Chem. Soc., Ray Commem. Vol.* 1933, 1.
45. J. L. Burmeister and F. Basolo, *Inorg Chem.* 1964, **3**, 1587.
46. P. M. Kiernan and A. Ludi, *J. Chem. Soc., Dalton Trans.* 1978, 1127.
47. R. S. Osborn and D. Rogers, *J. Chem. Soc., Dalton Trans.* 1974, 1002.
48. M. Textor and H. R. Oswald, *Z. Anorg. Allg. Chem.* 1974, **407**, 244.
49. P. Hoake and P. A. Cronin, *Inorg. Chem.* 1963, **2**, 879.
50. M. J. Blandamer, J. Burgess and J. G. Chambers, *J. Chem. Soc., Dalton Trans.* 1977, 60.
51. R. C. Conrad and J. V. Rund, *Inorg. Chem.* 1972, **11**, 129.
52. T. Boschi, G. Deganello and G. Carturan, *J. Inorg. Nucl. Chem.* 1969, **31**, 2423.
53. G. W. Bushell, K. R. Dixon and M. A. Khan, *Can. J. Chem.* 1974, **52**, 1367.
54. P. M. Kiernan and A. Ludi, *J. Chem. Soc., Dalton Trans.* 1978, 1127.
55. R. J. Mureinik and M. Bidani, *Inorg. Chim. Acta* 1978, **29**, 37.
56. R. J. Mureinik and M. Bidani, *Inorg. Nucl. Chem. Lett.* 1977, **13**, 625.
57. R. D. Gillard, L. A. P. Kane-Maguire and P. A. Williams, *Transition Met. Chem. (Weinheim, Ger.)* 1977, **2**, 55.
58. J. V. Rund, *Inorg. Chem.* 1968, **7**, 24.
59. A. J. Carty and P. C. Chieh, *J. Chem. Soc., Chem. Commun.* 1972, 158.
60. P. C. Chieh, *J. Chem. Soc., Dalton Trans.* 1972, 1643.
61. L. F. Power, *Inorg. Nucl. Chem. Lett.* 1970, **6**, 791.
62. R. A. Plowman and L. F. Power, *Aust. J. Chem.* 1971, **24**, 303.
63. R. A. Plowman and L. F. Power, *Aust. J. Chem.* 1971, **24**, 309.
64. G. M. Intille, C. E. Pfluger and W. A. Baker Jr., *J. Cryst. Mol. Struct.* 1973, **3**, 47.
65. R. D. Gillard, *Inorg. Chim. Acta* 1974, **11**, L21.
66. R. D. Gillard and B. T. Heaton, *J. Chem. Soc.* 1969, 451.
67. P. Moore, *Inorg. React. Mech.* 1979, **6**, 174.
68. J. Burgess, *Inorg. React. Mech.* 1979, **6**, 278.
69. J. Burgess and P. Moore, *Inorg. React. Mech.* 1981, **7**, 163.
70. P. Moore, *Inorg. React. Mech.* 1981, **7**, 200.
71. J. Burgess and P. Moore, *Inorg. React. Mech.* 1981, **7**, 208.
72. J. Burgess, *Inorg. React. Mech.* 1981, **7**, 228.
73. J. Burgess, *Inorg. React. Mech.* 1981, **7**, 287.
74. M. A. Jamieson, N. Serpone and M. Z. Hoffman, *Coord. Chem. Rev.* 1981, **39**, 121.
75. N. Serpone, M. A. Jamieson, M. S. Henry, M. Z. Hoffman, F. Bolletta and M. Maestri, *J. Am. Chem. Soc.* 1979, **101**, 2907.
76. M. S. Henry, *J. Am. Chem. Soc.* 1977, **99**, 6138.

77. M. S. Henry and M. Z. Hoffman, *Adv. Chem. Ser.* 1978, **168**, 91.
78. G. N. La Mar and G. R. Van Hecke, *Inorg. Chem.* 1973, **12**, 1767.
79. W. A. Wickramasinghe, P. H. Bird and N. Serpone, *Inorg. Chem.*, 1982, **21**, 2694.
80. Y. Kaizu and H. Kobayashi, *Bull. Chem. Soc. Japan* 1972, **45**, 470.
81. Y. Kaizu and H. Kobayashi, *Bull. Chem. Soc. Japan.* 1970, **43**, 2492.
82. M. S. Wrighton and D. L. Moore, *J. Organomet. Chem.* 1975, **97**, 405.
83. G. R. Dobson, *Acc. Chem. Res.* 1976, **9**, 300.
84. R. J. Angelici and J. R. Graham, *J. Am. Chem. Soc.* 1965, **87**, 5586.
85. J. R. Graham and R. J. Angelici, *J. Am. Chem. Soc.* 1965, **87**, 5590.
86. R. J. Angelici and J. R. Graham, *Inorg. Chem.* 1967, **6**, 988.
87. J. R. Graham and R. J. Angelici, *Inorg. Chem.* 1967, **6**, 992.
88. R. J. Angelici, S. E. Jacobsen and C. M. Ingemason, *Inorg. Chem.* 1968, **7**, 2466.
89. J. Burgess and S. F. N. Morton, *J. Chem. Soc., Dalton Trans.* 1972, 1717.
90. J. Burgess, J. G. Chambers and R. I. Haines, *Transition Met. Chem. (Weinheim, Ger.)* 1981, **6**, 145.
91. J. A. Connor and C. Overton, *Inorg. Chim. Acta* 1982, **65**, L1.
92. J. Burgess, A. J. Duffield and R. I. Haines, *Transition Met. Chem. (Weinheim, Ger.)* 1977, **2**, 276.
93. J. Burgess, A. J. Duffield and R. Sherry, *J. Chem. Soc., Chem. Commun.* 1980, 350.
94. M. J. Blandamer, J. Burgess, J. G. Chambers and A. J. Duffield, *Transition Met. Chem. (Weinheim, Ger.)* 1981, **6**, 156.
95. N. Serpone, Personal communication.
96. E. C. Constable, Manuscript in preparation.
97. R. D. Gillard, C. T. Hughes, L. A. P. Kane-Maguire and P. A. Williams, *Transition Met. Chem. (Weinheim, Ger.)* 1976, **1**, 226.
98. R. D. Gillard, C. T. Hughes and P. A. Williams, *Transition Met. Chem., (Weinheim, Ger.)* 1976, **1**, 51.
99. E. C. Constable and K. R. Seddon, Unpublished results.
100. R. D. Gillard, L. A. P. Kane-Maguire and P. A. Williams, *Transition Met. Chem. (Weinheim, Ger.)* 1977, **2**, 12.
101. R. D. Gillard, L. A. P. Kane-Maguire and P. A. Williams, *J. Chem. Soc., Dalton Trans.* 1977, 1039.
102. J. A. A. Sagüés, R. D. Gillard and P. A. Williams, *Inorg. Chim. Acta* 1980, **44**, L253.
103. R. D. Gillard and C. T. Hughes, *J. Chem. Soc., Chem. Commun.* 1977, 776.
104. E. C. Constable, Unpublished results.
105. E. C. Constable and J. Lewis, *Inorg. Chim. Acta* 1983, **70**, 251.
106. B. Bosnich and F. P. Dwyer, *Aust. J. Chem.* 1966, **19**, 2229.
107. B. Bosnich and F. P. Dwyer, *Aust. J. Chem.* 1966, **19**, 2235.
108. R. D. Gillard and P. A. Williams, *Transition Met. Chem. (Weinheim, Ger.)* 1977, **2**, 247.
109. A. A. Schilt, *J. Am. Chem. Soc.* 1963, **85**, 904.
110. S. H. Peterson and J. N. Demas, *J. Am. Chem. Soc.* 1976, **98**, 7880.
111. S. H. Peterson and J. N. Demas, *J. Am. Chem. Soc.* 1979, **101**, 6571.
112. A. A. Schilt, *Inorg. Chem.* 1964, **3**, 1323.
113. R. D. Gillard, *Inorg. Chim. Acta* 1974, **11**, L21.
114. C. Creutz and N. Sutin, *Proc. Natl. Acad. Sci.* 1975, **72**, 2858.
115. K. R. Seddon and E. A. Seddon, *The Chemistry of Ruthenium.* To be published.
116. K. Kalyanasundaram, *Coord. Chem. Rev.* 1982, **46**, 159.
117. E. C. Constable and K. R. Seddon, *J. Chem. Soc., Chem. Commun.* 1982, 34.
118. J. A. A. Sagüés, R. D. Gillard, R. J. Lancashire and P. A. Willaims, *J. Chem. Sco., Dalton Trans.* 1979, 193.
119. R. D. Gillard, R. J. Lancashire and P. A. Williams, *Transition Met. Chem. (Weinheim, Ger.)* 1979, **4**, 115.
120. D. J. Brown and S. F. Mason, *The Pyrimidines* (Edited by A. Weissberger). Wiley, New York (1962).
121. D. J. Brown, R. F. Evans and T. J. Batterham, *The Pyrimidines, Suppl.* 1 (Edited by A. Weissberger and E. C. Taylor). Wiley–Interscience, New York (1980).
122. R. D. Gillard and P. A. Williams, *Transition Met. Chem. (Weinheim, Ger.)* 1978, **3**, 334.
123. V. M. S. Gil, R. D. Gillard, P. A. Williams, R. S. Vagg and E. C. Watton, *Transition Met. Chem. (Weinheim, Ger.)* 1979, **4**, 14.
124. E. M. Smolin and L. Rapoport, *S-Triazines and derivatives* (Edited by A. Weissberger). Interscience, New York (1959).
125. V. M. S. Gil and A. M. P. Pereira, *Tetrahedron* 1971, **27**, 5619.
126. E. I. Lerner and S. J. Lippard, *J. Am. Chem. Soc.* 1976, **98**, 5397.
127. E. I. Lerner and S. J. Lippard, *Inorg. Chem.* 1977, **16**, 1546.
128. G. Nord, *Inorg. Chem.* 1976, **15**, 1921.

129. A. J. Deeming, R. Peters, M. B. Hursthouse and J. D. J. Backer-Dirks, *J. Chem. Soc., Dalton Trans.* 1982, 787.
130. K. Jackson, J. H. Ridd and M. L. Tobe, *J. Chem. Soc., Perkin Trans.* 2, 1979, 607.
131. K. Jackson, J. H. Ridd and M. L. Tobe, *J. Chem. Soc., Perkin Trans.* 2, 1979, 611.
132. J. A. A. Sagüés, R. D. Gillard and P. A. Williams, *Inorg. Chim. Acta* 1979, **36**, L411.
133. R. D. Gillard and P. A. Williams, *Transition Met. Chem. (Weinheim, Ger.)* 1979, **4**, 18.
134. P. A. Williams, *Transition Met. Chem. (Weinheim, Ger.)* 1979, **4**, 24.
135. H. A. Goodwin, R. N. Sylva, R. S. Vagg and E. C. Watton, *Aust. J. Chem.* 1969, **22**, 1605.
136. M. J. Janmohamed and G. H. Ayres, *Anal. Chem.* 1972, **44**, 2263.
137. R. S. Vagg, R. N. Warrener and E. C. Watton, *Aust. J. Chem.* 1969, **22**, 141.
138. G. A. Barclay, R. S. Gagg and E. C. Watton, *Acta. Crystallogr., Sect B* 1978, **33B**, 1833.
139. R. D. Johnston, R. S. Vagg and E. C. Watton, *Inorg. Chim. Acta* 1978, **26**, 103.
140. B. Martin and G. M. Waind, *J. Chem. Soc.* 1958, 4284.
141. B. Chiswell and S. E. Livingstone, *J. Inorg. Nucl. Chem.* 1964, **26**, 47.
142. R. E. DeSimone and R. S. Drago, *Inorg. Chem.* 1969, **8**, 2517.
143. K. R. Wunschel Jr. and W. E. Ohnesorge, *J. Am. Chem. Soc.* 1967, **89**, 2777.
144. C. M. Flynn Jr. and J. N. Demas, *J. Am. Chem. Soc.* 1974, **96**, 1959.
145. R. J. Watts, J. S. Harrington and J. Van Houten, *J. Am. Chem. Soc.* 1977, **99**, 2179.
146. R. D. Gillard, R. J. Lancashire and P. A. Williams, *J. Chem. Soc., Dalton Trans.* 1979, 190.
147. R. J. Watts and S. F. Bergeron, *J. Phys. Chem.* 1979, **83**, 425.
148. J. L. Kahl, K. Hanck and K. DeArmond, *J. Inorg. Nucl. Chem.* 1979, **41**, 495.
149. P. J. Spellane and R. J. Watts, *Inorg. Chem.* 1981, **20**, 3561.
150. W. A. Wickramasinghe, P. H. Bird and N. Serpone, *J. Chem. Soc., Chem. Commun.* 1981, 1284.
151. N. Serpone, Personal communication.
152. K. R. Seddon and J. E. Turp, Personal communication.
153. R. D. Gillard, Personal Communication.
154. N. R. Davies and F. P. Dwyer, *Trans. Faraday Soc.* 1952, **48**, 244.
155. N. R. Davies and F. P. Dwyer, *Trans. Faraday Soc.* 1953, **49**, 180.
156. R. G. Wilkins and M. J. C. Williams, *J. Chem. Soc.* 1957, 1763.
157. J. A. Broomhead and F. P. Dwyer, *Aust. J. Chem.*, 1963, **16**, 51.
158. F. Basolo, J. C. Hayes and H. M. Neumann, *J. Am. Chem. Soc.* 1953, **75**, 5103.
159. N. R. Davies and F. P. Dwyer, *Trans. Faraday Soc.* 1954, **50**, 1325.
160. T. Fujiwara and Y. Yamamoto, *Inorg. Nucl. Chem. Lett.* 1975, **11**, 635.
161. M. Yamamoto, T. Fujiwara and Y. Yamamoto, *Inorg. Nucl. Chem. Lett.* 1979, **15**, 37.
162. E. Iwamoto, T. Fujiwara and Y. Yamamoto, *Inorg. Chim. Acta* 1980, **43**, 95.
163. T. Fujiwara and Y. Yamamoto, *Inorg. Nucl. Chem. Lett.* 1979, **15**, 397.
164. R. D. Gillard and P. A. Williams, *Transition Met. Chem. (Weinheim, Ger.)* 1977, **2**, 14.
165. G. A. Lawrance and D. R. Stranks, *Inorg. Chem.* 1978, **17**, 1804.
166. B. Bosnich and D. W. Watts, *Inorg. Chem.* 1975, **14**, 47.
167. C. P. Cayley and D. W. Margerum, *J. Chem. Soc. Chem. Commun.* 1974, 1002.
168. T. Fujiwara and Y. Yamamoto, *Inorg. Chem.* 1980, **19**, 1903.
169. G. E. Humiston and J. E. Brady, *Inorg. Chem.* 1969, **8**, 1773.
170. A. Tatehata, T. Kumamaru and Y. Yamamoto, *J. Inorg. Nucl. Chem.* 1971, **33**, 3427.
171. Y. Yamamoto, K. Akabori and T. Seno, *Inorg. Nucl. Chem. Lett.* 1973, **9**, 195.
172. C. D. Schmulbach, F. Dachille and M. E. Bunch, *Inorg. Chem.* 1964, **3**, 808.
173. G. K. Schweitzer and J. M. Lee, *J. Phys. Chem.* 1952, **56**, 195.
174. T. L. J. Huang and D. G. Brewer, *Can. J. Chem.* 1981, **59**, 1689.
175. D. Rablen and G. Gordon, *Inorg. Chem.* 1969, **8**, 395.
176. R. H. Holyer, C. D. Hubbard, S. F. A. Kettle and R. G. Wilkins, *Inorg. Chem.* 1966, **5**, 622.
177. G. A. Barclay, R. S. Vagg and E. C. Watten, *Acta Crystallogr., Sect B* 1977, **33B**, 3487.
178. R. D. Gillard and R. J. Wademan, *J. Chem. Soc., Chem. Commun.* 1981, 448.
179. R. D. Gillard and R. J. Wademan, *J. Chem. Soc., Dalton Trans.* 1981, 2599.
180. O. Mønsted and G. Nord., *J. Chem. Soc., Dalton Trans.*, 1981, 2599.
181. K. R. Seddon and J. E. Turp, Personal communication.
182. J. G. Vanderhooft and R. D. Ernst, *J. Organomet. Chem.* 1982, **233**, 313.
183. G. Nord, A. C. Hazell, R. G. Hazell and O. Farver, *Inorg. Chem.*, Manuscript submitted.
184. S. Dholakia, R. D. Gillard and F. L. Wimmer, *Inorg. Chim. Acta*, 1982, **65** L121.
185. S. Dholakia, R. D. Gillard and F. L. Wimmer, *Inorg. Chim. Acta*, 1983, **69**, 179.

LANTHANIDE PERCHLORATE COMPLEXES OF 1-PHENYL-3-METHYL-4-PHENACYL-PYRAZOL-5-ONE

V. GIRI and P. INDRASENAN*
Department of Chemistry, University of Kerala, Trivandrum 695034, India

Abstract—Complexes of lanthanide perchlorates with 1-phenyl-3-methyl-4-phenacyl-pyrazol-5-one with the general formula: $[Ln(PMPP)_5ClO_4](ClO_4)_2$ (where Ln = La, Pr, Nd, Sm, Gd and Dy) have been synthesised and characterized. The physico–chemical studies indicate that the five ligands and one of the perchlorates are coordinated to the metal ion in a monodentate fashion to give approximately octahedral geometries for the complexes.

Ligands containing the C–O group are the largest group of compounds forming complexes with the lanthanides.[1] Probably the first series of lanthanide complexes with neutral oxygen donor ligands is that of anitpyrine.[2] Since then a variety of lanthanide complexes with ligands containing the pyrazolone ring have been reported.[1,3,4] Recently, Okafor[5] reported on the synthesis of some lanthanide complexes of 1 - phenyl - 3 - methyl - 4 - benzoyl - pyrazol - 5 - one. Now we are reporting on the synthesis and structure elucidation of some interesting lanthanide perchlorate complexes of 1 - phenyl - 3 - methyl - 4 - phenacyl - pyrazol - 5 - one (hereafter abbreviated to PMPP). PMPP acts as a unidentate ligand unlike the above 4-benzoyl compound,[5] which acts as a bidentate ligand. Moreover, one of the perchlorate groups is also coordinated to the metal ions in the present complexes and in this way they are very interesting.

EXPERIMENTAL

Preparation of lanthanide perchlorates. The perchlorates of La, Pr, Nd, Sm, Gd and Dy were prepared by dissolving a slight excess of the oxide (99.9% pure) in hot 60% aqueous perchloric acid. The undissolved oxides were filtered off and the perchlorates were crystallised out by evaporation.

Preparation of the ligand. 1 - phenyl - 3 - methyl-4 - phenacyl - pyrazol - 5 - one (PMPP) was prepared by the standard method.[6] Solutions of 1 - phenyl - 3 - methyl - pyrazol - 5 - one (0.01 mole) and freshly prepared phenacyl bromide (0.01 mole) in the minimum quantities of ethanol were mixed together in presence of fused sodium acetate (5 g) and the resulting mixture was refluxed

for 2 hr. The white solid formed was filtered, washed with ethanol and then with water and dried over phosphorus(V) oxide.

Preparation of the complexes. To a clear warm solution of the lanthanide perchlorate in *n*-pentanol a slight excess of the solid ligand was added in small quantities. The reaction mixture was heated carefully up to the boiling point of the solvent (138°C) for 10 min. The green solution obtained was filtered and the filtrate was concentrated to give a viscous mass. To this, solvent ether was added and it was stirred to separate solid complex. The supernatant liquid was poured off and the solid was washed with ether and dried in vacuum over phosphorus(V) oxide.

Analysis of the complexes. The lanthanide contents in the complexes were determined gravimetrically by the oxalate–oxide method[7] and the perchlorate contents by Kurz's method.[8]

Physical measurements. The molar conductances ($\sim 10^{-4}$ M solutions) of the complexes were determined at room temperature (28 ± 2°C) using an ELICO conductivity bridge type CM82 with dip type cell (type cc-03) having platinum electrodes. Magnetic susceptibility measurements were carried out also at room temperature by the Gouy method. The IR spectra of the complexes and the ligand were taken in KBr pellets on a Perkin–Elmer 397 IR Spectrophotometer in the range 4000–400 cm^{-1}. The molecular weights of the complexes ($\sim 10^{-4}$ M solutions) were determined by the cryoscopic method in nitrobenzene.[9]

RESULTS AND DISCUSSION

All the six complexes are non-hygroscopic solids. They are soluble in acetonitrile, nitrobenzene, methanol, ethanol, *n*-pentanol and dimethylformamide and are insoluble in benzene, carbo-

*Author to whom correspondence should be addressed.

Table 1. Elemental analyses and molecular weight data

Complex	% Metal		% Perchlorate		Molecular Weight	
	Found	Required	Found	Required	Found	Required
La	7.30	7.32	15.87	15.71	1845	1899
Pr	7.42	7.41	15.96	15.70	1915	1901
Nd	7.46	7.58	15.49	15.67	1895	1904
Sm	7.78	7.87	15.97	15.63	1911	1910
Gd	8.33	8.21	15.35	15.57	1910	1917
Dy	8.54	8.46	15.39	15.53	1933	1923

ntetrachloride, ether and water. The elemental analysis data (Table 1) indicate the following general formula for the complexes: $[Ln(PMPP)_5](ClO_4)_3$, where Ln = La, Pr, Nd, Sm, Gd and Dy.

The molar conductivity values (Table 2) of the complexes in nitrobenzene reveal that they behave as 2:1 electrolytes indicating that one of the perchlorate groups is coordinated to the metal ions. However, they behave as 3:1 electrolytes both in methanol and dimethylformamide indicating that the coordinated perchlorate group is replaced from the coordination sphere by the solvent molecule.

The magnetic data are also given in Table 2. The La complex is diamagnetic as is to be expected. It may be seen from Table 2 that the observed magnetic moments are generally found to agree with the theoretical values calculated by the Van Vleck formula.[10]

The important IR spectral bands are presented in Table 3. The side chain carbonyl stretching frequency in the free ligand occurs as a very strong band at $1675 \, cm^{-1}$ and the ring C=O frequency is shifted to $1610 \, cm^{-1}$. The discrepancy in the ring carbonyl frequency is due to the intermolecular H-bonding in the ligand.[11] In the complexes the side chain C=O frequency is shifted to $1655 \, cm^{-1}$

as a shoulder in the strong peak of the ring carbonyl frequency, which is practically unaltered. A lowering of $\sim 20 \, cm^{-1}$ in the side chain carbonyl frequency is attributed to the coordination of the metal ion through the side chain carbonyl oxygen rather than the ring carbonyl oxygen. It may be noted that the ring carbonyl frequency is lowered by $\sim 5 \, cm^{-1}$ and a shift of only $\sim 20 \, cm^{-1}$ is observed for the side chain carbonyl frequency on complexation. This may be explained as follows: Due to complexation the frequencies of the two carbonyl groups come closer and the coupling is more effective than in the free ligand. Hence the ring carbonyl band is lowered slightly and the frequency of the side chain carbonyl group is slightly raised, resulting in the small shift to the lower frequency region ($\sim 20 \, cm^{-1}$). The broad absorption band between $3300-2800 \, cm^{-1}$ in the spectra of the complexes as well as that of the ligand may be attributed to the H-bonding.[11] The existence of the H-bonding in the spectra of the complexes confirms that the ring carbonyl group is not involved in the coordination. Therefore, the ligand shows monodenticity coordinating through the oxygen of the side chain carbonyl group.

The IR spectra of the six complexes studied show a strong doubly split band with band maxima

Table 2. Conductivity and magnetic measurements data

Complex	Molar conductivity*		In dimethylformamide	Magnetic moment (BM)	
	In nitrobenzene	In methanol		Found	Calculated**
La	56.4	294.1	261.1	0.0	0.0
Pr	58.7	294.9	252.2	3.4	3.6
Nd	54.9	267.5	226.4	3.7	3.7
Sm	55.8	278.0	237.2	1.8	1.6
Gd	57.2	292.2	243.5	8.1	7.9
Dy	55.0	281.5	236.0	10.7	10.6

*$Ohm^{-1} \, Cm^2 \, mole^{-1}$; the concentration $\sim 10^{-3} \, M$.
**Calculated using the Van Vleck equation.

Table 3. Important IR spectral bands (in cm^{-1})

	C=O$^{(side\ chain)}$	C=O$^{(nuclear)}$	v_3 ClO$_4$	v_1 ClO$_4$	v_4 ClO$_4$
Ligand	1675 (s)	1610 (s)			
La Complex	1655 (sh)	1605 (s)	1105 (s) 1085 (s)	925 (m)	620 (s)
Pr Complex	1655 (sh)	1605 (s)	1100 (s) 1085 (s)	925 (m)	620 (s)
Nd Complex	1655 (sh)	1605 (s)	1100 (s) 1085 (s)	925 (m)	620 (s)
Sm Complex	1655 (sh)	1605 (s)	1110 (s) 1085 (s)	925 (m)	620 (s)
Gd Complex	1655 (sh)	1605 (s)	1110 (s) 1085 (s)	925 (m)	620 (s)
Dy Complex	1655 (sh)	1605 (s)	1100 (s) 1085 (s)	925 (m)	620 (s)

Abbreviations:—s = strong; sh = shoulder; m = medium.

at 1100 and 1085 cm^{-1} which is assigned to the v_3 vibration of the perchlorate group. This splitting of the asymmetric stretch shows that the perchlorate group is coordinated to the metal ion, the coordination probably being monodentate.[12] However, the splitting of v_3 band is not so clear and in some cases they are broad bands with two maxima at 1100 and 1085 cm^{-1}. A medium band at 925 cm^{-1} and a strong band at 620 cm^{-1}, which are unsplit, are assigned respectively to the v_1 and v_4 vibrations of the perchlorate groups.[12]

Based on the above physical measurements the present series of complexes have the following formula: [Ln(PMPP)$_5$ClO$_4$](ClO$_4$)$_2$ with a coordination number of six. The molecular weight determinations show that all the six complexes are monomers (Table 1) in solid state. The five ligand molecules and one of the perchlorate groups are coordinated to the metal ion in a monodentate fashion to give presumably a distorted octahedral geometry but an X-ray crystal structure is clearly needed to determine the actual configuration.

REFERENCES

1. D. K. Koppikar, P. V. Sivapulliah, L. Ramakrishnan and S. Soundararajan, *Structure and Bonding* 1978, **34**, 135.
2. A. Kolb, *Z. Anorg. Allg. Chem.* 1913, **83**, 143.
3. C. G. R. Nair and Jacob Chacko, *Curr. Sci. (India)* 1976, **45**, 452.
4. Jacob Chacko, C. P. Prabhakaran and C. G. R. Nair, *J. Inorg. Nucl. Chem.* 1976, **38**, 1555.
5. Emmanuel Chukwuemeka Okafor, *J. Inorg. Nucl. Chem.* 1980, **42**, 1155.
6. N. B. Das and A. S. Mittra, *Indian J. Chem.* 1978, **16B**, 638.
7. I. M. Kolthoff and P. S. Elving, *Treatise on Analytical Chemistry*, Part II, Vol. 8. Interscience, New York (1963).
8. E. Kurz, G. Kober and M. Berl. *Anal. Chem.* 1958, **30**, 1983.
9. W. G. Palmer, *Experimental Physical Chemistry*. The University Press, Cambridge (1954).
10. J. H. Van Vleck and N. Frank, *Phys. Rev.* 1927, **34**, 1494.
11. A. R. Katritzky and F. W. Maine, *Tetrahedron* 1964, **20**, 304; 307.
12. K. Nakamoto, *Infrared Spectra of Inorganic and Coordination Compounds*. Wiley, New York (1963).

OXIDATION OF L-CYSTEINE, MERCAPTOACETIC ACID AND β-MERCAPTOETHYLAMINE BY 12-TUNGSTOCOBALTATE(III)

G. ADEFIKAYO AYOKO and M. ADEGBOYEGA OLATUNJI*

Department of Chemistry, Ahmadu Bello University, Zaria, Nigeria

Abstract—The stoichiometries and kinetics of the reactions of 12-tungstocobaltate(III) with L-cysteine, mercaptoacetic (thioglycollic) acid and β-mercaptoethylamine have been investigated in aqueous perchloric acid solution over a wide concentration range and at an ionic strength of $1.0 \, mol \, dm^{-3}$ ($NaClO_4$). One mole each of the thiols is required to reduce 12-tungstocobaltate(III) to 12-tungstocobaltate(II) ions, with the disulphide of the thiol as the other product. The rates of reactions decrease with increasing acidity and there is no evidence for the formation of an intermediate complex of significant stability. The reactions are interpreted in terms of an outer-sphere mechanism.

INTRODUCTION

The use of heteropoly molybdates and tungstates as electron-dense stains for electron microscopy[1] has been known for a long time. In recent years, much attention has been focussed on the use of these complexes as antiviral agents[2,3] and as electron acceptors in studies of photosynthesis.[4-6] Very little work has been done on the redox reactions involving these heteropoly acids and their anions. Rasmussen and Brubaker[7] investigated the kinetics of the electron exchange between 12-tungstocobaltate(III) $[Co(III)O_4W_{12}O_{36}]^{5-}$ and 12-tungstocobaltate(II) $[Co(II)O_4W_{12}O_{36}]^{6-}$ anions, hereafter referred to as [Co(III)] and [Co(II)] respectively, while Lappin *et al.*[8] reported the reactions of $[CuW_{12}O_{40}]^{7-}$ anion with hexacyanoferrate(III) in perchlorate media. The redox reactions of [Co(III)] with ligands containing di-hydroxyl groups have also been studied by McAuley *et al.*[9] and except for the reactions of [Co(III)], the oxidant in this study, with thioureas[10] no other reaction of the oxidant with sulphur-containing organic ligands have been reported. This paper is therefore an account of the kinetic investigation of the reactions of [Co(III)] with sulphur-containing ligands such as L-cysteine, thioglycollic acid and β-mercaptoethylamine.

Previously, oxidation of many thiols by metal ions has been shown to proceed through the formation of inner-sphere complexes. In the aquo-cobaltic ion oxidation of α-mercaptocaboxylic acids,[11,12] electron transfer was preceded by the formation of transient species. Similar results were obtained in the thallium(III) oxidation of thiomalic acid,[13] Cr(VI) oxidation of L-cysteine,[14] thioureas,[15] penicillamine,[16] and gluthathione[16] and Fe(III) oxidation of mercaptocaboxylic acids.[17] However, in the ceric oxidation of α-thiols[18] and thioureas,[19] aquo-cobaltic oxidation of the thioureas,[20] and the reactions of [Co(III)] with thioureas,[10] there was no evidence for the formation of intermediate complexes prior to electron transfer. In the unlikely event that intermediate complex formation is important in the present study, the choice of thiols should make possible the investigation of the effectiveness of O, N and S as binding sites. For example, if oxygen of the carboxylic acid group is an important coordinating site, its absence in β-mercaptoethylamine should be reflected in the rate and thermodynamic parameters for complex formation.

In addition, the relative position of the various coordinating sites and in particular the size of the entire molecule may also affect these values. On the other hand, if there is no evidence for complex formation, it would be interesting to know how the mechanisms of these reactions relate to those of the same oxidant with other sulphur-containing ligands like thioureas,[10] where no evidence was found for the existence of an intermediate complex.

EXPERIMENTAL

Materials

Potassium 12-tungstocobaltate was prepared by the method of Baker and McCutcheon[12] and characterised for purity by its UV-visible spectra.[9] A stock solution of [Co(III)] was standardised using a spectrophotometric titration method. The titration was carried out with a standard solution of Fe(II) which quantitatively reduced [Co(III)] to [Co(II)].

L-Cysteine (BDH reagent), β-mercaptoethylamine hydrochloride (Koch Light) were used without further purification, but mercaptoacetic acid (Analar grade) was redistilled under reduced pressure and used as soon as possible after purification. Perchloric acid (Analar grade) was used to investigate the effect of hydrogen ions on the rates of reactions while sodium perchlorate (Fluka puriss) was employed in maintaining the ionic strength constant at $1.0 \, mol \, dm^{-3}$. Other chemicals were used as supplied.

Kinetics

The reactions of the three thiols were found to be very slow under the conditions employed in the kinetic investigation. Consequently, the rates of the various reactions were measured by following the decrease in the concentration of [Co(III)] with time at 390 nm using a Pye Unicam SP 8000 spectrophotometer. All measurements were made under pseudo-first order conditions using the following reactant concentrations:

$$[Co(III)] = 2 \times 10^{-4} \, mol \, dm^{-3}; \quad [thiol] = 2-40 \times 10^{-3} \, mol \, dm^{-3};$$

$$[H^+]_± = 0.02-0.10 \, mol \, dm^{-3} \quad and \quad I = 1.0 \, mol \, dm^{-3} \, (NaClO_4).$$

The reactions were studied at temperatures in the range 15.8–30.3°C. Temperature variation within a particular set of runs was not greater than 0.1°C.

Stoichiometry

The stoichiometries of the reactions were determined by spectrophotometric titration. Absorbances of solutions containing various concentrations of the thiols in the range $(0.80-9.60 \times 10^{-4} \, mol \, dm^{-3})$ and a constant initial concentration of [Co(III)] $(2.0 \times 10^{-4} \, mol \, dm^{-3})$ at $[H^+] = 0.05 \, mol \, dm^{-3}$ and $I = 1.0 \, mol \, dm^{-3}$ ($NaClO_4$) were measured at 390 nm after the reac-

---

*Author to whom correspondence should be addressed.

tions had gone to completion. The stoichiometries were then evaluated from plots of absorbance vs thiol concentration curves. Results were found to be independent of wavelength used. Similar results were obtained when the concentration of the thiol was kept constant at 2.0×10^{-4} mol dm^{-3} and those of [Co(III)] varies between 0.4–4.8×10^{-4} mol dm^{-3} using the same values of [H$^+$]$_0$ and ionic strength as in the titrations above.

RESULTS AND DISCUSSION

For each mole of [Co(III)], 0.92 ± 0.03 moles of L-cysteine, 0.94 ± 0.02 moles of β-mercaptoethylamine and 0.94 ± 0.04 moles of mercaptoacetic acid were oxidized. These are in reasonable agreement with reaction (1) where RSH represents a thiol.

$$2[Co(III)] + 2RSH \rightarrow 2[Co(II)] + RSSR + 2H^+. \quad (1)$$

Accurate knowledge of the reactant species is a requirement for a reasonable interpretation of kinetic data. An effort was therefore made to identify the important reactant species in these redox reactions. Spectra of [Co(III)] monitored over the acid concentration range employed in the kinetic investigations indicated that there was no reactive species of oxidant other than [CoO$_4$W$_{12}$O$_{36}$]$^{-5}$. For the thiols, the pK$_a$ values corresponding to the loss of a proton from an –SH and NH$_3^+$ group[22-24] are >8, whereas those of the carboxylic acid groups are ca. 2 for cysteine[14] and ca. 4 for mercaptoacetic acid.[17] Hence, in the acidity range [H$^+$] = 0.2–0.10 mol dm^{-3} employed in this work, the carboxylic acid is the predominant species, although a small proportion of the zwitterion formed from the dissociation of monoprotonated ligand (eqn 2) is also present in solution.

$$\overset{+}{N}H_3 \qquad \qquad \overset{+}{N}H_3$$
$$| \qquad \qquad \qquad |$$
$$HS\!-\!CH_2\!-\!C\!-\!CO_2H \overset{K_a}{\rightleftharpoons} HS\!-\!CH_2\!-\!C\!-\!CO_2^- + H^+.$$
$$| \qquad \qquad \qquad |$$
$$H \qquad \qquad \qquad H \qquad \qquad (2)$$
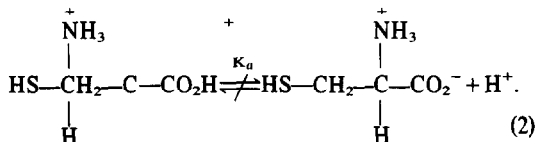
This is in line with conclusions reached by McAuley and Olatunji,[25] working under identical experimental conditions. Attempts were also made to determine the effect of these proton equilibria on the actual concentration of hydrogen ions present using the method employed by McAuley and Olatunji.[25] No significant effect was observed. This would tend to suggest that although the protonated ligand may be formed, the effective concentration of hydrogen ions remained essentially at the initial value, [H$^+$]$_0$.

Comparison of the initial absorbances in the kinetic investigations with those for [Co(III)] when no ligand was present showed no significant difference, indicating that no detectable intermediate was formed. Plots of log $(A_t - A_\infty)$ (where A_t and A_∞ are the absorbances at time t and at the end of the reaction respectively) vs time were linear to greater than 90% completion of the reactions. The strict linearity of these plots does suggest that there is no strong inhibition of the reactions by products and that the rate is first-order in [Co(III)] in each of the reactions investigated. Pseudo-first order rate constants, k_{obs}, obtained from gradients of these plots at various values of [H$^+$]$_0$ and thiol concentrations are presented in Table 1.

On plotting k_{obs} vs [RSH]^2 (where RSH is L-cysteine or mercaptoacetic acid), straight lines were obtained, suggesting that the rates of the redox reactions are
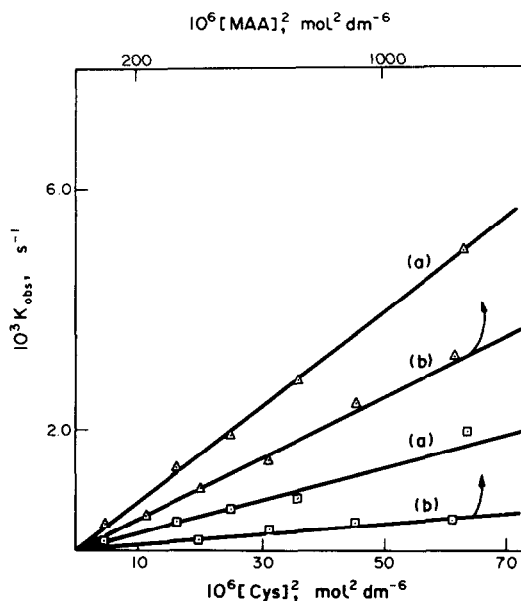
Fig. 1. The dependence of observed rate constant (k_{obs}) on the concentration of mercaptoacetic acid (MAA) and L-cysteine (cys) at 25°C. (A) L-cysteine. (B) Mercaptoacetic acid (top coordinate). [H$^+$] = 0.04 mol dm^3 ($\triangle$). (H$^+$) = 0.08 mol dm^3 ($\square$).

second-order in these thiols (Fig. 1). Plots of gradients of these lines as a function of [H$^+$]$_0^{-2}$ gave a straight line passing through the origin at constant temperature (Fig. 2). On the other hand, when RSH is mercaptoethylamine, plots of k_{obs}/RSH vs [RSH] (Fig. 3) indicate that two pathways are concurrently operative in the reaction, one being first-order in the ligand while the other has a second-order ligand dependence. Gradients of these plots vary in a linear manner with 1/[H$^+$]$_0$ at constant temperature (Fig. 4).

If the rate of protonation of the thiols is diffusion controlled, the rate of dissociation of such protonated
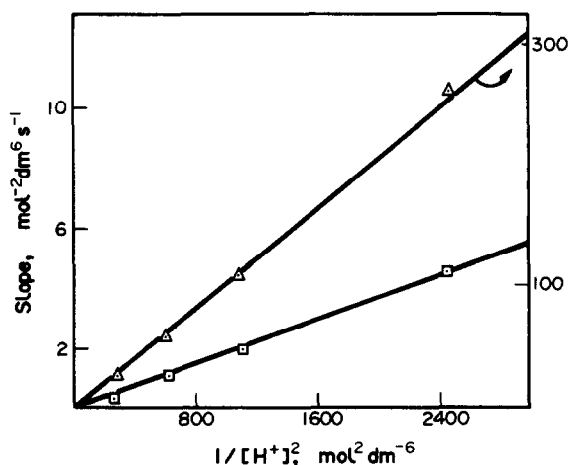
Fig. 2. Dependence of the gradients of plots of observed rate constant, k_{obs}, vs ligand concentrations (Fig. 1) on 1/[H$^+$]^2 for the reactions of mercaptoacetic acid and L-cysteine with [Co(III)]. ($\triangle$) L-Cysteine: $T = 20.1$°C (right-hand coordinate). · Mercaptoacetic acid: $T = 15.8$°C.

Table 1. Rate constants, k_{obs}, for the redox reactions. $[Co(III)] = 2.0 \times 10^{-4}$ mol dm^{-3}; $I = 1.0$ mol dm^{-3}; $\lambda = 390$ nm; [RSH] = L-cysteine, mercaptoacetic acid and β-mercaptoethylamine

(a) [RSH] = L-Cysteine, (T = 25.0°C)

$[H^+]_o$ mol dm^{-3}	10^3[RSH] Mol dm^{-3}	$10^3 k_{obs}$ s^{-1}	$[H^+]_o$ mol dm^{-3}	10^3[RSH] mol dm^{-3}	$10^3 k_{obs}$ s^{-1}
0.02	2.00	1.00	0.03	2.00	0.65
	3.00	2.90		4.00	2.38
	5.00	7.69		5.00	3.48
	6.00	11.05		6.00	4.75
				8.00	9.16
0.04	2.00	0.45	0.06	2.00	0.18
	4.00	1.40		4.00	0.65
	5.00	1.95		5.00	0.88
	6.00	2.79		6.00	1.44
	8.00	5.00		8.00	2.58
0.08	2.00	0.15			
	4.00	0.50			
	5.00	0.66			
	6.00	0.80			
	8.00	2.00			

(b) [RSH] = Mercaptoacetic acid (T = 25.5°C)

$[H^+]_o$	10^3[RSH]	$10^3 k_{obs}$	$[H^+]_o$	10^3[RSH]	$10^3 k_{obs}$
0.02	10.00	0.85	0.03	10.00	0.35
	15.00	1.56		15.00	0.84
	20.00	3.92		20.00	1.41
	25.00	5.92		25.00	2.63
	30.00	8.77		30.00	3.16
				35.00	4.23
0.04	10.00	0.27	0.06	15.00	0.25
	15.00	0.61		18.00	0.37
	20.00	1.07		20.00	0.48
	25.00	1.48		28.00	0.59
	30.00	2.40		30.00	0.75
	35.00	3.15		35.00	1.16
				40.00	1.60
0.08	20.00	0.19			
	25.00	0.36			
	30.00	0.46			
	35.00	0.50			
	40.00	0.56			

(c) [RSH] = β-mercaptoethylamine (T = 25.1°C)

$[H^+]_o$	10^3[RSH]	$10^3 k_{obs}$	$[H^+]_o$	10^3[RSH]	$10^3 k_{obs}$
0.04	10.00	0.23	0.06	10.00	0.19
	20.00	0.66		20.00	0.49
	25.00	0.80		25.00	0.63
	30.00	1.20		30.00	0.86
	35.00	1.48		35.00	1.01
0.08	10.00	0.18	0.10	10.00	0.61
	20.00	0.42		20.00	0.34
	25.00	0.58		25.00	0.44
	30.00	0.72		30.00	0.57
	35.00	0.90		35.00	0.68
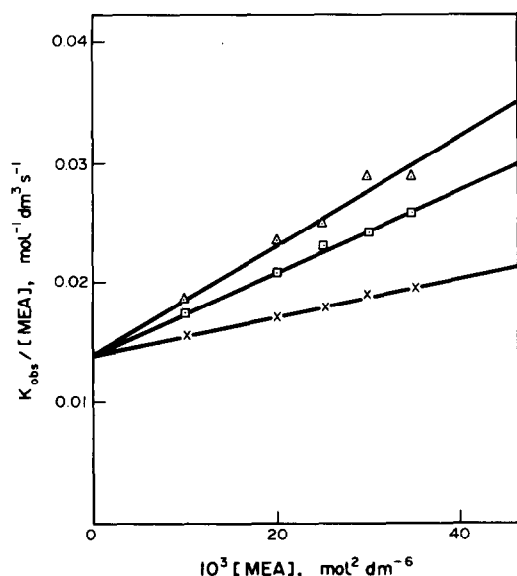
Fig. 3. The dependence of observed rate constant (k_{obs}) on ligand concentration for the reaction of [Co(III)] with β-mercapto-ethylamine (MEA) at 25°C. [H$^+$] = 0.06 mol dm^3 ($\triangle$). [H$^+$] = 0.08 mol dm^3 ($\square$). (H$^+$] = 0.10 mol dm^3 ($\times$).

species may be estimated from the dissociation constant of the thiol group.[14,16]

$$RSH \underset{k_{-d}}{\overset{k_d}{\rightleftharpoons}} RS^- + H^+ \qquad (3)$$

$$K_a = \frac{k_d}{k_{-d}} \qquad (4)$$

$$k_d = 10^{10} K_a . \qquad (5)$$

Since the value of K_a for the thiols[22-24] is approx. 10^{-7}–10^{-8}, the value of k_d obtained using eqn (5) is of the order of 10^2–10^3 s^{-1}. This value is much higher than the
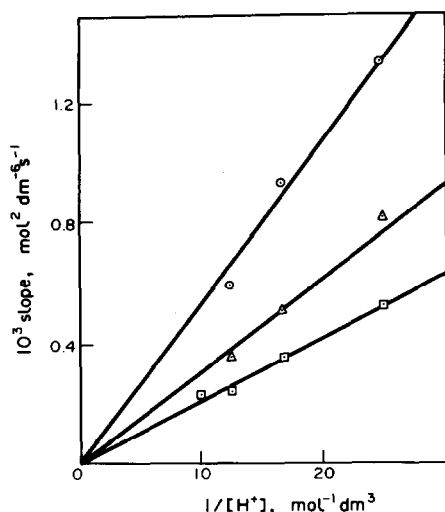
Fig. 4. Dependence of gradients of plots of K_{obs}/[MEA] vs [MEA] (Fig. 3) on 1/[H$^+$] for the reactions of [Co(III)] with mercaptoethylamine. T = 30.3°C (○); T = 25.0°C (△); T = 20.1°C (□).

observed rate constants, k_{obs}, for the redox steps; it is therefore reasonable to assume that dissociation of –SH precedes electron transfer.

From the observed experimental data, the mechanism below can be postulated for the reactions of L-cysteine and mercaptoacetic acid with 12-tungstocobaltate(III) ions, where the protons released are derived from the thiol group as shown above.

Mechanism I

$$2RSH \overset{K_a}{\rightleftharpoons} 2RS^- + 2H^+ \qquad (6)$$

$$[Co(III)] + RS^- \overset{K_{os}}{\rightleftharpoons} [Co(III)], RS^- \qquad (7)$$

$$[Co(III)], RS^- + RS^- \overset{k_1}{\longrightarrow} [Co(II)] + RSSR^- \qquad (8)$$

$$RSSR^- + [Co(III)] \overset{fast}{\rightleftharpoons} [Co(II)] + RSSR \qquad (9)$$
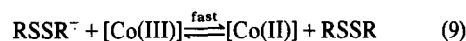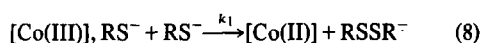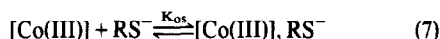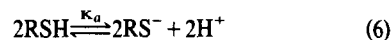
where K_{os} is the outer-sphere equilibrium constant. This reaction scheme is consistent with the rate of loss of [Co(III)] as expressed in eqn (10)

$$\frac{-d[Co(III)]_t}{dt} = \frac{k_1 K_{os} K_a [RSH]^2 [Co(III)]_t}{[H^+]^2 + K_{os} K_a^{1/2}[H^+][RSH]} \qquad (10)$$

If $[H^+]^2 \gg K_{os} K_a^{1/2}[H^+][RSH]$, then k_{obs} can be derived

$$k_{obs} = \frac{k_1 K_{os} K_a [RSH]^2}{[H^+]^2}. \qquad (11)$$

This is in good agreement with the observed data as shown in Figs. 1 and 2. Values of $k_1 K_{os} K_a = k_1'$[11] derived at different temperatures and the corresponding activation parameters are shown in Table 2.

An alternative mechanism in which dimerization of RSH with loss of protons to give RSSR^{2-} is proposed as a first step, followed by a rate-determining electron transfer reaction to give the product [Co(II)] and a dithio radical RSSR$^-$ is also in agreement with the observed data. This type of mechanism was, in fact, put forward by Carlyle[26] to explain the observed second-order dependence of the ligand HSO$_3^-$ on the rate of reduction of Fe(phen)$_3^{3+}$ ions. However, this mechanism is not likely to be operating in the present study in view of the kinetic inertness of the dithio anion[27] RSSR^{2-}. The favoured mechanism outlined above is similar to the one postulated by Olatunji[10] for the reactions of the same oxidant with the thioureas. However, the second pathway involving first-order dependence on ligand concentration observed by that author was not obtained in the present investigation.

The significance of second-order ligand-dependent processes has been discussed.[28] In a number of reactions,[14,16,26] recourse had to be made to this type of process in order to rationalize the observed kinetic parameters. For sulphur-containing one-electron reductants such as those under consideration (L-cysteine and mercaptoacetic acid), routes corresponding to such terms are considered important in providing a pathway for the generation of the disulphide product. However, a rate-determining dimerization process leading to the formation of a four-centred M$_2$S$_2$ complex[29] in the transition state, which yields the disulphide without the

Table 2. Dependence of $k_1{}^{11}$ on temperature where $k_1{}^{11} = k_1 K_{os} K_a$

L-Cysteine		Mercaptoacetic acid	
T/°C	k_1^{11}/s^{-1}	T/°C	$10^3 k_1^{11}/s^{-1}$
20.1	0.10	15.8	1.85
25.0	0.14	20.7	2.71
30.1	0.18	25.5	4.11
$\Delta H^{\ddagger}/kJ\ mol^{-1}$	42.7 ± 2		57.3 ± 3
$\Delta S^{\ddagger}/JK^{-1}\ mol^{-1}$	-113.3 ± 8		-91.7 ± 10

formation of a radical, is not deemed feasible in [Co(III)] reactions because of the structure and stability of the oxidant.

In the reaction of [Co(III)] with β-mercaptoethylamine, the two-term experimental rate law encountered appears to require two parallel reaction pathways leading to the disulphide product. Mechanisms consistent with these kinetic observations are embodied in the equations below

Mechanism II

$$[Co(III)] + RSH \overset{K_{os}}{\rightleftharpoons} [Co(III)], RS^- + H^+ \quad (12)$$

$$[Co(III)] + RSH \overset{k_2}{\longrightarrow} [Co(II)] + RS^{\cdot} + H^+ \quad (13)$$

$$[Co(III)], RS^- + RSH \overset{k_3}{\longrightarrow} [Co(II)] + RSSRH^{\cdot} \quad (14)$$

$$RSSRH^{\cdot} + [Co(III)] \rightleftharpoons [Co(II)] + RSSR + H^+ \quad (15)$$

$$2RS^{\cdot} \rightleftharpoons RSSR. \quad (16)$$
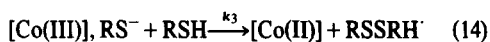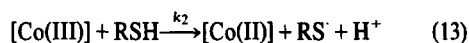
This mechanism gives the rate law:

$$\frac{-d[Co(III)]_t}{dt} = [Co(III)]_t[RSH]\left[\frac{K_{os}k_3[RSH]}{[H^+]} + k_2\right]. \quad (17)$$

From eqn (17), k_{obs} can be derived

$$k_{obs} = [RSH]\left[\frac{K_{os}k_3[RSH]}{[H^+]} + k_2\right]. \quad (18)$$

Rearranging eqn (18) gives eqn (19)

$$\frac{k_{obs}}{[RSH]} = \left[\frac{K_{os}k_3[RSH]}{[H^+]} + k_2\right]. \quad (19)$$

The linearity of the plots of $k_{obs}/[RSH]$ against [RSH] is in good agreement with this rate law (Figs. 3 and 4). Values of the rate and activation parameters derived from such plots are shown in Table 3.

Earlier results obtained from the reactions of cysteine[30,31] with $Fe(CN)_6{}^{3-}$ were also rationalized by a two-term rate expression. Interestingly, the rate constant for the first-order ligand-dependent pathway was found to increase with increasing temperature. A similar trend was observed by us in an earlier investigation of the oxidation of the thioureas[32] by $Fe(phen)_3{}^{3+}$ and $[Co(III)]$.[10]

According to Walling,[33] the values of entropy of activation ΔS^* within the range -83 to $-143\ KJ\ mol^{-1}$ obtained in the reaction of β-mercaptoethylamine with [Co(III)] suggested a mechanism involving free radicals. An obvious possibility for such a radical is $RS^{\cdot}$, but radiolysis studies have shown that thioradicals formed from cysteine[34] and a variety of thiols of simple and complex structures[35] are in equilibrium with the corresponding dithio radical anion, $RSSR^{-}$. In some instances, these species may be protonated to give $RSSRH^{\cdot}$. This is in excellent agreement with mechanism II where the radical $RSSRH^{\cdot}$ has been proposed as a shortlived product formed in reaction (14) and also in the oxidation of cysteine and related ligands[30,31] by $Fe(CN)_6{}^{3-}$.

In conclusion, the oxidations of L-cysteine, mercaptoacetic (thioglycollic) acid and β-mercaptoethylamine by [Co(III)] appear to follow a route leading to the forma-

Table 3. Dependence of k_2 and $k_3{}^{11}$ on temperature for the reaction of β-mercaptoethylamine with the oxidant, [Co(III)], where $k_3{}^{11} = K_{os}k_3$

T/°C	$k_2/mol^{-1}\ dm^3\ s^{-1}$	$10^5 k_3^{11}/mol^{-1}\ dm^3\ s^{-1}$
20.1	0.010	2.120
25.1	0.014	3.110
30.3	0.018	5.400
$\Delta H^*/kJ\ mol^{-1}$	42.3 ± 7	59.8 ± 7
$\Delta S^*/JK^{-1}\ mol^{-1}$	-133.6 ± 25	-123.0 ± 22

tion of [Co(II)] and disulphides as products without the formation of intermediate complexes of significant stability. A similarity in the modes of activation of these reactions and those of the thioureas[10] with the same oxidant is therefore implied. The thermodynamic parameters for the steps involving a second-order ligand dependence are quite similar to those obtained for the di-hydroxyl ligands[36]. This may be an indication that the mode of reactions with both sulphur- and oxygen-containing ligands are the same and independent of the active groups in these ligands. This type of behaviour would not be expected if the reactions proceeded by an inner-shpere mechanism.

REFERENCES

[1] G. B. Dermer, *J. Ultrastructure Res.* 1973, **45**, 183.
[2] J. C. Chermann, F. C. Sinoussi and C. Jasmin, *Biochem. Biophys. Res. Commun.* 1975, **65**, 1229.
[3] C. Jasmin, J. C. Chermann, G. Hervé, A. Tézé, P. Souchay, C. Boy-Loustan, M. Raynaud, F. Sinoussi and M. Raymond, *J. Nat. Cancer Inst.* 1974, **53**, 469.
[4] R. T. Giaquinta and R. A. Dilley, *Biochem. Biophys. Acta* 1975, **387**, 288.
[5] S. P. Berg and S. Izawa, *Biochem. Biophys. Acta* 1977, **460**, 206.
[6] M. G. Goldfield, R. I. Halilov and S. V. Hangulov, *Biochem. Biophys. Res. Commun.* 1978, **85**, 1199.
[7] P. G. Rasmussen and C. H. Brubaker, *Inorg. Chem.* 1964, **3**, 977.
[8] A. G. Lappin and R. D. Peacock, *Inorganica Chimica Acta* 1980, **46**, L71.
[9] Z. Amjad, U. Brodovitch and A. McAuley, *Can. J. Chem.* 1977, **55**, 3581.
[10] M. A. Olatunji, Ph.D. Thesis. University of Glasgow, Glasgow (1975).
[11] J. Hill, A. McAuley and W. F. Pickering, *Chem. Commun.* 1967, 573.
[12] J. Hill and A. McAuley, *J. Chem. Soc. (A)* 1968, 2405.
[13] Z. Amjad, G. Chambers and A. McAuley, *Can. J. Chem.* 1977, **55**, 3575.
[14] J. P. McCann and A. McAuley, *J. Chem. Soc. (A)* 1975, 783.
[15] M. A. Olatunji and A. McAuley, *J. Chem. Soc. Dalton Trans.* 1975, 682.
[16] M. A. Olatunji and A. McAuley, *Can. J. Chem.* 1977, **55**, 3335.
[17] A. G. Lappin and A. McAuley, *J. Chem. Soc. (A)* 1975, 1560.
[18] J. Hill and A. McAuley, *J. Chem. Soc. (A)* 1968, 156.
[19] U. D. Gomwalk and A. McAuley, *J. Chem. Soc. (A)* 1968, 2948.
[20] R. Shanker and A. McAuley, *Ibid.* 1973, 2321.
[21] L. C. W. Baker and T. P. McCutcheon, *J. Am. Chem. Soc.* 1956, **78**, 4503.
[22] E. M. Crook (Ed.), *Gluthatione, Biochem. Soc.* (London) Symposium No. 17. Cambridge University Press (1959).
[23] E. W. Wilson and R. B. Martin, *Arch. Biochem. Biophys.* 1971, **142**, 445.
[24] J. D. Morris, *A Biologist's Physical Chemistry*, 2nd Edn, Chap. 6. Edward Arnold, London (1974).
[25] M. A. Olatunji and A. McAuley, *Can. J. Chem.* 1977, **55**, 3328.
[26] D. W. Carlyle, *J. Am. Chem. Soc.* 1972, **94**, 4525.
[27] A. G. Gilmour and A. McAuley, *J. Chem. Soc. (A)* 1970, 1006.
[28] J. K. Beetle and G. P. Haight Jr., *Prog. Inorg. Chem.* 1972, **17**, 93.
[29] K. J. Ellis, A. G. Lappin and A. McAuley, *J. Chem. Soc. (A)* 1975, 1930.
[30] G. L. Bridgart, M. W. Fuller and I. R. Wilson, *J. Chem. Soc. (A)* 1973, 1274.
[31] G. L. Bridgart and I. R. Wilson, *Ibid.* 1973, 1281.
[32] M. A. Olatunji and A. McAuley, Unpublished data.
[33] C. Walling, *Free Radicals in Solution*, p. 38. Wiley, New York (1957).
[34] G. E. Adams, *Current Topics Radiation Res.* 1967, **3**, 35.
[35] W. Karmann, A. Granzow, G. Meissner and A. Henglein, *Internat. J. Radiation Phys. Chem.* 1968, **1**, 395.
[36] M. A. Olatunji and G. A. Ayoko, to be submitted for publication.

METAL COMPLEXES OF SCHIFF'S BASE DERIVED FROM SALICOYLHYDRAZINE AND BIACETYLMONOXIME

M. M. MOSTAFA*, M. A. KHATTAB and K. M. IBRAHIM

Department of Chemistry, Faculty of Science, Mansoura University AR, Egypt

Abstract—Biacetylmonoxime-salicoylhydrazone (BMSH) complexes of the types [Hg(BMSH)Cl₂] and [M(BMSH-H)₂], where M = Cu(II), Co(II), Ni(III), Mn(II), Zn(II), Cd(II) and UO₂(VI), have been prepared and characterized by conventional chemical and physical measurements. The IR spectra show that the ligand usually coordinates via carbonyl oxygen (C=O), azomethine nitrogen (C=N) and phenolic OH with replacement of hydrogen by metal ions, but acts as a bidentate molecule coordinating through (C=O) and (C=N) in the Hg(II) complex. The magnetic and spectral data of the Co(II) and Ni(II) complexes support octahedral stereochemistry, whilst tetragonally distorted octahedral geometry is suggested for the Cu(II) complex.

Our earlier work[1,2] on the complexes of hydrazone-oxime has been extended to the complexes of biacetyl-monoxime-salicoylhydrazone (BMSH) with some transition metal ions. Recently, Saha *et al.*[3] have isolated the Cu(II) complex of BMSH using ammonia as a buffering agent. However, no structural studies on transition metal complexes of BMSH have been undertaken to date. In the present paper, tentative structures are proposed for some complexes on the basis of molar conductance, elemental analyses, IR, magnetic and spectral data.

RESULTS AND DISCUSSION

The IR spectrum of BMSH shows three bands at 3410, 3340 and 3260 cm⁻¹ considered to be $\nu(OH)$ (phenolic), $\nu(OH)$ (oxime) and $\nu(NH)$ respectively. The existence of bands at lower wavenumbers in the spectrum of the ligand may be due to inter- or intra-molecular hydrogen bonding.[4] The observation of two weak and broad bands entered at 2280 and 1950 cm⁻¹ due to O—H—O stretching and bending vibrations[5,6] confirms the presence of in-

tramolecular hydrogen bonding which is presumed to be form between phenolic OH and carbonyl oxygen as shown in structure (I).
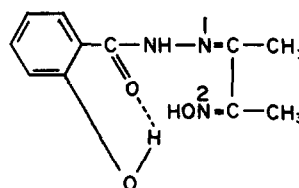
(I)

The complexes of this ligand which have been isolated from absolute ethanol and in presence of sodium acetate as a buffering agent are listed in Table 1. They are insoluble in non-polar solvents but dissolve in DMF and DMSO. Molar conductivities in DMF at 25°C (Table 1) indicate[7] these complexes to be non-electrolytes in this solvent.

The phenolic OH band at 3410 cm⁻¹ is not present in the spectra of the complexes (except the HgCl₂ complex). The band at 1240 ch⁻¹ is assigned to the phenolic (C–O) vibration in the spectrum of BMSH as reported in previous assignments[8,9] but is shifted to higher wavenumbers in the spectra of the complexes suggesting that the o-hydroxy group entered into bond formation

*Author to whom correspondence should be addressed. Present address: Chemistry Department, Illinois State University, Normal, IL 61716, U.S.A.

Table 1. Analytical and physical data for the complexes

Compound	Colour	M.P., °C	Calc. %				Found %				Λ_m† in DMF
			C	H	M	Cl	C	H	M	Cl	
[Co(BMSH-H)₂]	Brown	>360	50.10	4.58	11.17	–	50.46	4.68	11.05	–	35
[Ni(BMSH-H)₂]	Yellow	>360	50.12	4.58	11.12	–	50.66	4.20	11.27	–	3
[Mn(BMSH-H)₂]	Yellow	>360	50.48	4.62	10.49	–	50.42	3.99	10.81	–	11
[Cu(BMSH-H)₂]3H₂O	Green	>360	48.21	4.41	11.59	–	47.93	3.94	12.10	–	18
[Zn(BMSH-H)₂]	Yellow	>360	49.49	4.53	12.25	–	49.92	3.86	12.51	–	7
[Cd(BMSH-H)₂]	Yellow	>360	45.48	4.16	19.34	–	46.07	3.44	19.44	–	4
[UO₂(BMSH-H)₂]	Yellow	>360	35.87	3.01	32.32	–	35.54	2.88	32.62	–	9
[Hg(BMSH)Cl₂]	Yellow	>360	26.07	2.59	–	13.99	25.34	2.57	–	14.30	20

† in cm² ohm⁻¹ mol⁻¹

with displacement of hydrogen. Moreover, spot test identification of the phenolic OH[10] in metal complexes proves the replacement of hydrogen by metal ions.

The bands at 3340, 1310 and 945 cm^{-1} in the spectrum of the ligand attributable respectively to ν(OH) (oxime), $\nu(C=\overset{2}{N}+OH)$ and ν(NO) appear more or less at the same positions for the complexes indicating that neither NO nor $C=\overset{2}{N}$ groups take part in complex formation. Also, the presence of OH (oxime) in the complexes was detected by a spot test,[11] indicating that the oxime group does not participate in coordination. Strong evidence for the presence of a free -OH (oxime) in the complexes comes from the proton magnetic resonance spectra of solutions of the diamagnetic complexes in d$_7$-DMF. In, for example, a solution of [Cd(BMSH-H)$_2$], the -OH proton signal at 10.55 ppm downfield from TMS disappears upon addition of D$_2$O.

Medium and strong bands at 1630 and 1545 cm^{-1} are due respectively to the azomethine groups of the hydrazone $\nu(\overset{1}{C=N})$ and oxime $\nu(C=\overset{2}{N})$. The $\nu(C=N)$ band suffers a negative shift, while the $\nu(C=\overset{2}{N})$ band is shifted to higher wavenumbers indicating the involvement of only azomethine from the hydrazone moiety in coordination. Also, the positive shifts of the band at 1000 cm^{-1} due to ν(N-N)[12] can be taken as an evidence for the involvement of $\nu(C=\overset{1}{N})$ in bonding. The carbonyl band ν(C=O) at 1660 cm^{-1} is shifted to lower wavenumbers in all complexes suggesting that the carbonyl oxygen is also a potential site for bonding. The low frequency bands in the regions 430–410 and 365–320 cm^{-1} are tentatively assigned to ν(M-O)[13,14] and ν(M-N)[15] respectively.

The IR absorptions due to the UO$_2$ group are observed at 930 and 860 cm^{-1} as sharp bands corresponding[16] to the asymmetric stretching frequencies ν_3 and ν_1 respectively. These observations indicate that the UO$_2$ moiety is virtually linear.[16] All these observations together with the elemental analyses suggest structure (II) for all complexes except that of Hg(II) which may have structure (III). The mercury (II) complex shows ν(Hg-Cl) at 255 cm^{-1} which is in the region typically found for tetrahedral structures.[17]
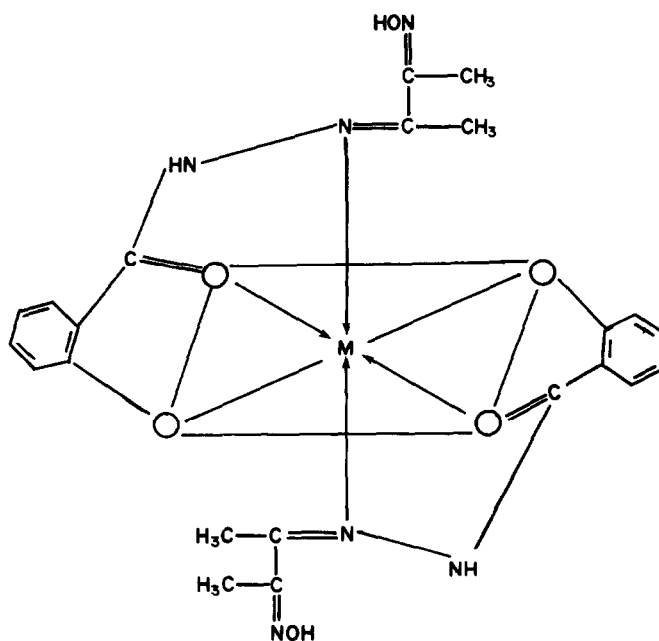
M=Cu (II), Co(II), Ni(II), Mn(II), Zn (II) and Cd (II)

(II)

Table 2. Spectral and magnetic properties of BMSH complexes

Compound	Magnetic moment μ_{eff}(B.M.)	Electronic spectra (in cm^{-1} × 10^3) Ligand field bands	Charge-transfer
[Co(BMSH-H)$_2$]	4.85	7.7, 15.3, 18.6; Dq=840, B=796, β=0.81	23.9, 30.8, 36.3
		7.3, 11.2, 15.1, 23.1, 25.8;	
[Ni(BMSH-H)$_2$]	3.32	Dq=730, B=802, β=0.77	29.6, 35.5
[Cu(BMSH-H)$_2$]3H$_2$O	1.79	14.6(sh), 16.9	22.7, 24.2
[Mn(BMSH-H)$_2$]	6.02		
[Zn(BMSH-H)$_2$]	diamag.		
[Cd(BMSH-H)$_2$]	diamag.		
[Hg(BMSH)Cl$_2$]	diamag.		
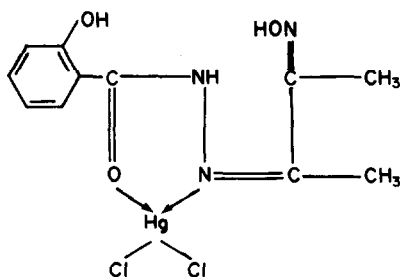
(III)

The magnetic moments and reflectance spectra of the complexes are listed in Table 2. The magnetic moment of the Cu(II) complex corresponded to the spin-only value for one unpaired electron and was in the range normally observed for Cu(II) complexes having an orbitally non-degenerate B_{1g} ground state, thereby indicating no metal–metal interaction. The electronic spectrum shows one broad band at $16,900 \, cm^{-1}$ with a shoulder at $14,600 \, cm^{-1}$ which may be assigned respectively to $^2B_{1g} \rightarrow ^2E_g$ and $^2B_{1g} \rightarrow ^2A_{1g}$ transitions. On this basis the Cu(II) complex seems to have tetragonally distorted octahedral geometry.[18] The three bands at 7,300, 11,200 and $23,100 \, cm^{-1}$ in the spectrum of the Ni(II) complex are assigned to $^3A_{2g} \rightarrow ^3T_{2g}$, $^3A_{2g} \rightarrow ^3T_{1g}(F)$ and $^3A_{2g} \rightarrow ^3T_{1g}(P)$ respectively,[19] while the band at $15,100 \, cm^{-1}$ may be assigned to the $^3A_{2g} \rightarrow ^1E_g$ transition.[20] The values of $10D_q$ and B have been calculated from the observed positions of the bands by using the equations for the d^8 system[21] which can be taken as evidence for an octahedral structure. Also, the value of the magnetic moment (3.32 B.M.) together with the ratio ν_2/ν_1 (1.53)[22] gives further support for the proposed octahedral geometry. The reflectance spectrum of the Co(II) complex shows three bands at 7700, 15,300 and $18,600 \, cm^{-1}$ which are assigned respectively to $^4T_{1g} \rightarrow ^4T_{2g}$, $^4T_{1g} \rightarrow ^4A_{2g}$ and $^4T_{1g}(P)$ transitions. The values of D_q, B and magnetic moment suggest an octahedral geometry[23,24] for the cobalt complex as well.

EXPERIMENTAL

BMSH was prepared by refluxing 1 mole of biacetylmonoxime with 1 mole of salicoylhydrazine in ethanol for 2 hr and crystallizing the product from ethanol; m.p. 250°C.

The complexes of Co(II), Ni(II), Mn(II), Cd(II), Zn(II), Hg(II) and UO$_2$(VI) were prepared using ethanolic solutions of the hydrated metal salts and adding a 2:1 mole ratio of ligand to metal salt in presence of sodium acetate as a buffering agent and heating the mixture under reflux for 30 min. The complexes were filtered hot, washed with ethanol and dried in a vacuum desiccator (CaCl$_2$). The same procedure was used in case of the Cu(II) complex but without adding sodium acetate.

The analyses for the metals and chloride were carried out by standard methods.[25] Carbon and hydrogen contents were determined by the Microanalytical Unit of Mansoura University.

The IR spectra were measured as nujol mulls between CsI discs and recorded on Pye Unicam SP.2000 and Perkin-Elmer 557 ($4000-200 \, cm^{-1}$) spectrophotometers. Electronic spectra were measured in the solid state using a Unicam SP.700 C spectrophotometer. Molar conductances in DMF were measured using a Tacussel conductivity bridge type CD6NG at room temperature (25°C). Magnetic moments were measured using the Gouy method at Liverpool University, UK, and were corrected for the diamagnetism of the component atoms using Pascal's constant.[26] Proton magnetic resonance spectra of the complexes were carried out on a Perkin-Elmer R12B (60 MHz) spectrophotometer.

REFERENCES

[1] A. M. Shallaby, M. M. Mostafa and M. M. Bekheit, *J. Inorg. Nucl. Chem.* 1978, **41**, 267.

[2] M. M. Mostafa, S. M. Hassan and G. M. Ibrahim, *J. Inorg. Nucl. Chem.* 1980, **42**, 285.

[3] N. Saha, K. M. Datta and B. N. Mallick, *J. Ind. Chem. Soc.* 1978, **LV**, 1311.

[4] C. N. Rao, *Chemical Applications of Infrared Spectroscopy.* Academic Press, New York (1967).

[5] R. Blinck and D. Hadzi, *J. Chem. Soc.* 1958, 4536.

[6] K. Burger, I. Ruff and F. Ruff, *J. Inorg. Nucl. Chem.* 1965, **27**, 179.

[7] W. J. Geary, *Coord. Chem. Revs.* 1971, **7**, 81.

[8] N. S. Biradar, B. R. Patil and V. H. Kulkarni, *J. Inorg. Nucl. Chem.* 1975 **37**, 1901.

[9] N. Bhave and R. B. Kharat, *J. Inorg. Nucl. Chem.* 1980, **42**, 977.

[10] R. Feigl, *Spot Tests in Organic Analysis.* Elsevier, Amsterdam (1966).

[11] R. L. Shriner, R. C. Fuson and D. Y. Curtin, *The Systematic Identification of Organic Compounds.* Wiley, London (1965).

[12] D. N. Sathanarayana and D. Nicholls, *Spectrochim. Acta* 1978, **34A**, 263.

[13] A. N. Speca, M. M. Karayanis and L. L. Pytlwski, *Inorg. Chem. Acta.* 1974, **9**, 87.

[14] M. P. Teotia, D. K. Rastogi and W. U. Malik, *Inorg. Chim. Acta.* 1973, **7**, 339.

[15] B. Beecroft, M. J. M. Campbell and R. Grzeskowiak, *J. Inorg. Nucl. Chem.* 1974, **36**, 55.

[16] L. Cattalini, U. Croatto, S. Degetto and E. Tondello, *Inorg. Chim. Acta Rev.* 1971, **5**, 19.

[17] J. R. Ferraro, *Low Frequency Vibrations of Inorganic and Coordination Compounds.* Plenum Press, New York (1971).

[18] M. J. M. Campbell and R. Grzeskowiak, *J. Chem. Soc., A* 1967, 396.

[19] C. K. Jørgensen, *Acta. Chem. Scand.* 1956, **10**, 887.

[20] A. B. P. Lever, *Inorganic Electronic Spectroscopy.* Elsevier, Amsterdam (1968).

[21] L. Sacconi, *Trans. Met. Chem.* 1968, **4**, 212.

[22] D. W. Meek, R. S. Drago and T. S. Piper, *Inorg. Chem.* 1962, **1**, 285.

[23] E. K. Barefield, D. H. Busch and S. M. Nelson, *Quart. Rev.* 1968, **22**, 457.

[24] J. Reedijk, W. L. Briessen and W. L. Groeneveld, *Rec. Trav. Chim.* 1969, **88**, 1094.

[25] A. I. Vogel, *A. Text Book of Quantitative Inorganic Analysis.* Longmans, London (1961).

[26] J. Lewis and R. G. Wilkins, *Modern Coordination Chemistry.* Interscience, New York (1960).

IRON(II) COMPLEXES OF PYRAZOL-4,5-DIONE-5-OXIMES

J. CHARALAMBOUS,* L. I. B. HAINES,* W. M. SHUTIE and F. B. TAYLOR
Department of Chemistry, The Polytechnic of North London, London N7 8DB, England

and

R. McGUCHAN
PERME, Waltham Abbey, Essex EN9 1BP, England

and

D. CUNNINGHAM
Department of Chemistry, University College Galway, Galway, Ireland

Abstract—The complexes Fe(po)₂·H₂O, Fe(Ppo)₂·H₂O and Fe(Ppo)₂·2py, where poH = 3 - methyl - 4 - oxime - 1H - pyrazole - 4,5 - dione and PpoH = 3 - methyl - 4 - oxime - 1 - phenyl - 1H - pyrazole - 4,5 - dione, have been prepared. The magnetic susceptibilities and Mössbauer spectra of the complexes have been investigated.

The reactions of 2-nitrosophenols (mono-oximes of 1,2-quinones) (LH) with metal salts or with metal carbonyls give neutral metal complexes of type ML$_n$ (*n* = 2 or 3).[1-3] In certain cases deoxygenation of the ligand can occur to give heterocyclic or other organic products. We now report on the reactions of the related ligands 3 - methyl - 4 - oxime - 1H - pyrazole - 4,5 - dione (poH) (**1**; R = H, R′ = CH₃) and 3 -
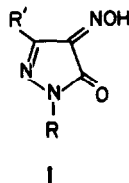
methyl - 4 - oxime - 1 - phenyl - 1H - pyrazole - 4,5 - dione (PpoH) (**1**; R = C₆H₅, R′ = CH₃) with iron(II) ammonium sulphate and with iron(O) pentacarbonyl. We also report on the properties and structure of the metal complexes which arise from these reactions. Complexes of copper(II), nickel(II), zinc(II), cadmium(II) and magnesium(II) derived from ligands of type **1** (R = H, C₆H₅, 4-(NO₂)C₆H₄, 4-ClC₆H₄, 2,4-(NO₂)₂C₆H₃; R′ = H, CH₃, C₆H₅) have been reported earlier.[4-6]

EXPERIMENTAL

The ligands were prepared as described in the literature.[7]

Interaction of 3 - methyl - 1 - phenyl - 4 - oxime - 1H - pyrazole - 4,5 - dione or 3 - methyl - 4 - oxime 1H - pyrazole - 4,5 - dione with iron(II) ammonium sulphate

3 - Methyl - 1 - phenyl - 4 - oxime - 1H - pyrazole - 4,5 - dione (2.0 g, 2 mol equiv.) and iron(II) ammonium sulphate (1.9 g, 1 mol equiv.) were stirred in ethanol–water (2 : 1) (120 cm³) (1 hr). Turquoise *bis*(3 - *methyl - 1 - phenyl - 4 - oximato - 1H - pyrazole - 4,5 - dione)iron(II) - monohydrate* (1.4 g, 59%), (Found: C, 50.2; H, 4.1; Fe, 11.7;

N, 17.1. C₂₀H₁₈FeN₆O₅ requires: C, 50.2; H, 3.8; Fe, 11.7; N, 17.6%), was filtered off, washed with water (2 × 100 cm³) and ethanol (2 × 100 cm³) and dried at 30°C/0.1 mm.

Unchanged 3 - methyl - 4 - oxime - 1H - pyrazole - 4,5 - dione (88%) (identified by IR) was recovered after stirring (4 hr) with the iron(II) salt in ethanol–water.

Interaction of 3 - methyl - 4 - oxime - 1H - pyrazole - 4,5 - dione with iron pentacarbonyl

3 - Methyl - 4 - oxime - 1H - pyrazol - 4,5 - dione (2.51 g, 1 mol equiv.) and iron pentacarbonyl (19.4 g, 5 mol equiv.) were heated under reflux for 12 hr in dry tetrahydrofuran (100 cm³) under nitrogen. The mixture was filtered to give dark green *bis*(3 - *methyl - 4 - oximato - 1H - pyrazol - 4,5 - dione)iron(II) - monohydrate* (1.49 g, 54%). (Found: C, 29.9; H, 2.8; Fe, 17.1, N, 25.9) C₈H₁₀FeN₆O₆ requires: C, 29.5; H, 3.1; Fe, 17.1; N, 25.8%) which was washed with tetrahydrofuran and dried at 30°C/0.1 mm. The washings were concentrated and filtered to give orange 2,4 - *dihydro - 4 - (5 - hydroxy - 3 - methyl - 1H - pyrazol - 4 - yl)imino - 5 - methyl - 3H - pyrazol - 3 - one* (0.14 g, 8%). (Found C, 47.1; H, 4.9; N, 33.6%; C₈H₉N₅O₂ requires: C, 46.9; H, 4.8; N, 33.8%), m.p. 265–67°C sub.; *m/e* 207 (M⁺).

Interaction of 3 - methyl - 1 - phenyl - 4 - oxime - 1H - pyrazole - 4,5 - dione with iron pentacarbonyl

3 - Methyl - 1 - phenyl - 4 - oxime - 1H - pyrazole - 4,5 - dione (2.04 g, 2 mol equiv.) and iron pentacarbonyl (0.98 g, 1 mol equiv.) were heated under reflux for 12 hr under nitrogen in dry tetrahydrofuran (100 cm³). Chromatography of the mixture (silica gel) gave, with toluene as eluant 2,4 - dihydro - 4 - (5 - hydroxy - 3 - methyl - 1H - pyrazol - 4 - yl) - imino - 5 - methyl - 1 - phenyl - pyrazol - 3 - one (0.41 g 66%), m.p. 185–7°C (*lit.*,[8] 183°C), (Found: C, 67.1; H, 5.1; N, 19.2%). Calc. for C₂₀H₁₇N₅O₂: C, 66.8; H, 4.8; N, 19.5%), *m/e* 359 (M⁺). Further elution with toluene gave 1,2,5 - oxadiazole[3,4-*d*] - 6 - methyl - 4 - phenyl - 4H - pyrazole (0.04 g, 6%), m.p. 86–8°C (*lit.*,[9] 91°C), *m/e* 200 (M⁺). Methanol eluted *bis*(5 - methyl - 1 - phenyl - 4 - oximato - 1H - pyrazol - 4,5 - dione)iron(II) - hydrate, (0.11 g, 14%) (identified by IR).

Interaction of bis(3 - methyl - 1 - phenyl - 4 - oximato 1H - pyrazole - 4,5 - dione)iron(II) - monohydrate with pyridine

Bis(3 - methyl - 1 - phenyl - 4 - oximato - 1H - pyrazole - 4,5 - dione)iron(II) - monohydrate (2.6 g) and pyridine (10 cm³) were stirred for 24 hr. *Bis*(3 - *methyl* - 1 - *phenyl* - 4 - *oximato* - 1H - *pyrazole* - 4,5 - *dione*)*iron*(*II*) - *dipyridine* (2.7 g, 79%) (Found: C, 57.7; H, 4.4; Fe, 8.6; N, 17.7. $C_{30}H_{26}FeN_8O_4$ requires C, 58.2; H, 4.2; Fe, 9.0; N, 18.1%) was filtered off, washed with diethyl ether (2 × 50 cm³) and dried at 30°C/0.1 mm.

Thermal gravimetric analysis data for $Fe(Ppo)_2 \cdot 2py$

Weight of sample: 206 mg. Weight loss: 55 mg (Calc. for 2 mol of pyridine per mol of adduct: 53 mg). Temperature of loss: 172–8°C.

Measurements

Magnetic susceptibility and thermogravimetric analysis data, also IR and NMR spectra were obtained as described earlier.[1] Mössbauer spectra were recorded on a constant acceleration Mössbauer spectrometer (J and P Engineering, Reading) using a [57]Co source in a rhodium matrix (Spire Corporation). The velocity calibration was based on the inner four lines of the spectrum of natural iron.

RESULTS AND DISCUSSION

The reaction of iron(II) ammonium sulphate with PpoH in aqueous ethanol gave a turquoise complex of stoichiometry $Fe(Ppo)_2 \cdot H_2O$. In contrast poH failed to react with the iron(II) salt under similar conditions. However, the complex $Fe(po)_2 \cdot H_2O$ was obtained along with some 2,4 - dihydro - 4 - (5 - hydroxy - 3 - methyl - 1H - pyrazol - 4 - yl)imino - 5 - methyl - 3H - pyrazol - 3 - one (2; R = H) from the reaction of the oxime with iron pentacarbonyl. The reaction of iron pentacarbonyl with PpoH afforded mainly 2,4 - dihy-

dro - 4 - (5 - hydroxy - 3 - methyl - 1 - phenyl - 1H - pyrazol - 4 - yl)imino - 5 - methyl - 2 - phenyl - 3H - pyrazol - 3 - one (2; R = C_6H_5), together with 1,2,5 - oxadiazole[3,4-*d*] - 6 - methyl - 4 - phenyl - 4H - pyrazole (3) and $Fe(Ppo)_2 \cdot H_2O$. The formation of the organic products can be rationalised in terms of de-oxygenation of the protonated ligands as discussed for analogous reactions of complexes of quinone mono-oximes.[10,11]
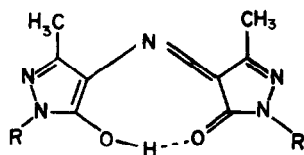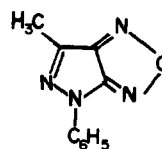
The complex $Fe(Ppo)_2 \cdot H_2O$ reacted with pyridine to give $Fe(Ppo)_2 \cdot 2py$. The thermal gravimetric analysis of the adduct showed that pyridine (2 mol/mol adduct) was lost at *ca.* 175°C. The room temperature magnetic moments (Table 1) of the hydrates and of

3

2
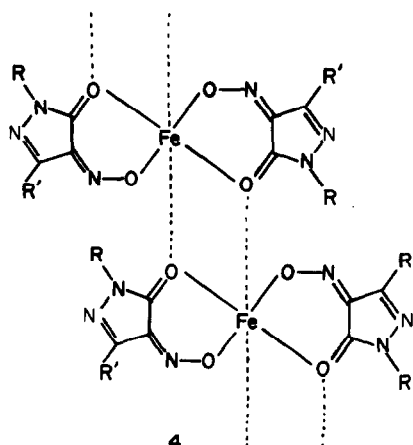
4

Table 1. Magnetic and Mössbauer data

$Fe(Ppo)_2 \cdot H_2O$										δ (mm s⁻¹)†	Δ (mm s⁻¹)†
T (K)	363	333	303	272	243	214	184	154	124		
$10^6\chi_A$	10443	11202	11383	12032	12789	13481	14437	14920	16367	1.19	2.58 at 300 K
μ_{eff}(B.M)	5.51	5.47	5.26	5.13	4.99	4.80	4.61	4.28	4.03	1.18	2.55 at 75 K
$-\theta$ (K)	280										
$Fe(Ppo)_2 \cdot 2py$											
T (K)	363	335	303	273	243	213	184	153	124		
$10^6\chi_A$	10399	11402	12515	13431	15650	17870	20688	24645	30768	1.10	2.51 at 300 K
μ_{eff}(B.M)	5.50	5.53	5.51	5.42	5.52	5.52	5.52	2.49	5.53		
$-\theta$ (K)	0										
$Fe(po)_2 \cdot H_2O$											
T (K)	363	333	302	273	244	214	183	153	123		
$10^6\chi_A$	10402	11121	11665	11828	12297	12858	13886	14771	16096	1.03	2.61 at 300 K
μ_{eff}	5.50	5.45	5.31	5.09	4.90	4.69	4.51	4.26	3.99	1.14	262 at 75 K
$-\theta$ (K)	316										

†The isomer shifts (δ) are given relative to iron foil. The errors in δ and Δ are of the order 0.02 and 0.03 mm s⁻¹ respectively.

the pyridine adduct lie between 5.2 B.M. and 5.4 B.M. and are indicative of high-spin iron(II).

The magnetic behaviour of the complexes was measured at variable field strength and at variable temperature (Table 1). All complexes follow the Curie–Weiss Law. The decreasing magnetic moment with temperature of the hydrates and their large negative Weiss constants indicate antiferromagnetic behaviour and suggest association (4). However the experimental data do not rule out the possibility of spin-orbit coupling. Some indirect support for association is provided by the insolubility of the complexes and the contrasting magnetic behaviour of the pyridine adduct. The room magnetic moment, the negligible Weiss constant and the lack of significant variation of magnetic moment within the temperature range used all suggest that the pyridine adduct is monomeric. The value of $\theta = 0$ for $Fe(Ppo)_2 \cdot 2py$ suggests that the pyridine adduct is magnetically dilute, indicating a pseudooctahedral structure. The Mössbauer parameters of all the complexes (Table) indicate that the materials are essentially free from iron(III) impurities, and are in accord with high-spin iron(II), and the structural suggestions.[12]

The high spin character of the iron complexes suggests that the ligand field exerted by po^- or Ppo^- is weak. This contrasts with the high ligand-field character of quinoneoximato ligands and is probably a consequence of the limited conjugation within chelated po^- or Ppo^- ligands.

REFERENCES

[1] J. Charalambous, N. A. Nassef and F. B. Taylor, *Inorg. Chim. Acta* 1978, **26**, 107.

[2] J. Charalambous, G. R. Soobramanien, A. Betts and J. Bailey, *Inorg. Chim. Acta* 1982, **60**, 151.

[3] D. K. Allen, J. Charalambous, L. I. B. Haines, M. H. Johri, D. S. Peat, J. Bailey and H. D. Matthewson, unpublished data.

[4] V. Hovorka and L. Sucha, *Coll. Czechoslov. Chem. Comm.* 1960, **25**, 1796.

[5] V. Hovorka and L. Sucha, *Coll. Czechoslov. Chem. Comm.* 1960, **25**, 1432.

[6] V. Hororka and L. Sucha, *Coll. Czechoslov. Chem. Comm.* 1964, **29**, 983.

[7] A. O. Fitton and R. K. Smalley, *Practical Heterocyclic Chemistry*, p. 24. Academic Press, London (1968).

[8] W. Hänsel, *Liebigs Ann. Chem.* 1976, 1380.

[9] E. Möhr, *J. Prakt. Chem.* 1909, **79**, 1.

[10] J. Charalambous, M. J. Kensett and J. M. Jenkins, *J. Chem. Soc. Chem. Commun.* 1977, 400.

[11] R. G. Buckley, J. Charalambous and E. G. Brain, *J. Chem. Soc. Perkin I* 1982, 1075.

[12] N. N. Greenwood and T. C. Gibb, *Mössbauer Spectroscopy*, p. 144. Chapman & Hall, London (1971). B. W. Dockum and W. M. Reiff, *Inorg. Chim. Acta* 1979 **35**, 285. M. M. Bishop and J. Lewis, *J. Chem. Soc. Dalton* 1980, 1390.

METAL CHELATES OF 1-ACETYLPYRIDINIUM CHLORIDE-4-PHENYL-3-THIOSEMICARBAZIDE

A. A. EL-ASMY and M. M. MOSTAFA*

Chemistry Department, Faculty of Science, Mansoura University, AR. Egypt

Abstract—The metal chelates of 1-acetylpyridinium chloride-4-phenyl-3-thiosemicarbazide [(APTS)]$^+$Cl$^-$ of the type [M(APTS)X$_2$]$^+$Cl$^-$ (M = Co(II), Ni(II), Cu(II), Zn(II) or Cd(II); X = Cl, Br or $\frac{1}{2}$SO$_4$) have been prepared and characterized on the basis of elemental analysis, molar conductance, IR, electronic spectra and magnetic studies. IR spectral studies showed that the ligand coordinates via thioketo and ^{1}NH groups. Magnetic and spectral studies suggest a tetrahedral structure for Ni(II), pseudo-tetrahedral for Co(II) and square planar and/or distorted tetrahedral for Cu(II) chelates.

INTRODUCTION

Our previous study[1-5] on the ligands containing thiosemicarbazide moiety are extended to 1-acetylpyridinium chloride-4-phenyl-3-thiosemicarbazide [(APTS)]$^+$Cl$^-$. Also, we have reported[1-5] the isolation of some metal complexes both in the keto and the enol forms of the same ligand by changing the pH of the solution using sodium acetate. In contrast to this observation, we prepared herein only the keto chelates even though the pH of the solution was changed. Moreover, the ligand coordinates exclusively via the thioketo and ^{1}NH groups forming a five membered ring around the metal ion. The isolated metal chelates are characterized by conventional physical and chemical studies. Finally, the stereochemistry of the chelates is discussed on the basis of magnetic and spectral studies.

EXPERIMENTAL

All the chemicals used are BDH quality. The ligand (I) was prepared by adding slowly phenyl isothiocyanate (13.5 cm^3) to a solution of (18.5 g) Girard's reagent P (carbohydrazidopyridinium chloride) in absolute ethanol. The mixture was refluxed on a water bath for a half-hour. The white product was crystallized from absolute ethanol and dried in a vacuum desiccator over anhydrous calcium chloride; m.p., 161°C.

(I)
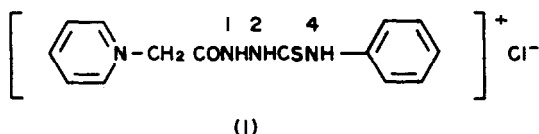
Preparation of the metal chelates

The metal chelates were prepared by adding equimolar amounts (10^{-2} moles) of APTS and the metal salts in absolute ethanol. The mixture was refluxed on a water bath for approximately a half-hour. The product was filtered off, washed with hot ethanol and diethylether respectively and finally dried in a vacuum desiccator over anhydrous calcium chloride. Even in presence of excess ligand attempts to prepare the bis-chelates were unsuccessful.

*Author to whom correspondence should be addressed. Present address: Chemistry Department, Illinois State University, Normal, IL 61761, U.S.A.

Analyses

Elemental analyses were carried out by the Microanalytical Unit of the Mansoura University. The metals and chloride contents were carried out by standard methods.[6]

Physical measurements

Molar conductance measurements were obtained with a Tacussel type CD6NG conductivity bridge using 10^{-3} M solutions in dimethylsulphoxide at 25°C. The electronic spectra of the metal chelates in DMSO, pyridine and nujol mull were recorded on a Pye Unicam SP.1800 spectrophotometer. The magnetic susceptibility measurements were carried out using Gouy method and HgCo(SCN)$_4$ as calibrant at Alexandria University, Egypt. Diamagnetic corrections were made using Pascal's constants.[7] IR spectra were recorded as nujol mulls on Pye Unicam SP.2000 spectrophotometer.

RESULTS AND DISCUSSION

Analytical results and some physical properties of the isolated metal chelates are listed in Table 1. The chelates [M(APTS)X$_2$]$^+$Cl$^-$ are stable in air and insoluble in common organic solvents, but quite soluble in DMF and DMSO. The molar conductance of the ligand in DMSO was found to be 54 Ω^{-1} cm^2 mole^{-1} which falls in the range reported for 1:1 electrolytes.[8] Also, the molar conductance values of the metal chelates in DMSO are in the range expected for 1:1 electrolytes (i.e. 25–70 Ω^{-1} cm^2 mole^{-1}).[8]. The relatively high value (70 Ω^{-1} cm^2 mole^{-1}) for [Ni (APTS)Cl$_2$]$^+$Cl$^-$ may suggest 1:2 electrolyte or more likely some dissociation of this complex in DMSO.

All the isolated metal chelates have the same general formula [M(APTS)X$_2$]$^+$Cl$^-$ irrespective of the divalent metal ion and the pH of the preparative mixture. The existence of the free ligand as a salt as well as the distribution of the positive charge over the cation may stabilize both the thioketo and carbonyl groups and thereby prevent the deprotonation. To explain the chelation via the thioketo and ^{1}NH and not through the carbonyl and ^{2}NH groups, we believe that the ^{2}NH is less basic than ^{1}NH. Also, the carbonyl group is under the influence of the tautomeric effect and/or hydrogen bonding which decreases the activity of the carbonyl oxygen as a coordination site. Both factors therefore favour chelation by the thioketo and

Table 1. Elemental analyses and some physical properties of $[M(APTS)X_2]^+Cl^-$ chelates

Compound	M.P. °C	Colour	% Calc.				% Found				Λ_m in DMSO*
			C	H	M	Cl	C	H	M	Cl	
$[(APTS)]^+Cl^-$	161	white	52.26	4.38	--	11.01	51.61	4.64		11.09	54
$[Cu(APTS)Cl_2]^+Cl^-$	145	deep green	36.86	3.10	14.07	23.31	36.51	3.15	14.28	23.69	52
$[Co(APTS)Cl_2]^+Cl^-$	235	green	37.25	3.13	12.91	23.56	36.58	3.49	12.95	22.90	50
$[Ni(APTS)Cl_2]^+Cl^-$	250	reddish brown	37.22	3.12	13.05	23.55	37.08	3.81	12.85	23.38	70
$[Cd(APTS)Cl_2]^+Cl^-$	205	white	33.28	2.79	22.25	21.05	34.07	2.54	21.72	21.53	32
$[Hg(APTS)Cl_2]^+Cl^-$	243	white	28.36	2.38	--	17.94	28.10	2.20	--	17.69	--
$[Cu(APTS)Br_2]^+Cl^-$	140	brown	30.84	2.58	11.65	--	30.58	2.23	11.83	--	43
$[Cd(APTS)Br_2]^+Cl^-$	236	white	28.30	2.37	18.92	--	28.18	2.80	18.80	--	35
$[Zn(APTS)Br_2]^+Cl^-$	224	white	30.72	2.57	11.94	--	30.78	2.08	11.60	--	27
$[Cu(APTS)SO_4]^+Cl^-$	194	deep green	34.93	2.93	13.19	--	34.11	2.84	12.59	--	41

*in $ohm^{-1} cm^2 mole^{-1}$

NH groups. In contrast to this, we have found[1-5] that similar neutral ligands were easily deprotonated in the presence of sodium acetate as a buffering agent.

IR spectral studies

The infrared spectrum of $[(APTS)]^+Cl^-$ indicates that it exists mainly in the keto form; it shows $v(CO)$ and $v(CS)$ bands at 1730 and 1290 cm^{-1} respectively and no bands above 3480 cm^{-1} as well as in the region 2600–2550 cm^{-1} which would be expected for the enol forms (IV) and (V).

$$RNHC=NNHCOR' \rightleftharpoons RNHCSNHNHCOR' \rightleftharpoons RNHCSNHN=CR'$$

HS (IV) (III) OH (V)
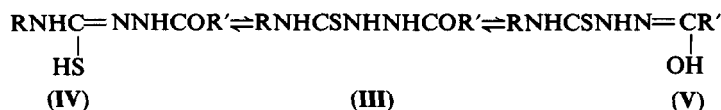
where R = phenyl and R' = —(—CH₂—N⟨⟩)Cl⁻.

The spectra of all these metal chelates are very similar. The band at 1730 cm^{-1} in the spectrum of the ligand is essentially unchanged in the spectra of the metal chelates. Also, the band at 1570 cm^{-1} due to $v(CO + NH)$ is not affected by chelation. These observations can be taken as evidence that the carbonyl group is not involved in coordination to the metal ions. The three bands at 1540, 1500 and 1460 cm^{-1} in the spectrum of the ligand are likely due to $v(-N-C=S)$ vibrations.[9] These bands are assigned as coupled modes principally of $\beta(NH)$ and $v(CN)$.[10] Also, the bands at 1290 and 790 cm^{-1} are due to $v(C=S)$ with contribution of $v(CN)$. The negative shifts of these bands to lower wavenumbers in the spectra of all metal chelates can be taken as evidence that the ligand coordinates via the thioketo group. The three $v(NH)$ mode of vibrations undergo a negative shift in the spectra of the metal chelates indicating the involvement of at least one of the $v(NH)$ groups in bonding. This supported by the small positive shifts of the band at 1020 cm^{-1} assigned to $v(N-N)$[11] in the spectrum of the ligand and the appearance of a new band at *ca.* 335 cm^{-1} which may be attributed to $v(M-N)$.[12] In summary, all these observations to-

gether with elemental analyses suggest that the ligand acts in a bidentate manner and coordinates via its thioketo and NH groups with the formation of a 5-membered rings around the central metal ion.

The stereochemistry of the metal chelates are assigned on the basis of their electronic spectra in nujol, DMSO as well as pyridine solutions and confirmed by magnetic measurements. The results of electronic spectra together with magnetic moments are reported in Table 2. The magnetic moment of the compound $[Co(APTS)Cl_2]^+Cl^-$ is found to be 4.62 B.M., which is acceptable for either tetrahedral or five coordinate structure depending on the extent of chlorine coordination. Both the spectra in nujol and DMSO are identical and show three bands at 14,700, 16,000 and 17,850 cm^{-1} which excludes a five coordinate structure.[13] The strong band at 14,700 cm^{-1} is assigned to $^4A_2\rightarrow^4T$ (P) transition, while the band at 17,900 cm^{-1} may be assigned to spin-forbidden transition[14] which is typically found for pseudo-tetrahedral structure around Co(II). On dissolution of the Co(II) chelate in pyridine the colour changes from green to brownish red and the spectrum exhibits four bands at 14,900; 15,900; 17,900 and 18,900 cm^{-1}. These values are different from those obtained in nujol and DMSO and are similar to those reported for six coordinate Co(II) complexes.[13] The spectra of Ni(II) chelate in nujol and DMSO exhibit a split band at 14,300 and 14,900 cm^{-1} along with a weak band at 12,200 cm^{-1} which support the presence of tetrahedral structure around Ni(II) ion. Also, the value of magnetic moment $\mu_{eff} = 3.38$ B.M., for Ni(II) ion suggests a tetrahedral structure around Ni(II). The spectrum of Ni(II) chelate in pyridine shows two bands at 18,900 and 13,500 cm^{-1} which are assigned respectively to $^3A_{2g}\rightarrow^3T_{1g}$ and $^3A_{2g}\rightarrow^1E_g$ transitions in octahedral

Table 2. Magnetic moments and electronic spectra of the metal chelates

Compound	$\mu_{eff.}$ (B.M.)	Medium	Electronic spectra (in cm^{-1} x 10^3)			
[Co(APTS)Cl$_2$]$^+$Cl$^-$	4.62	Nujol mull	13.7(sh),	14.8,	16.1, 17.9	
		DMSO	14.7,	16.0,	17.9	
		Pyridine	14.9,	15.9,	17.9, 18.9	
[Ni(APTS)Cl$_2$]$^+$Cl$^-$	3.38	Nujol mull	12.2,	14.3,	14.9, 18.9	
		DMSO	12.2,	14.3,	16.1, 18.5(sh)	
		Pyridine	13.5,	18.9		
[Cu(APTS)Cl$_2$]$^+$Cl$^-$	2.15	Nujol mull	11.9,	14.1,	16.9	
		DMSO	12.2,	14.3		
		Pyridine	12.2,	16.7		
[Cu(APTS)Br$_2$]$^+$Cl$^-$	1.93	Nujol mull	12.2(sh),	14.1,	16.1(sh),	19.0, 25.6
		DMSO	12.0(sh),	14.1		18.9, 25.6
		Pyridine	12.2(sh),	16.9		
[Cu(APTS)SO$_4$]$^+$Cl$^-$	1.84	Nujol mull	12.0,	14.1,	14.9(sh),	17.5(sh), 25.0
		DMSO	12.0,	14.1,	14.9(sh),	25.0
		Pyridine	12.2,	15.4(sh)		16.7

structure.[13] Two different types of spectra were recorded for Cu(II) chelates. The spectra of copper(II) chloride and sulphate chelates show a broad band centred at *ca.* 14,000 cm^{-1} with no discernible shoulders, while the bromide chelate shows three bands at 12,000(sh), 14,100 and 19,000 cm^{-1} which suggests a square planar for the former and pseudo tetrahedral for the latter. The band at 19,000 cm^{-1} in the spectrum of Cu(II) bromide may be attributed to Π(Br)→Cu(II).[15] Also, the bands at 25,000 and 25,600 cm^{-1} in the spectra of Cu(II) sulphate and bromide respectively are assumed to arise from charge transfer M→L.[16] Finally, the solution spectra in pyridine for Cu(II) chelates were also recorded and exhibit a broad band centred at ~16,000 cm^{-1} with a low energy shoulder. On this basis all the chelates in pyridine are seen to be tetragonally distorted.[17] The values of magnetic moments for the Cu(II) chelates are in a good agreement with those reported for d^9 configuration.[18,19]

REFERENCES

[1]M. M. Mostafa, A. M. Shallaby and A. A. El-Asmy, *J. Inorg. Nucl. Chem.* 1981, **43**, 2992.
[2]M. M. Mostafa, A. M. Shallaby and A. A. El-Asmy, *Trans. Met. Chem.* 1981, **6**, 303.
[3]M. M. Mostafa and A. A. El-Asmy, *J. Coord. Chem.*, in press.
[4]A. A. El-Asmy and M. M. Mostafa, *J. Coord. Chem.*, in press.
[5]A. M. Shallaby, M. M. Mostafa and A. A. El-Asmy, *Acta Chim. Hung.* in press.
[6]A. I. Vogel, *A Text Book of Quantitative Inorganic Analysis*. Longmans, London (1961).
[7]J. Lewis and R. G. Wilkins, *Modern Coordination Chemistry*. Interscience, New York (1960).
[8]W. J. Geary, *Coord. Chem. Rev.* 1971, **7**, 81.
[9]C. N. Rao and R. Venkatarghavan, *Spectrochim. Acta* 1962, **18**, 541.
[10]M. Mashima, *Bull. Chem. Soc. Japan* 1964, **37**, 974.
[11]A. Braibanti, F. Dellvalla, M. A. Pellinghelli and E. Leporati, *Inorg. Chem.* 1968, **7**, 1430.
[12]J. R. Ferraro and W. R. Walker, *Inorg. Chem.* 1965, **4**, 1382.
[13]A. B. P. Lever, *Inorganic Electronic Spectroscopy*. Elsevier, Amsterdam (1968).
[14]G. H. Faye J. L. Horwood, *Can. J. Chem.* 1967, **45**, 2335.
[15]J. C. T. Rendell and L. K. Thompson, *Can. J. Chem.* 1979, **54**, 1.
[16]R. B. Wilson, J. R. Wasson, W. E. Hatfield and D. J. Hodgson, *Inorg. Chem.* 1978, **17**, 641.
[17]M. J. M. Campbell and R. Grzeskowiake, *J. Chem. Soc.* 1967, 396.
[18]L. Sacconi, *Coord. Chem. Rev.* 1966, **1**, 126.
[19]M. Kato, H. B. Jonassen and J. C. Fanning, *Chem. Rev.* 1964, **64**, 99.

REACTIONS OF DIBORANE WITH AROMATIC HETEROCYCLES—2[1]

REACTIONS WITH NITROGEN-CONTAINING HETEROCYCLES RELATED TO PYRIDINE

PHILIP C. KELLER,[*2a] RONALD L. MARKS[2b] and JOHN V. RUND[2a]
Departments of Chemistry, University of Arizona, Tucson, AZ 85721, U.S.A.

and

Indiana University of Pennsylvania, Indiana, PA 15705, U.S.A.

Abstract—The reactions of solutions of B_2H_6 in ethers with a variety of aromatic heterocycles containing one or more six-membered rings with only one nitrogen per ring have been examined. Quinoline and isoquinoline form monoborane adducts which hydroborate in the presence of an excess of B_2H_6. Protonolysis gives the 1,2,3,4-tetrahydro-compounds in both cases. N-Methylquinolinium and N-methylisoquinolinium iodides both hydroborate. Hydroboration and halogen loss occur with 2-, 3- or 4-haloquinolines (chlorine or bromine). Prior to hydroboration 8-hydroxyquinoline forms a borane adduct which rapidly eliminates one equivalent of hydrogen in a probable intramolecular ring closure. Sodium 8-hydroxyquinolinate combines with B_2H_6 in an unsymmetrical cleavage reaction to form $B_2H_7^-$ or BH_4^-, and the same ring closed product formed by 8-hydroxyquinoline. Phenanthridine and N-methylphenanthridinium iodide both readily undergo hydroboration. The products formed by the latter with B_2H_6 are 5-methyl-5,6-dihydrophenanthridine–borane and an iodoborane etherate. 1,8-Naphthyridine forms a transient borane complex which rapidly undergoes hydroboration; protonolysis gives 1,2,3,4-tetrahydro-1,8-naphthyridine. 2,2′-Bipyridyl undergoes a complex reaction with one equivalent of BH_3 giving a mixture of bpy·$2BH_3$ and hydroborated products, but 4,4′-bipyridyl does not appear to hydroborate. 1,10- and 1,7-Phenanthroline both hydroborate giving a mixture of reduced products on protonolysis. Pyridine-borane and 2-phenylpyridine-borane both decompose in refluxing diglyme, but protonolysis gives no reduced products in either case.

During the past few years we have been interested in the reactions of diborane with rigid polydentate chelating ligands. In experiments with bases like 1,10-phenanthroline, 8-hydroxyquinoline and 1,8-naphthyridine we observed unexpectedly complex reactions which in most instances turned out to involve hydroboration of the heterocyclic aromatic ring. Since little is known of the reactions of diborane with aromatic heterocycles, we decided to explore this area for the purpose of determining the scope of this reaction. This and subsequent papers contain the results of our examination of the reactions of diborane with a wide variety of aromatic heterocycles. In this article we describe results with heterocycles containing one or more six-membered rings with only one nitrogen atom per ring.

RESULTS AND DISCUSSION

Quinoline, isoquinoline and their N-methyl cations

The stable monoborane complexes of quinoline (**I**) and isoquinoline (**II**) have been known for a number of years.

I

II
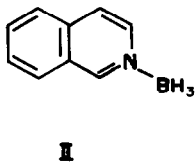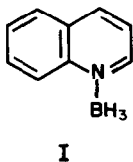
The adducts may be prepared by the direct reaction of the bases with stoichiometric quantities of diborane[3] or by displacement of borane from weak base complexes like $Me_2S·BH_3$.[4]

In a recent paper Martin *et al.* reported that quinoline and isoquinoline react with quantities of $Me_2S·BH_3$ *in excess* of that required for adduct formation to give complex mixtures of high melting point which the authors postulate as resulting from hydroboration of the heterocyclic ring.[4]

In another recent publication Nose and Kudo reported the reduction of quinoline, isoquinoline, and a number of their C-methyl derivatives by treatment with *two* equivalents of $THF·BH_3$ followed by hydrolysis with hydrochloric acid.[5] The authors propose that ring reduction occurs during the hydrolysis step by the action of B–H-containing intermediates. Although this is evidently the case when immediate hydrolysis is involved, the studies of Martin *et al.*[4] and the results presented in this article demonstrate that hydroboration occurs before hydrolysis when the reaction time is sufficient.

We have obtained results similar to those of Martin *et al.* in reactions of quinoline and isoquinoline with $THF·BH_3$ in excess of that required for simple adduct formation. Protonolysis gave the tetrahydro derivatives of quinoline (**III**) and isoquinoline (**IV**) in 34 and 50% yield, respectively.

We have also observed that yields of **III** and **IV** improve if reactions are carried out using borane complexes of somewhat stronger bases. Thus, treat-

III   IV
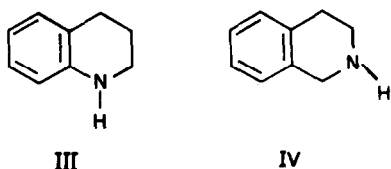
ment of quinoline with $Me_2S \cdot BH_3$ or $py \cdot BH_3$ followed by protonolysis gave III in 53 and 73% yields, respectively.

Reaction of quinoline with excess $THF \cdot BH_3$ followed by deuteronolysis with 20% DCl/D_2O then 50% CH_3COOD/D_2O gave the trideutero compound V.

V
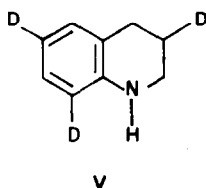
The presence of deuterium on the aromatic ring results from electrophilic aromatic substitution during workup. The position of the deuterium on the reduced ring reveals the site of the boron–carbon bond in the hydroborated intermediate.[6]

The first step in these reactions is undoubtedly coordination of BH_3 to the nitrogen lone pair. Once this site is blocked, the π-bonds in the heterocyclic ring are susceptible to attack by additional BH_3. In support of this hypothesis we studied the reactions of the N-methyl cation salts with diborane. The reactions in both cases were slower, taking *ca* 3 weeks at ambient temperature, but the usual workup gave the reduced products VI and VII in 34 and 51% yield, respectively.

VI   VII
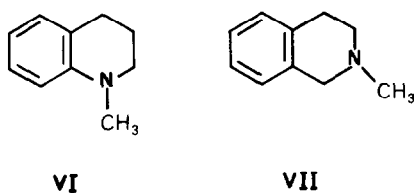
Scheme 1 illustrates the proposed reaction sequence for the case of quinoline. After initial hydroboration, reduction of the isolated CN double bond would probably follow easily by hydride shift from coordinated BH_3 to give an aminoborane. The final structure shown is an oversimplification since the BH_2 group on the 3-position and possibly the BH_2 group attached to nitrogen can engage in further hydroborations to form complex crosslinked products. That this situation probably exists is supported by our boron-11 NMR studies of heterocycle–excess borane solutions. Spectra usually comprise only very broad featureless signals, and no resolved quartets or triplets characteristic of amine–boranes or aminoboranes are present.

As an extension of this work, the reactions of diborane with the 2-, 3-, and 4-haloquinolines VIII, IX, and X were examined. In all cases heterocyclic ring reduction with loss of halogen occurred. After protonolysis and workup, VIII, and IX afforded 1,2,3,4-tetrahydroquinoline III in 4 and 37% yield, respectively. The 7-chloro derivative of III was obtained from X in 19% yield.

VIII   IX

X
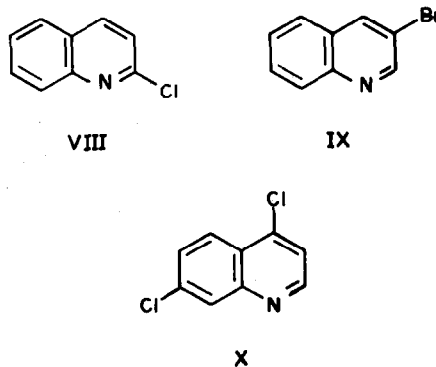
These results are consistent with the studies of Pasto and coworkers on haloborane eliminations in the hydroborations of halogen-substituted olefins.[7,8] Assuming boron–carbon bond formation at the 3-position, the situation with VIII and X would resemble that found by Pasto and Hickman in the hydroboration of 3-chlorocyclohexene.[7] In this system the principal hydroboration product was *trans*-2-
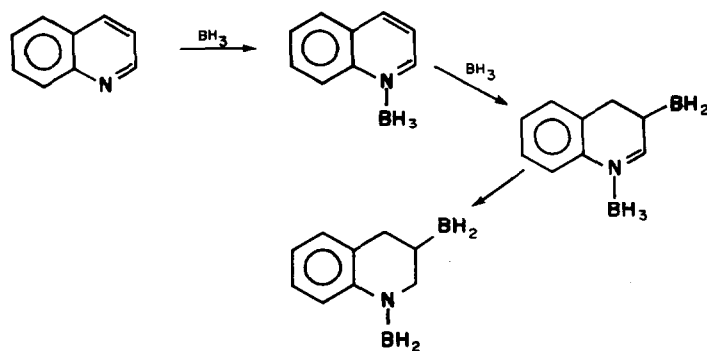
Scheme 1.
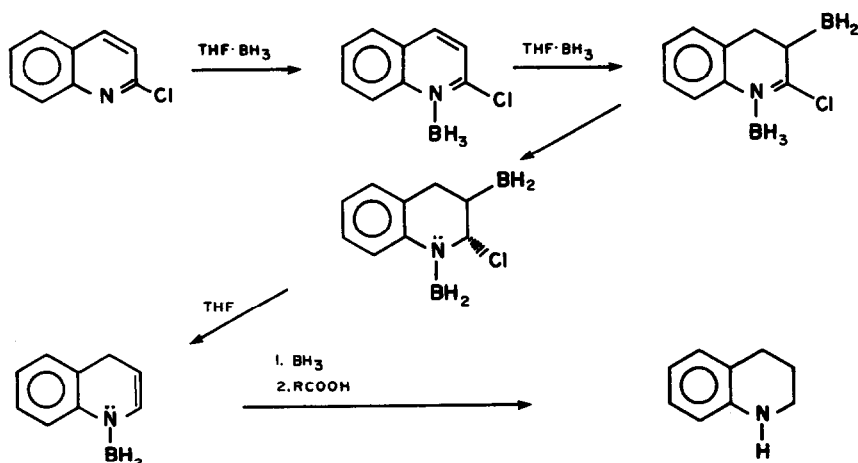
Scheme 2.

chlorocyclohexylborane from which BH_2Cl was readily eliminated in the presence of THF. The resulting cyclohexene subsequently underwent rapid hydroboration. This sequence is illustrated for the case of VIII in Scheme 2.

Again assuming boron addition at the 3-position, the hydroboration of IX would parallel the reaction found by Pasto and Snyder with 2-bromostyrene in which α-transfer rather than BH_2Br elimination occurred.[8] A possible sequence for IX is illustrated in Scheme 3. If BC bond formation occurred at the 4-position on IX, the situation would resemble Scheme 2.

8-Hydroxyquinoline and its sodium salt

Reaction with diborane is a two-stage process in which complexation and chelate formation are followed by a slower hydroboration. In the early stage of the reaction 8-hydroxyquinoline combines with one equivalent of BH_3 and rapidly evolves 1 mole of hydrogen. A boron-11 NMR spectrum of the reacting solution taken immediately after mixing shows a quartet and a triplet in addition to the signal of excess

diborane itself. During a period of 5 min at room temperature the triplet completely replaces the quartet, and hydrogen evolution ceases. Prompt hydrolysis yields only unaltered 8-hydroxyquinoline. These observations are consistent with the sequence shown in eqn (1). The borane complex XI gives rise to the

$$(1)$$

Scheme 3.
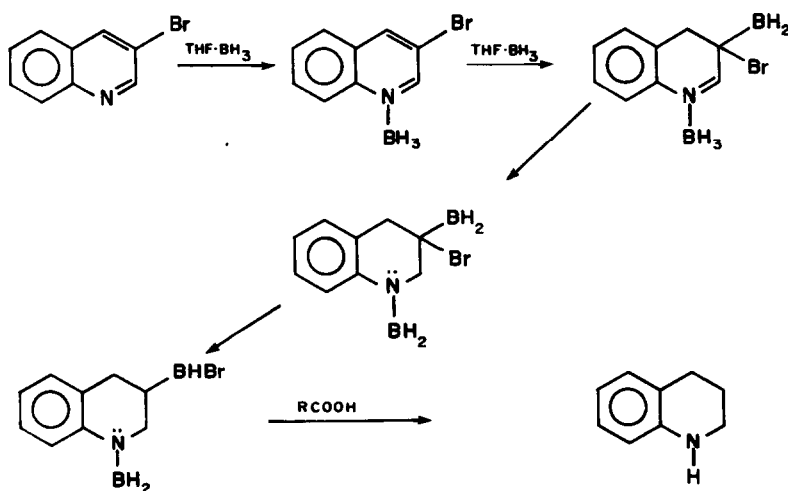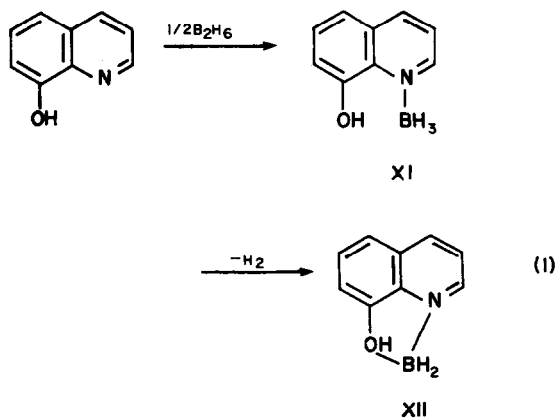
quartet in the boron-11 NMR spectrum. The complex then eliminates hydrogen, and we speculate that this step may be intramolecular giving the ring compound **XII**. Hydrolysis of **XII** would give unaltered 8-hydroxyquinoline.

The reaction of excess diborane with the salt sodium 8-hydroxyquinolinate proceeds in a similar manner. A boron-11 NMR spectrum run moments after initiation of the reaction shows the same triplet as that assigned to **XII** plus a relatively sharp singlet. The chemical shift of the latter depends directly on the quantity of excess diborane present and results from the rapid hydride ion exchange between B_2H_6 and $B_2H_7^-$.[9] These observations are consistent with the unsymmetrical cleavage reaction[10] (eqn 2) and the associated exchange reaction (eqns 3 and 4) shown.

Prompt hydrolysis again yields unaltered 8-hydroxyquinoline.

If these reactions are allowed to stand 24 hr before hydrolysis, no 8-hydroxyquinoline is recovered, and the triplet in the boron-11 NMR spectrum assigned to **XII** disappears and is replaced by a very broad featureless signal. Protonolysis affords small yields (7% with 8-hydroxyquinoline) of 1,2,3,4-tetra-hydro-8-hydroquinoline. Excess diborane is not necessary for the loss of **XII**, although it is consumed if present.

Phenanthridine and N-*methylphenanthridinium iodide*

Borane adds across the CN double bond in phenanthridine in THF at room temperature. Protonolysis gives 5,6-dihydrophenanthridine **XIII** in 53% yield. In the presence of excess diborane solid N-methylphenanthridinium iodide dissolves in a few hours in monoglyme, but requires several weeks in ethyl ether. Methanolysis of the resulting solution gives the tertiary amine **XIV** in 99% yield. A boron-11 NMR study of this reaction revealed that the hydroboration intermediate is the borane complex **XV**
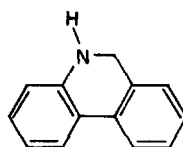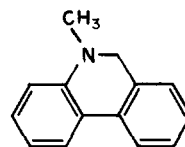
XIII   XIV
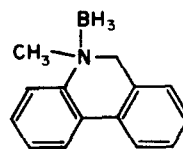
XV

(quartet, $\delta = -7.7$ ppm, $J = 81$ Hz). This was proved by isolation of the intermediate and comparison of its IR and boron-11 NMR spectra with those of the actual borane complex prepared from the tertiary amine **XIV**. In addition to the quartet assigned to **XV**, the boron-11 NMR spectrum contained a singlet ($\delta = 17.8$ ppm) and a sharp doublet ($\delta = 27.3$ ppm, $J = 160$ Hz) suggestive of the presence of the tri- and dialkoxyboranes $B(OR)_3$ and $HB(OR)_2$, respectively.[11]

These observations are consistent with the addition of the elements of BH_4^- across the CN double bond (eqn 5). The presence of the alkoxyboranes can be explained by an ether cleavage by the iodoborane[12] followed by known disproportionation reactions (eqns 6 and 7).[13] Cleavage of monoglyme could give several products, but with ethyl ether only ethyl iodide and ethoxyboranes would form. The isolation of ethyl iodide established the occurrence of ether cleavage.

XII   (2)

$$BH_4^- + 1/2\ B_2H_6 \longrightarrow B_2H_7^- \qquad (3)$$

$$B_2H_7^- + B_2H_6 \rightleftharpoons B_2H_6 + B_2H_7^- \qquad (4)$$

(5)

$$BH_2I\cdot OR_2 \longrightarrow RI + BH_2OR \qquad (6)$$

$$BH_2OR \longrightarrow HB(OR)_2,\quad B(OR)_3,\quad BH_3 \qquad (7)$$
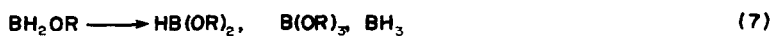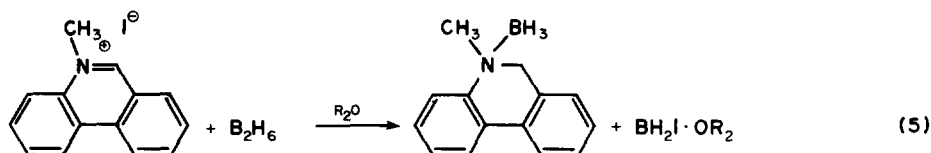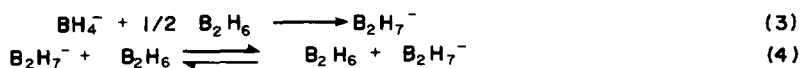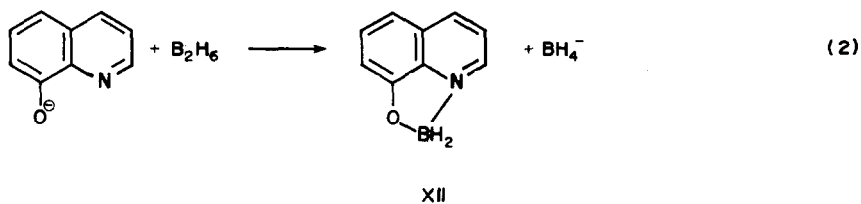
A similar addition of the elements of BH_4^- to an N-methyl iminium group has been reported by Yamada and Ikegami in the reaction of $THF \cdot BH_3$ with 1,2-dimethyl-3,4-dihydroisoquinolinium iodide XVI.[14] The product was found to be the tertiary amine–borane XVII, but no investigation of possible ether cleavage was undertaken.

XVI   XVII
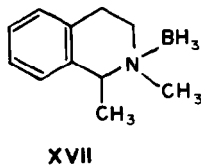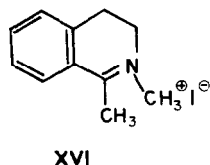
1,8-Naphthyridine

Boron-11 NMR study reveals that at low temperature 1,8-naphthyridine forms a borane complex of as yet undetermined stoichiometry. Above 0° the quartet signal of the adduct loses intensity, and an irreversible hydroboration occurs which is complete within 4 hr at room temperature. Approximately 1.19 mol of diborane is consumed per mol of 1,8-naphthyridine. The IR spectrum of the hydroboration product shows both BH terminal and bridge stretching. Protonolysis gives the 1,2,3,4-tetrahydro-derivative XVIII in 44% yield. Similar workup using CH_3COOD gives a product with deuterium in both the 3 and 4 positions on the saturated ring.

XVIII
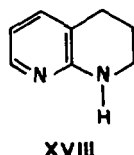
2,2′ and 4,4′-bipyridyl

Excess diborane reacts immediately with 2,2′-bipyridyl (bpy) in monoglyme to form an insoluble air-stable bis-borane complex $bpy \cdot 2BH_3$.[15] In an attempt to prepare and characterise the monoborane adduct $bpy \cdot BH_3$, we reacted bpy with one half mole of diborane in monoglyme. Surprisingly, the reaction proved to be more complex as evidenced by the precipitation of solid products over a 1–2-day period and the gradual coloring of the initially clear colorless solution to a deep orange–red. The IR spectrum of the insoluble material comprised all the absorptions of $bpy \cdot 2BH_3$ plus bands from an unidentified substance. The IR spectrum of the monoglyme-soluble products showed no BH stretching bands and was not that of bpy itself. Protonolysis of these products gave unaltered bpy and a mixture of partially reduced products (PMR and mass spectroscopic evidence). The further separation and characterisation of these materials was not pursued.

As with bpy, excess diborane reacts with 4,4′-bipyridyl in monoglyme to form an insoluble air-stable bisborane complex which regenerates 4,4′-bipyridyl on hydrolysis. Reaction of 4,4′-bipyridyl with one half mole of diborane gives no evidence for hydroboration, and hydrolysis regenerates unaltered 4,4′-bipyridyl in high yield.

In the case of the 2,2′-isomer it appears that $bpy \cdot BH_3$ may form initially, but a variety of more complex reactions including disproportionation and hydroboration subsequently occur. As pure speculation, we suggest that the difference in behavior of the 2,2′- and 4,4′-isomers toward one equivalent of BH_3 may hinge upon a chelate effect. Reduction of the 2,2′-isomer may be promoted by a hydride displacement from coordinated BH_3 assisted by a neighboring nitrogen lone pair (eqn 8).

further
hydroboration

(8)
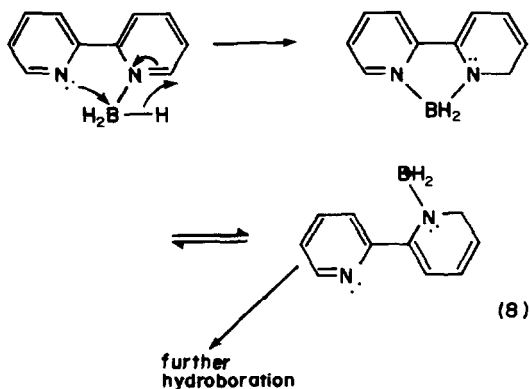
1,10- and 1,7-phenanthroline

Both bases react rapidly with diborane in a complex manner giving colored intermediates and complex stoichiometry. The products give broad, unresolved boron-11 NMR spectra and IR spectra showing both terminal and bridge BH stretching absorptions. Protonolysis gives poor yields of mixed tetra- and octahydrophenthrolines (mass spectral evidence). The further separation and characterisation of these substances was not pursued.

Pyridine and 2-phenylpyridine

The borane adducts of many pyridine (py) derivatives are relatively stable, well characterized substances. Pyridine–borane itself $(py \cdot BH_3)$ is commonly used as a reducing agent and is available commercially. Although these substances can be handled safely at room temperature, $py \cdot BH_3$ is known to undergo a violent reaction when heated.[16,17] To determine whether this process might be a hydroboration, we examined the products formed by heating diglyme solutions of $py \cdot BH_3$ and 2-phenylpyridine-borane. We found that refluxing diglyme solutions of $py \cdot BH_3$ as dilute as 0.29 M underwent violent exothermic reaction, suddenly generating large amounts of colorless insoluble material after induction periods of 30–45 min. The decomposition of 2-phenylpyridine-borane was not violent. Protonolysis gave no product at all in the case of $py \cdot BH_3$ and only a small amount of starting material with 2-phenylpyridine-borane. Substantial quantities of intractable materials were formed in both workup procedures. The decomposition reactions may involve a Lewis-acid promoted ring-opening polymerization rather than a hydroboration.[18]

Note on protonolysis procedure

In the early stages of this work we found that the standard protonolysis procedure of adding propionic

or acetic acid to cleave boron–carbon bonds in organoboranes[19] often resulted in the isolation of N-propyl or N-ethyl derivatives of reduced heterocycles. These products probably arise through the reducing action of intermediate acyloxyboranes formed by the action of the carboxylic acid on residual or unreacted borane. Processes of this type have been proposed by Gribble et al. in studies of amine alkylations using sodium borohydride in carboxylic acid media.[20] The problem of unwanted N-alkylation was circumvented by carrying out the protonolysis step with 50% aqueous acetic or propionic acid. The effect of the added water is most likely the rapid destruction of residual boranes or acyloxyboranes before reduction can occur.

EXPERIMENTAL

Reagents. The following were purchased from the Aldrich Chemical Co.: quinoline, isoquinoline, 2-chloroquinoline, 3-bromoquinoline, 4,7-dichloroquinoline, 8-hydroxyquinoline, phenanthridine, 2,2'-bipyridyl, 4,4'-bipyridyl, 1,10-phenanthroline, pyridine–borane, 2-phenylpyridine, THF·BH$_3$, and Me$_2$S·BH$_3$. 1,7-Phenanthroline was obtained from the Pfaltz and Bauer Chemical Co. Purification, dehydration, or conversion from hydrochloride salts of some of the above bases was performed as needed by standard methods. N-methylquinolinium iodide, N-methylisoquinolinium iodide, and N-methylphenanthridinium iodide were prepared by treating the appropriate base with CH$_3$I followed by standard purification. Diborane,[21] acetic acid-d,[22] and 1,8-naphthyridine[23] were prepared by standard methods. The solvents ethyl ether, monoglyme (1,2-dimethoxyethane), diglyme (bis(2-methoxyethyl) ether), tetrahydrofuran (THF), and methanol were purchased commercially and were dried by standard methods. For use on the vacuum line the first four were stored in evacuated bulbs over LiAlH$_4$ and were vacuum transferred directly into reaction vessels when needed.

Spectra. Boron-11 NMR spectra were obtained using a Varian HA-100 spectrometer operating at 32.1 MHz. Chemical shifts are relative to Et$_2$O·BF$_3$, and downfield shifts are positive. NMR reactions were performed in a vessel of about 10 ml volume designed to fit into the probe of the spectrometer. Proton NMR spectra were obtained with a Varian T60 spectrometer. IR spectra were obtained with a Perkin–Elmer 337 spectrophotometer. Mass spectra were run on a Hewlet-Packard 5930A spectrometer operated by the University of Arizona Analytical Center.

Methods. Standard high vacuum and inert atmosphere techniques were used in all small quantitative experiments.[24] On a larger scale the basic methods described by Brown et al. were employed.[25] In most cases the workup of hydroboration products was generally the same and involved preliminary refluxing with 50% acetic or propionic acid (see above) followed by treatment with aqueous NaOH until basic, extraction with CHCl$_3$, drying with MgSO$_4$, evaporation, and recrystallization or distillation as appropriate.

Quinoline and diborane

A freshly dried and distilled sample of 5.0 g (39 mmol) of quinoline was added to 116 cm^3 of 1M BH$_3$ in THF in a nitrogen filled dry box and the mixture was allowed to stand at room temperature for 5 days. The resulting yellow solution was concentrated under vacuum and treated with 100 cm^3 of methanol to destroy residual active hydride. The solution was again concentrated and worked up as described above. Vacuum distillation of the dried CHCl$_3$ extract gave 1.7 g (34%) of 1,2,3,4-tetrahydroquinoline (III) (b.p. 88–90° at 1 torr; identification by IR and PMR).

In an experiment similar to the above, the hydroborated

quinoline was treated with D$_2$O, then 20% DCl/D$_2$O to destroy active hydride and was then refluxed with 50% CH$_3$COOD/D$_2$O. Workup gave 3,6,8-trideuterio-1,2,3,4-tetrahydroquinoline (V). IR (neat, ν CD) 2251, 2166 cm^{-1}; PMR (neat) 1.78 (m, 1H), 2.69 (d, 2H, J6.3 Hz), 3.08 (d, 2H, J5.4 Hz), 3.75 (s, 1H), 7.02 and 7.07 (s, 2H combined); MS, m/e 136 [P$^+$], base peak at low ionization energy.

Isoquinoline and diborane

An experiment paralleling the above with 19 g (148 mmol) of isoquinoline and 220 cm^3 of 0.45M BH$_3$ in THF gave 9.78 g (50%) of 1,2,3,4-tetrahydroisoquinoline (IV), identified by comparison of IR and PMR spectra with an authentic sample. In a vacuum line experiment, 2.78 g (21.6 mmol) of isoquinoline in diglyme consumed 27.6 mmol of B$_2$H$_6$ (1:1.28 ratio).

N-*Methylquinolinium iodide and diborane*

Treatment of 22.2 g (82 mmol) of N-methylquinolinium iodie in 50 cm^3 of THF with 164 ml 1M BH$_3$ in THF for 3 weeks gave, after workup, 4.1 g (34%) VI by vacuum distillation (85° at 1 torr). The product was identified by IR, PMR and mass spectrometry.

N-*Methylisoquinolinium iodide and diborane*

Treatment of 22.2 g (82 mmol) of N-methylisoquinolinium iodide in 50 cm^3 THF with 164 ml 1M BH$_3$ in THF for 3 weeks gave, after workup, 6.2 g (51%) of VII, m.p. methiodide, 189–190°, lit. 190°.[26]

2-*Chloro-, 3-bromo- and 4,7-dichloroquinoline and diborane*

Reactions were carried out in the usual way with the quantities of reactants listed below. After standard workup the crude products were chromatographed in alumina using hexane, hexane–isopropanol (9:1), and hexane–isopropanol (3:1) as successive eluants. Much tarry material was retained on the column in all cases. Product identification was by IR and PMR.

Treatment of 5.07 g (31.0 mmol) of 2-chloroquinoline in 50 cm^3 THF with 95 ml 1M BH$_3$ in THF for 1 week at 25° gave after workup 0.161 g (3.9%) III.

Reaction of 4.97 g (23.9 mmol) of 3-bromoquinoline in 50 cm^3 THF with 72 ml 1M BH$_3$ in THF for 1 week at 25° produced after workup 1.17 g (36.7%) III.

Treatment of 5.08 g (25.7 mmol) of 4,7-dichloroquinoline in 50 cm^3 THF with 80 ml 1M BH$_3$ in THF for 1 week at 25° gave after workup 0.81 g (18.8%) of the 7-chloroderivative of III.

8-*Hydroxyquinoline and diborane*

A freshly-combined mixture of 0.131 g (0.906 mmol) of 8-hydroxyquinoline, 1 cm^3 monoglyme, and 1.2 mmol of B$_2$H$_6$ was allowed to warm from the solvent melting point to −5° in the NMR probe. The boron-11 NMR spectrum initially consisted of three approximately equal signals: that of unreacted B$_2$H$_6$, a triplet at 5.1 ppm, J, 112 Hz (XII), and a quartet at −11.1 ppm, J, 93 Hz (XI). Within 15 min the quartet had disappeared leaving the diborane signal and a greatly enhanced triplet. The evolution of hydrogen, which had been steady since the start of the reaction, stopped at this point. Over a 20-hr period at room temperature the triplet and the diborane signals were replaced by very broad featureless absorptions.

In a larger scale reaction, a 1.016-g (7.01 mmol) sample of 8-hydroxyquinoline dissolved in 20 cm^3 of monoglyme was allowed to react with 7.74 mmol of B$_2$H$_6$ at 25°. Vigorous hydrogen evolution ceased within 30 min leaving a clear yellow solution. The vessel was opened after standing several days and 7.35 mmol of hydrogen was collected. Vacuum fractionation of volatile products gave 0.99 mmol of recovered B$_2$H$_6$ (6.75 mmol consumed). The usual workup of the yellow, oily residue gave a low yield (<10%) of 1,2,3,4-tetrahydro-8-hydroxyquinoline m.p. 119–121°, lit. 122.5°.[27] Mass spec. parent ion m/e 149.

A similar experiment in which workup was performed 3 hr after initiation of the reaction gave only unchanged 8-hydroxyquinoline (62% recovery).

Sodium 8-hydroxyquinolinate and diborane

An NMR reaction was carried out using 0.129 g (0.774 mmol) of sodium 8-hydroxyquinolinate and 1.02 mmol of B_2H_6 in 1 cm³ of monoglyme. The solid dissolved readily giving a clear yellow solution. No hydrogen was produced. The boron-11 NMR consisted of a strong triplet identical with that of XII and a singlet due to $B_2H_7^- - B_2H_6$ exchange[10] at −20.7 ppm. After 24 hr the triplet had disappeared, and the spectrum comprised the $B_2H_7^- - B_2H_6$ exchange singlet and a very broad featureless absorption at lower field.

Phenanthridine and diborane

A 1.55-g (9.99 mmol) sample of phenanthridine was allowed to react with 13.9 cm³ of $1M$ BH_3 in THF at room temperature for 2 weeks. Workup gave 0.96 g (53%) of 5,6-dihydrophenanthridine (XIII), m.p. 122.5–123°, lit. 123°.[28] In a separate quantitative vacuum line experiment 0.358 g (2.00 mmol) of phenanthridine consumed 2.72 mmol B_2H_6 (1:1.36 ratio).

N-Methylphenanthridinium iodide and diborane

A 0.587-g (1.83 mmol) sample of N-methylphenanthridinium iodide was sealed in an all-glass vessel with 10 cm³ Et_2O and 1.83 mmol B_2H_6. The solid gradually dissolved over a 6-week period giving a clear colorless solution. Vacuum line separation of volatile products gave 0.27 mmol of unreacted B_2H_6 and a small amount of C_2H_5I (gas IR). A mass spectrum of the colorless solid residue showed it to be 5,6-dihydro-5-methylphenanthridine-borane (XV) (parent ion m/e 209). IR νBH (in cm⁻¹): 2400s, 2350s, 2255m. Treatment of XV with anhydrous methanol followed by vacuum evaporation of the clear colorless solution gave 0.409 g (99.4%) of the 5,6-dihydro compound XIV, m.p. 49–51°, lit 46–48°.[29] Reaction of 0.215 g (1.10 mmol) of XIV with 1.51 mmol B_2H_6 in monoglyme followed by separation of volatiles (0.56 mmol B_2H_6 consumed) gave a solid with an IR spectrum superimposable upon that of XV.

In a separate NMR reaction, a 0.283 g (0.878 mmol) sample of N-methylphenanthridinium iodide dissolved in 1 cm³ of monoglyme in the presence of 1.13 mmol B_2H_6 in 24 hr. The boron-11 NMR spectrum is described above.

1,8-Naphthyridine and diborane

A 0.622-g (4.79 mmol) sample of 1,8-naphthyridine in 10 cm³ of monoglyme was allowed to react with 7.36 mmol of B_2H_6 at room temperature for 24 hr. Vacuum line separation of volatile materials indicated the consumption of 5.71 mmol of B_2H_6. The involatile solid residue was air-sensitive and showed BH and BHB IR stretching bands at 2400, 2390, 2310, 2000 and 1880 cm⁻¹. Treatment of this residue with 50% acetic acid followed by the usual recovery procedure gave 0.283 g (44%) of the tetrahydro compound XVIII, identified by PMR.[30]

In an NMR experiment a 1.62-mmol sample of B_2H_6 was condensed on to 0.142 g (1.09 mmol) of 1,8-naphthyridine and 1 cm³ of monoglyme at −196°. The vessel was warmed until the solvent melted and was placed in the NMR probe cooled to −40°. The boron-11 NMR spectrum at this temperature consisted of a B_2H_6 signal and a broad quartet at approx. 7 ppm, J, 80 Hz. Upon warming to room temperature the quartet rapidly disappeared and was replaced by a broad unresolved signal.

4,4′-Bipyridyl and diborane

A 1.86-mmol sample of B_2H_6 was condensed into a vessel containing a solution of 0.208 g (1.33 mmol) of 4,4′-bipyridyl in 10 cm³ of monoglyme. As the solvent melted, a colorless solid formed and persisted at room temperature. No further change was seen. After 24 hr, fractionation of volatiles showed 1.37 mmol of B_2H_6 had been consumed

(complex composition bpy·1.03 B_2H_6). The colorless solid bisborane adduct was air stable and showed IR BH stretching bands at 2350 s, br; 2275 m, sh. Solvolysis in acidified ethanol and treatment with base gave unchanged 4,4′-bipyridyl.

In a long term experiment 2.09 mmol of B_2H_6, 0.226 g (1.45 mmol) of 4,4′-bipyridyl, and 10 cm³ of monoglyme were left to stand in a sealed Pyrex tube at room temperature for 1 yr. Solvolysis as above gave unchanged starting material (80%).

A sample of 0.217 g (1.39 mmol) of 4,4′-bipyridyl in 10 cm³ of monoglyme was allowed to react with 0.691 mmol of B_2H_6 in a sealed Pyrex tube. The solid-free, light-yellow solution was allowed to stand at ambient temperature for 1 yr prior to standard workup. Only starting material was recovered (91%).

2,2′-Bipyridyl and 0.5 equivalent of diborane

A 2.275-g (14.6 mmol) sample of 2,2′-bipyridyl in 10 cm³ of monoglyme was treated with 7.22 mmol of diborane in a 100-cm³ reaction vessel. The originally clear colorless solution turned dark orange over several hours and a colorless solid, identified as bpy·2BH₃ by its IR spectrum,[15] formed over a period of 2 days. The usual workup gave a dark red liquid product. The PMR of this material showed it to be a mixture of starting material and nonaromatic products. A mass spectrum of the mixture showed parent peaks at m/e 156 (bpy) and m/e 166 (a decahydro product). No further separation or characterization of the products was attempted.

1,10-Phenanthroline and diborane

A 0.106 g (0.588 mmol) sample of 1,10-phenanthroline in 5 cm³ of monoglyme was treated with 1.43 mmol of B_2H_6. The initially colorless mixture rapidly turned dark purple as the vessel came to room temperature, then changed to dark green over 1 hr and finally lightened to yellow with the formation of a solid of the same color after 24 hr. No further changes occurred and no hydrogen was evolved. A sample of the air-sensitive yellow solid showed BH stretching absorptions at 2580, 2470, 2410, 2360, 2310, 2030 and 1940 cm⁻¹. Fractionation of volatiles showed that 1.49 mmol of B_2H_6 had been consumed per mmol of 1,10-phenanthroline. Standard workup gave an air-stable oil which was chromatographed on alumina using benzene–chloroform (80/20) as an eluant to give a light yellow oil which was a mixture of tetra- and octa-hydro-1,10-phenanthrolines (MS parent ions m/e 184, 188) in less than 10% yield. No further separation was attempted.

1,7-Phenanthroline and diborane

A 0.363-g (2.01 mmol) sample of 1,7-phenanthroline in 10 cm³ of monoglyme was treated with 3.87 mmol of diborane. Reaction was evidenced by the appearance of yellow–brown crystals on standing 24 hr. After 3 days, fractionation of volatiles showed 1.65 mmol B_2H_6 absorbed per mmol phenanthroline. Standard workup gave a red–orange oil which was a mixture of tetra- and octahydro-derivatives (MS parent ions m/e 184, 188). No further separation or characterization was attempted.

Decomposition of pyridine–borane

A 0.560-g (6.02 mmol) sample of pyridine–borane in 21 cm³ of diglyme (0.29 M solution) was heated to reflux in a nitrogen atmosphere. After 45 min, cream-colored solid began to separate from solution. Within 4 min the formation of this material became so vigorous and exothermic that much of the solution and solid bumped to the top of the reflux condenser. On cooling, the products were subjected to standard workup. Nothing was recovered.

2-Phenylpyridine and diborane

A diglyme solution of 2-phenylpyridine-borane, formed by treating 4.0 g (25.8 mmol) of 2-phenylpyridine in 20 cm³ diglyme with 28.2 mmol of B_2H_6 followed by vacuum evap-

oration of excess B_2H_6, was refluxed in a nitrogen atmosphere for 2 days. The usual workup followed by distillation gave 1.2 g (30%) of unchanged 2-phenylpyridine and *ca* 1.5 g of tarry residue in the distilling flask.

REFERENCES

[1] For paper number 1 in this series, see: K. K. Knapp, P. C. Keller and J. V. Rund, *J.C.S. Chem. Comm.* 1978, 971.

[2a] University of Arizona. [2b] Indiana University of Pennsylvania.

[3] V. I. Mikheeva and E. M. Fedneva, *Zhur. Neorg. Khim.* 1956, **1**, 894; *Chem. Abstr.* 1957, **51**, 3347e.

[4] C. J. Faret, M. A. Chinsano, J. D. O'Brien and D. R. Martin, *J. Inorg. Nucl. Chem.* 1980, **42**, 165.

[5] A. Nose and T. Kudo, *J. Pharm. Soc. Japan* 1979, **99**, 1240.

[6] H. C. Brown and K. J. Murray, *J. Org. Chem.* 1961, **26**, 631.

[7] D. J. Pasto and J. Hickman, *J. Amer. Chem. Soc.* 1968, **90**, 4445.

[8] D. J. Pasto and Sr. R. Snyder, O.S.F., *J. Org. Chem.* 1966, **31**, 2773.

[9] D. F. Gaines, *Inorg. Chem.* 1963, **2**, 523.

[10] R. W. Parry and L. J. Edwards, *J. Am. Chem. Soc.* 1959, **81**, 3554.

[11] H. Nöth and B. Wrackmeyer, *Nuclear Magnetic Resonance Spectroscopy of Boron Compounds.* Springer-Verlag, Berlin (1978).

[12] R. W. Jotham and L. H. Long, *Chem. Commun.* 1967, 1288.

[13] A. B. Burg and H. I. Schlesinger, *J. Am. Chem. Soc.* 1933, **55**, 4020.

[14] S. Yamada and S. Ikegawi, *Chem. Pharm. Bull. (Tokyo)* 1966, **14**, 1382.

[15] P. C. Keller and J. V. Rund, *Inorg. Chem.* 1979, **18**, 3197.

[16] V. I. Mikheeva and E. M. Fedneva, *Russ. J. Inorg. Chem.* 1956, **1**, 15.

[17] R. A. Baldwin and R. M. Washburn, *J. Org. Chem.* 1961, **26**, 3549.

[18] V. A. Kargin and V. A. Kabanov, In *Kinetics and Mechanics of Polymerization* (Edited by K. C. Frisch and S. L. Reegen), Vol. 2, p. 359. Marcel Dekker, New York (1969).

[19] H. C. Brown and K. Murray, *J. Am. Chem. Soc.* 1959, **81**, 4108.

[20] G. W. Gribble *et al.*, *Ibid.* 1974, **96**, 7812.

[21] Diborane was prepared by treating $NaBH_4$ with warm polyphosphoric acid.

[22] Acetic acid-*d* was prepared by refluxing acetic anhydride with D_2O.

[23] W. W. Pandler and T. J. Kress, *J. Org. Chem.* 1967, **32**, 832.

[24] D. F. Shriver, *The Manipulation of Air Sensitive Compounds.* McGraw-Hill, New York (1969).

[25] H. C. Brown, G. W. Kramer, A. B. Levy and M. M. Midland, *Organic Synthesis Via Boranes.* Wiley-Interscience, New York (1975).

[26] L. G. Yudin, A. N. Kost, Yu. A. Berlin and A. E. Shipor, *Zhur. Obshchei Khim.* 1957, **27**, 3021.

[27] K. Bedall and O. Fischer, *Chem. Ber.* 1881, **14**, 1366.

[28] *Heterocyclic Compounds* (Edited by R. C. Elderfield), Vol. 4, p. 598. Wiley, New York (1952).

[29] P. Karrer, L. Szabo, H. J. V. Krishna and R. Schwyzer, *Helv. Chim. Acta* 1950, **33**, 294.

[30] W. L. F. Armarego, *J. Chem. Soc. (C)* 1967, 377.

ALLYLDIFLUOROPHOSPHITE-METAL CHEMISTRY: Ru COMPLEXES OF F₂POC₃H₅ AND THE CRYSTAL STRUCTURE OF (Ph₃P)₂(F₂POC₃H₅)Ru(CO)(Cl)H

JOHN W. GILJE*† and REINHARD SCHMUTZLER*

Lehrstuhl B für Anorganische Chemie der Technischen Universität, Pockelsstrasse 4, D-3300 Braunschweig, West Germany

and

W. S. SHELDRICK and V. WRAY

Gesellschaft für Biotechnologische Forschung mbH, Mascheroder Weg 1, D-3300 Braunschweig-Stöckheim, West Germany

Abstract—With several chloro ruthenium phosphine complexes, allyldifluorophosphite, F₂POC₃H₅, displaces triphenylphosphine to form new compounds in which it acts as a phosphorus donor ligand. The new complexes [PPh₃]₂[F₂POC₃H₅]Ru[CO][Cl][H], I, and [(PPh₃)₂(F₂POC₃H₅)₂RuCl₂]ₙ, II, have been characterized by chemical, spectroscopic, and, in the case of I, crystallographic means. This behaviour of F₂POC₃H₅ contrasts to its reactions with several platinum and palladium chloro complexes where it undergoes Arbuzov-type rearrangements.

Both PF₃ and phosphite esters, P(OR)₃, are important ligands in organometallic and coordination chemistry. Consequently, it is somewhat surprising that the metal chemistry of the organofluorophosphites, $F_nP(OR)_{3-n}$, $n = 1$ or 2, has not received much attention. In previous studies a few complexes in which compounds of the type $F_nP(OR)_{3-n}$ serve as conventional phosphorus ligands have been isolated.[1,2] Of greater interest, however, is the ability of certain organodifluorophosphites to undergo reactions, formally related to the classic "Michaelis–Arbuzov" reaction, producing complexes of F₂PO⁻.[3–8] The F₂PO⁻ ion is isoelectronic with PF₃, and is known to serve both as a monodentate ligand bonding through phosphorus and a bridging ligand in which both phosphorus and oxygen are coordinated.[3–9]

The lack of simple synthetic routes to F₂PO⁻ or its complexes has, no doubt, prevented a systematic evaluation of its ligand properties. Thus, the possibility that reactions of F₂POR could provide a general route to its preparation is an interesting question to explore. Previously square planar platinum group halides have been shown to effect the transformation in several cases.[3–8] In this note we would like to report the reaction of F₂POCH₂CH=CH₂ with several ruthenium complexes. Allyldifluorophosphite, F₂POC₃H₅, was chosen for these studies since it is the organodifluorophosphite which is known to form most easily F₂PO⁻ complexes via a Michaelis–Arbuzov reaction.

EXPERIMENTAL

All manipulations were carried out under a dry nitrogen or argon atmosphere using standard techniques. Solvents were dried and deoxygenated by appropriate means and distilled immediately before use. Published procedures were used to prepare F₂POC₃H₅,[1] (Ph₃P)₃Ru(CO)(H)(Cl),[10] (Ph₃P)₃RuCl₂,[11] and (Ph₃P)₄RuCl₂.[11]

NMR spectra were recorded on CDCl₃ solutions using a Varian XL-100 spectrometer. Chemical shifts are referenced to internal Si(CH₃)₄ for ¹H, external CCl₃F for ¹⁹F, and external 85% H₃PO₄ for ³¹P. Chemical shifts are positive to high frequency. IR spectra were obtained on Nujol mulls, KBr pellets and solutions using a Perkin–Elmer IR 4260 spectrometer. Elemental analysis was performed by Mikroanalytisches Laboratorium Beller, Göttingen, West Germany.

Reaction of (Ph₃P)₃Ru(H)(CO)(Cl) with F₂POC₃H₅. The preparation of (Ph₃P)₂(F₂POC₃H₅)Ru(CO)(H)(Cl), I

A 0.24 g sample of (Ph₃P)₃Ru(H)(CO)(Cl) was dissolved in 10 cm³ of CH₂Cl₂. From a syringe 0.46 g (3.6 mmol, about 0.5 cm³) of F₂POC₃H₅ was added to the solution. After 1 hr stirring the volume was reduced to about 3 cm³ by evaporation under vacuum; the mixture was then placed in a freezer at −20° for about 18 hr. After this period white crystals had formed. They were removed, washed with two 10-cm³ portions of diethylether and dried under vacuum to yield 0.12 g of (Ph₃P)₂(F₂POC₃H₅)Ru(CO)(Cl)(H)·H₂CCl₂. Anal. for C₄₁H₃₈Cl₃F₂O₂P₃Ru. Calc. C, 55.7; H, 4.02; P, 11.68. Found: C, 56.69; H, 4.43; P, 11.66%. IR ν(CO), 1985 cm⁻¹ (s); ν(Ru–H), 1915 cm⁻¹ (w).

Reaction of (Ph₃P)₃RuCl₂ with F₂POC₃H₅. The preparation of (Ph₃P)₂(F₂POC₃H₅)₂RuCl₂, II

A 1.06 g sample of (Ph₃P)₃RuCl₂ was dissolved in 20 cm³ of benzene and 0.9 cm³ of F₂POC₃H₅ added. Over a 1/2 hr period the initially very deeply coloured solution faded to a light yellow color and a pale yellow solid began to precipitate. After 24 hr the solution was filtered, the precipitate washed with four 10 cm³ portions of diethylether and dried

---
*Authors to whom correspondence should be addressed.
†Department of Chemistry, University of Hawaii Honolulu, HI 96822, U.S.A.

under vacuum to give 0.56 g of $(Ph_3P)_2(F_2POC_3H_5)_2RuCl_2$. Anal. for $C_{42}H_{40}Cl_2F_4O_2P_4Ru$. Calc. C, 53.16; H, 4.22; Cl, 7.49; P, 13.08. Found: C, 53.63; H, 4.35; Cl, 7.56; P, 13.00%.

Using the same procedure, II, can be obtained by the reaction of $(Ph_3P)_4RuCl_2$ with $F_2POC_3H_5$. II can be recrystallized from CH_2Cl_2 or $CHCl_3$.

RESULTS AND DISCUSSION

The reaction of $(Ph_3P)_3Ru(H)(CO)(Cl)$ with an excess of $F_2POC_3H_5$ at ambient temperature produces $(Ph_3P)_2(F_2POC_3H_5)Ru(H)(CO)(Cl)$, I. This white complex has been characterized by the usual analytical and spectroscopic methods. NMR data, obtained on freshly prepared $CDCl_3$ solutions, are summarized in Table 1, and are consistent with the proposed empirical formula for I. The 27.7 Hz coupling of the phosphorus in $F_2POC_3H_5$ with two equivalent PPh_3 phosphorus nuclei is typical of couplings between *cis* phosphorus ligands in octahedral complexes,[12] and the 224 Hz J(PRuH) coupling observed between F_2POC$_3$H$_5$ and the Ru–H is in the characteristic range for a phosphite *trans* to a hydride.[13] In the IR spectrum, a strong band at 1983 ± 3 cm^{-1} can be assigned as $\nu(CO)$ while a weak absorption at 1918 ± 5 cm^{-1} arises from ν(Ru–H). Thus, $\nu(C \equiv O)$ is shifted to a higher frequency in I than in the starting material, where it appears at about 1920 cm^{-1}. Such shifts are typical when a PPh_3 group is substituted by a better π-accepting ligand, and have previously been seen with phosphite, $P(OR)_3$, derivatives, $(Ph_3P)_{3-n}(P(OR)_3)_nRu(H)(CO)(Cl)$.[13] The IR spectrum also contains peaks virtually identical to those of free $F_2POC_3H_5$ and indicates that extensive ligand rearrangement has not occurred during the formation of I.

These data suggest that I is an octahedral complex derived from $(Ph_3P)_3Ru(H)(CO)(Cl)$ by substitution of the Ph_3P group trans to the hydride ligand by

$F_2POC_3H_5$. This structure has been confirmed by single crystal X-ray diffraction[14] and the resulting structure is shown in Fig. 1. It is noteworthy that $F_2POC_3H_5$ is coordinated through the phosphorus atom and that no interaction occurs between the allyl fragment and any other portion of the molecule.[14]

Reaction of $F_2POC_3H_5$ with both $(Ph_3P)_4RuCl_2$ and $(Ph_3P)_3RuCl_2$ produces a pale yellow complex of empirical formula $(Ph_3P)_2(F_2POC_3H_5)_2RuCl_2$, II. Between 750 and 4000 cm^{-1} the IR spectrum of II is essentially a superposition of the spectra of Ph_3P and $F_2POC_3H_5$, and thus strongly implies that no rearrangements have occurred in these ligands upon their coordination to ruthenium. NMR data indicate that II is an octahedral complex with *trans* $F_2POC_3H_5$ ligands located *cis* to two *cis* Ph_3P groups. If ^1H couplings are ignored, ^{19}F and ^{31}P spectra obtained on freshly prepared samples of II in $DCCl_3$ represent a well-resolved $A_2A_2'MM'XX'$ spin system. While the spectra are not first order, they can be analyzed and computer simulated, yielding the parameters given in Table 1. The 889.9 Hz coupling between phosphorus atoms in two equivalent $F_2POC_3H_5$ ligands indicates[12] that they are *trans* while the 53.3 Hz coupling between $F_2POC_3H_5$ and PPh_3 phosphorus atoms is characteristic of *cis* ligand configurations. The following stereochemistry for II is thus indicated

$$F_2POC_3H_5$$
$$Ph_3P \diagdown \;\Big|\; \diagup Cl$$
$$Ru$$
$$Ph_3P \diagup \;\Big|\; \diagdown Cl$$
$$F_2POC_3H_5$$
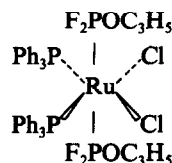
Whether II is monomeric or possesses an oligomeric, chloride-bridged, ionic structure similar to those of
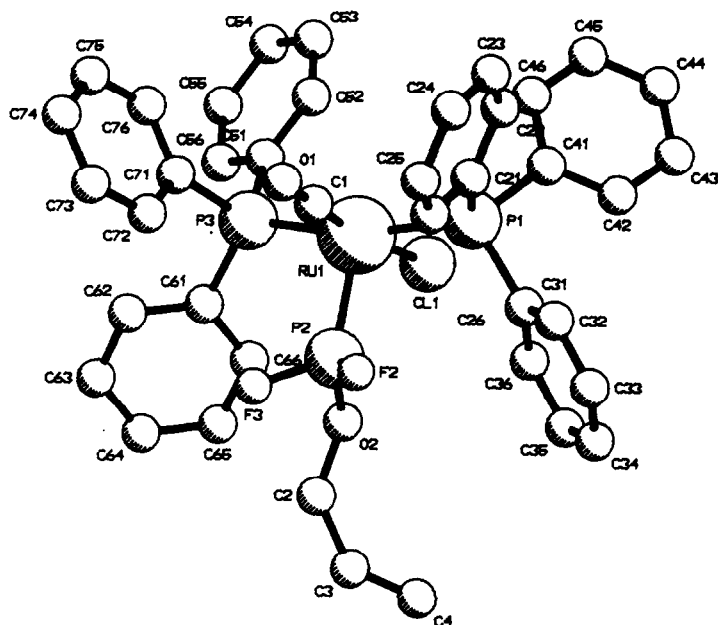
Fig. 1. Molecular structure of $(Ph_3P)_2(F_2POC_3H_5)Ru(H)(CO)(Cl)$.[14] A hydrogen atom (which was not located) is assumed to occupy the vacant position in the coordination sphere about ruthenium.

Table 1. NMR data[a]

[PPh$_3$]$_2$[F$_2$POC$_3$H$_5$]Ru[CO][Cl][H]:

Chemical Shifts:

^{19}F: -33.49 ppm (F$_2$P)

^{31}P: +130.10 ppm (F$_2$P)

  + 38.06 ppm (Ph$_3$P)

^{1}H:[b] -4.29 ppm (HRu)

Coupling Constants:

^{1}J(PF) = (-) 1286.8 Hz

^{3}J(PF) = 4.0 Hz

^{2}J(PhPRuPF) = 27.7 Hz

^{2}J(F$_2$PRuH) = 224 Hz

^{2}J(Ph$_3$PRuH) = 19.2 or 33.2 Hz[c]

^{3}J(F$_2$PRuH) = 33.2 or 19.2 Hz[c]

[(PPh$_3$)$_2$(F$_2$POC$_3$H$_5$)$_2$RuCl$_2$]$_n$

Chemical Shifts:

^{19}F: -37.09 ppm (F$_2$P)

^{1}H: see note (b)

^{31}P: +124.9 ppm (F$_2$P)

  + 22.7 ppm (Ph$_3$P)

Coupling Constants:[d]

^{1}J(PF) = -1258.6 Hz

^{3}J(F$_2$PRuPF) = 67.9 Hz

^{2}J(Ph$_3$PRuPF) = 53.3 Hz

^{2}J(F$_2$PRuPF) = 889.9 Hz

^{3}J(F$_2$PRuPPh) = ~6.1 Hz

[a]Spectra are second order. Chemical shifts and coupling constants have been obtained from theoretical spectra which have been matched to the experimental data by iterative calculations using a modified LAOCOON III program.

[b]The ^{1}H spectrum between 1–6 ppm was second order and qualitatively resembled the complex spectra expected for F$_2$POCH$_2$CH=CH$_2$. Between 7–9 ppm typical PPh$_3$ resonances occurred. No attempt was made to extract detailed spectral parameters, however.

[c]The Ru–*H* resonance appeared as a doublet of triplets. Since both *F*$_2$PRu*H* and (Ph$_3$P)$_2$Ru*H* couplings would generate triplet splittings, it was impossible to assign these couplings uniquely from the ^{1}H data. In order to enhance intensity, ^{31}P and ^{19}F spectra were obtained with [^{1}H] decoupling; consequently the assignment of these coupling constants is ambiguous.

[d]^{4}J(FF) and ^{2}J(Ph$_3$P Ru*P*Ph$_3$) were arbitrarily set to 10 Hz and 20 Hz, respectively; variations in these values did not affect the form of the spectrum at experimental resolution.

some other phosphine and phosphite ruthenium complexes[13,15] is not certain. However, after a few minutes the NMR spectra show changes and within 15–20 min the ^{19}F spectrum becomes a complex series of many weak resonances and the F$_2$POC$_3$H$_5$ resonances and couplings become unresolvable in the ^{31}P spectrum. This is not the result of decomposition of the F$_2$POC$_3$H$_5$ since **II** can be recrystallized from these solutions after concentration and cooling, or upon the addition of petroleum ether. Similar behavior has been noted in other mixed phosphine or mixed phosphine/phosphite ruthenium complexes and has been found to be the result of complex oligomerization and ligand interchange equilibria.[15] In all likelihood **II** enters into similar equilibria, but the exact details of these must await further study.

The formation of compounds **I** and **II** is noteworthy since they demonstrate that the F$_2$POC$_3$H$_5$ moiety can exist, coordinated to ruthenium, in media which undoubtedly contain Cl$^-$ and PPh$_3$. A Michaelis–Arbuzov reaction in which a nucleophile displaces an organo group from a coordinated organodifluorophosphite is consistent with the formation of F$_2$PO$^-$ in square planar platinum and palladium systems,[3,5] but obviously does not occur in the compounds studied here. Arbuzov-like rear-

rangements also occur in phosphite complexes. Recently these and some related intramolecular alkyl group exchanges have been shown to involve an oxidative alkyl migration to the metal.[16–18] The possibility that such a process could also be responsible for F$_2$PO$^-$ formation in F$_2$POR metal complexes, but is blocked in **I** and **II** by the unfavorable thermodynamics for the oxidation of Ru(II), is presently under investigation.

REFERENCES

[1] R. Schmutzler, *Chem. Ber.* 1963, **96**, 2435.
[2] A. Maisonnat, P. Kalck and R. Poilblanc, *Inorg. Chem.* 1974, **13**, 661.
[3] J. Grosse, R. Schmutzler and W. S. Sheldrick, *Acta. Cryst.* 1974, **B30**, 1623.
[4] J. Grosse and R. Schmutzler, *J.C.S. Dalton* 1976, 405.
[5] J. Grosse and R. Schmutzler, *Z. Naturforsch.* 1973, **28b**, 515.
[6] J. Grosse and R. Schmutzler, *J.C.S. Dalton* 1976, 412.

[7]S. Neumann, D. Schomburg and R. Schmutzler, *J.C.S. Chem. Commun.* 1979, 848.

[8]S. Hietkamp and R. Schmutzler, *Z. Naturforsch.* 1980, **35b**, 548.

[9]Th. Kruck, H. Jung, M. Höfler and H. Blume, *Chem. Ber.* 1976, **107**, 2145; and references therein.

[10]A. Ahmad, J. J. Levison, S. D. Robinson and M. F. Uttley, *Inorg. Syntheses* 1974, **15**, 45.

[11]P. S. Hallman, T. A. Stephenson and G. Wilkinson, *Inorg. Syntheses* 1970, **12**, 237.

[12]Y. Koie, S. Shinoda and Y. Sato, *Inorg. Nucl. Chem. Lett.* 1981, **17**, 147.

[13]M. Preece, S. D. Robinson and J. N. Wingfield, *J.C.S. Dalton* 1976, 613.

[14]J. W. Gilje, W. S. Sheldrick and R. Schmutzler, unpublished data. I crystallizes in the orthorhombic space group *Pna*2_1 with $a = 11.184(3)$, $b = 15.548(4)$,

$c = 23.137(6)$ Å, $z = 4$, and was refined to $R = 0.103$ for 1274 unique reflections (Mo$K\alpha$, $2\theta \leqslant 45°$) with $F_0^2 \geqslant 2.0\sigma(F_0^2)$ and with anisotropic temperature factors being introduced for the Ru. The small size of the best available crystal (volume $\sim 10^{-6}$ cm^3) limited the number of observable reflections and hence the quality of the X-ray analysis. A listing of positional parameters with isotropic or anisotropic temperature factors, bond lengths and angles, and observed and calculated structure factors have been deposited as Supplementary Data with the Editors from whom copies are available on request.†

[15]W. J. Sime and T. A. Stephenson, *J. Organomet. Chem.* 1978, **161**, 245.

[16]R. K. Pomeroy and R. F. Alex, *J.C.S. Chem. Commun.* 1980, 1114.

[17]V. W. Day, I. Tavanaiepour, S. S. Abdel-Meguid, J. F. Kirner, L.-H. Goh and E. L. Muetterties, *Inorg. Chem.* 1982, **21**, 657, and references therein.

[18]R. F. Alex and R. K. Pomeroy, *Organometallics* 1982, **1**, 453.

†Atomic co-ordinates have also been deposited at the Cambridge Crystallographic Data Centre.

SYNTHESIS AND CHARACTERIZATION OF LAYERED TETRAVALENT METAL TERPHENYL MONO- AND *BIS*-PHOSPHONATES

MARTIN B. DINES✠ and PETER C. GRIFFITH

Occidental Research Corporation, Irvine, CA 92713, U.S.A.

Abstract—The syntheses of *p*-terphenylphosphonic acid and *p,p"*-terphenyl-*bis*-phosphonic acid have been developed, and the resulting products were used to prepare layered Th(IV) and Zr(IV) phosphonates. The monoacidic terphenyl species formed a bilayered structure while the diacid created a pillared geometry. Mixed component phases were also produced. Synthesis, characterization, X-ray and thermal properties of these materials are discussed.

INTRODUCTION

Several reports of the preparation and properties of the tetravalent metal phosphonates $-M(O_3PR)_2-$ which have a layered structure and therefore access to the bulky $-R$ groups via intercalation have now appeared.[1–5] The terminal functions of the appended organic group can thus interact with guest species in a variety of selective sorption, ion-exchange or catalytic reactions. Furthermore, since the coexistence of more than one group between the layers is possible[3,6] polyfunctional systems can be conceived, microporosity can be incorporated (using pillaring cross-linking groups) and groups larger than the limiting cross-sectional area per site (about 24 Å² for the zirconium salts) can be included by adding compensatory small groups.

The synthesis of these compounds usually involves simple precipitation of the phosphonic acid with the metal ion. However, in many cases some of the most desirable $-R$ groups are not readily available as phosphonic acids, either commercially or via the simple Arbuzov or related reactions.[7] We have chosen one of the more difficult, and most useful, of the class, the polyaromatic mono- and *bis*-phosphonic derivatives, to illustrate how the layered compounds can be prepared and characterized. We focus upon the thorium salts because they are found to be generally more crystalline (i.e. they yield sharper X-ray diffraction reflections). The polyphenyl-*bis*-phosphonic acids are particularly good pillars because they are rigid and oriented perpendicularly between the lamellae. They are potentially valuable, therefore, in the architecture of microporosity in the interlayer regions.

Figure 1 shows a simplified structure of the layered phosphonates.

EXPERIMENTAL

All reagents and starting materials were obtained from commercial suppliers and used as received. Powder patterns were run on a Philips diffractometer using Cu K$_\alpha$ radiation. The thermogravimetry was performed on a DuPont DTA/TGA instrument, using air, and a heating rate of 20°/min.

p-Bromoterphenyl and p,p"-*dibromoterphenyl*. These com-

pounds were prepared by methods described in the literature,[8] and were actually obtained in the same reaction. They can be separated into pure components by selective extraction with hot ethanol. Each had the proper melting point.

Diethyl-p-terphenylphosphonate. *p*-Bromoterphenyl, 4.0 g (0.0129 mol), was slurried in 50 cm³ of *m*-diisopropylbenzene, heated to 140°C, and 100 mg of palladium dichloride were added to the solution. Then, while the reaction mixture was maintained at 160°C, 2.55 cm³ (0.0148 mol) of triethylphosphite were added over a period of 1 hr. This slow addition is required to prevent deactivation of the catalyst. After 3 hr at 160°C, the reaction mixture was cooled and the product fractionally distilled using a Kugelrohr at 170°C/0.4 torr, leading to a residual dark solid (4.0 g) which proved to be a 1:1 mixture of starting material and product. This assessment was made on grounds of both NMR and elemental analysis. Since we planned subsequently to hydrolyze and precipitate the phosphonate, this mixture was used without further purification. This "shortcut" could not be used in the case of the *bis*-phosphonic acid (*vide infra*), since contaminants would also react in later steps, unlike the case with bromoterphenyl.

p,p"-Terphenyl(bis)diethylphosphonate. Using the same route as before, 5.00 g (0.0129 mol) of dibromoterphenyl were added to 50 cm³ *m*-diisopropylbenzene and heated to 150°C. To the slurry which resulted, 0.220 g of palladium dichloride was added and the mixture brought to 160°C, whence 4.86 cm³ (0.0283 mol) triethylphosphite were added

Zr(O₃PR)₂
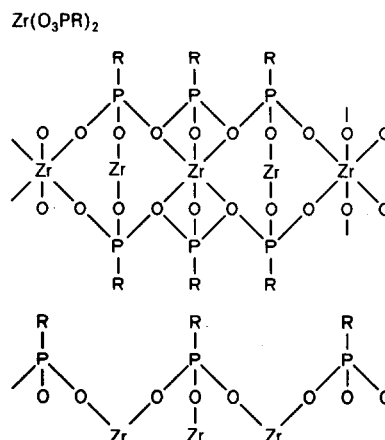
Fig. 1. Depiction of the framework sheet structure of the tetravalent metal phosphonates.

dropwise over 3 hr. (The addition was timed so that no triethylphosphite reflux occurred) Vacuum distillation (120°C/1 torr) of the solvent and phosphite left a dark solid which still contained some bromoaromatic, so the procedure was repeated to yield finally 5.8 g (90%) of solid having the appropriate NMR, but containing residual palladium. (Calcd. for $C_{26}H_{32}O_6P_2$: C, 62.1%, H, 6.43, P, 12.3; Found: C, 59.6, H, 6.01, P, 11.3, Pd, 3.1.) The palladium was removed in the next step, the hydrolysis of the phosphonic ester to the acid. When chromatography was attempted to purify the ester, much was lost on the column, presumably due to its association with the palladium.

Hydrolysis of the phosphonate esters and precipitation with thorium(IV). In the case of both phosphonate esters, the mono- and *bis*-substituted terphenyls, suitable conditions were sought for hydrolysis and separation of contaminating palladium. Furthermore, in the case of the mono-phosphonate, the product has to be freed of bromoterphenyl which was present (*vide supra*). The best conditions for hydrolysis were found to be heating for 1 hr in 30 cm³ of 30% HBr in acetic acid, cooling, and filtering to remove palladium and the product phosphonic acid. The latter was extracted into hot dioxane to which was added a solution of thorium nitrate in 80% dioxane/water. The resulting precipitate after refluxing for 20 hr. was washed with hot ethanol, then ether, and dried at 105°C for several hours. The phosphonic acid should always be in excess over the metal ion in the precipitation. This procedure led to a satisfactory product in the case of the *bis*-phosphonic acid (Calcd. for $Th(O_3PC_{18}H_{12}PO_3)$: C, 34.9%, H, 1.96; Found: C, 32.5, H, 3.00—other data in Results and Discussion); however, for the monophosphonic acid it remained to remove the significant contamination by bromoterphenyl. Based on the observation of two distinct weight loss processes in the thermogravimetric curve at 280 and 520°C, the first of which is sublimation of the bromoterphenyl, the product of precipitation in dioxane/water was heated in flowing helium at 240°C until no more material sublimed, leaving the product (Calcd. for $Th(O_3PC_{18}H_{13})_2$: C, 50.9, H, 3.09, Found: C, 52.3, H, 3.33).

Corresponding zirconium products were prepared in analogous reactions, using zirconyl chloride. Mixed component phases described in the text were prepared by precipitating combined solutions of the phosphonic acids.

RESULTS AND DISCUSSION

The general strategy for the preparation of both the bilayered, singly-bound terphenyl derivative and the cross-linking (monolayered) analogue is outlined in Fig. 2. Starting with the monobromo- and *p,p"*-dibromoaromatic, which are both formed by bromination of terphenyl and are separable due to their solubility difference in ethanol, the phosphorylated products can be made by a modified Arbuzov reaction (aryl halides required a group 8 metal catalyst,[9] see eqns 1 and 2).

Arbuzov reaction:

$$R-X + P(OR')_3 \rightarrow [R\overset{+}{-}P(OR')_3X^-] \rightarrow RPO(OR)_2$$
$$+ R'-X \quad (1)$$

Modified:

$$Ar-X + P(OR')_3 \xrightarrow{\text{Pd(II)}} [Ar-Pd-X] \rightarrow ArPO(OR')_2$$
$$+ R'-X. \quad (2)$$
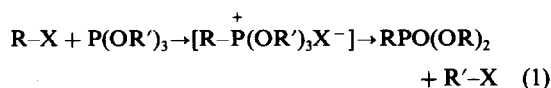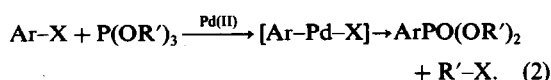
After hydrolysis to the phosphonic acid, the precipitation with tetravalent metal ion is carried out in an appropriate solvent system, i.e. one in which reactants
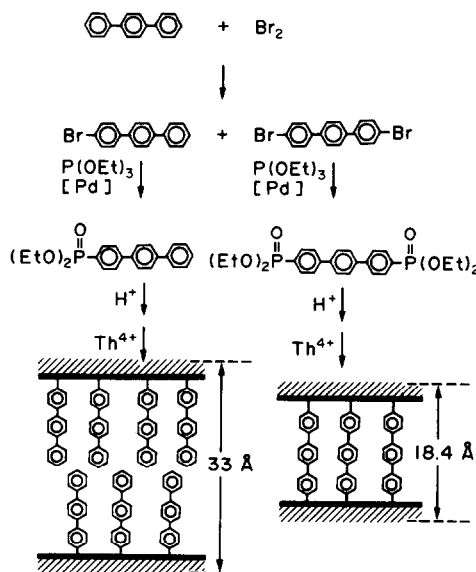
Fig. 2. The strategy for the preparation of the terphenyl compounds.

are all soluble. Given the nature of the aryl substituent, this was not achievable in straight aqueous media, as are most of the preparations of the layered metal(IV) phosphonates.

The choice of conditions for the precipitation (and purification) of the final products is not the only complication in the synthesis; we found it necessary to modify the preceding steps as well, and this is spelled out in the Experimental.

In the next sections we shall discuss some of the characterization of the products, compare the results of zirconium use to thorium, and touch upon some mixed composition compounds containing the terphenyl substituent.

$Th(O_3P\text{-}terphenyl)_2$

This product was prepared under conditions in which contaminating bromoterphenyl had to be removed. The presence of the halide was apparent in the thermogravimetric curve of the product of the thorium precipitation, which clearly showed two weight loss processes, at 280 and 520°C. The first weight loss is attributed to evaporation of the aryl bromide from the solid, the second is the decomposition of the layered phosphonate. The organic component is not intercalated in the thorium compound, as evidenced by its X-ray diffraction pattern, which shows the *d*-spacing series at about 33 Å. Since this is approximately the value expected for a bi-layered terphenyl structure, no guest is included in the crystalline product. This does not preclude the possibility of an amorphous or very poorly crystalline intercalated phase coexisting with the simple terphenyl-phosphonate.

On heating the impure product to 240°C in flowing helium, about half of the weight is lost, and the clean product results. The TGA now exhibits a single process at 520°C, and the XRD still has the 001 series corresponding to an interlayer distance of 33 Å (Fig. 3). This value is exactly that predicted based on a structure of non-interleaving perpendicularly oriented
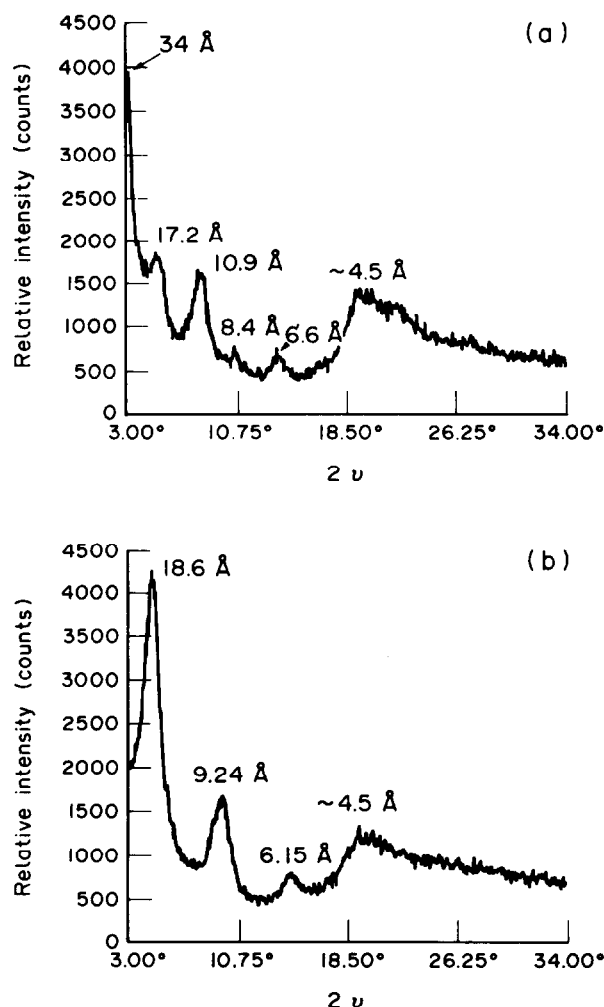
Fig. 3. X-ray diffraction powder patterns of the terphenyl compounds: A, Th(O₃P-terphenyl)₂; B, Th(O₃P-terphenyl-PO₃).

terphenyl groups appended from every site on the basal surface of a thorium-PO₃ sheet similar in structure to α-zirconium phosphate. The corresponding layer–layer spacings for mono- and diphenyl-substituted thorium phosphonates[6] are 15 and 24 Å, which make for a good linear relationship (Fig. 4). The slope, 9 Å/(2) phenyl groups, agrees with the value of 4.2 Å for -⬡- from CPK models.

Th(O₃P-*terphenyl*-PO₃)

The preparation and characterization of this product was actually more straightforward than the monophosphonate, because the starting material was purer. Although the thermogravimetric curve did not show any occluded organic as before, the decomposition process was not as sharp. Instead of a single narrow weight loss, there was a broadened continuous decomposition which occurred from 250 to 800°C, corresponding to the loss of the organic component (calcd loss for $C_{18}H_{12}$, 37%; found, 37.5%). The cause of this extended range may be the fact that the organic groups are doubly bound, and that deintercalation of the products of decomposition is inhibited, necessitating an edge-inwards process.

The XRD spacing found for the crosslinked terphenyl was 18.6 Å (see Fig. 3), which when compared with the diphenyl analogue[10] yields a slope of 4.1 Å per phenyl group, in good agreement with the model discussed for the monophosphonate. It is also interesting that the intercept, which implies a value for the thickness of the Th(O₃P-)₂ inorganic layer, is the same in both cases, 6.2 Å (Fig. 5). The corresponding value for the zirconium compounds is 5.4 Å, in close enough agreement (after correcting for the greater ionic radius of Th^{4+}) to suggest that both series have the α-zirconium phosphate sheet structure.

The value estimate for the pillar length of the terphenyl group (18.6–6.2 = 12.4 Å) suggests that this might be an attractive candidate for mixed component microporous products. Our only attempt at this, using the terphenyl-*bis*-phosphonate together with phenylphosphonic acid, led to a product whose X-ray powder pattern indicated that mostly a pure phase of the phenyl derivative had formed. This could occur if the rate of precipitation of the phenyl product is much faster than that of the *bis*-acid, a situation we have observed in other instances. In such situations mixed component products can often be formed by using excessive amounts of the slower
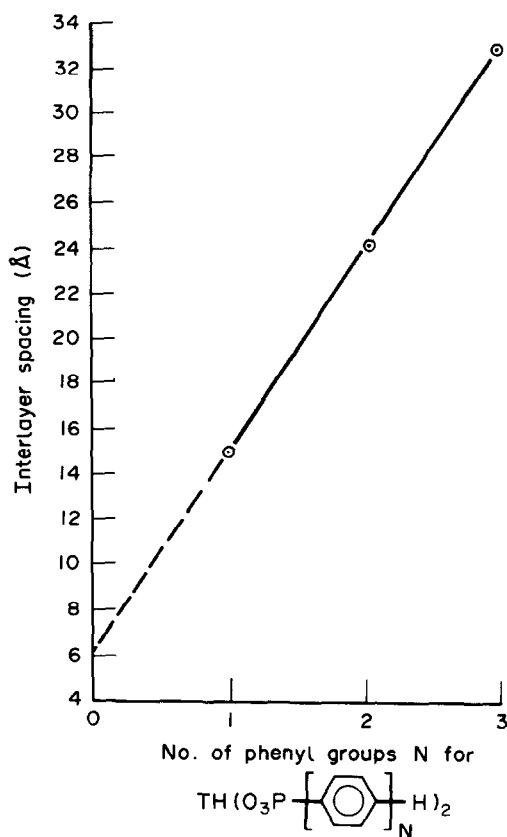
Fig. 4. Plot of the d-spacing (interlayer distance) for the series of thorium arylphosphonates.

Fig. 6. Representation of two alternative structures for the mixed component thorium phenyl/terphenyl phosphonate product. Top, ordered with the same group covering basal surfaces; bottom, ordered or disordered with variable basal content. In both cases, the interlayer distance corresponds to phenyl–terphenyl interactions dictating the interlayer distance.

Fig. 5. Plot of the d-spacings for the cross-linked thorium arylphosphonates.

precipitating species, but we did not explore this possibility in the case at hand.

Other terphenyl-containing products

Although the attempt at the preparation of a mixed-component cross-linked compound was not successful, it did prove possible to produce one containing a monophosphonate group, namely $Th(O_3PC_6H_5)(O_3PC_{18}H_{13})$. In this case, by co-precipitation of the corresponding phosphonic acids, a product having the correct analysis, and more significantly an X-ray powder pattern exhibiting predominantly the series of reflections for a d-spacing of 24.3 Å was afforded. This dimension is just what would be expected for a structure in which terphenyl groups oppose phenyl groups across the interlayer (i.e. $1/2(15 \text{ Å} + 33 \text{ Å})$. Two alternative ways this could be arranged are: (a) either one entire face contains one group and the other the opposite group (an ordered array), or (b) a random structure in which somehow terphenyls are fitted efficiently with phenyls (Fig. 6). We cannot differentiate experimentally between these alternatives, although one might expect that there would be density differences between the two structures.

The analogous zirconium compounds were prepared for most of the cases under discussion and true to our past experience, they were generally found to be of inferior crystallinity as implied by their poor XRD patterns.

REFERENCES

[1] G. Alberti, U. Costantino, S. Alluli and N. Tomassini, *J. Inorg. Nucl. Chem.* 1978, **40**, 1113.

[2] M. Dines and P. DiGiacomo, *Inorg. Chem.* 1981, **20**, 92.

[3] M. Dines, P. DiGiacomo, K. Callahan, P. Griffith, R. Lane and R. Cooksey, in *Chemically Modified Surfaces in Catalysis and Electrocatalysis* (Edited by J. Miller, Chap. 13, ACS Symposium Series 192. ACS (1982).

[4] L. Maya, *Inorg. Nucl. Chem. Lett.* 1979, **15**, 2811.

[5] M. Dines and P. Griffith, *J. Phys. Chem.* 1982, **86**, 571.

[6] M. Dines and P. Griffith, *Inorg. Chem.* 1983, **22**, 0000.

[7] R. F. Hudson, *Structure and Mechanism in Organophosphorous Chemistry*, p. 135ff. Academic Press, New York (1965).

[8] H. France, I. Heilbron and D. Hey, *J. Chem. Soc.* 1938, 1364.

[9] *German Pat.* 2,118,273 (CA 76: 34399).

[10] The diphenyl analogue—$Th(O_3P-C_{12}H_8-PO_3)$—was prepared from *p,p'*-dibromodiphenyl by the same means as described in this report.

PREPARATION AND CHARACTERIZATION OF DICHLOROBIS(N-ALKYL-SUBSTITUTED SALICYLIDENEAMINATO)MANGANESE(IV) COMPLEXES

TAKAYUKI MATSUSHITA* and TOSHIYUKI SHONO
Department of Applied Chemistry, Faculty of Engineering, Osaka University, Yamadaoka, Suita, Osaka 565, Japan

Abstract—A series of dichlorobis(N-alkyl-substituted salicylideneaminato)manganese(IV) complexes, $Mn(N-R-Xsal)_2Cl_2$, was prepared by the reaction of $Mn(N-R-Xsal)_2Cl$ complexes with hydrogen chloride, where R can be $n\text{-}C_8H_{17}$ (Oct), $n\text{-}C_{12}H_{25}$ (Dod), $n\text{-}C_{18}H_{37}$ (Octd), and $CH_2C_6H_5$ (Bz) and X can be 5-bromo, 5-nitro, and 5,6-benzo groups. These complexes were characterized by the magnetic susceptibilities, IR and electronic spectra, and cyclic voltammograms.

Manganese(III) and -(IV) complexes are of interest in relation to the biological redox systems catalyzed by manganese ions, which include the disproportionation of superoxide ion (O_2^-) by the manganese-containing superoxide dismutases and the photosynthetic oxygen evolution by water oxidation in green plants.[1,2] Although a number of manganese(III) complexes with various ligands have been investigated, very few manganese(IV) complexes have been isolated and characterized so far. The reason seems to be that manganese(IV) ion is a strong oxidizing agent and its complexes are unstable toward moisture.[3,4]

Previously we have found that a series of chloromanganese(III) complexes with the bidentate and tetradentate Schiff base ligands reacts with hydrogen chloride to give the corresponding dichloromanganese(IV) complexes as deep green crystals.[5] These complexes, however, are not stable toward water even in the solid state and decompose gradually to their reduced manganese(III) complexes. In an earlier paper we have shown that the dichloromanganese(IV) complexes with the bidenatae Schiff bases which were derived from salicylaldehyde and long-chain aliphatic monoamines such as $n\text{-}C_{12}H_{25}NH_2$ and $n\text{-}C_{18}H_{37}NH_2$ are more stable toward water than those derived from $n\text{-}C_3H_7NH_2$ and $n\text{-}C_4H_9NH_2$.[6]

Present paper describes the preparation and characterization of new dichloromanganese(IV) complexes as shown in Fig. 1.

EXPERIMENTAL

Preparation of Mn(III) Schiff Base Complexes, Mn(N-R-Xsal)$_2$Cl. Chlorobis(N - dodecyl - 5 - bromosalicylideneaminato)manganese(III), Mn(N - Dod - 5 - Brsal)$_2$Cl. N - Dodecyl - 5 - bromosalicylideneamine (N - Dod - 5 - BrsalH) was prepared by the condensation of 5-bromosalicylaldehyde and equimolar dodecylamine in tetrahydrofuran. This was recrystallized from ether. The other bidentate Schiff bases were prepared in a similar manner. Their melting points and analytical data are listed in Table 1.

To an ethanol solution (100 cm³) of N-Dod-5-BrsalH (7.37 g, 0.02 mol), Mn(III) $(CH_3CO_2)_3 \cdot 2H_2O$ (2.68 g, 0.01 mol) and LiCl (0.84 g, 0.02 mol) were added. The mixture was warmed at 60°C for 1 hr with stirring and then

evaporated to remove the solvent under reduced pressure. The resulting brown solids were collected on a glass filter, washed with small amounts of ethanol, and dried *in vacuo*. They were extracted with dichloromethane (150 cm³), and the solution was evaporated to give brown solids. They were recrystallized from acetonitrile.

The other manganese(III) complexes were prepared in a similar manner. The solvents employed for recrystallization were acetonitrile for Mn(N-Oct-5-Brsal)$_2$Cl, Mn(N-Oct-5,6-Benzosal)$_2$Cl, Mn(N-Dod-5,6-Benzosal)$_2$Cl, Mn(N-Oct-5-NO$_2$sal)$_2$Cl, and Mn(N-Dod-5-NO$_2$sal)$_2$Cl, acetone for Mn(N-Octd-5-Brsal)$_2$Cl and Mn(N-Octd-5,6-Benzosal)$_2$Cl, dichloromethane for Mn(N-Bz-5Brsal)$_2$Cl and Mn(N-Octd-5-NO$_2$sal)$_2$Cl, methanol for Mn(N-Bz-5-Brsal)$_2$Cl, and N,N-dimethylformamide for Mn(N-Bz-5-NO$_2$sal)$_2$OH. These complexes are soluble in dichloromethane, methanol, and acetonitrile, slightly soluble in ether, and insoluble in water. The analytical data for these complexes are given in Table 2.

Preparation of Mn(IV) Schiff Base Complexes, Mn(N-R-Xsal)$_2$Cl$_2$. Dichlorobis(N - dodecyl - 5 - bromosalicylideneaminato)manganese(IV), Mn(N-Dod-5-Brsal)$_2$Cl$_2$. To a 2-propanol (70 cm³) containing Mn(N-Dod-5-Brsal)$_2$Cl (1.0 g) was added a 2-propanol solution of hydrogen chloride (1.5 molar folds over the complex) at room temperature. The mixture was stirred for 1 hr to give deep green precipitates. They were collected on a glass filter, washed with 2-propanol, and dried *in vacuo*. They were recrystallized from benzene to give deep green crystals. The yield was *ca.* 0.2 g. This complex is soluble in dichloromethane, benzene, and acetone to give deep green colour. These solutions show no measurable change in colour allowing to stand for 1 hr in an aerial atmosphere. This complex

$$Mn(N\text{-}R\text{-}X\,sal)_2Cl_2$$

R	X
$n\text{-}C_8H_{17}$ (Oct)	5-Br
$n\text{-}C_{12}H_{25}$ (Dod)	5,6-Benzo
$n\text{-}C_{18}H_{37}$ (Octd)	5-NO$_2$
$CH_2C_6H_5$ (Bz)	
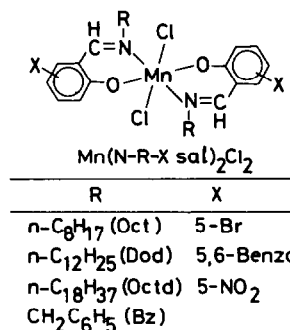
Fig. 1. Mn(IV) complexes.

Table 1. Melting points and analytical data for Schiff base ligands

Ligand	M.P. $^{\circ}C$	Found (Calcd) (%)		
		C	H	N
N-Dod-5-BrsaiH	24 - 25	61.51(61.95)	8.30(8.21)	3.83(3.80)
N-Octd-5-BrsaiH	50.5 - 51	65.98(66.36)	9.39(9.36)	3.07(3.10)
N-Dod-5,6-BenzosaiH	64.5	81.07(81.61)	9.80(9.53)	4.20(4.14)
N-Octd-5,6-BenzosaiH	82 - 82.5	82.25(82.41)	10.84(10.49)	3.37(3.31)
N-Dod-5-NO$_2$saiH	93 - 93.5	67.97(68.23)	9.05(9.04)	8.31(8.38)
N-Octd-5-NO$_2$saiH	99.5 - 100	71.69(71.73)	10.18(10.11)	6.78(6.69)

Table 2. Analytical data for manganese(III) Schiff base complexes

Mn(N-R-Xsai)$_2$Cl		Found (Calcd) (%)			
R	X	C	H	N	Mn
Oct	5-Br	50.88(50.54)	6.08(5.94)	3.96(3.93)	7.62(7.71)
Dod	5-Br	55.33(55.32)	7.12(7.09)	3.32(3.40)	6.74(6.66)
Octd	5-Br	60.06(60.45)	8.30(8.32)	2.84(2.82)	5.59(5.53)
Bz	5-Br	50.30(50.29)	3.40(3.32)	4.07(4.19)	8.32(8.22)
Oct	5,6-Benzo	69.52(69.66)	7.44(7.38)	4.19(4.28)	8.46(8.38)
Dod	5,6-Benzo	72.31(72.00)	8.56(8.41)	3.71(3.65)	7.13(7.16)
Octd	5,6-Benzo	74.19(74.45)	9.40(9.48)	2.96(2.99)	6.02(5.87)
Bz	5,6-Benzo	70.61(70.77)	4.69(4.62)	4.54(4.58)	9.02(8.99)
Oct	5-NO$_2$	55.50(55.86)	8.60(8.69)	6.63(6.56)	8.45(8.52)
Dod	5-NO$_2$	59.79(60.27)	7.77(7.72)	7.38(7.40)	7.11(7.25)
Octd	5-NO$_2$	64.80(64.88)	9.07(8.93)	5.95(6.05)	5.92(5.94)
Bz	5-NO$_2$ $^{a)}$	57.96(57.64)	4.06(3.97)	9.54(9.60)	9.38(9.42)

a) Values for Mn(N-Bz-5-NO$_2$sai)$_2$OH.

also is soluble in pyridine and methanol but these solutions change in colour from green to brown gradually.

The other dichloromanganese(IV) Schiff base complexes were prepared in a similar manner. The analytical data for the manganese(IV) complexes are given in Table 3.

Measurements. The melting points were determined by means of a Yanagimoto MP-1 melting point apparatus and uncorrected. The UV and VIS spectra were obtained by a Hitachi 340 spectrophotometer. The IR spectra were recorded on a Hitachi EPI-215 grating spectrophotometer in the 650–4000 cm^{-1} regions and on a Hitachi EPI-L grating spectrophotometer in the 200–700 cm^{-1} regions. The magnetic susceptibilities were measured by the Gouy method at room temperature. The cyclic voltammetry was performed with a Yanagimoto P-8 polarograph connected with a Yanagimoto P8-PT potentiostat. The working electrode was a platinum-inlay electrode, while the auxiliary electrode was a platinum wire. The reference electrode was a saturated calomel electrode which was inserted in an aqueous solution of 1 M KCl in a 100 cm^3 beaker connected with a conventional brown H-Type cell by means of a 4% agar-saturated KCl gel bridge. Tetrabutylammonium perchlorate, Bu$_4$NClO$_4$, was used as the supporting electrolyte (0.1 M). The dissolved oxygen was removed by passing N$_2$ gas through a sample solution for 20 min. The cyclic voltammograms were recorded under the following conditions: concentration of the complexes was 5×10^{-4} M, the scan rate was 0.06 V/s, and temperature was kept at 25°C.

Materials. All reagents were of reagent grade. The solvents were purified by a usual manner. Acetonitrile was distilled twice over diphosphorus pentaoxide prior to use. Benzene was distilled over sodium.

RESULTS AND DISCUSSION

Preparation. We reported previously the preparation and characterization of dichlorobis (N-butyl-substituted salicylideneaminato)manganese(IV) complexes, Mn(N-Bu-Xsal)$_2$Cl$_2$, where X can be H, 5-Br, 5-NO$_2$, and 5,6-Benzo groups.[5] These complexes were decomposed gradually to the reduced manganese(III) complexes by moisture allowing to stand in an aerial condition even in the solid state. Thus in order to obtain pure manganese (IV) complexes much care should be taken to remove trace amounts of water in the solvents used. In an earlier paper[6] we have reported that the manganese(IV) complexes incorporating long-chain alkyl groups such as n-C$_{12}$H$_{25}$ and n-C$_{18}$H$_{37}$ can be protected from attack of water. These

Table 3. Analytical data for manganese(IV) Schiff base complexes

| $Mn(N-R-Xsal)_2Cl_2$ | | | | Found (Calcd) (%) | | |
R	X	C	H	N	Cl	Mn
Oct	5-Br	48.28(48.15)	5.82(5.66)	3.74(3.74)	30.55(30.84)[a]	7.33(7.34)
Dod	5-Br	53.12(53.04)	6.90(6.79)	3.28(3.26)	26.56(26.81)[a]	6.52(6.38)
Octd	5-Br	57.92(58.37)	8.18(8.03)	2.81(2.72)	22.91(22.53)[a]	5.31(5.34)
Bz	5-Br	47.96(47.76)	3.26(3.15)	3.95(3.98)	32.62(32.77)[a]	7.80(7.80)
Oct	5,6-Benzo	66.39(66.08)	7.11(7.01)	4.42(4.06)	10.75(10.27)	8.11(7.95)
Dod	5,6-Benzo	68.58(68.82)	8.09(8.03)	3.50(3.49)	8.67(8.83)	7.05(6.84)
Octd	5,6-Benzo	71.44(71.73)	9.21(9.13)	2.91(2.88)	7.52(7.30)	5.70(5.66)
Bz	5,6-Benzo	66.69(66.89)	4.41(4.37)	4.45(4.33)	11.10(10.97)	8.54(8.50)
Oct	$5-NO_2$	52.74(52.95)	6.23(6.22)	8.39(8.24)	10.00(10.42)	8.10(8.07)
Dod	$5-NO_2$	57.74(57.57)	7.53(7.37)	7.05(7.07)	9.05(8.94)	6.93(6.93)
Octd	$5-NO_2$	62.24(62.49)	8.78(8.50)	5.92(5.83)	8.34(7.34)	5.69(5.72)
Bz	$5-NO_2$ [b]	50.19(50.42)	3.53(3.42)	8.22(8.25)	16.33(15.67)	8.56(8.09)

a) Cl + Br.   b) Inclusion of $(CH_2Cl_2)_{0.5}$ as a crystalline solvent.

findings led us to prepare a series of dichloromanganese(IV) Schiff base complexes having long-chain alkyl groups. All the manganese(III) complexes which were prepared have a composition of $Mn(N-R-Xsal)_2Cl$, with the exception of $Mn(N-Bz-5-NO_2sal)_2OH$ (Table 2). All the manganese(IV) complexes which were obtained have a composition of $Mn(N-R-Xsal)_2Cl_2$ (Table 3). The properties for the

manganese(III) and manganese(IV) complexes are summarized in Tables 4 and 5, respectively.

Melting points. The manganese(III) complexes having the long-chain alkyl groups showed low melting points without decomposition. As seen in Table 4, the longer the alkyl groups the lower melting points are obtained in the order of Bz > Oct > Dod > Octd. As to the substituents on the aromatic ring the melting

Table 4. Properties of manganese(III) Schiff base complexes

| $Mn(N-R-Xsal)_2Cl$ | | M.P. | μ_{eff}[a] | ν_{max}(log ε)[b] | $\nu(Mn-Cl)$[c] | $E_{p/2}$ vs. SCE[d] |
R	X	°C	BM	10^3 cm^{-1}	cm^{-1}	V Mn(III)→Mn(II)
Oct	5-Br	141 - 145	4.95	14.97 (2.72)	306	0.08
Dod	5-Br	122 - 123	4.92	14.93 (2.75)	305	0.08
Octd	5-Br	104 - 105	4.83	14.97 (2.75)	306	0.07
Bz	5-Br	229 - 230[f]	4.91	14.86 (2.77)	330	0.08
Oct	5,6-Benzo	136 - 137	4.91	15.11 (2.70)	306	-0.09
Dod	5,6-Benzo	109 - 110	4.83	15.15 (2.72)	305	-0.08
Octd	5,6-Benzo	94 - 95	4.82	15.13 (2.71)	305	-0.06
Bz	5,6-Benzo	208 - 209[f]	3.25	15.08 (2.70)	313	-0.07
Oct	$5-NO_2$	197 - 198	3.89	15.92 (2.84)	293	0.28
Dod	$5-NO_2$	181 - 182	3.79	15.67 (2.70)	294	0.25
Octd	$5-NO_2$	179 - 180	3.53	15.72 (2.72)	293	0.30
Bz	$5-NO_2$	220 - 222[f]	4.20	15.82 (2.65)	293	0.28
Oct	H [e]	154 - 155	4.93	15.20 (2.60)	317	-0.16

a) Measured at room temperature. b) Measured in dichloromethane. c) Measured in Nujol mulls. d) Measured in acetonitrile containing $(Bu)_4NClO_4$ (0.1 mol dm^{-3}) at 25 °C. e) In a previous work.[6] f) With decomposition.

Table 5. Properties of manganese(IV) Schiff base complexes

Mn(N-R-Xsal)₂Cl₂		M.P.	μ_{eff} [a]	ν_{max} (log ε) [b]	ν(Mn-Cl) [c]	$E_{p/2}$ vs. SCE [d]	
R	X	°C	BM	10^3 cm⁻¹	cm⁻¹	V	
						Mn(IV)→Mn(III)→Mn(II)	
Oct	5-Br	123 - 124	4.07	15.72 (3.72)	329	0.87	-0.12
Dod	5-Br	115 - 116	4.02	15.72 (3.73)	326	0.85	-0.10[f]
Octd	5-Br	111 - 112	4.07	15.67 (3.66)	337	0.85	-0.10[f]
Bz	5-Br	184 - 185	3.87	15.77 (3.55)	337	0.90	-0.03
Oct	5,6-Benzo	94 - 95	4.02	14.84 (3.68)	336	0.40	-0.13
Dod	5,6-Benzo	86 - 87	4.04	14.75 (3.77)	327	0.39	-0.13[f]
Octd	5,6-Benzo	83 - 84	3.91	14.75 (3.75)	326	0.40	-0.07[f]
Bz	5,6-Benzo	148 - 149	3.90	14.83 (3.77)	326	0.41	-0.07
Oct	5-NO₂	190 - 193	3.93	16.98 (3.72)	358	0.93	0.06
Dod	5-NO₂	185 - 190	4.06	17.01 (3.77)	354	0.92	0.06
Octd	5-NO₂	180 - 184	4.10	16.85 (3.74)	358	0.93	0.12[f]
Bz	5-NO₂	>280	3.94	17.12 (3.74)	355	1.00	0.21
Oct	H[e]	106 - 107	3.92	16.00 (3.62)	348	0.83	-0.12

a) Measured at room temperature. b) Measured in dichloromethane. c) Measured in
Nujol mulls. d) Measured in acetonitrile containing $(Bu)_4NClO_4$ (0.1 mol dm^{-3}) at 25 °C.
e) In a previous work.[6] f) Measured in a mixture of acetonitrile and dichloromethane
(1/1 volume ratio). All the melting points were observed with decomposition.

points are lowered in the order of 5-NO₂ > H > 5-Br > 5,6-Benzo groups. The melting points for Mn(N-R-sal)₂Cl which were prepared in a preceding work are 154-155, 129-130, 119.5-120, and 205-206°C for R = Oct, Dod, Octd and Bz, respectively. On the other hand, the melting points of the manganese(IV) complexes are lower than those of the corresponding manganese(III) complexes, and they decompose at near melting points, showing colour changes from green to brown (Table 5). As to the alkyl groups the melting points are lowered in the same order as that for the manganese(III) complexes, and as to the substituents on the aromatic ring they are lowered in the order of 5-NO₂ > 5-Br > H > 5,6-Benzo groups, with the exception of Mn(N-Bzsal)₂Cl₂. The melting points of Mn(N-R-sal)₂Cl₂ which were prepared in a preceding work are 106-107, 97.5-98.5, 94-95, and 112-113°C for R = Oct, Dod, Octd and Bz, respectively.

Magnetic properties. The magnetic moments for the manganese(III) complexes fall within the range of 4.82-4.95 BM, with the exception of Mn(N-Bz-5,6-Benzosal)₂Cl and all the 5-nitro derivatives (Table 4). These values are consistent with the spin-only value expected for a complex having a d^4 high-spin electron configuration. The lower values observed for the above complexes may be caused by antiferromagnetic interaction between manganese atoms due to a binuclear structure in which they are bridged by two phenolic oxygen atoms. No further investigation on magnetic properties for these complexes has been made.

The magnetic moments for the manganese(IV) complexes fall within the range of 3.87-4.10 BM

(Table 5). These values are consistent with the spin-only value expected for a complex having a d^3 electron configuration.

Electronic spectra. The electronic spectra of the manganese(III) complexes measured in dichloromethane show the absorption bands (log ε = 2.7) around 15000 cm⁻¹. These complexes may have a five-coordinate configuration around the central manganese atom in such a noncoordinating solvent.[7] Therefore, these bands can be assigned to a ligand field transition due to $d_{xy} \rightarrow d_{x^2-y^2}$. The absorption maxima are affected by the aromatic ring substituents and are shifted to higher energies in the order of 5-NO₂ > H > 5,6-Benzo > 5-Br groups (Table 4). The alkyl groups attached to the nitrogen atoms have little effect on the absorption maxima. On the other hand, the electronic spectra of the manganese(IV) complexes in dichloromethane show the more intense absorption bands (log ε = 3.7) in the range of 14700-17100 cm⁻¹ compared with those for the manganese(III) complexes. These bands can be assigned to a charge-transfer transition due to $Cl(p\pi) \rightarrow Mn(d\pi)$ from their intensities as discussed in the previous papers.[5,6] These absorption maxima are also affected by the aromatic ring substituents and are shifted to higher energies in the order of 5-NO₂ > H > 5-Br > 5,6-Benzo groups (Table 5). The alkyl groups have little effect on the absorption maxima as well as the manganese(III) complexes.

IR spectra. The IR spectra of the manganese(IV) complexes show almost the same pattern as those of the manganese(III) complexes in the region from 500 to 4000 cm⁻¹, but both spectra are significantly different in the region from 200 to 500 cm⁻¹. In this

region the absorption bands due to Mn–Cl stretching vibrations should be observed.[8] Both manganese(III) and manganese(IV) complexes showed one absorption band assignable to ν(Mn–Cl) (Tables 4 and 5). The frequencies for the manganese(IV) complexes are observed in higher energies compared with those for the corresponding manganese(III) complexes. This may be caused by the change in the oxidation state of the central manganese atom from Mn(III) to Mn(IV). The results that one absorption band due to ν(Mn–Cl) is observed for the manganese(IV) complexes imply that two chlorine atoms coordinate to the manganese atom as a *trans*-configuration. Thus we propose a *trans*-octahedral configuration for the manganese(IV) complexes investigated here as shown above.

Electrochemical properties. The cyclic voltammograms of the manganese(III) and manganese(IV) complexes were measured in acetonitrile. Some of the manganese(IV) complexes were measured in a mixture of acetonitrile and dichloromethane (1:1) owing to their poor solubility in acetonitrile. The current-potential curves for the manganese(III) complexes showed the one cathodic wave around 0.0 V (vs SCE) in the +1.2 to −0.8 V range. This can be assigned to the one-electron reduction from Mn(III) to Mn(II).[9] On the other hand, the current-potential curves for the manganese(IV) complexes showed the two-step cathodic waves around +0.9 and 0.0 V with similar wave heights. These waves can be assigned to the one-electron reductions from Mn(IV) to Mn(III) and from Mn(III) to Mn(II), respectively. The separations of the peak potentials between the cathodic wave and the corresponding anodic wave for both redox waves are larger than the 57 mV expected for a reversible

one-electron redox wave, so these electrode reactions may be irreversible. Thus the half-peak potentials ($E_{p/2}$) of the cathodic waves for the manganese(III) and manganese(IV) complexes are summarized in Tables 4 and 5, respectively. The reduction potentials for the manganese(III) complexes are affected by the aromatic ring substituents and are shifted to more positive potentials in the order of 5-NO_2 > 5-Br > 5,6-Benzo groups. And they are little affected by the alkyl groups. On the other hand, the reduction potentials for the manganese(IV) complexes are significantly affected by the aromatic ring substituents and are shifted to more positive potentials in the order of 5-NO_2 > 5-Br > 5,6-Benzo groups. These potential shifts can be explained by the electron-withdrawing ability of the substituent groups. And also the alkyl groups have little effect on the reduction potentials. These results are not inconsistent with those obtained in the electronic and IR spectra.

REFERENCES

[1] G. D. Lawrence and D. T. Sawyer, *Coord. Chem. Rev.* 1978, **27**, 173.
[2] K. Sawer, *Acc. Chem. Res.* 1980, **13**, 249.
[3] G. Davies, *Coord. Chem. Rev.* 1969, **4**, 199.
[4] W. Levason and C. A. McAuliffe, *Ibid.* 1972, **7**, 353.
[5] T. Matsushita, H. Kono and T. Shono, *Bull. Chem. Soc. Jpn.* 1981, **54**, 2646.
[6] T. Matsushita, Y. Hirata and T. Shono, *Ibid.* 1982, **55**, 108.
[7] L. J. Boucher and V. W. Day, *Inorg. Chem.* 1977, **16**, 1360.
[8] K. Nakamoto, *Infrared Spectra of Inorganic and Coordination Compounds*, p. 214. Wiley-Interscience, New York (1970).
[9] W. M. Coleman, R. R. Goehring, L. T. Taylor, J. G. Mason and R. K. Boggess, *J. Am. Chem. Soc.* 1979, **101**, 2311.

THE REACTION OF LITHIUM ALUMINIUM HYDRIDE WITH CARBON DIOXIDE OR SODIUM BICARBONATE

B. T. THOMPSON, T. N. GALLAHER* and T. C. DeVORE

James Madison University, Department of Chemistry, Harrisonburg, VA 22807, U.S.A.

Abstract—The reaction of $LiAlH_4$ with CO_2 or $NaHCO_3$ at elevated temperatures has been investigated. Methane and ethylene are the primary products of each reaction. These molecules are probably the "explosive" reaction products formed when CO_2 fire extinguishers are used on $LiAlH_4$ fires.

Recently several letters have appeared in the literature discussing the hazards of lithium aluminium hydride (LiAlH₄ or LAH) fires.[1-3] It was reported that burning LAH pellets could not be quenched in a nitrogen atmosphere and an intert gas such as argon was required to extinguish the fire safely. It was also noted that the use of a sodium bicarbonate or carbon dioxide (CO_2) fire extinguisher to extinguish a LAH fire formed "explosive" reaction products.[2-4] LAH is a common reducing reagent for both organic and inorganic reactions.[5,6] In addition, there has been a considerable amount of interest generated in C_1 chemistry.[7-10] The reaction of CO and CO_2 with H_2 in the presence of metal reducing catalysts can produce a variety of organic molecules ranging from methane to gasoline hydrocarbons.[7] Since LAH is such a good reducing agent and there are hazards in trying to extinguish a LAH fire, an investigation of the reaction of LAH with CO_2 and with $NaHCO_3$ was undertaken. This paper presents the results of this investigation.

EXPERIMENTAL

The apparatus used to investigate the LAH reactions has been described in detail previously.[11,12] Briefly, the reactions were carried out in a quartz tube attached to an MDC Manufacturing Company stainless steel 4-way cross vacuum flange. Two opposing sides of the flange were equipped with KBr windows to make an infrared gas cell. The entire system was maintained under vacuum by a liquid nitrogen trap, 2 in. oil diffusion pump and a rotary vacuum pump. An uncalibrated thermocouple gauge was used to monitor the pressure in the system. This cell was placed in the sample compartment of a Nicolet MX-1 Fourier Transform IR Spectrometer (FTIR). The spectra were taken using 1 min scans at 1 cm⁻¹ resolution as the reaction progressed. After completion of the reactions, the trapped gases were either allowed to flow back into the cell so spectra could be retaken or they were collected in a mass spectrometer sampling bulb. In most cases the IR spectrum was sufficient to identify the reaction products, however, mass spectra, taken on a Varian

EM-600, were occasionally used to confirm the product assignments.

All of the experiments were performed in essentially the same way. LAH or mixtures of LAH and various reactants were placed in the quartz tube and the system was evacuated to 0.1 Pa pressure. The tube was resistively heated with a nichrome wire. Sufficient CO_2 was added to the reaction mixture to produce a combined total pressure of 10^2 Pa and the spectrum was taken as the reaction proceeded.

RESULTS AND DISCUSSION

From the reaction of $LiAlH_4$ with CO_2, the following products were identified from the IR absorption bands (cm⁻¹) cited: CH_4 (3016, 1305); C_2H_4 (3100, 949); CO (2144). At approximately 400 K, small amounts of methane (CH_4) were formed. When the quartz tube was heated to 600 K, CH_4 and ethylene (C_2H_4) were rapidly formed. After prolonged heating which partially depleted the LAH, carbon monoxide bands also appeared in the spectrum. Reactions involving CO_2 and CO in solution with LAH have been investigated previously.[13-16] Apparently, the reaction products from solution are very different from the gas/solid reaction products found here. Cox *et al.*[16] reported that methane and carbon monoxide were not present as reduction products of the solution reaction. However, while carrying out methanolysis reactions using CO and LAH in solution, Martin *et al.* determined that methane was one of the reaction products.[14] The lower reaction temperatures ($\sim$ 373 K) of these solution reactions, solvent effects, stirring, etc. apparently can combine to yield a variety of different products. In the gas/solid reactions performed here, only CO, CH_4 and C_2H_2 have been observed as the reaction products.

The second experiment performed was the reaction between sodium bicarbonate and LAH. In this experiment the LAH and $NaHCO_3$ were mxied ($\sim$ 50/50, v/v) and placed in the quartz tube. This mixture was heated and the spectra were taken. As the mixture was warmed to 325 K, bands for H_2O (1600 cm⁻¹) and CO_2 (2350, 667 cm⁻¹) could be observed. As the temperature was increased, the bands

---

*Author to whom correspondence should be addressed.

for water decreased and bands for methane ($3016, 1305 \text{ cm}^{-1}$) and ethylene ($3100, 949 \text{ cm}^{-1}$) appeared in a manner similar to the CO_2/LAH experiments. $NaHCO_3$ is known to decompose at ~ 325 K to form H_2O and CO_2[17] which readily explains the observation of these bands in the spectra at these temperatures. The other products resulted from the reaction of CO_2 and LAH.

Differential Thermal Analysis (DTA) indicates that LAH decomposes through several steps.[18] The first of these occurs at 421–431 K where part of the hydrogen is evolved. As the LAH is heated to higher temperatures (~ 500–555 K) significant amounts of H_2 are evolved as the compound decomposes. Since no CH_4 was observed at temperatures lower than ~ 400 K, it was assumed that the reactions of LAH with CO_2 and $NaHCO_3$ must first proceed with the partial decomposition of the LAH to form finely divided Al metal. This Al would then react with CO_2 to form CO and aluminium oxide. The CO must then further react to form a CH_2 radical. This radical could either react with H_2 to form CH_4 or with additional CH_2 to form C_2H_4. To test this hypothesis another experiment was performed. In this experiment CO_2 and H_2 were passed over finely divided aluminium powder placed in the quartz tube. The tube was heated and the spectrum taken. No reaction was observed until the tube was heated to 650–800 K. At these temperatures the bands for CO_2 slowly disappeared and bands for CH_4, C_2H_4, CO and H_2O grew into the spectrum. It is interesting that H_2O was produced in this experiment since it was not observed in the LAH reactions with CO_2. One possible explanation of this observation is that any H_2O produced in the previous experiments rapidly reacted with LAH and thus was not observed. The Al formed from the thermal decomposition of LAH is expected to be more finely divided and hence more reactive than the Al powder used in these experiments. These results suggest that Al metal takes part in the reaction mechanism. Since H_2O was observed in this set of reactions, it is not certain if Al functions as a reactant or a catalyst. In either case, the first step of the reaction probably is

$$Al + CO_2 \rightarrow \text{``AlO''} + CO.$$
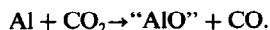
This is not unlike the mechanism proposed by Fontijn *et al.* for the reaction of Al atoms and CO_2.[19] This "AlO" may then react with hydrogen to reform the Al and H_2O or it may further react with CO_2 to form Al_2O_3. The failure to observe clearly Al_2O_3 suggests that the former may have occurred. However, since the total amount of Al_2O_3 formed is expected to be small, this cannot be taken as definite proof that Al is acting as a catalyst. The role of H_2 gas in the mechanism is also not known with certainty. It is likely that some of the hydrogenations occur on the Al surface. The reaction of hydrogen in the gas phase may also occur for some steps in the mechanism. The steps where each is the case could not be clearly established.

Bellama and MacDiarmid investigated the solid phase reactions of SiO_2, GeO_2, P_2O_5, As_2O_3 and Sb_2O_3, with LAH.[20] They found that these reactions produced the various hydrides of these elements. In addition, they reported that some of their samples of

LAH were contaminated with small quantities of diethylether and ethylene since they also observed these molecules in their system. Based on the results of the experiments performed here, it appears reasonable to suggest that they may have actually observed products from the reaction of the LAH with residual CO_2 in the reaction vessel. To test this hypothesis, one of their experiments was repeated using this apparatus. In this experiment SiO_2 and LAH were mixed ($\sim 50/50$, v/v), placed in the quartz tube, and heated. In addition to the expected silane (SiH_4) bands at 2188 and 909 cm^{-1}, bands for methane and ethylene were clearly visible in the spectrum even though no CO_2 was passed over this reaction mixture. No bands were observed which could be assigned to diethyl ether. It does, however, appear that Bellama and MacDiarmid may also have observed the reaction of LAH with residual CO_2 in their reaction vessel. Methane probably was not observed in their experiments because of a failure to trap it. Any methane produced may have been pumped out of their system with the evolved hydrogen.

CONCLUSION

Based on the results of these experiments, a reaction scheme may be written for the gas/solid reaction of CO_2 and LAH.

(1) $LiAlH_4 \xrightarrow{\sim 500 \text{ K}} Al + LiH + 3H_2$.

(2) $2Al + 3CO_2 \xrightarrow{\sim 500 \text{ K}} Al_2O_3 + 3CO$.

(3) $2Al + 3H_2 + 3CO \rightarrow Al_2O_3 + 3CH_2$.

(4) $CH_2 + H_2 \rightarrow CH_4$.

(5) $CH_2 + CH_2 \rightarrow C_2H_4$.

The formulas shown are meant to indicate only the overall stoichiometry of the reaction. As stated previously, it is not certain that Al_2O_3 forms directly from the reaction of Al and CO_2. It is possible that it could be produced by the sequence

(a) $Al + CO_2 \rightarrow \text{``AlO''} + CO$.

(b) $\text{``AlO''} + H_2 \rightarrow H_2O + Al$.

(c) $4H_2O + LiAlH_4 \rightarrow LiOH + Al(OH)_3 + 4H_2$.

(d) $2Al(OH)_3 \xrightarrow{\Delta} Al_2O_3 + 3H_2O$.

Since no H_2O was observed in the LAH reaction and the final products are largely the same, the simpler overall scheme (not involving H_2O) is proposed as the actual reaction sequence. Sapienza *et al.* have proposed a mechanism for the formation of methanol from the reaction of CO_2 and H_2 on metal oxide surfaces.[21] They propose that CO_2 is dissociated to CO and O which are chemisorbed on to the surface of the metal oxide. In the presence of H_2 the CO is reduced to methanol. No bands for methanol were observed in the spectra from these epxeriments. Whether the absence of methanol bands indicates that no Al_2O_3 is formed or that the H_2 is largely depleted by the time it forms cannot be determined from these experiments. CH_2 radical also was not observed. Its presence is inferred from the observation of only ethylene and methane as the reaction products. Additionally, the decomposition products of LAH have not been well characterized. Thus, while the proposed reaction scheme accounts for all of the products, many details of the mechanism still have not been established.

Based on these experiments, it appears that the

"explosive" reaction products reported for the burning LAH/CO₂ reaction are methane and ethylene. Both molecules would react explosively with oxygen in the air if ignited. A CH_4/C_2H_4/Air mixture could easily be ignited by the heat from the burning LAH. Additionally, when NaHCO₃ is used to put out a LAH fire, H_2O is formed. Normally this would be desirable for a fire extinguisher. In this case, however, it would only serve to aggravate the situation since LAH and H_2O react violently.

REFERENCES

[1] L. Metts. *Chem. Engng News* **3**, 1981, 3. 1981, 3.

[2] M. I. Grossman, *Chem. Engng News* **12**, 1981, 57.

[3] J. Deberitz, *Chem. Engng News* **15**, 1982, 3.

[4] National Research Council. Committee on Hazardous Substances in the Laboratory; H. O. House, Chairman, *Prudent Practices for Handling Hazardous Chemicals in Laboratories*, p. 70. National Academy Press, Washington, D.C. (1981).

[5] N. G. Gaylord, *Reductions with Complex Metal Hydrides*. Interscience, New York (1956).

[6] F. A. Cotton and G. Wilkinson, *Advanced Inorganic Chemistry*, 2nd Edn, p. 447. Interscience, New York (1966).

[7] T. Wilson, G. Lin, W. Wong, A. K. William, V. K. Wong and J. A. Gladysz, *J. Am. Chem. Soc.* 1982, **104**, 141 and references therein.

[8] D. J. Darensbourg and A. Rokicki, *J. Am. Chem. Soc.* 1982, **104**, 349, and references therein.

[9] B. Kirste and H. Kurreck, *J. Am. Chem. Soc.* 1980, **102**, 6181.

[10] J. Haggin, *Chem. Engng News* **28**, 1982, 31.

[11] T. C. DeVore and T. N. Gallaher, *Inorg. Chem.* submitted for publication.

[12] T. C. DeVore and T. N. Gallaher, *High Temp. Sci.* submitted for publication.

[13] A. E. Finholt and E. C. Jacobson, *J. Am. Chem. Soc.* 1952, **74**, 3943.

[14] J. F. Martin, A. J. Neale and H. S. Turner, *J. Chem. Soc.* 1956, 4428.

[15] R. F. Nystrom, W. H. Yanko and W. G. Brown, *J. Am. Chem. Soc.* 1948, **70**, 441.

[16] J. D. Cox, H. S. Turner and R. J. Warner, *J. Chem. Soc.* 1950, 3167.

[17] *The Merck Index* (Edited by M. Windholtz), 9th Edn, p. 1109. Merck, Rahway (1976).

[18] J. Block and A. P. Gray, *Inorg. Chem.* 1965, **4**, 304.

[19] A. Fontijn and W. Felder, *J. Chem. Phys.* 1977, **67**, 1561.

[20] J. M. Bellama and A. G. MacDiarmid, *Inorg. Chem.* 1968, **7**, 2070.

[21] R. S. Sapienza, L. D. Spaulding, J. R. Lynch and M. J. Sansone, *Report* 1978 BNL-24428, CONF-780902-3, 9pp. Fron *Energy Res. Abst.* 1978, **3**(23), Abst No. 54803.

VIBRATIONAL AND LUMINESCENCE SPECTRA OF A NEW BINUCLEAR URANYL COMPLEX [(C₂H₅)₄N]₂[UO₂F(NO₃)₂]₂

COLIN D. FLINT* and PETER A. TANNER

Department of Chemistry, Birkbeck College, University of London, London WC1E 7HX, England

Abstract—The preparation, vibrational and luminescence spectra of the title compound are described. The complex has bidentate nitrate groups and bridging fluoride ions. The spectra are assigned in detail and interpreted as showing couplings between the uranyl antisymmetric stretching modes and between the nitrate modes within the dimer, the coupling energy being $17 \, \text{cm}^{-1}$ in the former case. There is no clear evidence for electronic coupling involving the uranyl groups.

INTRODUCTION

During recent synthetic and spectroscopic studies of the coordination chemistry of the uranyl ion[1,2] we prepared a new uranyl complex of stoichiometry $[(C_2H_5)_4N]UO_2F(NO_3)_2$. A preliminary X-ray investigation[3] indicated that the compound is binuclear, fluorine-bridged with bidentate nitrate groups completing an in-plane six-fold coordination of the uranyl group. By contrast to the other fluorine-bridged uranyl complexes we have studied, the low-temperature luminescence spectrum is well resolved and free from traps. This permits a clear comparison of the uranyl vibrations and the nitrate vibrations observed in the luminescence spectra with those observed in the infrared and Raman Spectra.

EXPERIMENTAL

$[(C_2H_5)_4N]_2[UO_2F(NO_3)_2]_2$ was prepared as well-formed lime green crystals by the following method. A solution of 5 g uranyl nitrate in 20 cm³ of water was added to a solution prepared from tetraethylammonium hydroxide (2 cm³ of 25% aqueous solution) and hydrofluoric acid (0.5 cm³ of 40% aqueous solution) in 20 cm³ water and the mixture allowed to stand at room temperature. The initial lemon-yellow precipitate was discarded and the solution deposited crystals of the product after several days. Analysis: Calcd. for $[(C_2H_5)_4N]_2[UO_2F(NO_3)_2]_2$: C, 17.7; H, 3.7; N, 7.7; F, 3.5; U, 43.8%. Found: C, 17.5; H, 3.6; N, 7.6; F, 3.5; U, 43.9%.

Spectroscopic measurements

These were made as previously described.[4]

STRUCTURAL DATA

A preliminary X-ray study[3] shows that the compound $[(C_2H_5)_4N]_2[UO_2F(NO_3)_2]_2$ crystallises in the $P2_1/c - C_{2h}^5$ space group with two centrosymmetric binuclear units in the Bravais cell. The crystallographic site symmetry of the uranyl ion is therefore C_1 but nearly C_{2v}. The space group and number of formula units per Bravais cell are the same[5] as

those of the binuclear fluorine-bridged complex $Cs_4(UO_2)_2F_8 \cdot 2H_2O$.

RESULTS

The high-energy region of the 15 K luminescence spectrum is shown in Fig. 1. The relative intensities of features were observed to be independent of the exciting line, and the decay of emission from a 4 cm⁻¹ band width is exponential with a (e^{-1}) lifetime of 2.5 ms. The $\Pi_g \rightarrow \Sigma_g^+$ electronic origin of the uranyl ion is intense and the excited state is split into two components at $20\,547$, $20\,555$ cm⁻¹ due to the low site symmetry. These origins are only 200 cm⁻¹ to low energy of their positions in $(C_2H_5)_4N[UO_2(NO_3)_3]$ where the uranyl groups have an in-plane coordination of six oxygen atoms,[6] but more than 700 cm⁻¹ to high energy of the origins in $Cs_4(UO_2)_2F_8 \cdot 2H_2O$ where the uranyl groups have an in-plane coordination of five fluorine atoms. Between the origins and $20,250$ cm⁻¹ there is a complex group of incompletely resolved vibronic bands. The most intense features occur near 145, 200 and 250 cm⁻¹ from the origin. The first of these is almost coincident with a strong Raman shift (155 cm⁻¹) and by comparison with the Raman and luminescence spectra of $CsUO_2(NO_3)_3$ these probably correspond to one or more ligand bending modes. The remaining two strong bands shift some 15 cm⁻¹ to low vibrational wavenumber in the absorption spectrum and are therefore assigned as the uranyl rocking and bending modes. These bending and rocking modes are also observed in both the IR and Raman spectra. As usual the rock is stronger in the Raman and the bend in the IR spectrum. Other weaker bands in this region show smaller shifts in the absorption spectrum and are therefore attributed to uranyl-ligand stretching modes coupled to the rock and bend.

During our recent studies of bi-[1] and polynuclear[2] uranyl fluoride complexes, we correlated modes of vibration with those of the $UO_2F_5^{3-}$ monomer, neglecting specific assignments for U–F (bridge) modes. These vibrations are more conveniently studied in $[(C_2H_5)_4N]_2[UO_2F(NO_3)_2]_2$ due to the absence of U–F (terminal) bonds. The two bands at 405, 365 cm⁻¹ in the luminescence spectrum of

---
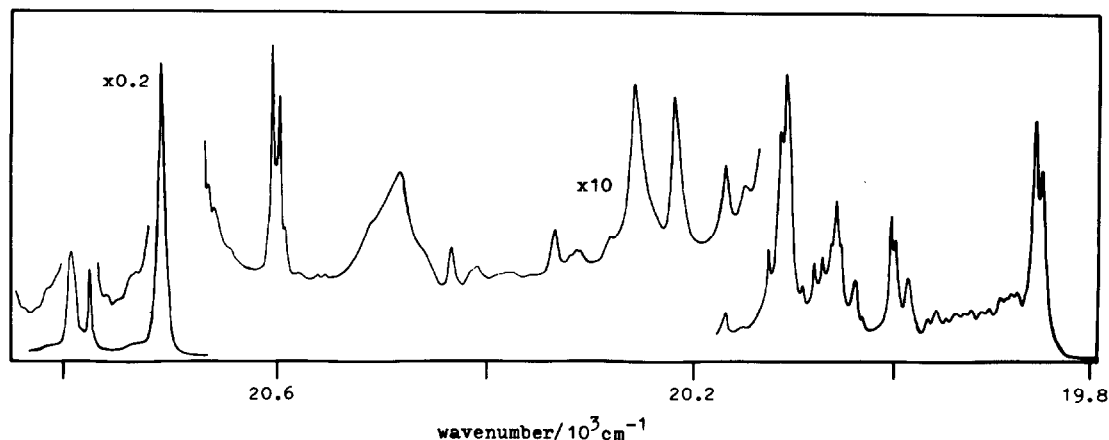
Fig. 1. The high energy part of the 457 nm-excited 15 K luminescence spectrum of $[(C_2H_5)_4N]_2[UO_2F(NO_3)_2]_2$.

$[(C_2H_5)_4N]_2[UO_2F(NO_3)_2]$ clearly involve motion of the bridging fluorides. The higher wavenumber band is strong in the IR spectrum whereas the other is barely detected; both bands are weak in the Raman spectrum. The 405 cm^{-1} mode is therefore assigned as the in-phase fluoride motion along the U–U axis and the 365 cm^{-1} mode as the corresponding anti-phase motion. The assignment of the two other motions with substantial uranium–fluoride stretch character is less certain. A mode at 315 cm^{-1} appears with moderate strength in the luminescence spectrum but weakly in the 120 K Raman spectrum. This is nearly but not exactly coincident with a strong 300 K IR band at 308 cm^{-1}. It is not certain whether these features are one or both of the expected modes. If the former is the case, the differences in wavenumber can be attributed to the different temperatures of measurement and selection rules. The remaining U–F mode may then lie in the complex vibronic structure below 300 cm^{-1}.

The O–U–O stretching vibrations in $[(C_2H_5)_4N]_2[UO_2F(NO_3)_2]$ are readily accounted for under a dimer model contrasting with our results from other binuclear uranyl systems.[1] For the O–U–O symmetric stretch (v_1), a centrosymmetric dimer model predicts the occurrence of one IR and one Raman band. This mode is observed at 854 cm^{-1} as the strongest band in the Raman spectrum but weakly in the IR spectrum (852 cm^{-1}). In luminescence, progressions in v_1 on the electronic origin

and all the vibronic features may be followed to at least six members, the modes with one quantum of v_1 being the most intense. The $\Pi_g \to \Sigma_g^+ + nv_1$ bands $(n = 2–6)$ exhibit the same splitting $(7.5 \pm 1.5$ cm$^{-1})$ as the electronic origin. However, for $n = 3$ these bands are accompanied by a third component at 5 cm^{-1} to high vibrational energy which moves further away and loses intensity in successive members (Fig. 2). The behaviour of the antisymmetric O–U–O stretch (v_3) is more complex. From studies of other binuclear uranyl complexes we expect the coupling between uranyl groups to be largest for this mode. In the 300 K IR spectrum v_3 occurs as a single band at 934 cm^{-1} but at 85 K a shoulder near 920 cm^{-1} becomes resolved. The luminescence spectrum in the region of the v_3 vibronic origin is rather different, consisting of a weaker, sharp feature at 921 cm^{-1} and a broader band at 938 cm^{-1} from the lower energy origin. We attribute these two bands to the in-phase (938 cm^{-1}) and antiphase components of the O–U–O antisymmetric stretch. It is curious, however, that the origin splitting is not resolved in the 921 cm^{-1} feature. The behaviour of successive members of the v_1 progression based on the v_3 vibronic origin raises further problems. For the $n = 1$ member of the $\Pi_g \to \Sigma_g^+ + nv_1 + v_3$ progression, three bands are resolved between 1775 and 1792 cm^{-1}, the separation of the lower energy components being 4 cm^{-1} (Fig. 2). For the $n = 2–5$ members the highest vibrational energy component of v_3 moves away from and loses
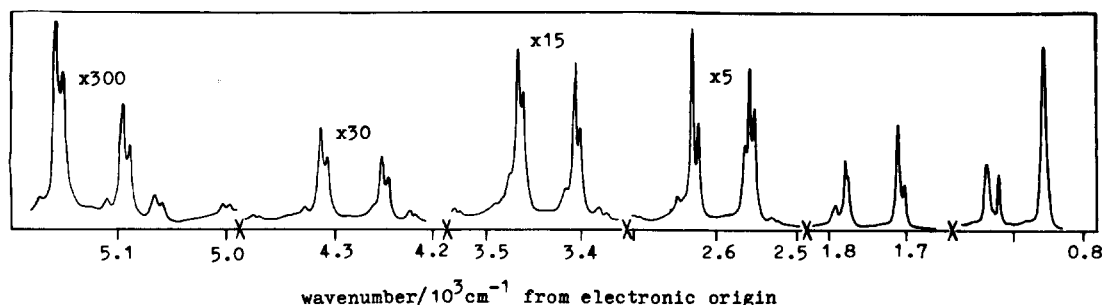
Fig. 2. The 15 K luminescence spectrum of $[(C_2H_5)_4N]_2[UO_2F(NO_3)_2]_2$ in the region of the $\Pi_g \to \Sigma_g^+ + nv_1$ and $\Pi_g \to \Sigma_g^+ + v_2 + (n-1)v_1$ transitions for $n = 1–6$. (The wavenumbers are measured from the lower energy electronic origin, 20,547 cm^{-1}. Note the scale discontinuities.)

Table 1. Internal nitrate vibrational modes in $[(C_2H_5)_4N]_2[UO_2F(NO_3)_2]_2$

Isolated Nitrate Mode		Binuclear Complex Mode	Observed Wavenumber/cm^{-1}		
D_{3h}	C_{2v}	C_i	Raman 85 K	Infrared 85 K	Luminescence 15 K
α_1' stretch	α_1	$2\alpha_g$, $2\alpha_u$	1023m 1030s	1024s 1032m	1030 1037
α_2'' o.o.p. bend	β_1	$2\alpha_g$, $2\alpha_u$	n.o.	808m 812m	804 810
ϵ_1' stretch	α_1	$2\alpha_g$, $2\alpha_u$	n.r.	1525sh 1531s 1550s 1563	1519 1528 1546 1559
	β_2	$2\alpha_g$, $2\alpha_u$	n.o.	1259s 1267w 1271w 1277ms 1282s	1254 1263 1276 1281
ϵ_1' bend	α_1	$2\alpha_g$, $2\alpha_u$	742s 748m	747s 752m	740 747 753
	β_2	$2\alpha_g$, $2\alpha_u$	706vw	n.o.	710

n.o. not observed; n.r. not recorded

o.o.p. out-of-plane

intensity relative to the other component. The splitting of $6.7 \pm 1.5\,\text{cm}^{-1}$ observed for the latter is the same as that of the electronic origin within experimental error. For the $\Pi_g \to \Sigma_g^+ + \nu_1 + \nu_3$ and $\Pi_g \to \Sigma_g^+ + 3\nu_1$ bands, the most reasonable assignment of the additional component in each case is to a Fermi resonance with nitrate modes.

All of the internal modes of the coordinated nitrate ions may be observed in either the IR or Raman spectra and also in the luminescence spectrum (Table). In most cases all four components expected for a centrosymmetric dimer may be resolved, together with additional features which may be due to Fermi resonances or unit cell group couplings. As expected the coupling between *cis* nitrate groups (as reflected by the separation of the two IR- or two Raman-active components) is larger than the *trans*-coupling across the bridge.

DISCUSSION

The most interesting feature of the spectroscopic behaviour of $[(C_2H_5)_4N]_2[(UO_2)F(NO_3)_2]_2$ is the coupling between the $UO_2F(NO_3)_2$ entities. We consider first the evidence for an electronic coupling between the uranyl groups. If significant this would produce a splitting of the electronic origin and of the progressions in ν_1 proportional to the square of the dipole strength of the individual lines, but no appreciable splitting of the vibronic origins. The constant splitting of the $\Pi_g \to \Sigma_g^+ + n\nu_1$ and $\Pi_g \to \Sigma_g^+ + \nu_3 + n\nu_1 (n \geqslant 2)$ transitions (which is equal to the origin splitting) is not consistent with this. This splitting must then be attributed to a site symmetry

splitting of the degenerate excited electronic state, although we are unable to give a convincing explanation for the absence of this splitting for several vibronic features, notably $\Pi_g \to \Sigma_g^+ + \nu_3$. A similar observation may be made[1] from the luminescence spectrum of $Cs_4(UO_2)_2F_8 \cdot 2H_2O$.

By contrast, the splitting of about $17\,\text{cm}^{-1}$ in $\nu_3[\nu_{as}(O-U-O)]$ in both the IR and luminescence spectra of $[(C_2H_5)_4N]_2[UO_2F(NO_3)_2]_2$ is attributed to a vibrational coupling within the dimer. This is consistent with our previous assignment[1] of the two *strong* IR ν_3 bands (split by $15\,\text{cm}^{-1}$) in $Cs_4(UO_2)_2F_8 \cdot 2H_2O$ to α_u, $\beta_u(C_{2h})$ unit cell group modes. The similar intensity of these two components cannot be explained under a centrosymmetric dimer model since the $\beta_{2g}(D_{2h})$, $\alpha_g(C_i)$ antiphase ν_3 dimer mode is IR-inactive, but this vibration gives rise to one IR-active and one IR-inactive mode under C_{2h} unit cell group rules, (the irreducible representation corresponding to the IR-active mode depends upon the location of the C_{2h} symmetry elements). The intensity of the antiphase intradimer ν_3 mode in $Cs_4(UO_2)_2F_8 \cdot 2H_2O$ thus arises from the interdimer coupling dipole. The same splitting of ν_3 in the IR spectra $(16 \pm 1\,\text{cm}^{-1})$ of $Cs_4(UO_2)_2F_8 \cdot 2H_2O$ and $[(C_2H_5)_4N]_2[UO_2F(NO_3)_2]$, but the very different intensity ratios of the two components are both consistent with structural data[3,5] since although the U–U intradimer distances are similar, the interdimer coupling in the latter compound is reduced due to shielding by the large organic cations.

The ν_3 antiphase mode is more intense (relative to the in-phase mode) in luminescence, rather than

in the IR absorption spectrum of $[(C_2H_5)_4N]_2 \cdot [UO_2F(NO_3)_2]_2$ since for the former process the selection rules are relaxed at the C_{2v} uranyl site. As in the luminescence spectrum of $Cs_4(UO_2)_2F_8 \cdot 2H_2O$, progressions are observed in the v_3 mode. The agreement between the IR and luminescence frequencies for the v_3 modes in $[(C_2H_5)_4N]_2[UO_2F(NO_3)_2]_2$ illustrates the small dispersion of these local dimer modes, by contrast to the $v_{as}(O–U–O)$ vibrations in other luminescence spectra.[1,2,7]

REFERENCES

[1] C. D. Flint and P. A. Tanner, *J. Chem. Soc. Faraday* 2 1981, **77**, 2339.
[2] C. D. Flint and P. A. Tanner, *J. Chem. Soc. Faraday* 2 1982, **78**, 839.
[3] Private Communication from Dr. A. Perrin, University of Rennes, France.
[4] C. D. Flint and P. A. Tanner, *J. Chem. Soc. Faraday* 2 1979, **75**, 1168.
[5] N. Dao, *Acta Crystallogr. Sect. B* 1972, **28**, 2011.
[6] P. Sharma, Thesis, University of London 1981.
[7] C. D. Flint and P. A. Tanner, *Inorg. Chem.* 1981, **20**, 4405.

STUDY OF THE COMPLEXES OF Np(V) WITH ORGANIC LIGANDS BY SOLVENT EXTRACTION WITH TTA AND 1, 10-PHENANTHROLINE

YASUSHI INOUE* and OSAMU TOCHIYAMA

Department of Nuclear Engineering, Faculty of Engineering, Tohoku University, Aramaki-aza-aoba, Sendai 980, Japan

Abstract—Complex formation constants of Np(V) with 22 organic ligands, 7 hydroxycarboxylic acids, 4 dicarboxylic acids, 4 aminocarboxylic acids, 3 pyridinecarboxylic acids, 8-hydroxyquinoline-5-sulfonic acid, IDA, NTA and EDTA, have been determined in 1M NaClO$_4$ at 25°C by using the solvent extraction method with TTA and 1, 10-phenanthroline. The factors influencing the stabilities of Np(V) complexes are discussed in connection with the linear structure of NpO$_2^+$.

The aqueous solution chemistry of actinides, particularly of U, Np, Pu and Am, offers us an enormous task because of its complicated features connected with redox, disproportionation, hydrolysis and complex formation reactions. Among the actinide ions, penta- and hexavalent actinides assume the form of dioxo ions called "yl" ions which are a special type of cations as regards complex chemistry. Although a vast amount of data exists on complex formation of actinides in solution, pentavalent actinides have not been so extensively studied because of their reduced reactivity with various ligands as a result of their low ionic potential.

Since the valence stability of Np(V) in aqueous solution makes neptunium a useful representative element for studying the aqueous complex chemistry of pentavalent actinides, we decided to study the complex formation of Np(V) with different organic ligands by using a solvent extraction technique. Recently, we succeeded in extracting Np(V) by the combined use of either thenoyltrifluoroacetone (TTA) and quaternary alkylammonium salts[1] or TTA and 1,10-phenanthroline (phen).[2] The former system has been successfully applied to the determination of stability constants of the complexes of Np(V) with several hydroxycarboxylic acids.[3] This system, however, has limited applicability because it does not allow the presence of large, hydrophobic anions such as perchlorate, or dissociated anions of organic acids because of their interaction with the quaternary alkylammonium cation. Although the synergistic enhancement of TTA extraction of Np(V) is somewhat smaller with phen than with quaternary alkylammonium salts, the TTA-phen system permits us to study the aqueous chemistry of Np(V) with fewer restrictions. By using this extraction system in the presence of 1M NaClO$_4$, we have obtained complex formation constants of Np(V) with 22 organic ligands including hydroxycarboxylic acids, dicarboxylic acids, aminocarboxylic acids and some other widely-known chelating reagents.

EXPERIMENTAL

Reagents. ^{239}Np tracer was prepared by milking from ^{243}Am (obtained from the Commissariat a l'Energie Atomique) by the method of Sill[4] and adjusted to the pentavalent state by evapora-

tion to dryness and dissolution in water.[5] TTA and 2-(N-Morpholino)ethanesulphonic acid monohydrate (MES) were obtained from Dojindo Laboratories (Kumamoto, Japan) and used as received. All the other reagents were of A.R. grade and used without further purification. The solutions of these chemicals were freshly prepared just prior to use.

Procedures. An aqueous solution (4 cm³) containing ^{239}Np, 1M sodium perchlorate, buffer reagents (a proper mixture of 0.05 M of MES and 0.05 M of THAM [Tris(hydroxymethyl)aminomethane] and a variable concentration of complex forming reagent was mixed in a glass tube with the same volume of organic solution containing the desired concentration of TTA and phen, and the tube was shaken mechanically for 15 min (140 times/min) at 25±1°C. The phases were separated and a 1-cm³ portion of each phase was pipetted into a counting tube and the γ-activity of each phase was measured in a well-type NaI(Tl) scintillation counter (Fuji Denki Model⁸ NHS2). The remaining part of the aqueous phase was used for pH measurement with a pH meter (Tōa Dempa HM-5BS) equipped with a glass electrode. Conditions adopted in the experiments are listed in Table 1.

Calculation of stability constants. The distribution ratio of neptunium in the absence of complexing agents, D$_0$, can be represented by[2]:

$$D_0 = K_{ex}[HT]_O[phen]_O{}^m/[H^+], \qquad (1)$$

where HT and phen denote the neutral form of TTA and phen, K$_{ex}$ the extraction constant, m number of molecules of phen in the extracted species, and O refers to the organic phase. From the published data of distribution constants of TTA and phen between water and organic solvents[6], [HT]$_O$ and [phen]$_O$ were assumed to be equal to the total added concentrations C$_{TTA}$ and C$_{phen}$ in the conditions adopted in the experiment. Contributions from the formation of water-soluble complexes of Np(V) with TTA anion to the log β (stability constant) values were estimated to be less than 0.02, using the reported value of the stability of Np(V)–TTA complexes[7], and were neglected under all conditions shown in Table 1. The distribution ratio D of Np(V) in the presence of a complexing agent (L) can be expressed by:

$$D = D_0/(1 + \sum_n \beta_n[L]^n), \qquad (2)$$

where the values of β_n are the overall formation constants of Np(V) complexes with ligand L (charges of ions are omitted for simplicity). [L] was evaluated from the total added concentration of ligand acid, C$_L$, by using the dissociation constants[8] listed in Table 2. In the calculation, the concentration of neutral acid in the organic phase was assumed to be negligibly small. Equation

---

*Author to whom correspondence should be addressed.

Table 1. Conditions used for solvent extraction

Symbol	c_{TTA}(M)	c_{phen}(M)	organic diluent	pH
A	2×10^{-2}	2×10^{-2}	isobutylmethylketone	5.8 ± 0.2
B	1×10^{-4}	2×10^{-2}	isopentylalcohol	7.5 ± 0.5
B'	1×10^{-3}	1×10^{-2}	isopentylalcohol	6.5 ± 0.3
C	2×10^{-3}	5×10^{-2}	dichloromethane	6.7 ± 0.3

Table 2. Stability constants of Np(V) complexes

Complexing agent	log β_n ($\pm \sigma$) n=1	n=2	n=3	method [a]	$[L]_{max}$
1. Glycolic acid (3.62) $CH_2(OH)COOH$	1.21(0.03) 1.21(0.21) 1.21(0.11) 1.14 1.51	1.70(0.01) 1.90(0.03) 1.74(0.03) 1.88		A B' C R sp	1.0 1.0 1.0
2. Lactic acid (3.64) $CH_3CH(OH)COOH$	1.11(0.08) 1.09 1.75	1.78(0.03) 1.60		A R sp	2.0
3. α-Hydroxybutyric acid (3.80) $CH_3CH_2CH(OH)COOH$	1.13(0.02) 1.10 1.62	1.51		C R sp	0.5
4. β-Hydroxybutyric acid (4.35) $CH_3CH(OH)CH_2COOH$	0.55(0.04) 0.67	0.98(0.01) 0.91		C R	0.6
5. α-Hydroxyisobutyric acid (3.77) $(CH_3)_2C(OH)COOH$	1.48(0.02) 1.55(0.07) 1.53(0.02) 1.35 1.99	2.19(0.01) 2.48(0.03) 2.35(0.02) 1.88 2.90	3.53	A B' C R cix	0.4 1.0 0.6
6. 2-Hydroxy-2-methylbutanoic acid (3.73) $CH_3CH_2C(CH_3)(OH)COOH$	1.60(0.02) 1.40	2.21(0.02) 1.98		C R	0.3
7. 2-Ethyl-2-hydroxybutanoic acid (3.63) $(CH_3CH_2)_2C(OH)COOH$	1.57(0.03) 1.57	2.06		C R	0.4
8. Oxalic acid (1.04,3.55) $(COOH)_2$	3.44(0.03) 3.67(0.01) 3.59(0.01) 3.42 3.74	5.83(0.03) 6.29(0.01) 6.16(0.01) 5.66 6.31		A B C R pH	0.06 8×10^{-3} 4×10^{-3}
9. Malonic acid (2.60,5.07) $HOOCCH_2COOH$	2.25(0.02) 2.26 2.75	3.61(0.02) 3.26		A R pH	0.6
10. Succinic acid (3.95,5.12) $HOOC(CH_2)_2COOH$	1.13(0.01) 1.29 1.72	1.50(0.01) 1.89	2.35(0.01)	B R pH	0.5
11. Glutaric acid (4.11,4.87) $HOOC(CH_2)_3COOH$	1.27(0.02) 1.18 1.43	1.44(0.02) 1.42	2.45(0.01)	B R sp	0.5
12. Glycine (2.35,9.75) H_2NCH_2COOH	3.17(0.01) 3.31	5.47(0.01) 5.44		B sp	0.02
13. DL-Alanine (2.31,9.84) $CH_3CH(NH_2)COOH$	3.30(0.01) 3.37	5.67(0.01) 5.77		B sp	0.05
14. L-Aspartic acid (2.00,3.67,9.62) $HOOCCH_2CH(NH_2)COOH$	0.70(0.05) 2.63	1.32(0.01) for $M(HL)_n$ 5.32 for ML_n		A A+B	0.5 0.5
15. L-Glutamic acid (2.39,4.21,9.55) $HOOC(CH_2)_2CH(NH_2)COOH$	0.76(0.03) 2.72	1.41(0.01) for $M(HL)_n$ 5.13 for ML_n		A A+B	0.5 0.5
16. Picolinic acid (0.86,5.17) C_5H_4NCOOH (2-)	3.45(0.02) 3.23 3.59	6.03(0.02) 5.59 6.54		A R sp	0.03

Table 2. (*Contd.*)

| Complexing agent | log β_n ($\pm \sigma$) | | | method [a] | $[L]_{max}$ |
	n=1	n=2	n=3		
17. Nicotinic acid (2.09,4.70) C_5H_4NCOOH (3-)	0.57(0.03)			C	0.5
18. Dipicolinic acid (2.13,4.51) $C_5H_3N(COOH)_2$ (2,6-)	7.07(0.02) 7.25(0.01)			C B	5×10^{-6} 5×10^{-6}
19. 8-Hydroxyquinoline-5-sulfonic acid (3.86,8.23) $C_9H_5N(OH)(SO_3H)$	5.42(0.01)	10.21(0.01)		C	1×10^{-4}
20. Iminodiacetic acid (1.88,2.56,9.35) $HN(CH_2COOH)_2$	5.64(0.01) 5.76(0.01) 6.27			B C ix	7×10^{-5} 8×10^{-5}
21. Nitrilotriacetic acid (1.97,2.43,9.33) $N(CH_2COOH)_3$	6.08(0.01) 6.30(0.01) 6.81			C B' ix	5×10^{-5} 3×10^{-5}
22. Ethylenedinitrilotetraacetic acid (2.0,2.68,6.11,10.17) $(HOOCCH_2)_2N(CH_2)_2N(CH_2COOH)_2$	4.46(0.01) 4.52(0.02) 5.30	for MHL for MHL for MHL		C B' ix	4×10^{-3} 1×10^{-3}

a) A, B, B', C: solvent extraction, see Table 1.
   R: solvent extraction with TTA + alkylammonium[3].
   sp: spectrophotometry at 25°C, $\mu = 1$, taken from Ref. 9 and references cited therein.
   cix: cation exchange[10] at $\mu = 0.05$.
   pH: potentiometry[11] at 20°C, $\mu = 1$.
   ix: ion exchange[12] at 25°C, $\mu = 0.1$.

(2) is equivalent to a linear function,

$$y = f(x), \tag{3}$$

where

$$y = 1/D,$$

$$f(x) = 1/D_0 + \sum_n (\beta_n/D_0)x^n$$

and

$$x = [L].$$

About twenty sets of data (x_i, y_i) were analyzed by the least-squares method to give β_n values. Since the counting-time of γ-activities was set to make the relative statistical errors of the total counts approximately constant, residuals of observed ratios, *y*, are expected to be proportional to the value of $1/D$ from error propagation rules. Although the observed value of $1/D$ is not error-free, this value gives a good basis for the estimate of the weight of the observation. Therefore least-squares fitting was carried out to minimize the following sum of the weighted squares of the residuals:

$$S = \sum_i \{y_i - f(x_i)\}^2/y_i^2. \tag{4}$$

When a polybasic acid is used as the complexing agent, there is the possibility of forming different types of complex; that is, the ligands in different stages of dissociation can react with Np(V). In this case, the proper form of complex is taken to be that which gives self-consistent values of stability constants when series of experiments are conducted at different values of pH.

RESULTS AND DISCUSSION

The results are listed in Table 2 together with literature values. The maximum concentration of the ligand adop-

ted in each series of experiment is shown in the last column of Table 2. Standard deviations, shown in parentheses, indicate that each series of experiment is of fairly high precision. However, comparison between the values obtained under different conditions (diluent, pH, concentration of extractants) reveals that the accuracy of the value is somewhat poorer than that expected from standard deviations. As a whole, the total error in log β_n remains less than 0.1, and therefore the present values agree well with literature values within the limits of the experimental error. Our two-solvent extraction systems, TTA plus alkylammonium salts and TTA plus phen, gave very similar values, although the former were a little smaller than the latter in almost every case. This may be attributed to the difficulty of correcting the effect of the formation of water-soluble complexes of Np(V) with TTA anion in the former system. The fact that the present values also agree well with those obtained by completely different techniques such as spectrophotometry or potentiometry, supports the validity of this extraction technique.

The results in Table 2 can be used to elucidate the factors influencing the stabilities of complexes—those common to chelates in general and those characteristic only of chelates involving dioxo ions.

The effect of the size of the chelate ring can be seen by comparing the stabilities of the chelates of hydroxycarboxylates, dicarboxylates and pyridinecarboxylates. The orders of stability are:

α-hydroxycarboxylate > β-hydroxycarboxylate,
oxalate > malonate > succinate ~ glutarate,

and

picolinate > nicotinate.
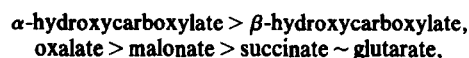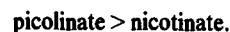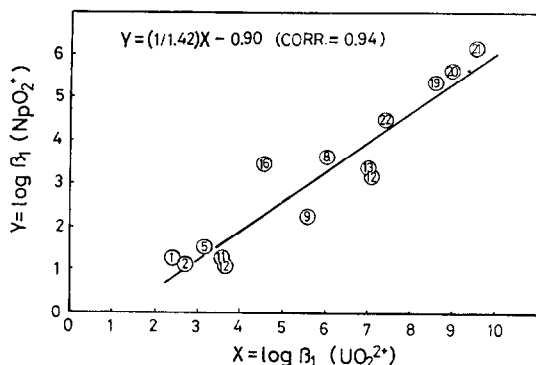
Fig. 1. Correlation between 1:1 chelate stability constants of UO_2^{2+} and NpO_2^+. Numbers correspond to the compounds listed in Table 2.
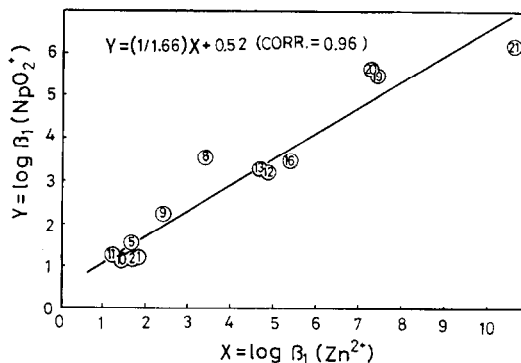
Fig. 2. Correlation between 1:1 chelate stability constants of Zn^{2+} and NpO_2^+. Numbers correspond to the compounds listed in Table 2. For 22, Zn^{2+} forms ML, while NpO_2^+ forms MHL. Dipicolinic acid (18) shows a large deviation from the line (log $\beta = 6.35$, 11.88 for Zn^{2+}).

These orders are consistent with the general rule that chelates with a five-membered ring are most stable. For these chelates with a five-membered ring, the nature of the donor atoms affects the stability sequence as follows:

sulfoxine(phenolic O^-, N)>dicarboxylate(O^-, O^-)$\geq$ aminocarboxylate(O^-, N)>hydroxycarboxylate(O^-, O).
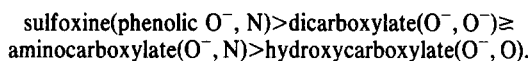
It is interesting to note the effect of the number of available coordination sites of the chelating agent. All the tri- or tetradentate ligands investigated give more stable chelates than bidentate ligands. However, these ligands give only 1:1 complexes suggesting that a steric effect opposes the formation of higher complexes. This steric hindrance can be considered to result from the fact that the pentavalent neptunium exists as very stable "yl" ions NpO_2^+ with two short covalent metal–oxygen bonds and can accommodate ligands only in the plane equatorial to "yl" bond.

Another point of interest is the comparison of the results for Np(V) with those for other metal ions. For this purpose, it is desirable to compare with other actinides, but we have little comparable data because the pentavalent state of other actinides is very unstable (except in the case of protactinium which behaves differently from other members of this group of elements). Instead, the stabilities of Np(V) complexes were compared with those of UO_2^{2+} and Zn^{2+} complexes because UO_2^{2+} is also a dioxo cation of similar type and complexes of Zn^{2+} have stability constants comparable to those of Np(V). Figures 1 and 2 clearly indicate that both UO_2^{2+} and Zn^{2+} give a good correlation of stabilities with Np(V). One reason is that all these complexes are considered to be formed by the interaction of a hard

acid and a hard base. Another reason is that we are comparing the values of log β_1, which are not affected by the steric factors. As a proof, stability constants of Np(V) with IDA, NTA and EDTA correlate better with those of UO_2^{2+} than those of Zn^{2+}. Moreover, UO_2^{2+} gives only 1:1 complexes with the above ligands, while Zn^{2+} gives higher complexes as well. Slopes in Figs. 1 and 2 indicate that NpO_2^+ in its complex-forming behaviour resembles cations with a charge between +1 and +2.

REFERENCES

[1]Y. Inoue, O. Tochiyama and I. Oda, *Inorg. Nucl. Chem.* 1979, **41**, 1375.
[2]Y. Inoue and O. Tochiyama, *Radiochim. Acta,* in press.
[3]Y. Inoue, O. Tochiyama and T. Takahashi, *Radiochim. Acta,* in press.
[4]C. W. Sill, *Anal. Chem.* 1966, **38**, 802.
[5]Y. Inoue and O. Tochiyama, *J. Inorg. Nucl. Chem.* 1977, **39**, 1443.
[6]J. Stary and H. Freiser, *IUPAC Equilibrium Constants of Liquid-Liquid Distribution Reactions*, Part IV: *Chelating Extractants.* Pergamon Press, Oxford (1978).
[7]J. Gross and C. Keller, *J. Inorg. Nucl. Chem.* 1972, **34**, 725.
[8]A. E. Martell and R. M. Smith, *Critical Stability Constants.* Plenum Press, New York (1977).
[9]C. Keller, *The Chemistry of the Transuranium Elements*, Verlag Chemie, Weinheim/Bergstr., Germany (1971).
[10]A. I. Moskvin, *Radiokhimiya* 1971, **13**(4), 582.
[11]L. Magon, A. Bismondo, G. Tomat and A. Cassol, *Radiochim. Acta* 1972, **17**, 164.
[12]S. H. Eberle and U. Wede, *J. Inorg. Nucl. Chem.* 1970, **32**, 109.

A POTENTIOMETRIC STUDY ON COMPLEX FORMATION OF CADMIUM(II) ION WITH 2-MERCAPTOACETIC AND 2-MERCAPTOPROPIONIC ACIDS

HARUO MATSUI*

Government Industrial Research Institute, Nagoya, Hirate-cho, Kita-ku, Nagoya 462, Japan

and

HITOSHI OHTAKI

Department of Electronic Chemistry, Tokyo Institute of Technology at Nagatsuta, Nagatsuta-cho, Midori-ku, Yokohama 227, Japan

Abstract—Complex equilibria between cadmium ions and 2-mercaptoacetic acid (H_2maa) or 2-mercaptopropionic acid (H_2mpa) have been studied in aqueous solutions containing 3 mol dm^{-3} LiClO$_4$ as a constant ionic medium at 25°C by potentiometric titration. Formation constants of mono-η and bis-2-mercaptoalkanoato)cadmium complexes were found to ge log K_{11} = 4.34 and log K_{12} = 2.15 for the cadmium-H_2maa complexes, and log K_{11} = 5.66 and log K_{12} = 2.85 for the cadmium-H_2mpa complexes, respectively. The protonated complexes, CdHmaa$^+$ and CdHmpa$^+$, and a mixed ligand complex, Cd(maa)(mpa)$^{2-}$, were also detected.

In a previous investigation on the complex formation between cadmium ions and glycine and α-alanine,[1] we found that the glycine complex is more stable than the α-alanine complex, in spite of the smaller basicity (or the larger dissociation constant) of the former ligand than the latter. Such a reverse trend of the formation constants of glycinate and α-alaninate complexes to the basicity of the ligands has also been observed for complexes with other divalent metal ions.[2] In the paper[1] we interpreted the result in terms of ligand–ligand interactions through the central metal ion, in which electron back-donation was assumed from the cadmium ion to oxygen and nitrogen atoms within the complexes. In the present work we have studied complex equilibria between cadmium ions and 2-mercaptoacetic acid {H_2maa, maa = (SCH$_2$COO)$^{2-}$} or 2-mercaptopropionic acid {H_2mpa, mpa = (CH$_3$CHSCOO)$^{2-}$}. These ligands have a sulphur atom which acts as a stronger electron-donor, as well as a stronger π-electron acceptor, than an oxygen or a nitrogen atom and can be regarded as SH-substituted compounds of glycine and α-alanine. The formation constant of the mixed ligand complex, Cd(maa)(mpa)$^{2-}$ has also been determined. In this study we detected protonated complexes CdHmaa$^+$ and CdHmpa$^+$, the CdHL-type complex having not been found in the previous cases with glycine and α-alanine.

EXPERIMENTAL

Cadmium perchlorate was prepared by dissolving CdO (99.99%, Mitsuwa Pure Chemicals Co., Osaka) in a 1:1 HClO$_4$ (reagent grade) solution. The purity of the cadmium oxide was checked by emission spectroscopy. The cadmium perchlorate was recrystallized twice from water. Lithium perchlorate was prepared according to the method of Biedermann and Ciavatta.[3] Lithium hydroxide was prepared by electrolysis of a 3 mol dm^{-3} LiClO$_4$ solution and used within 2 weeks after preparation. 2-Mercaptoacetic acid (88% in water) and 2-mercaptopropionic acid (99.8) were

obtained from Katayama Chemicals Co., Osaka, and concentrations of each reagent were determined by both pH titration and total organic carbon analysis by using a TOC analyzer, Model-GCT-12N, Sumitomo Chemicals Ind., Tokyo. An Orion Digital pH Meter Model 801 was used for pH-metric titrations of test solutions in combination with a Beckman glass electrode No. 40495 and a silver–silver chloride electrode. The method of the measurements was essentially the same as that described in previous papers.[1,4] The ratio of the total concentration of the ligand (or ligands) to that of cadmium ions was 5 in all the cases. During the pH-metric titrations the total concentration of perchlorate ions was kept constant at 3 mol dm^{-3} by using lithium perchlorate.

All the measurements were carried out under a nitrogen atmosphere at 25.00 ± 0.02°C in a liquid paraffin bath set in a room thermostated at 25.0 ± 1.5°C.

RESULTS AND DISCUSSION

The complex formation of 2-mercaptoacetic acid with metal ions has been investigated by Leussing[5] for manganese(II), cobalt(II), nickel(II), and zinc(II) in 1958. He found the formation of the M(maa) and M(mae)$_2^{2-}$ complexes, but did not examine reactions between cadmium ions and the ligand. In 1962, Cabrera and West[6] reported the formation of the polynuclear Cd$_2$(maa)$_3^{2-}$ complex in an ammoniacal aqueous solution at pH 10, but they did not report the formation of the 1:1 and 1:2 complexes in the solution. In the present work we found the 1:1 and 1:2 complexes, together with a protonated MHL-type complex, in solutions of pH 5–9 in the cadmium-H_2maa system. In the cadmium-H_2mpa system the same types of the complexes were found.

Typical results of titration curves of solutions of H_2mpa and cadmium–H_2mpa mixtures are shown in Fig. 1, in which the degree of neutralization X of H_2mpa in the solutions was plotted vs $-$ log [H$^+$] (X = $-$ H/C$_L$; H stands for the analytical excess of hydrogen ion and C$_L$ is the total concentration of the ligand). Similar results were obtained for the cadmium–H_2maa system.

The formation constants (K$_{11}$, K$_{12}$, and β_{pqrs}) of the

---

*Author to whom correspondence should be addressed.
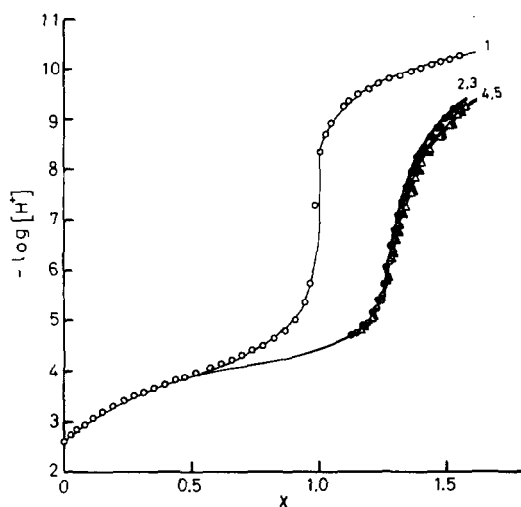
Fig. 1. Titration curves of 2-mercaptopropionic acid and cadmium(II)-2-mercaptopropionic acid solutions. Curve (1) C_{Cd}(mmol dm^{-3}) = 0.0, C_L(mmol dm^{-3}) = 41.05; (2) 3.130, 16.00; (3) 3.441, 17.76; (4) 4.168, 21.51; (5) 4.304, 22.21.

where H_2L and H_2L' denote 2-mercaptoacetic and 2-mercaptopropionic acids, respectively.

Calculations were carried out by using the SCOGS program[7] with an electronic computer FACOM M-160S. The results obtained are summarized in Table 1. The solid lines in Fig. 1 were calculated curves using the estimated constants.

The formation constants (K_{11}) of the cadmium complexes with H$_2$maa and H$_2$mpa are larger than those with glycine (Hgly) and α-alanine (Hala), respectively (see Table 1b). This indicates that a cadmium ion combines more strongly with a mercapto group than an amino group due to a stronger electron-donating ability of the former than the latter to the central cadmium ion. However, the electrostatic interactions between cadmium ions and the ligands must be considered. The large values of the formation constants (K_{11} and K_{12}) of the cadmium–H$_2$mpa complexes compared with those of the cadmium–H$_2$maa complexes may be caused by the stronger electron-donating ability of a sulphur atom in the former ligand than in the latter, due to the inductive effect of a methyl group introduced. In this case we did not see a reverse trend of the formation constants of the complexes to the dissociation constants of the ligands, which has been observed in the systems of glycine and α-alamine, and a usual relationship between the formation constants and the pK values of the ligands was found. The result may be explained as follows: since electron donation from the sulphur atom within

complexes are defined by the following equations:

$$\left.\begin{array}{l} Cd^{2+} + L^{2-} = CdL \\ K_{11} = [CdL]/([Cd^{2+}][L^{2-}]) \end{array}\right\} \quad (1)$$

$$\left.\begin{array}{l} CdL + L^{2-} = CdL_2^{2-} \\ K_{12} = [CdL_2^{2-}]/([CdL][L^{2-}]) \end{array}\right\} \quad (2)$$

$$\left.\begin{array}{l} p\,Cd^{2+} + q\,H^+ + r\,L^{2-} + s\,L'^{2-} = Cd_pH_qL_rL_s'^{(2p+q-2r-2s)+} \\ \beta_{pqrs} = [Cd_pH_qL_rL_s'^{(2p+q-2r-2s)+}]/([Cd^{2+}]^p[H^+]^q[L^{2-}]^r[L'^{2-}]^s) \end{array}\right\} \quad (3)$$
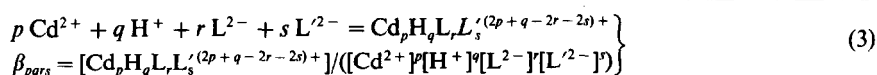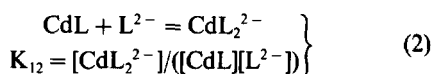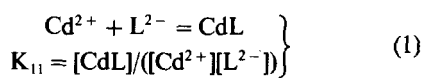
Table 1. Formation constant, $\beta_{pqrs} = [Cd_pH_qL_rL_s'^{(2p+q-2r-2s)+}]/([Cd^{2+}]^p[H^+]^q[L^{2-}]^r[L'^{2-}]^r)$, of cadmium complexes with 2-mercaptoacetic and 2-mercaptopropionic acids in 3 mol dm^{-3} LiClO$_4$ at 25°C*[1]

	H$_2$maa	H$_2$mpa	Hgly *[2]	Hala *[2]
a) Ionization constants.				
pK$_1$	3.83	3.96	2.76	2.81
pK$_2$	9.99	10.25	9.68	9.72
b) Formation constants of mono- and bis(2-mercaptoalkanoato)-cadmium complexes, protonated complexes, and mixed ligand complex.				
log K$_{11}$	4.34	5.66	4.01	3.69
log K$_{12}$	2.15	2.85	3.48	3.24
log β$_{1020}$ or log β$_{1002}$	6.49	8.51	7.49	6.93
log β$_{1110}$ or log β$_{1101}$	11.08	11.22	-	-
log β$_{1011}$	7.93		7.47	

*1   Standard deviations are ± 0.03.

*2   The values are obtained from Ref. 1.

2-mercaptopropionic acid is stronger than that from the ligand sulphur within 2-mercaptoacetic acid, the π-electron acceptability of the former may be relatively smaller than the latter. The effect of the electron donation may be more pronounced in this case than the electron-accepting effect, because of a strong electron-donating ability of sulphur atoms. The formation constants of H_2maa complexes with other divalent metal ions are also larger than those with Hgly.[5]

However, the second stepwise formation constants (K_{12}) of the complexes with cadmium and H_2maa or H_2mpa are smaller than those with the metal and glycine or α-alanine, respectively. This may be explained in terms of a smaller electrostatic interaction between the neutral 1:1 complex of the Cd(maa) or Cd(mpa) and a second entering ligand anion (maa^{2-} or mpa^{2-}) than that between a positively charged Cd(gly)$^+$ or Cd(ala)$^+$ and the relevant ligand.

The protonated complexes Cd(Hmaa)$^+$ and Cd(Hmpa)$^+$ were found in the both solutions of cadmium–H_2maa and –H_2mpa. The dissociation equilibria of the ligands can be described as follows:

wise formation constant of the mixed ligand complex from that of the corresponding parent complex is explained in terms of the so-called "entropy effect", and the increment is 0.6 in an ideal case.

The value of $\log K_{12} = 3.59$ observed for the reaction, Cd(maa) + mpa^{2-} = Cd(maa)(mpa)$^{2-}$, was considerably larger than the second stepwise formation constant of the Cd(mpa)$_2^{2-}$ ($\log K_{12} = 2.85$). The increment was much larger than the statistical value of 0.6. The increased constant at the second step of the formation of the Cd(maa)(mpa)$^{2-}$ complex from Cd(maa) and mpa^{2-} may be explained as follows: since maa^{2-} has a weaker electron-donating ability than mpa^{2-}, the charge density of the cadmium ion within the Cd(maa) complex is still low compared with that within the Cd(mpa) complex. Thus, the entering ligand mpa^{2-} can combine with the Cd(maa) complex more strongly than with Cd(mpa) to form the more stable complex of Cd(maa)(mpa)$^{2-}$ than Cd(mpa)$_2^{2-}$.

When the Cd(mpa) complex is formed at the first stage, the charge density at the cadmium ion within the complex is increased by a strong electron-

$$HSCH_2COOH \rightleftharpoons HSCH_2COO^- + H^+ \rightleftharpoons {}^-SCH_2COO^- + 2H^+$$

$$\underset{\underset{CH_3CHCOOH}{|}}{SH} \rightleftharpoons \underset{\underset{CH_3CHCOO^-}{|}}{SH} + H^+ \rightleftharpoons \underset{\underset{CH_3CHCOO^-}{|}}{S^-} + 2H^+$$

As is seen from Fig. 1, the complex formation between cadmium ions and H_2mpa is not observed until the hydrogen ion of the carboxyl group is almost fully dissociated. Therefore, we assumed that protons within the protonated complexes, Cd·(Hmaa)$^+$ and Cd(Hmpa)$^+$, were combined with the sulphur atom of the mercapto group. No polynuclear complex was found in the solution.

The formation constant of the mixed ligand complex Cd(maa)(mpa)$^{2-}$ was also determined. The formation constant of the mixed ligand complex lies between the values of the two parent complexes, thus, $\beta_{1002} > \beta_{1011} > \beta_{1002}$, although the relationship $\beta_{1011}^2 > \beta_{1020} \cdot \beta_{1002}$ still holds for the complex.

The second stepwise formation constant was evaluated to be $\log K_{12} = 3.59$ for the reaction, Cd(maa) + mpa^{2-} = Cd(maa)(mpa)$^{2-}$ and 2.27 for Cd(mpa) + maa^{2-} = Cd(maa)(mpa)$^{2-}$. The second stepwise formation of a mixed ligand complex is usually larger than that of the corresponding parent complex. The values of $\log K_{12}$ of the parent complexes are 2.15 and 2.85 for Cd(maa)$_2^{2-}$ and Cd(mpa)$_2^{2-}$, respectively. The increment of the step-

donation from mpa^{2-}, and therefore, the electron acceptability of the cadmium ion for the second entering ligand of maa^{2-} is decreased, which is a weaker ligand than mpa^{2-}. Therefore, the second stepwise formation constant of the Cd(maa)(mpa)$^{2-}$ complex from Cd(mpa) and maa^{2-} is smaller than that of the Cd(mpa)$_2^{2-}$, although the former value is still larger by 0.12 log unit than the second stepwise formation constant of the Cd(maa)$_2^{2-}$ complex ($\log K_{12} = 2.15$) due to the entropy effect.

REFERENCES

[1] H. Matsui and H. Ohtaki, Bull. Chem. Soc. Jpn. 1982, 55, 461.

[2] L. G. Sillén and A. E. Martell, Stability Constants of Metal-Ion Complexes, The Chemical Society, London (1964); Suppl. No. 1 (1971).

[3] G. Biedermann and L. Ciavatta, Acta Chem. Scand. 1962, 16, 2221.

[4] H. Matsui, J. Inorg. Nucl. Chem. 1981, 43, 2187.

[5] D. L. Leussing, J. Am. Chem. Soc. 1958, 80, 4180.

[6] A. M. Cabrera and T. S. West, Talanta 1962, 9, 730.

[7] I. G. Sayce, Talanta 1968, 15, 1397.

ORGANOTIN COMPLEXES OF
5-ARYLAZO-8-QUINOLINOLS

T. S. BASU BAUL, T. K. CHATTOPADHYAY and B. MAJEE*
Department of Chemistry, University of North Bengal, Darjeeling—734430, India

Abstract—5-Phenylazo-8-quinolinol (LH) forms di/tri-organotin complexes similar to the well-known organotin oxinates, but 5-(2'-carboxyphenylazo)-8-quinolinol (L'HH') forms three classes, viz., the carboxylate derivatives of the type $R_3SnL'H$, the quinolinolates of the type $R_2Sn(L'SnR_3')_2$ and $R_3SnL'SnR_3'$. The carboxylates, $R_3SnL'H$, are 5-coordinate complexes similar to other triorganotin arylazobenzoates and the quinolinolates, R_2Sn (L'H')$_2$, closely resemble the corresponding organotin oxinates. Unlike the oxinates, $R_2Sn(L'H')_2$ type complexes can, be made water soluble by treatment with aqueous $NaHCO_3$ whereby $R_2Sn(L'Na)_2$ type complexes are formed. The binuclear complexes of the type $R_2Sn(L'SnR_3')_2$ contain 5- and 6-coordinate organotin groups in the same ligand.

Although known for a long time as analytical reagents for qualitative detection of metal ions,[1–3] the extant literature contains no report of isolation and characterisation of metal or organometallic complexes of 5-arylazo-8-quinolinols (I). More recent studies on this group of compounds concern mainly the azo-hydrazone tautomeric equilibria[4–6] and bacteriocidal properties[7,8] although some of these compounds, particularly, 5-(2'-carboxyphenylazo)-8-quinolinol, appear to be suitable ligands for the preparation of a variety of a rare type of complex in which the two coordination sites (2'—COOH and 8–OH groups) are bonded to two different ions/groups. In this paper we report the preparation and electronic spectra of organotin complexes of 5-arylazo-8-quinolinols (I). Of particular interest is the diorganotin-5-(2'-carboxyphenyl azo)-8-quino-linolates which can be made water soluble through conversion into their sodium-salts by reaction with $NaHCO_3$. The corresponding triorganotin compounds are likely to find wide application as water soluble organotin biocides and attempts are therefore being made to prepare these compounds.
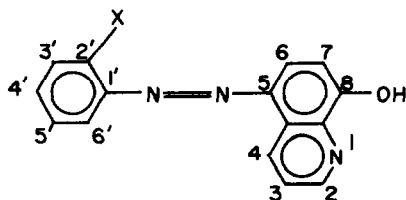
(I)

1. LH (X═H)
2. L'HH'(X═COOH)†

†H and H' refer to the hydroxyl and carboxyl protons respectively.

---

*Author to whom correspondence is to be addressed.

EXPERIMENTAL

(a) *Preparation of 5-arylazo-8-quinolinols* (I) *and their methyl derivatives.* The ligands LH and L'HH' were synthesised according to methods given in Ref. 2.

5-(2'-carbomethoxyphenyl)azo-8-quinolinol, L'MeH, was prepared by the method reported by Sawicki.[6]

Preparation of 5-(2'-carbomethoxyphenyl)azo-8-methoxyquinoline, L'Me₂. L'HH' was methylated by refluxing in MeOH and conc. H_2SO_4 as described by Vogel.[9] The product was purified by repeated crystallisation from ether. m.p. 112°C; PMR(δ), 3.78(COOCH₃), 4.03(Aryl–OCH₃); IR ν_{as}(OCO) 1730 cm⁻¹; ms *m/e* (M⁺), 321.

5-(2'-carboxyphenyl)azo-8-methoxyquinoline, L'MeH' was prepared by saponification of L'Me₂ using standard procedures.[10]

(b) *Preparation of organotin derivatives of 5-arylazo-8-quinolinols* (I). A few preparative details are given below:

(i) Ph₂SnL₂: A mixture of diphenyltin oxide (0.85 g) and LH (0.75 g) in 100 cm³ dry benzene was refluxed for 20 hr, cooled and filtered. The filtrate was concentrated and petroleum ether (60–80) added when the crude product separated out. This was purified by repeated crystallisation from benzene and petroleum ether (60–80). The pure product was obtained as orange crystals; m.p. 202°C; yield 80–82%.

(ii) Ph₃SnL'H: A mixture of Ph₃SnCl(2.03 g) and the Ag–salt of L'HH'(2.1 g) was refluxed in 250 cm³ dry benzene for 25 hr, cooled and filtered. Addition of petroleum ether to the concentrated filtrate yielded the crude product which was filtered and washed with hot petroleum ether, 2% NaHCO₃ and then with water. The product was crystallised from benzene and petroleum ether (60–80); m.p. > 300°C; yield 70–75%.

(iii) Ph₂Sn(L'H')₂: ¹HH' (2.5 g) was Soxhlet-extracted in 300 cm³ THF. To the solution was added 1.46 g. Ph₂SnCl₂ and few drops of pyridine. The reaction mixture was stirred at room temperature for 10 hr. THF was then distilled off, the solid washed with hot petroleum ether and extracted with cold benzene. Addition of petroleum ether (60–80) to the concentrated solution afforded the orange-red product which was again recrystallised from benzene and petroleum ether; d.p. 259°C; yield 40–45%.

(iv) Ph₂Sn(L'Me)₂: L'MeH(1.3 g) and Ph₂SnCl₂(0.73 g) were taken in 150 cm³ dry benzene containing a few drops of pyridine. The mixture was refluxed for 10 hr, cooled and filtered. Addition of petroleum ether to the concentrated filtrate yielded the crude product which was filtered, washed with hot petroleum ether, 2% NaHCO₃ and finally with water. The brown coloured compound was purified by repeated crystallisation from benzene and petroleum ether (60–80); m.p. 178°C; yield 50–55%.

(v) $Ph_2Sn(L'SnPh_3)_2$: A mixture of $Ph_2Sn(L'H')_2(1.0 g)$ and $(Ph_3Sn)_2O(0.83 g)$ in 200 cm³ dry benzene was refluxed for 15 hr, cooled and filtered. Addition of petroleum ether to the concentrated filtrate yielded the crude product which was filtered, washed with hot petroleum ether, 2% $NaHCO_3$ and finally with water. The solid was purified by repeated crystallisation from benzene and petroleum ether (60–80); m.p. > 300°C; yield 60–65%.

RESULTS AND DISCUSSION

(a) *Method of preparation of the organotin derivatives*

While the monobasic ligand LH, forms only one type of organotin complexes, viz. the organotin quinolinolates, the dibasic ligand L'HH' can form three types, viz. the organotin carboxylate, organotin quinolinolate and the binuclear di/triorganotin (triorganotincarboxyphenyl)azo-quinolinolates.

The organotin carboxylates are conveniently prepared by reactions (1) and (2):

$$R_3SnCl + L'HAg \longrightarrow R_3SnL'H + AgCl \qquad (1)$$

$$R_3SnOCOCH_3 + L'HH' \longrightarrow R_3SnL'H + CH_3COOH \qquad (2)$$
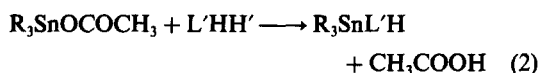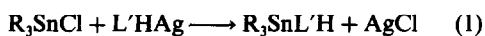
The quinolinolates were prepared by using reactions (3)–(6):

$$(Ph_3Sn)_2O + 2LH \longrightarrow 2Ph_3SnL + H_2O \qquad (3)$$

$$R_2SnX_2 + 2LH \longrightarrow R_2SnL_2 + 2HX \qquad (4)$$

$$R_2SnX_2 + 2L'HH' \longrightarrow R_2Sn(L'H')_2 + 2HX \qquad (5)$$

$$R_2SnX_2 + 2L'MeH \longrightarrow R_2Sn(L'Me)_2 + 2HX \qquad (6)$$
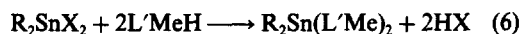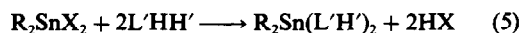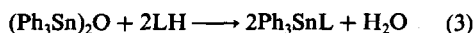
Addition of a small amount of pyridine to the reaction mixture to neutralise the acid formed in reactions (2) and (4)–(6) improves the yield. The binuclear di/tri-organotin (triorganotincarboxyphenyl)azoquinolinolates were prepared in 20–70% yield by reactions (7) and (8) which take place on refluxing the reactants in dry benzene.

$$(R_3'Sn)_2O + R_2Sn(L'H')_2 \rightarrow R_2Sn(L'SnR_3')_2 + H_2O \qquad (7)$$

$$(Ph_3Sn)_2O + L'HH' \rightarrow Ph_3SnL'SnPh_3 + H_2O \qquad (8)$$
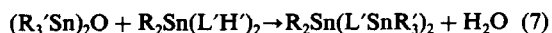
Reaction (9) and (10), were also tried for the preparation of the binuclear complexes:

$$2R_3'SnL'H + R_2SnCl_2 \longrightarrow R_2Sn(L'SnR_3')_2 + 2HCl \qquad (9)$$

$$R_2Sn(L'Ag)_2 + 2R_3'SnCl \longrightarrow R_2Sn(L'SnR_3')_2 + 2AgCl \qquad (10)$$
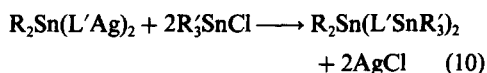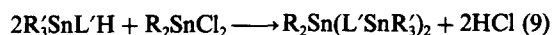
However, the yield in reaction (9) is not good although the reaction time is short. The reverse holds good for reaction (10).

Table 1. Analytical data

Compound*	Found (Calc.) (%)			
	C	H	N	Sn
1. $Ph_3SnL'H$	63.85 (63.58)	3.80 (3.89)	6.50 (6.54)	18.62(18.49)
2. $Bu_3SnL'H$	57.72(57.76)	6.30 (6.36)	7.28(7.22)	20.12(20.40)
3. Ph_3SnL	66.20(65.95)	4.10(4.02)	7.0(7.1)	19.80(19.62)
4. Ph_2SnL_2	65.50(65.25)	3.90(3.50)	10.90(10.95)	15.40(15.36)
5. Bu_2SnL_2	62.70(62.69)	4.90(4.79)	11.50(12.60)	16.30(16.22)
6. Oct_2SnL_2	66.60(65.05)	6.20(6.35)	9.70(9.72)	13.70(13.50)
7. Me_2SnL_2	59.50(60.20)	4.0(3.95)	13.0(13.20)	18.40(18.35)
8. $Ph_2Sn(L'H')_2$	60.92(61.63)	3.52(3.50)	9.79(9.80)	13.90(13.85)
9. $Bu_2Sn(L'H')_2$	58.75(58.77)	4.60(4.65)	10.12(10.28)	14.70(14.53)
10. $Oct_2Sn(L'H')_2$	61.95(62.02)	6.02(5.81)	9.15(9.04)	12.50(12.78)
11. $Me_2Sn(L'H')_2$	56.01(55.68)	3.50(3.54)	11.50(11.46)	16.23(16.20)
12. $Ph_2Sn(L'Me)_2$	62.42(62.39)	3.90(3.84)	9.36(9.49)	13.89(13.41)
13. $Bu_2Sn(L'Me)_2$	59.50(59.66)	4.52(4.97)	10.1(9.94)	14.12(14.05)
14. $Oct_2Sn(L'Me)_2$	63.57(62.71)	6.10(6.06)	7.97(8.78)	12.34(12.40)
15. $Me_2Sn(L'Me)_2$	57.10(56.78)	3.90(3.94)	10.73(11.04)	15.96(15.60)
16. $Ph_2Sn(L'SnPh_3)_2$	61.70(61.77)	3.70(3.73)	5.39(5.40)	22.50(22.91)
17. $Bu_2Sn(L'SnPh_3)_2$	60.70(60.59)	3.19(3.78)	5.72(5.58)	23.68(23.65)
18. $Oct_2Sn(L'SnPh_3)_2$	62.50(61.98)	5.25(5.04)	5.30(5.16)	21.89(21.90)
19. $Me_2Sn(L'SnPh_3)_2$	57.95(58.73)	3.50(3.77)	5.62(5.87)	25.10(24.9)
20. $Ph_2Sn(L'SnBu_3)_2$	57.25(56.89)	5.50(5.71)	6.12(5.85)	24.95(24.83)
21. $Bu_2Sn(L'SnBu_3)_2$	54.50(55.08)	6.62(6.45)	6.22(6.02)	25.79(25.54)
22. $Oct_2Sn(L'SnBu_3)_2$	56.92(57.36)	6.96(7.03)	5.50(5.57)	24.10(23.64)
23. $Ph_3SnL'SnPh_3$	62.50(63.0)	3.92(3.90)	4.10(4.24)	24.15(23.97)

* Me = CH_3, Bu = C_4H_9, Oct = C_8H_{17}, Ph = C_6H_5.

The diorganotin quinolinolates of the type $R_2Sn(L'H')_2$ can be easily converted into the corresponding Na-salts, $R_2Sn(L'Na)_2$ which are water soluble, by treatment with aqueous $NaHCO_3$. The Na-salts can also be crystallised from methanol.

(b) Electronic absorption spectra

Ligands and their organotin complexes in which the 8–OH group is present show two absorption bands in the visible region at ~ 400 nm and ~ 460–480 nm (Table 2) due to azo-hydrazone tautomerism, well-known in such systems.[5,6] The lower wavelength band must be assigned to the π–π^* transition of the azo form since all compounds in which the –OH group is methylated or complexed with organotin group and, thus, exist only in the azo form, show a single intense absorption at ~ 400 nm. The ~ 460–480 nm band must, therefore, be attributed to the hydrazone form in agreement with the earlier observations that the hydrazone form generally absorbs at a longer wavelength.[10] The solvent dependence of the relative intensities of the two bands are also consistent with the known trends in similar molecules.[6]

The relative intensities of the ~ 400 and ~ 460 nm bands show that the azo-hydrazone equilibrium in the carboxylate derivatives of the type $R_3SnL'H$ is considerably shifted towards the azo form compared to that in the corresponding methyl ester, $L'MeH$. In the latter, the hydrazone form is stabilised by the formation of a 6-membered ring due to intramolecular H-bonding (II).[6]

(II)
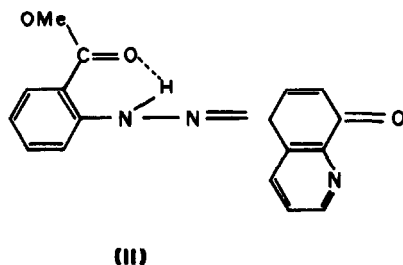
In the organotin complexes (III), the presence of N→Sn coordinate bond prevents the formation of any such intramolecular H-bond in the hydrazone form. The hydrazone form is, therefore, less favoured in the organotin complexes.
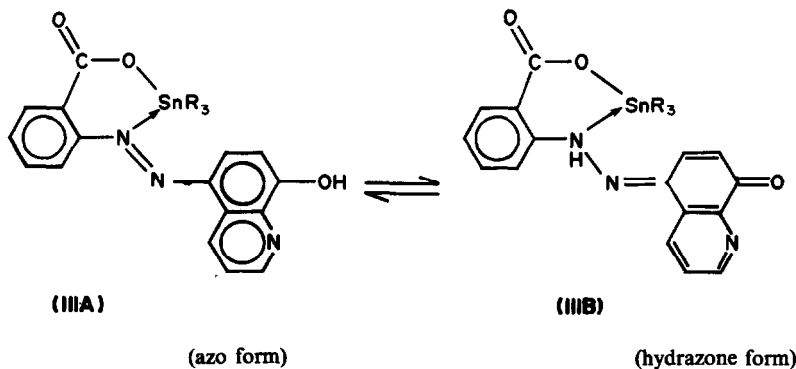
The large bathochromic shift of the π–π^* transition in the azo form in $R_3SnL'H$ type complexes (λ_{max}, ~ 420 nm) compared to that in the corresponding methyl ester $L'MeH$ (λ_{max}, 385 nm) is also consistent with the presence of N→Sn coordination.

Though the possibility of azo-hydrazone tautomerism is eliminated in the organotin quinolinolates of the type $R_2Sn(L'H')_2$, their electronic spectra (Table 2) are strongly influenced by the nature of solvent due to solute–solvent interaction through the carboxylic H-atom as shown by the following observations.

5 - (2' - carbomethoxyphenyl)azo - 8 - methoxyquinoline (IV), a model for the azo form, shows a single absorption maximum at 380 nm in polar as well as nonpolar solvents.

(IV)
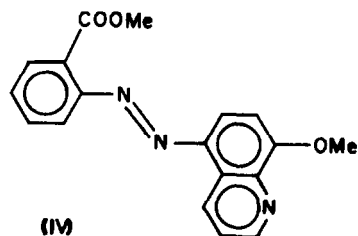
The corresponding organotin derivatives, $R_2Sn(L'Me)_2$, absorb at considerably longer wavelength (λ_{max}, 420 nm). The organotin complexes are, thus, structurally quite similar to the organotin oxinates[11–15] and should be formulated as shown in (V). On the other hand, complexes of the type $R_2Sn(L'H')_2$ in which the carboxyl group is free, absorb predominantly at 415–420 nm in donor solvents (acetone, methanol, DMSO, etc.) and at 480 nm

(V)

(IIIA)   **(IIIB)**

(azo form)   (hydrazone form)

T. S. BASU *et al.*
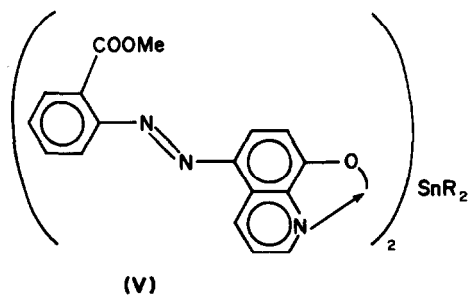
Table 2. IR and electronic spectral data of the organotin complexes of 5-arylazo-8-quinolinols (I)

Compound* (Mp.°C, yield %)	IR ν_{as} (OCO) cm^{-1}	Electronic spectra[j] (λ_{max} nm)	
		MeOH	C_6H_6
1. $Ph_3SnL'H$[a] (>300, 70-75)	1630	410 (480)	420
2. $Bu_3SnL'H$[b] (220, 35-40)	1635	410 (480)	420
3. Ph_3SnL[c] (176, 80-85.)	–	410	410
4. Ph_2SnL_2[d] (202, 80-82)	–	430	430
5. Bu_2SnL_2[d] (118, 60-65)	–	430	430
6. Oct_2SnL_2[d] (93, 65-70)	–	430	430
7. Me_2SnL_2[d] (187, 60-65)	–	430	430
8. $Ph_2Sn(L'H')_2$[e] (259[i], 40-45)	1725	415	480(420)
9. $Bu_2Sn(L'H')_2$[e] (163, 20-25)	1725	420	480(420)
10. $Oct_2Sn(L'H')_2$[e] (144, 30-35)	1725	410	480(420)
11. $Me_2Sn(L'H')_2$[e] (169, 35-40)	1730	410	480(420)
12. $Ph_2Sn(L'Me)_2$[f] (178, 50-55)	1720	420	420
13. $Bu_2Sn(L'Me)_2$[f] (174, 40-45)	1720	420	420
14. $Oct_2Sn(L'Me)_2$[f] (178, 40-50)	1720	420	420
15. $Me_2Sn(L'Me)_2$[f] (175, 45-50)	1720	420	420
16. $Ph_2Sn(LSnPh_3)_2$[g] (300, 60-65)	1630	420	420
17. $Bu_2Sn(LSnPh_3)_2$[g] (211[i], 30-35)	1630	410	415
18. $Oct_2Sn(LSnPh_3)_2$[g] (165[i], 30-30)	1630	410	415
19. $Me_2Sn(LSnPh_3)_2$[g] (175, 40-50)	1630	410	410
20. $Ph_2Sn(LSnBu_3)_2$[g] (242, 20-30)	1635	410	410
21. $Bu_2Sn(LSnBu_3)_2$[g] (162, 20-30)	1630	410	410
22. $Oct_2Sn(LSnBu_3)_2$[g] (182, 35-40)	1635	415	410
23. $Ph_3SnL'SnPh_3$[h] (180, 65-70)	1630	410	420

*Me = CH_3, Bu = C_4H_9, Oct = C_8H_{17}, Ph = C_6H_5. a, b, c, d, e, f, g and h refer to the reactions (1), (2), (3), (4), (5), (6), (7), and (8) respectively as the method of preparation.
i decomp. point.
j λ_{max} in parentheses are shoulders.

(VIA)

(VIB)
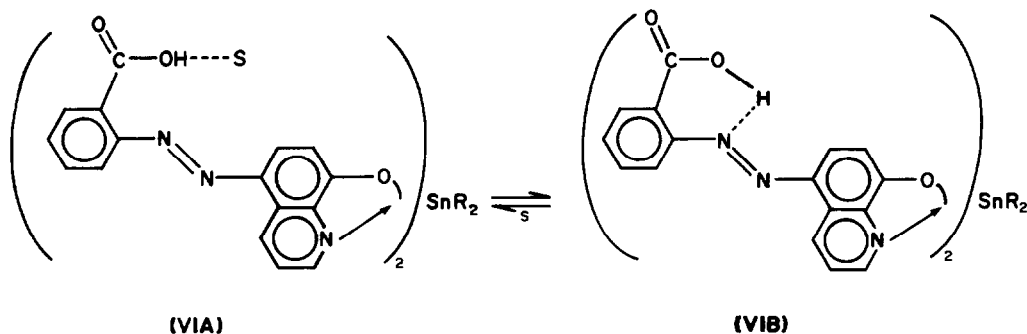
in nonpolar solvents. Since all compounds of this series in which the carboxylic proton has been replaced, e.g. $R_2Sn(L'Me)_2$, $R_3SnL'H$, $R_2Sn(L'SnR_3')_2$ have a single intense absorption at ~ 410 nm in all the solvents, the ~ 420 nm absorption in $R_2Sn(L'H')_2$ should be attributed to the structure (VIA) which is expected to exist in donor solvents (S) due to intermolecular H-bonding involving the carboxylic proton and the donor atom of the solvent. Since the H-atom is not directly involved in the π-system, such interaction will have little influence on the $\pi-\pi^*$ transition and consequently the absorption spectra closely resemble those of the corresponding carbomethoxy compounds in donor solvents (λ_{max}, $Ph_2Sn(L'H')_2 = 415$ nm; $Ph_2Sn(L'Me)_2$, 420 nm).

On the other hand, formation of an intermolecular H-bond involving the azo N-atom (VIB) would certainly result in a large bathochromic shift of the $\pi-\pi^*$ transition.[16,17] The 480 nm absorption should, therefore, be attributed to the species (VIB), the two forms (VIA) and (VIB) being in equilibrium. Clearly, the intramolecular H-bonded form (VIB) will be the main species in nonpolar solvents while donor solvents will tend to form solvent-solute or intermolecular hydrogen bond, thereby shifting the equilibrium towards the form (VIA).

In the binuclear derivatives of the type $R_2Sn(L'SnR_3')_2$ and $(R_3Sn)_2L'$, the possibility of azohydrazone tautomerism as well as intra-or intermolecular H-bonding involving the carboxyl group is eliminated. Consequently, the visible spectra shows a single absorption at 410 nm in both types of solvents. The bathochromic shift of the absorption maximum compared to that in the corresponding methyl derivative, $L'Me_2$ (λ_{max}, 380 nm) indicates the formation of $N \rightarrow Sn$ bond.

(c) *IR spectra*

Both in the organotin carboxylates $R_3SnL'H$ and the binuclear derivatives $(R_3Sn)_2L'$ and $R_2Sn(L'SnR_3')_2$, the asymmetric carboxyl stretch occurs at 1630–1650 cm^{-1} which is typical of 5-coordinate organotin arylazocarboxylates.[18,19] The binuclear derivatives $R_2Sn(L'SnR_3')_2$ which should be formulated as in (VII), therefore, constitute probably the first examples of mixed organotin complexes of polyfunctional ligands.

Interestingly, $\nu_{as}(OCO)$ occurs at 1730 cm^{-1} both in $R_2Sn(L'H')_2$ and $R_2Sn(L'Me)_2$ type compounds indicating the absence of intramolecular H-bonding

(VII)
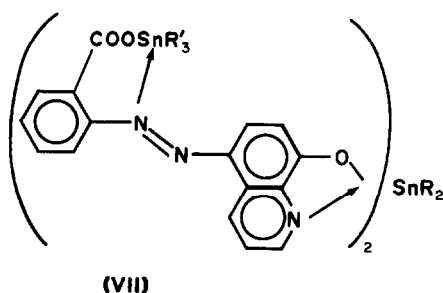
involving the –COOH group in the former in solid phase. This is somewhat surprising since the electronic spectra indicate presence of intramolecular H-bond in the solution phase. Presumably, the intermolecular interactions are more important in the solid phase so that intramolecular H-bonds are broken as in the polar solvents (VIA).

REFERENCES

[1] J. Matheus, *Ber.* 1888, **21**, 1644.
[2] F. J. Welcher, *Organic Analytical Reagents*, Vol. 1. Van Nostrand, London (1947).
[3] V. M. Ivanov and T. F. Rudometkina, *Zh. Anal. Khim.* 1978, **33**, 2426.
[4] Y. Matsunaga, *Bull. Chem. Soc. Japan*, 1971, **44**, 878.
[5] G. M. Badger and R. G. Buttery, *J. Chem. Soc.* 1956, 614.
[6] E. Sawicki, *J. Chem. Soc.* 1956, 743.
[7] R. N. Shreve and R. Bennett, *J. Am. Chem. Soc.* 1943, **65**, 2243.
[8] T. Matsuo, A. Musashi and Y. Naito, *J. Pharm. Soc. Japan*; 1952, **72**, 1456.
[9] A. I. Vogel, *A Text Book of Practical Organic Chemistry*. E.L.B.S. London (1971).
[10] J. Griffiths, *Colour and Constitution of Organic Molecules*. Academic Press, New York (1976).
[11] K. Kawakami and R. Okawara, *J. Organometal. Chem.* 1966, **6**, 249.
[12] K. Kawakami, Y. Kawasaki and R. Okawara, *Bull. Chem. Soc. Japan* 1967, **40**, 2693.
[13] W. Kitching, *J. Organometal. Chem.* 1966, **6**, 586.

[14]T. Tanaka, M. Kowura, Y. Kawasiki and R. Okawara, *J. Organometal. Chem.* 1964, **1**, 484.

[15]D. Blake, G. E. Coates and J. M. Tate, *J. Chem. Soc.* 1961, 756.

[16]W. C. J. Ross and G. P. Warwick, *J. Chem. Soc.* 1956, 1719.

[17]H. Suzuki, *Electronic Absorption Spectra and Geometry of Organic Molecules.* Academic Press New York (1967).

[18]B. Majee and S. Banerjee, *J. Organometal Chem.* 1977, **139**, 39.

[19]B. Majee, A. Roy and S. Banerjee, *Indian J. Chem.* 1978, **16A**, 542.

CYANO- AND THIOCYANATO-DERIVATIVES OF TETRAHALOPHOSPHONIUM IONS

KEITH B. DILLON* and ANDREW W. G. PLATT

Chemistry Department, University of Durham, South Road, Durham DH1 3LE, England

Abstract—Several cyano- and thiocyanato-derivatives of the ions PBr_4^+ and PCl_4^+, including some mixed species, have been obtained in solution by using liquid halogens as solvents, and identified by means of ^{31}P NMR spectroscopy. The method of pairwise interactions has proved very valuable for assigning structures to the various species.

INTRODUCTION

During the course of our recent investigations into pseudohalogeno-derivatives of simple phosphorus(V) species[1–6] we were naturally interested in preparing derivatives of the tetrahalophosphonium ions PBr_4^+ and PCl_4^+. The tetra-azidophosphonium ion $P(N_3)_4^{+7}$ and the series $PCl_{4-n}(N_3)_n^{+3}$ are the only known examples of pseudohalogeno-species derived from PCl_4^+, while no derivatives of PBr_4^+ have been reported. We describe here the identification by means of ^{31}P NMR spectroscopy of several cyano- and thiocyanato-species, including some mixed ions $PCl_xBr_yX_z^+$ ($x + y + z = 4$; $X = CN$ or NCS), derived from PBr_4^+ or PCl_4^+ and prepared in liquid halogens as solvents. The use of the pairwise additivity of chemical shifts[8–10] over a wide range of tetrahedrally-coordinated phosphorus(V) species has proved invaluable as an aid to structural assignment.

EXPERIMENTAL

All manipulations including NMR sample preparation were carried out either *in vacuo* or under an atmosphere of dry nitrogen. Chemicals of the best available commercial grade were used, in general without further purification, except as described below. Bromine and chlorine were dried over P_2O_5 before use. Zinc cyanide was dried by heating to 373K *in vacuo* for 5 hr. $P(CN)_3$ and cyanogen were prepared as described in a previous paper.[5] Anhydrous LiNCS was prepared by the method of Lee.[11] PBr_4BBr_4 was obtained by the action of BBr_3 on PBr_5 in a suitable inert solvent, and the salts PCl_4BCl_4 and PCl_4SbCl_6 were prepared by standard methods.[12] Reactions involving Cl_2 were carried out in thick-walled silica tubes which were sealed under vacuum. The $P(CN)_3/(CN)_2$ system was prepared in a similar manner.

^{31}P NMR spectra were recorded at 307.2K on the Fourier transform spectrometer as described previously.[3] Chemical shifts were measured relative to external H_3PO_4, with the downfield direction taken as positive. Where an entire series of compounds was observed, e.g. $PCl_{4-n}Br_n^+$ or $PBr_{4-n}(CN)_n^+$, the pairwise additivity parameters were refined by a least squares method and these "best fit" values were used in the calculation of chemical shifts.

RESULTS AND DISCUSSION

The formation of $P(N_3)_4^+$ by direct substitution is very dependent on the choice of solvent,[3,7] and $MeNO_2$ was found to be the only common solvent which promotes the reaction.[3] It is thus not surprising that the reactions of PBr_4^+ and PCl_4^+ with other pseudohalides depend greatly on the choice of solvent. Normal organic solvents were found not to

favour simple substitution reactions; some examples of the types of reaction we have observed therein are outlined in eqns (1)–(6).

$$PCl_4SbCl_6 + AgCN \xrightarrow[PhNO_2]{MeCN} PCl_3(CN)_3^- \quad (1)$$

or

$$PCl_4BCl_4 + AgCN \xrightarrow{PhNO_2} PCl_3 + ClCN \quad (2)$$

$$PCl_4SbCl_6 + AgNCS \xrightarrow[slow]{PhNO_2} SPCl_{3-n}(NCS)_n \quad (3)$$

$$PCl_4SbCl_6 + AgNCS \xrightarrow[rapid]{MeCN} SPCl_{3-n}(NCS)_n \quad (4)$$

$$PCl_4SbCl_6 + LiNCS \xrightarrow{MeNO_2} SPCl_{3-n}(NCS)_n \quad (5)$$

$$PCl_4BCl_4 + LiNCS \xrightarrow{MeNO_2} SPCl_{3-n}(NCS)_n + PCl_3 \quad (6)$$
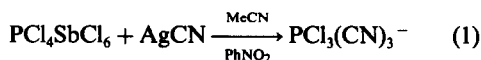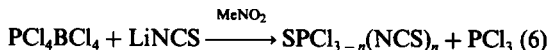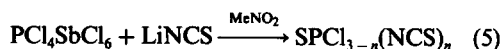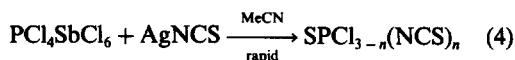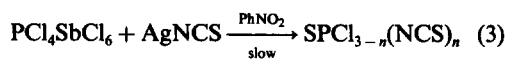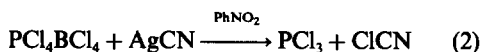
The phosphorus-containing products were identified by means of their characteristic ^{31}P NMR shifts,[5,13] and ClCN (eqn 2) by its gas phase IR spectrum. The usual reactions were either reduction to PCl_3 and/or (for thiocyanates) the formation of thiophosphoryl compounds, although PCl_4SbCl_6 reacted with AgCN in either MeCN or $PhNO_2$ to give the ion $PCl_3(CN)_3^{-5}$. The salts containing the PBr_4^+ ion were either insoluble (PBr_4PF_6), or decomposed readily to $PBr_3(PBr_5$ or PBr_4BBr_4) in normal organic solvents.

In liquid bromine, however, PBr_5 dissolves to give the PBr_4^+ cation (δ ^{31}P − 76.5 ppm), there being no possibility of reduction to phosphorus(III) species in such an oxidising medium. Since some of the reactions above led to reduction of phosphorus(V), the use of liquid halogens as solvent systems seemed feasible. Although side reactions of the metal pseudohalide with the solvent were sometimes apparent they were not always rapid, and reaction with the phosphonium ions often seemed to occur at a faster rate.

Cyano-derivatives of PBr_4^+ *and* PCl_4^+. The reaction of PBr_5 with $Zn(CN)_2$ in liquid bromine gave rise to four new resonances in the ^{31}P NMR spectrum (Table 1). Assignment of the signals is not straightforward as the shift of $P(CN)_4^+$ is to higher field of those of $PBr_2(CN)_2^+$ and $PBr(CN)_3^+$. The $P(CN)_4^+$ assignment was confirmed by measurements on a $P(CN)_3/(CN)_2$ system,[14] where in addition to resonances assigned to $P(CN)_3(\delta$ − 130.6 ppm)[15] and

Table 1. Calculated and observed shifts of $[PBr_{4-n}X_n]^+$ ions in Br_2

n	X=Cl		X=CN	
	δ calc. (p.p.m.)	δ obs. (p.p.m.)	δ calc. (p.p.m.)	δ obs. (p.p.m.)
0	-76.2	-76.5	-76.2	-76.5
1	-32.6	-32.9	-51.7	-49.3
2	8.5	8.5	-37.8	-40.3
3	47.2	47.1	-34.5	-33.3
4	83.2	83.2	-41.8	-41.9

$P(CN)_5(\delta - 98.4\,ppm)$, a higher frequency signal was observed at $\delta - 43.6\,ppm$, agreeing well with the value of $-41.9\,ppm$ in Br_2.

From these observations, and a series of measurements on the $PCl_5/ZnBr_2/Br_2$ system to obtain the shifts of the $PCl_{4-n}Br_n^{+}$[16,17] cations in Br_2 (Table 1), the pairwise additivity parameters Cl : Cl, Cl : Br, Br : Br, Br : CN and CN : CN can be evaluated. Thus to calculate the shifts for the series of cations $PBr_xCl_y(CN)_z^+$ $(x + y + z = 4)$ only the Cl : CN term needs to be found. This was evaluated from the shift of $PCl_3(CN)^+$ (δ 44 ppm), which was observed in the spectra from the reaction between PCl_4SbCl_6 and $Zn(CN)_2$ in Cl_2. All the phosphorus-containing species were insoluble in Cl_2 at room temperature, but the reaction proceeded slowly in the solid state, and the separate resonances due to solid state signals were resolvable because of the large chemical shift differences. $PCl_2(CN)_2^+$ was also observed at δ 11 ppm. PCl_5 also reacted with $Zn(CN)_2$ in Cl_2 to form $PCl_3(CN)^+$ (δ 44 ppm), but no further substitution occurred in this instance.

The reaction of $Zn(CN)_2$ with PCl_5 in Br_2 gave rise to a complex series of spectra. The main reaction observed was the formation of $PCl_{4-n}Br_n^+$ ions (from reaction of $Zn(CN)_2$ with the solvent), and these were the most intense peaks in the ^{31} NMR spectrum, but several resonances were apparent which could be ascribed to cyano-containing derivatives. The observed shifts and assignments are shown in Table 2. The $PCl_2(CN)_2^+$ resonance is likely to be masked by the strong peak due to $PCl_2Br_2^+$, but the failure to detect any signal from $PClBr(CN)_2^+$ must be due to low concentration as no other strong resonances are expected in the region of $-12.5\,ppm$, which is the calculated shift for this species.

Thiocyanato-derivatives. The reactions between both PBr_5 and PCl_5 with AgNCS in Br_2 as solvent were exothermic, and the ^{31}P NMR spectra of the resulting solutions showed several new species to be present, in addition to (for PCl_5) the series $PCl_{3-n}Br_n^+$. The formation of both thiophosphoryl compounds and cyano-substituted species as well as thiocyanato-derivatives was apparent, leading to complex spectra. Possible assignments are shown in Table 3, following calculation of the shifts by the pairwise interaction method, as outlined below.

As pairwise additivity parameters have been shown to be independent of charge and only influenced by the geometry of the compound[4,9,10] the known shifts of $POCl_{3-n}(NCS)_n$ and $POBr_{3-n}(NCS)_n$[18] can be utilised to obtain some of these parameters. (Al-

though the shifts of these compounds have not been quoted for Br_2 as solvent the values seem relatively independent of the solvent in this case, as shown by the checks described subsequently.) The calculation of the pairwise parameters is as follows:

$$
\begin{aligned}
Cl : Cl &= 13.9\,ppm \text{ (from } \delta\ PCl_4^+) \\
O : Cl &= -12.9\,ppm \text{ (from } \delta\ POCl_3) \\
Cl : NCS &= 3.6\,ppm \text{ (from } \delta\ PCl_3(NCS)^+) \\
\delta\ POCl_2(NCS) &= -21.0\,ppm \\
&= 2O:Cl + O:NCS + 2Cl:NCS \\
&\quad + Cl:Cl \\
\therefore O : NCS &= -16.5\,ppm \\
\delta\ POCl(NCS)_2 &= -41.5\,ppm \\
&= O:Cl + 2O:NCS + 2Cl:NCS \\
&\quad + NCS:NCS \\
\therefore NCS : NCS &= -16.5\,ppm.
\end{aligned}
$$

Thus all the data required for the calculation of δ $PCl_{4-n}(NCS)_n^+$ are available. A simple check that the above approach is reasonable is to calculate δ $PO(NCS)_3 = -58.2\,ppm$, which agrees well with the

Table 2. Assignments from the $PCl_5/Zn(CN)_2/Br_2$ system

δ obs. (p.p.m.)	Assignment	δ calc. (p.p.m.)
-76.5	PBr_4^+	-76.2
-52.7	$PBr_3(CN)^+$	-51.7
-45.7	$P(CN)_4^+$	-41.8
-32.9	PBr_3Cl^+	-32.6
-19.6	$PCl(CN)_3^+$	-18.3
-17.4	$PBr_2Cl(CN)^+$	-17.2
-1.0	-	-
1.1	-	-
8.5	$PBr_2Cl_2^+$	8.5
15.4	$PBrCl_2(CN)^+$	14.7
29.2	-	-
44.2	$PCl_3(CN)^+$	*
47.2	$PBrCl_3^+$	47.1
83.2	PCl_4^+	83.2

* observed value used to calculate Cl:CN parameter

Table 3. Assignments for the $PX_5/AgNCS/Br_2$ systems

(a) $PBr_5/AgNCS/Br_2$ system

δ obs. (p.p.m.)	Assignment	δ calc. (p.p.m.)
-76.2	PBr_4^+	-76.2
-62.2	$SPBr_2(NCS)$	-
-52.9	-	-
-50.9	$PBr_3(CN)^+$	-51.7
-41.1	$P(CN)_4^+$	-41.9
-38.4	$PBr_2(CN)_2^+$	-37.8
	or $PBr_3(NCS)^+$	-37.5
-33.1	$PBr(CN)_3^+$	-34.5
-26.7	$SPBr(NCS)_2$	-
-18.2	$P(NCS)_4^+$	-17.4
-15.8	$PBr_2(NCS)_2^+$	-14.8
-8.9	$SP(NCS)_3$	-
	or $PBr(NCS)_3^+$	-8.1

(b) $PCl_5/AgNCS/Br_2$ system

δ obs. (p.p.m.)	Assignment	δ calc. (p.p.m.)
-20.5	$P(NCS)_4^+$	-17.4
-8.2	$SP(NCS)_3$	-
3.6	$SPCl(NCS)_2$	-
	or $PCl(NCS)_3^+$	2.1
5.8	$PClBr(NCS)_2^+$	6.5
10.5	$PCl_2Br_2^+$	8.5
20.2	$PCl_2Br(NCS)^+$	24.9
24.2	$PCl_2(NCS)_2^+$	25.4
34.4	$SPCl_3$	-
44.0	$PCl_3(CN)^+$	-
46.0	PCl_3Br^+	47.2
52.0	$PCl_3(NCS)^+$	*
83.2	PCl_4^+	83.2

* observed shift used to calculate Cl:NCS parameter

observed value of -61.9 ppm.[13,18] The shift parameters required for the brominated derivatives were evaluated in a similar way. Thus

$$\delta\ PSBr_3 = -111.8\ \text{ppm gives S : Br as } -24.6\ \text{ppm}$$

$$\delta\ PS(NCS)_3 = -9.3\ \text{ppm gives S : NCS as } -0.2\ \text{ppm}$$

$$\delta\ PSBr_2(NCS) = -62.8\ \text{ppm}^{19}\ \text{gives Br : NCS as } -0.2\ \text{ppm}.$$

The values were checked by calculating δ for $PSBr(NCS)_2$ as -27.5 ppm, which compares well with the experimental value of -28.4 ppm.[19] Although there is ambiguity in a few of the assignments (Table 3), the majority of the observed peaks could be satisfactorily assigned.

Although the isolation of the species observed in these reactions is not feasible because of the complexity of the systems, the low concentration of some of the species and the likely instability of the compounds in the absence of oxidising media ($P(CN)_5$, for example, was observed to dissociate rapidly to $P(CN)_3$ and (presumably) $(CN)_2$ in CH_2Cl_2), they can be readily identified by solution ^{31}P NMR spectroscopy. This, combined with the use of the pairwise additivity method, allows the elucidation of the somewhat complex chemistry of these systems, giving an insight which would be difficult if not impossible to achieve by any other means. It is noteworthy that the parameters for the $PBr_{4-n}(CN)_n^+$ system correctly predict a maximum in the shift values for $n = 3$; a similar maximum (on the present sign convention) has been both observed and calculated previously for the six-coordinate species $PCl_{6-n}(N_3)_n^-$.[2,3]

REFERENCES

[1] K. B. Dillon, A. W. G. Platt and T. C. Waddington, *Inorg. Nucl. Chem. Lett.* 1978, **14**, 1511.
[2] K. B. Dillon, A. W. G. Platt and T. C. Waddington, *J. Chem. Soc. Chem. Commun.* 1979, 889.
[3] K. B. Dillon, A. W. G. Platt and T. C. Waddington, *J. Chem. Soc. Dalton Trans.* 1980, 1036.
[4] K. B. Dillon, A. W. G. Platt and T. C. Waddington, *J. Chem. Soc. Dalton Trans.* 1981, 2292.
[5] K. B. Dillon and A. W. G. Platt, *J. Chem. Soc. Dalton Trans.* 1982, 1199.
[6] K. B. Dillon and A. W. G. Platt, *J. Chem. Soc. Dalton Trans.*, 1983, In the press.
[7] A. Schmidt, *Chem. Ber.* 1970, **103**, 3923.
[8] T. Vladimiroff and E. R. Malinowski, *J. Chem. Phys.* 1967, **46**, 1830.
[9] J. S. Hartman and J. M. Miller, *Inorg. Chem.* 1974, 13, 1467.
[10] K. B. Dillon and J. M. Miller, unpublished work.
[11] D. A. Lee, *Inorg. Chem.* 1964, 3, 289.
[12] K. B. Dillon, R. N. Reeve and T. C. Waddington, *J. Chem. Soc. Dalton Trans.* 1977, 2382.
[13] V. Mark, C. H. Dungan, M. M. Crutchfield and J. R. Van Wazer, *Top. Phosphorus Chem.* 1967, **5**, 227.
[14] H. Gall and J. Schuppen, *Ber.* 1930, **63**, 482.
[15] K. B. Dillon, M. G. C. Dillon and T. C. Waddington, *J. Inorg. Nucl. Chem.* 1976, **38**, 1149.
[16] K. B. Dillon and P. N. Gates, *J. Chem. Soc. Chem. Commun.* 1972, 348.
[17] K. B. Dillon, T. C. Waddington and D. Younger, *Inorg. Nucl. Chem. Lett.* 1973, **9**, 63.
[18] E. Fluck, *Z. Naturforsch.* 1964, **19b**, 869.
[19] E. Fluck, H. Binder and F. L. Goldman, *Z. Anorg. Chem.* 1965, **338**, 58.

EXTRACTION OF NICKEL IN THE PRESENCE OF AMMONIA WITH β-DIKETONES CONTAINING PHENYL AND ALKYL GROUPS

HIDEO KOSHIMURA*
Tokyo Metropolitan Industrial Technical Institute, Nishigaoka 3-13-10, Kita-ku, Tokyo, Japan

and

TEIJI OKUBO
National Chemical Laboratory for Industry, Tukuba Research Center, Yatabe, Ibaraki 305, Japan

Abstract—The extraction of nickel chelates with β-diketones containing either alkyl or phenyl groups was examined in the absence and in the presence of ammonia in the aqueous solution, in order to define the effect of substituents and the coordinating effect of ammonia on the extraction.

In the extraction of nickel chelates in the presence of ammonia, the extracted species were identified to be [NiA$_2$(NH$_3$)$_2$] (A: β-diketone anion) and ammonia acts both as adduct-forming in the organic phase and as a masking reagent in the aqueous phase.

INTRODUCTION

The β-diketone derivatives which are represented by acetyl–acetone are commonly used as extractants in the solvent extraction of many metals. The distribution coefficients of nickel chelates with the β-diketones are known to be much smaller than those of other divalent metals with the corresponding reagents and the low extractability is attributable to hydrous nickel chelate in an organic phase.[1]

Yosida *et al.*[2] had reported that nickel chelates with di-propyonylmethane, di-*n*-butyrylmethane, di-iso-butyrylmethane, di-iso-valerylmethane and di-*n*-caproylmethane were in a dimeric octahedral structure, and these dimeric chelates were stable in the solid state. However, they appeared to be dimeric monohydrates and monomeric dihydrates in non-coordinating solvents according to spectroscopic studies. It was also known that nickel acetyl–acetonate combined with base adducts such as pyridine[3].

In the previous studies,[4] it was proved that the logarithmic values of the distribution coefficients for the alkyl-substituted β-diketones and their copper or iron chelates were a linear function of the number of additional carbon atoms in the molecule of common water immiscible solvents.

In this paper, the extraction of the nickel chelate with β-diketones containing either alkyl or phenyl groups was investigated both in the absence and in the presence of ammonia in an aqueous phase, in order to define the effect of substituents and the effect of ammonia on the extraction.

EXPERIMENTAL

Materials. Benzoylacetylacetone (BAA), di-benzoylmethane (DBM) and acetylacetone were obtained from Dojindo Co., Ltd. Alkyl-substituted β-diketones, dipropyonylmethane (DPrM), di-*n*-butyrylmethane (DNBM), di-*n*-valerylmethane (DNVM), di-*n*-caproyl-methane (DNCM), di-iso-butyrylmethane (DIBM), di-iso-

valerylmethane (DIVM), dipivaloylmethane (DPM) and pivaloylacetylmethane (PAM) were synthesized by a procedure similar to that of Adams *et al.*[5] and their compositions were confirmed by elementary analysis.

Stock solution of 10^{-4}M NiClO$_4$ was prepared by careful evaporation of the initial chloride solution with perchloric acid. The aqueous pH was controlled with borate buffer in the absence of ammonia, while an ammonium chloride solution was used in the presence of ammonia and perchloric acid or sodium hydroxide was used for pH adjustment.

Benzene of chemical grade was used as the diluent with no further purification. All the other reagents were reagent-grade and were used without further purification.

The ionic strength was kept at 0.10 with sodium perchlorate, which was not added, however, at the concentration of ammonium salt in excess of 0.1 M.

Procedure. An aqueous phase initially containing 10^{-4} M nickel was shaken with an equal volume of 0.10 M β-diketone in benzene. After contrifugation, the concentration of nickel in an aliquot of the organic phase was measured as an oxinate with spectrophotometry. The pH value of the aqueous phase was measured with a pH meter. The equilibrium of extraction was reached slowly in the absence and rapidly in the presence of ammonium salt, then the time of shaking was 2 days for the former and 5 hr for the latter. All experiments were carried out at 20°C.

Apparatus. Most of the apparatus used were essentially the same as that described previously.[4] A Toadempa HM 9A pH meter was used for the measurement of pH. Absorbances were measured with Yuniongiken SM 401 spectrophotometer.

RESULT AND DISCUSSION

The formation of nickel chelates in the aqueous solution is expressed as

$$\text{Ni}^{2+} + nA^- \rightleftharpoons \text{Ni}An^{(2-n)}$$

$$\beta_A = \frac{[\text{Ni}An]}{[\text{Ni}^{2+}][A^-]^n} \tag{1}$$
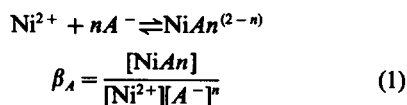
where A^- denotes the β-diketon anion and β_A is the stability constant. The distribution coefficient of the neutral chelate, P_M, between the two phases is defined

---

by:

$$P_M = \frac{[\text{Ni}An]\text{org}}{[\text{Ni}An]\text{aq}} \qquad (2)$$

where subscripts org and aq refer to the organic and aqueous phases respectively, which may be omitted, if not necessary. In a case where the organic phase contains only the $[\text{Ni}A_2]$ species, and the aqueous phase contains a series of metal chelates, the distribution ratio D is described as:

$$D = \frac{[\text{Ni}A_2]\text{org}}{[\text{Ni}^{2+}]\{1 + \Sigma\beta n[A^-]^n\}}. \qquad (3)$$

By introducing eqns (1) and (2), eqn (3) can be rewritten as:

$$D = \frac{P_M\beta_2[A^-]^2}{\{1 + \Sigma\beta n[A^-]^n\}}. \qquad (4)$$

When the concentration of the nickel chelates is sufficiently low as compared with that of the free nickel ions in the aqueous phase, the overall extraction equilibrium can be written as:

$$[\text{Ni}^{2+}] + 2[HA]\text{org} \rightleftharpoons [\text{Ni}A_2]\text{org} + 2[\text{H}^+]$$

$$\text{Kex}^{(1)} = \frac{[\text{Ni}A_2]\text{org}[\text{H}^+]^2}{[\text{Ni}^{2+}][HA]^2\text{org}} = D_1\frac{[\text{H}^+]^2}{[HA]^2\text{org}}. \qquad (5)$$
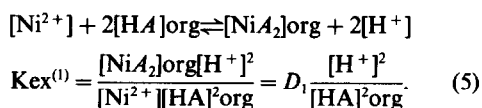
The distribution ratio can be described as:

$$D_1 = \frac{[\text{Ni}A_2]\text{org}}{[\text{Ni}^{2+}]} = \text{Kex}^{(1)}\frac{[HA]^2_{\text{org}}}{[\text{H}^+]^2}. \qquad (6)$$

Thus, when no aqueous chelate complex is formed, the distribution ratio is proportional to the square of the concentration of the chelating extractant in the
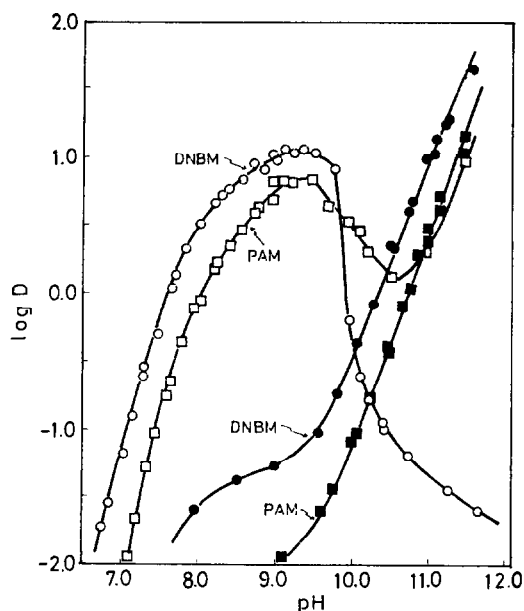
Fig. 2. Distribution ratios of nickel as a function of pH. Organic phase: DNBM, PAM 0.1 M benzene. Aqueous phase: blank dot 0.1 M NaClO$_4$; solid dot 1.0 M NH$_4$Cl.

organic phase and is inversely proportional to the square of the hydrogen ion concentration in the aqueous phase. However, when the distribution ratio is given by eqn (4), it can be described as:

$$D_1 = \text{Kex}^{(1)}\frac{[HA]^2_{\text{org}}[\text{H}^+]^{-2}}{\{1 + \Sigma\beta n[A^-]^n\}}. \qquad (7)$$

In addition, when the formation of metal hydrolysis products in the aqueous phase is not negligible over the pH range under consideration, eqn (7) can also be
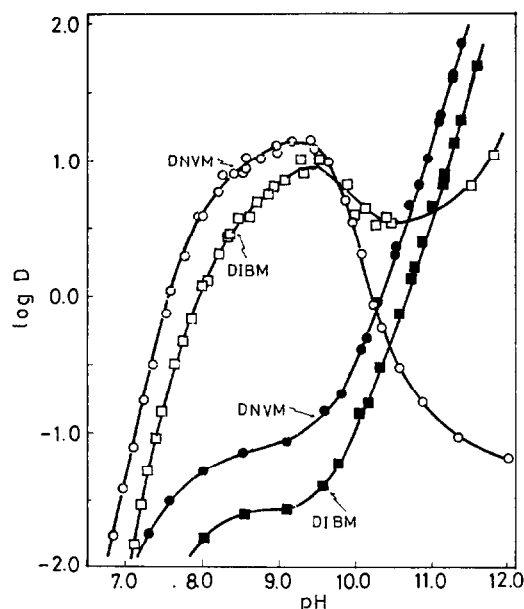
Fig. 1. Distribution ratios of nickel as a function of pH. Organic phase: DNVM, DIBM 0.1 M benzene. Aqueous phase: blank dot 0.1 M NaClO$_4$; solid dot 1.0 M NH$_4$Cl.
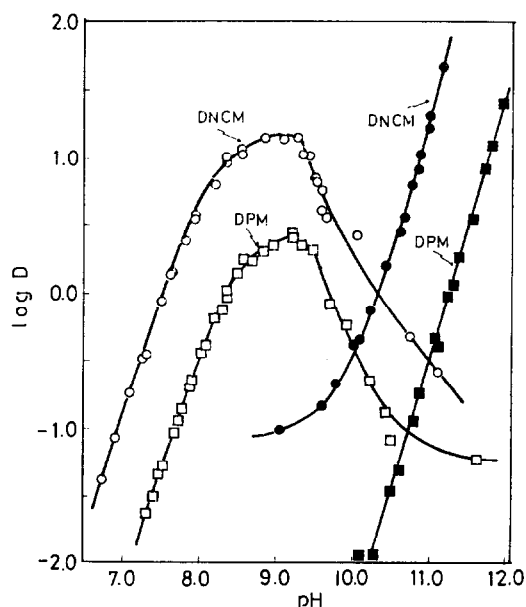
Fig. 3. Distribution ratios of nickel as a function of pH. Organic phase: DNCM, DPM 0.1 M benzene. Aqueous phase: blank dot 0.1 M NaClO$_4$; solid dot 1.0 M NH$_4$Cl.

defined as:

$$D_1 = \text{Kex}^{(1)} \frac{[HA]^2_{org}[H^+]^{-2}}{1 + \Sigma\beta n[A^-]^n + \Sigma\beta_j[OH]^j} \quad (8)$$

where β_j is the overall formation constants for nickel hydroxocomplexes.

In order to identify the distributed species, the distribution ratio was measured at different hydrogen ion concentrations for each of β-diketones. The experimental data were plotted for the values of log D vs pH. Figures 1–3 show several typical examples with a blank dot for the absence and a solid dot for the presence of ammonia in the aqueous phase.

At the absence of ammonia, the distribution ratio increased with the pH value over a weak alkaline region, approached to a maximum value at about pH 9.5, and then decreased rapidly for higher pH region. This probably ascribed the formation of nickel hydroxocomplexes and/or of intermediate complexes with the reagent in the aqueous phase. However, the extraction curves as straight lines of a slope $+2$ were obtained only in the lower region of the distribution ratio for each of β-diketones except for the AA and DPrM, indicating that the simple 1:2 chelate [NiA$_2$] was present in the organic phase.

On the basis of the distribution data, the values for the extraction constants were calculated, which are given in Table 1 together with the aqueous pH values needed for 50% extraction, the distribution coefficients and the acid dissociation constants for each of β-diketones used here. The values of Kex$^{(1)}$ for the AA and DPrM systems could not be calculated due to the poor extractability of the nickel chelates. The values of Kex$^{(1)}$ for the DIBM, PAM and DPM were also in good agreement with those in the previous paper.[6]

It has been attempted to calculate the values of the formation constants of nickel hydrolysis with the aid of eqn (8) and using the values of D, pH and Kex$^{(1)}$ for the DNBM system, as a series of nickel chelates in the aqueous phase were negligibly small. The mean values of the formation constants were therefore

obtained as $10^{4.6}$ for $\beta_{j(OH)}$ and $10^{9.2}$ for $\beta_{j(OH)_2}$, respectively.

The chelates extracted with the DIBM, DPM and PAM into the organic phase appeared pink, which was distinctive other β-diketones. Fackler and Cotton[7] referring to the above fact, had indicated that the *bis*-DIBM and the *bis*-DPM nickel chelates were anhydrous in non-coordination solvents by means of the spectroscopic studies. Accordingly, in the case with the DIBM, DPM and PAM, either all or only part of the extracted species was probably existed as an anhydrous form in the organic phase.

At the presence of ammonia in the aqueous phase, the distribution ratios of nickel chelates increased within the high pH region as shown in Figs. 1–3. Figure 4 shows the visible absorption spectra of the DNBM system as an example of the extracted nickel chelates in the organic phase both at the presence and absence of ammonia in the aqueous phase, in which the absorption peaks of these chelates were shown at 610 nm for the presence and 650 nm for the absence of ammonia. The spectral change which is observed when ammonia gas was bubbled through the organic solution containing the extracted chelate at the absence of ammonia was also quite similar to that of the DNBM chelate described above.

In order to examine the contribution of ammonia on the extraction, the distribution ratios of the DIVM system as an example of the nickel chelates were measured at different concentrations of ammonium chloride at a pH value and the results are shown in Fig. 5. The distribution ratios increased slightly with the increase in the molar concentration of ammonia and decreased rapidly as the further increase in the concentration of one.

The concentration of free ammonia after equilibrium was reached was calculated according to eqn (9):

$$[NH_3] = \frac{[NH_4^+] \text{ in}}{\left\{1 + \dfrac{[H^+]}{Ka}\right\}} \quad (9)$$

Table 1. Equilibrium data in extraction of nickel with β-diketone (20°C)

β-diketone	pKa [*]	log P$_{HA}$ [*]	log Kex(1)	log Kex(3)	log $\frac{Kex(3)}{Kex(1)}$	pH ½	
						0.1M NaClO$_4$	1.0M NH$_4$Cl
D N B M	9.67	2.88	−13.28	−14.90	−1.62	7.64	10.30
D I B M	9.82	3.04	−13.88	−15.41	−1.53	7.94	10.61
D N V M	9.72	4.15	−13.24	−14.85	−1.61	7.62	10.30
D I V M	9.88	4.05	−13.25	−14.65	−1.40	7.60	10.21
D P M	11.57	3.98	−14.48	−16.70	−2.22	8.38	11.28
D N C M	9.71	5.46	−12.80	−14.82	−2.02	7.52	10.32
P A M	10.00	2.18	−13.96	−15.75	−1.79	7.98	10.79
D B M	9.35 [**]	5.35 [**]	−11.02 [**]	−13.10	−2.08	6.4 [**]	7.82
B A M	8.96 [**]	3.06 [**]	−12.12 [**]	−13.71	−1.59	6.9 [**]	9.36

[*]   Quoted from ref (6)

[**]   Quoted from ref (9)
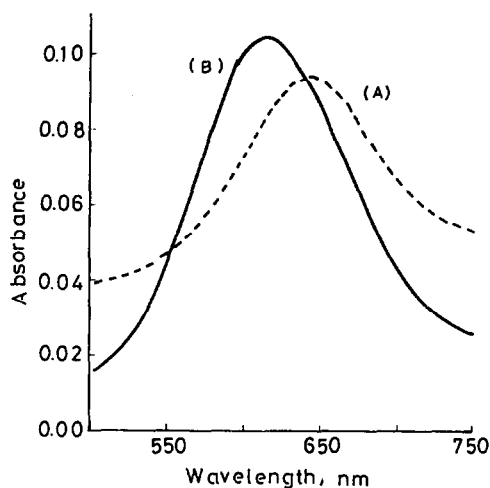
Fig. 4. The visible absorption spectra of the extracted nickel-DNBM chelate. Organic phase: DNBM 0.1 M benzene. Aqueous phase: (A) 0.1 M $NaClO_4$, pH 9.25; (B) 1.0 M NH_4Cl, pH 11.92. Concentration of nickel in organic phase, 1.47×10^{-2} M for (A), 1.26×10^{-2} M for (B).

Fig. 6. Correlation between the concentrations of nickel and ammonia in the organic phase. Organic phase, DIBM 0.1 M benzene. Aqueous phase, NH_4Cl 1.0 M, pH 11.92.

where Ka is the apparent association constant $(= 10^{-9.37})^8$ of ammonium ion and $[NH_4^+]_{in}$ denotes the initial concentration of ammonium salt.

Figure 6 also gives the concentration of ammonia in the organic phase at varying concentration of the nickel ions equilibrated with a 1.0 M NH_4Cl aqueous solution. Obviously, the concentration of ammonia increases in proportion to the nickel concentration with a slope 1.9. The fact that the ammonia dependence is 1.9 means that two mole of the ammonia are coordinated in one mole of the nickel β-diketone.

On the other hand, it was known that the equilibrium of the extraction for the system AA, BAM or DBM alone was reached slowly after being shaken for few days,[9] it was however observed in the presence
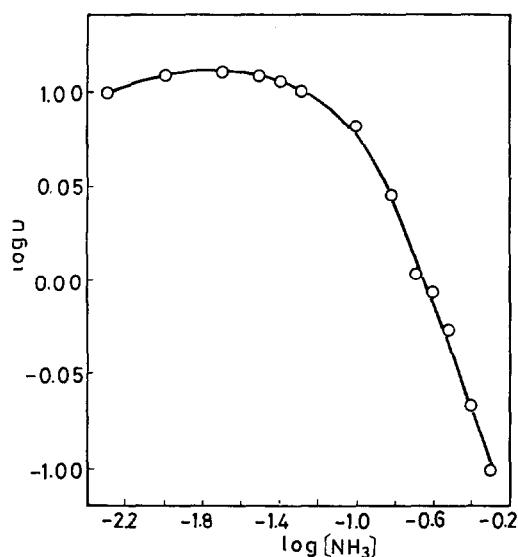
Fig. 5. Distribution ratios of nickel as a function of the concentrations of the ammonia in the aqueous phase. Organic phase, DIVM 0.1 M benzene. Aqueous phase, pH 9.37.

of ammonia, the equilibrium in the extraction was reached within less than 1 hr. Consequently, it may be considered that the nickel chelate was not extracted by the ligand exchange between the β-diketone anion and the coordinated ammonia in the ammine nickel complex, but was extracted by the ligand exchange between the β-diketone anion and the coordinated water in the nickel aquo complex, because the ligand exchange was easily formed with an activated water molecule when 1 and/or 2 mole of the ammonia molecules were coordinated to the nickel aquo complex. The stepwise extraction equilibrium in the presence of ammonia can be written as:

$$[Ni(NH_3)^{2+}] + 2[HA]_{org} \rightleftharpoons [NiA_2(NH_3)]_{org} + 2[H^+]$$

$$[Ni(NH_3)_2^{2+}] + 2[HA]_{org} \rightleftharpoons [NiA_{2A2}(NH_3)_2]_{org}$$
$$+ 2[H^+] \rightarrow [NiA_2(NH_3)_2]_{org} + 2[H^+]$$
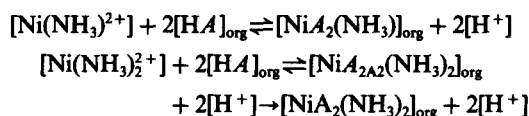
and thus

$$Kex^{(2)} = \frac{[NiA_2(NH_3)]_{org}[H^+]^2}{[Ni(NH_3)^{2+}][HA]_{org}^2}. \quad (10)$$

$$Kex^{(3)} = \frac{[NiA_2(NH_3)_2]_{org}[H^+]^2}{[Ni(NH_3)_2^{2+}][HA]_g^2}. \quad (11)$$

The distribution ratios in the presence of ammonia may be defined as:

$$D = \frac{[NiA_2]_{org} + [NiA_2(NH_3)]_{org} + [NiA_2(NH_3)_2]_{org}}{[Ni^{2+}] + [Ni(NH_3)^{2+}] + \cdots\cdots + [Ni(NH_3)_6^{2+}]}. \quad (12)$$

From eqns (6), (10) and (11), eqn (12) can then be rewritten as:

$$D = \frac{[HA]_{org}^2}{[H^+]^2} \cdot$$

$$\left[\frac{Kex^{(1)} + Kex^{(2)}\beta_1[NH_3] + Kex^{(3)}\beta_2[NH_3]^2}{1 + \Sigma\beta_n(NH_3)^n}\right]. \quad (13)$$
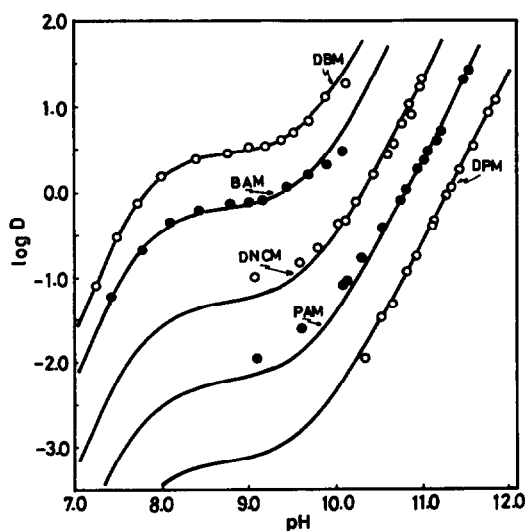
Fig. 7. Distribution ratios of nickel as a function of pH. Organic phase, reagent 0.1 M benzene. Aqueous phase, NH$_4$Cl 1.0 M. —, Calcd value; O, found value.
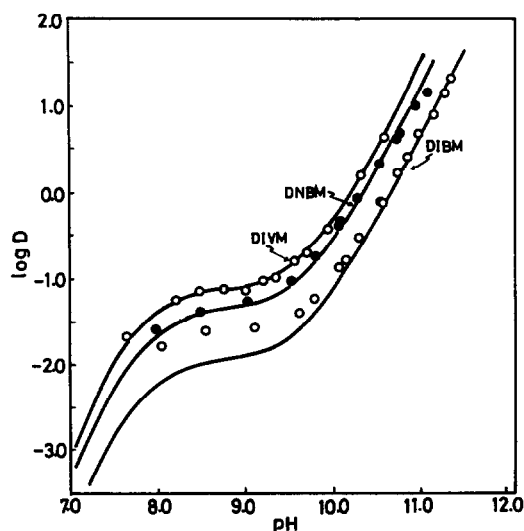
Fig. 8. Distribution ratios of nickel as a function of pH. Organic phase, reagent 0.1 M benzene. Aqueous phase, NH$_4$Cl 1.0 M. —, Calcd value; O, found value.

If the concentration of ammonia was comparatively high, eqn (13) may be reduced as:

$$D = \text{Kex}^{(3)} \cdot \frac{[HA]_{org}^2}{[H^+]^2} \cdot \frac{\beta_2 [NH_3]^2}{\{1 - \Sigma \beta_n (NH_3)^n\}} \qquad (14)$$

where β_n is the overall formation constants for ammine nickel complexes.

The distribution ratios of nickel chelates are then obtained as a function of the ammonia concentration. Equation (13) also suggests that the ammonia acts both as a masking reagents and simultaneously as an adduct forming ligands.

The values of Kex$^{(3)}$ for each of β-diketones were calculated from eqn (14) by employing the observed values of the pH, the distribution ratio, the ammonia concentration and the formation constants for ammin nickel complexes which had been known in the literature.[8] These results are given in Table 1. The results from the present study are shown in Figs. 7 and 8 in order to for the comparison of the behaviour of the distribution ratios for each of β-diketones with a rather wide pH region. The distribution curves show an almost similar tendency for each of β-diketones and a displacement is observed in the pH range of 9–10.

It may be considered that slight positive deviations from the curve for the DIBM system at low pH region are due to the formation of the adduct-comples [NiA_2(NH$_3$)] in the organic phase. Providing that the distribution ratios were compared with a fixed pH, it seems that the values of log D increases as the values of log Ka of corresponding β-diketones lower except for the DBM system. In addition, the synergistic effect with ammonia which is expressed as Kex$^{(3)}$/Kex$^{(1)}$ is approximately the same for β-diketones used here.

REFERENCES

[1]T. Sekine and R. Murai, Proc. Int. Solvent Extraction Conf. ISEC 77, Toronto, 1979, 457 pp.

[2]I. Yoshida, H. Kobayashi and K. Ueno, Bull. Chem. Soc. Japan 1972, **45**, 1411.

[3]J. P. Fackler, Jr., J. Am. Chem. Soc. 1962, **84**, 24.

[4]H. Koshimura, J. Inorg. Nucl. Chem., 1978, **40**, 865.

[5]C. R. Hauser and J. T. Adams, J. Am. Chem. Soc., 1944, **66**, 1220.

[6]H. Koshimura and T. Okubo, Anal. Chem. Acta, 1971, **55**, 163.

[7]F. A. Cotton and J. P. Fackler, Jr., J. Am. Chem. Soc. 1961, **83**, 2818.

[8]L. G. Sillén and A. E. Martell, Stability Constants of Metal-Ion Complexes, 151 pp. The Chemical Society, London (1964).

[9]J. Starý, The Solvent Extraction of Metal Chelates, Pergamon Press, Oxford (1964) 51 pp.

CHEMISTRY IN FUMING NITRIC ACIDS—I. NMR SPECTROSCOPIC STUDY OF PF₅, HPO₂F₂ AND P₄O₁₀ IN THE SOLVENT SYSTEM 44 wt.% N₂O₄ IN 100% HNO₃

C. CLIFFORD ADDISON, JOHN W. BAILEY, SIMON H. BRUCE, MICHAEL F. A.
DOVE, RICHARD C. HIBBERT and NORMAN LOGAN*
Department of Chemistry, University of Nottingham, University Park
Nottingham NG7 2RD, England

Abstract—^{31}P and ^{19}F NMR spectroscopy has been used to elucidate the nature of the interaction of PF$_5$, HPO$_2$F$_2$ and P$_4$O$_{10}$ with the solvent system 44 wt.% N$_2$O$_4$ in 100% HNO$_3$ ("High Density Acid", HDA). PF$_5$ generates the species PF$_6^-$, HPO$_2$F$_2$ and HF (with some H$_2$PO$_3$F present as a minor product). HPO$_2$F$_2$ gives rise to H$_2$PO$_3$F and HF (with smaller amounts of PF$_6^-$ also present). The ^{31}P NMR spectrum of P$_4$O$_{10}$ in HDA exhibits four resonances assigned to P(OH)$_4^+$, H$_4$P$_2$O$_7$, (HPO$_3$)$_4$ and a mixture of cyclic and branched phosphoric acids, respectively.

Fuming nitric acids have found widespread use over the last 40 yr as oxidiser components of liquid rocket propellants.[1] They possess a number of advantages in this role, namely, a high specific gravity (1.5 or greater), a convenient liquid range ($-40°C$, or lower, to $+80°C$), hypergolicity (spontaneous ignition) with a number of fuels and they are relatively cheap to manufacture. They have, however, several disadvantages, particularly their highly corrosive nature. 100% nitric acid undergoes the auto-ionisation (1)

$$2HNO_3 \rightleftharpoons NO_2^+ + NO_3^- + H_2O. \qquad (1)$$

The presence of NO$_2^+$, NO$_3^-$ and molecular H$_2$O in 100% HNO$_3$ was established by Raman spectroscopy.[2,3] ^{1}H NMR studies have shown that a rapid exchange takes place between the chemical species present.[4,5] Due to the presence of molecular H$_2$O the terms "pure" or "anhydrous" nitric acid are misleading; the term "analytically 100% nitric acid" is preferred and, if not specified, should be understood whenever HNO$_3$ or nitric acid is referred to in this paper. This acid is termed white fuming nitric acid (WFNA). WFNA is, however, unstable and undergoes thermal or photolytic decomposition (eqn 2).

$$2HNO_3 \xrightarrow{\Delta \text{ or } h\nu} N_2O_4 + H_2O + \tfrac{1}{2}O_2. \qquad (2)$$
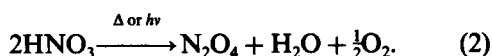
*Author to whom correspondence should be addressed.

This limits the suitability of WFNA as a propellant due to possible pressure build-up in tanks and uncertainty in the oxidising power. The addition of N$_2$O$_4$ improves the stability and storability of the oxidiser. Of particular interest is the mixture 44 wt.% N$_2$O$_4$ in 100% HNO$_3$. This composition gives the maximum density of any N$_2$O$_4$–100% HNO$_3$ mixture and is thus referred to as High Density Acid (HDA). N$_2$O$_4$–100% HNO$_3$ mixtures are highly corrosive towards the series 300 stainless steels and aluminium alloys used as containment materials for the oxidiser and thus small quantities (*ca.* 0.5 wt%) of a third component are added to inhibit corrosion. HF and PF$_5$ are found to be the most highly successful inhibitors thus far tried[6] but P$_4$O$_{10}$ and HPO$_2$F$_2$ are potential alternatives.

The purpose of the present study was to investigate the interaction of the solutes PF$_5$, HPO$_2$F$_2$ and P$_4$O$_{10}$ with the system 44 wt.% N$_2$O$_4$ in 100% HNO$_3$ (HDA), by means of ^{19}F and ^{31}P NMR spectroscopy. The chemical nature of the HDA medium is of considerable interest. N$_2$O$_4$ is known to undergo essentially complete ionic self-dissociation (eqn 3) at concentrations up to 1M ($\sim$9 wt.%) in 100% HNO$_3$[7]

$$N_2O_4 \rightleftharpoons NO^+ + NO_3^-. \qquad (3)$$

The proportions of the various species at higher concentrations of N$_2$O$_4$ are not precisely known, although a recent investigation by Raman spectroscopy in our laboratories[8] has confirmed the presence of the molecular species NO$^+$, NO$_3^-$,

HNO$_3$ and N$_2$O$_4$ in HDA, which is also known to contain small concentrations of NO$_2$ (as indicated by its orange colour) and H$_2$O (characteristic absorption in the near IR at 7117 cm^{-1}). The chemistry of HDA has been reviewed.[9] The present study enables the reactivity of this complex medium to be further elucidated.

EXPERIMENTAL

Materials

PF$_5$ was prepared by the controlled fluorination of red phosphorus. Any POF$_3$ impurity formed in the reaction was removed by holding the reaction vessel at $-78°C$ during the transfer of PF$_5$ to a steel storage vessel. Pure HPO$_2$F$_2$ was obtained from the commercial material (Koch–Light) by the method of DesMarteau et al.[10] The purity of samples prepared in this way was confirmed by ^{19}F NMR spectroscopy,

$$(\delta_{CFCl_3} = -87.3 \text{ ppm}, \quad J_{F-P} = 982 \text{ Hz}).$$

Commercial P$_4$O$_{10}$ (Albright and Wilson) was used without further purification.

HDA is prepared on a routine basis in our laboratories by mixing 100% HNO$_3$ and liquid N$_2$O$_4$. 100% HNO$_3$ was obtained by distillation under reduced pressure (10^{-2} Torr) of a 3:1 (v:v) mixture of concentrated sulphuric acid and 95% nitric acid. The product was collected and stored at low temperature (ca. $-20°C$). Commercial N$_2$O$_4$ (Air Products Ltd.) was purified by drying the liquid over P$_4$O$_{10}$ (1 day) followed by distillation in a slow oxygen stream through a P$_4$O$_{10}$ drying column. The purified N$_2$O$_4$ was collected as a colourless solid at $-78°C$. HDA, as prepared in our laboratories, was found to contain ca. 0.23 wt.% H$_2$O.[8]

Preparation of NMR samples

The samples were made up by weight in 6 mm o.d. fluorinated ethylene propylene (FEP) polymer tubes. These tubes were coupled to Kel–F vacuum valves so that samples could be degassed and volatile components added from a calibrated fluorocarbon polymer vacuum manifold. Finally, the FEP tubes containing the prepared solutions were heat sealed.

NMR spectra

All NMR spectra were obtained using a Bruker WM250 pulse Fourier transform spectrometer (^{19}F studies at 235.35 MHz and ^{31}P at 101.27 MHz). The FEP tubes were placed inside 10 mm dia. glass NMR tubes containing CDCl$_3$ (to provide a deuterium lock) in the outer annulus. Samples for ^{19}F

NMR investigations also contained CFCl$_3$ (as external standard) in the glass tube. All ^{31}P spectra were externally referenced to 85% H$_3$PO$_4$ by sample replacement. Relative concentrations of species were determined from measured peak integrals. The spectra were accumulated until a satisfactory signal-to-noise ratio was attained. For low concentrations of solutes (0.7 wt.% PF$_5$ and 1 wt.% P$_4$O$_{10}$) approx. 100,000 pulses (ca. 15 hr accumulation time) were required for the production of a high quality spectrum.

RESULTS AND DISCUSSION

(a) The PF$_5$–HDA system

The PF$_5$–HDA system was studied at PF$_5$ concentrations of 6 and 0.7 wt.% (PF$_5$ is used as an inhibitor in HDA at concentrations between 0.5 and 0.7 wt.%). The 6 wt.% mixture contained a white solid (although this did not interfere with the running of NMR spectra). This solid was identified on the basis of its IR spectrum and X-ray powder pattern as predominantly NO$^+$PF$_6^-$. The precipitation of NO$^+$PF$_6^-$ rather than NO$_2^+$PF$_6^-$ is to be expected since the self-dissociation of N$_2$O$_4$ supresses the self-dissociation of HNO$_3$ to the extent that the NO$_2^+$ concentration becomes very small in HDA. The 0.7 wt.% mixture was completely homogeneous.

The ^{19}F chemical shifts and coupling constants for the observed species (HF, H$_2$PO$_3$F, HPO$_2$F$_2$ and PF$_6^-$) are collected in Table 1. ^{31}P NMR spectroscopy demonstrated the absence of any other phosphorus-containing species in either mixture. The formation of the observed products may be rationalised using the following series of equations

$$2PF_5 + HNO_3 \rightarrow POF_3 + NO_2^+ + PF_6^- + HF \quad (4)$$

$$POF_3 + HNO_3 \rightarrow HPO_2F_2 + NO_2^+ + F^-. \quad (5)$$

$$HPO_2F_2 + HNO_3 \rightleftharpoons H_2PO_3F + NO_2^+ + F^-. \quad (6)$$

$$HPO_2F_2 + 4F^- + 2NO_2^+ \rightleftharpoons PF_6^- + NO_3^- \\ + HNO_3. \quad (7)$$
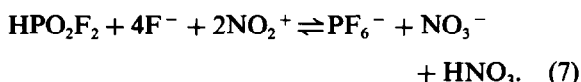
Neither POF$_3$ nor PF$_5$ was detected in the solution phase by NMR spectroscopy, presumably because they are very rapidly solvolysed in HDA. However, POF$_3$ has been observed (by NMR spectroscopy) in solution in other strongly acidic media (e.g. fluorosulphuric acid[12]) and we have observed it in the vapour phase above a 5 wt.% solution of PF$_5$ in HNO$_3$ (although it was not detected in the solution phase by NMR). A de-

Table 1. ^{19}F NMR parameters for the fluorine-containing species in the system PF$_5$–HDA

	$\delta(^{19}F)$/ppm*			J_{F-P}/Hz		
	0.7 wt.%	6 wt.%	†	0.7 wt.%	6 wt.%	†
PF$_6^-$	−70.6	−70.5	−73.0[11]	708	708	706[11]
HPO$_2$F$_2$	−84.0	−84.1	−87.2[12]	983	983	983[12]
H$_2$PO$_3$F	−76.6	−76.6	−77.3[12]	952	952	955[12]
HF	−157.0	−157.8	−200.9[11]	–	–	–
F$^-$	–	–	−126.1[11]	–	–	–

* relative to CFCl$_3$

† literature values

tailed NMR investigation of the PF$_5$–HNO$_3$ system has not yet been conducted but preliminary results indicate that the interaction of PF$_5$ with HNO$_3$ is similar to that with HDA except that, at PF$_5$ concentrations in excess of ca. 5 wt%, NO$_2^+$PF$_6^-$, rather than NO$^+$PF$_6^-$, is precipitated from solution. The variation with time of the concentrations of the observed species in the 0.7 wt.% mixture is displayed in Fig. 1. HF concentrations determined by direct integration were unreliable due to interference from a very broad signal (centred at

Fig. 1. Variation with time of species detected by ^{19}F NMR in a solution of 0.7 wt.% PF$_5$ in HDA. ○, HF (calculated)/2; ●, HPO$_2$F$_2$; △, PF$_6^-$; ▲, H$_2$PO$_3$F.

ca. −122 ppm) produced by the fluoroplastic NMR tube (see Fig. 2). The HF concentrations shown in Fig. 1 were therefore determined using the measured concentrations of H$_2$PO$_3$F, HPO$_2$F$_2$ and PF$_6^-$ and by assuming that the P:F ratio in the sealed system remained constant at 1:5.

Results from the 6 wt.% mixture indicate that the hydrolysis of HPO$_2$F$_2$ (as indicated by the rate of formation of H$_2$PO$_3$F) is concurrent with that of PF$_6^-$ (as indicated by the rate of formation of HPO$_2$F$_2$) although it is less rapid. In the 0.7 wt.% system (Fig. 1) the HPO$_2$F$_2$ and HF concentrations increase in a regular manner as the PF$_6^-$ concentration diminishes, whereas the H$_2$PO$_3$F concentration remains relatively small but slowly increases. Figure 1 also indicates that a stable (equilibrium) situation would eventually be reached in the 0.7 wt.% mixture.

(b) The HPO$_2$F$_2$–HDA system

The HPO$_2$F$_2$–HDA system was studied at initial HPO$_2$F$_2$ concentrations of 2.7, 4.1, 9.7 and 22.8 wt.% (all mixtures were homogeneous). At all concentrations the only observed species were HF, H$_2$PO$_3$F, HPO$_2$F$_2$ and PF$_6^-$. The ^{19}F NMR parameters of these species were similar to those observed in the PF$_5$–HDA system and were virtually independent of concentration. Typical ^{31}P NMR parameters are presented in Table 2. The major fluorophosphate species observed were HPO$_2$F$_2$ and H$_2$PO$_3$F (as opposed to PF$_6^-$ and HPO$_2$F$_2$ in the PF$_5$–HDA system). H$_2$PO$_3$F is formed by solvolysis of HPO$_2$F$_2$ (eqn 6) and the fluoride thus generated subsequently attacks HPO$_2$F$_2$ to form PF$_6^-$ (eqn 7). The observed PF$_6^-$ concentrations were never more than 11% of the corresponding H$_2$PO$_3$F concentration.

In HPO$_2$F$_2$–HDA mixtures and PF$_5$–HDA mixtures the chemical shift of the resonance ascribed to HF is in the region which corresponds to
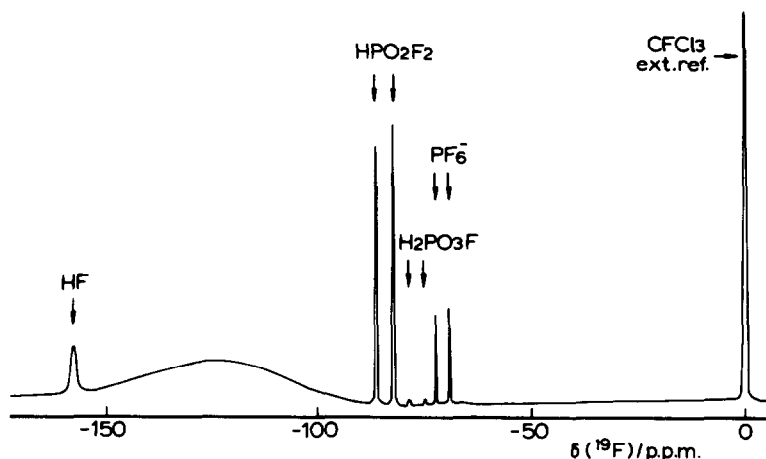
Fig. 2. ^{19}F NMR spectrum of 0.7 wt.% PF$_5$ in HDA after 83 days.

hydrogen-bonded HF molecules, rather than to HF$_2^-$ or F^{-13} (Table 1). The change in chemical shifts of the fluorophosphoric acids (Tables 1 and 2) in HDA with respect to the pure compounds, can be ascribed to solvation effects rather than protonation. Protonation of the phosphoryl oxygen of H$_2$PO$_3$F or HPO$_2$F$_2$ in 1:1 fluorosulphuric acid–antimony pentafluoride ("Magic Acid") substantially increases the coupling constants (^{1}J$_{F-P}$) for these species,[14] however, no such increase was observed in HDA. A solution of HPO$_2$F$_2$ (19 wt.%) in HNO$_3$ (at $-20°$C to inhibit the thermal decomposition of nitric acid) was also examined. In addition to the species observed in HDA, a weak peak at $+2.1$ ppm, assignable to protonated orthophosphoric acid,[15] was observed. The coupling constants of HPO$_2$F$_2$ (994 Hz) and H$_2$PO$_3$F (965 Hz) were higher than in HDA and are indicative of some degree of protonation of these species also.

(c) *The P$_4$O$_{10}$–HDA system*

Solutions at initial P$_4$O$_{10}$ concentrations of 4.2, 2.9 and 1 wt.% in HDA were examined. A solution

of P$_4$O$_{10}$ (4.3 wt.%) in 100% HNO$_3$ was also prepared for comparison purposes. The tubes containing ca. 4.2 wt.% P$_4$O$_{10}$ were stored at $-20°$C (freezer) between ^{31}P NMR measurements. This enabled a comparison of the two systems to be made (it being necessary to store the tube containing HNO$_3$ at $-20°$C to prevent thermal decomposition of the acid).

The results are summarised in Tables 3 and 4. Generally speaking, four ^{31}P resonances were observed for each solution (see Fig. 3). The low field peak at 2.0 ± 0.3 ppm has been assigned to protonated orthophosphoric acid (P(OH)$_4^+$).[15] A down-field shift is observed when protonation of the doubly bound oxygen takes place.[15] (This assignment is, however, made with some reservation because HPO$_2$F$_2$ and H$_2$PO$_3$F also show a ^{31}P downfield shift in HDA but no increase in coupling constant; see Section (a)). The peak at -11.75 ± 0.25 ppm can be assigned to diphosphoric acid, H$_4$P$_2$O$_7$. An aqueous solution of this acid has a shift of -10.6 ppm[16] and a solid sample rotating at the "magic angle" of 54°44′ resonates at -12 ppm.[17]

The position of the third peak is very close to that reported for tetrametaphosphoric acid $(-24.0$ ppm)[18] and this assignment is supported by the observation that under controlled conditions this acid is the principal hydrolysis product of P$_4$O$_{10}$. The position $(-26.7 \pm 0.6$ ppm) of the fourth peak is intermediate between that expected for cyclic (ca. -20 to -24 ppm) and branched (ca. -30 ppm) phosphate.[15] This peak (which is quite broad; ca. 230 Hz) is therefore tentatively assigned to a mixture of cyclic and branched phosphoric acids in fairly rapidly reversible equilibrium giving a single averaged signal. The variation with time of the proportions of the various

Table 2. ^{31}P NMR parameters for the fluorophosphate species in the HPO$_2$F$_2$–HDA system

	$\delta(^{31}$P)/ppm*		J$_{P-F}$/Hz	
		†		†
H$_2$PO$_3$F	−6.3	−8.3	950	952
HPO$_2$F$_2$	−16.3	−21.7	978	984
PF$_6^-$	−143	−145	706	715

* relative to 85% H$_3$PO$_4$

† literature values[11]

Table 3. Summary of ^{31}P NMR chemical shifts for the P_4O_{10}–HNO_3 and P_4O_{10}–HDA systems

	Time/days	$\delta(^{31}P)$/ppm*			
4.3 wt.%	17	+1.7,	−12.0,	−24.9,	−27.3
P_4O_{10} in HNO_3	33	+1.8,	−11.8,	−24.8,	−26.9
	66	+1.8,	−11.8,	−24.8,	−26.9
4.2 wt.%	17	+2.3,	−11.5,	−23.6,	−26.7
P_4O_{10} in HDA	48	+2.2,	−11.5,	−23.9,	−26.5
	101	+2.1,	−11.5,	−23.9,	−26.1
2.9 wt.%	6	+1.8,	−11.7,	−24.2,	−27.0
P_4O_{10} in HDA	43	+1.7,	−11.6		
1 wt.%	3	+1.7,	−11.8,	−24.1,	−26.7[†], −27.1[†]
P_4O_{10} in HDA	7	+1.8,	−11.7,	−24.1,	−26.9
	35	+1.8,	−11.7		

* relative to 85% H_3PO_4

[†] peaks overlap

products (expressed as % of total phosphorus present) is summarised in Table 4. A number of conclusions can be drawn from these results. Provided the initial concentration of P_4O_{10} in HDA is small (around 1 wt.%), complete conversion to protonated orthophosphoric acid $(P(OH)_4^+)$ would eventually be observed, whereas at higher initial P_4O_{10} concentrations an equilibrium mixture of phosphoric acids would ultimately be obtained. The attainment of this equilibrium position (or of complete hydrolysis of P_4O_{10}) appears to require a considerable length of time. This is probably due

Table 4. Variation with time of proportions of phosphoric acids in solutions of P_4O_{10} in HNO_3 and HDA

	Time/days	Phosphoric Acids (% of total P)			
		Ortho-	Di-	Tetrameta-	Cyclic + Branched
4.3 wt. %	17	34.6	55.6	3.5	6.3
P_4O_{10} in	33	41.9	54.4	1.5	2.2
HNO_3	66	45.2	50.2	1.4	3.4
4.2 wt. %	17	6.9	26.7	12.7	53.7
P_4O_{10} in	48	11.3	41.2	7.0	47.4
HDA	101	16.3	56.1	4.4	23.2
2.9 wt. %	6	16.4	44.4	10.4	28.8
P_4O_{10} in HDA	43	56.7	43.5	–	–
1 wt. %	3	9.2	24.6	8.5	57.7
P_4O_{10} in	7	47.7	40.7	1.0	10.6
HDA	35	90.8	9.2	–	–
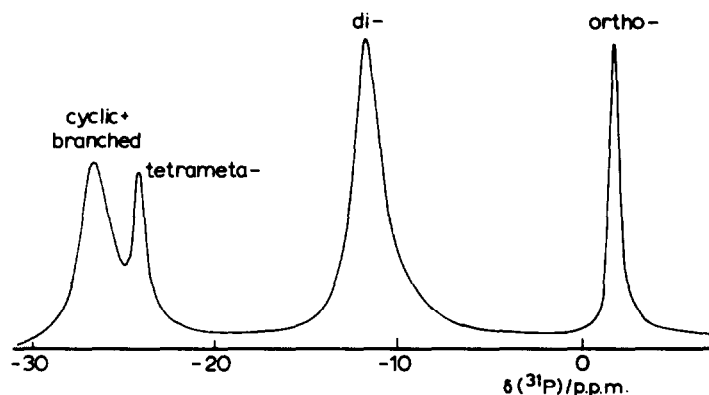
Fig. 3. ^{31}P NMR spectrum of 2.9 wt.% P_4O_{10} in HDA after 6 days (assignments to phosphoric acids).

to the resistance to hydrolysis of some of the cyclic and branched phosphoric acids present in the system. The hydrolysis of P_4O_{10} in 100% HNO_3 is more extensive and rapid than in HDA, although similar species are observed in both media.

SUMMARY

In the solvent system 44 wt.% N_2O_4 in 100% HNO_3 (HDA) the solutes PF_5, HPO_2F_2 and P_4O_{10} undergo what may be termed "hydrolysis" reactions. The hydrolysis of all three solutes is incomplete (except at low concentrations) equilibrium mixtures of fluorophosphate species (PF_5 and HPO_2F_2) or phosphoric acids (P_4O_{10}) being ultimately obtained. Reactions in HDA therefore more closely resemble those in aqueous solution,[19,20] than in strongly acidic media.[12,13,15]

REFERENCES

1. J. D. Clark, *Ignition: An Informal History of Liquid Rocket Propellants*. Rutgers University Press, New Brunswick (1972).
2. C. K. Ingold and D. J. Millen, *J. Chem. Soc.* 1950, 2612.
3. J. Chedin and S. Fenéant, *Comptes Rendus* 1947, **224**, 930.
4. G. C. Hood, O. Redlich and C. A. Reilly, *J. Chem. Phys.* 1954, **22**, 2067.
5. R. A. Ogg and J. D. Ray, *J. Chem. Phys.* 1956, **25**, 1285.
6. H. P. Heubusch, *U.S. Nat. Tech. Inform. Serv. AD Rep.* 1973, *No.* 77332/2GA, from Gov. Rep. Announcements (U.S.) 1974, **74**(7), 204.
7. J. D. S. Goulden, W. H. Lee and D. J. Millen, *J. Chem. Soc.* 1957, 734.
8. N. Logan and A. A. M. Moharum, unpublished results.
9. C. C. Addison, *Chem. Rev.* 1980, **80**, 21.
10. P. A. Bernstein, F. A. Hohorst, M. Eisenburg and D. D. DesMarteau, *Inorg. Chem.* 1971, **10**, 1549.
11. J. W. Emsley, J. Feeney and L. H. Sutcliffe, *High Resolution N.M.R. Spectroscopy*, Vol. 2, p. 881. Pergamon Press, Oxford (1966).
12. G. A. Olah and C. W. McFarland, *Inorg. Chem.* 1972, **2**, 845.
13. K. Schaumberg and C. Deverell, *J. Am. Chem. Soc.* 1968, **90**, 2495.
14. G. A. Olah and R. H. Schlosberg, *J. Am. Chem. Soc.* 1968, **90**, 2726.
15. K. B. Dillon and T. C. Waddington, *J. Chem. Soc.*, (*A*) 1970, 1146.
16. N. Muller, P. C. Lauterbur and J. Goldenson, *J. Am. Chem. Soc.* 1956, **78**, 3557.
17. E. R. Andrew and V. T. Wynn, *Proc. Roy. Soc.*, (*A*) 1966, **291**, 257.
18. M. M. Crutchfield, C. F. Callis, R. R. Irani and G. C. Roth, *Inorg. Chem.* 1962, **1**, 813.
19. M. Shima, K. Hamamoto and S. Utsumi, *Bull. Chem. Soc. Japan* 1960, **33**, 1386.
20. W. Lange and R. Livingston, *J. Am. Chem. Soc.* 1947, **69**, 1073.

³¹P AND ¹⁹⁵Pt NMR SPECTRA OF
[Pt(PPh₃)₂(μ-η²-C₂H₄₋ₙXₙ)] (n = 0 ... 4; X = CN, COOMe)

GIORGIO PELLIZER and MAURO GRAZIANI*

Istituto di Chimica, Università di Trieste, Italy

and

MAURIZIO LENARDA

Facoltà di Chimica Industriale, Università di Venezia, Italy

and

BRIAN T. HEATON*

Chemical Laboratory, University of Kent, Canterbury, CT2 7NH, England

Abstract—³¹P and ¹⁹⁵Pt NMR measurements on compounds of the type [Pt(PPh₃)₂ (μ-η²-C₂H₄₋ₙXₙ)] (n = 0 ...4; X = CN, COOMe) are reported and discussed.

The study of platinum complexes with unsaturated organic molecules has received attention for several years and there is still much activity in trying to distinguish and understand the resulting electronic and steric effects on varying the olefin and/or coordinated ligands. The complexes [Pt(PR₃)₂(μ-η²-ol)] (ol = olefin) have an approximately planar arrangement with a small dihedral angle between the PtC₁C₂ and PtP₁P₂ planes.[1–7]

The most widely accepted description of metal–olefin bonding was proposed by Dewar, Chatt and Duncanson. This model has been a stimulus to much synthetic, structural and mechanistic work. A metallacyclopropane model is also reported, sometimes in contrast with the former. In terms of resulting electronic structure within the M.O. approach the two models are equivalent and complexes with different olefins imply only different amounts of orbital mixing[8] but often the metallacyclopropane model is used as being synonymous with a strong metal–carbon interaction. Recently considerable theoretical effort has been devoted to obtaining detailed theoretical descriptions of the electronic structure of transition metal–olefin complexes.

NMR parameters of single compounds have been taken into consideration to get some insight into the electronic structure of the coordinated olefin. $^2J_{H,H}$ observed in [Pt(PPh₃)₂(C₂H₄)] is much nearer to the value found in cylcopropane than in free ethylene. On the other hand, $^1J_{Pt,C}$ is noticeably lower than one should expect for a σPt–C bond[9], but in this respect it should be noticed that the variation of $^1J_{Pt,C}$ in the series cis-[Pt(PPh₃)₂Et₂] (700 Hz), (PPh₃)₂Pt–CH₂–CH₂–CH₂ (400 Hz), [Pt(PPh₃)₂(C₂H₄)] (200 Hz) [10] parallels the strong decrease in $^1J_{C,C}$ observed in ethane (∼37 Hz) and cyclopropane (∼10 Hz).

The fact that, through olefin substitution it is possible to modulate the complex properties without essential changes in geometry around the platinum atom and with only minor variations in bond distances should simplify the recognition of the main factors responsible for the variations of molecular properties and thus reveal details of the electronic structure in the platinum–olefin region.

Calorimetric measurements have shown that the platinum–olefin bond in [Pt(PPh₃)₂(C₂(CN)₄)] is 156 kJ mole⁻¹ more stable than in [Pt(PPh₃)₂(C₂H₄)][11], although there is little variation in Pt–C distance with the Pt–P distance being slightly longer in the C₂(CN)₄ complex (2.289 Å) than in the C₂H₄ complex (2.267 Å).

*Author to whom correspondence should be addressed.

ESCA measurements have been reported for [Pt(PPh₃)₂(olefin)] (olefin = ethylene, tetrachloroethylene, tetrafluoroethylene, tetracyanoethylene) and for [Ni(PPh₃)₂(olefin)] (olefin = ethylene, acrylonitrile, methylacrylate).[12]

In order further to investigate the effect of olefin substitution in this type of compound we now report ³¹P and ¹⁹⁵Pt NMR measurements on the complexes [Pt(PPh₃)₂(C₂H₄₋ₙXₙ)], (n = 0 ... 4; X = CN and COOMe); ¹H NMR spectra of these complexes have already been reported.[13]

RESULTS AND DISCUSSION

The ³¹P and ¹⁹⁵Pt chemical shifts, together with the values obtained for $^1J_{Pt,P}$, for the cyano and carbomethoxy derivatives are shown in Tables 1 and 2, respectively.

Platinum–phosphorus coupling constants

Various reports have appeared on the ³¹P NMR of [Pt(PPh₃)₂(C₂H₄)] and the reported values of $^1J_{Pt,P}$ range from 3425 to 3694 Hz.[9,4-17] The reason for this rather large variation in $^1J_{Pt,P}$ is not obvious but the value is clearly much higher than is normally found (⩽2000 Hz) for cis-[Pt(PPh₃)₂R₂] (R = alkyl) [18]. Similar high values of $^1J_{Pt,P}$ have been found for phosphorus trans to carbon, which is part of a $\overline{Pt–C–X}$ three-membered ring, X = S,[19,20] X = C,[6,9,16] X = P,[21-23] and high values are also found in related alkyne complexes.[24]

Phosphorus ligands trans to 3-membered rings are thus associated with high values of $^1J_{Pt,P}$. The reason is however still obscure since, although Ph₃PPtPPh₃ bond angles trans to 3-membered rings are usually in the region of 110° giving rise

Table 1. ³¹P and ¹⁹⁵Pt NMR data for [Pt(PPh₃)₂(R₁R₂C = CR₃R₄)] in CDCl₃ at 25°C

R₁	R₂	R₃	R₄	δ_P[a](ppm)	δ_{Pt}[b](ppm)	$^1J_{Pt,P}$(Hz)	$^2J_{P,P}$(Hz)
H	H	H	H	33.8	-555	3718	
H	H	H	CN	29.2	-555	3973	36
				28.7		3476	
H	CN	H	CN	23.5	-487	3705	
H	CN	CN	CN	19.1	-424	3985	0
				20.1		3525	
CN	CN	CN	CN	15.3	-363	3745	

a.- with respect to external H₃PO₄; shifts to low fields positive

b.- with respect to 21.400 MHz at such a magnetic field that the protons in TMS resonate at exactly 100 MHz; shifts to low fields positive

Table 2. ³¹P and ¹⁹⁵Pt NMR data for [Pt(PPh₃)₂(R₁R₂C = CR₃R₄)] in CDCl₃ at 25°C[a]

R₁	R₂	R₃	R₄	δ_P(ppm)	δ_{Pt}(ppm)	$^1J_{Pt,P}$(Hz)	$^2J_{P,P}$(Hz)
H	H	H	H	33.8	-555	3718	
H	H	H	COOMe	27.4	-614	4089	39.7
				28.5		3575	
trans H	COOMe	H	COOMe	23.8	-642	3860	
H	COOMe	COOMe	COOMe	20.1	-616	3854	18.3
				22.5		3802	
COOMe	COOMe	COOMe	COOMe	20.2	-583	3754	

a. See footnotes in Table 1.

to values of $^1J_{Pt,P}$ *ca* 3400–3600 Hz, the complex [Pt(Ph$_2$PN(CHMePh)PPh$_2$)(C$_2$(CF$_3$)$_2$)], which has an extremely small value for PPtP angle (71.3°), still has a high value of $^1J_{Pt,P}$ (2929 Hz).[25]

Similar problems are associated with providing a plausible explanation for the small variation in $^1J_{Pt,P}$ on going from the ethylene to di- and tetra-substituted cyano and carbomethoxy derivatives since it has previously been found that there is a significant decrease in the value of $^1J_{Pt,P}$ *trans* to CH$_2$X in [Pt(PPh$_2$(CH$_2$)$_n$PPh$_2$)(CH$_2$X)Cl] ($n = 2$ and 3; X = H and CN) on going from the methyl to cyanomethyl derivative with a corresponding increase in the value of $^1J_{Pt,P}$ *cis* to CH$_2$X.[26] A bigger variation in $^1J_{Pt,P}$ is found in our unsymmetrically substituted derivatives, [Pt(PPh$_3$)$_2$(C$_2$H$_{4-n}$X$_n$)] ($n = 1$ and 3; X = CN and COOMe), but it is not possible to make an unambiguous assignment, although these results are similar to those found in the acyclic CH$_2$X derivatives. The apparent insensitivity of $^1J_{Pt,P}$ to cyanide or carbomethoxy substitution contrasts with the variations

observed in substituted alkyne derivatives[24,27] and with the strong *trans*-influence on the $^1J_{Pt,P}$ observed in [Pt(dppe)MeX]$^{n+}$ where X = neutral ($n = 1$) or anionic ($n = 0$) ligands.[28] We presently have no explanation for this difference in behaviour between alkyne and olefin complexes containing the Pt(PPh$_3$)$_2$ moiety.

Platinum chemical shifts.

In the CN substituted compounds the platinum is monotonically deshielded by increasing the number of substituents whilst the dependence is less marked and non monotonic in the case of the COOMe substitution. Analogous behaviour is found for CN and COOMe substituted acetylene complexes.[24]

The electronic charge on the metal is expected to decrease monotonically increasing the number of electron withdrawing substituents on the olefin. If the main factor responsible for the ^{195}Pt chemical shift variations within a series of complexes is the
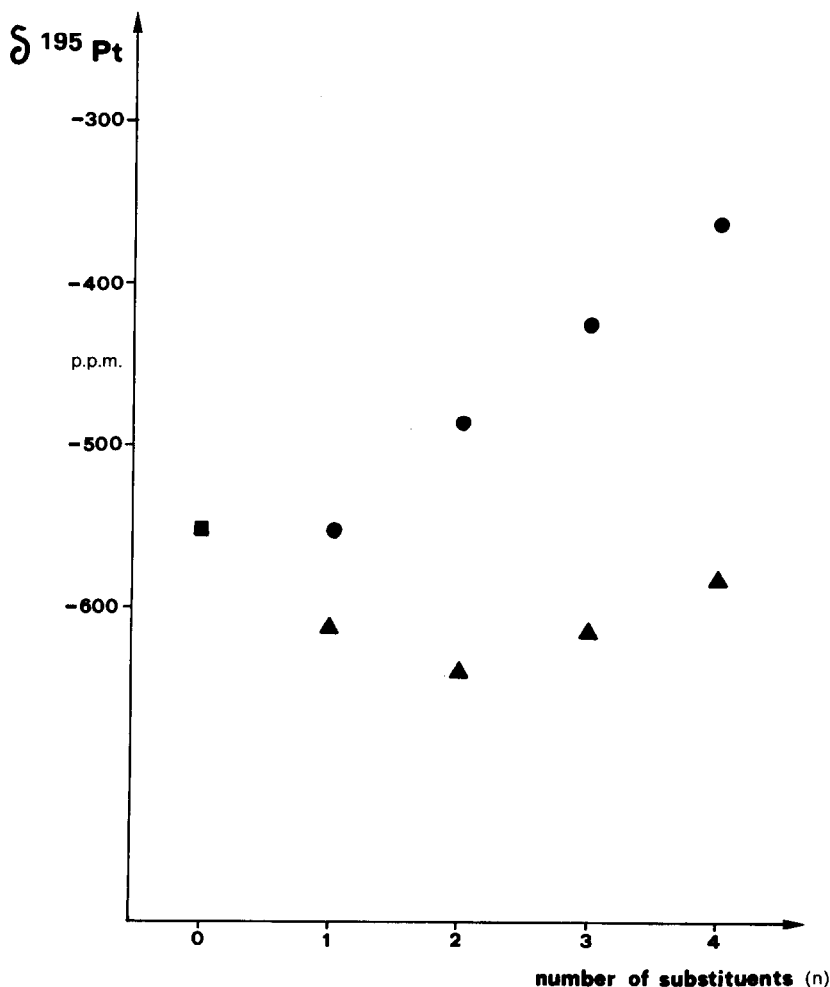
Fig. 1. $\delta(^{195}$Pt) values for Pt(PPH$_3$)$_2$(C$_2$H$_{4-n}$X$_n$) complexes. ●, CN or ▲, COOMe.

charge on the metal it would be difficult to explain the difference in trends observed for CN and COOMe in olefin and acetylene[24] derivatives.

According to the Ramsey formulae the paramagnetic contribution to the nuclear screening constant is connected with the existence of nonvanishing angular momentum mixed matrix elements from low lying monoelectronic states and depends on the value of these matrix elements and on $(\Delta E)^{-1}$.

Some relevant features of the electronic structure of [PtL$_2$(olefin)] compounds have been described by interacting the M.O.s of the L$_2$Pt fragment[8,29] with the suitable π and π^* olefin orbitals.

These descriptions show the existence of a low-lying empty M.O. built up from the b_2 orbital of PtL$_2$ fragment (mainly Ptd_x with some p_x character) and the olefin in antibonding combination. A relevant local paramagnetic contribution to the platinum screening constant can be ascribed to the above situation as the matrix element between this M.O., which has significant metal character, and some of the filled mainly d M.O.s can be rather large and ΔE is small.

Substitution of alkene hydrogens with CN groups decreases the π^* energy in the free olefin[7,8,30,31] and, assuming a constant geometry for the Pt(PPh$_3$)$_2$ fragment,[8] should mainly imply a lowering of the low-lying empty M.O. Thus, like in the alkyne complexes,[24] the experimental trend of platinum chemical shifts in the CN substituted olefins can be explained through a decrease in the relevant ΔE as the number of substituents increases. However, according to this explanation the platinum in the ethylene complex should resonate at higher fields than observed. Perhaps this discrepancy could be ascribed to the neglect of the $P_1\widehat{Pt}P_2$ angles variation.[1-3] An increase of this angle should cause[8] a decrease in energy and p_x character of the b_2 M.O. of the PtL$_2$ fragment and therefore a weakening of the interaction with the olefin π^* M.O. So, due to the particularly high value of $P_1\widehat{Pt}P_2$ angle the ethylene complex can have a low-lying empty M.O. with energy very close to that of the acrylonitrile complex despite the difference of the π^* energies in the two uncoordinated olefins.

Thus olefin substitution affects the energy of the relevant empty M.O. both through a variation of the free alkene empty level and through variation of the $P_1\widehat{Pt}P_2$ angle, the two effects being opposite in the cyano substituted compounds and the former being predominant from acrylonitrile to tetracyanoethylene. Carbomethoxy substitution is expected to cause small variations on the olefin π^* energies. No structural data on the $P_1\widehat{Pt}P_2$ angles are reported but it is possible that the two effects are almost in balance in this series of compounds and this could explain the observed ^{195}Pt shifts trend.

Phosphorus chemical shifts

Acceptable conclusions about phosphorus chemical shifts in metal complexes are usually difficult to establish due to the variety of factors which can play a determinant role.[18] This is even more so for the complexes reported in this paper as more structural parameters are needed to determine meaningful correlations. Nevertheless the increase of phosphorus shielding on increasing the number of olefin substituents observed both for CN and for COOMe and the similarity both in
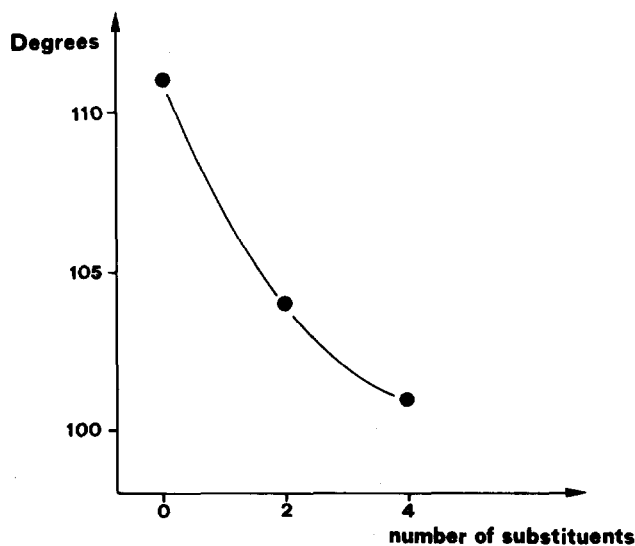
Fig. 2. P_1PtP_2 angle in complexes $Pt(PPh_3)_2(C_2H_{4-n}X_n)$.

trend and in magnitude with the phosphorus chemical shifts of [Pt(PPh$_3$)$_2$(acetylenes)] complexes revealed by inspection of the data reported in Ref. 24 are remarkable. If this behaviour is connected primarily with the local contributions to the screening constant of phosphorus, it should reflect a decrease in paramagnetic contribution as the lone pair electronic charge moves further from phosphorus atom. However, the previously mentioned variation of P$_1$P̂tP$_2$ angles suggests the possibility that the observed trends for phosphorus chemical shifts are linked with changes in geometrical factors and recent reports on platinum chemical shift anisotropy[32] in Pt(II) and Pt(IV) complexes indicate that the magnetic anisotropy of the platinum electron cloud has to be taken into consideration in an explanation of the above trends.

As expected ^{31}P NMR spectra of [Pt(PPh$_3$)$_2$ (olefin)] complexes with asymmetrically substituted olefins confirm that the alkene C–C axis does not lie in a plane perpendicular to the P$_1$PtP$_2$ plane and that no olefin rotation occurs with a speed significant in the NMR time scale.

EXPERIMENTAL

The complexes Pt(PPh$_3$)$_4$ and Pt(PPh$_3$)$_2$(C$_2$H$_4$) were prepared by literature methods.[33] Slightly modified literature methods were used for olefin synthesis,[34] except for commericially available products. All preparations were performed under an atmosphere of nitrogen or argon; work up was done in the air. All solvents were dried and degassed before use.

^{195}Pt and ^{31}P NMR spectra were recorded as described previously.[35,36]

REFERENCES

1. P. T. Cheng and S. C. Nyburg, *Can. J. Chem.* 1972, **50**, 912.
2. G. Bombieri, E. Forsellini, C. Panattoni, R. Graziani and G. Bandoli, *J. Chem. Soc. (A)* 1970, 1313.
3. C. Panattoni, R. Graziani, G. Bandoli, D. A. Clemente and U. Belluco *J. Chem. Soc. (B)* 1970, 371.
4. J. N. Francis, *J. Organometal. Chem.* 1971, **29**, 131.
5. D. R. Russell and P. A. Tucker, *J. Chem. Soc. Dalton* 1976, 2181.
6. R. B. Osborne, H. C. Lexis and J. A. Ibers, *J. Organometal. Chem.* 1981, **208**, 125.
7. S. D. Ittel and J. A. Ibers, *Adv. Organometal. Chem.* 1976, **14**, 33.
8. T. A. Albright, R. Hoffmann J. C. Thibeault and D. L. Thorn, *J. Am. Chem. Soc.* 1979, **101**, 3801.
9. N. C. Harrison, M. Murray, J. L. Spencer and F. G. A. Stone, *J. Chem. Soc. Dalton* 1978, 1337.

10. R. J. Klingler, J. C. Huffmann and J. K. Kochi, *J. Am. Chem. Soc.* 1982, **104**, 2147.
11. A. Evans, C. T. Mortimer and R. J. Puddephatt, *J. Organometal. Chem.* 1974, **72**, 25.
12^a. C. D. Cook, K. Y. Wan, U. Gelius, K. Hamrin, G. Johansson, E. Olsson, H. Siegbahn, C. Nordling and K. Siegbahn, *J. Am. Chem. Soc.* 1971, **93**, 1904; ^{b}C. A. Tolman, *Inorg. Chem.* 1973, **12**, 2770.
13. M. Lenarda, R. Ganzerla, A. Lisini, M. Graziani and T. Boschi, *Transition Met. Chem.* 1981, **6**, 199 and refs therein.
14. B. E. Mann and A. Musco, *J. Chem. Soc. Dalton* 1980, 776.
15. A. Sen and J. Halpern, *Inorg. Chem.* 1980, **19**, 1073.
16. R. G. Muzzo, T. J. McCarthy and G. M. Whitesides, *Inorg. Chem.* 1981, **21**, 1312.
17. R. S. Paonessa and W. C. Taylor, *Organometallics* 1982, **1**, 768.
18. P. S. Pregosin and R. W. Kunz, *^{31}P and ^{13}C NMR of Transition Metal Phosphine Complexes, NMR-16, Basic Principles and Progress* (Edited by P. Diehl, E. Fluck and R. Kosfield). Springer-Verlag, Berlin (1979).
19. J. W. Gosselink, G. Van Koten, A. L. Speck and A. J. M. Duisenberg, *Inorg. Chem.* 1981, **20**, 877.
20. R. Mason and D. W. Meek, *Angew. Chem. Int. Ed. (Engl.)* 1978, **17**, 183.
21. N. Bresciani, M. Calligaris, P. Delise, G. Nardin and L. Randaccio, *J. Am. Chem. Soc.* 1974, **96**, 5642.
22. S. Bresadola, B. Longato and F. Morandini, *J. Organometal. Chem.* 1977, **128**, C5.
23. J. C. T. R. Burckett-St. Laurent, P. B. Hitchcock, H. W. Kroto and J. F. Nixon, *J.C.S. Chem. Comm.* 1981, 1141.
24. Y. Koie, S. Shinoda and Y. Saito, *J. Chem. Soc. Dalton* 1981, 1082.
25. D. H. Farrar and N. C. Payne, *J. Organometal. Chem.* 1981, **220**, 251.
26. R. Ros, R. A. Michelin, R. Bataillard and R. Roulet, *J. Organometal. Chem.* 1977, **139**, 355.
27. G. Butler, C. Eaborn and A. Pidcock, *J. Organometal. Chem.* 1981, **210**, 403.
28. D. W. Meek and T. J. Mazanec, *Acc. Chem. Res.* 1981, **14**, 266.
29. D. M. P. Mingos, *J. Chem. Soc. Dalton* 1977, 602.
30. K. N. Houk and L. L. Munchausen, *J. Am. Chem. Soc.* 1976, **98**, 937.
31. M. A. M. Meester, H. Van Dam, D. J. Stufkens and A. Oskapi, *Inorg. Chim. Acta* 1977, **21**, 251.
32. D. M. Doddrell, P. F. Barron, D. E. Clegg and C. Bowie, *J.C.S. Chem. Comm.* 1982, 575.
33. F. R. Hartley, *The Chemistry of Platinum and Palladium.* Applied Science, London (1973).
34. W. Middleton and V. A. Engelhardt, *J. Am. Chem. Soc.* 1958, **80**, 2788.
35. C. Brown, B. T. Heaton, A. D. C. Towl, P. Chini, A. Fumagalli and G. Longoni, *J. Organometal. Chem.* 1979, **181**, 233.
36. B. T. Heaton, L. Longhetti, L. Garlaschelli and U. Sartorelli, *J. Organometal. Chem.* 1980, **192**, 431.

COMPLEXATION OF THE LANTHANIDES BY PYRAZINECARBOXYLATE

Gyu Shik Kim, Young Inn Kim[+], and Sock Sung Yun[*]

Department of Chemistry, Chungnam National University
Daejeon 300-31, Korea

(Received 2 March 1983)

ABSTRACT

The stability constants of the lanthanide pyrazinecarboxylate
complexes in aqueous solution have been determined in the ionic
medium of 1.0 M $NaClO_4$ at 25°C. The stability of the lanthanide
pyrazinecarboxylates is relatively larger than those of the
monodentate ligands, indicating that the heterocyclic 1-nitrogen
atom of the ligand is involved in the chelate formation.

INTRODUCTION

Relatively little attention has been given to the lanthanide
complexation with the heterocyclic carboxylic acids. The complexation
reactions in aqueous solution of trivalent lanthanide cations by
furoate[1], α-picolinate[2-4], α-picolinate N-oxides[2], and dipicolinate[5]
have been studied. The results[1-4] have shown that the heterocyclic
nitrogen atom of α-picolinate is involved in the chelate ring
structure whereas the heterocyclic ring oxygen of furoate does not.

To study the influence of the heterocyclic ring of the ligands
on the complexation, we have determined the stability constants for
the lanthanide pyrazinecarboxylate complexes in aqueous solution.
The potentiometric titration technique was employed in this study.

EXPERIMENTAL

<u>Chemicals</u>. Stock solutions of the lanthanide perchlorates were
prepared by dissolving the lanthanide oxides (Merck Co) in concentr-
ated $HClO_4$. Standardization of the stock solutions was accomplished
by EDTA titration with xylenol orange indicator in the acetate buffer.
The total ionic strength of the working solution was adjusted to 1.0 M
with $NaClO_4$. The stock solution of pyrazinecarboxylic acid (Aldrich
Chemical Co.) was prepared and standardized using the Acid-Base
titration method. The sodium pyrazinecarboxylate buffer solutions
were prepared in the buffer ratio of 0.4 with the standard NaOH
solution. Deionized water was used for the preparation of all
solutions.

[+]Present address: Department of Chemical Education, Busan National
University, Busan 607-00, Korea.

[*]Author to whom correspondence should be addressed.

. The electrode potential was measured using Fisher
Accumet 520 Digital pH/Ion meter and Fluke 8000-A Digital Multimeter
with the quinhydrone-Pt electrode and the salt bridge. About 200 mg
of quinhydrone (Merck Co) were added for every 15.0 ml of the solution
titrated. The pure platinum wire was cleaned occationally by immersion
in the chromic acid-conc. H_2SO_4 solution.

Procedure. The experimental procedure is essentially same as that
described by Choppin[6]. The measured e.m.f. values were used to
calculate the hydrogen ion concentrations. The titration was performed
in the conditions of $\mu = 1.0$ M $NaClO_4$ and t = $25^\circ C$.

Assuming that only mononuclear complexes are formed, the average
number of the ligands bound per cation, $\bar{n}$, is related to the stability
products, β_n, in the equation[6],

$$\bar{n} = \frac{\sum\limits_{n=1}^{N} n \cdot \beta_n [L]^n}{1 + \sum\limits_{n=1}^{N} \beta_n [L]^n}$$

where $[L]$ is the free ligand concentration. The initial values of β_n
were estimated by the graphical method of Bjerrum[7]. These initial
values of β_n along with $\bar{n}$ and $[L]$ were used for the iterative least
square analysis of above equation to obtain the final values of the
stability products, β_n. The calculations were performed on the IBM
370/1482 computer. All error limits are expressed in 95 % confidence
level.

RESULTS AND DISCUSSION

The dissociation constant of pyrazinecarboxylic acid, $pK_a = 2.76 \pm 0.05$,
was obtained by the titration with the base for the acid solution of 1.0 M
ionic strength at $25^\circ C$.

Figure 1 is the plot of the complex formation functions $\bar{n} = f(p[L])$,
where $p[L] = -\log[L]$, for some typical titrations. The curves approach
to around $\bar{n} = 3$, indicating the possible formation of the fourth complex,
ML_4^-. To check the possibility of the polynuclear complex formation,
the titrations for Sm^{3+} system were made at two different metal ion
concentrations, one at $C_M = 7.808$ mM and the other at $C_M = 3.904$ mM.
Figure 1 shows that these two curves are overlapped and thus no
measurable amount of the polynuclear complexes is formed.

Table 1 lists the values of the log of the stability products
for the some lanthanide(III) pyrazinecarboxylates. The variation in
the stability constants for the lanthanide pyrazinecarboxylates with
increasing atomic number of the cations is similar to those[2] for the
α-picolinate and α-picolinate N-oxide systems. This similarity would
suggest that the pyrazinecarboxylate ligand forms too the chelate
complexes with lanthanide ions.

Figure 1.   Complex formation curves, $\bar{n} = f(p[L])$, for the lanthanide pyrazinecarboxylates; Nd^{3+} ($\blacktriangle$), $Sm^{3+}(1C_m)$ ($\bigcirc$), Sm^{3+} ($\frac{1}{2}C_m$) ($\bullet$), Gd^{3+} ($\times$), Eu^{3+} ($\triangle$).
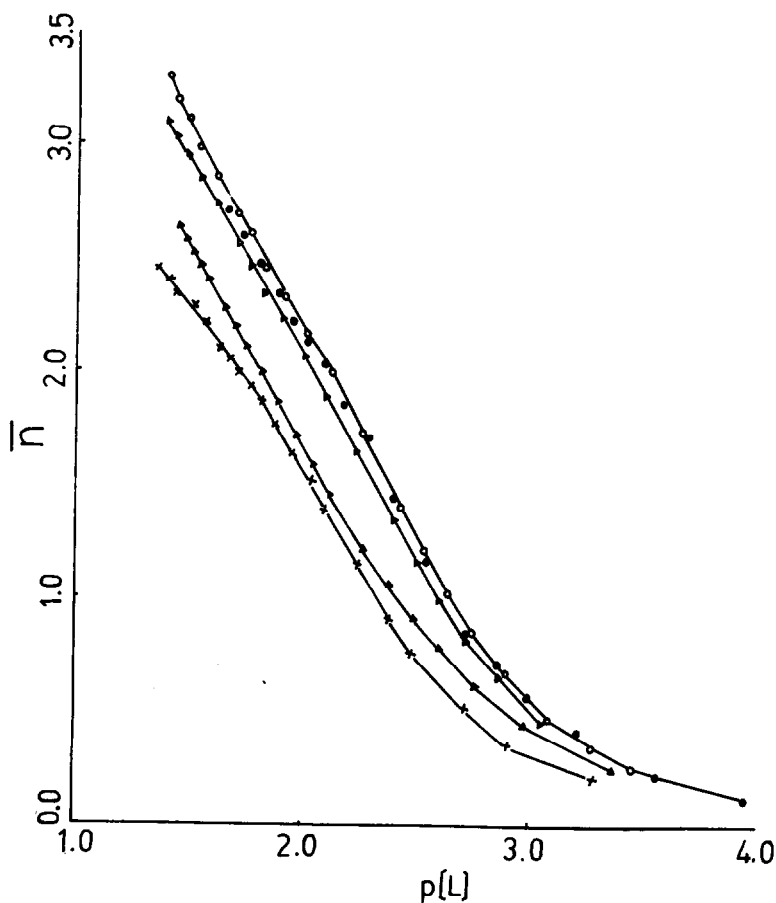
Choppin[4,8] has shown the linear relationship between the stability constants β_1 and the acid constants pK_a of the ligands for a number of lanthanide complexes in aqueous solution. Similarly, we have plotted the value of log β_1 against pK_a of the ligand for some Sm(III) complexes with monocarboxylate ligands in Figure 2. All the values[8,9,10] were

Table 1. Stability products of the lanthanide(III) pyrazine-
          carboxylates, $\mu = 1.0$ M (NaClO$_4$), t = 25.0°C.

M^{3+} ions	Log β_1	Log β_2	Log β_3
La	2.30 ± 0.03	4.09 ± 0.06	5.26 ± 0.08
Nd	2.77 ± 0.08	4.78 ± 0.13	6.27 ± 0.20
Sm	2.85 ± 0.09	5.22 ± 0.15	7.07 ± 0.20
Eu	2.82 ± 0.06	5.14 ± 0.10	6.86 ± 0.11
Gd	2.50 ± 0.06	4.58 ± 0.08	6.08 ± 0.10
Tb	2.77 ± 0.08	4.83 ± 0.14	6.82 ± 0.17
Ho	2.91 ± 0.09	4.91 ± 0.23	6.83 ± 0.26
Er	2.84 ± 0.03	4.95 ± 0.07	6.66 ± 0.11
Lu	2.98 ± 0.05	5.13 ± 0.10	7.07 ± 0.16

measured in 0.10 M NaClO$_4$ ionic medium beside those for the ligands
with the heterocyclic ring, in 1.0 M NaClO$_4$ for the pyrazinecarboxylate,
and 2.0 M NaClO$_4$ for the α-picolinate[2], α-picolinate N-oxide[2], and
furoate[1]. For the α-picolinate, two other values measured in 0.1 M[3]
and 0.5 M[4] NaClO$_4$ are also given.

However, the qualitative comparison of the values plotted in Figure
2 could be made since the stability constant of the complex is generally
increased with decreasing the ionic strength of the solution. It is
expected that the stability constants of the complexes for the hetero-
cyclic ligand systems would be somewhat larger at 0.1 M ionic strength
than the present data. The data for the pyrazinecarboxylate,
-picolinate, and α-picolinate N-oxide deviate above from the linear
correlation of log β_1 vs. pK$_a$ for the monodentate ligand systems,
whereas the furoate data fit the correlation well. This would mean
that these ligands beside the furoate form the chelate complexes with
the lanthanide cations. It has been reported[1] that the ring oxygen of
the furoate is not involved in formation of a chelate ring. Even though
the basicities of 1-nitrogen atom of the heterocyclic ring and 2-
carboxylate of the pyrazinecarboxylate ligand are greatly reduced by
the electron withdrawing effect of 4-nitrogen atom, it seems like that
the pyrazinecarboxylate ligand forms quite stable chelate complexes with
the lanthanide ions as the α-picolinate does. To obtain detailed
information on the complexation of the pyrazinecarboxylate in aqueous
solution, we are conducting a thermodynamic investigation on the
lanthanide pyrazinecarboxylates.

Figure 2. Relationship of log β_1 and pK_a of SmL^{2+} complexes where L = propionate (1), acetate (2), benzoate (3), thioacetate (4), methoxyacetate (5), chloroacetate (6), furoate (7), α-picolinate (μ = 0.1 M (8), 0.5 M (9), and 2.0 M (10)), α-picolinate N-oxide (11), and pyrazinecarboxylate (12).
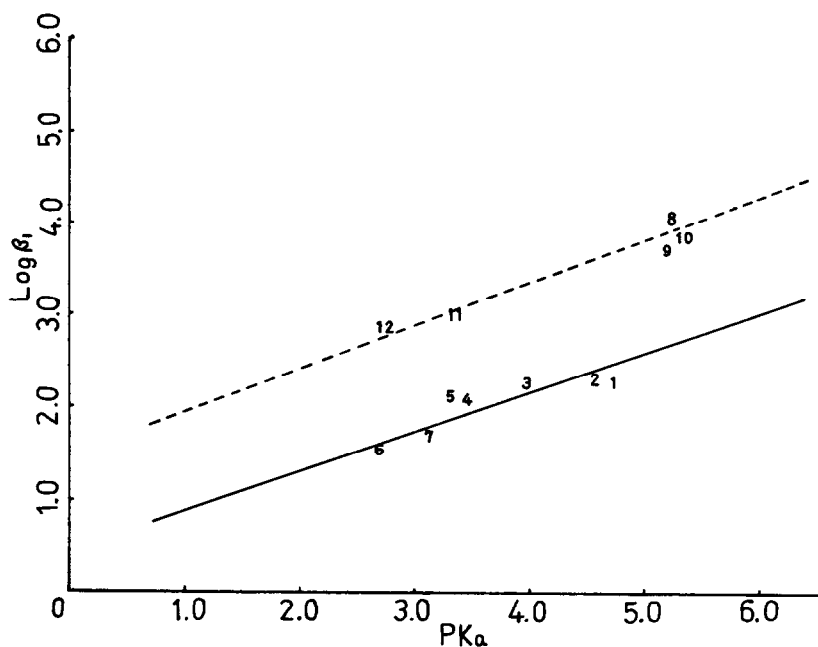
REFERENCES

[1] S. S. Yun, G. R. Choppin, and D. Blakeway, J. Inorg. Nucl. Chem., 1976, 38, 587.

[2] H. Yoneda, G. R. Choppin, J. L. Bear, and A. J. Graffeo, Inorg Chem., 1965, 4, 244.

[3] L. C. Thompson, Inorg. Chem., 1964, 3, 1319.

[4] T. F. Gritmon, M. P. Goedken, and G. R. Choppin, J. Inorg. Nucl Chem., 1977, 39, 2021.

[5] I. Grenthe, J. Am. Chem. Soc., 1961, 83, 360.

[6] G. R. Choppin and J. A. Chopoorian, J. Inorg. Nucl. Chem., 1961, 22, 97.

[7]L. Eeckhaut, F. Verbeek, H. Deelstra, and J. Hoste, *Anal. Chim. Acta.*, 1964, 30, 3690.

[8]G. R. Choppin, P. A. Bertrand, Y. Hasegawa, and E. N. Rizkalla, *Inorg. Chem.*, 1982, 21, 3722.

[9]R. S. Kolat and J. E. Powell, *Inorg. Chem.*, 1962, 1, 293.

[10]J. E. Powell, R. S. Kolat, and C. S. Paul, *Inorg. Chem.*, 1964, 3, 518.

NOTES

Polarographic study of mixed ligand complex stability constants and kinetic parameters of reduction of zinc(II)-tartrate—Thiocyanate system

Km. KRISHNA and S. K. JHA*
Department of Chemistry, Agra College, Agra, India

Abstract—The Zn-tartrate-thiocyanate system has been investigated polarographically and the composition and stability constants of mixed complexes formed have been determined.

Simple Zn-thiocyanate complexes have been reported[1,2] and Matsuda and Ayabe[3] studied the Zn-tartrate system polarographically and have reported the formation of four successive complexes. Since Zn is hexacoordinated when tartrate acts as a bidentate ligand, the maximum possible number of successive complexes can be three and not four as reported by Matsuda and Ayabe. From the survey of literature it is evident that so far no attempt has been made to determine the stability constants and kinetic parameters of reduction of simple Zn-tartrate and mixed Zn-tartrate-thiocyanate complexes. With this aim in view the present study has been undertaken.

EXPERIMENTAL

The studies were done at pH8, constant ionic strength $\mu = 2$ and a temperature of $25 \pm 0.1°C$. The d.m.e had the following characteristics: $m = 4.67$ mg/sec, $t = 2.4$ sec, $m^{2/3}t^{1/6} = 3.176$ mg$^{2/3}$ sec$^{-1/2}$, (in 0.1 M NaNO$_3$, open circuit) and $h_{corr} = 61.8$ cm. Rest of the experimental procedure was the same as reported earlier.[4,5]

RESULTS AND DISCUSSION

The stability constants of simple complexes of Zn-thiocyanate[1] and Zn-tartrate were determined prior to the study of mixed ligand system. Identical conditions were maintained in both the simple and mixed ligand systems. Since results of simple Zn-thiocyanate system have already been reported by the authors these are not being incorporated in the present paper.

1. Zn-*tartrate system*

A series of polarograms were obtained with increasing concentrations of tartrate (0–0.6 M). In each case a well-defined and diffusion-controlled wave was obtained. The slope values indicated that quasi-reversible reduction of Zn(II) becomes irreversible in the presence of ligand. The reversible half-wave potential ($E'_{1/2}$) was calculated by Gellings'[6] method.

The plot of $E'_{1/2}$ vs log [Tart^{2-}] is a smooth curve thereby showing the formation of successive complexes. Deford and Hume's method[7] modified by Irving[8] has been applied for determination of composition and stability constants of the complexes. The plots of $F_j[x]$ vs [x] (Fig. 1) clearly indicates that only three successive complexes are formed. If four complexes were possible $F_3[x]$ should not have been a straight line. Our results are also in accordance with well established fact that a hexacoordinated metal ion can form only three complexes with a bidentate ligand. A 1:4 complex as claimed by Matsuda and Ayabe will require the coordination number of Zn to be eight which is improbable. Three complexes are [Zn(Tart)], [Zn(Tart)$_2$]$^{2-}$ and [Zn(Tart)$_3$]$^{4-}$ with stability constants log $\beta_1 = 2.0$, log $\beta_2 = 3.0$ and log $\beta_3 = 4.3$. The percentage distribution of Zn(II) in its various forms as a function of [Tart^{2-}] is presented in Fig. 2.

---

*Address for all correspondence: Dr. S. K. Jha, 26/226, Balkabasti, Agra-282002, India.
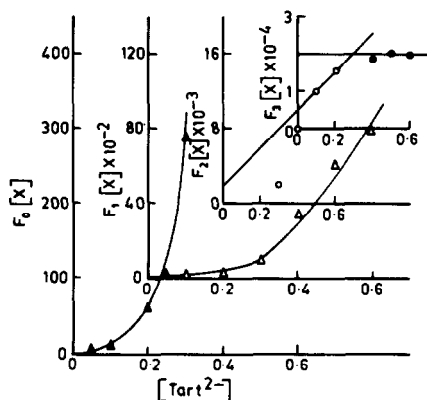
Fig. 1. $F_j[X]$ functions for Zn(II)-tartrate system. $F_0[X]$ ▲; $F_1[X]$ △; $F_2[X]$ ○; $F_3[X]$ ●.
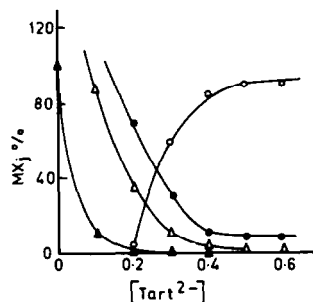
Fig. 2. Percentage distribution of Zn(II) in its various forms as a function of Tart^{2-}. M% ▲; MX$_1$% △; MX$_2$% ●; MX$_3$% ○.

2. Zn-*tartrate-thiocyanate system*

The concentration of tartrate has been varied from 0 to 0.6 M keeping concentration of thiocyanate constant at 0.1 M in one set and at 0.2 M in another. These two sets are referred as series I and Series II respectively in the Table 1. A perusal of slope values shows that the reduction of the mixed complexes are irreversible. Having calculated $E'_{1/2}$ by Gellings' method, the method of Schaap and McMasters[9] has been used to determine the composition and stability constants of the mixed complexes.

F_{ij} vs [Tart^{2-}] plots required to calculate the stability constants are presented in Fig. 3. Two mixed complexes viz. [Zn(Tart)(SCN)$_2$]$^{2-}$ and [Zn(Tart)$_2$(SCN)$_2$]$^{4-}$ with stability constants log $\beta_{12} = 3.65$ and log $\beta_{22} = 6.07$ are formed. The values are reproducible to $\pm 0.5\%$. The negative values[10] of β_{11} and β_{12} rule out the possibility of [Zn(Tart)(SCN)]$^{1-}$ and [Zn(Tart)$_2$(SCN)]$^{3-}$ species.

Assuming that Zn is hexacoordinated and tartrate is acting as a bidentate ligand and aforesaid two species are

Table 1. Polarographic characteristics and kinetic parameter (αn_a) of simple Zn(II)-tartrate and mixed Zn(II)-tart-SCN systems, $\mu = 2(NaNO_3)$; pH8; temperature $25 \pm 0.1°C$; for metal ion in absence of ligands under the experimental condition mentioned; $i_d = 7.48\ \mu A$, $-E_{1/2} = 0.990$ V vs SCE & $-E'_{1/2} = 0.980$ V vs SCE

[Tartrate] M	Simple Zn(II)-Tartrate Complexes				Mixed Zn(II)-Tart-SCN Complexes							
					Series I				Series II			
	i_d μA	$-E_{1/2}$ v S.C.E.	$-E'_{1/2}$ v S.C.E.	αn_a	i_d μA	$-E_{1/2}$ v S.C.E.	$-E'_{1/2}$ v S.C.E.	αn_a	i_d uA	$-E_{1/2}$ v S.C.E.	$-E'_{1/2}$ v S.C.E.	αn_a
0.10	7.32	1.040	1.020	0.738	6.51	1.015	1.010	0.88	6.24	1.050	1.040	0.80
0.20	7.13	1.060	1.030	0.738	6.51	1.040	1.030	0.82	6.07	1.075	1.070	0.98
0.30	6.97	1.080	1.050	0.702	6.33	1.050	1.045	0.95	6.07	1.100	1.040	0.92
0.40	6.80	1.090	1.070	0.632	6.07	1.080	1.070	0.53	6.07	1.105	1.100	0.86
0.50	6.80	1.110	1.080	0.630	6.07	1.090	1.080	0.52	4.92	1.115	1.110	0.62
0.60	6.64	1.130	1.100	0.590	5.80	1.100	1.090	0.68	4.75	1.125	1.120	0.59

ruled out, then the two mixed complexes existing in solution have the equilibria shown in Table 2. The equilibrium constants (log values) are given for each equilibrium. From these values of equilibrium constants (β) the tendency of a ligand to add to a complex and to substitute another ligand may be compared. The relative tendencies to substitute SCN^- and $Tart^{2-}$ can be compared (equilibria 6, 7 and 8). It shows that $Tart^{2-}$ has greater complexation tendency than SCN^-. From log values it is evident that formation of $[Zn(Tart)_2(SCN)_2]^{4-}$ (as per equilibria 7) is favoured over other mixed complexes being formed through equilibrium Nos. 3, 4, 5, 6, 8 and 9.

The stability of the mixed complexes, follows the order:

$$[Zn(Tart)(SCN)_2]^{2-} < [Zn(Tart)_2(SCN)_2]^{4-}.$$
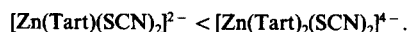
The mixing constants[11] for the reactions:

$$[Zn(Tart)] + [Zn(SCN)_2] \rightleftharpoons [Zn(Tart)(SCN)_2]^{2-} + Zn^{2+} \quad (1)$$

$$\tfrac{1}{2}[Zn(Tart)_2]^{2-} + [Zn(SCN)_2] \rightleftharpoons [ZN(Tart)(SCN)_2]^{2-} + \tfrac{1}{2}Zn^{2+} \quad (2)$$

$$[Zn(Tart)_2]^{2-} + [Zn(SCN)_2] \rightleftharpoons [Zn(Tart)_2(SCN)_2]^{4-} + Zn^{2+} \quad (3)$$
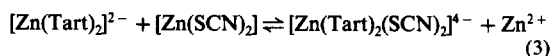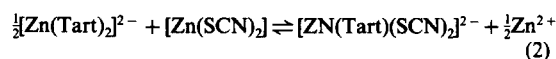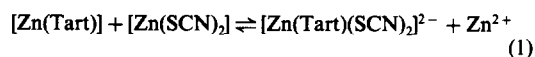
can be given by the relations:

$$K_M(1) = \beta_{12}/(\beta_{10}\ \beta_{02})$$

$$K_M(2) = \beta_{12}/(\beta_{20}^{1/2}\ \beta_{02})$$

$$K_M(3) = \beta_{22}/(\beta_{20}\ \beta_{02}).$$

The $\log K_M$ values for the reactions 1, 2 and 3 work out to be 1.05, 1.55 and 2.47 respectively. The positive values of mixing constants show that the mixed complexes $[Zn(Tart)(SCN)_2]^{2-}$ and $[Zn(Tart)_2(SCN)_2]^{4-}$ are more stable than simple mono and bis complexes.

αn_a values

"n" the total number of electrons involved in the electrode process as determined by the method of DeVries and Kroon[12] gives value close to 2 for both Zn-tartrate and mixed Zn-tart-SCN systems. This is in conformity with the earlier study of Matsuda and Ayabe.[3] When n is two the n_a the number of electrons involved in activation step can either be one or two. However, Meites[13] is of the opinion that only a single electron can be transferred at a time and a value exceeding 1 should merely mean that the successive steps are too nearly simultaneous to be distinguished on the time scale implicit in the polarographic measurement. The values of αn_a (Table 2) are decreasing in indiscrete manner and no two consecutive values have ratio of 2. Thus it can safely be concluded that it is α which is undergoing the change and not n_a.

αn_a values for simple Zn-tartrate system show a regular decrease while values for Zn-tart-SCN do not follow any order. According to Crow[14] in most of the systems studied polarographically a mobile equilibria exists between the various complexes and aquo–metal ion and different number of complexes are present at varying ligand concentration.

$$[Zn(Tart)_0]^{2+} + 2e \rightleftharpoons Zn$$
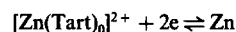
prevails while $[Tart^{2-}] \leq 0.1$ M, whereas at $[Tart^{2-}] > 0.1$ M the equilibrium, $[Zn(Tart)_2]^{2-} + 2e \rightleftharpoons Zn + 2Tart^{2-}$ operates and, therefore, at concentrations reported (Table 1), sequential decrease in αn_a values or in other words decrease in α with increasing ligand concentration signifying that reduction becomes more and more difficult is quite obvious. In case of mixed Zn-tart-

SERIES 1   SERIES 2
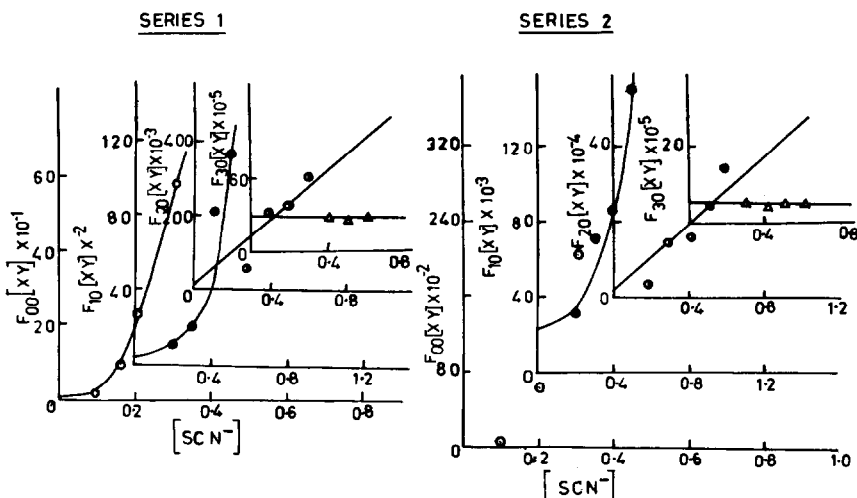
Fig. 3. $F_{ij}[XY)$ functions for Zn(II)-tartrate-thiocyanate system. $F_{00}[XY]$ O; $F_{10}[XY]$ ●; $F_{20}[XY]$ ◑; $F_{30}[XY]$ △.

Table 2. Equilibria involved in two mixed complexes and equilibrium constants β values

Equilibria		log β
1. $Zn^{2+} + Tart^{2-} + 2SCN^-$ ⇌	$[Zn(Tart)(SCN)_2]^{2-}$	3.65
2. $Zn^{2+} + 2Tart^{2-} + 2SCN^-$ ⇌	$[Zn(Tart)_2(SCN)_2]^{4-}$	6.07
3. $[Zn(SCN)_2] + Tart^{2-}$ ⇌	$[Zn(Tart)(SCN)_2]^{2-}$	3.05
4. $[Zn(Tart)] + 2SCN^-$ ⇌	$[Zn(Tart)(SCN)_2]^{2-}$	1.65
5. $[Zn(Tart)_2]^{2-} + 2SCN^-$ ⇌	$[Zn(Tart)_2(SCN)_2]^{4-}$	3.07
6. $[Zn(SCN)_3]^- + Tart^{2-}$ ⇌	$[Zn(Tart)(SCN)_2]^{2-} + SCN^-$	2.65
7. $[Zn(SCN)_3]^- + 2Tart^{2-}$ ⇌	$[Zn(Tart)_2(SCN)_3]^{4-} + SCN^-$	5.07
8. $[Zn(Tart)_3]^{4-} + 2SCN^-$ ⇌	$[Zn(Tart)_2(SCN)_2]^{4-} + Tart^{2-}$	1.77
9. $[Zn(Tart)(SCN)_2]^{2-} + Tart^{2-}$ ⇌	$[Zn(Tart)_2(SCN)_2]^{4-}$	2.42

SCN irregular values of an_a may be due to the facts that (i) probably from the mobile equilibria of various complexes more than one species are reduced at a time or (ii) at various ligand concentrations different species dominate the electrode process or both of these possibilities.

REFERENCES

[1]Km. Krishna, S. K. Jha, M. Singh, *J. Indian Chem. Soc.* 1980, **57**, 19.
[2]R. E. Frank, D. N. Hume, *J. Am. Chem. Soc.* 1953, **75**, 1736.
[3]H. Matsuda, Y. Ayabe, *Z. Elektrochem* 1962, **63**, 469.
[4]Km. Krishna, Anju Varshney, M. Singh, *J. Inorg. Nucl. Chem.* 1981, **43**, 2075.

[5]D. R. Crow, *Polarography of Metal Complexes*, p. 58. Academic Press, New York, (1969).
[6]P. J. Gellings, *Z. Elecktrochem, Ber. Bunsenges Phys. Chem.* 1962, **66**, 477, 481, 799; 1963, **67**, 167.
[7]D. D. DeFord, D. N. Hume, *J. Am. Chem. Soc.* 1951, **73**, 5321.
[8]H. Irving, *Advances in Polarography* (Edited by I. S. Longmuir), Vol. 1, p. 42. Pergamon Press, Oxford (1960).
[9]W. B. Schaap, D. L. McMasters, *J. Am. Chem. Soc.* 1961, **83**, 4699.
[10]R. G. Bidkar, D. G. Dhuley, R. A. Bhobe, *Current Sci.* 1976, **45**, 5.
[11]S. L. Jain, J. Kishan, R. C. Kapoor, *Indian J. Chem.* 1979, **18A**, 133.
[12]T. DeVries, J. L. Kroon, *J. Am. Chem. Soc.* 1953, **75**, 2484.
[13]L. Meites, *Polarographic Techniques*, p. 246. Interscience New York (1965).
[14]D. R. Crow *Polarography of Metal Complexes*, p. 58. Academic Press, New York (1969).

Synthesis and studies on dichloro iodo triphenylphosphine oxide nickel(III)

K. P. SARMA and RAJ K. PODDAR*

Department of Chemistry, North-Eastern Hill University, Bijni House, Shillong 793 003, India

Abstract—A new compound of nickel(III), [Ni(OPPh$_3$)Cl$_2$I] has been prepared by the action of nitrosyl chloride or chlorine gas on [Ni(PPh$_3$)$_2$I$_2$]. Various physical studies of the compound are reported.

During the investigation on the reactions of [Ni(PPh$_3$)$_2$X$_2$] (X = Cl, Br, I, NCS and NO$_3$) with nitrosyl chloride, it was found that the nickel(II) complexes gave dimeric species, viz. [Ni(PPh$_3$)XCl]$_2$ (X = Cl, Br, NCS, NO$_3$) and the oxidation of the liberated triphenylphosphine molecule to triphenylphosphine oxide.[1] However, reaction of [Ni(PPh$_3$)$_2$I$_2$] with nitrosyl chloride resulted in the oxidation of nickel(II) to nickel(III) with formation of [Ni(OPPh$_3$)Cl$_2$I]. In this work, the synthesis and studies of the complex [Ni(OPPh$_3$)Cl$_2$I] are reported.

EXPERIMENTAL

Diiodo bistriphenylphosphine nickel(II) was prepared according to the method of Venanzi.[2]

Preparation of dichloro iodo triphenylphosphine oxide nickel(III)

A suspension of powdered [Ni(PPh$_3$)$_2$I$_2$] (1 g) was taken in dry cyclohexane (50 cm^3) and nitrosyl chloride was bubbled slowly through the suspension for about 20 min while stirring the mixture. Slowly the suspended material went into solution. After discontinuing the bubbling of the gas, the mixture was stirred at room temperature for about 8 hr, when yellow compound (m.p. 100–105°d) separated out. During the reaction, colour of the solution changed from dark reddish brown to light red through green. The compound was filtered out and washed several times with dry diethyl ether and dried under vacuum. It was analysed for [Ni(OPPh$_3$)ICl$_2$]: Found: Ni, 10.95; Cl, 13.57; I, 24.12; P, 5.80; C, 40.68; H, 3.12; [N: (OPPh$_3$)ICl$_2$] requires: Ni, 10.97; Cl, 13.27; I, 23.74; P, 5.79; C, 40.37; H, 2.80%. The same compound was also obtained by using chlorine gas instead of nitrosyl chloride.

The mother liquor, after the separation of the compound, on concentration yielded triphenylphosphine oxide, characterised by m.p. (157°C) and IR spectrum ($v_{P=O}$ at 1185 cm^{-1}).

The total halide content in the compound was obtained by decomposing the compound with KNO$_3$, KOH mixture, acidifying with dil. nitric acid to make the solution just acidic and then precipitating as silver halide using silver nitrate. Chloride estimation was done by decomposing the compound with dilute nitric acid and heating for about 30 min to oxidise iodide to iodine and get liberated and then precipitating silver halide by silver nitrate. Iodide content was obtained by subtracting chloride content from the total halide content. For phosphorus estimation, the compound was decomposed with a mixture of sugar, KNO$_3$ and Na$_2$O$_2$ in a Parr–Bomb, extracted with water, acidified with slight excess of dilute sulphuric acid, heated to dryness, extracted again with water, filtered and estimated it as phosphate using ammonium molybdate.

IR spectra were recorded on Perkin–Elmer 297 in the range 4000–600 cm^{-1} and on Polytec FIR 30 spectrophotometer in the range 600–100 cm^{-1}. The UV-visible spectral studies were carried out on Beckman 26 spec-

trophotometer. The ESR spectrum was recorded at liquid nitrogen temperature using Varian E 104 spectrophotometer. The magnetic measurements were made by the Gouy method. Conductivity measurements in nitrobenzene was made on an Elico type CM 82 conductivity bridge. The oxidation state of nickel in the compound was determined iodometrically by the reduction of a known amount of the compound with aqueous potassium iodide solution, followed by titration of the liberated iodine with standard sodium thiosulphate solution.

RESULTS AND DISCUSSION

The compound was characterised by the elemental analyses and the physical studies mentioned above. The compound has the empirical formula [Ni(OPPh$_3$)Cl$_2$I]. The magnetic moment of the complex at room temperature was found to be 1.68 B.M., characteristic of nickel(III) having one unpaired electron. The conductivity measurements in acetonitrile and nitrobenzene solvents did not show any conductance, confirming that all the anions are coordinated to the metal ion.

The presence of triphenylphosphine oxide was confirmed by the infrared studies. A strong band at 1180 cm^{-1} could be assigned to $v_{P=O}$ of the triphenylphosphine oxide molecule[3] coordinated with the metal. After decomposing the complex with water, the liberated ligand was isolated and characterised as triphenylphosphine oxide (m.p. and IR spectrum). The IR spectrum in the region 600–100 cm^{-1} showed the presence of bands at 548, 520, 452, 365, 308 and 225 cm^{-1}. The bands at 548 and 520 cm^{-1} are due to triphenylphosphine oxide. The band at 452 cm^{-1} could be assigned to v_{Ni-O}, at 365 and 308 cm^{-1} to v_{Ni-Cl} (terminal) and at 225 cm^{-1} to v_{Ni-I} (terminal). These assignments are made in accordance with that of isotopically labelled nickel complexes, viz. [Ni(PPh$_3$)$_2$X$_2$] (X = Cl, Br, I).[4]

The ESR spectrum of a powdered sample at liquid nitrogen temperature showed two absorption lines from which the g-values calculated are, $g_\perp = 2.085$ and $g_\parallel = 2.430$. If we choose the z coordinate such that it bisects the ClNiCl angle and x and y coordinates perpendicular to the above, then a possible configuration is $(d_{x^2-y^2})^2 (d_{z^2})^2 (d_{xz})^2 (d_{yz})^\pm$. Following the detailed treatment of d^7 system with the above configuration,[5,6] we can predict $g_{zz} > g_{yy}$, which is observed experimentally too. Due to the lack of the availability of all the d–d-transitions, it is not possible to interpret the ESR data quantitatively, at present. On the basis of the observed g-values, we can make a tentative assignment of 25,000 cm^{-1} ($\epsilon = 70$) band to $d_{x^2-y^2} \rightarrow d_{yz}$ and 16,000 cm^{-1} ($\epsilon = 13$) band to $d_{z^2} \rightarrow d_{yz}$ transitions. Thus, the compound has a tetrahedral geometry with tetragonal distortions.

The complex, on treatment with triphenylphosphine in acetic acid resulted a dark brown crystalline compound with probable composition [Ni(PPh$_3$)$_2$ClI], with nickel in +2 oxidation state. The nickel(III) complex acts as a catalyst in the oxidation of triphenylphosphine to triphenylphosphine oxide. The catalytic oxidation reaction using the complex and triphenylphosphine in varying

---

*Author to whom correspondence should be addressed.

proportions (up to 1:25) in cyclohexane or nitrobenzene gave quantitative yield of the oxide. The method of reaction and characterization is similar to the one reported earlier.[7] The complex is found to oxidise cyclohexanol to cyclohenanone in pyridine solvent. More studies concerning the oxidising property of the complex are being carried out.

REFERENCES

1. K. P. Sarma and Raj K. Poddar, Trans. Met. Chem. (in press).
2. L. M. Venanzi, J. Chem. Soc. 1958, 719.
3. F. A. Cotton, R. D. Barnes and E. Bannister, J. Chem. Soc. 1960, 2199.
4. C. Udovich, J. Takemoto and K. Nakamoto, J. Coord. Chem. 1971, 1, 89.
5. A. H. Maki, N. Edelstein, A. Davison and R. H. Holm, J. Am. Chem. Soc. 1964, 86, 4580.
6. B. R. McGarvey, Can. J. Chem. 1975, 53, 2498.
7. R. K. Poddar and U. Agarwala, Inorg. Nucl. Chem. Lett. 1973, 9, 785.

On the nature of the peroxoborate ion in solution

CHRISTOPHER J. ADAMS* and IAN E. CLARK
Unilever Research Laboratory, Port Sunlight, Bebington, Wirral, Merseyside, L63 3JW, England

Abstract—The Raman spectra of alkaline lithium metaborate solutions containing H_2O_2 reveal lines attributable to a peroxoborate anion, $B(OH)_3OOH^-$, in equilibrium with $B(OH)_4^-$ and H_2O_2. There is no evidence for the formation of peroxoboric acids at low pH.

Sodium perborate is in widespread use as a bleaching agent in fabric washing products, but the chemistry of perborates has not been much investigated. There has recently been a determination of the crystal structure of the commercial material "sodium perborate tetrahydrate", showing that it contains dinuclear anions with double peroxo bridges (I),[1] and is therefore better formulated as $Na_2[B_2(O_2)_2(OH)_4].6H_2O$.

(I)

However, the nature of peroxoborate species in solution has remained elusive. Potentiometric titrations[2] and polarographic studies[3] suggest that alkaline perborate solutions display an equilibrium involving a hydroperoxotrihydroxoborate anion (II).

$$B(OH)_4^- + H_2O_2 \rightleftharpoons B(OH)_3(OOH)^- + H_2O$$

(II)

giving $K = \dfrac{[B(OH)_3(OOH)^-]}{[B(OH)_4^-][H_2O_2]}$

as ca. $25 \, mol^{-1} \, dm^3$ at 25°C. Other potentiometric investigations have been interpreted in terms of the formation of higher perborates in alkaline solution containing two or more peroxide groups for each boron atom[4]. In acid solu-

tions, the formation of peroxoboric acids has been postulated to explain the drop in pH when hydrogen peroxide is added to boric acid solutions[2].

We set out to use Raman spectroscopy to identify and characterise the peroxoboron species in aqueous solution and to monitor changes in the position of equilibrium with changes in solution composition. It soon became clear that solution concentrations of about 1 mol dm^{-3} were needed to facilitate the observation of spectra, and so the lithium borate/H_2O_2 system was chosen for investigation.

EXPERIMENTAL

Preparation of materials

Lithium metaborate, $LiB(OH)_4.6H_2O$, and sodium perborate tetrahydrate, $Na_2[B_2(O_2)_2(OH)_4].6H_2O$ were prepared from AnalaR reagents. Hydrogen peroxide, Na_2H_2EDTA, boric acid, and hydrochloric acid (all AR Grade) and lithium hydroxide (GPR) were used without further purification.

Preparation of solutions

The solutions were made up by dissolving lithium metaborate in the required concentration of hydrogen peroxide, and adding HCl or LiOH to adjust the pH. All the solutions contained EDTA (1×10^{-4} mol dm^{-3}) to inhibit the metal-catalysed decomposition of H_2O_2. The pH and H_2O_2 content were checked before and after measurement of spectra.

Raman spectra

The filtered solutions were contained in a quartz cell which had been cleaned with aqua regia. Sodium perborate was finely ground and packed into a glass capillary. The spectra were excited at 5145 Å by an Ar^+ laser and were recorded at room temperature (23 ± 1°C) using a Spex Ramalog 5M spectrometer.

RESULTS AND DISCUSSION

The Raman shifts and relative intensities measured in our experiments are listed in Table 1, and partial representative

---

*Author to whom correspondence should be addressed.

proportions (up to 1:25) in cyclohexane or nitrobenzene gave quantitative yield of the oxide. The method of reaction and characterization is similar to the one reported earlier.[7] The complex is found to oxidise cyclohexanol to cyclohenanone in pyridine solvent. More studies concerning the oxidising property of the complex are being carried out.

REFERENCES

1. K. P. Sarma and Raj K. Poddar, *Trans. Met. Chem.* (in press).
2. L. M. Venanzi, *J. Chem. Soc.* 1958, 719.
3. F. A. Cotton, R. D. Barnes and E. Bannister, *J. Chem. Soc.* 1960, 2199.
4. C. Udovich, J. Takemoto and K. Nakamoto, *J. Coord. Chem.* 1971, 1, 89.
5. A. H. Maki, N. Edelstein, A. Davison and R. H. Holm, *J. Am. Chem. Soc.* 1964, 86, 4580.
6. B. R. McGarvey, *Can. J. Chem.* 1975, 53, 2498.
7. R. K. Poddar and U. Agarwala, *Inorg. Nucl. Chem. Lett.* 1973, 9, 785.

On the nature of the peroxoborate ion in solution

CHRISTOPHER J. ADAMS* and IAN E. CLARK
Unilever Research Laboratory, Port Sunlight, Bebington, Wirral, Merseyside, L63 3JW, England

Abstract—The Raman spectra of alkaline lithium metaborate solutions containing H_2O_2 reveal lines attributable to a peroxoborate anion, $B(OH)_3OOH^-$, in equilibrium with $B(OH)_4^-$ and H_2O_2. There is no evidence for the formation of peroxoboric acids at low pH.

Sodium perborate is in widespread use as a bleaching agent in fabric washing products, but the chemistry of perborates has not been much investigated. There has recently been a determination of the crystal structure of the commercial material "sodium perborate tetrahydrate", showing that it contains dinuclear anions with double peroxo bridges (I),[1] and is therefore better formulated as $Na_2[B_2(O_2)_2(OH)_4].6H_2O$.

(I)

However, the nature of peroxoborate species in solution has remained elusive. Potentiometric titrations[2] and polarographic studies[3] suggest that alkaline perborate solutions display an equilibrium involving a hydroperoxotrihydroxoborate anion (II).

$$B(OH)_4^- + H_2O_2 \rightleftharpoons B(OH)_3(OOH)^- + H_2O$$

(II)

giving $K = \dfrac{[B(OH)_3(OOH)^-]}{[B(OH)_4^-][H_2O_2]}$

as *ca.* $25\,mol^{-1}\,dm^3$ at 25°C. Other potentiometric investigations have been interpreted in terms of the formation of higher perborates in alkaline solution containing two or more peroxide groups for each boron atom[4]. In acid solu-

tions, the formation of peroxoboric acids has been postulated to explain the drop in pH when hydrogen peroxide is added to boric acid solutions[2].

We set out to use Raman spectroscopy to identify and characterise the peroxoboron species in aqueous solution and to monitor changes in the position of equilibrium with changes in solution composition. It soon became clear that solution concentrations of about 1 mol dm^{-3} were needed to facilitate the observation of spectra, and so the lithium borate/H_2O_2 system was chosen for investigation.

EXPERIMENTAL

Preparation of materials

Lithium metaborate, $LiB(OH)_4.6H_2O$, and sodium perborate tetrahydrate, $Na_2[B_2(O_2)_2(OH)_4].6H_2O$ were prepared from AnalaR reagents. Hydrogen peroxide, Na_2H_2EDTA, boric acid, and hydrochloric acid (all AR Grade) and lithium hydroxide (GPR) were used without further purification.

Preparation of solutions

The solutions were made up by dissolving lithium metaborate in the required concentration of hydrogen peroxide, and adding HCl or LiOH to adjust the pH. All the solutions contained EDTA (1×10^{-4} mol dm^{-3}) to inhibit the metal-catalysed decomposition of H_2O_2. The pH and H_2O_2 content were checked before and after measurement of spectra.

Raman spectra

The filtered solutions were contained in a quartz cell which had been cleaned with aqua regia. Sodium perborate was finely ground and packed into a glass capillary. The spectra were excited at 5145 Å by an Ar^+ laser and were recorded at room temperature (23 ± 1°C) using a Spex Ramalog 5M spectrometer.

RESULTS AND DISCUSSION

The Raman shifts and relative intensities measured in our experiments are listed in Table 1, and partial representative

---

*Author to whom correspondence should be addressed.

Table 1. Raman spectra of alkaline perborate solutions

	A	B	C	D	E	F	G	H	I	
Solution Composition										
Borate, mol dm^{-3}	1.0	1.0	1.0	1.0	1.0	1.0	0.5	1.0	0.0	
Peroxide mol dm^{-3}	1.0	1.0	1.0	1.0	2.0	0.5	0.5	0	1.0	
pH	8.5	9.2	10.1	11.1	10.1	10.0	12.5	10.5	11.0	
Counterion	Li$^+$	Li$^+$	Li$^+$	Li$^+$	Li$^+$	Li$^+$	Li$^+$	Na$^+$	Na$^+$	
Spectra[a] and Assignments										
Peroxoborate	1250(2)	1250(2)	1250(4)	1250(1)	1250(3)	1250(2)				?dp
Peroxoborate	960(7)	960(8)	960(16)	960(12)	960(12)	960(9)				dp
B(OH)$_4^-$							945(5)			dp
Peroxoborate	895(66)	895(91)	887(100)	894(100)	895(69)	895(66)	900(90)			p
H$_2$O$_2$	877(100)	877(100)	887(100)	878(88)	875(100)	875(77)	880(32)		875(60)	p
OOH$^-$				855(27)			849(100)		850(40)	p
B(OH)$_4^-$				741(73)		743(75)		745(100)		p
Peroxoborate	733(38)	737(47)	737(60)	735(59)	734(38)	725(45)				p
Peroxoborate	715(25)	715(36)	716(38)	715(41)	715(28)	725(45)				p
B(OH)$_4^-$							580(9)			dp

a. Reported as Raman shift in cm^{-1} (Relative Intensity).

spectra are shown in Fig. 1. Our Raman shifts for Na$_2$[B$_2$(O$_2$)$_2$(OH$_4$)].6H$_2$O agree well with an earlier report[5], and so are not given in full detail.

Alkaline solutions

The first set of experiments to be discussed used solutions A–F with lithium metaborate concentrations 1.0 mol dm^{-3} and various pH and [H$_2$O$_2$] values. The Raman spectra show two broad features, at *ca.* 880 and 740 cm^{-1}, but the peak positions and the line shapes change as the solution composition changes. The spectra can be interpreted in terms of the known Raman lines of B(OH)$_4^-$, H$_2$O$_2$, B(OH)$_3$ and OOH$^-$, together with a set of lines (at 1250, 950, 890, 735 and 715 cm^{-1}) which cannot be attributed to any known polyborate[6]. The intensities of the new lines all respond in the same way to changes in solution composition, suggesting that they can all be attributed to a single peroxoborate anion present in the solutions.

Increasing the ratio of peroxide:borate much above 1 : 1 gives only the new set of Raman lines together with H$_2$O$_2$ and we are thus justified in formulating the anion as a monoperoxoborate. The spectrum of the anion in solution, however, is different from that of the solid sodium perborate tetrahydrate and so the centrosymmetric binuclear species (I) cannot be the anion in solution. (The most telling evidence is the absence of a strong polarised line at 960 cm^{-1}, associated in the solid with the *gerade* combination of the B(OH)$_2$ antisymmetric stretches.) By default, then, the spectra must be assigned to the B(OH)$_3$OOH$^-$ anion proposed by potentiometric titration.

The Raman line at 890 cm^{-1} is clearly a fundamental of the O–O stretching mode; the value of 890 cm^{-1} compares with that found for XOOH groups (e.g. 886 cm^{-1} for H$_2$SO$_5$)[7] rather than XOO$^-$ groups (849 cm^{-1} in OOH$^-$). The lines at 735 cm^{-1} and 950 cm^{-1} are respectively the symmetric and antisymmetric stretches of the B(OH)$_3$ unit, while the B–OOH stretch occurs at 715 cm^{-1} (close to the B–F stretch in [B(OH)$_3$F]$^-$)[6]. Finally the weak feature at 1250 cm^{-1} is assignable to the BOOH deformation mode.

The spectra show that peroxoborate formation reaches a maximum at pH *ca.* 10.2 but significant amounts are present between pH 8.5 and 11.1. At higher pH, hydrogen peroxide is removed as OOH$^-$ (solution D), and at lower pH the tetrahydroxoborate anion is converted into boric acid. In all
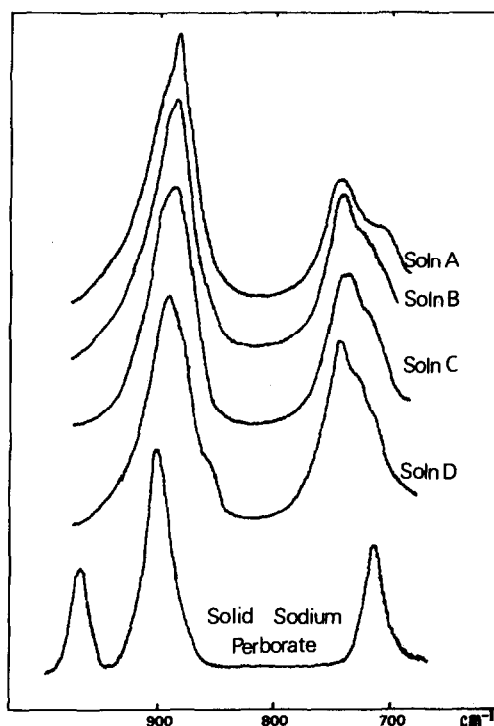
Fig. 1. Raman spectra of alkaline perborate solutions.

cases the proportion of peroxoborate falls as the concentration falls. A quantitative estimate of the equilibrium constant is impossible because of the overlap of the Raman lines, but the observations are consistent with a value of 20 mol^{-1} dm^3 as suggested by potentiometric titration.

Acid solutions

Solutions of boric acid with H$_2$O$_2$ (both 1 mol dm^{-3}) show only one intense Raman line at 875 cm^{-1}. This sharp line must include contributions from the symmetric BO$_3$ stretch of B(OH)$_3$ and the O–O stretch of H$_2$O$_2$, which

coincide at this frequency. There is thus no evidence for the formation of peroxoboric acids, and some other explanation must be found for the large pH changes noted by Edwards.[2]

SUMMARY

The Raman spectra of lithium metaborate–hydrogen peroxide solutions are consistent with the equilibrium $B(OH)_4^- + H_2O \rightleftharpoons B(OH)_3OOH^- + H_2O$ $(K \simeq 20\,mol^{-1}\,dm^3)$. There is no evidence for the formation of peroxoboric acids at low pH.

REFERENCES

[1] M. A. Carrondo and A. C. Skapsi, *Acta. Cryst.* 1978, **B34**, 3551.
[2] J. O. Edwards, *J. Am. Chem. Soc.* 1953, **75**, 6154.
[3] D. M. Kern, *J. Am. Chem. Soc.* 1955, **77**, 5458.
[4] P. J. Antikainen, *Suomen Kemistilehti* 1955, **28B**, 159.
[5] E. Koberstein, H. G. Bachman, H. Gebaver, G. Köhler, E. Lakatos and G. Nonnemacker, *Z. Anorg. Allg. Chem.* 1970, **374**, 125.
[6] L. Maya, *Inorg. Chem.* 1976, **15**, 2179; M. Maeda, T. Hirao, M. Kotaka and H. Kakihana *J. Inorg. Nucl. Chem.* 1979, **41**, 1217.
[7] J. L. Arnau and P. A. Giguere, *Can. J. Chem.* 1970, **48**, 3903.

Taft substituent constants for arene chromium dicarbonyl phosphine and arsine derivatives

THOMAS E. BITTERWOLF
Department of Chemistry, U.S. Naval Academy, Annapolis, MD 21402, U.S.A.

Abstract—A series of biphenyl, meta- and para-fluorobiphenyl complexes of chromiumtricarbonyl, chromiumdicarbonyltriphenylphosphine and chromiumdicarbonyltriphenylarsine have been prepared and their spectral and physical properties recorded. Taft substituent constants have been calculated for the coordinated arenes and the consequences of substituting a Group V ligand for a carbonyl are discussed.

For organometallic complexes, a comparison of the substituent constants of free and coordinated organic groups provides a quantitative measure of the electronic changes which occur upon complexation. For example, substituent constants for the arenechromiumtricarbonyl group have been measured by several groups using a variety of techniques.[1–6] The values of these substituent constants generally support the interpretation that complexation of a chromiumtricarbonyl to a phenyl group results in a significant increase in the inductive electron withdrawal by the coordinated phenyl and reduction of the resonance electron donation to a fraction of that of an uncoordinated phenyl.

As a consequence of our recent synthesis of a series of biphenylbis(chromiumdicarbonyl)-μ-diphosphine dimers, we have become interested in the changes in electronic character which occur when a carbonyl is removed and replaced by a Group V ligand. In order to determine these effects, we have measured the Taft substituent constants of arenechromiumdicarbonyl derivatives of triphenylphosphine and triphenylarsine.

RESULTS AND DISCUSSION

A set of nine compounds were prepared and examined in the present work. Biphenylchromiumtricarbonyl and its *m*- and *p*-fluorobiphenyl derivatives were prepared by the method of Top and Jaouen[7] and had properties consistent with the physical and spectral properties reported in the literature. Triphenylphosphine and triphenylarsine were introduced to the chromium by UV photolysis in benzene.[8] After recrystallization from petroleum ether, the compounds were examined for purity by HPLC using petroleum ether:tetrahydrofuran (3:2) as an elutant on a silica gel column. Elemental analyses and/or melting points of the compounds are presented in Table 1. UV-visible and IR spectra were recorded for all compounds and the major spectral features are summarized in Table 2. ^1H, ^{19}F and ^{31}P NMR results are also included in Table 2.

σ_I and σ_R^0 constants were calculated from the ^{19}F chemical shifts of *m*- and *p*-fluorobiphenyl derivatives relative to internal fluorobenzene using the equations presented by Taft *et al.*[9] These substituent constants are summarized in Table 3 for both benzene and chloroform as solvents.

Comparison of the UV-visible and IR spectra for compounds 1–3 indicates that for these compounds the electronic and vibrational changes brought about by the phosphine and arsine ligands are very similar. Introduction of a fluorine onto the uncoordinated ring of a biphenyl has little effect on either the electronic or vibrational spectra. ^{31}P NMR of the biphenyl and fluorobiphenylchromiumdicarbonyltriphenylphosphine compounds show only a small shift of the phosphorus resonance with introduction of the fluorine.

Gubin *et al.*[4] obtained Taft substituent constants for the phenylchromiumtricarbonyl group. These workers used a slightly modified form of the Taft equations, but obtained substituent constants in close agreement with those found in the present work. These constants show that coordination of a phenyl ring by a chromiumtricarbonyl enhances the electron withdrawing ability of the phenyl ring and sharply reduces the resonance contribution of the phenyl. The

coincide at this frequency. There is thus no evidence for the formation of peroxoboric acids, and some other explanation must be found for the large pH changes noted by Edwards.[2]

SUMMARY

The Raman spectra of lithium metaborate–hydrogen peroxide solutions are consistent with the equilibrium $B(OH)_4^- + H_2O \rightleftharpoons B(OH)_3OOH^- + H_2O$ $(K \simeq 20 \, mol^{-1} \, dm^3)$. There is no evidence for the formation of peroxoboric acids at low pH.

REFERENCES

[1] M. A. Carrondo and A. C. Skapsi, *Acta. Cryst.* 1978, **B34**, 3551.
[2] J. O. Edwards, *J. Am. Chem. Soc.* 1953, **75**, 6154.
[3] D. M. Kern, *J. Am. Chem. Soc.* 1955, **77**, 5458.
[4] P. J. Antikainen, *Suomen Kemistilehti* 1955, **28B**, 159.
[5] E. Koberstein, H. G. Bachman, H. Gebaver, G. Köhler, E. Lakatos and G. Nonnemacker, *Z. Anorg. Allg. Chem.* 1970, **374**, 125.
[6] L. Maya, *Inorg. Chem.* 1976, **15**, 2179; M. Maeda, T. Hirao, M. Kotaka and H. Kakihana *J. Inorg. Nucl. Chem.* 1979, **41**, 1217.
[7] J. L. Arnau and P. A. Giguere, *Can. J. Chem.* 1970, **48**, 3903.

Taft substituent constants for arene chromium dicarbonyl phosphine and arsine derivatives

THOMAS E. BITTERWOLF
Department of Chemistry, U.S. Naval Academy, Annapolis, MD 21402, U.S.A.

Abstract—A series of biphenyl, meta- and para-fluorobiphenyl complexes of chromiumtricarbonyl, chromiumdicarbonyltriphenylphosphine and chromiumdicarbonyltriphenylarsine have been prepared and their spectral and physical properties recorded. Taft substituent constants have been calculated for the coordinated arenes and the consequences of substituting a Group V ligand for a carbonyl are discussed.

For organometallic complexes, a comparison of the substituent constants of free and coordinated organic groups provides a quantitative measure of the electronic changes which occur upon complexation. For example, substituent constants for the arenechromiumtricarbonyl group have been measured by several groups using a variety of techniques.[1–6] The values of these substituent constants generally support the interpretation that complexation of a chromiumtricarbonyl to a phenyl group results in a significant increase in the inductive electron withdrawal by the coordinated phenyl and reduction of the resonance electron donation to a fraction of that of an uncoordinated phenyl.

As a consequence of our recent synthesis of a series of biphenylbis(chromiumdicarbonyl)-μ-diphosphine dimers, we have become interested in the changes in electronic character which occur when a carbonyl is removed and replaced by a Group V ligand. In order to determine these effects, we have measured the Taft substituent constants of arenechromiumdicarbonyl derivatives of triphenylphosphine and triphenylarsine.

RESULTS AND DISCUSSION

A set of nine compounds were prepared and examined in the present work. Biphenylchromiumtricarbonyl and its *m*- and *p*-fluorobiphenyl derivatives were prepared by the method of Top and Jaouen[7] and had properties consistent with the physical and spectral properties reported in the literature. Triphenylphosphine and triphenylarsine were introduced to the chromium by UV photolysis in benzene.[8] After recrystallization from petroleum ether, the com-

pounds were examined for purity by HPLC using petroleum ether:tetrahydrofuran (3:2) as an elutant on a silica gel column. Elemental analyses and/or melting points of the compounds are presented in Table 1. UV-visible and IR spectra were recorded for all compounds and the major spectral features are summarized in Table 2. ^{1}H, ^{19}F and ^{31}P NMR results are also included in Table 2.

σ_I and σ_R^0 constants were calculated from the ^{19}F chemical shifts of *m*- and *p*-fluorobiphenyl derivatives relative to internal fluorobenzene using the equations presented by Taft *et al.*[9] These substituent constants are summarized in Table 3 for both benzene and chloroform as solvents.

Comparison of the UV-visible and IR spectra for compounds 1–3 indicates that for these compounds the electronic and vibrational changes brought about by the phosphine and arsine ligands are very similar. Introduction of a fluorine onto the uncoordinated ring of a biphenyl has little effect on either the electronic or vibrational spectra. ^{31}P NMR of the biphenyl and fluorobiphenylchromiumdicarbonyltriphenylphosphine compounds show only a small shift of the phosphorus resonance with introduction of the fluorine.

Gubin *et al.*[4] obtained Taft substituent constants for the phenylchromiumtricarbonyl group. These workers used a slightly modified form of the Taft equations, but obtained substituent constants in close agreement with those found in the present work. These constants show that coordination of a phenyl ring by a chromiumtricarbonyl enhances the electron withdrawing ability of the phenyl ring and sharply reduces the resonance contribution of the phenyl. The

Table 1. Analytical data[a] and melting points

Compound	C	H	P	M.p. °C
1. $C_{12}H_{10}Cr(CO)_3$				84–85 (lit.[7], 85°C)
2. $C_{12}H_{10}Cr(CO)_2PPh_3$	73.75(73.28)	5.03(4.77)	5.92(5.92)	150–152°
3. $C_{12}H_{10}Cr(CO)_2AsPh_3$	67.51(67.72)	4.49(4.41)		146–148°
4. $m-FC_{12}H_9Cr(CO)_3$	58.40(58.44)	3.14(2.92)		101–103(lit.[4], 102–103°)
5. $m-FC_{12}H_9Cr(CO)_2PPh_3$	71.50(70.85)	4.64(4.43)	5.36(5.72)	130–132°
6. $m-FC_{12}H_9Cr(CO)_2AsPh_3$	65.38(65.53)	4.20(4.10)		139–140°
7. $p-FC_{12}H_9Cr(CO)_3$	58.48(58.44)	3.02(2.92)		117–118(lit.[4], 115–117°)
8. $p-FC_{12}H_9Cr(CO)_2PPh_3$	70.65(70.85)	4.50(4.43)	5.82(5.72)	144–146°
9. $p-FC_{12}H_9Cr(CO)_2AsPh_3$	64.35(64.53)	4.09(4.10)		135–137°

[a] Calculated values in parenthesis

Table 2. Spectral data

Compound	UV–Visible[a]	IR[b]	^1H NMR[b]	^{31}P NMR[b,d]	^{19}F NMR[b,e]	^{19}F NMR[a,e]
1	327(9480)[c]	1970,1900	4.86(2),4.56(3)			
2	342(8870)	1890,1832	5.15(2),4.89(3)	90.43		
3	337(6780)	1896,1835	5.20(2),4.83(3)			
4	327(9930)	1978,1902	5.62(2),5.46(3)		-1.34	-0.63
5	343(8470)	1895,1837	5.12(2),4.07(3)	90.13	-0.35	+0.16
6	338(7250)	1902,1850	5.06(2),4.79(3)		-0.31	+0.14
7	327(9825)	1890,1900	5.59(2),5.48(3)		-1.19	-0.50
8	341(8190)	1890,1836	5.08(2),4.71(3)	89.68	+1.08	+1.41
9	330(7030)	1897,1837	5.08(2),4.82(3)		+0.95	+1.35

[a] Benzene solvent. [b] Deuterochloroform solvent. [c] Extinction coefficient in parenthesis. [d] Relative to external 85% phosphoric acid. [e] Relative to external fluorobenzene.

Table 3. Taft substituent constants

Compound	Cholroform		Benzene	
	σ_I	$\sigma_R^°$	σ_I	$\sigma_R^°$
$C_6H_5Cr(CO)_3$	+0.27	+0.005	+0.173	+0.004
$C_6H_5Cr(CO)_2PPh_3$	+0.13	+0.048	+0.062	+0.042
$C_6H_5Cr(CO)_2AsPh_3$	+0.13	+0.043	+0.065	+0.047

present work demonstrates that substitution of either a triphenylphosphine or triphenylarsine for a carbonyl reverses both the inductive and resonance changes brought about by coordination. The inductive electron donating abilities of the phosphine and arsine substituted compounds are actually greater than that of the uncoordinated phenyl ring, and the resonance contribution of these compounds is intermediate between that of the chromiumtricarbonyl compound and the free arene.

Substituent constants calculated for the chromium compounds in both benzene and chloroform are presented in Table 3. Resonance constants for the two solvents were identical within experimental error, but the inductive electron withdrawal is increased in chloroform relative to its value in benzene. We suggest that the increased electron withdrawal in chloroform results from interaction of the strongly polar solvent with the electron rich chromium center.

Kursanov et al.[10] have recently reported on the reactivity of coordinated diarenes towards electrophilic hydrogen exchange. They found that the hydrogen exchange rate of biphenylchromiumtricarbonyl was an order of magnitude slower than that of biphenyl, but that biphenylchromiumdicarbonyltriphenylphosphine was an order of magnitude faster than that of the uncoordinated biphenyl. For the case of biphenylchromiumtricarbonyl, it

is inferred from the data that most of the hydrogen exchange occurs on the uncoordinated ring, while the data clearly show that hydrogen exchange occurs equally on the two rings of the triphenylphosphine substituted compound. The increased reactivity of the coordinated biphenyl to electrophilic hydrogen exchange when carbonyl is replaced by triphenylphosphine is entirely consistent with the changes in the substituent constant found in the present work.

EXPERIMENTAL

UV-visible spectra were recorded on a Cary 15 Spectrometer. IR spectra were recorded on a Perkin–Elmer 467 Grating Spectrometer. NMR spectra were recorded on a Varian FT-80 NMR Spectrometer. Analyses were conducted by Micro-Analysis, Inc. of Wilmington, DE.

REFERENCES

[1] B. Nichols and M. S. Whiting, *J. Chem. Soc.* 1959, 551.
[2] G. Klupman and F. Calderazzo, *Inorg. Chem.* 1967, 6, 977.
[3] S. P. Gubin and V. S. Khandkarova, *J. Organometal. Chem.* 1970, 22, 449.

[4]V. S. Khandkarova, S. P. Gubin and B. A. Kvasov, *J. Organometal. Chem.* 1970, **23**, 509.

[5]A. Z. Kreindlin, V. S. Khandkarova and S. P. Gubin, *J. Organometal. Chem.* 1975, **92**, 197.

[6]W. Adcock and G. L. Aldous, *J. Organometal. Chem.* 1980, **201**, 411.

[7]S. Top and G. Jaouen, *J. Organometal. Chem.* 1979, **182**, 381.

[8]W. Strohmeier and H. Hellmann, *Chem. Ber.* 1963, **96**, 2859.

[9]R. W. Taft, E. Price, I. R. Fox, I. C. Lewis, K. K. Andersen and G. T. Davis, *J. Am. Chem. Soc.* 1963, **85**, 709, 3146.

[10]A. A. Tsoy, N. N. Baranetskaya, V. N. Setkina and D. N. Kursanov, *J. Organometal. Chem.* 1981, **212**, 377.

COMMUNICATION

On the mechanism of the chromium(III)-periodate reaction

YOUSIF SULFAB

Department of Chemistry, University of Kuwait, Kuwait

We have previously reported an unusual second-order dependence on the concentration of aqua chromium(III) ion in its reaction with periodate in aqueous acidic solution.[1] The activated complex is believed to contain two chromium(III) species and one periodate ion. Simultaneous two one-electron transfer from the two chromium(III) species to iodine(VII), which is rate determining, is attained. The mechanism of this reaction was described by eqns (1)-(6)

$$H_4IO_6^- + H^+ \rightleftharpoons H_5IO_6 \quad (K_1) \quad (1)$$

$$Cr^{3+} + H_2O \rightleftharpoons CrOH^{2+} + H^+ \quad (K_h) \quad (2)$$

$$CrOH^{2+} + H_4IO_6^- \rightleftharpoons [Cr-(OH)-IO_5H_2]^+ + H_2O \quad (K_2) \quad (3)$$

$$[Cr-(OH)-IO_5H_2]^+ Cr^{3+} \rightleftharpoons$$
$$[Cr-(OH)-IO_4H-(OH)-Cr]^{4+} + H_2O \quad (K_3) \quad (4)$$

$$[Cr-(OH)-IO_4H-(OH)-Cr]^{4+} \rightarrow 2Cr(IV) + IO_3^- \quad \text{(slow)} \quad (5)$$

$$Cr(IV) + I(VII) \rightarrow Cr(VI) + IO_3^- \quad \text{(fast)}. \quad (6)$$
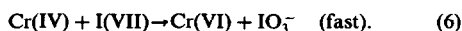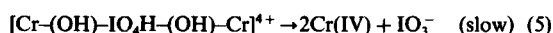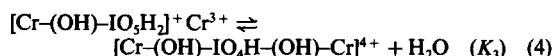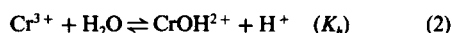
An alternative mechanism which also accounts for the second-order dependence on chromium(III) ion concentration was suggested.[2] This mechanism is described by eqns (7)-(9).

$$Cr(III) + I(VII) \rightleftharpoons Cr(V) + I(V) \quad k_1, k_{-1} \quad (7)$$

$$Cr(III) + Cr(V) \rightarrow 2Cr(IV) \quad k_2 \quad \text{(slow)} \quad (8)$$

$$Cr(IV) + I(VII) \rightarrow Cr(VI) + IO_3^- \quad \text{(fast)}. \quad (9)$$
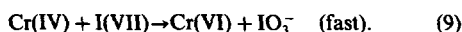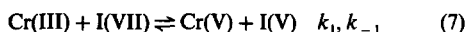
Applying the steady state approximation for Cr(V) the rate law given in eqn (10) is obtained.

$$-d[Cr(III)]/dt = \frac{k_1 k_2 [Cr(III)]^2 [I(VII)]}{k_2 [Cr(III)] + k_{-1} [IO_3^-]}. \quad (10)$$

In this mechanism step (7) is postulated as a reversible reaction with the equilibrium lying on the left side. Step (8) is considered the rate-determining reaction with step (9) following rapidly.

Table 1. Effect of addition of iodate on the chromium(III)-periodate reaction[†]

$10^2[IO_3^-]$M	k_2M^{-1}s^{-1}	$10^{-2}k_3$, M^{-2}s^{-1}
0.50	2.56 ± 0.02	2.56 ± 0.02
1.00	2.36 ± 0.02	2.36 ± 0.02
1.50	2.42 ± 0.03	2.42 ± 0.03
3.50	2.63 ± 0.04	2.63 ± 0.04

[†][IO_3^-] = 1.0×10^{-2} M, [Cr(III)] = 4.43×10^{-4} M, pH = 2.05 ± 0.01, Ionic strength $I = 0.50$ M and $T = 25.0 \pm 0.1°C$.

If $k_{-1}[IO_3^-] \gg k_2[Cr(III)]$ eqn (10) reduces to the form of eqn (11) which predicts retardation of the reaction rate by the deliberate addition of IO_3^-.

$$-d[Cr(III)]/dt = \frac{k_1 k_2 [Cr(III)]^2 [I(VII)]}{k_{-1}[IO_3^-]}. \quad (11)$$

The effect of addition of iodate on the reaction rate was investigated over the iodate concentration range $(0.50-3.5) \times 10^{-2}$ M at fixed reaction conditions. The results in Table 1 show that the initial addition of varying concentrations of iodate did not lead to any retardation of the reaction rate as indicated by the constancy of k_3. These results clearly indicate that iodate does not supress the rate of oxidation of aqua chromium(III) by periodate, and the alternative mechanism does not seem to operate. The mechanism in which two one-electron transfer, from two chromium(III) species, in a single activated state, seems to operate.

REFERENCES

[1] Ahmed Y. Kassim and Y. Sulfab, *Inorg. Chem.* 1981, **20**, 506.
[2] This mechanism was suggested by Professor Richard M. Noyes.

POLYHEDRON REPORT NUMBER 5

METAL–METAL BONDS AND METAL–CARBON BONDS IN THE CHEMISTRY OF MOLYBDENUM AND TUNGSTEN ALKOXIDES

MALCOLM H. CHISHOLM
Department of Chemistry, Indiana University, Bloomington, IN 47405, U.S.A.

CONTENTS

I. INTRODUCTION

Simple binary alkoxides of formula $M(OR)_n$ are known for most electro-positive metals and the majority of the transition elements and lanthanides. Mixed metal alkoxides are known for a variety of metals and some of these have quite remarkable properties. For example, the lanthanide elements and aluminum form an extensive series of isopropoxides of formula $MAl_3(OPr^i)_{12}$ which are volatile solids or liquids.

A characteristic feature of an alkoxy ligand is its ability to readily form bridges between two or even three metal atoms. Such oligomerization proceeds in order to satisfy the metal atom's desire to attain a preferred coordination geometry. Oligomerization may be suppressed by the use of sterically bulky alkoxy ligands and, in this way, unusual coordination numbers and geometries may be imposed. Many examples could be used to illustrate these simple concepts. I shall mention but a few.

(1) Alkoxides of niobium and tantalum in the +5 oxidation state exist as dimers when the alkoxy group is not too sterically demanding, e.g. MeO and EtO, as shown in **I** below. However, with bulky alkoxides, such as Bu^tO, monomeric five coordination is imposed.

(2) The ethoxides and methoxides of titanium (+4) adopt a tetrameric structure in the solid state, **II**, whereby each metal atom achieves an octahedral environment. In benzene solution, the titanium ethoxide dissociates to trimers, while with the bulky Bu^tO ligand, a monomeric $Ti(OBu^t)_4$ is found.

I

II

X = OMe, OEt
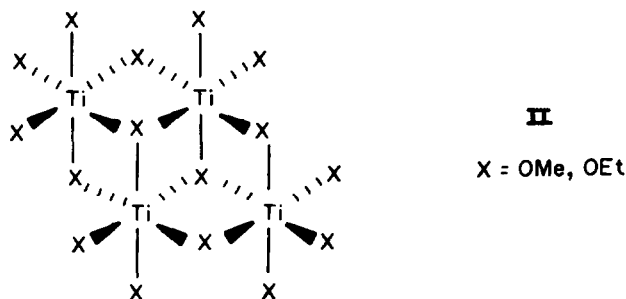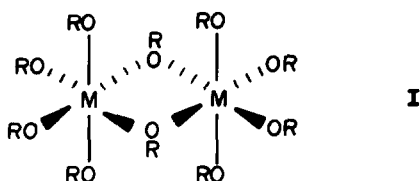
(3) Aluminium-tert-butoxide is a dimer, **III**, while the isopropoxide is a trimer when freshly distilled and a tetramer in the solid state, and when aged in solution, **IV**. Chromium(III), which is a similar size to aluminium(III), has a greater propensity for forming octahedral complexes because of the crystal field stabilization energy arising from the t_{2g}^3 orbital configuration in an O_h field. Cr(III) forms a non-volatile, non-hydrocarbon soluble isopropoxide $[Cr(OPr^i)_3]_n$ and based upon electronic spectral and magnetic properties, it is formulated as having a polymeric $Cr(3+)O_6$ lattice structure.

III

IV

X = OPr^i
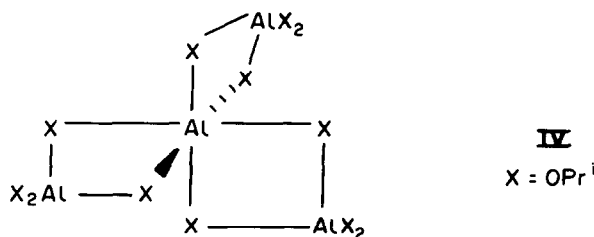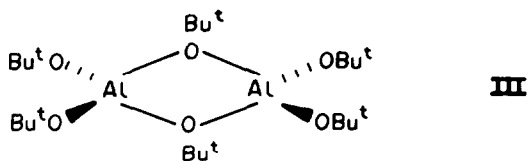
It should also be emphasized that alkoxide ligands may act as π-donor ligands, RO⇒M. This capability will have maximum effect for terminal alkoxy ligands and for transition metals in high oxidation states with vacant d orbitals of appropriate symmetry to receive π-electrons.

Metal alkoxides are in general a highly reactive group of complexes. The metal atoms are commonly susceptible to nucleophilic attack and the oxygen atoms are susceptible to electrophilic attack. Common reactions involving substrates with acidic hydrogens include hydrolysis with water, alcohol exchange with other alcohols or silanols, substitution reactions with organic acids or acid anhydrides, acyl halides, β-diketones, β-keto-esters, β-ketoamines and Schiff bases. Insertion reactions may also occur with unsaturated molecules such as CO_2, CS_2 and ArNCO.

The preparations, physico–chemical properties and chemical reactions of metal alkoxides have been extensively reviewed within the past few years.[1,2] The scope of this report is confined to the alkoxide chemistry of molybdenum and tungsten. Except in the oxidation state +6, where the metal atoms have no valence d electrons, the alkoxide chemistry of these elements is markedly different from that anticipated by Bradley's early theories for metal alkoxide polymers.[3,4] In all the lower oxidation states, the d^n valence electrons on the metal atoms are used to form metal–metal bonds which may be localized single or multiple bonds or delocalized into cluster bonding molecular orbitals. The formation of metal–metal bonds may modify or totally change the structural ground state of a molecule from that anticipated for a d^0 metal complex. Furthermore, metal–metal bonds provide a reservoir for electrons which may be "tapped" for oxidative-addition reactions or "filled" in reductive–elimination reactions.

One other area of chemistry that is emphasized concerns the use of alkoxy ligands in organometallic chemistry. Alkoxy ligands, which are strong π-donors and may readily interchange bonding modes between terminal and bridging (μ_2 and μ_3), are clearly very different from the now "classical" ligands in organometallic chemistry, such as tertiary phosphines, carbonyl, cyclopentadienes and olefins, all of which are soft and π-acceptors. We see a new facet of organometallic chemistry emerging in the area of early transition metal organoalkoxide chemistry.

II. CLASSES OF COMPOUNDS

1. d^3–d^3 dimers with M–M triple bonds

The addition of alcohols to hydrocarbon solutions of $Mo_2(NMe_2)_6$[5] leads to an extensive series of dinuclear alkoxides $Mo_2(OR)_6$, where $R = Bu^t$, Pr^i, CH_2Bu^t, $CH(Me)Ph$, $SiMe_3$ and SiE_3.[6] Polymeric compounds $[Mo(OR)_3]_n$ are obtained for sterically unencumbered alkoxy ligands such as OEt and OMe, but little is yet known about these compounds. The dinuclear alkoxides, $Mo_2(OR)_6$ are yellow–orange, hydrocarbon soluble, crystalline compounds. They sublime *in vacuo* in the temperature range 70–120°C at 10^{-4} Torr. In the mass spectrometer, they yield strong molecular ions, together with an extensive series of Mo_2-containing ions. They are diamagnetic and show only one type of alkoxy or trialkylsiloxy group in their ^1H and ^{13}C NMR spectra, independent of temperature. Only one compound, the neopentoxide, has been fully characterized by a single crystal X-ray study and its molecular structure is shown in Fig. 1. There is an unbridged Mo–Mo triple bond of distance 2.22 Å and the central Mo_2O_6 skeleton has virtual D_{3d} symmetry. There can be little, if any, doubt that the other alkoxides of formula $Mo_2(OR)_6$ adopt similar structures and, as such, are members of an extensive series of compounds containing M–M triple bonds (M = Mo, W) between tri-ligated metal atoms.[7]

Rather interestingly, alcoholysis reactions involving $W_2(NMe_2)_6$[8] do not lead to an extensive series of compounds of formula $W_2(OR)_6$.[9] Only $W_2(OBu^t)_6$ has been isolated, though amine adducts $W_2(OR)_6(HNMe_2)_2$ have been obtained for $R = Pr^i$ and CH_2Bu^t.[10] Tungsten appears to differ from molybdenum in three important respects with regard to the formation and stability of $M_2(OR)_6$ compounds. (1) Tungsten binds Lewis bases more tightly for a given alkoxy group, e.g. as in the isolation of $W_2(OR)_6(HNMe_2)_2$ noted above. (2) Tungsten is more readily oxidized to W(4+) alkoxides. Both of these points will be elaborated upon further in this article. (3) Whereas $Mo_2(OR)_6$ compounds readily sublime when heated *in vacuo*, $W_2(OBu^t)_6$ and the amine adducts $W_2(OR)_6(HNMe_2)_2$, where $R = SiMe_3$, Pr^i and CH_2Bu^t, decompose when heated *in vacuo* above 80°C.[9] In the mass spectrometer, however, $W_2(OR)_6{}^+$ ions are observed.[9]

Some mixed amido– or alkyl–alkoxy compounds containing M≡M bonds have been prepared. For example, treatment of $1,2$-$Mo_2X_2Y_4$ (M≡M), where X = Br and Y = CH_2SiMe_3 or X = Cl and Y = NMe_2, with LiOR (2 equivalents) yields compounds of formula $1,2$-$Mo_2(OR)_2Y_4$ where $R = Bu^t$ and Pr^i. The molecular structure of $1,2$-$Mo_2(OBu^t)_2(CH_2SiMe_3)_4$ deduced from a single crystal X-ray study reveals the *anti*-conformation[11] (see Fig. 2). Rather interestingly, the $1,1$-isomer, $(Bu^tO)_2(Me_3SiCH_2)Mo≡Mo(CH_2SiMe_3)_3$, is obtained from the addition of Bu^tOH to $1,1$-$Mo_2(NMe_2)_2(CH_2SiMe_3)_4$.[11]

Alcoholysis reactions involving $1,2$-$Mo_2R_2(NMe_2)_4$ proceed *via* elimination of $HNMe_2$ to give $1,2$-$Mo_2R_2(OR')_4$ compounds [R = Me, R' = Bu^t; R = CH_2SiMe_3, CH_2CMe_3 and R' = Bu^t, Pr^i, CH_2CMe_3 and Et], but when R contains β-hydrogens, elimination of one equivalent of alkane results in $Mo_2R(OR')_5$ compounds [R = Et and Pr; R' = Bu^t and Pr^i]. The mechanistic aspects of these reactions are discussed later.
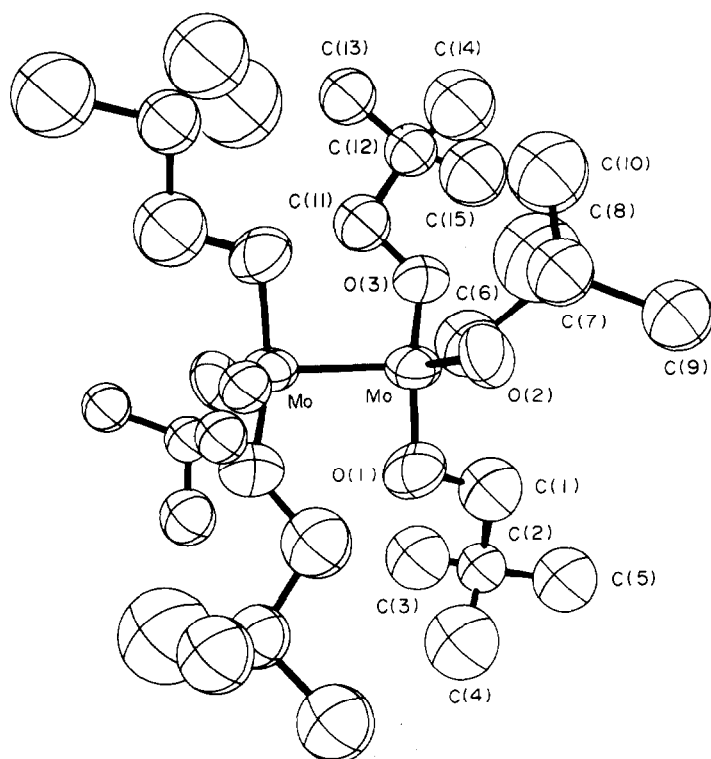
Fig. 1. An ORTEP view of the centrosymmetric $Mo_2(OCH_2Bu^t)_6$ molecule. Pertinent distances (Å) and angles (°) are: Mo–Mo = 2.222(2); Mo–O(1), –O(2), –O(3) = 1.905(6), 1.867(6), 1.855(6); Mo′–Mo–O(1), –O(2), –O(3) = 98.3(2), 105.5(2), 105.4(2).
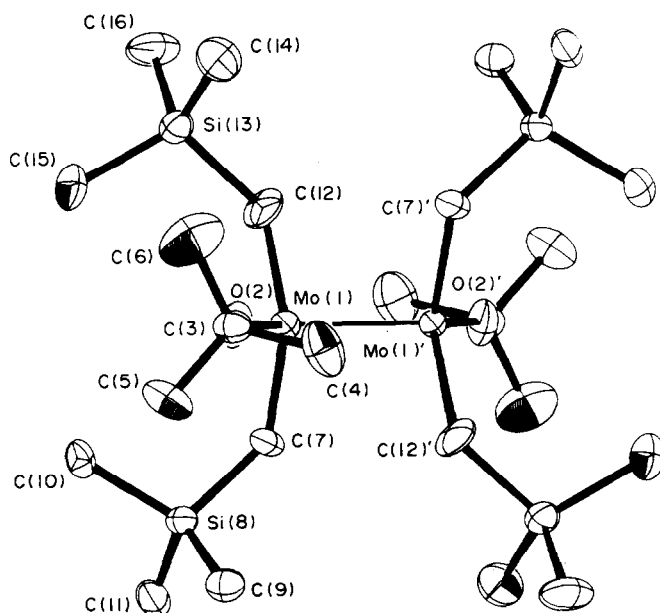
Fig. 2. An ORTEP view of the centrosymmetric $1,2\text{-}Mo_2(OBu^t)_2(CH_2SiMe_3)_4$ molecule. Pertinent distances (Å) and angles (°) are: Mo(1)–Mo(1)′ = 2.209(2); Mo(1)–O(2), –C(7), –C(12) = 1.865(8), 2.13(1), 2.14(1); Mo(1)′–Mo(1)–O(2), –C(7), –C(12) = 110.7(2), 100.0(3), 100.2(4).

The most striking feature of the aforementioned compounds of formula $M_2(OR)_6$ and $M_2X_n(OR)_{6-n}$ is the presence of the M–M triple bond, unsupported by bridging alkoxide ligands. Evidently the bridged $Al_2(OR)_6$ structure, **III**, is considerably higher in energy since compounds of formula $X_2YM\equiv MY_3$ and $XY_2M\equiv MXY_2$ do not readily isomerize in hydrocarbon solvents, even at $+100°C$.[11]

From calorimetric studies, it has been estimated that the formation of a pair of bridging OR ligands from two terminal OR ligands, $2Mo–OR\rightarrow Mo_2(\mu–OR)_2$, is favoured by $10–15\,kcal\,mol^{-1}$.[12] That bridges are not seen in these compounds, and that isomerizations which would be possible if bridged intermediates were energetically accessible, imply that the energy difference between $(RO)_3Mo\equiv Mo(OR)_3$ and $(RO)_2Mo(\mu–OR)_2Mo(OR)_2$ must be quite large and at least greater than $ca.\ 30\,kcal\,mol^{-1}$. This in turn must reflect upon the relative strengths of Mo–Mo bonds in the bridged and non-bridged structures.

The strength of $D(Mo\equiv Mo)$ in $Mo_2(OPr^i)_6$ has been estimated to be $90\,kcal\,mol^{-1}$ from calorimetric studies wherein the heat of formation of $Mo_2(OPr^i)_6$ is determined.[12] However, it is impossible to separate $D(Mo–OR)$ and $D(Mo\equiv Mo)$ in such calculations and thus an error in the assumption of $D(Mo–OR)$ is magnified six-fold in $D(Mo\equiv Mo)$. Since $D(Mo–OR)$ can be determined for a large number of mononuclear compounds, a reasonable estimate of $D(Mo–OR)$ in $Mo_2(OR)_6$ compounds can be obtained to $\pm 5\,kcal\,mol^{-1}$. The strength of the $Mo\equiv Mo$ bond may therefore be determined to lie within the range $60–120\,kcal\,mol^{-1}$, and so a value of $90–100\,kcal\,mol^{-1}$ seems most plausible.

A simple bonding picture for $M_2(OR)_6$ compounds can be constructed as follows. Letting the z axis be coincident with the M–M axis, the metal atomic d_{z^2} orbitals may interact to form σ and σ^* M–M molecular orbitals and d_{xz} and d_{yz} may form π and π^* orbitals. In oxidation state $+3$, each metal has the d^3 configuration and thus a M–M triple bond of configuration $\sigma^2\pi^4$ can be formed. Each metal may use s, p_x and p_y atomic orbitals to form three σ bonds with the OR ligands, and metal d_{xy}, $d_{x^2-y^2}$ and p_z atomic orbitals have the appropriate symmetry to form π-bonds with oxygen filled p atomic orbitals. It is clear from considerations of the short Mo–OR bond distances that there is considerable multiple bond character. (See also Part 7, this section).

This qualitative bonding scheme finds support from detailed calculations employing the SCF X_α–SW technique on $Mo_2(OH)_6$.[13] The orbital energies so calculated correlate well with the data obtained from He(I) and He(II) photoelectron spectroscopic studies. For $Mo_2(OCH_2Bu^t)_6$, the first ionization occurs at $ca.\ 7.2\,eV$ and the second at $8.0\,eV$, corresponding to ionizations from M–M π and σ bonding orbitals, respectively.

The electronic absorption spectra of $M_2(OR)_6$ compounds have recently been examined[14]. There are no absorption maxima in the visible region of the spectra: the colours (yellow or orange) are derived from higher energy absorptions tailing into the visible. The first absorption maximum, v_1, occurs at $360\,nm$ ($\epsilon\ ca.\ 1400$) for $Mo_2(POr^i)_6$ and can be assigned to a M–M π-to-M–Lπ^* transition (M–M π-to-M–M δ). The second absorption maximum, v_2, occurs at $210.5\,nm$ ($\epsilon\ ca.\ 22,400$) and is assigned to the M–M π-to-π^* transition. The spectrum of $W_2(OBu^t)_6$ is very similar with v_1 at $380\,nm$ ($\epsilon\ ca.\ 1600$) and v_2 at $210\,nm$ ($\epsilon\ ca.\ 13,000$). The spectrum of $W_2(OBu^t)_6$ also shows quite pronounced shoulders to low energy of these absorption maxima which can be assigned to the spin forbidden transitions to triplet states: $v_1' = 460\,nm$ ($\epsilon\ ca.\ 500$) and $v_2' = 250\,nm$ ($\epsilon\ ca.\ 6800$). The electronic absorption spectra of $Mo_2(OPr^i)_6$ and $W_2(OBu^t)_6$ are compared in Fig. 3.

2. d^2–d^2 dimers with M–M double bonds

The addition of alcohols to $Mo(NMe_2)_4$ leads to an extensive series of compounds of formula $[Mo(OR)_4]_n$.[15] The bulky tert-butoxide appears to be monomeric in benzene, but its structure is not known in the solid state. It is weakly paramagnetic, which contrasts with the diamagnetic monomeric four-coordinate compounds, MoX_4, where $X = NMe_2$[16] and SBu^t.[17] $Mo(OBu^t)_4$ is clearly a molecule worthy of further attention. The isopropoxide is dimeric and diamagnetic in hydrocarbon solutions, but in the presence of pyridine, a paramagnetic species, believed to be $Mo(OPr^i)_4(py)_2$ akin to $Mo(OSiMe_3)_4(HNMe_2)_2$,[15] is formed. In the solid state, an interesting dimeric structure is found.[18] Each molybdenum atom is in a distorted trigonal bipyramidal geometry. The two halves of the molecule share a common axial equatorial edge through the agency of alkoxy bridges as shown schematically in **V** below.

An ORTEP view of this molecule is shown in Fig. 4. The Mo–O distances show the expected

V

O = OPr^i
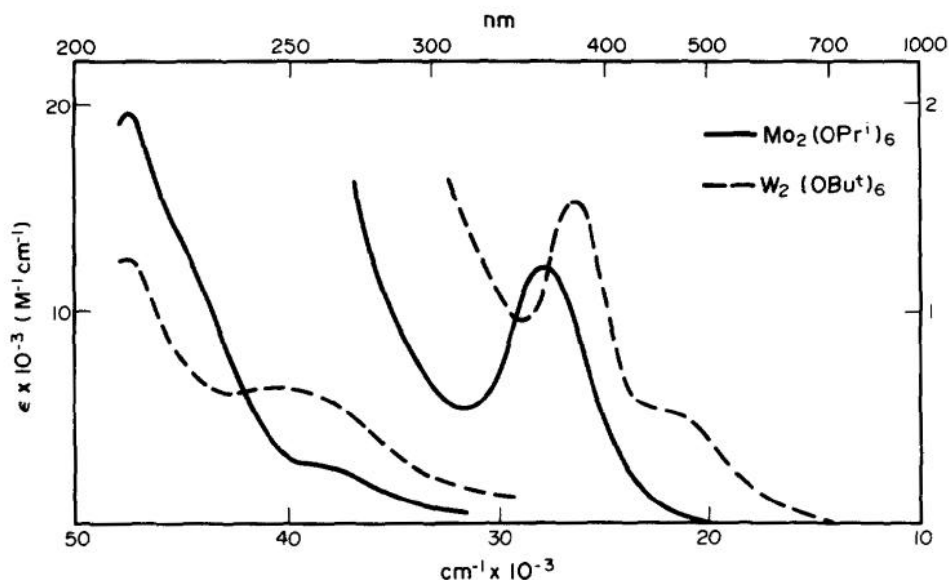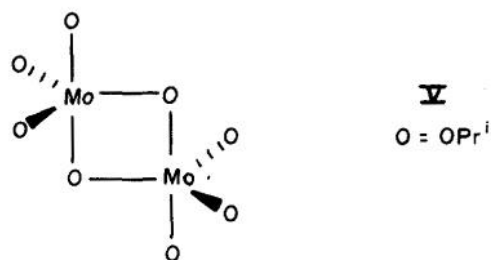
Fig. 3. Comparison of the electronic absorption spectra of Mo$_2$(OPr^i)$_6$ and W$_2$(OBu^t)$_6$ in hexane solutions.
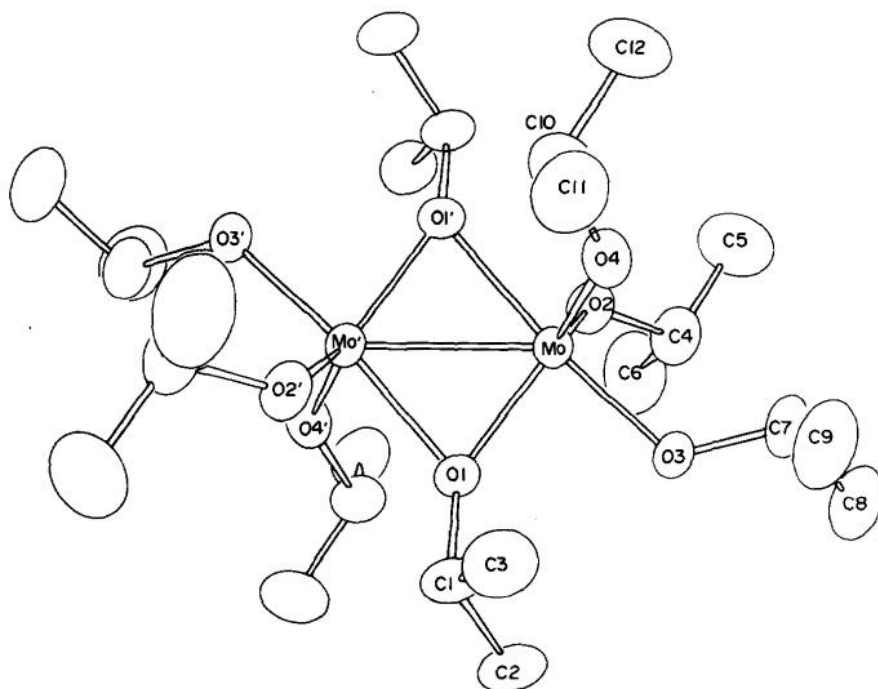
Fig. 4. An ORTEP view of the centrosymmetric Mo$_2$(OPr^i)$_8$ molecule. Pertinent distances are given in comparison with the Mo$_2$(OPr^i)$_6$(NO)$_2$ molecule in Fig. 18.

and general trend that terminal M–O distances are shorter than bridging ones, but we also find that the axial bonds are longer than the equatorial bonds within each set of terminal and bridging ligands. This also turns out to be a general trend in what is now quite an extensive series of dimeric molybdenum compounds whose structures are based on fused trigonal bipyramids.

The diamagnetism and the shortness of the Mo–Mo distance, 2.523(1) Å, are readily rationalized by the presence of an Mo–Mo double bond. This may be formulated in the following manner. Let the z axis be coincident with the axial O–Mo–O groups of each metal. Then the formation of five σ bonds to oxygen may use s, p_x, p_y, p_z and d_{z^2} atomic orbitals. This leaves two doubly degenerate d orbitals (d_{xz}, d_{yz}) and ($d_{x^2-y^2}$, d_{xy}) with the former lying lower in energy in a simple trigonal bipyramidal field. If we then choose the y axis to be coincident with the Mo–O (equatorial) bridging ligands, then the d_{yz} atomic orbitals can form M–M σ and σ^* orbitals; the d_{xz}–d_{xz} interaction will yield π and π^* orbitals. This simple picture predicts a M–M bonding configuration $\sigma^2\pi^2$ for a d^2–d^2 dimer. Note the degeneracy of the M–M π bonds, which is present in $X_3M\equiv MX_3$ compounds, is removed for a dimer of type V.

The M–M distances in the molecules $Mo_2(OPr^i)_8$ and $Mo_2(OPr^i)_6(NO)_2$ make an interesting comparison. The latter compound adopts a structure similar to that shown in V in which two axial OR groups are replaced by linear Mo–N–O groups.[19] If for the purposes of electron counting we use the formalism that a linear M–N–O group is equivalent to $M^-\leftarrow(NO^+)$, then the formal oxidation state of molybdenum is $+2$ in $Mo_2(OPr^i)_6(NO)_2$, resulting in a d^4–d^4 dimer. In terms of M–M bonding, this would lead to a totally non-bonding configuration $\sigma^2\pi^2\pi^{2*}\sigma^{*2}$ and the Mo-to-Mo distance, 3.335(2) Å, precludes an M–M bond. In fact, the d^4 electrons on each molybdenum reside in the (d_{xz}, d_{yz}) orbitals and are extensively used in backbonding to the NO π^* orbitals, as evidenced by the low $v(N-O)$ value, 1640 cm^{-1}.

Other alkoxides of Mo(4+) derived from alcoholysis reactions involving $Mo(NMe_2)_4$ are less well characterized. With decreasing size of the alkoxide ligand, there is a tendency to associate further in solution. For example, a cryoscopic molecular determination on the ethoxide gave a value close to that expected for a trimer, $[Mo(OEt)_4]_3$. In view of the tetranuclear structure of the tungsten analogue (discussed later), further studies of these $[Mo(OR)_4]_n$ compounds should be undertaken.

Dinuclear tungsten(IV) alkoxides of formula $W_2(OR)_8$ are presently not known. However, it seems that routes to such compounds should be forthcoming, even though $W(NMe_2)_4$ is not a known compound. For example, oxidative-addition reactions involving RO–OR and $W_2(OR)_6$ compounds might prove effective. The only simple d^2–d^2 dinuclear tungsten alkoxides are the green compounds of formula $W_2Cl_4(OR)_4(HOR)_2$.[20] These were first prepared by Wentworth and Clark from the reactions of $[Bu_4N]_3W_2Cl_9$ with alcohols and were incorrectly formulated as tungsten(III) compounds. $W_2Cl_4(OR)_2(HOR)_4$.[21] Later work, however, showed that these compounds could be prepared by a variety of routes including alcoholysis of WCl_4 and that they were in fact tungsten(IV) dimers.[22] The structure of $W_2Cl_4(OEt)_4(HOEt)_2$ was determined by a single crystal study and revealed the edge-shared octahedral geometry shown in VI.[20]

VI
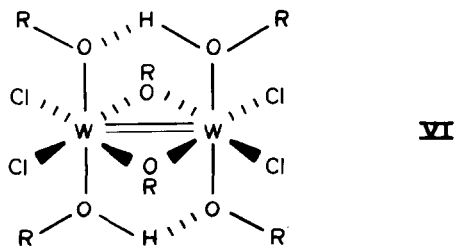
The fusing of two octahedral units along a common edge allows the metal t_{2g} atomic orbitals to interact to form one σ, one π and one δ bonding and anti-bonding set of molecular orbitals. The d^2–d^2 dimer thus provides a double bond of configuration $\sigma^2\pi^2$, which is compatible with the W–W distance of 2.479(1) Å.

There are a number of other dinuclear alkoxides of molybdenum and tungsten which are formed by addition reactions involving $M_2(OR)_6$ compounds that can be considered to have M–M double bonds. These are discussed later.

3. d^1–d^1 dimers with M–M single bonds

The only homoleptic M(5+) compound that is known for molybdenum and tungsten is $W(OPh)_5$, formed by the reduction of $W(OPh)_6$ with molecular hydrogen and Raney nickel.[23] In solution, a molecular weight determination yielded a value greater than a monomer, but less than a dimer. In view of the structural characterization of $M_2Cl_4(OR)_6$ compounds, it is possible that the phenoxide has an edge-shared W_2O_{10} moiety.

There are a number of reports in the early literature concerning compounds of empirical formula $WCl_2(OR)_3$ formed from reactions of WCl_6 with alcohols and under electrolysis. It is not clear that the early workers were correct in their formulations since various colours and magnetic properties were attributed to these compounds. However, more recently Cotton and Walton[24] have prepared an extensive series of $W_2Cl_4(OR)_6$ compounds by the oxidation of $W_2Cl_4(OR)_4(HOR)_2$ compounds using molecular oxygen or Ag^+ as oxidants.[24] Addition of halogens to $Mo_2(OPr^i)_6$ leads to $Mo_2X_4(OPr^i)_6$ compounds, where X = Cl, Br and I.[25] All of these compounds are orange crystalline solids. They are diamagnetic and show two types of OR ligands, consistent with the maintenance in solution of the structure found in the solid state, depicted by VII, for $Mo_2(OPr^i)_6X_4$ where X = Cl and Br[25] and for $W_2(OEt)_6Cl_4$.[24]
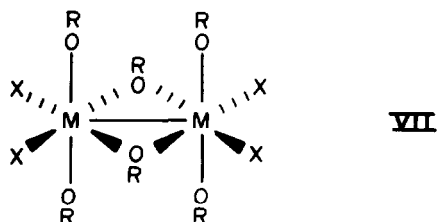
In all of the structurally characterized compounds of formula $M_2Cl_4(OR)_6$, the M–M distance is close to 2.71 Å, which is roughly 0.8 Å less than that of a M–M non-bonding distance found for the d^0–d^0 compound $[Nb(OMe)_5]_2$.[26]

A compilation of bond distances and assigned bond orders for a number of simple dinuclear alkoxides and their adducts or derivatives is given in Table 1. A fairly consistent picture emerges. Triple bonds of configuration $\sigma^2\pi^4$ have distances in the range 2.2–2.3 Å; double bonds, $\sigma^2\pi^2$, are all close to 2.5 Å; single bonds, σ^2, are close to 2.7 Å, while non-bonding distances for $M_2(\mu\text{–}OR)_2$-containing compounds are all greater than 3 Å, typically in the range 3.3–3.5 Å.

4. Trinuclear alkoxides

Since some of the alkoxides of molybdenum(IV) appear trimeric in solution, it is interesting to speculate that triangulo Mo_3 structures might be found for certain $[Mo(OR)_4]_n$ compounds. The six metal valence electrons not used in M–OR bonding could be used to form M–M bonds: $a^2 + e^4$. This situation is seen for $Mo_3O(OR)_{10}$ compounds, where R = Pr^i and CH_2Bu^t.[27] An ORTEP view of the central skeleton of the $Mo_3O(OCH_2Bu^t)_{10}$ molecule is shown in Fig. 5. The structure is closely related to a large group of triangulo Mo_3- and W_3-containing complexes with capping (μ_3-) oxo, sulphido and carbyne ligands.[28] In solution, the ^1H NMR spectra indicate that the solid state structure is maintained. Four types of alkoxy ligands are seen in the integral ratio 3:3:3:1, indicating that the molecule is not fluxional on the NMR time-scale.

5. Tetranuclear alkoxides

Addition of ethanol or methanol to hydrocarbon solutions of $W_2(NMe_2)_6$ yields the tetranuclear alkoxides $W_4(OR)_{16}$.[29,30] The structure of the ethoxide has been determined by an X-ray study and is shown in Fig. 6. The structure is of type II which is found for $[Ti(OR)_4]_4$ compounds where R = Me and Et,[31] but the W——W distances are all shorter than the analogous Ti——Ti

Table 1. Metal–metal distances and metal–metal bond orders in representative dinuclear alkoxides of molybdenum and tungsten

Compound	Bridging Ligands	M–M Distance ($\mathring{A}$)	Bond Order	Ref
$Mo_2(OCH_2Bu^t)_6$	none	2.222(2)	3	6
$Mo_2(OPr^i)_6(py)_2$	none	2.250(2)	3	47
$W_2(OPr^i)_6(py)_2$	none	2.334(1)	3	9
$Mo_2(OBu^t)_6(CO)$	$2OBu^t$, CO	2.498(1)	2	68
$Mo_2(OPr^i)_6(py)_2(CO)$	$2OPr^i$, CO	2.486(2)	2	69
$W_2(OPr^i)_6(py)_2(CO)$	$2OPr^i$, CO	2.499(3)	2	69
$Mo_2(OPr^i)_8$	$2OPr^i$	2.523(1)	2	16
$Mo_2(OCH_2Bu^t)_6Br_2(py)$	2OR, Br	2.534(1)	2	47
$W_2Cl_4(OEt)_4(HOEt)_2$	2OEt	2.483(1)	2	20
$[W_2(H)(OPr^i)_7]_2$	H, $2OPr^i$	2.446(1)	2	35
$Mo_2Cl_4(OPr^i)_6$	$2OPr^i$	2.731(1)	1	25
$W_2Cl_4(OEt)_6$	2OEt	2.715(1)	1	24
$[Mo(OPr^i)_3(NO)]_2$	$2OPr^i$	3.335(2)	0	19
$[W_2(H)(OPr^i)_7]_2$	2OR	3.407(1)	0	35
$[W(OMe)_4NPh]_2$	2OMe	3.47(1)	0	a

^{a}A.J. Nielson and J.M. Waters, Polyhedron 1982, 1, 561.

distances. Evidently in $W_4(OEt)_{16}$, the eight tungsten valence electrons are used to form delocalized M–M bonds.

The central centrosymmetric M_4X_{16} unit formed by four fused octahedral units appears quite common in coordination compounds and in ternary metal oxides. A mixed oxo-alkoxy–pyridine compound, $Mo_4(\mu_3$-$O)_2(\mu_2$-$O)_2(O)_4(\mu_2$-$OPr^i)_2(OPr^i)_2(py)_4$, has been structurally characterized.[30] $Ag_8W_4O_{16}$[32] and $Ba_{1.14}Mo_8O_{16}$[33] also have M_4O_{16} subunits. The molybdenum oxide contains two types of M_4 units differing most significantly in the M–M distances. This difference can be correlated with the number of bonding cluster electrons: 8 vs 10. The M_4X_{16} framework has been found to accommodate 0, 4, 8 and 10 cluster bonding electrons. The changes in M–M distances as a function of the number of cluster electrons are summarized in Table 2. It is clear that molybdenum and tungsten use their d^n electrons to form M–M bonds. The nature of the M–M bonding in the 8 and 10 electron clusters has recently been the subject of a Fenske–Hall calculation by Cotton and Fang.[34] They rationalized the elongation of two M——M distances, which accompanies the change from the 10 electron to the 8 electron cluster, in terms of a second order Jahn–Teller distortion.

Aside from the solid state structural parameters, the presence of M–M cluster bonding electrons drastically alters the solution behaviour of $M_4(OR)_{16}$ compounds. Whereas $[Ti(OEt)_4]_4$ dissociates in benzene solution to trimers, the tungsten compound retains its tetranuclear nature as evidenced
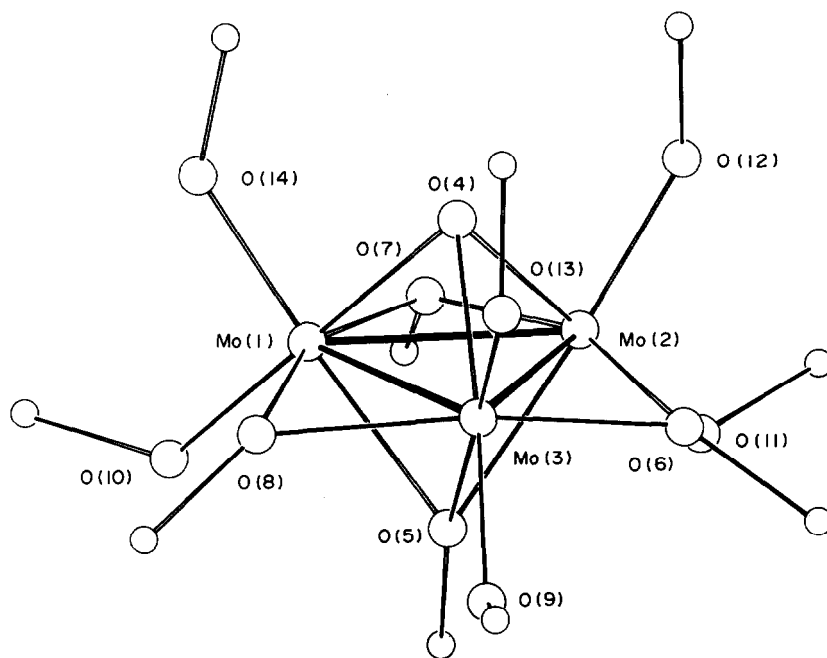
Fig. 5. An ORTEP view of the central $Mo_3O(OC)_{10}$ skeleton of the $Mo_3O(OCH_2Bu^t)_{10}$ molecule. All atoms are assigned arbitrary thermal parameters. Each molybdenum atom is in a distorted octahedral environment with respect to six directly bonded oxygen atoms. Pertinent bond distances in Å (averaged) are: Mo–Mo = 2.529(9), Mo–μ_3O(oxo) = 2.03(3), Mo–μ_3OR = 2.21(3), Mo–μ_2OR = 2.02(3), Mo–OR (terminal) *trans* to O(4) = 1.94(2), Mo–OR (terminal) *trans* to μ_3OR = 1.85(3).
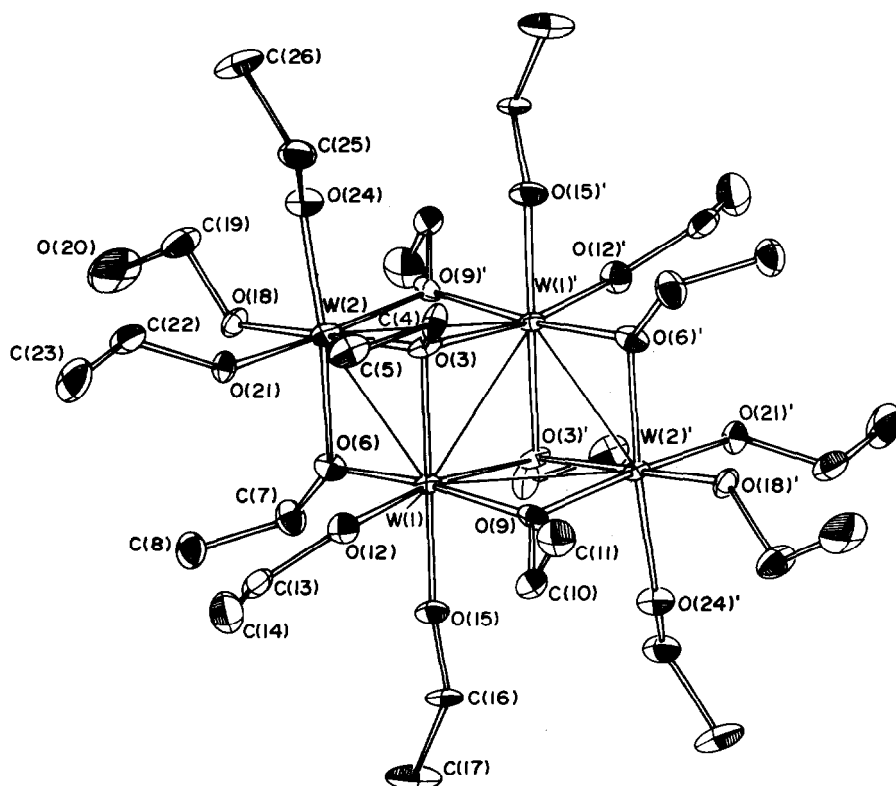
Fig. 6. An ORTEP view of the centrosymmetric $W_4(OEt)_{16}$ molecule emphasizing the local WO_6 octahedral geometry for each tungsten atom. Pertinent W–W and W–O distances are given in Tables 2 and 3, respectively.

Table 2. M–M distances (Å) found in compounds which are structurally related to $W_4(OEt)_{16}$[a]

Compound	M(2)–M(1)'	M(1)–M(2)	M(1)–M(1)'	Number of M_4 Cluster Electrons	Ref.
$[Ti(OEt)_4]_4$	3.34	3.50	3.42	0	31
$Ag_8W_4O_{16}$	3.32	3.23	3.49	0	32
$Mo_4O_8(OPr^i)_4(py)_4$	3.47	2.60	3.22	4	30
$Mo_4Cl_4O_6(OPr^n)_6$	3.43	2.67	not given	4	b
$W_4(OEt)_{16}$	2.65	2.94	2.76	8	30
$Ba_{1.14}Mo_8O_{16}$	2.54	2.84	2.56	8	33
$Ba_{1.14}Mo_8O_{16}$	2.61	2.57	2.58	10	33

(a) Distances are quoted to ±0.01 Å; the labelling scheme for M(1), M(2) and M(1)' is shown below and is such that M(1) and M(2) have, respectively, two and three terminal groups. (b) S.A. Koch and S. Lincoln, *Inorg. Chem.* 1982, **21**, 2904.
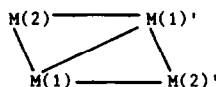
by cryoscopic molecular weight determinations. Also, the ^{1}H NMR spectrum of $W_4(OMe)_{16}$ shows eight sharp resonances of equal intensity, which is exactly what is predicted by a consideration of the centrosymmetric solid state structure of $W_4(OEt)_{16}$.

From reactions between $W_2(NMe_2)_6$ and Pr^iOH, a most intriguing hydrido–alkoxide, $W_4(\mu-H)_2(OPr^i)_{14}$, has been isolated and characterized.[35] The central $W_4(\mu-H)_2O_{14}$ skeleton of this molecule is shown in Fig. 7. The molecule is centrosymmetric and the eight electrons available
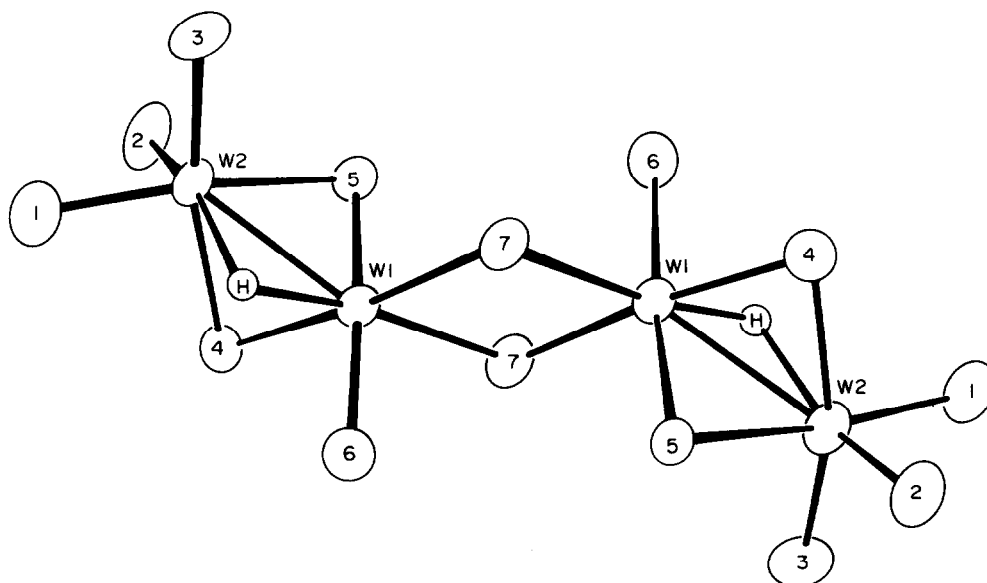
Fig. 7. An ORTEP view of the central skeleton of the centrosymmetric $W_4(\mu-H)_2(OPr^i)_{14}$ molecule. Some pertinent distances (Å) and angles (°) are: W(1)——W(1)' = 3.407(1), W(1)–W(2) = 2.446(1) and W(2)–W(1)–W(1)' = 142. The W–OR distances are within the range reported in Table 3 for terminal and μ_2–OR ligands.

for M–M bonding are evidently used to form two localized M–M double bonds: W(1)–W(2) = W(1)′–W(2)′ = 2.446(1) Å. The central distance, W(1)——W(1)′ = 3.407(1) Å, is typical of a non-bonding distance in $M_2(\mu_2\text{–OR})_2$-containing compounds (see Table 1). The molecule may thus be viewed as a dimer of dinuclear compounds: $[W_2(\mu\text{–H})(OPr^i)_7]_2$. It is interesting to speculate why $W_4(\mu\text{–H})_2(OPr^i)_{14}$ adopts a chain structure rather than a cluster based on the $W_4(OEt)_{16}$ structure in which a pair of μ_2 or μ_3 OEt ligands are replaced by hydrides.

A cryoscopic molecular weight determination in benzene indicates that a tetranuclear structure is maintained in solution. However, in contrast to the rigid (NMR timescale) structure of $W_4(OR)_{16}$ compounds (R = Me and Et), $W_4(\mu\text{–H})_2(OPr^i)_{14}$ is highly fluxional. In the ^1H NMR spectrum, only one type of OPr^i ligand is observed in the temperature range $-60°$ to $+80°C$. Evidently some fluxional process rapidly scrambles all the OPr^i ligands. This process also exchanges the two types of tungsten atoms, which are in formal oxidation states $+4\frac{1}{2}$ and $+3\frac{1}{2}$, since the hydride resonance at $\delta = 7.87$ ppm shows only one coupling to ^{183}W, $I = \frac{1}{2}$, 14.5 natural abundance. From the relative intensities of the satellites to the central hydride resonance, it is evident that the hydride ligand bridges two equivalent tungsten atoms; the hydride ligands are not scrambled over all four tungsten atoms. One can readily accommodate these observations by a fluxional process in which the molecule essentially "turns itself inside-out". A cleavage of one of the central W(1)–μ–OR bridges could be followed by a succession of bridge$\rightleftharpoons$terminal OPr^i exchanges to give an intermediate of the type shown in **VIII** below. From such an intermediate, a return to the chain structure could occur with exchange of W(1) and W(2). It is, however, still quite remarkable that $W_4(\mu\text{–H})_2(OPr^i)_{14}$ is so labile to OPr^i scrambling.
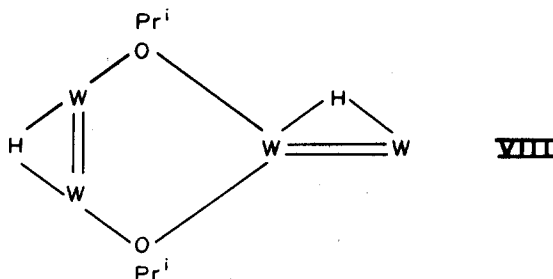
Three further types of tetranuclear alkoxides have recently been found for compounds of formula $Mo_4X_4(OR)_8$, where X = F, Cl and Br. These are described later since they are formed in X-for-OR exchange reactions involving $Mo_2(OR)_6$ compounds. It should be noted, however, that each of these structures is possible for a compound of formula $Mo_4(OR)_{12}$ and, since the $Mo_2(OR)_6$ (M≡M) structure is only realized with bulky R groups, the structures of the polymeric compounds $[Mo(OEt)_3]_n$ and $[Mo(OMe)_3]_n$ are clearly worthy of investigation.

6. Hexanuclear alkoxides

In methanol as solvent, molybdenum(II) halides react with NaOMe to give $Na_2Mo_6X_8(OMe)_6$ compounds, where X = Cl and Br.[36] Based on spectroscopic data, these compounds can reasonably be formulated as $Mo_6(\mu_3\text{–X})_8^{4+}$-containing clusters in which six OMe ligands are terminally bonded to each molybdenum atom and radiate from the centre of an idealized Mo_6-octahedral unit. Under more forcing conditions (150°C, NaOMe melt), a yellow–brown crystalline compound of formula $Na_2Mo_6(OMe)_{14}$ is obtained.[36] This compound is pyrophoric in air and shows two types of OMe ligands in the ^1H NMR spectrum in the integral ratio 3:4, which is consistent with a cube–octahedral relationship for a $Mo_6(\mu_3\text{–OMe})_8^{4+}$ moiety with six terminal OMe ligands. A full structural study seems warranted for this 24-electron Mo_6 cluster compound.

7. Physical evidence for RO-to-M π-bonding

Direct evidence for RO-to-M multiple bonding can be seen in a large number of structural studies. For terminal alkoxy ligands, the C_{sp^3}–O distances average 1.44(2) Å. Given that this is a

single bond distance and that the radius of C_{sp^3} is 0.77 Å, then the covalent radius of oxygen (single bond) is placed at 0.67 Å. The covalent radius of molybdenum or tungsten may be reasonably estimated from M–C_{sp^3} distances. For example, in compounds of formula 1,2-$M_2R_2(NMe_2)_4$[37] or 1,2-$Mo_2(OBu^t)_2(CH_2SiMe_3)_4$,[38] where the M–$C_{sp^3}$ distances are 2.17(2) Å, the single bond covalent radius for M is determined to be 1.40 Å. This then sets $d_{(Mo-O)} = r_M + r_0 = 2.06$ Å. This value is in fact typical of M–μ–OR distances, but considerably longer than any seen for terminal M–OR groups which fall in the range 1.80–1.96 Å. In $Mo_2(OCH_2Bu^t)_6$, the average Mo–O distance is 1.88(2) Å.[6] In this molecule, it is the metal δ-type orbitals, d_{xy} and $d_{x^2-y^2}$, which are primarily involved in π-bonding and an average Mo–O bond order of 1.66 is thus expected to correlate with this distance. Upon addition of another ligand, one of the in-plane orbitals becomes used in σ-bonding. Typically in $M_2(OR)_6L_2$ compounds, the M–O distances are in the range 1.90–1.96 Å, consistent with a net decrease in π-bonding. On the other hand, in 1,2-$Mo_2(OBu^t)_2(CH_2SiMe_3)_4$, where each alkoxy group may be fully involved in π-bonding, the Mo–O distance is shorter. A listing of terminal and bridging M–OR bond distances is given in Table 3.

Table 3. Representative M–O distances (Å) in molybdenum and tungsten alkoxides[a]

Compound	M–O (terminal)	Mo–O (μ_2)	Mo–O (μ_3)	Ref
$Mo_2(OCH_2Bu^t)_6$	1.905(6) 1.867(6) 1.855(6)			6
$Mo_2Cl_4(OPr^i)_6$	1.815(3) 1.808(3) 1.819(3) 1.814(3)	2.020(3) 2.013(3) 2.014(3) 2.016(3)		25
$W_2Cl_4(OEt)_6$	1.820(4) 1.828(4)	2.011(4) 2.013(4)		24
$Mo_2(OPr^i)_8$	1.976(3) (axial) 1.884(3) (eq) 1.872(3) (eq)	2.111(3) (axial) 1.958(3) (eq)		16
$Mo_3O(OCH_2Bu^t)_{10}$[a]	1.94(2) (trans to O) 1.85(2) (trans to OR)	2.02(3)	2.21(3)	27
$Mo_4Cl_4(OPr^i)_8$[a]		1.981(4) 2.078(4)		50
$Mo_4Br_4(OPr^i)_8$[a]	1.84(1)	2.02(2)	2.15(1)	50
$W_4(OEt)_{16}$[a]	1.93(3)	2.04(3)	2.18(2)	30
$Mo_2(OBu^t)_6(CO)$	1.88(1) 1.89(1)	2.09(1) 2.07(1)		68
$Mo_2(OPr^i)_6(py)_2(CO)$	1.909(6) 1.920(5)	2.098(6) 2.113(6)		69
$W_2(OPr^i)_6(py)_2(CO)$	1.91(2) 1.92(2)	2.12(2) 2.15(2)		69
$[W(OMe)_4NPh]_2$	1.92(1) 1.97(1) 2.02(1)	2.04(1) (trans to OMe) 2.14(1) (trans to NPh)		b

[a]Averaged where appropriate.

[b]A.J. Nielson and J.M. Waters, Polyhedron 1981, 1, 561.

Of course, many factors may influence an individual M–O distance, particularly the oxidation state of the metal, the *trans*-ligand and steric and electronic properties of adjacent ligands.[39] It is, however, safe to say terminal RO-to-Mo or -W distances are always shorter than would be expected from considerations of single bond radii.

The influence of RO-to-M π-bonding may be shown in the spectroscopic properties of adjacent ligands. (1) In $Mo(OBu^t)_2(py)_2(CO)_2$,[40] the low values of $v(CO)$, 1906 and 1776 cm^{-1}, arise because π-donor ligands enhance t_{2g}^4 backbonding to carbonyl π^* orbitals. (2) In $MoO_2(OPr^i)_2(bpy)$,[41] which contains the *cis*-Mo(6+)O$_2$ moiety and a pair of mutually *trans* OPr^i ligands, the oxo and OPr^i ligands compete to fill (π-donate with) the vacant Mo t_{2g} orbitals. There is an abundance of π-electrons to do this job. An oxo group may be a six electron donor and usually a *cis*-Mo(6+)O$_2$ group will contain two Mo–O groups of bond order 2.5. It has been noted that Mo–O bond distance, Mo–O bond order and ^{17}O chemical shifts correlate linearly for terminal Mo–O groups.[42] In $MoO_2(OPr^i)_2(bpy)$, the Mo–O (oxo) distances, 1.71(1) Å (averaged), and the ^{17}O chemical shift value of 878 ppm are longer and lower, respectively, than the values anticipated for a *cis*-Mo(6+)O$_2$ function in octahedral complexes. The maximum Mo–O π bond order of 1.5 is evidently not attained because some RO-to-Mo π-bonding occurs. The latter, however, is relatively small as evidenced by the rather long Mo–OPr^i distances, 1.93(1) Å (averaged).[41]

III. CHEMICAL REACTIONS

By far the most extensively studied group of alkoxides of molybdenum and tungsten are the dinuclear compounds of formula $M_2(OR)_6$ (M≡M). Their reactions are discussed in detail and, where appropriate, related reactions involving other alkoxides are noted.

1. *Lewis base association reactions*

In hydrocarbon solutions, $M_2(OR)_6$ compounds (M≡M) react with N and P donor ligands, L, according to the equilibrium reaction (1) shown below.[6,9,10,43,44]

$$M_2(OR)_6 + 2L \rightleftharpoons M_2(OR)_6L_2; \text{ K.} \tag{1}$$

The position of equilibrium is very sensitive to the nature of R and L and for related compounds $K_W > K_{Mo}$. Also, tungsten prefers to coordinate P donors relative to N donors, provided steric factors permit coordination. Several adducts have now been structurally characterized. All structures are based on conformations of **IX**.
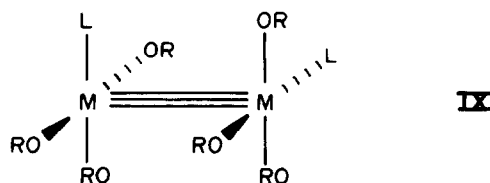
Each metal atom is coordinated to four atoms which lie roughly in a plane; the two metal atoms are united by a triple bond and the two halves of the molecule adopt a conformation which is determined by ligand–ligand interactions across the M–M bond. In general, steric repulsive interactions favour staggered conformations, but for $W_2(OPr^i)_6(HNMe_2)_2$, a near eclipsed geometry is found. In the latter case, N–H——OR hydrogen bonding occurs across the M–M bond similar to that found in $W_2Cl_4(OR)_4(HOR)_2$ compounds.[20] Some pertinent structural data for these Lewis base adducts are given in Table 4.

The equilibrium (1) may be monitored by NMR spectroscopy as a function of temperature. At room temperature in toluene-d_8, $Mo_2(OPr^i)_6$ and pyridine react rapidly and reversibly to give $Mo_2(OPr^i)_6(py)_2$. On lowering the temperature, the equilibrium position shifts in favour of the adduct and pyridine dissociation–association becomes slow on the NMR time-scale. The spectrum of the adduct at *ca.* −25°C, 220 MHz, indicates two types of OPr^i ligands in the integral ratio 2:1, consistent with *cis* and *trans* Pr^{i}O–W–*py* groups. At this temperature, rotation about the M–M

Table 4. Comparison of M–M, M–N, M–O bond distances (Å) and relevant bond angles (°) in selected $M_2(OR)_6L_2$ compounds[a]

Compound	M–M	M–N(av)	M–M–L(av)	L–M–M–L	$M–O^t$	$M–M–O^t$	$M–O^c$(av)	$M–M–O^c$(av)	Ref
$W_2(OPr^i)_6(HNMe_2)_2$	2.339(1)	2.28	90.6	95.0	1.90	110.1	1.96	100	43
$W_2(OPr^i)_6(py)_2$	2.334(1)	2.27	91.8	58.6	1.92	105.7	1.94	102	9
$W_2(OCH_2Bu^t)_6(pyMe-4)_2$	2.328(2)	2.27	97.4	127.2	1.94	99.2	1.92	107	43
$W_2(OEt)_6(DMEDA)$	2.296(2)	2.28	90.0	48.3	1.89	106.8	1.94	102	43
$W_2(OCH_2Bu^t)_6(PMe_3)_2$	2.362(2)	2.52	90.2	114.0	1.95	113.3	1.96	104	b
$Mo_2(OPr^i)_6(py)_2$	2.250(2)	2.32	92.7	56.5	1.90	104.3	1.95	104	43
$Mo_2(OCH_2Bu^t)_6(py)_2$	2.222(1)	2.31	95.1	44.5	1.96	105.8	1.94	103	43
$Mo_2(OSiMe_3)_6(HNMe_2)_2$	2.242(1)	2.28	94.6	110.0	1.94	101.6	1.95	103	c
$Mo_2(OCH_2Bu^t)_6(DMEDA)$	2.218(1)	2.31	91.1	51.3	1.92	101.6	1.96	102	43

[a]Abbreviations are as follows: py = pyridine; pyMe-4 = 4-methylpyridine; DMEDA = $Me_2NCH_2CH_2NMe_2$; O^t = oxygen trans to L; O^c = oxygens cis to L. [b]M.J. Chetcuti, M.H. Chisholm and J.C. Huffman, results to be published. [c]M.H. Chisholm, F.A. Cotton, M.W. Extine and W.W. Reichert, J. Am. Chem. Soc. 1978, 100, 153.

bond is rapid, but at lower temperatures and at higher magnetic field strengths (below $-50°C$, 360 MHz), three OPr^i ligands are seen in the integral ratio $1:1:1$. The spectrum is thus consistent with the adoption of a structure having C_2 symmetry akin to that found in the solid state.[43] For some compounds, e.g. $Mo_2(OCH_2Bu')_6(py)_2$, low temperature spectra have been obtained indicative of freezing out two conformations, each having C_2 symmetry for the $M_2O_6N_2$ skeleton; furthermore, restricted rotations about Mo–L bonds are observed.[43]

For P donor ligands (PMe_3, PMe_2Ph, PPh_3, $Me_2PCH_2CH_2PMe_2$ and $Ph_2PCH_2CH_2PPh_2$), the equilibrium (1) may also be monitored by ^{31}P NMR spectroscopy. For specific combinations of alkoxide and P donor ligands, it is possible to observe high temperature limiting spectra corresponding to free phosphine and low temperature spectra corresponding to the adducts. This is because the favourable enthalpy of binding in (1) may be offset at higher temperatures by the negative entropy of binding. The ^{31}P chemical shifts of free and coordinated phosphines differ by ca. 25 ppm. At intermediate temperatures, a single broadened resonance is observed. The position of this resonance is dependent upon the relative concentrations of coordinated and free phosphine and the line shape is influenced by the rate of exchange. The ^{31}P NMR spectra of the ditungsten adducts show interesting satellite features due to couplings (one and two bond) to ^{183}W, $I = \frac{1}{2}$, 15% natural abundances (see Fig. 8).
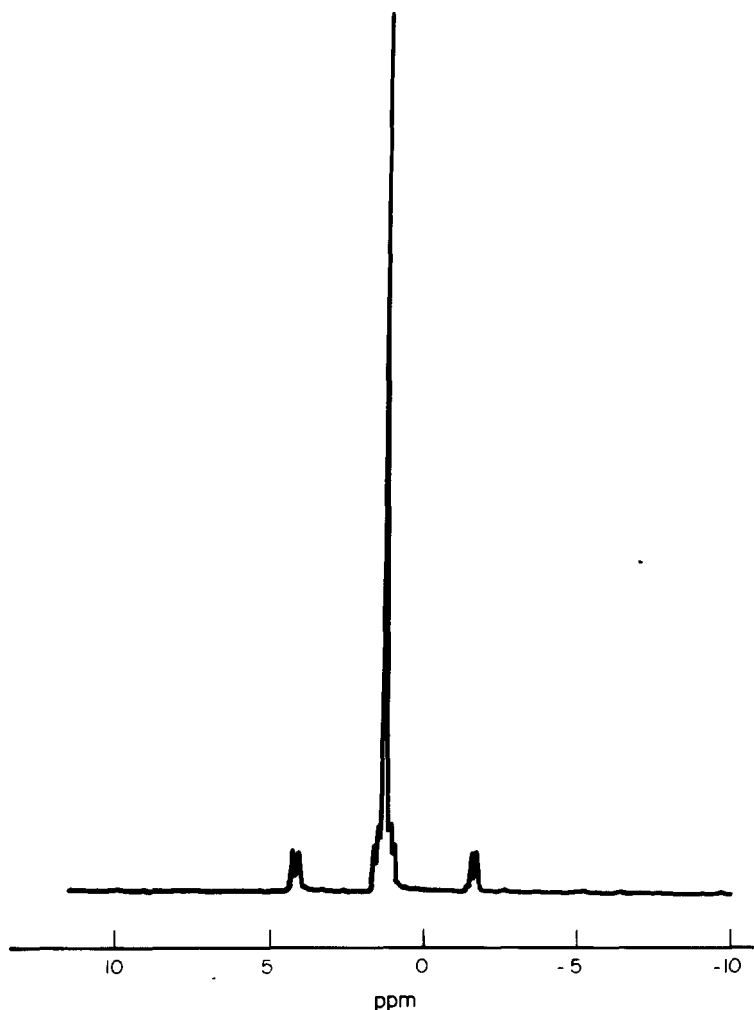
Fig. 8. ^{31}P NMR spectrum (40.5 MHz, 25°C, toluene-d_8 solvent) of $W_2(OCH_2Bu')_6(PMe_3)_2$. Chemical shift $\delta = 1.5$ ppm relative to external H_3PO_4 (85% aq); $^1J_{183W-31P} = 240$ Hz, $^2J_{183W-31P} = 20$ Hz and $^3H_{31P-31P} = 5.4$ Hz.

The equilibrium (1) may also be monitored by UV-visible spectroscopy. All the adducts of formula $M_2(OR)_6L_2$ are more intensely coloured than the parent $M_2(OR)_6$ compounds. On adduct formation, the lowest energy transition of the $M_2(OR)_6$ compounds, v_1, which corresponds to M–M π-to-M–L π^*, $(d_{xy}, d_{x^2-y^2})$ splits into two bands. One band moves to higher energy and the other to lower energy: it is the latter which is responsible for absorption in the visible region.

One other intriguing aspect to emerge from studies of (1) is the finding that $M_2(OR)_6L$ species are unstable with respect to disproportionation to $M_2(OR)_6$ and $M_2(OR)_6L_2$. This leads to a cooperative phenomenon. For the sequence depicted by (2), where M_2 represents $M_2(OR)_6$ and M_2L_2 represents $M_2(OR)_6L_2$, both of which are in equilibrium, the second addition of L occurs more rapidly than the first, $k_2 > k_1$. Similarly in the dissociation reaction, the second loss of L is more rapid than the first, $k_{-1} > k_{-2}$.

$$M_2 + L \underset{k_{-1}}{\overset{k_1}{\rightleftharpoons}} M_2L$$

$$M_2L + L \underset{k_{-2}}{\overset{k_2}{\rightleftharpoons}} M_2L_2. \tag{2}$$

This observation is quite contrary to what would be expected from simple considerations of both steric factors and Lewis acid–Lewis base concepts. The origin of the relative instability of $M_2(OR)_6L$ compounds must be electronic, but at present it is not clearly understood.

In contrast to Lewis base association reactions involving $M_2(OR)_6$ compounds which retain the $M{\equiv}M$ bond, $Mo_2(OPr^i)_8$ (M=M) reacts with Lewis bases to give $Mo(OPr^i)_4L_2$ compounds. The latter are paramagnetic and are most likely related to the $Mo(OSiMe_3)_4(HNMe_2)_2$ molecule which has a central MoO_4N_4 skeleton of octahedral geometry in the solid state[15] as is shown in Fig. 9.

2. M–OR bond insertion reactions

$M_2(OR)_6$ compounds react rapidly and reversibly with CO_2, both in hydrocarbon solutions and in the solid state, to give mixed alkoxide–alkylcarbonato compounds according to eqn (3)[45,46]

$$M_2(OR)_6 + 2CO_2 \rightleftharpoons M_2(OR)_4(O_2COR)_2. \tag{3}$$

The mechanism of CO_2 insertion in (3) involves a direct pathway: it does not require a catalyst such as ROH.[46] The alkylcarbonato compounds, $M_2(OR)_4(O_2COR)_2$ are quite stable at room
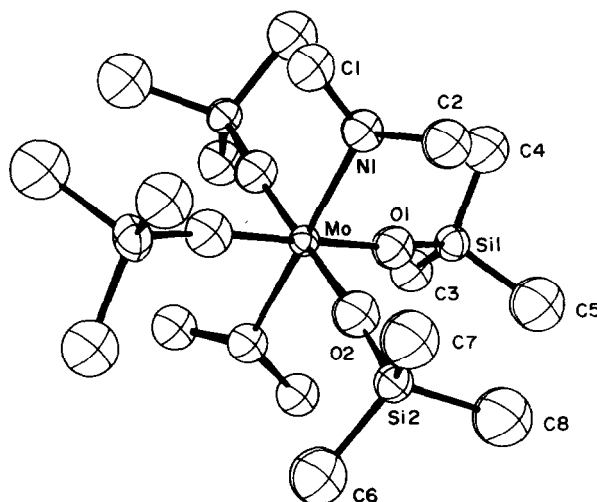
Fig. 9. An ORTEP view of the centrosymmetric $Mo(OSiMe_3)_4(HNMe_2)_2$ molecule showing the *trans* octahedral geometry of the MoO_4N_2 skeleton. Pertinent distances (Å) and angles (°) are: Mo–O(1), –O(2), –N(1) = 1.950(4), 1.951(4), 2.219(4); O(1)–Mo–O(1)′, –O(2), –O(2)′, –N(1), –N(1)′ = 180.0(3), 89.2(1), 90.8(1), 94.6(1), 85.4(1); Mo–O(1)–Si(1) = 170.8(2); Mo–O(2)–Si(2) = 174.2(2).

temperature, but readily and reversibly lose CO_2 when heated to 60–80°C. In solution, however, the alkylcarbonato compounds readily lose CO_2 according to (3) and must be maintained under an atmosphere of CO_2 (25°C) if the equilibrium is to favour the insertion product.

The solid state molecular structure of $Mo_2(OBu^i)_4(O_2COBu^i)_2$ was determined by an X-ray study and revealed the *cis*-bridged geometry depicted by **X**. The presence of a pair of bridging O_2CX groups imposes a near-eclipsed conformation as is shown in Fig. 10.
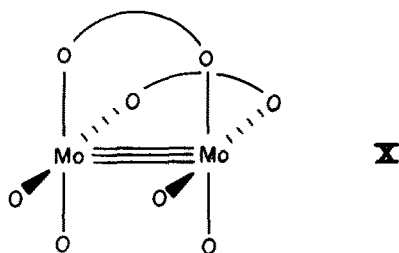
The ^1H NMR spectra of $M_2(OR)_4(O_2COR)_2$ compounds (R = $CHMe_2$ and CH_2CMe_3) are consistent with the presence of a *cis*-bridged O_2COR structure in solution. Specifically, for the Mo–OR ligands, the methyl groups are diastereotopic for the isopropoxy compound, giving rise to a pair of doublets, and the methylene protons are diastereotopic for the neopentoxide, which gives rise to an AB quartet.
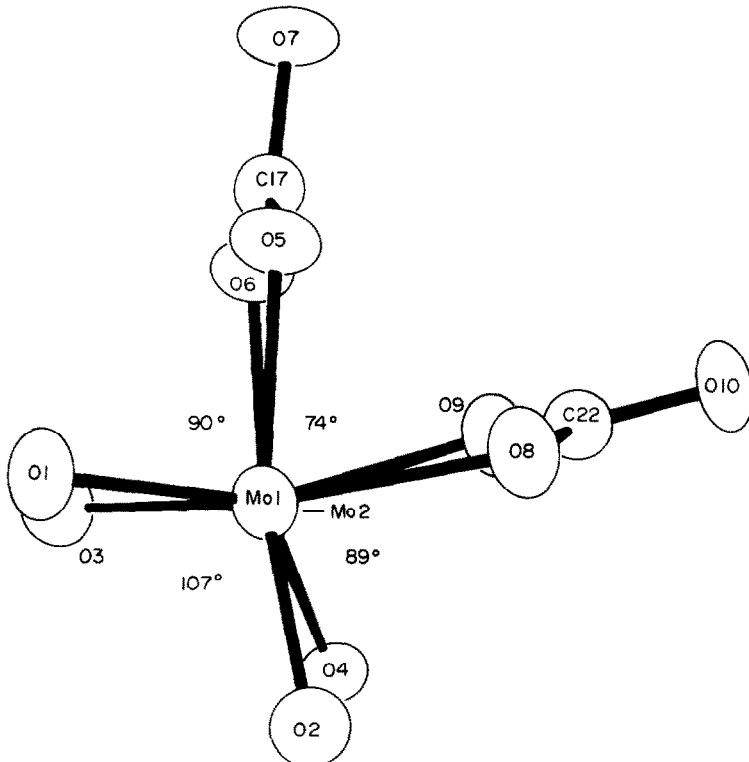
Fig. 10. An ORTEP view of the central skeleton of the $Mo_2(OBu^i)_4(O_2COBu^i)_2$ molecule viewed down the Mo–Mo bond showing the near eclipsed geometry caused by the presence of the *cis*-bridging O_2COR ligands. Some pertinent distances (Å) are: Mo–Mo = 2.241(1); Mo–OBu^i = 1.88(2), Mo–O–(alkylcarbonate) = 2.12(2).

$M_2(OR)_6$ compounds have also been found to react with alkyl- and aryl-cyanates, $R'NCO$, to give insertion products $M_2(OR)_4\{OC(OR)NR'\}_2$. This insertion reaction is irreversible and the products are quite stable in solution. The ^1H NMR spectra are generally consistent with the *cis*-bridged, head-to-tail structure found for $Mo_2(O_2CH_2CMe_3)_4(OC(OCH_2CMe_3)NPh)_2$ in the solid state,[47] which is represented by **XI** below.
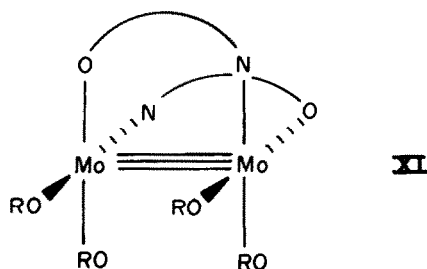
3. *Ligand exchange reactions*

A number of closely related compounds to those depicted by **X** and **XI** have been obtained from protolysis reactions in which a bidentate ligand is substituted for an OR group. For example, the reactions between 1,3-diaryltriazines and $Mo_2(OR)_6$ compounds give $Mo_2(OR)_4(ArN_3Ar)_2$ compounds and related reactions involving 2-hydroxypyridine yield $Mo_2(OR)_4(O-N)_2$ where O–N is the dianion derived from deprotonation of 2-hydroxypyridine.[48] The structural characterization of $Mo_2(OPr^i)_4(O-N)_2$ revealed the *cis*-bridged, head-to-tail geometry depicted by **XI** in the solid state and ^1H NMR studies are consistent with this structure being maintained in solution.

Bidentate ligands generally bridge the Mo≡Mo bond when formation of a five-membered ring is achieved, e.g. as is found for $RCOO^-$, $ArNNNAr^-$ and $R'NC(OR)O^-$ ligands. However, reactions between $M_2(OR)_6$ compounds and 2,4-pentanedione, acacH, proceed to give $M_2(OR)_4(acac)_2$ derivatives in which the acac ligands are bidentate, but are chelated to each metal. The structure of $Mo_2(OCH_2CMe_3)_4(acac)_2$ found in the solid state is shown in Fig. 11. Presumably
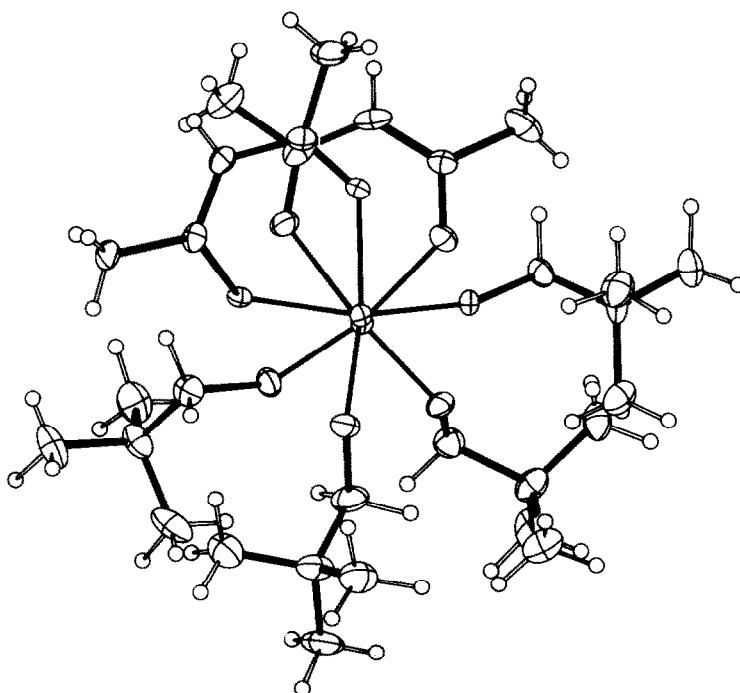
Fig. 11. An ORTEP view of the $Mo_2(OCH_2Bu^t)_4(acac)_2$ molecule looking down the Mo–Mo bond showing the staggered conformation. Some pertinent distances (Å) are Mo–Mo = 2.237(1), Mo–OR = 1.89(1) (averaged) and Mo–O–(acac) = 2.08(2) (averaged). The Mo–Mo–O angles fall in the range 97–104°.

the formation of the six-membered ring is favoured relative to the seven-membered ring which would be required if acac⁻ were to span the Mo≡Mo bond. Using unsymmetrically substituted acac⁻ ligands which form A–B-type chelates, three geometric isomers are possible, each having an enantiomer. However, in solution we have only been able to observe two isomers, probably because extremely facile rotation about the Mo≡Mo bond rapidly interconverts two isomers on the ^{1}H NMR time-scale.

4. *Halide-for-alkoxide exchange*

From the reaction between $Mo_2(OBu^t)_6$ and PF_3 in hydrocarbon solvents, a black crystalline product of empirical formula $MoF(OBu^t)_2$ was isolated.[49] During one such preparation, crystals suitable for an X-ray study were obtained and, when this was undertaken, the unit cell was found to contain a mixture of molecules $Mo_4F_4(OBu^t)_8$ and $Mo_4F_3(OBu^t)_8(NMe_2)$ in the ratio 1:2. The presence of the NMe_2 group, which was not anticipated, can reasonably be traced to incomplete alcoholysis in the preparation of $Mo_2(OBu^t)_6$ from $Mo_2(NMe_2)_6$. The structure of the $Mo_4F_4(OBu^t)_8$ molecule is shown in Fig. 12. The central Mo_4 unit is a bisphenoid with two short Mo–Mo distances, 2.24 Å, and four long Mo–Mo distances, ca 3.75 Å. The molecule may be viewed as two Mo≡Mo units brought together through the agency of fluoride bridges. Each $Mo_2(OBu^t)_4(\mu\text{-F})_2$ unit (M≡M) has a geometry very similar to that found in $Mo_2(OBu^t)_4(O_2COBu^t)_2$.[46] The $Mo_4F_3(OBu^t)_8(NMe_2)$ molecule has one $\mu\text{-NMe}_2$ group in place of a μ–F group, but this produces a negligible effect on the M–M distances in the Mo_4 moiety.

In search of a more general route to mixed halide–alkoxide compounds, we have initiated studies of the reactions between $Mo_2(OPr^i)_6$ and acetyl halides.[50] In hexane, $Mo_2(OPr^i)_6$ and CH_3COX (X = Cl and Br) produce black crystalline compounds of empirical formula $Mo_4X_3(OPr^i)_9$. These compounds are only very sparingly soluble in hexane, but are appreciably soluble in toluene. ^{1}H NMR spectra recorded in toluene-d_8 and benzene-d_6 are consistent with that
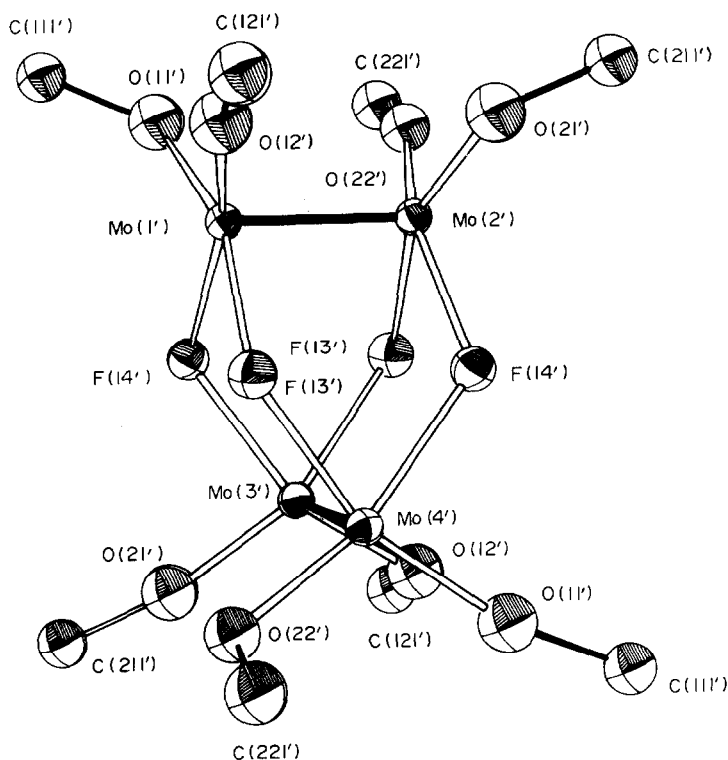
Fig. 12. An ORTEP view of the central skeleton of the $Mo_4(OBu^t)_8(\mu_2\text{-F})_4$ molecule. Pertinent distances (Å) are: Mo(1′)–Mo(2′) = 2.262(2), Mo(3′)–Mo(4′) = 2.263(2), Mo(1′)–Mo(3′) = 3.743(2), Mo(1′)–Mo(4′) = 3.730(2), Mo(2′)–Mo(3′) = 3.713(2), Mo(2′)–Mo(4′) = 3.700(2), Mo–μ–F = 2.10(2) (averaged) and Mo–O = 1.94(2) (averaged).

expected for a $Mo_4(\mu_2\text{-}X)_3(\mu_2\text{-}OPr^i)(OPr^i)_8$ structure akin to that described above for $Mo_4F_3(NMe_2)(OBu^t)_8$.

A further reaction between $Mo_4X_3(OPr^i)_9$ and CH_3COX or a direct reaction between $Mo_2(OPr^i)_6$ and CH_3COX (2 equiv) in toluene yield black crystalline compounds of empirical formula $MoX(OPr^i)_2$. These compounds are only very sparingly soluble in toluene and little is known about their solution properties. The solid state molecular structures are fascinating, however. For the chloride,[50] there is a square of molybdenum atoms with eight bridging (μ_2)OPr^i ligands, four lying above and four lying below thĕ Mo_4 plane. The Mo–Cl bonds are terminal and radiate from the centre of the Mo_4-square (see Fig. 13). The central $Mo_4O_8Cl_4$ unit has virtual D_{4h} symmetry. The Mo–Mo distance of 2.37 Å implies strong Mo–Mo bonding. The compound is diamagnetic and, in a formal sense, may be viewed as an inorganic analogue of cyclobutadiene formed by the coupling of two Mo≡Mo units.

Quite remarkably, the structure of the bromide, $Mo_4Br_4(OPr^i)_8$, is different from that of the chloride just discussed. The bromide contains a butterfly or opened-tetrahedron of molybdenum atoms with five relatively short Mo–Mo distances, ca. 2.5 Å, and one long distance, 3.1 Å.[50] The Mo–Br groups are all terminal, but the Mo–OPr^i groups are terminal (2) and doubly (4) and triply (2) bridging as shown in Fig. 14.

The $Mo_4X_4(OPr^i)_8$ structures, where X = Cl and Br, may be viewed as subunits of the well known $Mo_6(\mu_3\text{-}X)_8^{4+}$ unit.[51-53] In both of the alkoxide structures, the oxygen atoms lie roughly at the corners of an idealized O_8 cube. The four molybdenum atoms occupy positions at four faces of the cube such that two opposite faces are vacant (X = Cl) or two adjacent faces are vacant (M = Br) relative to the $Mo_6(\mu_3\text{-}X)_8^{4+}$ geometry.
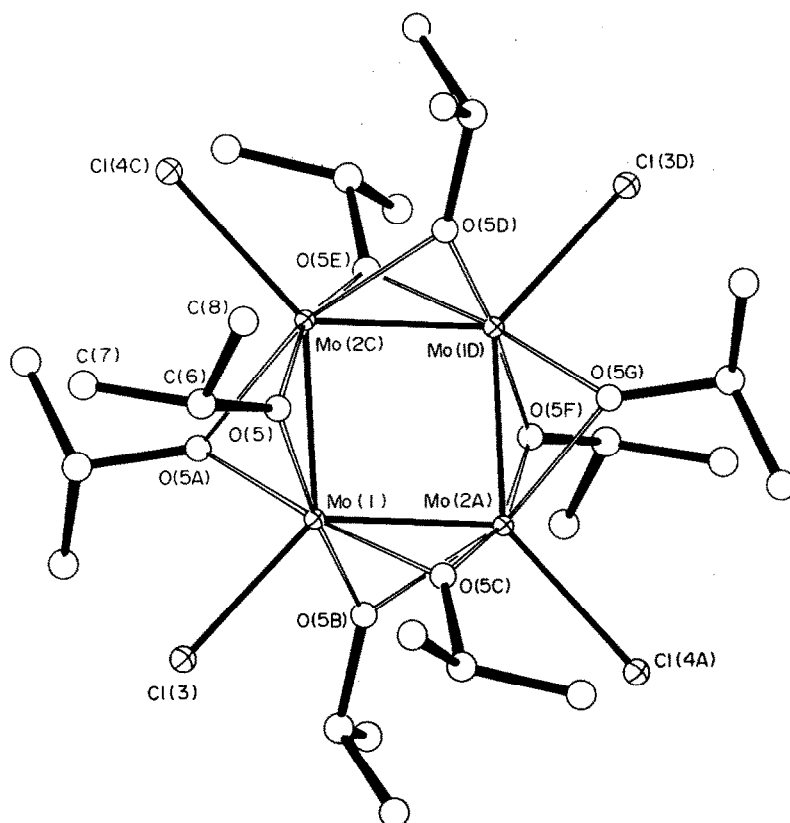
Fig. 13. An ORTEP view of the $Mo_4Cl_4(OPr^i)_8$ molecule. The molecule has a crystallographically imposed C_2 axis, which contains Cl(3)–Mo(1)–Mo(1D)–Cl(3D), and a mirror plane, which contains Cl(4C)–Mo(2C)–Mo(2A)–Cl(4A) and relates atoms O(5) and O(5D), O(5A) and O(5E), etc. Pertinent bond distances (Å) and angles are: Mo(1)–Mo(2C) = 2.378(2), Mo(1)–Cl(3) = 2.442(5), Mo(1)–O(5) = 1.981(4), Mo(2C)–O(5) = 2.078(4); Mo(2C)–Mo(1)–Mo(1D) = 91.4(1); Mo(1)–Mo(2C)–Mo(1D) = 88.5(1); Cl(3)–Mo(1)–O(5) = 93.3(1).
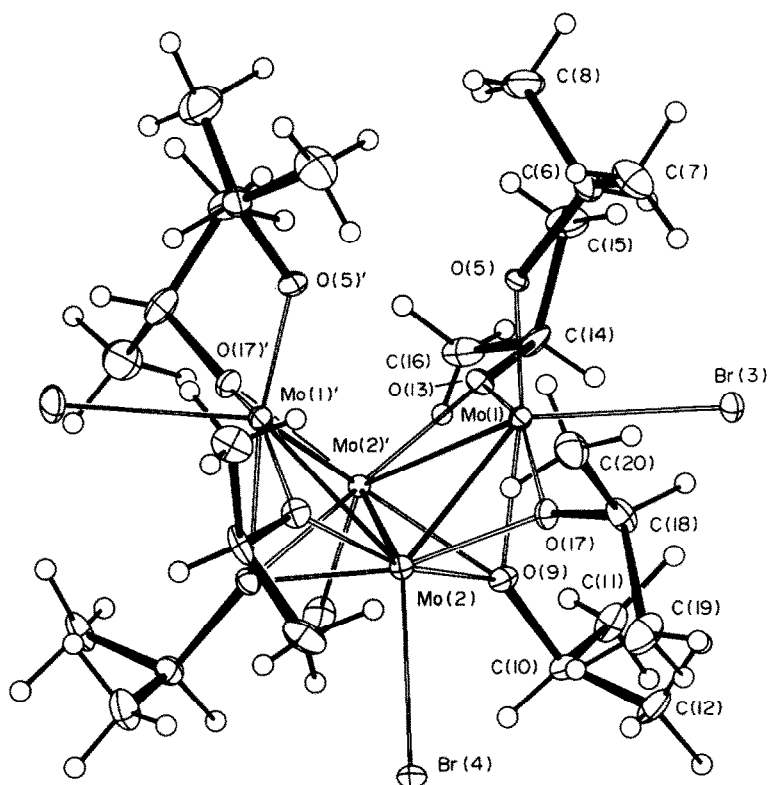
Fig. 14. An ORTEP view of the $Mo_4Br_4(OPr^i)_8$ molecule which has C_{2v} symmetry. Some pertinent distances (Å) and angles (°) are: $Mo(1)-Mo(2) = 2.513(1)$, $Mo(2)-Mo(1)' = 2.516(1)$; $Mo(2)-Mo(2)' = 2.481(1)$; $Mo(1)-Br(3) = 2.596(1)$; $Mo(2)-Br(4) = 2.568(1)$; $Mo-OR = 1.84(1)$ (terminal), $2.02(1)$ (μ_2) and $2.15(1)$ (μ_3) (averaged); $Mo(1)-Mo(2)-Mo(1)' = 81.6(1)$; $Mo(1)-Mo(2)-Mo(2)' = 60.5(1)$.

It seems likely that the $Mo_4X_4(OPr^i)_8$ molecules will be reactive toward further association reactions: $M_2 + M_4 \rightarrow M_6$, etc. It may ultimately be possible to systematically interconvert M_2 (multiple bond), M_4 (cluster) and M_6 (octahedral) complexes. It should also be noted that McCarley et al.[54] have coupled two $Mo\equiv Mo$ bonds to form a rectangular Mo_4^{8+} containing compound: $2Mo_2Cl_4(PR_3)_2(HOMe)_2 \rightarrow Mo_4Cl_4(\mu_2-Cl)_4(PR_3)_4 + 4MeOH$. The M–M distances are alternating long and short, indicative of single and triple bonds, respectively, in a simple valence bond description.

At this point, it is worth noting the variety of M_4-alkoxide structures that have been found for molybdenum and tungsten: $Mo_4F_4(OBu^i)_8$,[49] $Mo_4Cl_4(OPr^i)_8$,[50] $Mo_4Br_4(OPr^i)_8$,[50] $W_4(OEt)_{16}$[30] and $W_4(\mu-H)_2(OPr^i)_{14}$.[35] In each structure, M–M bonding is clearly important, but it is not clear what factors are responsible for the adoption of one geometry relative to another. Why do the $Mo_4X_4(OR)_8$ structures differ for X = F, Cl and Br, and why are two localized W=W bonds found in $W_4(\mu-H)_2(OPr^i)_{14}$, rather than an 8-electron W_4 cluster of the type seen in $W_4(OEt)_{16}$? These questions provide the stimulus for further studies in the area.

5. Oxidative-addition reactions

Compounds with M–M multiple bonds have a source of electrons which may be tapped for oxidative processes. A number of simple stepwise M–M bond order transformations have been observed.[55] Oxidative-addition reactions involving $Mo_2(OPr^i)_6$ ($M\equiv M$) have been noted to give $(Mo=Mo)^{8+}$-containing compounds as shown in eqn (4).

$$Mo_2(OPr^i)_6 + X_2 \rightarrow Mo_2(OPr^i)_6X_2 \qquad (4)$$
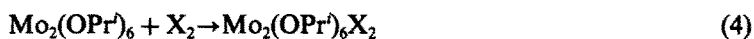
where $X = Pr^iO^{11}$ or $PhCOO$.[41,56]

The structure and bonding in $Mo_2(OPr^i)_8$ has already been discussed. The structure of $Mo_2(OPr^i)_6(O_2CPh)_2$ has not been determined by a single crystal study, but NMR characterization suggests the edge-shared octahedral geometry shown in XII.

XII

O = OR

$\overset{\frown}{O \quad O}$ = $PhCO_2$
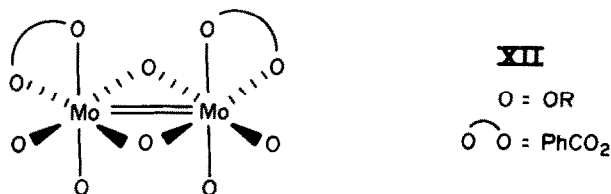
The direct addition of halogens X_2, where $X = Cl$, Br and I, to hydrocarbon solutions of $Mo_2(OPr^i)_6$ gives edge-shared octahedral complexes with Mo–Mo single bonds, $Mo_2(OPr^i)_6X_4$, VII.[25] Attempts to prepare $Mo_2(OPr^i)_6X_2$ (M=M) compounds by the careful addition of one equivalent of the halogen were unsuccessful and there is evidence that such compounds are unstable with respect to disproportionation to $Mo_2(OR)_6$ and $Mo_2(OPr^i)_6X_4$ compounds. However, from the reaction between $Mo_2(OR)_6$ and $PhCHBr_2$ in hexane/pyridine solvent mixtures, compounds of formula $Mo_2(OR)_6Br(py)$ have been isolated.[57] The neopentoxide has been shown to have an interesting confacial bioctahedral geometry involving two μ_2-OR and one μ-Br ligand (see Fig. 15). The Mo–Mo distance, 2.534(1) Å, is consistent with the presence of a $(Mo=Mo)^{8+}$ unit. However, in a formal sense, the oxidation states of the two molybdenum atoms differ, $Mo(4\frac{1}{2}+)$ and $Mo(3\frac{1}{2}+)$. The ^1H NMR spectra in toluene-d_8 are consistent with the maintenance of this structure in solution.

A number of other substrates react with $M_2(OR)_6$ compounds to give adducts which may be viewed as products of redox reactions. For example, orthoquinone ligands can behave as neutral, -1 (semiquinones) or -2 (catecholate) ligands.[58] The adducts with $M_2(OR)_6$ compounds, either 1:1 or 2:1, are often highly coloured, presumably due to low energy charge transfer, either MLCT or LMCT. Tetrachloroorthoquinone, which is known to be a good oxidizing agent $(C_6Cl_4O_2 + 2e^- = C_6Cl_4O_2^{2-}, -0.78$ V$)$ has been found to react with $Mo_2(OR)_6$ compounds to give
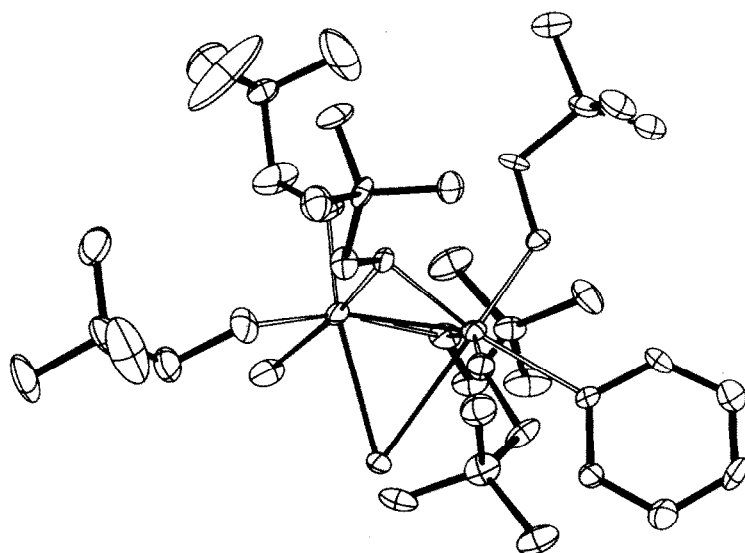
Fig. 15. An ORTEP view of the $Mo_2(OCH_2Bu^t)_6Br_2(py)$ molecule showing the confacial bioctahedral geometry. Some pertinent distances (Å) are: Mo–Mo = 2.534(1), Mo–Br (terminal) = 2.584(1), Mo–Br (μ_2) = 2.73(1) (averaged), Mo–N = 2.257(6). The Mo–O distances are all within the range commonly found for terminal and μ_2 ligands as shown in Table 3.
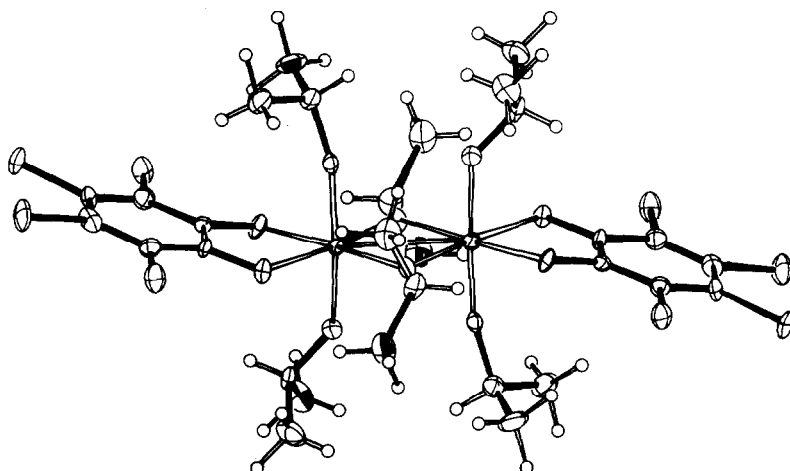
Fig. 16. An ORTEP view of the $Mo_2(OPr^i)_6(O_2C_6Cl_4)_2$ molecule emphasizing the edge-shared octahedral geometry. The Mo–Mo distance is 2.754(2) Å and the Mo–O distances (averaged) are 1.83(1) (terminal OR), 2.01(1) $-\mu$–OR) and 2.02(1) Å $(O_2C_6Cl_4)$.

2:1 adducts $Mo_2(OR)_6(O_2C_6Cl_4)_2$, which may best be viewed as d^1–d^1 dimers. The structure of the isopropoxide is shown in Fig. 16. From a consideration of the Mo–Mo, Mo–O and C–O (quinine) distances, this is clearly a Mo_2^{10+}-containing compound.

$W_2(OPr^i)_6(py)_2$ also reacts with benzil and 2,3-butanedione to give 2:1 adducts of formula $W_2(OR)_6(R_2'C_2O_2)_2$. The structures of the compounds where R = Pr^i and R' = p-tolyl and methyl have been determined in the solid state.[60] The structure of the 2,3-butanedione derivative is shown in Fig. 17. Once again, the W–W, W–O and C–C distances (2,3-butanedione ligand) are indicative of a d^1–d^1, W_2^{10+}-containing molecule. Most notably, the C–C double bond is evidenced by the 1.33(1) Å bond distance which demonstrates the importance of the resonance form **XIIIb** relative to **XIIIa**.
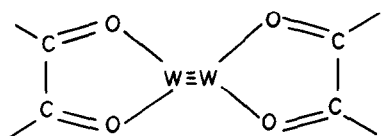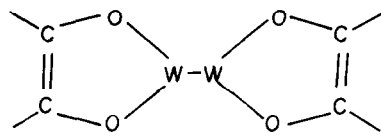
XIIIa   **XIIIb**

In these reactions which oxidize the $(M{\equiv}M)^{6+}$ unit, it is interesting to note that oxidation occurs more readily for tungsten than molybdenum. This is seen, for example, in the alcoholysis reactions of $M_2(NMe_2)_6$ compounds. Whereas molybdenum forms an extensive series of $Mo_2(OR)_6$ compounds, tungsten is readily oxidized to the +4 oxidation state as in the formation of $W_4(\mu-H)_2(OPr^i)_{14}$[35] and $W_4(OEt)_{16}$.[30] The oxidation of the $(W{\equiv}W)^{6+}$ unit may be blocked by strongly coordinating ligands such as pyridine, $MeN(H)CH_2CH_2N(H)Me$ and PMe_3 which give adducts $W_2(OR)_6L_2$ or $W_2(OR)_6(L-L)$ when alcoholysis of $W_2(NMe_2)_6$ is carried out in their presence.[10] The oxidative-addition step presumably proceeds through an unsaturated and reactive intermediate of the form $W_2(OR)_6(HOR)$. This type of oxidative-addition finds a parallel in the recent work of Brown and Nubel.[61] $1,2-Re_2(CO)_8(X-H)_2 \rightarrow Re_2(CO)_8(X-H) \rightarrow Re_2(CO)_8(\mu-H)(\mu-X)$ where X–H = H_2O and C_6H_5N (pyridine).

A number of other reactions with unsaturated organic molecules (π-acceptors such as CO, $RC{\equiv}CR$) lead to adducts which may be viewed as oxidative-addition products. These are discussed later.
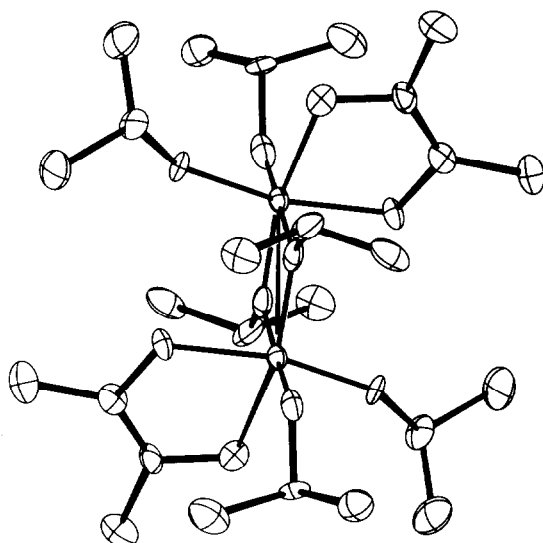
Fig. 17. An ORTEP view of the $W_2(OPr^i)_6(O_2C_2Me_2)_2$ molecule. The W–W distance is 2.754(1) Å and the distances (Å) associated with the $W-O_2C_2Me_2$ moiety are: (averaged) W–O = 1.94(4), C–O = 1.34(2); C–C (central) = 1.35(1).

6. M–M cleavage reactions

$M_2(OR)_6$ compounds react with NO (2 equiv) in hydrocarbon solvents to cleave the M≡M bond. In a formal sense, the M–M σ and π bonds are broken to form two M–N σ bonds and four M–N π bonds (Md-to-NO π^*) as shown in eqn (5).

$$M≡M + 2X \longrightarrow 2M≡X. \tag{5}$$

The molecular structure of $[Mo(OPr^i)_3NO]_2$ deduced from an X-ray study[19] is shown in Fig. 18. Each molybdenum atom is in a distorted trigonal bipyramidal geometry. The molecule is

(a)

$Mo_2(O-i-Pr)_8$
Skeleton

(b)

$Mo_2(O-i-Pr)_6(NO)_2$
Skeleton
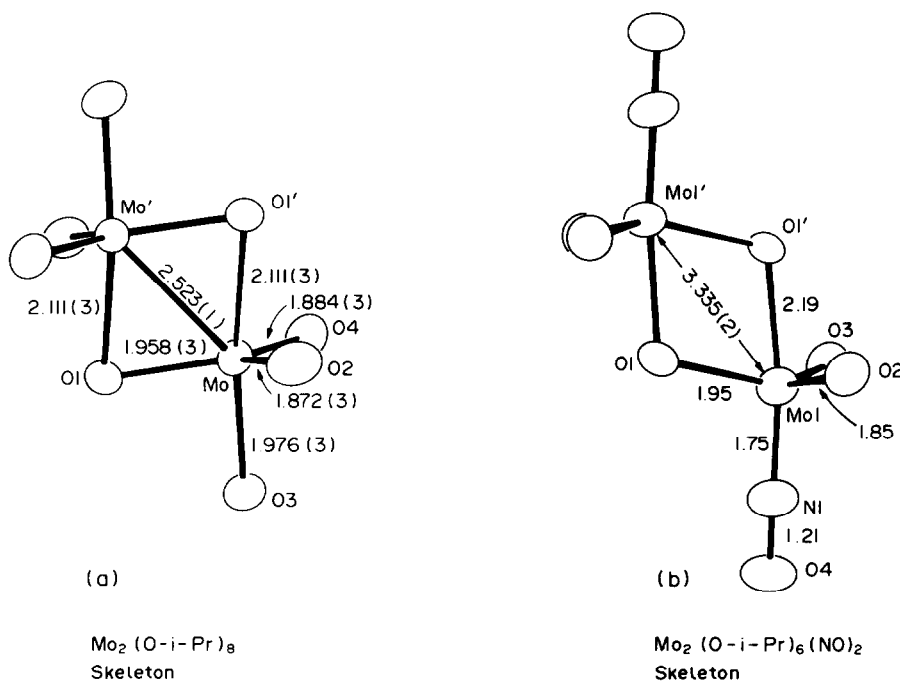
Fig. 18. Comparison of some structural parameters for the centrosymmetric molecules $Mo_2(OPr^i)_8$ and $Mo_2(OPr^i)_6(NO)_2$.

centrosymmetric with linear terminal Mo–N–O groups which occupy axial positions. The two halves of the molecule are joined along a common equatorial axial edge by a pair of μ–OPr^i ligands. The Mo-to-Mo distance is 3.335 Å, typical of a non-bonding M——M distance spanned by a pair of μ–OR ligands (see Table 1). The lack of any M–M bond in $M_2(OR)_6(NO)_2$ compounds can also be seen in their reactions with donor ligands such as pyridine, which leads to $M(OR)_3(NO)(py)$ compounds.[62] The structure of the $W(OBu^i)_3(NO)(py)$[63] molecule is shown in Fig. 19. Again, the local trigonal bipyramidal geometry is seen and extensive $W(d_{xz}, d_{yz})^4$-to-NO π^* bonding is evident from the extremely short W–NO distance and the low value of $v(NO)$, 1555 cm^{-1}. For a series of related $M_2(OR)_6(NO)_2$ compounds, the $v(NO)$ values fall ca. 1720 (M=Cr), 1640 (M = Mo) and 1550 (M = W), which reflects the relative ability of the group 6 metals to backbond to the π-acceptor NO ligand in their oxidation state 3+ (or 2+ if we count $M^-\leftarrow(NO^+)$ for a linear M–N–O group).

Another cleavage of the M≡M bond has recently been reported by Schrock et al.[64] in the reaction between $W_2(OBu^i)_6$ and alkynes as shown in eqn (6)

$$W_2(OBu^i)_6 + RC{\equiv}CR \rightarrow 2(Bu^iO)_3W{\equiv}CR \tag{6}$$
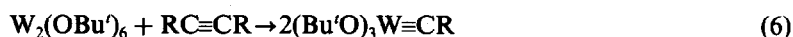
where R = Me, Et, Pr.

The reaction appears to be specific to $W_2(OBu^i)_6$: other alkoxides of W_2^{6+} and related dimolybdenum compounds give different products as will be discussed later. Also, the cleavage of the W≡W bond in (6) is not observed in reactions with ethyne. Closely related to (6) is the cleavage of the W≡W bond in reactions involving nitriles, eqn (7).[64]

$$W_2(OBu^i)_6 + RC{\equiv}N \rightarrow (Bu^iO)_3W{\equiv}N + (Bu^iO)_3W{\equiv}CR \tag{7}$$
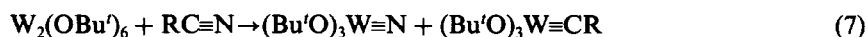
where R = Me, Ph and PhCH$_2$.

If the alkylidyne ligand is counted as a 3-ligand like nitride N^{3-}, then reactions (6) and (7) may be viewed as oxidative-cleavages of the M≡M bond.

Other $W_2(OR)_6$ compounds will react with nitriles to give nitrides, i.e. the reaction is not specific to the Bu^iO ligand, but we have not been able to use (7) to prepare other $(RO)_3W{\equiv}CR'$ compounds. It appears that the alkylidynes may themselves react with nitriles to give nitrides and alkynes. $Mo_2(OR)_6$ compounds do not react with nitriles to give nitrides. Once again the greater reactivity of the W≡W bond, relative to Mo≡Mo, is seen with respect to oxidation.

The molecular structures of the $(Bu^iO)_3W{\equiv}X$ compounds, where X = CMe and N, have been determined in the solid state and are shown in Figs. 20 and 21, respectively.[65] A comparison with
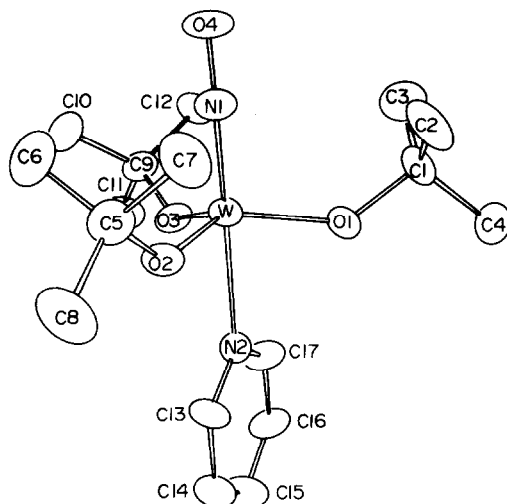
Fig. 19. An ORTEP view of the $W(OBu^i)_3(NO)(py)$ molecule. Some pertinent distances (Å) and angles (°) are W–NO = 1.732(8), W–N(py) = 2.323(7), W–O = 1.88(1) (averaged); W–N–O = 179.2(8), N–W–N = 177.0(3), O–W–N(NO) = 100(1) (averaged).
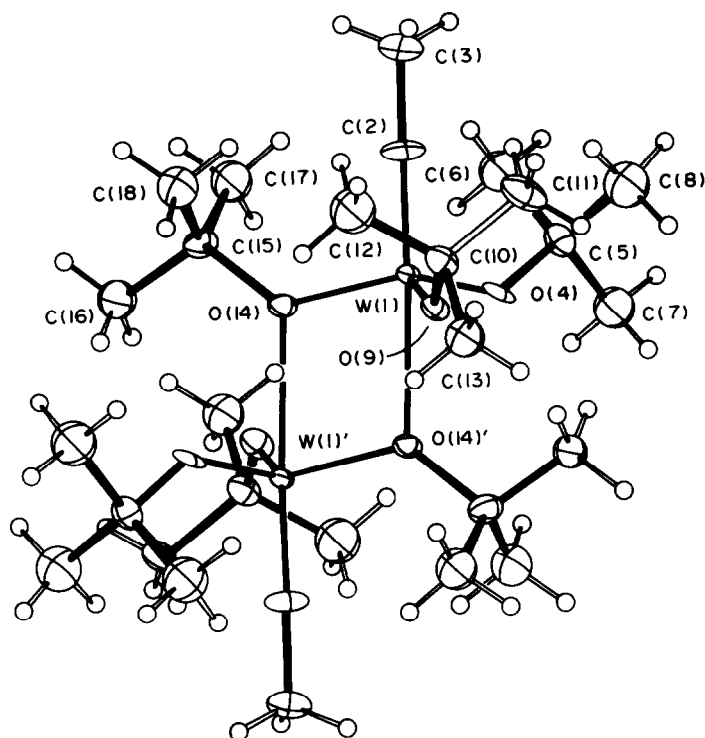
Fig. 20. An ORTEP view of the centrosymmetric [(Bu'O)₃W≡CMe]₂ molecule. Pertinent bond distances (Å) and angles (°) are: W(1)–O(4), –O(9), –O(14), –C(2) = 1.886(4), 1.897(4), 1.934(4) and 1.759(6); W(1)'–O(14) = 2.484(4); C(2)–W(1), –O(4), –O(9), –O(14) = 102.3(2), 101.2(2) and 102.8(2); W(1)–C(2)–C(3) = 179.8(6).

the structures of [Mo(OPr')₃NO]₂ and W(OBu')₃(NO)(py), shown in Figs. 18 and 19, is most interesting. (Bu'O)₃W≡N crystallizes in the hexagonal space group $P6_3cm$ yielding a beautiful view down the C axis, as shown in Fig. 22.

Closely related to (6) and (7) is the cleavage of a M≡M bond by reaction with O₂ to give two M=O bonds, eqn (8).[27,41]

$$Mo_2(OPr')_8 + O_2 \rightarrow 2MoO(OPr')_4. \tag{8}$$
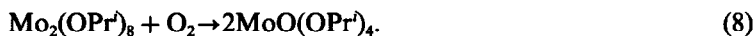
Reaction (8) is extremely rapid and quantitative. However, addition of molecular oxygen to
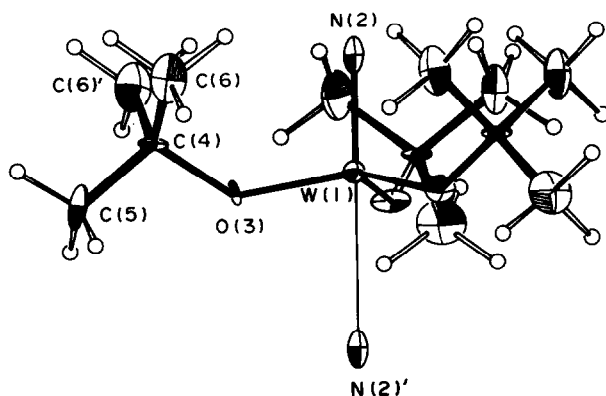
Fig. 21. An ORTEP view of the repeating unit along the C axis in the [(Bu'O)₃WN]ₓ polymer. Pertinent distances (Å) and angles (°) are: W(1)–N(2) = 1.740(15); W(1)–O(3) = 1.872(7); W(1)–N(2)' = 2.661(15); N(2)–W(1)–O(3) = 101.6(2); W(1)–O(3)–C(4) = 136.6(8).
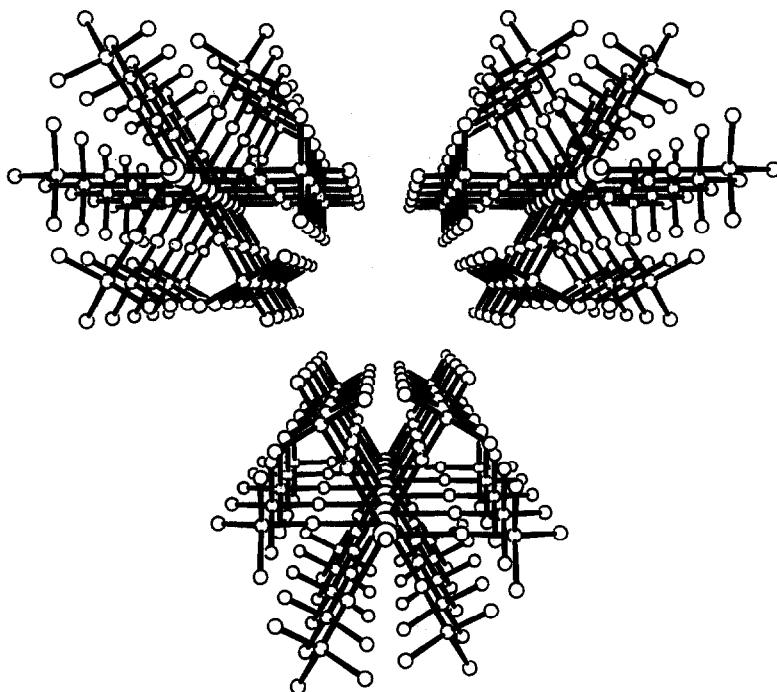
Fig. 22. View of the [W(OBu^t)$_3$N]$_x$ polymer viewed down the C axis from a point at $x = 1/3$, $y = 2/3$. Five cells along the C axis are shown. Hydrogen atoms have been omitted. In the space group $P6_3cm$, there is a hexagonal network of tungsten atoms perpendicular to the C axis.

$M_2(OR)_6$ compounds leads to a variety of products, depending on the metal and the steric properties of the alkoxy ligands.

For molybdenum, the overall reaction proceeds according to (9), but many intermediates may be detected or isolated where $R = Pr^i$ and CH_2CMe_3.[66,41]

$$Mo_2(OR)_6 + 2O_2 \rightarrow 2MoO_2(OR)_2 + 2RO \qquad (9)$$
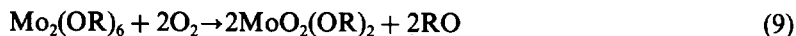
$R = Bu^t$, Pr^i and CH_2CMe_3.

The compound $MoO_2(OBu^t)_2$ is monomeric; the related isopropoxy and neopentoxy compounds are oligomers $[MoO_2(OR)_2]_n$ of, as yet, unknown structures. A clean synthesis of the latter compounds involves the addition of excess of ROH ($R = Pr^i$, CH_2CMe_3) to $MoO_2(OBu^t)_2$. Addition of pyridine or 2,2'-bipyridine to $[MoO_2(OR)_2]_n$ compounds yields monomeric octahedral complexes. The molecular structure of $MoO_2(OPr^i)_2(bpy)$ in the solid state reveals the cis-MoO_2 group with mutually trans OPr^i ligands as shown in Fig. 23.[41]

The addition of molecular oxygen to $Mo_2(OR)_6$ compounds, where $R = Pr^i$ and CH_2CMe_3, leads initially to green solutions containing the triangulo $Mo_3O(OR)_{10}$ compounds (see Fig. 5). A clean, direct synthesis of these compounds is by the addition of $MoO(OR)_4$ to $Mo_2(OR)_6$ compounds, eqn (10). This simple redox reaction redistributes the six electrons available for metal–metal bonding from $\sigma^2\pi^4$ in M≡M to $a^2 + e^4$ in the triangulo Mo_3^{12+} unit.

$$Mo_2(OR)_6 + MoO(OR)_4 \rightarrow Mo_3O(OR)_{10} \qquad (10)$$

$R = Pr^i$ and CH_2CMe_3.

Further reaction of $Mo_3O(OR)_{10}$ with O_2 leads to cleavage of the Mo_3 unit and elimination of RO˙ which abstracts H from solvent. A hexanuclear chain compound $Mo_6O_{10}(OPr^i)_{12}$ has been isolated and structurally characterized.[67] A view of this fascinating molecule is shown in Fig. 24. The average oxidation state of molybdenum is +5.33. Four electrons are available for metal–metal bonding and these are used to form two localized Mo–Mo single bonds, as is evidenced by the two short Mo–Mo distances, 2.585(1) Å, compared to the four long distances, 3.3 Å. These electrons are reactive toward further oxidation by molecular oxygen: $Mo_6O_{10}(OPr^i)_{12} + O_2 \rightarrow 6MoO_2(OPr^i)_2$.
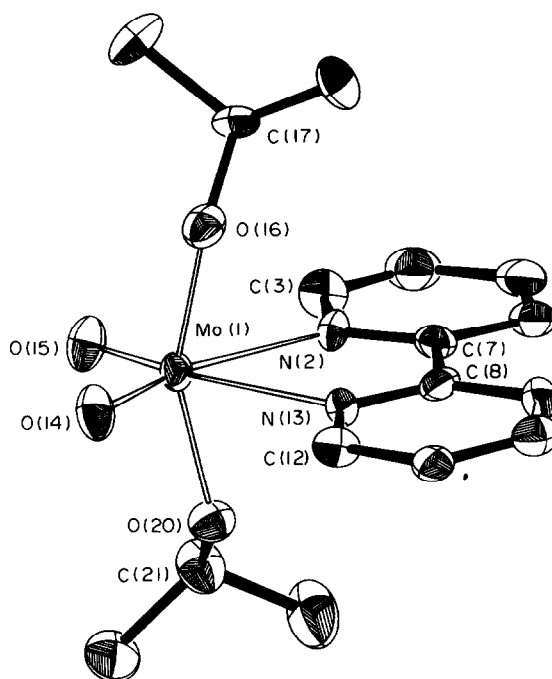
Fig. 23. An ORTEP view of the $MoO_2(OPr^i)_2(bpy)$ molecule. Some pertinent bond distances (Å) and angles (°) are: Mo(1)–O(14), –O(15), –O(16), –O(20), –N(2), –N(13) = 1.69(1), 1.72(1), 1.91(1), 1.94(1), 2.37(1) and 2.35(1); O(14)–Mo(1)–O(15) = 108.0(3), O(14)–Mo(1)–O(16) = 96.6(3), O(14)–Mo(1)–O(20) = 96.7(3), O(16)–Mo(1)–O(20) = 160.9(3), N(2)–Mo(1)–N(13) = 69.2(3).

For tungsten, the story is much simpler, but quite different from molybdenum as is shown in eqn (11).[41]

$$W_2(OR)_6 + 3/2O_2 \rightarrow W_2O_3(OR)_6 \tag{11}$$
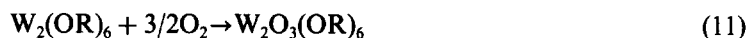
R = Bu^t, Pr^i and CH_2CMe_3.

The structures of $W_2O_3(OR)_6$ compounds are not known and, in solution, only one OR group is seen in the NMR spectra. A cryoscopic molecular weight determination in benzene indicated that $W_2O_3(OBu^t)_6$ is extensively (60%) dissociated, presumably to $WO_2(OBu^t)_2$ and $WO(OBu^t)_4$. The mass spectra of $W_2O_3(OR)_6$ compounds show only mononuclear ions and may be viewed as a superimposition of fragments derived from $WO(OR)_4$ and $WO_2(OR)_2$. A plausible structure for $W_2O_3(OR)_6$ compounds can be based on a confacial bioctahedral unit with two bridging OR ligands and one bridging oxo group.

IV. METAL–CARBON BONDS

1. Reactions with carbon monoxide

Carbon monoxide reacts rapidly with hydrocarbon solutions of $M_2(OR)_6$ compounds at 1 atm, 25°C. In some cases, the reactions produce $M(CO)_6$ compounds and oxidized metal containing species, i.e. CO induces disproportionation. The detailed course of the reaction depends upon the metal, Mo vs W, and on the steric properties of the alkoxy ligand. In the case of $Mo_2(OBu^t)_6$, the stoichiometric reaction (12) has been established and has been shown to proceed via an initial reversible reaction (13).[68]

$$2Mo_2(OBu^t)_6 + 6CO \rightarrow Mo(CO)_6 + 3Mo(OBu^t)_4 \tag{12}$$

$$Mo_2(OBu^t)_6 + CO \rightleftharpoons Mo_2(OBu^t)_6(\mu\text{-}CO). \tag{13}$$
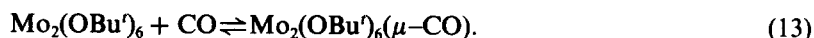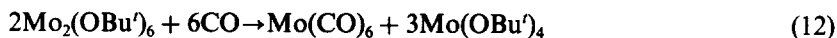
The dark purple crystalline compound $Mo_2(OBu^t)_6(\mu\text{-}CO)$ adopts a structure in which each molybdenum atom is in a square based pyramidal geometry. The two halves of the molecule are joined by a μ_2–CO ligand which occupies the apical position and a pair of μ_2–OBu^t ligands which
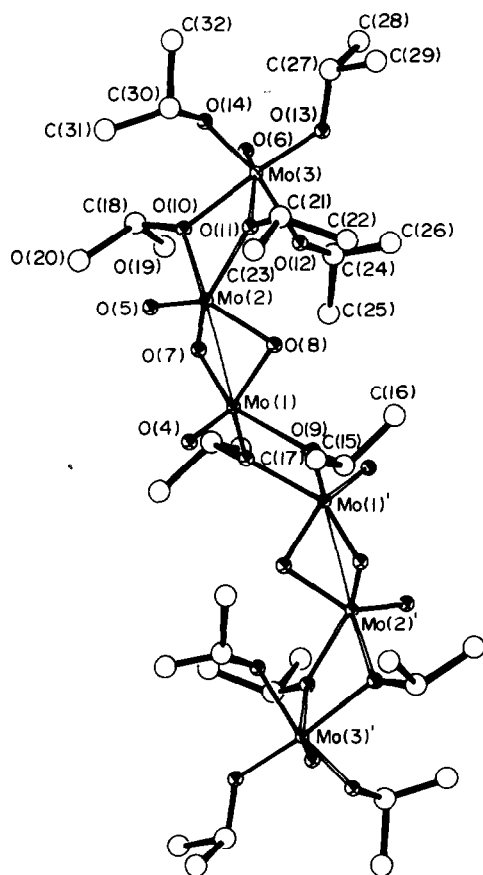
Fig. 24. An ORTEP view of the centrosymmetric molecule $Mo_6O_{10}(OPr^i)_{12}$. Some pertinent bond distances (Å) and bond angles (°) are: $Mo(1)-Mo(2) = Mo(1)'-Mo(2)' = 2.585(1)$; $Mo(1)-Mo(1)' = 3.353(1)$, $Mo(2)-Mo(3) = Mo(2)'-Mo(3)' = 3.285(1)$, $Mo(1)'-Mo(1)-Mo(2) = 146.5(1)$, $Mo(1)-Mo(2)-Mo(3) = 134.3(1)$; Mo–oxo (terminal) = 1.68 (averaged); Mo–oxo $(\mu_2) = 1.93$ (averaged); Mo–OR (terminal) = 1.86 (averaged), Mo–OR $(\mu_2) = 2.05$–2.19.

are basal with respect to the fused square based pyramids. The central skeleton of this beautiful molecule is shown in Fig. 25.

Since the bridging carbonyl ligand can be counted as a one-electron donor to each metal, the addition of CO transforms a d^3–d^3 dimer to a d^2–d^2 dimer and thus a M–M triple to a double bond. The Mo–Mo distance, 2.498(1) Å is consistent with this assignment. The C–O triple bond is also reduced to a C–O double bond: $(M{\equiv}M)^{6+} + CO{\rightarrow}(M{=}M)^{8+}(\mu-CO^{2-})$.

In the presence of donor ligands, such as pyridine, it is possible to isolate an extensive series of compounds of formula $M_2(OR)_6L_2(\mu-CO)$ from reactions between $M_2(OR)_6$ compounds and CO.[69] These compounds are closely related to $Mo_2(OBu^t)_6(\mu-CO)$, having a donor ligand *trans* to the M–C bond of the bridging CO ligand. In solution, the donor ligands are labile to reversible dissociation and, on the NMR time-scale, bridge $\rightleftharpoons$ terminal OR group exchange is rapid. However, at low temperature and high magnetic field strengths, low temperature limiting spectra are obtained which are consistent with the structures observed in the solid state. The donor ligands serve the important role of suppressing the kinetically facile disproportionation reactions which occur in the presence of excess CO. Also, CO dissociation from $Mo_2(OR)_6(\mu-CO)$ is blocked when the dimer is ligated.

These μ_2–CO compounds show anomalous spectroscopic properties (see Table 5). The values of $v(CO)$ are unprecedentedly low for μ_2–CO ligands in neutral molecules. Also, the ^{13}C carbonyl chemical shifts appear below 300 ppm, which is out of the range of bridging carbonyl ligands in organometallic compounds. From simple symmetry considerations, it can be seen that the M–M
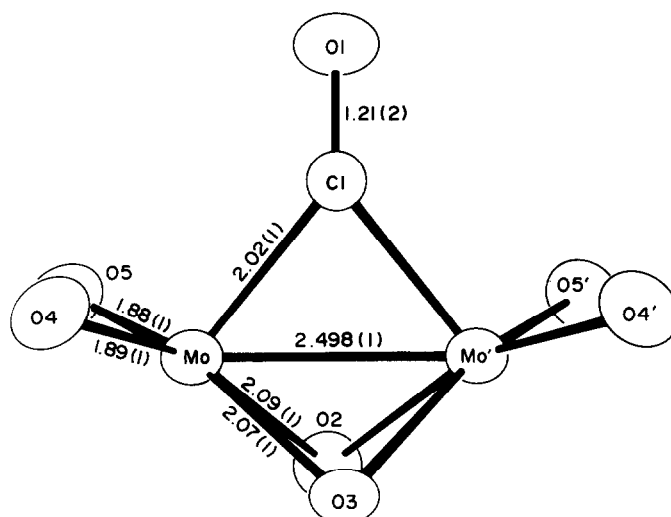
Fig. 25. Central skeleton of the $Mo_2(OBu^i)_6(\mu\text{–CO})$ molecule showing some of the pertinent distances.

π bond can interact strongly with the C=O π^* orbital. These molecules are inorganic analogues of cyclopropenones and show a significant contribution of the resonance shown in **XIV**.
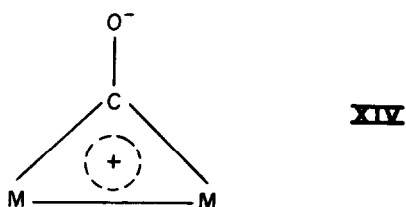
The resonance form **XIV** is equivalent to an oxycarbyne ligand bridging two metal atoms and suggests that the μ–CO ligand might behave as a good Lewis base. This has actually been demonstrated in the isolation of a molecule of formula $W_4(OPr^i)_{12}(py)_2(CO)_2$ formed in the reaction between CO and $W_2(OPr^i)_6(py)_2$.[70] This intriguing complex may be viewed as a dimer of dimers

Table 5. Some characterization data for the $M_2(OPr^i)_6(py)_2(\mu\text{–CO})$ compounds[a]

	M = Mo	M = W
$\nu(CO)$ cm^{-1}	1655	1555
$\nu(^{13}CO)$ cm^{-1}	1637	1532
$\delta(^{13}CO)$ ppm	325.7	310.4 $J_{183W-13C}$ = 170 MHz
d(C–O) Å	1.19(1)	1.22(2)
d(M–CO) Å	2.06(1)	2.04(2)
d(M–M) Å	2.486(2)	2.490(3)

[a]All data taken from ref. 69.
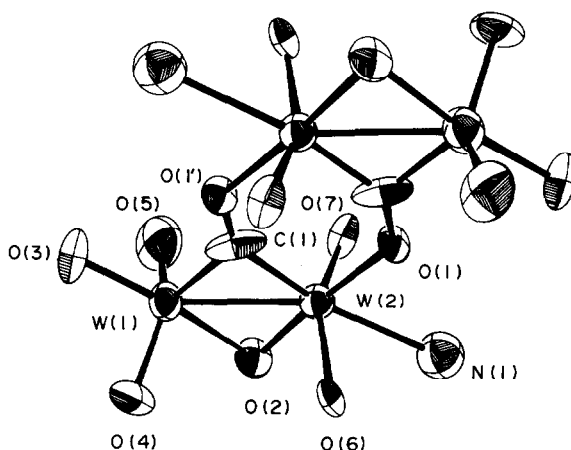
Fig. 26. An ORTEP view of the central $W_4O_{12}(CO)_2N_2$ skeleton of the centrosymmetric $W_4(OPr^i)_{12}(py)_2(CO)_2$ molecule. Some key bond distances are: $W(1)-W(2) = 2.654(1)$, $W(1)-C(1) = 2.00(3)$, $W(2)-C(1) = 1.91(3)$, $C(1)-O(1)' = 1.33(3)$ and $W(2)-O(1) = 2.01(1)$ Å.

formed by the loss of one pyridine from $W_2(OPr^i)_6(py)_2(CO)$: $2W_2(OPr^i)_6(py)_2(CO) \rightarrow$ $W_4(OPr^i)_{12}(py)_2(CO)_2 + 2py$. Figure 26 shows the essential details of this molecule.[70]

Four points should be noted. (1) The W–W distance of 2.654(1) Å is close to that of a single bond distance found in edge-shared octahedral complexes of $W(5+)$, e.g. 2.715(1) Å in $W_2(OEt)_6Cl_4$ and certainly longer than the $W{=}W$ bond in $W_2(OEt)_4(HOEt)_2Cl_4$[24] and $W_2(OPr^i)_6(py)_2(CO)$. (2) The W–O (carbonyl) distance of 2.02 Å is much shorter than would be expected for a simple donor $O{\rightarrow}W$ distance. The W–O distance is approaching a W–OR terminal distance. (3) The C–O bond distance of 1.32 Å is close to that expected for a $C_{(sp^2)}$–O single bond distance. (4) The W–C (carbonyl) distance is shorter by *ca.* 0.1 Å than it is in the $W_2(OPr^i)_6(py)_2(\mu{-}CO)$ molecule. All four points are indicative of the importance of the resonance forms **XVa** and **XVb**.
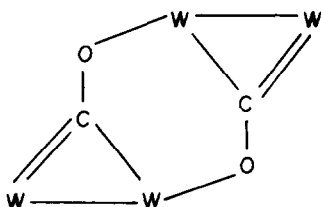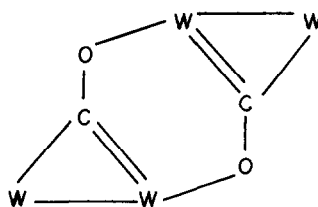
XV a   **XV b**

Thus, in a simple sequence, the $W{\equiv}W$ and $C{\equiv}O$ bonds are transformed to single bonds, W–W and C–O, respectively. In a further reaction with $W_2(OPr^i)_6$, it appears that an additional two-electron reduction of the CO ligand occurs to give carbido and oxotungsten clusters. It is not yet clear how this proceeds: the stoichiometry of the reaction is not known. The structural characterization of $W_4(OPr^i)_{12}(NMe)(C)$, a molecule derived from the degradation of $W_2(OPr^i)_6(HNMe_2)_2$, reveals[71] the butterfly W_4C unit shown in Fig. 27 and bears a striking resemblance to the "iron-butterfly", $Fe_4(C)(CO)_{13}$.[72]

In the presence of excess CO, two other carbonyl compounds have been isolated and structurally characterized. $Mo(OBu^i)_2(py)_2(CO)_2$ is formed in the reaction between $Mo_2(OBu^i)_6$ and CO, in the presence of pyridine, and has a distorted octahedral geometry based on **XVI**.[40]

This molecule is characterized by unusually low $v(CO)$ values, 1906 and 1776 cm^{-1}, for *cis* dicarbonyl $Mo(2+)$ containing compounds. In part, this may be understood in terms of the RO

BuO
|
py,,, | ,,CO
'Mo'
py | CO
|
BuO

XVI
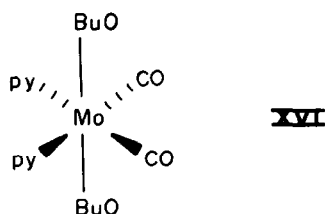
π-donating ability of the RO ligands. The C–Mo–C angle is also unusually small, 72°, and this presumably influences the magnitude of the CO coupling which is exceedingly large, $\Delta = 140 \text{ cm}^{-1}$.

Cotton and Schwotzer[70] have isolated a compound of formula $W_2(OPr^i)_6(CO)_4$ from the reaction between $W_2(OPr^i)_6(py)_2$ and CO. This molecule has the edge-shared octahedral geometry shown in **XVII**.

R   O
O   C
| |
RO,,, | ,,,\\\ R ,,,,, | ,,CO
      O
W(1)   W(2)
RO | O | CO
      O   R
      R   C
O   O
R

XVII
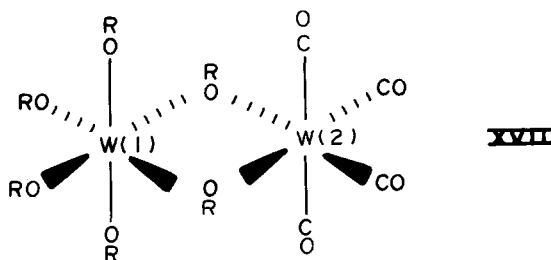
The W–W distance is greater than 3 Å, too long to indicate any W–W bonding. Also, the W–O distances associated with the $W_2(\mu_2\text{-}OPr^i)_2$ group are asymmetric, averaging 1.92 and 2.10 Å to W(1) and W(2), respectively. The compound may be viewed as a W(6+)–W(O) dimer in which a pair of alkoxy groups act as neutral ligands to a $W(CO)_4$ group. It is easy to see how $W(CO)_6$ and $W(OPr^i)_6$ could be derived by the further reaction with two equivalents of CO. In the reaction between CO and $Mo_2(OPr^i)_8$, an adduct, $Mo_2(OPr^i)_8(CO_2)_2$, was isolated[40] and was proposed to have the similar structure shown in **XVIII** based on the appearance of two CO bands at 1940 and 1820 cm^{-1}.
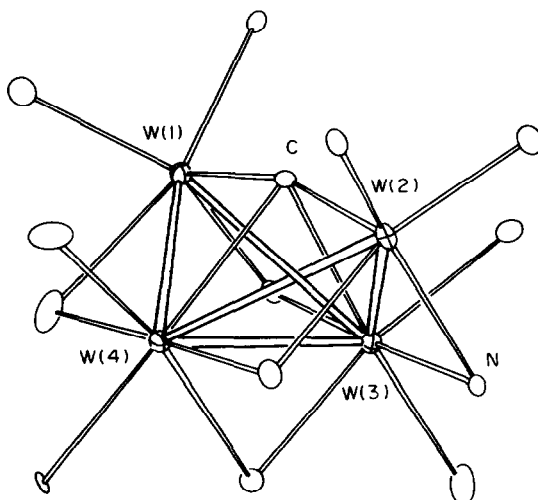
Fig. 27. ORTEP view of the central $W_4(C)(N)O_{12}$ skeleton of $W_4(\mu_4\text{-}C)$–$(\mu_2\text{-}NMe)(OPr^i)_{12}$. Some pertinent bond distances (Å) are: W(1)–W(3) = 2.799(2), W(1)–W(4) = 2.814(2), W(2)–W(3) = 2.822(1), W(2)–W(4) = 2.747(2), W(3)–W(4) = 2.795(2), W(1)–C = 1.91(1), W(2)–C = 1.96(1), W(3)–C = 2.25(1), W(4)–C = 2.24(1), W–O (terminal OR) = 1.90 (averaged), W–μ_2O (bridging OR) = 2.05 (averaged), W–μ–N = 1.94 (averaged).

XVIII
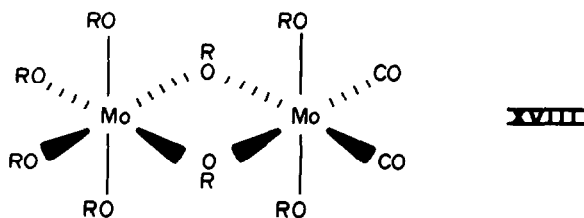
If for the sake of electron counting we split the bridge asymmetrically, this may be viewed as a Mo(6+)——Mo(2+) dimer. $Mo_2(OPr^i)_8(CO)_2$ would then be related to $Mo(OBu^t)_2(py)_2(CO)_2$, **XVI**.

2. *Addition of alkynes*

Hydrocarbon solutions of $Mo_2(OR)_6$ compounds (R = Bu^t, Pr^i and CH$_2$Bu^t) react rapidly with the sterically unencumbered alkynes, CH≡CH, MeC≡CH and MeC≡CMe. Ethyne produces an insoluble polymer of grey–black metallic appearance; propyne yields a yellow powdery material and but-2-yne gives a rubbery material. The detailed nature of these polymers are not known at present. The polymerization processes are very rapid at room temperature and, in an attempt to moderate these reactions and investigate the mechanism of polymerization, we carried out alkyne additions in the presence of donor ligands such as pyridine. This approach yielded a number of interesting compounds containing alkyne or alkyne fragments. For the isopropoxy ligand, compounds of formula $Mo_2(OPr^i)_6(py)_2(\mu-C_2RR')$ were isolated (R = R' = H, Me and R = Me, R' = H). The structure of $Mo_2(OPr^i)_6(py)_2(\mu-C_2H_2)$ is shown in Fig. 28, wherein a close resemblance can be seen to the $Mo_2(OPr^i)_6(py)_2(CO)$ molecule. In solution, these molecules are fluxional and show rapid reversible dissociation of pyridine on the NMR time scale.

With the less sterically demanding neopentoxy ligand, flyover compounds are formed and a view of the structurally characterized compound $Mo_2(OCH_2Bu^t)_6(py)(\mu-C_4H_4)$ is shown in Fig. 29. A number of interesting points emerge from a consideration of this structure. Whereas it is possible to view the $Mo_2(OPr^i)_6(py)_2(\mu-C_2H_2)$ molecule as a d^3-d^3 dimer with the bridging alkyne acting as a four-electron donor, in the $\mu-C_4H_4$ compound, the dimolybdenum center has clearly been oxidized. The Mo–Mo distance, 2.69(1) Å, is approaching that of a single bond distance. If the $\mu-C_4H_4$ ligand is counted as a 2-ligand with respect to Mo(1) and merely a η^4-diene to Mo(2), then the formal oxidation state of Mo(1) is $+4\frac{1}{2}$ and that of Mo(2) is $+3\frac{1}{2}$. The Mo(1)–μ–O distance, 2.06(2) Å, is notably shorter than the Mo(2)–μ–O distance, 2.17(2) Å, and the Mo(1)–N(pyridine)
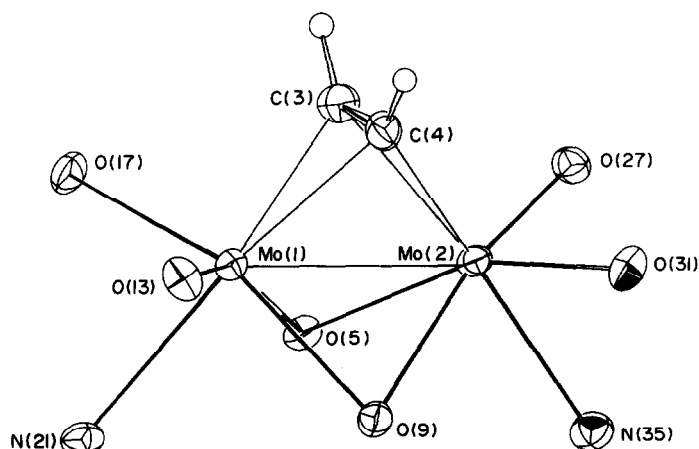
Fig. 28. An ORTEP view of the central $Mo_2O_6N_2(\mu-C_2H_2)$ skeleton of the $Mo_2(OPr^i)_6(py)_2(\mu-C_2H_2)$ molecule. Some bond distances (Å) (averaged where appropriate) are: Mo–Mo = 2.554(1), Mo–O (terminal) = 1.94(2), Mo–O(μ_2) = 2.15(1), Mo–N = 2.31(1), Mo–C = 2.09(1) and C–C ($\mu-C_2H_2$) = 1.368(6).
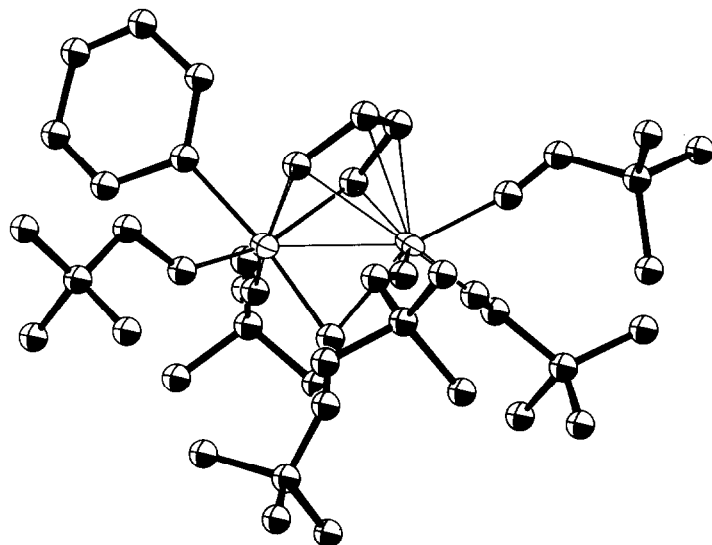
Fig. 29. An ORTEP view of the $Mo_2(OCH_2Bu^t)_6(\mu\text{-}C_4H_4)(py)$ molecule. Some pertinent bond distances (Å) (averaged where appropriate) are: Mo–Mo = 2.69(1), Mo–O = 1.92(2), Mo–O (μ_2) = 2.15(2), Mo–N = 2.15(1), Mo–C (σ) = 2.12(2), Mo–C (π) = 2.37(2); C–C $(\mu\text{-}C_4H_4)$ = 1.45(2).

distance, 2.15(3) Å, is significantly shorter than those in $Mo_2(OPr^i)_6(py)_2(\mu\text{-}C_2H_2)$ which average 2.31(1) Å. In solution (toluene-d_8), the molecule is not fluxional on the NMR time scale and the pyridine ligand does not exchange with free pyridine. Only at +90°C do these processes become sufficiently rapid to cause line broadening.

The nature of the formation of the $\mu\text{-}C_4H_4$ ligand is evidently a simple coupling process since the ^1H NMR spectrum of the $\mu\text{-}C_4H_2D_2$ ligand formed from the addition of C_2H_2 to $Mo_2(OCH_2Bu^t)_6(py)_2(\mu\text{-}C_2H_2)$, is an AX spectrum whereas that of the protio ligand $\mu\text{-}C_4H_4$ is an AA'XX' spectrum at 220 MHz.

The possible role of these compounds in alkyne polymerization was investigated by a variety of labelling studies which showed that they were only involved in alkyne trimerization to give benzenes, e.g. as in eqns (14) and (15).[73]

$$Mo_2(OPr^i)_6(py)_2(MeC_2H) + 3HC{\equiv}CH \rightarrow Mo_2(OPr^i)_6(py)_2(HC_2H) + C_6H_5Me \qquad (14)$$

$$Mo_2(OCH_2Bu^t)_6(py)(\mu\text{-}C_4H_4) + 3DC{\equiv}CD \rightarrow Mo_2(OCH_2Bu^t)_6(py)(\mu\text{-}C_4D_4) + C_6H_4D_2. \qquad (15)$$
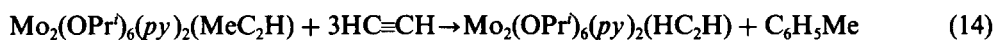
The catalytically active species in the polymerization process, which is kinetically more rapid than cyclotrimerization, is not yet known. It could conceivably be a carbene, vinylidene or carbyne function,[74] all of which could be derived from an alkyne.

Analogous reactions involving $W_2(OR)_6L_2$ compounds with C_2H_2 have led to the isolation of simple adducts $W_2(OR)_6(py)_2(\mu\text{-}C_2H_2)$ where R = Bu^t and Pr^i.[43] The isopropoxide is isostructural with its molybdenum analogue and shows similar solution behaviour. However, its reactivity is somewhat different. Addition of more ethyne leads to $W_2(OPr^i)_6(\mu\text{-}C_4H_4)(C_2H_2)$ presumably via an intermediate $W_2(OPr^i)_6(py)(\mu\text{-}C_4H_4)$ analogous to $Mo_2(OCH_2Bu^t)_6(py)(\mu_2\text{-}C_4H_4)$. Similarly, addition of 2-butyne to $W_2(OPr^i)_6(py)_2$ proceeds ultimately to give $W_2(OPr^i))_6(\mu\text{-}C_4Me_4)(C_2Me_2)$. The solid state structures of the compounds $W_2(OPr^i)_6(\mu\text{-}C_4R_4)(C_2R_2)$ where R = H and Me have been determined by X-ray studies and their dynamic solution behaviour investigated by variable temperature NMR studies. An ORTEP view of the $W_2(OPr^i)_{16}(\mu\text{-}C_4H_4)(C_2H_2)$ compound is given in Fig. 30 which provides the basis for a comparison with the $Mo_2(OCH_2Bu^t)_6(py)(\mu\text{-}C_4H_4)$ molecule. The W–W distance is 2.877(1) Å, indicative of a relatively weak M–M bond. This distance is ca. 0.2 Å longer than that in $Mo_2(OCH_2Bu^t)_6(py)(\mu\text{-}C_4H_4)$, consistent with the view that metal d electrons are effectively tied up in backbonding to the π-acceptor ligands. Tungsten, relative to molybdenum, is more easily oxidized and, in this instance, is reluctant to eliminate a benzene molecule.
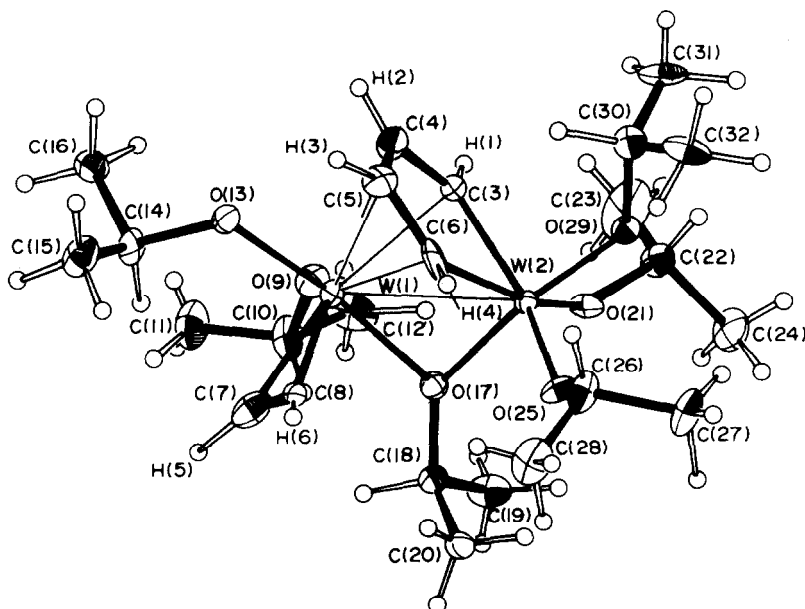
Fig. 30. An ORTEP view of the $W_2(OPr^i)_6(\mu-C_4H_4)(C_2H_2)$ molecule. Some pertinent bond distances (Å), averaged where appropriate, are: W(1)–W(2) = 2.877(1), W(2)–C(3), –C(6) = 2.11(1), 2.14(1); W(1)–C(3), –C(4), –C(5), –C(6) = 2.42(1), 2.42(1), 2.40(1), 2.37(1); W(2)–C(7), –C(8) = 2.09(1), 2.06(1). The W–O distances fall within the range of W–OR terminal and μ_2 reported in Table 3.

As noted earlier, $W_2(OBu^t)_6$ reacts with 2-butyne to give $(Bu^tO)_3W{\equiv}CMe$.[64] Cotton and Schwotzer[70] have characterized $[(Bu^tO)_2W(\mu-CPh)]_2$ and $W_2(OBu^t)_4(\mu-C_2Ph_2)_2$ compounds from reactions involving $W_2(OBu^t)_6$ and $PhC{\equiv}CPh$. The structure of the former compound is similar to that observed for $[(Me_3SiCH_2)_2W(\mu-CSiMe_3)]_2$,[76] while the latter contains a planar W_2O_4 moiety with terminal OBu^t ligands with two skewed bridging μ–acetylene ligands. It is evident that a wide variety of products are derived from reactions involving alkynes and $M_2(OR)_6$ compounds and that steric and electronic factors and reaction conditions are critical in controlling the course of the reaction.

3. Alkyl–alkoxides of dimolybdenum $(M{\equiv}M)$

Two approaches to the synthesis of mixed alkyl–alkoxides of dimolybdenum $(M{\equiv}M)$ have been taken. One involves metathetic reactions wherein an alkyl ligand or an alkoxy ligand is introduced to the dimetal center, e.g. as in (16)[11] and (17).[77]

$$1,2\text{-}Mo_2Br_2R_4 + 2LiOR' \rightarrow 1,2\text{-}Mo_2(OR')_2R_4 + 2LiCl \tag{16}$$

where $R = CH_2SiMe_3$, $R' = Bu^t$ or Pr^i.

$$Mo_2(OBu^t)_6 + 2ZnMe_2 \rightarrow 1,2\text{-}Mo_2Me_2(OBu^t)_4 + \tfrac{1}{2}[Zn(Me)OBu^t]_4. \tag{17}$$

The other approach involves the alcoholysis of $1,2\text{-}Mo_2R_2(NMe_2)_4$ compounds. The latter reaction yield products dependent on the nature of the alkyl ligand as is shown in (18) and (19).[78]

$$1,2\text{-}Mo_2R_2(NMe_2)_4 + R'OH \rightarrow 1,2\text{-}Mo_2R_2(OR')_4 + 4HNMe_2 \tag{18}$$
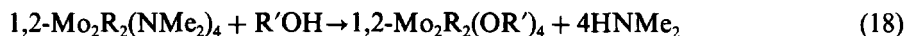
where $R = Me$, $R' = Bu^t$; $R = CH_2CMe_3$, CH_2SiMe_3 and $R' = Bu^t$, Pr^i, CH_2CMe_3 and Et.

$$1,2\text{-}Mo_2R_2(NMe_2)_4 + R'OH \rightarrow Mo_2R(OR')_5 + RH + 4NMe_2 \tag{19}$$

where $R = Et$ and Pr; $R' = Bu^t$ and Pr^i.

The rate of alcoholysis is dependent on the steric factors of R and R', being much slower for bulky combinations. Alcoholysis is faster for $Mo-NMe_2$ groups than for Mo–R groups, but the thermodynamically favoured products in (18) and (19) are $Mo_2(OR')_6$ compounds, and these are

ultimately formed under prolonged alcoholysis. For example, while $Mo_2Me_2(NMe_2)_4$ reacts rapidly with $Bu'OH$ to give $Mo_2Me_2(OBu')_4$, further reaction to give $Mo_2Me(OBu')_5$ and $Mo_2(OBu')_6$ occurs more slowly.

The failure to isolate or even detect $Mo_2R_2(OR')_4$ compounds, where $R = Et$ and Pr and $R' = Bu'$ and Pr^i, suggested a β-hydrogen elimination pathway was involved. This was confirmed and delineated in the following reactions.[78] (1) When $Mo_2(CH_2CD_3)_2(NMe_2)_4$ and $Mo_2\{CH(CD_3)_2\}_2(NMe_2)_4$ were allowed to react with $Bu'OH$, the eliminated alkanes were CH_2DCD_3 and CD_3CHDCD_3, respectively. (2) When $Mo_2(CH_2CH_3)_2(NMe_2)_4$ was allowed to react with $Bu'OD$, the resulting ethyl complex was $Mo_2(CH_2CH_2D)(OBu')_5$. Evidently the elimination of alkane involves the transference of a β-hydrogen (or deuterium) from one alkyl group to the α-carbon of the other, and the resultant ethyl ligand is formed from the hydrogen atom (deuterium) of the hydroxyl group of the alcohol and a coordinated alkene. A reductive–elimination and oxidative–addition sequence of the type schematically represented by (20a, b and c) is implicated.

$$Et–Mo\equiv Mo–Et \rightarrow Mo\equiv Mo + C_2H_6 + C_2H_4 \qquad (20a)$$

$$Mo\equiv Mo + ROH \rightarrow RO–Mo\equiv Mo–H \qquad (20b)$$

$$RO–Mo\equiv Mo–H + C_2H_4 \rightarrow RO–Mo\equiv Mo–Et. \qquad (20c)$$
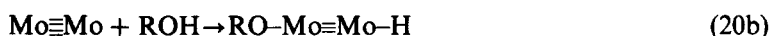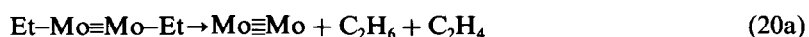
Each step has precedence in the dinuclear chemistry of molybdenum and tungsten. (1) Reductive elimination by alkyl group disproportionation has been observed in the reactions between $Mo_2Et_2(NMe_2)_4$ and CO_2, reaction (21).[79]

$$Mo_2(CH_2CD_3)_2(NMe_2)_4 + CO_2 \rightarrow Mo_2(O_2CNMe_2)_4 + CH_2{=}CD_2 + CH_2DCD_3. \qquad (21)$$

(2) Oxidative-addition of ROH to a $W–W$ triple bond is seen in the formation of $W_4(\mu–H)_2(OPr^i)_{14}$.[35] (3) Insertion of alkenes into metal hydrides is, of course, well documented in organometallic chemistry and $W_2(\mu–H)_2(OPr^i)_{14}$ reacts reversibly with ethylene.[35]

Further evidence for the sequence in (20) is seen in the observation that $Mo_2Bu_2^i(NMe_2)_4$ reacts with Pr^i OH to give an intense blue solution which by ^1H NMR can be seen to contain a Mo_2-hydride ($\delta = 6.7$ ppm). This probably is a confacial bioctahedral compound: $Mo_2(OPr^i)_3(\mu–H)(\mu–OPr^i)_2(HNMe_2)_3$. Addition of ethylene gives $Mo_2Et(OPr^i)_5$.

One other interesting feature of (19) concerns the insertion step forming the alkyl. In reactions involving $Mo_2R_2(NMe_2)_4$ with $Bu'OH$, where $R = Pr^i$, Pr^n and Bu^i, the products are $Mo_2Pr^i(OBu')_5$ and $Mo_2Bu^i(OBu')_5$. In the reaction between $Mo_2Pr_2^n(NMe_2)_4$ and Pr^iOH, the initially formed compound is $Mo_2Pr^i(OPr^i)_5$ which, in the absence of donor ligands such as $HNMe_2$, is quite stable. However, upon addition of donor ligands, $HNMe_2$ or py, isomerization to $Mo_2Pr^n(OPr^i)_5$ is observed. It is apparent that (1) the insertion of the alkene ligand occurs with kinetic control and (2) that isomerization of the alkyl ligand by a β-hydrogen elimination process does not readily occur for $Mo_2R(OR')_5$ compounds, but that this may be promoted by a Lewis base association reaction.

It is possible to rationalize these observations in the following way. (1) The metal–hydride insertion step occurs across the M–M bond and thus the conformational preference for alkene coordination with its alkyl substituent(s) distal to the M–M bond will generate, upon hydride insertion, the most highly substituted carbon being σ-bonded to molybdenum. (2) The strongly π-donating RO ligands will effectively tie up empty molybdenum atomic orbitals which would otherwise be available for M----H–C interactions leading to M–H and alkene. This stabilization of β-hydrogen containing alkyls has been discussed in detail in connection with $M_2R_2(NMe_2)_4$ compounds.[37] (3) In the presence of donor ligands, the coordination of a ligand to one metal activates the other toward β-hydrogen abstraction. This may be viewed as another aspect of the cooperative binding of $M_2(OR)_6$ compounds, reaction (2), discussed previously.

A common intermediate of the type shown in **XIX** can be envisaged.

When $X = R$ (alkyl), elimination of alkane occurs. When $X = OR$, insertion will lead to $Mo_2\{CH(CH_3)R'\}(OR)_5$, where $R' = H$ or Me. A subsequent isomerization of the alkyl ligand may occur in the presence of L providing the alkene can ultimately gain access to a position with the alkyl group(s) over the M–M bond. Alternatively, if the Lewis base coordinates to the $Mo(OR)_3$

R'
CH₃ ════ H
        OR   X
    Mo ════ Mo   **XIX**
L'   │   RO' │
    RO   RO
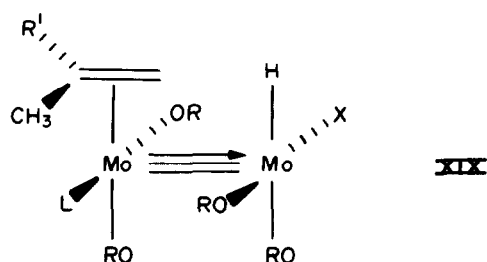
end of the molecule, β-hydrogen abstraction followed by an insertion to give the isomerized alkyl may occur at the other metal. Clearly more work is required to delineate the intricacies of these reactions.

4. Olefin– and acetylene–metathesis reactions

One of the most fascinating reactions to capture the minds of organic and organometallic chemists within recent years is the olefin metathesis reaction.[80,81] There is now a large body of evidence to support the intimate mechanism originally proposed by Chauvin[82] which is depicted by (22).

$$M{=}CHR + R'CH{=}CH_2 \rightarrow M \underset{\underset{R'}{\overset{|}{CH}}}{\overset{\overset{R}{\overset{|}{CH}}}{<}} CH_2 \rightarrow M{=}CHR' + RCH{=}CH_2 \qquad (22)$$
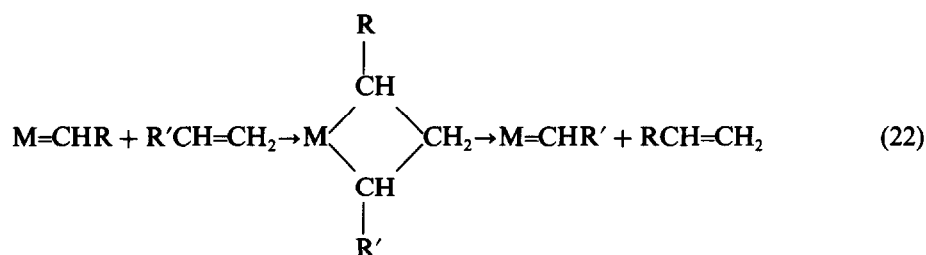
Schrock et al.[83] have shown that niobuim and tantalum alkylidene complexes can indeed promote olefin metathesis. One of the terminating steps and breakdown in the catalytic cycle involves a β-hydrogen elimination step either from the metallacycle or from the alkylidene complex as shown in (23) and (24).

$$M \underset{CH_2}{\overset{CH_2}{<}} CH_2 \rightarrow M + \underset{CH_2}{\overset{CH_3}{>}} CH \qquad (23)$$

$$M{=}C \overset{H}{\underset{CH_2R}{<}} \rightarrow M + CH_2{=}CHR. \qquad (24)$$
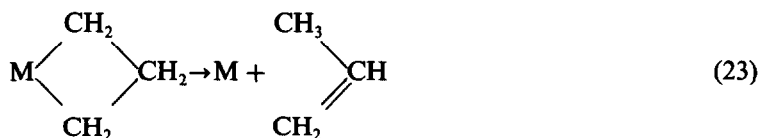
In both (23) and (24), β-hydrogen abstraction is followed by reductive elimination of alkene by C–H bond formation. The net effect is a 1,2-H atom shift. Schrock et al. have shown that these competing β-hydrogen abstraction reactions can be greatly suppressed by replacing Cl by RO ligands.[84] Tungsten(VI) oxo, imido and alkoxy alkylidene complexes are amongst the best homogeneous olefin metathesis catalysts known.[83] The role of the ancillary π-donor ligands in the olefin metatesis reaction has recently been the subject of a theoretical study: the so-called spectator group effect.[85]

The alkoxy–alkylidyne complexes $(Bu^tO)_3W{\equiv}CR$ are efficient alkyne metathesis catalysts. There is good evidence to support the view that alkyne metathesis proceeds via the intermediacy of the tungstenacyclobutadiene as shown in eqn (25).

$$M \equiv CR + R'C \equiv CR' \longrightarrow \quad \text{[structure]} \quad \longrightarrow M \equiv CR' + R'C \equiv CR \qquad (25)$$
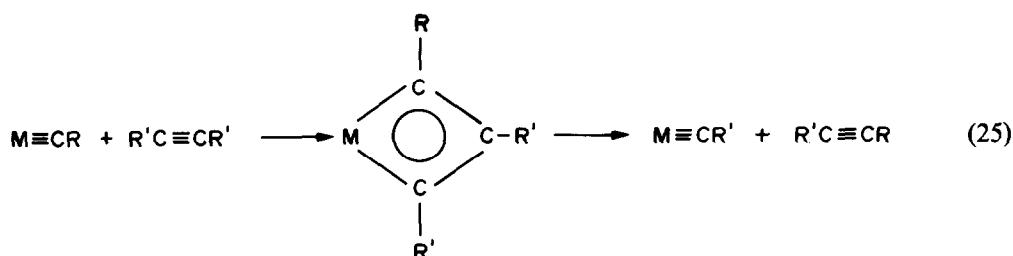
When chloride ligands are on tungsten, a tungstencyclobutadiene complex, **XX**, has been isolated and structurally characterized[86] and found to have a trigonal bipyramidal geometry with one W–Cl and two W–C bonds in the equatorial plane.

XX
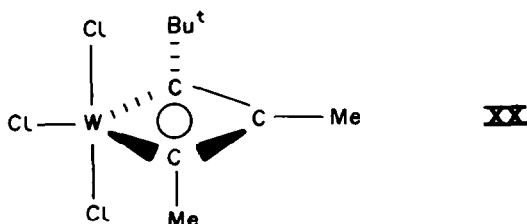
Further reaction with another molecule of dimethylacetylene gives $(\eta^5\text{-}C_5Me_4R)WCl_3$: tungsten is reduced from $+6$ to $+4$. However, when alkoxy ligands are present, the alkylidyne complex is stabilized relative to the metallacyclobutadiene and the ultimate formation of the π-cyclopentadiene $W(4+)$ complex is not observed. Interestingly, one Bu^{t}O ligand can be introduced into the equatorial site replacing Cl in **XX**, but a further Bu^{t}O for Cl substitution reforms the alkylidyne complex, eqn (26).

$$\text{[structure]} \quad \xrightarrow{\text{LiOBu}^t} \quad (Bu^tO)_3W \equiv CR \qquad (26)$$
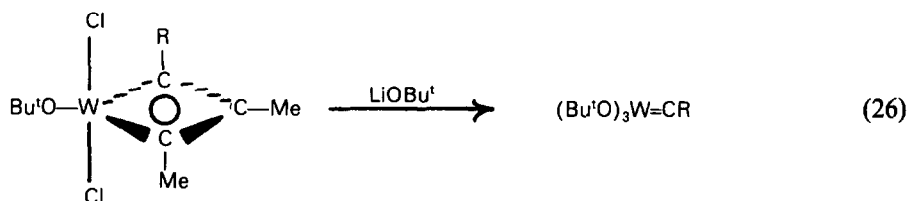
where $R = Bu^t$ or Me

The Bu^{t}O ligands favour the alkylidyne ligand, relative to the metallacyclobutadiene; they suppress β-hydrogen elimination and favour the oxidation state $+6$ for tungsten.

V. CONCLUDING REMARKS

Metal–metal bonds are pervasive in the chemistry of molybdenum and tungsten alkoxides. They may modify structures found for d^0 metal alkoxides as is seen for $W_4(OEt)_{16}$ or may provide for totally new geometries as is seen for the $M_2(OR)_6$ compounds. Metal–metal bonds provide a reservoir of electrons for redox chemistry: the reservoir may be tapped in oxidative-addition reactions and may be filled in reductive–elimination processes. Alkoxide ligands may act as four- or two-electron donors and may readily change between terminal and bridging positions. This allows for the facile interconversion of saturated and unsaturated metal centers. As π-donor ligands, they can enhance backbonding to π-acid ligands on the same metal; they can tie up vacant metal d orbitals and suppress metal–hydride abstraction from coordinated alkyl ligands and they stabilize metals in high oxidation states. A variety of steric control may be engineered by suitable choice of alkyl group and this may greatly influence structure, M–M bonding and the reactivity

of coordinated ligands. This is well illustrated in the reactions of $MeC{\equiv}CMe$ with $W_2(OBu^t)_6$ and $W_2(OPr^i)_6$ which lead to $(Bu^tO)_3W{\equiv}CMe$ and $W_2(OPr^i)_6(\mu-C_4Me_4)(MeC_2Me)$. It is now clear that an extensive organometallic chemistry can be supported in the absence of ligands commonly employed in organometallic chemistry.

REFERENCES

1. D. C. Bradley, R. C. Mehrotra and P. D. Gaur, *Metal Alkoxides*. Academic Press, London (1978).
2. R. C. Mehrotra, *Advances in Inorganic and Radiochemistry*. In press.
3. D. C. Bradley, *Nature (Lond.)* 1958, **182**, 1211.
4. D. C. Bradley, *Coord. Chem. Rev.* 1967, **2**, 299.
5. M. H. Chisholm, F. A. Cotton, B. A. Frenz, W. W. Reichert, L. W. Shive and B. R. Stults, *J. Am. Chem. Soc.* 1976, **98**, 4469.
6. M. H. Chisholm, F. A. Cotton, C. A. Murillo and W. W. Reichert, *Inorg. Chem.* 1977, **16**, 1801.
7. M. H. Chisholm and F. A. Cotton, *Acct. Chem. Res.* 1978, **11**, 356.
8. M. H. Chisholm, F. A. Cotton, M. W. Extine and B. R. Stults, *J. Am. Chem. Soc.* 1976, **98**, 4477.
9. M. Akiyama, M. H. Chisholm, F. A. Cotton, M. W. Extine, D. A. Haitko, D. Little and P. E. Fanwick, *Inorg. Chem.* 1979, **18**, 2266.
10. M. J. Chetcuti, M. H. Chisholm, J. C. Huffman and J. Leonelli, *J. Am. Chem. Soc.* 1983, **105**, 292.
11. M. H. Chisholm, K. Folting, J. C. Huffman and I. P. Rothwell, *Organometallics* 1982, **1**, 252.
12. K. J. Cavell, J. A. Connor, G. Pilcher, M. A. Ribeiro da Silva, M. D. M. C. Ribeiro da Silva, H. A. Skinner, Y. Yirmani and M. T. Zafarani-Moattar, *J.C.S. Farad. Trans.* 1981, **77**, 1585.
13. F. A. Cotton, G. G. Stanley, B. Kalbacher, J. C. Green, E. Seddon and M. H. Chisholm, *Proc. Natl Acad. Sci., U.S.A.* 1977, **74**, 3109.
14. M. H. Chisholm and E. Kober, results to be published.
15. M. H. Chisholm, W. W. Reichert and P. Thornton, *J. Am. Chem. Soc.* 1978, **100**, 2744.
16. M. H. Chisholm, F. A. Cotton and W. W. Reichert, *Inorg. Chem.* 1978, **17**, 2944.
17. S. Otsuka, M. Kamata, K. Hirotsu and T. Higuchi, *J. Am. Chem. Soc.* 1981, **103**, 3011.
18. M. H. Chisholm, F. A. Cotton, M. W. Extine and W. W. Reichert, *Inorg. Chem.* 1978, **17**, 2944.
19. M. H. Chisholm, F. A. Cotton, M. W. Extine and R. L. Kelly, *J. Am. Chem. Soc.* 1978, **100**, 3354.
20. L. B. Anderson, F. A. Cotton, D. DeMarco, A. Fang, W. H. Isley, B. W. S. Kolthammer and R. A. Walton, *J. Am. Chem. Soc.* 1981, **103**, 5078.
21. P. W. Clark and R. A. D. Wentworth, *Inorg. Chem.* 1969, **8**, 1223.
22. C. H. Brubaker, Jr. and W. J. Reagan, *Inorg. Chem.* 1970, **9**, 827.
23. H. Funk, H. Matschiner and H. Nauman, *Z. Anorg. All. Chem.* 1965, **340**, 75.
24. F. A. Cotton, D. DeMarco, B. S. W. Kolthammer and R. A. Walton, *Inorg. Chem.* 1981, **20**, 3048.
25. M. H. Chisholm, J. C. Huffman and C. C. Kirkpatrick, *Inorg. Chem.* 1981, **20**, 871.
26. A. A. Pinkerton, D. Schwartzenback, L. G. Hubert-Pfalzgraf and J. G. Reiss, *Inorg. Chem.* 1976, **15**, 1196.
27. M. H. Chisholm, K. Folting, J. C. Huffman and C. C. Kirkpatrick, *J. Am. Chem. Soc.* 1981, **103**, 5967.
28. A. Muller, R. Jostes and F. A. Cotton, *Angew. Chem., Int. Ed. Engl.* 1980, **19**, 875.
29. M. H. Chisholm, J. C. Huffman and J. Leonelli, *J. Chem. Soc., Chem. Commun.* 1981, 270.
30. M. H. Chisholm, J. C. Huffman, C. C. Kirkpatrick, J. Leonelli and K. Folting, *J. Am. Chem. Soc.* 1981, **103**, 6093.
31. J. A. Ibers, *Nature (Lond.)* 1963, **197**, 686.
32. P. M. Skarstad and S. Geller, *S. Matl Res. Bull.* 1975, **10**, 791.
33. R. E. McCarley, M. H. Luly, T. R. Ryan and C. C. Torardi, *A.C.S. Symp. Series* 1981, **155**, 41.
34. F. A. Cotton and A. Fang, *J. Am. Chem. Soc.* 1982, **104**, 113.
35. M. Akiyama, M. H. Chisholm, F. A. Cotton, M. W. Extine, D. A. Haitko, J. Leonelli and D. Little, *J. Am. Chem. Soc.* 1981, **103**, 779.
36. P. Nannelli and B. P. Block, *Inorg. Chem.* 1968, **7**, 2423.
37. M. H. Chisholm, D. A. Haitko and J. C. Huffman, *J. Am. Chem. Soc.* 1981, **103**, 4046.
38. M. H. Chisholm, K. Folting, J. C. Huffman and I. P. Rothwell, *Organometallics* 1982, **1**, 251.
39. T. G. Appleton, H. C. Clark and L. E. Manzer, *Coord. Chem. Rev.* 1972, **10**, 335.
40. M. H. Chisholm, J. C. Huffman and R. L. Kelly, *J. Am. Chem. Soc.* 1979, **101**, 7615.

41. C. C. Kirkpatrick, Indiana University, Ph.D. Thesis, 1982.
42. K. F. Miller and R. A. D. Wentworth, *Inorg. Chem.* 1979, **18**, 984.
43. J. Leonelli, Indiana University, Ph.D. Thesis, 1982.
44. M. J. Chetcuti, M. H. Chisholm and J. Stewart, results to be published.
45. M. H. Chisholm, F. A. Cotton, C. A. Murillo and W. W. Reichert, *J. Am. Chem. Soc.* 1977, **99**, 1652.
46. M. H. Chisholm, F. A. Cotton, M. W. Extine and W. W. Reichert, *J. Am. Chem. Soc.* 1978, **100**, 1727.
47. M. H. Chisholm, J. C. Huffman and A. L. Ratermann, results to be published.
48. M. H. Chisholm, K. Folting, J. C. Huffman and I. P. Rothwell, *Inorg. Chem.* 1981, **20**, 2215.
49. M. H. Chisholm, J. C. Huffman and R. L. Kelly, *J. Am. Chem. Soc.* 1979, **101**, 7100.
50. M. H. Chisholm, R. J. Errington, K. Folting and J. C. Huffman, *J. Am. Chem. Soc.* 1982, **104**, 2025.
51. L. J. Guggenberger and A. W. Sleight, *Inorg. Chem.* 1969, **8**, 2041.
52. P. Healy, D. L. Kepert, D. Taylor and A. H. White, *J. Chem. Soc., Dalton Trans.* 1973, 646.
53. H. Schafer, H. G. von Schnering, *Angew. Chem.* 1971, **385**, 75.
54. R. N. McGinnis, T. R. Ryan and R. E. McCarley, *J. Am. Chem. Soc.* 1978, **100**, 7900.
55. M. H. Chisholm and I. P. Rothwell, *Progr. Inorg. Chem.* 1981, **29**, 1.
56. M. H. Chisholm, J. C. Huffman and C. C. Kirkpatrick, *Inorg. Chem.* In press.
57. M. H. Chisholm, J. C. Huffman and A. L. Ratermann, *Inorg. Chem.* Submitted.
58. C. G. Pierpont and R. M. Buchanan, *Coord. Chem. Rev.* 1981, **38**, 45.
59. T. P. Blatchford, M. H. Chisholm, J. C. Huffman and K. Folting, results to be published.
60. M. H. Chisholm, J. C. Huffman and A. L. Ratermann, submitted.
61. T. L. Brown and P. O. Nubel, *J. Am. Chem. Soc.* 1982, **104**, 4955.
62. D. C. Bradley, F. A. Cotton, M. H. Chisholm, P. E. Fanwick, D. A. Haitko, D. Little, C. W. Newing and R. L. Kelly, *Inorg. Chem.* 1980, **19**, 3010.
63. M. H. Chisholm, F. A. Cotton, M. W. Extine and R. L. Kelly, *Inorg. Chem.* 1979, **18**, 116.
64. R. R. Schrock, M. L. Listerman and L. G. Sturgeoff, *J. Am. Chem. Soc.* 1982, **104**, 4291.
65. M. H. Chisholm, D. M. Hoffman and J. C. Huffman, *Inorg. Chem.* In press.
66. M. H. Chisholm, K. Folting, J. C. Huffman, C. C. Kirkpatrick and A. L. Ratermann, *J. Am. Chem. Soc.* 1981, **103**, 1305.
67. M. H. Chisholm, K. Folting, J. C. Huffman and C. C. Kirkpatrick, *J. Chem. Soc., Chem. Commun.* 1982, 188.
68. M. H. Chisholm, F. A. Cotton, M. W. Extine and R. L. Kelly, *J. Am. Chem. Soc.* 1979, **101**, 7645.
69. M. H. Chisholm, J. C. Huffman, J. Leonelli and I. P. Rothwell, *J. Am. Chem. Soc.* 1982, **104**, 7030.
70. F. A. Cotton and W. Schwotzer, private communication.
71. M. H. Chisholm, J. C. Huffman and J. Leonelli, results to be published.
72. J. S. Bradley, G. B. Ansell, M. E. Leonwicz and E. W. Hill, *J. Am. Chem. Soc.* 1981, **103**, 4968.
73. M. H. Chisholm, J. C. Huffman and I. P. Rothwell, *J. Am. Chem. Soc.* 1982, **104**, 4389.
74. T. J. Katz and S. J. Lee, *J. Am. Chem. Soc.* 1980, **102**, 422.
75. M. H. Chisholm, D. M. Hoffman and J. C. Huffman, submitted for publication.
76. M. H. Chisholm, F. A. Cotton, M. W. Extine and C. A. Murillo, *Inorg. Chem.* 1978, **17**, 696.
77. M. H. Chisholm and R. J. Tatz, results to be published.
78. M. H. Chisholm, J. C. Huffman and R. J. Tatz, *J. Am. Chem. Soc.* 1983, **105**, 2075.
79. M. J. Chetcuti, M. H. Chisholm, K. Folting, D. A. Haitko and J. C. Huffman, *J. Am. Chem. Soc.* 1982, **104**, 2138.
80. T. J. Katz, *Adv. Organometal. Chem.* 1977, **16**, 283.
81. R. H. Grubbs, *Progr. Inorg. Chem.* 1978, **24**, 1.
82. J. L. Herrison and Y. Chauvin, *Makromol. Chem.* 1970, **141**, 161.
83. R. R. Schrock, *A.C.S. Symp. Series* 1983, **221**, 369 and references therein.
84. R. R. Schrock, S. M. Rocklage, J. D. Fellman, G. A. Rupprecht and L. W. Messerle, *J. Am. Chem. Soc.* 1981, **103**, 1440.
85. A. K. Rappe and W. A. Goddard, III, *J. Am. Chem. Soc.* 1982, **104**, 448.
86. R. R. Schrock, S. F. Redersen, M. R. Churchill and H. J. Wasserman, *J. Am. Chem. Soc.* 1982, **104**, 6808.

ADDENDUM

Since the submission of this Report, two particulary significant findings have been made which warrant mention here.

(1) From the reaction between $Mo_2(Bu^i)_2(NMe_2)_4$ and Pr^iOH in hexane/pyridine solvent, the crystalline compound $Mo_2(OPr^i)_4(py)_4$ has been isolated and structurally characterized.[87] This compound is the first M–M quadruple bond supported by RO ligands[88] and its isolation in the reaction between $Mo_2(Bu^i)_2(NMe_2)_4$ and Pr^iOH supports

the proposed reductive–elimination sequence **20a**. The molecular structure of $Mo_2(OPr^i)_4(py)_4$ is depicted in **XXI** below and is typical in conformation to that seen for many other $Mo_2X_4L_4(M \equiv M)$ compounds.[88]
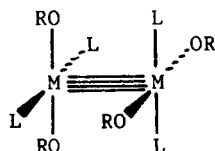
XXI

Of particular note, however, are the Mo–Mo distances, 2.195(1)Å, and the Mo–O distances, 2.030(3) Å (averaged). The Mo–Mo distance is the longest thus far seen for a Mo–Mo quadruple bond[88] and the Mo–O distances are the longest known for Mo–OR (terminal) bonds (see Table 3). The lengthening of these bonds can be understood in terms of the mutual influence of alkoxy-π-donor ligands and the Mo–Mo quadruple bond. The metal d orbitals are used to form M–M bonds, $d_{z^2}(\sigma)$, d_{xz}, $d_{yz}(\pi)$ and $d_{xy}(\delta)$, and metal ligand bonds, $d_{x^2-y^2}$, along with s and p_x and p_y. The Mo–OR σ-bonds are thus not supplemented by RO-to-Mo π bonds: the observed Mo–OR distances are close to the value 2.06 Å predicted for d(Mo–O) as a single bond in $Mo_2R_2(OR)_4$ compounds (see section entitled *Physical Evidence for RO-to-M π-Bonding*). To the extent that RO-to-Mo π-bonding does occur in $Mo_2(OPr^i)_4(py)_4$, this will weaken and lengthen the Mo–Mo bond, since it will destabilize the M–M π and δ bonds.

(2) Though $W_2(OPr^i)_6(py)_2(\mu\text{-}C_2H_2)$ is isostructural with its molybdenum analogue (Fig. 28), the compound believed to be $W_2(OBu^i)_6(py)_2\text{-}(\mu\text{-}C_2H_2)$ has now been shown to be $W_2(OBu^i)_6(py)(\mu\text{-}C_2H_2)$ with a solvent molecule of pyridine in the unit cell.[89] Each tungsten atom is in a distorted trigonal bipyramidal geometry. There is a perpendicular acetylene bridge (perpendicular to the M–M bond) which occupies a common equatorial bridging position and a bridging OBu^t ligand which provides a common axial site as shown schematically in **XXII** below.
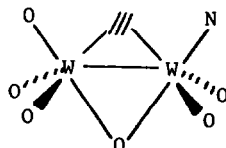
XXII

Of further interest are the W–W distance, 2.667(1) Å, and the C–C (acetylene) distance, 1.441(14) Å, both of which are longer than those in $W_2(OPr^i)_6(py)_2(\mu\text{-}C_2H_2)$. It is, of course, not clear whether this has any relevance to the fact that $W_2(OBu^t)_6$ and $MeC \equiv CMe$ react to give two equivalents of $(Bu^tO)_3W \equiv CMe$, eqn (6). However, we have found that, whereas $W_2(OBu^t)_6$ and $MeC \equiv N$ react to give methylcarbyne and nitrido tungsten compounds, eqn (7), the addition of $MeC \equiv N$ to $W_2(OR)_6(\mu\text{-}C_2R_2)$ compounds yields $W_2(OR)_6(\mu\text{-}NC_4R_2Me_2N)$ compounds containing a ligand derived from coupling one $C \equiv C$ and two $C \equiv N$ bonds.[90] For example, $MeC \equiv CMe$ and $MeC \equiv N$ give the ligand which may be viewed as the deprotonated 4-anion of **XXIII** below.
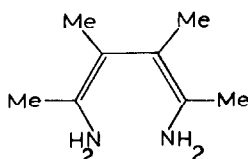
XXIII

87. M. H. Chisholm, J. C. Huffman and R. J. Tatz, *J. Chem. Soc.*, Chem. Commun., submitted.
88. F. A. Cotton and R. A. Walton, *Multiple Bonds Between Metal Atoms*. Wiley, New York (1982).
89. M. H. Chisholm, D. M. Hoffman and J. C. Huffman, results to be published.
90. M. H. Chisholm, D. M. Hoffman and J. C. Huffman, *J. Chem. Soc.*, Chem. Commun., submitted.

COMPLEXES OF ZINC, CADMIUM AND MERCURY(II) WITH THE ZWITTER-IONIC FORM OF NN'-ETHYLENEBIS (SALICYLIDENEIMINE)

H. A. TAJMIR-RIAHI*

Department of Chemistry, University of Aburayhan-Birouni, Tehran P.O. Box 2719, Iran

Abstract—The Schiff base NN'-ethylenebis(salicylideneimine), H_2 salen reacts with hydrous and anhydrous Zinc, Cadmium and Mercury(II) salts to give complexes $M(H_2$ salen$)X_2 \cdot nH_2O$ (M = Zn, Cd, Hg; X=Cl, Br, I, NO_3; M=Zn, X_2=SO_4; n = 0-2). Spectroscopic and other evidence indicated that; (i) halide and sulphate are coordinated to the metal ion, whereas the nitrate group is ionic in mercury nitrate compound and covalently bonded in zinc and cadmium nitrato complexes, (ii) the Schiff base is coordinated through the negatively charged phenolic oxygen atoms and not the nitrogen atoms, which carry the protons transferred from phenolic groups on coordination, (iii) therefore the coordination numbers suggested are 4-, in mercury and 4- or 6- in zinc and cadmium Schiff base complexes.

Schiff bases derived from salicylaldehyde, such as NN'-ethylenebis (salicylideneimine), H_2 salen are well known as poly-dentate ligands[1,2] coordinating in two ways.

In the first (and better understood), the ligand is ionised by removal of the phenolic protons giving complexes such as Zn(salen).[3] In the second the Schiff base is apparently either un-ionised[4,5] or partly ionised.[6] In this case the metal ion has class A character: lanthanides,[4,5] actinides,[7] Ti(IV),[8] Zr(IV),[9] Sn(IV),[10,11] Co(II)[12] and Fe(III).[13] Typical examples are TiCl$_4$(H$_2$ salen),[8] UCl$_4$(H$_2$ salen)thf[7] (thf = tetrahydrofuran) and LaCl$_3$(H$_2$ salen)$_2$.[4] There has been no report on un-ionised Schiff base complexes of the class B metal cations such as Zn,[11] Cd[11] and Hg.[11] Although many examples (Bullock and Tajmir-Riahi references therein)[4] of the second type are known, until very recently the structures of this type of complex were unknown. Some authors[14] have supposed that the Schiff base is coordinated through the phenolic oxygen since an enol-imine(I) to ketoenamine(II) tautometric conversion is possible; evidence for this came from IR and UV spectroscopy. From essentially identical IR results, other workers[4,7-11] suggest that the Schiff base is coordinated only through the azomethine nitrogen atoms, with the ligand remaining in the enol-imine form in the complexes.

Recently we have reported[15] the structure of Ca(H$_2$L)(NO$_3$)$_2$, H$_2$L=NN' - propane - 1.3 - diylbis (salicylideneimine), (H$_2$sal-1,3pd), in which the Schiff base is best described by the third tautomer(III), namely, the charge-separated (zwitter-ionic) form. Coordination takes place through the negatively charged oxygen atoms only (not the nitrogen atoms, which carry the proton transferred from the phenolic groups on coordination) and bi-dentate nitrate groups.

The changes observed on comparing the IR spectra of this compound and the free Schiff base in the C=N stretching region are the same for the complexes discussed in this work as for the other compounds.[4,5,7-11]

*Correspondence to: Department of Chemistry, Université de Montréal, Montréal, Québec H3C3VI, Canada.

(I)   (II)

(III)
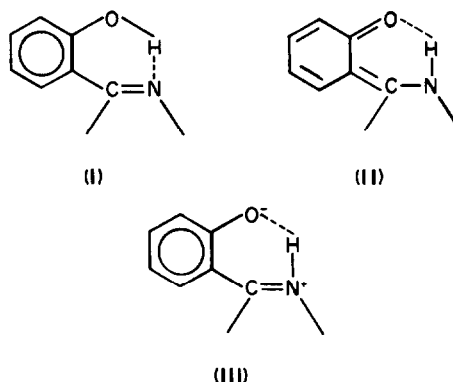
RESULTS AND DISCUSSION

The thirteen new complexes (M=Zn, Cd, Hg) with H$_2$salen which have been prepared are shown with analytical data and millimolar conductance in Table 1. The low molar conductivities[16] of 1×10^{-3}M solutions of the halide and sulphate complexes in dimethylformamide, dimethylsulphoxide and butanol (in the range 5–30 Ω^{-1} cm^2) indicate non-electrolytic behaviour, while the nitrate complexes show considerable dissociation in these solvents (Λ_M = 83–155 Ω^{-1} cm^2), this is due to some ligand exchange between the strong donors DMF, DMSO and the weakly bonded nitrate group in the coordination sphere of these metal ions in these solvents.[17]

IR spectroscopy

(a) 4000–2000 cm^{-1}. In this region, the free Schiff base shows a strong intramolecular hydrogen bonding (O–H . . . . N)[4] which gives rise to a broad absorption near 2700 cm^{-1}; this band shifts to 3000 cm^{-1} in the spectra of metal complexes as the hydrogen bonding arrangements change (O . . . . H$^+$—N).[15]

On examining the IR spectra of the complexes with fully ionised Schiff base, there is neither absorption near 2700 or at 3000 cm^{-1}; in these complexes only the aliphatic and aromatic C–H vibrations are observed. For the hydrated complexes an additional broad band near 3400 cm^{-1} was assigned to water molecules.

Table 1. Analytical[a] and conductance[b] data for H_2 salen complexes

Complexes	M%	X%	N%	$M \times 10^3$	Λ_M[b]
Zn(H_2 salen)Cl_2	16.25(16.16)	17.35(17.55)	7.04(6.92)	1.00(c)	13.7
Zn(H_2 salen)Br_2	13.10(13.24)	32.25(32.38)	5.70(5.67)	1.00(c)	17.5
Zn(H_2 salen)I_2	11.30(11.12)	43.10(43.20)	4.50(4.76)	1.00(d)	5.5
Zn(H_2 salen)(NO_3)$_2$·$2H_2O$	13.15(13.25)	24.90(25.13)	— —	1.00(c)	155.0
Zn(H_2 salen)SO_4	15.10(15.22)	22.20(22.35)	6.40(6.52)	1.00(e)	27.2
Zn salen	19.60(19.72)	— —	8.44(8.44)	1.00(c)	1.1
Cd(H_2 salen)Cl_2	24.70(24.89)	15.65(15.72)	6.30(6.20)	1.00(c)	24.5
Cd(H_2 salen)Br_2	20.80(20.79)	29.35(29.60)	5.30(5.18)	1.00(c)	27.5
Cd(H_2 salen)I_2	17.85(17.71)	39.80(40.00)	4.25(4.39)	1.00(c)	29.5
Cd(H_2 salen)(NO_3)$_2$·$2H_2O$	20.60(20.79)	22.75(22.94)	— —	1.00(c)	132.0
Cd salen	29.50(29.69)	— —	7.19(7.39)	1.00(c)	2.9
Hg(H_2 salen)Cl_2	37.35(37.17)	12.90(13.15)	5.00(5.18)	1.00(c)	26.8
Hg(H_2 salen)Br_2	31.75(31.91)	25.30(25.45)	4.60(4.48)	1.00(c)	8.5
Hg(H_2 salen)I_2	27.90(27.76)	34.95(35.12)	4.00(3.87)	1.00(c)	12.9
Hg(H_2 salen)(NO_3)$_2$·$2H_2O$	31.55(31.85)	19.50(19.78)	— —	1.00(e)	83.5
Hg salen	43.05(42.99)	— —	5.80(6.00)	1.00(c)	1.5

[a]Calc. analyses in parentheses; [b]millimolar conductance values in c DMF, d butanol, e DMSO.

(b) 2000–600 cm^{-1}. The main features of this region relevant to the present discussion for the ligand and the complexes are listed in Table 2. A strong absorption band at 1630 cm^{-1} was assigned to C=N stretching frequency in the free ligand which shifts to a higher frequency at about 1650 cm^{-1} in metal complexes ($\Delta \bar{\nu}$ 8–35 cm^{-1}). It has been found[18] that C=N$^+$ groups have in general higher frequencies than the parent C=N groups, thus the results are consistent with the presence of charge-separated forms and these and the other complexes[4,5,7–11,14,15] are likely to be structurally related in that the coordination takes place through the nega-

tively charged phenolic oxygen atoms rather than the positively-charged nitrogen atoms of the azomethine groups. A sharp absorption at 1280 cm^{-1} assignable to C–O stretching vibration in the free base changes little on complex formation ($\Delta \bar{\nu} - 10$ to $+17$ cm^{-1}). The C–O stretching vibration must include considerable contributions from the skeletal vibrations of the aromatic ring and because the vibration changed little in the complexes it was suggested[15] that the bonding arrangements of the oxygen atoms were the same in the free Schiff base and the metal complexes.

On comparing the IR spectra of these complexes with

Table 2. Selected IR bands (cm^{-1}) for the ligand and metal complexes

Ligand	Complexes	C=N	C-O	M-O (ligand)	Other bands		
H_2salen		1630 s	1280 s				
	Zn(H_2salen)Cl_2	1665 s	1285 vs	515 s	290	vs	Zn-Cl
	Zn(H_2salen)Br_2	1660 s	1275 vs	500 s	240	s	Zn-Br
	Zn(H_2salen)I_2	1645 s	1285 s	505 s	---		
	Zn(H_2salen)SO_4	1665 vs	1297 vs	520 s	270	m	Zn-O_2SO_2
	Zn(H_2salen)(NO_3)$_2$·$2H_2O$	1650 vs	1280 vs	510 s	350	s	Zn-ONO_2
	Cd(H_2salen)Cl_2	1638 vs	1280 vs	510 m	295	m	Cd-Cl
	Cd(H_2salen)Br_2	1640 vs	1285 vs	520 s	210	m	Cd-Br
	Cd(H_2salen)I_2	1642 s	1280 s	510 s	---		
	Cd(H_2salen)(NO_3)$_2$·$2H_2O$	1648 vs	1285 vs	520 s	240	s	Cd-ONO_2
	Cd(salen)	1620 bs	1315 vs	505 s	580	s	Cd-N
	Hg(H_2salen)Cl_2	1635 s	1285 s	510 s	245	m	Hg-Cl
	Hg(H_2salen)Br_2	1648 s	1270 s	500 s	240	s	Hg-Br
	Hg(H_2salen)I_2	1640 s	1290 s	480 m	---		
	Hg(H_2salen)(NO_3)$_2$·$2H_2O$	1640 s	1290 m	505 m	---		
	Hg(salen)	1610 vs	1275 s	520 m	550	s	Hg-N

s, strong; b, broad; v, very; m, medium.

the fully ionised Schiff base compounds one can see that the C=N stretching vibration of the free ligand has fallen on complex formation and the C–O stretching vibration increased to a higher frequency (Table 2). Therefore the results are consistent with those of the structurally known ionised complexes such as U(salen)Cl$_2$·2thf[7,19] where the coordination took place via the phenolic oxygen atoms and the nitrogen atoms of the azomethine groups.

Nitrate complexes

The IR spectra of Hg(H$_2$ salen)(NO$_3$)$_2$·2H$_2$O showed a broad and strong absorption band centered at 1370 cm^{-1} which was related to the presence of the ionic nitrate[20] in this compound, whereas the absence of the said absorption in the spectra of the Zn(H$_2$ salen)(NO$_3$)$_2$·2H$_2$O and Cd(H$_2$ salen)(NO$_3$)$_2$·2H$_2$O with the presence of the strong absorption from ν_1 (1480–1500 cm^{-1}), ν_2(1020–1030 cm^{-1}), ν_4(1280–1300 cm^{-1}) and ν_6(820 cm^{-1}) was indicative of the coordinated nitrate group in C$_{2v}$ symmetry[21,22] in these two nitrato complexes. The weak fundamentals ν_4 (720 cm^{-1}) of the ionic nitrate and ν_3 and ν_5 of bonded nitrato group were masked by the strong ligand absorption (700–800 cm^{-1}).

Sulphate complex

On comparing the spectra of the free ligand and the halide complexes with the sulphate compound, the sulphate spectra were dominated by the strong absorption from ν_3(1190, 1155 and 1120 cm^{-1}), ν_1(998 cm^{-1}), ν_2(450 cm^{-1}) and ν_4(610, 640 cm^{-1}) of the sulphate group in C$_{2v}$ symmetry.[23,24] Therefore the sulphate group must act as a chelated ligand in this compound.

(c) 600–200 cm^{-1}. A broad band in the spectra of the halide complexes around 200–300 cm^{-1} may be associated with metal–halide stretching vibrations[25,26] (Table 2). However conclusive evidence regarding the bonding of M–O[25] of the ligand has been provided by the occurrence of the strong absorption band at about 500 cm^{-1} in the spectra of the metal complexes (Table 2). The metal-oxygen[25] stretching vibrations of the coordinated anions (nitrato and sulphato) were found near 250–350 cm^{-1} in the spectra of zinc and cadmium complexes. A sharp, strong absorption around 550–600 cm^{-1} in the spectra of the fully ionised Schiff base complexes, M(salen), is attributed to M–N stretching.[27]

CONCLUSION

On the basis of the properties of the complexes studied here, some features can be emphasized: (a) the ligand is coordinated through the phenolic oxygen atoms only, (b) the halides and sulphate are bonded to the metal ions, (c) the nitrate group has shown ionic character in the mercury nitrate compound but covalently bonded in the corresponding zinc and cadmium Schiff base complexes, (d) therefore the mercury ion would be 4-coordinated in these series of Schiff base complexes whereas the zinc and cadmium ions could have 4-coordination in halo and sulphato and 6-coordination in nitrato (except for Hg(II)nitrate) complexes with possible tetrahedral or octahedral geometry around these metal cations.

EXPERIMENTAL

Materials

All the chemicals were reagent grade. The ligand was prepared by routine method.[3]

Preparation of the complexes

Most of the complexes were prepared by the addition of the stoichiometric amount of the hydrous or anhydrous metal ion salt in absolute ethanol or methanol (containing 1% water) to a hot solution of the ligand in absolute ethanol. A yellow precipitate formed almost immediately. This was filtered off and washed with hot ethanol and ether several times and dried (CaCl$_2$). The complexes are not soluble in common organic solvents, only dissolve in dimethylformamide, dimethylsulphoxide and slightly hot alcohol. Many unsuccessful attempts were made to prepare the Schiff base complexes of cadmium and mercury sulphate due to the insolubility of CdSO$_4$ and HgSO$_4$ in alcohol.

Analysis of the complexes

The metal ions were determined complexometrically,[28] halides as silver halide and sulphate ion as BaSO$_4$, nitrate was analyzed by precipitation with nitron[28] and nitrogen was estimated by Kejeldahl's method.[28]

Vibrational spectra

IR spectra were obtained on Perkin–Elmer 598 (4000–200 cm^{-1}) using Nujol and Hexachlorobutadien mulls technique with KBr and polyethylene disks.

Conductance measurements

Conductivity measurements were made in 10^{-3} M dimethylformamide, dimethylsulphoxide and butanol solutions at 25°C with a CDM2e conductivity meter (Radiometer, Copenhagen).

REFERENCES

1. R. H. Holm, G. W. Everett and A. Chakravorty *Progress in Inorganic Chemistry*, 1966, 7, 83.
2. M. D. Hobday and T. D. Smith, *Coordin. Chem. Rev.* 1973, 9, 311.
3. C. S. Marvel, S. A. Aspey and E. A. Dudley, *J. Am. Chem. Soc.* 1956, 78, 4905.
4. J. I. Bullock and H. A. Tajmir-Riahi, *J. Chem. Soc. (Dalton)* 1978, 36.
5. J. I. Bullock and H. A. Tajmir-Riahi, *Inorg. Chim. Acta* 1980, 38, 141.
6. H. A. Tayim, M. Absi, A. Darwish and S. K. Thabet, *Inorg. Nuclear Chem. Let.* 1975, 11, 395.
7. L. Doretti, F. Madalosso, S. Sitran and S. Faleschini, *Inorg. Nuclear Chem. Lett.* 1976, 12, 817.
8. N. S. Biradar and V. H. Kulkarni, *Rev. Roumaine Chim.* 1970, 15, 1993.
9. V. A. Kogan, V. P. Sokolov and O. A. Osipov, *Russ. J. Inorg. Chem.* 1968, 13, 1195.
10. V. A. Kogan, O. A. Osipov, V. L. Minkin and V. P. Sokolov, *Russ. J. Inorg. Chem.* 1965, 10, 45.
11. L. V. Orlova, A. D. Garnovskii, O. A. Osipov and I. I. Kukushkina, *Zhur. Obschei Khim.* 1968, 38, 1850.
12. P. Bamfield, *J. Chem. Soc.* 1967, (A), 804.
13. A. van den Bergen, K. S. Murray, K. J. O'Connor, N. Rehak and B. O. West, *Austral. J. Chem.* 1968, 21, 1505.
14. G. Condorelli, I. Fragala, S. Guiffrida and A. Cassol, *Z. Anorg. Allg. Chem.* 1975, 412, 251.
15. J. I. Bullock, H. A. Tajmir-Riahi, M. F. C. Ladd and D. C. Povey, *Acta Cryst.* 1979, B35, 2013.
16. W. J. Geary, *Coord. Chem. Rev.* 1971, 7, 81.
17. J. V. Quagliano, J. Fujita, G. Franz, D. J. Phillips, J. A. Walmsley and S. Y. Tyree, *J. Am. Chem. Soc.* 1961, 83, 3770.
18. C. Sandorfy, *The Chemistry of the Carbon–Nitrogen Double Bond* (Edited by S. Patai), p. 42 (1970).
19. F. Calderazzo, C. Floriani, M. Pasquali, M. Cesari and G. Perego, *Gazz. Chim. Ital.* 1976, 106, 127.
20. B. M. Gatehouse and A. E. Comyns, *J. Chem. Soc.* 1958, 3966.

21. C. C. Addison, N. Logan, S. C. Wallwork and C. D. Garner, *Quart. Rev.* 1971, **25**, 289.
22. J. I. Bullock, *J. Inorg. Nucl. Chem.* 1967, **29**, 2257.
23. K. Nakamoto, J. Fujita, S. Tanaka and M. Kobayashi, *J. Am. Chem. Soc.* 1957, **79**, 4904.
24. C. G. Barraclough and M. L. Tobe, *J. Chem. Soc.* 1961, 1993.

25. M. W. G. DeBolster and W. L. Groeneveld, *Rec. Trav. Chim.* 1971, **90**, 477, 687.
26. G. E. Coates and D. Ridley, *J. Chem. Soc.* 1964, 166.
27. B. B. Mohapatra, B. K. Mohapatra and S. Guru, *J. Inorg. Nucl. Chem.* 1978, **40**, 1178.
28. A. I. Vogel, *A Text-Book of Quantitative Inorganic Analysis,* 3rd Edn. Longmans, London (1961).

A RADIOCHEMICAL INVESTIGATION OF YbCl$_3$–(AlCl$_3$)$_n$ COMPLEXES IN THE GAS PHASE

G. STEIDL, F. DIENSTBACH and K. BÄCHMANN*

Fachbereich Anorganische Chemie und Kernchemie, Technische Hochschule Darmstadt, 6100 Darmstadt, Federal
Republic of Germany

Abstract—The vapour densities of complex species in the YbCl$_3$/AlCl$_3$ system were investigated by using tracer ^{169}Yb. The results obtained allowed a description of the equilibria in the vapour phase in the temperature range from 500 to 1000 K. The equilibrium constants according to YbCl$_{3(s)}$ + n*Al$_2$Cl$_{6(g)}$⇌YbAl$_{2n}$Cl$_{6n+3(g)}$ were fitted to expressions of the form log K_p = A + (B/T) and the thermodynamic values of ΔH and ΔS were calculated.

$$YbCl_{3(s)} + 0.5\ Al_2Cl_{6(g)} \rightleftharpoons YbAlCl_{6(g)} \qquad \Delta H_{298} = 149.9(\pm 13)kJ/mol$$
$$\Delta S_{298} = 124.4(\pm 13)J/mol\ K$$

$$YbCl_{3(s)} + 1.0\ Al_2Cl_{6(g)} \rightleftharpoons YbAl_2Cl_{9(g)} \qquad \Delta H_{298} = 87.5(\pm 13)kJ/mol$$
$$\Delta S_{298} = 47.7(\pm 13)J/mol\ K$$

$$YbCl_{3(s)} + 1.5\ Al_2Cl_{6(g)} \rightleftharpoons YbAl_3Cl_{12(g)} \qquad \Delta H_{298} = 27.6(\pm 4)kJ/mol$$
$$\Delta S_{298} = -11.5(\pm 8)J/mol\ K$$

$$YbCl_{3(s)} + 2.0\ Al_2Cl_{6(g)} \rightleftharpoons YbAl_4Cl_{15(g)} \qquad \Delta H_{298} = 0(\pm 4)kJ/mol$$
$$\Delta S_{298} = -65.9(\pm 10)J/mol\ K.$$
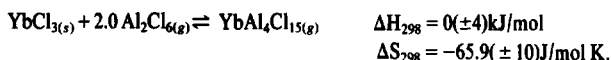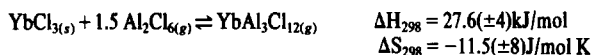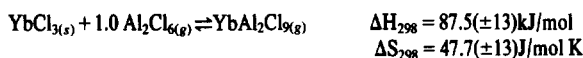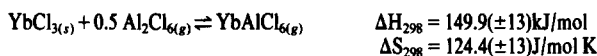
The formation of gaseous complexes has gained in significance in the preparative chemistry and in industrial problems. Slightly volatile halides can be transported chemically through temperature gradients and the combination of this chemical transport together with other reactions leads to new synthetic routes.[1–3] The halides of the lanthanides are important in the development of high pressure discharge tubes. The halides are decomposed in the plasma and reformed near the wall. To increase the saturation of the halides the addition of complex formers is necessary, e.g. CeI$_3$ + NaI + CsI.[4–6]

A further field of application of gaseous complexes is the separation of lanthanides and actinides by gas chromatography of the aluminium chloride complexes.[7–9] Like many other complexes[1] the aluminium chloride–lanthanide chloride system presents a special problem containing several complexes.[10–16] The general methods used to investigate these aluminium chloride–lanthanide chloride systems and to determine the thermodynamic values are UV-Vis spectrometry[10,11,17] and entrainment, quenching and chemical transport experiments[14] and mass spectrometric investigations.[16] The applications of these methods are limited. At temperatures above 850 K spectrometric methods are not useful because the AlCl$_3$ attacks the cell. At temperatures lower than 650 K it is difficult to investigate the complex systems because of the small absorbances measured. Mass spectrometric investigations allow pressures up to 10^{-1} atm only.[18,19] The entrainment experiments are limited to low pressures, too.

To get further information on the equilibrium and on the thermodynamic data of the lanthanide chloride–aluminium chloride system we have applied a new method suggested by Peterson *et al.*[12] The basic idea is to use a heated quartz tube and to measure the radioactivity of ^{169}YbCl in the vapour as a function of the temperature, knowing the amount of solid YbCl$_3$, ^{169}YbCl$_3$ and AlCl$_3$ at the start of the experiments. The γ-counting rate of ^{169}Yb is related to the vapour density of the complexes in the gas. The vapour pressure of pure YbCl$_3$ is negligible in the temperature range measured. The advantages of this measuring system are:

(a) The method is useful for volatile inorganic species, which are not accessible to spectrometric techniques.

(b) The method allows investigation of the system at low temperatures and at low complex concentrations by adding elevated amounts of tracer ^{169}Yb (important for the determination of the vapour density of the large YbAl$_4$Cl$_{15}$-complex).

(c) The method allows measurement of the vapour densities of the complexes at elevated temperatures (1000 K) and pressures (5 atm).

In the present study we have investigated the YbCl$_3$–AlCl$_3$-system in the temperature range from 500 to 1000 K. Like the other lanthanide chloride–aluminium chloride complexes YbCl$_3$ can be expected to react with AlCl$_3$ according to the general equation

$$YbCl_{3(s)} + n^*Al_2Cl_{6(g)} \rightleftharpoons YbAl_{2n}Cl_{6n+3(g)}. \qquad (1)$$

The occurrence of the gaseous complex is responsible for increased concentrations of the lanthanide in the gas phase.

EXPERIMENTAL

AlCl$_3$ was prepared by passing chlorine over analytical grade aluminium metal at temperatures of 600 K. The chlorine was dried by passage through sulphuric acid and phosphorus pentoxide. The aluminium chloride was sublimed under a chlorine atmosphere into a quartz tube and flushed with dry helium (99.999%, passed through a cold trap at −190°C).

---

*Author to whom correspondence should be addressed.
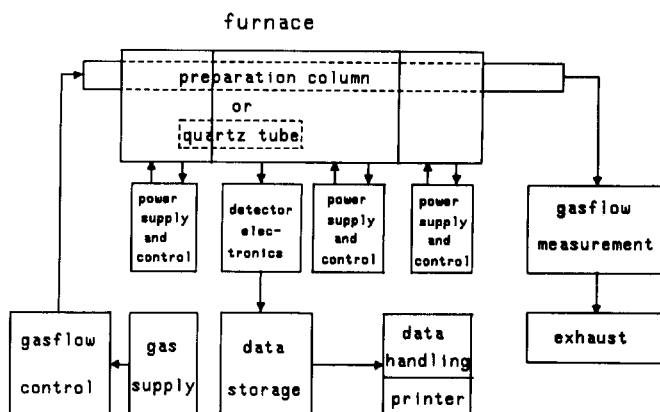
furnace

Fig. 1. Schematic diagram of the experimental section.

In order to prepare $YbCl_3$, dry Yb_2O_3 was transferred to a quartz tube containing a great excess of $AlCl_3$ (Fig. 1). The tube was flushed with helium, evacuated and sealed, then placed in a furnace and slowly heated to 600 K. Yb_2O_3 reacted with $AlCl_3$ according to equation

$$Yb_2O_{3(s)} + Al_2Cl_{6(g)} \longrightarrow Al_2O_{3(s)} + 2YbCl_{3(s)}. \qquad (2)$$
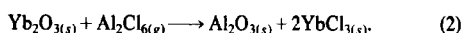
This method was worked out and reported by Papatheodorou *et al.*[11] for preparing some lanthanide chlorides and $ThCl_4/AlCl_3$ by reaction of the corresponding oxide with $AlCl_3$. Under a helium atmosphere known amounts of $YbCl_3$, irradiated $^{169}YbCl$, and $AlCl_3$ were transferred to a helium flushed cylindrical quartz tube. The quartz tube was evacuated and sealed, then placed into a furnace surrounded by a shield of lead bricks except for a detection slot (Fig. 2). (Size of the quartz tube: $\emptyset_i = 6.5$ cm, $1 = 30$ cm, volume = 40 cm³.)

The furnace consists of three resistance-heated, 1 mm thick Kantal wires around a ceramic tube (26 mm I. D., 35 mm O. D.). The furnace is insulated with a 40 mm thick "ceramic fibre felt", which guarantees a sufficient uniform temperature distribution inside the ceramic tube. Thermocouples are used for temperature measurement and control. The three parts of the oven have separate temperature controls allowing as well isothermal as temperature-programmed operation with constant heating and cooling rates.[20] The temperature gradient along the furnace was adjusted so that the temperature of the detection point was 3–4°C higher than that of the sample containing the end of the tube. The non-volatilized portion of the $YbCl_3$, thus, remained outside of the detection volume. Reported temperatures were those of the cooler end of the tube, because the equilibrium between Al_2Cl_6 and $YbCl_3$ was established over the condensed phase.[12] In the temperature range measured the vapour pressure of pure $YbCl_3$ did not contribute to the γ-ray measuring.[21]
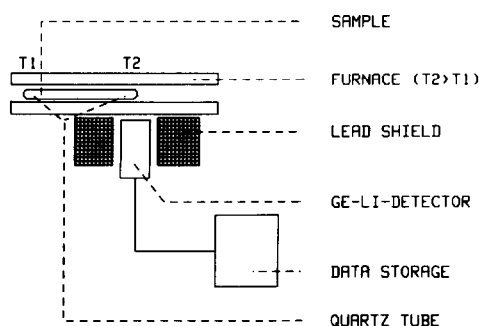
Fig. 2. Schematic diagram of the experimental set-up.

For the detection of the radioactive compound a Ge–Li-detector was used, placed outside the furnace at the opposite side of the cool end of the quartz tube. It was surrounded by lead bricks so that only the γ-rays of a small section were detected and the background counting rate was less than 1% of the maximum counting rate obtained when all the $YbCl_3$ was in the vapour phase.

The γ-rays of $^{169}YbCl_3$ were measured several times for ascending and descending temperatures. To calculate the concentration of ytterbium chloride in the vapour phase the average values of the γ-countings of every measuring point were used.

The experiments were evaluated for temperatures between 500 and 1000 K only. At temperatures below the triple point of $AlCl_3$ (T ~ 460 K) a solid vapour interface can exist.[12] The solids which are present can be $AlCl_3$, $LnCl_3$ (Ln = lanthanides) and/or a solid solution of the two.[15] At temperatures between 460 and 500 K a region of liquid–vapour equilibrium exists.[11–13] A break in the plot of the complexed metal ion quantity vs the temperature curve indicates the physical change of the condensed phase from solid to liquid.[12,13,22] The nature of these phases in the vicinity of the triple point are not well known.[12] The reaction of $AlCl_3$ with quartz was investigated by Schäfer *et al.*[23] Despite favourable thermodynamics the reaction does not occur to any significant extent below 1000 K.

In order to determine the vapour complex density and thermodynamics of the $AlCl_3/YbCl_3$-system the following experiments were performed: Five different $YbCl_3$ and $AlCl_3$ weight-ins the γ-peak contents of ^{169}Yb in dependence of the corresponding temperatures are recorded in 5 K intervals from 500 to 1000 K. To maintain equilibrium, ascend and descend rates of 0.4 K/min are sufficient for high reactant concentrations, for lower $AlCl_3$ weight-ins, ascend rates lower than 0.1 K/min are necessary. The γ-peaks are evaluated automatically by an "ND-66 Multichannel Analyzer System" and recorded by a PDP-11 system processor. The partial pressure of aluminium chloride is calculated from the known amounts of $AlCl_3$, corrected for the $AlCl_3$, which combines with ytterbium chloride and that part which forms the dimerisation according to

$$2 AlCl_{3(g)} \rightleftharpoons Al_2Cl_{6(g)}$$
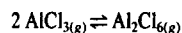
using literature data[13] for the equilibrium constant of the dissociation. Some aluminium chloride vapour pressures and corresponding temperatures of the experiments are given in Table 1.

The weight-in of $AlCl_3$ and $YbCl_3$ is chosen in such a manner that at temperatures of about 1000 K all the $YbCl_3$ is in the vapour phase. Thus, the maximum number of the γ-counting rate is proportional to the weight-in. Assuming a linear function between the γ-counting rate and the $YbCl_3$ present in the vapour phase it is possible to determine the partial pressure of the complexed ions.

3. RESULTS AND DISCUSSION

Assuming that only monolanthanide complexes were formed in the AlCl$_3$/LnCl$_3$-system, the LnAl$_3$Cl$_{12}$-complex was established to be the main complex in the temperature range from 500 to 1000 K.[13,14] Thus, the predominant vapour complex in the AlCl$_3$/YbCl$_3$-system was assumed to

$$(YbCl_3)_m * 1.5 \, Al_2Cl_6 \quad (m = 1).$$

The assumption ($m = 1$) as well has been used for the transition metal chloroaluminate complexes supported by mass spectrometric studies,[16,18] as for the investigation of NdCl$_3$,[13] SmCl$_3$,[11] GdCl$_3$,[14] and EuCl$_3$[10] AlCl$_3$-systems. For higher temperatures and low AlCl$_3$ pressures the formation of gas complexes with lower molecular weight (LnAl$_2$Cl$_9$, LnAlCl$_6$) became prevalent; at low temperatures, however, a complex according to

$$YbCl_3 + 2Al_2Cl_6 \rightleftharpoons YbAl_4Cl_{15} \qquad (3)$$

was supposed to exist in detectable quantities beside the 1.5-complex. The thermodynamics of the equivalent NdAl$_4$Cl$_{15}$-complex were determined by Øye and Gruen.[13]

In the temperature range from 500 to 1000 K the equilibrium of the vapour phase could best be rationalized by considering that two or more different YbCl$_3$/AlCl$_3$ complexes should coexist.[1] In agreement with these considerations the experimentally determination of the stoichiometric factor n according to

$$YbCl_3 + n*Al_2Cl_6 \rightleftharpoons YbAl_{2n}Cl_{6n+3} \qquad (1)$$

decreased from 1.8 to 0.95 with increasing temperature. Since $P_c \ll P\,Al_2Cl_6$ (P_c = pressure of the complexed vapour phase), the equilibrium constant of reaction (1) is

$$K_n = P_c/(P_{Al_2Cl_6})^n.$$

Between 670 and 770 K the stoichiometric factor n was nearly constant indicating the dominance of the YbAl$_3$Cl$_{12}$ complex. Assuming that only very small amounts of complexes other than YbAl$_3$Cl$_{12}$ were present in this temperature range, plots of the logarithm of the equilibrium constant $K_{1.5}$ vs $1/T$ according to

$$YbCl_{3(g)} + 1.5 \, Al_2Cl_{6(s)} \rightleftharpoons YbAl_3Cl_{12(g)} \qquad (4)$$
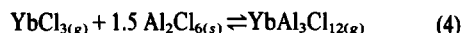
should as well be a linear function of $1/T$ as coincidence for different AlCl$_3$/YbCl$_3$ weight-ins. These conditions are sufficiently fulfilled in a first convergence and the equilibrium constant of the reaction (4) was fitted to an expression (Temp = 680–750 K) of the form

$$\lg K_{1.5} = A_{1.5} + (B_{1.5/T}) \qquad (5)$$

with

$$K_{1.5} = \frac{P_{YbAl_3Cl_{12}}}{(P_{Al_2Cl_6})^{1.5}} \qquad (6)$$

and

$$P_{YbAl_3Cl_{12}} = Pctot$$

(Pctot = sum of the partial pressures of the complexes)

Requiring $\lg K$ to be a linear function of $1/T$ with eqns (5) and (6) the partial pressure of the YbAl$_3$Cl$_{12}$-complex is given by eqn (7):

$$P_{YbAl_3Cl_{12}} = 10 \exp\,[A_{1.5} + (B_{1.5}/T)] * (P_{Al_2Cl_6})^{1.5}. \qquad (7)$$

The assumption that YbAl$_3$Cl$_{12}$ was the only complex present in the temperature range from 670 to 770 K was not exactly fulfilled. The larger complex—YbAl$_4$Cl$_{15}$—was present in small amounts, too. We tried to eliminate this interference. Knowing the approximate partial pressure of

Table 1. AlCl$_3$ and Al$_2$Cl$_6$ partial pressures at the start and the end of the experiments

Exp.	$P_{Al_2Cl_6}^{523}$ [atm]	$P_{AlCl_3}^{523}$ [atm]	$P_{Al_2Cl_6}^{873}$ [atm]	$P_{AlCl_3}^{873}$ [atm]
1	1.91	0.0054	2.02	2.94
2	1.46	0.0047	1.44	2.48
3	1.04	0.0040	0.91	1.99
4	0.51	0.0028	0.34	1.21
5	2.86	0.0067	——	——

the 1.5-complex from eqn (7) and assuming that the complexes with lower molecular weights did not contribute to the partial pressure Pctot at temperatures lower than 750 K

$$P_{YbAl_4Cl_{15}} = Pctot - P_{YbAl_3Cl_{12}} \qquad (8)$$

and the equilibrium constant of the YbAl$_4$Cl$_{15}$-complex according to reaction (3) in the temperature range from 550 to 600 K is

$$K_{2.0} = (Pctot - P_{YbAl_3Cl_{12}}/(P_{Al_2Cl_6})^{2.0} \qquad (9)$$

$$= P_{YbAl_4Cl_{15}}/(P_{Al_2Cl_6})^{2.0}$$

and

$$lg\, K_{2.0} = A_{2.0} + (B_{2.0}/T). \qquad (10)$$
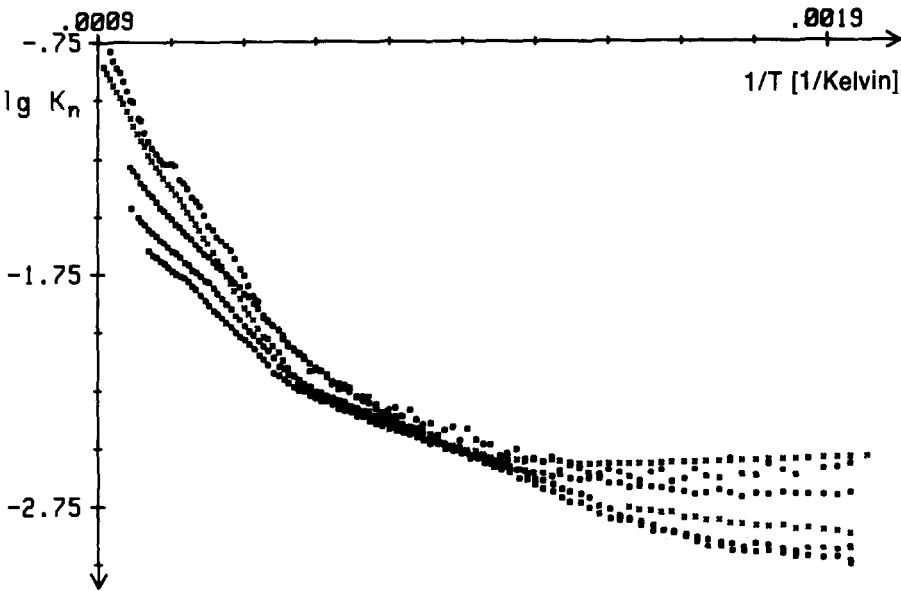
Fig. 3. Gaseous equilibrium of $YbCl_{3(s)} + nAl_2Cl_{6(g)} \rightleftharpoons YbAl_{2n}Cl_{6n+3(g)}$ lg Kn in dependence of 1/T (for different weight-ins).
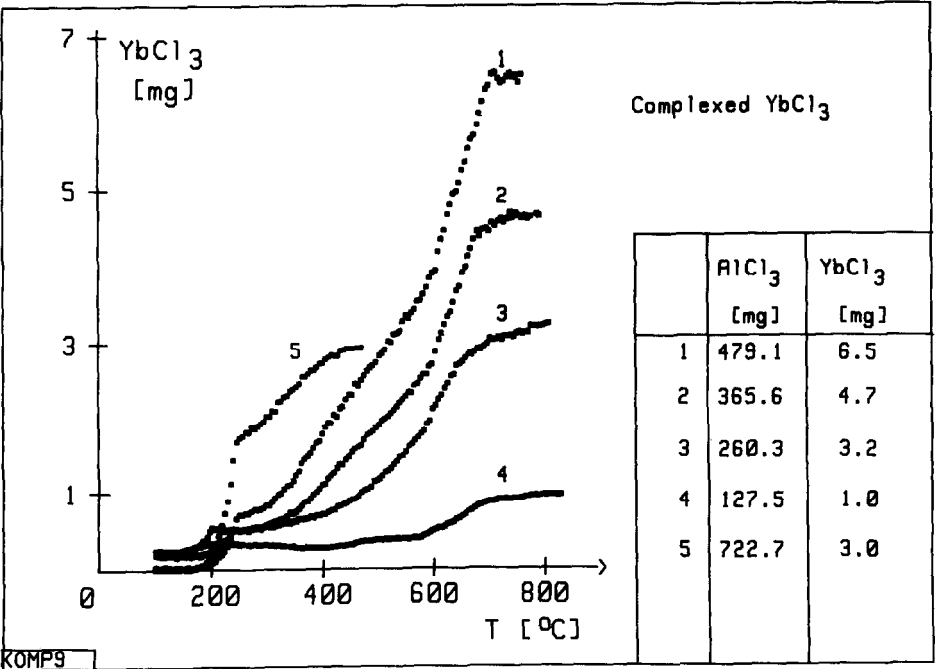
Fig. 4. Complexed YbCl$_3$ for different weight-ins in dependence of the temperature T.

The partial pressure $P_{YbAl_3Cl_{12}}$ is calculated from eqn (7). The values of $A_{2.0}$ and $B_{2.0}$ were determined from the plot of lg $K_{2.0}$ vs $1/T$. Knowing the values of $A_{2.0}$ and $B_{2.0}$ new values of $A_{1.5}$ and $B_{1.5}$ were determined with

$$P_{YbAl_3Cl_{12}} = Pctot - P_{YbAl_4Cl_{15}} \qquad (ii)$$

and eqns (5) and (6).

The partial pressure $P_{YbAl_4Cl_{15}}$ is calculated from eqn (7b)

$$P_{YbAl_4Cl_{15}} = 10 \exp[(A_{2.0} + \left(\int \Delta C_p \, d \ln T/R * \ln 10\right))$$
$$+ (B_{2.0}/T + \left(\int \Delta C_p \, dT/R * \ln 10 * T\right))] * (P_{Al_2Cl_6})^{2.0} \qquad (7b)$$

with $\Delta Cp = 3$ cal/K for reaction (3). This iteration method was repeated till the values of $A_{2.0}$, $B_{2.0}$, $A_{1.5}$ and $B_{1.5}$ became constant. For temperatures below 750 K the vapour pressures then could be represented by:

$$A_{1.5} = -0.60 \quad B_{1.5} = -1442$$

$$A_{2.0} = -3.35 \quad B_{2.0} = -30.$$

Using

$$\lg K = \frac{\Delta S}{R * \ln 10} - \frac{\Delta H}{R * T * \ln 10} \qquad (12)$$

the thermodynamic data were calculated and listed in Table 2 with

$$\Delta C_p = 0 \text{ cal/K} \quad \text{for reaction (4)}$$

and

$$\Delta C_p = +3 \text{ cal/K} \quad \text{for reaction (3).}$$

The complexes with lower molecular weights did coexist at higher temperatures, each in significant amounts. The approximation method used for the determination of the larger complexes (YbAl$_4$Cl$_{15}$ and YbAl$_3$Cl$_{12}$) is not practicable for the smaller complexes.

To determine the thermodynamic values of the complexes YbAlCl$_6$ and YbAl$_2$Cl$_8$ we set:

$$PC21 = P_{YbAlCl_6} + P_{YbAl_2Cl_9}$$
$$= Pctot - P_{YbAl_3Cl_{12}} - P_{YbAl_4Cl_{15}} \qquad (13)$$

and

$$PC21 = K_{1.0} * (P_{Al_2Cl_6})^{1.0} + K_{0.5} * (P_{Al_2Cl_6})^{0.5} \qquad (14)$$

with

$$\lg K_{1.0} = A_{1.0} + (B_{1.0}/T)$$

and

$$\lg K_{0.5} = A_{0.5} + (B_{0.5}/T)$$

$P_{YbAl_3Cl_{12}}$ is calculated from eqn (7), $P_{YbAl_4Cl_{15}}$ is calculated from eqn (7b).

Knowing the partial pressures PC21 from eqn (13) as a function of temperature, the constants $A_{1.0}$, $B_{1.0}$, $A_{0.5}$ and $B_{0.5}$ were varied and computer processed. With

$$10 \exp(A_{1.0} + B_{1.0}/T) * (P_{Al_2Cl_6})^{1.0}$$
$$+ 10 \exp(A_{0.5} + B_{0.5}/T) * (P_{Al_2Cl_6})^{0.5} = PC21t \qquad (15)$$

the partial pressures PC21t were determined theoretically for every measuring point.

The best fit would be when the difference (D) between the sum of the measured partial pressures (PC21) and the sum of the theoretically determined partial pressures (PC21t) became zero:

$$\sum(PC21 - PC21t) = \sum|D| = 0. \qquad (16)$$

Table 2. Thermodynamic functions for the reaction LnCl$_{3(s)}$ + n*Al$_2$Cl$_{6(g)}$ $\rightleftharpoons$ LnAl$_{2n}$Cl$_{6n+3}$(y) at 298 K

COMPLEXES	ΔH_{298} [kJ/mol]	ΔS_{298} [J/mol K]	LIT.
LnCl$_3$ * 0.5 Al$_2$Cl$_6$	204.7	136.9	theoret.
YbCl$_3$ * 0.5 Al$_2$Cl$_6$	149.9 ± 13	124.4 ± 13	this work
NdCl$_3$ * 0.5 Al$_2$Cl$_6$	157.0 ± 13	110.3 ± 13	[16]
LnCl$_3$ * 1.0 Al$_2$Cl$_6$	100.9	45 ± 5	theoret.
YbCl$_3$ * 1.0 Al$_2$Cl$_6$	87.5 ± 13	47.7 ± 13	this work
YbCl$_3$ * 1.5 Al$_2$Cl$_6$	27.6 ± 4	−11.5 ± 8	this work
GdCl$_3$ * 1.5 Al$_2$Cl$_6$	35.8 ± 8	11.0 ± 11	[14]
SmCl$_3$ * 1.5 Al$_2$Cl$_6$	28.1 ± 1	− 4.2 ± 1	[11]
NdCl$_3$ * 1.5 Al$_2$Cl$_6$	45.2 ± 1	8.4 ± 1	[13]
YbCl$_3$ * 2.0 Al$_2$Cl$_6$	0 ± 4	−65.9 ± 10	this work
NdCl$_3$ * 2.0 Al$_2$Cl$_6$	0 ± 1	−67 ± 2	[13]

Equation (16) is fulfilled with

$A_{1.0} = 2.0$ $B_{1.0} = -4300$ $(\Delta C_p = -4\text{cal/K})^*$ [16]

$A_{0.5} = 5.5$ $B_{0.5} = -7300$ $(\Delta C_p = -2\text{cal/K})^*$ *estimated.

The thermodynamic values were calculated from eqn (19) shown in Table 2.

Figure 5 shows the amounts of complexed $YbCl_3$ in dependence of the corresponding temperature for experiment 1. The values of ΔH and ΔS for some lanthanide complexes are compared in Table 2. To estimate the thermodynamic values of the formation of the complexes a method is used suggested by Schäfer.[1] For

$$0.5\, Yb_2Cl_{6(g)} + 0.5\, Al_2Cl_{6(g)} \rightleftharpoons YbAlCl_{6(g)} \quad (19)$$
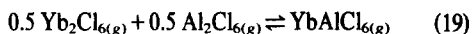
we set according to experience $\Delta H° \cong 0$ $\Delta S° \cong 0$ and $\Delta C_p \cong 0$.[1]

From the combination of the dimerisation[1] and the sublimation of $YbCl_3$ (eqn 20, 21) follows eqn (18).

$YbCl_{3(g)} \rightleftharpoons 0.5\, Yb_2Cl_{6(g)}$ $\Delta H_{(298)} = -24.8\,\text{kcal/mol}$
$\qquad\qquad\qquad\qquad\qquad \Delta S_{(298)} = -17.3\,\text{cal/mol K}$ (20)
$YbCl_{3(f)} \rightleftharpoons YbCl_{3(g)}$ $\Delta H_{(298)} = 73.7\,\text{kcal/mol}$
$\qquad\qquad\qquad\qquad\qquad \Delta S_{(298)} = 50\,\text{cal/mol K}$ (21)
$YbCl_{3(f)} + 0.5\, Al_2Cl_{6(g)} \rightleftharpoons YbAlCl_{6(g)}$
$\qquad\qquad\qquad\qquad\qquad \Delta H_{(298)} = 48.9\,\text{kcal/mol}$
$\qquad\qquad\qquad\qquad\qquad \Delta S_{(298)} = 32.7\,\text{cal/mol K}$ |(18)
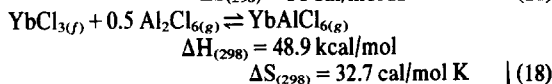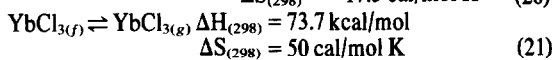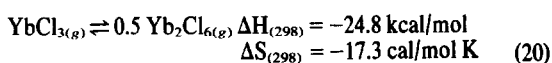
$$\Delta C_p = -4\,\text{cal/K}. \quad [16]$$

From our experiment we determine for reaction (18)

$\Delta S_{950} = 25.12(\pm3)\text{cal/mol K} \triangleq 105.2(\pm13)\text{J/mol K}$
$\Delta H_{950} = 33.2(\pm3)\text{kcal/mol} \triangleq 139.0(\pm13)\text{kJ/mol}$
$\Delta S_{298} = 29.7(\pm3)\text{cal/mol K} \triangleq 124.4(\pm13)\text{J/mol K}$
$\Delta H_{298} = 35.8(\pm3)\text{kcal/mol} \triangleq 149.9(\pm13)\text{kJ/mol}.$

Schäfer *et al.*[16] determined the entropies and enthalpies of the equivalent $NdAlCl_6$-complex by mass spectroscopy (T = 1123 K) resulting:

$$\Delta S_{298} = 26.3(\pm3)\text{cal/K}$$

and

$$\Delta H_{298} = 37.5(\pm3)\text{kcal.}$$

These data give good correspondence with our experiments and the data calculated theoretically.
For the reaction

$$YbCl_{3(f)} + 1.0\, Al_2Cl_{6(g)} \rightleftharpoons YbAl_2Cl_{9(g)} \quad (12)$$
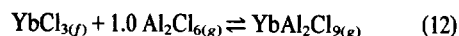
we estimate the entropy to be the same as the entropy of the divalent chloride compounds (ΔS 11 ± 1 cal/mol). With eqn (31) and

$$2YbCl_{3(g)} \rightleftharpoons 2*0.5\, Yb_2Cl_{6(g)}$$
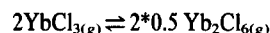
the enthalpy of reaction (12) is

$$73.7 - 2*(-24.8\,\text{cal/mol}) \longrightarrow \Delta H_{298} = 24.1\,\text{kcal/mol.}$$

From our experiments follows the reaction (12)

$\Delta S_{950} = 9.1(\pm3)\,\text{cal/mol K}$ $38.2(\pm13)\text{J/mol K}$
$\Delta H_{950} = 19.6(\pm3)\text{kcal/mol}$ $82.1(\pm13)\text{kJ/mol}$
$\Delta S_{298} = 11.4(\pm3)\text{cal/mol K}$ $47.7(\pm13)\text{J/mol K}$
$\Delta H_{298} = 20.9(\pm3)\text{kcal/mol}$ $87.5(\pm13)\text{J/mol}$

with

$$\Delta C_p = -2\,\text{cal/mol (estimated).}$$

The experimental data are in good agreement with our calculated data; experimental data of other $LnAl_2Cl_9$ are not available.
For the reaction

$$LnCl_{3(s)} + 1.5\, Al_2Cl_{6(g)} \rightleftharpoons LnAl_3Cl_{12(g)} \quad (22)$$
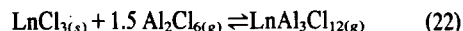
we determined for Ln = Yb ($\Delta C_p = 0$)

$$\Delta S_{298} = -2.8(\pm2)\text{cal/mol K}$$
$$-11.5(\pm8)\text{J/mol K.}$$
$$\Delta H_{298} = +6.6(\pm1)\text{kcal/mol}$$
$$+27.6(\pm4)\text{kJ/mol.}$$

In Table 2 the thermodynamic values are listed.

weight-in :

AlCl₃   : 479.1 mg
YbCl₃   :   6.5 mg

1. experimental
2. calculated
3. YbCl₃ * 2.0 Al₂Cl₆
4. YbCl₃ * 1.5 Al₂Cl₆
5. YbCl₃ * 1.0 Al₂Cl₆
6. YbCl₃ * 0.5 Al₂Cl₆
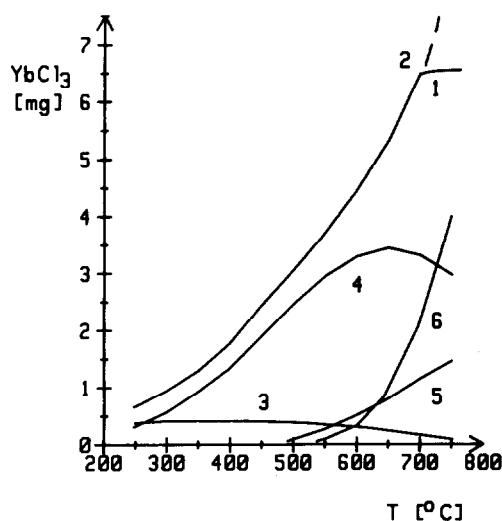
Fig. 5. Amount of $YbCl_3$ in the vapour dependence of the temperature T.
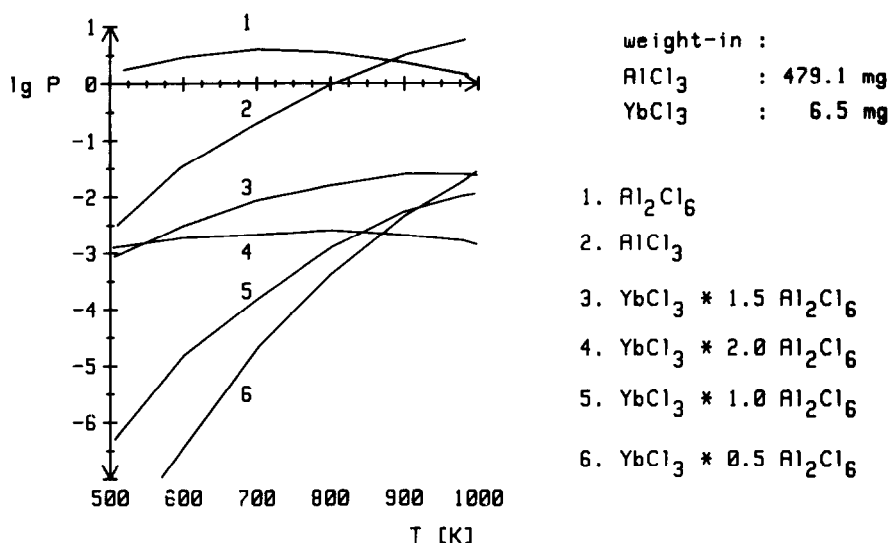
Fig. 6. Partial pressures in the system YbCl₃*(AlCl₃)ₙ.

The entropies and enthalpies of the 1,5-complex appear very close to the data which Papatheodorou *et al.*[11] obtained. Compared with the thermodynamic values of the equivalent $NdAl_3Cl_{12}$[10] and $GdAl_3Cl_{12}$[14] a difference is observed. Papatheodorou *et al.*[11] consider this difference to be attributed to experimental uncertainties or bonding and structure differences of the vapour complexes.

From the changing of the stoichiometric factor and from the plot of the logarithm of the equilibrium constant (lgK_n) against the temperature ($1/T$) we conclude the existence of a large complex ($YbAl_4Cl_{15}$) according to eqn (3).

$$YbCl_{3(s)} + 2.0Al_2Cl_{6(g)} \rightleftharpoons YbAl_4Cl_{15(g)} \qquad (3)$$
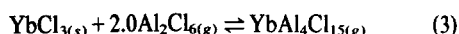
In the temperature range from 520 to 600 K and with $\Delta C_p = +3$ cal/K we determined ΔH_{298} and ΔS_{298} of reaction (3)

$$\Delta S_{298} = -16.0(\pm 3)\text{cal/mol}$$
$$-65.9(\pm 10)\text{J/mol K}$$

$$\Delta H_{298} = 0(\pm 1)\text{kcal/mol}$$
$$0(\pm 4)\text{kJ/mol}$$

The thermodynamic data are compared in Table 1 with those of the equivalent $NdAl_4Cl_{15}$-complex, investigated by Øye and Gruen.[12] Our data are in accordance with the data Øye and Gruen obtained.

CONCLUSION

From our experiments follows the existence of four different ytterbium chloride–lanthanide chloride complexes ($YbAlCl_6$, $YbAl_2Cl_9$, $YbAl_3Cl_{12}$, $YbAl_4Cl_{15}$). We have determined the thermodynamic data of the complexes formed in the YbCl₃/AlCl₃-system in the temperature range from 500 to 1000 K. In accordance with former investigations of the LnCl₃/AlCl₃-systems the $YbAl_3Cl_{12}$ complex is found to be the main complex in the temperature range from 500 to 900 K (Figs. 5 and 6). The dominance of this complex leads to elevated statistical errors in the

determination of the thermodynamic values of the other vapour species; the existence of a large complex ($YbAl_4Cl_{15}$) at lower temperatures, however, and the appearance of $YbAlCl_6$ and $YbAl_2Cl_9$ at elevated temperatures is evident.

With ascending temperatures and low aluminium chloride pressures the existence of the $YbAlCl_6$-complex is favoured, probably that is the reason why Schäfer *et al.*[16] cannot find any fragments of the $NdAl_2Cl_9$ complex by mass spectrometric investigations in the NdCl₃/AlCl₃-system at temperatures of 1123 and 1150 K. With our data we determine theoretically the partial pressure of the $YbAl_2Cl_9$-complex to be less than 1% compared with the partial pressure of $YbAlCl_6$ under the experimental conditions Schäfer and Flörke[16] used.

Our experiments confirm the existence of a $YbAl_4Cl_{15}$-complex, equivalent to $NdAl_4Cl_{15}$ recorded by Øye and Gruen.[13]

The method is very useful for the investigations of volatile inorganic complex species, in particular it is possible to describe the equilibrium in the vapour phase within a great temperature range and with elevated AlCl₃/Al₂Cl₆-pressures, facilitating the determination of the thermodynamic data of the secondary complexes.

REFERENCES

[1] H. Schäfer, *Angew. Chemie Int. Ed. Engl.* 1976, **15**, 713.
[2] H. Schäfer, *Z. Anorg. Allg. Chemie* 1974, **403**, 116.
[3] F. P. Emmenegger, *J. Cryst Growth* 1972, **17**, 31.
[4] K. N. Semenenko, T. N. Naumora, L. N. Gorokhov and A. V. Novoselova, *Dokl. Akad. Nauk SSR* 1964, **154**, 169.
[5] E. S. Kotora, A. L. Kuzmenko and G. I. Novikov, *Russ, J. Phys. Chem.* 1972, **46**, 1690.
[6] I. T. Buraya, O. G. Polyachenok and G. I. Novikov, *Russ. J. Phys. Chem.* 1974, **48**, 952.
[7] T. S. Zvarova and I. Zvara, *J. Chromatogr.* 1969, **44**, 604.
[8] T. S. Zvarova, *Radiochem. Radioanal. Lett.* 1972, **11/2**, 113.
[9] G. Steidl, Diplomarbeit, Technische Hochschule Darmstadt (1978).
[10] M. Sorlie and H. A. Øye, *J. Inorg. Nucl. Chem.* 1978, **40**, 493.

[11]G. N. Papatheodorou and G. H. Kucera, *Inorg. Chem.* 1979, **18**, 385.

[12]E. J. Peterson, J. A. Caird, J. P. Hessler, H. R. Hoekstra and C. W. Williams, *J. Phys. Chem.* 1979, **83**, 2458.

[13]H. A. Øye and D. M. Gruen, *J. Am. Chem. Soc.* 1969, **91**, 2229.

[14]M. Cosandey and F. P. Emmenegger, *J. Electrochem. Soc.* 1979, **126**, 1601.

[15]W. T. Carnall, J. P. Hessler, H. R. Hoekstra and C. W. Williams *J. Chem. Phys.* 1978, **68**, 4304.

[16]H. Schäfer and U. Flörke, *Z. Anorg. Allg. Chem.* 1981, **479**, 89.

[17]J. A. Caird, W. T. Carnall, J. P. Hessler and C. W. Williams, *J. Phys. Chem.* 1981, **74**, 798.

[18]H. Schäfer and U. Flörke, *Z. Anorg. Allg. Chem.* 1980, **469**, 172.

[19]H. Schäfer and U. Flörke, *Z. Anorg. Allg. Chem.* 1980, **462**, 173.

[20]J. Rudolph and K. Bächmann, *Mikrochim. Acta* 1979, I, 477.

[21]D. Brown, *Halides of Lanthanides and Actinides.* Wiley-Interscience, London (1968).

[22]F. P. Emmenegger, *Inorg. Chem.* 1977, **16**, 343.

[23]H. Schafer, *Z. Anorg. Allg. Chem.* 1978, **445** 129.

FORMATION AND THERMODYNAMIC PROPERTIES OF MIXED COMPLEXES OF Cd(II) WITH THIOUREA AND NITRITE OR THIOSULPHATE IONS AS LIGANDS

ATHOS BELLOMO, DOMENICO DE MARCO* and ALESSANDRO DE ROBERTIS
Istituto di Chimica Analitica, Universita di Messina, Via dei Verdi, 98100 Messina, Italy

Abstract—Formation and thermodynamic parameters of mononuclear mixed complexes $Cd(SCN_2H_4)_n(NO_2)_p^{2-p}$ and $Cd(SCN_2H_4)_n(S_2O_3)_p^{2(1-p)}$ in aqueous solution were investigated by potentiometric measurements at different temperatures and $\mu = 1$ for KNO_3.

NOTATION

Tu thiourea
Ts thiosulphate ion
Nt nitrite ion
X Nt or Ts
n index referred to Tu molecules coordinated
P index referred to Nt molecules coordinated
$\Delta G^*, \Delta H^*, \Delta S^*$ overall free energy, enthalpy and entropy changes (respectively in Kcal/mole, Kcal/mole and cal/mole/deg.)
$\Delta G^\circ, \Delta H^\circ, \Delta S^\circ$ free energy, enthalpy and entropy changes for the coordination of single Tu, Nt or Ts ligand (complex + Y = complexY, with Y = Tu, Nt, or Ts).

The equilibrium data on mixed complexes gives information about the thermodynamics of addition or displacement reactions. By means of the inter-

pretation of these quantities, changes in substrata structure (i.e. as produced by coordinated ligands) and solvent effects on the reactions can be deduced.

In aqueous solution, Cd(II) behaves like a "soft" or "class B" acid[1] and usually forms complexes of low thermodynamic stability.[2-6] Therefore, reactions of substrata complexes of this ion must depend considerably on coordination and solvation of various reaction terms.

On cadmium complexes with thiourea, nitrite or thiosulphate there are notes on equilibria with one ligand.[2-10] This paper refers to $Cd(II)–SCN_2H_4–NO_2^-$ and $Cd(II)–SCN_2H_4–S_2O_3^{2-}$ mixed complexes.

EXPERIMENTAL

Experimental parts and calculations are referred to in previous works[11-13] and will be summarized.

In every system the final ΔG^*, ΔH^* and ΔS^* data are based on 250–300 titrations (about 2500–3000 experimental points) covering four or five temperatures.

Function (1) (in tabulated form) in dependance on [Tu] and [X] was obtained by non-linear analytical extrapolation of values measured at finite $[Cd(II)]_{tot}$ by using the following

---

*Author to whom correspondence should be addressed.
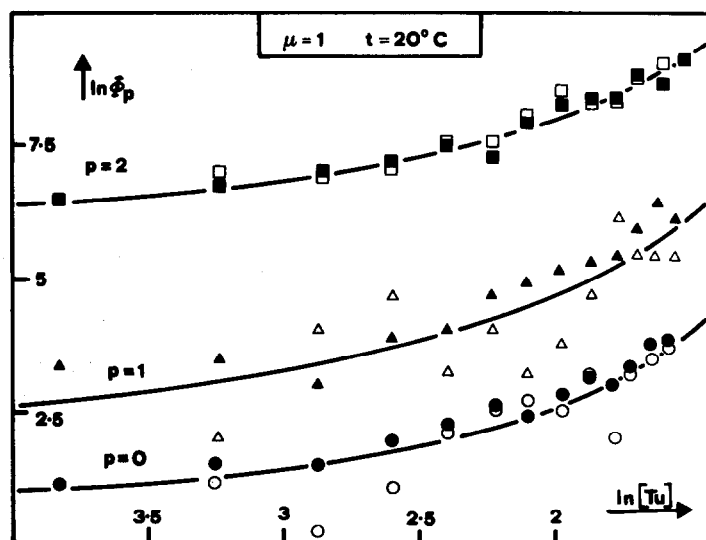
Fig. 1. Relation between ln Φ_p and ln Tu at 20°C and $\mu = 1$ for the system Cd(II)–Tu–Nt.

potentiometric system (2).

$$\ln \alpha_0 = \lim_{[\text{Cd(II)}]_{\text{tot}} \to 0} \ln \left([\text{Cd(II)}]_{\text{tot}} / [\text{Cd(II)}]_{\text{free}} \right) \qquad (1)$$

$$\text{Cd/Cd(II)} /\!/ \text{KNO}_3 \text{sat} /\!/ \text{SCE}. \qquad (2)$$

Responses and reversibility of this cell were tested previously.[11] Electrode potentials were measured using an Amel mod. 333 potentiometer. The complexes identified by successive divided differences method[14] applied in two successive stages on linear transform eqn (1). Enthalpy and entropy changes were calculated by linear fitting of Gibbs–Helmoltz equation on the experimental data $\{\Delta G^\circ, T\}$.

All calculations were computerized by using our programs on HP 9825 desk computer.

Cd(II) and ligands concentration ranges are reported in the following scheme:

$$5 \times 10^{-3}\,\text{M} \le [\text{Cd(II)}]_{\text{tot}} \le 7 \times 10^{-2}\,\text{M}$$

$$0\,\text{M} \le [\text{SCN}_2\text{H}_4]_{\text{tot}} \le 0.5\,\text{M}$$

$$0\,\text{M} \le [\text{NO}_2^-]_{\text{tot}} \le 0.2\,\text{M}$$

$$0\,\text{M} \le [\text{S}_2\text{O}_3^{2-}]_{\text{tot}} \le 4.5 \times 10^{-2}\,\text{M}.$$

In order to have very meaningful $\ln \beta$ values, only solutions having $[\text{Cd(II)}]_{\text{tot}} < ([\text{Tu}]_{\text{tot}} + [\text{X}]_{\text{tot}})/4$ were considered. The cadmium solutions were as nitrate salt, nitrite as potassium salt and thiosulphate as sodium salt. Thiourea purified by recrystallization from ethanol was used for thiourea solutions. Ionic strength was kept constant ($\mu = 1$) by adding suitable amounts of KNO_3.

RESULTS AND DISCUSSION

Formation of mono and di-coordinated complexes with nitrite ion were found in the system $\text{Cd(II)}-\text{SCN}_2\text{H}_4-\text{NO}_2^-$. Figure 1 refers (on logarithmic diagram) to experimentally deduced dependence of conditional constants ($\phi_P = \sum_n \beta_{(n,p)}[\text{Tu}]^n$) and Tu concentration. Empty symbols are the values obtained by successive non-linear extrapolations, whereas filled ones correspond to the values obtained by non-linear least squares fitting. The sharp functional dependence of ϕ_p parameter on $[\text{SCN}_2\text{H}_4]$ is consistent with successive coordination of two thiourea molecules independently of substratum.

The number of simple cadmium complexes with thiourea (CdTu_n^{2+}, $n = 1-2$) is in apparent contrast with the one previously found[11] where a tetracoordinated cadmium–thiourea complex was found.[7-10] This suggests that the highest Cd–Tu complex may be tetracoordinate. Because of uncertainties in the measurements ($\simeq 5\%$)[12] and low thermodynamic stability of complexes, it is preferred to describe the function (1) by the least number of certainly identifiable terms. In any case, Fig. 1 clearly shows the first derivative of experimental dependence of $\ln \phi_p$ ($p = 0$) on $\ln [\text{Tu}]$ (as evaluated at the upper limit), is still increasing.

In the system $\text{Cd(II)}-\text{SCN}_2\text{H}_4-\text{S}_2\text{O}_3^{2-}$ dicoordinate complex with thiourea and a sharp dependence of $\phi_n = \sum \beta_{(m,p)}[\text{S}_2\text{O}_3^{2-}]^p$ on $[\text{S}_2\text{O}_3^{2-}]$ (Fig. 2) was found.

Table 1 refers to identified complexes and their formation parameters. Data in regular type are the most probable deduced from primitive experimental data; the ones starred are interpolated on $\{\Delta G^\circ, T\}$. By using the standard deviation of ΔH° and ΔS°, standard errors on ΔG° can be deduced.[14]

Binary diagrams of Figs. 3(a) and (b) refer to only mononuclear complexes. Although they are deduced from the most probable starred data, because of the experimental errors, the boundaries of different surfaces are shaded.

In the system $\text{Cd(II)}-\text{SCN}_2\text{H}_4-\text{NO}_2^-$, Cd(II) is mainly in hydrated form. The only mixed complex with analytical importance (because of its high percentage) is $\text{Cd(SCN}_2\text{H}_4)_2(\text{NO}_2)_2$.

In the system $\text{Cd(II)}-\text{SCN}_2\text{H}_4-\text{S}_2\text{O}_3^{2-}$ for $-2.9 \le p[\text{S}_2\text{O}_3^{2-}] \le -1.4$ and $-1.5 \le p[\text{SCN}_2\text{H}_4] \le -0.5$ there are the surfaces relative to the mixed complexes $\text{Cd(SCN}_2\text{H}_4)(\text{S}_2\text{O}_3)_2^{2-}$, $\text{Cd(SCN}_2\text{H}_4)_2(\text{S}_2\text{O}_3)$ and $\text{Cd(SCN}_2\text{H}_4)_2(\text{S}_2\text{O}_3)_2^{2-}$. Figure 4 refers to the changes of thermodynamic functions in some reactions of complexes as derived from the most probable values of Table 1. The successive coordination of a
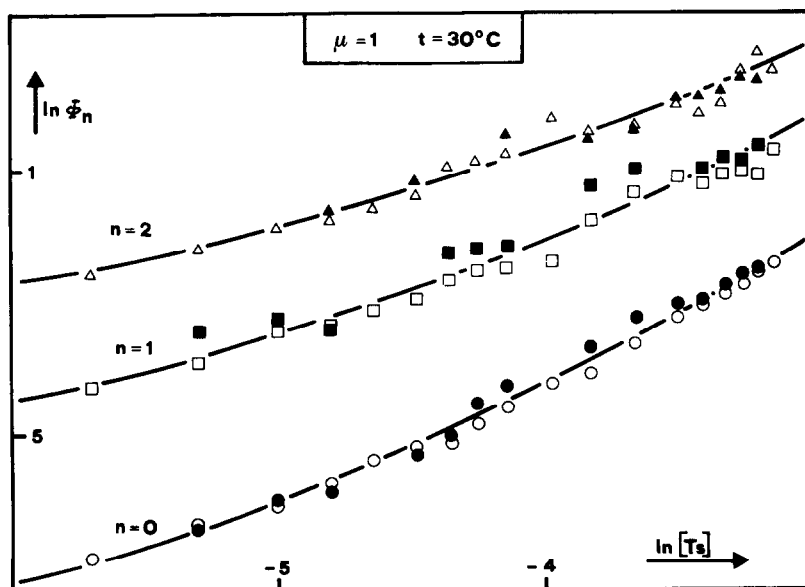
Fig. 2. Relation between $\ln \Phi_n$ and $\ln \text{Ts}$ at 30°C and $\mu = 1$, for the system of Cd(II)–Tu–Ts.

Table 1. Thermodynamic formation parameters of $CdN_pTu_m^{2-p}$ complexes

Formula	t = 10°C log β	t = 10°C $-\Delta G°$	t = 20°C log β	t = 20°C $-\Delta G°$	t = 25°C log β	t = 25°C $-\Delta G°$	t = 30°C log β	t = 30°C $-\Delta G°$	t = 35°C log β	t = 35°C $-\Delta G°$	t = 40°C log β	t = 40°C $-\Delta G°$	log β*	$-\Delta G°*$	$\Delta H°*$	$\Delta S°*$
$CdTu^{2+}$	1.87	2.42	1.59 / 1.79	2.13 / 2.40	1.61 / 2.87	2.20 / 3.82	0.95 / 2.05	1.31 / 2.85	1.54 / 1.51	2.18 / 2.12	1.42	2.00	1.8	2.39	-7.52 ± 8	-17 ± 26
$CdTu_2^{2+}$	2.84	3.68	2.72 / 3.55	3.65 / 4.77	2.72 / 3.00	3.71 / 4.10	2.23 / 2.63	3.09 / 3.65	2.28 / 2.42	3.22 / 3.42	—	—	2.74	3.72	-12.68 ± 6	-30 ± 20
$CdNt^{+}$	—	—	1.23	1.66	1.66	2.22	1.33	1.85	1.12	1.58	0.71	1.03	1.36	1.86	-13.2 ± 7	-38 ± 23
$CdNtTu^{+}$	—	—	2.37	3.18	2.59	3.47	2.64	3.67	2.50	3.53	2.00	2.87	2.46	3.40	-6.7 ± 7	-11.2 ± 22
$CdNtTu_2^{+}$	—	—	3.73	5.00	3.86	5.17	3.37	4.67	3.32	4.68	3.27	4.70	3.52	4.95	-11.4 ± 3	-22 ± 11
$CdNt_2$	—	—	2.71	3.63	2.37	3.19	2.48	3.44	2.07	2.92	2.04	2.92	2.46	3.39	-13.5 ± 4	-34 ± 12
$CdNt_2Tu$	—	—	3.83	5.15	3.63	4.87	3.51	4.86	2.97	4.18	2.70	3.87	3.60	4.90	-24 ± 3	-64 ± 11
$CdNt_2Tu_2$	—	—	4.86	6.52	5.24	7.03	5.65	7.84	4.47	6.30	4.60	6.6	5.13	6.91	-10.3 ± 13	-11 ± 44
$CdTs$	3.63	4.70	3.75	5.03	3.61	4.93	3.41	4.73	3.93	5.55	—	—	3.72	5.01	$+1.8 \pm 5$	$+23 \pm 16$
$CdTsTu$	4.67	6.05	3.93	5.28	5.17	7.04	4.80	6.66	4.07	5.74	—	—	4.52	6.17	-2.68 ± 12	$+12 \pm 42$
$CdTsTu_2$	5.72	7.41	5.76	7.72	5.71	7.79	5.88	8.16	4.98	7.02	—	—	5.60	7.63	-8.14 ± 8	-2 ± 26
$CdTs_2^{2-}$	5.86	7.59	5.6	7.51	5.64	7.7	5.55	7.7	5.81	8.19	—	—	5.69	7.76	-1.56 ± 3	$+21 \pm 10$
$CdTs_2Tu^{2-}$	7.24	9.38	6.93	9.29	7.85	10.7	7.03	9.75	6.95	9.8	—	—	7.20	9.82	-2.9 ± 9	$+23 \pm 32$
$CdTs_2Tu_2^{2-}$	8.43	10.41	8.85	11.88	7.89	10.8	7.71	10.7	7.16	10.10	—	—	7.92	10.80	-22 ± 9	-32 ± 32
$CdTs_3^{4-}$	8.01	8.35	7.74	10.38	7.81	10.6	7.42	10.30	7.61	10.79	—	—	7.46	10.18	$+16.16 \pm 9$	$+88 \pm 30$

(*) Most probable values at t = 25°C
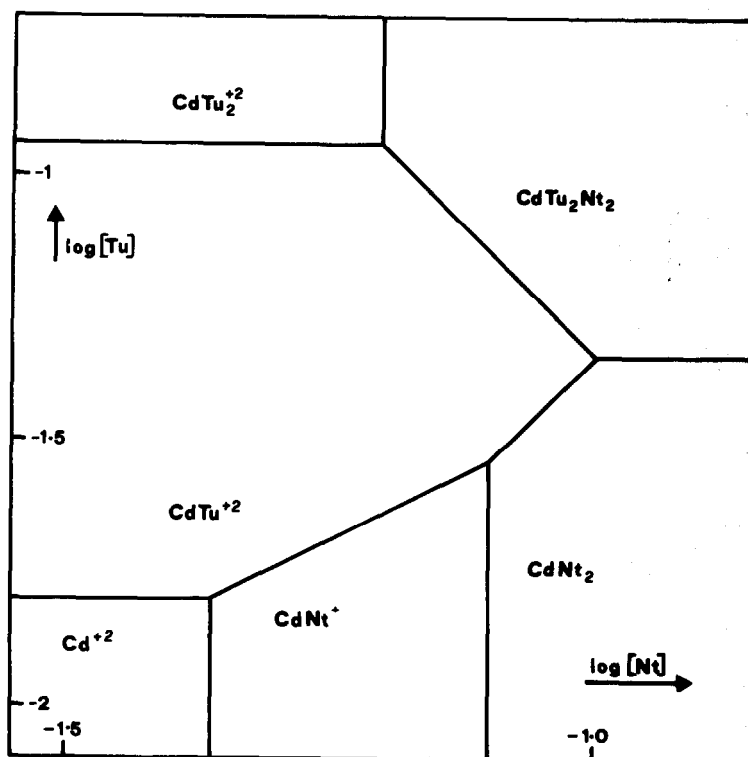
Fig. 3(a) Distribution diagram of mononuclear complexes in the system Cd(II)–Tu–Nt, at 25°C and $\mu = 1$.
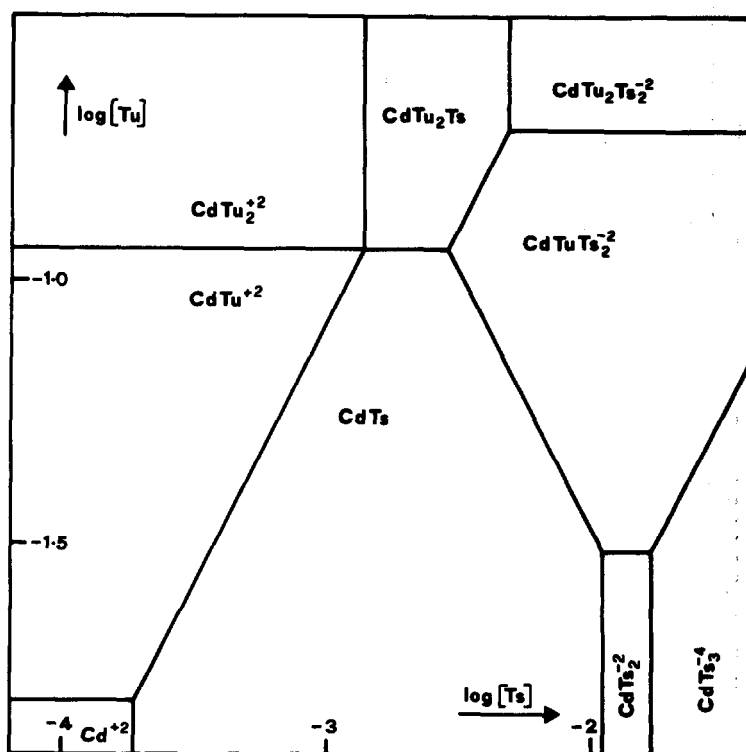
Fig. 3(b). Distribution diagram of mononuclear complexes in the system Cd(II)–Tu–Ts, at 25°C and
$\mu = 1$.
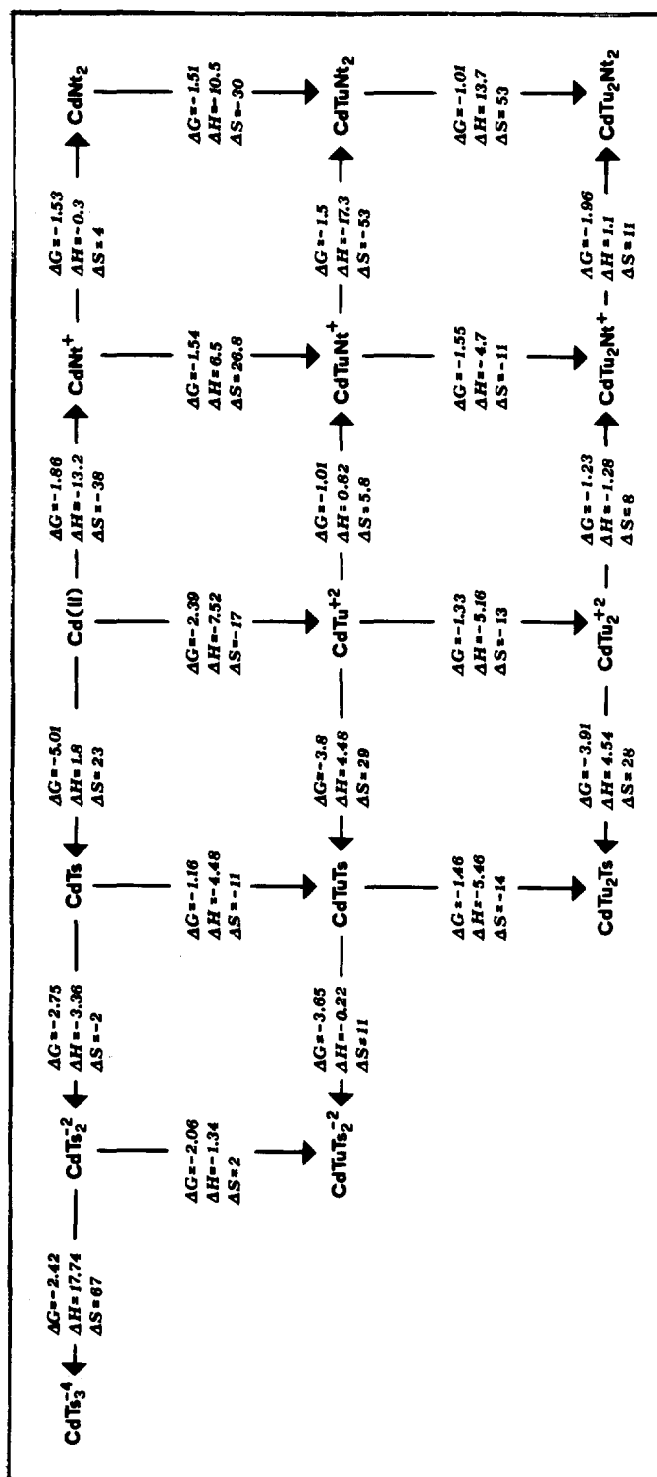
Fig. 4. Diagram of partial free energy, enthalpy and entropy change.

single ligand is represented by an arrow while ligand displacement can be deduced along two opposite arrows.

The coordination of one thiourea or nitrite ligand causes nearly the same free energy losses ($\simeq$ 1–2 Kcal/mole). It seems the nature of coordinated groups does not have much influence on partial $\Delta G^{\ominus}$ values, which are dependent on coordination number of substratum reagent. In fact the $\Delta G^{\ominus}$ increases with the coordination number of substratum. In the coordination of thiosulphate ion the free energy losses are most evident ($\simeq$ 3–5 Kcal/mole) and are modified in a positive way by coordination number.

According to the experimental results, the coordination of Tu to complex substrata of Cd(II) shows the following stability sequence: $NO_2^- < SCN_2H_4 < S_2O_3^{2-}$.

Enthalpy changes for similar reactions show a different sequence. The coordination of $S_2O_3^{2-}$ has more positive $\Delta H^{\ominus}$ changes in respect to the values relative to the other two ligands. In the coordination of SCN_2H_4 or NO_2^- $\Delta H^{\ominus}$ is dependent on substrata and it is not possible to define an unequivocal sequence. Consequently, the higher stability of thiosulphate coordination comes from the entropy change.

At least, the direct relation between $\Delta S^{\ominus}$ and $\Delta H^{\ominus}$ ($\Delta S^{\circ} \gtrless 0 \Rightarrow \Delta H^{\ominus} \gtrless 0$) confirms the results of previous work.[11]

REFERENCES

[1] R. G. Pearson, *Hard and Soft Acid and Bases*. Dowden, Hutchinson and Ross, Stroudburg (1973).

[2] K. B. Yatsimirskii and V. P. Vasiliev, *Instability Constants of Complex Compounds*. Pergamon Press, New York (1960).

[3] S. F. Ashcroft and C. T. Mortimer, *Thermochemistry of Transition Metal Complexes*. Academic Press, London and New York (1970).

[4] *Stability Constants*, Special Publication, No. 17. The Chemical Society, London (1971).

[5] *Stability Constants*, Special Publication, No. 25. The Chemical Society, London (1971).

[6] D. D. Perrin, *Stability Constants of Metal-ion Complexes*, Part B. Pergamon Press, Oxford (1979).

[7] P. Gerdin, *Acta Chem. Scand.* 1966, **20**, 2771.

[8] T. J. Lane, C. S. C., J. A. Ryon and E. F. Britten, *J. Am. Chem. Soc.* 1958, **20**, 315.

[9] H. Persson, *Acta Chem. Scand.* 1970, **24**(10), 3729.

[10] D. R. Gottard, B. D. Lodam, S. O. Aiayi and M. J. Campbell, *J. Chem. Soc.* A, 1969, 506.

[11] D. De Marco, A. Bellomo and A. De Robertis, *J. Inorg. Nucl. Chem.* 1980, **42**, 599.

[12] D. De Marco, A. Bellomo and A. De Robertis, *ibid.* 1981, **43**, 137.

[13] D. De Marco, A. Bellomo and A. De Robertis, *Atti Soc. Pelor. Sci. Fis. Mat. Nat.* in press.

[14] F. B. Hildebrand, *Analisi Numerica*. C. E. A. Milano (1967).

FORMATION AND PROPERTIES OF *n*-ALKYLAMMONIUM COMPLEXES WITH LAYERED TRI- AND TETRA-TITANATES

H. IZAWA†, S. KIKKAWA* and M. KOIZUMI
The Institute of Scientific and Industrial Research, Osaka University, Osaka 567, Japan

Abstract—The formation of *n*-alkylammonium complexes was studied using $Na_2Ti_3O_7$ and $K_2Ti_4O_9$ and the results for both compounds were compared. Alkylammonium complexes could be obtained from $H_2Ti_3O_7$ and $H_2Ti_4O_9 \cdot H_2O$, which were prepared by HCl treatment of $Na_2Ti_3O_7$ and $K_2Ti_4O_9$ respectively. The complexes were formed by exchange of H^+ with alkylammonium ions. Molecular intercalation of alkylamine was also possible with $H_2Ti_4O_9 \cdot H_2O$. However, alkylammonium complexes were not formed directly from $Na_2Ti_3O_7$ and from $K_2Ti_4O_9$. Orientations of alkylammonium ions in the interlayer are also discussed in relation to the structure of the titanate layers.

Organic intercalations have been thoroughly investigated for clay minerals and for transition metal dichalcogenides.[1-3] However, there have been few studies on synthetic layered oxides. Organic complexes were first investigated for $Na_2Ti_2O_5$, $K_4Nb_6O_{17}$ and $NaUO_2V_3O_9$.[4-6] They were obtained by direct exchange of the interlayered alkali metals with alkylammonium. These investigations did not pay attention to the structure of host layers. Most of the host materials have flat layers.

In recent years, we found that $HTiNbO_5$ could absorb alkylammonium into its interlayer;[7] $HTiNbO_5$ was prepared by the ion exchange of $KTiNbO_5$. The tilting angle of the alkyl chain to the basal plane was 71° in $HTiNbO_5$ complexes. It was much larger than 56° which is the value found for clay minerals and transition metal dichalcogenides.[2,3] The tilting angle might be different because the $TiNbO_5$ layer is uneven. It was not clear whether the organic complex was produced by the exchange of H^+ with alkylammonium cations or by the intercalation of alkylamine which then formed alkylammonium with the interlayered proton taken into the interlayer at an earlier stage.

There is a series of alkali titanates having general formula $A_2Ti_nO_{2n+1}$ where A is an alkali metal and $1 \leq n \leq 8$. $K_2Ti_4O_9$ and $Na_2Ti_3O_7$ have layers which are basically built up from four or three units of TiO_6 octahedra as depicted in Fig. 1. Their structures belong to the monoclinic system. All Ti_3O_7 layers stacking in the *a*-direction are constructed by exactly the same arrangement of three TiO_6 blocks in $Na_2Ti_3O_7$. Sodium ions are distributed equally in every Ti_3O_7 block. In $K_2Ti_4O_9$, every two Ti_4O_9 layers have the same configuration of Ti_4O_9 units. The convex and concave arrays are opposite in neighbouring layers. Potassium ions are accommodated in a widely opened space in the interlayer. Ion exchange and dehydration of these compounds have been studied.[8] All sodium ion were substituted with proton in trititanate. In tetratitanate, half of the potassium ions

were exchanged with proton but the other half were substituted with H_3O^+ probably for structural reasons. The difference in structure between $Na_2Ti_3O_7$ and $K_2Ti_4O_9$ and the presence of water in the latter may affect the formation of alkylammonium complexes.

This paper deals with the formation of alkylammonium complexes of trititanate and of tetratitanate from the viewpoint of reaction mechanism and of structure. The reaction was firstly investigated with $Na_2Ti_3O_7$, $K_2Ti_4O_9$ and their HCl-treated products using *n*-propylamine or *n*-propylammonium as intercalants. The rate of reactions and the properties of products were then examined with various alkylammonium ions having different lengths of alkyl chain.

EXPERIMENTAL

$Na_2Ti_3O_7$ was prepared by heating a mixture of Na_2CO_3 and TiO_2 in the molar ratio 1:3 at 800°C for 20 hr and for another 20 hr after grinding. $K_2Ti_4O_9$ was obtained by the reaction of K_2CO_3 and TiO_2 in the ratio 1:3.5, using the same heat treatment as in the case of $Na_2Ti_3O_7$. The hydrolyses of $Na_2Ti_3O_7$ (ca. 0.75 g) and $K_2Ti_4O_9$ (ca. 1 g) were performed in 200 cm³ of 0.5 M HCl at 60°C for 3 days. The acid solution was changed every day in order to remove alkali completely from the compounds. The products were washed with distilled water and dried in vacuum at 30°C. Hereafter we denote $Na_2Ti_3O_7$, $K_2Ti_4O_9$ and their acid-treated products as Na–, K–, NaH– and KH–types, respectively.

These materials (*ca.* 50 mg) were respectively sealed in glass tubes with 50% aqueous solution of *n*-propylamine (*ca.* 2 ml). *n*-Propylamine (>98% pure) was supplied by Nakarai Chemical Co. Ltd. *n*-Propylamine has a large dissociation constant of $pK_a = 10.53$, so that most would be ionized as *n*-propylammonium in the presence of water.[9] Durations of reaction were about a month at 60°C. The glass tubes were shaken well during the reaction to keep the reaction homogeneous. We also investigated whether NaH– and KH–type compounds can intercalate *n*-propylamine molecules with or without addition of water. Exchange of the interlayered H^+ or H_3O^+ was also investigated in 50% aqueous solutions of *n*-alkylammonium salts having various lengths of alkyl chain.

Excess alkylammonium ions were removed when the reactions were completed. The products were washed with

*Author to whom correspondence should be addressed.
†Permanent address: Research Laboratory, Osaka Cement Co. Ltd., Minamiokajima, Osaka 551, Japan.

741
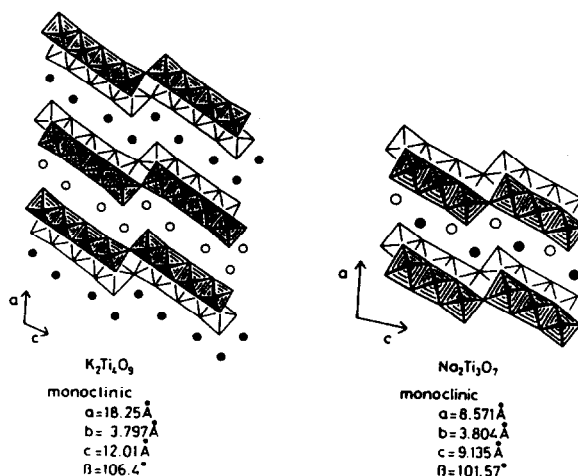
Fig. 1. Schematic crystal structures of $K_2Ti_4O_9$ and $Na_2Ti_3O_7$ and their crystal data.[11,12]

acetone and dried in air. The products were characterized by X-ray powder diffraction. C, H and N contents were determined by conventional chemical analysis.

RESULTS AND DISCUSSION

Formation of alkylammonium-titanate complexes

Exchange of interlayered cation with n-propylammonium was investigated with Na-, K-, NaH- and KH-type compounds. The amounts of n-propylammonium in the complexes were determined by C, H, N chemical analysis on the products from NaH- and KH-compounds. They were plotted against run duration as shown in Fig. 2, and reached a maximum within a week. The lattice parameter, a, which can be related to basal spacing, expanded from 8.08 to 16.63 Å on the formation of the n-propylammonium complex of NaH-compound, and from 18.77 to 34.15 Å in the case of the KH-compound. The expansions suggest that n-propylammonium is accommodated in the interlayer regions. The reaction did not proceed homogeneously. Both the original and the final a-parameters were observed in X-ray diffraction photographs of the compounds during the exchange reactions. On the other hand, there were no changes in the X-ray diffraction patterns of Na- and K-type compounds even after three weeks. The aqueous solution of n-propylamine is basic, while NaH- and KH-type compounds behave as Lewis acids. Acid-base interaction might enhance the exchange reactions with n-propylammonium cations.

Experiments were carried out to determine whether the reactions of NaH- or KH-compounds with n-propylamine proceed by exchange of interlayered H^+ with n-propylammonium or by intercalation of n-propylamine which then forms propylammonium within the interlayer. The NaH-compound did not react with n-propylamine without the presence of water, as shown in Fig. 3. However, the propylammonium complex was formed when water was added to the reaction system. These results suggest that the complex could be obtained by the exchange of H^+ with n-propylammonium. On the other hand, the propylammonium complex could be easily prepared from the KH-compound even if water was not added to the reaction system.

The n-alkylammonium complexes were formed more rapidly from the KH-compound than from the NaH-compound. The amount of interlayered propylammonium for the KH-compound reached its maximum value within a day, as shown in Fig. 3. In

o : KH-type·n-C$_3$H$_7$NH$_2$·H$_2$O
● : NaH-type·n-C$_3$H$_7$NH$_2$·H$_2$O
◇ : K-type, Na-type·n-C$_3$H$_7$NH$_2$·H$_2$O
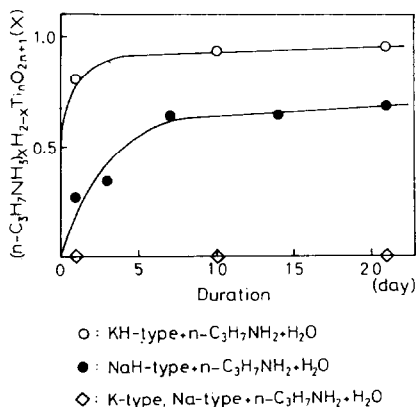
Fig. 2. Reaction of n-propylammonium ions with $Na_2Ti_3O_7$ and $K_2Ti_4O_9$ and their HCl-treated products.

o : KH-type·n-C$_3$H$_7$NH$_2$·H$_2$O
● : KH-type·n-C$_3$H$_7$NH$_2$
◇ : NaH-type·n-C$_3$H$_7$NH$_2$·H$_2$O
◆ : NaH-type·n-C$_3$H$_7$NH$_2$
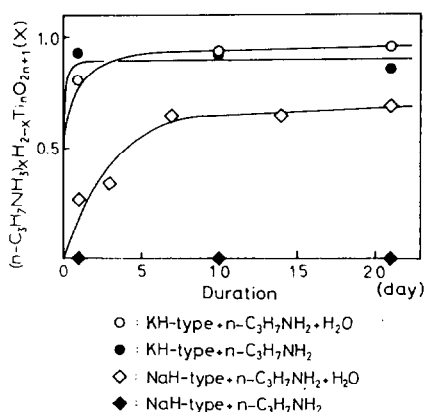
Fig. 3. Effect of water on the reaction of n-propylamine with $H_2Ti_3O_7$ and $H_2Ti_4O_9$·H_2O.

the case of the NaH-compound, it still continued to increase after one day, and the reaction was completed in a week. The rate of reaction was much affected by the length of the alkyl chain, because alkylammonium ions had to diffuse through the interlayer space: the rate decreases with increase in length of alkyl chains. It took one month to obtain the maximum amount of n-$C_6H_{13}NH_3^+$ in the interlayer region of NaH-compound. However, the reaction with the KH-compound finished within a week.

The KH-compound has a composition of $H_2Ti_4O_9 \cdot H_2O$, which can be rewritten as (H^+, H_3O^+)Ti_4O_9. Hydroxonium ions, H_3O^+, are probably located in the wide interlayer space of tetratitanate as is K^+ in $K_2Ti_4O_9$. The parts of the Ti_4O_9 layers which do not accommodate interlayered ions face very closely to each other. Absorption of alkylammonium increases the interlayer distance and decreases the repulsive force between neighbouring $Ti_4O_9^{2-}$ layers. The interlayered water in the KH-compound may also keep the interlayer space open, so that it is easy for tetratitanate to be intercalated by alkylamine, forming alkylammonium with the interlayered proton. It is already known that prior intercalation of a smaller molecule makes additional intercalation of a larger species possible.[10] This ion exchange is obviously possible in the case of the KH-compound as shown in Fig. 3. In conclusion, the KH-alkylammonium complex can probably be obtained through both mechanisms, ion exchange and molecular intercalation.

Structure of the complexes

The C, H and N percentages and the chemical formulae for tri- and for tetratitanate are listed in Tables 1 and 2 respectively. The ratios of C/N in the products are almost the same as the values for corresponding alkylammoniums. These results lead
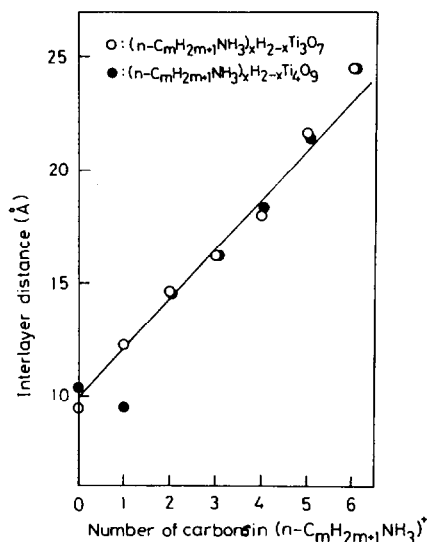
Fig. 4. Interlayer distances of alkylammonium-titanate complexes as a function of carbon number in the alkyl chain.

Table 1. C, H, N contents and chemical formulae of n-alkylammonium-trititanate complexes

C(wt%)	N(wt%)	H(wt%)	$(n\text{-}C_mH_{2m+1}NH_3)_xH_{2-x}Ti_3O_7$
——	4.30	1.99	$(NH_4)_{0.87}H_{1.13}Ti_3O_7$
3.45	3.90	2.37	$(CH_3NH_3)_{0.83}H_{1.17}Ti_3O_7$
5.67	3.39	2.33	$(C_2H_5NH_3)_{0.68}H_{1.32}Ti_3O_7$
8.09	3.22	2.86	$(n\text{-}C_3H_7NH_3)_{0.68}H_{1.32}Ti_3O_7$
10.51	3.25	3.26	$(n\text{-}C_4H_9NH_3)_{0.69}H_{1.31}Ti_3O_7$
16.18	3.28	4.14	$(n\text{-}C_6H_{13}NH_3)_{0.76}H_{1.24}Ti_3O_7$

Table 2. C, H, N contents and chemical formulae of n-alkylammonium-tetratitanate complexes

C(wt%)	N(wt%)	H(wt%)	$(n\text{-}C_mH_{2m+1}NH_3)_xH_{2-x}Ti_4O_9 \cdot yH_2O$
——	2.73	1.70	$(NH_4)_{0.72}H_{1.28}Ti_4O_9 \cdot 1.06H_2O$
2.82	3.25	2.10	$(CH_3NH_3)_{0.89}H_{1.11}Ti_4O_9 \cdot 0.75H_2O$
5.25	3.26	3.01	$(C_2H_5NH_3)_{0.91}H_{1.09}Ti_4O_9 \cdot 2.09H_2O$
8.15	3.32	2.95	$(n\text{-}C_3H_7NH_3)_{0.92}H_{1.08}Ti_4O_9 \cdot 0.86H_2O$
10.69	3.17	3.61	$(n\text{-}C_5H_9NH_3)_{0.97}H_{1.03}Ti_4O_9 \cdot 1.53H_2O$
14.69	3.62	4.27	$(n\text{-}C_5H_{11}NH_3)_{1.14}H_{0.86}Ti_4O_9 \cdot 1.52H_2O$
13.89	3.13	4.02	$(n\text{-}C_6H_{13}NH_3)_{0.88}H_{1.12}Ti_4O_9 \cdot 1.56H_2O$

Table 3. Lattice parameters of n-alkylammonium-titanate complexes

n-alkylammonium	trititanate				tetratitanate			
	a (Å)	b (Å)	c (Å)	β(deg.)	a (Å)	b (Å)	c (Å)	β(deg.)
ammonium	9.45	3.75	9.05	95.0	21.54	3.78	11.60	105.0
methylammonium	12.55	3.78	9.23	102.0	19.60	3.78	11.54	104.0
ethylammonium	15.06	3.78	9.27	103.0	30.60	3.78	11.78	108.0
propylammonium	16.63	3.76	9.27	103.0	34.15	3.78	11.78	108.0
butylammonium	18.31	3.76	9.21	100.0	37.92	3.78	11.54	104.0
pentylammonium	22.01	3.76	9.21	100.0	44.07	3.78	11.54	104.0
hexylammonium	24.91	3.76	9.21	100.0	50.59	3.78	11.54	104.0

Parameters, a, b, c, were initially calculated using reflections 100, 020 and 002. The value of β was estimated using the parameters of a, b and c and reflections 101, 10$\bar{1}$ and/or 20$\bar{1}$ of trititanate complexes. Lattice parameters of tetratitanate complexes were similarly calculated using reflections of 200, 020, 003, 101 and 301. The values were then refined by the least squares method for all diffraction lines. Accuracy might be not so good for the longer alkylammonium complexes as for ethylammonium because they showed only a few X-ray diffraction lines.

to the conclusion that alkylammonium ions were absorbed in the titanates without decomposition during the reactions. Chemical formulae presented in Table 1 suggest that less than half of the interlayered protons were substituted by alkylammonium in $H_2Ti_3O_7$. X-Ray powder diffractions of all the products could be indexed as monoclinic, having almost the same lattice parameters as those of $H_2Ti_3O_7$ except for a. The parameters are summarized in Table 3. The unit cell in the basal plane has a dimension of $b \cdot c = 3.8 \times 9.2 \, \text{Å}^2$ for trititanate. Two alkyl chains standing perpendicularly to the Ti_3O_7 layer can be accommodated in one Ti_3O_7 unit of the basal plane because the van der Waals radius of an alkyl group is about 2 Å. However, judging from the results given in Tables 1 and 3, it is reasonable to estimate that half of the protons were substituted for alkylammonium, forming double layers in the interlayer region. Alkylammonium and proton stand alternately within the same layer. In the case of $H_2Ti_4O_9 \cdot H_2O$, Table 2 suggests that only the proton was exchanged with alkylammonium, leaving H_3O^+ as it was in the interlayer. Alkylammonium and hydroxonium stand alternately in the same interlayer, forming a double layer of these ions. Such an arrangement is also acceptable judging from the unit cell size of $b \cdot c = 3.8 \times 12 \, \text{Å}^2$.

Interlayer distances of the alkylammonium complexes are plotted against the numbers of carbons in alkylammonium chains, as presented in Fig. 4. They were roughly estimated as $a \sin \beta$ in trititanate and $a/2 \sin \beta$ in tetratitanate. They increase almost linearly with the number of carbon atoms, having a gradient of 2.1 Å/carbon number. The alkyl chains grow by 1.27 Å per added carbon. The gradient therefore suggests that the interlayered alkylammonium ions form double layers with their terminal NH_3^+ groups pointing to the host $(Ti_3O_7)^{2-}$ and $(Ti_4O_9)^{-2}$ layers. The inclination angle of the alkyl chain to the basal plane is $\sin^{-1}(2.1/1.27 \times 2) \approx 57°$. This value is about the same as those observed for intercalation compounds prepared using materials with flat layers such as clay minerals. The structure of the host $(Ti_3O_7)^{2-}$ and $(Ti_4O_9)^{2-}$ layers does not seem to affect greatly the tilting of alkyl chains in the interlayer. The interlayer distance of the methylammonium-tetratitanate complex was well off the line presented in Fig. 4, and was not very different from the value for the ammonium complex.

The ammonium ion is spherical having an ionic radius of 1.5 Å; methylammonium has a length of about 5 Å because the van der Waals radius of an alkyl group is 2 Å and the covalent bond distance between C–N is 1.5 Å. The dimensions of the unit cell are $b \cdot c = 3.8 \times 12 \, \text{Å}$ in the basal plane of tetratitanate. Methylammonium ions can lie horizontally in the basal plane. Ethylammonium cannot have the same configuration as methylammonium because its length of 6.5 Å is greater than half the c-parameter. In the case of trititanate, the unit cell is not large enough to accommodate even methylammonium when keeping its alkyl chain horizontal. Thus all the alkylamonium ion, $C_mH_{2m+1}NH_3^+$, have the same orientations in the series $m = 0$–6.

In summary, alkylammonium complexes were obtained from $H_2Ti_3O_7$ and $H_2Ti_4O_9 \cdot H_2O$. The interlayered proton was exchanged with alkylammonium. Molecular intercalation was also possible with tetratitanate. Slopes of alkyl chains in the complexes were not much different from those of flat layered materials, in spite of the convex and concave features of uneven host layers in the titanates.

REFERENCES

[1] R. E. Grim, Clay Mineralogy, 2nd Edn. McGraw Hill, New York (1968).
[2] A. Weiss, Angew. Chem. 1934, 47, 539.
[3] R. Schöllhorn, E. Sick and A. Weiss, Z. Naturforsch. 1973, 28b, 168.
[4] A. Weiss and A. Weiss, Angew. Chem. 1960, 72, 413.
[5] G. Lagaly and K. Beneke, J. Inorg. Nucl. Chem. 1976, 38, 1513.
[6] K. Beneke, U. Grosse-Brauckmann, G. Lagaly and A. Weiss, Z. Naturforsch. 1973, 28b, 408.
[7] S. Kikkawa and M. Koizumi, Mat. Res. Bull. 1980, 15, 533.
[8] H. Izawa, S. Kikkawa and M. Koizumi, J. Phys. Chem. 1982, 86, 5023.
[9] M. Kotake (Editor), Constants of Organic Compounds, pp. 584. Asakura Publishing Company, Tokyo (1963).
[10] G. W. Brindley and S. Ray, Am. Mineralogist 1964, 49, 106.
[11] M. Dion, Y. Piffard and M. Tournoux, J. Inorg. Nucl. Chem. 1978, 40, 917.
[12] S. Andersson and A. D. Wadsley, Acta Cryst. 1961, 14, 1245.

HALOMETALLATES OF 1-METHYL-4,4-DIMERCAPTO-PIPERIDINIUM. EVIDENCE OF STRONG HYDROGEN BONDS WITH PARTICIPATING THIOL GROUPS

H. BARRERA and F. TEIXIDOR*

Departament de Química Inorgànica, Universitat Autònoma de Barcelona, Bellaterra, Barcelona, Spain

Abstract—Chlorometallates of transition and B subgroup elements are readily prepared and precipitated by reaction of the corresponding metallic salts with 1-methyl-4,4-dimercaptopiperidinium chloride. These chlorometallates investigated were $[ZnCl_4]^{2-}$, $[CdCl_3]^-$, $[CoCl_4]^{2-}$, $[CuCl_5]^{3-}$ and $[FeCl_4]^{2-}$. Strong S–H . . . Cl interactions, but not N–H . . . Cl, have been evidenced by IR spectroscopy in the zinc, cadmium and cobalt complexes. The S–H and N–H absorptions are observed at $\simeq 2480\,cm^{-1}$ and $3060\,cm^{-1}$, respectively. Partial deuteration of the $[ZnCl_4]^{2-}$ complex with d_1-methanol, shifted these IR signals to 1800 and $2260\,cm^{-1}$, clearly evidencing a X-hydrogen type of bond. The S–H . . . Cl interaction is smaller in the $[FeCl_4]^{2-}$ complex, and practically nonexistent in the $[CuCl_5]^{3-}$ complex.

Ambidentate ligands which may, in principle, coordinate through nitrogen or sulfur have received considerable interest. A great deal of work has been done with β-mercaptoamines[2] and recently with 1-methyl-4-mercaptopiperidine.[2,3] However, amino-*gem*-dithiols, i.e. ligands with two thiol groups on the same carbon and an amine group in the molecule, have not been studied.

We report in this communication the syntheses of halocomplexes of the first transition series and I-B and II-B subgroups, which are crystallized as salts of 1-methyl-4,4-dimercaptopiperidinium, an amino-*gem*-dithiol cation. These compounds (the copper compound excepted), display strong S–H . . . Cl interactions. In addition, the N–H bond is very little externally perturbed if at all. The complexing ability of the 1-methyl-4,4-dimercaptopiperidine ligand will be the object of a following communication.

EXPERIMENTAL

General

IR spectra were determined on a Beckman IR-20A as KBr pellets. The IR spectral data are listed in Table 1. The UV-visible spectra were recorded on a Beckman, Acta III. The 1-methyl-4-piperidone (Fluka) was distilled before use. The *gem*-dithiol 1-methyl-4,4-dimercaptopiperidine

was prepared according to a reported method.[4] Hydriodic acid (Merck) was purified by the hypophosphorous acid method.[5] Unless specifically mentioned all other reagents and solvents were commercial grade and were used without further purification. Elemental analyses were performed in our laboratories. All melting points are uncorrected.

$[C_6H_{14}NS_2]X$ (X = Cl, Br, I)

Bromide (**II**) and iodide(**III**) salts of $[C_6H_{14}NS_2]$ have been prepared following the procedure used for chloride(**I**).[4] Hydriodic acid (57%) and hydrobromic acid (48%) have been utilized instead of hydrogen halides.

$[C_6H_{14}NS_2]_2[ZnCl_4]$ (IV)

A solution containing 2 g (14.6 mmol) of $ZnCl_2$ finely divided in ethanol and 1.5 cm³ of hydrochloric acid (36%) was slowly poured into a stirred solution of 2 g of $[C_6H_{14}NS_2]Cl$ (10 mmol) in ethanol previously filtered. A white, crystalline solid separated, m.p. 116.5°C (dec). Found: Zn, 12.2; Cl, 26.4; S, 23.3. Calc: Zn, 12.2; Cl, 26.5; S, 23.9%.

$[C_6H_{14}NS_2]CdCl_3.1.5H_2O$ (V)

A stream of hydrogen chloride was passed through a methanolic solution of 1 g (4.4 mmol) of $CdCl_2.2.5H_2O$, for 5–10 min. A methanolic solution of 1.3 g (6.5 mmol) of $[C_6H_{14}NS_2]Cl$ was

---

*Author to whom correspondence should be addressed.

Table 1. IR spectral data

Compound	
I	2940(s), 2910(s), 2680(vs), 2600(s), 2580(s), 2540(s), 2460(vs), 1465(vs), 1440(m), 1415(m), 1400(m), 1300(m), 1260(m), 1160(m), 1090(m), 1050(s), 1040(m), 985(m), 965(s), 800(s), 760(m).
II	2940(s), 2920(s), 2700(vs), 2470(vs), 1470(vs), 1400(vs), 1310(m), 1270(m), 1170(m), 1090(m), 1060(vs), 980(s), 960(s), 800(s), 770(m).
III	2940(s), 2720(vs), 2470(vs), 1460(vs), 1400(s), 1310(m), 1265(m), 1170(m), 1050(s), 1030(m), 980(m), 970(m), 960(m), 800(m), 760(m).
IV	3060(vs), 2480(s), 1470(vs), 1450(s), 1410(m), 1380(s), 1365(s), 1315(m), 1170(s), 1120(m), 1050(m), 1030(m), 1000(s), 980(s), 820(m), 760(m), 300(s,sh), 270(vs,sh).
V	3440(m,b), 3050(vs), 2470(s), 1460(vs), 1445(s), 1410(m), 1370(s), 1310(m), 1170(m), 1050(m), 1030(m), 980(s), 970(s), 950(m), 820(m), 760(m), 340(w), 280(w,sh), 250(w).
VI	3440(m,b), 3060(vs), 2500(s), 2480(s), 1470(vs), 1450(s), 1410(m), 1370(vs), 1310(m), 1270(m), 1160(vs), 1120(s), 1080(m), 1050(s), 1030(s), 990(vs), 970(vs), 820(s), 800(m), 760(s), 490(w), 470(vw), 330(m,sh), 310(s,sh), 295(s,sh), 285(vs).
VII	3400(s,b), 2950(s), 2680(s), 2580(s,b), 1470(s), 1440(m), 1310(m), 1260(m), 1160(m), 1050(m), 1030(m), 970(s), 800(m), 740(m), 301(w), 300-250(w,b).
VIII	3400(s,b), 3000(s,b), 2980(s), 2760(s), 2500(s), 1470(vs), 1420(m), 1370(m), 1310(m), 1260(m), 1170(m), 1060(m), 1030(m), 1000(m), 980(s), 760(w), 280(s).

treated in the same way. Both solutions were mixed and, upon partial removal of the solvent at room temperature by means of a rotary evaporator, white crystals of (V) separated. After the first crystals were formed the vessel containing them was separated from the rotary evaporator and cooled with ice–water until no more precipitation was observed. The white crystals were filtered and washed with cold methanol containing hydrogen chloride. Found: Cd, 27.2; Cl, 26.3; S, 15.4. Calc: Cd, 27.4; Cl, 26.0; S, 15.6%.

$[C_6H_{14}NS_2]_2CoCl_4.H_2O$ (VI)

The method described for (V) was used with few variations (ethanol as solvent and $CoCl_2.6H_2O$ as the metallic salt) to synthesize (VI). The precipitation of blue crystals takes several days unless

ether is added (m.p. = 117°C (dec)). Found: Co, 10.6; Cl, 25.8; S, 23.4. Calc: Co, 10.7; Cl, 25.9; S, 23.4%.

$[C_6H_{14}NS_2]_3CuCl_5.3H_2O$ (VII)

A stream of hydrogen chloride was passed through a ethanolic solution of 2 g (9.7 mmol) of $CuCl_2.4H_2O$ until a yellowish red coloration is obtained ($\simeq 20$ min). An ethanolic solution of 2 g (10 mmol) of $[C_6H_{14}NS_2]Cl$ was saturated with hydrogen chloride as before.

Upon mixing, a yellow precipitate separated. It was filtered, washed with ethanol containing some hydrogen chloride and dried under vacuum. The compound is yellow but becomes greenish unless kept in anhydrous atmosphere. Found: Cu, 8.03; Cl, 22.4. Calc: Cu, 8.05; Cl, 22.5%.

[C₆H₁₄NS₂]₂FeCl₄.H₂O (VIII)

A stream of hydrogen chloride was passed through a solution of 2 g (10 mmol) of [C₆H₁₄NS₂]Cl in degassed absolute ethanol. In another vessel were introduced 1 g (5 mmol) of FeCl₂.4H₂O, a small piece of pure metallic ion and enough degassed absolute ethanol to dissolve the metallic salt. Hydrogen chloride was passed during a 10-min period. By mixing both solutions a pale yellow solid immediately separated. The precipitation was complete in a 3–4 hr period. The solid was filtered and rinsed, first with cold degassed absolute ethanol containing some HCl, finally with dry ether. The solid was dried under vacuum. Found: Fe, 10.1; Cl, 25.9. Calc: Fe, 10.2; Cl, 26.0%.

Partial deuteration of [C₆H₁₄NS₂]₂ZnCl₄ (IX)

Compound (VII) was dissolved in d_1-methanol. After 2 hr the resulting solution was rotoevaporated down to dryness yielding a white solid.

RESULTS

Reaction of metallic salts of transition and B sub-groups elements: ZnCl₂; CdCl₂.2.5H₂O; CoCl₂.6H₂O; CuCl₂.4H₂O; FeCl₄.4H₂O with 1-methyl-4,4-dimercaptopiperidinium chloride yields, in alcohols and in presence of hydrogen chloride, halometallates of 1-methyl-4,4-dimercaptopiperidinium. In absence of hydrogen chloride metal complexation would take place *via* sulphur.

The identity of the species containing the anions [CoCl₄]²⁻, [ZnCl₄]²⁻ and [FeCl₄]²⁻ was definitively established by their elemental analysis and far IR spectroscopy (Table 1). Besides, the absorptions centered at $\simeq$ 685 nm, $\epsilon \simeq$ 700 in VI, are in good concordance with literature data for [CoCl₄]²⁻ complexes.[6] Unfortunately, not so much spectroscopic information is available regarding the structures of (V) and (VII). Discrete species [CuCl₅]³⁻ are known to exist in the series [M(NH₃)₆]CuCl₅. However, most of the compounds whose stoichiometry could indicate the presence of the anion [CuCl₅]³⁻ are actually made up of [CuCl₄]²⁻ and Cl⁻.[7] According to literature data, the most energetic absorptions due to [CuCl₄]²⁻ and [CuCl₅]³⁻ species happen to be between 280–305 and 256–280 cm⁻¹, respectively.[7] The corresponding absorption in (VII) is at 301, and the next one at 287 cm⁻¹ favouring, therefore, a [CuCl₄]²⁻/Cl⁻ species. The existence of Cd–Cl bonds in (V), is clearly proved by IR absorptions at 280 cm⁻¹. However, the IR information is not sufficient to choose among the different structural possibilities of the trichlorocadmiates.

DISCUSSION

Complexes having *gem*-dithiol ligands have not been described in the literature. The scarcity of *gem*-dithiols, and the sulfur atom tendency to form bridges between two metal atoms poses serious difficulty to use them as complexing ligands. We have evidenced this difficulty using the ligand 1-methyl-4,4-dimercaptopiperidine to complex VIIIB and IIB transition metal ions.[8] However, the N-methyl-4,4-dimercaptopiperidinium ion has been shown to be very efficient to precipitate halocomplexes of VIIIB, IB and IIB metal ions.

An interesting point about some of these salts is the formation of hydrogen bonds S–H . . . Cl, and the existence of non externally perturbed H–N bonds. We arrived to this conclusion upon observation of the IR spectra of these complexes in the 3500–2000 cm⁻¹ range. Strong absorptions at $\simeq$ 3060 and $\simeq$ 2480 cm⁻¹ stand out in the spectra of (IV), (V) and (VI). Deuteration of (IV) by means of d_1-methanol, and IR spectral analysis of the deuterated sample indicated that these absorptions were due to hydrogen participating bonds, where the hydrogen atom is easily replacable by deuterium. Two new bands at 2260 and 1800 cm⁻¹ were observed as a result of the deuteration. The ratios of frequencies between the corresponding former and new bands are 3060/2260 = 1.35 and 2480/1800 = 1.37 in good agreement with the expected ratios for N–H or S–H: 1.37 and 1.39, respectively. Accordingly, the absorptions at 3060 and 2480 cm⁻¹ in IV are due to bonds having labile hydrogens, i.e. in this case S–H or N–H. The IR spectrum of (IV) in the 3200–2200 cm⁻¹ range is depicted in Fig. 1. We have attributed the absorption at 3060 cm⁻¹ to the N–H bond, for the S–H bond absorbs at 2600–2570 cm⁻¹ when it is not externally perturbed. Moreover, the S–H absorption moves to lower wavenumbers when the proton
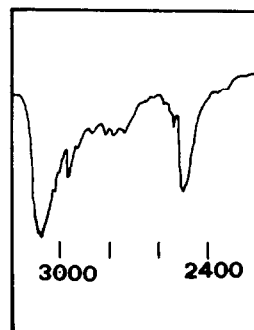
Fig. 1. IR spectrum of [C₆H₁₄NS₂]₂[ZnCl₄] in the range 3200–2200 cm⁻¹.

is participating in a hydrogen bond. According to Chenon and Sandorfy's prediction this absorption at 3060 cm^{-1} corresponds to a non-externally perturbed N–H bond.[9,10].

Absorptions near 2500 cm^{-1} are observed in the IR spectra of amine halohydrates (e.g. 2510 cm^{-1} in triethylammonium chloride)[9] and are attributed to hydrogen bonds N–H ... Cl. However, the N–H absorption at 3060 cm^{-1} in (IV), (V), (VI) suggests that N–H does not participate, at least strongly, in hydrogen bond formation and consequently, no N–H bonds would be expected around 2500 cm^{-1} for these compounds. Therefore, we assign the absorption at 2480 cm^{-1} to the S–H bond. The unusual strong intensity of the S–H absorption in these spectra is attributed to hydrogen bond formation. Supporting our assignation are the strong absorptions at 2400 and 2520 cm^{-1}, that are observed in 1,1-dimethyl-4-mercaptopiperidinium chloride and 1,1-dimethyl-4-mercaptopiperidinium trichloroestannate, respectively.[11] None of these compounds has a N–H bond that could give rise to these absorptions.

The assignation is further corroborated comparing the position of this absorption in $[C_6NSH_{14}]_2[CoCl_4]$ and $[C_6NS_2H_{14}]_2[CoCl_4]$. As may be seen in Fig. 2, the cations are identical except

(a)   (b)
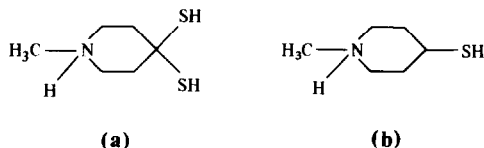
Fig. 2. The cations 1-methyl-4,4-dimercaptopiperidinium (A), and 1-methyl-4-mercaptopiperidinium (B). Piperidine hydrogens have been omitted for clarity.

that one is a *gem*-dithiol, and the other is a monothiol. Because both salts have the same anion, any difference in the position of the S–H absorption must be due to the cation. It is generally accepted that the strength of the hydrogen bond is dependent on the acidity of the proton and the electronegativity of the two elements bonded by hydrogen. The pK_1 of 1-methyl-4-mercaptopiperidine is 9.5^{12} and the pK_1 of 1-methyl-4,4-dimercaptopiperidine, calculated from the former using Taft and Hammett's parameters is 7.5.[13] These pK values suggest that the strongest hydrogen bond should take place in $[C_6NS_2H_{14}]_2[CoCl_4]$. This compound should, therefore, display a SH absorption at lower frequency and with higher intensity than $[C_6NSH_{14}]_2[CoCl_4]$. The experimental results are $2530(m) \text{ cm}^{-1}$ for

$[C_6NSH_{14}]_2[CoCl_4]$[14] and $2480(s) \text{ cm}^{-1}$ for $[C_6NS_2H_{14}]_2[CoCl_4]$ in concordance with our interpretation. We believe, therefore, that in compounds (IV), (V) and (VI) there is a hydrogen bond *via* SH connecting the halocomplex and the cation.

The IR spectrum of $[C_6NS_2H_{14}]_3[CuCl_5]$ displays absorptions at $2680(s)$ and $2580(s) \text{ cm}^{-1}$ but none of both above discussed. These absorptions at 2680 and 2580 are in the typical range for ammine halohydrates and are indicative of a hydrogen bond via N–H. In $[C_6NS_2H_{14}]_2[FeCl_4]$ it is probable that both types of hydrogen bond via S–H and N–H coexist because the IR absorption at $3000(s, b)$ and $2500(s)$ suggest a S–H hydrogen bond type and the absorption at 2760 a bond of the N–H type.

As can be seen from the former discussion all halocomplexes described here, except $[CuCl_5]^{3-}$, manifest a tendency to form hydrogen bonds via SH. This trend is very clear in the $[CoCl_4]^{2-}$, $[ZnCl_4]^{2-}$ and $[CdCl_3]^{-}$ but not so much in $[FeCl_4]^{2-}$. On the contrary, $[CuCl_5]^{3-}$ does not show it since the hydrogen bond is formed via N–H. The reason may be that $[CuCl_5]^{3-}$ is actually made up of $[CuCl_4]^{2-}$ and Cl^{-}.

REFERENCES

1. [a]M. Akbar Ali and S. E. Livingstone, *Coord. Chem. Rev.* 1974, **13**, 101; [b]L. K. Tiwari, S. Jain and A. Kumar, *Indian J. Chem.* 1977, **15A**, 310; [c]L. K. Tiwari, A. Kumar and S. Jain, *Indian J. Chem.* 1978, **16A**, 495.
2. J. C. Bayón, J. L. Briansó, M. C. Briansó and P. González-Duarte, *Inorg. Chem.* 1979, **18**, 3478.
3. M. C. Briansó, J. L. Briansó, W. Gaete, J. Ros and C. Suñer, *J. Chem. Soc., Dalton Trans.* 1981, 853.
4. H. Barrera and R. R. Lyle, *J. Org. Chem.* 1962, **27**, 41.
5. W. Conrad Fernelius, *Inorg. Synth.* 1946, **II**, 210.
6. F. A. Cotton and G. Wilkinson, *Advanced Inorganic Chemistry*, p. 772. Wiley, New York (1980).
7. See D. W. Smith, *Coord. Chem. Rev.* 1976, **21**, 93.
8. F. Teixidor and H. Barrera, to be submitted.
9. B. Chenon and C. Sandorfy, *Can. J. Chem.* 1958, **36**, 1181.
10. Chenon and Sandorfy predicted the N–H non-externally perturbed absorption between 3000 and 3200 cm^{-1}.
11. J. Serrat, J. Real, J. Vives and P. González-Duarte, Private communication.
12. H. Barrera, J. C. Bayón, P. González and J. Sola, *J. Chim. Phys. Chim. Biol.* 1979, **76**, 987.
13. G. B. Barlin and D. D. Perun, *Quart Rev.* 1966, **20**, 75.
14. J. Ros, Tesi Doctoral, Universitat Autònoma de Barcelona (1981).

STRUCTURES AND REARRANGEMENTS OF
CLOSO-BORON HYDRIDES

DARRYL J. FULLER and DAVID L. KEPERT*

School of Chemistry, University of Western Australia, Nedlands, Western Australia,
Australia

Abstract—The bonding in *closo*-boron hydrides, $B_nH_n^{2-}$ (where $n = 5$–12), is considered to be the sum of all possible $n(n - 1)/2$ boron–boron interactions. The bonding energy u between any pair of boron atoms is taken to depend only upon the internuclear distance d, and to be given by $u = 1/d^2 - 1/d$. This scheme can be used to rationalize details of molecular geometry and also allows the relative importance of various intramolecular rearrangement pathways to be assessed. This method is compared with alternative approaches to treating the bonding in these molecules.

In a recent paper[1] we have proposed a new approach which may be used for the prediction of the structures and the intramolecular rearrangement pathways for the *closo*-boron hydrides, $B_nH_n^{2-}$. It is assumed that every boron atom is directly bonded to every other boron atom, the bonding depending only upon the interatomic distance. A convenient relation between the bonding energy u_{ij} and the interatomic distance d_{ij} between boron atoms i and j is of the form:

$$u_{ij} = \frac{1}{d_{ij}^x} - \frac{1}{d_{ij}^y}. \tag{1}$$

The total bonding energy of the molecule is then:

$$U = \sum_{ij} u_{ij}. \tag{2}$$

Fitting this function vs the known crystal structures of $[Zn(NH_3)_4][B_8H_8]^2$ and $Rb_2[B_9H_9]^3$ yields $x \sim 2$ and $y \sim 1$. A particular advantage of this approach is its extreme simplicity which allows structures to be calculated without imposing any symmetry on the molecule and allows a wide range of reaction coordinates to be examined for the intramolecular rearrangement of these compounds.

In this work we complete the analysis of the *closo*-boron hydrides and compare the results with those obtained from experiment and with those obtained from PRDDO calculations by Lipscomb *et al.*[4-7] and from MNDO calculations by Dewar and McKee.[8] Future work will extend this approach to *nido-*, *arachno-* and *hypho*-compounds.

RESULTS

$B_5H_5^{2-}$

The structure calculated for $B_5H_5^{2-}$ using a 2:1 potential is a trigonal bipyramid, the distances between the boron atoms and the polyhedral centre being $r_{eq} = 1.220$ and $r_{ax} = 1.445$ ($r_{eq}/r_{ax} = 0.844$). The bonding energy $U = -2.4692$. A trigonal bipyramidal D_{3h} symmetry was assumed for the PRDDO calculations,[5] the resulting structural parameters being $r_{eq} = 1.06$ Å, $r_{ax} = 1.19$ Å and $r_{eq}/r_{ax} = 0.89$. The $B_5H_5^{2-}$ anion is experimentally unknown.

$B_6H_6^{2-}$

The present calculations show that the regular octahedron is the stable geometry, $r = 1.352$, $U = -3.6928$. The octahedral structure is the experimentally observed structure for $(Me_4N)_2[B_6H_6]$,[9] $r = 1.20$ Å, and is also that found from PRDDO[4,5] calculations, $r = 1.20$ Å, and from MNDO[8] calculations, $r = 1.225$ Å.

Using the 2:1 potential the trigonal prism lies 0.0371 units higher in energy, $r = 1.381$, $U = -3.6557$, the angles the polyhedral centre-

boron atom vectors make with the three-fold axis being 50.6°. The PRDDO and MNDO calculations show the trigonal prism is 728 kJ mol^{-1} and 296 kJ mol^{-1} respectively less stable than the octahedron. A lower symmetry (C_s) transition state for the rearrangement of $B_6H_6^{2-}$ with an activation energy of 347 kJ mol^{-1} located from the PRDDO calculations could not be located using our model.

$B_7H_7^{2-}$

Using the 2:1 potential the pentagonal bipyramid was found to be the stable geometry for $B_7H_7^{2-}$ with $r_{eq} = 1.489$, $r_{ax} = 1.229$, $r_{eq}/r_{ax} = 1.212$. A pentagonal bipyramidal structure was assumed for the PRDDO calculations[5] yielding $r_{eq} = 1.35$ Å, $r_{ax} = 1.13$ Å, $r_{eq}/r_{ax} = 1.20$. The pentagonal bipyramid was also found from MNDO calculations,[8] $r_{eq} = 1.399$ Å, $r_{ax} = 1.190$ Å, $r_{eq}/r_{ax} = 1.176$. These three sets of results are in approximate agreement but in contrast to early EHT calculations[10,11] which assumed pentagonal bipyramidal stereochemistry with $B_{eq} - B_{eq} = 1.80$ Å, the stable structure being found at $r_{eq}/r_{ax} = 0.92$. The structure of $B_7H_7^{2-}$ is experimentally unknown although ^{11}B NMR spectra are consistent with a pentagonal bipyramidal structure.[10]

Using the 2:1 potential, the capped octahedron and the capped trigonal prism lie 0.0085 and 0.0087 energy units above the pentagonal bipyramid (Tables 1 and 2). The capped trigonal prism lies 106 (or 148)[12] kJ mol^{-1} above the pentagonal bipyramid from the MNDO calculations.

$B_8H_8^{2-}$

The D_{2d} dodecahedron is the most stable structure calculated using $x = 2$, $y = 1$. The calculated stereochemical parameters, $r_A = 1.563$, $r_B = 1.351$, $r_A/r_B = 1.157$, $\phi_A = 35.6°$, $\phi_B = 107.4°$ are in agreement with the known crystal structure of $[Zn(NH_3)_4][B_8H_8]^2$: $r_A = 1.51$ Å, $r_B = 1.31$ Å, $r_A/r_B = 1.15$, $\phi_A = 31.1°$, $\phi_B = 105.7°$. The dodecahedral structure is similarly found to be the most stable stereochemistry from PRDDO[7] and MNDO[8] calculations, the structural parameters again being reasonable ($r_A = 1.476$ Å, $r_B = 1.257$ Å, $r_A/r_B = 1.17$, $\phi_A = 31.6°$, $\phi_B = 103.1°$ and $r_A = 1.495$ Å, $r_B = 1.388$ Å, $r_A/r_B = 1.078$, $\phi_A = 33.9°$, $\phi_B = 102.5°$ respectively).

The 2:1 potential shows the bicapped trigonal prism to be the next most stable stereochemistry at 0.0013 energy units above the dodecahedron.[1] The bicapped trigonal prism was also found to be

Table 1. Structural parameters (degrees) for seven-atom polyhedra[a]

polyhedron	symmetry	atom	ϕ	θ	r
pentagonal bipyramid	D_{5h}	A	(0.0)		1.229
		B	(90.0)	(0.0)	1.489
capped octahedron	C_{3v}	A	(0.0)		1.790
		B	65.0	(0.0)	1.395
		E	125.0	(60.0)	1.333
capped trigonal prism	C_{2v}	A	(0.0)		1.737
		B	70.2	47.8	1.431
		F	138.5	(0.0)	1.290

[a]Values in parentheses are enforced by symmetry or by choice of axes.

Table 2. Bonding energies for seven-atom polyhedra

polyhedron	U	$U-U$(pentagonal bipyramid)
pentagonal bipyramid	-5.1048	0.0000
capped octahedron	-5.0962	0.0085
capped trigonal prism	-5.0961	0.0087

the next most stable stereochemistry from the PRDDO and MNDO calculations, at 15 and 8 kJ mol^{-1} respectively above the dodecahedron.

$B_9H_9{}^{2-}$

The results using the $x = 2$, $y = 1$ potential for $B_9H_9{}^{2-}$ have also been reported previously.[1] The tricapped trigonal prism is the most stable structure, with $r_{cap} = 1.633$, $r_{prism} = 1.423$, $r_{cap}/r_{prism} = 1.148$ and $\phi = 46.6°$. The tricapped trigonal prismatic structure was assumed for the PRDDO calculations,[5] which yielded $r_{cap} = 1.57$ Å, $r_{prism} = 1.42$ Å, $r_{cap}/r_{prism} = 1.11$, $\phi = 51.2°$. In contrast, the MNDO calculations[8] yield the capped square antiprism as the most stable structure, with the tricapped trigonal prism being less stable by 98 kJ mol^{-1}. The 2:1 potential calculations show that the capped square antiprism is less stable than the tricapped trigonal prism by 0.0021 energy units.[1]

The experimentally observed structure in $Rb_2[B_9H_9]$[3] is a tricapped trigonal prism, $r_{cap} = 1.630$ Å, $r_{prism} = 1.434$ Å, $r_{cap}/r_{prism} = 1.14$, $\phi = 50.1°$. In $[B_9H_7(SMe_2)_2]$[13] one sulphur atom is attached to a prism boron atom and the other

sulphur atom to the *trans*-capping atom. For all nine boron atoms, $r_{cap} = 1.63$ Å, $r_{prism} = 1.44$ Å, $r_{cap}/r_{prism} = 1.13$, $\phi = 52°$. If only the seven BH groups are considered, $r_{cap} = 1.63$ Å, $r_{prism} = 1.46$ Å, $r_{cap}/r_{prism} = 1.11$, $\phi = 52°$ and if only the two $BSMe_2$ groups are considered, $r_{cap} = 1.63$ Å, $r_{prism} = 1.33$ Å, $r_{cap}/r_{prism} = 1.23$, $\phi = 52°$.

$B_{10}H_{10}{}^{2-}$

With the imposition of no symmetry elements, the $x = 2$, $y = 1$ potential yields the bicapped square antiprism as the stable structure for $B_{10}H_{10}{}^{2-}$. The calculated structural parameters, $r_{cap} = 1.729$, $r_{antiprism} = 1.480$, $r_{cap}/r_{antiprism} = 1.17$, $\phi = 63.0°$, may be compared with $r_{cap} = 1.84$ Å, $r_{antiprism} = 1.51$ Å, $r_{cap}/r_{antiprism} = 1.22$, $\phi = 60°$, observed for a variety of bicapped square antiprismatic molecules (Table 3). A bicapped square antiprism was the assumed structure for the PRDDO calculations,[5] which yielded $r_{cap} = 1.75$ Å, $r_{antiprism} = 1.46$ Å, $r_{cap}/r_{antiprism} = 1.20$, $\phi = 60.3°$. A bicapped square antiprism was similarly obtained from MNDO calculations,[8] $r_{cap} = 1.822$ Å, $r_{antiprism} = 1.540$ Å, $r_{cap}/r_{antiprism} = 1.18$, $\phi = 60.7°$.

A number of approaches were used to consider

Table 3. Structural parameters (degrees and Å) for bicapped square antiprismatic molecules

	r_{cap}	$r_{antiprism}$	$\dfrac{r_{cap}}{r_{antiprism}}$	ϕ	cap-centre-cap	Ref
$Cu_2[B_{10}H_{10}]$	1.86	1.51	1.24	60	179	14
$Rb_2[B_{10}H_9 \cdot B_{10}H_9]$[a]	1.83	1.49	1.23	60.4	175.3	15
$(Et_3NH)_2[(B_{10}H_9)_2NO]$[b]	1.85	1.53	1.21	60.3	178.5	16
$(Me_4N)_2[B_{10}H_7Cl_3]$[c]	1.82	1.52	1.20	61.1	176.8	17
$[(Ph_3P)_2Cu]_2[B_{10}H_{10}]CHCl_3$[d]	1.82	1.49	1.22	59.8	179.5	18
$[B_{10}H_8(SMe_2)_2]$[e]	1.84	1.51	1.22	60.5	177.4	19

[a]   Two bicapped square antiprisms are linked through BHB bridges to antiprism atoms. Neglecting these atoms, $r_{cap}/r_{antiprism} = 1.83/1.49 = 1.23$, $\phi = 60.2°$/

[b]   The nitrosyl group links two bicapped square antiprisms through capping atoms. Neglecting these atoms, $r_{cap}/r_{antiprism} = 1.87/1.53 = 1.23$, $\phi = 60.2°$.

[c]   One chlorine atom is attached to a capping atom and two chlorine atoms to antiprism atoms. For the BCl groups, $r_{cap}/r_{antiprism} = 1.86/1.46 = 1.27$, $\phi = 60.2°$. For the BH groups, $r_{cap}/r_{antiprism} = 1.78/1.54 = 1.16$, $\phi = 61.0°$.

[d]   Each copper atom asymmetrically bridges a capping site and an antiprism site, $Cu-H_{cap} = 1.86$Å, $Cu-H_{antiprism} = 2.07_5$Å. For these four chemically similar boron atoms, $r_{cap}/r_{antiprism} = 1.82/1.46 = 1.25$, $\phi = 59.3°$.

[e]   The SMe_2 group is attached to one capping atom, and one of the antiprism boron atoms is bonded to the other half of the dimer. For all other BH groups, $r_{cap}/r_{antiprism} = 1.89/1.51 = 1.25$, $\phi = 60.8°$.

possible intermediates for the intramolecular rear-rangement of $B_{10}H_{10}^{2-}$, including those based on classical geometrical polyhedra and those based on fragments of close packing.

There are no regular polyhedra available for a cluster of ten atoms in which all vertices are identical, all edges are identical, and all faces are identical. There are two semiregular polyhedra in which all vertices are identical, that is, all boron atoms are the same. These are the pentagonal prism with regular pentagonal and square faces and the pentagonal antiprism with regular pentagonal and equilateral triangular faces (Fig. 1).

Five non-uniform convex polyhedra can be constructed with regular polygons as faces (Fig. 2). These have more than one type of vertex, that is, there are boron atoms in different environments. The bicapped square antiprism has 16 triangular faces, the sphenocorona has two square and 12 triangular faces, the bicapped cube has four square and eight triangular faces, the bidiminished icosahedron has two pentagonal and ten triangular faces, and the capped tridiminished icosahedron has three pentagonal and seven triangular faces. The detailed shapes of these polyhedra change using the $x = 2$, $y = 1$ potential, the structural parameters being listed in Table 4. The bidiminished icosahedron does not exist as a minimum under the constraints of C_{2v} symmetry with the two mirror planes containing four atoms and two atoms respectively, but turns into a sphenocorona with substantial creasing of the two pentagonal faces ABDIC and ABEJF (Fig. 2b).

A capped tridiminished icosahedron (Fig. 2e) is a particular case of a general series of structures with C_{3v} symmetry and can be considered as a $1:3:3:\bar{3}$ stack (Fig. 3a). A "tetracapped trigonal prism" (Fig. 3b) is closely related, being a $1:3:\bar{3}:3$ stack; this polyhedron is not convex if constructed from equilateral triangles. Both of these polyhedra grossly distort using a $2:1$ potential to form the "trirhombohedron" containing three rhomboidal and ten triangular faces (Fig. 3c and Table 4). For a "hard sphere model" trirhombohedron, that is, one in which all edge lengths are identical, the dimensions of each rhomboidal face is given by $ABE = 72.0°$, $BAC = 108.0°$, and the ratio of the
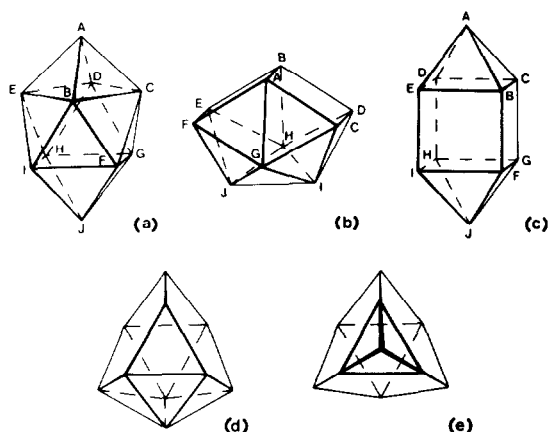
Fig. 2. (a) Bicapped square antiprism. (b) Spheno-corona. (c) Bicapped cube. (d) Bidiminished ico-sahedron. (e) Capped tridiminished icosahedron.

long diagonal to an edge is $BC/AB = (\sqrt{5} + 1)/2$. This ubiquitous "golden ratio" is also found in other rhombic polyhedra. For example the rhombic triacontahedron consists of 30 equal rhomboids in which the ratio of the *long diagonals* to the *short diagonals* is $(\sqrt{5} + 1)/2$. It may be noted that a trirhombohedron can be considered as half a regular icosahedron fused to half a rhombohedron (Fig. 4). Alternatively, a trirhombohedron can be formed if one face of a regular icosahedron is coalesced to a point. The trirhombohedron created using the $x = 2$, $y = 1$ bireciprocal potential is slightly distorted with a small creasing of each rhomboid along a long diagonal, the dihedral
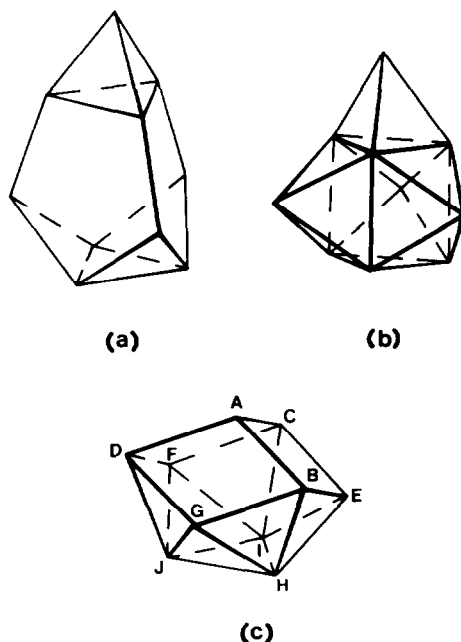
Fig. 3. (a) Capped tridiminished icosahedron. (b) Tet-racapped trigonal prism. (c) Trirhombohedron.
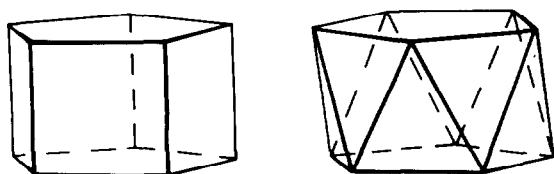
Fig. 1. Pentagonal prism and pentagonal antiprism.

Table 4. Structural parameters (degrees) for ten-atom polyhedra[a]

polyhedron	symmetry	atom	φ	θ	r
bicapped square antiprism	D_{4d}	A	(0.0)		1.729
		B	63.0	(0.0)	1.480
pentagonal prism	D_{5h}		57.9	(0.0)	1.561
pentagonal antiprism	D_{5d}		59.1	(0.0)	1.557
sphenocorona	C_{2v}	A	28.8	(0.0)	1.676
		C	71.5	58.5	1.665
		G	103.4	(0.0)	1.421
		I	138.3	(90.0)	1.291
bicapped cube	D_{4h}	A	(0.0)		1.923
		B	58.4	(0.0)	1.462
trirhombohedron	C_{3v}	A	(0.0)		1.407
		B	62.2	(0.0)	1.727
		E	84.9	(60.0)	1.526
		H	133.6	(0.0)	1.390
scarab prism	C_{2v}	A	30.3	(0.0)	1.657
		C	82.6	49.7	1.286
		G	139.9	44.2	1.801
scarab antiprism	C_{2h}	A	45.8	(0.0)	1.305
		C	58.5	99.0	1.637
		E	(90.0)	44.6	1.871
edge-shared bioctahedron	D_{2h}	A	31.9	(90.0)	1.492
		C	(90.0)	59.9	1.810
		G	(90.0)	(0.0)	1.136
large tetrahedron	T_d	A	(0.0)		1.291
		B	(54.7)	(0.0)	1.993
dsd transition state	C_2	A	36.3	(0.0)	2.005
		E	77.1	43.3	1.582
		G	83.1	139.7	1.167
		I	140.0	66.3	1.278

[a]Values in parenthesis are enforced by symmetry or by choice of axes.

angle between ABC and BCE (Fig. 3c) being 176.7°.

Rhomboidal semiregular polyhedra formed from rhomboids and regular polygons are not usually considered in classical accounts of polyhedra but are nevertheless encountered in chemistry. For example a central gold atom is surrounded by a trirhombohedral arrangement of gold atoms in [Au{Au(ligand)}$_{10}$].[20] The simplest examples of rhomboidal semiregular polyhedra are those formed by the face-sharing of polyhedra which have been chosen so that the dihedral angle between adjacent equilateral triangular faces is 180.0°. Two simple examples are shown in Fig. 5, the face-sharing of an octahedron and a tetrahedron to form a "capped octahedron" with
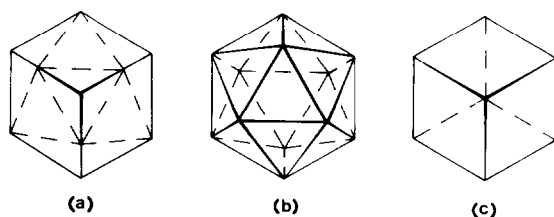
Fig. 4. (a) Trirhombohedron. (b) Icosahedron. (c) Rhombohedron.
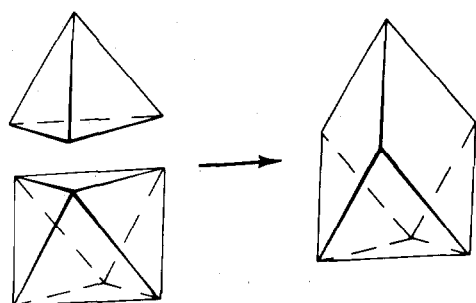
(a)
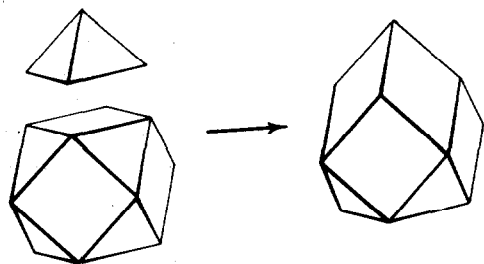
(b)

Fig. 5. (a) Face-sharing of an octahedron and a tetrahedron to form a "capped octahedron". (b) Facesharing of a cuboctahedron and a square pyramid to form a "capped cuboctahedron".

(a)   (b)

Fig. 6. (a) Regular pentagon. (b) Scarab.

four triangular and three rhomboidal faces, and the face-sharing of a cuboctahedron and a square pyramid to form a "capped cuboctahedron" with four triangular, five square and four rhomboidal faces. Other polyhedra composed of rhomboids and regular polygons may be formed by contraction of parallelohedra as discussed by Coxeter.[21]

Two additional stereochemistries can be generated by removal of some of the applied symmetry elements from the pentagonal prism and the pentagonal antiprism respectively. It is generally observed that removal of five-fold axes from polyhedra with pentagonal faces results in linkage across the 1,3-positions to form a "scarab" (Fig. 6). Removal of the five-fold axis from the pentagonal prism so that the symmetry is reduced from D_{5h} to C_{2v} results in the formation of the more stable scarab prism (Fig. 7a and Table 4). This polyhedron is very slightly concave, the dihedral angle between the trapezoidal CFJG face and the triangular ACF face being 180.8°. A similar process generates the C_{2h} scarab antiprism from the D_{5d} pentagonal antiprism (Fig. 7b and Table 4). This again results in creasing of the scarab faces, the dihedral angle between ADHI and AEI now being 169.2° for a 2:1 potential.

Other stereochemistries for ten atom clusters can

be generated by taking fragments of close packing, by the linking of octahedra, or by the capping of octahedra. The edge-shared bioctahedron (Fig. 8a and Table 4) is formed from two octahedra, ACDHGI and BEFGHJ, sharing the GH edge. Alternatively it can be considered as a tetracapped octahedron (ABGHIJ as the octahedron, CDEF as the capping atoms). The structure can be considered as a fragment of close packing, the close packed layers being ABCGF and DHEIJ. The layers are slightly buckled, the dihedral angle between ABG and ACG being 172.8°. This arrangement of metal atoms is observed in $V_{10}O_{28}^{6-}$.[22]

The most symmetrical ten-atom cluster is the large tetrahedron (Fig. 8b and Table 4). It can also be considered as a tetracapped octahedron (ADEFGJ as the octahedron, BCHI as the capping atoms), or as a fragment of cubic close packing (layers being B, ADG and CEHJIF). For a 2:1 potential the large triangular faces are slightly convex, the dihedral angle between ABD and ADE being 176.6°.

The last plausible intermediate to consider for the rearrangement of a bicapped square antiprism is that formed when two adjacent triangular faces flatten out and distort to form a square as in a "diamond-square-diamond" (dsd) transition

(a)   (b)
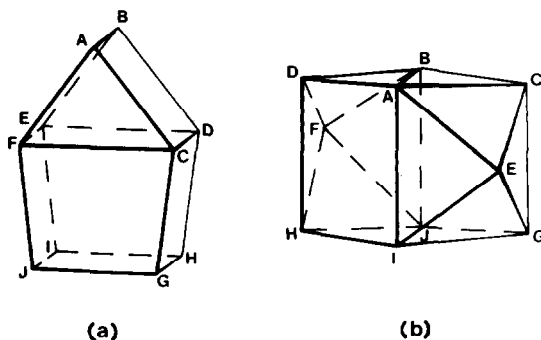
Fig. 7. (a) Scarab prism. (b) Scarab antiprism.

state.[23] If only a single square face is enforced, the resulting *dsd* transition state is shown in Fig. 9. The dihedral angle between the triangular faces BEG and EGI (and the symmetry related DFH and FHJ) is 176.1° so that the structure approaches a polyhedron formed from one square face, two rhomboidal faces and ten triangular faces.

(a)

(b)
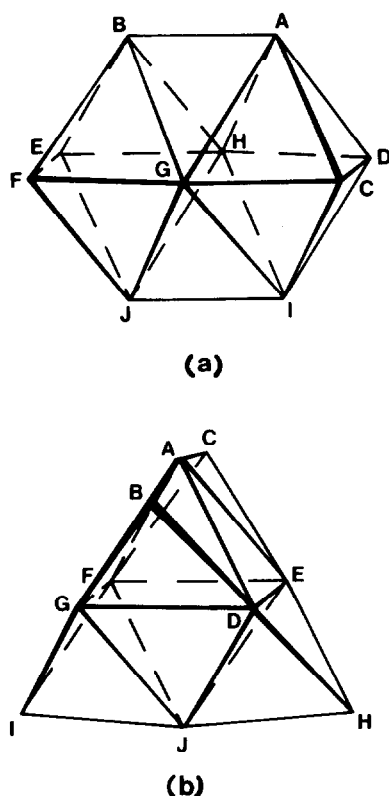
Fig. 8. (a) Edge-shared bioctahedron. (b) Large tetrahedron.

The bonding energies of these ten-atom polyhedra calculated using a 2:1 potential are given in Table 5. The most stable polyhedron is the bicapped square antiprism containing only triangular faces. The calculated transition states for the rearrangement of the bicapped square antiprism is the trirhombohedron with three rhomboidal faces, which is preferred to the sphenocorona with two square faces. All other polyhedra are much less stable. The relation between the two possible transition states is shown in Fig. 10; sliding the top edge of the sphenocorona as indicated by the arrows transforms the square faces into two of the rhomboidal faces of the trirhombohedron. Experiments which will distinguish between these two transition states are not easy to envisage, for example rearrangement of the bisubstituted bicapped square antiprismatic $[B_{10}H_8(\text{ligand})_2]$ will lead to the same mixture of isomers through either intermediate.

$B_{11}H_{11}^{2-}$

With no applied symmetry, the structure calculated for $B_{11}H_{11}^{2-}$ using the 2:1 energy potential is the octadecahedron of C_{2v} symmetry (Fig. 11). This polyhedron can be considered to be formed from an icosahedron by coalescing one edge to form a vertex, atom B in Fig. 11. This boron atom has six close boron neighbours. The changes in bonding energy arising from moving this atom are extremely small and a detailed consideration of the stereochemical parameters is not warranted. The structural parameters quoted in Table 6 are those obtained from calculations in which only a single mirror plane was assumed. The structure of

Table 5. Bonding energies for ten-atom polyhedra

polyhedron	$\underline{U}$	$\underline{U} - \underline{U}_{\text{bicapped square antiprism}}$
bicapped square antiprism	-10.6933	0.0000
trirhombohedron	-10.6883	0.0050
sphenocorona	-10.6871	0.0062
dsd transition state	-10.6427	0.0506
edge shared bioctahedron	-10.6208	0.0725
scarab antiprism	-10.6146	0.0787
bicapped cube	-10.6089	0.0844
pentagonal antiprism	-10.5947	0.0987
scarab prism	-10.5766	0.1167
pentagonal prism	-10.5682	0.1252
large tetrahedron	-10.5064	0.1870
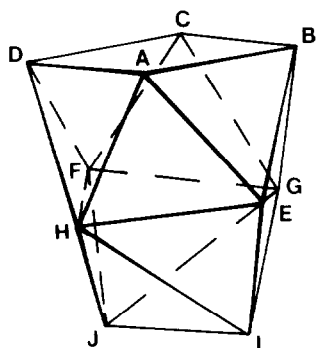
Fig. 9. *dsd* Transition state.
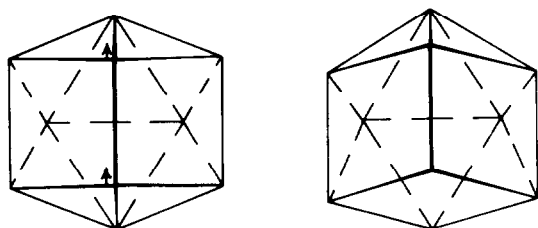
Fig. 10. Relation between the sphenocorona and the trirhombohedron.

Fig. 11. Octadecahedron.

(a)

(b)

Fig. 12. (a) Capped pentagonal antiprism. (b) Scarabheptadecahedron.

the rearrangement of the octadecahedron of C_{2v} symmetry. The MNDO calculations[8] also show the C_{2v} structure to be the most stable, with the C_s structure 2 kJ mol^{-1} higher in energy. Within the precision of the PRDDO calculations[6] both of these structures were found to be within approximately 10 kJ mol^{-1} of each other.

$B_{12}H_{12}^{2-}$

The $x = 2$, $y = 1$ potential function leads to the expected icosahedral structure for $B_{12}H_{12}^{2-}$ with $r = 1.586$.[1] The icosahedral structure was also found from MNDO calculations, with $r = 1.728$ Å.[8] Icosahedral symmetry was assumed for the PRDDO calculations[5] which yielded $r = 1.65$ Å. Icosahedral structures are observed for $K_2[B_{12}H_{12}]$[25] and $(Et_3NH)_2[B_{12}H_{12}]$,[26] with $r = 1.688$ and 1.694 Å respectively. Examination of a large number of possible pathways for the intramolecular rearrangement of $B_{12}H_{12}^{2-}$ reveals that face rotation with the formation of a C_{3h} icosahedron as intermediate is preferred, with an activation energy of 0.0587 energy units.[1] A similar but not identical intermediate was found from MNDO calculations with an activation energy of 376 kJ mol^{-1}.

$B_{11}H_{11}^{2-}$ is not known, although this octadecahedral structure is observed in $(Et_4N)_2[B_{11}H_9Se_3]$[24] in which the Se_3 ring links atoms D and G (Fig. 11).

The stereochemical parameters of other eleven-atom polyhedra are given in Table 6. The pentacapped trigonal prism, capped pentagonal prism and capped pentagonal antiprism are obviously related to classic geometric polyhedra. Lowering of symmetry of the capped pentagonal antiprism so that only one mirror plane is retained results in the pentagonal face forming a *scarab*, EACDB in Fig. 12, with the formation of a *scarab*-heptadecahedron or capped sphenocorona.

Table 7 shows that the *scarab* heptadecahedron of C_s symmetry is the favoured transition state for

DISCUSSION

Theoretical calculations on boron hydrides which allow geometrical optimisation of a particular structure are presently restricted to the empirical $x = 2$, $y = 1$ potential used in this work and the semi-empirical MNDO and PRDDO methods.

The MNDO calculations yield the incorrect structure for $B_9H_9^{2-}$. The PRDDO calculations using full geometrical optimisation appear to have been carried out only for $B_6H_6^{2-}$, $B_8H_8^{2-}$, and $B_{11}H_{11}^{2-}$. The very simple 2:1 potential has allowed structures to be calculated with no implied symmetry

Table 6. Structural parameters (degrees) for eleven-atom polyhedra[a]

polyhedron	symmetry	atom	ϕ	θ	r
octadecahedron	C_{2v}	A	(0.0)		2.029
		B	53.8	(0.0)	1.439
		D	53.1	90.5	1.652
		F	106.9	(0.0)	1.963
		G	102.7	56.7	1.608
		I	112.4	132.4	1.308
		K	167.0	(0.0)	1.383
pentacapped trigonal prism	D_{3h}	A	(0.0)		1.379
		B	59.6	(0.0)	1.752
		E	(90.0)	(60.0)	1.312
capped pentagonal prism	C_{5v}	A	(0.0)		2.011
		B	53.8	(0.0)	1.738
		G	113.3	(36.0)	1.411
capped pentagonal antiprism	C_{5v}	A	(0.0)		1.758
		B	60.0	(0.0)	1.654
		G	117.4	(36.0)	1.477
scarabheptadecahedron	C_s	A	46.0	51.2	1.520
		C	(46.0)	137.1	1.668
		E	73.3	(0.0)	2.098
		F	104.5	(180.0)	1.302
		G	102.9	101.3	1.454
		I	112.3	35.4	1.644
		K	180.5	(180.0)	1.381

[a]Values in parentheses are enforced by symmetry or by choice of axes.

Table 7. Bonding energies for eleven-atom polyhedra

polyhedron	U	U-U(octadecahedron)
octadecahedron	-12.9635	0.0000
scarabheptadecahedron	-12.9602	0.0032
pentacapped trigonal prism	-12.9425	0.0210
capped pentagonal antiprism	-12.9405	0.0230
capped pentagonal prism	-12.8996	0.0639

Table 8. Activation energies (arbitrary units) for the rearrangement of $B_nH_n^{2-}$

ion	transition state	E_{act}
$B_6H_6^{2-}$	trigonal prism	0.0371
$B_7H_7^{2-}$	capped octahedron	0.0085
	capped trig. prism	0.0087
$B_8H_8^{2-}$	bicap. trig. prism	0.0013
$B_9H_9^{2-}$	capped sq. antipr.	0.0021
$B_{10}H_{10}^{2-}$	trirhombohedron	0.0050
	sphenocorona	0.0062
$B_{11}H_{11}^{2-}$	scarabheptadecahedron	0.0032
$B_{12}H_{12}^{2-}$	$\underline{C_{3h}}$ icosahedron	0.0587
	$\underline{D_{3h}}$ icosahedron	0.0587

and has allowed a great diversity of rearrangement pathways to be examined. In some instances reaction intermediates have been located which have not been considered by previous workers, namely the capped octahedron for the rearrangement of $B_7H_7^{2-}$, the trirhombohedron for the rearrangement of $B_{10}H_{10}^{2-}$, and the C_{3h} icosahedron for the rearrangement of $B_{12}H_{12}^{2-}$.

The activation energies for the intramolecular rearrangement of $B_nH_n^{2-}$, in arbitrary units, are shown in Table 8. Experimental data is in general, but not exact, agreement with this qualitative order. There appears to be no experimental information on $B_6H_6^{2-}$ or substituted compounds. The ^{11}B NMR spectrum of $B_7H_7^{2-}$ in water shows a 5:2 pattern of boron atoms consistent with a rigid pentagonal bipyramidal structure at room temperatures.[10] The ^{11}B NMR spectrum of $Na_2[B_8H_8]$ in 1,2-dimethoxyethane at $-32°C$ shows a 2:4:2 pattern consistent with a bicapped trigonal prism but not a dodecahedron. The spectrum collapses above $46°C$ as expected for a stereochemically non-rigid molecule, the detailed behaviour depending both on choice of solvent and cation.[27] The ^{11}B NMR spectrum of $(Me_3S)_2[B_9H_9]$ in water is reported to show boron atoms in the ratio 3:6 indicating a tricapped trigonal prismatic structure.[28] However, the ^1H NMR spectrum of $[B_9H_7(SMe_2)_2]$ shows rapid rearrangement at room temperature with two distinct dimethylsulphide groups at low temperature.[13] The halide complexes $B_9X_9^{2-}$ also show two types of boron atoms,[29] whereas the oxidised B_9Br_9 shows only a ^{11}B NMR singlet.[30] Disubstituted derivatives of $B_{10}H_{10}^{2-}$ have been extensively studied, the compounds only rearranging above $200°C$.[31,32] The most extensive data is for

$[B_{10}H_8(NMe_2)_2]$;[31] equilibrium between all possible bicapped square antiprismatic isomers is established in the melt after 30 min at $300°C$. For the single pathway $2,3-[B_{10}H_8(MNe_3)_2] \rightarrow 1,6-[B_{10}H_8(NMe_3)_2]$ at $230°C$, $\Delta H^{\neq} \sim 150\,kJ\,mol^{-1}$. The ^{11}B NMR spectrum of $(Et_4N)_2[B_{11}H_{11}]$ in dimethylformamide/acetone/methanol mixtures from -70 to $30°C$ shows only a single boron atom indicating rapid rearrangement.[33] Since all boron atoms in an icosahedron are identical, information can only be obtained from substituted derivatives of $B_{12}H_{12}^{2-}$. They are exceptionally resistant to rearrangement, for example $1,7-[B_{12}H_{10}(NMe_3)_2]$ remains mostly unchanged after five minutes in the melt at $400°C$.[31]

REFERENCES

1. D. J. Fuller and D. L. Kepert, *Inorg. Chem.* 1982, **21**, 163.
2. L. J. Guggenberger, *Inorg. Chem.* 1969, **8**, 2771.
3. L. J. Guggenberger, *Inorg. Chem.* 1968, **7**, 2260.
4. T. A. Halgren, I. M. Pepperberg and W. N. Lipscomb, *J. Am. Chem. Soc.* 1975, **97**, 1248.
5. D. A. Dixon, D. A. Kleir, T. A. Halgren, J. H. Hall and W. N. Lipscomb, *J. Am. Chem. Soc.* 1977, **99**, 6226.
6. D. A. Kleier, D. A. Dixon and W. N. Lipscomb, *Inorg. Chem.* 1978, **17**, 166.
7. D. A. Kleier and W. N. Lipscomb, *Inorg. Chem.* 1979, **18**, 1312.
8. M. J. S. Dewar and M. L. McKee, *Inorg. Chem.* 1978, **17**, 1569.
9. R. Schaeffer, Q. Johnson and G. S. Smith, *Inorg. Chem.* 1965, **4**, 917.
10. F. Klanberg, D. R. Eaton, L. J. Guggenberger and E. L. Muetterties, *Inorg. Chem.* 1967, **6**, 1271.
11. E. L. Muetterties and B. F. Beier, *Bull. Soc. Chim. Belg.* 1975, **84**, 397.

12. An energy difference of 25.4 kcal mol^{-1} is quoted in the text of Ref. 8, but 35.4 kcal mol^{-1} is quoted in Table V of Ref. 8.

13. D. D. Bray, R. M. Kabbani and E. H. Wong, *Acta Cryst.* 1982, **B38**, 957.

14. R. D. Dobrott and W. N. Lipscomb, *J. Chem. Phys.* 1962, **37**, 1779.

15. B. G. DeBoer, A. Zalkin and D. H. Templeton, *Inorg. Chem.* 1968, **7**, 1085.

16. C. H. Schwalbe and W. N. Lipscomb, *Inorg. Chem.* 1971, **10**, 160.

17. F. E. Scarbrough and W. N. Lipscomb, *Inorg. Chem.* 1972, **11**, 369.

18. J. T. Gill and S. J. Lippard, *Inorg. Chem.* 1975, **14**, 751.

19. O. P. Anderson and A. P. Schmitt, *Inorg. Chem.* 1977, **16**, 1630.

20. P. Bellon, M. Manassero and M. Sansoni, *J. Chem. Soc. Dalton* 1972, 1481.

21. H. S. M. Coxeter, *Twelve Geometric Essays*, Chap. 4. Southern Illinois University Press (1968).

22. D. L. Kepert, *The Early Transition Metals*. Academic Press, London (1972).

23. W. N. Lipscomb, *Science* 1966, **153**, 373.

24. G. D. Friesen, J. L. Little, J. C. Huffman and L. J. Todd, *Inorg. Chem.* 1979, **18**, 755.

25. J. A. Wunderlich and W. N. Lipscomb, *J. Am. Chem. Soc.* 1960, **82**, 4427.

26. G. Shoham, D. Schomburg and W. N. Lipscomb, *Cryst. Struct. Comm.* 1980, **9**, 429.

27. E. L. Muetterties, R. J. Wiersema and M. F. Hawthorne, *J. Am. Chem. Soc.* 1973, **95**, 7520.

28. F. Klanberg and E. L. Muetterties, *Inorg. Chem.* 1966, **5**, 1955.

29. E. H. Wong and R. M. Kabbani, *Inorg. Chem.* 1980, **19**, 451.

30. D. Saulys and J. A. Morrison, *Inorg. Chem.* 1980, **19**, 3057.

31. W. R. Hertler, W. H. Knoth and E. L. Muetterties, *J. Am. Chem. Soc.* 1964, **86**, 5434.

32. W. H. Knoth, W. R. Hertler and E. L. Muetteries, *Inorg. Chem.* 1965, **4**, 280.

33. E. I. Tolpin and W. N. Lipscomb, *J. Am. Chem. Soc.* 1973, **95**, 2384.

SYNTHESIS AND SPECTRAL STUDIES OF
MIXED COPPER(II) DIPEPTIDE COMPLEXES
OF IMIDAZOLE AND RELATED NITROGEN DONORS

S. V. DESHPANDE and T. S. SRIVASTAVA*

Department of Chemistry, Indian Institute of Technology Powai, Bombay 400 076, India

Abstract—Eight mixed copper(II) complexes of the type [Cu(II)(D)(HL)], where D = anion of glycylglycine, glycyl-L-tyrosine or glycyl-L-phenylalanine, and HL = imidazole, 1-methylimidazole, 2-methylimidazole or benzimidazole have been prepared and characterised. The visible and EPR spectral studies of these complexes indicate that they are monomeric having five coordinate square pyramidal geometry (possibly distorted) about Cu(II). The dipeptide behaves as terdentate ligand in these complexes with amino, ionised amide nitrogen and carboxylate oxygen donor atoms approximately tetragonally disposed about Cu(II). The magnetic and bonding parameters obtained by detailed EPR spectral analysis coupled with electronic absorption spectral data suggest that imidazole, 1-methylimidazole, 2-methylimidazole or benzimidazole occupies the fourth position in the tetragonal plane and water molecule occupies an axial position about Cu(II) in solid state and in solution.

Current interest in the study of Cu(II) complexes with imidazole ligand has emphasised the importance of the bond between copper and imidazole from histidine residues of blue copper proteins and nonblue proteins.[1-3] The X-ray structural studies of poplar plastocyanine[4] and *pseudomonas aeruginosa azurin*[5] have revealed that imidazoles from histidine residues of these proteins are involved in the bonding of Cu(II) at the active site. It is also known that the imidazole acts as a bridging ligand at the active site of the bovine erythrocyte superoxide dismutase which catalyses the conversion of superoxide to peroxide.[6,7] The study of a series of model Cu(II) complexes has suggested a distorted square pyramidal configuration at the copper site in galactose oxidase, in oxyhemocyanine and in magnetically coupled ion pairs believed to constitute type **III** copper.[8] Recently, many low molecular weight complexes of Cu(II) containing imidazole ligand(s) have been proposed as models of active site of copper proteins.[9-11] In view of the importance of Cu(II)-imidazole complexes as models for copper proteins, we report here the synthesis and spectral properties of several mixed monomeric Cu(II) dipeptide complexes of imidazole, 1-methylimidazole, 2-methylimidazole and benzimidazole.

EXPERIMENTAL

Materials

Glycylglycine (Gly.Gly), glycyl-L-tyrosine (Gly.Tyr) and glycyl-L-phenylalanine (Gly.Phe) were purchased from Sigma, U.S.A. Imidazole (imH), 2-methylimidazole (2-MeimH) and benzimidazole (BzimH) were bought from SISCO, India. 1-methylimidazole (1-Meim) was obtained from Aldrich, U.S.A. Other commercially available reagent grade chemicals were used without further purification.

Synthetic procedures

Cu(Gly.Gly).3H$_2$O (**Ia**). This complex was prepared by the method described earlier.[12] The product was recrystallised from water.

Cu(Gly.Tyr).4H$_2$O (**IIa**). This was prepared by the method of Dehand *et al.*, and recrystallised from water.[13]

Cu(Gly.Gly)(imH).2H$_2$O (**Ib**) *and* Cu(Gly.Gly)(1-Meim).H$_2$O (**Ic**). These complexes were pre-

---

pared by the methods of Driver and Walker[14] and recrystallised from 50% methanol.

Cu(Gly.Gly)(2-MeimH).2H$_2$O (Id). The blue copper hydroxide was prepared by adding excess of 6N NaOH to a solution of 0.170 g of copper chloride in 15 cm^3 of water. This precipitate was filtered and washed with distilled water to get it free from chloride ions. The precipitate was suspended in 20 cm^3 of water to which 2-methylimidazole (0.083 g) and glycylglycine (0.132 g) were added. The solution was stirred for 1 hr and then filtered. The deep blue filtrate was concentrated to a small volume and kept in a refrigerator for 1 day. The deep blue needle crystals obtained were filtered, washed with cold water and dried in a vacuum desiccator over anhydrous calcium chloride. Found: C, 30.9; H, 5.1; N, 17.2. Calc. for [C$_8$H$_{12}$N$_4$O$_3$Cu].2H$_2$O: C, 30.82; H, 5.13; N, 17.98%.

Cu(Gly.Gly)(BzimH).H$_2$O (Ie). A solution of 0.118 g of benzimidazole in 20 cm^3 of methanol was added to a solution of 0.248 g of (Ia). The resulting solution was incubated at room temperature for 1 day. The sky blue fibre-like crystals obtained were filtered and washed with ice cold water. The product was recrystallized from 50% methanol. The crystals were filtered, washed with cold ethanol and dried in air. Found: C, 41.0; H, 4.1; N, 16.7. Calc. for [C$_{11}$H$_{12}$N$_4$O$_3$Cu].H$_2$O: C, 40.06; H, 4.25; N, 16.99%.

Cu(Gly.Tyr)(imH).H$_2$O (IIb). Glycyl-L-tyrosine (0.238 g, 10^{-3} M) and imidazole (0.68 g, 10^{-3} M) were added to a freshly prepared copper hydroxide (10^{-3} M) suspended in 30 cm^3 of water. This mixture was stirred for 30 min at 60°C and then boiled for 2 min. The mixed solution was filtered to remove unreacted copper hydroxide. The deep blue filtrate was concentrated to 15 cm^3, on a water bath. The resulting solution was kept at room temperature for 2 hr. The sky-blue crystals obtained were filtered. This product was recrystallized from water. The crystals obtained were filtered, washed with cold water, methanol and then diethyl ether. They were finally dried in air. Found: C, 43.9; H, 4.5; N, 14.4. Calc. for [C$_{14}$H$_{16}$N$_4$O$_4$Cu].H$_2$O: C, 43.58; H, 4.66; N, 14.53%.

Cu(Gly.Tyr)(2-MeimH).H$_2$O (IIc). This complex was prepared by the addition of glycyl-L-tyrosine (0.238 g, 10^{-3} M) and 2-methylimidazole (0.083 g, 10^{-3} M) to a freshly prepared copper hydroxide (10^{-3} M) suspended in 25 cm^3 of 50% aqueous methanol. This mixture was stirred for 2 hr and then filtered. The deep blue solution was concentrated to a small volume and kept frozen for 12 hr. The deep blue needle crystals obtained were

filtered, washed with cold water, methanol and finally with diethyl ether. The crystals were finally dried in air. Found: C, 44.8; H, 4.8; N, 13.8. Calc. for [C$_{15}$H$_{18}$N$_4$O$_4$Cu].H$_2$O: C, 45.06; H, 5.01; N, 14.02%.

Cu(Gly.Tyr)(BzimH).3.5H$_2$O (IId). Glycyl-L-tyrosine (0.238 g, 10^{-3} M) and benzimidazole (0.118 g, 10^{-3} M) were added to a suspension of 10^{-3} M copper hydroxide in methanol–water mixture (2:1) (v/v). The mixture was heated on a water bath for 30 min with occasional stirring and then filtered. When this filtrate was cooled, shining sky blue crystals were obtained. They were filtered, washed with cold water, methanol and diethyl ether. The product was recrystallized from 70% methanol. The crystals obtained were dried in air. Found: C, 45.2; H, 5.3; N, 11.0. Calc. for [C$_{18}$H$_{18}$N$_4$O$_4$Cu]3.5H$_2$O: C, 44.95; H, 5.20; N, 11.66%.

Cu(Gly.Phe)(imH).H$_2$O (IIIa). The complex was prepared by the same method as described for (Ib). This was recrystallised from 50% aqueous ethanol solution when dark blue crystals were obtained. Found: C, 45.9; H, 4.5; N, 14.9. Calc. for [C$_{14}$H$_{16}$N$_4$O$_3$Cu].H$_2$O: C, 45.47; H, 4.88; N, 15.16%.

Physical measurements

The electronic absorption spectra of the Cu(II) complexes were recorded using Perkin–Elmer (model 402) spectrophotometer. The matched quartz cells of 10 mm pathlength were used. The complexes were dispersed in Nujol and their IR spectra were recorded on Perkin–Elmer (model-577) IR spectrophotometer in the range of 4000–600 cm^{-1}. This instrument was calibrated using polystyrene film.

The magnetic susceptibility measurements at room temperature were performed on a Gouy balance following the procedure described elsewhere.[15] The electron paramagnetic resonance (EPR) spectra of the Cu(II) complexes in solution at room temperature and at low temperature (77 K) were recorded on Varian E-112 ESR spectrometer (X-band) by using TCNE (g = 2.00277) as g marker. The EPR spectra of all complexes except (IIc) and (IId) were measured by dissolving them in a mixture of ethyleneglycol and water in the ratios of 1:1 and 2:1 (v/v). The room temperature solution spectra of the Cu(II) complexes were measured using Varian aqueous solution cell, E-248. The EPR spectra of (IIc) and (IId) were taken in dimethyl sulphoxide (DMSO). The pH of aqueous solutions was adjusted using dilute NaOH solution.

RESULTS AND DISCUSSION

Eight Cu(II) dipeptide complexes such as (**Ib**, **Ic**, **Id**, **Ie**, **IIb**, **IIc**, **IId** and **IIIa**, with imidazole, 1-methyl-imidazole, 2-methylimidazole and benzimidazole) have been prepared and characterised by elemental analysis, and by IR, visible and EPR spectroscopy. The IR spectra of these complexes show a strong band between 1575 and 1591 cm^{-1}. This can be assigned to peptide carbonyl stretching band with ionisation of peptide N–H hydrogen.[16] The N–H bending vibrations were observed between 1597 and 1633 cm^{-1}. The N–H stretching vibrations of NH_2 group, imidazole, 2-methylimidazole and benzimidazole were observed between 3066 and 3466 cm^{-1}. The O–H stretching vibration of phenol group in complexes containing Gly.Tyr was observed between 3552–3628.[17] The effective magnetic moments (μ_{eff}) of Cu(II) complexes at room temperature are given in Table 1. The magnetic moments are in the range of 1.80–2.00 B.M. These values indicate that they are magnetically dilute systems.[18]

The electronic absorption spectra of the Cu(II) complexes were taken in different solvents in the range of 400–850 nm. The absorption maxima with their extinction coefficients (ϵ) are given in Table 1. All the complexes show only one broad band in the visible region, which is assigned to d–d transition of the Cu(II) complexes.[18] The fairly high extinction coefficient observed for this transition is indicative of presence of square pyramidal geometry about Cu(II). The d–d transitions of adducts of

imidazole, 1-methylimidazole and 2-methylimidazole and benzimidazole with (**Ia**) and (**IIa**) occur at higher energies than of (**Ia**) and (**IIa**) respectively. This may be attributed to stronger ligand fields of imidazole and related nitrogen donors than of water.[19] The slightly higher position of absorption bands of (**Ic**) and (**Id**) as compared to the Cu(Gly.Gly) adduct of imidazole (**Ib**) is probably due to increase of steric hindrance, which may result in longer Cu–N bonds and thus relatively lowering the 10 Dq values.[20]

The absorption spectra of Cu(II) complexes also show some absorption at 850 nm. The percentage ratio of ϵ_{850} and ϵ_{max} is also measured and they are given in Table 1. This percentage varies between 2 and 9 in Cu(II) dipeptide adducts of imidazole and related nitrogen donors. These lower values suggest that these nitrogen bases are substituting for an equatorial water in Cu(II) dipeptide complexes with dipeptides still behaving terdentate ligands.[21] However, the 1:1 complex of $CuCl_2$ and Gly.Gly shows a λ_{max} at 770 nm with the percentage ratio of ϵ_{850} and ϵ_{max} as 75. In this complex, the Gly.Gly binds Cu(II) quite differently[22,23] and supports the terdentate binding of dipeptide to Cu(II) in Cu(II) dipeptide adducts of imidazole and related nitrogen donors.

The EPR spectra of Cu(II) complexes at room temperature are isotropic due to tumbling motion of the molecules. The isotropic g value, g_0, is calculated at the centre of the spectrum of the four lines. The isotropic nuclear hyperfine constant, A_0,

Table 1. Visible absorption spectral and magnetic data of copper(II) complexes

Compound	λ_{max} in nm in different solvents(ϵ)			$\dfrac{\epsilon_{850}}{\epsilon_{max}}$ x 100	μ_{eff} (K)
	Water^{a}	Methanol	DMSO		B.M.
Ia	640(85)	–	–	10	1.92(300)
Ib	613(87)	616(95)	–	8	1.86(300)
Ic	618(87)	608(95)	–	5	1.85(298)
Id	630(87)	622(102)	–	2	1.84(300)
Ie	620(125)	620(107)	610(115)	9	1.82(300)
IIa	635(75)	–	–	14	1.90(300)
IIb	620(74)	600(91)	574(110)	5	1.87(298)
IIc	630	–	590(110)	8	–
IId	–	–	600(87)	7	1.94(300)
IIIa	615(87)	595(98)	510(110)	5	1.80(303)

^{a}The pH of the solution was between 6.7 to 7.1

is expressed in cm^{-1} and is calculated between two adjacent lines of the spectrum.[24] The EPR spectra of the complexes in glassy state at 77 K show three well resolved peaks of low intensity in the low field region and intense unresolved peaks are obtained in the high field region. The $g_\parallel$ and $A_\parallel$ values were accurately calculated from this spectrum while $g_\perp$ and $A_\perp$ values were evaluated using the following equations.[25] The EPR parameters thus

$$g_1 = \frac{3g_0 - g_\parallel}{2} \quad \text{and} \quad A_1 = \frac{3A_0 - A_\parallel}{2}$$

obtained are given in Table 2.

The X-ray structural studies of (Ia, Ib and IIa) reveal that they have distorted square pyramidal geometry about Cu(II).[9,13,19] Similar structures are expected for other Cu(II) complexes. The $g_\parallel$ values of these complexes are also greater than corresponding $g_\perp$ values,[18,26] and therefore, they have an unpaired electron in $d_{x^2-y^2}$ molecular orbital. Considering an approximate D_{4h} symmetry in these complexes, the metal ligand σ-bonding parameter α^2, was calculated by using the following relationship[27]

$$\alpha^2 = \frac{1}{8}[-14(A_\parallel + K)/P + 11(g_\parallel - g_e) + 9(g_0 - g_e)]$$

where P = dipole coefficient = $0.036\,cm^{-1}$ for free Cu^{2+} ion. K represents the Fermi contact term

which is calculated by using the relationship

$$K = -A_0 + P(g_0 - g_e).$$

The out-of-plane σ-bond strength, α'^2, was calculated by using the relationship

$$\alpha^2 + \alpha'^2 - 2\alpha\alpha'S = 1$$

where S is the overlap integral which is taken as 0.093.[28] The bonding parameters, β'^2 and β^2, which represent in-plane and out-of-plane π-bond strengths respectively, were calculated by Kevilson and Neiman method.[28] The charge density in the 4s orbital or the 4s contribution to the ground state can be represented by ϵ'^2 and is calculated by the method of Rockenbauer.[27] The values of α^2, $\alpha'^2 \cdot \beta_1^2$, β^2 and ϵ'^2 are given in Table 3.

The metal ligand in-plane σ-bonding, α^2, is completely ionic if $\alpha^2 = 1$ and it is completely covalent if $\alpha^2 = 0.5$. The α^2 values of these Cu(II) complexes fall in the range of 0.71–0.82. These values are indicative of appreciable in-plane covalence. The substitution of a water molecule by imidazole in (Ia) lowers its α^2 value and thus introduces more in-plane covalency. The trend can be explained in terms of imidazole substituting for equatorial water in (Ia).[28] Similar changes were observed in Cu(II) dipeptide adducts of other nitrogen bases. The values of in-plane π-bonding, β_1^2, for the Cu(II) complexes vary in the range of 0.79–0.90. The trend of β_1^2 values is opposite to that observed for α^2 values, which is indicative of competitive mechanism of in-plane σ- and π-bonding in these Cu(II) complexes. The values of out-of-plane π-bonding, β^2, vary in the range of

Table 2. Magnetic parameters of copper(II) complexes

Compound	$g_\parallel$	$g_\perp$	g_0	$A_\parallel \times 10^4$ cm^{-1}	$A_\perp \times 10^4$ cm^{-1}	$A_0 \times 10^4$ cm^{-1}
Ia	2.250	2.068	2.128	185	16	70
Ib	2.238	2.061	2.120	167	7	57
Ic	2.230	2.064	2.120	164	7	56
Id	2.236	2.065	2.122	164	13	59
Ie	2.234	2.067	2.122	167	27	71
IIa	2.243	2.059	2.120	183	17	69
IIb	2.226	2.064	2.118	165	10	62
IIc	2.221	2.051	2.107	176	33	79
IId	2.226	2.056	2.112	177	36	81
IIIa	2.228	2.061	2.116	172	7	59

Table 3. Ligand field energies, bonding parameters and ϵ'^2 of copper(II) complexes

Compound	ΔE cm^{-1}	α^2	α'^2	β_1^2	β^2	ϵ'^2
Ia	15625	0.82	0.27	0.80	0.86	0.30
Ib	16313	0.78	0.31	0.83	0.84	0.38
Ic	16181	0.76	0.33	0.82	0.89	0.37
Id	15873	0.76	0.34	0.84	0.91	0.33
Ie	16129	0.71	0.39	0.89	0.98	0.16
IIa	15748	0.81	0.28	0.80	0.77	0.31
IIb	16129	0.77	0.32	0.81	0.89	0.34
IIc	16949	0.71	0.39	0.88	0.82	0.13
IId	16667	0.71	0.39	0.90	0.87	0.11
IIIa	16260	0.78	0.30	0.79	0.83	0.38

0.83–0.93 showing little to appreciable out-of-plane π-bonding.

The $g_\parallel$ values of Cu(II) dipeptide adducts of the imidazole and related nitrogen donors decrease as compared to the $g_\parallel$ values of the corresponding Cu(II) dipeptides (see Table 2). This variation is also explained in terms of imidazole, 1-methylimidazole, 2-methylimidazole or benzimidazole substituting for an equitorial water in (Ia) or (IIa).[29] This is also supported by the conclusion obtained above by trends of α^2 values as well as X-ray structural studies of (Ib).[26] The isotropic spectra of these nitrogen base adducts at room temperature shows even superhyperfine lines at the highest field of Cu hyperfines with ^{14}N hyperfine constant of about 11 gauss. This supports the presence of three nitrogen donors in the equitorial plane of Cu(II) ions in these complexes. These conclusions are further supported in solution also by the change of electronic absorption maximum of (Ia) from 640 to 610 nm in its imidazole adduct (Ib). If the imidazole binds at apical position by displacing an apical water molecule from (Ia), the absorption maximum may shift to longer wavelength due to the pentammine effect.[30] The blue shifts on adduct formation by other nitrogen donors have also been observed (see Table 1). These observations are in contrast with the suggestion of Hartzell et al.[31] that the imidazole occupies an apical position in (Ib).

The theoretical straight line plot of ϵ'^2 the $4s$ contribution to the ground state, against α^2 for these Cu(II) complexes, assuming approximate D_{4h} symmetry, was obtained by using empirical equation

$$\epsilon'^2 = 1.06\ \alpha^2 - 0.567$$

suggested by Rochenbauer.[27] This plot is given in Fig. 1. If ϵ'^2 values are obtained using eqn (15) from the Rockenbauer's paper,[27] the points fall near, above and below the theoretical straight line (see Fig. 1). Actually, the above analysis was applied to Cu(II) complexes having tetragonal ligand field (square planar). If ϵ'^2 values calculated from eqn (15) are plotted vs corresponding α^2 values, the points divert upward in rhombic distortion and downward in tetrahedral distortion. If a similar plot is made of Cu(II) complexes having square pyramidal geometry, by analogy, the points divert upward in rhombic distorted square pyramidal configuration and downwards in tetrahedral distorted square pyramidal configuration[32] or distortion towards configuration intermediate between square pyramidal and trigonal bipyramidal. The rhombic distortion seems to be present in (Ib, Ic, Id and IIb), but distortion towards tetrahedron or intermediate configuration is present in (IIc) and (IId). This may be because of steric crowding due to bulky substituents on dipeptide and imidazole.

The Cu(II) dipeptide complexes with imidazole and other nitrogen donors have distorted square pyramidal geometry about Cu(II) in these complexes. The dipeptide occupies three coordination positions and imidazole (or other nitrogen donor) occupies fourth position in the tetragonal plane, and the apical position is occupied by water.
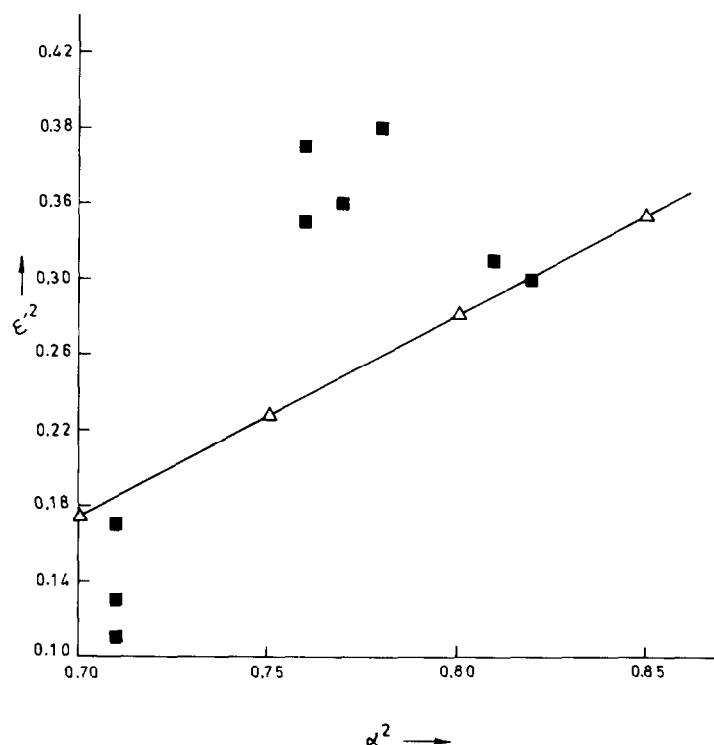
Fig. 1. Plot of α^2 vs ϵ'^2 for Cu(II) complexes.

REFERENCES

1. A. E. G. Cass and H. A. O. Hill, *Biological Roles of Copper, Ciba Foundation Symposium* 79 (New Series), pp. 71–91. Excerpta Medica (1980).
2. J. K. Markley, E. L. Ulrich, S. P. Berg and D. W. Krogman, *Biochemistry* 1975, **14**, 4428.
3. T. B. Friedman, J. S. Loehr and J. M. Loehr, *J. Am. Chem. Soc.* 1976, **98**, 2809.
4. P. M. Colman, H. C. Freeman, J. M. Guss, M. Murta, V. A. Norris, J. A. M. Ramshaw and M. P. Venkatappa, *Nature* 1978, **272**, 319.
5. E. T. Adam, R. R. Stenkamp, L. C. Sieker and L. H. Jemsen, *J. Mol. Biol.* 1978, **123**, 35.
6. J. S. Richardson, K. A. Thomas, B. H. Rubin and D. C. Richardson, *Proc. Natl. Acad. Sci., U.S.A.* 1976, **72**, 1349.
7. I. Fridovich, *Advances in Inorganic Biochemistry* (Edited by G. L. Eichhorn and D. L. Merzilli), p. 67. Elsevier–North-Holland, New York (1979).
8. A. R. Amundsen, J. Whelan and B. Bosnik, *J. Am. Chem. Soc.* 1977, **99**, 6730.
9. R. Osterberg, *Coord. Chem. Rev.* 1974, **12**, 309.
10. Y. Nakao, W. Mori, T. Sakurai and A. Nakahara, *Inorg. Chim. Acta* 1981, **55**, 103.
11. S. J. Lippard, C. L. O'Young, J. C. Dewan and H. R. Lilienthal, *J. Am. Chem. Soc.* 1978, **100**, 7291.
12. A. R. Manyak, C. B. Murphy and A. E. Martell, *Arch. Biochem. Biophys.* 1955, **59**, 373.
13. J. Dehand, J. Jordanoo and F. Keck, *Inorg. chim. Acta* 1977, **21**, L-33.
14. R. Driver and W. R. Walker, *Austr. J. Chem.* 1968, **21**, 671.
15. B. N. Figgis and J. Lewis, *Modern Coordination Chemistry* (Edited by J. Lewis and R. G. Wilkins), pp. 400–454. Interscience, New York (1960).
16. K. Nakamoto, *Infrared and Raman Spectra of Inorganic and Coordination Compounds*, 3rd Edn, pp. 314–317. Wiley, New York (1978).
17. J. R. Dyer, *Applications of Absorption Spectroscopy of Organic Compounds*, pp. 33–38. Prentice-Hall, New Jersey (1965).
18. B. J. Hathaway, *J. Chem. Soc. Dalton Trans.* 1972, 1196.
19. R. J. Sundeberg and R. B. Martin, *Chem. Rev.* 1974, **74**, 471.
20. W. J. Eilbeck, F. Holmes, C. E. Taylor and A. E. Underhill, *J. Chem. Soc. (A)* 1968, 128.
21. M. C. Lim, E. Sinn and R. B. Martin, *Inorg. Chem.* 1976, **15**, 807.

22. M. K. Kim and A. E. Martell, *Biochemistry*, 1964, 3, 1169.
23. A. Nakahara, O. Yamauchi and Y. Nakao, *Bio-organic Chemistry* (Edited by E. E. Van Tamelen), Vol. IV, pp. 349–383. Academic Press, New York (1978).
24. G. F. Bryce, *J. Phys. Chem.* 1966, **70**, 3549.
25. H. M. McConnel, *J. Chem. Phys.* 1956, **25**, 709.
26. B. J. Hathaway and D. E. Billing, *Coord. Chem. Rev.* 1970, **5**, 143.
27. A. Rockenbauer, *J. Mag. Res.* 1979, **35**, 429.
28. D. Kevilson and R. Neiman, *J. Chem. Phys.* 1961, **35**, 149.
29. R. Barbucci and M. J. M. Campbell, *Inorg. Chim. Acta.* 1976, 27, 109.
30. B. J. Hathaway and A. A. G. Tomlinson, *Coord. Chem. Rev.* 1970, **5**, 1.
31. R. E. Viola, C. R. Hartzell and J. J. Villafranca, *J. Bioinorg. Chem.* 1979, **10**, 293.
32. P. I. Fareday, D. Hodgson, S. Tyagi and B. J. Hathaway, *Inorg. Nucl. Chem. Lett.* 1981, **17**, 243.

THE FORMATION OF FLUORIDE
COMPLEXES OF TITANIUM(IV)

LIBERATO CIAVATTA* and ADRIANA PIROZZI
Istituto di Chimica dell'Università, Via Mezzocannone 4, 80134 Napoli, Italy

Abstract—The complex formation equilibria between titanium(IV) and fluoride ions have been studied at 25°C in 3 M(Na)Cl ionic medium by measuring, with an ion selective electrode for F^-, the free HF concentration in acid Ti(IV) solutions. The $[H^+]$ was kept within 0.25 and 1 M where the predominant form of uncomplexed metal is the dihydroxotitanium(IV) ion, $Ti(OH)_2^{2+}$. The potentiometric data have been explained by assuming $Ti(OH)_2F^+$, TiF_4 and $HTiF_6^-$, with equilibrium constants given in Table 3. Within the accuracy of the present e.m.f. study, ± 0.2 mV, no evidence for intermediate complexes bearing 2, 3 and 5 F^- was found.

From a special series of measurements, carried out by replacing a large part of the Cl^- with ClO_4^-, it is concluded that no appreciable amount of Ti(IV)–Cl complexes is formed at the 3 M level employed as ionic medium.

NOTATION

a concentration of HF
A total fluoride concentration
B total titanium concentration
f_i activity coefficient of the i species
$F_{i,n}$ activity coefficient quotient, eqn (5)
h concentration of H^+
H analytical concentration excess of H^+, $= [Cl^-] - [Na^+] - 2B$
K_n formation constant for all species containing n F^-, eqn (9)
Z average number of fluoride ions bound per titanium atom, $= (A - a - [F^-] - [HF_2^-])/B$
$\beta_{i,n}$ formation constant for $Ti(OH)_iF_n^{4-i-n}$, eqn (4)

When not stated, concentrations and equilibrium constants are expressed on the molar scale.

Previous measurements[1] with the redox Ti(IV)/Ti(III) couple in chloride solution have shown the predominance of the hydroxotitanium(IV) ion, $Ti(OH)_2^{2+}$, in the acidity range from 0.25 to 2 M. This result is the starting point of the present investigation aiming at the elucidation of the complex formation equilibria between $Ti(OH)_2^{2+}$ and HF.

METHOD

This work describes the determination of [HF] a, using an ion specific electrode for fluoride, in a series of acid titanium(IV) chloride solutions of various A and B values. The acidity levels, H, were chosen between 0.25 and 1 M. From the primary data the function $Z(\log a)_{B,H}$, which forms the basis of the following treatment, was calculated.

In the attempt to minimize the activity coefficient variation of the reacting species the chloride concentration was maintained at the 3 M level by introducing sodium chloride. Thus the test solution (TS) had the general composition: B M Ti(IV), A M F^-, H M H^+, $(3 - 2B - H)$ M Na^+, 3 M $Cl^- = TS$. As the reference state 3 M NaCl is taken and the activity coefficient of a reacting species is defined to tend to

unity as the composition of TS approaches this pure salt solution. We recall at this stage that no certain conclusions on the number of Cl^- bound to Ti(IV) species can be drawn from data obtained in a constant Cl^- medium. To gain an idea of the extent to which Ti(IV) associates with Cl^- a special series of measurements was performed by replacing 2.7 M of Cl^- with ClO_4^-.

The a values in TS were measured with cell(I)

$$- EF/TS, Q.QH_2(s)/Pt + \qquad (I)$$
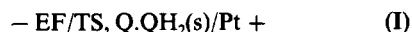
where EF indicates the ion specific electrode for F^- and $Q.QH_2$ stands for quinhydrone.

The e.m.f. of cell(I) may be written, in V, at 25°C

$$E = E_0' + 0.05916 \log(af_{HF}) + E_q \qquad (1)$$

in which E_0' is a constant, and E_q is a small correction term accounting for the basicity of p-benzoquinone[2] and for f_Q and f_{QH_2}. In each experiment H was kept constant while Z was successively varied. Since $B < 0.1H$, the composition of TS changed only slightly. Consequently, for H constant we may neglect the variation of f_{HF} and of E_q and calculate $\log a$ by the simplified form of (1), eqn (2), where E_0 includes the f_{HF} and E_q terms,

$$E = E_0 + 0.05916 \log a. \qquad (2)$$

The measurements were carried out as potentiometric titrations. First, E_0 was determined in the absence of titanium. Since in the chosen experimental conditions practically all the fluoride is present in form of HF[3], E_0 was calculated by putting $a = A$ in eqn (2). In any case E_0 proved to be constant within ± 0.1 mV in the A range from 10^{-3} to 0.1 M. Then the complex formation was followed (i) by increasing the A/B ratio while B was kept constant, or (ii) by decreasing the A/B values. The coincidence of data obtained with these different procedures served as a criterion for true equilibrium. With the known E_0 and using (2) a could be calculated for each point. Finally, Z was obtained from $(A - a)/B$ being the concentration of F^- and HF_2^- negligible in our solutions.

EXPERIMENTAL

Materials and analysis

Titanium(IV) chloride solutions were made from $TiCl_4$ p.a. quality furnished by C. Erba. This product was found to contain trace amounts of Fe(III), less than 0.05%, which may be considered unimportant for our purposes.

A series of 0.8 M stock solutions was prepared by adding $TiCl_4$ to ice cold 6 M HCl and was stored in a refrigerator at 4°C. Storage at low temperature proved convenient due to the appreciable HCl vapour tension at room temperature. Periodical controls of the acid concentration indicated HCl losses of less than 0.3% in 6 months.

The [Ti(IV)] in the stock solutions was determined gravimetrically (a) as TiO_2 by precipitating titanium hydroxide with gaseous ammonia and then igniting it at 800°C or (b) as oxinate according to Berg and Teitelbaum.[4] Accurate results can be attained with the last procedure provided the oxinate is protected by moisture during cooling and weighing. The results of analyses agreed to within 0.1%.

The total chloride concentration of the stock solutions was obtained gravimetrically as AgCl and by Volhard's method. The results coincided within 0.1%.

The analytical concentration excess of H^+ was found from $H = [Cl^-] - 2[Ti(IV)]$.

Solutions of *hydrochloric acid* were prepared by diluting the p.a. product Merck and were standardized against $KHCO_3$ using methyl red as visual indicator. The results agreed better than 0.1%.

Sodium fluoride was obtained as described previously.[3]

Sodium chloride Merck p.a. was ignited in a platinum vessel at 360°C in an electric oven.

Sodium perchlorate and *perchloric acid* solutions were prepared and analysed as described in a previous work.[5]

The *quinhydrone* Merck p.a. was recrystallised from water and was dried over H_2SO_4. No Fe(III) and Cl^- ions could be detected in the final product.

Details of the e.m.f. measurements

All the e.m.f. measurements were performed in a paraffin oil thermostat kept at $25 \pm 0.02°C$.

The fluoride electrode used, Metrohm, consisted of a membrane of LaF_3 doped with europium(II) ions. The electrode, 5 min after the addition of reagents, acquired a potential which remained constant within ± 0.2 mV for 12 hr. To check the Nernstian response to the HF concentration, the e.m.f. of cell (I) was measured in acid solutions, $H > 0.25$ M, as a function of a in the interval from 10^{-3} and 0.1 M. In any case E_0 values constant to ± 0.1 mV were found.

The titration vessel was a gold cup which assured chemical inertia against TS and furthermore a rapid thermal equilibrium. Cell arrangements made of plastic material achieved the bath temperature in more than 1 hr. A Teflon-coated magnetic bar served for stirring. The burette tips and other parts which might come into contact with fluoride solutions were constructed by Teflon or Plexiglas. Fluoride solutions were added with a polythene weighing burette.

The e.m.f. values of cell(I) were measured, with a precision of 0.01 mV, with a Dynamco Ltd. 2022 digital voltmeter.

DATA AND CALCULATIONS

The $Z(\log a)_{B,H}$ data, which form the basis of the calculations, are collected in Table 1. In Fig. 1 are represented the measurements for $H = 0.5$ M.

At each of the studied H levels the Z values were found to tend to 6 as a increases. Furthermore data of different B fell practically on the same curve. These features of the $Z(\log a)$ functions suggest mononuclear complexes with 6 maximum coordination. However, as the plot of Fig. 1 shows, the formation function is accomplished within less than $2 \log a$
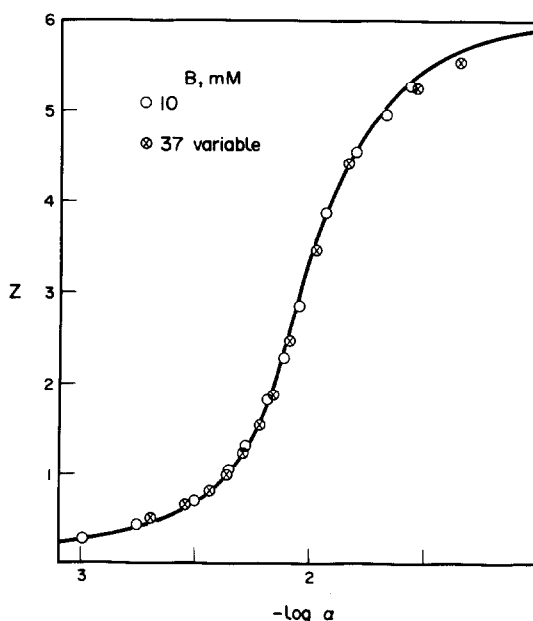
Fig. 1. Z, the average number of fluoride ions bound per titanium atom, as a function of $\log a$ in solutions of $H = 0.5$ M. The curve has been calculated by assuming $B = 0.01$ M and the constants of Table 3.

units, indicating the limited range of existence for intermediate complexes.

The calculations of the number of OH^- and F^- ions in the predominating complexes and the corresponding equilibrium constants were performed in three steps. First, data of constant H were treated separately. By this approach the number of F^- in the complexes and the conditional constants K_n were computed. Then the OH^- groups and preliminary values of $\beta_{t,n}$ were estimated by examining the variation of K_n with H. Finally, the equilibrium constants were refined with numerical procedures based on the principle of the least-squares.

Treatment of data of constant H

In this section the $Z(\log a)_H$ data are considered separately.

In the presence of only mononuclear complexes Z may be expressed by

$$Z = \frac{\sum n\beta_{t,n}F_{t,n}h^{-p}a^n}{1 + \sum \beta_{t,n}F_{t,n}h^{-p}a^n} \quad (3)$$

in which n, t and $p = (n + t - 2)$ are integers, $\beta_{t,n}$ is the equilibrium constant for

$$Ti(OH)_2^{2+} + n\,HF \rightleftarrows Ti(OH)_tF_n^{4-n-t} + p\,H^+ \quad (4)$$

and $F_{t,n}$ is the activity coefficient quotient

$$F_{t,n} = \frac{f_{HF}^n f_{Ti(OH)_2^{2+}}}{f_{t,n}f_{H^+}^p}. \quad (5)$$

At constant H we may use the approximation $F_{t,n} = $ constant without introducing any appreciable error.

In order to find n of the main complexes the experimental data were confronted with normalised

Table 1. Survey of measurements

$$\overline{H} = 0.25 \text{ M}$$

a) $Z(-\log a)_{B=0.01294}$

0.251(3.313);0.566(2.845);0.884(2.578);1.30(2.413);2.13(2.256);
2.73 (2.173); 3.24(2.110); 3.80(2.044);4.35(1.956);4.78(1.854);
5.07 (1.739); 5.20(1.648).

b) $Z(-\log a, B\times10^3)$

0.517(2.898,22.05);0.656(2.758,21.16);0.779(2.646,20.39);
0.969(2.536,19.33); 1.24(2.437,18.03); 1.67(2.334,16.27);
1.94(2.290,15.32); 2.30(2.243,14.25); 2.70(2.191,13.27);
3.27(2.126,11.88); 4.08(2.015,10.28); 5.15(1.804, 8.27);
5.44(1.628, 7.09); 5.59(1.455, 5.68); 5.69(1.312, 4.09).

$$H = 0.50 \text{ M}$$

a) $Z(-\log a)_{B=0.0100}$

0.268(3.000);0.423(2.755);0.691(2.498);0.991(2.355);1.30(2.275);
1.83(2.180); 2.28(2.111); 2.86(2.045); 3.88(1.931);4.54(1.800);
4.95(1.670); 5.27(1.570).

b) $Z(-\log a, B\times10^3)$

0.505(2.687,37.29);0.660(2.542,34.10);0.833(2.432,31.11);
1.03(2.347,28.32); 1.24(2.285,25.82); 1.55(2.217,22.81);
1.88(2.162,20.27); 2.48(2.086,16.79); 3.48(1.969,12.84);
4.44(1.829,10.03); 5.25(1.540, 6.71); 5.56(1.352, 4.33).

$$H = 1.00 \text{ M}$$

$Z(-\log a, B\times10^3)$

0.221(2.760,41.23);0.335(2.569,37.85);0.447(2.438,34.84);
0.692(2.295,29.74); 1.05(2.191,24.50); 1.47(2.118,20.36);
1.82(2.069,17.73); 2.25(2.022,15.27); 2.73(1.970,13.15);
3.13(1.920,11.63); 3.53(1.869,10.36); 3.94(1.818, 9.22);
4.14(1.770, 8.54); 4.61(1.666, 7.08); 5.10(1.501, 4.97).

$$H = 0.516 \text{ M}, \quad 2.7 \text{ M ClO}_4^-, 0.3 \text{ M Cl}^-$$

$Z(-\log a, B\times10^3)$

0.204(3.260,23.54);0.258(3.138,23.01);0.326(3.015,22.38);
0.407(2.889,21.65);0.479(2.758,20.69);0.609(2.631,19.58);
0.772(2.518,18.33);0.960(2.432,17.09); 1.21(2.349,15.67);
1.54(2.279,14.15); 1.93(2.216,12.67); 2.31(2.165,11.45);
2.56(2.136,10.77); 2.85(2.102,10.05); 3.23(2.063, 9.24);
3.68(2.009, 8.35); 3.94(1.973, 7.87); 4.22(1.930, 7.37);
4.49(1.877, 6.85); 4.76(1.803, 6.25); 4.98(1.725, 5.63);
5.21(1.604, 4.67); 5.33(1.486, 3.58); 5.43(1.413, 2.76);
5.59(1.347, 1.91).

model functions representing different hypotheses. For the calculations some assumptions had to be made about the dependence of h upon B and Z. Since $B < 0.1H$, h must be close to H and therefore it is sufficient to estimate only a lower and a higher limit for h. We have postulated the validity of the inequalities

$$H < h \le H + BZ \qquad (6)$$

in which the upper limit comes from the hypothesis that $p = n$ in (4). The results of the next section show that in our solutions h never exceeds $H + BZ$.

On the basis of (3) and (6) two types of functions, $G(a)$ and $\Phi(w)$, were constructed

$$\log G(a) = \log\left(\sum nK_n a^{n-6}\right) > \log Z +$$
$$0.434 \int_0^a (Z/a)\,da - 6\log a \qquad (7)$$

$$\log \Phi(w) = \log\left(\sum nK_n w^{n-6}\right) \le \log Z +$$
$$0.434 \int_0^w (Z/w)\,dw - 6\log w \qquad (8)$$

where K_n, the conditional constant, is defined by

$$K_n = \sum \beta_{i,n} H^{-p} F_{i,n} \qquad (9)$$

and

$$w = a(1 + BZ/H)^{-1}. \qquad (10)$$

The integrals $\int_{a_0}^{a} (Z/a)\,da$ as well as $\int_{w_0}^{w} (Z/w)\,dw$, where a_0 and w_0 denote the lowest measured values, were evaluated by the trapezoidal rule, thus no smoothing was involved. To obtain $\int_0^{a_0} (Z/a)\,da$ and $\int_0^{w_0} (Z/w)\,dw$ the parabola fitting the lowest three $(Z/a) = f(a)$ and $(Z/w) = f(w)$ points was assumed to represent the experimental points at values where no data are available.

In any case the same n values were obtained if either $G(a)$ or $\Phi(w)$ was employed to approximate the data. In order to save space only the functions originating from (7) are given. At each acidity studied a satisfactory agreement, within the limits of experimental error, could be found between the $\log G(a)(\log a)$ data and the normalised functions $Y(\log v)_L$ in which

$$Y = \log G - \log K_6 = \log (6 + 4Lv^{-2} + v^{-5}) \quad (11)$$

$$\log v = \log a + (1/5)\log K_6 - (1/5)\log K_1 \quad (12)$$

$$L = K_4(K_6^3 K_1^2)^{-(1/5)}. \qquad (13)$$

On the other hand large systematic trends were observed with any other model representing the presence of only three complexes. We may thus conclude that the data of present accuracy are explained with the formation of $Ti(OH)_t F^{3-t}$, $Ti(OH)_p$, F_4^{-t} and $Ti(OH)_t F_6^{-t-2}$.

The conditional constants given in Table 2 were computed, using (11)–(13), from the differences $\log G - Y$, $\log v - \log a$ and L read off in position of best fit. Practically coincident results for K_1 and K_4 were obtained with either (7) or (8), whereas $\log K_6$ values higher than 0.3 units were found when (7) was replaced by (8). The discrepancy however introduces no uncertainty in the evaluation of n of the main species.

The most probable number of OH$^-$ *in* $Ti(OH)_t f_n^{4-t-n}$

To evaluate t in the reaction products the dependence on H of the apparent constants was examined according to (9). Clearly, correct conclusions on t and $\beta_{t,n}$ may be reached only if we are able to estimate the activity coefficient changes caused by the replacement of a large part of the medium ion Na$^+$ with H$^+$. However, since from structural considerations p is expected to be a small integer, the determination of t of the predominating species should be only slightly influenced putting $F_{t,n} = 1$ in (9). On the other hand, activity coefficient variations cannot be neglected if the evaluation of t for minor complexes and if more accurate $\beta_{t,n}$ are required. The calculations presented in this section assume $F_{t,n} = 1$. Medium effects are taken into account in the next section as it was impossible to consider them simultaneously with the evaluation of t.

The plots of $\log K_1$ and $\log K_4$ against $\log H$ could be well described by straight lines of slope 1 and 2, respectively, thus indicating the presence of $Ti(OH)_2F^+$ and TiF_4. The constants $\beta_{2,1}$ and $\beta_{0,4}$ of Table 3 were calculated as the average of $\log K_1 + \log H$ and $\log K_4 + 2 \log H$.

Analysis of the $K_6(H)$ function led to different conclusions. The quantity $\log K_6 + 3 \log H$, evaluated using approximation (8) was found to be constant indicating the formation of $HTiF_6^-$ with a constant $\beta_{-1,6}$ given in Table 3. On the contrary $K_6 H^{-3}$ values obtained using (7) showed a systematic trend with H which might be due to either medium effects or additional species. Most probably, as it will result from the treatment of the next section, the trend stems from the approximation $F_{-1,6} = $ constant.

Refinement of the equilibrium constants

The calculations of the previous sections were based on equations of limited validity and moreover on the assumption that no significant activity coefficient changes occur when Na$^+$ is exchanged with H$^+$. It was therefore desirable to prove the

Table 2. The conditional constants, K_n, in 3 M (Na, H)Cl media

H, M	$\log K_1$	$\log K_4$	$\log K_6$ eq (7)	$\log K_6$ eq (8)
0.25	2.86 ±0.05	9.58 ±0.1	13.06 ±0.03	13.40 ±0.03
0.50	2.50 ±0.05	8.83 ±0.1	12.25 ±0.03	12.45 ±0.03
1.00	2.20 ±0.05	8.29±0.08	11.55 ±0.03	11.57 ±0.02

Table 3. Survey of equilibrium constants, $\beta_{t,n}$

Method	$\log \beta_{2,1}$	$\log \beta_{0,4}$	$\log \beta_{-1,6}$
Dependence of K_n on H, eq (9)	2.20 ± 0.05	8.4 ± 0.1	11.57 ± 0.03
Least-squares, 3 M NaCl	2.28 ± 0.03	8.34± 0.02	11.41 ± 0.01
Least-squares, 2.7 M ClO$_4^-$	2.38 ± 0.03	8.57± 0.02	11.77 ± 0.01

formation of minor species and to refine the constants with more exact procedures.

The experimental data were treated with Sillén's powerful least-squares method Letagrop.[6] The computation consisted in the minimization of the sum

$$U = \sum (Z_c - Z)^2 \qquad (14)$$

where Z_c designates values of Z calculated with a certain set of assumed constants.

As a first run we tested the hypothesis involving the formation of $Ti(OH)_2F^+$, TiF_4 and $HTiF_6^-$. Then we took account for medium changes according the specific interaction theory (SIT).[7,8] The molal activity coefficient γ_i of the species i, defined so that $\gamma_i \to 1$ as the molality of i, m_i, tends to zero in the solvent salt 3.2 m NaCl, may be expressed in NaCl–HCl mixtures of constant chloride molality by

$$\log \gamma_i = (b(i, H^+) - b(i, Na^+)) m_{H^+} \qquad (15)$$

in which b is the symbol of the interaction coefficient. According to the theory $b = 0$ for positively charged i. As a consequence the formation equilibria of $Ti(OH)_2F^+$ and TiF_4 should not be sensibly affected by the substitution of Na^+ with H^+ since, as supported by the estimates of the next section, reagents and products are neutral or positively charged. On the contrary the equilibrium leading to $HTiF_6^-$ should be influenced to the extent to which $b(HTiF_6^-, H^+)$ differs from $b(HTiF_6^-, Na^+)$. In other words the medium effects are accounted for by

$$\log F_{-1,6} = \xi H \qquad (16)$$

where ξ includes interaction coefficients as well as conversion terms from molality to molarity. Being not able to guess the probable ξ value, we considered it as an unknown parameter to be determined simultaneously with $\beta_{-1,6}$. When ξ was adjusted to vary together with the constants $\beta_{2,1}$, $\beta_{0,4}$ and $\beta_{-1,6}$ U decreased by more than 50%. The minimum was found with $\xi = 0.17$ and the constants listed in Table 3. These are seen to agree well with the graphical evaluation. The uncertainty of the Letagrop constants is 3 times the standard deviation and is lower of the maximum error estimated by curve-fitting.

As the most important measure of the fit between experimental data and the proposed model let us consider Fig. 2, where $(Z_c - Z)/Z$ is plotted as a function of Z. From a total 67 points 33 are found to show positive and 34 negative deviations. The average positive deviation amounts to 3.7%, the average negative to 2.9%. The magnitude and the sign of the deviations do not exhibit appreciable trend with H and Z.

Calculations were carried out also by assuming, besides $Ti(OH)_2F^+$, TiF_4 and $HTiF_6^-$, other conceivable species like $Ti(OH)F^{2+}$, $Ti(OH)_2F_2^{2+}$, TiF_5^-. However no significant lower minima were afforded to make plausible the presence of detectable amounts of such minor species in the concentration range investigated.

The influence of the Cl^- ions on the complex formation

The probable number of Cl^- ions bound to $Ti(OH)_2^{2+}$ and to the fluoride complexes can be
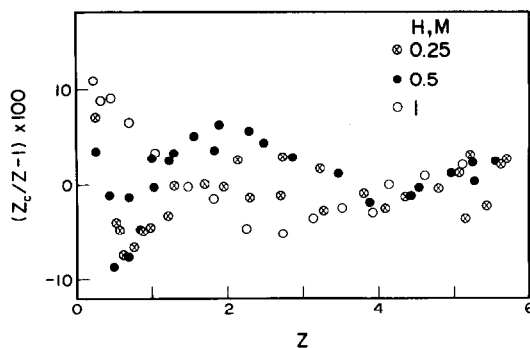
Fig. 2. Illustration of the fit between experimental data and the model represented by the equilibrium constants of the second row of Table 3 and $\xi = 0.17$ (eqn 16). Points for 3 M Cl^-: $(Z_c/Z - 1) \times 100$ as a function of Z.

estimated from the differences between equilibrium constants determined in solutions where Cl^- is replaced by ClO_4^-. If we neglect as first approximation changes of the activity coefficients and postulate that $Ti(OH)_2^{2+}$ and the $Ti(OH)_iF_n^{4-i-n}$ species do not form complexes with ClO_4^-, then we may conclude from the small difference between the constants valid in 3 M NaCl and those found from the special measurements in 2.7 M ClO_4^-, 0.3 M Cl^- medium, given in Table 3, that titanium chloride complexes are hardly detectable in 3 M NaCl.

In order to explain quantitatively the magnitude of the $\beta_{i,n}(ClO_4^-) - \beta_{i,n}(Cl^-)$ differences, the variation of the activity coefficients when Cl^- is replaced by ClO_4^- was evaluated with the SIT.[7,8] By assimilating $Ti(OH)_2^{2+}$ and $Ti(OH)_2F^+$ to Mg^{2+} and Li^+, respectively, and setting equal to zero the interaction coefficients of neutral species, the constants

$$\log \beta_{2,1} = 2.5_1 \pm 0.10$$

$$\log \beta_{0,4} = 8.7_4 \pm 0.10$$

$$\log \beta_{-1,6} = 11.7_6 \pm 0.10$$

were estimated to hold in 3 M $NaClO_4$. For the calculations the interaction coefficients listed in Ref. 8 were employed. The coincidence of experimentally determined with predicted constants corroborates the hypothesis that chloride complexes are formed in negligible extent in 3 M NaCl solutions.

Comparison with the results of previous work

The fluoride complex formation has been the subject of a number of investigations.

In 1952, Kleiner[9] determined spectrophotometrically, in 0.1 M HNO_3, temperature not stated, the equilibrium constant for $[TiO(H_2O_2)]^{2+} + F^- \rightleftarrows TiOF^+ + H_2O_2$ which, combined with the constant of $TiO^{2+} + H_2O_2 \rightleftarrows [TiO(H_2O_2)]^{2+}$, yielded $\log ([TiOF^+] [TiO^{2+}]^{-1}[F^-]^{-1}) = 6.44$.

In 1960, one of the present authors, in cooperation with Caglioti and Liberti,[10] measured, at 25°C in 3 M $NaClO_4$, using a quinhydrone half-cell, the competition of F^- for H^+ and Ti(IV) in the acidity range from 0.05 to 0.2 M. By assuming that no protons were involved in the reaction of TiO^{2+} with F^- the data were explained with $TiOF_n^{2-n}$, $n = 1, 2, \ldots 4$.

The results of the present work prove, however, the inadequacy of that assumption and led the present authors to undertake a recalculation of the earlier (B, H^*, A, h) data. Here H^* stands for the H^+ analytical concentration excess counting H_2O, Ti^{4+} and F^- as zero level. The function

$$R = \frac{A + h - (H^* + 2B)}{B}$$

$$= \frac{\sum P[Ti(OH)_t F_n^{4-t-n}]}{[Ti(OH)_2^{2+}] + \sum [Ti(OH)_t F_n^{4-t-n}]} \quad (17)$$

was first constructed. Then the various hypotheses were tested by minimizing the error sum $\sum (R_c - R)^2$ in which R_c is a value calculated with a set of assumed constants. For $R > 2$ the constants of the third row of Table 3 gave ($R_c - R$) values of the expected order of magnitude, e.g. a few percent, whilst deviations as large as 20% were observed for lower R. In consideration of the inferior acidity the deviations were ascribed to additional species. As a matter of fact, $Ti(OH)_2F_2$ and TiF_6^{2-}, with equilibrium constants, respectively, of $10^{4.5}$ M^0 and $10^{10.9}$ M^{-2}, improved considerably the fit. A practically coincident minimum was, however, obtained by replacing $Ti(OH)_2F_2$ with $Ti(OH)_3F$ and probably a better agreement would involve other conceivable species. In conclusion these results are in substantial concordance with those of the present work, although the limited accuracy of the earlier measurements does not allow an independent and unequivocal interpretation. Nabivanets[11] as well as Parpiev and Maslennikov[12] have studied the distribution equilibria between titanium chloride solutions and ion exchange resins. Nabivanets explained his data in 0.2 M HCl in terms of $TiOF_n^{2-n}$, $n = 1, \ldots 4$, while Parpiev and Maslennikov estimated from measurements in 0.5 M HCl a constant of about 6.3×10^3 for $TiF_5^- + F^- \rightleftarrows TiF_6^{2-}$. A satisfactory explanation of the distribution data is made difficult by the lack of experimental details.

DISCUSSION

Most often the titanyl ion, formulated here as $Ti(OH)_2^{2+}$, has been assumed to describe the ti-

tanium(IV) solution chemistry. The results of the present work show, on the contrary, how the central group loses its identity through the removal of OH^- by F^-. As a consequence a quantitative explanation of the successive complexation equilibria can be achieved only using approaches suitable for the investigation of a ternary system $(Ti(IV) - H^+ - F^-)$, i.e. the knowledge of two variables, h and a, in as wide a range as possible.

It is intended to extend the study to acidities enclosing the limits from 0.05 to 10 M. At $h < 0.25$ M, in addition to hydrolytic species, the complexes $Ti(OH)_2F_2$ and $Ti(OH)_2F_3^-$ are favoured. On the other hand, measurements obtained in the $h > 1$ M range should contain information on TiF_n^{4-n} with $n < 4$. In a new attack of the system one should provide e.m.f. data more accurate than 0.2 mV. The detection of TiF_5^-, whose limited range of existence has to be connected with structural changes from TiF_4 to $HTiF_6^-$, is committed to the improvement of the potentiometric measurements.

REFERENCES

[1] L. Ciavatta, D. Ferri and G. Riccio, To be published.
[2] G. Biedermann, Acta Chem. Scand. 1956, 10, 1340.
[3] L. Ciavatta, Arkiv Kemi 1963, 21, 129.
[4] R. Berg and M. Teitelbaum, Z. analyt. Chem. 1930, 81, 1.
[5] L. Ciavatta, D. Ferri, I. Grenthe and F. Salvatore, Inorg. Chem. 1981, 20, 463.
[6] L. G. Sillén, Acta Chem. Scand. 1962, 16, 159.
[7] G. Biedermann, On the Nature of Sea Water, Dahlem Konferenzen, Berlin, 1975.
[8] L. Ciavatta, Ann. Chim. (Rome) 1980, 70, 551.
[9] K. E. Kleiner, Zhur. Obshchei Khim. 1952, 22, 17, as quoted in C.A. 46, 6027b.
[10] V. Caglioti, L. Ciavatta and A. Liberti, J. Inorg. Nucl. Chem. 1960, 15, 115.
[11] B. I. Nabivanets, Ukr. Khim. Zhur. 1966, 32, 886, as quoted in C.A. 65, 19360b.
[12] N. A. Parpiev and I. A. Maslennikov, Uzb. Khim. Zhur. 1967, 11, 21, as quoted in C.A. 69, 54827t.

COMPLEXES OF VITAMIN B₆—XV†
QUATERNARY COMPLEXES INVOLVING PYRIDOXAMINE, GLYCINE AND ETHYLENEDIAMINE WITH Co(II), Ni(II), Cu(II) and Zn

HAYAT M. MARAFIE, MOHAMMED S. EL-EZABY* and AHMAD S. SHAWALI‡
Department of Chemistry, Faculty of Science, University of Kuwait, Kuwait

Abstract—The formation constants of quaternary Co(II), Ni(II), Cu(II) and Zn complexes comprising pyridoxamine as a first, glycine as a second and ethylenediamine as a third ligand were determined by pH-metric titration at I = 0.5 M NaNO₃ and 30°. The complexes are generally protonated in which the ligands may act as bidentate as well as monodentate. The formation of the quaternary species is discussed in relation to pertinent binary and ternary species. The validity of the Van Panthaleon van Eck equation was also tested.

Pyridoxamine (Pm), glycine (Gly) and ethylenediamine (en) are of considerable interest in biological studies, since they are present in significant amounts in all cells. Pyridoxamine, a vitamin B₆ compound, may act as a coenzyme for reactions of carbonyl compounds.[1] Glycine is one of the amino acids constituting proteins and has been of considerable interest as models for metal-proteins reactions.[2] Ethylenediamine and other polyamines were found to be involved in catalytic reactions and act in the transfer of metal ions in peptide complexes.[3] These ligands were proved to form stable binary complexes with some divalent metal ions.[4,5] They have been involved in some ternary complex formation with Co(II), Ni(II), Cu(II), Zn and Cd ions.[4,5] However, quaternary complexes comprising the three ligands were not studied. These complex equilibria may act as a model for the cluster of ligands around a trace metal ion in biological systems. They may describe the functions of some vitamin B₆-dependent enzymes. In addition, they may give a clue for their role in humans if the complexes are introduced as chemotherapeutic agents.

EXPERIMENTAL

Materials

Pyrodoxaminedihydrochloride   [Pm(HCl)₂]
(Fluka AG), and glycine (Gly) (BDH) was used as

---

†Part XIV. Kinetics and Reaction Mechanism of the Interaction of Pyridoxal-5-phosphate with Cu(II)-Pyridoxamine Complexes, *Inorg. Chim. Acta.* in press.

‡Present address: Chemistry Department, Faculty of Science, Cairo University, Cairo, Egypt.

*Author to whom correspondence should be addressed.

supplied. Ethylenediamine (en) was purified by distillation under reduced pressure. The concentration of the stock solutions of the ligands (0.1 M) were checked potentiometrically. Only en (0.1 M) was acidified with HNO₃ (0.2 M). The concentration of the stock solutions of Co(II), Ni(II), Cu(II) and Zn nitrates were checked complexometrically, by using potentiometric methods, utilizing a Radiometer Cupric Selective Electrode.[6]

Equipment

A Radiometer pH-meter model 63, equipped with Radiometer combination electrode type GK 2301C was used to follow the pH during the titration of sample solutions of ligands in the absence or presence of metal ions. A Radiometer autoburette model ABU 12 was used to deliver the titrant (0.1 M carbonate-free NaOH).

Methods

Titrations were carried out as previously described.[7] The concentration of the ligands never exceeded twice that of the metal ions. Titration data were taken at 30°C and at an ionic strength of 0.5 M NaNO₃. Purified nitrogen was surged in the solutions of Co(II) system during titration. The direct pH-meter readings were used in the calculations. The pK$_w$ value was taken as 13.75 at I = 0.5 and T = 30°C[8].

The MINIQUAD-75 program was used to assess the titration data.[9] The procedures for selecting the correct equilibrium model were described in previous report.[7] All equilibrium constants were calculated from at least six titration curves of different concentration ratios of metal ions and ligands.
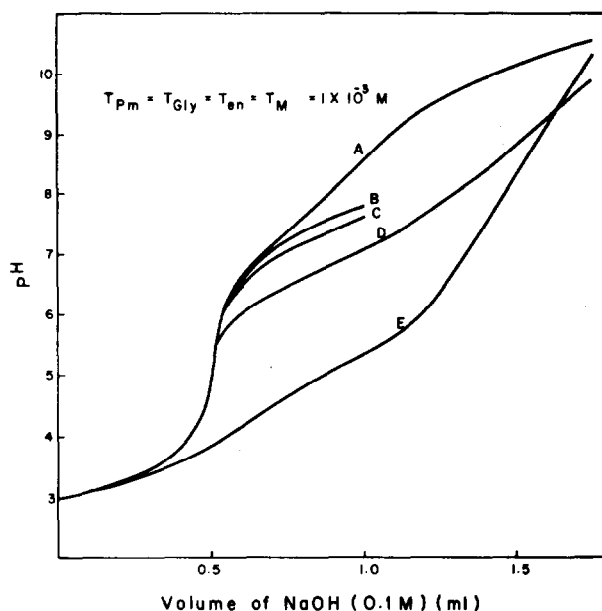
Fig. 1. Typical titration curve of the quaternary systems involving Pm, Gly and en with various metal ions. A, ligands only; B, Zn; C, Co(II); D, Ni(II); and E, Cu(II).

RESULTS AND DISCUSSION

Figure 1 shows typical titration curves for Co(II), Ni(II), Cu(II) and Zn in the presence of equivalent amounts of Pm, Gly and en. Precipitation occurs above pH 8.0 only in Zn system when the composition ratio is $1:1:1:1$, (Pm : Gly : en : Zn). The quaternary complex formation may be represented by the following reaction,

$$l \, Pm^- + p \, Gly^- + q \, en + r \, M^{2+} + s \, H^+ \rightleftharpoons$$

$$(M_r Pm_l Gly_p en_q H_s)^Z \quad (1)$$
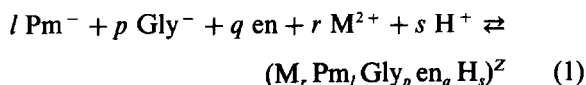
where l, p, q, r and s are the stoichiometric coefficients and $Z = (2r + s) - (l + p)$.

In order to determine the formation constants of the equilibria represented by reaction (1) using program MINIQUAD-75, the relevant constants of the binary and ternary complexes should be known together with the protonation constants of the ligands. However, not all these constants were determined.[4,5] The only systems which were not investigated were those of M-Gly-en. Table 1 depicts the values of the ternary complex formation constants for Co(II), Ni(II), Cu(II) and Zn with Gly and en determined under the experimental conditions of this work. Some of the values were estimated assuming that the difference in the formation constants between e.g. 01110 and 01111 is independent of the metal type Cu(II) is excepted) and that log β's for different metal ternary complexes is linear function of the sum of the log

of the 1st protonation constants of their ligands (Fig. 2).

The values of formation constants of the quaternary systems expressed for the equilibrium reaction (1) are recorded in Table 2. At least 20 sets of complexes for each system were examined using MINIQUAD-75. The criteria of model choice were as previously reported.[7] Table 2 shows that most of the quaternary complexes are protonated even at higher pH's than in ternary and binary species indicating that the protons may be located on the Pm moiety as in $1:1:1:1:1$ and $1:1:1:1:2$ and
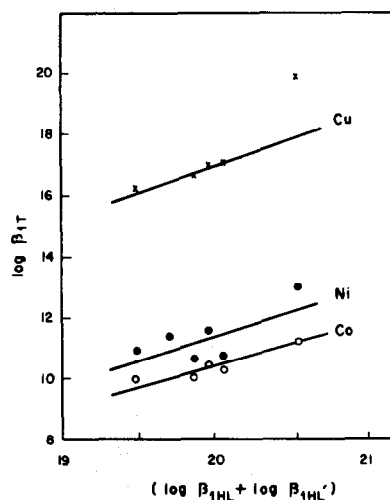
Fig. 2. The formation constants of the ternary species in the log forms in their dependence on the sum of log forms of the 1st protonation constants of the ligands.

Table 1. The formation constants of the ternary complexes of Co(II), Ni(II), Cu(II) and Zn involving Gly and en at I = 0.5 M $NaNO_3$ and T = 30°C. n = number of data points, σ = standard deviation

M	l	p	q	r	s	log β(σ)	n	pH range	Reported
Co(II)	0	1	1	1	0	11.05*	228	6.1 - 8.2	
	0	1	1	1	1	18.17*			
	0	1	1	1	2	26.05 (.01)			
Ni(II)	0	1	1	1	0	11.38 (.05)	299	6.0 - 8.0	12.55
	0	1	1	1	1	19.26*			
	0	1	1	1	2	26.38 (.01)			
	0	1	2	1	0	16.19 (.02)			15.51
	0	2	1	1	0				18.45
Cu(II)	0	1	1	1	0	16.20*	261	2.7 - 6.9	
	0	1	1	1	1				
	0	1	1	1	2	27.54 (.01)			
	0	2	1	1	4	44.64 (.01)			
	0	2	1	1	2	34.34 (.04)			
	0	1	2	1	4	48.15 (.01)			
Zn(II)	0	1	1	1	0	10.23(.02)	201	6.1 - 8.2	
	0	1	1	1	1	18.11 (.01)			
	0	1	1	1	2	25.23*			
	0	1	2	1	0	15.79 (.01)			

* Est. values.

on Gly or en or both as in 1 : 1 : 1 : 1 : 3 and 1 : 1 : 1 : 1 : 4. Moreover, the existence of quaternary species with two ligand molecules of the same kind could not be proved.

A good linear relationship is found between log formation constants of the quaternary complexes (log β_{1Q}) and the second ionization potential (I_2) of the metal ions under consideration (Zn is excepted) which prove the validity of Van panthaleon van Eck equation[10] (Fig. 3).

$$\log \beta_{1Q} = A(I_2 - B) \qquad (2)$$

where A and B are constants depending on the ligand and the experimental conditions but independent of metal ions; A depends on the number of donor atoms and the polarizability of ligands, while B is characteristic of the donor atoms. The values of A decreases as the number of protons increases in the complex. They are 3.14, 2.56 and 0.8 for 1 : 1 : 1 : 1 : 1, 1 : 1 : 1 : 1 : 2 and

1 : 1 : 1 : 1 : 4, respectively. This observation indicates a decrease in the number of the ligating atoms, as the number of protons increases in the complex. This linear relationship of log β_{1Q} on I_2 made it possible to predict values of log β_{1Q} of Cu(II) system for 1 : 1 : 1 : 1 : 0 and 1 : 1 : 1 : 1 : 3, species (Table 2). The difficulty in obtaining an equilibrium model including the latter two species for Cu(II) system may be due to structural factors. In case of the 1 : 1 : 1 : 1 : 0 species an octahedral structure should be expected which is not as stable as in the Ni(II) and Co(II) systems. On the other hand, steric hindrance may be excercised more in the Cu(II) square planar complex of 1 : 1 : 1 : 1 : 3 species. It is unfortunate that log β_{1Q} for Zn complexes cannot be fitted in the above linear relationship invalidating eqn (2).

The affinity of the ternary complexes M Pm Gly H_s, M Pm en H_s and M Gly en H_s to the ligands en, Gly⁻ and Pm⁻, respectively, to form the quaternary complex species, 1 : 1 : 1 : 1 : sH may be

Table 2. Log values of quaternary complexes of Cu(II), Ni(II), Co(II) and Zn involving Pm, Gly and en at I =). 5 M NaNO$_3$ and T = 30°C. S = sum of squared residuals, Xi^2 = Chi square

M	Stoichiometric coefficients l p q r s	logβ(σ)	(S)x10^7	Xi^2	R	n	pH range
Co(II)	1 1 1 1 4	48.39(.01)	31	15	0.010	166	7.3-9.5
	1 1 1 1 3	40.36(.01)					
	1 1 1 1 2	32.91(.01)					
	1 1 1 1 1	23.56(.01)					
	1 1 1 1 0	14.64(.01)					
Ni(II)	1 1 1 1 4	48.14(.01)	12.6	477	0.015	245	6.3-10.2
	1 1 1 1 3	40.98(.02)					
	1 1 1 1 2	34.38(.01)					
	1 1 1 1 1	26.26(.01)					
	1 1 1 1 0	17.20(.01)					
Cu(II)	1 1 1 1 4	50.22(.01)	3.2	20	0.007	201	4.0-9.5
	1 1 1 1 3	43.2*					
	1 1 1 1 2	39.77(.01)					
	1 1 1 1 1	32.46(.01)					
	1 1 1 1 0	25.5*					
Zn(II)	1 1 1 1 4	48.82(.01)	1.9	46	0.009	128	7.1-9.5
	1 1 1 1 3	41.19(.01)					
	1 1 1 1 2	33.77(.01)					
	1 1 1 1 1	25.40(.01)					
	1 1 1 1 0	16.25 (.01)					

* Est. value.
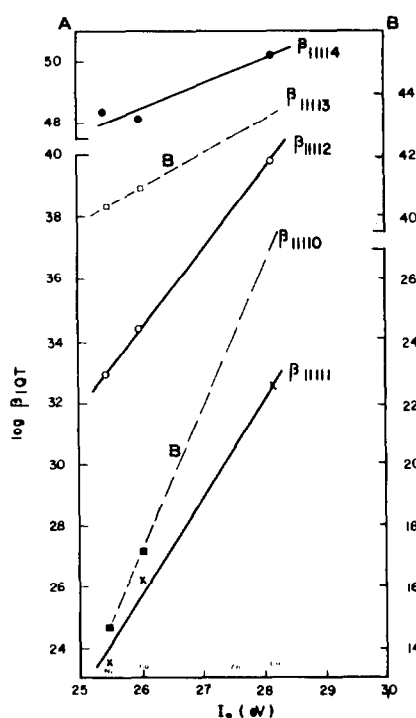
Fig. 3. The dependence of log β_{1Q} on the ionization potential (I$_2$) of the metal ions for different quaternary species.

visualized if one considers the following equilibria:
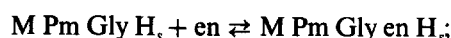
$$M\ Pm\ Gly\ H_s + en \rightleftarrows M\ Pm\ Gly\ en\ H_s;$$

$$K^I = \beta_{1Q}/\beta_{MPmGlyH_s} \qquad (3)$$

$$M\ Pm\ en\ H_s + Gly^- \rightleftarrows M\ Pm\ Gly\ en\ H_s;$$

$$K^{II} = \beta_{1Q}/\beta_{M\ Pm\ en\ H_s} \qquad (4)$$
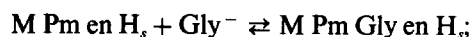
$$M\ Gly\ en\ H_s + Pm^- \rightleftarrows M\ Pm\ Gly\ en\ H_s;$$

$$K^{III} = \beta_{1Q}/\beta_{M\ Gly\ en\ H_s} \qquad (5)$$

where $\beta_{M\ Pm\ Gly\ H_s}$, $\beta_{M\ Pm\ en\ H_s}$ and $\beta_{M\ Gly\ en\ H_s}$ are the formation constants of the ternary complexes.[4,5] Table 3 lists the log values of K^I, K^{II} and K^{III} whenever their calculation is permissible. It appears that reactions (3) and (5) are more favorable than reaction (4).

The formation of quaternary complex may also arise from the interaction of three different binary complexes or one binary species with one ternary species or even from the combination of two different ternary complexes.

Different combination of binary complexes may lead to the formation of the 1 : 1 : 1 : 1 : sH quaternary complex. However, a detailed description

Table .3. Log K values expressed by eqns (3)–(14)

Stoichiometric coefficients l p q r s	log K	Co	Ni	Cu	Zn
1 1 1 1 0	log K^{I}	4.15	5.66	8.51	-
1 1 1 1 1		5.18	6.69	7.85	-
1 1 1 1 0	log K^{II}	3.41	4.18	5.65	5.88
1 1 1 1 1		3.78	4.69	5.23	6.48
1 1 1 1 0	log K^{III}	3.59	5.82	9.30 .	6.59
1 1 1 1 1		5.39	7.76	-	7.29
1 1 1 1 0	log K^{IV}	-1.08	-2.70	-3.51	-0.47
1 1 1 1 1		-1.19	-1.16	-2.61	-0.55
1 1 1 1 0	log K^{Va}	-4.99	-5.55	-4.88	-3.69
1 1 1 1 1		-13.04	-12.90	-16.45	-10.19
1 1 1 1 0	log K^{Vb}	-5.76	-6.59	-7.96	-3.95
1 1 1 1 1		-4.80	-6.41	-11.24	-2.33
1 1 1 1 0	log K^{Vc}	-4.64	-4.44	-4.61	-2.50
1 1 1 1 1		-3.72	-4.27	-7.89	-1.08
1 1 1 1 0	log K^{VI}	-2.02	-0.70	-1.12	-
1 1 1 1 1	(n=0,m=1)	-1.55	-0.19	-1.54	-
1 1 1 1 1	(n=1,m=0)	-0.99	0.33	-1.78	-
1 1 1 1 2	(n=0,m=2)	0.85	1.08	0.25	-
1 1 1 1 2	(n=1,m=1)	-0.09	-0.10	-1.85	-
1 1 1 1 3	(n=1,m=2)	-	-	-	2.20
1 1 1 1 4	(n=1,m=3)	-	-	-1.90	-
1 1 1 1 0	log K^{VII}	-2.13	-0.17	-	-
1 1 1 1 1	(n=0,m=1)	-0.33	1.01	-	-
1 1 1 1 1	(n=1,m=0)	-1.10	.86	-	-
1 1 1 1 2	(n=0,m=2)	1.14	2.01	2.96	-
1 1 1 1 2	(n=1,m=1)	1.13	1.10	-	-
1 1 1 1 3	(n=1,m=2)	0.70	0.58	-	-
1 1 1 1 3	(n=3,m=0)	-	-	-	1.15
1 1 1 1 0	log K^{VIII}	-1.75	0.49	0.52	1.80
1 1 1 1 1	(n=0,m=1)	0.05	1.67	-	3.07
1 1 1 1 1	(n=1,m=0)	-1.28	1.00	0.10	2.40
1 1 1 1 2	(n=1,m=1)	0.95	2.27	-	2.89
1 1 1 1 2	(n=0,m=2)	1.52	2.67	3.45	4.32
1 1 1 1 2	(n=2,m=0)	1.12	2.27	-	3.92
1 1 1 1 3	(n=1,m=2)	0.52	0.72	-0.50	3.19
1 1 1 1 3	(n=2,m=1)	1.45	0.99	-	3.46
1 1 1 1 4	(n=2,m=2)	1.60	1.03	1.02	3.97
1 1 1 1 0	log K^{IX}	-1.47	-0.84	-0.92	0.14
1 1 1 1 1	(n=1,m=0)	-1.58	0.70	-0.02	-1.16
1 1 1 1 1	(n=0,m=1)	-0.33	0.34	-	1.40
1 1 1 1 2	(n=0,m=2)	1.80	1.34	2.01	2.66
1 1 1 1 2	(n=1,m=1)	-0.65	0.94	-	-1.65
1 1 1 1 3	(n=1,m=2)	0.22	0.42	-0.62	1.95
1 1 1 1 0	log K^{X}	-1.36	-1.37	-2.07	-1.19
1 1 1 1 1		-0.99	-0.86	-2.49	1.73

HAYAT M. MARAFIE *et al.*

Table 3. (*Contd*)

Stoichiometry coefficients l p q r s	log K	Co	Ni	Cu	Zn
1 1 1 1 2		0.79	0.41	-0.68	3.31
1 1 1 1 0	log K^{XI}	-2.60	-2.03	-2.56	
1 1 1 1 1		-0.70	-1.00	-3.22	-
1 1 1 1 3		-	-	-	0.54
1 1 1 1 0	log K^{XII}	-1.26	1.05	3.20	0.96
1 1 1 1 1	(n=1,m=0)	0.34	1.22	0.19	2.67
1 1 1 1 1	(n=0,m=1)	0.54	2.23	-	2.23
1 1 1 1 2	(n=0,m=2)	2.01	3.23	6.13	3.48
1 1 1 1 2	(n=1,m=1)	1.89	1.46	-	3.08
1 1 1 1 3	(n=1,m=2)	1.46	0.94	-0.41	3.38
1 1 1 1 0	log K^{XIII}	-0.81	-0.41	-1.24	1.71
1 1 1 1 1		-0.34	0.07	-1.66	2.31
1 1 1 1 2		2.06	1.34	0.15	3.83
1 1 1 1 0	log K^{XIV}	-1.29	-1.04	-1.16	-
1 1 1 1 1		-0.26	2.84	-1.82	-
1 1 1 1 3		-	-	-	1.86

of these equilibria depends on the availability of different species. The forthcoming analysis will deal only with symmetric combination of binary complexes. The proton will be assumed to be located on the Pm since most of the binary complexes of Gly and en are unprotonated;

$$MLH_s + ML' + ML'' \rightleftarrows MLL'L''H_s + 2M$$

$$K^{IV} = \beta_{1Q}/\beta_{1ML'}\beta_{1ML''}\beta_{1MLH_s} \qquad (6)$$

$$M(LH_s)_2 + M(L')_2 + M(L'')_2 \rightleftarrows MLL'L''H_s + LH_s + ML' + ML''$$
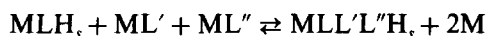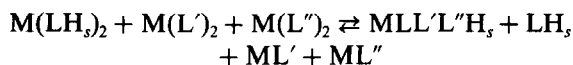
$$K^{V}_{(a)} = \beta_{1Q}\beta_{1ML'}\beta_{1ML''}/\beta_{2MLH_s}\beta_{2ML'2ML''} \qquad (7a)$$

or

$$\rightleftarrows MLL'L''H_s + ML' + MLH_s + L''$$

$$K^{V(b)} = \beta_{1Q}\beta_{1ML'}\beta_{1MLH_s}/\beta_{2MLH_s}\beta_{2ML'}\beta_{2ML''} \qquad (7b)$$

or

$$\rightleftarrows MLL'L''H_s + MLH_s + ML'' + L'$$

$$K^{V(c)} = \beta_{1Q}\beta_{1MLH_s}\beta_{1ML''}/\beta_{2MLH_s}\beta_{2ML'}\beta_{2ML''} \qquad (7c)$$

where LH_s, L' and L'' stand for PmH_s, Gly and en, and β_{1ML}, $\beta_{1ML''}$ and β_{1MLH_s} are the formation constants of the monobility species and β_{2ML}, $\beta_{2ML''}$ and β_{2MLH_s} are the formation constants of the dibinary species. The values of log K^{IV} and K^{V} are depicted in Table 3. It seems that quaternary complex formation are not enhanced via the interaction of

binary species since most of the values of log K^{IV} and log K^{V} are negative. However, it has been proved that ternary complexes of systems involving Pm, Gly and en with Co(II), Ni(II), Cu(II) and Zn can generally coexist with binary species involved in these systems[4, 5]. So it may be reasonable to discuss the formation of $1:1:1:1:sH$ quaternary complexes from the point of the interaction of the $1:1:1:1:sH$ ternary species. This may be viewed from the following equilibria,

$$MLL'H_n + MLL''H_m \rightleftarrows MLL'L''H_s + MLH_t$$
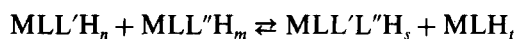
$$K^{VI} = \beta_{1Q}\beta_{1MLH_t}/\beta_{1MLL'H_n}\beta_{1MLL''H_m} \qquad (6)$$

$$MLL'H_n + ML'L''H_m \rightleftarrows MLL'L''H_s + ML'H_t$$
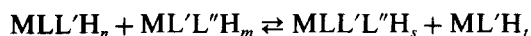
$$K^{VII} = \beta_{1Q}\beta_{1ML'H_t}/\beta_{1MLL'H_n}\beta_{1ML'L''H_m} \qquad (7)$$

$$MLL''H_n + ML'L''H_m \rightleftarrows MLL'L''H_s + ML''H_t$$
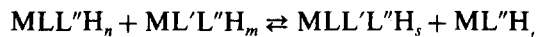
$$K^{VIII} = \beta_{1Q}\beta_{1ML''H_t}/\beta_{1MLL''H_n}\beta_{1ML'L''H_m} \qquad (8)$$

where $\beta_{1MLL'H_m}$, $\beta_{1MLL''H_m}$, $\beta_{1ML'L''H_M}$ and $\beta_{1MLLL''H_n}$ are the formation constants for the ternary species mentioned in the above equilibria and $n + m = s + t$ (the number of hydrogen atoms). The values of log K's are recorded in Table 3. Although, other ternary species than $1:1:1:sH$ may be also involved in quaternary complex formation, yet they are of minor importance due to their lower relative concentrations.[4,5]

Since some binary species may exist with some ternary species, their interactions are unavoidable.
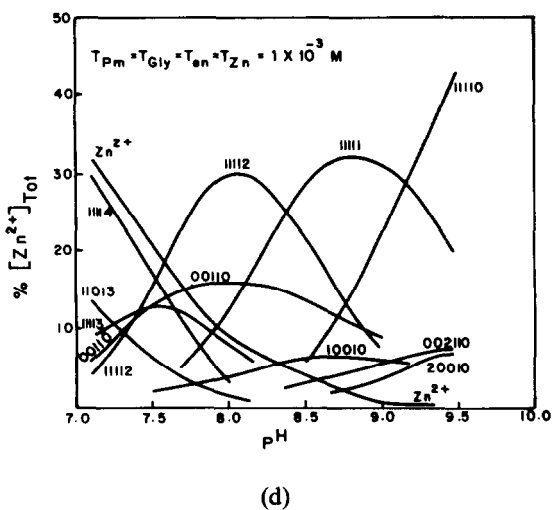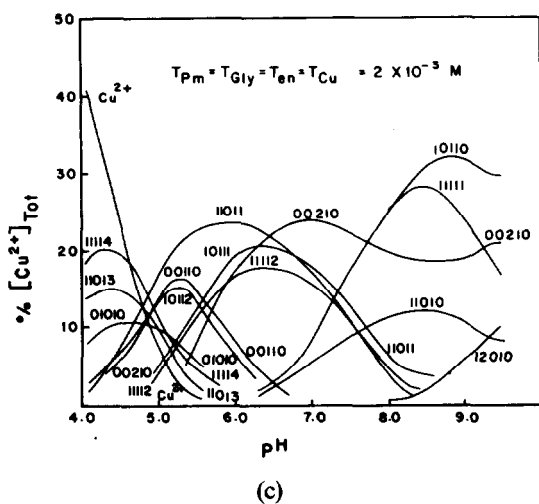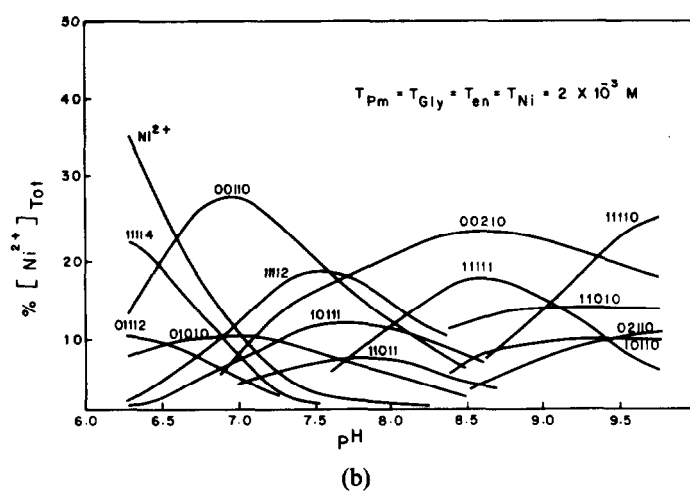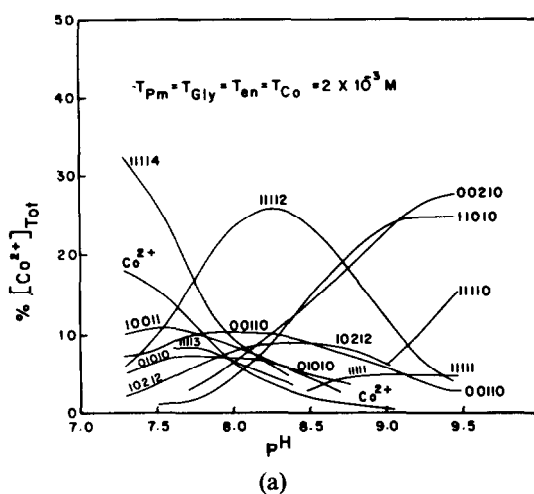
Fig. 4. Distribution diagrams of the quaternary system as function of pH. (a) Co-Pm-Gly-en, (b) Ni-Pm-Gly-en, (c) Cu-Pm-Gly-en, (d) Zn-Pm-Gly-en.

The following possibilities are only representative and probably the most important;

$$MLH_n + ML'L''H_m \rightleftarrows MLL'L''H_s + M,$$

$$K^{IX} = \beta_{1Q}/\beta_{1MLH_n}\beta_{1MLL'L''H_m} \qquad (9)$$

$$ML' + MLL''H_s \rightleftarrows MLL'L''H_s + M,$$

$$K^{X} = \beta_{1Q}/\beta_{1ML'}\beta_{1MLL''H_s} \qquad (10)$$

$$ML'' + MLL'H_s \rightleftarrows MLL'L''H_s + M,$$
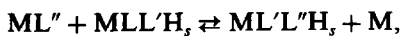
$$K^{XI} = \beta_{1Q}/\beta_{1ML''}\beta_{1MLL'H_s} \qquad (11)$$

$$M(LH_n)_2 + ML'L''H_m \rightleftarrows MLL'L''H_s + MLH_n$$
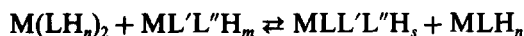
$$K^{XII} = \beta_{1Q}\beta_{1MLH_n}/\beta_{2MLH_n}\beta_{1ML'L''H_m} \qquad (12)$$

$$ML'_2 + MLL''H_s \rightleftarrows MLL'L''H_s + ML$$
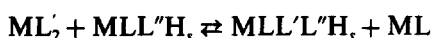
$$K^{XIII} = \beta_{1Q}\beta_{1ML}/\beta_{1MLL''H_s}\beta_{2ML'} \qquad (13)$$

$$ML''_2 + MLL'H_s \rightleftarrows MLL'L''H_s + ML''$$
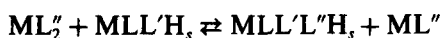
$$K^{XIV} = \beta_{1Q}\beta_{1ML''}/\beta_{2ML''}\beta_{1MLL'H_s}, \qquad (14)$$

The values of $\log K^{IX-XIV}$ are shown in Table 3. There is a certain degree of enhancement of quaternary complex formation through some of the above equilibria specially for $1:1:1:1:2$ species.

If we assume that chemical and electrical attraction between the metal ion and the ligand are independent of ligands already attached, then the magnitude of the stepwise formation constants are determined by statistical considerations. The ratio of the three constants for a bidentate ligand in an octahedral complex is $K_1:K_2:K_3 = 12/1 : 5/2 : 4/15.^{11}$

The ratio which interests us is that between the stepwise formation constant of a tris-complex and that of a bis-complex. This amounts to $8/75$ ($= -0.97$ in log form). Upon consulting Table 3, the values of $\log K^{I-III}$ and most of $\log K^{VI-XIV}$ are greater than -0.97 which indicate various degrees of enhancement of quaternary complex formulation. Only those of $\log K^{IV-V}$ are much less than the statistical value indicating dehancement of quaternary complex formation. The conclusion which may be extracted from these results is that quaternary complexes cannot be simply formed from the interaction of only binary complexes and that ternary complexes should exist for their effective formation. A general conclusion, however, cannot be drawn to rationalize the negative values occurred less than -0.97 among those of $\log K^{VI-XIV}$. The interesting result which is observed for Zn system is that about 95% of the $\log K^{VI-XIV}$ values obtained are highly positive, which means that crystal field stabilization energy is not the only

governing factor in the enhancement of quaternary complex formation.

Figures 4(a–d) show the distribution curves of the binary, ternary and quaternary complexes involving Pm, Gly and en with the metal ions under consideration as function of pH. As it has been mentioned previously,[5] these curves are dependent on the initial concentration of the reactants. In equal concentration of M : Pm : Gly : en a mixture of binary, ternary and quaternary complexes may exist in various ratios. Of course, highly protonated quaternary species (containing 2 protons or more) are present in acidic media and the less protonated (containing 2 protons or less) are in neutral or basic solutions. The predominance of quaternary species may be arranged according to the type of metal ions in their systems as Zn > Co(II) > Ni(II) > Cu(II). In other words, the distribution of Cu(II) among different complexes in Cu(II)-system is more or less identical and there is no preference to quaternary species opposite to what is in Zn system. This may be explained as due to the fact that Zn with a filled d-shell and no ligand field stabilization energy may accommodate the distorted geometry (which may also be acquired by Co, Ni and Cu) without destabilization.

It is worth mentioning that most of the quaternary complexes are positively charged which make them susceptible for easier transportation in biological fluids.

REFERENCES

1. D. E. Metzler, Biochemistry. Academic Press, New York (1977).
2. G. L. Eichorn, Inorganic Biochemistry, Vol. 1. Elsevier, Amsterdam (1973), and Refs therein.
3. H. Sigel, Metal Ions in Biological Systems, Vol. 1. Marcel Dekker, New York (1974), and Refs therein.
4. M. S. El-Ezaby, H. M. Marafie and S. Fareed, J. Inorg. Biochem. 1979, 11, 317.
5. H. M. Marafie, M. S. El-Ezaby, B. Abd. El-Nabey and N. Kittaneh, Trans. Metal. Chem. 1982, 7, 227.
6. Instruction Manual for Cupric Selectrode Type F1112 Cu, Radiometer A/s Copenhagen (1972).
7. M. S. El-Ezaby and T. E. El-Khalafawy, J. Inorg. Nucl. Chem. 1981, 43(4), 831.
8. L. G. Sillen and A. E. Martell, Stability Constants of the Metal Ion Complexes, Spec. Publ. No. 7 (1964), and Supplement No. 1, Spec. Publ. No. 25 (1971). The Chemical Society, London.
9. P. Gans, A. Sabatini and A. Vacca, Inorg. Chim. Acta, 1976, 18, 237.
10. M. T. Beck, Chemistry of Complex Equilibria. Van Nostrand–Reinhold, New York (1970).
11. B. Sen, Anal. Chim. Acta, 1962, 27, 518.

FOURIER TRANSFORM HETERONUCLEAR MAGNETIC TRIPLE RESONANCE IN COMPLEX SPIN SYSTEMS—III†

SYMMETRICAL DITERTIARY PHOSPHINE COMPLEXES OF GROUP VI METAL CARBONYLS

GEOFFREY T. ANDREWS, IAN J. COLQUHOUN and WILLIAM McFARLANE*
Chemistry Department, City of London Polytechnic, Jewry Street, London EC3N 2EY, England

Abstract—Magnetic multiple resonance experiments of the types $^{13}C-\{^{31}P, {}^{1}H\}$, $^{13}C-\{^{1}H\}$ and $^{31}P-\{^{183}W, {}^{1}H\}$ have been used to determine the magnitudes and signs of P–C and P–P coupling constants in the symmetrical complexes $LM(CO)_4$ ($L = Ph_2P(CH_2)_nPPh_2$, $Ph_2PN(H)PPh_2$, $(Ph_2P)_2C=CH_2$, *cis*-$Ph_2PCH=CHPPh_2$; M = Cr, Mo, W; $n = 1$–4). A knowledge of the signs of the couplings shows that they display a systematic pattern of behaviour according to metal atom and ring size and this may have diagnostic value. ^{13}C, ^{31}P and ^{183}W chemical shifts are also reported.

INTRODUCTION

Proton and more recently ^{13}C and ^{31}P NMR spectroscopy has played an important part in the development of the chemistry of phosphine complexes of metal carbonyls. Not only can the technique be used to establish molecular structure and stereochemistry, it can also in principle be used to probe intimate details of electronic distribution and the factors which determine this. For this latter purpose ^{13}C and ^{31}P are probably more valuable than proton NMR, since the shieldings and coupling constants for these two nuclei are more directly affected by the metal atom and are also less subject to external influences such as changes of solvent. However, ordinary proton-decoupled spectra seldom yield all the information necessary for a proper assessment of the relationship between the NMR parameters and electronic structure, and in this paper we describe the results of multiple resonance experiments upon a series of chelating tertiary biphosphine complexes of group VI metal carbonyls which resolve this difficulty. In particular, the magnitudes of the two-bond coupling constants between ^{31}P and the ^{13}C nuclei of the carbonyl groups show a complex pattern of variation[1–4] whose dependence upon the metal and upon the stereochemical relationships can be understood only if the *signs* of the couplings are also known. Additionally, the important homonuclear phosphorus–phosphorus couplings are not normally available directly from simple ^{31}P spectra when the ligands are chemically symmetrical. In order to get the signs of the $^{31}P-^{13}C$ coupling constants it is necessary to perform $^{31}P-\{^{13}C\}$ or $^{13}C-\{^{31}P\}$ selective multiple resonance experiments,[5] the latter being generally the more convenient,[6] but neither type of experiment has been usual in previous work. For the $^{31}P-^{31}P$ couplings considerable effort[7,8] in the past has gone into making complexes with unsymmetrical ligands such as $R_2P(CH_2)_nPR_2'$ where

R and R′ are sufficiently different (e.g. Et and Ph) for there to be a substantial chemical shift difference between the two kinds of phosphorus so as to allow $^2J(PP)$ to be read off directly from the essentially first-order spectra. This method is synthetically demanding and does not give the sign of $J(PP)$. The multiple resonance approach used here is easier synthetically and gives the sign of $J(PP)$ in complexes of symmetrical ligands of possibly greater fundamental importance; it is based upon using spin-tickling experiments[9] for the indirect detection of weak transitions in the spectra from species which are chemically but not magnetically symmetric.[5,6] All of the complexes studied are of the type *cis*-$LM(CO)_4$ with M = Cr, Mo, or W, and L = $(Ph_2P)_2CH_2$ (*dppm*), $(Ph_2P)_2C=CH_2$ (*gem-pp*), $(Ph_2P)_2NH$ (*dpnp*), $Ph_2P(CH_2)_2PPh_2$ (*dppe*), *cis*-$Ph_2PCH=CHPPh_2$ (*cis-vpp*), $Ph_2P(CH_2)_3PPh_2$ (*dppp*), or $Ph_2P(CH_2)_4PPh_2$ (*dppb*). They have octahedral co-ordination at the metal and thus contain two types of CO group—axial and equatorial as in (I). With the exception of [4] and the three *dpnp* derivatives all have been previously reported.[10–13]

(I)
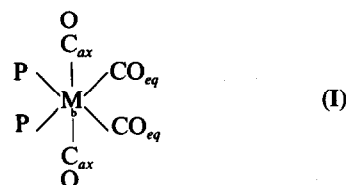
EXPERIMENTAL

All solutions of ligands and their complexes were prepared and manipulated under an atomsphere of gaseous dry dinitrogen. The ligands were made as described elsewhere[6] and were purified by recrystallization; the complexes[10–13] were made by refluxing together stoichiometric amounts of ligand and the appropriate metal hexacarbonyl in diglyme for 12 hr, followed by removal of the diglyme *in vacuo* and recrystallization from $CHCl_3/MeOH$ (1:1). New complexes were: *gem-pp*$Cr(CO)_4$ [4]: Found: C 64.1; H 3.9; $C_{30}H_{22}CrO_4P_2$ requires: C 64.3; H 3.9%. m.p. 197–198°. *dpnp*

---

†For Part II see Ref. 6.
*Author to whom correspondence should be addressed.

$Cr(CO)_4$ [7]: Found: C 61.1; H 3.8; $C_{28}H_{21}CrO_4P_2$ requires: C 61.2; H 3.8%. m.p. 194°. *dpnp* $Mo(CO)_4$ [8]: Found: C 56.5; H 3.6; $C_{28}H_{21}MoO_4P_2$ requires: C 56.7; H 3.5%. m.p. 216°. *dpnp* $W(CO)_4$ [9]: Found: C 49.1; H 3.1; $C_{28}H_{21}WO_4P_2$ requires: C 49.4; H 3.1%. m.p. 205°. The others had properties identical to those previously reported.

The NMR measurements were performed at 22°C upon concentrated solutions in dichloromethane containing ca. 10% C_6D_6 to provide a locking signal for the spectrometer. This was a JEOL FX-60 Fourier transform instrument operating at measuring frequencies of 59.8, 15.0 and 24.2 MHz for ^1H, ^{13}C and ^{31}P respectively. The probes of the spectrometer were modified[5] to permit ^1H-$\{^{31}P\}$, ^{13}C-$\{^{31}P, ^1H\}$ and ^{31}P-$\{^{183}W, ^1H\}$ multiple resonance experiments, the additional radio frequency being provided by a GenRad model 1061 frequency synthesizer which was locked to the master oscillator of the spectrometer. $Cr(acac)_3$ was added to the solutions to facilitate observations of the ^{13}CO signals. Samples were examined in 10 mm o.d. tubes, and prior to Fourier transformation the f.i.d. was weighted so as to maximise the signal-to-noise ratio while retaining sufficient resolution for the purpose in hand.

METHODS AND RESULTS

The proton-decoupled ^{31}P NMR spectra of the complexes (I) consist of a single line due to an A_2 spin system from which it is not possible to derive a value of $J(PP)$ when the two phosphorus atoms are *chemically* equivalent, as is the case with all the molecules studied here. However, the presence of ^{13}C ($I = \frac{1}{2}$, natural abundance 1.1%) at a particular site can lower the *magnetic* symmetry so that the relevant spin system becomes AA'X (A, A' = ^{31}P, X = ^{13}C) and more information is available.[14] It is convenient to distinguish three general cases.

(i) J(*PP*) *is zero or very small*. The main ^{31}P peak (from molecules containing ^{12}C) is flanked by ^{13}C satellites whose positions give the magnitudes of the two ^{31}P-^{13}C coupling constants, and the ^{13}C spectrum is a doublet of doublets. Neither spectrum gives the relative signs of the two ^{31}P-^{13}C coupling constants.

(ii) J(*PP*) *is of moderate size*. The magnitude of $J(PP)$ can be obtained from the positions of the ^{13}C satellites in the ^{31}P spectrum, and their intensity pattern normally makes it possible to get the relative signs of the two ^{31}P-^{13}C coupling constants. The ^{13}C spectrum is a symmetrical five-line pattern having half its intensity in two lines separated by N, the algebraic sum of the two ^{31}P-^{13}C coupling constants, and the remainder in a central ine and two weaker outer lines whose positions depend upon $J(PP)$ and the ^{31}P-^{13}C couplings. Analysis of this pattern can also give a good indication of the magnitude of $J(PP)$.

(iii) J(*PP*) *is large*. The ^{13}C satellites in the ^{31}P spectrum are again in positions which give the values of the various coupling constants, but four of them are too weak to be detected and the other four are close to the central main peak and may be obscured by its wings. The ^{13}C spectrum is a triplet with almost a 1:2:1 intensity distribution, the small amount of intensity missing from the central line being in two outer lines at approx. $\pm J(PP)$, but which are too weak to be detected by normal observation.

The transition between cases (ii) and (iii) depends upon the relative values of the three coupling constants involved, and also upon the capabilities of the spectrometer, but as a very rough guide $|J(PP)| = 50$ Hz usually represents the maximum value that can be measured from a normal spectrum.

For case (ii) it is possible to use straightforward selective heteronuclear double resonance experiments[15] (under conditions of complete proton decoupling) to compare the sign of $J(PP)$ with that of either of the two ^{31}P-^{13}C couplings. Either ^{31}P-$\{^{13}C, ^1H_{noise}\}$ or ^{13}C-$\{^{31}P, H_{noise}\}$ experiments can be used, but the latter are generally more convenient since they avoid the severe dynamic range problems associated with detecting the weak ^{13}C satellites in the presence of a strong ^{31}P signal from molecules containing no ^{13}C. An important feature of this approach is that it can also be applied to case (iii) and used to determine the positions of *all* of the lines including the very weak ones even though only the strong ones are detected directly. This is because no matter how weak a particular line is, it is possible to increase the amplitude of the heteronuclear irradiating field to such a level that tickling effects will be transferred to a strong observed line, and a systematic search over a suitable range of trial frequencies will than give the position of the normally unobservable weak line.[5]

In the complexes studied in the present work the sites where the presence of ^{13}C can lead to the above kind of magnetic inequivalence are the equatorial CO groups, any of the positions in the phenyl groups, and certain of the backbone carbons of the bidentate phosphine ligands. However, a ^{13}C in an axial CO group or a symmetric central position in the backbone (i.e. in *dppm*, *gem-pp*, or *dppp*) leads to an A_2X spin system from which it is not possible to determine either $J(AA)[= J(PP)]$ or the sign of $J(AX)[= J(PC)]$. However, this latter parameter can often be inferred by comparison with another similar coupling.

The experiments involving the aromatic carbons are particularly valuable because they permit almost all of the signs of the coupling constants to be put onto an absolute basis. In practice, the signals from the non-protonated carbons bound to phosphorus were too weak (owing to the long relaxation times and absence of any n.O.e.) to be used conveniently in this way, whilst the couplings to the *para*-carbons were too small. However, in the case of the *ortho*-carbons the determination of $J(PP)$ also gave its sign relative to $N(PC)[= ^2J(PC) + ^4J(PC)]$. Since $^4J(PC) \ll ^2J(PC)$ the sign of $N(PC)$ is also that of $^2J(PC)$ which was found to be positive by comparison with $^3J(PH)$ [itself known[16] to be positive] in a selective ^{13}C-$\{^1H\}$ decoupling experiment. Similar considerations apply to the *meta*-carbons with the added security that $^5J(PC)$ is even smaller. The signs of the various other ^{31}P-^{13}C couplings were then related to that of $J(PP)$ in each complex. At high power levels the ^{31}P irradiation gives complete decoupling in the ^{13}C spectra, and the simplification achieved in this way can be a valuable aid to assignment in certain cases, although this was not really necessary in the present work.

The peaks of the ^{31}P spectra of the tungsten complexes are flanked by satellites arising from coupling to ^{183}W ($I = \frac{1}{2}$, natural abundance = 14%); ^{31}P-$\{^{183}W, ^1H_{noise}\}$ experiments gave the tungsten resonance frequency and hence $\delta(^{183}W)$. The sign of $^1J(PW)$ can be reliably taken as positive in this type

Table 1. Coupling constants in group VI metal carbonyl complexes[a]

No.	Complex[j]	$^2J(PP)$	$J(PC_{b-bone})$[c]	$^2J(P-CO_{ax})$[h] cis	$^2J(P-CO_{eq})$ cis	$^2J(P-CO_{eq})$ trans	$^1J(PW)$
1	dppm Cr(CO)₄	-13.0	18.3	12.8	-12.1	- 7.7	-
2	" Mo(CO)₄	+25.5	19.2	8.7	- 8.4	+23.2	-
3	" W(CO)₄	+30.5	24.4	6.8	- 7.4	+21.6	+201.2
4	gem-rpp Cr(CO)₄	+47 (b)	13.7,7.8	12.2	(∓)17.1(i)		-
5	" Mo(CO)₄	+76 (b)	14.6,6.1	8.3	(±)16.6(i)		-
6	" W(CO)₄	+84 (b)	20.9,6.1	6.8	(±)16.6(i)		+210.9
7	dpnp Cr(CO)₄	-38 (b)	-	13.1	(∓)18.3(i)		-
8	" Mo(CO)₄	0 (b)	-	8.9	(∓) 9.8	(±)25.1	-
9	" W(CO)₄	0	-	7.0	(∓) 8.0	(±)23.4	+207.5
10	dppe Cr(CO)₄	+ 2.9	N=40.0 (d)	13.4	-12.7	- 4.7	-
11	" Mo(CO)₄	-10.8	23.8,16.1(f)	8.9	- 9.1	+25.3	-
12	" W(CO)₄	- 4.0	27.3,14.5(f)	6.8	- 6.7	+23.9	+229 (b)
13	cis-vpp Cr(CO)₄	+ 5.5 (b)	34.7,29.8(f)	13.2	(∓)12.7	(∓) 3.4	-
14	" Mo(CO)₄	+ 8.7	N=62.5 (d)	8.8	- 8.2	+26.3	-
15	" W(CO)₄	+19.8	N=64.5	6.6	- 5.8	+24.4	+233 (b)
16	dppp Cr(CO)₄	-33.7	N=27.8(e)5.8	13.4	-12.1	- 6.9	-
17	" Mo(CO)₄	-28.6	21.5,5.8,0.9	9.0	- 9.4	+23.5	-
18	" W(CO)₄	-21.5	24.3,4.8,2.1 (g)	7.0	- 7.7	+22.6	222.2
19	dppb Cr(CO)₄	-27.0	15.7,4.9,2.0 (g)	13.2	(∓)17.6(i)		-
20	" Mo(CO)₄	-21.5	17.1,7.8,1.0 (g)	8.3	(±)16.6(i)		-
21	" W(CO)₄	-15.0	22.2,6.3,0.4 (g)	7.0	- 6.4	+24.2	+230.7

Notes:
(a) In Hz, ±0.2Hz unless otherwise noted. Signs without parentheses are absolute, those with parentheses have been assigned by comparison with a closely related coupling.
(b) ±0.5Hz
(c) nJ listed for increasing values of n.
(d) N = ¹J + ²J.
(e) N = ¹J + ³J.
(f) ¹J and ²J of like sign, but their assignment is uncertain.
(g) ¹J and ³J are of like sign.
(h) All are probably negative.
(i) Sum of cis and trans couplings.
(j) See text for meanings of abbreviations.

Table 2. ^{13}C chemical shifts[a] in phosphine ligands of group VI metal carbonyl complexes

No.	Complex[b]		Phenyl Groups				C_{b-bone}[c]
		C_1	C_2	C_3	C_4	
1	dppm Cr(CO)$_4$	136.9	131.5	129.1	130.6	47.3
2	" Mo(CO)$_4$	137.0	131.5	129.1	130.6	48.7
3	" W(CO)$_4$	135.9	131.9	128.9	130.6	51.4
4	gem-pp Cr(CO)$_4$	133.7	132.8	129.0	130.7	152.1,127.5
5	" Mo(CO)$_4$	133.5	133.2	129.0	130.8	154.1,130.3
6	" W(CO)$_4$	132.9	133.0	128.9	130.8	156.3,132.4
7	dpnp Cr(CO)$_4$	138.7	129.9	128.4	130.2	-
8	" Mo(CO)$_4$	138.8	130.5	128.6	130.4	-
9	" W(CO)$_4$	137.8	130.3	128.5	130.5	-
10	dppe Cr(CO)$_4$	138.2	132.1	129.5	130.4	28.4
11	" Mo(CO)$_4$	137.8	132.5	129.5	130.7	27.9
12	" W(CO)$_4$	135.6	131.8	128.9	130.2	29.7
13	cis-vpp Cr(CO)$_4$	136.9	131.6	129.0	130.3	148.9
14	" Mo(CO)$_4$	137.1	132.1	129.1	130.4	148.0
15	" W(CO)$_4$	136.4	132.0	129.0	130.5	149.4
16	dppp Cr(CO)$_4$	138.1	132.1	129.4	129.7	30.9,20.0
17	" Mo(CO)$_4$	138.2	132.2	128.7	129.9	31.6,20.1
18	" W(CO)$_4$	137.6	132.3	130.1	130.2	31.2,20.5
19	dppb Cr(CO)$_4$	139.0	131.8	128.3	129.4	32.1,23.6
20	" Mo(CO)$_4$	138.5	131.9	128.4	129.4	30.3,23.6
21	" W(CO)$_4$	138.3	132.0	128.4	129.6	31.1,23.5

Notes:

(a) In ppm (±0.1 ppm) to high frequency of Me$_4$Si.

(b) See text for meanings of abbreviations.

(c) When two figures are given the first refers to carbon bound to phosphorus.

of compound.[17] Tables 1–4 list the NMR parameters of these complexes.

DISCUSSION

(a) Coupling constants

The main factors which are known to affect nuclear spin-coupling constants involving phosphorus are the effective nuclear charge and hybridization of phosphorus and of the other nucleus, and the geometry of the coupling path.[18] With the possible exception of the three derivatives [7–9] of *dpnp* all of the complexes examined here must have very comparable effective nuclear charges at phosphorus since in each case the phosphorus is bound to the metal atom, to two

phenyl groups, and to a carbon atom which may be either sp^3 or sp^2 hybridized. The phosphorus hybridization will be between p^3 and sp^3 in all of the compounds, and although it will be affected by changes in the interbond angles at phosphorus brought about by different ring sizes, this effect is likely to be relatively unimportant. Support for this contention is provided by the narrow range of variation for any particular metal atom of the coupling $^2J(P-CO_{ax})$ for which the relevant PMC interbond angle is 90° and should be little affected by alterations in the size of the chelate ring. It thus seems reasonable to attribute the major trends in the phosphorus-phosphorus and phosphorus-carbonyl couplings to

Table 3. Carbonyl ^{13}C, ^{31}P and ^{183}W chemical shifts in group VI metal complexes

No	Complex [a]	CO_{ax} [b][c]	CO_{eq} [b][d]	$\delta(^{31}P)$ [e]	$\Delta\delta(^{31}P)$ [f]	$\delta(^{183}W)$ [g]
1	dppm Cr(CO)$_4$	222.6	229.7	26.0	49.6	–
2	" Mo(CO)$_4$	211.0	219.5	1.5	25.1	–
3	" W(CO)$_4$	203.6	211.0	-23.5	0.1	527
4	gem-pp Cr(CO)$_4$	222.9	229.7	50.1	54.0	–
5	" Mo(CO)$_4$	211.4	219.1	26.4	30.3	–
6	" W(CO)$_4$	203.9	210.4	7.8	11.7	477
7	dpnp Cr(CO)$_4$	220.7	228.2	96.2	53.6	–
8	" Mo(CO)$_4$	209.6	218.2	69.6	27.0	–
9	" W(CO)$_4$	201.9	209.6	45.7	3.1	482
10	dppe Cr(CO)$_4$	221.5	230.4	79.4	91.9	–
11	" Mo(CO)$_4$	209.9	218.0	54.7	67.2	–
12	" W(CO)$_4$	201.9	208.8	40.1	52.6	192
13	cis-vpp Cr(CO)$_4$	219.3	229.0	88.0	111.1	–
14	" Mo(CO)$_4$	208.4	217.2	63.9	87.0	–
15	" W(CO)$_4$	200.4	208.1	49.8	72.9	150
16	dppp Cr(CO)$_4$	222.0	226.9	41.0	58.3	–
17	" Mo(CO)$_4$	208.6	213.2	20.4	37.3	–
18	" W(CO)$_4$	203.2	206.0	-0.1	17.2	326
19	dppb Cr(CO)$_4$	221.9	225.9ₐ	48.0	63.0	–
20	" Mo(CO)$_4$	210.4	214.9	29.2	44.2	–
21	" W(CO)$_4$	203.0	205.6	11.3	26.3	367

Notes:

(a) See text for meaning of abbreviations.
(b) In ppm (±0.1 ppm) to high frequency of Me$_4$Si.
(c) Carbonyl trans to carbonyl.
(d) Carbonyl trans to phosphorus.
(e) In ppm (±0.1 ppm) to high frequency of external 85% H$_3$PO$_4$.
(f) Coordination chemical shift (see ref. 10) in ppm.
(g) In ppm (±2 ppm) to high frequency of W(CO)$_6$, for which Ξ (^{183}W) = 4.151878 MHz.

geometrical and electronic changes in the through-bond coupling path(s).

(i) $^2J(PP)$. This coupling can be regarded as being the sum of through-metal and "backbone" contributions as suggested by Grim et al.[7] For the complexes of dppb the backbone contribution will be over five sigma bonds and can probably be ignored, so that the observed coupling is a good measure of the through-metal component. Furthermore, for these complexes and those of dppp there is likely to be little or no distortion of the interbond angle at the metal atom due to the constraints of the chelate ring. The uniform difference in $^2J(PP)$ between the three complexes of dppb and the corresponding ones of

dppp, which is essentially independent of the metal atom, may thus be ascribed to a backbone contribution of -6.8 ± 0.3 Hz in the latter complexes. This may be compared with a value of ± 1.0 Hz in the free ligand dppp itself[6] where there is no special rigid stereochemical relationship between the two phosphorus atoms. In cis-$(Me_3P)_2M(CO)_4$ where the PMP interbond angles are likely to be close to 90° and there can be no backbone contribution $J(PP)$ has values of -36, -29.7 and -25.0 Hz for M = Cr, Mo and W respectively.[19]

By contrast, a comparison of the complexes having a five-membered chelate ring with those of dppb does show a significant dependence upon the metal atom,

Table 4. Coupling constants between ^{31}P and ^{13}C in phenyl groups of group VI metal carbonyl complexes[a]

No.	Complex [b]	$^1\underline{J}(PC)$, $^3\underline{J}(PC)$ [c]	$^2\underline{J}(PC)$, $^4\underline{J}(PC)$ [c]	$^3\underline{J}(PC)$, $^5\underline{J}(PC)$ [c]	$^4\underline{J}(PC)$ [d]
1	dppm Cr(CO)$_4$	36.7	+12.7,−0.6	9.8	<2.0
2	dppm Mo(CO)$_4$	37.0	+14.9,−0.9	10.0	<2.0
3	dppm W(CO)$_4$	42.3	13.4	10.2	<2.0
4	gem-pp Cr(CO)$_4$	39.0	11.7	9.8	<1.5
5	gem-pp Mo(CO)$_4$	37.8	14.0	11.0	<1.5
6	gem-pp W(CO)$_4$	44.0	13.2	10.3	<1.5
7	dpnp Cr(CO)$_4$	43.1,−3.4	13.4	10.4	2
8	dpnp Mo(CO)$_4$	32.4,(∓)6.8	15.3,0	10.4,0	1.8
9	dpnp W(CO)$_4$	38.5,−6.9	15.3,−0.7¯	10.7,0	2.2
10	dppe Cr(CO)$_4$	36.6	+9.7,−0.1	8.8	1.8
11	dppe Mo(CO)$_4$	35.0	+12.5,−0.3	9.2	1.7
12	dppe W(CO)$_4$	39.0	+9.7,−0.1	12.2	1.8
13	cis-vpp Cr(CO)$_4$	37.4,2.9	11.2,<0.5	9.5,<0.5	1.9
14	cis-vpp Mo(CO)$_4$	35.5,2.6	12.2,0.5	9.3,0.5	<1.5
15	cis-vpp W(CO)$_4$	41.5,2.5	11.2,0.5	10.3,<0.5	<1.5
16	dppp Cr(CO)$_4$	37.3	8.8	10.6	<3.5
17	dppp Mo(CO)$_4$	34.8	12.0	9.1	<2.0
18	dppp W(CO)$_4$	38.5,2.5	+11.9,−0.5	9.2	<3.0
19	dppb Cr(CO)$_4$	32.8,3.3	9.3,0.5	8.8,0	<1.5
20	dppb Mo(CO)$_4$	31.3,2.4	11.2,0.2	8.8,0	<1.5
21	dppb W(CO)$_4$	37.9,1.9	11.2,0	9.0,0	<1.5

Notes: (a) In Hz, ± 0.2 Hz.   Signs are given only when definitely known.

(b) For meanings of abbreviations see text.

(c) When there is only one entry it refers to $\underline{N}(PC)$, the algebraic sum of the two coupling·constants.

(d) Strictly $\underline{N}(PC)$, but it is reasonable to assume $^6\underline{J}(PC)$ = 0.

the changes of *dppb* → *dppe* being + 16.2, + 17.5 and + 20.5 Hz for Cr, Mo, and W respectively, while for *dppb* → *cis-vpp* the corresponding changes are + 27.0, + 30.2 and + 34.8 Hz. This is certainly consistent with there being significant (different) backbone contributions in the complexes of *dppe* and *cis-vpp*, but it should also be noted that the presence of two sp^2 hybridized carbon atoms in the chelate ring formed by *cis-vpp* will seriously affect the conformational mobility of its complexes and hence will produce greater constraints upon the PMP interbond angle than in the case of *dppe*. For the complexes with a four-membered ring the differences are even greater, the chromium complex being the most discrepant, as is to be expected if through-metal interactions are beginning to play a major role.

Although it can hardly be doubted that there are two separate paths available for the coupling mechanism, a problem with this type of analysis is that changes in the geometry of the ring are likely to affect both paths. Thus the smaller size of chromium compared with molybdenum and tungsten will affect the conformation of the chelate ring and hence of the ligand backbone—values of *J*(PP) are known to be very sensitive to such conformational effects. Nonetheless, it does emerge clearly from this study that in the sequence chromium, molybdenum, tungsten there is a progressive positive increment in $^2J(PP)$ for all types of complex studied. In view of the diversity of types of backbone involved it seems reasonable to attribute the major part of this change to the through-metal contribution. For the four-membered chelate rings the difference between $^2J(PP)$ for the chromium and molybdenum complexes is much greater than for the molybdenum and tungsten: this is reasonable since in these complexes the PMP interbond angle is constrained to be substantially less (typically it is 70°) than its "normal" value of 90° and

is very sensitive to the PM bond lengths which are quite similar for molybdenum and tungsten.[20] It is of course well-known that $^2J(PP)$ is strongly dependent upon the hybridization of an intermediate carbon atom, and on theoretical grounds it is believed that differences in the energies of the various metal electronic excitations will affect this coupling and may cause it to change sign. It is also clear from our results that it is essential to determine the sign of $^2J(PP)$ *experimentally*. Previously, it has been usual[3] simply to rely upon the expected algebraic increase in the sequence Cr, Mo, W, to estimate the signs, but evidently this would not necessarily have predicted the negative sign in compound [1].

(ii) $^2J(^{31}P-^{13}CO)$. The symmetry of the complexes is such that it was possible to obtain only the magnitude of $^2J(P-CO_{ax})$ and not its sign. However, comparison with the other similar *cis* couplings $^2J(P-CO_{eq})$ of known sign in these complexes makes it obvious that in all cases the sign is actually negative. Indeed, the magnitudes of the two kinds of *cis* P–CO coupling run so closely parallel that it is feasible to use the value of $^2J(P-CO_{ax})$ to estimate $^2J(P-CO_{eq})$ in those complexes where it was possible to measure only the sum of the *cis* and *trans* P–CO$_{eq}$ couplings and hence to obtain a good estimate of the *trans* $^2J(P-CO_{eq})$. For the six complexes to which this applies the calculated values are: [4], -4.9; [5], $+24.9$; [6], $+23.4$; [7], -5.2; [19], -4.4; [20], $+24.9$ Hz; all probably correct to within 1 Hz.

Our results demonstrate that for all the chromium complexes the *cis*- and *trans* P–CO couplings are negative, while for the molybdenum and tungsten complexes the *cis*-couplings are still negative but the *trans* are positive. This could constitute a useful assignment aid. It had been previously observed that in *cis*-(PH$_3$)$_2$Cr(CO)$_4$ the *cis* and *trans* P–CO couplings are of opposite sign although their absolute signs were unknown.[2] It is perhaps worth noting that for the complexes with a four-membered chelate ring two paths are in principle available for the P–CO coupling: the two-bond P–M–C one, and the four-bond P–C–P–M–C route which is not necessarily negligible, especially when there is a fixed geometry. However, the relative insensitivity of the P–CO coupling to chelate ring size suggests that in fact the four-bond route is unimportant. The most striking feature of the behaviour of $J(P–CO)$ is that in the sequence Cr, Mo, W there are algebraic increases of *ca.* 4 and 2 Hz respectively for the *cis* relationship, whereas the changes are *ca.* $+30$ and -2 Hz for the *trans*. These changes are much more consistent throughout the series of complexes than the changes in $J(PP)$, suggesting that the previously observed correlation between the two types of coupling may not be of very great generality.[3] It has been proposed elsewhere[21] that geminal coupling constants can be represented by an expression which for our complexes will take the form

$$^2J(P-M-C) = S \cdot {}^1J(PM) \cdot {}^1J(MC) \qquad (1)$$

where S depends upon the hybridization and electronic excitations of the intermediary atom M. In the tungsten complexes there is a rough correlation between the *trans* $^2J(P-CO_{eq})$ coupling and $^1J(PW)$ which is in agreement with eqn (1), but not for the *cis*

$^2J(P-CO)$ couplings. Thus it is probably reasonable to apply the mean electronic excitation energy approximation to the *trans* couplings, which are relatively large and positive, but not to the *cis*, which are smaller and negative. In this context it would be very interesting to know the signs and magnitudes of the geminal $^{13}C-^{13}C$ couplings between the carbonyl groups.

(iii) $^1J(^{183}W-^{31}P)$. This coupling increases with increasing size of the chelate ring, i.e. with increasing PWP interbond angle, and as pointed out above is broadly paralleled by *trans* $^2J(^{31}P-CO)$.

(iv) $J(^{31}P-^{13}C)_{backbone}$. The most striking feature of the one-bond couplings is that the differences between the tungsten and molybdenum complexes are greater than those between the molybdenum and chromium ones. For sp^3 hybridized phosphorus one-bond P–C couplings are normally positive and fairly large, while for p^3 they are negative and fairly small. Thus $^1J(PC)$ can be regarded as indicative of phosphorus hydribization, and shows it to be intermediate between p^3 and sp^3 in these complexes as expected. However, it is surprising that the phosphorus hybridizations in the molybdenum and tungsten complexes differ sufficiently to produce the observed differences in $^1J(PC)$. In this connection it must be realized that particularly for the complexes with smaller rings the nominally one-bond P–C couplings will in fact be made up of contributions from the true one-bond pathway and also from a route *via* the metal atom. This latter contribution will depend upon the electronic excitations involving the metal atom which may well differ significantly for molybdenum and tungsten.

The longer-range P–C$_{backbone}$ couplings will depend upon the above factors and also upon the stereochemical constraints of the ring; further discussion is not warranted at present. In principle the P–C couplings of the phenyl groups can also provide a guide to phosphorus hybridization and again provide evidence for significant differences between the phosphorus hybridizations in the molybdenum and tungsten (and also the chromium complexes).

(b) *Chemical shifts*

As has been discussed elsewhere[11] the tungsten chemical shifts in these complexes are sensitive to the size of the chelate ring, but the precise nature of the relationship is complex. Thus a four-membered ring experiences a large shift to high frequency, and a five-membered ring a large shift to low frequency, compared with an unstrained ring or no ring at all. This feature may be of diagnostic value, since it should be possible to use $\delta(^{183}W)$ to distinguish between small-ring monomers and large-ring dimers which might otherwise have very similar NMR parameters. The newly reported phosphorus coordination shifts, $\Delta\delta(^{31}P)$, also show the same marked dependence upon ring size and metal atom that was previously noted by Grim for *dppm*, *dppe* and *dppp* complexes.[10]

For any particular metal atom the ^{13}C chemical shifts of the axial carbonyl groups are quite insensitive to the size of the chelate ring, whilst those of the equatorial carbonyls do show some effect. This is reasonable, since for an axial CO group the P–M–C interbond angle will always be very close to 90° and

hence any through-space shielding effect will be essentially constant, whilst for an equatorial CO group this interbond angle and the concomitant shielding effect will be much more variable, according to the size of the chelate ring.

REFERENCES

[1] P. S. Braterman, D. W. Milne, E. W. Randall and E. Rosenberg, *J. Chem. Soc., Dalton* 1973, 1027.

[2] G. M. Bodner, *Inorg. Chem.* 1975, **14**, 2694.

[3] G. M. Bodner, M. P. May and L. E. McKinney, *Inorg. Chem.* 1980, **19**, 1951.

[4] I. J. Colquhoun, S. O. Grim, W. McFarlane, J. D. Mitchell and P. H. Smith, *Inorg. Chem.* 1981, **20**, 2516.

[5] I. J. Colquhoun and W. McFarlane, *J. Magn. Reson.* 1978, **31**, 63; I. J. Colquhoun, S. O. Grim, W. McFarlane and J. D. Mitchell, *J. Magn. Reson.* 1981, **42**, 186.

[6] I. J. Colquhoun and W. McFarlane, *J. Chem. Soc., Dalton* 1982, 1915.

[7] S. O. Grim, R. C. Barth, J. D. Mitchell and J. Delgaudio, *Inorg. Chem.* 1977, **16**, 1776.

[8] R. B. King and J. C. Cloyd, *Inorg. Chem.* 1975, **14**, 1550.

[9] R. Freeman and W. A. Anderson, *J. Chem. Phys.* 1962, **37**, 2053.

[10] S. O. Grim, W. L. Briggs, R. C. Barth, C. A. Tolman and J. P. Jesson, *Inorg. Chem.* 1974, **13**, 1095.

[11] G. T. Andrews, I. J. Colquhoun, W. McFarlane and S. O. Grim, *J. Chem. Soc., Dalton* 1982, 2353.

[12] R. B. King and C. A. Eggers, *Inorg. Chem. Acta* 1968, **2**, 33.

[13] S. S. Sandhu and A. K. Mehta, *J. Organomet. Chem.* 1974, **77**, 45.

[14] J. W. Emsley, J. Feeney and L. H. Sutcliffe, *High Resolution Nuclear Magnetic Resonance Spectroscopy.* Pergamon Press, Oxford (1965).

[15] W. McFarlane, *Ann. Rev. N.M.R. Spectroscp.* 1968, **1**, 135.

[16] W. McFarlane, *Org. Magn. Reson.* 1969, **1**, 3.

[17] W. McFarlane and D. S. Rycroft, *J. Chem. Soc., Chem. Commun.* 1973, 336.

[18] E. G. Finer and R. K. Harris, *Progr. N.M.R. Spectroscp.* 1971, **6**, 61.

[19] J. G. Verkade, *Coord. Chem. Rev.* 1972, **9**, 1.

[20] K. K. Cheung, T. F. Lai and K. S. Mok, *J.C.S.(A)*, 1971, 1644; M. J. Bennett, F. A. Cotton and M. D. LaPrade, *Acta Cryst.* 1971, **27B**, 1899.

[21] C. J. Jameson, *J. Amer. Chem. Soc.* 1969, **91**, 6232.

SELF-REDUCTION OF CHLOROHEMIN IN PYRIDINE: COMPARISON WITH THE PHOTOREDUCTION PROCESS

P. ZANELLO

Istituto di Chimica Generale dell'Universita' di Siena, Siena, Italy

C. BARTOCCI,* A. MALDOTTI and O. TRAVERSO

Centro di Studio sulla Fotochimica e Reattività degli Stati Eccitati dei Composti di Coordinazione del C.N.R., Istituto Chimico dell'Università di Ferrara, Ferrara, Italy

Abstract—The self-reduction of chlorohemin in pure pyridine has been investigated by voltammetric techniques. The results obtained indicate that the self-reduction follows a first-order kinetic rate law. The reduction is strongly inhibited by the presence of chloride ions suggesting that the monopyridine protoporphyrin iron(III) $[Fe(III)(PP)(py)]^+$ axial complex is the species undergoing self-reduction. In oxygenated solution the process is strongly retarded since the oxidation of the $Fe(II)PP$ intermediate strongly competes with the formation of a stable $Fe(II)(PP)(py)_2$ complex. The results are discussed in the light of those obtained in a previous investigation on the photochemistry of chlorohemin under similar conditions.

It is well known that, in a number of biological systems, cytochromes, heme-containing iron-proteins, play a fundamental role in electron transfer processes. However, the means by which these proteins carry out their redox catalyst function is not clear and to date has been the subject of many investigations.[1-4]

The study of the iron porphyrin complex redox behaviour appears to be very useful in view of the construction of model systems capable of mimicking the features of biological redox processes. In a recent paper Bartocci *et al.*[5] have reported on the photoreduction process of chlorohemin [Fe(III)Protoporphyrin(IX) chloride, Fe(III) solvent, the authors attempted to simulate the solvent, the authors attempted, to simulate the aprotic environment of the heme-containing protein socket. In that paper it was observed that Fe(III)(PP)Cl underwent photoreduction yielding a dipyridine Fe(II)protoporphyrin(IX) complex as the final product. A slow thermal reduction, giving rise to the same final product obtained in the photochemical process, occurred when chlorohemin was dissolved in pyridine. This process has previously been observed by several authors,[6-8] during their investigations on Fe(III)porphyrin

complexes in pyridine solution. However, different explanations have been given and the possibility that impurities were responsible for this reduction were not ruled out.

In order to contribute to clarifying this unexplained self-reduction process, a re-investigation of this phenomenon was carried out.

EXPERIMENTAL

Materials

The supporting tetraethylammonium perchlorate† and tetraethylammonium chloride (Carlo Erba) electrolytes were dried in a vacuum oven and used without further purification. Chlorohemin, iron(III) protoporphyrin(IX) chloride [Fe(III)(PP)Cl] was recrystallized following the reported[9] glacial acid method. Imidazole (BDH) and phenyl-*tert*-butyl nitrone (PBN)(Aldrich) were used without further purification. Spectroscopic grade pyridine (Merck) was dried with calcium hydride, twice distilled and used within 24 hr after purification. Nitrogen (99.99%) was employed to remove oxygen from the tested solutions. When necessary, ultrapure oxygen was bubbled through the solutions.

Apparatus

In all the voltammetric experiments, a P.A.R. Model 170 Electrochemistry System was used as a polarizing unit. A water-jacketed cell maintained

---

*Author to whom correspondence should be addressed.

†Caution.

at a selected temperature ($\pm$ 0.1C) by a Haake FE water thermostat was employed. Cyclic voltammetric tests were performed with a platinum microelectrode surrounded by a platinum spiral counter electrode. The potential of the working microelectrode was probed by a Luggin capillary reference electrode compartment. An electrode with periodical renewal of the diffusion layer was obtained by moving the solid electrode with a time-controlled knocker. All potential values refer to a saturated aqueous calomel electrode.

Electron spin resonance measurements were performed using a Bruker 220 SE spectrometer, equipped with accessory for variable temperatures.

Irradiation equipment and procedures were as previously reported.[5]

RESULTS AND DISCUSSION

In the potential range of the iron(III)–iron(II) couple, the cyclic voltammetric response of a de-aerated pyridine solution just after the addition of chlorohemin shows a cathodic peak to which an anodic peak is directly associated. As previously pointed out,[6] the charge-transfer involves a simple one-electron quasi-reversible step ($E_{1/2}$ = + 0.06 V, ΔE_p = 110 mV at 0.2 V/sec, i_{pa}/i_{pc} = 1.0).

The occurrence of a de-aerated hemin solution self-reduction reaction in time has been investigated by d.c. voltammetry using a platinum electrode with periodical renewal of the diffusion layer. As an example, the voltammetric responses obtained at 25°C at two different times are reported in Fig. 1. (Timing starts after the addition of hemin to pre-deaerated pyridine solutions.) Plots of the Fe(II)/Fe(III) ratio as a function of time at different temperatures are represented in Fig. 2. These ratios were calculated using cathodic and anodic limiting currents. Thus one can see that the self-reduction of chlorohemin in de-aerated pyridine is highly dependent on temperature.

In the concentration range of chlorohemin from 1.10×10^{-4} to 2.0×10^{-3} mol dm^{-3} the same trends hold. This datum, together with those reported in previous investigations,[8] indicates that a first-order reaction is involved in the self-reduction. A rate constant of 1.3×10^{-5} sec^{-1} was computed at 25°C, a value which is very close to that previously obtained (1.1×10^{-5} sec^{-1}) by spectrophotometric techniques.[8]

The influence of di-oxygen on the reduction rate of chlorohemin has been tested by bubbling ultra-pure oxygen (P_{O_2} = 1 atm) in the voltammetric cell. The results can be seen in Fig. 3. When the oxygenated solution was successively de-aerated, the self-reduction occurred again at the same rate as in the case of chlorohemin added to de-aerated pyridine.

Since the addition of chloride ions noticeably prevents the self-reduction of chlorohemin, the process was carried out in the presence of tet-
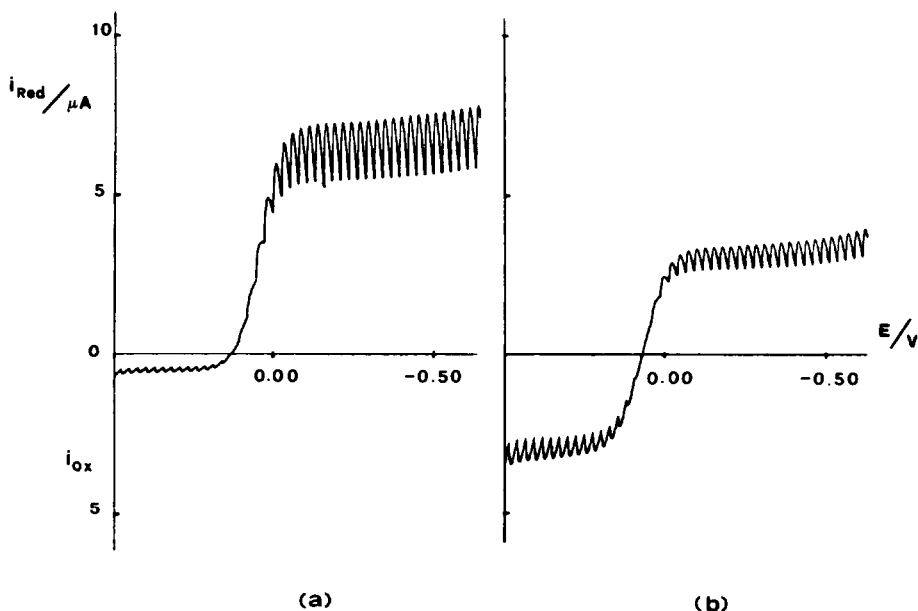
Fig. 1. D.c. voltammetric curves recorded for a pyridine solution containing chlorohemin (1.20×10^{-3} mol dm^{-3}) and [NEt$_4$][ClO$_4$] (0.1 mol dm^{-3}). (a) After 1 hr. (b) After 23 hr. Platinum working microelectrode, t = 25°C.
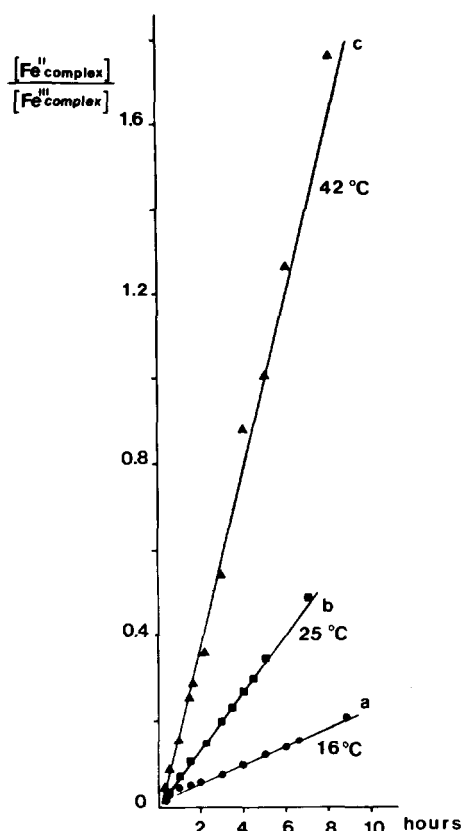
Fig. 2. Rate of reduction of chlorohemin in de-aerated pyridine solution at different temperatures. Chlorohemin concentrations are: curve a, 1.35×10^{-3} mol dm^{-3}; curve b, 1.20×10^{-3} mol dm^{-3}; curve c, 1.29×10^{-3} mol dm^{-3}. Supporting electrolyte, [NEt]$_4$[ClO$_4$] (0.1 mol dm^{-3}).

Fig. 3. Comparison between the rate of reduction of chlorohemin in de-aerated pyridine solution (curve a) and in pyridine saturated with dioxygen ($P_{O_2} = 1$ atm). Chlorohemin concentrations are: curva a, 1.00×10^{-3} mol dm^{-3}; curve b, 9.7×10^{-4} mol dm^{-3}, $t = 25°C$.

Scheme 1.

raethylammonium chloride (0.1 mol dm^{-3}) as supporting electrolyte. The data at 25°C indicate that under these experimental conditions the reduction of chlorohemin occurs to a degree quite similar to that reported in Fig. 3 for the influence of dioxygen. It must be noted that in the presence of an excess of chloride the reduction wave of chlorohemin shifts to more negative potentials ($E_{1/2} = -0.07$ V), indicating that chloride ions stabilize chlorohemin with respect to the reduction. An explanation for this result can be given by taking into consideration the fact that chloride influences the equilibria when chlorohemin is dissolved in pyridine, as reported by Bartocci et al.[5] (Scheme 1). It is evident from this scheme that an excess of chloride ions shifts the equilibria towards chloride complexes 2 and 3. The drastic lowering of the reduction rate observed under these conditions is clear evidence that the pyridine complex (1) undergo self-reduction more easily than the chlo-

ride complexes (2 and 3). The low self-reducibility of these species is an indication that Fe(III)-porphyrin chloride complexes are more stable than the corresponding Fe(II) complexes. Accordingly, by assuming the concentration of chloro-complexes to be negligible in the absence of free chloride ions, the shift of $E_{1/2}$ observed in the presence of excess [Cl$^-$] suggests that the stability constant of iron(III) chloride complexes is roughly 10^2 greater than that of the corresponding iron(II) complexes.

It is well known[6,7] that the reduction of chlorohemin in pyridine is strongly inhibited by the presence of an excess of imidazole, due to the formation of a bis-imidazole Fe(III)porphyrin

complex. D.c. voltammetric experiments carried out using pyridine chlorohemin solutions containing 0.1 mol dm^{-3} imidazole indicated that no iron(II) was formed within 7 hr. The shift of half-wave potential ($E_{1/2} = -0.56$ V), indicating that the stability constant of the imidazole iron(III) complex is 10^{10} greater than that of the corresponding imidazole iron(II) complex, accounts for the great stability of chlorohemin solutions in the presence of imidazole.

In order to detect the formation of radical intermediates during the self-reduction process, freshly prepared pyridine solutions of chlorohemin containing 5×10^{-2} M phenyl-*tert*-butyl nitrone (PBN) as a spin trap,[10] have been kept in an ESR cavity. No ESR signals indicating the formation of PBN radical adducts were observed at room temperature even after eight hours. This behaviour appears to be quite different from that observed by Bartocci *et al.* in the photoreduction investigation[5] where clear evidence of formation of pyridyl radicals was obtained by ESR trapping experiments. Identical results were obtained at 40°C, under conditions where the self-reduction rate was observed to be about three times faster than at room temperature (Fig. 2). In order to verify that the lack of detection of radical species is due to the PBN adduct instability, solutions of Fe(III)(PP)Cl in pyridine were irradiated both at room temperature (25°C) and at 40°C. In both cases ESR signals characteristic of pyridyl radical adducts with PBN appeared after a few minutes. No appreciable decrease in the signal intensity, which would indicate the decomposition of the adduct, was observed within 3 hr. The above results suggest that no appreciable amount of radical species are trapped by PBN during self-reduction. The observed discrepancy between photochemical and thermal reduction could simply be accounted for by assuming that an impurity reduces Fe(III) to Fe(II). However, this hypothesis may be ruled out since the reaction can go to completion, and in the wide range tested, it is not dependent on the chlorohemin concentration. Another, more plau-

sible, explanation should be that, although the final reduction products are identical, the photochemical and thermal systems do not follow exactly the same reaction coordinate. In a previous paper,[5] the primary photochemical process was identified as an intramolecular electron transfer from the axial pyridine to iron. Since the two electrons of the nitrogen of the coordinated pyridine are held in a strong σ bond, it is very likely that a π electron of the aromatic ring is involved in the electron transfer to central iron. As a consequence, the radical species formed in the primary photochemical act should be a π-type radical cation, which, by reacting with pyridine solvent, gives rise to the formation of a pyridyl radical, which is intercepted by the powerful radical scavenger, PBN. Unlike the photochemical reduction, the primary process in the self-reduction of chlorohemin should be an intermolecular electron transfer from pyridine solvent to iron. In this case the transfer of an electron of the *lone pair* of the pyridine nitrogen to metal appears to be the most probable event, and a pyridine N-radical cation should be the species formed in the primary act. The lack of formation of PBN paramagnetic adducts observed in the self-reduction process can then be explained in terms of a different fate of the N-radical cation in comparison with the π radical cation, i.e. the first could give rise to a different, very fast process, before giving radical species capable of being trapped by PBN. As a matter of fact, it is reported[11] that a pyridine N-radical cation can react very rapidly with pyridine to give bipyridine species rather than pyridyl radicals.

The pronounced effect of oxygen in slowing the reduction reaction (see results) can be explained in terms of an oxidation of the Fe(II)(PP)py complex, which is formed in the primary event (Scheme 2) in competition with pyridine axial coordination. This conclusion is substantiated by the finding that the final product Fe(II)(PP)(py)$_2$ oxidation cannot be responsible for the observed lowering of the reduction reaction because oxygen very slowly oxidizes this complex.[12]

$$\text{Fe (III) (PP) (py)}^+ + \text{py} \longrightarrow \text{Fe (II)(PP)(py)} + \text{py}^+$$

$$\text{py}^+ + \text{py} \xrightarrow{\text{very fast}} \text{products}$$

$$\text{Fe (II)(PP)(py)} + \text{py} \longrightarrow \text{Fe (II) (PP)(py)}_2$$

$$\text{Fe (II)(PP)(py)} + \text{O}_2 \longrightarrow \text{Fe (III)(PP)(py)}^+ + \text{O}_2^-$$
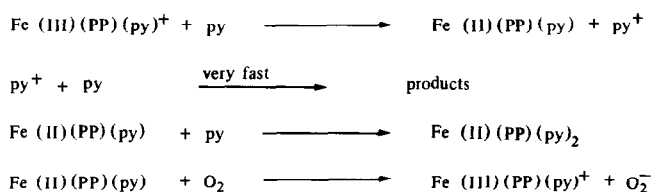
Scheme 2.

REFERENCES

1. H. A. Harbuyr and R. H. L. Marks, In *Inorganic Biochemistry* (Edited by G. L. Eichhorn), Vol. 2, p. 902. Elsevier, Amsterdam (1973).
2. C. Creutz and N. Sutin, *Proc. Natl. Acad. Sci., U.S.A.* 1973, **70**, 1701.
3. W. G. Miller and M. A. Cusanovitch, *Biophys. Struct. Mech.* 1975, **1**, 97.
4. F. R. Salemme, *Ann. Rev. Biochem.* 1977, **46**, 299.
5. C. Bartocci, A. Maldotti, O. Traverso, C. A. Bignozzi and V. Carassiti, *Polyhedron* 1983, **2**, 97.
6. L. A. Constant and D. G. Davis, *Anal. Chem.* 1975, **47**, 2253.
7. L. M. Epstein, D. K. Straub and C. Maricondi, *Inorg. Chem.* 1967, **6**, 1720.
8. M. Brody, S. B. Broyde, C. C. Yeh and S. S. Brody, *Biochemistry* 1968, **7**, 3007.
9. J. H. Furhop and K. M. Smith, In *Porphyrins and Metalloporphyrins* (Edited by K. M. Smith), p. 809. Elsevier, Amsterdam (1975).
10. E. G. Janzen, *Acc. Chem. Res.* 1971, **4**, 1.
11. A. Ledwith and P. J. Russel, *J. Chem. Soc. Perkin II*, 1974, 582.
12. W. S. Caughey, In *Inorganic Biochemistry* (Edited by G. L. Eichhorn), Vol. 2, p. 827. Elsevier, Amsterdam (1973).

SOME TRIMETHYL PHOSPHINE AND TRIMETHYL PHOSPHITE COMPLEXES OF TUNGSTEN(IV)

ERNESTO CARMONA,* LUIS SÁNCHEZ and MANUEL L. POVEDA

Departamento de Química Inorgánica, Facultad de Química, Universidad de Sevilla, Sevilla, Spain

and

RICHARD A. JONES,* and JOHN G. HEFNER

Chemistry Department, University of Texas at Austin, Austin, TX 78712, U.S.A.

Abstract—Direct reduction of WCl_6 with PMe_3 in toluene at 120°C in a sealed tube affords the complexes $[WCl_4(PMe_3)_x]$ ($x = 2, 3$). $[WCl_4(PMe_3)_3]$ abstracts oxygen from equimolar amounts of water in wet acetone or tetrahydrofuran to give $[WOCl_2(PMe_3)_3]$ in very high yields. This procedure has been successfully applied to the high yield synthesis of other known oxotungsten(IV) complexes, $[WOCl_2(PR_3)_3]$ ($PR_3 = PMe_2Ph$ and $PMePh_2$). Metathesis reactions of $[WOCl_2(PMe_3)_3]$ with NaX give $[WOX_2(PMe_3)_3]$ (X = NCO, NCS) and $[WOX_2(PMe_3)]$ (X = Me_2NCS_2). The synthesis of the trimethylphosphite analogue, $[WOCl_2(P(OMe)_3)_3]$, is also described and the structures of the new complexes assigned on the basis of IR and ^1H and ^{31}P NMR spectroscopy.

In recent years we have been interested in the preparation and properties of trimethylphosphine complexes of Group VI metals, particularly molybdenum. This work has resulted in the synthesis of dinitrogen, ethylene, acyl and related complexes,[1,2] with the metal in oxidation states 0 or +2. Adequate starting reagents for these preparations are the chlorophosphine complexes $[MoCl_3(PMe_3)_3]$ and $[MoCl_2(PMe_3)_4]$. A natural extension of this work was the preparation of the tungsten analogues. However, at the time our work started little was known on the chemistry of trimethylphosphine derivatives of tungsten chlorides. In our search for a suitable starting material we have found that the tungsten(IV) complexes $[WCl_4(PMe_3)_x]$ ($x = 2, 3$) can be prepared in high yields by the PMe_3 reduction of WCl_6 in toluene, at 120°C in a sealed Carius tube. While our work was in progress Sharp and Schrock[3a] reported the preparation of these and other related complexes, including the metal–metal bonded dimer $[W_2Cl_4(PMe_3)_4]$. In this paper we wish to report our synthesis for the W(IV) complexes, $[WCl_4(PMe_3)_x]$ ($x = 2, 3$), and their facile conversion into the oxo species $[WOCl_2(PMe_3)_3]$ by oxygen abstraction from water in wet acetone or tetrahydrofuran (THF). The preparations and properties

of the oxo-trimethylphosphite analogue, $[WOCl_2(P(OMe)_3)_3]$, and other related complexes are also reported. We finally show the generality of the oxygen abstraction process for the conversion of $[WCl_4(PR_3)_2]$ complexes into the corresponding oxo-derivatives $[WOCl_2(PR_3)_3]$, by applying it to the synthesis of the known compounds $[WOCl_2(PR_3)_3]$ ($PR_3 = PMe_2Ph$, $PMePh_2$), previously prepared in rather low yields.[4] The reactions leading to these complexes are summarized in the Scheme.

RESULTS AND DISCUSSION

(1) *Tetrachlorobis- and tris-(trimethylphosphine) tungsten(IV)*

Although previous attempts to prepare $[WCl_4(PR_3)_2]$ complexes, directly from WCl_6 without reducing agents other than the phosphine in either cold or boiling THF yielded only oily materials,[4] it was later shown[5] that these complexes can be obtained in good yields by carrying out the reaction in boiling benzene (eqn 1)

$$WCl_6 + 3PR_3 \xrightarrow[\text{reflux}]{C_6H_6} [WCl_4(PR_3)_2] + R_3PCl_2 \quad (1)$$
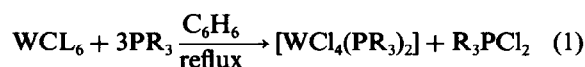
($PR_3 = PMe_2Ph$, $PMePh_2$).

We have successfully applied this procedure to the synthesis of the trimethylphosphine analogue,

---

*Authors to whom correspondence may be addressed.
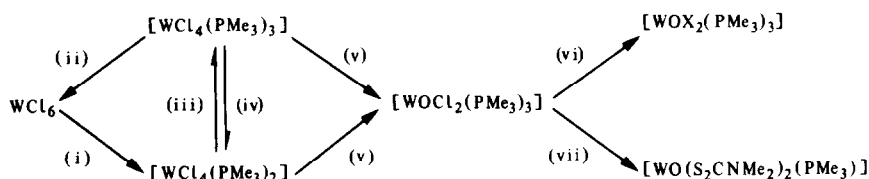
Scheme. (i) PMe₃ (less than 3 equiv), toluene, 120°C, 12–18 hr; (ii) as in (i), excess PMe₃; (iii) PMe₃, THF or toluene; (iv) reflux in toluene; (v) H₂O, PMe₃, THF or acetone, 40–50°C, 3 hr; (vi) KNCO or KNCS, THF, 3–4 hr; (vii) anhydrous NaS₂CNMe₂, THF, 3 hr.

[WCl₄(PMe₃)₂]. The reaction is best carried out in a sealed tube to avoid loss of volatile PMe₃. Thus, when WCl₆ and PMe₃ (*ca.* 1:2.5 molar ratio) are reacted in toluene at 120°C in a Carius tube, [WCl₄(PMe₃)₂] is formed in high yields. Using more than 3 equiv of PMe₃ a mixture of red [WCl₄(PMe₃)₂] and red–purple [WCl₄(PMe₃)₃] is obtained. These complexes can be easily converted into one another, addition of PMe₃ to solutions of the former causing precipitation of the latter, while moderate heating of solutions of [WCl₄(PMe₃)₃] produces loss of PMe₃ and formation of [WCl₄(PMe₃)₂]. Both complexes are moderately stable to air in the solid state but decompose quickly in solution. [WCl₄(PMe₃)₂] is monomeric in solution (cryoscopically in benzene) and paramagnetic with $\mu_{eff} = 1.87$ M.B. (Evans's method[6]), in the range expected for this type of complex [7]. Despite its paramagnetism it shows a relatively sharp NMR signal at $\delta - 25.2$ ppm. [WCl₄(PMe₃)₃] gives also a sharp NMR signal ($\delta - 8.2$ ppm) but its low solubility has precluded solution molecular weight and magnetic moment determinations. As mentioned above these two complexes have been independently prepared[3a] from WCl₄ and PMe₃. The crystal structure of [WCl₄(PMe₃)₃] has been determined.[3b]

(2) Oxotungsten(IV) complexes

Complexes of composition [WOCl₂(PR₃)₃] are known[4] for several monotertiary phosphines (PR₃ = PMe₂Ph, PMePh₂, PEt₂Ph) and were prepared in rather poor yields (*ca.* 30%) by reaction of WCl₆ with the phosphine in ethanol for PR₃ = PMe₂Ph, and in the presence of zinc in the case of the less reducing phosphines PMePh₂ and PEt₂Ph. We have now prepared the trimethylphosphine analogue [WOCl₂(PMe₃)₃] in 80% yield by an oxygen–atom abstraction reaction between [WCl₄(PMe₃)ₓ] (x = 2, 3) and stoicheiometric amounts of water, in the presence of an excess of PMe₃ to accept the generated hydrogen chloride, (eqn 2)

$$[\text{WCl}_4(\text{PMe}_3)_2] + \text{H}_2\text{O} + 3\text{PMe}_3$$

$$\rightarrow [\text{WOCl}_2(\text{PMe}_3)_3] + 2\text{HCl·PMe}_3. \quad (2)$$
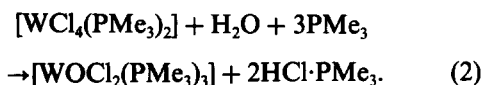
Stirring a solution of [WCl₄(PMe₃)₂], or a suspension of [WCl₄(PMe₃)₃], in wet acetone or THF, at 40–50°C in the presence of PMe₃, produces a change in colour to dark-blue and precipitation of a white microcrystalline solid, identified as [HPMe₃]⁺Cl⁻ by comparison of its IR and NMR spectra with those of an authentic sample. When the reaction is complete and after work up, moderately air-stable dark blue crystals of [WOCl₂(PMe₃)₃] can be collected. This compound has been prepared independently by Wilkinson *et al.*[8] The IR spectrum of the complex shows absorptions characteristic of the PMe₃ ligands but no band due to $\nu(\text{W}=\text{O})$ can be observed. This is very likely due to overlapping with the strong, broad absorption centred at 940 cm⁻¹, characteristic of coordinated trimethylphosphine.[9] As in other related complexes[4] [WOCl₂(PMe₃)₃] is monomeric in benzene solution and diamagnetic. The ¹H NMR spectrum in CH₂Cl₂ shows a triplet at δ 1.57 and a doublet at 1.60 ppm (intensity ratio 2:1). This spectrum may be interpreted in terms of a *meridional* arrangement of the phosphine ligands and this along with the fact that the IR spectra of the complexes [WOX₂(PMe₃)₃] X = NCO, NCS) show two bands due to $\nu(\text{C–N})$ of the X ligands (see later) suggest stereochemistry as in I.

(1)
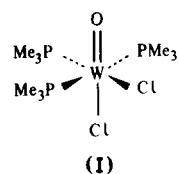
The procedure described above for the preparation of [WOCl₂(PMe₃)₃] is of general use and can be applied to the high yield synthesis of other known oxotungsten(IV) complexes. Thus, [WOCl₂(PMe₂Ph)₃], initially prepared in 25% yield by reaction of WCl₆ with PMe₂Ph in ethanol,[4] is obtained in *ca.* 75% yield by interaction of [WCl₄(PMe₂Ph)₂] with equimolecular amounts of water, in the presence of PMe₂Ph (see Experimental Section). Similarly, [WOCl₂(PMePh₂)₃] can be prepared by this same procedure in *ca.* 70%

yield, (eqn 3)

$$[WCl_4(PR_3)_2] + H_2O + 3PR_3$$

$$\rightarrow [WOCl_2(PR_3)_3] + 2HCl \cdot PR_3 \qquad (3)$$
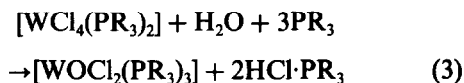
($PR_3 = PMe_2Ph$, 75%; $PR_3 = PMePh_2$, 70%).

The trimethylphosphite derivative, $[WOCl_2\{P(OMe)_3\}_3]$, can be isolated in *ca.* 80% yield, as purple crystals, by the sodium amalgam reduction of $WOCl_4$ in the presence of $P(OMe)_3$. The IR spectrum has $\nu(W=O)$ at 955 cm^{-1}, and the ^1H NMR shows a multiplet at δ 3.82, that provides no information with regard to the stereochemistry of the complex. The $^{31}P\{^1H\}$ NMR spectrum consists of a triplet at δ 134.88 [$^2J(P-P) = 23.5$ Hz; $^1J(W-P) = 316.9$ Hz] and a doublet at 128.08 ($^1J(W-P) = 257.0$ Hz]. This is consistent with either a *facial* or a *meridional* distribution of the phosphite ligands.

Metathesis reactions of the chlorotrimethylphosphine complex $[WOCl_2(PMe_3)_3]$ with the appropriate potassium pseudohalide, yield $[WO(NCO)_2(PMe_3)_3]$ and $[WO(NCS)_2(PMe_3)_3]$ as dark blue crystalline materials. The Nujol-mull IR spectra show two strong bands at 2230 and 2190 cm^{-1} (cyanate complex) and 2060 and 2040 cm^{-1} (thyocyanate complex) attributed to $\nu(C-N)$ of the NCO and NCS ligands respectively. This and the appearance of the ^1H methyl resonances for these complexes as a triplet and a doublet (intensity ratio 2:1) strongly support structure of the type **I**.

The ease of the metathetical replacement of the chlorine atoms in $[WOCl_2(PMe_3)_3]$, provided an opportunity to synthesize the related oxodithiocarbamatetungsten(IV) complexes $[WO(S_2CNR_2)_2(PMe_3)]$ by similar procedures. Compounds of this type are to our knowledge unknown, although for both Mo and W a series of complexes of composition $[MO(S_2CNR_2)_2(R^1C_2R^2)]$ has been reported.[10,11] While for M = Mo these complexes are usually prepared by reaction of the known $[MoO(S_2CNR_2)_2]$ with the appropriate ligands,[10] for tungsten the corresponding $[WO(S_2CNR_2)_2]$ are still unknown, and the acetylene complexes $[WO(S_2CNR_2)_2(R^1C_2R^2)]$ have been obtained by the intermetal oxygen–atom transfer reaction[11] depicted in eqn (4),

$$[W(S_2CNR_2)_2(CO)(R^1C \equiv CR^2)]$$

$$+ [Mo_2O_3\{S_2P(OEt)_2\}_4] \rightarrow [WO(S_2CNR_2)_2(R^1C$$

$$\equiv CR^2)] + 2[MoO(S_2P(OEt)_2)_2] + CO. \qquad (4)$$
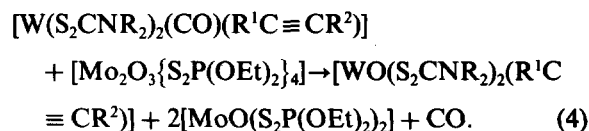
The complex oxodichlorotris(trimethylphosphine)tungsten(IV), $[WOCl_2(PMe_3)_3]$, reacts with anhydrous NaS_2CNMe_2, in THF, at room temperature to afford dark red crystals of $[WO(S_2CNMe_2)_2(PMe_3)]$ in *ca.* 70% yield. In addition to absorptions due to the PMe_3 ligand, the IR spectrum of this moderately air-stable solid is characterized by a strong band at 930 cm^{-1} due to the W=O stretch and two absorptions at 1540 and 1515 cm^{-1} which are assigned to the C=N stretch of the coordinated dithiocarbamate ligands. While the $^{31}P\{^1H\}$ NMR spectrum is a singlet at temperatures between 25° and $-80°C$ (δ -19.8 ppm, $^1J(W-P) = 210.9$ Hz) the ^1H NMR spectrum shows temperature dependence. At 35°C (CD_2Cl_2) the spectrum consist of three methyl signals at δ 3.81, 3.66 and 3.34 ppm (intensity ratio 1:1:2) for the dithiocarbamate groups and a doublet at 1.44 ppm ($^2J(P-H) = 9.2$ Hz) for the PMe_3 protons. Upon lowering the temperature, the singlet at 3.34 broadens, and at 20°C gives rise to an unresolved doublet. On further cooling this signal becomes a sharp doublet of resonances, no additional changes being observed down to $-80°C$. At this temperature four distinct ^1H methyl resonances at 3.81, 3.66, 3.37 and 3.30 ppm are observed for the $Me_2NCS_2^-$ ligands. This spectrum is consistent with structure type **II**.

(II)
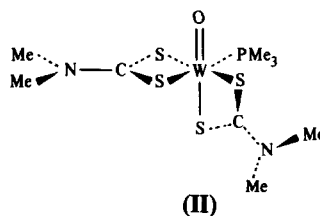
Although a more detailed NMR study is required before any definite conclusion can be reached, it is tempting to assume that the averaging of the two low temperature methyl signals at 3.37 and 3.30 ppm, to give a singlet at 3.34 ppm in the 35°C spectrum, is due to fast exchange of the two methyl groups of the monodentate dithiocarbamate ligand in the short-lived 5-coordinate intermediate, $[WO(S_2CNMe_2)(SC(=S)NMe_2)(PMe_3)]$, formed by rupture of the W–S bond trans to oxygen. This assumption is supported by the high *trans*-influence of the oxo ligand which is well documented in this type of complex.[11,12]

EXPERIMENTAL

surements. Magnetic susceptibilities were obtained in solution by the Evans method.

All preparations and other operations were carried out under oxygen-free nitrogen following conventional Schlenk techniques. Solvents were dried and degassed before use.

The light petroleum used had b.p. 40–60°C. PMe₃ was prepared according to the literature method.[13] The complexes [WCl₄(PR₃)₂] (PR₃ = PMe₂Ph, PMePh₂) were prepared by a slight modification of the method of Galyer and Wilkinson.[5] Details of the preparations are given below. NaS₂CNMe₂ was dried by heating at 90°C under vacuum for 6–7 days.

Tetrachlorobis(trimethylphosphine)tungsten(IV)

A thick-walled 250 cm³ Carius tube, provided with a stirring-bar, was charged with WCl₆ (19.8 g, *ca.* 50 mmol). Toluene (100 cm³) and PMe₃ (14.0 cm³, *ca.* 140 mmol) were successively added via syringe, the resulting mixture frozen at liquid nitrogen temperature and the tube sealed under *vacuo*. The mixture was allowed to reach room temperature and then heated at 120°C for 12–18 hr, with occasional shaking to facilitate the reaction. The resulting dark red solution was transferred while hot (boiling water external bath) and the remaining solid extracted with several portions of hot toluene until no more [WCl₄(PMe₃)₂] was left (*ca.* 4 × 75 cm³). The solution was reduced in volume (to *ca.* 100 cm³) and cooled at −30°C overnight. 14 g of well formed red crystals impurified by relatively small amounts of a yellow powder (Cl₂PMe₃)[14] were obtained. Another crop (4 g) of less pure product was recovered from the mother liquor. The total yield of crude, but pure enough for most synthetic purposes, [WCl₄(PMe₃)₂] was *ca.* 75%. The compound can be purified by recrystallisation from hot toluene. [Found C, 15.4 (15.1); H, 3.9 (3.8); Cl, 29.4 (29.7)% *M*, 462 (444).]

IR (KBr) bands at: 2980, 2940, 1410, 1290, 1275, 1250, 1095, 1010, 935, 835, 785, 720, 650 cm⁻¹. NMR data ¹H(C₆H₆): −25.2 bs. $\mu_{eff} = 1.86 \, \mu_B$.

Tetrachlorotris(trimethylphosphine)tungsten(IV)

To a magnetically stirred solution of [WCl₄(PMe₃)₂] (0.95 g, *ca.* 2 mmol) in THF an excess of PMe₃ (0.3 cm³, *ca.* 3 mmol) was slowly added. Dark red–purple microcrystals of the title compound immediately formed. The mixture was kept overnight at −30°C to complete crystallisation, the resulting solid filtered off, washed with petroleum or Et₂O and vacuum dried. The yield was *ca.* 90%. Recrystallisation can be achieved from hot toluene in a closed flask to avoid loss of PMe₃. [Found C, 19.5 (19.5); H, 5.0 (4.9); Cl, 25.6 (25.6)%.]

IR (KBr) bands at: 2980, 2950, 1420, 1295, 1230, 1100, 950, 850, 800, 780, 730, 665 cm⁻¹. NMR data ¹H(C₆H₆): −8.2 bs.

Oxodichlorotris(trimethylphosphine)tungsten(IV)

To a stirred solution of [WCl₄(PMe₃)₂] (0.95 g, *ca.* 2 mmol) in THF or acetone (40 cm³), PMe₃ (0.7 cm³, *ca.* 7 mmol) was added. Immediate formation of red purple microcrystals of [WCl₄(PMe₃)₃] was observed. To the resulting suspension were added a few drops of deoxygenated water and the mixture stirred at 45°C. the reaction was followed by the disappearance of insoluble [WCl₄(PMe₃)₃] and more water added if required. A large excess of water should be avoided since considerable decomposition takes place. The stirring was continued at this temperature until all the initial [WCl₄(PMe₃)₃] had been taken into solution (*ca.* 2 hr) and then for another hour. The mixture was evaporated to dryness and the residue extracted with Et₂O (40 cm³). Filtration and cooling at −30°C afforded the title compound as dark-blue crystals in *ca.* 80% yield. [Found C, 21.5 (21.5); H, 5.5 (5.4)%. *M*, 490 (499).]

IR (Nujol mull) bands at: 1375, 1300, 1280, 1260, 950, 850, 800, 720, 660 cm⁻¹.

NMR. ¹H (C₆H₆): 1.57t (18), *J*(P-H)ap = 4 Hz; 1.60d (9), *J*(P-H) = 10 Hz.

Oxodichlorotris(dimethylphenylphosphine)tungsten (IV)

The complex [WOCl₂(PMe₂Ph)₃] was prepared in *ca.* 75% yield as dark blue crystals (from hot ethanol) following a procedure identical to that described above for [WOCl₂(PMe₃)₃]. The parent complex, [WCl₄(PMe₂Ph)₂] was prepared as follows:

To a suspension of WCl₆ (4.8 g, *ca.* 12 mmol) in benzene (100 cm³) were added 4 cm³ of PMe₂Ph (*ca.* 30 mmol). A grey oil formed in the bottom of the flask making stirring difficult. The mixture was refluxed for 12–18 hr when a red solution and a brown solid were obtained. The solid was decanted, the solution filtered while still hot and then evaporated until precipitation took place. Complete precipitation was achieved by addition of Et₂O (*ca.* 20 cm³) and cooling at −30°C overnight. Yield 60%.

The complex [WCl₄(PMePh₂)₂] was similarly prepared and reacted with water under the conditions mentioned above, to give mauve crystals (from Et₂O–THF) of [WOCl₂(PMePh₂)₃] in 80% yield. Both oxocomplexes were identified by comparison of their IR and ¹H NMR spectra with those of authentic samples.[4]

Oxochlorotris(trimethylphosphite)tungsten(IV)

Freshly prepared WOCl₄ (3.62 g, *ca.* 5.63 mmol)

was loaded into a 500 cm³-pressure bottle with four equivalents of Na–Hg amalgam (1.5 cm³ of a *ca.* 1% in Na). The contents were pumped on for *ca.* 1 hr. The pressure vessel was cooled to −78°C and degassed THF (150 cm³) and P(OMe)₃ (5.3 cm³, *ca.* 45 mmol) were added. The bottle was pressurized to 40 psi with hydrogen. The reaction vessel was allowed to warm slowly to room temperature and stirred for 12 hr. The volatile materials were removed under vacuum leaving a purple oil. This was extracted into Et₂O (50 cm³), filtered, evaporated to *ca.* 25 cm³ and cooled at −20°C. Purple crystals of [WOCl₂(P(OMe)₃)₃] were collected and dried under vacuum. Yield: 80%. [Found C, 17.0 (16.8); H, 4.2 (4.2); Cl, 10.9 (11.0); P, 14.4 (14.4)%.]

IR (Nujol mull) bands at: 2855, 1371, 1309, 1267, 1188, 1021, 955, 669 cm⁻¹.

NMR: ¹H (C₆D₆): 3.82 mult. ³¹P{¹H} (C₆D₆): 134.88t, ²J(P–P) = 23.5 Hz, ¹J(W–P) = 316.9 Hz; 128.08d, ¹J(W–P) = 257.0 Hz.

Oxobis (cyanate) tris (trimethylphosphine) tungsten (IV)

[WOCl₂(PMe₃)₃] (0.5 g, *ca.* 1 mmol) and dried (100°C, 24 hr) KCNO (0.2 g, excess) were stirred at room temperature in THF (40 cm³) over a period of 3–4 hr. The solvent was then stripped *in vacuo* and the residue extracted with 50 cm³ of Et₂O. The resulting suspension was centrifuged and small dark blue needles of [WO(NCO)₂(PMe₃)₃] were collected in *ca.* 80% yield by cooling at 0°C overnight. [Found C, 25.7 (25.8); H, 5.3 (5.3)%].

IR (Nujol mull) bands at: 2230, 2190, 1375, 1350, 1335, 1300, 1285, 950, 725, 665, 620 cm⁻¹.

RMN: ¹H (CH₂Cl₂): 1.60t (18), J(P–H)ₐₚ = 4 Hz; 1.70d (9), J(P–H) = 8 Hz.

Metathesis with KSCN was accomplished in a similar way to give small blue crystals of [WO(NCS)₂(PMe₃)₃] (from Et₂O–THF) in *ca.* 80% yield. [Found C, 24.4 (24.3); H, 5.0 (5.0)%.]

IR (Nujol mull) bands at: 2060, 2040, 1380, 1305, 1290, 1260, 965, 945, 835, 720, 665 cm⁻¹.

RMN: ¹H (CH₂Cl₂): 1.80t (18), J(P–H)ₐₚ = 4 Hz; 1.88d (9), J(P–H) = 8 Hz.

Oxobis(N,N - dimethyldithiocarbamate)trimethyl - phosphinetungsten(IV)

30 cm³ of THF were syringed into a mixture of [WOCl₂(PMe₃)₃] (0.5 g, *ca.* 1 mmol) and anhydrous NaS₂CNMe₂ (0.5 g, excess). The dark blue crystals of the tungsten compound dissolved immediately giving a dark red solution. The mixture was stirred for *ca.* 3 hr at room temperature and the solvent was

removed *in vacuo*. Extraction with 30 cm³ of a 1:1 mixture of Et₂O:CH₂Cl₂ and centrifugation afforded a dark red solution from which dark red crystals of [WO(S₂CNMe₂)₂(PMe₃)] were collected in *ca.* 70% yield after partial removal of the solvent and cooling at −30°C. [Found C, 22.2 (20.9); H, 4.4 (4.1); N, 5.7 (5.4)%.]

IR (Nujol mull) bands at: 1545, 1520, 1400, 1390, 1280, 1275, 1240, 1150, 1140, 1050, 1040, 950, 935, 930, 895, 850, 830, 730, 720, 660 cm⁻¹.

¹NMR: ¹H (CD₂Cl₂, −80°C): 3.81s (3); 3.66s (3); 3.37s (3); 3.30s (3); 1.44d (9), J(P–H) = 9.2 Hz. ³¹P{¹H} (CD₂Cl₂, −80°C): −19.8; J(W–P) = 210.9 Hz.

REFERENCES

1. E. Carmona, J. M. Marín, M. L. Poveda, J. L. Atwood and R. D. Rogers, *Polyhedron* 1983, **2**, 185; E. Carmona, J. M. Marín, M. L. Poveda, J. L. Atwood and R. D. Rogers, *J. Am. Chem. Soc.* in the press.
2. E. Carmona, L. Sánchez, M. L. Poveda, J. M. Marín, J. L. Atwood and R. D. Rogers, *J. Chem. Soc., Chem. Comm.* 1983, 161.
3. ªP. R. Sharp and R. R. Schrock, *J. Am. Chem. Soc.* 1980, **102**, 1430; ᵇJ. L. Atwood and R. D. Rogers, personal communication.
4. A. V. Butcher, J. Chatt, G. J. Leigh and P. L. Richards, *J. Chem. Soc., Dalton Trans.* 1972, 1064.
5. A. L. Galyer, Ph.D. Thesis. Imperial College, London (1976); A. L. Galyer and G. Wilkinson, unpublished results.
6. D. F. Evans, *J. Chem. Soc.* 1959, 2003.
7. C. A. McAuliffe and W. Levason, In *Phosphine, Arsine and Stibine Complexes of the Transition Elements*. Elsevier, Amsterdam (1979); Z. Dori, *Prog. Inorg. Chem.* 1981, **28**, 239.
8. Kwok W. Chiu, David Lyons and G. Wilkinson, *Polyhedron* 1983, **2**, 803.
9. See for instance H. F. Klein and H. H. Karsch, *Chem. Ber.* 1976, **109**, 2524.
10. W. E. Newton, J. W. McDonald, J. L. Corbin, L. Ricard and R. Weiss, *Inorg. Chem.* 1980, **19**, 1997.
11. J. L. Templeton, B. C. Ward, G. J.-J. Chen, J. W. McDonald and W. E. Newton, *Inorg. Chem.* 1980, **20**, 1248.
12. D. Coucouvanis, *Prog. Inorg. Chem.* 1979, **26**, 301.
13. W. Wolfsberger and H. Schmidbaur, *Synth. React. Inorg. Metal Org. Chem.* 1974, **4**, 149.
14. R. Appel and H. Schöler, *Chem. Ber.* 1977, **110**, 2382.

TRIMETHYLPHOSPHINE COMPLEXES OF TUNGSTEN(O) AND (IV). X-RAY CRYSTAL STRUCTURES OF TRIMETHYLPHOSPHINE TRIS (PHENYLACETYLENE) TUNGSTEN(O); BIS(TRIMETHYLPHOSPHINE) TETRAKIS (METHYLISOCYANIDE) TUNGSTEN(O), AND OXODICHLOROTRIS (TRIMETHYLPHOSPHINE) TUNGSTEN (IV)

KWOK W. CHIU, DAVID LYONS and GEOFFREY WILKINSON*

Chemistry Department, Imperial College of Science and Technology, London, SE7 2AY,
England

and

MARK THORNTON-PETT and MICHAEL B. HURSTHOUSE*

Chemistry Department, Queen Mary College, London, E1 4NS, England

Abstract—The reduction of $WCl_4(PMe_3)_3$ by sodium amalgam in presence of phenylacetylene gives $W(PMe_3)(PhC\equiv CH)_3$ (*A*). Reduction in presence of methylisocyanide gives $W(PMe_3)_2(MeNC)_4$ (*B*), while in presence of excess PMe_3 in tetrahydrofuran under hydrogen, $WH_2Cl_2(PMe_3)_4$ (*C*) is formed. The reaction of $WCl_2(PMe_3)_4$ with methanol in tetrahydrofuran gives mixtures of $WH_2Cl_2(PMe_3)_4$ and $WOCl_2(PMe_3)_3$ (*D*).
The structures of A, B, and D have been determined by X-ray diffraction.

RESULTS AND DISCUSSION

1. *Reductions of tris(trimethylphosphine)tetrachlorotungsten*

(a) *Phenylacetylene.* The interaction of WCl_4 $(PMe_3)_3$,[1] and excess phenyl acetylene with sodium amalgam in tetrahydrofuran gives a pale yellow complex, $W(PMe_3)(PhC\equiv H)_3$ (*A*). Other compounds of the type $WX(RC\equiv CR')$, $X = CO$, MeCN or PMe_2Ph have been obtained from $W(CO)_3(MeCN)_3$.[2,3] The new complex is slightly soluble in petroleum but very soluble in benzene and toluene. The solid is moderately stable in air but solutions are sensitive. No $C\equiv C$ stretching frequency could be identified in the IR spectrum although for similar W or Mo compounds bands are reported around $1750\,cm^{-1}$.[2,4] The ^1H, ^{31}P and ^{13}C NMR spectra are in agreement with those expected for the structure (Fig. 1) as determined by X-ray diffraction. The $^{13}C\{^1H\}$ spectrum shows a doublet at $\delta\,201.4\,ppm$ $(^2J_{C-P} = 5\,Hz$; $^1J_{C-W} = 41\,Hz)$ assigned to $PhC\equiv CH$; a doublet at

$\delta\,164.2\,ppm$ $(^2J_{C-P} = 16\,Hz$; $^1J_{C-W} = 32.8\,Hz)$ assigned to $PhC\equiv CH$; singlets at $\delta\,142$, 130.2, 127.8 and 127.5 ppm corresponding to the 1, 2, 3 and 4 carbons of the phenyl ring; a doublet at $\delta\,17.5\,ppm$ $(^1J_{C-P} = 14.7\,Hz)$ due to PMe_3. These assignments are confirmed by the off-resonance ^{13}C spectrum where the peaks at $\delta\,201.4$ and 142 ppm remain as singlets while the peak at $\delta\,164.2\,ppm$ is a doublet of doublets and can be assigned to $PhC\equiv CH$.

A diagram of the molecular structure of *A* is given in Fig. 1, whilst selected geometry parameters are given in Table 1. The complex has an approximate three-fold axis of symmetry coincident with the W–P axis, and the acetylenic groups are aligned in such a way that the three WC_2 planes are approximately parallel to this axis (making angles of 2, 0 and 2°). The acetylenic carbon atoms are bonded almost symmetrically to the tungsten atom with all six W–C bonds equal within the limits of experimental error. The geometry of the phenylacetylenes are modified in the expected manner, with the formal $C\equiv C$ bonds lengthened to $\sim 1.30\,\text{Å}$ and the Ph groups bent away to give a $C\equiv C-C$ angle of $\sim 138°$. The structure and molec-

---

*Authors to whom correspondence should be addressed.
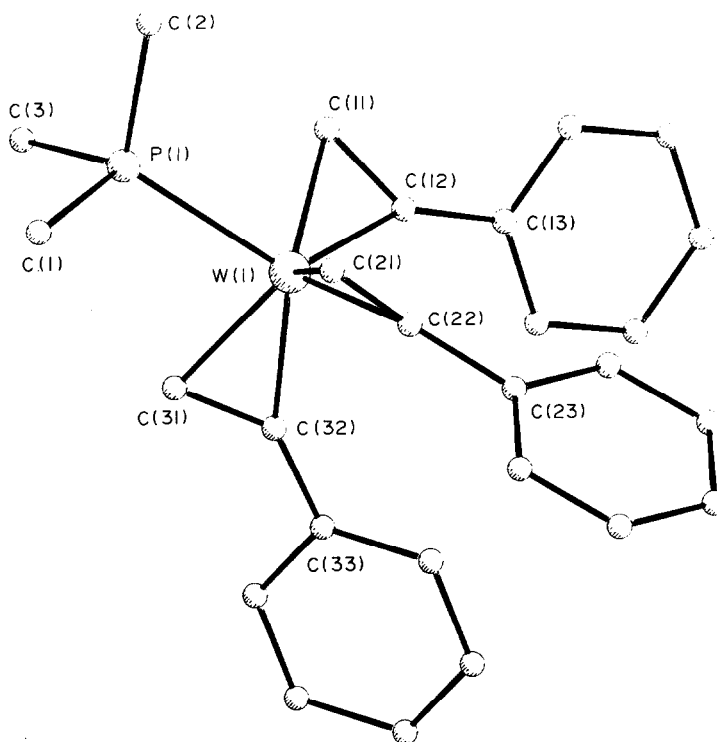
Fig. 1. Single molecule of $(Me_3P)W(PhC \equiv CH)_3$.

Table 1. Selected molecular geometry parameters for $(Me_3P)W(PhC \equiv CH)_3$

(a) **Bond Lengths.**

W–P(1)	2.455(4)		
W–C(11)	2.076(13)	W–C(12)	2.078(13)
W–C(21)	2.093(25)	W–C(22)	2.035(19)
W–C(31)	2.070(23)	W–C(32)	2.072(23)
C(11)–C(12)	1.299(22)	C(12)–C(13)	1.448(17)
C(21)–C(22)	1.336(24)	C(22)–C(23)	1.457(16)
C(31)–C(32)	1.292(19)	C(32)–C(33)	1.447(22)

(b) **Bond Angles.**

P(1)–W–C(11)	84.9(4)	P(1)–W–C(12)	121.3(5)
P(1)–W–C(21)	85.5(4)	P(1)–W–C(22)	123.3(6)
P(1)–W–C(31)	82.9(5)	P(1)–W–C(32)	119.3(5)
C(11)–C(12)–C(13)	138(1)		
C(21)–C(22)–C(23)	138(2)		
C(31)–C(32)–C(33)	137(2)		

ular geometry parameters are closely analogous to those of the complex $(OC)W(HC\equiv CPh)_3$.[3b] The electronic structure of complexes of this type has been discussed previously by Tate *et al.*[3a] who suggested that the complex could be regarded as an eighteen electron system if two of the acetylenes were acting as 4-electron donors (i.e. donating both pairs of π electrons). The structural, and presumably electronic equivalence of all three acetylenes suggests that the unused pair is delocalised into a non-bonding MO (actually of a'_2 symmetry.[3a]

(b) *Methylisocyanide*. Reduction of WCl_4 $(PMe_3)_3$ in presence of MeNC gives an orange, air sensitive complex *trans*-$W(PMe_3)_2(MeNC)_4$ (B), which is very soluble in hydrocarbons.

This complex was shown by X-ray structure analysis to have an octahedral *trans*-phosphine structure. The crystal structure contains two independent centrosymmetric molecules which differ only in the crystallographic orientation of the equatorial $W(CNMe)_4$ groups. A diagram of the unit cell contents are given in Fig. 2, whilst selected molecular geometry parameters are given in Table 2. In view of the low precision of this structure

determination (see Experimental) it is not possible to discuss these parameters in any detail.

In solution both ^1H and $^{31}P\{^1H\}$ NMR spectra indicate that there is a mixture of *cis* and *trans* isomers in a ratio 1:3 at 25°C; the ^1H spectrum is essentially unchanged from -80 to $+75$°C. The ^1H NMR assigned to the *trans* isomer has a triplet at δ 1.8 $(^2J_{P-H} + {}^4J_{P-H} = 5.2\,Hz)$ for the PMe_3 groups and a multiplet at δ 2.84 for *Me*NC. The *cis* isomer has a doublet at δ 1.54 $(^2J_{P-H} + {}^4J_{P-H} = 5.2\,Hz)$ for PMe_3 and two multiplets at δ 2.85 and 2.83 for *Me*NC.

The $^{31}P\{^1H\}$ spectrum has two singlets at δ -25.5 ppm $(^1J_{P-W} = 286\,Hz)$ for the *trans* and δ -34.0 ppm $(^1J_{P-W} = 220\,Hz)$ for the *cis* isomer.

Orange red products are also obtained using Bu^{t}NC but we have been unable to isolate pure compounds. No other phosphine isocyanides appear to exist but a variety of carbonyl compounds $W(CO)_n(PR_3)_m$, $n + m = 6$ are known.[5]

(c) *Trimethylphosphine under hydrogen*. The reduction of $WCl_4(PMe_3)_3$ under hydrogen in presence of excess PMe$_3$ produces the air sensitive pale yellow $WH_2Cl_2(PMe_3)_4$ (C), whose analogue, $WH_2Cl_2(PMe_2Ph)_4$, has recently been reported.[6]
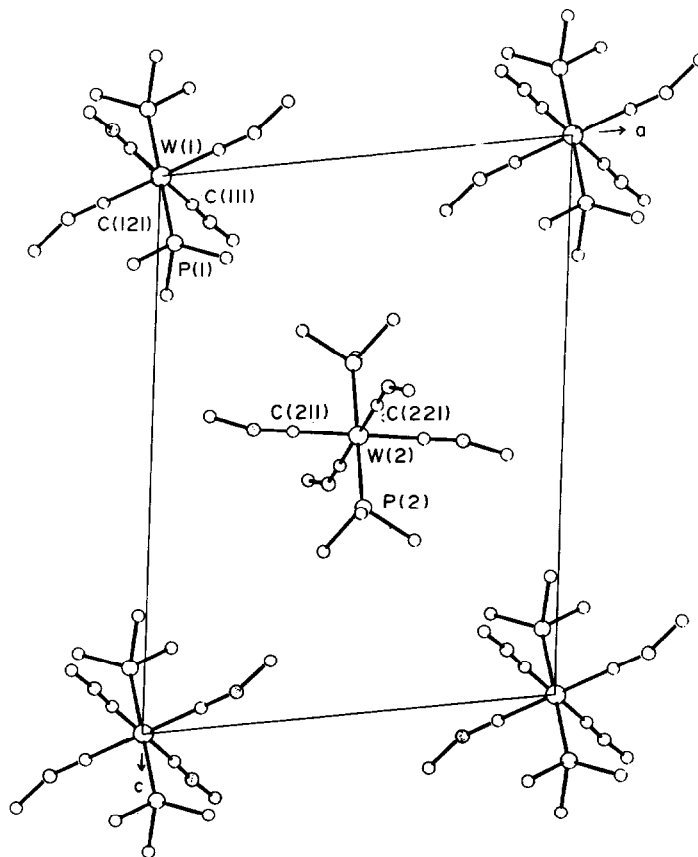
Fig. 2. Unit cell diagram of *trans*-$W(PMe_3)_2(MeNC)_4$.

Table 2. Selected molecular geometry parameters for trans-W(PMe$_3$)$_2$(MeNC)$_4$

(a) Bond Lengths

	Molecule 1	Molecule 2
W-P	2.38(1)	2.43(1)
W-C(X11)	2.23(4)	2.07(3)
W-C(X21)	2.03(3)	2.05(4)
C(X11)-N(X11)	1.14(4)	1.21(3)
C(X21)-N(X21)	1.21(3)	1.25(3)
N(X11)-C(X12)	1.29(4)	1.35(3)
N(X21)-C(X22)	1.41(3)	1.41(4)

(b) Bond Angles

	Molecule 1	Molecule 2
P-W-C(X11)*	91(1)	91(1)
P-W-C(X21)	87(1)	93(1)
C(X11)-W-C(X21)	89(1)	91(1)
W-C(X11)-N(X11)	176(3)	177(3)
W-C(X21)-N(X21)	179(3)	177(3)
C(X11)-N(X11)-C(X12)	172(4)	166(4)
C(X21)-N(X21)-C(X22)	164(4)	147(4)

*For the numbering of atoms in the isocyanides, X = 1, 2 for molecules

1, 2 respectively.

The compound is also obtained by the reaction of WCl$_2$(PMe$_3$)$_4$ with methanol (see below). The compound is very soluble in aromatic hydrocarbons and crystallises well from diethylether. The spectroscopic data is consistent with the structure (1) which is confirmed by preliminary X-ray crystallographic data. Thus, the IR has peaks at 1985 and 1936 cm^{-1} for W–H while the ^{1}H NMR spectrum shows a multiplet at δ 1.44 for PMe$_3$ groups and a triplet of doublets of doublets at δ -3.44 ($^2J_{P-H} = 37.7$ Hz, 42.1 Hz and 60.6 Hz) with an AA'B$_2$X$_2$ spin system for W–H. The ^{31}P{^{1}H} spectrum shows two triplets with an A$_2$B$_2$ spin system at δ -17.06 ppm ($^2J_{P-P} = 16$ Hz, $^1J_{P-W} = 174.4$ Hz) and δ -23.65 ($^2J_{P-P} = 16$ Hz, $^1J_{P-W} = 194$ Hz).

2. Oxodichlorotris(trimethylphosphine)tungsten(IV)

The complex trans-WCl$_2$(PMe$_3$)$_4$[1] is quite unreactive and can be recovered unchanged after treatment with methyllithium or Grignard reagents in ether although it does react with tri-

methylaluminium to give an alkylidyne.[7] However, it reacts readily with methanol alone or in tetrahydrofuran on refluxing to give mixtures of WH$_2$Cl$_2$(PMe$_3$)$_4$ and the purple air-stable WOCl$_2$(PMe$_3$)$_3$ (D).[8] Similar complexes, MOCl$_2$ (PR$_3$)$_3$, M = Mo, W, have long been known for different phosphines.[9,10]

This oxo complex is found to have a *meridional* arrangement of the three phosphines with one of the two chlorines *trans* to the oxo-function. The unit cell contains two independent molecules (a diagram of one of which is given in Fig. 3) whose geometries (Table 3) are essentially equal, within the limits of experimental error. All geometry parameters are close to expected values. The *trans*-influence of the oxo-function on the opposing W–Cl bond and the other chlorine on the opposing W–P bond are noticeable but are not very large. The spectroscopic data for the oxo complex is consistent with the structure determined by X-ray diffraction. The reaction presumably involves an initial oxidative addition of methanol followed by
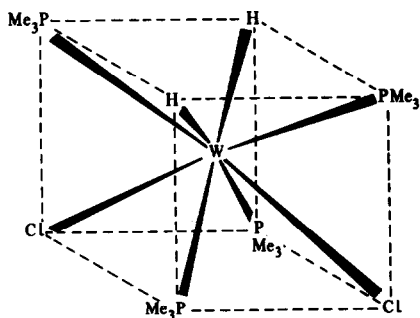
(1)

further reactions of the intermediate methoxide which we have been able to detect spectroscopically but have been unable to isolate. The oxidative addition of methanol to the tungsten(II) species $WH_2(PMe_3)_5$ leading to $WH_3(OMe)(PMe_3)_4$ has previously been established.[11]

EXPERIMENTAL

Microanalysis were by Pascher (Bonn).

Spectrometers. NMR. Perkin–Elmer R32 (^1H), Bruker WM 250 (^1H 250 MHz, ^{31}P 101.2 MHz, ^{13}C 62.9 MHz, 28°C). ^1H data referenced to Me_4Si, $^{31}P\{^1H\}$ to external 85% H_3PO_4 in ppm.

IR. Perkin–Elmer 627; data in cm^{-1}.

All operations were performed under oxygen-free nitrogen or argon or *in vacuo*, and all solvents except methanol were dried over sodium and distilled from sodium benzophenone under nitrogen immediately before use. Methanol was dried over magnesium methoxide and distilled under nitrogen. Petroleum had b.p. 40–60°C. Melting points were determined in sealed tubes under nitrogen (uncorrected).

$WCl_2(PMe_3)_4$ and $WCl_4(PMe_3)_3$ were prepared according to the literature[1].

Trimethylphosphine   tris(phenylacetylene)   tungsten(O) (A)

To $WCl_4(PMe_3)_3$ (1.31 g, 2.36 mmol) suspended in thf (100 cm^3) was added excess phenylacetylene (1.2 cm^3, 10.9 mmol), and the mixture was added to thf (50 cm^3) containing sodium amalgam (1.0 g, 10 cm^3 Hg). The mixture was stirred overnight at room temperature, when the solution was filtered, and evaporated under vacuum. The residue was extracted into petroleum (2 × 40 cm)^3), the solution filtered, concentrated to *ca.* 60 cm^3 and cooled to − 10°C to give pale yellow crystals. Yield: 0.6 g, 50%; m.p., 148–9°C. [Found: C 57.4 (57.2), H 4.8 (4.8), Cl < 0.2 (0), P 5.9 (5.5)%. *M* 550 (566)].

IR: 3078w, 3060w, 3007w, 1970w, 1900w, 1820w, 1635m, 1625m, 1620m, 1610m, 1591w, 1570w, 1480s, 1442s, 1418m, 1303m, 1282m, 1191w, 1170w, 1156w, 1070m, 1027m, 1005m,
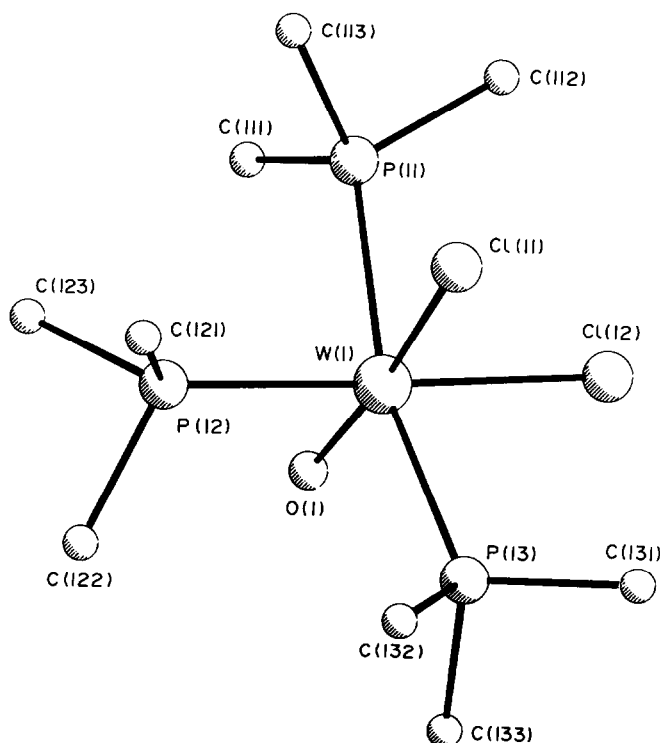
Fig. 3. Structure of the molecule of $WOCl_2(PMe_3)_3$.

Table 3. Selected molecular geometry parameters for $WOCl_2(PMe_3)_3$

		Molecule 1	Molecule 2
(a)	**Bond Lengths (Å)**		
	W — O		1.67(1)
	W—Cl(X1)	2.492(3)	2.483(6)
	W—Cl(X2)	2.473(4)	2.475(3)
	W—P(X1)	2.504(4)	2.499(4)
	W—P(X2)	2.468(3)	2.473(3)
	W—P(X3)	2.510(5)	2.517(4)
(b)	**Bond Angles (deg)**		
	O—W—Cl(X1)	171.6(3)	170.7(3)
	O—W—Cl(X2)	98.0(3)	98.6(3)
	O—W—P(X1)	97.1(4)	94.9(3)
	O—W—P(X2)	85.7(3)	97.2(3)
	O—W—P(X3)	96.7(4)	96.1(3)
	P(X1)—W—P(X3)	164.4(1)	161.2(1)
	P(X2)—W—Cl(X2)	176.3(1)	174.2(2)
	Cl(X2)—W—P(X3)	84.4(2)	81.1(1)
	Cl(X2)—W—P(X1)	86.5(2)	82.2(1)
	P(X2)—W—P(X1)	93.2(2)	96.8(1)
	P(X2)—W—P(X3)	95.1(2)	98.9(1)
	Cl(X1)—W—Cl(X2)	90.3(2)	90.7(2)
	P(X1)—W—Cl(X1)	84.4(1)	86.6(2)
	P(X2)—W—Cl(X1)	86.0(1)	83.5(2)
	P(X3)—W—Cl(X1)	82.9(1)	85.0(2)

998m, 987m, 950s, 935s, 918m, 850m, 842m, 825m, 815m, 796w, 750s, 735m, 690s, 678w, 640w, 620w, 575m, 550w, 500w, 482w.

NMR. ^{1}H (C_6D_6): 9.43 d, 8.27 d, 7.89 d, 7.25 m, 7.13 m, (15) *Ph*C≡CH; 1.57 s (3), PhC≡C*H*; 1.54 s (9), P*Me$_3$*.

^{31}P{^{1}H}(C_6H_6 + 10% C_6D_6): 0.62 s ($^1J_{W–P}$ = 140 Hz)*P*Me$_3$.

^{13}C: see text.

Tetrakis(methylisocyanide) trans *bis(trimethylphosphine) tungsten(O)* (B)

To $WCl_4(PMe_3)_3$ (0.5 g, 0.9 mmol) suspended in thf (50 cm^3) was added excess MeNC (0.5 cm^3, 5.0 mmol), and sodium amalgam (0.5 g Na, 6 cm^3 Hg) in thf (50 cm^3). The mixture was stirred overnight at room temperature. After filtration the solution was evaporated under vacuum, the residue extracted into petroleum (40 cm^3), and the solution filtered, concentrated to *ca.* 10 cm^3 and cooled to − 20°C to give orange crystals. Yield, 0.36 g, 80%; m.p., 110°C. [Found: C33.2 (33.6), N

10.7 (11.4), H 6.0 (6.0), P 11.6 (12.4)%. *M* 480 (500)].

IR. 2118w, 1970sbr, 1830vsbr, 1406w, 1390m, 1380m, 1290m, 1270m, 955s, 938s, 750w, 662m.

NMR. See text.

Tetrakis(trimethylphosphine)   *dichlorodihydridotungsten(IV)* (C)

To a suspension of $WCl_4(PMe_3)_3$ (0.8 g, 1.44 mmol) in thf (20 cm^3) was added excess trimethylphosphine (0.5 cm^3, 5 mmol) and the slurry transferred to a pressure bottle containing sodium amalgam (0.5 g in 2 cm^3 Hg) at − 78°C. After pressurisation with hydrogen (9 atm) the suspension was allowed to warm slowly, and then stirred for 2 hr at room temperature. The resulting green solution was filtered, evaporated under reduced pressure and the residue extracted with diethyl ether (50 cm^3), the solution filtered, concentrated and cooled slowly to − 20°C to give yellow crystals. Yield: 0.36 g (*ca.* 51%); m.p. (decomp.) *ca.*

180°C. [Found: C 25.7 (25.7), H 6.77 (6.77), Cl 12.7 (12.6), P 21.8 (22.1)%. M 550 (561)].

IR. 1985w, 1936s, 1475m, 1432s, 1420s, 1400m, 1300m, 1280m, 1270m, 1100m, 1030w, 940vsbr, 860m, 850m, 820w, 800w, 720s, 665m.

NMR. See text.

4, 5, 6-*Tris*(*trimethylphosphine*)-2, 3-*cis*-*dichloro*-1 -*oxo* *tungsten*(*IV*) (D)

Dried methanol (20 cm³) was added to *trans*-WCl$_2$(PMe$_3$)$_4$ (1.5 g, 2.68 mmol) in thf (50 cm³) at room temperature. The solution was stirred *ca.* 16 hr when the solvent was removed and the residue extracted into toluene (2 × 30 cm³). The orange red extract was filtered, evaporated and the residue extracted into diethylether (2 × 40 cm³). This ether solution was filtered, concentrated to *ca.* 30 cm³ and cooled to − 10°C to give purple crystals of WOCl$_2$(PMe$_3$)$_3$, which were collected. The

filtrate was further concentrated and cooled to − 20°C to give pale yellow crystals, WH$_2$Cl$_2$ (PMe$_3$)$_4$, identical to that prepared as above. (Yield: 0.5 g, 35%).

For WOCl$_2$(Me$_3$)$_3$, Yield: 0.4 g, 30%, m.p., 134–5°C. [Found: C 21.6 (21.7), H 5.5 (5.4), Cl 13.7 (14.2), P. 19.1 (18.6), O 3.0 (3.2)%. M 470 (499)].

IR. 1475w, 1420m, 1300m, 1285m, 1210w, 950vsbr (W = O), 855m, 730s, 715msh, 667m.

NMR. ^{1}H (C$_6$D$_6$): δ 1.44 m.

^{31}P{^{1}H}(C$_6$H$_6$ + 10% C$_6$D$_6$): δ − 24.0 d (2), $^1J_{W-P}$ = 343 Hz, $^2J_{P-P}$ = 4.2 Hz; δ − 30.1 t (1), $^1J_{W-P}$ = 446 Hz, $^2J_{P-P}$ = 4.2 Hz.

Crystallographic studies

Crystals of all three compounds were sealed under argon in Lindemann capillaries. All crystallographic measurements were made using a CAD4 diffractometer, operating in the $\omega/2\theta$ scan

Table 4. Crystal data and details of refinement

	Compound A	Compound B	Compound D
(1) Crystal Data			
Formula	C$_{27}$H$_{27}$PW	C$_{14}$H$_{30}$N$_4$P$_2$W	C$_9$H$_{27}$Cl$_2$OP$_3$W
Formula weight	566.36	500.26	499.02
Crystal System	Tetragonal	Monoclinic	Monoclinic
a/Å	22.140(4)	12.484(4)	17.222(3)
b/Å	22.140(4)	10.408(1)	12.824(4)
c/Å	10.141(7)	10.989(5)	19.279(3)
β/deg		97.46(3)	115.84(1)
V/Å³	4970	2189	3832
Sapce group	I$\bar{4}$	P2$_1$/c	P2$_1$/c
Z	8	4	8
Dz/g cm^{-3}	1.51	1.52	1.73
Linear Abs. Coeff/cm^{-1}	45.09	51.85	62.5
Crystal size/mm³			
(2) Data Collection			
ω scan width/deg	0.8 + 0.35 tan θ	0.8 + 0.35 tan θ	0.8 + 0.35 tan θ
θ$_{min}$, θ$_{max}$/deg	2.0, 25	1.5, 27.0	1.5, 25.0
Total data	4740 (± h,k,ℓ)	5249	7286
Total unique	2463	4767	6746
Total observed [F$_o$ > 3σ(F$_o$)]	2269	1877	4611
(3) Refinement			
Number of parameters	227	163	200
Weighting scheme coeff g in ω = 1/[σ²(F$_o$) + g|F$_o$|²]	0.0005	*	0.0007
Final R = Σ|ΔF|/Σ|F$_o$|	0.039	0.061	0.057
Final R' = Σω|ΔF|²/Σω|F$_o$|²	0.042		0.056

*Unit weights used

mode, with monochromated Mo–$K\alpha$ radiation ($\lambda = 0.71069$ Å) in a manner previously described in detail.[12] All data were corrected for absorption empirically.[13] The structures were determined using standard heavy atom procedures and refined by full matrix least-squares methods. Computers, programs and sources of scattering factor data were also as given in Ref. 12.

For compound A all non-hydrogen atoms were refined with anisotropic thermal parameters but the phenyl rings were refined as rigid bodies with hexagonal geometry, and the hydrogen atoms included in idealised positions (C–H = 1.08Å) and assigned a common, overall U_{iso} parameter (= 0.15Å^2). Unfortunately the acetylenic protons could not be located and were not included. For compound B, the refinement was difficult due to excessive pseudo-symmetry and some disorder in the orientation of the PMe_3 groups. The unit cell contains two independent, centrosymmetric molecules, centred at 0, 0, 0 and $\frac{1}{2}$, $\frac{1}{2}$, 0, and in addition to the heavy atom pseudo-centring, the linear P–W–P units are also approximately parallel. However, the set of equatorial $CNMe$ groups have different orientations in the two molecules and this allowed the pseudo symmetry to be broken, albeit weakly. Stable refinement could only be achieved by retaining isotropic thermal parameters for all but the metal atoms, and by constraining the P–C bonds to standard values (1.84 ± 0.02Å). As a result the structure has not been determined with high precision.

For compound D, high thermal motion and/or disorder in the PMe_3 groups also caused some problems in refinement and for this structure the P–C distances were also constrained during refinement, for which two blocks were used (one molecule per block).

Details of the crystal data, intensity measurement and refinement procedures are given in Table 4. Computer programs and sources of scattering factor data are as given previously.[13]

Tables of atomic coordinates, thermal parameters, bond lengths and angles and lists of F_o/F_c values have been deposited as supplementary data with the Editor, from whom copies are available on request. Atomic coordinates have also been deposited with the Cambridge Crystallographic Data Base.

REFERENCES

1. P. R. Sharp and R. R. Schrock, *J. Am. Chem. Soc.* 1980, **102**, 1403.
2. For references see R. Davis and L. A. P. Kane-Maguire, In *Comprehensive Organometallic Chemistry* (Edited by G. Wilkinson, F. G. A. Stone and E. W. Abel), Vol. 3, p. 1375. Pergamon Press, Oxford (1982).
3. (a) D. P. Tate, J. M. Augl, W. M. Ritchey, B. L. Ross and J. G. Grasselli, *J. Am. Chem. Soc.* 1964, **86**, 3261. (b) R. M. Laine, R. E. Moriarty and R. Bau, *J. Am. Chem. Soc.* 1972, **94**, 1402.
4. R. Bowerbank, M. Green, H. P. Kirsch, A. Mortreaux, L. E. Smart and F. G. A. Stone, *J. Chem. Soc., Chem. Commun.* 1977, 245.
5. R. Mathieu, M. Lenzi and R. Poilblanc, *Inorg. Chem.* 1970, **9**, 2030.
6. M. E. Fackley and R. L. Richards, *Transition Met. Chem.* 1982, **7**, 1.
7. P. R. Sharp, S. J. Holmes, R. R. Schrock, M. R. Churchill and H. J. Wesserman, *J. Am. Chem. Soc.* 1981, **103**, 965; S. J. Holmes, D. N. Clark, H. W. Turner, and R. R. Schrock, *J. Am. Chem. Soc.* 1982, **104**, 6322.
8. Independently synthesised by E. Carmona, personal communication; see *Polyhedron* 1983, **2**, 797.
9. A. V. Butcher and J. Chatt, *J. Chem. Soc.* (*A*) 1970, 2652.
10. A. V. Butcher, J. Chatt, G. J. Leigh and R. L. Richards, *J. Chem. Soc., Dalton Trans.* 1972, 1064.
11. K. W. Chiu, R. A. Jones, G. Wilkinson, A. M. R. Galas, K. M. A. Malik and M. B. Hursthouse, *J. Chem. Soc., Dalton Trans.* 1981, 1204.
12. M. B. Hursthouse, R. A. Jones, K. M. A. Malik and G. Wilkinson, *J. Am. Chem. Soc.* 1970, **101**, 4128.
13. A. C. T. North, D. C. Phillips and F. J. Mathews, *Acta Cryst.* 1968, **A24** 351.

ISOELECTRONIC REAGENTS. II. STANDARD FORMATION
ENTHALPIES OF PHENYL AND pFLUOROPHENYL IODINE DICHLORIDES

M. CARTWRIGHT and A.A. WOOLF*

School of Chemistry, University of Bath,
Bath BA2 7AY, UK

Abstract – The formation heats $\Delta H_f^o PhICl_2(c)$
= 21.7 kJ mol^{-1} and $\Delta H_f^o pFC_6H_4ICl_2(c)$ = −173.0 kJ mol^{-1}
were determined by reaction of iodides with excess
chlorine in methyl cyanide. These heats are used to
show:

(i)   that thermal or photo-decompositions of aryl
       iodine dichlorides are kinetically controlled,

(ii)   the greater halogenating ability of aryl
       iodine dichlorides than Ph_3ACl_2 (A = P, As,
       Sb) compounds, and

(iii) the weakening of halogenating ability with
       phenylation.

INTRODUCTION

In Part I[1] previously unrelated fluorinating reagents
such as $PhIF_2$, Ph_3PF_2 and XeF_2 were shown to be period-
ically related as isoelectronic molecules E_3AF_2, where
E represents a bonded or non-bonded electron pair and A
a main group element. They were arranged in order of
fluorinating ability by estimating the magnitude of
reduction couples as approximated by enthalpy
differences $\Delta H_f^o(E_3AF_2) - \Delta H_f^o(E_3A)$.

In this paper we start a quantitative study on the
halogenating ability of the corresponding series of di-
chlorides by measuring heats of formation of the well
known aryl iodine dichlorides.[2] This will enable
kinetic effects to be distinguished from equilibrium
control when these reagents are used.

EXPERIMENTAL

Materials

Phenyl and p-fluorophenyl iodine dichlorides were
made in high yields (>95%) by passing dichlorine into
ice-cold solutions of iodides in methylene chloride.
The precipitates were vacuum dried (1-2 hrs at
1.33 Nm^{-2}) and analysed iodometrically after adding

aqueous KI to solutions of the dichloride in CCl_4. At
room temperatures the loss of oxidising power per day
was 0.5% for $PhICl_2$ over a week, and 0.04% for
$pFC_6H_4ICl_2$ over a 40 day period. Hence samples were
used soon after preparation or were stored at $-10^\circ C$
before use.

Calorimetry

A glass isoperibol calorimeter was used at $25^\circ C$ with
solids or liquids held in PTFE screw-capped glass
cylinders closed with polythene foils. For heats of
gas absorption a 'bell' fitment, described previously,
held the gas prior to solution.[3]

Two strategies were adopted for determining heats of
formation of the iodine dichlorides; direct formation
from iodide and chlorine, and interaction of the
iodine dichloride with reductants. In the direct
formation the heats of chlorine dissolution in con-
ventionally purified methyl cyanide were inconsistent.
The presence of chlorine-consuming impurities left
after distillation had also been noted when $MeNO_2$ was
used as solvent.[4] Consistent heats of solution,
approaching values expected from Raoult's Law, were
only obtained after prechlorination, which consisted of
saturating the conventionally purified MeCN with
chlorine and leaving for 2 days before refractionating.
Approximately one fifth of the mid-fraction was again
saturated with chlorine and then added to the remainder
of this fraction. The heat of solution of chlorine in
an ideal solvent should approach the latent heat of
evaporation of chlorine (20.4 kJ mol^{-1}) or the heat
derived from the Clapeyron-Clausius equation over the
range $5-30^\circ C$ (20.0 kJ mol^{-1}). The value obtained in
MeCN of 23.1 kJ mol^{-1} compares with 17.8 kJ mol^{-1} in
CCl_4,[5] which is regarded as an 'ideal' solvent.

Even when solvent chlorination effects had been
eliminated, the heats of addition of chlorine to excess
of PhI were inconsistent. The heats of successive
additions decreased from values greater than, to values
less than, the heat of the inverse reaction in MeCN
(i.e. PhI into excess of Cl_2). This effect was caused
by slow chlorination of excess PhI with the generated
$PhICl_2$ as demonstrated by the gradual loss in the
ability of mixed $PhICl_2$-PhI solutions in MeCN to
liberate I_2 from KI.

Addition of aliquots of PhI to 20% saturated solutions
of Cl_2 in MeCN gave consistent heats, but at higher
concentrations values were unreliable because of
appreciable degassing of solutions.

The alternative technique, in which the redox couple $ArICl_2/ArI$ is combined with another couple, requires rapid quantitative reactions at $25°C$ and well defined accessible starting materials and products. The $SnCl_2/SnCl_4$ and I^-/I_2 or I_2/I^+ couples would normally meet the requirements, and indeed both $SnCl_2$ and KI are readily oxidised by $ArICl_2$. The data collected in Table 2 leads to heats inconsistent with those derived by direct chlorination.

Another reductant tried was sodium sulphite. This reaction, carried out in a mixed solvent ($MeCN-H_2O$) to maintain solution homogeneity, proceeded smoothly and reproducibly. Direct measurement of the heat of solution of Na_2SO_3 in the mixed solvent, which is liable to errors because of oxidation by dissolved oxygen, was avoided by using iodine as oxidant. The equation (3), used to calculate the heat of formation of the aryl iodine dichloride, was the difference between the redox reactions (1) and (2), with all components in solution apart from the added solid phases indicated (c).

$$pFC_6H_4ICl_2(c) + Na_2SO_3 + H_2O \rightarrow pFC_6H_4I + Na_2SO_4 + 2HCl \qquad (1)$$

$$Na_2SO_3 + I_2(c) + H_2O \rightarrow Na_2SO_4 + 2HI \qquad (2)$$

$$pFC_6H_4ICl_2(c) + 2HI \rightarrow pFC_6H_4I + 2HCl + I_2(c) \qquad (3)$$
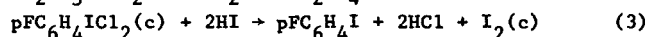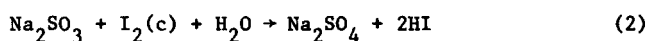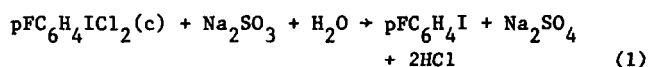
The enthalpies obtained differed considerably from those determined by direct chlorination, and this was finally traced to the participation of the iodosulphite ion SO_2I^- in reaction (2). These results and the occurrence of iodosulphites in other reactions will be discussed in detail elsewhere.

Decomposition of phenyl iodine dichlorides

Compacted samples sealed in tubes appended to evacuated boro-silicate bulbs were decomposed in the dark at constant temperature ($\pm1°$) in a stirred-air oven of large thermal capacity. The size of bulb was chosen to keep the final pressure below 2 atmos., assuming 1 mole of HCl was formed per mole of polyhalide. Other specimens were irradiated under a mercury u.v. lamp in sealed silica tubes at $20°C$ until the sample had completely liquefied. Hydrogen chloride was removed in vacuo at $-30°C$, and the residual liquids were weighed by difference after washing out the removed tube-appendix with petroleum ether ($60-80°C$ range). Free iodine was extracted and estimated with excess aqueous thiosulphate or sulphurous acid solutions. The organic phase was separated through phase separating paper, dried with molecular seive (Linde 3A) and the

components separated on a Carbowax (15% chromosorb
W-AW-DCMS) column at 125°. Products were identified by
peak enhancement, retention times and i.r. spectra
where appropriate. The concentrations of the com-
ponents relative to iodobenzene were assessed by
comparison with synthetic mixtures. Results are
summarized in Table 3. At the higher temperatures
some solid product had sublimed onto the upper part of
the bulbs. It was not identified but probably
consisted of chlorinated di- and poly-phenyls. This
was supported by the iodine balance obtained at the
highest temperature. The iodine displaced as a % of
that originally present in the polyhalide was greater
than the measured % of non-iodinated products.
Analogous products were isolated from the $p\text{-}FC_6H_4ICl_2$
thermal and catalysed ($SnCl_4$) decompositions and were
identified by mass spectrometry.

RESULTS AND DISCUSSION

The standard heats of formation were calculated as
$\Delta H_f^o PhICl_2(c) = 21.7$ kJ mol^{-1} and $\Delta H_f^o pFC_6H_4ICl_2(c)$
$= -173.0$ kJ mol^{-1} using the data from oxidative
addition of dichlorine in Table 1 and the auxiliary
heats $\Delta H_f^o PhI(l) = 114.5$ kJ mol^{-1} and $\Delta H_f^o pFC_6H_4I(l)$
$= 81.7$ kJ mol^{-1}.[6] The latter has not been reported but
can be estimated by group-additivity methods, or more
simply by averaging the values for $\Delta H_f^o pFC_6H_4F(l)$ and
$\Delta H_f^o pIC_6H_4I(l)$. Some estimates of heats of melting and
vapourization are required also. Thus the heat of
fusion of pIC_6H_4I was taken as 1.17 times that of
the ortho-compound[7] from which $\Delta H_f^o pIC_6H_4I(l)$ was
estimated as 177.3 kJ mol^{-1}. The heat of vapouriz-
ation of pFC_6H_4I was estimated as 45.6 kJ mol^{-1} using a
Trouton constant of 100 kJ mol^{-1} K^{-1}. For the group
additivity method we accept Benson's C_B-H additivity
increment of 13.8 kJ,[8] but use C_B-F, C_B-I and C_B-Cl
values of -183 ± 2, 92.5 ± 0.6, -17.1 ± 0.6 kJ, about
4 kJ less than Benson's value since they are derived
from the mono- and di-halobenzenes heats rather than
from a more extended range of compounds. This leads to
$\Delta H_f^o pFC_6H_4I(l) = -80.9$ kJ mol^{-1}, compared to a value of
-82.4 kJ mol^{-1} by averaging dihalide values. Hence a
mean value of -81.7 kJ mol^{-1} is probably correct to
± 1 kJ. [These estimates can be cross-checked using the
iso-electronic heat method[9] in which heats of OH and F
compounds are equated, i.e.

$\Delta H_f^o pIC_6H_4OH(c) = -95.4$ kJ mol^{-1} $\pm 5.4 \approx \Delta H_f^o pIC_6H_4F(c)$
and a heat of fusion estimate of 17 kJ mol^{-1}.]

In reductions with stannous chloride or iodine, reactions additional to the expected simple reactions must occur (see Table 2).

$$ArICl_2 + SnCl_2 \rightarrow ArI + SnCl_4;$$
$$ArICl_2 + I_2 \rightarrow ArI + 2ICl; \text{ or}$$
$$3ArICl_2 + I_2 \rightarrow 3ArI + 2ICl_3.$$
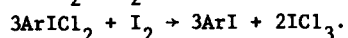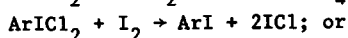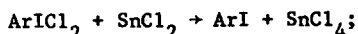
It is probable that the stannic chloride formed reacts with $ArICl_2$ to produce a reactive salt such as $ArICl^+SnCl_5MeCN^-$, which can ring chlorinate the former to some extent as well as the aryl iodide. It is significant that in experiments with $Ar = pFC_6H_4$ the results neatly divide into groups above and below the ratio $ArICl_2/SnCl_2 = 2$, the limiting ratio required to completely form the salt. The reality of substitution reactions in this system was confirmed by gas chromatographic examination of products which were the same as those formed by thermal or photo-decomposition of $ArICl_2$. Salt formation was indicated by the large heat of mixing and increase in electrical conductivity when solutions of $pFC_6H_4ICl_2$ and $SnCl_4$ in MeCN were mixed. Even more complications could arise with the iodine oxidation, since as well as salt formation and substitution reactions, equilibration of I_2 with ICl and Cl^- could produce mixtures of ions such as I_3^-, I_2Cl^- and ICl_2^-, dependent on the iodine and chloride ion concentrations.

The decomposition of phenyl iodine dichloride can now be considered from a thermodynamic viewpoint. The decomposition products of thermal and photochemical decompositions can result from simple dissociation, A, the reverse of the formation reaction, from aromatic substitution, B, and from halogen displacement, C. The product distribution classified as A, B or C products is shown in Table 4. The enthalpies of these reaction types have been evaluated in Table 5.

The free energies for A and B can be approximated by adding a $T\Delta S^o$ term of about 66 kJ mol^{-1} to the enthalpy values due to the release of a mole of gas. The large endo-ergic value for A means that the PhI content in the decomposition reactions is far from equilibrium. Higher temperatures and longer periods of heating move the reactions closer to equilibrium with increasing participation of the most exo-ergic displacements, C, as shown in the last column of Table 5. Substitution reactions predominate under mild irradiation conditions and would be expected to be susceptible to catalysis as was illustrated in the thermochemical measurements with stannic chloride formed in situ.

Keefer and Andrews[4] claimed to have measured dissociation constants for reaction A in various solvents. They obtained a K value of 4.2×10^{-4} at 298 K for $PhICl_2$ in $MeNO_2$. The equivalent ΔG^o value of 19.3 kJ mol^{-1} is quite incompatible with our thermochemical measurements for reaction A. However, it is very much closer to the ΔG^o value for reaction B and we suggest that they were actually observing the substitution reaction rather than the dissociation. The experimental technique they used does not preclude this possibility. They measured the original oxidising power of the solution iodometrically to obtain iodobenzene dichloride concentrations and then observed the disappearance of the $PhICl_2$ absorption at 380 nm ($\varepsilon = 105$) at which wavelength PhI has an ε value of only 0.05. They did not consider any substitution products. These would also be unobserved, since the ε values for the ClC_6H_4I isomers are only 0.01 - 0.03. Perhaps the most revealing indication of substitution is the slight increase in the rate of equilibration by HCl and the tremendous effect of ICl. The last observation ties in with the inconsistencies we encountered in measuring heats of reaction of $PhICl_2$ with I_2 where the ICl formed caused substitution. Indeed, the interpretation of results in this and their subsequent series of papers can be questioned, if substitution reactions are involved to any appreciable extent.

The halogenating ability of E_3AX_2 compounds (X = halogen) has been placed in a sequence according to the central atom A:

P < Sb $\sim$ As $\sim$ Te < Se < S < I < Br < Cl $\sim$ Xe < Kr, mainly from qualitative observations.[1] It is therefore of interest to check part of this sequence with the new data. Chlorinating couples expressed in enthalpy values are collected in Table 6. (In making comparisons between isoelectronic reagents it is reasonable to assume that entropy changes will cancel approximately and that 'enthalpy couples' can be employed.)

The aryl iodine dichlorides are almost identical in reduction potentials and this was confirmed by showing that the equilibrium

$$C_6H_5ICl_2 + FC_6H_4I \rightleftharpoons C_6H_5I + FC_6H_4ICl_2$$
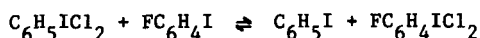
could be approached from either side as shown by in situ proton and fluorine magnetic resonance measurements. Phenyl iodine dichloride in methyl cyanide solutions is almost as powerful an oxidant as solid iodine trichloride.

The relative values of the other couples are also compatible with the known chemistry. Thus the weakest oxidant, Ph_3PCl_2, is unable to oxidise tetrachloroethene. Indeed, Ph_3PCl_2 is prepared quantitatively[10] by the reverse reaction: $Ph_3P + C_2Cl_6 \rightarrow Ph_3PCl_2 + C_2Cl_4$ or by using the more powerful oxidant $PhICl_2$ in MeCN.

Similarly, it is reported that Ph_3Sb is chlorinated with ferric chloride and Ph_3P by cupric chloride. This contrasts with the ability of $PhICl_2$ to dissolve iron or ferrous chloride, and copper or cuprous chloride. Sulphuryl chloride has been used in the preparation of Ph_3ACl_2 (A = As, Sb)[11] and we have shown that it can also chlorinate Ph_2S. (The SO_2Cl_2/SO_2 couple will be less negative than shown in Table 6 when in solutions such as methyl cyanide.) Heats of formation of E_3ACl_2 compounds in earlier groups can be determined using the greater chlorinating ability of the $PhICl_2/PhI$ couple.

Phenyl iodine dichloride is often referred to as an I(III) compound in the literature. This description violates the usual assignment rules for oxidation stated because it implies that the phenyl group is negatively charged with respect to iodine. Sanderson, using his electronegativity equalization method, has assigned charges to phenyl compounds of different elements and shown that phenyls are positive with respect to less electronegative elements.[12] Hence the oxidation state of iodine in $PhICl_2$ should be less than in ICl_3 and this is confirmed by the reduction potentials shown in Table 6. In general, phenylation of interhalogens and other E_3AX_2 compounds would be expected to moderate their reactivity, as the oxidation state on the central atom is lowered.

REFERENCES

[1] M. Cartwright and A.A. Woolf, J. Fluorine Chem., 1981, 19, 101.

[2] D.F. Banks, Chem. Rev., 1966, 66, 243. M. Fieser and L.F. Fieser, Reagents for Organic Synthesis, Vols. 1, 2, 3, 4 and 6, J. Wiley, New York, 1967-77.

[3] M. Cartwright and A.A. Woolf, J. Fluorine Chem., 1979, 13, 353.

[4] R.M. Keefer and L.J. Andrews, J. Amer. Chem. Soc., 1958, 80, 5350.

[5] W. Gerrard, Solubility of Gases in Liquids, Plenum Press, New York, 1976.

[6] J.B. Pedley and J. Rylance, N.P.L. Computer Analysed Thermochemical Data, Univ. of Sussex, 1977. CODATA Bulletin 28, Recommended Key Values for Thermodynamics, 1978.

[7] A. Bondi, Physical Properties of Molecular Crystals, Liquids and Glasses, J. Wiley, New York, 1968.

[8] S.W. Benson, Thermochemical Kinetics, 2nd ed., p.281, J. Wiley, New York, 1976.

[9] A.A. Woolf, J. Fluorine Chem., 1978, 11, 307.

[10] R. Appel and H. Schoeler, Ber., 1977, 110, 2382.

[11] A.J. Banister and L.F. Moore, J. Chem. Soc., 1968A, 1137.

[12] R.T. Sanderson, Inorganic Chemistry, p.386, Reinhold, New York, 1967.

Table 1. Heats of reaction of ArI with excess Cl_2 in MeCN

Reaction	Weight/g	Heat/J	Reaction heat/kJ mol^{-1}
PhI into MeCN/Cl_2*	0.9457	224.4(0)	48.4(1)
	0.7408	166.2(1)	45.7(7)
	0.6997	165.5(4)	48.2(7)
	0.9046	217.7(5)	49.1(0)
	0.8640	198.1(4)	46.7(8)
		Mean:	47.6(7) σ 1.36
pFC_6H_4I into MeCN/Cl_2	1.5082	296.7(0)	43.7(0)
	2.3068	474.7(2)	45.6(9)
	1.8322	304.9(7)	41.8(7)
	0.7894	152.6(4)	42.9(3)
	1.0599	198.8(7)	41.6(7)
	0.8249	168.6(2)	45.3(8)
		Mean:	43.5(4) σ 1.71
Cl_2 into MeCN/Cl_2**	0.1338	42.86	22.7(1)
	0.1118	37.54	23.8(2)
	0.1384	43.64	22.3(6)
	0.0581	19.15	23.3(7)
		Mean:	23.0(7) σ 0.65
$PhICl_2$ into MeCN/Cl_2	Mean heat of solution		-22.1(5) σ 1.68
$pFC_6H_4ICl_2$ into MeCN/Cl_2	Mean heat of solution		-24.7(0) σ 0.80

* The calorimetric fluid was 250 ml of CH_3CN 20% saturated with Cl_2.

** The weights were determined iodometrically.

Table 2. Unsuccessful methods for determining $\Delta H_f^\circ (PhICl_2)_c$

Reaction	Weight /g	Reaction heat /kJ mol^{-1}
Successive additions	0.5701*	72.0
of Cl$_2$ into	0.8159	68.3
0.098M PhI in CH$_2$Cl$_2$	0.6387	51.0
PhICl$_2$ into CH$_2$Cl$_2$		Mean heat of soln −23.9 σ 2.5
PhI into CH$_2$Cl$_2$		Mean heat of soln −1.25 σ 0.2
Successive additions	0.4423	91.8
of Cl$_2$ into MeCN	0.4690	84.3
purified by	0.4775	68.0
distillation		
I$_2$ into excess PhICl$_2$ i	0.2364	91.7
in MeCN (250 ml)	0.2791	41.1
i 1.757 g PhICl$_2$	0.2317	54.1
ii 1.608 g PhICl$_2$ ii	0.2813	10.8
	0.1825	6.3
	0.2588	−8.6
SnCl$_2$ into excess	0.3968	227.5
pFC$_6$H$_4$ICl$_2$ in MeCN i	0.2906	224.6
(220 ml)	0.2830	242.8
i 2.079 g pFC$_6$H$_4$ICl$_2$	0.1848	224.1
ii 1.970 g pFC$_6$H$_4$ICl$_2$ ii	0.3101	224.7
	0.2138	257.8
	0.1537	256.3
SnCl$_4$ into MeCN		Mean heat of soln 157.5 σ 2.0
PhI into MeCN		Mean heat of soln −3.1 σ 0.4
SnCl$_4$ solution in MeCN		
(0.6654 molal)	0.1186	139.5
into PhICl$_2$ in MeCN	0.1159	138.3

* Weights determined iodometrically.

Table 3. Decomposition products of $C_6H_5ICl_2$

Conditions		C_6H_5Cl	$1,4C_6H_4Cl_2$	$1,2C_6H_4Cl_2$	C_6H_5I	$1,2,4C_6H_3Cl_3$	pC_6H_4ICl	oC_6H_4ICl
				Products % w/w				
Closed tube,								
1.	hν, 31 hr at 20°C	0.30	1.71	0.84(5)	11.6	0.44	47.8	37.3
Closed tube, dark								
2.	4 hr at 100°C	0.63	3.1	1.43	18.6	1.22	40.3	34.8
3.	1 hr at 124°C	1.13	2.55	1.36	33.1	0.73	32.8	28.3
4.	0.25 hr at 157°C	2.26	3.25	1.86	36.5	0.80	28.5	26.8
5.	74 hr at 157°C	6.14	14.4(5)	10.0(5)	19.9	2.43	21.7	25.3
Open tube, daylight								
	5 min at 124°C	0.8	1.33	0.70	31.6	0.13	33.6	31.8

Table 4. Decomposition of $C_6H_5ICl_2$ classified into
dissociation (A), substitution (B) and
displacement (C) reactions*

Conditions	Product distribution /mole %			Reaction ratios		
	A	B	C	B/A	C/A	C/(A+B)
hν, 31 hr at 20°C	13.0	81.8	5.2	6.29	0.40	0.055
Dark, 4 hr at 100°C	20.3	70.1	9.6	3.45	0.47	0.106
Dark, 1 hr at 124°C	35.3	55.8	8.9	1.58	0.25	0.098
Dark, 0.25 hr at 157°C	38.1	49.3	12.6	1.29	0.33	0.144
Dark, 74 hr at 157°C	18.4	37.3	44.3	2.03	2.41	0.795

* Recognised by products, i.e. for A, PhI; for B, chloro-iodo
compounds; for C, chloro-compounds.

Table 5. Enthalpies of decomposition reactions of
phenyl iodine dichloride

	Reaction	$\Delta H°$/kJ mol^{-1}
A)	$PhICl_2(c) \rightarrow PhI(l) + Cl_2(g)$	92.8
B)	$PhICl_2(c) \rightarrow$ I-⟨C$_6$H$_4$⟩-Cl(c) + HCl(g)	−54.9
	" $\rightarrow$ " (1) "	−34.5
C)	I-⟨C$_6$H$_4$⟩-Cl(c) + $\frac{1}{2}Cl_2$(g) $\rightarrow$ Cl-⟨C$_6$H$_4$⟩-Cl(c) + $\frac{1}{2}I_2$(c)	−101.4
	" " $\rightarrow$ " (1) "	−83.0

Table 6. Enthalpy difference for chlorinating couples

Couple	$\Delta H^{\circ}(XCl_2 - X)/kJ\ mol^{-1}$
$pFC_6H_4ICl_2(c) - pFC_6H_4I(l)$	-91.3
$PhICl_2(c) - PhI(l)$	-92.8
$ICl_3(c) - ICl(l)$	-65.6
$(PhICl_2 \rightarrow PhI + Cl_2)$ in MeCN solution	-67.6
$SO_2Cl_2(l) - SO_2(g)$	-97.3
$2 \times [FeCl_3(c) - FeCl_2(c)]$	-114.6
$C_2Cl_6(c) - C_2Cl_4(l)$	-153.2
$2 \times [CuCl_2(c) - CuCl(c)]$	-160.6

A COMPARATIVE STUDY OF CUPRIC COMPLEXES
OF DICARBOXYLIC ACIDS AND ACID-AMIDES LIGANDS

Philippe ARRIZABALAGA [a] and Paule CASTAN[*]

Laboratoire de Chimie de Coordination du CNRS, 205 route de Narbonne,
31400 Toulouse, France

and

Patrick SHARROCK

Département de Chimie, Université de Sherbrooke, Quebec J1K 2R1, Canada

ABSTRACT – A bis(succinamato)copper(II) complex has been synthetized as well as several cyclic acid-amide ligand complexes. These compounds were characterized by elemental and thermogravimetric analyses, infrared and EPR spectroscopies. Analogous dicarboxylic acids give complexes of 1/1 stoichiometry which are thermally more stable than the acid-amide complexes. All the reported compounds show triplet state EPR spectra similar to cupric acetate. There is no evidence for a participation of the amide functions in cupric ion complexation.

INTRODUCTION

Metal salts of carboxylic acids are well known and several reviews have appeared on copper carboxylates,[1-3] magnetic and spectroscopic studies on copper dicarboxylates have also been reported.[4] We have been interested in carboxylic acid-amides difunctional ligands as sources of new metal complexes. Even though copper-biuret compounds have been known for a long time[5-7] and copper binding to deprotonated peptide-amide groups is well documented,[7] very few cupric salts of amides have been synthesized.[9,10]

We wish to report the first synthesis of a metal salt of succinamic acid and of several analogous cyclic dicarboxylic acid and carboxylic acid-amide salts of copper(II).

The dicarboxylic acids here examined and their abbreviations are respectively; cyclohexane 1,2 dicarboxylic acid (cyclohexane diA.); 4-cyclohexene 1,2 dicarboxylic acid (cyclohexene diA.); cyclopentane 1,1 diacetic acid (cyclopentane diA.). The carboxylic acid-amide are; succinamic acid (suc); cyclohexane 1-carboxylic acid 2-carboxamide (cyclohexane A.A.); and cyclopentane 1-acetic acid 1-acetamide (cyclopentane A.A.).

EXPERIMENTAL SECTION

Infrared spectra were recorded using a Perkin Elmer Model 577 spectrometer calibrated with a polystyrene film in the 4000–200 cm^{-1} range using KBr disks. The ESR spectra were obtained with a conventional X-band Bruker ER-200D spectrometer. Thermogravimetric analyses were carried out under nitrogen atmospheres with a Setaram electrobalance and a programmable furnace set at 3°C increase per minute.

[a] Present address : Laboratoire de Chimie Physique, Université de Genève, 30 quai Ernest-Ansermet, 1211 Genève 4, Suisse.

SYNTHESIS

1. Carboxylic acid-amide ligands

Dry ammonia is bubbled into a saturated 100 ml dimethoxypropane solution of the dicarboxylic anhydride (obtained commercially from Aldrich). A precipitate forms which is collected, washed with water and leached with boiling acetone to remove any dicarboxylic acid formed. Elemental analyses are in good agreement with the proposed formula for the resulting compounds.

2. Dicarboxylic acid complexes

The dicarboxylates were synthesized by adding aqueous cupric sulphate to potassium hydroxide neutralized solutions of the dicarboxylic acids. The resulting blue-green precipitates were filtered off and leached with boiling acetone to remove excess ligand.

3. Carboxylic acid-amide complexes

The carboxylic acid-amide complexes were obtained by reacting stoichiometric quantities of the ligand adjusted to pH 7 and cupric chloride. The desired precipitates were washed with water and then with acetone. All elemental analysis are in good agreement with the proposed formula listed in Table 1.

Table 1. Thermogravimetric results

Compound [a]	Decomposition range (°C)	T max (°C) [b]	Weight left (%) [c]
$Cu(Suc)_2$	220–380	240,260,350	33.7
$Cu(cyclohexane\ A.A.)_2$	240–310	240,310	20.0
$Cu(cyclohexene\ A.A.)_2$	220–280	240,310	23.5
$Cu(cyclohexanediA).H_2O$	280–350	320	28.7
$Cu(cyclohexenediA).H_2O$	210–330	300	28.3
$Cu(cyclopentanediA).H_2O$	270–400	280,380	34.6

[a] abbreviations defined in text
[b] temperatures of maxima observed in the derivative of the thermogravimetric curve
[c] percentage calculated as weight remaining at 500°C/weight of starting hydrated complex

RESULTS AND DISCUSSION

The first result obtained from analytical data is that succinamic acid, like the other studied cyclic carboxylic acid-amide ligands, forms anhydrous bis-complexes with copper in analogy with acetic acid itself. This suggests that the amide functions are not implied in curpic salt formation. Indeed, acetamide is only known to form adducts with copper. Valeramide represents one example where it is claimed the deprotonated amide function forms a

copper acetate-like dimeric salt at basic pH.[11] It may be emphasized that biuret itself which is known to form the well-known violet complex with copper which is the prototype for the complexation of four deprotonated amide nitrogens (from two biuret ligands) only gives this type of reaction in strongly alkaline solutions.[5-7] In fact, biuret does not deprotonate at pH<11.5.

The infrared spectra are expected to give some more informations on the nature of the sites actually involved in bonding in the carboxylic acid-amide complexes. The strong band at 1660-1680 cm^{-1} has been interpreted as the amide I band and due to the C=O (amide) stretching modes. This band remains unaltered in position and intensity in the complexes excluding a coordination by the amidic carbonyl. This fact is supported by the presence in the spectra of the complexes as well as of the ligands of the two strong absorption bands at 3410-3200 cm^{-1} which are due to the asymmetric and symmetric N-H stretching vibrations of the amide groups, unaffected upon complexation. The assignments of the symmetric and asymmetric carboxylate stretching frequencies are at wave numbers very similar to those reported for dimeric Cu(II) carboxylates[12] i.e. at ca. 1600 and 1410 cm^{-1}, respectively. However, it has been difficult to ascertain the positioning of the ν_a vibration due to its overlapping with the amide II band of the amide group.

The cyclic dicarboxylates form hydrated monoligand complexes, where the water molecules appear to be coordinated to the cupric ions because they are lost in the temperature range 110-120°C. These complexes are insoluble in common solvents which suggest they are polymeric like the other known analogues.[4]

The thermogravimetric results show that the acid-amide complexes are less thermally-stable than the corresponding diacid complexes. This can be attributed in part to the lower decomposition temperature of the non-coordinated amide groups and also to the higher stability of the polymeric network in the dicarboxylate salts. The temperatures of maximum decomposition (see Table 1) reveal that the introduction of one double-bond in the cyclohexane ring for the dicarboxylate complexes lowers the thermal stability some 20°C. The cyclopentane dicarboxylate is partially degraded at even lower temperatures showing that stress in the ligand is responsible for the lower decomposition temperatures. The same observation is obtained by comparing cyclohexane and cyclopentane acid-amide complexes. The acid-amide complexes decompose in a multistep process, pointing to the alteration of the ligands followed by decomposition of the complexes formed with the intermediate carboxylic acid function. The final weight corresponds to the presence of a mixture of copper, copper oxide and traces of graphite.

The EPR results can be interpreted in a straightforward manner by attributing a dimeric copper-acetate like structure for the compounds. Thus, the main features of the EPR spectra yield the parameters of the paramagnetic triplet states obtained by coupling two doublet state cupric ions. Monomeric impurities are present in varying amounts, with the corresponding absorptions near 3000 gauss. The decrease in intensity and improved resolution at low temperature is compatible with a thermally accessible triplet state above the ground singlet state.

The EPR parameters are similar to those usually obtained for dimeric carboxylates and the results are presented in Table 2. The D values vary between .336 cm^{-1} and .357 cm^{-1}, with

E values quite small, the largest one, 77 gauss (.0072 cm^{-1}) being observed for the succinamate complex. This shows the copper ions are essentially in a square planar environment with little rhombic distortion. The observed hyperfine values are less than 70 gauss, which corresponds, as expected, to half the normal value, as obtained for the monomer impurity signals for example. There is a good agreement between the g values observed for the monomer impurities (Table 3) and the g values calculated from the spectra for the triplet state dimers (Table 2). Further data would be needed (structural information, magnetic susceptibilities), in order to find any trends in g or D values or to explain the lack of resolution in some cases.

Table 2. Electron paramagnetic resonance parameters derived from triplet spectra of dimer copper compounds

Compound	$g /\!/$	$g \perp$	$\overline{g}$	D, cm^{-1}	E', G	$A /\!/, G$
Cu(Suc)$_2$	2.348	2.062	2.157	.336	77	68.5
Cu(cyclohexane A.A.)$_2$	2.436	2.162	2.253	.357	-	-
Cu(cyclopentane A.A.)$_2$	2.362	2.068	2.166	.340	28	66.2
Cu(cyclohexanediA).H$_2$O	2.385	2.088	2.187	.339	52	-
Cu(cyclohexenediA).H$_2$O	2.381	2.076	2.177	.345	53	-
Cu(cyclopentanediA).H$_2$O	2.392	2.096	2.195	.346	-	67

Table 3. Electron paramagnetic resonance parameters derived from monomer impurity signals

Compound	$g /\!/$	$g \perp$	$\overline{g}$	$A /\!/, G$
Cu(Suc)$_2$	2.334	2.077	2.164	140
Cu(cyclohexane A.A.)$_2$	2.358	2.077	2.171	150
Cu(cyclopentane A.A.)$_2$	2.352	2.076	2.168	130
Cu(cyclohexanediA).H$_2$O	2.388	2.081	2.183	-
Cu(cyclohexenediA).H$_2$O	2.357	2.066	2.163	145
Cu(cyclopentanediA).H$_2$O	-	-	2.166	-

In general, however, it may be stated the EPR spectra are characteristic of carboxylate salts of copper, with no direct influence of the amide functions. Perhaps, the amide groups occupy the axial coordination positions on copper, accounting for the minimal interdimer exchange resulting in well resolved dicopper hyperfine structure, as illustrated in the spectrum of the copper(II) succinamic acid complex (Fig. 1) compared to the copper(II) cyclohexene dicarboxylic complex (Fig. 2).
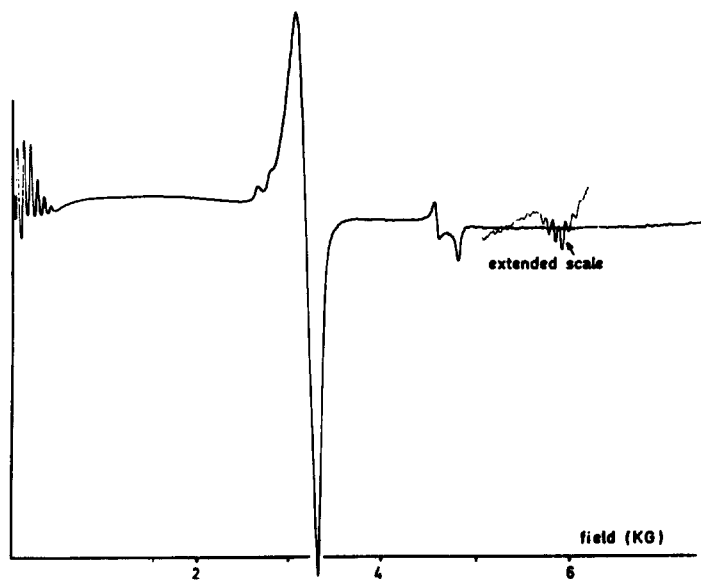
Fig. 1. EPR spectrum of the succinamic acid copper(II) complex recorded at 85 K.
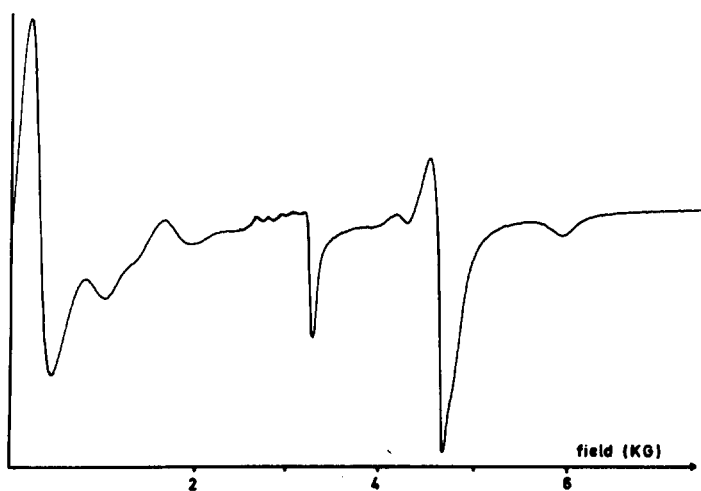
Fig. 2. EPR spectrum of copper(II) cyclohexene dicarboxylate, recorded at 123 K.

CONCLUSION

The difunctional ligands used show no evidence for participation of the carboxamide group in complex or chelate formation. The formulae, infrared spectra as well as EPR spectra all point to a typically carboxylate-like behaviour for the ligands. The carboxylic acid-amide complexes are less thermally stable than the corresponding dicarboxylates. Further work is planned with metal ions with higher affinities for the carboxamide functions.

REFERENCES

[1] M. Melnik, Coord. Chem. Rev., 1982, **42**, 259.

[2] R.W. Jotham, S.F.A. Kettle and J.A. Marks, J. Chem. Soc. Dalton Trans., 1972, 428.

[3] P.O. Ikekwere and K.S. Patel, J. Inorg. Nucl. Chem., 1981, **43**, 1085.

[4] P. Sharrock, M. Dartiguenave and Y. Dartiguenave, Bioinorg. Chem., 1978, **9**, 3.

[5] G. Wiedemann, Justus Liebigs Am. Chem., 1848, **182**, 741.

[6] R. Sanyal, P. Srivastava and B.K. Banerjea, J. Inorg. Nucl. Chem., 1975, **37**, 343.

[7] H.C. Freeman, J.E.W. Smith and J.E. Taylor, Acta Crystallogr., 1961, **14**, 407.

[8] H. Sigel and R.B. Martin, Chem. Rev., 1982, **83**, 385.

[9] M. Nonoyama and K. Nonoyama, J. Inorg. Nucl. Chem., 1981, **43**, 2567.

[10] N.N. Srivastava, R.C. Tewari, U.C. Srivastava, G.B. Bhargava and A.N. Vishnoi, J. Inorg. Nucl. Chem., 1976, **38**, 1897.

[11] Y.Y. Kharitonov, R.I. Machkhosvichi and N.B. Generalova, Zh. Neorg. Khim., 1973, **18**, 2866.

[12] M. Kato, M.B. Jonassen and J.C. Fanning, Chem. Rev., 1964, **64**, 99.

Reaction of 2,5-(Dibenzothiazolin-2-yl)thiophene with Some Metal Ions

A.S. Salameh and H.A. Tayim[*]

Department of Chemistry, American University of Beirut

Beirut, Lebanon

Abstract

2,5-(Dibenzothiazolin-2-yl)thiophene has been synthesized by the reaction of 2,5-thiophenedicarboxaldehyde and o-aminobenzenethiol. It reacts as a neutral ligand with Pd(II). However, it reacts as a dianion with Cu(II), Ag(I), Cd(II), Pb(II) and Zn(II), suggesting that the ligand is bonded as the conjugate base of the Schiff base 2,5-thiophenediylbis{N-(pheylen-2-thiol)aldimine}. Its behavior with Hg(II), Ru(III), Pt(II), Rh(III) and Ni(II) involves the opening of one of the thiazoline rings of the ligand.

Introduction

We have been investigating the coordination compounds of Schiff bases derived from the condensation of heterocyclic mono- and dialdehydes with o-aminobenzenethiol and o-aminophenol. The reaction of 2,5-thiophenedicarboxaldehyde with o-aminobenzenethiol did not afford the expected Schiff base (I)(SBH$_2$), but rather the poly-heterocyclic compound 2,5-(dibenzothiazolin-2-yl)-thiophene(II) (LH$_2$). The synthesis of this ligand and the results of its reactions with several metal salts are reported hereby.

Experimental

Preparation of 2,5-(dibenzothiazolin-2-yl)thiophene(II). A solution of thiophene-2,5-dicarboxaldehyde[1] (1.4 g, 0.01 mole) in ethanol (7 ml) was treated with a solution of o-aminobenzenethiol (3.13 g, 0.025 mole) in ethanol (6 ml). The mixture was refluxed with stirring for 30 min, then cooled. The pale yellow product obtained was filtered, washed with cold ethanol and dried. It melted at 115° forming a solid on the sides of the capillary tube, which melted at 200-250°. Yield: 3.2 g, 90%. The compound is insoluble in water, but soluble in ether, chloroform, hot methanol, hot ethanol and acetone. Found: C, 60.83; H, 3.90; N, 7.88; S, 26.97. Calcd. for C$_{18}$H$_{14}$N$_2$S$_3$: C, 60.98; H, 3.98; N, 7.90; S, 27.14%. ν_{NH} at 3350 cm^{-1}.

---

* Author to whom correspondence should be addressed; present address:
  Department of Chemistry, University of Petroleum & Minerals, Dhahran, Saudi Arabia.

829

Reactions of the ligand with metal ions. The reactions of the ligand (II) with
several metal ions were attempted. Metal ions that afforded isolable complexes
are classified into three categories according to the method of synthesis of
their corresponding complexes.

(i) Metal ions whose compounds react with the ligand upon mixing: These
include $CuCl_2 \cdot 2H_2O$, $HgCl_2$, $AgClO_4$, $RuCl_3 \cdot 3H_2O$, $Pb(CH_3COO)_2$, $RhCl_3 \cdot 3H_2O$ and
$Pd(C_6H_5CN)_2Cl_2$. In a typical reaction of these salts with the ligand, a hot
(almost boiling) solution of the ligand in ethanol was added to a hot solution
of the metal salt in ethanol. The ligand-to-metal molar ratio was 2:1. Immediate
precipitation of the complex took place. The product was filtered, washed with
hot ethanol and dried in vacuo.

(ii) Metal ions which required refluxing: The reactions of $Cu(CH_3COO)_2 \cdot H_2O$
and $Ni(acetylacetonate)_2 \cdot H_2O$ with the ligand were carried out by refluxing the
solution of the ligand and the metal salt in ethanol for one hour. The precipi-
tates that formed were filtered off, washed with ethanol, then ether and dried
in vacuo over P_2O_5.

When the complex of Ag(I), obtained by the reaction of $AgClO_4$ with the
ligand immediately upon mixing of hot ethanolic solutions of the reactants, was
further refluxed for one hour, a different complex was obtained.

(iii) Metal ions which afforded complexes upon mixing hot ethanolic solutions
of the reactants, then cooling the reaction mixture. These include $Cd(CH_3OOO)_2 \cdot$
$2H_2O$, $FeCl_3 \cdot 6H_2O$ and $Zn(CH_3COO)_2 \cdot 2H_2O$. The reaction of aqueous K_2PtCl_4 with the
ethenolic solution of the ligand required stirring overnight at room temperature.

The complexes thus synthesized are listed in Table 1 along with their colors
and melting points. Table II lists the elemental analyses of these complexes.

Oxidation of 2,5-(dibenzothiazolin-2-yl)thiophene: Air was passed through a hot
ethanolic solution of 2,5-(dibenzothiazolin-2-yl)thiophene (1.00 g in 80 ml) with
stirring for 10 hours. In another procedure oxygen gas was passed through an
identical solution with stirring for 3 1/2 hours. The yellow solid formed was
filtered off and recrystallized from benzene to yeild 0.63 g (64%) of a compound
melting at 235-237° with decomposition. The IR spectrum did not show a v_{N-H} at
3350 cm^{-1}. Found: C, 61.90; H, 3.01; N, 7.86; S, 26.93. Calcd. for $C_{18}H_{12}N_2S_3$:
C, 61.68; H, 2.88; N, 7.99; S, 27.45%. The product was identified as 2,5-(di-
benzothiazol-2-yl)thiophene(III) (L).

Reaction of 2,5-(dibenzothiazol-2-yl)thiophene(III) with Pd(II): The oxidation
product of 2,5-(dibenzothiazolin-2-yl)thiophene(II) in hot benzene (0.140 g,
0.4 mole in 18 ml) was treated with a hot filtered solution of dichlorobis(ben-
zonitrile)palladium(II) (0.077 g, 0.2 mmole in 4 ml benzene). The precipitate
which formed immediately was filtered off, washed with hot benzene and ether
respectively; and dried in vacuo over P_2O_5. It melted with decomposition at

TABLE I

Reaction of Some Metal Ions With 2,5-(Dibenzothiazolin-2-yl)thiophene(II)(LH$_2$)

Metal Salt	Product	Color	Decomposition Point(^{O}C)
CuCl$_2$.2H$_2$0	Cu(SB)*1/2H$_2$0	Brown	147-149
Cu(CH$_3$000)$_2$.H$_2$0	Cu(SB)	Black	195-198
HgCl$_2$	Hg(SBH)**Cl.2H$_2$0	Dark-Red	128-133
AgClO$_4$(Reflux)	Ag$_3$(SB)(SBH)	Reddish-Brown	235-236
FeCl$_3$.6H$_2$0	L.†1/2 H$_2$0	Yellow	233-236
RuCl$_3$.3H$_2$0	Ru(SBH)Cl$_2$.2H$_2$0	Dark Brown	>360
Cd(CH$_3$COO)$_2$.2H$_2$0	Cd(SB)	Orange	311-314
Pb(CH$_3$COO)$_2$	Pb(SB).1/2 C$_2$H$_5$OH	Reddish-Brown	190-194
Pd(C$_6$H$_5$CN)$_2$Cl$_2$	Pd(LH$_2$)Cl$_2$.2H$_2$0	Light Brown	175-178
Zn(CH$_3$COO)$_2$.2H$_2$0	Zn(SB).2H$_2$0	Reddish-Black	178-180
K$_2$PtCl$_4$	Pt(SBH)(LH$_2$)Cl.2H$_2$0	Olive Green	230-240
RhCl$_3$.3H$_2$0	Rh(SBH)Cl$_2$.1/2 H$_2$0	Brown	>360
Ni(acac)$_2$***.H$_2$0	Ni(SBH)$_2$	Brownish Black	185-192
AgClO$_4$	Ag$_3$(SBH)$_2$ClO$_4$.4H$_2$0	Wine-Red	245-246

*SB is the dianion of SBH$_2$(I);   (**) SBH is anion (IV)
(***) acac = acetylacetonate ;   † L is the oxidition product III of LH$_2$

340-343°. Found: C, 40.95; H, 2.27; N, 5.56; S, 18.03; Cl, 12.40. Calcd. for Pd(L)Cl$_2$.1/2 H$_2$0: C, 40.27; H, 2.06; N, 5.22; S, 17.92; Cl, 13.21.

Elemental analyses were carried out by Pascher, Mikroanalytisches Laboratorium, Bonn, Germany; the IR spectra were run using a Perkin-Elmer 621 Grating Spectrophotometer. Potassium bromide pellets were used. Melting and decomposition points (uncorrected) were taken using a Mel-Temp apparatus.

TABLE II

Elemental Analyses of the Complexes of 2,5-(Dibenzothiazolin-2-yl)thiopene

Compound	%C	%H	%N	%S	%Cl
			Analyses †		
Cu(SB)[*].1/2 H_2O	50.93(50.86)	2.95(3.08)	6.74(6.59)	22.70(22.63)	
Cu(SB)[**]	51.47(51.96)	2.99(2.91)	6.89(6.73)	22.54(22.54)	
Hg(SBH)Cl.$2H_2O$	34.48(34.55)	2.37(2.74)	4.77(4.48)	14.01(15.37)	6.66(5.69)
Ag_3(SBH)$_2$ClO$_4$.$4H_2O$	34.90(35.97)	2.20(2.85)	4.60(4.66)	15.80(16.00)	2.17(2.95)
Ag_3(SB)(SBH)	43.32(42.00)	2.45(2.45)	5.75(5.44)	18.32(18.69)	
L.1/2 H_2O	60.40(60.13)	3.14(3.08)	7.82(7.79)	25.80(26.76)	
Ru(SBH)Cl$_2$.$2H_2O$	38.52(38.50)	2.88(2.05)	5.31(4.99)	16.69(17.13)	13.57(12.63)
Pd(LH$_2$)Cl$_2$.$2H_2O$	38.25(38.07)	2.76(3.19)	5.37(4.93)	16.73(16.94)	10.60(12.49)
Ru(SBH)Cl$_2$.1/2 H_2O	40.91(40.31)	2.81(2.63)	4.97(5.23)	17.88(17.94)	13.55(13.22)
Pt(SBH)(LH$_2$)Cl.$2H_2O$	43.82(44.36)	2.62(3.20)	6.17(5.75)	19.15(19.74)	3.26(3.64)
Pb(SB).1/2 C_2H_5OH	40.67(39.16)	2.54(2.59)	5.26(4.81)	17.20(16.51)	
Cd(SB)	45.91(46.50)	2.71(2.60)	6.08(6.03)	19.97(20.69)	
Zn(SB).$2H_2O$	53.69(53.59)	3.27(3.72)	6.98(6.95)	23.19(23.82)	
Ni(SBH)$_2$	56.28(56.48)	3.27(3.42)	7.45(7.32)	24.69(25.13)	

* From CuCl$_2$.$2H_2O$ ** From Cu(CH$_3$COO)$_2$.H_2O † (Calc. values)

Results and Discussion

The condensation of 2,5-thiophenedicarboxaldehyde with o-aminobenzenethiol was attempted with the intention of preparing the corresponding Schiff base, 2,5-thiophenediylbis-{N-(pheylen-2-thiol)aldimine)(I)(SBH$_2$).
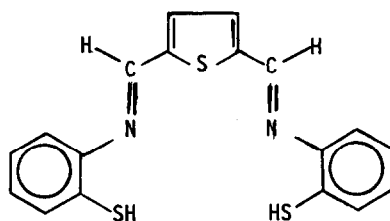
I (SBH$_2$)

However, the dithiazoline compound 2,5-(dibenzothiazolin-2-yl)thiophene(II) was obtained instead.
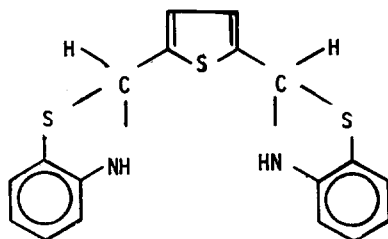
II (LH$_2$)

The identity of the dithiazoline(II), which has not hitherto been reported, is confirmed by its elemental analysis and by its IR spectrum. The spectrum contains a band at 3350 cm^{-1} characteristic of v_{NH}, and does not have a band at 2600 cm^{-1} suggesting the absence of SH bond and thus ruling out structure I. A similar behavior has been reported[2] for the condensation of 2,6-pyridinedicarboxaldehyde with o-aminobenzenethiol, except that the product isolated was the oxidized form, dithiazole. The formation of the dithiazoline was proposed as an intermediate. In the case of 2,5-thiophenedicaroxaldehyde, 2,5-(dibenzothiazol-2-yl)thiophene(III) could only be formed by the oxidation of the dithiazoline with air, oxygen or an oxidizing agent such as Fe^{+++}.
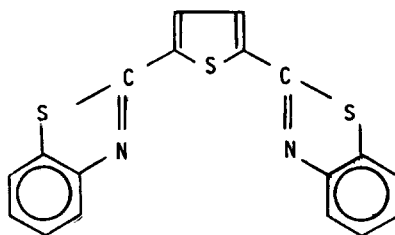
III (L)

The identity of the dithiazole(III) is confirmed by its elemental analysis and its IR spectrum. The v_{N-H} present in the spectrum of the dithiazoline at 3350 cm^{-1} disappeared upon oxidation, and instead, a band at 1590 cm^{-1} appeared, indicating the presence of a C=N bond.

The formation of the dithiazoline is most likely preceded by the formation of the Schiff base(I) which then rearranges to the dithiazoline. The rearrangement and interconversion of dithiazoline to dithiazole are influenced by the metal ions. The behavior of dithiazoline in its reactions with the metal ions investigated thus varied with the nature of the metal. Copper(II), Zinc(II), cadmium(II) and lead(II) afforded complexes of the form M(SB) where the ligand behaved as a tetradentate dithiolate Schiff base having structure(I) with the loss of the two acidic protons. This is suggested by the stoichiometry of the

complexes (ruling out structure(III) and the absence of v_{NH} in the IR spectra
of the complexes (thus ruling out structure(II)).

Ring-opening in the dithiazoline(II) was encountered with Hg(II), Ag(I),
Ru(III), Rh(III) and Ni(II) where the ligand adopted the anionic form(IV)(SBH).
The IR spectra of the complexes showed bands around 3350 cm^{-1} (v_{NH}) and 1590 cm^{-1}
($v_{C=N}$). Structure IV for the ligand in these complexes is substantiated by the
X-ray structure determination[3] of a Zn(II) complex with the 2,6-pyridine analogue
of our ligand.
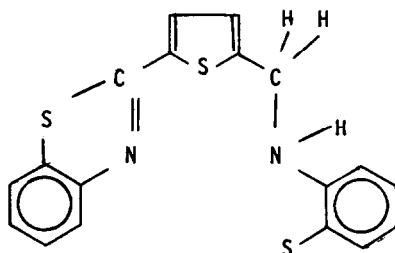
IV (SBH)

The reaction of the dithiazoline(II) with Pd(II) afforded $Pd(LH_2)Cl_2 \cdot 2H_2O$
in which the ligand has not rearranged. The IR spectrum of the complex showed
a band at 3350 (v_{NH}), and no bands due to v_{SH} or $v_{C=N}$. Decomposition of the
complex with aqueous KCN followed by extraction with $CHCl_3$ afforded the di-
thiazoline(II). The oxidized form, the dithiazole(III) reacted with Pd(II) to
yield $Pd(L)Cl_2 \cdot 1/2 H_2O$. The decomposition of the complex with aqueous potassium
cyanide produced the dithiazole(III). The reaction of Pt(II) with the dithia-
zoline(II) afforded the complex $Pt(SBH)(LH_2)Cl \cdot 2H_2O$ in which one of the thiazoline
rings in one of the ligands must have opened to account for the divalence of
platinum.

The reaction of the dithiazoline with Fe(III) did not result in the forma-
tion of a complex, but the ligand was oxidized to the dithiazole(III) which was
isolated and identified by comparison with the authentic compound obtained from
the air-oxidation of the dithiazoline.

References

1. Toy Sone, Bull. Chem. Soc. Japan, 1964, 37, 1197.
2. S.E. Livingstone and J. D. Nolan, J. Chem. Soc. Dalton, 1972, 218
3. D.C. Liles, M. McPartlin, and P. A. Tasker, J. Am. Chem. Soc., 1977, 99, 7704.

NOTES

REMARK ON PLUTONIUM DISPROPORTIONATION REACTIONS

G. L. Silver

Monsanto Research Corp., Mound Plant,* Miamisburg, Ohio 45342

Abstract - The course of a plutonium disproportionation reaction can be approximated by a succession of equilibrium valence state arrangements whose acidities are intermediate between the final solution acidity and the acidity for which the initial oxidation state configuration would have represented equilibrium.

In his interesting review of the kinetics of the lighter actinides, Newton[1] observes that the rate of a reaction such as

$$2Pu^{4+} + 2H_2O = Pu^{3+} + PuO_2^+ + 4H^+ \quad (K = K_1) \tag{1}$$
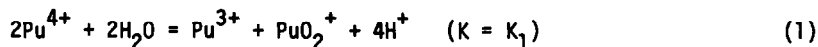
is slow, whereas the rate of the reaction

$$Pu^{4+} + PuO_2^+ = Pu^{3+} + PuO_2^{2+} \quad (K = K_2) \tag{2}$$

is relatively rapid, and under most circumstances a plutonium system will be near equilibrium with respect to it at all times. If this hypothesis is true, the expression

$$Q_2 = \frac{[Pu^{3+}][PuO_2^{2+}]}{[Pu^{4+}][PuO_2^+]} \approx K_2 \tag{3}$$

is a constraint upon the plutonium system whether or not the system is at equilibrium. Another constraint which always applies to plutonium systems is mass conservation

$$[Pu^{3+}] + [Pu^{4+}] + [PuO_2^+] + [PuO_2^{2+}] = T \tag{4}$$

where T is the total plutonium concentration, and may be taken as unity so that oxidation states in brackets may be conveniently interpreted as fractions of the total plutonium. Still another constraint which always applies to a plutonium system is charge conservation[2]

$$(6-N)[PuO_2^{2+}] + (5-N)[PuO_2^+] + (4-N)[Pu^{4+}] + (3-N)[Pu^{3+}] = 0 \tag{5}$$

in which N is the plutonium oxidation number. Equations (3), (4), and (5) constitute a system of three equations in the four unknowns $[Pu^{3+}]$, $[Pu^{4+}]$, $[PuO_2^+]$, and $[PuO_2^{2+}]$. If one further constraint upon the plutonium system were available, the system could be solved as a system of four equations in the four unknown fractions representing the various oxidation states.

If the composition of a nonequilibrium plutonium system is known at a certain time, and if the final, equilibrium composition is also known, it is ordinarily true that every species passed

from its initial value to its final value in a smooth, continuous manner. If the fraction of
a plutonium oxidation state likewise does not pass through a maximum or a minimum during
transit to equilibrium, then every intermediate value assumed by it between the initial and
final compositions corresponds to a unique arrangement of oxidation states. Since valence
state rearrangement reactions do not produce extrema in the fractions of all of the oxidation
states, it is possible to select arbitrary, unique, intermediate fractional values for at
least one of these oxidation states. Thus the fourth constraint upon the plutonium system
can be selected as

$$[Pu^{4+}] = \text{a unique value allowed by continuity} \qquad (6)$$

The continuity constraint is given in terms of $[Pu^{4+}]$ as an example; another oxidation state
could have been selected provided it passes from its initial to its final value in a contin-
uous, single-valued manner. Equation (6) states that if the initial fraction of $[Pu^{4+}]$ were
1.0 (pure tetravalent plutonium), and its final value 0.4 (after extensive disproportion-
ation), then there must have been an instant when its fraction was any chosen intermediate
value such as 0.65. Thus it is possible to approximate the courses of plutonium valence
rearrangement reactions by solving Equations (3)-(6) as a set of four equations in four
unknowns. (By "course" is meant the succession of oxidation state distributions correspond-
ing to the passage from initial state to the equilibrium state.) This method is considerably
easier than the conventional method of solving a pair of simultaneous differential equa-
tions[1]. The accuracy of the method is limited only by the accuracy of the approximation
$Q_2 \approx K_2$, where K_2 is the equilibrium constant for Equation (2), and Q_2 is the actual, non-
equilibrium concentration quotient for this reaction.

There is another, more interesting method of plotting the course of oxidation state rearrange-
ment reactions. It is to be observed that the solution acidity does not enter Equations (3)-
(6). The consequence of this is that the courses of rearrangement reactions are approximately
independent of the acidity, and that the error in this consequence is no greater than the
error in the hypothesis that $Q_2 = K_2$. Nowhere in the literature of plutonium chemistry does
this implication seem to have been noticed.

When calculating equilibrium oxidation state distributions, it is customary to use the solu-
tion acidity as one of the defining parameters[3]. Equations (3)-(5) are always satisfied in
this computation, and values for the fractions of oxidation states are the results of such
calculations. But the process may be turned around, so that Equations (3)-(5) are still
satisfied, and the fraction of one oxidation state, say $[Pu^{4+}]$, is given some value which it
must have momentarily assumed. The resulting nonequilibrium oxidation state distribution can
be made to fit the equation

$$K_1 = \frac{[Pu^{3+}][PuO_2^+][H^+]^4}{[Pu^{4+}]^2} \qquad (7)$$

so that a value of $[H^+]$ can be obtained. This value of $[H^+]$ (which is not the actual value
of the solution acidity) and the given value of N are sufficient to define an equilibrium
valence state distribution; this equilibrium distribution is identical to the distribution
known to be nonequilibrium for the actual solution acidity. In other words, the course of a

rearrangement reaction can be plotted by calculating the succession of equilibrium oxidation state distributions for acidities intermediate between the actual solution acidity and the acidity for which the initial nonequilibrium oxidation state distribution would have represented equilibrium. The observation that nonequilibrium distributions of plutonium valence states are a succession of equilibrium states for other (intermediate) acidities also seems to have been overlooked, but its value as an approximation is not worse than the approximation $Q_2 = K_2$ on which Newton comments favorably.

Many years ago, data were obtained on the passage to equilibrium of a solution initially containing about 50% each of pentavalent and hexavalent plutonium[4]. The oxidation number of this solution was therefore close to 5.5, and acidity is reported as $0.5\underline{M}$ HCl. From the data in the reference containing this information, it is possible to approximate $K_1 \approx (2.1)(10^{-4})$ and $K_2 \approx 8.5$ in this medium. The alpha coefficients[5,6] for the plutonium oxidation states may all be taken as unity, because their actual values (which are greater than unity) are reflected in the experimentally determined values of K_1 and K_2 in $0.5\underline{M}$ HCl. A solution which has the equilibrium composition of 50% each PuO_2^+ and PuO_2^{2+} has a very low acidity: for this purpose $[H^+] = 0.01\underline{M}$ is low enough to represent the initial acidity. Plotted in Figure 1 are equilibrium compositions for a succession of solutions whose equilibrium acidities are taken between $0.01\underline{M}$ and the final, actual solution acidity of $0.5\underline{M}$. The course predicted by this diagram may be compared to the experimentally determined course in $0.5\underline{M}$ HCl; it will be found that the agreement is striking[4]. This bears out as reasonable the hypothesis that generally $Q_2 \approx K_2$ and the consequence of this hypothesis that the course of a disproportionation reaction is well approximated by a succession of equilibrium states whose acidities are intermediate between the final, actual solution acidity, and the acidity for which the initial oxidation state distribution would have represented equilibrium.

REFERENCES

1. T. W. Newton, The Kinetics of the Oxidation-Reduction Reactions of Uranium, Neptunium, Plutonium, and Americium in Aqueous Solutions, Technical Information Center, Office of Public Affairs, U. S. Energy Research and Development Administration, 1975, p. 45.
2. G. L. Silver, J. Inorg. Nucl. Chem. (1974), 36, 939.
3. G. L. Silver, Radiochimica Acta, (1974), 21, 54.
4. R. E. Connick, in The Transuranium Elements, Part I, G. T. Seaborg, J. J. Katz and W. M. Manning (Eds.), McGraw-Hill Book Company, New York, NY, 1949, p. 270.
5. A. Ringbom, J. Chem. Ed., (1958), 35, 282.
6. G. L. Silver, Marine Chemistry (1983), 12, 91.
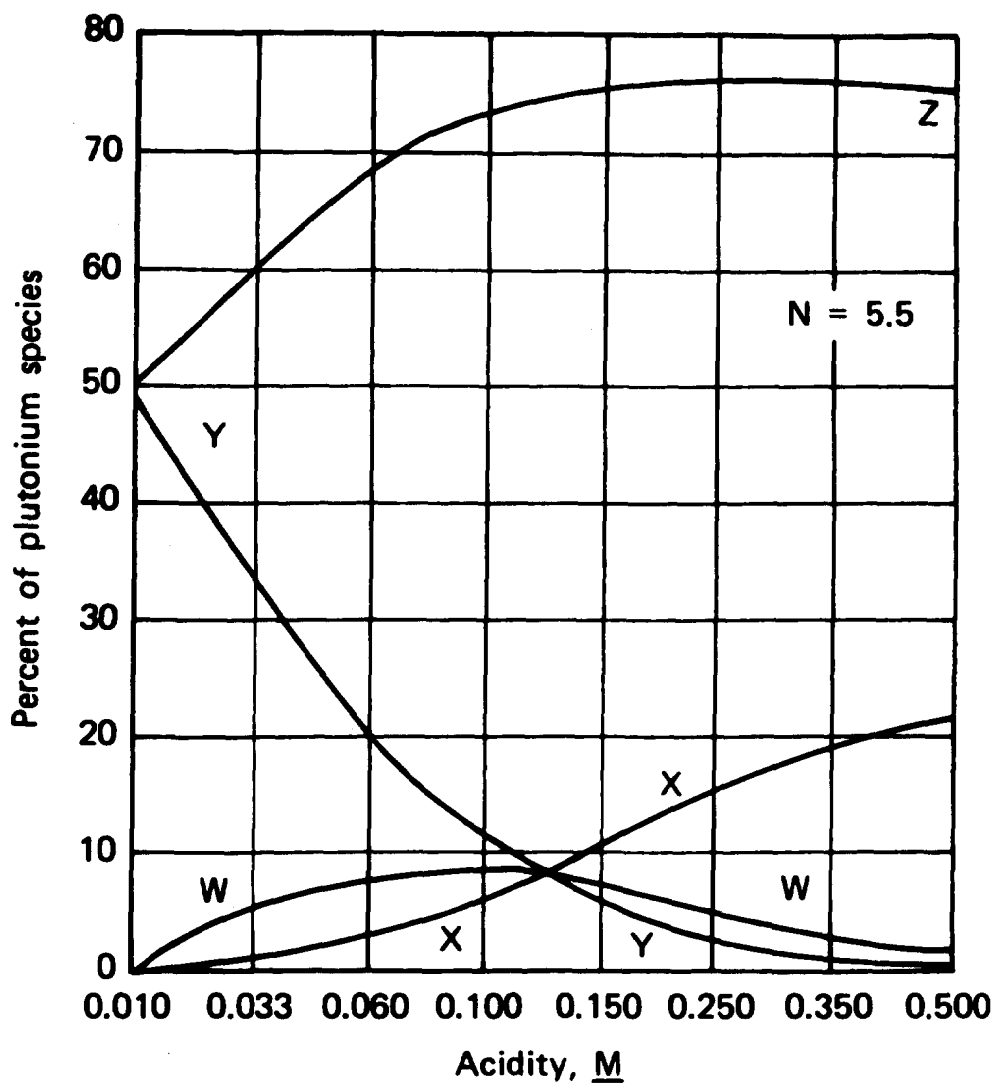
Figure 1.   The course of a plutonium rearrangement reaction in 0.5$\underline{M}$ hydrochloric acid.   The equilibrium distribution of the four plutonium valence states for plutonium oxidation number 5.5 is plotted vs. increasing acidity.   (W = $[Pu^{3+}]$; X = $[Pu^{4+}]$; Y = $[PuO_2^+]$; Z = $[PuO_2^{2+}]$)

SYNTHESIS OF NEW MIXED LIGAND COMPLEXES OF COPPER(II) DITHIOCARBAMATES

K.K.M. YUSUFF*, K. MUHAMMAD BASHEER and M. GOPALAN
Department of Chemistry, University of Calicut, Kerala, 673 635, India

Abstract: New mixed ligand complexes of copper(II) dithiocarbamates of the general formula, $[CuCl(R_2dtc)L]$ or $[CuCl(R'dtc)L]$ (R=CH_3 or C_2H_5, R' = $(CH_2)_5$, dtc =-NCSS⁻ and L = Pyridine, 3-picoline or 4-picoline), have been prepared by the reaction of bis(dithiocarbamato)di-μ-chloro-dicopper(II) complexes with pyridine or picolines. The complexes are found to be non-electrolytes in nitrobenzene. Magnetic susceptibilities, i.r. and electronic spectra of the complexes are reported. A psuedo-tetrahedral structure is suggested for these complexes.

INTRODUCTION

A series of bis(dithiocarbamato)di-μ-chloro-dicopper(II) (A) have been synthesized[1,2]. It was found that ligands like pyridine and picolines are able to break the chlorine bridges in these type of complexes to form some hitherto unknown mixed ligand complexes of copper(II). The preparation and some physico-chemical studies of the new complexes are presented here.
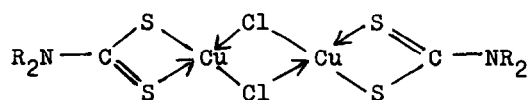
(A)

EXPERIMENTAL

Bis(dithiocarbamato)di-μ-chloro-dicopper(II) complexes were synthesized as described in the literature[1].

Physico-chemical measurements:

The molar conductances of the complexes (10^{-3}M solution) in pure dry nitrobenzene was determined at $30\pm2°C$ with a Toshniwal conductivity bridge using platinum electrodes.

Magnetic susceptibilities were determined at room temperature ($30\pm2°C$) by the Gouy Method using $Hg[Co(NCS)_4]$ as calibrant[3].

Electronic spectra of the complexes were recorded in the solid state by a mull technique following a procedure recommended by Venanzi[4] on a DMR-21 recording spectrophotometer.

---

*Author to whom all correspondence should be directed. Present address: Department of Applied Chemistry, University of Cochin, Cochin 682 002, Kerala, India.

The i.r. spectra in the region 400-4000 cm^{-1} were recorded on a Perkin-Elmer 257 infrared spectrophotometer. The far i.r. spectra (Nujol mull) in the region 200-600 cm^{-1} were recorded on a Beckman IR-12 infrared spectrophotometer.

Synthesis:

All the complexes were prepared by same general method given below. About 2 gms. of bis(dithiocarbamato)di-μ-chloro-dicopper(II) was dissolved in the minimum quantity of appropriate bases (pyridine, 3-picoline or 4-picoline) with vigorous stirring. The solution was filtered and kept for one hour. Diethyl ether was then added to precipitate the complex. The crystalline complex seperated was filtered, washed with ether and dried over anhydrous calcium chloride.

Analysis:

Copper, Chlorine and Nitrogen in the complexes were estimated using standard procedures[5].

Table 1

Analytical and Magnetic Susceptibility data of Complexes

Compound	weight percent found (calcd.)			$\mu_{eff.}$ at $303\pm2°K$
	Cu	Cl	N	
$[CuCl((CH_3)_2dtc)Py]$	21.41(21.30)	12.02(11.89)	9.34(9.39)	1.96
$[CuCl((CH_3)_2dtc)3\text{-Pic.}]$	20.12(20.35)	11.01(11.35)	8.91(8.97)	2.07
$[CuCl((CH_3)_2dtc)4\text{-Pic.}]$	19.93(20.35)	11.20(11.35)	8.88(8.97)	2.02
$[CuCl((C_2H_5)_2dtc)Py]$	19.36(19.47)	10.72(10.86)	8.52(8.59)	2.01
$[CuCl((C_2H_5)_2dtc)3\text{-Pic.}]$	18.52(18.66)	10.27(10.42)	8.18(8.23)	2.09
$[CuCl((C_2H_5)_2dtc)4\text{-Pic.}]$	18.57(18.66)	10.32(10.42)	8.14(8.23)	2.05
$[CuCl((CH_2)_5dtc)Py]$	18.62(18.78)	10.52(10.48)	8.25(8.28)	2.07
$[CuCl((CH_2)_5dtc)3\text{-Pic.}]$	17.90(18.03)	9.92(10.06)	7.85(7.95)	2.09
$[CuCl((CH_2)_5dtc)4\text{-Pic.}]$	18.20(18.03)	9.95(10.06)	7.92(7.95)	2.03

Py = Pyridine; 3-Pic. = 3-Picoline; 4-Pic. = 4-Picoline

RESULTS AND DISCUSSION

The analytical data of the complexes show that they have the general formula, $[CuCl(R_2dtc)L]$ or $[CuCl(R'dtc)L]$, where R = CH$_3$ or C$_2$H$_5$; R' = (CH$_2$)$_5$;

dtc = -NCSS⁻ and L = Pyridine, 3-picoline or 4-picoline. Our attempts to
prepare the mixed ligand complexes with 2-picoline met with failure. This
may be due to the steric strain caused by the methyl group in the 2-position,
which blocks the stable bond formation.

The complexes are moderately soluble in benzene, nitrobenzene, chloro-
form and carbon tetrachloride. They are almost insoluble in acetone,
diethyl ether and alcohol. All of them decompose on keeping, as indicated
by the tarnishing of colour and also by the poor analytical data given
by the older samples.

Conductance behaviour:

The molar conductance values of the complexes are around 4.5 $ohm^{-1}cm^2$
$mole^{-1}$, which indicate that the complexes are non-electrolytes in nitrobenzene.

Magnetic behaviour:

The magnetic moment (μeff.) values, tabulated in Table 1, indicate the
presence of one unpaired electron and the absence of metal-metal interaction.
The fairly high values suggest a psuedo-tetrahedral structure for these
complexes. In a completely undistorted tetrahedron, copper(II) should have
a room temperature magnetic moment of about 2.2 B.M.[6].

Electronic Spectra:

The electronic spectra of the complexes show bands around 23300 cm^{-1},
15900 cm^{-1} and 8300 cm^{-1}. The band around 23300 cm^{-1} is intense and is,
therefore, a charge transfer band. The small band around 8300 cm^{-1} may be
due to the psuedo-tetrahedral nature of the complexes[7,8].

I.R. Spectra:

Most of the bands in the spectrum of free pyridine or picolines are
almost reproduced with only minor shifts or splittings in the i.r. spectra
of the complexes[9]. The same is the case with the bands of dithiocarbamato
ligand. However, there is considerable amount of overlapping between the
bands of these two ligands.

The C-N stretching frequency usually occurs around 1500 cm^{-1} in metal
dithiocarbamato complexes[10]. In these mixed ligand complexes also, the
C-N stretching frequency appears around 1500 cm^{-1}. The region 950-1050 cm^{-1}
is associated with the C-S stretching frequency. According to Ugo and
Bonati[11], the presence of only one band in this region indicates a comple-
tely symmetric bidentate bonding by the dithiocarbamato ligand. In the
case of the present mixed ligand complexes, this region also contains vibra-
tions due to the bases. Therefore, more than one band in the 950-1050 cm^{-1}
region do not imply an unsymmetric bonding of the dithiocarbamato ligand in
these complexes. Instead, it would be more realistic to assume a symmetric
bidentate bonding in all these complexes.

The i.r. spectra in the region 200-400 cm^{-1} provide information regarding

the nature of metal ligand vibrations. All the complexes show a medium band around 360 cm^{-1} and a strong band around 300 cm^{-1} which can be assigned to Cu-S and Cu-Cl stretching vibrations respectively[12,13]. The band around 280 cm^{-1} in the pyridine derivatives and 260 cm^{-1} in the picoline derivatives may be attributed to Cu-N stretching vibration.

Acknowledgement

REFERENCES

(1) C.G.R. Nair and K.K.M. Yusuff, J. Inorg. Nucl. Chem., 1977, 39, 281.

(2) R.H. Furneaux and Ekk Sinn, Inorg. Chem., 1977, 16, 1809.

(3) B.N. Figgis and J. Lewis, in J. Lewis and R.G. Wilkins (Eds.), Modern Coordination Chemistry, Interscience, New York, 1960.

(4) G. Dyer, J.G. Hartley and L.M. Venanzi, J. Chem. Soc., 1965, 1293.

(5) A.I. Vogel, A. Text Book of Quantitative Inorganic Analysis, Longmans-Green, London, 1968.

(6) B.N. Figgis and J. Lewis, Progr. Inorg. Chem., 1964, 6, 217.

(7) L. Sacconi and M. Ciampolini, J. Chem. Soc., 1964, 276.

(8) S.J. Gruber, C.M. Harris and E. Sinn, J. Inorg. Nucl. Chem., 1968, 30, 1805.

(9) N.S. Gill, R.H. Nuttal, D.E. Scaife and D.W.A. Sharp, J. Inorg. Nucl. Chem., 1961, 18, 79.

(10) D.A. Brown, W.K. Glass and M.A. Burke, Spectrochim. Acta, 1976, 32A, 137.

(11) F. Bonati and R. Ugo, J. Organometal. Chem., 1967, 10, 257.

(12) K. Nakamoto, Infrared Spectra of Inorganic and Coordination Compounds, 2nd Edit., Wiley-Interscience, 1970.

(13) D.M. Adams, Metal-ligand and Related Vibrations, Arnold, London, 1967.

COMMUNICATIONS

A NOVEL DIMERIC ORGANOIMIDO TUNGSTEN(VI) COMPOUND.

X-RAY CRYSTAL AND MOLECULAR STRUCTURE OF

$[W(NBu\text{-}tert.)(\mu_2\text{-}NPh)Cl_2(tert.\text{-}BuNH_2)]_2$.

D.C. Bradley*, R.J. Errington, M.B. Hursthouse*,

A.J. Nielson and R.L. Short

Department of Chemistry, Queen Mary College,

Mile End Road, London E1 4NS

Abstract. The reaction of tetrachloro-phenylimido-tungsten(VI)
$[W(NPh)Cl_4]$ with tert.-butyltrimethylsilylamine $[tert.Bu(Me_3Si)NH]$ gave
the dimeric complex $[W(NBu\text{-}tert.)(\mu_2\text{-}NPh)Cl_2(tert.\text{-}BuNH_2)]_2$ which was
shown by X-ray crystallography to contain bridging phenylimido and non-
bridging (nearly linear) tertiary butylimido groups together with tertiary
butylamine ligands coodinated to octahedral tungsten. The tert.-butylamine
NH_2 protons were non-equivalent due to N-H....Cl bridging within the dimer.

*Authors to whom correspondence may be addressed.

A number of interesting organoimido complexes of molybdenum and tungsten have been synthesized and characterized in recent years.[1] Among the d^o W(VI) species are the monomeric tetrahedrally coordinated $W(NEt)_2(NEt_2)_2$ [2] and $W(NBu-tert.)_2(HNBu-tert.)_2$ [3], the dimeric 5-coordinated (TBP) $[W(NBu-tert.)(\mu_2-NBu-tert.)Me_2]_2$ [4] and the trimeric octahedrally coordinated $[W(NPh)(\mu_2-O)Me_2(PMe_3)_2]_3$ [5]. We have shown that $W(NPh)Cl_4$ (1) is a useful starting for synthesizing a range of W(VI), W(V) and W(IV) phenylimido complexes[5,6,7] and accordingly the ligand $tert.Bu(Me_3Si)NH$ (2) was selected as a means of re-placing two chlorines by a tert.-butylimido group in a reaction with (1) to produce a tungsten complex containing two different organoimido groups.

From the reaction involving (1) and (2) in 1:2 mole ratio the orange crystalline product $[W(NPh)(NBu-tert.)Cl_2(H_2NBu-tert.)]$ (3) was isolated. The ^1H nmr spectrum showed two distinguishable tert.-butyl groups as singlets ($\delta 1.28$ and 1.37) and two widely separated broad doublets ($\delta 3.38$ and 6.26; ^2J, 12Hz) which were assigned to two non-equivalent protons of the NH_2 groups. Moreover, the infrared spectrum showed two sharp bands in the ν_{NH} stretching region (3243 and 3142 cm^{-1}) confirming the non-equivalence of the NH protons. The structure of (3) was determined by a single crystal X-ray study.

Crystal Data: $W_2Cl_4N_6C_{28}H_{50}$, M = 980.26, monoclinic, space group $P2_1/c$, cell dimensions $\underline{a}$ = 10.063(3), $\underline{b}$ = 14.189(4), $\underline{c}$ = 13.287(3)Å, β = 97.40(2), V = 1881.4Å^3, Z = 2, D_c = 1.730 g cm^{-3}, λ(Mo-Kα) = 0.71073Å, μ(Mo-Kα) = 65.549 cm^{-1}, F(000) = 952.

The structure was solved by the heavy atom method, and refined by least square with anisotropic thermal parameters for all non-hydrogen atoms and iso-tropic for phenyl and amine hydrogen. Other hydrogens had fixed thermal para-

meters. The final R value is 0.031 (Unit weights). Tables of atomic positional

and thermal parameters and Fo/Fc values have been deposited as supplementary

data with the Editor, from whom copies are available on request.[†]

The structure (Figure) shows (3) to be dimeric with very unsymmetrical

phenylimido bridges [W-N, 1.895(3) and 2.324(3)$\overset{o}{A}$] and practically linear tert.-

butylimido groups [W-N, 1.729(4); $\overset{\frown}{\text{CNW}}$ 168.3(3)^o]. Of particular interest in

the structure is the present oc strong hydrogen bonding by one of the NH_2

protons to a chlorine on the neighbouring tungsten atom thus explaining the non-

equivalence noted in the nmr and infrared spectra. Another feature of interest

is the pronounced _trans_-influence of the tert.-butylimido groups acting as a

4-electron donor (N W) which allows the phenylimido nitrogen to π-donate only

where it is _cis_ to the tert.-butylimido nitrogen and thus produces the unsym-

metrical bridge. Interestingly a similar strong _trans_-influence was exerted

by the non-bridging phenylimido-nitrogen in the trimer [$W_3(NPh)_3(\mu_2-O)_3Me_6$

$(PMe_3)_3$] which led to very unsymmetrical WOW bridging.[5] It is clearly signifi-

cant that the unsymmetrical imido bridge (W-N, 1.842, 2.288$\overset{o}{A}$) in the dimer

[$W(NBu-tert.)(\mu_2-NBu-tert.)Me_2]_2$ involving 5-coordinated tungsten has the long

bond _trans_ to the linear non-bridging imido group (W-N, 1.736$\overset{o}{A}$)[4] whereas

symmetrical imido bridges are found in tetrahedral complexes such as

[$Ti(\mu_2-NBu-tert.)(NMe_2)_2]_2$ [1] where there is no possibility of a trans-influence

occurring.

[†] Footnote

Atomic coordinates have also been deposited with the Cambridge Crystallo-

graphic Data Centre.

References

1. W.A. Nugent and B.L. Haymore, <u>Coord.Chem.Rev.</u>, 1980, <u>31</u>, 123.

2. D.C. Bradley, M.H. Chisholm and M.W. Extine, <u>Inorg.Chem.</u>, 1977, <u>16</u>, 1791.

3. W.A. Nugent and R.L. Harlow,, <u>Inorg.Chem.</u>, 1980, <u>19</u>, 777.

4. D.L. Thorn, W.A. Nugent and R.L. Harlow, <u>J.Amer.Chem.Soc.</u>, 1981, <u>103</u>,
    357; see also [Mo(OBu-tert.)$_2$(NAr)(μ_2-NAr)]$_2$, M.H. Chisholm, K. Folting,
    J.C. Huffman and A.L. Ratermann, <u>Inorg.Chem.</u>, 1982, <u>21</u>, 978.

5. D.C. Bradley, M.B. Hursthouse, K.M. Abdul Malik and A.J. Nielson.
    <u>J.C.S.Chem.Comm.</u>, 1981, 103.

6. D.C. Bradley, M.B. Hursthouse, K.M. Abdul Malik, A.J. Nielson and R.L.
    Short, submitted to <u>J.Chem.Soc.(Dalton Trans.)</u>.

7. A.J. Nielson and J.M. Waters, <u>Polyhedron</u>, 1982, <u>1</u>, 561.
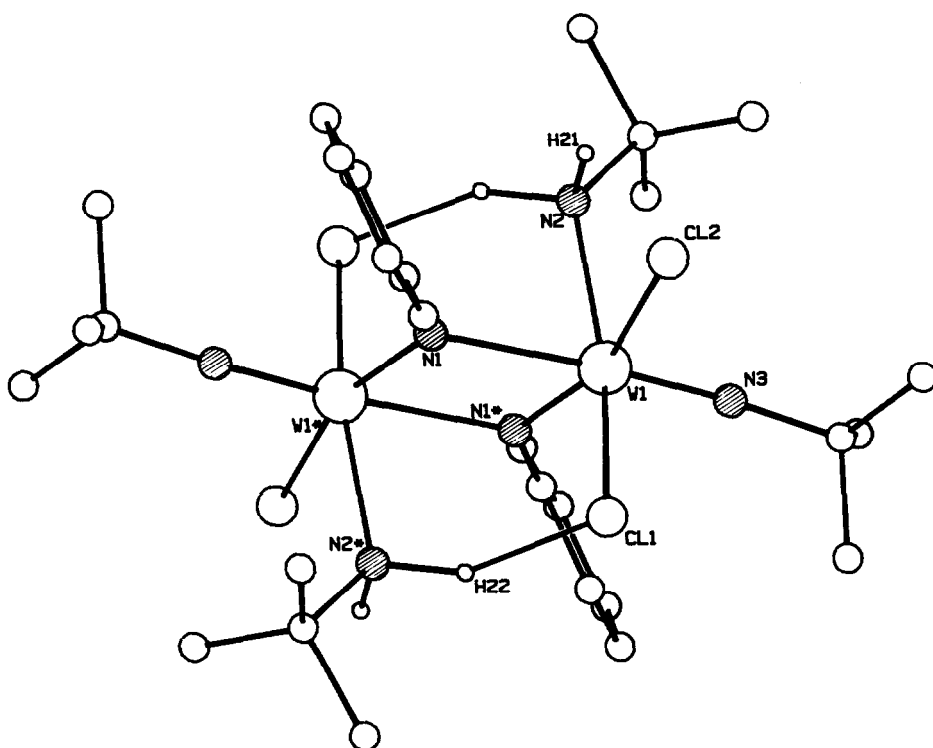
Figure The Structure of W(NBu^t)(μ_2-NPh)Cl$_2$(Bu^{t}NH$_2$)

Important Bond Lengths (Å) and Angles (deg) are:-

W(1)-Cl(1) 2.398(1),   W(1)-Cl(2) 2.462(1),   W(1)-N(1) 2.324(3)

W(1)-N(1)* 1.895(3),   W(1)-N(2) 2.223(3),   W(1)-N(3) 1.729(4)

N(1)-W(1)-N(1)*   76.5(1),   Cl(1)-W(1)-N(1)   85.7(1)

Cl(1)-W(1)-N(1)* 97.8(1),   Cl(1)-W(1)-N(2)   158.0(1)

Cl(1)-W(1)-Cl(2) 86.3(0),   N(3)-W(1)-Cl(1)   93.3(1)

N(3)-W(1)-Cl(2)   97.8(1),   N(3)-W(1)-N(2)   104.0(1)

N(3)-W(1)-N(1)*   99.3(1),   N(3)-W(1)-N(1)   175.4(1)

A NOVEL TRINUCLEAR ORGANOIMIDO VANADIUM(V) COMPOUND.

CRYSTAL AND MOLECULAR STRUCTURE OF

$[V_3Cl_2(NBu\text{-}tert.)_3(\mu_2\text{-}NPh)_3(\mu_3\text{-}PhNCONHBu\text{-}tert.)]$

D.C. Bradley*, M.B. Hursthouse*, A.N. de M. Jelfs and R.L. Short

Department of Chemistry, Queen Mary College,

Mile End Road, London E1 4NS

Abstract. From the reaction involving $V(NPh)Cl_3$ and $tert.Bu(Me_3Si)NH$ the trinuclear complex $[V_3Cl_2(NBu\text{-}tert.)_3(\mu_2\text{-}NPh)_3(\mu_3\text{-}PhNCONHBu\text{-}tert.)]$ has been isolated and its structure determined by single-crystal X-ray diffraction. The molecule contains non-bridging (nearly linear) tert.-butyl imido groups, bridging phenylimido groups and a novel triple-bridging (through oxygen) PhNCONHBu-tert. ligand.

* Authors to whom correspondence may be addressed.

A recent review revealed that only a few authentic organoimido vanadium compounds have been characterized.[1,2,3] We have found that trichloro-phenyl-imidovanadium(V) (1) is readily prepared by the reaction of $VOCl_3$ with phenyl-isocyanate and that it is a useful starting material for synthesizing phenyl-imidovanadium compounds by replacement of the chlorine with other ligands. In attempting to prepare a vanadium complex containing two different organoimido ligands we have investigated the reaction of (1) with the unsymmetrical amine (tert.-Bu)(Me$_3$Si)NH which may be deprotonated and/or de-trimethylsilylated in reacting with V-Cl bonds. A crystalline product [V_3Cl_2(NBu-tert.)$_3$(μ_2-NPh)$_3$-(μ_3-PhNCONHBu-tert.)] was isolated and a single crystal X-ray structure deter-mination was carried out.

Crystal Data: $V_3OCl_2N_8C_{11}H_{56}$, M = 901.69, triclinic, a = 11.334(2), b = 11,420(2), c = 20.775(7)Å, α = 100.20(2), β = 75.55(2), γ = 111.21(1)$^\circ$, V = 2416.3Å^3, space group P$\bar{1}$, Z = 2, D_c = 1.24 g cm^{-3}, μ(Mo-Kα) = 7.38 cm^{-1}, (λMo-Kα = 0.71069Å), F(000) = 940.

The structure was solved by direct methods and refined by least-squares, with anisotropic thermal parameters for all non-hydrogen atoms and hydrogen positions calculated in idealised positions and assigned an overall, refined, isotropic thermal parameter. The final R and R_w values are 0.0495, 0.0475 with w = 1/[α^2(F) + 0.0005F^2]. Tables of atomic positional and thermal para-meters and Fo/Fc values have been deposited as supplementary data with the Editor, from whom copies are available.[†]

The structure (Figure) shows several interesting features. Thus the basic nucleus of the structure is a $(VN)_3$ ring in which the metal atoms are bridged by phenylimido groups [V-N = 1.853(9) - 1.912(8)A]. Each vanadium atoms is bonded to a nearly linear non-bridging tert.-butylimido group [V-N = 1.608(9), 1.611(8), 1.648(8)A] and two of the vanadiums, which are chemically equivalent, are each bonded to a chlorine [V-Cl = 2.254(4), 2.254(4)Å]. The third vanadium is bonded to the phenylamido nitrogen [V-N = 1.965(1)Å] of the unexpected ligand (tert.-BuNHCONPh)⁻, whose oxygen is triply bridging all three metal atoms [V-O = 2.252(7), 2.263(7), 2.287(6)Å]. The source of this ligand is a matter for conjecture but the structure suggests its formation _via_ insertion of PhNCO into a V-NHBu-tert. bond. The phenyl isocyanate may have been retained in the V(NPh)Cl₃ from its preparation and this aspect is the subject of continuing research.

Each vanadium is exhibiting a highly distorted trigonal bipyramidal configuration with the tert.-butylimido ligand and the oxygen of tert.-BuNHCONPh in the axial positions. The near-linear CNW groups show that the tert.-butylimido groups are acting as 4-electron donors with triple-bond character and bond lengths similar to that found in V(NR)(OSiMe₃)₃ (R = adamantyl, V-N = 1.614Å), in which the vanadium is 4-co-ordinated.[2] It is noteworthy that the bridging phenyl imido nitrogens are all _cis_ to the tert.-butylimido nitrogen which clearly exerts a powerful _trans_-influence on the triple-bridging ocygen.

References

1.   W.A. Nugent and B.L. Haymore,   Coord.Chem.Rev., 1980, 31, 123.

2.   W.A. Nugent and R.L. Harlow,   J.C.S.Chem.Comm., 1979, 342.

3.   N. Wiberg, H.W. Haring and U. Schubert,   Z.Naturforsch, 1980, 35b, 599.
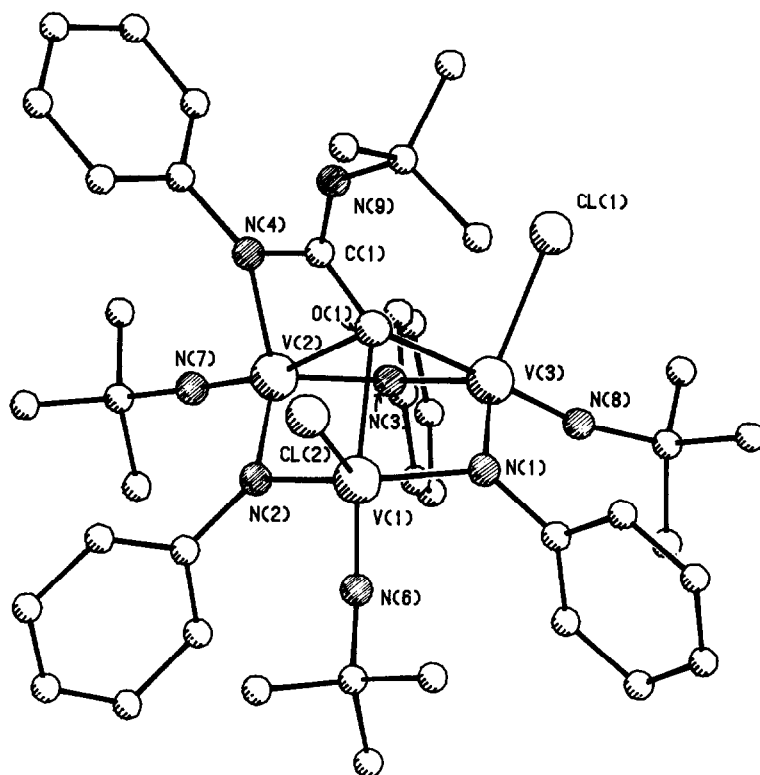
Figure   The Molecular Structure of $V_3Cl_2(NBu^t)_3(\mu_2\text{-}NPh)_3(\mu_3\text{-}PhNCONHBu^t)$

Selected Bond Lengths are:-

V(1)-N(1)	1.898(9),	V(1)-N(2)	1.912(8),	V(1)-N(6)	1.611(8),
V(2)-N(2)	1.853(9),	V(2)-N(3)	1.870(9), ·	V(2)-N(3)	1.648(9),
V(3)-N(3)	1.902(7),	V(3)-N(1)	1.909(8),	V(3)-N(3)	1.608(9),
V(2)-N(4)	1.965(8),	V(1)-O(1)	2.263(7),	V(2)-O(1)	2.287(6),
V(3)-O(1)	2.252(7),	V(1)-Cl(1)	2.254(4),	V(3)-Cl(1)	2.254(5).

Direct ¹H NMR assignment of [Co(III)(edta)]⁻

OLIVER W. HOWARTH

Department of Chemistry & Molecular Sciences, University of Warwick, Coventry,
CV4 7AL England

Abstract—Direct assignment of the ¹H NMR spectrum of the ethylenedinitrilo–NNN′N′-tetra-acetato-cobalt(III) anion [Co(III)(edta)]⁻, illustrates the value of n.O.e. difference and 2-D n.O.e. spectroscopy in coordination chemistry.

In 1971, Sudmeier *et al.*[1] assigned the ¹H NMR spectrum of aqueous [Co(III)(edta)]Cl on the basis of a theoretical argument concerning the relative rates of deuteriation of the glycinate protons. This assignment has been used as a starting point for many further papers on related compounds[2, 3]. We now confirm it directly *via* the nuclear Overhauser enhancement (n.O.e.) difference spectra[4] shown in the figure. Irradiation of resonance *b* gives not only the expected enhancement at *a* but also one at *c*, and similarly irradiation at *e* not only affects *f* but also *d*. The minor disturbances at other positions arise from imperfect subtraction, and do not integrate significantly. Unfortunately, the selectivity of n.O.e. difference spectroscopy is insufficient to penetrate the crowded region around δ 3.8. However, a 2D-n.O.e. experiment[5] confirms the absence of unreasonable dipolar interactions (such as *df*) as well as the presence of the above near-neighbour relationships. The two

methods clearly have considerable value in non-labile coordination chemistry.

REFERENCES

1. J. L. Sudmeier, A. J. Senzel and G. L. Blackmer, *Inorg. Chem.* 1971, **10**, 90.
2. O. W. Howarth, P. Moore and N. Winterton, *J. Chem. Soc., Dalton Trans.*, 1974, 2271 and refs contained therein.
3. O. W. Howarth, P. Moore and N. Winterton, *J. Chem. Soc., Dalton Trans.* 1975, 360.
4. J. H. Noggle and R. E. Schirmer, *The Nuclear Overhauser Effect*. Academic, New York (1971).
5. J. Jeener, B. H. Meier, P. Bachmann and R. R. Ernst, *J. Chem. Phys.* 1979, **71**, 4546.
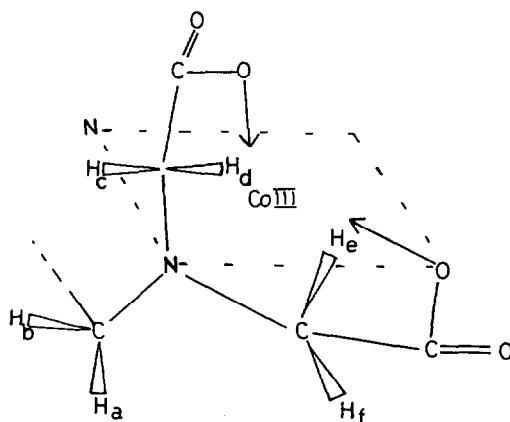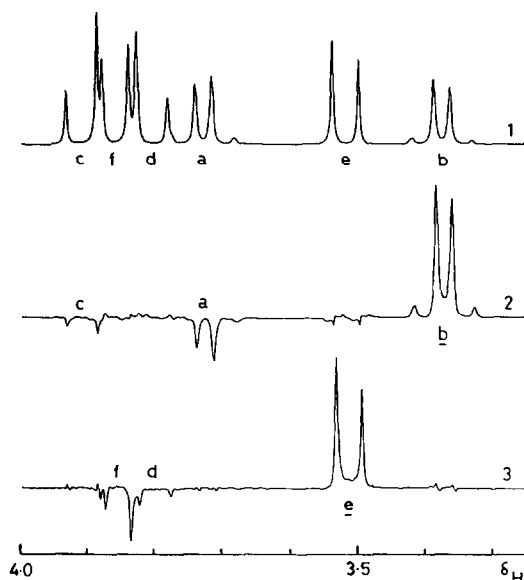
Fig. 1. 400 MHz ¹H NMR spectrum of title compound, labelled according to the half-structure shown. Two *ab* quartets and one *aa′ bb′* near-quartet are resolved. 2. Irradiation of backbone resonance *b* affects not only *a* but also *c*. 3. Irradiation of *e* affects *d* as well as *f*, thus confirming the assignment.

ERRATUM

R. D. Gillard, M. F. Pilbrow, S. Leonard, M. C. Rendle, and C. F. H. Tipper: The reaction of carbon monoxide with platinum ylids. *Polyhedron* 1982, **1**, 689.

The reference numbers attached to types of compound in the Introduction (p. 689) are not all correct.

(**II**) is missing, and (**I**) appears twice.

To clarify this, the correct codes are:

[X₂PtCH₂CH₂(pyridine)₂]	(**I**) platina(IV)cyclobutane
[X₂Pt{CH(py)CH₂CH₃}(py)]	(**II**) platinum(II) ylid
[X₄Pt{CH(py)CH₂CH₃}(py)]	(**III**) platinum(IV) ylid
[Cl₂Pt{CH(py)CH₂CH₃}(CO)]	(**IV**) platinum carbonyl ylid.

The numbers appearing in Scheme 1 (p. 690) are correct.

HISTORICAL SKETCHES

NIKOLAĬ SEMENOVICH KURNAKOV, THE REACTION (1893) AND THE MAN (1860–1941) A NINETY-YEAR RETROSPECTIVE VIEW

GEORGE B. KAUFFMAN

Department of Chemistry, California State University, Fresno, CA 93740, U.S.A.

Abstract—Kurnakov's classic thiourea reaction, proposed ninety years ago and still used to differentiate *cis* from *trans* isomers of dipositive platinum and palladium, represents his best known contribution to coordination chemistry. The circumstances surrounding its discovery, its implications, and its relationship to Peyrone's and Jørgensen's reactions and Chernyaev's *trans* effect are discussed. A brief discussion of Kurnakov's other studies of coordination compounds, and a short biography are also provided.

[The] stability [of the platinum compounds of thiourea prepared by me] and their close relationships to other complex platinum salts permits a closer investigation into their nature and an important expansion of our conceptions of complex bases in general . . . in individual cases the ability to form salts of general formula PtX₂·2U·2A (in which A = NH₃) [and U = thiourea] serves as a characteristic indication for differentiating the isomeric salt[s] PtX₂·2A.[1]

These words, written in 1893, the same year that Alfred Werner's coordination theory[2] was published, occur in one of the first major systematic studies of the coordination compounds of platinum undertaken in Russia. Entitled *On Complex Metallic Bases*[3] and serving as his inaugural dissertation for the Professorship of Inorganic Chemistry at the St. Petersburg Mining Institute, this experimental and theoretical study by Nikolaĭ Semenovich Kurnakov (1860–1941) represents not only his first major work but also his most widely-known contribution to coordination chemistry. Published first in Russian and then in German translation,[1] it provided the nineteenth-century coordination chemist with a simple diagnostic test for differentiating *cis* from *trans* isomers of dipositive platinum or palladium—a test still used today for this purpose.[4]

THE REACTION

The first decade following Kurnakov's graduation as Mining Engineer from the Mining Institute in 1882 was devoted largely to research in halurgy (salt manufacture), metallurgy, and assaying, carried out both in the laboratory and in the plants and factories that he visited. His second research period (1891–1902), devoted to the structure and properties of coordination compounds, began with the complexes ("double compounds") of silver(I) nitrate and mercury(I) nitrate with thiourea, $CS(NH_2)_2$.[5] After a short study comparing the solubilities of the chlorides of the luteocobaltic ($CoCl_3 \cdot 6NH_3$; modern, $[Co(NH_3)_6]Cl_3$), purpureocobaltic ($CoCl_3 \cdot 5NH_3$; modern, $[Co(NH_3)_5Cl]Cl_2$), and roseopentamminecobaltic ($CoCl_3 \cdot 5NH_3 \cdot H_2O$; modern, $[Co(NH_3)_5H_2O]Cl_3$) series (1892),[6] he returned in 1893 to the ligand thiourea for the subject of his dissertation. Since platinum had been and still continues to be one of the most valuable of Russia's natural resources, it is not surprising that Kurnakov chose the complexes of platinum with thiourea for the main part of this experimental work. Throughout his long scientific career, he retained his interest in this noble metal; not only did he later become Director of the Institute for the Study of Platinum and Other Noble Metals following the death of its founder Lev Aleksandrovich Chugaev (1873–1922),[7] but also, because of his development of coordination theory and application of complexes to the refining of the platinum metals, he is regarded as one of the founders of the platinum industry of the U.S.S.R.[8]

In his first part of *On Complex Metallic Bases*[1] Kurnakov found that addition of excess aqueous potassium tetrachloroplatinate(II) ($PtCl_2 \cdot 2KCl$; modern, K_2PtCl_4) to aqueous thiourea (tu) caused precipitation of the compounds $PtCl_2 \cdot 2tu$ (reddish-yellow *trans*-$[Pt(tu)_2Cl_2]$, which he correctly recognized as analogous to the chloride of Reiset's second base, *trans*-$[Pt(NH_3)_2Cl_2]$):

Изъ химической лабораторіи Горнаго Института.

О сложныхъ металлическихъ основаніяхъ.

Н. Курнакова.

Глава I. Металлическія соединенія тіокарбамида.

Способность тіокарбамида или тіомочевины къ сочетаніямъ съ металлическими солями является весьма ясно выраженной. Уже Рейнольдсъ [1]), открывшій тіомочевину при изомерномъ превращеніи роданистаго аммонія, описалъ характерныя соединенія:

$$AuCl.2CSN_2H_4$$
$$PtCl_2.HCl.2CSN_2H_4,$$
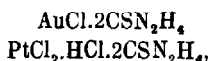
образующіяся при дѣйствіи тіомочевины на растворы хлорныхъ солей золота и платины. Впослѣдствіи Клаусъ [2]), Мали [3]), Преторіусъ-Зейдлеръ [4]), Ратке [5]) и др. получили попутно при своихъ изслѣдованіяхъ надъ тіомочевиною и ея производными многочисленныя сочетанія съ солями свинца, кадмія, ртути, олова, висмута, серебра, таллія и мѣди. Всѣ эти соединенія заключаютъ тіомочевину въ видѣ цѣлыхъ частицъ и имѣютъ составъ, выражаемый слѣдующей общей формулой:

$$MX_m.nCSN_2H_4 \text{ или } MX_m.nu,$$
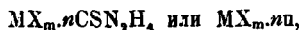
если обозначить для краткости $CSN_2H_4 = u$. Въ извѣстныхъ до настоящаго времени соляхъ коэффиціентъ n измѣняется въ предѣлахъ отъ 1 до 4 (на одинъ атомъ металла).

Особенно замѣчательны мѣдныя соединенія, изслѣдованныя Ратке. При взаимодѣйствіи съ солями окиси мѣди тіомочевина реагируетъ сначала, какъ возстановитель, по уравненію:

$$CSN_2H_4 + 2CuCl_2 = 2CuCl + (CSN_2H_4)_2Cl_2$$
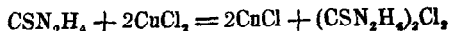
Образующаяся CuCl вступаетъ затѣмъ въ сочетаніе съ новымъ количествомъ тіомочевины и даетъ сложную соль. Такимъ образомъ, смѣшивая на холоду разведенные растворы тіомочевины и хлорной

[1]) L. E. Reynolds, Ann. Chem. Parm. 150, 232 (1869).
[2]) Claus, Ann. Chem. Pharm. 179, 132; Berl. Ber. 9, 226,
[3]) Maly, Berl. Ber. 9, 172.
[4]) Praetorius-Seidler, Journ. f. pract. Chem. (2) 21, 143.
[5]) Rathke, Berl. Ber. 14, 1780; 17, 297.

химич. общ. 36

Fig. 1. The first page of Kurnakov's classic paper "O Slozhnykh Metallicheskykh Osnovaniiakh" (On Complex Metallic Bases) J. Russ. Phys. Chem. Soc. 1893, 25, 565 (Ref. 1).

$$K_2\begin{bmatrix} Cl & & Cl \\ & Pt & \\ Cl & & Cl \end{bmatrix} + 2tu \rightarrow \begin{bmatrix} tu & & Cl \\ & Pt & \\ Cl & & tu \end{bmatrix}$$

+ 2KCl *(modern formulation)* (1)
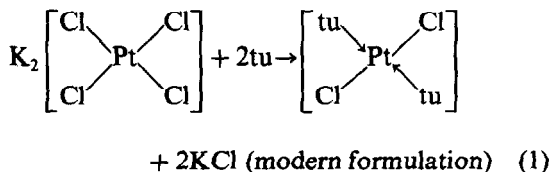
and PtCl$_2$·tu (an orange–yellow water-insoluble substance, which was not obtained in a pure state and was not further investigated). Warming either of these compounds with excess thiourea transformed them into the soluble white compound PtCl$_2$·4tu([Pt(tu)$_4$]Cl$_2$), which Kurnakov correctly recognized as related to the chloride of Reiset's first base ([Pt(NH$_3$)$_4$]Cl$_2$). Kurnakov also prepared

the very stable PtCl$_2$·4tu directly by adding a warm, concentrated solution of K$_2$PtCl$_4$ to a warm, saturated solution of thiourea. He also prepared the bromide, sulphate, nitrate, hexachloroplatinate(IV) and tetrachloroplatinate(II) of the [Pt(tu)$_4$]$^{2+}$ ion as well as the palladium salt PdCl$_2$·4tu ([Pd(tu)$_4$]Cl$_2$). Substituted thioureas (methyl-, ethyl-, *sym*-diethyl- and triethylthiourea), thioacetamide (CH$_3$·CS·NH$_2$), and xanthogenamide (NH$_2$·CS·OC$_2$H$_5$) gave similar salts with 2 or 4 moles of base per mole of PtCl$_2$. Kurnakov correctly recognized that the thiourea was monodentate and bonded to the metal atom through the sulphur atom rather than through one

of the nitrogen atoms, a conclusion that has since been confirmed by studies of IR spectra.[9]

But it was Kurnakov's preparation of the $PtCl_2$ "salts of mixed bases" (those containing both thiourea and either ammonia or pyridine) that furnished the basis for what has since become known as Kurnakov's reaction or Kurnakov's test:

> The chloride salt of Reiset's second base (platosammine chloride) is especially interesting. . . . In the presence of thiourea β-$PtCl_2$·$2NH_3$ quickly dissolves on warming with formation of a colourless solution, from which snow-white needles of the mixed compound $PtCl_2$·$2NH_3$·$2CSN_2H_4$ separates on evaporation or treatment with hydrochloric acid. This compound apparently has the composition of the type of salt of Reiset's first base $PtCl_2$·$4NH_3$, in which 2 molecules of NH_3 are replaced by 2 molecules of CSN_2H_4. This formation is completely analogous to the formation of $PtCl_2$·$4NH_3$ from β-$PtCl_2$·$2NH_3$ and ammonia.[1]

In modern formulation,

$$\begin{bmatrix} H_3N & Cl \\ & Pt \\ Cl & NH_3 \end{bmatrix}_{trans} + 2tu \rightarrow \begin{bmatrix} H_3N & tu \\ & Pt \\ tu & NH_3 \end{bmatrix}_{trans} Cl_2$$

Kurnakov's Reaction   (2)

$$\begin{bmatrix} H_3N & Cl \\ & Pt \\ Cl & NH_3 \end{bmatrix}_{trans} + 2NH_3 \rightarrow \begin{bmatrix} H_3N & NH_3 \\ & Pt \\ H_3N & NH_3 \end{bmatrix} Cl_2$$

(3)
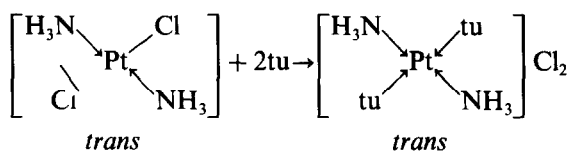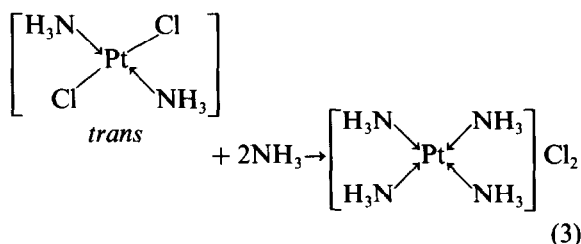
On the other hand, Kurnakov observed:

> It is noteworthy that the isomeric α-compounds, platosemidiammine chloride α-$PtCl_2$·$2NH_3$ of Peyrone and platosemidipyridine chloride α-$PtCl_2$·$2C_5H_5N$, apparently do not form mixed salts as do the β-compounds, at least not under the same conditions.

> Peyrone's salt and platosemidipyridine chloride dissolve easily on warming with thiourea. Ammonia or pyridine are here split off, and yellow solutions are formed, from which, on addition of hydrochloric acid, the salt $PtCl_2$·$4U$ is precipitated in yellow needles (recognizable by its behaviour with H_2SO_4 and Na_2PtCl_6). The same result is also obtained at room temperature.[1]

In modern formulation,

$$\begin{bmatrix} A & Cl \\ & Pt \\ A & Cl \end{bmatrix}_{cis} + 4tu \rightarrow \begin{bmatrix} tu & tu \\ & Pt \\ tu & tu \end{bmatrix} Cl_2 + 2A$$

Kurnakov's Reaction   (4)
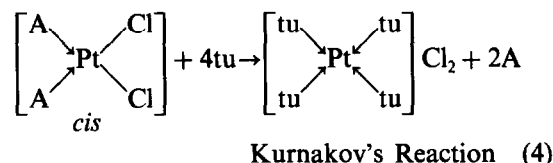
($A = NH_3$ or pyridine).

Thus replacement by thiourea (or thioacetamide) occurs with all the ligands of the cis isomer but only with the acid radicals of the trans compound. Inasmuch as the isomers yield easily distinguishable, characteristically different products and by-products (eqns 2 and 4), reaction with thiourea or thioacetamide (Kurnakov's reaction) may be used to differentiate cis from trans isomers of Pt(II) and Pd(II).

Kurnakov's reaction, useful as it is, however, was not the first discovered example of directive influences in substitution reaction of coordination compounds. For example, the syntheses of two of the longest known platinum isomers, viz. platosemidiammine chloride or Peyrone's salt[10] (α- or cis-[Pt(NH_3)_2Cl_2]) and platosammine chloride or Reiset's second chloride[11] (β- or trans-[Pt(NH_3)_2Cl_2]), involve such influences. Their preparative reactions[12] were known as Peyrone's reaction[10] and Jørgensen's reaction,[13] respectively, and were said to exemplify Peyrone's rule (cis orientation) and Jørgensen's rule (trans orientation):

Peyrone's reaction

$$K_2 \begin{bmatrix} Cl & Cl \\ & Pt \\ Cl & Cl \end{bmatrix} + 2NH_3 \rightarrow$$

$$\begin{bmatrix} H_3N & Cl \\ & Pt \\ H_3N & Cl \end{bmatrix} + 2KCl \qquad (5)$$

cis

Jørgensen's reaction

$$\begin{bmatrix} H_3N & NH_3 \\ & Pt \\ H_3N & NH_3 \end{bmatrix} Cl_2 + 2HCl \rightarrow$$

$$\begin{bmatrix} H_3N & Cl \\ & Pt \\ Cl & NH_3 \end{bmatrix} + 2NH_4Cl \qquad (6)$$

trans
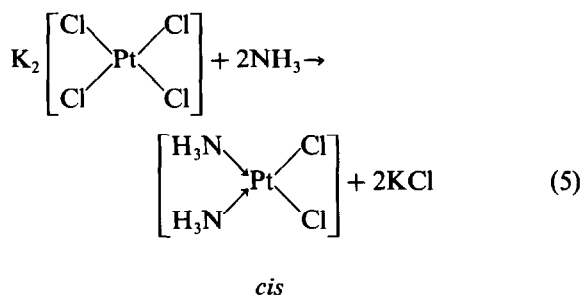
These reactions played crucial roles in Werner's proof of the square planar configuration for platinum(II)[2] and, along with Kurnakov's reaction, were valuable weapons in the inorganic stereochemist's arsenal. Kurnakov recognized that his synthesis of trans-[Pt(tu)$_2$Cl$_2$] by the action of thiourea on potassium tetrachloroplatinate(II) (eqn 1) constituted an exception to Peyrone's rule (eqn 5), which predicted formation of the cis isomer. Actually, the conflict is apparent rather than real, for Peyrone's reaction, Jørgensen's reaction, and Kurnakov's reaction are all specialized cases of a more general principle underlying the directive influence of coordinated ligands, which was not enunciated until well into the third decade of the twentieth century.

Although Werner[2] recognized the principle of "trans elimination" as early as 1893, it was not until 1926 that Il'ya Il'ich Chernyaev (1893–1966)[14] pointed out the general regularity of what he called the trans effect in order to describe the influence of a coordinated ligand on the practical ease of preparing compounds in which the group trans to it had been replaced.[15] Chernyaev theorized that a negative group coordinated to a metal atom labilizes the bond of any group trans to it, and thus he explained not only the empirically formulated Peyrone's, Jørgensen's, and Kurnakov's reactions but also many other features of the reactions of dipositive and tetrapositive platinum and palladium and of other metals as well. He postulated that electronegative ligands have a greater "trans influence" than neutral ligands, and his original trans-directing series has been extended to include a variety of ligands:

$$CN^- \sim CO \sim C_2H_4 \sim NO \sim H^- > CH_3$$
$$\sim SC(NH_2)_2 \sim SR_2 \sim PR_3 > SO_3H^-$$
$$> NO_2^- \sim I^- \sim SCN^- > Br^- > Cl^-$$
$$> C_5H_5N > RNH_2 \sim NH_3 > OH^-$$
$$> H_2O.[16]$$
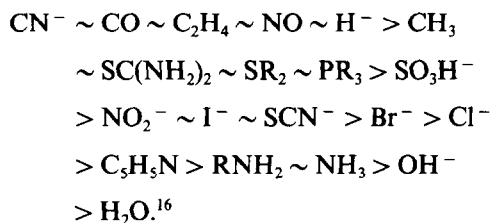
Thus the formation of cis-diammines by reaction of ammonia or amines with tetraacidoplatinates(II) (eqn 5) is essentially due to the fact that the trans influence of ammonia or amines is less than the trans influence of the anions. Similarly, the course of Kurnakov's reaction is explained by the weak trans influence of ammonia and amines and the strong trans influence of thiourea, which, after displacement of the acid radicals in the cis-diammines (eqn 4) labilizes the ammonia or amine molecules so that they are also substituted by thiourea, while in trans-diammines

(eqn 2) the two ammonia or amine molecules are not labilized by thiourea and cannot be displaced by it.[17] Chernyaev's trans effect also explains not only the course of reaction (1) but also why Kurnakov's test fails with complexes containing ligands of strong trans effect. For example, the trans effect of thiourea is balanced by the trans effect of phosphorus-containing ligands, and cis-[Pt{(C$_2$H$_5$)$_3$P}$_2$Br$_2$] dissolves readily in cold aqueous thiourea to yield cis-[Pt(tu)$_2${(C$_2$H$_5$)$_3$P}$_2$]Br$_2$ rather than [Pt(tu)$_4$]Br$_2$ as predicted by eqn (4).[18]

At the time that Kurnakov was working on his dissertation, the Blomstrand–Jørgensen chain theory[19] was still the most widely accepted of the various theories of the structure of complexes,[20] and Werner's coordination theory was just being proposed. In his dissertation Kurnakov rejected Kekulé's outdated theory of molecular compounds[20] and critically reviewed the various theories that had been proposed to explain the structure of complexes. Like Werner, he noted the changes in chemical function of both metal and acid radicals in salts brought about by the combination of such salts with ammonia, water, or other bases, and he likewise noted the similarities between hydrated metal salts and metal–ammonia compounds. Nevertheless, in his opinion, none of the theories was completely satisfactory although each served to explain various facets of the problem.

Thus Kurnakov occupied an intermediate position between the old and new theories. While he did not find it possible to agree totally with the Blomstrand–Jørgensen chain theory, he likewise did not completely accept Werner's views. In each theory he found a sound core of ideas, which, nevertheless, in his opinion, could not explain all the known facts. According to the chain theory, in complex compounds the acid radicals were bonded to the metal through one or more (a chain) of neutral ligands. For example, the chloride of Reiset's second base was written

$$Pt \begin{matrix} NH_3-Cl \\ \\ NH_3-Cl \end{matrix} \quad .$$
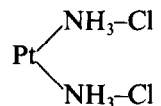
According to Werner's coordination theory, the anions were directly bonded to only the metal, and the neutral ligands were similarly bonded:

$$\begin{matrix} Cl & & NH_3 \\ & Pt & \\ H_3N & & Cl \end{matrix} \quad .$$

trans
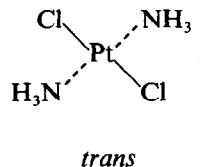
Kurnakov, however, thought that the anions were simultaneously bonded to both the metal atom and the neutral molecules:

$$\begin{array}{ccc} Cl & & NH_3 \\ & \diagdown Pt \diagup & \\ | & & | \\ H_3N & \diagup \diagdown & Cl \end{array}.$$
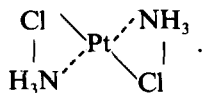
In support of this assumption he pointed to the fact that the chemical reactivities of halogens, hydroxide, and other acid substituents depend not only upon the metal to which they are bonded but upon the other groups to which the metal is bonded as well. He regarded complexes as intermediate between chemical compounds of fixed composition and phases of varying composition, a harbinger of his later "berthollide-daltonide" dichotomy (1914).[21]

Kurnakov did not limit himself to studying the synthesis and properties of coordination compounds, but he investigated physical properties of important theoretical significance such as colour, index of refraction (later useful in studies of dipole moment), crystal form, solubility, and acidic and basic properties (later developed more fully by A. A. Grinberg). For example, in 1898 he published an article on "The Relation Between the Colour and the Constitution of Haloid Double Salts", in which he investigated the change in colour caused by the introduction of water, ammonia, or other neutral ligands into inorganic salts.[22] In the following years he synthesized and studied hydrated lithium bromocuprite,[23] and he prepared new complexes of palladium(II) chloride[24] and nickel(II) chloride[25] with ethylenediamine. After a hiatus of three decades he returned to studies of coordination compounds of platinum. He studied derivatives of tetraammineplatinum(II) chloride,[26] the so-called "ice isotherms"[27] and the equilibrium[28] in the ternary system: $NaCl–PtCl_4–H_2O$, the latter two studies being examples of his technique of physicochemical analysis. He also drew a number of important inferences concerning the similarity between complex ions and simple metal ions, which was later confirmed by Chugaev's demonstration of the analogy between the $[Pt(NH_3)_5Cl]^{3+}$ ion and Ba^{2+} and Pb^{2+} ions.[29]

Nikolaĭ Semenovich Kurnakov is regarded as the founder of a new chemical discipline—physicochemical analysis—and it is his later works in this field that are immediately thought of when his name is mentioned. Yet, as Il'ya Il'ich Chernyaev has observed,

if Kurnakov had produced nothing but his early work on complex compounds, his name

would not be forgotten. . . . Kurnakov's work on complex compounds played an immense part in the development of the chemistry of complex compounds, both in its experimental and theoretical aspects.[4]

THE MAN

Nikolaĭ Semenovich Kurnakov was born in Nolinsk, Vyatka province, on 6 December (24 November, O.S.), 1860, but spent his childhood in the village of Zhedrin, Nizhegorodskaĭa province.[30] His father, an army officer, died in 1868, leaving him with his mother (Varvara Alekseevna Kurnakova, née Mezentseva) and brother. From 1871 to 1877 he received a high school education at the military gymnasium at Nizhni Novgorod (now Gorkiĭ). Distantly related to the great organic chemist Markovnikov, he made an early choice of a career, setting up a home laboratory at the age of fourteen. Immediately after graduation, he entered the St. Petersburg Mining Institute, where independent research under chemists Sushin and Lisenko and mineralogist Yeremyev resulted in his first publication, a crystallographic study of alum and Schlippe's salt $(Na_3SbS_4·9H_2O)$.[31] After graduation from the Factory Section in 1882 with the degree of Mining Engineer, he was retained by the chemical laboratory of the institute.

Kurnakov's interest in chemical industry would not permit him to remain exclusively a laboratory worker, and he now began the first of his many trips to plants and factories. In the summer of 1882, together with Prof. N. A. Iôssa, he investigated the smelting operations at the Altai (Siberia) refineries. The following year, during a trip abroad, he toured the laboratories of the Freiburg Akademie where he attended the lectures of Winkler and Richter. A detailed study of salt manufacturing in Prussia, Lorraine, Württemberg, Baden, Bavaria, and the Austrian Tyrol made during the summer of 1884 resulted the following year in his dissertation for the position of *Adiunkt* (Assistant) in metallurgy, halurgy, and assaying, a post which he held for eight years. This work, "Isparitel'nye Sistemy Solïanykh Varnits" (Evaporative Systems of Salt Boilers), containing the germs of Kurnakov's subsequent studies of salt equilibria, appeared long before van't Hoff's research on the Stassfurt salt beds. The eighties were years of great developments in physical chemistry; Kurnakov's work was in keeping with this trend.

Further scientifically fruitful summer travels included: a chemical study of therapeutic mineral muds in the Crimean salt lakes (1894), which resulted in Kurnakov's introduction of the coefficient of metamorphization, a new and im-

portant unit for the characterization of natural salt solutions; a study of firedamp (methane) in the Donets Basin anthracite mines (1895);[32] work as an expert at the All-Russian Industrial and Artistic Exhibition at Nizhni Novgorod (1896); a visit to Germany and France to study methods for the investigation of detonating (oxyhydrogen) gas (1898); a trip as a delegate to the International Congress of Chemical and Mining Industries and as a member of the Commission of Experts at the World's Fair, both in Paris (1900).

In 1893 Kurnakov was appointed Professor of Inorganic Chemistry following the successful defense of his dissertation "On Complex Metallic Bases",[3] discussed in detail above. In 1899 he was appointed a member of the Mining and Scientific Mining Institute, and he organized the teaching of physical chemistry at the Saint Petersburg Electrotechnical Institute. In 1902 he was appointed Professor of General Chemistry at the St. Petersburg Polytechnic Institute, which he had organized together with Mendeleev and Menschutkin; he held this post until 1930.

During the first decade of the twentieth century, Kurnakov was concerned with the solution of industrial problems such as platinum refining, metallic alloys, metallography, and salt manufacturing. In 1909 he was awarded the degree of Doctor of Chemical Sciences *honoris causa* by Moscow University, became a contributing editor of the *Zeitschrift für anorganische Chemie*, and was appointed a member of the Mining and Scientific Committee. In 1910 he directed studies of the Russian Council on Platinum Refining, and the following year he went abroad to study methods of transporting warm sulphur waters. In connection with his work on the Russian Commission for the Study of Toxic Properties of Commercial Ferrosilicon, he carried out chemical–metallographic studies of alloys of iron with aluminum, phosphorus and silicon.[33]

Official recognition abroad followed recognition at home. In 1912 Kurnakov was elected a council member of the Société chimique and became a member of the Russian Department of the Inter-national Commission on the Nomenclature of Inorganic Compounds. As a delegate of the Russian Physical-Chemical Society, he participated in the meetings of the International Association of Chemical Societies held at Berlin (1912) and Brussels (1913). In 1913 he was elected vice-president of the Russian Metallurgical Society and became Ordinary Academician in chemistry at the Russian Academy of Sciences. The laboratory of the academy had been inactive for a number of years, but it experienced a rebirth as a result of Kurnakov's extraordinary organizational talent.

World War I brought new tasks for Kurnakov. He was instrumental in the creation of a number of new institutes and commissions. In 1915, together with fellow academicians V. I. Vernadskiĭ and A. E. Fersman, he organized and became assistant chairman of Komissiĭa po Izucheniĭu Estestvenno Proizvodstvennykh Sil Rossii, KEPS (Commission for the Study of Russian Natural Productive Sources), at the Academy. At KEPS, he established a Salt Commission, and the study of salt solutions and related problems occupied much of his time for the next few years.

Upon mobilization, Kurnakov became chairman of the newly-created Artillery Commission for the Study of Asphyxiating Gases where he conducted research both in the field and laboratory on the physiological action of war gases. From 1916 to 1918 he participated in the work of the chemical plant of the Military Industrial Committee in Petrograd. During the Civil War following the October (1917) Revolution, a trying period of frost, famine, and other disasters, when all organized life was completely disrupted, research continued in Kurnakov's laboratories. He even organized an expedition to investigate the formation of Glauber's salt ($Na_2SO_4 \cdot 10H_2O$) at Kara–Bogaz–Gol Bay.[34]

In 1919 he organized and became director (a position held until 1927) of the Gosudarstvennyĭ Institut Prikladnoĭ Khimii, GIPKh (State Institute of Applied Chemistry) with facilities located at Vasil'yevskiĭ Island on the Neva at Petrograd, which had grown out of the first Russian labora-
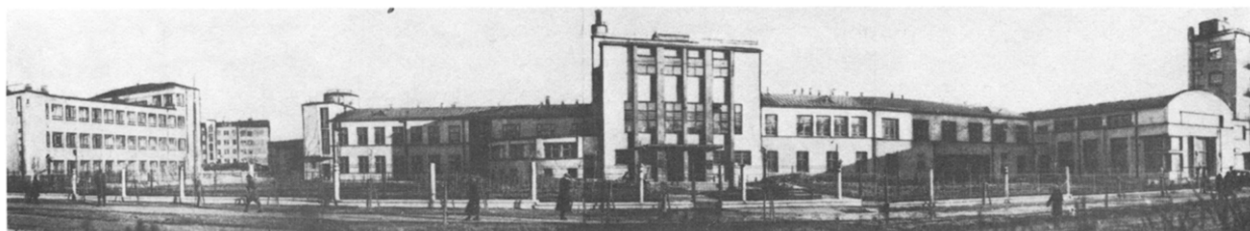
Fig. 2. The N. S. Kurnakov Institute of General and Inorganic Chemistry, Leninskiĭ Prospect 31, Moscow (by courtesy of the late Academician Il'ya Il'ich Chernyaev).

tory founded by Mikhail Vasil'yevich Lomonosov (1711–1765). Here scientific workers from the provinces gathered, especially during the summers, to work under Kurnakov's guidance. In the fall they returned home with ideas and projects for the next few years. In this manner, Kurnakov disseminated his ideas and expanded his rapidly growing school.

In 1918 at KEPS Kurnakov founded and became director of the Institut Fiziko-Khimicheskogo Analiza (Institute of Physicochemical Analysis), and the following year he became editor of its *Izvestiia Instituta Fiziko-Khimicheskogo Analiza* (now *Izvestiia Sektora Fiziko-Khimicheskogo Analiza*); he held both positions until his death. The first volume of this journal contained a classic in halurgy, viz. Kurnakov and Zhemchuzhnyĭ's study of natural salt deposits of marine origin.[35] The year 1922 saw Kurnakov become director of the General Chemistry Laboratory of the Academy, director of the Platinum Institute at KEPS upon Chugaev's death, and a member of the Göttingen Akademie.

In 1934 the Institute of Physicochemical Analysis, the Platinum Institute, and the General Chemistry Laboratory of the Academy merged into the Institut Obshchei i Neorganicheskoĭ Khimii, IONKh (Institute of General and Inorganic Chemistry). with headquarters in Moscow and with Kurnakov as its director. IONKh rapidly became one of the leading scientific research institutes in the U.S.S.R. and a center for physicochemical investigations of metallurgy, halurgy, precious metals, organic substances, and other economically significant problems.[36] Following Kurnakov's death in 1941, it was renamed the N. S. Kurnakov Institute.

From 1920 to the end of his life there were few chemical or metallurgical conferences in which Kurnakov failed to participate as chairman, lecturer, or delegate. He was chairman of the Chemical Association of the Academy of Sciences of the U.S.S.R. (1930–1938) and vice-president of the D. I. Mendeleev All-Union Society. In addition to his industrial consulting, in which he gave technical advice to plants and factories throughout the U.S.S.R., he was extremely active in public affairs.

Kurnakov's contributions were recognized on numerous occasions by the Soviet government. He received the First Mendeleev Prize (1936), the Order of the Red Banner for Labor (1939), and the title of Meritorious Worker of Science of the Russian Soviet Federated Socialist Republic (1940), and the Stalin Prize, First Class, for the fourth edition of his book *Introduction to Physicochemical Analysis*,[37] dedicated to the memory

Fig. 3. President of the USSR, Mikhail Ivanovich Kalinin (1875–1946), right, presenting the medal of the Order of Lenin to Academician Nikolaĭ Semenovich Kurnakov (1860–1941) in 1940. Photograph by P. Troshkin, courtesy of the late Academician Chernyaev.

of his closest friend, his wife Anna Mikhailovna, who for more than half a century had accompanied him everywhere and supported him in all his endeavors. The Kurnakovs had two children—a son Dr. Nikolaĭ Nikolaevich Kurnakov (born in 1889), a chemist who worked at the Baikov Metallurgical Institute of the Academy of Sciences of the

Fig. 4. On 15 August 1951, Kurnakov's portrait appeared on a 40–kopek postage stamp, part of a commemorative issue honouring outstanding figures of Russian art and science. Legend reads "N. S. Kurnakov, outstanding Russian chemist, Founder of Physicochemical Analysis". Scott catalogue No. 1573.

U.S.S.R., and a daughter Vera Nikolaevna Kurnakova (born in 1898), who died at the age of 23 while still a student.

His wife's death in 1940 had serious effects on Kurnakov's health. Ignoring the cancer which was soon to claim his life, he continued his full work schedule almost to the very end, and when his colleagues inquired as to the state of his health, which was visibly deteriorating, he quickly shifted the conversation to scientific topics. At the beginning of March, 1941 he entered the sanitorium at Barvikha where he died on 19 March. His work is continued by an extensive school of scientists armed with new research methods, new apparatus, new theories, and new applications which he himself had created. The two-volume *Collection of the Selected Works of N. S. Kurnakov*[38] contains a complete list of his works published through 1939, and the three volumes of his *Selected Works*[39] appeared in 1960–1963. The majority of the works of one of Russia's most distinguished and versatile chemists, even those published almost a century ago, are still of great theoretical and practical interest today.

REFERENCES

1. N. S. Kurnakov, *J. Russ. Phys. Chem. Soc.* 1893, **25**, 565, 693; *J. Prakt. Chem.* 1894, [2]**50**, 481; 1895, [2]**51**, 249; 1895, [2]**52**, 177, 490.
2. A. Werner, *Z. Anorg. Chem.* 1893, **3**, 267. For an English translation see G. B. Kauffman, *Classics in Coordination Chemistry—1. The Selected Papers of Alfred Werner*, pp. 9–88. Dover Publications, New York (1968).
3. N. S. Kurnakov, *O Slozhnykh Metallicheskikh Osnovaniakh*, Inaugural Dissertation. Gornyĭ Institut, St. Petersburg (1893).
4. G. G. Urazov and V. Nikolaeva, *Uspekhi Khim.* 1939, **8**, 785; G. G. Urazov, *Izvest. Fiz.-Khim. Anal., Inst. Obshchei i Neorg. Khim., Akad. Nauk S.S.S.R.* 1948, **16**, 5; I. I. Chernyaev, *Izvest. Sektora Platiny i Drugikh Blagorodnykh Metal., Inst. Obshchei i Neorg. Khim., Akad. Nauk S.S.S.R.* 1948, **21**, 7; O. E. Zvyagintsev, *ibid.* 1954, **28**, 133; I. N. Lepeshkov, *Russ. J. Inorg. Chem.* 1960, **5**, 1153.
5. N. S. Kurnakov, *J. Russ. Phys. Chem. Soc.* 1891, **23**, 559; *Ber.* 1891, **24**, 3956.
6. N. S. Kurnakov, *J. Russ. Phys. Chem. Soc.* 1892, **24**, 629.
7. G. B. Kauffman, *J. Chem. Educ.* 1963, **40**, 656; *Platinum Metals Rev.* 1973, **17**, 144.
8. G. B. Kauffman, *Platinum Metals Rev.* 1982, **26**, 129.
9. A. Yamaguchi, R. B. Penland, S. Mizushima, T. J. Lane, C. Curran and J. V. Quagliano, *J. Am. Chem. Soc.* 1958, **80**, 527; K. Swaminathan and H. M. N. H. Irving, *J. Inorg. Nucl. Chem.* 1964, **26**, 1291.
10. M. Peyrone, *Ann. Chem.* 1844, **41**, 1.
11. J. Reiset, *Ann. Chim. Phys.* 1844, [3]**11**, 417; *Compt. Rend.* 1844, **18**, 1100.
12. G. B. Kauffman and D. O. Cowan, *Inorg. Syn.* 1963, **7**, 239.
13. S. M. Jørgensen, *J. Prakt. Chem.* 1886, [2]**33**, 489; *Z. Anorg. Chem.* 1900, **24**, 153.
14. V. A. Golovnya, T. N. Leonova, W. Craig and G. B. Kauffman, *Ambix* 1976, **23**, 187; G. B. Kauffman, *Platinum Metals Rev.* 1976, **20**, 126; *J. Chem. Educ.* 1977, **54**, 86.
15. I. I. Chernyaev, *Izv. Inst. Izucheniĩ Platiny i Drug. Blagorodn. Metal.* 1926, **4**, 243; *Ibid.* 1927, **4**, 118. For an English translation of the second paper see G. B. Kauffman, *Classics in Coordination Chemistry—3. Twentieth Century Papers (1904–1935)*. pp. 151–195. Dover Publications, New York (1978).
16. J. E. Huheey, *Inorganic Chemistry. Principles of Structure and Reactivity*, 1st Edn, p. 424. Harper and Row, New York (1972).
17. A. A. Grinberg, *Vvedenie v Khimiyu Kompleksnykh Soedinenii*, 2nd Edn, pp. 301. Leningrad, Moscow (1951). *An Introduction to the Chemistry of Complex Compounds* (Translated by J. R. Leach, Edited by D. H. Busch and R. F. Trimble), pp. 138, 224. Addison-Wesley, Reading, Mass. (1962).
18. A. A. Grinberg, Z. A. Razumova and A. D. Troiskaya, *Bull. Acad. U.R.S.S., Ser. Chim.* **1946**, 253; A. A. Grinberg and Z. A. Razumova, *Zhur. Obshch. Khim.* 1947, **18**, 282; A. D. Troiskaya, *Zhur. Priklad. Khim.* 1953, **26**, 781.
19. G. B. Kauffman, *J. Chem. Educ.* 1959, **36**, 521; *Chymia* 1960, **6**, 180; *Classics in Coordination Chemistry—2. Selected Papers (1798–1899)*, pp. 93–102. Dover Publications, New York (1976).
20. G. B. Kauffman, *J. Chem. Educ.* 1972, **49**, 813; *Ibid.* 1974, **51**, 522.
21. N. S. Kurnakov, *Bull. Acad. Sci. St. Petersburg* **1914**, 321; N. V. Ageev, *Ann. sect. anal. phys.-chim., Inst. chim. gén. (U.S.S.R.)* 1943, **16**, 119.
22. N. S. Kurnakov, *Z. Anorg. Chem.* 1898, **17**, 207.
23. N. S. Kurnakov and A. A. Sementschenko, *Z. Anorg. Chem.* 1899, **19**, 335.
24. N. S. Kurnakov and N. I. Grozdarev, *Z. Anorg. Chem.* 1899, **22**, 384.
25. N. S. Kurnakov, *Z. Anorg. Chem.* 1900, **22**, 466.
26. N. S. Kurnakov and I. A. Andreevskiĭ, *Z. Anorg. Chem.* 1930, **189**, 137.
27. N. S. Kurnakov and M. I. Ravich, *Ann. Inst. Anal. Phys.-Chim. (U.S.S.R.)* 1935, **7**, 225.
28. N. S. Kurnakov and E. A. Nikitina, *J. Gen. Chem. (U.S.S.R.)* 1940, **10**, 577.
29. L. A. Chugaev and N. Vladimirov, *Compt. Rend.* 1915, **160**, 840; L. A. Chugaev, *Z. Anorg. Allgem. Chem.* 1924, **137**, 1; *Izv. Inst. Izucheniĩu Platiny i Drug. Blagorodn. Metal.* 1926, **4**, 1.
30. G. B. Kauffman, *J. Chem. Educ.* 1962, **39**, 44; Yu. I. Solov'ev and O. E. Zvyagintsev, *Nikolaĭ Semenovich Kurnakov: Zhizn' i Deyatel'nost'*, Izdatel'stvo Akademii Nauk S.S.S.R., Moscow (1960); Yu. I. Solov'ev, In *Dictionary of Scientific Biography* (Ed-

ited by C. C. Gillispie), Vol. 7, pp. 529–530. Charles Scribner's Sons, New York (1973).

31. N. S. Kurnakov, *Zapiski Min. Obshch.* 1880, **16**, 210, 331.

32. N. S. Kurnakov, *J. Russ. Phys. Chem. Soc.* 1902, **34**, 654.

33. N. S. Kurnakov, G. G. Urazov and G. S. Elin, *J. Russ. Phys. Chem. Soc.* 1913, **45**, 676; N. S. Kurnakov and G. G. Urazov, *Z. Anorg. Chem.* 1922, **123**, 89; *Rev. metal.* 1923, **20**, 451.

34. N. S. Kurnakov and S. F. Zhemchuzhnyï, *Material, Akad. Nauk S.S.S.R.* 1930, **73**, 339.

35. N. S. Kurnakov and S. F. Zhemchuzhnyï, *J. Russ. Phys. Chem. Soc.* 1916, **48**, 634; 1919, **51**, 1; *Bull. Acad. Sci. Russ.* **1918**, 1855.

36. N. S. Kurnakov, *Uspekhi Khim.* 1936, **4**, 957.

37. N. S. Kurnakov, *Vvedenie v Fiziko-Khimicheskiĭ Analiz*, 4th Edn. Akademiia Nauk S.S.S.R., Moscow (1940).

38. *Sobranie Izbrannykh Rabot N. S. Kurnakova*, 2 vols. Moscow, Leningrad (1938–1939).

39. *Izbrannye Trudy N. S. Kurnakova*, 3 vols. Moscow (1960–1963).

SYNTHESIS, CHARACTERISATION AND THERMAL PROPERTIES OF HYDRAZINIUM METAL OXALATE HYDRATES. CRYSTAL AND MOLECULAR STRUCTURE OF HYDRAZINIUM COPPER OXALATE MONOHYDRATE

D. GAJAPATHY, S. GOVINDARAJAN, K. C. PATIL and H. MANOHAR*

Department of Inorganic and Physical Chemistry, Indian Institute of Science,
Bangalore 560 012, India

Abstract—Complexes of the formula $(N_2H_5)_2M(C_2O_4)_2 \cdot nH_2O$ where M = Co, Ni, Cu and $n = 3, 2, 1$ respectively have been prepared and their spectral, magnetic and thermal properties investigated. The copper complex, $(N_2H_5)_2Cu(C_2O_4)_2 \cdot H_2O$ has a square planar geometry with no coordination of hydrazinium cations as confirmed by a single crystal X-ray study. Nickel and cobalt form octahedral complexes and X-ray powder patterns reveal that the complexes are not isomorphous.

Of the complexes containing positively charged ligands, those with the hydrazinium cation are of increasing interest.[1,2] Preparation and thermal study of metal double fluorides with hydrazinium cation have been reported.[3-12] A few chloride complexes of copper,[2] cadmium[13] and tin[14] with $N_2H_5^+$ cation have also been studied.

Another group of complexes containing $N_2H_5^+$ is the series of metal hydrazinium sulphates,[1,15-19] $M(N_2H_5)_2(SO_4)_2$ where M = Cr, Mn, Fe, Co, Ni, Cu, Zn, Cd and Mg. Double sulphates of lighter rare earths (La–Sm) with $N_2H_5^+$ have been studied in this laboratory.[20] A few hydrazinium metal hydrazidocarbonate hydrates have also been mentioned in the literature.[21,22] However no complexes containing $N_2H_5^+$ with oxalate have been reported. We report in this paper the preparation, characterization, magnetic and thermal properties of hydrazinium metal oxalate hydrates $(N_2H_5)_2M(C_2O_4)_2 \cdot nH_2O$ where M = Co, Ni, Cu and $n = 3, 2, 1$ respectively, and the crystal structure of hydrazinium copper oxalate monohydrate.

EXPERIMENTAL

Preparation of the compounds

Aqueous solutions of hydrazinium oxalate $(N_2H_5)_2C_2O_4$ and the corresponding metal nitrate hydrates, in the ratio 4:1 are mixed at room temperature and the mixture cooled to 5°C when the crystals of the respective hydrazinium metal oxalate hydrates separate out. The rate of formation of the product is in the increasing order Co < Ni < Cu. The crystals are immediately washed with small quantity of ice cold water and air dried. Except for the cobalt compound these compounds are quite stable in air. Hydrazinium cobalt oxalate trihydrate slowly decomposes in air in the course of a few days. Efforts to prepare the corresponding Mn, Fe and Zn compounds using a similar procedure resulted only in the formation of simple metal oxalates.

Conventional chemical analysis of all the three samples was done. Hydrazine content was estimated by titrating against standard KIO_3 under Andrews condition.[23] Metal contents were determined by EDTA titrations. Oxalate in the compounds was precipitated as calcium oxalate which was dissolved in dilute H_2SO_4 and titrated against standard $KMnO_4$. Water content in the samples was obtained by the method of difference and was further confirmed by thermogravimetry.

Physical measurements

IR spectra (4000–200 cm^{-1}) of the complexes were recorded in Nujol mull using a Perkin–Elmer PE 599 spectrophotometer. Reflectance spectra were recorded on Shimadzu UV-210A double beam spectrophotometer using MgO as a reference material. Magnetic susceptibility values were measured at room temperature by the Gouy method and corrected with Pascal constants. ESR spec-

---

*Author to whom correspondence should be addressed.

trum of the copper compound in the powder form was recorded on a Varian E 109 ESR spectrometer.

Differential thermal analysis (DTA) of the samples was recorded on an instrument described elsewhere[24] fitted with an omniscribe strip chart recorder. Thermogravimetric analysis (TG) was carried out on a Stanton Redcroft TG–750 thermobalance. Both the thermal experiments were done in air, with platinum cups as sample holders and a heating rate of $10°C\,min^{-1}$.

Crystallography of $(N_2H_5)_2Cu(C_2O_4)_2 \cdot H_2O$

Crystal data. $(N_2H_5)_2Cu(C_2O_4)_2 \cdot H_2O$, $M = 323.54$, monoclinic, $P2_1/n$, $a = 3.592(1)$, $b = 7.855(2)$, $c = 19.143(3)$ Å, $\beta = 94.3(3)°$, $Z = 2$, $D_c = 1.995\,g\,cm^{-3}$, $D_m = 1.99\,g\,cm^{-3}$, $F_{000} = 326$, $\mu(MoK\alpha) = 15.6\,cm^{-1}$.

X-Ray data collection and structure analysis

A crystal of dimensions $0.20 \times 0.25 \times 0.62$ mm was used for data collection. The unit cell dimensions and the intensities of all independent reflections with $\theta(MoK\alpha) < 32°$ were determined by standard experimental methods using an Enraf–Nonius CAD-4 diffractometer equipped with a graphite monochromator. Corrections were applied for Lorentz-polarisation and secondary extinction effects but not for absorption, since μ is small. 1550 independent reflections with $I \geqslant 3\sigma(I)$ were used in the subsequent analysis.

Copper positions were determined from a three-dimensional Patterson map and the remaining non-hydrogen atoms were located in subsequent Fourier maps. Atomic positions and thermal parameters were refined by full matrix least squares methods using the SHELX-76 program.[25] A difference Fourier synthesis at the end of the refinement gave peaks corresponding to all hydrogen atoms of the $N_2H_5^+$ group. Hydrogen atoms of disordered water could not be located. The final refinement including hydrogen atoms of $N_2H_5^+$ ion with an isotropic temperature factor $(5\,Å^2)$ converged at $R = 0.058$ and $R_w = 0.068$.

Atomic coordinates, thermal parameters and a table of Fo, Fc values have been deposited with the Editor as supplementary material. Atomic scattering factors and anomalous dispersion corrections were taken from Ref 26. The extinction coefficient g [(eqn 17.17) in Stout and Jensen[27]] was 5.8333×10^{-5}. The weighting function employed was $w = 0.5/(\sigma^2F + 0.023|F|^2)$.

Results and discussion

The results of chemical analysis (Table 1) of the samples agree well with the assigned composition of $(N_2H_5)_2M(C_2O_4)_2 \cdot nH_2O$ where M = Co, Ni, Cu and $n = 3, 2, 1$ respectively.

Infrared spectral data are tabulated (Table 2) and assigned on the basis of earlier work.[1,2,28–31] IR spectra of the complexes show absorptions corresponding to bidentate oxalate[28] at 1720–1650 cm^{-1}. The presence of hydrazine as a cation is revealed by the characteristic bands at 2650 cm^{-1} corresponding to the NH stretching of NH_3^{+} [29] and wagging vibrations of NH_3^+ at 1100 and 1085 cm^{-1}.[30] The N–N stretching frequency of $N_2H_5^+$ is known to occur $\sim 965\,cm^{-1}$ [31] and when hydrazinium ion is acting as a ligand ν_{N-N} invariably absorbs at 1005 cm^{-1}.[1,2]

Reflectance spectral data and the room temperature magnetic susceptibility values of the complexes are given in Table 3. These data furnish supporting evidence about the geometry of the complexes.

X-Ray powder patterns of the complexes indicate that they are not isomorphous. The d-spacings of the complexes are listed in Table 4.

Thermoanalytical curves of all the three complexes are shown in Figs. 1(a) and (b).

$(N_2H_5)_2[Cu(C_2O_4)_2]H_2O$

The IR spectrum of this complex does not offer conclusive evidence about the coordination of $N_2H_5^+$ to the metal. The spectrum exhibits two absorptions at 975 and 980 cm^{-1}. The assignment

Table 1. Analytical data

Compound	Colour	% Metal Found	% Metal Calc	% Hydrazine Found	% Hydrazine Calc	% Oxalate Found	% Oxalate Calc
$(N_2H_5)_2Co(C_2O_4)_2 \cdot 3H_2O$	Pink	16.34	16.60	17.90	18.03	50.00	49.59
$(N_2H_5)_2Ni(C_2O_4)_2 \cdot 2H_2O$	Dark blue	17.45	17.50	18.97	19.01	52.40	52.27
$(N_2H_5)_2Cu(C_2O_4)_2 \cdot H_2O$	Blue	19.87	19.64	19.40	19.78	53.80	54.40

Table 2. IR spectra data (cm^{-1})

$(N_2H_5)_2Co(C_2O_4)_2 \cdot 3H_2O$	$(N_2H_5)_2Ni(C_2O_4)_2 \cdot 2H_2O$	$(N_2H_5)_2Cu(C_2O_4)_2H_2O$	Assignment
3500 b	3500 b 3400 s	3620 b 3550 b	asym. OH stretching
3315 s	3380 s 3260 m 3130 m	3330 m 3265 w	asym. NH stretching sym. NH stretching
2660 w	2660 w	2650 w	NH stretching of NH$_3^+$
1725 s	1720 b	1710 w	asym OCO stretching
1625 b	1650 b	1690 s 1650 b	NH$_2$ bending and OH bending
1550 w		1510 w	Bending of NH$_3^+$
1430 m 1335 m	1440 s 1310 s	1405 s	sym. OCO stretch
1300 m	1290 s	1280 s	NH$_2$ wagging
1150 s 1100 s	1150 s 1085 m	1125 m 1100 s 1085 m	NH$_2$ twisting and wagging of NH$_3^+$
965 s	1010 s 1000 s	980 s 975 s	N-N stretching
	895 w	895 w	OCO bending
805 s	800 s	800 s	OCO deformation
615 w	630 s		NH$_2$ rocking
465 m	495 s	495 m	M-O stretching
370 m	390 w		M-N stretching

Table 3. Electronic spectral and magnetic data

Compound	Electronic spectra		μ eff(26°C)
	cm^{-1}	Assignment	BM
$(N_2H_5)_2Cu(C_2O_4)_2 \cdot H_2O$	15,100	$^2B_{1g} \rightarrow {}^2E_g$	1.86
	30,100	charge transfer	
$(N_2H_5)_2Ni(C_2O_4)_2 \cdot 2H_2O$	16,600	$^3A_{2g} \rightarrow {}^3T_{1g}(F)$	3.10
	26,300	$^2A_{2g} \rightarrow {}^3T_{1g}(P)$	
	30,700	charge transfer	
$(N_2H_5)_2Co(C_2O_4)_2 \cdot 3H_2O$	19,200	$^4T_{1g}(F) \rightarrow {}^4T_{1g}(P)$	5.00
	21,500		
	29,400	charge transfer	

of these absorptions is rather difficult since the observed frequency is too high for ionic $N_2H_5^+$ ($v_{N-N} = 965$ cm^{-1}) and too low for coordinated $N_2H_5^+$ ($v_{N-N} = 1005$ cm^{-1}).

Reflectance spectrum of the complex shows the $d-d$ transition at 15,100 cm^{-1} which favours square planar stereochemistry of Cu(II).[32]

The ESR spectrum of the complex is shown in Fig. 2. The lower g value ($g = 2.11$) is also in accordance with the square planar geometry around Cu(II).[33]

However the unequivocal proof about the coordination environment of the metal comes from a single crystal X-ray study of the complex. The crystal contains discrete $N_2H_5^+$ ions, $[Cu(C_2O_4)_2]^{2-}$ ions and water molecules. The copper atom lies on a centre of symmetry, with square planar coordination of oxygens from two bidentate oxalate groups (Fig. 3). The $N_2H_5^+$ ion is not coordinated to the copper. Selected interatomic bond distances and angles are listed in Table 5.

The Cu–O(1) distance (1.944 (2) Å) is slightly longer than Cu–O(2) distance (1.926 (2) Å). The bite angle of the bidentate ligand [O(1)–Cu–O(2)] is 85.5°. The oxalate group is planar and Cu(II) is out of this plane by 0.1 Å. As expected, coordi-

Table 4. X-Ray powder diffraction data (*d*-spacing in Å)

$(N_2H_5)_2Co(C_2O_4)_2 \cdot 3H_2O$	$(N_2H_5)_2Ni(C_2O_4)_2 \cdot 2H_2O$	$(N_2H_5)_2Cu(C_2O_4)_2 \cdot H_2O$
7.618 vs	8.115 w	7.286 vs
7.144 s	7.314 vs	4.954 m
5.965 w	6.530 s	4.077 m
5.753 s	6.299 m	3.931 s
3.935 m	6.151 s	3.633 m
3.807 s	5.340 s	3.576 m
3.780 m	5.039 w	3.232 m
3.652 m	4.796 m	3.184 m
3.614 m	4.484 m	3.154 s
3.556 m	4.320 s	3.028 w
3.257 s	4.004 m	2.992 m
3.053 m	3.702 m	2.788 w
3.005 w	3.604 m	2.644 m
2.944 w	3.562 m	2.592 m
2.895 m	3.363 m	2.529 w
2.806 w	3.314 m	2.475 w
2.536 m	3.255 w	2.423 m
2.400 w	3.121 m	2.374 w
2.369 w	3.028 s	2.161 w
2.349 w	2.962 s	2.122 w
2.337 w	2.614 m	2.087 w
2.281 w	2.529 m	2.045 w
2.201 w	2.449 w	1.672 m
1.861 w	2.391 w	
1.823 w	2.344 w	
1.809 w	2.304 w	
1.769 w	2.243 w	
1.703 w	2.220 m	
	2.085 w	
	2.058 m	

vs = very strong,   s = strong,   m = medium,   w = weak
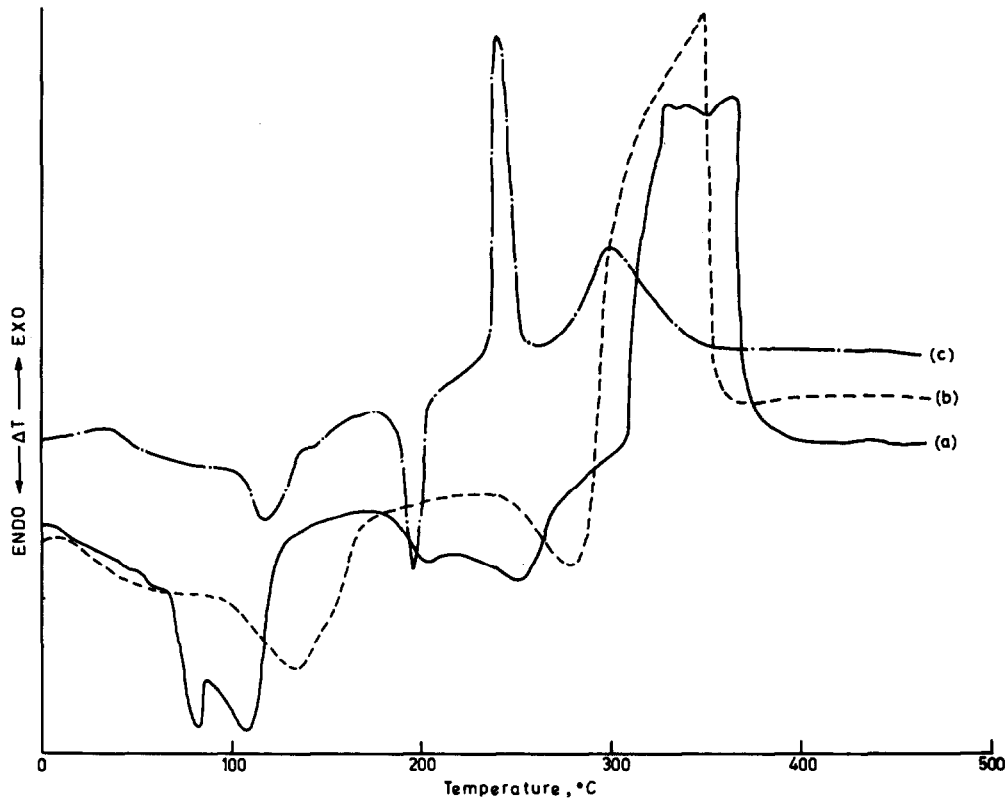
Fig. 1(a). DTA curves of (a) $(N_2H_5)_2Co(C_2O_4)_23H_2O$. (b) $(N_2H_5)_2Ni(C_2O_4)_22H_2O$. (c) $(N_2H_5)_2Cu(C_2O_4)_2H_2O$.
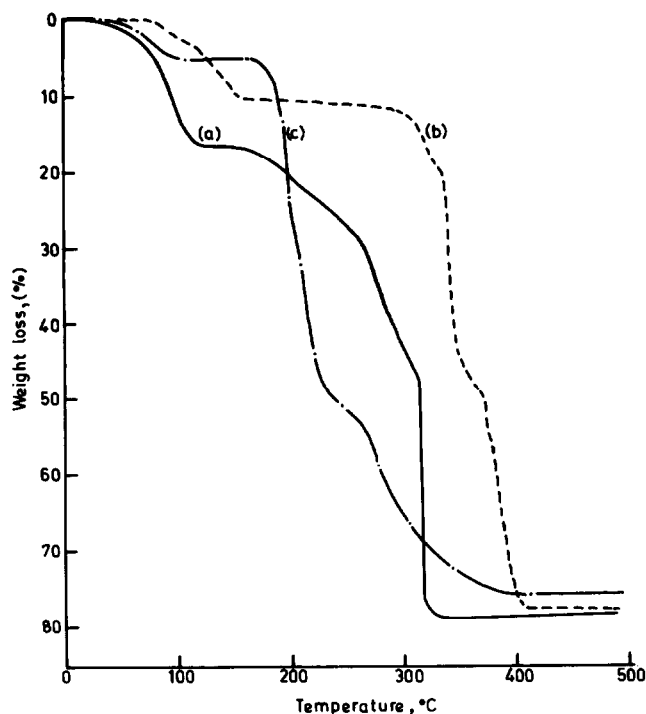
Fig. 1(b). TGA curves of (a) $(N_2H_5)_2Co(C_2O_4)_2 \cdot 3H_2O$. (b) $(N_2H_5)_2Ni(C_2O_4)_2 \cdot 2H_2O$. (c) $(N_2H_5)_2Cu(C_2O_4)_2 \cdot H_2O$.
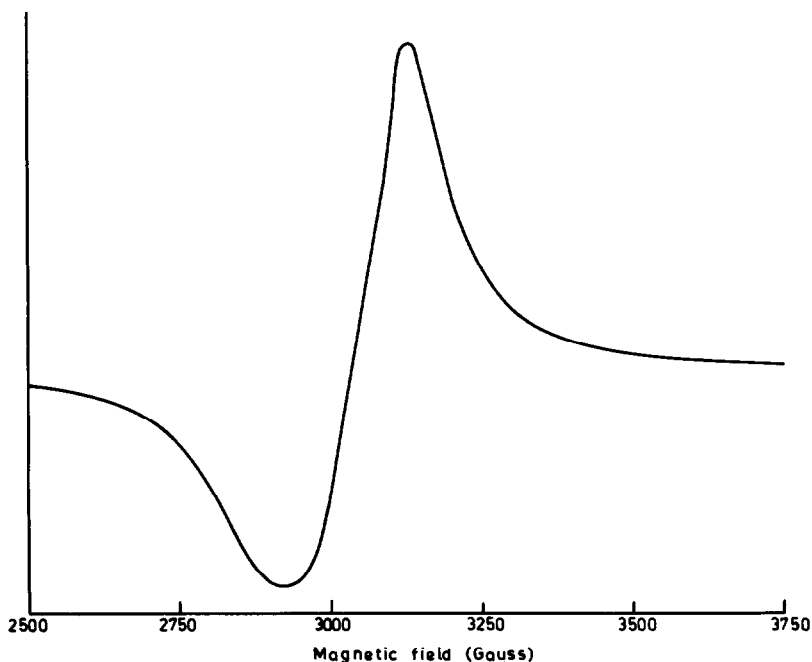
Fig. 2. EPR spectrum of $(N_2H_5)_2Cu(C_2O_4)_2 \cdot H_2O$.

nated C–O distances (1.284 and 1.270 Å) are slightly longer than the free C–O distances (1.229 and 1.239 Å). The C–C–O bond angles (114.1–115.5°) are substantially smaller than the exterior angles (118.8–119.7°) due to the steric restrictions on the planar five-membered chelate ring. In the $N_2H_5^+$ ion, the NH_3 group is staggered with respect to the NH_2 group and its lone pair. The observed N(1)–N(2) bond distance of 1.429(4) Å is in agreement with the values reported for similar compounds, e.g. 1.427(3) Å in $N_2H_5LiSO_4$ and 1.435(9) Å in $N_2H_5[Sc(N_2H_3COO)_4] \cdot 3H_2O$.

In the crystal there is a network of hydrogen
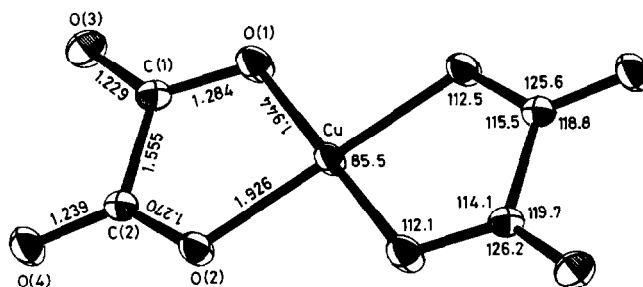
Fig. 3. The $Cu(C_2O_4)_2^{2-}$ anion in $(N_2H_5)_2Cu(C_2O_4)_2 \cdot H_2O$.

Table 5. Bond distances (Å) and bond angles (deg.) in $(N_2H_5)_2Cu(C_2O_4)_2 \cdot H_2O$

Cu	–	O(1)	1.944(2)	O(1)	– Cu	– O(2)	85.5(1)
Cu	–	O(2)	1.926(2)	C(1)	– O(1)	– Cu	112.1(2)
C(1)	–	O(1)	1.284(4)	C(2)	– O(2)	– Cu	112.5(2)
C(2)	–	O(2)	1.270(3)	C(1)	– C(2)	– O(2)	115.5(2)
C(1)	–	O(3)	1.229(4)	C(2)	– C(1)	– O(1)	114.1(2)
C(2)	–	O(4)	1.239(4)	C(1)	– C(2)	– O(4)	118.8(3)
C(1)	–	C(2)	1.555(4)	C(2)	– C(1)	– O(3)	119.7(3)
N(1)	–	N(2)	1.429(4)	O(3)	– C(1)	– O(1)	126.2(3)
				O(4)	– C(2)	– O(2)	125.6(3)

bonds involving the $N_2H_5^+$ ion, lattice water and oxalate oxygens (Fig. 4). The hydrogen bond lengths are in the range 2.84 to 3.10 Å. The molecules are stacked one above the other along *a* axis with separation of 3.6 Å, the unit cell translation *a*.

The DTA curve of hydrazinium copper oxalate shows an endotherm at 119°C corresponding to dehydration; another endotherm at 198°C where the anhydrous compound melts sharply and an exotherm at 238°C in which the anhydrous hydrazinium copper oxalate decomposes to give copper oxalate which further decomposes exothermically at 305°C to give CuO.

The   decomposition   scheme   of
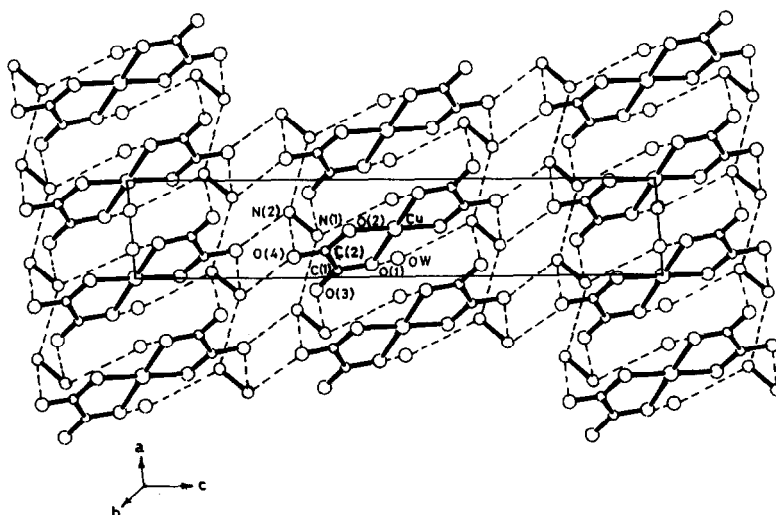
Fig. 4. Packing diagram of $(N_2H_5)_2Cu(C_2O_4)_2 \cdot H_2O$—view down *b*.

$(N_2H_5)_2Cu(C_2O_4)_2 \cdot H_2O$ in air can be represented as follows. The DTA peak temperatures for each step are indicated.

$$(N_2H_5)_2[Cu(C_2O_4)_2]H_2O \xrightarrow{119°C(endo)}$$

$$(N_2H_5)_2[Cu(C_2O_4)_2] + H_2O \quad (1)$$

$$(N_2H_5)_2[Cu(C_2O_4)_2] \xrightarrow{238°C(exo)}$$

$$CuC_2O_4 + 2NH_3 + N_2 + 2CO_2 + 2H_2O \quad (2)$$

$$CuC_2O_4 \xrightarrow{305(exo)} CuO + 2CO_2. \quad (3)$$
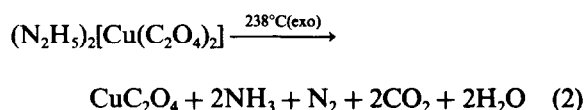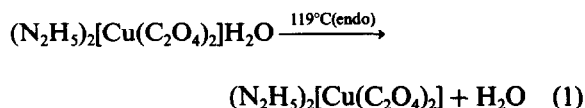
The percentage weight losses observed in TG for these steps are 5.5, 52.0 and 75 respectively. The calculated percentage weight losses of 5.6, 53.2 and 75.4 for these steps are in good agreement with the observed values.

$[(N_2H_5)_2Ni(C_2O_4)_2]2H_2O$

The IR spectrum of this complex shows ν_{N-N} at 1000, 1010 cm^{-1} proving the coordination of $N_2H_5^+$ to the metal unambiguously and suggesting an octahedral geometry. Supporting evidence for an octahedral environment around Ni(II) is furnished by the reflectance spectrum. The bands at 16,600 and 26,300 cm^{-1} can be assigned to $^3A_{2g} \rightarrow {^3T_{1g}}(F)$ and $^3A_{2g} \rightarrow {^3T_{1g}}(P)$ transitions respectively which are characteristic of octahedral geometry around Ni(II).[34] Magnetic susceptibility value ($\mu_{eff} = 3.1$ BM) is in accordance with that of a high spin complex of nickel. A single crystal X-ray study of the complex could not be carried out as the crystal showed twinning rendering the X-ray investigation difficult.

Thus based upon IR, UV spectra and magnetic susceptibility data, the proposed structure of hydrazinium nickel oxalate dihydrate is represented as follows:
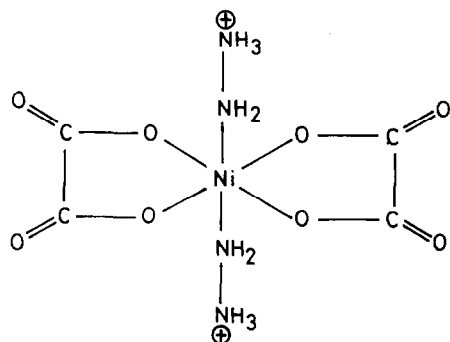
The nickel complex decomposes in three steps. In the first step water is lost endothermically at 124°C. The anhydrous complex further decomposes to give nickel oxalate monohydrazinate. This is observed as an endotherm with peak temperature of 280°C. The final step corresponds to the decomposition of nickel oxalate monohydrazinate to nickel oxide (NiO). This decomposition is exothermic at 342°C.

$$[(N_2H_5)_2Ni(C_2O_4)_2]2H_2O \xrightarrow{124°C(endo)}$$

$$[(N_2H_5)_2Ni(C_2O_4)_2] + 2H_2O \quad (4)$$

$$[(N_2H_5)_2Ni(C_2O_4)_2] \xrightarrow{280°C(endo)} NiC_2O_4 \cdot N_2H_4$$

$$+ NH_3 + 1/2N_2 + 2CO_2 + 3/2H_2O \quad (5)$$

$$NiC_2O_4 \cdot N_2H_4 \xrightarrow{342°C(exo)}$$

$$NiO + 2CO_2 + NH_3 + 1/2N_2 + 1/2H_2O. \quad (6)$$
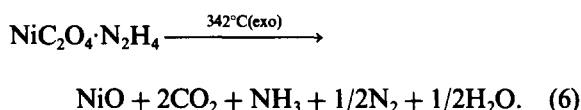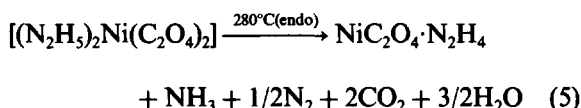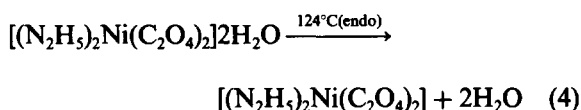
Thermogravimetric analysis data are in accordance with the DTA results. The TG curve shows three distinct steps with percentage weight losses of 10.5, 47 and 77 corresponding to the formation of the anhydrous compound, $NiC_2O_4 \cdot N_2H_4$ and NiO respectively. The calculated percentage weight losses for these steps are 10.7, 46.9 and 77.8 respectively.

$(N_2H_5)_2[Co(C_2O_4)_2]3H_2O$

The fact that hydrazinium cobalt oxalate trihydrate is not isomorphous either with the copper or nickel analogue suggests that the geometry around Co^{2+} is different from the other two. IR absorption of ν_{N-N} at 965 cm^{-1} clearly shows that $N_2H_5^+$ is outside the coordination sphere. Magnetic susceptibility value ($\mu_{eff} = 5.0$) shows that the complex is high spin and could have octahedral or tetrahedral geometry.

It has been shown previously[35] that orbital contributions in tetrahedral Co(II) complexes decrease as the ligand varies from I$^-$ towards CN$^-$ in the spectrochemical series I$^-$ < Br$^-$ < Cl$^-$ < OH$^-$ < NO$_3^-$ < C$_2$O$_4^{2-}$ < H$_2$O < NH$_3$ < CN$^-$. Hence tetracoordinated Co(II) complexes are given tetrahedral structures only if the values of magnetic moments are in the range 4.2–4.7 BM.[36] The observed magnetic moment of 5.00 BM in the present case of cobalt complex thus rules out the possibility of tetrahedral geometry.

Additional evidence against a tetrahedral structure comes from the visible absorption spectrum. All tetrahedral cobaltous complexes are known to exhibit a characteristic intense multicomponent band in the 13,300–16,600 cm^{-1} region associated

with $^4A_2 \rightarrow ^4T_1(P)$ transition in tetrahedral geometry, whereas no band is observed in this specified region in the reflectance spectrum of the cobalt complex. The electronic spectrum of hydrazinium cobalt oxalate trihydrate shows bands at 21,500 and 19,200 cm^{-1} assigned to $^4T_{1g}(F) \rightarrow ^4T_{1g}(P)$ which is usually split due to spin-orbit coupling in the $^4T_{1g}(P)$ state. The electronic spectrum is comparable with the spectrum of octahedral Co(II) complexes as reported by Ballhausen and Jorgensen[37] with a double band having centre of gravity ~20,000 cm^{-1}. The pink colour of the complex is also indicative of octahedrally coordinated Co(II).[38]

Cotton and Holm[39,40] have claimed that planar complexes of type [CoO$_4$] may also be of high spin and have μ_{eff} values in the range 4.8–5.2 BM. Based on energy level diagram for Co(II) in a ligand field of D$_{4h}$ symmetry, they have shown that planar spin-free complexes are possible if the four donor atoms provide a weak enough ligand field.

The foregoing evidence leads us to conclude that the cobalt complex reported herein might have planar Co(C$_2$O$_4$)$_2^{2-}$ anions which aggregate to form a chain structure with pairs of long Co–O bonds between anions making it octahedral. The structure could be represented as
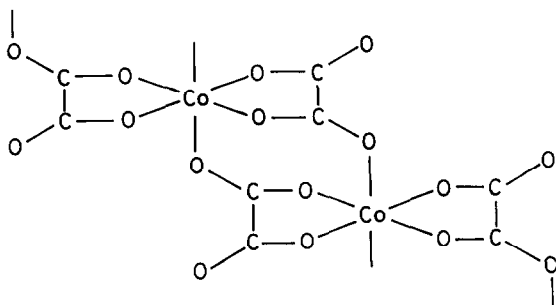
Such a structure is known to exist in propylene diammonium bis(oxalato)cuprate (II).[41] Single crystal X-ray study of the Co complex could not be carried out to confirm the proposed structure as the compound is unstable.

Hydrazinium cobalt oxalate trihydrate decomposes in a manner similar to the nickel compound

$$(N_2H_5)_2[Co(C_2O_4)_2]3H_2O \xrightarrow{84°C(endo),\ 102°C(endo)}$$

$$(N_2H_5)_2[Co(C_2O_4)_2] + 3H_2O \quad (7)$$

$$(N_2H_5)_2[Co(C_2O_4)_2] \xrightarrow{210°C(endo),\ 254°C(endo)} CoC_2O_4$$

$$\cdot N_2H_4 + NH_3 + 1/2N_2 + 2CO_2 + 3/2H_2O \quad (8)$$

$$CoC_2O_4 \cdot N_2H_4 \xrightarrow{310-370°C(broad\ exo)}$$

$$Co_3O_4 + 3NH_3 + 3/2N_2 + 6CO_2 + 3/2H_2O. \quad (9)$$
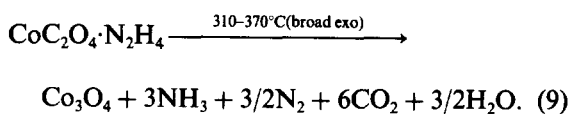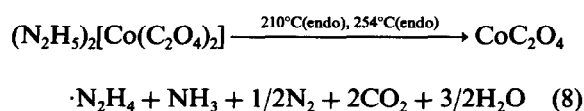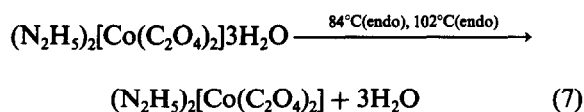
This decomposition scheme is supported by the TG data; percentage weight losses observed being 16, 49 and 78 which tally with the calculated percentage weight losses for the above steps 15.2, 49.6 and 77.7 respectively.

REFERENCES

1. A. Nieuwpoort and J. Reedijk, *Inorg. Chim. Acta* 1973, **7**, 323.
2. D. B. Brown, J. A. Donner, J. W. Hall, S. R. Wilson, R. B. Wilson, D. J. Hodgson and W. A. Hatfield, *Inorg. Chem.* 1979, **18**, 2635.
3. J. Slivnik, A. Rahten and J. Macek, *Proc. Eur. Therml. Anal. 1st.* 1976, 227.
4. J. Siftar and P. Bukovec, *Monatsh. Chem.* 1970, **101**, 1184.
5. P. Bukovec and J. Siftar, *Monatsh. Chem.* 1971, **102**, 94.
6. J. Slivnik, J. Macek, A. Rahten and B. Sedej, *Thermochim. Acta* 1980, **39**, 21.
7. M. R. Anderson, I. D. Brown and S. Vilminot, *Acta. Cryst.* 1973, **B29**, 2625.
8. J. Slivnik, J. Pezdic and B. Sedej, *Monatsh. Chem.* 1967, **98**, 204.
9. J. Slivnik, B. Volavsek, *Sci. Tech. Aerosp. Rep.* 1969, **7**, 1647.
10. J. Slivnik and P. Glavic, *J. Inorg. Nucl. Chem.* 1970, **32**, 2939.
11. J. Slivnik, A. Rahten, J. Macek and B. Sedej, *Vestn. Slov. Kem. Drus.* 1979, **26**, 19.
12. A. Lari-Lavassani, *C. R. Hebd, Seances Acad. Sci. Ser. C*, 1978, **286**, 585.
13. A. Braibanti and A. Tiripicchio, *Gazz. Chim. Ital.* 1966, **96**, 1580.
14. W. Pugh and A. M. Stephen, *J. Chem. Soc., Part IV*, 1952, 4138.
15. C. K. Prout and H. M. Powell, *J. Chem. Soc.* 1961, 4177.
16. K. C. Patil, R. Soundararajan and V. R. Pai Verneker, *Proc. Indian Acad. Sci. (Chem. Sci.)*, 1978, **87A**, 281.
17. K. C. Patil, S. Govindarajan and H. Manohar, *Synth. React. Inorg. Met. Org. Chem.* 1981, **11**, 245.
18. K. C. Patil, S. Govindarajan, R. Soundararajan and V. R. Pai Verneker, *Proc. Indian Acad. Sci., (Chem. Sci.)*, 1981, **90**, 421.
19. B. Banerjee, P. K. Biswas and N. Ray Chaudhri, *Thermochim. Acta* 1981, **47**, 15.
20. S. Govindarajan, Ph.D. Thesis. Indian Institute of Science, Bangalore 1983.
21. J. Slivnik, A. Rihar and B. Sedej, *Monatsh. Chem.* 1967, **98**, 200.
22. J. Slivnik and A. Rihar, *Monatsh. Chem.* 1972, **103**, 1572.

23. A. I. Vogel, *A Textbook of Quantitative Inorganic Analysis*, 3rd Edn, p. 380. Longman, London (1962).
24. K. Kishore, V. R. Pai Verneker and M. R. Sunitha, *J. Appl. Chem. Biotechnol.* 1977, **27**, 415.
25. G. M. Sheldrick, SHELX-76, Program for Crystal Structure Determination. Cambridge University, Cambridge (1975).
26. *International Tables for X-ray Crystallography*, Vol. IV, Tables 2.2.A and 2.1.C. Kynoch Press, Birmingham (1974).
27. G. H. Stout and L. H. Jensen, *X-Ray Structure Determination*, p. 412. Macmillan, London (1968).
28. N. F. Curtis, *J. Chem. Soc., Part IV*, 1963, 4109.
29. J. Lindgren, J. De Villepin and A. Novak, *Chem. Phys. Lett.* 1969, **3**, 84.
30. V. Schettino and R. E. Salmon, *Spectrochim. Acta* 1974, **30A**, 1445.
31. A. Braibanti, F. Dallavalle, M. A. Pellinghelli and E. Laporati, *Inorg. Chem.* 1968, **7**, 1430.
32. J. Malaviya, P. R. Shukla and L. N. Srivastava, *J. Inorg. Nucl. Chem.* 1973, **35**, 1706.
33. J. S. Tiwari, S. C. Sinha and P. K. Ghosh, *Technology* 1969, **6**, 105.
34. D. Nicholls and R. Swindells, *J. Inorg. Nucl. Chem.* 1968, **30**, 2211.
35. R. H. Holm and F. A. Cotton, *J. Chem. Phys.* 1959, **31**, 788.
36. L. Sacconi, M. Ciampolini, F. Maggio and F. P. Cavasino, *J. Am. Chem. Soc.* 1962, **84**, 3246.
37. C. J. Ballhausen and C. K. Jorgensen, *Act. Chem. Scand.* 1955, **9**, 397.
38. F. A. Cotton and R. H. Holm, *J. Am. Chem. Soc.* 1960, **82**, 2983.
39. F. A. Cotton and R. H. Holm, *J. Am. Chem. Soc.* 1960, **82**, 2979.
40. R. H. Holm and F. A. Cotton, *J. Inorg. Nucl. Chem.* 1960, **15**, 63.
41. D. R. Bloomquist, J. J. Hansen, C. P. Landee, R. D. Willett and R. Buder, *Inorg. Chem.* 1981, **20**, 3308.

SPECTROSCOPIC CHARACTERIZATION OF SUPERPARAMAGNETIC PARTICLES OF THERMOLYTIC PRODUCTS OF FERRIC SULPHATE HYDRATES

P. C. MORAIS and K. SKEFF NETO*

Grupo de Física Molecular e Magnetismo, Departamento de Física, Universidade de Brasília 70910-Brasília-DF, Brasil

Abstract—Superparamagnetic particles of chemically pure samples, in the system $Fe(OH)SO_4/Fe(OH)SO_4 \cdot (H_2O)$, are produced by thermal decomposition of ferric sulphate hydrates. The control of particle size distribution is achieved by successive hydration and dehydration processes monitored by X-ray diffraction, electron microscopy, Mössbauer and IR spectroscopy. The particle size modification is related for the particle growth and two mechanisms are suggested thereon.

Thermal treatments induces oxidation of Fe^{2+} ion to Fe^{3+} in sulphate hydrates. This well-known phenomenon has been reported by many workers.[1-9] The thermal decomposition of Fe^{2+} compounds can be probed by several techniques including Mössbauer spectroscopy, because of its high sensitivity to the valence state of the iron in solids. The oxidation mechanism is that Fe^{2+} is oxidized into Fe^{3+} by hydroxyl radicals which originate from the water of crystallization.[10] However, this mechanism does not specify the chemical formulae of the thermal decomposition products. The present report deals with an investigation of thermal decomposition products of ferrous sulphate monohydrate using Mössbauer, IR and X-ray diffraction. The main thermolytic product is a ferric specimen identified as $Fe(OH)SO_4$.

In an aqueous-vapour atmosphere this compound gives a hydrate $Fe(OH)SO_4(H_2O)_2$ which was confirmed by chemical and spectroscopic analysis. The process of hydration is monitored by X-ray diffraction, Mössbauer and IR spectroscopy. Heating of $Fe(OH)SO_4(H_2O)_2$ reconverts it to $Fe(OH)SO_4$ but the drying process induces a change in volume and alters significantly their magnetic properties. In the present paper we analyze the change on the particle size distribution based on electron microscopy patterns and magnetic measurements. The Mössbauer effect has proved to be a unique tool for the measurement of such magnetic preperties.

Another important reason for applying the Mössbauer technique is that no external field must be applied to the sample and the zero-field magnetization may be determined with great accuracy.

EXPERIMENTAL

Analytically pure $FeSO_4(H_2O)$ was used as the original material to obtain the $FeSO_4(H_2O)_4$. This compound is grown from aqueous solution of $FeSO_4(H_2O)_7$ at constant temperature within the range 54–64°C according to the literature.[11] $FeSO_4(H_2O)$ was obtained from the aqueous solution of $FeSO_4(H_2O)_7$ at constant temperature within the range 80–100°C in vacuum for a few days. On heating $FeSO_4(H_2O)$ in air up to 180°C a mixture of compounds was obtained.[12] However, the Mössbauer spectra at room temperature of $FeSO_4(H_2O)$ heated at 250°C for several days shows a pure well resolved doublet with I.S. (Fe) = 0.44 mm/s and Q.S. = 1.45 mm/s as depicted in Fig. 1, spectrum $AB(250)_0$.

This compound was called A (250) or $AB(250)_0$ and in the laboratory atmosphere the Mössbauer spectra changes slowly over a period of several months, but in an aqueous-vapour atmosphere (75%) the process of hydration is speeded up and at the end of 22 days we obtain another pure compound. This compound was called B(250) or $AB(250)_{22}$ and shows a pure well resolved doublet at room temperature as shown in Fig. 1. Compounds A (250) and B(250) show, at room temperature, essentially the same I.S. but a different quadrupole splitting. The Q.S. of B(250) is 0.97 mm/s.

The compounds A(250) and B(250) were

*Author to whom correspondence should be addressed.
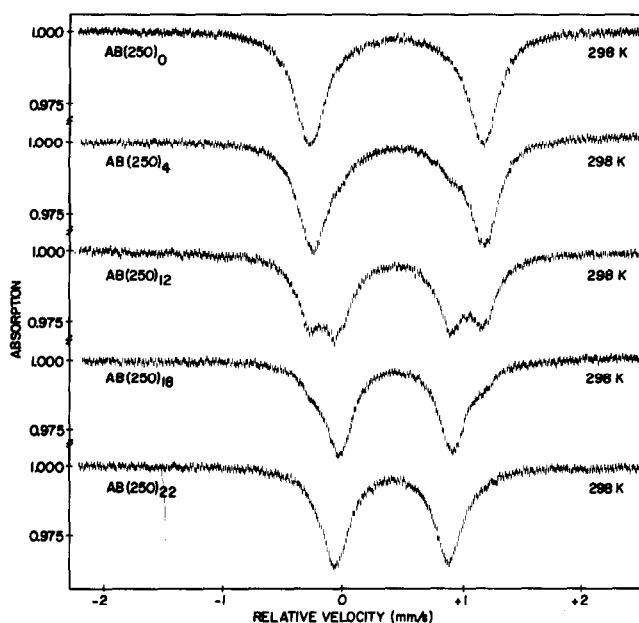
Fig. 1. Mössbauer spectra of AB(250)$_d$, at room temperature, after $d = 0$, 4, 12, 18 and 22 days of hydration.

DISCUSSION

identified by chemical and spectroscopic measurements as $Fe(OH)SO_4$ and $Fe(OH)SO_4(H_2O)_2$ respectively.[13] The Mössbauer parameters were determined using computer fitting and are listed in Table 1. The process of hydration was monitored, at room temperature, by X-ray diffraction, Mössbauer and IR spectroscopy as shown in Figs. 1–3. During the process of hydration several samples of A(250) were collected after 0, 4, 12, 18 and 22 days of hydration. These samples were heated at 200°C, for several days until the total dehydration so that the final products were $Fe(OH)SO_4$. The Mössbauer spectra of such products at 77 K are depicted in Fig. 4. This process of hydration and subsequent dehydration was followed by electron microscopy and is shown in Figs. 5(a)–(c).

The presence of $FeSO_4(H_2O)$, in the vacuum treatment at room temperature of $FeSO_4(H_2O)_4$, can be confirmed by reported Mössbauer parameters.[6,7] A schematic sequence on the thermal and aqueous-vapour treatments is shown below. Here A(250) is the same

$$FeSO_4(H_2O)_7 \rightarrow FeSO_4(H_2O)_4 \rightarrow FeSO_4(H_2O)$$
$$\downarrow$$
$$BA(250)_d \leftarrow AB(250)_d \leftarrow A(250)$$
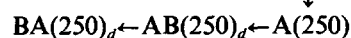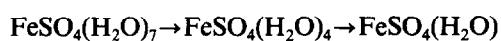
as $AB(250)_0$, $AB(250)_{22}$ is the same as B(250) and $BA(250)_d$ are chemically $Fe(OH)SO_4$. The subscript "d" that appears on $AB(250)_d$ may be referred as the days of hydration in an aqueous-vapour atmosphere (75%) at room temperature.

Table 1. The Mössbauer parameters of the A(250), B(250) and those of butlerite

Sample	T(K)	Hint (Koe)	Q.S. (mm/s)	I.S.* (mm/s)	Ref.
A(250)	298	0	1.45	0.44†	[12]
B(250)	298	0	0.97	0.42†	[13]
$Fe(OH)SO_4 \cdot 2H_2O$ ((butlerite)	300	0	0.94	0.42	[22]

*Relative to Fe at 298 K.
†The accuracy is 0.02 mm/s.
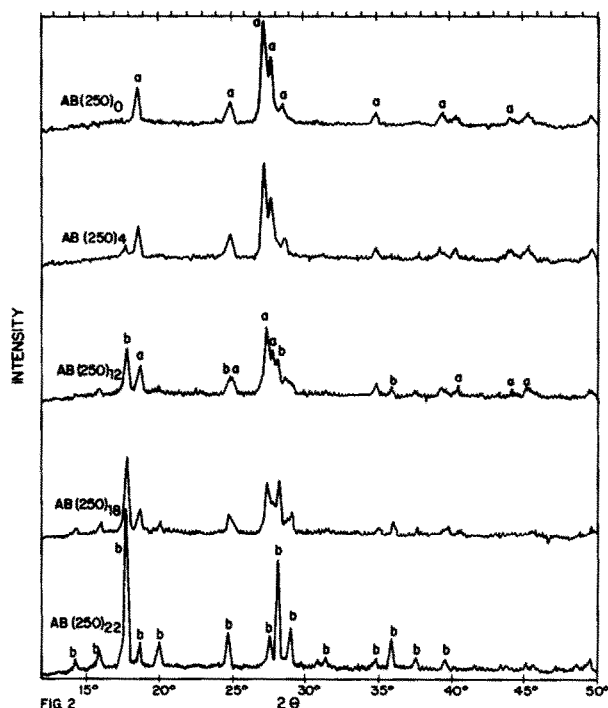
Fig. 2. X-Ray diffraction patterns of $AB(250)_d$, at room temperature, a denotes the diffraction peak related to $Fe(OH)SO_4$ and b denotes the diffraction peak related to $Fe(OH)SO_4(H_2O)_2$.
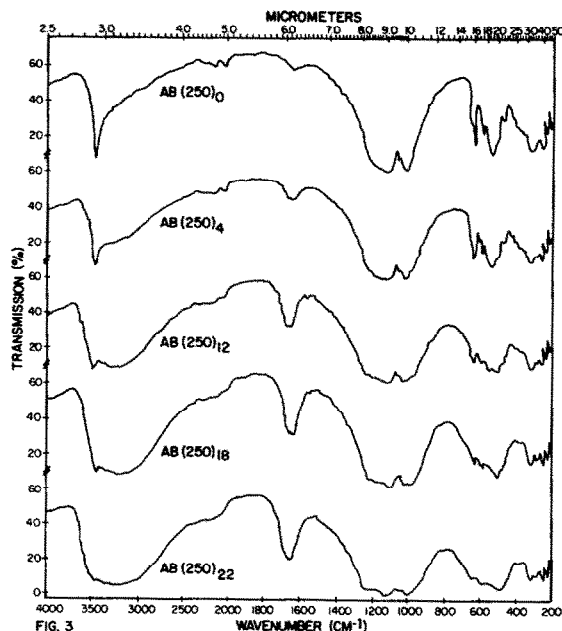
Fig. 3. IR spectra of $AB(250)_d$, at room temperature, after $d = 0$, 4, 12, 18 and 22 days of hydration.

Comparing the Mössbauer parameters of B(250) compound and those of Butlerite (Table 1) we can conclude that B(250) compound is the Butlerite

whose structure has been determined by Fanfani.[14]

In Fig. 1 we show the Mössbauer spectra sequence in the process of hydration at room temperature which convert $Fe(OH)SO_4$ into $Fe(OH)SO_4(H_2O)_2$. Here we represent the process of hydration by

$$Fe(OH)SO_4 \rightarrow x\ Fe(OH)SO_4,$$
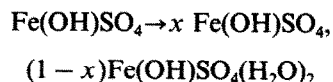
$$(1 - x)Fe(OH)SO_4(H_2O)_2$$

where "x" is related to "d" parameter with $0 \le x \le 1$. The intermediate Mössbauer spectra, for which $0 < x < 1$, shows a superposition of $Fe(OH)SO_4$ and $Fe(OH)SO_4(H_2O)_2$. As shown in Table 1 the values of Q.S. for $AB(250)_0$ and $AB(250)_{22}$ samples is large for the high spin ferric compounds and it is characteristic for Fe–O–Fe bridge compounds.[15]

The X-ray diffraction pattern sequence in the process of hydration, taken at room temperature, is shown in Fig. 2. Here the observed diffraction pattern of $AB(250)_{22}$ sample agree exactly with those of Butlerite listed in the ASTM file. It is worth mentioning that the diffraction pattern of $AB(250)_0$ sample shown in Fig. 2, which we identified as pure $Fe(OH)SO_4$, have not been re-
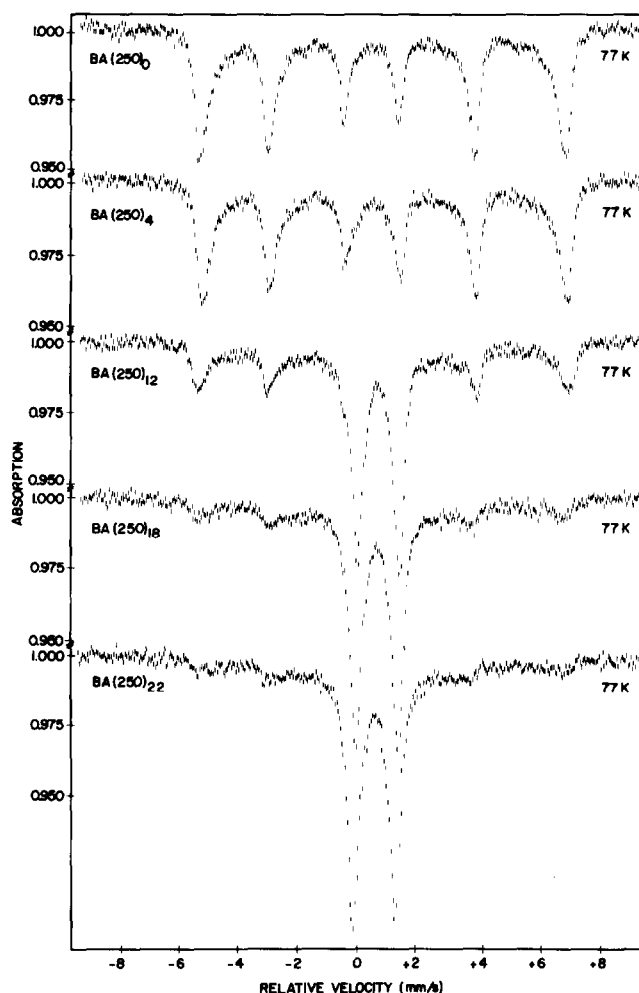
Fig. 4. Mössbauer spectra of BA(250)$_d$, at 77 K, for $d = 0$, 4, 12, 18 and 22.

ported hitherto. The intermediate diffraction patterns shows a superposition of that Fe(OH)SO$_4$ and Fe(OH)SO$_4$(H$_2$O)$_2$. Besides the diffraction peaks of Fe(OH)SO$_4$(H$_2$O)$_2$ denoted by "b" in Fig. 2, there are other peaks which are denoted by "a" and related to Fe(OH)SO$_4$.

In order to gain more information about the process of hydration of Fe(OH)SO$_4$, the IR spectra sequence was obtained at room temperature and is shown in Fig. 3. Here the absorption in the region of 1100 cm^{-1} is indicative of the presence of SO$_4^{2-}$ ion in inorganic compounds.[16] The absorption about 1650 and 3450 cm^{-1} corresponds to HOH bending mode and OH stretching of water respectively. This characterizes the Fe(OH)SO$_4$(H$_2$O)$_2$ compound as the AB(250)$_{22}$ sample. The very little absorption near 1650 cm^{-1} and a sharp absorption at 4380 cm^{-1} characterize the Fe(OH)SO$_4$ compound as the AB(250)$_0$ sample. The intermediate IR spectra shows a superposition of AB(250)$_0$ and AB(250)$_{22}$ samples.

It is worth noting what would happen in the process of hydration and subsequent dehydration of Fe(OH)SO$_4$. Here the process of dehydration, by heating at 200°C for various days, may be represented by
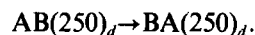
$$AB(250)_d \rightarrow BA(250)_d.$$

The samples, namely BA(250)$_d$, collected during the process of hydration for $d = 0$, 4, 12, 18, 22 and heated as described above, show the same IR, Mössbauer and X-ray diffraction pattern at room temperature. These spectra show the same patterns as AB(250)$_0$ sample at room temperature. However, as we may expect, the Mössbauer spectra of BA(250)$_d$ samples depict different magnetic interactions at 77 K (see Fig. 4). The interesting fact about the foregoing result is that the process of hydration and dehydration induces a modification on the particle size distribution and change significantly their magnetic properties. In Fig. 4 the
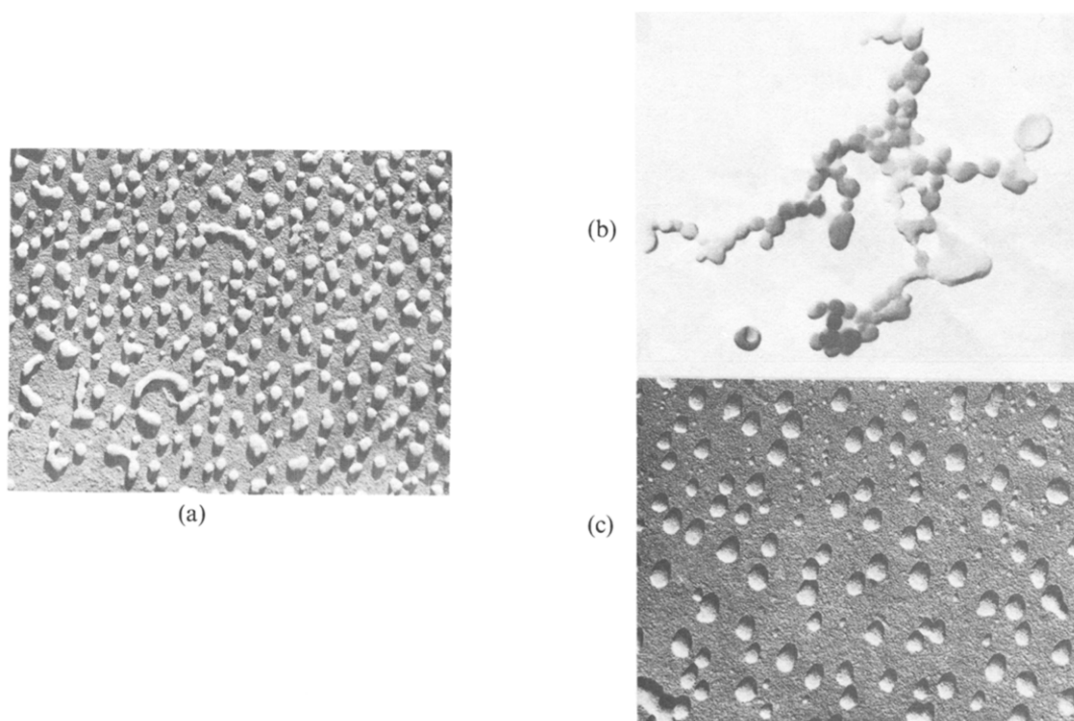
Fig. 5. Electron microscopy patterns. (a) $AB(250)_0$ sample $(44.000x)$. (b) $AB(250)_4$ sample $(113.000x)$. (c) $BA(250)_4$ sample $(44.000x)$.

hfs lines broaden when the days of hydration (d) increase and the low resolution results in merging of the six hyperfine structure components into two lines. This variation of the Mössbauer spectra offers an evidence of superparamagnetic behavior of the $Fe(OH)SO_4$ particles.[17,18] Another behaviour clearly displayed in Fig. 4 is the increase of the internal field (H_0), as the days of hydration, to a maximum and subsequent decrease. This behaviour was associated with the growth of the $Fe(OH)SO_4$ particles as a function of "d" and the presence of a maximum in the value of the internal field (H_0) was associated with the existence of a critical diameter.[13]

The process of evolution in the particle size distribution may be suggested by the analysis of electron microscopy patterns shown in Fig. 5 and by the evolution of the X-ray diffraction sequence shown in Fig. 2. In Fig. 2 the narrowing of the X-ray lines during the process of hydration is an indication of a recrystalization process. In Fig. 5 we show the electron microscopy patterns of $AB(250)_0$, $AB(250)_4$ and $BA(250)_4$ which represents the process of hydration of $Fe(OH)SO_4$ for 4 days and subsequent heating at 200°C for various days until the total dehydration. In this process the diameter of particles has grown approx. 75%. Here the dimensional changes during drying process occur because the particles are brought into close

contact and porosity is reduced. The driving force is due to the decrease of total surface energies which comes about because of the particle contact and particle growth. The atoms in the small particles are transferred to the larger particles, and the pores are replaced by solid material.[19] The electron microscopy patterns, X-ray diffraction sequence and the magnetic nature of the samples suggest two distinct but concurrent mechanisms to this mass transfer in the process of the particle growth in accordance with Burke[20] and Mackenzie and Shuttleworth.[21] They are illustrated schematically in Fig. 6. Burke[20] analyzed the diffusion mechanism (Fig. 6a) which involves the movement of atoms and the countermovement of lattice vacancies. There is an accompanying shrinkage of bulk volume which maintains contact of the
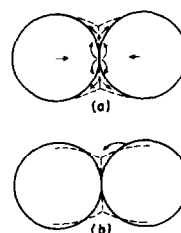
Fig. 6. Schematic of mass transfer mechanisms. (a) Diffusion.[19] (b) Liquid phase.[20]

particle and brings the particle centers closer together. Mackenzie and Shuttleworth[21] studied the liquid phase sintering (Fig. 6b) which involves the removal of ions or atoms from surfaces of higher energy and depositing them on surfaces of lower energy. The highest-energy surfaces are those with small radii of convex curvature: the lowest-energy surfaces are those with small radii of concave curvature.

CONCLUSION

We have analyzed the process of production of chemically pure samples in form of small particles. By means of successive hydration and dehydration we can control adequately the particle size distribution. This is an important point because the magnetization in an amorphous material is very sensitive to the particle size distribution. In the present work we used the chemical system $Fe(OH)SO_4/Fe(OH)SO_4(H_2O)_2$ for two reasons; firstly the process of successive hydration and dehydration is chemically reversible and secondly the $Fe(OH)SO_4$ exhibit superparamagnetic properties.

The use of several techniques for monitoring the process of dimensional changes is very important because they ensure the reversible character in the chemical transformation. The Mössbauer spectroscopy shows the superparamagnetic behavior and the electron microscopy depict the particle size distribution. The particle size control in the process of growth was oriented by the mechanism suggested herein.

REFERENCES

1. B. C. Frazer and P. J. Brown, *Phys. Rev.* 1972, **125**, 1283.
2. C. E. Johnson, W. Marshall and G. J. Perlow, *Phys. Rev.* 1962, **126**, 1503.
3. J. C. Boyat and G. Bassi, *Compt. Rend* 1963, **256**, 1482.
4. A. J. Nozik and M. Kapla, *Phys. Rev.* 1967, **159**, 273.
5. K. Chandra and S. P. Puri, *Phys. Rev.* 1968, **196**, 272.
6. A. Vértes and B. Zsoldos, *Acta Chim. Acad. Scient. Hung.* 1970, **65**, 3.
7. A. Vértes, T. Székely and T. Tarnoczy, *Acta Chim. Acad. Scient. Hung.* 1970, **63**, 1.
8. P. K. Gallaghar, D. W. Johnson and F. Scherey, *J. Am. Ceram. Soc.* 1970, **53**, 566.
9. V. K. Garg, S. P. Puri, *J. Chem. Phys.* 1971, **54**, 209.
10. P. Gütlich, S. Odar, B. W. Fitzsimmons and N. E. Erickson, *Radiochimica Acta* 1968, **10**, 147.
11. K. Skeff Neto and V. K. Garg, *Radiochem. Radional. Lett.* 1973, **15**, 357.
12. K. Skeff Neto and V. K. Garg, *J. Inorg. Nucl. Chem.* 1975, **37**, 2287.
13. P. C. Morais and K. Skeff Neto, *J. Appl. Phys.* 1983, **54**(1), 307.
14. L. Fanfani, A. Nunzi and P. F. Zanazzi, *Am. Min.* 1971, **56**, 751.
15. H. Schugar, C. Walling, R. B. Jones and H. B. Gray, *J. Am. Chem. Soc.* 1967, **89**, 3712.
16. R. A. Nyquist and R. O. Kagel, *Infrared Spectra of Inorganic Compounds*, pp. 264–299. Academic Press, New York (1971).
17. K. Skeff Neto, I. C. Cunha Lima, N. S. Almeida and L. C. M. Miranda, *J. Phys. C* 1978, **11**, 695.
18. K. Skeff Neto, L. C. M. Miranda, *Solid State Commun.* 1978, **28**, 43.
19. D. MacLean, *Grain Boundaries in Metals.* Oxford University Press, London (1957).
20. J. E. Burke, *Recrystallization and Sintering in Ceramics, Ceramic Fabrication Processes.* Wiley, New York (1958).
21. J. K. MacKenzie and R. Shuttleworth, *Proc. Phys. Soc. London* 1949, **B62**, 833.
22. N. Sakai, H. Sekizawa and K. Ôno, *J. Inorg. Nucl. Chem.* 1981, **43**, 1731.

NICKEL(II) COMPLEXES OF PHTHALIC HYDRAZIDE OR ITS ANION, AND THEIR REACTION WITH OXYGEN AND NITROGEN-DONOR LIGANDS

M. ARSHAD ALI BEG* and S. ASHFAQ HUSAIN

PCSIR Laboratories, Karachi 39, Pakistan

Abstract—The reaction of phthalic hydrazide(H_2PH) with Ni(II) salts yields complexes of the type $[NiHPH)_2(H_2O)_2]2H_2O(I)$. Reaction of this complex with acetylacetone(acac) and ethylenediamine(en) gives mononuclear complexes of type $[NiHPH)(acac)_2(H_2O)]H_2O(II)$ and $[Ni(HPH)_2(en)_3(H_2O)]H_2O(IV)$ respectively and with monoethanolamine (MEA), aniline(An) and *p*-phenylenediamine(*p*-Phda) it gives trinuclear complexes of type $[Ni_3(PH)_7(MEA)_4 (H_2O)_3]3H_2O(III)$, $[Ni_3(HPH)_4(An)(H_2O)_7]H_2O(V)$ and $[Ni_3(HPH)_5(p-Phda)(H_2O)_7]H_2O(VI)$ respectively. The complexes have been characterized on the basis of infrared and electronic spectra and magnetic properties as containing octahedral Ni(II) and anionic hydrazide ligand.

Ligand field parameters have been calculated and compared with chromophores containing oxygen and nitrogen donor atoms. Analysis of electronic spectra, calculated Dq values and IR absorptions strongly indicate the presence of NiN_2O_4, $NiNO_5$, NiO_6 and NiN_3O_3 chromophores.

Coordination properties of acyclic hydrazides[1-10] towards metal ions have extensively been investigated. They act as neutral, anionic mono-, bi-, tri- or tetradentate ligands depending on the structure and reaction conditions. There are relatively few reports on the coordination compounds of cyclic hydrazides with metal ions. The *o*-aminophthalhydrazide and anthracene hydrazides[11-14] are some such ligands, the chemiluminescent reactions of which have been noted in the complex formation with some metal ions. *o*-Aminophthalhydrazide has been suggested to act as a bidentate ligand coordinating through carbonyl oxygen and amino nitrogen atoms to form a six membered chelate ring whereas anthracene hydrazide has been suggested to act as a monodentate ligand bonding possibly through carbonyl oxygen.[11]

In spite of the above studies very little information is available on the interaction of phthalic hydrazide with metal ions. Phthalic hydrazide is known to exist in the lactam-lactim form with 1-hydroxyphthalazine-4-one as its most stable tautomer[15] in the solid state and in neutral solutions.
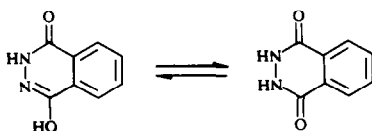
In alkaline aqueous solutions it acts as a weak acid and exists in anionic form by liberating at least one proton. Accordingly the mono-metallic salts of Na^+ and Ag^+ ions of this ligand have been reported.[16] In an earlier study[17] Co(II) ion was reported to be chelated by anionic coordination in dilactim, i.e. 1,4-dihydroxyphthalazine form. The bidentate monoanionic and tetradentate bianionic coordination through oxygen and nitrogen of lactim group of the ligand has been suggested for the Co(II) complex containing metal/ligand ratios of 1:2 and 1:1 respectively.

The bis-phthalhydrazidato-diaquo-Co(II) complex of type $[Co(HPH)_2(H_2O)_2]$ like other diaquo metal chelates such as metal-quinolinates[18,19] and β-diketonates[20] has been found to form adducts with other nitrogenous bases, e.g. bipyridyl and ethylenediamine[17] by replacing the water molecules. These bases have been found to act as bidentate ligands.

The present paper is an extension of the previous studies and is concerned with the preparation and characterization of Ni(II) complex of phthalic hydrazide and its reaction with acetylacetone(acac), monoethanolamine(MEA), ethylenediamine(en), aniline(An) and *p*-phenylenediamine(*p*-Phda). Phthalic hydrazide, hereafter, is abbreviated as H_2PH and HPH to represent neutral and monoanionic form of the ligand respectively. The Lewis acidity of the parent complex towards the adducting ligands, their mode of bonding and the influence on stereochemistries of the complexes formed with different bases have been studied.

EXPERIMENTAL

Preparation of the ligand and complexes

Phthalic hydrazide (H_2PH) was prepared and purified by the methods reported in literature.[15,21]

Bis-phthalic hydrazidato-diaquo Ni(II) dihydrate $[Ni(HPH)_2(H_2O)_2]2H_2O(I)$ was obtained as a green solid using the method reported previously for bis-phthalic hydrazidato-diaquo Co(II) complex.[17] An aqueous solution of $NiCl_2 \cdot 6H_2O$ (10 mM) was mixed with one of

---

*Author to whom correspondence should be addressed.

phthalic hydrazide H_2PH (20 mM) in dilute aqueous ammonia at room temperature. The pH of the reaction medium was adjusted between 5.5 and 7.0. The resulting green precipitates were filtered, washed with water, ethanol and finally with ether and dried under vacuum over P_2O_5. Homogeneity of the product was ensured by correct maintenance of pH.

Complexes of $[Ni(HPH)_2(H_2O)_2]2H_2O$ (I) were obtained by refluxing the suspension of the latter (453 mg, 1 mM) for 1 hr in a methanolic solution of acetylacetone (10 mM) or of amine (2 mM) or in aqueous solution of ethylenediamine (2 mM). The resulting solution was filtered and its volume was reduced. Acetylacetone, aniline and p-phenylenediamine complexes were deposited immediately on cooling while the monoethanolamine and ethylenediamine complexes were precipitated on adding a methanol:ether mixture (1:5, v/v) to their cool solutions. The resulting solid produce was then washed with ethanol followed by an ethanol–ether mixture and finally with ether and dried under vacuum over P_2O_5. The acetylacetone(acac) and aniline(An) complexes of type $[Ni(HPH)(acac)_2(H_2O)]H_2O$ (II) and $[Ni_3(HPH)_4(An)(H_2O)_7]H_2O$ (V) were obtained as green solids while the monoethanolamine(MEA), ethylenediamine(en) and p-phenylenediamine(p-Phda) complexes of type $[Ni_3(HPH)_7(MEA)_4(H_2O)_3]3H_2O$ (III), $[Ni(HPH)_2(en)_3(H_2O)]H_2O$ (IV) and $[Ni_3(HPH)_5(p$-$Phda)(H_2O)_7]H_2O$ (VI) were obtained as violet, red and brown solids respectively.

Physical measurements

Electronic spectra were recorded with a Beckman DK-2 recording spectrophotometer. IR spectra of KBr pellets were recorded with a Perkin–Elmer spectrophotometer model 621 (4000–200 cm^{-1}) at the University of Western Ontario, London, Canada while one of the authors (MAAB) was on a CIDA–NRC Research Associateship. Room temperature magnetic susceptibility measurements were carried out by Gouy method using $HgCo(NCS)_4$ as calibrant. The diamagnetic corrections were made using the appropriate Pascal's constants. Elemental analyses were carried out by Chemalytics, Inc. Laboratories, U.S.A. Nickel in complexes was determined by colorimetric method[22] using dimethylglyoxime.

RESULTS AND DISCUSSIONS

Phthalic hydrazide (H_2PH) prepared by the method of Drew and Hatt[21] exhibits spectra similar to that reported in literature[15] for 1-hydroxyphthalazine-4-one.

The latter is the preferred tautomer as against the dilactim form, i.e. 1,4-dihydroxy-phthalazine mentioned previously.[17] Assignment of the IR spectral bands of metal complexes therefore has to take into account the metal bonded lactim group and the free C=O and NH vibrations.

Appearance of the bands due to NH and C=O groups in the complexes suggests that the lactim–lactam structure of the ligand does not change on complexation with Ni(II) ion and it is the lactim group which is involved in
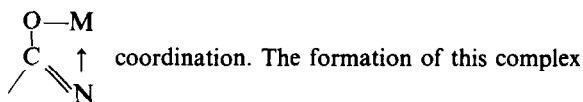
coordination. The formation of this complex in the presence of ammonium hydroxide in the pH range 5.5–7.0 is apparently favourable to monobasic coordination through a lactim group. The mode of bonding seems analogous to the monobasic bidentate behaviour of 8-hydroxyquinoline,[23] possessing phenolic OH and C=N donor groups in its metal chelates which are formed at the same pH range and also in the presence of ammonium hydroxide.

Bonding through nitrogen of the lactim group with another metal ion may not be favoured in this pH range but may be expected at pH > 7.0 as it has been reported in the metal complexes of nucleic acid bases[24,25] such as uracil and thymine (dilactam). The reaction of the metal ion with phthalic hydrazide may preferentially adopt the following scheme.
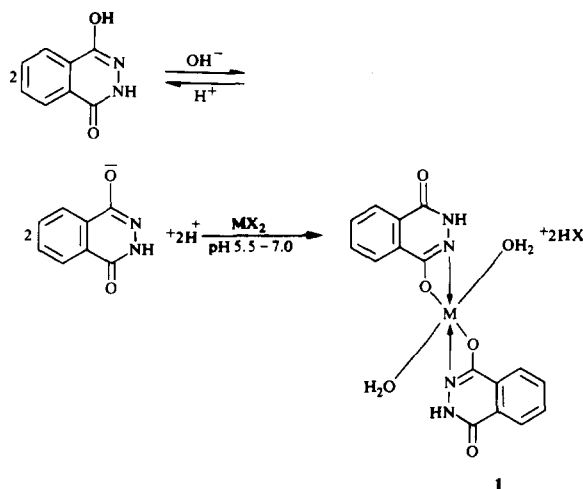
Phthalic hydrazide, according to the above scheme, behaves as a monoanionic bidentate ligand in the formation of Ni(II) complex which is a green solid and according to analytical data can be formulated as $[Ni(HPH)_2(H_2O)_2]2H_2O$ (I). This complex like the Co(II) complex[17] and the diaquo Ni(II)-quinolinate[23] is precipitated in the pH range of 5.5–7.0 and likewise forms addition compounds with other oxygen and nitrogen donor ligands. Reaction products are obtained as solids having colours different from those of the parent complex(I). The reaction of the diaquo-Ni(II) complex(I) with acetylacetone and ethylenediamine yield the mononuclear complexes of type $[Ni(HPH)(acac)_2(H_2O]H_2O$ (II) and $[Ni(HPH)_2(en)_3(H_2O)]H_2O$ (IV) respectively while from the reactions with monoethanolamine, aniline and p-phenylenediamine trinuclear complexes of the type $[Ni_3(HPH)_7(MEA)_4(H_2O)_3]3H_2O$ (III), $[Ni_3(PH)_4(An)(H_2O)_7]H_2O$ (V) and $[Ni_3(PH)_5(p$-$Phda)(H_2O)_7](H_2O)$ (VI) respectively are obtained. The analytical results are reported in Table 1.

The complexes are stable under laboratory conditions and decompose above 350°C. They are slightly soluble in methanol, ethanol and water and are insoluble in other organic solvents. Poor solubility of these complexes does not permit the study of their NMR spectra.

Table 1. Analytical data

No.	COMPOUND	COLOUR	C% Calc.	C% Found	H% Calc.	H% Found	N% Calc.	N% Found	Ni% Calc.	Ni% Found
I	[Ni(HPH)$_2$(H$_2$O)$_2$]2H$_2$O	Green	42.42	42.34	4.00	3.94	12.36	12.23	12.96	13.11
II	[Ni(HPH)(acac)$_2$(H$_2$O)]H$_2$O	Green	47.51	47.52	5.31	5.35	6.17	6.32	12.90	12.78
III	[Ni$_3$(HPH)$_7$(MEA)$_4$(H$_2$O)$_3$]3H$_2$O	Violet	46.40	46.35	4.56	4.87	15.22	15.08	10.63	10.49
IV	[Ni(HPH)$_2$(en)$_3$(H$_2$O)]H$_2$O	Brick red	44.24	43.96	6.41	6.53	23.44	23.68	9.83	9.57
V	[Ni$_3$(HPH)$_4$(An)(H$_2$O)$_7$]H$_2$O	Green	43.15	43.05	3.43	3.47	11.91	11.78	16.65	16.43
VI	[Ni$_3$(HPH)$_5$(p.Phda)(H$_2$O)$_7$]H$_2$O	Dark brown	44.86	45.02	3.84	3.52	13.64	13.55	14.29	14.39

Magnetism and electronic spectra

Magnetic moments of complexes (I–VI) are found in the range of 3.10–3.6 B.M. (Table 2) and these are consistent with octahedral Ni(II) complexes.[26] Support to this assignment is obtained from the electronic spectra and their assignment (Table 2). Appearance of spin-forbidden band due to $^3A_{2g} \rightarrow ^1E_g$ transition possibly suggests the presence of spin-orbit coupling[27] as is evident from the values of magnetic moment. Similarly since all the three spin-allowed bands are noted, the presence of weak octahedral field[27–29] around the metal ion can be suggested.

Parameters Dq, B' and β' have been calculated by numerical method[28] by fitting v_1 and sum of v_2 and v_3 bands from the observed data. A close agreement has been found between observed and calculated transition energies of v_2 and v_3.

The Dq value of [Ni(HPH)$_2$(H$_2$O)$_2$]2H$_2$O(I) is consistent with NiN$_2$O$_4$ chromophore[27,30–32] in literature, such as those of diaquo Ni(II) complexes of nicotinic and picolinic acid.[32] The trinuclear amine complexes (III, V and VI) of parent compound (I) shows the Dq values to be consistent with NiNO$_5$ chromophore[31,33] whereas the mononuclear amine complex (VI) and acetylacetone complex (II) agree with NiN$_3$NO$_3$[31,34] and NiO$_6$[27,30,31] chromophores respectively. These chromophores, hereafter have been confirmed by IR spectra.

The lower intensity of first d–d band (v_1) as compared with that of second (v_2) suggests a trans arrangement[34] for water molecules leaving the cis positions in octahedral structures of parent complex (I) and trinuclear amine complexes (V and VI), naturally for phthalic hydrazide. In complexes (II, III and IV) the intensities of these bands seem to be consistent with the trans occupation of phthalic hydrazide (HPH) and cis[34] position of water or adducting ligands.

IR spectra

The spectrum of phthalic hydrazide (H$_2$PH) is in accord with the published data[15] and corresponds with the monolactim form, i.e. 1-hydroxy phthalazine-4-one and analogous maleic hydrazide.[35]

Appearance of vNH, vC=O, vC=N and vC=O bands in all the complexes (I–IV) (Table 3) suggests the persistance of lactam-lactim structure of phthalic hydrazide. The strong vC=N and weak ring vibration bands of phthalic hydrazide (H$_2$PH), like those of nucleic acid bases,[36,37] are shifted to higher frequencies in the parent complex [Ni(HPH)$_2$(H$_2$O)$_2$]2H$_2$O(I) by exhibiting the bands at 1605, 842 and 560 cm^{-1} respectively. In acetylacetone and amine complexes (II–VI) these bands are shifted to lower frequencies as compared to parent complex (I). These results suggest the bonding through nitrogen C=N group of phthalic hydrazide (HPH) in parent complex (I) but in its complexes (II–VI) it may not be suggested.

The disappearance of strong OH band of free phthalic hydrazide at 1300 cm^{-1} and appearance of vM–O bands, like those of metal-β-diketonates,[38] in the 455–450 cm^{-1} region in all the complexes (I–VI) indicate coordination through enolic carbonyl oxygen of phthalic hydrazide which may behave as an anionic ligand, forming chelate ring in (I).

The vM–O band of parent complex (I) at 455 cm^{-1}, like those of metal-β-keto-enolates,[20,39,40] is shifted to lower frequency in its complex (II–VI) due to adduct formation.

The energies of vNH and vC=O bands of free phthalic hydrazide remain unchanged but those of δNH in- and out-of-plane modes are shifted to higher frequencies by 30 and 25 cm^{-1} respectively in parent complex (I). These results indicate that the above two groups are not donors in this complex. They remain hydrogen bonded (C=O ... HN) as is evidenced by the solid state spectrum of free ligand[41,42] and this supports the coordination through C=N and C–O groups, as concluded above. The higher shifts of δNH bands may possibly be the result of coupling with vC=O band as has been noted in metal complexes of nucleic acid bases such as those of thymine.[24]

In acetylacetone, monoethanolamine and ethylenediamine complexes (II, III and IV) the vNH and δNH bands of parent complex (I) are shifted to higher and lower frequencies respectively and vC=O band to higher frequency in (II) and lower frequencies in (III and IV). These results do not suggest coordination through NH and C=O groups; the hydrogen bonding of the type (C=O ... HN) in parent complex (I), may be broken possibly due to axial coordination of phthalic hydrazide (HPH) through the enolic carbonyl group, as concluded above. The shifting of vC=O band in (III and IV) to lower frequencies by 18–6 cm^{-1} may suggest the formation of hydrogen bonding possibly with hydrogen of coordinated water in monoethanolamine complex (III) and with hydrogen of free amino group[43–45] of ethylenediamine complex (IV) when water or ethyl-

Table 2. Magnetic moments, electronic spectra and ligand field parameters

No.	COMPOUND	μ_{eff} B.M.	SOLVENT	CHROMOPHORE	ν_1=10Dq $^3A_{2g} \to {}^3T_{2g}(F)$	$\to E_{1g}$	ν_2 $^3 \to T_{1g}(F)$	ν_3 $^3 \to T_{1g}(P)$	B'	β'
I	$[Ni(HPH)_2(H_2O)_2]2H_2O$	3.28	Ethanol	NiN_2O_4	9.62 (1.71)	13.50 (1.76)	15.20 (1.81)	24.10 (2.02)	0.70	0.67
II	$[Ni(HPH)(acac)_2(H_2O)]H_2O$	3.34	Methanol	NiO_6	8.33 (1.15)	11.76 (0.82)	14.29 (0.91)	24.10 (1.26)	0.89	0.86
III	$[Ni_3(HPH)_7(MEA)_4(H_2O)_3]3H_2O$	3.35	Methanol	$NiNO_5$	8.10 (1.35)	12.50 (1.28)	13.89 (1.28)	24.27 (1.99)	0.92	0.89
IV	$[Ni(HPH)_2(en)_3(H_2O)]H_2O$	3.10	Water	NiN_3O_3	10.53 (0.93)	12.82 (0.78)	16.53 (0.84)	24.51 (1.90)	0.63	0.61
V	$[Ni_3(HPH)_4(An)(H_2O)_7]H_2O$	3.36	Methanol	$NiNO_5$	8.46 (1.50)	15.38 (1.60)	14.04 (1.54)	23.70 (2.13)	0.82	0.79
VI	$[Ni_3(HPH)_5(p.Phda)(H_2O)_7]H_2O$	3.33	Ethanol	$NiNO_5$	8.33 (1.40)	12.63 (1.47)	13.16 (1.50)	23.92 (2.11)	0.81	0.77

Note: Band position in kK

Log ξ in parentheses

Table 3. IR spectral data

No.	COMPOUND	νOH Free	νOH Coord	νNH2 Free	νNH2 Coord. asym.	νNH2 Coord. sym.	νNH	νC-O	νC-N	δNH in-plane (δNH2)
	H2PH						3125s	1658s	1598s	1550s
I	[Ni(HPH)2(H2O)2]2H2O	3645w,br	3504w,br				3125s	1660s	1605s	1580vs
II	[Ni(HPH)(acac)2(H2O)]H2O		3500s,br 3475s,br				3164s	1665s 1614s (acac)	1602s	1575w
III	[Ni3(HPH)7(MEA)4(H2O)3]3H2O	3653w,br	3506w,br 3390w,br 3280s 3260s (MEA)	3214s			3130s	1642vs	1597s	1572s
IV	[Ni(HPH)2(en)3(H2O)]H2O	3653w,br	3570w 3473s	3365s 3332s	3320s 3284s 3238s	3164s	3132s	1654s		1573s
V	[Ni3(HPH)4(An)(H2O)7]H2O	3618w,br	3586w		3278s	3178s	3108s	1958s	1606s	1580s 1576s
VI	[Ni3(HPH)5(p.Phda)(H2O)7]H2O	3600w,br	3504w	3404w	3240s	3160s	3114s	1665s	1602m	1575s

No.	COMPOUND	Ring νC-O (asym.νC-C-C)	νC-N (CH2wagg)	δOH in-plane	NH2 wagg (NH2 twist)	(νC-C+νC-O) CH2 rock	δNH out-of-plane	pr(H2O)
	H2PH	1450s	1370s	1300			860s	
I	[Ni(HPH)2(H2O)2]2H2O	1440s	1370s				885w	822w
II	[Ni(HPH)(acac)2(H2O)]H2O	(1515s) 1455s	1375s			(930m)	880w	820m
III	[Ni3(HPH)7(MEA)4(H2O)3]3H2O	1460s 1004s(MEA)	1370s 1160s(MEA)			898w	870w	820m
IV	[Ni(HPH)2(en)3(H2O)]H2O	1450s	(1390s) 1375s		(1018s)	980w	872w	
V	[Ni3(HPH)4(An)(H2O)7]H2O	1440s	1360s 1203s		1065w		876w	823w
VI	[Ni3(HPH)5(p.Phda)(H2O)7]H2O	1450s	1352s 1214s		1130w		872w	

No.	COMPOUND	NH2 rock	pw(H2O)	Ring vib.	νM-O	νM-OH2	νM-N
	H2PH			815s 550w			
I	[Ni(HPH)2(H2O)2]2H2O		655m 645m	842w 560w	455w	376w	330m
II	[Ni(HPH)(acac)2(H2O)]H2O		652w	825s 560w	452w 296w(acac)	375w	
III	[Ni3(HPH)7(MEA)4(H2O)3]3H2O	744m	650s	800s 562w	430s 540w (MEA)	375w	328w
IV	[Ni(HPH)2(en)3(H2O)]H2O	740w	658m	838m 558w	453w	366w	493w 313w
V	[Ni3(HPH)4(An)(H2O)7]H2O	758w	656w	842s 575s	453w	366w	342w 326w
VI	[Ni3(HPH)5(p.Phda)(H2O)7]H2O		650w 630w	838 565	444w	370w	340w 312w

s, strong; vs, very strong; m, medium; w, weak

enediamine is at one of the axial position along with the axially occupied phthalic hydrazide (HPH). Appearance of some new and broad νNH bands in the 3365–3332 and 3320–3280 cm⁻¹ regions in (IV) indicates the presence of hydrogen bonded and metal bonded NH2 groups due to monodentate[46] behaviour of ethylenediamine which seems to be consistent with above conclusion. CH2 twisting, CH2 rocking, NH2 rocking and νM–N bands appear as they do in ethylenediamine complexes of metal-β-diketonates[46,47] and of metal salts[48-49] at 1390, 1018, 980, 740 and 493 cm⁻¹ respectively which suggests the bonding of ethylenediamine with metal ion.

The trinuclear monoethanolamine complex (III) exhibits new bands due to νOH, νNH and νC–O modes at 3280–3260, 3214 and 1004 cm⁻¹ respectively which are at lower frequencies as compared with free mono-

thanolamine as has been noted in complexes of metal salts.[50,51] Coordination is apparently taking place through NH_2 and OH groups of monoethanolamine which may behave as a bridging ligand between the two metal ions.

The acetylacetonate complex (II) of (I), like the metal–acetylacetonates and their adducts[39,48] exhibits the bands at 1614, 1515 and 296 cm^{-1} due to $\nu C=O$, $\nu C-C-C$ and $\nu M-O$ modes respectively. This observation suggests a bidentate coordination of acetylacetonate anion with the metal ion.

In trinuclear aniline and p-phenylenediamine complexes (V and VI), the νNH and $\nu C-N$ bands of parent complex (I) are shifted to lower frequencies by 17–10 and 18–10 cm^{-1} respectively. It is therefore reasonable to suggest that coordination occurs through NH group of phthalic hydrazide (HPH) which may behave as a bridging ligand between the two metal ions through the enolic carbonyloxygen. The appearance of νNH and $\nu C-N$ bands, like the aromatic amine complexes of metal salts[52,53] in the 3278–3160 and 1214–1203 cm^{-1} regions respectively suggests the bonding of these amines with the metal ions. The new band due to free νNH_2 mode at 3404 cm^{-1} in (VI) indicates the monodentate behaviour of p-phenylenediamine.

The complexes (I–VI), like other aquo complexes[38,54,55] exhibit the νOH, $\rho w(H_2O)$, $\rho r(H_2O)$ and $\nu M-OH_2$ bands in the 3504–3500, 770–630, 822 and 376–375 cm^{-1} regions respectively thereby indicating the coordination of water molecules with the metal ion.

CONCLUSION

Phthalic hydrazide appears to behave as a monobasic ligand (HPH) in all the complexes (I–VI). It acts as a bidentate chelating ligand in parent compound (I) and bidentate bridging ligand in aniline and p-phenylenediamine complexes (V) and (VI) of (I) possibly occupying cis positions of the octahedral framework while aniline and p-phenylenediamine seem to act as monodentate ligands occupying $trans$ positions. In acetylacetone, monoethanolamine and ethylenediamine complexes (II, III and IV) of (I), these ligands seem to behave as a bidentate chelating, bidentate bridging and monodentate ligands respectively, possibly occupying cis, cis and $trans$ positions respectively while the phthalic hydrazide anion (HPH$^-$) acts as a monodentate ligand occupying the $trans$ position.

REFERENCES

1. M. E. Iskander, L. El-Sayed, A. E. M. Hefnay and S. E. Zayan, J. Inorg. Nucl. Chem. 1976, 38, 2209.
2. R. C. Aggrawal, T. Parshad and B. N. Yadan, J. Inorg. Nucl. Chem. 1975, 37, 899.
3. M. A. A. Beg and B. Bilquis, Pak. J. Sci. Ind. Res. 1970, 12, 340.
4. M. A. A. Beg and B. Bilquis, Rev. Roumain. Chim. 1970, 15, 1860.
5. M. A. A. Beg, S. A. Hussain and B. Bilquis, Pak. J. Sci. Ind. Res. 1971, 14, 447.
6. R. C. Paul and S. L. Chadha, Spectrochim. Acta 1967, 23A, 1249.
7. M. F. Iskander, S. E. Zayan, M. A. Khalifa and L. El-Sayed, J. Inorg. Nucl. Chem. 1974, 36, 551.
8. L. El-Sayed and M. F. Iskander, J. Inorg. Nucl. Chem. 1971, 33, 435.
9. A. D. Ahmed and N. R. Chaudhri, J. Inorg. Nucl. Chem. 1971, 33, 189.
10. A. D. Ahmed and N. R. Chaudhri, J. Inorg. Nucl. Chem. 1969, 31, 2545.
11. T. G. Burdo and W. R. Seitz, Anal. Chem. 1975, 47, 1639.
12. H. Ojima, Nippon Kagaku Zasshi, 1961, 82, 973, Chem. Abstr. 1962, 57, 217f.
13. A. K. Babko and L. I. Dubovenko, Ukr. Khim. Zh. 1963, 29, 1083; Chem. Abstr. 1964, 60, 7509g.
14. A. K. Babko and N. M. Lukovskaya, Ukr. Khim. Zh. 1964, 30, 508; Chem. Abstr. 1964, 61, 6442h.
15. J. A. Elvidge and A. P. Redman, J. Chem. Soc. 1960, 1710.
16. F. M. Rowe and A. T. Petters, J. Chem. Soc. 1933, 1331.
17. M. A. A. Beg and S. A. Hussain, Pak. J. Sci. Ind. Res. 1972, 15, 353.
18. K. S. Bhatki, A. T. Rane and H. Freiser, Inorg. Chem. 1978, 17, 2215.
19. L. L. Merrit, Anal. Chem. 1953, 25, 718.
20. J. M. Haigh, N. P. Slabbert and D. A. Thornton, J. Inorg. Nucl. Chem. 1970, 32, 3635.
21. H. K. Drew and H. H. Hatt, J. Chem. Soc. 1937, 16.
22. A. I. Vogel, A Text Book of Quantitative Inorganic Analysis. Green, London (1961).
23. N. Ohkaku and K. Nakamoto, Inorg. Chem. 1971, 10, 798.
24. M. Goodgame and K. W. Johns, J. Chem. Soc. Dalton 1977, 1680.
25. T. J. Kistenmacher, T. Sorrell and L. G. Marzilli, Inorg. Chem. 1975, 14, 2479.
26. B. N. Figgis and J. Lewis, Prog. Inorg. Chem. 1964, 6, 197.
27. A. B. P. Lever, Inorg. Electronic Spectroscopy. Elsevier, Amsterdam (1968).
28. D. K. Rastogi, K. G. Sharma, S. K. Dua and M. P. Teotia, J. Inorg. Nucl. Chem. 1975, 37, 685.
29. A. B. P. Lever, J. Chem. Educ. 1968, 45, 711.
30. C. K. Jorgensen, Absorption Spectra and Chemical Bonding in Complexes. Pergamon Press, Oxford (1964).
31. R. C. Rosenberg, C. A. Root and H. B. Gray, J. Am. Chem. Soc. 1975, 97, 21.
32. K. Kleinstein, G. A. Webb, J. Inorg. Nucl. Chem. 1971, 33, 405.
33. C. Preti and G. Tosi, Aust. J. Chem. 1979, 32, 989.
34. A. K. Srivastava and F. Tarli, J. Inorg. Nucl. Chem. 1977, 39, 1973.
35. B. H. P. Fritz and P. Berkert, Chem. Ber. 1975, 108, 478.
36. S. Schirotake and T. Sakaguchi, Chem. Pharm. Bull. 1978, 26, 2941.
37. S. Schirotake, Chem. Pharm. Bull. 1980, 28, 956.
38. Z. Jawarska, C. I. Jose and J. Urbanski, Spectrochim. Acta 1974, 30A, 1161.

39. G. Marcotrigiano, R. Battistauzzi and G. C. Pellacani, *Can. J. Chem.* 1972, **50**, 2557.
40. N. K. Misra and D. V. Ramana Rao, *J. Inorg. Nucl. Chem.* 1969, **31**, 3875.
41. P. Sohan, *Acta. Chim. Acad. Sci. (Hung)* 1964, **40**, 317, *Chem. Abstr.* 1965, **63**, 1344e; **62**, 14457d.
42. S. F. Mason, *J. Chem. Soc.* 1957, 4874.
43. G. Marain, *Bull. Chem. Soc. Japan* 1965, **38**, 2073.
44. G. Narain and P. Shukla, *Aust. J. Chem.* 1967, **20**, 227.
45. G. Narain, *J. Inorg. Nucl. Chem.* 1966, **28**, 2403.
46. T. Kurauchi, N. Matsui, Y. Nakamura, S. Ooi, S. Kairaguchi and H. Kuroga, *Bull. Chem. Soc. Jpn.* 1974, **47**, 3049.
47. Y. Nisbikawa, Y. Nakamura and S. Kawaguchi, *Bull. Chem. Soc. Jpn.* 1972, **45**, 155.
48. K. Nakamoto, *Infrared Spectra of Inorganic and Coordination Compounds.* Wiley Interscience, New York (1970).
49. R. W. Berg and K. Rasmussen, *Spectrochim. Acta* 1974, **30A**, 1881.
50. D. G. Brannon, R. H. Morrison, J. L. Hall, G. L. Humpherey and D. N. Zimmermah, *J. Inorg. Nucl. Chem.* 1971, **33**, 981.
51. M. S. Masoud, *J. Inorg. Nucl. Chem.* 1977, **39**, 413.
52. M. A. Jungbauter and C. Curran, *Spectrochim. Acta* 1965, **21**, 641.
53. M. S. Barvinok and I. S. Bukhareva, *Russ. J. Inorg. Chem.* 1965, **10**, 464.
54. C. Preti and G. Tosi, *Spectrochim. Acta* 1978, **34A**, 269.
55. C. Preti and G. Tosi, *Spectrochim. Acta* 1975, **31A**, 1139.

NUCLEAR MAGNETIC RESONANCE STUDY OF ALUMINUM CHLORIDE-n-BUTYLPYRIDINIUM CHLORIDE MELTS

FRANCIS TAULELLE and ALEXANDER I. POPOV*
Department of Chemistry, Michigan State University, East Lansing, MI 48824, U.S.A.

Abstract—High resolution proton and ^{13}C-NMR measurements were used to follow the variation of the n-butylpyridinium (BP^+) cation spectra in BP^+Cl^-–$AlCl_3$ molten mixtures. The mole fraction of $AlCl_3$ was varied between 0.45 and 0.60. It was found that chemical shifts and proton coupling constants are significantly affected by the BP^+–Cl^- and BP^+–$AlCl_4^-$ associations. Analysis of the NMR results shows that in the melts the ionic association into ion pairs is essentially quantitative. Lithium-7 NMR of $BPCl$–$AlCl_3$–$LiCl$ melt shows that when the mole-fraction of $AlCl_3$ is < 0.50 (basic melt) $LiCl_2^-$ ion is formed, while in the acidic melts the Li^+ ion probably interacts with two $AlCl_4^-$ ions to form $LiAl_2Cl_8^-$ ion.

The Lewis acid-base properties of molten mixtures of aluminum chloride and various chloride ion donors, such as alkali chlorides or alkylpyridinium chlorides, have been studied by several investigators.[1–10]

Various electrochemical techniques as well as electronic and vibrational spectroscopies, were used to characterize acid-base behavior of various solutes in these melts. The results of the above studies have been recently summarized by Mamantov and Osteryoung.[9]

Though acid-base properties are fairly well known for individual $AlCl_3$–MCl or $AlCl_3$–RCl mixtures, an absolute comparison of acid strengths of different mixtures is still very difficult and, in fact, an evaluation of cation–anion interactions is necessary to compare acid strengths of different MCl–$AlCl_3$ melts. For example, it has been shown[3,10] that the equilibria occurring in the above molten mixtures

$$2AlCl_4^- \rightleftarrows Al_2Cl_7^- + Cl^- \tag{1}$$

and

$$2Al_2Cl_7^- \rightleftarrows Al_2Cl_6 + 2AlCl_4^- \tag{2}$$
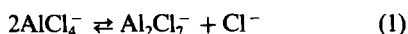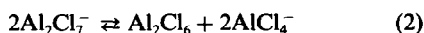
are strongly dependent on cation–anion associations,

$$M^+ + Cl^- \rightleftarrows M^+Cl^- \tag{3}$$

$$M^+ + AlCl_4^- \rightleftarrows M^+AlCl_4^- \tag{4}$$

$$M^+ + Al_2Cl_7^- \rightleftarrows M^+Al_2Cl_7^- \tag{5}$$
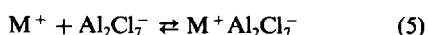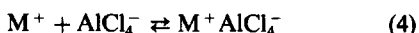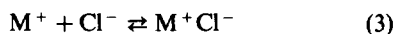
which, in turn, obviously depend on the nature of M^+. Therefore, equilibria (3)–(5), govern the acidity of the melt which is expressed as pCl^-. No quantitative and thermodynamically valid comparison of acid-base equilibria in aluminum chloride melts are possible without a knowledge of the equilibrium constants of reactions (3)–(5).

We and others have shown that multinuclear NMR is a powerful probe of the immediate chemical environment of ions and of organic ligands in aqueous and nonaqueous solutions.[11,12] It seemed reasonable to extend the use of this technique to studies of ionic associations in molten salt mixtures.

Osteryoung et al.[13] reported the variation in the room temperature proton and ^{13}C-NMR spectra of 1:1 and 1:2 butylpyridinium:aluminum chloride mixtures as they were progressively diluted with benzene. Since our interest is primarily focused on cation–anion interactions in $AlCl_3$–BP^+Cl^-–M^+Cl^- melts, it was of interest to us to determine precisely how the high resolution ^1H and ^{13}C spectra of the BP^+ cation vary with a change in the $AlCl_3/BP^+Cl^-$ ratio and, consequently, how the conformation of the organic cation is affected by the change in the acid-base characteristics of the melt. The use of a high field instrument under optimal resolution conditions was an indispensable prerequisite for such studies.

We also wish to report an initial investigation of alkali cation influence on the equilibria (1)–(5) in ternary melts. The ternary system studied was the $AlCl_3$–$BPCl$–$LiCl$ mixture. Lithium-7 NMR was used as a probe of the environment of the Li^+ ion.

EXPERIMENTAL

(1) Reagents

n-Butylpyridinium chloride was prepared by the method of Osteryoung et al.[14] The product was recrystallized twice from acetonitrile–ethylacetate mixture and dried under vacuum. After preparation the salt was kept in sealed ampules under inert atmosphere until used.

Aluminum chloride was sublimed in inert atmosphere in the presence of metallic aluminum as described previously;[15] CH_3NO_2-d_3 (Aldrich, gold label) was used as received. Lithium chloride (Alfa) was dried at 200°C for ~12 hr. All weighings, transfers and preparations of CH_3NO_2 solutions were carried out in a dry-box under nitrogen atmosphere. The concentrations of water and of oxygen in the dry-box atmosphere were less than 10 ppm.

(2) NMR measurements

Proton and ^{13}C NMR measurements were performed on a Bruker WM-250 spectrometer operating in the Fourier

---

*Author to whom correspondence should be addressed.

transform mode at a field strength of 58.7 kG and frequencies of 250.13 and 62.09 MHz respectively. Lithium-7 NMR spectra were obtained on a Bruker WH-180 F.T. spectrometer at a field strength of 42.28 kG and a frequency of 69.96 MHz. It was convenient to follow the probe temperature by monitoring temperature-sensitive ^{1}H chemical shifts of ethylene glycol as described by Bombi and Sachetto.[16] Ethylene glycol, in a 5-mm NMR tube, was placed concentrically in a 10-mm NMR tube containing D_2O as the lock. The rate of spinning and the heat flow were carefully adjusted and the proton spectrum of ethylene glycol was recorded when thermal equilibrium was attained. The sample temperature was calculated from the relationship given below which is corrected for field strength of our spectrometer.

$$\text{Temperature} = 466.40 - 0.402\Delta v \text{ K.} \qquad (6)$$

Equation (6) was checked at three different temperatures in the 25–100°C temperature range, with a copper-constantan thermocouple inside ethylene glycol (without spinning) and experimental differences were within ±0.5°C.

Resolution enhancement was performed on proton spectra by using Gaussian multiplication.[17] Bruker's LAOCOON program version has allowed coupling constant evaluation and comparison between experimental and theoretical spectra. Proton and ^{13}C chemical shifts were referenced to external TMS, except for one basic mixture (55% BPCl–45% AlCl₃) for which external and internal TMS peaks were measured. This difference was used to correct the shifts from external referencing.

Lithium-7 chemical shifts were referenced to an external aqueous 0.1 M LiCl solution. The chemical shifts were determined with an accuracy of 5×10^{-2} ppm.

RESULTS AND DISCUSSION

In order to obtain some detailed information on the behavior of the butylpyridinium cation in molten salt media, we obtained proton and ^{13}C NMR spectra in the BPCl–AlCl₃ melt as well as of BPCl in nitromethane solution. This solvent was selected since it has the best properties of the common organic solvents we tried, in terms of solubility and spectral resolution. The spectra of the CD_3NO_2 solution and of the BPCl–AlCl₃ 1:1 mixture are shown in Fig. 1. The latter spectrum is very similar to the one obtained by Osteryoung et al.[13]

In order to obtain highest possible resolution, we used a sweep width of 2500 Hz, aquisition of the F.I.D. in the quadrature mode, quadrature phase detection, memory size of 32 K, Gaussian filtering with zero filling up to 128 k. Under these conditions the mean line width was reduced from about 2.5 Hz shown in Fig. 1 to 0.25 Hz for the CD_3NO_2 solution and about 0.8 Hz for the molten salt.

PROTON NMR

The high resolution proton spectra are shown in Fig. 2. The results indicate that the resonances most sensitive to ionic association are those of protons on the carbons 2,6 (Fig. 2a), 3.5 (Fig. 2c) and α-CH_2 (Fig. 2d). Figure 2(a) shows that the 2,6 pattern is quite

^{1}H After Resolution Enhancement

BPCl in CD_3NO_2 BPCl-AlCl₃ (1:1)

Fig. 2. Resolution-enhanced proton spectra of BPCl and of 1:1 BPCl:AlCl₃ melt at room temperature and 40°C respectively. A, 2.6; B, 4; C, 3.5; D, αCH_2; E, βCH_2; F, γCH_2; G, δCH_3 protons.

Fig. 1. Proton and ^{13}C NMR spectra of BPCl solution in CD_3NO_2 at room temperature and of a 1:1 BPCl:AlCl₃ mixture at 40°C. A, ^{1}H of BPCl; B, ^{1}H of melt; C, ^{13}C of BPCl; D, ^{13}C of melt.

detailed in CD_3NO_2 solution and somewhat less so in the melt. It is seen that these protons mainly couple with the 3,5 and 4 protons. However, two small inner peaks were observed. They were well defined in CD_3NO_2 but seen as shoulders in the molten salt. Simulation experiments show that this splitting does not originate from a coupling between protons of the pyridine ring but rather from the coupling of the 2,6-protons with those of the α-CH_2 group.

On Fig. 2(c) the 3,5 pattern shows a quite marked difference between CD_3NO_2 solution and the molten salt. For the latter the pattern is better defined, indicating a simpler coupling system.

In the case of the α-CH_2 protons (Fig. 2d), the linewidth is much greater. This broadening could be due to the coupling with the 2,6-protons or to the relaxation of the ^{14}N nucleus.

In all cases a change in the BP^+ cation association from that with Cl^- to that with $AlCl_4^-$ anion (at higher $AlCl_3$ mole fractions), significantly affects not only the ^1H chemical shift but also, as shown in Table 2, the coupling constants, which differ in nitromethane solution and in the melt.

It should be noted that with the above described resolution enhancement it was possible to determine ^1H chemical shifts with a precision of 4×10^{-4} ppm in CD_3NO_2 solutions and 10^{-3} ppm in the melt.

^{13}C NMR

The ^{13}C decoupled spectra are rather simple (Fig. 1c and 1d) and the chemical shifts can be measured accurately without enhanced resolution. The precision of the chemical shift measurements was better than $\pm 10^{-2}$ ppm. The inversion of position 2 and 6 with 4 resonance, when compared to ^1H NMR has been previously explained[13] as the difference between paramagnetic and diamagnetic dominating effect respectively in ^{13}C and ^1H magnetic resonance experiments.

It is interesting to note that nitrogen couples more strongly with 2- and 6-carbons in the molten salt than in the CD_3NO_2 solution.

VARIATION OF ^1H AND ^{13}C SPECTRA WITH BPCl/AlCl₃ RATIO

Our main reason for seeking high resolution spectra of BPCl was to see how the resonance frequencies of

Table 2. Proton coupling constants of *n*-butylpyridinium chloride in nitromethane solution and in equimolar BPCl–AlCl₃ melt

Coupling	J_{H-H} (Hz) in CD_3NO_2	J_{H-H} (Hz) in Melt
J2.3 or J5.6	6.76	6.71
J2.4 or J4.6	1.28	1.44
J3.4 or J4.5	7.51	7.86
Jαβ	6.88	7.28
Jβγ	6.75	7.43
Jγδ	7.13	7.60

the cationic protons and carbons were affected as the melt changed from a basic to an acidic composition. Consequently, proton and ^{13}C measurements were carried out at 40°C in the $AlCl_3$ mole fraction range 0.45 to 0.60. Figures 3 and 4 show the variation of ^1H and ^{13}C chemical shifts with composition.

All ^1H and ^{13}C nuclei are sensitive to the composition of the melt, albeit to a different extent. The 2,6 and α-CH_2 protons and carbons show the highest sensitivity. The plots of chemical shift against concentration consist in most cases of two straight lines intersecting at the 1:1 BPCl/AlCl₃ mole ratio.

When we have a rapid exchange of NMR-active nuclei between several different sites, the observed chemical shift is given by the expression:

$$\delta_{obs} = \sum_i \delta_i X_i \tag{7}$$

where δ_i is the chemical shift of site i and X_i is the mole fraction of the species i. In the case of the BPCl–AlCl₃ system, when the mixture is basic (i.e. $AlCl_3 < 50$ mole %) only $PB^+AlCl_4^-$ and BP^+Cl^- species are present. On the acidic side we have $BP^+AlCl_4^-$ and $BP^+Al_2Cl_7^-$. Therefore, in the former case eqn (7) becomes

$$\delta_{obs} = \frac{N}{1-N}\delta_{BPAlCl_4} + \frac{1-2N}{1-N}\delta_{BPCl} \tag{8}$$

while on the acidic side we have,

Table 1. Proton and ^{13}C chemical shifts of *n*-butylpyridinium chloride in nitromethane solutions and in equimolar PBCl–AlCl₃ melt

| $^1H/^{13}C$ | ^1H Shifts | | ^{13}C Shifts | |
	CD_3NO_2	Melt	CD_3NO_2	Melt
10	0.967	0.980	13.18	13.30
9	1.435	1.470	19.48	19.07
8	2.073	2.133	33.93	32.76
7	4.986	4.739	61.57	62.19
3,5	8.197	8.208	128.76	128.77
4	8.693	8.675	146.13	145.78
2,6	9.564	8.921	145.81	144.07

^{1}H Shifts in BPCl—AlCl$_3$ Mixtures at 40°C
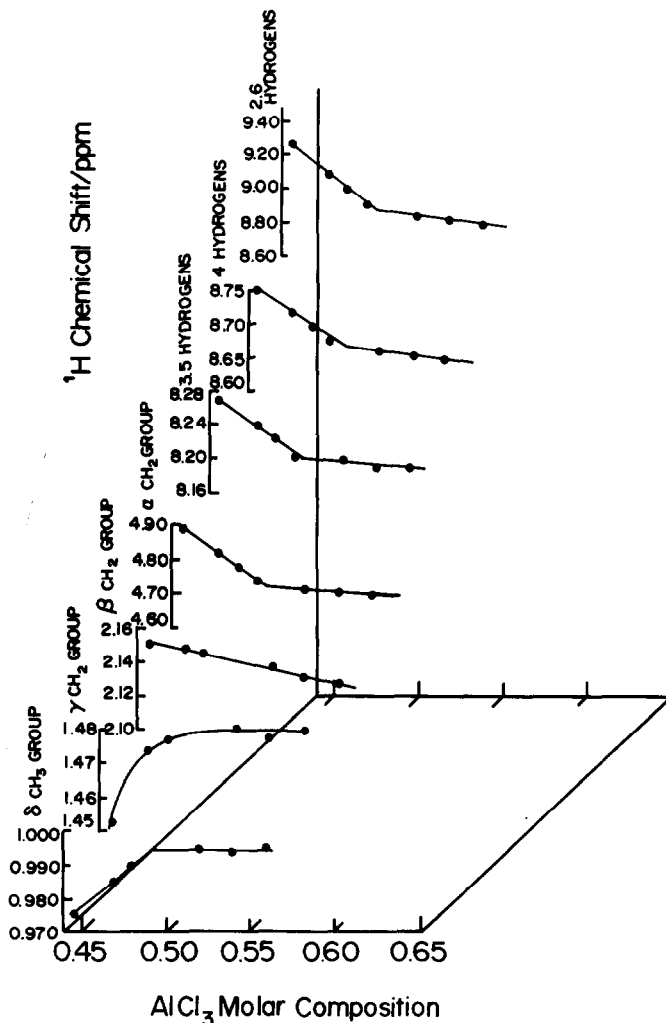
Fig. 3. Variation of ^{1}H chemical shifts of the BPCl:AlCl$_3$ mixture with composition at 40°C.

$$\delta_{obs} = \left(2\frac{N}{1-N}\right)\delta_{BPAlCl_4} + \frac{2N-1}{1-N}\delta_{BPAl_2Cl_7} \quad (9)$$

where N is AlCl$_3$ molar composition and can be expressed as:

$$N = \frac{n^0_{AlCl_3}}{n^0_{AlCl_3} + n^0_{BPCl}} \quad (10)$$

with $n^0_{AlCl_3}$ and n^0_{BPCl} representing the stoichiometric number of moles of AlCl$_3$ and butylpyridinium chloride respectively.

Since in the mixtures used in this investigation the fractions (N/1 − N), (1 − 2N/1 − N) and (2N − 1/1 − N) are essentially linear functions of N, it can be concluded that the ionic association into ion pairs is essentially quantitative. The ionic transport in these melts must involve migration of the BP$^+$ cation and/or the anions from one ion pair to another by a chain mechanism and not, as is usually assumed, by free ions.

LITHIUM-7 NMR MEASUREMENTS

Lithium chloride (mole fraction 10^{-2}) was introduced into a series of BPCl-AlCl$_3$ mixtures of variable composition. The NMR tubes were then sealed and allowed to stay overnight at 120°C so as to dissolve the LiCl. On cooling the tubes to room temperature, it was noted however, that only the melt with 45 mole % AlCl$_3$ and those above 50.5 mole % were completely homogeneous. The ^{7}Li signal was still observable in the 47 and 50% melts although not all the LiCl was dissolved, but not in the 48 or 49.5% melts.

The results shown in Fig. 5 clearly indicate that the Li$^+$ ion exists in very different environments on the acidic and the basic sides. The ^{7}Li chemical shifts in these two media differ by 2.4 ppm which is very large for this nucleus where the total chemical shift range is ~ 6 ppm.[18] Moreover, the lines are narrow on the acidic side (~ 1 Hz) and 3–4 times broader on the basic side, indicating a decrease in symmetry around the lithium nucleus.

Since on the basic side an excess of chloride ion is necessary to dissolve LiCl, the solubility is probably
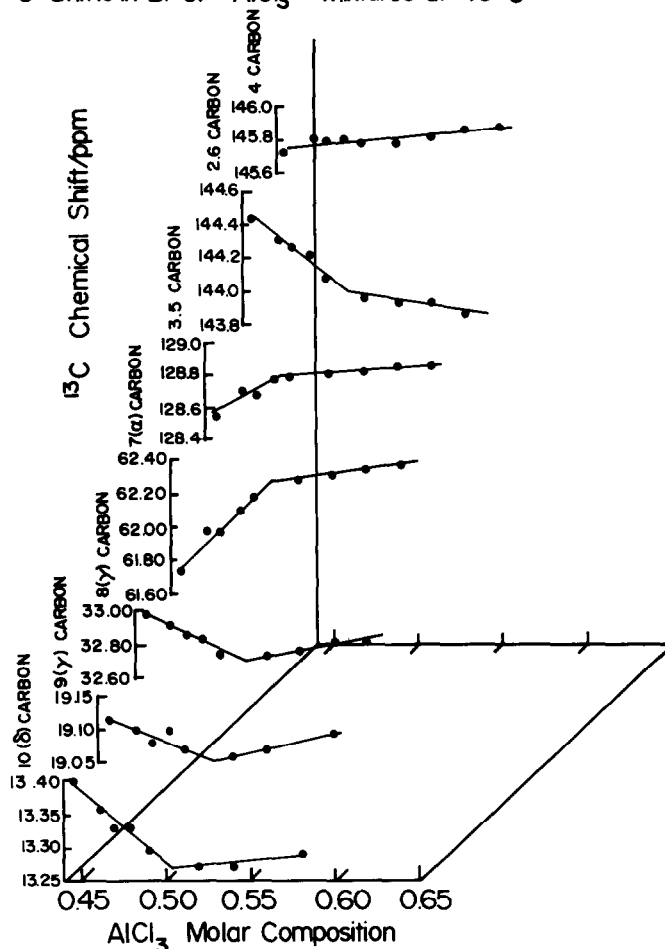
Fig. 4. Variation of ^{13}C chemical shifts of the BPCl:AlCl$_3$ mixture with composition at 40°C.

due to the formation of a lithium chloride complex

$$LiCl + Cl^- \rightleftharpoons LiCl_2^-. \tag{11}$$
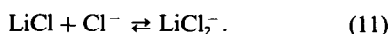
On the other nand, on the acidic side we probably have the equilibrium

Fig. 5. Variation of the ^{7}Li chemical shift with composition of the BPCl:AlCl$_3$ mixture at 25°C. Mole fraction of LiCl $= 10^{-2}$.

$$LiCl + Al_2Cl_7^- \rightleftharpoons Li^+ + 2AlCl_4^-. \tag{12}$$
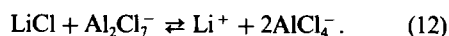
Rytter *et al.* studied by Raman spectroscopy[19] MCl–AlCl$_3$ molten mixture containing 50–75 mole % AlCl$_3$. The authors found that in the case of a LiCl–AlCl$_3$ 50–50 mixture, the T$_d$ symmetry of AlCl$_4^-$ was distorted to C$_{2v}$; they proposed the structure
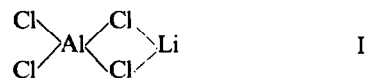
It seems equally likely that on the acidic side lithium can interact with two tetrachloroaluminates to give
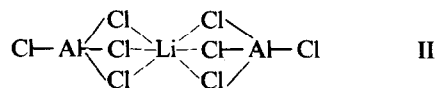
If we assume that tetrahedral and octahedral environments are most probable for the lithium ion, an octahedral environment can be proposed for the acidic side leading to a higher symmetry and narrower NMR lines, while on the basic side Li$^+$ is in a tetrahedral environment which still gives a narrow resonance line but broader than the previous one. It follows from such an assumption that the only complex fulfilling these conditions in the basic range is

$LiCl_2AlCl_4^{2-}$, with the structure

$$III$$
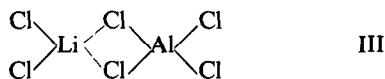
since LiX_2^- species are known for the fluoride;[20] likewise a similar ion HCl_2^- has been identified in low temperature molten pyridinium chlorides.[21]

It can be seen from the above results that multinuclear NMR can indeed offer a novel view on equilibria in molten salt mixtures and can very efficiently complement studies of these systems by other physicochemical techniques. More detailed NMR studies of $MCl–BPCl–AlCl_3$ systems and others are underway at this time in our laboratory.

REFERENCES

[1]B. Tremillon and G. Letisse, *J. Electroanal. Chem.* 1968, **17**, 371.

[2]B. Tremillon and G. Letisse, *J. Electroanal. Chem.* 1968, **17**, 387.

[3]G. Torsi and G. Mamantov, *Inorg. Chem.* 1971, **10**, 1900.

[4]G. Toris and G. Mamantov, *Inorg. Chem.* 1972, **11**, 1439.

[5]L. G. Boxall, H. L. Jones and R. A. Osteryoung, *J. Electrochem Soc.* 1973, **120**, 223.

[6]R. J. Gale, B. Gilbert and R. A. Osteryoung, *Inorg. Chem.* 1978, **17**, 2728.

[7]R. J. Gale and R. A. Osteryoung, *Inorg. Chem.* 1979, **18**, 1603.

[8]J. S. Wilkes, J. A. Levitsky, R. A. Wilson and C. L. Hussey, *Inorg. Chem.* 1982, **21**, 1263.

[9]G. Mamantov and R. A. Osteryoung, *Characterization of Solutes in Nonaqueous Solvents* (Edited by G. Mamantov), Chap. 11. Plenum Press, New York (1978).

[10]A. Hjuler, A. Mahan, J. H. VonBarner and N. J. Bjerrum, *Inorg. Chem.* 1982, **21**, 402.

[11]A. I. Popov, *Pure and Aphl. Chem.* 1979, **51**, 101, and refs listed therein.

[12]J. D. Lin and A. I. Popov, *J. Am. Chem. Soc.* 1981, **103**, 3773.

[13]J. Robinson, R. C. Bugle, H. L. Chum, D. Koran and R. A. Osteryoung, *J. Am. Chem. Soc.* 1979, **101**, 3776.

[14]R. J. Gale, B. Gilbert and R. A. Osteryoung, *Inorg. Chem.* 1978, **17**, 2728.

[15]F. Taulelle, C. Piolet and B. Tremillon, *J. Electroanal. Chem.* 1982, **134**, 131.

[16]C. Piccini-Leopardi, O. Fabre and J. Reisse, *Org. Mag. Res.* 1976, **8**, 233.

[17]A. G. Ferridge and J. C. London, *J. Mag. Res.* 1978, **31**, 337.

[18]A. I. Popov, *Pure Appl. Chem.* 1975, **41**, 275.

[19]E. Rytter, H. A. Fye, S. J. Cyvin and B. N. Cyvin, *J. Inorg. Nucl. Chem.* 1973, **35**, 1185.

[20]J. H. Burns and W. R. Busing, *Inorg. Chem.* 1965, **4**, 1510.

[21]C. A. Angell and J. W. Shuppert, *J. Phys. Chem.* 1980, **84**, 538.

STEREOCHEMICAL NONRIGIDITY OF THE SQUARE COMPLEX (PPh₃)₂Pt(HgGePh₃)(GePh₃)

Yu. K. GRISHIN,* V. A. ROZNYATOVSKY and Yu. A. USTYNYUK
Department of Chemistry, Moscow State University, Moscow 117234, U.S.S.R.

and

S. N. TITOVA, G. A. DOMRACHEV and G. A. RAZUVAEV
Institute of Chemistry, Academy of Science of the U.S.S.R., Gorky, U.S.S.R.

Abstract—^{31}P, ^{195}Pt and ^{199}Hg NMR spectra of complex $(PPh_3)_2Pt(HgGePh_3)(GePh_3)$ (I) have been studied. The spectra at temperatures below $-40°C$ prove that (I) is a *cis*-isomer with the square-planar coordination of the Pt atom. The reversibility of temperature dependences of spectra, insensitivity of line shape to the solvent, concentration and presence of free phosphine establish the fluxional behaviour of (I). The activation parameters of the intramolecular rearrangement which is realized, most probably, through a digonal twist, are: $\Delta G_{298}^{\neq} = 51.5 \pm 2.9$ kJ/mol, $\Delta H^{\neq} = 59.3 \pm 2.9$ kJ/mol, $\Delta S^{\neq} = 26.2 \pm 9.7$ J/mol · K.

Bivalent Pd and Pt can form with phosphine ligands square-planar complexes $MX_2(PR_3)_2$ whose *cis*- and *trans*-isomers in solution are able to transform into one another.[1-4] Isomerization rate greatly depends on the medium. The process is catalyzed by very small admixtures of free phosphine. For platinum complexes it proceeds according to the intermolecular mechanism with the rupture of the Pt–P bond which manifests itself in the disappearance of ^{195}Pt–^{31}P satellites in the NMR spectra at fast-exchange limit. Isomerization is most likely to proceed via a five-coordinated intermediate in the form of a square pyramid belonging to stereochemically nonrigid structure[5,6] or via an ion intermediate.[3] The *bis*-(triphenylphosphine)nickel (II) complex $(PPh_3)_2NiCl_2$ is paramagnetic and has a tetrahedral structure.[7,8] But a number of four-coordinated complexes of Ni(II)[9,10] exist in solution as equilibrium mixtures of diamagnetic planar and paramagnetic tetrahedral isomers. In dilute solutions of inert solvents there occurs interconversion between planar and tetrahedral forms via a digonal twist. So, in the process of ligand exchange *cis-trans*-isomerization may proceed according to the intramolecular mechanism with a low activation barrier. For square complexes of platinum there has been suggested[11] such a mechanism for photochemical isomerization but hitherto no intra-

molecular isomerization processes have been revealed under thermal conditions. Teplova *et al.*[12] who investigated ^{31}P NMR spectra of four-nuclear complex of *cis*-$(PPh_3)_2Pt(HgMPh_3')(M'Ph_3')$, M, M' = Ge, Sn; Ph = C_6H_5, Ph$' = C_6F_5$, which have the distorted planar-square structure, suggested that they are susceptible to isomerization in solution. The present work contains the results of ^{31}P, ^{195}Pt, ^{199}Hg NMR investigations of a previously obtained[13] complex $(PPh_3)_2Pt(HgGePh_3)(GePh_3)$ (I).

EXPERIMENTAL

Complex I[13] was dissolved in pure THF and toluene and the solutions placed in sample tubes (10 mm and 8 mm O.D.) under vacuum. The concentration of the solutions of THF (pure and with the addition of 4 vol% of $(CD_3)_2CO$) ranged within 0.003–0.03 M. The solutions in toluene were close to a saturation at room temperature. PPh₃ was commercial (CHEMAPOL) and used without further purification, $Pt(PPh_3)_3$ and $Pt(PPh_3)_4$ were synthesized using a literature method.[14]

Proton decoupled ^{31}P (40.32 MHz), ^{199}Hg (17.84 MHz) and ^{195}Pt (21.41 MHz) FT NMR spectra were recorded on a multi-nuclear spectrometer JEOL FX-100 using from 8 to 16 K real points and applying digital quadrature detection and internal ^{2}D-lock.

^{31}P NMR spectra were obtained with 60° flip angle (22 μs), 5500 Hz frequency range from 1.5 to 3s acquisition time and pulse delay is using from 1000 to 25,000 transitions. ^{199}Hg NMR spectra

---

*Author to whom correspondence should be addressed.

were measured with 75° flip angle (24 μs), 20 KHz frequency range, *ca.* 0.4 s acquisition time, using from 60,000 to 190,000 transients. [195]Pt NMR spectra were taken with 75° flip angle (44 μs), 20 KHz frequency range, *ca.* 0.4 s acquisition time, using from 20,000 to 46,000 transients. Chemical shifts were measured from 80% H_3PO_4 (^{31}P NMR spectra), neat $(CH_3)_2Hg$ ([199]Hg NMR spectra) and saturated Na_2PtCl_6 solution in D_2O ([199]Pt NMR spectra) as external standards and are given on the δ-scale (the positive sign corresponds to a downfield shift) without corrections for bulk susceptibility. The temperature in the sample was controlled with an accuracy of ± 1°C.

RESULTS AND DISCUSSION

The parameters of ^{31}P, [199]Hg and [195]Pt NMR spectra are listed in Table 1. The proton decoupled ^{31}P and [199]Hg NMR spectra of complex I at temperatures below −40°C are given in Fig. 1(a) and 2(a). For isotopomers which do not contain magnetic metal isotopes ^{31}P atoms yield a spectrum of the AB type with a characteristic two-bond through metal coupling [2]J(P–P) unambiguously proving *cis*-configuration I with non-equivalent phosphorus atoms.[15] We failed to discover signals of the *trans*-isomer and if it is present in the solution its relative content cannot actually exceed 2–3%. In the ^{31}P NMR spectra one can distinctly see [195]Pt and [199]Hg satellites corresponding to the AB-parts of the ABM and ABMX systems from various isotopomers.† Of interest is the fact that

---

†In Fig. 1(a) the ABMX subspectrum is practically invisible, its observation calls for a more prolonged accumulation.

[199]Hg satellites are somewhat broadened ($\Delta v_{1/2} \approx 20$ Hz), so the two-bond P–P coupling in them is not resolved. When the temperature was lowered down to −80°C their line width slightly increased.

The broadening of the satellites may arise from relaxation of the [199]Hg via chemical shift anisotropy mechanism as it has been demonstrated for [195]Pt[16] and [205]Tl[17] and recently for [199]Hg.[18] The chemical shift anisotropy contribution to the [199]Hg spin-lattice relaxation in a linear mercury arrangement can be significant even at low magnetic field,[19] its effect becomes more substantial at low temperatures.

The [1]J(Pt–P) values of complex I (see Table 1) range within those typical of Pt(II) square complexes. These values imply that the $Hg(GePh_3)$ group has a smaller *trans*-influence than the $GePh_3$ group.[15] One should note a considerable difference of two [2]J(Hg–P) coupling, the *trans*-interaction manifests itself to a greater extent. The magnitude of this coupling constant may serve an independent indicator of mutual arrangement of mercury and phosphorus atoms. It has already been discovered that [2]J(Hg–P) *trans* and [2]J(Hg–P) *cis* in the iridium octahedral complex differ almost by 10 times.[20] This property is typical of other [2]J(M–P) and, in particular, of [2]J(P–P),[15] [2](Sn–P).[21,22] Two geminal couplings [2]J(Hg–P) in complex I which follows from the values of the averaged parameters of [199]Hg satellites spectra at fast-exchange limit, discussed below have opposite signs which is the case with [2]J(P–P)[15].

The [199]Hg-{^{1}H} NMR spectrum Fig. 2(a) and the [195]Pt-{^{1}H} NMR spectrum similar to it at low temperatures being a superposition of the M-parts of the ABM and ABMX systems provide addi-

---

Table 1. NMR-parameters for $(PPh_3)_2Pt(HgGePh_3)(GePh_3)$

Solvent	°C	Chemical shifts, ppm			Coupling constants, Hz			
		[31]P	[199]Hg	[195]Pt	[2]J(P–P)	[1]J(Pt–P)	[2]J(Hg–P)[c]	[1]J(Hg–Pt)
THF[a]	−49	49.1 34.3	−259.1	−4750	10.7	2762 ± 2 2503 ± 2	1878 ± 4 (trans) 328 ± 4 (cis)	8180 ± 20
	59	42.1	d,e	d	−	2621 ± 2	781 ± 2	d
Toluene[b]	−40	49.8 35.4	−281.0	−4733	10.5	2748 ± 3 2488 ± 3	1835 ± 6 (trans) 320 ± 6 (cis)	8130 ± 40
	90	43.4	−349.0	−4746	−	2614 ± 1	762 ± 1	8120 ± 20

a A concentration of 0.013 M. b For a saturated solution. c [2]J(Hg–P)*cis* and [2]J(Hg–P)*trans* have opposite sings (see the text). d Not measured. e −311 ppm at 25°C
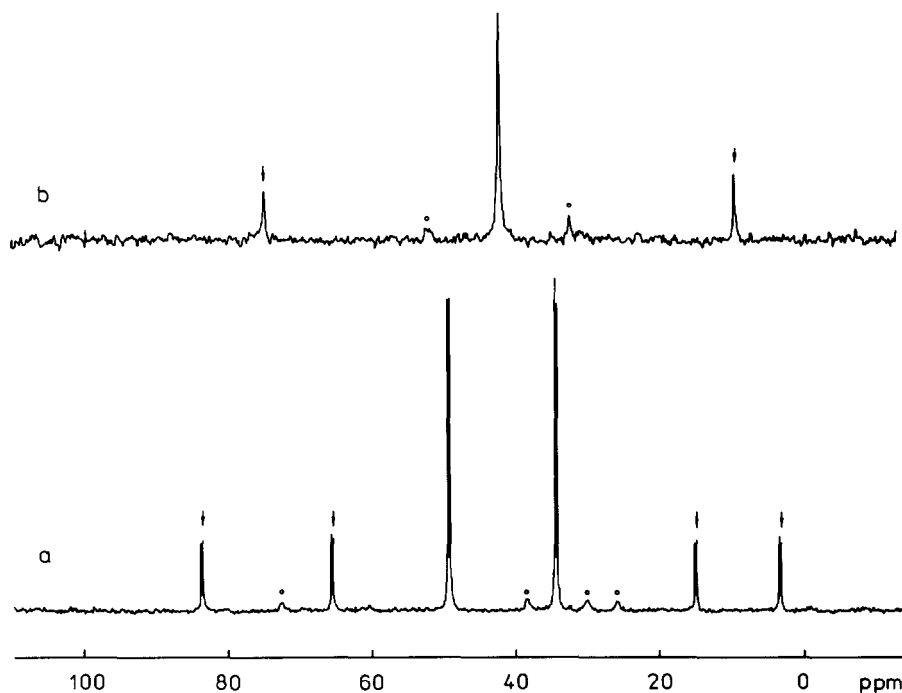
Fig. 1. $^{31}P-\{^1H\}$ NMR spectra of complex $(PPh_3)_2Pt(HgGePh_3)(GePh_3)$. (a) At $-49°C$. (b) At $+59°C$, 0.013 M, THF. Arrows point to the ^{195}Pt satellites, circles—to ^{199}Hg satellites.
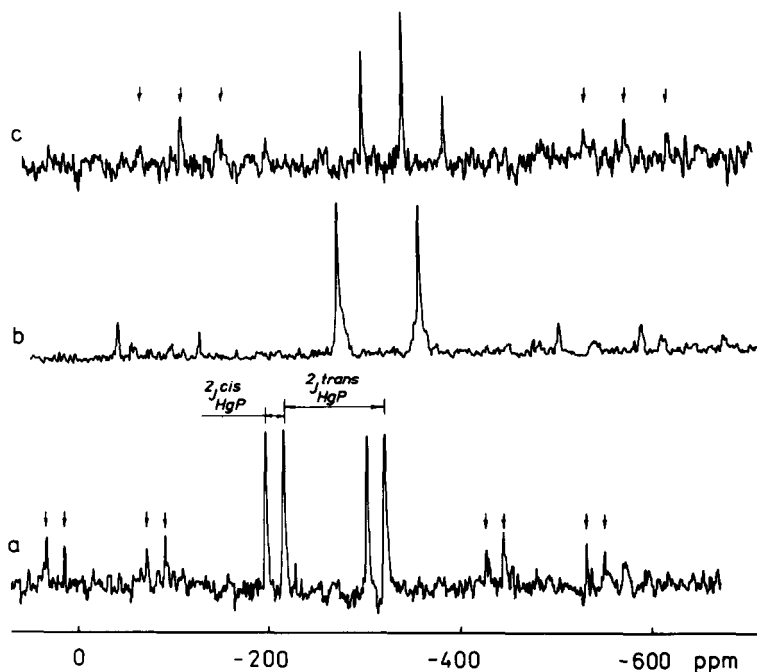
Fig. 2. $^{199}Hg-\{^1H\}$ NMR spectra of complex $(PPh_3)_2Pt(HgGePh_3)(GePh_3)$. (a) At $-40°C$, 0.03 M, THF. (b, c) At 25°C and 90°C, saturated solution on toluene. Arrows point to the ^{195}Pt satellites.

tional information on the structure of complex I and the presence of the Pt–Hg bond. Besides splitting due to the interaction with the ^{31}P nuclei of two phosphine groups in them there are coupling $^1J(Hg-Pt)$ exceeding 8000 Hz. Up to now such

constants have not yet been measured. As was observed in ^{31}P NMR spectrum discussed above the ^{199}Hg satellites in the ^{195}Pt NMR spectrum are broadened at low temperatures as well.

Data of the ^{199}Hg and ^{195}Pt chemical shifts for the

compounds containing Pt–Hg bonds are unknown. The ^{199}Hg chemical shifts change in a wide range depending on the metal type at the mercury atom and the substituent at the metal.[23-26] For digermyl mercury derivatives ^{199}Hg shielding changes by more than 1200 ppm, from 500 ppm for $(Et_3Ge)_2Hg$[25] down to -700 ppm for $(Ph_3Ge)_2Hg$.[26] Since ^{199}Hg chemical shifts in first approximation are additive the data obtained for I illustrate Pt(II) effect on ^{199}Hg shielding. Complex I is noted for a somewhat larger ^{195}Pt shielding with respect to *cis*-$PtCl_2(PEt_3)_2$[27] which corresponds to an upfield shift of 255–275 ppm. It is noteworthy that the replacement of one halogen for GeH_2Cl group[27] or $SnCl_3^-$ group[21] in *cis*-$PtCl_2(PEt_3)_2$ causes a still stronger upfield shift.

The spectra of complex I have a reversible temperature dependence which reveals the fluxional behaviour of the molecule in the NMR timescale. A temperature rise results in typical of exchange process evolutions of the resonance line shapes corresponding to rearrangements AB⇌BA, ABM⇌BAM and ABMX⇌BAMX. At 60°C the ^{31}P NMR spectrum (Fig. 1b) displays a rather narrow signal from two phosphine groups of the isomer which contains no ^{199}Hg and ^{195}Pt magnetic isotopes. The satellites of these isotopes under such fast exchange conditions are also averaged, but they have an asymmetric broadening which is related to the difference of ^1J(Pt–P) and ^2J(Hg–P) couplings for two phosphine groups. At the further increase of the temperature the satellites' widths become equal (90°C, toluene). The parameters under fast exchange are close to arithmetic mean values obtained from the corresponding low temperature parameters (see Table 1). At room temperature the ^{199}Hg NMR spectrum (Fig. 2b) corresponds to intermediate exchange rates, and at 90°C (Fig. 2c) there occurs an averaged spectrum including platinum satellites. Similar changes are observed in the ^{195}Pt NMR spectra.

The temperature dependence of the spectra, and the observation of spin–spin couplings between magnetic isotopes of phosphorus, platinum and mercury at fast-exchange limit show that the dynamic process in I is intramolecular. It is taking place without a rupture of Pt–P and Pt–Hg bonds. Good evidence in favour of the latter conclusion is the similarity of the temperature dependence of the line shape in the ^{31}P NMR spectra of very diluted solutions of I in two very different solvents—THF and toluene. This is also proved by the study of the line shape at several temperatures for solutions of

---

†According to the ^{31}P spectra at -80°C the PPh_3 content cannot exceed 1%.

I in THF at concentrations of 0.003 and 0.03 M testifying to the absence of concentration dependence of the exchange rate.

Finally, the catalytic mechanism should be ruled out. It might be supposed that in the solutions there exist small admixtures of free phosphine† which is a dissociation product of $Pt(PPh_3)_4$[28] employed in the synthesis of I. There have been investigated solutions of I with equimolar $Pt(PPh_3)_4$ and $Pt(PPh_3)_3$ additions, as well as with greater PPh_3 quantities. The experiments have shown that these substances whose content exceeds by far the amounts necessary for catalysis did not perceptibly influence the character and kinetic of the process in question.

Thus, the phenomenon described is conditional by the fluxional nature of complex I. The fact that the ^{31}P and ^{195}Pt chemical shifts and the coupling ^1J(Pt–P) at fast-exchange limit are close to the averaged values of parameters of low temperature spectrum shows that no paramagnetic tetrahedral complex is taking part in the equilibrium. The degenerate rearrangement involved is of intramolecular character, its probable mechanism being a digonal twist with the transition state close to the tetrahedral structure. Thus, $(PPh_3)_2Pt(HgGePh_3)(GePh_3)$ is a stereochemically nonrigid molecule.

We can also note the temperature dependence of ^{199}Hg chemical shift of I, which is *ca.* -0.5 ppm/K. Very high sensitivity of ^{199}Hg shielding of mercury compounds to medium and temperature are well-known.[29-31] The temperature dependence of δHg is rather complicated. For example, according to our data, for solution $[(CF_3)_3Ge]_2Hg$ and $(CF_3)_2Hg$ in toluene it is *ca.* -0.1 ppm/K, for $(Et_3Si)_2Hg$ in THF it is *ca.* 0.8 ppm/K. The ^{199}Hg signal of Et_2Hg (as a pure liquid) moves upfield in the temperature range from -50 to $+25$°C $(-0.3$ ppm/K).

From the temperature dependence of the ^{31}P line shapes (sub-spectrum AB, THF, 0.013 M) the following activation parameters were obtained: $\Delta G_{298}^{\neq} = 51.5 \pm 2.9$ kJ/mol, $\Delta H^{\neq} = 59.3 \pm 2.9$ kJ/mol, $\Delta S^{\neq} = 26.2 \pm 9.7$ J/mol·K. The positive values of $\Delta S^{\neq}$ obtained for I is in good agreement with the data of La Mar and Sherman[9] which show that the tetrahedral-planar equilibrium for complex $[RP(Ph)_2]_2NiX_2$ is characterized by a larger values of entropy for the tetrahedral state.

REFERENCES

1. L. Cattalini and M. Martelli, *J. Am. Chem. Soc.* 1969, **91**, 312.
2. P. Haake and R. M. Pfeiffer, *J. Am. Chem. Soc.* 1970, **92**, 4996.

3. D. G. Cooper and J. Powell, *J. Am. Chem. Soc.* 1973, **95**, 1102.

4. D. A. Redfield, L. W. Cary and J. H. Nelson, *Inorg. Chem.* 1975, **14**, 50.

5. E. L. Muetterties, *Rec. Chem. Prog.* 1970, **31**, 51.

6. J. P. Jesson and E. L. Muetterties, In *Dynamic Nuclear Magnetic Resonance Spectroscopy* (Edited by L. M. Jackman and F. A. Cotton), p. 253. Academic Press, New York (1975).

7. L. M. Venanzi, *J. Chem. Soc.* 1958, 719.

8. F. A. Cotton, O. D. Faut and D. M. L. Goodgame, *J. Am. Chem. Soc.* 1961, **83**, 344.

9. G. N. La Mar and E. O. Sherman, *J. Am. Chem. Soc.* 1970, **92**, 2691.

10. R. H. Holm, In *Dynamic Nuclear Magnetic Resonance Spectroscopy* (Edited by L. M. Jackman and F. A. Cotton), p. 317. Academic Press, New York (1975).

11. P. Haake and T. A. Hylton, *J. Am. Chem. Soc.* 1969, **84**, 3774.

12. T. N. Teplova, L. G. Kuzmina, Yu. T. Struckhov, V. I. Sokolov, V. V. Bashilov, M. N. Bochkarev, L. P. Maiorova and P. V. Petrovski, *Koordin. Khim.* 1980, **6**, 134.

13. S. N. Titova, V. T. Bychkov, G. A. Domrachev, T. N. Konkina, Yu. A. Sorokin and G. A. Razuvaev, *Zh. Obsh. Khim.* 1982, **52**, 1580.

14. L. Malatesta and C. Cariello, *J. Chem. Soc.* 1958, 2323.

15. P. S. Pregosin and R. W. Kunz, *³¹P and ¹³C NMR of Transition Metal Phosphine Complexes.* Springer-Verlag, Berlin (1979).

16. J.-Y. Lallemand, J. Soulié and J.-C. Cottard, *J. Chem. Soc. Chem. Commun.* 1980, 436.

17. F. Brady, R. W. Matthews, M. J. Forster and D.

G. Gillies, *J. Chem. Soc. Chem. Commun.* 1981, 911.

18. R. Benn, H. Günther, A. Maercker, V. Menger and P. Schnaitt, *Angew. Chem.* 1982, **94**, 314.

19. D. G. Gillies, L. P. Blaauw, G. R. Hays and A. D. H. Clague, *J. Magn. Res.* 1981, **42**, 420.

20. P. I. Van Bliet, J. Kuyper and K. Vrieze, *J. Organometal. Chem.* 1976, **122**, 99.

21. P. S. Pregosin and S. N. Sze, *Helv. Chim. Acta* 1978, **61**, 1848.

22. G. Buller, C. Eaborn and A. Pidcock, *J. Organometal. Chem.* 1979, **181**, 47.

23. M. J. Albright, *Abstracts of 19th Experimental NMR Conference.* Blacksburg, VA (1979).

24. S. Cradock and E. A. V. Ebsworth, N. S. Hosmane and K. M. Mackay, *Angew. Chem.* 1975, **87**, 207.

25. Yu. A. Strelenko, Yu. K. Grishin, V. T. Bychkov and Yu. A. Ustynyuk, *Zh. Obshch. Khim.* 1979, **49**, 1172, viz. *J. Gen. Chem. USSR*, 1979, **49**, 1025.

26. M. N. Bochkarev, N. L. Ermolaev, G. A. Razuvaev, Yu. K. Grishin and Yu. A. Ustynyuk, *J. Organometal. Chem.* 1982, **229**, C1.

27. D. W. W. Anderson, E. A. V. Ebsworth and D. W. H. Rankin, *J. Chem. Soc., Dalton* 1973, 2370.

28. C. A. Tolman, W. G. Seidel and D. N. Gerlach, *J. Am. Chem. Soc.* 1972, **94**, 2669.

29. M. A. Sens, N. K. Wilson, P. D. Ellis and J. D. Odom, *J. Magn. Res.* 1975, **19**, 323.

30. Yu. A. Strelenko, O. K. Sokolikova, Yu. K. Grishin and Yu. A. Ustynyuk, *Dokl. Akad. Nauk SSSR* 1980, **252**, 924.

31. Yu. K. Grishin, Yu. A. Strelenko, L. A. Margulis, Yu. A. Ustynyuk, L. S. Golovchenko, D. N. Kravtsov and A. S. Peregudov, *Dokl. Akad. Nauk SSSR* 1979, **249**, 892.

32. P. Peringer, *Inorg. Chim. Acta* 1980, **39**, 67.

NMR (^{195}Pt AND ^{13}C) CONTRIBUTION TO THE STUDY OF SOME Pt(II), Pt(IV) AND MIXED-VALENCE THIOAMIDO COMPLEXES

JEAN-MICHEL BRET, PAULE CASTAN,* GERARD COMMENGES and
JEAN-PIERRE LAURENT
Laboratoire de Chimie de Coordination du CNRS, Associé à l'Université Paul Sabatier, 205 route de
Narbonne, 31400 Toulouse, France

Abstract—The ^{195}Pt and ^{13}C chemical shifts (δ_{Pt} and δ_C) are reported for platinum(II), platinum(IV) and class II mixed-valence complexes, with general formula [PtL$_4$]X$_2$, *cis*- and *trans*-PtL$_2$X$_2$, PtL$_2$X$_4$ and Pt$_2$L$_4$X$_6$ (where L may be thiourea, 2-imidazolidine-thione, tetrahydro 2-pyrimidinethione, thiocaprolactam, pyridine-2-thione and tetramethylthiourea, and X may be Cl or Br). The ^{195}Pt chemical shifts can be understood in view of ^{13}C data in terms of variations of electronegativities and σ-donor abilities of ligands attached to platinum.

Thiourea and its derivatives have played an important rôle in the early development of platinum chemistry. The thiourea complexes of platinum(II) first synthesized by Kurnakov at the end of the last century have afforded a large contribution to the knowledge of substitution reactions in square planar complexes with a particular reference to the *trans*-effect of these ligands.[1] In spite of their interest, these complexes have not yet been included in the numerous ^{195}Pt resonance works,[2,3] and little[4-6] has been done on magnetic shielding of platinum nuclei in compounds involving *s*-bonded ligands, these being almost limited to thiocyanates.

Recently, we have isolated some complexes involving coordination of thiourea and related ligands to platinum(II) and platinum(IV).[7] Furthermore, halogeno complexes of general formula PtL$_2$X$_3$ (where L = thioamido ligands, X = halogen) have been obtained.[8-10] They are reminiscent of the PtA$_n$X$_3$ complexes (A = monodentate or bidentate aminoligands, n = 2 or 1, X = halogen) which, according to physical measurements,[11-18] and particularly to X-ray determination,[19] are actually considered as "class II mixed-valence compounds" according to the classification of Robin and Day.[20]

In fact, direct proofs (XPS data) of the mixed-valence character of the thiomido complexes (PtL$_2$X$_3$)$_2$ have been reported in a previous paper,[8,9] however the precise structure of these complexes seems to be dependent on experimental conditions, at least when ethylene thiourea is involved as a ligand. Synthetic details, largely discussed in our last paper,[9] suggest that two isomeric mixed-valence complexes may be obtained: either [PtL$_4$][PtX$_6$] or [PtL$_2$X$_2$][PtL$_2$X$_4$]. Intermediate compounds, isolated during the course of the preparation, support this assumption. From the great sensitivity of the ^{195}Pt chemical shift, it may be inferred that NMR may provide indirect informations on the nature of these compounds, at least in solution.

Finally this work is devoted to the NMR behaviour (^{13}C and ^{195}Pt) of the single-valence complexes of platinum(II) and platinum(IV) and to the mixed-valence compounds obtained with the reactive –NH–C=S group in ligands such as thiourea (tu), 2-imidazolidine-thione (etu) (ethylenethiourea), tetrahydro 2-pyrimidinethione (tpt), thiocaprolactam (tcp), pyridine-2-thione (pyt) and tetramethylthiourea (tmt).

EXPERIMENTAL

NMR measurements

All NMR spectra were recorded on a WH250 Brucker spectrometer operating in the Fourier transform mode and equipped with wide band probe (23–103 MHz).

The complexes were dissoved in DMSO-d_6, the ^{2}H resonance of which provided the field/frequency locking signal. ^{1}H noise modulated decoupling ensured complete proton decoupling of the spectra.

^{13}C *spectra*. Typical parameters for ^{13}C spectra were: pulse width 20 μsec, impulse delay 1 sec; 2000–5000 accumulations were usually necessary to achieve a satisfactory signal to noise ratio. The ^{13}C shifts were measured relative to the solvent DMSO-d_6, however, δ values reported are quoted with respect to TMS.

^{195}Pt *spectra*. Typical parameters for ^{195}Pt spectra were: pulse width 20 μsec, impulse delay 1 sec; 500–3000 transients were collected. All the previous papers reporting ^{195}Pt chemical shifts mention use of different compounds as reference zero. We have adopted the convention suggested by Kerrisson,[21] which conforms to that of the IUPAC using ^{195}Pt of H$_2$PtCl$_6$ in D$_2$O solution as external zero reference at 53 770 768 MHz. The dependence of the chemical shift of the solvent was examined in the case of H$_2$PtCl$_6$ by use of solutions in DMSO-d_6.

Solutions for NMR spectra were nearly saturated and data were collected on freshly prepared samples. The data given were quite reproducible and there was no evidence of solvolysis or decomposition of the complexes during the course of the measurements.

The chemical shifts are given in Tables 1–3. A *positive* shift implies that the sample resonance occurs at a *higher frequency* and that the ^{195}Pt nucleus is less shielded than in reference.

Preparation of the complexes

The platinum complexes were prepared as previously described.[7-9] Their purities were checked by chemical analysis, IR, NMR and also XPS spectroscopy for the mixed-valence compounds.

*Author to whom correspondence should be addressed.

Table 1. ^{195}Pt^a and ^{13}C^b (C=S) chemical shifts of platinum(II) complexes in DMSO solution

Ligands		tu	etu	ptu	tcp	pyt	tmtu	Assignment
	^{13}C (C=S)	183.4	184.5	176.9	209.7	177.6	192.8	
Complexes	^{13}C (C=S)	174.3	173.5	167.9	155.2	161.9	176.9	
PtL$_2$Cl$_2$	^{195}Pt	-3483	-3421	-3432	-3611	-3420	-3389	trans
		-3779	-3697	-3738		-	-	cis
	^{13}C (C=S)	175.3	175.0	168.5	157.2	165.2	180.0	
PtL$_2$Br$_2$	^{195}Pt	-3793	-3722	-3771	-	-	-	trans
		-3980	-3872	-3929	-3875	-3946	-3930	cis
[PtL$_4$]Cl$_2$	^{13}C (C=S)	179.4	181.6	169.9	197.6	174.4	183.8	
	^{195}Pt	-4045	-3882	-3883	-3970	-3993	-3928	

^{a}In ppm relative to H$_2$PtCl$_6$ in D$_2$O.
^{b}In ppm relative to TMS.

Table 2. ^{195}Pt^a and ^{13}C^b chemical shifts of platinum(IV) complexes in DMSO solution

Ligands		etu	tmtu	Assignment
	^{13}C (C=S)	184.5	192.8	
Complexes	^{13}C (C=S)	157.7	156.2	[PtL$_4$Cl$_2$]$^{2+}$
PtL$_2$Cl$_4$	^{195}Pt	+430	+430	[PtCl$_6$]$^{2-}$
		-3867	-3887	[PtL$_4$Cl$_2$]$^{2+}$
	^{13}C (C=S)	164.2	170.9	[PtL$_4$Br$_2$]$^{2+}$
PtL$_2$Br$_4$	^{195}Pt	-1430	-1434	[PtCl$_6$]$^{2-}$
		-3939	-3858	[PtL$_4$Br$_2$]$^{2+}$

^{a}In ppm relative to H$_2$PtCl$_6$ in D$_2$O.
^{b}In ppm relative to TMS.

RESULTS

Platinum(II) compounds. On the basis of IR and NMR data, it has been already inferred that, in the platinum(II) complexes, coordination of the thio-amido ligands occurs through the sulphur atom.[7,22-24] This bonding scheme has been definitively established by X-ray determination in the case of the (PtL$_4$)Cl$_2$ complexes (L = thiourea or dimethylthiourea).[25,26]

The data reported in Table 1 afford a new proof of the occurrence of a Pt–S bond in the PtL$_2$X$_2$ complexes as well as in the (PtL$_4$)Cl$_2$ ones since, in all cases, the C=S nucleus suffers an important high field shift with respect to the free ligand. Concerning the

configuration of the PtL$_2$X$_2$ complexes, very few data have been published. They are essentially deduced from far IR spectra. The presence of two ν(Pt–Cl) bands in the range of 300 cm^{-1}, split by 15–30 cm^{-1}, is taken as a proof for the *cis*-configuration.

Bearing in mind that interconversion between *cis* and *trans* isomers may occur quite readily in solution and that this study may not very easily be extended to the solid state, the ^{195}Pt resonance spectra for some of the PtL$_2$Cl$_2$ complexes herein investigated display two lines separated by *ca.* 290 ppm. These lines are attributed to the *cis* and *trans* isomers.

Considering the results already obtained for the

Table 3. ^{195}Pt^a and ^{13}C^b (C=S) chemical shifts of mixed-valence complexes in DMSO solution

Ligands			tu	etu	ptu	tcp	pyt	tmtu	Assignment
Complexes	^{13}C (C=S)		183.4	184.5	176.9	209.7	177.6	192.8	
	^{13}C (C=S)		175.3	181.1	170.0	196.9	174.4	184.0	
[PtL$_4$][PtCl$_6$]	^{195}Pt		+430	+430	+430	+433	+431	+430	[PtCl$_6$]$^{2-}$
			−3975	−3859	−3885	−	−3930	−3915	[PtL$_4$]$^{2+}$
[PtL$_4$][PtBr$_6$]	^{195}Pt		−1430	−1430	−1429	−1430	−1430	−1430	[PtBr$_6$]$^{2-}$
			−4009	−3886	−3926	−3960	−3957	−3930	[PtL$_4$]$^{2+}$
[PtL$_2$Cl$_2$][PtL$_2$Cl$_4$]	^{13}C			174.2				177.5	PtL$_2$Cl$_2$
				157.1				158.0	[PtL$_4$Cl$_2$]$^{2+}$
	^{195}Pt			+430				+425	PtCl$_6$$^{2-}$
				−3421				−3423	PtL$_2$Cl$_2$
				−3844				−3887	PtL$_4$Cl$_2$$^{2+}$

^{a}In ppm relative to H$_2$PtCl$_6$ in D$_2$O.
^{b}In ppm relative to TMS.

(R$_3$P)$_2$PtCl$_2$[27,28] and the low field shift (ca. 500 ppm observed between the *trans* complex and its *cis*-homologue, and those of Goodfellow et al.[29] for a series of trimethyl phosphine and related ligands complexes, we attribute the lines which appear at about 3700 and 3900 ppm to the *cis* isomers in the PtL$_2$Cl$_2$ and PtL$_2$Br$_2$ complexes, respectively.

While no significant changes in the platinum-ligand bond strength occur by replacement of a ligand by another, quite similar δ values are observed for all the *cis* (or *trans*) complexes except for the thio-caprolactam complexes. In this case, the only line observed strictly lies between the values expected for a *cis* and a *trans* isomer, respectively. Moreover the δ ^{195}Pt change (264 ppm) in going from this chloro complex to the *cis*-bromo complex is consistent neither with *cis* configuration ($\Delta\delta$ ^{195}Pt ca 180 ppm) nor *trans* configurations ($\Delta\delta^{195}$Pt ca. 315 ppm). This behaviour may be related to the steric hindrance of the thiocaprolactam ring which distorts the interbond angles from the idealized right-angle square planar geometry. Similar effects have been already observed for platinum in cycloalkanes derivatives[27] and for other heavier nuclei such as ^{207}Pb.[27]

Platinum(IV) compounds. We succeeded in preparing four complexes which have been identified by chemical analysis, IR spectroscopy and XPS measurements, as PtL$_2$X$_4$ species (X being Cl or Br and L = imidazolidine-2-thione and tetramethylthiourea).

Surprisingly, the ^{195}Pt resonance spectra of these species comprise two lines, indicating the occurrence of two types of platinum nuclei. In each case the shift of the low-field signal is identical with the shift of the corresponding [PtX$_6$]$^{2-}$ entity (+430 ppm for chloro and −1430 ppm for bromo complexes). It is very likely that when a PtL$_2$X$_4$ complex is in solution, a Pt(II)-catalysed Pt(IV) substitution reaction occurs, attended by the formation of a [PtX$_6$]$^{2-}$ [PtL$_4$X$_2$]$^{2+}$ species. This type of reaction has been recently de-

scribed by Scott.[30] Another possible explanation would be the formation of complexes in which one or more solvent molecules would have been introduced in the coordination sphere. Due to the fact that similar data have been obtained in two solvents (DMSO and DMF), we consider this possibility as unlikely. At first sight, one may consider that the chemical shift (ca. −3800 ppm) attributed to the platinum nucleus in the [PtL$_4$X$_2$]$^{2+}$ entity, is rather low for a platinum(IV). However, it is not unusual that the resonance of a platinum(IV) species occurs at a lower field than that of a platinum(II) analogue. The simplest example of such a behaviour refers to the couple [PtCl$_6$]$^{2-}$ (δ ^{195}Pt = 0 ppm in D$_2$O), [PtCl$_4$]$^{2-}$ (δ ^{195}Pt = −1620 ppm in D$_2$O).

The ^{13}C spectra show one signal only for the C=S nucleus which is strongly shielded with respect to the free ligand.

Mixed-valence compounds. As already reported, two types of compounds have been obtained. Their mixed-valence nature has been unambiguously established from XPS measurements.

In the case of the [PtL$_4$][PtX$_6$] complexes, the analysis of the NMR spectra is straightforward since these spectra are merely the sum of the spectra relating to the isolated entities [PtL$_4$]$^{2+}$ and [PtX$_6$]$^{2-}$.

The behaviour of the other type of mixed-valence compounds is more surprising at first sight. Instead of the two lines expected on the basis of a [L$_2$PtCl$_2$][L$_2$PtCl$_4$] formulation, three lines are observed in the ^{195}Pt spectra. However, one of them (δ = 3421 ppm) is unambiguously attributable to the platinum(II) moiety [L$_2$PtCl$_2$]. Accordingly, the remaining two lines (δ ^{195}Pt = + 430 and − 3844 ppm) would be due to the platinum(IV) moiety which would give rise in solution to a redistribution reaction analogous to the reaction mentioned for the Pt(IV) complexes (*vide supra*). This behaviour is not surprising since the specific character of mixed-valence complexes is known to disappear in solution where

their component entities recover their individuality. The two lines observed for $\delta_{C=S}$ in the ^{13}C spectra support this assumption.

DISCUSSION

Viewing the whole set of data relating to ^{195}Pt resonance (Tables 1–3), some general remarks can be made.

First of all, the two isomers, *cis*- and *trans*-PtL$_2$X$_2$ are easily distinguished, as their related Pt resonances are separated by *ca.* 280 ppm (X = Cl) and *ca.* 180 ppm (X = Br). On the basis of the correlation between the wavelength absorption and the ^{195}Pt chemical shifts of the PtL$_2$X$_2$ complexes, the Pt lines are expected to move towards higher field when going from the chloro to the bromo complexes. This trend is actually observed; however, the difference is less pronounced for the *cis*-PtL$_2$X$_2$ than for the *trans* isomers. A similar observation has already been made in the case of a number of PtL$_2$X$_2$ complexes (L = SR$_2$, PR$_3$, AsR$_3$).

Theoretically, the magnetic shielding in a nucleus may be ascribed in terms of local "paramagnetic" σ_p, and diamagnetic σ_d contributions.[31–33] For metals, the dominance of the σ_p is well acknowledged and an evaluation of this term has been performed by Dean and Green[34] through a modification of Ramsey's equation. σ_p depends on (i) the asymmetry of the electronic distribution with the 5d and 6p orbitals of the platinum atom, (ii) the mean inverse cube of the distance between these electrons and the nucleus, (iii) the magnitude of the energy of the ligand field transition (ΔE). Assuming that changes in (i) and (ii) are small, a correlation between metal shielding and ΔE is expected but interpretations of ^{195}Pt chemical shift variations on this basis have met very limited success.[27,6] A possible interpretation is that changes in ΔE do not necessarily dominate changes in the ^{195}Pt shielding. Moreover, attempts to include other contributions such as changes in $\langle r^{-3} \rangle$ due to the contraction of 5d orbitals turns out very modestly rewarded.

This stated, we will use a more empirical approach based on the joint consideration of ^{195}Pt and ^{13}C data. In this respect, it is noteworthy that satisfactory correlations of δ ^{13}C with substituent electronegativities have been found in many series of organic compounds. Substituent inductive effects may primarily affect the diamagnetic term (σ_d) but electronic withdrawal by a substituent on platinum may also modify the electronic imbalance among valence orbitals and cause a change in the paramagnetic contribution.[35]

In our analysis, we have first to consider the rôle of the oxidation state. It is generally assumed that the magnitude of related contributions for platinum complexes is a few tens of ppm at most and may therefore be neglected;[36] nevertheless, the trend usually observed for greater shielding in Pt(IV) complexes than in Pt(II) complexes is explained on the basis of a contraction of Pt(IV) 5d orbitals with respect to Pt(II) ones due to the greater charge on the metal. However, this explanation does not hold for the couple [PtI$_6$]$^{2-}$/[PtI$_4$]$^{2-}$. Considering the three couples [PtX$_6$]$^{2-}$/[PtX$_4$]$^{2-}$ (X = Cl, Br, I), we suggest that the

changes in the ^{195}Pt chemical shifts are better related to the inductive effects of six and four halogens, respectively. The chemical shift difference between Pt(IV) and Pt(II) decreases when Cl is replaced by Br in accordance with a lowering of the substituent electronegativity. When this electronegativity is further decreased—(PtI$_6$)$^{2-}$/(PtI$_4$)$^{2-}$—the order of the chemical shifts is even reversed (− 6300 and − 5420 ppm, respectively).

Thus, it seems that the deshielding of the platinum nucleus is first due to the electronegativity of the group attached to platinum as this will affect the electron density around the nucleus and/or the electronic imbalance among valence orbitals.

To apply this approach to our complexes, we must notice that the thiourea ligands are neutral π acid, since sulphur has vacant d orbitals which can accept electron density from filled metal orbitals to form a kind of π bonding that supplements the σ bonding arising from lone-pair donation. In the case of etu and tmtu complexes, the two entities [Pt^{II}L$_4$]$^{2+}$ and [Pt^{IV}L$_4$Cl$_2$]$^{2+}$ display almost the same ^{195}Pt chemical shift, i.e. − 3882 and − 3844 ppm respectively, while the corresponding C=S shifts are noticeably different. When going from the free ligand L to the [Pt^{II}L$_4$]$^{2+}$ complex, the thiocarbonyl carbon suffers a small shielding (*ca.* 4 ppm) which contrasts with the strong effect (*ca.* 27 ppm) related to the [Pt^{IV}L$_4$Cl$_2$]$^{2+}$ complex. These effects are consistent with a lowering of the C=S bond order, the change being small in the former case and more pronounced in the latter.

This decrease in the thiocarbonyl bond order may be related to two causes: either the possible backdonation of metal electrons towards ligands or the increase of the σ donor ability of sulphur towards platinum(IV) with respect to platinum(II). Backdonation would imply a high electron density on the metal atom which is not consistent with a high oxidation state. Thus, an increase of the σ donor ability of sulphur seems likely and it is suggested that this effect would balance the inductive influence of the two chlorine atoms yielding almost equal charge densities around platinum(II) and (IV). It is noteworthy that a very similar behaviour is observed in the case of platinum(II) and platinum(IV) cyano complexes for which the C≡N nucleus is more shielded in [Pt(CN)$_6$]$^{2-}$ (δ ^{13}C *ca.* 85 ppm) than in [Pt(CN)$_4$]$^{2-}$ (δ ^{13}C *ca.* 125 ppm),[37] in agreement with a greater donor ability towards Pt(IV) than towards Pt(II).

In a family of platinum(II) compounds, the same trend is observed. The shielding of the ^{195}Pt nucleus is increased in going from PtL$_2$Cl$_2$ to PtL$_2$Br$_2$ and [PtL$_4$]$^{2+}$. This effect is consistent with an increase of the charge on the metal dependent upon a decrease of the ligands electronegativity which causes the metal-ligand bond to become more covalent.

The data observed for the ^{13}C chemical shifts are quite in agreement with those noted for ^{195}Pt ones. When comparing the $\delta_{C=S}$ changes in the same ligand family we can observe that increasing the shielding of the platinum atom causes a subsequent low field shift in the corresponding thiocarbonyl carbon atoms. This implies a greater charge transfer from sulphur towards platinum for PtL$_2$Cl$_2$ than for the other compounds, observable either by ^{195}Pt or by ^{13}C NMR spectroscopy.

REFERENCES

[1] F. R. Hartley, *The Chemistry of Platinum and Palladium.* Applied Science, London (1973).

[2] R. Garth Kidd and R. J. Goodfellow, In *NMR and the Periodic Table* (Edited by R. K. Harris and B. E. Mann). Academic Press, London (1978) (for general review of ^{195}Pt nuclear magnetic resonance).

[3] P. S. Pregosin, *Coord. Chem. Rev.* 1982, **44**, 247 (for general review of ^{195}Pt nuclear magnetic resonance).

[4] S. J. Andersson and R. J. Goodfellow, *J. Chem. Soc. Dalton Trans.* 1977, 1683.

[5] S. J. Andersson, P. L. Goggin and R. J. Goodfellow, *J. Chem. Soc. Dalton Trans.* 1976, 1959.

[6] W. McFarlane, *J. Chem. Soc. Dalton Trans.* 1974, 324.

[7] P. Castan and J.-P. Laurent, *Trans. Met. Chem.* 1980, **5**, 154.

[8] P. Arrizabalaga, P. Castan and J.-P. Laurent, *Chem. Phys. Lett* 1980, **76**, 548.

[9] J.-M. Bret, P. Castan and J.-P. Laurent, *Inorg. Chim. Acta* 1981, **51**, 103.

[10] J. -M. Bret, P. Castan and J.-P. Laurent, *Inorg. Chim. Acta* 1981, **54**, L237.

[11] R. J. H. Clark, M. L. Franks and W. R. Tromble, *Chem. Phys. Lett.* 1976, **41**, 287.

[12] R. J. H. Clark and P. Turtle, *J. Chem. Soc. Dalton* 1978, 1622.

[13] D. Layek and G. C. Papavassiliou, *Z. Naturforsch.* 1980, **35b**, 339.

[14] G. C. Papavassiliou and D. Layek, *Z. Naturforsch.* 1980, **35b**, 676.

[15] G. C. Papavassiliou, D. Layek and T. Theophanides, *J. Raman Spect.* 1980, **9**, 69.

[16] A. J. Cohen and N. Davidson, *J. Amer. Chem. Soc.* 1951, **73**, 1955.

[17] L. V. Interrante, K. W. Browall and F. P. Bundy, *Inorg. Chem.* 1974, **13**, 1158.

[18] N. Natsumoto, M. Yamashita and S. Kida, *Bull. Chem. Soc. Japan* 1978, **51**, 2334.

[19] C. Brosset, *Arkiv. Kemi, Mineral Geol.* 1948, **25A**, 19.

[20] M. B. Robin and P. Day, *Adv. Inorg. Chem. Radiochem.* 1967, **10**, 247.

[21] S. J. Kerrisson and P. J. Sadler, *J. Mag. Res.* 1978, **31**, 328.

[22] N. S. Kurnakov, *Isvest. Akad. Nauk SSSR* 1963, 57.

[23] T. Tarantelli and C. Furlani, *J. Chem. Soc. (A)* 1968, 1715.

[24] Yu. N. Kukushkin, V. V. Sibirskaya, V. N. Samuseva, V. V. Sturkov, V. G. Pogareva and T. K. Mikhal'chenko. *Zh. Obsch. Khim.* 1977, **47**, 1402.

[25] R. L. Girling, K. K. Chatterjee and E. L. Amma, *Inorg. Chim. Acta* 1973, **12**, 557.

[26] F. Bachechi, L. Zambonelli, G. Marcotrigiano, *J. Cryst. Mol. Struct.* 1977, **7**, 11.

[27] J. D. Kennedy, W. McFarlane, R. J. Puddephatt and P. J. Thompson, *J. Chem. Soc. Dalton Trans.* 1976, 874.

[28] D. W. Anderson, E. A. V. Ebsworth and D. W. Rankin, *J. Chem. Soc. Dalton Trans.* 1973, 2370.

[29] P. L. Goggin, R. J. Goodfellow, S. R. Haddock, B. F. Taylor and I. R. H. Marshall, *J. Chem. Soc. Dalton Trans.* 1976, 459.

[30] G. M. Summa and B. A. Scott, *Inorg. Chem.* 1980, **19**, 1079.

[31] N. F. Ramsey, *Phys. Rev.* 1950, **78**, 699.

[32] N. F. Ramsey, *Phys. Rev.* 1951, **83**, 540.

[33] N. F. Ramsey, *Phys. Rev.* 1952, **86**, 243.

[34] R. R. Dean and J. C. Green, *J. Chem. Soc. (A)* 1968, 3047.

[35] C. J. Jameson and H. S. Gutowsky, *J. Chem. Phys.* 1964, **40**, 1714.

[36] W. G. Schneider and A. D. Buckingham, *Discuss. Faraday Soc.* 1962, **34**, 147.

[37] C. Brown, B. T. Heaton and J. Sabounchei, *J. Organomet. Chem.* 1977, **142**, 413.

SOME NOVEL TRIORGANOTIN(IV) DERIVATIVES OF β, δ-TRIKETONES

ANIL KUMAR and B. P. BACHLAS*

Department of Chemistry, University of Rajasthan, Jaipur 302004, India

and

JEAN-CLAUDE MAIRE

Université de Droit, D'Economie et de Sciences D'Aix-Marseille, Facult'e des Sciences et
Techniques de Saint-Jéromé Laboratoire des Organometallique, 13397 Marseille Cedex 4,
France

Abstract—Thirty triorganotin(IV) derivatives of the type $R_3Sn(R'COCHCOCH_2COR'')$
and $[R_3Sn]_2$ ($R'COCHCOCHCOR''$) (where $R = CH_3$, C_2H_5, $n-C_3H_7$, $n-C_4H_9$, and C_6H_5
and $R' = R'' = CH_3$, C_6H_5 or $R' = C_6H_5$, $R'' = CH_3$) have been synthesised by the
interaction of R_3SnCl with mono- or disodium salt of 2, 4, 6-heptanetrione, 1-phenyl-1,
3, 5-hexanetrione and 1, 5-diphenyl-1, 3, 5-pentanetrione in 1:1 and 2:1 molar ratios,
respectively. The complexes have been examined by their molecular weight, IR, PMR and
elemental analyses and their tentative structures assigned. Both "Z" and "E" forms have
been identified in the 1:1 complexes in equilibrium with the enol form containing five
coordinate tin. The 2:1 derivatives contain one five- and other four coordinated tin(IV)
except the phenyl analogue where both the tins are five coordinated.

There has been an upsurge of interest in the
development of the chemistry of β,
δ-triketones,[1-15] their Schiff's bases[9,16] and
compartmental ligands.[17-19] These ligands
readily form homo- as well as hetero-bimetallic
complexes. However, no work appears to have
been done on the triorganotin(IV) derivatives of β,
δ-triketones. The work on diorganotin(IV) has
been recently completed in our laboratories.[20] In
the present communication we report the syntheses
and characterisation of thirty new derivatives of β,
δ-triketones.

EXPERIMENTAL

The syntheses of the ligands and their character-
isation are reported earlier.[21,22] All the reac-
tions were carried out under anhydrous conditions.
Carbon and hydrogen were analysed on a Col-

man Carbon–Hydrogen Analyser. IR spectra were
measured in Nujol mulls or neat between the range
of 4000–200 cm^{-1} using CsI optics on
Perkin–Elmer Model 577 spectrophotometer. The
PMR spectra were recorded on a Perkin–Elmer
R12B Spectrometer (60 MHz) in $CDCl_3$ or CCl_4
solutions using TMS as a reference.

Synthesis of trimethyltin -mono(2, 4, 6-*hepta-
netrionate*)

A benzene solution of trimethyltin chloride (0.01
mole) was added to the mono sodium salt of 2, 4,
6-heptanetrione (0.01 mole), prepared by the direct
interaction of the latter with sodium isopropoxide
(0.01 mole) in benzene. The mixture was refluxed
for 2 hr. The sodium chloride so formed was
filtered out and the solvent stripped off under
vacuum.

The complex is red viscous liquid which solidifies
on keeping. It is soluble in chloroform and other
polar and non-polar solvents. The compound de-
composes above 150°C. Found: Mol. Wt., 284; C,

*Author to whom correspondence should be ad-
dressed.

A. KUMAR *et al.*

Table 1. Preparation and properties of triorganotin(IV)-mono(β, δ-triketonates)

	Wt. of R_3SnCl* (g)	Wt. of ligand* (g)	Colour and state	Yield (g)	M.P. °C	% of C Found (Calc.)	% of H Found (Calc.)	% of Sn Found (Calc.)	Mol.Wt. in freezing benzene Found (Calc)
(i) $(CH_3)_3Sn(CH_3COCHCOCH_2COCH_3)$	2.98	2.13	Red solid	3.31	Decompose 150	39.02 (39.39)	5.69 (5.94)	38.38 (38.92)	284 (304)
(ii) $(C_2H_5)_3Sn(CH_3COCHCOCH_2COCH_3)$	1.20	0.71	Red viscous liquid	1.34	-	-	-	34.03 (34.20)	320 (347)
(iii) $(\underline{n}-C_3H_7)_3Sn(CH_3COCHCOCH_2COCH_3)$	1.41	0.71	Red viscous liquid	1.44	-	-	-	30.11 (30.34)	366 (391)
(iv) $(\underline{n}-C_4H_9)_3Sn(CH_3COCHCOCH_2COCH_3)$	1.62	0.71	Light red viscous liquid	1.99	-	-	-	27.25 (27.52)	408 (431)
(v) $(C_6H_5)_3Sn(CH_3COCHCOCH_2COCH_3)$	1.92	0.71	Yellow brown viscous liquid	2.13	-	60.82 (61.13)	4.63 (4.92)	23.92 (24.16)	465 (491)
(vi) $(CH_3)_3Sn(C_6H_5COCHCOCH_2COCH_3)$	1.99	2.04	Light brown solid	3.22	90	48.79 (49.09)	5.21 (5.49)	32.18 (32.34)	349 (367)
(vii) $(C_2H_5)_3Sn(C_6H_5COCHCOCH_2COCH_3)$	1.20	1.02	Brown solid	1.92	130	-	-	28.72 (29.01)	382 (409)
(viii) $(\underline{n}-C_3H_7)_3Sn(C_6H_5COCHCOCH_2COCH_3)$	1.41	1.02	Light red crystalline solid	2.14	100	55.61 (55.90)	6.96 (7.14)	26.27 (26.32)	430 (451)

	Compound		Physical state		m.p. (°C)	C% Found (Calcd)	H% Found (Calcd)	Sn% Found (Calcd)	Mol. wt. Found (Calcd)
(ix)	$(n\text{-}C_4H_9)_3Sn(C_6H_5COCHCOCH_2COCH_3)$	1.62	Brown viscous liquid	2.25	-	-	-	24.28 (24.06)	468 (493)
(x)	$(C_6H_5)_3Sn(C_6H_5COCHCOCH_2COCH_3)$	1.92 / 1.02	Dirty yellow solid	2.51	>300d	64.85 (65.13)	4.58 (4.73)	21.90 (21.45)	526 (553)
(xi)	$(CH_3)_3Sn(C_6H_5COCHCOCH_2COC_6H_5)$	0.99 / 1.33	Yellow crystalline solid	1.92	95	55.53 (55.98)	5.28 (5.16)	28.02 (27.65)	402 (429)
(xii)	$(C_2H_5)_3Sn(C_6H_5COCHCOCH_2COC_6H_5)$	1.20 / 1.33	Brown solid	2.07	128	58.35 (58.63)	5.72 (5.98)	25.39 (25.18)	-
(xiii)	$(n\text{-}C_3H_7)_3Sn(C_6H_5COCHCOCH_2COC_6H_5)$	1.41 / 1.33	Yellow crystalline solid	2.26	102	60.29 (60.84)	6.52 (6.67)	22.95 (23.12)	491 (513)
(xiv)	$(n\text{-}C_4H_9)_3Sn(C_6H_5COCHCOCH_2COC_6H_5)$	1.62 / 1.33	Brown viscous liquid	2.12	-	-	-	21.49 (21.37)	424 (555)
(xv)	$(C_6H_5)_3Sn(C_6H_5COCHCOCH_2COC_6H_5)$	1.62 / 1.33	Creamish solid	2.52	did not melt up to 360	68.12 (68.32)	6.02 (6.22)	19.46 (19.28)	587 (615)

* Both the reactants were taken in 1:1 molar ratio and refluxed for two hours.

Table 2. Preparation and properties of bis[triorganotin(IV)]-mono(β, δ-triketonates)

	Wt. of R_3SnCl* (g)	Wt. of ligand* (g)	Colour and state	Yield (g)	M.P. °C	% of C Found (Calc.)	% of H Found (Calc.)	% of Sn Found (Calc.)	Mol.Wt. in freezing benzene Found (Calc.)
(i)	$[(CH_3)_3Sn]_2(CH_3COCHCOCHCOCH_3)$ 1.99	0.71	Red viscous liquid	1.52	-	33.12 (33.38)	5.46 (5.60)	50.30 (50.74)	449** (467)
(ii)	$[(C_2H_5)_3Sn]_2(CH_3COCHCOCHCOCH_3)$ 2.41	0.71	Red viscous liquid	2.35	-	-	-	42.82 (43.01)	528** (551)
(iii)	$[\underline{n}\text{-}C_3H_7)_3Sn]_2(CH_3COCHCOCHCOCH_3)$ 2.83	0.71	Red viscous liquid	2.62	-	-	-	37.13 (37.31)	-
(iv)	$[\underline{n}\text{-}C_4H_9)_3Sn]_2(CH_3COCHCOCHCOCH_3)$ 3.25	0.71	Red viscous liquid	3.12	-			32.71 (32.95)	689 (720)
(v)	$[(C_6H_5)_3Sn]_2(CH_3COCHCOCHCOCH_3)$ 2.71	0.50	Yellow solid	2.63	>360d	61.12 (61.47)	4.33 (4.55)	28.05 (28.25)	-
(vi)	$[(CH_3)_3Sn]_2(C_6H_5COCHCOCHCOCH_3)$ 1.99	1.02	Yellow crystalline solid	2.08	132	40.54 (40.80)	5.24 (5.32)	44.61 (44.80)	499 (529)
(vii)	$[(C_2H_5)_3Sn]_2(C_6H_5COCHCOCHCOCH_3)$ 2.41	1.02	Light red crystalline solid	2.65	94	46.58 (46.95)	6.18 (6.56)	38.19 (38.66)	586 (613)
(viii)	$[\underline{n}\text{-}C_3H_7)_3Sn]_2(C_6H_5COCHCOCHCOCH_3)$ 2.83	1.02	Orange solid	3.22	54	-	-	34.12 (34.00)	673 (698)

				m.p.	C	H	Sn	Mol. wt.
(ix)	$[(\underline{n}\text{-}C_4H_9)_3Sn]_2(C_6H_5COCHCOCHCOCH_3)$ 3.25 1.02	Red viscous liquid	3.70	–	–	–	30.56 (30.34)	749 (782)
(x)	$[(C_6H_5)_3Sn]_2(C_6H_5COCHCOCHCOCH_3)$ 3.85 1.02	Brown solid	4.15	>360d	63.61 (63.90)	4.58 (4.46)	26.21 (26.30)	854 (902)
(xi)	$[(CH_3)_3Sn]_2(C_6H_5COCHCOCHCOC_6H_5)$ 1.99 1.33	Creamish solid	2.56	127	46.13 (46.67)	4.92 (5.10)	40.14 (40.10)	563 (591)
(xii)	$[(C_2H_5)_3Sn]_2(C_6H_5COCHCOCHCOC_6H_5)$ 1.20 0.66	Light red crystalline solid	1.51	99	51.15 (51.52)	5.98 (6.26)	34.89 (35.11)	650 (676)
(xiii)	$[(\underline{n}\text{-}C_3H_7)_3Sn]_2(C_6H_5COCHCOCHCOC_6H_5)$ 2.83 1.33	Orange solid	3.53	105	–	–	31.24 (31.22)	–
(xiv)	$[(\underline{n}\text{-}C_4H_9)_3Sn]_2(C_6H_5COCHCOCHCOC_6H_5)$ 3.25 1.33	Red viscous liquid	3.95	–	–	–	28.43 (28.11)	805 (844)
(xv)	$[(C_6H_5)_3Sn]_2(C_6H_5COCHCOCHCOC_6H_5)$ 3.85 1.33	Yellow solid	4.19	>360d	67.91 (68.50)	4.08 (4.39)	24.57 (24.61)	–

*   Both the reactants were taken in 2:1 molar ratios and refluxed for four hours.

**   In boiling methanol, d for decomposed material.

39.02; H, 5.69; Sn, 38.38. Calc. for (CH₃)₃Sn(CH₃COCHCOCH₂COCH₃); Mol. Wt., 304; C, 39.39; H, 5.94; Sn, 38.92%.

Similarly the reactions of triethyltin-, tri-*n*-propyltin-tri-*n*-butyltin- and triphenyltin chlorides with 2, 4, 6-heptane-trione, 1-phenyl-1, 3, 5-hexanetrione and 1, 5-diphenyl-1, 3, 5-pentanetrione have been carried out. Their details of syntheses and identifications are given in Table 1.

Synthesis of bis[trimethyltin-mono(2,4,6-heptanetrionate)]

Trimethyltin chloride (0.02 mole) taken in 20 cm³ of benzene was added to the benzene suspension of disodium salt of 2, 4, 6-heptanetrione (0.01 mole) in isopropanol. The reaction mixture was allowed to reflux for 4–5 hr to complete the reaction. Sodium chloride formed during the reaction was removed by filteration. From the filtrate binary benzene-isopropanol azeotrope was fractionated out between the temperature range 68–80°C and the compound was isolated by removing the last traces of solvent under vacuum.

Bis(trimethyltin) -mono (2, 4, 6-heptanetrionate) was found to be soluble in methanol and other polar solvents but insoluble in non-polar solvents. It is monomeric in refluxing methanol and non-electrolyte in nitrobenzene. Found: Mol. Wt., 449; C, 33.12; H, 5.46; Sn, 50.30. Calc. for [(CH₃)₃Sn]₂(CH₃COCHCOCHCOCH₃); Mol. Wt., 467; C, 33.38; H, 5.60; Sn, 50.74%.

Likewise the reactions of triethyltin-, tri-*n*-propyltin tri-*n*-butyltin- and triphenyltin chlorides with disodium salt of 2, 4, 6-heptanetrione, 1-phenyl-1, 3, 5-hexanetrione and 1, 5-diphenyl-1, 3, 5-pentanetrione in 2:1 molar ratio have been carried out and their analytical results are given in Table 2.

RESULTS AND DISCUSSION

The triorganotin mono (β, δ-triketonates) and bis(triorganotin)-mono (β, δ-triketonates) are either yellow–brown coloured viscous liquids or crystalline solids, soluble in common organic polar and non-polar solvents, except the bis-derivatives of 2, 4, 6-heptanetrione. They decompose around 35–45°C. Both 1:1 and 2:1 products are monomeric in freezing benzene and non-electrolyte in nitrobenzene.

Infrared spectra of triorganotin-mono (β, δ-triketonates) show prominent bands in the region 3400–3200 and 1700–1500 cm⁻¹. The former has been assigned to the νOH. The strong intensity bands around 1680–1650 cm⁻¹ are assigned to the free carbonyl group. The band around 1600 cm⁻¹ has been assigned to the coordinated carbonyl groups.[7,23] The νC = O of the non-chelated carbonyl group is also slightly shifted in comparison to those of free ligands, presumably due to the shift in keto-enol equilibrium.

However in the IR spectra of bis-triorganotin)-mono (β, δ-triketonates) marked lowering in νC = O without splitting have been observed, indicating thereby coordination of all the carbonyl oxygens to the central tins.[23]

The presence of metal–oxygen[24] and metal–carbon is revealed by the presence of strong to medium intensity bands in the region 730–600 and 590–500 cm⁻¹, respectively. The presence of two bands in the latter region clearly reveals non-linear nature of -SnR₃ groups Tables 3 and 5.

The PMR spectra (Table 4) of triorganotin-mono (β, δ-triketonates) reveal the presence of tautomeric methine signal at δ, 7.15–7.3 ppm. This signal is a far more shifted downfield than the one due to free ligands. Such a situation has emerged because of the delocalisation of π-electrons (I),

(I)

"Z" form
(II)

"E" form
(III)
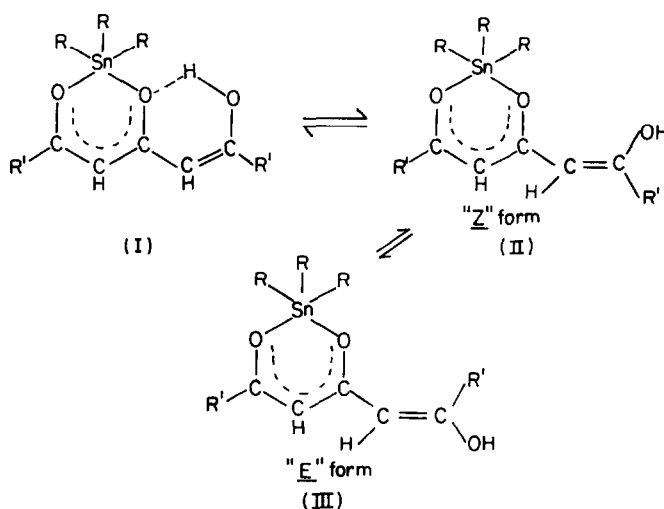
Table 3. Diagnostic IR bands of triorganotin-mono(β, δ-triketonates)

Compound	$\nu_{C=O}$	$\nu_{C=O}$	ν_{as} Sn–O	ν_s Sn–O	ν_{as} Sn–C	ν_s Sn–C
$R_3Sn(CH_3COCHCOCH_2COCH_3)$						
R = CH_3	1670s	1600s	720w	670b	620s	520m
R = C_2H_5	1675s	1608s	725w	675b	590w	525m
R = $\underline{n}$-C_3H_7	1660s	1600b	710w	670–660b	600m	540–510b
R = $\underline{n}$-C_4H_9	1650s	1590s	700w	680s	600w	510w
R = C_6H_5	1660s	1595s	715m	665m	610w	540s
$CH_3COCH_2COCH_2COCH_3$	1715s	–	–	–	–	–
$R_3Sn(C_6H_5COCHCOCH_2COCH_3)$						
R = CH_3	1670w	1600w	735s	580b	540w	450s
R = C_2H_5	1675w	1600m	720m	670m	585m	500w
R = $\underline{n}$-C_3H_7	1670s	1590s	720s	660m	580m	520m
R = $\underline{n}$-C_4H_9	1670s	1590s	700s	670m	610m	525w
R = C_6H_5	1680s	1600s	715s, 700m	670w	600s, 550w	500m, 475m
$C_6H_5COCH_2COCH_2COCH_3$	1700s	–	–	–	–	–
$R_3Sn(C_6H_5COCHCOCH_2COC_6H_5)$						
R = CH_3	1670w	1600m	720s	650w	560w	490s
R = C_2H_5	1680m	1590s	720m	640m	540m	510s
R = $\underline{n}$-C_3H_7	1675s	1590s	735s	660w	580m	520m
R = $\underline{n}$-C_4H_9	1670m	1590m	710m	600m	550w	470m
R = C_6H_5	1665m	1600s	690s	620w	550m	495w
$C_6H_5COCH_2COCH_2COC_6H_5$	1680s	–	–	–	–	–

Annotation: s = sharp, m = medium, b = broad and w = weak.

Table 4. PMR data for $R_3Sn(CH_3COCHCOCH_2COCH_3)$ at room temperature

Compound	Chemical shift in δ values			
	Aromatic	=CH	–CH_2	–CH_3[*]
$CH_3COCH_2COCH_2COCH_3$	–	5.28, 5.7	3.55, 3.85	2.1, 2.45
$(CH_3)_3Sn(CH_3COCHCOCH_2COCH_3)$	–	7.15, 5.8, 5.4	–	2.00
$(\underline{n}$-$C_4H_9)_3Sn(CH_3COCHCOCH_2COCH_3)$	–	7.3, 5.78 5.22	–	1.80–2.40
$(C_6H_5)_3Sn(CH_3COCHCOCH_2COCH_3)$	7.20–7.70	6.1, 5.4	–	2.00–2.20

* Methyl group at the terminal of the ligand molecule.

Table 5. Diagnostic IR bands of bis(triorganotin)-mono(β, δ-triketonates)

Compound	$\nu_{C=O}$	ν_{as} Sn–O	ν_s Sn–O	ν_{as} Sn–C	ν_s Sn–C
$[R_3Sn]_2$ $(CH_3COCHCOCHCOCH_3)$					
R = CH_3	1600s	730m	670b	600w	530–520b
R = C_2H_5	1600s	740m	670–660b	610w	530–520b
R = $\underline{n}$-C_3H_7	1600s	710m	680–670b	600s	510m
R = $\underline{n}$-C_4H_9	1600s	750m	680s	610b	530–510b
R = C_6H_5	1610s	730s, 700s	660m	600w	520w
$[R_3Sn]_2$ $(C_6H_5COCHCOCHCOCH_3)$					
R = CH_3	1600m	725s	680m	600w	550s
R = C_2H_5	1600s	720s	670b	600w	540s
R = $\underline{n}$-C_3H_7	1630s	710s	680s	580s	510m
R = $\underline{n}$-C_4H_9	1610s	720s	690s	600b	500b
R = C_6H_5	1600s	730s, 700s	680s	600w	550w, 500w
$[R_3Sn]_2$ $(C_6H_5COCHCOCHCOC_6H_5)$					
R = CH_3	1590s	700s	680m	540s	510w
R = C_2H_5	1600s	710m	670b	600b	520m
R = $\underline{n}$-C_3H_7	1610s	710m	660m	610s	510b
R = $\underline{n}$-C_4H_9	1600s	725s	680s	590w	530–510b
R = C_6H_5	1600s	720s	680m	600w	500s

Annotation: s = sharp, m = medium, b = broad and w = weak.

implying coordination of both the terminal and central carbonyl groups to the central tin.

The CH_2 signals were found at δ, 5.8 and 5.4 ppm, respectively is implying that the vinylic proton is under two magnetically non-equivalent environments, the "Z" and "E" forms. These two forms are in equilibrium. In the "Z" form the vinylic proton is nearer to the alkyl group (II) because of the shielding effect of the alkyl group while the peak appearing in the downfield region is attributed to the vinylic proton of "E" form in which it is deshielded (III).

The PMR chemical shift data of some of the bis(triorganotin)-mono (β, δ-triketonates) are given in Table 6. The methylene signals appearing at δ, 3.5–4.3 ppm in the unchelated ligands,[25] altogether disappear in the chelates, implying involvement of all the three carbonyl groups in chelation. The methine signals shift towards lower magnetic field as compared to free ligand, implying delocalisation of π-electrons throughout the framework. Further appearance of two methine signals at δ, 7.15–7.5 and 5.75–6.0 ppm indicate two types of methine protons. In the former case

(IV)

(R = alkyl group)

(V)
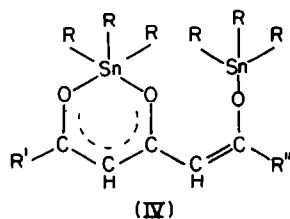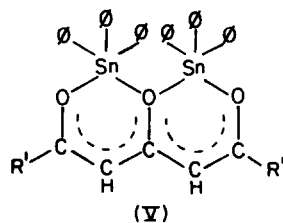
($\emptyset$ is phenyl)

Table 6. PMR data for $[R_3Sn]_2(\beta, \delta$-triketonates) at room temperature

Compound	Chemical shift in δ values			
	Aromatic	-CH	CH$_2$	CH$_3^*$
$\left[(CH_3)_3Sn\right]_2(CH_3COCHCOCHCOCH_3)$	-	7.15,5.75	-	1.7-2.20
$\left[(\underline{n}\text{-}C_3H_7)_3Sn\right]_2(CH_3COCHCOCHCOCH_3)$	-	7.20,5.95	-	1.95-2.30
$\left[(\underline{n}\text{-}C_4H_9)_3Sn\right]_2(CH_3COCHCOCHCOCH_3)$	-	7.5,6.05	-	1.90-2.40
$\left[(C_6H_5)_3Sn\right]_2(CH_3COCHCOCHCOCH_3)$	7.2-7.7	-	-	1.90-2.10
$\left[(CH_3)_3Sn\right]_2(C_6H_5COCHCOCHCOCH_3)$	6.8,7.4	6.0	-	1.80
$\left[(\underline{n}\text{-}C_3H_7)_3Sn\right]_2(C_6H_5COCHCOCHCOCH_3)$	7.35,7.95	6.0	-	1.80
$\left[(CH_3)_3Sn\right]_2(C_6H_5COCHCOCHCOC_6H_5)$	6.8,7.35	5.90	-	-
$\left[(\underline{n}\text{-}C_3H_7)_3Sn\right]_2(C_6H_5COCHCOCHCOC_6H_5)$	7.35,8.00	6.0	-	-

* Methyl group at the terminals of the ligand molecule.

one of the trialkyl tin forms a part of the chelated ring, embracing two oxygens of the central and terminal carbonyl groups, stabilized through the π-electron delocalisation, imparting quasi-aromaticity.[26,27] In such a situation the methine proton is deshielded (IV), allowing the formation of penta-coordinated tin, while the second trialkyltin is attached to the oxygen of the terminal carbonyl group and it is four coordinated.

Further in the complexes (V) of triphenyltin there is only one CH proton signal, implying that each of the triphenylstannyl groups attached to the two of the three carbonyl groups forming homo bimetallic complex. The explanation of this strange situation can be advanced on the basis of the $-$ I effect of the phenyl group, resulting in the enhancement of the electron accepting property of tin(IV). As a result of this central oxygen becomes three-coordinated and on account of the ring current both the CH protons are rendered magnetically equivalent. The methine signal also merges into the those of the phenyl groups.

REFERENCES

1. F. Sagara, H. Kobayashi and K. Ueno, *Bull. Chem. Soc., Japan* 1968, **41**, 266.
2. Y. Taguchi, F. Sagara, H. Kobayashi and K. Ueno, *Bull. Chem. Soc., Japan* 1970, **43**, 2470.
3. D. P. Murtha and R. L. Lintvedt, *Inorg. Chem.* 1970, **9**, 1532.
4. F. Sagara, H. Kobayashi and K.Ueno, *Bull. Chem. Soc., Japan* 1972, **45**, 794.
5. F. Sagara, H. Kobayashi and K. Ueno, *Bull. Chem. Soc., Japan* 1972, **45**, 900.
6. J. M. Kuszaj, B. Tomlonovic, D. P. Murtha, R. L. Lintvedt and M. D. Glick, *Inorg. Chem.* 1973, **12**, 1297.
7. F. Sagara, H. Kobayashi and K. Ueno, *Bull. Chem. Soc., Japan* 1973, **46**, 484.
8. R. L. Lintvedt, L. L. Borer, D. P. Murtha, J. M. Kuszaj and M. D. Glick, *Inorg. Chem.* 1974, **13**, 18.
9. B. K. Tomlonovic, R. L. Hough, M. D. Glick and R. L. Lintvedt, *J. Am. Chem. Soc.* 1975, **97**, 2925.
10. M. D. Glick, R. L. Lintvedt, T. J. Anderson and J. L. Mack, *Inorg. Chem.* 1976, **15**, 2258.
11. M. D. Glick and R. L. Lintvedt, *Structural and magnetic studies of polynuclear transition metal β-polyketonates*, Prog. Inorg. Chem. 1976, **21**, 233.
12. D. E. Fenton, S. E. Gayda and P. Holmes, *Inorg. Chim. Acta*, 1977, **21**, 187.
13. B. Bogdanovic and M. Yus, *Angew, Chem.* 1979, **91**, 742.
14. A. Kumar, H. Sharma, V. Sharma and B. P. Bachlas, *J. Ind. Chem. Soc.* 1982, **LIX**, 280.
15. R. L. Lintvedt, M. J. Heeg, N. Ahmad and M. D. Glick, *Inorg. Chem.* 1982, **21**, 2350.
16. T. Yano, T. Ushigima, M. Sasaki, H. Kobayashi and K. Ueno, *Bull. Chem. Soc., Japan* 1972, **45**, 2452.
17. R. L. Lintvedt, M. D. Glick, B. K. Tomlonovic and D. P. Gavel, *Inorg. Chem.* 1976, **15**, 1646.
18. M. D. Glick, R. L. Lintvedt, D. P. Gavel and B. Tomlonovic, *Inorg. Chem.* 1976, **15**, 1654.
19. R. L. Lintvedt and N. Ahmad, *Inorg. Chem.* 1982, **21**, 2356.
20. Y. Maire, Anil Kumar, H. Sharma, B. P. Bachlas and J. C. Maire, *Bull. Chim. Soc., France* (communicated).
21. J. N. Collie and A. A. B. Reilley, *J. Chem. Soc.* 1922, **121**, 1984.

22. M. L. Miles, T. M. Harris and C. R. Hauser, *J. Org. Chem.* 1965, **30**, 1007.
23. L. J. Bellamy, *The Infrared Spectra of Complex Molecules*. Methuen, London (1966).
24. M. M. McGrady and R. S. Tobias, *J. Am. Chem. Soc.* 1965, **87**, 1909.
25. D. Backer, C. W. Dudley and C. Oldham, *J. Chem. Soc.* A, 1970, 2605.
26. J. P. Collman, In *Adv. Chem. Ser. No.* 37, 1963, 78.
27. R. C. Mehrotra, R. Bohra and D. P. Gaur, *Metal β-Diketonates and Allied Derivatives*. Academic Press, London (1978).

ON THE TRI-*n*-OCTYLAMMONIUM CHLOROCOMPLEXES OF Sn(II) IN BENZENE SOLUTION

CLAUS FISCHER* and HARALD WAGNER

Central Institute of Solid State Physics and Material Research, Academy of Sciences of
the GDR, Dresden, GDR

and

VLADIMIR V. BAGREEV

V.I. Vernadsky Institute of Geochemistry and Analytical Chemistry, USSR Academy of
Sciences, Moscow, U.S.S.R.

Abstract—Loading experiments in the extraction system $TOAH^+Cl^-$/benzene–$SnCl_2$–HCl and measurements of the IR spectra and the specific conductivities κ of the extracts revealed the occurrence of two Sn(II)complexes: $TOAH^+SnCl_3^-$ (1:1-complex) and $(TOAH\ldots Cl\ldots HTOA)^+SnCl_3^-$ (2:1-complex). The shift of the νNH frequencies of these complexes with N-deuteration, expressed by the ratio $\nu HN/\nu ND$, amounts to 1.33 and 1.28 respectively. This agrees very well with corresponding values of complexes with analogous or similar composition.

A few studies have been published on the extraction of Sn(II) with long-chain amine salts from halide solution[1-3] and only in one of those studies[3] supposed extractable Sn(II) containing species were mentioned in the form of general gross formulas. All investigations were performed without exclusion of oxygen. This doubtless caused the formation of considerable quantities of Sn(IV),[4] and therefore the results of these studies cannot reflect the true behaviour of pure Sn(II) compounds.

The present work deals with the occurrence and the composition of tri-*n*-octylammonium chlorocomplexes of Sn(II). By analogy with preceding studies[5-7] investigations were performed including loading experiments in the system $TOAH^+Cl^-$/C_6H_6–$SnCl_2$–HCl (TOA = tri-*n*-octylamine) as well as IR spectroscopic and conductivity measurements of the Sn(II) containing extracts.

EXPERIMENTAL

The reagents $SnCl_2 \cdot 2H_2O$, HCl and C_6H_6 were of analytical grade. Tri-*n*-octylamine (pract., $d_4^{20}0.82$;

n_D^{20} 1.4476) was supplied by Fluka AG (Switzerland), deuterobenzene (Benzol-D$_6$, b.p.$_{760}$80.1°C; 99.2 ± 0.1 at% D) by the Zentralinstitut für Isotopen- und Strahlenforschung Leipzig, deuterium chloride (20% DCl in D_2O; 99.9%) by VEB Berlin-Chemie, Berlin-Adlershof.

The loading experiments, the preparation of the extracts and the measurements of the IR spectra and specific conductivities were carried out as described earlier.[5-7] All operations with Sn(II) were performed with freshly prepared solutions under an atmosphere of pure argon. The distribution coefficients $D_{Sn(II)}$ were determined by iodometric titration of aliquot parts of the aqueous phase after equilibration. The chloride concentrations of the organic phase were determined by argentometric titration according to Volhard's method after a preceding back extraction shaking 5 cm³ of the organic phase twice with 10 cm³ 1M H_2SO_4/1 M $HClO_4$ for 5 min and then boiling 3 cm³ of the back extract with 6 cm³ conc. HNO_3. Anhydrous $SnCl_2$ was prepared by reaction of $SnCl_2 \cdot 2H_2O$ with acetic anhydride.[8]

LOADING EXPERIMENTS AND PREPARATION OF THE EXTRACTS

Solutions of 0.125–1.76 M $SnCl_2$ in 6 M HCl were extracted by solutions of 0.25 M $TOAH^+Cl^-$

---

*Author to whom correspondence should be addressed.

in benzene (phase ratio $V_w/V_{org} = 1$; $t = 20$ min). The extraction isotherm is given in Fig. 1. It indicates the formation of a pure 1:1-complex at Sn(II) initial concentrations $\geqslant 0.5$ M under the extraction conditions used. This is confirmed by the molar ratio TOA: $Sn(II)_{(org)}$:$Cl_{(org)} = 0.98:1:2.79$, which approximates the theoretical ratio of the 1:1-complex 1:1:3 quite well. The corresponding molar ratio found at the Sn(II) initial concentration 0.125 M, 2.02:1:3.87, approximates the theoretical ratio of a 2:1-complex (2:1:4) indicating the formation of this complex at lower Sn(II) concentrations in the organic phase.

Using this knowledge of the extraction conditions extracts were prepared for the measurements of the IR spectra. The preparation conditions are given in Table 1. For measurements of the specific conductivity κ extracts No. 1 and No. 3 were also prepared with benzene as diluent and a Sn(II)

concentration of 0.1 M was set up by dilution with additional benzene (Table 1).

IR SPECTRA, CONDUCTIVITY MEASUREMENTS AND DISCUSSION

The IR spectra of the extracts were taken in the range 1800–3800 cm^{-1}. They are given in Fig. 2. The wave numbers of the νNH and νND absorptions are summarized in Table 2.

The IR spectra of the non-deuterated extract No. 1 with the stoichiometry TOA:Sn(II) = 1:1 exhibits a strong νNH band at 3030 cm^{-1} indicating only a weak cation–anion interaction by H-bond. The position of the band agrees very well with those of the 1:1-complexes of the trivalent ions of In, Ga and Fe, $TOAH^+MCl_4^-$[†], and is nearly identical with the νNH frequency of $TOAH^+CuCl_3^-$ (3015 cm^{-1}).[7] Furthermore there is complete agreement concerning the shift of this band with N-deuteration. The ratios νNH/νND for the 1:1-complexes of Sn(II), Cu(II) and Fe(III) are 1.33–1.34. Therefore the suggested structure of the 1:1-complex $TOAH^+SnCl_3^-$ is proved by the IR spectroscopic data as well as by the molar ratio of TOA, Sn(II) and Cl in the extract.

The stoichiometric data of the 2:1-extracts would permit complexes with the structures $(TOAH...Cl...HTOA)^+SnCl_3$ or $(TOAH^+)_2 SnCl_4^{2-}$. However, the peaks of the νNH vibration of the non-deuterated extract No. 3 at 2500, 2558 and 2613 cm^{-1} unambiguously confirm the structure $(TOAH ... Cl ... HTOA)^+SnCl_3^-$, because
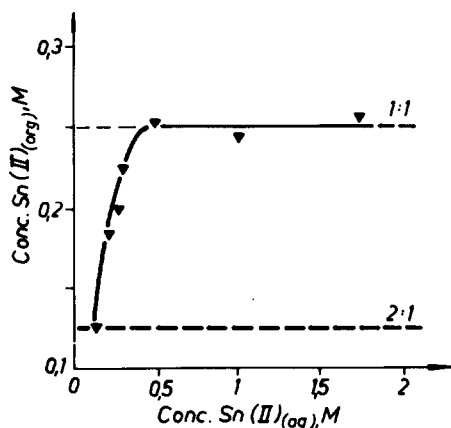
Fig. 1. Extraction isotherms for SnCl$_2$, extracted from 6 M HCl with 0.25 M TOAH$^+$Cl$^-$/benzene. (- - - - Molar ratio TOA:Sn(II)$_{org}$).

[†]Complexes are here and subsequently written in monomeric form.

Table 1. Preparation of the extracts for the IR spectra

No.	Sn(II) bearing complex	Extract composition, M			Diluent	Initial organic phase,M (H$_2$O or D$_2$O)	Initial aqueous phase,M	D$_{Sn(II)}$ detd.
		TOA	Sn(II)	Cl				
1	(TOAH$^+$)SnCl$_3^-$	0.25	0.254	0.71	C$_6$D$_6$	0.25 TOAH$^+$Cl$_6^-$	0.50 SnCl$_2$ 6 HCl	1.03
2	(TOAD$^+$)SnCl$_3^-$	0.25	0.254	0.71	C$_6$H$_6$/C$_6$D$_6$[+)]	0.25 TOAD$^+$Cl$_6^-$	0.50 SnCl$_2$ DCl	
3	(TOAH..Cl..HTOA)$^+$SnCl$_3^-$	0.25	0.124	0.48	C$_6$D$_6$	0.25 TOAH$^+$Cl$_6^-$	0.125 SnCl$_2$ 6 HCl	124
4	(TOAD..Cl..DTOA)$^+$SnCl$_3^-$	0.25	0.124	0.48	C$_6$H$_6$/C$_6$D$_6$[+)]	0.25 TOAD$^+$Cl$_6^-$	0.125 SnCl$_2$ DCl	

[+)] Extracts were duplicated with the diluents C$_6$H$_6$ and C$_6$D$_6$, resp.

it had been shown earlier,[7] that these frequencies are characteristic for the cation (TOAH ... Cl ... HTOA)$^+$. The shoulder at 3030 cm^{-1} indicates the presence of small quantities of 1:1-complex in the extract, due to the equilibrium

(TOAH ... Cl ... HTOA)$^+$SnCl$_3^-$ $\rightleftharpoons$ TOAH$^+$ SnCl$_3^-$ + TOAH$^+$Cl$^-$. The ratio vNH/vND amounts to 1.28, which is also in a very good agreement with other complexes involving the group (TOAH ... Cl ... HTOA)$^+$ (2:1-complex
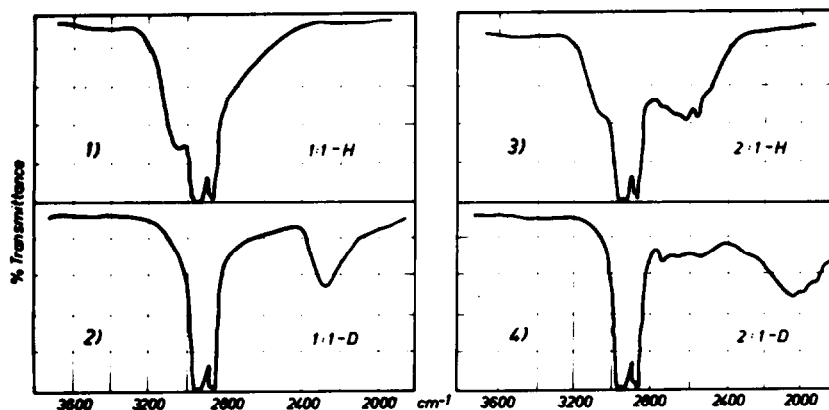
Fig. 2. IR spectra of the extracts. (The numbers refer to Table 1.)

Table 2. Wave numbers (in cm^{-1}) of the vNH and vND absorptions

No. (acc. to Table1)	Complex		v NH	v ND	v NH/ v ND
1	TOAH$^+$SnCl$_3^-$	1:1	3030 s		1.33
2	TOAD$^+$SnCl$_3^-$	1:1		2278 m	
3	(TOAH...Cl...HTOA)$^+$SnCl$_3^-$	2:1	2500 w, sh		
			2558 m		
			2613 m		
			(3030)vw, sh$^{+)}$		
4	(TOAD...Cl...DTOA)$^+$SnCl$_3^-$	2:1			1.28
				1992 m	
				2046 m	
				(2280) vw$^{+)}$	

$^{+)}$ Due to small quantities of 1:1-complex

Table 3. Specific conductivity data κ. (Metal concentration: 0.1 M; diluent: benzene)

Complexes	$\kappa/\Omega^{-1}\text{cm}^{-1}$/ at 25 ± 0.02 °C	
1:1-Complexes		
TOAH$^+$FeCl$_4^-$	2.75 x 10^{-5}	/5/
TOAH$^+$SnCl$_3^-$	2.18 x 10^{-5}	(extract No. 1)
TOAH$^+$CuCl$_3^-$	1.84 x 10^{-5}	/7/
2:1-Complexes		
(TOAH...Cl...HTOA)$^+$FeCl$_4^-$	6.02 x 10^{-5}	/5/
(TOAH...Cl...HTOA)$^+$SnCl$_3^-$	7.18 x 10^{-5}	(extract No. 3)
(TOAH$^+$)$_2$CuCl$_4^-$	1.54 x 10^{-5}	/7/

of Fe(III); 3:1-complexes of Cu, Zn and Co) and with the 2:1-complexes of Cu, Zn and Co.[7]

The specific conductivity data κ of the Sn(II) bearing extracts are given in Table 3 together with the data of the corresponding Fe(III) and Cu(II) bearing extracts determined earlier [5–7]. They confirm the statements on the structure of Sn(II) complexes deduced by the IR spectra.

The 1:1-complex $TOAH^+SnCl_3^-$ exhibits a value between those of the equally composed complex $TOAH^+CuCl_3^-$ and the corresponding complex $TOAH^+FeCl_4^-$. The κ value of the 2:1-complex $(TOAH \ldots Cl \ldots HTOA)^+SnCl_3^-$ is near to that of the complex $(TOAH \ldots Cl \ldots HTOA)^+FeCl_4^-$ having the same cation, but is clearly distinguished from that of the 2:1-complex $(TOAH^+)_2CuCl_4^{2-}$ according to its different structure.

REFERENCES

1. A. R. Selmer-Olsen, *Acta Chem. Scand.* 1966, **20**, 1621.
2. M. Y. Mirza, M. Ejaz, A. R. Sani, S. Ullah and M. Rashid, *Anal. Chim. Acta* 1967, **37**, 402.
3. B. N. Laskorin, V. S. Ulyanov, R. A. Sviridova, G. N. Melikhova and I. D. Akimova, *Zh. Prikl. Chim.* 1975, **48**, 1221.
4. I. S. Levin, V. A. Tarasova, V. A. Varnek and T. F. Rodina, *Zh. Neorg. Chim.* 1977, **22**, 761; I. S. Levin and V. A. Tarasova, *ibid.* 1977, **23**, 1324.
5. C. Fischer, H. Wagner and V. V. Bagreev, *J. Inorg. Nucl. Chem.* 1977, **39**, 513.
6. C. Fischer, H. Wagner and V. V. Bagreev, *J. Inorg. Nucl. Chem.* 1980, **42**, 891.
7. C. Fischer, H. Wagner and V. V. Bagreev, *Polyhedron*, to be published.
8. G. Brauer, *Handbuch der Präparativen Anorganischen Chemie*, Vol. 1, p. 646. F. Enke Verlag, Stuttgart (1960).

TETRAGONAL DISTORTIONS AND VIBRONIC COUPLING IN HEXAFLUORO NICKEL(II) AND COPPER (II) COMPLEXES

ROMAN BOČA*, PETER PELIKÁN, MARTIN BREZA and JÁN GAŽO

Departments of Inorganic Chemistry and Physical Chemistry, Slovak Technical University, CS-812 37 Bratislava, Czechoslovakia

Abstract—Two parameters, axial (R_a) and equatorial (R_e) metal–ligand distances, describe the tetragonal distortions of the NiF_6^{4-} and CuF_6^{4-} complexes under study. The experimental values of R_a plotted vs R_e exhibit a smooth curve type dependence valid for MF_6 chromophore of solid state compounds. In the model study it becomes explained by analyzing the shape of the adiabatic potential surface (APS) of the form of $E_T(R_a, R_e)$. Around the energy minima the map of numerical values (obtained by the quantum-chemical CNDO–UHF and INDO–UHF methods) was transformed to an analytic form from which the quantitative characteristics of APS were obtained in a new, simple way. The set of equatorial–axial parameters as well as the set of vibronic parameters were evaluated and discussed in more detail.

Fluoro complexes of M = Cr, Mn, Fe, Co, Ni, Cu and Zn belong to the transition metal complexes containing MX_6 chromophore in which the octahedral geometry is often disturbed so that tetragonal or orthorhombic distortions appear.[1–4] It was found that the mean axial (R_a) and the mean equatorial (R_e) metal ligand distances in these complexes are mutually dependent. In tetragonal bipyramids (the coordination number 4 + 2, 6 or 2 + 4), for a given chromophore, they show correlation along a smooth curve: the longer R_a, the shorter R_e, and vice versa.[5–8] Such a dependence R_a vs R_e also occurs in NiF_6^{4-} and CuF_6^{4-} coordination polyhedra in the solid state.[7,8] A more detailed understanding of particular factors operating in such distortion and dependences requires further re-solutions of several problems. Some of them form the subject of the present communication.

METHOD

Theoretical study of the stereochemistry of MF_6^{4-} type complexes poses the following problems.

(i) The shape of the adiabatic potential surface (APS) for the free MF_6^{4-} ion must be examined. It depends, in general, on fifteen degrees of freedom (internal coordinates). If only the tetragonal distortions within the symmetry point group of D_{4h} are considered, this number becomes reduced to

only two, so that APS will be considered as a simple function of the $E_T(R_a, R_e)$ type (E_T being the total molecular energy following from quantum-chemical calculations). For extreme distortions such as $R_a \to \infty$ the square-planar arrangement of the central atom, viz. MF_4^{2-} complex, is approached while for $R_e \to \infty$ the MF_2 molecule becomes linear. The numerical values of E_T were obtained by semiempirical CNDO/2 and INDO methods. The original CNDO/2 parametrization[9] extended to transition metals[10] for the Gouterman–Zerner basis set of valence atomic orbitals was used.[11] Additional Slater–Condon parameters[9,12] for the INDO method and some scaled radial integrals[13] were adapted in the program.[14] The self-consistent-field procedure for canonical molecular orbitals converges rapidly: *ca.* 13 cycles are required in order to obtain the electronic energy on the threshold of 10^{-4} eV.

(ii) The detailed form of APS depends on the electronic state of the system under study. For the non-degenerate state of A_{1g} a single energy minimum is exhibited in the octahedral geometry ($R_a^0 = R_e^0 = R_0$). For the doubly degenerate state of E_g a double energy minimum is found within the $E_T(R_a, R_e)$ picture. The first minimum corresponds to an elongated tetragonal bipyramid ($R_a^0 > R_e^0$) while the second minimum to its compressed form ($R_a^0 < R_e^0$).[3,5] The nature of this situation follows from the Jahn–Teller theorem or, more precisely, from the $E_g - e_g$ and $E_g - (a_{1g} + e_g)$ vibronic

---

*Author to whom correspondence should be addressed.

Table 1. Mutual relationships between equatorial–axial parameters and vibronic parameters in square bipyramidal systems

Equatorial – axial parameters	Vibronic parameters
$R_a^0 = (de - 2bf)/(4cf - e^2)$	
$R_e^0 = (be - 2cd)/(4cf - e^2)$	
$R_e = R_0 + (\sqrt{2}\,Q_1 + Q_2)/\sqrt{12}$	$Q_1 = 2(2R_e + R_a)/\sqrt{6} - R_0\sqrt{6}$
$R_a = R_0 + (\sqrt{2}\,Q_1 - 2Q_2)/\sqrt{12}$	$Q_2 = 2(R_e - R_a)/\sqrt{3}$
	$Q_3 = 0$
$k_{aa} = (\partial^2 E_T/\partial R_a^2) = 2c$	$T_{11} = (\partial^2 E_T/\partial Q_1^2) = (k_{ee} + 2k_{ae} + k_{aa})/6$
$k_{ee} = (\partial^2 E_T/\partial R_e^2) = 2f$	$T_{22} = (\partial^2 E_T/\partial Q_2^2) = (k_{ee} - 4k_{ae} + 4k_{aa})/12$
$k_{ae} = (\partial^2 E_T/\partial R_a \partial R_e) = e$	$T_{12} = (\partial^2 E_T/\partial Q_1 \partial Q_2) = (k_{ee} - k_{ae} - 2k_{aa})/6\sqrt{2}$
$(d_a)_e = (k^{-1})_{ae}/(k^{-1})_{ee} = -k_{ae}/k_{aa}$	$K_a = T_{11}$
$(d_e)_a = (k^{-1})_{ea}/(k^{-1})_{aa} = -k_{ae}/k_{ee}$	$K_e = (T_{22}^{(1)} + T_{22}^{(2)})/2$
	$Y = -T_{11}Q_1^0 - T_{12}Q_2^0$
	$Z = sT_{12}$
	$A = s(T_{12}Q_1^0 + T_{22}Q_2^0)$ $s = -1$ for $E_T^{(1)}$
	$B = -s(T_{22} - K_e)/2$ $s = +1$ for $E_T^{(2)}$

coupling, respectively, as it will be discussed below.

(iii) The nearest region of the individual minima may be described by an analytic form of APS which in the harmonic approximation takes the form:

$$E_T(R_a, R_e) = a + bR_a + cR_a^2 + dR_e + eR_aR_e + fR_e^2 \tag{1}$$

Then the equilibrium coordinates, R_i^0, and the harmonic force constants, k_{ij}, may be evaluated (Table 1).

(iv) The ability of a coordination polyhedron to undergo tetragonal distortions (called here its plasticity[2]) may be expressed using the interaction displacement coordinates, $(d_i)_j$; their expressions are listed in Table 1. Applying the minimum energy coordinate approach,[15,16] the interaction displacement coordinates measure in the internal coordinate space the change in remaining coordinates (say R_a), required to minimize the total energy, following a fixed displacement of a selected coordinate (say R_e).

(v) Starting from the octahedral geometry towards the dissociation limit cases (MF_4^{2-} or MF_2) a reaction path is questionable. First, the selected coordinate R_a was systematically displaced by a certain step of ΔR_a. Then the corresponding optimum value of R_e^{opt} was found so that the complex relaxed to the local energy minimum. Thus a valley

on APS was found. Pairs of values $\{R_a^c = R_a^0 + n\Delta R_a; R_e^{opt}\}$ correlate along a smooth curve, where with increasing R_a^c the value of R_e^{opt} decreases. The procedure was repeated for fixed displacements of R_e and thus the second part of the valley (or the correlation curve R_a vs R_e) was obtained.

(vi) The principal factors operative in the stabilization of the complex equilibrium geometry may be analyzed on the basis of the energy partitioning. The one-centre, E_A, and the two-centre, E_{AB}, terms easily can be re-summarized:

$$E_T = \sum_A E_A + \sum_{A<B} E_{AB} = E_{mono} + E_{L-L} + E_{M-L} \tag{2}$$

where E_{mono} means the total one-centre term, E_{L-L} is the ligand–ligand and E_{M-L} the metal–ligand energy term. The corresponding formulae for the CNDO–UHF and INDO–UHF methods used are described elsewhere.[17]

(vii) In order to re-derive an analytic form of the APS in the double minimum case of the E_g state, the following assumptions were accepted: the normal vibrations (Q_1—symmetric stretching, Q_2—tetragonal distortion, Q_3—orthorhombic distortion) were considered in the harmonic approximation, and the vibronic Hamiltonian included the $E_g - (a_{1g} + e_g)$ coupling up to quadratic terms. Then the resulting first-order analytic formula for
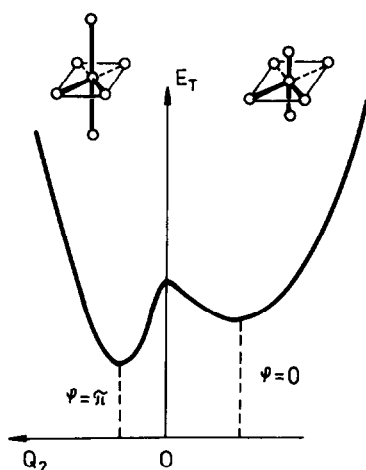
Fig. 1. A cut of the Mexican hat type APS for $Q_1 = $ const. and $Q_3 = 0$.

APS (see appendix) is:

$$E_T^{1,2}(Q_1, Q_2; Q_3 = 0) = E_T(Q_1^0, Q_2^0) + YQ_1 + \tfrac{1}{2}K_aQ_1^2$$
$$+ \tfrac{1}{2}(K_e + 2sB)Q_2^2 + s(A - ZQ_1)Q_2 \quad (3)$$

where $s = \pm 1$. The meaning of this formula is illustrated in Fig. 1. A simple fitting of the type of

$$E_T(Q_1, Q_2) = a' + b'Q_1 + c'Q_1^2$$
$$+ d'Q_2 + e'Q_1Q_2 + f'Q_2^2 \quad (4)$$

leads to the determination of a'–f' parameters, so that the elastic force constants K_a and K_e, as well as the vibronic constants Y, Z, A and B can be evaluated.

(viii) Finally, the harmonic approximation of the energy minima in the form (1) can be combined

Table 2. Fine mapping of the adiabatic potential surface $E_T(R_a, R_e)$ in the NiF_6^{4-} ion by the INDO method[a]

R_a	R_e				
m=1:	1.94	1.95	1.96	1.97	1.98
2.04	0.28803	0.30057	0.29762	0.27974	0.24752
2.03	0.28810	0.30268	0.30176	0.28589	0.25567
2.02	0.28181	0.29845	0.29957	0.28574	0.25754
2.01	0.26889	0.28762	0.29080	0.27902	0.25285
2.00	0.24908	0.26990	0.27517	0.26545	0.24133
1.99			0.25238	0.24475	0.22270
1.98				0.21664	0.19666
1.97				0.18080	0.22121
m=1:	1.98	1.99	2.00	2.01	2.02
2.00	0.24133	0.20336	0.15030		
1.99	0.22270	0.18523	0.19108		
1.98	0.19666	0.21870	0.22630	0.21830	0.19530
1.97	0.22121	0.24658	0.25571	0.24922	0.22773
1.96	0.24147	0.26838	0.27904	0.27408	0.25410
1.95	0.25537	0.28383	0.29604	0.29261	0.27415
1.94	0.26265	0.29267	0.30642	0.30454	0.28761
1.93	0.26301	0.29460	0.30991	0.30958	0.29420
1.92		0.28934	0.30623	0.30745	0.29362
1.91		0.27660	0.29506	0.29785	0.28557
m=3:	1.97	1.98	1.99	2.00	
2.00	2.95801	2.97017	2.96681	2.94855	
1.99	2.96230	2.97622	2.97464	2.95812	
1.98	2.95998	2.97569	2.97587	2.96112	
1.97	2.95078	2.96828	2.97026	2.95728	

[a] Total energy $E_T(R_a,R_e) = -5\,200.0 - E'$(eV), where E' is listed in the table, separately for the spin multiplicity of $m = 1$ and $m = 3$. R_a and R_e are in 10^{-10} m. Energy minima are underlined.

with the double minimum type of the analytic potential (3). Then, after simple algebraic operations, the one-to-one correspondence between the set of equatorial–axial parameters and the set of vibronic parameters can be obtained (Table 1).

RESULTS

The APS of the form $E_T(R_a, R_e)$ was mapped using the step of $\Delta R = 1$ pm (Table 2, for CuF_6^{4-} see Ref. 6). Nine or more points of E_T around the energy minimum were used in order to obtain the six constants a–f of eqn (1) applying the least-squares method. The high correlation coefficient for the two-dimensional paraboloid type regression (greater than 0.9999) indicated that the harmonic approximation was well fulfilled.

The principal results obtained for the $^3A_{1g}$ and ^1E_g states of the complex NiF_6^{4-} and for the ^2E_g state of the complex CuF_6^{4-} are collected in Table

3. Although the high-spin state is preferable for NiF_6^{4-}, the CNDO–UHF method yields only a poor value for the energy separation $\Delta = E_T(^1E_g) - E_T(^3A_{1g}) = 0.007$ eV in the optimum octahedral configuration. This failure vanishes if the INDO–UHF method is used: $\Delta = 2.782$ eV. The other quantities are less sensitive to the method (CNDO vs INDO) used. For example, in the CuF_6^{4-} complex the calculated minimum points (R_a^0, R_e^0) are (1.977, 1.984) and (1.958, 1.986) for the INDO method compared with (1.991, 1.964) and (1.954, 1.982) for the CNDO method.

The interaction displacement coordinates were used in the definition of the minimum energy coordinates:

$$D_a = R_a + (d_e)_a R_e$$
$$D_e = R_e + (d_a)_e R_a \qquad (5)$$

Table 3. Calculated characteristics of APS

Quantity	NiF$_6^{4-}$						CuF$_6^{4-}$	
	INDO			CNDO			CNDO	
	$^3A_{1g}$	^1E_g		$^3A_{1g}$	^1E_g		^2E_g	
	I=II	I	II	I=II	I	II	I	II
(1) Equatorial – axial parameters								
R_0	1.985	1.981		1.989	1.989		1.973	
R_a^0	1.985	2.030	1.929	1.989	2.032	1.944	1.991	1.954
R_e^0	1.985	1.954	2.005	1.989	1.965	2.010	1.964	1.982
E_{JT}	–	0.108	0.115	–	0.085	0.087	0.017	0.017
k_{aa}	67.250	63.325	71.750	66.864	64.964	70.566	73.897	76.462
k_{ae}	17.738	20.365	15.560	15.924	17.649	13.775	18.599	16.699
k_{ee}	152.250	152.233	153.483	149.364	146.161	151.365	167.496	168.763
$-(d_e)_a$	0.117	0.134	0.101	0.107	0.121	0.091	0.111	0.099
$-(d_a)_e$	0.264	0.322	0.217	0.238	0.272	0.195	0.252	0.218
(2) Vibronic parameters								
Q_1^0		-0.0030	-0.0031		-0.0037	-0.0038	-0.0009	-0.0009
Q_2^0		-0.0875	-0.0877		-0.0769	0.0761	-0.0321	0.0319
K_a	42.496	42.715	42.726	41.346	41.070	41.580	46.432	46.437
K_e	29.192	29.263		29.427	29.748		33.188	
Y	–	0.181	0.190	–	0.141	0.191	0.047	0.047
A	–	2.365	2.766	–	2.148	2.403	1.039	1.091
Z	0.001	0.615	0.657	0.034	0.167	0.417	0.130	0.101
B	–	1.129		–	0.898		0.399	

[a] $R_0, R_a^0, R_e^0, Q_1^0, Q_2^0$ are in units of 10^{-10} m; E_{JT} in eV; Y and A in 10^{10} eV.m^{-1}; $k_{aa}, k_{ae}, k_{ee}, K_a, K_e, Z, B$ in 10^{20} eV.m^{-2} .

For example, the value of $(d_e)_a = -0.117$ means that R_e will be compressed by 11.7% of the length, if R_a is stretched. Similarly, R_a would be compressed by 26.4% relative to a given stretching of R_e, as follows from the value of $(d_a)_e = -0.264$ for the complex NiF_6^{4-}. Therefore, the interaction displacement coordinates may be accepted as quantitative characteristics in describing the plasticity of coordiantion polyhedra (the ability to undergo tetragonal distortions) in the harmonic approximation. It seems (Table 3) that the first minimum (the elongated bipyramid) corresponds to a somewhat softened, more plastic complex compared with the second minimum (the compressed form).

To open discussion of calculated vibronic parameters it must be mentioned that the formula (3) represents a cut of a Mexican hat type[3,28] of the APS. If the calculated numerical map of the APS values is consistent with such an approximate analytic form of the APS, then some additional relations will hold: the same values of vibronic parameters K_a, Y, A and Z are to be obtained for both minima. This condition is satisfactorily fulfilled for CNDO calculations of CuF_6^{4-} and INDO calculations of NiF_6^{4-}. Moreover, the vibronic parameters presented for CuF_6^{4-} are not too far from those previously reported elsewhere.[19] That method, however, was rather time consuming as it was based on the non-linear regression and a complicated functional minimization. The non-zero values of Q_1^0 indicate that the actual form of the APS is more complex compared with the simple Mexican hat type with a warping (as considered, for example, in Ref. 18).

The calculated value of K_a (the rigidity against the a_{1g}-type stretching of Q_1) is significantly higher in comparison with K_e (the rigidity vs the e_g-type distortion of Q_2). Thus the Q_2 mode may be considered as a soft mode, so that the tetragonal distortion is preferable over the symmetric expansion (compression) of an octahedron. The linear vibronic constant Y (proportional to $\partial \hat{V}/\partial Q_1$) is significantly lower in comparison with A (proporitonal to $\partial \hat{V}/\partial Q_2$), so that the linear vibronic coupling $E_g - e_g$ predominates over the $E_g - a_{1g}$ admixture. Simultaneosly, the quadratic vibronic constant Z (proportional to $\partial^2 \hat{V}/\partial Q_1 \partial Q_2$) is lower in comparison with B (proportional to $\partial^2 \hat{V}/\partial Q_2^2$) so that the prevailing of the $E_g - e_g$ vibronic coupling again is indicated.

The harmonic form of (1) or (4) leads to the following condition for the local energy minima

$$(\partial E_T/\partial R_a)_{R_e} = b + eR_e + 2cR_a = 0 \qquad (6)$$

so that an R_a vs R_e curve adopts a linear form:

$$R_a = -b/2c - R_e(e/2c) \qquad (7)$$

for fixed displacements of R_e. Since $e/2c = k_{ae}/k_{aa}$ is positive, the dependence is represented by a descending straight line. Analogically, the second dependence is obtained for fixed displacements of R_e:

$$R_a = -d/e - R_e(2f/e) \qquad (8)$$

Such a prediction is acceptable only in the nearest region of the energy minimum, because for larger displacements either $R_e \leq 0$ or $R_a \leq 0$ is obtained. In reality, the $R_e^{min} > 0$ occurs as square-planar complexes MF_4^{2-} (for $R_a \rightarrow \infty$) and $R_a^{min} > 0$ would lead to linear molecules MF_2 (for $R_a \rightarrow \infty$). Therefore, in order to obtain a correct form of the R_a vs R_e dependence at least the cubic or higher degree terms must be considered in the analytic form of APS.

Figure 2 represents the calculated dependence R_a vs R_e between the limiting MF_4^{2-} and MF_2 cases in the harmonic approximation. Also the experimental points (as they result from the X-ray structure data[20]) were included in Fig. 2. This leads to the previously reported finding[6] that the experimentally observed structures of tetragonal bipyramids are situated along the valley of the adiabatic potential surface. Thus an intrinsic disposition of the MX_6^{4-} type complex to undergo tetragonal distortions rather than to adopt an ideal octahedral configuration lies in the shape of APS. Interactions in the solid state probably amplify the manifestation of this disposition. The free-particle APS E_T is to be modified by an additional lattice potential V_L which depends on the crystal packing as well as on the quality of actual ions.[22] The most probable location of a minimum of $E_T + V_L$ lies along the valley of E_T, or in the other words, along the correlation curve R_a vs R_e. It cannot be ruled out that the free-parcicle distortions (like in the CuF_6^{4-} complex) owing to the local Jahn–Teller effect can be amplified by cooperative effects in the solid state.[3]

Finally, the energy partitioning (Fig. 3) shows that the ligand–ligand interaction E_{L-L} is insensitive to geometry changes. On the contrary, the metal-ligand interaction energy appears to be the crucial term in stabilizing the equilibrium geometry. This term consists of two contributions: the interaction energy of metal–equatorial ligands, E_{M-F_e}, and metal–axial ligands, E_{M-F_a}. These contributions exhibit a reciprocal dependence along the valley: the higher the first term, the lower the
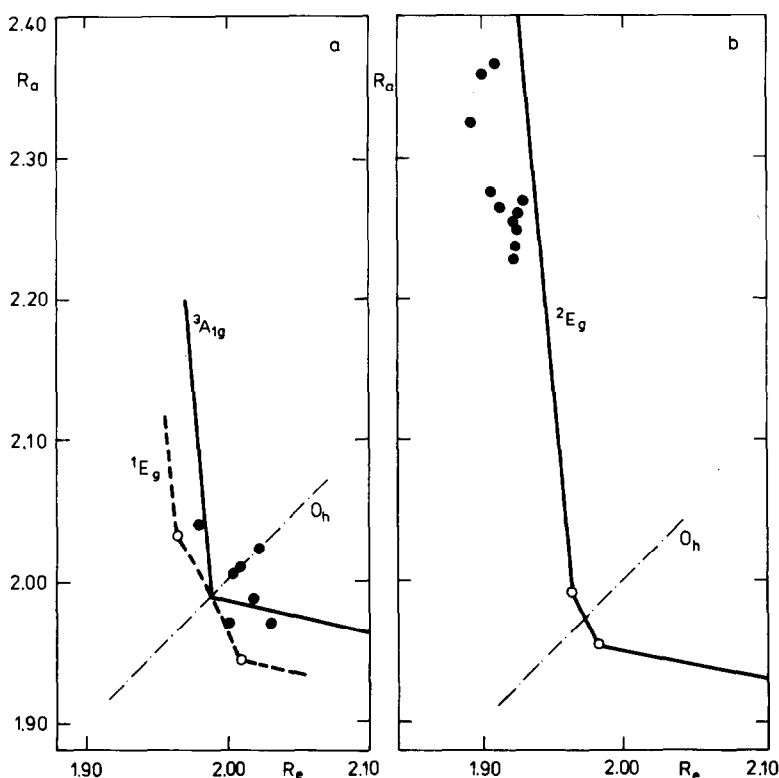
Fig. 2. The R_a vs R_e dependence by the CNDO calculations. ●, experimental structure data; ○, calculated positions of energy minima for the free complex. (a) NiF_6^{4-}. (b) CuF_6^{4-}.

second term, and vice versa. This leads to the conception to consider the R_a vs R_e dependences as a consequence of the mutual influence of ligands mediated via the central atom,[23] in this particu-

lar case as a manifestation of the equatorial–axial influence.[5]

Fig. 3. The energy terms along the valley of APS. (a) NiF_6^{4-}. (b) CuF_6^{4-} in $^3A_{1g}$ state. (b) CuF_6^{4-} in ^2E_g state. The double minimum course of E_T for CuF_6^{4-} is not distinghished in the given scale.

REFERENCES

1. B. J. Hathaway, *Struct. Bonding (Berlin)* 1973, **14**, 49.
2. J. Gažo, I. B. Bersuker, J. Garaj, M. Kabešová, J. Kohout, H. Langfelderová, M. Melnik, M. Serátor and F. Valach, *Coord. Chem. Rev.* 1976, **19**, 253.
3. D. Reinen and C. Friebel, *Struct. Bonding (Berlin)* 1979, **37**, 1.
4. B. Hathaway, M. Duggan, A. Murphy, J. Mullane, C. Power, A. Walsh and B. Walsh, *Coord. Chem. Rev.* 1981, **36**, 267.
5. J. Gažo, R. Boča, E. Jóna, M. Kabešová, Ľ. Macášková, J. Šima, P. Pelikán and F. Valach, *Coord. Chem. Rev.* 1982, **43**, 87.
6. R. Boča and P. Pelikán, *Inorg. Chem.* 1981, **20**, 1618.
7. R. Boča, *Chem. Zvesti* 1981, **35**, 769.
8. R. Boča and P. Pelikán, *Chem. Zvesti* 1982, **36**, 35.
9. J. A. Pople and D. L. Beveridge, *Approximate Molecular Orbital Theory.* McGraw-Hill, New York (1970).
10. D. W. Clack, N. S. Hush and J. R. Yandle, *J. Chem. Phys.* 1972, **57**, 3503.
11. R. Boča and M. Liška, Program MOSEMI, unpublished work, Slovak Technical University.
12. T. Anno and H. Teruya, *J. Chem. Phys.* 1970, **52**, 2840.

13. P. Pelikán, M. Liška, R. Boča and L. Turi Nagy, *Chem. Zvesti* 1978, **32**, 607.

14. R. Boča, Program PCILO3, submitted to Q.C.P.E.

15. B. I. Swanson, *J. Am. Chem. Soc.* 1976, **98**, 3067.

16. B. I. Swanson and S. K. Satija, *J. Am. Chem. Soc.* 1977, **99**, 987.

17. M. Liška, P. Pelikán and J. Gažo, *Koord. Khim.* 1979, **5**, 978.

18. I. B. Bersuker, *Coord. Chem. Rev.* 1975, **14**, 357.

19. P. Pelikán, M. Breza and M. Liška, *Inorg. Chim. Acta* 1980, **45**, L1.

20. Experimental structure data. NiF$_2$: J. W. Stout and S. A. Reed, *J. Am. Chem. Soc.* 1954, **76**, 5279; W. H. Baur, *Naturwiss.* 1957, **44**, 349; W. H. Baur, *Acta Cryst.* 1958, **11**, 488. K$_2$NiF$_4$: D. Baltz and K. Plieth, *Z. Elektrochem.* 1955, **59**, 545. Ba$_2$NiF$_6$: H. G. von Schnering, *Z. Anorg. Allg. Chem.* 1967, **353**, 13. KNiF$_3$: cited in D. Reinen, *J. Solid State Chem.* 1979, **27**, 71. RbNiF$_3$ and CsNiF$_3$: D. Babel, *Z. Anorg. Allg. Chem.* 1969, **369**, 117. CuF$_2$: C. Billy and H. M. Haendler, *J. Am. Chem. Soc.* 1957, **79**, 1049. K$_2$CuF$_4$: D. Reinen and S. Krause, *Inorg. Chem.* 1981, **20**, 2750. NaCuF$_3$ and K$_2$CuF$_4$: R. Haegele and D. Babel, *Z. Anorg. Allg. Chem.* 1974, **409**, 11. K$_3$Cu$_2$F$_7$ and K$_2$CuF$_4$: E. Herdtweck and D. Babel, *Z. Anorg. Allg. Chem.* 1981, **474**, 113. BaCuF$_4$: J.-M. Dance, *Mat. Res. Bull.* 1981, **16**, 599. Na$_2$CuF$_4$: D. Babel, *Z. Anorg. Allg. Chem.* 1965, **336**, 200. Ba$_2$CuF$_6$: C. Friebel, *Z. Naturforsch.* 1974, **29b**, 634; D. Reinen and H. Weitzel, *Z. Naturforsch.* 1977, **32b**, 476. KCuF$_3$: A. Okazaki and Y. Suemere, *J. Phys. Soc. Jpn.* 1961, **16**, 176; A. Okazaki, *J. Phys. Soc. Jpn.* 1969, **27**, 518; K. Tanaka, M. Konishi and F. Marumo, *Acta Cryst.* 1979, **B35**, 1303.

21. J. H. Ammeter, *Nouv. J. Chim.* 1980, **4**, 631.

22. J. H. Ammeter, L. Zoller, J. Bachmann, P. Baltzer, E. Gamp, R. Bucher and E. Deiss, *Helv. Chim. Acta* 1981, **64**, 1063.

23. J. Gažo, *Zh. Neorg. Khim.* 1977, **22**, 2936.

24. J. S. Griffith, *The Theory of Transition-Metal Ions.* University Press, Cambridge (1964).

APPENDIX

Complete vibronic coupling $E_g - (a_{1g} + e_g)$

The first-order perturbation theory yields an aditional term $\epsilon(Q)$ to the harmonic part of APS:

$$E_T(Q_1, Q_2, Q_3) = E_T(Q_1^0, Q_2^0, Q_3^0) + \tfrac{1}{2}K_aQ_1^2 + \tfrac{1}{2}(Q_2^2 + Q_3^2)K_e + YQ_1$$
$$- \sqrt{(A - ZQ_1)^2(Q_2^2 + Q_3^2) + B^2(Q_2^2 + Q_3^2)^2 + 2B(A - ZQ_1)Q_2(Q_2^2 - 3Q_3^2)}$$

$$E_T(Q) = E_T(Q_0) + \frac{1}{2}\sum_m K_mQ_m^2 + \epsilon(Q).$$

This is an eigenvalue of the 2×2 type of secular equation

$$\det(\mathbf{U} - \epsilon\mathbf{1}) = 0$$

where the perturbation covers linear and quadratic

terms of the Taylor expansion of the electron-nuclear operator $\hat{V}(q, Q)$:

$$U_{ij} = \left\langle \psi_i \right| \sum_m \left[\frac{\partial \hat{V}(q, Q)}{\partial Q_m}\right]_0 Q_m$$
$$+ \frac{1}{2}\sum_{m,n} \left[\frac{\partial^2 \hat{V}(q, Q)}{\partial Q_m \partial Q_n}\right]_0 Q_m Q_n \left| \psi_j \right\rangle$$

in the basis set of the electronic doublet ψ_i, $\psi_j \in E_g$. Considering only the a_{1g} (Q_1) and e_g (Q_2, Q_3) type of normal vibrations, for the matrix **U** it holds:

$$\mathbf{U} = X_aQ_1\mathbf{C}_1 + X_e(Q_2\mathbf{C}_2 + Q_2\mathbf{C}_3) + \frac{1}{2}X_{aa}Q_1^2\mathbf{C}_1$$
$$+ X_{ae}(Q_1Q_2\mathbf{C}_2 + Q_1Q_3\mathbf{C}_3) + v\frac{1}{2\sqrt{2}}X_{ee}$$
$$\times [(Q_2^2 + Q_3^2)\mathbf{C}_1 + (Q_3^2 - Q_2^2)\mathbf{C}_2 + 2Q_2Q_3\mathbf{C}_3]$$

where

$$\mathbf{C}_1 = \frac{1}{\sqrt{2}}\begin{pmatrix} 1 & 0 \\ 0 & 1 \end{pmatrix} \quad \mathbf{C}_2 = \frac{1}{\sqrt{2}}\begin{pmatrix} -1 & 0 \\ 0 & 1 \end{pmatrix}$$
$$\mathbf{C}_3 = \frac{1}{\sqrt{2}}\begin{pmatrix} 0 & 1 \\ 1 & 0 \end{pmatrix}.$$

Here X_a and X_e are the linear vibronic constants and X_{aa}, X_{ee} and X_{ae} being the quadratic vibronic constants of the given type of symmetry (a_{1g} or e_g). The expression of $\langle \psi_i|[\partial^2\hat{V}(q, Q)/\partial Q_m\partial Q_n]_0|\psi_j \rangle$ type integral through a vibronic constant X_{ab} multiplied by a certain coefficient is based on the Wigner formula.[24]

The above equations may be re-written using the substitutions of

$$K_a = K_1 + X_{aa}/\sqrt{2}$$
$$K_e = K_2 + 2B$$
$$Y = X_a/\sqrt{2}$$
$$A = -X_e/\sqrt{2}$$
$$Z = X_{ae}/\sqrt{2}$$
$$B = X_{ee}/4$$

so that for an analytic form of APS the previously reported formula[19] (except the term containing Y) holds:

Using the polar coordinates of $\rho = (Q_2^2 + Q_3^2)^{1/2}$ and $\varphi = \text{arctg}(Q_3/Q_2)$ the vibronic correction term may be re-written as:

$$\epsilon(Q) = YQ_1 - \rho[(A - ZQ_1)^2 + B^2\rho^2$$
$$+ 2B(A - ZQ_1)\rho \cos 3\varphi]^{1/2}.$$

Within the $E_T(\rho, \varphi; Q_1 = \text{const.})$ picture such an APS

corresponds to a Mexican hat type function with warping. Notice, the direct product of two t-type vibrations (e.g. $t_{2g} \times t_{2g}$) yields a component within the e_g-type representation, so that some quadratic terms $\langle \psi_i | [\partial^2 V(q, Q)/\partial Q_m \partial Q_n]_0 | \psi_j \rangle$ for $Q_m, Q_n \in t_{2g}, t_{2u}, t'_{1u}, t''_{1u}$ are non-zero. Therefore, strictly speaking, an admixture of $E_g - (t_{2g} + t_{2u} + t'_{1u} + t''_{1u})$ coupling takes place.

For a vanishing coordinate Q_3 (the case of only a tetragonal distortion) it is valid that $U_{12} = 0$, so that the eigenvalues of the secular equation directly correspond to its diagonal elements U_{11} and U_{22}. Then the final formulae are obtained:

$$E_T^{(1)}(Q_1, Q_2, Q_3 = 0) = E_T(Q_1^0, Q_2^0) + YQ_1 + \tfrac{1}{2}K_a Q_1^2$$

$$+ AQ_2 - ZQ_1 Q_2 + \tfrac{1}{2}(K_e + 2B)Q_2^2$$

$$E_T^{(2)}(Q_1, Q_2, Q_3 = 0) = E_T(Q_1^0, Q_2^0) + YQ_1 + \tfrac{1}{2}K_a Q_1^2$$

$$- AQ_2 + ZQ_1 Q_2 + \tfrac{1}{2}(K_e - 2B)Q_2^2.$$

LIGAND EFFECTS ON THE REDOX POTENTIALS OF METAL CARBONYLS

RELATIONSHIP TO CO FORCE CONSTANTS IN MANGANESE(I) DERIVATIVES

J. W. HERSHBERGER and J. K. KOCHI*

Department of Chemistry, Indiana University, Bloomington, IN 47405, U.S.A.

Abstract—The reversible oxidation potentials E^0 of a single series of methylcyclopentadienyldicarbonylmanganese(I) derivatives η^5-MeCpMn(CO)$_2$L are measured for a wide variety of ligand types, including L = alkyl and aromatic amines, alkyl cyanide and isocyanide, alkene, alkyl and aryl phosphines and phosphites. The relationship of E^0 with the carbonyl force constants evaluated by the Cotton–Kraihanzel method is presented.

Oxidation and reduction are important properties of metal carbonyls since they can strongly influence the rates and course of reactions. For example, ligand substitutions and rearrangements of carbonylmetal derivatives have been shown to proceed rapidly when they are induced simply by either a one-electron oxidation or reduction.[1-5] As such, it is important to ascertain the functional relationship between the structure of metal carbonyl and its redox potential. Indeed Treichel *et al.*[6,7] recognized a linear relationship between the potential $E_{1/2}$ for the one-electron oxidation of a series of manganese carbonyls [Mn(CO)$_{6-n}$(CNR)$_n$]$^+$ with the number of alkyl and aryl isocyanide ligands varying from $1 < n < 6$. Moreover, Sarapu and Fenske[8] have analyzed the bonding properties of the methyl isocyanide and carbonyl ligands in [Mn(CO)$_{6-n}$(CNMe)$_n$]$^+$ for $0 < n < 6$ via approximate molecular orbital calculations, and have found that the values of $E_{1/2}$ do correlate extremely well with the calculated HOMO energies. It is noteworthy that they found the approximate force constants for the carbonyl stretching frequencies v(CO) evaluated by the Cotton–Kraihanzel method[9] to also correlate with the computed electron occupation of the carbonyl 5σ and 5π orbitals.

Similar relationships between the oxidation potential and the degree of substitution in the mixed carbonyl/acetonitrile complexes of chromium and tungsten, i.e. Cr(CO)$_{6-n}$(NCMe)$_n$ and W(CO)$_{6-n}$(NCMe)$_n$, have also been noted.[10,11] Several recent studies have discussed the correlation of the oxidation potentials of various metal carbonyl derivatives with the infrared data, particularly the carbonyl stretching frequencies.[12-18] Such studies have encompassed a variety of ligands, including such nitrogen-centred ones as dinitrogen, alkyl and aryl cyanides, ammonia, cyanide, thiocyanate, and azide, etc. in addition to carbon monoxide and the halides [12, 14]. The effects of phosphorus-centred ligands such as alkyl and aryl phosphines and phosphites on the potentials of metal carbonyls have also been examined.[15,16] In this context, the studies of Connelly and Kitchen[16] are particularly pertinent, since they showed that the oxidation potentials for the series of manganese carbonyls η^5-MeCpMn(CO)$_{3-b}$L$_n$ with L = phosphorus(III) alkyls, aryls, alkoxides, phenoxides, etc. were directly related to the Cotton–Kraihanzel force constants derived from the carbonyl stretching frequencies.

In order to examine the general effect associated with the use of a wide variety of ligand types on the oxidation potential of a metal carbonyl, we focussed our attention on the mono-substitution products of η^5-MeCpMn(CO)$_3$. The choice of this carbonylmetal system is particularly appropriate since the one-electron oxidation is usually reversible and allows the oxidation potential E^0 to be determined. Moreover, by focussing on a single carbonylmetal system, i.e. η^5-MeCpMn(CO)$_2$L we hoped to minimize ambiguities related to the evaluation of the force constants based on the Cotton–Kraihanzel method.[9]

---

*Author to whom correspondence should be addressed.

EXPERIMENTAL

Synthesis of carbonylmanganese derivatives η^5-MeCpMn(CO)$_2$L

The monosubstituted carbonylmanganese derivatives η^5-MeCpMn(CO)$_2$L listed in Table 1 were prepared from η^5-MeCpMn(CO)$_2$(THF), which was generated *in situ* by irradiation of a solution of the parent tricarbonyl complex in tetrahydrofuran (THF) under argon.[19]

$$+ \quad \text{(1)}$$
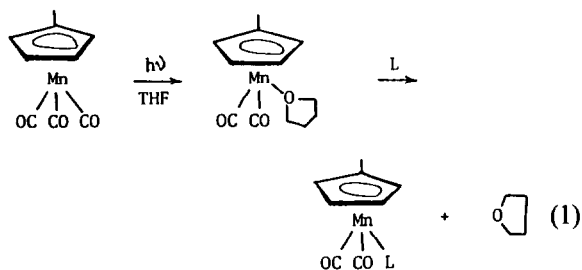
The photochemical reactor consisted of a 300 cm^3 cylindrical flask with a 100 watt medium pressure Hg lamp contained in a quartz immersion well.

All preparative reactions and ligand exchange studies were carried out by benchtop manipulations under either a nitrogen or an argon atmosphere in Schlenk flasks. Many of the manganese complexes employed in this study are generally air sensitive, both in the solid state as well as in solutions. In a typical procedure, a solution of 2 g of (η^5-C$_5$H$_4$Me)Mn(CO)$_3$ in 300 cm^3 THF was deaerated, and irradiated for 50 min at 0°C. The IR spectrum of the solution indicated that ~90% of the starting material was converted to (η^5-C$_5$H$_4$Me)Mn(CO)$_2$(THF).[26] One equivalent of the appropriate ligand (L = py, MeCN, piperidine, PPh$_3$, P(C$_6$H$_4$Me-p)$_3$, P(C$_6$H$_4$Cl-p)$_3$ P(OMe)$_3$, P(OPh)$_3$, PEt$_3$, P(Me)Ph$_2$, P(OMe)Ph$_2$, CNCMe$_3$, Me$_2$-SO, AsPh$_3$, and SbPh$_3$) was added, and the solution stirred for several hours at ambient temperatures. During this period, the deep purple color of the tetrahydrofuran complex gave way to the yellow or orange color of the product. The THF was removed at reduced pressure, and the residue was taken up in ethyl ether. [When the product was not soluble in ether, chloroform was employed.] Filtration of the solution, followed by crystallization from a mixture of ether and hexane or chloroform and ethanol afforded crystalline products in 30–70% yield. For L = PEt$_3$ and P(OMe)$_3$, the products were oils, which were purified by chromatography on Florisil according to the literature description.[16] For L = SO$_2$, sulphur dioxide gas (1 atm.) was bubbled through the solution of (η^5-C$_5$H$_4$Me)Mn(CO)$_2$

Table 1. Methylcyclopentadienyldicarbonylmanganese(I) derivatives

L	IR†	m.p., °C‡ (lit)	Found C%	H%	X%	Calc. C%	H%	X%
1 CO	2024, 1946	oil						
2 PEt$_3$	1937, 1874	oil [16]						
3 PPh$_3$	1944, 1884	118–119 (119–120) [23]						
4 P(C$_6$H$_4$Me-p)$_3$	1939, 1879	184–186	70.38; 5.82			70.44 5.71		
5 P(C$_6$H$_4$Cl-p)$_3$	1946 1887	156–158	56.10; 3.45		(Cl, 19.28)	56.20 3.45		(Cl, 19.14)
6 P(Me)Ph$_2$	1940, 1878	57–58 (55–57) [24]						
7 P(OMe)Ph$_2$	1944, 1884	64–66	62.41 5.16			62.08 4.96		
8 P(OMe)$_3$	1947, 1892	oil [16]						
9 P(OPh)$_3$	1970, 1910	75–77 (75–76) [22]						
10 MeCN	1950, 1886	73 (dec)	52.07 4.26		(N, 6.34)	51.97 4.36		(N, 6.06)
11 NC$_5$H$_5$ (py)	1934, 1868	72–73 (75) [21]						
12 HN(CH$_2$)$_5$	1929, 1860	71–72 (71–73) [20]						
13 Norbornene	1969, 1910	65–66	63.56 6.00			63.38 6.03		
14 CNCMe$_3$	1954, 1908	53–54.5	57.09 5.78		(N, 5.23)	57.15 5.90		(N, 5.13)
15 THF	1927, 1850§							
16 Me$_2$SO	1960, 1896	64–66 (66) [25]						
17 SO$_2$	2018, 1976	90 (dec) (73) [25]						
18 AsPh$_3$	1941, 1881	117–119 (118–120) [16]						
19 SbPh3‖	1940, 1884	99–100	57.79 4.19			57.50 4.08		

†Carbonyl stretching frequencies in cm^{-1}.
‡Melting points are uncorrected.
§The IR spectrum was recorded in THF.
‖The IR spectrum of this compound is reported in Ref. 26.

(THF) in THF with rapid stirring. The reaction was complete at room temperature within a few minutes. Crystallization of the product from a mixture of ether and hexane afforded orange crystals in 53% yield based on $(\eta^5\text{-}C_5H_4Me)Mn(CO)_3$. Since THF is not readily displaced from $(\eta^5\text{-}C_5H_4Me)Mn(CO)_2(THF)$ by norbornene, $(\eta^5\text{-}C_5H_4Me)Mn(CO)_2(norbornene)$ was prepared directly by the irradiation of $(\eta^5\text{-}C_5H_4Me)Mn(CO)_3$ (2.0 g) in 300 cm³ of toluene containing a 20-fold excess of norbornene. The product was purified by crystallization from n-heptane, and obtained in 59% yield.

The microanalyses included in Table 1 were performed either by Midwest Microlabs, Ltd., Indianapolis, Indiana, or by Galbraith Laboratories, Inc., Knoxville, Tennessee.

The infrared spectra of the series of $\eta^5\text{-MeCpMn(CO)}_2L$ were measured in heptane solution on a Perkin–Elmer model 298 spectrophotometer.

Electrochemical measurements were performed on a Princeton Applied Research Model 173 potentiostat equipped with a Model 176 current-to-voltage converter, which provided a feedback compensation for ohmic drop between the working and reference electrodes. The high impedance voltage follower amplifier (PAR Model 178) was mounted external to the potentiostat to minimize the length of the connection to the reference electrode for low noise pickup. Cyclic voltammetry was carried out in a cell designed according to Van Duyne and Reilley.[27] The configuration of this cell is convenient for low temperature experiments since the lower portion of the cell containing the working solution could be easily submerged in the desired cold bath contained in a Dewar flask. The distance between the Pt electrode and the tip of the salt bridge was less than 2 mm to minimize ohmic drop. The reference electrode was isolated from the cold bath and maintained at room temperature ($\sim 25°C$). The voltammograms were recorded on a Houston Series 2000 X–Y recorder. CV scans were measured several minutes after agitation to ensure thermal equilibration. Electrode aging was not a serious problem in this study. Between experiments the platinum wire was soaked briefly in concentrated nitric acid, rinsed with distilled water, and dried at 110°C.

RESULTS AND DISCUSSION

The electrochemical behaviour of the manganese carbonyls in Table 1, was examined by cyclic voltammetry (CV) carried out at a stationary platinum microelectrode in acetonitrile solutions containing 0.1 M tetraalkylammonium perchlor-

ates as supporting electrolytes. The initial anodic scans for the cyclic voltammorgrams of the pyridine, triphenylphosphine, and carbon monoxide derivatives of $MeCpMn(CO)_2L$ in Fig. 1 are all characterized by ratios of the anodic and cathodic currents $(i_p{}^a/i_p{}^c)$ of unity and by anodic and cathodic peak separations $(E_p{}^a - E_p{}^c)$ of near 60 mV for reversible one-electron processes, i.e.

$$MeCpMn(CO)_2L \underset{}{\overset{E^0}{\rightleftharpoons}} MeCpMn(CO)_2L^+ + e^-. \quad (2)$$

Hereafter the average value $(E_p{}^a + E_p{}^c)/2$ will be taken as the measure of the oxidation potential E^0.[28]

The cyclic voltammetry of the piperidine and pyridine derivatives could not be examined in acetonitrile solutions owing to a rapid electrocatalytic ligand substitution described elsewhere.[29] Accordingly, the cyclic voltammograms for these complexes were recorded for acetone solutions containing 0.1 M TEAP. The difference in solvent effects between acetonitrile and acetone on E^0 for these complexes appears to be minimal since an examination of several alkyl and aryl phosphine and phosphite complexes indicated the values of E^0 to be virtually solvent independent.

The magnitude of the reversible oxidation potentials E^0 of the series of $MeCpMn(CO)_2L$ listed in Table 2 is strongly dependent upon the nature of the coordinated ligand L. Thus the nitrogen-centred ligands such as amines and nitriles effect the most negative values in the range, $-0.04\,V < E^0 < 0.19\,V$. The reversible potentials of alkyl and aryl phosphine complexes are clustered around 0.5 ± 0.1 V, but those of corresponding phosphites are significantly more positive. Among carbon-centred ligands, the values of E^0 become progressively more positive in the order: alkene (norbornene, 0.44 V) < isocyanide (tert-BuNC, 0.53 V) ≪ carbon monoxide (1.15 V). In-
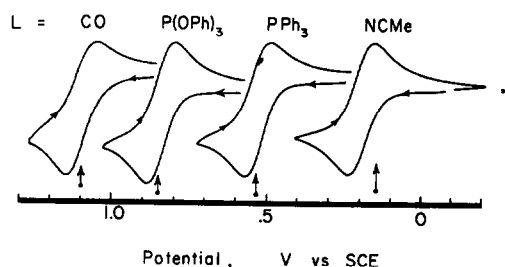
Fig. 1. Variation in E^0 for various $MeCpMn(CO)_2L$ as shown by the reversible cyclic voltammograms recorded at 100 mV s⁻¹ in acetonitrile containing 0.1 M tetraethylammonium perchlorate at 22°C [CO derivative measured at 200 mV s⁻¹ and −28°C].

Table 2. The cyclic voltammetric parameters of η^5-MeCpMn(CO)$_2$L[a]

	L	Solvent	E_p^{ox} (V)	E^0 (V)	i_p^a/i_p^c
1	CO	MeCN[e]	1.15	1.10	1.0
2	PEt$_3$	Me$_2$CO	0.44	0.40	1.0
3	PPh$_3$	MeCN	0.55	0.52	1.0
4	PPh$_3$	Me$_2$CO	0.55	0.52	1.0
5	P(C$_6$H$_4$Me-p)$_3$	MeCN	0.53	0.50	1.0
6	P(C$_6$H$_4$Cl-p)$_3$	MeCN	0.64	0.60	1.0
7	P(Me)Ph$_2$	MeCN	0.53	0.49	1.0
8	P(OMe)Ph$_2$	MeCN	0.65	0.62	1.0
9	P(OMe)$_3$	MeCN	0.72	0.68	1.0
10	P(OPh)$_3$	MeCN	0.91	0.85	1.0
11	MeCN	Me$_2$CO[b]	0.18	0.12	1.0
12	MeCN	CH$_2$Cl$_2$[c]	0.20	0.15	1.0
13	MeCN	MeCN	0.22	0.19	1.0
14	NC$_5$H$_5$ (py)	Me$_2$CO	0.14	0.11	1.0
15	HN(CH$_2$)$_5$	Me$_2$CO	0.02	-0.04	1.1
16	norbornene	MeCN[d]	0.49	0.44	1.1
17	CNCMe$_3$	MeCN	0.58	0.53	1.0
18	CNCMe$_3$	Me$_2$CO	0.59	0.54	1.0
19	THF	THF[f]	0.09	h	
20	Me$_2$SO	MeCN	0.73	h	
21	SO$_2$	Me$_2$CO	1.06[g]	h	
22	AsPh$_3$	MeCN	0.55	h	
23	SbPh$_3$	MeCN	0.65	h	

[a] Cyclic voltammetry performed at a Pt microelectrode with solutions 10^{-3} M in substrate and 0.1 N in supporting electrolyte (tetraethyl-ammonium perchlorate for MeCN or acetone, tetrabutylammonium per-chlorate for THF or CH$_2$Cl$_2$). Unless otherwise noted, the scan rate was 100 mV s^{-1} and T = 22 °C. Potentials reported relative to the Cp$_2$Fe/Cp$_2$Fe$^+$ couple taken to have (E_p^{ox} + E_p^{red})/2 = 0.31 V in all solvents. [b] Scan rate = 50 mV s^{-1}, T = -55 °C. [c] Scan rate = 800 mV s^{-1}. [d] Scan rate = 200 mV s^{-1}, T = -50 °C. [e] Scan rate = 200 mV s^{-1}, T = -28 °C. [f] Scan rate = 30 mV s^{-1}. [g] Value difficult to reproduce owing to the rapid deactivation of the Pt electrode. Experimental error in voltage is ± 0.01 V. [h] Irreversible CV wave.

deed the potential of the carbon monoxide complex MeCpMn(CO)$_3$ is the most positive of the derivatives listed in Table 2. We can deduce from these trends that the ease with which various MeCpMn(CO)$_2$L are oxidized is qualitatively dependent on the σ-donor property of L and by its π-acidity. For example, among complexes with nitrogen ligands, E^0 becomes progressively more negative with increasing base strengths of L in the order: acetonitrile < pyridine ≪ piperidine. Moreover, we infer from the significantly more negative value of E^0 for MeCpMn(CO)$_2$-(CNBu-t) compared to the E^0 for MeCpMn(CO)$_3$ that the ligand basicities are in the order: t-butyl isocyanide > carbon monoxide, as elaborated by Sarapu and Fenske[8] for the series of Mn(CO)$_{6-n}$(CNMe)$_n^+$.

From the IR data presented in Table 1, we applied the method of Cotton and Kraihanzel[9] to derive the carbonyl force constants for these

carbonyl–manganese complexes. The derived force constants k(CO) are listed in Table 3, and they are plotted vs the reversible oxidation potentials in Fig. 2. The extensive scatter of the points indicate no general correlation of k(CO) with E^0 for this single series of carbonylmanganese derivatives. However a closer inspection reveals a limited correlation among the various phosphorus(III) ligands. Thus the arbitrary line drawn in Fig. 2 includes only those phosphine and phosphite ligands with a correlation coefficient of 0.86 [30]. The complexes derived from the nitrogen-centred ligands such as piperidine, pyridine and acetonitrile as well as the carbon-centred ligands such as t-butyl isocyanide, norbornene and carbon monoxide clearly lie beyond any reasonable relationship with those containing phosphorus(III) ligands.[31]

The oxidation potentials of a series of chromium

Table 3. Carbonyl force constants for η^5-MeCpMn(CO)$_2$L[a]

L	k(CO) (mdyn $\overset{\circ}{A}^{-1}$)	L	k(CO) (mdyn $\overset{\circ}{A}^{-1}$)
1 CO	15.71	11 NC$_5$H$_5$ (py)	14.60
2 PEt$_3$	14.66	12 HN(CH$_2$)$_5$	14.50
3 PPh$_3$	14.80	13 norbornene	15.19
4 P(C$_6$H$_4$Me-p)$_3$	14.72	14 CNCMe$_3$	15.06
5 P(C$_6$H$_4$Cl-p)$_3$	14.83	15 THF	14.41
6 P(Me)Ph$_2$	14.72	16 Me$_2$SO	15.01
7 P(OMe)Ph$_2$	14.80	17 SO$_2$	16.10
8 P(OMe)$_3$	14.88	18 AsPh$_3$	14.75
9 P(OPh)$_3$	15.20	19 SbPh$_3$	14.76
10 MeCN	14.86		

[a] Experimental force constant error: ± 0.02 mdyn $\overset{\circ}{A}^{-1}$
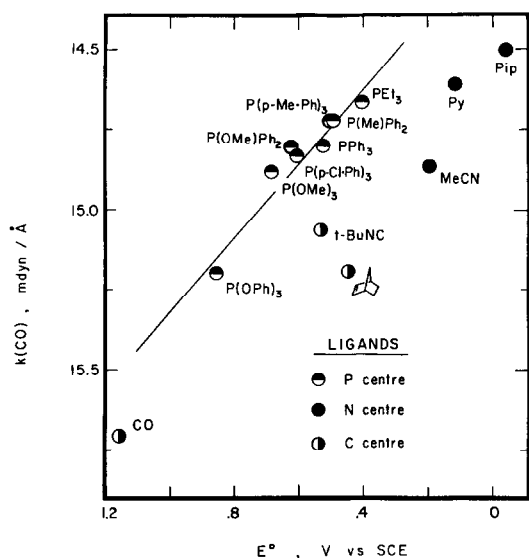
Fig. 2. Relationship between E^0 of MeCpMn(CO)$_2$L and the Cotton–Kraihanzel carbonyl force constant for various ligands L containing phosphorus(III) centres, nitrogen centres (pip = piperidine, py = pyridine), and carbon centres as labelled. The least squares line is arbitrarily drawn only through the phosphorus(III) derivatives, see text.

Fig. 3. Comparative effects of phosphorus(III)-, nitrogen-, and carbon-centred ligands on E^0 on the series of MeCpMn(CO)$_2$L and (OC)$_5$CrL. [Data for t-Bu-NC(OC)$_5$Cr taken from Ref. 18.]

carbonyls with the Cr(CO)$_5$ moiety bound to a variety of ligands L are also known [3, 32]. Figure 3 shows the relationship between the oxidation potentials of the manganese dicarbonyls MeCpMn(CO)$_2$L with those of the corresponding chromium pentacarbonyls (OC)$_5$CrL for some of the representative ligands included in Fig. 2. The reasonable correlation is consistent with HOMO energies of both series of complexes which are affected in similar ways by amine, phosphine,

isocyanide and carbonyl ligands with different σ- and π-bonding characteristics. However the small slope indicates that the effect in the chromium carbonyls is attenuated to about a half of that in the manganese carbonyls. Thus the carbonyl force constants in (OC)$_5$CrL are also unlikely to be measures of their oxidation potentials when a broad series of donors are considered. In this connection, the recent empirical approach by Chatt et al.[13] to the prediction of redox potentials based on linear free energy relationships appears to be a more inclusive method.

REFERENCES

1. J. Bezems, P. H. Rieger and S. Visco, J. Chem. Soc. Chem. Commun. 1981, 265.

2. D. P. Summers, J. C. Luong and M. S. Wrighton, *J. Am. Chem. Soc.* 1981, **103**, 5238.

3. J. W. Hershberger, R. J. Klingler and J. K. Kochi, *J. Am. Chem. Soc.* 1982, **104**, 3034.

4. A. M. Bond, D. J. Darensbourg, E. Mocellin and B. J. Stewart, *J. Am. Chem. Soc.* 1981, **103**, 6827.

5. A. M. Bond, B. S. Grabaric and J. J. Jackowski, *Inorg. Chem.* 1978, **17**, 2153.

6. P. M. Treichel, D. W. Firich and G. P. Essenmacher, *Inorg. Chem.* 1979, **18**, 2405. See also D. A. Bohling, J. F. Evans and K. R. Mann, *Ibid.* 1982, **21**, 3546.

7. P. M. Treichel, G. E. Direen and H. J. Mueh, *J. Organomet. Chem.* 1972, **44**, 339.

8. A. C. Sarapu and R. F. Fenske, *Inorg. Chem.* 1975, **14**, 247.

9. (a) F. A. Cotton and C. S. Kraihanzel, *J. Am. Chem. Soc.* 1962, **84**, 4432. (b) For a discussion of the problems, see L. M. Bower and M. H. B. Stiddard, *Inorg. Chim. Acta* 1967, **1**, 231; L. H. Jones, *Inorg. Chem.* 1968, **7**, 1681; F. A. Cotton, *Inorg. Chem.* 1968, **7**, 1683.

10. C. J. Pickett and D. Pletcher, *J. Organomet. Chem.* 1975, **102**, 327.

11. A. Seurat, P. Lemoine and M. Gross, *Electrochim. Acta* 1980, **25**, 675.

12. J. Chatt, G. J. Leigh, H. Neukomm, C. J. Pickett and D. R. Stanley, *J. Chem. Soc., Dalton Trans.* 1980, 121.

13. J. Chatt, C. T. Kan, G. J. Leigh, C. J. Pickett and D. R. Stanley, *J. Chem. Soc., Dalton Trans.* 1980, 2032.

14. G. T. Leigh, R. H. Morris, C. J. Pickett, D. R. Stanley and J. Chatt, *J. Chem. Soc., Dalton Trans.* 1981, 800.

15. N. G. Connelly, Z. Demidowicz and R. L. Kelly, *J. Chem. Soc., Dalton Trans.* 1975, 2335.

16. N. G. Connelly and M. D. Kitchen, *J. Chem. Soc., Dalton Trans.* 1977, 931.

17. The relationship between $E_{1/2}(red)$ and CO stretching frequencies in metal carbonyls has been discussed: D. DeMontauzon and R. Poilbanc, *J. Organomet. Chem.* 1976, **104**, 99.

18. A direct correlation between $E_{1/2}(ox)$ and $\lambda(max)$ for the M→CNR charge transfer transition has been reported for $(RNC)_nM(CO)_{6-n}$ (M = Mo, Cr) with varying R: J. A. Connor, E. M. Jones, G. K. McEwen, M. K. Lloyd and J. A. McCleverty, *J. Chem. Soc., Dalton Trans.* 1972, 1246.

19. Cf. P. J. Giordano and M. S. Wrighton, *Inorg. Chem.* 1977, **16**, 160.

20. Cf. V. W. Strohmeier and K. Gerlach, *Z. Naturforsch. B.* 1960, **15**, 675.

21. V. W. Strohmeier and J. F. Guttenberger, *Z. Naturforsch. B* 1966, **18**, 80.

22. D. A. Brown, H. J. Lyons and A. R. Manning, *Inorg. Chim. Acta* 1970, **4**, 428.

23. R. S. Nyholm, S. S. Sandhu and M. H. B. Stiddard, *J. Chem. Soc.* 1963, 5917.

24. P. M. Treichel, W. H. Douglas and W. K. Dean, *Inorg. Chem.* 1972, **11**, 615.

25. V. W. Strohmeier, J. F. Guttenberger and G. Popp, *Chem. Ber.* 1965, **98**, 2248.

26. A. R. Manning, *J. Chem. Soc. A* 1971, 106.

27. R. P. Van Duyne and C. N. Reilley, *Anal. Chem.* 1972, **44**, 142.

28. R. J. Klingler and J. K. Kochi, *J. Phys. Chem.* 1981, **85**, 1731.

29. J. W. Hershberger and J. K. Kochi, *J. Chem. Soc. Chem. Comm.* 1982, 212.

30. The least squares slope is $1.14\,mdyn\,Å^{-1}\,V^{-1}$ with an intercept of $14.2\,mdyn\,Å^{-1}$.

31. The anodic CV peak potential E_p (measured at a scan rate of $100\,mV\,s^{-1}$) shows a similar correlation with k(CO), and includes all the derivatives listed in Table 1. The line for the phosphorus(III) ligands has a slope of $1.08\,mdyn\,Å^{-1}\,V^{-1}$ with an intercept of $14.1\,mdyn\,Å^{-1}$. The correlation coefficient of 0.94 is slightly better than that in Fig. 2.

32. See also Ref. 12.

EPR ON TRICHLORO-NITROSYL-BIS(DIMETHYLPHENYLPHOSPHINE)TECHNETIUM(II) $TcCl_3(NO)(PMe_2Ph)_2$

REINHARD KIRMSE*

Department of Chemistry, Karl-Marx-University, 7010 Leipzig, Liebigstr. 18, G.D.R.

and

BERND LORENZ and KLAUS SCHMIDT

Central Institute of Isotope and Radiation Research, 7050 Leipzig, Permoserstr. 15, G.D.R.

Abstract—The d^5 low-spin Tc(II) complex trichloro-nitrosyl-bis(dimethylphenylphosphine)technetium(II) was studied by EPR at $295 \geqslant T \geqslant 27.2$ K. In the room-temperature spectrum well-resolved ^{99}Tc hyperfine splitting is observed indicating a ground state for the unpaired electron which is well separated from other orbital states. At low temperatures the spectrum can be fitted by an axial spin Hamiltonian. The analysis of the ^{99}Tc hyperfine splitting shows remarkable covalent interactions with the "in-plane" ligands. The ^{31}P superhyperfine splitting observed was used to get information about the overall spin density distribution in the molecular orbital of the unpaired electron.

Although coordination compounds of technetium have attracted a growing interest in view of the relevance to the field of nuclear medicine,[1] their chemistry is much less known than that of the corresponding neighbouring elements. This holds true especially for compounds in which Tc possesses low formal oxidation states. In addition, as found for nitrosyl-molybdenum(II) complexes[2] low-valent Tc nitrosyl complexes are expected to form highly active precatalysts for olefin metathesis.

In this paper we report an EPR study on the d^5 low-spin $(S = 1/2)$ complex trichloro-nitrosyl-bis (dimethylphenylphosphine) technetium (II), $TcCl_3(NO)(PMe_2Ph)_2$ (I). This study has been made to get some information about (a) the bonding situation in this compound and (b) the kind of EPR spectra to be obtained for the d^5 low-spin configuration of Tc^{2+}. There are very few well-characterized Tc(II) compounds only,[3-11] the first of which was prepared by Fergusson and Nyholm.[3] From some of the compounds—$[Tc(NH_3)_4(NO)(H_2O)]Cl_3$,[6] $[Tc_2Cl_8]^{3-}$,[9] —the EPR spectra of the undiluted isolated compounds were obtained. However, they consist of a broad unresolved line only. For $(n\text{-}Bu_4N)[Tc(NO)Br_4]$ and $(n\text{-}Bu_4N)_2[Tc(NO)(NCS)_5]$[10] the liquid-solution EPR spectra were obtained, but the spin Hamiltonian parameters were not given. Very recently, the first well-resolved frozen-solution EPR spectra were reported[11] for the Tc^{2+} low-spin complexes $[Tc(NH_3)_4(NO)H_2O]^{3+}$ and $[TcCl_5(NO)]^{2-}$. Ligand hyperfine interactions could not be detected. In addition, EPR spectra were reported for some compounds containing Tc in the oxidation states $+4$[12,13] and $+6$.[14,15]

Considering the radioactivity of Tc, EPR appears to be a very suitable method for investigating paramagnetic Tc complexes because only very small amounts of the compounds are needed. Nevertheless, Tc is one of the transition metals the EPR behaviour of which is almost unknown.

The preparation of (I) has not yet been reported in the literature, therefore, its synthesis will briefly be described in the experimental part.

(1)

---
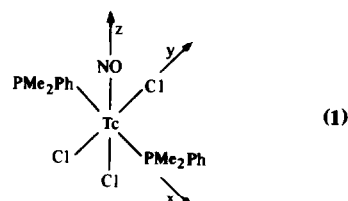
*Author to whom correspondence should be addressed.

EXPERIMENTAL

Synthesis of trichloro-nitrosyl-bis(dimethyl-phenylphosphine)technetium(II), $TcCl_3(NO)$ $(PMe_2Ph)_2$.

$TcCl_3(PMe_2Ph)_3$[16] (0.66 g = 1.06 mM) in benzene (120 cm^3) was boiled while NO was bubbled through the solution for 1 hr. Within 5–10 min the colour of the solution turned from orange to blue–green. After 1 hr the solvent was removed and the dark green oil was dissolved in 10 cm^3 CH_2Cl_2, filtered and treated with methanol (100 cm^3). After standing overnight black–green crystals of $TcCl_3(NO)(PMe_2Ph)_2$ were obtained. Yield: 340 mg (62%); m.p. 175–177°C. The compound can be recrystallized from CH_2Cl_2/CH_3OH.

Found: C, 37.4; N, 2.6; Tc, 19.2; Cl, 21.0. $C_{16}H_{22}Cl_3NOP_2Tc$ requires: C, 37.54; N, 2.73; Tc, 19.35; Cl, 20.79%. Vis. spectrum in CHCl$_3$: λ_{max} in nm (ϵ_{max} in 1 mol^{-1} cm^{-1}): 614 (930) and 710 (615) sh.

IR: in KBr, ν_{NO} 1770 and 1795 cm^{-1}; in CHCl$_3$, ν_{NO} = 1805 cm^{-1}.

EPR measurements. EPR spectra were recorded at room temperature, T = 130 and 27.2 K (using liquid neon) in the X-band ($\nu \approx 9.3$ GHz) with an E-112 spectrometer (Varian, U.S.A.). 10^{-3}–10^{-4} M solutions of $TcCl_3(NO)(PMe_2Ph)_2$ in CHCl$_3$ were used.

RESULTS

The X-band EPR spectrum of a CHCl$_3$ solution of (I) recorded at T = 295 K is shown in Fig. 1. It consists of 10 hyperfine lines resulting from hyperfine interaction with the ^{99}Tc nucleus (^{99}Tc, nuclear spin I = 9/2). The $m_I^{Tc} = \pm 1/2$ lines which are the smallest ones show the presence of further hyperfine interactions due to the ^{31}P ligand nuclei. However, this splitting is poorly resolved only.
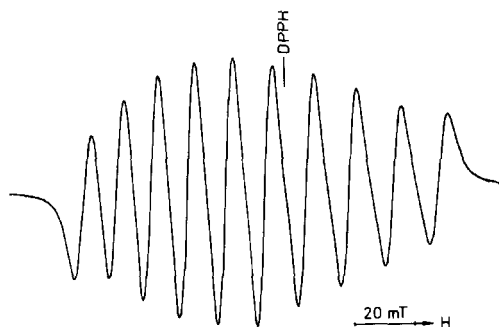
Fig. 1. X band room-temperature EPR spectrum of $TcCl_3(NO)(PMe_2Ph)_2$ in CHCl$_3$.
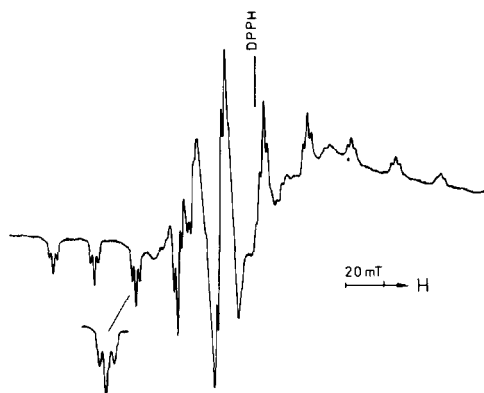
Fig. 2. X band EPR spectrum of $TcCl_3(NO)(PMe_2Ph)_2$ in CHCl$_3$. T = 27.2 K.

In Fig. 2 the EPR spectrum of a frozen solution of (I) at T = 27.2 K is reproduced. The general features of the spectrum are characteristic for an axially symmetric, randomly oriented S = 1/2 system with parallel and perpendicular sets of ^{99}Tc hyperfine lines, as described by the spin Hamiltonian

$$\hat{H}_{sp} = \beta_e[g_{\parallel}H_z\hat{S}_z + g_{\perp}(H_x\hat{S}_x + Hy\hat{S}_y)] + A_{\parallel}^{Tc}\hat{I}_z\hat{S}_z$$
$$+ A_{\perp}^{Tc}(\hat{I}_x\hat{S}_x + \hat{I}y\hat{S}_y)$$
$$+ Q'\left[\hat{I}_z^2 - \frac{1}{3}I(I+1)\right], \qquad (1)$$

where $g_{\parallel}$, $g_{\perp}$, $A_{\parallel}^{Tc}$ and $A_{\perp}^{Tc}$ are the principal values of the $\tilde{g}$ and the ^{99}Tc hyperfine interaction tensor $\tilde{A}^{Tc}$ and Q' is the ^{99}Tc quadrupole coupling constant. These parameters were obtained by use of the usual second-order expressions;[17] Q' is small and was neglected. The $\tilde{g}$ tensor was found to be nearly isotropic within the experimental error.

In the parallel part of the spectrum the ^{99}Tc hyperfine lines are split into well resolved triplets (intensity ratio 1:2:1) arising from interaction of the unpaired electron with two equivalent ^{31}P nuclei of the phosphine ligands. ^{31}P superhyperfine splitting ("shfs") is also resolved in the perpendicular part of the spectrum. Some further resolution is to be seen on the parallel lines which should be due mainly to the interaction of the unpaired electron with the equatorial ^{35,37}Cl nuclei and, possibly, the ^{14}N nucleus of the NO ligand. Considering the linewidth this splitting was found to be smaller than 0.5 mT. The perpendicular part of the spectrum did not show any further resolution. The measured spin Hamiltonian parameters are listed in Table 1. No differences have been found between the parameters derived at T = 130 and 27.2 K.

Table 1. EPR Parameters† for $TcCl_3(NO)(PMe_2Ph)_2$ (Hyperfine coupling constants are given in $10^{-4}\,cm^{-1}$)

$\tilde{g}$	$\tilde{A}(Tc)$	$\tilde{A}(P)$
$g_{\parallel} = 2.045 \pm 0.003$	$A_{\parallel} = 214.8 \pm 2.0$	$A_{\parallel} = 23.6 \pm 1.0$
$g_{\perp} = 2.049 \pm 0.005$	$A_{\perp} = 89.2 \pm 5.0$	$A_{\perp} = 19.1 \pm 0.5$
$g_{av}\ddagger = 2.048$	$A_{av} = 131.1$	$A_{av} = 20.6$
$g_0 = 2.052 \pm 0.003$	$a_0 = 125.6 \pm 1.0$	

†Anisotropic data obtained from the 27.2 K spectrum; isotropic data (g_0, a_0) are measured at $T = 295$ K.

‡$g_{av} = (g_{\parallel} + 2g_{\perp})/3$, $A_{av} = (A_{\parallel} + 2A_{\perp})/3$.

DISCUSSION

The spectra observed are in agreement with what is expected for a Tc d^5 low-spin complex. The theory of EPR in the $d^5(t_{2g}^5)$ configuration was first put forward by Stevens[18] and then in more complete form by Bleaney and O'Brien.[19] The d^5 system is treated as a d^1 system via the hole formalism. The combined action of a low-symmetry ligand field and spin-orbit interaction resolves the sixfold degeneracy of the $^2T_2$ ground term producing three well-separated Kramers' doublets which can be written as follows[20] assuming tetragonal quantization as suggested by the structure of the complex under study:

$$-|1\rangle = \frac{1}{\sqrt{2}}(d_{xz} + id_{yz}) \tag{2a}$$

$$|-1\rangle = \frac{1}{\sqrt{2}}(d_{xz} - id_{yz}) \tag{2b}$$

$$\xi_1 = id_{xy} = \frac{1}{\sqrt{2}}(|2\rangle - |-2\rangle). \tag{2c}$$

The "effective" symmetry of the first coordination sphere of (I) can be assumed to be an axial one because of the symmetry of the tensor parameters $\tilde{g}$, $\tilde{A}_{Tc}$ of the spin-Hamiltonian observed experimentally (Table 1). Therefore, we are concerned with two different ground state situations depending on the sign and the magnitude of the ligand-field perturbation component: (a) the ground state is mainly determined by ξ_1 (2c), the other orbital states $(-|1\rangle, |-1\rangle)$ are much higher concerning their energy $(\gtrsim 10^4\,cm^{-1})$, (b) the unpaired electron occupies one of the orbital states (2a) or (2b) which are separated by spin-orbit interaction only, if axial symmetry will be assumed. Due to the magnitude of the spin-orbit coupling constant λ of Tc^{2+} $(\lambda(Tc^{2+}) = 850\,cm^{-1})$[21] case

(b) would result in a relatively small separation of (2a) and (2b) and, therefore, in short electron spin-lattice relaxation times for (I) not allowing the observation of well-resolved EPR spectra at room temperature. Therefore, according to the experimental results the ground state must be a Kramers' doublet which consists mainly of ξ_1 (2c). The assumption of a "d_{xy}" ground state is also in agreement with the ^{99}Tc hyperfine structure observed.

An interpretation of the $\tilde{g}$ tensor components in terms of molecular orbital coefficients is extremely difficult for the present case because there are more unknown quantities (ordering of energy levels and energy separations between the levels giving important contributions to the $\tilde{g}$ components, the large number of MO coefficients to be considered) than experimentally obtained ones. A comparison of the experimental spin Hamiltonian parameters with those calculated using the MO coefficients and transition energies obtained from semiempirical MO calculations (preferably Extended Hückel MO calculations) can be very helpful for these purposes.[22-24] However, good results are restricted to $3d$ metals; for $4d$ or $5d$ metals the discrepancies found are too large for a useful interpretation.[25,26] Therefore, in the following only the hyperfine interactions will be analyzed which are mainly magnetic in character allowing us to draw conclusive statements about the MO of the unpaired electron.

The ^{99}Tc *hfs* can be used to estimate the degree of covalency of the equatorial (x, y) Tc-ligand bonds. Applying the formalism given by McGarvey.[27]

$$A_{\parallel}(Tc) = -K - \frac{4}{7}\beta^2 P + (g_{\parallel} - g_e)P + \frac{3}{7}(g_{\perp} - g_e)P \tag{3a}$$

$$A_{\perp}(Tc) = -K + \frac{2}{7}\beta^2 P + \frac{11}{14}(g_{\perp} - g_e)P \tag{3b}$$

$$A_{av}(Tc) = -K + (g_{av} - g_e)P, \qquad (3c)$$

where K is a measure of the Fermi contact interaction and $P = (-)200 \times 10^{-4}\,cm^{-1}$,[27] one arrives at a value of $\beta^2 \approx 0.77$; $K = -141.1 \times 10^{-4}\,cm^{-1}$. β^2 is a measure of covalancy of the equatorial Tc-ligand bonds in the MO of the unpaired electron (contributions of the axial ligands to this MO are expected to be small because of symmetry considerations, therefore, they are neglected):

$$\psi_{MO} = \beta|4d_{xy}\rangle - \beta'|\phi_L\rangle. \qquad (4)$$

The value obtained for β^2 clearly indicates the presence of covalent interactions between Tc and the equatorial ligands.

Additional information about delocalization of "unpaired spin density" can be obtained from ligand hyperfine interactions. In the spectra a well-resolved *shfs* due to the ^{31}P nuclei of the phosphine ligands was observed which is predominantly isotropic in character. From the isotropic ^{31}P *shfs* the coefficient of the P 3s orbital "C_s" in the MO of the unpaired electron can be calculated. Using eqn (5) and $A_{av}(P)_{calc} = (8\pi/3)g_e g_N \beta_e \beta_N |\Psi_{3s}(O)|^2 = 3395 \times 10^{-4}\,cm^{-1}$,[28] C_s is found to be 0.078. This corresponds to a spin density of $C_s^2 \times 100 = 0.61\%$ in the phosphorus 3s orbital.

$$A_{av}(P)_{exp} = A_{av}(P)_{calc} \cdot C_s^2 \qquad (5)$$

In a similar way by means of eqn (6) the anisotropic part of the ^{31}P *shfs* can be analyzed to estimate the P 3p orbital contribution "C_p" to the MO of the unpaired electron.

$$A_{||}(P) - A_{av}(P) = \frac{4}{5}g_e g_N \beta_e \beta_N \langle r^{-3}\rangle_{2p} \cdot C_p^2. \qquad (6)$$

With $[A_{||}(P) - A_{av}(P)] = 3.0 \times 10^{-4}\,cm^{-1}$ and $\frac{4}{5}g_e g_N \beta_e \beta_N \langle r^{-3}\rangle_{3p} = 191.4 \times 10^{-4}\,cm^{-1}$[28] C_p is found to be 0.125. C_s^2 and C_p^2 can be used to estimate the hybridization degree "n^2" of the P 3s and 3p orbitals: $C_s^2/C_p^2 = (1 - n^2)/n^2$. A value of $n^2 = 0.72$ is obtained which is close to what is expected for sp^3 hybridization $[n^2(sp^3) = 0.75]$. This value, however, can be considered as being a rough estimation only because a correction concerning the contribution of the dipolar term $A_d(P) = g_e g_N \beta_e \beta_N / R^3$ (R = Tc–P bond length) has not been made; although, assuming $R \approx 230\,pm$ a value of $A_d^P \approx 0.85 \times 10^{-4}\,cm^{-1}$ will be calculated. A more detailed consideration appears to be not useful because of the magnitude of the experimental error which is $\pm 1.0 \times 10^{-4}\,cm^{-1}$. In contrast to this the C_s value derived from the isotropic

^{31}P *shfs* can be considered as being a good one because of the magnitude of $A_{av}(P)$ much exceeding that of the experimental error.

The predominantly isotropic character of the ^{31}P *shfs* tensor is not unexpected for the complex under study. The ^{13}C *shfs* tensors observed in a single-crystal study for the equatorial CN^- ligands of the d^5 low-spin π acceptor complex $[Cr(CN)_5NO]^{3-}$ the bonding properties of which should be closely related to those of $TcCl_3(NO)(PMe_2Ph)_2$ show a similar behaviour.[29] However, the contribution of the C 2s orbitals to the MO of the unpaired electron—$C_s \approx 0.1$—is found to be larger than that derived for the corresponding P 3s orbitals of (I) indicating more covalent interactions in $[Cr(CN)_5NO]^{3-}$. Unfortunately, for $[Mn(CN)_5NO]^{2-}$ which would be of most interest for comparison purposes, ^{13}C data are not available.[30] A comparison[23] of the electronic structures and the magnetic hyperfine interactions analyzed for the d^5 isoelectronic sequence of pentacyanonitrosyls from vanadium to iron indicates a decrease of spin delocalization as one moves from left to right in the periodic table.

It should be noted, that in the parallel part of the frozen solution EPR spectrum poorly resolved hyperfine interactions due to the $^{35,37}Cl$ nuclei and (less probably) the ^{14}N nucleus of the NO ligand could be detected. Assuming the extent of electron spin delocalization to the chlorine and the phosphine ligands to be of a similar magnitude a value of $A_{av}(Cl) \approx 9 \times 10^{-4}\,cm^{-1}$ will be expected. The actual isotropic $^{35,37}Cl$ splitting is smaller than the predicted one. Due to the less pronounced π acceptor properties of the Cl ligand with respect to PRR$_2'$ this is not unexpected. A contribution of the dipolar part to the $^{35,37}Cl$ *shfs* can be neglected because of its smallness. Considering the ^{14}N *shfs* detected for $[Mn(CN)_5NO]^{2-}$,[30] the corresponding isotropic value for (I) should not exceed $4 \times 10^{-4}\,cm^{-1}$. This value is smaller than that estimated for $A_{av}(Cl)$, therefore, the ^{14}N *shfs* is not expected to be resolved in the spectra of $TcCl_3(NO)(PMe_2Ph)_2$. *Shfs* interactions due to $^{35,37}Cl$ and/or ^{14}N were also not observed in the spectra obtained for $[Tc(NO)Cl_5]^{2-}$ and $[Tc(NH_3)_4(NO)H_2O]^{3+}$ recently reported.[11]

More insight in the bonding situation of $TcX_3(NO)(PR_3)_2$ complexes could be obtained if complexes with $X = Br$ (the $^{79,81}Br$ *shfs* coupling constants are expected to be larger by a factor 4 or 5 than the $^{35,37}Cl$ splittings because of the larger nuclear magnetic moments of $^{79,81}Br$) or diamagnetically diluted single-crystals of (I) would be available. However, we did not succeed in preparing $TcBr_3(NO)(PR_3)_2$, and single-crystals of (I)

could not be grown because of the lack of a suitable host lattice.

REFERENCES

1. P. Valk, J. McRae, A. J. Bearden and P. Hambright, *J. Chem Educ.* 1976, **53**, 542.
2. R. Taube and K. Seyferth, *Z. Anorg. Allg. Chem.* 1977, **437**, 213.
3. J. E. Fergusson and R. S. Nyholm, *Nature* 1959, **183**, 1039.
4. J. E. Fergusson and R. S. Nyholm, *Chem. & Ind.* 1960, 347.
5. J. E. Fergusson and J. H. Hickford, *Aust. J. Chem.* 1970, **23**, 453.
6. R. A. Armstrong and H. Taube, *Inorg. Chem.* 1976, **15**, 1904.
7. J. E. Fergusson and P. F. Heveldt, *J. Inorg. Nucl. Chem.* 1976, **38**, 2231.
8. U. Mazzi, D. A. Clemente, G. Bandoli, L. Magon and A. A. Orio, *Inorg. Chem.* 1977, **16**, 1042.
9. V. I. Spitzyn, A. F. Kuzina, A. A. Oblova, S. V. Kryuchkov and L. I. Belyaeva, *Dokl. Akad. Nauk SSSR* 1977, **237**, 1412.
10. C. Orvig, A. Davison and A. G. Jones, *J. Labelled Compd. Radiopharm.* 1981, **18**, 148.
11. G. C. Yang, M. W. Heitzmann, L. A. Ford and W. R. Benson, *Inorg. Chem.* 1982, **21**, 3242; see also (liquid solution spectra): M. W. Heitzmann, G. C. Yang, L. A. Ford and W. R. Benson, *J. Labelled Compd. Radiopharm.* 1981, **18**, 535.
12. W. Low and P. M. Llewellyn, *Phys. Rev.* 1958, **110**, 842.
13. G. Römelt and K. Schwochau, *Z. Naturforsch.* 1967, **22a**, 519.
14. M. Kawashima, M. Koyama and T. Fujinaga, *J. Inorg. Nucl. Chem.* 1976, **38**, 801.
15. R. Kirmse, J. Stach and H. Spies, *Inorg. Chim. Acta* 1980, **45**, L 251.
16. U. Mazzi, G. de Paoli, P. di Bernardo and L. Magon, *J. Inorg. Nucl. Chem.* 1976, **38**, 721.
17. B. Bleaney, *Philos. Mag.* 1951, **42**, 441.
18. K. W. H. Stevens, *Proc. Roy. Soc., Ser. A* 1953, **219**, 542.
19. B. Bleaney and M. C. M. O'Brien, *Proc. Phys. Soc., Ser. B* 1956, **69**, 1216.
20. J. S. Griffith, *The Theory of Transition Metal Ions*, p. 364. Cambridge, University Press, London (1961).
21. T. M. Dunn, *Trans. Faraday Soc.* 1961, **57**, 1441.
22. C. P. Keijzers and E. de Boer, *Molec. Phys.* 1975, **29**, 1007; 1743.
23. P. T. Manoharan, S. Vijava, J. R. Shock and M. T. Rogers, *J. Chem. Phys.* 1975, **63**, 2507.
24. J. Stach, R. Kirmse, S. Wartewig and R. Böttcher, *Z. Chem.* 1979, **19**, 205.
25. J. G. M. van Rens, Thesis. Nijmegen (1974).
26. A. Nieuwpoort, Thesis. Nijmegen (1975).
27. B. R. McGarvey, *J. Phys. Chem.* 1967, **71**, 51.
28. J. E. Wertz and J. R. Bolton, *Electron Spin Resonance—Elementary Theory and Practical Applications.* McGraw-Hill, New York (1972).
29. H. A. Kuska and M. T. Rogers, *J. Chem. Phys.* 1964, **40**, 910; 1965, **42**, 3034.
30. P. T. Manoharan and H. B. Gray, *Inorg. Chem.* 1966, **5**, 823.

ON THE NET CHARGES IN CYCLOPENTADIENYL METAL COMPOUNDS

NATALIYA A. OGORODNIKOVA and AVTANDIL A. KORIDZE*

A. N. Nesmeyanov Institute of Organo-Element Compounds, Academy of Sciences,
Vavilov Street 28, Moscow, U.S.S.R.

Abstract—An attempt was made to estimate the net charges of a number of cyclopentadienyl metal compounds on the basis of ^{19}F NMR data for p-fluorophenylcyclopentadienyl metal compounds. The investigated compounds can be clearly divided into four groups according to the polarity of metal–cyclopentadienyl bond: covalent compounds (derivatives of Fe, Ru, Os, Rh and Pd) with a net charge on the η-C_5H_5 ring in the range from -0.19 to -0.29, the so-called ionic compounds (derivatives of Li, Na and K) with a net charge on the ring $-0.64 \div -0.72$, and compounds with an intermediate character of the bond (derivatives of Cu, Mg and Tl) with a net charge of $-0.44 \div -0.46$; the net charge on the rings of cyclopentadienyl manganese tricarbonyl and -rhenium tricarbonyl is near to zero. When the effective charge on the ring is near -0.44 the cyclopentadienyl metal compounds are able to dissociate into ions in solution.

The problem of the net charges even in a such well studied molecule as ferrocene has for a long time been a subject of some controversy. According to various quantum-chemical calculations the values of the net charges vary largely not only in absolute values but in sign as well, from -0.64 to $+1.80$ (see data summarized in Ref. 1).

In previous works we investigated m- and p-fluorophenylcyclopentadienyl compounds of transition and non-transition metals by ^{19}F NMR technique and estimated the electronic effects of the corresponding metal cyclopentadienyl groups as substituents in the benzene ring.[2] We studied in detail the effect of alkali metal cation, the coordinating ability of the solvent, complexing agents (TMEDA, crown-ethers), and concentration on the equilibrium between tight and solvent separated ion pairs. On the basis of data obtained for $LiC_5H_4C_6H_4F$-$m(-p)$ and $NaC_5H_4C_6H_4F$-p in hexamethylphosphoramide (HMPA) solution, electronic effect of the $C_5H_4^\ominus$-substituent as a "free ion" has been determined.[2b]

In this paper we attempt to estimate the metal–cyclopentadienyl bond polarity, based on the ^{19}F NMR data of respective fluorophenylcyclopentadienyl organometallic compounds.

RESULTS AND DISCUSSION

Our approach to estimating the net charges in cyclopentadienyl metal compounds on the basis of ^{19}F NMR data of p-fluorophenylcyclopentadienyl derivatives is based on a known linear dependence between calculated charge densities in fluorobenzenes and their ^1H, ^{13}C and ^{19}F NMR chemical shifts.[3] Thus, there is a correlation between ^{13}C chemical shifts of para-carbon atom in monosubstituted benzenes and total electron density on the carbon atom,[3a] excellent correlation between ^{19}F chemical shifts in p-fluorosubstituted benzenes and ^{13}C chemical shifts of para carbon atom in substituted benzenes[3a] and correlation between ^{19}F chemical shifts and p-^{13}C–F chemical shifts in p-fluorosubstituted benzenes.[3a]

Therefore to plot a linear dependence of the net charges on fluorine screening in p-fluorophenylcyclopentadienyl derivatives of metals, it is necessary to have data on charge distribution at least in two such derivatives. The two simplest systems were chosen: "free" p-fluorophenylcyclopentaidenyl anion[2b] and its lithium derivative.

The choice of lithium cyclopentadienyl as one of the reference system is based on the assumption that the extent of charge separation in LiC_5H_5 when going from common solvents (ethers, acetonitrile) to isolated molecule is only slightly changed. Such assumption is substantiated by the

following experimental data. The ^{19}F chemical shifts in lithium p-fluorophenylcyclopentadienyl are independent of concentration and are practically the same for such solvents as acetonitrile and THF,[2b] that have different donor centers, different "donor number" and dielectric constants. The ^{13}C chemical shifts of lithium cyclopentadienyl in these solvents, 103.8 ppm in CH_3CN, 103.2 ppm in THF,[4] and 103.59 ppm in 3:1 mixture of dimethoxyethane–deuterobenzene[5] practically coincide. The $^1J(^{13}C, \, ^1H)$ coupling constants of lithium cyclopentadienyl in these solvents, 159.5, 159.6 and 159.4 Hz respectively,[4,5] are also practically the same.

One more evidence follows from the analysis of ^{7}LiNMR data[6] according to which the ^{7}Li chemical shift of lithium cyclopentadienyl in dioxane, THF, dimethoxyethane and diglyme is essentially constant, $8.35 \div 8.68$ ppm. In this respect lithium cyclopentadienyl differs from all other studied carbanions (1-phenylallyl, 1,3-diphenylallyl, triphenylmethyl, indenyl, fluorenyl),

---

†In calculations we used known data on electron affinity values, determined by minimum energy of the electron detachment from a negative ion (Table 2).

for which the range of ^{7}Li chemical shifts in these solvents exceeds 8 ppm (from 0.66 to 8.99 ppm).

To calculate the net charge in the lithium cyclopentadienyl molecule we used eqn (1), obtained by Matcha and King[7] for determining the effective charge transfer of atoms in alkali metal halides:

$$f = 0.974448 - 0.00435(IP_m - EA_x). \qquad (1)$$

Here IP_m is the ionization potential of the metal and EA_x represents the halogen electron affinity.

First of all it was necessary to check the validity of eqn (1) for evaluating the net charges in organometallic compounds for which quantum-chemical data is available.

Table 1 lists the net charges for isolated molecules of organic derivatives of the alkai metals, calculated according to eqn (1).† The polarity of metal carbanion bond in benzyl, cyclopentadienyl and ethynyl compounds of alkali metals is higher than that of the metal–hydrogen atom bond in metal hydrides. Metal acetylides appear to be the most polar from all the listed compounds, being similar in polarity with alkali metal iodides.[7]

To our knowledge data on molecular orbital calculations of the net charges for organic deriva-

Table 1. The effective charge (atomic units) on the metal atoms in alkali metal compounds[a]

Radical	Li	Na	K	Rb	Cs
H	0.54	0.56	0.64	0.65	0.68
CH_3	0.48	0.50	0.58	0.59	0.62
$C_6H_5CH_2$	0.55	0.58	0.65	0.66	0.69
CH_2CHCH_2	0.52	0.55	0.62	0.63	0.66
$NCCH_2$	0.62	0.65	0.72	0.74	0.76
C_5H_5	0.64	0.66	0.73	0.75	0.77
$CH_3C_5H_4$	0.63	0.65	0.72	0.74	0.76
$HC\equiv C$	0.74	0.77	0.84	0.85	0.88
CH_3O	0.62	0.64	0.71	0.73	0.76
$(CH_3)_3CO$	0.64	0.67	0.74	0.76	0.78
$(CH_3)_3CCH_2O$	0.65	0.67	0.75	0.76	0.79
C_6H_5O	0.69	0.71	0.79	0.80	0.83
$o-CH_3C_6H_4O$	0.69	0.71	0.79	0.80	0.83
$o-ClC_6H_4O$	0.71	0.73	0.81	0.82	0.85
C_6H_5S	0.70	0.72	0.80	0.81	0.84
HS	0.68	0.71	0.78	0.80	0.82
CH_3S	0.64	0.67	0.74	0.75	0.78
CD_3S	0.64	0.67	0.74	0.75	0.78
C_2H_5S	0.65	0.67	0.75	0.76	0.79
$n-C_3H_7S$	0.66	0.68	0.75	0.77	0.79
$iso-C_3H_7S$	0.66	0.68	0.75	0.77	0.80
$n-C_4H_9S$	0.66	0.68	0.76	0.77	0.80
$tert-C_4H_9S$	0.66	0.69	0.76	0.77	0.80
$n-C_5H_{11}S$	0.66	0.69	0.76	0.78	0.80

[a] In calculations we used the values of ionization potentials of metals, listed in ref. (7).

Table 2. Electron affinity (EA) of radicals estimated by minimal energy of electron photodetachment from a negative ion

Radical	EA		References
	eV	kcal/mol	
H	0.7539±0.002	17.4	13
CH$_3$	0.08±0.03	1.8±0.7	14
C$_6$H$_5$CH$_2$	≤ 0.88±0.06	≤ 20.4±1.5	15
CH$_2$CHCH$_2$	0.550±0.054	12.7±1.2	16
NCCH$_2$	1.507±0.018	38.4±0.4	16
C$_5$H$_5$	1.786±0.020	41.2	17
CH$_3$C$_5$H$_4$	≤ 1.67±0.04	≤ 38.5	18
HC≡C	2.94±0.10	67.8	19
CH$_3$O	1.59±0.04	36.7±0.9	20
(CH$_3$)$_3$CO	1.87±0.01	43.1±0.2	20
(CH$_3$)$_3$CCH$_2$O	1.93±0.06	44.5±1.4	20
C$_6$H$_5$O	≤ 2.36±0.06	≤ 54.4±1.4	21
o-CH$_3$C$_6$H$_4$O	≤ 2.36±0.06	≤ 54.4±1.4	21
o-ClC$_6$H$_4$O	≤ 2.58±0.08	≤ 59.5±1.8	21
C$_6$H$_5$S	≤ 2.47±0.06	≤ 57.0±1.4	21
HS	2.31±0.01	53.3±0.2	22
CH$_3$S	1.861±0.004	42.91±0.09	22
CD$_3$S	1.856±0.006	42.80±0.14	22
C$_2$H$_5$S	1.953±0.006	45.04±0.14	22
n-C$_3$H$_7$S	2.00±0.02	46.1±0.5	22
iso-C$_3$H$_7$S	2.02±0.02	46.6±0.5	22
n-C$_4$H$_9$S	2.03±0.02	46.8±0.5	22
tert-C$_4$H$_9$S	2.07±0.02	47.7±0.5	22
n-C$_5$H$_{11}$S	2.09±0.02	48.2±0.5	22

tives of Na, K, Rb and Cs are not available. The results of available calculations of the extent of charge separation in organolithium compounds are listed below.

With methyllithium the following values of the net charges on Li atom have been estimated: + 0.37,[8a] + 0.14,[8b] + 0.35,[8c] + 0.56[8d] (ab initio), + 0.37[8e] and + 0.45.[8f] The value + 0.48 (Table 1) obtained by the eqn (1) is in a good agreement with the majority of theoretical data. The net charge + 0.74 on Li atom in ethynyllithium, evaluated by the equation (1), coincides with the calculated charges +0.74[9a] and + 0.78[9b] (ab initio). In the case of allyllithium the calculated values of the effective charges on Li atom are +0.44,[10a] +0.16[10b] (ab initio), and + 0.12[10c] as compared with +0.52 value found by eqn (1). Thus the values of net charges obtained by eqn (1) for various organolithium compounds are in agreement with the available theoretical data.

On this basis we assumed the value − 0.64 calculated by eqn (1) for the net charge of the ring in lithium cyclopentadienyl (this value corresponds to ^{19}F chemical shift 11.1 ppm of lithium p-fluorophenylcyclopentadienyl[26]) and the value

− 1.0 corresponding to the fluorine chemical shift 17.9 ppm of lithium (sodium) p-fluorophenylcyclopentadienyl in HMPA ("free" cyclopentadienyl anion).[2b] So we obtained the relationship (2) defining the dependence of a bond polarity of cyclopentadienyl metal compounds on fluorine chemical shift in corresponding p-fluorophenyl derivatives

$$f = 0.05 - 0.053(\delta\,^{19}\mathrm{F}) \qquad (2)$$

where f is the net charge of cyclopentadienyl ring (in a.u.) and $\delta\,^{19}$F denotes fluorine NMR chemical shift in ppm relative to fluorobenzene.

In accordance with the relationship (2) the net charge of cyclopentadienyl ring in ferrocene is equal to − 0.26 and consequently the iron atom has partial charge of + 0.52 (Table 3). This value is in a good agreement with calculated + 0.682[11]. The net charges on Ru and Os atoms in ruthenocene and osmocene only slightly differ from the charge on the iron atom in ferrocene.

As it is seen from Table 3 the data for metallocenes of the iron subgroup are in a good agreement with the results obtained by Alexanyan et al.[12] in studying the extent of charge separation

Table 3. Effective charges (atomic units) in cyclopentadienyl compounds of metals and ^{19}F NMR chemical shifts in their p-fluorophenyl derivatives

Compound	^{19}F NMR chemical shifts[a]			Effective charges	
	Solvent	$\delta(^{19}F)$	Ref.	Ring	Metal
LiC_5H_5	HMPA	17.9	2[b]		-1.0[b]
NaC_5H_5	HMPA	17.8	2[b]		-1.0[b]
LiC_5H_5	THF	11.1	2[b]		(-0.64)[c] +0.64
NaC_5H_5	THF	12.3	2[b]	-0.69	(-0.66)[c] +0.69
KC_5H_5	THF	12.7	2[b]	-0.72	(-0.73)[c] +0.72
$Mg(C_5H_5)Br$	THF	7.8	2[a]	-0.46	
$Cu(C_5H_5)(PEt_2Ph)$	THF	7.5	2[e]	-0.45	
$Tl(C_5H_5)$	THF	7.4	2[a]	-0.44	
$Pd(C_5H_5)(C_3H_5)$	CCl_4	4.6	2[a]	-0.29	
$Fe(C_5H_5)_2$	THF	4.0	2[c]	-0.26	$+0.52$
$Ru(C_5H_5)_2$	C_6H_6	3.85	2[c]	-0.25	$+0.50$
$Os(C_5H_5)_2$	C_6H_6	3.76	2[c]	-0.25	$+0.50$
$Rh(NBD)(C_5H_5)$	CCl_4	3.47	23	-0.23	
$Rh(cyclo-C_6H_8-1.3)-(C_5H_5)$	CCl_4	3.31	23	-0.23	
$Rh(COD)(C_5H_5)$	CCl_4	2.72	23	-0.19	
$Mn(C_5H_5)(CO)_3$	CCl_4	-0.04	2[d]	-0.05	
$Re(C_5H_5)(CO)_3$	CCl_4	-0.59	2[d]	-0.02	
$[Fe(C_5H_5)_2 H]^+$	HBF_3OH	-0.3	24	-0.03	
$Mo(C_5H_5)_2(NO)I$	CS_2	-1.63	25	$+0.04$	

[a] Recorded for $\sim 0.1M$ solutions in ppm relative to C_5H_5F, the positive sign indicates the shift into strong field.

[b] Adopted on the basis of measurement of ^{19}F NMR chemical shifts of p-fluorophenylcyclopentadienyl compounds of Li and Na[2b],^{7}Li NMR chemical shifts of LiC_5H_5[6], ^{13}C NMR chemical shifts and $^{13}C,^1H$ coupling constants in LiC_5H_5 and NaC_5H_5[4].

[c] Calculated by equation (1).

through analysis of absorption band intensities in vibrational spectra of sandwich compounds. The authors came to a conclusion that the bond polarity in all studied systems (bis-cyclopentadienyl derivatives of Mg, Ca, V, Cr, Mn, Fe, Co, Ni, Ru and Os) for both covalent compounds and compounds traditionally considered as ionic (derivatives of Mg, Ca and Mn) do not exceed 0.6. Unfortunately this technique does not permit a determination of the sign of the charge on the metal.

In the case of monocyclopentadienyl organometallic compounds containing other ligands as well, our approach can only help to evaluate the net charge in the ring. As it is seen from Table 3 the polarity of palladium–cyclopentadienyl and rhodium–cyclopentadienyl bonds in $Pd(C_5H_5)$ (C_3H_5) and $Rh(dien)(C_5H_5)$ complexes is closely similar to that in ferrocene, ruthenocene and osmocene. The charge of the ring in cyclopentadienyl manganese tricarbonyl and -rhenium tricarbonyl is close to zero just as in iron protonated ferrocene and $Mo(C_5H_5)_2(NO)I$.

The organometallic compounds $Cu(C_5H_5)$ (PEt$_2$Ph), $Mg(C_5H_5)Br$ and TlC_5H_5 occupy the intermediate position between the covalent derivatives of iron, ruthenium, osmium, rhodium and palladium on the one hand, and mostly ionic derivatives of alkali metals on the other hand; the net charge of the ring in these compounds is practically the same -0.45, -0.46 and -0.44 respectively.

The stereochemical approach used in our earlier work[2a] (it consists in a comparative ^{13}C NMR study of diastereotopy of cyclopentadienyl carbons in $TlC_5H_4CH(Me)Ph$, $KC_5H_4CH(Me)Ph$, and $Fe(C_5H_5)C_5H_4CH(Me)Ph$) reveals that the thallous compound in THF solution is predominantly in the form of tight ion pairs. Thus beginning with the net charge in the ring of -0.44 the cyclopentadienyl derivatives of metals may dissociate into ions in solutions.

The net charge values obtained for cyclopentadienyl compounds of metals are in a good agreement with the relative reactivity of these compounds and with their physical properties and calculated characteristics.

It should be noted that neither our conclusions

nor our quantitative appraisals are significantly changed when other reference points and other solvents are used to plot the straight line. The absolute value of the net charge of cyclopentadienyl ring in ferrocene molecule according to the relationship obtained from the value of fluorine chemical shift of "free" anion and passing through zero (fluorobenzene), is only 0.04 less than the value 0.26 adopted in discussion. With relationship obtained from fluorine chemical shifts of "free" anion and $LiC_5H_4C_6H_4F\text{-}p$ in acetonitrile this value is higher by 0.06.

Thus, on the basis of ^{19}F NMR data for p-fluorophenylcyclopentadienyl metal compounds an attempt was made to evaluate the net charges of a number of cyclopentadienyl metal compounds. According to the polarity of metal–cyclopentadienyl bond the investigated compounds can be divided into four groups: covalent compounds (derivatives of Fe, Ru, Os, Rh and Pd) with the partial charge on C_5H_5 ring in the range from -0.19 to -0.29; the so-called ionic compounds (derivatives of Li, Na and K) with a charge on the ring from -0.64 to -0.72, and compounds with an intermediate character of the bond (derivatives of Cu, Mg and Tl) with a charge on the ring close to -0.45; the net charge of the ring in cyclopentadienyl manganese tricarbonyl and -rhenium tricarbonyl is near to zero. The cyclopentadienyl derivatives of metals may dissociate into ions in solutions when the effective charge on the ring is close to value of -0.44.

REFERENCES

1. [a]N. M. Klimenko, *Structure of Molecules and Chemical Bonding*, Vol. 6. Quantum Chemical Calculations of Transition Metal Complexes. VINITI, Moscow (1978). [b]D. Schmitz, J. Fleischhauer, U. Meier, W. Schleker and G. Schmitt, *J. Organometal. Chem.* 1981, **205**, 381.
2. [a]A. A. Koridze, N. A. Ogorodnikova and P. V. Petrovsky, *J. Organometal. Chem.* 1978, **157**, 145; [b]N. A. Ogorodnikova, A. A. Koridze and S. P. Gubin, *J. Organometal. Chem.* 1981, **215**, 293; [c]S. P. Gubin, A. A. Koridze, N. A. Ogorodnikova, A. A. Bezrukova and B. A. Kvasov, *Izv. Akad. Nauk SSSR, Ser. Khim.* 1981, 1170; [d]S. P. Gubin, A. A. Koridze, N. A. Ogorodnikova and B. A. Kvasov, *Doklady AN SSSR* 1972, **205**, 346; [e]A. A. Koridze, P. V. Petrovsky, A. S. Peregudov and N. A. Orogodnikova, *Izv. Akad. Nauk SSSR, Ser. Khim.* 1980, 2613.
3. [a]W. J. Hehre, R. W. Taft, R. D. Topsom, *Prog.* *Phys. Org. Chem.* 1976, **12**, 159; [b]G. E. Maciel and J. J. Natterstad, *J. Chem. Phys.* 1965, **42**, 2427.
4. N. A. Ogorodnikova and A. A. Koridze, *Izv. Akad. Nauk SSSR, Ser. Khim.* in press.
5. P. Fischer, J. Stadelhofer and J. Weidlein, *J. Organometal. Chem.* 1976, **116**, 65.
6. R. H. Cox and W. H. Terry, *J. Magn. Resonance* 1974, **14**, 317.
7. R. L. Matcha and S. C. King, *J. Amer. Chem. Soc.* 1976, **98**, 3420.
8. [a]N. C. Baird, R. F. Barr and R. K. Datta, *J. Organometal. Chem.* 1973, **59**, 65; [b]N. J. Fitzpatrick, *Inorg. Nucl. Chem. Lett.* 1974, **10**, 263; [c]M. F. Guest, I. H. Hillier and V. R. Saunders, *J. Organometal. Chem.* 1972, **44**, 59; [d]A. Streitweiser, Jr., J. E. Williams, S. Alexandratos and J. M. McKelvey, *J. Am. Chem. Soc.* 1976, **98**, 4778; [e]G. R. Peyton and W. H. Glaze, *Theor. Chim. Acta* 1969, **13**, 259; [f]A. H. Cowley and W. D. White, *J. Amer. Chem. Soc.* 1969, **91**, 34.
9. [a]A. Hinchliffe, *J. Mol. Struct.* 1977, **37**, 145; [b]A. Veillard, *J. Chem. Phys.* 1968, **48**, 2012.
10. [a]T. Clark, E. D. Jemmis, P. v. R. Schleyer, J. S. Binkley and J. A. Pople, *J. Organometal. Chem.* 1978, **150**, 1; [b]A. Borgini, G. Cainelli, G. Cardillo, P. Palmieri and A. Umani-Ronchi, *J. Organometal. Chem.* 1976, **110**, 1; [c]E. R. Tidwell and B. R. Russel, *J. Organometal. Chem.* 1974, **80**, 175.
11. E. M. Shustorovish and M. E. Dyatkina, *Doklady Akad. Nauk SSSR* 1959, **128**, 1234.
12. [a]V. T. Alexanyan, T. I. Arsenieva, N. N. Vyshinsky, I. I. Grinvald and A. N. Smirnov, *Izv. Akad. Nauk SSSR, Ser. Khim.* 1981, 299; [b]V. T. Alexanyan, N. N. Vyshinsky, I. I. Grinvald and T. I. Arsenieva, *Izv. Akad. Nauk SSSR, Ser. Khim.* 1981, 303; [c]V. T. Alexanyan and I. I. Grinvald, *J. Mol. Struct.* 1982, **90**, 35.
13. D. Feldman, *Phys. Lett. A* 1975, **53A**, 82.
14. G. B. Ellison, P. C. Engelking and W. C. Lineberger, *J. Am. Chem. Soc.* 1978, **100**, 2556.
15. J. H. Richardson, L. M. Stephenson and J. I. Brauman, *J. Chem. Phys.* 1975, **63**, 74.
16. A. H. Zimmerman and J. I. Brauman, *J. Am. Chem. Soc.* 1977, **99**, 3565.
17. P. C. Engelking and W. C. Lineberger, *J. Chem. Phys.* 1977, **67**, 1412.
18. J. H. Richardson, L. M. Stephenson and J. I. Brauman, *J. Chem. Phys.* 1973, **59**, 5068.
19. B. K. Janousek and J. I. Brauman, *J. Chem. Phys.* 1979, **71**, 2057.
20. B. K. Janousek, A. H. Zimmerman, K. I. Reed and J. I. Brauman, *J. Am. Chem. Soc.* 1978, **100**, 6142.
21. J. H. Richardson, L. M. Stephenson and J. I. Brauman, *J. Am. Chem. Soc.* 1975, **97**, 2967.
22. B. K. Janousek, K. I. Reed and J. I. Brauman, *J. Am. Chem. Soc.* 1908, **102**, 3125.
23. A. A. Koridze, *Koord. Khimia* 1982, **8**, 380.
24. T. E. Bitterwolf and A. C. Ling, *J. Organometal. Chem.* 1977, **141**, 355.
25. A. A. Koridze, A. I. Yanovsky, Yu. L. Slovokhotov, V. T. Andrianov and Yu. T. Struchkov, *Koord. Khim.* 1982, **8**, 541.

THE SOLUBILITY OF URANIUM(IV) HYDROUS OXIDE IN SODIUM HYDROXIDE SOLUTIONS UNDER REDUCING CONDITIONS

JACK L. RYAN* and DHANPAT RAI
Pacific Northwest Laboratory, P.O. Box 999, Richland, WA 99352, U.S.A.

Abstract—The solubility of hydrous UO_2 in sodium hydroxide solutions containing sodium dithionite and/or Zn metal powder as reductants has been measured. The results provide no firm evidence for any amphoteric behavior of U(IV) but do set an upper limit of $K \leq 2 \times 10^{-23}$ for the hypothetical reaction:

$$U^{4+}(aq) + 5H_2O \rightleftharpoons U(OH)_5^- + 5H^+.$$
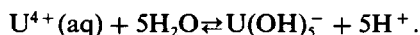
The results provide no evidence for such a reaction.

The hydrolysis behavior of metal cations is a field about which a very large degree of uncertainty exists. In particular, much of the experimental data[1] are highly questionable because of inadequate or improper experimental technique, sparcity of data points, and wide scatter in the data. Often later authors have used such poor or limited experimental data to arrive at conclusions different from and often much beyond those that the original authors were willing to make. An example of this is the calculation of the formation constants of the lanthanide tetrahydroxo complexes[1] from data on the solubility of the $Ln(OH)_3$ in NaOH solutions in which some of the original workers indicated that the experimental results were not adequate for any calculation of species formed[2] and from data of other workers that clearly does not show such a dependence of solubility on NaOH concentration or mean ionic activity[2-4] as to be able to conclude that the $Ln(OH)_4^-$ ions are even being formed.

The solubilities of the actinides at near neutral pH values are of particular importance to the geological disposal of nuclear waste. In particular, the solubility of tetravalent actinides is of importance under the reducing conditions expected in several of the proposed repository environments such as deep basalt or granite. Under these conditions, tetravalent species of U, Np and perhaps Pu become important. There has been a large effort exerted towards prediction of solubilities and modeling of actinide migration behaviour on the basis

of hydrolysis and complex formation equilibria. Much of this equilibrium hydrolysis data has come from limited and poor experimental results or has been estimated by extrapolation from other hydrolysis constants of the same metal ions by what might be considered reasonable but certainly unproven methods.

Specifically, with the tetravalent actinides, almost all of the hydrolysis data for mononuclear species beyond the MOH^{3+} species is based on old and questionable work by Gayer and Leider[5] on the solubility of what they called uranium (IV) hydroxide [actually hydrous U(IV) oxide.[6] Hydrous U(IV)oxide, $UO_{2(am)}$, is *very* easily air-oxidized, and their preparation and handling of the material leaves considerable doubts that they measured U(IV) in solution at all. In addition, their solutions were settled for 3–5 days without filtration. (It is the present authors' observation that centrifuging at 1500 G for up to 1 hr will not totally remove the Tyndall Effect from even fresh suspensions of crystalline UO_2.) They measured U concentrations at six NaOH concentrations, and after discarding two data points that did not fit their conclusions, used only four points to arrive at a first power dependence on OH^- concentration (0.14 to 0.48 M) and calculated an equilibrium constant for formation of $H_3UO_4^-$. Baes and Mesmer[1] assumed this species to be $U(OH)_5^-$ instead of $H_3UO_4^-$ and, making the totally erroneous assumption that Gayer and Leider had used $UO_2(c)$ instead of amorphous hydrous UO_2 (referred to as "$U(OH)_4$" by gayer and Leider,[5] calculated the fifth hydrolysis constant of U(IV). Then, using measured values for the first hydro-

lysis constant and the perhaps not completely unreasonable but certainly completely unproven assumption that the logarithms of the stepwise hydrolysis constants are linear with respect to the number of hydroxide ions, they calculated values for the formation constants of the $U(OH)_2^{2+}$, $U(OH)_3^+$, and $U(OH)_4(aq)$ species. Actually such a concept could be very strongly questioned on several grounds such as for example the fact that there certainly does not appear to be a uniform progression in the hydrolysis of the actinide M^{5+} or M^{6+} ions where *very* strong hydrolysis to the MO_2^+ and MO_2^{2+} ions occurs with little apparent stability for less hydrolyzed species along with a much lower tendency to further hydrolysis. In fact, the tendency of pentavalent and hexavalent actinides to form oxo rather than hydroxo species, and the fact that the tetravalent actinides precipitate as hydrous oxides rather than hydroxides[6] raises a question of whether complexes such as $U(OH)_4(aq)$ and $U(OH)_5^-$ exist at all.

Langmuir[7] repeated the same hydrolysis constant estimates for U(IV) made by Baes and Mesmer[1] including the erroneous assumption that there was no free energy change in forming $UO_2(c)$ from the amorphous "$U(OH)_4$" solid used by Gayer and Leider.[5] He calculated free energies of formation for $U(OH)_2^{2+}$, $U(OH)_3^+$, $U(OH)_4(aq)$, and $U(OH)_5^-$. It is interesting that Langmuir made the opposite assumption further on in his paper[7] to conclude that $UO_{2(am)}$, which is indeed the same as "$U(OH)_4$," is at least 7.6 kcal/mole less stable than $UO_2(c)$ and may more likely be 12.8 kcal/mole less stable. These erroneous formation constants[7] have been further used,[8] apparently without critical review, to calculate the solubility of amorphous UO_2, as a function of pH. The preposterous conclusion, in terms of well-known U(IV) chemistry, was reached and published[8] that uranium solubility at low (10^{-80}) oxygen fugacity would increase above about pH 4.5 reaching 1 g/L at pH 9.8, and 10 g/L at pH 10.8. Such conclusions appear to be the result of a total loss of contact with the reality of known actinide behaviour and a total preoccupation with the computer manipulation of formation constant data without regard to its validity.

Others[9-12] have repeated similar estimates of U(IV) hydrolysis constants or free energies of formation often giving additionally estimates of entropies, extrapolating to other tetravalent actinides, or giving values as a function of ionic strength. Most of these values are the same or very near those reported by Baes and Mesmer[1] and are based on the limited and questionable results of Gayer and Leider.[5]

Tremaine et al.[13] have made a careful attempt to measure the solubility of $UO_2(c)$ under non-oxidizing conditions at high pH. They used de-aereated and H_2 saturated LiOH solutions (about 0.003 and 0.04 M) in a flow apparatus with concentration of U by ion exchange followed by neutron activation analysis. Their U solubilities were in the range of about 5×10^{-8} to $1.7 \times 10^{-7} M$ (seventy-fold lower than the values predicted for these OH$^-$ concentrations for $UO_2(am)$ by Gayer and Leider's[5] results). Their U analyses were apparently near their detection limit due to ^{18}F interference which is directly proportional to the LiOH concentration. Also, they have shown[13] by X-ray photoelectron spectra that during their flow solubility runs below 150°, oxidation of the UO_2 surface beyond the initial 0.3 U(VI)/U(IV) (corresponding to two monolayers of UO_3) occurred up to at least 0.76 U(VI)/U(IV). Their solutions apparently also contained somewhat less than 1% carbonate relative to hydroxide, and they showed based on literature stability constants, that at $10^{-8} M$ CO_3^{2-} and 10^{-5} atm O_2 the U(VI)/U(IV) ratio in solution should be 10^7. Despite this, they have interpreted their results based on only two OH$^-$ concentrations in terms of the predominant solution species being $U(OH)_5^-$. It is our opinion that they cannot possibly have measured U(IV) solubility as long as U(VI) solid is clearly present, and it is known that U(VI) has a solubility of $\geq 10^{-3} M$ in LiOH solutions in this concentration range[14] (as it also has in $(C_3H_7)_4NOH$[15] and $(C_4H_9)_4NOH$[16] solutions).

The present work reports results of a study of the solubility of amorphous, hydrous UO_2 under anoxic, reducing, alkaline conditions at 25°. Sodium dithionite and metallic zinc were used as reductants in this study.

EXPERIMENTAL

Reagents

Water was in all cases deaerated by boiling following by thorough sparging at 25° with Ar($> 99.99\%$). A new bottle of reagent grade pellets of NaOH was opened in an Ar atmosphere, and a stock 10.5 M NaOH solution was prepared under Ar. An analysis showed 0.0152 M carbonate. A 7.5% excess of $BaCl_2$ was added, and the closed container was allowed to stand for two weeks under Ar to achieve complete precipitation and settling of the $BaCO_3$. Sodium dithionite was from Sigma Chemical and a 1 M stock solution was prepared under Ar immediately before it was used to make up the first series of solubility solutions.

U(IV) stock solution was prepared by dissolving Hanford reactor grade uranium metal in 12 M HCl (initially with solution cooling but finally with heating to 100°). The hot solution was centrifuged while slow H_2 evolution was still occurring from black residues. The solution (~ 500 g U(IV)/L and ~ 2 M HCl) was then filtered through an 250 nm Millipore Solvinert filter and stored under Ar.

General procedure

All solutions were made up and handled in an Ar atmosphere, and all solution containers were kept closed except for the minimum times necessary for makeup and sampling. Sodium hydroxide solutions (20 cm^3) were made by dilution of the stock solution, followed immediately by addition of reductant, and then of the U(IV) solution. The total U present was 0.25 mg/cm^3, and by adding it as such a concentrated stock solution, its precipitation and the neutralization of excess acid would be expected to consume only 0.005 M OH$^-$, which is 10% of the lowest hydroxide concentration used. All the sealed containers of solution plus hydrous UO$_2$ were shaken vigorously for 13 or 16 days at room temperature (21 $\pm$ 2°). At the end of this equilibration period, the still-sealed containers were centrifuged for 30 min at > 1000 G. Each container was then opened under Ar and the supernatant solution was quickly sampled by syringe. A membrane filter was immediately attached to the syringe, and the solution forced slowly through the filter. The filters in all cases except the ≥ 10 M NaOH solutions were Nuclepore Ultrafilter®, Type F, No. 1F7257, which has a 20,000 molecular weight cutoff for globular proteins (~ 2 nm pore size), and is resistant to OH$^-$ solutions. Insufficient flow of ≥ 10 M NaOH could be obtained with this filter, and Millipore Solvinert® filters UGWP with 250 nm pore size were used for these solutions.

Uranium analysis

Uranium analyses were made by laser-induced fluorescence using a Scintrex® model UA-3 uranium analyzer with the known addition technique.[17,18] The samples were pretreated by addition of excess NaOCl (while still basic so that the dithionite would not decompose before it was oxidized) and were then acidified and, except for the samples containing only Zn as reductant, taken to dryness. The residues (principally Na salts) were taken up in dilute HNO$_3$ and analyzed. The samples containing Zn only as reductant showed a high fluorescence before addition of the buffered complexant used in the method if they had been dried so were taken only to near dryness. The principal

purpose of the drying was to remove excess acid to avoid over-consuming the buffering capacity of the complexant.

Known U standards were, after addition of NaOH, Na$_2$S$_2$O$_4$, etc. taken through the above procedure with accurate recovery. These standards and those used in the known addition technique were prepared from NBS uranium metal standard. Reagent blanks corresponding approximately in composition to some of the samples yielding results below 10^{-8} M were run and gave approximately 80% of the sample values (instrument scale readings were also very low for these) indicating that the true values for samples below 10^{-8} M are in all cases less than those shown.

RESULTS AND DISCUSSION

Tremaine, et al.[13] have estimated, based on earlier stability constant estimates[19] using the Gayer and Leider[5] data for U(OH)$_5^-$, that $K = 3 \times 10^{55}$ for the reaction:

$$U(OH)_5^- + CO_3^{2-} + \tfrac{1}{2}O_2 + 3H^+ \rightleftarrows UO_2CO_3(aq) + 4H_2O. \quad (1)$$
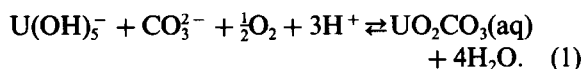
A reasonable estimate for the carbonate concentration at their highest LiOH concentration (0.04 M) would be about 2×10^{-4} M. This would mean that an O$_2$ fugacity of less than 10^{-26} would be required to maintain a U(VI)/U(IV) ratio of one in solution. Any lower stability of U(OH)$_5^-$ (as reflected by lower U(IV) solubility) would lower the required O$_2$ fugacity by two orders of magnitude for each order of magnitude lower U(IV) solubility. This alone points to the impossibility of Gayer and Leider's results being correct since they used no reductant for O$_2$ removal at all. It is also extremely improbable that the H$_2$ used by Tremaine et al.[13] could be a kinetically sufficient reductant to achieve such low fugacities, especially at temperatures below 150°C.

The dithionite ion is known to be a strong reductant with $E_B^\circ = 1.12 V$[19] for the reaction:

$$S_2O_4^{2-} + 4OH^- \rightleftarrows 2SO_3^{2-} + 2H_2O + 2e^-. \quad (2)$$
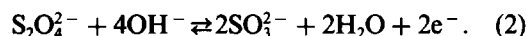
It is known that alkaline dithionite solution reacts with oxygen rather rapidly,[20] and it was found that when 1–10 g U(VI)/L solutions in (C$_3$H$_7$)$_4$NOH were warmed with dithionite (or the related Rongolite), reduction and precipitation of U(IV) hydrous oxide occurred. Based on the above potential, it can be shown that the thermodynamic equilibrium oxygen fugacity in NaOH solutions above 0.01 M and containing 50% oxidized dithionite would be below 10^{-90}. Zinc metal is slightly

more reducing with $E_B^\circ = 1.216V^{19}$ for the reaction:

$$Zn + 4OH^- \rightleftarrows ZnO_2^{2-} + 2H_2O + 2e^- \qquad (3)$$
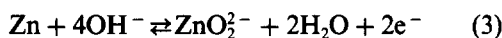
and the ZnO_2^{2-} ion is sufficiently stable[19], with $K = 1 \times 10^{-29}$ for:

$$Zn(OH)_2 \rightleftarrows ZnO_2^{2-} + 2H^+ \qquad (4)$$
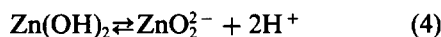
to maintain small amounts of Zn in solution and not form $Zn(OH)_2$ at the OH^- concentrations of interest here. Zn metal will also thermodynamically keep O_2 fugacity below 10^{-90} above $0.01\ M$ NaOH, but because it is a solid may not be kinetically adequate. Using the reductants discussed above, solubility measurements were made in three series of solutions. The principal series was in dithionite solution while fewer measurements were made with zinc metal or zinc metal plus dithionite.

Carbonate was removed from the stock $10.5\ M$ NaOH with $BaCl_2$ at an $0.0012\ M$ excess. If activity coefficients are neglected (they should be greater than one in $10.5\ M$ NaOH), a CO_3^{2-} concentration in this stock solution of $5 \times 10^{-6}\ M$ is obtained based on the published[21] solubility product for $BaCO_3$. The values for the individual solutions will vary with the dilution factor from this stock solution.

Table 1 gives measured total uranium concentrations in the dithionite containing solutions of NaOH in contact with hydrous UO_2. The solubilities are shown in Figure 1 along with those of Gayer and Leider[5] as a function of mean ionic activity of NaOH using activity coefficient data of Hamer and Wu.[22] The solid line corresponds to the formation constant reported by Gayer and Leider. Over the concentration range where the Gayer and Leider measurements were made, the values measured here are all 10^3 to 10^4-fold lower than those of Gayer and Leider and all values are, as discussed in the experimental section, almost at the reagent blank level so they must be considered at the detection limit and are upper limits on the true solubility. Since they are upper limits, no significance can be placed on a possible slope in this region. At higher NaOH concentrations, there is greater than an order of magnitude scatter in the total U concentration data so again a slope cannot be determined.

Table 2 gives measured total uranium concentrations in NaOH solutions containing metallic zinc powder and hydrous UO_2. These results are also shown in Fig. 1 as a function of mean ionic activity of NaOH. The measured solubilities with Zn as a reductant are higher at low NaOH concentrations and lower at high NaOH concentrations than those with dithionite as the reductant. It was observed that at $10\ M$ NaOH, most of the sodium dithionite actually precipitated from solution. Also, because of the increasing stability of the

Table 1. Measured U(IV) hydrous oxide solubility in NaOH-0.05 M $Na_2S_2O_4$ solutions

NaOH Molarity	U Molarity
0.045	3.6×10^{-8}
0.070	4×10^{-9}
0.095	5×10^{-9}
0.145	9×10^{-9}
0.295	8×10^{-9}
0.50	7×10^{-9}
0.65	7×10^{-9}
0.80	8×10^{-9}
1.00	2.4×10^{-7}
2.00	2.5×10^{-8}
3.00	1.9×10^{-7}
5.0	6.7×10^{-5}
7.0	1.3×10^{-5}
10.0	1.5×10^{-4}
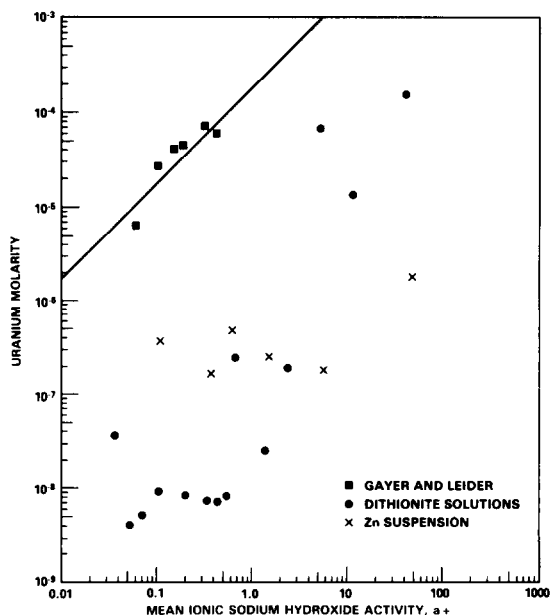
Fig. 1. Measured apparent solubilities of hydrous U(IV) oxide in sodium hydroxide solutions. Results of Gayer and Leider are from Ref. 5. Dithionate solutions were initially 0.05 M $Na_2S_2O_4$ and Zn suspensions were initially 1.6 mg Zn/cm³.

Table 2. Measured U(IV) hydrous oxide solubility in initially 1.6 mg Zn/cm³ suspensions in NaOH

NaOH Molarity	U Molarity
0.153	5.0×10^{-7}
0.55	1.64×10^{-7}
1.05	4.6×10^{-7}
2.10	2.48×10^{-7}
5.2	1.81×10^{-7}
10.5	1.81×10^{-6}

Table 3. Measured U(IV) hydrous oxide solubility in NaOH-0.05 M Na₂S₂O₄ solutions containing initially 1.6 mg Zn/cm³

NaOH Molarity	U Molarity
0.145	5.46×10^{-8}
0.50	7.98×10^{-7}
1.00	8.82×10^{-7}
2.00	2.28×10^{-6}
5.0	8.4×10^{-6}

ZnO_2^{2-} ion relative to $Zn(OH)_2$ or ZnO at high hydroxide concentrations, it might be expected that any coating initially present or forming on the Zn surface might be more readily removed at higher alkalinity making Zn kinetically more effective at the higher hydroxide concentrations. At lower (< 1 M) NaOH concentration, the higher apparent solubilities with Zn reductant may be due to poorer kinetics of oxygen scavenging or might possibly be due to uranium complexing by ZnO_2^{2-} ion. In any case, all values are much below those predicted by the results of Gayer and Leider.[5]

Table 3 gives measured total uranium concentrations in NaOH solutions containing both dithionite and Zn metal powder. Despite the fact that the values in Table 3 are all at least two orders of magnitude lower than predicted by the results of Gayer and Leider, they are higher in all cases but one than the values for dithionite alone, and in all but one other case than values for Zn alone. The reason for this is not clear; the dithionite stock solution was 2 weeks old when used to make up the solutions used for the data of Table 3, whereas it was less than 1 hr old when used for make up of solutions in Table 1. Also, it was visually observed that the finer Zn particles dissolved during equilibration in the Zn-only suspensions (Table 2), whereas they did not appear to react at all in the dithionite–zinc mixtures (Table 3) indicating preferential consumption of dithionite in the latter.

Overall, it is much more probable that erroneously high results rather than erroneously low results will be obtained in the solubility experiments described here. In all cases here, solubility was approached from the over-saturated side. As noted earlier, very low oxygen fugacities are expected to be required to maintain U(IV) in these alkaline solutions, and since U(VI) is much more soluble than U(IV), high values would be expected if incomplete oxygen scavenging occurred. In this regard, the higher observed solubilities in dithionate solutions above 1 M OH⁻ may be due to poorer oxygen scavenging, U(VI) reduction, or precipitation kinetics in these increasingly viscous solutions. It should also be noted that CO_3^{2-} concentration is proportional to OH⁻ concentration in these solutions, and carbonate complexing is expected to increase the stability of U(VI). Any-cross-contamination resulting from working in the same inert atmosphere chamber for solution makeup with very concentrated U solutions and for solution sampling and filtering would also yield an erroneously high result.

The only way that low results could be expected would be if the analytical method did not respond to the total uranium present. All of the results given are based on more than one analysis (many on several with good agreement). In all cases, analysis was based on the technique of known addition whereby appropriate standards were added after the sample reading was obtained and a new reading measured. In addition, in many cases standards were added either to aliquots of samples which had not been pretreated or to NaOH-Na₂S₂O₄ solution, and these were taken through the entire procedure with excellent standard recovery. In order to show that soluble U was not removed by ion exchange or other reaction with the filter material, the solution shown in Table 1 as 0.295 M NaOH was, after initial sampling for filtration, resealed, and was centrifuged at > 1000 G for 24 hr and a sample taken without filtering analyzed $1.3 \times 10^{-8} M$ U vs $8 \times 10^{-9} M$ (or background level) with filtering. Thus, it must be concluded that the solubility values of $< 10^{-8} M$ in the range 0.1 to 1 m NaOH in dithionite solution are real, and that the results of Gayer and Leider are at least four orders of magntiude too high.

CONCLUSIONS

Based on the above discussion, only the lowest measured U concentrations at a given NaOH concentration should be considered as an upper

limit for U(IV) solubility. The results do not provide solid evidence for any amphoteric behavior of U(IV) despite the measured solubility values being higher above 1 M NaOH. It is by no means certain that the measured U in any of these solutions was present as U(IV). The data presented indicate that the solubility of U(IV) hydrous oxide is at least four orders of magnitude lower than predicted by the results of Gayer and Leider,[5] and that their equilibrium constant for the formation of $U(OH)_5^-$, if such indeed is a dominant species at all in this OH^- concentration range, is at least four orders of magnitude too large. In other words, $K \leq 1.7 \times 10^{-8}$ for the reaction:

$$UO_2(am) + 2H_2O + OH^- \rightleftarrows U(OH)_5^-. \quad (5)$$
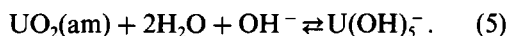
Using the conservative value of Langmuir[7] for the free energy of formation of amorphous UO_2 and assuming that this applies to the 2-week old precipitated hydrous UO_2 used here, gives a limit for $\Delta G_f \geq -379.4$ kcal/mole for $U(OH)_5^-$. Using $\Delta G_f = -126.9$ kcal/mole for $U_{(aq)}^{4+}$[7,23], yields a value of $K \leq 2 \times 10^{-23}$ for the reaction:

$$U^{4+}(aq) + 5H_2O \rightleftarrows U(OH)_5^- + 5H^+ \quad (6)$$

vs a value of 10^{-16} reported by Baes and Mesmer.[1] Such a value yields a solubility of crystalline UO_2 as U(IV) of $< 10^{-14} M$ at 1 M NaOH.

REFERENCES

1. C. F. Baes, Jr. and R. E. Mesmer, *The Hydrolysis of Cations*. Wiley, New York (1976).
2. R. S. Tobias and A. B. Garrett, *J. Am. Chem. Soc.* 1958, **80**, 3532.
3. B. N. Ivanov-Emin, E. N. Siforova, M. M. Fisher and V. M. Kampos, *Russ. J. Inorg. Chem.* 1966, **11**, 258.
4. B. N. Ivanov-Emin, E. N. Siforova, V. M. Kampos and E. B. Lafert, *Russ. J. Inorg. Chem.* 1966, **11**, 1054.
5. K. M. Gayer and H. Leider, *Can. J. Chem.* 1957, **35**, 5.
6. R. Prasud, M. L. Beasley and W. O. Milligan, *J. Electronmicroscopy (Tokyo)* 1967, **16**, 101.
7. D. Langmuir, *Geochimica et Cosmochimica Acta* 1978, **42**, 547.
8. A. E. Ogard and C. J. Duffy, *Nucl. Chem. Waste Management* 1981, **2**, 169, and C. J. Duffy and A. E. Ogard, *Uraninite Immobilization and Nuclear Waste*, LA-9199-MS. Los Alamos National Laboratory, Los Alamos, NM (1982).
9. B. Allard, H. Kipatsi and J. O. Liljenzin, *J. Inorg. Nucl. Chem.* 1980, **42**, 1015.
10. R. J. Lemire and P. R. Tremaine, *J. Chem. Eng. Data* 1980, **25**, 361.
11. S. L. Phillips, *Hydrolysis and Formation Constants at 25°C*. LBL-14313, Lawrence Berkeley Laboratory, Berkeley, CA (1982).
12. B. Allard, *Solubilities of Actinides in Neutral or Basic Solutions*, In *Proc. of the Actinides 81 Conf.* (Edited by N. Edelstein). Pergamon Press, Oxford (in press).
13. P. R. Tremaine, J. D. Chen, G. J. Wallace and W. A. Bovin, *J. Sol'n Chem.* 1981, **10**, 221.
14. B. Tomazic, V. Zutic and M. Branica, *Inorg. Nucl. Chem. Lett.* 1969, **5**, 271.
15. J. L. Ryan, *MTP Int. Rev. Sci., Series One* 1972, **7**, 342.
16. C. Musikas, *Radiochem. Radioanal. Lett.* 1972, **11**, 307.
17. J. C. Robbins, *CIM Bulletin*, May 1978, **71**, 61.
18. J. C. Robbins, *Laser-Induced Fluorescence for Uranium Analysis of Geological Materials*. Presented to Geo-Analysis '78, Ottawa, Ontario, Canada, (May 1978).
19. W. M. Latimer, *The Oxidation States of the Elements and their Potentials in Aqueous Solutions*, 2nd Edn. Prentice Hall, New Jersey (1952).
20. F. Fieser, *J. Am. Chem. Soc.* 1924, **46**, 2639.
21. L. G. Sillen and A. E. Martell, *Stability Constants of Metal-Ion Complexes*. The Chemical Society, London (1964).
22. W. J. Hamer and Y. C. Wu, *J. Phys. Chem. Ref. Data* 1972, **1**, 1047.
23. J. Fuger and F. L. Oetting, *The Chemical Thermodynamics of Actinide Elements and Compounds*—II. *The Actinide Aqueous Ions*, p. 28. Atomic Energy Agency, Vienna (1976).

NOTES

Quantum chemical calculation of $S_2O_8^{2-}$, SO_4^{2-} and $SO_4^{\cdot-}$ by INDO/$_2$ method

G. P. PIROUMIAN, G. G. GRIGORIAN and N. M. BEYLERIAN*
Yerevan State University, Yerevan 375049, U.S.S.R.

Abstract—Electron density distribution on atomic bonds S–O and O–O in persulphate ion for two different –O–O– bond lengths — 1.5 and 2.0Å using INDO/$_2$ method with parameters proposed by Pople on the BESM-6 computer have been calculated.

The results of the calculations show that the electron density is lowest on –O–O– bond, which is in accordance with experimental data. The calculations based on the assumption that $d_{O-O} \to \infty$ lead to the conclusion that the homolytic cleavage of –O–O– bond in $S_2O_8^{2-}$ ion is more probable.

In spite of the wide application of peroxides there are not many works concerning the theoretical study of their electronic structure.

The initial works deal the simplest peroxide—the hydrogen peroxide. Penney and Sutherland[1] showed the non-symmetrical distribution of charges on the –O–O– bond. Amako and Griguers[2] had calculated the length of the –O–O– bond and the angle O–OH.

Dialkyl peroxides and hydroperoxides were investigated by Ohkubo and Okado[3] who showed the –O–O– bond to be little "populated". They concluded that the peroxide bond may be attacked by nucleophilic agents. Similar data were received by Vanezawa, Kato and Yamamoto[4] and by Silbert *et al.*[5] The latter work carries the conclusion that olefins, which are π-donors, fill the lowest nonbonding orbitals of the –O–O– bond. Kucher and his colleagues[6-9] calculated the electronic structure of H_2O_2, organic peroxides and the corresponding radicals to find a relationship between electronic structure and reactivities.

The electron density and other quantum chemical parameters of benzoyl peroxide were calculated[10] and a "deficiency" of electrons was estimated in the –O–O– bond.

The ion $S_2O_8^{2-}$ has not been studied quantum chemically in spite of its wide application in many radical-chain reactions.

According to Beylerian[11] the passage of one or two electrons occurs from metal cations, having variable valence to the –O–O– bond when oxidizing with peroxides, particularly with persulphate. According to this hypothesis a complex is formed between $S_2O_8^{2-}$ and M^{n+} as a result of charge transfer from the cation to the –O–O– bond.

The aim of the present work is to calculate the $S_2O_8^{2-}$ ion and to verify the reality of the existence of electron "deficiency" on the –O–O– bond in the $S_2O_8^{2-}$ ion. The calculation was carried out through the INDO/$_2$ method with parameters proposed by Pople[12] on the BESM-6 computer.

In this method the measure of the bond strength is the value b_{AB}.[13,14]

$$b_{AB} = \sum_j^B \sum_i^A P_{ij} S_{ij},$$

where P_{ij} are the bond orders between atomic orbitals with i, j numbers, and S_{ij} are the overlapping integrals of the orbitals with i, j numbers.

The over-all indexes of bond energies in which the noneqiuivalence of different kinds of overlapping orbitals energy is considered,[15] is determined by the following formula:

$$E_{AB}^R = \sum_j^B \sum_i^A H_{ij}(P_{ij}^\alpha + P_{ij}^\beta),$$

where H_{ij} are matrix elements of frame Hamiltonian, P_{ij}^α and P_{ij}^β are matrix elements of the electron density with α and β spins correspondingly.

The geometrical parameters of $S_2O_8^{2-}$ ion were taken from Ref. 16.

In the calculations of the electron density on –O–O– bond the length of this bond was varied: 1.5; 2.0 and ∞ Å. The calculated data for the bond length $d_{O-O} = 1.5$Å, which corresponds to the crystal structure value of the ion $S_2O_8^{2-}$, are listed in Table 1.

The charge distribution on the atoms in the $S_2O_8^{2-}$ ion at $d_{O-O} = 1.5$Å is illustrated on Fig. 1.

From the results of Table 1 and Fig. 1 it is obvious that the electron density on –O–O– bond is minimum, the data concerning the bond strengths shows that the weakest is the –O–O– bond too, which breaks.

Further calculations have been carried on for $d_{O-O} = 2.0$Å (see the data of Table 2).

The charge distribution on the atoms in the $S_2O_8^{2-}$ ion at $d_{O-O} = 2.0$Å is illustrated on Fig. 2.

From the data of Table 2 and Fig. 2 we conclude that when the length becomes 2.0Å from 1.5Å E_{A-B}^R and b_{A-B} for

*Author to whom correspondence should be addressed.

Table 1. The calculated data for the bonds $A–B$ when $d_{O-O} = 1.5$ Å

A – B	P_{ij}	S_{ij}	b_{AB}	H_{ij}	E_{A-B}^R
S – O	1,1044	0,3431	0,3789	−0,5471	−0,6042
O – O	0,8820	0,3513	0,3099	−0,3663	−0,3011
O – S	1,1044	0,3431	0,3789	−0,5471	−0,6042

Table 2. The calculated data for the bonds $A-B$ when $d_{O-O} = 2.0$ Å

A – B	P_{ij}	S_{ij}	b_{A-B}	H_{ij}	E^R_{A-B}
S – O	1,1368	0,3431	0,3900	–0,5471	–0,6219
O – O	1,0238	0,2645	0,2708	–0,0899	–0,0920
O – S	1,1368	0,3431	0,3900	–0,5471	–0,6219
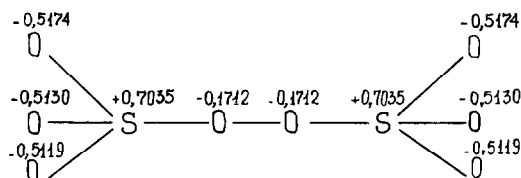
Fig. 1. The charge distribution on the atoms in the $S_2O_8^{2-}$ ion at $d_{O-O} = 1.5$Å.

(a)   (b)
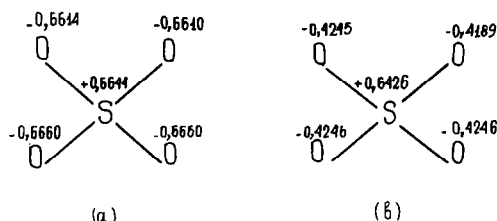
Fig. 3. The charge distribution on the atoms in SO_4^{2-} (a) and SO_4^{-} (b).
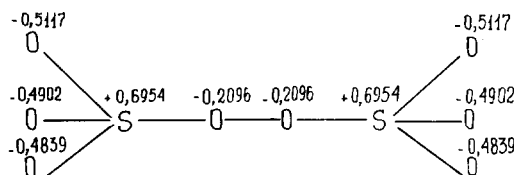
Fig. 2. The charge distribution on the atoms in the $S_2O_8^{2-}$ ion at $d_{O-O} = 2.0$Å.

–O–O– bond diminish. It confirms the proposition about the ease of –O–O– homolysis in $S_2O_8^{2-}$ ion. In the case when $d_{O-O} = 2.0$Å, $S_{ij} = 0.2645$ and for $d_{O-O} = 1.5$Å, $S_{ij} = 0.3513$. It is deduced, that when the overlapping is more the bond strength is more too. At 2.0Å the electron density is more than when the –O–O– bond length is equal to 1.5Å.

It is probable that as a result of the increase in bond length the repulsion between oxygen atoms decreases and the formed "deficiency" is fullfilled owing to partly delocalisation of both electrons in the $S_2O_8^{2-}$ ion.

The rupture of –O–O– bond can lead to either the formation of SO_4^{-}, if the –O–O– bond ruptures homolytically, or SO_4^{2-}, if the rupture occurs heterolytically.

The charge distribution on the atoms in SO_4^{2-} and SO_4^{-} is illustrated on Fig. 3.

The values of E_Σ for SO_4^{-} and SO_4^{2-} are as follows:—

$$E_\Sigma(SO_4^{-}) = -80.5426 \text{ a.u.}$$

$$E_\Sigma(SO_4^{2-}) = -80.0606 \text{ a.u.}$$

The calculated results, which are shown on Fig. 3 and the values E_Σ of SO_4^{-} and SO_4^{2-} show, that E_Σ for SO_4^{-} is less than for SO_4^{2-} on one side, and the electrons are delocalised in the all system, on the other.

Therefore the quantum chemical calculations show that there is a "deficiency" of the negative charge on the –O–O– bond in the ion $S_2O_8^{2-}$ and it has been concluded that a

nucleophilic attack on the –O–O– bond is theoretically possible.

REFERENCES

[1] W. G. Penney and G. B. Sutherland, J. Chimie Phys. 1934, 2, 402.

[2] J. Amako and P. A. Griguere, Can. J. Chem. 1962, 1, 765.

[3] K. Ohkubo and M. Okado, Bull. Chem. Soc. Japan 1971, 44, 2869.

[4] T. Vanezawa, U. Kato and O. Yamamoto, Bull. Chem. Soc. Japan 1967, 40, 30.

[5] G. S. Silbert, L. P. Witnauer, D. Swern and C. Riociuti, J. Am. Chem. Soc. 1959, 81, 3244.

[6] R. V. Koutcher, I. A. Opeyda, A. F. Dmitruk and V. V. Lobanov, Reports of Academy Sciences of U.S.S.R. 1974, 218, 612 (in Russian).

[7] I. A. Opeyda and R. V. Koutcher, Reports of Academy Sciences 1969, 187, 138 (in Russian).

[8] I. A. Opeyda, A. F. Dmitruk and R. V. Koutcher, Theor. Exper. Chem. 1972, 3, 385 (in Russian).

[9] R. V. Koutcher, A. A. Turovski, N. A. Turovski, N. V. Dzumedzey and A. F. Dmitruk, Reports of Academy Sciences 1973, 210, 3 (in Russian).

[10] O. Kikuchi, A. Hiyama, H. Yoshida and K. Suzuki, Bull. Chem. Soc. Japan 1978, 51, 11.

[11] N. M. Beylerian, Doctorate Thesis. Yerevan State University (1974).

[12] J. A. Pople, G. A. Segal and K. Hase, Theor. Chim. Acta 1973, 31, 3215.

[13] S. Ehrenson and S. Seltzer, Theor. Chim. Acta 1971, 20, 17.

[14] J. W. Mc'Iver, P. B. Coppens and D. Nowak, Chem. Phys. Lett. 1971, 11, 82.

[15] H. Fisher and H. Kollmar, Theor. Chim. Acta 1970, 16, 163.

[16] B. F. Ormont, The Structures of Inorganic Compounds. Nauka, Moscow (1950) (in Russian).

Tetrahedral metal complexes of [MW$_{12}$O$_{40}$]-type (M=Al^{III}, Zn^{II}) with dodecatungstate as tetrahedral ligand

KENJI NOMIYA and MAKOTO MIWA*

Department of Industrial Chemistry, Faculty of Engineering, Seikei University, Musashino-shi, Tokyo 180, Japan

Abstract—Tetrabutylammonium salts of 12-heteropolytungstates with central metal ions in a tetrahedral oxygen environment, MW$_{12}$O$_{40}$ (M=Al, Zn), have been prepared and their spectroscopic data (IR, UV and MCD) presented. IR studies in acetonitrile solution suggest that the tetrahedral structure around AlO$_4$ moiety is largely distorted, whereas the ZnO$_4$ moiety retains excellent tetrahedral symmetry.

Recently we have reported the syntheses and the spectroscopic properties of tetrahedral transition–metal complexes of [MW$_{12}$O$_{40}$]-type with dodecatungstate as tetrahedral ligand; M=Cu, Fe, Co and Co.[1,2] As an additional work, we have prepared the [AlW$_{12}$O$_{40}$]$^{5-}$ and [ZnW$_{12}$O$_{40}$]$^{6-}$ anions as tetrabutylammonium salts. These compounds were first prepared by Brown and Mair,[3–6] but no spectroscopic data have yet been reported. As a continuity of structural studies of tetrahedral complexes series of heteropolyanion, we have measured their IR spectra in a solid and in a solution, UV and MCD spectra and compared with the results of other tetrahedral complexes.

EXPERIMENTAL

Spectral measurements were performed by previously reported methods.[1,2]

H$_2$[(C$_4$H$_9$)$_4$N]$_4$[ZnW$_{12}$O$_{40}$]. Preparation of 12-tungstozincate acid was performed by modification of the method of Brown and Mair[5]. Appropriate volume of nitric acid (1 mol dm^{-3}) was added to Na$_2$WO$_4$·2H$_2$O (11.3 g, 3.4 × 10^{-2} mol) dissolved in water (80 cm^3), adjusted to pH of about 5, and the solution kept at 80–90°C with mechanical stirring, into which Zn(NO$_3$)$_2$·6H$_2$O (2.0 g, 6.7 × 10^{-3} mol) in water (140 cm^3) was added slowly over 20 hr. The solution was cooled, concentrated to about 50 cm^3, set aside overnight and filtered. The filtrate was extracted with 12N-sulphuric acid (200 cm^3) and diethyl ether (100 cm^3). The lowest layer, containing ether-adduct of the product and metatungstic acid, was taken out, added to an equal volume of water, and the ether was removed by evaporation. The solution was evaporated to dryness

and dried several hours on a steam-bath. During the drying, metatungstic acid was converted to yellow tungsten oxide, insoluble in water. The residual system was extracted with water and filtered. The process was repeated until no more yellow compound was formed. From the final aqueous solution repeated more than ten times, colourless solid 12-tungstozincate acid was obtained. The solid was added to the aqueous solution containing excess tetrabutylammonium bromide, which has been acidified by nitric acid. The precipitate was washed thoroughly with water and recrystallized from acetonitrile. Yield 3.5 g (colourless). Found: C, 19.92; H, 3.70; N, 1.46. Calc. for H$_2$[(C$_4$H$_9$)$_4$N]$_4$[ZnW$_{12}$O$_{40}$]: C, 19.79; H, 3.76; N, 1.44%.

H[(C$_4$H$_9$)$_4$N]$_4$[AlW$_{12}$O$_{40}$]. 12-Tungstoaluminate acid was prepared and purified by modification of the method of Mair and Waugh.[3] Appropriate volume of nitric acid (1 mol dm^{-3}) was added to Na$_2$WO$_4$·2H$_2$O (28.0 g, 8.5 × 10^{-2} mol) dissolved in water (240 cm^3), adjusted to pH of about 5.5, and the solution refluxed, and into which Al(NO$_3$)$_3$·9H$_2$O (5.0 g, 1.3 × 10^{-2} mol) in water (200 cm^3) was added drop by drop over 20 hr. The solution was cooled, concentrated to about 50 cm^3, stored at 6°C overnight, and filtered. The filtrate was extracted with 12N-sulphuric acid and ether. By the similar work-up to the preceding preparation, colourless solid of 12-tungstoaluminate acid was obtained (8.3 g) and converted to the tetrabutylammonium salt. It was washed thoroughly with water and recrystallized twice from acetonitrile. Found: C, 19.82; H, 3.88; N, 1.47. Calc. for H[(C$_4$H$_9$)$_4$N]$_4$[AlW$_{12}$O$_{40}$]: C, 19.98; H, 3.77; N, 1.46%.

[(C$_4$H$_9$)$_4$N]$_4$[SiW$_{12}$O$_{40}$] and [(C$_4$H$_9$)$_4$N]$_3$[PW$_{12}$O$_{40}$] were prepared by the usual methods. Found: C, 19.86; H, 3.82; N, 1.51. Calc. for [(C$_4$H$_9$)$_4$N]$_4$[SiW$_{12}$O$_{40}$]: C, 19.99; H, 3.78; N, 1.46%. Found: C, 15.77; H, 3.10; N, 1.12%. Calc. for [(C$_4$H$_9$)$_4$N]$_3$[PW$_{12}$O$_{40}$]: C, 15.99; H, 3.03; N, 1.17%.

*Author to whom correspondence should be addressed.

RESULTS AND DISCUSSION

In the preparation of M=Zn and Al compounds, adjusting the pH of the starting solution with nitric acid significantly influenced the yields. However, the pH ranges allowed are relatively wide and the yields comparatively high, e.g. in comparison with the preparation of M=Cu compound.[1] Free acids have many solvated water molecules and to dry completely is difficult. When the tetrabutylammonium is employed as a counter cation, isolation and treatment become convenient and solvation can be avoided.

IR spectra. The IR spectrum of the metal–oxygen stretching region in $[ZnW_{12}O_{40}]^{6-}$ anion (Fig. 1) measured by a KBr disk shows three prominent bands, v(W–O, terminal) at $940\,cm^{-1}$, v(W–O–W, octahedral edge-sharing) at $870\,cm^{-1}$, overlapped band of $v_3(F_2)$ by Zn–O stretching motion in a tetrahedral ZnO_4 and v(W–O–W, octahedral corner-sharing) at $770\,cm^{-1}$, and one small band; $v_4(F_2)$ by O–Zn–O angle bending motion in ZnO_4 unit at $440\,cm^{-1}$. The overlapping of $v_3(F_2)$ and v(W–O–W, corner-sharing) bands has been also observed in the cases of $[MW_{12}O_{40}]$ compounds with M=Cu(II), Fe(III), Co(II) and Co(III). Because of its triply degenerate mode for perfect T_d symmetry, the spectral shape of $v_4(F_2)$ band directly reflects whether the symmetry of a ZnO_4 moiety is regular T_d or not. For such a discrimination, the spectrum of a solution rather

than of a solid is preferable, since the effects of crystal packing and/or environment are eliminated. The IR spectrum recorded in acetonitrile solution shows that the overlapped band at $770\,cm^{-1}$ is slightly separated and the $v_4(F_2)$ band retains symmetrical envelope without significant splitting. Thus, the ZnO_4 moiety can be expected to have regular tetrahedral symmetry.

On the other hand, the IR spectrum of $[AlW_{12}O_{40}]^{5-}$ anion in the solid (Fig. 2) is composed of four prominent bands and one doubly split band; the former are v(W–O, terminal) at $955\,cm^{-1}$, v(W–O–W, octahedral edge-sharing) at $885\,cm^{-1}$, which has a small shoulder at $925\,cm^{-1}$, v(W–O–W, octahedral corner-sharing) and $v_3(F_2)$ by Al–O stretching motion in AlO_4 unit, which appear at 810 and $770\,cm^{-1}$, respectively, or vice versa, and the latter $v_4(F_2)$ by O–Al–O bending motion in the AlO_4 unit at $475\,cm^{-1}$. The separation of v(W–O–W, corner-sharing) and $v_3(F_2)$ bands in the solid-state spectrum has also appeared in the $[MW_{12}O_{40}]$ with M=Si and P, but not M=Cu(II), Fe(III), Co(II) and Co(III). The spectrum measured in acetonitrile solution, as a whole, appears to be sharpened and shows the following characteristics; (1) v_4 band is doubly split as in the solid-state spectrum, (2) both v(W–O–W, corner-sharing) and v_3, with broadened envelope in the solid-state spectrum, are split, and (3) the small shoulder at $925\,cm^{-1}$ accom-
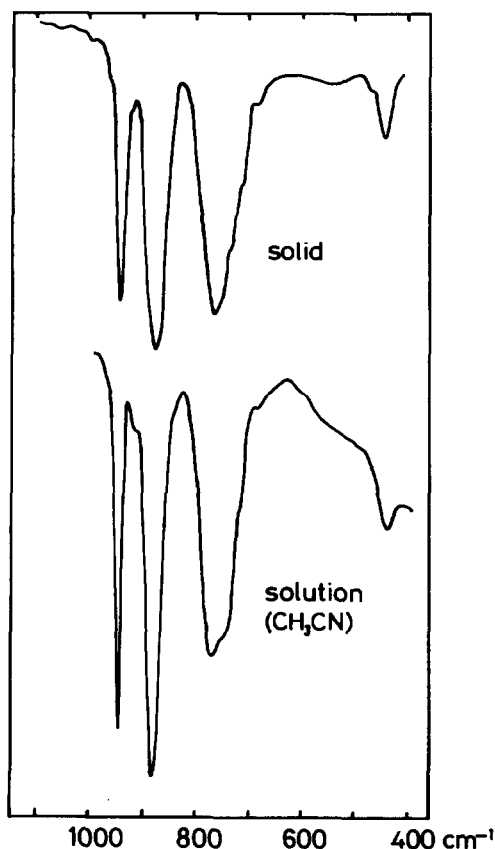
Fig. 1. IR spectra of tetrabutylammonium salt of $[ZnW_{12}O_{40}]^{6-}$ anion in a solid (KBr disk) and in acetonitrile solution.
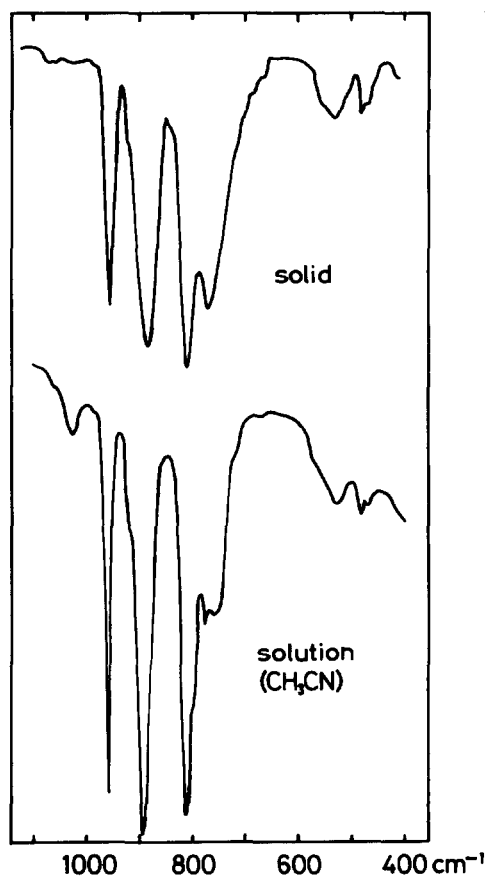
Fig. 2. IR spectra of tetrabutylammonium salt of $[AlW_{12}O_{40}]^{5-}$ anion in a solid (KBr disk) and in acetonitrile solution.

panied with the ν(W–O–W, edge-sharing) is also observed.

The splitting of $\nu_3(F_2)$ and $\nu_4(F_2)$ bands show the lowering of symmetry in the tetrahedral AlO$_4$ moiety. Since the ν_3 and ν_4 modes are essentially independent of each other, the degeneracy of them in only one mode will be possibly split by the distortion of symmetry around the MO$_4$ unit. This has been observed in the M=Si and P compounds. However, since the ν_3 and ν_4 bands in the M=Al compound are simultaneously split, the distortion of AlO$_4$ moiety may be different from those of SiO$_4$ and PO$_4$ units. The shoulder or splitting components of corner- and edge-sharing bands of W–O–W stretching may reflect that the symmetry of W$_{12}$O$_{40}$ skeleton is also lowered.

Recently Akitt and Farthing have investigated the course of preparation of [AlW$_{12}$O$_{40}$]$^{5-}$ using ^{27}Al–NMR technique and discussed all species formed during the preparation.[7] They pointed out from the appearance of two ^{27}Al resonances in the spectrum of final product that the preparation seemed to produce two 1:12 anions, and they suggested the possibilities of its cause as follows; structural difference leading to distortion of the symmetry around the AlO$_4$ unit, protonation of the anion to give a [H$_3$AlW$_{12}$O$_{40}$]$^{2-}$, replacement of counter cation by H$_3$O$^+$, and a combination of these possibilities. Our results explicitly supported the possibility of the structural difference.

UV and MCD spectra. UV and MCD spectra in acetonitrile solution of four tetrabutylammonium salts, [MW$_{12}$O$_{40}$] with M=Al, Zn, Si and P, are shown in Figs.

Fig. 4. UV and MCD spectra of tetrabutylammonium salts of [MW$_{12}$O$_{40}$] anions in acetonitrile solution; full line for M=Si and dotted line for M=P.

3 and 4. Absorption bands at $37–38 \times 10^3$ cm^{-1} are due to the charge transfer transition within dodecatungstate lattice and are commonly observed in the dodecatungstate compounds, whether the central atom is a transition metal or not. The intensities of the Zn and Al compounds (ϵ 3.41×10^4 and 3.75×10^4, respectively) are relatively small in comparison with those of Si and P compounds (ϵ 5.08×10^4 and 5.24×10^4, respectively). MCD spectra in the UV region show apparently two positive and one negative components, where the negative one appears near the position of absorption maximum and exists between two positive ones. The positive component of high frequency region in the Zn compound has not been measured, because of spectral noise, but such a component will probably exist. This MCD pattern is characteristic of the dodecatungstates and can be distinguished from that of dodecamolybdates, which is composed of only two positive components. The intensity of each component changes with central atom, especially those of Zn compound are very small. This may be related to the strong interaction between central Zn ion and dodecatungstate lattice, the excellent T$_d$ symmetry of the ZnO$_4$ moiety, and/or a combination of them. The W–O charge transfer band, observed as one absorption, has been further resolved and found to be significantly influenced by the central metal.

Fig. 3. UV and MCD spectra of tetrabutylammonium salts of [MW$_{12}$O$_{40}$] anions in acetonitrile solution; full line for M=Al and dotted line for M=Zn.

REFERENCES

1. K. Nomiya, M. Miwa, R. Kobayashi and M. Aiso, *Bull. Chem. Soc. Jpn.* 1981, **54**, 2983.

2. K. Nomiya, R. Kobayashi and M. Miwa, under submission.

3. J. A. Mair and J. L. T. Waugh, *J. Chem. Soc.* 1950, 2372.

4. D. H. Brown, *J. Chem. Soc.* 1962, 3281.

5. D. H. Brown and J. A. Mair, *J. Chem. Soc.* 1958, 2597.

6. D. H. Brown, *J. Chem. Soc.* 1962, 3189.

7. J. W. Akitt and A. Farthing, *J. Chem. Soc. Dalton Trans.* 1981, 1615.

A NEW TETRAHEDRALLY DISTORTED COPPER(II) COMPLEX DERIVED FROM

DISULPHIDE COUPLED N-(2-ETHANETHIOL)SALICYLIDENEIMINE

D. M. ROUNDHILL

Department of Chemistry, Tulane University, New Orleans, LA 70118, USA

Abstract - Copper(II) acetate reacts with N-(2-ethanethiol)salicylideneimine forming an ONNO chelate of α,α'-(diethylenedisulphide)-N,N'-disalicylideneimine with an uncoordinated disulphide. This copper(II) complex can also be obtained in higher yield if the thiol is first oxidized to disulphide with iodine. The geometry about copper(II) is distorted from planar to a flattened tetrahedron.

In the presence of copper(II) ions, thiols are rapidly oxidized to disulphides with the simultaneous reduction of copper to the monovalent state. Nevertheless, in view of the fact that blue copper proteins have a thiolato ligand directly bonded to copper(II),[1,2] interest remains high in exploring synthetic routes to such model complexes. Despite considerable effort toward this goal, there still remain very few well documented examples of a synthetic compound having such a coordinate linkage.[3] Many literature examples of compounds prepared from the interaction of thiols and copper(II) salts cannot be treated as valid biomimetic examples of blue copper proteins because the products have been only poorly characterized. In many cases the complexes have copper in a monovalent or mixed valence state, and only in a few cases is copper divalent. One such example is the complex N-(2-thiophenolato)-R-salicylideneimine pyridine copper(II).[4] Using this compound as a guideline we have explored the possibility of preparing an analogous copper(II) complex having an aliphatic thiolato ligand. We have thus used the compound N-(2-ethanethiol)-salicylideneimine for complexation with cupric ion.

EXPERIMENTAL

Electronic spectra were measured on a Cary 17 spectrophotometer. EPR measurements were made on a Varian E3 spectrometer. Reagents were used as supplied.

The compound N-(2-ethanethiol)salicylideneimine was prepared by first dissolving 2-aminoethanethiol hydrochloride (2.50 g, 0.022 mol) in the minimum quantity of methanol. This solution was then added to potassium acetate (5.89 g) which was dissolved in the minimum volume of ethanol. After filtration of potassium chloride, salicylaldehyde (2.51 g, 0.024 mol) was added to the filtrate, and the solution warmed for 10-15 min.[5] The resulting solution of N-(2-ethanethiol)salicylideneimine was added to copper acetate (2.45 g, 0.012 mol) dissolved in hot methanol. The precipitate which formed was extracted with hot pyridine, and the complex precipitated as a green powder by addition of hexane or diethyl ether. The filtered solid was washed with a little methanol then diethyl ether. Yield 1.4 g, 28%. Found: C, 51.23, 51.32; H, 4.35, 4.31; N, 6.77, 6.96; S, 15.56. Calc. for $C_{18}H_{18}CuN_2O_2S_2$: C, 51.23; H, 4.30; N, 6.64; S, 15.20%.

Alternatively the complex may be prepared by allowing the warm solution of N-(2-ethanethiol)salicylideneimine (0.024 mol) to cool, and then adding iodine crystals followed by copper acetate. Benzene and water were added as necessary to keep the solution homogeneous. Iodine addition was continued until there remained a faint purple colouration in the benzene layer. A dilute aqueous solution of sodium thiosulphate was then added to remove excess iodine, and the organic product extracted with benzene. The benzene solvent was removed by rotary evaporation and the residue containing α,α'(diethylenedisulphide)-N,N'-disalicylideneimine (0.012 mol) was dissolved in a methanol-acetone mixture. This solution was added to a solution of copper acetate (3.8 g, 0.019 mol) in hot methanol, and the green solid product filtered. Yield 3.6 g, 71%. The product is identical with that prepared from N-(2-ethanethiol)salicylideneimine.

RESULTS AND DISCUSSION

The compound N-(2-ethanethiol)salicylideneimine is a potential tridentate ligand which can be used to prepare thiolato complexes of metals such as nickel(II).[5] Reaction of this compound with copper(II) acetate yields a green complex in rather low yield. The electronic spectrum of this complex as a solution in pyridine shows absorptions at 10,700 cm^{-1} (ε 55), 14,900 cm^{-1} (ε 110), 21,300 cm^{-1} (ε 260), along with two intense ligand centred charge transfer bands at 27,000 cm^{-1} and 34,240 cm^{-1}. The solid state EPR

spectrum at 293K and 77K shows a broad line of width 104 ± 5 gauss centred at g = 2.090(3), a reasonable position for g_1 in copper(II) complexes.[6] Since this complex can be prepared in high yield from the disulfide it is very unlikely that the structure of this complex has a thiolato copper(II) bond. The low yield of complex when prepared from N-(2-ethanethiol)salicylideneimine [28% based on $Cu(OAc)_2 \cdot H_2O$] is a consequence of the thiol group being oxidized to disulphide, with reduction of cupric ion to the cuprous state. The oxidation product, α,α'-(diethylenedisulfide)-N,N'-disalicylideneimine, is a tetradentate ONNO ligand. Verification of this ligand structure has been made by prior oxidation of N-(2-ethanethiol)salicylideneimine to α,α'-(diethylenedisulfide)-N,N'-disalicylideneimine with iodine, followed by its use to prepare the identical copper(II) complex in higher yield (71% based on disulphide ligand). These reactions are shown in the scheme.
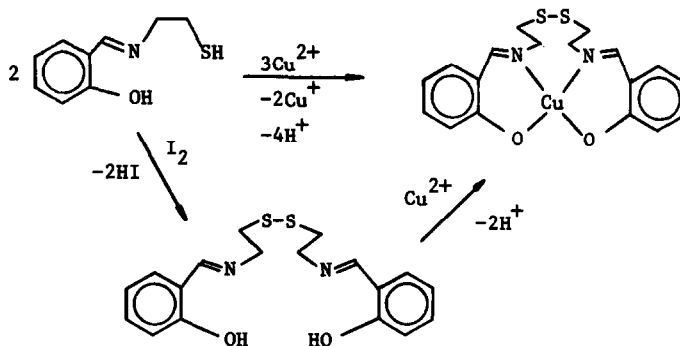
Scheme

Molecular models suggest that conformational strain about the diethylenedisulphide backbone of the ligand makes a planar coordination geometry about copper unfavourable, and that a tetrahedral distortion would be sterically preferable. Comparison of the electronic spectrum of this new complex with other copper(II) salicylideneimine complexes supports this contention. Increasing the steric bulk of the N-alkyl substituent causes a distortion from planar (R = n-Pr) to flattened tetrahedral (R = t-Bu).[7,8] This change is reflected in a progressive shift of the d-d electronic bands to lower energy as the copper(II) coordination geometry distorts from planar. Comparison of the electronic spectrum of this new complex with that for R = n-Pr, which has λ_{max} = 17,000 cm^{-1} (ϵ 110), or for R = t-Bu, with λ_{max} = 8,500 (ϵ 20), 13,400 (ϵ 260), 20,800 (ϵ1,500), supports a structure with a distortion from planarity approaching that found for the t-butyl substituted complex.[9,10,11]

REFERENCES

1. P. M. Colman, H. C. Freeman, J. M. Guss, M. Murata, V. A. Norris, J. A. M. Ramshaw and M. P. Venkatoppa, *Nature (London)* 1978, 272, 319.

2. E. I. Solomon, J. W. Hare and H. B. Gray, *Proc. Natl. Acad. Sci. USA* 1976, 73, 1389.

3. J. L. Hughey IV, T. G. Fawcett, S. M. Rudich, R. A. Lalancette, J. A. Potenza and H. J. Schugar, *J. Am. Chem. Soc.* 1979, 101, 2617.

4. W. W. Fee, J. D. Pulsford and P. D. Vowles, *Aust. J. Chem.* 1973, 26, 675.

5. G. R. Brubaker, J. C. Latta and D. C. Aquino, *Inorg. Chem.* 1970, 9, 2608.

6. I. Bertini, A. Dei and A. Scozzafava, *Inorg. Chem.* 1975, 14, 1526.

7. L. Sacconi, *Coord. Chem. Rev.* 1966, 1, 126.

8. T. P. Cheeseman, D. Hall and T. N. Waters, *J. Chem. Soc. A.* 1966, 685.

9. J. Ferguson, *J. Chem. Phys.* 1961, 35, 1612.

10. L. Sacconi and M. Ciampolini, *J. Chem. Soc.* 1964, 276.

11. R. C. Rosenberg, C. A. Root, P. K. Bernstein and H. B. Gray, *J. Am. Chem. Soc.* 1975, 97, 2092.

RELATIONSHIPS BETWEEN INTERATOMIC DISTANCES AND ELECTRON NUMBERS FOR
D_{3h} TRICAPPED TRIGONAL PRISMATIC 9-ATOM CLUSTER SYSTEMS

MARION E. O'NEILL and KENNETH WADE

Chemistry Department, Durham University, South Road, Durham DH1 3LE (UK)

ABSTRACT

The polyhedron edge-bonding or -antibonding characteristics of the nondegenerate tenth and eleventh MO's of D_{3h} tricapped trigonal prismatic 9-atom homonuclear clusters like B_9Cl_9, $B_9H_9^{2-}$, Ge_9^{2-}, Sn_9^{3-} and Bi_9^{5+} can be used to rationalize the edge lengths in such clusters. Skeletal bonding is strongest, and the clusters are nearest to spherical, when there are 20 skeletal bonding electrons present, as in the cases of $B_9H_9^{2-}$ and Ge_9^{2-}. Species with one or two more or fewer electrons have expanded structures based on longer and thinner trigonal prisms.

INTRODUCTION

Most <u>closo</u> borane-type clusters like the anions $B_nH_n^{2-}$ and carboranes $C_2B_{n-2}H_n$ (n = 5 → 12) have (n + 1) skeletal electron pairs to hold their n atoms together. However, species in which the (n + 1)'th and (n + 2)'th MO's (the HOMO and LUMO of $B_nH_n^{2-}$) are non-degenerate can in principle suffer loss or gain of one or two electrons without a change of symmetry from that of the <u>closo</u> shape appropriate for (n + 1) pairs.[1] The D_{2d} dodecahedral shape of $B_8H_8^{2-}$ [2], the D_{3h} tricapped trigonal prismatic shape of $B_9H_9^{2-}$ [2], and the C_{2v} octadecahedral shape of $B_{11}H_{11}^{2-}$ [3], are all compatible with n, (n + 1) or (n + 2) skeletal electron pairs, the strongest bonding (and so most compact shape) being when there are (n + 1) pairs. We have elsewhere[1] pointed out in preliminary form that the differences between B_8Cl_8 [4] and $B_8H_8^{2-}$ [2], or between B_9Cl_9 [5] and $B_9H_9^{2-}$ [2], are consistent with the B-B bonding or antibonding characteristics of the HOMO's of $B_8H_8^{2-}$ [6] and $B_9H_9^{2-}$ [2]. Our emphasis in that earlier paper was on 8-atom clusters. Here, we illustrate and develop our argument with particular reference to 9-atom clusters, and consider how it can be extended to allow clusters of one element to be compared with those of another element of different atomic radius.

FRONTIER ORBITALS OF D_{3h} TRICAPPED TRIGONAL PRISMATIC CLUSTERS.

Molecular orbital treatments of $B_9H_9^{2-}$ [2] and of related clusters M_9^{2-} (where M = a Group IV element such as Ge, Sn or Pb)[7-9] have shown that there is a significant energy gap between the tenth and eleventh MO's, the former (the HOMO) being of a'_2 symmetry and predominantly bonding in character, the latter (the LUMO) being of a''_2 symmetry and predominantly antibonding in character. The combinations of p atomic orbitals (tangentially orientated with respect to the pseudo-spherical cluster surface) that contribute to these MO's are shown in the Figure, from which it is apparent that while the HOMO is bonding for edges of types g and h, and antibonding for edges of type f, the LUMO is precisely the reverse, bonding for edges of type f, but antibonding for edges of types g and h. Adding one or two electrons to D_{3h} $B_9H_9^{2-}$ or related clusters, or taking one or two electrons away from such a system, is expected to cause the same type of distortion if the D_{3h} symmetry is retained. Edges of type f (which surround the triangular prism faces) are expected to shorten, while those of

HOMO-a'$_2$ skeleton   LUMO-a"$_2$
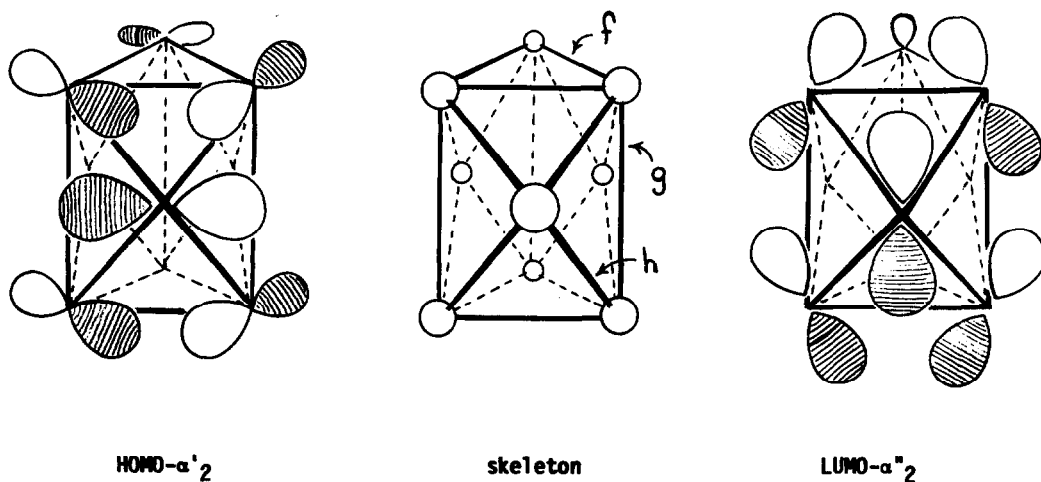
Figure. D_{3h} tricapped trigonal prismatic skeleton of the 9-atom clusters B_9Cl_9, $B_9H_9^{2-}$, $C_2B_7H_9$, Sn_9^{3-} and Bi_9^{5+}, with the frontier orbitals of $B_9H_9^{2-}$.

Table. Polyhedral edge lengths in some D_{3h} 9-atom tricapped trigonal prismatic clusters with from eighteen to twenty-two skeletal electrons

Species	Skeletal electrons	Edge Lengths (pm)				Ref.
		f	g	h	f/g	
B_9Cl_9	18	180	208	175	0.87	5
$B_9H_9^{2-}$	20	188	181	171	1.04	2
$C_2B_7H_9$	20	197	177	170*	1.11	13
Ge_9^{2-}	20	267	295**	256	0.91**	10
Sn_9^{3-}	21	306	330	294	0.93	11
Bi_9^{5+}	22	324	374	309	0.87	12

*   Distance to capping boron; h for capping carbon is 161 pm.

**   This anion is very distorted, with one long bond of type g - see text.

types g (the prism length) and h (the links to the capping atoms) are expected to lengthen. The effect is to convert the pseudo-spherical ten electron pair system into an ellipsoidal system elongated along the 3-fold axis.

INTERATOMIC DISTANCES IN D_{3h} TRICAPPED TRIGONAL PRISMATIC CLUSTERS

The interatomic distances in a series of homonuclear D_{3h} tricapped trigonal prismatic clusters[2,5,10-12], and in the related C_{2v} symmetry carborane $C_2B_9H_{11}$,[13] are listed in the Table. The first two entries, B_9Cl_9[5] and $B_9H_9^{2-}$[2], show precisely the difference expected-- the trigonal prism of the former is longer and narrower than that of the latter. The data for the carborane $C_2B_7H_9$,[13] in which the carbon atoms occupy capping positions, when compared with those for $B_9H_9^{2-}$, show that the main effect of the carbon atoms is to drain electronic charge from the prism ends, lengthening the edges of type f and so making the prism even fatter.

Comparison with clusters of elements other than boron is facilitated by calculating the ratio of the prism edge parameters f/g. Since f is expected to shorten and g to lengthen as electrons are added or removed, this ratio provides a more sensitive guide to the effect of changing the electron numbers,[9] than the interatomic distances themselves do and allows comparisons to be made between the boron systems just considered and related metal clusters containing larger atoms. At present, there is unfortunately a dearth of information on the structures of closo anionic clusters M_9^{2-} (M = Ge, Sn or Pb).[7,8] Though these anions are believed to feature in the solution chemistry of alkali metal alloys of these metals,[7] the anions M_9^{4-}, with nido capped square antiprismatic structures, have been much more thoroughly structurally characterized. The one anion M_9^{2-} that has been structurally characterized is Ge_9^{2-},[10] and it has C_{2v} symmetry, one edge of the trigonal prism (type g) being 30 pm longer than the other two. The reason for this distortion from the ideal D_{3h} geometry is not clear, but a consequence is that the ratio of edge lengths f/g is much lower than might have been expected for a system that is believed to contain ten skeletal bond pairs (the charge on the anion was inferred from the shape and from the number of cations present).

The remaining two clusters in the Table, the odd electron system Sn_9^{3-}[11] and the eleven pair cluster Bi_9^{5+}[12] both have low values of f/g as expected for species with elongated narrow trigonal prisms, the degree of distortion from the 'ideal' geometry being greatest, again as expected, for Bi_9^{5+}, which contains two antibonding electrons, whereas Sn_9^{3-} contains only one.

With the exception of Ge_9^{2-}, which is anyway very distorted from D_{3h} symmetry, these 9-atom D_{3h} clusters thus show the sensitivity of shape to electron numbers that is expected from simple frontier orbital considerations. Structural characterisation of further examples, particularly closo systems M_9^{2-} (M = Ge, Sn or Pb), and related 19 electron clusters if these can be prepared, would help test the generality of the arguments outlined here.

ACKNOWLEDGEMENT

REFERENCES

1. M. E. O'Neill and K. Wade, <u>Inorg. Chem</u>. 1982 21, 461.

2. L. J. Guggenberger, <u>Inorg. Chem</u>. 1968 7, 2260; 1969 8, 2771.

3. F. Klanberg and E. L. Muetterties, <u>Inorg. Chem</u>. 1966 5, 1955.

4. G. S. Pawley <u>Acta Crystallogr</u>. 1966 20, 631.

5. M. B. Hursthouse, J. Kane and A. G. Massey, <u>Nature</u> 1970 228, 659; M. B. Hursthouse, personal communication.

6. D. A. Kleir and W. N. Lipscomb <u>Inorg. Chem</u>. 1979 18 1312.

7. J. D. Corbett <u>Progr. Inorg. Chem</u>. 1976 21 129.

8. L. L. Lohr <u>Inorg. Chem</u>. 1981 20 4229.

9. R. C. Burns, R. J. Gillespie, J. A. Barnes and M. J. McGlinchey, <u>Inorg. Chem</u>. 1982 21, 806.

10. C. H. E. Belin, J. D. Corbett and A. Cisar <u>J. Am. Chem. Soc</u>. 1977, 99, 7163.

11. J. D. Corbett and S. C. Critchlow (personal communication) have determined the structure of the anion Sn_9^{3-} and carried out EHMO calculations on this and related species that broadly support the arguments presented here. However, they find that, in the LUMO of Sn_9^{2-} and the HOMO of Bi_9^{5+}, the contribution made by the p orbitals of the capping atoms is the reverse of that shown in our figure, i.e. σ-bonding, π-antibonding, and so overall net <u>bonding</u>, even though the bonds to the capping atoms increase proportionately in length as the twenty-first and twenty-second skeletal electrons are added.

12. A. Hershaft and J. D. Corbett, <u>Inorg. Chem</u>. 1963, 2, 979.

13. T. F. Koetzle, F. E. Scarbrough and W. N. Lipscomb, <u>Inorg. Chem</u>. 1968, 7, 1076.

COMMUNICATIONS

ISOCYANIDE INSERTION REACTION IN ALKYLCOMPLEXES OF IRON:
A DIHAPTOIMINOACYL DERIVATIVE OF IRON (II)

Giuseppe Cardaci*, Gianfranco Bellachioma

Department of Chemistry, University of Perugia, 06100 Perugia Italy

Pierfrancesco Zanazzi

Institute of Mineralogy, University of Perugia, 06100 Perugia Italy

Abstract: The dihaptoiminoacyl complex $[Fe(CO)_2(PMe_3)_2(\eta^2\text{-}CMe=N\text{-}CMe_3)]^+$ I^- was obtained by reaction of $[Fe(CO)_2(PMe_3)_2MeI]$ and tertbutylisocyanide. The structure of the complex was determined by an X-ray structure analysis.

Isocyanides are structurally similar and isoelectronic with carbon monoxide; therefore an understanding of isocyanide insertion[1] may help our understanding of CO insertion[2]. Moreover, isocyanide insertion is not an equilibrium reaction and can give polyinsertion[3]. When there is a choice within one molecule, isocyanide insertion prevails over CO insertion, though its calculated activation energy is higher than for CO insertion[4]. This can be explained by acid catalysis[4]. Another reason may be the action of the metal, which acts as an acid toward the nitrogen atom to stabilize the dihaptostructure as an insertion intermediate. Two examples of dihaptoiminoacyl complexes are described in the literature[5]. We here describe the preparation of a complex of iron (II) showing this structure (Scheme 1).

Scheme 1 (L=PMe₃)
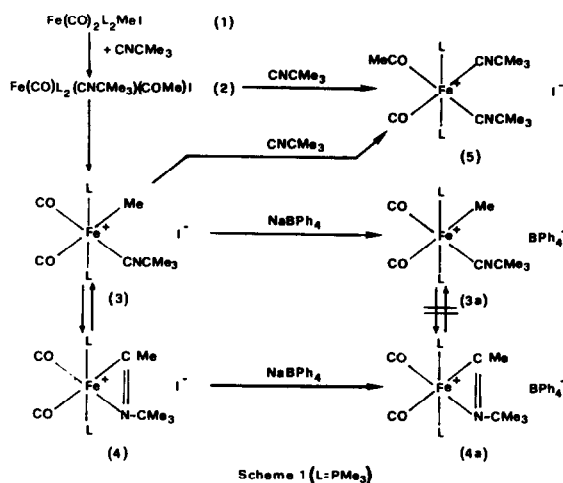
The reaction of $[Fe(CO)_2(PMe_3)_2MeI]$ (1) with tert-butylisocyanide in benzene (molar ratio 1/1) quickly yields $[Fe(CO)(PMe_3)_2(CNCMe_3)(COMe)I]$ (2), which ionizes to the complex $[Fe(CO)_2(PMe_3)_2(CNCMe_3)Me]^+$ I^- (3);(3) reaches an equilibrium with the dihaptoiminoacyl complex $[Fe(CO)_2(PMe_3)_2(\eta^2\text{-}CMe=NCMe_3)]^+$ I^- (4). With an excess of tert-butylisocyanide the reaction proceeds to the complex $[Fe(CO)(PMe_3)_2(CN\text{-}CMe_3)_2(COMe)]^+$ I^- (5). The complexes (3) and (4) cannot be isolated because equilibrium between them is established in the solid state, too; on the other hand the complex (4a) can be precipitated from a tetrahydrofurane solution of (3a) and (4a) obtained by exchange with $NaBPh_4$ in methanol. The elemental analyses of the complexes (4a) and (5) are in agreement with the proposed formulation.

(4a) crystallizes in the monoclinic system with a = 29.832(4), b = 12.174(3), c = 10.650 (3) Å, β = 91.45(2)°, U = 3866.6 Å^3, D_c = 1.045 g.cm^{-3}, Z = 4, space group $P2_1/n$. Intensity data were measured with a Philips PW 1100 diffractometer, using $MoK\alpha$ radiation, μ = 4.7 cm^{-1}.
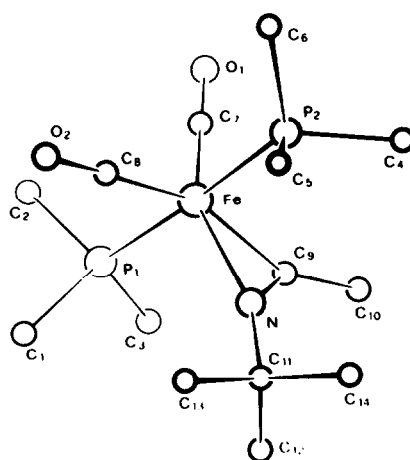
Fig. 1

The structure was solved by direct method and refined by full matrix least squares method to R = 0.075 for 1628 observed reflections and 149 parameters[§]

The molecular structure of complex (4a) is shown in Fig. 1.

In addition to the Fe-PMe$_3$ and Fe-CO groups, an iminoacyl (Me-C=N-CMe$_3$)group bonded to the metal atom is observed. Relevant internuclear distances and angles are: Fe-C$_9$ = 1.940(13)Å; Fe-N = 2.007(10)Å; C$_9$-N = 1.211(14)Å; C$_9$-C$_{10}$ = 1.496(19)Å; N-C$_{11}$ = 1.523(16)Å; C$_{10}$-C$_9$-N = 139.1(13); C$_9$-N-C$_{11}$ = 137.4(12); C$_9$-Fe-N = 35.7(4). The increase of the angles C$_{10}$-C$_9$-N and C$_9$-N-C$_{11}$ with reference to a normal η^1-iminoacyl structure[5a,6] and the similar bond distances Fe-N and Fe-C$_9$ indicate a dihaptoiminoacyl structure as found in the previously described complexes[5].

The structures of the complexes (3), (4) and (5) are supported by i.r. and [1]H n.m.r. spectra (Tab. 1).

Table 1: i.r. (cm^{-1}) and ^{1}H n.m.r. (ppm)data in CH$_2$Cl$_2$

Complex	ν_{CO}	ν_{COMe}	ν_{CN}	τ_{Me}	τ_{COMe}
(2) (B)	1938(s)	1584(m)	2146(s)		7.65(s)
(3)	2027(s),1983(s)		2172(s)	8.94(t) $J_{H,P}$= 7.8 cps	
(4)	2012(s),1950(s)		1750(m)	7.04(t) $J_{H,P}$= 2.4 cps	
(5)	1982(s)	1600(s)	2175(s),2140(s)		7.56(s)

B = benzene solution; s = strong, m = medium for the i.r. spectrum;

s = singlet, t = triplet for the ^{1}H n.m.r. spectra.

In particular complex (4) shows two i.r. CO stretchings, no i.r. band in the range 2100-2200 cm^{-1}(C≡N stretchings) or in the range 1500-1600 cm^{-1} (C=N stretchings). The band at 1750 cm^{-1} is assigned to the C=N of the η^2-dihaptoiminoacyl structure. A comparison with the band observed in the other two dihapto complexes (ν_{CN}= 1654 cm$^{-1,5b}$ and ν_{CN}= 1680 cm$^{-1,5a}$), indicate that this band is strongly influenced by the dihapto structure.

The shift is to a higher frequency with respect to the C=N stretching. This trend is opposite to that observed in the dihaptoacyl complexes[7] and corresponds to the effect observed on the double bond of the cyclopropene derivatives[8]. Since the structure of cyclopropene and dihaptoiminoacyl metal are very similar, the strengthening of the double bond may be due to the partial sp hybridization on the C and N atoms, observed in cyclopropene[8] and to the quaternary iminium salt $>$C=N$<$ structure, for which a shift to higher frequencies of the C=N stretching is observed[9].

REFERENCES

[1] A. Wojcicki, Adv. Organometal. Chem. 1974, 12, 31.

[2] F. Calderazzo, Angew. Chem. Internat. Ed. 1977, 16, 299; A. Wojcicki, Adv. Organometal. Chem. 1973, 11, 87.

[3] J. Yamamoto and H. Yamazaky, J. Organometal. Chem. 1975, 90, 329.

[4] H. Berke and R. Hoffmann, J. Am. Chem. Soc. 1978, 100,7224.

[5] a) R.D. Adams and D.F. Chodosh, J. Am. Chem. Soc. 1977, 99, 6544; idem, Inorg. Chem. 1978, 17, 41; idem, J. Organometal. Chem. 1976, 122,C 11; b) W.R. Roper, G.E. Taylor, J.M. Waters and L.J. Wright, J. Organometal. Chem. 1978, 157, C 27.

[6] K.P. Wagner, P.M. Treichel and J.C. Calabrese, J. Organometal. Chem. 1974, 71, 299.

[7] G. Fachinetti, C. Floriani, F. Marchetti and S. Merlino, J. Chem. Soc. Chem. Comm. 1976, 522; W.R. Roper, G.E. Taylor, J.M. Waters and L.J. Wright, J. Organometal. Chem. 1979, 182, C 46.

[8] M.K. Kemp and W.H. Flygare, J. Am. Chem. Soc. 1967, 89, 3925; W.R. Bernett, J. Chem. Ed. 1967, 44, 17.

[9] R. Merenyi, "Structure Determination of iminium salts by physical methods", in "Advances in Organic Chemistry" Ed. H. Bohme and H.G. Viehe, Wiley interscience New York, 1976, Vol. 9, part 1, pp. 23-105.

[§] Atomic coordinates, bond lenghts and angles and lists of F$_o$/F$_c$ values have been deposited as supplementary material with the Editor, from whom copies are available on request. Atomic coordinates have also been deposited with the Canbridge Crystallographic Data Center.

Refutation of the synthesis of tetrakis(cyclopentadienyl)cerium(IV)

G. B. DEACON,* T. D. TUONG and D. G. VINCE†
Chemistry Department, Monash University, Clayton, Victoria 3168, Australia

Abstract—Reaction of sodium cyclopentadienide with dipyridinium hexachlorocerate(IV) in tetrahydrofuran yields tris(cyclopentadienyl)cerium(III) and not tetrakis(cyclopentadienyl)cerium(IV).

The synthesis of tetrakis(cyclopentadienyl)cerium(IV) by reaction of $(pyH)_2[CeCl_6]$ with sodium cyclopentadienide has been reported.[1]

$$(pyH)_2[CeCl_6] + 4Na(C_5H_5) \rightarrow$$

$$(C_5H_5)_4Ce + 4NaCl + 2(pyH)Cl. \quad (1)$$
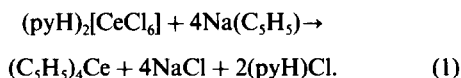
It has also been claimed that the same reagents (different stoichiometry) and reaction of $(C_5H_5)_4Ce$ with $(pyH)_2[CeCl_6]$ yield tris(cyclopentadienyl)cerium(IV) chloride,[2] from which a range of $(C_5H_5)_3CeX$ (e.g. X = alkyl or aryl,[3] alkoxide,[4] BH_4[5] compounds have been derived. Tetrakis(cyclopentadienyl)cerium (IV) was reported to be stable to water and dilute acids,[1] by contrast with organolanthanides in more stable oxidation states.[6,7] The compound was said to be "chemically stable" but the stability to air was not specifically mentioned.[1] The occurrence of (1) is surprising in view of the formation of tris-(cyclopentadienyl)cerium(III) from cerium tetrafluoride and $(C_5H_5)_2Mg$,[8] but receives some support from the preparation of $(C_5H_5)_3Ce(OPr^i)$ from $Ce(OPr^i)_4$ and $(C_5H_5)_2Mg$.[9] However, the properties of $(C_5H_5)_3Ce(OPr^i)$ from this source (colour, volatility, IR absorptions)[9] differ from those of the same compound prepared by alcoholysis of $(C_5H_5)_4Ce$ or $(C_5H_5)_3CeCl$,[4] and it is not easy to reconcile cleavage of $(C_5H_5)_4Ce$ by isopropanol[4] with stability to water and dilute acids.[1] These contradictions and inconsistencies have led us to reinvestigate the reported synthesis[1] of tetrakis(cyclopentadienyl)cerium(IV).

EXPERIMENTAL

Reactions were carried out under purified (with BASF 3/11 oxygen-removal catalyst and molecular sieves) nitrogen in Schlenk assemblies, and solids were handled under purified nitrogen in Vacuum Atmospheres HE 43-2 or CSIRO dry boxes. Tetrahydrofuran and petro-

leum ether were purified as described previously.[10] Dipyridinium hexachlorocerate(IV)[11] and solutions of sodium cyclopentadienide in tetrahydrofuran[12] (standardized by acidolysis) were prepared by published methods. Infrared spectra of compounds as Nujol mulls were recorded with Jasco IRA-1 or Perkin–Elmer 257 or 180 spectrophotometers. The magnetic moment was determined at room temperature by the Gouy method for a sample sealed under nitrogen.

Reaction of dipyridinium hexachlorocerate(IV) with sodium cyclopentadienide

A solution of sodium cyclopentadienide (25 mmol) in tetrahydrofuran (19 cm³) was added to a suspension of dipyridinium hexachlorocerate(IV) (5.06 mmol) in tetrahydrofuran (120 cm³) under purified nitrogen at room temperature. The mixture turned dark brown within 1.5 min and brown–black in 3–4 min. After heating under reflux for 3 hr, a white precipitate and yellow solution were obtained, and no change was observed during further heating (16 hr). Filtration and evaporation to dryness (pyridine evolved with the volatiles) gave a dirty-yellow precipitate with an infrared spectrum in agreement with that of a sample of tris-(cyclopentadienyl)(tetrahydrofuran)cerium(III) (prepared by the thallous cyclopentadienide transmetallation route),[13] which was largely insoluble in petroleum ether (see reported behaviour of $(C_5H_5)_4Ce^i$). Sublimination (210–235°C, 10^{-3} mm) gave tris-(cyclopentadienyl)cerium(III) [47%; IR identical with a sample from sublimation of authentic $(C_5H_5)_3Ce(thf)$], not decomposed at 360°C, lit.[12] m.p. 435°C, $\mu = 2.30$ BM, lit.[12] $\mu = 2.46$ BM, with the known[12] violent air sensitivity.

RESULTS AND DISCUSSION

Reaction of dipyridinium hexachlorocerate(IV) with sodium cyclopentadienide (mole ratio 1:5) in refluxing tetrahydrofuran gave the highly air-sensitive tris-(cyclopentadienyl)cerium(III) [reaction (2)],

$$2(pyH)_2[CeCl_6] + 12Na(C_5H_5) \rightarrow$$

$$2(C_5H_5)_3Ce + (C_5H_5)_2 + 4C_5H_6 + 12NaCl + 4py \quad (2)$$

---
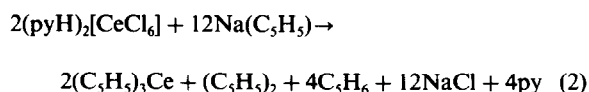
*Author to whom correspondence should be addressed.

†Present address: Nobel Group, ICI Australia Operations Pty. Ltd., Deer Park, Victoria, 3023, Australia.

and not the reported[1] tetrakis(cyclopentadienyl)cerium(IV) [reaction (1)]. Although a longer reaction time (19 hr) was used than that reported (10–12 hr),[1] the appearance of the reaction mixture was unchanged from 3→19 hr. The evolution of pyridine [see eqn (2)] is hardly surprising, since sodium cyclopentadienide is a strong base and the pyridinium ion an acid.

Apart from refutation of the synthesis of $(C_5H_5)_4Ce$, the present results also cast doubts on reported preparations of tris(cyclopentadienyl)cerium(IV) compounds (e.g. [2–5]) especially those derived from $(C_5H_5)_4Ce$.[2,4] Published syntheses of tetra(fluorenyl)cerium(IV)[14] and dicycloheptatrienylcerium(IV) dichloride[15] by the same workers also could not be repeated.[7]

REFERENCES

1. B. L. Kalsotra, S. P. Anand, R. K. Multani and B. D. Jain, *J. Organomet. Chem.* 1971, **28**, 87.
2. B. L. Kalsotra, R. K. Multani and B. D. Jain, *Israel J. Chem.* 1971, **9**, 569.
3. B. L. Kalsotra, R. K. Multani and B. D. Jain, *J. Inorg. Nuc. Chem.* 1973, **35**, 311.
4. S. Kapur and R. K. Multani, *J. Organomet. Chem.* 1973, **63**, 301.
5. S. Kapur, B. L. Kalsotra, R. K. Multani and B. D. Jain, *J. Inorg. Nucl. Chem.* 1973, **35**, 1689.
6. T. J. Marks, *Prog. Inorg. Chem.* 1978, **24**, 51.
7. H. Schumann, *Organometallic compounds with lanthanide–carbon sigma bonds—one of the last problems in organometallic chemistry*. In *Organometallics of the f-Elements* (Edited by T. J. Marks and R. D. Fischer), pp. 81–112. Reidel, Dordrecht (1979).
8. A. F. Reid and P. C. Wailes, *Inorg. Chem.* 1966, **5**, 1213.
9. A. Greco, S. Cesca and G. Bertolini, *J. Organomet. Chem.* 1976, **113**, 321.
10. G. B. Deacon, W. D. Raverty and D. G. Vince, *J. Organomet. Chem.* 1977, **135**, 103.
11. D. C. Bradley, A. K. Chatterjee and W. Wardlaw, *J. Chem. Soc.* 1956, 2260.
12. J. M. Birmingham and G. Wilkinson, *J. Amer. Chem. Soc.* 1956, **78**, 42.
13. G. B. Deacon, A. J. Koplick and T. D. Tuong, *Polyhedron* 1982, 1, 423, and unpublished results.
14. B. L. Kalsotra, R. K. Multani and B. D. Jain, *J. Inorg. Nucl. Chem.* 1972, **34**, 2679.
15. B. L. Kalsotra, R. K. Multani and B. D. Jain, *J. Organomet. Chem.* 1971, **31**, 67.

BOOK REVIEW

Organotransition Metal Chemistry: Applications to Organic Synthesis. Stephen G. Davies, Pergamon Press, Oxford, 1982, pp. xv and 411

Organic compounds of the main Group elements have been employed in organic synthesis for at least a century. The more recent development of organotransition metal chemistry as a coherent discipline is now pointing the way to the exploitation of these compounds in a wide range of versatile organic transformations. Coordination of an unsaturated ligand to a transition metal often significantly modifies the reactivity of the ligand. Arenetricarbonyl chromium complexes, for example, are activated to attack by nucleophiles compared with the free arenes, so that a sequence of reactions involving complex formation, addition of a carbanion followed by oxidative removal of the transition metal permits nucleophilic substitution of an arene. Free alkenes normally react by electrophilic addition. η^2-alkene dicarbonylcyclopentadienyliron cations, however, add nucleophiles, and the resulting substituted alkyl group can readily be removed from the metal in a variety of ways. An important feature of reactions especially valuable in synthesis of organotransition metal complexes is the high degree of regio- and stereoselectivity with which they often proceed.

Dr. Davies is a young organic chemist who is actively engaged in research on organotransition metal compounds and their applications in organic synthesis, and is therefore well qualified to write a book on the subject. He begins with a useful general introduction considering the structures of organotransition metal complexes and the bonding within them. For a system to be useful in synthesis, complex formation and subsequent removal of the metal function must proceed readily and in high yield. Such processes are covered clearly and systematically. The versatility and range of the methods already available to the organic chemist are brought out by chapters on organometallics as protecting groups, as electrophiles and nucleophiles, in coupling and cyclisation reactions and in isomerisation of olefins and acetylenes. Organotransition metal reagents can be employed either stoicheiometrically or as catalysts. Examples of the latter method include catalysed oxidation, hydrogenation and carbonylation of alkenes and of other unsaturated organic compounds. The use of chiral complexes in effecting asymmetric syntheses is also covered.

This book is recommended. As the author states in the Preface, coverage cannot be comprehensive. The work, however, provides a clear and wide ranging account of the possibilities and potential of this exciting new area of chemistry. It could be read with profit by organic and organometallic chemists, and by postgraduate and advanced undergraduate students. The price however, will probably prevent purchase by the latter group. The book is reproduced directly from the typescript. The index could be more comprehensive, although this is counteracted by the systematic organisation of the subject matter.

PAUL POWELL

CHEMISTRY OF SUBSTITUTED SULPHURIC ACIDS — XVII. COMPLEXES OF V(III), Cr(III), Mn(II) AND Fe(II) METHYLSULPHATES

SUNITI KUMAR SHARMA*, R. K. MAHAJAN, B. KAPILA and V. P. KAPILA

Department of Chemistry, Panjab University, Chandigarh 160 014, India

Abstract—V(III), Cr(III), Mn(II) and Fe(II) methylsulphates form stable donor-acceptor complexes with nitrogen donors. 1:1 and 1:2 complexes with bipyridyl have been prepared in respect of trivalent salts and 1:2 and 1:4 metal:base complexes have been obtained in respect of divalent metal salts with bipyridyl and pyridine respectively. Electronic spectra suggest an octahedral geometry around metal ions. IR spectra of the anhydrous metal methylsulphates have been studied and assigned. The changes in the IR spectra of the methylsulphate group in different stereochemical situations have been observed.

Paul *et al.*[1–4] have prepared and characterized a few transition and non-transition metal methylsulphates. Johnson *et al.*[5] reported the complexes of some divalent transition metal methsulphates. The preparation and characterisation of the complexes of the methylsulphates of title metal ions is being reported now.

EXPERIMENTAL

Vanadium(III), chromium(III) and manganese-(II) methylsulphates were prepared as described earlier.[1] Iron(II) methylsulphate was obtained in the same way by solvolyzing $FeCl_2$ with anhydrous CH_3SO_3H. Anhydrous methylsulphuric acid was prepared conductometrically.[2]

The bipyridyl complexes were prepared by shaking a stoichiometric amount of the reactants in methanol. The contents of the reaction mixture were concentrated and the complex precipitated and washed with solvent ether. The complexes of divalent metal methylsulphates with pyridine were obtained by dissolving the anhydrous salt in excess base and then metathesizing with solvent ether. The pyridine complexes of trivalent metal methylsulphates were prepared in an analogous manner except that no precipitating/washing solvent was used; instead the excess base was pumped off by prolonged evacuation at 70°C. All the compounds were ascertained for their composition by elemental analyses. The IR spectra were run as nujol mulls on IR 621. The electronic spectra of the solids were recorded as nujol mulls by the transmittance method on DMR–21 at I.I.T. Madras. The electronic spectra of the pyridine complexes of V(III) could not be recorded as they did not offer mulls of sufficient consistency. The magnetic moments were obtained by Gouy's method at room temperature. Allowance for diamagnetic corrections has been made in all cases. The solution spectra were recorded on a Beckman DB recording spectrophotometer. In Table 1 are recorded the magnetic moments, colour and analytical data of the compounds.

DISCUSSION

The divalent and trivalent transition metal methylsulphates have an octahedral $M[O_6]$ chromophore.[1] This is explained on the basis of the presence of bridging CH_3SO_3 groups in these compounds. Recent investigations[6] on some bifunctional titanium(IV) compounds suggest that the CH_3SO_3 group is an excellent bridging group.

The coordination number, stereochemistry, etc., of the complexes, in question, have been deduced on the basis of electronic and IR spectral data.

Electronic spectra and magnetic moments. The complex, $V(CH_3SO_3)_3 . 2Bipy$ has bands at 16.0 and 18.7 kK(v_1) and a band at 30.3 kK (v_3) whereas $V(CH_3SO_3)_3 . Bipy$ has bands at 14.9 (v_1) and 25.0 and 28.6 kK (v_3). The splitting of v_1 or v_3 bands is

*Author to whom correspondence should be addressed.

Table 1. Analytical data of V(III), Cr(III), Mn(II) and Fe(II) methylsulphates and their complexes

Compound	Colour	$\mu_{eff.}$ (B.M.)	Metal	Nitrogen	Sulphur
			Analysis % Found (Calculated)		
1. $V(CH_3SO_3)_3$	Yellowish-Green	2.68	15.73(15.18)	–	29.02(28.57)
2. $V(CH_3SO_3)_3.3Py$	Green	2.57	9.09(8.90)	7.14(7.32)	16.48(16.75)
3. $V(CH_3SO_3)_3.Bipy$	Jade-green	2.69	10.73(10.36)	5.61(5.69)	19.09(19.51)
4. $V(CH_3SO_3)_3.2Bipy$	Violet	2.97	7.77(7.87)	8.88(8.64)	14.37(14.81)
5. $Cr(CH_3SO_3)_3$	Dark green	3.73	15.88(15.43)	–	27.76(28.49)
6. $Cr(CH_3SO_3)_3.3Py$	Green	4.21	9.74(9.06)	7.16(7.31)	16.33(16.72)
7. $Cr(CH_3SO_3)_3.Bipy$	Light green	3.90	10.26(10.55)	5.70(5.67)	20.00(19.47)
8. $Cr(CH_3SO_3)_3.2Bipy$	Light green	3.67	7.78(8.01)	8.53(8.62)	14.28(14.79)
9. $Mn(CH_3SO_3)_2$	White	5.46	22.24(22.45)	–	26.88(26.12)
10. $Mn(CH_3SO_3)_2.4Py$	White	5.63	9.53(9.80)	9.82(9.98)	12.06(11.41)
11. $Mn(CH_3SO_3)_2.2Bipy$	Light pink	6.19	9.73(9.87)	10.01(10.05)	11.24(11.49)
12. $Fe(CH_3SO_3)_2$	Light grey	4.90	22.41(22.76)	–	25.89(26.02)
13. $Fe(CH_3SO_3)_2.4Py$	Pale yellow	5.65	10.12(9.96)	9.48(9.96)	11.98(11.39)
14. $Fe(CH_3SO_3)_2.2Bipy$	Cherry red	6.10	10.53(10.13)	9.91(10.03)	11.23(11.47)

ascribable to the presence of low symmetry ligand fields in these compounds. The position of these bands is indicative of octahedral vanadium(III) species.[7] In as much as bipyridyl is a bidentate donor, it may be concluded that the 1:2 complex has a $V[O_2N_4]$ chromophore and the 1:1 complex, $V[O_4N_2]$ chromophore. A bridging methylsulphate provides the fourth oxygen atom in the latter case. The proposition of an ionic $CH_3SO_3^-$ group seems obligatory in the case of the bis(bipyridyl) complex. Unfortunately, due to the insolubility of these compounds in conventional organic solvents, no conductometric investigations could be carried out to ascertain the existence of ionic groups.

The electronic spectra of the chromic complexes reveal the following bands: $Cr(CH_3SO_3)_3.2Bipy$: 14.7 and 16.0 (v_1) and 22.2 kK (v_2); $Cr(CH_3SO_3)_3$. Bipy: 15.9 (v_1) and 21.7 kK (v_2); $Cr(CH_3SO_3)_3.3Py$: 15.7 and 16.3 (v_1), 22.2 (v_2) and 30.8 kK (v_3). The v_3 band in the case of the first two complexes seems to have been lost under the envelope of charge transfer bands. The proposition of octahedral chromophores seems obligatory in the light of these observations.

The electronic spectra of the complexes of manganese(II) exhibit the following bands: Mn-$(CH_3SO_3)_2.4Py$: 13.3, 15.6 and 20.0 kK and $Mn(CH_3SO_3)_2.2Bipy$: 13.8, 15.0, 20.0 and 28.6 kK, but these bands are not revealing in that the band intensities could not be measured and hence no assignments could be made.

Iron(II) methylsulphate which has been pre-pared and characterized during the course of present studies, has two bands at 6.9 and 9.3 kK, arising out of the splitting of the ^5E_g excited state due to Jahn–Teller distortion.[7] The pyridine complex has bands at 8.9 and 12.5 kK whereas the bipyridyl complex has bands at 8.5 and 11.0 kK. The position of these bands consigns a coordination number of six to the ferrous compounds. The red colour of the bipyridyl complex seems to arise because of charge transfer bands occuring in the high energy region of the visible spectrum. Thus the solution spectrum of this complex in ethylenecarbonate (in which it does not furnish ionizable CH_3SO_3 groups) reveal three intense bands at 19.5, 20.5 and 28.6 kK of intensity 2980, 2250 and 1950 $Lmole^{-1}cm^{-1}$ respectively. These are recognised as metal→ligand C.T. bands. On the basis of simplified energy level diagram depicting metal t_{2g} and ligand π^* orbitals,[7] a 10 Dq value of 9.1 kK is approximated for the mixed ligand field which is well within the range of the 10 Dq values of similar systems.

The magnetic moments (obtained at room temperature) of all the compounds are in compliance with those expected from high-spin systems.

IR spectra

The CH_3SO_3 group can act as monodentate, tridentate or a bidentate ligand. In view of this, it is necessary to foresee the changes in vibrational spectrum of the methylsulphate group in different stereochemical dispositions.

Table 2. IR spectra of transition metal methylsulphates and some of their complexes (cm^{-1})

Assignments (a)	Compounds*									Assignments (b)
	1ᵃ	3ᵃ	9ᵃ	12ᵃ	7ᵃ	2ᵇ	6ᵇ	10ᵇ	14ᵇ	
(M-O) str.	-	-	235 255	375	{210 230}†		210 220	210 230		(M-N) str.
SO₃ rock	345 365	310	325 340	342 350	320 360	310	320	340	340	S-CH₃ wag
						335	360	350	350	S-CH₃ torsion
(V-O) str.	430	425	-	-	-	430	-	-	380	(M-O) str.
SO₃ sym. bend	525	530	-	530	510	510	510	510	510	(S-O**) wag.
SO₃ asym. bend	570	570	540	545	535	520	530	520	532	(SO₂) rock
						535	570	530	550	(SO₂) bend
S-CH₃ str.	785	770	780	780	780	770	780	770	780	S-CH₃ str.
SO₃ sym. str.	1030	1000	1050	1050	1010	1020	1030	1030	1060	(S-O**) str.
SO₃ asym. str.	1270	1130 1260	1200	1190	1130 1250	1140	1130	1150	1165	(SO₂) sym. str.
						1250	1260	1240	1240	(SO₂) asym. str.

* Numbers refer to the serial number of the compounds in Table 1.
** Coordinating oxygen atom of the methylsulphate group.
† These band positions are for (M-N) str.

(a) The symmetry of an isolated CH₃SO₃ group is lowered from C_{3v} to C_s if it is acting as a unidentate ligand. This lowering in symmetry is expected to bring about perceptible changes in the vibrational spectrum of the methylsulphate ion. Thus the three E modes, viz., SO₃ (asym. str.), SO₃(asym. bend) and S–C(wag), may split to give rise to six bands.[5]

(b) A tridentate CH₃SO₃ group has C_{3v} symmetry which implies that it will have the vibrational spectrum similar to that of the free ion.

(c) Although a bridging methylsulphate group has a larger number of bands than the possibility (b) above, but the presence of a bridging group should be acknowledged, only if other supplementary data[8] are available.

It may be possible, therefore, to use, to some extent, IR spectrum of CH₃SO₃ group for a diagnosis of its mode of coordination. The IR spectra of the anhydrous methylsulphates of the title ions have not been studied previously and are being assigned now (Table 2). It is noteworthy that the bivalent salts have just six fundamentals (3A + 3E)

ascribable to a C_{3v} symmetry (b) for the CH₃SO₃ group. A similar situation has been observed by Johnson et al. (loc.cit.). IR spectra of a few representative complexes are also tabulated. The assignments marked (b) in Table 2 are based on the assumption of monodentate CH₃SO₃ groups.

REFERENCES

1. R. C. Paul, V. P. Kapila, Miss N. Palta and S. K. Sharma, Indian J. Chem. 1974, 12, 825.
2. R. C. Paul, V. P. Kapila and S. K. Sharma, J. Inorg. Nucl. Chem. 1974, 36, 1933.
3. R. C. Paul, V. P. Kapila and S. K. Sharma, Indian J. Chem. 1974, 12, 651.
4. R. C. Paul, V. P. Kapila, R. Kumar and S. K. Sharma, J. Inorg. Nucl. Chem. 1980, 42, 281.
5. N. C. Johnson, J. T. Turk, W. E. Bull and H. G. Mayfield (Jr.), Inorg. Chim. Acta. 1977, 25, 235.
6. S. K. Sharma, R. K. Mahajan and V. P. Kapila, Indian J. Chem. In press.
7. A. B. P. Lever, Inorganic Electronic Spectroscopy. Elsevier Publishing Company, New York (1968).
8. M. R. Rosenthal, J. Chem. Educ. 1973, 50, 331.

THERMAL DECOMPOSITION OF OXOVANADIUM(IV) COMPLEXES WITH SUBSTITUTED PYRIDINES

R. LOZANO*, J. MARTINEZ, A. MARTINEZ and A. DOADRIO LÒPEZ

Departamento de Química Inorgánica, Facultad de Farmacia, Universidad Complutense de Madrid,
Madrid (3), Spain

Abstract—The kinetics of decomposition of solid complexes of bis(dibenzoylmethanato) oxovanadium(IV) with pyridine and several methyl, dimethyl and aminopyridines has been studied using differential scanning calorimetry. Activation energies have been determined and, in general show an increase with increasing basicity of the ligands. A linear relationship exists between pK_b values of the bases and the temperatures for the decomposition, except for the complexes obtained with 4 aminopyridine and 4 methylpyridine. These complexes are less stable than expected from the basicity of the ligands. These observations are discussed in terms of the nature of the metal–ligand bond.

The use of thermal methods of analysis as a technique for studying bonding and structure of coordination compounds has increased greatly in the last few years.[1] Most of the thermal studies have been limited to a determination of temperatures appropriate for drying or ignition for analysis, but some of the more recent ones have yielded a considerable volume of kinetic and thermodynamic data for reactions in solid state.[2–8]

Bowman and Rogers[9] and House *et al.*[10,11] have determined the correlation between the stability of the various transition-metal complexes with pyridine and substituted pyridines with the ligand basicity and steric factors. They found that thermal stability increased with ligand basicity and that steric effects influenced stability in a predictable manner, i.e. when methyl groups blocked the co-ordinating position, the stability decreased.

Wendlant[12] reported a decreasing trend in thermal stability as the ligand on copper(II) sulphate changed from ethylenediamine to 1,2-propanediamine and to 1,3-propanediamine.

To determine the decomposition reactions and the thermal parameters associated with them complexes of bis(dibenzoylmethanato) oxovanadium(IV) with pyridine and several substituted pyridines, were prepared in the present work. We were also interested in determining the relationship between the basicity of the ligands and the temperatures and activation energies of decomposition of the solid complexes.

EXPERIMENTAL

(a) *Materials.* Vanadium(IV) oxide sulphate, dibenzoylmethane (dbm), pyridine, 3-methylpyridine, 4-methylpyridine, 3,5-dimethylpyridine, 3-aminopyridine and 4-aminopyridine were Merck commercial products. The solvents used to prepare the complexes were Carlo Erba or Merck.

(b) *Analytical procedures.* Elemental analyses were performed with a Perkin–Elmer model 240 B. Vanadium was determined by Atomic Absorption with a Perkin–Elmer model 430 Atomic Absorption Spectrophotometer after de-

composing the complexes with concentrated HNO_3 and concentrate H_2SO_4 mixture (1:1).

The analytical data for the complexes are shown in Table 1.

(c) *Methods.* Thermal measurements were performed using a Mettler HE-20 thermobalance and a Mettler T.A. 3000 system with a Differential Scanning Calorimeter model DSC 20, samples of about 5 mg being used so as to render insignificant the degree of temperature non-uniformity within the sample. Aluminium pan was used under a dry nitrogen atmosphere. The scanning rate used was 2°C/min, and the instrument calibration was checked periodically with standard samples of indium. In all cases several runs were made and the results are shown, in Table 2.

(d) *Preparation of complexes.* The complexes of pyridine (Py), 3-methylpyridine (3-MP), 4-methylpyridine (4-MP), 3,5-dimethylpyridine (3,5-DMP), 3 aminopyridine (3-AP) and 4 aminopyridine (4-AP) with bis(dibenzoylmethano) oxovanadium(IV), VO(dbm)$_2$, were prepared as follows:

$VO(C_6H_5-CO-CH=CO-C_6H_5)_2$
Bis(dibenzoylmethano) oxovanadium(IV), (VO(dbm)$_2$) was prepared from a warm ethanol solution (15 cm³) of 0.886 g (3.95 mmol) of dibenzoylmethane which was mixed with a warm solution of 0.5 g (1.97 mmol) of vanadyl sulphate in water (10 cm³) and ethanol (5 cm³) with stirring. Lastly, NaOH 2N is added drop by drop till reaching pH = 5. Green solid was formed, which was filtered *in vacuo*, washed with ethanol and water and recrystallized from cloroform–ether solution. Green crystals were obtained and dried over P$_2$O$_5$. Yield: 79%.
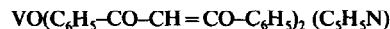
$VO(C_6H_5-CO-CH=CO-C_6H_5)_2$ (C$_5$H$_5$N)
This adduct can be prepared by two ways:
(a) A solution of 0.5 g (1.97 mmol) of vanadyl sulphate in a mixture of water (5 cm³) and ethanol (3 cm³) was prepared. Another solution of 0.886 g (3.95 mmol) of dibenzoylmethane in ethanol (15 cm³) was prepared. This solution was added to the first with vigorous stirring. Lastly, 1 cm³ of pyridine was added to the resulting solution and a brown solid was formed after *ca.* 24 hr at room temperature. This solid was filtered *in vacuo*, washed with water and ethanol mixture (1:1) and dried over P$_2$O$_5$. Yield: 86%.
(b) VO(dbm)$_2$ previously synthesized was dissolved in a ethanol solution of pyridine (1 cm³) with heating. After *ca.* 24 hr at room temperature, a brown solid was formed which was separated by filtration *in vacuo* and washed repeatedly with a water–ethanol mixture, (1:1), so that one obtains a brown power which was dried over P$_2$O$_5$. Yield: 83%.
A similar preparation was realised for the corresponding

---

*Author to whom correspondence should be addressed.

Table 1. Analytical data

COMPOUND	% CALCULATED				% FOUND			
	C	H	N	V	C	H	N	V
VO(dbm)$_2$	70.17	4.28	----	9.88	69.94	4.13	----	9.59
VO(dbm)$_2$.Py	70.94	4.56	2.36	8.61	71.10	4.60	2.38	8.69
VO(dbm)$_2$,3-MP	71.28	4.78	2.31	8.41	70.94	4.86	2.29	8.37
VO(dbm)$_2$,4-MP	71.28	4.78	2.31	8.41	71.68	4.80	2.35	8.55
VO(dbm)$_2$,3,5-DMP	71.61	5.00	2.25	8.25	71.86	5.20	2.27	8.66
VO(dbm)$_2$,3-AP	68.89	4.59	4.59	8.35	68.97	4.62	4.65	8.59
VO(dbm)$_2$,4-AP	68.89	4.59	4.59	8.35	69.15	4.67	4.63	8.50

complexes with 3-MP, 4-MP, 3,5-DMP, 3-AP and 4-AP as ligands.

DISCUSSION

The primary objectives of the present study were to determine the nature of the decomposition relations
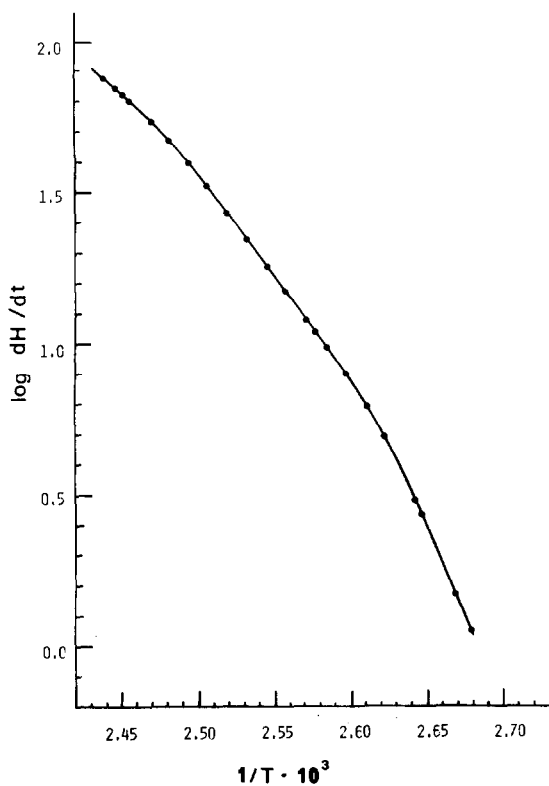
Fig. 1. Arrhenius plot of log(dH/dt) vs 1/T for VO(dbm)$_2$ 3-MP.

for a series of complexes of VO(dbm)$_2$ with pyridine and substituted pyridines, and to investigate the relationship between the basicity of the ligands and the kinetics of decomposition of the solid complexes.

The analytical data in Table 1 show that all the complexes obtained contain one molecule of ligand. The formula which most closely fits the analyses is VO(dbm)$_2$L, where L is pyridine or a substituted pyridine.

The DSC curves corresponding to the decomposition of the complexes showed only a single endothermic peak. The mass loss accompanying the endothermic transition corresponded to the loss of pyridine or a substituted pyridine in all cases with the residue being VO(dbm)$_2$. Data for the thermal parameters and mass loss determinations are shown in Table 2.

The peak temperature that corresponded to the loss of the molecule of ligand:

$$VO(dbm)_2L \rightarrow VO(dbm)_2 + L$$
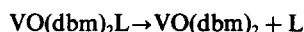
was used in the correlations. This temperature is underlined in the Table 2.

The activation energies were estimated by the method of Thomas and Clarke.[13] A plot of log dH/dt vs 1/T, Fig. 1, obtained from DSC data, was indeed found to be linear for $\alpha = 0.025$ to $\alpha = 0.211$ (see Table 2).

When the decomposition proceeds in the linear region over the range of temperature scanned by a calorimeter, the use of equation:

$$-\log k = -\log(dH/dt)(1/A)$$
$$= +\frac{E_A}{2.303RT} - \log C \qquad (1)$$

(k = rate constant; A = total area of DSC peak) to compute rate constants is justified. Moreover, the activation energy derived from Arrhenius plots repre-

Table 2. Thermal data for decomposition of VO(dbm)$_2$L

Compound	Peak Temp (°C)	% Mass loss		ΔH (Kcal/mol)	Activation Energy (Kcal/mol)	Range of α	pK_b
		Calcd	Expt				
VO(dbm)$_2$PY	108.2	13.34	13.28	17.09	15.14	0.14-0.70	8.87 *
VO(dbm)$_2$3-MP	137.6	15.34	15.10	19.18	31.34	0.03-0.21	8.32 *
VO(dbm)$_2$4-MP	108.1	15.34	15.31	22.34	24.68	0.03-0.41	7.98 *
VO(dbm)$_2$3,5-DMP	161.4	17.25	17.53	22.25	26.29	0.22-0.72	7.85 *
VO(dbm)$_2$3-AP	182.9	15.44	15.39	16.89	42.39	0.08-0.59	7.49 #
VO(dbm)$_2$4-AP	212.9	15.44	15.41	23.91	28.12	0.02-0.69	4.88 *

* Reference 16
# Experimental value
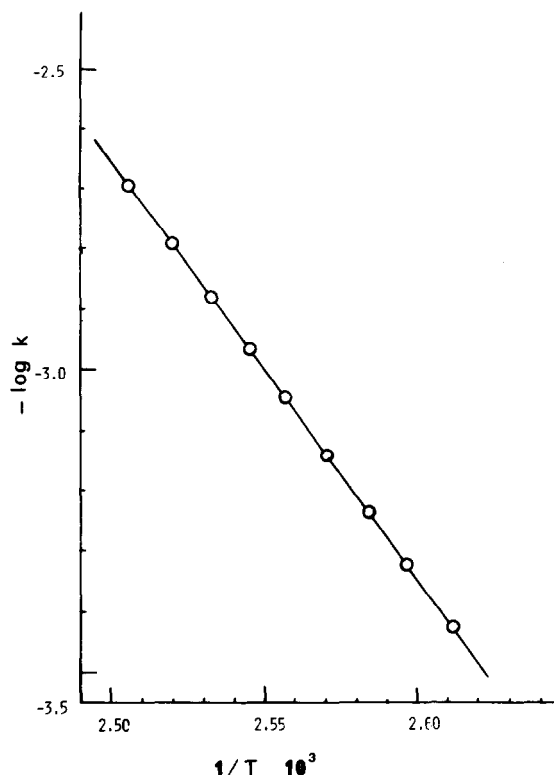
Fig. 2. Arrhenius plot constructed from DSC data using
equation (1) to VO(dbm)$_2$ 3-MP complex.

sents the true activation energy for interfacial reaction. Figure 2 shows the Arrhenius plots constructed from DSC data using the equation (1) for VO(dbm)$_2$ (3-MP).

Pyridine and the substituted pyridines used in this study, excluding 4 aminepyridine, provide only a relatively narrow range of basicities, but the effects on the kinetics of decomposition of solid complexes are quite large. Substituted pyridines and pyridine, listed in order of decreasing base strength, were:

4-AP > 3-AP > 3.5-DMP > 4-MP > 3-MP > Py.

The pK$_b$ value reflects the basicity of the ligand

towards the proton. It may be assumed, then, that the pK$_b$ of the ligand provides a measure of the ability of the ligand to form σ bonds to metal ions[14,15] In general, as can be seen from the data in Table 2, the greater the basicity and the higher the temperature to produce the loss of the ligand. The outstanding exceptions are the 4-AP and 4-MP complexes which will be discussed later.

The plot of pK$_b$ vs decomposition temperature presented in Fig. 3, shows that, except for the 4-AP and 4-MP complexes, a very satisfactory correlation was obtained. It is obvious from this figure that temperature is linearly related to the basicity for the ligands not containing a substituent group in the 4 position. It is also readily apparent that the ligands with a methyl and an amino group in the 4 position has a pronounced effect on the stability of the solid oxovanadium(IV) complexes. This effect is not reflected by the basicity of the ligand and can be due to the existence of the resonance structures of the types:

Fig. 4. Resonance forms.

When the pyridine ring contains a methyl and an amino group in the 4 position, the complexes obtained with these ligands are less stable and decompose more easily than those not containing a substituent group in the 4 position. Since the basicity toward the proton is a reliable measure of the σ bonding and electrostatic effects, one can say that there must be a significant difference in the tendency to form metal–ligand π bonds when a methyl or an amino group are in the 4 position of a pyridine ring and however the complexes containing 4-MP and 4-AP as ligand appear to be less stable than expected from the basicity of the ligand.

In general, the greater basicity the higher activation energy for the decomposition of the complexes (Table 2). The three complexes that appear not to follow this pattern are those of 4-AP, 4-MP and 3,5-DMP,
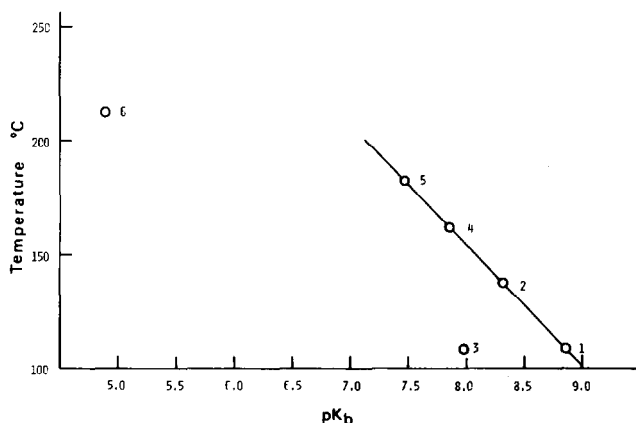
Fig. 3. Temperature for decomposition of the Vanadium oxo-complexes function of pK$_b$. Points 1–6 correspond to complexes of Py, 3-MP, 4-MP, 3,5-DMP, 3-AP and 4-AP respectively.

which present lower values of activation energy than expected from the basicity of the ligands. The explanation of this behaviour may be due to the existence of resonance forms, as we have seen previously to the complexes with 4-AP and 4-MP as ligand, and the steric factors or inductive effect exercised by the methyl groups to the complex with 3,5-DMP as ligand.

REFERENCES

[1] W. W. Wendlandt and J. P. Smith, *The Thermal Properties of Transition Metal Ammine Complexes*. Elsevier Amsterdam (1967).

[2] G. G. T. Guarini and R. Spinicci, *J. Ther. Anal.* 1972, **4**, 435.

[3] R. S. Botell, H. Chang and D. A. Lusardi, *J. Inorg. Nucl. Chem.* 1979, **41**, 909.

[4] J. E. House, *Thermoch. Acta* 1980, **40**, 225.

[5] C. A. Jepsen and J. E. House, *J. Inorg. Nucl. Chem.* 1981, **43**, 9531.

[6] N. Ghiassee, P. G. Clay and G. N. Walton, *J. Inorg. Nucl. Chem.* 1981, **43**, 2909.

[7] C. E. Bamberger, K. Brookhart and P. R. Robinson, *Inorg. Chim. Acta* 1982, **57**, 161.

[8] G. S. Harris and J. S. MacKechie, *Polyhedron* 1982, 1, 215.

[9] P. B. Bowman and L. B. Rogers, *J. Inorg. Nucl. Chem.* 1966, **28**, 2215.

[10] Abbas Akhavein and J. E. House Jr., *J. Inorg. Nucl. Chem.* 1970, **32**, 1479.

[11] Ramzi Farran and J. E. House Jr., *J. Inorg. Nucl. Chem.* 1972, **34**, 2219.

[12] W. W. Wendlandt, *J. Inorg. Nucl. Chem.* 1963, **25**, 833.

[13] J. M. Thomas and T. A. Clarke, *J. Chem. Soc. (A)* 1968, 457.

[14] R. K. Murmann and F. Basolo, *J. Amer. Chem. Soc.* 1955, **77**, 3884.

[15] W. R. May and M. M. Jones, *J. Inorg. Nucl. Chem.* 1963, **25**, 507.

[16] *Handbook of Chemistry and Physics*. 53rd Edn. Weast (1972–1973).

KINETICS OF OXIDATION OF HYPOPHOSPHITE ION BY Au(III) IN HYDROCHLORIC ACID MEDIUM

KALYAN KALI SENGUPTA,* BISWANATH BASU, SHIPRA SENGUPTA and
SANGHAMITRA NANDI
Department of Chemistry, Jadavpur University, Calcutta 700032, India

Abstract—Hypophosphite ion is oxidised by Au(III) in aqueous hydrochloric acid to give phosphorus acid and Au(I). The kinetics of the reaction has been studied spectrophotometrically in the UV region at different temperatures. The oxidation of hypophosphorous acid is first order with respect to both Au(III) and substrate. Hydrogen ion has no effect on the rate in acid media (0.15–1.0) M. The energy and entropy of activations are $128 \pm 3.0 \, kJ \, mol^{-1}$ and $135.8 \pm 6.5 \, JK^{-1} \, mol^{-1}$ respectively. The results are interpreted in terms of the probable formation of intermediate Au(II).

The kinetics of the oxidation of $H_2PO_2^-$ by various metal ion oxidants in acidic and alkaline media have been published.[1–4] Au(III) compounds which are toxic in nature were used earlier[5] in the treatment of tuberculosis. However, the toxic nature of the treatment was reduced by using hypophosphite as an antidote. The mechanism of oxidation of hypophosphite ion by Au(III) has not received attention. Au(III) as an oxidant is of interest because it may behave as an one equivalent or a two equivalent oxidant in the reaction with hypophosphite ion. Since Au(III) chloride is unstable with respect to substitution[6] in alkaline aqueous medium, the reaction has been studied in hydrochloric acid solution over a wide range of experimental conditions.

EXPERIMENTAL

Reagents. The materials employed were of highest purity available. Sodium hypophosphite (NaH_2PO_2) was of E. Merck grade. Chloroauric acid (Johnson–Matthey) was used to prepare solutions of Au(III). The concentration of Au(III) was determined gravimetrically[7] and the solution was stored in the dark and used under subdued lighting conditions. Hydrochloric acid was prepared by dilution of (B.D.H.) AnalaR grade stock solution and was analysed by titration with NaOH. Lithium chloride, sodium chloride and potassium chloride were (B.D.H.) AnalaR grade materials. All the solutions were made in doubly distilled water.

Absorption spectra of Au(III) solution. The absorption spectrum of Au(III) solution in 0.1–2.0 M hydrochloric acid in the concentration range $(0.25–1.5) \times 10^{-4} \, M$ was recorded in the UV region. The spectral pattern remained unaltered with changes in the concentration of Au(III). The spectra showed two very strong bands in the ultraviolet region[8] (227 nm, $\epsilon = 35,750$ and 315 nm, $\epsilon = 5400$ $M^{-1} cm^{-1}$). Beer's law has been found to be valid in the concentration range studied.

Kinetic measurements. The reaction was carried out under pseudo-first order conditions, i.e. at high concentration of hypophosphite ion compared to that of Au(III) concentrations. The rates were determined by following the decrease in the optical density of Au(III) at 315 nm in a Perkin–Elmer (Hitachi 200) spectrophotometer equipped with thermostated holders. Other reactants and products of the reaction had negligible absorption at this wavelength. The reactants were separately equilibrated to temperature,

mixed externally and immediately transferred into a cell of path length 1 cm. There is an initial period of disturbance at the beginning of the reaction after which the reaction obeyed good first order kinetics (Fig. 1). Pseudo-first order rate constant (k_{obs}) was determined from the slope of linear portion of logarithm (optical density) vs time plot. The rate constants obtained from different determinations were within $\pm 5\%$ of each other.

RESULTS

Stoichiometry and product analysis: Au(III) was mixed with a large excess of hypophosphite ions and kept for 2 hr at $[H^+] = 1.0$ M. Analysis[9] of unreacted reductant indicated the following stoichiometry.

$$Au(III) + H_3PO_2 + H_2O \rightarrow Au(I) + H_3PO_3 + 2H^+. \quad (1)$$
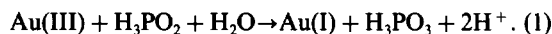
Phosphite ion was identified by thin layer chromatography[10] on silica gel G (E. Merck) using the
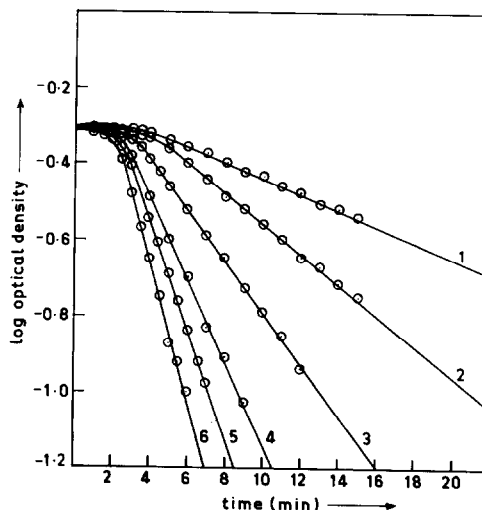
Fig. 1. Typical pseudo-first order plots for the oxidation of hypophosphite ion by Au(III) in HCl solution. $[Au(III)] = 1.0 \times 10^{-4} M$, $[H]^+ = 1.0 M$, Temp = 50°C and $[H_2PO_2^-] = (1) \, 0.5 \times 10^{-2}$, (2) 1.0×10^{-2}, (3) 2.0×10^{-2}, (4) 3.0×10^{-2}, (5) 4.0×10^{-2}, (6) $5.0 \times 10^{-2} M$.

*Author to whom correspondence should be addressed.

mixture of methanol, ammonia, trichloroacetic acid and water as the solvent system. A control TLC experiment was also done together with hypophosphite, phosphite and phosphate from which it was confirmed that hypophosphite ion was converted only to the phosphite stage (R_f value $= 0.74$ and lit. R_f value[4b] $= 0.75$). There is no evidence of a redox reaction between the H_3PO_3 and Au(III) under the condition of the experiment. However when Au(III) was in large excess to that of the substrate and the reaction mixture was stored for several hours, further oxidation of phosphorous acid occurred leading to the formation of phosphoric acid. Gold metal is sometimes generated[6] by further reduction of Au(I) by excess of reductant and/or by the disproportionation at lower acidities (< 0.2 M). However, we have no evidence for the formation of gold metal during 2 hr in $[H^+] = 1.0$ M.

Test with vinyl compound. A solution of Au(III) (1 cm³, 1×10^{-3} M) was added to a solution containing substrate solution (2 cm³, 1.0×10^{-1} M), HCl (5 cm³, 2.0 M) and acrylamide (2 cm³, 40% w/v) and the total volume was adjusted to 10 cm³. The addition of a large volume of methanol gave a suspension indicating that the reaction of Au(III) and hypophosphite ion in acid medium induces the polymerization of acrylamide whereas neither Au(III) nor hypophosphorous acid alone induces appreciable polymerization.

Effects of reactant concentration. The reaction was studied at different Au(III) concentrations. The average pseudo-first order rate constants are $(3.04 \pm 0.12) \times 10^{-4}$ sec^{-1} at [Au(III)], [$H_2PO_2^-$], [H^+] and temperature of $(0.125 - 1.25) \times 10^{-4}$ M, 2.0×10^{-2} M, 1.0 M and 35°C respectively. This indicates that pseudo-first order rate constant is independent of initial Au(III) concentration. Several other experiments were also carried out at constant acidity and Au(III) concentrations but varying concentrations of the substrate. The rate of reaction was found to increase with increase in substrate concentration (Table 1). The plots of k_{obs} against [substrate] are linear at different temperatures passing through the origin indicating that order with respect to substrate is unity (Fig. 2) and kinetic evidence for 1:1 complex formation is insignificant. The oxidation of hypophosphite ion was also studied in hydrochloric acid medium (0.15–1.0) M. The ionic strength was held constant at 1.0 M by the addition of sodium chloride. Hydrogen ion has no effect on the rate of reaction.

Effect of salts. The influence of addition of three different salts such as lithium chloride, sodium chloride and potassium chloride was investigated. The reaction was studied at [$H_2PO_2^-$], [Au(III)] and [H^+] of 1.0×10^{-2}, 1.0×10^{-4} and 1.0 M respectively where salt concentrations were varied between the limits (0.2–1.0) M. The reaction rate is independent of added salt-concentrations. The present observation is similar to that obtained by Moodley and Nicol[12] in the oxidation of Pt(II) by Au(III) and suggests that the path involving higher chlorocomplex of Au(III) is not significant. Moreover, participation of aquo and hydroxo complexes like $AuCl_3(H_2O)$ and $AuCl_3(OH)^-$ are unlikely[13] since in those cases the rate would have decreased with the increase in both hydrogen and

Table 1. Effect of hypophosphite ion concentration on pseudo-first order rate constants at [Au(III)] and [H^+] of 1.0×10^{-4} and 1.0 M respectively and at different temperatures

Temp. °C	[Substrate] $\times 10^2$ M	$k_{obs} \times 10^4$ sec^{-1}	$\dfrac{k_{obs}}{[\text{substrate}]} \times 10^2$ M^{-1} sec^{-1}
35	0.5	0.65	1.30
	1.0	1.23	1.23
	2.0	3.04	1.52
	3.0	3.66	1.22
	4.0	6.22	1.56
	5.0	7.05	1.41
40	0.5	1.61	3.22
	1.0	3.25	3.25
	2.0	6.12	3.06
	3.0	9.82	3.27
	4.0	12.5	3.13
	5.0	15.6	3.11
45	0.5	3.25	6.50
	1.0	6.43	6.43
	2.0	12.5	6.25
	3.0	18.1	6.03
	4.0	24.8	6.21
	5.0	31.7	6.31
50	0.5	7.82	15.6
	1.0	14.9	14.9
	2.0	26.9	13.45
	3.0	42.6	14.2
	4.0	55.3	13.8
	5.0	70.0	14.0
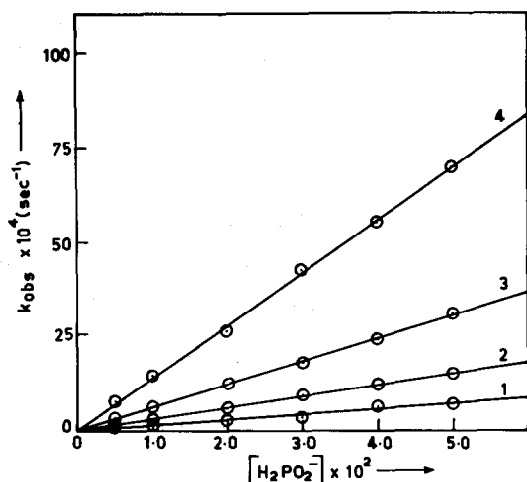
Fig. 2. Variation of pseudo-first order rate constants with substrate concentrations at different temperatures. Plots of k_{obs} against substrate concentrations. $[Au(III)] = 1.0 \times 10^{-4}$ M and $[H^+] = 1.0$ M (1) 35°, (2) 40°, (3) 45°, (4) 50°C.

chloride ion concentrations as shown below

$$AuCl_4^- + H_2O \rightleftharpoons AuCl_3(H_2O) + Cl^- \qquad (2)$$

$$AuCl_3(H_2O) \rightleftharpoons AuCl_3(OH)^- + H^+. \qquad (3)$$
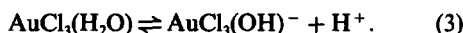
Activation parameters. The second order rate constants (k_2) at different temperatures were calculated. The values of k_2 are $(1.37 \pm 0.2) \times 10^{-2}$, $(3.17 \pm 0.11) \times 10^{-2}$, $(6.3 \pm 0.25) \times 10^{-2}$ and $(14.35 \pm 1.5) \times 10^{-2} (M^{-1} \sec^{-1})$ at 35, 40, 45 and 50°C respectively. The energy of activation was calculated from log k_2 vs $1/T$ plot and has been found to be 128 ± 2.0 kJ mol^{-1}. The value of $\triangle S^*$ has been calculated to be 135.8 ± 6.5 JK^{-1}mol^{-1}.

DISCUSSION

Hypophosphite ion is oxidised to phosphorous acid stage in acid solution and further oxidation of phosphorous acid was very slow under the conditions of experiment. The addition of ammonium molybdate to the reaction mixture failed to precipitate ammonium phosphomolybdate just after the kinetic experiment indicating the absence of phosphate ion. This has been confirmed from the TLC experiment which again indicated that phosphorous acid is the product of oxidation. Hypophosphorous acid oxidations are characterised by equilibria involving active and inactive forms[2,3,11] and the active form is known to be a better electron donor than the normal form of the substrate. Hypophosphorous acid which ionises according to the equilibria.

$$H_3PO_2 \overset{K_1}{\rightleftharpoons} H^+ + H_2PO_2^- \qquad (4)$$

has a dissociation constant (K_1) of 1.0×10^{-1}. This will remain in the undissociated form in the presence of sufficient acid (~ 1.0 M). Again HAuCl$_4$ remains in equilibrium with H$^+$ and AuCl$_4^-$ in hydrochloric acid

solution $(K_2 = 1.0 \pm 0.1)$ as follows.[12,14,15]

$$H AuCl_4 \overset{K_2}{\rightleftharpoons} H^+ + AuCl_4^-. \qquad (5)$$

In the present study hydrogen ion has no effect on the rate of reaction. So even if both dissociated and undissociated species are present, they appear to have the same kinetic properties. It is suggested that the reacting oxidising species attacks the undissociated molecule of the substrate. The reaction between a metal ion and a ligand usually prefers a complex formation rather than second order mechanism[16] and the energy of activation of the former process is smaller than that of the simple second order mechanism. In the oxidation of hypophosphorous acid by some metal ions,[3-5] it has been shown that the intermediate complex is formed between the active form of the substrate and the oxidising agent

$$H_3PO_2(\text{active}) + \text{Oxidant(ox)} \overset{\text{fast}}{\underset{\text{slow}}{\rightleftharpoons}} H_3PO_2 \cdot Ox$$
$$\rightarrow \text{Reaction Product.}$$
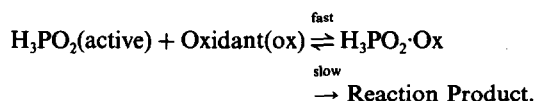
On the other hand, in the oxidation of hypophosphorous acid by hexachloroiridate(IV)[17] kinetic evidence failed to give an indication of the formation of an intermediate complex between hypophosphorous acid and Ir(IV). Likewise, complex formation between hypophosphorous acid and Au(III) has not been observed in the present study and the rate is strictly proportional both to hypophosphorous acid and Au(III) concentrations. This is supported by the high energy of activation obtained in this study as compared to the earlier studies where 1:1 intermediate complexes were formed between metal ion and hypophosphorous acid prior to electron transfer.[1,3,4] However, Au(III) may be reudced in either one electron change or by two electron change in the slow step. The observed polymerization in acrylamide is strongly indicative of free radical intermediates in the present study. It is, therefore, suggested that the initial reaction of active form of hypophosphorous acid with Au(III) takes place producing free radicals thereby reducing Au(III) into Au(II). The evidence for the existence of Au(II) as a reaction intermediate has also been shown in earlier studies.[12,14,17] The free radical further reacts with another Au(III) and by fast step (8) gives phosphorous acid. Au(II) undergoes disproportionation and gives Au(III) and Au(I). The reaction takes place as follows where step (6) is slow and all other steps are fast.

$$(6)$$

$$+ Au(II) + H^+ \qquad (7)$$

$$[(HO)_2P:]^+ + H_2O \rightarrow H_3PO_3 + H^+ \qquad (8)$$

$$2Au(II) \rightarrow Au(III) + Au(I). \qquad (9)$$
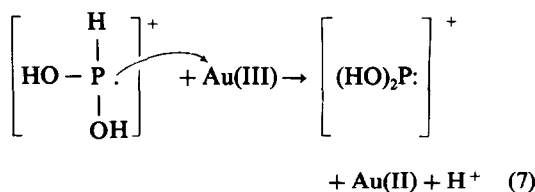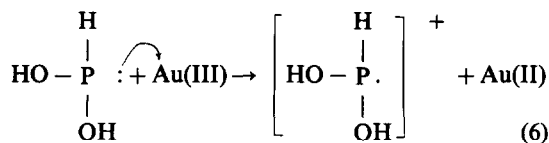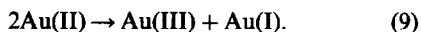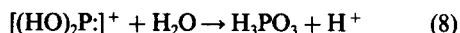
Thus the following two electron mechanism (step 10) may be ignored in the present reaction.

$$\begin{array}{c} H \\ | \\ HO - P \\ | \\ OH \end{array} : + Au(III) \xrightarrow{slow} [(HO)_2P:^+]^+ + Au(I) + H^+. \qquad (10)$$
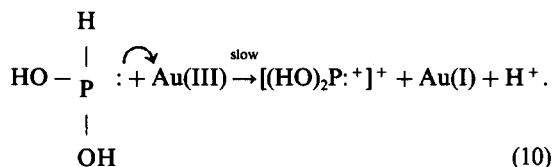
In the photolysis[18] of tetrachloroaurate(III)-oxalate system in aqueous acidic solution $AuCl_2^-$ and Au(O) were obtained from $AuCl_4^-$, whereas in the thermal decomposition of tetrachloroaurate(III)-oxalate system only $AuCl_2^-$ was obtained.[19] According to a number of authors[20] colloidal gold was formed when $HAuCl_4$ was exposed to UV light or sunlight and its formation was enhanced when the irradiation was carried out in the presence of reducing species for a long time. Regardless of which mechanism (6) or (10) is correct one piece of information is obtained with certainity that in hydrochloric acid solution further reduction of Au(I) does not occur under kinetic conditions and in this respect the present result is in agreement with that reported earlier by Moodley and Nicol.[12]

REFERENCES

[1a] S. K. Mishra and Y. K. Gupta, *J. Inorg. Nucl. Chem.* 1967, **29**, 1643; [b] K. S. Gupta and Y. K. Gupta, *J. Chem. Soc. (A)* 1970, 256.

[2] W. K. Jenkins and D. M. Yost, *J. Inorg. Nucl. Chem.* 1959, **11**, 297.

[3] R. L. Carrol and K. B. Thomas, *J. Am. Chem. Soc.* 1966, **88**, 1376.

[4a] J. Paton and C. H. Brubaker, *Inorg. Chem.* 1973, **12**, 1402; [b] K. K. Sen Gupta, J. K. Chakladar and A. K. Chatterjee, *J. Inorg. Nucl. Chem.* 1973, **35**, 901.

[5] B. F. G. Johnson and R. Davis, *The Chemistry of Copper, Silver and Gold.* p. 729. Pergamon Press, London (1975).

[6] F. A. Cotton and G. Wilkinson, *Advanced Inorganic Chemistry*, 3rd End., p. 1054. Wiley Eastern, New Delhi (1979).

[7] S. C. Soundar Rajan and N. Appala Raju, *J. Indian Chem. Soc.* 1973, **50**, 110.

[8] A. K. Gangopadhyay and A. Chakravorty, *J. Chem. Phys.* 1961, **35**, 2206.

[9] A. I. Vogel, *A Text Book of Quantative Inorganic Analysis*, p. 411. Longmans Green & Co., London (1964).

[10] E. Stahl, *Thin Layer Chromatography*, p. 482. Academic Press, New York (1965).

[11] E. Benzvi, *J. Phys. Chem.* 1963, **67**, 2698.

[12] K. G. Moodley and M. J. Nicol, *J. Chem. Soc. (Dalton)* 1977, 993.

[13] F. H. Fry, G. A. Hamilton and J. Turkevich, *Inorg. Chem.* 1966, **5**, 1943.

[14] H. G. Forsberg, II. Widdel and L. G. Erwall, *J. Chem. Educ.* 1960, **37**, 44.

[15] K. K. Sen Gupta and B. Basu, *Trans. Metal Chem.* in press.

[16] H. Taube, *J. Chem. Educ.* 1968, **45**, 452.

[17] K. K. Sen Gupta, S. Maiti and S. P. Ghosh, *Indian J. Chem.* 1980, **19A**, 869.

[18] B. S. Maritz, R. Van Eldik and J. A. Van Den Berg, *J. South African Chem. Inst.* 1975, **28**, 14.

[19] V. P. Kazakov, A. I. Matveeva, A. M. Erenburg and B. I. Peshchevitskii, *Russ. J. Inorg. Chem.* 1965, **10**, 563.

[20] V. Balzani and V. Carassiti, *Photochemistry of Coordination Compounds*, p. 273. Academic Press, London (1970).

PROTON NMR SPECTRA AND STRUCTURE OF CHLORO TIN(IV) TERNARY COMPLEXES OF 8-QUINOLINOL AND ITS 5,7 DICHLORO AND 2 METHYL-5,7 DICHLORO DERIVATIVES

J. L. NIETO*

Instituto de Estructura de la Materia, Consejo Superior de Investigaciones Científicas, Serrano 119, Madrid-6, España

and

A. M. GUTIERREZ

Departamento de Química Analítica, Facultad de Ciencias Químicas, Universidad Complutense, Madrid-3, España

Abstract—The low temperature ^{1}H NMR spectra in *d*-chloroform of the ternary complexes bis-(8-quinolinato) tin(IV) dichloride, bis-(5,7 dichloro-8-quinolinato) tin(IV) dichloride, and bis-(2 methyl-5,7-dichloro-8-quinolinato) tin(IV) dichloride have been obtained. The spectra showed that for the three complexes, only two configurations were appreciably populated, their free energy differences being equal to 0.28, 0.08 and − 0.04 kcal/mol respectively. The proton chemical shifts, the ^{1}H–^{1}H coupling constants and some of the ^{1}H–^{119}Sn coupling constants have been obtained for each complex in the two configurations. An approximate computation of chemical shifts, including aromatic ring magnetic anisotropies and electric effects from polar groups, allowed the identification of the two configurations as the *cis-cis-trans* and the *cis-trans-cis* (with respect to Cl, N and O atoms), the former being the more populated one.

Some structural studies on solutions of organotin(IV) substituted 8-quinolinols can be found in the literature.[1–3] Nevertheless, complexes of this type not involving metal–carbon bonds have received much less attention, mainly due to their low solubilities.[4,5] With the use of high field NMR spectrometers, the sensitivity problems are greatly reduced, and the pattern of NMR lines simplified, so it is now possible to extend structural studies to this type of complexes.

Recently, a detailed study on the complexation of tin(IV) by 8-quinolinol and its derivatives has been reported,[6] and we have considered it interesting to investigate further the structure of these complexes by proton NMR.

In this paper, we report the low temperature ^{1}H NMR spectra in *d*-chloroform of the ternary complexes, bis-(8-quinolinato) tin(IV) dichloride (Cl_2SnQ_2), bis-(5,7-dichloro-8-quinolinato) tin(IV) dichloride $(Cl_2Sn(CQ)_2)$ and bis-(2-methyl-5,7-dichloro-8-quinolinato) tin(IV) dichloride $(Cl_2Sn(MQ)_2)$. From their analyses, the chemical shifts and the ^{1}H–^{1}H and ^{1}H–^{119}Sn coupling constants were obtained. With the help of an approximate computation of chemical shifts, the different configurations that coexist in solution were also identified.

EXPERIMENTAL

Preparation of complexes

Details of the synthesis and purification of the complexes were reported previously.[6]

Proton NMR spectra

They were recorded at 360 MHz in the Fourier mode on a Bruker WM-360 pulse spectrometer. *D*-chloroform of the highest degree of deuteration

---

*Author to whom correspondence should be addressed.

available (99.98%, Stohler Isotope Inc.) was used to reduce the dynamic range problem originated by the residual signal from the protonated solvent. Saturated solutions corresponding to 3.0, 5.1 and 0.5 mM respectively, flip angles of 70°, 16 K of memory, 10000 scans and a relaxation delay between pulses of 2 sec were used. When needed, digital filtering of the free induction decay was used to improve signal to noise ratio (line broadening factor of 1 Hz). Alternatively, the Gauss–Lorentz multiplication was used to enhance resolution in some spectra. The chemical shifts were measured with respect to the chloroform signal, and assigned a value of 7.300 ppm. Low temperature spectra (− 30°C) were obtained with the standard Bruker accessory by flushing the sample with cool N_2 gas. The temperature was calibrated with a methanol thermometer[7] and the precision of the regulator was ± 0.5°C.

Other nuclei NMR spectra

The NMR spectra of nuclei other than proton could give supplementary information on the structure of the complexes, so attempts were made to obtain ^{13}C and [119]Sn spectra. A ^{13}C NMR spectrum of the most soluble complex (Cl_2SnQ_2) was obtained on an overnight accumulation, but the poor signal to noise ratio prevented any detailed study. Although the [119]Sn nucleus is a more sensitive one, its larger line width precludes the obtaining of spectra at these very low concentrations. In fact, our attempts to obtain a [119]Sn low temperature NOE suppressed NMR spectrum of the above mentioned complex were not successful.

Calculation of shieldings

The effect of the anisotropy of one 8-quinoline ring on the shieldings of the five protons of the other ring in the five configurations of the complex has been calculated by the method of Johnson–Bovey.[8] A FORTRAN program written in our laboratory that, from a known geometry (bond lengths and angles), calculates the shieldings originated by a phenyl ring on selected atoms, has been used. In the absence of aromaticity values for the 8-quinoline ring, the approach of two phenyl rings of additive effects was employed. An approximate geometry for the *cis-cis-trans* configuration was obtained from the dimethyl bis(8-quinolinato) tin(IV);[9] for the other configurations the geometry of the 8-quinoline ring was maintained, and right angles around the tin atom were used.

The polar Sn–Cl bonds can only affect the shielding of very close protons, and the effects will depend on the relative orientation of the Sn–Cl and C–H bonds. An inspection of a molecular model

showed that this effect can be of importance for the proton H2 in the *cis-trans-cis* configuration, and less important although noticeable for the proton H7 in the *cis-cis-trans* configuration. For other protons within the molecule the effects are very small, and in addition they tend to cancel each other in most cases. The shieldings were computed by the method of Buckingham,[10] with the approximate geometries already mentioned and $\mu(Sn–Cl) = 3.5$ D taken from the $(CH_3)_3SnCl$.[11]

Shieldings of appreciable intensity due to Van der Waals dispersions,[12,13] could arise only from atoms very close to each other. The two H2 protons in the *trans-cis-cis* configuration were the only potential candidates, and its effect if any, is to decrease their shieldings. However, any attempt to evaluate Van der Waals effects in this molecule remains speculative, because the lack of a precise knowledge of both the polarizability α of the C–H2 bond, and the distance between the two H2 protons, that directly affect the computed shieldings. Other through-space effects like magnetic anisotropies and electric moments involving the N and O atoms will not produce noticeable shieldings on any proton because of the large distances involved.

RESULTS AND DISCUSSION

Proton NMR spectra

The 360 MHz ^{1}H NMR spectra at low temperature of the three complexes are shown in Fig. 1; the spectra of the free ligands were also obtained and the centres of the multiplets are indicated in the figure. Some of the free ligand spectra at 100 MHz in d_6-dimethylsulphoxide, and at 220 MHz in d-chloroform have been reported previously.[4,14]

Three features are readily recognized on these spectra. First, two set of signals of unequal intensity are observed for each complex showing that two configurations are present. Second, satellite lines appear at both sides of every line, corresponding to the couplings of protons to the tin atom; the coupling constants are not large enough to distinguish between [1]H–[117]Sn and [1]H–[119]Sn couplings. Due to the poor signal to noise ratio, tin-proton couplings are observed only for two of the complexes (Tables 1 and 2). Third, only minor intensity lines from impurities of the free ligands appear in the spectra, except for the $Cl_2Sn(MQ)_2$ complex that partially decomposes when dissolved unless an excess of free MQ is added.[6] In the NMR spectrum of this last complex three additional very low intensity lines appear in the region 2.8–3.6 ppm, that must correspond to the methyl groups of the other three less populated configurations of the complex. At 360 MHz the spectra are nearly first
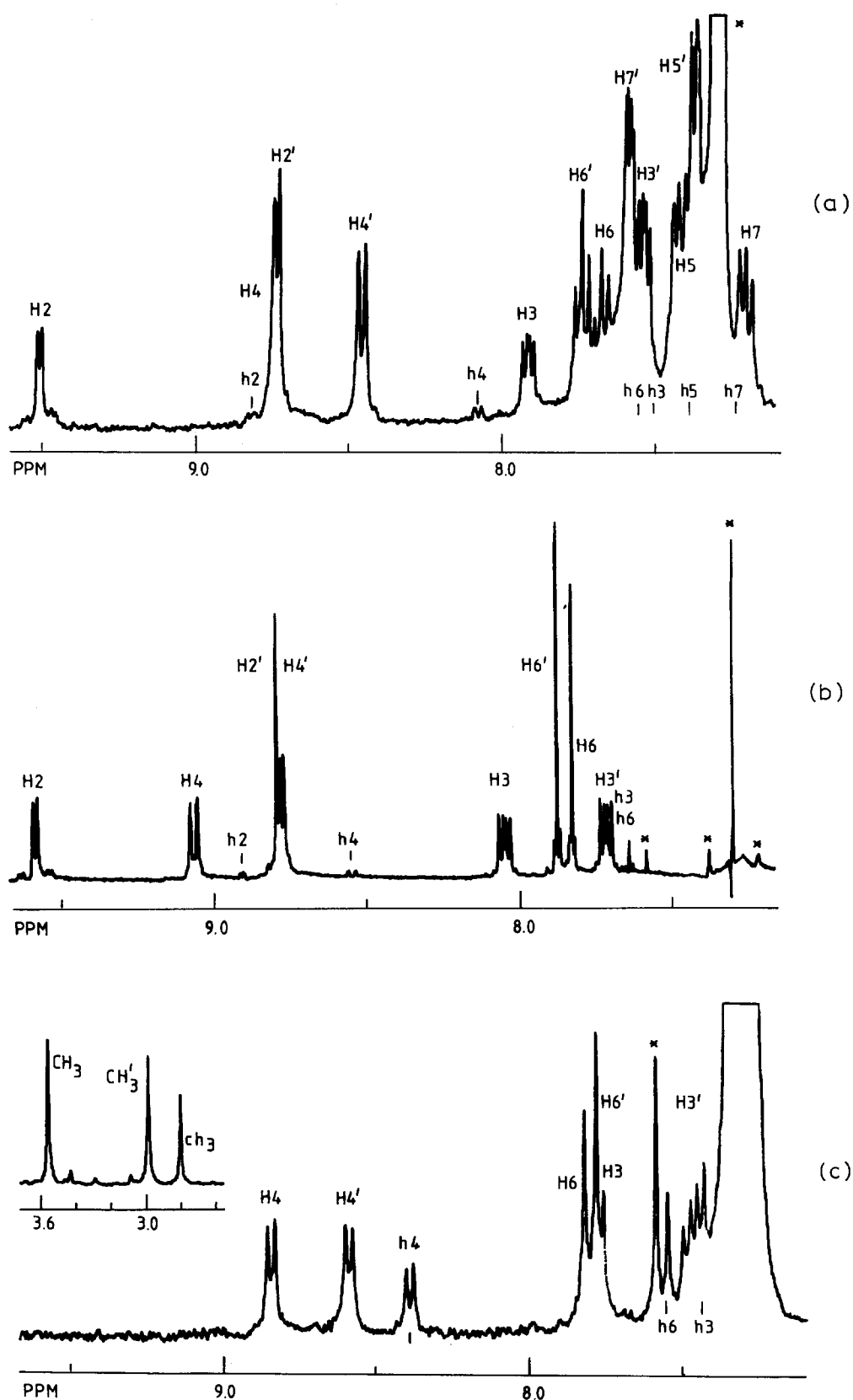
Fig. 1. 360 MHz ^{1}H NMR spectra at $-30°C$ of the complexes in $CDCl_3$ (a) Cl_2SnQ_2, 3.0 mM, (b) $Cl_2Sn(CQ)_2$, 5.1 mM, (c) $Cl_2Sn(MQ)_2$, 0.5 mM. Lower case letters mark the free ligands' resonances, apostrophes distinguish between the two configurations of each complex, and the asterisks mark lines from the solvent.

Table 1. Proton chemical shifts (δ, ppm from Cl_3CH) and $^1H-^1H$ and $^1H-^{119}Sn$ coupling constants (J, Hz) of the two configurations of the Cl_2SnQ_2 complex, 3.0 mM in Cl_3CD, $-30°C$ (360 MHz)
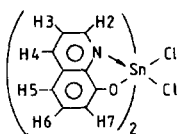
	Free ligand δ	Configuration I			Configuration II		
		δ	$\Delta\delta$*	$J(^1H-^{119}Sn)$**	δ	$\Delta\delta$	$J(^1H-^{119}Sn)$
H2	8.826	9.510	.68	32.8	8.736	-.09	18.5
H3	7.489	7.918	.43	11.8	7.542	.05	10.8
H4	8.207	8.739	.53	--	8.460	.25	--
H5	7.382	7.419	.04	--	7.378	.00	--
H6	7.503	7.681	.18	--	7.744	.24	--
H7	7.224	7.197	.03	--	7.591	.37	--
J_{23}	4.3	4.8			4.9		
J_{24}	1.4	1.0			1.3		
J_{34}	8.4	8.3			8.3		
J_{56}	8.3	8.2			8.3		
J_{57}	0.9	--			--		
J_{67}	7.6	7.8			7.4		
Intensity		0.36			0.64		

* $\Delta\delta=\delta-\delta$ (free ligand). $\delta(Cl_3CH)$=7.300 ppm.
** Some of the $^1H-^{119}Sn$ couplings could not be obtained due to overlapping of lines and to the solvent peak.

Table 2. Proton chemical shifts (δ, ppm from Cl_3CH) and $^1H-^1H$ and $^1H-^{119}Sn$ coupling constants (J, Hz) of the two configurations of the $Cl_2Sn(CQ)_2$ complex, 5.1 mM in Cl_3Cd, $-30°C$ (360 MHz)
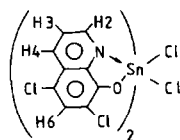
	Free ligand δ	Configuration I			Configuration II		
		δ	$\Delta\delta$*	$J(^1H-^{119}Sn)$	δ	$\Delta\delta$	$J(^1H-^{119}Sn)$
H2	8.922	9.581	.66	33.2	8.788	-.13	20.6
H3	7.703	8.053	.35	12.3	7.721	.02	10.0
H4	8.541	9.067	.53	7.3	8.784	.24	7.9
H6	7.608	7.832	.22	6.2	7.881	.27	7.1
J_{23}	4.3	4.9			5.0		
J_{24}	1.7	--			--		
J_{34}	8.8	8.4			8.3		
Intensity		0.46			0.54		

* $\Delta\delta=\delta-\delta$ (free ligand). $\delta(Cl_3CH)$=7.300 ppm.

order, so they can be straightforwardly analyzed, the chemical shifts and coupling constants being shown in Tables 1–3.

As a general rule, the NMR lines of the complexes are shifted downfield with respect to the lines of the free ligands, with the only exception of the proton H2 in the more populated configuration. In addition to other effects, the coordination of chloride atoms to the tin atom could contribute appreciably to this general downfield shift, as the same effect has been reported in the ^{13}C spectra of chloroderivatives of alkyltin compounds.[15] The $^1H-^1H$ coupling constants are very similar in the two configurations of each complex, and these in turn are very close to the coupling constants of the free ligands, although slight differences beyond the experimental error are detected, in particular for the J_{23} coupling.

Tin-proton coupling constants for protons H2 and H3 are of the same order of magnitude as those reported for aryltin compounds.[16] In both complexes, Cl_2SnQ_2 and $Cl_2Sn(CQ)_2$, the $^3J(^{119}Sn-^1H)$ couplings for protons H2 and H3 were smaller in the more populated configuration, thus reflecting a variation in the dihedral angle Sn–C–C–H. Although a Karplus type relationship between the dihedral angle and the vicinal $^{119}Sn-^{13}C$ coupling constant has been established,[17] an analogous relationship for the $^3J(^{119}Sn-^1H)$ is not yet available, so that the variation cannot be evaluated quantitatively. Conversely, the $^3J(^{119}Sn-^1H)$ couplings in a given configuration are very similar, in the two complexes, which indicates that the dihedral angle Sn–C–C–H is maintained.
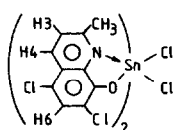
Stereochemistry

These hexacoordinated complexes of the type $M(L-L')_2X_2$ can exist in five different configurations[18] in solution, enantiomers being indistinguishable from the NMR point of view. The cis-cis-cis (with respect to Cl, N and O atoms) configuration has no symmetry (point group C_1), the two 8-quinoline rings are not equivalent and it should give two set of NMR signals of identical intensity. In the other four configurations, cis-trans-cis (C_2), cis-cis-trans (C_2), trans-cis-cis (C_{2v}) and trans-trans-trans (C_{2h}), the two 8-quinoline rings are equivalent and only one set of NMR signals are expected for each configuration. As only two sets of unequal intensity signals are observed for the three complexes, the presence of the cis-cis-cis configuration can be definitively discarded, and only two of the remaining four possible configurations are appreciably populated and coexist in solution. To identify them a more detailed analysis of the experimental chemical shifts is required.

The lines in the NMR spectra of the complexes are shifted with respect to their positions in the free ligand. Two types of effect contribute to these shifts. The first effect is the change in the shielding of the protons due to the coordination of the 8-quinoline ring and the chloride to the tin atom ("through bond" shifts). The second effect is the change in the shieldings due to the proximity of anisotropic groups ("through-space" shifts). The net result of these two contributions is the shift we measure in the spectrum. As "through-bonds" shieldings are difficult to evaluate a priori, no values obtained in similar tin(IV) complexes being available, the "through space" shieldings cannot be obtained by the differences in frequency between "coordinated" and "free" 8-quinoline ring protons. However, it is reasonable to suppose that these "coordination shifts" are of similar magnitude for the five different configurations of a given complex so, if chemical shift differences between configurations are considered, only through space effects do have influence. These effects can be approximately evaluated, and the comparison between observed and computed differences of chemicals shifts will provide a means to identify the configurations that coexist in solution.

Table 4 shows the shieldings computed for the five protons of the 8-quinoline ring, in the five configurations of the Cl_2SnQ_2 complex (details are

Table 3. Proton chemical shifts (δ, ppm from Cl_3CH) and $^1H-^1H$ coupling constants (J, Hz) of the two configurations of the $Cl_2Sn(MQ)_2$ complex, 0.5 mM and − 30°C (360 MHz)

	Free ligand δ	Configuration I		Configuration II	
		δ	$\Delta\delta$*	δ	$\Delta\delta$
H3	7.462	7.772	.31	7.486	.02
H4	8.401	8.843	.44	8.589	.19
H6	7.553	7.822	.27	7.784	.23
CH_3	2.803	3.561	.76	2.991	.19
J_{34}	8.5	8.6		8.7	
Intensity		0.52		0.48	

* $\Delta\delta=\delta-\delta$ (free ligand) . $\delta(Cl_3CH)=7.300$ ppm.

given in the experimental part). The computed differences of shieldings among all possible pairs of configurations are shown in Table 5, that also includes the comparison with the experimental differences obtained from the NMR spectra. Four of the six pairs can be readily excluded and in the remaining two, the cis-cis-trans configuration is included, so its presence is definitively confirmed. It can be seen that the agreement of the pair cis-cis-trans and cis-trans-cis is very good, so the presence of the cis-trans-cis as the second configuration is strongly favoured. Although the agreement of the pair trans-cis-cis and cis-cis-trans

is considerably worse, it cannot be completely excluded on the basis of this calculation alone, due to the approximate character of both the geometry and the calculation of shieldings. Two additional reasons support the absence of the trans-cis-cis configuration. First, the experimental differences of shieldings between the two configurations are very similar for the three complexes we studied here, which indicates that the configurations that coexist in solution are the same in the three cases. In the case of the $Cl_2Sn(MQ)_2$ complex, it is very unlikely that the trans-cis-cis configuration could be appreciably populated, because of steric hin-

Table 4. Computed shieldings (ring anisotropies and polar groups effects) of the five configurations of the Cl_2SnQ_2 complex

No.	Configuration	Shielding* σ (ppm)					
		H2	H3	H4	H5	H6	H7
1	cis-cis-cis	-.17	-.11	-.10	-.05	.01	.09
		1.20	.40	.12	.02	-.03	-.08
2	cis-trans-cis	-.12	-.06	-.06	-.04	-.01	.03
		(-.35)					
3	cis-cis-trans	.31	.42	.26	.10	-.02	-.15
							(-.07)
4	trans-trans-trans	-.21	-.08	-.06	-.05	-.06	-.12
5	trans-cis-cis	-.49	-.14	-.07	-.05	-.05	-.09

* Negative signs denote diminution of shielding. Numbers in parenthesis are the only appreciable shieldings originated by nearby Cl-Sn polar bonds, calculated by the method of Buckingham[10]. Ring anisotropy shieldings were calculated following Johnson-Bovey[8], with approximate geometries.

Table 5. Computed chemical shift differences among all possible pairs of configurations of the Cl_2SnQ_2 complex and comparison with the experimental differences obtained for the three complexes

	a	b	Chemical shift differences (ppm)					
			H2	H3	H4	H5	H6	H7
$\Delta\delta^*_{ab}$ (computed)	3	2	.78	.48	.32	.14	-.01	-.25
	4	2	.26	-.02	.00	-.01	-.05	-.15
	2	5	.02	.08	.01	.01	.04	.12
	3	4	.52	.50	.32	.15	.04	-.10
	3	5	.80	.56	.33	.15	-.03	-.13
	4	5	.28	.06	.01	.00	-.01	-.03
$\Delta\delta^{**}_{I-II}$ (experimental)	Cl_2SnQ_2		.77	.38	.28	.04	-.06	-.34
	$Cl_2Sn(CQ)_2$		.79	.33	.28	--	-.05	--
	$Cl_2Sn(MQ)_2$		.57 (methyl)	.29	.25	--	.04	--

* $\Delta\delta_{ab}=\sigma_a-\sigma_b$, where σ's are computed shieldings and a and b refer to the numbering of configurations, both shown in Table IV.

** $\Delta\delta_{I-II}=\delta(config.I)-\delta(config.II)$; I and II refer to the two configurations of Tables I-III.

drance of the methyl groups. Second, it has been reported on other tin(IV) dichloride complexes[19,20] that the *cis* halogen configuration is favoured against the *trans*.

From all the reasons discussed we conclude that the three complexes studied here adopt the same two configurations in solution, the *cis-cis-trans* and the *cis-trans-cis*, the former being the more populated one. Free energy differences between them, obtained through the relationship[21] $\Delta G^0 = - RT \ln (p_2/p_1)$ where p_2/p_1 is the population ratio measured in the NMR spectra, were 0.28, 0.08 and $- 0.04$ kcal/mol respectively. As the temperature is raised, the two configurations begin to exchange more rapidly thus originating a broadening and shifting of lines in the NMR spectrum.

REFERENCES

1. K. Kawakami and R. Okawara, *J. Organomet. Chem.* 1966, **6**, 249.
2. L. Roncucci, G. Faraglia and R. Barbieri, *J. Organomet. Chem.* 1966, **6**, 278.
3. C. D. Barsode, P. Umapathy and D. N. Sen, *J. Ind. Chem. Soc.* 1976, **53**, 761.
4. B. C. Baker and D. T. Sawyer, *Anal. Chem.* 1968, **40**, 1947.
5. B. C. Baker and D. T. Sawyer, *Inorg. Chem.* 1969, **8**, 1160.
6. A. M. Gutierrez, A. Sanz-Medel and R. Gallego, *Anal. Chim. Acta* 1983, **149**, 259.
7. R. Duerst and A. Merbach, *Rev. Sci. Instr.* 1965, **36**, 1896.
8. C. E. Johnson and F. A. Bovey, *J. Chem. Phys.* 1958, **29**, 1012.
9. E. O. Schlemper, *Inorg. Chem.* 1967, **6**, 2012.
10. A. D. Buckingham, *Can. J. Chem.* 1960, **38**, 300.
11. A. L. McClellan, *Tables of Experimental Dipole Moments.* Freeman, San Francisco (1963).
12. A. A. Bothner-By, *J. Mol. Spectrosc.* 1960, **5**, 52.
13. W. T. Raynes, A. D. Buckingham and H. J. Bernstein, *J. Chem. Phys.* 1962, **36**, 3481.
14. A. Corsini, W. J. Louch and M. Thompson, *Talanta* 1974, **21**, 252.
15. T. N. Mitchell, *Org. Mag. Res.* 1976, **8**, 34.
16. V. S. Petrosyan, *Progr. NMR Spectrosc.* 1977, **11**, 79.
17. D. Doddrell, I. Burfitt, W. Kitching, M. Bullpitt, C. Lee, R. J. Mynott, J. L. Considine, H. G. Kuivila and R. H. Sarma, *J. Am. Chem. Soc.* 1974, **96**, 1640.
18. R. H. Holm, In *Dynamic Nuclear Magnetic Resonance Spectroscopy* (Edited by L. M. Jackman and F. A. Cotton). Academic Press, New York (1975).
19. J. A. S. Smith and E. J. Wilkins, *J. Chem. Soc. (A)* 1966, 1749.
20. N. Serpone and R. C. Fay, *Inorg. Chem.* 1967, **6**, 1835.
21. W. A. Thomas, *Ann. Rep. NMR Spectrosc.* 1968, **1**, 43.

ESCA STUDIES ON THE STRUCTURE OF AMORPHOUS ADDITION COMPLEXES OF TIN DICHLORIDE WITH AROMATIC SCHIFF BASES

G. MARLETTA

Istituto Dipartimentale di Chimica e Chim. Ind., Università di Catania,
Vole A. Doria 6, 95125 Catania, Italy

and

P. FINOCCHIARO, E. LIBERTINI and A. RECCA*

Facoltà di Ingegneria, Università di Catania, V. le A. Doria 6, 95125 Catania, Italy

Abstract—The ESCA characterization of three similar new amorphous addition complexes of tin dichloride with tetradentate aromatic Schiff bases has been carried out. The results support the previously proposed ionic structure.

The solid state structure of addition products is generally an interesting problem, since their various properties are strictly related to it.

In this paper we present a peculiar case of solid state influence on the complexing properties of similar compounds.

The syntheses and characterization of our interest new addition complexes 1–3 of $SnCl_2$ with aromatic Schiff bases L_1-L_3 has been reported in a previous paper.[1]

L1; n = 2   1; $(SnCl_2)_2L_1$
L2; n = 4   2; $(SnCl_2)_2L_2$
L3; n = 6   3; $(SnCl_2)_2L_3$

Elemental analysis, IR, Mass Spectrometry and Conductance Measurements indicate the presence of 1:2 (ligand: $SnCl_2$) adducts, with an ionic type structure.

The nature of the chemical structure of these compounds was to be checked in the solid state, being the most important previously used techniques operating in the gas-phase (MS) and in solution (Conductance measurements).

As references compounds uncomplexed polymeric systems 4–6 have been used.

EXPERIMENTAL

Compounds 1–3 and polymers 4–6 have been prepared following the procedure described in literature.[1,2]

The Esca spectra were obtained with a KRATOS ES-300 electron Spectrometer. The measurements were performed with $Al_{K\alpha1,2}$ photon source. The vacuum in the analysis chamber was better than 10^{-8} Torr. The samples were stable in
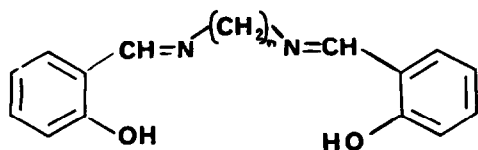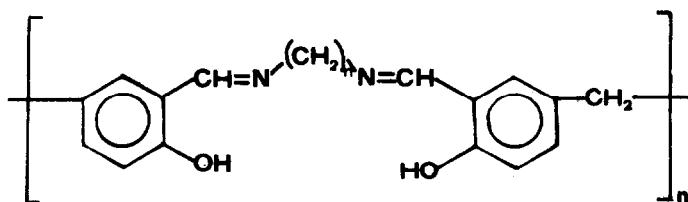
4 : n = 2
5 : n = 4
6 : n = 6

*Author to whom correspondence should be addressed.

vacuum. Each sample was introduced into the Spectrometer both as powder stripped onto an Indium strip as well as powder pellets obtained under reduced pressure (rotary pump) and attached to a Ni–Cr wire with a silver glue.

The N 1s, O 1s, S_n $3d_{5/2}$ and Cl 2p peaks were monitored at different times of irradiation in order to detect eventual reduction processes. No sign of reduction was found for powder pellets.

RESULTS AND DISCUSSION

The Binding Energies (B.E.) of the main peaks of the compounds 1–6 are reported in Table 1.

The B.E. values of Sn $3d_{5/2}$ peak and its separation from Cl 2p and C 1s peaks are in the range of values reported for Sn (II) and Sn (IV) ions.[9] However, we found that the Sn B.E.'s[9] are lower than expected for Sn (II) chelates. This fact suggests that a higher electron density is present on the Sn ions.

The internal distances and the relative abundances of Sn 3d and Cl 2p peaks remain constant for all the adducts.

It is worth noting that while the Sn 3d peaks have a F.W.H.M. of 2.0–2.1 eV in accordance with the presence of one kind of Sn ion, the Cl_{2p} peaks are instead broad and somewhat different in shape with respect to the characteristic Cl doublet.

This fact suggests that more than one chlorine ion could be present.[8] The Sn/O ratio is about the same for the adducts 1 and 3 whereas in the case of adduct 2 it is slightly lower indicating, probably, a greater difficulty of the ligand to complex with $SnCl_2$ in this case.

There is no evidence of structure effects on the Sn and Cl B.E.'s or peak shapes on going from 1 to 3 adducts.

The C 1s bands are asymmetric in shape being a convolution of two peaks which should be separated of about 1.6 eV in energy.

In accordance with the literature,[3,4] the peak of lower energy (and higher intensity in our spectra) could be attributed to the aromatic carbons (284.8 eV) and in the same region is expected to fall the peak arising from the –CH_2– groups nonbonded to the nitrogens.

The peak at higher B.E. (and lower intensity in our spectra) is attributed to the C=N groups. In fact the B.E. values observed are almost the same to those reported in the literature.[3-5]

To this class of carbon atoms are also belonging the CH_2–N, groups.

The C 1s bands show an intensity decrease of the unresolved component at higher B.E. on going from 1 to 3 adducts. This is in accordance with the relative weight increase of the –CH_2– groups for compounds 2 and 3. The comparison with the corresponding polymers 4–6 shows that the complexation induces only minor variations in the features of C 1s bands for the compounds 2 (showing a small increasing in F.W.H.M. of the peak) and 3 (showing a more marked asymmetry) with respect to 5 and 6 polymers. The compound 1 does not show any difference with respect to 4.

The complexation is found instead to affect strongly the O 1s and N 1s spectral features.

The N 1s peaks (Fig. 1) are very large and asymmetric in shape. The reference compounds 4–6 show on the contrary a symmetric and narrower shape. The observed increasing of F.W.H.M. are of about 0.8–1.1 eV on going from 4–6 to 1–3 compounds. In general the centroid of the whole N 1s band in the 1–3 compounds is shifted by 0.7–1.3 eV from compound 1 to 3.

The N 1s bands seem to be constituted by two distinct peaks (in various relative ratios) with about the same internal shift for all the adducts (Table 1).

The peak at lower B.E. is attributed to the non-complexed nitrogen atoms (as confirmed by

Table 1.[a]

Compound	O$_{1s}$		N$_{1s}$		Sn$3d_{\frac{5}{2}}$	Cl$_{2p\frac{3}{2}}$
1	532.8	531.5	400.2	398.8	486.8	198.6
2	532.5	531.1	400.2	398.9	486.6	198.5
3	532.8	531.4	400.2	398.7	486.8	198.7
4	532.3	–	–	398.7	–	–
5	532.5	–	–	398.9	–	–
6	532.4	–	–	398.9	–	–

[a] The values are referred to a C1s bond (B.E. 284.8) according to references 6–7.

N_{1s}

(a)

(b)

(c)

UNCORRECTED K.E.
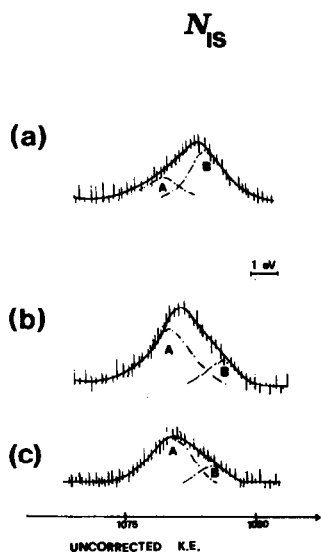
Fig. 1. N 1s peaks of adducts 1(a), 2(b), 3(c).

the very close value of the uncomplexed polymers **4–6**), while the peak at higher B.E. to the complexed nitrogen atoms. In fact, the B.E. values are comparable with those observed for Schiff base metal complexes.[6,7] The positive chemical shift for N 1s is found consistent with a decrease in electron density on the nitrogen site upon coordination to the metal.

The compound **1** shows an almost non-bonded nitrogen; on the contrary in compounds **2** and **3** the nitrogen is in prevalence bonded.

The O 1s peaks of compounds **1–3** show a symmetric shape and a homogeneous B.E. shift towards lower values, with respect to the reference compounds **4–6**. A slight increase of F.W.H.M. can be seen when considering compounds **1–3** with respect to **4–6** (2.5–2.8 eV vs 2.0–2.3 eV). This fact could be explained with the existence of a lower intensity component corresponding to the no bonded oxygen in compounds **4–6** and of a higher intensity component shifted of 1.3–1.4 eV at lower B.E. values.

In accord with such negative O 1s shift we think that in all the cases the –OH linkage is replaced by –Ō–Sn^{2+} and that for adducts **2–3** the proton could become bonded to the nitrogens.

The higher B.E. component could be due to two different contributing factors:

(a) Water contamination, comparable for the three compounds; in fact the B.E. of the water O 1s peak should be close to that one of non-bonded O 1s component.[6]

(b) An excess of base with respect the Sn available.

On the basis of the previous observations some considerations can be made about the solid state nature of our adducts:

(i) That most of the oxygen sites are complexed with the tin in all the adducts.

(ii) The Sn/Cl ratio and the relative B.E.'s are almost the same in the three compounds.

(iii) In adduct **1** most of the nitrogen sites are non-complexing, while most of them are complexing in compounds **2** and **3**.

(iv) No correlation is found for oxygen vs nitrogen bonding.

The ESCA findings support then a picture[6] of such solids as having a disordered structure of an ionic type:

$$[(L-Sn)^{2+}]SnCl_4{}^{2-}$$
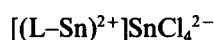
in which the oxygen sites are almost completely complexed, while the nitrogen sites are more or less complexed in connection with the different molecular structure, probably due to the different steric hindrance. In fact, the length of the aliphatic chain seems to influence the availability of the nitrogens for the complexation.

The fact that the nitrogen sites are less complexed in adduct **1** with respect to **2** and **3** could be connected to the experimental finding that during the synthesis of such adducts the precipitation is immediate for compounds **2** and **3** while it occurs after some minutes in the case of compound **1**.[1]

Since in the tin (II) chemistry there is no evidence for the formation of $SnCl_4{}^{2-}$ anion we feel that both $SnCl_3{}^-$ and Cl^- are present, as suggested also by the broad Cl_{2p} peaks.[8]

REFERENCES

1. F. A. Bottino, P. Finocchiaro, E. Libertini and A. Recca, *J. Coord. Chem.* 1983, **12**, 303.
2. F. A. Bottino, P. Finnocchiaro, E. Libertini, A. Reale and A. Recca, *Inorg. Nucl. Chem. Letters* 1980, **16**, 417.
3. D. T. Clark, In *Characterization of Metal and Polymer surfaces* (Edited by L. H. Lee), Vol. 2. Academic Press, New York (1977).
4. R. Holm and S. Storp, *SIA–Surf. Interf. Anal.* 1980, **2**, 96.
5. D. T. Clark, W. J. Feast, W. K. R. Musgrave and I. Ritchie, *J. Polym. Sci. Polym. Chem. Ed.* 1975, **13**, 857.
6. J. G. Dillard and L. T. Taylor, *J. Electron Spectry* 1974, **3**, 455.

7. J. H. Burness, L. T. Taylor and J. G. Dillard, *J. Electron Spectry* 1976, **8**, 483.

8. J. R. Ebner, D. L. McFadden, D. R. Tyler and R. A. Walton, *Inorg. Chem.* 1976, **15**, 3014; D. T. Clark, D. B. Adams, D. Briggs, *Chem. Commun*, 1971, **12**, 602;

P. M. A. Sherwood, *J. Chem. Soc. Dalton Trans.* 1976, **10**, 803.

9. P. Umapathy, S. Badrinarayanan and A. P. B. Sinha, *J. Electron Spectry* 1983, **28**, 261.

2-AMINO-5-PICOLINE N-OXIDE COMPLEXES
FORMED FROM VARIOUS COPPER(II) SALTS

DOUGLAS X. WEST

Department of Chemistry, Illinois State University, Norman, IL 61761, U.S.A.

Abstract—Copper(II) complexes with 2-amino-5-picoline N-oxide (2am5PicO = L), $CuL_4X_2(X = ClO_4, BF_4,$ and $NO_3)$, CuL_2X_2 (X = Cl, Br) and $CuLX_2$ (X = Cl) have been isolated and characterized using spectral methods (i.e. IR, UV-vis and ESR). Coordination occurs via the N-oxide oxygen exclusively with the amine functional group showing only slight tendency to involve itself in hydrogen bonding to the anions. The halide complexes involve the halide ions in the coordination spheres while the polyatomic anions are not bound directly to copper. The latter compounds have monomeric, 4-coordinate CuO_4 chromophores while the former solids are apparently polymeric. Evidence for N-oxide bridging ligands in the CuL_2X_2 solids and halogen bridging in the $CuLX_2$ solid is presented.

2-alkylaminipyridine N-oxides have been shown to bond to Cu(II) primarily as monodentate ligands via the N-oxide oxygen.[1] In contrast, 2-dialkylaminopyridine N-oxides coordinate most commonly as bidentate ligands involving the amine group as well.[2] Previous workers[3] have reported the preparation and the infrared spectra of a number of transition metal complexes of the unsubstituted 2-aminopyridine N-oxide. Because of my interest in 2-substituted pyridine N-oxide complexes, additional copper complexes of this ligand were prepared and characterized by a variety of spectral methods.[4] Recently a similar study with the ligand 2-amino-4-picoline N-oxide has been communicated[5] and there were significant differences in the complexes of this methyl substituted ligand compared to 2-aminopyridine N-oxide (2amPyO). A study of the metal ion complexes of the various 2-amino-picoline N-oxides was therefore initiated, and the Cu(II) complexes of 2-amino-5-picoline N-oxide (2am5PicO) are reported here. Comparisons between these new Cu(II) solids and the previously reported ones are included. It is believed that this is the first report on metal ion complexes of 2am5PicO.

EXPERIMENTAL

The 2am5PicO was prepared by oxidizing 2-amino-5-picoline (Aldrich) with *m*-chloroperoxybenzoic acid Aldrich in acetone[6]. The preparation and characterization of the complexes were performed in an analogous manner to previous studies from this laboratory.[1,2,4,5]

RESULTS AND DISCUSSION

The unique solids isolated with 2am5PicO and the various Cu(II) salts are shown in Table 1 along with their colours, decomposition temperatures and some elemental analyses. Compounds of analogous stoichiometry and colour were isolated with 2am4PicO except for the nitrate. However, as opposed to 2am4PicO, solids analogous to $Cu(2am4PicO)_2(ClO_4)_2$ and $Cu(2am4PicO)Br_2$ have not been achieved despite repeated attempts. Molar conductivity values obtained from acetonitrile solutions are also included in Table 1. Complexes with polyatomic anions are 1 : 2 electrolytes and the halide solids are non-electrolytes.[7] Based on the similarity of colour to previously studied compounds, the complexes isolated with 4 : 1 ligand to Cu(II) mole ratios would be expected to have the four ligands bound via the N-oxide oxygens to give CuO_4 chromophores. The remaining complexes may involve bidentate ligand bonding, participation of the anion in the coordination sphere, polynuclear complex formation or some combination of these. The results of the solid state spectral studies are shown in Tables 2(IR), 3(electronic) and 4(ESR).

The two stretching modes associated with the amine function are found at higher frequencies than for the previous ligand indicating that this amino group is considerably less involved in intermolecular[8] hydrogen bonding. However, the spectra of the complexes formed from the perchlorate and tetrafluoroborate salts show both bands shifted to substantially higher energies

Table 1. Colours, decomposition temperatures, partial elemental analyses and molar conductivities for the various copper(II) complexes of 2-amino-5-picoline N-oxide(L)

Compound	Color	Dec. Pt (^{o}C)	% Calcd C	% Calcd H	% Found C	% Found H	Λ^a (ohm^{-1}cm^2 mol^{-1})
$CuL_4(ClO_4)_2$	green	>250	38.0	4.3	37.2	4.2	242
$CuL_4(BF_4)_2$	green	230	39.3	4.4	39.2	5.0	234
$CuL_4(NO_3)_2$	green	210	42.1	4.7	41.4	4.7	236
CuL_2Cl_2	brown	178	37.7	4.2	38.1	4.7	24
$CuLCl_2$	red brown	196	27.8	3.1	28.5	3.5	21
CuL_2Br_2	red brown	172	30.6	3.4	29.6	3.7	57

a. ca. 10^{-3} M solutions in CH_3CN.

confirming, not only non-coordination of the amine group, but also indicating little, if any, hydrogen bonding of this function to the polyatomic anions. Since coordinated amines generally have their bands at much lower energies (e.g. $v_a(NH_2) = 3250$ cm^{-1} when complexed to Cu(II)[9]), the lower energies of these bands for the remaining compounds are more likely due to an association with the anions as was suggested for analogous solids in previous studies.[4,5]

For 2amPyO[4] and 2am4PicO[5] the v_{NO} band was assigned to strong bands at 1195 and 1191 cm^{-1}, respectively, but this region of the spectrum of the free 2am5PicO is devoid of any bands. At higher energy there is a band of medium intensity located at 1245 cm^{-1} while a band at 1270 cm^{-1} is assignable to δCH (in plane)[10]. In the spectra of the metal complexes v_{NO} is assigned to a weak band at

comparable energies to the previous complexes.[1,4,5] The relatively high energy for v_{NO} compared to an unsubstituted ring (i.e. $v_{NO} = 1243$ cm^{-1} for pyridine N-oxide[11]) may arise from steric effects in the solid caused by the weakly hydrogen bonding amine group as well as the methyl group in the 5-position. δ_{NO} assignments are omitted from Table 2 since this band is not much shifted in the spectra of the complexes from its 838 cm^{-1} position in the ligand spectrum.

At this point the various spectral results of Tables 2–4 will be discussed for the different compounds (or pairs of compounds).

$CuL_4(ClO_4)_2$ and $CuL_4(BF_4)_2$. Both the ESR and the electronic spectra of these two compounds suggest that they have nearly identical Cu(II) centres and that the anions are not coordinated to the Cu(II). Confirming this is the presence of a

Table 2. IR band assignments for 2am5PicO and its copper(II) complexes

Compound	$v_a(NH_2)$	$v_s(NH_2)$	v_{NO}*	v_{CuO}	v_{CuX}
L=2am5PicO	3410m	3290w	1245sh		
$CuL_4(ClO_4)_2$	3476m	3354m	1200w	409s	
$CuL_4(BF_4)_2$	3488m	3379m	1192w	408s	
$CuL_4(NO_3)_2$	3423w,b	3310w,b	1210w	407s	
CuL_2Cl_2	3400w,b	3270w,b	1200w	407w 372s	292sh 283m 274sh
$CuLCl_2$	3400m	3302m	1210w	410w	322m 302s 288m
CuL_2Br_2	3412m 3392sh	3282m 3240sh	1195w	411w 380w	260m 230s

*see text

Table 3. Electronic band assignments (kK) for the various copper(II) complexes of 2-amino-5-picoline N-oxide(L)

Compound	$O(\pi) \rightarrow Cu(d)$	$X \rightarrow Cu(d)$	d–d
$CuL_4(ClO_4)_2$	23.15		16.05,14.29sh
$CuL_4(BF_4)_2$	23.04		15.92,14.29sh
$CuL_4(NO_3)_2$	23.25		15.92,13.89sh
CuL_2Cl_2	23.25	19.61sh	12.66
$CuLCl_2$	23.42	19.18	17.64sh,9.33
CuL_2Br_2	23.42	18.52	10.42

Table 4. Electron spin resonance parameters for the copper(II) complexes of 2-amino-5-picoline N-oxide(L)

Compound	Temp.	$g_{//}(g_3)$	$g_{\perp}(g_2,g_1)$	g_{ave}
$CuL_4(ClO_4)_2$	RT	2.243	2.052	2.116
	77K	2.237	2.053	2.114
$CuL_4(BF_4)_2$	RT	2.243	2.054	2.117
	77K	2.237	2.054	2.115
$CuL_4(NO_3)_2$	RT	2.247	2.058	2.121
	77K	2.246	2.056	2.119
CuL_2Cl_2	RT		g_{iso}=2.112	2.112
	77K	2.222*	2.041	2.101
$CuLCl_2$	RT	2.045	2.238,2.185	2.156
	77K	2.044	2.234,2.181	2.153
CuL_2Br_2	RT		g_{iso}=2.115	2.115
	77K		g_{iso}=2.091+	2.091

*$A_{//}$=155G
+hyperfine and/or superhyperfine lines present

relatively broad band at 1065 cm^{-1} and a sharp band at 618 cm^{-1} in the spectrum of the perchlorate solid and similarly shaped bands at 1015 and 519 cm^{-1} in the spectrum of the tetrafluoroborate solid with the two pairs of bands assignable to v_3 and v_4 of approximately tetrahedral AX_4 species.

The v_{CuO} modes for these two solids are lower in energy than that assigned in the analogous complexes of 2am4PicO (i.e. 415–420 cm^{-1})[5] but slightly higher than the 405 cm^{-1} found for 2amPyO.[4] The higher energy of the two methyl substituted ligands is probably due to the greater electron density these substituents contribute to the ring. The 4-position being more favourable for this donation to the ring nitrogen must cause the higher values for v_{CuO} in the complexes of 2am4PicO. Another factor which could cause this higher en-

ergy is the greater steric hindrance provided by the methyl substituents to the axial coordination of the polyatomic anions.

As opposed to the orthorhombic powder spectrum of the analogous complexes for 2am4PicO[5] the ESR spectra of these solids are the typical axial type associated with a $d_{x^2-y^2}$ ground state. The value of $g_{||}$ for these complexes is slightly lower than was found for the analogous 2amPyO complexes lending support to the stronger planar bonding suggested from the Cu–O stretching frequencies. Therefore, the 5-methyl group while sterically hindering anions from interacting with the Cu(II) centre due to the "propeller-like" positions of the rings[12] does not cause significant distortion of the CuO_4 plane due to interactions between Cu(II) centres in the powder.

Solution electronic and ESR spectra indicate a

change of species in this matrix when compared to the powder spectra. For example, 10^{-3} M acetonitrile solutions show a symmetrical d–d band at ca. 15.0 kK. This shift to lower energy is probably caused by the axial addition of solvent molecules. On long standing the solution ESR spectra show a variety of Cu(II) centres. But immediate freezing of a methanol solution of the tetrafluoroborate salt yielded a spectrum whose principal species has $g_{\parallel} = 2.248$, $g_{\perp} = 2.055$ and $g_{av} = 2.119$. Additionally, $A_{\parallel}$ is ca. 175 G and is indicative of a very strong planar bonding of the four oxygen atoms. The similarity of the various g-values to the values found in the powder spectrum confirms this strong planar bonding in the powder and suggests little interaction between neighbouring centres.

While the 2amPyO showed only a broad featureless d–d envelope,[4] the complexes of 2am4PicO[5] and these solids show a low energy shoulder. Resolution of the shoulder suggests that these complexes have less tetragonal distortion (i.e. are closer to 4-coordinate).[13] Coupling the energy of the shoulder to $g_{\parallel}$ and the energy of the main band to $g_{\perp}$ allows the calculation of orbital reduction factors, k^2, and employing the equations used by previous authors[14] yields values of 0.71 for both $k_{\perp}$ and $k_{\parallel}$. This value indicates that little π-bonding is involved in the metal–ligand bonds.

In Table 5 pertinent spectral information is collected for the CuO$_4$ chromophores prepared with Cu(ClO$_4$)$_2$ and the various 2-aminopyridine N-oxides. The larger alkyl substituents on N appear to strengthen the bonding to Cu(II) based on higher energies for v_{dd} and lower values of $g_{\parallel}$. This

is probably due to greater steric hindrance which prevents interactions of the Cu(II) centre with the perchlorate anions or ligands on neighbouring Cu centres. Substitution on the ring may have a similar effect but other 2-aminopicoline N-oxide complexes and, 2-aminolutidine N-oxides, need to be studied.

Cu(L)$_4$(NO$_3$)$_2$. With 2am4PicO a nitrate solid of suitable purity was not obtained[5] whereas CuL$_3$(NO$_3$)$_2$ and CuL$_2$(NO$_3$)$_2$ were isolated with 2amPyyO[4] so that, comparisons for this nitrate solid are limited to the perchlorate and tetrafluoroborate solids of this study. The data for the three compounds in Tables 3 and 4 suggest little difference in their nature and, therefore, ionic character for the nitrate ions. Confirming this is the assignment of the following bands (cm^{-1}) associated with ionic nitrate:[15] $v_1 = 1018$ m, $v_2 = 819$ s, $v_3 = 1351$ s and $v_4 = 722$ m. Further, a single weak band is observed at 1752 cm^{-1} which is assignable to $v_1 + v_4$ of ionic nitrate.[15, 16]

CuL$_2$Cl$_2$ and CuL$_2$Br$_2$. Analogous compounds with similar colours were isolated with 2am4PicO.[5] The non-electrolytic character in acetonitrile suggests coordination of both halogen atoms. It should be noted that the energies of the v_{N-H} bands in these complexes are consistent with non-coordination of the amine function. For CuL$_2$Br$_2$ the extra shoulders on the v_{NH} bands may be indicative of some structural differences in Cu(II) centres in the lattice which is caused by steric effects.

Additionally, both v_{CuO} and v_{CuX} for each compound have at least two bands assignable to them

Table 5. Spectral information of copper(II) complexes of 2-aminopyridine N-oxides and 2-aminopicoline N-oxides (CuO$_4$ chromophores)

Compound[a]	v_{NO}(cm^{-1})	v_{CuO}(cm^{-1})	v_{dd}(kK)	$g_{\parallel}$	g_{av}	Ref
[Cu(2amPyO)$_2$](ClO$_4$)$_2$	1198	406	16.75	2.254	2.123	4
[Cu(M)$_4$(ClO$_4$)$_2$]	1189	405	15.63	2.239	2.115	1a
[Cu(E)$_4$(ClO$_4$)$_2$]	1188	400	16.31	2.242	2.114	1b
[Cu(P)$_4$(ClO$_4$)$_2$]	1182	390	16.67	2.240	2.112	1c
[Cu(IP)$_4$(ClO$_4$)$_2$]	1190	409	16.95	2.229	2.113	1d
[Cu(2am4PicO)$_2$](ClO$_4$)$_2$	1199	416	16.72, 14.08sh	2.190[b]	2.119	5
[Cu(2am5PicO)$_2$](ClO$_4$)$_2$	1194	409	16.05, 14.79sh	2.243	2.116	present work

b. highest g-value of an orthorhombic spectrum

a. M = 2-methylaminopyridine N-oxide
E = 2-ethylaminopyridine N-oxide
P = 2-propylaminopyridine N-oxide
IP = 2-isopropylaminopyridine N-oxide

which indicates a possible mixture of species. Very recently a single crystal X-ray study of the chloride solid with 2-methylaminopyridine N-oxide has been reported[17] and it was found, upon recrystallization from a mixture of methanol and triethylorthoformate, to have a dimer structure. Briefly, the two copper atoms are bridged by two N-oxide ligands and each Cu(II) has one monodentate N-oxide ligand and one chloride ligand completing its planar portion. A second chloro ligand is in an axial position yielding a distorted square pyramid and the two pyramids are related by an inversion centre. However, this material yielded a weak monomer signal with resolved $g_\parallel$ feature suggesting that the diamagnetic dimer was serving as host for a monomeric impurity.

The ESR signal for this chloro complex also shows a resolved feature while the bromo solid has an isotropic spectrum at both temperatures with clear resolution of hyperfine (or superhyperfine) features over most of the isotropic line. Neither sample shows any features in the ($g \sim 4$) where the $\Delta M = 2$ transitions of dimers are observed. However, the observance of the resolved $g_\parallel$, as well as the fact that the spectra are a factor of more than 100 times less intense than those complexes formed from Cu(II) salts with polyatomic anions, suggest that these features are due to a monomeric impurity. Therefore, the ESR spectra are a measure of the monomer while the remaining spectral studies deal with the more concentrated dimer. In the IR spectrum of CuL_2Br_2 the additional bands found for the N–H stretching frequencies could be due to a monomeric species.

Immediate freezing of the chloro complex dissolved in methanol yields a mixture of species. The principal species present has parameters of $g_\parallel = 2.301$, $g_\perp = 2.063$ and $g_{av} = 2.146$ with $A_\parallel = 148\,G$ which do not agree with the powder values. However, these values are not inconsistent with the 4-coordinate CuO_2Cl_2 monomer which would be formed by symmetrical dissociation of a dimer analogous to the Pavkovic and Wille structure.[17]

Other infrared bands that might be expected to be observed at two different energies if the dimer structure of these complexes is analogous to that found by Pavkovic and Wille[17] are the following: ν_{NO}, ν_{CuO} and ν_{CuCl}. While two different bands are expected for the ν_{NO} mode because of bridging and non-bridging N-oxide ligands, the weakness of the bands in the spectra makes the assignment to various types of N-oxide ligands unattractive. However, both the Cu–O and Cu–X stretching frequencies have multiple bands and the lower band assigned to ν_{CuO} is likely due to a bridging

N-oxide. Additionally, the energies of the Cu–X stretching modes are consistent with terminal rather than bridging halogens suggesting a N-oxide dimer rather than a halogen bridged one.[18]

$Cu(2am5PicO)Cl_2$. While there are certainly a number of dimers of the $(CuL_2X_2)_2$ stoichiometry,[19] there have also been a large number of polymeric species of the stoichiometry $CuLX_2$ reported. In some cases these species include a solvent molecule in their coordination to reach a 5-coordinate centre at each Cu(II)[20], while in other cases a chain of dimers, often one-dimensional, has been found.[21] With this in mind it should be pointed out that again for this compound there is no indication of amine coordination based on the IR spectrum of the solid and the solid can be expected to be polymeric.

Analogous compounds formed from 2am4PicO[5] and copper(II) chloride or bromide were considered to have halogen bridges with the remaining halogen and the N-oxide ligand completing a distorted tetrahedral environment for the Cu(II) centres. Inspection of the bands assigned to ν_{CuCl} shows that the bands are higher in energy than usually assigned to a bridging halogen (i.e. $250\,cm^{-1}$).[18,22] However, for bridged tetrahedral centres the ν_{CuCl} bands would be expected to be higher in energy than for those bridging Cu(II) centres of higher coordination number. For example, ν_{CuCl} for chloro ligands bridging tetrahedral centres have been reported by one group[23] to be in the range $260–270\,cm^{-1}$ and by other authors[24] as high as $275–282\,cm^{-1}$. Additionally, $Cu_2Cl_6^{2-}$ ions with different cations have been studied extensively and it has been shown that distortion of the Cu(II) ions from square planar toward tetrahedral, which is caused by increases in cation size, causes an increase in CuCl (bridging) frequency.[25] Therefore, a structure analogous to that proposed for the 2am4PicO complexes[5] would be possible with the band at $288\,cm^{-1}$ assigned to the bridging Cu–Cl stretching mode and the other bands due to terminal $\nu_{Cu–Cl}$. Since these bands are at higher energy than was found for the previous complexes,[5] greater distortion towards tetrahedral symmetry would be expected for the present complex. Consistent with this is the low energy of the main d–d transition at $9.33\,kK$.

The ESR spectrum is essentially that of a "reversed" monomer which is thought for six-coordinate Cu(II) to be due to a d_{z^2} ground state or more commonly to tetragonally elongated complexes with adjacent Cu(II) centres aligned at right angles to each other with strong exchange interactions.[26] However, once again the ESR signal in the $g = 2$ region is quite weak and is likely due to

a monomeric impurity of lower coordination number than six.

An immediate freezing of a methanolic solution of this solid gives $g_3 = 2.332$, $g_2 = 2.095$, $g_1 = 2.070$ and $g_{av} = 2.166$ with A_3 ca. 115 G. While this species has a "typical" $d_{x^2-y^2}$ ground state spectrum, its average g-value is not greatly different from the 2.153 of the solid at the same temperature. It may be that the spectra are representative of the same species, but lacking the strong exchange interactions in the solution.[26] Compared to the previous chloro species in this study, $Cu(2am5PicO)Cl_2$ is either more tetrahedrally distorted or has a larger coordination number.

In conclusion, the ligand does not function as a bidentate group in any of the complexes, and the solids isolated from copper halide salts appear to yield dimeric products with monomeric impurities. Additionally, it has been found that the methyl group in the 5-position does not significantly alter the stereochemistry of the complexes when compared to the 2amPyO[4] and in contrast to the findings for 2am4PicO.[5]

REFERENCES

1. D. X. West and H-H. Wang, *J. Inorg. Nucl. Chem.* 1979, **41**, 1719; 1980, **42**, 1656, D. X. West and K. Duffield, *J. Inorg. Nucl. Chem.* 1981, **43**, 1517; D. X. West and J. B. Sedgwick, *J. Inorg. Nucl. Chem.* 1981, **43**, 2307.
2. D. X. West and W-H. Wang, *J. Inorg. Nucl. Chem.* 1980, **43**, 958; 1981, **43**, 1511.
3. H. Sigel and H. Brintzinger, *Helv. Chim. Acta* 1963, **46**, 701.
4. D. X. West, *J. Inorg. Nucl. Chem.* 1981, **43**, 3169.
5. D. X. West, *Inorg. Chim. Acta* 1981, **71**, 251.
6. L. W. Deady, *Synth. Comm.* 1977, **7**, 509.
7. W. J. Geary, *Coord. Chem. Rev.* 1971, **7**, 81.
8. M. C. R. Symons and D. X. West, unpublished results.
9. N. B. Singh and J. Singh, *J. Inorg. Nucl. Chem.* 1978, **40**, 919.
10. A. R. Katritzky and A. R. Hands, *J. Chem. Soc.* 1958, 2195.
11. S. Kida, J. V. Quagliano, J. A. Walmsley and S. Y. Tyree, *Spectrochim. Acta* 1963, **19**, 189.
12. S. F. Pavkovic, private communication.
13. I. M. Procter, B. J. Hathaway and P. Nicholls, *J. Chem. Soc.(A)* 1968, 1678; D. E. Billing and B. J. Hathaway, *J. Chem. Soc.(A)* 1968, 1516; J. I. Bullock, R. J. Hobson and D. C. Povey, *J. Chem. Soc. (Dalton)* 1974, 2307 and D. E. Billing and A. E. Underhill, *J. Inorg. Nucl. Chem.* 1968, **30**, 2147.
14. R. S. Naidu and R. R. Naidu, *J. Inorg. Nucl. Chem.* 1979, **41**, 1625.
15. N. M. Karayannis, C. M. Mikulski, L. L. Pytlewski and M. M. Labes, *Inorg. Chem.* 1974, **13**, 1146.
16. A. B. P. Lever, E. Mantovani and B. S. Ramaswamy, *Can. J. Chem.* 1971, **49**, 1957.
17. S. F. Pavkovic and S. L. Wille, *Acta Cryst.* 1982, **B38**, 1605.
18. I. S. Ahuja, R. Singh and C. R. Rai, *Trans. Met. Chem.* 1977, **2**, 257; M. Biddau, M. Massacesi, R. Pinna and G. Ponticelli, *Trans. Met. Chem.* 1978, **3**, 153; and J. A. C. Van Ooyen and J. Reedijk, *J. Chem. Soc. Dalton* 1978, 1170.
19. W. E. Marsh, W. E. Hatfield and D. J. Hodgson, *Inorg. Chem.* 1982, **21**, 2679 and references therein.
20. E. D. Estes and D. J. Hodgson, *Inorg. Chem.* 1976, **15**, 348; D. A. Krost and G. L. McPherson, *J. Am. Chem. Soc.* 1978, **100**, 987.
21. D. D. Swank and R. D. Willett, *Inorg. Chem.* 1980, **19**, 2321.
22. I. S. Ahuja, R. Singh and R. Sriamulu, *Trans. Met. Chem.* 1978, **3**, 185.
23. S. S. Sandhu, S. S. Tandon and H. Singh, *J. Inorg. Nucl. Chem.* 1979, **41**, 1239.
24. M. M. Aly and Z. H. Khalil, *J. Inorg. Nucl. Chem.* 1980, **42**, 1261.
25. W. E. Estes, J. R. Wasson, J. W. Hall and W. E. Hatfield, *Inorg. Nucl. Chem.* 1978, **17**, 3657.
26. I. Bertini, D. Gatteschi and A. Scozzafava, *Coord. Chem. Rev.* 1979, **29**, 67.

STUDIES ON YELLOW AND COLOURLESS MOLYBDOPHOSPHATE COMPLEXES IN THE AQUEOUS SOLUTION BY LASER RAMAN SPECTROSCOPY

KATSUO MURATA* and SHIGERO IKEDA

Department of Chemistry, Faculty of Science, Osaka University, Toyonaka, Osaka 560,
Japan

Abstract—Yellow and colourless complexes of molybdophosphate were investigated by the use of laser Raman spectroscopy. Two kinds of yellow molybdophosphates were identified in the weakly acidic solutions: 12-molybdophosphoric and 11-molybdophosphoric acid which are in equilibrium in solution at pH 1–2. When excess phosphate is present, the colourless molybdophosphate is formed. This complex exists in the solutions of pH 4–1 under the condition of excess phosphate ([P]/[Mo] > 2). This complex was confirmed to be $P_2Mo_5O_{23}^{6-}$ and is so stable that the yellow molybdophosphate is converted into the colourless by excess phosphate.

Heteropolymolybdate anion plays an important role in analytical chemistry. Most reliable method for the analysis of such elements P, Si, As and Ge is based on the formation of polynuclear hetero-polymolybdate complexes.[1-4] The formation process of heteropoly acid has been studied by various methods.[5-8] The condition, the acidity below pH 1 and the excess molybdate, were frequently requested for the determination of micro amounts of phosphorus.[9-12] The basic idea to establish the optimum condition applied for the chemical analysis has still not been completely understood. Javier *et al.* showed that on the basis of kinetic data the formation mechanism of molybdophosphoric acid was related, at the initial stage, to the interaction between phosphate and Mo(VI) followed by polymerization to form 12-molybdophosphoric acid.[13] But its formation mechanisms from isopolymolybdate is not fully understood. The purpose of the present study is to find out some species of molybdophosphate complexes and to clarify the formation mechanism of 12-molybdophosphoric acid in the aqueous solution by the use of laser Raman spectroscopy.

EXPERIMENTAL

Reagent and apparatus

Polynuclear molybdophosphate complexes were produced by means of the mixed solutions of

phosphate and molybdate. The acid used for the preparation of the solution is hydrochloric acid because both perchloric and sulphuric acid interfere with the measurements of Raman spectra of polynuclear molybdate complex. Raman spectra were measured with a JASCO R750 triple mono-chromator and JASCO R800, using 514.5 nm (Ar+ laser) as the excitation source. In order to measure quantitatively the intensity of Raman lines, an internal standard of sodium nitrate was used. The Raman lines to be observed were calibrated with those of indene.[14]

RESULTS AND DISCUSSION

(a) Yellow molybdophosphate complexes

Acidification of the mixed solutions of phosphate and molybdate leads to the formation of some molybdophosphate complexes from colourless to yellow colour. Yellow 12-molybdophosphoric acid is mostly useful in analytical chemistry. But the formation behaviour of molybdophosphate complexes has not been well understood because of complexity. The spectrophotometric investigation does not tell much about the configurational information of the chemical species in the aqueous solution. Raman measurements were attempted to obtain the acidic condition for the formation of 12-molybdophosphoric acid. Figure 1 shows three kinds of Raman spectra: (1) solid 12-molybdophosphoric acid, (2) the dissolved aqueous solution of 12-molybdo-

phosphoric acid, and (3) the acidified mixed solutions of phosphate and molybdate ($[P] = 1.0 \times 10^{-2}$ M, $[Mo] = 1.2 \times 10^{-1}$ M). Raman spectrum of 12-molybdophosphoric acid solution(2) is analogous to that of solid 12-molybdophosphoric acid(1), but is different in the intensity of the peak at 996 cm^{-1} and 975 cm^{-1}. The intensity of the peak at 996 cm^{-1} in the solution is lower than that of the solid one, and the intensity of the peak at 975 cm^{-1} is higher than that of solid 12-molybdophosphoric acid. This implies that 12-molybdophosphoric acid to be dissolved undergoes a little change in the solution. Although Raman spectra of the acidified mixed solutions vary with the acidity as shown in Fig. 1 (3), Raman spectra of the mixed solutions of pH 1.17–0.5 M HCl are similar to that of 12-molybdophosphoric acid solution(2). Hence 12-molybdophosphoric acid can also be produced in these acidic mixed solutions.

The authors focussed carefully the ν_1 line of molybdate observed over 900–1000 cm^{-1}. Raman spectra of the acidified 30 solutions (pH 6.52–2 M HCl) of molybdophosphate were normalized by the use of an internal standard (0.08 M NaNO$_3$). Concerning the mixed solutions of pH 6.52–5.15, influence of acidity on Raman spectra is similar to the case of the solutions of molybdate alone.[15] Namely the peak at 897 cm^{-1} due to MoO$_4^{2-}$ species decreases with acidification, whereas the peak at 940 cm^{-1} due to Mo$_7$O$_{24}^{6-}$ species increases. The interaction between phosphate and molybdate does not appear to be prominent, but careful observation allows us to find fine changes on Raman spectra of the mixed solution. The Raman line broadening (at 940 cm^{-1}) becomes eminent. These are much broader than those obtained from isopolymolybdate alone.[15] This must be due to the superposition of molybdophosphate complex and heptamolybdate Mo$_7$O$_{24}^{6-}$. This is also described in the next section of colourless molybdophosphate complexes.

Further acidification of the mixed solutions leads to the shift of the peak to the much higher wavenumber, and the mixed solutions become faint yellow. Then the peak at 975 cm^{-1} appears and its intensity increases in the solutions of pH 4.59–2.27 (Z = 1.48–1.70). On further acidification, the peak at 975 cm^{-1} decreases, and the peak at 996 cm^{-1} appears. The increase of the intensity at 996 cm^{-1} is based on the formation of 12-molybdophosphoric acid.[16,17] These mixed solutions exhibit characteristic yellow colour. Raman spectra indicate two species of yellow coloured molybdophosphate are main complexes in these solutions. One species at 996 cm^{-1} is
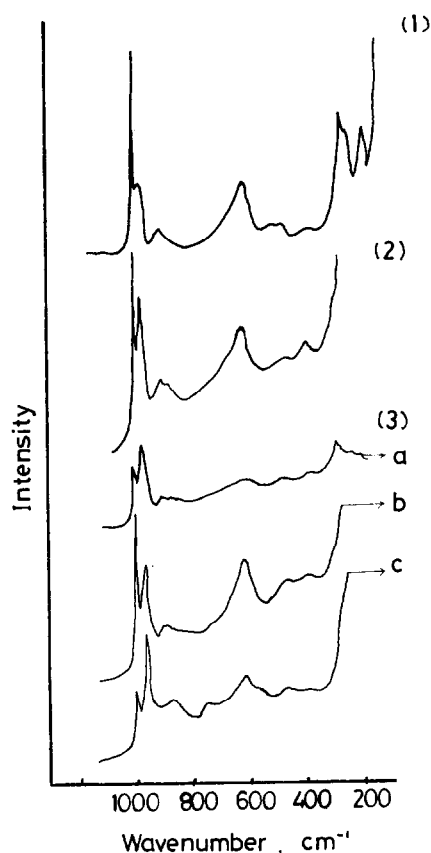
Fig. 1. Raman spectra of 12-molybdophosphoric acid in the solutions and the solid state. (1) Solid 12-molybdophosphoric acid. (2) The dissolved aqueous solution of 12-molybdophosphoric acid. (3) The acidic mixed solutions of phosphate and molybdate ($[P] = 1.0 \times 10^{-2}$ M, $[Mo] = 1.2 \times 10^{-1}$ M), (a) pH 1.46, (b) pH 1.01, (c) 1 M HCl.

12-molybdophosphoric acid. Another species has the peak at 975 cm^{-1}. In order to clarify the latter species, two precipitates of tetraethylammonium salt were obtained from the solutions of pH 2.1 and pH 1 by addition of tetraethylammonium chloride solution. The results of elementary analysis for these precipitates are given in Table 1. The precipitate from pH 1 is 12-molybdophosphate salt, as expected. The precipitate from pH 2.1 is not 9-molybdophosphate, which is known to be P$_2$Mo$_{18}$O$_{62}^{6-}$ in the solid,[18] but 11-molybdophosphate. Thus the species at 975 cm^{-1} is considered to be 11-molybdophosphoric acid. When the mixed solutions of phosphate and molybdate are acidified, 12-molybdophosphoric acid is produced via the formation of 11-molybdophosphoric acid. 12-molybdophosphoric acid is equilibrated with 11-molybdophosphoric acid in the mixed solutions of pH 1.99–1.05(Z = 1.72–2.06). 12-molybdophosphoric acid decomposes above 2 M acidity to

Table 1. Elementary analysis of tetraethylammonium molybdophosphate obtained from the solutions of pH 2.1 and pH 1

Precipitate from pH 1	Precipitate from pH 2.1
$[(C_2H_5)_4N]_3PMo_{12}O_{40}$	$[(C_2H_5)_4N]_3PMo_{11}O_{37}$

	Precipitate from pH 1		Precipitate from pH 2.1	
	$[(C_2H_5)_4N]_3PMo_{12}O_{40}$		$[(C_2H_5)_4N]_3PMo_{11}O_{37}$	
	Calcd	Found	Calcd	Found
C	13.03 %	13.01 %	13.92 %	14.03 %
H	2.73	2.80	2.90	3.04
N	1.90	1.95	2.03	2.12
P	1.40	1.39	1.49	1.43
Mo	52.02	52.33	51.02	49.97
			$[(C_2H_5)_4N]_3PMo_9O_{31}$	
			Calcd	Found
C			16.18 %	14.03 %
H			3.37	3.04
N			2.36	2.12
P			1.47	1.43
Mo			48.50	49.97

transform to cationic molybdate species, whose intense Raman line appears at $953\,cm^{-1}$.

(b) *Effect of phosphate concentration and colourless molybdophosphate complex*

The concentration of phosphate is also important in the formation of molybdophosphate complexes. The present author[19] and Hori[20] pointed out that excess phosphate leads to the formation of colourless or pale yellow molybdophosphate. This would be attributed to the transformation into the lower polymerized molybdophosphate species. The authors investigated the influence of phosphate concentration on Raman spectra of pH 1 molybdate solutions. The increase of phosphate concentration results in the increase of the intensity at $996\,cm^{-1}$ and the decrease of the intensity at $955\,cm^{-1}$. This clearly indicates that the phosphate added reacts with the polynuclear molybdate species[15] $Mo_{12}O_{37}^{2-}$ to produce 12-molybdophosphoric acid. The polynuclear molybdate species having the peak at $955\,cm^{-1}$ is closely correlated to the formation of 12-molybdophosphoric acid. The further increase in the concentration of

$$PO_4^{3-} + Mo_{12}O_{37}^{2-} + 2H^+ \rightleftarrows PMo_{12}O_{40}^{3-} + H_2O$$
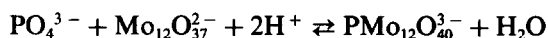
phosphate, however, brings about the decrease of the intensity at $996\,cm^{-1}$ and the increase at $970\,cm^{-1}$. This implies that the excess phosphate produces 11-molybdophosphate. The further addition of excess phosphate induces the peak at $945\,cm^{-1}$ accompanying the disappearance of the peak at $970\,cm^{-1}$. The colouration of these mixed solutions becomes colourless via pale yellow. Colourless molybdophosphate can be stable and pre-

sent in the mixed solutions of the wide pH range. Only one species of colourless molybdophosphate having the peak at $945\,cm^{-1}$ is present in the mixed solutions of pH 4–1. As previously described [section (a)], Raman spectra of molybdophosphate change variously with the acidity in the solutions. But the excess phosphate results in no shift of the peak at $945\,cm^{-1}$ in the mixed solutions of pH 4–1. This colourless molybdophosphate was confirmed to be $P_2Mo_5O_{23}^{6-}$ species by the elementary analysis of tetraethylammonium salt obtained from pH 3. Found: C, 15.03; H, 3.81; N, 2.17; P, 4.76; Mo, 37.49. Calcd for $[(C_2H_5)_4N]_2H_4P_2Mo_5O_{23}\cdot6H_2O$: C, 14.98; H, 4.37; N, 2.18; P, 4.83; Mo, 37.43. The existence of this species $P_2Mo_5O_{23}^{6-}$ in the solution is also supported from the appearance of the break point at $[Mo]/[P] \approx 2.5$ in the plots, where the intensity at $945\,cm^{-1}$ is plotted against phosphate concentration. Therefore it is assumed that excess phosphate brings about the following equilibria.

$$11PMo_{12}O_{40}^{3-} + PO_4^{3-} \rightleftarrows 12PMo_{11}O_{37}^{3-}$$

$$5PMo_{11}O_{37}^{3-} + 17PO_4^{3-} \rightleftarrows 11P_2Mo_5O_{23}^{6-}.$$
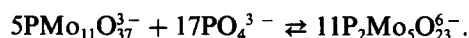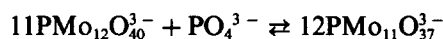
As seen in the above description, there are two significant factors affecting the formation of molybdophosphate complexes in the aqueous solution. One is phosphate concentration, and another is acidity in the aqueous solution. When excess phosphate ($[P]/[Mo] > 2$) is present in the mixed solution of phosphate and molybdate, the species of $P_2Mo_5O_{23}^{6-}$ exists mainly in the solution of wide pH range (pH 4–1). The species of $P_2Mo_5O_{23}^{6-}$ is so stable that the addition of excess phosphate can transform 12-molybdophosphoric acid formed into 11-molybdophosphoric acid or colourless $P_2Mo_5O_{23}^{6-}$. But in the presence of equivalent amounts of phosphate ($[Mo]/[P] = 12$), the species of molybdophosphate complex varies with the acidity in the solution. Two kinds of species as the yellow molybdophosphoric acid are present in the solutions above $Z = 1.5$. The formation of 12-molybdophosphoric acid is predominant in the solution of $Z = 2.0$ and 11-molybdophosphoric acid predominantly forms in the solution of $Z = 1.7$.

The question is raised what isopolymolybdate species is mainly concerned to the formation of each molybdophosphate complex. In our previous works,[15] the formation of some isopolymolybdate species was clarified by the use of Raman spectroscopy. The formation curves of each isopolymolybdate and molybdophosphate are plotted against Z value of the solution in Fig. 2. It can be seen that the formation of $P_2Mo_5O_{23}^{6-}$, $PMo_{11}O_{37}^{3-}$

and $PMo_{11}O_{37}^{3-}$ is correlated with the species of $Mo_7O_{24}^{6-}$, $Mo_8O_{26}^{4-}$ and $Mo_{12}O_{37}^{2-}$ ($Mo_6O_{19}^{2-}$), respectively.
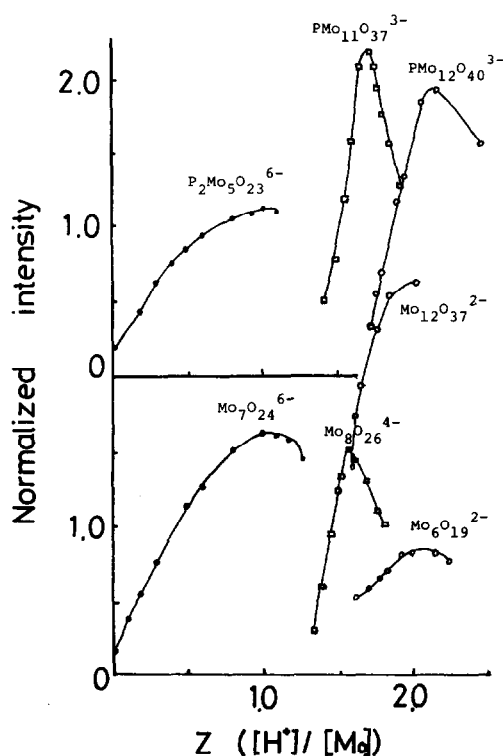
Fig. 2. Formation behaviour of each species in isopoly- and heteropoly molybdates by plotting the intensity of Raman line against Z value of solutions. (The formation of each species was followed at each Raman line: $Mo_7O_{24}^{6-}$, 940 cm^{-1}; $Mo_8O_{26}^{4-}$, 970 cm^{-1}; $Mo_{12}O_{37}^{2-}$, 955 cm^{-1}; $Mo_6O_{19}^{2-}$, 980 cm^{-1}; $P_2Mo_5O_{23}^{6-}$, 945 cm^{-1}; $PMo_{11}O_{37}^{3-}$, 975 cm^{-1}; $PMo_{12}O_{40}^{3-}$, 996 cm^{-1}) [P] = 1.0 × 10^{-2} M. [Mo] = 1.2 × 10^{-1} M, [NO$_3^-$] = 8.0 × 10^{-2} M.

REFERENCES

1. I. M. Kolthoff and E. B. Sandell, *Textbook of Quantitative Inorganic Analysis*, 3rd. Edn, pp. 382, 684. Macmillan, New York (1964).
2. I. M. Kolthoff and P. J. Elving (Ed.), *Treatise on Analytical Chemistry*, Part II, Volume 5, Phosphorus (W. Rieman III, J. Benken Kamp) (1961).
3. G. Eckert, *Z. Anal. Chem.* 1958, **161**, 421.
4. E. Ebner, *Z. Anal. Chem.* 1964, **206**, 106.
5. P. Krumholz, *Z. Anorg. Chem.* 1933, **212**, 91.
6. P. Souchay, *Ann. Chim.* 1944, **19**, 102; 1945, **20**, 73; 1947, **2**, 203.
7. G. Jander and K. F. Jahr, *Koll. Beihefte* 1934, **41**, 297.
8. H. Buchwald, P. J. Coope and W. P. Thistlewalte, *J. Inorg. Nucl. Chem.* 1956, **3**, 300.
9. D. F. Boltz and M. G. Mellon, *Anal. Chem.* 1948, **20**, 749.
10. A. H. Ennor and H. Rosenberg, *Biochem. J.* 1952, **52**, 594.
11. R. B. Heslop and E. F. Person, *Anal. Chim. Acta* 1967, **39**, 209.
12. P. Pokalns, *Anal. Chim. Acta* 1968, **40**, 1.
13. A. C. Javier, S. R. Crouch and H. V. Malmstadt, *Anal. Chem.* 1968, **40**, 1922.
14. P. J. Hendra and E. J. Loader, *Chem. and Ind.* 1968, 718.
15. K. Murata and S. Ikeda, *Spectrochim. Acta* in press.
16. C. Rocchiccioli–Deltcheff, R. Thouvenot and R. Franck, *Spectrochim. Acta* 1976, **32A**, 587.
17. M. S. Kasprzak, S. R. Crouch and G. E. Leroi, *Appl. Spectrosc.* 1978, **32**, 537.
18. (a) G. A. Tsigdinos, *Heteropoly Compounds of Molybdenum and Tungsten*. Climax Molybdenum Co. Bull. Cdb-12a. (b) T. J. R. Weakley, *Struc. Bonding* 1974, **18**, 131.
19. K. Murata and T. Kiba, *J. Inorg. Nucl. Chem.* 1970, **32**, 1667.
20. T. Hori, *J. Inorg. Nucl. Chem.* 1977, **39**, 2173.

α-PYRIDINECARBOXYLATE COMPLEXES OF RHODIUM

J. V. HERAS,* E. PINILLA and M. MARTINEZ

Departamento de Química Inorgánica e Instituto de Química Inorgánica "Elhuyar" del
C.S.I.C., Facultad de Ciencias Químicas, Universidad Complutense de Madrid,
Madrid (3), Spain

Abstract—The complex Rh(pyc)(NBD) (pyc = α-pyridinecarboxylate anion, NBD = 2,5-norbornadiene) reacts with carbon monoxide with displacement of the diolefin and formation of $Rh(pyc)(CO)_2$. Addition of triarylphosphines to the latter compound causes the formation of complexes of the type $Rh(pyc)(CO)[P(p\text{-}RC_6H_4)_3]$ (R = F, Cl, Me, MeO). The addition of iodine, bromine or methyl iodide to solutions of the monocarbonyl derivatives leads to the formation of $RhX_2(pyc)(CO)[P(p\text{-}RC_6H_4)_3]$ (X = I, Br) and $RhMeI(pyc)(CO)[P(p\text{-}RC_6H_4)_3]$ complexes.

Organometallic square-planar rhodium(I) complexes with asymmetric chelating anionic ligands having N and O as donor atoms have been reported. Those derived from Schiff's bases,[1-5] β-ketoamines,[6] 8-oxyquinoline[7-10] and aminoacids[11, 12] have been intensively investigated. On the contrary, the ability of the α-pyridinecarboxylate(pyc) group to act as a bidentate ligand has been scarcely studied, and as far as we know only the $Rh(pyc)(CO_2)$ has been described.[7]

In this paper we report the synthesis and reactions of several α-pyridinecarboxylate rhodium(I) complexes. Some oxidative addition reactions are reported. It is noteworthy to point out that previous attempts to convert some square-planar rhodium(I) complexes with salicylaldimine Schiff's bases[1] into octahedral rhodium(III) derivatives by oxidative addition reactions were unsuccessful.

EXPERIMENTAL

IR spectra were recorded on a Perkin–Elmer 325 spectrophotometer (over the 4000–200 cm^{-1} range) using KBr discs. Conductivities were measured using approx. 3×10^{-4} M acetone solution with a Philips PR 9500 conductimeter.

Synthesis of Rh(pyc)(NBD)

A stoichiometric amount of α-pyridinecarboxylic acid (Hpyc) was added to a C_6H_6 suspension of the RhCl(NBD)$_2$ complex. After addition of excess of Na_2CO_3 and stirring for 4 hr at room temperature, the yellow solid formed was filtered off, recrystallized from CH_2Cl_2:Et_2O, washed with Et_2O and air dried.

Synthesis of Rh(pyc)(CO$_2$)

Carbon monoxide was bubbled through a solution of the complex Rh(pyc)(NBD) in CH_2Cl_2 at room temperature for 30 min. After concentration, the Rh(pyc)(CO)$_2$ complex was precipitated by adding cold Et_2O. This was filtered off and recrystallized from CH_2Cl_2:Et_2O, and vacuum-dried.

Rh(pyc)(CO)[P(p-RC$_6$H$_4$)$_3$] complexes

The addition of a stoichiometric quantity of $P(p\text{-}RC_6H_4)_3$ to a yellow solution of Rh(pyc)(CO)$_2$, in the minimum amount of CH_2Cl_2, caused evolution of CO and the colour intensified. The solution was stirred at room temperature for 10 min and crystallization was induced by the addition of n-hexane. The solids thus obtained were recrystallized from CH_2Cl_2:n-hexane and vacuum-dried.

Rh(pyc)X$_2$(CO)[P(p-RC$_6$H$_4$)$_3$ complexes

A slight excess over the stoichiometric of X_2 (X = I, Br) was added to a CH_2Cl_2 solution of the corresponding Rh(pyc)(CO)[P(p-RC$_6$H$_4$)$_3$] complex. The solution was stirred for 1 hr at room temperature and crystallization was induced by the addition of Et_2O. The brown solid was filtered off, recrystallized from CH_2Cl_2:Et_2O and vacuum-dried.

Rh(pyc)MeI(CO)[P(p-RC$_6$H$_4$)$_3$] complexes

The above method was also used for the prepa-

---

*Author to whom correspondence should be addressed.

ration of these complexes, using MeI instead of I_2, but the reaction time was 4 hr.

RESULTS AND DISCUSSION

Rhodium(I) complexes

Reaction of $RhCl(NBD)_2$[13] in benzene with an equimolecular amount of α-pyridinecarboxylic acid in the presence of sodium carbonate gave a good yield of yellow solid which was identified as Rh(pyc)(NBD) (NBD = 2,5-norbornadiene, pyc = α-pyridinecarboxylate anion). The bubbling of carbon monoxide through a dichloromethane solution of this complex, causes the displacement of the coordinated diolefin according to eqn (1):

$$Rh(pyc)(NBD) + 2CO \rightarrow Rh(pyc)(CO)_2 + NBD. \quad (1)$$
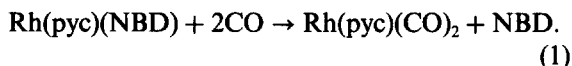
The violet dicarbonyl derivative has been previously prepared by Ugo et al.[7] by reaction of $[RhCl(CO)_2]_2$ with the anionic ligand.

Monocarbonyl complexes of the type $Rh(pyc)(CO)[P(p\text{-}RC_6H_4)_3]$ can be prepared by addition of triarylphosphines to solutions of $Rh(pyc)(CO)_2$ in dichloromethane, according to eqn (2):

$$Rh(pyc)(CO)_2 + P(p\text{-}RC_6H_4)_3 \rightarrow$$
$$Rh(pyc)(CO)[P(p\text{-}RC_6H_4)_3] + CO \quad (2)$$

$$(R = MeO, Me, F, Cl).$$
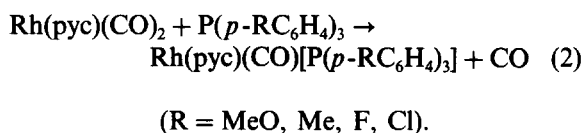
The reaction most likely proceeds via the formation of the pentacoordinated complex $Rh(pyc)(CO)_2[P(p\text{-}RC_6H_4)_3]$, which was not detected. When the reaction was performed with a stoichiometric amount or excess of diphosphine, poorly characterized yellow products without coordinated carbon monoxide were obtained.

Only one $v(CO)$ vibration was observed for all $Rh(pyc)(CO)[P(p\text{-}RC_6H_4)_3]$ complexes. It can reasonably be assumed that the isomer obtained present the phosphine trans to the pyridine nitrogen, due to the stronger trans effect of this atom. In fact an X-ray diffraction study on the related complex $Rh(oxyquinolate)(CO)PPh_3$ show the phosphine group to be trans to the heterocyclic nitrogen.[14] An inverted correlation between $v(CO)$ and the basicity of the triarylphosphine seems to be observed (Table 1). The increasing basicity of the phosphines could increase the extent of Rh–C back-bonding and, therefore, the $v(CO)$ are shifted to lower values.

The presence of the asymmetric $v(C=O)$ band of the carboxylic group in the range 1660–1680 cm^{-1} for all the above mentioned complexes, show that

this group acts as monodentate, ruling out pentacoordinated structures. Furthermore, the $v(C=O)$ values for these complexes support square-planar coordination.

All the complexes are stable in air at room temperature and were obtained in high yields. Elemental analyses (carbon, hydrogen and nitrogen) and IR data are collected in Table 1. The violet $Rh(pyc)(CO)_2$ derivative is dichroic in the solid state,[7] but Rh(pyc)(NBD) and Rh(pyc)$(CO)[P(p\text{-}RC_6H_4)_3]$ complex present yellow colour. consistent with the lack of any intermolecular rhodium-rhodium interactions in the solid state, arising from steric reasons.

Oxidative addition reactions with iodine, bromine and methyliodide

Because the relatively low value of the $v(C=O)$ band in $RH(pyc)(CO)[P(p\text{-}RC_6H_4)_3]$ complexes should give an indication of the nucleophility of these rhodium(I) complexes, we were interested to explore some oxidative addition reactions.

The addition of a slight excess of iodine, bromine or methyl iodide to dichloromethane solutions of $Rh(pyc)(CO)[P(p\text{-}RC_6H_4)_3]$ complexes leads to the formation of hexacoordinated rhodium(III) complexes (eqns 3 and 4):

$$Rh(pyc)(CO)P(p\text{-}RC_6H_4)_3 + X_2 \rightarrow$$
$$RhX_2(pyc)(CO)[P(p\text{-}RC_6H_4)_3] \quad (3)$$

$$(X = I, Br)$$

$$Rh(pyc)(CO)P(p\text{-}RC_6H_4)_3 + MeI \rightarrow$$
$$RhMeI(pyc)(CO)[P(p\text{-}RC_6H_4)_3], \quad (4)$$
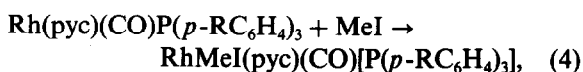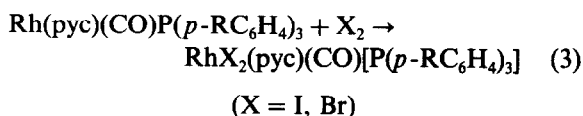
As expected for these types of oxidative addition reactions, the $v(CO)$ vibration of the oxidation products is shifted in every case towards higher energies relative to the parent compound. This shift is in the 110–125 cm^{-1} range for the complexes formed by addition of iodine or bromine, and in the 80–95 cm^{-1} range for the $RhMeI(pyc)(CO)[P(p\text{-}RC_6H_4)_3]$ derivatives. The oxidative addition reactions with methyliodide, are slow enough to show that the rate of reaction increases for the more basic phosphines. The presence of a single sharp $v(CO)$ absorption in the IR spectra seems to point to the presence of only one isomer in the solid state. These complexes show the asymmetric $v(C=O)$ band of the monodentate carbonyl group in the range 1665–1680 cm^{-1}. They are stable in air at room temperature and were obtained in high yields (Table 1). All the complexes described in this paper are non-conducting in acetone or have negligible conductivity.

Table 1. Analytical, IR data and yields for the rhodium complexes

Complex	Found(Calcd.)%			$\nu(C \equiv O)$ (cm^{-1})	Yield (%)
	C	H	N		
Rh(pyc)(NBD)	50.3 (49.3)	4.0 (3.8)	4.6 (4.4)	----	85
Rh(pyc)(CO)$_2$	34.4 (34.2)	1.4 (1.4)	5.4 (5.0)	----	73
Rh(pyc)(CO)P(p-ClC$_6$H$_4$)$_3$	48.0 (48.5)	2.6 (2.6)	2.4 (2.3)	1974	78
Rh(pyc)(CO)P(p-FC$_6$H$_4$)$_3$	53.2 (52.8)	2.9 (2.8)	2.6 (2.5)	1973	75
Rh(pyc)(CO)P(p-MeC$_6$H$_4$)$_3$	60.9 (60.4)	4.9 (4.5)	2.7 (2.5)	1966	75
Rh(pyc)(CO)P(p-MeOC$_6$H$_4$)$_3$	54.6 (55.6)	4.7 (4.1)	2.1 (2.3)	1965	78
RhI$_2$(pyc)(CO)P(p-ClC$_6$H$_4$)$_3$	34.4 (34.4)	1.8 (1.8)	1.6 (1.6)	2085	89
RhI$_2$(pyc)(CO)P(p-FC$_6$H$_4$)$_3$	36.4 (36.5)	2.0 (1.9)	1.7 (1.7)	2085	82
RhI$_2$(pyc)(CO)P(p-MeC$_6$H$_4$)$_3$	41.5 (41.5)	3.1 (3.1)	1.6 (1.7)	2085	83
RhI$_2$(pyc)(CO)P(p-MeOC$_6$H$_4$)$_3$	40.9 (39.2)	3.2 (2.9)	1.4 (1.6)	2080	86
RhBr$_2$(pyc)(CO)P(p-ClC$_6$H$_4$)$_3$	37.2 (38.5)	1.9 (2.0)	1.6 (1.7)	2100	70
RhBr$_2$(pyc)(CO)P(p-FC$_6$H$_4$)$_3$	41.0 (41.1)	2.0 (2.1)	1.8 (1.9)	2107	68
RhBr$_2$(pyc)(CO)P(p-MeC$_6$H$_4$)$_3$	49.2 (49.9)	3.1 (3.4)	1.7 (1.9)	2097	75
RhBr$_2$(pyc)(CO)P(p-MeOC$_6$H$_4$)$_3$	42.9 (43.9)	3.2 (3.2)	1.6 (1.8)	2097	60
RhMeI(pyc)(CO)P(p-ClC$_6$H$_4$)$_3$	41.2 (41.1)	2.6 (2.5)	1.9 (1.8)	2065	70
RhMeI(pyc)(CO)P(p-FC$_6$H$_4$)$_3$	44.1 (43.9)	3.0 (2.7)	2.1 (2.0)	2065	75
RhMeI(pyc)(CO)P(p-MeC$_6$H$_4$)$_3$	50.2 (49.8)	4.2 (4.0)	2.1 (2.0)	2050	88
RhMeI(pyc)(CO)P(p-MeOC$_6$H$_4$)$_3$	47.3 (46.6)	3.8 (3.7)	1.9 (1.9)	2050	80

REFERENCES

1. R. J. Cozens, K. S. Murray and B. O. West, *J. Organometal. Chem.* 1971, **27**, 399.
2. Yu. S. Varshavskii, T. G. Cherkasova, O. A. Osipov, N. P. Bednyagina, A. D. Garnovskii, R. I. Oglobina, G. K. Mitina and G. N. Liponova, *Russ. J. Inorg. Chem.* 1972, **17**, 726.
3. N. Platzer, N. Goasdone and R. Bonnaire, *J. Organometal. Chem.* 1978, **160**, 455.
4. J. T. Mague and M. O. Nutt. *J. Organometal. Chem.* 1977, **63**, 166.
5. M. Valderrama and L. A. Oro, *J. Organometal. Chem.* 1981, **218**, 241.
6. F. Bonati and R. Ugo, *Chim. Ind., Milan* 1964, **46**, 1339.
7. R. Ugo, G. La Monica, S. Cenini and F. Bonati, *J. Organometal. Chem.* 1968, **11**, 159.
8. Yu. S. Varshavskii, T. G. Cherkasova and N. A. Buzina, *Russ. J. Inorg. Chem.* 1972, **17**, 1150.
9. Yu. S. Varshavskii, T. G. Cherkasova, N. A. Buzina and V. A. Kormer, *J. Organometal. Chem.* 1974, **77**, 107.

10. R. Usón, L. A. Oro, M. Sanau, P. Lahuerta and K. Hildenbrand, *J. Inorg. Nucl. Chem.* 1981, **43**, 419.
11. D. Dowerah and M. M. Singh, *Transition Met. Chem.* 1976, **1**, 294; *J. Chem. Res. (S)*, 1979, 38.
12. Z. Nagy-Magos, P. Kvintovics and L. Markó, *Transition Met. Chem.* 1980, **5**, 186.

13. E. W. Abel, M. A. Bennett and G. Wilkinson, *J. Chem. Soc.* 1959, 3178.
14. L. G. Kuzmina, Yu. S. Varshavskii, N. G. Bokki, Yu. T. Struchkov and T. G. Cherkasova, *Zh. Strukt. Khim.* 1971, **12**, 653; *J. Struct. Chem.* 1971, **12**, 593.

COORDINATION CHEMISTRY OF NEW SULPHUR CONTAINING LIGANDS—26. EIGHT COORDINATE VANADIUM(IV) AND MOLYBDENUM(IV) COMPLEXES OF 2-AMINO-1-CYCLOPENTENEDITHIOCARBOXYLATE[1]

ROBERT D. BEREMAN* and JAY R. DORFMAN

Department of Chemistry, North Carolina State University, Raleigh, NC 27650, U.S.A.

Abstract—The new difunction ligand, 2-amino-1-cyclopentenedithio-carboxylate(L), was prepared and its coordination chemistry examined to gain further insight into the reactivity of "aromatic" dithio type ligands. Reaction with $MoCl_4py_2$ and $VOSO_4$, led to the surprising eight coordinate products ML_4. The sp^2 hybridization of the ring carbon to which the CS_2 moiety is bonded apparently yields a pseudo-aromatic effect on the reactivity of this ligand. The physical properties of these new compounds are discussed.

We have been very interested in the design and syntheses of new dithiolate and dithiocarbamate as well as new monothiocarbamate ligands where non-traditional reactivity could be expected. In particular, we have shown that the suppression of the importance of potential resonance contributions (Scheme 1) to the ground state electronic structures of these classes of ligands yield novel transition element complexes.[1–5] Our work has concentrated on systems where Form C in Scheme 1 played an unimportant role in the coordination chemistry. This was accomplished in various ways but normally by the design of a peripheral ligand structure whose inherent resonance structure suppressed this form (Scheme 2).

We chose to extend this study by the in-vestigation of a new ligand, 2-amino-1-cyclopentenedithiocarboxylate (ACDA)[6–8] (Fig. 1). This ligand is interesting because of its potential dual bidentate coordinate possibilities (NS vs S_2) and because a resonance structure leading to other possible resonance structures is suppressed by the presence of the double bond involving the bridgehead ring carbon (Scheme 3). It was anticipated, that this ligand would have a parallel reactivity to dithiobenzoate and pyrroledithiocarbamate. One of the very special reactions of this class of ligands
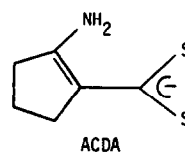
*Author to whom correspondence should be addressed.

ACDA

Fig. 1.
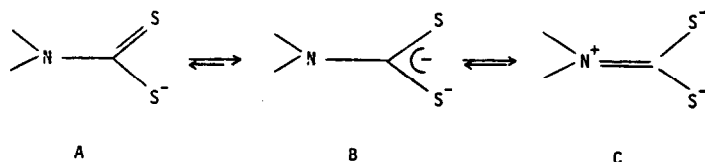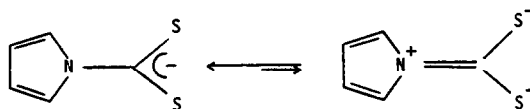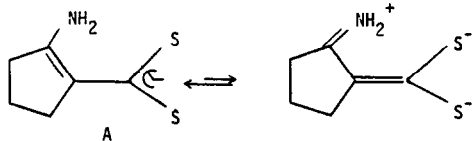
Scheme 1

Scheme 2

Scheme 3.

is that of stabilizing eight-coordinate vanadium(IV) coordination compounds over the vanadyl, $V = O^{+2}$ unit.[9] For that reason, we have investigated this and the Mo(IV) system.

EXPERIMENTAL

Materials

All solvents were of reagent grade and were freshly distilled before use. $VOSO_4 \cdot 2H_2O$ was obtained from the Fisher Scientific Co. and used without further purification. $MoCl_4 \cdot 2py$ was obtained from the Climax Molybdenum Co. and was handled under an argon atmosphere using Schlenk techniques. Methylene chloride was dried over calcium chloride and stored over 4Å molecular sieves.

Preparation of compounds

(1) ACDA was prepared as previously described.[6-8]

(2) $V(ACDA)_4 \cdot 1.5H_2O$

The procedure used here was similar to that of Piovesana and Cappuccilli[10]. 2.102 g of ACDA was dissolved in 150 cm^3 of diethyl ether. The reaction mixture was stirred for 15 minutes to allow complete dissolution. 1.313 g of vanadyl sulphate was dissolved in a 50:50 v/v ethanol‖H_2O solvent system. The vanadyl solution was added dropwise to the dithioacid solution over a 15 min period. Gradually, the solution of the dithioacid (initially yellow) turns brown, then red–brown. The reaction was stirred for a total of 18 hr. A red–brown solid was collected, washed with ice-cold H_2O and dried for 60 min. (Yield—42%).

Table 1 lists the analytical data for this compound and the forthcoming compound.

(3) 0.220 g of ACDA was dissolved in 200 cm^3 of methanol which was degassed by successive freeze-thaw cycles. To this solution was added (dropwise) a methanol solution containing 0.137 g of $MoCl_4 \cdot 2py$ (py = pyridine). The solution, initially yellow, immediately turned blue and was allowed to stir for several hours. The blue–black solid was collected and dried by suction filtration washed with cold methanol, and dried in vacuo for one hour. The compound is air-stable and the blue–black colour is characteristic of 8-coordinate Mo^{4+} sulphur systems.[1] (Yield—77%). Elemental Analyses were determined by Atlantic Microlabs, Atlanta, Ga (see Table 1).

Spectroscopic measurements

All IR, optical, and esr spectra were recorded as described previously.[1-5] Second order corrections were applied to the calculation of all g values.[11]

RESULTS AND DISCUSSIONS

ACDA was reacted with vanadyl sulphate to ascertain if a labilization of the vanadyl (VO^{2+}) unit would be observed. This is a reaction which occurs when the aromatic dithiocarbamates are reacted with vanadyl salts, and is rather unusual owing to the well-known marked stability of the VO^{2+} unit. For example, direct reaction of the VO^{2+} ion with $R_2NCS_2^-$ in water gives "normal" $VO(R_2NCS_2)_2$ complexes which are five-coordinate (approximate C_{2v} symmetry).[12,13] Eight-coordinate $V(R_2NCS_2)_4$ complexes are obtained from insertion reactions of CS_2 and $V(NR_2)_4$ in dry cyclohexane, under dry, oxygen-free conditions.[14] Apart from these complexes, the vast majority of complexes involved with V(IV) chemistry incorporate the VO^{2+} unit. The usual rationale proposed for formation of non-vanadyl V(IV) complexes has been insertion of CS_2^- into the oxo-vanadium bond.[9,15] Thus, if this premise is indeed true, resonance form B(Scheme 3) should make little contribution towards the electronic structure of ACDA. To investigate this property, IR spectroscopy was employed to prove the nature of the C–S bonds. A strong band in the vicinity of 1225 cm^{-1} and a medium-intensity band at about 670 cm^{-1} have been identified by various workers as $\nu(C = S)$ and $\nu(C–S)$, respectively, in aliphatic

Table 1. Elemental analyses

Compound	Colour	%C Calc. (Found)	%H Calc. (Found)	%S Calc. (Found)
$V(ACDA)_4 \cdot 1.5H_2O$	red–brown	40.56 (40.55)	4.93 (4.98)	36.05 (36.07)
$Mo(ACDA)_4$	blue–black	39.56 (39.48)	4.40 (4.44)	35.16 (35.28)

dithioacids.[16] If a monodentate ligand were present in the putative $VL_4(L = ACDA)$ complex, frequencies closely approximating the above values would be expected. Instead, as noted in Table 2, there are two fairly strong absorptions at 900 and 950 cm^{-1}. This would strongly suggest the presence of a delocalized CS_2^- moiety. These assignments are also in accord with previous work on Ni^{2+} complexes of ACDA.[8] The characteristic bands in the IR corresponding to the $v(N-H)$ absorptions are found at 3210 and 3280 cm^{-1} in VL_4 and are within 10 cm^{-1} of the same absorptions found in ACDA. This verifies the premise that the $-NH_2$ moiety remains intact (no deprotonation occurring) and that coordination to the vanadium is unlikely. The bands attributed to $v(N-H)$ usually shift their position rather significantly to lower energy upon coordination to a transition metal. In addition, the VO^{2+} unit has a strong characteristic absorption in the IR in the range $1000-1500 \text{ cm}^{-1}$.[1,15,18] There is no such intense band in the IR spectrum of $V(ACDA)_4$. Finally, the vanadyl analog of this compound has been reported as being a green solid, but the elemental analysis obtained was not satisfactory.[19] The analysis for $V(ACDA)_4$, which is a red-brown solid, is in excellent agreement with the theoretical values (see Experimental

Section). Taken together, these pieces of data support the proposed 8-coordinate VL_4 structure. The optical data for VL_4 in CH_2Cl_2 shows a weak band at 12.1 kK and a shoulder at 19.8 kK as the only ligand field features. Both the optical data and the colour of the complex are in agreement with similar properties observed for other VS_8 chromophores.[9,20]

The VL_4 complex is presumably a V(IV) complex (d^1 system), and thus lends itself to ESR studies. The spin Hamiltonian parameters for V(A-CDA)$_4$ are summarized in Table 3. The ESR spectra of this compound both at room temperature and in frozen glasses resulted in well resolved metal hyperfine structure. The eight-line pattern is characteristic of $^{51}V(I = 7/2)$ systems. The observation that $g_\perp > g_\parallel$ is consistent with other 8-coordinate V(IV) systems, while the metal hyperfine splitting values of 150G and 53G for $A_\parallel$ and $A_\perp$, respectively, are indicative of a covalent system, and further support the presence of 8-coordination.[9,20] During the optical and ESR experiments, the colour of the solutions are the same as that of the compound in the solid state. However, over a period of about one hour, the solution changes colour from red-brown to yellow, which is the colour of the uncomplexed (ACDA) ligand. This would suggest that the VL_4 complex gradually decomposes over this time period.

These data support the predominant resonance form for ACDA as form A. This structure induces the formation of a delocalized CS_2^- unit which does indeed labilize the VO^{2+} moiety forming an 8-coordinate VL_4 complex. The mode of formation probably involves withdrawal of electron density from the $V=O$ bond by the π-system of ACDA-SH, but without further mechanistic studies, this only remains a suggestion based on similar compounds.[9,20] Single crystals of VL_4 are currently being grown for the purposes of unequivocally proving the presence of the 8-coordinate system. It is apparent that as a result of the unusual electronic character of ACDA-SH, the reactivity patterns resemble those of the aro-

Table 2. Selected IR data for $V(ACDA)_4^a$

Band (cm^{-1})	Intensity^b	Assignment
3290	(w)	v (N-H)
3210	(w)	v (N-H)
1615	(s)	v (C=C)
1290	(m)	v (C--N)
950	(m)	v (C----S)
900	(m)	v (C----S)
460	(m)	v (V-S)

a. Spectra obtained as nujol mulls.

b. (w) = weak; (s) = strong; (m) = medium.

Table 3. ESR data for $V(ACDA)_4$

Solvent	$<g>^a$	$<a>_V^{a,b}$	$g_{\parallel}$	$A_{\parallel}^b$	$g_{\perp}$	$A_{\perp}^b$
CH_4Cl_2	1.967	85.0	1.931	150.0	1.986	53.0
Toluene	1.968	84.8	1.933	150.2	1.985	52.8

^{a} Isotropic values obtained from solution spectra at room temperature.

^{b} Hyperfine splitting values in units of gauss.

matic carboxylates and aromatic dithiocarbamates, rather than aliphatic dithioacids.

To further investigate the reactivity of ACDA, this ligand was reacted with a Mo^{4+} salt, specifically $MoCl_4$ (pyridine)$_2$. The first report of the synthesis of Mo-dithio complexes appeared in 1971 when $Mo(IV)(R_2Dtc)_4$ complexes were obtained by CS_2 insertion into $Mo(NR_2)_4$ complexes.[21] Nieuwpoort et al. have obtained $Mo(IV)(R_2Dtc)_4$ complexes with R = Me, Et, i–Pr, and Ph[22]. The optical spectra of these compounds show six absorptions between 10.0 and 25.0 kK, and assignments are complicated.[22]

The IR spectrum of the product of $MoCl_4$(pyridine)$_2$ and ACDA shows two absorptions at 3210 and 3300 cm^{-1} which are assigned as ν(N–H) bands. In addition, there is no band in the 2400–2600 cm^{-1} range which is where ν(S–H) absorptions are usually found. The lack of a strong absorption in the 900–1000 cm^{-1} region is good evidence for the lack of any Mo = 0 bonds. In addition, there is no evidence of any pyridine in this compound as the very characteristic bands attributable to ν(C–H) and ν(C = C) in pyridine are also absent. The optical spectrum of this compound is very similar to other reported 8-coordinate $Mo^{4+}(d^2)$ systems[23,24] (Fig. 2). of $Mo(S_8)$ chromophores.[23] The suggested strucpound is dark blue–violet, a common characteristic of $Mo(S_8)$ chromophores[23]. The suggested structure of $Mo(ACDA)_4$ is somewhat unusual in that, as noted earlier, a limited number of $Mo(S_8)$ systems have been reported. What is novel here is the, initial source of Mo^{4+}, namely

$MoCl_4$(pyridine)$_2$. This appears to be the first report of a $Mo(S_8)$ system generated, using this reagent.

In conclusion, the reactivity of ACDA appears to parallel that of aromatic dithiocarbamates and the aromatic carboxylates. This chemistry is a result of the resonance-induced formation of a distinct CS_2^- moiety as a component of the ligand. In the aromatic carboxylates and dithiocarbamates, this $-CS_2^-$ unit is induced as a result of the peripheral aromatic system which must remain intact. In ACDA–SH, the $-CS_2^-$ formation is presumably due to the fact that this resonance contributor avoids the formation of any positive charge building upon the electronegative primary nitrogen(amine) atom. It is thus suggested that aliphatic dithioacids may behave as analogous aromatic systems do, if the peripheral electronic nature of the ligand induces the formation of the appropriate resonance form.

REFERENCES

1. R. D. Bereman, D. M. Baird, C. T. Vance, J. Zubietta and J. Hutchinson, Inorg. Chem. 1983, 22, 0000. (No. 25 in this series).
2. R. D. Bereman, D. M. Baird and W. Hatfield, J. Inorg. Nucl. Chem. 1982, 43, 2729.
3. R. D. Bereman, D. M. Baird, J. Bordner and J. R. Dorfman, Inorg. Chem. 1982, 21, 2365.
4. R. D. Bereman, D. M. Baird, J. Bordner and J. R. Dorfman, Polyhedron 1983, 2, 25.
5. R. D. Bereman, D. M. Baird and C. Moreland, Polyhedron 1983, 2, 59.
6. B. Bordas, P. Sohar, G. Matolcsy and P. Berencsi, J. Org. Chem. 1972, 37, 1727.
7. G. D. Shields, Ph.D. Thesis. State University of New York at Buffalo (1978).
8. K. Nag and D. S. Joardar, Inorg. Chem. Acta 1975, 14, 133.
9. R. D. Bereman and D. N. Nalewajek, J. Inorg. Nucl. Chem. 1978, 40, 1309.
10. M. F. Corrigan, K. S. Murray, B. O. West and J. R. Pilveoq, Aust. J. Chem. 1977, 30, 2455.
11. D. J. Kosman and R. D. Bereman, Biological applications of electron spin resonance spectroscopy. Spectroscopy in Biochemistry. CRC Press, Boca Rotan, Florida (1981).
12. B. J. McCormick, Inorg. Chem. 1968, 7, 1965.
13. G. Vigee, J. Selbin, J. Inorg. Nucl. Chem. 1969, 31, 3187.

= Mo(dtb)$_4$.

----- = Mo(ACDA-SH)$_4$.

*(dtb) = dithiobenzoate
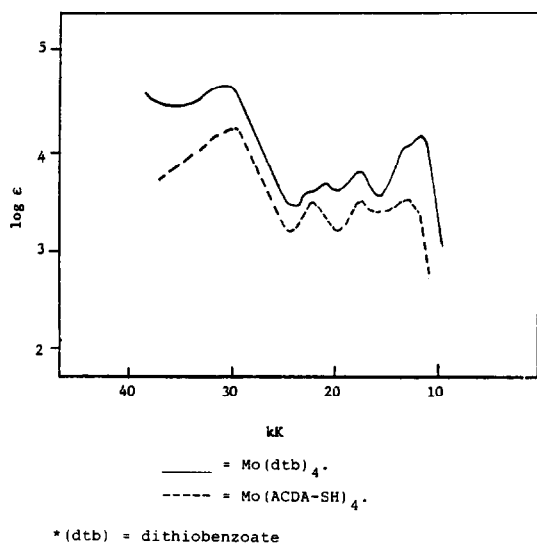
Fig. 2. Absorption spectra of $Mo(ACDA)_4$ and $Mo(dtb)_4$.

14. D. C. Bradley, R. H. Moss and K. D. Sales, *Chem. Commun.* 1969, 1255.
15. D. Coucouvanis, *Prog. Inorg. Chem.* 1979, **26**, 301.
16. B. Bak, L. Hansen-Nygaard and C. Pedersen, *Acta Chem. Scand.* 1958, **12**, 1451.
17. R. S. Drago, *Op. Cit.* p. 177.
18. R. P. Burns, F. P. McCullough and G. A. McAuliffe, *Adv. Inorg. Radiochem.* 1980, **23**, 211.
19. S. N. Choi and J. R. Wasson, *Inorg. Chem.* 1975, **14**, 1964.
20. O. Piovesana and G. Cappuccilli, *Inorg. Chem.* 1972, **11**, 1543.
21. D. C. Bradley and M. H. Chisholm, *J. Chem. Soc. A*, 1971, 2741.
22. A. Nieuwpoort, H. M. Claessen and J. G. M. Van der Linden, *Inorg. Nucl. Chem. Lett.* 1975, **11**, 869.
23. O. Piovesana and L. Sestili, *Inorg. Chem.* 1974, **13**, 2745.
24. D. M. Baird, Ph.D. Thesis. State University of New York, Buffalo (1981).

ESR STUDIES ON THE REACTIVE CHARACTER OF THE RADICAL ANIONS, SO_2^-, SO_3^- AND SO_4^- IN AQUEOUS SOLUTION

TOSHIHIKO OZAWA* and TAKAO KWAN†

Faculty of Pharmaceutical Sciences, University of Tokyo, Hongo, Bunkyo-ku, Tokyo 113, Japan

Abstract—The reactive characteristics of the oxy anion radicals of sulphur, SO_2^-, SO_3^- and SO_4^- were investigated by use of the rapid-mixing flow technique coupled with electron spin resonance (ESR) which can detect the radicals having a lifetime of 5–100 msec. The SO_2^- reduced the aromatic nitro compounds to the corresponding anion radicals, but did not abstract the hydrogen from the saturated compounds nor add to the unsaturated compounds. The SO_3^- could add to the compounds having C=C bond, but did not abstract the hydrogen from the saturated compounds nor reduce the aromatic nitro compounds. The SO_4^- could abstract the hydrogen from the saturated compounds and also add to the unsaturated compounds having C=C bond, but did not reduce the aromatic nitro compounds. These differences of the reactivity towards the organic substrates were discussed on the basis of the difference in the distribution of the unpaired electron density of each radical anion.

It is well known that the rapid-mixing flow technique coupled with electron spin resonance (ESR) is useful to detect the short-lived radicals having a lifetime longer than a few msec. In previous papers, by use of this technique we have reported that the sulphite radical anion (SO_3^-), which is generated from Ce^{4+}-$NaHSO_3$ system, can add to the compounds having C=C[2], C≡C[3] and C=S[4] bonds to give the corresponding secondary radicals, respectively. Also, we have found that the reactive character of SO_3^- towards the compounds having C=C bond is different from that of the sulphate radical anion (SO_4^-) due to Norman *et al.*[4] and have briefly suggested that this difference may be caused by the difference in the distribution of the unpaired electron density of each radical anion.[1]

In order to clarify the reactive characters of these oxy anion radicals of sulphur in detail, we have further examined the reactions of SO_2^-, SO_3^- and SO_4^- with a number of organic substrates by use of the rapid-mixing flow technique. In this paper, we report these results.

EXPERIMENTAL

Materials. $Ce(NO_3)_4 \cdot 2NH_4NO_3$, $NaHSO_3$, $TiCl_3$ and $Na_2S_2O_8$ were purchased from Wako Pure Chemical Ind. Ltd. and used without further purification. $Na_2S_2O_4$ was obtained from Nakarai Chemicals Ltd. Organic substrates were purchased from a commercial source and used without further purification. Sulphuric acid, NaOH, and other chemical reagents were of commercial GR grade.

ESR measurements. ESR measurements were carried out on a JEOL–PE–1X ESR spectrometer (*X*-band) with 100 kHz field modulation in conjunction with a JEOL mixing chamber. The rapid mixing flow apparatus which we used was the same as that reported previously and enabled us to detect radicals having a lifetime of 5–100 msec[5–7]. The hyperfine coupling constants and the *g*-values were calibrated with an aqueous solution of Fremy's salt ($g = 2.0055$, $a^N = 13.0$ G)[8] kept in a capillary tube attached to the sample.

Procedure. All solutions were prepared from triply distilled water, and their pH was adjusted by

*Author to whom correspondence should be addressed. Present address: National Institute of Radiological Sciences, 9–1, Anagawa-4-chome, Chiba-shi 260, Japan.

†Faculty of Pharmaceutical Sciences, University of Teikyo, Sagamiko-cho, Tsukui-gun, Kanagawa 199–01, Japan.

an aqueous solution of sulphuric acid or NaOH.

For the generation of SO_3^-, $Ce(NO_3)_4 \cdot 2NH_4NO_3$ and $NaHSO_3$ were used. The SO_2^- was generated by dissolving $Na_2S_2O_4$ in an aqueous alkaline solution. This radical is stable for more than 5 hr at room temperature.[7] The SO_4^- was obtained by the $TiCl_3$–$Na_2S_2O_8$ system, according to the method reported by Norman et al.[4]

To investigate the reaction of SO_3^- with organic substrates, two aqueous solutions were mixed: one (a) contained 0.01 M Ce^{4+} acidified to pH 2.5 by sulphuric acid and the other (b) 0.1 M $NaHSO_3$ containing various organic substrates of 0.02–0.3 M concentrations.

In the reactions of SO_2^- with organic substrates, the following two solutions were mixed: one (c) contained 0.1 M $Na_2S_2O_4$ at the pH range of 7.5–9.0 and the other (d) 0.02–0.3 M organic substrates at the pH range of 7.5–9.0.

For the reactions of SO_4^- with organic substrates at pH 2.5, one solution (e) contained $TiCl_3$ (0.01 M) and the other (f) contained $Na_2S_2O_8$ (0.1 M) and the organic substrates (0.01 M–0.3 M) which was acidified to pH 2.5 by sulphuric acid.

RESULTS

Abstraction reaction of hydrogen from saturated compounds. No change was observed in the ESR spectrum of SO_3^- (singlet line at $g = 2.0022$)[7] when the solution (b) containing the saturated

compounds such as methanol, ethanol and iso-propanol were allowed to mix with the solution (a). Likewise, in the reactions of SO_2^-, the ESR spectrum due to SO_2^- (singlet line at $g = 2.0055$)[7] was not affected by addition of these compounds. These results suggest that both SO_3^- and SO_2^- are inactive to the abstraction of hydrogen from the saturated compounds.

On the other hand, methanol radical $(\cdot CH_2OH)$[9] was observed when high concentration of methanol (0.3 M) was contained in the solution (f) and was allowed to mix with the solution (e). This radical may be formed by the following reactions,[4]

$$Ti^{3+} + S_2O_8^{2-} \rightarrow Ti^{4+} + SO_4^- + SO_4^{2-} \quad (1)$$

$$SO_4^- + CH_3OH \rightarrow HSO_4^- + \cdot CH_2OH. \quad (2)$$
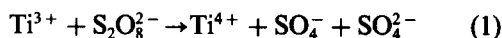
This result indicates that SO_4^- is active to the abstraction of hydrogen from the saturated compounds.

Addition reactions to the compounds having C=C bond. In the reactions of SO_2^-, no spectral change could be observed by mixing the solution (c) with the solution (d) containing the olefinic compounds such as allyl alcohol, crotonic acid and fumaric acid.

The ESR spectrum of SO_3^- was completely consumed when allyl alcohol was added to the
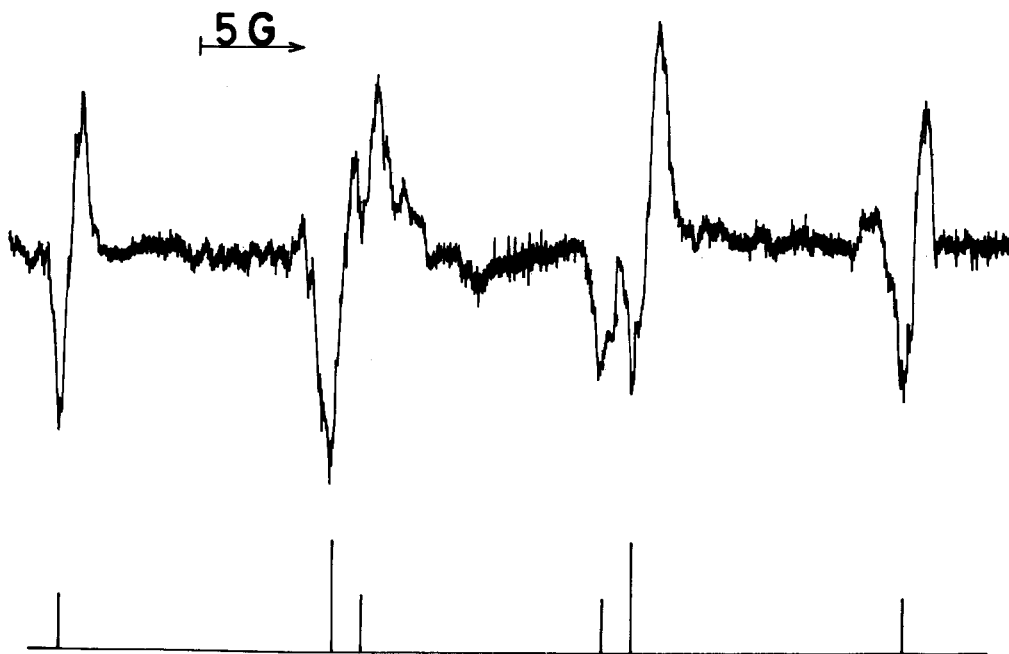
Fig. 1. ESR spectrum observed during the reaction of SO_3^- with acrylic acid in aqueous solution at pH 2.5.

Table 1. Hyperfine coupling constants (gauss) and g-values for the radicals derived from the reaction of SO_3^- with the compounds having C=C bond

Substrate	Radical	Hyperfine splitting const. (gauss)			g
		a(α-H)	a(β-H)	a_{Me}^H	
$HO_2CCH=CHCO_2H$	$^-O_3SCH(CO_2H)\dot{C}HCO_2H$	20.7	8.1	–	2.0033
$CH_2=CHCO_2H$	$^-O_3SCH_2\dot{C}HCO_2H$	20.4	15.9	–	2.0034
$CH_2=CMeCO_2H$	$^-O_3SCMe(CO_2H)\dot{C}H_2$	23.1	–	–	2.0032
$MeCH=CHCO_2H$	$^-O_3SCH(Me)\dot{C}HCO_2H$	20.3	6.6	0.76	2.0033
$Me_2C=CHCO_2H$	$^-O_3SCMe_2\dot{C}HCO_2H$	20.5	–	–	2.0033
$CH_2=CHOCOCH_3$	$^-O_3SCH_2\dot{C}HOCOCH_3$	20.0	13.7	1.40	2.0035

Ce^{4+}-$NaHSO_3$ system, but no secondary radical could be observed. This result may indicate that SO_3^- reacts with olefinic compounds even if the secondary radicals were not observed. Perhaps the secondary radical may be formed, but not in detectable concentration. The secondary radicals were detected when acrylic acid, methacrylic acid, 3, 3-dimethylacrylic acid, crotonic acid, fumaric acid and vinyl acetate were respectively added to the Ce^{4+}-$NaHSO_3$ system. The assigned structures and the ESR parameters were summarized in Table 1.

Figure 1 shows the ESR spectrum observed by the reaction of SO_3^- with acrylic acid. Under the same experimental conditions, only very weak unanalysable resonance was detected with styrene, and there was no detectable ESR absorption with the, following compounds; acrylamide, acrolein, crotonaldehyde and acrylic acid methyl ester.

On the other hand, when crotonic acid or allyl alcohol was added to the Ti^{3-}-$Na_2S_2O_8$ system at pH 2.5, the secondary radicals shown in Table 2 were observed. Acrylic acid gave only very weak, unanalysable resonance, and fumaric acid, acrylamide, acrolein and crotonaldehyde gave no detectable ESR absorption.

Aromatic nitro compounds. Neither SO_3^- nor SO_4^- could react with aromatic nitro compounds

such as nitrobenzene, 1, 2-dinitrobenzene and p-nitrobenzoic acid.

On the other hand, when p-nitrobenzoate was allowed to mix with the SO_2^- solution at pH 9.0, the ESR spectrum of SO_2^- was completely consumed and simultaneously the secondary radical was observed (Fig. 2). This spectrum can be analyzed in terms of the parameters: $a^N(1) = 13.01$ G, $a^H(2) = 3.41$ G and $a^H(2) = 1.41$ G. These values are almost identical to those accepted for the p-nitrobenzoate anion radical.[10] Similar anion radicals were respectively observed by the reaction
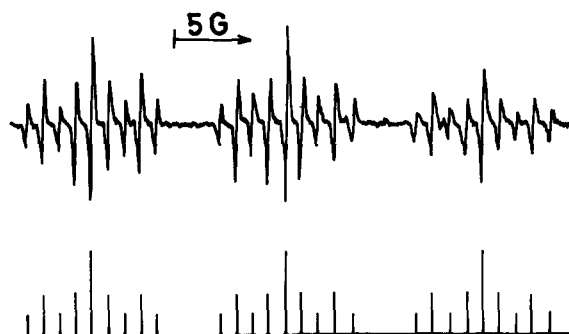
Fig. 2. ESR spectrum observed during the reaction of SO_2^- with p-nitrobenzoate in aqueous solution at pH 9.0.

Table 2. Hyperfine splitting constants (gauss) for the radicals from the reaction of SO_4^- with the unsaturated compounds having C=C bond

Substrate	Radical	Hyperfine splitting const. (gauss)		
		a(α-H)	a(β-H)	a_{Me}^H
$MeCH=CHCO_2H$	$Me\dot{C}HCH(OSO_3^-)CO_2H$	21.5	14.8	25.1
$CH_2=CHCH_2OH$	$^-OSO_3CH_2\dot{C}HCH_2OH$	21.9	24.0	–
			17.6	

Table 3. Comparison of the reactivities between SO_2^-, SO_3^- and SO_4^- towards the organic substrates

Substrate	Secondary radicals observed from		
	SO_2^-	SO_3^-	SO_4^-
CH_3OH	–	–	$\cdot CH_2OH$
$CH_2=\overset{\displaystyle CH_3}{\underset{\displaystyle }{C}}-COOH$	–	$\cdot CH_2-\overset{\displaystyle CH_3}{\underset{\displaystyle SO_3^-}{C}}-COOH$	$CH_2-\overset{\displaystyle CH_3}{\underset{\displaystyle OSO_3^-}{\overset{\displaystyle}{C}}}\cdot-COOH$
$\overset{\displaystyle H_3C}{}C=C\overset{\displaystyle H}{\underset{\displaystyle COOH}{}}$ (with H, COOH)	–	$^-O_3S-\overset{H_3C}{\underset{H}{C}}-\overset{H}{\underset{COOH}{C}}\cdot$	$\cdot\overset{CH_3}{\underset{H}{C}}-\overset{}{\underset{COOH}{C}}H-OSO_3^-$
$\overset{\displaystyle HOOC}{}C=C\overset{\displaystyle H}{\underset{\displaystyle COOH}{}}$	–	$^-O_3S-\overset{HOOC}{\underset{H}{C}}-\overset{H}{\underset{COOH}{C}}\cdot$	–
$\overset{\displaystyle H}{}C=C\overset{\displaystyle H}{\underset{\displaystyle CH_2OH}{}}$	–	–	$^-O_3SO-\overset{H}{\underset{H}{C}}-\overset{H}{\underset{CH_2OH}{C}}\cdot$
nitrobenzene	anion radical	–	–

SO_2^- with nitrobenzene[11] or 1, 2-dinitrobenzene.[12] In these reactions, since the ESR spectrum due to the SO_2^- completely disappeared, anion radicals may be formed according to the following reaction.

$$R\text{-}C_6H_4NO_2 + SO_2^- \rightarrow (R\text{-}C_6H_4NO_2)^{\cdot -} + SO_2 \quad (3)$$
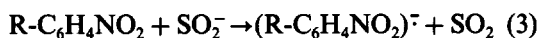
DISCUSSION

In Table 3 the reaction characteristics of the oxy anion radicals of sulphur, SO_2^-, SO_3^- and SO_4^- towards the organic substrates are summarized. From Table 3, it is apparent that these anion radicals which combine with the different number of oxygen have the different reactive character towards the organic substrates. That is, SO_4^- which has the four oxygen atoms in the radical molecule is so reactive that it can abstract the hydrogen from the saturated compounds, whereas SO_2^- which has only the two oxygen atoms in the radical molecule is not so reactive that it can abstract the hydrogen from the saturated compounds or add to the compounds having the C=C bond. The reactive character of SO_3^- is intermediate between those of SO_4^- and SO_2^-. It can add to the compounds having the C=C bond, but can neither abstract the hydrogen from the saturated compounds nor reduce the aromatic nitro compounds.

Further, it is noted that the type of the addition to the compounds having C=C bond differs considerably between SO_3^- and SO_4^- (Table 3).

Table 4. The distribution of the unpaired electron density of SO_2^-, SO_3^- and SO_4^- radical anoins

Atom Radical	S	O
SO_2^-	0.75	0.135
SO_3^-	0.62	0.13
SO_4^-	~0	0.25

The distribution of the unpaired electron density of these oxygen anion radicals of sulphur, (SO_2^-)[13], (SO_3^-)[14] and (SO_4^-)[15] has already been reported in irradiated crystals or powders. These are shown in Table 4. As is shown in Table 4, the unpaired electron density in sulphur atom decreases with the increase of the number of the oxygen combined with the sulphur atom. In the SO_4^- radical, the unpaired electron density on the sulphur atom is nearly zero, being equally distributed over the four oxygen atoms as shown by one of the four equivalent canonical structures (Fig. 3). Therefore, SO_4^- has the property of an oxygen radical and facilitates both the C–O bond formation to the C=C bond and the abstraction of hydrogen from the saturated compounds.

On the other hand, the unpaired electron density of SO_2^- is highly localized on the sulphur atom. Then, since SO_2^- is thought to act as a sulphur radical, and sulphur atom rather than an oxygen atom would take part in the reactivity of SO_2^-.
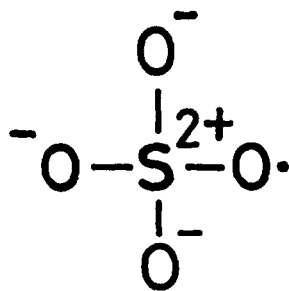
Fig. 3. A canonical structure of SO_4^-.

The distribution of the unpaired electron density for SO_3^- is similar to that for SO_2^-, but the electron density on the sulphur atom for the former is smaller than that for the latter. These facts suggest that SO_3^- has the weaker character as a sulphur radical, as compared with SO_2^-. Accordingly, SO_3^- may not have a reducing ability. However, since the addition reactions of SO_3^- to the C=C bond occur through the C–S bond formation,[1] SO_3^- is thought to be a sulphur radical rather than an oxygen radical.

From the results mentioned above, it is concluded that the difference in the characteristics of the reactivities between these three oxy anion radicals of sulphur, SO_2^-, SO_3^- and SO_4^- arises at least partly from the different distribution of the unpaired electron density among them, as suggested previously by us.[1]

REFERENCES

1. T. Ozawa, M. Sato and T. Kwan, *Chem. Lett.* 1972, 591.
2. T. Ozawa and T. Kwan, *J. Chem. Soc., Chem. Commun.* 1983, 80.
3. T. Ozawa, M. Setaka, H. Yamamoto and T. Kwan, *Chem. Pharm. Bull.* 1974, **22**, 962.
4. R. O. C. Norman, P. M. Storey and P. R. West, *J. Chem. Soc.* (B), 1970, 1087.
5. M. Setaka, Y. Kirino, T. Ozawa and T. Kwan, *J. Catal.* 1969, **15**, 209.
6. T. Ozawa, Y. Kirino, M. Setaka and T. Kwan, *Nippon Kagaku Zasshi* 1971, **92**, 304.
7. T. Ozawa, M. Setaka and T. Kwan, *Bull. Chem. Soc. Jap.* 1971, **44**, 3473.
8. J. Q. Adams, S. W. Nicksic and J. R. Thomas, *J. Chem. Phys.* 1966, **45**, 654.
9. W. T. Dixon and R. O. C. Norman, *J. Chem. Soc.* 1963, 3119.
10. P. L. Kolker and W. A. Waters, *J. Chem. Soc.* 1964, 1136.
11. D. H. Geske and A. H. Maki, *J. Am. Chem. Soc.* 1960, **82**, 2671.
12. A. H. Maki and D. H. Geske, *J. Chem. Phys.* 1960, **33**, 825.
13. R. A. Schoonhyedt and J. H. Lunsford, *J. Phys. Chem.* 1972, **76**, 323.
14. G. W. Chantry, A. Horsfield, J. R. Morton, J. R. Rowlands and D. H. Whiffen, *Mol. Phys.* 1962, **5**, 217.
15. M. C. R. Symons and S. B. Barnes, *J. Chem. Soc.* (A) 1970, 2000.

SYNTHESIS, PROPERTIES AND CRYSTAL STRUCTURE OF BIS(THIOBENZOATO-S) SELENIUM(II)

G. ARAVAMUDAN*, T. SUBRAHMANYAN, M. SESHASAYEE and
G. V. N. APPA RAO

Chemistry Department/Physics Department, Indian Institute of Technology,
Madras 600 036, India

Abstract—The synthesis, properties and crystal structure of bis(thiobenzoato)selenium(II) are described. The complex is formed on interaction of selenium(IV) in acid medium with thiobenzoic acid. It is highly stable towards most metal ions. Crystal structure analysis and ir spectroscopic study indicate that the selenium is covalently bonded to sulphur with weak secondary interactions between selenium and oxygen which complete an S_2O_2 coordination around selenium. There are no intermolecular interactions in the crystal structure.

The oxidation state selenium(II) is unstable and under weak complexation conditions selenium(II) will disproportionate to Se(IV) and Se(O). Thus $SeCl_2$ and $SeBr_2$ have been observed only in the gas phase. However, interaction of selenium(IV), with many sulphur(-II) compounds yields selenium(II) complexes of the sulphur ligands which in many cases are quite stable. The sulphur ligand generally reduces the selenium(IV) to selenium(II) getting itself oxidised generally to the corresponding disulphide. Excess of sulphur ligand would form stable complexes with selenium(II). The ligands which have been successfully used to stabilize selenium(II) are thiocyanate,[1] thiosulphate,[2] mercaptocarboxylic acids,[3-5] dithiocarbamates[6,7] aryl sulphonate[8] and xanthate.[9] Structural work has shown interestingly low coordination number and extensive covalent bonding in the complexes. Data on the reactivity patterns are sparse. Recent electrochemical work[10] has highlighted the extraordinary stability of the complexes of selenium(II) with mercaptocarboxylic acids. In the present work the interaction of selenium(IV) with a bidentate ligand monothiobenzoic acid was studied. The thiobenzoate anion has both oxygen and sulphur sites for coordination. Complexes of thiobenzoic acid with transition metals[11-15] and tin(IV)[16] have only been reported earlier. The formation, structural and reactivity aspects of the selenium(II) complex of thiobenzoic acid reported in this work highlight

the extreme soft acid character of selenium(II) featuring strong sulphur coordination of the ligand.

EXPERIMENTAL

Materials and methods

The chemicals used in synthetic and reaction studies were of AnalaR grade. Thiobenzoic acid used was 99% pure. Solution of the acid in methanol was freshly prepared and stored under nitrogen. Microanalyses were done by CSIRO, Melbourne, Australia. Molecular weight of the selenium(II) complex isolated was determined by Mechrolab. Model 301A vapour pressure Osmometer calibrated with benzil using benzene as solvent. IR Spectra were recorded in the range 600–4000 cm^{-1} in a Perkin–Elmer 257 unit and in the range 100–1000 cm^{-1} in a Polytech FIR 30 unit. UV-visible spectra were recorded in a Carl–Zeiss DMR 21 Spectrophotometer. Radiochemical measurements using ^{75}Se tracer were made in a Frieseke–Hofner γ-ray spectrometer provided with a 440 multichannel analyzer and a Naithal crystal.

The molar ratio of interaction between selenium(IV) and thiobenzoic acid in acid medium was determined by three different methods, viz spectrophotometry, radiochemical titration and redox potentiometry.

Spectrophotometry

The products of interaction between selenium(IV) and thiobenzoic acid showed an absorption maximum at 355 nm in benzene solution.

---

*Author to whom correspondence should be addressed.

Selenium(IV) was not extracted into benzene and freshly prepared thiobenzoic acid in benzene showed little absorption at 355 nm. Solutions of H_2SeO_3 (0.05 M in 2 N sulphuric acid medium) and to thiobenzoic acid (0.05 M) in methanol) were mixed in various ratios. 5 cm^3 of 2 N sulphuric acid and 10 cm^3 methanol were added. Benzene was added in small portions and the benzene extracts were collected and made up to 50 cm^3. The absorbance of the benzene extract was measured at 355 nm using a 5 cm cell. The absorbance vs mole ratio plot shown in Fig. 1(a) indicates the interaction ratio to be 1:4.

Radiochemical titration

^{75}Se tracer in the form of H_2SeO_3 was used. To 10 cm^3 of 0.05 M H_2SeO_3 solution in 1 M sulphuric acid labelled with ^{75}Se tracer were added different volumes of 0.05 M solution of thiobenzoic acid in methanol. The interaction products were then extracted into benzene and the activity of ^{75}Se in the benzene phase was measured. The radiochemical graph 1(b) indicates that the activity in the benzene phase levels off when the selenium(IV) to thiobenzoic acid ratio reaches 1:4.

Redox potentiometry

A solution containing 0.25 mM of selenium(IV) in 20 cm^3 methanol and 20 cm^3 2 N sulphuric acid in a beaker was titrated against a solution of 0.1 M thiobenzoic acid in methanol taken in a burette. A platinum foil was used as redox indicator electrode with saturated calomel electrode as reference. In another series of measurements the titration was done after the addition of 20 cm^3 1 M potassium bromide. The potential readings were studied. The potentiometric curves (Fig. 1c) indicate a marked inflection at 1:4 selenium(IV) to thiobenzoic acid ratio. The addition of potassium bromide helped to give an increased break apparently due to the increased oxidation potential of selenium(IV) in presence of bromide.

Suitable crystals of the selenium complex were

†Atomic Co-ordinate have also been deposited into the Cambridge Crystallographic Data Centre.

obtained by the following method for the structural analysis.

Forty cm^3 0.1 M thiobenzoic acid in methanol were added to a solution containing 2 mM of H_2SeO_3 dissolved in 125 cm^3 methanol. The precipitate formed was extracted into benzene. On evaporation of the benzene extract at room temperature two types of crystals, one needlelike and pale yellow (selenium complex) and the other stubby and colourless (the disulphide) were obtained.

Crystal data

Monoclinic, $C2/c$, $a = 24.244(4)$, $b = 4.2692(7)$, $c = 14.452(7)$ Å, $\beta = 109.95(3)°$, $V = 1406.05$ Å^3, $D_c = 1.69$ g cm^{-3}, $Z = 4$, $\mu = 6.03$ mm^{-1}. 1840 reflections with $I > 3\sigma(I)$ were recorded using a CAD-4 single crystal X-ray diffractometer with Cu$K\alpha$ radiation ($\lambda = 1.5418$ Å). Structure was solved by Patterson and difference Fourier methods. Full matrix leastsquares refinements with 1012 unique reflections gave final $R = 0.051$, $R_w = 0.054$, where the weighting scheme used was $w = 0.0422/[\sigma^2(F_0) + 0.0605|F_0|^2]$. Final difference Fourier maps gave the locations of all the hydrogen atoms which were subsequently refined. All calculations were carried out by use of SHELX-76 program.[17] Atomic parameters have been deposited with the Editor as supplementary data,† derived dimensions are given in Table 1. The molecular structure of the complex is shown in Fig. 2.

RESULTS AND DISCUSSION

Synthesis and general characteristics

The interaction between selenium(IV) and thiobenzoic acid was found to occur readily in strongly
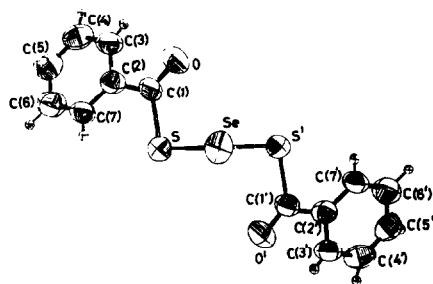
Fig. 2. Perspective view of the molecule.
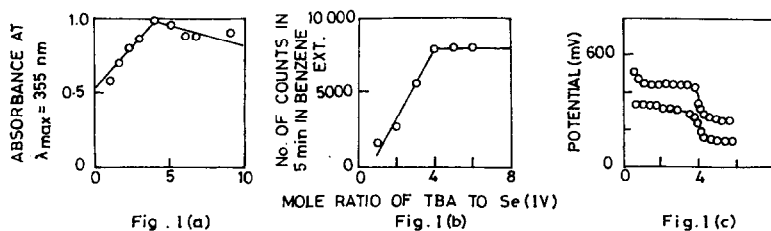
Fig. 1. Interaction ratio of selenium(IV) and thiobenzoic acid by: (a) Spectrophotometry. (b) radiochemical titrations. and (c) Redox potentiometry.

Table 1. Bond lengths (Å) and bond angles (°) with estimated standard deviations in parentheses

Se-S	2.174(1)
S-C(1)	1.827(5)
C(1)-O	1.187(7)
C(1)-C(2)	1.472(6)
S-Se-S'*	105.0(1)
Se-S-C(1)	102.1(2)
S-C(1)-O	121.6(3)
O-C(1)-C(2)	124.7(4)
S-C(1)-C(2)	113.7(4)
C(1)-C(2)-C(3)	118.7(5)
C(1)-C(2)-C(7)	123.5(5)

*Unprimed and primed atoms indicate equivalent positions

x y z and x̄ y 1/2 - z

acidic medium. There was no interaction in alkaline condition. The results of the study under acidic condition to find the interaction ratio are given in Figs. 1(a)–(c). All the three techniques, viz. spectrophotometry, radiochemical titration and redox potentiometry, unequivocally indicate the selenium(IV)-thiobenzoic acid interaction ratio as 1:4 and this considered in conjunction with the occurrence of a redox reaction as revealed by potentiometry suggests that the reaction could be represented as

$$H_2SeO_3 + 4C_6H_5COSH \rightarrow (C_6H_5COS)_2Se$$
(A)

$$+ C_6H_5COSSCOC_6H_5 + 3H_2O.$$
(B)
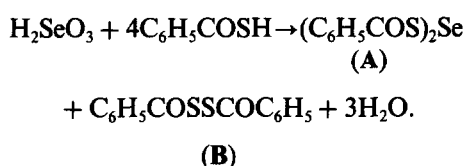
The compounds bis(thiobenzoato)selenium(II) (A) and the dibenzoyl disulphide (B) had different crystal habits and were isolated by fractional crystallisation using benzene as solvent. (B) was more soluble than (A). Found, complex (A): Se 22.0; S 18.0; C 47.1; H 2.72; Calc. for $C_{14}H_{10}O_2S_2Se$: Se 22.35; S 18.15; C 47.57; H 2.85%; Found, Disulphide (B): S 23.3; C60.3; H 3.09%; Calc. for $C_{14}H_{10}O_2S_2$: S 23.37; C 61.28; H 3.673%.

Bis(thiobenzoato)selenium(II) was highly soluble in most polar and non-polar organic solvents. The complex was indefinitely stable both in the solid state and solutions of organic solvents under anhydrous conditions. It melted at 120°C and decomposed to selenium and disulphide at 130°C. Aqueous methanolic solutions of the complex were unaffected by non-oxidising acids, but even mild

Table 2. Structural comparison of S-ligated Se(II) compounds

Compound	Se-S(Å)	S-Se-S(°)	Coordination	Ref.
Se(SCN)₂	2.21	101	Two sulphurs	1
Ba[Se(S₂O₃)₂]3H₂O	2.181, 2.178	104	Two sulphurs	2
Se(SCH₂·CH₂COOH)₂	2.180(3)	105	Two sulphurs	5
Se(SO₂C₆H₅)₂	2.20	105	Two sulphurs	8
Se(SCO C₆H₅)₂	2.174	105	Two sulphurs	This work
Se(S₂CNC₄H₈O)₂	2.282 2.782 2.314 2.791	70.5 84.6 69.7 135.0	Four sulphurs (Planar trapezoid)	7
Se(S₂COMe)₂	3.50 3.60 2.21 2.17	80.0 91.2 87.6 100.8	Four sulphurs	9

alkali solutions readily decomposed the selenium(II) complex into the red selenium and disulphide. Keeping the complex in contact with excess of thiobenzoic acid in aqueous methanol solutions resulted in slow formation of selenium. This is due to the reducing action of the hydrogen sulphide formed under these conditions as a result of slow hydrolysis[18] of thiobenzoic acid.

The stability of the selenium complex (dissolved in methanol) towards metal ions was demonstrated by its being unaffected by the addition of even large excess of Cu(II), Co(II) and Ni(II). Ag(I) caused displacement of selenium and subsequent complicated redox reactions only at higher temperatures, but not at 30°C. The selenium complex reacted with Hg(II) at room temperature and this work is being reported separately. The selenium(II) complex was also not affected by addition of iodide which is one of the best soft bases. The stability of the selenium-thiobenzoato complex is comparable with that of selenium(II)-carboxyliphatic thiolato complexes.[10] Addition of thioglycollic acid or β-mercaptopropionic acid to solutions of bis-(thiobenzoato)selenium(II) in methanol resulted in the formation of selenium. Thus even though the complexes of selenium(II) with thiobenzoate and β-mercaptopropionate[5] are individually quite stable, admixtures of the two complexes are unstable. This feature occurs in many mixed ligand systems in the chemistry of tellurium(II)[19] also.

Structure

The complex bis(thiobenzoato)selenium(II) was monomeric in solution as shown by vapour pressure osmometry using benzene as solvent.

The IR spectrum of selenium(II) complex (A) taken in KBr in the region 600–4000 cm^{-1} was virtually identical with that of dibenzoyldisulphide (B). This indicates the absence of oxygen coordination in the selenium complex. The $\nu_{C=O}$ for thiobenzoic acid, the dibenzoyldisulphide and the selenium complex were observed at 1690, 1685 and 1685 cm^{-1} respectively. The ν_{C-S} which occurs at 960 cm^{-1} for the sodium thiobenzoate occurs at 900 cm^{-1} in (A) and (B). This indicates that the Se–S interaction in (A) is strong and comparable to that observed for Pd–S[14] and Hg–S[11] interactions in their respective thiobenzoate complexes. The ν_{S-H} occurs as a weak band at 2560 cm^{-1} in thiobenzoic acid. This absorption is not noticed in the selenium complex. The far IR spectra of (A) and (B) are very similar excepting for an additional strong absorption at 212 cm^{-1} in (A). This is assigned to $\nu_{Se-S°}$. Thus IR data suggest strong selenium to sulphur bonding and little or no selenium–oxygen interaction in similarity with the Pd and Hg complexes

of thiobenzoic acid and in contrast with the nickel(II) complex of thiobenzoic acid in which both sulphur and oxygen are known to be coordinated from IR spectral,[11] magnetic and X-ray results.[12] The conclusions from IR and molecular weight studies of the selenium complex are fully corroborated by the results of X-ray structural analysis discussed below.

The thiobenzoate group is essentially unidentate and is covalently linked to the selenium through the sulphur. The selenium–sulphur distance (2.174 Å) is close to 2.11 Å (which is the sum[21] of the single covalent radii) and the S–Se–S angle is 105°. Both the Se–S distance and the S–Se–S angle are comparable with those reported for in the other sulphur-ligated two-coordinated selenium(II) complexes listed in Table 2. The two carbonyl oxygens are *trans* to each other with respect to the S–Se–S plane. The two Se–O distances are equal (3.11 Å). This Se–O distance in the complex is much longer than 1.80 Å the sum of the single covalent radii of Se and oxygen but well within the van der Waals Se–O distance[20] (3.42 Å). Hence, these contacts may well indicate weak Se–O secondary interactions of the type discussed by Alcock[20] in many other Se compounds. The Se–O secondary interaction in the complex is weaker than the Se–S secondary interactions noticed in the dithiocarbamate[6] and xanthate complexes[9] of Se(II). The SeS_2O_2 unit forms a pyramid with Se atom at the apex and the other four atoms forming a quadrilateral base, which is planar within 0.1 Å. The Se atom is considerably lifted out of the basal plane, the deviation being 1.28 Å. This is to be contrasted with the SeS_4 geometry in the dithiocarbamate and xanthate complexes of Se, wherein the SeS_4 is very nearly planar trapezoidal. This is attributed to the different bites of the Se–O and Se–S groups and the extent of secondary interactions. The lone pair of electrons in Se occupy positions above Se away from the S_2O_2 plane. They do not take part in any intermolecular interactions in this complex.

The C–O and C–S distances are 1.187 and 1.827 Å and compare well with other published values in similar compounds. The average C–H distance is 0.83(5) Å and the average C–C–H angle is 119(4)°. The two phenyl rings are nearly parallel to each other making an angle of 4.6(7)°.

REFERENCES

1. S. M. Ohlberg and P. A. Vaughan, *J. Am. Chem. Soc.* 1954, **76**, 2649.
2. K. Maroy, *Acta Chem. Scand.* 1972, **26**, 45.
3. H. E. Ganther, *Biochem.* 1968, **7**, 2898.

4. E. R. Clark and A. J. Collett, *J. Inorg. Nucl. Chem.* 1976, **36**, 3680.
5. G. V. N. Appa Rao, M. Seshasayee, G. Aravamudan, T. Nageswara Rao and P. N. Venkatasubramanian, *Acta Cryst.* 1982 (in press).
6. S. Husebye and G. Helland-Madsen, *Acta Chem. Scand.* 1970, **24**, 2273.
7. O. P. Anderson and S. Husebye, *Acta Chem. Scand.* 1970, **24**, 3141.
8. S. Furberg and P. Oyum, *Acta Chem. Scand.* 1954, **8**, 1701.
9. N. J. Brondmo, S. Esperas, H. Graver and S. Husebye, *Acta Chem. Scand.* 1973, **27**, 713.
10. T. Nageswara Rao, G. Aravamudan and R. Narayan, *Electrochim. Acta*, 1982, **27(8)**, 985.
11. V. V. Savant, J. Gopalakrishnan and C. C. Patel, *Inorg. Chem.* 1970, **9**, 748.
12. G. Melson, N. Crawford and B. Geddes, *Inorg. Chem.* 1970, **9**, 1123.
13. R. O. Gould, T. A. Stephenson and M. A. Thompson, *J. Chem. Soc. Dalton* 1978, 769.
14. John A. Goodfellow, T. A. Stephenson and M. C. Cornock, *J. Chem. Soc. Dalton* 1978, 1195.
15. John A. Goodfellow and T. A. Stephenson, *Inorg. Chim. Acta*, 1980, **41**, 19.
16. R. C. Mehrotra, G. Srivastava and N. Vasanta, *Inorg. Chim. Acta*, 1981, **47**, 125.
17. G. M. Sheldrick, SHELX-76, Program for Crystal Structure Determination, Cambridge University, England, 1975.
18. A. J. Hall and D. P. N. Satchell, *Chem. Ind.* 1974, 527.
19. P. R. Sethuraman, M. R. Udupa and G. Aravamudan, *J. Inorg. Nucl. Chem.* 1973, **35**, 3291.
20. N. W. Alcock, *Advances in Inorganic and Radiochem.* 1972, **15**, 1.
21. L. Pauling, *Nature of the Chemical Bond*. Cornell University Press, Ithaca, New York (1960).

THE FORMATION AND CRYSTAL AND MOLECULAR STRUCTURES OF HEXA(μ-ORGANOTHIOLATO)TETRACUPRATE(I) CAGE DIANIONS: BIS-(TETRAMETHYLAMMONIUM)HEXA-(μ-METHANETHIOLATO)TETRACUPRATE(I) AND TWO POLYMORPHS OF BIS(TETRAMETHYLAMMONIUM)HEXA-(μ-BENZENETHIOLATO)-TETRACUPRATE(I)

IAN G. DANCE*

School of Chemistry, University of New South Wales, Kensington, N.S.W. 2033, Australia

and

GRAHAM A. BOWMAKER, GEORGE R. CLARK and JEFFREY K. SEADON
Department of Chemistry, University of Auckland, Auckland, New Zealand

Abstract—X-Ray analysis shows that the crystalline compounds $(Me_4N)_2[Cu_4(SMe)_6]$ (**1**), $(Me_4N)_2[Cu_4(SPh)_6]$ (**2**) and $(Me_4N)_2[Cu_4(SPh)_6]EtOH$ (**3**) all contain the [*tetrahedro*-Cu_4^I-*octahedro*-$(SR)_6]^{2-}$ molecular cage. Very well developed pale yellow crystals of (**2**) and (**3**) can be obtained directly from a mixture of copper(II) salt and excess benzenethiol with tertiary amine in alcohol. The substituents R of the $[Cu_4(SR)_6]^{2-}$ cage remove the high symmetry of the Cu_4S_6 core, and allow three configurational isomers for the cage. All known instances of this cage structure occur as the isomer which minimises the number of close contacts of substituents over the surface of the cage. Despite this, there remain intra-cage repulsive interactions between substituents, greater for R=Ph than for R=Me, which cause distortions primarily in the S–Cu–S angles which range from 105–144°. Cu–S distances are coupled, apparently electronically, to opposite S–Cu–S angles. The stereochemical analysis is extended to all known $Cu_4(SR)_6$ cages, and to alternative cage structures.

Anionic complexes $[Cu_2^IX_3]_n^{n-}$, X being a monodentate monoanionic ligand, can possess the high symmetry molecular cage structure *tetrahedro*-M_4-*octahedro*-X_6 in which each ligand bridges the edges of the tetrahedral array of M, and each metal has trigonal coordination. This structure occurs in $(Ph_3MeP)_2Cu_4I_6$,[1] in two crystalline modifications of $(Me_4N)_2[Cu_4(SPh)_6]$,[2] and in $[Cu_4(SPh)_6]^{2-}$ crystallised with Ph_4P^+.[3]

An alternative molecular cage structure type with the same stoichiometry, $[Cu_8X_{12}]^{4-}$, and the same coordination numbers, is *hexahedro*-Cu_8-*icosahedro*-X_{12} in which copper atoms as a cube lie in the faces of an X_{12} icosahedron. This structure is known only for complexes with chelating dithiolate ligands[4,5] and for related compounds with a central spherical ligand.[6–8] We have suggested[2] than an empty cage $[Cu_8(SR)_{12}]^{4-}$ with

unconnected thiolate groups would be insufficiently rigid for independent existence, a suggestion supported by the observation of increasing distortions in the series of empty cages $[M_4(SR)_6]^{2-}$, $[M_5(SR)_7]^{2-}$, $[M_6(SR)_8]^{2-}$.[9,10] It has also been suggested[4] that $[Cu_8(SPh)_{12}]^{4-}$ does not form due to repulsions between phenyl groups over the surface of the S_{12} icosahedron, but this is partially refuted by the occurrence of $[ClZn_8(SPh)_{16}]^-$ in which there is an icosahedral array of bridging SPh groups.[11] Nevertheless there remain questions about the packing of substituents R over the surfaces of molecular cages maintained by bridging ligands RS^-. We have prepared $(Me_4N)Cu_2(SMe)_3$ (**1**), with the smallest substituent R, and report here that it contains the $[Cu_4(SMe)_6]^{2-}$ molecular cage, as suggested by infrared data.[12]

Several different methods of synthesis of $[Cu_4(SR)_6]^{2-}$ have been employed. We present here previously unpublished details of our syntheses of

---

*Author to whom correspondence should be addressed.

(Me$_4$N)$_2$[Cu$_4$(SPh)$_6$] **(2)** and its solvate (Me$_4$N)$_2$[Cu$_4$(SPh)$_6$]EtOH **(3)**, and also full details of the crystal structures of **(1)**, **(2)** and **(3)**. Compound **(2)** contains two crystallographically independent [Cu$_4$(SPh)$_6$]$^{2-}$ cages, denoted **(2a)** and **(2b)**, and therefore when (Ph$_4$P)$_2$[Cu$_4$(SPh)$_6$]^3 **(4)** is included, structural information is available for five independent molecules [Cu$_4$(SR)$_6$]$^{2-}$. This geometrical data is compared and interpreted in this paper.

The high symmetry (T$_d$) possible for the *tetrahedro*-Cu$_4$-*octahedro*-S$_6$ core of these molecules must be largely if not totally removed by the substituents R. Configurational isomerism is possible due to inversion at bridging sulphur, and is discussed here. Deviations from idealised molecular geometry are examined in terms of substituent interactions over the surface of the cage.

RESULTS AND DISCUSSION

Synthesis. The preparation of (Me$_4$N)$_2$[Cu$_4$(SMe)$_6$] **(1)** involved[12] addition of NaSMe solution in ethanol to a solution of tetramethylammonium chlorocuprate(I) complexes in ethanol/acetonitrile. The MeS$^-$/Cu(I) ratio was 4.2, and the product obtained as colourless crystals.

The preparation of (Me$_4$N)$_2$[Cu$_4$(SPh)$_6$], which is pale yellow, involved addition of copper(II) salt solution to a solution containing thiol, tertiary amine as deprotonating agent, and tetramethylammonium chloride, again using alcohol/acetonitrile solvent systems, eqn (1). At room temperature copper(II) is

$$Cu^{2+} + PhSH + R_3N + Me_4N^+ \xrightarrow{CH_3CN/ROH}$$

$$[Cu_4(SPh)_6]^{2-}(Me_4N^+) + PhSSPh + R_3NH^+ \quad (1)$$
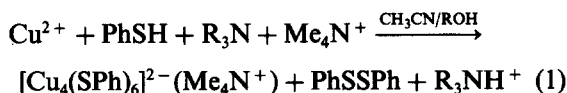
very rapidly reduced by thiolate, and precipitates as CuSR unless excess thiolate is present. The solutions from which crystallisation of **(2)** and **(3)** (and (Me$_4$N)$_2$[Cu$_5$(SPh)$_7$]^9) occurred contained PhS$^-$/Cu(I) in ratios of 2.9–5.0, as well as PhSSPh and halide ion which are not competitive ligands.

This method allows direct production of well-formed crystals of **(2)** and **(3)**. The yields are low, and it is very likely that other, more soluble, [Cu$_x$(SPh)$_y$]$^{x-y}$ species are present in the yellow solutions. The crystallisation solutions are initially supersaturated, and it appears that nucleation rates, in addition to the PhS$^-$/Cu(I) ratio and the solvent composition, influence the variable distribution of crystalline product between **(2)** and **(3)** and (Me$_4$N)$_2$[Cu$_5$(SPh)$_7$].

(Ph$_4$P)$_2$[Cu$_4$(SPh)$_6$] **(4)** has been prepared by re-

actions **(2)**, **(3)** and **(4)**,[3]

$$[Cu(CH_3CN)_4]^+ + KSPh + Ph_4P^+$$

$$\xrightarrow[Et_2O]{CH_3CN} [Cu_4(SPh)_6]^{2-}(Ph_4P^+) \quad (2)$$

$$[Cu(CH_3CN)_4]^+ + [Cu(SPh)_3]^{2-}(Ph_4P^+)$$

$$\xrightarrow[Et_2O]{CH_3CN} [Cu_4(SPh)_6]^{2-}(Ph_4P^+) \quad (3)$$

$$[Cu_8(dts)_6]^{4-} + KSPh$$

$$\xrightarrow[Et_2O]{CH_3CN} K_2dts(s) + [Cu_4(SPh)_6]^{2-}(Ph_4P^+). \quad (4)$$
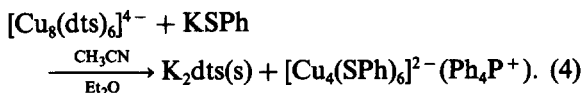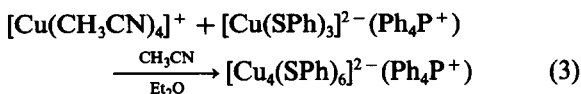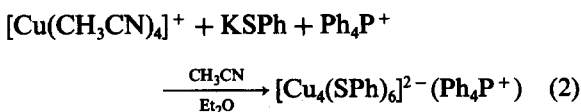
Molecular structure. Each molecular cage [Cu$_4$(SR)$_6$]$^{2-}$ contains a tetrahedron of copper atoms, with a doubly-bridging thiolate ligand across each of the six edges of the tetrahedron such each copper atom has approximately trigonal planar CuS$_3$ coordination. The Cu$_4$S$_6$ core can also be described as an octahedron of sulphur atoms with copper atoms lying at the midpoints of four faces of the octahedron, that is *tetrahedro*-Cu$_4$-*octahedro*-S$_6$ (Fig. 1a).

(a)

(b)
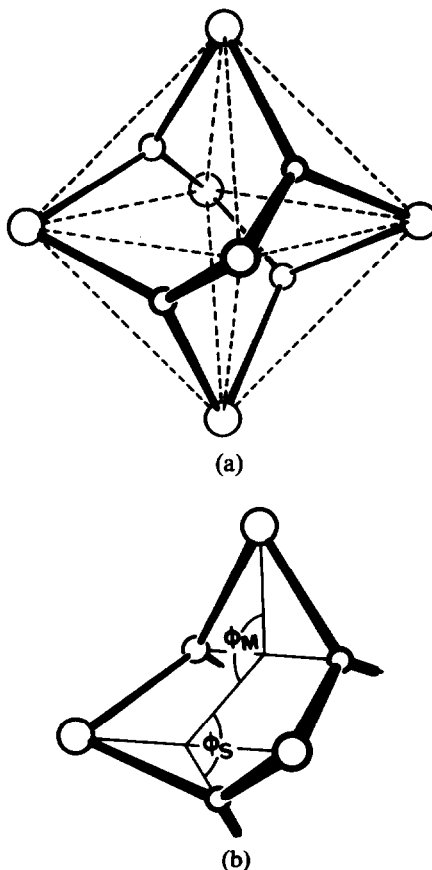
Fig. 1. (a) The *tetrahedro*-Cu$_4$-*octahedro*-S$_6$ core of cages [Cu$_4$(SR)$_6$]$^{2-}$. (b) The dihedral angles ϕ_M, ϕ_S in the cycles Cu$_3$S$_3$ of Cu$_4$S$_6$. The larger circles are sulphur.

An alternative description of the Cu_4S_6 core recognises four fused Cu_3S_3 cycles, each in chair conformation but distorted because the intracycle angles at Cu and S are 120° and 70.53° respectively. The distortion of the Cu_3S_3 cycle from ideal chair conformation is shown also by the dihedral angles ϕ_M and ϕ_S at the Cu–Cu and S–S chords of the cycle (see Fig. 1b), which are 115.2 and 80.0° respectively instead of the ideal 125.3°.

The configurational isomerism of $M_4(SR)_6$ due to inversion at bridging thiolate can be described in terms of the directions of the S–C vectors referenced to the four M_3S_3 cycles in pseudo-chair conformation. At each S atom the S–C vector is axial (a) to one and equatorial (e) to the other of the two chairs it shares, and the isomers are then classified in terms of the distribution of axial and equatorial S–C vectors in each of the four chairs. There are three distributions: I {aaa, aae, aee, eee}; II {aae, aae, aae, eee}; III {aae, aae, aee, aee}, shown diagramatically in Figs. 2(c)–(e). Each of the stereoisomers is enantiomeric; II has symmetry C_3, while I and III are asymmetric.

(c)

(d)

(a)

(e)

(b)
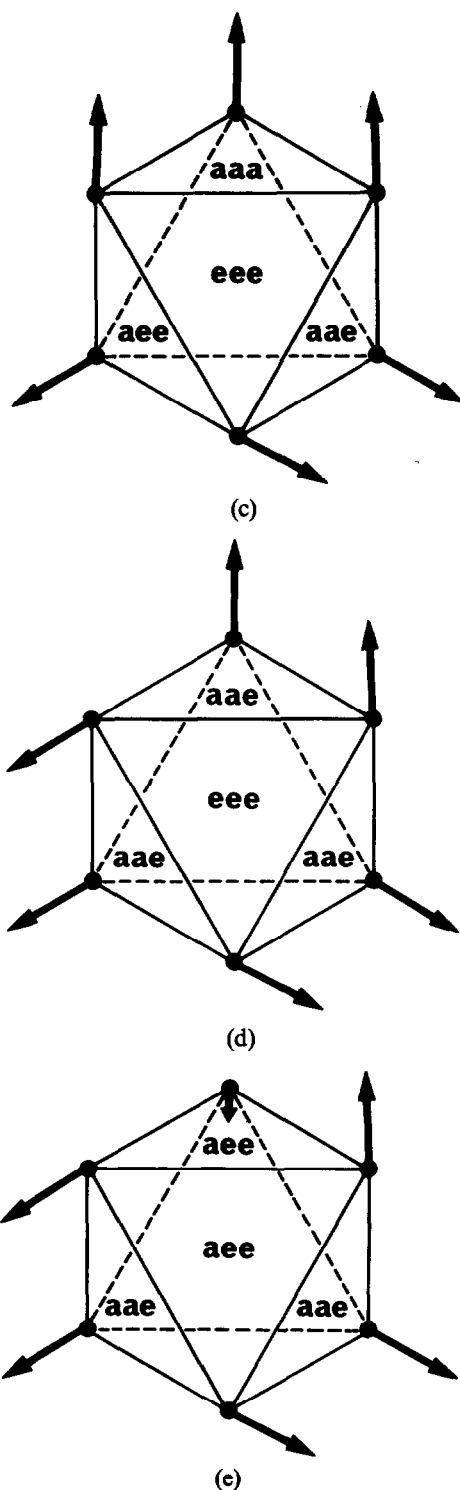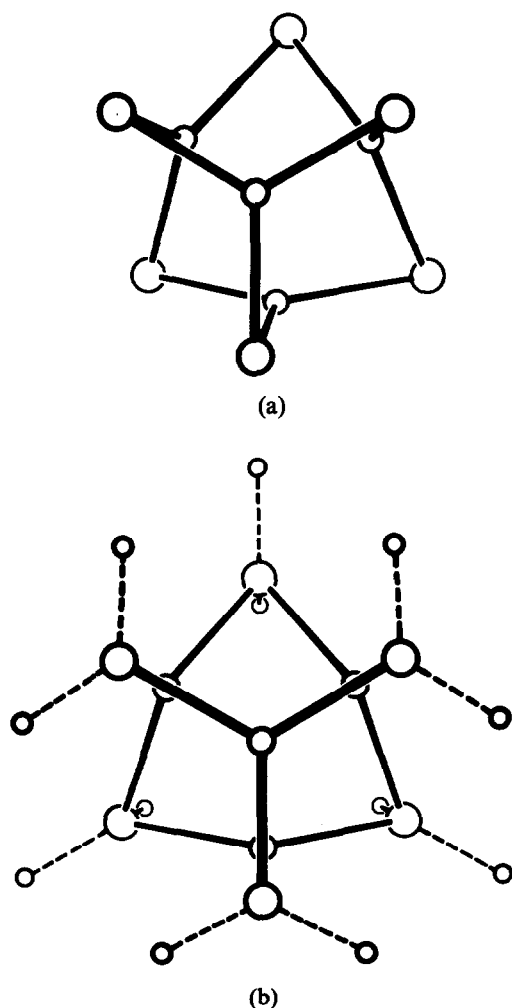
Fig. 2. (a) The M_4S_6 core, view direction close to a threefold axis. (b) $M_4(S–C)_6$, view direction parallel to the threefold axis of part (a), showing alternative directions of S–C vectors at each sulphur atom. (c), (d), (e) Diagrammatic representations, oriented as in part (b), of the configurational isomers according to the direction (arrows) of S–C bonds with respect to the S_3 triangles of the four M_3S_3 cycles; a, axial, e, equatorial; the central letter triplet refers to the underside S_3 triangle; (c) isomer I, (d) isomer II, (e) isomer III.

The molecule $[Cu_4(SMe)_6]^{2-}$ and the three independent $[Cu_4(SPh)_6]^{2-}$ molecules in (2) and (3) all occur as isomer III. This isomer occurs also in $(Ph_4P)_2[Cu_4(SPh)_6]$ (4).[3] All four crystals are centrosymmetric, containing both enantiomers of isomer III. In view of these five occurrences of the one asymmetric configurational isomer, the presentation and analysis of molecular geometry and dimensions is made with all molecules in equivalent orientation and with the same atom labelling scheme. Figure 3 shows the four molecules (1), (2a), (2b), (3), all oriented in the same manner as the isomer diagram of Fig. 2(e), and the atom labelling.[13]

The close similarity in overall configuration of the three $[Cu_4(SPh)_6]^{2-}$ molecules (2a), (2b), (3), shown in Fig. 3, cannot be attributed to influences of crystal environment, which are quite different. Figure 3 shows that there is more variation in the conformations of phenyl rings due to rotation about S–C bonds than in the orientations of the S–C vectors relative to the molecular cage framework. Nevertheless, the complete shape of molecule (2a) is very similar to that of (3). The greatest differences between the structures occur in the conformations of rings 2 and 4, and 3 and 6. These are the two pairs of ligands which are the contiguous axial pairs in the isomer {aae, aae, aee,
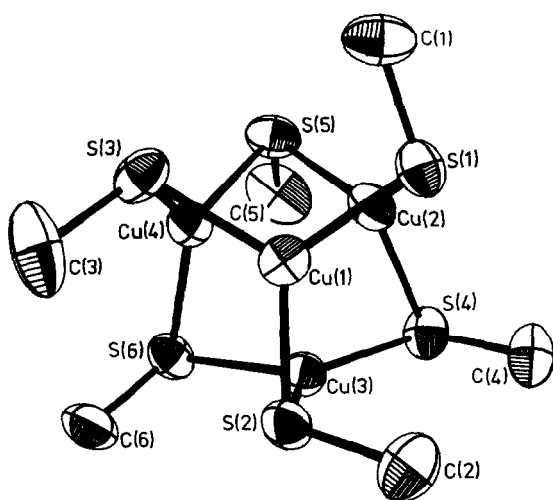
(3a)
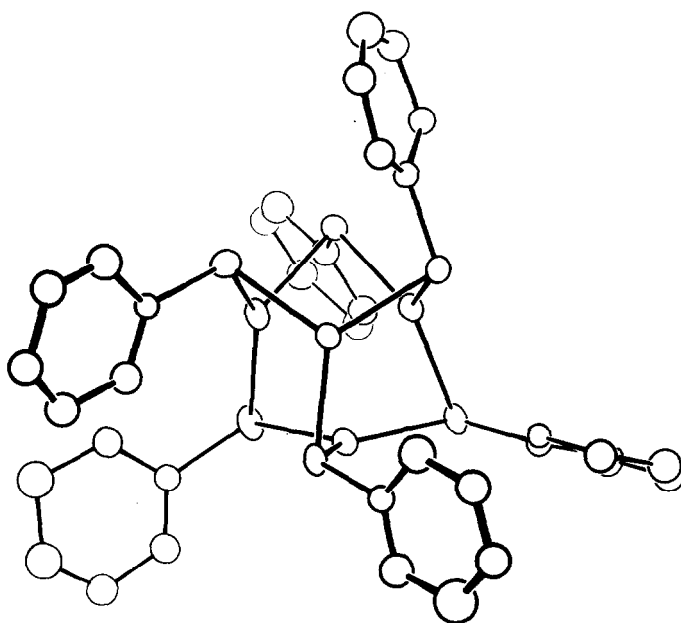
(3b)
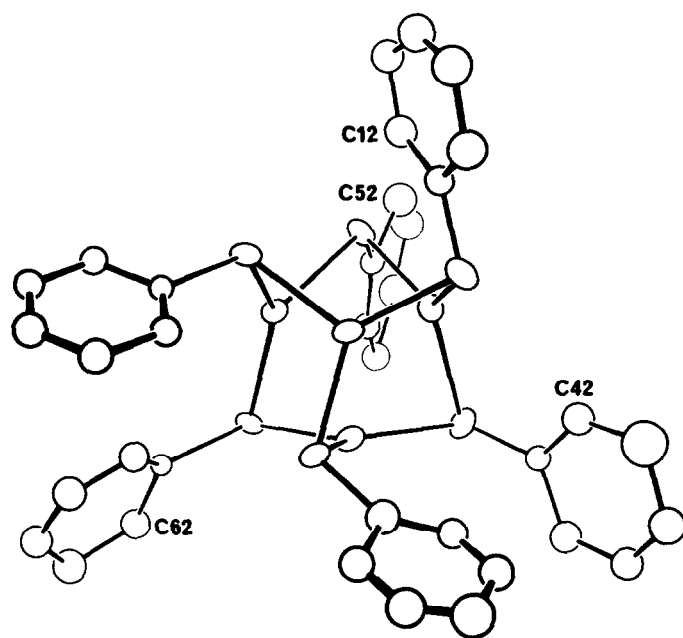
(3c)
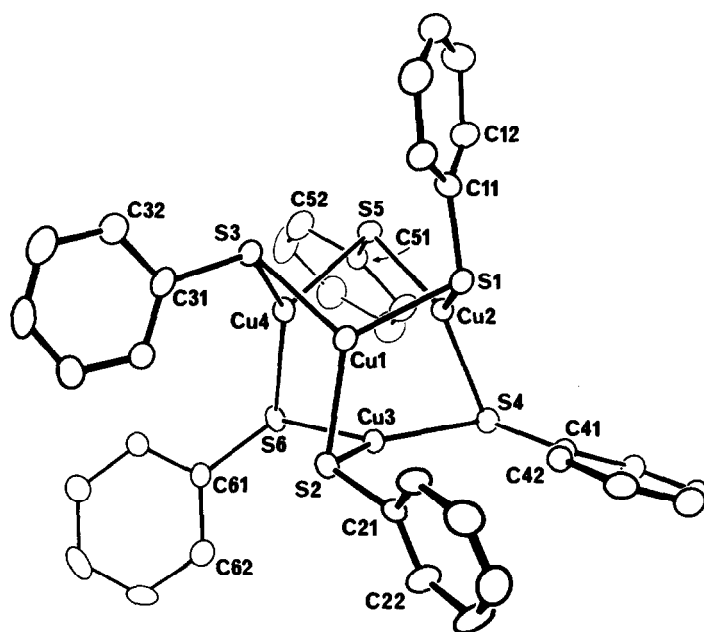
(3d)

Fig. 3. The four molecules $[Cu_4(SR)_6]^{2-}$, all oriented as Fig. 2(e). (a) $[Cu_4(SMe)_6]^{2-}$ (1). (b) $[Cu_4(SPh)_6]^{2-}$, molecule (2a). (c) $[Cu_4(SPh)_6]^{2-}$, molecule (2b). (d) $[Cu_4(SPh)_6]^{2-}$ (3). A common atom labelling scheme applies to all molecules, with cyclic numbering Cnm, m 1 to 6, on phenyl rings.

aee}, III. It may be noted that threefold propeller conformation of PhS ligands occurs around Cu1 and Cu2.

Intramolecular dimensions are presented and compared in Table 1. The mean values of the large populations of nominally equivalent dimensions are unexceptional. However, the main feature of

the set of cage dimensions is the occurrence of large and significant variances and excursions from mean values. In fact the cage framework is appreciably distorted from the tetrahedro-Cu_4-octahedro-S_6 ideal, and the details of the distortions allow some insight into the bonding forces in $[Cu_4(SR)_6]^{2-}$. The sample standard deviations

s,[14] (0.16Å) and range (3.67–4.33Å), of the S–S distances are proportionally much larger than the corresponding values (0.06, 2.64–2.85Å) for the Cu–Cu distances. Concomitant with this, the angles S–Cu–S (s 9.5; range 104.9–143.7°) are much more variable than angles Cu–S–Cu (s 1.6; range 70.2–76.7°). There is substantial angular flexibility in the cage bonds, occurring primarily as flapping variation of the bridging arms, affecting the S–S distances, rather than breathing variation of the CuS_3.planes affecting the Cu–Cu distances.

More detailed examination of these angular variations reveals that they are at least partly due to intramolecular repulsions between thiolate substituents. The standard deviation of S–S in $[Cu_4(SMe)_6]^{2-}$ is 0.10Å, while in the $[Cu_4(SPh)_6]^{2-}$ cages it is 0.18Å, consistent with more influential repulsive interactions between the larger phenyl groups. In all structures the S6–Cu4–S3 and S2–Cu3–S4 angles are larger than the remainder, and these are the only two angles which are subtended by an axial–axial pair of ligands. In the $[Cu_4(SPh)_6]^{2-}$ cages these two angles are 7–15° greater than the corresponding values for $[Cu_4(SMe)_6]^{2-}$. Concomitant with this, the S–Cu–S angles subtended by equatorial–equatorial pairs of

Table 1. Intramolecular dimensions (Å, degrees)

	(1)	(2a)	(2b)	(3)	(4) [a]
Cu1 - S1	2.276(2)	2.286(9)	2.272(9)	2.297(2)	2.274
Cu1 - S2	2.247(2)	2.247(10)	2.286(8)	2.276(2)	2.301
Cu1 - S3	2.284(2)	2.260(10)	2.309(10)	2.307(2)	2.310
Cu2 - S1	2.250(3)	2.299(10)	2.252(10)	2.292(2)	2.279
Cu2 - S4	2.304(3)	2.263(11)	2.303(9)	2.282(2)	2.306
Cu2 - S5	2.275(3)	2.265(10)	2.278(10)	2.258(2)	2.276
Cu3 - S2	2.281(3)	2.273(8)	2.290(9)	2.263(2)	2.271
Cu3 - S4	2.272(3)	2.299(8)	2.327(9)	2.265(2)	2.262
Cu3 - S6	2.315(3)	2.335(9)	2.329(10)	2.319(2)	2.316
Cu4 - S3	2.262(3)	2.250(10)	2.316(9)	2.288(2)	2.253
Cu4 - S5	2.293(3)	2.345(8)	2.349(7)	2.346(2)	2.338
Cu4 - S6	2.278(3)	2.286(10)	2.268(8)	2.265(2)	2.242

Mean (48) [b] = 2.287Å   s [c] = 0.027Å

	(1)	(2a)	(2b)	(3)	(4)
S1 - Cu1 - S2	123.1(1)	127.4(3)	131.7(4)	124.63(9)	115.8
S2 - Cu1 - S3	122.0(1)	120.4(3)	113.5(3)	122.97(9)	127.7
S3 - Cu1 - S1	114.7(1)	111.9(3)	114.4(3)	111.47(9)	116.1
S1 - Cu2 - S4	117.2(1)	117.9(3)	121.9(4)	119.71(9)	120.5
S4 - Cu2 - S5	115.9(1)	128.0(3)	115.5(4)	122.31(9)	117.1
S5 - Cu2 - S1	126.7(1)	114.0(3)	122.6(3)	117.75(9)	121.7
S2 - Cu3 - S4	127.7(1)	132.9(3)	135.4(4)	138.67(9)	138.1
S4 - Cu3 - S6	118.8(1)	104.9(3)	108.7(3)	111.49(8)	103.8
S6 - Cu3 - S2	113.0(1)	121.5(3)	115.7(3)	109.38(8)	117.8
S3 - Cu4 - S5	120.4(1)	108.2(3)	107.9(3)	107.26(9)	101.2
S5 - Cu4 - S6	111.1(1)	109.7(3)	116.2(3)	108.64(8)	120.8
S6 - Cu4 - S3	128.2(1)	141.7(3)	135.7(3)	143.69(9)	137.8

Mean (48) [b] = 119.9°   s = 9.5°

[a] From reference 3   [b] Mean excluding values from compound (4)

[c] $s = [\Sigma \Delta^2 / (n-1)]^{\frac{1}{2}}$

Table 1(b).

	(1)	(2a)	(2b)	(3)
Cu1 - S1 - Cu2	74.44(5)	75.5(3)	73.1(3)	76.67(7)
Cu1 - S2 - Cu3	73.67(5)	74.0(3)	73.0(2)	76.36(7)
Cu1 - S3 - Cu4	72.02(5)	73.1(3)	74.4(3)	70.18(7)
Cu2 - S4 - Cu3	72.14(6)	73.1(3)	73.1(3)	70.98(7)
Cu2 - S5 - Cu4	73.00(6)	72.4(3)	73.1(2)	75.27(7)
Cu3 - S6 - Cu4	74.83(7)	74.8(3)	71.3(3)	76.40(7)

Mean (24)   =   73.6°   s =   1.7°

	(1)	(2a)	(2b)	(3)
S1 - C11	1.88(1)	1.82(3)	1.76(3)	1.775(8)
S2 - C21	1.88(1)	1.66(3)	1.81(4)	1.766(8)
S3 - C31	1.81(1)	1.72(3)	1.76(3)	1.783(8)
S4 - C41	1.85(1)	1.84(3)	1.69(3)	1.783(8)
S5 - C51	1.78(1)	1.82(3)	1.82(3)	1.771(8)
S6 - C61	1.83(1)	1.78(3)	1.82(2)	1.777(8)

Mean (24)   =   1.79Å   s   =   0.05Å

	(1)	(2a)	(2b)	(3)
Cu1--Cu2	2.738(2)	2.806(5)	2.693(5)	2.846(1)
Cu1--Cu3	2.715(2)	2.721(6)	2.721(6)	2.806(1)
Cu1--Cu4	2.673(2)	2.686(6)	2.797(7)	2.641(1)
Cu2--Cu3	2.694(2)	2.716(6)	2.758(5)	2.640(1)
Cu2--Cu4	2.717(2)	2.722(5)	2.756(6)	2.812(1)
Cu3--Cu4	2.791(2)	2.806(7)	2.679(6)	2.835(1)

Mean (24)   =   2.74Å   s   =   0.06Å

Table 1(c).

	(1)	(2a)	(2b)	(3)
S1--S2	3.977(3)	4.06(1)	4.16(1)	5.040(3)
S1--S3	3.839(3)	3.77(1)	3.85(1)	3.804(3)
S1--S4	3.886(3)	3.91(1)	3.98(1)	3.955(3)
S1--S5	4.045(3)	3.83(1)	3.97(1)	3.895(3)
S2--S3	3.969(3)	3.91(1)	3.84(1)	4.027(3)
S2--S4	4.088(3)	4.19(1)	4.27(1)	4.237(3)
S2--S6	3.833(3)	4.02(1)	3.91(1)	3.740(3)
S3--S5	3.954(3)	3.72(1)	3.77(1)	3.731(3)
S3--S6	4.085(3)	4.29(1)	4.24(1)	4.326(3)
S4--S5	3.882(3)	4.07(1)	3.87(1)	3.976(3)
S4--S6	3.948(3)	3.67(1)	3.78(1)	3.789(3)
S5--S6	3.770(3)	3.79(1)	3.92(1)	3.746(3)

Mean (48) = 3.94Å   s = 0.16Å

	(1)	(2a)	(2b)	(3)
Cu1 - S1 - C11	104.4(3)	102(1)	103(1)	108.2(3)
Cu2 - S1 - C11	106.3(3)	112(1)	112(1)	108.3(3)
Cu1 - S2 - C21	107.1(4)	114(1)	118(1)	110.4(3)
Cu3 - S2 - C21	114.1(4)	117(1)	109(1)	111.4(3)
Cu1 - S3 - C31	109.7(4)	110(1)	113(1)	112.1(3)
Cu4 - S3 - C31	110.3(4)	112(1)	113(1)	115.7(3)
Cu2 - S4 - C41	101.7(3)	109(1)	110(1)	108.4(3)
Cu3 - S4 - C41	110.4(3)	112(1)	114(1)	113.2(3)
Cu2 - S5 - C51	103.5(4)	113(1)	110(1)	115.3(3)
Cu4 - S5 - C51	104.9(3)	105(1)	111(1)	101.0(3)
Cu3 - S6 - C61	102.9(3)	114(1)	113(1)	104.2(2)
Cu4 - S6 - C61	109.0(3)	116(1)	113(1)	110.5(3)

Mean (48) = 110.0°   s = 4.3°

ligands are consistently small in the $[Cu_4(SPh)_6]^{2-}$ cages, but not in $[Cu_4(SMe)_6]^{2-}$. Statistical consideration of all S–Cu–S angles in the $[Cu_4(SPh)_6]^{2-}$ cages according to substituent relative configuration yields:

a–a substituents, mean 138.0° (s 4.1°)
a–e substituents, mean 118.3° (s 6.2°)
e–e substituents, mean 108.1° (s 2.1°)

Corresponding mean values of S–Cu–S for $[Cu_4(SMe)_6]^{2-}$ are 128.0 (0.4); 118.0(5.4); 119.6(1.1) respectively. It can be concluded that intramolecular repulsions between phenyl substituents cause large angular distortions at trigonal copper, that corresponding repulsions between methyl substituents are much less, and that *inter*-molecular interactions between substituents also induce angular distortions primarily at the copper atoms.

The Cu–S distances in Table 1 range from 2.247 to 2.349Å, a difference almost as large as that between digonally (2.160Å) and trigonally (2.270Å) coordinated copper in $[Cu_5(SPh)_7]^{2-}$.[9] In the $[Cu_4(SR)_6]^{2-}$ structures the Cu–S distances reflect the variation of opposite S–Cu–S angles in the distorted trigonal coordination
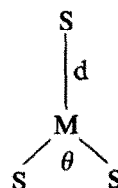
A plot of all 48 pairs d,θ reveals fair linear correlation, with some distinction between the SMe and SPh compounds. Linear regression, d = aθ + b, yields a = 2.90 × 10^{-3}Å deg^{-1}, b = 1.93 Å, r(correlation coefficient) = 0.84, for the 12 Cu–SCH$_3$ bonds in (1), and a = 2.05 × 10^{-3}Å deg^{-1}, b = 2.04Å, r = 0.75, for the 36 Cu-SPh bonds in (2a), (2b) and (3). This geometrical phenomenon must be largely electronic in origin. The regression analyses yield Cu–SCH$_3$ = 2.278 Å and Cu–SPh = 2.290 Å for ideal trigonal coordination.

All copper atoms in the five [Cu$_4$(SR)$_6$]$^{2-}$ molecules are located slightly *outside* the linked S$_3$ coordination planes of the S$_6$ octahedron. Details are given in Table 2, the mean displacement for all 20 copper atoms being 0.07Å. This effect will relieve slightly the acute angles at the sulphur atoms. We see no geometrical reason for including significant bonding interactions between copper atoms in [Cu$_4$(SR)$_6$]$^{2-}$, particularly in view of the outward displacements of the copper atoms, and the Cu–Cu distances (Table 1) which are long, as we have argued previously.[1,9]

Table 2. Molecular plane calculations

(A) Displacements (Å) of copper atoms from S$_3$ coordination planes: all displacements are to the outside of the S$_6$ octahedron.

	(1)	(2a)	(2b)	(3)	(4)
Cu1	0.05	0.08	0.08	0.13	0.06
Cu2	0.05	0.04	0.03	0.06	0.08
Cu3	0.08	0.12	0.07	0.09	0.06
Cu4	0.06	0.09	0.07	0.08	0.04

(B) Angles between S-C vectors and normals to CuSCu planes

Vector/plane	(1)	(2a)	(2b)	(3)
S1-C11/Cu1, S1, Cu2	19.4	22.7	22.9	23.6
S2-C21/Cu1, S2, Cu3	16.6	32.8	30.4	27.0
S3-C31/Cu1, S3, Cu4	15.0	26.6	29.2	29.8
S4-C41/Cu2, S4, Cu3	11.2	26.3	28.3	26.1
S5-C51/Cu2, S5, Cu4	17.8	24.5	25.7	25.9
S6-C61/Cu3, S6, Cu4	10.8	32.4	29.0	22.9
Mean (s[a])	15.1(3.5)[b]	27.0(3.1)[c]		

(C) Acute angles[d] between the normals to phenyl ring planes and the CuSCu planes

Ring	(2a)	(2b)	(3)
1	69.4	84.2	64.4
2	56.9	77.2	60.3
3	89.8	59.7	82.4
4	89.5	66.1	85.3
5	78.2	85.3	77.0
6	61.6	85.0	68.2

[a] s = [$\Sigma\Delta^2$/(n-1)]$^{\frac{1}{2}}$ [b] For [Cu$_4$(SMe)$_6$]$^{2-}$, (1), only

[c] For [Cu$_4$(SPh)$_6$]$^{2-}$, (2a), (2b), (3).

[d] This angle may range only between 90° and the complement of the corresponding angle

The geometrical structure around the sulphur atoms in $[Cu_4(SR)_6]^{2-}$ molecules also relates to the bonding in the cage and the difference between alkyl- and aryl-thiolate ligands in bridging positions. The stereochemistry at sulphur is necessarily distorted from pseudotetrahedral by the very acute Cu–S–Cu angle, which is 73.5 for both ligand types. However the data in Table 2 on the angles between the S–C vectors and the normals to the CuSCu planes at the bridging thiolate ligands show clear distinction between $[Cu_4(SMe)_6]^{2-}$, where the mean value of this angle is 15.1° (s 3.5°), and the molecules $[Cu_4(SPh)_6]^{2-}$ where the mean value is 27.0° (s 3.1°). The latter value is closer to the tetrahedral ideal of 35.3°. Close examination reveals that in both cases the acuteness of bonding at the bridging sulphur is clearly not due to steric repulsions between the substituents (in fact in $[Cu_4(SMe)_6]^{2-}$ the more acute bonding occurs at S4 and S6 where it *decreases* intramolecular separations between methyl groups). The differentiation between bridging methanethiolate and bridging benzenethiolate is more likely to be electronic in origin.

Angles relating to rotation of the SPh rings about the S–C vectors are also contained in Table 2. The similarity of conformation between molecules (2a) and (3) is again apparent.

In (3) the ethanol is not hydrogen bonded, and is poorly defined crystallographically.

Alternative cage structures. $[Cu_4(SR)_6]^{2-}$ is the smallest three-dimensional cage structure known and possible with monodentate ligands. There are limitations to the flexibility of the cage framework, and the angular distortions reported here are smaller than those observed in larger cage structures with bridging thiolate ligands.[9,10] The correlation of angular distortion with cage size allows straightforward rationalisation of the non-observation of the *hexahedro*-Cu₈-*icosahedro*-(SR)₁₂ cage structure shown in Fig. 4. The connectivity of linked coordination trigonal planes in $[Cu_4(SR)_6]^{2-}$ is around empty triangles as shown schematically in Fig. 5(a), while in $[Cu_8(SR)_{12}]^{4-}$ the coordination triangles are linked around empty quadrilaterals (Fig. 5b). The flexibility of the latter arrangement is much greater than that of the former. Indeed, $[Ag_6(SPh)_8]^{2-}$ contains four coordination trigonal planes linked as in Fig. 5(b), but with additional struts (additional digonal metal atoms bridging vertices) as shown schematically in Fig. 5(c), and yet is still very heavily distorted in the crystal.[10] Hypothetical $[Cu_8(SR)_{12}]^{4-}$, without such support, would have insufficient rigidity for independent existence. The Cu_8S_{12} framework oc-
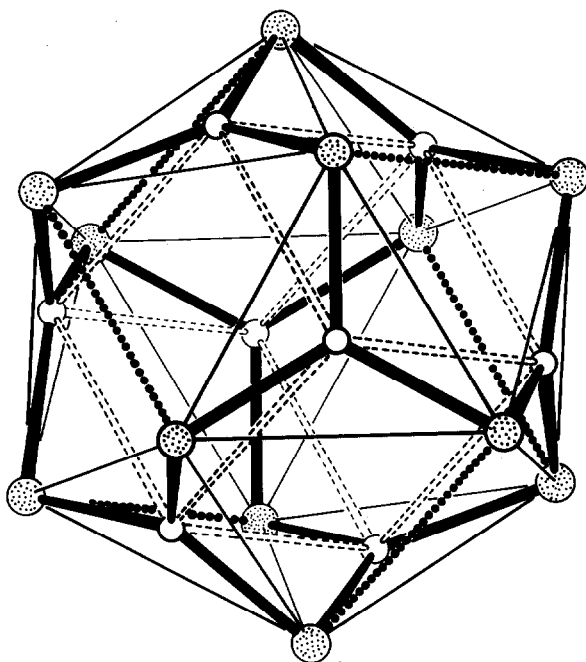
Fig. 4. The idealised *hexahedro*-M₈-*icosahedro*-SR)₁₂ structure. The six chelate linkages between sulfur atoms are denoted as . . . . . .

curs only when the quadrilaterals of Fig. 5(b) are braced (by chelation) as shown in Fig. 5(d) and Fig. 4.

An alternative means of structural stabilisation is a central spherical ligand.[6–8,11,15] We note that the compounds $(Me_4N)_2[Cu_4(SR)_6]$ R = Me, Ph crystallised from solutions containing excess Cl⁻ which might have served this function, but it appears that three bridging thiolate ligands saturate the coordination of copper(I) in these compounds.

Two other instances of the *tetrahedro*-Cu₄-*octahedro*-S₆ cage structure have been reported. One occurs with the monodentate thiocarbonyl ligand thiourea (tu) in $[Cu_4(tu)_6]$ $(NO_3)_4 4H_2O$.[16] Geometrically the $[Cu_4(tu)_6]^{4+}$ cage is similar to the $[Cu_4(SR)_6]^{2-}$ cage, in the pyramidal stereochemistry around bridging sulphur and the adoption of configurational isomer III, {aae, aae, aee, aee}. In addition, there is a' variability of S–Cu–S angles in $[Cu_4(tu)_6]^{4+}$, and the Cu atoms are further (0.07, 0.20, 0.23, 0.36Å) outside their trigonal coordination planes, a difference which leads to longer Cu–Cu distances (2.83–3.09Å).

The similarity of geometrical structure in $[Cu_4(tu)_6]^{4+}$ and $[Cu_4(SR)_6]^{2-}$ prompts inquiry about similarity of bonding at bridging sulphur. This would require substantial delocalisation of positive charge onto peripheral atoms in $[Cu_4(tu)_6]^{4+}$. The greater Cu–Cu distances in

$[Cu_4(tu)_6]^{4+}$ and the observation that these copper atoms will coordinate to additional thiourea ligands yielding $[Cu_4(tu)_9]^{4+}$ [16] and $[Cu_4(tu)_{10}]^{4+}$,[17] support the expected difference in bonding between uncharged thiourea and anionic thiolate in $[Cu_4(tu)_6]^{4+}$ and $[Cu_4(SR)_6]^{2-}$.

The Cu_4S_6 cage core also occurs in the chelate complex $[Cu_4(SP(Ph)_2NP(Ph)_2S)_3]^{+}$,[18] in which the ligand restricts the cage geometry.

EXPERIMENTAL

Synthesis. The preparation of (1) has been described.[12] Reagent grade solvents and reactants were used, without any special purification. All solutions were prepared and maintained in an atmosphere of dinitrogen.

Three compounds, $(Me_4N)_2[Cu_4(SPh)_6]$ (2), as pale yellow blocks, $(Me_4N)_2[Cu_4(SPh)_6]EtOH$ (3), as very pale yellow needles, and $(Me_4N)_2$ $[Cu_5(SPh)_7]^9$, crystallise from solutions of very similar composition, and frequently crystallise simultaneously from the one preparative solution. On the basis of a large number of preparative experiments it appears that solvent composition, temperature, and rate of nucleation are the main factors which determine the predominant product, but it has not yet been possible to devise reproduceable methods for crystallisation of (2) or (3) alone. In practice this is not a serious deficiency, as both compounds can be grown directly from the

(5c)

(5d)
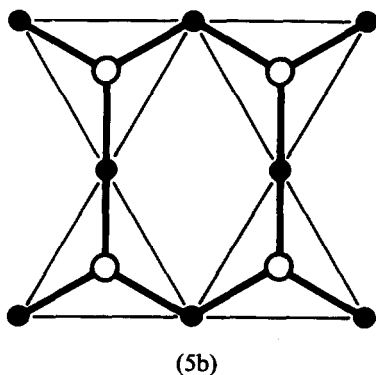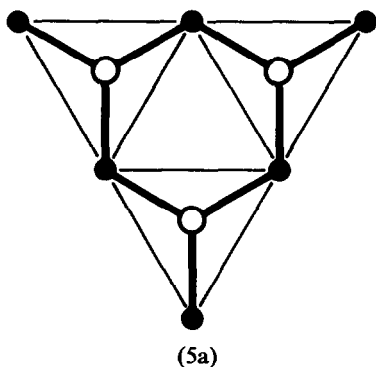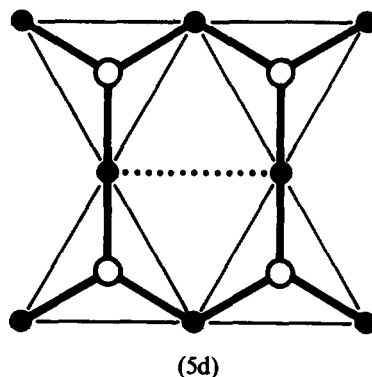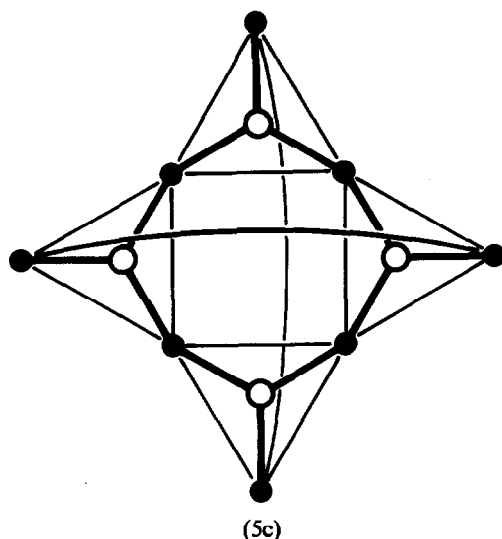
Fig. 5. Schematic planar representations of linkage modes for $Cu(\mu$-SR$)_3$ coordination triangles in related structure types: (a) around empty triangles in $Cu_4(SR)_6$; (b) around empty quadrilaterals in hypothetical $M_8(SR)_{12}$; (c) around a square in $Ag_6(SR)_8$ but braced with additional connections; (d) around quadrilaterals but stabilised by chelation (...) in $M_8(S ... S)_6$.

(5a)

(5b)

reaction mixture as large crystals which can be easily separated manually.

The following are representative experiments.

(a) A solution containing benzenethiol (6.0 g, 54 mmol), tri-*n*-butylamine (9.5 g, 51 mmol) and tetramethylammonium chloride (4.5 g, 41 mmol) in a mixture of absolute ethanol (100 cm³), methanol (50 cm³) and acetonitrile (30 cm³), was prepared at 50°C. To this a solution of copper(II) nitrate trihydrate (3.3 g, 13.7 mmol) in absolute ethanol (50 cm) was added rapidly with efficient stirring. Any precipitated CuSPh redissolved within about 2 min at 50°C, when the flask was sealed and allowed to cool slowly without disturbance. Crystallisation began almost immediately, and was allowed to continue for 3 days at room temperature. The product for (3.6 g) was separated,

washed with chloroform, and dried in nitrogen at 1 atm. It consisted of approximately equal amounts of pale yellow blocks (**2**) and needles (**3**).

(b) A yellow solution with the following composition was prepared as in (a): PhSH (6.0 g), Bu$_3$N (9.5 g), Me$_4$NCl (4.5 g), Cu(NO$_3$)$_2$3H$_2$O (2.4 g, 9.9 mmol), absolute ethanol (250 cm^3), methanol (25 cm^3), acetonitrile (50 cm^3). Crystallisation began soon after the commencement of cooling from 60°C, and was completed during 2 days at 0°C. The product, washed with CHCl$_3$ and dried with nitrogen gas, was almost totally (**2**) as well formed pale yellow blocks. Yield *ca.* 2.5 g. This crystallisation mixture contained a higher PhS$^-$/Cu ratio than in (a).

(c) In similar manner the following yellow solution containing *n*-propanol was prepared: PhSH (6.0 g), Bu$_3$N (9.5 g), Me$_4$NCl (4.5 g), Cu(NO$_3$)$_2$3H$_2$O (2.4 g), absolute ethanol (70 cm^3), *n*-propanol (180 cm^3), methanol (25 cm^3) acetonitrile (75 cm^3). Crystallisation began 1 hr after slow cooling from 60°, and was allowed to continue for 2 days at room temperature. The product contained mainly beautiful large blocks of (**2**), together with smaller bright yellow blocks of (Me$_4$N)$_2$[Cu$_5$(SPh)$_7$].

Needles of (**3**) contain solvent which is readily lost on pumping or open exposure at room temperature. *Anal.* (**2**): Calc. for (Me$_4$N)$_2$Cu$_4$(SPh)$_6$: C, 49.98; H, 5.15; N, 2.65; Cu, 24.03; S, 18.19. Found: C, 49.86; H, 5.31; N, 2.70; Cu, 24.00; S, 18.36.

The presence of ethanol in (**3**) was established by diffraction analysis, for which a single crystal was sealed in a capillary tube together with crushed crystals of the same compound.

Crystals of (**2**) and (**3**) react with oxygen, developing a dark brown coating after 24 hr at room temperature. Both compounds are soluble in acetonitrile and acetone to give pale yellow solutions, and in pyridine to give a strongly yellow solution, all solutions being decomposed rapidly by oxygen. Recrystallisation of (**2**) or (**3**) is complicated by dissociation to CuSPh, which is insoluble.

Crystallography. The following general information applies to the three crystals. Data were collected at 294 K; scattering factors for uncharged atoms were from International Tables,[19] all least squares calculations minimised $\Sigma w(|F_0| - |F_c|)^2$; residuals quoted are $R = \Sigma \|F_0| - |F_c\|/\Sigma|F_0|$, $R_w = [\Sigma w(|F_0| - |F_c|)^2/\Sigma w|F_0|^2]^{1/2}$; in both SPh compounds phenyl ring hydrogen atoms were maintained at calculated positions with thermal parameters equal to those of connected atoms; a common atom labelling scheme is used for the three crystals (see Fig. 3).

Compound (**1**). (Me$_4$N)$_2$[Cu$_4$(SMe)$_6$], C$_{14}$H$_{42}$-Cu$_4$N$_2$S$_6$, M = 685.00; colourless hexagonal plates, trigonal space group P3c1 (no. 158); a = 16.777(2), c = 17.540(2)Å, γ = 120°, U = 4275.5Å, D$_M$ = 1.60 gcm^{-3} (flotation in *n*-hexane/1,3-dibromopropane), Z = 6, D$_{calc}$ = 1.60 gcm^{-3}; F(000) = 2112. Nickel filtered CuK$_\alpha$ radiation, λ = 1.5418Å, μ = 74.2 cm^{-1}; crystal habit {001}{110}{120} {$\bar{1}$21}($\bar{1}\bar{1}$1), specimen dimensions 0.33 × 0.32 × 0.20 mm. Intensity data (Siemens AED diffractometer) to θ_{max} 65° by $\theta/2\theta$ scan, with intensity standard decreasing 1→0.9. Decay and analytical absorption corrections were applied, I = N$_p$ − N$_b$, σ(I) = [N$_p$ + N$_b$ + (0.04N$_p$)^2]$^{1/2}$, yielding 2380 unique reflections with I/σ(I) > 2.58.

Structure determination was effected by MULTAN and difference Fourier methods. It was found that one cation (N4) occupied a general position while the second was situated about a set of special positions. Each atom lying on the threefold axis was assigned a multiplicity of one-third. Refinement of parameters, initially with unit weights and isotropic temperature factors for all atoms, returned R = 0.158. In subsequent least squares w = 4|F$_0$|^2/σ^2(F$_0^2$) and anisotropic temperature factors were assigned to the copper and sulfur atoms, converging at R = 0.057. The carbon atoms attached to N3 and the tetramethylammonium ions on special positions did not refine well, and therefore were repositioned by difference Fourier and not refined further. The final refinement, with anisotropic temperature factors assigned to all non-hydrogen atoms in the anion and in the cation at general position, converged at R = 0.041, R$_w$ = 0.046.

Compound (**2**). (Me$_4$N)$_2$[Cu$_4$(SPh)$_6$], C$_{44}$H$_{54}$-Cu$_4$S$_6$N$_2$, M = 1057.47, pale yellow blocks, monoclinic space group P2$_1$/c, a = 23.733(3), b = 12.428(2), c = 35.853(4)Å, β = 106.84(2)°, U = 1.0121 × 10^{4}Å^3, Z = 8, D$_{calc}$ = 1.39 gcm^{-3}. Nickel filtered CuK$_\alpha$ radiation, μ = 43.7 cm^{-1}, crystal habit {100}{001}{101}{102}, specimen dimensions 0.17 × 0.25 × 0.31 mm. Intensity data (Siemens AED diffractometer) by $\theta/2\theta$ scan, with corrections for absorption and for intensity loss due to appreciable crystal decay, 7234 intensity measurements yielded 4110 unique reflections with I/σ(I) > 2.58.

The structure was determined by MULTAN and Fourier methods, and refined by blocked matrix least squares, w = [σ(F$_0$)]$^{-2}$. Refinement with anisotropic temperature factors for copper and sulfur atoms converged at R = 0.111, R$_w$ = 0.089 for 3598 reflections with sinθ/λ > 0.2. A difference Fourier revealed peaks (maximum electron density

$2.6\text{e}\text{Å}^{-3}$) near the copper atoms, attributed to errors in the data caused by the X-radiation damage to the crystal, and also some evidence for a partially occupied alternative Me_4N^+ cation site. In view of the limited quality of the data, further modelling of the structure was not attempted. In the final least squares cycle all positional parameters for atoms bonded together were included in the same block: $R = 0.105$, $R_w = 0.085$ (3598 data, $\sin\theta/\lambda > 0.2$).

Compound (3). $(Me_4N)_2[Cu_4(SPh)_6].C_2H_5OH$, $C_{46}H_{60}Cu_4S_6N_2O$, $M = 1103.54$, pale yellow needles losing solvent on exposure, monoclinic spacegroup $P2_1/a$, $a = 19.125(2)$, $b = 15.433(1)$, $c = 17.500(2)\text{Å}$, $\beta = 103.73(1)°$, $U = 5017.6\text{Å}^3$, $Z = 4$, $D_{calc} = 1.46\,\text{gcm}^{-3}$. Monochromatised MoK_α radiation, crystal habit $\{011\}$, $\{001\}$, $\{100\}$, specimen dimensions $0.20 \times 0.22 \times 0.38$ mm, specimen sealed in capillary with crushed sample to prevent solvent loss, intensity data (Syntex $P_{\bar{1}}$ diffractometer) by $\theta/2\theta$ scan. Corrections for absorption, found by psi-cans to cause less than 6% variation in F^2 (2.5% in F), were not applied. The data set contained 3370 independent reflections with $I > 2\sigma(I)$. The structure was solved by MULTAN and Fourier methods, and refined normally $(w = [\sigma(F)]^{-2})$ with anisotropic thermal parameters for all non-hydrogen atoms. The oxygen and carbon atoms of the ethanol were not well defined, with large thermal motion. On completion of refinement, $R = 0.044$, $R_w = 0.054$, and $[\Sigma w(\Delta F)^2/(m - n)]^{1/2} = 1.21$, for 3370 reflections (m) and 532 variables (n).

Atomic coordinates and thermal parameters for the three structures have been deposited with the Editor as supplementary material; copies are available on request. Atomic coordinates have been deposited with the Cambridge Crystallographic Data Centre.

REFERENCES

1. G. A. Bowmaker, G. R. Clark and D. K. P. Yuen, *J. Chem. Soc. Dalton* 1976, 2329.
2. I. G. Dance and J. C. Calabrese, *Inorg. Chim. Acta* 1976, **19**, L41.
3. D. Coucouvanis, C. N. Murphy and S. K. Kanodia, *Inorg. Chem.* 1980, **19**, 2993.
4. F. J. Hollander and D. Coucouvanis, *J. Am. Chem. Soc.* 1977, **99**, 6268.
5. P. J. M. W. L. Birker and G. C. Verschoor, *J. Chem. Soc. Chem. Comm.* 1981, 322.
6. P. J. M. W. L. Birker and H. C. Freeman, *J. Am. Chem. Soc.* 1977, **99**, 6890.
7. H. J. Schugar, C. C. Ou, J. A. Thich, J. A. Potenza, T. R. Felthouse, M. S. Haddad, D. N. Hendrickson, W. Furey and R. A. Lalancette, *Inorg. Chem.* 1980, **19**, 543.
8. (a) P. J. M. W. L. Birker, *Inorg. Chem.*, 1979, **18**, 3502; (b) P. J. M. W. L. Birker, J. Reedijk and G. C. Verschoor, *Inorg. Chem.* 1981, **20**, 2877.
9. I. G. Dance, *Austral. J. Chem.* 1978, **31**, 2195.
10. I. G. Dance, *Inorg. Chem.* 1981, **20** 1487.
11. I. G. Dance, *J. Chem. Soc. Chem. Comm.* 1980, 818.
12. G. A. Bowmaker and L. C. Tan, *Aust. J. Chem.* 1979, **32**, 1443.
13. The code to convert atom labels used for $(Ph_4P)_2[Cu_4(SPh)_6]^3$ to those used here is Cu1→Cu4, Cu2→Cu1, Cu3→Cu2, Cu4→Cu3, S1→S5, S2→S1, S3→S6, S4→S6, S4→S2, S5→S4, S6→S3.
14. $s = [\Sigma\Delta^2/(n - 1)]^{1/2}$.
15. H. B. Bürgi, H. Gehrer, P. Strickler and F. K. Winkler, *Helv. Chim. Acta*, 1976, **59**, 2558.
16. E. H. Griffith, G. W. Hunt and E. L. Amma, *J. Chem. Soc. Chem. Comm.*, 1976, 432.
17. I. G. Dance and A. E. Landers, in preparation.
18. C. P. Huber, M. L. Post and O. Siiman, *Acta Cryst.*, 1978, **B34**, 2629.
19. *International Tables for X-ray Crystallography*, Vol. IV, Tables 2.2A and 2.3.1. Kynoch Press, Birmingham (1974).

LIGAND EXCHANGE PROCESSES IN SOME IRON–SULPHUR-CARBONYL AND -NITROSYL COMPLEXES

ANTHONY R. BUTLER, CHRISTOPHER GLIDEWELL,* ANDREW R. HYDE
JOSEPH McGINNIS and JULIE E. SEYMOUR
Chemistry Department, University of St. Andrews, St. Andrews, Fife KY16 9ST, Scotland

Abstract—The complex $[Fe_2(SMe)_2(CO)_6]$ undergoes stepwise exchange with Et_2S_2 to yield successively $[Fe_2(SMe)(SEt)(CO)_6]$ and $[Fe_2(SEt)_2(CO)_6]$. Carbonyl complexes $[Fe_2(SR)_2(CO)_6]$ are efficiently converted to the nitrosyls $[Fe_2(SR)_2(NO)_4]$ by the action either of NO gas or of methanolic sodium nitrite: the analogous species $[Fe_2S_2(CO)_6]$, $[Fe_2S_2(CO)_6]^{2-}$, and $[Fe_3S_2(CO)_9]$ all, with methanolic nitrite, yield $[Fe_4S_3(NO)_7]^-$. This anion, $[Fe_4S_3(NO)_7]^-$, reacts with sulphur to give the cubane-like $[Fe_4S_4(NO)_4]$: the synthesis of its selenium analogue, $[Fe_4Se_3(NO)_7]^-$ is described. The complexes $[Fe_2(SR)_2(NO)_4]$ (R = Me, Et, Pr^n, Pr^i, Bu^t, $PhCH_2$) all consist of two isomers in solution, presumed to have structures of C_{2h} and C_{2v} symmetry: activation parameters for the $C_{2h} \rightleftharpoons C_{2v}$ reaction are reported.

In recent years a wide range of iron–chalcogen-carbonyl complexes, containing terminal carbonyl ligands bonded to an iron–chalcogen core, have been synthesized:[1–7] these complexes have been studied primarily from the standpoints of structural characterization in the solid state,[7–11] and in the case of the *S*-alkylated complexes $[Fe_2(SR)_2(CO)_6]$, of their fluxional behaviour in solution.[5,6] Closely analogous to, and formally isoelectronic with the $[Fe_2(SR)_2(CO)_6]$ are the nitrosyls $[Fe_2(SR)_2(NO)_4]$:[12,13] these are the esters of Roussin's red salt $[Fe_2(S_2)_2(NO)_4]^{2-}$,[14] and the structure of the ethyl ester in the solid state has been determined.[15] A further analogy between the carbonyls and nitrosyls is provided by the anion $[Fe_2S_2(CO)_6]^{2-}$,[16,17] whose chemistry has been compared with that of $[Fe_2S_2(NO)_4]^{2-}$.

We have demonstrated[18] a simple method for converting $[Fe_2(SMe)_2(CO)_6]$ into $[Fe_2(SMe)_2(NO)_4]$, and have sought to exploit this type of conversion as a means of preparing a range of derivatives $[Fe_2(SR)_2(NO)_4]$, from the readily accessible carbonyls: one of our objectives was to explore routes to suitably functionalised nitrosyl complexes which might have solubility characteristics similar to those of the salts of $[Fe_4S_3(NO)_7]^-$,

which are freely soluble both in water and in many of the common organic solvents.[14] In the present paper we report upon the exchange reactions of $[Fe_2(SR)_2(CO)_6]$ with disulphides $R_2'S_2$; on the nitrosylation not only of $[Fe_2(SR)_2(CO)_6]$, but of a number of other iron–sulphur-carbonyl species also; on the inter-conversion of some tetra-iron complexes; and finally on the results of a variable-temperature NMR study of $[Fe_2(SR)_2(NO)_4]$ for R = Me, Et, Pr^n, Pr^i, Bu^t, and $PhCH_2$.

RESULTS AND DISCUSSION

Di-iron complexes

An attractive possibility for the synthesis of compounds $[Fe_2(SR)_2(CO)_6]$ in cases where the thiol RSH and the disulphide RSSR are of low volatility is the exchange reaction with $[Fe_2(SMe)_2(CO)_6]$ (eqn 1).

$$Fe_2(SMe)_2(CO)_6 + RSSR \rightarrow$$
$$Me_2S_2 + Fe_2(SR)_2(CO)_6. \quad (1)$$
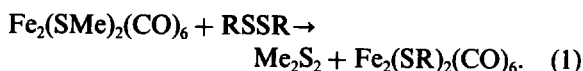
This possibility was investigated initially for the case of R = Et. Although $[Fe_2(SEt)_2(CO)_6]$ is indeed formed, the reaction does not proceed as shown in eqn (1); when the composition of the reaction mixture was monitored over time by mass spectrometry, it was clear that the product initially formed was the mixed alkyl thiolate disulphide

---

*Author to whom correspondence should be addressed.

$[Fe_2(SMe)(SEt)(CO)_6]$, and that the formation of the di-ethyl product was very much slower (eqn 2).

$$Fe_2(SMe)_2(CO)_6 \xrightarrow{Et_2S_2} Fe_2(SMe)(SEt)(CO)_6$$

$$\xrightarrow{Et_2S_2} Fe_2(SEt)_2(CO)_6. \qquad (2)$$
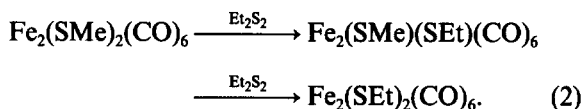
A number of distinct mechanistic possibilities for the formation of the intermediate $[Fe_2(SMe)(SEt)(CO)_6]$ were examined: exchange between Me_2S_2 and Et_2S_2 to yield MeSSEt was found to be extremely slow, and could therefore be ruled out. For effective exchange between pairs of disulphides, catalysis by SH^- or SR^- is necessary.[19] Similarly, it was found that in the reaction between $[Fe_2(SMe)_2(CO)_6]$ and $[Fe_2(SEt)_2(CO)_6]$, the formation of $[Fe_2(SMe)(SEt)(CO)_6]$ was very much slower, under identical conditions, than the formation of the mixed compound from $[Fe_2(SMe)_2(CO)_6]$ and Et_2S_2: this observation, and the fact that a mechanism involving exchange between the two di-iron complexes would require the formation of $[Fe_2(SEt)_2(CO)_6]$ to precede, rather than follow, the formation of $[Fe_2(SMe)(SEt)(CO)_6]$, allows the elimination of this possibility.

There remains the possibility of the stepwise replacement of SR groups, with concommitant formation of EtSSMe (eqn 3).

$$Fe_2(SMe)_2(CO)_6 + Et_2S_2 \longrightarrow EtSSMe$$
$$+ Fe_2(SMe)(SEt)(CO)_6. \qquad (3)$$
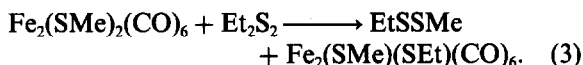
This was confirmed by the identification by GC/MS of EtSSMe amongst the reaction products, and by following the rate of its formation alongside the rate of formation of $[Fe_2(SMe)(SEt)(CO)_6]$. Since simple thiols RSH do not participate in such an exchange process, despite the volatility of MeSH (eqn 4):

$$Fe_2(SMe)_2(CO)_6 + RSH \nrightarrow MeSH$$
$$+ Fe_2(SMe)(SR)(CO)_6 \qquad (4)$$
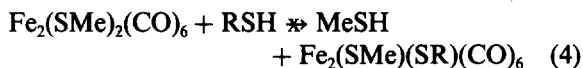
we conclude that the exchange depends upon the supernucleophilicity (α effect) arising from the two adjacent sulphur atoms (eqn 5).

Having demonstrated the occurrence of RS exchange we then turned to a more complex RSSR species, the disulphide $(MeOCOCH_2S)_2$ derived from methylthioglycolate by oxidation.[19] Surprisingly this showed no exchange with $[Fe_2(SMe)_2(CO)_6]$ under conditions in which Et_2S_2 had reacted readily: possibly the carboxyl groups reduce the nucleophilicity of the disulphide group sufficiently to prevent effective reaction. Consequently, in order to attempt the preparation of $[Fe_2(SCH_2COOMe)_2(CO)_6]$, we reverted to the reaction of $Fe_2(CO)_{12}$ with R_2S_2:[12] when the disulphide was in 5-fold excess, the desired product was obtained, although contaminated with the excess of the disulphide. On the other hand when the $Fe_3(CO)_{12}$ was in 2.5 fold excess, the compound $[Fe_2(SCH_2COOMe)_2(CO)_6]$ was formed in only very low yield, after 2 hr reflux and the major products were $[Fe_2S_2(CO)_6]$ and $[Fe_3S_2(CO)_9]$: on longer reflux (e.g. 5 hr), $[Fe_2(SCH_2COOMe)_2(CO)_6]$ increased in abundance at the expense of $[Fe_2S_2(CO)_6]$ and $[Fe_3S_2(CO)_9]$. This reaction is thus rather reminiscent of those, studied by King,[20] of $Fe_3(CO)_{12}$ and episulphides. The product of King's reactions turned out[11] to be a 1:1 compound of $[Fe_2S_2(CO)_6]$ and $[Fe_3S_2(CO)_9]$: this compound survived sublimation unchanged, although in our own system the two components are readily separable by chromatography. The results of the $[Fe_3(CO)_{12}/(SCH_2COOMe)_2$ reaction suggested that the compounds $[Fe_2S_2(CO)_6]$ and $[Fe_3S_2(CO)_9]$ might be intermediates: alternatively their disappearance as the reaction proceeds could be due simply to decomposition rather than to consumption by reaction with R_2S_2 with concommitant formation of $[Fe_2(SR)_2(CO)_6]$. We find in fact that the reactions of $[Fe_2S_2(CO)_6]$ and of $[Fe_3S_2(CO)_9]$ with $(SCH_2COOMe)_2$ do not yield any $[Fe_2S_2(SCH_2COOMe)_2]$ so that these iron-sulphur carbonyls are not intermediates in the formation of the Roussin-type ester. On the other hand both are formed by reaction of $Fe_3(CO)_{12}$ with elemental sulphur, and both slowly decompose (presumably to carbon monoxide and iron sulphides) on reflux alone: their formation therefore represents merely a side reaction in this process.

Finally we note for the sake of completeness that

$$(5)$$
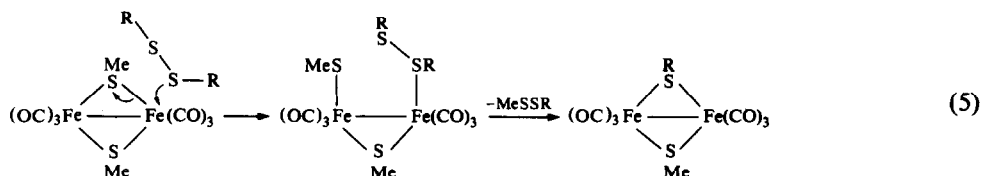
Table 1. Nitrosation reactions

Reactant	Method [a]	Product	Yield/%
$Fe_2(CO)_9$	A	$Fe(CO)_2(NO)_2$	b
$Fe_3(CO)_{12}$	A	$Fe(CO)_2(NO)_2$	b
$Fe_2(SMe)_2(CO)_6$	A	$Fe_2(SMe)_2(NO)_4$	33
$Fe_2(SMe)_2(CO)_6$	B	$Fe_2(SMe)_2(NO)_4$	29[c]
$Fe_2(SEt)_2(CO)_6$	A	$Fe_2(SEt)_2(NO)_4$	33
$Fe_2S_2(CO)_6$	A	$Fe_4S_3(NO)_7^-$	79
$Fe_2S_2(CO)_6$	B	No reaction	-
$Fe_2S_2(CO)_6^{-2}$	A	$Fe_4S_3(NO)_7^-$	82
		$Fe_2S_2(NO)_4^{-2}$	9
$Fe_2S_2(CO)_6^{-2}$	B	d	-
$Fe_3S_2(CO)_9$	A	$Fe_4S_3(NO)_7^-$	53
$Fe_3S_2(CO)_9$	C	$Fe_4S_3(NO)_7^-$	81
$Fe_3S_2(CO)_9$	B	No reaction	-

a. For identification of procedures A, B, C, see experimental part.

b. Volatile product; yield not measured.

c. Yield for room temperature reaction: yield rises to 92% if mixture refluxed

     during passage of NO (see text).

d. Trace only of nitrosylated product, not identified.

$[Fe_2(SMe)_2(NO)_4]$ can be prepared by reaction of Me_2S_2 with $Fe(NO)_2(CO)_2$ (eqn 6)

$$2Fe(NO)_2(CO)_2 + Me_2S_2 \rightarrow Fe_2(SMe)_2(NO)_4 + 4CO. \tag{6}$$
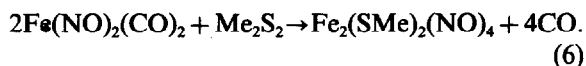
This preparation is entirely analogous to that for the selenium–iron complex $[Fe_2(SeEt)_2(NO)_4]$, reported by Hieber and Beck.[21] This reaction, and that of $Hg[Fe(CO)_3NO]_2$ with elemental sulphur to yield $[Fe_4S_4(NO)_4]$,[22] both conducted under reflux at high temperature, both involve complete displacement of carbonyl ligands and complete retention of nitrosyl ligands, and, as such, must testify to the extreme robustness of the (FeNO) fragment in these complexes. This very strong binding of the nitrosyl ligand to iron has been remarked upon previously,[23] and seems, in diamagnetic complexes at least, not to be dependent upon any particular formal oxidation state of the iron: in all these systems, the nitrosyl is formally present as NO^+.

Nitrosylation reactions

Reaction of $Fe(CO)_5$ with nitrite in alkaline aqueous methanol yields[24] the anion $[Fe(CO)_3NO]^-$, readily isolable as its mercury derivative

$Hg[Fe(CO)_3NO]_2$: further treatment of the anion with nitrite in the presence of a weak acid, such as acetic acid yields the neutral $[Fe(CO)_2(NO)_2]$, where the overall reaction represents replacement of three carbonyl groups with two nitrosyl groups. Since many of the known iron–sulphur-carbonyl complexes contain $Fe(CO)_3$ fragments in which all the carbonyl ligands are terminal,[7,9–11,15] we have explored the reactions of a number of such complexes with methanolic nitrite. The results of this study are summarised in Table 1, along with those for some similar nitrosation reactions which use NO as the nitrosating agent.

The binary carbonyls $Fe_2(CO)_9$ and $Fe_3(CO)_{12}$ were studied first, to establish the generality of this procedure: both carbonyls yield $[Fe(CO)_2(NO)_2]$ as the only iron-nitrosyl product. The complexes $[Fe_2(SR)_2(CO)_6]$ (R = Me, Et) both readily yield the analogous nitrosyl with Procedure A (see Experimental for details), as does $[Fe_2(SMe)_2(CO)_6]$ when subjected to Procedure B, (nitrosation by NO gas). At room temperature or below, the use of NO gas in an organic medium does not effect complete conversion of $[Fe_2(SMe)_2(CO)_6]$ to $[Fe_2(SMe)_2(NO)_4]$, but separation of the two complexes was readily achieved by fractional crystallisation. However if

the mixture is refluxed during the passage of the NO gas, no carbonyl complex remains, and the conversion is almost quantitative, giving a 92% yield of [Fe$_2$(SMe)$_2$(NO)$_4$].

The complexes [Fe$_2$S$_2$(CO)$_6$], [Fe$_2$S$_2$(CO)$_6$]$^{2-}$, and [Fe$_3$S$_2$(CO)$_9$] all yield the anion of Roussin's black salt,[14] [Fe$_4$S$_3$(NO)$_7$]$^-$ in good yield when nitrosylated according to Procedure A: in the case of [Fe$_2$S$_2$(CO)$_6$]$^{2-}$ as reactant the anion [Fe$_4$S$_3$(NO)$_7$]$^-$ is accompanied by a low yield of [Fe$_2$S$_2$(NO)$_4$]$^{2-}$, the anion of Roussin's red salt.[14] Reaction of these three complexes with NO gas in an inorganic solvent (Procedure B) effects negligible nitrosylation, whereas reaction of [Fe$_3$S$_2$(CO)$_9$] with NO gas in an alkaline medium again gave an excellent yield of [Fe$_4$S$_3$(NO)$_7$]$^-$. In addition to these observations, we note that the action of NO gas upon [Fe$_2$(SCF$_3$)$_2$(CO)$_6$] has been reported[25] to give [Fe$_2$(SCF$_3$)$_2$(NO)$_4$]. In view of the readily available carbonyl complexes [Fe$_2$(SR)$_2$(CO)$_6$], this preparation of the analogous nitrosyl species provides an efficient alternative route to these complexes.

While we cannot suggest with confidence the identity of any intermediates in these nitrosylation reactions, we note that an equimolar mixture of [Fe$_2$(SMe$_2$)(CO)$_6$] and [Fe$_2$(SEt)$_2$(CO)$_6$], when nitrosylated by procedure A gave no evidence for the formation of the mixed species [Fe$_2$(SMe)(SEt)(NO)$_4$], despite a 4 hr reflux. This suggests that the Fe$_2$S$_2$ framework remains intact, with no formation either of monomeric fragments [Fe(SR)(CO)$_3$] or [Fe(SR)(NO)$_2$] or of ions RS$^-$ + Fe(CO)$_3^+$ or Fe(NO)$_2^+$: in contrast the μ-iodo complex Fe$_2$I$_2$(NO)$_4$ has been shown to ionise completely to Fe(NO)$_2^+$ and I$^-$.[26]

Tetra-iron complexes

The first example of a tetra-nuclear iron-sulphur nitrosyl to be characterised was the anion [Fe$_4$S$_3$(NO)$_7$]$^-$ of Roussin's black salt,[14] the crystal structures of two of whose salts have been determined[27,28] Reaction of salts of this anion with elemental sulphur in refluxing toluene leads to formation of the cubane-like complex [Fe$_4$S$_4$(NO)$_4$], first prepared by reaction of Hg[Fe(CO)$_3$NO]$_2$ with elemental sulphur.[22] This reaction could be simply the completion of the Fe$_4$S$_4$ framework by addition of a sulphur to the existing Fe$_4$S$_3$ framework, or alternatively, it might proceed by means of a large scale fragmentation and subsequent re-formation of the iron–sulphur skeleton.

The reaction of the mercurial Hg[Fe(CO)$_3$NO]$_2$ with elemental selenium similarly yields a black, rather labile compound whose IR and UV spectra are very similar to those of [Fe$_4$S$_4$(NO)$_4$] [ν(NO),

1785 cm^{-1}; λ(max), 270 nm] and which may be the analogous [Fe$_4$Se$_4$(NO)$_4$], although we have not succeeded in obtaining an analytical sample of this material. On brief (e.g. 2hr) reflux of the mercurial with selenium, no such compound is formed. Reaction of salts of [Fe$_4$S$_3$(NO)$_7$]$^-$ with elemental selenium in refluxing toluene again gives a material having the characteristic IR and UV spectra of the cubane species. This latter could be either [Fe$_4$S$_3$Se(NO)$_4$] if the reaction simply involves framework completion, or it could be a more complex mixture of species [Fe$_4$S$_x$Se$_{4-x}$(NO)$_4$] if the reaction proceeds by fragmentation and reformation. Further study of this point is in progress.

In contrast to its reaction with elemental sulphur, the mercurial Hg[Fe(CO)$_3$NO]$_2$ reacts with aqueous methanolic polysulphide solutions at room temperature to yield salts of [Fe$_4$S$_3$(NO)$_7$]$^-$; these conditions are not sufficiently vigorous to effect the further conversion of [Fe$_4$S$_3$(NO)$_7$]$^-$ to [Fe$_4$S$_4$(NO)$_4$]. We note that the reverse conversion of [Fe$_4$S$_4$(NO)$_4$] to [Fe$_4$S$_3$(NO)$_7$]$^-$ has also been effected.[28]

Just as reaction of a solution of ammonium sulphide and nitrite with iron(II) yields salts of [Fe$_4$S$_3$(NO)$_7$]$^-$, so also a solution of sodium hydrogen-selenide and nitrite reacts with iron(II) to yield the anion [Fe$_4$Se$_3$(NO)$_7$]$^-$, characterised spectroscopically and by elemental analysis of its tetraphenylarsonium salt. Further study of this material is in progress and will be reported upon in due course.

NMR spectra

In Table 2, we record the ^{1}H and ^{13}C NMR assignments for [Fe$_2$(SMe)$_2$(CO)$_6$] and [Fe$_2$(SEt)$_2$(CO)$_6$]: the proton data for the methyl derivative have been reported previously.[2,5,6] The ^{13}C shifts of the methyl groups are of interest for the large difference between the two non-equivalent methyl carbons in the *anti* isomers. This phenomenon is observed also for the methylene carbons in the *anti* isomer of [Fe$_2$(SEt)$_2$(CO)$_6$] where one of the CH$_2$ carbons has a chemical shift similar to those of the methyl carbons in this compound: off-resonance decoupling was required to assign the shifts in the *anti* isomer. For neither of these compounds were we able to establish by NMR methods the activation parameters for the *anti* $\rightleftharpoons$ *syn* interconversion, as at elevated temperatures, decomposition was sufficiently rapid to prevent the recording of adequate NMR spectra. Conversion of either isomer of either compound to an equilibrium mixtura of *syn* and *anti* isomers is quite rapid, being complete for example after 10 min reflux in benzene solution. At ambient temperatures the carbonyl groups ex-

Table 2. NMR assignments for $Fe_2(SR)_2(CO)_6$, $(R = Me, Et)^a$

Compound	$\delta(CH_3)$	$\delta(CH_2)$	$\delta(CH_3)$	$\delta(CH_2)$	$\delta(CO)$	$^3J(HCCH)$
$Fe_2(SMe)_2(CO)_6$						
syn	2.13		20.3		209.7	
anti	1.63		8.0		208.7	
	2.17		21.6			
$Fe_2(SEt)_2(CO)_6$						
syn	1.33	2.45	18.0	32.9	210.2	7.3
anti	1.11	2:15	17.5	19.6	209.5	7.3
	1.38	2.45	17.7	33.9		

a. Chemical shifts in p.p.m., from Me_4Si; J in Hz; spectra recorded in $CDCl_3$ at 310 K.

hibit fluxional behaviour: the low temperature behaviour has been discussed.[6]

Table 3 contains ^1H and ^{13}C chemical shifts for the analogous nitrosyl species [$Fe_2(SR)_2(NO)_4$]: we have not yet succeeded in recording ^{14}N or ^{15}N shifts for this series. These are two points of particular interest associated with these data. First, there is for the examples of $R = CH_3$, C_2H_5 and $PhCH_2$, a considerable solvent-induced chemical shift difference observed for the protons on changing the solvent from chloroform-d to toluene-d_8. In the methyl derivative this shift is *ca.* 0.6 p.p.m., and in the ethyl derivatives *ca.* 0.4 p.p.m. for the methyl protons and *ca.* 0.5 p.p.m. for the methylene protons: in the benzyl derivative, the solvent shift for the methylene protons is *ca.* 0.35 p.p.m., and for the phenyl protons which appear as a single unresolved absorption at 80 MHz, the shift is again 0.35 p.p.m. In every case, the proton chemical shift is lower in toluene than in chloroform, but the solvent-induced shifts in the ^{13}C resonances seem to be very modest in magnitude. A possible interpretation of the large proton solvent-induced shifts is in terms of the paratropic ring current in the solvent toluene, but this idea requires rather specific mean orientations of the solvent molecules around a solute molecule: we have not yet investigated systematically the solvent effects on the chemical shifts of these complexes. Regardless of the solvent, there is a steady shift to low field of the C–S resonance as R varies from Me to Bu^t.

The second noteworthy feature is the observation of the splitting of many, but not all, of the proton and carbon signals. For example, when R = Me, two similar spectra, of identical intensity are observed in toluene, but only one in chloroform. Similar splittings have been observed previously,[29] and interpreted in terms of equally abundant C_{2v} and C_{2h} isomers. The observation of a

single spectrum is due either of accidentally identical chemical shifts or to fast equilibration between isomers, rather than to the presence of a single isomer. In our preliminary account of the formation of [$Fe_2(SMe)_2(NO)_4$] from [$Fe_2(SMe)_2(CO)_6$],[18] we observed only a single ^1H spectrum, having chosen chloroform as our NMR solvent. This observation, together with that of apparent chromatographic homogeneity, led us to the belief that only one isomer was present: since the X-ray analysis of [$Fe_2(SEt)_2(NO)_4$] revealed the presence only of the C_{2h} isomer,[15] we inferred that this was the isomer present in solution. This belief of a single isomer was strengthened by the observation of only a single ^{13}C chemical shift in chloroform solution (Table 3).

However, it is clear from the spectra in toluene solution that there are indeed two isomers present in solution for all of this series, and using variable-temperature ^1H spectroscopy we have measured the activation energies in toluene solution for the $C_{2h} \rightleftharpoons C_{2v}$ isomerisation process. The relevant data, all derived from solutions in toluene-d_8 are given in Table 4. Distinct coalescence temperatures were determined for the CH_3 and CH_2 protons in the ethyl compounds, giving $\Delta G^\ddagger$ values identical within experimental uncertainty. Replacement of one hydrogen in the methyl derivative by an alkyl group to give the ethyl or *n*-propyl derivatives causes a modest reduction in $\Delta G^\dagger$ of some 2.5 kJ mol^{-1}: double replacement to yield the *iso*-propyl derivative causes a much bigger reduction in $\Delta G^\ddagger$ of almost 20 kJ mol^{-1}. When all three hydrogens have been replaced, as in the *t*-butyl derivative, no splitting of the ^1H signal is observed in toluene solution even at 223 K, suggesting for any reasonable values of Δv, an upper limit for $\Delta G^\ddagger$ in this case of around 50 kJ mol^{-1}.

Our observation (see above) that [$Fe_2(SR)_2$-

Table 3. NMR assignments for $Fe_2(SR)_2(NO)_4$[a]

Compound	Solvent	$\delta(^1H)$/p.p.m.	$\delta(^{13}C)$/p.p.m.	Assignment
$Fe_2(SMe)_2(NO)_4$	$CDCl_3$	2.83	27.45	CH_3
	$C_6D_5CD_3$	2.16, 2.23	26.95, 27.18	CH_3
$Fe_2(SEt)_2(NO)_4$	$CDCl_3$	1.53, 1.58	19.14	CH_3
		3.07, 3.10	39.45, 40.15	CH_2
	$C_6D_5CD_3$	1.13, 1.16	18.98	CH_3
		2.53, 2.63	39.49, 40.19	CH_2
$Fe_2(SPr^n)_2(NO)_4$	$CDCl_3$	1.11	13.11	CH_3
		1.96	27.33	$CH_3CH_2CH_2$
		3.02, 3.05	47.33, 47.66	$CH_3CH_2CH_2$
	$C_6D_5CH_3$	0.84	12.93	CH_3
		1.61	27.50	$CH_3CH_2CH_2$
		2.64, 2.68	47.48, 47.91	$CH_3CH_2CH_2$
$Fe_2(SPr^i)_2(NO)_4$	$CDCl_3$	1.54, 1.57	27.64	CH_3
		3.04, 3.07	49.70, 50.63	CH
	$C_6D_5CD_3$	1.26[b]	27.47	CH_3
		2.69[b]	49.94, 50.92	CH
$Fe_2(SBu^t)_2(NO)_4$	$CDCl_3$	1.45	34.14	CH_3
		-	52.95	Me_3C
	$C_6D_5CD_3$	1.23[c]	33.96	CH_3
		-	57.05	Me_3C
$Fe_2(SCH_2Ph)_2(NO)_3$	$CDCl_3$	4.18, 4.22	48.63, 49.37	CH_2
		7.43	128.2, 129.1	Ph
	$C_6D_5CD_3$	3.82, 3.85	d	CH_2
		7.07	d	Ph

a. Data at 308 K, chemical shift in p.p.m. from Me_4Si.

b. $\delta(^1H)$ at 233 K: 1.23, 1.27, 2.47 p.p.m.

c. No splitting observed even at 223 K.

d. Not studied.

Table 4. ^1H coalescence data for $Fe_2(SR)_2(NO)_4$[a]

Compound	Signal	T_c/K[b]	$\Delta\nu$/Hz	$\Delta G^{\ddagger}$/kJ mol^{-1}
$Fe_2(SMe)_2(NO)_4$	CH_3	357(1)	5.8(3)	78.3(4)
$Fe_2(SEt)_2(NO)_4$	CH_3CH_2	332(1)	2.0(2)	75.6(5)
	CH_3CH_2	348(1)	6.9(3)	75.8(4)
$Fe_2(SPr^n)_2(NO)_4$	$CH_3CH_2CH_2$	338(1)	3.4(3)	75.5(5)
$Fe_2(SPr^i)_2(NO)_4$	$(CH_3)_2CH$	263(1)	2.8(4)	59.3(6)
$Fe_2(SCH_2Ph)_2(NO)_4$	$PhCH_2$	341(1)	2.7(2)	76.8(5)

a. All spectra measured in $C_6D_5CD_3$

b. T_c taken from ^1H spectra.

(NO)$_4$] undergoes neither dissociation to form monomeric [Fe(SR)(NO)$_2$] nor ionisation to Fe(NO)$_2^+$ and SR$^-$ makes it virtually certain that the rate processes we have observed are indeed those for the C$_{2h} \rightleftharpoons$ C$_{2v}$ isomerisation. We intend to report further on the interesting solvent dependence of these spectra in a future communication.

EXPERIMENTAL

Literature methods were employed for the preparation of [Fe$_2$S$_2$(CO)$_6$][1], [Fe$_2$S$_2$(CO)$_6$]$^{2-}$,[16] [Fe$_3$S$_2$(CO)$_9$][1], [Fe$_2$(SMe)$_2$(CO)$_6$]^2 and Hg[Fe(CO)$_3$NO]$_2$;[24] [Fe$_2$(SEt)$_2$(CO)$_6$] was prepared in a manner similar to that for [Fe$_2$(SMe)$_2$(CO)$_6$] and for each of these compounds, two isomers were separable by chromatography. Evidence was obtained for a third, minor, component in the chromatography of [Fe$_2$(SMe)$_2$(CO)$_6$], but adequate characterisation was not achieved owing to the tiny amount of material isolated.

NMR spectra were recorded using Varian CFT-20 and Bruker WP-80 instruments. For both [Fe$_2$(SMe)$_2$(CO)$_6$] and [Fe$_2$(SEt)$_2$(CO)$_6$] full NMR spectral assignments (^{1}H and ^{13}C) were made for both isomers, by use of off-resonance decoupling: the NMR spectral data for these compounds are given in Table 2.

Nitrosylation, Procedure A

In a typical reaction, the carbonyl complex (24 mmol) and sodium nitrite (6.0 g) were added to a solution of sodium hydroxide (10.0 g) in a mixture of water (50 cm^3) and ethanol (25 cm^3). The mixture was then stirred and refluxed under nitrogen for 4 hr. After cooling to ca. 30°C, the mixture was acidified with 1 : 1 acetic acid/water (approx. 30 cm^3). The resulting mixture was evaporated to dryness: the solid was extracted firstly with CH$_2$Cl$_2$ (6 × 50 cm^3), and secondly with water (2 × 100 cm^3). The methylene chloride extract was washed with water (2 × 50 cm^3), dried over Na$_2$SO$_4$, and evaporated to dryness: recrystallisation from 1 : 1 CH$_2$Cl$_2$/MeOH yielded Fe$_2$(SR)$_2$(NO)$_4$. Tha aqueous extract was extracted with ether (4 × 50 cm^3), and the ether layer was dried over Na$_2$SO$_4$, and evaporated to yield Na[Fe$_4$S$_3$(NO)$_7$]: to the residual aqueous layer was added an aqueous solution of Ph$_4$As$^+$Cl$^-$; the resulting precipitate was filtered off, and dissolved in CH$_2$Cl$_2$; after drying over Na$_2$SO$_4$ and evaporation, recrystallisation from CH$_2$Cl$_2$ yielded (Ph$_4$As)$_2$[Fe$_2$S$_2$(NO)$_4$].

Procedure B

Typically, the carbonyl complex (10 mmol) was dissolved in CH$_2$Cl$_2$ (50 cm^3), and the solution

purged with nitrogen. Nitric oxide was bubbled through the solution for 1 hr, and the solution was evaporated to dryness. The work-up then follows that described for Procedure A. When the substrate was [Fe$_2$(SMe)$_2$(CO)$_6$] the product was a mixture of [Fe$_2$(SMe)$_2$(CO)$_6$] and [Fe$_2$(SMe)$_2$(NO)$_4$], separated by differential crystallisation using light petroleum (b.p. 40/60°C).

Procedure C

This was similar to Procedure A, except that the nitrogen gas stream was replaced by a nitric oxide stream, and the sodium nitrite was omitted from the reaction medium.

Preparation of salts of Fe$_4$Se$_3$(NO)$_7^-$

(a) Sodium salt

A mixture of 7 g selenium and 50 cm^3 water was stirred under N$_2$: a solution of 7 g NaBH$_4$ in 50 cm^3 water was added dropwise with stirring. Vigorous evolution of H$_2$ occurred, and after this had subsided the solution was allowed to cool, giving a clear grey solution above a precipitate of Na$_2$B$_4$O$_7$.10H$_2$O. NaNO$_2$ (8 g) was added with stirring, and the solution turned dark red. The solution was boiled and 20 g of FeSO$_4$.7H$_2$O in 160 cm^3 water was added in one portion, followed by slow addition of 35 cm^3 of 25% NH$_3$ solution. The solution was then boiled for 30 mins, filtered hot, cooled, and filtered a second time. The cold filtrate was extracted with ether, and the dried extracts evaporated to yield the sodium salt of Fe$_4$Se$_3$(NO)$_7^-$.

(b) Ph$_4$As$^+$ salt

Equimolar quantities of Na[Fe$_4$Se$_3$(NO)$_7$] and Ph$_4$AsCl.H$_2$O were dissolved in water, and the solutions mixed. The whole was extracted with chloroform, and the dried extract was evaporated. The resulting solid was recrystallised from methanol to yield Ph$_4$As[Fe$_4$Se$_3$(NO)$_7$] as shiny black crystals. Found: C, 27.2; H, 1.8; N, 9.2; Fe, 22.3; Se, 22.6. Calc. for C$_{24}$H$_{20}$AsFe$_4$N$_7$O$_7$Se$_3$: C, 27.4; H, 1.9; N, 9.3; Fe, 21.2; Se, 22.5%. UV/visible spectrum: λ/nm(ϵ/lmol^{-1}cm^{-1}): 570(2700), 432(10000), 360(16000), 279(27000). IR spectrum, ν(NO)/cm^{-1}: 1790 m, 1690 s, 1720 m.

Iron and selenium were determined by atomic absorption, using the hydride method for selenium.

REFERENCES

1. W. Hieber and J. Gruber, Z. Anorg. Allgem. Chem. 1955, 296, 91.
2. R. B. King, J. Amer. Chem. Soc. 1962, 84, 2460.
3. R. B. King and M. B. Bisnette, Inorg. Chem. 1965, 4, 482.

4. G. Bor, *J. Organometallic Chem.* 1968, **11**, 195.

5. L. Maresca, F. Greggio, G. Sbrignadello and G. Bor, *Inorg. Chim. Acta* 1971, **5**, 667.

6. R. D. Adams, F. A. Cotton, W. R. Cullen, D. L. Hunter and L. Michichuk, *Inorg. Chem.* 1975, **14**, 1395.

7. L. F. Nelson, F. Y.-K. Lo, A. D. Rae and L. F. Dahl, *J. Organometallic Chem.* 1982, **225**, 309.

8. L. F. Dahl and C. H. Wei, *Inorg. Chem.* 1963, **2**, 328.

9. L. F. Dahl and P. W. Sutton, *Inorg. Chem.* 1963, **2**,·1067.

10. C. H. Wei and L. F. Dahl, *Inorg. Chem.* 1965, **4**, 1.

11. C. H. Wei and L. F. Dahl, *Inorg. Chem.* 1965, **4**, 493.

12. K. A. Hofmann and O. F. Weide, *Z. Anorg. Allgem. Chem.* 1895, **9**, 295.

13. Wang Guang-hui, Zhang Wen-xin and Chai Wen-gang, *Acta Chimica Sinica* 1980, **38**, 95.

14. F. Z. Roussin, *Ann. Chim. Phys.* 1858, **52**, 285.

15. J. T. Thomas, J. H. Robertson and E. G. Cox, *Acta Cryst.* 1958, **11**, 599.

16. D. Seyferth and M. K. Gallagher, *J. Organometallic Chem.* 1981, **218**, C5.

17. D. Seyferth and R. S. Henderson, *J. Organometallic Chem.* 1981, **204**, 333.

18. A. R. Butler, C. Glidewell and J. McGinnis, *Inorg. Chim. Acta* 1982, **64**, L77.

19. D. T. McAllan, T. V. Cullum, R. A. Dean and F. A. Fidler, *J. Am. Chem. Soc.* 1951, **73**, 3627.

20. R. B. King, *Inorg. Chem.* 1962, **2**, 326.

21. J. Hieber and W. Beck, *Z. Anorg. Allgem. Chem.* 1960, **305**, 274.

22. R. S. Gall, C. T.-W. Chu and L. F. Dahl, *J. Amer. Chem. Soc.* 1974, **96**, 4019.

23. C. Glidewell and J. McGinnis, *Inorg. Chim. Acta*, 1982, **64**, L171.

24. W. Hieber and H. Beutner, *Z. Anorg. Allgem. Chem.* 1963, **320**, 101.

25. J. L. Davidson and D. W. A. Sharp, *J. Chem. Soc. (Dalton)* 1973, 1959.

26. G. Piazza and G. Innorta, *J. Organometallic Chem.* 1982, **240**, 257.

27. G. Johansson and W. N. Lipscomb, *Acta Cryst.* 1958, **11**, 594.

28. C. T.-W. Chu and L. F. Dahl, *Inorg. Chem.* 1977, **16**, 3245.

29. T. B. Rauchfuss and T. D. Weatherill, *Inorg. Chem.* 1982, **21**, 827.

STUDIES IN THE FLEXIBILITY OF MACROCYCLIC LIGANDS. CRYSTAL AND MOLECULAR STRUCTURE OF 2,13-DIMETHY1-3,6,9,12,18-PENTAAZABICYCLO (12.3.1) OCTADECA-(18),14,16-TRIENE-DICHLOROION (III) HEXAFLUOROPHOSPHATE

MICHAEL G. B. DREW*, DAVID A. RICE* and SIDIK BIN SILONG

Department of Chemistry, University of Reading, Whiteknights,
Reading RG6 2AD, England

Abstract—The crystal structure of the title compound $[FeL^2Cl_2][PF_6]$ is reported. Crystals are monoclinic with $a = 11.747(9)$, $b = 16.051(11)$, $c = 11.964(10)$Å, $\beta = 98.1(1)°$, $Z = 4$, Spacegroup $P2_1/n$. 1173 independent reflections above background have been refined to R 0.09. The coordination geometry around the Fe(III) ion is pentagonal bipyramidal with the two chlorine atoms in axial positions [Fe–Cl 2.348(7), 2.354(7)Å]. The five donor nitrogen atoms of the macrocycle form a pentagonal girdle with lengths in the range 2.20(2)–2.25(2)Å. The macrocycle conformation is compared to that found in $[CuL^2]^{2+}$ and $[CoL^2Cl]^{2+}$ where the $5N$ donor set provides respectively trigonal bipyramidal and square pyramidal environments and also to that found in the comparable 7–coordinate $[FeL^1(NCS)_2]^+$ where L^1 is the related pentaene.

The coordinative properties of macrocyclic ligands are dependent upon a number of factors. Three of the most important ones are the size of the "hole" or site in the ring, the degree of flexibility of the ligand and finally the nature of the donor atoms; i.e. do they form a "hard" or "soft" set. In this study we wished to extend our investigation into the effects of changing the flexibility of the ligand while keeping the donor set constant and to investigate whether the hole size of the macrocycle varied with conformation.

Suitable ligands for our comparative study are L^1 and its reduced form L^2 in which the imine groups have been hydrogenated.

The rigid 15–membered macrocycle L^1 forms complexes with metal ions ranging in ionic radii from 0.64Å (Fe^{3+}) to 1.18Å (Pb^{2+}); these being synthesised by allowing 3,6–diazaoctane 1,8–diamine to react with 2,6–diacetylpyridine (1:1 molar ratio) in the presence of a metal ion. The list of ions that have been successfully used are Mg^{2+}, Mn^{2+}, Fe^{3+}, Fe^{2+}, Co^{2+}, Zn^{2+}, Sn^{2+}, Cd^{2+}, and Pb^{2+}.[1-4] In these structures, L^1 forms a pentagonal girdle around the metal and with two axial anions
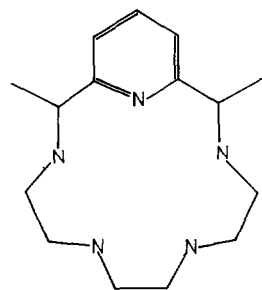
L^2
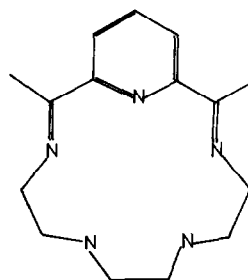
L^1

provides a pentagonal bipyramidal environment for the metal. Ni^{2+} and Cu^{2+} ions are unsuited to this geometry and their complexes cannot be prepared directly by template synthesis but only by

---

*Authors to whom correspondence should be addressed.

1053

trans-metallation. Crystal structures of several compounds including L^1 have been reported namely $[(FeL^1(NCS)_2) \cdot (ClO_4)]$,[1] $[FeL^1(NCS)_2]$,[2] $[FeL^1(H_2O)Cl \cdot (ClO_4)]$,[3] $[(Mg(L^1)(H_2O)_2)Cl_2]$.[4] The rigid nature of L^1 ensures that the specific stereochemistry preferred by the ion cannot necessarily be fulfilled.

However the macrocycle L^1 can be hydrogenated to give the more flexible macrocycle L^2. We have studied the structures of L^2 complexes with the aim of observing the effect of the increased flexibility on going from L^1 to L^2. Two structures we have reported are $[(CuL^2)(PF_6)_2]$[5] in which the donor atoms form a trigonal bipyramid and $[(CoL^2Cl)(ClO_4)_2]$[5] where an approximate square pyramid is formed by the donor atoms of the ligand. Both Cu^{2+} and Co^{3+} have preferred stereochemistries arising from their d^n configuration and so these structures cannot be directly compared to the 7–coordinate L^1 analogues.

However we now present a study of an Fe^{3+} complex of L^2 that via comparison with the structure of $[(FeL^1(NCS)_2)(ClO_4)]$[2] allows a discussion of the effect of flexibility on the mode of coordination. The Fe^{3+} ion being high spin has no CFSE effect to mask ligand preferences as have Cu^{2+} and Co^{3+}.

DISCUSSION OF THE STRUCTURE

The geometry of the cation $[FeL^2Cl_2]^+$ is illustrated in Fig. 1, together with the atomic numbering scheme. The iron atom which is in the cavity of the macrocycle has an approximately pentagonal bipyramidal coordination sphere; the chlorine atoms being in the axial sites.

The geometry of the macrocycle can be compared with that of the unsaturated L^1 in $[FeL^1(NCS)_2]$. The maximum deviation of a contributing atom from the FeN_5 plane is 0.23 Å in the
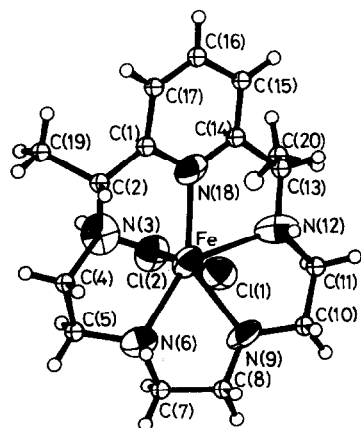
L^2 structure compare compared to 0.11 Å in L^1. The mean Fe–N distance in the present structure is 2.252 Å compared to 2.228 Å. This increase is presumably a consequence of the increase in the two C–N bond lengths and the resultant puckering which creates a larger hole for the metal ion. We have calculated the macrocycle hole sizes using the criterion of Tasker et al.[7] This method involves calculating the macrocycle hole size as twice the mean distance of the donor atoms from their centroid. In these pentagonal bipyramidal structures the values are 4.50 Å for L^2 and 4.45 Å for L^1.

A comparison of the torsion angles in the two structures in Table 2 shows considerable agreement with the variations as expected concentrated on the C(2)–N(3) and N(12)–C(13) bonds. The values found for $[FeL^2Cl_2]$ are not particularly strained and confirm the stability of the saturated complex.

The 7–coordinate structure observed for $[FeL^2Cl_2]$ is particularly interesting as both 5- and

Table 1. Dimensions in the coordination sphere

FE	–	CL(2)			2.348(7)
FE	–	CL(1)			2.354(7)
FE	–	N(3)			2.244(23)
FE	–	N(9)			2.323(17)
FE	–	N(12)			2.252(21)
FE	–	N(18)			2.203(20)
FE	–	N(6)			2.239(19)
CL(2)	–	FE	–	N(3)	87.2(4)
CL(2)	–	FE	–	CL(1)	177.0(3)
N(3)	–	FE	–	CL(1)	90.9(4)
CL(2)	–	FE	–	N(9)	84.6(5)
N(3)	–	FE	–	N(9)	146.9(8)
CL(1)	–	FE	–	N(9)	95.9(5)
CL(2)	–	FE	–	N(12)	97.5(5)
N(3)	–	FE	–	N(12)	142.0(7)
CL(1)	–	FE	–	N(12)	85.4(5)
N(9)	–	FE	–	N(12)	71.0(7)
CL(2)	–	FE	–	N(18)	95.0(5)
N(3)	–	FE	–	N(18)	71.8(7)
CL(1)	–	FE	–	N(18)	86.5(5)
N(9)	–	FE	–	N(18)	140.8(7)
N(12)	–	FE	–	N(18)	70.2(6)
CL(2)	–	FE	–	N(6)	93.4(5)
N(3)	–	FE	–	N(6)	78.1(7)
CL(1)	–	FE	–	N(6)	83.9(5)
N(9)	–	FE	–	N(6)	74.4(7)
N(12)	–	FE	–	N(6)	142.5(7)
N(18)	–	FE	–	N(6)	144.4(7)

Fig. 1.

Table 2.

Torsion Angles(degrees)			$[FeL^2Cl_2]^+$	$[CoL^2Cl]^{2+}$	$[CuL^2]^{2+}$	$[FeL^1Cl_2]^+$
N(18) - C(1) - C(2) - N(3)			-17.5	-25.5	1.6	-3.6
N(18) - C(1) - C(2) - C(19)			-143.2	-152.0	132.9	-179.6
C(1) - C(2) - N(3) - C(4)			163.0	161.4	121.3	-177.2
C(19) - C(2) - N(3) - C(4)			-71.9	-71.3	-8.8	-1.2
C(2) - N(3) - C(4) - C(5)			-175.3	-169.0	-172.3	162.8
N(3) - C(4) - C(5) - N(6)			59.5	47.7	34.5	43.5
C(4) - C(5) - N(6) - C(7)			178.3	83.1	-129.3	-178.6
C(5) - N(6) - C(7) - C(8)			174.7	-81.3	80.2	170.8
N(6) - C(7) - C(8) - N(9)			-59.1	-43.0	54.6	-57.7
C(7) - C(8) - N(9) - C(10)			172.3	-90.2	80.5	172.4
C(8) - N(9) - C(10) - C(11)			-173.8	78.6	-150.2	-178.8
N(9) - C(10) - C(11) - N(12)			55.3	50.7	53.2	47.4
C(10) - C(11) - N(12) - C(13)			-178.7	77.3	-169.3	157.9
C(11) - N(12) - C(13) - C(14)			172.4	-103.1	88.2	-178.4
C(11) - N(12) - C(13) - C(20)			47.8	130.3	-148.6	-2.7
N(12) - C(13) - C(14) - N(18)			-22.1	-9.2	24.4	-3.4
C(20) - C(13) - C(14) - N(18)			104.9	109.5	-98.0	-179.3

6-coordinate structures are possible. Nuclear charge on the high spin Fe(III) ion combined with its relatively large radius and lack of octahedral CFSE are factors which favour the coordination of the two additional monodentate anions.

The two metal ions Fe^{3+} and Co^{3+} have similar ionic radii (0.65, 0.61 Å) and yet very different stereochemistries are observed with L^2. In $[CoL^2Cl]^{2+}$ the macrocycle is folded and the metal is 6-coordinate. The folding reduces the hole size from 4.50 to 3.74 Å; the Co–N distances fall within the range 1.81–2.00 Å. So one possible reason is that the small increase in size going from Co^{3+} to Fe^{3+} makes this conformation unsuitable. In addition, the CFSE values for Co^{3+} favour octahedral (– 24 Dq) over pentagonal bipyramidal (– 15.5 Dq). Examination of the torsion angles in the octahedral conformation show no obvious strains. The $[CuL^2]^{2+}$ complex ion is trigonal bipyramidal. The Cu^{2+} ion forms a variety of stereochemistries and CFSE values for a range of them are – 6.0 Dq (octahedral), – 14.3 Dq (square planar), – 9.2 Dq (square pyramidal) – 7.1 Dq trigonal bipyramidal) and – 4.9 Dq (pentagonal bipyramidal). Thus the order of favoured stereochemistries is square-planar (S) > square pyramidal (SP) > trigonal bipyramid (TBP). The square planar conformation is unlikely as it is doubtful that a square planar array of nitrogen atoms could be provided by L^2 as any such system

designed to provide such an array would bring a fifth atom into close proximity. However as is apparent from the Co structure, L^2 can provide a square pyramidal environment for a metal. Indeed looking at the torsion angles that are observed in $[CuL^2]^{2+}$ we can conclude that the TBP conformation is particularily strained. In particular the C(19)–C(2)–N(3)–C(4) and C(4)–C(5)–N(6)–C(7) angles of – 8.8° and – 129.3° signify eclipsed conformations. On the basis of CFSE and macrocycle conformation then, the TBP is less favoured than the SP.

The only conclusion we reach is that the hole size provided by the macrocycle in the TBP conformation is more suited to the size of the Cu^{2+} ion. Thus the macrocycle hole size provided by the TBP conformation is 4.05 A, considerably larger than for the SP conformation (3.74 A). As the Cu^{2+} ion radius at 0.73 Å is somewhat larger than Co^{2+} then it would seem that the larger hole provided by the macrocycle in the TBP conformation is necessary for complexation.

CONCLUSIONS

By comparison of the three structures $[CoL^2Cl]^{2+}$, $[CuL^2]^{2+}$ and $[FeL^2Cl_2]^+$ we have shown that both crystal field affects, and the size of hole are important in the deciding of the stereochemistries observed with the flexible macrocycle ligand L^2. This work also examines the method of

Tasker *et al.*[7] for the calculation of macrocycle hole size. Unlike the examples in Ref. 7, the present work demonstrates how the size can vary considerably (3.74–4.10 Å) with the conformation of the macrocycle. It seems clear therefore that the calculation can only be used with rigid macrocycles or when the conformation has been established by X-ray diffraction.

EXPERIMENTAL

Preparation. The ligand was synthesized following the method of Ref. 6 and recrystallised from an acetonitrile–diethyl ether mixture.

Crystal data

$C_{15}H_{27}N_5Cl_2PF_6F_e$, $M = 548.9$, Monoclinic, $a = 11.747(9)$, $b = 16.051(11)$, $c = 11.964(10)$ Å, $\beta = 98.1(1)°$, $U = 2233.3$ Å^3, $d_c = 1.64$, $d_m = 1.63$, $Z = 4$, $\lambda(Mo-K\alpha) = 0.7107$ A, $\mu = 10.69$ cm^{-1}. Spacegroup $P2_1/n$ from the systematic absences $h0l$, $h + l = 2n + 1$, $0k0$, $k = 2n + 1$.

A crystal of approximate shape 0.12*0.75* 1.00 mm was mounted on a Stoe STADI2 diffractometer and intensity data was collected via variable width w scan. Background counts were 20s and the scan rate of 0.033°/s was applied to a width of $(1.5 + \sin \mu / \tan \theta)$. The maximum 2θ value was 45°. 1948 independent reflections were measured of which 1173 with $I > 2\sigma(I)$ were included in subsequent calculations. The structure was determined by heavy atom methods. The structure was refined using full matrix least square methods with Fe, Cl, N, P anisotropic and F, C isotropic. The PF_6^- anion was disordered. Two rigid octahedra were refined with occupancy factors of x and 1-x. x refined to 0.70(2). The hydrogen atoms in the cation were placed in trigonal or tetrahedral positions but were given a common thermal parameter. Apart from those on methyl groups which were refined as rigid groups but those on the same carbon atom were given a common thermal parameter weighting scheme was chosen to give equivalent values of $w\Delta^2$ over ranges of F_0 and $\sin \theta / \lambda$. This was $w = 1/(\sigma^2(F) + 0.003 \, F^2)$ where $\sigma(F)$ was taken from counting statistics. Scattering factors were taken from Ref 8. Calculations were made using Shelx76[9] on the CDC7600 Computer at the University of Manchester Computer Centre. The final R value was 0.09 (R_W 0.09). Dimensions in the metal coordination sphere are given in Table 1. Atomic parameters, thermal parameters and a list of structure factors have been deposited with the Editor as supplementary material; copies are available on request. Atomic coordinates have also been deposited with the Cambridge Crystallographic Data Centre.

REFERENCES

1. M. G. B. Drew, A. H. Othman, P. B. A. McIlroy and S. M. Nelson, *J. Chem. Soc. Dalton* 1975, 2507.
2. M. G. B. Drew, J. Grimshaw, P. D. A. McIlroy and S. M. Nelson, *J. Chem. Soc. Dalton* 1976, 1388.
3. M. G. B. Drew, A. H. Othman, P. D. A. McIlroy and S. M. Nelson, *Acta Cryst.* 1976, **A31**, S140.
4. M. G. B. Drew, A. H. Othman, S. G. McFall and S. M. Nelson, *J. Chem. Soc. Chem. Comm.* 1975, 818.
5. M. G. B. Drew and S. Hollis, *Inorg. Chim. Acta* 1978, **29**, L231.
6. M. C. Rakowski, M. Rycheck and D. H. Busch, *Inorg. Chem.* 1975, **14**, 1194.
7. K. Drummond, K. Henrick, M. F. L. Kanagasundraram, L. F. Lindoy, M. McPartlin and P. A. Tasker, *Inorg. Chem.* 1982, **21**, 3923.
8. G. M. Sheldrick, Shelx76, Program for Crystal Structure Determination, University of Cambridge, England.
9. *International Tables for X-ray Crystallography*, Vol. IV. Kynoch Press, Birmingham (1974).

NOTE

Synthesis and spectroscopic studies of europium chelate complexes

GILBERTO F. DE SÁ

Departamento de Física e Departamento de Química, da Universidade Federal de Pernambuco, Cidade
Universitária, 50000 Recife, PE—Brasil

Abstract—The synthesis of the mixed complexes of the europium ion with 2-pyridylcarbinol-N-oxide,
and 2,2′-dipyridyl and 1,10-phenanthroline were prepared. The compounds, were characterized by means
of chemical analyses, vibrational spectra, molar conductivities, and electronic spectra. The emission of the
[EuL₃, phen] complex at 10 K is very intense and an assignment of the point symmetry of the Eu(III) ion
has been made.

The complexes formed between transition metal ions and 2-pyridylcarbinol-N-oxide (HL) have been discussed recently.[1] The present note deals with the synthesis and some spectroscopic properties of the mixed complexes formed between the europium ion, 2-pyridylcarbinol-N-oxide, and 1,10-phenanthroline or 2,2′-dipyridyl. In principle, complexes of the formula LnL₃ (which have not been isolated) are coordinately unsaturated and could function as "shift reagents".[2] The utility of the shift depends, of course, on their ability to bind one or more additional ligands which have a site of Lewis basicity.

To a warm ethanolic solution of 3.0 mmol. of HL were successively added 10 cm³ of an ethanolic solution containing 1.0 mmol. of lanthanide perchlorate and 15 cm³ of an ethanolic solution containing 1.0 mmol of 2,2′-bipyridyl or 1,10-phenanthroline. The solution was evaporated under vacuum to an oily residue. This was triturated with several portions of petroleum until a solid began to form. The solution was then cooled to −5°C for 24 hr. The compound was purified by recrystallization from dioxane. The vibrational spectra and molar conductivities were obtained and discussed as previously reported.[3] Emission spectra were obtained with a Spex 1702 double monochromator using an Argon laser as excitation source at 4765 and 4880 Å.[4]

The analytical data for the europium, carbon, hydrogen, and nitrogen of the compounds were performed by PCR, Inc. and by the microanalytical Lab. of the UPS. Experimental data are in good agreement with the theoretical values (Found: C, 54.72; H, 4.91; N, 8.93; Eu, 19.37. Calc. for [EuL₃, phen]: C, 54.85; H, 4.82; N, 8.88; Eu, 19.28%) and (Found: C, 52,26; H, 4.94; N, 9.61; Eu, 20.74. Calc. for [EuL₃, bipy]: C, 52.06; H, 4.88; N, 9.48; Eu, 20.58%).

The [EuL₃, bipy] complex shows highly intense fluorescence, that can be just observed with sunlight. The results obtained from the measurements of the emission spectrum of the [EuL₃, phen] complex at 10 K are shown in Table 1 along with the suggested assignments of the $^5D_0 \rightarrow {}^7F_{1,2}$ transitions. The most intense transitions is $^5D_0 \rightarrow {}^7F_2$, followed by $^5D_0 \rightarrow {}^7F_1$ and by a weak $^5D_0 \rightarrow {}^7F_0$. The $^5D_0 \rightarrow {}^7F_0$ (~580.4 nm) transition is strictly forbidden in D_2 symmetry if it is considered to be of electric dipole origin, however this has now been discussed.[5] In fact, the inclusion of J mixing to evaluate the matrix elements of the "pseudo-quadrupolar" interaction[6–8] may be of great value in interpreting the $^5D_0 \rightarrow {}^7F_0$ intensity as observed in the present work.

The dominant geometries for eight coordination complexes are those derived from the square anti-

Table 1. Allowed transitions between selected states in D_{4d}, D_{2d} and D_2 symmetries.

Transition	D_{4d}	D_{2d}	D_2	Assignments (nm)		
$^5D_0 \rightarrow {}^7F_1$	$A_1 \rightarrow A_2$	$A_1 \rightarrow A_2$	$A \rightarrow B_1$			
		$A_1 \rightarrow E$	$A \rightarrow B_2$	590.9	592.9	595.6
			$A \rightarrow B_3$			
$^5D_0 \rightarrow {}^7F_2$	$A_1 \rightarrow E_2$	$A_1 \rightarrow B_2$	$A \rightarrow B_1$			
		$A_1 \rightarrow E$	$A \rightarrow B_2$	614.5	615.4	616.7
			$A \rightarrow B_3$			

(HL)
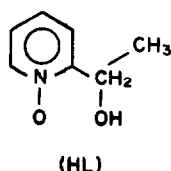
prism (D_{4d}) or the dodecahedron (D_{2d}).[9] Both of these can give rise to structures that possess D_2 symmetry. A summary of the crystal-field splitting for the dominant angular momenta, J, in D_{4d}, D_{2d} and D_2 symmetries together with the transition allowed for magnetic dipolar selection rules ($^5D_0 \rightarrow {}^7F_1$) or electric dipolar selection rules ($^5D_0 \rightarrow {}^7F_2$) appears in Table 1. The emission spectrum is in agreement with what would be expected of Eu^{3+} in a D_2 environment but unfortunately it is not possible to choose between the structure which is derived from antiprism and that which is derived from the dodecahedron.

The spectra of [EuL$_3$, phen] and [EuL$_3$, bipy] in solution show that the ions preserve the same symmetry. This is confirmed by the emission spectra of the powders at room temperature which show the same broadening as the solution fluorescence spectra, indicating a vibronic induced and solvent interaction broadening. At similar concentrations these europium complexes were tested and are more effective shift reagents than the often used Eu(fod)$_3$.[10] However, the low solubility of the former in the usual deuterated solvents their use as a appropriate shift reagents. At the moment, other solvents are being examined.

In conclusion, the interpretation of vibrational spectra and the conductivity data agree with the formulation [EuL$_3$, bipy] and [EuL$_3$, phen] for the complexes and complement the octacoordination structure with D_2 symmetry predicted from the splittings of the fluorescent transitions.

REFERENCES

[1] S. A. Body, R. E. Kohrman and D. X. West, *J. Inorg. Nucl. Chem.* 1976, **38**, 1605, and references therein.
[2] C. C. Hinckley, *J. Am. Chem. Soc.* 1969, **91**, 5160.
[3] G. F. de Sá, A. A. de Gama, M. A. de F. Gomes and R. Ferreira, *Proc. XVIII Intern. Conf. Coord. Chem.* 1977, **1**, 254.
[4] G. F. de Sá and M. A. V. de Almeida, *J. Coord. Chem.* 1980, **10**, 35.
[5] O. L. Malta, *Molec. Phys.* 1981, **42**, 65.
[6] C. K. Jørgensen and B. R. Judd, *Molec. Phys.* 1964, **8**, 281.
[7] R. D. Peacock, *J. Mol. Struct.* 1978, **46**, 203.
[8] O. L. Malta and G. F. de Sá, *Chem. Phys. Lett.* 1980, **74**, 101.
[9] E. L. Mutterties and C. M. Wright, *Quart. Rev. (London)* 1967, **21**, 109.
[10] R. E. Rondeaux and R. E. Sievers, *J. Am. Chem. Soc.* 1973, **93**, 1522.

NOTE

Spin-crossover phenomena in tris(trifluoronicotinoylacetonato) iron (III)

A. A. ADIMADO
Department of Chemistry, University of Ibadan, Ibadan, Nigeria

Abstract—Tris(trifluoronicotinoylacetonato) iron(III) has been shown to exhibit spin-crossover phenomenon between $^6A_{1g}$ and $^2T_{2g}$ terms which are about 322 cm^{-1} apart.

Tris (dialkyldithiocarbamato) iron(III) complexes first reported by Cambi et al.[1–3] are probably the most extensively studied examples of iron(III) showing the spin-crossover phenomenon between the $^6A_{1g}$ and $^2T_{2g}$ terms. High-spin, low-spin and intermediate spin situations can be attained and the thermal equilibrium between the two extreme cases have also been examined in suitable examples.[4,5] Tweedle and Wilson[6] studying magnetic properties of [Fe(Sal$_2$trien)]PF$_6$ in acetone solution reported $\Delta H = 4.62$ kcal mol^{-1} and an entropy, $\Delta S = 16.46$ e.u. for the $^2T_{2g} \rightleftarrows {}^6A_{1g}$ equilibrium. This process in the solid state is estimated to have a spin–state lifetimes,[6] $\tau \gtrsim 10^{-7}$ s.

The first examples of iron(III) β-diketonates exhibiting this phenomenon were found in tris(monothio-β-diketonato) iron(III) complexes,[7] having moments of 4.35–5.75 B.M. at 300K and 2.24–2.80 B.M. at 87K. These are complexes with FeS$_3$O$_3$ chromophores. In this work, the magnetic behaviour of tris(trifluoronicotinoylacetonato) iron(III) has been examined between 87 and 300K; and some thermodynamic parameters have been calculated in order to compare the FeS$_3$O$_3$ and FeO$_6$ chromophores.

EXPERIMENTAL

The ligand 4,4,4-trifluoro-1-(3-pyridyl)-1,3-butanedione (Htfpybd) was obtained from Eastman Organic Chemicals. The preparation of the iron(III) complex, Fe(tfpybd)$_3$ is reported elsewhere.[8] C$_{27}$H$_{15}$F$_9$FeN$_3$O$_6$, mpt., 189–190°. Found: C, 45.62 H, 2.52 N, 5.46 Fe, 7.85. Calc: C, 45.96 H, 2.29 N, 5.96 Fe, 7.92%. The magnetic susceptibility values were measured between 300 and 80K using a Gouy balance. At 293K, the susceptibilities ($\chi_A/10^6$) at field strength 6310, 5804 and 3304 Gauss gave values 5802, 5835 and 5819 c.g.s. units respectively. The susceptibilities are therefore independent of field strength and suggest the absence of ferromagnetic impurities in Fe(tfpybd)$_3$ complex.

RESULTS AND DISCUSSION

Iron(III) has a high-spin $^6A_{1g}$ ground state with a normal moment of about 5.92 B.M. which corresponds to five unpaired electrons whilst its low-spin $^2T_{2g}$ ground state with a normal moment of about 2.30 B.M. corre-

sponds to one unpaired electron. Since the $^2T_{2g}$ ground state retains some orbital angular momentum, moments may range in value from μS to μS + L, the exact value depending on the temperature of measurements and the magnitude of the spin-orbit coupling.

Assuming a dynamic $^2T_{2g} \rightleftarrows {}^6A_{1g}$ process is operative in the solid state:

$$^2T_{2g} \rightleftarrows {}^6A_{1g} \qquad (1)$$

If α is the fraction or population of high-spin state then $(1 - \alpha)$ represents low-spin state.

$$\mu_{obs}^2 = \alpha(5.92)^2 + (1 - \alpha)(2.30)^2 \qquad (2)$$

$$\text{Keq} = \frac{\alpha}{1 - \alpha}. \qquad (3)$$

The variation of ln Keq with the T^{-1} can be used to obtain ΔH and ΔS changes. A typical plot for Fe (tfpybd)$_3$ is presented in Fig. 1. The best straight line was obtained by the least-squares fitting procedure and the average deviation from the least squares calculations is $\pm 15\%$. The magnetic moment of Fe(tfpybd)$_3$ at 293K was found to be 3.69 B.M., independent of field strength, and corresponds to only 27% of the high-spin form.

A plot of ln Keq with T^{-1} yields $\Delta H = 0.92$ kcal mol^{-1} and $\Delta S = 1.68$ cal mol^{-1} K^{-1} (Table 2). Assuming that ΔH values obtained in Table 2 are a measure of the $^2T_{2g} - {}^6A_{1g}$ separation, it is observed that the $^6A_{1g}$ term in the FeO$_6$ chromophore lies at 322 cm^{-1} above the ground $^2T_{2g}$ term whilst this varies between 170 and 685 cm^{-1} for the FeS$_3$O$_3$ chromophore. This separation compares favourably with those of FeS$_6$ chromophore in dithiocarbamates, quoted by Ewald et al.[5] (500 cm^{-1}), Hall and Hendrickson[9] (204 cm^{-1}).

The observed entropy change of 1.68 e.u. for Fe (tfpybd)$_3$ is small as expected but not that predicted by change in spin multiplicity alone ($\Delta S = R\ln 3$) which gives a theoretical value of 2.16 cal mol^{-1} K^{-1}. Although only electronic entropy predominantly contributes to the $^2T_{2g} \rightleftarrows {}^6A_{1g}$ process, there could be some other effects such as changes in bond lengths and/or angles which cause the deviations of ΔS from the
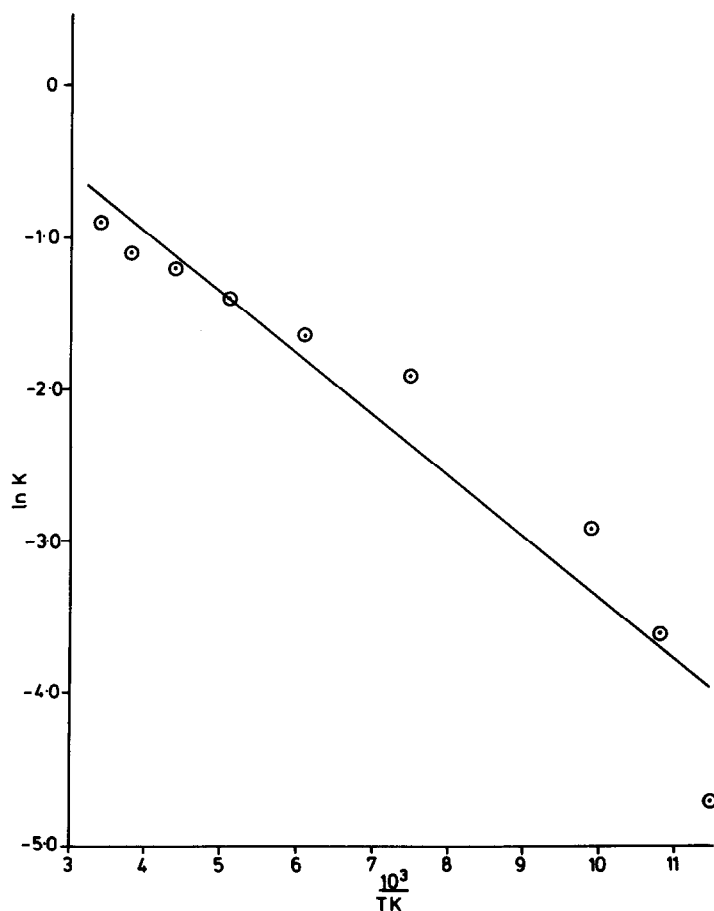
Fig. 1. Plots of ln K vs reciprocal of temperature.

Table 1. Magnetic behaviour of Fe(tfpybd)₃

T/K	$10^6 \chi$/c.g.s	μ_{obs}/B.M.	ln K	10^3/TK
293	5814	3.69	-0.95	3.41
261	5990	3.54	-1.13	3.83
229	6544	3.46	-1.24	4.37
197	7038	3.33	-1.42	5.08
165	7789	3.21	-1.60	6.06
133	8758	3.05	-1.86	7.52
101	8541	2.63	-2.85	9.90
93	8204	2.47	-3.57	10.75
87	7908	2.35	-4.85	11.49

DNC = 216.3 x 10^{-6} c.g.s.

Table 2. Some thermodynamic data

Compound	Chromophore	% High-Spin form	ΔH kcal mol^{-1}	$^2T_{2g}$-$^6A_{1g}$ cm^{-1}	ΔS e.u.
Fe(C₅H₄N.CO.CH.CO.CF₃)₂	FeO₆	27	0.92	322	1.68
Fe(C₆H₅CO.CH.CS.CH₃)₃*	FeS₃O₃	46	1.96	685	6.79
Fe(C₆H₅CS.CH.CO.CH₃)₃*	FeS₃O₃	93	0.49	170	6.37
Fe(C₆H₅CS.CH.CS.CH₃)₆*	FeS₃O₃	80	0.99	348	5.54

*Magnetic data from Ref (7) were used in the various calculations.

theoretically expected value. A quantitative interpretation of these effects is not possible as there does not appear to be any correlation between the entropy and the population of the high-spin forms.

REFERENCES

1. L. Cambi and L. Szego, *Ber. Dtsch. Chem. Ges.* 1931, **64**, 2591.
2. L. Cambi and L. Szego and A. Cagnasso, *Atti. Accad. Lincei* 1932, **15**, 226; 329.
3. L. Cambi and L. Malatesta, *Ber. Dtsch. Chem. Ges.* 1937, **70**, 2067.
4. A. H. White, E. Kokot, R. Roper, H. Waterman and R. L. Martin, *Austral. J. Chem.* 1964, **17**, 294.
5. A. H. Ewald, R. L. Martin, E. Sinn and A. H. White, *Inorg. Chem.* 1969, **8**, 1837.
6. M. F. Tweedle and L. J. Wilson, *J. Amer. Chem. Soc.* 1976, **98**, 4824.
7. M. Cox, J. Darken, B. W. Fitzsimmons and A. W. Smith, L. F. Larkworthy and K. A. Rogers, *J. Chem. Soc. (Dalton)* 1972, 1192.
8. K. S. Patel and A. A. Adimado, *J. Inorg. Nucl. Chem.* 1981, **43**, 1165.
9. G. T. Hall and D. N. Hendrickson, *Inorg. Chem.* 1976, **15**, 607.

NOTE

Complex formation of 1,4,7,10-tetraoxacyclododecane with alkali metal ions studied by ^{13}C spectroscopy

EILIF AMBLE and ERIK AMBLE*†
Kjemisk Institutt, Universitetet i Oslo, Oslo 3, Norway

Abstract—Complex formation of 1,4,7,10-tetraoxacyclododecane (12-crown-4) with lithium, sodium and potassium salts in methanol solution was investigated. The strong influence of complexing on the chemical shift of the single ^{13}C NMR line permitted titration of the ligand with alkali metal salts. Concentration stability constants of the complexes were obtained by a computerized iterative least squares method. Na^+ and K^+ form both 1 : 1 and 1 : 2 complexes, $\log K_1 = 2.1$ and $\log K_2 = 3.8$, $\log K_1 = 1.7$ and $\log K_2 = 2.4$ respectively. Li^+ is complexed weakly. Assuming 1 : 1 stoichiometry the complex stability constant is estimated to be < 1.

NMR spectroscopy has been extensively applied to investigate complex formation between alkali and alkaline earth metal ions and electrically neutral ligands.[1-3] Recently the conformations of free and complexed oligoethers have been studied using ^{13}C NMR spectroscopy.[4] Significant chemical shift differences were observed due to conformational rearrangements following complex formation. These findings were interpreted on the basis of empirical γ and δ-effects on the chemical shift.[5] The most dramatic upfield ^{13}C chemical shift was found for 1,4,7,10-tetraoxacyclododecane (12-crown-4).[6,7] It was therefore possible to study in some more detail the complexing of various alkali metal salts with 12-crown-4. We report here our efforts to determine quantitatively the complex stabilities by least squares approximation of the obtained data.

PRINCIPLE OF THE METHOD

The interaction between the ligand 12-crown-4 (L) and alkali metal ions (M) taking into account both 1:1 and 1:2 complexes is defined by eqns (1)–(4).

$$L + M \rightleftharpoons LM \tag{1}$$

$$LM + L \rightleftharpoons L_2M \tag{2}$$

$$K_1 = \frac{[LM]}{[L][M]} \tag{3}$$

$$K_2 = \frac{[L_2M]}{[L]^2 \cdot [M]} \tag{4}$$

If the exchange rate between the three different environments of the ligand is rapid, the observed chemical shift δ_{obs} represents a weighed average and eqn (5) is valid.

$$\delta_{obs} = \frac{[L]}{[L_0]} \delta_L + \frac{[LM]}{[L_0]} \delta_{LM} + \frac{2 \cdot [L_2M]}{[L_0]} \delta_{L_2M} \tag{5}$$

where $[L_0] = [L] + [LM] + 2 \cdot [L_2M]$, $[M_0] = [M]$

$+ [LM] + [L_2M]$, δ_L, δ_{LM} and Δ_{L_2M} are the chemical shifts of the free ligand, the 1 : 1 and the 1 : 2 complex respectively.

The induced chemical shift by complex formation $\Delta\delta_{obs} = \delta_{obs} - \delta_L$ is expressed by eqn (6).

$$\Delta\delta_{obs} = \frac{[LM]}{[L_0]} \Delta\delta_{LM} + \frac{2 \cdot [L_2M]}{[L_0]} \Delta\delta_{L_2M} \tag{6}$$

where $\Delta\delta_{LM}$ and $\Delta\delta_{L_2M}$ are the chemical shifts of the complexes relative to δ_L.

Substitution of [L], [L_2M] and [M] in eqns (1)–(4) by [LM] yields

$$\left\{K_2 - 4 \cdot \frac{K_2^2}{K_1^2}\right\}[LM] - \left\{4 \cdot \frac{K_2}{K_1} - K_1 + 2\right.$$

$$\times K_2[M_0]\Big\}[LM] + \{K_2[L_0](2[M_0] - [L_0]) - K_1([L_0]$$

$$+ [M_0]) - 1\}[LM] + K_1[L_0][M_0] = O. \tag{7}$$

From eqn (7) [LM] can be calculated as a function of experimental values $[M_0]$ and $[L_0]$ for assumed values of K_1 and K_2.

The experimental procedure consists of measuring $\Delta\delta_{obs}$ as a function of changing concentrations $[M_0]$ while $[L_0]$ is kept constant, leading to titration curves shown in Fig. 1. The accompanying variations in ionic

Fig. 1.

---
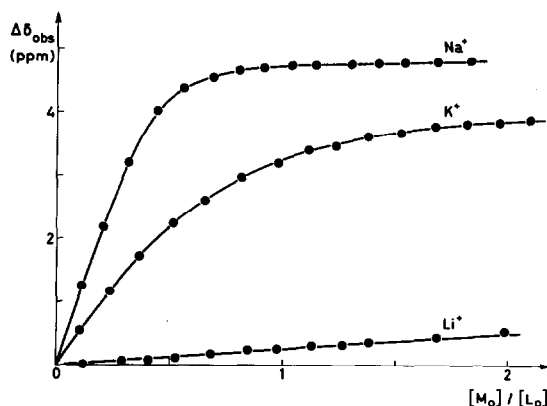
*Author to whom correspondence should be addressed.
†Present address: Rumen Kjemi A/S, P.B. 23 Refstad, Oslo 5, Norway.

strength are neither expected to influence the ^{13}C chemical shifts nor the complexation constants over the titration range.[5,8] Therefore, approximation of these data by calculated values of $\Delta\delta_{obs}$ based on eqns (6) and (7) is possible and yields K_1, K_2, $\Delta\delta_{LM}$ and $\Delta\delta_{L_2M}$.

The mathematical analysis of the data represents an extension of the method of Creswell and Allred for 1:1 complexes. With assumed values for K_1 and K_2 values for [LM] can be calculated for all data points using eqn (7). Only real roots [LM] $\leq$ [M$_0$] have physical significance. Least squares approximation of $\Delta\delta_{obs}$ (eqn 6) using these calculated values for [LM] yields estimates for $\Delta\delta_{LM}$ and $\Delta\delta_{L_2M}$.

In principle this procedure can be repeated with new values for K_1 and K_2 until the best fit and hence the optimal K_1 and K_2 are found. However, considerable computing time can be saved by applying a modified trial and error iteration. It is easily seen that the amount of 2:1 complex is predominant for small values of [M$_0$]. This means that K_2 is dominating on the lower part of the titration curve. Therefore only one of the two constants K_1 and K_2 is varied at a time and only the part of the data used where this constant has a substantial impact on the value of $\Delta\delta_{obs}$. When e.g. an optimal K_2 for a chosen K_1 is found using the lower part of the titration curve, i.e. small [M$_0$]/[L$_0$], this value for K_2 is used for the determination of an improved value for K_1 using the upper part of the data. This procedure of shifting between the two parts of the data is repeated with new values of K_1 and K_2 until the best pair of stability constants and the corresponding values of $\Delta\delta_{LM}$ and $\Delta\delta_{L_2M}$ are found.

RESULTS AND DISCUSSION

The ^{13}C NMR chemical shift of the single line of 12-crown-4 was measured in solutions containing varying amounts of alkali metal salts. Plots of the induced chemical shift $\Delta\delta_{obs}$ vs the relative metal ion concentration [M$_0$]/[L$_0$] are shown in Fig. 1. As it is seen the three alkali metal ions gave rise to very different titration curves.

Sodium ions had a strong effect on $\Delta\delta_{obs}$ already at low concentrations. The plot rises almost linearly until 0.5 equivalents have been added. After a sharp bend only small changes were observed. These findings indicate that the formation of a 2:1 sandwich complex is preferred.

Increasing concentrations of potassium ions also led to substantial induced chemical shifts. However, the plot exhibits a smaller curvature. It is thus not possible to estimate visually which complex stoichiometry is predominant.

Finally upon addition of Li$^+$ only very small induced chemical shifts were observed.

The results of the iterative least squares analysis of these data are listed in Table 1.

It is seen that both sodium and potassium ions lead to 1:1 complexes with comparable strength. Note also that the induced upfield shifts $\Delta\delta_{LM}$ are similar suggesting that 12-crown-4 adopts essentially the same conformation in both complexes.

However, sodium forms a considerably more stable sandwich 2:1 complex than potassium, the calculated values for log K_2 being 3.8 for Na$^+$ and 2.4 for K$^+$. Furthermore the values for the induced chemical shift is by far the biggest in the 2:1 complex with Na$^+$.

Table 1.

	Na$^+$	K$^+$
log K_1	2.1	1.7
log K_2	3.8	2.4
$\Delta\delta_{LM}$	66.5 Hz	65.5 Hz
$\Delta\delta_{L_2M}$	82.3 Hz	58.5 Hz

Both results reflect the ideal size of 12-crown-4 for the formation of a sandwich complex with sodium ions in solution, as it has been suggested on the basis of X-ray crystallography.[11–13]

The smaller upfield shift observed for the 2:1 complex with K$^+$ and the weaker binding of this ion are in good accord with the necessary conformational adjustment of the ligand to this bigger ion.

The data from Li$^+$ titration could not be analyzed by the described method. However, an estimate for K_1 was obtained under the hypothesis that only a 1:1 complex is formed and that its chemical shifts is similar to the one of the other 1:1 complexes. Using these assumptions, a comparison of the observed shifts with values calculated for various K_1 values lead to the estimate: $K_1 < 1$. This result leads to the surprising conclusion that 12-crown-4 faces strong competition by methanol in solvating Li$^+$, demonstrating that this twelve membered ring system is not ideal for complexing such a small ion.

It has thus been shown that simple estimates based on correlations between ring size and ionic radius, which would predict a rather stable 1:1 lithium complex, are not possible when conformational changes accompany complex formation.

In conclusion we claim to have demonstrated that ^{13}C NMR might be a useful tool for the quantitative determination of complexing of crown ethers and their amino analogues.[14]

REFERENCES

[1] J. M. Lehn, J. P. Sauvage and B. Dietrich, J. Amer. chem. Soc. 1970, 92, 2916.
[2] R. L. Bodner, M. S. Greenberg and A. I. Popov, Spectroscopy Lett. 1972, 5, 489.
[3] R. Büchi and E. Pretsch, Helv. Chim. Acta 1977, 60, 114.

[4]J. Krane, E. Amble, J. Dale and K. Daasvatn, *Acta Chem. Scand.* 1980, **B34**, 255.

[5]G. Borgen, J. Dale, K. Daasvatn and J. Krane, *Acta Chem. Scand.* 1980, **B34**, 249.

[6]G. Borgen, J. Dale and G. Teien, *Acta Chem. Scand.* 1979, **B33**, 15.

[7]J. Dale, *Israel J. Chem.* 1980, **20**, 3.

[8]E. T. Roach, P. R. Handy and A. I. Popov, *Inorg. Nucl. Chem. Lett.* 1973, **9**, 339.

[9]J. Creswell and A. L. Allred, *J. Phys. Chem.* 1962, **66**, 1469.

[10]K. L. Gammon, S. H. Smallcombe and J. H. Richards, *J. Am. Chem. Soc.* 1972, **94**, 4573.

[11]F. A. Anet, J. Krane, J. Dale and K. Daasvatn, *Acta Chem. Scand.* 1973, **27**, 3395.

[12]F. P. van Remoortere and F. P. Boer, *Inorg. Chem.* 1974, **13**, 2071.

[13]F. P. Boer, M. A. Neuman, F. P. van Remoortere and E. C. Steiner, *Inorg. Chem.* 1974, **13**, 2826.

[14]M. J. Calverley and J. Dale, *Acta Chem. Scand.* 1982, **B36**, 241.

[15]H. Stamm, W. Lamberty and J. Stafe, *Tetrahedron* 1976, **32**, 2045.

NOTE

Correlation of closo-carborane ^{11}B–H spin-coupling constants with structural features including cage "umbrella" angle

WILEY JARVIS, Z. JEAN ABDOU and THOMAS ONAK*

Department of Chemistry, California State University, Los Angeles, CA 90032, U.S.A.

Abstract—The magnitude of $^1J(^{11}B^1H)$ values for the closo-carboranes are correlated to structural characteristics. Among the various parameters considered, both the number of adjacent cage carbon atoms and cage "umbrella" angle appear to contribute significantly to changes in the observed spin-coupling constants with smaller cage umbrella angles contributing to higher $J(^{11}B–H)$ values. A derived empirical method enables the prediction, or confirmation, of certain NMR assignments in those instances where some uncertainty previously existed.

Previous investigations of element–hydrogen spin–spin coupling have well established that the numerical value of $^1J(XH)$ becomes greater with increasing s-orbital character of the X–H bond. In the cases of compounds containing boron–hydrogen bonds two studies[1,2] have attempted to relate $^1J(^{11}B^1H)$ with MO-determined element s-orbital electron population. However, within the closo polyhedral carborane series $C_2B_nH_{n+2}$, only three of these compounds ($n = 3$–5) have heretofore been considered in this manner. And although the obtained correlations were reasonably satisfactory, an extension of these MO approaches to other isomers within these polyhedral systems and to the remainder of the series, $n \leqslant 10$, would have very limited quantitative predictive value. Until easily accessible and accurate values of s-electron populations become available we present another approach, empirical in nature, for the prediction of $^1J(^{11}B^1H)$ values of closo-carboranes. In the present study, certain structural characteristics of the cage compounds are correlated with the magnitude of $^1J(^{11}B^1H)$.

EXPERIMENTAL AND DATA

Nuclear magnetic resonance data

Although apparent $^1J(^{11}B^1H)$ constants for the closo-carboranes (Fig. 1) listed in Table 1, column 6, have been previously reported in the literature, it was highly desirable for the purpose of the present study to establish these values within an error of $\leqslant \pm 2$ Hz. The literature values for each of the following: $1,5\text{-}C_2B_3H_5,$[3,4] $1,2\text{-}C_2B_4H_6,$[4] $1,6\text{-}C_2B_4H_6,$[4,5] $2,4\text{-}C_2B_5H_7,$[3,6–9] $1,7\text{-}C_2B_6H_8,$[10] $1,6\text{-}C_2B_7H_9,$[11,12] $1,6\text{-}C_2B_8H_{10},$[9,12]

$2,3\text{-}C_2B_9H_{11},$[13–15] $1,2\text{-}C_2B_{10}H_{12},$[16] $1,7\text{-}C_2B_{10}H_{12}$[16] and $1,12\text{-}C_2B_{10}H_{12},$[17] were rechecked by ^{11}B and ^{1}H NMR spectra which were recorded by, variously, Varian HA-100 and Bruker WP-60 spectrometers in our laboratories as well as by the Bruker WM-500 spectrometer at the Southern California Regional Facility, California Institute of Technology. The average estimated error for the observed J values reported in Table 1 is within $\pm 1\%$ ($\sim 80\%$ confidence), within $\pm 1.5\%$ (with $> 95\%$ confidence).

Structural data

Umbrella angles, Table 1, column 4, were calculated from known structural coordinates for all of the cited closo-carboranes: $1,5\text{-}C_2B_3H_5,$[18] $1,2\text{-}C_2B_4H_6,$[18] $1,6\text{-}C_2B_4H_6,$[18] $2,4\text{-}C_2B_5H_7,$[18] $1,7\text{-}C_2B_6H_8,$[19] $1,6\text{-}C_2B_7H_9,$[20] $1,6\text{-}C_2B_8H_{10},$[21] $2,3\text{-}C_2B_9H_{11},$[22] $1,2\text{-}C_2B_{10}H_{12},$[18] $1,7\text{-}C_2B_{10}H_{12}$[18] and $1,12\text{-}C_2B_{10}H_{12}.$[18] These calculations were performed using PROPHET computer programs (CRYST, EDITMODEL, MAST) made available by the National Institutes of Health. It is estimated that the reliability of the structural data used for the calculated umbrella angles results in an error within $\pm 0.5\%$ of values of θ (for the definition of θ, see below).

RESULTS AND DISCUSSION

An examination of the data in Table 1 (see columns 3, 4 and 6) leads to the conclusion that the value of $^1J(^{11}BH)$ is dependent (a) on the number of cage carbon atoms, C, bonded to the boron atom of the B–H bond under consideration, and (b) on the magnitude of a cage "umbrella" angle, θ. The term "umbrella" angle describes the (average) interior angle of a conical, or near-conical, shaped figure having the boron atom of a

---

*Author to whom correspondence should be addressed.
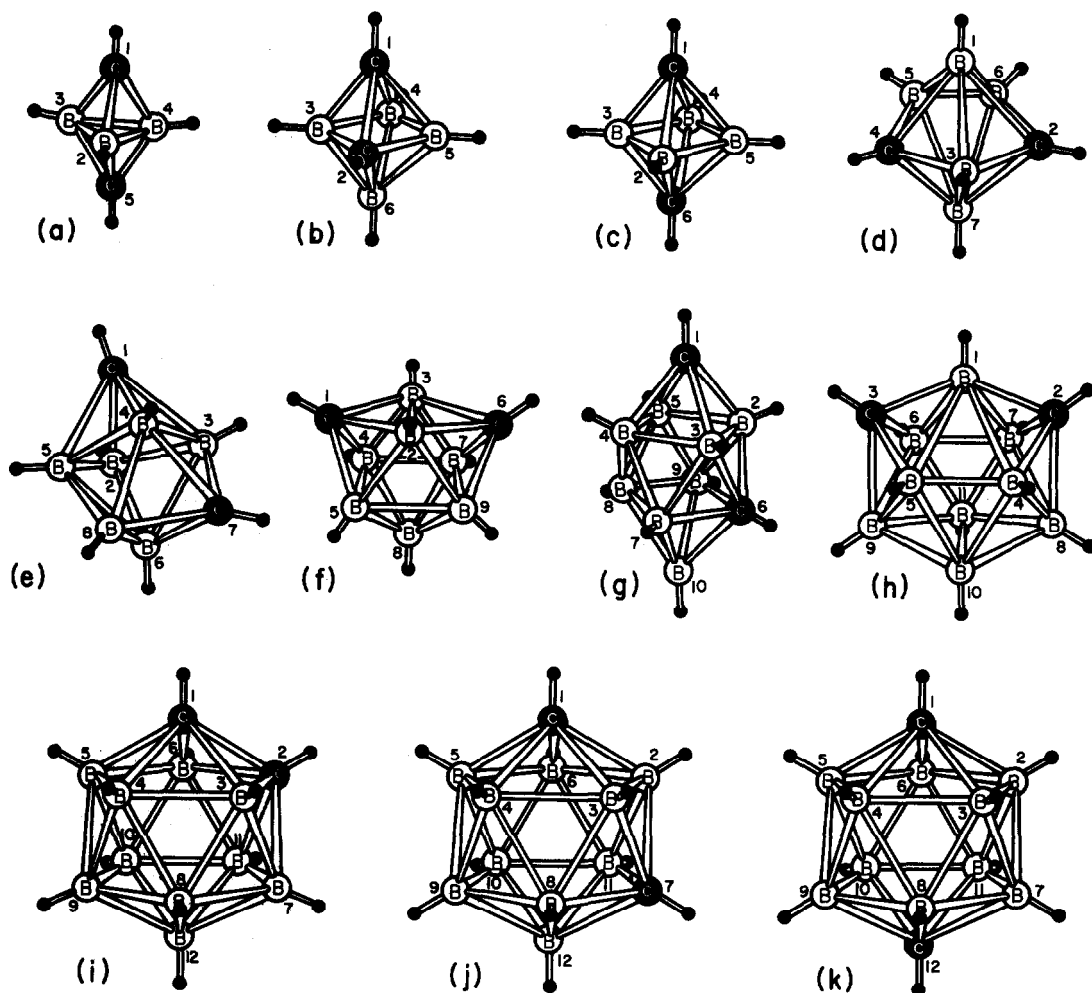
Fig. 1. Cage Structures of the closo-carboranes. (a) $1,5\text{-}C_2B_3H_5$, (b) $1,2\text{-}C_2B_4H_6$, (c) $1,6\text{-}C_2B_4H_6$, (d) $2,4\text{-}C_2B_5H_7$, (e) $1,7\text{-}C_2B_6H_8$, (f) $1,6\text{-}C_2B_7H_9$, (g) $1,6\text{-}C_2B_8H_{10}$, (h) $2,3\text{-}C_2B_9H_{11}$, (i) $1,2\text{-}C_2B_{10}H_{12}$, (j) $1,7\text{-}C_2B_{10}H_{12}$ (k) $1,12\text{-}C_2B_{10}H_{12}$.

given B–H bond at the apex, and bonds to neighbouring cage atoms as the radial frame:
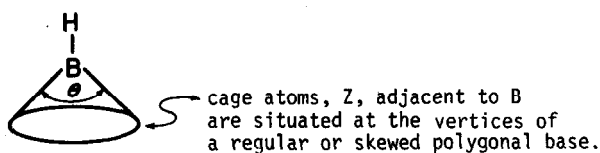
The value of θ is determined by averaging values of 2β for all B–Z bonds of any given boron:
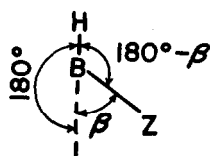
The concept of using an "umbrella angle" for the present study involving cage carborane compounds can be considered similar to the use of C–C–C interatomic bond angles in correlating J(CH) values for organic ring systems.[23] In the latter studies it was found, of course, that smaller C–C–C angles resulted in higher J(CH) values; the simple explanation for this correlation involves greater p-orbital involvement of the CH carbon atom electrons toward ring C–C bonding resulting in greater s-orbital density in the CH bond external to the ring.[23] An extension of this reasoning to cage carboranes is consistent with the association of smaller umbrella angles with larger J(^{11}B–H) values for any particular boron site. A study of Table 1, cf columns 4 and 6, bears this out.

Linear relationships of the type J(^{11}B–H) = Aθ + B, when applied to the data in Table 1, columns 3, 4 and 6, yield:

$$J(^{11}\text{B–H}) = -2.08(\theta) + 394 \quad \text{when } C = 0 \quad (1)$$

$$J(^{11}\text{B–H}) = -0.0621(\theta) + 172 \text{ when } C = 1 \quad (2)$$

$$J(^{11}\text{B–H}) = -0.333(\theta) + 214 \quad \text{when } C = 2 \quad (3)$$

Table 1. Data, C, θ, $^1J(^{11}B-H)$, for the closo carboranes in Fig. 1

(1) Compound	(2) Position of cage boron	(3) Number of Adjacent Carbons, C	(4) Umbrella Angle, θ	(5) Calculated $^1J(^{11}B^1H)$ using eq (4)	(6) Observed J (Hz)
$1,5-C_2B_3H_5$	2,3,4	2	77.2	189	188
$1,2-C_2B_4H_6$	3,5	2	86.6	186	185
	4,6	1	88.1	166	162
$1,6-C_2B_4H_6$	2,3,4,5	2	85.6	186	186
$2,4-C_2B_5H_7$	1,7	2	97.7	182	179
	3	2	91.4	185	184
	5,6	1	90.2	166	168
$1,7-C_2B_6H_8$	2,8	1	95.2	166	168
	3,4	2	102	181	171
	5,6	1	104	166	168
$1,6-C_2B_7H_9$	2,3	2	105	180	176
	4,5,7,9	1	106	165	162
	8	0	110	165	164
$1,6-C_2B_8H_{10}$	2,3	2	109	179	180
	4,5	1	111	165	--
	7,9	1	111	165	--
	8	0	111	163	--
	10	1	100	166	183
$2,3-C_2B_9H_{11}$	1	2	116	176	171
	4,5,6,7	1	111	165	167
	8,9	1	112	165	172 (or 150)
	10,11	0	118	149	150 (or 172)
$1,2-C_2B_{10}H_{12}$	3,6	2	114	177	178
	4,5,7,11	1	116	165	164
	8,10	0	117	151	151
	9,12	0	117	151	151
$1,7-C_2B_{10}H_{12}$	2,3	2	114	177	178
	4,6,8,11	1	116	165	165
	5,12	1	116	165	162
	9,10	0	117	151	151
$1,12-C_2B_{10}H_{12}$	2-11	1	116	165	165

where C is the number of contiguous cage carbon atoms. Fusing the three separate equations into a single expression gives eqn (4):

$$^1J(^{11}BH) = \frac{-2.08(13.4)^{C^2}(\theta)}{449^C} + \frac{394(1.69)^{C^2}}{3.87^C}. \quad (4)$$

This relationship predicts with reasonable precision J(^{11}B–H) values (Table 1, column 5) for nearly all BH sites in the neutral *closo*-cage compounds.

In the case of $2,3-C_2B_9H_{11}$ there previously existed some uncertainty about the chemical shift assignments (and also therefore J values) of B(8,9) and B(10,11); the observed J(BH) values for the two doublets were observed to be 172 and 150 Hz. Since the areas for each were identical, unambiguous assignments were not possible. It is clear from the calculated J(BH) values using eqn (4), that the higher J(BH) can be assigned to cage

positions 8 and 9 and the lower J(BH) value thus belongs to positions 10 and 11.

Though the area "2" B–H resonances for the 1,2- and 1,7-isomers of $C_2B_{10}H_{12}$ have been previously assigned from substituent studies[16] ambiguity still exists; but it is reassuring that the J(BH) values predicted from eqn (4), are in complete accord with this assignment, (Table 1, cf columns 5 and 6).

Two predicted J(BH) values, those for the B(3,4)-H of $1,7-C_2B_6H_8$ and the B(10)-H of $1,6-C_2B_8H_{10}$, are sufficiently different from the reported experimental values to warrant comment. The $1,7-C_2B_6H_8$ is the only *closo*-carborane in the present study in which there is strong suspicion of rapid cage fluxional behaviour.[24,25] Thus the application of eqn (4), to this situation, where an umbrella angle is obtained from static geometrical data, may be unreasonable. Incomplete experimental data and assignments for $1,6-C_2B_8H_{10}$ makes speculation

difficult for the J(BH) discrepancy, experimental vs predicted.

The magnitude of J values for all the compounds mentioned here could show some dependence on variables other than those, C and θ, in eqn (4). However, our attempts to correlate the available coupling constant data with parameters such as cage-atom coordination number and cage bond delocalization (e.g. antipodal effects)[26] were inefficacious and did not indicate any discernible dependency of $^1J(^{11}B^1H)$ on these particular factors.

Also, an attempt to relate $^1J(^{13}C^1H)$, for the cage carbon atoms, to any or all of the parameters discussed above proved unproductive due to the scarcity of available data points.

REFERENCES

1. J. Kroner and B. Wrackmeyer, *J. Chem. Soc. Faraday Trans. II*, 1976, **72**, 2283.
2. T. Onak, J. B. Leach, S. Anderson, M. J. Frisch and D. Marynick, *J. Magnetic Resonance* 1976, **23**, 237.
3. R. N. Grimes, *J. Am. Chem. Soc.* 1966, **88**, 1895.
4. T. Onak and E. Wan, *J. C. S. Dalton* 1974, 665.
5. T. Onak, R. P. Drake and G. B. Dunks. *Inorg. Chem.* 1964, **3**, 1686.
6. J. F. Ditter, E. B. Klusman, R. E. Williams and T. Onak, *Inorg. Chem.* 1976, **15**, 1063.
7. T. Onak, F. J. Gerhart and R. E. Williams, *J. Am. Chem. Soc.* 1963, **85**, 3378.
8. R. Warren, D. Paquin, T. Onak, G. Dunks and J. R. Spielman, *Inorg. Chem.* 1970, **9**, 2285.
9. G. Dunks, Private communication.
10. G. B. Dunks, Ph.D. Dissertation, 1970.
11. G. B. Dunks and M. F. Hawthorne, *Inorg. Chem.* 1970, **9**, 893.
12. Prior unpublished studies carried out in these laboratories.
13. V. Chowdry, W. R. Pretzer, D. N. Rai and R. W. Rudolph, *J. Am. Chem. Soc.* 1973, **95**, 4560, see footnote 12.
14. F. R. Scholer, R. Brown, D. Gladkowski, W. F. Wright and L. J. Todd, *Inorg. Chem.* 1979, **18**, 921.
15. F. N. Tebbe, P. M. Garrett and M. F. Hawthorne, *J. Am. Chem. Soc.* 1968, **90**, 869.
16. T. E. Fielding, Ph.D. Dissertation, 1971; A. R. Garber, G. M. Bodner, L. J. Todd and A. R. Siedle, *J. Magnetic Resonance* 1977, **28**, 383.
17. T. A. Babushkina, V. V. Khrapov, V. A. Brattsev, Yu V. Gol'tyapin and V. I. Stanko, *Zhurnal Strukturnoi Khimii* 1973, **14**, 1018, English Trans. p. 959.
18. T. F. Koetzle and W. N. Lipscomb, *Inorg. Chem.* 1970, **9**, 2743.
19. H. Hart and W. N. Lipscomb, *Inorg. Chem.* 1968, **7**, 1070.
20. T. F. Koetzle, F. E. Scarbrough and W. N. Lipscomb, *Inorg. Chem.* 1968, **7**, 1076.
21. T. F. Koetzle and W. N. Lipscomb, *Inorg. Chem.* 1970, **9**, 2279.
22. C. Tsai, Ph.D. Dissertation, 1968.
23. C. S. Foote, *Tetrahedron Letters* 1963, 579; P. Lazlo and P.v.-R. Schleyer, *J. Am. Chem. Soc.* 1964, **86**, 1171.
24. R. E. Williams and F. J. Gerhart, *J. Am. Chem. Soc.* 1965, **87**, 3513.
25. E. L. Muetterties, E. L. Hoel, C. G. Salentine and M. F. Hawthorne, *Inorg. Chem.* 1965, **14**, 950.
26. T. Onak, *Boron Hydride Chemistry* (Edited by E. L. Muetterties), pp. 349–382. Academic Press, New York (1975); G. A. Beltram and T. P. Fehlner, *J. Am. Chem. Soc.* 1979, **101**, 6237; T. Onak and W. Jarvis, *J. Magnetic Resonance* 1979, **33**, 649; T. Onak, Polyhedral Organoboranes. In *Comprehensive Organometallic Chemistry* (Edited by G. Wilkinson, F. G. A. Stone and E. W. Abel), Vol. 1, pp. 411–457. Pergamon Press, New York (1982).

NOTE

Synthesis and characterization of sodium-tetramethylammonium decamolybdate

EWA K. HODOROWICZ and STANISLAW A. HODOROWICZ*
Department of Chemistry, Jagiellonian University, Krakow, Poland

Abstract—Sodium-tetramethylammonium decamolybdate in acidified solution has been crystallized. Chemical analysis, thermogravimetric and X-ray studies have been performed.

When normal tungstate or molybdate solutions are acidified, various polyanions of increasing degrees of condensation are obtained according to different acidifications and other conditions. In the recent years using specific organic cations new forms have been isolated.[1] In particular, Souchay et al.[2] described the formation of dodecatung state $[H_{16}W_{12}O_{48}]^{8-}$ in aqueous solution acidfied to $Z = 1.33$ (the degree of acidity Z is defined as $Z = [H^+]/[W]$) in the presence of tetramethylammonium ions. In our investigations we have found that in conditions similar to those used by Souchay two different forms of polytungstate crystallized. One of these species was formulated as metadodecatungstate $[N(CH_3)_4]_6W_{12}O_{39}(H_2O)_6$,[3] and the other as sodium tetramethylammonium decatungstate $Na_6[N(CH_3)_4]_3[W_{10}O_{34}(OH)](H_2O)_8$.[4,5] Now we report new data for polymolybdate precipitated from solution under the above-mentioned conditions.

EXPERIMENTAL

The crystallization was carried out at concentration 0.250 M molybdate and the degree of acidity $Z = 1.33$. First a sodium molybdate dihydrate (POCh Gliwice, Poland) solution in 2 M tetramethylammonium chloride was prepared. This solution was treated with the calculated amount of 1 N HCl in 2 M tetramethylammonium chloride and next it was left for crystallization at 25°C. After several days a white crystalline precipitate was obtained, filtered off, washed with ethanol, dried in the air and placed in a desiccator over $CaCl_2$.

The crystals were then examined microscopically. No difference in the form of crystals was observed. All crystals were very small plates.

The precipitate was analyzed chemically. Molybdenum was determined by the gravimetric method after Busev[6] as $PbMoO_4$. Sodium was determined indirectly as

Na$_2$O from the sum of the MoO_3 and Na_2O. The nitrogen, carbon and hydrogen were determined on a Perkin–Elmer automatic CHNO analyzer.† The compound was subjected to X-ray powder diffraction analysis in a 100-m Guinier–Hägg camera equipped with a quartz monochromator to provide clean Cu-K$_{\alpha 1}$ radiation. Platinum powder ($a = 3.9238 \pm 0.0003$ Å, 25°C) was used as an internal standard. Quantitative intensity data were obtained on a DRON-2 (Burevestnik, U.S.S.R.) diffraction with nickel-filtered copper radiation.

The thermogravimetric measurements were performed in the air and in argon within the temperature range 25–800°C using model OD-12, MOM Budapest derivatograph. Samples of 300 mg were heated at rates 5°/min and the galvanometer sensitivity DTA = 1/3 and DTG = 1/3. The density of the crystals was determined by the pycnometric method using carbon tetrachloride.

RESULTS AND CONCLUSIONS

The result of analysis: Mo = 50.03 ± 0.1%, $MoO_3 + Na_2O = 84.05 \pm 0.05\%$, N = 2.21 ± 0.02%, C = 7.55 ± 0.02% and H = 2.25 ± 0.04% indicate that the molar ratio $MoO_3 : Na_2O : N : C : H$ is equal to 3.30 : 0.92 : 1 : 3 : 3.98 : 14.15.

The powder patterns obtained are very similar to those of previous reported sodium-tetramethylammonium decatungstate.[4] They can be indexed in the orthorhombic system with lattice parameters $a = 16.43(2)$, $b = 21.67(3)$ and $c = 13.78(3)$ Å. These parameters were derived by the least-squares procedure from a refinement based on 25 coincidence-free reflections. Table 1 lists the population of both experimental and theoretical interplanar spacings for 34 successive reflections.

The density of crystals at temperature 25 ± 0.5°C is 2.57 ± 0.02 gcm^{-3}. The volume of the unit cell is 4908 Å^3 and its mass is 12613×10^{-24} g. The multiplicities possible of the molecules per unit cell for the ortho rhombic system are only 1, 2, 4 and 8. For these values the molecular weights are 7598, 3799, 1899 and 950, respectively. By comparison of these data with the results of chemical analysis the most probable formula for the

*Author to whom correspondence should be addressed.

†These measurements were carried out in the Regional Laboratory of Physicochemical Analysis and Structural Research, Jagiellonian University, Kraków, Poland.
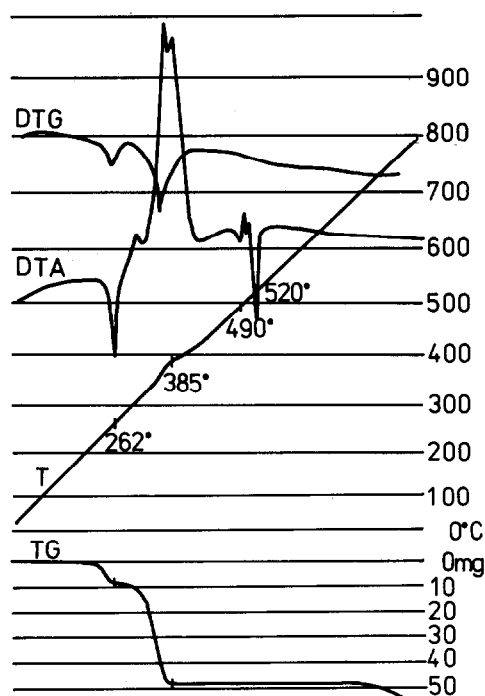
Fig. 1. Thermal analysis curves for sodium-tetramethylammonium decamolybdate under air.

compound obtained seems to be a decamolybdate, $3Na_2O \times 1.5[N(CH_3)_4]_2O \times 10MoO_3 \times 3.5H_2O$. Calculated values for this formulae are: $Mo = 49.\overset{.}{5}9\%$, $Na_2O + MoO_3 = 84.01\%$, $N = 2.17\%$, $C = 7.45\%$, $H = 2.24\%$; molecular weight 1935; X-ray density $2.62\ gcm^{-3}$.

Thermal analysis curves are given in Fig. 1. The TG curve shows that the loss in mass occurs in two steps. The endothermal effect with a minimum at 265°C corresponds to the loss of three water molecules. The DTA exothermic peak above 300°C (it was endothermic in argon) is connected with decomposition of the tetramethyl ammonium cation and probably with further dehydration. A quite new diffraction pattern, probably of the crystalline phase $3Na_2O \times 10MoO_3$, appears over the temperature range 300–400°C. Above 490°C further structural changes occur and then new phase melts at 520°C.

The results obtained show that in sodium molybdate solutions acidified to $Z = 1.33$, in the presence of tetramethylammonium chloride only decamolybdate $3Na_2O \times 1.5[N(CH_3)_4]_2O \times 10MoO_3 \times 3.5H_2O$ is formed. This compound is not reported so far in the literature and it is presumably a true analogue* of the sodium-tetramethylammonium decatungstate $Na_6[N(CH_3)_4]_3[W_{10}O_{34}(OH)] \times 8H_2O$.

Further investigations of water bonding and structure

Table 1. Interplanar spacings and intensities for first 34 diffraction lines of complex investigated

$d_{obs.}$	$I_{max}, \%$	h	k	l						$d_{calcd.}$
10.54	4	1	0	1						10.56
9.51	100	1	1	1						9.49
8.53	14	0	2	1						8.52
7.66	30	2	1	0						7.68
5.50	2	1	2	2						5.48
4.86	3	3	2	0						4.88
4.83	6	1	4	1						4.82
4.43	5	1	0	3						4.42
4.03	5	4	1	0						4.03
3.87	10	4	1	1						3.87
3.84	8	4	2	0						3.84
3.70	3	2	5	1						3.69
3.58	30	1	5	2						3.58
3.52	22	4	0	2						3.52
3.36	5	3	4	2						3.36
3.176	5	2	0	4,	4	3	2,	4	4 1	3.177, 3.171, 3.184
3.046	40	2	2	4						3.049
2.935	2	5	1	2						2.938
2.864	4	1	4	4						2.863
2.817	6	3	2	4						2.816
2.780	12	1	7	2						2.783
2.720	15	1	0	5						2.719
2.637	5	1	2	5						2.637
2.560	7	2	5	4						2.560
2.525	8	4	6	2						2.524
2.494	7	0	6	4						2.493
2.446	4	6	4	0						2.444
2.427	8	1	4	5						2.429
2.385	90	2	6	4						2.385
2.274	7	1	0	6,	4	1	5			2.275, 2.276
2.209	10	7	1	2						2.210
2.134	42	6	1	4						2.134
1.996	36	4	1	6						1.996
1.908	28	2	1	7						1.907

The observed intensity is the average of two independent measurements

of sodium-tetramethylammonium decamolybdate are in progress.

REFERENCES

1. J. Fuchs, *Naturforsch.* 1973, **28b**, 389.
2. B. Le Meur and P. Souchay, *Rev. Chim. Minerale* 1972, **9**, 501.
3. J. Chojnacka, E. Hodorowicz and K. Stadnicka, *Roczniki Chemii* 1977, **51**, 1593.
4. J. Chojnacka and E. Hodorowicz, *J. Inorg. Nucl. Chem.* 1981, **43**, 3175.
5. E. Hodorowicz and S. Sagnowski, *Ibid.* 1981, **43**, 3179.
6. A. I. Busev, *Analytical Chemistry of Molybdenum, Israel Program for Scientific Translations*, p. 123. Jerusalem (1964).

NOTE

Ion-pairing and optical activity of diastereomeric zinc(II) 1, 10-phenanthroline, S-valinate systems

A. DECINTI* and G. LARRAZÁBAL

Departamento de Análisis Químico, Facultad de Ciencias Básicas y Farmacéuticas, Universidad de Chile, Santiago, Chile

Abstract—A series of S-valinatobis(1, 10-phenanthroline)zinc salts in methanolic solution have been prepared and their conductivities and ORD spectra measured. A positive linear correlation of optical rotation with conductance was found for salts of non-chelating counter anions. From the application of the Yoe-Jones method on the system Zn, phen, S-val$^-$, Cl$^-$ it was concluded that the counter anion dependence of the optical activity is connected mainly with heterocyclic ligand counter anion exchange equilibria.

A previous report from this laboratory described the preparation and optical properties of 1:2:1 mixed complex salts of zinc, 1, 10-phenanthroline and chiral aminoacidates.[1] In methanol these compounds exhibit aromatic exciton activity which presumably arises from a small difference in stability of the diastereomeric forms of the 1:2:1 mixed chelate ions. The intensity of such an effect depends upon the chiral ligand and, to a lesser extent, on the counter anion.[2]

A comparative study of counter anion effects on the optical activity of the above diastereomeric systems may provide evidence on ion pair associations in hydroxylic solvents as well as on the ligand ability of some anions. In this work we studied the counteranion dependence of the optical activity of the system Zn:1, 10-phenanthroline:S-valinate = 1:2:1, with a number of organic and inorganic anions in methanol. Preliminary results on this subject have been reported.[2] However, modifications of the preparative procedures and more data have slightly changed the earlier preliminary results.

EXPERIMENTAL

Salts of the mixed chelate ion [Zn(phen)$_2$(S-val)]$^+$ were prepared as 7.07×10^{-3} M solutions in methanol by the following reactions:

$$ZnSO_4 \cdot 7H_2O + \tfrac{1}{2}Ba(OH)_2 \cdot 8H_2O + 2phen \cdot H_2O$$

$$+ \tfrac{1}{2}BaX_2 \cdot 2H_2O + S\text{-valH} \rightarrow$$

$$[Zn(phen)_2(S\text{-val-}]X + BaSO_4 + 15H_2O$$
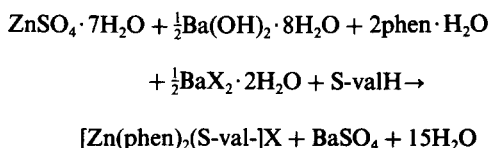
where X$^-$ = Br$^-$, Cl$^-$ or CH$_3$CO$_2^-$, and

$$ZnSO_4 \cdot 7H_2O + Ba(OH)_2 \cdot 8H_2O + 2phen \cdot H_2O$$

$$+ \tfrac{1}{n}H_nX + S\text{-valH} \rightarrow$$

$$[Zn(phen)_2(S\text{-val})]X\frac{1}{N} + BaSO_4 + 19H_2O,$$
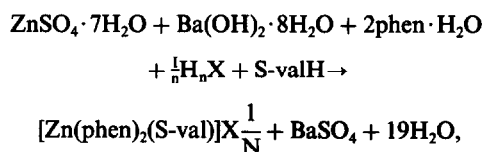
where X = gly$^-$, S-val$^-$, benzoate, salicylate$^-$, salicylate^{2-}, o-phthalate, m-nitrobenzoate, p-nitro benzoate, o-amino benzoate, m-amino benzoate or p-amino benzoate. The nitrate was obtained from bromide by metathesis with silver nitrate.

Stoichiometric mixtures of chromatographically homogeneous-S-valine and appropriate analytic reagent grade chemicals were stirred ultrasonically in methanol at room temperature and were heated to boiling point for 10 min. After cooling this procedure was repeated to ensure completion of reaction. Barium sulfate was removed by suction filtration. The solutions were reduced by evaporation to appropriate volumes and were standardized to 7.07×10^{-3}M Zn(II) at 25°C. At least three preparations were made with each counteranion. The optical rotatory dispersion spectra (ORD) of these solutions were run at 25°C over the range 330–400 nm on a modified Perkin–Elmer 141 polarimeter using a thermostated cell. Conductivity measurements at 25°C were made using a Wayne Kerr B 221 universal bridge, with an immersion cell (cell constant = 1.44). Differences in the small amounts of water derived from the salts did not affect the measurements.

The accuracy of the preparative procedures was tested gravimetrically or by counteranion exchange. Schematically, these were: SO$_4^{2-}$/Cl$^-$, SO$_4^{2-}$/p-amino benzoate, Br$^-$/NO$_3^-$, Cl$^-$/NO$_3^-$, salicylate^{2-}/salicylate$^-$ and S-valinate/acetate.

---

*Author to whom correspondence should be addressed.

The dependences of optical activity and conductivity on complex ion concentration were studied by diluting solutions of the chloride form of the cation salt. Yoe and Jones's molar-ratio type studies[3] of optical activity and conductivity of the system Zn, phen, S-val$^-$, Cl$^-$ were also performed. These experiments were carried out on series of individual preparations.

RESULTS AND DISCUSSION

A nearly linear concentration dependence of optical rotation over a range of the UV region was observed for chloride salt solutions (Fig. 1). Hence, the equivalent specific rotation of the diastereomeric system in presence of each counteranion reflects the concentration of 1:2:1 species, i.e. free cations plus paired cations. An essential requirement of this assumption is that ion-pairing between the 1:2:1 diastereomeric cations and the counterions does not significantly affect the exciton coupling, such an interaction being merely electrostatic or of the solvent structure-enforced ion-pairing type.[4] The aromatic anions o-amino benzoate, m-nitrobenzoate and p-nitrobenzoate made the samples almost opaque below 355 nm, modifying the typical shape of the ORD spectra. Although this effect might be attributed to some type of charge transfer interaction involving the aromatic systems, there is a long wavelength tail of the UV spectra of these anions giving considerable absorbance up to 355 nm. Hence, the changes in the typical shape of the ORD spectra in the presence of these anions were assumed to be unrelated to aromatic exciton coupling. However, in order to include the benzoate derivatives in the counteranion series, α values at 400 nm were used; but for the concentration ratio dependence studies, α values at 355 nm or 350 nm were used.

The equivalent specific rotation ($[\Phi]_{400\,nm}^{25°}$) and equivalent conductance (Λ) data are listed in Table 1 with the average deviations. There are two points to be made about these data: (1) The [Φ] and Λ values tend to exhibit

parallel dependences on the counteranion nature. (2) The potentially chelating counteranions give the lowest [Φ] and Λ values. A linear correlation of these data by regression analysis is shown in Fig. 2, where the least squares line was calculated excluding the chelating anions. This figure shows that the effects of chloride, bromide and nitrate on the optical activity of the system are very similar. The conductivity sequence $NO_3^- > Br^- > Cl^-$ follows the limiting ionic conductance of these ions in methanolic solutions.[5,6] On the other hand, the decrease of optical rotation of the diastereomeric system in the presence of SO_4^{2-} or a carboxylate counterion could be ascribed to greater ligand-counteranion exchange, which decreases the equilibrium concentrations of the 1:2:1 species. The presence in the system of S-val$^-$ as a counteranion excludes the effects of the chiral ligand-counteranion exchange equilibrium. Hence, the point for specific rotation and conductance values of the S-val$^-$ counteranion salt falling close to the correlation line (Fig. 2) suggests that for non chelating counteranions the main exchange equilibria must involve the heterocyclic ligand. The deviation from the least squares line for the glycinate salt could be ascribed to a glycinate-S-valinate exchange resulting in approximately half of the S-valinate being outside the coordination sphere. (The S-val$^-$: gly$^-$ equivalent specific rotation ratio is 1.97, whereas the similar equivalent conductance ratio is 0.99.) Furthermore, the deviation observed for o-phthalate could be indirect evidence for formation of a seven membered Zn-o-phthalate chelate ring.

These considerations agree with evidence on the system Zn, phen, S-val$^-$, Cl$^-$, Fig. 3 and 4. Figure 3 shows that the species which predominantly account for the optical activity of the system are the 1:2:1 diastereomeric complexes; the increase of conductivity with increasing [phen]:[Zn] can be ascribed to a 1, 10-phenanthroline-chloride exchange. Also, this increase
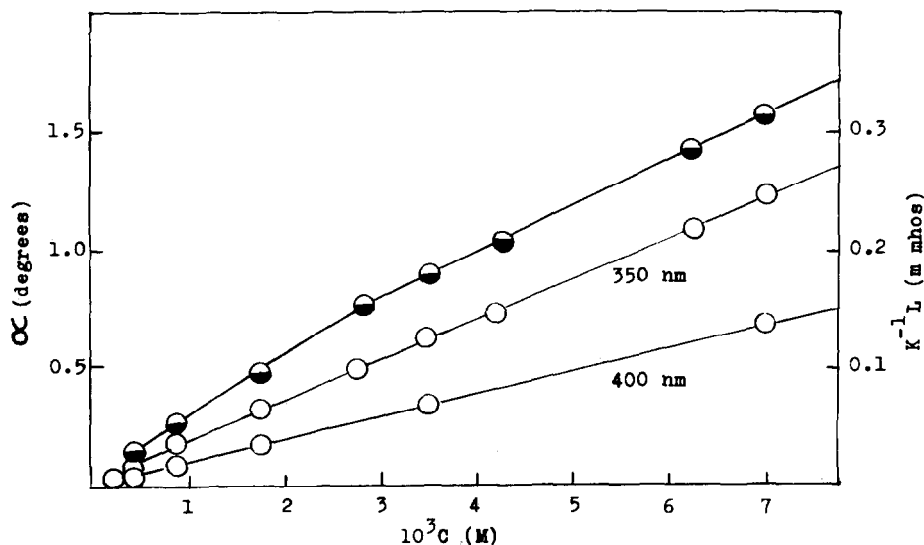
Fig. 1. Concentration dependence of optical rotation (1 = 2 cm) and conductivity (cell constant = 1.44) of [Zn(phen)$_2$(S-val)]Cl in methanol at 25°C.

Table 1. Equivalent specific rotation and equivalent conductance data of salts of $[Zn(phen)_2(S\text{-val})]^+$ in methanol at 25°C

X^{n-}	$\left[\Phi\right]_{400\ nm}^{25°}$	$\Lambda\ (7.07 \times 10^{-3}\ M)$
Br^-	4845 ± 36	67.2 ± 0.4
Cl^-	4795 ± 43	64.4 ± 0.4
NO_3^-	4788 ± 36	69.9 ± 1.9
p-Nitrobenzoate	4534 ± 74	53.4 ± 0.4
Acetate	4455 ± 70	53.6 ± 0.4
m-Nitrobenzoate	4434 ± 63	50.1 ± 1.4
Salicylate$^-$	4286 ± 50	48.9 ± 0.4
Benzoate	4158 ± 30	48.9 ± 0.6
m-Aminobenzoate	4010 ± 80	44.0 ± 1.0
o-Aminobenzoate	3663 ± 20	43.0 ± 0.2
p-Aminobenzoate	3623 ± 60	43.3 ± 0.8
SO_4^{2-}	3430 ± 30	30.6 ± 0.4
S-Valinate	2752 ± 30	19.6 ± 0.4
Salicylate^{2-}	2652 ± 50	24.5 ± 0.4
o-Phthalate^{2-}	2086 ± 43	15.8 ± 0.2
Glycinate	1400 ± 30	19.8 ± 0.4
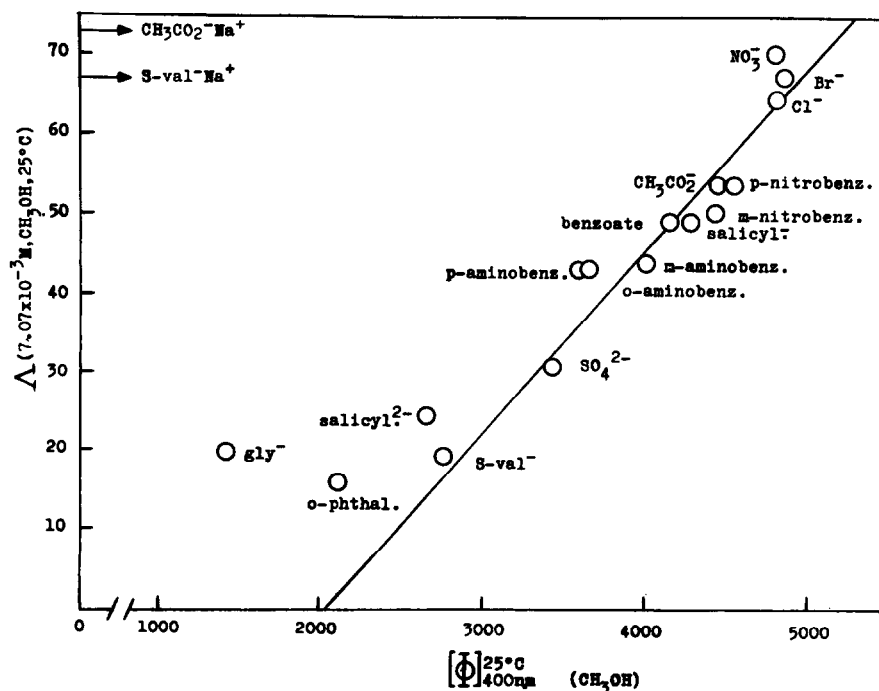
Fig. 2. Correlation of equivalent specific rotation with equivalent conductance for salts of $[Zn(phen)_2(S\text{-val})]^+$. (Correlation coefficient = 0.94.) Conductances of 7.07×10^{-3} M sodium salts in methanol have been included as reference data.
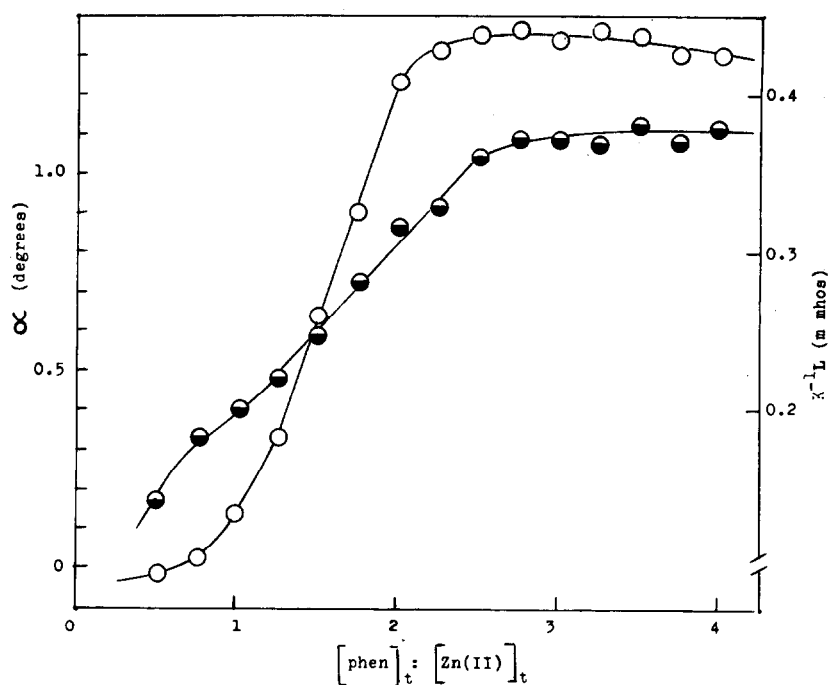
Fig. 3. Effects of the [phen]$_{total}$:[Zn(II)]$_{total}$ molar-ratio an optical rotation (0) and conductivity of the system 7.07×10^{-3} M Zn(II): S-val^{-}: Cl^{-}: phen = 1:1:1:x. (α at 350 nm and $1 = 2$ cm).
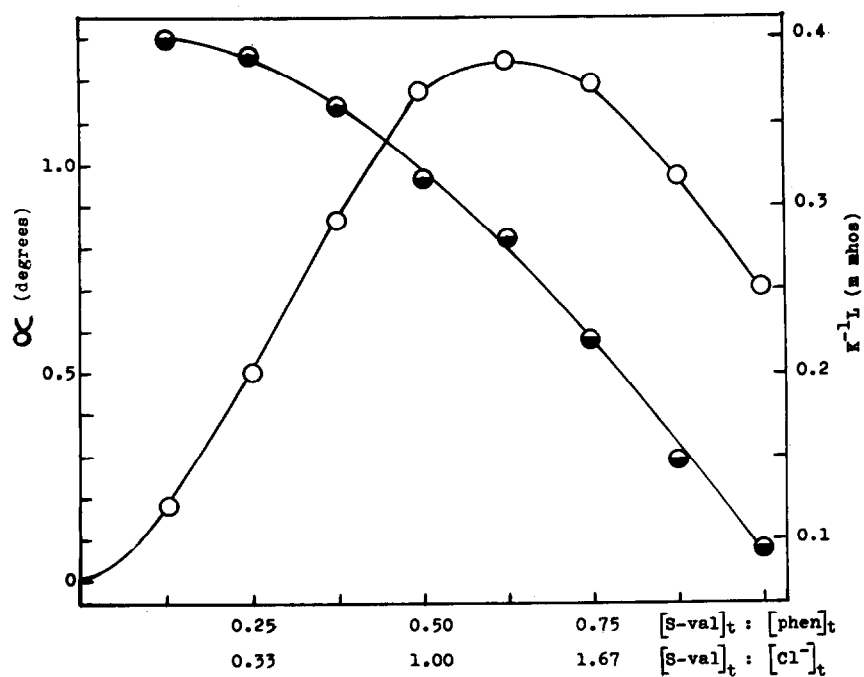
Fig. 4. Optical rotation (open circles) and conductivity of the system 7.07×10^{-3} M Zn(II): phen:S-val^{-}:Cl^{-} = 1:2:x:y as a function of the [S-val^{-}]$_{total}$:[Cl^{-}]$_{total}$ molar-ratio. (α at 355 nm and $1 = 2$ cm). ($x + y = 7.07 \times 10^{-3}$ M).

of conductivity suggests that the 1:2:1 species form less stable ion pairs than [Zn(phen)(S-val)]⁺. (For the latter species formation of a pentacoordinate inner complex with chloride ion is also possible.) The base strength dependent sequence observed for some univalent counteranions of similar size, i.e. the benzoates, tends to support the view that 1:1:1 species is involved in an inner sphere ion-pairing interaction (Fig. 5). The results in Fig. 4 conclusively confirm the preponderance of equilibria involving diastereomeric 1:2:1 cations as causes of residual exciton activity. Moreover, the concentration dependences shown in Figs. 3 and 4

suggest that S-valinate has a greater chelating ability than 1, 10-phenanthroline in methanol.

For non chelating univalent counterions (X⁻) the results may be treated using the following approximations:

Mass balance of 1:2:1 species gives

$$[\Delta^+] + [\Delta^+X^-] + [\Lambda^+] + [\Lambda^+X^-]$$
$$= ([\Delta^+] + (\Lambda^+])(1 + K_2[X^-]) \quad (1)$$

where Δ^+ and Λ^+ are the diastereomeric helical mixed chelate ions, and the same ion pair formation constant,
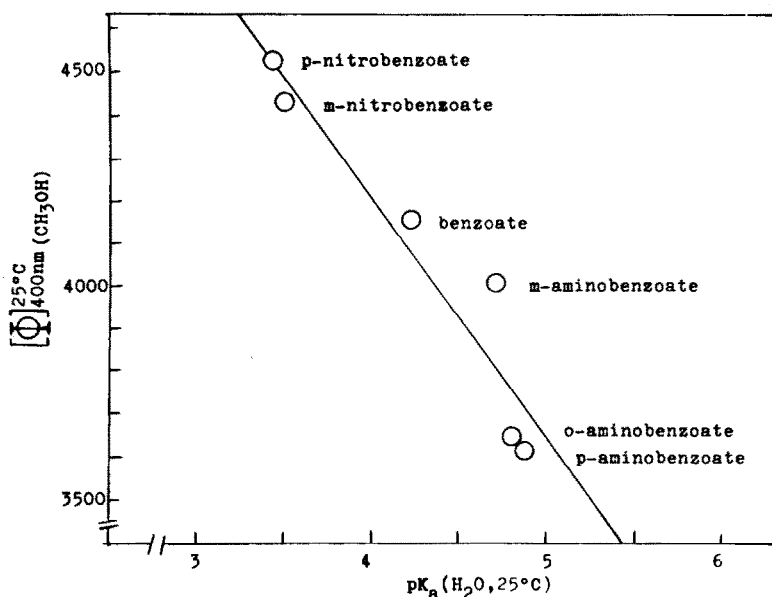
Fig. 5. Correlation of equivalent specific rotation (at 400 nm) with pK_a for some carboxylate salts of $[Zn(phen)_2(S\text{-val})]^+$. (Correlation coefficient = 0.95.)
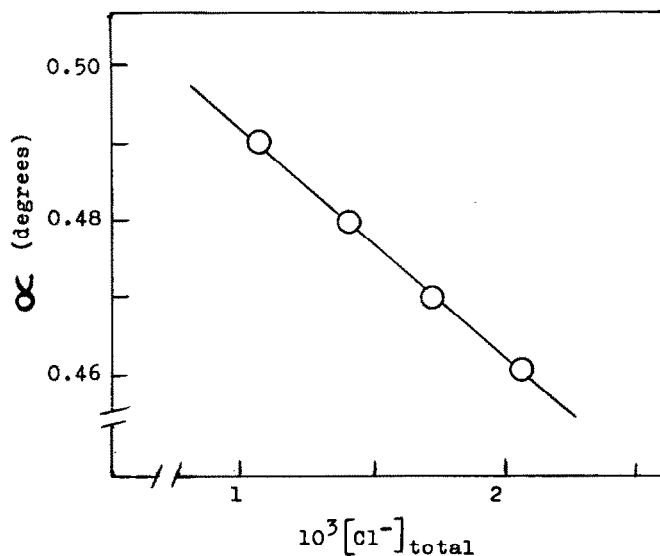
Fig. 6. Effect of tetraethylammonium chloride on the optical activity of S-valinato bis(-phenanthroline)zinc(II) chloride in methanol. (α at 350 nm, 20°C and l = 5 cm; 1.06×10^{-3} M.)

K_2, is assumed for both. By introducing the formation constants

$$K_\Delta = \frac{[\Delta^+]}{[Zn(phen)(S\text{-val})^+][phen]} \quad (2)$$

and

$$K_\Lambda = \frac{[\Lambda^+]}{[Zn(phen)(S\text{-val})^+][phen]}. \quad (3)$$

Equation (1) becomes

$$[\Delta^+] + [\Delta^+X^-] + [\Lambda^+] + [\Lambda^+X^-] = [Zn(phen)$$

$$(S\text{-val})^+][phen](K_\Delta + K_\Lambda)(1 + K_2[X^-]). \quad (4)$$

If the ion-pairing of the $1:1:1$ species is also considered, eqn (4) becomes

$$\frac{[\Delta^+] + [\Delta^+X^-] + [\Lambda^+] + [\Lambda^+X^-]}{[Zn(phen)(S\text{-val})^+] + [Zn(phen)(S\text{-val})^+X^-]}$$

$$= \frac{[Zn(phen)_2(S\text{-val})^+]_{total}}{[Zn(phen)(S\text{-val})^+]_{total}}$$

$$= \frac{(K_\Delta + K_\Lambda)(1 + K_2[X^-])[phen]}{1 + K_1[X^-]}. \quad (5)$$

In this approximation the equilibria involving S-valinate exchange are disregarded. According to this scheme, the residual excitonic activity should increase with the concentration of heterocyclic base, in agreement with results (Fig. 3). Moreover, according to Fig. 3, $K_1 > K_2$. Hence a decrease of excitonic optical activity should result from an increase of counteranion concentration, as shown in Fig. 6 for the effect of tetraethylammonium chloride.

The specific rotation of the system in the presence of each counteranion may be represented by

$$[\Phi]_{exp} \sim \frac{1}{C}([\Delta^+] + [\Delta^+X^-])[\Phi_{e\Delta}]$$

$$\frac{1}{C}([\Lambda^+] + [\Lambda^+X^-])[\Phi_{e\Lambda}] + [\Phi_a] \quad (6)$$

where $[\Phi_{e\Delta}]$ and $[\Phi_{e\Lambda}]$ are the excitonic contributions of the diastereomeric chelates; $[\Phi_a]$ is the contribution of the chelated S-val$^-$ ($1:2:1$ species plus $1:1:1$ species); C is the total concentration of Zn(II), and all the S-val$^-$ is assumed to be chelated. Combination of eqns (2)–(4) and (6) gives

$$[\Phi]_{exp} \sim \frac{[Zn(phen)_2(S\text{-val})^+]_{total}(K_\Delta[\Phi_{e\Delta}] + K_\Lambda[\Phi_{e\Lambda}])}{C(K_\Delta + K_\Lambda)} + [\Phi_a]. \quad (7)$$

Hence, the specific excitonic rotation for the equilibrium mixture of diastereomeric cations would be

$$[\Phi_{em}] \sim \frac{K_\Delta[\Phi_{e\Delta}] + K_\Lambda[\Phi_{e\Lambda}]}{K_\Delta + K_\Lambda}. \quad (8)$$

According to these approximations the diastereomeric mixture could be treated as a single optically active species since

$$[Zn(phen)_2(S\text{-val})^+]_{total} \sim ([\Phi]_{exp} - [\Phi_a])C/[\Phi_{em}].$$

Specific rotation and conductance appear to be linearly correlated in the counteranion series (Fig. 2) probably because they depend in a similar way upon the concentration of $1:2:1$ species. If the equilibrium system in a $1:2:1$ cation salt solution is regarded as a mixture of $1:2:1$ and $1:1:1$ cation salts, the conductance should increase with the $(1:2:1):(1:1:1)$ total concentration quotient since $K_1 > K_2$ and the effects of ion-pairing on conductance tend to predominate over the differences in equivalent specific anionic conductances (as can be noticed on comparing conductances of the complex salts with conductances of sodium salts, Fig. 2). Hence, eqn (5) would be also in agreement with the correlation shown in Fig. 2.

REFERENCES

1. S. Bunel, G. Larrazábal and A. Decinti, *J. Inorg. Nucl. Chem.* 1981, **43**, 2781.
2. A. Decinti and G. Larrazábal, *Bol. Soc. Chil. Quim.* 1982, **XXVII**, 55.
3. J. H. Yoe and A. L. Jones, *Ind. Eng. Chem. Anal. Ed.* 1944, **16**, 111.
4. R. M. Diamond, *J. Phys. Chem.* 1963, **67**, 2513.
5. A. Weissberger and B. W. Rossiter, *Physical Methods of Chemistry.* Wiley, New York (1971).
6. R. A. Robinson and R. H. Stokes, *Electrolyte Solutions.* Butterworths, London (1959).

NOTE

Adducts of tin tetrahalides with monodentate Schiff bases

JOSÉ A. GARCÍA-VÁZQUEZ,* MANUEL LÓPEZ-BECERRA and JOSÉ R. MASAGUER

Departamento de Química Inorgánica, Facultad de Ciencias, Universidad Autónoma, Canto Blanco,
Madrid (34), Spain

Abstract—Complexes of tin tetrachloride and tetrabromide with N-(dimethylphenyl)benzalaldimines have been synthesized and characterized by electronic, infrared and Raman spectroscopy. The vibrational data have been interpreted in terms of *trans*-octahedral structure.

Transition metal complexes of Schiff bases which apart from the imine group have other functional group, usually –OH, sufficiently near to the N donor atom to be able to form a chelate ring, have been studied extensively.[1-3] Comparatively little attention has been given to systems in which the Schiff base is a monodentate ligand and the metal is a non-transitional element.[4,5]

In this work we describe the preparation and characterization of the complexes resulting from the reaction of tin tetrachloride and tetrabromide with Schiff bases derived from benzaldehyde and substituted anilines.

In Scheme 1, $R = 2,3$-di-CH_3(**I**); $2,4$-di-CH_3(**II**); $2,5$-di-CH_3(**III**); $2,6$-di-CH_3(**IV**); $3,4$-di-CH_3(**V**) and $3,5$-di-CH_3(**VI**).
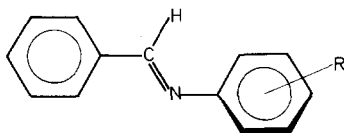
Scheme 1.

EXPERIMENTAL

Tin(IV) chloride and bromide were Merck products; benzaldehyde and amine was a Fluka product. Pure reagents and solvents (C. Erba) have been used and, when necessary, have been purified and/or dried according to standard procedures. Schiff bases were prepared by refluxing equimolecular amounts of the amine and aldehyde in benzene until the theoretical amounts of water was collected in a Dean–Stark trap followed by distillation of the product under reduced pressure.

The preparation of complexes has been carried out in a dry-box under N_2 atmosphere, using anhydrous solvents, according to the following procedure; 2 mmole of

SnX₄, dissolved in about 25 cm³ of carbon tetrachloride, was added dropwise to a solution of the appropiate amount of the Schiff base (4 mmole in 25 cm³ of CCl_4) under continuous stirring and the mixture was kept stirring at room temperature for about 3–5 hr. The precipitate was filtered off, washed with carbon tetrachloride and cyclohexane, and dried *in vacuo* at room temperature. The tin was estimated gravimetrically as SnO_2. The C, H and N analyses were made with a conventional microanalyzer.

The electronic spectra were recorded on a Pye Unicam SP8-100 spectrometer. IR spectra were recorded with a Perkin–Elmer 180 spectrophotometer. The adducts were prepared as Nujol mulls and placed between CsI or polyethylene windows. The Raman spectra were recorded in a Jarrell–Ash spectrophotometer model 25–300, using HE–Ne laser (25 mw, 623.8 nm line) and placing the sample into capillary tubes in order to avoid hydrolysis.

RESULTS AND DISCUSSION

The elemental analyses (Table 1) indicate the general formulae of the complexes to be $SnX_4 \cdot 2L$ where $X = Cl$ or Br.

The UV absorption spectrum of Schiff bases in different solvents shows the existence of several bands. The lowest energy band *ca.* 320 nm have been assigned to $\pi_1 \rightarrow \pi_1^*$ transition of imine group. The second one *ca.* 260 nm has been reported to be due to the transition within the phenyl ring orbitals of the benzal portion $(\pi_2 \rightarrow \pi_2^*)$.[6-8] It was not possible to observe the $n \rightarrow \pi^*$ imine transition band, probably because they are included in the envelope of a higher intensity band.[6] It is obvious that none of these transitions will be pure as a consequence of conjugation of the unshared pair of electrons on the nitrogen atom with the π orbitals of the imine and phenyl groups.

In the complexes a bathocromic shift takes place for these transitions (Table 2) probably due to the localization of nitrogen lone-pair electrons as the complex is form. A similar behaviour has been found by

---

*Author to whom correspondence should be addressed.

Table 1. Analytical and physical data for tin(IV) complexes

Compound		C	H	N	Sn	m.p., °C	Colour
SnCl$_4$·2L	Calc.%	53.06	4.45	4.12	17.48		
L = (I)	Found %	52.31	4.30	4.40	17.34	183 d	yelow
L = (II)		54.31	4.65	3.82	17.04	135 d	yelow
L = (III)		52.05	4.41	4.16	17.44	178 d	yelow
L = (IV)		53.18	4.22	3.67	17.42	168 d	white
L = (V)		52.82	4.21	3.93	17.42	170	yelow
L = (VI)		52.81	4.18	4.04	17.50	166	yelow
SnBr$_4$·2L	Calc.%	42.05	3.27	3.53	13.85		
L = (I)	Found %	42.22	3.26	3.35	14.08	136	yelow
L = (II)		41.66	3.25	3.00	13.71	77	yelow
L = (III)		41.05	3.32	3.24	14.00	145	yelow
L = (IV)		41.84	3.32	3.35	13.66	114	white
L = (V)		42.45	3.42	3.33	14.20	168 d	yelow
L = (VI)		42.27	3.41	3.24	13.96	194 d	yelow

Table 2. UV spectral data on $\pi \to \pi^*$ transitions (nm)

Ligand No	Cyclohexane			1,2 Dichloroethane		
	Ligand	Cl$_4$Sn.2L	Br$_4$Sn.2L	Ligand	Cl$_4$Sn.2L	Br$_4$Sn.2L
(I)	260, 327	263, 330	262, 329	262, 326	268, 334	263, 330
(II)	260, 331	265, 336	263, 334	266, 332	276, 342	268, 335
(III)	262, 331	265, 334	264, 333	262, 332	274, 334	268, 333
(IV)	252, 332	352, 334	253, 334	252, 332	268, 334	260, 333
(V)	262, 325	263, 332	262, 327	264, 325	272, 348	268, 334
(VI)	262, 320	263, 326	263, 324	265, 320	278, 344	265, 331

Table 3. IR (Raman) spectra results in the $\nu(C=N)$ region (cm^{-1})

Ligand	Ligand	SnCl$_4$·2L	SnBr$_4$·2L
(I)	1631 vs (1629 vs)	1645 m (1646 m)	1642 m (1641 m)
(II)	1630 vs (1629 s)	1649 vs (1646 vs)	1642 s
(III)	1630 vs (1634 vs)	1646 m (1647 m)	1646 m (1644 m)
(IV)	1639 vs (1638 vs)	1646 vs	1641 vs
(V)	1629 vs (1621 m)	1654 m (1655 m)	1654 s (1650 s)
(VI)	1628 s (1618 s)	1656 m (1655 m)	1654 s (1648 s)

Table 4. Relevant IR and Raman absorption of complexes and tentative assignments

| Compound | (Sn-X) | | | (Sn-N) |
	E_u	A_{1g}	B_{1g}	A_{2u}
$SnCl_4 \cdot 2L$				
L = (I)	328 vs	295 vs	250 w	310 m
L = (II)	320 vs	301 vs	255 w	295 m
L = (III)	332 vs	296 vs	251 m	312 s
L = (IV)	330 vs			300 s
L = (V)	323 vs, 330 sh	298 vs	254 w	303 sh
L = (VI)	325 vs	303 s	267 w	305 m
$SnBr_4 \cdot 2L$				
L = (I)	232 vs, 200 sh	189 vs	148 w	305 m
L = (II)	225 vs, 205 sh			310 m
L = (III)	220 vs, 205 sh	189 vs	15? w	308 m
L = (IV)	228 vs, 210 sh			318 s
L = (V)	230 vs, 200 sh	208 s	155 w	312 m
L = (VI)	205 vs	190 vs	148 w	312 m

Brocklehurst[7] when the nitrogen lone pair electrons are localized by protonation or nitrone formation. This shift may be interpreted as indicative of the bond of the imino-nitrogen to the metal.

The ligand band in the region 1623–1639 cm^{-1} in infrared and Raman to which a high $v(C=N)$ contribution may be assigned shifts to higher frequencies in all the adducts (Table 3) indicating that the coordination of SnX_4 is effected through the azomethine nitrogen of the ligands and this may be interpreted as a consequence of increased bond order in the carbon to nitrogen link. An analogous behaviour has been found for several adducts of Schiff bases.[9,10]

For these adducts, there are two probable configurations; one is the cis-form with C_{2v} symmetry for the skeleton and the other is the trans-form with D_{4h} symmetry. In theory a trans configuration having two stretching modes, one $v(Sn-X)(E_u)$ and one $v(Sn-N)(A_{2u})$ IR active, and three stretching modes, two $v(Sn-X)(A_{1g} + B_{1g})$ and one $v(Sn-N)(A_{1g})$ Raman active that should be readily distinguishable from a cis molecule with six IR and Raman active vibrations, four $v(Sn-X)(2A_1 + B_1 + B_2)$ and two $v(Sn-N)(A_1 + B_2)$. However as can be seen (Table 4), the number of the bands and their position suggest that these complexes have a trans-configuration or D_{4h} symmetry. The IR spectra are strikingly similar in the metal–halogen stretching region and are characterized by an intense band with a weak shoulder which appears in the region 320–330 cm^{-1} for chloride complexes and ca. 100 cm^{-1} lower for bromide complexes. The appearance of a shoulder band may indicate the splitting of the doubly degenerate Sn-X stretching mode (E_u) due to lowering of the D_{4h} symmetry in the solid state.[11] The $v(SnCl)$ are in good agreement with the range predicted by several authors[11-13] for the six-coordinated adducts of tin tet-

rachloride (usually 360–300 cm^{-1}). Also the ratio $v(SnBr)/v(SnCl)$ comes out to be 0.63–0.71 which is within the range accepted for complexes having similar coordination. The band at ca. 300 cm^{-1} in the spectra of $SnCl_4 \cdot 2L$ and $SnBr_4 \cdot 2L$ is tentatively assigned to the $v(SnN)$, since the positions of these bands are not likely to be different in the two spectra. The Raman spectra of these complexes confirm these conclusions. An intense Raman line, non-coincident with the strong IR band and at lower frequency accompanied by a weaker line at ca. 50 cm^{-1} to lower frequency appears in each case. This is the same type of spectrum as that found for other SnX_4 adducts.[14,15] The strong Raman line can be assigned to the A_{1g} $v(Sn-X)$ mode and it weaker counterpart to the B_{1g} mode of a trans D_{4h} skeleton. The frequency shift of the A_{1g} mode of a trans adduct accompanying the halogen substitution, also confirms our assignment by the constancy of the ratio $v(SnBr)/v(SnCl)$; this ratio is close to $(\mu_{Br}/\mu_{Cl})^{\frac{1}{2}} = 0.66$, as expected in the harmonic potential approximation.[14]

REFERENCES

1. R. H. Holm, G. W. Everett and A. Chakravorty, Prog. Inorg. Chem. 1966, 7, 83.
2. L. Sacconi, Coord. Chem. Rev. 1966, 1, 126.
3. S. Yamada, Coord. Chem. Rev. 1966, 1, 415.
4. V. A. Kogan, A. S. Egorov and O. A. Osipov, Russ. J. Inorg. Chem. 1973, 18, 1106.
5. V. A. Kogan, A. S. Egorov and O. A. Osipov, Russ. J. Inorg. Chem. 1974, 19, 980.
6. H. H. Jaffe, S. Yeh and R. W. Gardner, J. Mol. Spectrosc. 1958, 2, 120.
7. P. Brocklehurst, Tetrahedron 1962, 18, 299.
8. W. F. Smith, Tetrahedron 1963, 19, 445.
9. A. S. Egorov, V. A. Kogan, V. A. Bren and O. A. Osipov, Zh. Obshch. Khim. 1975, 45, 2478.

10. L. Doretti, F. Madalosa, S. Sitran, S. Faleschini and P. A. Vigato, *Inorg. Nucl. Chem. Lett.* 1977, **13**, 607 and refs. therein.

11. N. Ohkaku and K. Nakamoto, *Inorg. Chem.* 1973, **12**, 2440.

12. F. Farona and J. G. Grasselli, *Inorg. Chem.* 1967, **6**, 1675.

13. M. Webster and H. E. Blayden, *J. Chem. Soc. A,* 1969, 2443.

14. S. J. Ruzicka and A. E. Merbach, *Inorg. Chim. Acta* 1976, **20**, 221.

15. A. J. Carty, T. Hinsperger, L. Mihichuk and H. D. Sharma, *Inorg. Chem.* 1970, **9**, 2573.

NOTE

PREPARATIONS OF SOME TRIBUTYLTIN PHOSPHATES

J.L. LECAT and M. DEVAUD*

I. N. S. C. I. R., BP 08, 76130 MONT SAINT AIGNAN, FRANCE

ABSTRACT

Different complex tributyltin organophosphates have been prepared; in some cases the organotin cation is directly linked to the phosphate group, in other cases it is linked to a carboxylate or to a thioate function in a RO–P substituent. The direct phosphorylation of a tributyltin hydroxy salt is only possible for a marked covalent salt. Intramolecular rearrangements were observed.

The combination of the tributyltin group (a well-known fungicide) to an organophosphate with similar properties gives the compound a wide spectrum of toxicity. Numerous organotin phosphates have therefore already been described in the literature[1-3]. We report here on the syntheses of some new tributyltin organophosphates which are in fact parents of organophosphorus pesticides. They were prepared by direct action of organophosphorus acid or salt on bis(tributyltin)oxide (TBTO) or tributyltin chloride (TBTCl). Direct phosphorylation of a tributyltin hydroxy salt was found to be difficult and could be used only in a few cases.

EXPERIMENTAL

^1H and ^{31}P NMR chemical shifts are expressed in δ units, referenced to TMS and a 85% H_3PO_4 solution. Butyl protons are not reported.

Chromatograms (glc) were carried out on a SE30 column at 150°C, allowing the identification of Bu_4Sn and TBTCl formed in some reactions.

The C, H, N analyses are reported in the table.

The tributyltin compounds used in this work were prepared by adding TBTO (0.1 mole) to a solution of acid (0.2 mole) in acetone or benzene (100 cm^3) in the presence of calcium sulphate[9] (10g) under refluxing conditions for 3h. The product was isolated after filtration and evaporation of the solvent.

Bis(tributyltin) 2-aminoethyl phosphate 1 was obtained by decantation after addition of 50 cm^3 of acetone solution of TBTCl (11.6 g, 35.6 mmol) to 100 cm^3 of aqueous solution of dipotassium 2-aminoethyl phosphate (3,9g, 17.8 mmol)– NMR:δ ppm: 3.7 t(2) 2.75 t(2)

Tributyltin bis(2-bromophenylamido)phosphate 3 Potassium bis(2-bromophenylamido)phosphate (prepared by action of 2-bromoaniline (37.2g, 0.216 mole) on phosphoryl trichloride (15.3g, 0.1 mole) in 200 cm^3 of ether at 0°C, followed by hydrolysis in 200 cm^3 of alcoholic potassium hydroxide (0.1 mole)) and TBTCl (0.1 mole) were heated for 30 min in refluxing ethanol. After KCl filtration and ethanol evaporation, compound 3 was recovered as a liquid.

* Author for correspondence

Tributyltin bis(dimethylamido)phosphate 4 was precipitated by adding 100 cm^3 of acetone
solution of TBTCl (33.8 mmol) to 50 cm^3 of an aqueous solution of the potassium salt(33.8
mmol) obtained from hydrolysis of bis(dimethylamido)chlorophosphate- NMR:δ ppm: 2.45 d(12)

Tributyltin ethyl (diethoxydithiophosphoryl)succinate 5 - The hydrogen ester was obtained by
the Chen method[4]. Compound 5 was prepared by action of TBTO on the hydrogen ester under
acetone reflux and in the presence of calcium sulphate - NMR:δ ppm: 4.2 m(7) 2.95 d(2)

Bis(tributyltin) 2,4,5-trichlorophenyl thiophosphate 6 - The thiophosphorylation was carried
out according to the literature[8]. Two equivalents of triethylamine and of tributyltin
glycolate were then introduced at - 17°C. After stirring for 90 min at room temperature, the
mixture was treated with a 2% sodium carbonate solution and then extracted by petroleum
ether. After evaporation of solvent, compound 6 was isolated in liquid form.

Phosphorylation of tributyltin compounds - The phosphorylation was carried out by adding
28.6 mmol of each of the two reactants, potassium carbonate (15g) and in some cases copper
powder (0.1g) in 150 cm^3 of solvent (PhH or THF). After stirring for 2h, the mixture was
filtered, evaporated and analysed.

Tris(tributyltin) tris(2,3,5-trichloro-S-pyridyl) tetra(thiophosphate) 15 - Chlorpyrifos
(5g, 14.2 mmol) and tributyltin glycolate (10.4g, 28.5 mmol) were heated at 130°C for 2h
under reduced pressure. Compound 15 slowly precipitated after addition of methanol-
Molecular weight by vapour osmometry : Found (1620 ± 200)g, Calc.: 1810g.

Table: Analytical Data, Found% (Calc.%)

Compound	Formula		C	H	N
1	$C_{26}H_{60}NO_4PSn_2$	liquid	43.8(43.42)	8.4(8.41)	1.7(1.95)
3	$C_{24}H_{37}Br_2N_2O_2PSn$	liquid	42.0(41.47)	5.8(5.37)	3.9(4.03)
4	$C_{16}H_{39}N_2O_2PSn$	F=173°C	43.6(43.56)	8.1(8.91)	6.0(6.34)
5	$C_{22}H_{45}O_6PS_2Sn$	liquid	42.4(42.66)	7.2(7.32)	
6	$C_{30}H_{56}Cl_3O_3PSSn_2$	liquid	41.3(41.34)	6.6(6.47)	
15	$C_{51}H_{84}Cl_9N_3O_9P_4S_4Sn_3$	solid	34.1(33.83)	4.7(4.67)	3.0(2.32)

RESULTS AND DISCUSSION

Compounds 1, 3 and 4 were obtained by action of the potassium salt on TBTCl. The
structure of 1 was corroborated by the disappearance of ν(P=O) band and the value of ^{31}P
chemical shift[7]. 1 was slowly hydrolysed, the appearance on the IR spectrum of the two
deformations δ(NH$_2$) and δ(NH$_3^+$) at 1670 and 1590 cm^{-1}, which were also observed for the
potassium hydrogen salt, is consistent with the following reaction:

$$(NH_2CH_2CH_2O)PO(OSnBu_3)_2 + H_2O \longrightarrow (NH_2CH_2CH_2O)PO(OH)(OSnBu_3) + 1/2 \text{ TBTO} \qquad (1)$$

$$\underset{1}{} \qquad\qquad\qquad\qquad \underset{2}{}$$

$$\delta^{31}P = -4.9 \text{ ppm} \qquad\qquad\qquad \delta^{31}P = -6.4 \text{ ppm}$$
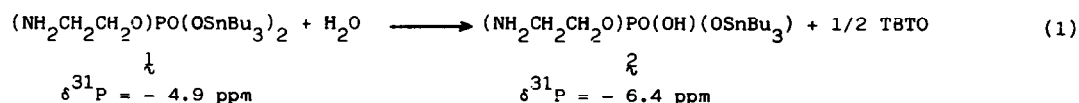
The two amidophosphates 3 and 4 are easy to prepare and stable. Their structures
were monitored by their IR spectra.

Compound 5 was synthesized by action of TBTO on the organophosphorus acid in the
presence of calcium sulphate as drying agent[9]. The IR spectrum showed that the carboxylate
group is monodentate and that there is no coordination between the ester function and the
tin atom:

$(EtO)_2PS(S-CHCOOEt \quad)$ $\nu(C=O) = 1740 \ cm^{-1}$ $\nu_{as}(COO) = 1660 \ cm^{-1}$

           $|$
   $\underset{\sim}{5}$ $CH_2COOSnBu_3$ $\nu(P=S) = 830-810 \ and \ 660 \ cm^{-1}$
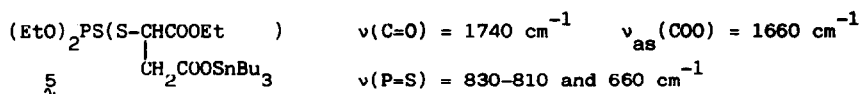
The third method of preparation investigated was the direct phosphorylation of a tributyltin compound.

The phosphorylation of two equivalents of tributyltin glycolate by dichloro-2,4, 5-trichlorophenyl thiophosphate was probably accompanied by the rapid hydrolysis of the condensation product in the course of preparation. The compound $\underset{\sim}{6}$ which was formed underwent a slow intramolecular rearrangement which was revealed by gas chromatographic analysis.

$$(Cl_3C_6H_2O)PS(OSnBu_3)_2 \quad \longrightarrow \quad (Cl_3C_6H_2O)SP\underset{O}{\overset{O}{\diagup}}SnBu_2 + Bu_4Sn \qquad (2)$$

       $\underset{\sim}{6}$ $\underset{\sim}{7}$
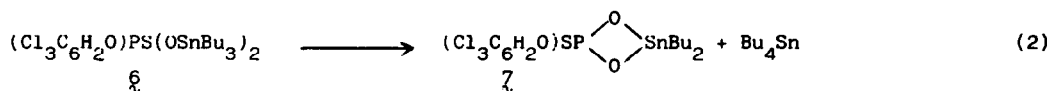
The action of tributyltin 2-hydroxyethane thioate on chlorophosphates of general formula Y_2PXCl with $X = S$ or O and $Y = OEt$, OCH_2CCl_3 or NMe_2 depends on the solvent and the Y substituent.

For $X = S$ and $Y = OEt$, compound $\underset{\sim}{8}$ was obtained in benzene in the presence of potassium carbonate and copper powder. In the absence of copper, an isomerisation P=S/P=O, responsible of the appearance of the $\nu(P=O)$ at $1250 \ cm^{-1}$, was observed. In THF, the partially isomerised potassium salt, revealed by its IR spectrum, was isolated.

$(EtO)_2PSCl$

    $+$

$HOCH_2CH_2SSnBu_3$

$\overset{PhH, \ Cu}{\longrightarrow} (EtO)_2PS(OCH_2CH_2SnBu_3) \quad \underset{\sim}{8} \quad \nu(P=S) = 815-790, \ 675 \ cm^{-1}$

                                                (3)

$\overset{THF}{\longrightarrow} (EtO)PO(OK)(SCH_2CH_2OH) + (EtO)PS(OK)(OCH_2CH_2OH) \quad \underset{\sim}{9}$

      $\nu(OH)=3400 \ cm^{-1} \quad \nu(PO_2^-)=1145 \ cm^{-1} \quad \nu(P=S)=790-760,660 \ cm^{-1}$
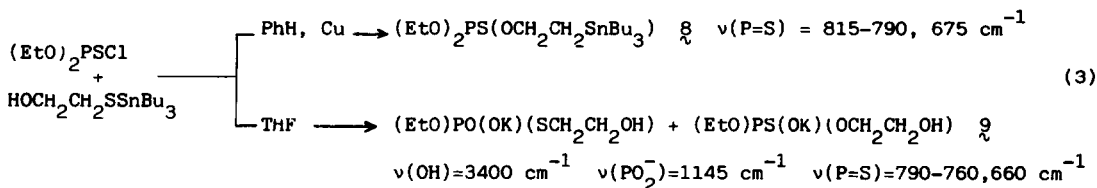
For $X = O$ and $Y = OCH_2CCl_3$, in the same conditions, potassium bis(2,2,2-trichlordethyl)phosphate $\underset{\sim\sim}{10}$ always precipitated. The second product of the reaction was the initial organotin compound or TBTCl in the presence of copper powder. The great insolubility of the salt $\underset{\sim\sim}{10}$ is responsible for the lack of reaction with TBTCl.

For $X = O$ and $Y = NMe_2$, product $\underset{\sim\sim}{11}$ decomposes slowly following reaction (4). The 1,4-dithiacyclohexane was identified by its NMR spectrum; its formation possibly involved a sulphonium cation[5].

$$(Me_2N)_2PO(OCH_2CH_2SSnBu_3) \quad \longrightarrow \quad (Me_2N)_2PO(OSnBu_3) + S\underset{CH_2CH_2}{\overset{CH_2CH_2}{\diagup \diagdown}}S \qquad (4)$$

      $\underset{\sim\sim}{11}$ $\underset{\sim}{4}$
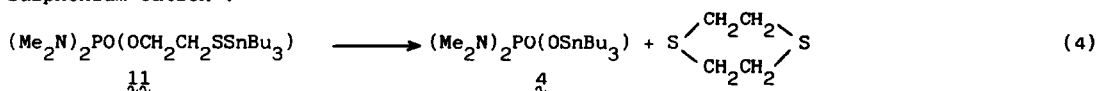
Similarly, the phosphorylation of tributyltin 4-amino salicylate did not give the desired product. In THF, the dipotassium salt $\left[NH_2C_6H_3(COOK)O\right]PS(OEt)(OK)$ $\underset{\sim\sim}{12}$ of the O-phosphorylated product precipitated. In benzene, both hydroxy and amino functions reacted; the 4-amino salicylic acid which was formed crystallised. In the remaining liquid there was, as well, a slow rearrangement between TBTCl formed in the reaction and compound $\underset{\sim\sim}{13}$ according to reaction (5).

$$(EtO)_2PSNH\!-\!\!\!\langle\bigcirc\rangle\!\!-\!COOSnBu_3 + TBTCl \longrightarrow (EtO)_2PSNH\!-\!\!\!\langle\bigcirc\rangle\!\!-\!COO\!-\!SnBu_2 + Bu_4Sn \qquad (5)$$

  $\underset{\sim\sim}{13}$ $OPS(OEt)_2$ $\underset{\sim\sim}{14}$ $|$

                                                               $OPS(OEt)O$

$\delta^{31}P$ ppm : $\underset{\sim\sim}{12}$: $- 57.3$ $\underset{\sim\sim}{13} + \underset{\sim\sim}{14}$: $- 68.8$ -60.8 and $- 56.5$
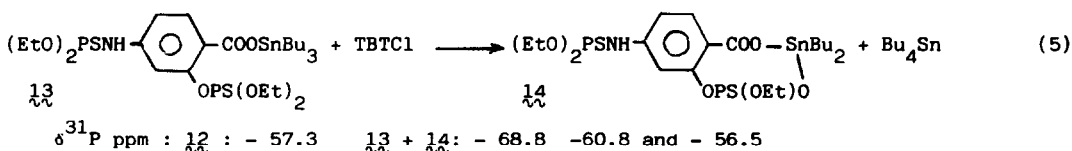
Tetrabutyltin was detected by its chromatographic peak. The constitution of the mixture $\underset{\sim\sim}{13} + \underset{\sim\sim}{14}$ was monitored by the ^{31}P spectra. The ^{31}P chemical shift decreases when an OR group

is replaced by a NR_2 group; it increases in an ionic salt or in an aromatic phosphate[7]. We therefore attribute the major signal at - 68.8 ppm to the structure $Ar-NH-PS(OEt)_2$, the signal at - 60.8 ppm to the group $Ar-O-PS(OEt)_2$ and the signal at - 56.5 ppm to the ionic group $Ar-O-PS(OEt)^-$.

In the same conditions, 4-nitro-2-hydroxy, 2,4-dihydroxy and 4-hydroxy benzoate of tributyltin gave the potassium salt of the acid only.

These different experiments showed that the direct phosphorylation of a tributyl-tin hydroxy salt does not generally give the expected product because the nucleophilic attack on the phosphorus atom can occur by the salt function if this is too ionic. For this reason, the best results were obtained in benzene solutions.

The transesterification of an organic commercial phosphate $(RO)_2PSY$ by tributyl-tin glycolate was not successful.The desired product $(RO)_2PSY(OCH_2COOSnBu_3)$ which was formed transiently was solvolysed by the ROH alcohol resulting from the reaction, and hydrolysed by water formed by dehydration of glycolate. In the case of chlorpyrifos, we isolated the unknown tetra(thiophosphate) 15.

The direct substitution of an ethyl group in triethylphosphate by trimethyltin has been achieved recently by heating trimethyltin halogenide with the phosphate[6]. We observed that this reaction cannot work with the tributyltin moiety, possibly because the covalent character of the tributyltin halogenide is too high.

In conclusion, we must underline the difficulties entailed in the preparation of complex tributyltin phosphates. The most stable compounds are monotributyltin which contain an amido group and could constitute products with interesting anti-fouling properties.

REFERENCES

[1] J.L. Lefferts, K.C. Molloy, J.J. Zuckerman, I. Haiduc, H. Curtui, C. Guta and D. Ruse, Inorg. Chem., 1980, 19, 1662 and 2861 and enclosed references

[2] B.P. Singh, G.Srivastava and R.G. Mehrotra, J. Organometal. Chem., 1979, 171, 35 and Synth. React. Inorg. Metal. Org., 1982, 12, 105

[3] K.C. Molloy, F.A.K. Nasser and J.J. Zuckerman, Inorg. Chem., 1982, 21, 1711

[4] P.R. Chen, W.P. Tucker and W.C. Dauterman, J. Agr. Food Chem., 1969, 17, 86

[5] T.R. Fukuto and E.M. Stafford, J. Amer. Chem. Soc., 1957, 79, 6083

[6] J. Kowalski and J. Chojnowski, J. Organometal. Chem., 1980, 193, 191

[7] A.J.R. Jones and A.R. Katrisky, Angew. Chem. Internat. Edn., 1962, 1, 32

[8] R.H. Rigterink and E.E. Kenaga, J. Agr. Food Chem., 1966, 14, 304

[9] G.B. Kushlefsky, Ger. Offen, 2, 257, 825 - Chem. Abstr., 1977, 87, 118366

NOTE

REACTIONS OF 2-THIAZOLIN-2-YLTHIOPHENE WITH SOME METAL IONS

H.A. Tayim[*]
Department of Chemistry, University of Petroleum & Minerals
Dhahran, Saudi Arabia

and

A.S. Salameh
Department of Chemistry, American University of Beirut
Beirut, Lebanon

Abstract

The condensation of o-aminobenzenthiol with 2-thiophenecarboxaldehyde
yields 2-thiazolin-2-ylthiophene rather than the expected Schiff base.
However, upon reaction with metal ions, the thiazoline rearranges to
the expected thiolate Schiff base. Complexes of the Schiff base with
Ni(II), Cu(II), Zn, Cd, Pb(II), Ag(I) and Pd(II) have been isolated
and characterized.

It is well established now that the condensation of an aldehyde with an aminethiol, such as
o-aminobenzenthiol, does not yield the Schiff base as would the amine if no thiol group was
present. The sulphur atom of the thiol group tends to form another S-C bond. Cyclization
takes place with the resulting formation of a thiazole (as in the case of 2,6-pyridinedicar-
boxaldehyde[1]) or a thiazoline (as in the case of 2,5-thiophenedicarboxaldehyde[2]).The purpose
of the present work was to check the behaviour of 2-thiophenecarboxaldehyde and to investi-
gate the reactions of the resulting thiazoline or thiazole with metal ions.

Experimental

Preparation of 2-thiazolin-2-ylthiophene: A solution of 2-thiophenecarboxaldehyde 6.72g,
0.06 mole) in ethanol (12 cm^3) was treated with o-aminobenzenethiol (7.50g, 0.06 mole) in
ethanol (12 cm^3). The mixture was refluxed for 3½ hrs. Concentration of the solution led
to the formation of a pale yellow product which was recrystallized from ethanol. Yield;6.92g
(53%). M.pt. 94-95°C. Found: C, 60.53; H, 3.69; N, 6.48; S, 29.36. Calc. for $C_{11}H_9NS_2$;
C, 60.24; H, 4.13; N, 6.39; S, 29.24%. IR spectrum: ν_{NH} at 3300 cm^{-1}.

Oxidation of 2-thizaoline-2-ylthiophene: Oxidation was carried out by bubbling air for four
hrs in a benzene solution of 2-thizaoline-2-ylthiophene. The oxidation product was 2-thia-
zol-2-ylthiophene. Found: C,60.83; H, 3.30; N, 6.46; S, 29.51. Cal. for $C_{11}H_7NS_2$; C, 60.80;
H, 3.25; N, 6.45; S, 29.14%. No band was observed in the IR spectrum above 3100 cm^{-1}, indi-
cating the absence of ν_{NH}.

---

[*] Author to whom correspondence should be addressed.

<u>Reactions of 2-thiazoline-2-ylthiophene with metal ions</u>: The ligand was reacted with the metal ions investigated according to the following procedures:

(i) A hot solution of the ligand (0.219 g, 1 mmole) in ethanol (7 cm^3) was added to a hot solution of the metal salt (0.4 mmoles) in ethanol (10 cm^3). The precipitate that was formed was filtered off, washed with ethanol and ether, respectively, and dried in vacuo over P_2O_5. This procedure was followed for the reactions of $CuCl_2.2H_2O$, $Pb(CH_3COO)_2$, $Cd(CH_3COO)_2.2H_2O$, $Zn(CH_3COO)_2.2H_2O$ and $Cu(CH_3COO)_2.H_2O$. Acetone was used as a solvent in the reaction of $Cu(ClO_4)_2.6H_2O$.

The same procedure was applied for the reaction of $AgClO_4$ except that the reaction mixture had to be stirred for two hours at room temperature in order to precipitate the product.

(ii) The reaction of the ligand with dichloro-bis-(benzonitrile)palladium(II) was carried out by stirring a mixture of benzene solutions of the ligand and the Pd(II) complex for one hour at room temperature. The product obtained was filtered off and washed with benzene, then dried in vacuo over P_2O_5.

(iii) Bis-(acetylacetonato) nickel(II) was reacted with the ligand by mixing boiling benzene solutions of Ni(accac)$_2$.H$_2$O and the ligand. An immediate wine-red colouration was observed. The mixture was concentrated in a hot water bath and petroleum ether (110-120°C) was added. The reddish-brown precipitate that separated was filtered off, washed with petroleum ether, and dreid in vacuo over P_2O_5.

Results and Discussion

The reaction of 2-thiophenecarboxaldehyde with <u>o</u>-aminobenzethiol afforded a product whose IR spectrum shows a band at 3300 cm^{-1} (assigned to ν_{NH}) but no absorption at 2600 cm^{-1} (the ν_{SH} region). Thus the Schiff base 2-thiophen-2-yl-{N(phenylen-2-thiol)aldimine} $\underset{\sim}{I}$ is ruled out. By comparison with the behaviour of 2,5-thiophenedicarboxaldehyde[2] the product is characterized as 2-thiazolin-2-ylthiophene($\underset{\sim}{II}$). This is further substantiated by the absence of $\nu_{C=N}$ in the IR spectrum of the product. The $\nu_{C=N}$ band is observed in the oxidized product 2-thiazol-2-ylthiophene($\underset{\sim}{III}$) at 1590 cm^{-1}. The ν_{NH} disappeared in the thiazole($\underset{\sim}{III}$). Both the thiazoline $\underset{\sim}{II}$ and the thiazole $\underset{\sim}{III}$ have not hitherto been reported.

$$\underset{\sim}{I} \qquad\qquad\qquad \underset{\sim}{II} \qquad\qquad\qquad \underset{\sim}{III}$$
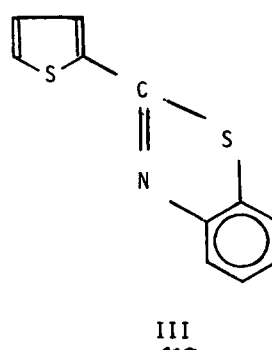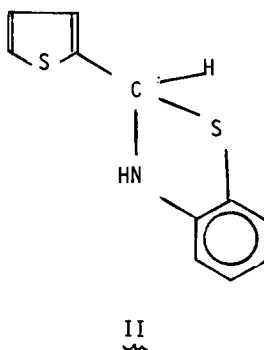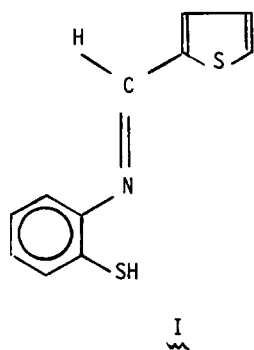
TABLE I

Reactions of Some Metal Ions with 2-Thiazoline-2-ylthiophene

Melt Salt	Product	Colour	Decomposition point($^\circ$C)
$CuCl_2 \cdot 2H_2O$	$Cu(SB)Cl$	Mustard	185-190
$Cu(CH_3COO)_2 \cdot 2H_2O$	$Cu(SB)(CH_3COO) \cdot 1/2H_2O$	Dark Brown	155°
$Cu(ClO_4)_2 \cdot 6H_2O$	$Cu_3(SB)_4(ClO_4)_2 \cdot 2H_2O$	Brown	238-240
$Pb(CH_3COO)_2$	$Pb(SB)_2$	Yellow	225-228
$Cd(CH_3COO)_2 \cdot 2H_2O$	$Cd(SB)(CH_3COO) \cdot 1/2H_2O$	Yellow	285-290
$Zn(CH_3COO)_2 \cdot 2H_2O$	$Zn(SB)_2$	Orange-Red	230
$AgClO_4$	$Ag_4(SB)_3ClO_4 \cdot H_2O$	Yellow	180
$Ni(acac)_2 \cdot H_2O$	$Ni(SB)_2 \cdot H_2O$	Reddish-Brown	153-157
$Pd(C_6H_5CH)_2Cl_2$	$Pd(SB)Cl \cdot H_2O$	Red	over 360

TABLE II

Element Analyses of the Reaction Products of 2-Thiazoline-2-ylthiophene with Metal Ions

Compounds	Analyses* %				
	C	H	N	S	Cl
$Cu(SB)Cl$**	42.53(41.63)	2.45(2.54)	4.60(4.42)	19.80(20.21)	10.57(11.17)
$Cu(SB)(CH_3COO) \cdot 1/2H_2O$	44.41(44.62)	3.17(3.46)	4.62(4.00)	19.33(18.33)	
$Cu_3(SB)_4(ClO_4)_2 \cdot 2H_2O$	40.58(40.39)	2.85(2.47)	4.66(4.33)	18.95(19.79)	4.89(5.48)
$Pb(SB)_2$	40.43(41.03)	2.62(2.51)	4.31(4.35)	19.20(19.92)	
$Cd(SB)(CH_3COO) \cdot 1/2H_2O$	39.19(39.15)	2.89(3.03)	3.73(3.51)	16.02(16.08)	
$Zn(SB)_2$	52.28(52.67)	3.34(3.22)	5.66(5.59)	24.94(25.57)	
$Ag_4(SB)_3ClO_4 \cdot H_2O$	32.35(32.92)	2.15(2.18)	3.67(3.49)	16.30(16.00)	3.10(2.95)
$Ni(SB)_2 \cdot H_2O$	52.96(51.47)	3.66(3.53)	5.29(5.46)	23.85(24.98)	
$Pd(SB)Cl \cdot H_2O$	34.28(34.93)	2.44(2.66)	3.97(3.70)	16.86(16.97)	9.38(11.23)

* (Calc); ** SB is 2-thiophen-yl-{N-(phenylen-2-thiolate)aldimine}

The results of the reactions of 2-thiozolin-2-ylthiophene II with some metal ions are listed in Tables I and II along with the elemental analyses of the reaction products. The behaviour of 2-thiazoline-2-ylthiophene II is distinctly different from that of the corresponding 2,6-pyridine dithiazole (and dithiazoline) and 2,5-thiophene dithiazoline. The reactions of transition metal ions with 2,6-pyridine dithiazole result generally in the formation of complexes in which the thiazole rings remain intact. The ligand behaves simply as a disubstituted pyridine bonded to the metal through the pyridine nitrogen[1]. With 2,5-thiophene dithiazoline, however, one or both of the thiazoline rings may open, depending on the stoichiometric requirements of the complexes[2]. This may be due to the reluctance of the thiophene sulphur atom to bond to the metal ions. It has been observed that while

2,6-pyridinedicarboxaldehyde readily forms complexes with several transition metal ions[3], no complexes could be obtained from the reaction of 2,5-thiophenedicarboxaldehyde with metal ions[4].

The reactions of 2-thiazolin-2-ylthiophene with the metal ions investigated in this work are invariably accompanied with the opening of the thiazoline ring and the re-arrangement of the ligand to the Schiff base 2-thiophen-yl-{N-(phenylen-2-thio)aldimine}(I). Thus the complexes obtained were of the form MSBX (M = Cu, Pd; X = Cl; M = Cu, Cd; X = acetate) and M(SB)$_2$ (M = Pb, Zn, Ni). SB stands for the conjugate base of the Schiff base I. The perchlorates of Cu(II) and Ag(I) afforded the complexes Cu$_3$(SB)$_4$(ClO$_4$)$_2$·2H$_2$O and Ag$_4$(SB)$_3$ClO$_4$·H$_2$O, respectively. The Schiff base ligands in these latter complexes bridge the metal ions. No absorption above 3100 cm^{-1} occurred in the spectra of the an-hydrous complexes, indicating the absense of NH bonding. Moreover, $\nu_{C=N}$ was invariably observed about 1590 cm^{-1}. These observations along with the elemental analyses, support the formulation of the ligand as the anion of the Schiff Base I.

The complex Pd(SB)Cl·H$_2$O was decomposed with aqueous KCN and the organic ligand was recovered. It was identified as the original thiazoline II. Thus in the absence of metal ions the free Schiff base apparently rearranges in a fast reaction to the more favoured thiazoline.

References

1. A.S. Salameh, H.A. Tayim and B.C. Uff; Polyhedron; 1982, 1, 543.

2. A.S. Salameh and H.A. Tayim; Polyhedron, in Press.

3. A.S. Salameh, B.C. Uff; Y.S. Saikaly and H.A. Tayim; J. Inorg. Nucl. Chem.1980, 42, 43.

4. H.A. Tayim and A.S. Salameh, Unpublished work.

NOTE

Preparation and Thermal Decomposition of Dineophylplatinum(II) Complexes; δ-Hydrogen

Migration Controlled by the Nature of Ancillary Ligands.[+]

By David C. Griffiths and G. Brent Young,*

Chemistry Department, Imperial College of Science and Technology,

London, SW7 2AY.

The novel complexes $L_2Pt(CH_2CMe_2Ph)_2$ $[L_2 = 1,5$-cod, $2,2'$-bipy, $2,2'$-bipym; $L = PEt_3$, $PPh_3]$ readily undergo cyclisations to afford $L_2Pt(2\text{-}C_6H_4CMe_2CH_2)$ with elimination of tert-butylbenzene at rates dependent on L_2; reaction is fastest for the bulky monodentate Ph_3P, while chelating ligands generally decrease lability.

Hydrogen migrations provide some of the major rearrangement paths for organotransition metals. The[1] β-elimination is especially facile for alkyl-metals and has received much attention.[1] Where this option is suppressed, however, it may be supplanted by an α-hydrogen abstraction[2] or, as has emerged more recently, migration from a more remote γ-[3] or δ-carbon.[3,4] We now report a δ-elimination from a novel dialkylplatinum(II) precursor L_2PtR_2, which affords a platinacyclopent-2-ene. We have discovered that the facility of the transformation is critically dependent, inter alia, on the ancillary ligand L (Scheme).

Dineophyl(1,5-cyclooctadiene)platinum(II), 1a, is obtained as colourless crystals from the reaction of excess neophylmagnesium chloride with (cod)PtCl$_2$ in tetrahydrofuran at temperatures not exceeding ambient (yield 68%). ^{1}H n.m.r. parameters appear in Table 1. Particularly diagnostic of 1a are the 1:4:1 triplets at 3.87 ppm $[^2J_{Pt-H} = 38$ Hz] and 2.24 ppm $[^2J_{Pt-H} = 88$ Hz], characterising the platinum-bound alkene and methylene hydrogens, respectively.

When a toluene solution of 1a is heated, smooth quantitative conversion to the platinacyclopentene 2a is observed, with concomitant liberation of an equivalent amount of tert-butylbenzene. These events may be followed conveniently by ^{1}H n.m.r. spectroscopy; 2a has two distinct platinum-bound alkene environments which generate 1:4:1 resonance patterns at 4.64 $[^2J_{Pt-H} = 44$ Hz] and 5.08 ppm $[^2J_{Pt-H} = 37$ Hz], while the metallacyclic methylene hydrogens appear at 2.29 ppm $[^2J_{Pt-H} = 88$ Hz] (Table 1).[5]

The diene ligand in 1a can be replaced by a variety of nitrogen and phosphorus donor ligands. Treatment of a chloroform solution of 1a with 2,2'-bipyridyl yields 1b. If reaction is conducted at room temperature, however, metallacyclisation occurs at an appreciable rate and 2b is the predominant product. Optimal preparation of bright red, crystalline 1b involves reaction at 10°C in toluene with a large excess (ca. 50-fold) of 2,2'-bipyridyl and with rigorous exclusion of air.[6] Reaction is complete in 4 days. In notable contrast toluene solutions of the corresponding 2,2'-bipyrimidyl derivative 1c

---

[+]"neophyl" = 2-methyl-2-phenylpropyl

*To whom correspondence should be addressed.

are thermally inert at ambient temperatures, even in air. Wine-red crystals are recovered after 10 days' reaction of equivalent 1a and bipyrimidyl. Temperatures in excess of 40 C are required to generate 2c at significant rates. In the ^{1}H n.m.r. spectrum of a toluene-d_8 solution, the methylene triplet at 2.73 ppm for 1c is replaced by another at 2.88 ppm (ultimately of 50% relative intensity) while the methyl resonance of tert-butylbenzene (1.14 ppm) appears simultaneously.

Displacement of 1,5-cyclooctadiene by tertiary phosphine ligands is much more rapid; metathesis is complete at 20°C in 2-24 hours. Dineophyl-bis(triethylphosphine)platinum(II), 1d, can be isolated as colourless prisms. This derivative undergoes cyclisation at 35°C in toluene to give 2d. In this case, ^{31}P n.m.r. spectroscopy is more convenient as a reaction monitor; the 1:4:1 triplet for 1d gives way to a corresponding triplet of AB quartets, characteristic of 2d (Table 1).

Interaction of 1a with triphenylphosphine, on the other hand, leads directly to 2e. The intermediate dialkyl 1e is too labile even at 0°C to be isolated. It can, however, be detected as a transient intermediate by ^{31}P n.m.r. spectroscopy (Table 1) in freshly mixed solutions of 1a and a large (ca. 5-fold) excess of triphenylphosphine.

The metallacyclisations conform to first order kinetics. Rate constants are presented in Table 2 (reaction of 1d is too rapid at 60°C for its rate to be reliably measured by ^{31}P n.m.r. spectroscopy). We are now engaged in extensive kinetic studies aimed at elucidating the mechanism of the rearrangement but some preliminary comments are pertinent.

Although decomposition solvents and temperatures do not coincide, the indications are that neophyl complex 1d is appreciably more labile than its neopentyl-[3b] and 2,2-dimethylbutylplatinum[4d] analogues. Cyclisation of 1d to give 2d is retarded by the presence in solution of triethylphosphine, in accord with a pathway in which phosphine dissociation normally occurs prior to cyclisation.[3b,4d] Significantly, ring-closure in complexes with chelating ligands, 1a-1c, is uniformly much slower, although we have yet to examine fully the effect of a bidentate diphosphine for more legitimate comparison.[7]

The rate constant for formation of 2e from 1e is estimated to be $\geq 4.0 \times 10^{-4}$ sec^{-1} at ambient temperature, in the presence of a five-fold excess of triphenylphosphine. Under analogous conditions, cyclisation of 1d is negligibly slow. The two phosphines differ appreciably in bulk[8] and the contribution of steric congestion in controlling cyclisation and elimination in related dineopentylplatinum complexes has been emphasised.[9] Whether the rate-difference reflects easier phosphine dissociation or crowded transition state geometry has yet to emerge. Electronic disparities, moreover, cannot be entirely discounted.

Bipyridyl and the nominally isosteric bipyrimidyl, however, do create different electronic environments at the metal, on the evidence of u.v./visible spectra. The lowest energy metal ligand charge transfer transition ($d\pi$-π*) which appears at 477 nm for 1b is shifted to lower energy at 502 nm in the bipyrimidyl analogue 1c.[10] In spite of this , we detect no significant rate-difference in their metallacyclisations.

Related cyclisations of dialkylplatinum complexes have been proposed to involve transient hydridoalkylplatinum(IV) intermediates,[3,4] and a hydridoiridium(III) product of neophyl cyclisation has recently been isolated.[3c] The thermal rearrangement of 1a is remarkable for its cleanness, in view of the lability of cyclooctadiene derivatives of Pt(IV) towards alkene loss,[11] and the complicated thermolytic behaviour of previously observed (cod)PtR$_2$.[12]

Under the relatively mild conditions required for these reactions, the metallacyclopent-2-ene is the only significant organometallic product. At present, we detect neither metallacyclobutane formation[3] (via attack on ligand methyl substituents) nor rearrangement to 2-tert-butylphenylplatinum species,[13] to any appreciable extent. Moreover, we have observed no coupling or deuterium-abstraction products ascribable to free radical participation. The rates and products of thermal decomposition of 1 are, however, affected by the presence of dioxygen, and by the use of halo-carbon solvents. The mechanistic significance of these observations is being explored. We are, in addition, studying the related, but comparatively less labile, asymmetric dialkyl $L_2Pt(Me)(CH_2CMe_2Ph)$, 3, which affords 2 by elimination of methane.

References and Notes

1.   P.S. Braterman and R.J. Cross, Chem. Soc. Rev., 1973, 2, 271; M.C. Baird, J. Organomet. Chem. 1974, 64, 289; P.J. Davidson, M.F. Lappert and R. Pearce, Chem. Rev., 1976, 76, 219; R.R. Schrock and G. W. Parshall, ibid., 1976, 76, 243.

2.   See, e.g., R.R. Schrock, Acc. Chem. Res., 1979, 12, 98, and references therein.

3. (a) R.A. Andersen, R.A. Jones, and G. Wilkinson, J. Chem. Soc., Dalton Trans. 1978, 446; (b) P. Foley, R. DiCosimo and G.M. Whitesides, J. Am. Chem. Soc., 1980, 102, 6713; (c) T.H. Tulip and D.L. Thorn, ibid., 1981, 103, 2448; for a review, see S.D. Chappell and D.J. Cole-Hamilton, Polyhedron, 1982, 1, 739.

4. (a) J.A. Duff, B.L. Shaw, and B.L. Turtle, J. Organomet. Chem., 1974, 66, C18; (b S.D. Chappel and D.J. Cole-Hamilton, J. Chem. Soc., Chem. Commun., 1980, 238; (c) S.D. Chappell, D.J. Cole-Hamilton, A.M.R. Galas and M.B. Hursthouse, J. Chem. Soc., Dalton Trans., 1982, 1867; (d) R. DiCosimo, S.S. Moore, A.F. Sowinski, and G.M. Whitesides, J. Am. Chem. Soc., 1982, 104, 124.

5.   Satisfactory elemental analyses have been obtained for all the new dialkyl and metallacycloalkylplatinum complexes.

6.   Toluene solutions of $(bipy)Pt(CH_2CMe_2Ph)_2$ decompose readily by a different path in the presence of air; D.C. Griffiths and G.B. Young, unpublished observations.

7.   Preliminary examinations indicate that the analogous complexes where $L_2 =$ bis(diphenylphosphino)methane [^1J(Pt-P) = 1263 Hz], 1,2-bis(diphenylphosphino ethane [^1J(Pt-P) = 1584 Hz] and 1,2-bis(dimethylphosphino)ethane [^1J(Pt-P) = 1634 Hz] are uniformly less labile than 1d. Toluene solutions are unchanged after 6 hours at 60°C.

8.   The cone angle θ for Et_3P is 132° while that for Ph_3P is 145°; C.A. Tolman, Chem. Rev., 1977, 77, 313.

9.   J.A. Ibers, R. DiCosimo and G.M. Whitesides, Organometallics, 1982, 1, 13.

10.   This is a generally observed difference between (bipy)PtR$_2$ and   (bipym)PtR$_2$; V.F. Sutcliffe and G.B. Young, submitted to Polyhedron;   cf. also R.R. Ruminski and J.D. Petersen, Inorg. Chem., 1982 21, 3706;   C. Overton and J.A. Connor, Polyhedron, 1982, 1, 53.

11.   See, e.g., H.C. Clark, and L.E. Manzer, J. Organomet. Chem., 1973, 59, 411.

12.   G.B. Young, and G.M. Whitesides, J. Am. Chem. Soc., 1978, 100, 5808.

13.   B. Akermark and A. Ljungqvist, J. Organomet. Chem., 1978, 149, 97; R.F. Heck, ibid., 1972, 37, 389.

Table 1

N.M.R. Characteristics of Neophylplatinum and Platinacyclopentene Complexes.[a,b]

COMPOUND	δ ^{1}H ppm: Hydrocarbyl Ligands (J_{Pt-H}) [Assignment]		
	CH$_2$	CH$_3$	Aromatic
1a (C$_8$H$_{12}$)Pt(CH$_2$CMe$_2$Ph)$_2$ [c]	2.23 (88)	1.53(6)	7.45 dd ($J_{H_2-H_3}$ = 8) [H$_2$] 7.17–6.92 m [H$_3$,H$_4$]
2a (C$_8$H$_{12}$)Pt(2-C$_6$H$_4$CMe$_2$CH$_2$) [d]	2.29 (89)	1.44	7.26–700 m
1b (bipy)Pt(CH$_2$CMe$_2$Ph)$_2$	2.78 (86)	1.78	7.68 dd ($J_{H_2-H_3}$ = 7) [H$_2$] 7.04–6.64 m [H$_3$,H$_4$]
2b (bipy)Pt(2-C$_6$H$_4$CMe$_2$CH$_2$)	2.91 (96)	1.81	7.31–6.84 m
1c (bipym)Pt(CH$_2$CMe$_2$Ph)$_2$	2.74 (87)	1.78	7.68 dd ($J_{H_2-H_3}$ = 8) [H$_2$] 6.78–6.60 m [H$_3$,H$_4$]
2c (bipym)Pt(2-C$_6$H$_4$CMe$_2$CH$_2$)	2.87 (97)	1.76	7.25–6.98 m
1d (Et$_3$P)$_2$Pt(CH$_2$CMe$_2$Ph)$_2$ [f,h]	2.26 tm (64)	1.73	7.65 dd ($J_{H_2-H_3}$ = 7) [H$_2$] 7.38–7.15 m [H$_3$,H$_4$]
2d (Et$_3$P)$_2$Pt(2-C$_6$H$_4$CMe$_2$CH$_2$) [f,i]	2.14 tt (56) ($^2J_{Pt-H}$ = 6 Hz)	1.73	7.27–7.16 m
1e (Ph$_3$P)$_2$Pt(CH$_2$CMe$_2$Ph)$_2$ [j]	g	g	g
2e (Ph$_3$P)$_2$Pt(2-C$_6$H$_4$CMe$_2$CH$_2$) [f,k]	2.37 tt (62) ($^2J_{Pt-H}$ = 5 Hz)	1.71	e

Footnotes to Table 1.

a; All spectra recorded in d^8-toluene unless otherwise stated.

b; Coupling constants in Hz if observed.

c; alkene CH: $\delta H = 3.87$, $^2J(Pt-H) = 38$;

d; alkene CH: $\delta H_1 = 5.08$, $\delta H_2 = 4.64$, $^2J(Pt-H_1) = 38$, $^2J(Pt-H_2) = 42$.

e; Obscured.

f; ^1H spectrum recorded in d^6-benzene.

g; Complex too labile at ambient temperature to be observed by ^1H n.m.r.
(see text).

h; δP: 0.74 ppm; $^1J(Pt-P) = 1678$

i; δP_1: 13.25 ppm; $^1J(Pt-P_1) = 1833$; δP_2: 10.62 ppm; $^1J(Pt-P_2) = 1857$;
$^2J(P_1-P_2) = 13$

j; δP: 27.17 ppm; $^1J(Pt-P) = 1668$.

k; δP_1: 35.02 ppm; $^1J(Pt-P_1) = 1949$; δP_2 34.72 ppm; $^1J(Pt-P_2) = 1813$;
$^2J(P_1-P_2) = 9$

Table 2

First Order Rate Constants for Rearrangement 1→2.[a]

Complex 1	T (°C)	k (sec^{-1} x 10^5)
1a $(C_8H_{12})Pt(CH_2CMe_2Ph)_2$	60	3.0
1b $(bipy)Pt(CH_2CMe_2Ph)_2$	60	1.8
1c $(bipym)Pt(CH_2CMe_2Ph)_2$	60	1.8
1d $(Et_3P)_2Pt(CH_2CMe_2Ph)_2$	35	22.3

[a] Thermal decomposition carried out in toluene, under argon.
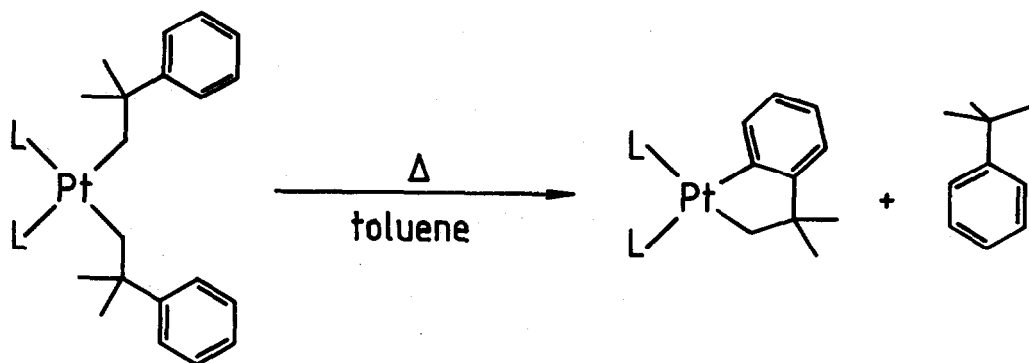
(a) L_2 = 1,5-cyclooctadiene (cod)

(b) L_2 = 2,2'-bipyridyl (bipy)

(c) L_2 = 2,2'-bipyrimidyl (bipym)

(d) L = triethylphosphine

(e) L = triphenylphosphine

COMMUNICATION

REACTIONS OF ETHYL- AND PHENYLLANTHANIDE σ COMPLEXES WITH N,N-DIMETHYLBENZAMIDE AND BENZALDEHYDE

KAZUHIRO YOKOO, YUZO FUJIWARA,[*] TOSHIHIRO FUKAGAWA and HIROSHI TANIGUCHI

Department of Applied Chemistry, Faculty of Engineering, Kyushu University, Fukuoka 812, Japan

Abstract—Metallic Pr, Nd and Dy reacted with iodoethane at room temperature or 65°C in tetrahydrofuran (THF) but Gd, Ho and Er did not. The reaction of PhLnI complexes (Ln=Eu, Sm, Yb) with N,N-dimethylbenzamide gave benzophenone in good yields whilst the reaction of EtSmI with benzaldehyde afforded reduction and coupling products of benzaldehyde.

The formation of complexes of type RLnI by the lanthanides (Ln) such as Ce, Sm, Eu and Yb was first reported by Evans et al.[1] We have reported reactions of phenylytterbium iodide (PhYbI) with carbonyl compounds.[2,3] We wish to report here the reactivity of Pr, Nd, Gd, Dy, Ho and Er to iodoethane, and the reactions of RLnI with N,N-dimethylbenzamide and benzaldehyde.

Each lanthanide metal was allowed to react with iodoethane in THF at room temperature or 65°C. The results are listed in Table 1, and the data in the table show that Pr, Nd and Dy react with iodoethane to give coloured solutions which presumably contain EtLnI σ complexes, whereas Gd, Ho and Er did not react.

Table 1. Reactivity of rare earth metals to iodoethane

Ln	Pr	Nd	Gd	Dy	Ho	Er
Reacts	yes[a]	yes[b]	no[b]	yes[b]	no[b]	no[b]

[a]Reaction temp: room temperature. [b]Reaction temp: 65°C.

That Yb reacts easily with organic halides such as iodoethane or iodobenzene to give divalent RYbI σ-complexes[1] is due to filled f^{14} electronic configuration of Yb^{2+}.

The chemical behaviour of RLnI, prepared in situ, toward N,N-dimethylbenzamide and benzaldehyde was investigated. The reactions of PhYbI complexes with dimethylbenzamide gave benzophenone in good yields. The results are summarized in Table 2. For comparison, the

Table 2. Reactions of PhLnI with N,N-dimethylbenzamide

Run	Ln mg-atom	PhI mmol	Temp °C	Yield of Ph_2CO, %
1	Eu 0.75	0.5	-20	63[a,c]
2	Eu 0.75	0.5	r.t.	57[a]
3	Yb 0.5	0.75	r.t.	60[b,c]
4	Sm 0.5	0.75	65	-
5	Mg 0.5	0.75	r.t.	20[b]

[a]Yields are based on metal. [b]Yields are based on PhI. [c]Refluxed for 2 h.

result with the Grignard reagent, phenylmagnesium iodide, is also listed (run 5), which shows that the reactivity of Eu and Yb complexes toward the benzamide is higher than that of the Grignard reagent. The RSmI complex did not react with the benzamide (run 4) but it was

found to cause reduction and coupling of benzaldehyde to give benzyl alcohol, benzoin, benzyl benzoate, and hydrobenzoin in 10, 18, 8 and 1% yields, respectively. This reductive nature of Sm^{2+} is attributed to the lower potential of Sm: Sm^{3+}/Sm^{2+} -1.55 V, Yb^{3+}/Yb^{2+} -1.15 V and Eu^{3+}/Eu^{2+} -0.43 V.[1] In the reaction of RSmI with PhCHO, one electron transfer from Sm^{2+} to

$$Et-Sm-I \quad + \quad PhCHO \xrightarrow[\text{r.t.}]{\text{THF}} PhCH_2OH \quad + \quad \underset{\underset{OH \quad O}{|}}{Ph-\overset{H}{\underset{|}{C}}-\overset{O}{\underset{||}{C}}-Ph} \quad + \quad \underset{\underset{H}{|}}{Ph-\overset{O}{\underset{||}{C}}-O-\overset{H}{\underset{|}{C}}-Ph}$$

$$+ \quad \underset{\underset{OH \quad OH}{|\quad|}}{Ph-\overset{H}{\underset{|}{C}}-\overset{H}{\underset{|}{C}}-Ph}$$
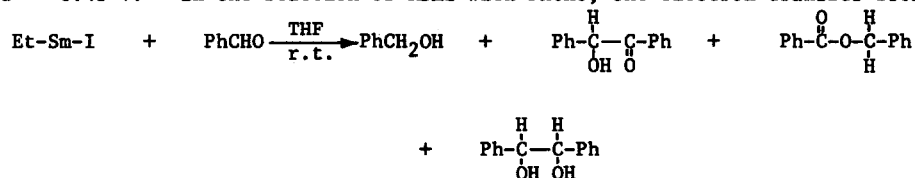
PhCHO would occur to give a radical anion $Ph-\overset{\cdot}{C}H-O^-$ which undergoes the coupling reaction.[4]

EXPERIMENTAL

Metals

Samarium, gadolinium and ytterbium were ca. 40 mesh powders from Research Chemicals. Praseodymium, neodymium, dysprosium, holmium and erbium ingots (Research Chemicals) were freshly cut.

Reaction of lanthanide metals with iodoethane

In a 50-cm³ centrifuge tube, 0.5 mg-atom of lanthanide metal and a magnetic stirring bar were placed under air and the tube was sealed with a serum cap. After the tube was dried by heating under nitrogen, 1 cm³ of THF, which was freshly distilled under nitrogen from sodium benzophenone ketyl, was added by a syringe. Then 1.0 mmol of iodoethane was added slowly to the tube at room temperature or 65°C and the mixture was stirred at room temperature or 65°C (see Table 1). Colour of the resulting solutions are light brown (Pr), grey (Nd) and grey-green (Dy).

Reaction of PhLnI with N,N-dimethylbenzamide

In the similar manner as above, reactions were performed adding dimethylbenzamide (0.5 mmol) to the THF solution of PhLnI, prepared from lanthanide metal and iodobenzene at -20°C in 3 cm³ of THF. The mixtures were stirred overnight and then in some cases (see Table 2) refluxed for 2 h. The resulting mixtures were quenched by 2N-HCl and the products were extracted by ether. From the ethereal layer benzophenone was obtained and sometimes a trace amount of triphenylcarbinol was also detected by GLC.

Reaction of EtSmI with benzaldehyde

Reaction was carried out using Sm (0.5 mg-atom), iodoethane (1.0 mmol) and benzaldehyde (0.5 mmol) in THF (2 cm³) at room temperature with stirring overnight. The products were separated by medium-pressure column chromatography (silica gel) and identification of the products was done by comparison with authentic samples.

REFERENCES

[1] D. F. Evans, G. V. Fazakerley and R. F. Phillips, *J. C. S. Chem. Commun.*, 1970, 244 ; *J. Chem. Soc. A*, 1971, 1931.

[2] T. Fukagawa, Y. Fujiwara, K. Yokoo and H. Taniguchi, *Chem. Lett.*, 1981, 1771.

[3] T. Fukagawa, Y. Fujiwara and H. Taniguchi, *Chem. Lett.*, 1982, 601.

[4] P. Girard, R. Couffignal and H. B. Kagan, *Tetrahedron Lett.*, 1982, 22, 3959.

COMMUNICATION

CATIONIC CARBONYL COMPLEXES OF MANGANESE (I) WITH NITRILES AND DINITRILES

F.J. García Alonso, V. Riera*

Department of Inorganic Chemistry, University of Valladolid, Spain

(Received 5 May ; accepted 16 June 1983)

ABSTRACT The reaction of $Mn(CO)_5OClO_3$ with nitriles, L, and dinitriles, L-L, in a wide variety of conditions affords cationic pentacarbonyls, $[Mn(CO)_5(L)]ClO_4$ and $[Mn(CO)_5(L-L)]ClO_4$ and fac-tricarbonyls, $[Mn(CO)_3(L)_3]ClO_4$ and $[(CO)_3Mn(\mu L-L)_3Mn(CO)_3](ClO_4)_2$

RESULTS AND DISCUSSION The reaction of $Mn(CO)_5OClO_3$ with nitriles, (1/3 molar ratio) in refluxing $CHCl_3$ gave cationic tricarbonyl derivatives fac-$[Mn(CO)_3(L)_3]ClO_4$[1], (L: EtCN, $CH_2=CHCH_2CN$, PhCN, $PhCH_2CN$). In CH_2Cl_2 at room temperature the reaction gave a mixture of pentacarbonyls $[Mn(CO)_5(L)]ClO_4$ (which are initially formed) and the tricarbonyls fac-$[Mn(CO)_3(L)_3]ClO_4$; from the resulting solutions pure pentacarbonyls were isolated in low yield; by using equimolecular ratio, at -10°C, the formation of fac-tricarbonyl was greatly reduced, but the yields were not improved due to the low solubility of the precursor neutral perchlorate. All attempts to promote further substitution have failed; use of EtOH as solvent led to the formation of a fac-tricarbonyl derivative, possibly fac-$[Mn(CO)_3(EtOH)_3]ClO_4$, not previously described, which could not be characterized since it was obtained as an oil by solvent evaporation; IR (cm^{-1}) ν CO (CH_2Cl_2) 2040 s, 1935 br,s.

Similar reactions with dinitriles L-L, (L-L: $NCCH_2CN$, $NCCH_2CH_2CN$, $NCCH_2CH_2CH_2CN$, $o-C_6H_4(CN)_2$), in CH_2Cl_2 at room temperature in 1/3 ratio led to precipitation of white-yellow solids, identified by IR spectroscopy as mixtures of the corresponding penta- and tricarbonyl derivatives. Attempts to separate pure pentacarbonyls by succesive recrystallizations were unsuccesful, although analytical data are very close to the expected for $[Mn(CO)_5(L-L)]ClO_4$. The $Mn(CO)_5OClO_3$ reacted with a three fold excess of dinitriles L-L in refluxing $CHCl_3$ giving, through the intermediate pentacarbonyls, the tricarbonyls fac-$[(CO)_3Mn(\mu L-L)_3Mn(CO)_3](ClO_4)_2$, which must be dimers in accordance with conductivity data at various concentrations, and their structures are probably those in which the dinitriles are bridging two $Mn(CO)_3$ groups.

The pentacarbonyls show four ν CO bands in CH_2Cl_2 or in $CHCl_3$. Although uncommon, since IR spectra of pentacarbonyls usually exhibit only three absorptions $(2 A_1 + E)$ in the ν CO region, this behaviour is not unique and some pentacarbonyls can be found in the literature with four ν CO bands[2]. Using the Cotton-Kraihanzel method[2], the B_1 band which is not IR active for rigorous C_{4v} symmetry, must appear at 2106 cm^{-1} which supports the view that the band at 2122 cm^{-1} may be the B_1 mode. The weak ν CN absorptions of coordinated nitriles, at higher wavenumbers than that of free ligands, indicate that all the nitriles and dinitriles are bound to the metal through the nitrogen.

EXPERIMENTAL All the reactions were carried out under N_2 and in absence of light.

Preparation of $[Mn(CO)_5(L)]ClO_4$ (General method) A mixture of $Mn(CO)_5OClO_3$[3] in

---

* Author for correspondence

CH_2Cl_2, obtained from 0.3 g (1.09 mmol) of $Mn(CO)_5Br$, and L was stirred. The yellow oil which results from the removal of the solvent in vacuo, was washed with Et_2O to extract the unreacted L and the fac-$[Mn(CO)_3(L)_3]ClO_4$. The resulting solid was recrystallized from $CH_2Cl_2/EtOH$. IR (cm^{-1}) $\overline{V}$ CO $(CH_2Cl_2$ or $CHCl_3)$ 2165 w, 2122 w, 2080 s, 2045 m, for all the pentacarbonyls. The specific conditions for each reaction (neutral perchlorate/ligand mol ratio, solvent, time, temperature and yield), analytical and conductivity data for the catio-nic pentacarbonyls were as follows:

L: EtCN, 1/2.5, $CHCl_3$, 8 h, room temperature, 39%. M.P. 87°C. Λ_M 92 S cm^2 mol^{-1}.(The solvent used for all conductivity measurements was $MeNO_2$).$\overline{V}$ CN (nujol) 2315 cm^{-1}.Found C 27.49, H 1.59, N 3.97. Calc. C 27.49, H 1.44, N 4.00 %. L: $CH_2=CHCH_2CN$, 1/2.2, $CHCl_3$, 9 h, room temperature, 21%. M.P. 96°C. Λ_M 93 S cm^2 mol^{-1}. $\overline{V}$ CN (nujol) 2310 cm^{-1}. Found C 29.20, H 1.41 N 3.31. Calc. C 29.30, H 1.39, N 3.87%. L: $PhCH_2CN$, 1/1, CH_2Cl_2, 33 h, -10°C, 25%.M.P.92°C. Slope 143^4. $\overline{V}$ CN (nujol) 2317 cm^{-1}. Found C 38.55, H 1.82, N 3.78. Calc. C 37.94, H 1.71, N 3.40%.

         Preparation of $[Mn(CO)_3(L)_3]ClO_4$ L: EtCN. To a solution of $Mn(CO)_5OClO_3$ (prepared from 0.3 g, 1.09 mmol, of $Mn(CO)_5Br$) in 40 cm^3 of $CHCl_3$, 0.2 cm^3 (2.49 mmol) of EtCN was added. After refluxing 2 h, the solvent was removed under reduced pressure. The residue was washed with hexane to extract unreacted L. Yield 65%. M.P. 98°C. Slope 200^4. IR (cm^{-1}) $\overline{V}$ CO (CH_2Cl_2) 2070 s, 1977 br,s; $\overline{V}$ CN (nujol) 2300. Found C 35.06, H 3.63, N 10.17. Calc. C 35.71, H 3.74, N 10.40%. L: PhCN. It was obtained by the procedure above described. Yield 65%. M.P. 97°C. Λ_M 93 S cm^2 mol^{-1}. IR (cm^{-1}) $\overline{V}$ CO $(CHCl_3)$ 2070 s, 1983 br,s; $\overline{V}$ CN (nujol) 2270. Found C 53.12, H 2.79, N 7.67. Calc. C 52.62, H 2.76. N 7.50%. L: $CH_2=CHCH_2CN$ and $PhCH_2CN$. They were not characterized because of the formation of uncrystallizable oils. Their IR spec-tra (CH_2Cl_2) in the $\overline{V}$ CO region are the same (cm^{-1}) 2070 s, 1985 br,s.

         Preparation of fac-$[(CO)_3Mn(\mu$ L-L$)_3Mn(CO)_3](ClO_4)_2$ L-L: $NCCH_2CH_2CN$. A mixture of $Mn(CO)_5OClO_3$ (from 0.25 g (0.91 mmol) of $Mn(CO)_5Br$) in 50 cm^3 of $CHCl_3$ and 0.218 g (2.73 mmol) of $NCCH_2CH_2CN$ was refluxed for 18 h. The resulting oil was washed with CH_2Cl_2 and Et_2O. Yield 50%. Recrystallized from Me_2CO/Et_2O. It blackens at 188°C without melting. Slope 316^4. IR (cm^{-1}) $\overline{V}$ CO (Me_2CO) 2065 s, 1983 br,s; $\overline{V}$ CN (nujol) 2310. Found C 30.09, H 1.70, N 11.70. Calc. C 30.15, H 1.69, N 11.72%. L-L: $o-C_6H_4(CN)_2$. It was prepared using a similar proce-dure. Yield 38%. It blackens at 193°C. Slope 367^4. IR (cm^{-1}) $\overline{V}$ CO (Me_2CO) 2075 s, 1955 br,s; $\overline{V}$ CN (nujol) 2275. Found C 42.09, H 1.17, N 9.53. Calc. 41.82, H 1.40, N 9.75%. For L-L: $NCCH_2CN$ and $NCCH_2CH_2CH_2CN$ the complexes could not be purified.

NOTES AND REFERENCES

1.- For a review of the field, see Comprehensive Organometallic Chemistry. G. Wilkinson, F.G.A. Stone, E. Abel. Vol. 4,pp 31-32. Pergamon Press. Oxford. U.K. 1982

2.- F.A. Cotton and C.S. Kraihanzel, J. Am. Chem. Soc.,1962, 84, 4432

3.- R. Usón, V. Riera, J. Gimeno, M. Laguna and M.P. Gamasa, J. Chem. Soc., (Dalton)., 1979,996

4.- Slope of the straight line which results from plotting Λ_0 $-\Lambda_e$ versus $\sqrt{Ce}$, where Λ_e is the equivalent conductivity, Λ_0 is Λ_e at infinite dilution, and Ce is the equivalent concen-tration. The value 143 and 200 are in the expected range for 1:1 electrolytes and the values 316 and 367 are in the expected range for 1:2 electrolytes when $MeNO_2$ is used as solvent.- R.D. Feltham and R.G. Hayter, J. Chem. Soc. 1964, 4587

BOOK REVIEW

Gmelin Handbook of Inorganic Chemistry. 8th Edition Sn—Organotin Compounds. Part 10. Mono- and Diorganotin-Sulfur Compounds. Published by the Gmelin Institute for Inorganic Chemistry of the Max Planck Society for the Advancement of Science. Springer-Verlag. Springer–Heidelberg–New York. 1983. xi + 352 pp. DM 993. US $ approx. 397.20.

Previous volumes on organotin compounds in this series have dealt with tetraalkyltins, trialkyltin hydrides, and alkyltin halides and pseudohalides. Volume 9 covered trialkyltin-sulphur compounds, and this companion volume covers the mono- and di-alkyltin compounds of sulphur, and the few organo–selenium and organotin–tellurium compounds which are known; and it ends with the sentence: "Organotin–Polonium Compounds: No organotin–polonium compound has yet been prepared". The literature is covered up to the end of 1980.

This volume follows the established form for the series, which is now written wholly in English. The entry for $(CH_3)_2Sn(SCH_3)_2$, the first in the book can serve as an example. It covers more than two pages and includes 17 references. The first paragraph deals with the preparative methods the second with physical properties, and the third with spectroscopic properties. ^1H NMR, and IR and Raman data are tabulated. Two paragraphs then cover chemical reactions, and the final one deals with applications: indeed the industrial applications provide an important aspect of this volume, as the dialkyltin organosulphur compounds are widely used as stabilisers of p.v.c.

Related compounds are collected together in tables, and there is a formula index covering 70 pages.

Organotin chemists who have access to these volumes are indeed fortunate, and will salute the industry of Herbert and Ingeborg Schumann who write them. The next volumes, which will cover the centrally-important organotin–oxygen compounds are eagerly awaited.

A. G. DAVIES

DEPOLYMERIZATION KINETICS OF $Ru_4(OH)_4^{8+}$ AND CHARACTERIZATION OF THE REACTION PRODUCT: DIMERIC Ru(III) ION

W. D'OLIESLAGER*, L. HEERMAN and M. CLARYSSE

Laboratorium voor Radiochemie, Katholieke Universiteit Leuven, Celestijnenlaan 200F, 3030 Heverlee, Belgium

Abstract—Perchloric acid solutions of $Ru_4(OH)_4^{8+}$ were prepared by the controlled-potential reduction of Ru(IV) at platinum electrodes in a high-speed coulometric cell. The solution spectrum of $Ru_4(OH)_4^{8+}$ is reported. Tetrameric Ru(III) ion decomposes in a reaction which is first-order with respect to its concentration, but independent of the acidity, to another species of the same valence state which is believed to be a dimeric ion ($Ru_2(OH)_2^{4+}$ or similar).

Electrochemical reduction of this species yields Ru^{2+} which can be reoxidized only to Ru^{3+}, the most stable of the Ru(III)-aquo ions.

Ruthenium(IV) exists in non-complexing media (e.g. acid perchlorate solutions) as a tetrameric ion, formulated as $Ru_4(OH)_{12}^{4+}$ (or $Ru_4O_6^{4+}$, etc.).[1,2] On platinum rotating disk electrodes, two reversible waves are observed for the reduction steps Ru(IV)→Ru(3.5)→Ru(III), each wave being the sum of two one-electron steps:[3]

products possibly are formed in less acidic solutions. The further reduction of tetrameric Ru(III)-ion to Ru(II) occurs at more cathodic potentials and can be observed only on mercury electrodes.[4-6] According to this scheme, tetrameric Ru(III)-ion slowly decomposes into another more stable species of the same valence state which was

1st wave

$$Ru_4(OH)_{12}^{4+}(IV) \xrightarrow{\underline{0.650\ V}} Ru_4(OH)_{10}^{5+}(3.75) \xrightarrow{\underline{0.656\ V}} Ru_4OH_8^{6+}(3.5)$$
$$\overline{\qquad\qquad 0.653\ V \qquad\qquad}$$

2nd wave

$$Ru_4(OH)_8^{6+}(3.5) \xrightarrow{\underline{0.493\ V}} Ru_4(OH)_6^{7+}(3.25) \xrightarrow{\underline{0.455\ V}} Ru_4OH_4^{8+}(III)$$
$$\overline{\qquad\qquad 0.469\ V \qquad\qquad}$$

$$Ru_4(OH)_4^{8+}(III) \xrightarrow{k_1} 2Ru_2(OH)_2^{4+}(III). \qquad (1)$$
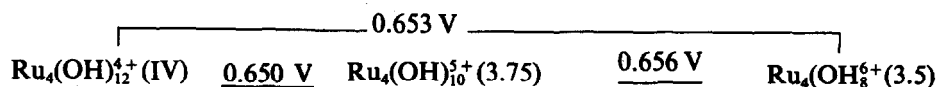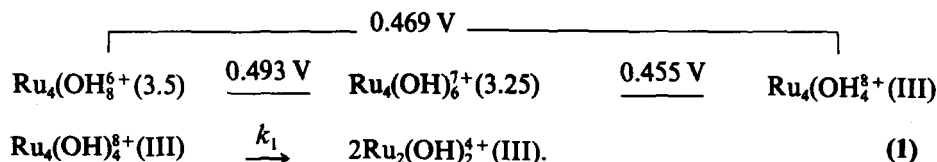
Potentials (vs. nhe) and species are given for 1.0 M HClO₄ solutions (the high charge on these ions most probably is reduced by perchlorate complex or ion-pair formation); more hydrolized

hypothesized to be a dimeric species (*vide infra*).[3] The existence of such a follow-up chemical reactions was already indicated by Wehner and Hindman[7] who noticed profound changes in the UV absorption spectrum of Ru(III) solutions prepared by electrolytic reduction of Ru(IV) at platinum electrodes, when stored at 0°C under an inert atmosphere (see also Refs. 1 and 3).

*Author to whom correspondence should be addressed.

This paper reports on the depolymerization kinetics of $Ru_4(OH)_4^{8+}$ and on the electrochemical reduction of its decomposition product (dimeric Ru(III)-ion).

EXPERIMENTAL

Acid perchlorate solutions of Ru(IV) were prepared and analyzed as described previously.[3]

Solutions of tetrameric Ru(III)-ion for spectrophotometric studies were prepared, in an air thermostat under inert atmosphere, by electrolysis at a platinum gauze electrode in a high-speed coulometric cell ($p \simeq 3.5 \times 10^{-2} sec^{-1}$; for a definition of p, see Bard[8]); complete electrolysis was achieved in about 180–200 sec. The solution was then transferred immediately to a spectrophotometer cell and the spectral changes were recorded as a function of time (Beckman Acta M IV spectrophotometer). The spectrum of $Ru_4(OH)_4^{8+}$ was obtained by recording a spectrum immediately after the preparative electrolysis and correcting it for the small amount of dimer (less than 5% at 0°C) already formed during the electrolysis time. The concentration of the dimer was estimated by treating the mass transfer and the follow-up chemical reaction during the electrolysis as a system of consecutive first-order reactions using experimental values of p and k_1 (*vide infra*).

Electrochemical experiments were carried out using a PAR Model 303 SMDE (static mercury drop electrode) and a PAR Model 174A polarographic analyzer; other experimental details have been reported elsewhere.[3]

RESULTS AND DISCUSSION

The spectra of tetrameric and dimeric Ru(III)-ions are shown in Fig. 1. The spectrum of dimeric Ru(III) contains a single peak at 290 nm ($\epsilon_D^{290} = 2360 \pm 50$), in agreement with the work of Wallace and Propst[1] (Wehner and Hindman[7] reported a peak at 300 nm). The spectrum of tetrameric Ru(III)-ion, not previously reported in the literature, exhibits plateaus at 285–310 nm and 390–405 nm ($\epsilon_T^{400} = 730 \pm 10$) (the formal molar absorptivities were calculated using the analytical concentration of ruthenium, C_{Ru}).

The depolymerization kinetics of tetrameric Ru(III)-ion was studied by recording the spectral changes at 290 nm and plotting $\log(\epsilon_D^{290}C_{Ru} - A^{290})$ vs time, as is shown in Fig. 1, inset; from the mass balance and the postulate of additive absorbances it follows that $(\epsilon_D^{290}C_{Ru} - A^{290})$ is proportional to the concentration of $Ru_4(OH)_4^{8+}$ (this is true, irrespective of whether the product of the follow-up chemical reaction is a dimeric ion or not). Such plots were linear over at least two to three half-
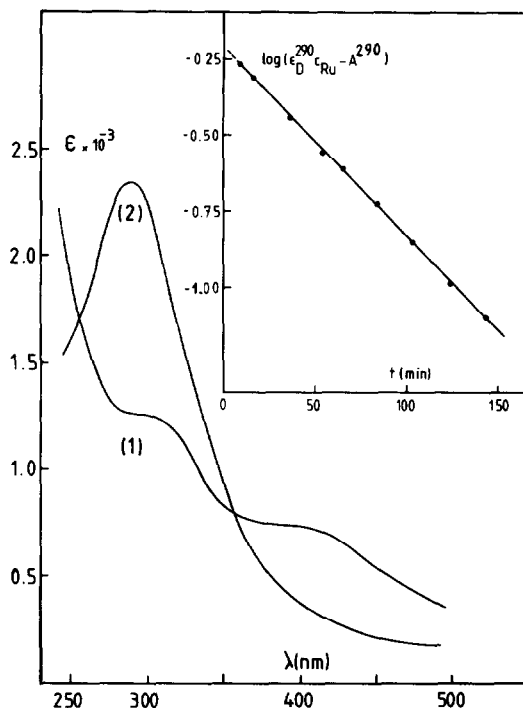
Fig. 1. Absorption spectrum of (1) $Ru_4(OH)_4^{8+}$ and (2) $Ru_2(OH)_2^{4+}$ in 1.0 M $HClO_4$ solution. Inset. Decomposition kinetics of $Ru_4(OH)_4^{8+}$: plot of $\log(\epsilon_D^{290}C_{Ru} - A^{290})$ vs time (0°C).

lives, as expected for a reaction that is first order with respect to the concentration of $Ru_4(OH)_4^{8+}$. The rate constant k_1 was found to be independent of the solution acidity over the range $0 \leq pcH \leq 2$. Values of k_1 are 2.37 (± 0.03) $\times 10^{-4} sec^{-1}$(0°C), 9.82(± 0.20) $\times 10^{-4} sec^{-1}$ (15°C) and 2.47 (± 0.06) $\times 10^{-3} sec^{-1}$(25°C); the energy of activation is calculated as 63 kJ/mole. Furthermore, it was established by direct potentiometry (using glass electrodes) that protons are neither consumed nor liberated in the reaction. These facts seem to suggest that the stoichiometry of the follow-up chemical reaction is adequately represented by (1); it must be stressed however that an unquestionable proof of the existence of a dimeric Ru(III) aquoion has not been given thus far.

Methods such as ion exchange, solvent extraction and potentiometry cannot be used, at least in perchloric acid solutions, to investigate the ionic nature of this Ru(III) species since it is slowly oxidized by perchlorate ion (Wehner and Hindman[7] already implicitly dismissed the possibility that the species is a chloro-complex, chloride being produced in the oxidation reaction).

Some indirect evidence for the existence of a dimeric Ru(III) species was obtained from the following experiment.

A solution of 2, 2'-bipyridine in toluene

$(10^{-3}$ M) was added to a solution of "stable" Ru(III) (absorption maximum at 290 mμ). The organic ligand was slowly extracted into the aqueous phase with formation of an intensely green coloured complex. The aqueous phase was then 50-fold diluted with acetonitrile and the spectrum was recorded; the complex absorbs at 410 nm and 640 nm. According to Weaver et al.,[9] a high intensity, low energy band at about 650 nm is characteristic for oxo-bridged dimers such as $[(bipy)_2(H_2O)RuORu(H_2O)(bipy)_2]^{4+}$ (these authors preferred the diaquo-μ-oxo formulation over the di-μ-hydroxy formulation proposed by Dwyer et al.[10] for similar 1, 10-phenanthroline complexes).

The electrochemical reduction of dimeric Ru (III) has been studied by polarography (sampled DC) and cyclic voltammetry. Over the acidity range $0 \le pcH \le 2$, a single polarographic wave is observed with $E_{\frac{1}{2}} = -0.290$ V vs SCE (for 1.0 M $HClO_4$ solutions and $t = 1$ s). The electrode reaction involves one electron per ruthenium atom and, therefore, corresponds with the reduction step dimeric Ru(III)→Ru(II). The number of electrons involved in the reduction was estimated by comparing the diffusion current with the diffusion currents for the reduction steps of Ru(IV) under identical conditions of concentration, drop time, etc., a direct determination by controlled potential

coulometry is impossible since Ru(II) is oxidized by perchlorate ion during the experiment. The half-wave potential is independent of the ruthenium concentration but shifts to more negative values if the solution acidity is decreased $(dE_{\frac{1}{2}}/dlog c_{H^+} = -0.044$ V/decade). Furthermore, the half-wave potential shifts to more negative values for shorter drop times $(dE_{\frac{1}{2}}/dlog t = -0.022$ V/decade), which indicates the irreversibility of the electron transfer process. The cyclic voltammogram obtained for a solution of dimeric Ru(III) at the HMDE, shown in Fig. 2, exhibits a single reduction peak A on the first scan but the corresponding anodic peak is absent on the reverse sweep (as expected for an irreversible reaction); instead, a new reversible couple B/C is produced which can be identified with the Ru^{3+}/Ru^{2+} couple $(E_{\frac{1}{2}} = 0.002$ V vs SCE) in good agreement with the measurements of Mercer and Buckley.[11] During successive scans, the height of peak A decreases while the height of peaks B/C increases; similarly, the ratio of the peak heights A/B(C) increases at slower scan rates. These observations are in agreement with a reaction scheme where the irreversible charge transfer step is followed by a chemical reaction, such as

$$(Ru-O + Ru)^{4+} \xrightarrow[\text{irreversible}]{2e^-,\,6H^+} (Ru-\overset{\overset{\displaystyle H}{|}}{O}-Ru)^{3+}$$

$$\xrightarrow[k_2]{1H^+} 2Ru^{2+}.$$
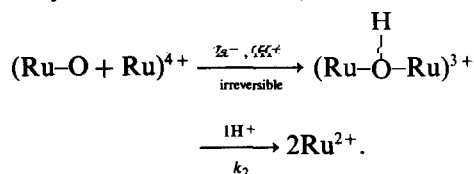
Obviously, the overall reaction is the reduction of dimeric Ru(III) to Ru^{2+} which can be reoxidized to Ru^{3+}, the most stable of the Ru(III)-aquo-ions.

REFERENCES

1. R. M. Wallace and R. C. Propst, J. Am. Chem. Soc. 1969, 91, 3779.
2. C. Brémard, G. Nowogrocki and G. Tridot, Bull. Soc. Chim. Fr., 1974, 392.
3. J. Schauwers, F. Meuris, L. Heerman and W. D'Olieslager, Electrochim. Acta 1981, 26, 1065.
4. L. W. Niedrach and A. D. Tevebaugh, J. Am. Chem. Soc. 1951, 73, 2835.
5. D. K. Atwood and T. De Vries, J. Am. Chem. Soc. 1962, 84, 2659.
6. L. N. Lazarev and J. S. Khvorostin, Russ. J. Inorg. Chem. 1968, 13, 1297.
7. P. Wehner and J. C. Hindman, J. Am. Chem. Soc. 1950, 72, 3911.
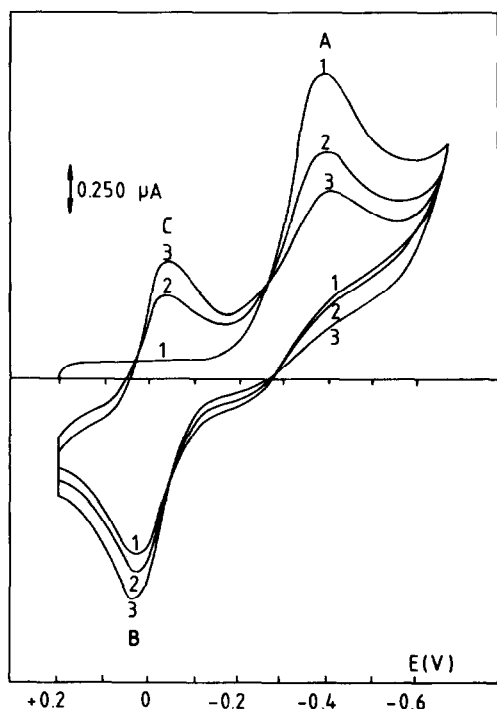
8. A. J. Bard and K. S. V. Santhanam, *Electroanalytical Chemistry* (Edited by A. J. Bard), Vol. 4, p. 215. Marcel Dekker, New York (1970).

9. T. R. Weaver, T. J. Meyer, S. Ajao Adeyemi, G. M. Brown, R. P. Eckberg, W. E. Hatfield, E. C. Johnson, R. W. Murray and D. Untereker, *J. Am. Chem. Soc.* 1975, **97**, 3039.

10. F. P. Dwyer, H. A. Goodwin and E. C. Gyarfas, *Aust. J. Chem.* 1963, **16**, 544.

11. R. R. Buckley and E. E. Mercer, *J. Phys. Chem.* 1966, **70**, 3103.

COMPARISON OF FREE AND METAL COORDINATED 1,4-DISUBSTITUTED-1,4-DIAZA-1,3-BUTADIENES

CRYSTAL AND MOLECULAR STRUCTURES OF 1,4-DICYCLOHEXYL-1,4-DIAZA-1,3-BUTADIENE AND *TRANS*-[DICHLORO(TRIPHENYLPHOSPHINE)(1,4-DI-TERT-BUTYL-1,4-DIAZA-1,3-BUTADIENE)PALLADIUM(II)]

JAN KEIJSPER, HENK VAN DER POEL, LOUIS H. POLM, GERARD VAN KOTEN*, KEES VRIEZE

Anorganisch Chemisch Laboratorium, J. H. Van 't Hoff Instituut, University of Amsterdam, Nieuwe Achtergracht 166, 1018 WV Amsterdam, The Netherlands

and

PAUL F. A. B. SEIGNETTE, RONALD VARENHORST and CASPAR STAM
Laboratorium voor Kristallografie, J. H. Van 't Hoff Instituut, University of Amsterdam, Nieuwe Achtergracht 166, 1018 WV Amsterdam, The Netherlands

Abstract—The crystal and molecular structures of c-Hex-DAB (c-hexyl-N=C(H)–C(H)=N-c-hexyl; DAB = 1,4-diaza-1,3-butadiene) and of trans-[PdCl$_2$(PPh$_3$)(t-Bu-DAB)] are reported. Crystals of c-Hex-DAB are monoclinic with space group $C_{2/c}$ and cell constants: $a = 24.70(1)$, $b = 4.660(2)$, $c = 12.268(3)$ Å, $\beta = 107.66(4)°$, $Z = 4$. The molecule has a flat E-s-trans-E structure with bond lengths of 1.258(3) Å for the C=N double bond and 1.457(3) Å for the central C–C′ bond. These bond lengths and the N=C–C′ angle of 120.8(2)° indicate that the C- and N-atoms are purely sp^2-hybridized and that there is little or no conjugation within the central DAB skeleton. Crystals of trans-[PdCl$_2$(PPh$_3$)(t-Bu-DAB)] are triclinic with space group $P\bar{1}$ and cell constants: $a = 17.122(3)$, $b = 18.279(3)$, $c = 10.008(5)$ Å, $\alpha = 96.77(2)$, $\beta = 95.29(3)$, $\gamma = 109.79(2)$. $Z = 4$. The t-Bu-DAB ligand is coordinated to the metal via one lone pair only. In this 2e; σ-N coordination mode the E-s-trans-E conformation of the free DAB-ligand is still present and the bonding distances within the DAB-ligand are hardly affected. [C=N: 1.261(10) Å; C–C′: 1.479(10) Å (mean).] The Pd–N-, N=C- and central C–C′-bond lengths are compared with those found in other metal -R–DAB complexes.

During the last few years much attention has been paid to the coordination properties of cumulated and conjugated hetero double bond systems such as:

pseudo allenes, e.g. (R)N=C(H)–N(R)$^-$,[1a,2] O=C(R)–O$^-$,[1a,2] (R)N=N–N(R)$^-$,[1a,2] (R)(R′)C=S=O,[1b] (R)N=S=O,[2c] (R)N=S=N(R);[2c]

pseudo butadienes, e.g. (R)N=C(H)–C(OEt)=O,[1c] (R)N=N–N=N(R),[1d,2a,b] (R)N=C(H)–C(H)=N(R).[2a,2b,3]

The use of 1,4-disubstituted-1,4-diaza-1,3-butadiene (R–DAB), a member of the group of α-diimines (see Fig. 1), has been especially successful and many new R–DAB-metal complexes have been synthesized.[3,4,8,9]

If one compares R–DAB with other α-diimines, it is clear that the R–DAB ligand is much more versatile in coordination behaviour. It is not only possible to donate the free electron pair on each of the nitrogen atoms, but also to use the π-electrons for coordination. As expected this use has not been observed for 2,2′-bipyridine and 1,10-phenanthroline, because here the π-electrons are part of an aromatic system. With R–DAB as a ligand, changes on the metal centre can be accommodated by changing the coordination
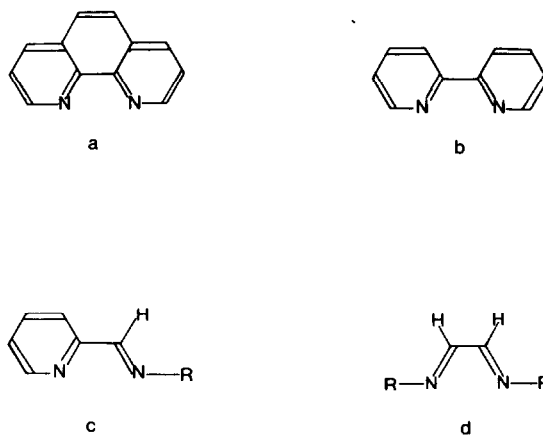
Fig. 1. Some well known α-diimines. 1,10-phenanthroline (a), 2,2′-bipyridine (b), pyridinealdimine (c), R–DAB (d).

mode of R–DAB. For example, loss of a CO-group from CoMn(CO)$_7$(R–DAB) results in a change of the R–DAB coordination from the 4e; σ-N, σ-N′- to the 6e; σ-N, σ-N′, η^2-C=N′-coordination mode.[3]

The various coordination modes of R–DAB are shown in Fig. 2. Figure 2(a) illustrates the σ-N monodentate (2e donor mode) which has been postulated in

_____

*Author to whom correspondence should be addressed.
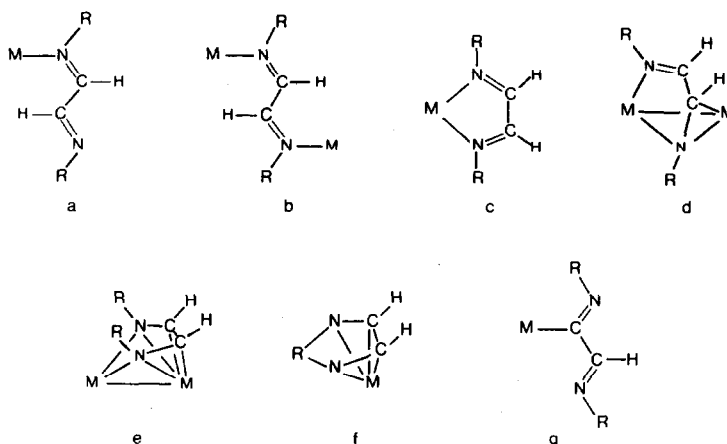
Fig. 2. The coordination modes of the R–DAB ligand: 2e; σ-N (a), 4e; σ-N, σ-N' bridging (b), 4e; σ-N, σ-N' chelating (c), 6e; σ-N, σ-N', η^2-C=N' or σ-N, μ-N', η^2-C=N' (d), 8e; σ-N, σ-N', η^2-C=N, η^2-C=N' (e), 4e; η^2-C=N, η^2-C=N' (f), 2e; σ-C (g).

e.g. *trans*-[PdCl$_2$(*t*-Bu–DAB)$_2$][5] and is found in *trans*-[PdCl$_2$(PPh$_3$)(*t*-Bu–DAB)] (this report). Until now the σ-N, σ-N'-bridging (4e donor) mode (Fig. 2b) has only been found in d^8-metal complexes of Pt(II), Pd(II), Rh(I), e.g. in [{PtCl$_2$(PBu$_3$)}$_2$(*t*-Bu–DAB)].[4] The σ-N, σ-N'-chelate (4e donor) mode (Fig. 2c) is the most common one and has been found in many low-valent metal complexes.

Relatively few examples are known in which the R–DAB also uses its π-electrons for coordination, though in the last few years the number has been growing rapidly. The σ-N, σ-N', η^2-C=N' or σ-N, μ-N', η^2-C=N' coordination (6e donor) mode, depicted in Fig. 2(d), has been observed in MM'(CO)$_6$(DAB) (M=M'=Fe, Ru, Os; M=Mn, Re; M'=Co) and Ru$_2$(CO)$_4$(DAB)$_2$ complexes.[3,6,7] The σ-N, σ-N', η^2-C=N, η^2-C=N' coordination (8e donor) mode (Fig. 2e) in which the DAB uses its maximum number of 8 electrons for coordination has been found in Ru$_2$(CO)$_4$(μ-C$_2$H$_2$)(DAB), Ru$_4$(CO)$_8$(DAB)$_2$ and Mn$_2$(CO)$_6$(DAB).[8–10]

The bonding situation recently found in Ru$_3$(CO)$_9$(*c*-Hex–DAB) can best be described as being intermediate between the 6e- and 8e-donor mode[11] because one C=N side of the DAB is strongly η^2-C=N bonded, while the other side is bonded only very weakly.†

In the free R–DAB ligand the conformation at the C=N bonds is the E(*anti*) one. This conclusion was based on IR, NMR, and dipole-moment measurements[14–16,19] and on an electron diffraction study in the gas phase on *t*-Bu–DAB.[17] This configuration is also found in all metal-R–DAB complexes. The conformation of the C–C'-bond is not quite clear. In the gas phase 20% of the *t*-Bu–DAB molecules has a *s-trans* conformation (torsion τ = 180°), while 80% has a gauche conformation

(τ = 65°).[17] In solution conformations are present with torsion angles between 90 and 140° according to dipole-moment measurements.[16] Such a torsion around the C–C' bond is also found in diketones.[18] IR, Raman, UV and PES measurements on the other hand support the conclusion that the free R–DAB molecule predominantly exists in a *s-trans* conformation.[14,19,20] MO calculations on R–DAB and related hetero-butadienes such as biacetyl[21] and 2,2'-bipyridine[22] also give the *s-trans* conformer as the most stable one.[23]

In order to obtain both the conformation of the free ligand in the solid state, as well as precise bond lengths and angles, we have carried out an X-ray study of *c*-Hex–DAB: *c*-Hex–N=C(H)–C(H)=N-*c*-Hex. The data on bond lengths and angles obtained are more precise than those obtained earlier via a diffraction study in the gas phase on *t*-Bu–DAB.[17] Accordingly we have now a better point of reference for the interpretation of the molecular distances in the R–DAB ligand in a great number of metal-R–DAB complexes for which the crystal structures are known.

In order to see if 2e; σ-N-coordination affects the geometry of, or bonding distances within the R–DAB ligand, we have also completed an X-ray investigation on *trans*-[PdCl$_2$(PPh$_3$)(*t*-Bu–DAB)]. This compound's crystal structure also represents the first example in which the R–DAB ligand is bonded in the 2e; σ-N bonding mode fashion (Fig. 2a). This coordination mode as well as the dynamic properties of *trans*-[MCl$_2$(PR$_3$)(*t*-Bu–DAB)] (M = Pt, Pd; R = aryl) in solution have already been put forward on basis of ^{1}H, ^{13}C-, ^{31}P-, ^{15}N- and ^{195}Pt–NMR measurements.[5,24]

†Other bonding possibilities are: η^2-C=N, η^2-C=N' coordination mode (4e-donor) (Fig. 2f), which has been proposed for cyclic α-diimine systems,[12] while in 1,4-diaza-1,3-butadiene-2-yl-complexes there is a bond between a central C-atom of the R–DAB and the metal (Fig. 2g).[13]

EXPERIMENTAL

Syntheses

Synthesis of *c*-Hex–DAB,[24] and *trans*-[PdCl$_2$(PPh$_3$)(*t*-Bu–DAB)][5] have been carried out according to literature methods. Recrystallization from diethyl ether and dichloromethane/pentane, respectively, yielded single crystals suitable for X-ray measurements.

Data collection and structure determination of 1,4 - di-cyclohexyl - 1,4 - diaza - 1,3 - butadiene, $C_{14}H_{24}N_2$

Crystals of c-Hex–DAB are monoclinic with space group $C_{2/c}$ with 4 molecules in a unit cell of dimensions $a = 24.70(1)$, $b = 4.660(2)$, $c = 12.268(3)$ Å and $\beta = 107.66(4)°$. A total of 1150 intensities were measured on a NONIUS CAD 4 diffractometer using graphite mono-chromated CuK_α radiation, 326 of which were below the 2.5σ(I) level and were treated as unobserved. No absorption correction was applied (crystal dimensions $0.3 \times 0.3 \times 0.05$ mm; $\mu = 4.54$ cm^{-1}). The structure was solved by means of the symbolic addition programme set SIMPEL.[25] Refinement proceeded by block-diagonal least-squares calculations, anisotropic for C and N, isotropic for H. The H-atoms were located in a ΔF-synthesis. The final R value for the 824 observed reflexions was 0.055. A weighting scheme $\omega = (0.66 + F_0 + 0.011\ F_0^2)^{-\frac{1}{2}}$ was used and extinction corrections

$$F^{corr} = F\left(1 + g\frac{1 + \cos^4 2\theta}{1 + \cos^2 2\theta/\sin 2\theta}\right)^{-\frac{1}{4}}$$

with $g = 1.2 \times 10^{-5}$ were applied.†

trans-[PdCl$_2$(PPh$_3$)(t-Bu–DAB)], $C_{28}H_{35}Cl_2N_2PPd$

Crystals of the title compound are triclinic with space-group P$\overline{1}$ and cell constants $a = 17.122(3)$, $b = 18.279(3)$, $c = 10.008(5)$ Å, $\alpha = 96.77(2)$, $\beta = 95.29(3)$, $\gamma = 109.79(2)$. There are four molecules in the unit cell, that is two in the asymmetric unit. A total of 7979 reflexions were measured on a NONIUS CAD 4 diffractometer using graphite mono-chromated MoK_α radiation, 1762 of which were less than 2.5σ(I) and were treated as unobserved. No absorption correction was applied (crystal dimensions $0.4 \times 0.2 \times 0.25$ mm; $\mu = 8.90$ cm^{-1}) The positions of the two Pd-atoms in the asymmetric unit were derived from an E^2-Patterson synthesis. A ΔF-synthesis based on the contributions of the Pd-atoms revealed the remaining non-hydrogen atoms except those of the methyl groups. These showed up in a subsequent ΔF-synthesis as rather diffuse peaks. Anisotropic block-diagonal least-squares refinement reduced R to 0.057. A ΔF-synthesis at this stage indicated the hydrogen atoms, except those of the tert-butyl groups, and made clear that these methyl groups are subject to disorder. Since it was not possible to devise a satisfactory description for this disorder we have not introduced it in the model. Continued refinement with 34 non-methyl hydrogen atoms fixed at their calculated positions, converged to R = 0.049 for the 6217 observed reflexions. A weighting scheme $\omega = (1.0 + F_0 + 0.018\ F_0^2)^{-\frac{1}{2}}$ was used and the anomolous scattering of Pd was taken into account. Computer programmes were taken from the X-RAY system[26] and PLUTO.[27]†

RESULTS AND DISCUSSION

The molecular geometries of c-Hex–DAB and *trans*-[PdCl$_2$(PPh$_3$)(t-Bu–DAB)] are depicted together with the atomic numbering in Figs. 3 and 4 respectively.

†*Supplementary Material* consists of a list of the final coordinates and equivalent isotropic thermal parameters and anisotropic thermal parameters of c-Hex–DAB and of *trans*-[PdCl$_2$(PPh$_3$)(t-Bu–DAB)]. Copies are available on request from the Editor at Queen Mary College. Atomic coordinates have also been deposited with the Cambridge Crystallographic Centre.

Molecular geometry of c-Hex–DAB

The bond distances and angles of c-Hex–DAB are listed in Table 1. In the solid state the molecular geometry of the R–DAB molecule is centrosymmetric with a flat E-s-$trans$-E conformation; deviations from the least-squares plane through C(2)–N(1)=C(1)–C(1')=N(1')–C(2') are less than 0.002(2) Å. This conformation is different from that found in the gas phase[17] (*vide supra*), but corresponds well with that predicted by MO-calculations.[23] The bond distances of C(1)–C(1') and C(1)–N(1) (1.457(3) and 1.258(3) Å respectively) are very near to the C(sp^2)–C(sp^2) and C(sp^2)=N(sp^2) standard single and double bond lengths (1.48 and 1.27 Å, respectively)[28] which would imply little conjugation in the central N=C–C=N-part of the c-Hex–DAB molecule. The cyclohexyl ring is in a chair conformation with an average C–C distance of 1.517(6) Å and an average C–C–C angle of 111.4(4)°. The angle between the planar part C(3)C(4)C(6)C(7) of the cyclohexyl ring and the flat N=C–C=N part is 88°.

Molecular geometry of trans-[PdCl$_2$(PPh$_3$)(t-Bu–DAB)]

The crystal structure of this compound contains two independent, but very similar molecules, A and B. Some bond lengths and -angles are listed in Table 2.†

The Pd-coordination plane in *trans*-[PdCl$_2$(PPh$_3$)(t-Bu–DAB)] is approximately square planar; deviations from the least-squares plane through Pd, Cl(1), Cl(2), N(1) and P are less than 0.091(1) and 0.109(2) for molecules A and B re-
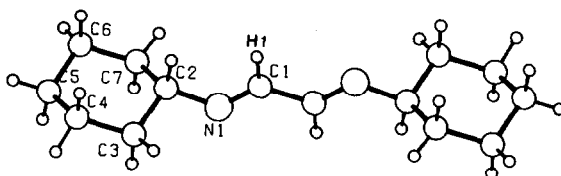
Fig. 3. Molecular geometry of c-Hex–DAB with atomic numbering.
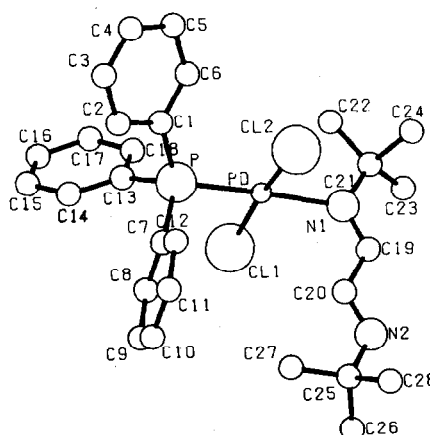
Fig. 4. Molecular geometry of *trans*-[PdCl$_2$(PPh$_3$) (t-Bu–DAB)] with atomic numbering.

Table 1. Bond lengths (Å) and bond angles (°) with ESD's in parentheses in *c*-Hex–DAB

Table 1 : Bond lengths (Å) and bond angles (°) with e.s.d.'s in parentheses in c-Hex–DAB.

C(1)–C(1')	1.457(3)	N(1)–C(1)–C(1')	120.8(2)
C(1)–N(1)	1.258(3)	C(1)–N(1)–C(2)	117.7(2)
N(1)–C(2)	1.456(3)	N(1)–C(2)–C(3)	109.2(2)
C(2)–C(3)	1.518(3)	N(1)–C(2)–C(7)	108.9(2)
C(2)–C(7)	1.521(3)	C(3)–C(2)–C(7)	110.7(2)
C(3)–C(4)	1.524(3)	C(2)–C(3)–C(4)	111.3(2)
C(4)–C(5)	1.513(4)	C(3)–C(4)–C(5)	111.6(2)
C(5)–C(6)	1.509(4)	C(4)–C(5)–C(6)	111.6(2)
C(6)–C(7)	1.519(3)	C(5)–C(6)–C(7)	111.2(2)
		C(2)–C(2)–C(6)	112.0(2)

Table 2. Some bond lengths (Å) and bond angles (°) with ESD's in parentheses in *trans*-[PdCl₂(PPh₃)(*t*-Bu–DAB)]

	Molec.A	Molec.B		Molec.A	Molec.B
Pd – Cl(1)	2.303(3)	2.309(3)	Cl(1)–Pd–Cl(2)	171.13(8)	170.15(8)
Pd – Cl(2)	2.300(2)	2.292(3)	Cl(1)–Pd–P	90.51(8)	80.88(8)
Pd – P	2.241(2)	2.244(2)	Cl(1)–Pd–N(1)	89.5 (1)	90.4 (2)
Pd – N(1)	2.130(7)	2.126(5)	Cl(2)–Pd–P	90.75(8)	91.81(8)
P – C(1)	1.831(8)	1.824(9)	Cl(2)–Pd–N(1)	88.8 (2)	88.7 (2)
P – C(7)	1.821(7)	1.818(6)	P–Pd–N(1)	177.3 (2)	178.7 (2)
P – C(13)	1.826(8)	1.822(7)	Pd–P–C(1)	118.6 (2)	115.9 (2)
N(1)–C(19)	1.265(10)	1.265(12)	Pd–P–C(7)	105.9 (3)	107.9 (3)
N(1)–C(21)	1.494(8)	1.494(9)	Pd–P–C(13)	116.5 (3)	116.2 (3)
N(2)–C(20)	1.238(12)	1.275(12)	C(1)–P–C(7)	107.3 (3)	106.9 (3)
N(2)–C(25)	1.484(9)	1.496(9)	C(1)–P–C(13)	100.6 (4)	100.6 (4)
C(19)–C(20)	1.485(10)	1.472(10)	C(7)–P–C(13)	107.3 (4)	108.8 (4)
			Pd–N(1)–C(19)	119.1 (5)	117.6 (5)
			Pd–N(1)–C(21)	119.3 (5)	120.8 (5)
			C(19)–N(1)–C(21)	121.5 (7)	121.6 (6)
			N(1)–C(19)–C(20)	124.1 (8)	122.4 (8)
			C(19)–C(20)–N(2)	118.6 (8)	118.6 (8)
			C(20)–N(2)–C(25)	119.6 (7)	119.0 (7)

spectively. This coordination plane makes an angle of 87.4° (mean) with the N=C–C=N plane. The conformation of the 2*e*; σ-N coordinated *t*-Bu–DAB molecule is the *E-s-trans-E* one, which is the same as in the free ligand.

The N=C–C=N skeleton is approximately planar; deviations from the least squares plane are less than 0.005(6) and 0.029(8) Å for molecules A and B, respectively.

The above mentioned coordination mode of the *t*-Bu–DAB-ligand brings the H(20) atom into the neighbourhood of the Pd-atom, above the coordination plane. The calculated distances are 2.60 and 2.58 Å for molecules A and B, respectively, which is less than the sum of Van der Waals radii for Pd and H, being 3.1 Å.[29] This geometry is similar to that found in [*trans*-{PtCl₂(PBu₃)}₂(*t*-Bu–DAB)] in which the *t*-Bu–DAB is bridged bonded[4] (see Fig. 2b). The extreme low field shift (9.91 ppm) of this H(20) atom

in ¹H NMR measurements indicates that the same conformation is present in solution.[5] The Pd ... H interaction can be best described as a very weak one.[4,5]

The Pd–Cl bond distances are comparable with those found in other complexes with a *trans* Cl–Pd(II)–Cl configuration: they all fall in the range 2.29–2.31 Å,[30] being equal to the sum of the covalent radii for Pd and Cl.[29]

The Pd–P bond distances (2.241(2) and 2.244(2) for molecules A and B respectively) compare well with other Pd(II)–P distances in complexes in which there is a nitrogen donor ligand *trans* to the phosphine.[31] The Pd–N bond distances of 2.130(7) and 2.126(5) Å for molecules A and B respectively are exceptionally long. In other Pd(II) complexes with a P-atom in *trans* position, Pd(II)–N bond distances are normally 2.06 Å[31a] and in Pd(II)Cl₂(imine)₂ complexes, Pd–N(imine) bond distances are found between 2.01

and 2.05 Å.[30] The longest previous Pd(II)–N(sp^2) bond distance, to our knowledge, is 2.092(9) Å found in [PdBr(PPh$_3$)(pyridine)]$_2$.[31b]

Comparison of structural data of the N=C–C=N-skeleton in free and metal coordinated R–DAB ligands may provide an answer as to the extent of σ- and π-bonding operative in their complexes.

Figure 5 shows that π-backbonding in either the σ-N-monodentate or σ-N, σ-N′-chelate coordination fashion, comprises interaction of the ligands LUMO with a filled metal d-orbital. Any contribution of this backbonding would then lead to (i), shortening of the M–N- and C–C′- and (ii), lengthening of the C=N-bondlengths.† These trends have indeed been observed for the C=N- and C–C′- but not for the M–N-bond lengths‡ in a variety of complexes where π-backbonding can be expected to be operative.[2b] This expectation is justified by the presence in these complexes of a metal in a low formal oxidation state in combination with either a R–DAB ligand with enhanced π-accepting properties (e.g. if R = aryl)[35] or other ligands with poor π-accepting capacity. In trans-[PdCl$_2$(PPh$_3$)(t-Bu–DAB)] none of the features favouring π-backbonding are present. This seems to be reflected by the similarity of the C=N- and C–C′-bond lengths in σ-N-bonded t-Bu–DAB, i.e. 1.265(10) and 1.478(10) Å, when compared with those found for free c-Hex–DAB, i.e. 1.258(3) and 1.457(3), respectively. Such data indicate that in the absence of π-backbonding, pure σ-N-coordination does not affect the C=N- and C–C′-bond lengths. This conclusion is supported by the C=N- and C–C′-distances found in e.g. [PtCl$_2$(PBu$_3$)]$_2$(t-Bu–DAB)[4] and [PtCl$_2$(C$_2$H$_3$C$_6$H$_5$)(t-Bu–DAB)][2b] containing σ-N, σ-N′ bridge and σ-N, σ-N′-chelate bonded t-Bu–DAB ligands, respectively.

M   DAB
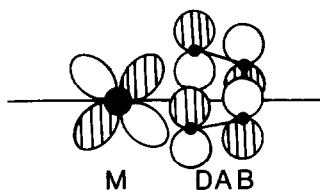
Fig. 5. π-Backbonding from a filled d orbital to the LUMO of the R–DAB ligand in a R–DAB-metal complex.

---

†This bond length behaviour in the metal-heterobutadiene system is particularly found in metal-tetraaza-1,3-butadiene complexes. Tetraaza-1,3-butadiene, R–N=N–N=N–R, has a LUMO with the same character as that of R–DAB and an even stronger π-backbonding capacity,[32] which results in shorter M–N- and central N–N′- and long N=N-bond lengths in their complexes.[1d]

‡In [MnBr(CO)$_3$(c-Hex–DAB)] the C=N-, C–C′- and Mn–N-bond lengths are 1.28, 1.49 and 2.05 Å, respectively,[33] whereas in [Mn(t-Bu–DAB)$_2$] these bond lengths are 1.32, 1.38 and 2.06 Å.[34]

REFERENCES

[1a] A. F. M. J. van der Ploeg, G. van Koten and K. Vrieze, Inorg. Chem. 1982, 21, 2026 and references therein. [b] J. W. Gosselink, A. M. F. Brouwers, G. van Koten and K. Vrieze, J. Chem. Soc. Dalton Trans. 1982, 397. [c] A. de Cian and R. Weiss, J. Chem. Soc. Chem. Commun. 1976, 249. [d] P. Overbosch, G. van Koten, D. M. Grove, A. L. Spek, A. J. M. Duisenberg Inorg. Chem. 1982, 21, 3253 and references therein.

[2a] G. van Koten and K. Vrieze, Recl. Trav. Chim. Pays-Bas, 1981, 100, 129. [b] G. van Koten and K. Vrieze, Advances in Organometallic Chemistry, 1982, 21, 152. [c] K. Vrieze and G. van Koten, Recl. Trav. Chim. Pays-Bas 1980, 99, 145.

[3] L. H. Staal, J. Keijsper, G. van Koten, K. Vrieze, J. A. Cras and W. P. Bosman, Inorg. Chem. 1981, 20, 555 and references therein.

[4] H. van der Poel, G. van Koten and K. Vrieze, Inorg. Chim. Acta, 1980, 39, 197.

[5] H. van der Poel, G. van Koten and K. Vrieze, Inorg. Chem., 1980, 19, 1145.

[6] L. H. Staal, L. H. Polm, R. W. Balk, G. van Koten, K. Vrieze and A. M. F. Brouwers, Inorg. Chem., 1980, 19, 3343.

[7] H. W. Frühauf, A. Landers, R. Goddard and C. Krüger, Angew. Chem. 1978, 90, 56.

[8] L. H. Staal, L. H. Polm, K. Vrieze, F. Ploeger and C. H. Stam, Inorg. Chem. 1981, 20, 3590.

[9] L. H. Staal, G. van Koten, K. Vrieze, F. Ploeger, C. H. Stam, Inorg. Chem. 1981, 20, 1830.

[10] R. D. Adams, J. Am. Chem. Soc. 1980, 102, 7476.

[11] J. Keijsper, G. van Koten and K. Vrieze, to be published.

[12] H. tom Dieck, I. W. Renk and H. P. Brehm, Z. Anorg. Allg. Chem. 1970, 379, 169.

[13] B. Crociani, G. Bandolini and D. A. Clemente, Ibid. 1980 184, 269 and references therein.

[14] H. tom Dieck and I. W. Renk, Chem. Ber. 1971, 104, 92.

[15] J. M. Kliegman and R. K. Barnes, Tetrahedron Lett. 1969, 24, 195.

[16] O. Exner and J. M. Kliegman, J. Organomet. Chem. 1971, 36, 2014.

[17] I. Hargittai and R. Seip, Acta Chem. Scand. 1976, 30A, 540.

[18] P. H. Cureton, C. G. Lefèvre and R. J. W. Lefèvre, J. Chem. Soc. 1961, 4447.

[19] H. Bock and H. tom Dieck, Chem. Ber. 1967, 100, 228.

[20] H. tom Dieck and K. D. Franz, Angew. Chem. 1975, 87, 244.

[21] J. Tyrrell, J. Am. Chem. Soc. 1979, 101, 3766.

[22] O. Borgen, B. Mestvedt and I. Kauvik, Acta Chem. Scand. 1979, 30A, 43.

[23] J. Reinhold, R. Benedix, P. Birner and H. Hennig, Inorg. Chim. Acta 1979, 33, 209.

[24] H. van der Poel, G. van Koten, D. M. Grove, P. S. Pregosin and K. A. Ostaja Starzewski, Helv. Chim. Acta 1981, 64, 1174.

[25] A. R. Overbeek and H. Schenk, In Computing in Crystallography (Edited by H. Schenk, R. Olthof, H. van Koningsveld and G. C. Bassi). Delft University Press, Delft (1978).

[26] J. M. Stewart, The X-RAY system. Tech. Rep. TR 446 Computer Science Center; University of Maryland, College Park, Maryland (1976).

[27] W. D. S. Motherwell PLUTO, Program for plotting crystal and molecular structures. University of Cambridge (1976).

[28] M. Bruke–Laing and M. Laing, Acta Cryst. 1976, B32, 3216.

[29] L. Pauling, The Nature of the Chemical Bond, 3rd Edn. Cornell University Press, New York (1960).

[30a] F. W. B. Einstein and J. S. Field, Acta Cryst. 1979, B35, 1696. [b] A. M. Manotti Lanfredi, A. Tiripicchio, G. Natile, F. Gasparrini and B. Galli, Cryst. Struct. Commun. 1979, 8, 611. [c] L. G. Kuzmina and Y. T. Struchkov, Ibid. 1979, 8, 715. [d] Y. Yamane, T. Ashida, H. Suzuki, K. Itok and Y. Ishii, Bull. Chem. Soc. Jpn 1978, 51, 3161.

[31a] G. J. Palenik, M. Mathew, W. L. Steffen and G. Beran,

J. Am. Chem. Soc. 1975, **97**, 1059. [b]K. Nakatsu, K. Kinoshita, H. Kanda, K. Isobe, Y. Nakamura and S. Kawaguchi, *Chem. Lett.* 1980, 913.

[32]W. C. Trogler, C. E. Johnson and D. E. Ellis, *Inorg. Chem.* 1981, **20**, 980.

[33]A. J. Graham, D. Akrigg and B. Sheldrick, *Cryst. Struct. Commun.* 1977, **6**, 57.

[34]B. Bruder, Ph.D. Thesis 1979. University of Frankfurt, Frankfurt am Main.

[35]H. tom Dieck and J. W. Renk, *Chem. Ber.* 1972, **105**, 1419.

A DYNAMIC NUCLEAR MAGNETIC RESONANCE STUDY OF 1,3-INTRAMOLECULAR SHIFTS IN PENTA-CARBONYL-CHROMIUM(O) AND -TUNGSTEN(O) COMPLEXES OF β-2,4,6-TRIMETHYL-1,3,5-TRITHIAN, 1,3,5-TRITHIAN, 1,3-DITHIAN AND 2-METHYL-1,3-DITHIAN: THE X-RAY CRYSTAL STRUCTURE OF [W(CO)₅{SCH(Me)SCH(Me)SCH(Me)}]

EDWARD W. ABEL,* GARY D. KING, KEITH G. ORRELL, GRAHAM M. PRING and
VLADIMIR SIK
Department of Chemistry, University of Exeter, Exeter EX4 4QD, England

and

T. STANLEY CAMERON
Chemistry Department, Dalhousie University, Halifax, Nova Scotia, Canada B3H 3JB

Abstract—Variable temperature ^{1}H NMR spectroscopy has been used in the study of 1,3-intramolecular shifts of the M(CO)₅ moiety in complexes of the general formula [M(CO)₅L], (M = Cr or W), L = SCH₂SCH₂SCH₂, SCH₂SCH₂CH₂CH₂ and SCH(Me)SCH₂CH₂CH₂. For the 1,3,5-trithian complexes precise energy barriers for the process have been obtained by detailed computer simulation of the static and dynamic spectra. Our results suggest that the magnitude of ΔG$^+$ (298.15 K) for the 1,3-shift is largely dependent upon the skeletal flexibility of the ligand system. In this context we have investigated the X-ray crystal structure of the highly substituted trithian complex [W(CO)₅{β-SCH(Me)SCH(Me)SCH(Me)}].

In 1975 Schenk and Schmidt[1] reported a novel fluxional phenomenon in the Group VI metal pentacarbonyl complexes of β-2,4,6-trimethyl–1,3,5-trithian; [M(CO)₅{SCH(Me)SCH(Me)SCH(Me)}] (M = Cr and W). Line shape changes in the 60 MHz ^{1}H NMR spectra between − 10 and + 30°C implied an equilibration of the three methylene protons, along also with the equilibration of the three methyl groups. This was suggested to be a consequence of an intramolecular commutation of the M(CO)₅ moiety over all three donor sulphur atoms. The analogous motion was not, however, observed in the unsubstituted ring complexes [M(CO)₅(SCH₂SCH₂SCH₂)] (M = Cr and W); the NMR ^{1}H spectra at + 30°C were consistent with the heterocyclic ligand 1,3,5-trithian coordinating to a M(CO)₅ group via a single sulphur atom.

By detailed computer simulation of static and dynamic spectra we have previously calculated and reported[2] accurate Arrhenius and Eyring activation parameters for the above "1,3-shift" of an M(CO)₅ moiety in the complexes [M(CO)₅{SCH(Me)SCH(Me)SCH(Me)}] (M = Cr and W). It was postulated that these complexes undergo 1,3-shifts rapidly at room temperature, whereas those of the 1,3,5-trithian and 1,3-dithian are static at this temperature, because of the ring conformation of β-2,4,6-trimethyl-1,3,5-trithian. We suggested that steric factors force the M(CO)₅ group into an axial

position, the corresponding equatorial conformer being highly unfavoured. In the axial complex the other sulphur lone pairs are ideally placed for a facile 1,3-shift. By contrast, in the other (non-methyl substituted) complexes, ring reversal and inversion of configuration at the sulphur atoms (both processes are fast at room temperature), change the relative positions of the M(CO)₅ group and sulphur atom lone pairs, thus reducing the probability of a 1,3-shift.

We now report the X-ray crystal structure of [W(CO)₅{SCH(Me)SCH(Me)SCH(Me)}], confirming ease of access for the 1,3-shift of the W(CO)₅ moiety. Furthermore, we have now carried out dynamic NMR studies on the complexes [M(CO)₅L] (M = Cr or W; L = SCH₂SCH₂SCH₂, SCH₂SCH₂CH₂CH₂ and SCH(Me)SCH₂CH₂CH₂, which are found to undergo 1,3-shifts at well above room temperature. Accurate energy barriers (ΔG$^+$) have been obtained for this process in the two complexes of 1,3,5-trithian, and are compared with the corresponding β-trimethyl-trithian complexes.

EXPERIMENTAL

Preparations

Ligands were prepared using literature procedures 1,3,5-trithian,[3] β-2,4,6-trimethyl-1,3,5-trithian,[4] 1,3-dithian,[5] 2-methyl-1,3-dithian.[6] The complexes [M(CO)₅{SCH(R)SCH(R)SCH(R)}](M = Cr or W, R = H or Me) and [M(CO)₅(SCH₂SCH₂SCH₂)] (Me = Cr or W) have been previously reported.[7,8] [M(CO)₅{SCH(Me)SCH₂CH₂CH₂}] (M = Cr or W), are hitherto unknown and were prepared by a general method for the synthesis of [M(CO)₅L] complexes described by Connors *et al.*[9]

*Author to whom correspondence should be addressed.

All reactions and manipulations were performed under an atmosphere of dry nitrogen. Freshly distilled nitrogen purged anhydrous solvents were used, as solutions of the complexes were noted to decompose rapidly on exposure to air. The yellow crystalline solids were however fairly stable in the atmosphere, and were all obtained in 30–60% yield (Table 1).

Spectroscopic studies

IR spectra of the metal carbonyl region of the complexes were obtained on a Perkin–Elmer 299B spectrophotometer. Variable Temperature NMR spectra were recorded at 5–10°C intervals on a JEOL MH-100 spectrometer. A JES–VT-3 unit was used to control the probe temperatures, which were measured, using a Comark digital thermometer type 5000 attached to a Cu/Cu–Ni thermocouple, to an accuracy of at least $\pm 1°C$.

Due to the decomposition of solutions of the complexes in air, all NMR samples were made up by adding the crystalline complex to an NMR tube fitted with a Taperlok (Wilmad Glass Co. Inc.) joint. The appropriate solvent (C_6D_6 or C_2Cl_4) and hexamethyldisiloxane were then distilled into the tube under vacuum, which was then filled with dry nitrogen.

Crystallographic studies

Crystal data: $C_{11}H_{12}O_5S_3W$; triclinic, $a = 9.704(4)$, $b = 13.041(2)$, $c = 14.073(3)Å$, $\alpha = 88.55(2)$, $\beta = 72.85(3)$, $\gamma = 81.39(3)°$, space group $P\bar{1}$, $Z = 4$, $D_c = 1.988\,\text{g cm}^{-3}$, $F(000) = 960$. Mo-K_{α_1} radiation, $\lambda = 0.71069Å$, $\mu = 69.30\,\text{cm}^{-1}$. Data collection: Nonius CAD4 four circle diffractometer. 3140 independent reflections of which 2427 had $I > \sigma(I)$. The three standard reflections showed an uneven and unrecoverable loss of intensity (averaging about 10%) during collection.

Structure solution and refinement

The structure was solved using a multi solution tangent formula procedure[10] and was refined with a full matrix least squares analysis. Hydrogen atoms were located geometrically, and the refinement, with anisotropic temperature parameters on all non-hydrogen atoms, converged with $R = 0.081$.†

RESULTS

The Crystal Structure of [W(CO)$_5$ $\{\beta$-$\dot{S}CH(Me)SCH(Me)\dot{S}CH(Me)\}]$.

The crystal of the above complex contains two unique molecules I and II, as shown in Fig. 1.

In each of these the tungsten atom has an octahedral coordination sphere with the carbonyl groups at five sites and a sulphur atom of the methyl substituted trithian ligand at the sixth position. Selected bond lengths and bond angles are given in Table 2.

In both complex molecules the ligand is the β-form of 2,4,6-trimethyl-1,3,5-trithian, which has the chair conformation, and three methyl groups in the equatorial positions. The S–C, and similarly C–Me bond lengths are not significantly different (mean 1.81(4) and 1.52(6)Å respectively) in I and II. These compare with mean lengths of 1.81(8) and 1.51(3)Å in the free ligand.[11] The coordinated sulphur atom uses only one

of its lone pairs of electrons to form the W–S bond, namely the pair that is "axial" with respect to the ligand methyl groups. The sum of the interbond angles at this sulphur atom is 328(2)° and 331(2)° for molecules I and II respectively, demonstrating its near exactly tetrahedral nature.

The W–S bond lengths (mean 2.553(5)Å) compare well with 2.556(8)Å in a similar bond in thiomorpholin-3-thione-pentacarbonyltungsten,[12] and it is only slightly less than the sum of the covalent radii values of sulphur and tungsten (1.04 and 1.58Å respectively).[13,14]

Any distinction between W–C bonds of the carbonyl groups *cis* and *trans* to the ligand atom is not well defined, in comparison with those in structures reported for some analogous complexes.[12,15,16] Consequently, there is no really observable *trans* effect. The variation in W–C ($1.84(3) - 2.11(3)Å$) of the four pseudo planar carbonyl groups may well reflect the erratic decomposition of the crystal, it was originally a gold orange and changed to an opaque black under the action of X-rays.

The two unique molecules differ essentially in a rotation of 23° about the W–S bond; an equivalent OC–W–S–C(Me) torsional angle in the two molecules is 173° and 150° for molecules I and II respectively. This places the two methyl groups closest to the tungsten atom in an approximately staggered conformation relative to the *cis* carbonyl groups.

Variable temperature ^1H NMR studies

The spectra of each type of ligand complex are best described individually.

1,3,5-Trithian complexes

The spectra of these complexes [M(CO)$_5$ ($\dot{S}CH_2SCH_2SCH_2$)] at room temperature are as reported previously.[1] The occurrence of two singlets in an intensity ratio of 2 : 1 (with the most intense resonance at high frequency) is consistent with: (i) The trithian ligand coordinating via one of its sulphur atoms to the single M(CO)$_5$ moiety, (ii) the complexes undergoing rapid sulphur atom inversion and six-membered ring reversal to equilibrate axial hydrogen environments on individual ring methylene groups.[2]

Increase of temperature above ambient caused identical changes in both the chromium and tungsten complexes. The two ^1H singlets were observed to broaden and coalesce (*ca.* 75 and 87°C for the chromium and tungsten complexes respectively), eventually giving rise to a sharp singlet on further increase in probe temperature. A non-exchanging sharp singlet, attributable to the free ligand, was observed throughout the temperature range studied.

The above reversible spectral changes, along with the absence of free ligand exchange imply an equilibration of all methylene hydrogen environments by an intramolecular commutation of the M(CO)$_5$ moiety over all sulphur atom coordination sites via a series of 1,3-shifts. A diagrammatical representation of this is given in Fig. 2 (the M(CO)$_5$ group is shown axial to the ligand for reasons to be discussed later).

The full dynamic nuclear spin problem for this system is shown in Fig. 2. A lack of long-range coupling, however, permits the reduction of the complex situation to a simple A(66.6%) $\rightleftharpoons$ B(33.3%)

---

†Copies of atomic co-ordinates, thermal parameters and observed and calculated structure factors has been deposited as supplementary material with the Editor from whom copies are available on request. Atomic co-ordinates have also been deposited at the Cambridge Crystallographic Data Centre.

Table 1. Characterization for six-membered sulphur heterocyclic ring complexes of chromium and tungsten carbonyls

Complex	m.p./°C	Analysis[a]		Metal Carbonyl Stretch in cm^{-1} (Infrared)[b]		
		C	H	$A_1(m)$	E(vs)	$A_1(s)$
[W(CO)$_5${SCH(Me)SCH(Me)SCH(Me)}]	102-103	26.3(26.2)	2.35(2.40)	2078	1945	1932
[W(CO)$_5$(SCH$_2$SCH$_2$SCH$_2$)]	110	21.1(20.8)	1.24(1.31)	2078	1943	1937
[Cr(CO)$_5$(SCH$_2$SCH$_2$SCH$_2$)]	100	29.1(29.1)	2.04(1.83)	2069	1943	1940
[W(CO)$_5$(SCH$_2$SCH$_2$CH$_2$CH$_2$)]	72-73	24.1(24.3)	1.36(1.82)	2070	1945	1938
[Cr(CO)$_5$(SCH$_2$SCH$_2$CH$_2$CH$_2$)]	51	34.6(34.6)	2.32(2.58)	2065	1948	1941
[W(CO)$_5${SCH(Me)SCH$_2$CH$_2$CH$_2$}]	82(d)	26.2(26.2)	2.18(2.20)	2072	1944	1934
[Cr(CO)$_5${SCH(Me)SCH$_2$CH$_2$CH$_2$}]	69(d)	36.8(36.8)	3.21(3.10)	2069	1943	1938

[a] Calculated values in parentheses.

[b] Recorded in n-hexane, spectra calibrated against polystyrene film.
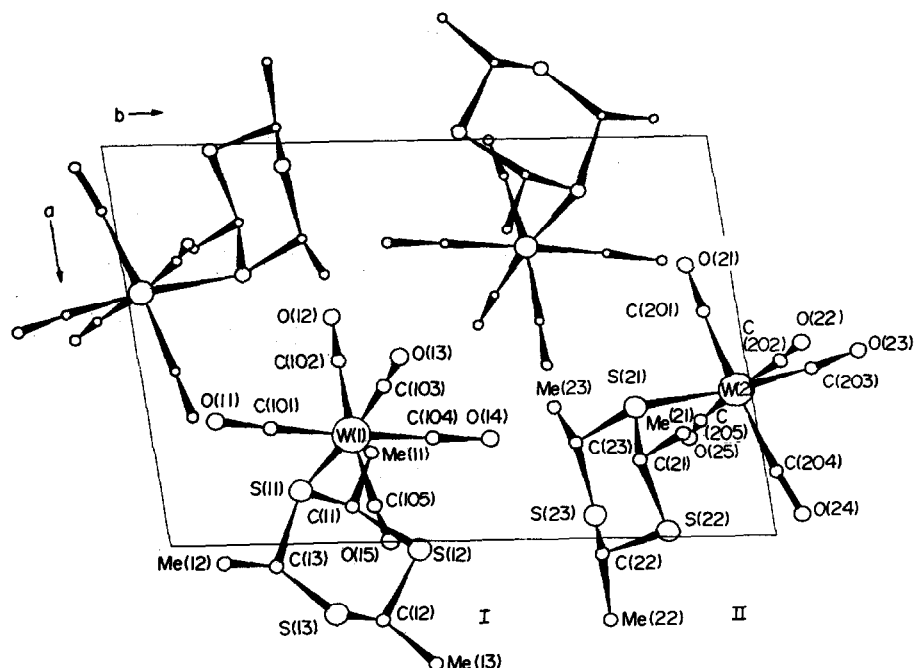
Fig. 1. Crystal structure of [W(CO)$_5$$\{\overline{SCH(Me)SCH(Me)SCH(Me)}\}$] showing the two unique molecular conformations (I and II).

Fig. 2. Dynamic nuclear spin problem for the 1,3-shift process in the complexes [M(CO)$_5$($\overline{SCH_2SCH_2SCH_2}$)] (M = Cr or W).

problem. This allows spectra to be simulated using the DNMR8 computer program. A visual comparison of experimental and computer simulated spectra, until "best-fits" were obtained, yielded the rate of the 1,3-shift at the various temperatures investigated. A series of experimental spectra of the complex [Cr(CO)$_5$($\overline{SCH_2SCH_2SCH_2}$)] and their computer simulation is illustrated in Fig. 3. The static NMR parameters utilized in the computations are given in Table 3. Plotting these rate constant data

Fig. 3. Variable-temperature ^{1}H NMR spectra of the complex [Cr(CO)$_5$($\overline{SCH_2SCH_2SCH_2}$)] and their computer syntheses.

Table 2. Selected bond lengths (Å) and bond angles ( ) in [W(CO)₅{β-$\overline{SCH(Me)SCH(Me)SCH(Me)}$}]

a) bond lengths

W(1)-S(11)	2.553(6)	W(2)-S(21)	2.553(7)
W(1)-C(101)	1.87(3)	W(2)-C(201)	1.97(3)
W(1)-C(102)	2.06(3)	W(2)-C(202)	2.00(3)
W(1)-C(103)	1.92(3)	W(2)-C(203)	1.87(3)
W(1)-C(104)	1.84(3)	W(2)-C(204)	2.07(3)
W(1)-C(105)	2.11(3)	W(2)-C(205)	2.03(3)

b) bond angles

S(11)-W(1)-C(101)	87(1)	S(21)-W(2)-C(201)	84.6(8)
S(11)-W(1)-C(102)	86.1(8)	S(21)-W(2)-C(202)	93(1)
S(11)-W(1)-C(103)	174.1(8)	S(21)-W(2)-C(203)	173(1)
S(11)-W(1)-C(104)	95.8(9)	S(21)-W(2)-C(204)	99.1(8)
S(11)-W(1)-C(105)	99.5(8)	S(21)-W(2)-C(205)	92.8(8)
C(101)-W(1)-C(102)	93(1)	C(201)-W(2)-C(202)	91(1)
C(101)-W(1)-C(103)	89(1)	C(201)-W(2)-C(203)	90(1)
C(101)-W(1)-C(104)	178(1)	C(201)-W(2)-C(204)	176(1)
C(101)-W(1)-C(105)	92(1)	C(201)-W(2)-C(205)	92(1)
C(102)-W(1)-C(103)	90(1)	C(202)-W(2)-C(203)	84(1)
C(102)-W(1)-C(104)	87(1)	C(202)-W(2)-C(204)	90(1)
C(102)-W(1)-C(105)	173(1)	C(202)-W(2)-C(205)	174(1)
C(103)-W(1)-C(104)	89(1)	C(203)-W(2)-C(204)	87(1)
C(103)-W(1)-C(105)	85(1)	C(203)-W(2)-C(205)	91(1)
C(104)-W(1)-C(105)	89(1)	C(204)-W(2)-C(205)	87(1)
W(1)-C(101)-O(11)	175(2)	W(2)-C(201)-O(21)	173(3)
W(1)-C(102)-O(12)	175(2)	W(2)-C(202)-O(22)	174(3)
W(1)-C(103)-O(13)	177(2)	W(2)-C(203)-O(23)	177(3)
W(1)-C(104)-O(14)	174(2)	W(2)-C(204)-O(24)	173(2)
W(1)-C(105)-O(15)	176(3)	W(2)-C(205)-O(25)	169(2)

Table 3. ¹H NMR parameters for the methylene protons in the complexes [M(CO)₅($\overline{SCH_2SCH_2SCH_2}$)] (M = Cr or W)

Complex	Solvent	Δν(AB)/Hz	p(A) [a]	p(B) [a]	T_2^*/s [b]
[Cr(CO)₅($\overline{SCH_2SCH_2SCH_2}$)]	C_6D_6	20.26	0.66	0.33	0.127
[W(CO)₅($\overline{SCH_2SCH_2SCH_2}$)]	C_2Cl_4	19.85	0.66	0.33	0.133

[a] Populations.

[b] Effective transverse relaxation time, $T_2^* = (\pi\Delta\nu_{\frac{1}{2}})^{-1}$ (where $\Delta\nu_{\frac{1}{2}}$ is the natural line width at half height).

according to the Arrhenius and Eyring equations (using least squares fitting), yielded the activation parameters for the 1,3-shift process. These are reported in Table 4 along with those previously obtained[2] for the complexes [M(CO)₅{$\overline{SCH(Me)SCH(Me)SCH(Me)}$}] (Me = Cr or W).

The Arrhenius plot for the intramolecular 1,3-shift in the pentacarbonylchromium(O) complex of 1,3,5-trithian is shown in Fig. 4.

1,3,-Dithian and 2-methyl-1,3-dithian complexes

The room temperature ¹H NMR spectra in C_6D_6

of the complexes [M(CO)₅($\overline{SCH_2SCH_2CH_2CH_2}$)] (M = Cr or W), show a singlet and three complex multiplets in an intensity ratio of 1:1:1:1. The latter are attributable to the -(CH₂)₃-portion of the heterocyclic ligand. An examination of molecular models shows this to be an AA′BB′CC′ spin system. This simplified system is generated from the room temperature equilibration of two ABCDEF type spin systems by rapid ring reversal and ligand sulphur atom inversion (see Fig. 5). These belong to the two structures possible for each of the 1,3-dithian complexes; the M(CO)₅ moiety can be axial or equatorial

Table 4. Arrhenius and Eyring transition state parameters for 1,3-shifts in the complexes $[M(CO)_5\{SCH(R)SCH(R)SCH(R)\}]$ (M = Cr or W; R = H or Me)

Complex	E_a/kJ mol^{-1}	$\log_{10} A$	$\Delta H^{\ddagger}$/kJ mol^{-1}	$\Delta S^{\ddagger}$/J K^{-1} mol^{-1}	$\Delta G^{\ddagger}$/kJ mol^{-1} [a]
$[Cr(CO)_5\{SCH(Me)SCH(Me)SCH(Me)\}]$ [b]	75.68 ± 2.70	14.53 ± 0.46	73.60 ± 2.70	26.18 ± 8.72	65.80 ± 0.08
$[W(CO)_5\{SCH(Me)SCH(Me)SCH(Me)\}]$ [b]	73.16 ± 3.65	13.62 ± 0.63	70.67 ± 3.66	7.38 ± 12.12	68.47 ± 0.02
$[Cr(CO)_5\{SCH_2SCH_2SCH_2\}]$	80.62 ± 0.94	13.63 ± 0.14	77.80 ± 0.92	6.71 ± 2.72	75.80 ± 0.11
$[W(CO)_5\{SCH_2SCH_2SCH_2\}]$	81.37 ± 1.63	13.32 ± 0.24	78.41 ± 1.63	0.27 ± 4.60	78.33 ± 0.26

[a] $\Delta G^{\ddagger}$ was calculated for T = 298.15 K.

[b] Ref. 2.

Fig. 4. Arrhenius plot for the 1,3-shift process in the complex [Cr(CO)$_5$($\overline{SCH_2SCH_2SCH_2}$)].

Fig. 5. The effect of ring reversal and sulphur inversion on the -(CH$_2$)$_3$-nuclear magnetic spin system in the complexes [M(CO)$_5$($\overline{SCH_2SCH_2CH_2CH_2}$)] (M = Cr or W).

to the ligand ring. Thus, equatorial and axial protons on methylene C$_4$ (and likewise those on C$_5$ and C$_6$) achieve chemical (but not magnetic) equivalence as a result of the above two rapid fluxions, generating a "pseudo-plane" of symmetry in the ligand ring. However, in the methyl substituted complexes [M(CO)$_5$$\{$$\overline{SCH(Me)SCH_2CH_2CH_2}$$\}$] (M = Cr or W), the substituent on C$_2$ destroys this symmetry element, which results in the retention of an ABCDEF spin system. This explains the considerably increased complexity of the -(CH$_2$)$_3$-multiplets observable in the room temperature spectra of the 2-methyl-1,3-dithian complexes.
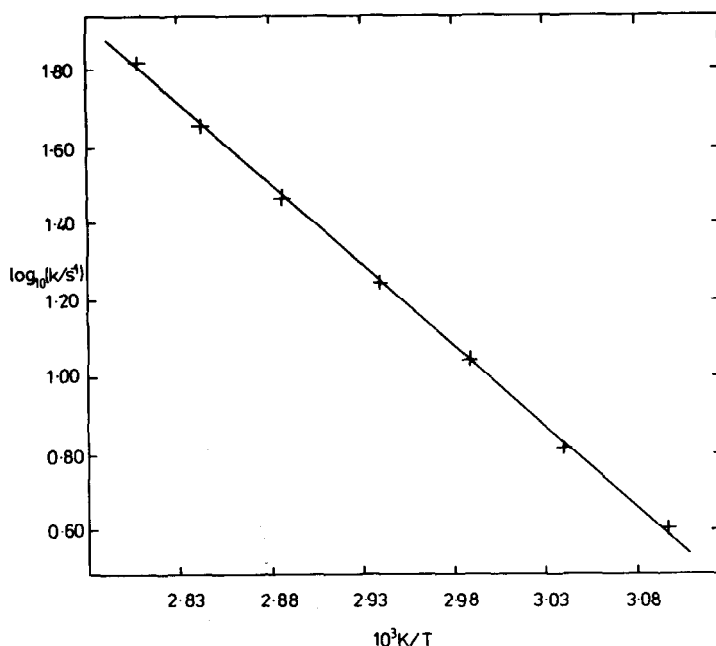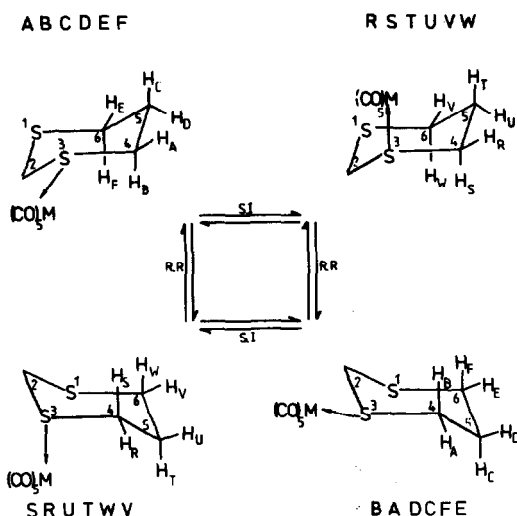
Heating C$_6$D$_6$ solutions of the above four complexes to ca. 90°C resulted in only a slight broadening of the multiplets, but changing the solvent to

d^8-toluene, and increasing the temperature to 120°C produced extensive changes in the spectra line shapes. The resonances arising from the methylene protons on C$_4$ and C$_6$ (which occur at high frequency w.r.t. the C$_5$ multiplet) were observed to partially coalesce, and simultaneously the C$_5$ methylene proton multiplet broadened.

Such spectral changes are consistent with the commencement of the equilibration of the two 4,6-carbon methylene environments; AA'BB'CC' ⇌ CC'BB'AA' in the 1,3-dithian complexes (see Fig. 6), ABCDEF ⇌ EFCDAB in the 2-methyl-1,3-dithian complexes. This indicates that the M(CO)$_5$ moiety has started to commute between the two 1,3-positional sulphur atoms. Unfortunately a further rise in the probe temperature produced braodened free ligand lines in the spectra indicative of the commencement of *inter*molecular ligand exchange and thermal degradation of the complexes. This is also indicated by the irreversible colour change of the solutions from yellow to brown. As total coalescence could not be obtained we were unable to carry out a full line shape analysis, and can report only the qualitative observation of 1,3-shifts without numerical data for activation parameters. It

A A'B B'C C' ⇌ C C'B B'A A'
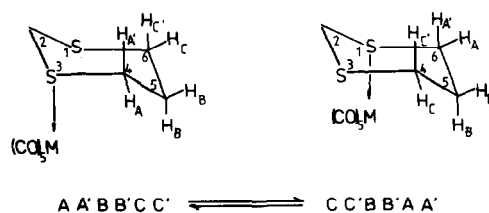
Fig. 6. The effect of M(CO)$_5$ 1,3-shifts on the -(CH$_2$)$_3$-environment in the complexes [M(CO)$_5$ $\overline{SCH_2SCH_2CH_2CH_2}$)] (M = Cr or W).

is notable, however, that ΔG^+ for a shift in the 1,3-dithian complex is higher than in the corresponding 1,3,5-trithan complex; a factor which may be associated with the reduced probability of access to a suitably placed sulphur atom for the 1,3-shift.

DISCUSSION

Of all the activation parameters, ΔG^+ has been recognised as the least susceptible to temperature and rate errors.[17] We therefore base our discussion of the relative ease of 1,3-shifts in these complexes upon the ΔG^+ (298.15 K) values listed in Table 4.

The intramolecular nature of the 1,3-shift in these complexes is indicated by the absence of exchange with added free ligand, and is confirmed by the numerical values of $\log_{10}A$ and ΔS^+ (Table 4), these being all close to 13 and 0 respectively.

The X-ray crystal structure of the complex pentacarbonyl-β-2,4,6-trimethyl-1,3,5-trithiantungsten(O) would appear to confirm our previous reasoning[2] as to why the $M(CO)_5$ moiety undergoes rapid 1,3-shifts at ambient temperatures in the complexes $[M(CO)_5 \{\overline{SCH(Me)SCH(Me)SCH(Me)}\}]$ (M = Cr or W), but not in those of 1,3,5-trithian etc. The rigid chair conformation of β-2,4,6-trimethyl-1,3,5-trithian with all methyl groups equatorial, forces the $M(CO)_5$ group to adopt exclusively the sterically less hindered axial position. Low temperature ^1H NMR spectra of the complexes $[M(CO)_5\{\overline{SCH(Me)SCH(Me)SCH(Me)}\}]$ (M = Cr and W) showed the predominance ($> 95\%$) of one of the two possible conformers, thereby virtually certainly confirming the retention of the solid state conformation in solution. In such a structure the axial lone pairs of unco-ordinated sulphur atoms are held at a constant distance from the $M(CO)_5$ moiety, and further, are directed in such a way as to greatly facilitate a 1,3-shift via an easily accessible seven coordinate intermediate. In the complexes $[M(CO)_5(\overline{SCH_2SCH_2SCH_2})]$ [M = Cr or W], however, ring reversal and ligand sulphur atom inversion interconvert conformers of similar ground state energy, thus changing the ideal relative positioning of $M(CO)_5$ groups and sulphur lone pairs. This increase in ligand "flexibility" makes the probability of a commutation more remote, and is reflected by an increase in ΔG^+ of ca. $10\,kJ\,mol^{-1}$ between the trimethyl substituted and the unsubstituted trithian complexes.

The suggestion that ligand "flexibility" is a major influential factor in determining the magnitude of ΔG^+ for 1,3-shifts across a $-S-CH_2-S-$ ligand system, is further supported by the following examples

of pentacarbonyltungsten complexes which are ordered in terms of increasing flexibility, and also increasing ΔG^+ values

$[W(CO)_5\overline{SCH(Me)SCH(Me)SCH(Me)}]$,

$$68.47 \pm 0.02,^2;$$

$[W(CO)_5(\overline{SCH_2SCH_2SCH_2})]$, 78.33 ± 0.26^{18};

$[W(CO)_5(\overline{SCH_2SCH_2SCH_2SCH_2})]$, 83.44 ± 0.58^{19};

$[W(CO)_5(MeSCH_2SMe)]$, 84.65 ± 0.66^{20}; $kJ\,mol^{-1}$.
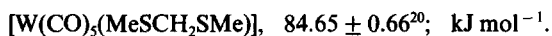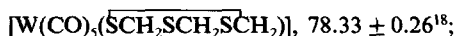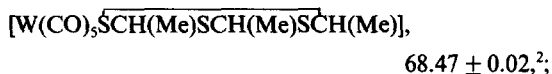
In all of these classes of complex it is notable that activation energies for pentacarbonylchromium complexes are consistently ca. $3\,kJ\,mol^{-1}$ lower than their tungsten analogues.

REFERENCES

[1] W. A. Schenk and M. Schmidt, Z. Anorg. Allg. Chem. 1975, **416**, 311.
[2] E. W. Abel, M. Booth, K. G. Orrell and G. M. Pring, J.C.S. Dalton 1981, 1944.
[3] R. W. Bost and E. W. Constable, Org. Synth., Coll. 1943, **2**, 610.
[4] E. W. Campaigne, N. F. Chamberlain and B. E. Edwards, J. Org. Chem. 1962, **27**, 135.
[5] E. J. Corey and D. Seebach, Org. Synth. 1970, **50**, 72.
[6] E. J. Corey and B. W. Erickson, J. Org. Chem. 1971, **36**, 3553.
[7] W. A. Schenk and M. Schmidt, Naturwiss. 1971, **58**, 96.
[8] H. G. Raubenheimer, S. Lotz, H. W. Viljeon and A. A. Chalmers, J. Organomet. Chem. 1978, **152**, 73.
[9] J. A. Connor, E. M. Jones and G. K. McEwen, J. Organomet. Chem. 1972, **43**, 357.
[10] G. Sheldrick, X-ray System Report. University Chemical Laboratory, Lensfield Road, Cambridge, England (1976).
[11] K. Sekido, J. Itoh, T. Noguchi and S. Hirokawa, Bull. Chem. Soc. Japan 1981, **54**, 1881.
[12] M. Cannas, G. Carta, A. Cristini and G. Marongiu, Acta. Cryst. 1975, **B31**, 2909.
[13] L. Pauling, The Nature of the Chemical Bond, 3rd Edn., p. 255. Cornell University Press (1960).
[14] M. Elder and D. Hall, Inorg. Chem. 1969, **8**, 694.
[15] M. Cannas, G. Carta, D. DeFilipo, G. Marongiu and E. F. Trogu, Inorg. Chim. Acta 1974, **10**, 145.
[16] M. Cannas, G. Carta, G. Marongiu and E. F. Trogu, Acta Cryst. 1974, **B30**, 2252.
[17] G. Binsch and H. Kessler, Angew. Chem. Int. Ed. Eng. 1980, **19**, 411.
[18] See Table 4 of this paper.
[19] G. D. King, University of Exeter. Results to be published.
[20] T. E. McKenzie, University of Exeter, Results to be published.

INTERACTIONS OF ANTIMONY(III) HALIDES WITH AMIDES AND TETRAMETHYLUREA IN 1,2-DICHLOROETHANE SOLUTION

CLAUDIO AIROLDI*, PEDRO L. O. VOLPE and JOSEFA M. M. de M. LIRA†

Instituto de Química, Universidade Estadual de Campinas, 13100 Campinas, São Paulo, Brasil

Abstract—The interactions of SbCl₃, SbBr₃ and SbI₃ with N,N-dimethylformamide (DMF); N,N-dimethylacetamide (DMA) and tetramethylurea (TMU) have been studied in 1,2-dichloroethane solution. The equilibrium constants and the respective variations of enthalpy for 1:1 and 1:2 species were obtained by means of the incremental calorimetric titration technique. From ΔH_i° values, the acidity order $SbCl_3 > SbBr_3 > SbI_3$ and the basicity order $TMU > DMA > DMF$ were established. The ionization in solution such as autocomplex formation and halides displacement are discussed using conductometric titration values.

The majority of *p*-block elements in lower valence states have a lone electron pair which gives rise to an irregular coordination in the adduct formed. This lone pair of electrons in antimony(III) halides is considered to be predominantly of *s*-character, due to the fact that in SbX_3 molecules the X–Sb–X angles are 97–99°.[1] These figures indicate that the Sb–X bond involves mainly the metal *p*-orbitals. The lone pair leads to a high electron density close to the metal, in spite of the difference in electronegativities of the atoms in the metal–halide bond and consequently, it should be difficult to accommodate a Lewis base in the coordination sphere. For 1:1 adduct formation a rehybridisation is required to arrange the new ligand in a trigonal–bipyramidal geometry, where the lone pair is lying in an equatorial position. Identically, with two molecules of bases an octahedral geometry is formed, the lone pair occupying one site of coordination. X-Ray structure determinations of SbCl₃ adducts of aniline[2], tetramethylthiourea[3] and triphenylarsine[4] illustrate this behaviour, where the strain of the lone pair causes a highly distorted geometry.

The Lewis acid properties of these metal halides are displayed by an increase in coordination number of the metal through the formation of a σ ligand–metal bond. In solution this behaviour can be illustrated by the interaction of SbCl₃ with some aliphatic and aromatic amides.[5] Molecular adducts are formed in 1:1 and 1:2 stoichiometries, these reactions being followed by vibrational spectroscopy. The relative donor ability of the amides toward $SbCl_3$ as a fixed acid was established by means of carbonyl and antimony–chloride frequency shifts. Thus, in benzene the order is DMA > DMF > NMA (NMA = N-methylacetamide), which reverses in a polar solvent such as chloroform. In agreement with these results,

in an aprotic solvent the basicity order TMU⟩DMA⟩DMF was recently obtained using a calorimetric technique.[6]

Thermodynamic parameters involving the equilibrium between SbX_3, dissolved in 1,2-dichloroethane and a series of ligands have been calorimetrically obtained.[7] Among these ligands, there are oxygen donors such as pyridine N-oxide, dimethyl sulphoxide and triphenylphosphine oxide, which showed successive formation of 1:1 and 1:2 adducts in distinct steps, where $X_1 > X_2$. No abrupt difference was observed in the enthalpies of these steps of coordination. The ligands Ph_3PO and C_5H_5NO gave high stability constants at the first step of complexation, in comparison with the analogous phosphorus and nitrogen donors, which presented small enthalpies of formation. However, three moles of aliphatic amines reacted quantitatively with metal–halides to produce very large exothermic enthalpy changes. In this case, it was suggested that the aliphatic amines are coordinated to the halogen in the adducts rather than to the metal.

In this paper, SbX₃ were calorimetrically titrated with N,N-dimethylformamide (DMF); N,N-dimethylacetamide (DMA) and tetramethylurea (TMU) in the assumed inert solvent 1,2-dichloroethane. From the incremental calorimetric titration results, the stability constants and the variation of enthalpy for the two steps of coordination of these oxygen donors ligands were calculated.

EXPERIMENTAL

Materials. All solvents for preparation of metal halides, for calorimetry and for conductance measurements were carefully dried, distilled and stored over molecular sieves. N,N-dimethylformamide;[8] N,N-dimethylacetamide[9] and tetramethylurea[10] were previously distilled and dried over barium oxide or sodium carbonate. After standing overnight these solvents were distilled through an efficient column under reduced pressure, collecting the fractions at 36°C and 30 mmHg; 30°C and 6 mmHg and 80°C and 30 mmHg for DMF, DMA and TMU, respectively. After distillation these solvents were stored over molecular sieves. All the manipulations concerning the metal halides were

---

*Author to whom correspondence should be addressed.
†Permanent address: Departamento de Química—CCEN, Universidade Federal da Paraíba, Campus I—Cidade Universitária, 58000 João Pessoa, Paraíba, Brasil.

carried out under an atmosphere of dry nitrogen on a vacuum line or in a dry-box. Antimony chloride (Carlo Erba) was purified by sublimation in vacuum, giving a melting point of 73°C, literature 73°C.[11] Antimony tribromide was prepared from the reaction of antimony with an excess of bromine in carbon disulphide under an atmosphere of nitrogen. When the antimony vanished, the solution was pumped to dryness and the solid was crystallized twice in carbon disulphide to give a product of melting point 96°C, literature 96°C.[12] Antimony triiodide was prepared by means of a direct reaction of the metal and iodine in benzene. After filtration the product was dried *in vacuo* and recrystallized in toluene, giving a melting point 170°C, literature 170°C.[12]

Calorimetric measurements. All calorimetric experiments were performed with the solvent 1,2-dichloroethane by means of a LKB 8700-2 precision calorimetric system. The titrand solution at $(25.00 \pm 0.05°C)$ was incrementally added to $90.0 \, \text{cm}^3$ of the desired solution, already in the calorimeter vessel and the heat recorded or described previously.[13,14] The calorimeter's performance was checked using the enthalpy of titration of hydrochloric acid with tris(hydroxyamino)methane.[15] The metal halides were titrated twice with each of the three ligands. In a typical example, an $SbCl_3$ solution $(1.30 \times 10^{-2} \, \text{moles} \cdot \text{l}^{-1})$ was titrated with a DMF solution of $0.15 \, \text{moles} \cdot \text{l}^{-1}$. A new titration of the same $SbCl_3$ solution was carried out with a DMF solution $1.16 \, \text{moles} \cdot \text{l}^{-1}$. The final volume in each case was *ca.* $100 \, \text{cm}^3$ and the relative number of moles of $SbCl_3$ to the number of ligand was 1.3/1 and 10/1 with between 15 and 25 points.

The net enthalpy for each increment of titrand (Q_A) was calculated after subtracting the heat of dilution. The effect produced by the ligand solution was determined when its solution was added to $90.0 \, \text{cm}^3$ of 1,2-dichloroethane (Q_B). The heat of dilution of the metal halide solution was calculated after the addition of solvent to the calorimeter vessel containing $90.0 \, \text{cm}^3$ of the halide solution (Q_C). Thus, the variation of enthalpy due to the chemical reaction (Q_{obs}) can be obtained by: $Q_{obs} = Q_A - Q_B - Q_C$. The K_1, K_2, ΔH_1 and ΔH_2 values are related to the interactions of metal halides (SbX_3) with the ligands (L):

$$SbX_3 + L = SbX_3 \cdot L; \quad K_1, \; \Delta H_1^\circ$$

$$SbX_3 \cdot L + L = SbX_3 \cdot 2L; \quad K_2, \; \Delta H_2^\circ$$
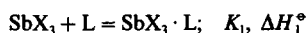
where $K_1 = |SbX_3 \cdot L|/|SbX_3||L|$ and $K_2 = |SbX_3 \cdot 2L|/|SbX_3 \cdot L||L|$. A previously described procedure of calculation was followed to find, K_1, K_2, ΔH_1° and ΔH_2° values. This method consists in adjusting the points of the titrations of the calculated curve (Q_{calc}) to the experimental one (Q_{obs}). In this procedure the function $U = \Sigma (Q_{obs} - Q_{calc})^2$ is minimized by using a least square programme.[13,14]

Conductance measurements. The metal halides were conductometrically titrated at $(25.00 \pm 0.02°C)$ with the ligands in 1,2-dichloroethane to high concentration of metal halide/ligand; i.e. about 1/10. In these series of measurements a Metrohm Herisau Konduktoskop E 365 bridge was used.

RESULTS AND DISCUSSION

The progress of the reaction between the metal halides SbX_3 (X = Cl, Br, I) and the ligands L (L = DMF, DMA, TMU) was studied in 1,2-dichloroethane, which is considered to be a very poor interacting solvent. The results of a typical calorimetric titration are listed in Table 1 and the enthalpies of dilutions Q_B and Q_C are given in Tables 2 and 3, respectively. The plot of the heat obtained against the volume is presented in Fig. 1. From these incremental calorimetric titrimetry values the thermo-

Table 1. Titration of $90.0 \, \text{cm}^3$ of $SbCl_3$ solution $(1.30 \times 10^{-2} \, \text{M})$ with 0.15 M DMF solution

V/cm^3	$- Q_{obs}/J$	$- \Sigma Q_{obs}/J$
90.00	0	0
90.25	0.44	0.44
90.54	0.88	1.32
90.78	0.66	1.98
91.29	1.50	3.48
91.85	1.29	4.77
92.65	2.07	6.84
93.45	1.75	8.59
94.45	2.20	10.79
95.46	1.86	12.65
96.67	2.13	14.78
98.17	2.09	16.87
100.00	1.76	18.63

Table 2. Dilution of $90.0 \, \text{cm}^3$ of DMF solution (0.15 M) with 1,2-dichloroethane

V/cm^3	Q_{obs}/J	$\Sigma Q_{obs}/J$
90.00	0	0
90.49	0.46	0.46
91.14	0.53	0.99
91.91	0.56	1.55
92.70	0.56	2.11
93.63	0.64	2.75
94.84	0.68	3.43
96.02	0.69	4.12
97.29	0.73	4.85
98.74	0.79	5.64
100.00	0.74	6.38

Table 3. Dilution of $90.0 \, \text{cm}^3$ of $SbCl_3$ solution $(1.30 \times 10^{-2} \, \text{M})$ with 1,2-dichloroethane

V/cm^3	Q_{obs}/J	$\Sigma Q_{obs}/J$
90.00	0	0
90.63	0.28	0.28
91.72	0.38	0.66
93.15	0.36	1.02
95.15	0.38	1.40
97.44	0.38	1.78
100.00	0.43	2.21

dynamic parameters of Table 4 were calculated. In an attempt to obtain information about the ionic behaviour in 1,2-dichloroethane, the metal halides were conductometrically titrated in the same range of concentration as that carried out in the calorimetry measurements. The plot of Fig. 2 represents the ionic character of the metal halides when titrated with tetramethylurea. The curves of distribution of $SbBr_3$, $SbBr_3 \cdot DMF$ and $SbBr_3 \cdot 2DMF$ species in Fig. 3

Table 4. Stability constants and the corresponding variation of enthalpies for interactions of antimony halides with the ligands

Acid	Base	K_1/mol^{-1} ℓ	$-\Delta H_1^\ominus/kJ\ mol^{-1}$	K_2/mol^{-1}	$-\Delta H_2^\ominus/kJ\ mol^{-1}$
$SbCl_3$	DMF	1160 ± 1	26.8 ± 0.1	216 ± 1	28.9 ± 0.1
	DMA	460 ± 1	36.4 ± 0.1	1915 ± 1	31.7 ± 0.1
	TMU	79 ± 1	58.7 ± 0.1	25 ± 1	38.0 ± 0.1
$SbBr_3$	DMF	473 ± 1	28.9 ± 0.2	4228 ± 2	21.1 ± 0.2
	DMA	$(900 \pm 4)10^5$	39.4 ± 0.2	100 ± 2	29.2 ± 0.2
	TMU	800 ± 1	42.8 ± 0.2	1375 ± 2	44.3 ± 0.2
SbI_3	DMF	$(320 \pm 2)10^3$	27.9 ± 0.2	$(110 \pm 2)10^4$	17.6 ± 0.2
	DMA	$(140 \pm 2)10^5$	28.6 ± 0.2	$(170 \pm 2)10^4$	19.7 ± 0.2
	TMU	$(600 \pm 2)10^3$	33.5 ± 0.2	$(98 \pm 2)10^4$	21.2 ± 0.2
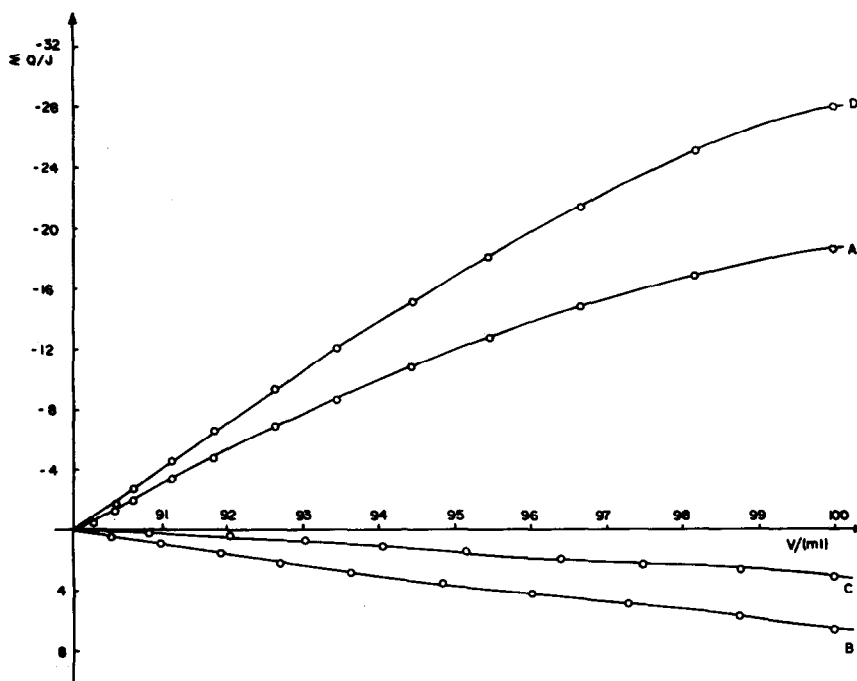
Fig. 1. Calorimetric titration of $90.0\ cm^3$ of a 1.30×10^{-2} M solution of $SbCl_3$ with 0.15 M DMF solution. The experimental points in curves A, B and C represent the summation of Q_A's, Q_B's and Q_C's, respectively. The calculated points in curve D represent the summation of the Q_{obs}.
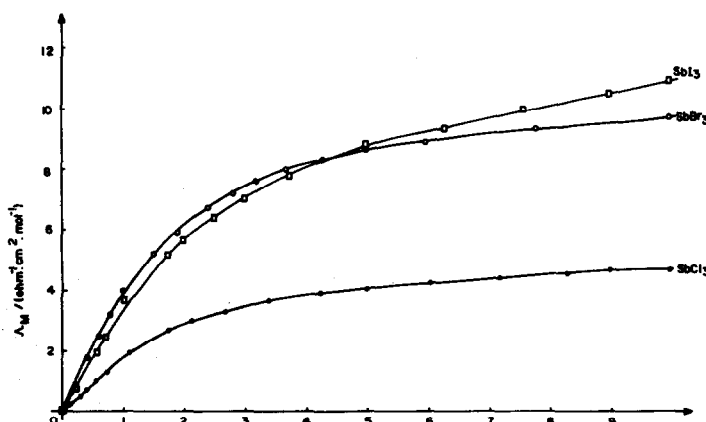
Fig. 2. Conductometric titration of $90.0\ cm^3$ of metal halides with TMU in 1,2-dichloroethane: 1.42×10^{-2} M $SbCl_3$ and 0.99 M TMU; 1.31×10^{-2} M $SbBr_3$ and 0.99 M TMU; 3.03×10^{-3} M SbI_3 and 0.28 M TMU.
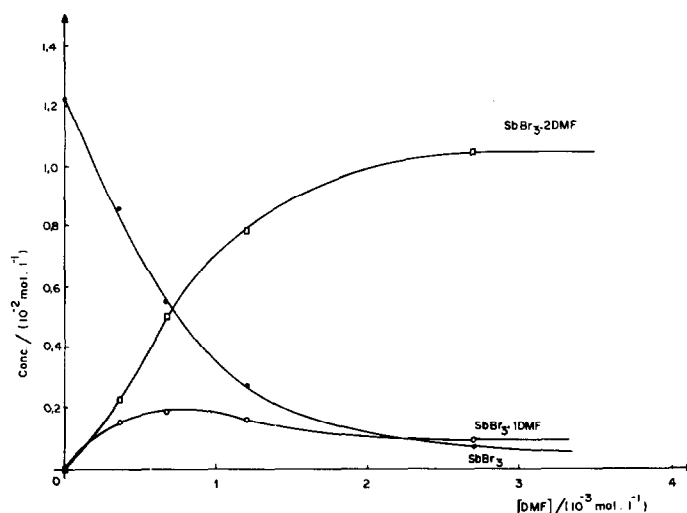
Fig. 3. Distribution curve of SbBr$_3 \cdot$2DMF and SbBr$_3 \cdot$DMF adducts in the SbBr$_3$–DMF system in 1,2-dichloroethane at 298 K.

were calculated from values of K_1 and K_2 obtained from the titrations.

The halides SbX$_3$ (X = Cl, Br) interact exothermically with the amides. However, SbI$_3$ produces an endothermic effect in this process except with DMA in high concentration. In all cases the dilution leads to an endothermic effect more pronounced with SbI$_3$, in spite of its lower concentration, due to its reduced solubility in the solvent.

Calorimetric measurements between SbX$_3$ and DMA have been previously obtained[16] with the following $\Delta H_1^{\ominus}$ values: −35.98 (SbCl$_3$), −30.96 (SbBr$_3$) and −31.80 (SbI$_3$) kJ mol^{-1}, which are comparable with our results. From these values the authors did not establish any acidity order for these metal halides. In the mean time, our $\Delta H_1^{\ominus}$ results (Table 4) demonstrate that TMU is a more suitable base to differentiate the acidity properties of the metal halides, giving the order SbCl$_3$ > SbBr$_3$ > SbI$_3$, as is also observed with triphenylphosphine oxide.[7] This behaviour is associated with the donor number of the ligands.[17] Whereas DMF and DMA have the values 26.6 and 27.8, respectively, leading to similar enthalpies; TMU with donor number 31, leads to a different $\Delta H_1^{\ominus}$ values.

The enthalpies values listed in Table 4 show an increase from DMF to TMU, reflecting the increasing donor number of these ligands. In all cases the basicity order TMU > DMA > DMF can be proposed, since any metal halide is fixed as acceptor. This sequence of basicity is clearly seen with SbCl$_3$. On the other hand, the same sequence was previously established for the interaction of this acid with the above bases by means of the reactions in condensed phase,[6] viz.   SbCl$_3$(s) + L(ℓ) = SbCl$_3 \cdot$ L(ℓ, s); $\Delta H_R^{\ominus}$: −27.82 ± 0.15; −37.96 ± 0.16 and −44.86 ± 0.27 kJ mol^{-1} for DMF, DMA and TMU, respectively.

The metal halides in the concentration range of the calorimetric titrations give the same specific conductivity of the net solvent, thus they maintained their

characteristic molecular properties in this medium. Although the metal halides present some degree of dissociation during the conductometric titrations with the ligands, the molar conductivity is much below that of 1:1 electrolyte type behaviour.[18] Figure 2 shows a conductometric titration of SbX$_3$ with TMU. The conductance results reveal the donor–acceptor complex formation, which depends on the donor properties of the ligand, the polarizability and the energy of Sb–X bond. The highest conductance values observed for SbI$_3$ (Fig. 2) fit very well with the most basic ligand and the characteristics of Sb–I bond.

The stability constant values of K_1, for the formation of the adducts of SbCl$_3$, increase from TMU to DMF, which is the inverse order of the donor ability of the ligands. This enhancement of the equilibrium constant in that sequence suggests that the autocomplex should be formed, producing ionic species in solution, with a consequent decrease of the amount of the adduct formed. This fact can be explained in considering the equations of formation of adduct and autocomplex:[19]

$$SbCl_3 + L \rightleftharpoons SbCl_3 \cdot L;$$

$$K_1 = [SbCl_3, \cdot \ L]/[SbCl_3][L]$$
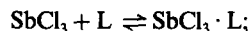
$$2SbCl_3 \cdot L \rightleftharpoons SbCl_2L_2^+ + SbCl_4^- ;$$

$$K_e = [SbCl_2L_2^+][SbCl_4^-]/[SbCl_3 \cdot L]^2.$$

The autocomplex is more easily formed with TMU due to its highest donor power. In this way the K_1 value turns out to be the smallest among these values. For the second step of complexation TMU and DMF present $K_2 < K_1$, which are normally interpreted by statistical effects. Thus, K_2 values for both ligands suggest the predominance of SbCl$_3 \cdot$ 2L species in solution due to the reaction SbCl$_3 \cdot$ L + L $\rightleftharpoons$ SbCl$_3 \cdot$ 2L. However, the highest K_2 value for DMA indicates an ionization in solution with the

displacement of chloride: $SbCl_3 \cdot DMA + DMA$ $\rightleftarrows [SbCl_2 \cdot 2DMA]^+ + Cl^-$. These results corroborate with that found in the conductance titrations, where DMA presents a higher conductance in comparison with other ligands. This behaviour also affects the interaction of $SbBr_3$ and DMA, where the K_1 value suggests the presence of ionic species in solution due to autocomplex formation: $2SbBr_3 \cdot DMA \rightleftarrows [SbBr_22DMA]^+ + [SbBr_4]^-$. A decrease of this constant is observed with DMF and TMU; such results indicating the predominance of the formation of the adduct: $SbBr_3 + L \rightleftarrows SbBr_3 \cdot L$. In examining K_2 for this system, higher values are shown for TMU and DMF. The displacement of bromide for these bases can be suggested as: $SbBr_3 \cdot L + L \rightleftarrows [SbBr_2 \cdot 2L]^+ + Br^-$. The lowest K_2 value for DMA favours an equilibrium in the course of adduct formation $SbBr_3 \cdot DMA \cdot + DMA$ $\rightleftarrows SbBr_3 \cdot 2DMA$.

The equilibrium constants involving the ligands and SbI_3 are all large in value (Table 4). The first species formation suggests that it might have an auto-association in solution. As previously described ionized species should prevail in solution, being more accentuated with DMA. For the second step of complexation, for all cases, an ionization occurs with exchange of ligand, with predominance of ionic species in solution. This fact is consistent with the conductometric data which show that SbI_3 presents the highest degree of conductivity among the metal halides and that DMA more easily displaces the halides from SbX_3. The conductivity order for the trihalides is $SbI_3 > SbBr_3 > SbCl_3$ and for the amides the displacement order of halide is $DMA > TMU > DMF$.

REFERENCES

[1] A. F. Wells, *Structural Inorganic Chemistry*, 4th Edn, p. 703. Clarendon Press, Oxford (1975).
[2] R. Hulme and J. C. Scruton, *J. Chem. Soc. A* 1968, 2448.
[3] I. Lindqvist, *Inorganic Adduct Molecules of Oxo-Compounds*. Springer-Verlag, New York (1968).
[4] E. Hough and D. G. Nicholson, *J.C.S. Dalton Trans.* 1981, 2083.
[5] M. van Canteren-Thevissen and Th. Zeegers-Huyskens, *Inorg. Chim. Acta* 1979, **32**, 33.
[6] C. Airoldi, *Inorg. Chem.* 1981, **20**, 998.
[7] M. J. Gallagher, D. P. Graddon and A. R. Sheikh, *Thermochim. Acta* 1978, **27**, 269.
[8] G. Durgaprasad, D. N. Sathyanarana and C. Patel, *Bull. Chem. Soc. Japan* 1971, **44**, 316.
[9] C. D. Schulbach and R. S. Drago, *J. Am. Chem. Soc.* 1960, **82**, 4484.
[10] A. Luttringhaus and H. W. Dirksen, *Angew. Chem. Int. Edn* 1964, **3**, 260.
[11] J. C. Bailar Jr., H. J. Hemeléus, R. Nyholm and A. F. Trotman-Dickenson, *Compresensive Inorganic Chemistry*, Vol. 2, p. 578. Pergamon Press, Oxford (1973).
[12] G. Brauer, *Handbook of Preparative Inorganic Chemistry*, 2nd Edn, Vol. 1. Academic Press, New York (1963).
[13] P. L. O. Volpe, A. P. Chagas and C. Airoldi, *J. Inorg. Nucl. Chem.* 1980, **42**, 1321.
[14] C. Airoldi, P. L. O. Volpe and A. P. Chagas, *Polyhedron* 1982, **1**, 49.
[15] J. J. Christensen, D. P. Wrathall and M. Izatt, *Anal. Chem.* 1968, **40**, 175.
[16] V. Gutmann and H. Czuba, *Monatsh. Chem.* 1969, **100**, 788.
[17] V. Gutmann, *The Donor–Acceptor Approach to Molecular Interactions*. Plenum Press, London (1978).
[18] W. J. Geary, *Coord. Chem. Rev.* 1971, **7**, 81.
[19] V. Gutmann, *Topics in Current Chemistry*, Vol. 27, p. 59. Springer-Verlag, New York (1972).

MAGNETIC AND ELECTRONIC CHARACTERIZATION OF 2:1 COPPER(II) COMPLEXES OF A SERIES OF AMINOCARBOXYLIC ACIDS

N. F. ALBANESE† and H. M. HAENDLER*

Department of Chemistry, University of New Hampshire, Durham, NH 03824, U.S.A.

Abstract—Copper(II) complexes with L-(−)-proline, pipecolinic acid, picolinic acid, anthranilic acid, 4-chloranthranilic acid, 3,5,-dichloroanthranilic acid, 4-nitroanthranilic acid, N-phenyl-anthranilic acid, and flufenamic acid anions were prepared and characterized. The copper complexes of the anions of proline, pipecolinic acid, and picolinic acid are soluble in polar solvents and display frozen solution EPR spectra with axial resonance parameters. The copper complexes of the ring-substituted anthranilates are highly insoluble or only slightly soluble in a few solvents. The EPR spectra of the copper-doped zinc(II) analogues of these complexes display various degrees of rhombicity in their EPR parameters. The N-substituted anthranilates form insoluble complexes in aqueous solution which readily dissolve in organic solvents and undergo dimerization.

The anion of anthranilic acid (o-aminobenzoic acid) is a unique ligand which forms highly insoluble complexes suitable for gravimetric determination of transition metals. Despite the insolubility of anthranilate complexes, the bis(anthranilato)copper(II) complex is pharmacologically active as an anti-inflammatory agent[2], and rhodium and other metal complexes with the anthranilate anion have unusual catalytic properties.[3]

In 1975, Lange and Haendler[4] reported the crystal and molecular structure of bis(anthranilato)copper(II). The local coordination geometry is a distorted octahedron, with two amino nitrogens and two carboxylate oxygens occupying the equatorial coordination sites in a *trans* configuration. A carbonyl oxygen from a ligand on an adjacent complex molecule occupies each axial coordination site. The polymeric, carboxylate-bridged network is further stabilized by hydrogen bonds, and undoubtedly accounts for the unusual insolubility of this complex.

A study of the copper(II) complexes with a series of aminocarboxylate ligands that are structurally related to anthranilic acid is reported here. The objective of this study is the comparison of the electronic and magnetic properties of these complexes, and the correlation of these properties with structural differences. Due to the insolubility of some of these complexes, the complexes were studied in both solution and the solid state. Further X-ray crystallographic study has been initiated.

EXPERIMENTAL

Preparation of complexes

Aqueous solutions of the ligands were prepared by dissolving the free acid in a slight excess of dilute sodium hydroxide solution and adjusting the pH to 6–7 with dilute acid. The filtered ligand solution was added to an aqueous solution of copper(II) acetate in a 2:1 ligand–metal mole ratio. The complexes, except those of L-(−)-proline and pipecolinic acid, precipitated immediately as fine powders. The prolinato and pipecolinato complexes are extremely water soluble, but were isolated by gradual addition of less polar organic solvents to the aqueous solution. The products were collected by vacuum filtration, washed, and air dried. Copper-doped zinc(II) and nickel(II) complexes were prepared in the same manner, using approx. 5 mol% copper(II) acetate in nickel (II) or zinc(II) acetate.

Reagent grade methanol and benzene were stored over 4A molecular sieves and used without further purification to prepare solutions of the complexes. Reagent grade dioxane was not pretreated. N,N'-dimethylformamide (DMF) was carefully prepurified immediately prior to use.[5]

Table 1. Ligands and corresponding complexes

Parent Ligand	IUPAC Name	Empirical Formula of Complex	Color of Solid Complex	% Composition Calculated		% Composition Observed	
				M	N	M	N
L-(−)-proline	L-pyrrolidine-2-carboxylic acid	$Cu(pro)_2 \cdot 2H_2O$	dark purple	19.4	8.5	18.7	8.2
pipecolinic acid	2-piperidine-carboxylic acid	$Cu(pip)_2 \cdot 2H_2O$	blue	17.9	7.9	17.8	7.8
picolinic acid	2-pyridine-carboxylic acid	$Cu(pic)_2$	purple	20.6	9.1	20.9	9.1
anthranilic acid	o-aminobenzoic acid	$Cu(anth)_2$	light green	18.9	8.3	19.4	7.9
		$Ni(anth)_2$	pale blue	17.8	8.5	17.6	8.2
		$Zn(anth)_2$	pale green	19.3	8.3	19.2	8.8
4-chloro-anthranilic acid	2-amino,4-chlorobenzoic acid	$Cu(canth)_2$	light green	15.7	6.9	14.8	6.8
		$Zn(canth)_2$	white	16.1	6.9	15.8	7.0
3,5-dichloro-anthranilic acid	2-amino,3,5-dichloro-benzoic acid	$Cu(dcanth)_2 \cdot 2H_2O$	light green	12.5	5.5	12.5	6.5
		$Zn(dcanth)_2$	yellow green	13.7	5.9	13.9	5.8
4-nitro-anthranilic acid	2-amino,4-nitrobenzoic acid	$Cu(nanth)_2$	grey	14.9	13.2	14.9	13.2
		$Zn(nanth)_2$	yellow	15.3	13.1	15.4	13.2
N-phenyl-anthranilic acid	N-phenyl-2-aminobenzoic acid	$Cu(panth)_2$	tan	13.0	5.7	12.6	5.9
		$Cu(panth)_2 \cdot MeOH$ (b)	dark green	12.2	5.4	12.3	5.5
		$Cu(panth)_2$ (c)	dark brown	13.0	5.7	13.5	5.7
		$Ni(panth)_2$	light green	12.2	5.8	12.0	5.5
		$Zn(panth)_2$	orange	13.3	5.7	13.6	5.5
flufenamic acid	N-(α,α,α-trifluoro-m-tolyl)-2-aminobenzoic acid	$Cu(fluf)_2$	tan	10.2	4.5	9.6	4.0
		$Cu(fluf)_2 \cdot MeOH$ (d)	dark green	9.7	4.3	9.6	4.6
		$Cu(fluf)_2$ (c)	reddish brown	10.2	4.5	10.0	4.6
		$Ni(fluf)_2$	yellow green	9.5	4.5	9.6	4.7
		$Zn(fluf)_2$	salmon pink	10.4	4.5	10.2	4.4

a) Nickel and zinc complexes doped with 5 mol% copper

b) Prepared by recrystallization of $Cu(panth)_2$

c) Prepared by thermal decomposition of corresponding methanol solvate

d) Prepared by recrystallization of $Cu(fluf)_2$

Hereafter, the complexes are designated by the empirical formulae listed in Table 1 with the ligand abbreviations shown.

Elemental analysis

Composition of the complexes was determined by C,H,N and metal analysis. Metal content was determined gravimetrically by the anthranilate or ethylenediamine method.[1]

Magnetic susceptibility

The magnetic susceptibility of complexes in the solid state was measured by the Gouy method.[6] Measurements were performed at room temperature in a magnetic field of 5.8 kG. The calibration constant, β, was determined using $HgCo(CNS)_4$ and checked against $(NH_4)_2Fe(SO_4)_2 \cdot 6H_2O$. Susceptibilities were corrected for the temperature independent paramagnetism of the copper(II) ion ($N_\alpha = 60 \times 10^{-6}$ cgsu).

Visible spectroscopy

Solution spectra were recorded on the Cary 14 scanning spectrophotometer using matched quartz cells (1 cm pathlength) with pure solvent in the reference beam. Diffuse powder reflectance data were collected using a Beckman Model DU Quartz Spectrophotometer with reflectance attachment 2580. The reflectance was measured relative to the reflectance of magnesium carbonate.

X-Ray diffraction

X-Ray powder diffraction photographs were taken with a Philips 57.3 mm camera, and were exposed with nickel-filtered Cu K_α radiation ($\lambda = 1.5418$ Å). Samples were contained in 0.3 mm glass capillaries.

Electron Paramagnetic Resonance (EPR) spectroscopy

EPR spectra were recorded on the Varian E-4 spectrometer operating at X-band frequency (9.5 GHz) with 100 kHz field modulation. The

magnetic field was calibrated with a proton nuclear magnetic resonance gaussmeter. Diphenyl-picrylhydrazine (DPPH, $g_0 = 2.0037 \pm 0.0002$)[7] was used as a microwave frequency marker. Cylindrical quartz tubes (3 mm I.D.) were used to contain all powder samples, all dioxane and benzene solutions at room temperature, and all solutions at liquid nitrogen temperature. A quartz flat cell was used for DMF and methanol solutions at room temperature. Instrument settings were selected to avoid power saturation, overmodulation, and lineshape distortion.

EPR parameters were refined by computer simulation of spectra using a FORTRAN program for $S = \frac{1}{2}$ systems.[8] Simulations were performed with a nitrogen hyperfine interaction from two magnetically equivalent nitrogen donor atoms with couplings of $8-10 \times 10^{-4}$ cm^{-1}. Additional refinement was achieved by including various hydrogen atom hyperfine couplings of $1-4 \times 10^{-4}$ cm^{-1}.

The temperature dependence of the intensity of the spin triplet EPR signal of Cu(panth)$_2$·MeOH and Cu(fluf)$_2$·MeOH was measured with a Bruker VT2000 variable temperature controller and Bruker ER200D spectrometer. A nonlinear least-squares program was used to obtain values of $-2J$ by fitting the experimental signal intensity data to the Bleaney–Bowers equation[9]

$$\chi_m = \frac{g^2 N \beta^2}{3kT} \cdot \frac{1}{1 + \frac{1}{3}\exp(-2J/kT)} + N_\alpha$$

where the signal intensity is proportional to the molar susceptibility, χ_m.

Calculation of bonding parameters

Molecular orbital theory has been applied to the interpretation of EPR spectra of transition metal complexes. The theory and derivation of the equations that follow are discussed more completely elsewhere.[10-15]

In D_{4h} symmetry, assuming a $d_{x^2-y^2}$ ground state, the g and A values are predicted by

$$g_\parallel - 2.0023 = \frac{-8\lambda\alpha\beta_1}{\Delta E_{d_{x^2-y^2}\to d_{xy}}} \{\alpha\beta_1 - \alpha'\beta_1 S$$
$$- \alpha(1 - \beta^2)^{1/2} T(n)/2\}$$

$$g_\perp - 2.0023 = \frac{-2\lambda\alpha\beta}{\Delta E_{d_{x^2-y^2}\to d_{xz,yz}}} \{\alpha\beta - \alpha'\beta S$$
$$- \alpha'(1 - \beta^2)^{1/2} T(n)/2\}$$

$$A_\parallel = P\{\alpha^2(-K_0 - \tfrac{4}{7}) + (g_\parallel - 2.0023)$$
$$+ \tfrac{3}{7}(g_\perp - 2.0023)\}$$

where λ is the spin orbit coupling constant, which is less than the free ion value $\lambda_0 = 828$ cm^{-1}, S is the overlap integral, $T(n)$ is a function primarily of $s-p$ hybridization of ligand orbitals, P is the electron–nuclear dipole coupling term, which is less than the free ion value $P_0 = 0.36$ cm^{-1}, and $K_0 = 0.43$ is the Fermi contact term. Typical values of S and $T(n)$ are 0.076 and 0.333 for oxygen donor atoms, and 0.093 and 0.220 for nitrogen donor atoms, respectively.[11] The energies of the individual electron transitions $(\Delta E_{d_{x^2-y^2}\to dxy}$, $\Delta E_{d_{x^2-y^2}\to dxz,yz}$, etc.) were approximated by the energies from the absorption peaks in the visible spectra of the complexes in solution or in the reflectance spectra of the complexes as polycrystalline solids. The so-called bonding parameters are the mixing coefficients of the molecular orbital wavefunctions constructed by taking linear combinations of ligand atomic orbitals and metal 3d orbitals. The primed symbols refer to ligand antibonding orbitals, and the unprimed symbols to metal antibonding orbitals. Normalization of orbitals yields $\alpha^2 + \alpha'^2 = 1$ for in-xy-plane σ-bonding orbitals (neglecting overlap), $\beta_1^2 + \beta_1'^2 = 1$ for in-xy-plane π-bonding orbitals, and $\beta^2 + \beta'^2 = 1$ for out-of-xy-plane π-bonding orbitals. When α^2, β_1^2, or β^2 is equal to one, bonding in the corresponding orbital is ionic; values of 0.5 indicate that bonding is covalent. The degree of covalency can be used to compare the molecular structure of a series of related complexes in similar media.

When xy-anisotropy in g is observed, the above equations must be replaced by the ones appropriate for crystal field symmetries lower than D_{4h}. In D_{2h} symmetry the in-xy-plane anisotropy arises from splitting of the d_{xz} and d_{yz} orbital energy levels, while in C_{2v} symmetry the anisotropy is also due to mixing of $d_{x^2-y^2}$ and d_{z^2} orbital character. The equations which predict the g and A values are[11,12]

$$g_z - 2.0023 = \frac{-8\lambda\alpha^2\beta_1^2(\cos^2\delta)}{\Delta E_{d_{x^2-y^2}\to d_{xy}}}$$

$$g_y - 2.0023 = \frac{-2\lambda\alpha^2\beta^2(\cos\delta + \sqrt{3}\sin\delta)^2}{\Delta E_{d_{x^2-y^2}\to d_{xz}}}$$

$$g_x - 2.0023 = \frac{-2\lambda\alpha^2\gamma^2(\cos\delta - \sqrt{3}\sin\delta)^2}{\Delta E_{d_{x^2-y^2}\to d_{yz}}}$$

$$A_z = P[-K\alpha^2 - (\tfrac{4}{7})\alpha^2(\cos 2\delta) + (\tfrac{3}{7})\lambda\alpha^2\gamma^2(\cos 2\delta$$
$$+ (\sqrt{3}/3)\sin 2\delta)/\Delta E_{yz} + (\tfrac{3}{7})\lambda\alpha^2\beta^2(\cos 2\delta$$
$$- (\sqrt{/3})\sin 2\delta)/\Delta E_{xz} + 8\lambda\alpha^2\beta_1^2$$
$$\times (\cos^2\delta)/\Delta E_{xy}]$$

where β^2 and γ^2 are the bonding parameters for out-of-xy-plane π-bonding via the d_{xz} and d_{yz} orbitals, respectively, and $\cos \delta$ and $\sin \delta$ are coefficients for $d_{x^2-y^2}, d_{z^2}$ orbital mixing. In D_{2h} symmetry $\cos \delta = 1$ and $\sin \delta = 0$.

The bonding parameters were calculated by an iterative method. A $d_{x^2-y^2}$ ground state was assumed in all cases. All calculations employed $\lambda_0 = 828 \, \text{cm}^{-1}$ because it is difficult to predict the extent of reduction of the spin orbit coupling constant. If no xy-anisotropy in g was observed, the equations for D_{4h} symmetry were used. If xy-anisotropy in g was observed, the equations for C_{2v} symmetry were used, starting with $\cos \delta = 1$. If β_1^2, β^2, or γ^2 was greater than one, the degree of mixing was increased by small increments to obtain the best fit.

RESULTS

Stoichiometry of the complexes

Complexes with a 2:1 ligand–metal mole ratio were prepared. The results of elemental analysis for N and metal content are in agreement with the empirical formulae listed in Table 1. IR spectra of the complexes in Nujol mulls between KBr plates were recorded on a grating spectrophotometer. The amine stretching vibrations of every copper, nickel, and zinc complex were shifted to lower frequency relative to the corresponding free acid, demonstrating that coordination through nitrogen occurs in each complex.

X-Ray powder patterns

The diffraction data are compiled elsewhere.[16] For each ligand it was found that the powder patterns of the corresponding copper and zinc complexes were different. The Ni(panth)$_2$ complex, as prepared, is amorphous. The powder patterns of Ni(anth)$_2$ and Zn(anth)$_2$ are the same, but the powder pattern of Ni(fluf)$_2$ differs from that of Zn(fluf)$_2$.

Single crystals of bis(pipecolinato)copper(II) dihydrate have been grown and a full X-ray structure determination is in progress.

Solubility

The solvents used to test solubility were DMF, methanol, dioxane, and benzene, listed in decreasing order of dielectric constant. Cu(canth)$_2$, like Cu(anth)$_2$, is insoluble in each of these solvents, whereas Cu(pro)$_2 \cdot 2H_2O$, Cu(pip)$_2 \cdot 2H_2O$, and Cu(pic)$_2$ are soluble only in methanol, DMF, and water. Cu(panth)$_2$ and Cu(fluf)$_2$ are insoluble in water, but soluble in all the organic solvents. The complexes Cu(panth)$_2 \cdot$MeOH and Cu(fluf)$_2 \cdot$MeOH were obtained from methanol solutions of

Cu(panth)$_2$ and Cu(fluf)$_2$, respectively. Cu(d-canth)$_2 \cdot 2H_2O$ and Cu(nanth)$_2$ were slightly soluble in DMF and dioxane, but not in methanol or benzene.

Visible spectra

The spectral data are listed in Table 2. Cu(pro)$_2 \cdot 2H_2O$, Cu(pip)$_2 \cdot 2H_2O$, and Cu(pic)$_2$ absorb around 600 nm in DMF and methanol solution. All the other soluble complexes absorb at much longer wavelengths. The spectra of the benzene and dioxane-soluble complexes are dominated by an intense absorption below 400 nm which is presumably a ligand band or ligand–metal charge transfer band. A shoulder on this intense band is observed near 400 nm for Cu(panth)$_2$ in dioxane and Cu(fluf)$_2$ in benzene. Powder reflectance data are also listed in Table 2. Well-resolved peaks at 675, 625, and 575 nm were observed for Cu(pro)$_2 \cdot 2H_2O$. The reflectance data of the dimeric complexes, Cu(panth)$_2 \cdot$MeOH and Cu(fluf)$_2 \cdot$ MeOH, exhibit peaks near 675 and 475 nm. The other complexes exhibit a single broad peak in their reflectance data.

Magnetic susceptibility

The magnetic susceptibility data for the polycrystalline complexes are summarized in Table 3. The magnetic moments of the copper complexes are in the range 1.8–2.0 B.M., excluding Cu(p-anth)$_2 \cdot$MeOH and Cu(fluf)$_2 \cdot$MeOH. The observed moment of Cu(anth)$_2$ falls between values of 1.84[17] and 2.0 B.M.[18] previously reported for this complex. The reduced room temperature magnetic moments of Cu(panth)$_2 \cdot$MeOH and Cu(fluf)$_2 \cdot$MeOH are indicative of spin–spin coupling and suggest that these complexes have a dimeric structure similar to that of copper(II) acetate, which has a room temperature magnetic moment of 1.39 B.M.[19] Grigor'eva et al.[20] observed room temperature magnetic moments of 1.35 and 1.40 B.M., respectively, for N - 2,3 - dimethyl - phenyl - anthranilate and flufenamate complexes isolated from aqueous DMF solution.

The observed magnetic moments of Ni(anth)$_2$ and Ni(panth)$_2$ fall within the range of values typically observed for nickel(II) complexes with octahedral geometry (i.e. 2.9–3.4 B.M.).[21] Magnetic moments of 3.2 and 3.4 B.M. were reported previously for Ni(anth)$_2$.[18,22] Although the observed magnetic moment of Ni(fluf)$_2$ is lower than those typically observed for complexes with tetrahedral or octahedral geometry, square planar complexes are normally diamagnetic.[21] Dimerization or polymerization leading to antiferromagnetic spin coupling is suggested, but addi-

Table 2. Visible spectral data

Complex	DMF λ_{max}	ϵ	MeOH λ_{max}	ϵ	Dioxane λ_{max}	ϵ	Benzene λ_{max}	ϵ	Powder Reflectance Data, λ_{max}
$Cu(pro)_2 \cdot 2H_2O$	596	47	600	73	-	-	-	-	675, 625, 575
$Cu(pip)_2 \cdot 2H_2O$	592	79	596	95	-	-	-	-	650
$Cu(pic)_2$	627	35	630	68	-	-	-	-	600
$Cu(anth)_2$	-	-	-	-	-	-	-	-	650
$Cu(canth)_2$	-	-	-	-	-	-	-	-	675
$Cu(dcanth)_2 \cdot 2H_2O$	750	86	-	-	663	81	-	-	700
$Cu(nanth)_2$	675	77	-	-	675	15	-	-	700
$Cu(panth)_2$ (b)	738	112	731	66	668	252	682	49	c
$Cu(panth)_2$ (d)	729	135	732	70	669	256	688	73	c
$Cu(panth)_2 \cdot MeOH$	738	138	736	68	669	247	688	63	675, 475
$Cu(fluf)_2$ (b)	759	74	725	78	672	166	711	44	c
$Cu(fluf)_2$ (d)	753	81	731	73	671	213	718	56	c
$Cu(fluf)_2 \cdot MeOH$	753	92	738	60	675	242	709	62	675, 475

a) λ_{max} in nm, ϵ in $cm^{-1}M^{-1}$

b) Original complex from aqueous solution

c) No major peaks resolved

d) Product from thermal decomposition of corresponding methanol adduct

Table 3. Powder susceptibility data

Complex	$T(^{\circ}K)$	$\chi(10^6)$	$\chi_{dia}(10^6)$	$\chi'_m(10^3)$	$\mu_{eff}(B.M.)$
$Cu(pro)_2 \cdot 2H_2O$	294	3.72	-142.7	1.36	1.8
$Cu(pip)_2 \cdot 2H_2O$	298	3.71	-165.9	1.49	1.8
$Cu(pic)_2$	298	4.52	-56.9	1.45	1.8
$Cu(anth)_2$	297	4.36	-71.4	1.54	1.9
$Cu(canth)_2$	298	3.72	-111.6	1.62	1.9
$Cu(dcanth)_2 \cdot 2H_2O$	298	2.63	-166.9	1.51	1.9
$Cu(nanth)_2$	299	4.08	-91.4	1.83	2.0
$Cu(panth)_2$ (b)	296	2.85	-106.2	1.50	1.8
$Cu(panth)_2$ (c)	293	3.34	-106.2	1.74	2.0
$Cu(panth)_2 \cdot MeOH$	292	1.44	-128.6	0.88	1.4
$Cu(fluf)_2$ (b)	293	2.41	-150.2	1.65	1.9
$Cu(fluf)_2$ (c)	293	2.26	-150.2	1.56	1.9
$Cu(fluf)_2 \cdot MeOH$	296	0.980	-172.5	0.82	1.3
$Ni(anth)_2$	295	11.7	-71.4	3.44 (d)	2.9
$Ni(panth)_2$	295	8.00	-106.2	3.57 (d)	2.9
$Ni(fluf)_2$	295	1.53	-150.2	0.59 (d)	1.2

a) Corrected for T.I.P. of Cu(II), $N_\alpha = 60 \times 10^{-6}$.

b) Original complex from aqueous solution.

c) Product from thermal decomposition of methanol solvate.

d) Corrected for presence of 5 mol% copper(II) and T.I.P. of nickel(II), $N_\alpha = 500 \times 10^{-6}$.

tional work on these nickel complexes is warranted.

EPR spectra of the undiluted powders

The parameters from the room temperature EPR spectra of the magnetically undiluted polycrystalline copper(II) complexes are summarized in Table 4. According to the classification scheme of Hathaway and Billing,[11] the spectra of $Cu(pip)_2 \cdot 2H_2O$, $Cu(panth)_2$, and $Cu(fluf)_2$ are isotropic whereas $Cu(pro)_2 \cdot 2H_2O$ has a lineshape corresponding to an "exchanged-coupled" spectrum. Sastry and Sastry[23] demonstrated that a small ferromagnetic exchange coupling occurs in crystalline $Cu(pro)_2 \cdot 2H_2O$ with $2J = +0.108 \, cm^{-1}$. The spectrum of $Cu(dcanth)_2 \cdot 2H_2O$ has rhombic parameters. In the other complexes which have $g_1 \geq 2.04$, the copper atom is probably in an axially symmetric environment of square planar or elongated octahedral geometry. The observed g-values of $Cu(anth)_2$ are in excellent agreement with values reported by Ismailov.[17]

The EPR spectra of $Cu(fluf)_2 \cdot MeOH$ and $Cu(p-anth)_2 \cdot MeOH$ exhibit zero field splitting (Fig. 1) characteristic of the triplet state of copper(II) dimers. A low intensity signal near 3200 G that appears at low temperature is the singlet state absorption of residual monomer species. Only four principal $\Delta m_s = \pm 1$ resonance fields are expected in the triplet spectrum when the rhombic component of the zero field splitting is zero.[24] The four resonance fields in each spectrum are $H_{Z1} = 0$, $H_{X1} = 378$, $H_{X2} = 4622$ and $H_{Z2} = 5757G$ for $Cu(fluf)_2 \cdot MeOH$, and $H_{Z1} = 0$, $H_{X1} = 541$, $H_{X2} = 4622$ and $H_{Z2} = 5465G$ for $Cu(panth)_2 \cdot MeOH$. Averaged values of D calculated from[24]

Table 4. Powder g-values

Complex	g_1	g_2	g_3
$Cu(pro)_2 \cdot 2H_2O$	2.06	2.17	-
$Cu(pip)_2 \cdot 2H_2O$	2.11	-	-
$Cu(pic)_2$	2.06	2.17	-
$Cu(anth)_2$	2.07	2.25	-
$Cu(canth)_2$	2.07	2.25	-
$Cu(dcanth)_2 \cdot 2H_2O$	2.06	2.19	2.31
$Cu(nanth)_2$	2.05	2.26	-
$Cu(panth)_2$	~2.1	-	-
$Cu(fluf)_2$	~2.1	-	-

a) Estimated uncertainty: ± 0.005.
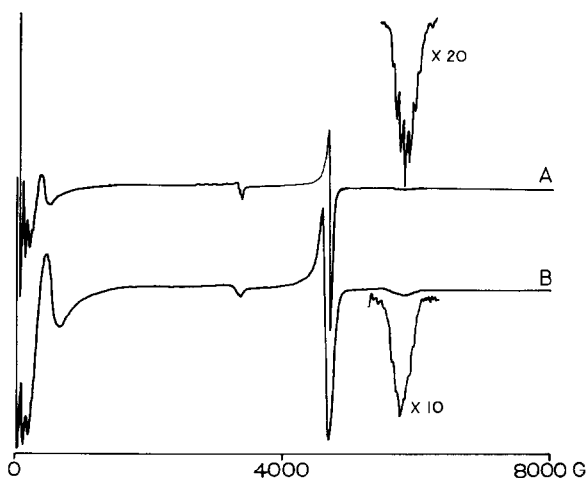
Fig. 1. EPR spectra of polycrystalline $Cu(p-anth)_2 \cdot MeOH$ (A), and $Cu(fluf)_2 \cdot MeOH$ (B) at liquid nitrogen temperature.

$$H_{X1}^2 = (g_e/g_x)^2(H_0 - D/(g_e\beta))H_0$$

$$H_{X2}^2 = (g_e/g_x)^2(H_0 + D/(g_e\beta))H_0$$

$$H_{Z1}^2 = (g_e/g_z)^2(H_0 - D/(g_e\beta))^2$$

$$H_{Z2}^2 = (g_e/g_z)^2(H_0 + D/(g_e\beta))^2$$

are $0.30 \pm 0.03 \, cm^{-1}$ for $Cu(panth)_2 \cdot MeOH$, and $0.28 \pm 0.01 \, cm^{-1}$ for $Cu(fluf)_2 \cdot MeOH$ using $g_x = g_y = 2.07$, $g_z = 2.34$ (assumed values) and $hv = 0.3195 \, cm^{-1}$ (from the DPPH frequency mark).

The magnitude of the zero field splitting is temperature independent, but at liquid nitrogen temperature, the copper hyperfine structure in the H_{Z1} and H_{Z2} resonance fields is well-resolved. The seven-line pattern arises from the interaction of two equivalent $I = \frac{3}{2}$ copper nuclei with the triplet state ($S = 1$) of the two unpaired electrons in the dimer unit. The observed splitting is about $70-80G$ or roughly $a_\parallel/2$. The singlet–triplet energy separation ($-2J$) obtained from the least-squares non-linear regression fit of the temperature dependence of the signal amplitude of the H_{X2} resonance field to the Bleaney–Bowers equation is $213 \, cm^{-1}$ for $Cu(fluf)_2 \cdot MeOH$, and $375 \, cm^{-1}$ for $Cu(p-anth)_2 \cdot MeOH$ (Fig. 2). Grigor'eva et al. reported $-2J = 240 \, cm^{-1}$ for the flufenamate complex.[20]

EPR spectra of dilute solutions

EPR parameters from spectra of dilute solutions are listed in Table 5. In methanol and DMF solution at room temperature, the prolinato, pipecolinato, and picolinato complexes display the typical isotropic spectrum of copper with four hyperfine lines arising from the interaction of the

Fig. 2. Temperature dependence of EPR signal amplitude of Cu(panth)$_2$·MeOH (A), and Cu(fluf)$_2$·MeOH (B), showing experimental data and nonlinear least-squares fit.

Table 5. EPR parameters for dilute solution

Complex	Solvent	Isotropic[b]		Anisotropic[c]						Bonding Parameters[c,d]			
		g_0	A_0	g_x	g_y	g_z	A_x	A_y	A_z	α^2	β_1^2	β^2	γ^2
Cu(pro)$_2$·2H$_2$O	DMF	2.116	81.7	2.050	2.050	2.251	18.7	18.7	190.1	0.82	0.81	0.66	—
	MeOH	2.120	71.6	2.054	2.054	2.263	8.5	8.5	178.4	0.81	0.87	0.72	—
Cu(pip)$_2$·2H$_2$O	DMF	2.115	74.1	2.050	2.050	2.245	18.4	18.4	186.0	0.81	0.82	0.69	—
	MeOH	2.117	70.5	2.056	2.056	2.249	15.5	15.5	181.9	0.81	0.84	0.74	—
Cu(pic)$_2$	DMF	2.124	73.0	2.064	2.064	2.262	9.7	9.7	191.1	0.85	0.78	0.76	—
	MeOH	2.126	68.8	2.059	2.059	2.265	12.2	12.2	189.1	0.85	0.80	0.71	—
Cu(dcanth)$_2$·2H$_2$O	DMF	~2.13[e]	~57.0[e]	2.060	2.060	2.369	20.0	20.0	147.0	0.84	0.93	0.66	—
Cu(nanth)$_2$	DMF	~2.10[e]	~80.0[e]	2.054	2.054	2.282	17.0	17.0	172.0	0.82	0.82	0.64	—
Cu(panth)$_2$	DMF	—	—	2.070	2.070	2.370	9.0	9.0	147.0	0.84	0.96	0.71	—
	MeOH	—	—	2.070	2.087	2.381	< 5.0	15.0	143.0	0.80	0.97	0.69	0.86
	Dioxane	—	—	2.066	2.181	2.368	8.0	25.0	162.0	0.88	0.95	1.2	1.2
Cu(fluf)$_2$	DMF	—	—	2.069	2.069	2.373	12.0	12.0	145.0	0.84	0.94	0.70	—
	MeOH	—	—	2.052	2.091	2.382	< 5.0	15.0	144.0	0.80	0.97	0.51	0.91
	Dioxane	—	—	2.060	2.188	2.365	< 5.0	25.0	164.0	0.88	0.94	1.1	1.2

a) Solutions about 1.5×10^{-3} M. Values of g and A refined by computer simulation. Estimated uncertainty in g-values is $\pm$ 0.001. The copper hyperfine couplings are reported as isotope-weighted averages (69.09% ^{63}Cu, 30.91% ^{65}Cu) in units of 10^{-4} cm^{-1}. Estimated uncertainty in A_z is $\pm$ 0.5×10^{-4} cm^{-1}; greater incertainty in Ax, Ay.

b) From spectra recorded at room temperature ($\sim$22°C).

c) From spectra recorded at liquid nitrogen temperature.

d) See text for definitions.

e) Approximate values not refined by simulation.

unpaired electron with the copper nucleus. The corresponding anisotropic frozen solution spectra have axial parameters (Table 5). Axial symmetry is most commonly observed for copper(II) complexes, especially with amino acids.[11,25-28] For these three complexes, the solvent has a more pronounced effect on the g and A values than does the ligand. Ammeter et al.[29] described the dependence

of g-values, hyperfine coupling constants, and electron transition energies on the host lattice for bis(picolinato)copper(II).

The room temperature EPR spectra of Cu(n-anth)$_2$ and Cu(dcanth)$_2$·2H$_2$O in DMF are broadened, and the copper hyperfine structure is poorly resolved. The frozen solution spectrum of the dichloroanthranilate complex suggests the pres-

ence of more than one species. The frozen solution spectrum of the nitroanthranilate complex more closely resembles the spectra of the prolinate, pipecolinate, and picolinate complexes than that of the dichloroanthranilate complex.

The room temperature EPR spectra of CuL_2 and $CuL_2 \cdot MeOH$ ($L =$ panth or fluf) complexes in methanol and DMF are severely broadened. In benzene and dioxane, a broad absorption in the $1500-2000G$ region probably arises from forbidden transitions of loosely coupled dimers. Relatively sharp features near $3200G$ in the dioxane spectra suggest that monomers are also present. At liquid nitrogen temperature, the frozen solution spectra of these complexes in DMF, methanol, and dioxane are the typical anisotropic spectra characteristic of monomeric copper(II) complexes. In frozen benzene solution, a broad isotropic signal near $3130G$ was observed for the N-phenylanthranilate complex, whereas no signal could be detected for the flufenamate complex. Evidently, association of complex molecules occurs in solution, but solvents with coordinating ability can disrupt aggregate or dimer formation.

EPR spectra of copper-doped zinc(II) complexes

Parameters from the EPR spectra of the polycrystalline copper-doped zinc(II) host complexes at liquid nitrogen temperature are listed in Table 6. The degree of xy-anisotropy is greatest for the dichloroanthranilate and nitroanthranilate complexes. The degree of $d_{x^2-y^2} - d_{z^2}$ orbital mixing appears to be the greatest for the nitroanthranilate complex. The spectra from the $Zn(panth)_2$ and $Zn(fluf)_2$ host complexes are different in overall appearance compared to the other anthranilates. The linewidths are narrower, the xy-anisotropy is small or zero, $g_\| > 2.4$, and σ-bonding orbitals have reduced covalent character ($\alpha^2 \sim 0.82$ vs

$\alpha^2 \sim 0.75$ for the anthranilates). In-xy-plane π-bonding has very little covalent character in all these complexes ($\beta_1^2 \sim 1.0$).

DISCUSSION

Complexes described in this series can be separated into the following categories

(1) *Five-membered chelate ring structures.* These complexes which include $Cu(pro)_2 \cdot 2H_2O$, $Cu(pip)_2 \cdot 2H_2O$, and $Cu(pic)_2$, bear little relation to $Cu(anth)_2$ and the other complexes in solubility and spectral characteristics. The EPR parameters of these complexes are axially symmetric with $g_\perp = 2.05-2.06$, $g_\| = 2.25-2.26$, $A_\| = 178-191 \times 10^{-4}\,cm^{-1}$ and $\alpha^2 = 0.81-0.85$, $\beta_1^2 = 0.78-0.87$ and $\beta^2 = 0.66-0.76$. Visible absorption maxima are around $600\,nm$ in solution. X-Ray crystallographic studies of $Cu(pic)_2 \cdot 2H_2O$, in which the water molecules are interstitial, and of $Cu(pro)_2 \cdot 2H_2O$ have shown that the local coordination geometry of each complex in the solid state is elongated octahedral.[30,31] However, the axial bond lengths in these complexes are much longer than the axial bond length in $Cu(anth)_2$.[4]

(2) *Monomeric six-membered chelate ring structures.* The variously substituted anthranilate ligands form complexes of this type, but the N-substituted anthranilates also form dimeric complexes. With the exception of $Cu(nanth)_2$ in DMF which has $g_\| = 2.282$ and thus probably has elongated octahedral geometry as do the prolinate, pipecolinate, and picolinate complexes, these complexes have $g_\| > 2.3$, $A_\| > 170 \times 10^{-4}\,cm^{-1}$ and exhibit various degrees of xy-anisotropy. Two types of coordination geometry are evident.

(a) *Distorted tetrahedral.* This geometry probably occurs for the dichloroanthranilate, N-phenylanthranilate, and flufenamate complexes in solution. These complexes are characterized by

Table 6. EPR parameters for copper(II) in zinc(II) host complexes

Complex	EPR Parameters[a]						Bonding Parameters[b]				
	g_x	g_y	g_z	A_x	A_y	A_z	α^2	β_1^2	β^2	γ^2	$\cos\delta$
$Zn(anth)_2$	2.039	2.096	2.318	14.0	14.0	143.0	0.74	0.99	0.67	0.85	0.995
$Zn(canth)_2$	2.053	2.089	2.318	12.0	12.0	145.0	0.76	0.95	0.90	0.76	0.995
$Zn(dcanth)_2$	2.036	2.142	2.342	28.0	40.0	126.0	0.75	1.01	0.94	0.91	0.98
$Zn(nanth)_2$	2.008	2.148	2.311	29.0	58.0	112.0	0.76	1.02	0.97	0.66	0.925
$Zn(panth)_2$	2.069	2.069	2.438	≤ 5.9	≤ 5.9	122.6	0.85	1.2	0.77	——	——
$Zn(fluf)_2$	2.058	2.087	2.402	≤ 0.8	≤ 1.8	142.6	0.82	1.08	0.60	0.92	1.00

a) From spectra of polycrystalline samples recorded at liquid nitrogen temperature. Parameters refined by computer simulation. Estimated uncertainty in g is ± 0.001. Copper hyperfine couplings are reported as isotope-weighted averages in units of $10^{-4}\,cm^{-1}$. Estimated uncertainty in A_z is $\pm 0.5 \times 10^{-4}\,cm^{-1}$. Greater uncertainty in A_x and A_y.

b) See text for definitions.

$g_\parallel = 2.36\text{–}2.38$, $A_\parallel = 143\text{–}164 \times 10^{-4}\,\text{cm}^{-1}$, and exhibit a pronounced solvent dependency in their EPR parameters. The EPR parameters show xy-anisotropy when the complexes are in MeOH and dioxane solution, but not in DMF. The N-phenyl-anthranilate and flufenamate complexes in dioxane show greatly reduced covalent character in both σ- and π-bonding orbitals compared to all the other complexes in Table 5. Numerically, the shift to larger $g_\parallel$ values observed for these complexes is related to their smaller electron transition energies relative to the prolinate, pipecolinate, and pico-linate complexes.

The $d_{x^2-y^2}$ ground state is not easily distinguished from the d_{xy} ground state in C_4, C_{4h}, D_4, D_{4h}, C_{4v}, or D_{2d} symmetry on the basis of EPR parameters without the benefit of polarized single-crystal electronic spectra. However, the visible and EPR spectral data are consistent with distorted tetrahedral geometry for these complexes. The geometry is probably more nearly square planar or elongated octahedral when DMF is the solvent. The weaker donor solvents, MeOH and dioxane, probably allow twisting of bond angles in the equatorial plane to a more tetrahedral arrangement. The tetrahedral distortion is more evident in dioxane than in MeOH.

(b) *Rhombically-distorted elongated octahedral*. This geometry probably occurs in the zinc host complexes with the anthranilate, chloro-anthranilate, dichloroanthranilate, and nitro-anthranilate ligands. The EPR parameters of the copper(II) ion in these host environments are strongly dependent on the nature of the ligand substituents, and show pronounced xy-anisotropy, some degree of $d_{x^2-y^2} - d_{z^2}$ orbital mixing, little covalent character in the in-xy-plane π-bonding orbitals, and variable covalent character in the out-of-xy-plane π-bonding orbitals. This degree of variation in the EPR parameters would not be expected if the octahedral coordination environment was completed by "axial" coordination of carboxylate oxygens from adjoining complex molecules as it is in Cu(anth)$_2$.[4] Thus, the chloro and nitro substituents are probably involved in coordination, although whether they occupy "axial" or "equatorial" sites, and whether *cis* or *trans* configurations occur must be determined by full X-ray crystal and molecular structure analysis.

(3) *Dimeric structures*. The N-substituted an-thranilates form dimeric as well as monomeric complexes in solution and in the solid state. The Cu(panth)$_2$·MeOH and Cu(fluf)$_2$·MeOH complexes in the solid state exhibit zero field splittings in their triplet EPR spectra and exchange energies comparable to those of copper(II) acetate and

other carboxylate-bridged dimers.[19,32] It was suggested in earlier studies that the dimer might be held together by bridging hydrogen bonds between the amine group and the carboxylate oxygen (i.e. $-\text{N-H}\text{---O=C-}$).[20,33–35] However, hydrogen bond-bridged dimers of copper(II) complexes with amino alcohols exhibit small exchange energies ($-2J < 100\,\text{cm}^{-1}$) and large copper–copper separations ($> 5\,\text{Å}$).[36] X-ray crystallography showed that the copper–copper separation in CuL$_2$·DMF (HL = N-(2,3-dimethylphenyl)-anthranilic acid) is $2.613\,\text{Å}$.[37,38]

The EPR parameters of the copper(II) ion in the zinc host complexes Zn(panth)$_2$ and Zn(fluf)$_2$, are distinct in that $g_\parallel > 2.4$. Whereas the copper(II) ion in zinc(II) acetate has $g_\parallel = 2.344$,[39] the typical range of $g_\parallel$ values for dimeric copper(II) carbox-ylates is $2.32\text{–}2.42$.[32] Thus, the zinc complexes are probably carboxylate-bridged dimers. Possible structures for the water-insoluble monomeric Cu(panth)$_2$ and Cu(fluf)$_2$ complexes and the corresponding nickel(II) complexes are not obvious from the data presented above.

CONCLUSION

The copper(II) complexes of ligands which are structurally related to anthranilic acid display a wide variation in solubility behaviour and magnetic characteristics. Further X-ray crystallographic work is warranted.

REFERENCES

1. A. I. Vogel, *Textbook of Quantitative Inorganic Analysis*. Wiley, New York (1966).
2. J. R. J. Sorenson, *J. Med. Chem.* 1976, **19**, 135.
3. N. L. Holy, *J. Org. Chem.* 1979, **44**, 239.
4. B. A. Lange and H. M. Haendler, *J. Solid State Chem.* 1975, **15**, 325.
5. J. A. Riddick and W. B. Bunger, *Techniques of Chemistry—Organic Solvents, Physical Properties and Methods of Purification*, 3rd Ed, pp. 836–840. Wiley–Interscience, New York (1970).
6. W. L. Jolly, *The Synthesis and Characterization of Inorganic Compounds*. Prentice-Hall, New Jersey (1970).
7. J. E. Wertz and J. R. Bolton, *Electron Spin Resonance—Elementary Theory and Practical Applications*, McGraw-Hill, New York (1972).
8. L. K. White and R. L. Belford, *J. Am. Chem. Soc.* 1976, **98**, 4428.

9. B. Bleaney and K. D. Bowers, *Proc. Roy. Soc. (A)* 1952, **214**, 451.

10. D. Kivelson and R. Neiman, *J. Chem. Phys.* 1961, **35**, 149.

11. B. J. Hathaway and D. E. Billing, *Coord. Chem. Rev.* 1970, **5**, 143.

12. A. Bencini, I. Bertini, D. Gatteschi and A. Scozzafava, *Inorg. Chem.* 1978, **17**, 94.

13. G. F. Kokoszka and H. C. Allen, Jr., *J. Chem. Phys.* 1965, **42**, 3683.

14. A. Abragam and M. H. L. Pyrce, *Proc. Roy. Soc. (A)* 1951, **206**, 164.

15. A. Maki and B. R. McGarvey, *J. Chem. Phys.* 1958, **29**, 31, 35.

16. N. F. Albanese, Ph.D. Dissertation, University of New Hampshire, 1979.

17. G. Ismailov, V. V. Zelentsov and Yu. V. Yablokov, *Russ. J. Inorg. Chem.* 1972, **17**, 1202.

18. S. S. Sandhu, B. S. Manhas, M. R. Mittal and S. S. Parmar, *Indian J. Chem.* 1969, **7**, 286.

19. M. Kato, H. B. Jonassen and J. C. Fanning, *Chem. Rev.* 1964, **64**, 99.

20. A. S. Grigor'eva, V. V. Zelentsov, E. E. Kriss and A. K. Stroesku, *Russ. J. Inorg. Chem.* 1978, **23**, 1493.

21. F. A. Cotton and G. Wilkinson, *Advanced Inorganic Chemistry—A Comprehensive Text.* Interscience, New York (1972).

22. S. E. Livingstone, *J. Chem. Soc.* **1956**, 1042.

23. B. A. Sastry and G. S. Sastry, *Ind. J. Pure Appl. Phys.* 1973, **11**, 474.

24. J. R. Wasson, C.-I. Shyr and C. Trapp, *Inorg. Chem.* 1968, **7**, 469.

25. H. Yokoi, M. Sai, T. Isobe and S. Ohsawa, *Bull. Chem. Soc. Jpn* 1972, **45**, 2189.

26. H. Yokoi, M. Sai and T. Isobe, *Ibid.* 1972, **45**, 3488.

27. H. Yokoi, *Ibid.* 1974, **47**, 639.

28. H. C. Allen, Jr., M. J. Mandrioli and J. W. Becker, *J. Chem. Phys.* 1972, **56**, 997.

29. J. Ammeter, G. Rist and Hs. H. Guenthard, *J. Chem. Phys.* 1972, **57**, 3852.

30. N. Shamala and K. Venkatesan, *Cryst. Struct. Commun.* 1973, **2**, 5.

31. R. Faure, H. Loiseleur and G. Thomas-David, *Acta Crystallogr. (B)* 1973, **29**, 1890.

32. J. Catterick and P. Thornton, *Adv. Inorg. Chem. Radiochem.* 1977, **20**, 291.

33. E. E. Kriss, A. S. Grigor'eva, K. B. Yatsimirskii, Yu. A. Fialkov and E. S. Endel'man, *Russ. J. Inorg. Chem.* 1976, **21**, 931.

34. K. B. Yatsimirskii, E. E. Kriss and A. S. Grigor'eva, *Dokl. Akad. Nauk. SSSR* 1975, **221**, 153.

35. E. E. Kriss, A. S. Grigor'eva and K. B. Yatsimirskii, *Russ. J. Inorg. Chem.* 1975, **20**, 727.

36. J. A. Bertrand, E. Fujita and D. G. Vanderveer, *Inorg. Chem.* 1980, **19**, 2022.

37. A. S. Grigor'eva, E. E. Kriss and K. B. Yatsimirskii, *Proc. XIXICCC*, Prague, Czechoslovakia, 4–8 Sept. 1978.

38. K. B. Yatsimirskii, M. G. Mys'kiv, A. S. Grigor'eva, E. E. Kriss and E. I. Gladyshevskii, *Dokl. Akad. Nauk SSSR* 1979, **247**, 1204.

39. G. F. Kokoszka and H. C. Allen, Jr., *J. Phys. Chem.* 1965, **42**, 3693.

ON THE TRI-*n*-OCTYLAMMONIUM CHLORO COMPLEXES OF Cu(II), Zn(II) AND Co(II) IN BENZENE SOLUTION

CLAUS FISCHER* and HARALD WAGNER

Central Institute of Solid State Physics and Material Research, Academy of Sciences of the
G.D.R., Dresden, G.D.R.

and

VLADIMIR V. BAGREEV

V. I. Vernadsky Institute of Geochemistry and Analytical Chemistry, U.S.S.R. Academy
of Sciences, Moscow, U.S.S.R.

Abstract—Extracts with tri-*n*-octylammonium chloro complexes of Cu(II), Zn(II) and Co(II) of various compositions, including the *N*-deuterated compounds, were prepared and investigated by IR spectroscopy and conductivity measurements. Besides the well-known 2:1-complexes $(TOAH^+)_2MCl_4^{2-}$, for which new assignments of νNH frequencies are given, complexes with a stoichiometric ratio TOA:M > 2 were found. Their cations contain the groups $(TOA\ldots Cl\ldots HTOA)^+$ and $TOAH^+$ and they are supposed to be 3:1-complexes $(TOA\ldots Cl\ldots HTOA)^+ TOAH^+ MCl_4^{2-}$. The IR spectrum of the 1:1-complex $TOAH^+ CuCl_3^-$ is given. The occurrence of the analogous 1:1-complex $TOAH^+ ZnCl_3^-$ could not be detected under the preparative conditions used.

In preceding studies[1,2] the occurrence and conditions of formation of various extractable halo complexes in the system tri-*n*-octylammonium chloride/C_6H_6 or $C_6D_6 - MX_3 - HX[M = In(III)$, Fe(III) or Ga(III); X = Cl, Br or I] were investigated by means of loading experiments, IR spectroscopic investigations and measurements of the conductivity of the metal bearing extracts.

With the knowledge derived from these studies work was extended to the corresponding chloro complexes of Cu(II), Zn(II) and Co(II).

Previous solvent extraction studies[3–7] on such systems (or similar ones) stated the formation of 2:1-complexes $(R_3NH^+)_2MCl_4^{2-\dagger}(M = Cu$, Zn or Co). Aguilar *et al.*[8,9] proposed in the case of Zn besides the 2:1-complex a 3:1-complex $(R_3NHCl)_3ZnCl_2$, based on distribution data treated by means of the LETAGROP program. IR spectroscopic investigations on the 2:1-complexes

were performed with the aim to elucidate their structure.[4,5,10–12] However, the published data concerning the positions and assignments of the νNH frequencies are uncertain or contradictory and therefore reliable conclusions cannot be drawn.

The present study involves the investigation of Cu(II), Zn(II) or Co(II) bearing TOA extracts of various compositions by IR spectroscopy and conductivity measurements to determine the type of the complexes formed. For the sake of completion and extension of the arguments, analogous extracts were prepared starting from the corresponding *N*-deuterated systems (among them also Fe(III) bearing extracts).

EXPERIMENTAL

The reagents $CuCl_2.2H_2O$, $ZnCl_2$, $CoCl_2.6H_2O$, HCl and C_6H_6 were of analytical grade. Deuterium chloride (20% DCl in D_2O, 99.9%) was supplied by VEB Berlin–Chemie, Berlin–Adlershof. Quality and supply of the other reagents used are given elsewhere.[1,2]

---

*Author to whom correspondence should be addressed.

†Complexes are here and subsequently written in monomeric form.

Table 1. Preparation of the extracts for the IR spectra

No.	Complex[+]	Extract composition, M TOA	M^{II}	Cl	Diluent	Initial org. phase, M	Initial aqueous phase, M (H_2O or D_2O)	D_M^{II} detd.
1	Cu-2:1 H	0.25	0.127	0.52	C_6H_6/C_6D_6	0.25 TOAH$^+$Cl$^-$	2 $CuCl_2$ 3 LiCl^2 1 HCl	0.068
2	Cu-2:1 D	0.25	0.127	0.52	C_6H_6/C_6D_6	0.25 TOAD$^+$Cl$^-$	2 $CuCl_2$ 3 LiCl^2 1 DCl	
3	Cu-1:1 H	0.25	0.25		C_6D_6			
4	Cu-1:1 D	0.25	0.25		C_6H_6			
5	Cu-3:1 H^{++}	0.25	0.083		C_6H_6/C_6D_6			
6	Cu-3:1 D[++]	0.25	0.083		C_6H_6/C_6D_6			
7	Zn-2:1 H	0.25	0.124	0.51	C_6H_6/C_6D_6	0.25 TOAH$^+$Cl$^-$	0.5 $ZnCl_2$ 1 HCl^2	0.33
8	Zn-2:1 D	0.25	0.124	0.51	C_6H_6/C_6D_6	0.25 TOA	0.5 $ZnCl_2$ 1 DCl^2	
9	Zn-1:1 H(?)	0.25	0.20	0.68	C_6H_6/C_6D_6	0.25 TOA	5 $ZnCl_2$ 1 HCl^2	0.042
10	Zn-1:1 D(?)	0.25	0.20	0.68	C_6H_6/C_6D_6	0.25 TOA	5 $ZnCl_2$ 1 DCl^2	
11	Zn-3:1 H^{++}	0.25	0.083		C_6H_6/C_6D_6			
12	Zn-3:1 D[++]	0.25	0.083		C_6H_6/C_6D_6			
13	Zn-2:1 H	0.125	0.0625		CCl_4			
14	Zn-3:1 H^{++}	0.1875	0.0625		CCl_4			
15	Zn-3:1 H^{++}	0.25	0.0625		CCl_4			
16	Co-2:1 H	0.25	0.129	0.52	C_6H_6/C_6D_6	0.25 TOAH$^+$Cl$^-$	0.25 $CoCl_2$ 12 LiCl^2 0.5 DCl	1.06
17	Co-2:1 D	0.25	0.129	0.52	C_6H_6/C_6D_6	0.25 TOAD$^+$Cl$^-$	0.25 $CoCl_2$ 12 LiCl^2 0.5 DCl	
18	Co-3:1 H^{++}	0.25	0.083		C_6H_6/C_6D_6			
19	Co-3:1 D[++]	0.25	0.083		C_6H_6/C_6D_6			
20	Fe-1:1 D	0.25	0.25		C_6H_6/C_6D_6	0.25 TOA	3 $FeCl_3$ 6 DCl^3	0.091
21	Fe-2:1 D	0.25	0.124		C_6H_6/C_6D_6	0.25 TOA	0.125 $FeCl_3$ 6 DCl^3	97

[+] H: non-deuterated; D: N-deuterated   [++] 3:1-complexes supposed

Other preparation conditions: **No. 3:** 4 ml extract No. 1 +67 mg anhydrous $CuCl_2$ (24 h, 20 °C), some unsoluble residue remained. No. 4: do., but 4 ml extract No. 2. **No. 5:** 2 ml extract No. 1 +1 ml 0.25 M TOAH$^+$Cl$^-$. **No. 6:** 2 ml extract No. 2 +1 ml 0.25 M TOAD$^+$Cl$^-$. **No. 11:** 2 ml extract No.7 +1 ml 0.25 M TOAH$^+$Cl$^-$. **No. 12:** 2 ml extract No. 8 +1 ml 0.25 M TOAD$^+$Cl$^-$. **No. 13:** Prepn. according to extract No. 7, 10 ml diluted with 10 ml CCl_4. **No. 14:** do., 10 ml diluted with 5 ml 0.25 M TOAH$^+$Cl + 5 ml CCl_4. **No. 15:** do., 10 ml diluted with 10 ml 0.25 TOAH$^+$Cl$^-$. **No. 18:** 2 ml extract No. 16 +1 ml 0.25 M TOAH$^+$Cl$^-$. **No. 19:** 2 ml extract No. 17 +1 ml 0.25 M TOAD$^+$Cl$^-$.

The preparation of the extracts and the measurements of the IR spectra and conductivities were carried out as described earlier[1,2] The distribution coefficients D_M were determined using ^{64}Cu, ^{65}Zn and ^{60}Co, respectively. The extracts prepared for IR spectroscopy and their preparation conditions are compiled in Table 1. In most cases these extracts were duplicated with benzene and deuterobenzene as diluents, written in Table 1 "C_6H_6/C_6D_6". In the deuterated systems (aqueous phases with D_2O and DCl) $CuCl_2$, $ZnCl_2$ and

$CoCl_2$ were used as anhydrous salts. The extracts for the conductivity measurements were prepared in the same or an analogous way, respectively, but with benzene as diluent only.

IR SPECTRA

The IR spectra of the extracts were taken in the range 1800–3800 cm^{-1}. They are given in Figs. 1 and 2. The wave numbers of the νNH and νND absorptions are summarized in Table 2.

The νNH bands of the 2:1-complexes
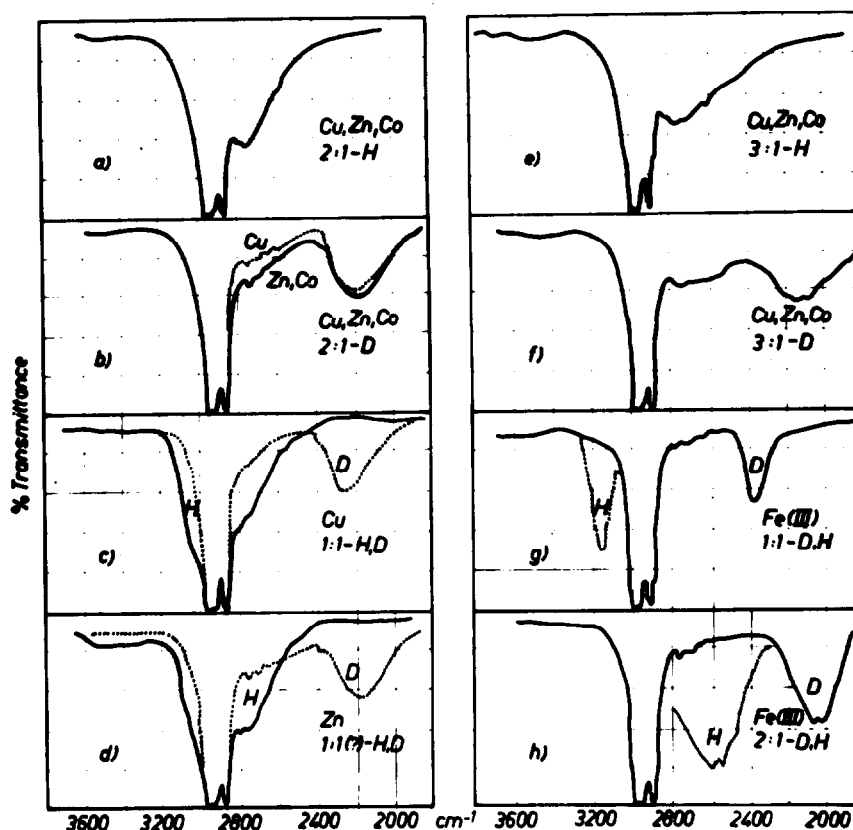
Fig. 1. IR spectra of the extracts (the numbers refer to Table 1). (a) 1, 7, 15. (b) ···· 2; ———8, 17. (c) ———3; ····· 4. (d) ———9; ····· 10. (e) 5, 11, 18. (f) 6, 12, 19. (g) ——— 20; ····· taken from (1). (h) ——— 21; ···· taken from (1).

$(TOAH^+)_2MCl_4{}^{2-}$ (M = Cu, Zn and Co, resp.) appear in the spectra uniformly as a double peak at $2740/2790\ cm^{-1}$, moreover, an evident broadening of the νCH bands in the short wave region at $3000\ cm^{-1}$ is observed. The IR spectra of the deuterated complexes $(TOAD^+)_2MCl_4{}^{2-}$, however, show only a single νNH band at $2180\ cm^{-1}$ (Zn, Co) and $2190\ cm^{-1}$ (Cu), respectively. Hence it follows that the νNH band in the spectra of the non-deuterated complexes is perturbed by over-

lapping with absorptions of the octyl groups, and thus the peaks occurring in this region do not reflect true shape and position of the νNH band. The peak at $2740\ cm^{-1}$ has to be considered as a coincidental amplification by a vibration which is to be assigned to the octyl groups, because it occurs in the IR spectrum of the free TOA, too. Thus the assignments given in earlier work[10] could not be confirmed.

The spectra of the 2:1-complexes show very weak absorptions at 3520, 3635 and $3680\ cm^{-1}$ indicating very small quantities of water in the extracts. The assignments for such absorptions were given in Ref.[2]

The IR spectra of the extracts with a stoichiometry which approximates that of the 1:1-complexes of Cu and Zn respectively, exhibit essential differences. In the Cu bearing non-deuterated extract the νNH band, in spite of the nearness to the strong νCH absorptions, is found at $3015\ cm^{-1}$, i.e. in the region expected for an 1:1-complex. The corresponding band of the deuterated extract is the νNH band at $2260\ cm^{-1}$. Its
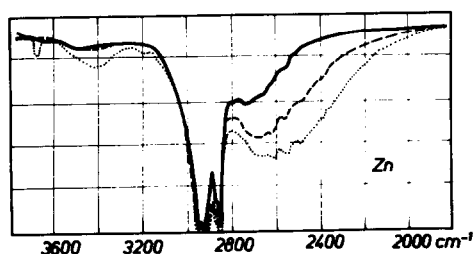
Fig. 2. IR spectra of Zn bearing extracts with different molar ratios TOA:Zn (diluent: CCl_4). ——— 2:1; ——— 3:1; ······4:1.

Table 2. Wave numbers (in cm^{-1}) of the νNH and νND absorptions

No. (acc. to Table 1)	Complex (M = Cu, Zn and Co, resp.)	ratio	ν NH	ν ND	$\frac{\nu \text{NH}}{\nu \text{ND}}$
1 7 16	(TOAH$^+$)$_2$MCl$_4^{2-}$	2:1	2790 s[+]		1.28
2 8 17	(TOAD$^+$)$_2$MCl$_4^{2-}$	2:1		2180 s(Zn,Co) 2190 s(Cu)	
3	TOAH$^+$CuCl$_3^-$	1:1	3015 sh		1.33
4	TOAD$^+$CuCl$_3^-$	1:1		2260 s	
9	TOAH$^+$ZnCl$_3^-$ (?)	1:1(?)	2790 s[+]		1.28
10	TOAD$^+$ZnCl$_3^-$ (?)	1:1(?)		2180 s	
5 11 18	(TOAH...Cl...HTOA)$^+$TOAH$^+$MCl$_4^{2-}$	3:1[++]	2500 sh 2558 w,br 2615 m 2790[+]s		1.28
6 12 19	(TOAD...Cl...DTOA)$^+$TOAD$^+$MCl$_4^{2-}$	3:1[++]		1998 w 2043 s 2170 s	
-	TOAH$^+$FeCl$_4^-$ [+++]	1:1	3122 s		1.34
20	TOAD$^+$FeCl$_4^-$	1:1		2330 s	
-	(TOAH...Cl...HTOA)$^+$ FeCl$_4^-$ [+++]	2:1	2500 sh 2555 s,br 2610 s		1.28
21	(TOAD...Cl...DTOA)$^+$ FeCl$_4^-$	2:1		2000 s 2045 s	

+) Apparent frequency; ++) 3:1-complex supposed; +++) Taken from /1/

position is clearly distinguished from the position of the corresponding νND band of the 2:1-complex of Cu (2190 cm^{-1}). Absorptions between 2700 and 2800 cm^{-1} point to considerable quantities of 2:1-complex in the extract. In general, however, these IR spectra demonstrate the existence of the 1:1-complex TOAH$^+$CuCl$_3^-$ (or TOAD$^+$CuCl$_3^-$).

The Zn bearing extracts show a different picture. Their νNH and νND absorptions coincide almost entirely with those of the corresponding 2:1-complexes, although the stoichiometric ratio TOA:M of the extracts approximates 1(0.25 M TOA; 0.20M Zn$_{(org)}$). Absorptions corresponding to the 1:1-complex of Cu are detectable only as broadenings of the νNH bands and the νND band respectively, when a direct comparison of the spectra is performed. It is obvious, that in the case of Zn the equilibrium of the reaction

$(\text{TOAH}^+)_2\text{MCl}_4^{2-}{}_{(org)} + \text{MCl}_{2(w)} \rightleftharpoons 2\text{TOAH}^+ \text{MCl}_3^-{}_{(org)}$

is shifted strongly to the left side of the equation. A simultaneous extraction of ZnCl$_2$.nH$_2$O, indicated by the occurrence of a νOH band at 3460 cm^{-1}, suggests a complex stoichiometry of approximately 1:1. To elucidate the question, whether there are additional complexes with molar ratio TOA:M > 2 besides the well-known 2:1-complexes of Cu, Zn and Co or not, extracts with a stoichiometric ratio TOA:M = 3:1 were

prepared. The IR spectra of the non-deuterated extracts show, besides the absorption at 2790 cm^{-1}, the three peaks of the νNH vibration at 2500 (as shoulder), 2558 and 2615 cm^{-1}. These three peaks appear with almost constant frequencies in the IR spectra of all complexes comprising the group (TOAH... Cl... HTOA)$^+$.[1,2] This points to the existence of a further complex, which must comprise that group. The increased absorption in the region about 2400 cm^{-1} (compared with the IR spectra of the 2:1-complexes) and a weak νOH band at 3420 cm^{-1} indicate the presence of quantities of the simple salt TOAH$^+$Cl$^-$.H$_2$O. This involves that equimolar quantities of 2:1-complex are present due to the extract stoichiometry 3:1.

Figure 2 shows the IR spectra of Zn bearing extracts with molar ratios TOA:Zn 2:1, 3:1 and 4:1. Carbon tetrachloride was used here as diluent. With increasing excess of TOA the intensity of the νNH band in the region about 2500–2615 cm^{-1} increases, too. The extract with the stoichiometry 4:1 exhibits an even greater increase in the absorption in the region about 2400 cm^{-1}, compared with the spectrum of the extract 3:1. Moreover, νOH bands of associated and free H$_2$O respectively appear distinctly at 3420 and 3680 cm^{-1}. This indicates the presence of considerable quantities of TOAH$^+$Cl$^-$.H$_2$O in the extract.

Going back to Fig. 1 there can be seen in the spectra of the deuterated extracts with the stoichiometric ratio 3:1 that, apart from the weak shoulder at 2500 cm^{-1}, the νNH bands at 2558 and 2615 cm^{-1} are uniformly shifted to 1998 and 2043 cm^{-1} (νND). Thus it is clearly shown, that these peaks indeed mutually represent the group (TOAH...Cl...HTOA)$^+$ or (TOAD...Cl...DTOA)$^+$ and belong together. The absorption at 2170 cm^{-1}, which is likewise to be assigned to a νND vibration, corresponds to the νNH absorption at 2790 cm^{-1} in the spectrum of the non-deuterated extract.

The Fe(III) bearing extracts confirm the assignments stated for the νNH and νND bands. There is a good agreement between the νNH/νND ratios of the 1:1-complexes of Fe(III) and Cu. The same holds for the 2:1-complex of Fe(III) on the one hand and for the complexes of Cu, Zn and Co comprising the group. (TOAH...Cl...HTOA)$^+$ or (TOAD...Cl...DTOA)$^+$ on the other. The shift of the νNH band of the 2:1-complex of Fe(III) with deuteration shows the correlation of the peaks of this band very distinctly.

CONDUCTIVITY MEASUREMENTS

Earlier[13] it was pointed out for the case of some trivalent metals that there is an unambiguous correlation between the values of the specific conductivity κ (and of the dielectric constant ϵ, too) and the molar ratio TOA:Metal$_{(org)}$, which offers an additional possibility to characterize and identify the extracted species. Thus κ values of the extracts were also determined in the present work. They are given in Table 3.

The measured values of κ show a distinct decrease in the order Fe(III)-complexes > 3:1-complexes > 2:1-complexes. The top values for Fe(III) are not surprising, because it is well known, that complexes with such univalent anions exhibit essentially higher κ values than corresponding complexes with bivalent anions.[13] The values of the extracts with the stoichiometry 3:1 are clearly differentiated from those of the 2:1-complexes thus indicating another kind of complex. A striking difference is observed among the 2:1-complexes, where the κ value of the Cu-complex considerably exceeds the nearly equal values of the Zn- and Co-complexes. The κ value of the extract with the 1:1-complex of Cu is somewhat higher than that of the 2:1-complex, but does not reach the value of the 1:1-complex of Fe(III). Therefore it may be supposed that this extract consists of a mixture of 1:1- and 2:1-complex. This assumption agrees with the IR spectroscopic findings. The extract which should contain the 1:1-complex of Zn has a κ value somewhat lower than the value of the 2:1-complex thus giving no evidence for the existence of the 1:1-complex.

CONCLUSION

It has been shown, that in addition to the well-known 2:1-complexes (TOAH$^+$)$_2$MCl$_4^{2-}$ of Cu, Zn and Co complexes bearing these metals can occur, which exhibit an increased stoichiometric ratio TOA:M and include the group (TOAH...Cl...HTOA)$^+$. The occurrence of this group and the simultaneously detectable TOAH$^+$-group in extracts with the stoichiometric ratio 3:1 are certainly not complete evidence for the existence of a defined 3:1-complex with the composition (TOAH...Cl...HTOA)$^+$TOAH$^+$MCl$_4^{2-}$. On the other hand Aguilar *et al.*[8,9], as already mentioned, proposed 3:1-complexes as a result of their work on the system R$_3$NH$^+$Cl$^-$/C$_6$H$_6$ − ZnCl$_2$ − LiCl − HCl (R = *n*-hexyl, *n*-octyl and *n*-dodecyl, resp.) with Zn concentrations from tracer amounts

Table 3. Specific conductivity data κ of the extracts. (Metal concentration: 0,1 M; diluent: benzene)

Complex	Metal	κ/Ω^{-1} cm^{-1}/at 25 $\pm$ 0.02°C
2:1	Fe(III)	6.02 × 10^{-5}‡
1:1	Fe(III)	2.75 × 10^{-5}‡
3:1†	Cu	2.14 × 10^{-5}
3:1†	Zn	1.85 × 10^{-5}
3:1†	Co	1.72 × 10^{-5}
1:1	Cu	1.84 × 10^{-5}
2:1	Cu	1.54 × 10^{-5}
2:1	Zn	8.89 × 10^{-7}
2:1	Co	6.21 × 10^{-7}
(1:1(?)	Zn	3.44 × 10^{-7})

†Complex supposed.
‡Taken from[1]

up to 0.0135 M. The increasing concentration of $(TOAH \ldots Cl \ldots HTOA)^+$-groups when going from the 3:1 to the 4:1 ratio is the result of the equilibrium between $TOAH^+$, $TOAH^+Cl^-$ and $(TOAH \ldots Cl \ldots HTOA)^+$ and does not necessarily show a distinguishable 4:1-complex.

A striking constancy of the ratios $\nu NH/\nu ND$ is observed for all complexes investigated. Complexes with weak H bonds ($\nu NH > 3000\ cm^{-1}$) exhibit the ratio 1.33–1.34, such with medium strong H bonds ($\nu NH\ 2500$–$2800\ cm^{-1}$) 1.28 (see ref.,[14] due to the well-known weakening of the H-bond by deuteration. This is valid not only for the complexes with Cu, Zn, Co and Fe(III), but also for corresponding complexes bearing the elements Sn(II, IV) and Sb(III, V).[15] Knowing the constancy of these ratios the apparent frequencies of the νNH vibration of some complexes at $2790\ cm^{-1}$ can be corrected into true frequencies: Cu-2:1-complex $2800\ cm^{-1}$; Zn- and Co-2:1-complex $2790\ cm^{-1}$; Cu-, Zn- and Co-3:1-complex $2780\ cm^{-1}$. The reasons for the essentially higher κ value of the Cu-2:1-complex (in comparison with those of the Zn- and Co-2:1-complexes) are not clear. The differences of the strength of the H bonds as shown by the νNH frequencies are insignificant. Statements on the anion structures in complexes of the type $(R_3NH^+)_2MCl_4^{2-}$ ($CuCl_4^{2-}$: D_{2d}[4], C_{2v}[5]; $ZnCl_4^{2-}$: not clear; $CoCl_4^{2-}$: C_{2v}[5], cannot verify the particular behaviour of the Cu-2:1-complex, too.

REFERENCES

[1] C. Fischer, H. Wagner, V. V. Bagreev and E. S. Stojanov, *J. Inorg. Nucl. Chem.* 1977, **39**, 513.
[2] C. Fischer, H. Wagner and V. V. Bagreev, *J. Inorg. Nucl. Chem.* 1980, **42**, 891.
[3] M. L. Good, S. E. Bryan, F. F. Holland jr. and G. J. Maus, *J. Inorg. Nucl. Chem.* 1963, **25**, 1167.
[4] T. Sato and K. Adachi, *J. Inorg. Nucl. Chem.* 1969, **31**, 1395.
[5] M. G. Kuzina, A. A. Lipovsky and S. A. Nikitina, *Zh. Neorg. Khim.* 1971, **16**, 2461.
[6] O. V. Singh and S. N. Tandon, *J. Inorg. Nucl. Chem.* 1974, **36**, 2083.
[7] T. Sato and T. Kato, *J. Inorg. Nucl. Chem.* 1977, **39**, 1205.
[8] M. Aguilar, *Chemica Scripta* 1973, **4**, 207; 1974, **5**, 213.
[9] M. Aguilar and M. Muhammed, *J. Inorg. Nucl. Chem.* 1976, **38**, 1193.
[10] W. E. Keder, A. S. Wilson and L. L. Burger, *Symposium on Aqueous Reprocessing Chemistry for Irradiated Fuels.* Brussels, Belgium, 23–26 April (1963).
[11] U. A. Th. Brinkman, G. de Vries and E. van Dalen, *Z. Anorg. Allg. Chemie* 1967, **351**, 73.
[12] T. Sato, *J. Inorg. Nucl. Chem.* 1967, **29**, 547.
[13] C. Fischer and V. V. Bagreev, *Z. Chem.* 1974, **14**, 247.
[14] G. C. Pimentel and A. L. McClellan, *The Hydrogen Bond*, p. 111. W. H. Freeman and Co., San Francisco (1960).
[15] C. Fischer, H. Wagner and V. V. Bagreev, unpublished.

REARRANGEMENT OF 2-(2-THIENYL)BENZOTHIAZOLINE IN THE PRESENCE OF THIOPHILIC METAL IONS

L. F. CAPITÁN-VALLVEY* and P. ESPINOSA

Department of Analytical Chemistry, Faculty of Sciences, University of Granada, Granada, Spain

Abstract—2-(2-thienyl)Benzothiazoline and 2-(2-thienyl)benzothiazol have been synthesized and characterized by several techniques (IR, NMR, UV–VIS, MS) and elemental analysis. The reactions of a solution of 2-(2-thienyl)benzothiazoline with Zn, Cd, Hg(II) and Pb(II) ions have been studied. The spectral studies of the isolated complexes showed that the rearrangement of the benzothiazoline to the Schiff base, N-2-mercaptophenyl-2'-methyleneimine, had occurred. The factors influencing this rearrangement are discussed. Several complexes of 2-(2-pyridyl)benzothiazoline with Cd and Pb(II) were synthesized for purposes of comparison.

It has been well established that condensation of *o*-aminobenzenethiol with a carbonyl compound does not normally lead to the isolation of the corresponding Schiff base, but thiazoline or benzothiazoline is obtained.[1–4] However, several workers[2–13] have shown that in alkaline solution or in the presence of metal ions the cyclic structure of the above thiazoline or benzothiazoline rearranges to give Schiff base metal complexes. The role played by the metal ion in these rearrangements has been discussed by Thompson[14] and Lindoy.[15]

We are interested in the study of the complexing abilities and analytical applications of heterocyclic azomethines derived from pyridine - 2 - aldehyde, thiophen - 2 - aldehyde and pyrrol - 2 - aldehyde. Some results have been previously reported.[16–18] In this paper, we present some of the results found in the study of 2 - (2 - thienyl)benzothiazoline.

RESULTS AND DISCUSSION

Structure and spectral and thermal properties of the ligand

Condensation of *o*-aminobenzenethiol with thiophen - 2 - aldehyde in ethanol results in formation of 2 - (2 - thienyl)benzothiazoline (**I**).

The IR spectrum of (**I**) shows a band of medium intensity at 3280 cm^{-1} assignable to N–H stretching vibration[1,4,18] and an intense band at 920 cm^{-1} due to the C–S–C linkage.[19] The appearance of

these bands and the absence of v(S–H) IR absorption band in the region 2600–2550 cm^{-1} confirm the existence of benzothiazoline structure. Two bands of medium intensity at 1585 and 1545 cm^{-1} can be assigned to the thiazoline ring vibrations.

The NMR spectrum of (**I**) shows the NH proton signal as a broad signal at 4.5 ppm. No signals, even weak, of the open ring tautomer (**II**) can be detected. The other protons of (**I**) appear as a complex multiplet centered at 7.32 ppm. The integration curve is correct (1:8).

The mass spectrum of (**I**) shows the molecular peak (M˙$^{+}$) at m/e 219 (45%) and the base peak (M˙$^{+}$ − 2). Other important peaks are: 218 (60.2%), 136 (22.6%), 108 (34.4%), 83 (20.6%) and 45 (24.7%).

The thermal behaviour of (**I**) has also been studied. The DTG curve shows an endothermic peak at 96°C (melting of the compound) followed by a small exothermic effect at 127°C that was supposed to be due to the transformation in 2 - (2 - thienyl)benzothiazol (**III**) by the loss of an hydrogen molecule from (**I**) (Scheme 1).

By heating (**I**) at 127°C an intense orange crystalline compound is formed. In the IR spectrum of this compound the following was observed: (1) the absence of an absorption which can be assigned to v(N–H) mode, (2) three strong bands at 1477, 1436 and 1417 cm^{-1}, and two bands of medium intensity at 1590 and 1540 cm^{-1} (benzene and thiazol ring vibrations),[30] (3) a strong band at 913 cm^{-1}

---

*Author to whom correspondence should be addressed.
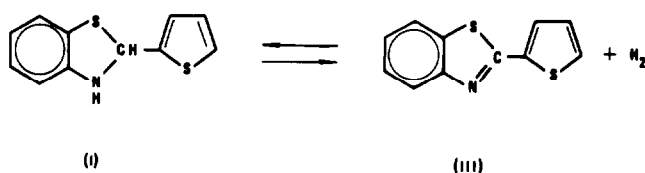
Scheme 1.

assignable to the C–S–C linkage. The synthesis of 2 - (2 - thienyl)benzothiazol (see Experimental) and further comparison of the IR and NMR spectra of both compounds confirm our previous supposition.

The electronic spectrum of (I) (Fig. 1) shows a band at 318 nm ($\epsilon = 12210\ 1.\ mol^{-1}\ cm^{-1}$) and an inflexion (shoulder) at 255 nm ($\epsilon = 9600\ 1.\ mol^{-1}\ cm^{-1}$) which fully support the typical spectrum of the cyclic form of benzothiazoline.[21,22] The position of this band remains unchanged with the pH.

Conversion to the Schiff base form is favoured by treatment of a solution of (I) in ethanol with alkali or sodium ethoxide. The addition of base is accompanied by the appearance of an intense band in the visible region (Fig. 2). We attribute this band to absorption by the sodium salt of the rearranged form (Schiff base) of the ligand (n–π^* or π–π^* transitions of the double bond of the azomethine group). The addition of a large excess of sodium leads to an increase in intensity and a small bathochromic shift of this band. This is in accord with the observations of other authors.[3,4,7,22-24]

Therefore, we conclude that in solution the ligand exists as an equilibrium mixture of (I) and (II) where the benzothiazoline form seems to predominate almost exclusively. There is a partial conversion to the Schiff base form in the presence of a large excess of sodium. This conversion is being studied quantitatively; our results will be reported in due course.

Rearrangement of the ligand in the presence of metal ions

Reaction of a solution of (I) in ethanol with zinc acetate at room temperature yields a red crystalline complex whose composition is $Zn(C_{11}H_8NS_2)_2$. The IR spectrum of this complex does show absorp-
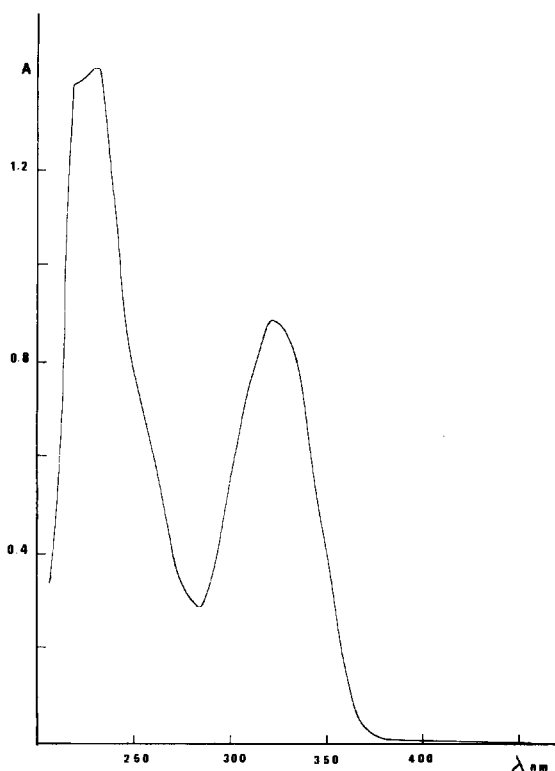
Fig. 1. Electronic spectrum of 2 - (2 - thienyl) benzothiazoline in ethanol (conc. $7'3.10^{-5}$ M).
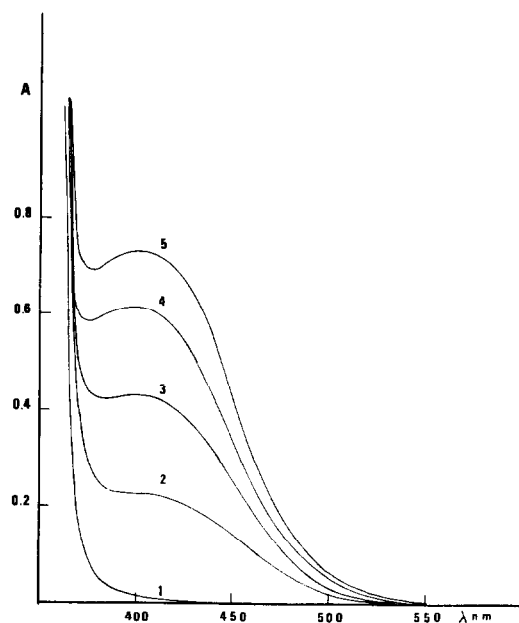
Fig. 2. Absorption spectra of 2 - (2 - thienyl) benzothiazoline (conc. 10^{-3} M): (1) In ethanol; (2) In ethanol containing Na conc. 3×10^{-3} M; (3) *Idem.*, 6×10^{-3} M; (4) *Idem.*, 1.2×10^{-2} M; (5) *Idem.*, 1.8×10^{-2} M.
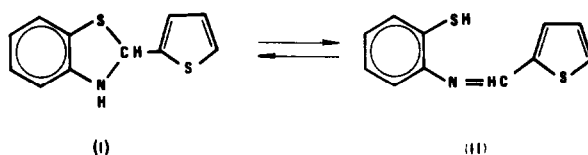
Scheme 2.

tions at 1585, 1566, 1557 and 1548 cm⁻¹ (Table 1) which can be ascribed to imine and aromatic ring vibrations. On the other hand, no C–S–C linkage band (characteristic of the closed ring structure) appears. These results indicate that the zinc ions promote the rearrangement of (I), so that the zinc complex of the tautomeric Schiff base is obtained (Scheme 3).

(IV) was also prepared by reaction of thiophen - 2 - aldehyde with a suspension of bis(o-aminobenzenethiolo) zinc in ethanol. However, the reaction progress slowly and it is difficult to establish its mechanism. Finally, (IV) was obtained by reaction of thiophen - 2 - aldehyde and o-aminobenzenethiol in the presence of zinc acetate. The mass spectrum of (IV) exhibited the band of isotopic peaks centred around the major peaks at m/e 500 (^{64}Zn), 502 (^{66}Zn) and 504 (^{68}Zn).

Reaction of a solution of (I) in ethanol with cadmium acetate yields a yellow compound whose composition is Cd_2 $(C_{11}H_8NS_2)_2$ $(CH_3–COO)$, (V). The IR spectrum of (V) shows two strong broad bands at 1548 and 1410 cm⁻¹ assignable to v(C=O)

and v(C–O) of the carboxylate vibrations, respectively. The position of these bands and the Δv value (138 cm⁻¹) indicate the presence of a bridging acetate group in the molecule of this complex.[25-28] Another important question is to determine the nature of the ligand in this complex. The IR spectrum exhibits no band at 920 cm⁻¹ (in the 1000–900 cm⁻¹ range only two very weak bands appear). The absence of this band suggests that in the presence of Cd ions (I) rearranges to give the Schiff base complex (V) (Scheme 4). The band corresponding to a complexed C=N stretching mode could not be identified because of the presence of a broad intense band (due to the v(C=O) vibration) in the same spectral region. Unfortunately, (V) was insufficiently soluble in nonpolar solvents for NMR studies and insufficiently volatile for mass spectral characterisation.

(V) was also obtained allowing to occur the formation of the ligand (from thiophen - 2 - aldehyde and o-aminobenzenethiol) in the presence of cadmium acetate.

The treatment of a strongly basic solution of (I)

Table 1. Selected IR data[a]

Compound	v N–H, cm⁻¹	Aromatic Vib. and C=N, cm⁻¹				v(C=O), cm⁻¹	v(C–O), cm⁻¹	C–S–C link. vib., cm⁻¹
I	3280 (m)							920 (s)
IV	–	1585(s)	1566(s)	1557(sh)	1548(w)	–	–	–
V	–	1589(w)	1570(w)			1548(s,b)	1410 (s,b)	–
VI	+	1598 (s)	1589(w)	1569(s)	1550(w)	–	–	–
VII	–	1603(s)	1590 (m)	1568(s)	1550(w)	–	–	–
VIII	–	1596(s)		1566(m)	1551(w)	–	–	–

a Key : s, strong ; m, medium ; sh, shoulder ; b, broad ; w, weak
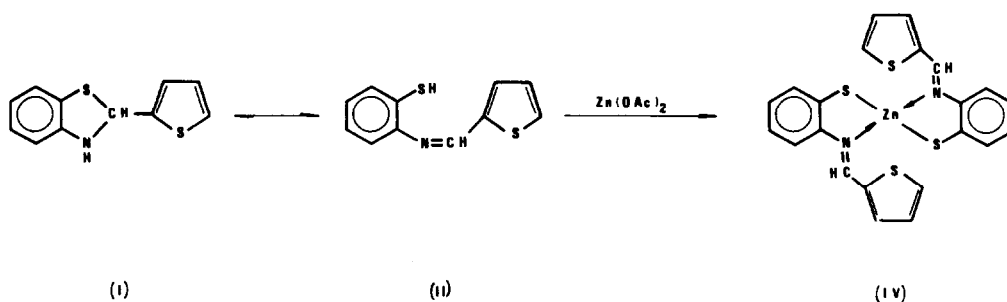
Scheme 3.
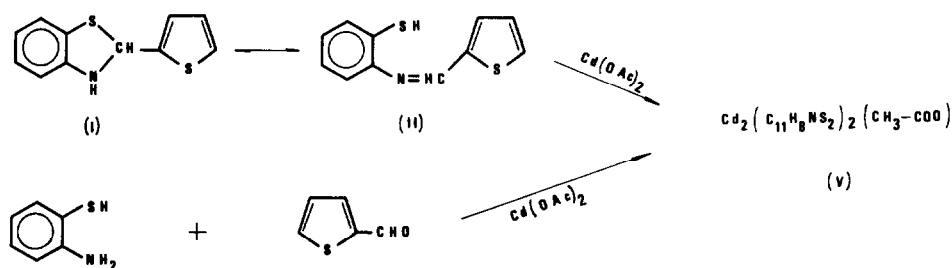
Scheme 4.

in ethanol with cadmium acetate yields (V) from an orange solution. However, the colour of the reaction solution seems to indicate the existence of another different complex. This complex could only be isolated by reaction of a large excess of thiophen-2-aldehyde with a suspension of bis(o-aminobenzenethiolo) cadmium in ethanol. The orange crystalline compound thus obtained has the composition $Cd(C_{11}H_8NS_2)_2$, (VI) (Scheme 5). It can be seen from the IR data (Table 1) that the reaction occurs to yield the corresponding Schiff base complex.

Thiophen - 2 - aldehyde reacted with o-aminobenzenethiol in the presence of mercury and lead acetates, respectively, to give crystalline complexes of the type $M(C_{11}H_8NS_2)_2$. The mercury complex (VII) can also be obtained by reaction of thiophen - 2 - aldehyde with a suspension of bis(o-aminobenzenethiolo) mercury (II) in ethanol (see Experimental). The IR data do show that in

both complexes the ligand has rearranged to the imine form (Scheme 6).

On the other hand, there is no indication in any of the previous complexes of participation in bonding of the thiophen sulphur atom.

As mentioned above the complexes (V), (VI), (VII) and (VIII) are of light colour and (IV) is intense red, and all contain the ligand in the imine form. Lindoy and Livingstone,[3] in a study of the rearrangement of 2-(2-pyridyl)benzothiazoline by metal ions, have pointed out that the light colour of the complexes suggests that the benzothiazoline has not rearranged to the Schiff base. In this case, they have postulated that the solids contain the deprotonated form of benzothiazoline as ligand. In order to find spectral evidences useful in our study, we have synthesized the following complexes of 2 - (2 - pyridyl)benzothiazoline : Acetato (N - 2 - thiolophenyl - 2' - pyridylmethyleneimine) cad-

(VI)

Scheme 5.

M = Hg . VII
M = Pb . VIII
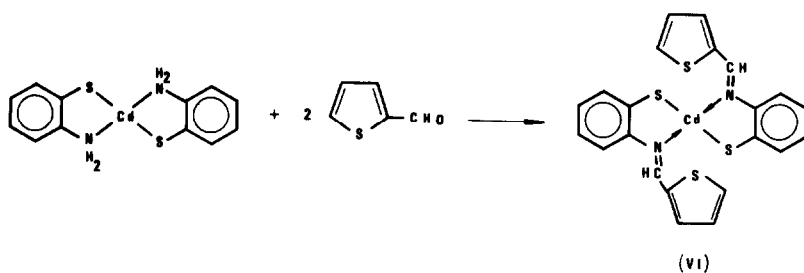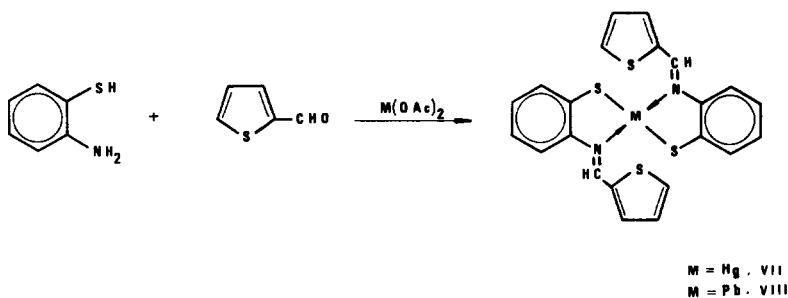
Scheme 6.

mium, **(IX)** (yellow); Chloro 2 - (2 - pyridyl)benzo-thiazolinato cadmium, **(X)** (yellow); Bis (N- 2 - thiolophenyl-2′ - pyridylmethyleneimine) cadmium, **(XI)** (intense red); Acetato bis (N - 2 - thiolophenyl - 2′ - pyridylmethyleneimine) lead (II), **(XII)** (intense red). On the basis of IR and UV–VIS spectra it is not possible distinguish the arrangement of the ligand in each of these complexes. However, from the IR spectra of **(IX)** and **(XII)** we think that a bridging acetate group is present in both complexes [**(IX)**: $v(C=O)$ and $v(C–O)$ appear at 1562 and 1405 cm^{-1} respectively, $\Delta v = 157$ cm^{-1}; **(XII)**: $v(C=O)$ and $v(C–O)$ appear at 1540 and 1400 cm^{-1} respectively, $\Delta v = 140$ cm^{-1}].

Finally, we suggest the use of **(I)** as colorimetric reagent for the ions determination in view of the intense colours of some complexes in DMF (Table 2). Thabet and Tabibian[29] reported a highly sensitive and selective method for the micro-determination of zinc, and we have studied the use of the ligand for determination of Hg(II) by extraction of the complex into chloroform ($\lambda = 364$ nm, $\epsilon = 6200$ l. mol^{-1} cm^{-1}) with successful results.

EXPERIMENTAL

Analyses and physical measurements

Chemical analyses were performed by Department of Analyses and Instrumental Techniques (University of Granada). Conductance measurements were made with a Conductivity Meter Radiometer Type CDM 2e. Thermogravimetric measurements were performed with a Setaram GDTD-10 thermoanalyzer fitted with a B-70 electrobalance with thermocouples of Pt/Pt–Rh in an alumine base. IR spectra were recorded with a Beckman 4240 IR Spectrophotometer in the 4000–250 cm^{-1} range using the KBr pellets technique. UV–VIS spectra were recorded with a Beckman Acta III Spectrophotometer using 1 cm quartz cells. NMR spectra were recorded with a Hitachi Perkin–Elmer

R-20 NMR equipment in CDCl$_3$ using TMS as internal reference. MS spectra were recorded with a Hewlett–Packard 5930 A Mass Spectrometer (70 eV).

Syntheses

2 - (2 - thienyl)benzothiazoline. This ligand was prepared by two routes: (1) As Thabet and Tabibian previously reported.[29] These authors recrystalized the compound from low-boiling petroleum ether. However, we use more successfully a mixture of low-boiling petroleum ether–ethanol (4:1); m.p. 94–95°C; yield 50%. Found: C, 60.66; H, 3.97; N, 6.39. Calc. for C$_{11}$H$_9$NS$_2$:C, 60.24; H, 4.13; N, 6.39%. (2) Thiophen - 2 - aldehyde (0.05 mol) in ethanol (20 cm^3) was added to o-aminobenzenethiol (0.05 mol) in ethanol (20 cm^3). The solution was heated under reflux for 30 min, then allowed to cool and finally 40 cm^3 of distillated water (cooled to 5°C) was added slowly with stirring. The suspension was let stand at 0°C for several hours and by this time a pale yellow crystalline compound had formed. This product was repeatedly washed with a mixture ethanol–water (1:1); m.p. 95–96°C; yield 75%. Found: C, 60.40; H, 4.10; N, 6.45%.

2 - (2 - thienyl)benzothiazol. This compound was prepared using the method of Miller *et al.*[20] in the preparation of other benzothiazoles.

FeCl$_3$ (0.444 g) in ethanol (15 cm^3) was added to 2 - (2 - thienyl)benzothiazoline (0.5 g) in ethanol (20 cm^3). The solution was heated under reflux, then it was allowed to cool at room temperature and distillated water (cooled to 5°C) was added; the product formed as yellow crystals. Found: C, 60.7; H, 3.4; N, 6.6. Calc. for C$_{11}$H$_7$NS$_2$: C, 60.8; H, 3.25; N, 6.45%.

The NMR spectrum of this compound exhibits only a complex multiplet centered at 8.05 ppm.

Bis(N - 2 - thiolophenyl - 2′ - thienylmethyleneimine) zinc. Zinc acetate dihydrate (0.11 g) in ethanol (15 cm^3) was added to 2 - (2 - thienyl) benzothiazoline (0.25 g) in ethanol (20 cm^3). Red crystals of the complex were deposited from an intense red solution. Then, the red crystals were separated by suction, washed with ethanol and distillated water, and dried *in vacuo* over CaCl$_2$; yield 0.114 g (45.3%). Found: C, 52.70; H, 3.27; N, 5.60; Zn, 13.00. Calc. for Zn(C$_{11}$H$_8$NS$_2$)$_2$: C, 52.64; H, 3.21; N, 5.58; Zn, 13.02%.

This compound was prepared as above except that the formation of the ligand from thiophen - 2 - aldehyde and o-aminobenzenethiol (1.25 g) was carried out in the presence of zinc acetate dihydrate (1.12 g) in hot ethanol (40 cm^3); yield 2.1 g. Found: C, 52.80; H, 3.34; N, 5.61; Zn, 12.96%.

Table 2. Electronic spectral data[a]

Compound	λ max nm	$\mathcal{E}$ l.mol^{-1}.cm^{-1}
IV	449	5400
V	426	4850
VI	420	4600
VII	365	6300
VIII	425	1600
XII	487	2150

a Key : In DMF

Finally this compound was also prepared by condensing thiophen - 2 - aldehyde (2 cm³) with a suspension of bis(o-aminobenzenethiolo) zinc† (0.313 g) in ethanol (50 cm³). The resulting suspension was heated for 6 hr. The product formed as red crystals; yield 60%. Found: N, 5.56; Zr 12.95%.

Acetato[bis(N - 2 - thiolophenyl - 2' - thienylmethyleneimine) cadmium]. Cadmium acetate dihydrate (0.14 g) in ethanol (10 cm³) was added to 2 - (2 - thienyl)benzothiazoline (0.23 g) in ethanol (20 cm³). A pale yellow compound was deposited from intense orange solution. The complex was separated by suction, washed with ethanol and ethanol–water (1:1), and dried *in vacuo* over CaCl₂; yield 0.43 g (48.9%). Found: C, 40.10; H, 2.9; N, 3.76; Cd, 31.00. Calc. for Cd₂(C₁₁H₈NS₂)₂–(CH₃COO): C, 40.01; H, 2.66; N, 3.89; Cd, 31.20%.

This compound was also prepared as follows: thiophen - 2 - aldehyde (0.46 g) and o-aminobenzenethiol (0.53 g) were refluxed together in ethanol (20 cm³) for 5 min. Cd(CH₃COO)₂. 2H₂O (0.82 g) in ethanol (20 cm³) was then added and the mixture was heated for 20 min. The mixture was then cooled and filtered. The pale yellow compound obtained was washed with ethanol–water (1:1), and dried *in vacuo* over CaCl₂; yield 60%. Found: C, 40.20; H, 2.84; N, 3.8; Cd, 30.9%.

Bis (N - 2 - thiolophenyl - 2' - thienylmethyleneimine) cadmium. This compound was prepared by condensing thiophen - 2 - aldehyde (4 g) with a suspension of bis(o-aminobenzenethiolo) cadmium† (0.5 g) in ethanol (40 cm³). The resulting suspension was refluxed for 8 hr. The product formed as orange crystals was filtered and washed with ethanol; yield 60%. Found: C, 48.23; H, 2.84; N, 4.96; Cd, 21.00. Calc. for Cd(C₁₁H₈NS₂)₂: C, 48.13; H, 2.94; N, 5.10; Cd, 20.47%.

Bis (N - 2 - thiolophenyl - 2' - thienylmethyleimine) mercury(II). This compound was prepared allowing that the formation of the ligand from thiophen - 2 - aldehyde (0.22 g) and o-aminobenzenethiol (0.25 g) was carried out in the presence of mercury acetate (0.32 g) in hot ethanol (50 cm³). The complex formed as yellow crystals; yield 0.383 g (60%). Found: C, 42.00; H, 2.63; N, 4.44. Calc. for Hg(C₁₁H₈NS₂)₂: C, 41.5; H, 2.53; N, 4.4%.

This compound was also prepared by condensing thiophen - 2 - aldehyde (1.5 g) with a suspension of bis (o-aminobenzenethiolo) mercu-

ry(II)† (0.5 g) in ethanol (30 cm³); yield, 100%. Found: C, 41.8; H, 2.59; N, 4.40%.

Bis (N - 2 - thiolophenyl - 2' - thienylmethyleneimine) lead(II). Thiophen - 2 - aldehyde (1.1 g) and o-aminobenzenethiol (1.2 g) were refluxed together in ethanol (30 cm³) for 5 min. Pb(CH₃–COO)₂·3H₂O (1.86 g) in ethanol–water (5:1, 30 cm³) was then added and the mixture was refluxed for a further 30 min. The resulting solution was cooled at room temperature. The orange–yellow product which precipitated was filtered off, washed with ethanol–water and dried *in vacuo* over CaCl₂; yield, 60%. Found: C, 40.76; H, 2.64; N, 4.35; Pb, 32.73. Calc. for Pb(C₁₁H₈NS₂)₂: C, 41.04; H, 2.50; N, 4.35; Pb, 32.18%.

Aceto [bis (N - 2 - thiolophenyl - 2' - pyridylmethyleneimine) lead (II)]. Pyridine - 2 - aldehyde (1.6 g) and o-aminobenzenethiol (1.9 g) were refluxed together in ethanol (20 cm³) for 10 min. Pb(CH₃–COO)₂. 3 H₂O (4.8 g) in ethanol–water (6:1, 35 cm³) was then added and the mixture was refluxed for a further 60 min. The intense red solution was let stand at 0°C for several hours. The complex formed as intense red crystals; yield; 60%. Found: N, 6.20; Pb, 46.16. Calc. for Pb₂(C₁₂H₉N₂S)₂(CH₃–COO): N, 6.23; Pb, 46.04%.

Bis (N - 2 - thiolophenyl - 2' - pyridylmethyleneimine) cadmium. Cd(NO₃)₂·4H₂O (0.16 g) in ethanol (10 cm³) was added to an alkaline solution of 2 - (2 - pyridyl)benzothiazoline (0.22 g) in ethanol (25 cm³). Intense red crystals of the complex were deposited from a deep red solution; yield, 60%. Found: N, 10.20; Cd, 21.12. Calc. for Cd(C₁₂H₉N₂S)₂: N, 10.39; Cd, 20.85%.

Acetato (N - 2 - thiolophenyl - 2' - pyridylmethyleneimine)cadmium. This compound was prepared as previously described.³ Found: N, 7.8; Cd, 31.76. Calc. for C₂₆H₂₁N₄O₂S₂Cd₂: N, 7.88; Cd, 31.64%.

Chloro 2 - (2 - pyridyl)benzothiazolinato cadmium. This compound was prepared as previously described.³ Found: N, 7.70; Cd, 31.8. Calc. for C₁₂H₉N₂SCdCl: N, 7.76; Cd 31.12%.

Molar conductance data (ohm⁻¹ cm² mol⁻¹)*in DMF at* 25°C. (IV), Λ = 3; (V), Λ = 2.8; (VI), Λ = 0.5; (VII), Λ = 2; (VIII), Λ = 2.5; (XII), Λ = 2.4. In view of Λ_M values, the complexes can be regarded as non-electrolytes.

REFERENCES

¹R. G. Charles and H. Freiser, *J. Organometal Chem.* 1953, **18**, 422.

²H. Jadamus, Q. Fernando and H. Freiser, *J. Am. Chem. Soc.* 1964, **86**, 3056.

†This compound was prepared as previously described.²

[3] L. F. Lindoy and S. E. Livingstone, *Inorg. Chim. Acta* 1967, **1**, 365.

[4] E. Uhlemann and V. Pohl, *Z. Chem.* 1969, **9**, 385; ibid *Z. anorg. allg. chem.* 1973, **397**, 162.

[5] P. Pfeiffer, W. Offermann and A. Werner, *J. Prakt. Chem.* 1942, **159**, 313.

[6] L. F. Lindoy and S. E. Livingstone, *Inorg. Chem.* 1968, **7**, 1149.

[7] E. Bayer and E. Breirmaier, *Chem. Ber.* 1969, **102**, 728.

[8] C. J. Jones and J. A. McCleverty, *J. Chem. Soc. (A)* 1971, 38.

[9] L. F. Lindoy and D. H. Busch, *J. C. S. Chem. Comm.* 1972, 683; *Inorg. Chem.* 1974, **13**, 2494.

[10] S. E. Livingstone and J. D. Nolan, *J. C. S. Dalton* 1972, 218.

[11] J. R. Dilworth, C. A. McAuliffe and B. J. Sayle, *J. C. S. Dalton* 1977, 849.

[12] D. C. Liles, M. McPartlin and P. A. Tasker, *J. Am. Chem. Soc.* 1977, **99**, 7704.

[13] T. J. Kemp, P. A. Lampe, P. Moore and G. R. Quick, *J. C. S. Dalton* 1981, 2137.

[14] M. C. Thompson and D. H. Busch, *J. Am. Chem. Soc.* 1964, **86**, 213.

[15] L. F. Lindoy, *Quarterly Reviews* 1971, **XXV**, No. 3, 379.

[16] F. Capitán, F. Salinas and L. F. Capitán-Vallvey, *An. Quim.* 1977, **73**, 1308; ibid 1978, **74**, 276.

[17] F. Capitán, F. Salinas and L. F. Capitán-Vallvey, *Bull. Soc. Chim. France* 1979, **1–2**, 36; ibid 1979, **5–6**, 185.

[18] F. Capitán, F. Salinas and L. F. Capitán-Vallvey, *Bull. Soc. Quim. Perú* 1977, **XLIII**, (2), 69.

[19] C. A. Rice, C. G. Benson and C. A. McAuliffe, *Inorg. Chim. Acta* 1982, **59**, 33.

[20] P. E. Miller, G. L. Oliver, J. R. Dann and J. W. Gates, *J. Org. Chem.* 1957, **22**, 664; C. A. 52, 2031 e.

[21] F. J. Goetz, *J. Heterocyclic Chem.* 1968, **5**, 509.

[22] R. K. Sharma, R. V. Singh and J. P. Tandon, *J. Inorg. Nucl. Chem.* 1980, **42**, 1267.

[23] E. Bayer, *Angew. Chem.* (Int. Edit.) 1964, **3**, 325.

[24] S. N. Poddar and N. S. Das, *Indian J. Chem.* 1976, **14A**, 589.

[25] K. Itoh and H. J. Bernstein, *Can. J. Chem.* 1956, **34**, 170.

[26] M. Kato, H. B. Jonassen and J. C. Fanning, *Chem. Rev.* 1964, **64**, 99.

[27] M. M. Aly and Z. H. Khalil, *J. Inorg. Nucl. Chem.* 1980, **42**, 1261.

[28] L. F. Capitán-Vallvey, C. Jimenez and L. Cuadros, *Can. J. Chem.* 1982, **60**, 1713.

[29] S. Thabet and O. Tabibian, *Anal. Chim. Acta* 1966, **34**, 228; S. Thabet and P. W. West, *Anal. Chim. Acta* 1967, **37**, 246.

[30] M. Conte, R. Guglielmetti and J. Metzger, *Bull. Soc. Chim. France* 1967, **8**, 2834.

METAL CHELATES OF AZO-PYRIDAZINE DYES—II

CHELATING TENDENCIES OF DIACETYL-, BENZIL- AND BENZOYLETHANE-MONOHYDRAZONE-3-HYDRAZINO-4-BENZYL-6-PHENYLPYRIDAZINE

EMIL N. RIZKALLA*
Faculty of Science, Ain Shams University, Abbassia, Cairo, Egypt

and

ATEF A. T. RAMADAN and MAGDY H. SEADA
Faculty of Education, Ain Shams University, Roxy, Cairo, Egypt

Abstract—The diacetyl-(DAHP), benzil-(BHP) and benzoylethane-(BEHP) derivatives of 3-hydrazino-4-benzyl-6-phenylpyridazine have been prepared and characterized. Their acid-base properties and their equilibria with transition metal ions in 75% dioxan–water solvent at 30°C have been investigated by pH titrimetry. The role of proton and metal ion solvation by the organic solvent has been discussed in view of the results obtained for the lanthanide-BHP systems in different media. Probable structures of the metal chelates are given based on potentiometric data and spectral results for the solid copper chelates. The possibility of forming MHL species were inferred from electronic absorption measurements at different pH values. The use of BHP as an analytical reagent for the determination of copper spectrophotometrically or as a metallochrom indicator in the complexometric titration of Cu(II) ion is also discussed.

Previous studies[1] in this laboratory of the sequestering properties of benzoylacetone derivative of 3-hydrazino-4-benzyl-6-phenylpyridazine (BAHP, structure I) with transition and lanthanide metal ions have demonstrated quantitatively the capability of forming *bis*-chelates with the ligand behaving as a monoprotic acid. Under drastic conditions of reflux with copper salts, the ligand loses two gram equivalents of hydrogen-probably those of the enolic and hydrazo groups-and behave as a diprotic species.

These class of compounds are related structurally to the corresponding azo-pyrazolone dyes (structure II)[2,3] and differs only in the positions of the azo (or hydrazo) group relative to the nitrogenous nucleus. Although both types of ligands are capable of forming strong (N=N)→M bonds, however, the simultaneous participation of the pyrazolone ring nitrogen in the coordination

with the metal ion is questionable particularly in the presence of an acidic or basic group (A) ortho to the azo group.

I
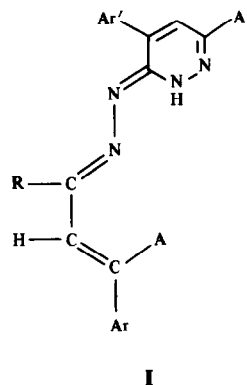
In the present report, the chelating ability of the diacetyl (DAHP), benzoylethane (BEHP) and benzil (diphenylethanedione; BHP) derivatives of the chromophoric nucleus 3-hydrazino-4-benzyl-6-

---

*Author to whom correspondence should be addressed.

II
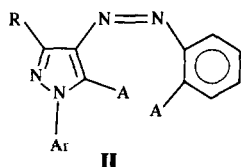
phenylpyridazine have been measured. Each compound retains at least a portion of the basic structure of **BAHP**, namely the hydrazino-pyridazine group but substituting the β-diketone with either a ketonic compound or a diketyl derivative.

crystals obtained were filtered, washed with ethanol and recrystallised from benzene. The average yield in each case is approx. 70%. The elemental analysis results for C, H and N are shown in Table 1.

(ii) *Preparation of the copper complexes*

A mixture of equimolar amounts of the ligand and copper nitrate in 75% dioxan–water solvent was refluxed for 30 min. After a while, the complex separated as a purple solid. This was filtered, washed with ether and dried under vacuum. The full analysis of the species prepared is shown in Table 1.

III   **IV**

DAHP $(X = CH_3 —$; $Y = CH_3 — \overset{O}{\overset{\|}{C}} —$);

BEHP $(X = C_2H_5 —$; $Y = C_6H_5$);

BHP $(X = C_6H_5 —$; $Y = C_6H_5 — \overset{O}{\overset{\|}{C}} —$);
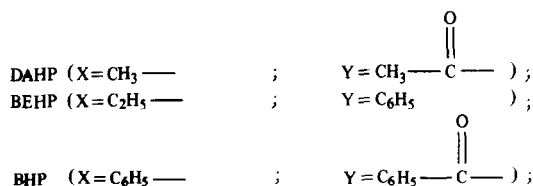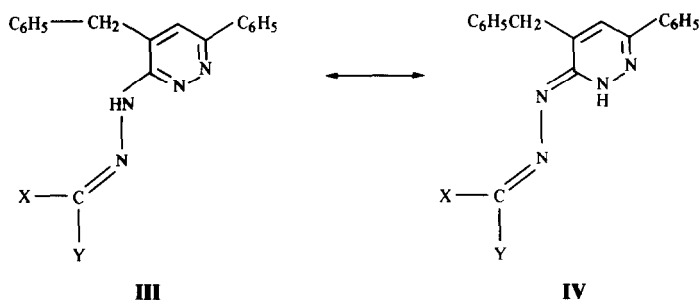
EXPERIMENTAL

(i) *Preparation of the solid ligands*

DAHP, BEHP and BHP were prepared by refluxing an ethanolic solution of the 3-hydrazino-pyridazine derivative[4] with the stoichiometric amounts of diacetyl, benzoylethane or benzil solution in ethanol, for 1 hr. The yellow

(iii) *Reagents and materials*

Stock solutions of the metal nitrates were prepared and standerdised using EDTA in the presence of a suitable indicator.[5] Purification of dioxan was carried out as described earlier.[1] Methanol was purified by refluxing the commercial products with barium oxide for few hours followed

Table 1. Analytical data for the ligands and their copper complexes

Species and Formula	%C		%H		%N		%M	
	Calc	Found	Calc	Found	Calc	Found	Calc	Found
DAHP ; $C_{21}H_{20}N_4O$	73.26	72.99	5.81	5.79	16.28	16.17		
BEHP ; $C_{26}H_{24}N_4$	79.59	79.53	6.12	6.05	14.29	14.23		
BHP $C_{31}H_{24}N_4O$	79.49	79.51	5.13	5.10	11.97	12.00		
$Cu(BEHP)(NO_3)(H_2O)$	58.37	58.31	4.68	4.66	13.10	13.04	11.88	11.82
$Cu(BHP)(NO_3)(H_2O)$	60.93	61.22	4.10	4.09	11.47	11.45	10.40	10.45

by distillation.[6] Dimethylformamide was purified by following the procedure recommended by Mo-skalyk, et al.[7] Acidic impurities of formic acid were removed by stirring the crude reagent with Dowex-1 resin in the hydroxyl form.

(iv) Procedures

Potentiometric titrations and the experimental conditions are essentially the same as described in the first part of this series.[1] The temperature was 30°C and the ionic strength was maintained at 0.10 M with KNO_3. In all cases, the metal to ligand ratio was kept at 1:2 with the metal concentration 10^{-3} M. All the measurements were taken either in 75% (v/v) dioxan–water, dimethylformamide–water or methanol–water solvent. In the case of dioxan–water solvent measurements, the value of

hydrogen ion concentration was derived from pH values after adding a correction of 0.28.[8] Values of the activity coefficients, γ_+, for the hydrogen ion in methanol–water or DMF–water were calculated from the extended Debye–Hückel equation

$$\log \gamma_+ = -\frac{|Z_1 Z_2| 1.29 \times 10^6 \sqrt{2\mu}}{(\epsilon T)^{3/2}} \Big/ \left(1 + \frac{35.56°\alpha°\sqrt{2\mu}}{(\epsilon T)^{1/2}}\right)$$

where, μ = ionic strength, T = absolute temperature, Z_1 and Z_2 are the charges for the positive and negative ions and $\alpha°$ = the mean ionic parameter. The value of 6 Å was used for $\alpha°$.[10] The dielectric constant, ϵ, for the mixed solvent was calculated using the relationship
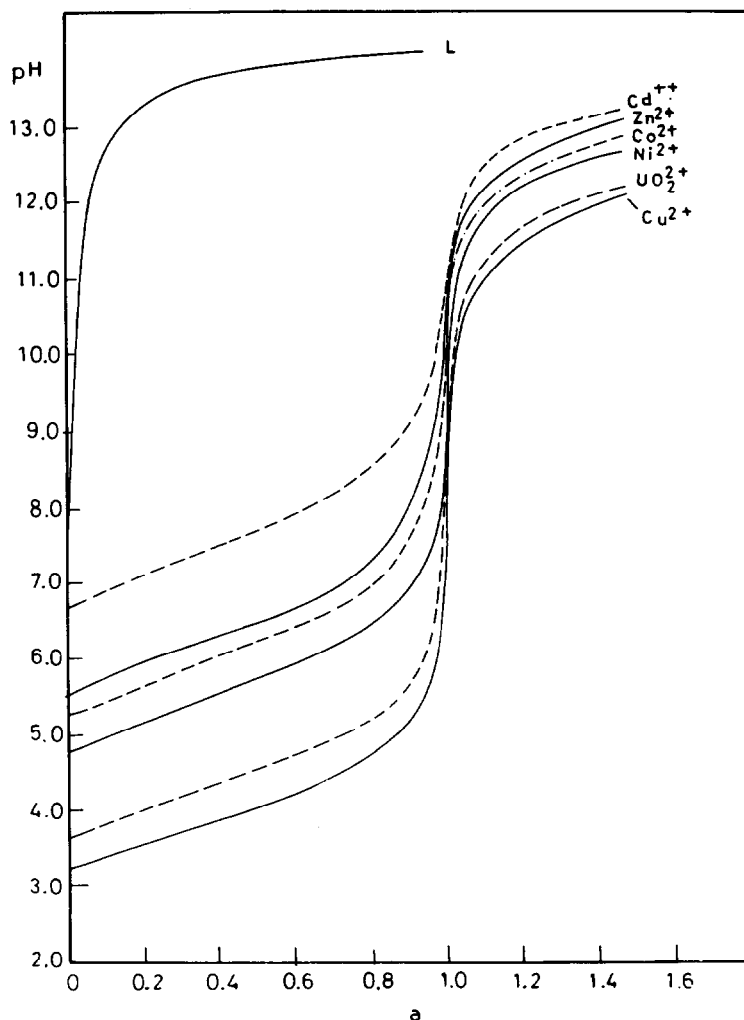
Fig. 1. Potentiometric Titration cruves of BHP and its complexes with Co(II), Ni(II), Cu(II), Zn(II), Cd(II) and UO_2^{2+} ions at 30°C in 75% dioxan–water solvent. [L] = Free ligand, a = moles of base added per mole of BHP, [M] = 10^{-3} M; [L] = 2×10^{-3} M.

$$P_{12} = P_1 f_1 + P_2 f_2$$

$$= f_1 (M_1/d_1)\left(\frac{\epsilon_1 - 1}{\epsilon_1 + 2}\right) + f_2 (M_2/d_2)\left(\frac{\epsilon_2 - 1}{\epsilon_2 + 2}\right)$$

$$= \frac{\epsilon - 1}{\epsilon + 2} \cdot \frac{f_1 M_1 + f_2 M_2}{d_{12}}$$

where P_i = molar polarization, f_i = mole fraction, M_i = molecular weight and d = density.

The final values obtained for γ_+ are 0.619 and 0.615 in the case of methanol–water and DMF–water respectively.

IR spectra were recorded on a Perkin–Elmer 437 spectrometer ($4000-300\ cm^{-1}$) using potassium bromide discs. The electronic spectra were measured with a prolabo UV-visible spectrometer using 1 cm matched quartz cells and at 25°C.

RESULTS

(i) Potentiometric results

Representative plots for the titration curves of BHP ligand in the absence and in the presence of divalent metal ions are shown in Fig. 1. Closely related plots were also obtained for either the same ligand in different solvents or for other ligands in 75% (v/v) dioxan–water solvent. In all cases, the

metal–ligand titration curves show the presence of an inflection at $a = 1$ (a = moles of base added per mole of ligand). This suggests that the ligands are only monoprotic through the dissociation of the hydrazo group hydrogen. The values of the acid dissociation constants, K^H were calculated as described previously[1] and are summarised in Table 2.

The titration curves of DAHP and BEHP ligands in the presence of copper(II) ions showed a distinct inflection at $m = 1$ (m = moles of base added per mole of metal ion) in addition to that at $m = 2$ to account for the stepwise formation of ML and ML_2 species. Such features were not observed with other cations where only one overlapping buffer region between $m = 0$ to $m = 2$ was observed. The calculation of the overall equilibrium constants were carried out using standard procedures based on the calculation of the average number of ligand bound per metal ion, $\bar{n}_L$ and the free ligand concentration, [L], then minimising the residuals in the equation,

$$\frac{\bar{n}_L}{(1 - \bar{n}_L)[L]} + \beta_{102} \frac{(\bar{n}_L - 2)[L]}{(1 - \bar{n}_L)} - \beta_{101} = 0$$

using a least squares method.

Table 2. Acid dissociation constants for the ligands DAHP, BEHP and BHP

Ligand	log K^H		
	Dioxan-water	Methanol-water	DMF-water
DAHP	12.94		
BEHP	13.75		
BHP	13.72	11.07	11.52

Table 3(a). Formation constants for DAHP, BEHP and BHP complexes with the divalent metal ions. (30°C, $\mu = 0.10$ M KNO_3)

Metal Ion	DAHP*		BEHP*		BHP*		BHP**	
	log β_{101}	log β_{102}	log β_{101}	log β_{102}	log β_{101}	log β_{102}	log β_{101}	log β_{102}
Co^{2+}	10.62	20.24	10.13	--	10.14	19.70	6.99	13.34
Ni^{2+}	11.07	21.25	9.30	17.88	10.61	20.67	7.48	14.37
Cu^{2+}	12.12	23.43	11.41	21.20	12.32	24.12	9.50	17.73
Zn^{2+}	10.21	19.48	8.97	--	9.82	19.11	6.78	12.89
Cd^{2+}	9.41	17.78	7.78	--	8.65	16.70	6.37	12.15
UO_2^{2+}	11.77	22.63	11.81	--	11.80	23.09	8.90	16.67

* Measurements were obtained in 75% dioxan-water solvent.

** Measurements were obtained in 75% DMF-water solvent.

The log of the formation constants of the divalent metal ion complexes with the different dyes are presented in Table 3(a). Values of $\log \beta_{102}$ for the bis chelates of Co, Zn, Cd and UO_2 ions with BEHP are not included because of the tendency of these species to hydrolyse in the region of its formation. For the same reason, only the values of $\log \beta_{101}$ are quoted in Table 3(b) for the lanthanide complexes with BHP in the different solvents.

(ii) *Spectral results*

The absorption characteristics of the free ligands resemble basically those of BHP[1]. The $\pi \rightarrow \pi^*$ transition shows a marked bathochromic shift accompanied by a decrease in the absorption intensity in the case of DAHP, whereas for the benzil derivative, the molar absorptivity is slightly enhanced compared to that of BAHP. A parallel behaviour was also observed for the trend in

Table 3(b). Formation constants for BHP complexes with lanthanide ions at 30°C; $\mu = 0.10$ M KNO_3

Metal Ion	$\log \beta_{101}$		
	DMF-water 75% (v/v)	Methanol-water 75% (v/v)	Dioxan-water 75% (v/v)
La^{3+}	5.52	6.55	8.19
Ce^{3+}	5.63	6.75	8.35
Pr^{3+}	5.74	6.95	8.52
Nd^{3+}	5.91	7.31	8.73
Sm^{3+}	6.08	7.65	9.05
Eu^{3+}	6.28	7.70	9.25
Gd^{3+}	6.39	7.61	9.14
Tb^{3+}	6.29	7.59	9.08
Dy^{3+}	6.43	7.67	9.52
Ho^{3+}	6.49	7.75	9.78
Er^{3+}	6.54	7.78	9.99
Tm^{3+}	6.63	7.79	10.04
Yb^{3+}	6.68	7.87	10.08
Lu^{3+}	6.64	7.74	10.01

Table 4. Absorption spectra of the ligands and their metal complexes in 75% dioxan–water solvent

Species	max nm	$\log \epsilon$ *	Assignment
H(DAHP)	255	4.42	$\pi \rightarrow \pi^*$, (K-Band)
	360	4.27	$n \rightarrow \pi^*$, (R-Band)
H(BHP)	250	4.74	$\pi \rightarrow \pi^*$, (K-Band)
	360	4.41	$n \rightarrow \pi^*$, (R-Band)
H(BAHP)	220	4.65	$\pi \rightarrow \pi^*$, (K-Band)
	291	4.26	$n \rightarrow \pi^*$, (R-Band)
Ni-BHP	510	3.78	$\pi \rightarrow d$
	535 sh	3.71	$d \rightarrow \pi$
Co-BHP	580(broad)	3.60	$d \rightarrow \pi$
Cu-BHP	530	4.00	$d \rightarrow \pi$
Co-DAHP	440-480 sh.	3.16-3.40	$\pi \rightarrow d$
	510-520 sh.	3.58-3.62	
	540	3.67	$d \rightarrow \pi$
Cu-DAHP	463-472 sh.	3.49-3.56	$\pi \rightarrow d$
	492	3.67	$d \rightarrow \pi$
UO_2-DAHP	550(broad)	3.50	CT

* Values for the metal complexes are apparant and estimated for the 1:2 metal : ligand ratio except for UO_2-DAHP where the ratio is 1:1.

$n \to \pi^*$ transition. Table 4 summarises all the results obtained. At fixed ligand concentration, the absorbance was found to be pH dependent with a slight blue shift in the absorption maxima at high alkali concentration, $(-\log[H^+] = 12 - 14)$. The results were analysed for the calculation of the dissociation constant of BHP in 75% dioxan–water using the following equation[11],

$$A = A_L - \frac{[H^+](A - A_{HL})}{K^H}$$

where A, A_L and A_{HL} stands for the absorption of the mixture, anionic and neutral dye species respectively. The value of $\log K^H$ obtained was found to be 13.78 compared to 13.72 as obtained potentiometrically.

The UV spectral properties of the metal complexes are similar to that of the proton complex with a significant lowering in ϵ_{max} and a blue shift in λ_{max}(20 nm). In the visible region, the spectra of the complex solutions displayed an additional assymetric band as is shown in Fig. 2.

The solid ligands and their copper complexes were characterised by infrared spectroscopy. Important band groups and their assignments are summarised in Table 5.

(iii) Analytical studies

BHP was used as a reagent for the determination of copper(II) ions by means of three different ways.

In the first method, absorbances were recorded for Cu(II) solutions $(0.6$–$6.0 \mu g/cm^3)$ in the presence of sufficient excess of the reagent and at the wavelength 530 nm. The results adhere well to Beer–Lambert law with a standard deviation of 0.004. Alternatively, the purple coloured Cu–BHP (1:1) mixture was titrated spectrophotometrically at λ_{max} using standard EDTA solution as the titrant
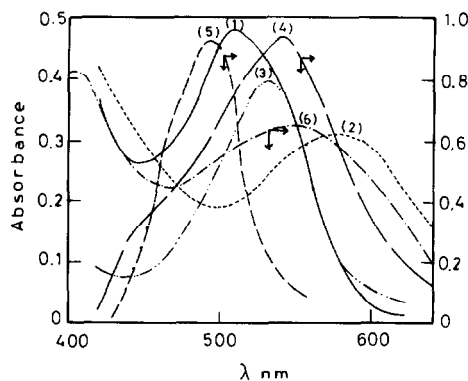
Fig. 2. Electronic absorption spectra of M-BHP and M-DAHP Chelates in 75% dioxan-water at the optimum pH. (1) [Ni] = 8×10^{-5}M; [BHP] = 16×10^{-5}M. (2) [Co] = 8×10^{-5}M; [BHP] = 16×10^{-5}M. (3) [Cu] = 4×10^{-5}M; [BHP] = 8×10^{-5}M. (4) [Co] = 1×10^{-4}M; [DAHP] = 2×10^{-4}M. (5) [Cu] = 1×10^{-4}M; [DAHP] = 2×10^{-4}M. (6) [UO$_2$] = 1×10^{-4}M; [DAHP] = 1×10^{-4}M.

Table 5. Selected band groups in the IR spectra and their tentative assignments, cm^{-1}

Assignment	DAMP	BEHP	BHP	Cu-BEHP	Cu-BHP
ν_{HOH}				3381 sb	3300-3500 sb
ν_{NH}	3220 mb	–	3250wb	–	–
ν_{CH}	2920 m	3015m	3016 m	3000m	3048 m
		2944m	2977 m		
$\nu_{C=O}$	1632 s	–	1640 s	–	–
$\nu_{C=C}, \nu_{C=N}$	1583 s	1588 m	1600 s	1568 s	1580 s
	1570 s		1544 s		1565 s
$\nu_{N=N}$	1420 s	1436 s	1400 m	1392 s	1390 m
ν_{M-O}				512 w	652 w
$\nu_{MN}, \nu_{MN'}$				488 m	488 m
				412 m	436 m

s = strong; m = medium; w = weak; b = broad.

and both the titrant and titrand were buffered to pH 8. Finally, when a few crystalls of the solid ligand were added to a warm solution of Cu(II) (0.02–0.10 M), a purple colour was obtained which turns bluish green at the equivalent point when titrating with a standard EDTA solution. In the latter case, BHP serves as indicator. The results obtained are in excellent agreement with those obtained following standard procedures.

All measurements were carried out in 75% dioxan–water solvent.

DISCUSSION

(i) Protonation equilibria

Among the various tautomeric forms of BAHP, tautomer **I** has been shown to adhere well with both spectral and potentiometric results.[1] Further evidence for this assignment is gained from the results reported here for the homologous species DAHP, BHP and BEHP. The presence of a strong ketocarbonyl stretching, $v(C = O)$ at 1630–1640 cm^{-1} and a broad band in the region of 3220–3250 cm^{-1} assigned to $v(N–H)$ suggests that the keto form of BHP and DAHP (structure **IV**) is the dominant one. This is supported by the absence of the bands characteristic of the OH group stretching frequency in the IR spectra of the two species.

A comparison of the pK^H value of BAHP with those obtained for DAHP, BEHP and BHP under similar experimental conditions, reflects at least partially, the differences in the basicity of the enolic OH group of the benzolylacetone segment in BAHP and the protonated pyridazine nitrogen in the other cases. The difference amounts to one log unit in the case of DAHP and 1.8 log units for BEHP and BHP species. The lower basicity of DAHP is accounted for by the stabilization of the anionic ligand by the coplanarity of the whole conjugated system. The non-coplanarity of the two phenyl groups as imposed by the stereochemistry of the benzil segment in BHP is also indicated from the relatively low molar absorptivity of this species.

It has been shown by Kole and Chaudhury[10] that protonation constants in mixed aqueous solvents decreases with, (a) increasing the dielectric constant of the solvent; (b) decreasing the extent of hydrogen bonding in water by the organic solvent and (c) increasing the proton solvation by the organic solvent. These effects are prominent at solvent contents greater than 60%. It has been indicated also[12] that dioxan molecules progressively breakdown the hydrogen bonded structure of water whereas, methanol can form hydrogen bonded associations with water. This effect in addition to the low dielectric constant of dioxan–water solvent compared to that of methanol–water or DMF-water would perhaps rationalise the relative pK^H values of BHP in the different solvents as is shown in Table 2.
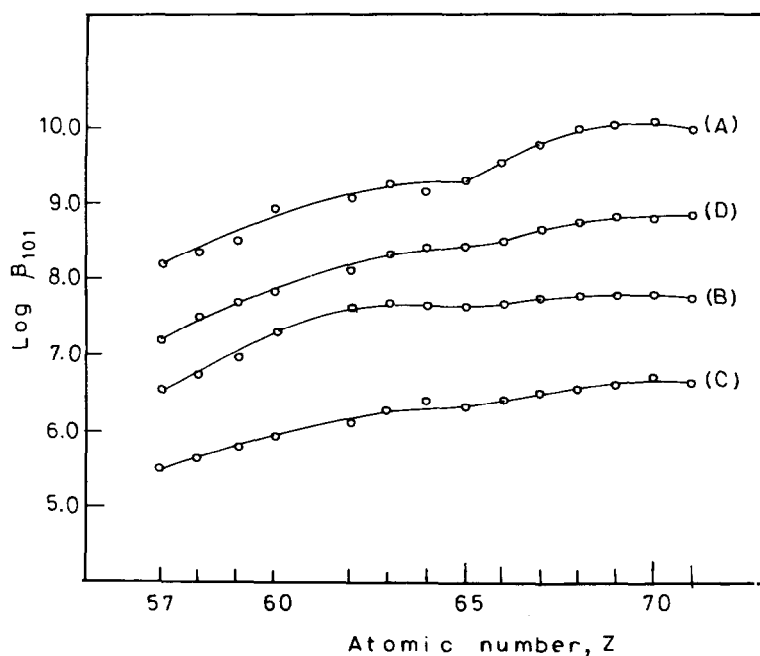
Fig. 3. Log β_{ML} as a function of the atomic number Z for the various rare earth complexes. (A) Ln–BHP in 75% dioxan–water. (B) Ln–BHP in 75% methanol–water. (C) Ln–BHP in 75% DMF-water. (D) Ln–BAHP in 75% dioxan–water.

(ii) Complexation studies

The role of metal solvation is apparent in the comparison of the equilibrium constants, β_{101} for the different lanthanide-BHP chelates in the various solvents (see Table 3(b)). Although the order of increasing $1/\epsilon$ values of the media is,

dioxan–water > methanol–water $\simeq$ DMF–water

the values of β_{101} are markedly greater in methanol-water than in DMF-water. This is perhaps, due to the strong solvating power of methanol over DMF to the lanthanide ions which are hard acids.

The trend in the formation constants of Ln-BHP complexes reported here are much the same as reported previously for BAHP ligand (see Fig. 3). The major differences between both systems are related to the difference in basicities of the two ligands which determine the absolute magnitude of β_{101} values and also to the size of the chelate ring formed.

With azo ligands, the azo group can coordinate to lanthanide and actinide ions, particularly when additional complex stabilization is afforded by the presence of a second donor atom in a position favourable for chelation. Thus, in the isostructural PAR complexes [4-(2-pyridylazo)resorcinol], the uranyl ion was shown to coordinate to the pyridine nitrogen, the azo nitrogen farthest from the pyridine nitrogen, and the ortho phenolic group, forming a tridentate 1:1 chelate.[13] Based on similarity in ligand structure, it is expected that BHP and DAHP form complexes of a similar nature. However, a comparison of β_{101} values with those reported for PAR or PAN analogues[14] suggest that BHP and DAHP act as rather bidentate ligands. The complete disappearance of the carbonyl stretching band in the IR spectra of the solid UO$_2$-BHP and UO$_2$-DAHP complexes[15] is indicative of a chelation with the enolic form (Structure V).

$$Ar = C_6H_5$$
$$Ar' = C_6H_5 CH_2 ——$$
$$X = C_6H_5 \text{ (in BHP)}$$
$$= CH_3 \text{ (in DAHP)}$$

V
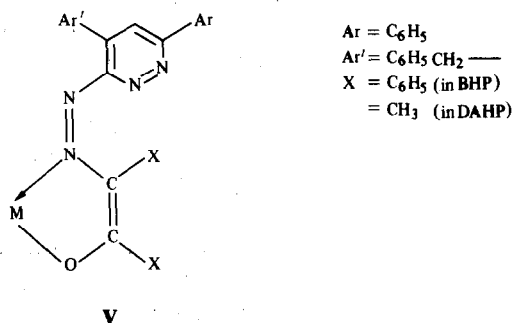
With transition elements, the relative stabilities of the 1:1 metal complexes are the same for the three ligands and are in agreement with the order found with other ligands, Cu(II) > Ni(II) > Co(II) > Zn(II) > Cd(II) except with BEHP where Ni(II) and Co(II) exchange places.

The copper(II) complexes were isolated from solution as the monohydrate 1:1 chelate, CuL(H$_2$O). Attempts to isolate the 1:2 chelates were unsuccessful. However, evidences are obtained from both potentiometric and spectral data for the presence of the 1:2 species in solution. The absence of the ketocarbonyl stretching, $v(C = O)$, and the observed shift in $v(C = N)$ and $v(N = N)$ in the IR spectra of Cu–BHP suggests the formation of a chelate of similar structure to that given above. The change in band position can be attributed to the shift of electron density when the ligand behaves as a bidentate N, O-donor.

The behaviour of BEHP appears curious at first. The ligand forms complexes with the transition elements of a comparable stability to those formed with BHP, BAHP and DAHP which suggest the participation of the available two donor centers (the azo and the pyridazine ring nitrogens) in coordination. If that is acceptable, then the only reason for the non-participation of the BHP/or DAHP pyridine nitrogens in bonding to metal ions is perhaps the preferable trans-arrangement of the vinyl and pyridazine moieties around the azo group which give no access of the simultaneous coordination of the three sites with the metallic centre.

The UV-visible spectra of the different complex systems show the presence of a complex band in the region of 440–580 nm. The intensity of this band is a function of both the molar ratio and the pH of the medium. With nickel and copper species, two overlapping exist in the pH region 3–6, whereas for cobalt complexes, the two absorption maxima are quite separate. Plots of the mole fraction (α_{ML} and α_{ML_2}) calculated from potentiometric data are also presented for the sake of comparison. Obviously, even in the absence of CoL or CoL$_2$ species or in the presence of insignificant concentrations of CuL or CuL$_2$ complexes, i.e. in moderately acidic media, the mixture of the metal and the ligand absorbs strongly. To account for this anomalously, the number of absorbing species in solution were determined by applying Coleman et al.[16] graphical method to the different data of BHP and DAHP complexes at several wavelengths and at the different relevant pH's. Typical plots at the overlapping regions are given in Fig. 5. The analysis revealed that only one absorbing species exists in moderately acidic region (ca. pH 3). Increasing the pH to 4(in the case of Cu and Ni complexes) or 5(in the case of Co chelates) two absorbing species were found as indicated by
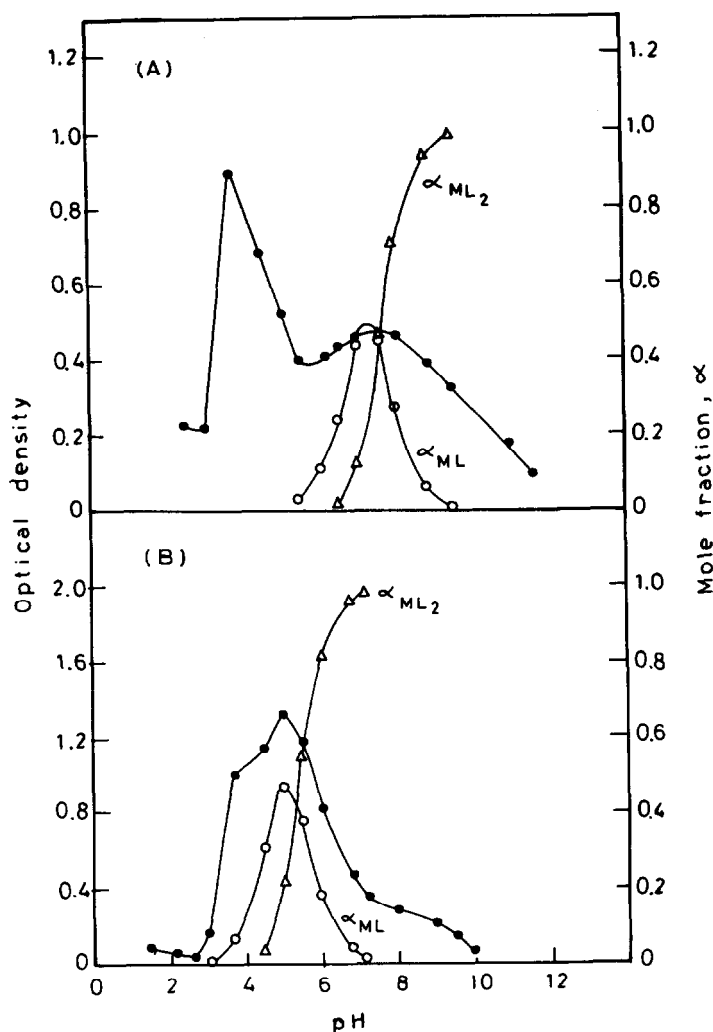
Fig. 4. Absorption-pH and mole fraction-pH plots for (A) Co–BHP species at $\lambda = 580$ nm.
(B) Cu–BHP species at $\lambda = 540$ nm.
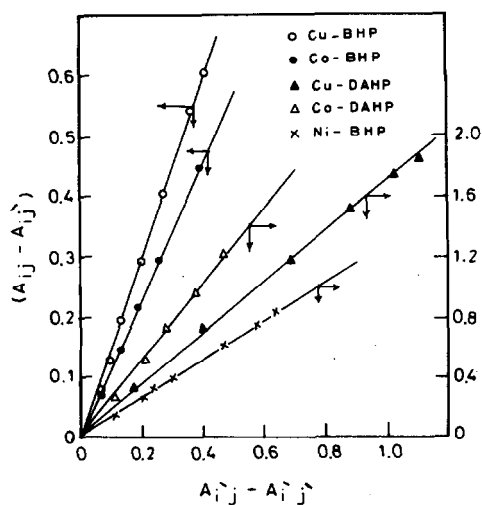
Fig. 5. Coleman *et al.* plots for the different BHP and DAHP chelates.

the linear plots shown in Fig. 5. Since the free ligands absorb far below this region of the spectrum, perhaps the only possible absorbing species in moderately acidic media is that formed between the metal ions and the acid ligands, MHL species. At very high acidities, protons compete with the metal ions for the available nitrogen donor sites and no complexes are formed, whereas in strong alkaline media, complex hydrolysis might account for the decrease in optical density.

By analogy, these bands are of a charge transfer origin. BHP and DAHP being a better π acceptor that BAHP, their charge transfer bands are expected at lower energy. Thus for the same metal ion, the order of increasing the energy of $d \rightarrow \pi$ transition is;

$$M(BAHP) > M(DAHP) > M(BHP).$$

Whereas, for the same ligand, the following order holds,

$$CoL > NiL \simeq CuL$$

which is the same order of metal reductibility.

The bands observed for Cu and Co chelates with BHP are quite broad and perhaps the $\pi \to d$ transitions in these cases are obscured and collapsed with those of the $d \to \pi$ origin. In general, when the metal ion was fixed, the energy of transition follows an order similar to that advanced in the previous paragraph.

For uranyl(VI) ion, an electron transfer takes place within the ion, from the oxygens of the uranyl group to the central uranium ion. This transfer involves much higher energy than that reported here (see Fig. 2). Coordination with ligands which are very prone to transfer electrons were found to cause the electron transfer bands to move further into the visible spectrum. Such an effect is brought about by the thiocyanate ion[17] and is likely to take place here with DAHP.

REFERENCES

1. A. A. T. Ramadan, M. H. Seada and E. N. Rizkalla, *Talanta*, 1983, **30**, 245.
2. F. A. Snavely, W. C. Fernelius and B. P. Block, *J. Am. Chem. Soc.* 1957, **79**, 1028.
3. F. A. Snavely, B. D. Krecker and C. G. Clark, *J. Am. Chem. Soc.* 1959, **81**, 2337.
4. H. Jahine, H. A. Zaher, A. Sayed and M. H. Seada, *Indian J. Chem.* 1977, **15B**, 352.
5. T. S. West, *Complexometry with EDTA and Related Reagents*. Broglia Press, London (1969).
6. J. Kucharsky and L. Šafařik, *Titrations in Non-Aqueous Solvents*. Elsevier, Amsterdam (1965).
7. R. E. Moskalyk, L. G. Chatten and M. Pernarowski, *J. Pharm. Sci.* 1961, **50**, 179.
8. H. M. N. H. Irving and U. S. Mahnat, *J. Inorg. Nucl. Chem.* 1968, **30**, 1215.
9. H. S. Harned and B. B. Owen, *The Physical Chemistry of Electrolytic Solutions*. Reinhold, New York (1958).
10. N. Kole and A. K. Chaudhury, *J. Inorg. Nucl. Chem.* 1981, **43**, 2471.
11. A. Albert and E. P. Serjeant, *Ionisation Constants of Acids and Bases*. Chapman & Hall, Edinburgh (1971).
12. A. Gergely and T. Kiss, *J. Inorg. Nucl. Chem.* 1977, **39**, 109.
13. U. Casellato, M. Vidali and P. A. Vigato, *Inorg. Chim. Acta* 1976, **18**, 77.
14. L. G. Sillén and A. E. Martell, *Stability Constants of Metal Ion Complexes*. The Chemical Society, London (1971).
15. Unpublished results.
16. J. S. Coleman, L. P. Varga and S. H. Mastin, *Inorg. Chem.* 1970, **9**, 1015.
17. S. Ahrland, *Acta Chem. Scand.* 1949, **3**, 1067.

TRANSITION METAL COMPLEXES WITH 1-METHYL-4,4-DIMERCAPTOPIPERIDINE

H. BARRERA and F. TEIXIDOR*

Departament de Química Inorgànica, Universitat Autònoma de Barcelona, (Bellaterra),
Barcelona, Spain

Abstract—The syntheses of $Co(AH_2)_2X_2$ ($AH_2 = $ 1-methyl-4, 4-dimercaptopiperidine, X = Cl, Br, I, acetate, propanate, perchlorate, nitrate and sulphate), $M(AH_2)$ Cl_2 (M = Cd, Zn) are described. According to IR and UV-visible data it seems most probable that the amino*gem*-dithiol (AH_2) coordinates Co via both sulphur atoms, but Zn and Cd via one sulphur. A square pyramidal geometry about Co and a tetrahedral geometry about Zn and Cd are proposed. In no case has coordination via nitrogen been found. Strong X–H. . .N hydrogen bonds have been observed in most of these complexes.

Complexes containing mercaptoamines as ligands have been extensively studied.[1,2] However no complexes have been reported containing a *gem*-dithiol ligand, i.e. two thiol groups on the same carbon atom. This lack of research about these type of complexes may be due to the few *gem*-dithiols known, their general tendency to lose SH_2 and the tendency of sulphur to form bridges between two metals.

In an attempt to gain insight into the coordination chemistry of the dithiols we undertook a research using the readily synthesized 1-methyl-4,4-dimercaptopiperidine. The precipitating ability of the cation 1-methyl-4,4-dimercaptopiperidinium with halometallates of transition metal ions has been just recently reported.[3] It is interesting to mention the strong S–H. . .X hydrogen bonds detected in these salts. In the present paper we report on the coordinating ability of this ligand toward Co^{2+}, Zn^{2+} and Cd^{2+} ions.

EXPERIMENTAL

General

IR spectra were obtained on a Beckman IR-20A as KBr pellets. The IR spectral data are listed in Table 2. The UV-visible spectra were recorded on a Beckman, Acta III. Conductivity measurements were determined on a CDM-3 Radiometer Copenhaguen Conductivimeter in Dimethylform-

amide. The 1-methyl-4-piperidine (Fluka) was distilled before use. The preparation of 1-methyl-4,4-dimercaptopiperidine ($C_6NS_2H_{13}$) has been described previously.[4] All metallic salts were either commercially available or were synthesized according to Pascal's methods.[5] Solvents were used as received. The complexes were analyzed as follows: S as barium sulphate; Co, Zn and Cd as anthranilate; Cl as AgCl; C, H and N in a Perkin–Elmer 240 analyser. Results are given in Table 1.

Syntheses of complexes $Co(AH_2)_2X_2$ where X = Cl, Br, I, SCN, CH_3COO, CH_3CH_2COO

Throughout this paper the ligand $C_6NS_2H_{13}$ is symbolized as AH_2. The analytical formula and the analyses (calculated and observed) of the compounds are indicated in Table 1.

(*a*) $Co(AH_2)_2Cl_2$ *and* $Co(AH_2)_2X_2$ (X = Br, I, SCN). To a beaker containing $CoCl_2 \cdot 6H_2O$ (1.5 g) in methanol was added, with continuous stirring, 1-methyl-4,4-dimercaptopiperidine (2.3 g) in 60–100 cm^3 of methanol containing 5–10 cm^3 of acetic acid. A solid precipitated immediately and was collected by filtration and washed with methanol and ethyl ether. The dark green solid was dried under vacuum for 30 min. M.p. = 210°C(dec.).

With slight variations, compounds $Co(AH_2)_2Br_2$, $Co(AH_2)_2I_2$ and $Co(AH_2)_2(SCN)_2$ were prepared following the procedure for $Co(AH_2)_2Cl_2$. The salts used were $CoBr_2 \cdot 6H_2O$, $CoI_2 \cdot 2H_2O$ and $Co(SCN)_2 \cdot 4H_2O$, respectively. In this latter case butanoic acid was used instead of acetic acid.

---

*Author to whom correspondence should be addressed.

Table 1. Compounds prepared and analyses

Compound	Analyses (Found)						Analyses (Calculated)					
	C,	H,	N,	S,	M,	X	C,	H,	N,	S,	M,	X
$Co(AH_2)_2Cl_2$	32,9	5,74	6,13	28,1	12,7		31,6	5,70	6,14	28,1	12,9	
$Co(AH_2)_2Br_2$	26,6	4,84	5,10	23,6	10,8		26,4	4,77	5,14	23,5	10,8	
$Co(AH_2)_2I_2$	22,5	4,07	4,20	19,9	9,18		22,5	4,07	4,20	19,9	9,22	
$Co(AH_2)_2(SCN)_2$	33,5	5,13			11,8		23,5	5,19			11,8	
$Co(AH_2)_2(CH_3COO)_2 \cdot H_2O$	36,7	6,36	5,39	24,6	11,3		36,8	6,52	5,37	24,6	11,3	
$Co(AH_2)_2(CH_3CH_2COO)_2$	40,6	6,69	5,34	24,1	11,1		40,7	6,78	5,27	24,1	11,1	
$Co(AH_2)_2(ClO_4)_2$	25,4	4,67	4,79	21,7	10,0		24,7	4,45	4,79	21,9	10,1	
$Co(AH_2)_2(NO_3)_2$				25,8	11,6					25,2	11,6	
$Co(AH_2)_2SO_4 \cdot 2H_2O$	27,7	5,61	5,16	30,8	11,0		27,7	5,78	5,39	30,8	11,3	
$Zn(AH_2)Cl_2 \cdot 2H_2O$				18,7	19,8	20,7				19,1	19,5	21,1
$Cd(AH_2)Cl_2 \cdot H_2O$				17,6	31,4	19,7				17,6	30,9	19,5

Table 2. IR spectral data

Compound	
$Co(AH_2)_2Cl_2$	2970(s), 2900(m), 2710(s), 1460(s), 1440(m), 1410(m), 1270(s), 1260(m), 1050(m), 1030(m), 970(s), 420(s), 380(w), 360(w).
$Co(AH_2)_2Br_2$	2970(s), 2900(m), 2570(s), 1470(s), 1440(m), 1410(m), 1270(s), 1260(m), 1050(m), 1030(m), 980(s), 420(s), 410(m,sh), 380(w), 360(w).
$Co(AH_2)_2I_2$	2980(s), 2750(s), 1460(s), 1430(m), 1420(m), 1390(m), 1260(s), 1250(m), 1040(m), 1020(m), 970(s), 420(s), 410(m,sh), 380(w), 360(w).
$Co(AH_2)_2(SCN)_2$	2970(s), 2750(s), 2090(s), 1470(s), 1430(m), 1420(m), 1260(m), 1030(m), 980(s), 420(s), 410(m,sh), 380(w), 360(w).
$Co(AH_2)_2(CH_3COO)_2$	3030(m), 2970(s), 2750(s), 1730(s,b), 1580(m,b), 1460(s), 1450(m), 1420(s), 1260(s), 1250(m), 1030(m), 980(s), 770(s,b), 460(m), 420(s), 410(m,sh), 380(w), 360(w).
$Co(AH_2)_2(CH_3CH_2COO)_2$	2960(s), 2750(s), 1580(s), 1460(s), 1450(m), 1410(s), 1370(m), 1300(m), 1270(m), 1260(m), 1060(m), 1040(m), 980(s), 420(s), 380(w), 360(w).
$Co(AH_2)_2SO_4$	3300(m,b), 2960(s), 2720(s), 1460(s), 1430(m), 1420(m), 1400(m), 1260(m), 1250(m,sh), 1140(sh), 1120(s), 1050(m), 1030(m), 970(s), 620(s), 420(s).
$Co(AH_2)_2(ClO_4)_2$	3420(m,b), 2960(s), 2720(s), 1460(m), 1420(m), 1260(m), 1150(s), 1110(sh), 1090(m), 970(m), 640(m), 630(s), 420(w), 410(sh).
$Co(AH_2)_2(NO_3)_2$	3040(m), 2950(m), 2720(m), 1450(m), 1430(sh), 1380(sh), 1350(s), 1330(m), 1290(m), 1260(m), 1250(m), 1040(m), 1020(m), 970(s), 420(m), 410(m), 380(w), 360(w).
$Zn(AH_2)Cl_2$	3420(m,b), 2990(s,b), 2710(s), 1720(m), 1460(s), 1250(m), 1150(m), 1050(m), 1030(m), 970(sh), 960(s), 800(m), 750(m), 360(sh), 330(sh), 280(m,b).
$Cd(AH_2)Cl_2$	3420(m,b), 3000(s,b), 2750(s), 1720(s), 1460(s), 1250(m), 1210(m), 1160(m), 1080(m), 1050(m), 1040(m), 960(s), 800(m), 750(m), 750(s).

(b) $Co(AH_2)_2(CH_3CO_2)_2$ and $Co(AH_2)_2(CH_3CH_2CO_2)$. The general features of these syntheses were as before. In particular $Co(CH_3CO_2)_2 \cdot 4H_2O$ was dissolved in acetic acid and $Co(CH_3CH_2CO_2)_2 \cdot 3H_2O$ in propionic acid. Isopropanol was used as the ligand solvent containing, in the former acetic acid and in the latter, propionic acid.

(c) $Co(AH_2)_2(ClO_4)_2$. Under vigorous stirring, Na $ClO_4(2.5\,g)$ were added to AH_3 Cl $(2\,g)$ in $120\,cm^3$ of ethanol. A precipitate of NaCl formed within minutes. When the precipitation was complete, NaOH$(0.2\,g)$ in ethanol was added and the suspension was filtered. Upon addition of $Co(ClO_4)_2 \cdot 6H_2O(2\,g)$ in ethanol to the filtrate, a dark green solid separated which was collected by filtration. The solid was washed three times with ethanol and dried thoroughly with dry-air.

(d) $Co(AH_2)_2(NO_3)_2$. The above procedure for $Co(AH_2)_2Cl_2$ was used to synthesize this compound. However butanoic acid was used instead of acetic acid. The solid was washed and dried as done in the ClO_4^- compound.

(e) $Co(AH_2)_2SO_4$. Equimolar amounts of a saturated solution of $NaHSO_4$ and $AH_2(2\,g)$, both in methanol, were mixed and, after standing for a while, filtered. To the filtrate, a recently prepared solution of $CoSO_4 \cdot 7H_2O$ was added. Immediately a green solid precipitated which was filtered, washed three times with methanol and dried at the vacuum line.

(f) $Zn(AH_2)Cl_2 \cdot 2H_2O$. In a beaker, were mixed two ethanolic solutions of $ZnCl_2$ $(0.6\,g)$ and AH_3 Cl $(1\,g)$, containing NaOH$(0.1\,g)$. Upon the mixing, a white solid separated which was filtered, washed with ethanol and ether and dried with dry air passing through the filter. Finally, the solid was dried at the vacuum line.

This compound is at first soluble in water but after a few minutes decomposes precipitating a solid.

(g) $Cd(AH_2)Cl_2 \cdot H_2O$. In a beaker were mixed two ethanolic solutions of $CdCl_2 \cdot 2,5H_2O$ $(1\,g)$, containing both of them a small amount of hydrogen chloride. Immediately a white solid separated which was filtered, washed with cold ethanol containing a small amount of hydrogen chloride and, finally, with ether.

The correct drying conditions for this compound have not been found. Its stoichiometry was determined by comparison of the atomic ratios of Cd, S and Cl.

It was proved that upon varying the drying conditions, the only variable element was sulphur, while the ratio Cl/Cd remained constant and averaged 1.99.

In order to know the ratio S/Cd all the solid resulting in one synthesis was placed wet in a 500 cm^3, round bottomed flask and treated with $120\,cm^3$ of Br_2–KBr[6] solution containing $CuCl_2(0.4\,g)$. Immediately the flask was tightly closed and thoroughly stirred for 1 hr. After cooling it at 0°C, concentrated $HNO_3(100\,cm^3)$ was carefully added. The resulting solution was gently heated for 1 hr and then evaporated to 50–60 cm^3. While continuing the heating, concentrated hydrochloric acid was added until no nitrogen dioxide vapours were apparent. The resulting solution was diluted to approx. 1 l. and SO_4^{2-} and Cd^{2+} analyzed from it.

RESULTS AND DISCUSSION

Cobalt complexes

The reaction of cobalt salts with 1-methyl-4,4-dimercaptopiperidine in ethanol, yields dark green solids whose stoichiometry has been determined to be $Co(AH_2)_2X_2$, where X = Cl, Br, I, SCN, acetate, propanate, ClO_4, NO_3 and $\frac{1}{2}SO_4$. All of the cobalt complexes discussed here gave very similar IR spectra (Table 2). Of these, it is important to note the strong absorptions at $\simeq 435\,cm^{-1}$ and $\simeq 2730\,cm^{-1}$ assigned to $\nu(M-S)$ and $\nu(N-H)$, respectively. This latter absorption exhibits an hypsochromic shift from $2710\,cm^{-1}$ (Cl) to $2750\,cm^{-1}$ (Br, I, SCN) attributed to hydrogen bond formation (N-H...Y). The frequency of the M-S absorption is high compared to other already reported $\nu(M-S)$ IR data. However, the presence of this band in all these spectra, independently of the X groups poses little doubt to its assignment. The IR spectral analysis of the X groups suggests that these are somehow coordinated. For instance, the $\nu(C-N)$ absorption band in $Co(AH_2)_2(SCN)_2$ occurs at $2090\,cm^{-1}$, while it is known to be at $2053\,cm^{-1}$ in KSCN.[7] In addition, the frequency separation between the asymmetric and symmetric modes of vibration of the OCO group in the acetate and propanoate complexes, $\Delta \simeq 160\,cm^{-1}$, suggest a monodentate coordination,[8,9] as it is thought of the sulphate and perchlorate complexes. However, the IR analysis of the nitrato compound suggest a non-coordinated nitrate group.

The 10^{-3}M conductivity values of these complexes $Co(AH_2)_2X_2$ in DMF at 25°C are indicated in Table 3. Comparison of them with accepted values for common types of electrolytes[10] suggest a molecular type of compound for the acetate and propanoate complexes but ionic for the others. However, excepting the perchlorate, which is on the lower side for 1:2 electrolytes, the iodide and thiocyanate complexes fall within the 1:1 type.

More structural information about these complexes is derived from the visible spectra, either in

Table 3. Conductivity values[a]

Complex	Assumed molecular weight	M
$Co(AH_2)_2I_2$	639	80
$Co(AH_2)_2(SCN)_2$	501	65
$Co(AH_2)_2(CH_3COO)_2 \cdot H_2O$	521	11
$Co(AH_2)_2(CH_3CH_2COO)_2$	531	12
$Co(AH_2)_2(ClO_4)_2$	584	130

(a) All conductivities were taken at 25°C and were calculated assuming a molecular weight given by the empirical formula.

the solid phase or in solution. A broad and symmetrical band, centered at 594 ± 1 nm, has been observed in all of the solid phase spectra of these complexes. This band shifted to 600 nm ($\epsilon = 2000$) when the spectra were recorded in DMF solution.

This visible spectral information clearly suggests the existence of a common chromophere in all of these $Co(AH_2)_2X_2$ complexes. Consequently, the X groups would not be coordinated to the cobalt and the conductivity and IR data would be explained by considering strong N–H...X hydrogen bonds as pointed out before. Besides, the high molar absorbance ($\epsilon \simeq 2000$, at 600 nm) can neither be explained by a centrosymmetric nor by a tetrahedral metal environment. We suggest that the square pyramidal geometry (Fig. 1) as exemplified by some dithiocarbamate complexes $Cu(R_2Dtc)_2$, $Cd(Et_2Dtc)_2$[11] could be consistent with the visible and IR data.

Zinc and cadmium complexes

The reaction of zinc and cadmium chlorides with 1-methyl-4, 4-dimercaptopiperidinium chloride in ethanol, yields white solids whose stoichiometry has been determined to be $Zn(AH_2)Cl_2 \cdot 2H_2O$ and $Cd(AH_2)Cl_2 \cdot H_2O$. The IR spectra of these solids

(Table 2) show, among others, absorptions at $2710\ cm^{-1}$, attributed to a N–H bond, and at the interval $255-325\ cm^{-1}$, attributed to terminal M–Cl[12] bonds in tetrahedrally coordinated complexes.[13]

Even though the M–S absorptions cannot be clearly identified in these IR spectra, we assume that the amino-dithiol moiety is coordinated to the metal by comparison with the IR spectra of $[AH_3]_2ZnCl_4$ and $[AH_3]CdCl_3$[3] salts, where 1-methyl-4, 4-dimercaptopiperidinium is the cation.

The amino-*gem*-dithiol-metal interaction takes place via sulphur of sulphurs, as is shown by the existence of an N–H band in the IR spectra of these complexes.

The existence of M-halogen bonds and the known tendency of the thiolate group to form bridges between metal atoms makes us believe that the structure of these Zn and Cd complexes may be as depicted in Fig. 2 with only one S atom of each ligand moiety binding the two metals. A structure like this has been observed by X-ray diffraction studies for $Zn(LH)Cl_2$,[2d] where LH is 1-methyl-4-mercaptopiperidine.
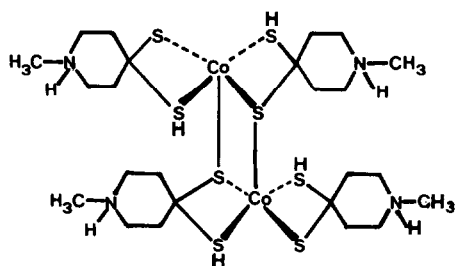
Fig. 1. Proposed structure for the $Co(AH_2)_2X_2$ complexes. A fifth coordination is obtained bonding the metal ion and one sulfur of a second $Co(AH_2)_2X_2$ moiety.
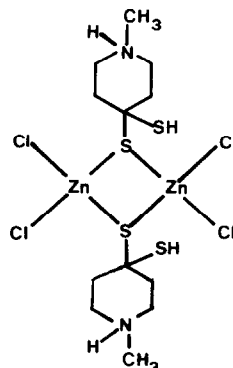
Fig. 2. Proposed structure for the $Zn(AH_2)Cl_2$ and $Cd(AH_2)Cl_2$ complexes.

CONCLUSION

The study of the Co, Zn and Cd complexes of 1-methyl-4,4-dimercaptopiperidine has permitted insight into the coordination behaviour of a *gem*-dithiol ligand. Attempts to get crystals suitable for an X-ray diffraction study have been unsuccessful. It is mostly due to the high insolubility in suitable solvents. As a consequence, the complete characterisation of the coordination is not yet known. However, it seems most probable, based on spectroscopic data that this ligand coordinates either via only one sulphur, bridging two metals, or via both sulphurs acting as a chelating agent.

REFERENCES

1. (a) D. C. Jicha and D. H. Bush, *Inorg. Chem.* 1962, **1**, 872; *Idem* 1962, **1**, 878; *Idem* 1962, **1**, 884; (b) M. Albou Ali and S. E. Livingstone, *Coord. Chem. Rev.* 1974, **13**, 101.
2. (a) L. K. Tiwari, S. Jain and A. Jymar, *Indian J. Chem.* 1977, **15A**, 310; (b) L. K. Tiwari, A. Kumar and S. Jain, *Indian J. Chem.* 1978, **16A**, 495; (c) J. C. Bayón, J. L. Briansó, M. C. Briansó and P. González-Duarte, *Inorg. Chem.* 1979, **18**, 3478; (d) M. C. Briansó, J. L. Briansó, W. Gaete, J. Ros and C. Suñer, *J. Chem. Soc.* Dalton Trans. 1981, 853.
3. H. Barrera and F. Teixidor, Accepted for publication in *Polyhedrom.*
4. H. Barrera and R. R. Lyle, *J. Org. Chem.* 1962, **27**, 641.
5. P. Pascal, *Nouveau Traité de Chimie Minérale.* Masson & Cie, Paris.
6. This solution was prepared by mixing KBr (160 g) with 100 cm³ of a saturated solution of Br₂ in water. After stirring thoroughly the mixture, water was added up to 2 l.
7. K. Nakamoto, *Infrared Spectra of Inorganic and Coordination Compounds*, 2nd Edn. Wiley, New York (1970).
8. P. O. Whimp and N. F. Curtis, *J. Chem. Soc. (A)* 1966, 867.
9. The Δ value is almost the same either for ionic or monodentate acetate. As a consequence, a $\Delta = 160\,cm^{-1}$ also could indicate ionic acetate or propanate group, however the conductivity measurements seem to favor a monodentate coordination via hydrogen bond.
10. W. J. Geary, *Coord. Chem. Rev.* 1971, **7**, 81.
11. D. Concouvanis, *Progr. Inorg. Chem.* 1970, **11**, 234 and Refs therein.
12. G. C. Pellacani, G. Peyronell, G. Pollacci and R. Cronati, *J. Inorg. Nucl. Chem.* 1976, **38**, 1619.
13. D. M. Adams, *Metal-Ligand and Related Vibrations.* Arnold, London (1967).

TERNARY COMPLEXES OF MIXED N/O DONOR LIGANDS IN SOLUTION

P. RABINDRA REDDY* and M. HARILATHA REDDY

Department of Chemistry, Osmania University, Hyderabad 500 007, India

Abstract—The stability constants of the ternary Cu(II), Ni(II), Co(II), Mn(II), Mg, Ca and Zn complexes containing xanthosine and, as a second ligand, glycine have been determined in aqueous solution by potentiometric titration [$\mu = 0.10$ M(KNO$_3$), 35°C]. The stability constants of the binary system containing the above metal ions and xanthosine in a 1:2 ratio were also determined to compare the effect of the secondary ligand on a 1:1 metal–xanthosine system. The $\Delta \log K$ (defined as the difference in the overall: 1:1 stability constants and corresponding 1:1 binary complexes) values are more positive for 1:2 metal–xanthosine system than the 1:1:1 metal–xanthosine–glycine system. This difference in stability may be due to the "stacking" interaction in the 1:2 metal–xanthosine system.

Investigations of the stability of ternary complexes will help toward understanding the driving forces that lead to the formation of such complexes in biological systems. Although binary and ternary complexes of nucleotides in solution have received much attention during recent years.[1–11] very little is known about the nucleoside complexes. Because of the importance of nucleosides, which provide a link between purine and pyrimidine bases and nucleotides, in understanding the nature of metal nucleic acid interactions in biological systems, we have undertaken a programme to systematically investigate the interaction of various metal ions with nucleosides in solution. Mixed ligand complexes containing Cu(II) are relatively well investigated.[12,13] Much less is known about other metal ions, especially about those which are of basic biological importance like Mg, Ca or Zn. Therefore, in this paper we have carried out a detailed physicochemical studies on the interaction of Cu(II), Ni(II), Co(II), Mn(II), Mg, Ca and Zn with xanthosine and glycine in a 1:1:1 ratio to see how the stabilityof mixed ligand complexes varies with in a series of metal ions. We have also studied 1:2 metal–xanthosine complexes with a view to understand the effect of the same secondary ligand as compared to the different secondary ligand on 1:1 metal–xanthosine system.

The stability constants of the 1:1:1 ternary complexes of xanthosine are lower than those observed for 1:2 metal–xanthosine system, which

is expected on the basis of the stacking interaction in the latter. All measurements were made at 35° ± 0.1°C and 0.10 M(KNO$_3$) ionic strength.

EXPERIMENTAL AND CALCULATIONS

Xanthosine and glycine were obtained from Sigma Chemical Company (U.S.A). Transition and alkaline earth metal ions were of Analar Grade and were standardised volumetrically by titration with disodium salt of EDTA in the presence of a suitable indicator as outlined by Schwarzenbach.[14]

The experimental method employed consisted of a potentiometric titration of metal and xanthosine in a 1:2 ratio or metal ion, xanthosine and glycine in a 1:1:1 ratio at 35° ± 0.1°C with standard NaOH solution. The experimental conditions maintained were similar to those described in our previous work.[7]

The acid dissociation constants of xanthosine and glycine were calculated by the usual algebraic method. The stability constants of 1:2 metal–xanthosine complexes were determined by the help of the equations described earlier.[10]

In order to calculate the stability constants of the ternary complexes of Cu(II) and Ni(II) with xanthosine and glycine, in a 1:1:1 ratio, the following equations were used (omitting charges)

$$M + H_2L + HA \overset{K^{M}_{MHLA}}{\rightleftharpoons} MHLA + 2H^+ \quad (1)$$

together with the related equilibria

$$M + HL + A \rightleftharpoons MHLA \quad (2)$$

$$K_{MHLA}^{M} = \frac{T_M - [M]}{[M][HL][A]}. \quad (3)$$

However, for the ternary complexes of Co(II), Mn(II), Mg, Ca and Zn with xanthosine and glycine the following equations were used.

$$MA + H_2L \overset{K_{MHLA}^{MA}}{\rightleftharpoons} MHLA + H^+ \quad (4)$$

related equilibria

$$MA + GL \overset{K_{MHLA}^{MA}}{\rightleftharpoons} MHLA \quad (5)$$

$$K_{MHLA}^{MA} = \frac{T_M - [M]}{[MA][HL]} \quad (6)$$

where MA = 1:1 metal–glycine complex; H_2L = xanthosine; HA = glycine; T_M = total metal ion species present in solution; and [M] = concentration of the free metal ion.

The concentrations of various species involved in the above equations were obtained by setting up suitable material balanced equations and solving for the unknowns. The details were given in our earlier publications.[8]

RESULTS AND DISCUSSION

In Fig. 1(d) is given the mixed ligand titration curve of Cu(II)-xanthosine and glycine in a 1:1:1 ratio, which shows an inflection at $m = 2$ (where "m" is the moles of base added per mole of metal ion) indicating simultaneous formation of 1:1:1 mixed ligand complex in the buffer region between $m = 0$ and $m = 2$. Accordingly, it was assumed that a monoprotonated 1:1:1 complex is formed in this buffer region. The constant K_{MHLA}^{M} was calculated with the help of eqn (3). Similar titration curve was also obtained for Ni(II) and the constants thus calculated are given in Table 1.

Figure 1(c) gives the mixed ligand titration curve of Zn-xanthosine and glycine system in a 1:1:1 ratio. The constant K_{MHLA}^{MA} formed from 1:1 metal–galcine complex in the buffer region between $m = 1$ and $m = 2$ was calculated by eqn (6) and presented in Table 1.

Similar trends were obtained for Co(II), Mn(II), Mg and Ca. The constants for these systems are included in Table 1.
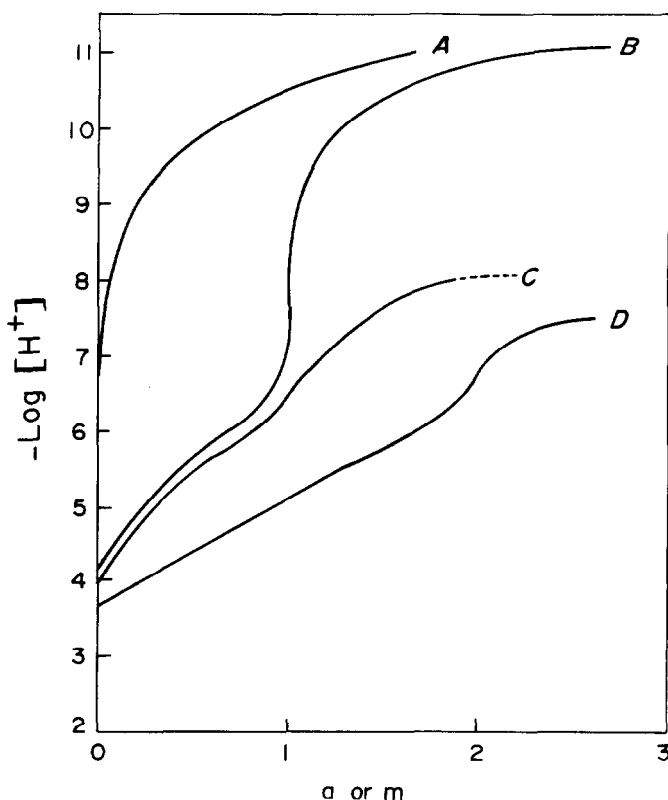
Fig. 1. Potentiometric titration curves for Cu(II) and Zn–xanthosine–glycine system in a 1:1:1 ratio at 35°C, $\mu = 0.10$ M(KNO$_3$). A = Free glycine; C = Zn–xanthosine–glycine; D = Cu(II)–xanthosine–glycine; m = moles of base added per mole of metal ion (for curves C & D); a = moles of base added per mole of ligand (for curves A & B). ---, Precipitation.

Table 1. Stability constants of complexes containing 1:1 and 1:2 ratios of metal ions and xanthosine, 1:1 ratio of metal ions with glycine and 1:1:1 ternary metal complexes of xanthosine with glycine. Temp. $= 35°C$; $\mu = 0.10 \ M(KNO_3)$

Metal (II) ion	Metal-xanthosine		Metal-Glycine	Metal-Xanthosine-Glycine		Δlog K
	log K^M_{MHL} (1:1)*	log $K^M_{MH_2L_2}$ (1:2)*	log K^M_{MA} (1:1)*	log K^M_{MHLA} (1:1:1)**	log K^{MA}_{MHLA} (1:1:1)**	
Cu	3.06	6.36	8.61	12.8	--	1.13
Ni	2.92	5.90	5.92	10.9	--	2.06
Zn	2.21	5.25	5.50	--	2.8	0.59
Co	2.51	5.38	5.22	--	3.0	0.49
Mn	2.57	5.76	3.85	--	2.8	0.23
Mg	2.23	5.07	3.40	--	2.5	0.27
Ca	2.21	5.15	3.58	--	2.6	0.39

* The constants are accurate to $\pm$ 0.06 log K unit.
** The constants are accurate to $\pm$ 0.1 log K unit.

Glycine	pK$_{2a}$	= 9.75 $\pm$ 0.02
Xanthosine	pKa	= 5.56 $\pm$ 0.02
	pK$_{2a}$	= 9.90 $\pm$ 0.02

In Table 1 are also given the stability constants of binary (metal–xanthosine and metal–glycine) complexes and $\Delta \log K$ values, calculated as the difference in the overall 1:1:1 stability constants and 1:1 constants. Although the constants of Cu(II), Ni(II), Co(II), Mn(II) and Zn glycine systems are available in the literature, we have remeasured these constants as it is preferable to determine the binary and ternary complexes under the same conditions. Otherwise the experimental difference might show up in $\Delta \log K$ (Defined as the difference in the overall 1:1:1 stability constants and corresponding 1:1 binary complexes). However, our values agree well with those from literature. The stability constants of Mg and Ca glycine systems have been determined for the first time.

It is worthwhile here to mention briefly the theoretical value of $\Delta \log K$ and its origin. In a ternary system containing metal ion and two ligands (bidentate), H_2A and H_2L with significant difference in complexing capabilities, simple complex with one of the ligands is formed which has the more complexing tendency as compared to the other. However, if there is only small difference in the complexing tendencies between the two ligands the following type of complex will result.

$$M + A + L \rightleftharpoons MLA.$$
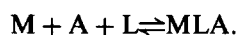
The reaction may proceed either of the following

equilibria

$$M + A \rightleftharpoons MA$$

$$MA + L \rightleftharpoons MAL$$

$$M + L \rightleftharpoons ML$$

$$ML + A \rightleftharpoons MLA.$$
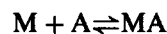
In dilute solutions the possibility of having other species like hydroxo, polymeric, etc. can be ignored. Therefore, we have left with equilibrium constant which represent the overall or stepwise mixed ligand complex depending upon the system under investigation. The difference in stability between a binary complex and ternary complex is usually explained in terms of $\Delta \log K$.

$$\Delta \log K = \log K^{MA}_{ML} - \log K^M_{ML}$$

or

$$\log K^{ML}_{MLA} - \log K^M_{MA}.$$

Thus, if $\Delta \log K$ values are positive the ternary complexes are more stable than the corresponding binary complexes and if the values for $\Delta \log K$ are negative the binary complexes are more stable than the ternary complexes. However, the negative val-

ues for $\Delta \log K$ does not preclude the formation of ternary complexes. The stability of mixed ligand complex formation is also determined by the reproportionate constant from statistical consideration. Under these conditions when there is no interaction between MAL, MA$_2$ and ML$_2$, there is possibility of 50% formation of MAL, while binary complexes MA$_2$ and ML$_2$ are formed to the extent of only 25% each.

Thus in a mixed system, the probability of formation of mixed ligand complexes more than that of the binary complexes. A detailed discussion on this subject is found in an article by Sigel.[15]

It can be seen from the table that the ternary complexes are more stable than the binary complexes, resulting in the positive values of $\Delta \log K$ for all the metal ions studied. This is because the destabilization caused by ligand repulsion is smaller in a mixed ligand complex than in the binary complex. In the ternary systems, generally the reaction between the metal ion and the secondary ligands containing heteroaromatic nitrogen and oxygen donors result in the formation of more stable complexes than the ligands containing pure nitrogen and oxygen donor atoms. In this context, it is important and of interest to compare the $\Delta \log K$ values for 1:2 metal–xanation system with those of 1:1:1 metal–xanthosine N, N-tetramethylethylene diamine, α–α'-bipyridyl, 1, 10-phenanthroline and 5-sulphosalicyclic acid.[10] The $\Delta \log K$ values for the former are more positive than the latter cases. These results support the above observation. Similar observations were also made by Sigel.[16]

The above arguments can also be extended successfully to metal–xanthosine–glycine system. In this system there seems to be two types of interactions for the metal ions studied as is evident from the titration curves (Fig. 1c, d). The Cu(II) and Ni(II) form one type of complexes and Co(II), Mn(II), Mg, Ca and Zn form another type. Hence, we have chosen only the latter type for comparison with 1:2 metal–xanthosine system since in both the cases we have a similar type of complexes. The $\Delta \log K$ values of Co(II), Mn(II), Mg, Ca and Zn for 1:2 metal–xanthosine system are more positive than the corresponding $\Delta \log K$ values 1:1:1 metal–xanthosine–galcyine system, though in both the cases we have mixed N/O donor atoms in the secondary ligand. These differences in the stabilities are expected because of the fact that the glycine is an aliphatic ligand and therefore, cannot take part in stacking interaction with xanthosine in 1:1:1 ternary complex. On the other hand, xanthosine can take part in stacking interaction in 1:2 system. These results once again confirm out earlier observations[10] that, in the ternary complexes the extent of stacking interaction rather than the nature of the metal ion is more important in deciding the $\Delta \log K$ values.
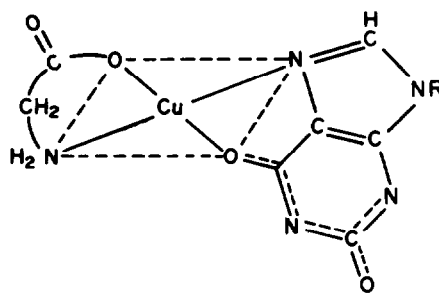
Fig. 2. Possible (tentative) structure of Cu(II)–xanthosine-glycine system in solution. R = ribose.

It is important here to mention that it is a well established fact that purine and pyrimidine bases, nucleosides and nucleotides associate extensively in aqueous solution by a mechanism involving vertical stacking of bases. The divalent metal ions like Mg and Zn promote stacking by a factor of about 4 in nucleoside 5'-triphosphates.[17] Therefore, in the case of 1:2 xanthosine system also the stacking is expected to be promoted by divalent metal ions though to a lesser extent as compared to the nucleotides. Although we have an oxo group in xanthosine, we expect an alternating stacking arrangement with a partially overlapped orientation so that H-8 and H-1' can be both shielded to a similar extent. Here not only the steric hindrance of the ribosyl group is reduced but also the repulsion between the dipole moments of the adjacent bases expected in the straight stack is reduced. We could not compare the $\Delta \log K$ values for Cu(II) and Ni(II) systems as they form different types of complexes with xanthosine and glycine as explained above.

The $\Delta \log K$ value of Ni(II)–xanthosine–glycine complex is more positive than the Cu(II)–xanthosine–glycine complex indicating a more stable ternary complex of Ni(II). The instability of Cu(II)–xanthosine–glycine complex may be due to its low coordination number as compared to the Ni(II) complex.

Based on this we propose a possible (tentative) structure of Cu(II)–xanthosine–glycine complex in solution (Fig. 2).

REFERENCES

1. M. M. Taqui Khan and A. E. Martell, *J. Am. Chem. Soc.* 1966, **88**, 668.
2. R. M. Izatt, J. J. Christensen and J. H. Rytting, *Chem. Rev.* 1971, **71**, 439.
3. M. M. Taqui Khan and P. Rabindra Reddy, *J. Inorg. Nucl. Chem.* 1972, **34**, 967.

4. M. M. Taqui Khan and P. Rabindra Reddy, *J. Inorg. Nucl. Chem.* 1973, **35**, 2813.

5. M. M. Taqui Khan and P. Rabindra Reddy, *J. Inorg. Nucl. Chem.* 1975, **37**, 771.

6. M. M. Taqui Khan and P. Rabindra Reddy, *J. Inorg. Nucl. Chem.* 1976, **38**, 1234.

7. P. Rabindra Reddy, K. Venugopal Reddy and M. M. Taqui Khan, *J. Inorg. Nucl. Chem.* 1976, **38**, 1923.

8. P. Rabindra Reddy, K. Venugopal Reddy and M. M. Taqui Khan, *J. Inorg. Nucl. Chem.* 1978, **40**, 1265.

9. H. Sigel, *J. Inorg. Nucl. Chem.* 1977, **39**, 1903.

10. P. Rabindra Reddy, K. Venugopal Reddy and M. Taqui Khan, *J. Inorg. Nucl. Chem.* 1979, **41**, 423.

11. H. Sigel, *J. Am. Chem. Soc.* 1975, **97**, 3209.

12. H. Sigel, In *Metal Ions in Biological Systems* (Edited by H. Sigel), Marcel Decker, New York (1973). Vol. 2, p. 63 and refs therein.

13. K. Bhattacharya, *J. Sci. Ind. Res.* 1981, **40**, 382.

14. G. Schwarzenbach, In p. 77. Interscience, New York (1957).

15. H. Sigel, *Ang. Chem. Int. Ed. Engl.* 1975, **14**, 394.

16. H. Sigel, B. E. Fischer and B. Prijs, *J. Am. Chem. Soc.* 1977, **99**, 4489.

17. K. HG. Scheller, F. Hofstetter, P. R. Mitchell, B. Prijs and H. Sigel, *J. Am. Chem. Soc.* 1981, **103**, 247.

BIS(INDENYL)TITANIUM(IV) AND ZIRCONIUM(IV) COMPLEXES OF MONOFUNCTIONAL BIDENTATE SALICYLIDIMINES

B. KHERA, A. K. SHARMA and N. K. KAUSHIK*
Department of Chemistry, University of Delhi, Delhi 7, India

Abstract—Dichlorobis(indenyl)-titanium(IV) and -zirconium(IV), $(C_9H_7)_2TiCl_2$ and $(C_9H_7)_2ZrCl_2$, react with bidentate Schiff bases such as salicylidene aniline, salicylidene-*o*-toluidine, salicylidene-*m*-toluidine and salicylidene-*p*-toluidine in a 1:1 molar ratio in refluxing tetrahydrofuran in the presence of triethylamine to yield complexes of the type $(C_9H_7)_2Ti(SB)Cl$ and $(C_9H_7)_2Zr(SB)Cl$, respectively where SB is the anion of the corresponding Schiff base, SBH. The new derivatives have been characterised on the basis of their elemental analyses, conductance measurements and spectral (IR, ^{1}H NMR and electronic) studies.

Schiff bases derived from the reaction of salicylaldehyde with primary amines represent a versatile series of ligands, the metal complexes of which have been widely studied.[1–3] Some Schiff base derivatives of bis(cyclopentadienyl)titanium(IV) and bis(cyclopentadienyl) zirconium(IV) with bidentate, terdentate and quadridentate Schiff bases are known.[4–7] Recently, we have reported[8,9] some reactions of dichloro bis(cyclopentadienyl)-titanium(IV) and bis(cyclopentadienyl) zirconium(IV) with N-aryl salicylidimines. However, reactions of bis(indenyl)-titanium(IV)- and bis(-indenyl)zirconium(IV)-dichlorides with Schiff bases have not been reported previously. The present work describes the reactions of bis(-indenyl)titanium(IV) and bis(indenyl)zirconium(IV) with bidentate Schiff bases derived from salicylaldehde and aniline, *o*-, *m*- or *p*-toluidine. The main interest in the preparation of such compounds is the attachment of Schiff base ligand to the titanium or zirconium atom in the presence of bulky idenyl groups, which due to some steric factors might have some effect on the structure of the complexes. However, various physico-chemical studies carried out for these complexes show the coordination to the central metal atom through nitrogen of azomethine group and oxygen of phenolic -OH group.

EXPERIMENTAL

Reagents and general techniques

All the reagents used were of analytical grade. Bis(indenyl)titanium(IV)dichloride and bis(indenyl)zirconium(IV)dichloride, $(C_9H_7)_2TiCl_2$ and $(C_9H_7)_2ZrCl_2$, were prepared by the reaction of indenyl thallium(I) and titanium tetrachloride or zirconium tetrachloride in 2:1 molar ratio in tetrahydrofuran. THF (Baker AR) was dried over sodium metal and then boiled under reflux until it gave a blue colouration with Ph_2CO. It was finally dried by distillation from $LiAlH_4$. *n*-Hexane (BDH) was dried by refluxing over sodium metal followed by distillation and triethylamine was dried as reported in the literature.[10] Nitrobenzene for conductance measurements was purified by the method described by Fay *et al.*[11] Titanium and zirconium were determined gravimetrically as their oxides and chlorine was estimated as silver chloride. Nitrogen was estimated by standard method as described by Vogel.[12]

Conductance measurements were made in nitrobenzene at 20 ± 0.05°C using a Systronic Digital Direct Reading Conductivity Meter Type 304. IR spectra were recorded in "KBr pellets" in the 4000–200 cm^{-1} region using a Perkin–Elmer 621 spectrophotometer. The proton NMR spectra were recorded at ambient temperature (20°C) at a sweep width of 900 Hz with a Perkin–Elmer R-32 spectrometer. Chemical shifts (δ, ppm) are expressed relative to an internal reference of TMS (1% by volume). Electronic spectra of the complexes in

---

*Author to whom correspondence should be addressed.

acetone were recorded on Perkin–Elmer UV-visible spectrophotometer, Model554.

Preparation of Schiff bases

To an appropriate amine (6 mmole) in 60 cm³ of freshly distilled ethanol, salicylaldehyde (5 mmole) in 60 cm³ of freshly distilled ethanol was added dropwise with vigorous stirring. There was immediate precipitation of products but the mixture was refluxed for half an hour, then cooled in an ice bath and filtered. The product was recrystallised by addition of 40 cm³ of hot ethanol. The mixture was cooled in an ice bath, filtered, and washed with sodium-dried diethyl ether and the Schiff base was dried *in vacuo*. The yield was approx. 90%.

Preparation of the complexes

All operations were carried out under strictly anhydrous conditions. The Schiff base (4 mmole) was added to a solution of $(C_9H_7)_2TiCl_2$ or $(C_9H_7)_2ZrCl_2$, (4 mmole) in 40 cm³ of dry tetrahydrofuran. To this triethylamine, Et_3N (6 mmole) was added and the mixture was refluxed (68°C) for about 10–12 hr. Precipitated $Et_3N \cdot HCl$ was removed by filtration and the volume of the filtrate was reduced to *ca.* 30 cm³ by evaporating the solvent under reduced pressure at room temperature. The crystals of the product were obtained by adding about 75 cm³ of dry *n*-hexane.

RESULTS AND DISCUSSION

Dichloro-bis-(indenyl)titanium(IV) and dichloro-bis-(indenyl)zirconium(IV), react with bidentate Schiff bases in 1:1 molar ratio to yield complexes of the type $(C_9H_7)_2Ti(SB)Cl$ and $(C_9H_7)_2Zr(SB)Cl$, respectively according to the following equation:

$$(C_9H_7)_2MCl_2 + SBH + Et_3N \xrightarrow[68°C]{THF}$$
$$(C_9H_7)_2M(SB)Cl + Et_3N \cdot HCl$$
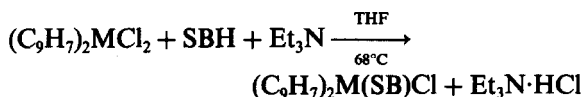
(M = Ti(IV) or Zr(IV); (SB)⁻ represents the anion of the corresponding bidentate Schiff base SBH).

All the Schiff base complexes crystallise as yellow to yellowish–brown crystals. They are highly soluble in common organic solvents, viz., benzene, THF, acetone, dichloromethane, nitrobenzene and chloroform. Electrical conductance measurements in nitrobenzene show them to be non-electrolytes and to be susceptible to hydrolysis. The analytical and physical data of the complexes are given in Table 1.

The assignments of characteristic IR frequencies for $(C_9H_7)_2M(SB)Cl$ complexes are listed in Table 2. Absorption bands indicating the presence of indenyl groups are found at *ca.* 3100 cm⁻¹ ν(C–H), 1450 cm⁻¹ ν(C–C), 1020 cm⁻¹ δ i.p. (C–H) and 815 cm⁻¹ δ o.p. (C–H). Appearance of these indenyl bands in the Schiff base derivatives indicate that electrons in these groups remain delocalised and π-bonded (η^5) to the metal.[13] Apart from this, the bands at *ca.* 355 and 440 cm⁻¹ may be assigned to ν(M–Cl) and metal-ring vibrations,[14] respectively.

A strong band at *ca.* 1625 cm⁻¹ is observed in the spectra of Schiff bases, which is characteristic of the azomethine (–HC=N–) group. Coordination of the nitrogen to the metal atom would, however, be expected to reduce the electron density in the

Table 1. Analytical and physical data

Complex	Dec.temp.[a] (°C)	Conductance[b] M × 10³ = 0.5	Elemental analyses % Found (Calc.)		
			Ti/Zr	N	Cl
$(C_9H_7)_2Ti(sal-aniline)Cl$	174–176	0.26	9.42(9.27)	2.75(2.69)	6.97(7.06)
$(C_9H_7)_2Ti(sal-o-toluidine)Cl$	167–169	0.22	9.17(9.03)	2.67(2.54)	6.78(6.71)
$(C_9H_7)_2Ti(sal-m-toluidine)Cl$	160–161	0.30	9.17(8.98)	2.67(2.60)	6.78(6.63)
$(C_9H_7)_2Ti(sal-p-toluidine)Cl$	203–206	0.28	9.17(8.94)	2.67(2.59)	6.78(6.69)
$(C_9H_7)_2Zr(sal-aniline)Cl$	126–127	0.20	16.47(16.38)	2.53(2.46)	6.42(6.33)
$(C_9H_7)_2Zr(sal-o-toluidine)Cl$	180–182	0.24	16.06(15.88)	2.47(2.33)	6.27(6.36)
$(C_9H_7)_2Zr(sal-m-toluidine)Cl$	185–186	0.24	16.06(15.92)	2.47(2.42)	6.27(6.20)
$(C_9H_7)_2Zr(sal-p-toluidine)Cl$	128–130	0.28	16.06(16.01)	2.47(2.28)	6.27(6.16)

[a] Uncorrected values; [b] in ohm⁻¹ cm² mole⁻¹

Table 2. Characteristic IR bands and ^{1}H NMR data

Complex	IR (cm^{-1})		^{1}H NMR (δ, ppm)			
	γ(C=N)	ν(C-O)	C_9H_7	Aromatic ring protons	(-CH=N)	-CH$_3$
$(C_9H_7)_2$Ti(sal-aniline)Cl	1610	1300	6.50	7.65(m)	8.65(s)	-
$(C_9H_7)_2$Ti(sal-o-toluidine)Cl	1600	1300	6.62	7.60(m)	8.60(s)	2.08(s)
$(C_9H_7)_2$Ti(sal-m-toluidine)Cl	1600	1290	6.72	7.64(m)	8.60(s)	2.12(s)
$(C_9H_7)_2$Ti(sal-p-toluidine)Cl	1605	1310	6.70	7.62(m)	8.62(s)	2.18(s)
$(C_9H_7)_2$Zr(sal-aniline)Cl	1600	1295	6.70	7.50(m)	8.68(s)	-
$(C_9H_7)_2$Zr(sal-o-toluidine)Cl	1610	1300	6.58	7.62(m)	8.70(s)	2.10(s)
$(C_9H_7)_2$Zr(sal-m-toluidine)Cl	1605	1295	6.60	7.70(m)	8.60(s)	2.16(s)
$(C_9H_7)_2$Zr(sal-p-toluidine)Cl	1595	1310	6.65	7.66(m)	8.62(s)	2.20(s)

(m) = multiplet, (s) = singlet

azomethine link and thus lower the (C=N) frequency. In the Schiff base complexes, this band is very slightly shifted to the lower side in our studies (ca. 1600 cm^{-1}), showing the presence of coordination through the azomethine nitrogen.[4-7,15] A high intensity band at ca. 1275 cm^{-1} in the Schiff bases can be assigned to the phenolic C-O stretching.[4] In the complexes, the C-O stretching vibrations appear at 1310-1300 cm^{-1}. This shift to higher frequency indicates bonding of the ligand to the metal through oxygen. This is further supported by the disappearance of the broad v (O-H) band in the 3300-3150 cm^{-1} region in the complexes.

Bands at 560-540 cm^{-1} and 525-425 cm^{-1} can be tentatively assigned to M-O and M-N bands, however, specific assignments are difficult.[4]

The ^{1}H HMR spectra of the complexes were taken in deutero-chloroform. Chemical shifts for the protons in δ scale are listed in Table 2. The signal due to azomethine proton appears at ca. δ 8.60 ppm, showing a downfield shift as compared to the corresponding Schiff base ligand (δ 8.45 ppm) indicating its deshielding as a result of coordination through nitrogen of the azomethine group to metal. The signals due to indenyl protons overlap with that of aromatic proton signals of Schiff base and result in a complex multiplet in the range δ 6.58-7.70 ppm. The δ values of methyl protons in case of Schiff base complexes derived from salicylaldehyde and o-, m-, or p-toluidine occur at around δ 2.10 ppm.

The disappearance of the phenolic -OH proton signal in the Schiff base complexes indicates its deprotonation and having taken part in the bond formation to metal through oxygen.

The UV spectra of the complexes were recorded in chloroform. The bands appearing at ca. 250, 320 and 385 nm are due to the $\pi - \pi^*$ (benzoid), $\pi - \pi^*$ (azomethine) and $\eta - \pi^*$ (azomethine) electronic transitions, respectively. In the ligands (Schiff bases) the first two bands were observed at the same positions, whereas the third band was observed at ca. 425 nm. This hypsochromic shift in the Schiff base complexes may be due to the donation of the lone pair of electrons by the nitrogen of the azomethine group to the central metal atom.[5]

The visible spectra of the complexes in chloroform show a single band in the 24,800-24,300 cm^{-1} region. Absence of a d-d transition rules out the presence of an unpaired electron in the metal ion confirming the quadrivalent state of these metals.[16-18] On the basis of elemental analyses and spectral studies, the structure assigned to the $(C_9H_7)_2$M(SB)Cl complexes will involve the Schiff base bonding in the bidentate mode.

REFERENCES

1. L. Sacconi, *Coord. Chem. Rev.* 1966, **1**, 126.
2. S. Yamada, *Coord. Chem. Rev.* 1966, **1**, 415.
3. R. H. Holm and G. W. Everett, *Prog. Inorg. Chem.* 1966, **7**, 83.
4. G. Gupta, R. Sharan and R. N. Kapoor, *Transition Met. Chem.* 1978, **3**, 282.
5. R. K. Sharma, R. V. Singh and J. P. Tandon, *J. Inorg. Nucl. Chem.* 1980, **42**, 1382.
6. G. Gupta, R. Sharan and R. N. Kapoor, *Bull. Chem. Soc. Japan* 1979, **52**, 3088.
7. G. Gupta, R. Sharan and R. N. Kapoor, *Indian J. Chem.* 1979, **18A**, 58.
8. A. K. Sharma, B. Khera and N. K. Kaushik, *Acta Chimica* 1983 (accepted for publication).
9. A. K. Sharma, B. Khera and N. K. Kaushik, *Synth. React. Inorg. Met.-Org. Chem.* 1983, **13**(4).
10. A. I. Vogel, *A Text Book of Practical Organic Chemistry*, 4th Edn. Longmans–Green, London (1978).
11. R. C. Fay and R. N. Lowry, *Inorg. Chem.* 1967, **6**, 1512.
12. A. I. Vogel, *A Text Book of Quantitative Inorganic Analysis*, 4th Edn. Longmans–Green, London (1978).
13. E. R. Lippincott and R. D. Nelson, *J. Chem. Phys.* 1953, **21**, 1307.
14. R. S. P. Coutts and P. C. Wailes, *J. Organometal. Chem.*, 1975, **84**, 47.
15. J. Uttamchandani and R. N. Kapoor, *Transition Met. Chem.* 1978, **3**, 79.
16. N. K. Kaushik, B. Bhushan and G. R. Chhatwal, *J. Inorg. Nucl. Chem.* 1980, **42**, 457.
17. N. K. Kaushik, A. K. Sharma and G. S. Sodhi, *Indian J. Chem.* 1981, **20**, 847.
18. A. K. Sharma and N. K. Kaushik, *Synth. React. Inorg. Met.-Org. Chem.* 1981, **11**, 685.

KINETICS AND MECHANISM OF SOME FAST ANATION REACTIONS OF A SERIES OF SUBSTITUTED dien COMPLEXES OF PALLADIUM(II). TEMPERATURE AND PRESSURE DEPENDENCIES IN WEAKLY ACIDIC AQUEOUS SOLUTION[1]

E. L. J. BREET†, R. van ELDIK* and H. KELM
Institute for Physical Chemistry, University of Frankfurt, Robert-Mayer-Str. 11,
6000 Frankfurt/Main, F.R.G.

Abstract—Anation reactions of the type $[Pd(L)(H_2O)]^{2+} + X^- \rightarrow [Pd(L)X]^+ + H_2O$ with L = 1, 4, 7-Et$_3$dien, 1, 1, 7, 7-Me$_4$dien and 1, 1, 4, 7, 7-Me$_5$dien and $X^- = Cl^-$, Br^-, I^- and N_3^- have been studied kinetically as a function of $[X^-]$, temperature and pressure (up to 1 kbar). Second-order anation rate constants decrease with an increase in the size of L, and are accompanied by an increase in $\Delta H^{\ne}$. For a given L the sequence $Cl^- < Br^- < I^- < N_3^-$ holds, and the values of $\Delta S^{\ne}$ and $\Delta V^{\ne}$ are consistent with an associative mechanism. The results are discussed with reference to similar anation reactions previously investigated.

During the past few years this laboratory has undertaken various studies on the kinetics and mechanism of substitution reactions of diethylenetriamine (dien) and substituted dien complexes of platinum(II) and palladium(II).[2-10] One of the aims of these studies was to determine the effect of steric hindrance on the rate and corresponding mechanism of substitution. The majority of these reactions are fast, so that with conventional kinetic techniques we were limited to the investigation of a few systems only. The recent addition of a high-pressure stopped-flow system[10] to our instrumentation, has allowed us to substantially expand the series of complexes previously investigated. We have now undertaken detailed kinetic studies of series of fast anation and substitution reactions of some dien and substituted dien complexes of palladium(II).

We planned to study anation reactions for all the complexes listed in Table 1, but some reactions are so fast that we could perform kinetic measurements for three complexes only, viz. [Pd(1,4,7-Et$_3$dien)(H$_2$O)]$^{2+}$, [Pd(1,1,7,7-Me$_4$dien)(H$_2$O)]$^{2+}$ and [Pd(1,1,4,7,7-Me$_5$dien)(H$_2$O)]$^{2+}$, in addition to those already investigated, viz. [Pd(1,1,4-Et$_3$-

dien)(H$_2$O)]$^{2+}$, [Pd(1,1,7,7-Et$_4$dien)(H$_2$O)]$^{2+}$ and [Pd(4-Me-1,1,7,7-Et$_4$dien)(H$_2$O)]$^{2+7,10}$. In this paper we report on the temperature and pressure dependencies of some anation reactions of these complexes in weakly acidic aqueous solution. A comparison between these results and the previously reported kinetic data permits some interesting mechanistic conclusions.

EXPERIMENTAL

A series of palladium(II) substituted dien complexes (Table 1) was prepared according to standard literature procedures.[11] The preparation of the complexes was simplified by isolating them as perchlorates. In a similar effort to simplify the tedious preparative procedure for the 1, 4, 7-Me$_3$dien complex we succeeded in isolating the species [Pd(1, 4, 7-Me$_3$dien)Cl$_2$]HCl, the details of which are reported elsewhere.[12] The complexes were subjected to chemical analysis,[13] the results of which are summarized in Table 1.

For the present study each complex was converted from the chloro into the aquo form by the addition of an equivalent amount of AgClO$_4$ to a hot solution of the complex and removal, on cooling, of the AgCl precipitate by filtration through a Sartorius membrane filter (0.1 μm pore size). The UV-visible spectral data presented in Table 2 for the chloro, aquo and hydroxo species (the latter two prepared in solution only), as well as for the species produced during anation by Cl^-,

Table 1. Analysis of substituted dien complexes

Complex	%C Calc.	%C Found	%H Calc.	%H Found	%N Calc.	%N Found	%Cl Calc.	%Cl Found
[Pd(dien)Cl]Cl	17.1	17.2	4.7	4.6	15.0	14.9	25.3	25.0
[Pd(1,4,7-Me$_3$dien)Cl$_2$]HCl	23.4	23.5	5.6	5.5	11.7	11.8	29.6	29.3
[Pd(1,4,7-Et$_3$dien)Cl]ClO$_4$	28.0	27.9	5.9	5.7	9.8	9.9	16.5	16.4
[Pd(1,1,7,7-Me$_4$dien)Cl]ClO$_4$	24.0	23.7	5.3	5.2	10.5	10.4	17.7	17.2
[Pd(1,1,4-Et$_3$dien)Cl]ClO$_4$	28.0	28.0	5.9	6.0	9.8	9.7	16.5	16.5
[Pd(1,1,4,7,7-Me$_5$dien)Cl]ClO$_4$	26.1	26.1	5.6	5.4	10.1	10.2	17.1	17.0

Table 2. Spectral data for substituted *dien* complexes

Complex and Spectral Property (λ in nm and ε in $dm^3\ mol^{-1}\ cm^{-1}$)		Chloro Species	Aquo Species	Hydroxo Species	Species Produced during Anation by Cl⁻**	Br⁻	I⁻	N$_3$⁻
[Pd(*dien*)Cl]Cl	λ	330 / 330 [11] / 331 [6]	313	309	332	341 / 342 [6]	369 / 370 [6]	317
	ε	460 ± 1 / 460 [11] / 490 [6]	511 ± 2	410 ± 4	478	468 / 520 [6]	590 / 540 [6]	1 725
[Pd(1,4,7-Me$_3$*dien*)Cl$_2$]HCl*	λ	339 [12] / 342 [11]	321	309	339	350	387	315
	ε	671 ± 5 [12] / 635 [11]	862 ± 10	525 ± 18	681	594	699	2 153
[Pd(1,4,7-Et$_3$*dien*)Cl]ClO$_4$	λ	334	323	310	341	352	390	316
	ε	759 ± 7	963 ± 4	598 ± 3	740	650	744	2 338
[Pd(1,1,7,7-Me$_4$*dien*)Cl]ClO$_4$	λ	332	320	313	340	352	388	315
	ε	810 ± 2	1 088 ± 16	644 ± 9	799	654	665	1 888
[Pd(1,1,4-Et$_3$*dien*)Cl]ClO$_4$	λ	341	327	317	345	354	386	321
	ε	708 ± 4	825 ± 7	562 ± 5	735	665	806	2 250
[Pd(1,1,4,7,7-Me$_5$*dien*)Cl]ClO$_4$	λ	338 / 339 [11] / 339 [6]	326	312	346	360	404	317
	ε	865 ± 1 / 775 [11] / 820 [6]	1 174 ± 22	683 ± 3	850	691	713	2 419

*yields the same species in aqueous solution as the complex [Pd(1,4,7-Me$_3$*dien*)Cl]Cl prepared by the authors of ref. 11 (cf. ref. 12)

**differ somewhat from the data for the chloro species since the slight hydrolysis of these species in aqueous solution is excluded here by an excess of free chloride ion

Br⁻, I⁻, and N$_3$⁻, were obtained using a Perkin–Elmer 555 spectrophotometer. The acid dissociation constants of the aquo species reported in Table 3 were determined spectrophotometrically since deprotonation of the dien ligand led to complications at high pH in the normal titrimetric procedure. The method is based on the relation pH = pK + log{$(A_{aquo} - A)/(A - A_{hydroxo})$}, where A_{aquo} and $A_{hydroxo}$ are the absorbances of the aquo and hydroxo species respectively and A the absorbances at various pH during the titration. Solutions titrated were at an ionic strength of 0.1 mol dm^{-3}, adjusted with NaClO$_4$, so as to be in agreement with all subsequent kinetic experiments. All pH measurements were obtained using a Metrohm E520 pH meter.

Table 3. Acid dissociation pK values of substituted dien aquo complexes

Complex	pK
[Pd(dien)(H₂O)]²⁺	7.38 ± 0.01
[Pd(1,4,7-Me₃dien)(H₂O)]²⁺	7.05 ± 0.01
[Pd(1,4,7-Et₃dien)(H₂O)]²⁺	7.24 ± 0.01
[Pd(1,1,7,7-Me₄dien)(H₂O)]²⁺	7.54 ± 0.01
[Pd(1,1,4-Et₃dien)(H₂O)]²⁺	7.12 ± 0.01
[Pd(1,1,4,7,7-Me₅dien)(H₂O)]²⁺	7.29 ± 0.02

The kinetic experiments were performed on an Aminco stopped-flow system at ambient pressure and on the recently described[10] high-pressure stopped-flow system at pressures up to 1 kbar. The pseudo-first-order rate constants k_{obs} were determined in the usual way from six successive kinetic runs, a linearity standard of at least three half-lives being set for the corresponding plots. Chemicals of analytical reagent grade were used throughout the study and test solutions were prepared using doubly distilled water.

RESULTS AND DISCUSSION

The results of the chemical analysis of the synthesized complexes are in excellent agreement with the theoretically expected values as shown by the entries in Table 1. The measured UV-visible spectral data compare favourably with the available literature data according to Table 2. The pK values of all the aquo species in Table 3 fall within a narrow range of values as expected.

The anation reactions were studied at pH = 5 so that only aquo species were present in solution and no complication from the possible participation of hydroxo species could occur. These reactions were expected to exhibit, contrary to the two-term rate-law usually observed for substitution reactions of square planar complexes,[14] a first-order dependence on the entering ligand concentration. Thus k_{obs} was measured initially as a function of [X⁻] (X⁻ = entering ligand) at 25°C to confirm, as indicated in Table 4, that $k_{obs} = k_{anation}[X^-]$. In the subsequent measurements of the temperature and pressure dependencies of k_{obs} (Tables 4 and 5) only

one [X⁻] was considered. These measurements could, however, only be performed for the species [Pd(1,1,7,7-Me₄dien(H₂O)]²⁺ and [Pd(1,4,7,7-Me₅-dien)(H₂O)]²⁺ {and previously[10] for the species [Pd(1,1,4-Et₃dien)(H₂O)]²⁺}, since the anation reactions are so fast that for the species [Pd(1,4,7-Et₃dien)(H₂O)]²⁺ a single value of k_{obs} (Table 4) and for the species [Pd(1,4,7-Me₃dien)(H₂O)]²⁺ and [Pd(dien)(H₂O)]²⁺¹⁰ no data at all could be obtained despite the extremely low concentration and temperature conditions. This demonstrates the tremendous effect the steric hindrance, brought about by the dien ligand substituents, has on the anation rate.

The kinetic data presented in Tables 4 and 5 show some interesting tendencies. The value of $k_{anation}$ increases significantly with increasing nucleophilicity of the entering ligand according to the series Cl⁻ < Br⁻ < I⁻ < N₃⁻. The sequence is, with the exception of the azide ion (see further discussion), in agreement with the n_{Pt} values[15] usually observed for these ligands. The increase in $k_{anation}$ is accompanied by a decrease in the activation parameters $\Delta H^\ddagger$ and $\Delta S^\ddagger$ determined by application of the Eyring equation. Similarly the values of $\Delta V_{exp}^\ddagger$, calculated from the slopes of the linear plots of $\ln k_{obs}$ versus pressure, show a decrease along the quoted series and parallel the tendency in $\Delta S^\ddagger$ (Table 5). The significantly negative values of $\Delta S^\ddagger$ and $\Delta V_{exp}^\ddagger$ emphasize the associative nature of the anation process. In this respect it should be borne in mind that $\Delta V_{exp}^\ddagger$ is a composite quantity consisting of contributions from $\Delta V_{intr}^\ddagger$, due to changes in bond lengths and angles, and

Table 4. Temperature dependence of anation reactions of substituted *dien* complexes. [Complex] = 1×10^{-3} mol dm⁻³, ionic strength = 0.1 mol dm⁻³, wavelength = 320 nm (X = Cl, Br), 400 nm (X = I, N₃)

Complex	X⁻	$[X^-]$ mol dm⁻³	k_{obs}/s^{-1} 10,4°C	17,4°C	25,0°C	30,8°C	$k_{anation}$ dm³ mol⁻¹ s⁻¹ at 25°C	$\Delta H^{\ddagger}$ kcal mol⁻¹*	$\Delta S^{\ddagger}$ cal K⁻¹ mol⁻¹*
[Pd(1,4,7-Et₃dien)(H₂O)]²⁺	Cl⁻	1×10^{-2}	70,4 ± 1,5						
[Pd(1,1,7,7-Me₄dien)(H₂O)]²⁺	Cl⁻	1×10^{-2}	7,96 ± 0,16	11,5 ± 0,3	19,4 ± 0,5	25,9 ± 1,4	1 908 ± 50	9,5 ± 0,4	−11,7 ± 1,4
		2×10^{-2}			37,5 ± 1,9				
	Br⁻	1×10^{-2}	12,9 ± 0,3	19,1 ± 0,3	32,1 ± 0,3	41,3 ± 0,5	3 126 ± 119	9,3 ± 0,3	−11,2 ± 1,1
		2×10^{-2}			60,8 ± 2,6				
	I⁻	1×10^{-2}	37,6 ± 0,5	58,5 ± 2,3	87,1 ± 4,5	109 ± 4	8 081 ± 893	8,1 ± 0,4	−13,2 ± 1,4
		2×10^{-2}			149 ± 3				
	N₃⁻	1×10^{-2}	107 ± 5	153 ± 3				7,7 ± 0,4	−12,8 ± 1,1
[Pd(1,1,4,7,7-Me₅dien)(H₂O)]²⁺	Cl⁻	1×10^{-2}	2,20 ± 0,06	3,71 ± 0,12	6,25 ± 0,05	8,22 ± 0,30	629 ± 19	10,6 ± 0,6	−10,1 ± 2,0
		3×10^{-2}			18,4 ± 0,5				
		5×10^{-2}			32,5 ± 1,5				
	Br⁻	1×10^{-2}	4,24 ± 0,13	6,85 ± 0,23	11,0 ± 0,3	13,9 ± 0,3	1 087 ± 19	9,5 ± 0,5	−12,9 ± 1,8
		2×10^{-2}			21,5 ± 0,8				
	I⁻	1×10^{-2}	22,5 ± 0,7	33,7 ± 0,6	42,6 ± 1,9	66,8 ± 1,6	4 162 ± 144	7,9 ± 1,2	−15,0 ± 4,0
		2×10^{-2}			81,2 ± 3,2				
	N₃⁻	1×10^{-2}	32,8 ± 1,2	51,2 ± 0,8	69,9 ± 1,4	87,9 ± 1,7	6 678 ± 443	7,4 ± 0,6	−15,9 ± 2,1
		2×10^{-2}			127 ± 4				

*presented in non SI-units for direct comparison with available literature data

Table 5. Pressure dependence of anation reactions of substituted dien complexes. [Complex] = 1×10^{-3} mol dm^{-3}, [X$^-$] = 1×10^{-2} mol dm^{-3}, ionic strength = 0.1 mol dm^{-3}, temperature = 25°C, wavelength = 320 nm (X = Cl, Br), 400 nm (X = I, N$_3$).

Complex	X$^-$	k_{obs}/s^{-1}						$\Delta V^{\ddagger}_{exp}$/cm^3 mol^{-1}
		1 bar*	50 bar	250 bar	500 bar	750 bar	1000 bar	
[Pd(1,1,7,7-Me$_4$dien)(H$_2$O)]$^{2+}$	Cl$^-$	19.1 ± 0.5	18.1 ± 0.4	19.0 ± 0.1	20.5 ± 0.6	22.2 ± 2.4	23.8 ± 0.3	- 7.2 ± 0.2
	Br$^-$	31.3 ± 1.2	29.1 ± 0.4	30.8 ± 0.1	33.2 ± 0.3	35.5 ± 0.4	39.2 ± 0.5	- 7.6 ± 0.3
	I$^-$	80.8 ± 8.9	63.2 ± 2.1	69.4 ± 3.9	72.6 ± 0.7	84.1 ± 0.4	90.4 ± 2.2	- 9.3 ± 0.8
[Pd(1,1,4,7,7-Me$_5$dien)(H$_2$O)]$^{2+}$	Cl$^-$	6.29 ± 0.19	6.18 ± 0.04	6.47 ± 0.10	6.77 ± 0.08	7.00 ± 0.15	7.55 ± 0.18	- 4.9 ± 0.4
	Br$^-$	10.9 ± 0.2	10.1 ± 0.1	10.9 ± 0.4	11.9 ± 0.2	12.6 ± 0.2	13.5 ± 0.3	- 7.3 ± 0.4
	I$^-$	41.6 ± 1.4	38.5 ± 1.4	45.4 ± 0.8	47.5 ± 0.7	53.0 ± 1.9	58.1 ± 1.1	- 9.9 ± 1.2
	N$_3^-$	66.8 ± 4.4	51.4 ± 0.4	54.1 ± 0.5	58.6 ± 2.9	69.4 ± 0.5	80.2 ± 1.2	-11.7 ± 1.2

* excluded from calculation of $\Delta V^{\ddagger}_{exp}$ since measurements at ambient and at elevated pressure were performed with different equipment

Table 6. Rate and activation parameters for anation of various complexes by chloride ion. [Complex] = 1×10^{-3} mol dm^{-3}, ionic strength = 0.1 mol dm^{-3}

Complex	$k_{anation}$/dm^3 mol^{-1} s^{-1} at 25°C	$\Delta H^{\ddagger}$/kcal mol^{-1}*	$\Delta S^{\ddagger}$/cal K^{-1} mol^{-1}*	$\Delta V^{\ddagger}_{exp}$/cm^3 mol^{-1} at 25°C
[Pd(1,1,7,7-Me$_4$dien)(H$_2$O)]$^{2+}$	1980 ± 50	9.5 ± 0.4	-11.7 ± 1.4	-7.2 ± 0.2
[Pd(1,1,4-Et$_3$dien)(H$_2$O)]$^{2+}$	1558 ± 7	10.5 ± 0.7	- 8.7 ± 2.3	-2.7 ± 0.2
[Pd(1,1,4,7,7-Me$_5$dien)(H$_2$O)]$^{2+}$	629 ± 19	10.6 ± 0.6	-10.1 ± 2.0	-4.9 ± 0.4
[Pd(1,1,7-Et$_4$dien)(H$_2$O)]$^{2+}$	4.19 ± 0.06	13.4 ± 0.4	-10.7 ± 1.2	-3.0 ± 0.2
[Pd(4-Me-1,1,7,7-Et$_4$dien)(H$_2$O)]$^{2+}$	2.27 ± 0.01	16.8 ± 0.4	- 0.3 ± 1.3	-7.7 ± 0.5

* presented in non SI-units for direct comparison with available literature data

$\Delta V_{\text{solv.}}^{+}$, due to changes in solvation during the formation of the transition state. On the one hand it is reasonable to argue that $\Delta V_{\text{solv}}^{+}$ should be positive due to charge neutralization during the anation process and constant for the various entering ligands on account of their similar charge. On the other hand it is expected that $\Delta V_{\text{intr}}^{+}$ should be negative and should depend on the size of the entering ligands. It follows that $\Delta V_{\text{intr}}^{+}$ outweighs $\Delta V_{\text{solv}}^{+}$ to produce an overall negative value for $\Delta V_{\text{exp}}^{+}$ and that the trend in $\Delta V_{\text{exp}}^{+}$ can be ascribed to an increasing negative contribution from $\Delta V_{\text{intr}}^{+}$ along the series $Cl^- < Br^- < I^- < N_3^-$.

Alternatively, ion-pairing[16] may play a significant role during anation, resulting in a mechanism

$$[Pd(L)(H_2O)]^{2+} + X^- \overset{K}{\rightleftharpoons} \{Pd(L)(H_2O)^{2+} \cdot X^-\}$$
$$\swarrow k$$
$$Pd(L)X^+ + H_2O$$
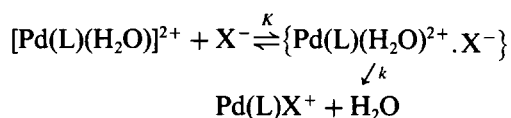
for which $k_{\text{obs}} = kK[X^-]/(1 + K[X^-])$. The rate-law simplifies to $k_{\text{obs}} = kK[X^-]$ in our case where no appreciable curvature in the k_{obs} vs $[X^-]$ plots (Table 4) is observed. It follows that $k_{\text{anation}} = kK$ and $\Delta V_{\text{exp}}^{+} = \Delta \bar{V}(K) + \Delta V^+(k)$ with $\Delta \bar{V}(K)$ being expected positive due to charge neutralization during ion-pair formation. The significantly negative values of $\Delta V_{\text{exp}}^{+}$ (Table 5) suggest that $\Delta V^+(k)$ should be even more negative to outweigh the positive contribution from $\Delta \bar{V}(K)$ and thus confirm the associative character of the anation process.

Table 6 summarizes the present kinetic data obtained for anation by Cl^- with those previously measured for some other palladium(II) substituted dien complexes. The reactivity decreases in the order 1, 4, 7-Et$_3$dien > 1, 1, 7, 7-Me$_4$dien > 1, 1, 4-Et$_3$dien > 1, 1, 4, 7, 7-Me$_5$dien > 1, 1, 7, 7-Et$_4$dien > 4-Me-1, 1, 7, 7-Et$_4$dien and is accompanied by an increase in ΔH^+. This is ascribed to a corresponding increase in the extent of steric hindrance along the quoted series. The results illustrate the similarity in the steric behaviour of methyl and ethyl groups and the importance of the position of substitution (see 1, 4, 7-Et$_3$dien and 1, 1, 4-Et$_3$dien). The values of ΔS^+ and $\Delta V_{\text{exp}}^{+}$ are such that no definite tendency can be assigned. For instance, the more negative value of $\Delta V_{\text{exp}}^{+}$ for the anation of the species [Pd(4-Me-1,1,7, 7-Et$_4$dien)(H$_2$O)]$^{2+}$ is in agreement with le Noble's hypothesis[17] regarding more sterically hindered associative reactions having "later" or more product-like transition states, but it is in disagreement with the suggestion by the almost zero value

of ΔS^+ that the anation process is less associative (i.e. more dissociative). Moreover, the first and the last entry of $\Delta V_{\text{exp}}^{+}$ in Table 6 are almost the same, strongly emphasizing the prevailing associative process for the series of complexes quoted. The magnitude of $\Delta V_{\text{exp}}^{+}$ can once again be interpreted in terms of positive and negative contributions from $\Delta V_{\text{solv}}^{+}$ and $\Delta V_{\text{intr}}^{+}$, or $\Delta \bar{V}(K)$ and $\Delta V^+(k)$, respectively as discussed above.

Finally, a comparison of the results of this investigation with those reported for the anation of the species [Pt(dien)(H$_2$O)]$^{2+4,18}$ highlights an interesting difference. The order of reactivity $I^- > Br^- > N_3^- > Cl^-$ reported[4] for this species differs from the order of reactivity $N_3^- > I^- > Br^- > Cl^-$ found in the present study. The markedly higher nucleophilicity of the azide ion in the case of the palladium(II) systems has also been observed in other studies[4,5] and should be explained in terms of the inherent nature of the sterically hindered complexes. Unfortunately, the reactivity order for the extremely fast anation reactions of the corresponding species [Pd(dien)(H$_2$O)]$^{2+}$ cannot be determined to aid in the understanding of this feature.

REFERENCES

1. A preliminary report on this and subsequent work was presented at the 22nd International Conference on Coordination Chemistry, Budapest, 1982, Abstract No. Tu P 71.
2. D. A. Palmer and H. Kelm, *Inorg. Chim. Acta* 1976, **19**, 117.
3. W. Rindermann, D. A. Palmer and H. Kelm, *Inorg. Chim. Acta* 1980, **40**, 179.
4. M. Kotowski, D. A. Palmer and H. Kelm, *Inorg. Chim. Acta* 1980, **44**, L113.
5. D. A. Palmer and H. Kelm, *Inorg. Chim. Acta* 1975, **14**, L27.
6. M. Kotowski, Ph.D. Thesis. Frankfurt/Main (1977).
7. D. A. Palmer, R. Schmidt, R. van Eldik and H. Kelm, *Inorg. Chim. Acta* 1978, **29**, 261.
8. D. A. Palmer and H. Kelm, *Aust. J. Chem.* 1979, **32**, 1415.
9. D. A. Palmer and H. Kelm, *Inorg. Chim. Acta* 1980, **39**, 275.
10. R. van Eldik, D. A. Palmer, R. Schmidt and H. Kelm, *Inorg. Chim. Acta* 1981, **50**, 131.
11. W. H. Baddley and F. Basolo, *J. Am. Chem. Soc.* 1966, **88**, 2944.

12. E. L. J. Breet and R. van Eldik, *Inorg. Chim. Acta* 1983, **76**, L301.
13. C, H, N and Cl analyses performed by Hoechst Analytical Laboratory, Frankfurt/Main.
14. M. L. Tobe, *Inorganic Reaction Mechanisms*, 45. Nelson, London (1972).
15. Ref. 14, p. 51.
16. J. B. Goddard and F. Basolo, *Inorg. Chem.* 1968, **7**, 936.
17. T. Asano and W. J. le Noble, *Chem. Rev.* 1978, **78**, 407.
18. H. B. Gray and R. J. Olcot, *Inorg. Chem.* 1962, **1**, 481.

SOLVENT EXTRACTION OF COPPER(II), NICKEL(II), COBALT(II), ZINC(II), AND IRON(III) BY HIGH MOLECULAR WEIGHT HYDROXYOXIMES

L. CALLIGARO, A. MANTOVANI and U. BELLUCO*

Istituto di Chimica Industriale, Facoltà di Ingegneria, Università di Padova, Via Marzolo,
9, 35100 Padova, Italy

and

M. ACAMPORA

Istituto di Chimica Fisica, Università di Padova, Via Loredan 4, 35100 Padova, Italy

Abstract—The effects of pH have been examined on the extraction of the title ions by complexing with LIX-64N in kerosene. The extent of metal extraction as a function of pH is: Cu(II) < Fe(III) < Ni(II) < Zn(II) < Co(II). Stripping of all metal ions but cobalt with sulphuric acid from loaded kerosene complexing solutions is easily accomplished. Oxidation of Co(II) to Co(III) in the organic phase prevents stripping of this metal ion.

Solvent extraction processes represent a technique of high significance in the hydrometallurgical field.[1-3] Extraction of metal ions into a water insoluble organic phase can only be effected if the metal ions are transferred as neutral species. Suitable to this purpose are acidic chelating extractants containing long chain alkyl groups to increase the lipophilicity of both complexes and ligands. To this class of ligands belong the substituted *ortho*-hydroxyoximes produced by General Mills Inc. and marketed as LIX reagents.[4-6] Since these reagents are known to be specific for copper extraction from acidic solutions,[6-8] most investigations have dealt with this metal and scarce information is available on the extraction of other metals. The present research partially fulfils these requirements, extending the solvent extraction process by the LIX-64N reagent to Cu(II), Ni(II), Co(II), Zn(II), and Fe(III) metal ions. Back extraction of some metal ions from kerosene solutions with sulphuric acid has also been studied.

EXPERIMENTAL

Apparatus

The extraction apparatus consists of a series of 100 cm³ round flasks magnetically stirred and immersed in a water bath set at 22°C. Metal analyses were performed on a Perkin–Elmer 380 atomic

absorption spectrophotometer. The pH measurements were taken on a Radiometer PHM28c pHmeter calibrated at pH 4.00 and pH 8.00 using buffer solutions.

Reagents

LIX-64N (General Mills Inc.) was used as a chelating extraction reagent and white kerosene (Fluka) as a diluent. Throughout a 10% (v/v) solution of this solvent (commercially available) was employed. $CuSO_4 \cdot 5H_2O$, $Fe_2(SO_4)_3 \cdot H_2O$, $NiSO_4 \cdot 7H_2O$, $ZnSO_4 \cdot 7H_2O$, and $CoSO_4 \cdot 7H_2O$ (Carlo Erba, Reagent grade) were dissolved in distilled water and used as 2.5×10^{-2} M solutions; a 8.33×10^{-3} M solution was however used for the iron salt, owing to its different stoichiometry. The pH of the aqueous phase was adjusted using concentrated solutions of sulphuric acid and sodium hydroxide. All solutions were adjusted to an ionic strength of 0.1 M with Na_2SO_4.

Extraction procedure

The distribution of the single metal ions between equal phase volumes (10.0 cm³) was examined at various hydrogen ion concentrations. 10.0 cm³ portions of each aqueous metal ion solution were adjusted at various pH using both H_2SO_4 and NaOH and added to 10.0 cm³ of 10% kerosene LIX-64N solution. Flasks were capped and mixtures magnetically stirred for 2 hr to reach equilibrium. The contents of each flask were then

---

*Author to whom correspondence should be addressed.

transferred to a separatory funnel and allowed to separate for *ca.* 1/2 hr. pH and metal concentration of the decanted aqueous layer were then determined. The metal ion contents in the organic phase were calculated as the difference between the starting aqueous soution concentration and the residual contents after equilibration. To achieve more accurate data concerning selective separations of couples of ions (e.g. Cu–Ni) the above procedure was slightly modified. The aqueous solutions were prepared mixing up two equal portions (10.0 cm^3) of the Cu and Ni solutions, each having the same concentration used for single experiments (i.e. 2.5×10^{-2} M) and the volume of the organic phase containing the chelating ligand was doubled. Thus, a constant LIX-64 N/metal ion ratio was always used.

Back extraction

The efficiency of aqueous sulphuric acid solutions in stripping the metal ions from loaded kerosene phases was determined by shaking equal volumes (10.0 cm^3) of kerosene solutions and sulphuric acid at various concentrations. After *ca.* 2 hr the mixtures were allowed to separate in a separatory funnel and the metal ion contents of the aqueous phases measured.

Loading capacity of LIX-64N

Since LIX-64N is a commercial solution of a mixture of an aromatic 2 - hydroxy - benzophenoneoxime (LIX-65N) and of an aliphatic α-hydroxyoxime (LIX-63) (the latter in small proportion, *ca.* 5%) in a high molecular weight hydrocarbon solvent,[9] the content of the active chelating ligand cannot be directly determined. The matter is also complicated by the existence of a *syn-anti* equilibrium, where the *syn* isomer is inactive. The loading capacity of the extractant solution was therefore chosen as active ligand concentration, the loading capacity being defined as the maximum amount of Cu(II) that a solution of the LIX reagent can accept when contacted with an infinite amount of a concentrated aqueous solution of Cu(II). This was experimentally determined by contacting successively 50 cm^3 of the LIX solution with several aqueous solutions of CuSO$_4$ 0.1 M at pH of *ca.* 6 (a value for which the extraction of Cu(II) is highest and the ligand cannot receive any more Cu(II) ions. See Fig. 1). The copper contained in the saturated organic phase was then stripped with five 20.0 cm^3 portions of 1 M H$_2$SO$_4$.

The molar amount of the active LIX reagent was considered to be twice the Cu(II) ion present in the stripped solution, since a complex of the type Cu(LIX)$_2$ is assumed to be formed in the kerosene

phase. On this basis the titre of the commercial LIX-64N stock solution was determined as 1.02 M.

RESULTS AND DISCUSSION

LIX-Reagents, which were introduced about twenty years ago by General Mills for the hydrometallurgical refining of copper, are in general high molecular weight hydroxyoximes. In particular, LIX-64N is a blending of 2 - hydroxy - 5 - nonylbenzophenone oxime (LIX-65N) and 5,8 - diethyl - 7 - hydroxydodecan - 6 - one oxime (LIX-63), the latter being the minor component (typical ratio 20:1 by weight).[4,9]
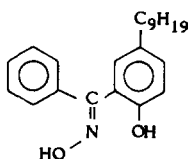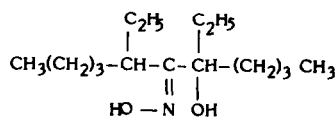
LIX-65N   LIX-63

Both reactants behave as acidic monoprotic ligands, HR, so that the extraction of divalent metal ions can be represented by the following equation:

$$M^{2+}_{(a)} + 2HR_{(o)} \rightleftharpoons MR_{2(o)} + 2H^+_{(a)} \qquad (1)$$

(where the subscripts (*a*) and (*o*) denote aqueous and organic phases, respectively). Previous studies showed that LIX-63 serves mainly to enhance the kinetics of extraction and has little or no effect on copper extraction, at least up to pH 4.[6,10]

Dependence of extraction ease on pH

Formation of uncharged metal complexes with LIX-64N reagent is largely dependent on the acid content of the aqueous phase, as can be seen from equilibrium (1). The distribution of a metal ion in an organic phase containing such reagents is therefore strictly controlled by the acidity of the solutions. Results from contacting equal volumes of kerosene and aqueous phases are shown in Fig. 1 as a plot of the percentage extraction vs the final pH of the aqueous phase.

Owing to the different charge (Fe^{3+} is likely to afford a complex of the type FeR$_3$), in order to get comparable data the iron concentration was chosen such that the amount of the chelating ligand was twice that stoichiometrically required, as for other divalent cations. Results of extraction from solutions containing single ions (Fig. 1) emphasize that all the metal ions investigated form stable complexes with LIX-64N in neutral or even acidic solutions. By properly choosing the pH ranges,
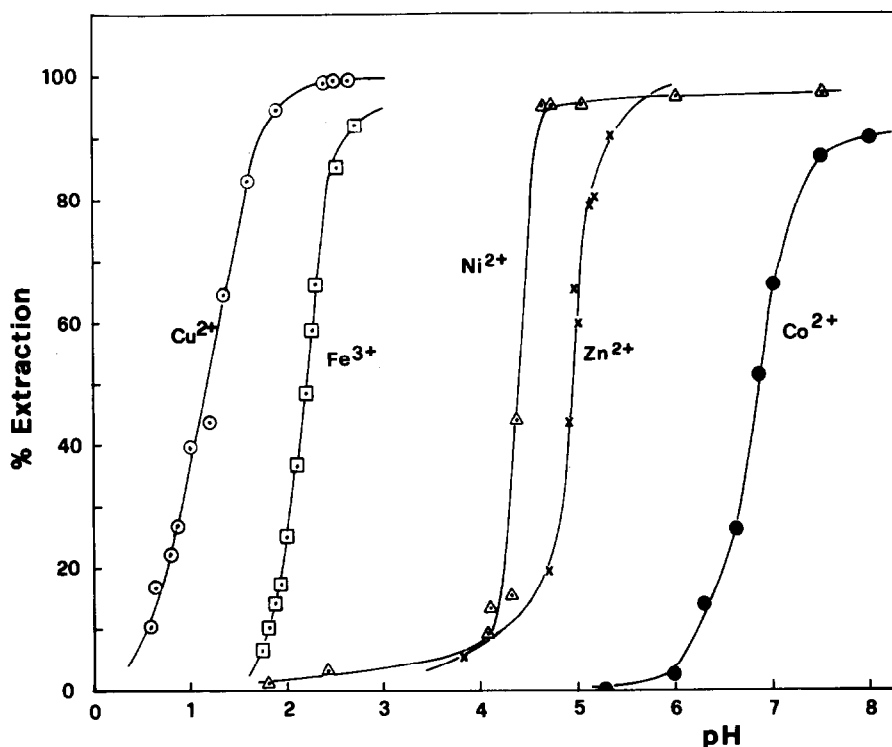
Fig. 1. Extraction of 2.5×10^{-2} M solutions of Cu(II), Ni(II), Co(II), Zn(II), and of a 1.67×10^{-2} M solution of Fe(III) with 0.1 M LIX-64N in kerosene; $a/o = 1$.

they can be selectively separated from each other. The extent of metal extraction as a function of pH, Cu(II) < Fe(III) < Ni(II) < Zn(II) < Co(II), is in strict agreement with the stability constants of the related salicylaldoxime complexes of these ions.[11] The most striking deviation is represented by Co(II), which although having been reported to have the same stability constant as Zn(II), is extracted at much higher pH values. The extraction of these ions by salicylaldoxime in benzene also compares well with the behaviour reported in Fig. 1 for the LIX-64N reagent.

The parallelism found for LIX-64N and salicylaldoxime is in agreement with the proposal of the same structure for the complexes obtained by both chelating ligands, which is quite an expected result. The structure below is thus proposed for the Cu(II) complex:[6,13]
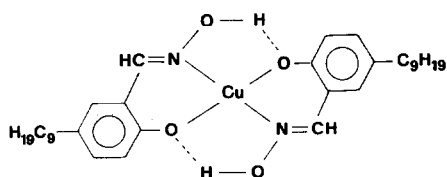
The distribution plot of Cu(II) agrees also with that reported by Flett et al. for LIX-65N. To get more reliable data on selectivity, in one case an extraction study of an equimolecular mixture of two ions, namely Cu(II) and Ni(II), has been carried out. The results reported in Fig. 2 closely

resemble the corresponding curves of Fig. 1, thus confirming their reliability and showing that the extraction of copper is essentially unaffected by the presence of nickel, and vice versa.

The results and experimental conditions from this study prove of straight forward application to large scale commercial metal recovery processes. In
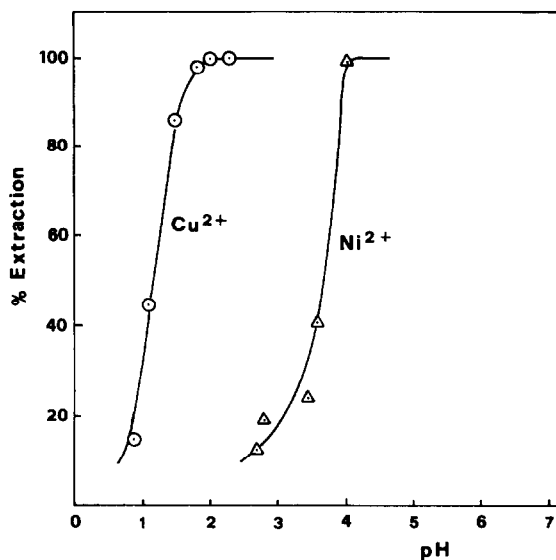
Fig. 2. Extraction of an aqueous equimolecular mixture of Cu(II) and Ni(II) (1.25×10^{-2} M) with 0.1 M LIX–64N in kerosene; $a/o = 1$.

fact, the ions studied undergo practically complete extraction in kerosene in a single run. Low solubility in water (reducing losses to a minimum) is also satisfied by kerosene, which thanks to its low volatility, can be used at quite high temperatures, a condition often required to speed up extraction in industrial applications. The ligand and metal complexes, also have low aqueous solubility in the pH range explored. At pH 1.8 the following data have been reported:[14]
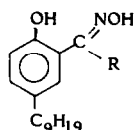
	R=H	R = Ph$_3$(LIX-65N)	LIX-63	Cu(LIX-65N)$_2$
Solubility (10^6 M mol l/l)	6.8	1.0	15.5	0.13

A slight increase in solubility is expected for alkaline solutions of these ligands, where dissociation of the phenolic OH group takes place yielding ionic species of enhanced solubility in water. For instance, when R = H (see the structure above), the following behaviour was observed:[14]

pH	< 8	10.5	11.5	12.5
Solubility (10^6 M)	< 7	40	140	> 380

Although these values are expected not to be reached in a two phase system because of the favourable distribution of the chelating ligand in the organic phase[15,16] use of ligands of this type at higher pH values than those explored in this work is not advised. Moreover, precipitation of metal hydroxides in neutral to alkaline solutions can make the extraction more difficult.

BACK EXTRACTION (OR STRIPPING) OF METAL IONS FROM KEROSENE SOLUTIONS

For use in industrial applications, ease of recovery of metal from the organic phase and regeneration of the reagent for recycle are essential. This can be accomplished by stripping the kerosene solutions of the complexes with sulphuric acid, thus obtaining a concentrated aqueous solution of the metal ions and an organic phase containing the chelate reagent, which can be recycled. It should be pointed out that the metals requiring higher pH values in the extraction process require lower acid concentration in their back extraction from the organic phase. In this respect, nickel(II) and copper(II) (Fig. 3) have a regular behaviour whilst cobalt(II) is hardly stripped from the organic solutions.

Indeed, even concentrated sulphuric acid has no significant effect on the extracted cobalt complex. This fact may be attributed to the oxidation of Co(II) to Co(III) and the formation of stable
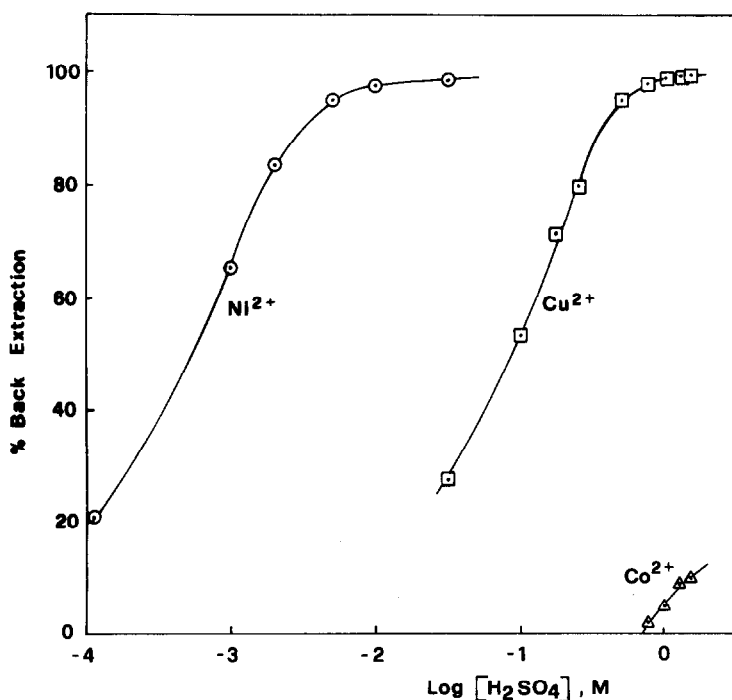
Fig. 3. Back extraction of 0.1 M LIX-64N kerosene solutions loaded with Cu(II), Ni(II) and Co(II) by sulphuric acid.

μ-peroxo-complexes in the organic phase.[17,18] The stripping process is favourable and complete for Cu(II) and Ni(II) under relatively mild conditions. By controlling the concentration of the sulphuric acid it is also possible to effect a further separation of the metal ions. When diluted acid is employed only nickel(II) is stripped, rejecting both copper(II) and cobalt(II) ions. Spot experiments carried out on Fe(III), and Zn(II) kerosene solutions indicate the reversibility for these systems.

CONCLUSIONS

Substituted salicylaldoximes, such as LIX-64N, proved to be highly selective copper(II), nickel(II), zinc(II), and iron(III) ions. The availability of the chelating extractants will both allow metal ion recovery from low grade solutions and separation in purification processes. The only drawback highlighted by this study is the irreversibility of cobalt(II) extraction.

REFERENCES

1. J. Monhemius, *Chem. Ind.* 1981, 410.
2. G. A. Davies, *Chem. Ind.* 1981, 420.
3. D. S. Flett, *Chem. Ind.* 1981, 427.
4. E. Uhlig, *Coord. Chem. Rev.* 1982, **43**, 299.
5. A. W. Ashbrook, *Coord. Chem. Rev.* 1975, **16**, 285.
6. D. S. Flett, D. N. Okuhara and D. R. Spink, *J. Inorg. Nucl. Chem.* 1973, **35**, 2471.
7. D. S. Flett, *Acc. Chem. Res.* 1977, **10**, 99.
8. A. W. Ashbrook, *Anal. Chim. Acta* 1972, **58**, 115 and references therein.
9. J. S. Preston, *J. Inorg. Nucl. Chem.* 1980, **42**, 441.
10. K. S. Koppiker and N. Maity, *Anal. Chim. Acta* 1975, **75**, 239.
11. K. Burger and I. Egyed, *J. Inorg. Nucl. Chem.* 1965, **27**, 2361.
12. I. Dahl, *Anal. Chim. Acta* 1968, **41**, 9.
13. A. Chakravorthy, *Coord. Chem. Rev.* 1974, **13**, 1 and references therein.
14 H. J. Foakes, J. S. Preston and R. J. Whewell, *Anal. Chim. Acta* 1978, **97**, 349.
15. J. S. Preston and Z. B. Luklinska, *J. Inorg. Nucl. Chem.* 1980, **42**, 431.
16. S. P. Carter and H. Freiser, *Anal. Chem.* 1980, **52**, 511.
17. P. Guesnet, J. L. Sabot and D. Bauer, *Proc. Int. Solv. Extraction Conf.*, Liege, 1980, Paper 80–119.
18. A. G. Sykes and J. A. Weil, *Progress in Inorg. Chem.* 1970, **13**, 1.

CHEMICAL SHIFT AND QUADRUPOLE COUPLING OF THE ^{27}Al NMR SPECTRA OF LiAlO$_2$ POLYMORPHS

D. MÜLLER* and W. GESSNER
Central Institute of Inorganic Chemistry of the Academy of Sciences of the G.D.R.,
DDR–1199 Berlin–Adlershof, German Democratic Republic

and

G. SCHELER
Department of Physics of the Friedrich Schiller University, DDR–6900 Jena,
German Democratic Republic

Abstract—^{27}Al chemical shift data of polycrystalline LiAlO$_2$ polymorphs, obtained from high field measurements in combination with magic-angle spinning techniques, have been used for the determination of the Al coordination in the α-, β-, and γ-phase. The β-phase was shown to have only tetrahedrally coordinated Al atoms. In addition quadrupole coupling data have been derived from analysis of low field NMR spectra of ^{27}Al in order to characterize the symmetry of the Al sites. The NMR results are discussed with regard to the crystal structure of the phases.

^{27}Al nuclear magnetic resonance can provide structural information about the environment of the Al nuclei in polycrystalline and amorphous samples using either quadrupole coupling data or chemical shifts. In the first case the quadrupole moment (eQ) of the Al nucleus is used as a sensitive probe for the electric field gradient (EFG) at the nuclear site. The resulting quadrupole coupling constant e^2qQ/h (h is Planck's constant, and $eq = V_{zz}$) is a measure of the size of the electric field gradients, and the EFG tensor is characterized by the asymmetry parameter $\eta = (V_{xx} - V_{yy})/V_{zz}$ (V_{ii} denotes components of the EFG tensor in the principal coordinate system with $|V_{xx}| \leq |V_{yy}| \leq |V_{zz}|$).

In the other case the magnetic shielding of the aluminium by its electronic environment is investigated. As it has been shown recently,[1-3] the second way proves to be a convenient method for the identification of AlO$_4$ tetrahedra and AlO$_6$ octahedra. So in aluminates and aluminium oxides

AlO$_6$ groups provide shifts between 0 and 20 ppm, AlO$_4$ units give rise to lines between 60 and 80 ppm. Furthermore, in addition to their dependence on the special Al coordination, the chemical shifts were also shown to be dependent on the type of nuclei present in the second coordination sphere.[4] The determination of the ^{27}Al chemical shifts, usually complicated by the dominant quadrupolar broadening in solids, was facilitated at high magnetic fields in combination with magic-angle spinning technique (MAS) which greatly suppresses quadrupolar line broadening.[5,6] The quadrupole coupling data are usefully determined at low magnetic fields.

For a systematic NMR investigation both at high and low magnetic fields the three known polymorphs of LiAlO$_2$ were chosen which have different crystal structures with different kinds of Al coordination. In such a system, all phases have the same chemical composition, possible additional influences by various cations being eliminated.

In the trigonal α-LiAlO$_2$ the Li and Al atoms

---

*Author to whom correspondence should be addressed.

have octahedral coordination,[7] in the tetragonal γ-phase (space group $P4_12_12$) both are tetrahedrally coordinated.[8] For the third modification, β-LiAlO$_2$, conflicting structures have been proposed. So Chang and Margrave[9] quote a monoclinic structure for the β-LiAlO$_2$, containing Li and Al atoms in mixed tetrahedral and octahedral coordination, whereas it is classified by Sachenko–Sakun *et al.*[10] and West[11] as orthorhombic and isostructural with β-LiGaO$_2$ (space group $Pna2_1$) with only tetrahedrally coordinated atoms.[12]

Quadrupole coupling data of LiAl$_5$O$_8$, a modified spinel form, have been reported by Stauss.[13]

EXPERIMENTAL

The low field ^{27}Al NMR measurements were carried out on a wide-line NMR spectrometer KRB 35 at frequencies of 4, 9 and 16 MHz. The first derivatives of the spectra were recorded. The high field measurements were carried out at the Friedrich–Schiller-University of Jena on a FKS 176 FT–NMR spectrometer supplemented with a 6.4 T superconducting magnet. The spectra were recorded at 70.4 MHz with static samples and in combination with the MAS-technique using a spinning rate of about 2.7 kHz. $\pi/6$ pulses of 1.6 μs duration were used. Up to 5000 FID's were accumulated with a repetition time of 0.5 s.

The chemical shifts, δ (ppm), measured relative to an external standard of aqueous AlCl$_3$ solution are denoted by a positive sign for low field shifts. The reproducibility of the chemical shift values was 1 ppm. The quadrupole coupling constants, the dipolar broadening, and asymmetry parameters were derived by a least-square fitting from the low field spectra, recorded at different magnetic fields, with an accuracy of 0.1 MHz, 0.5 kHz and 0.05, respectively.

The preparation of the samples is described elsewhere.[14]

RESULTS AND DISCUSSION

Figure 1 shows the derivative ^{27}Al NMR spectra of the three LiAlO$_2$ polymorphs recorded at low magnetic field (9 MHz, respectively 16 MHz) with conventional continuous wave technique. The corresponding spectra, recorded using pulsed NMR techniques, partially showed incorrect lineshapes due to the blocking of the receiver by the r.f. pulses. Therefore they were not suitable for the determination of the quadrupole parameters. The lineshape of the powder-pattern of the central (1/2, −1/2) spin transition perturbed by second-order quadrupole effects was computed according to
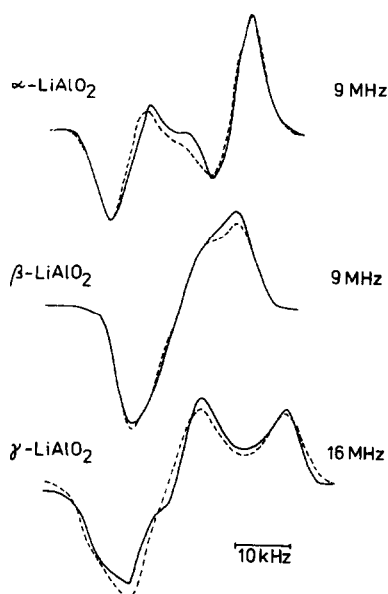
Fig. 1. ^{27}Al NMR spectra of the LiAlO$_2$ polymorphs obtained at 9 and 16 MHz. (——— experimental spectrum; ‐‐‐‐ computed lineshape; parameters are given in Table 1).

Narita *et al.*[15] The quadrupole coupling constant and asymmetry parameter were derived by a least-squares fitting.[16] Dipolar broadening was considered using a Gaussian convolution function with a peak-to-peak width of 2β of the derivative. The results are given in Table 1.

The corresponding high field spectra, shown in Fig. 2, illustrate the expected decrease of the quadrupolar broadening of the spectra with increasing magnetic fields. Therefore, at high fields correct lineshapes of the spectra could be obtained by pulsed NMR. The spectra, additionally narrowed by magic angle spinning of the samples, are also shown in Fig. 2. These MAS spectra allow an approximate determination of the chemical shifts. Considering the residual quadrupole shifts, the exact isotropic chemical shifts ($δ_{iso}$) can be determined using the quadrupole coupling parameters derived from the low field spectra (see Table 1). The value of $δ_{iso}$ can be determined either from the fitted high field spectra of the static sample or can be calculated directly adding a correction term[5,16]

$$δ_{corr} = 3 \times 10^4 \cdot \frac{1}{5}\left(1 + \frac{η^2}{3}\right)$$

$$\times \left(\frac{e^2qQ}{hν_0}\right)^2, \text{(ppm)} \qquad (1)$$

where $ν_0$ is the resonance frequency (MHz).

The chemical shifts $δ_{exp}$, experimentally obtained from the MAS spectra, the so-calculated correction

Table 1. ^{27}Al NMR data of the LiAlO$_2$ polymorphs

Phase	e^2qQ/h (MHz)	η	chemical shift (ppm)			2β [c] (kHz)
			δ_{exp}	δ_{corr} [a]	δ_{iso} [b]	
α	2.8	0.05	7	9.5	17	5.2
β	1.8	0.55	79	4	83	5.6
γ	3.2	0.70	67.5	14.5	82	6.0

[a] Correction calculated acc. equation (1); see text

[b] $\delta_{iso} = \delta_{exp} + \delta_{corr}$

[c] peak-to-peak width of a Gaussian convolution function
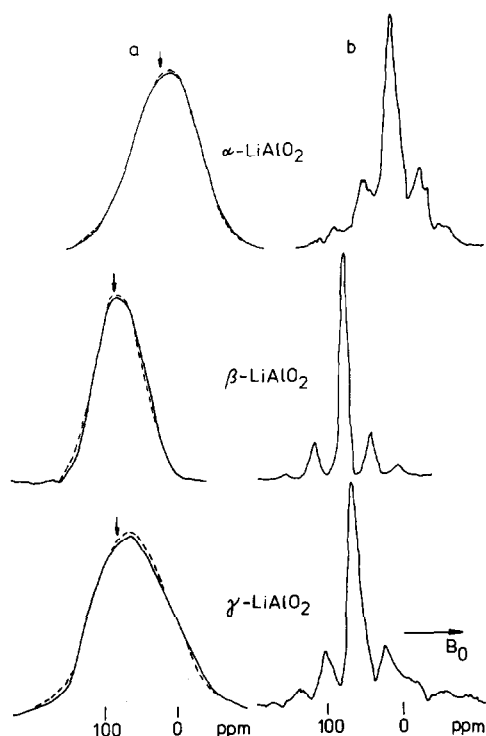
Fig. 2. High field ^{27}Al NMR spectra of the LiAlO$_2$ polymorphs obtained at 70.4 MHz. (a) Spectra of the static sample (----- computed lineshape using the quadrupole coupling data). Resulting locations of δ_{iso} are marked. (b) MAS spectra.

terms δ_{corr}, and the resulting exact isotropic chemical shifts δ_{iso} are also given in Table 1.

Chemical shifts

The chemical shifts of 17 and 82 ppm unambiguously reflect the octahedral Al coordination in the α-phase, and the tetrahedral Al coordination in the γ-phase of LiAlO$_2$, respectively. Likewise the chemical shift of 83 ppm in β-LiAlO$_2$ is a certain

evidence that the Al atoms in this phase are tetrahedrally coordinated. The comparison of the intensities of the NMR spectra of the various LiAlO$_2$ polymorphs showed comparable quantities. By this means it is checked that all of the Al nuclei are detected. Such an analysis is necessary since in some cases, mainly observed with 6-coordinated Al,[17] certain distorted Al–O structural groups could not be detected by NMR because of extreme line broadening. Thus it can be concluded that only tetrahedrally coordinated Al atoms exist in β-LiAlO$_2$. By this the NMR studies confirm the conclusions of Sachenko–Sakun et al.[10] and West[11] who classified the β-LiAlO$_2$ as orthorhombic with tetrahedral Al atoms only. A detailed discussion of this result in connection with the results of other methods is given elsewhere.[14]

As it can be seen from Figs. 1 and 2, the spectrum of β-LiAlO$_2$, compared to those of the other modifications, shows the smallest half-width of the resonance line indicating small distortions, i.e. minor electric field gradients, at the Al sites in this phase. This is also reflected in the quadrupole coupling constant of 1.8 MHz, compared to values of 2.8 and 3.2 MHz for the other phases. Corresponding to the small quadrupole coupling constant also a small, above-mentioned correction of the chemical shift value δ_{exp} results according to eqn (1). Whereas the experimentally found chemical shifts of γ- and β-LiAlO$_2$ actually differ more than 10 ppm, after the necessary correction only one common value of about 82 ppm results for both phases which approaches the value of Al(OH)$_4^-$ ions in alkaline solutions. Therefore the variation of δ_{exp} is to be assigned to residual quadrupole shifts and not to different magnetic shieldings of the Al nuclei. Thus the corrected ^{27}Al NMR chemical shifts seem to provide, apart from the direct coordination number, no information

about the further AlO_4 environment in this case. It has to be considered, however, that there are indeed different phases but the same kind of cations. So possible influences of the cations on the Al–O bonding and accordingly on the chemical shift are eliminated.

Quadrupole coupling parameters

Further information on the structure can be derived from the quadrupole coupling constant e^2qQ/h and the asymmetry parameter η. Whereas, as discussed above, the quadrupole coupling constant of β-$LiAlO_2$ distinctly contrasts, the asymmetry parameter in the different phases also point to different symmetries of the Al sites.

For the octahedrally coordinated Al in the α-phase an asymmetry parameter of 0.05 was derived which requires axial symmetry in the electric field gradients (zero asymmetry parameter). According to the trigonal structure of α-$LiAlO_2$[7] this axial field gradient can be assigned to a shortening of the AlO_6 octahedra along a threefold axis (along c-direction). The distortion of the octahedron is reflected in the two different interatomic O–O distances within the edges but not in the Al–O distance which is equal for all oxygen atoms (1.90 Å).[7] The two extremely different kinds of interatomic O–O distances of 2.80 and 2.58 Å are obviously the reason for the large quadrupole coupling constant of 3.2 MHz.

In the cases of the other two phases with tetrahedral Al coordination asymmetry parameters of 0.7 and 0.55, respectively, were obtained indicating nonaxial symmetry of the Al sites. This is in accordance with the structures of γ- and β-$LiAlO_2$ referring to the proposal of orthorhombic symmetry in β-$LiAlO_2$ as confirmed by our chemical shift data. In both structures there is no n-fold rotation axis with $n > 2$ for the AlO_x polyhedra hence $\eta \neq 0$ is required. Only in the case of the γ-$LiAlO_2$ (space group $P4_12_12$)[8] a twofold axis exists for the AlO_4 groups which requires $\eta \neq 0$, too.

Both structures consist of infinite three-dimensional arrays of AlO_4 and LiO_4 tetrahedra. Whereas in the case of the β-phase the tetrahedra have only vertices in common, in the γ-phase each AlO_4 tetrahedron shares one of its edges with another LiO_4 tetrahedron and each vertex of the tetrahedron is shared with two additional tetrahedra, one of each kind. Therefore in the latter case a significant distortion of the AlO_4 results which is reflected in a distinct decrease of one of

the O–Al–O bond angles to 101.7°, and correspondingly in a shortening of one of the six edges of the tetrahedron with an interatomic O–O distance of 2.737 Å compared with the average of the remaining five, nearly identical O–O distances of 2.900 Å.[8] This is apparently the reason for the great coupling constant of 3.2 MHz in the case of γ-$LiAlO_2$, whereas in the case of the β-$LiAlO_2$ the exclusive connection of the tetrahedra via vertices, having nearly equal O–O distances, explains the small quadrupole coupling constant of 1.8 MHz.

This illustrates that, although having a crystal structure with a higher symmetry, special structural groups can be subject to stronger distortions. So general conclusions concerning the electric field gradients at the Al sites in AlO_x polyhedra cannot be derived from the knowledge of the type of crystal structure but from a detailed analysis of the neighbouring atoms only.

REFERENCES

1. D. Müller, W. Gessner, H. J. Behrens and G. Scheler, *Chem. Phys. Lett.* 1981, **79**, 59.
2. V. M. Mastikhin, O. P. Krivoruchko, B. P. Zolotovskii and R. A. Buyanov, *React. Kinet. Lett.* 1981, **18**, 117.
3. C. A. Fyfe, G. C. Gobbi, J. S. Hartman, J. Klinowski and J. M. Thomas, *J. Phys. Chem.* 1982, **86**, 1247.
4. D. Müller, D. Hoebbel and W. Gessner, *Chem. Phys. Lett.* 1981, **84**, 25.
5. H. J. Behrens and B. Schnabel, *Physica* 1982, **114B**, 185.
6. E. Kundla, A. Samoson and E. Lippmaa, *Chem. Phys. Lett.* 1981, **83**, 229.
7. M. Marezio and J. P. Remeika, *J. Chem. Phys.* 1966, **44**, 3143.
8. M. Marezio, *Acta Cryst.* 1965, **19**, 396.
9. C. H. Chang and J. L. Margrave, *J. Am. Chem. Soc.* 1968, **90**, 2020.
10. L. K. Sachenko–Sakun, I. V. Guseva and V. A. Kolesova, *Z. Neorg. Chim.* 1967, **12**, 3220.
11. A. R. West, *Z. Kristallogr.* 1975, **141**, 422.
12. M. Marezio, *Acta Cryst.* 1965, **18**, 481.
13. G. H. Stauss, *J. Chem. Phys.* 1964, **40**, 1988.
14. W. Gessner and D. Müller, *Z. Anorg. Allg. Chem.* in press.
15. K. Narita, J. Umeda and H. Kusumoto, *J. Chem. Phys.* 1966, **44**, 2719.
16. D. Müller, *Ann. d. Phys.* in press.
17. F. v. Lampe, D. Müller, W. Gessner, A.-R. Grimmer and G. Scheler, *Z. Anorg. Allg. Chem.* 1982, **489**, 16.

NOTE

SYNTHESIS AND CHARACTERISATION OF ReOCl₃(DTO)₂ AND ReOCl₃(MBT)₂ COMPLEXES†

V. YATIRAJAM* and M. LAKSHMI KANTAM

Department of Chemistry, Kurukshetra University, Kurukshetra 132119, India

Abstract—New complexes of Re(V) with dithiooxamide and 2-mercaptobenzothiazole with the general formula $ReOCl_3L_2$, were prepared starting from potassium perrhenate. The compounds were characterised by chemical analysis, optical spectra and magnetic susceptibilities.

Many complexes of the general formula $ReOX_3L_2$ are known.[1] We report below the preparation of two new complexes of the type $ReOX_3L_2$ where X = Cl, and L is DTO† or MBT† by reacting the ligand with H_2ReOCl_5 in acetic acid. Complexes of these ligands with some transition metals[2,3] are known, but not with rhenium(V).

EXPERIMENTAL

Measurements and materials

Spectra were recorded on Beckman DU-2, Beckman IR-20, Brucker IFS 113 as applicable. Magnetic susceptibilities were determined by the Gouy method and conductivities on a Philips bridge PR 9500/90. Standard methods were used for determining the elements. The ligands were recrystallised from ethanol. Petroleum ether (60–80°) and other pure chemicals were used after thorough drying. Experiments were carried out in a glove box under dry nitrogen.

Preparations

$ReOCl_3(DTO)_2$—0.500 g of potassium perrhenate and 0.200 g of hydroquinone were dissolved in 16.7 cm³ of conc. HCl and vigorously shaken. The pure yellow solution of $ReOCl_5^{2-}$ ion[4] was then mixed with 46 cm³ of saturated magnesium chloride solution and extracted with 30 cm³ methyl ethyl ketone. The ketone layer was then mixed well with 15 cm³ each of acetic acid and acetic anhydride, while cooling under the tap. The cold solution was shaken with 30 cm³ petroleum ether. Two layers formed. The lower yellow layer was mixed with 10 cm³ each of acetic acid and acetic anhydride. After standing for 2 hr, the solution was shaken with (25 + 15) cm³ petroleum ether, the lower viscous yellow layer of H_2ReOCl_5 was diluted with 20 cm³ acetic acid–HCl.

To the above solution, 0.415 g DTO dissolved in 150 cm³ acetic acid–HCl, was added. An orange–brown precipitate formed immediately. It was filtered, washed with acetic acid–HCl followed by petroleum ether and

dried for 6 hr under vacuum over sodium hydroxide. Yield is 90%. The compound is somewhat soluble in acetone and only slightly soluble in nitromethane and acetonitrile.

$ReOCl_3(MBT)_2$—To an acetic acid solution of H_2ReOCl_5 obtained as above from 0.450 g potassium perrhenate and 0.170 g hydroquinone, was added 0.549 g MBT in 104 ml acetic acid–HCl and 13 cm³ acetic anhydride. The dark green precipitate was washed and dried as for the DTO complex. Yield is 75%. The compound is highly soluble in acetone but less so in dichloromethane, benzene and ethanol.

RESULTS AND DISCUSSION

Both the compounds analyse satisfactorily to the general formula $ReOCl_3L_2$.

$ReOCl_3(DTO)_2$ gave Re, 32.56(33.90); S, 22.30(23.30); Cl, 18.68(19.34)%.

$ReOCl_3(MBT)_2$ gave Re, 28.05(28.97); S, 19.56(19.93); Cl, 16.04(16.51).

Calculated values, in parentheses. The complexes show $\mu_{eff} = 0.50, 0.35$ B.M. at 292K respectively. The conductance (Ω^{-1} cm² mol⁻¹ at 292K) of the DTO complex is 62 in acetone and of the MBT complex, 21 in acetonitrile. The compounds are thus neutral molecules with but slight ionisation of chloride in the solvents. As Re(V) is normally 6-coordinated, the ligands must be present as monodentate neutral molecules in the complexes.

$ReOCl_3(DTO)_2$ shows IR absorption peaks (in cm⁻¹) at 3400m, sh, b, 3160s, sh, b, 1660m, sh, b, 1590m, b, 1485s, 1410w, 1308w, b, 1235w, 1010m, 985m, 790m, b, 680w, b, 600m, 333w, 311.2w, 284.4w, 194.3m, b. The assignments are made following Scott and Wagner[5] and Suzuki.[6] A decrease in the ν(C=S) and an increase in the ν(CN) and ν(NH), point to coordination of sulphur to the metal. Changes in the position and breadth of (NH) bands in the complex, point definitely to monodentate bonding of the ligand through the S atom and extensive participation of the H atoms of NH_2 in intramolecular and intermolecular hydrogen bonding with chlorine in the complex. The electronic spectrum of the complex

---

†DTO–Dithiooxamide, MBT–2-mercaptobenzothiazole.

*Author to whom correspondence should be addressed.

shows λ_{max} (in nm) at 330(10, 104) and 450(2965) while that of the ligand shows at 330(3140) and 490(22), the ϵ's are in parentheses.

ReOCl$_3$(MBT)$_2$ shows IR absorption peaks (cm^{-1}) at 3400m, b, 3005w, 1600w, 1580w, 1500s, 1432s, 1350m, 1315w, 1275m, 1012s, 975s, 858w, 327w, 292m, 260w, 235w, 217m, 189w. These show that hydrogen is present on N and that MBT is coordinated to Re(V) through S of the thioketo group. The electronic spectrum of the complex shows λ_{max} (in nm) at 340(7837) and 720(28) while the ligand[7] shows at 330(2253) only.

Both the complexes show two bands in their IR spectra assignable to v(ReCl). Hence, they are *cis*-isomers.[8]

REFERENCES

1. G. Rouschias, *Chem. Rev.* 1974, 531.
2. M. F. El-Shazly, T. Salem, M. A. El-Sayed and S. Hedwey, *Inorg. Chim. Acta.* 1978, **29**, 155.
3. S. C. Jain and R. Rivest, *J. Inorg. Nucl. Chem.* 1967, **29**, 2787.
4. Harjinder Singh, *Chemistry of Rhenium*, Ph.D. Thesis. Kurukshetra University (1976).
5. T. A. Scott and E. L. Wagner, *J. Chem. Phys.* 1959, **30**, 465.
6. I. Suzuki, *Bull. Chem. Soc. Jpn.* 1962, **35**, 1286, 1449.
7. A. I. Busev, L. N. Lamakina and T. I. Ignat'eva, *Russ. J. Inorg. Chem.* 1976, **21**, 269.
8. E. A. Allen, N. P. Johnson, D. T. Rosevear and G. Wilkinson, *J. Chem. Soc. A.* 1969, 788.

NOTE

TRANS-1,2-DITHIOOXALATE AS BRIDGING LIGAND—II†

THE X-RAY CRYSTAL STRUCTURE OF
μ-1,2-DITHIOOXALATO-BIS[BIS(TRIPHENYLPHOSPHINE)SILVER(I)]

LJUBO GOLIČ and NADA BULC
Department of Chemistry, Edvard Kardelj University, Yu-61001 Ljubljana, Yugoslavia

and

WOLFGANG DIETZSCH*
Sektion Chemie, Karl-Marx-Universität, DDR-7010 Leipzig, Liebigstraße 18, G.D.R.

Abstract—The X-ray structure of $(Ph_3P)_2Ag(SOC_2SO)Ag(PPh_3)_2$ shows this complex as the second authentic example containing a bridging *trans*-1,2-dithiooxalate ligand. The compound crystallizes in the monoclinic space group $P2_1/c$ with $a = 13.159(2)$, $b = 11.895(2)$, $c = 20.939(5)$ Å, $\beta = 101.35(2)°$ and $Z = 2$. The structure was solved by Patterson and Fourier methods for 5649 diffractometer data and refined to a final R value of 0.066 for 3545 observed reflections. The dimensions of the dithiooxalate bridge are compared with those of the corresponding *trans*-dithiooxalate in $(Ph_4As)_4[(O_2C_2S_2)_2In(SOC_2SO)In(S_2C_2O_2)_2]$. Differences between structures containing bridging *trans*-dithiooxalate or bridging *cis*-dithiooxalate, respectively, are discussed.

The classical sulphur ligand 1,2-dithiooxalate has been a subject of considerable recent interest, because the presence of four donor atoms in the dianion causes more than one possibility of coordination to the metal ions: 1,2-dithiooxalate is able to act as terminal SS- or OO-bonded ligand but also as bridging ligand between different or equal metal ions, respectively. X-ray structure analyses of compounds of the heterometallic type show that the thermodynamically favoured coordination is the *cis*-arrangement of the ligands whose sulphur donor atoms are bonded by the more thiophilic metal ion.[1] If the 1,2-dithiooxalate dianion acts as a quadridentate bridging ligand linking two equal metal ions a *trans*-arrangement of the ligand is expected.[2] Recently we reported on the synthesis and X-ray structure of the first authentic example containing such a planar *trans*-dithiooxalate bridge connecting two distorted InS_2O octahedra in the complex compound $(Ph_4As)_4[(O_2C_2S_2)_2In(SOC_2SO)In(S_2C_2O_2)_2]$.[3] In this paper we present a new synthesis and X-ray structure of the compound $(Ph_3P)_2Ag(SOC_2SO)Ag(PPh_3)_2$, first prepared by Coucouvanis and Piltingsrud in 1973,[2] containing a similar dithiooxalate bridge. The question was, which differences arise from the linking of different coordination spheres around the silver(I) ions and the indium(III) ions, respectively.

EXPERIMENTAL

Tris(triphenylphosphine)silver(I)chloride (1.86 g; 2 mmol) was dissolved in 25 cm³ pyridine. In this solution 495 mg (2.5 mmol) potassium 1,2-dithiooxalate were suspended with vigorous stirring. Careful addition of water in drops produced a transparent brown solution. After slow addition of more water the compound was deposited as yellow–brown crystals which were recrystallized by dissolving in 10 cm³ pyridine and slow addition of ethanol. The yield was nearly 100% referred to $(Ph_3P)_3AgCl$. The complex darkens from 140°C and melts at 167–170°C.

This synthesis is useful also in the case of the isomeric ligand 1,1-dithiooxalate,[4] producing a brown crystalline complex (m.p. 139–141°C), or for the reaction between $(Ph_3P)_2AuCl·O.5C_6H_6$ and 1,2-dithiooxalate causing a light-yellow product (m.p. 151°C).

Crystallography of $(Ph_3P)_2Ag(SOC_2SO)Ag(PPh_3)_2$

Crystals suitable for diffraction studies were grown from a concentrated pyridine solution of the complex covered with a layer of isopropanol and stored at 0°C over 24 hr. The investigated crystal had the shape of a thin plate with the dimensions $0.48 \times 0.32 \times 0.05$ mm.

Crystal data. $C_{74}H_{60}Ag_2O_2P_4S_2$, $M = 1384.94$, monoclinic, $a = 13.159(2)$, $b = 11.895(2)$, $c = 20.939(5)$ Å, $\beta = 101.35(2)°$, $U = 3213.4$ Å³; space group $P2_1/c$, $Z = 2$, $T = 293(1)K$, $D_c = 1.4319$ g·cm⁻³, $F(000) = 706$, $\mu(Mo–K_a) = 0.808$ mm⁻¹.

---

†Part I see Ref. 3.
*Author to whom correspondence should be addressed.

Table 1. Comparison of selected bond lengths (Å) and angles (°) of complexes containing *trans*- and *cis*-1,2-dithiooxalate bridging ligands, respectively

$(Ph_3P)_2Ag(SOC_2SO)Ag(PPh_3)_2$		$(Ph_4As)_4^-$ $[(O_2C_2S_2)_2In(SOC_2SO)In(S_2C_2O_2)_2]^3$		$M[(O_2C_2S_2)Ag(PPh_3)_2]_3$ [1b]	M = Al	M = Fe	
Ag–O	2.510(6)	In–O	2.334(7)	Al–O$_1$	1.895(8)	Fe–O$_1$	1.996(6)
				Al–O$_2$	1.883(8)	Fe–O$_2$	2.010(6)
Ag–S	2.513(2)	In–S	2.634(4)	Ag–S$_1$	2.566(3)		2.566(3)
				Ag–S$_2$	2.612(2)		2.607(3)
Ag–P$_1$	2.458(2)				2.465(4)		2.455(2)
Ag–P$_2$	2.488(2)				2.492(3)		2.480(2)
C–C	1.561(11)		1.545(16)		1.55(2)		1.52(1)
C–S	1.717(8)		1.705(11)		1.66(1)		1.67(1)
C–O	1.213(9)		1.238(14)		1.28(1)		1.27(1)
P$_1$–Ag–S	116.0(1)			P$_1$–Ag–S$_1$	111.6(2)		111.9(1)
P$_2$–Ag–O	88.9(1)			P$_2$–Ag–S$_2$	98.0(1)		99.6(1)
P$_1$–Ag–P$_2$	122.2(1)						
O–Ag–S	73.8(1)	O–In–S	74.01(22)	S$_1$–Ag–S$_2$	113.4(2)		115.2(1)
					83.2(1)		83.3(1)
O–C–S	121.7(6)		122(1)	O$_1$–C$_1$–S$_1$	123.7(6)		121.2(4)
				O$_2$–C$_2$–S$_2$	124.7(6)		123.6(4)
O–C–C	120.3(7)		121(1)	O$_1$–C$_1$–C$_2$	112.0(9)		113.5(6)
				O$_2$–C$_2$–C$_1$	110.4(9)		112.2(6)
S–C–C	118.0(5)		118(1)	S$_1$–C$_1$–C$_2$	124.4(7)		125.2(5)
				S$_2$–C$_2$–C$_1$	124.9(7)		124.1(5)

Data collection. CAD4 diffractometer, Mo–K_α radiation ($\lambda = 0.71069\text{Å}$, graphite monochromator), scan method $\omega - 2\theta$, measured reflections 15004 ($1° < \theta < 20°$ $\pm h$, $\pm k$, $\pm l$; $20° < \theta < 25°$ $+h$, $+k$, $\pm l$), 564 σ unique reflections, 3545 of them observed [$I > 29(I)$].

Structure solution and refinement

The structure was solved by heavy atom method using all 5649 unique diffractometer data. The Patterson map revealed the positions for Ag atoms. From the subsequent Fourier maps the residual non-hydrogen atoms were estimated. The refinement of all positions including the anisotropic temperature factors gave a final $R = \Sigma|\Delta F|/\Sigma|F_o| = 0.066$ and $R_w = [\Sigma w(\Delta F)^2/\Sigma w F_o^2]^{1/2} = 0.070$, respectively, with 4656 contributing reflections. The positions of the phenyl-hydrogen atoms were calculated and have been included as fixed atom contribution in the structure factor calculation. A table containing a complete summary of the data collection and refinement, tables of atomic co-ordinates, anisotropic thermal parameters and lists of F_o/F_c have been deposited with the Editor as supplementary material. Computer, programs and sources of scattering factor data are given in Ref. 3.

RESULTS AND DISCUSSION

The synthesis of the complex $(Ph_3P)_2Ag(SOC_2SO)Ag(PPh_3)_2$ in pyridine–water guarantees a complete reaction of the starting compound $(Ph_3P)_3AgCl$, if an excess of potassium dithiooxalate is used, and provides well formed crystals of the desired compound whereas the non-reacting dithiooxalate remains in solution. As shown in Fig. 1 the complex contains two silver(I) ions connected by a planar 1,2-dithiooxalate bridging ligand in *trans*-arrangement. Additionally each silver atom is coordinated to two phosphorus atoms of triphenylphosphine ligands. Thus, the central metal ions are surrounded by four donor atoms causing distorted tetrahedral AgP_2SO skeletons. As in the complex salt $(Ph_4As)_4[(O_2C_2S_2)_2In(SOC_2SO)In(S_2C_2O_2)_2]$ the bridging dithiooxalate ligand contains the inversion centre of the whole molecule. Some of the more important bond-lengths and angles are listed in Table 1 for comparison with the corresponding values of the indium compound. It is to be seen that the distances and angles in the *trans*-dithiooxalate ligands of both molecules show no difference greater than three times their estimated stan-

dard deviations. However, stronger deviations appear if the 1,2-dithiooxalate is bonded in *cis*-arrangement between different metal ions, e.g. aluminium(III) and silver(I) or iron(III) and silver(I), respectively,[1b] (see also Table 1). Whereas the C–C distances and the O–C–S angle are very similar in the four compared molecules, the C–O distances and the S–C–C angles are somewhat smaller and the C–S distances and O–C–C angles somewhat greater in the case of the *trans*-arrangement of the bridging ligands. The most surprising result is the similarity of the Ag–O and Ag–S distances in the structure under investigation. The last is typical for covalent silver(I)-sulphur bonding[5] and near the sum of covalent radii (2.57 Å), whilst the Ag–O distance is longer as that found in the Ag(I)-monothiocarbamate hexamer $[AgSOCN(C_3H_7)_2]_6$ having a threefold nonplanar AgS_2O-coordination (Ag–O 2.34–2.38 Å).[6] However, the distance is quite similar to the values in the two *bis*-complexes of silver(I) with 8-hydroxy–quinoline (Ag–O 2.451(4)–2.505(5) Å)[7] and pyridinecarboxylate-2(Ag–O 2.524(4) Å)[8] containing distorted tetrahedral AgO_2N_2 cores.

Because the In–O and In–S distances in the other structure with a *trans*-dithiooxalate bridge differ as expected, the equality found for Ag–O and Ag–S distances should be assumed to be a result of the different coordination geometry around the central metal ions: in the silver complex the bridging dithiooxalate links tetrahedra, in the indium complex, however, octahedra.

The Ag–S distance is considerably shorter in the complex containing the *trans*-dithiooxalate than those found in the two *cis*-dithiooxalate heterometallic compounds. Interestingly, the Ag–P_1 and Ag–P_2 bond lengths, which were found to be different, show a very similar behaviour in all three complexes compared.

REFERENCES

1. (a) D. Coucouvanis, N. C. Baenziger and S. M. Johnson, *J. Am. Chem. Soc.* 1973, **95**, 3875; (b) F. J. Hollander and D. Coucouvanis, *Inorg. Chem.* 1974, **13**, 2381; (c) F. J. Hollander, M. Leitheiser and D. Coucouvanis, *Inorg. Chem.* 1977, **16**, 1615.
2. D. Coucouvanis and D. Piltingsrud, *J. Am. Chem. Soc.* 1973, **95**, 5556.
3. L. Golič, N. Bulc and W. Dietzsch, *Inorg. Chem.* 1982, **21**, 3560.
4. W. Stork and R. Mattes, *Angew. Chem.* 1975, **87**, 452.
5. G. F. Gaspari, A. Mangia, A. Musatti and M. Nardelli, *Acta Cryst.* 1968, **B24**, 367.
6. P. Jennische and R. Hesse, *Acta Chem. Scand.* 1971, **25**, 423.
7. J. E. Fleming and H. Lynton, *Can. J. Chem.* 1968, **46**, 471.
8. J.-P. Delaume, R. Faure and H. Loiseleur, *Acta Cryst.* 1977, **B33**, 2709.

Fig. 1. The molecular structure of $(Ph_3P)_2Ag(SOC_2SO)$-$Ag(PPh_3)_2$.

NOTE

EPR DETECTION OF [Cu(*mnt*)X₂]²⁻†—A POSSIBLE HALOGENIDE STABILIZED INTERMEDIATE IN LIGAND EXCHANGE REACTIONS

J. STACH,* U. ABRAM, R. KIRMSE and W. DIETZSCH
Department of Chemistry, Karl-Marx-University, 7010 Leipzig, Liebigstr. 18, G.D.R.

and

VERA K. BELYAEVA and I. N. MAROV
Institute of Geochemistry and Analytical Chemistry, Academy of Sciences, Moscow, Vorob'evskoje chaussee 47a, U.S.S.R.

Abstract—During the reaction of $[Cu(mnt)_2]^{2-}$ with CuX_2 (X = Cl, Br) $[Cu(mnt)X_2]^{2-}$ species are formed and characterized EPR spectroscopically supporting a dissociative mechanism for ligand exchange reactions between $[Cu(mnt)_2]^{2-}$ and other Cu(II), Ni(II) and Pd(II) complexes which contain unsaturated dichalcogeno ligands.

In suitable solvents the reaction of $[Cu(mnt)_2]^{2-}$ with four-membered ring chelates of Cu(II), Ni(II) or Pd(II) containing unsaturated sulphur or selenium ligands (1) is characterized by quantitative formation of the mixed ligand complexes.[1,2]

$$[Cu(mnt)_2]^{2-} + ML_2 \rightarrow [Cu(mnt)L]^- + [M(mnt)L]^-$$
(1a)

$$[Cu(mnt)_2]^{2-} + [ML_2']^{2-} \rightarrow [Cu(mnt)L']^{2-}$$
$$+ [M(mnt)L']^{2-}$$
(1b)
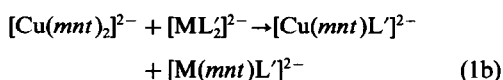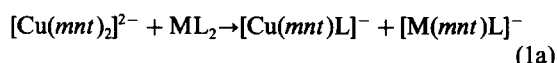
Unfortunately, the reactions between the corresponding copper complexes are too fast to be followed by a conventional EPR experiment. However, ligand exchange reactions of $[Cu(mnt)_2]^{2-}$ with the more inert Ni(II) and Pd(II) species are slow enough to be easily followed by EPR. The increase of the reaction rate with the temperature and after adding of Cu^{2+} ions, and the decrease in presence of the noncoordinated ligands

observed by EPR for the system $[Cu(mnt)_2]^{2-} + [Pd(i\text{-}mns)_2]^{2-}$ ($i\text{-}mns = (CN)_2C = CSe_2^{2-}$) suggest a dissociative start mechanism of the exchange reaction as given by the eqns (2) and (3).[3]

$$[Cu(mnt)_2]^{2-} \rightarrow [Cu(mnt)]_s + mnt^{2-}$$
(2)

$$[Pd(i\text{-}mns)_2]^{2-} \rightarrow [Pd(i\text{-}mns)]_s + i\text{-}mns^{2-}.$$
(3)
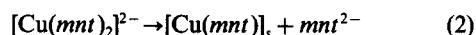
The solvated mono-chelates $[Cu(mnt)]_s$ and $[Pd(i\text{-}mns)]_s$ appear to be the important species in the following chain reaction.

In this paper we report the EPR detection† of Cu(II) sulphur ligand mono-chelates stabilized by halogenide
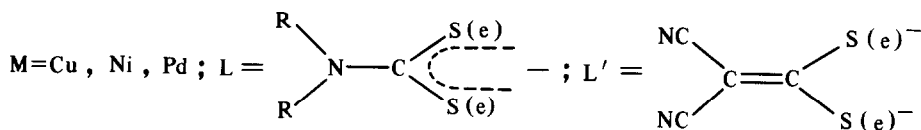
$$M=Cu, Ni, Pd ; L = \text{(structure)} \quad - ; L' = \text{(structure)}$$

copper complexes are too fast to be followed by a conventional EPR experiment. However, ligand exchange reactions of $[Cu(mnt)_2]^{2-}$ with the more inert Ni(II) and Pd(II) species are slow enough to be easily followed by EPR. The increase of the reaction rate with the temperature and after adding of Cu^{2+} ions, and the decrease in presence of the noncoordinated ligands

ligands instead of solvent molecules, which are regarded as essential members in a dissociative ligand exchange mechanism: $[Cu(mnt)X_2]^{2-}(X = Cl, Br)$. Up to now only EPR spectra of CuLX and $[CuLX_2]^-$ chelates with L = dichalcogenocarbamate have been described by several authors.[4-13]

The $[Cu(mnt)X_2]^{2-}$ species could be obtained according to the reaction given in eqn (4).

---
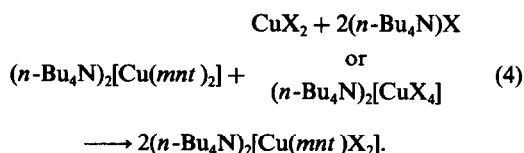
*Author to whom correspondence should be addressed.
†$mnt = (CN)_2C_2S_2^{2-}$, maleonitriledithiolate, X = Cl, Br.
‡EPR spectra were recorded with a VARIAN E-112 spectrometer operating at X band frequency.

$$(n\text{-}Bu_4N)_2[Cu(mnt)_2] + \begin{array}{c} CuX_2 + 2(n\text{-}Bu_4N)X \\ \text{or} \\ (n\text{-}Bu_4N)_2[CuX_4] \end{array}$$
(4)

$$\longrightarrow 2(n\text{-}Bu_4N)_2[Cu(mnt)X_2].$$

Table 1. EPR parameters of $[Cu(mnt)X_2]^{2-a}$, $[CuLX_2]^{-b}$ and $CuLX^c$ species; a_0 in $10^{-4}\,cm^{-1}$; L = diethyldithiocarbamate

	g	a_0^{Cu}	a_0^{X}	c_s^2
$Cu(mnt)Cl_2^{\ 2-}$	2.074	68.5	8.9	0.0060
$Cu(mnt)Br_2^{\ 2-}$	2.062	73.2	45.7	0.0061
$CuLCl_2^{\ -}$	2.072	71.6	7.7	0.0052
$CuLBr_2^{\ -}$	2.065	77.1	38.6	0.0051
$CuLCl$	2.070	72.5	7.7	0.0052
$CuLBr$	2.065	75.2	35.7	0.0047

[a]experimental errors: $g \pm 0.002$; $a_0^{Cu} \pm 0.5$ for X = Cl, ± 1.0 for X = Br; $a_0^X \pm 0.5$ for X = Cl, ± 1.0 for X = Br.
[b]values from Ref. 8.
[c]values from Ref. 12.
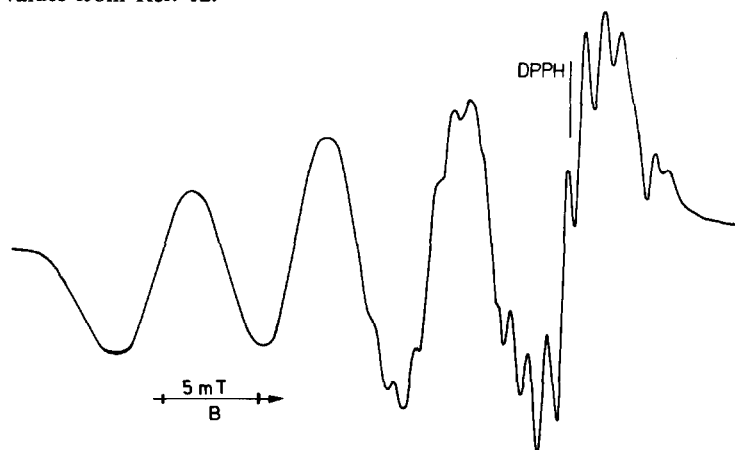
Fig. 1. EPR spectrum of $[Cu(mnt)Cl_2]^{2-}$ at $T = 235$ K; solvent: acetonitrile; frequency: 9.51 GHz.

If tetra-n-butylammonium salts are not present during reaction (4) black scarcely soluble $Cu[Cu(mnt)_2]^{14,15}$ is deposited.

The room-temperature EPR spectrum of a solution containing $[Cu(mnt)Cl_2]^{2-}$ anions consists of the typical[63,65] Cu hyperfine structure (hfs) quartet. In the spectrum recorded at $T = 235$ K an additional hfs due to the interaction of the unpaired electron with $^{35,37}Cl$ nuclei ($^{35,37}Cl$, I = 3/2) can be observed. The copper hfs lines are split into seven $^{35,37}Cl$ ligand hfs components clearly resolved for the $m_I = +3/2$ copper hfs line as shown in Fig. 1 indicating the presence of two Cl atoms in the first coordination sphere.

The solution EPR spectrum observed for $[Cu(mnt)Br_2]^{2-}$ species at room temperature consists of a quartet of seven hfs lines arising from the interaction of the unpaired electron with $^{63,65}Cu$ and two $^{79,81}Br$ nuclei both having I = 3/2. Due to the values of the coupling constants a_0^{Cu} and a_0^{Br} the hfs lines are partially overlapped. The $^{63,65}Cu$ as well as the $^{79,81}Br$ isotopic splitting is not resolved because of the experimental line width. The assignment made is given in the stick spectrum of Fig. 2.

The g values and the hfs coupling constants derived from the spectra are given in Table 1. For comparison Table 1 contains also the EPR parameters found for

CuLX and $[CuLX_2]^-$ complexes (L = dithiocarbamate). $[Cu(mnt)X]^-$ species could not be observed during our investigations.

The isotropic $^{35,37}Cl$ and $^{79,81}Br$ hfs can be used to obtain an estimate of the halogen 3s and 4s contribution to the MO of the unpaired electron. The isotropic ligand hfs splitting is given by the familiar expression

$$a_0(X) = \frac{8\pi}{3} g_e g_N \beta_e \beta_N |\Psi(0)|^2 c_s^2$$

where c_s is the coefficient of the halogen 3(4)s orbital in the MO containing the unpaired electron. $|\Psi(0)|^2$ is the 3s(Cl), 4s(Br) electron density at the nucleus. The evaluation of c_s^2 is accomplished[16] by taking the ratio of the observed isotropic $^{35,37}Cl$ and $^{79,81}Br$ ligand hfs splitting, a_0^{obsd}, to that calculated for an unpaired electron residing in a Cl 3s ($a_0^{calc}(^{35}Cl) \sim 155, 0$ mT) and a Br 4s orbital ($a_0^{calc}(^{81}Br) \sim 780, 0$ mT):

$$c_s^2 = \frac{a_0^{obsd}}{a_0^{calc}}.$$

The values estimated are given in Table 1. The c_s^2 values derived are small for all complexes studied and suggest a distorted tetrahedral coordination geometry for the
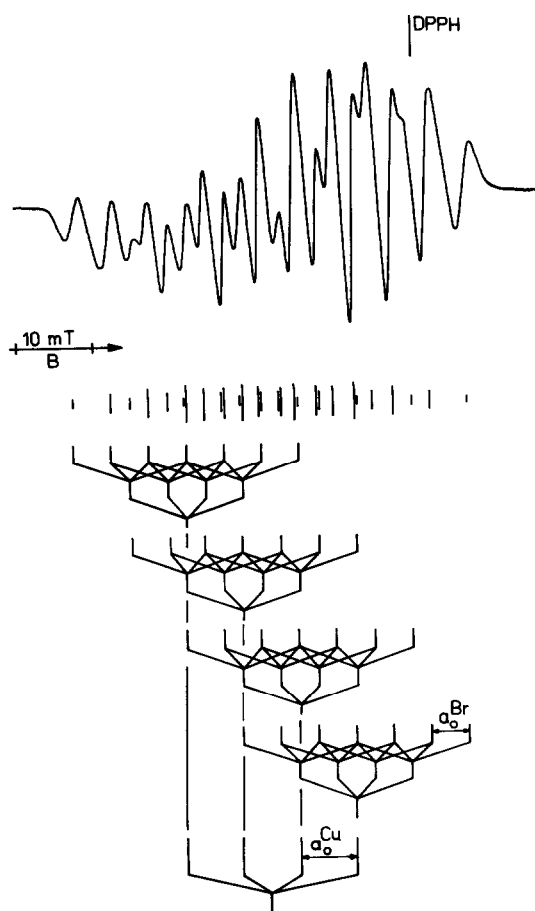
Fig. 2. EPR spectrum of [Cu(mnt)Br$_2$]$^{2-}$ at room temperature in acetonitrile; frequency: 9.51 GHz.

CuS$_2$X$_2$ chromophores. This is also reflected by the isotropic copper hfs coupling which is noticeably reduced with respect to that observed for planar [Cu(mnt)$_2$]$^{2-}$.[17] For tetrahedrally distorted [Cu(mnt)$_2$]$^{2-}$ characterized by a dihedral angle of 47.4° between the planes of the ligands an isotropic copper hfs coupling of (−) 68.4 × 10^{-4} cm^{-1} has been found.[18] A quantitative analysis of the MO of the unpaired electron for [Cu(mnt)X$_2$]$^{2-}$ requires knowledge of the corresponding anisotropic hfs data. Unfortunately, the latter values could not be estimated because frozen solution spectra allowing their determination could not be obtained.

REFERENCES

1. W. Dietzsch, J. Reinhold, R. Kirmse, E. Hoyer, I. N. Marov and V. K. Belyaeva, *J. Inorg. Nucl. Chem.* 1977, **39**, 1377.
2. W. Dietzsch, J. Lerchner, J. Reinhold, J. Stach, R. Kirmse, G. Steimecke and E. Hoyer, *J. Inorg. Nucl. Chem.* 1980, **42**, 509.
3. I. N. Marov, M. H. Wargaftig, V. K. Belyaeva, G. A. Evtikova, E. Hoyer, R. Kirmse and W. Dietzsch, *Z. Neorg. Khim.* 1980, **25**, 188.
4. H. C. Brinkhoff, J. A. Cras, J. J. Steggerda and J. Willemse, *Rec. Trav. Chim. Pays-Bas* 1969, **88**, 633.
5. H. C. Brinkhoff, *Rec. Trav. Chim. Pays-Bas* 1971, **90**, 377.
6. H. C. Brinkhoff, Thesis, Nijmegen (1970).
7. R. M. Golding, A. D. Rae, B. J. Ralph and L. Sullgoi, *Inorg. Chem.* 1974, **13**, 2499
8. R. M. Golding, C. M. Harris, K. J. Jessop and W. C. Tennant, *Austr. J. Chem.* 1972, **25**, 2567.
9. N. D. Yordanov and D. Shopov, *J. Inorg. Nucl. Chem.* 1976, **38**, 137.
10. R. H. Furneaux and E. Sinn, *Inorg. Nucl. Chem. Lett.* 1966, **12**, 501.
11. J. A. Cras and J. Willemse, *J. Inorg. Nucl. Chem.* 1977, **39**, 1225.
12. W. J. Newton and B. J. Tabner, *J. Chem. Soc. Dalton Trans.* **1981**, 466.
13. P. M. Soloshenkin, A. V. Iwanov, N. I. Kopitzia and F. A. Shwengler, *Dokl. Acad. Nauk* (U.S.S.R.) 1982, **266**, 139.
14. M. Kaneko and G. Manecke, *Makromol. Chem.* 1974, **175**, 3401.
15. T. Yoshimura, W. Storck and G. Manecke, *Makromol. Chem.* 1977, **178**, 75.
16. P. W. Atkins and M. C. R. Symons, *The Structure of Inorganic Radicals.* Elsevier, New York (1967).
17. A. H. Maki, N. Edelstein, A. Davison and R. H. Holm, *J. Am. Chem. Soc.* 1964, **86**, 4580.
18. D. Snaathorst, H. M. Doesburg, J. A. A. J. Rerenboom and c. P. Jeijzers, *Inorg. Chem.* 1981, **20**, 2526.

NOTE

ALUMINIUM TRIS(FLUOROSULPHATE)

SUKHJINDER SINGH and RAJENDAR D. VERMA*
Department of Chemistry, Panjab University, Chandigarh 160014, India

Abstract—Aluminium tris(fluorosulphate) is prepared by the reaction of aluminium tris(trifluoroacetate) and fluorosulphuric acid. The IR spectrum indicates a polymeric structure containing bridging bidentate fluorosulphate groups, giving hexacoordination around aluminium. Aluminium tris(fluorosulphate) forms coordination compounds with pyridine and bipyridyl.

Gallium,[1] indium[2] and thallium[2] tris-fluorosulphates are known. However, only a partially substituted fluorosulphate of aluminium,[3] and a 1:3 complex with MeCN,[4] $Al(SO_3F)\cdot3MeCN$ have been reported. Therefore, we have prepared and characterized aluminium tris(fluorosulphate).

The reaction between metal trifluoroacetates and fluorosulphuric acid has proved quite useful for obtaining fluorosulphates.[5,6] The reaction between aluminium tris(trifluoroacetate) and fluorosulphuric acid in a 1:3 molar ratio in sulphuryl chloride at 10°C yielded $Al(SO_3F)_3$ in a fast and clean reaction.

$$Al(O_2CCF_3)_3 + 3HSO_3F \rightarrow Al(SO_3F)_3 + 3CF_3CO_2H$$
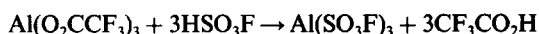
$Al(SO_3F)_3$ is a very hygroscopic, white powder, stable for days in dry conditions, but is readily hydrolysed. It is insoluble in the usual non-coordinating organic solvents as well as in fluorosulphuric acid suggesting a polymeric nature.

$Al(SO_3F)_3$ reacts with mulling agents such as nujol and hexachlorobutadiene. Therefore, its IR spectrum was recorded as a thin film of the solid between silver chloride plates. The average value of two strong broad bands (1360 and 1180 cm^{-1}) lies around 1270 cm^{-1}, which is usually the value expected for bidentate bridging fluorosulphate groups as shown in $X_2Sn(SO_3F)_2$; X=Me,[7,8] Cl,[9] for which a structural determination has verified bridging fluorosulphate groups. Not only the stretching but also the deformation modes of the SO_3F group in $Al(SO_3F)_3$ compare well with the corresponding modes in tin(IV) derivatives.[7–9] The νS–F at 812 cm^{-1} as a strong band confirms the presence of only one type of fluorosulphate group. These assignments suggest that the aluminium in $Al(SO_3F)_3$, is octahedrally coordinated as expected.[10–12] Close resemblance of the IR spectrum of $Al(SO_3F)_3$ with that of $Ga(SO_3F)_3$[1] and $In(SO_3F)_3$[2] suggest a similar conformation of the SO_3F groups in these compounds.

The νS–O at 1420, 1290 and 1015 cm^{-1} indicate a monodentate[13] fluorosulphate group in $Al(SO_3F)_3\cdot3Py$. Thus, aluminium retains hexacoordination in this complex. The various νS–O values; 1410, 1375, 1280, 1180, 1080 and 1005 cm^{-1} and two values of νS–F; 850 and 830 cm^{-1} reveal the presence of both mono- and bidentate SO_3F groups in $Al(SO_3F)_3\cdot bipy$. The appearance of a weak band at 1235 cm^{-1} and shift of the bands at 1578, 601 and 403 cm^{-1} to 1610, 630 and 440 cm^{-1} in pyridine complex indicate the coordination of pyridine to aluminium.[14] A band which is not present in free bipyridyl, but has been found in several of its chelated complexes,[15] appears at 1335 cm^{-1} and a band at 990 cm^{-1} is intensified and shifts to 1020 cm^{-1} in $Al(SO_3F)_3\cdot bipy$ on coordination.

EXPERIMENTAL

Freshly distilled fluorosulphuric acid (1.8 g, 18 mmol) was transferred to a suspension of aluminium tris(trifluoroacetate) (2.196 g, 6 mmol) in 30 cm^3 of sulphuryl chloride, while the reaction vessel was immersed in liquid nitrogen. The temperature of the vessel was slowly allowed to rise to 0°C and the contents stirred magnetically for 6 hr at 10°C. The contents were filtered under dry N_2, repeatedly washed with sulphuryl chloride followed by tetrachloromethane. Finally, $Al(SO_3F)_3$ was obtained as a pure white powder in almost quantitative yield after removal of all volatiles under vacuum. Found: Al, 8.41; S, 29.85; F, 17.34; $Al(SO_3F)_3$ requires Al, 8.33; S, 29.63; F, 17.59%. IR (cm^{-1}): 1360sb, 1180sb, 1080s, 812vs, 645w, 609w, 542vs, 440w, 420mw.

Complexes $Al(SO_3F)_3\cdot3Py$ and $Al(SO_3F)_3\cdot bipy$ were prepared by stirring $Al(SO_3F)_3$ suspended in tetrachloromethane or benzene with the ligand in the required stoichiometric ratio or in excess for 20 hr under dry N_2 at room temperature, filtered, washed with the respective solvent and finally dried *in vacuo*. Found: Al, 4.19; S, 16.85; F, 10.44; C, 31.58; H, 2.56; N, 7.40; $Al(SO_3F)_3\cdot3Py$ requires Al, 4.81; S, 17.11; F, 10.16; C, 32.09; H, 2.67; N, 7.49%.

IR (cm^{-1}): 1610s, 1540m, 1525m, 1485m, 1465m,

*Author to whom correspondence should be addressed.

1420w, 1290s, 1255w, 1235w, 1015m, 935w, 778s, 750s, 680m, 630m, 595w, 580w, 550s, 440m. Found: Al, 5.39; S, 20.81; F, 11.46; C, 25.63; H, 1.80; N, 5.59; $Al(SO_3F)_3 \cdot bipy$ requires Al, 5.62; S, 20.00; F, 11.88; C, 25.00; H, 1.67; N, 5.83%. IR (cm^{-1}): 1610s, 1590m, 1555m, 1525s, 1470m, 1450m, 1410w, 1375w, 1335w, 1280sb, 1180m, 1080m, 1020s, 1005mw, 850m, 830m, 775s, 750s, 680m, 650m, 610w, 600w, 585w, 570m, 550s, 440w, 420m, 390w.

Fluorosulphuric acid, ligands and the solvents were purified as described earlier.[2,5,6] $Al(O_2CCF_3)_3$ was prepared by the method reported by Cady and Hara.[16] The IR spectra were obtained on Perkin–Elmer 621 spectrophotometer.

REFERENCES

1. A. Storr, P. A. Yeats and F. Aubke, *Can. J. Chem.* 1972, **50**, 452.
2. R. C. Paul, R. D. Sharma, S. Singh and R. D. Verma, *J. Inorg. Nucl. Chem.* 1981, **43**, 1919.
3. E. Hayek, J. Puschman and A. Czaloun, *Monatsh* 1954, **85**, 359.
4. E. Hayek, A. Czaloun and B. Krismer, *Monatsh* 1956, **87**, 742.
5. S. Singh, M. Bedi and R. D. Verma, *J. Fluorine Chem.* 1982, **20**, 107.
6. R. C. Paul, S. Singh and R. D. Verma, *J. Fluorine Chem.* 1980, **16**, 153.
7. F. H. Allen, J. A. Lerbscher and J. Trotter, *J. Chem. Soc. (A)* 1971, 2507.
8. P. A. Yeats, J. R. Sams and F. Aubke, *Inorg. Chem.* 1972, **11**, 2634.
9. P. A. Yeats, B. L. Poh, B. F. E. Ford, J. R. Sams and F. Aubke, *J. Chem. Soc. (A)* 1977, 2188.
10. J. A. A. Ketalaar, *Z. Kristallog, Kristallgeom.* 1933, **85**, 119.
11. A. F. Wells, *Structural Inorganic Chemistry*, 3rd Edn. University Press, Oxford (1962).
12. C. T. Prewitt, R. D. Shannon, D. B. Rogers and A. W. Sleight, *Inorg. Chem.* 1969, **8**, 1985.
13. H. A. Carter, S. P. L. Jones and F. Aubke, *Inorg. Chem.* 1970, **9**, 2485.
14. N. S. Gill, R. H. Nuttall, D. E. Scaife and D. W. A. Sharp, *J. Inorg. Nucl. Chem.* 1961, **18**, 79.
15. L. Doretti, S. Sitran, P. Zanella and G. Faraglia, *Inorg. Nucl. Chem. Lett.* 1973, **9**, 7.
16. R. Hara and G. H. Cady, *J. Am. Chem. Soc.* 1954, **76**, 4285.

NOTE

PREPARATION AND NMR SPECTRA DIAMINOTETRAARYLOXYCYCLOTRIPHOSPHAZENES

MEISETSU KAJIWARA* and YASUO KURACHI

Department of Applied Chemistry, Faculty of Engineering, Nagoya University, Nagoya, 464
Japan

Abstract—New diaminotetraaryloxycyclotriphosphazenes $N_3P_3(NH_2)_2(OR)_4$ were prepared by the reaction between $N_3P_3(NH_2)_2Cl_4$ and RONa in THF solvent and ^{31}P NMR data showed geminal compounds were formed.

Many organo derivatives of hexachlorocyclotriphosphazene have been synthesized[1] and proton or phosphorus NMR spectroscopy had been used for elucidating the structure of cyclophosphazene derivatives in solution. In this report the synthesis of new derivatives of hexachlorocyclotriphosphazene and their proton and phosphorus NMR spectra are described.

EXPERIMENTAL

$(NPCl_2)_3$ was prepared by the method of Kajiwara.[2] The melting point of $(NPCl_2)_3$ was 112° C.

$N_3P_3(NH_2)_2Cl_4$ was prepared by the method of Geral.[3]

$N_3P_3(NH_2)_2(OR)_4$ were synthesized by the reaction between $N_3P_3(NH_2)_2Cl_4$ and RONa in THF solvent. The aryloxy compound e.g. C_6H_5OH, HOC_6H_4F-p, HOC_6H_4Cl-p or $HOC_6H_4CH_3-p$ (0.08 mol) and 0.08 mol sodium, respectively, were placed in three-necked flask with 200 cm³ of THF. After the sodium had dissolved, 0.016 mol of $N_3P_3(NH_2)_2Cl_4$ (dissolved in 100 cm³ of THF) was added and the mixture was refluxed with stirring for two days. After work up involving stirring of solvent, extraction with ether followed by evaporation to dryness. The product was recrystallized from benzene.

Analysis

^1H–NMR spectra of the derivatives were measured with Niphon Denshi Model C 60 HL instrument, with tetramethylsilane or D. S. S as an internal standard. ^{31}PNMR specra of the derivatives was recorded on Niphon Denshi Model–60 type spectrometer using a sample tube (8 mm), chloroform solvent and H_3PO_4 as the reference at 24.3 MHz and 20° C.

RESULTS AND DISCUSSION

The results of chemical analysis and the yields are summarized in Table 1.

All of the derivatives are colourless crystalline solids soluble in organic solvents.

The NMR data of the compounds is summarized in Table 2. The chemical shifts of the proton in N–H can often provide a diagnostic test for geminal and non-genimal structure in cyclotriphosphazene derivatives with primary amino substituents.[4] The N–H resonances for the non-geminal compounds occurred at 4.1–4.4 ppm, whereas the geminal compounds displayed resonances at 3.1–3.8 ppm.[5] In the case of $N_3P_3(NH_2)_2(OR)_4$ compounds, δ N–H occurs at

Table 1. The results of chemical analysis and the yield of diaminotetraaryloxycylotriphosphazenes

$N_3P_3(NH_2)_2(OR)_4$ R		Elemental analysis (%)			mp (°C)	Yield (%)
		N	C	H		
C_6H_4Cl-p	Calc	10.34	42.57	2.98	147–147.5	87
	Found	10.64	42.74	3.21		
C_6H_4F-p	Calc	11.45	47.15	3.30	114–115	89
	Found	11.45	46.91	3.43		
$C_6H_4CH_3-p$	Calc	11.76	56.47	5.42	120–121	87
	Found	11.85	56.76	5.54		

Table 2. H^1 and ^{31}P NMR data for diaminotetraaryloxycyclotriphosphazenes

Compound	^1H-NMR (ppm)				^{31}P-NMR (ppm)		
	NH_2 (br)	OC_6H_5 (multiplets)	OC_6H_4	CH_3	ΓNH_2 (A)	P(OR) (B)	J_{AB}
$N_3P_3(NH_2)_2(OC_6H_5)_4$	2.3	7.3			-8.65	-16.50	1.48
$N_3P_3(NH_2)_2(OC_6H_4F-p)_4$	2.4		6.7-7.6		-8.75	-15.60	1.58
$N_3P_3(NH_2)_2(OC_6H_4Cl-p)_4$	2.4		7.0-7.4		-8.35	-15.5	1.52
$N_3P_3(NH_2)_2(OC_6H_4CH_3-p)_4$	2.3		7.0	1.3	-13.47	-16.87	0.73

2.3–2.4 ppm, so geminal compounds may be inferred. ^{31}P–NMR spectroscopy is used to confirm the geminal or non-geminal structure. The ^{31}P chemical shift of P–NH$_2$ in $N_3P_3(NH_2)_2Cl_4$[6] was recorded at -9.03 ppm and -18.3 ppm, respectively. It is found that the compound gives an AB$_2$ type spectrum and is the geminal structure. The ^{31}P NMR of the other compounds are summarized in Table 2.

It is assumed that ^{31}P chemical shifts and P–P coupling constants do not depend on electronegativity in the substituent groups. The ^{31}P chemical shifts and P–P coupling constants, for a large number of cyclophosphazene derivatives have been determined.[7] Also, it has been suggested that change in electronegativity, π–bonding, and bond angles influence ^{31}P chemical shifts.[8] In addition, the chemical shifts of a particular phosphorus atom may be affected by the substituents elsewhere on the ring. Finer[9] and Schuman[10] have proposed that coupling constants correlate with the electronegativity of substituents. As shown in Table 2, ^{31}P chemical shifts and coupling constants of the derivatives, except $N_3P_3(NH_2)_2(OC_6H_4CH_3-p)_4$, give similar values since electronegativity, π–bonding or bond angles within the substituents are similar. On the other hand, the $N_3P_3(NH_2)_2(OC_6H_4CH_3-p)_4$ P–P coupling constant is smaller than the other derivatives. This means that

factors such as stereochemistry of the substituent may also contribute to chemical shift or coupling constant.

REFERENCES

1. Robert E. Singler, Gary L, Hangnaure and Richard W. Sicka, *ACS Symp Ser.* 1982, 193; V. V. Kireev, G. I. Mitropolskaya and Z. K. Zinovick, *Usp. Khim.* 1982, **51(2)**, 266.
2. H. Saito and M. Kajiwara, *J. Chem. Soc. Japan* 1963, **66**, 618.
3. R. F. Gerald, K. F. Marlene, C. D. Ronald and M. Theald, *Inorg. Syn.* 1973, **14**, 23.
4. R. N. Das, R. A. Shaw and M. Wood, *J. Chem. Soc.* 1973, 709.
5. M. Hasan, R. A. Shaw and M. Wood, *J. Chem. Soc.* 1975, 2202.
6. G. R. Feistel and T. Moeller, *J. Inorg. Nucl. Soc.* 1967, **29**, 2731.
7. C. W. Allen, *J. Mag. Reson.* 1971, **5**, 435.
8. F. Heatley, F and S. M. Todd, *J. Chem. Soc.* 1966, 1152.
9. E. C. Finer and R. K. Haris, *Prog. Nucl. Magn. Reson. Specto* 1971, **6**, 61.
10. K. Schuman and A. Schmidpeter, *Phosphorus* 1973, **3**, 51.

FORMATION AND TRANSFORMATION OF ALKOXY-DERIVED BaGeO$_3$

OSAMU YAMAGUCHI,[*] MICHIHARU KI, TAKAYA NIIMI AND KIYOSHI SHIMIZU

Department of Applied Chemistry, Faculty of Engineering, Doshisha University, Kyoto 602

Japan

Abstract——Beta-BaGeO$_3$, being high-temperature form, are formed metastably at 630-660 °C from an amorphous material prepared by the simultaneous hydrolysis of barium and germanium alkoxides. The transformation of BaGeO$_3$ can be summarized as follows; amorphous BaGeO$_3$

$$\xrightarrow[780-840°C]{} \alpha\text{-BaGeO}_3 \underset{1130-1150°C}{\overset{1180-1200°C}{\rightleftarrows}} \beta\text{-BaGeO}_3 \xrightarrow[1270°C]{} \text{melt.}$$

On cooling from the melt, β-BaGeO$_3$ can be retained at room temperature.
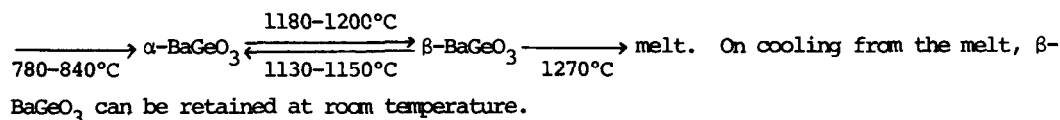
INTRODUCTION

Barium metagermanate, BaGeO$_3$, exists in at least two polymorphic modifications: a low-temperature α-form having a hexagonal pseudowollastonite-type structure and a high-temperature β-form having an orthorhombic pyroxene-type structure. There have been conflicting information in the literature concerning the formation and transformation of BaGeO$_3$. Roth[1] reported at first that α-BaGeO$_3$ changes to a different type of structure when heated with the addition of 1% Fe$_2$O$_3$. Liebau[2] showed that β-BaGeO$_3$ is formed by melting α-BaGeO$_3$ with the addition of 2% Fe$_2$O$_3$. Grebenshchikov et al.[3] reported that in the absence of mineralizers, α-BaGeO$_3$ remains unchanged at all temperatures, and β-BaGeO$_3$ is formed by the addition of BaSiO$_3$. Moreover, the transformation of BaGeO$_3$ in the presence of 2% Fe$_2$O$_3$ were studied by Grebenshchikov et al.[4] Reversible transformations of α- into β-BaGeO$_3$ and of β- into an undefined phase designated as the δ-form were observed at 1065 and 1160 °C, respectively. On the other hand, according to the results of Guha et al.,[5] β-BaGeO$_3$ is formed without addition of mineralizers, and in contrast to the Grebenshchikov et al. data[4] the transformations of α⇌δ and δ⇌β occur at 1100 and 1200 °C, respectively. However, no high-temperature X-ray analysis in the experiment of Guha et al.[5] was carried out for the identification of polymorphic modifications.

In the present study, it was found that β-BaGeO$_3$ is formed metastably at lower temperatures from an amorphous material prepared by the simultaneous hydrolysis of barium and germanium alkoxides. On the basis of this result, the transformation of BaGeO$_3$ was studied by thermal and high-temperature X-ray diffraction analysis.

EXPERIMENTAL

Germanium isopropoxide, Ge(OC$_3$H$_7$)$_4$, was a pure grade. Barium isopropoxide, Ba(OC$_3$H$_7$)$_2$, was synthesized by heating 99.9% barium metal in an excess of dehydrated 2-propanol for 5 h at 82 °C in a nitrogen atmosphere. The mixed alkoxides prepared in the mole ratio Ba^{2+}: Ge^{4+} =1:1 were refluxed for 20 h at the same conditions and then hydrolyzed by adding dropwise aqueous ammonia solution with stirring at 25 °C. After the termination of dropping, the resulting suspension was further stirred for 1 h at 20-25 °C. The hydrolysis product was separated from the suspension by centrifugation and dried at 80 °C under reduced pressure. The powder obtained is termed starting powder. Its average particle size, as determined by electron microscopy, was ca. 400 Å.

Thermal analyses (t.g., d.t.a.) were carried out in air at a rate of 10 °C min^{-1}. α-Alumina was used as a standard material in d.t.a. The specimens in the heating and cooling processes at a rate of 10 °C min^{-1} were identified by high-temperature X-ray diffractometry using nickel-filtered Cu-K$_\alpha$ radiation.

RESULTS AND DISCUSSION

Thermal analysis

Thermogravimetric examination of the starting powder showed a weight loss of 11.6% up to 360 °C, attributed to the loss of ammonia, surface-absorbed 2-propanol, absorbed water, and hydrated water.[6]

Figure 1(a) shows the d.t.a. curve of the starting powder in the heating process. Four peaks were observed at 630-660 °C, 780-840 °C, 1180-1200 °C, and 1270-1300 °C. They were sharp, so that the onset and end temperatures could be determined accurately. High-temperature X-ray diffraction analysis confirmed that the first exothermic peak (630-660 °C) is due to the crystallization of β-BaGeO$_3$ from an amorphous phase, and the second (780-840 °C) to the transformation of β- into α-BaGeO$_3$. The first and second endothermic peaks (1180-1200 °C and 1270-1300 °C) were found to be due to the transformation of α- into β-BaGeO$_3$ and the melting of β-BaGeO$_3$, respectively. In the cooling process from the melt, no peaks due to the transformation, except for the solidification, appeared in the d.t.a. curve. However, on cooling from the temperatures between 1200 and 1260 °C an exothermic peak was observed at 1130-1150 °C, corresponding to the transformation of β- into α-BaGeO$_3$ (Figure 1(b)).

X-Ray analysis

The starting powder was amorphous, no significant change in structure being recognized up to the temperature of the first exothermic peak (630-660 °C) in d.t.a. Pure BaGeO$_3$ derived from alkoxide showed the existence of two polymorphic modifications throughout the heating process; β-BaGeO$_3$ at 660-780 °C and 1200-1260 °C, and α-BaGeO$_3$ at 840-1180 °C. The third modification, δ-BaGeO$_3$, was not detected up to the melting temperature. In the present study, β-BaGeO$_3$ was crystallized metastably at 630-660 °C from an amorphous phase. The diffraction pattern of β-BaGeO$_3$ obtained by heating for 1 h at 700 °C was measured at room temperature using the standard X-ray diffractometer. The scanning speed of 1/4° min^{-1} of the goniometer was selected to satisfy the accuracy of d-spacing. Table 1 shows the observed values of d-spacing and relative intensity, in comparison with the Grebenshchikov *et al.* data.[4] Our powder pattern was more complex than that reported by them. All diffraction lines could be reasonably indexed by a orthorhombic unit cell[2] with a=4.59, b=5.70 and c=12.78 Å. The lattice parameters are little larger than those of β-BaGeO$_3$ (a=4.58, b=5.68 and c=12.76 Å)[2] formed by melting α-BaGeO$_3$ with the addition of 2% Fe$_2$O$_3$. On the other hand, the X-ray diffraction pattern of α-BaGeO$_3$ was identical with the reported one.[4] The reversible transformation of α-$\rightleftharpoons$ β-BaGeO$_3$ was observed at 1180-1200 °C and 1130-1150 °C. The X-ray diffraction pattern of β-BaGeO$_3$ observed at 1200-1260 °C was the same as that described above. Efforts to obtain β-BaGeO$_3$ at room temperature by rapid quenching from the temperatures between 1200 and 1260 °C failed to produce α-BaGeO$_3$ in the X-ray diffraction pattern. However, β-BaGeO$_3$ could be retained at room temperature on cooling from the melt, in agreement with the results of Liebau[2] and Guha *et al.*[5] From the thermal and X-ray data, the transformation of pure BaGeO$_3$ derived from alkoxide can be summarized as follows.

$$\text{Amorphous BaGeO}_3 \xrightarrow[630-660°C]{} \beta\text{-BaGeO}_3 \xrightarrow[780-840°C]{} \alpha\text{-BaGeO}_3 \underset{1130-1150°C}{\overset{1180-1200°C}{\rightleftharpoons}} \beta\text{-BaGeO}_3$$

$$\xrightarrow[1270°C]{} \text{melt}$$
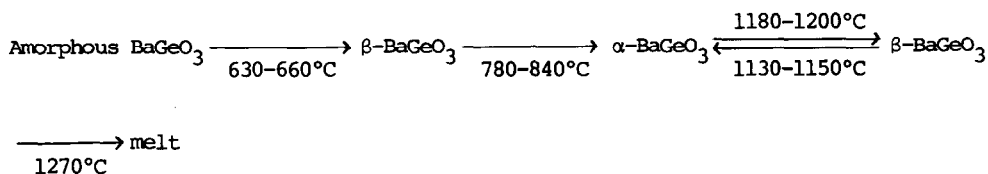
REFERENCES

1 R. S. Roth, *Am. Mineral.*, 1955, **40**, 32.

2 F. Liebau, *Neus Jahrb Mineral.*, 1960, **94**, 1209.

3 R. G. Grebenshchikov, N. A. Toropov and V. I. Shitova, *Izv. Akad. Nauk. SSSR, Neorg. Mater.*, 1965, **1**, 1130.

4 R. G. Grebenshchikov, V. I. Shitova and N. A. Toropov, *Izv. Akad. Nauk. SSSR, Neorg. Mater.*, 1967, 3, 1620.

5 J. P. Guha, D. Kolar and A. Porenta, *J. Therm. Anal.*, 1976, 9, 37.

6 O. Yamaguchi, T. Kanazawa and K. Shimizu, *J. Chem. Soc., Dalton Trans.*, 1982, 1005.

Table 1. X-Ray diffraction data of β-BaGeO$_3$

Present data			Grebenshchikov's data	
$d/\text{Å}$	I/I_0	hkl	$d/\text{Å}$	I/I_0
6.37	6	002	–	–
4.25	5	012	–	–
3.73	12	102	–	–
3.57	19	110	–	–
3.44	100	111	–	–
3.41	71	013	3.37	31
3.19	32	004	–	–
3.12	15	103,112	3.14	100
–	–	–	2.99	6
2.85	25	020	–	–
2.78	20	014,021	–	–
2.74	29	113	–	–
2.62	12	104	2.60	8
–	–	–	2.53	8
2.379	17	114	2.37	11
2.292	22	200	–	–
2.259	12	122	2.26	11
2.124	8	210,024	–	–
2.103	17	123	–	–
2.075	14	115	2.08	14
2.016	3	203,212	–	–
1.929	10	106	1.93	8
1.901	11	213,025	–	–
1.861	10	204	–	–
1.823	3	116	–	–
1.782	6	220	–	–
1.769	8	214	–	–
1.752	12	130	–	–
1.735	14	017	1.74	33
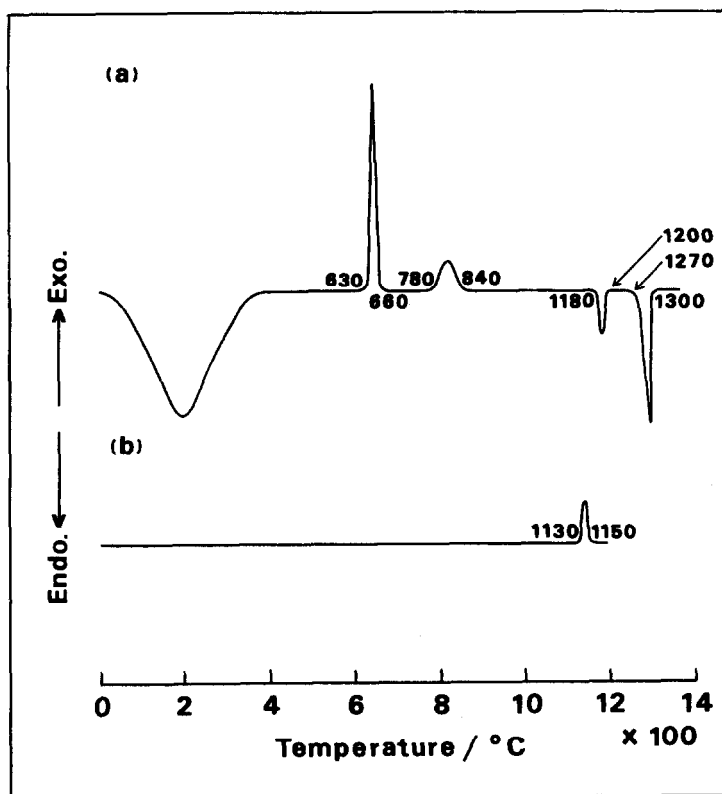
Fig. 1. D.t.a. curves of the starting powder. (a) Heating process, (b) cooling process. Sample weight = 120 mg.

NOTE

DIAZA-CROWN-N,N-DIALKANOIC ACIDS COPPER(II) AND DICOPPER(II) COMPLEXES

R.A.Koliński[a] and J.Mroziński[b]

[a]Institute of Organic Chemistry, Polish Academy of Sciences, 01224 Warszawa,
[b]Institute of Chemistry, Wrocław University, 50383 Wrocław, Poland

Abstract—Twelve-, fifteen-, and eighteen-membered diaza-crown-N, N'-dialkanoic acids LH_2 and their inner salt copper(II) complexes CuL and dicopper complex $[CuL(3) . CuCl_2 . CH_3OH]_n$ were obtained. The complexes of 15- and 18-membered ligands contain Cu^{2+} ion inside the ring.

Relatively few synthetic inner salt complexes of macrocyclic ligands are known, due to the scarcity of suitable ligands. This suggested a study of diaza-crown-N,N-dialkanoic acids, the compounds containing a macrocycle and two aminoacid moieties. We now report the synthesis and the structure of some copper(II) inner complexes of these ligands.

Diaza-crown-N,N-dialkanoic acids were obtained by alkylation of aminogroups of 12-, 15-, and 18-membered diaza-crown ethers with ethyl bromoacetate or ethyl DL-2-bromopropionate, followed by hydrolysis of ester groups by refluxing an aqueous solution of the diester. The following diacids were obtained:
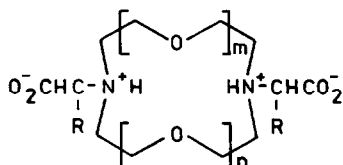
L(1)H_2, m=n=1, R=H, m.p.446–8 dec.,
L(2)H_2, m=1,n=2, R=H, m.p.446–8 dec.,
L(3)H_2, m=n=2, R=H, m.p.444–6 dec.[1],
L(4)H_2, m=n=2, R=CH$_3$, m.p.436–8 dec.,

L(4)H_2 has the meso-configuration.

Aminoacids L(1)H_2 – L(4)H_2 all contain zwitterionic structures as demonstrated by their ^{1}H NMR and IR spectra (νCO_2^- antisymmetric 1640 cm^{-1}).

The reaction of acids L(1)H_2 – L(4)H_2 with many copper(II) salts (chloride, bromide, perchlorate, acetate, etc.) in a 1 : 1 molar ratio in water or methanol produces CuL complexes. The absence of the anion(s) of the copper salt used in the reaction products confirms their inner salt structure. Reaction of acid L(3)H_2 with copper(II) chloride in a 1 : 2 molar ratio in methanol gives a dicopper complex $[CuL(3).CuCl_2.CH_3OH]_n$. Properties of the complexes are given in Table 1.

IR spectra of CuL complexes contain a very strong absorption band at 1640 cm^{-1} assigned to the antisymmetric νCO_2^- vibration. The assignment of the symmetric νCO_2^- band is difficult, because of its weak intensity and splitting especially in the spectra of centrosymmetric complexes. The frequency of the νCO_2^- band in complexes is the same as in the zwitterionic form of the parent aminoacids, which demonstrates their inner salt character and the unidentate coordination of the carboxylate groups $-C{\overset{O}{\underset{O-Cu}{}}}-$. The dicopper complex

Table 1. Properties of solid diaza-crown-N,N'-dialkanoate copper(II) complexes

Compound[a]	Colour	IR spectrum[b], cm^{-1} $\nu\,CO_2^-$, antisym.	Electronic spectrum[c], nm Charge transfer	$d \rightarrow d$	μ^d_{eff} B.M.	Point group of symmetry
CuL(1) $C_{12}H_{20}CuN_2O_6$	blue	1645vs,br	268br	666br	1.80	C_1 or C_2
CuL(2) $C_{14}H_{24}CuN_2O_7$	blue	1640vs,br	258 298sh	690sh 760	1.88	C_1
CuL(3) $C_{16}H_{28}CuN_2O_8$	violet	1645vs,br	266 286	540 620	1.80	$C_i^{\,e}$
CuL(4-meso) $C_{18}H_{32}CuN_2O_8$	violet	1640vs,br	277br	536 634	1.78	$C_i^{\,e}$
[CuL(3).CuCl$_2$.CH$_3$OH]$_n^{\,f}$ $C_{17}H_{32}Cu_2N_2O_9$	green-blue	1570vs,br^g	264 284 ca.400sh	ca.550sh >800		

^{a}All compounds gave correct elemental analysis. ^{b}Paraffin oil mulls. ^{c}Reflectance spectrum.
^{d}Gouy method, at ambient temperature. ^{e}From X-ray structure determination. ^{f}Polymeric compound.
^{g}CH$_3$OH: νOH 3490 cm^{-1},m,sharp.

has a single νCO_2^- band at 1570 cm^{-1}, which indicates a bridged coordination of the carboxylate groups $-C\overset{O-Cu-}{\underset{O-Cu-}{}}$. The presence of methanol is proved by the occurrence of the νOH band at 3490 cm^{-1} and by elemental analysis.

Electronic spectra of these complexes contain very broad $\underline{d}\rightarrow\underline{d}$ transition bands characteristic of tetragonally distorted $\underline{d}^9$ copper(II) complexes.

The effective magnetic moment values of CuL complexes lie appreciably above the spin-only value due to the mixing-in of some orbital angular momentum from the excited states $\underline{via}$ spin-orbit coupling.

EPR spectra of compounds CuL contain strong signals typical of rhombic symmetry with g_1, g_2, and g_3 components of the g tensor. Those of the dicopper complex indicate weak exchange interactions between the copper centres.

Starting from the known structure of ligands a variety of structures could be proposed for CuL complexes. The main structural features are: the metal ion inside the ring or outside the ring and the $\underline{cis}$ or $\underline{trans}$ (OONN or ONON, respectively) configuration of the coordination sphere and the carboxylate groups.

The Cu^{2+} cation (ionic radius r = 73 pm) is too large to get inside the 12-membered ring cavity (r = ca.60 pm). Taking into account the known structures of 12-membered ligands complexes[2] we propose the $\underline{cis}$ configuration for the CuL(1) complex with the Cu^{2+} cation located above the ring "plane". The point group of symmetry should be C_1 or C_2 depending on the ring conformation.

The Cu^{2+} cation fits very well into the 15-membered ring cavity (r = ca.80 pm). Therefore we propose the $\underline{trans}$ configuration for the CuL(2) complex with the Cu^{2+} cation inside the ring. The molecule is asymmetric because the ligand is asymmetric.
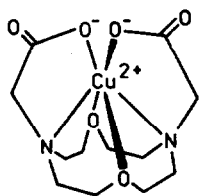
CuL(1)
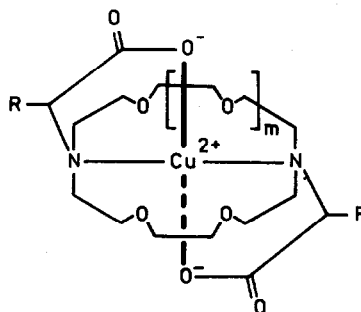
CuL(2),m=0,R=H ; CuL(3),m=1,R=H

CuL(4-meso),m=1,R=CH$_3$
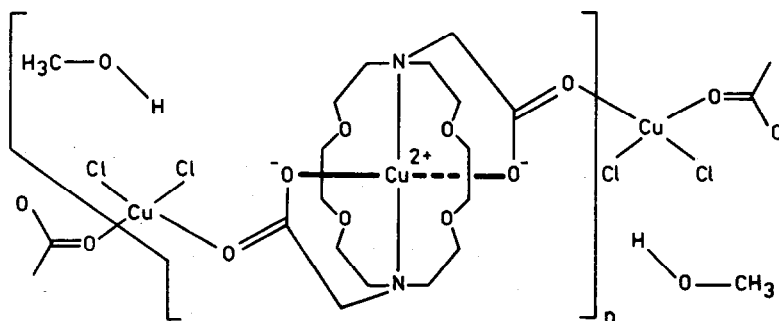
$\left[CuL(3), CuCl_2 \cdot CH_3OH\right]_n$

Complexes CuL(3) and CuL(4-_meso_) are _trans_ centrosymmetric molecules containing Cu^{2+} cation inside the ring, as shown by X-ray structure determination[3,4].

The structure of the dicopper complex was elucidated by X-ray analysis[5]. This shows a polymeric structure with an additional binding of the CO_2^- groups of the CuL(3) complex to the Cu^{2+} cation of the $CuCl_2$.

R e f e r e n c e s

[1] S.Kulstad and L. Å. Malmsten, _Acta Chem. Scand_. 1979, _B33_, 469.

[2] N.F.Curtis in _Coordination Chemistry of Macrocyclic Compounds_ (edited by G.A.Melson), pp.236, 303, Plenum, New York (1979).

[3] P.Gluziński, J.W.Krajewski, Z.Urbańczyk-Lipkowska, J.Bleidelis, and A.Mishnov, _Cryst.Struct. Comm_. 1982, _11_, 1589; T.Uechi, I.Ueda, M.Tazaki, M.Takagi, and K.Ueno, _Acta Cryst_. 1982, _B38_, 433.

[4] P.Gluziński, J.W.Krajewski,Z.Urbańczyk-Lipkowska,and M.Dobler,in preparation.

[5] P.Gluziński, J.W.Krajewski, Z.Urbańczyk-Lipkowska, G.D.Andreetti, and G.Boccelli, _Acta Cryst_. 1983, _B39_, in press.

NOTE

REDUCTIVE NITROSYLATION OF TETRAOXOMETALLATES. PART VIII[1]. A VIRTUALLY SINGLE STEP SYNTHESIS OF AZIDO-NITROSYL DERIVATIVES OF CHROMIUM(I) DIRECTLY FROM CHROMATE IN AQUEOUS-AEROBIC MEDIA.

R. G. Bhattacharyya[*] and G. P. Bhattacharjee,

Department of Chemistry, Jadavpur University,

Calcutta 700 032, India.

Abstract — Azido-nitrosyl complexes and their derivatives of the types $[Cr(NO)(N_3)_5]^{3-}$ and $[Cr(NO)(N_3)_2(L-L)]$ [L-L = 2,2' bipyridine (bipy) and 1,10 phenanthroline (phen)] were synthesised directly from chromate ion using hydroxylamine hydrochloride, azide ion and hydroxyl ion and other appropriate ligands virtually in a single step process in an aqueous aerobic medium. The compounds are characterised by IR, molecular weight, molar conductance, magnetic susceptibility, esr and electronic spectral data.

Reductive nitrosylation of chromate ions using hydroxylamine and cyanide ions in an alkaline medium generating the $\{Cr(NO)\}^{2+}$ moiety has long been known[2]. Recently it has been shown[3] that such a reaction using hydroxylamine and thiocyanate ion can be achieved in a slightly acidic or near neutral medium, and it has now been realised that an excess of hydroxylamine hydrochloride is necessary for leading such reactions to completion[4,5]. It has been found that although hydroxylamine is the source of the nitrosyl group, use of another reducing anion (viz, cyanide, thiocyanate or oxalate ion) in conjunction with hydroxylamine is necessary for the progress of this type of reactions[6]. Such a reductive nitrosylation reaction using hydroxylamine and azide ion was unknown until very recently[1(b),7]. In fact, azido-nitrosyl complexes of metals are quite rare[1(b),7-9] owing to the mutual interaction of azide ion and nitric oxide producing dinitrogen and dinitrogen monoxide. Herein is described, for the first time, the reductive nitrosylation reaction of chromate ion using hydroxylamine hydrochloride and azide ion in an alkaline medium and generation of $\{Cr(NO)\}^{2+}$ moiety as is evident by synthesizing $[Cr(NO)(N_3)_5]^{3-}$ and $[Cr(NO)(N_3)_2(L-L)]$ directly from chromate ion in an aqueous aerobic medium.

EXPERIMENTAL

Preparation and characterization of the complexes : In a solution of NaOH (2 g in 25 cm^3 of H_2O) was dissolved K_2CrO_4 (0.5 g ; 2.6 mmol) and to this solution were added $NH_2OH.HCl$ (2.7 g ; 38.8 mmol) and NaN_3 (1.7 g ; 26.2 mmol) portionwise with constant stirring at 60-70° for 30 m. The deep red-violet solution (pH≈11) was cooled to room temperature and the pH of the

---

[*] Author for correspondence.

solution was lowered down to 6.5-7.0 with 6 M HCl. The clear solution (Solution A) was filtered out from any solid residue.

1. $[Cr(NO)(N_3)_2(bipy)]$:

The solution A was added to a hot aqueous (20 cm^3) solution of bipy (0.6 g ; 3.85 mmol) with stirring and the mixture was then cooled at 0° for 1 h and then again stirred at room temperature for another 1 h. The separated deep brown solid was filtered off, washed with water, ethanol and ether and dried over fused CaCl$_2$ at a reduced pressure. The substance was then extracted with anhydrous acetone and acetone was removed by evaporation. The dry mass was then crystallised from acetone-ether mixture as deep brown crystals. Yield : 0.54 g (65 %). M.P. 165°(d). Found : C, 37.5 ; H, 2.6 ; N, 39.0 ; Cr, 15.7 ; M.W. (DMF, Osmometric) 297. C$_{10}$H$_8$N$_9$OCr requires : C, 37.3 ; H, 2.5 ; N, 39.1 and Cr, 16.1 % . M.W. 322. IR : ν_{NN}2040(s), ν_{NO}1665(s), ν_{CrN}(NO) 610(w) and ν_{CrN}(bipy) 375(m),   400(sh) cm^{-1}. λ_{max} (in CH$_3$CN) 620 (ϵ_{max} = 50), 482 (60) and 370 (230) nm. μ_{eff} = 1.9 B.M.

2. $[Cr(NO)(N_3)_2(phen)]$:

The same method as described under (1) was followed using phen instead of bipy. Yield : 0.55 g (62 %). M.P. 177°(d). Found : C, 42.0 ; H, 2.2 ; N, 36.0 ; Cr, 14.7 ; M.W. 320. C$_{12}$H$_8$N$_9$OCr requires : C, 41.6 ; H, 2.3 ; N, 36.4 and Cr, 15.0 % . M.W. 346. IR : ν_{NN}2030(s), ν_{NO}1650(s), 1680(s) (1625 cm^{-1} (s) in CH$_3$CN solution). ν_{CrN}(NO) 615 (w) and ν_{CrN}(phen) 390(m), 415(sh) cm^{-1}. λ_{max}(CH$_3$CN) 616 (40), 502 (45) and 372 (270) nm. μ_{eff} = 2.0 B.M.

3. $(Ph_4P)_3[Cr(NO)(N_3)_5]$:

The solution A was added dropwise to a hot aqueous (25 cm^3) solution of (C$_6$H$_5$)$_4$ PBr (3.8 g ; 9.0 mmol) with stirring at the room temperature for 1 h. A chocolate brown precipitate was obtained which was filtered off, washed with water, ethanol, ether and dried over fused CaCl$_2$ at a reduced pressure. The compound was extracted with anhydrous acetone and the extract was evaporated to dryness. The dried mass was then crystallised from acetone-ether mixture when deep brown needles were obtained. Yield : 1.86 g (55 %). M.P. 190°(d). Found : C, 66.3 ; H, 4.2 ; N, 16.7 ; P, 6.9 ; Cr, 4.1. C$_{72}$H$_{60}$N$_{16}$P$_3$OCr requires : C, 66.0 ; H, 4.6 ; N, 17.1 ; P, 7.1 and Cr, 4.0 % . IR : ν_{NN} 2080(s), 2040(s), ν_{NO} 1660(s), ν_{CrN}(NO) 610(w) and ν_{CrN}(N$_3^-$) 365(w) cm^{-1}. λ_{max}(CH$_3$CN) 720 (20), 600 (105), 450 (350) and 342 (470) nm. μ_{eff} = 2.0 B.M.

RESULTS AND DISCUSSION

While in the case of thiocyanato-nitrosyl complexes the reductive nitrosylation of chromate ions becomes smooth and almost quantitative in an acidic or near neutral medium[4], the reaction being facile also in an alkaline medium[6], the same reaction with hydroxylamine and azide ions proceeds more effectively in an alkaline medium. The azido-nitrosyl chromium complexes prepared in the acidic medium are always impure and a purification by column chromatography is essential. However, irrespective of the reaction route the

yield of the azido-nitrosyl complexes are much lower than the analogous thiocyanato-nitrosyl complexes owing possibly to the intrinsic instability of the azido-nitrosyl complexes of metals and the instability of the azide ions in the reaction medium. However, the isolated complexes are quite stable as solid as well as in solution in organic solvents, unlike the corresponding rhenium complexes which are prone to decomposition in solution phase[7]. The isolation of the complexes is also rather easy and does not involve the separation of sticky solid as a crude reaction product as occurs in the cases of the analogous osmium complexes[1(b)].

The tetraphenylphosphonium salt is, as expected, found to be 3 : 1 electro-lyte (Λ_M = 380 ohm^{-1} cm^2 mol^{-1})[10]. Other complexes are non electrolytes and monomeric. Assuming the NO^+ formalism, the formal oxidation state of chromium in these complexes should be +1 (i.e. possessing $\{Cr(NO)\}^5$ moiety) which is manifested by their magnetic moment values (see experi-mental section) and esr spectra (g_{av} for all the complexes are 2.0). The esr spectra of the polycrystalline solid as well as of the acetonitrile solution of the complexes show only one line, the lack of ligand hyperfine coupling to the nitrosyl nitrogen atom as well as coupling to the spin active ^{53}Cr contrasting with the results found for some analogous com-plexes, viz., $[Cr(NO)(L_5)]^Z$ (Z = +2 for L = NH$_3$[11,12] or OH$_2$[12] ; Z = -3 for L = CN[12]) and paralleling some others, viz, $[Cr(NO)(CH_3CN)_5]$ (ref. 13), the thiocyanato-[3,4] and a few cyano-nitrosyl[12,14] derivatives. The local symmetry of the $[CrN(N_2)(N_2)]$ (in bipy and phen complexes) and $[CrN(N)_5]$ (the Ph$_4$P$^+$ salt) chromophores may approximate to C_{4v} and generate an M.O. configuration, $(e)^4$ $(b_2)^1$ (see ref. 15). So, the electronic transitions responsible for the three uv - vis bands in the L-L complexes may be desig-nated as $b_2 \longrightarrow e$ (π^* NO), $b_2 \longrightarrow b_1$ and $b_2 \longrightarrow a_1$. The hexaco-ordinated anionic complex, however, possesses an extra very weak band (brought out by Gaussian analysis from an weak inflection) at a quite low energy (720 nm) not observed in the pentacoordinated cases as well as in the analogous thiocyanato complex[4,6]. Whether this is due to $b_2 \longrightarrow e$ transition or due to any other transition is difficult to say. It may also be pointed out that the positions of the $d \longrightarrow \pi^*$ NO transitions in the present L-L series are comparable with the analogous thiocyanato complexes[4] which is quite natural when one compares the position of thio-cyanate and azide ions in the spectrochemical series.

ACKNOWLEDGEMENT

REFERENCES

1.   (a) Part VII. R. G. Bhattacharyya, G. P. Bhattacharjee and A. M. Saha, Trans. Met. Chem. (In press). (b) Part VI. R. G. Bhattacharyya and A. M. Saha, Inorg. Chim. Acta., (In press).

2.   W. P. Griffith, J. Lewis and G. Wilkinson, J. Chem. Soc., 1959, 872.

3.   S. Sarkar and A. Müller, Z. Naturforsch., 1978, 33b, 1053.

4.   R. G. Bhattacharyya, G. P. Bhattacharjee and P. S. Roy, Inorg. Chim. Acta., 1981, 54, L263.

5.   R. G. Bhattacharyya and P. S. Roy, Trans. Met. Chem., 1982, 7, 285.

6.   R. G. Bhattacharyya, G. P. Bhattacharjee and P. S. Roy, Unpublished observations.

7.   R. G. Bhattacharyya and P. S. Roy, J. Coord. Chem., 1982, 12, 129.

8.   P. D. Douglas and R. D. Feltham, J. Amer. Chem. Soc., 1972, 94, 5254.

9.   J. A. Broomhead, J. R. Budge, W. D. Grumley, T. R. Norman and M. Sterns, Austral. J. Chem., 1976, 24, 275.

10.   W. J. Geary, Coord. Chem. Rev., 1971, 7, 81.

11.   P. T. Manoharan, H. A. Auska and M. T. Rogers, J. Amer. Chem. Soc., 1967, 89, 4564.

12.   B. A. Goodman, J. B. Raynor and M. C. R. Symons, J. Chem. Soc.(A), 1968, 1973.

13.   S. Clamp, N. G. Connelly, G. E. Tailor and T. S. Louttit, J. Chem. Soc. Dalton Trans., 1980, 2162.

14.   R. G. Bhattacharyya, G. P. Bhattacharjee and N. Ghosh, Polyhedron, (In press).

15.   J. H. Enemark and R. D. Feltham, Coord. Chem., Rev., 1974, 13, 339.

NOTE

Synthesis, Reactions and Catalytic Activities of a Cationic
Acrylonitrile-Rhodium(I) Complex

T. Kwon, J.C. Woo and C.S. Chin*

Department of Chemistry, Sogang University, Mapo-gu, Sinsu-dong
Seoul 121, Korea

Abstract: Reaction of $RhCl(CO)(Ph_3P)_2$ (Ph_3P = triphenylphosphine) with $AgClO_4$ in acrylonitrile at $30°C$ produces a new cationic rhodium(I) complex, $[Rh(CH_2CHCN)(CO)(Ph_3P)_2]ClO_4$ (1) and AgCl. The ^1H-NMR and IR spectra of 1 suggest that acrylonitrile is coordinated to rhodium through the π-system of the vinyl group. The complex 1 reacts with molecular hydrogen to give a propionitrile-rhodium(I) complex, $[Rh(CH_3CH_2CN)(CO)(Ph_3P)_2]ClO_4$ (2) where the coordination of propionitrile through nitrogen is suggested by the ^1H-NMR and IR spectral data. The coordinated acrylonitrile in 1 is readily replaced with triphenylphosphine and propionitrile to give $[Rh(CO)(Ph_3P)_3]ClO_4$ and 2, respectively. The complex 1 is catalytically active for the hydrogenation and polymerization of acrylonitrile at $25°C$ under the atmospheric pressure of hydrogen.

The reaction of $IrCl(CO)(Ph_3P)_2$ with $AgClO_4$ in acrylonitrile produces AgCl precipitate and the clear yellow solution which is catalytically active for the polymerization of acrylonitrile under nitrogen at room temperature.[1] Subsequently, we have become interested in the reaction of the rhodium analog, $RhCl(CO)(Ph_3P)_2$ with $AgClO_4$ in acrylonitrile.

We wish to report the synthesis, reactions and catalytic activities of a new cationic rhodium(I) complex, $[Rh(CH_2CHCN)(CO)(Ph_3P)_2]ClO_4$ (1) which has been identified by elemental analyses, conductivity measurements, ^1H-NMR and IR spectral data. There have been a few other cationic acrylonitrile-rhodium(I) complexes reported (e.g., $[Rh(C_8H_{12})(CH_2CHCN)]ClO_4$, $[Rh(C_8H_{12})(CH_2CHCN)(Ph_3P)]ClO_4$) with their catalytic activities for the hydrogenation of olefins.[2]

The addition of $AgClO_4$ into the yellow solution of $RhCl(CO)(Ph_3P)_2$ in acrylonitrile under nitrogen immediately produced AgCl precipitate.[3] The yellow solution obtained by the removal of AgCl turned orange within one hour and eventually dark brown within three hours at $30°C$ under nitrogen. The addition of hexane to this dark brown solution resulted in brown solid of $[Rh(CH_2CHCN)(CO)(Ph_3P)_2]ClO_4$ (1) (eq. 1).[4] The complex 1 is stable in the solid state in air and in solution under nitrogen, and soluble in polar organic solvents (acrylonitrile, chloroform, dichloromethane) but insoluble in non polar solvents (benzene, hexane).

$$RhCl(CO)(Ph_3P)_2 + AgClO_4 + CH_2CHCN \longrightarrow$$
$$[Rh(CH_2CHCN)(CO)(Ph_3P)_2]ClO_4 + AgCl \qquad (1)$$
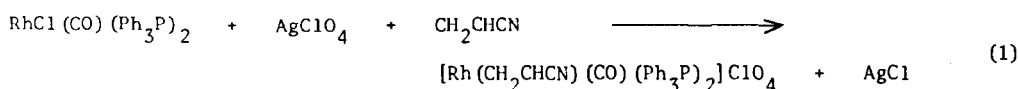
The molar conductance $(120\ ohm^{-1}cm^2mol^{-1})$ of $\underline{1}$ $(4.0 \times 10^{-5}\underline{M}$ in acrylonitrile) shows that the complex $\underline{1}$ is a 1:1 electrolyte.[5]

The formation of a π-bonding between acrylonitrile and rhodium is suggested by the IR spectrum of $\underline{1}$. The nitrile stretching frequency, ν_{CN} of acrylonitrile in $\underline{1}(2220\ cm^{-1}$, Nujol) is lower than that of free acrylonitrile $(2230\ cm^{-1})$. The decrease in ν_{CN} indicates that the acrylonitrile in $\underline{1}$ is coordinated to rhodium through the π-system of the vinyl group since it is well known that ν_{CN} of acrylonitrile increases upon coordination to a metal through nitrogen.[6] A very strong and broad absorption band at ca. $1100\ cm^{-1}$ (Nujol) attributable to the anionic tetrahedral ClO_4 group[7] supports that $\underline{1}$ is an ionic compound as confirmed by the conductivity data (see above). The ν_{CO} and ρ_{CH_2} (CH_2CHCN) in $\underline{1}$ appear at 1995 (very strong) and 950 (medium) cm^{-1} (Nujol), respectively.

The acrylonitrile hydrogens of $\underline{1}$ give rise to a multiplet at ca. δ = 5.75 ppm (vs. TMS, in $CDCl_3$) shifted upfield ca. 0.25 ppm from those (at ca. δ = 6.0 ppm) of free acrylonitrile. The multiplet due to the phenyl hydrogens of triphenylphosphine is seen at ca. δ = 7.5 ppm. The chemical shift of acrylonitrile in $\underline{1}$ and the ratio (10:1) of phenyl hydrogens to acrylonitrile hydrogens clearly suggest $Rh(CH_2CHCN)(Ph_3P)_2$ moiety in $\underline{1}$. The upfield shifts (0.25 ppm) observed for the acrylonitrile hydrogens in $\underline{1}$ are understood in terms of the increase in electron density at acrylonitrile due to its π-acceptor charactor through the π-system of the vinyl group as suggested by the IR data. The low oxidation state of rhodium in $\underline{1}$ probably facilitates the electron flow from the metal to the π-system of the vinyl group in the coordinated acrylonitrile. The hydrogens of acrylonitrile coordinated through nitrogen show downfield shifts relative to those of free acrylonitrile.[6,8] No complexes of coordinated acrylonitrile through the π-system of the nitrile group have been reported thus far.[6]

The complex $\underline{1}$ reacts with molecular hydrogen in chloroform at $25^\circ C$ to give the propionitrile-rhodium(I) complex, $[Rh(CH_3CH_2CN)(CO)(Ph_3P)_2]ClO_4$ $(\underline{2})$ (eq. 2).[9]

$$[Rh(CH_2CHCN)(CO)(Ph_3P)_2]ClO_4 \quad + \quad H_2 \quad \longrightarrow$$
$$[Rh(CH_3CH_2CN)(CO)(Ph_3P)_2]ClO_4 \tag{2}$$
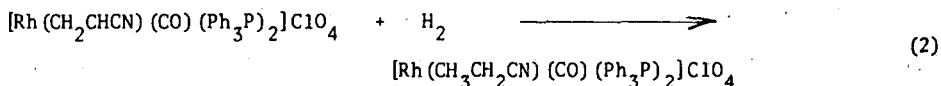
The IR spectral data provide the information on the nature of the bonding between metal and nitrile. It is well established that the bonding of a nitrile to a transition metal through nitrogen increases ν_{CN} relative to ν_{CN} of the nitrile uncoordinated, whereas the bonding through the π-system of the $C{\equiv}N$ group is characterized by a decrease in ν_{CN}.[6] The ν_{CN} of propionitrile in $\underline{2}$ is seen at $2260\ cm^{-1}$ (Nujol) while that of free propionitrile is seen at $2248\ cm^{-1}$,[10] which suggests that the propionitrile in $\underline{2}$ is coordinated through nitrogen. The ν_{CO} $(1970\ cm^{-1}$, Nujol) observed for $\underline{2}$ is significantly lower than that (1995 cm^{-1}) for $\underline{1}$. This may be the reflection of stronger Rh-CO bond in $\underline{2}$ than in $\underline{1}$. The IR spectrum of $\underline{2}$ also shows a strong and broad band at $1100\ cm^{-1}$ (Nujol) suggesting the anionic tetrahedral ClO_4 group in $\underline{2}$ as seen for $\underline{1}$.[7]

The ^{1}H-NMR spectrum of $\underline{2}$ shows the methyl hydrogens of the coordinated propio-
nitrile at $\delta = 0.53$ ppm (triplet, vs. TMS, $CDCl_3$) and the methylene hydrogens at
$\delta = 1.97$ ppm (quartet), while free propionitrile shows those at $\delta = 1.22$ and $\delta = 2.38$
ppm, respectively. The moiety of $Rh(CH_3CH_2CN)(Ph_3P)_2$ is evident in $\underline{2}$ from the
chemical shifts of the hydrogens of propionitrile and the ratio of the phenyl hydro-
gens at ca. $\delta = 7.5$ ppm to the hydrogens of propionitrile. The methyl hydrogens
of propionitrile in $\underline{2}$ are shielded more upon coordination to rhodium(I) than the
methylene hydrogens (1.22 - 0.53 = 0.69 ppm and 2.38 - 1.97 = 0.41 ppm, respectively).
The hydrogens of saturated nitriles coordinated to d^6 transition metals (Ru(II), Rh
(III)) showed downfield shifts relative to those of the free nitriles,[8] while those
coordinated to d^8 transition metal (Ir(I)) showed upfield shifts.[11,12] The upfield
shifts observed for $\underline{2}$ may be due to the facile electron flow from the electron rich
rhodium(I) to propionitrile. The spin coupling between ^{103}Rh and the hydrogens of
coordinated propionitrile has not been observed.

Acrylonitrile in $\underline{1}$ is readily replaced by propionitrile or triphenylphosphine
to give $\underline{2}$ or $[Rh(CO)(Ph_3P)_3]ClO_4$[13] in chloroform under nitrogen at 25°C (eq. 3).

$$[Rh(CH_2CHCN)(CO)(Ph_3P)_2]ClO_4 \quad + \quad L \quad \longrightarrow$$

$$[Rh(CO)(Ph_3P)_2L]ClO_4 \quad + \quad CH_2CHCN \qquad (3)$$
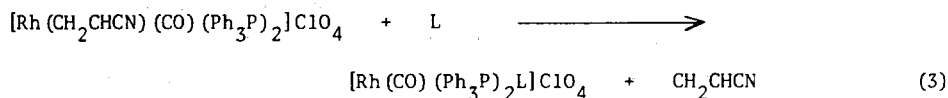
$$L = CH_3CH_2CN, \quad Ph_3P$$

The reaction of $\underline{1}$ with molecular hydrogen to produce $\underline{2}$ (eq. 2) has prompted us
to investigate the catalytic activity of $\underline{1}$ for the hydrogenation of acrylonitrile.
It has been found that the acrylonitrile solution of $\underline{1}$ under hydrogen (P_{H_2} = 700 mmHg)
at 25°C catalytically produces propionitrile and polyacrylonitrile. For example,
a 10 ml of acrylonitrile solution of $\underline{1}$ (0.12 g, 0.15 mmole) under hydrogen (P_{H_2} = 700
mmHg) produces 7.5 mmoles of propionitrile and 0.12 g (ca. 2.3 mmoles of acryloni-
trile monomer) of insoluble beige polyacrylonitrile[14] for 100 hours at 25°C.

References

(1) J. C. Woo, S. H. Kim and C. S. Chin, J. Polym. Sci., 20, 1947-1948 (1982).

(2) R. Uson, L. A. Oro, J. Jartigas and R. Sariego, J. Organomet. Chem., 179, 65-72
(1979).

(3) 0.203 g of AgClO$_4$ (0.98 mmol), 0.675 g of RhCl(CO)(Ph$_3$P)$_2$ (0.98 mmol) and 15 ml
of CH$_2$CHCN were used.

(4) The brwon solid was thoroughly washed with benzene. The yield was 0.687 g or
81% based on [Rh(CH$_2$CHCN)(CO)(Ph$_3$P)$_2$]ClO$_4$. Anal. Calcd for RhC$_{40}$H$_{33}$NClO$_5$

P_2: C, 59.46; H, 4.12; N, 1.73, Cl, 4.39; P, 7.67.

Found: C, 59.21; H, 4.20; N, 1.81; Cl, 4.31; P, 7.71. The complex 1 can also

be prepared by the reaction of $Rh(ClO_4)(CO)(Ph_3P)_2$[7] with acrylonitrile.

(5) Molar conductance of a standard 1:1 electrolyte $[(C_3H_7)_4N]PF_6$ in acrylonitrile
at 25° is 130 ohm^{-1} cm^2 mol^{-1}.

(6) S. J. Bryan, P. G. Huggett and K. Wade, Coordination Chem. Review, 40, 149-189
(1982).

(7) J. Peone, Jr. and L. Vaska, Angew. Chem. Int. Ed., 10, 511-512 (1971).

(8) R. D. Foust, Jr. and P. C. Ford, J. Am. Chem. Soc., 94, 5686-5697
(1972).

(9) 0.16 g(0.2 mmol) of 1 dissolved in 10 ml of chloroform was stirred under hydro-
gen(P_{H_2} = 700 mmHg) at 25°C for 24 hours during which time no visual change
was observed. Addition of hexane(ca. 25 ml) to the solution resulted in brown
solid(2) which was collected by filtration and washed thoroughly with benzene.
The yield was 0.12 g or 74% based on $[Rh(CH_3CH_2CN)(CO)(Ph_3P)_2]ClO_4$.
Anal. Calcd for $RhC_{40}H_{35}NClO_5P_2$: C, 59.31; H, 4.35; N, 1.73; Cl, 4.38; P, 7.65.
Found: C, 59.09; H, 4.21; N, 1.86; Cl, 4.40; P, 7.77. The molar conductance
of 2 is 120 ohm^{-1} cm^2 mol^{-1} in acrylonitrile at 25°C when [2] = 4.0 × 10^{-5} M.
The complex 2 can also be prepared by the reaction of $RhCl(CO)(Ph_3P)_2$ with
$AgClO_4$ in propionitrile under nitrogen at 30°C(refer the experimental details
for the preparation of 1 in text and ref. 4).

(10) R. D. Foust, Jr. and P. C. Ford, Inorg. Chem., 11, 899-901 (1972).

(11) C. A. Reed and W. R. Roper, J. Chem. Soc., Dalton, 1365-1370 (1973).

(12) C. J. Moon and C. S. Chin, unpublished results: ^{1}H-NMR of $[Ir(CH_3CH_2CN)(CO)(Ph_3P)_2]ClO_4$ in chloroform shows a triplet at δ = 0.57 ppm and a quartet at
δ = 2.02 ppm.

(13) L. Vaska and J. Peone, Jr., Suomen Kemistilehti, B44, 317-320 (1971).

(14) Polyacrylonitrile was separated by filtration and identified by the infrared
spectrum. In the absence of 1, polyacrylonitrile was not obtained under the
same experimental conditions(25°C, P_{H_2} = 700 mmHg).

NOTE

HETEROPOLYBLUES: RELATIONSHIP BETWEEN METAL-OXYGEN-METAL BRIDGES AND
REDUCTION BEHAVIOUR OF OCTADECA(MOLYBDOTUNGSTO)DIPHOSPHATE ANIONS.

J.P. CIABRINI, R. CONTANT[*] AND J.M. FRUCHART.
Laboratoire de Physicochimie Inorganique, ERA 608, Université Pierre et
Marie Curie, Tours 54-55, 4, place Jussieu, 75230 Paris Cedex 05

Abstract: The reduction behaviour of $P_2W_{18-n}Mo_nO_{62}^{6-}$ anions that can undergo
one or two-electron reduction steps has been rationnalized by taking
Mo^V-O-Mo^V angle and its deformation ability into consideration.

INTRODUCTION

Among the numerous heteropolyanions known[1] to easily give heteropolyblues
by reduction $P_2Mo_{18}O_{62}^{6-}(P_2Mo_{18})$ and As_2Mo_{18} are the only two that undergo
two-electron reduction steps even in the absence of protonation process.
Garvey and Pope[2] explain this particular behaviour by the chirality of
P_2Mo_{18} owing to an intramolecular rearrangement of short and long $Mo-O-Mo$[3a]
bonds.

We have investigated the reduction processes of some $P_2W_{18-n}Mo_n$ and
$PW_{12-n}Mo_n$ polyanions that we recently prepared by stereospecific methods[4,5].
The Garvey and Pope interpretation was reconsidered by taking the influence
of the positions of molybdenum atoms on the reduction pattern into account.

EXPERIMENTAL

Preparation. $K_6P_2W_{15}Mo_3O_{62}$. To a mixture of molar hydrochloric acid(125 ml)
and molar sodium molybdate(15 ml) solutions were added $Na_{12}P_2W_{15}O_{56}$(20 g)
then, after dissolution, potassium chloride(25 g).The yellow precipitate
was filtered off and recrystallised from acidulous water(50 ml; pH 2).
Anal. Calcd for $K_6P_2W_{15}Mo_3O_{62}$,14 H_2O : K 5.11 ; Mo 6.28 ; P 1.35 ; W 60.1 ;
H_2O 5.49. Found: K 5.15 ; Mo 6.26 ; P 1.35 ; W 59.7 ; H_2O 5.50
All other compounds were prepared by previously published methods[4,5,6].
$Na_{12}P_2W_{15}O_{56}$ has been first erroneously described as $P_2W_{16}^{6-}$. Analytical
procedures were given previously[4].
Reduction. Phosphopolyanion solutions(5.10^{-3}mol.l^{-1}) were electrochemically
reduced at pH 1 to obtain two-electron blues and at suitable higher pH to
obtain four-electron blues. The polarogramms were recorded on Radiometer

PO4 polarograph with rotating glass-imbedded carbon rod electrode. The halfwave potentials depending on the nature and the concentration of the counterions, the measurements were made in molar Na^+ solutions.

RESULTS AND DISCUSSION

Halfwave potentials, measured under conditions where the reduced anions are not protonated, are given in table 1. α_1-$P_2W_{17}Mo$ that contains the molybdenum atom in an equatorial site is more reducible than P_2Mo_{18} as $PW_{11}Mo$ is more reducible than PMo_{12}. On the other hand when the molybdenum atom is in a "cap" M_3O_{13}, it is less reducible than P_2Mo_{18}. This agrees with Pope et al[7,8] proposal that P_2W_{18} is initially reduced at one one of the twelve equivalent equatorial tungsten atoms. Moreover it should be the same for P_2Mo_{18}. Indeed, all the $P_2W_{18-n}Mo_n$ compounds that contain equatorial molybdenum atoms are more reducible than P_2Mo_{18} while $P_2W_{15}Mo_3$ that contains molybdenum atoms only in a M_3O_{13} group is less reducible than P_2Mo_{18}.

Table 1. Half-wave potentials(V vs. S.C.E.)

Species	$E_{1/2}$ at pH 4.7		ΔE^a	$E_{1/2}$ at pH 13	
	0-I	I-II		II-III	III-IV
P_2W_{18}	+0.04	-0.13	0.17	-0.51	-0.67
α_1-$P_2W_{17}Mo$ (4)[b]	+0.39	-0.05	0.44	-0.52	-0.64
α_2-$P_2W_{17}Mo$ (1)	+0.23	-0.20	0.43	-0.48	-0.59
$P_2W_{15}Mo_3$ (1,2,3)	+0.26	+0.06	0.20	-0.35	-0.70
$P_2W_{14}Mo_4$ (4,9,10,15)	+0.48(0-II)		0.05	-0.39	-0.60
A-$P_2W_{13}Mo_5$ (1,4,9,10,15)	+0.47(0-II)		0.04	-0.36	-0.60
B-$P_2W_{13}Mo_5$ (1,4,9,10,16)	+0.46	+0.35	0.11	-0.38	-0.60
$P_2W_{12}Mo_6$ (1,4,9,10,15,16)	+0.45(0-II)		0.03	-0.36	-0.58
P_2Mo_{18}	+0.32(0-II)		0.00	-0.18(II-IV)	
PW_{12}	-0.02	-0.29	0.27	-0.70	-0.94
$PW_{11}Mo$	+0.55	-0.20	0.75	-0.77	-0.96
PW_9Mo_3	+0.60	+0.26	0.34	-0.38	-0.98
PMo_{12}	+0.44	+0.27	0.17	-0.19	-0.38

[a] $\Delta E = E_{1/2}(0-I)-E_{1/2}(I-II)$ was calculated from $E_{3/4}-E_{1/4}$ for bielectronic waves. Then it is only an order of magnitude. [b] Arabic numerals in parenthesis refer to the positions of molybdenum atoms[9] (figure 1).
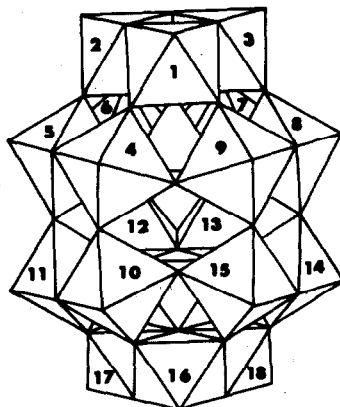
Figure 1. Idealized structure of a-$P_2W_{18}O_{62}$. a-$P_2Mo_{18}O_{62}$ has the same framework but the Mo-O-Mo bonds are alternatively short and long [3a].

Furthermore it appears that P_2Mo_{18} is not the only phosphopolyanion that undergoes two-electron reduction step; three other compounds studied here behave likewise. According to Garvey and Pope[2] interpretation, it is possible that in a group of molybdenum atoms the Mo-O-Mo bonds would be alternatively short and long but this effect should be the same in PMo_{12}[3b] and $P_2W_{15}Mo_3$ for which odd states of reduction were observed (table 1).

As the four anions that undergo two electron reductions contain at least a group of four corner-sharing MoO_6 octahedron, i.e. located in 4,9,10 and 15 positions, we assume that, in such a group, the stabilizing effect of antiferromagnetic spin pairing overcome the destabilizing effect of increasing charge. Indeed, if we consider, as usual, that electrons are introduced in metal atom d_{xy} orbitals perpendicular to the metal-terminal oxygen direction, the more d_{xy} orbitals overlap the more d electrons are strongly coupled. The largest overlap between d_{xy} orbitals and bridging oxygen 2p orbitals would occur for linear M-O-M bonds; this borderline case has been observed by Jeannin, Launay et al[10] on the $\left| W_4O_8Cl_8(H_2O)_4 \right|^{2-}$ anion where the two d electrons are strongly coupled in an antiferromagnetic way.

In P_2M_{18} compounds the M(4)-O-M(10) angle between the two PM_9 half-anion[3a] is 162°. As often as several molybdenum atoms are concerned the angle can open by rearrangement of short and long Mo-O-Mo bonds. Then ΔE(table 1) the difference between the first and second reduction potentials would decrease as the deformation ability of Mo(4)-O-Mo(10) bonds would increase (P_2Mo_{18} < $P_2W_{12}Mo_6$ < A-$P_2W_{13}Mo_5$ < $P_2W_{14}Mo_4$ < B-$P_2W_{13}Mo_5$ < P_2W_{18}). For instance, if we compare the two $P_2W_{13}Mo_5$ formally deriving from $P_2W_{12}Mo_6$ by replacing one molybdenum by one tungsten atom in position 16(A) or 15(B), the latter would more enhance the rigidity of the molybdenum group and then increase ΔE.

This interpretation, based on d_{xy} orbitals overlap and deformation ability of Mo-O-Mo bonds, can explain in the same way why P_2Mo_{18} and As_2Mo_{18} undergo second and third two-electron reduction steps[11] since they contain three groups of four corner-sharing MoO_6. For $P_2W_{18-n}Mo_n$(n = 4,5 or 6) compounds the first four electrons are introduced in the same group of molybdenum atoms, then the effect of increasing charge overcome the effect of spin pairing.

In PMo_{12} the splitting ΔE is about the same as in $P_2W_{15}Mo_3$ where the MoO_6 octahedrons are edge-shared but it is weaker than in PW_9Mo_3 where the MoO_6 are corner-shared with a theoretical Mo-O-Mo angle of 151°. Likewise $SiW_{12-n}Mo_n$ (n = 2 or 3)[9c] exhibit larger splittings[12] than $SiMo_{12}$ and even than SiW_{12}. All this agrees with the first two electrons introduced in the same M_3O_{13} group of XM_{12}, the two M^VO_6 octahedrons being then edge-shared.

The conclusion is that, for X_2M_{18} polyanions, the splitting of two-electron reduction steps into one-electron reduction steps varies with the M^V-O-M^V angle between the two XM_9 half-anions, If several MoO_6 octahedrons are corner shared the short and long Mo-O bonds can rearrange to favor angle opening and weaker splitting. Then the reduction behaviour of P_2Mo_{18} and As_2Mo_{18} is not an exception but merely a borderline case.

REFERENCES AND NOTES

1 T. J. R. Weakley, Structure and Bonding, 1974, 18, 131.

2 J. P. Garvey and M. T. Pope, Inorg. Chem. 1978, 17, 1115.

3 R. Strandberg, Acta Chem. Scand. 1975, A29, [a]350, [b]359.

4 R. Contant and J. P. Ciabrini, J. Inorg. Nucl. Chem. 1981, 43, 1525.

5 R. Massart, R. Contant, J. P. Ciabrini, J. M. Fruchart and M. Fournier,

   Inorg. Chem. 1977, 16, 2916.

6 R. Contant and J. P. Ciabrini, J. Chem. Res. 1977, (S)222 (M)2601.

7 G. M. Varga, E. Papaconstantinou and M. T. Pope, Inorg. Chem. 1970, 9, 662.

8 R. Acerete, S. Harmalker, C. F. Hammer, M. T. Pope and L. C. W. Baker,

   J. C. S. Chem. Comm. 1979, 777.

9a In $P_2W_{15}Mo_3O_{62}^{6-}$ the three molybdenum atoms are in one M_3O_{13} "cap" as the

    vanadium atoms in the related compound $P_2W_{15}V^{IV}V^VO_{62}^{10-}$ (S. P. Harmalker and

    M. T. Pope, J. Am. Chem. Soc. 1981, 103, 7381). The lack of a M_3O_{13} group

    in $P_2W_{15}O_{56}^{12-}$ is confirmed by the formation of $Co_2P_4W_{30}O_{112}^{20-}$ and

    $Co_4(H_2O)_2P_4W_{30}O_{112}^{16-}$ complexes (J. P. Ciabrini, Thèse, Paris 1982).

9b The proposed structures of $P_2W_{18-n}Mo_n$(n = 4,5 or 6) have been confirmed by

    solving the X-ray structure of a tetramer of $P_2W_{12}^6$. It is formed by four

    entities P_2W_{12} identical with that we have

    proposed in $P_2W_{12}Mo_6^6$ (A. Tézé and R. Contant, to be published).

9c It is now established (F. Robert and A. Tézé, Acta Cryst. 1981, B37, 318)

    that molybdenum atoms in SiW_9Mo_3 and $SiW_{10}Mo_2$ (α and β isomers [12]) belong

    to different M_3O_{13} groups and that MoO_6 octahedrons are corner-shared. It

    should be the same in PW_9Mo_3.

10 Y. Jeannin, J. P. Lanay, C. Sanchez, J. Livage and M. Fournier, Nouveau J.

    Chim. 1980, 4, 587.

11 R. Contant and J. M. Fruchart, Revue Chim. Minér. 1974, 11, 123.

12 J. M. Fruchart, G. Hervé, J. P. Launay and R. Massart, J. Inorg. Nucl.

    Chem. 1976, 38, 1627.

NOTE

THE ^{1}H AND ^{2}H NMR SPECTRA OF HFeCo$_3$(CO)$_{12}$

G.E. Hawkes and E.W. Randall*

Department of Chemistry, Queen Mary College,
Mile End Road, London, El 4NS

S. Aime, R. Gobetto, D. Osella

Istituto di Chimica Generale ed Inorganica,
Universita di Torino, Corse Massimo d'Azeglio 48,
19125 Torino, Italy

Abstract - The detection of the ^{2}H resonance of

^{2}HFeCo$_3$(CO)$_{12}$ led to the detection of the broader

^{1}H resonance of the ^{1}H isotopomer. The shift is

-21.4 ppm.

In the past twenty years it has been widely demonstrated

that ^{1}H NMR spectroscopy is a simple, accurate and

effective method for the detection of a hydrido-ligand

in a metal complex.[1] Difficulties can arise in this method

however if the metal which is involved has a nucleus, M,

possessing an electric quadrupole moment. This is the

case if the nuclear magnetic spin quantum number, I, of

the metal has a value greater than ^{1}/2. Examples are

^{59}Co (I=^{7}/2) and ^{55}Mn (I=^{5}/2). Moderately rapid

relaxation of M caused by the electric quadrupole

relaxation mechanism, at a rate denoted $(T_{qM})^{-1}$, can then

broaden the hydrido ^{1}H resonance if M and H are scalar

spin coupled (J_{HM}). In the limit that the ^{1}H multiplet

has collapsed to a single broad Lorentzian line, the

1235

proton relaxation time T_2-H is given by [2]

$$(T_2\text{-H})^{-1} = I(I+1)4\pi^2 J_{HM}^2 T_{qM}/3$$

T_2-H can be so short that the ^{1}H resonance is very difficult to detect since the line is very broad. This has been the case for example with $HMCo_3(CO)_{12}$ [M=Fe,Ru,Os], so that the nature of the hydride ligand in solutions of these compounds has remained unknown.[3,4,5] Even in the case of the solids there was initial uncertainty concerning the bonding which was eventually elucidated by X ray and neutron diffraction studies of $HFeCo_3(CO)_9$ [$P(OCH_3)_3$].[6,7,8] These showed that the hydrido ligand occupied a μ_3-coordination site below the tricobalt face. Renewed attempts to detect the hydrido signal in the ^{1}H NMR spectra were unsuccessful. These employed low temperatures to increase the 'thermal decoupling' effect, on the presumption that broadening was because the collapse of multiplet structure was only partial.[9]

We report here a novel method for the measurement of the ^{1}H shift in these cases by the use of surrogate ^{2}H NMR spectra of a deuteriated sample.[10] A chloroform solution of $^2HFeCo_3(CO)_{12}$ gave a ^{2}H signal with a line-width of 35 Hz at 294 K. The technique works because the value of $^1J_{HM}$ for the ^{2}H isotopomer is smaller by a factor of 6.51 than the value in the ^{1}H isotopomer, and therefore the value of T_2-H is expected by equation 1 to be $(6.57)^2$, i.e., 42.38 times larger for the ^{2}H resonance

than for the ^{1}H resonance. Thus the contribution to the

^{2}H line-width from the H-metal interaction should be 42.38

times smaller for ^{2}H than for ^{1}H. A complication is that

since the ^{2}H nucleus possesses its own quadrupole moment,

the ^{2}H line-width might be dominated by this effect. The

fact that the width did not increase when the temperature

was raised to 333 K suggests that this is so. The value

of 35 Hz for the ^{2}H line-width however is still quite low

and if it was all attributed to the effect of the ^{59}Co

then the corresponding ^{1}H line-width would be

35 x 42.38 = 1483 Hz, a figure which should constitute

only an upper limit. Even a line of this width should be

detectable with high resolution instrumentation, however,

and it was indeed found by the use of a wide spectral

width (150 ppm) such as normally employed for example in

the detection of broad resonances of paramagnetic

complexes. At 302 K the width was measured as

approximately 550 Hz and the shift as ca. -21 ppm. The

line width decreased to 500 Hz at 292 K. The

corresponding ^{2}H line width is calculated as 13 Hz,

rather less than the value measured. The difference of

22 Hz must be due to the quadrupole relaxation of ^{2}H

itself. Use of a correlation time τ_c of 20 ps gives

the electric quadrupole coupling constant for ^{2}H as

150 kHz if axial asymmetry is assumed.

The hydrido shifts measured for ^{1}H and ^{2}H are the

same (within the rather large errors arising from the

large ^{1}H line-widths) as expected in the absence of

primary isotope effects on shieldings.[11] The value of
-21.4 ppm relative to TMS is surprisingly within the
normal region of absorption of μ_2-bridging
hydrides.[1,12] It is noticeably to high field of the
resonances for other μ_3-face bridging hydrides:[13,14]
$(\mu_3-H)_4 Re_4 (CO)_{12}$ at -5.1 ppm; $\left[(\mu_3-H)(IrLL'H_2)_3 \right]$
$\left[PF_6 \right]_2$ at -3.9 ppm. It is different also from the case
of $HFeCo_2 (CO)_9 CH$ which probably has a μ_3-hydride
structure although there is no report of a crystal
structure determination. For this compound the value
-9.81 ppm has been reported[15] and considerable
broadening of the hydrido resonance was ascribed to
the effect of the ^{59}Co nuclei.

Clearly the question now arises concerning what
is the range of shift values which μ_3-hydrido
resonances can have as the cluster types and the
metals vary.

The use of surrogate ^2H-spectra should
constitute an important method in studies of this
sort, and in more general investigations of hydrido
derivatives of cobalt, manganese and other
quadrupolar metals.

REFERENCES

1   H.D. Kaesz and R.B. Saillant, Chem. Rev., 1972,

    72, 231.

2   see J.M. Lehn and J.P. Kintzinger in 'Nitrogen

    NMR', eds., M. Witanowski and G.A. Webb, Plenum,

    London, (1973); N.C. Pyper, Mol. Phys., 1971, 21,

    977.

3   M.J. Mays and R.N.F. Simpson, J. Chem. Soc. A,

    1968, 1444.

4   J. Knight and M.J. Mays, J. Chem. Soc. A, 1970,

    711.

5   J.W. White and C.J. Wright, J. Chem. Soc. A, 1971,

    2843.

6   B.T. Huie, C.B. Knobler and H.D. Kaesz, J. Chem.

    Soc. Chem. Comm., 1975, 684.

7   B.T. Huie, C.B. Knobler and H.D. Kaesz, J. Am.

    Chem. Soc., 1978, 100, 3059.

8   R.G. Teller, R.D. Wilson, R.K. McMullan,

    T.F. Koetzle and R. Bau, J. Am. Chem. Soc., 1978,

    100, 3071.

9   S. Aime, L. Milone, G. Gervasio and E. Rosenberg,

    Trans. Met. Chem., 1976, 1, 177.

[10]   Deuteriation was achieved by dissolving $[Co(Me_2CO)_6]^{2+}[FeCo_3(CO)_{12}]^-$ (200 mg) in DClP 37% solution in D_2O (10 ml). Extraction with warm cyclohexane afforded the deuterido cluster derivative.

[11]   H.H. Mantsch, H. Saito and I.C.P. Smith, Prog. NMR Spect. (Eds. J. Emsley, J. Feeney and L.H. Sutcliffe) 1977, Vol. 11, 211.

[12]   A.P. Humphries and H.D. Kaesz, _Prog. Inorg. Chem._, 1973, 25, 145.

[13]   R.B. Saillant, G. Barcelo and H.D. Kaesz, _J. Am. Chem. Soc._, 1970, 92, 5739.

[14]   D.F. Chodosh, R.H. Crabtree, H. Felkin and G.E. Morris, _J. Organometallic Chemistry,_ 1978, 161, C67.

[15]   R.A. Epstein, H.W. Withers and G.L. Geoffroy, _Inorg. Chem._ 1979, 18, 942.

COMMUNICATION

THE PREPARATION AND CRYSTAL STRUCTURE OF BIS(BIS(DIPHENYL-PHOSPHINO)ETHANE)CARBONYLFORMYLOSMIUM(II) HEXAFLUOROANTIMONATEDICHLOROMETHANE (1/1)

GARRY SMITH and DAVID J. COLE-HAMILTON*
Donnan Laboratories, University of Liverpool, P.O. Box 147, Liverpool L69 3BX, England

and

MARK THORNTON-PETT and MICHAEL B. HURSTHOUSE
Chemistry Department, Queen Mary College, Mile End Road, London E1 4NS, England

Abstract—Reaction of *trans*[Os(CO)$_2$(dppe)$_2$]$^{2+}$ with [KHB(OPr^i)$_3$] gives the formyl complex *trans*-[Os(CHO)(CO)(dppe)$_2$][SbF$_6$] which is thermally very stable; the crystal structure shows it to have *trans* stereochemistry and a long Os–C bond.

We have recently reported[1] the successful isolation of cationic formyl complexes of ruthenium from the action of monohydridic reducing agents on [Ru(CO)$_2$(P–P)$_2$]$^{2+}$

(P–P = Ph$_2$P(CH$_2$)$_n$PPh$_2$, n = 1, dppm; n = 2, dppe). Although these formyl complexes are sufficiently inert for isolation and characterisation, they decompose with half-lives of < 15 min in solution at room temperature.[2] We now report the isolation of an analogous osmium complex which is substantially more inert.

*Author to whom correspondence should be addressed.
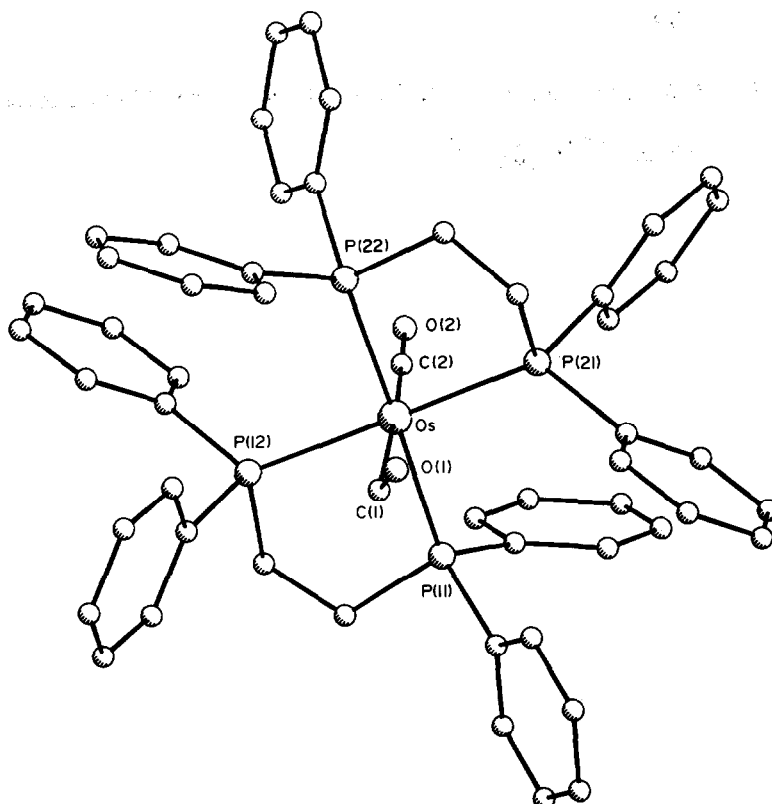
Fig. 1. Solid state structure and atomic numbering scheme for the cation of *trans*-[Os(CHO)(CO)(dppe)$_2$][SbF$_6$]·CH$_2$Cl$_2$. C(1)–O(1), 1.181(11); Os–C(1), 2.155(28); Os–Ĉ(1)–O(1),130.7(27); C(2)–O(2), 1.096(35); Os–C(2), 1.983(32); Os–Ĉ(2)–O(2), 173.0(28); C(1)–Ôs–C(2), 172.1(11). Angles in °, lengths in Å.

Treatment of *trans*[Os(CO)₂(dppe)₂][SbF₆]₂, prepared from [OsCl₂(dppe)₂], CO and excess Ag[SbF₆], with excess [KHB(OPrⁱ)₃] leads to the formation of *trans*-[Os(CHO)(CO)(dppe)₂][SbF₆] which has been fully characterised spectroscopically.† The complex is very much more thermally stable than its ruthenium analogue. For example, only 60% conversion to *trans*-[OsCl(CO)(dppe)₂]⁺ is observed on refluxing *trans*-[Os(CHO)(CO)(dppe)₂][SbF₆] in CHCl₃ under N₂ atmosphere for 5 days, the remaining 40% being mostly unchanged formyl.

In view of the scarcity of information on the structures of transition metal formyls[3-5] in general and cationic formyls in particular, *trans*-[Os(CHO)(CO)(dppe)₂][SbF₆]·CH₂Cl₂ was studied by X-ray diffraction methods.‡ The structure of the cation (Fig. 1) shows the presence of mutually *trans* carbonyl

(NO)(PPh₃)] (1.225 Å)[4] but longer than that of [Rh-(CHO)(octaethylporphyrin)] (1.175 Å)[5] which is unusual in many ways, including its preparation[6] by insertion of CO into a rhodium hydrogen bond.

Metal formyl complexes are normally believed to have contributions to their structures from the two resonance forms shown in Fig. 2. We assume that the observed short C=O bond length arises from a lesser contribution from form II on account of the positive charge already present on the metal.

Consistent with this, the Os–C bond length (2.155 Å) is comparable with those observed for Os–C single bonds (2.15 Å)[7] but much longer than Os=C as found in [Os(PPh₃)₂(CO)₂(CC₆H₅Me)] (1.90 Å).[8] This contrasts with the M–C bond length of, e.g. [Re(C₅H₅)(CHO)(NO)(PPh₃)] which is closer to the value found for Re=C in carbene complexes.[4,9]
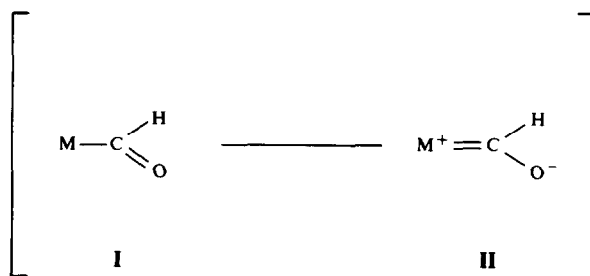
Fig. 2. Possible resonance forms for metal formyl complexes.

and formyl groups, the two being easily distinguished by an Os–Ĉ–O of 130.7° for the formyl ligand, similar to those reported for anionic (134°)[3] or neutral (130, 128°)[4,5] metal formyl complexes.

The formyl C=O bond length (1.181 Å) is somewhat shorter than those observed for [Et₄N][Fe(CHO)(CO)₃ (3,5-Me₂C₆H₃O)₃P] (1.195 Å)[3] and [Re(C₅H₅)(CHO)

---

†IR max. cm⁻¹: 2558w(ν_{C-H}), 1965vs and 1960vs($\nu_{C=O}$) {$\nu_{C=O}$ = 1970, CH₂Cl₂ soln}, 1558vs($\nu_{C=O}$); NMR: ¹H; δ14.45qu, J_{PH} = 4.9 Hz, (C*H*O); 5.32s(C*H*₂Cl₂); ³¹P δ17.85s.

‡Crystal data: Os(CHO)(CO)(Ph₂PCH₂CH₂PPh₂)₂· SbF₆·CH₂Cl₂, F.wt = 1363.9, orthorhombic, a = 22.361(4), b = 20.209(2), c = 11.940(2) Å, V = 5369 Å³, space group $Pn2_1a$ (alternative setting of $Pna2_1$, No. 33), Z = 4, D_c = 1.65 g cm⁻³, μ(Mo-K_α) = 29.64 cm⁻¹, R = 0.059 for 2301 observed [$I > 1.5\sigma(I)$] reflections (3861 unique) measured on a diffractometer. The atomic coordinates, thermal parameters and bond lengths and angles have been deposited as supplementary data with the Editor, from whom copies are available on request. Atomic co-ordinates have also been deposited with the Cambridge Crystallographic Data centre.

REFERENCES

1. G. Smith and D. J. Cole-Hamilton, *J. Chem. Soc. Chem. Commun.* 1982, 490.
2. G. Smith, L. H. Sutcliffe and D. J. Cole-Hamilton, Manuscript in preparation.
3. C. P. Casey, S. M. Neumann, M. A. Andrews and D. R. McAlister, *Pure Appl. Chem.* 1980, **52**, 625.
4. W. K. Wong, W. Tam, C. E. Strouse and J. A. Gladysz, *J. Chem. Soc. Chem. Commun.* 1979, 530.
5. B. B. Wayland and B. A. Woods, *J. Am. Chem. Soc.* 1982, **104**, 302.
6. B. B. Wayland and B. A. Woods, *J. Chem. Soc. Chem. Commun.* 1981, 700.
7. A. J. Schultz, J. M. Williams, R. B. Calvert, J. R. Shapley and G. D. Stucky, *Inorg. Chem.* 1979, **18**, 319.
8. W. R. Roper, J. M. Waters, L. J. Wright and F. van Meurs, *J. Organometal. Chem.* 1980, **201**, C27.
9. J. A. Gladysz, *Adv. Organometal. Chem.* 1982, **20**, 1.

INTERACTION OF ARYLDIAZONIUM SALTS WITH SOME SCHIFF-BASE COMPLEXES OF COBALT AND RUTHENIUM

NICHOLAS FARRELL*, MARIA N. DE OLIVEIRA BASTOS and ANTONIO A. NEVES

Departamento de Química, Universidade Federal de Minas Gerais, Belo Horizonte
MG 30.000, Brasil

Abstract—The interaction of aryldiazonium ions with some Schiff-base complexes of cobalt and ruthenium have been studied. With cobalt, one-electron oxidation of [Co(II)Salen] occurred; with [Co(I)Salen] the corresponding Co(III)-aryl complexes were isolated. In the case of ruthenium oxidation also occurs, [Ru(Salen)(CO)py] gave the corresponding monocation. The results, especially for ruthenium, are in contrast to the stabilisation of both nitrosyl and aryldiazonium adducts in analogous porphyrin complexes.

We have recently begun a study of the interaction of aryldiazonium ions with metal complexes of macrocycles and other quadridentate donor ligands and have reported on the preparation of aryldiazonium–ruthenium porphyrin species of the type [Ru(porphyrin)(N$_2$Ar)L]BF$_4$. To compare the effects of differing donor atoms in the equatorial plane we next studied the reactions of Schiff-base complexes† and this paper summarises our results on cobalt and ruthenium systems.

EXPERIMENTAL

All solvents were dried by usual methods and distilled under nitrogen. All reactions were carried out under a nitrogen atmosphere. The starting complexes of cobalt(II) were prepared by standard procedures[2,3] and the cobalt(I) Schiff base solutions generated *in situ* by the literature method.[4] Diphenyliodonium chloride was purchased from Aldrich Chemical Company Inc. and used without further purification.

IR spectra were recorded on a Perkin–Elmer 457 spectrometer for samples pressed in KBr discs. Visible spectra were recorded using a Cary-17 spectrophotometer. Elemental analyses were car-

ried out at the Centro de Tecnologia do Estado de Minas Gerais (CETEC), Belo Horizonte, Brasil.

N, N′-ethylenebis (salicylideneiminato) cobalt (III) tetrafluoroborate

To a stirred suspension of Co(Salen) (0.975 g, 0.003 mol) in CH$_2$Cl$_2$ (25 cm^3) was added a suspension of PhN$_2$BF$_4$ (0.58 g, 0.003 mol) in CH$_2$Cl$_2$ (25 cm^3). The mixture was stirred for 1 hr at reflux temperature during which time a red–brown solid precipitated. The solid was filtered off, washed with CH$_2$Cl$_2$ and recrystallised from acetone–ether to give a dark powder (yield, 45%). Found: C, 45.3; H, 3.92; N, 6.31. [C$_{16}$H$_{16}$N$_2$O$_3$BF$_4$Co] requires: C, 44.65; H, 3.72; N, 6.5%. Identical results were obtained using the *p*-NO$_2$ and *p*-OCH$_3$ salts and when acetone was used as solvent in place of dichloromethane. The iodo salt was prepared by metathesis with excess KI in acetone and compared with an authentic sample prepared by the literature method.[11]

Preparation of cobalt (III) Schiff-base aryl complexes

A stirred suspension of PhN$_2$BF$_4$ (0.192 g, 0.001 mol) in CH$_2$Cl$_2$ (15 cm^3) was added slowly to a filtered solution of [Co(I)Salen], (0.325 g, 0.001 mol) in THF (20 cm^3) at −10°C. The initial red–brown colour of the reaction mixture remained unaltered after 2 hr of stirring, when water (50 cm^3) was added to give a red–brown solid. This was filtered off and purified by chromatography on

---

*Author to whom correspondence should be addressed.

†Abbreviations used in this paper: H$_2$Salen = N,N′-ethylenebis (salicylideneimine); H$_2$Acacen = N,N′-ethylenebis(acetylacetonediimine).

a neutral alumina column by elution in CH$_3$OH–CHCl$_3$ (1:3). The orange–red solid obtained upon evaporation was treated with pyridine to give the yellow–orange product (yield = 40%). Found: C, 55.5; H, 4.60; N, 6.70. Calc for [C$_{27}$H$_{24}$N$_3$O$_2$Co]; C, 55.95; H, 4.16; N, 6.99%. The IR spectrum of this product was identical with that of an authentic sample.[4] In a similar manner [Co(Acacen)Ph(H$_2$O)],[5] Found: C, 57.44; H, 6.54; N, 7.41. Calc for [C$_{18}$H$_{25}$N$_2$O$_3$Co]: C, 57.4; H, 6.64; N, 7.44; [Co(Salen)(p-NO$_2$Ph)py], CH$_3$OH. Found: C, 58.03; H, 4.80; N, 10.8% [C$_{28}$H$_{29}$N$_4$O$_5$Co] requires: C, 58.33; H, 5.03; N, 9.7%; [Co(Salen)(m-NO$_2$Ph)py]. Found: C, 61.06; H, 4.25; N, 10.1% [C$_{27}$N$_{25}$N$_4$O$_4$Co] requires: C, 61.6; H, 4.37; N, 10.65%, were prepared in 30–50% yields. Use of Ph$_2$I$^+$Cl$^-$ (0.316 g; 0.001 mol) in CH$_3$OH (10 cm^3) gave a red–brown solution with [Co(I)Salen] from which a red–brown solid was precipitated by addition of ether. This solid when recrystallised from pyridine gave the yellow–orange [Co(Salen) (Ph)py], identical with the authentic sample.[4]

Carbonylpyridine-N,N′ ethylenebis(salicylideneiminato)-ruthenium(II)

The complex [Ru(CO)Salen]$_2$, obtained as a precipitate from the reaction between Ru$_3$(CO)$_{12}$ and H$_2$Salen in refluxing toluene, was dissolved in pyridine and the solution heated under reflux for 16 hr, when the solvent was evaporated giving a yellow–green solid. Found: C, 54.6; H, 4.27; N, 8.53. Calc for [C$_{22}$H$_{21}$N$_3$O$_4$Ru]: C, 54.9; H, 4.31; N, 8.88%.

Carbonylpyridine N,N′ ethylenebis(salicylideneiminato)-ruthenium(III) tetrafluoroborate

The complex [Ru(Salen)(CO)py], (0.25 g; 0.503 mmol) was suspended in CHCl$_3$ (50 cm^3) and excess aryldiazonium salt added. The suspension was maintained under reflux for 16 hr, after which the cooled solution was filtered and concentrated to half-volume whereupon a green solid precipitated in 50% yield. Found: C, 43.80; H, 3.44; N, 7.09. Calc for [Ru(Salen)(CO)py]BF$_4$, 0.5 CHCl$_3$: C, 43.49; H, 3.46; N, 6.77%. A similar procedure using Et$_3$O$^+$BF$_4^-$ in place of ArN$_2^+$ BF$_4^-$ resulted in an identical product.

RESULTS AND DISCUSSION

Cobalt

The complexes studied were those of H$_2$Salen and H$_2$Acacen: The reactions of Co(II)Salen with p-XC$_6$H$_4$N$_2$BF$_4$, (X = H, NO$_2$, OCH$_3$), in either chloroform or acetone at room temperature all

gave the same product, characterised by IR spectroscopy and elemental analysis as the product of one-electron oxidation, [Co(III)(Salen)(H$_2$O)]BF$_4$. The formulation was confirmed by metathesis with I$^-$ and comparison of the IR spectrum with that of an authentic sample of [Co(Salen)I] formed by oxidation of [Co(II)Salen] with I$_2$.[4] A similar reaction occurs for [Co(II)acacen)(H$_2$O)$_2$]. This mode of reaction has been observed previously for aryldiazonium ions with [Cr(C$_6$Me$_6$)(CO)$_2$(PPh$_3$)] giving the corresponding monocation.[6]

In an attempt to prepare Co(III)-aryldiazenato complexes we next considered oxidative addition of Co(I) species. When C$_6$H$_5$N$_2$BF$_4$ in acetone was added to the green solution of Na[Co(I)Salen] in tetrahydrofuran[2] at room temperature the colour of the solution immediately changed to red–brown and upon work-up as described in the Experimental Section of σ-aryl complex [Co(Salen) (Ph)py] was obtained. Use of lower temperatures followed by precipitation with diethyl ether failed to isolate the presumed aryldiazenato intermediate. The use of aryldiazonium ions as arylating agents has been described previously for [IrCl(CO)(PPh$_3$)$_2$][7] and by Nesmeyanov's group with complexes such as [FePh(Cp)(CO)$_2$].[8] Extrusion of dinitrogen from isolated aryldiazenato complexes [Pt(N$_2$Ar)(PEt$_3$)$_3$]$^+$$^{(9)}$, and [RhCl$_2$(N$_2$Ar) (PPh$_3$)$_3$],[10] also gave the corresponding σ-aryl derivatives. Use of the diphenyliodonium salt, Ph$_2$I$^+$Cl$^-$, instead of PhN$_2^+$, also gave the σ-phenyl complex in good yield. With [Co(I)Acacen] the known[5] [Co(Acacen)(Ph)H$_2$O] was readily isolated.

To test the generality of this reaction and to study the effect of substituents on the phenyl ring in stabilizing the Co(III)-N$_2$Ar species the reactions of [Co(I)Salen] were investigated with XC$_6$H$_4$N$_2$BF$_4$ (X=p-NO$_2$, p-OCH$_3$ and m-NO$_2$). In the case of the p-NO$_2$ salt the initial red–violet colouration of the reaction mixture persisted for some time on warming to room temperature but the final product isolated was [Co(Salen) (p-NO$_2$C$_6$H$_4$)py] as dark crystals. Similarly the m-NO$_2$ salt gave a black crystalline solid with an IR spectrum very similar to the p-NO$_2$ derivative. An unusual reaction, however, occurred using p-CH$_3$OC$_6$H$_4$N$_2$BF$_4$. In this case the dark-brown solid which precipitated from the reaction mixture was identified by elemental analysis and IR spectrum to be [Co(III)Salen]BF$_4$, representing a formal two-electron oxidation. We have not as yet investigated the mechanism of this reaction but the observation agrees in general with the deactivating role of methoxy in nucleophilic aromatic substitution.

A formal two-electron oxidation occurs in the formation of the Ir(III)-tetrazene complex, $[Ir(CO)(PPh_3)_2(N_4Ar_2)]BF_4$ from $[Ir(Cl(CO)PPh_3)_2]$ and aryldiazonium ion in benzene/ethanol.[11] A mechanism involving attack of ArN_2^+ on an Ir(I)–N₂Ar moiety has been proposed;[12] a similar situation in the cobalt case could also account for the observed result.

The results outlined in the Scheme are in accord with the known chemistry of these cobalt complexes, but do underline again the utility of aryldiazonium and diphenyliodonium salts as phenylating agents in inorganic chemistry especially where the standard Grignard or aryllithium route is inaccessible and usually are made from the less reactive aryl halides.[13]

Initial results on dimethylglyoxime and porphyrin complexes of cobalt also indicate that this reactivity is in fact general. Thus reduction of $[CoCl(dmg)_2py]$ to Co(I) by $NaBH_4$, destruction of excess borohybride with acetone and reaction with $PhN_2^+BF_4$ gave the known[14] $[Co(dmg)_2Ph(py)]$. With Co(II)(TPP) in CH_2Cl_2 treatment with ArN_2^+ gave visible spectra indicative of oxidation, the Soret band moving from 412 to 435 nm. Attempts to prepare phenyl derivatives by reduction with Na/Hg in pyridine[15] and subsequent reaction with ArN_2^+ did not however give a pure product but instead a mixture of species with very similar R_f values.

$$Co(II)(L_4) \xrightarrow{\text{Na/Hg}} Na[Co(I)(L_4)]^-$$

$$\downarrow ArN_2^+ \qquad\qquad p\text{-}OCH_3C_6H_4N_2^+ \quad \downarrow ArN_2^+$$

$$[Co(III)(L_4)]^+ \xleftarrow{\qquad} Co(III)\text{-}Ar(L_4).$$
$$\xrightarrow{ArMgX}$$
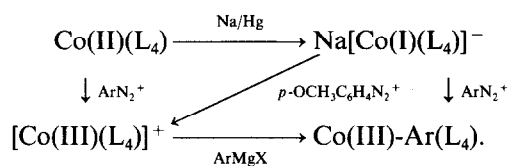
Ruthenium

As the porphyrin species studied[1] were of the type $[Ru(porphyrin)(CO)L]$ we studied the synthesis of similar Schiff-base complexes using H_2Salen. The dimeric $[Ru(Salen)(CO)]_2$ has been prepared from $Ru_3(CO)_{12}$ and the base in DMF[16] while use of $[RuCl_2(PPh_3)_3]$ gives $[Ru(Salen)(PPh_3)_2]$ from which a number of derivatives may be prepared.[17,18]

We have found that use of the same solvent system as that used for porphyrins[19,20] gives a very clean and simple route to the dimer with yields of 80–85%. Thus upon reaction of H_2Salen with $Ru_3(CO)_{12}$ in refluxing toluene the yellow [Ru(Salen)(CO)]₂ precipitates upon formation. The complex isolated is analytically pure and may be used without further purification. Upon dissolution in solvents such as pyridine under reflux the yellow–green [Ru(Salen)(CO)py] is formed. The $v(CO)$ of this complex ($1930 \, cm^{-1}$) is comparable with that of such derivatives as $[Ru(pyr_2en)(CO)PPh_3]$ ($1940 \, cm^{-1}$).[17]

When $[Ru(Salen)(CO)py]$ was allowed to react with $C_6H_5N_2^+BF_4^-$ or $p\text{-}NO_2C_6H_4N_2^+BF_4^-$ in chloroform the initial yellow–green solution turned green and upon addition of ether a green solid was isolated. Elemental analysis and the IR spectrum [$v(CO) = 1950$, $v_{asym}(BF_4) = 1050 \, cm^{-1}$] were also indicative of one-electron oxidation of the Ru(II) centre to Ru(III). An identical product was obtained using $Et_3O^+BF_4^-$ which has also been shown to effect 1-e oxidation in inert metal complexes.[21] The IR bands attributable to the base move only slightly and are essentially identical to those reported for $[Ru(Salen)(CO)]_2$.

The assignment of 1-e oxidation is consistent with the chemistry observed previously but the very slight increase in $v(CO)$ is unusual. Very few carbonyl complexes with planar Schiff-base ligands are in fact known; the Fe(II)/Fe(III) complexes which might be expected to serve as comparison are not known because of lack of reactivity even at high pressures,[16] and points up an interesting difference with the phthalocyanine and porphyrin ligands where the carbonyl adducts are of course formed readily. The affinity of CO for Ru(II) is well documented; indeed oxidation of the corresponding ruthenium–carbonyl–porphyrin complexes results in cation radicals from oxidation of the macrocycle rather than the metal centre.[22] The low value of $v(CO)$ in the Salen species may be explained by a strong σ-donation to the Ru–CO bond. Further studies with different Schiff bases and oxidising agents are in progress to determine the generality of this point, as indeed very few Ru(III)-carbonyl complexes are known.

The analogy between the nitrosyl and aryldiazonium ions has been much discussed.[23] Reaction of NO with $Ru(Salen)(PPh_3)_2$ gives an oxobridged species; coordinated nitrite from oxidation of the nitrosyl group is also formed.[24] The results for Schiff-bases are in contrast to the stabilisation of both nitrosyl[25] and aryldiazonium adducts in the Ru-porphyrin series; consistent with the good σ-donor properties of the porphyrin ligand and the greater ease of oxidation of the Schiff bases. The use of metal–macrocycle complexes is becoming of increasing interest in the study of the coordination chemistry of small molecules, where donor atoms in the equatorial plane and physicochemical properties such as redox potentials, etc. can be systematically varied. The consistent differences found in this work encourage this approach.

REFERENCES

1. N. Farrell and A. A. Neves, *Inorg. Chim. Acta* 1981, **54**, L53.
2. R. H. Bailes and M. Calvin, *J. Am. Chem. Soc.* 1947, **69**, 1886.
3. G. W. Everett and R. H. Holm, *J. Am. Chem. Soc.* 1966, **88**, 2442.
4. C. Floriani, M. Puppis and F. Calderazzo, *J. Organomet. Chem.* 1968, **12**, 209.
5. H. A. Hill, K. G. Morullee, G. Pellizer, G. Mestroni and G. Costa, *J. Organomet. Chem.* 1968, **11**, 167.
6. N. G. Connelly and Z. Demidowicz, *J. Organomet. Chem.* 1974, **73**, C31.
7. N. Farrell and D. Sutton, *Can. J. Chem.* 1977, **55**, 360.
8. A. N. Nesmeyanov, Y. A. Chapovskii, I. V. Polovyanyuk and L. G. Makharova, *J. Organomet. Chem.* 1967, **7**, 329.
9. A. W. B. Garner and M. J. Mays, *J. Organomet. Chem.* 1974, **67**, 153.
10. K. R. Laing, S. D. Robinson and M. F. Uttley, *J. Chem. Soc. (Dalton)* 1973, 2713.
11. F. W. B. Einstein, A. B. Gilchrist, G. W. Rayner-Canham and D. Sutton, *J. Am. Chem. Soc.* 1972, **94**, 645.
12. N. Farrell and D. Sutton, *J. Chem. Soc. (Dalton)* 1978, 2124.
13. K. L. Brown, A. W. Awtrey and R. Legates, *J. Am. Chem. Soc.* 1978, **100**, 823.
14. G. N. Schrauzer, *Inorg. Synth.* 1968, **11**, 61.
15. N. W. Whitlock Jr. and B. K. Bower, *Tetrahedron Lett.* 1965, 4827.
16. F. Calderazzo, C. Floriani, R. Henzi and F. L'Eplatteinier, *J. Chem. Soc. (A)* 1969, 1378.
17. J. R. Thornback and G. Wilkinson, *J. Chem. Soc. (Dalton)* 1978, 110.
18. K. S. Murray, A. M. van der Bergen and B. O. West, *Aust. J. Chem.* 1978, **31**, 203.
19. B. C. Chow and I. A. Cohen, *Bioinorg. Chem.* 1971, **1**, 57.
20. M. Tsutsui, D. Ostfeld and L. M. Hoffman, *J. Am. Chem. Soc.* 1971, **93**, 1820.
21. C. Eaborn, N. Farrell, J. L. Murphy and A. Pidcock, *J. Chem. Soc. (Dalton)* 1976, 58.
22. G. M. Brown, F. R. Hopf, T. G. Meyer and D. G. Whitten, *J. Am. Chem. Soc.* 1975, **97**, 5385.
23. D. Sutton, *Chem. Soc. Rev.* 1975, **4**, 663.
24. M. A. A. F. de C. T. Carrando, P. R. Rudolf, A. C. Skapski, J. R. Thornback and G. Wilkinson, *Inorg. Chim. Acta.* 1977, **24**, L95.
25. A. Antipas, J. W. Buchler, M. Gouterman and P. D. Smith, *J. Am. Chem. Soc.* 1978, **100**, 3015.

RUTHENIUM(II) COMPLEXES WITH MONO AND DITERTIARY ARSINES AND PHOSPHINES AND THEIR REACTION WITH SMALL MOLECULES

M. M. TAQUI KHAN*
Department of Chemistry, Osmania University, Hyderabad 500 007, India

and

RAFEEQ MOHIUDDIN
Department of Chemistry, University College for Women, Hyderabad, India

Abstract—Dichlorotetrakis(dimethylsulphoxide)ruthenium(II) reacts with $AsPh_3$, $AsMePh_2$, $AsMe_2Ph$ and $SbPh_3$ in ethanolic hydrochloric acid solution to yield the complexes $RuCl_2(DMSO)_2(AsPh_3)_2$, $RuCl_2(DMSO) L_2$ (L = $AsMePh_2$, $AsMe_2Ph$, $SbPh_3$) respectively. The treatment of ruthenium(II) blue solution with $AsMePh_2$, $AsMe_2Ph$ and $SbPh_3$ in alcohol resulted in the formation of the complexes; $RuCl_2L_3$ (L = $AsMePh_2$, $AsMe_2Ph$ and $SbPh_3$), respectively.

The reaction of $RuCl_2(DMSO)_4$ with the bidentate ligands 1,2 bis(diphenylarsino)methane (DPAM), 1,2 bis(diphenylarsino)ethane (DPAE) and 1,2 bis(diphenylphosphino)methane (DPPM). 1,2 bis(diphenylphosphino)ethane (DPPE), in ethanol gave the complexes $RuCl_2(DPAM)_2$, $RuCl_2(DPAE)_2$, $RuCl_2(DPPM)_2$ $RuCl_2(DPPE)_2$, respectively. The complexes thus obtained undergo reaction with carbon monoxide, hydrogen, molecular nitrogen and nitric oxide to yield a variety of mixed ligand complexes.

During the last decade extensive research has been carried out on ruthenium(II) complexes of tertiary phosphines especially Wilkinsons's complex $RuCl_2(PPh_3)_3$.[1,2] In contrast to the tertiary phosphine complexes, there are very few reports on ruthenium(II) complexes with monotertiary arsines. Some of these complexes include $RuCl_2(AsMePh_2)_4$[3] and $RuCl_2(AsMe_2Ph)_4$[4] that were obtained by the interaction of $RuCl_3$ with $AsMePh_2$ or $AsMe_2Ph$, respectively. However, $RuCl_3$ is not a very good source of ruthenium(II) since reduction to the ruthenium(II) state by the less basic arsine ligands in high boiling solvents invariably results in the formation of either polymers or chlorobridged

dimers.[5] Thus, reaction of $RuCl_3$ with ethyl-diphenylarsine in the presence of acid yielded $Ru_2Cl_3(AsEtPh_2)_6Cl$ with triple chloro bridges.[6]

A number of ruthenium(II) complexes were reported with bidentate ligands. Thus interaction of ruthenium(III) halide with o-phenylene-bisdimethylarsine(diars) produces $RuX_2(diars)_2$.[7] Similar preparative method with the ditertiary phosphines, diphos, (1,2 bis(diphenylphosphino)ethane, 1,2 bis(diphenylphosphine)methane and o-phenylenebis(dimethylphosphine) gave $RuCl_2(diphos)_2$.[8] The diarsine complexes prepared by this method include *trans*-$RuCl_2(DPAE)_2$ and *trans*-$RuCl_2$ (DPAM)$_2$ (DPAE = 1,2 bis(diphenylarsino) ethane, DPAM = 1,2 bis(diphenylarsino) methane).[9]

In the present work attempts were made to prepare monomeric ruthenium(II) complexes with a variety of monodentate arsines and bidentate

*Present address: Central Salt & Marine Chemicals Research Institute, Bhavnagar 364 002, Gujarat, India.

phosphines and arsines. The complex RuCl$_2$ (DMSO)$_4$[10,11] was employed as a suitable starting material for the synthesis of Ru(II) complexes with mono and bidentate phosphines and arsines. The blue solution[12] prepared by the reduction of RuCl$_3$ with zinc amalgam was also employed successfully for the synthesis of Ru(II) complexes with monodentate ligands. The Ru(II) complexes thus obtained activate small molecules like H$_2$, N$_2$, CO and NO to yield a variety of mixed ligand complexes of mono or bidentate ligands with the small molecules.

EXPERIMENTAL

The ligands, triphenylstibine, 1,2-bis(diphenylphosphino)methane (DPPM),1,2-bis(diphenylarsino)methane (DPAM),1,2-bis(diphenylphosphino)ethane (DPPE),1,2-bis(diphenylarsino) ethane (DPAE) were obtained from Ventron Corp., U.S.A. Triphenylarsine was from Maybridge Chemical Co., U.K. The arsine ligands, methyldiphenylarsine and dimethylphenylarsine were prepared by reacting the respective methyliodoarsines with methylmagnesium bromide in dry ether. Methyliodoarsine and dimethyliodoarsine were prepared by standard methods.[13] The reaction products were purified by vacuum distillation. Hydrated ruthenium trichloride (RuCl$_3$·3H$_2$O) was purchased from Alfa Ventron, U.S.A. and also from Johnson Matthey (England). The complexes RuCl$_2$(DMSO)$_4$[10,11] and RuCl$_2$(PPh$_3$)$_3$[1,2] were synthesized by published procedures. All organic solvents and acids used were BDH Analar grade.

The gases used in this work, carbon monoxide and nitric oxide were prepared and purified by standard procedures. Pure molecular hydrogen was obtained by electrolysis of a 20% solution of sodium hydroxide in a U-tube fitted with nickel electrodes and the gas dried by passing through a calcium chloride tower. Nitrogen gas obtained commercially was freed from oxygen and moisture by passing through vanadium(II) sulphate and alkaline pyrogallol solutions and finally through ascarite. Vanadium(II) sulphate solution was prepared by reduction of vanadyl(IV) sulphate solution by passing the solution through a column filled with zinc amalgam. All the complexes reported in this work were prepared under purified nitrogen atmosphere using the Schlenk tube technique.

The elemental analysis of the elements carbon, hydrogen and chlorine was performed by the Microanalytical service, CSIRO Australia and Chemalytics Inc., Tempe, Arizona, U.S.A., IR spectra were recorded on a Beckman IR-12 spec-

trophotometer. The NMR spectra were recorded on Varian A-60 and HA-100 spectrometers. The electronic spectra were measured in methanol-chloroform or dichloromethane solvents using Cary Model-14 and Carl Zeise DMR-2 spectrometers. Conductance data were obtained in dimethylacetamide (DMA) solution using a systronic conductance bridge and a cell which had been calibrated with 0.1 M aqueous potassium chloride solution.

PREPARATIONS

(1) *Dichlorobis(dimethylsulphoxide)bis(triphenylarsine)ruthenium(II)*

A solution of 0.24 g (0.5 mmol) of RuCl$_2$(DMSO)$_4$ in 10 cm^3 of ethanol and 3 cm^3 of concentrated hydrochloric acid was refluxed for about 15 min. To the hot solution was added an ethanolic solution of triphenylarsine (0.612 g, 2 mmol) and refluxed for about 6 hr. The colour of the solution changed from orange to brown. The solution was evaporated to a small volume under reduced pressure and the orange brown complex was precipitated by dissolving in acetone and reprecipitating with ether. The same complex was also prepared by heating 0.24 g of RuCl$_2$(DMSO)$_4$ and excess of triphenyl arsine (1.530 g, 5 mmol) dissolved in a mixture of ethanol and hydrochloric acid (70 and 7 cm^3 respectively) in a sealed tube at 70°C for about 48 hr. At the end of the reaction period a green complex separated which was filtered and washed with methanol. The complex was recrystallised from dichloromethane and acetone.

(2) *Dichloro(dimethylsulphoxide)tris(diphenylmethylarsine)ruthenium(II)*

About 0.24 g (0.5 mmol) of RuCl$_2$(DMSO)$_4$ was dissolved in 10 cm^3 of ethanol and 3 cm^3 of concentrated hydrochloric acid was added and the solution refluxed for about 15 min. To the hot solution was added methyldiphenylarsine (0.9 gm, 3 mmol) in 20 cm^3 of ethanol and refluxed for about 6 hr. The colour of the solution changed from scarlet-red to brown. The solution was evaporated to a small volume and the chocolate brown complex was precipitated by the addition of petroleum ether and recrystallised from dichloromethane and ether.

(3) *Dichloro(dimethylsulphoxide)tris(dimethylphenylarsine)ruthenium(II)*

A solution of 0.24 g (0.5 mmol) of RuCl$_2$ (DMSO)$_4$ in 10 cm^3 of ethanol and 3 cm^3 of concentrated hydrochloric acid was refluxed for

about 15 min. To the hot solution was added a solution of dimethylphenylarsine (0.846 g, 3 mmol) and refluxed for about 6 hr. The solution was evaporated to a small volume and cooled to −25°C by keeping in dry ice. The orange complex was precipitated by the addition of petroleum ether (40–60 grade). The complex was recrystallised from dichloromethane and ether.

(4) Dichloro{dimethylsulphoxide}tris{triphenylstibine}ruthenium(II)

A mixture of $RuCl_2(DMSO)_4$ (0.24 g, 0.5 g, 0.5 mmol) and triphenylstibine (0.704 g, 2 mmol) in 30 cm³ of ethanol was refluxed for about 3 hr. The solution turned yellowish orange from brown. The pink powder separated was filtered and washed with methanol. The complex was re-crystallised either from alcohol or dichloromethane.

(5) Dichlorotris(methyldiphenylarsine)ruthenium-(II)

(6) Dichlorotris(dimethylphenylarsine)ruthenium-(II)

These complexes were prepared by the addition of 6 mmol of methyldiphenyl or dimethylphenylarsine to an alcoholic blue solution obtained by refluxing ruthenium trichloride (0.208 g, 1 mmol) with zinc amalgam for 30 min. Zinc was removed from the solution and 3–4 cm³ of hydrochloric acid added. The mixture was further refluxed in the presence of the appropriate ligand for 3–4 hr. For the methyldiphenylarsine complex, solvent was removed under vacuum and the brown complex precipitated by the addition of acetone and recrystallised from dichloromethane and ether. The dimethylphenyl arsine complex separated as yellow crystals was filtered, washed with acetone and methanol and recrystallised from alcohol.

(7) Dichlorotris(triphenylstibine)ruthenium(II)

Ruthenium trichloride (0.208 g, 1 mmol) was refluxed with zinc amalgam in alcohol for about 30 min. Zinc was removed and to the blue solution triphenylstibine (1.408 g, 4 mmol) in alcohol was added. The solution was refluxed for about $2\frac{1}{2}$ hr. A pink coloured solid separated which was filtered and washed with methanol. The complex was recrystallised from alcohol.

(8) Dichlorobis{1,2-bis(diphenylarsino)methane} ruthenium(II)

(9) Dichlorobis{1,2-bis(diphenylphosphino)methane}ruthenium(II)

To a solution of $RuCl_2(DMSO)_4$ (0.242 g, 0.5 mmol) in 10 cm³ of ethanol, was added a solution of the appropriate ligand (1 mmol) in 30 cm³ of ethanol. The mixture was refluxed for about 4 hr. Lemon yellow crystals in the case of $RuCl_2(DPPM)_2$ and orange crystals in case of $RuCl_2(DPAM)_2$ were filtered, washed with methanol and ether. The complexes were recrystallised from dichloromethane.

(10) Dichlorobis{1,2-bis(diphenylphosphino)ethane}ruthenium(II)

This complex was prepared by a method simpler than that of Chatt and Hayter.[8] 1,2 bis (diphenylphosphino)ethane (0.796 g, 2 mmol) in 20 cm³ of ethanol was added to a solution of $RuCl_2(DMSO)_4$ (0.242 g, 0.5 mmol) in 15 cm³ of ethanol and the solution refluxed for about 2 hr. The colour changed from dark orange to bright lemon-yellow. The lemon-yellow crystals separated were filtered and washed with methanol. The complex was recrystallised from dichloromethane.

(11) Dichlorobis{1,2-bis(diphenylarsino)ethane}-ruthenium(II)

This complex was earlier reported by Mague and Mitchener.[9] The complex was synthesized by a method simpler than earlier reported whereby the refluxing time was reduced and a good yield was obtained. The complex $RuCl_2(DMSO)_4$, (0.484 g, 1 mmol) was dissolved in 10 cm³ of ethanol and 1,2 bis(diphenylarsino)ethane (0.480 g, 1 mmol) in 30 cm³ of ethanol were refluxed for about 2 hr. Orange yellow crystals separated, which were filtered and washed with methanol. The complex was recrystallised from dichloromethane.

(12) Dichloro-dicarbonyl(dimethylsulphoxide)(triphenylarsine)ruthenium(II).

(13) Dichloro-dicarbonyl-bis(methyldiphenylarsine)ruthenium(II).

(14) Dichloro-dicarbonyl-bis(dimethylphenylarsine)ruthenium(II).

(15) Dichloro-dicarbonyl-bis(triphenylstibine)ruthenium(II).

(16) Dichloro-carbonyl-tris(triphenylstibine)ruthenium(II).

(17) Dichloro-dicarbonyl-bis{1,2-bis(diphenylarsino)methane}ruthenium(II).

(18) Dichloro-dicarbonyl-bis{1,2-bis(diphenylphosphino)methane}ruthenium(II)

(19) *Chloro-carbonyl-bis{1,2-bis(diphenylphos-Phino)ethane}ruthenium(II)chloride.*

(20) *Chloro-carbonyl-bis{1,2-bis(diphenylarsino)-ethane}ruthenium(II).*

In a general method of preparation of the carbonyls, about 0.02 mmol of the complex (1–4), (8–11) was dissolved in dry chloroform and a stream of carbon monoxide was passed through the solution until there was no further colour change. The solutions were concentrated to a small volume and the carbonyls (12–20) precipitated by the addition of petroleum ether, filtered and dried.

(21) *Hydrido-chloro-bis(dimethylsulphoxide)bis-(triphenylarsine)ruthenium(II).*

(22) *Hydrido-chloro-(dimethylsulphoxide)tris(methyldiphenylarsine)ruthenium(II).*

(23) *Hydrido-chloro-(dimethylsulphoxide)tris(dimethylphenylarsine)ruthenium(II).*

(24) *Hydrido-chloro-tris(methyldiphenylarsine)ruthenium(II).*

Molecular hydrogen was bubbled through a 0.02 m molar dimethylformamide solution of complexes (1)/(3), (5), for about 12 hr at 40°C. The dark brown hydrides were isolated by removing the solvent under vacuum and precipitation by petroleum ether.

(25) *Hydrido(dinitrogen)bis(dimethylsulphoxide)-bis(triphenylarsine)ruthenium(II)chloride*

(26) *Hydrido(dinitrogen)dimethylsulphoxide-tris-(methyldiphenylarsine)ruthenium(II)chloride.*

Molecular hydrogen was passed through a 0.02 m molar dimethylformamide solution of the complexes (1) and (2) and molecular nitrogen bubbled through the solution for about 24 hr. The mixed ligand hydrido-dinitrogen complexes were isoalted by removing the solvent under vacuum and addition of petroleum ether.

(27) *Dichloro-nitrosyl-(dimethylsulphoxide)bis(triphenylarsine)ruthenium(II).*

(28) *Dichloro-nitrosyl-(dimethylsulphoxide)bis(methyldiphenylarsine)ruthenium(II).*

(29) *Dichloro-nitrosyl-(dimethylsulphoxide)bis(dimethylphenylarsine)ruthenium(II).*

(30) *Dichloro-nitrosyl-(dimethylsulphoxide)bis(triphenylstibene)ruthenium(II).*

(31) *Dichloro-nitrosyl-tris(methyldiphenylarsine)-ruthenium(II).*

(32) *Dichloro-nitrosyl-bis(diphenylphosphinomethane)ruthenium(II).*

(33) *Dichloro-nitrosyl-bis(diphenylarsinoethane)-ruthenium(II).*

Nitric oxide was passed through a 0.02 mmol chloroform solution of complexes (1–5), (9) and (11) for about 24 hr until there was no further colour change. The solutions were concentrated to a small volume and the nitrosyls precipitated by the addition of petroleum ether.

RESULTS AND DISCUSSION

Tables 1 and 2 present the analytical data and the molar conductivities of the ruthenium(II) complexes with mono and bidentate tertiary arsines and phosphines. IR spectra of these complexes are given in Table 3. The NMR and electronic spectra of some of the complexes are given in Tables 4 and 5 respectively.

A brown complex (1) was obtained by the displacement of two molecules of coordinated DMSO by $AsPh_3$ from $RuCl_2(DMSO)_4$. X-Ray structure of the parent complex $RuCl_2(DMSO)_4$ had indicated two different types of coordination of DMSO groups; three DMSO groups are bonded through sulphur and one through oxygen to the metal ion[14] with *cis*-chlorides. When $RuCl_2(DMSO)_4$ reacts with triphenylarsine the weakly O-bonded DMSO group gets displaced first followed by one of the S-bonded DMSO groups to give the complex $RuCl_2(DMSO)_4(AsPh_3)_2$ with *cis*-chlorides. The νM-Cl is expected to give two bands. Although a sharp peak is obtained at $320\,cm^{-1}$ the other band must have been masked by the DMSO peak. The band at $1075\,cm^{-1}$ indicative of S-bonded DMSO was observed but no band appeared around $900\,cm^{-1}$ which could be attributed to O-bonded DMSO.[15] The metal–arsine and metal–sulphur absorptions overlap in the complex and the peak at $480\,cm^{-1}$ could not be assigned unequivocally to any of these vibrations. The complex is assigned a C_h geometry as shown in Fig. 1.

A green modification of complex (1) was obtained when $RuCl_2(DMSO)_4$ and triphenylarsine were refluxed in a sealed tube. The preparation in the sealed tube was attempted with an idea to completely displace dimethylsulphoxide by triphenylarsine in $RuCl_2(DMSO)_4$ complex. The green complex shows an IR spectrum identical to that of the brown complex.

Two geometrical isomers are possible for the complex $RuCl_2(DMSO)_2(AsPh_3)_2$, one with *cis* dispositions of DMSO, triphenylarsine and *cis* chlorides (Fig. 1) and the other with *cis* dispositions of DMSO, the chloride and *trans* disposition of triphenylarsine (Fig. 2).

Table 1. Analytical data for ruthenium(II) complexes

S.No.	Complex	Colour	Analysis[+] (%) C	H	Cl	M.P. °C	Molar Conductance in DMA. (Ohms^{-1}.,Cm^2,equi^{-1})
1.	RuCl$_2$(DMSO)$_2$(AsPh$_3$)$_2$	Orange brown	51.13 (51.13)	4.20 (4.40)	8.60 (7.60)	106*	25.12
2.	RuCl$_2$(DMSO)(AsMePh$_2$)$_3$	Chocolate brown	49.70 (50.10)	4.30 (4.50)	9.80 (7.30)	118*	16.62
3.	RuCl$_2$(DMSO)(AsMe$_2$Ph)$_3$	Yellowish green	38.05 (39.19)	4.75 (4.90)	9.20 (8.92)	130*	23.86
4.	RuCl$_2$(DMSO)(SbPh$_3$)$_3$	Pink	51.40 (51.33)	3.94 (3.90)	4.80 (5.40)	239	11.25
5.	RuCl$_2$(AsMePh$_2$)$_3$	Brown	46.76 (48.78)	4.49 (4.31)	6.90 (7.85)	165*	14.90
6.	RuCl$_2$(AsMe$_2$Ph)$_3$	Yellow	41.65 (40.11)	4.87 (4.60)	8.88 (9.88)	191*	31.78
7.	RuCl$_2$(SbPh$_3$)$_3$	Pink	53.40 (52.64)	3.83 (3.65)	5.50 (5.76)	250*	37.70
8.	RuCl$_2$(DPAM)$_2$	Orange	53.78 (52.68)	3.86 (3.76)	5.40 (6.36)	215	30.38
9.	RuCl$_2$(DPPM)$_2$	Lemon Yellow	59.67 (62.50)	4.38 (4.46)	5.86 (6.97)	260*	32.50
10.	RuCl$_2$(DPPE)$_2$	Yellow	64.08 (64.08)	4.99 (4.97)	6.54 (7.33)	260*	12.00
11.	RuCl$_2$(DPAE)$_2$	Orange	54.42 (54.64)	4.34 (4.20)	5.50 (6.21)	255*	20.41

* decomposed

(+ calculated values in paranthesis)
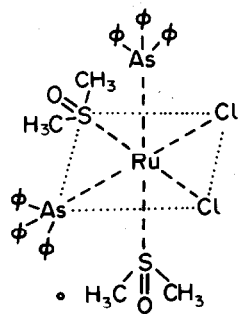
Fig. 1.
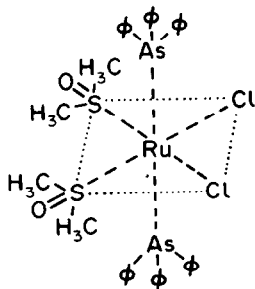
Fig. 2.

The brown isomer will have a C_h symmetry while the green isomer will have a C_{2v} symmetry. The two isomers cannot be distinguished on the basis of IR spectra which indicate cis-chlorides in both the complexes. Dipole moment measurements gave almost identical values within experimental error of 1.18 Debye for the brown and 1.3 Debye for the green isomers, respectively. This is expected because both the compounds have cis-chlorides, and a cis or trans disposition of other less polar groups cannot make a significant difference in dipole moments. However, these two isomers were characterized on the basis of their NMR spectra. The NMR spectrum of the brown complex with non-equivalent sets of ligands exhibited two multiplets of equal intensity at 2.15τ and 2.65τ which may be assigned to the phenyl protons of cis-triphenylarsines. The methyl protons of cis-DMSO groups also appeared as two multiplets at 6.65τ and 7.75τ. The NMR spectrum of the brown compound thus supports a C_h symmetry for the complex.

In the NMR spectrum of the green isomer of (1) the phenyl protons of triphenylarsine exhibit a

Table 2. Analytical data for ruthenium(II) complexes

S.No.	Complex	Colour	ANALYSIS[+] (%)				
			C	H	Cl	O	N
12.	RuCl$_2$(CO)$_2$(DMSO)(AsPh$_3$)$_2$	Yellow	43.03 (43.13)	2.40 (2.45)	11.00 (11.60)	7.20 (7.84)	-
13.	RuCl$_2$(CO)$_2$(AsMePh$_2$)$_2$	Yellow	52.03 (52.41)	4.00 (4.05)	11.00 (11.07)	4.55 (4.99)	-
14.	RuCl$_2$(CO)$_2$(AsMe$_2$Ph)$_2$	Yellow	36.02 (36.48)	3.05 (3.71)	11.03 (11.99)	5.02 (5.40)	-
15.	RuCl$_2$(CO)$_2$(SbPh$_3$)$_2$	Orange	52.80 (53.20)	3.50 (3.69)	8.00 (8.74)	3.50 (3.94)	-
16.	RuCl$_2$(CO)(SbPh$_3$)$_3$	Orange	56.00 (56.63)	3.40 (3.82)	9.00 (9.06)	2.00 (2.04)	-
17.	RuCl$_2$(CO)$_2$(DPAM)$_2$	Yellow	53.00 (53.24)	3.45 (3.75)	5.85 (6.05)	2.45 (2.73)	-
18.	RuCl$_2$(CO)$_2$(DPPM)$_2$	Yellow	62.25 (62.65)	4.05 (4.45)	6.30 (7.13)	3.00 (3.21)	-
19.	[RuCl(CO)(DPPE)$_2$]Cl	Yellow	63.25 (63.85)	4.60 (4.32)	7.00 (7.12)	1.40 (1.60)	-
20.	[RuCl(CO)(DPAE)$_2$]Cl	Yellow	54.08 (54.26)	4.00 (4.09)	6.00 (6.05)	1.26 (1.36)	-
21.	RuHCl(DMSO)$_2$(AsPh$_3$)$_2$	Dark brown	52.89 (53.00)	4.80 (4.74)	3.81 (3.92)	3.42 (3.53)	--
22.	RuHCl(DMSO)(AsMe$_2$Ph)$_3$	Dark brown	51.82 (51.93)	5.00 (4.35)	3.80 (3.74)	1.70 (1.68)	-
23.	RuHCl(DMSO)(AsMe$_2$Ph)$_3$	Dark brown	41.00 (40.93)	5.00 (5.25)	4.30 (4.56)	1.99 (2.10)	-
24.	RuHCl(AsMePh$_2$)$_3$	Dark brown	51.00 (50.71)	4.35 (4.60)	4.00 (4.03)	-	-
25.	[RuHN$_2$(DMSO)$_2$(AsPh$_3$)$_2$]Cl	Brown	51.30 (51.42)	4.30 (4.60)	3.60 (3.80)	3.50 (3.42)	2.87 (2.99)
26.	[RuHN$_2$(DMSO)AsMePh$_2$]Cl	Brown	50.30 (50.43)	4.61 (4.71)	3.50 (3.64)	1.70 (1.64)	2.75 (2.87)
27.	RuCl$_2$(NO)(DMSO)(AsPh$_3$)$_2$	Chocolate brown	51.20 (51.12)	4.00 (4.03)	7.35 (7.95)	2.68 (2.58)	1.47 (1.57)
28.	RuCl$_2$NO(DMSO)(AsMePh$_2$)$_2$	Brown	43.60 (43.75)	4.00 (4.16)	9.03 (9.24)	4.05 (4.16)	1.73 (1.82)
29.	RuCl$_2$(NO)(DMSO)(AsMe$_2$Ph)$_2$	Brown	34.00 (33.54)	4.21 (4.34)	11.07 (11.02)	5.01 (4.96)	2.04 (2.17)
30.	RuCl$_2$(NO)(DMSO)(SbPh$_3$)$_2$	Buff	46.03 (46.34)	3.70 (3.65)	7.05 (7.21)	3.05 (3.25)	1.44 (1.42)
31.	RuCl$_2$(NO)(AsMePh$_2$)$_3$	Chocolate brown	50.00 (49.60)	4.50 (4.38)	8.00 (7.98)	1.82 (1.79)	1.60 (1.57)
32.	RuCl$_2$(NO)(DPPM)$_2$	Brown	61.68 (61.85)	4.75 (4.53)	7.43 (7.32)	1.72 (1.65)	1.47 (1.44)
33.	RuCl$_2$(NO)(DPAE)$_2$	Brown	53.05 (53.15)	4.10 (4.08)	6.08 (6.04)	1.38 (1.36)	1.21 (1.19)

(+) Calculated values in parenthesis.

single multiplet at 3.6τ and methyl protons of DMSO a multiplet at 8.8τ. This is in accord with a trans-deposition of the triphenylarsine and cis disposition of DMSO and chloride groups in the compound with a point group C_{2v}.

The electronic spectrum of the brown isomer of (1) gives charge transfer bands characteristic of the presence of both DMSO[16] and triphenylarsine[17a,b] in the coordination sphere of the metal ion. The electronic spectrum of DMSO gives absorption bands at 200 and 210 nm that can be assigned to the $\sigma - \sigma^*$ and $n - \pi^*$ transitions of the ligand,

Table 3. IR spectra of ruthenium(II) complexes (3000–200 cm^{-1})

S.No.	Complex	γ(M-Cl)cm^{-1}	γ(M-DMSO)cm^{-1}	γ $\begin{array}{c}\text{(M-L)cm}^{-1}\\\text{(L=P or As)}\end{array}$	Other bands cm^{-1}
1.	RuCl$_2$(DMSO)$_2$(AsPh$_3$)$_2$	320(s)	480(s),1025(m), 1075(m),1430(s)	480(s)	660(m)690(s),735(s),1000(m), 1485(m)
2.	RuCl$_2$(DMSO)(AsMePh$_2$)$_2$	324(s)	480(s),1025(s), 1075(s),1435(s)	480(s)	660(m)690(m),735(s),800(s), 1000(m), 1485(m).
3.	RuCl$_2$(DMSO)(AsMe$_2$Ph)$_3$	330(s)	485(s),1065(s), 1430(s)	485(s)	670(w),695(m),730(s),800(s), 990(m)
4.	RuCl$_2$(DMSO)(SbPh$_3$)$_3$	275(s)	470(m),1010(s), 1060(s),1420(s)	450(m)	670(w),690(w),730(s),990(s), 1180(m),1290(m),1470(s).
5.	RuCl$_2$(AsMePh$_2$)$_3$	270(w),330(m)		480(s)	685(s),730(m),740(sn),835(m), 990(w),1420(s),1470(m)
6.	RuCl$_2$(AsMe$_2$Ph)$_3$	235(m),315(s)		425(m),475(m)	590(s),685(s),720(s),845(s), 875(s),1020(s),1070(s), 1230(s),1385(m),1475(s).
7.	RuCl$_2$(SbPh$_3$)$_3$	260(w),275(m)		455(m), 465(m)	650(m),675(m),710(s),985(w), 1050(w),1420(s),1470(s).
8.	RuCl$_2$(DPAM)$_2$	230(m),270(s)		330(s), 485(s)	585(m),615(m),690(s),735(s)
9.	RuCl$_2$(DPPM)$_2$	230(m),275(s)		510(s) 545(m)	620(m),690(m),710(m),740(m), 775(s)
10.	RuCl$_2$(DPPE)$_2$	320(m)		510(s) 530(v.s)	660(w),690(s),715(s),730(m), 740(m)
11.	RuCl$_2$(DPAE)$_2$	320(m)		450(m), 460(s), 500(s) 540(m)	565(m),610(w),690(v.s)730(v.s) 740(v.s)

Table 4. Proton NMR spectra of ruthenium(II) complexes*

S.No.	Complex	Phenyl protons	Methyl protons	Methylene protons	Methyl/Methylene protons
1.	RuCl$_2$(DMSO)$_2$(AsPh$_3$)$_2$ (Brown) (Green	2.15(m) 2.65(m) 3.60(m)	6.55(m) 7.75(m) 8.80(m)		
2.	RuCl$_2$(DMSO)(AsMePh$_2$)$_3$	2.80(m)	8.30(m) 8.75(m)		4.20(m) 5.30(m) 6.50(m)
3.	RuCl$_2$(DMSO)(AsMe$_2$Ph)$_3$	2.55(m)	8.13(m),8.57(m)		6.69(m),7.10(m)
4.	RuCl$_2$(DMSO)(SbPh$_3$)$_3$	1.75(m),2.76(m)	6.50(m)		
5.	RuCl$_2$(AsMePh$_2$)$_3$	2.50(m),2.90(m)	8.30(m),8.65(m)		
6.	RuCl$_2$(AsMe$_2$Ph)$_3$	3.90(m),3.97(m)	8.70(m),8.97(m)		
7.	RuCl$_2$(SbPh$_3$)$_3$	3.70(m),4.00(m)			
8.	RuCl$_2$(DPAM)$_2$	3.30(br),3.95(mbr)		5.87(d)	
9.	RuCl$_2$(DPPM)$_2$	3.96(m)		5.80(d),8.70(t)	
10.	RuCl$_2$(DPPE)$_2$	4.10(m)		7.26(m),8.47(m)	
11.	RuCl$_2$(DPAE)$_2$	4.10(m)		7.80(s),8.63(s)	

(*) τ values: S = singlet; d = doublet; t = triplet; b = broad; m = multiplet.

respectively. The $n - \pi^*$ transition undergoes a red shift in the sulphur coordinated complex and is exhibited at 230 nm ($\epsilon 2.8 \times 10^4$) in the brown complex. The electronic spectrum of triphenylarsine shows absorption bands at 215 and 248 nm assigned to $\sigma - \sigma^*$ and $n - \pi^*$ transitions.

These bands are considerably red-shifted in the coordinated arsine at 250 and 270 nm, respectively with an increase in intensity. The absorption band at 290 nm in (1) appears to be a metal ligand (DMSO) charge transfer band. The transitions at 410 and 520 nm can be assigned to $d - d$ transi-

Table 5. Electronic spectra of ruthenium(II) complexes

S.No.	Complex	Absorption (nm)	λ max (cm⁻¹)	E(M⁻¹cm⁻¹)	Assignment
1.	RuCl₂(DMSO)₂(AsPh₃)₂	230	43478	2.831×10^4	C.T.
		250	40000	2.6506×10^4	C.T.
		270	37037	1.6867×10^4	C.T.
		290	34482	7.8313×10^3	C.T.
		410	24390	1.02101×10^3	$1A_1 \to 1T_2$
		520	19230	2.4024×10^2	$1A_1 \to 1T_1$
2.	RuCl₂(DMSO)(AsMePh₂)₃	230	43478	2.3248×10^4	C.T.
		246	40650	1.1908×10^4	C.T.
		264	37878	1.8471×10^3	C.T.
		302	33112	9.5541×10^3	C.T.
		412	24271	8.882×10^2	$1A \to 1T_2$
		300	20000	8.5987×10^2	
		640	15625	4.44162×10^2	$1A_1 \to 1T_1$
3.	RuCl₂(DMSO)(SbPh₃)₃	230	43478	4.6666×10^4	C.T.
		250	40000	3.1250×10^4	C.T.
		272	36764	2.2083×10^4	C.T.
		302	33112	2.000×10^4	C.T.
		410	24390	7.4626	$1A_1 \to 1T_2$
		580	19685	3.73134×10^2	$1A_1 \to 1T_1$
4.	RuCl₂(AsMePh₂)₃	252	29682	1.26903×10^4	C.T.
		265	37735	1.16279×10^4	C.T.
		302	33112	7.0778×10^3	C.T.
		370	27027	1.11223×10^2	$1A_1 \to 1E_1$
		510	19607	4.0444×10^2	$1A_1 \to 1B_1$
		705	14184	1.76946×10^2	$1A_1 \to 1A_2$
5.	RuCl₂(SbPh₃)₃	263	38022	2.3342×10^2	C.T.
		298	33557	2.71167×10^4	C.T.
		303	33003	2.12063×10^4	C.T.
		434	22988	8.67550×10^2	$1A_1 \to 1E_1$
		540	18518	8.01320×10^2	$1A_1 \to 1B_2$
		770	12987	1.42838×10^2	$1A_1 \to 1A_2$
6.	RuCl₂(DPPE)₂	240	41666	2.29532×10^4	C.T.
		250	40000	2.41228×10^4	C.T.
		312	32051	2.04670×10^3	C.T.
		372	26881	1.02309×10^2	$1A_1 \to 1T_2$
		440	22727	1.00847×10^2	$1A_1 \to 1T_1$
7.	RuCl₂(DPAE)₂	245	40816	2.33937×10^4	C.T.
		260	38416	2.10870×10^2	C.T.
		378	26455	5.42850×10^2	$1A_1 \to 1T_2$
		432	23148	3.29000×10^2	$1A_1 \to 1T_1$

*C.T. = charge transfer bands.

tions in the complex corresponding to $1A_1 \to 1T_2$ and $1A_1 \to 1T_1$, respectively. The 10 Dq value calculated from these transitions comes to 20,518 cm⁻¹.

Carbonylation of complex (1) (brown isomer) resulted in the formation of the cis-dicarbonyl complex (13) by the displacement of a coordinated DMSO and triphenylarsine groups. The displacement is expected on the basis of the high trans-effect of DMSO and the arsine groups. The formation of the cis-dicarbonyl is indicated by the appearance of strong peak at 2010 cm⁻¹ accompanied by a peak of medium intensity at 1985 cm⁻¹ corresponding to the carbonyls trans to arsine and DMSO groups, respectively.

Hydrogenation of (1) (brown isomer) resulted in the formation of hydride (23) which exhibited a strong M–H peak around 1960 cm⁻¹. The hydride

is formed by the displacement of a coordinated chloride by hydride. The IR absorption bands corresponding to DMSO and triphenylarsine in complex (1) remain intact in the hydrido complex. On passing molecular nitrogen through the solution of the hydrido complex a hydrido-dinitrogen complex (26) is formed, as indicated by the total disappearance of metal-halogen band and the appearance of the characteristic dinitrogen peak around 2150 cm⁻¹; the hydrido peak was observed at 1940 cm⁻¹ in the complex. The hydrido and dinitrogen stretching frequency in this complex are similar to those observed in the complex $RuH_2(N_2)(PPh_3)_3$.[18]

Treatment of complex (1) with nitric oxide resulted in the formation of $RuCl_2(NO)(DMSO)$ (AsPh₃)₂ which showed a strong absorption band

characteristic of coordinated nitrosyl at 1850 cm^{-1}. The NO frequency in this complex could be compared to other ruthenium nitrosyl complexes where NO may be considered to be coordinated as NO^{+}[19].

Six coordinate complexes of the type RuCl$_2$-(DMSO)L$_3$, (L=AsMePh$_2$, AsMe$_2$Ph, SbPh$_3$)

Complexes (2–4) were obtained by the displacement of one weakly O-bonded and two S-bonded dimethylsulphoxide groups from RuCl$_2$(DMSO)$_4$ by the tertiary arsine or stibine. The remaining DMSO group is S-bonded in these complexes as confirmed by the presence of a strong band in the IR spectra of the complexes around 1075 cm^{-1} and the absence of bands around 900 cm^{-1} which could be assigned to O-bonded DMSO group. Since tertiary arsine and DMSO absorb in the region 400–500 cm^{-1}, the band at 480 cm^{-1} could not be assigned to either of these alone. The νM–Cl frequency in complexes (2–4) appear as a single peak at 324, 330 and 275 cm^{-1}, respectively, indicating a *trans* geometry of the coordinated chlorides. The complexes have very low dipole moments (0.77 and 1.15 Debye units for complexes 2 and 3, respectively) and are non-conducting in DMA (Table 1).

In complex (2) the phenyl protons of methyldiphenyl arsine merge and appear as a broad multiplet centered at 2.8τ. The methyl protons appear as two multiplets of 1:2 intensity at 8.3τ and 8.75τ, respectively and can be assigned to *meridional* arsines. The methyl protons of DMSO appeared at a lower field than the methyl protons of arsine (between 4.2τ and 6.5τ). The multiplets of methyl protons may be explained on the basis of a long range spin interaction of the methyl protons of DMSO with the methyl protons of arsine and vice versa.

The NMR spectrum of complex (3) is very well resolved as far as methyl protons are concerned, the phenyl protons again merge to give a broad multiplet centred at 2.55τ. The methyl protons of the *meridionally* disposed dimethylphenylarsine ligand are observed as two multiplets of 1:2 intensity at 8.13τ and 8.57τ. The methyl protons of DMSO are exhibited as multiplets centred at 6.69τ. The integration of NMR spectra are consistent with the proposed formulations.

The phenyl protons of triphenylstibine are well resolved (Table 3) in the NMR spectrum of complex (4) and appear as two multiplets at 1.75τ and 2.76τ in the ratio of 1:2. The methyl protons of DMSO appear at 6.5τ. The probable structure for

L = Asmeph$_2$, Asme$_2$ph, Sbph$_3$
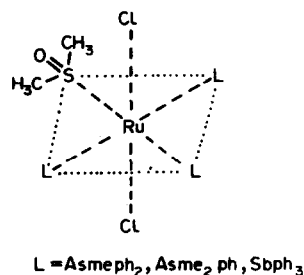
Fig. 3.

these complexes is given in Fig. 3. The complexes have *meridional* disposition of arsine or stibine ligands with *trans* chlorides and conform to C$_{2v}$ symmetry.

The electronic spectra of complexes (2) and (4) (Table 4) show ligand-to-metal charge transfer bands due to DMSO and methyldiphenyl arsine or triphenylstibine. The absorption bands appear around the same region as in complex (1). Thus absorption at 230 nm could be assigned to ligand–metal charge-transfer in DMSO and bands at 246, 264 nm and 250, 272 nm in complexes (2) and (4) respectively may be assigned to ligand–metal charge-transfer in the arsine and stibine ligand, respectively. The absorption bands at 302 nm may be due to metal–ligand (DMSO) charge-transfer bands. The transitions around 400 and 500 nm can be assigned to d–d transition in the complex corresponding to 1A$_1$→1T$_2$ and 1A$_1$→1T$_1$ transitions, respectively. The 10 Dq value of complexes (2) and (4) calculated from these transitions are 21,067 and 20,861 cm^{-1}, respectively.

Cis-dicarbonyls (13–15) were obtained from complexes (2–4) by the displacement of DMSO and one of the arsine or stibine groups. The dicarbonyls were confirmed by the appearance of peaks around 2010 cm^{-1} and 2200 cm^{-1}, 1950 and 2010 cm^{-1}, 1980 cm^{-1} and 2040 cm^{-1} respectively in complexes (13–15).

Reaction of complexes (2) and (3) with molecular hydrogen yielded hydrido complexes (22) and (23) by the displacement of a coordinated chloride by a hydride. The hydrides Ru(H)Cl(DMSO)(AsMePh$_2$)$_3$ and Ru(H)Cl(DMSO)(AsMe$_2$Ph)$_3$ show strong absorption peaks around 1960 and 1920 cm^{-1} respectively. No hydride was obtained with complex (4) in accord with a much lower acidity of stibine as compared to arsine ligands. Treatment with nitrogen, of the hydrido complex (22) resulted in the formation of the hydrido-dinitrogen complex (26). The characteristic dinitrogen peak appeared at 2150 cm^{-1} and the hydrido

peak at 1960 cm^{-1}. The other hydrides failed to react with molecular nitrogen.

When nitric oxide was passed through complexes (2)–(4), nitrosyl complexes (28)–(30) were obtained. The NO stretching frequency appeared at 1810 and 1850 cm^{-1} respectively in complexes (28)–(30). Nitric oxide with high *trans*-effect prefers to be in a *trans* position to a ligand with a low *trans*-effect. Hence it could not occupy a position *trans* to DMSO. A position *trans* to tertiary arsine or stibine looks more feasible for the ligand which may be considered to be coordinated as NO$^+$ in these complexes.

Five coordinate complexes of the type RuCl$_2$L$_3$
(L = AsMePh$_2$, AsMe$_2$Ph *or* SbPh$_3$)

These three complexes (5)–(7) were obtained by the interaction of ruthenium blue solution with methyldiphenyl arsine, dimethylphenylarsine or triphenylstibene. Molecular weights of the these complexes in nitrobenzene indicated them to be monomers. The presence of two bands in νM–Cl region at 270, 330 cm^{-1} in complex (5) 235 and 315 cm^{-1} in complex (6) and 260 and 275 cm^{-1} in complex (7) (Table 3), shows two *cis* chlorides in these complexes. There are many bands in the region 425–490 cm^{-1} assigned to νM-L vibrations (L = As or Sb). The complexes are diamagnetic. Two structures may be considered for these complexes; a square pyramid with *cis* chlorides and two mutually *trans* and a *cis* arsine (Fig. 4a) and a trigonal bipyramid with two axial and one equatorial arsine (Fig. 4b). The two proposed structures cannot be distinguished on the basis of NMR since arsines have the same environment in both the structures. For both the structures one should observe in the NMR spectra two singlets of 1:2 intensity due to methyl protons of two arsine groups. Because of *cis* interactions with equatorial arsines, two multiplets of 1:2 intensity are observed at 8.3τ and 8.65τ in complex (5) and 8.75τ and 8.97τ in complex (6), respectively. Likewise, phenylprotons also appear as two multiplets at

2.5τ and 2.9τ and 3.9τ and 3.97τ, respectively. In a similar manner the NMR spectrum of complex (7) shows multiplets in a 1:2 ratio at 3.7τ and 4.1τ.

A square pyramidal arrangement of ligands with two *cis* chlorides and a *meridional* arrangement of ligands however seems to be a much better arrangement from a steric view point than the trigonal bipyramidal arrangement. Based on a square pyramidal arrangement of the ligands three spin-allowed transitions are possible, 1A$_1$→1A$_2$, 1A$_1$→1B$_2$, 1A$_1$→1E$_1$, the first transitions 1A$_1$→1A$_2$ should give the 10 Dq value approximately and it is 14,000 cm^{-1} in complex (5).

The electronic spectrum of complex (7) shows three d–d transitions at 770, 540, 434 nm which can be assigned to the transitions 1A$_1$→1A$_2$, 1A$_1$→1B$_2$ and 1A$_1$→1E$_1$ in a square pyramidal configuration as in complexes (5) and (6). The bands at 263, 298 and 303 nm are charge-transfer bands as in complexes (5) and (6). Based on the lowest energy transitions 1A$_1$→1A$_2$ the 10 Dq value in this complex is 12,987 cm^{-1}. Complex (7) reacted with carbon monoxide to yield a monocarbonyl (16) which exhibits a single strong band at 1950 cm^{-1}.

Complex (5) reacted with molecular hydrogen to yield a hydrido complex (24). As in the other hydrido complexes (21)–(24) complex (24) is formed by the displacement of a chloride from complex (5). The hydride exhibits a strong peak at 1920 cm^{-1}. Complexes (6) and (7) failed to react with molecular hydrogen.

Reaction of complex (5) with nitric oxide yielded the nitrosyl complex (31) which showed a strong band around 1910 cm^{-1} corresponding to a coordinated NO$^+$ in this complex.

Cis-RuCl$_2$(DPAM)$_2$

The complex was obtained from RuCl$_2$(DMSO)$_4$ by the displacement of all DMSO groups by the chelating agent. Mague and Mitchener[9] had prepared the complex *trans*-RuCl$_2$(DPAM)$_3$ by the interaction of hydrated ruthenium trichloride with excess of DPAM. In this complex, one of the

L=AsMePh$_2$, AsMe$_2$Ph, SbPh$_3$

(a)   (b)

Fig. 4.

DPAM was reported to be bidentate and the other two monodentate.[9] The complex reported in this work was thus obtained from a different route and is different in composition and structure from that reported by Mague and Mitchener.[9] The absence of DMSO peaks in the IR spectrum is an evidence of complete displacement of DMSO from RuCl$_2$(DMSO)$_4$. Thus the ligand DPAM seems to act as a bidentate ligand. The peaks at 330 and 485 cm^{-1} may be assigned to νM–As vibrations of the coordinated diarsine. The complexes with chelated DPAE or DPAM lack a centre of symmetry in the molecule and diarsine groups are coordinated as cis or trans and more than one νM–As stretching frequency are observed. The cis or trans geometry in these complexes is based mostly on the observed νM–Cl stretching frequency. The bands at 230 and 270 cm^{-1} in complex (8) may be associated with the M–Cl vibrations of the cis chlorides in the complex. The M–Cl frequencies are lower than complexes with trans-halogen since in this case the chlorides are trans to arsenic. A cis disposition of the two arsines in the complex is confirmed by the NMR spectrum which shows methylene protons as a doublet at 5.06τ. The doublet arises due to two non-equivalent methylene protons of a chelated diarsine group. The position of methylene resonance at 8.7τ is in accord with the bidentate coordination of DPAM. In the complex RuCl$_2$(DPAM)$_3$ the peaks due to the methylene protons of bidentate diarsine molecule were observed[9] at 5.17τ and those due to monodentate diarsine at 7.28τ. The arrangement of a chelated diarsine is thus in accord with the earlier observations.[9] There are two groups of phenyl protons one due to two mutually trans diarsine and another one due to two mutually cis diarsine groups. These two groups give rise to a complicated A$_2$B$_2$ pattern where many of the peaks overlap and appear as a broad multiplet centred at 3.5τ and many peaks in the 3.95–4.43τ region. Integration of phenyl and methylene protons however is in agreement with the proposed formulation of the complex. The probable structure for the complex is given in Fig. 5.
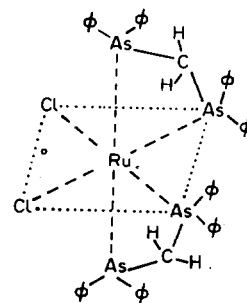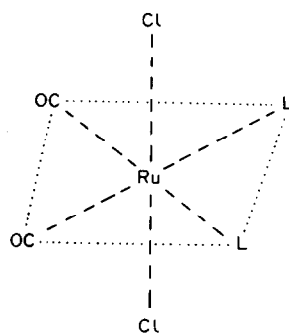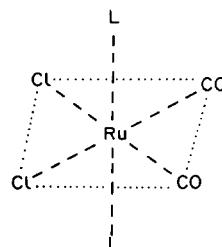
The electronic spectrum of RuCl$_2$(DPAM)$_2$ show ligand–metal charge-transfer bands at 245 and 270 nm (Table 5). The d–d transition in the complex was observed at 460 nm which can be assigned to the $1A_1 \rightarrow 1T_2$ transition.

Carbonylation of the complex yielded a dicarbonyl RuCl$_2$(CO)$_2$(DPAM)$_2$ (17). The IR spectrum of the dicarbonyl shows strong bands at 1935 and 2000 cm^{-1} associated with cis dicarbonyls. The dicarbonyls may be considered to have formed by

Fig. 5.

the opening of the DPAM chelate ring resulting in two molecules of DPAM acting as monodentate ligand. Mague and Mitchener[9] have prepared the compound RuCl$_2$(CO)$_2$(DPAM)$_2$ by the interaction of RuCl$_2$(DPAM)$_3$ with carbon monoxide. The configuration of the compound was proposed to be a mixture of (a) and (b) in Fig. 6.

The compound RuCl$_2$(CO)$_2$(L)$_2$ obtained in this investigation from cis-RuCl$_2$(DPAM)$_2$ is expected to have configuration 6(b) since carbonylation is expected to open the bidentate chelate rings of DPAM without any rearrangement of the halogens

(a)

(b)

L = DPAM

Fig. 6.

which is necessary in forming 6(a). The carbonyl frequencies of 2000 and 1930 cm^{-1} are in accord with a *cis* disposition of carbonyl groups to halogens.

Cis-RuCl$_2$(DPPM)$_2$

This complex is also prepared from RuCl$_2$(DMSO)$_4$ and diphos as other bidentate diphosphine or diarsine complexes. A complex of similar composition trans RuCl$_2$(DPPM)$_2$ was earlier reported by Chatt and Hayter[8] and later by Mague and Mitchener.[9] The former workers[8] prepared the complex directly from hydrated ruthenium trichloride and DPPM and the latter from red ruthenium carbonyl solution and DPPM. In this complex, the ligand is coordinated as a bidentate group. The procedure employed in this work for the preparation of RuCl$_2$(DPPM)$_2$ is more convenient than the earlier methods and gives the *cis* compound in a higher yield than the *trans* compound. As in the case of interaction of other chelated ligands with RuCl$_2$(DMSO)$_4$ interaction of DPPM with RuCl$_2$(DMSO)$_4$ results in complete displacement of DMSO by chelated phosphine as indicated by absence of peaks corresponding to coordinated DMSO in the IR spectrum of the complex.

The peaks at 420, 510, 545 cm^{-1} were assigned to vM–P vibrations of coordinated disphosphines (Table 3). The bands at 230, 275 cm^{-1} were indicative of a *cis* geometry for the chlorides.

The NMR spectrum of complex 9 exhibits peaks of equal intensity for methylene protons at 5.8τ and 8.7τ. This could be assigned to a bidentate and a monodentate phosphine ligand. On the basis of two modes of coordination for the complex, there are two structures possible for the complex. One is square pyramid (Fig. 7a) with two mutually *cis* phosphorus, a *trans* phosphorus and two mutually *cis* chlorides and the other one is a trigonal bipyramid (Fig. 7b) type of structure in which two phosphorus atoms (of two ligands) and a chloride are equitorial and a phosphorus and chlorine in axial position. In both the cases, there are two non-equivalent methylene groups due to the two modes of coordination of the ligand and two peaks due to methylene protons are expected in the NMR spectrum. Phenyl protons appear as a broad multiplet centered at 3.96τ. As in the case of other five coordinate complexes (5)–(7), the NMR as well as the electronic spectra of the complexes cannot decide between the two possibilities. On steric grounds the square pyramidal arrangement (7a) seems to be a better possibility than the trigonal bipyramid (7b).
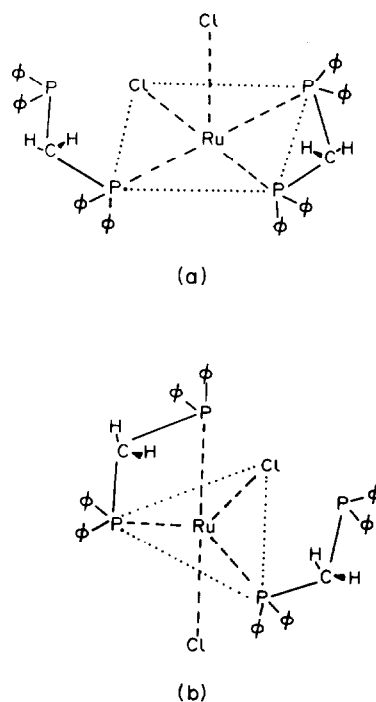

(a)

(b)

Fig. 7.

On carbonylation of (9), a *cis*-dicarbonyl of RuCl$_2$(DPPM)$_2$ is formed which shows strong bands at 1960 and 2000 cm^{-1}. As in the case of (8), the dicarbonyl formation may involve the rupture of a bidentate chelate ring and as such has two monodentate ligands in *trans* disposition as that of RuCl$_2$(CO)$_2$(DPAM)$_2$. The carbonylation of RuCl$_2$(DPPM)$_2$ can be expected to be more facile on the basis of a square pyramidal configuration rather than a trigonal bipyramid (Fig. 8a). In the former case one of the carbons monoxide molecules can add to the vacant coordination position on the metal ion and the other opens up the chelated DPPM groups to form RuCl$_2$(CO)$_2$(DPPM)$_2$. A trigonalbipyramidal structure requires rearrangement of various groups. Mague and Mitchener[9] have reported a cationic monocarbonyl species [RuCl(CO)(DPPM)$_2$]Cl by the interaction of *trans*-RuCl$_2$(DPPM)$_2$ with carbon monoxide (Fig. 8b). In this case the displacement of a chloride seems to be easier than rupture of a DPPM group to form the carbonylated complexes. The formation of a dicarbonyl or monocarbonyl thus seems to depend very much on the geometry of the starting material.

Complex (9) reacted with nitric oxide to yield a nitrosyl complex RuCl$_2$(NO)(DPPM)$_2$ (32). The formation of a nitrosyl complex is confirmed by the appearance of a single band around 1825 cm^{-1}. A nitrosyl group gets added to the vacant coordi-
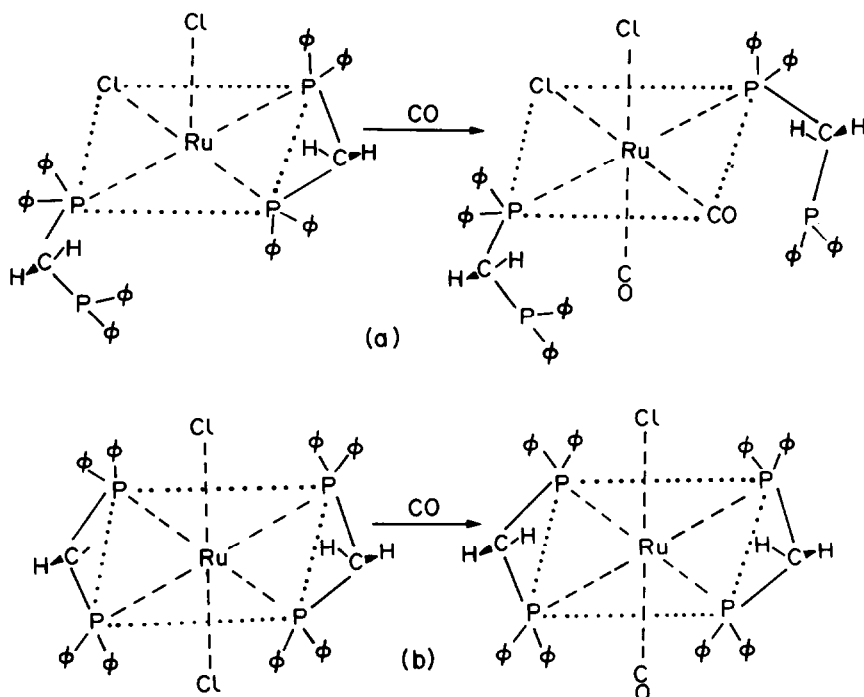
Fig. 8.

nation position on the metal ion to give a six coordinated species.

RuCl$_2$(DPPE)$_2$ and RuCl$_2$(DPAE)$_2$

These two complexes were prepared by the reaction of RuCl$_2$(DMSO)$_4$ with chelated phosphine or arsine. The complex RuCl$_2$(DPPE)$_2$ was previously obtained by Chatt and Hayter[8] by the direct reaction of hydrated ruthenium trichloride in ethanol with DPPE and the complex RuCl$_2$(DPAE)$_2$ was synthesized by Mague and Mitchener[9] by the reaction of Ru(CO)$_n$Cl$_3$ with DPAE. The method adopted in this work is different and more convenient than those of previous investigations[8,9] and gave a higher yield of the complexes. All the four DMSO groups from RuCl$_2$(DMSO)$_4$ are replaced by the bidentate chelating ligands to form RuCl$_2$L$_2$ (L = DPPE or DPAE). This is confirmed by the absence of peaks due to coordinated DMSO in the IR spectra of these complexes. The bands in the region 400–500 cm^{-1} may be assigned to the coordinated phosphorus or arsenic. The *trans* configuration of the complexes is confirmed by a single νM–Cl peak at 320 cm^{-1} in both the complexes.

The *trans* geometry of the chloride groups allow only *trans* disposition of the bidentate ligand. This fact is confirmed by the NMR spectra of the two complexes. The NMR spectrum of the complex RuCl$_2$(DPPE)$_2$ shows a multiplet at 4.1τ due to the

phenyl protons of the phosphine. The peaks due to the methylene protons are observed as multiplets at 7.26τ and 8.47τ in a ratio of 1:2. The methylene protons in the chelated ligand do not seem to be equivalent because in the five membered chelate ring methylene protons are expected to be above and below the plane containing the metal ion and the two phosphorus atoms. The configuration of the protons seems to be fixed in the ring since a flip-flop mechanism would give rise to a single methylene peak. The methylene triplet is expected because of the spin coupling of the protons by ^{31}P. In the NMR spectrum of the free ligand, the methylene protons are observed as one triplet at 8.07τ. This triplet arises due to splitting of equivalent methylene proton peak by the two phosphorus atoms. The NMR spectrum of complex RuCl$_2$(DPAE) shows a similar pattern to RuCl$_2$(DPPE). The only difference is that the methylene protons appear as two singlets since there is no splitting by arsenic. In the free ligand also there is a singlet due to equivalent methylene protons. The phenyl protons merge together and appear as a broad multiplet centered at 4.1τ in the complex. The integration of the phenyl and methylene protons in the two complexes is consistent with the proposed structures for these complexes (Fig. 9).

The electronic spectrum of RuCl$_2$(DPPE)$_2$ gave the ligand–metal charge-transfer bands at 240 and
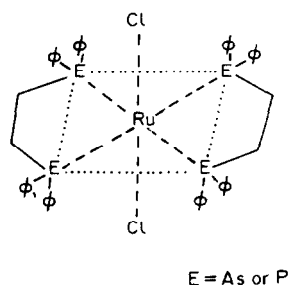
E = As or P

Fig. 9.

250 nm (Table 5). The d–d transitions in the complex are observed at 372 and 440 nm which can be assigned to $1A_1 \rightarrow 1T_2$ and $1A_1 \rightarrow 1T_1$ transitions, respectively. The 10 Dq value calculated for the complex is 23,770 cm^{-1}. The electronic spectrum of RuCl$_2$(DPAE)$_2$ gave ligand–metal charge-transfer bands at 245 and 260 nm. These charge-transfer bands can be compared to the monoarsine (Table 5) complexes that give bands around 240–250 and 260–270 nm. These bands may be assigned in a manner similar to other spin paired octahedral complexes as (10). The 10 Dq value calculated for the complex is about 23,935 cm^{-1}. On comparing the 10 Dq value calculated for the chelating phosphine and arsine complexes to those of non-chelating arsine and DMSO complexes, it may readily be seen that chelation gives a much higher 10 Dq values (about 400 cm^{-1} more than non-chelated compounds). This indicates extra stability and much higher ligand field strength of the chelated ligands as compared to the monodentate ligands.

Carbonylation of complexes (10) and (11) yielded the monocarbonyls (19) and (20), respectively. These carbonyls can be considered to be cationic species obtained by the displacement of a coordinated chloride from the coordination sphere of the metal ion. The monocarbonyls (19) and (20) exhibit single sharp peaks at 1950 and 1925 cm^{-1}, respectively. The complexes are cationic as indicated by their conductivities in DMA (1:1 electrolyte). Displacement of carbon monoxide from Ru(CO)$_2$Cl$_n$ by DPAE gives rise to RuCl$_2$(DPAE)$_2$.[9] The coordination of DPAE or DPPE to the metal ion seems to be stronger than carbon monoxide since the chelating ligands can displace carbon monoxide from the coordination sphere of the metal ion. In the case of complexes (10) and (11) however a coordinated chloride is displaced in the presence of excess of carbon monoxide from the coordination sphere of the

metal ion to form cationic monocarbonyl species. These cationic carbonyl complexes are prepared for the first time and their formation seems to be a general phenomenon in the reactions of chelated phosphine or arsine complexes with carbon monoxide.

Complex RuCl$_2$(DPAE)$_2$ reacted with nitric oxide yielding a nitrosyl complex RuCl$_2$(NO)(DPAE)$_2$ (33). The nitrosyl group shows a band at 1825 cm^{-1} in the complex. The nitrosyl formation may involve the rupture of a bidentate chelate ring and as such may have bidentate and monodentate DPAE ligand and a seven coordinate geometry for ruthenium.

REFERENCES

1. T. A. Stephenson and G. Wilkinson, J. Inorg. Nucl. Chem. 1966, 28, 945.
2. R. K. Poddar and U. Agarwala, Indian J. Chem. 1971, 9, 477.
3. Dwyer Humpoletz and R. S. Nyholm, J. Proc. Roy. Soc. N.S.W. 1946, 80, 217.
4. J. Chatt, B. L. Shaw and A. E. Field, J. Chem. Soc. 1964, 3466.
5. R. K. Poddar and U. Agarwala, J. Inorg. Nucl. Chem. 1973, 35, 567.
6. E. G. Leelamani and G. K. N. Reddy, Inorg. Nucl. Chem. Lett. 1975, 5, 11.
7. R. S. Nyholm and G. J. Sutton, J. Chem. Soc. 1958, 567.
8. J. Chatt and R. G. Hayter, J. Chem. Soc. 1961, 896.
9. J. T. Mague and J. P. Mitchener, Inorg. Chem. 1972, 11, 2714.
10. B. R. James, E. Ochial and G. L. Rempal, Inorg. Nucl. Chem. Lett. 1971, 7, 781.
11. I. P. Evans, A. Spencer and G. Wilkinson, J. Chem. Soc. (Dalton), 1973, 204.
12. D. Rose and G. Wilkinson, J. Chem. Soc. (A) 1970, 1791.
13. G. J. Burrows and E. E. Turner, J. Chem. Soc. 1921, 426.
14. A. Mercer and J.-Trotter, J. Chem. Soc. Dalton 1975, 2480.
15. R. S. McMillan, A. Mercer, B. R. James and J. Trotter, J. Chem. Soc. Dalton 1975, 1006.
16. C. N. R. Rao, U.V. and Visible Spectroscopy Chemical Applications, p. 33. Butterworth, London (1967).
17a. C. N. R. Rao, J. Ramachandran and A. Balasubramaniam, Can. J. Chem. 1961, 39, 171; b. H. H. Jaffe, J. Chem. Phys. 1954, 22, 1430.
18. R. O. Harris, N. K. Hota, L. Dadavoy and J. M. C. Yuen, J. Organometal. Chem. 1973, 54, 259.
19. S. D. Robinson and M. F. Uttley, J. Chem. Soc. Dalton 1972, 1.

SPECTROSCOPIC AND BIOLOGICAL STUDIES ON PALLADIUM(II) COMPLEXES WITH N-ETHYL AND N-PROPYLIMIDAZOLE

M. BIDDAU, M. MASSACESI and G. PONTICELLI*

Istituto di Chimica Generale, Inorganica ed Analitica Via Ospedale 72, 09100 Cagliari,
Italy

G. DEVOTO

Cattedra di Chimica A, Facoltà di Medicina, Istituto Medicina del Lavoro,
Via S. Giorgio 12, 09100 Cagliari, Italy

and

I. A. ZAKHAROVA

N. S. Kurnakov Institute of General and Inorganic Chemistry, Academy of Sciences,
Leninsky Prospect 31, 117071 Moscow, U.S.S.R.

Abstract—Palladium(II) halide complexes with N-ethylimidazole (N–EtIm) and N-propylimidazole (N–PropIm) with general formulae $Pd(L)_2X_2$ and $Pd(L)_4X_2$ (X = Cl, Br, I) were prepared and characterized by spectroscopic methods and conductivity measurements. These complexes are diamagnetic and have square planar stereochemistry. The $Pd(L_2)X_2$ derivatives, are non-conductors, and have *trans*-structures except for the *cis*-$Pd(N–EtIm)_2Br_2$. The biological activity of water soluble Pd(II) compounds is also reported.

Imidazole is a heterocyclic penta-atomic ring isomer of pyrazole, with an aromatic character; the tautomeric nature of the imidazole is missing when the hydrogen of the imine atom is substituted with an alkyl group. The N-alkylimidazoles are basic substances which form salts with acids.

Imidazole is used as an analgesic, antipyretic and antiflammatory agent.[1] In previous papers we have characterized N-ethylimidazole and N-propyl-imidazole complexes with copper(II), nickel(II), cobalt(II)[2] and successively with zinc, cadmium and mercury(II) salts.[3]

Recently Reedijk *et al.* have prepared Pd(II) and Pt(II) complexes with imidazole and N-methylimidazole.[4]

The present paper reports the preparation and characterization of the complexes of general formula $Pd(L)_nX_2$ where L = N-ethylimidazole

(N–EtIm), N-propylimidazole (N–propIm) $n = 2$, 4; X = Cl, Br and I.

The aim of this work is to control different stoichiometrical formulas, to establish the stereochemistry of the isolated compounds and to evaluate their biological activity.

RESULTS AND DISCUSSION

The isolated metal complexes with analytical data and other physical properties are listed in Table 1, the far IR data in Table 2, the summarized electronic spectra are shown in Table 3 and the biological data are reported in Table 4.

The compounds, obtained by refluxing or by mixing from water the metal salt and the ligand, are of the $[Pd(L)_4]X_2$, and $Pd(L)_2X_2$ types. The $Pd(L)_2X_2$ non-conducting derivatives are insoluble in water, while the $[Pd(L)_4]X_2$ are generally soluble in water.

All the complexes are crystalline, diamagnetic, soluble in MeOH, DMF, $EtNO_2$ and MeCN.

The vibrational modes of N–EtIm and

---

*Author to whom correspondence should be addressed.

M. BIDDAU *et al.*

Table 1. Analytical and physical properties

Compound	Colour	M.p °C	Found(calcd)%			Λ_M (cm$^2\Omega^{-1}$mole^{-1})	
			C	H	N		
Pd(N-EtIm)$_2$Cl$_2$	white	140	32.6(32.5)	4.3(4.4)	15.0(15.2)	9	EtNO$_2$
Pd(N-EtIm)$_2$Br$_2$	yellow	201	26.4(26.2)	3.5(3.5)	12.4(12.2)	16	MeOH
[Pd(N-EtIm)$_4$]Cl$_2$·2H$_2$O	pale yellow	175	39.8(40.2)	5.9(6.1)	18.6(18.7)	dec	
[Pd(N-EtIm)$_4$]Br$_2$	white	190	36.8(36.9)	4.9(4.8)	17.0(16.8)	"	
[Pd(N-EtIm)$_4$]I$_2$	white	152	32.2(32.2)	4.4(4.3)	14.8(15.0)	"	
Pd(N-PropIm)$_2$Cl$_2$	yellow	158	36.1(36.2)	5.1(5.1)	14.0(14.1)	13	MeOH
Pd(N-PropIm)$_2$Br$_2$	ochre	145	29.9(29.6)	4.3(4.1)	11.7(11.5)	14	MeOH
[Pd(N-PropIm)$_4$]Cl$_2$	white	101	46.2(46.6)	6.5(6.5)	17.9(18.1)	dec	
[Pd(N-PropIm)$_4$]Br$_2$	white	154	40.6(40.8)	5.6(5.7)	15.5(15.8)	"	
[Pd(N-PropIm)$_4$]I$_2$	pale yellow	132	36.0(36.0)	4.9(5.2)	13.9(13.9)	"	

Table 2. Far IR spectra (450–200 cm^{-1})*

Compound	✓(M–X)	Other vibrations Pd–X bendings and Pd–L stretch. and bend.
N–EtIm		412m, 344wbr, 279w, 244w
Pd(N–EtIm)$_2$Cl$_2$	334sbr, 326mbr	428sh, 377m, 254w
Pd(N–EtIm)$_2$Br$_2$	230vsbr	427mbr, 360wbr, 300vs, 285vs
[Pd(N–EtIm)$_4$]Cl$_2$·2H$_2$O		428m, 371m, 282s, 259m
[Pd(N–EtIm)$_4$]Br$_2$		432sh, 371m, 282s, 259m
[Pd(N–EtIm)$_4$]I$_2$		432sh, 395sbr, 252w, 235wbr, 142w, 138sh
N–PropIm		424w, 362w, 290w
Pd(N–PropIm)$_2$Cl$_2$	343–338vsbr	428w, 373mbr, 309msbr, 270vs,
Pd(N–PropIm)$_2$Br$_2$	263s	416ms, 300sh, 297vs, 278sh, 241mw
[Pd(N–PropIm)$_4$]Cl$_2$		390wbr, 381wbr, 295vwbr
[Pd(N–PropIm)$_4$]Br$_2$		386w, 275vw
[Pd(N–PropIm)$_4$]I$_2$		395sh, 378sh, 325s, 296m, 140w, 131w

* For the iodide derivatives the range is 450–100 cm^{-1}.

Table 3. Reflectance electronic spectra (d–d bands and Δ_1 ranges in cm^{-1})

Compound		ν_1	Δ_1
Pd(N–EtIm)$_2$Cl$_2$		25,000	27,100
Pd(L)$_2$X$_2$	L = N–EtIm; X = Br, I	23,800 – 26,650	25,900 – 28,750
	L = N–PropIm; X = Cl, Br		
[Pd(N–EtIm)$_4$]Cl$_2$·2H$_2$O		26,450	28,550
[Pd(L)$_4$]X$_2$	L = N–EtIm; X = Cl, Br	26,000 – 28,600	28,100 – 30,700
	L = N–PropIm; X = Cl, Br, I		

N–PropIm in the near and mid IR spectra appear noticeably unchanged on passing from the spectra of the free ligands to those of the complexes.

Table 4. Inhibitory activity of the palladium(II) complexes

Complex	Inhibitory activity % (±2) 10^{-4}M
Pd(N–PropIm)$_2$Cl$_2$	41
[Pd(N–EtIm)$_4$]Br$_2$	16
[Pd(N–EtIm)$_4$]I$_2$	15
[Pd(N–PropIm)$_4$]Cl$_2$	20
[Pd(N–PropIm)$_4$]Br$_2$	32
[Pd(N–PropIm)$_4$]I$_2$	35

The medium absorption bands within the 3430–3400 cm^{-1}, v(OH) and 1670–1625 cm^{-1}, δ(HOH), ranges are present in [Pd(N–EtIm)$_4$]Cl$_2$·2H$_2$O.

The complex loses all the water at 110°C before its decomposition. From a detailed analysis of the IR spectrum, we have found that the rocking, twisting and wagging modes ascribable to coordinated water are absent, according to the literature data.[5]

The Pd(N–EtIm)$_2$Cl$_2$ and Pd(N–PropIm)$_2$Cl$_2$, non-conductors, in the far IR spectrum show respectively two bands at 334 and 326 cm^{-1} and a broad band in the 343–336 cm^{-1} assigned to v (Pd–Cl) terminal for cis-square planar compounds in C$_{2v}$ stereochemistry.[6,7]

In the far IR region the spectrum of the Pd(N–PropIm)$_2$Br$_2$ derivative shows a band whose position of the metal halogen stretching is diagnostic of terminal halides for trans-square planar compounds in D$_{2h}$ stereochemistry.[8]

The reflectance spectra of the $Pd(L)_2X_2$ compounds confirm the square planar geometry.[9] The band $v_1 = {}^1A_{1g} \rightarrow {}^1B_{1g}$ falls in the 26,450–25,000 cm^{-1} range and $\Delta_1 = v_1 + 3.5\,F_2$ in the 28,750–25,900 cm^{-1} range.[10]

The palladium(II) derivatives $[Pd(L)_4]X_2$ decompose in MeCN or EtNO$_2$, probably for rearrangement of the complexes. In the far IR spectra of these complexes the bands in the expected range for the $v(M-X)$ stretching vibrations are absent, so that the two halogens are outside the coordination sphere. The $[Pd(L)_4]X_2$ complexes, according to the electronic spectra (Table 3), are square planar.

The band in the 28,600–26,000 cm^{-1} range may be assumed to the $v_1 = {}^1A_{1g} \rightarrow {}^1B_{1g}$ transition and increases in the expected order: $Pd(L_2)X_2 < [Pd(L)_4]X_2$.

By assuming a value of $F_2 = 10\,F_4 = 600$ cm^{-1} for the Slater–Condon interelectronic repulsion parameters for these palladium(II) complexes,[8] it is possible to derive from the first spin allowed $d-d$ transition the values of Δ_1 by $\Delta_1 = v_1 + 3.5\,F_2$. The splitting parameter is in the 30,700–28,100 cm^{-1} range.

BIOLOGICAL ACTIVITY

In a previous paper[11] we have studied the inhibitory activity of the $M(L)_2X_2$ complexes (M = Pd(II), Pt(II); L = isox and its methyl and/or phenyl derivatives; X = Cl, Br) on the membrane bonded to Ca, Mg dependent ATP-ase.

The Pd(II) complexes have a higher effect than the Pt(II) compounds and the chloride derivatives show greater inhibitory activity than the bromide compounds.

Successively we have extended this study to the $M(L)_2X_2$ (L = BO and MeBO, where BO = benzoxazole; X = Cl, Br).[12] Also in this case for the complexes soluble in water, C_2H_5OH and CHCl$_3$ the inhibitory effect is similar to the isoxazole derivatives.

Recently we have isolated the $Pd(ox)(L)_n$ complexes (ox = oxalate, $n = 2,1$; L = above cited heterocyclic ligands).[13]

In the monomeric $Pd(ox)(L)_2$ (L=N–MeIm, N–EtIm and N–PropIm) the inhibitorial effect decreases in the order N–PropIm > N–EtIm > N–MeIm for the major length of the ligand chain.

In the dimeric $Pd(ox)(L)$ (L = isox, 3,5-diMeisox, 2-MeBO and 2,5-diMeBO) this activity increases with the steric hyndrance of the heterocyclic ligand and is generally higher than the $Pd(ox)(L)_2$ derivatives.

In Table 4 are listed the results of the inhibitory activity of the Pd(II) complexes 10^{-4} M in saline aqueous solution (NaCl, MgCl$_2$) on the Ca, Mg-dependent ATP-ase.

The N–PropIm complexes have inhibitory effect higher than the N–EtIm derivatives. This fact can be explained by the length of the N–PropIm chain that renders soluble the complex in the lipidic part of the enzyme.

$Pd(N–PropIm)_2Cl_2$ has as activity almost double that of $[Pd(N–PropIm)_4]Cl_2$, because in the first case the coordinated chlorides are replaced by the water molecules and successively by the thiolic groups.

The $[Pd(L)_4]X_2$ have activity that increases in the sequence I > Br > Cl; in fact the counteranion reduces its size and then its interaction in the same way.

The inhibitory activity values of these complexes are smaller than the $M(L)_2X_2$ (L = isox and its derivatives) compounds[11] because the imidazole ligands derivatives have stronger bonds with respect to the coordinate halides in the isoxazole complexes.

As far as the inhibitory mechanism the irreversible interaction of the imidazole derivatives complexes occurs with the sulphur anion of the thiol group of the enzyme that replaces the ligands in the square planar compounds.

EXPERIMENTAL

The N-ethylimidazole and N-propylimidazole purum were purchased from the BASF Company.

Starting materials

Palladium(II) salts were commercially available or were prepared according to the literature methods.

Preparation of the complexes

The complexes were prepared as in Ref. 11 or from water.

Analyses

Carbon, hydrogen and nitrogen have been determined with a Perkin–Elmer 240 elemental analyser.

IR spectra

The IR spectra have been recorded in the 4000–200 cm^{-1} range with Perkin–Elmer 325 and 180 spectrophotometers. The spectra in the 4000–450 cm^{-1} range were obtained using KBr discs, or Nujol mull; the far IR spectra in the 450–200 cm^{-1} with CsI discs for all compounds except to the iodide derivatives (450–100 cm^{-1}).

Electronic spectra

The electronic spectra were recorded with a Shimadzu MPS-50L spectrophotometer in the solid state in the 40,000–15,000 cm^{-1} range.

Conductivity measurements

These measurements were carried out with WTW LBR conductivity bridge at 25°C for 10^{-3} M solutions in MeOH and $EtNO_2$.

Biological analyses

The extraction method of the sarcoplasmatic reticulum (SR) containing Ca, Mg dependent ATP-ase, the ferment activity and the SH groups determination by amperometric titrations were published elsewhere.[11]

REFERENCES

1. P. Puig Parellada, G. Garzia Gasulla and P. Puig-Muset, *Pharmacol.* 1973, **10**, 161.
2. M. Massacesi and G. Ponticelli, *J. Inorg. Nucl. Chem.* 1974, **36**, 2209.
3. M. Biddau, M. Massacesi, R. Pinna and G. Ponticelli, *Spectrochim. Acta* 1981, **37A**, 315.
4. C. G. Van Kralingen, J. K. De Ridder and J. Reedijk, *Inorg. Chim. Acta* 1979, **36**, 69.
5. K. Nakamoto, *Infrared Spectra of Inorganic and Coordination Compounds.* Wiley, New York (1963).
6. D. M. Adams, *Metal Ligands and Related Vibrations.* Arnold, London (1967).
7. J. R. Ferraro, *Low Frequency Vibrations of Inorganic and Coordination Compounds.* Plenum Press, New York (1971).
8. D. M. Adams, J. Chatt, J. Gerrat and A. D. Westland, *J. Chem. Soc.* 1964, 734.
9. A. B. P. Lever, *Inorganic Electronic Spectroscopy*, (Edited by N. F. Lappert) Elsevier, Amsterdam, (1968).
10. A. R. Latham, V. C. Hascall and H. B. Gray, *Inorg. Chem.*, 1965, **4**, 788.
11. I. A. Zakharova, Ja. V. Salyn, L. V. Tatjanenko, Yu. Sh. Moshkovsky and G. Ponticelli, *J. Inorg. Biochem.*, 1981, **15**, 89 and references therein.
12. M. Massacesi, R. Pinna, M. Biddau, G. Ponticelli and I. A. Zakharova, *Inorg. Chim. Acta*, 1983, **3**, 151.
13. G. Devoto, M. Biddau, M. Massacesi, R. Pinna, G. Ponticelli, L. V. Tatjanenko and I. A. Zakharova, *J. Inorg. Biochem.* in press.

THE PRODUCTION OF $Cr(NH_3)_6^{3+}$ FROM THE ACID CATALYSED HYDROLYSIS OF $Cr(NH_3)_5(NCO)^{2+}$

DAVID YANG and DONALD A. HOUSE*

Department of Chemistry, University of Canterbury, Christchurch, New Zealand

Abstract—The rate of the reaction

$$Cr(NH_3)_5(NCO)^{2+} + H_3O^+ \longrightarrow Cr(NH_3)_6^{3+} + CO_2 + \text{other Cr(III) products}$$

has been investigated at 40–65°C with $[HClO_4]$ varying from 0.04 to 0.6 M ($\mu = 0.6\,M$, $NaClO_4$). The observed rate law has the form: $-d[Cr(NH_3)_5(NCO)^{2+}]/dt = k_{obs}[Cr(NH_3)_5(NCO)^{2+}]$ where $k_{obs} = a[H^+]^2\{1 + b[H^+]^2\}^{-1}$ and at 55.0°C, $a = 0.36\,M^{-1}s^{-2}$ and $b = 6.9 \times 10^{-3}\,M^{-1}s^{-1}$. The rate of loss of $Cr(NH_3)_5(NCO)^{2+}$ increases with increasing acidity to a limiting value (at $[H^+] \sim 0.5\,M$) but the yield of $Cr(NH_3)_6^{3+}$ decreases with increasing $[H^+]$ and increases with increasing temperature. In the kinetic studies the maximum yield of $Cr(NH_3)_6^{3+}$ was 35% but a synthetic procedure has been developed to give a 60% yield.

The major acid hydrolysis product of $M(NH_3)_5(NCO)^{2+}$ is $M(NH_3)_6^{3+}$ and the kinetics of this reaction have been measured for M = Co(III)[1,2] Ru(III)[3] and Rh(III).[3] At low acid concentrations ($< 0.1\,M$) the rate law $-d[M]/dt = k[M][H^+]$ is observed,[1–3] but at higher acidities, some deviation from this is found.

Recently, the synthesis of $Cr(NH_3)_5(NCO)^{2+}$ has been described,[4] and this too, hydrolyses in acid to give $Cr(NH_3)_6^{3+}$.[4] In our hands, however, the yield of hexammine from the reaction of $[Cr(NH_3)_5(NCO)](NO_3)_2$ in $HClO_4$ or HNO_3 was never greater than 20%. In this paper we describe kinetic data for the loss of $Cr(NH_3)_5(NCO)^{2+}$ in acid media and present conditions to produce a reasonable yield (60%) of $Cr(NH_3)_6^{3+}$.

EXPERIMENTAL

$[Cr(NH_3)_5(NCO)](NO_3)_2$ was prepared as described by Schmidtke and Schönherr.[4] The bright orange crystalline nitrate salt had visible absorption and IR spectral parameters similar to those

described in the literature. Cr Calc, 17.2% Cr Found, 17.1%.

Kinetic studies and product analysis

Solutions (6.6 mM) of $Cr(NH_3)_5(NCO)^{2+}$ were prepared by dissolving 100 mg of the nitrate salt (F.W. = 303) in water (20 cm³) and adding appropriate volumes of $HClO_4$ and $NaClO_4$ solutions to give 50 cm³ $\mu = 0.6\,M$, $[H^+] = 0.04 - 0.6\,M$. The rate of complex decomposition was measured spectrophotometrically (1 cm cells) at constant temperature either by repetitive scans or fixed wavelength (490 nm) techniques. No isosbestic points were maintained in the spectral scan envelope (700–300 nm), but satisfactory "infinity" readings (7–8 half-lives) were obtained.

Pseudo-first-order rate constants were calculated from the expression

$$kt = \ln \frac{A_0 - A_\infty}{A_t - A_\infty}$$

where A_0, A_t and A_∞ are the absorbances (490 nm) at time zero, time, t, and at the end of the reaction (> 7 half lives).

At the end of the reaction, the sample used for

―――――――――――――――――
*Author to whom correspondence should be addressed.

spectrophotometric analysis was returned to the bulk flask (which had been maintained at the appropriate temperature for the duration of the spectrophotometric measurements) and the solution was stored at $-5°C$ for at least 24 hr. During this time, all the $Cr(NH_3)_6^{3+}$ present crystallised as the perchlorate salt and $10 cm^3$ aliquots of the now pink coloured solution were removed for total Cr analysis.[5] The difference between the $[Cr]_{initial}$ $(6.6 mM)$ and the $[Cr]$ in the mother liquor allowed an estimate of the amount of $Cr(NH_3)_6^{3+}$ produced. The $[Cr]$ in the mother liquor of a control containing 100 mg of $[Cr(NH_3)_6](ClO_4)_3$ dissolved $50 cm^3$ of 0.04 M $HClO_4$, 0.56 M $NaClO_4$ was too small to be of any significance $(<0.1 mM)$.
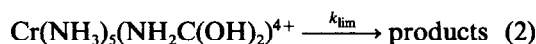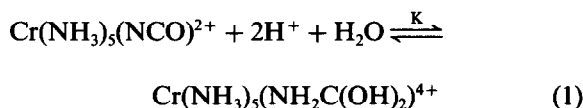
Synthesis of $[Cr(NH_3)_6](ClO_4)_3$

A solution of $NaClO_4·H_2O$ (45 g) in water $(500 cm^3)$ with $5.0 cm^3$ of 60% $HClO_4$ added was heated to 85°C. 3 g of $[Cr(NH_3)_5NCO](NO_3)_2$ were rapidly added to the stirred solution and the temperature was maintained for exactly 6.0 min before rapid cooling in ice. After 24 hr at $-5°C$ the yellow crystalline product (2.7 g, 60%) was removed from the faintly pink coloured mother liquor by filtration, and washed successively with 2-propanol and ether, and air dried. Calc for $[Cr(NH_3)_6](ClO_4)_3$: Cr, 11.5%. Found: Cr, 11.5%.

Synthesis of cis-$[CrCl(NH_3)_4(OH_2)]Cl_2$

$[Cr(NH_3)_5(NCO)](NO_3)_2$ (2 g) was dissolved in HCl (6 M, $30 cm^3$) and warmed (40°C) until pink crystals deposited (20 min). The solution was cooled to room temperature, and the filtered product (1.5 g, 93%) washed with isopropanol and then ether and air dried. Calc for $[CrCl(NH_3)_4(OH_2)]Cl_2$: Cr, 21.3%. Found: Cr, 21.4%.

RESULTS AND DISCUSSION

Tables 1 and 2 list values for the pseudo-first-order rate constants (k_{obs}) for the loss of $Cr(NH_3)_5(NCO)^{2+}$ in acid conditions at various temperatures, together with yields of $Cr(NH_3)_6^{3+}$. Figure 1 shows a plot of k_{obs} vs $[H^+]$ at various temperatures. The non-linearity and limiting values at high $[H^+]$ suggest that the $[H^+]$ dependence on the reaction rate is unique for H^+ catalysed decompositions of $M(NH_3)_5(NCO)^{2+}$ complexes.[1-3] Activation energy plots for $\ln(k_{obs})$ vs $T(K)^{-1}$ at any particular $[H^+]$ are linear and Table 3 presents the calculated kinetic parameters, with a systematic trend to lower activation energies (and more negative activation entropies) with increasing acidity. The data in Table 2 indicate the decomposition reaction is characterised by a positive salt effect and linear plots of k_{obs}^{-1} vs $[H^+]^{-2}$ (Fig. 2) give slope (k_{lim}^{-1}) and intercept $([k_{lim}K]^{-1})$ (Table 4) for the reaction scheme:[2,3]

$$Cr(NH_3)_5(NCO)^{2+} + 2H^+ + H_2O \overset{K}{\rightleftharpoons}$$

$$Cr(NH_3)_5(NH_2C(OH)_2)^{4+} \qquad (1)$$

$$Cr(NH_3)_5(NH_2C(OH)_2)^{4+} \xrightarrow{k_{lim}} products \qquad (2)$$

where

$$k_{obs} = k_{lim}K[H^+]^2\{1 + K[H^+]^2\}^{-1}. \qquad (3)$$

Values of K (eqn 1) increase with increasing temperature and the associated thermodynamic parameters are given in Table 4.

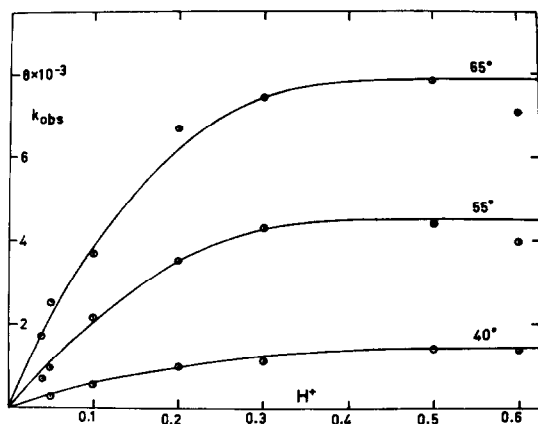The yield of $Cr(NH_3)_6^{3+}$ (Tables 1 and 2) increases with increasing temperature, and decreasing $[H^+]$ and is independent of ionic strength.

Fig. 1. Plots of k_{obs} vs $[H^+]$ for the decomposition of $Cr(NH_3)_5(NCO)^{2+}$ in $HClO_4$ ($\mu = 0.6 M$) at 40, 55 and 65°C.
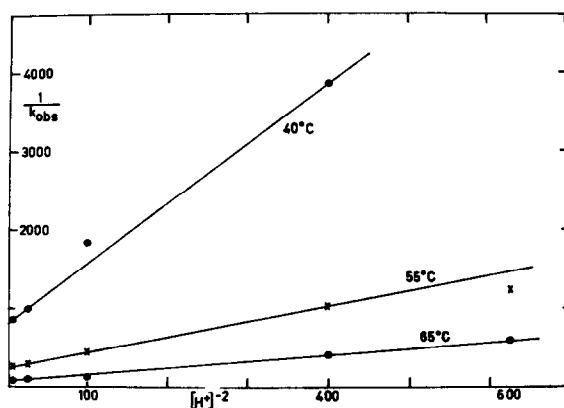

Fig. 2. Plots of $[k_{obs}]^{-1}$ vs $[H^+]^{-2}$ for the decomposition of $Cr(NH_3)_5(NCO)^{2+}$ in $HClO_4$ ($\mu = 0.6 M$) at 40, 55 and 65°C.

Table 1. Pseudo-first-order rate constants ($10^3 k_{obs}$, s^{-1}) for the loss of Cr(NH$_3$)$_5$(NCO)$^{2+}$ in HClO$_4$ ($\mu = 0.6$ M, NaClO$_4$)^{a,b} and % Cr(NH$_3$)$_6^{3+}$ produced

[H$^+$] [M]	40.0°C	55.0°C	65.0°C
0.04		0.68±0.03(27.0)	1.71±0.40(30.8)
		[0.52]	[1.16]
0.05	0.26±0.01(22.3)	0.95±0.07(30.9)	2.52±0.32(35.3)
	[0.21]	[0.77]	[1.71]
0.10	0.55±0.04	2.17±0.18	3.69±0.36
	[0.60]	[2.14]	[4.60]
0.20	1.00±0.10	3.54±0.27(20.0)	6.69±0.41
	[1.13]	[3.84]	[8.00]
0.30	1.13±0.11(9.2)	4.32±0.13(11.0)	7.40±0.64(16.8)
	[1.35]	[4.52]	[8.70]
0.50	1.42±0.14	4.39±0.21(5.0)	7.83±0.50(9.1)
	[1.50]	[4.97]	[10.1]
0.60	1.39±0.09	3.96±0.16^c	7.06±0.05^c(12.7)
	[1.52]	[5.05]	[10.2]

a Mean ± the standard deviation of at least three determinations. Numbers in parenthesis are the % Cr(NH$_3$)$_6^{3+}$ formed. [Cr(NH$_3$)$_5$(NCO)]$^{2+}$ = 6.6 mM. b Numbers in square brackets are $10^3 k_{obs}$(calc) using the expression k_{obs}(calc) = $\{k_{lim} K[H^+]^2\}\{1 + K[H^+]^2\}^{-1}$ with values of k_{lim} and K taken from Table 4. c One determination.

Table 2. Pseudo-first-order rate constants ($10^3 k_{obs}$, s^{-1}) for the loss of Cr(NH$_3$)$_5$(NCO)$^{2+}$ in HClO$_4$ at variable ionic strength and initial concentrations, T = 55.0°C^a

[H$^+$] M	μ^b M	complex$_i$ mM	$10^3 k_{obs}$ s^{-1}	Ref.
0.1	0.6	6.6	2.17±0.18	c
0.1	0.6	9.9	1.84 (25.8)	d
0.1	0.6	13.2	1.85 (27.0)	d
0.1	0.6	16.5	1.57 (30.5)	d,e
0.04	0.04	6.6	0.36 (?)	d,f
0.04	0.6	6.6	0.68±0.03(27.0)	c
0.1	0.1	6.6	1.14 (?)	d,f
0.1	0.6	6.6	2.17±0.18(25.8)	c
0.2	0.2	6.6	2.90 (14.4)	d
0.2	0.6	6.6	3.54±0.27(20.0)	c
0.3	0.3	6.6	3.34 (11.5)	d
0.3	0.6	6.6	4.32±0.13(11.0)	c
0.5	0.5	6.6	4.03 (5.2)	d
0.5	0.6	6.6	4.39±0.21(5.0)	c

a Numbers in parenthesis are % Cr(NH$_3$)$_6^{3+}$ formed. b Total [ClO$_4^-$]. c From Table 1. d Single determination with an estimated error of ±5%. e [Cr(NH$_3$)$_6$](ClO$_4$)$_3$ deposited during the kinetic run. f No [Cr(NH$_3$)$_6$](ClO$_4$)$_3$ deposited at these low ClO$_4^-$ concentrations.

Table 3. Calculated kinetic parameters for the acid hydrolysis of $Cr(NH_3)_5(NCO)^{2+}$ in $HClO_4$
$(\mu = 0.6\,M)$ at 298.2 K

[H⁺] [M̲]	$10^4\underline{k}$ (s^{-1})	$10^4\underline{k}_{calc}$[a] (s^{-1})	E_a $(kJ\ mol^{-1})$	$\Delta S^{\#}$ $(J\ K^{-1}\ mol^{-1})$
0.04	0.31	[0.34]	83.4±12	−60±24
0.05	0.553	[0.51]	79.2±3	−69±6
0.10	1.57	[1.55]	67.5±3	−99±6
0.20	2.71	[3.12]	68.3±2	−92±4
0.30	3.13	[3.86]	68.3±4	−91±8
0.50	4.45	[4.37]	60.7±2	−133±4
0.60	4.56	[4.48]	57.8±2	−123±4

a̲ See footnote b̲, Table 1.

Although the maximum yield of $Cr(NH_3)_6{}^{3+}$ under the reaction conditions used was only 35%, we have extrapolated these trends to develop a synthetic procedure where yields of 60% of the hexaammine can routinely be obtained from the easily prepared $[Cr(NH_3)_5(NCO)](NO_3)_2$.

Unfortunately we have been unable to characterise the other Cr(III) complexes formed. Absorption spectra of the resulting pink solutions (after precipitation of $Cr(NH_3)_6{}^{3+}$) indicate a complex mixture of $Cr(NH_3)_x(OH_2)_{6-x}^{3+}$ ($x \neq 5$) but the ratio of the products ($x = 1$–4) could not be determined. We can exclude $Cr(NH_3)_5(OH_2)^{3+}$ as a product on three accounts:

(a) The $ClO_4{}^-$ salt of this complex is reasonably insoluble, but no $[Cr(NH_3)_5(OH_2)](ClO_4)_3$ was detected.

(b) Treatment of the pink solution with concentrated HCl did not produce any of the very HCl insoluble $[Cr(NH_3)_5Cl]Cl_2$.

(c) The major product of the reaction between $Cr(NH_3)_5(NCO)^{2+}$ and $6\,M$ HCl is cis-$[CrCl(NH_3)_4(OH_2)]Cl_2$.

Table 5 lists the reported visible absorption spectral parameters for various $Cr(NH_3)_x(OH_2)_{6-x}^{3+}$ species, together with selected data for the red $Cr(NH_3)_x(OH_2)_{6-x}^{3+}$ complex mixtures produced in the reaction between $Cr(NH_3)_5NCO^{2+}$ and H^+. Inspection of these data suggest that di- and tri-ammines are the most likely products and that,

Table 4. Calculated limiting values for rate and equilibrium constants

T (°C)	[K]	$10^4\underline{k}_{lim}$[a,f] (s^{-1})	$\underline{K}$[b] $(M^{-1}\ s^{-1})$	ΔH^{o}[c] $(kJ\ mol^{-1})$	ΔS^{o}[d] $(J\ K^{-1}\ mol^{-1})$	K_{calc}[e]
25.0	298.2	4.76	48.2	9.6	64.4	48.2
40.0	313.2	16.0	59.5			58.1
55.0	328.2	52.6	68.7			68.7
65.0	338.2	106.0	76.8			76.3

a̲ Estimated from the intercept of k_{obs}^{-1} vs $[H^+]^{-2}$ plots.

b̲ Estimated from the slope of k_{obs}^{-1} vs $[H^+]^{-2}$ plots.   c̲ Estimated from the slop of lnK vs T^{-1} plot.   d̲ Calculated from the expression $RT\ ln\ K_{298} = T\Delta S^{o}-\Delta H^{o}$.   e̲ Calculated from the expression $RT\ ln\ K_T = T\Delta S^{o}-\Delta H^{o}$ using the values of ΔS^{o} and ΔH^{o} in the Table.

f̲ Kinetic activation parameters for k_{lim} are $E_a = 65.3 \pm 1$ kJ mol^{-1}, $\Delta S^{\#} = -98 \pm 2$ J K^{-1}mol^{-1}.

Table 5. Visible absorption spectral parameters for $Cr(NH_3)_x(OH_2)_{6-x}^{3+}$ species[a]

x	λ_{max}	λ_{max}	$10^6 k_H (70°C)$ (s^{-1})	Ref.	Product Mixture [b],[c],[d]			
					$[H^+]$ (M)	λ_{max}	λ_{max}	T (°C)
6	465	350	47.5[i]	e	0.04	525	387	55
	(40)	(33)				(15.9)	(14.9)	
5	480	359	47.2	e	0.10	517	381	55
	(35.1)	(30.3)				(21.0)	(17.0)	
c-4	595	366	24.2	f	0.20	517	381	55
	(35.8)	(26.8)				(19.9)	(16.3)	
t-4	470	369	44.4	f	0.30	515	397	55
	(21.5)	(32.1)				(22.1)	(17.4)	
fac-3	513	374	7.6	f	0.50	512	376	55
	(36.6)	(22.6)				(24.3)	(18.6)	
mer-3	502	376	23.5	f	0.60	510	374	55
	(26.3)	(26.8)				(26.5)	(20.4)	
c-2	526	386	3.4	g	0.05	523	385	40
	(27.0)	(21.3)				(18.3)	(15.1)	
t-2	522	387	17.5	g,h	0.05	526	388	55
	(21.3)	(24.6)				(17.1)	(15.4)	
1	547	396	1.1	g	0.05	525	387	65
	(19.9)	(18.6)				(16.2)	(15.4)	
0	574	407		g				
	(13.2)	(15.5)						

[a] λ in nanometers, values in parenthesis are molar extinction coefficients (ε, M^{-1} cm^{-1}). c = cis-, t = trans-.
[b] $[Cr(NH_3)_6](ClO_4)_3$ precipitated by storage at $-5°C$ for at least 24 hours before spectral analysis. [c] $[Cr(III)]_t$ determined spectrophotometrically by alkaline oxidation to CrO_4^{2-} with H_2O_2. Mean of 3 determinations ($\varepsilon \pm 0.2$ M^{-1} cm^{-1}). [d] $\mu = 0.6$ M (NaClO$_4$).
[e] Ref. 9. [f] Ref. 8. [g] Ref. 6. [h] Ref. 7. [i] Kinetic data from Table 4, ref. 9.

like the production of $Cr(NH_3)_6^{3+}$, the product ratio depends on both $[H^+]$ and temperature. In addition, Table 5 also lists rate constants for the thermal rupture of successive Cr–NH$_3$ bonds in HClO$_4$ media.[6,8-10] If di- and tri-ammines are indeed produced, it is obvious that their rate of formation from the parent pentaammine must be strongly catalysed with respect to thermal Cr–NH$_3$ bond rupture. It has been observed previously,[11,12] that weakly acidic leaving groups (e.g. NO$_2^-$) can catalyse Cr–NH$_3$ bond rupture in acidic media and it is possible that the CO$_2$ produced in the acid

decomposition of $Cr(NH_3)_5(NCO)^{2+}$ behaves in a similar fashion.

CONCLUSION

Comparison of the data obtained here with those obtained for other $M(NH_3)_5(NCO)^{2+}$ systems is difficult because of different rate laws, but at a constant $[H^+]$ the order of reactivity is $Rh^3 > Co^{1,2} > Ru^3 \gg Cr$.

In the case of Rh, Co and Ru, there is good evidence[2,3] for an intermediate N-bonded carbamate complex and the mechanism proposed here

(eqns 1 and 2) incorporates such a protonated species for the Cr(III) system. It is possible that the rapid loss of NH_3 could be attributed to chelation of the carbamate (*cf.* oxalate)[13] and this could account for the isolation of *cis*-[$CrCl(NH_3)_4$ (OH_2)]Cl_2. Indeed $Cr(NH_3)_4\left(\begin{array}{c}/NH_2\\ \backslash O\end{array}\right\rangle C{=}O\,\Big)^{2+}$ or $Cr(NH_3)_4\left(\begin{array}{c}/O\backslash\\ \backslash O\end{array}\right\rangle C{-}NH_2\Big)^{2+}$ could also be included as potential components of the unknown red reaction products.

REFERENCES

1. R. J. Balahura and R. B. Jordan, *Inorg. Chem.* 1970, **9**, 1567.
2. D. A. Buckingham, D. J. Francis and A. M. Sargeson, *Inorg. Chem.* 1974, **13**, 2630.
3. P. C. Ford, *Inorg. Chem.* 1971, **10**, 2153.
4. H. H. Schmidtke and T. Schönherr, *Z. Anorg. Allg. Chem.* 1978, **443**, 225.
5. D. A. House, *Acta Chem. Scand.* 1972, **26**, 2847.
6. L. Mønsted and O. Mønsted, *Acta Chem. Scand.* 1973, **27**, 2121.
7. D. A. House, *Aust. J. Chem.* 1969, **22**, 647.
8. L. Mønsted and O. Mønsted, *Acta Chem. Scand.* 1974, **28**, 23.
9. L. Mønsted and O. Mønsted, *Acta Chem. Scand.* 1974, **28**, 569.
10. L. Mønsted and O. Mønsted, *Acta Chem. Scand.* 1974, **28**, 1040.
11. T. C. Matts and P. Moore, *J. Chem. Soc. Chem. Comm* 1969, 29.
12. T. C. Matts and P. Moore, *J. Chem. Soc., A* 1969, 219.
13. Othman Nor and A. G. Sykes, *J. Chem. Soc., Dalton* 1973, 1232.

HYDROLYSIS OF CYANO(PYRROLYL-1)BORATES

JÓZSEF EMRI* and BÉLA GYÖRI
Department of Inorganic and Analytical Chemistry, Lajos Kossuth University, H-4010
Debrecen, Hungary

Abstract—The kinetics and mechanism of the hydrolysis of several cyano(pyrrolyl-1)borates in aqueous medium has been investigated. The hydrolysis of cyanophenyl(pyrrolyl-1)-borates, cyano(tripyrrolyl-1)borate and cyanohydro(pyrrolyl-1)borates proceeds via two kinds of reactions; (a) a special H^+ ion catalyzed reaction (A-1 mechanism) and (b) a H^+ ion concentration–independent process of S_N1 mechanism. In acidic medium the $[BH_2(NC_4H_4)CN]^-$ anion is reversibly protonated at the α-carbon of the pyrrolyl group and a product with composition $C_4H_5N \cdot BH_2CN$, stable towards hydrolysis is also formed.

In the H^+ ion catalyzed reaction the B–N bond very likely breaks, whereas upon the $[H^+]$ ion concentration–independent reaction a B–CN cleavage occurs. The presence of the cyano substituent significantly increases the hydrolytic stability of the B–N bond, whereas the pyrrolyl-1-substitution remarkably decreases the stability of the B–CN bonding.

In previous papers we have described the kinetics and mechanism of the hydrolysis of phenyl(pyrrolyl-1)borates[1] and hydro(pyrrolyl-1)-borates.[2] In this paper we wish to report on the study of the hydrolysis of several cyano(pyrrolyl-1)borates ($[BH_n(NC_4H_4)_{3-n}CN]^-$ and $[B(C_6H_5)_n(NC_4H_4)_{3-n}CN]^-$, where $n = 0, 1, 2$).

The kinetics and mechanism of the hydrolysis of the borates is significantly changed and modified by the presence of the cyano group. For example, the rate-constant of the hydrolysis of $[BH_3CN]^-$ anion[3] is about 10^8-fold lower than that of the BH_4^- anion.[4] Concomitant to the hydrolysis in D_2O such a rapid B–H isotopic exchange reaction takes place in the case of $[BH_3CN]^-$ that the $[BD_3CN]^-$ salts[3] can be isolated with good yields, whereas H-exchange of low degree has been observed upon hydrolysis of BH_4^- anion.[5] In this paper the effect of the cyano substituent on the kinetics and mechanism of the hydrolysis of (pyrrolyl-1)borates is described.

EXPERIMENTAL

The preparation of the borates utilized, $Na[B(C_6H_5)_2(NC_4H_4)CN]$, $Na[B(C_6H_5)(NC_4H_4)_2CN]$, $Na[B(NC_4H_4)_3CN] \cdot 1.5 \ C_4H_8O_2$, $K[BH_2(NC_4H_4)CN] \cdot C_4H_8O_2$ and $Na[BH(NC_4H_4)_2CN] \cdot 3 \ C_4H_8O_2$ have been described previously.[6,7]

The buffers used have been prepared in the usual manner using analytical grade chemicals from Reanal and Merck. The ionic strengths of the buffers was adjusted to $0.1 \ \text{mole/dm}^3$ or $1.0 \ \text{mole/dm}^3$ with NaCl. The pH values of the buffers was determined with a Radiometer model PHM-4 pH-meter. In the case of $K[BH_2(NC_4H_4)CN]$ at $[H^+] > 0.01$ mole/dm^3 the pH value was calculated on the basis of the HCl concentration, while at $[H^+] < 0.01$ mole/dm^3 the pH was measured, and the pH of a solution containing $0.010 \ \text{mole/dm}^3$ of HCl was acknowledged 2.00.

Kinetic measurements

The rate of hydrolysis of the cyano(pyrrolyl-1)-borates was followed by spectrophotometric (a) and complexometric (b) methods. The measurements were carried out at 25°C (or at 17.5 and 35°C) using samples thermostated to ± 0.1°C.

---

*Author to whom correspondence should be addressed.

(a) The concentration of the cyano(pyrrolyl-1)-borates in the buffer solutions was $2 \times 10^{-4} - 4 \times 10^{-4}$ mole/dm^3. The light absorption of the samples was determined using a Beckman Acta M–IV spectrophotometer at 250 nm (Na[B(C$_6$H$_5$)$_2$(NC$_4$H$_4$)CN]), 240 nm (Na[B(C$_6$H$_5$)(NC$_4$H$_4$)$_2$CN], Na[BH(NC$_4$H$_4$)$_2$CN] and Na[B(NC$_4$H$_4$)$_3$CN]) and 247 nm (K[BH$_2$-(NC$_4$H$_4$)CN]). The solid borate samples were dissolved in the buffer with rapid stirring and the change of absorption was followed for a period of 1–2 half-life time. The absorption of the hydrolysis products was measured when eight times the half-life of the reaction had elapsed.

(b) In neutral and alkaline media the progress of the hydrolysis was followed by measuring the free CN$^-$ ion concentration of the solution. For these experiments 0.02 mole/dm^3 solutions of the borates in the buffers were used. The free CN$^-$ ion concentration was determined by means of 0.1 mole/dm^3 AgNO$_3$ solution. For the determination of the end-point the I$^-$ ion indicator method was applied.

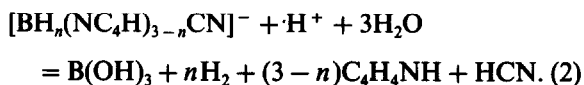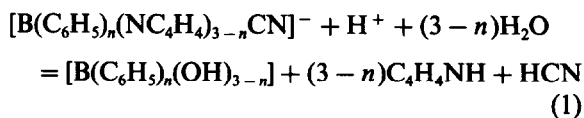*Examination of the influence of acetic acid on the rate of hydrolysis*

The rate of the hydrolysis of Na[B(NC$_4$H$_4$)$_3$CN] at 25°C was measured in pH = 4.07 buffers with 0.1 ionic strength at different acetic acid concentrations (0.015, 0.15 and 0.35 mole/dm^3). The following values were obtained for the pseudo-first-order rate constants: 3.26×10^{-4}; 3.08×10^{-4} and 2.97×10^{-4} s^{-1}.
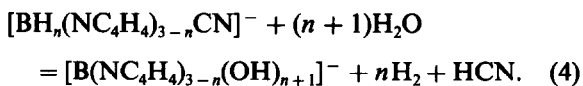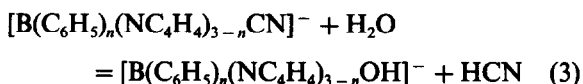
Determination of the activation parameters

The rate of hydrolysis was measured in pH = 5.36; 4.40; 3.90; 3.61 and 3.38 buffers and in the case of Na[B(NC$_4$H$_4$)$_3$CN] in pH = 3.90; 3.38; 2.43; 2.11 and 1.90 buffers at 17.5, 25.0 and 35.0°C. With the knowledge of the measured pseudo-first-order rate constants and the H$^+$ ion concentration, both the H$^+$ ion concentration-dependent and H$^+$ ion concentration-independent rate constants were determined. The actual [H$^+$] values were calculated from the measured pH values at 17.5, 25.0 and 35.0°C. The activation parameters were calculated in the usual manner from a plot of log k vs T^{-1} according to the Eyring equation using the determined values of the rate constants.

RESULTS AND DISCUSSION

The cyano(pyrrolyl-1)borates decompose slowly in aqueous acidic media, according to eqns (1) and (2) ($n = 0, 1, 2$):

$$[B(C_6H_5)_n(NC_4H_4)_{3-n}CN]^- + H^+ + (3-n)H_2O$$
$$= [B(C_6H_5)_n(OH)_{3-n}] + (3-n)C_4H_4NH + HCN \quad (1)$$

$$[BH_n(NC_4H_4)_{3-n}CN]^- + \cdot H^+ + 3H_2O$$
$$= B(OH)_3 + nH_2 + (3-n)C_4H_4NH + HCN. \quad (2)$$

In contrast with the hydrolysis of the other (pyrrolyl-1)-borates,[1,2] cyano(pyrrolyl-1)borates hydrolyse slowly also in strongly alkaline medium (0.1 mole/dm^3 NaOH) but pyrrole does not form upon the hydrolysis (Fig. 1). In neutral and alkaline medium this process takes place as shown by the following equations ($n = 0, 1, 2$):

$$[B(C_6H_5)_n(NC_4H_4)_{3-n}CN]^- + H_2O$$
$$= [B(C_6H_5)_n(NC_4H_4)_{3-n}OH]^- + HCN \quad (3)$$

$$[BH_n(NC_4H_4)_{3-n}CN]^- + (n+1)H_2O$$
$$= [B(NC_4H_4)_{3-n}(OH)_{n+1}]^- + nH_2 + HCN. \quad (4)$$

Since the spectrum of the borate significantly differs from that of the hydrolysis products in the range 220–270 nm, the rate of the hydrolysis of the cyano(pyrrolyl-1)borates can be readily followed by spectrophotometry. The measurement of the cyanide ion concentration is also a good method for determining the rate of hydrolysis in alkaline medium.
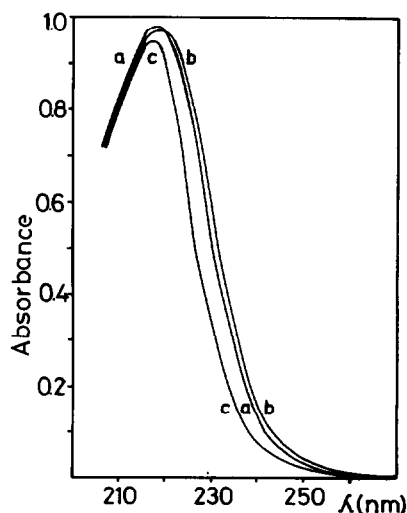
Fig. 1. The change of the spectrum of K[B(NC$_4$H$_4$)$_3$CN] ($c = 1.4 \cdot 10^{-4}$ mole/dm^3) upon hydrolysis in 0.1 mole/dm^3 NaOH solution: (a) before hydrolysis; (b) after hydrolysis; (c) after hydrolysis and adjustment of the pH first to acidic range (3–4) and then to the original value.

According to our studies the hydrolysis of cyano-(pyrrolyl-1)borates in aqueous buffers can be described as a kinetically pseudo-first-order reaction:

$$-\frac{d[B^-]}{dt} = k_1^{hydr}[B^-] \qquad (5)$$

where B^- denotes the cyano(pyrrolyl-1)borate and k_1^{hydr} is the pseudo-first-order rate constant. The measured k_1^{hydr} values of the cyano(pyrrolyl-1)-borates in aqueous buffers are summarized in Tables 1 and 3.

In acidic media the k_1^{hydr} values of the $[B(C_6H_5)_n(NC_4H_4)_{3-n}CN]^-$ anions ($n = 0, 1, 2$) and the $[BH(NC_4H_4)_2CN]^-$ anion varies linearly with the H^+ ion concentration (Table 1) and it can be expressed by the following equation:

$$k_1^{hydr} = k_H[H^+] + k_1 \qquad (6)$$

where k_H is the second-order rate constant of the acid-catalyzed process and k_1 is the first-order rate

constant of the H^+ ion concentration-independent reaction. The values of the k_H and k_1 rate constants, determined from the data given in Table 1, and also the ΔH^+ and ΔS^+ values, calculated from the k_H and k_1 constants are summarized in Table 2.

The rate-determining step in the H^+ ion-catalyzed hydrolysis of cyano(pyrrolyl-1)borates may be the cleavage of the B–CN or the B–N bond (in the case of borates containing B–H bond the cleavage of this bond may be also rate-determinant). We believe that in the reaction of the cyano(pyrrolyl-1)borate with H^+ ion the B–N bond is cleaved since the formation of pyrrole and the corresponding amine borane was observed in the reaction between cyano(pyrrolyl-1)borates and pyridine hydrochloride in non-aqueous solvents.[7,8]

On the contrary, the rate-determining step of the H^+ ion concentration-independent reaction can be only the cleavage of the B–CN bonding, as no formation of pyrrole can be observed in alkaline medium (Fig. 1), and also, the value of k_1^{hydr}, measured in alkaline medium, is equivalent with

Table 1. Pseudo-first-order hydrolysis rate constants (k_1^{hydr}) of cyano(pyrrolyl-1)borates in aqueous buffers at 25°C ($\mu = 0.1$) determined by spectrophotometric (pH < 8.8) and complexometric methods (pH > 8.8). (Ph = C_6H_5; Pyl = 1-NC_4H_4)

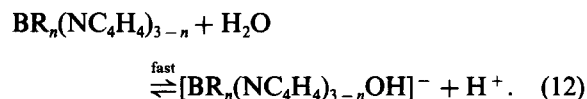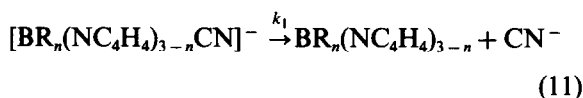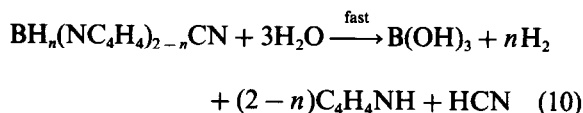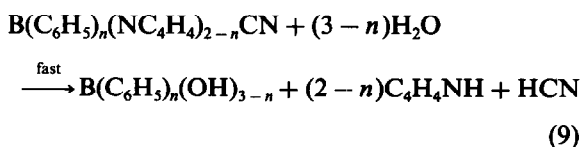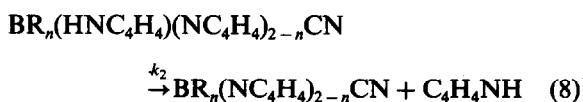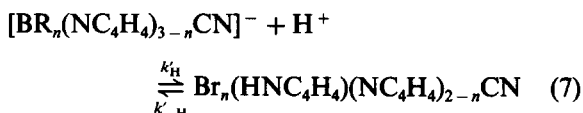| pH	k_1^{hydr} [s^{-1}]			
	$[BPh_2Py1CN]^-$	$[BPhPyl_2CN]^-$	$[BPyl_3CN]^-$	$[BHPyl_2CN]^-$
1.90	–	–	$1.8 \cdot 10^{-3}$	–
2.11	–	–	$1.2 \cdot 10^{-3}$	$4.6 \cdot 10^{-2}$
2.43	–	–	$7.5 \cdot 10^{-4}$	$2.2 \cdot 10^{-2}$
3.05	$5.9 \cdot 10^{-3}$	$4.8 \cdot 10^{-3}$	$4.2 \cdot 10^{-4}$	–
3.38	$2.9 \cdot 10^{-3}$	$2.6 \cdot 10^{-3}$	$3.6 \cdot 10^{-4}$	$2.7 \cdot 10^{-3}$
3.61	$1.8 \cdot 10^{-3}$	$1.7 \cdot 10^{-3}$	–	$1.6 \cdot 10^{-3}$
3.90	$9.8 \cdot 10^{-4}$	$1.3 \cdot 10^{-3}$	$3.1 \cdot 10^{-4}$	$9.1 \cdot 10^{-4}$
4.19	$6.0 \cdot 10^{-4}$	$9.1 \cdot 10^{-4}$	–	$5.2 \cdot 10^{-4}$
4.40	$4.3 \cdot 10^{-4}$	$7.9 \cdot 10^{-4}$	–	$3.8 \cdot 10^{-4}$
4.64	$3.0 \cdot 10^{-4}$	–	–	$2.9 \cdot 10^{-4}$
5.36	$2.2 \cdot 10^{-4}$	$6.4 \cdot 10^{-4}$	–	$1.8 \cdot 10^{-4}$
8.8	–	–	$3.3 \cdot 10^{-4}$	–
9.3	$1.6 \cdot 10^{-4}$	$6.1 \cdot 10^{-4}$	$3.3 \cdot 10^{-4}$	$1.2 \cdot 10^{-4}$
9.9	$1.7 \cdot 10^{-4}$	$5.9 \cdot 10^{-4}$	–	–
11.2	–	–	$3.2 \cdot 10^{-4}$	$1.1 \cdot 10^{-4}$
12.6 [a]	$1.8 \cdot 10^{-4}$	$6.0 \cdot 10^{-4}$	$3.2 \cdot 10^{-4}$	$1.2 \cdot 10^{-4}$

[a] NaOH–NaCl buffer

Table 2. Rate constants (k_H, k_1) and activation parameters of the hydrolysis of cyano(pyrrolyl-1)-borates at 25°C. ($\mu = 0.1$; Ph = C_6H_5; Pyl = 1-NC_4H_4)

Parameters (units)	Values			
	$[BPh_2PylCN]^-$	$[BPhPyl_2CN]^-$	$[BPyl_3CN]^-$	$[BHPyl_2CN]^-$
k_H (mole$^{-1} \cdot$dm$^3 \cdot$s^{-1})	6.4 ± 0.3	4.7 ± 0.2	0.117 ± 0.003	6.2 ± 0.4
$\Delta H^{\ddagger}$ (KJ$\cdot$mole^{-1})	80 ± 3	58 ± 3	65 ± 2	-
$\Delta S^{\ddagger}$ (J$\cdot$mole$^{-1} \cdot$K^{-1})	31 ± 6	-37 ± 6	44 ± 5	-
k_1 (s^{-1})	$(1.7 \pm 0.1) \cdot 10^{-4}$	$(6.1 \pm 0.2) \cdot 10^{-4}$	$(3.2 \pm 0.1) \cdot 10^{-4}$	$(1.2 \pm 0.1) \cdot 10^{-4}$
$\Delta H^{\ddagger}$ (KJ$\cdot$mole^{-1})	91 ± 3	89 ± 3	87 ± 2	-
$\Delta S^{\ddagger}$ (J$\cdot$mole$^{-1} \cdot$K^{-1})	-14 ± 6	-8 ± 6	-21 ± 5	-

that of k_1 determined for the process in acidic medium (Table 1), where the formation of pyrrole can be detected.

Studies with cyano(amino)borates ($[BH_2(NR_2)CN]^-$ anions), having analogous structure with that of the cyano(pyrrolyl-1)-borates, have shown that the rate-determining step of the hydrolysis is also the cleavage of the B–CN bond.[9]

According to the above experimental data, the hydrolysis of cyano(pyrrolyl-1)borates of type $[BR_n(NC_4H_4)_{3-n}CN]^-$ (where R = C_6H_5, $n = 1, 2$; R = H, $n = 0, 1$) can be described by the following equations:

$$[BR_n(NC_4H_4)_{3-n}CN]^- + H^+$$

$$\underset{k'_{-H}}{\overset{k_H}{\rightleftharpoons}} Br_n(HNC_4H_4)(NC_4H_4)_{2-n}CN \quad (7)$$

$$BR_n(HNC_4H_4)(NC_4H_4)_{2-n}CN$$

$$\overset{k_2}{\rightarrow} BR_n(NC_4H_4)_{2-n}CN + C_4H_4NH \quad (8)$$

$$B(C_6H_5)_n(NC_4H_4)_{2-n}CN + (3-n)H_2O$$

$$\overset{fast}{\longrightarrow} B(C_6H_5)_n(OH)_{3-n} + (2-n)C_4H_4NH + HCN$$
$$(9)$$

$$BH_n(NC_4H_4)_{2-n}CN + 3H_2O \overset{fast}{\longrightarrow} B(OH)_3 + nH_2$$

$$+ (2-n)C_4H_4NH + HCN \quad (10)$$

$$[BR_n(NC_4H_4)_{3-n}CN]^- \overset{k_1}{\rightarrow} BR_n(NC_4H_4)_{3-n} + CN^-$$
$$(11)$$

$$BR_n(NC_4H_4)_{3-n} + H_2O$$

$$\overset{fast}{\rightleftharpoons} [BR_n(NC_4H_4)_{3-n}OH]^- + H^+. \quad (12)$$

Since the borate is only weakly basic (i.e. $k'_{-H} \gg k'_H$), the Bodenstein principle can be applied for the reaction, namely, the concentration of $BR_n(HNC_4H_4)(NC_4H_4)_{2-n}CN$ remains small and quasi-constant all the time during the reaction.

At the same time—similarly to the reactions of phenyl(pyrrolyl-1)borates[1]—the reaction between the borate and the H$^+$ ion is a specific acid-catalyzed process (the rate of the hydrolysis is independent of the acid concentration), thus one can also assume that $k'_{-H} \gg k_2$.

As the hydrolysis takes place according to eqns (8) and (11) thus, the following expression can be given for the k_1^{hydr} value (eqn 5) on the basis of the

above considerations:

$$k_1^{hydr} = k_2 \frac{k'_H}{k'_{-H}} [H^+] + k_1. \qquad (13)$$

Equation (6), obtained from the experimental data, is practically identical with eqn (13), namely, the k_H value in eqn (6) is identical with the $k_2(k'_H/k'_{-H})$ value in eqn (13).

The hydrolysis involving the loss of CN^- ion (eqn 11) may be of S_N1 or S_N2-type process. However, the determined great ΔH^+ values and the small ΔS^+ values (Table 2) make the S_N1 mechanism more probable. This mechanism is also supported by the change of the k_1 values measured for $[B(NC_4H_4)_3CN]^-$ in dioxane–water mixtures (Fig. 2), since plotted $\log k_1$ vs $\log [H_2O]$ the slope is 5.7, whereas a value of about 2 would be eexpected if the process were of S_N2-type mechanism.[10]

Our studies have shown that the hydrolysis of $[BH_2(NC_4H_4)CN]^-$ under alkaline and weakly acidic conditions takes place similarly to that of the other cyano(pyrrolyl-1)-borates (Table 3).

Contrary to the results with the other cyano(pyrrolyl-1)-borates (Table 1) the k_1^{hydr} rate constant for $[BH_2(NC_4H_4)CN]^-$ approaches a constant value in more strongly acidic media (Table 3). Also, parallel with the relative decrease of the rate of the hydrolysis such a spectral change of the solution is observable which indicates the formation of a stable amine borane $(C_4H_5N \cdot BH_2CN)$ containing a pyrrolyl group protonated at the
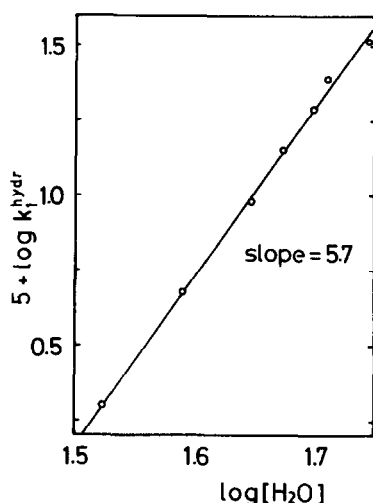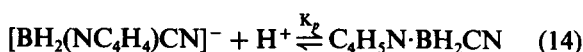

Fig. 2. The change of the rate constant (k_1) of the hydrolysis of $K[B(NC_4H_4)_3CN]$ in water–dioxane mixtures of 0.1 mole/dm³ NaOH concentration at 25°C as a function of the water-concentration.
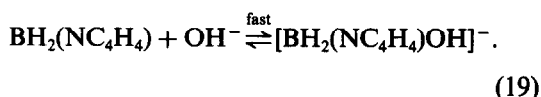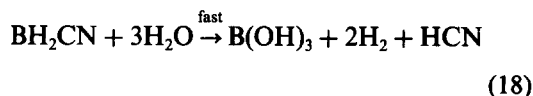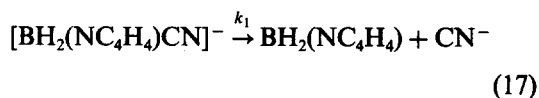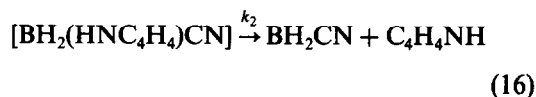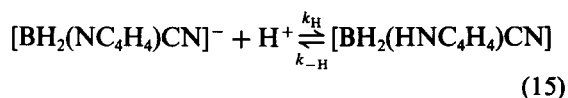
Table 3. Pseudo-first-order hydrolysis rate constants (k_1^{hydr}) of $KBH_2(NC_4H_4)CN$ in aqueous HCl. (a) H_3PO_4–KH_2PO_4, (b) KH_2PO_4–Na_2HPO_4, (c) buffers at 25°C (ionic strength 1.0) determined by spectrophotometric method

pH	Buffers	k_1^{hydr} [s⁻¹]
0.023	a	$5.5 \cdot 10^{-5}$
0.325	a	$5.6 \cdot 10^{-5}$
0.682	a	$5.6 \cdot 10^{-5}$
0.996	a	$5.2 \cdot 10^{-5}$
1.292	a	$4.9 \cdot 10^{-5}$
1.553	b	$4.1 \cdot 10^{-5}$
1.602	a	$3.9 \cdot 10^{-5}$
1.824	a	$3.2 \cdot 10^{-5}$
1.854	b	$3.4 \cdot 10^{-5}$
1.921	a	$3.1 \cdot 10^{-5}$
2.097	a	$2.6 \cdot 10^{-5}$
2.149	b	$2.2 \cdot 10^{-5}$
2.456	b	$1.4 \cdot 10^{-5}$
2.745	b	$8.9 \cdot 10^{-6}$
5.9	c	$1.5 \cdot 10^{-6}$
6.9	c	$1.6 \cdot 10^{-6}$
7.9	c	$1.5 \cdot 10^{-6}$

α-position, arising from the reaction between $[BH_2(NC_4H_4)CN)]^-$ and the H^+ ion.[7] The formation of similar compounds, containing a-protonated pyrrolyl group, can be observed in more concentrated sulphuric acid solutions of $L \cdot BH(NC_4H_4)CN$-type amine boranes[8] $(L = amine)$ and of the $[BH(NC_4H_4)(CN)_2]^-$ anion.[11]

In the reaction of the $[BH_2(NC_4H_4)CN]^-$ anion with the H^+ ion first either the B–H or the B–N bond is cleaved. According to our results the cleavage of the B–N bond was more probable since neither hydrogen gas evolution was observed upon the reaction of the borate with acid in non-aqueous medium, nor could B–H exchange be detected upon hydrolysis in D_2O.[7] If the hydrolysis proceeds via the cleavage of the B–N bond, protonation at the N atom of the pyrrolyl group gives rise to hydrolysis. At the same time, protonation at the carbon atom results in a stable borane complex with composition $C_4H_5N \cdot BH_2CN$, since according to earlier results[12] the rate of the H-exchange at the N atom of the pyrrole derivatives is about 1000-fold greater than at either carbon atom. On the basis of these considerations the hydrolysis of the $[BH_2(NC_4H_4)CN]^-$ anion can be described by the following equations:

$$[BH_2(NC_4H_4)CN]^- + H^+ \overset{K_2}{\rightleftharpoons} C_4H_5N \cdot BH_2CN \qquad (14)$$

$$[BH_2(NC_4H_4)CN]^- + H^+ \underset{k_{-H}}{\overset{k_H}{\rightleftharpoons}} [BH_2(HNC_4H_4)CN]$$

$$\text{(15)}$$

$$[BH_2(HNC_4H_4)CN] \overset{k_2}{\rightarrow} BH_2CN + C_4H_4NH$$

$$\text{(16)}$$

$$[BH_2(NC_4H_4)CN]^- \overset{k_1}{\rightarrow} BH_2(NC_4H_4) + CN^-$$

$$\text{(17)}$$

$$BH_2CN + 3H_2O \overset{fast}{\rightarrow} B(OH)_3 + 2H_2 + HCN$$

$$\text{(18)}$$

$$BH_2(NC_4H_4) + OH^- \overset{fast}{\rightleftharpoons} [BH_2(NC_4H_4)OH]^-.$$

$$\text{(19)}$$

According to eqns (14)–(19), to the preceding results obtained from the hydrolysis studies with the other cyano-(pyrrolyl-1)borates, and also, taking into consideration the following relationship between the total concentration of the non-hydrolysed borate (C_B), the concentration of the borate (B^-) and the concentration of the pro-tonated product (HB):

$$C_B = [B^-] + [HB] = [B^-](1 + K_p[H^+]) \quad (20)$$

the k_1^{hydr} value can be given by eqn (21):

$$k_1^{hydr} = \frac{k_2 k_H/k_{-H}[H^+] + k_1}{1 + K_p[H^+]}. \quad (21)$$

After calculation of the k_1 values, the parameters of eqn (21) were determined by the method described earlier[2] using the data of Table 3. The resulting values are summarized in Table 4. The K_p value (80) obtained from the kinetic measurements is in good agreement with that ($K_p = 69$) determined by the spectrophotometric method.[7]

Comparing the k_H values of the phenyl(pyrrolyl-1)-borates[11] and the hydro(pyrrolyl-1)borates[2] with that of the corresponding cyano derivatives (Tables 3 and 4) it can be established that a H–CN or C_6H_5–CN substituent exchange in the molecule results in a 4–5 orders of magnitude decrease in the value of k_H, but in the case of $[BH_2(NC_4H_4)CN]^-$ a 7 orders of magnitude decrease was observed. Thus the hydrolytic stability of the $[BH_2(NC_4H_4)CN]^-$ anion is much larger than has been expected on the basis of the substituent effect. However, this extra-stability is in good accordance

Table 4. Rate constants (k_H, k_1) and protonation constant (K_p) of the hydrolysis of $KBH_2(NC_4H_4)CN$ at 25°C (ionic strength 1.0)

Rate constants (units)	Values
$k_2 \dfrac{k_H}{k_{-H}}$ (mole^{-1}·dm^3·s^{-1})	$(4.8 \pm 0.3) \cdot 10^{-3}$
k_1 (s^{-1})	$(1.6 \pm 0.1) \cdot 10^{-6}$
K_p (mole^{-1}·dm^3)	80 ± 6

with the results of the H-exchange studies in D_2O: in the case of the $[BH_2(NC_4H_4)CN]^-$ anion the pyrrolyl group can be entirely deuterated[7] whereas only partial deuteration can be observed with the other anions.[2,11] We believe that in the case of the hydrolysis of the cyano(pyrrolyl-1)borates a close connection exists between the alteration of the rate of the hydrolysis from the linear substituent-effect, and the degree of deuteration of the pyrrolyl group of the borate. Similar explanation can be given also for finding that the hydrolytic ability of the $[B(C_6H_5)_2(NC_4H_4)CN]^-$ anion is somewhat larger than that expected according to the linear substituent effect (Table 2).

Contrary to the other (pyrrolyl-1)borates[1,2] the hydrolysis of the cyano(pyrrolyl-1)borates involves a novel reaction—the hydrolytic loss of cyanide anion—which does not take place upon the hydrolysis of the BH_3CN^- ion, but does proceed in the case of amine boranes[9] ($[BH_2(NR_2)CN]^-$ anions). The data summarized in Tables 2 and 4 clearly show that the rate of the S_N1-type hydrolysis (k_1) of the cyano(pyrrolyl-1)-borates increases with the increasing number of the pyrrolyl groups of the molecule. A similar change is characteristic also for the Lewis-acid character of the (pyrrolyl-1)-boranes,[13] namely, the value of the k_1 constants (Tables 2 and 4) is primarily determined by the Lewis-acid character of the borane attached to the CN group.

REFERENCES

1. J. Emri, B. Györi and P. Szarvas, Z. Anorg. Allg. Chem. 1973, 400, 321.

2. J. Emri and B. Györi, *Polyhedron* 1982, **1**, 673.
3. M. M. Kreevoy and J. E. C. Hutchins, *J. Am. Chem. Soc.* 1969, **91**, 4329.
4. R. E. Davis, E. B. Bromels and C. L. Kibby, *J. Am. Chem. Soc.* 1962, **84**, 885.
5. M. M. Kreevoy and J. E. C. Hutchins, *J. Am. Chem. Soc.* 1972, **94**, 6371.
6. P. Szarvas, B. Györi, J. Emri and Gy. Kovács, *Magy. Kém. Foly.* 1971, **77**, 495.
7. B. Györi, J. Emri and L. Szilágyi, *J. Organometal Chem.* 1978, **152**, 13.
8. B. Györi and J. Emri, *J. Organometal Chem.* 1982, **238**, 159.
9. C. Weidig, S. S. Uppal and H. C. Kelly, *Inorg. Chem.* 1974, **13**, 1763.
10. E. Tommila, *Acta Chem. Scand.* 1955, **9**, 975.
11. J. Emri and B. Györi, to be published.
12. D. M. Muir and M. C. Whiting, *J. Chem. Soc. Perkin II* 1975, 316; 1976, 388. G. P. Bean and T. J. Wilkinson, *J. Chem. Soc. Perkin II* 1978, 72.
13. P. Szarvas, B. Györi and J. Emri, *Acta Chim. Acad. Sci. Hung.* 1971, **70**, 1.

PHOTOCHEMICAL PRODUCTION OF CHROMATE(VI) IONS FROM SOME CHROMIUM(III) COMPLEXES[1]

ADAM MARCHAJ and ZOFIA STASICKA*

Institute of Chemistry, Jagiellonian University, 30–060 Kraków, Poland

and (in part)

DETLEF REHOREK

Sektion Chemie, Karl-Marx-Universität, 7010 Leipzig, D.D.R.

Abstract—Complexes of the type $[Cr(CN)_{6-x}(OH)_x]^{3-}$ were found to produce the chromate(VI) ions upon exposure to UV radiation in alkaline medium. The quantum yields are reported and possible mechanism is discussed.

Chromium(III) complexes are generally known to undergo substitution and substitution-related photoreactions. Photoredox reactions of these compounds are apparently rare. Only in few cases such processes were reported and then reduction to chromium(II) species was concluded.[2-9]

The cyanide complex, $[Cr(CN)_6]^{3-}$, has received perhaps more detailed study than that of any other ligand and photosubstitution of the CN^- ligand was inferred as the only mode by all authors[5,10-17] except Fleischauer[4] who suggested also a redox behaviour from his flash experiments. Our previous study[18] has revealed that under special conditions photosubstitution has been accompanied by a redox process in the case of hexacyanochromate(III) and hydroxocyanochromates(III).

We now report details of the redox photodecomposition of chromium(III) complexes with CN^- and OH^- ligands.

RESULTS AND DISCUSSION

Spectral changes recorded upon exposure of aerated alkaline solutions of cyanochromates(III) were found to depend strongly on the energy of radiation. This is illustrated in Fig. 1(a) and 1(b) for $[Cr(CN)_6]^{3-}$ and $[Cr(CN)_5OH]^{3-}$, respectively. Other hydroxocyanochromates(III) could not be

studied photochemically due to their high thermal instability. However, similar photochemical behaviour was also detected in the case of the $[Cr(CN)_3(OH)_3]^{3-}$, the most stable member of this group. In all these systems exposure to radiation within LF bands (see Table 1) resulted only in absorption changes characteristic of substitution products (see Ref. 18), whereas irradiation within LMCT bands (Table 1) generated also another species absorbing at $26.8 \times 10^3 \, cm^{-1}$ and $36.6 \times 10^3 \, cm^{-1}$.

This new photochemical mode was observed not only in the case of cyanochromates(III) but also in highly alkaline solutions of other chromium(III) salts. These were characterized by two LF bands at $16.8 \times 10^3 \, cm^{-1}$ ($\epsilon = 29 \, dm^3 \, mole^{-1} \, cm^{-1}$) and $23.3 \times 10^3 \, cm^{-1}$ ($\epsilon = 30 \, dm^3 \, mole^{-1} \, cm^{-1}$) and a continuous increasing absorption towards higher wave numbers (Fig. 1c). Species prevailing in such a solution were as yet not fully defined, among others it was formulated earlier as $[CrO_2(H_2O)_n]^-$.[29] For the sake of convenience, the complexes studied here are formulated as $[Cr(CN)_{6-x}(OH)_x]^{3-}$, where $x = 0, 1, 3$ or 6.

Spectral characteristic of the product generated upon exposure to radiation from CT bands in all systems studied fitted that of the CrO_4^{2-} ions (see Fig. 1d). This conclusion was confirmed also by chemical analysis. The rate of the chromate(VI) production was found to depend on concentration of the OH^- ions and molecular oxygen in solution. However, considerable amounts of CrO_4^{2-} were

---

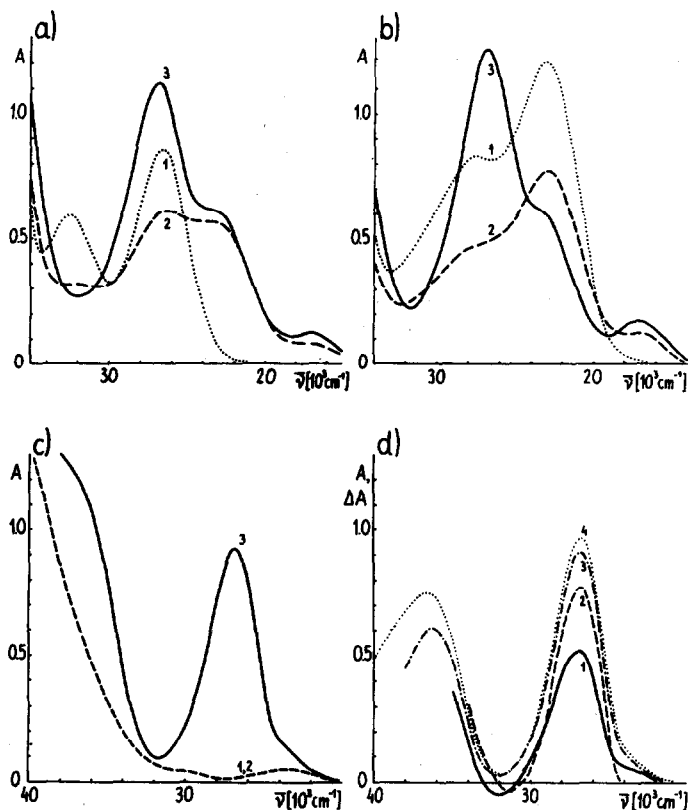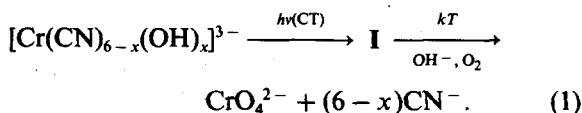*Author to whom correspondence should be addressed.

Fig. 1. Absorption changes observed in continuous photolysis of oxygenated alkaline (1 M KOH) solutions of: (a) $[Cr(CN)_6]^{3-}$ (10^{-2} M, $t_{irr} = 2$ min); (b) $[Cr(CN)_5OH]^{3-}$ (10^{-2} M, $t_{irr} = 5$ min); and (c) $[CrO_2(H_2O)_n]^-$ (10^{-3} M, $t_{irr} = 20$ min). Curves 1, in Figs. 1(a–c), refer to unirradiated solutions, curves 2—to solutions irradiated within LF bands ($\bar{\nu} \leqslant 32 \times 10^3$ cm^{-1}); and curves 3—to solutions irradiated within both, LF and CT, ranges (up to $\bar{\nu} \approx 37 \times 10^3$ cm^{-1}). In Fig. 1(d) the difference spectra, $(A_3 - A_2)$ from Fig. 1(a) (curve 1), Fig. 1(b) (curve 2) and Fig. 1(c) (curve 3) are compared with the spectrum of 10^{-4} M CrO_4^{2-} in 1 M KOH (curve 4).

observed also in aqueous unbuffered aerated solutions of $[Cr(CN)_6]^{3-}$ due to increase in pH in consequence of photoaquation. Some traces of Cr(VI) were also detected in de-aerated* alkaline solutions of $[Cr(CN)_{6-x}(OH)_x]^{3-}$.

Quantum yields of the CrO_4^{2-} production (Table 2) were found to depend strongly on the number of the CN^- ligands in the complex. The redox process at 265 nm was observed in the case of cyanochromates(III) to be accompanied by substitution. Its quantum yield could not be, determined however, with sufficient precision due to significant overlap of the product spectra with dominating absorption from the CrO_4^{2-} ions (see curves 3 in Figs. 1a, b). For hexacyanochromate(III) the substitution quantum yield under conditions quoted in Table 2 was roughly estimated as 0.06 ± 0.03.

Flash photolysis (time resolution 20 μs, detection within $14 < \bar{\nu} < 35 \times 10^3$ cm^{-1}) did not reveal any transient product preceding substitution in de-aerated as well as in aerated alkaline solutions of cyanochromates (see Fig. 2a). Since the experiments were carried out under conditions appropriate to detect transient absorption characteristic of hydrated electron (e.g. Ref. 31), its generation in the system seems to be improbable.

Chromate(VI) absorption was recorded not earlier than within seconds upon flashing of aerated samples (Figs. 2a and b) indicating that the CrO_4^{2-} ions are generated in secondary thermal processes at the expense of intermediates(I) absorbing weakly in the visible region, according to overall reaction

$$[Cr(CN)_{6-x}(OH)_x]^{3-} \xrightarrow{h\nu(CT)} \mathbf{I} \xrightarrow[OH^-, O_2]{kT}$$

$$CrO_4^{2-} + (6-x)CN^-. \tag{1}$$

The intermediate species, **I**, could be observed only upon flashing of the $[Cr(CN)_6]^{3-}$ complex in the

---

*The presence of traces of oxygen in the system cannot be excluded.

Table 1. Electronic spectra of cyanochromates(III) in alkaline solution

Complex	$\bar{\nu}$ max $[10^3$ cm$^{-1}]$	ε [dm^3 mole^{-1} cm^{-1}]	Assignment [d]
[Cr(CN)$_6$]$^{3-}$ pH 5.8 – 14	26.5 [a,b] 32.6 [a,b]	86 60	$^4A_{2g} \longrightarrow {}^4T_{2g}$ $^4A_{2g} \longrightarrow {}^4T_{1g}$ } d – d $t_{2g} \longrightarrow e_g$
	38.1 [a]	5400	$\begin{cases} ^4A_{2g} \longrightarrow {}^4A_{1u} \\ ^4A_{2g} \longrightarrow {}^4E_{1u} \\ ^4A_{2g} \longrightarrow {}^4T_{1u} \\ ^4A_{2g} \longrightarrow {}^4T_{2u} \end{cases}$ CTL$\rightarrow$M $t_{1u} \longrightarrow t_{2g}$
	43.5 45.8 48.4	1700 3100 3900	$\begin{cases} ^4A_{2g} \longrightarrow {}^4A_{1g} \\ ^4A_{2g} \longrightarrow {}^4E_{1g} \\ ^4A_{2g} \longrightarrow {}^4T_{1g} \\ ^4A_{2g} \longrightarrow {}^4T_{2g} \end{cases}$ CTL$\rightarrow$M $t_{1g} \longrightarrow t_{2g}$
[Cr(CN)$_5$OH]$^{3-}$ pH 14	23.0 [c] 27.5 [c] 41.2	120 78 4100	

[a] see also Refs. 19, 20;   [b] see also Refs. 11, 21 – 24;   [c] see also Ref. 25;

[d] based on SINDO/FEMP calculations [26,27]; the assignment of d – d bands is consistent with other reports [11,19, 21-23], whereas CTL$\rightarrow$M character of the more energetic transitions was suggested earlier by Schläfer et al [28], although Alexander and Gray [19], basing on SCCC MO method, assigned the band at 38.1x10^3 cm^{-1} to t_{2g} [M] $\longrightarrow t_{1u}$ π^* [L].

Table 2. Quantum yields of chromate(VI) production at 265 nm (1 M KOH, saturated with oxygen, T = 295 ± 0.5 K)

Complex	Concentration, [M]	Quantum yield, [mole Einstein^{-1}]
[Cr(CN)$_6$]$^{3-}$	2 x 10^{-3}	0.057 ± 0.002
[Cr(CN)$_5$OH]$^{3-}$	2 x 10^{-3}	0.025 ± 0.002
[CrO$_2$(H$_2$O)$_n$]$^-$	1 x 10^{-2}	0.007 ± 0.002

presence of an excess of the CN^- ions. Then, a short-lived absorption with a maximum at $\sim 30.5 \times 10^3$ cm^{-1} was recorded (Fig. 2c) that fitted into that characteristic of the [Cr(CN)$_6$]$^{4-}$ complex in solution.[25,30] Rapid decay of the [Cr(CN)$_6$]$^{4-}$ absorption when the [OH$^-$]/[CN$^-$] ratio in solution is higher than 5[25] would be responsible for the lack of any transient absorption in our experiments carried out in absence of the excess CN^-.

These results have led us to believe that CT photochemistry of the [Cr(CN)$_{6-x}$(OH)$_x$]$^{3-}$ complexes proceeds through photoreduction pathway.

This conclusion is consistent with the LMCT character of the transitions (see Table 1) and is

supported by the quantum yield values (Table 2) corresponding with the reported earlier[25] tendency of the chromium(III) complexes to be reduced to the Cr(II) ones in alkaline medium.

Subsequent fate of chromium(II) species generated photochemically would depend on the presence of oxygen in the system. In aerated solution, chromium(III) complexes should be rapidly regenerated. However, chromium(II) compounds are known[32] to be oxidized by molecular oxygen not only to chromium(III) but also to chromium(VI) with presumable generation of O_2^- and/or O_2^{2-} ions. The latter are used to oxidize Cr(III) compounds in alkaline medium to the CrO_4^{2-} ions for analytical purposes. Hydrogen peroxide was
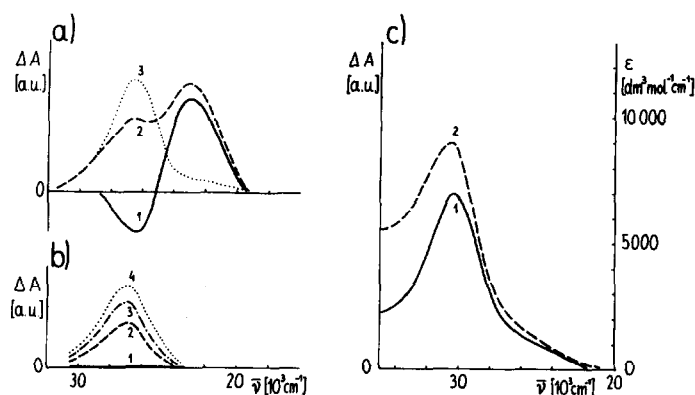
Fig. 2. Absorption changes recorded upon flashing of: (a) $[Cr(CN)_6]^{3-}$ (2×10^{-4} M) in oxygenated 0.01 M NaOH: curves 1 and 2—difference spectra $(A_t - A_o)$, recorded at delay times, t, between 20 μs and 0.2 s (curve 1) and at 200 s (curve 2), curve 3—difference spectrum $(A_{200s} - A_{20\mu s})$; (b) $[CrO_2(H_2O)_n]^-$ (2×10^{-3} M) in oxygenated 1 M NaOH: curves 1–4—difference spectra $(A_t - A_o)$ for t between 20 μs and 1 s (no changes), 22, 120 and 600 s, respectively; (c) $[Cr(CN)_6]^{3-}$ (2×10^{-4} M) in de-aerated 0.02 M NaOH and 0.05 M KCN curve 1 (left scale)—difference spectrum $(A_{10\mu s} - A_{300\mu s})$, curve 2 (right scale)—spectrum of the $[Cr(CN)_6]^{4-}$ complex according to Ref. 25.

reported[30] also to produce chromate(VI) from alkaline cyanochromates(II). We have found that the $[Cr(CN)_{6-x}(OH)_x]^{3-}$ complexes are transformed to the CrO_4^{2-} ions by an excess of H_2O_2 at room temperature (with the exception of $[Cr(CN)_6]^{3-}$ that needs to be heated).

Thus, reductive properties of generated photochemically chromium(II) species would be responsible for chromium(VI) production in secondary thermal processes.

On the other hand, chromium(II) complexes were reported[25] to catalyze substitution of hexacyanochromate(III) in aqueous alkaline cyanide media. Thus, the substitution proceeding upon exposure of the $[Cr(CN)_6]^{3-}$ complex to CT radiation would be a consequence of the catalytic properties of chromium(II) species generated photochemically, although population of the $^4T_{2g}$ level could not be excluded as well.

The photoreduction pathway should be accompanied by generation of ligand or/and sol-

vent radical. In aqueous solution of the $[Cr(CN)_{6-x}(OH)_x]^{3-}$ complexes, where $x \neq 6$, these could be the $\cdot CN$ and $\cdot OH$ radicals, whereas for $x = 6$, the only one possible would be $\cdot OH$.

Unfortunately, due to the high concentration of OH^- ions and relatively high radiation energy necessary for the redox process to proceed, our scavenging experiments did not lead to unequivocal detection of any radical in aqueous solution.

On the other hand, use of ESR spin trapping technique in methanolic solution of $K_3[Cr(CN)_6]$/crown ether has revealed that photochemical decay of the $[Cr(CN)_6]^{3-}$ signal ($g = 1.992$, 43.3 G linewidth) was accompanied by generation of spin adducts of the $\cdot OCH_3$ and $\cdot CH_2OH$ radicals (Table 3). This would be consistent with the intermolecular pathway

$$[Cr(CN)_6]^{3-} \xrightarrow{\frac{h\nu(CT)}{CH_3OH}} [Cr(CN)_6]^{4-} + \cdot OCH_3 + H^+ \quad (2)$$

Table 3. Hyperfine splitting constants of spin adducts (in mT) generated in photolyzed solutions of $K_3[Cr(CN)_6]$/18-crown-6

Radical	Spin trap	Solvent	a_N	a_H	
$\cdot OCH_3$	DMPO	CH_3OH / NaOH	1.36 ± 0.02	0.76 ± 0.02	/1H/
$\cdot CH_2OH$	DMPO	CH_3OH / NaOH	1.60 ± 0.02	2.27 ± 0.02	/1H/
$\cdot CH_2OH$	ND	CH_3OH / CH_2Cl_2 (5 : 1 v/v)	1.37 ± 0.02	0.79 ± 0.02	/2H/

Abbreviations : DMPO = 5,5-dimethylpyrroline-1-oxide;   ND = nitrosodurene.

followed by

$$\cdot OCH_3 + CH_3OH \longrightarrow \cdot CH_2OH + CH_3OH \quad (3)$$
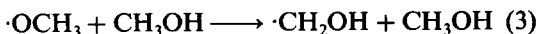
although the $\cdot OCH_3$ radical production in a secondary thermal process cannot be excluded, as well. Besides the $\cdot OCH_3$ and $\cdot CH_2OH$ radicals, other signals were also detected which could be assigned to radicals generated from spin trap and crown ether in reaction with reducing or oxidizing species.

The results obtained in methanolic medium as well as those from aqueous solutions induced us to postulate that CT photochemistry of the $[Cr(CN)_{6-x}(OH)_x]^{3-}$ complexes proceeds through intermolecular reduction

$$[Cr(CN)_{6-x}(OH)_x]^{3-} \xrightarrow[\text{SH}]{hv(CT)}$$

$$[Cr(CN)_{6-x}(OH)_x]^{4-} + \cdot S + H^+ \quad (4)$$
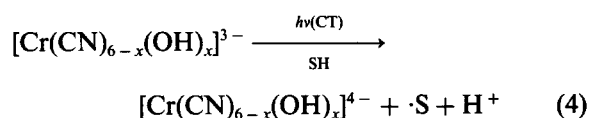
where $SH = H_2O$ or CH_3OH. Secondary thermal reactions of the chromium(II) complexes would be responsible for the chromate(VI) production in aerated alkaline solutions and (at least in part) for aquation accompanying the redox process.

EXPERIMENTAL

Materials. Cyano- and hydroxo-cyano-chromates(III) were prepared according to the methods described earlier.[18] The $[CrO_2(H_2O)_n]^-$ complex was obtained in solution from chromium potassium alum, $KCr(SO_4)_2 \cdot 12H_2O$, using an excess of KOH or NaOH. The solution was irradiated not before stopping its spectral changes. Alkalis were purified from carbonates, other chemicals were best available commercial reagents without further purification. For flash experiments water was purified adequately to observe the absorption of hydrated electron.

Apparatus and procedure. Techniques used for flash and continuous irradiations were described elsewhere.[18,33]

ESR spectra were recorded at room temperature using a JEOL JES-3BQ spectrometer. Irradiations were performed directly within the ESR cavity by a 200-W high pressure mercury lamp (HBO 200, Narva, Berlin). The light $\bar{v} < 28 \times 10^3 cm^{-1}$ was cut off by means of 1 cm of saturated $NiSO_4$ solution and 2 mm of the Schott glass UG 5.

REFERENCES

1. Taken in part from a thesis submitted by A. Marchaj to the Chemistry Department of the Jagiellonian University in partial fulfillment of the requirements for the Ph.D. degree in Chemistry, 1982. Presented in part at the 3rd *Symp. Photochemical and Thermal Reactions of Coordination Compounds*, Mogilany–Kraków, Poland, May 1980 and at the 22nd *Int. Conf. Coordination Chemistry*, Budapest, Hungary, August 1982.
2. V. Balzani and V. Carassiti, *Photochemistry of Coordination Compounds*, p. 91. Academic Press, London (1970).
3. R. L. Lintvedt, In *Concepts of Inorganic Photochemistry* (Edited by A. W. Adamson and P. D. Fleischauer), p. 309. Wiley–Interscience, New York (1975).
4. P. D. Fleischauer, Ph.D. Dissertation, University of Southern California 1968, as cited in A. W. Adamson, W. L. Waltz, E. Zinato, D. W. Watts, P. D. Fleischauer and R. D. Lindholm, *Chem. Rev.* 1968, **68**, 541.
5. D. C. McCain, *Inorg. Nucl. Chem. Letters* 1969, **5**, 873.
6. P. D. Fleischauer, A. W. Adamson and G. Sartori, *Progr. Inorg. Chem.* 1972, **17**, 1.
7. G. B. Porter and J. Van Houten, *Inorg. Chem.* 1979, **18**, 2053.
8. G. J. Ferraudi and J. F. Endicott, *Inorg. Chim. Acta* 1979, **37**, 219.
9. G. J. Ferraudi, D. B. Yang and C. Kutal, *J. Chem. Soc., Chem. Commun.* 1979, 1050.
10. L. Moggi, F. Bolletta, V. Balzani and F. Scandola, *J. Inorg. Nucl. Chem.* 1966, **28**, 2589.
11. A. W. Adamson, *J. Phys. Chem.* 1967, **71**, 798.
12. A. Chiang and A. W. Adamson, *J. Phys. Chem.* 1968, **72**, 3827.
13. H. F. Wasgestian, *Z. Phys. Chem. (Frankfurt am Main)* 1969, **67**, 39.
14. H. F. Wasgestian, *J. Phys. Chem.* 1972, **76**, 1947.
15. N. Sabbatini and V. Balzani, *J. Am. Chem. Soc.* 1972, **94**, 7587.
16. N. Sabbatini, M. A. Scandola and V. Carassiti, *J. Phys. Chem.* 1973, **77**, 1307.
17. V. Carassiti, N. Sabbatini, M. A. Scandola and A. Maldotti, *Atti Acad. Sci. Ist. Bologna, Cl. Sci. Fis. Rend.* 1976, **13**, 103.
18. A. Marchaj and Z. Stasicka, *Polyhedron*, 1983, **2**, 485.
19. J. J. Alexander and H. B. Gray, *J. Am. Chem. Soc.* 1968, **90**, 4260.
20. E. Blasius and H. Augustin, *Z. Anorg. Allg. Chem.* 1975, **417**, 55.
21. H. Kuroya and R. Tsuchida, *J. Chem. Soc. Japan* 1940, **61**, 597.
22. R. Krishnamurthy and W. B. Schaap, *Inorg. Chem.* 1963, **2**, 605.
23. R. Krishnamurthy, W. B. Schaap and J. R. Perumareddi, *Inorg. Chem.* 1967, **6**, 1338.
24. H. L. Schläfer, H. Gausmann and C. H. Möbius, *Inorg. Chem.* 1969, **8**, 1137.

25. L. Jeftić and S. Feldberg, *J. Phys. Chem.* 1971, **75**, 2381.

26. E. Wasielewska, To be published.

27. A. Gołębiewski, M. Witko, *Acta Phys. Pol.* 1980, **A57**, 585.

28. H. L. Schläfer, H. Wagener, H. F. Wasgestian, G. Herzog and A. Ludi, *Ber. Bunsenges. Phys. Chem.* 1971, **75**, 878.

29. M. Anbar and E. J. Hart, *J. Phys. Chem.* 1965, **69**, 973.

30. G. Davies, N. Sutin and K. O. Watkins, *J. Am. Chem. Soc.* 1970, **92**, 1892.

31. Z. Stasicka and A. Marchaj, *Coord. Chem. Rev.* 1977, **23**, 131.

32. J. Piccard, *Ber.* 1913, **46**, 2477.

33. T. Jarzynowski, T. Senkowski and Z. Stasicka, *Polish J. Chem.* 1981, **55**, 3.

SOLVOLYTIC BEHAVIOUR AND THE SOLUBILITIES OF VARIOUS INORGANIC COMPOUNDS, LEWIS ACIDS AND BASES IN FUSED MONOBROMO ACETIC ACID SOLVENT SYSTEM—II

J. K. PURI, JASWINDER KAUR and VIJAY SHARMA
Department of Chemistry, Panjab University, Chandigarh 160014, India

and

JACK M. MILLER*
Department of Chemistry, Brock University, St. Catharines, Ontario, Canada L2S 3A1

Abstract—Solubilities and the solvolytic behaviour of various inorganic compounds, Lewis acids and bases in fused monobromoacetic acid at $60 \pm 0.5°C$ are discussed. Ionic compounds are fairly soluble, iodides and thiocyanates being comparatively more soluble than chlorides and bromides. Tetraalkyl ammonium halides are highly soluble in this solvent. Conductometric and spectroscopic studies of various Lewis acids and bases in fused monobromoacetic acid indicate their solvolytic behaviour and their subsequent ionization. The solvolyses products $BBr_3 \cdot CH_2BrCOOH$ and $SbCl_5 \cdot CH_2BrCOOH$ have been observed to be the strongest Bronsted acids. Auto-ionization of this solvent has been supported by acid/base titrations.

Very little is known about fused monobromoacetic acid as solvent compared to acetic acid,[1] monochloroacetic acid,[2–5] sulphuric acid,[6] disulphuric acid,[7] or fluorosulphuric acid.[8] Earlier work on the solubility of substances in monobromoacetic acid is very limited. It has a convenient working range (6 b.p. 208°C, m.p. 48.5°C, dipole moment 2.90 at 35°C and specific conductance value $1.35 \times 10^{-3} ohm^{-1} cm^{-1}$). From freezing point, viscosity and density data of the mixture of $SnBr_4$ and $CH_2BrCOOH$ it has been reported[9] that there is no interaction between these two components. However in the case of $SbBr_3$–$CH_2BrCOOH$ system some chemical interaction has been proposed (*loc. cit.*). This is unreasonable since $SnBr_4$ is a stronger

acceptor than $SbBr_3$. Although monobromoacetic acid is moderately acidic in nature, very few adducts with nitrogen and oxygen donor molecules are known,[10,11] which seems surprising. A quantitative method for the estimation of organic tertiary bases has been established,[12] but no attempt has yet been made to isolate their addition compounds with monobromoacetic acid or to characterize them. Therefore, in view of the very favourable properties of fused monobromoacetic acid an attempt has been made to study it as a non-aqueous solvent. In this paper, we report the results of a study of the solubilities of various compounds, Lewis acids and bases and their solvolytic behaviour in fused monobromoacetic acid.

EXPERIMENTAL

Monobromoacetic acid was prepared and purified by the method reported earlier.[13] The best

---

*Author to whom correspondence should be addressed.

available commercial A.R. grade samples were used for solubility determinations. Lewis acids used were either commercially available or were prepared in the laboratory by standard methods. Organic tertiary bases were purified by distillation over potassium hydroxide pellets before use.

Quantitative determination of the solubilities of various solutes were made by taking a known amount of the salt and monobromoacetic acid in a small stoppered flask. Monobromoacetic acid was added in such an amount that there was always an excess of the solid undissolved. Each experiment was carried out in a dry box flushed continuously with dry nitrogen. The flasks were closed tightly, spring retainers on the standard taper stoppers. These flasks were rotated continuously in a thermostat maintained at $60 \pm 0.5°C$ for about 38 hr; to ensure that the equilibrium was established. After this the contents were filtered quickly in the dry box. Careful estimation of the cations by standard methods allowed the solubility of the substance in grams per 100 g of the solvent to be determined. From the qualitative study of the solubilities, the substances were extremely low

solubilities have been considered to be insoluble, while others which are soluble to an extent of either less than 5% or 5–10% have been termed as sparingly soluble and fairly soluble respectively. The colour of the saturated solution at equilibrium and the thermal changes during the dissolution have been observed as shown in Table 1.

Solvates of Lewis acids and bases were prepared by taking excess of monobromoacetic acid dissolved in hot benzene in a flask and adding Lewis acid or base in small amounts with constant shaking of the solution till a solvate separated. It was then quickly filtered in a dry atmosphere, washed with anhydrous hot benzene to remove the excess of monobromoacetic acid, finally washed with anhydrous methylene chloride and then dried under vacuum. In the case of the boron tribromide solvate, both the compounds were mixed in equimolar amounts in liquid SO_2 and then the solution was slowly restored to room temperature and a white solid was obtained on evaporating the solvent. In certain cases the bases form solvates which are separated as a second liquid phase. Excess of the solvents were decanted and the last traces of the solvent

Table 1. Solubilities of various solutes in fused monobromoacetic acid at $60 \pm 0.5°C$

Solute	Solubility gms/ 100 gms of solvent	Colour of the solution	Solute	Solubility gms/ 100 gms of solvent	Colour of the solution
$CH_2BrCOOK$	10.63	Colourless	$CH_2BrCOONa$	9.42	Colourless
$AlCl_3$	14.70	Colourless	$AlBr_3$	10.00	Light yellow
BBr_3	Miscible	Colourless	$SnCl_4$	Miscible	Colourless
$SnBr_4$	4.95	Dark brown	Ethyl acetate	Miscible	Colourless
$TiCl_4$	Miscible	Yellow	$SbCl_5$	Miscible	Colourless
$FeCl_3$	6.10	Colourless	$AsCl_3$, $POCl_3$, PCl_3, PBr_3	Miscible	Colourless
$SbCl_3$	10.50	Colourless	$TeCl_4$	0.24	Yellow
$BiCl_3$	5.80	Colourless	$SeCl_4$	1.50	Colourless
H_2SeO_4	Soluble	Colourless	SO_3	Miscible	Colourless
Br_2	Miscible	Yellow	$NiCl_2$, $BaCl_2$, $CdCl_2$, $SnCl_2$, $ZnCl_2$	Insoluble	–
$COCl_2$	1.16	Light pink	$(C_6H_5)_3As$	4.45	Colourless
$(C_6H_5)_3P$	4.86	Colourless	$(C_6H_5)_3Sb$	4.32	Colourless
α-Picoline, quinoline	Miscible	Light yellow	CF_3COOH, HNO_3	Soluble	Light yellow
Triethylamine	Miscible	Light yellow	Aniline	Miscible	Yellow
Isoquinoline	Miscible	Light yellow	$(C_4H_9)_4NI$	72.6	Reddish brown
$HgCl_2$, $HgBr_2$, $CdBr_2$	Insoluble	Colourless	KI	0.80	Colourless
$(CH_3)_4NBr$	52.80	Colourless	$SOCl_2$, S_2Cl_2	Miscible	Colourless
NH_4CNS	11.50	Colourless	2,2'-bipyridine	20.30	Colourless
Pyridine, piperidine	Miscible	Light yellow	KBr	1.40	Colourless
KCl	3.48	Colourless	KIO_3	55.40	Brown
$KMnO_4$	10.20	Pink	$KBrO_3$	13.20	Light Yellow

were removed under vacuum. After keeping the liquid solvates for a couple of days, needle shaped compounds separate. All these compounds have been characterized by elemental analysis and are reported in Table 2.

The conductance measurements in mono-bromoacetic acid were made in a specially designed cell with a y-shaped jacket and a cell constant of 0.678 cm^{-1} kept in a thermostat at $60 \pm 0.5°C$. The solutions were prepared directly in a conductance cell. The conductance was measured using a precision conductivity bridge (Phillips PR-9500). The infrared spectra of various solvates were recorded using a Perkin–Elmer Model 337 spectrophotometer either as neat liquids or as Nujol mulls.

RESULTS AND DISCUSSION

Fused monobromoacetic acid has a comparatively high dipole moment and low dielectric constant compared to acetic and monochloroacetic acids, which helps in the dissolution of various ionic compounds. The solubility of various solutes in monobromoacetic acid has been checked at $60 \pm 0.5°C$ and their values are given in Table 1. It has been noted that the chlorides of Mn, Ba, Pb,

Ni, Co and Cu, etc. are insoluble in it. Iodides and thiocyanates of these elements are more soluble. Anhydrous chlorides of Li, Na, K, NH_4, Ca, Sr are also insoluble. The low dielectric constant of monobromoacetic acid accounts for its being a poor solvent for these ionic compounds. Non-metals like S, Se, Te, phosphorus and the oxides of iron, chromium, aluminium, copper and lead are also insoluble. It is interesting to note that the anhydrous acetates of Na, K, Li and Cs are fairly soluble while those of Ca, Mg, Ba, Sr, Zn, Cd are insoluble. Tetramethyl ammonium chloride and bromide are highly soluble. When these compounds are added in excess, corresponding mono-bromoacetates separated out. Lewis acids and bases are fairly soluble in monobromoacetic acid. Chlorides of Zn, Ca, Mg form solvates of composition $MCl_2 \cdot 2CH_2BrCOOH$ when dissolved in monobromoacetic acid. Phosphorous and arsenic halides are miscible with monobromoacetic acid in all proportions without the separation of any compound. However, antimony and bismuth trichlorides form solids of composition $MCl_3 \cdot CH_2BrCOOH[M = Sb, Bi]$. Selenium and tellurium tetrachlorides undergo reduction when

Table 2. Analysis of various adducts of Lewis acids and bases with fused monobromoacetic acid

| Compound | Physical state | | M. pt. (°) | Elemental Analysis | | | | Molar Conductance in nitrobenzene (ohm^{-1}cm^{-2}mole^{-1}) |
| | State | Colour | | % Found | | % Required | | |
				Halogen	Metal	Halogen	Metal	
$FeCl_3 \cdot CH_2BrCOOH$	Solid	Brown	96-97	61.50	18.59	62.00	18.60	13.0
$AlCl_3 \cdot CH_2BrCOOH$	Solid	White	92-93°	63.23	8.00	64.80	9.90	15.1
$AlBr_3 \cdot CH_2BrCOOH$	Solid	Light Yellow	-	79.20	6.20	80.00	6.65	22.6
$TiCl_4 \cdot CH_2BrCOOH$	Solid	Light Yellow	196	66.20	14.90	67.70	14.58	18.0
$SnBr_4 \cdot CH_2BrCOOH$	Solid	Light Yellow	202	83.10	2.16	84.50	2.06	13.5
$SnCl_4 \cdot 2CH_2BrCOOH$	Solid	Black	182°C	55.10	20.21	56.20	21.50	14.5
$SnCl_4 CH_2BrCOOH$	Solid	Black	-	65.30	31.07	66.60	29.75	15.5
$SbCl_5 \cdot CH_2BrCOOH$	Liquid	Light Yellow	177°(B.P.)	47.23	26.20	48.80	27.93	17.2
$SbCl_3 \cdot CH_2BrCOOH$	Liquid	Light Yellow	-	54.30	32.90	55.50	33.19	13.6
$BBr_3 \cdot CH_2BrCOOH$	Solid	White	-	82.50	-	81.52	2.50	14.5
$C_5H_5N \cdot CH_2BrCOOH$	Solid	White	85(D)	25.90	(6.78)	36.69	(6.42)	16.53
$(C_2H_5)_3N \cdot CH_2BrCOOH$	Solid	White	95(D)	32.00	(5.40)	33.33	(5.83)	18.50
$\alpha-C_6H_7N \cdot CH_2BrCOOH$	Solid	White	112-115	33.63	(6.00)	34.48	(6.03)	9.10
$C_5H_{11}N \cdot CH_2BrCOOH$	Solid	White	147	34.23	(6.17)	35.71	(6.20)	15.00
$(C_2H_5)_3 \cdot C_6H_4N \cdot 2CH_2BrCOOH$	Solid	Bluish White	-	47.00	(3.60)	46.00	(4.00)	12.00
$C_7H_7N \cdot 2CH_2BrCOOH$	Solid	White	-	30.40	(4.90)	29.80	(5.20)	13.00
$(CH_3)_2 C_6H_5N \cdot 2CH_2BrCOOH$	Solid	Green	-	20.30	(3.42)	21.00	(3.50)	10.00
$C_{10}H_8N_2 \cdot 2CH_2BrCOOH$	Solid	Pink	135	34.57	(9.26)	34.93	(8.77)	23.31

In brackets ( ) the values are given for % Nitrogen in the base;   D = Decomposed

heated with monobromoacetic acid but $FeCl_3$ and $AlCl_3$ are highly soluble in it. Tetrahalides of tin and titanium, and pentahalides of antimony and phosphorus are completely miscible with mono-bromoacetic acid in all proportions. The substances which are soluble are generally Lewis acids and give coloured solutions probably due to the formation of solvates or complexes and which has been shown conductometrically in this solvent. Qualitative tests show that the solubilities of most of the solutes increase with rise in temperature. Only strong Lewis acids form adducts with mono-bromoacetic acid.

Organic tertiary bases (Table 1) are highly soluble in monobromoacetic acid. Varying amounts of heat are produced when these two compounds are mixed. Solid compounds of bases with fused monobromoacetic acid have been isolated from their solutions in carbon tetrachloride. Mono-bromoacetates of alkali metals are highly soluble in monobromoacetic acid, while monobromoacetates of alkaline earth metals are only sparingly soluble.
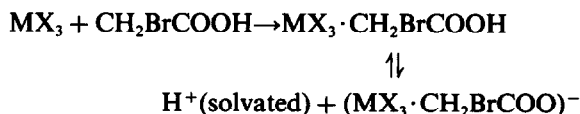
The auto-ionization of fused monobromoacetic acid has already been suggested as;

$$2CH_2BrCOOH \rightleftharpoons CH_2BrCOOH_2^+ + CH_2BrCOO^-. \tag{1}$$
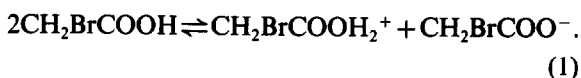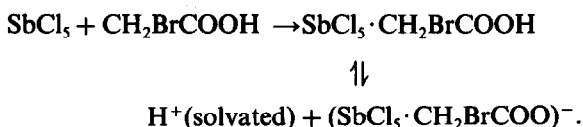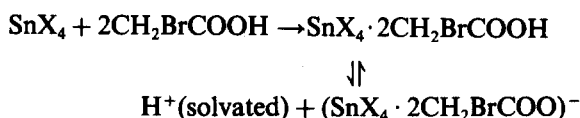
According to the solvent system concept, those solutes which directly or indirectly produce the cations characteristic of the auto-ionization of the solvent shall be acids of the system and the solutes which produce directly or indirectly the anions characteristic of the auto-ionization of the solvent shall be the bases of the system.

Lewis acids are fairly soluble in fused mono-bromoacetic acid and form highly conducting solutions. The breaks in their conductance composition curves (Fig. 1) have been observed at the molar ratios of Lewis acid: solvent of 1:1 and 1:2 and which corresponds to the solvate formation. The

high conductance of solutions containing these solvates may be supported by the ionization of these adducts as;

$$MX_3 + CH_2BrCOOH \rightarrow MX_3 \cdot CH_2BrCOOH$$
$$\updownarrow$$
$$H^+(\text{solvated}) + (MX_3 \cdot CH_2BrCOO)^-$$

(where $X = Cl, Br., M = Al, B$)

$$SnX_4 + 2CH_2BrCOOH \rightarrow SnX_4 \cdot 2CH_2BrCOOH$$
$$\updownarrow$$
$$H^+(\text{solvated}) + (SnX_4 \cdot 2CH_2BrCOO)^-$$

$$SbCl_5 + CH_2BrCOOH \rightarrow SbCl_5 \cdot CH_2BrCOOH$$
$$\updownarrow$$
$$H^+(\text{solvated}) + (SbCl_5 \cdot CH_2BrCOO)^-.$$

The nature of these solutions and the formation of these adducts has been further supported by isolating these solvates as shown in Table 2. Only very strong acceptor molecules form solvates with monobromoacetic acid. Except $SnCl_4$ and $SnBr_4$ which form solvates in this solvent in a 1:2 mole ratio all other metal halides form solvates in 1:1 mole ratios and show that monobromoacetic acid acts as a mono-dentate ligand in these solvates. All these compounds are moisture sensitive, have high melting points and are insoluble in polar solvents, but are soluble in various aprotic solvents. Molar conductance values of the milimolar solutions show them to be quite ionic in nature.

There are some references to solvates of Lewis acids with various aprotic solvents and molar conductance values of milimolar solutions show them to be quite ionic in nature.

There are some references to solvates of Lewis acids with various carboxylic acids but IR

Table 3. Shift of carbonyl stretching frequency in fused monobromoacetic acid on complex formation

Compound	Observed Carbonyl frequency (cm^{-1})	$\Delta\nu$ cm^{-1}	Compound	Observed Carbonyl frequency (cm^{-1})	$\Delta\nu$ cm^{-1}
$CH_2BrCOOH$	1720	–	$CH_2BrCOOH \cdot SbCl_5$	1640	80
$CH_2BrCOOH \cdot TiCl_4$	1650	70	$CH_2BrCOOH \cdot SnCl_4$	1672	48
$CH_2BrCOOH \cdot SnBr_4$	1654	66	$CH_2BrCOOH \cdot AlCl_3$	1664	56
$CH_2BrCOOH \cdot AlBr_3$	1660	60	$CH_2BrCOOH \cdot FeCl_3$	1678	62
$CH_2BrCOOH \cdot SbCl_3$	1675	45	$CH_2BrCOOH \cdot BBr_3$	1645	75
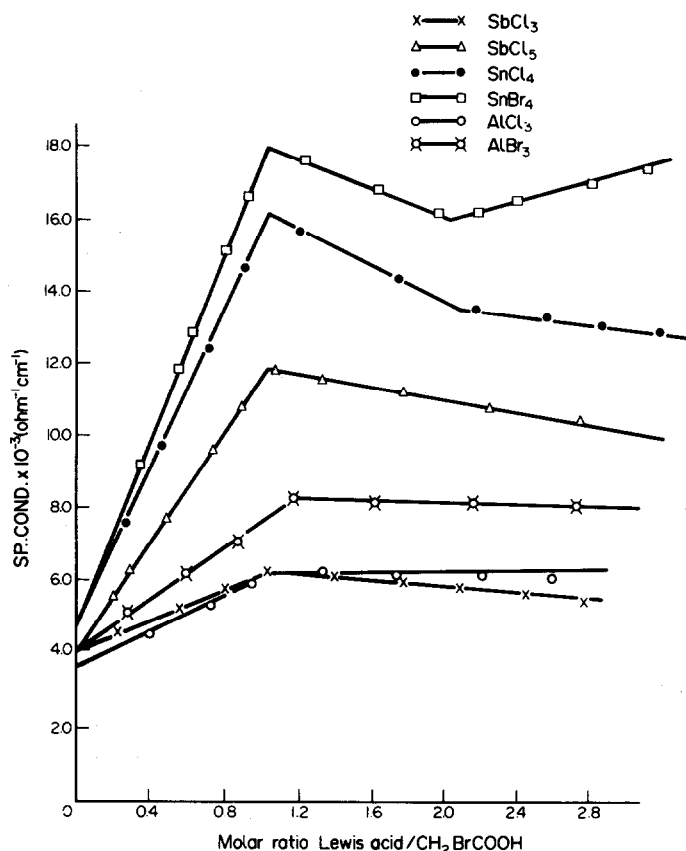
Fig. 1. Conductance composition curves of Lewis acids in CH_2Br–COOH at $60°C \pm 0.5°C$.

spectral evidence in support of their formation are very limited.[14,15] Monobromoacetic acid has a sharp intense band at 1720 cm^{-1} which may be attributed to carbonyl stretching mode.[16] A broad absorption band at 3430 cm^{-1} may be assigned to hydrogen bonded hydroxyl group. Pure carboxylic acids are known to have peaks near 1400 and 1300 cm^{-1} which arise from O–C vibrations but coupled with –OH vibrations in-plane bending vibrations.[17] It is therefore not possible to study the O–C vibrations of these adducts as has been described in the case of the adducts of the esters.[18] Changes in the frequency due to carbonyl group of the ligand on adduct formation have been noted.

On adduct formation with Lewis acids the absorption band due to –OH group of the monobromoacetic acid becomes very sharp. In the case of very weak acceptors like ferric chloride and antimony trichloride, the stretching frequency for the –OH group for the various adducts is at the same position as has been reported for the –OH group of the monomeric acid. It is quite resonable to assume that in these adducts the intermolecular hydrogen bonded structure of the ligand is ruptured. On adduct formation the withdrawal of

electrons from the carbonyl oxygen weakens the hydrogen bond and strengthens the adjacent –OH bond.

The carbonyl stretching frequency in the cases of aldehydes,[19] ketones,[20] amides[21] and esters[18] are lowered on complex formation with various acceptor molecules. With the withdrawal of electrons from the carbonyl group, the double bond character of the carbonyl group is reduced and the carbonyl frequency is lowered, accompanied by a corresponding increase in the O–C stretching mode. But if the ethereal oxygen is to be the donor site, a reverse effect would be expected. The present studies show that there is decrease in the $v(C=O)$ frequency of the ligand on adduct formation and thus the carbonyl oxygen of monobromoacetic acid is the donor site. If the lowering of the (C=O) stretching mode is a measure of the acceptor strength of the Lewis acids, then from Table 3 it is quite clear that the order of their acceptor strength is;
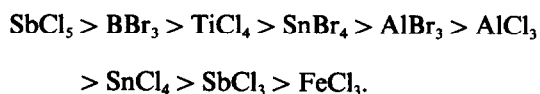
$$SbCl_5 > BBr_3 > TiCl_4 > SnBr_4 > AlBr_3 > AlCl_3$$

$$> SnCl_4 > SbCl_3 > FeCl_3.$$

Table 4. Principal IR bands (cm^{-1}) of the adducts of monobromoacetic acid with organic bases

Pyridine BrA	Piperidine BrA	α-Picoline BrA	Quinoline BrA
2942 (W), 2730 (S), 2150 (M)	2940 (W), 2732 (S), 2170 (M)	2941 (W), 2829 (S),	2945 (W), 2715 (S), 2195(M)
1620 (S), 1605 (S)	1622 (S), 1608 (S)	2142 (M), 1625 (S)	1635 (S), 1612 (S), 1530 (M)
1505 (S), 1482 (S)	1508 (S), 1487 (S)	1606 (S), 1510 (S)	1488 (S), 1410 (M)
1435 (M), 1383 (S)	1431 (M), 1380 (S)	1485 (S), 1434 (M)	1388 (M), 1325 (M)
1320 (S), 1250 (MS)	1329 (S), 1254 (MS)	1385 (S), 1325 (S)	1240 (S), 1170 (M)
1204 (MS), 1165 (MS)	1200 (MS), 1160 (MS)	1251 (MS), 1206 (MS)	1062 (M), 1044 (S)
1050 (M), 1035 (S)	1052 (M), 1030 (S)	1169 (MS), 1057 (M)	1025 (S), 1005 (S)
1025 (S), 1002 (S)	1022 (S), 1000 (S)	1032 (S), 1020 (S)	995 (S), 885 (S)
995 (S), 890 (S)	998 (S), 882(S)	1004 (S), 996 (S)	780 (S), 690 (vs)
755 (S), 682 (vs)	725 (S), 679 (Vs)	884 (S), 751 (S) 685 (Vs)	

M = medium   S = strong   W = weak   Vs=very strong

The adduct $BBr_3.CH_2BrCOOH$ when dissolved in fused monobromoacetic acid forms further solvate;

$$BBr_3 \cdot CH_2BrCOOH + CH_2BrCOOH$$
$$\updownarrow$$
$$CH_2BrCOOH_2^+ + (CH_2BrCOOBBr_3)^-.$$
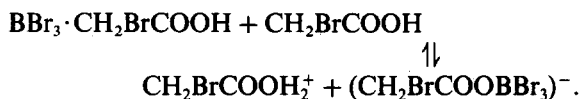
This behaviour has been supported by its molar conductance value, infra-red spectral measurements of the solid and also from its behaviour in solutions. Boron tribromide and aluminium trihalide adducts with monobromoacetic acid give absorption bands at 525, 540, 520 and 540 cm^{-1} respectively. The bands at 540 cm^{-1} are analogous to the degenerate ν_4(M–Cl) bending mode in MCl_4[20,21][M = B, Al]. These bands may be assigned to the change in the local symmetry from T_d to C_{3v} for the boron and aluminium. In these compounds a strong absorption band is also observed at 1100 cm^{-1} which may be due to a M–Br stretching mode analogous to ν_4 but this is coupled with the M–O stretching mode which also occurs in the same region.[22] In the case of the $SbCl_5.CH_2BrCOOH$ compound, a new band, not present in the ligand appears at 412 cm^{-1} which may be attributed to the Sb–O stretching mode.[23] The absorption bands at 342 cm^{-1} and 630 cm^{-1} may be attributed to Sb–Cl stretching modes in an octahedral environment of the metal.[24] Antimony, therefore, has achieved an octahedral environment by combining with the carbonyl-oxygen of the monobromoacetic acid as;

$$SbCl_5 \cdot CH_2BrCOOH + CH_2BrCOOH$$
$$\rightleftharpoons CH_2BrCOOH_2^+ + (SbCl_5.CH_2BrCOO)^-.$$
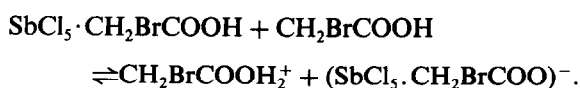
In the case of adducts of the tetrachlorides of tin and titanium, the metal–oxygen stretching modes are observed at 390 cm^{-1} and 460 cm^{-1} respectively. These stretching modes are observed at the same region as has been reported in literature.[25,26] The metal–chlorine stretching mode is observed at 380 cm^{-1} with a shoulder at 362 cm^{-1}. A sharp absorption band at 295 cm^{-1} may also be assigned to Sn–Cl stretching mode. As the Sn–O stretching mode of the spectrum is simpler than Sn–Cl stretching mode, the ligands are probably disposed at *trans*-positions to each other.[27] It is therefore probable that the tetrachlorides of tin and titanium acquire a co-ordination number of six by combining with two molecules of mono-bromoacetic acid with *trans*-disposition of the ligands.

Table 2 show that a large number of bases form solvates with monobromoacetic acid. Their solution behaviour in bromoacetic acid has been shown by IR spectral studies where only the principal spectra of these complexes are discussed. It has been noted that during complexation the bands of the pure compounds undergo the same changes and in the same order as reported for pyridinium chloride[28] complexes of acetyl chloride and pyridine.[29]

Bases are known to form complexes with Lewis acids where the nitrogen atom of the tertiary bases donates electrons to the vacant orbital of the central metal atom. Their IR spectra have been changed on donation. Here we discuss the formation of pyridinium, picolinium, quinolinium ions in monobromoacetic acid and their formation has been supported by their IR spectra when compared with the reported IR spectra of pyridine chloride.

Table 4 show the various bands obtained in case of pyridine, quinoline, picoline and piperidine and their assignment is according to Wimsprest and Bersten.[30] The C–H stretching mode of pyridine shifts to lower region on its adduct formation with monobromoacetic acid. The lowering of this band has been assigned to the co-ordination of pyridine through the nitrogen atom. Presently this band is found as a broad band at 2730 cm^{-1}. In pure pyridine, this band is observed at 3002 cm^{-1}. A broad absorption band at 2942 cm^{-1} is assigned to the –CH$_2$ group of monobromoacetic acid. The strong absorption bands at 1580, 1570, 1480 and 1440 cm^{-1} in pyridine are due to the C⸺C and C⸺N symmetric and antisymmetric stretching vibrations. Evidently the donation of electrons by the nitrogen of pyridine will increase the double bond character of the C⸺C and C⸺N bands owing to the reduced electron density on the nitrogen. New bands are found in the adduct C$_5$H$_5$N·CH$_2$BrCOOH at 1620, 1605, 1505, 1482 cm^{-1} are nearly at the same position as those of the pyridinium ion (*loc. cit.*). Two strong bands in the adduct at 1383 and 1320 cm^{-1} are at the same position as those of pyridinium ions. Pyridine has a very weak band at 1375 cm^{-1} which is intensified and shifts a little in the pyridinium ion complex. A new absorption peak is observed at 1435 cm^{-1} in the compound may be assigned to the N–H stretching frequency. The absorption peaks

at 1250, 1204 and 1165 cm^{-1} are due to the C–H in-plane deformation bands of pyridine which are present at 1222, 1150 and 1075 cm^{-1} in the free base. The shift to higher frequency is based on the withdrawal of electron density from the C–H bond. The next three bands at 1050, 1025 and 1002 cm^{-1} found in the adduct are at the same position as in pyridinium ion. These bands arise from the deformation of the pyridine ring. They appear at 1035 and 995 cm^{-1} on complex formation. Strong bands at 890 cm^{-1} in the spectrum of the complex is present in pyridine at 885 cm^{-1} as a weak band. Two bands at 751 and 680 cm^{-1} in the complex are in the same position as in (PyH)$^+$Cl$^-$ (755, 682 cm^{-1}) while pure pyridine absorbs at 785 and 705 cm^{-1}. Similar spectral changes have been observed in complexes with other tertiary organic bases as shown in Table 4. Thus all the changes in the spectra correspond to the formation of the protonated N cations as;

$$C_5H_5N + CH_2BrCOOH \rightleftharpoons C_5H_5N \cdot CH_2BrCOOH$$
$$+ \updownarrow$$
$$C_5H_5N\overset{+}{H} + CH_2BrCOO^-$$
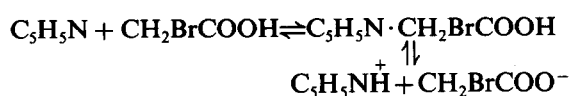
Similarly the adducts of monobromoacetic acid with 2, 2'-bi-pyridyl and 1, 10-phenanthroline have been prepared and characterized by their elemental analysis (Table 2). Both these compounds are susceptible to the hydrolytic attack but are quite
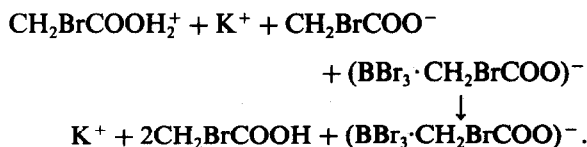
Table 5. IR spectra (cm^{-1}) of the adducts of 2, 2'-bipyridine and 1, 10-phenanthroline with monobromoacetic acid

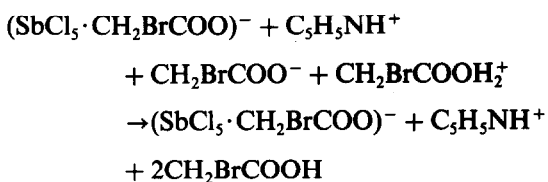| 2,2'-Bipyridine		2,2'-Bipyridine.CH$_2$BrCOOH	1,10-phenanthrolene		C$_{12}$H$_8$N$_2$.CH$_2$BrCOOH
3086		4000	3099 C–H stretching		3590
			3077		3100
3078	C–H stretching	3098		modes	
3061	modes	3081			
3054		3078			
1580		1620	1580 C=C		1620
1552		1692	1565 and		1590
1450	Phenyl nuclear	1490	1505 C≡N	stretching mode	1520
1405	stretching mode	1498	1450		1468
1060	In-plane hydrogen	1060	1418 Ring Vibration		1418
1042	bonding	1042	1355		1430
			1250		
990	Ring breathing	1025	995		1015
770	Ring (–H) out-of-plane bend	770	860 out-of-plane (–H) on		860
730			hetrocyclic ring		
670	Ring bend	670	740 out-of-plane (–H)		710
620		620	of central ring		

stable in a dry atmosphere. Molar conductance values of their milimolar solutions indicate them to be ionic. The infra-red spectra of these compounds have also been tabulated in Table 5 along with the fundamental vibrations of the pure ligand. All the spectral changes as shown in Table 5 suggest that 2, 2′-bipyridinium ion is formed on complex formation with monobromoacetic acid.

From the above studies, it is evident that the adducts of acids and bases with fused monobromoacetic acid are ionic in nature and it is reasonable to assume that ions are formed when these solvates are dissolved in fused monobromoacetic acid and both behave as solvo acids and solvo bases producing ions specific to the auto-ionization of the solvent. It is therefore of interest to carry out acid/base titrations in fused monobromoacetic acid conductometerically and visually. Crystal violet, malachite green and benzanthrone have been used to detect the end points in the case of visual titrations. Change in colour of the indicators near the end points are very sharp. The results are reproducible and the indicators can

act reversibly. Figure 2 illustrates the conductometric titration curves of boron tribromide adduct with monobromoacetic acid and various bases. Acid/base neutralization reactions may be suggested as;

$$CH_2BrCOOH_2^+ + K^+ + CH_2BrCOO^-$$
$$+ (BBr_3 \cdot CH_2BrCOO)^-$$
$$\downarrow$$
$$K^+ + 2CH_2BrCOOH + (BBr_3 \cdot CH_2BrCOO)^-.$$

Similarly in case of SbCl$_5$, the reaction may be suggested as;

$$(SbCl_5 \cdot CH_2BrCOO)^- + C_5H_5NH^+$$
$$+ CH_2BrCOO^- + CH_2BrCOOH_2^+$$
$$\rightarrow (SbCl_5 \cdot CH_2BrCOO)^- + C_5H_5NH^+$$
$$+ 2CH_2BrCOOH$$

Decrease in the conductance of the solution upon addition of the acid solution is due to the
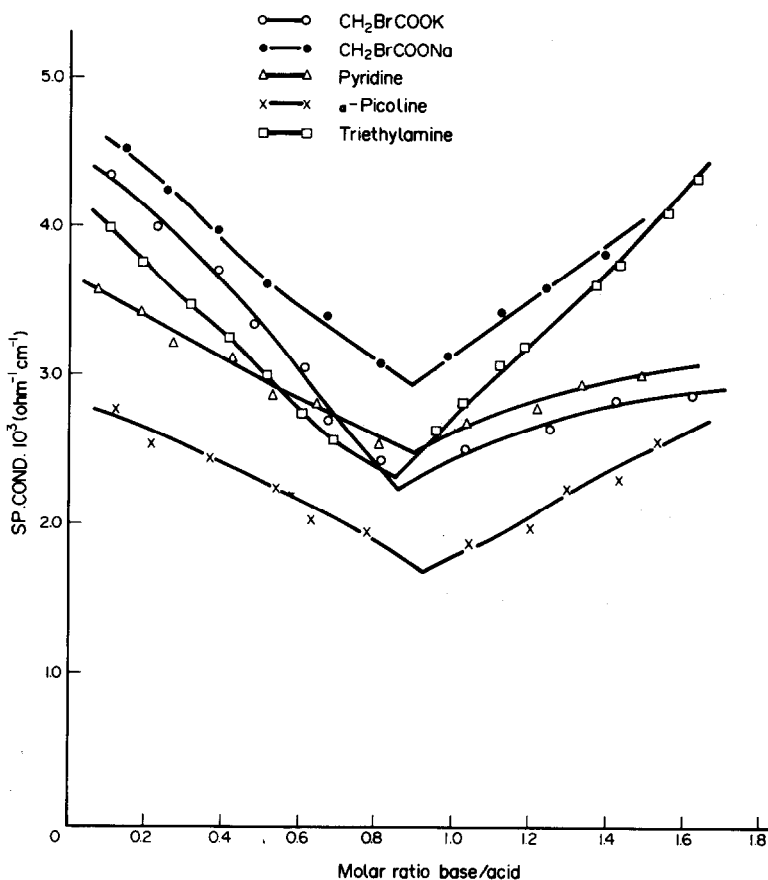
Fig. 2. Conductometric titrations between BBr$_3$CH$_2$BrCOOH and bases in fused monobromoacetic acid at 60°C ± 0.5°C.

removal of CH_2BrCOO^- ions. After the molar ratio acid:base of 1:1, when there is complete removal of CH_2BrCOO^- ions further addition of $CH_2BrCOOH_2^+$ ions causes an increase in the conductance of the solution. The presence of only one break in the conductance composition curve shows that $SbCl_5 \cdot CH_2BrCOOH$ and $BBr_3 \cdot CH_2BrCOOH$ behave as monobasic acids.

In the case of stannic chloride and titanium tetrachloride adducts, there are two breaks in the conductance-composition curves corresponding to the molar ratio acid:base of 1:1 and 1:2 confirming the dibasic character of these adducts which ionize as;

$$MX_4 \cdot 2CH_2BrCOOH + CH_2BrCOOH$$

$$\rightarrow CH_2BrCOOH_2^+$$

$$+ (MX_4 \cdot CH_2BrCOOH \cdot CH_2BrCOO)^-$$
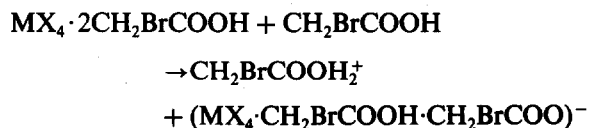
and subsequently ionize as:

$$(MX_4 \cdot CH_2BrCOOH \cdot CH_2BrCOO)^-$$

$$+ CH_2BrCOOH$$

$$\downarrow$$

$$CH_2BrCOOH_2^+ + [MX_4(CH_2BrCOO)_2]^{2-}.$$
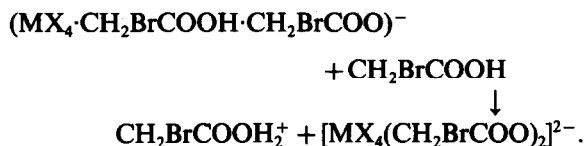
All these studies support the ionic behaviour of monobromoacetic acid and suggest its mode of ionizations as:

$$2CH_2BrCOOH \rightleftharpoons CH_2BrCOOH_2^+ + CH_2BrCOO^-.$$

REFERENCES

1. A. I. Popov, *The Chemistry of Non-aqueous Solvents* (Edited by J. J. Lagowski), p. 241. Academic Press, New York, (1970).
2. T. N. Sumarokova, I. Litvyak and Valezhanina, *Zhur. Fiz. Khim* 1960, **34**, 2725.
3. T. N. Sumarokova, I. Litvyak and T. V. Medvedeva, *Zhur. Obshch. Khim.* 1960, **30**, 1698.
4. O. A. Osipov, G. S. Samofalova and E. I. Glushko, *Zhur. Obshch. Khim* 1957, **27**, 1428.
5. M. I. Usanovich and T. Sumarokova, *Zhur. Obshch. Khim* 1951, **21**, 1214.
6. R. J. Gillespie and E. A. Robinson, *Non-aqueous Solvent System* (Edited by T. C. Waddington), p. 117. Academic Press, London (1965).
7. R. C. Paul and V. P. Kapila, *J. Ind. Chem. Soc.* 1977, **54**, 321.
8. J. Barr, R. J. Gillespie and R. C. Thompson, *Inorg. Chem.* 1964, **3**, 1149.
9. T. N. Sumarokova and N. Khakhlova, *Zhur. Obshch. Khim* 1957, **51**, 6302.
10. L. E. Swearinger and R. F. Ross, *J. Phys. Chem.* 1934, 1085.
11. A. S. Naumova, *Zhur. Obshch. Khim* 1949, **19**, 1222.
12. L. Genevois and G. Mandillon, *Comp. Rend Biol* 1935, **118**, 1353.
13. J. K. Puri, Miss Jaswinder Kaur, Vijay Sharma and Jack M. Miller, *Can. J. Chem.* 1983 (communicated).
14. I. Lindquist and M. Zackerson, *J. Inorg. Nucl. Chem.* 1961, **17**, 69.
15. M. F. Lappert, *J. Chem. Soc.* 1962, 542.
16. J. E. Katon, T. P. Carll and F. F. Bentley, *Appl. Spectroscopy*, 1971, **25**(2), 229.
17. L. J. Bellamy, *The Infra-red Spectra of Complex Molecules*, 2nd Edn. Wiley, New York (1958).
18. M. F. Lappert, *J. Chem. Soc.* 1961, 817.
19. R. C. Paul, H. R. Singhal and S. L. Chadha, *J. Chem. Soc. (A)* 1969, 1849.
20. R. C. Paul, R. Parkash and S. S. Sandhu, *Ind. J. Chem.* 1966, **4**, 426.
21. R. C. Paul and R. Dev, *Ind. J. Chem.* 1967, **5**, 267.
22. J. G. Jones, *Inorg. Chem.* 1966, **5**, 1229.
23. D. Cook, J. J. Kuh and G. A. Olah, *J. Chem. Phys.* 1960, **33**, 1669.
24. J. R. Beattie, *Quart Rev. (London)* 1963, **17**, 282.
25. G. Matsubayashi, J. Tanaka and R. Okawara, *J. Inorg. Nucl. Chem.* 1968, **30**, 1831.
26. T. Tanaka, Y. Matsumara, R. Okawara, Y. Musha and S. Kinumaki, *Bull. Chem. Soc. (Japan)* 1968, **41**, 1494.
27. R. Dev. Ph.D. Thesis, Panjab Univ. Chandigarh, India (1967).
28. N. N. Greenwood and K. Wade, *J. Chem. Soc.* 1958, 1667.
29. R. C. Paul and S. L. Chadha, *Spectrochim Acta* 1966, **22**, 615.
30. J. K. Wilmshurt and H. J. Bernstein, *Can J. Chem.* 1957, **35**, 1185.

SPECTRAL INTENSITY ANALYSIS OF THE Sm^{3+}-POCl$_3$-ZrCl$_4$ SYSTEM

K. BUKIETYŃSKA* and B. RADOMSKA

Institute of Chemistry, University of Wroclaw, 50-383 Wroclaw, Poland

Abstract—The solution absorption spectra of the Sm^{3+}-POCl$_3$-ZrCl$_4$ system were recorded within the 40,000-4000 cm^{-1} range. A number of absorption bands in solution in the near-IR region were considered taking advantage of the optical transparency of the solvent. It was proved that only in this case the Judd–Ofelt parameters Ω_λ are physically significant and can be determined with relatively good accuracy.

Spectral intensity data for the Sm^{3+} ion are scarce. Application of the Judd–Ofelt equations[1,2] to the analysis of the intensity of f–f transitions leads usually to high errors in the evaluated Ω_2 parameter, the error being sometimes one order higher than the Ω_2 values.[3–5] A satisfactory set of intensity parameters of Sm^{3+} has been reported only for the Sm^{3+}–DClO$_4$, Sm^{3+}–TBP solutions and the Sm^{3+}–KNO$_3$–LiNO$_3$ eutectic.[6–8] We have studied the Sm^{3+} ion spectra in POCl$_3$–ZrCl$_4$ solutions. The large transparent range (down to 4000 cm^{-1}) in the near-IR region for this aprotic solvent made it possible to observe $4f$–$4f$ transitions, which in protic solvents are very difficult to measure because of the existence of relatively strong and broad absorption bands in this region due to the overtones of OH, NH and other similar groups. This holds particularly for the Sm^{3+} ion because relatively intense absorption bands (with the hypersensitive one: $^4F_{1/2} \leftarrow {}^6H_{3/2} \approx 6400$ cm^{-1}) occur in this region.

EXPERIMENTAL

Freshly precipitated samarium carbonate, prepared from Sm$_2$O$_3$ (Merck 99.9%), was dissolved in a solution containing 60% of trifluoroacetic acid (Reachim). The excess carbonate was filtered off; after evaporation samarium trifluoroacetate crystallized. The product was dried under vacuum over P$_2$O$_5$ at 330 K for about 150 hr,[9,10] then it was monitored by IR spectroscopy and analysed.

We further used ZrCl$_4$ (Merck zur Synthese 99%) and POCl$_3$ (Merck), freshly distilled in a stream of dry nitrogen. Sm(CF$_3$COO)$_3$–

POCl$_3$–ZrCl$_4$ solutions were prepared by dissolving Sm(CF$_3$COO)$_3$ in the POCl$_3$–ZrCl$_4$ mixture under dry nitrogen atmosphere as described by Brecher and French.[11] The solutions were slightly heated for 10 hr to remove the volatile impurities. The concentration of Sm^{3+} ions was determined as follows: samples of the solution were evaporated to dryness and then treated with warm HClO$_4$. The insoluble residue (with Zr) was filtered off and the amount of samarium was determined gravimetrically as oxalate. The Sm^{3+}:Zr^{4+} molar ratio could be calculated from the amount of ZrCl$_4$ and Sm(CF$_3$COO)$_3$ used in the preparation.

Absorption spectra were recorded over the 40,000-4000 cm^{-1} region with a Cary 14 spectrophotometer, with POCl$_3$ as standard.

RESULTS AND DISCUSSION

The experimental oscillator strengths were calculated by graphical integration of the absorption bands (with correction for the base line) using an appropriate programme. From the experimental oscillator strengths, the Ω_Ω parameters were calculated using the least-squares method from the equation:[1,2,12]

$$P = x \frac{8\pi^2 mc}{3h} \sigma \sum_{\lambda=2,4,6} \frac{\Omega_\lambda (f^n \psi J \| U^{(\lambda)} \| f^n \psi' J')^2}{2J+1}$$

where P = the oscillator strength of the transition, x = Lorentz field correction for the refractivity of the medium, σ = the wavenumber (in cm^{-1}), J, J' = the total quantum numbers of the initial and final states respectively, $(f^n \psi J \| U^{(\lambda)} \| f^n \psi' J')^2 = U(\lambda)$ = the squares of the matrix elements of the unit tensor operator.[13] The root-mean square deviation (rms) were determined from the differences

---

*Author to whom correspondence should be addressed.

between the experimental oscillator strengths and those calculated from the evaluated set of Ω_λ parameters.

In all the investigated spectra of Sm^{3+} ions in $POCl_3$–$ZrCl_4$ solutions (similarly to those of Dy^{3+} in $POCl_3$–$ZrCl_4$), a rise of the spectral base line is observed in the UV region down to 24,000 cm^{-1}. This fact makes accurate measurements in this spectral region very difficult. The changes in the base line cause the variations of the oscillator strength values from one solution to another. It is difficult to decide what effect is responsible for this phenomenon. However the application of $POCl_3$ as solvent made it possible to determine with good accuracy the oscillator strength values for the bands within the near-IR region (transitions to the $^6H_{13/2}$; $^6F_{1/2}$, $^6H_{15/2}$, $^6F_{3/2}$; $^6F_{5/2}$; $^6F_{7/2}$ and $^6F_{9/2}$ levels). It is possible to leave out the UV part of the spectrum since a sufficient set of oscillator strengths is available in this case.

Experimental oscillator strengths values and those calculated from the Judd–Offelt equation for the Sm^{3+}–$POCl_3$–$ZrCl_4$ solutions with different Sm^{3+} concentrations are presented in the Table 1. The rms deviations of the oscillator strengths and evaluated sets of the intensity parameters are also included. The evaluated sets of the Ω_λ parameters reproduce relatively well the experimental set of the oscillator strengths values. The advantage of using the aprotic solvent in the investigation of the spectral intensity of the Sm^{3+} ion consist in the fact

that, aside from the relatively intense bands in the near IR, most of the 4f–4f transitions of the Sm^{3+} ion give rise to the rather weak absorption bands. For the transitions at wave number higher than 7500 cm^{-1}, the U(2) matrix element values are small (they do not exceed 0.022) and the total of all the U(2) values for about 100 transitions within the 7500–48,300 cm^{-1} spectral range is over 30 times smaller than that for the five transitions within the 4200–7500 cm^{-1} energy range. Moreover, the interpretation of the Sm^{3+} spectrum becomes complicated by the high density of the energy levels in the visible –UV regions. There it is necessary to assign arbitrarily the centres of gravity for a rather large number of states for each of the complex band envelopes observed up 20,000 cm^{-1}.[8] Thus, those observables are of little value in the fitting procedure and the omission of this group of bands seems to be quite reasonable.

We found that if the transitions with higher U(2) and U(4) matrix elements values transitions: $^6F_{5/2} \leftarrow {}^6H_{5/2}$ and $^6F_{3/2}\,{}^6H_{15/2}\,{}^6F_{1/2} \leftarrow {}^6H_{5/2}$ are included in the set of absorption bands used for the calculations, the values of the Ω_λ parameters for the Sm^{3+}–$POCl_3$–$ZrCl_4$ solutions are insensitive to variations of the fitting procedure. This was proved by repeating the fitting procedure with omission of one or two absorption bands. If however the $^6F_{5/2} \leftarrow {}^6H_{5/2}$ and/or $^6F_{3/2}\,{}^6H_{15/2}\,{}^6F_{1/2} \leftarrow {}^6H_{5/2}$ transitions were excluded from the considered absorption bands, the values of the Ω_2 and Ω_4 parameters

Table 1. The experimental and calculated oscillator strengths and Ω_λ parameters values for the Sm^{3+} in $POCl_3$–$ZrCl_4$ solutions. $c_{Sm^{3+}}:c_{Zr^{4+}} = 1:1.5$

Energy level	Spectral region (cm^{-1})	max (cm^{-1})	$10^6 P$					
			exp.	calc.	exp.	calc.	exp.	calc.
$^4I_{15/2}$ $^4G_{9/2}$ $^4M_{17/2}$ $^4F_{5/2}$	23250 – 21950	22780 22210	0.26	$\{$0.18 $\{$0.01*	0.29	$\{$0.18 $\{$0.01*	0.33	$\{$0.18 $\{$0.01*
$^4I_{13/2}$ $^4I_{11/2}$ $^4M_{15/2}$ $^4I_{9/2}$	21950 – 20200	21530	1.82	1.18	1.89	1.16	1.86	1.16
$^4G_{7/2}$	20200 – 19720	20010	0.03	0.09	0.03	0.08	0.04	0.08
$^4F_{11/2}$	11050 – 9900	10610	0.36	0.42	0.37	0.41	0.38	0.41
$^6F_{9/2}$	9700 – 8700	9260	2.54	2.61	2.47	2.56	2.53	2.58
$^6F_{7/2}$	8550 – 7600	8110	3.88	4.08	3.79	4.01	3.77	4.01
$^6F_{5/2}$	7580 – 6860	7250	2.73	2.62	2.71	2.59	2.68	2.55
$^6F_{3/2}$ $^6H_{15/2}$ $^6F_{1/2}$	6860 – 5880	6720 6550 6450	2.10	2.13	2.17	2.19	2.09	2.11
$^6H_{13/2}$	5750 – 4300	5120	0.29	0.26	0.28	0.25	0.30	0.26
$10^{20}\Omega_2$ (cm^2)			3.44$\pm$1.14		3.67$\pm$1.39		3.67$\pm$1.39	
$10^{20}\Omega_4$ (cm^2)			9.76$\pm$1.10		9.60$\pm$1.34		9.47$\pm$1.20	
$10^{20}\Omega_6$ (cm^2)			5.86$\pm$0.49		5.76$\pm$0.61		5.80$\pm$0.54	
10^7 rms			2.86		3.23		3.12	
$c_{Sm^{3+}}$ (M)			0.070		0.226		0.260	

*Calculated magnetic-dipole oscillator strength.[13]

varied significantly and were determined with a low accuracy (if the $^6F_{3/2}\,^6H_{15/2}\,^6F_{1/2} \leftarrow\,^6H_{5/2}$ transitions were excluded then $\Omega_2 = 58.5 \pm 18.6$). This means that when those important transitions are omitted, the Ω_2 and Ω_4 parameter values will become simply fitting parameters with no physical meaning.

From these results we are led to conclude definitely that a reasonable set of Ω_λ parameters can be evaluated for the Sm^{3+} ion (similarly as for the Dy^{3+}[14]) only if the near-IR region is available to measurements. To avoid the danger of evaluation of Ω_λ values devoid of physical meaning for the Sm^{3+} ion it is always necessary to consider transitions in the near-IR region.

REFERENCES

1. B. R. Judd, *Phys. Rev.* 1962, **127**, 750.
2. G. S. Ofelt, *J. Chem. Phys.* 1962, **37**, 511.
3. N. A. Kazanskaja, *Opt. Spekt.* 1970, **29**, 1101.
4. R. D. Peacock, *Mol. Phys.* 1973, **25**, 817.
5. K. Bukietyńska and G. R. Choppin, *J. Chem. Phys.* 1970, **52**, 2875.
6. W. T. Carnall, P. R. Fields and K. Rajnak, *J. Chem. Phys.* 1968, **49**, 4412.
7. D. E. Henrie and C. E. Smyser, *J. Inorg. Nucl. Chem.* 1977, **39**, 625.
8. W. T. Carnall, J. P. Hessler and F. Wagner, *J. Phys. Chem.* 1978, **82**, 2152.
9. B. Mathur and T. R. Bhat, *Z. Anorg. Allgem. Chem.* 1966, **343**, 220.
10. J. E. Roberts, *J. Amer. Chem. Soc.* 1961, **83**, 1087.
11. C. Brecher and K. W. French, *J. Phys. Chem.* 1973, **77**, 1370.
12. J. A. Axe, *J. Chem. Phys.* 1963, **39**, 1154.
13. W. T. Carnall, P. R. Fields and K. Rajnak, *J. Chem. Phys.* 1968, **49**, 4424.
14. K. Bukietyńska and B. Radomska, *Chem. Phys. Lett.* 1981, **79**, 162.

STERIC EFFECTS IN THE COMPLEXATION KINETICS OF COPPER(II) WITH *RAC*-5,5,7,12,12,14-HEXAMETHYL-1,4,8,11-TETRAAZACYCLOTETRADECANE IN BASIC AQUEOUS MEDIA

FU-TANG CHEN, CHUNG-SHIN LEE and CHUNG-SUN CHUNG*
Department of Chemistry, National Tsing Hua University, Hsinchu, Taiwan 300,
Republic of China

Abstract—Copper(II) reacts with *rac*-5,5,7,12,12,14-hexamethyl-1,4,8,11-tetraaza-cyclotetradecane (tet-b) in strongly basic aqueous media to give [Cu(tet-b) (OH) (blue)]$^+$ which contains trigonal bipyramidally co-ordinated Cu^{2+} with the tet-b ligand in its most stable, folded form. The kinetics of formation of this blue complex have been studied at $25.0° \pm 0.1°C$ using the stopped-flow technique. Second-bond formation is proposed as the rate-determining step for tet-b reaction with $Cu(OH)_3^-$ and $Cu(OH)_4^{2-}$. Possible mechanisms for the reaction and the steric effects resulting from the methyl groups on the alkyl backbone of the macrocyclic ligand are considered.

In order to account for the remarkable kinetic effects of ligand cyclization upon complex formation rate constants, a number of papers have dealt with various aspects of the kinetics of incorporation of metal ions into macrocyclic ligands.[1-10] As recently demonstrated,[5] the comparative behaviour of the closely correlated open-chain and cyclic ligands indicates that ligand cyclization itself has only a relatively small influence upon the complex formation rate-constants. Instead, the more significant kinetic effects arise from the substitution at the nitrogen donor atoms of the open-chain ligands or on the alkyl backbone of the cyclic compounds.[5]

In the current investigation, we have attempted to study the steric effects resulting from alkyl substitutions on the alkyl backbone of the macrocyclic ligand in complexation reaction. To accomplish this we have studied the kinetics of copper (II) reacting with unprotonated *rac*-5,5,7,12,12,14-hexamethyl-1,4,8,11-tetraazacyclotetradecane (tet-b, see Chart 1) in strong NaOH solutions.

Under these conditions the copper is present as a mixture of soluble hydroxide species,[5-11] and the ligand is essentially unprotonated.[12] Thus the reaction studied may therefore be represented by the formulation in eqn (1).

$$Cu(OH)_x^{2-x} + \text{tet-b} \xrightarrow{k_{obsd}}$$

$$[Cu(\text{tet-b})(OH)(\text{blue})]^+ + (x-1)OH^- \quad (1)$$
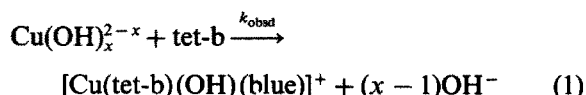
In marked contrast to the reactions of 1,4,8,11-tetraazacyclotetradecane (cyclam, see Chart 1) and *meso*-5,12-dimethyl-1,4,8,11-tetraazacyclotetradecane (Me$_2$cyclam, see Chart 1), tet-b reacts with copper(II) in basic aqueous media to give initially a blue 5-coordinate complex [Cu(tet-b)(OH)(blue)]$^+$ with the ligand in its most stable, folded form.[13] This kinetically controlled blue product is readily converted to the more thermodynamically stable red isomers, and the kinetics of this blue-to-red interconversion has recently been reported.[14,15]
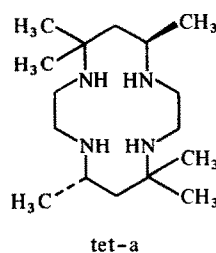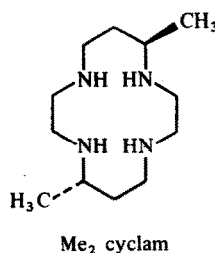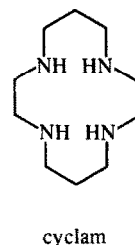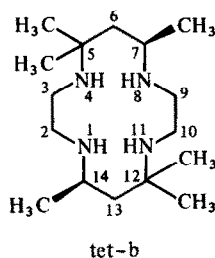

tet-b

cyclam

Me$_2$ cyclam

tet-a

Chart 1.

*Author to whom correspondence should be addressed.

EXPERIMENTAL

Reagents. The macrocyclic ligand tet-b was prepared by using the procedure described by Hay, Lawrance, and Curtis;[16] m.p. 102–105° (lit. m.p. 97–105°[17]). Found: C, 64.47; H, 12.64; N, 18.34. Calc. for $C_{16}H_{36}N_4 \cdot H_2O$: C, 63.53; H, 12.66; N, 18.52%. The ligand stock solutions were standardized by spectrophotometric mole ratio plots with standard Cu(II) solution.

The salt $Cu(ClO_4)_2 \cdot 6H_2O$ was recrystallized twice from water and standardized by titration with ethylenediaminetetraacetate. $NaNO_3$ was recrystallized twice before use. A saturated solution of sodium hydroxide (reagent grade) was prepared to precipitate sodium carbonate. A sample of this was diluted with freshly boiled, distilled, deionized water and stored in a Nalgene Teflon bottle. It was standardized against weighed amounts of potassium hydrogen phthalate.

Kinetic measurements. The reactions were monitored at 270 and 670 nm using a Union Giken RA-401 stopped-flow spectrophotometer. The temperature was maintained at $25.0° \pm 0.1°C$. Ionic strength was controlled at 1.0 mol dm^{-3} by using $NaNO_3$. The rate constants were obtained by a linear least-squares fit of the data by using the IBM 1130 computer.

RESULTS

In the $[OH^-]$ range of the measurements the ligand is essentially unprotonated, while the copper(II) is present as $Cu(OH)_3^-$ and $Cu(OH)_4^{2-}$.[5] The reactions were studies as a function of NaOH concentration at $25.0° \pm 0.1°C$ in an attempt to resolve the individual rate contributions of $Cu(OH)_3^-$ and $Cu(OH)_4^{2-}$. Studies were carried out under pseudo-first-order conditions by using at least a tenfold excess of ligand or copper(II) ion. The observed pseudo-first-order rate constants are given in Table 1. Plots of k'_{obsd} vs [tet-b] and k'_{obsd} vs $[Cu(OH)_x^{2-x}]$ give straight lines as shown in Figs. 1 and 2 respectively. The reaction was found to be first order with respect to each reactant and to proceed to completion according to the rate expression in eqn (2). The second-order rate constants are given in Table 1.

$$d[Cu(tet\text{-}b)(OH)(blue)^+]/dt = k_{obsd}$$
$$[Cu(OH)_x^{2-x}]_T[tet\text{-}b] \qquad (2)$$

As shown in Table 1, values of k'_{obsd} decreased as $[OH^-]$ increased. The rate of formation can be represented by eqn (3). Here L is tet-b.

$$\text{Rate} = k_{obsd}[Cu(OH)_x^{2-x}]_T[L] = k^L_{Cu(OH)_3}$$
$$\times [Cu(OH)_3^-][L] + k^L_{Cu(OH)_4}$$
$$\times [Cu(OH)_4^{2-}][L]. \qquad (3)$$

Table 1. Observed rate constant values for copper(II) reacting with tet-b in basic solution at $25.0° \pm 0.1°C$, $I = 1.0 \text{ mol dm}^{-3}$ ($NaNO_3 + NaOH$)

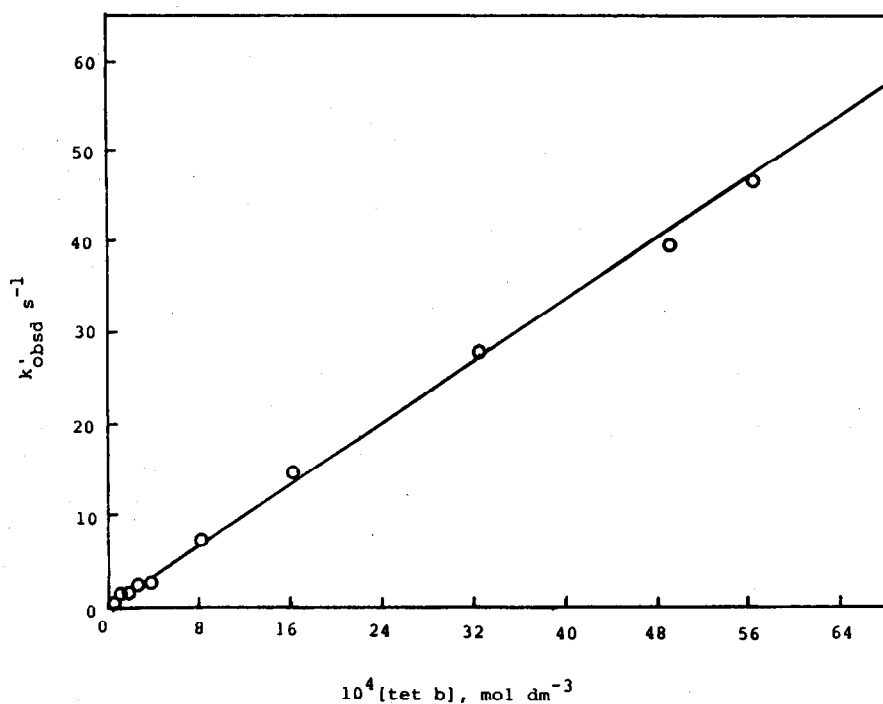| $10^5[Cu(OH)_x^{2-x}]_T$ mol dm^{-3}	$10^5[tet\ b]$ mol dm^{-3}	$[NaOH]$ mol dm^{-3}	k'_{obsd} s^{-1}	$10^{-4}k_{obsd}$ $\text{dm}^3 \text{ mole}^{-1}s^{-1}$
1.04	20.1	0.02	5.48	2.73
1.04	30.5	0.02	8.24	2.70
1.04	40.3	0.02	10.7	2.66
1.04	20.1	0.05	4.02	2.01
1.04	40.3	0.05	7.98	1.98
1.04	20.1	0.05	4.07	2.02
1.04	20.1	0.10	2.92	1.45
1.04	10.2	0.20	0.833	0.866
1.04	15.1	0.20	1.36	0.901
1.04	20.1	0.20	1.88	0.935
1.04	25.6	0.20	2.16	0.844
1.04	30.1	0.20	2.93	0.973
1.04	40.4	0.20	3.71	0.718
1.04	80.6	0.20	6.93	0.860
1.04	167	0.20	14.1	0.844
1.04	325	0.20	28.1	0.865
1.04	495	0.20	39.4	0.796
1.04	564	0.20	46.5	0.824
10.8	1.03	0.20	0.991	0.918
24.5	1.03	0.20	2.46	1.00
43.5	1.03	0.20	3.75	0.837
87.2	1.03	0.20	7.13	0.818
107	1.03	0.20	9.17	0.857
158	1.03	0.20	13.4	0.848
1.04	20.2	0.40	0.981	0.485
1.04	40.3	0.40	1.99	0.495
1.04	20.2	0.50	0.818	0.405
1.04	80.4	0.50	3.36	0.418
1.04	40.3	0.80	1.12	0.279
1.04	20.1	1.00	0.480	0.239

Fig. 1. The effect of tet-b concentration on the observed pseudo-first order rate constant for the reaction of $Cu(OH)_x^{2-x}$ with tet-b, $[Cu(OH)_x^{2-x}] = 1.04 \times 10^{-5} \, mol \, dm^{-3}$ 25.0°C, $[OH^-] = 0.20 \, mol \, dm^{-3}$, and $I = 1.0 \, mol \, dm^{-3}$ $(NaOH + NaNO_3)$.

Using the reported concentration equilibrium constants,[5,18] the resolved rate constants can be obtained from eqn (4).

$$k_{obsd}(1 + K_4^C[OH^-]) = k_{Cu(OH)_3}^L + k_{Cu(OH)_4}^L K_4^C[OH^-] \quad (4)$$

A plot of eqn (4) is shown in Fig. 3, and the values thus obtained are listed in Table 2 along with the reported values for cyclam, Me$_2$cyclam, and meso-5,5,7,12,12,14-hexamethyl-1,4,8,11-tetraazacyclotetradecane (tet-a, see Chart 1).[5,18]
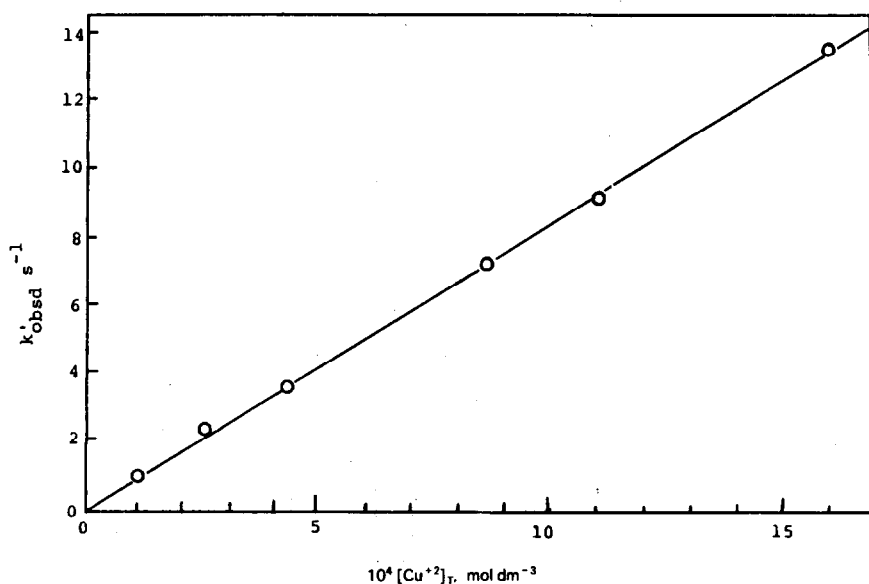

Fig. 2. The effect of $Cu(OH)_x^{2-x}$ concentration on the observed pseudo-first order rate constant for the reaction of $Cu(OH)_x^{2-x}$ with tet-b, $[tet-b] = 1.03 \times 10^{-5} \, mol \, dm^{-3}$,   25.0° ± 0.1°C, $[OH^-] = 0.20 \, mol \, dm^{-3}$ and $I = 1.0 \, mol \, dm^{-3}$ $(NaOH + NaNO_3)$.
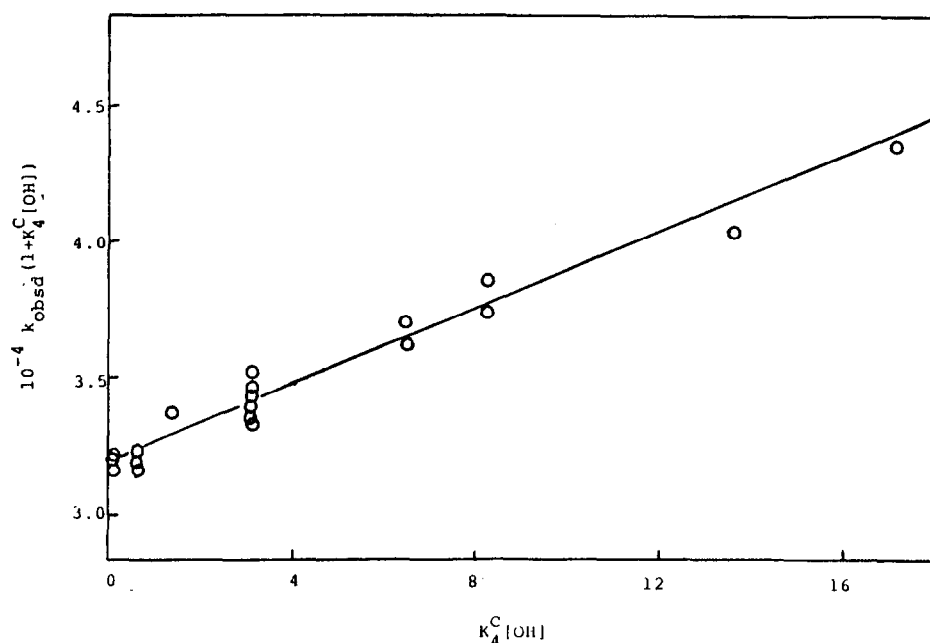
Fig. 3. Plot of eqn (4) to resolve the rate constants for the reaction of tet-b with $Cu(OH)_3^-$ and $Cu(OH)_4^{2-}$.

Table 2. Resolved formation rate constants for hydroxycuprate(II) species reacting with unprotonated macrocyclic tetraamines at $25.0° \pm 0.1°C$

Ligand	$k^L_{Cu(OH)_3}, dm^3mol^{-1}s^{-1}$	$k^L_{Cu(OH)_4}, dm^3mol\ s^{-1}$
tet b	3.2×10^4	1.1×10^2
Cyclam[a]	2.7×10^6	3.8×10^4
Me$_2$cyclam[a]	5.6×10^5	0.9×10^4
tet a[b]	$\sim 10^4$	$< 10^2$

[a] Reference 5.   [b] Reference 18.

DISCUSSION

As shown in Table 2, the resolved rate constants decrease with increasing methyl substitutions on the alkyl backbone of the cyclic ligands, and the difference increases dramatically for the highly substituted ligands, tet-b and tet-a. This trend indicates that the reactions exhibit a significant degree of association with the incoming nucleophile at the point of the rate-determining step.

The position of the rate-determining step is an important consideration in comparing the reactivities of closely related multidentate ligands with metal ions. The kinetics of Cu(II) reacting with a series of open-chain and cyclic polyamines have been studied by Lin *et al.*[5] For the reactions of cyclam and Me$_2$cyclam, Jahn-Teller (tetragonal) inversion following the first copper–nitrogen bond

formation is proposed as the rate-determining step with $Cu(OH)_3^-$, while second copper–nitrogen bond formation is proposed as the rate-determining step with $Cu(OH)_4^{2-}$.[5]

In the reaction of tet-b, the formation of Cu–N(1) or Cu–N(8) bond is expected to be faster than the formation of Cu–N(4) or Cu–N(11) bond on steric grounds. Accordingly, the first-coordinate-bond formation with N(1) or N(8) is expected to represent the predominant reaction route for the $Cu(OH)_x^{2-x}$ reaction with tet-b. The second-bond formation is the formation of Cu–N(4) or Cu–N(11) bond. As pointed out by Turan and Rorabacher,[19] alkyl substitution at sites three or more atoms removed from the donor atom undergoing coordinate-bond formation has little effect upon the ligand reactivity. Therefore, only·

one of the six methyl groups on the alkyl backbone of tet-b has significant effect upon the ligand reactivity at the point of first coordinate-bond formation. If Jahn–Teller inversion following the first-bond formation were the rate-determining step for the $Cu(OH)_x^{2-x}$ reaction with tet-b, the observed difference of the resolved rate constants between tet-b and cyclam should be mainly attributable to the steric effect of a C-substituted methyl group. The small ratios $k^{tet-b}_{Cu(OH)_3}/k^{cyclam}_{Cu(OH)_3}$ and $k^{tet-b}_{Cu(OH)_4}/k^{cyclam}_{Cu(OH)_4}$ strongly suggest that the first coordinate-bond formation may not be the rate-determining step for the tet-b reaction with $Cu(OH)_3^-$ or $Cu(OH)_4^{2-}$.

It is extremely unlikely for copper(II) to maintain a coordination number of 7 with three amine groups of tet-b and three OH^- groups. The fact that $Cu(OH)_4^{2-}$ appears as a reactant indicates that the rate-determining step occurs prior to the third coordinate-bond formation.[5] Furthermore, chelate effect and the stable copper–amine bonds also suggest that the rate-determining step occurs prior to the third-bond formation.[20] Thus these kinetic results lead to the postulate that second-bond formation is the rate-determining step for tet-b reacting with $Cu(OH)_3^-$ and $Cu(OH)_4^{2-}$.

It is interesting to note that first-bond formation is the rate-determining for the $Cu(OH)_3^-$ reaction

with cyclam or Me$_2$cyclam, while the second-order formation is the rate-determining for the $Cu(OH)_3^-$ reaction with tet-b. This sterically induced shift in the rate-determining step can readily be explained by the reaction mechanism proposed by Rorabacher and Margerum shown in Fig. 4.[5] As discussed previously, the second-bond formation is the formation of Cu–N(4) or Cu–N(11) bond, and the large steric effects resulting from the methyl groups on tet-b related to the crowding of coordinated water molecules and the high-energy barrier to internal rotation are expected to retard the formation of the second Cu–N bond (k_{2a}) and to accelerate the reelongation of the Cu–N bond (k_{-1b}). This would greatly improve the chances that $k_{-1b} > k_{2a}$, resulting in a shift of the rate-determining step to the point of second-bond formation. Similar sterically induced shift in the rate-determining step for Ni(II)–diamine reactions has been reported.[19]

Another interesting aspect of this study is the geometry of the product. In marked contrast to the reactions of $Cu(OH)_x^{2-x}$ with cyclam and Me$_2$cyclam,[21] $Cu(OH)_x^{2-x}$ reacts with tet-b to form initially a blue complex. This blue complex has been neutralized and isolated as [Cu(tet-b)]$_2$Cl(ClO$_4$)$_3$ which contains 5-coordinate (trigonal-bipyramidal) copper and with the tet-b ligand in its

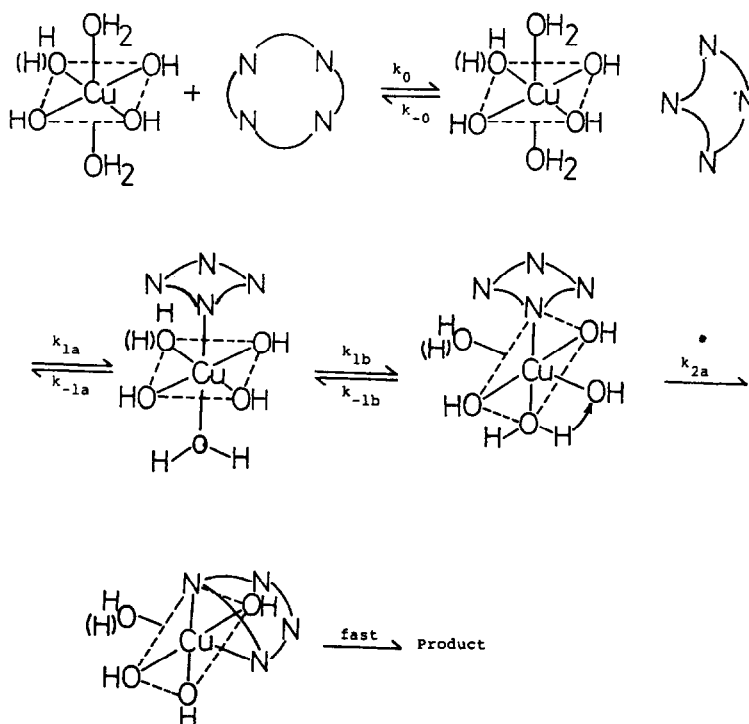

Fig. 4. Detailed mechanism proposed by Rorabacher and Margerum (Ref. 5) for $Cu(OH)_3^-$ (or $Cu(OH)_4^{2-}$) reacting with a tetraamine macrocyclic ligand showing sequential bonding and Jahn–Teller inversion steps.

most stable, folded form.[13] Chloride ion, which occupies one of the positions in the trigonal plane, dissociates from the copper in dilute solution but the electronic spectral characteristics of the complex in aqueous solution are similar to those of the crystals.[22] The blue complex is the kinetically controlled product, and is readily converted to the more thermodynamically stable red isomer in basic solution. The thermodynamics and kinetics of this blue-to-red interconversion have recently been reported.[14,23]

Assuming an initial coordination number of six for $Cu(OH)_x^{2-x}$ the coordination number of the blue product indicates that at some point in this reaction the formation of a copper–nitrogen bond has caused the loss of two coordinated water molecules. As pointed out by Margerum,[21] it is energetically more favourable if the multiple desolvation step occurs after the coordination of several strong donor groups. In order to relieve the steric congestion attributable to the methyl groups and to avoid multiple desolvation occurring prior to the rate-determining step, this highly substituted macrocyclic ligand folds in the complexation reaction with $Cu(OH)_x^{2-x}$, resulting in the formation of the blue species.

In addition to the reaction of $Cu(OH)_x^{2-x}$ with tet-b, unstable blue intermediates were also observed in the reactions of copper(II) with highly substituted macrocyclic tetraamines such as *meso*-5,5,7,12,12,14-hexamethyl-1,4,8,11-tetraazacyclotet radecane, *rac*-5,7,7,12,12,14-hexamethyl-1,4,8,11-tetraazacyclotetradecane, *meso*-5,7,7,12,12,14-hexamethyl-1,4,8,11-tetraazacyclotetradecane, and 5,7,12,14-tetraethyl-5,12-dimethyl-1,4,8,11-tetra-azacyclotetradecane.[24] Similar to the reaction of tet-b, some degree of ligand twisting or folding may be necessary to avoid multiple desolvation occurring prior to the rate-determining step. The formation of the blue species is a consequence of the folding or twisting of the macro-cyclic ligand. The kinetics of the blue-to-red interconversions of copper(II) complexes of these ligands have recently been reported.[24-26] It is interesting that such blue intermediates were not observed for the $Cu(OH)_x^{2-x}$ reaction with the less sterically hindered ligands such as cyclam and $Me_2cyclam$.[21]

In conclusion, the steric effects attributable to the substituted methyl groups on tet-b retard the forward steps and accelerate the backward steps of the complexation reaction of tet-b with copper(II), resulting in a shift of the rate-determining step to the point of second-bond formation, and a folding of the macrocyclic ligand.

REFERENCES

1. D. K. Cabbiness and D. W. Margerum, *J. Am. Chem. Soc.* 1969, **91**, 6540; 1970, **92**, 2151.
2. M. Kodama and E. Kimura, *J. Chem. Soc., Dalton* 1977, 1473.
3. T. A. Kaden, *Helv. Chim. Acta* 1971, **54**, 2307.
4. R. W. Hay and C. R. Clark, *J. Chem. Soc., Dalton* 1977, 1148.
5. C.-T. Lin, D. B. Rorabacher, G. R. Cayley and D. W. Margerum, *Inorg. Chem.* 1975, **14**, 919.
6. B.-F. Liang and C.-S. Chung, *J. Chin. Chem. Soc.* 1979, **26**, 85.
7. T. A. Kaden, *Chimia* 1969, **23**, 193.
8. L. Hertli and T. A. Kaden, *Helv. Chim. Acta* 1974, **57**, 1328.
9. W. Steinmann and T. A. Kaden, *Helv. Chim. Acta* 1975, **58**, 1358.
10. R. Buxtorf and T. A. Kaden, *Helv. Chim. Acta* 1974, **57**, 1035.
11. L. A. McDowell and H. L. Johnston, *J. Am. Chem. Soc.* 1963, **58**, 2009.
12. C.-L. Luo, C.-H. Chen and C.-S. Chung, *J. Chin. Chem. Soc.* 1979, **26**, 61.
13. R. A. Bauer, W. R. Robinson and D. W. Margerum, *J. Chem. Soc. Chem. Commun.* 1973, 289.
14. B.-F. Liang, D. W. Margerum and C.-S. Chung, *Inorg. Chem.* 1979, **18**, 2001.
15. C.-S. Chung, *Proc. Natl. Sci. Counc.* 1981, **5**, 240.
16. R. W. Hay, G. A. Lawrance and N. F. Curtis, *J. Chem. Soc, Perkin* 1975, **1**, 591.
17. N. F. Curtis, *J. Chem. Soc.* 1964, 2644.
18. D. K. Cabbiness, Ph.D. Thesis. Purdue University, 1970.
19. T. S. Turan and D. B. Rorabacher, *Inorg. Chem.* 1972, **11**, 288.
20. C.-S. Chung, *Inorg. Chem.* 1979, **18**, 1321.
21. D. W. Margerum, G. R. Cayley, D. C. Weatherburn and G. K. Pagenkopb, *ACS Monogr.* 1978, No. 174.
22. D. W. Margerum and R. A. Bauer, unpublished work.
23. B.-F. Liang and C.-S. Chung, *J. Chem. Soc., Dalton* 1980, 1349.
24. B.-F. Liang, Ph.D. Thesis, Tsing Hua University, 1980.
25. B.-F. Liang and C.-S. Chung, *Inorg. Chem.* 1980, **19**, 1867.
26. B.-F. Liang and C.-S. Chung, *Inorg. Chem.* 1981, **20**, 2152.

SYNTHESIS AND CHARACTERIZATION OF TWO Ni(II) COMPLEXES WITH FURFURAL S-METHYLTHIOSEMICARBAZONE

VUKADIN M. LEOVAC,* VLADIMIR DIVJAKOVIĆ and DRAGOSLAV PETROVIĆ

Faculty of Sciences, University of Novi Sad, I. Djuričića 4, 21000 Novi Sad, Yugoslavia

and

GYULA ARGAY and ALAJOS KÁLMÁN

Central Research Institute of Chemistry, Hungarian Academy of Sciences, H-1525 Budapest, POB 17, Hungary

Abstract—Synthesis of two Ni(II) complexes with furfural S-methylthiosemicarbazone (HL) of the formula $[Ni(HL)_2(H_2O)_2](ClO_4)_2$ (**A**) and $[Ni(HL)_2(ClO_4)_2]$ (**B**) are reported. Compound **A** was obtained from an ethanolic solution of $Ni(ClO_4)_2 \cdot 6H_2O$ and HL, whilst compound **B** was produced by heating compound **A** to 378 K. An X-ray analysis of the complex **A** showed that it has a *trans*(H_2O)-*trans*(HL) octahedral configuration in which HL behaves as a bidentate (NN) ligand. On the basis of the IR and electronic spectra as well as the magnetism, it was found that the compound **B** has also an octahedral configuration in which, HL and ClO_4 groups, are coordinated.

The synthesis and structural investigations of a considerable number of complexes of transition metals with S-methylthiosemicarbazide[1,2] and different S-methylthiosemicarbazones[3–9] have been recently reported. It has been established that S-methylthiosemicarbazide[1,2] and acetone S-methylthiosemicarbazone[3] behave as bidentate (NN) ligands. On the other hand, the products obtained by a condensation reaction of S-methylthiosemicarbazide with salicyladehyde[4–7] and 8-quinolinaldehyde[8,9] behave as tridentate (NNO) and (NNN) ligands, respectively. Studying further these complexes of 3d elements with S-methylthiosemicarbazones we report here the syntheses, IR and electronic spectra of two Ni(II) complexes with the new furfural S-methylthiosemicarbazone $[Ni(HL)_2(H_2O)_2](ClO_4)_2$ and $[Ni(HL)_2(ClO_4)_2]$ as well as the crystal structure analysis of the first complex, where HL = furfural S-methylthiosemicarbazone†:
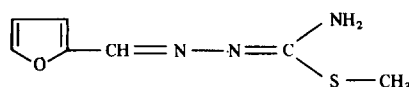
EXPERIMENTAL

Elemental analysis. For the elemental analysis the air-dry substance was used. Nickel was determined as bis(dimethylglyoximato)-nickel(II) after decomposing the complex by heating with 5.0 cm³ of conc. HNO_3 and 3–4 drops of conc. H_2SO_4. Nitrogen was determined as N_2 according to Dumas' method; carbon and hydrogen were determined by combustion into CO_2 and H_2O, respectively.

Magnetic susceptibility measurements. Magnetic susceptibility was measured at 300 K according to the Faraday method using $Hg[Co(NCS)_4]$ as calibrant; diamagnetic corrections were made by employing Pascal's constants.[10]

IR and electronic spectra. IR spectra were recorded with Carl–Zeiss model Specord IR 75 in KBr. Electronic spectra were measured in reflection mode on monochromator SPM-2 (Zeiss–Jena) using a reflection cell of the type R-45/0. Samples were prepared to comply with the

---

*Author to whom correspondence should be addressed.

†This ligand can be coordinated as a monoanion (L⁻) resulting from deprotonation of the NH₂-group (unpublished results).

hypothesis of theory.[11] MgO powder was used as a white standard.

Preparation of ligand. The ligand, furfural S-methylthiosemicarbazone was obtained by heating with refluxing the ethanolic solution of the stoichiometric amounts of S-methylthiosemicarbazide hydrogen iodide,[12] furfural and $Na_2CO_3 \cdot 10H_2O$. After completing the reaction (3 hr) the solution was filtered and its amount reduced to a small volume by heating with warm air. The yellowish crystals of the ligand, formed at room temperature, were filtered out and washed with ethanol and ether. Yield: 60%.

Preparation of complexes. $[Ni(HL)_2(H_2O)_2]$ $(ClO_4)_2$. A mixture consisting of 0.6 g of $Ni(ClO_4)_2 \cdot 6H_2O$ and 0.5 g of furfural S-methylthiosemicarbazone was dissolved by heating in 4.0 cm³ of ethanol and left at room temperature for about 50 hr. The resulting green–grey crystals were filtered off and washed with ethanol and ether. Yield: 0.6 g. Found: Ni, 8.76; C, 26.06; H, 3.17; N, 13.01; H_2O, 5.42; Calc. for $[Ni(HL)_2(H_2O)_2](ClO_4)_2$: Ni, 8.89; C, 25.47; H, 3.36; N, 12.73; H_2O, 5.45%; $\mu_{eff} = 3.18$ B.M. (300 K).

$[Ni(HL)_2(ClO_4)_2]$. Heating the powdered crystals of $[Ni(HL)_2(H_2O)_2](ClO_4)_2$ at 378 K produced the anhydrous complex $[Ni(HL)_2(ClO_4)_2]$. This transformation was accompanied by a change of colour from green–grey into yellow–green. The new compound is air stable. Found: Ni, 9.39; C, 27.08; H, 2.82; N, 13.61; Calc. for $[Ni(HL)_2(ClO_4)_2]$: Ni, 9.41; C, 26.94; H, 2.91; N, 13.46; $\mu_{eff} = 3.29$ B.M. (300 K).

Crystal structure analysis of $[Ni(HL)_2$ $(H_2O)_2](ClO_4)_2$. Crystal data of the complex are: $NiC_{14}H_{22}N_6O_{12}S_2Cl_2$, $M_r = 660.04$, triclinic $P\bar{1}$, $a = 7.938(2)$, $b = 12.039(3)$, $c = 7.807(2)$ Å,

solved by direct methods using MULTAN and refined by full-matrix least-squares techniques. All non-hydrogen atoms were refined with anisotropic thermal parameters; H atoms were kept with fixed values for both positional and isotropic thermal parameters. The positions of all H atoms were located from a difference map. The least-squares refinement converged to a final $R = 0.062$. The ESD of an observation of unit weight was $S = 5.63$ for the observed reflections. The correction for extinction was applied with the refined value of $g = 0.35624 \times 10^{-7}$. Atomic scattering factors including the corrections for anomalous dispersion were taken from International Tables for X-ray Crystallography. Final atomic coordinates, thermal parameters and list of F_o/F_c values have been deposited with the Editor as supplementary material; copies are available on request. Bond distances and angles are given in Table 1.

RESULTS AND DISCUSSION

Descriptions of the crystal structure. As shown by Fig. 1 the lattice consists of discrete complex cations $[Ni(HL)_2(H_2O)_2]^{2+}$ and ClO_4^- bound together by hydrogen bonds. However, the Ni(II) is screened completely from the anions. Ni(II), situated at a centre of symmetry, is surrounded pseudo-octahedrally by four N and two O atoms. The four nitrogen atoms: N(1), N(1), N(3) and N(3) form a plane around Ni with a mean Ni....N distance of 2.112(5) Å, which is in a good agreement with those found in high-spin Ni(II) complexes with four coplanar N donors.[13] The apical positions of the octahedron are occupied by two water molecules at a distance of 2.119(5) Å from Ni(II). Each water molecule maintains two hydrogen bonds with the ClO_4^- ions

		H...A	D...A	DH...A
O(W)–H(W)1 ... O(3)	$1-x, \bar{y}, \bar{z}$	1.97(2)	2.92(1) Å	173(1)°
O(W)–H(W)2 ... O(4)	x, y, z	2.06(1)	2.84(1)	139(1).

$\alpha = 99.34(2)$, $\beta = 110.44(2)$, $\gamma = 105.74(2)°$; $V = 645.0(7)$ Å³, $D_c = 1.70$ g cm⁻³, $D_o = 1.75$ g cm⁻³, $Z = 1$, $\mu_{(MoK_\alpha)} = 11.8$ cm⁻¹, $F(000) = 338$.

X-Ray diffraction data and accurate cell dimensions were measured on an automated Enraf–Nonius CAD–4 diffractometer using graphite monochromated MoK_α radiation and the ω-2θ scan mode. Of the 2286 unique reflections recorded with $2\theta < 50°$, 1818 were regarded as observed $I > 4\sigma(I)$. No absorption correction was applied. The intensity statistics suggested the centrosymmetric space group $P\bar{1}$. The structure was

These infinite chains are formed along the [100] direction. They are crosslinked by a third hydrogen bond built up between N(2)–H(N2) bonds pointing outward from the complexes and O(1) atoms of the anions.

N(2)–H(N2) ... O(1) $1-x, \bar{y}, 1-z$

2.22(1)   2,95(1)   139(1)°

Of ClO_4^- only O(2) is not involved in hydrogen bonding which is shown by the shortest Cl–O distance (1.348(4) Å). As it is apparent from the

Table 1. Bond distances and bond angles of $[Ni(HL)_2(H_2O)_2](ClO_4)_2$

Ni - N(1)	2.002(3) Å	C(4) - C(7)	1.336(7) Å
Ni - N(2)	2.223(3)	C(4) - O(8)	1.352(6)
Ni - O_w	2.119(3)	C(7) - C(6)	1.406(7)
S - C(1)	1.754(4)	C(6) - C(5)	1.310(10)
S - C(2)	1.795(5)	C(5) - O(8)	1.420(7)
N(1)- C(1)	1.265(5)	Cl - O(1)	1.380(5)
N(2)- C(1)	1.364(6)	Cl - O(2)	1.348(4)
N(2)- N(3)	1.387(4)	Cl - O(3)	1.358(4)
N(3)- C(3)	1.269(5)	Cl - O(4)	1.367(7)
C(3)- C(4)	1.427(6)		

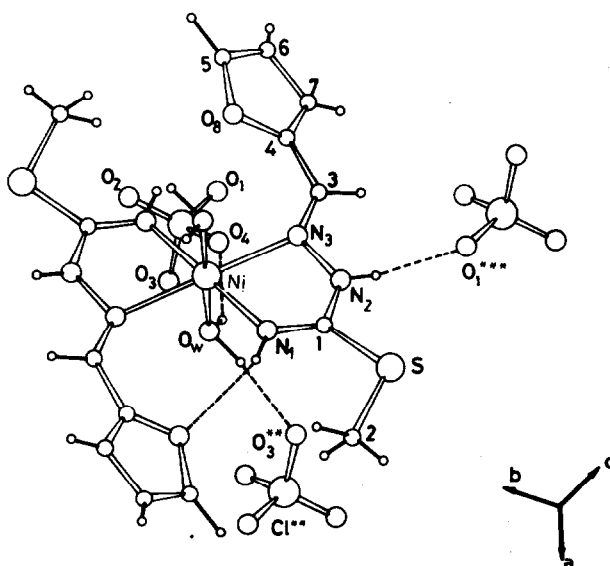|			
N(1) - Ni - N(3)	77.7(2)°	O(8) - C(4) - C(3)	126.8(7)°
N(1) - Ni - O_w	91.3(2)	O(8) - C(4) - C(7)	112.0(7)
N(3) - Ni - O_w	88.4(2)	C(6) - C(7) - C(4)	104.9(8)
C(2) - S - C(1)	101.3(4)	C(5) - C(6) - C(7)	110.1(9)
S - C(1)- N(1)	129.7(6)	C(8) - C(5) - C(6)	107.8(9)
S - C(1)- N(2)	111.2(5)	C(5) - O(8) - C(4)	105.1(7)
N(1) - C(1)- N(2)	119.0(5)	O(1) - Cl - O(2)	116.3(5)
Ni - N(1)- C(1)	117.2(5)	O(1) - Cl - O(3)	110.6(5)
C(1) - N(2)- N(3)	118.7(6)	O(1) - Cl - O(4)	107.1(6)
N(2) - N(3)- Ni	104.7(4)	O(2) - Cl - O(3)	109.7(6)
C(3) - N(3)- Ni	140.0(5)	O(2) - Cl - O(4)	112.6(6)
C(4) - C(3)- N(3)	126.6(7)	O(3) - Cl - O(4)	99.3(7)
C(7) - C(4)- C(3)	121.2(7)		

Fig. 1. A perspective view of the crystal lattice showing the coordination polyhedron around Ni(II) sitting at a centre of symmetry and some of the symmetry equivalent ClO_4^- tetrahedra. Atomic numbering is given with molecular fragments at (x, y, z). Bare numbers are for carbon atoms unless indicated otherwise. The numbering of H atoms is omitted. Symmetry equivalent atoms are labelled as follows: *, $= \bar{x}, \bar{y}, \bar{z}$; ** $= 1 - x, \bar{y}, \bar{z}$; *** $1 - x, \bar{y}, 1 - z$.

vigorous thermal motion of the ClO_4 tetrahedra the mean Cl–O bond length (1.363(4) Å) should be significantly shorter than that which is expected theoretically (1.45 Å)[14] and observed at low temperature. In accordance with the positions of H atoms around N(1) and N(2) inferred from difference Fourier synthesis the C(1)–N(1) double bond (1.265(5) Å) together with the low S–C(1)–N(2) angle (111.2(5)°) suggest that the new furfural S-methylthiosemicarbazone ligand predominantly assumes the *imido* form. No such localized C(1) = N(1) double bond has been found in other transition metal complexes with different S-methylthiosemicarbazone ligands.[3,6,7,9]

The thiosemicarbazide moiety together with C(3) and C(4) atoms lie roughly in the same plane (0.9744X + 0.1509Y − 0.1669Z = − 0.0966). The maximum deviation (0.18 Å) from this plane is shown by N(2). The furan ring is practically planar, the maximum displacement from the best plane (0.7281X + 0.5221Y − 0.4441Z = − 1.2517) is about 0.02 Å. The dihedral angle between these two least squares planes is 36.1(4)°. The two symmetry related ($\bar{1}$) ligands are bound together by a pair of weak hydrogen bond formed between the N(1)–H(N1) moiety and the ether oxygen O(8) of the symmetry related furan ring and vice versa.

$$H \ldots O = 2.37(1), \quad N \ldots O = 3.00(1) \text{ Å}$$

$$NH \ldots = 127(1)°.$$

Magnetic and spectral data. Both compounds are paramagnetic and their effective magnetic moments (3.18 B.M. for $[Ni(HL)_2(H_2O)_2](ClO_4)_2$ and 3.29 B.M. for $[Ni(HL)_2(ClO_4)_2]$) are within the limits characteristic for hexacoordinated Ni(II).[15] These values are in agreement with the unequivocally determined octahedral configuration for $[Ni(HL)_2(H_2O)_2](ClO_4)_2$ and with the supposed structure (based on the spectroscopic data) for $[Ni(HL)_2(ClO_4)_2]$. In Fig. 2 the fragments of the IR spectra for both complexes are depicted. It can be seen for $[Ni(HL)_2(H_2O)_2](ClO_4)_2$ in the region of 1150–1080 cm^{-1} there is a considerably wide very intense triplet band which can be assigned to the v_3 vibrations of ClO_4 group. It is known from the literature[15,16] that the ionically bonded perchlorate has around 1100 cm^{-1} a characteristic wide band of strong intensity which often shows tendency for splitting. The last is more pronounced in complexes which is the consequence of deformation of T_d symmetry of ClO_4 group, which is, on the other hand, caused by its coordination or, by presence of hydrogen bonds. With respect to the unequivocally determined ionic character of ClO_4 group in the complexes, the structure of $v_3(ClO_4)$ band is doubt-
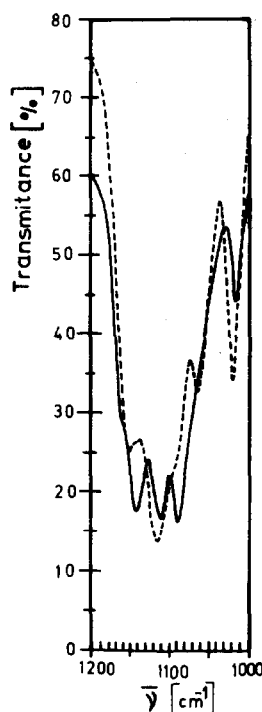

Fig. 2. Fragments IR spectra of:——$[Ni(HL)_2(H_2O)_2]$ $(ClO_4)_2$;---$[Ni(HL)_2(ClO_4)_2]$.

lessly, a consequence of the identified hydrogen bonds of these groups and atoms.

In contrast to this the $v_3(ClO_4)$ band in the IR spectrum of $[Ni(HL)_2(ClO_4)_2]$ is split into one band of very strong intensity at 1115 cm^{-1} on the one hand, and two somewhat weaker bands at 1150 and 1065 cm^{-1}, on the other hand. This is most probably due to the effect of coordination of the perchlorate group. In this way the paramagnetism of the compound can be also explained and supports the postulated octahedral configuration consisting of the two molecules of the bidentate furfural S-methylthiosemicarbazone and two ClO_4 groups.

It can be expected that the octahedral structure of this complex would be expected to be more tetragonally deformed compared to the starting aquo-complex; the same is indicated by the higher value of its magnetic moment.

The diffusion-reflection spectra are shown in Fig. 3. The reflectance spectra indicate unequivocally, the identical type of coordination of the central ion. Their array and the number of absorption maxima indicate the octahedral coordination of Ni(II). The Ni(II) ion involves the system $3d^8$ system. The first three maxima (1, 2, 3) can be attributed to the energy levels on a diagram of the Tanabe-Sugano type,[17] with the symmetry corresponding to the octahedral crystal field (Table 2).
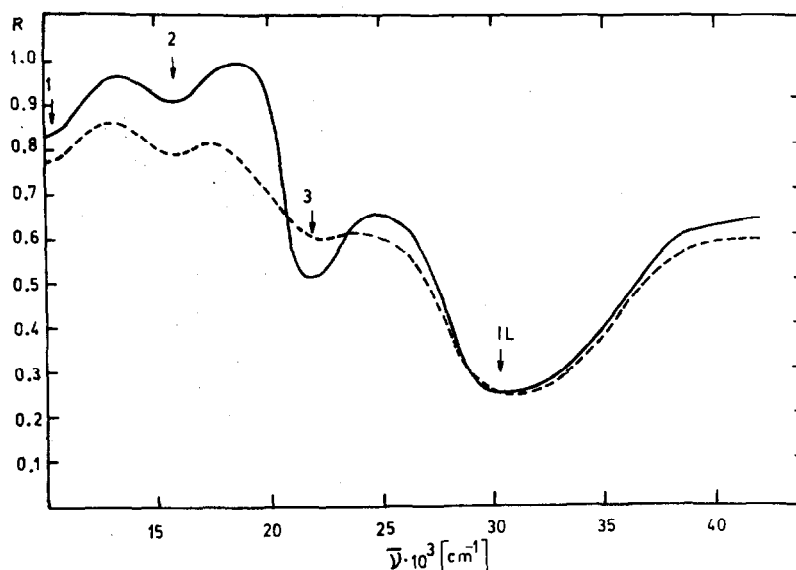
Fig. 3. Reflection spectrum of: —— $[Ni(HL)_2(H_2O)_2](ClO_4)_2$; – – – $[Ni(HL)_2(ClO_4)_2]$.

Table 2. Electronic spectral data

Complex	Transitions $[cm^{-1} \cdot 10^3]$			cm^{-1}	
	$^3A_{2g} \rightarrow {}^3T_{2g}(F)$	$^3A_{2g} \rightarrow {}^3T_{1g}(F)$	$^3A_{2g} \rightarrow {}^3T_{1g}(P)$	Dq	B
$[Ni(HL)_2(H_2O)_2](ClO_4)_2$	9.8	16.0	22.5	980	910
$[Ni(HL)_2(ClO_4)_2]$	9.6	15.8	22.5	960	950

The parameters of crystal field strength (Dq) and Racah parameters (B) were determined using a pair of equations derived from the theory of the crystal field,[18] are shown in Table 2.

The small difference in the values of the energy levels and other parameters, are probably due to difference in the strength of the ligand field of H_2O molecules and ClO_4 group.

It can be supposed that the band at 30,700 cm^{-1} (IL) results from a transition of the intraligand character since it was also detected in the spectrum of the free ligand of similar type.[19]

REFERENCES

1. V. Leovac, M. Babin, V. Canić and N. V. Gerbeleu, Z. Anorg. Allg. Chem. 1980, 471, 227.
2. V. Divjaković and V. Leovac, III Congresso Italo-Jugoslavo. Parma (1979).
3. V. Divjaković, B. Ribar, V. M. Leovac and N. V. Gerbeleu, Z. für Kristallogr. 1981, 154, 83.
4. V. M. Leovac, N. V. Gerbeleu and M. D. Revenko, Zhur. Neorg. Khim. 1978, 23, 1272.
5. V. M. Leovac, N. V. Gerbeleu and V. D. Canić, Zhur. Neorg. Khim. 1982, 27, 918.
6. V. Divjaković, V. M. Leovac, B. Ribar, Gy. Argay and A. Kálmán, Acta Cryst. 1982, B38, 1738.
7. A. F. Petrović, B. Ribar, D. Petrović, V. M. Leovac and N. V. Gerbeleu, J. Coord. Chem. 1982, 11, 239.
8. N. V. Gerbeleu, V. M. Leovac and M. D. Revenko, Zhur. Neorg. Khim. 1978, 23, 2452.
9. D. Petrović, B. Ribar, S. Carić and V. Leovac, Z. für Kristallogr. 1979, 150, 3.
10. B. Figgis and J. Lewis, The Magnetochemistry of Complex Compounds in Modern Coordination Chemistry (Edited by J. Lewis and R. G. Wilkins). Interscience, New York (1960).
11. P. Kubelka and F. Munk, Z. Tech. Physik. 1931, 12, 593.
12. M. Freund and T. Paradies, Ber. Deut. Chem. Ges. 1901, 34, 3114.
13. A. E. Shvelashvili and M. A. Porai-Koshits, Stereochemistry of Coordination Compounds of Some Metals with Cycleforming Amines (in Russian). Tbilisi (1979).
14. A. Kálmán, J. Chem. Soc.(A) 1971, 1857.

15. F. A. Cotton and G. Wilkinson, *Advanced Inorganic Chemistry*. Wiley-Interscience, New York (1971).

16. K. Nakamoto, *Infrared Spectra of Inorganic and Coordination Compounds*. Wiley-Interscience, New York (1970).

17. Y. Tanabe and S. Sugano, *J. Phys. Soc. Japan* 1954, **9**, 753.

18. A. P. Bogdanov, V. V. Zelentsov and V. M. Podalko, *Zhur. Neorg. Khim.* 1977, **10**, 2811.

19. D. Obadović, V. Leovac, D. Petrović and S. Carić, *Review of Research*, Vol. 9, p. 364. Faculty of Sciences, University of Novi Sad (1979).

POTENTIOMETRIC DETERMINATION OF THE STABILITY CONSTANTS OF A MODEL (Na$^+$ + K$^+$)ATPase COMPLEX

GRAHAM E. JACKSON* and MARK J. KELLY

Department of Inorganic Chemistry, University of Cape Town, Rondebosch 7700, South Africa

Abstract—Formation constants for the binary and ternary Mn(II)–nitrilotriacetic acid (NTA) and adenosine triphosphate (ATP) which model the action of (Na$^+$ + K$^+$)ATPase have been determined at 25°C and $I = 150$ mmole dm^{-3} NaCl. The results are interpreted in terms of the known stabilities of the enzyme complexes and it is concluded that metal–ion chelation of ATP alone is not enough for hydrolysis to occur. A substantial stabilisation of the ternary complex occurs, possibly through bridging sodium ions.

An important facet in the normal functioning of a biological cell is the maintenance of a Na and K concentration gradient across the cell membrane. As the cell membrtane is permeable to these ions via a passive transport mechanism, the cell requires an energy dependent, active transport mechanism to maintain the ionic balance against the concentration gradient. It is believed that the active transport mechanism, the so-called sodium pump, involves Na$^+$ and K$^+$ activated adenosinetriphosphatase,[1,2] a membrane bound metaloenzyme.

Grisham and Mildvan[1] have proposed a mechanism for the action of (Na$^+$ + K$^+$)ATPase. An essential part of this proposal is coordination of manganese(II) to the enzyme and subsequent coordination of ATP to form a ternary complex. Using nuclear magnetic resonance techniques one tight binding site for manganese(II) with a dissociation constant, K_D, of 0.88 μM has been found.[1] Kinetic studies have given an activator constant K_A of the same value, thus identifying the single tight manganese(II) binding site as the active site of the enzyme.[3]

Dissociation constants for ternary Mn(II)–(Na$^+$ + K$^+$)ATPase–phosphate and methylphosphonate[1] complexes have also been determined. However, because of the rapidity of ATP hydro-

lysis no ternary ATP complex has been studied. In an attempt then, to throw more light onto the role of the metal-ion in the sodium pump mechanism, the stability constants of ternary Mn(II)–model (Na$^+$ + K$^+$)ATPase–ATP have been determined. In choosing a simple molecule as a model for the enzyme cognizance was taken of the known strength of Mn-enzyme binding. This dictated the use of a multidentate mixed nitrogen, oxygen donor ligand, e.g. nitrilotriacetic acid (NTA).

RESULTS AND DISCUSSION

Protonation constants were determined for ATP and found to agree with the literature (Table 1). Formation curves (Fig. 1) for the Mn(II)–ATP system at different total metal and ligand concentrations were non-superimposable indicating the presence of protonated and/or hydroxo species. Final MINIQUAD[4] refinement resulted in the model given in Table 1. While the agreement between the experimental and theoretical formation curves is acceptable, at higher pH values there are reproducible systematic deviations. The low "crystallographic" R factor indicates the basic correctness of the model while the high χ^2 suggests the existence of further minor species. The introduction of hydroxo species did not result in a significant[5] improvement in the model and hence were discarded. The final results are in good agreement with the literature considering the different experimental conditions.

*Author to whom correspondence should be addressed.

Table 1. Formation constants determined in this study at 25°C, $I = 150$ mmol dm^{-1} NaCl; σ denotes standard deviation in $\log \beta$, n the number of experimental observations, R the MINIQUAD crystallographic R factor and χ^2 the statistical chi-squared function for normal distribution of residuals. The general formula of a complex is expressed by $M_p^{2+}(NTA)_q^{3-}(ATP)_{q'}^{4-}H_r$

p	q	q'	r	Log $\beta pqq'r$ Experimental	Literature[10]	σ	n	R	χ^2
0	0	1	1	6.39	6.42[b]	0.002	128	0.00309	52.5
0	0	1	2	10.44	10.57[a]	0.003			
1	0	1	0	4.72	4.76[a]	0.054	179	0.0083	38.95
1	0	1	1	9.19	8.90[a]	0.074			
1	0	1	2	12.73	-	0.099			
0	1	0	1	9.34	9.65[a]	0.005	55	0.0048	4.04
0	1	0	2	11.87	12.13[a]	0.013			
0	1	0	3	13.95	13.93[a]	0.002			
1	1	0	0	7.15	7.46[a]	0.006	83	0.00427	17.60
1	2	0	0	10.20	10.94[a]	0.018			
1	1	1	0	9.12	-	0.068	155	0.00397	257.94
1	1	1	1	15.57	-	0.140			

[a] 25°C $I = 0.1$ mol dm^{-3} [b] 25°C $I = 0.15$ mol dm^{-3}

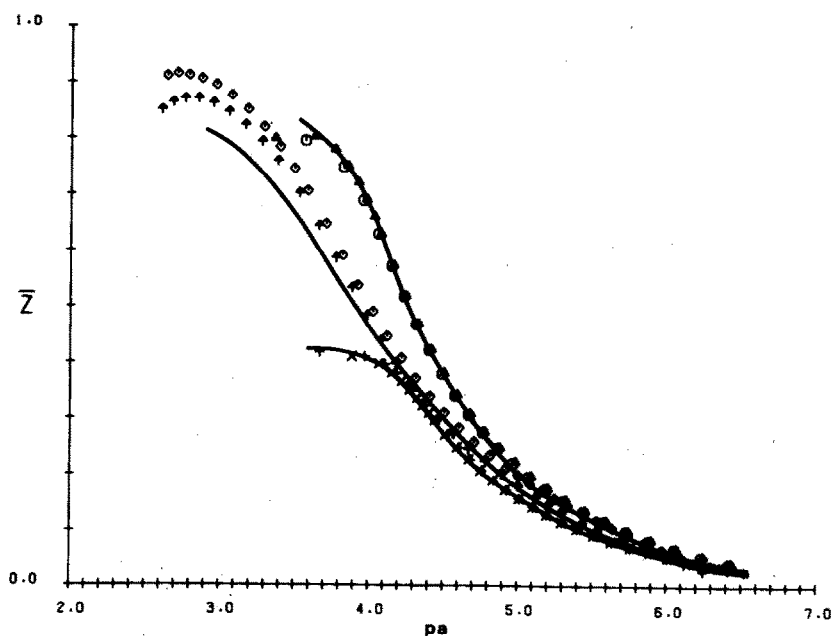

Fig. 1. Metal complex formation curves for the Mn(II)–ATP system at 25°C and $I = 150$ mmol dm^{-3} NaCl. The symbols represent different combinations of total ligand and total metal concentrations. The full lines represent corresponding theoretical curves obtained using the constants given in Table 1.

A similar set of experiments was carried out using NTA instead of ATP. In this case the formation curves were all superimposable indicating simple stepwise, mononuclear complex formation. MINIQUAD refinement resulted in a model and constants (Table 1) in very good agreement with the literature.

Potentiometric data from titrations of manganese(II), NTA and ATP with base were used to refine constants for the ternary system. Conditions were varied so as to maximise the formation of ternary species and minimise the formation of binary metal complexes. Again the final model (Table 1), as exemplified by the very low R value, is in good agreement with the experimental data. The high value for χ^2 may be a result of inadequately defining the binary Mn(II)–ATP system.

In order to compare the formation constants of our model system with results obtained for the native enzyme system it is necessary to calculate the association constants for the various interactions of a pH of 7.4. This can be done using the appropriate equations, e.g.
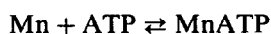
$$Mn + ATP \rightleftarrows MnATP$$

$$K_a = \frac{[MnATP]}{[Mn][ATP]}$$

where [ATP] = total concentration of uncomplexed ATP. In this way K_a, for the model system, is calculated to be 2.07 log units. This does not compare well with association constants of 5.32 and 5.14 log units for complexation of inorganic phosphate and methylphosphate respectively, to the Mn–ATPase complex.[1] However the stability of these latter two complexes is far greater than ATP with Mn(II) on its own (log $K_a = 4.7$). Since the presence of a bulky ligand (the $Na^+ + K^+$)ATPase protein molecule) on the metal centre is expected to destabilize any subsequent chelation (as shown by the model system) there must be a very substantial interaction between ATP and the protein in the ternary $(Na^+ + K^+)$ATPase–Mn(II)–ATP complex, i.e. coordination to the Mn(II) alone cannot account for the stability of the complex. Grisham and Mildvan[1] have postulated the existence of bridging sodium ions between the phosphate residues of ATP and the protein. However it is difficult to envisage such an electrostatic interaction stabilizing the complex by a factor of 10^4.

Of special interest is the amount of ternary complex formed at physiological pH. To this end a species distribution diagram (Fig. 2) was constructed. This shows that at no time is an appreciable amount of the Mn(II)–ATP complex formed. Rather initial coordination is to NTA followed, at higher pH, by formation of the ternary Mn(II)–NTA–ATP complex. An essential feature of the proposed Grisham and Mildvan[1] sodium pump mechanism is the deprotonation of the ternary complex upon migration to the outer surface of the cell membrane. In our model system this
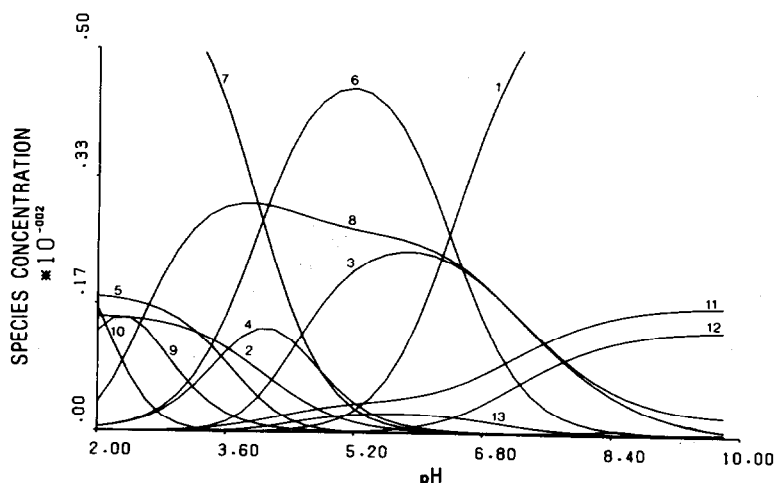
Fig. 2. Species distribution diagram for the ternary Mn(II)/NTA/ATP system. Total concentrations of Mn(II), NTA and ATP are: 3.3×10^{-3}, 3.3×10^{-3}, 7.9×10^{-3} mol cm^{-3} respectively. Using the notation (IIII) to represent species $ATP^{4-} \cdot NTA^{3-} \cdot Mn^{2+} \cdot H^+$: 1 = (1000), 2 = (0010), 3 = (1010), 4 = (1011), 5 = (1012), 6 = (1001), 7 = (1002), 8 = (0101), 9 = (0102), 10 = (0103), 11 = (0110), 12 = (1110) and 13 = (1111).

deprotonation does take place but at a physiologically unrealistic pH of 6.5. Even so the duplication of this feature is encouraging.

In conclusion, although our simple model of $(Na^+ + K^+)$ATPase is not in good quantitative agreement with the enzyme system, it does duplicate several of the essential features, viz. (i) coordination of ATP to the metal–ion, (ii) increased stability due to interaction with the protein and (iii) deprotonation of the complex at higher pH.

EXPERIMENTAL

Stock solutions of nitrilotriacetic acid (Merck) and manganese(II) chloride were standardised by a Gran[6] plot and compleximetric (EDTA) titration respectively. ATP (Merck) being unstable, was weighed directly into the titration vessel. All solutions were prepared using degassed, glass distilled water.

Potentiometric titrations were carried out as described in Ref. 7, all studies being performed at $25.00° + 0.05°C$ and $I = 150$ mmol dm^{-3} in NaCl. The electrode system was calibrated using the MAGEC[8] approach. Protonation curves for the ligands were obtained at different total ligand concentrations while metal complex formation curves were obtained at different metal:ligand ratios and for different total ligand and total metal concentrations. All titrations were repeated at least twice to check the reproducibility of the system. The data was treated to MINIQUAD[4] least squares analysis and the resulting "best" set of constants checked using the PSEUDOPLOT[9] approach.

REFERENCES

1. C. M. Grisham and A. S. Mildvan, *J. Biol. Chem.* 1974, **249**, 3187.
2. J. G. Nørby and J. Jensen, *Biochem. Biophys. Acta* 1971, **253**, 104.
3. J. P. Slater, I. Tamir, L. A. Loeb and A. S. Mildvan, *J. Biol. Chem.* 1972, **247**, 6784.
4. A. Sabatini, A. Vacca and P. Gans, *Talanta* 1974, **21**, 53.
5. A. Vacca, A. Sabatini and M. A. Gristina, *Coord. Chem. Rev.* 1972, **8**, 45.
6. G. Gran, *Int. Cong. Analyt. Chem.* 1952, **77**, 661.
7. G. V. Fazakerley, G. E. Jackson and P. W. Linder, *J. Inorg. Nucl. Chem.* 1976, **38**, 1397.
8. P. M. May, D. R. Williams, P. W. Linder and R. G. Torrington, *Talanta* 1982, **29**, 249.
9. A. M. Corrie, G. K. R. Makar, M. L. D. Touche and D. R. Williams, *J. Chem. Soc. Dalton* 1975, 105.
10. A. E. Martell and R. E. Smith, *Critical Stability Constants*. Plenum Press, New York (1974).

THIOCYANATO ADDUCTS OF CHROMIUM(II) CARBOXYLATES AND THE MOLECULAR STRUCTURE OF TETRAETHYL-AMMONIUM TETRA-μ-PROPIONATODIISOTHIO-CYANATODICHROMATE(II)

PETER D. FORD, LESLIE F. LARKWORTHY,* DAVID C. POVEY
and ANDREW J. ROBERTS
Department of Chemistry, University of Surrey, Guildford GU2 5XH, England

Abstract—X-Ray crystallographic studies on $[NEt_4]_2[Cr_2[(O_2CC_2H_5)_4(NCS)_2]$ show that the Cr–Cr separation (2.467 Å) in the dinuclear anion is one of the longest known. The thiocyanato groups are N-bonded, and the results emphasize the known sensitivity of the quadruple Cr–Cr bond to the nature of the axial ligands. The compound crystallises in the tetragonal space group $P4/mnc$ with two molecules per unit cell, the dimensions of which are $a = b = 9.785(1)$, $c = 21.186(2)$ Å. Magnetic investigations from room to liquid nitrogen temperature on the tetra-μ-propionato complex and on $[NMe_4]_2$ $[Cr_2(O_2CCH_3)_4(NCS)_2]$ show that both complexes have been obtained free from paramagnetic chromium(III) impurities. Their weak paramagnetic susceptibilities (χ_{Cr} is approx. 200×10^{-6} cm^3 mol^{-1} at 295 K and 50×10^{-6} cm^3 mol^{-1} at 90 K) are inherent, and are ascribed to temperature independent paramagnetism at low temperature plus paramagnetism arising from slight population of the triplet state ($2J \simeq 700$ cm^{-1}, $g = 2$, $N\alpha = 50 \times 10^{-6}$ cm^3 mol^{-1}) at higher temperatures.

The preparation of the first dichromium carboxylato complex with axially bonded anions, $[NEt_4]_2[Cr_2(O_2CCH_3)_4(NCS)_2]$, was recently reported.[1] From its reflectance spectrum and a correlation[2] between the band frequencies and Cr–Cr separations in known compounds, it was suggested[1] that the Cr–Cr separation in this compound should be among the longest known. Single crystal investigations have now shown that this is true for the analogous compound $[NEt_4]_2$ $[Cr_2(O_2CCH_2CH_3)_4(NCS)_2]$.

RESULTS AND DISCUSSION

Structure of the dinuclear anions

The carboxylato-bridged dinuclear structure of the anions in $[NEt_4]_2[Cr_2(O_2CCH_2CH_3)_4(NCS)_2]$ is represented in Fig. 1. The anions have $4/m$ symmetry, with the linear N-bonded thiocyanato ligands along the four fold axis defined with the Cr–Cr bond. Coordination of thiocyanate through nitrogen increases the N–C bond length (1.168 Å,

Table 1) and decreases the C–S bond length (1.614 Å) compared with the free ion values (1.149 and 1.689 Å).[3] This is the usual effect of coordination through nitrogen. All Cr–O bond lengths
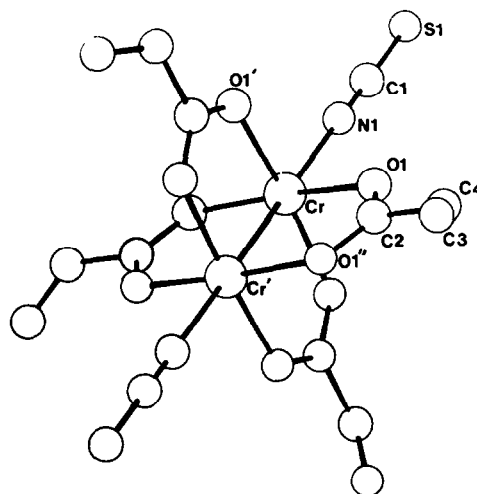

Fig. 1. The structure of the anions in $[NEt_4]_2$-$[Cr_2(O_2CCH_3)_4(NCS)_2]$.

*Author to whom correspondence should be addressed.

Table 1. Bond lengths and angles of $[NEt_4]_2[Cr_2(O_2CCH_2CH_3)_4(NCS)_2]$

Bond lengths (Å)				Bond angles (°)			
Anion							
Cr -Cr'	2.467(3)	N(1)-C(1)	1.168(9)	O(1)-Cr -O(1)'	89.8		
Cr -O(1)	2.019(4)	C(1)-S(1)	1.614(7)	Cr'-Cr -O(1)	86.5	N(1)-Cr-O(1)	93.5
Cr -N(1)	2.249(3)			Cr -O(1)-C(2)	121.6		
O(1)-C(2)	1.257(5)	N(2)-C(5)	1.518(9)	O(1)-C(2)-O(1)"	123.9		
C(2)-C(3)	1.504(9)	C(5)-C(6)	1.502(9)	O(1)-C(2)-C(3)	118.0		
C(3)-C(4)	1.229(10)			C(2)-C(3)-C(4)	119.1		
Cation[a]							
N(2)-C(5)	1.518(5)			C(6)-C(5)-N(2)	115.0		
C(5)-C(6)	1.503(10)						

a The tetraethylammonium cations possess 222 point symmetry.

are equal (2.019 Å), and very close to the average value (2.018 Å) in $[Cr_2(O_2CCH_3)_4(OH_2)_2]^4$. The Cr–O bonds of the CrO_4 units are bent towards the Cr–Cr bond (Cr'–Cr–O = 86.5°) presumably because the Cr–Cr bond length (2.467 Å) is greater than can be accommodated without distortion by the bite of the carboxylato ligands.

Extensive crystallographic investigations[5] have emphasized how the length of the Cr–Cr bond is primarily dependent upon whether axial ligands are present. Axial ligands donate electron density into the $d_{z^2} - d_{z^2}\sigma^*$ antibonding orbital and so lengthen the bond, the effect being greater with more strongly donating (basic) ligands. The nature of the bridging ligands is secondary, but the Cr–Cr bond is longer when weakly donating bridges are present.

Tetra-μ-carboxylato dichromium(II) complexes show a range of Cr–Cr bond distances from 2.28 Å in $[Cr_2(O_2CC_{14}H_9)_4(DME)_2]$ (DME = 1,2-dimethoxyethane) to 2.54 Å in $[Cr_2(O_2CCF_3)_4(Et_2O)_2]$, and in all cases axial ligands are present. Excluding the trifluoroacetate complex, which is exceptional in the weak donor nature of the bridge, the thiocyanato complex has the longest Cr–Cr bond.

N-bonded thiocyanate is usually considered a σ-donor, with a weaker ligand field than ammonia or pyridine, and, as isothiocyanic acid is a strong acid[3], NCS^- is a weak base. Nevertheless, since the Cr-Cr bond in the thiocyanato adduct is longer than in the pyridine (2.369 Å) and pyrazine (2.342 Å) adducts of chromium(II) acetate[5], NCS^- has greater donor strength than these amines towards the Cr–Cr bond. This may be because the charge and weak π-donor ability of NCS^- offset its lower basicity.

The Cr-Cr bond is considerably shorter than the Cu–Cu bond (2.643 Å)[6] in the analogous copper(II) dimer, $[NMe_4]_2[Cu_2(O_2CCH_3)_4(NCS)_2]$, and the Cr–N bond (2.249 Å) is somewhat longer than the Cu–N bond (2.08 Å), but in other respects the two structures have similar geometry.

Magnetic investigations

Owing to the difficulty in preventing oxidation, it has been uncertain whether the weak paramagnetism of chromium(II) acetate samples is inherent or arises from traces of chromium(III) impurities. The magnetic behaviour over a temperature range of one sample of chromium(II) acetate monohydrate[7a] could be reproduced by assuming strong interactions in a dinuclear structure $\{2J = 1250°(869\,cm^{-1})\}$, and 0.3% Cr^{3+} impurity ($\mu_{eff} = 3.87$ B.M., independent of T). Similar behaviour was found[1] for $[NMe_4]_2[Cr_2(O_2CCH_3)_4(NCS)_2]$. On the other hand, unpublished magnetic susceptibility measurements on $[Cr_2(O_2CCH_3)_4(OH_2)_2]$ are said[2] to show that the ground state consists of filled shells, and the weak paramagnetism of $[Cr_2(O_2CCH_3)_4(NH_3)_2]$ was ascribed[8] to temperature independent paramagnetism. Since molecular orbital calculations suggest[9] that the highest filled level lies some $5000\,cm^{-1}$ below the first excited level, population of the triplet state is expected to be insignificant at room temperature, and quadruply bonded Cr_2^{4+} species should be diamagnetic or at the most exhibit some temperature independent paramagnetism.

Samples of $[NMe_4]_2[Cr_2(O_2CCH_3)_4(NCS)_2]$ and $[NEt_4]_2[Cr_2(O_2CCH_2CH_3)_4(NCS)_2]$, after correction for the diamagnetism of the ligands, gave small positive values of χ_{Cr} which decreased as the tem-

perature was lowered (Table 2). There is no increase in χ_{Cr} at low temperatures in contrast to the behaviour of the acetate, $[Cr_2(O_2CCH_3)_4(OH_2)_2]^{7a}$, the new stearate (see Experimental), and the earlier preparation[1] of $[NEt_4]_2[Cr_2(O_2CCH_3)_4(NCS)_2]$, which all showed increases in χ_{Cr} at low temperatures due to small amounts of chromium(III) impurities. The data for $[NMe_4]_2[Cr_2(O_2CCH_3)_4(NCS)_2]$ and $[NEt_4]_2[Cr_2(O_2CCH_2CH_3)_4(NCS)_2]$ can be approximately reproduced over the available temperature range by substitution of $J = 375 \, cm^{-1}$ (NMe$_4$ salt), $J = 320 \, cm^{-1}$ (NEt$_4$ salt), $g = 2$ and $N\alpha = 50 \times 10^{-6} \, cm^3 \, mol^{-1}$ in the expression

$$\chi_{Cr} = \frac{Ng^2\beta^2}{kT}\left[\frac{1}{3+x^2}\right] + N\alpha$$

where $x = \exp(J/kT)$, to which the full expression[7b] for antiferromagnetic interaction in a binuclear chromium(II) complex ($S = 1$ or 2) reduces when J is large. Errors are large[7a] in measurements on weakly paramagnetic compounds but in these preparations paramagnetic impurities have been avoided so that the weak paramagnetism must be inherent. The singlet–triplet separation ($2J$) is of the order of $700 \, cm^{-1}$ which is inconsistent with the molecular orbital calculations[9] and the tentative assignment[2] of the $\delta \to \delta^*$ transition to a weak band at approx. $16000 \, cm^{-1}$.

Spectroscopic investigations

The IR spectra of the complexes contain absorption bands (Table 3) characteristic[3] of N-bonded NCS^- groups in agreement with the crystal structure determination.

A detailed analysis[2] of the low temperature polarised single-crystal absorption spectrum of $[Cr_2(O_2CCH_3)_4(OH_2)_2]$ has shown that there are dominant absorption bands at approx. $21000 \, cm^{-1}$ (Band I) and approx. $30,000 \, cm^{-1}$ (Band II). Band I has been assigned to the $\delta \to \pi^*$ transition of the binuclear system intensified by vibronic coupling, and band II to charge transfer from a non-bonding π-orbital of the carboxylate ligand to the π^* metal orbital. The energies of bands I and II in a limited series of quadruply bonded dichromium complexes comprising the carbonate $[NH_4]_4[Cr_2(CO_3)_4(OH_2)_2] \cdot H_2O$ (Cr–Cr = 2.214 Å[10] and some carboxylato complexes {of which $[Cr_2(O_2CH)_4(C_5H_5N)_2]^{11}$ showed the longest Cr–Cr separation (2.408 Å)} have been found [2] to decrease linearly with increasing Cr–Cr separation. Bands I and II in the powder reflectance spectra of the thiocyanate adducts (Table 3) are at lower frequencies than any in the above series in agreement with the greater Cr–Cr separation (2.467 Å).

The diffuse reflectance spectra of Cs_4 $[Cr_2(SO_4)_4(OH_2)_2] \cdot 2H_2O^{12}$, $[Cr_2(O_2CCH_3)_4(NH_3)_2]^8$ $[Cr_2(stearate)_4(OH_2)_2]$ are included in Table 3. From the frequencies the Cr–Cr separation

Table 2. Variation with absolute temperature of molar susceptibilities χ_{Cr}(cm^3 mol^{-1}) and effective magnetic moments μ_{eff}(B.M.) of the thiocyanato adducts and $[Cr_2\{O_2C(CH_2)_{16}CH_3\}_4(OH_2)_2]$

$[NMe_4]_2[Cr_2(O_2CCH_3)_4(NCS)_2]^a$			$[NEt_4]_2[Cr_2(O_2CCH_2CH_3)_4(NCS)_2]^a$		
$10^6\chi_{Cr}$	μ_{eff}	T	$10^6\chi_{Cr}$	μ_{eff}	T
174	0.64	295.1	231	0.74	294.5
142	0.55	262.5	190	0.63	262.5
101	0.43	231.2	173	0.57	233.5
83	0.36	199.0	115	0.43	199.0
61	0.29	168.0	97	0.36	168.5
46	0.22	135.5	71	0.28	135.5
50	0.20	103.5	65	0.22	103.5
21	0.12	89.0	52	0.19	89.0
Diamagnetic correction			Diamagnetic correction		
$= 156 \times 10^{-6} cm^3 mol^{-1}$			$= 215 \times 10^{-6} cm^3 mol^{-1}$		

a The molar susceptibilities are based on half the molecular weights corresponding to these formulae.

Table 3. Diffuse reflectance spectra (cm^{-1}) of complexes and IR absorptions (cm^{-1}) of iso-thiocyanato groups

Compound	Electronic Spectra II[a]				I[a]		IR Spectra ν(CN)		ν(CS)		δ(NCS)
[NMe$_4$]$_2$[Cr$_2$(O$_2$CCH$_3$)$_4$(NCS)$_2$]	34800b	33900sh	28600b		24700w	19000vb	2079vs	2030sh	779w		474w
[NEt$_4$]$_2$[Cr$_2$(O$_2$CCH$_3$)$_4$(NCS)$_2$]	35300b	33800sh	28700b		24900sh	18700vb	2070vs		790m[b]		475w
[NEt$_4$]$_2$[Cr$_2$(O$_2$CC$_2$H$_5$)$_4$(NCS)$_2$]	39100sh 36000b	33000sh	29200b		24900sh	18500vb	2079vs		810w 775sh	784m[b]	475vw
Cs$_4$[Cr$_2$(SO$_4$)$_4$(OH$_2$)$_2$].2H$_2$O[c]	43100 35600		30100 29400sh	26300sh	18100vb					
[Cr$_2$(stearate)$_4$(OH$_2$)$_2$]	40000vb		30000b	28400sh	21900vb						
[Cr$_2$(O$_2$CCH$_3$)$_4$(NH$_3$)$_2$][d]	37000b		29000b		19500vb						

a. See text and reference 2.
b. A medium intensity band due to the [NEt$_4$] groups renders the ν(CS) assignment uncertain.
c. Reference 12; spectrum re-recorded.
d. Reference 8.

would be expected to decrease in the order given, with the separation in the amine being approx. 2.5 Å commensurate with the high basicity of ammonia. The stearate is likely to have as short a Cr–Cr bond as the carbonate complex. Unfortunately, crystallographic data are not available for these three complexes.

EXPERIMENTAL

In the preparation[1] of [NEt$_4$]$_2$[Cr$_2$(O$_2$CCH$_3$)$_4$(NCS)$_2$], chromium(II) acetate monohydrate was extracted into a hot ethanolic solution of tetraethylammonium thiocyanate. The thiocyanate solution was obtained by mixing equimolar solutions of tetraethylammonium chloride and potassium thiocyanate in ethanol, followed by centrifugation to remove the precipitated chloride. This procedure was satisfactory with the acetate, but the corresponding propionate was not obtained pure. In the present work the tetraethylammonium and tetramethylammonium thiocyanates were first isolated.

To prepare [NMe$_4$]NCS equimolar amounts of the alkylammonium bromide (10.00 g) and potassium thiocyanate (6.31 g) were refluxed in absolute ethanol (150 cm^3). Potassium bromide was filtered off from the hot solution using a fine filter paper, the solution reduced to half volume, allowed to cool to room temperature, and residual KBr filtered off. Crystalline tetramethylammonium

thiocyanate was obtained by cooling the filtrate overnight in a refrigerator. It was twice recrystallised from a minimum of absolute ethanol. In the preparation of tetraethylammonium thiocyanate, the crude product was obtained by the slow addition of dried ether to the ethanolic solution. The hygroscopic thiocyanate was recrystallised from a minimum volume of a 5:2:3 mixture of ethanol, acetone and ether.

The monohydrates of chromium(II) acetate and chromium(II) propionate crystallised when a solution of chromium(II) bromide obtained from hydrobromic acid and the metal was filtered into a solution containing the sodium carboxylate in small excess. Previously,[13] spectroscopically pure chromium has been used in the preparation of chromium(II) salts, but the less expensive electrolytically produced metal (99.5%) supplied by BDH Chemicals Limited has been found satisfactory.

Preparation of ditetramethylammonium tetra-μ-acetatodiisothiocyanatodichromate (II)

Chromium(II) acetate monohydrate (1.54 g) was extracted by boiling ethanol (125 cm^3) containing an equimolar amount of tetramethylammonium thiocyanate (1.07 g). The suspension was refluxed for about 30 m, and, as the thiocyanato complex proved to be almost insoluble in ethanol, it was filtered off and dissolved in boiling, dry methanol (150 cm^3). On cooling, violet crystals appeared.

These were filtered off, washed with cold ethanol, and dried by continuous pumping for 2 hr. Yield = 55%. Found: C, 35.8; H, 6.00; N, 9.13. $C_9H_{18}N_2O_4SCr$ requires C, 35.8; H, 6.00; N, 9.27%.

Preparation of ditetraethylammonium tetra-μ-propionatodiisothiocyanatodichromate (II)

Chromium(II) propionate monohydrate (1.22 g) was extracted by boiling ethanol (100 cm³) containing an equimolar amount (0.75 g) of tetraethylammonium thiocyanate, and the solution refluxed for 1 hr. Violet crystals were obtained on slow cooling. The crystals were filtered off and dried as above. Since the complex oxidises only slowly, it was possible to select a crystal suitable for X-ray investigation in air and seal it under nitrogen in a Lindemann capillary to prevent long term oxidation. Yield = 65%. Found: C, 46.8; H, 7.98; N, 7.27. $C_{15}H_{30}N_2O_4SCr$ requires C, 46.6; H, 7.82; N, 7.25%.

Preparation of tetra-μ-stearatodichromium (II) dihydrate

To prepare the stearate $[Cr_2(O_2C(CH_2)_{16}CH_3)_4(OH_2)_2]$, sodium stearate was extracted with boiling water into a solution of chromium(II) bromide prepared as for the acetate and propionate. The orange product was filtered off, washed with cold water and dried as above. The insolubility of the stearato complex in common solvents frustrated attempts to prepare a thiocyanate adduct. Yield = 60%. Found: C, 68.45; H, 11.1. $C_{36}H_{72}O_5Cr$ requires C, 67.9; H, 11.4%.

The IR spectrum contained a broad water absorption at 3400 cm⁻¹. The sample was contaminated with approx. 2% of chromium(III) impurity since its magnetic behaviour paralleled that of the earlier preparation[1] of $[NEt_4]_2[Cr_2(O_2CCH_3)_4(NCS)_2]$, but with values of χ_{Cr} approximately twice as large ($\mu_{eff} = 0.9$ B.M. at 294 K and 0.6 B.M. at 90 K).

Physical measurements

Magnetic measurements were carried out from room to liquid nitrogen temperature by the Gouy method. Because of their very weak paramagnetism, about 1.2 g of the samples was packed into wide bore (5 mm) quartz tubes, and since traces of oxidation can markedly affect the magnetic results this was done in all-glass apparatus within an inert atmosphere box. The box, fitted with a re-circulatory gas purification system, was manufactured by Faircrest Engineering Ltd., Croydon.

Electronic spectra were recorded on a Beckman Acta MIV recording spectrophotometer provided

with a diffuse reflectance attachment. A lithium fluoride reference was used and the samples were sealed under nitrogen. Infrared spectra of nujol mulls were recorded on a Perkin–Elmer 577 spectrophotometer.

CRYSTALLOGRAPHIC STUDIES

Crystal data

$[C_{14}H_{20}N_2O_8Cr_2S_2][(C_2H_5)_4N]_2$, M = 768.97, tetragonal, $a = b = 9.785(1)$, $c = 21.186(2)$ Å, $U = 2028.5$ Å space group $P4/mnc$, $Z = 2$, $D_c = 1.26$ g. cm⁻³, D_m not measured, F(000) = 816, $\mu(Mo-K_\alpha = 6.3$ cm⁻¹.

Data collection

Enraf Nonius CAD4 diffractometer, Mo–K_α radiation. ($\lambda = 0.71069$ Å, graphite monochromator), crystal sealed under nitrogen in a Lindemann glass capillary, $\theta/2\theta$ scan mode, $1.0° \leqslant \theta \leqslant 25.5°$, 1905 data measured as orthorhombic, reduced to 1001 unique reflexions, 541 observed [$I \geqslant 2.50\,\sigma(I)$]; uncorrected for absorption but corrected for crystal decay during measurement (intensity of reference reflexion dropped by 17%).

Structure solution and refinement

The structure was solved by the heavy atom method and refined by full matrix least squares to a final conventional R-factor of 0.046 [weighting scheme used: $W = 1/[\sigma^2(F_0) + 0.04\,F_0^2]$. Non-hydrogen atoms were assigned anisotropic thermal parameters and all hydrogen atoms from the tetraethylammonium cation were located from a difference map and included in the refinement with isotropic thermal parameters. The positioning of the terminal carbon atom C(4) has proved extremely difficult. Electron density maps persistently located this atom off the mirror plane (*xyo*) thus producing a sec-butyrate although microanalyses do not support this. We are forced to conclude that this atom is disordered and a fixed occupancy of 0.5 has been assigned. The C(3)–C(4) bond length is very short and as such must be regarded as artificial although attempts to fix the C(4) atom at a more reasonable position resulted in a large increase in its thermal parameters. Its refined position is, therefore, one which produces a minimum in the R-factor.

REFERENCES

1. L. F. Larkworthy and A. J. Roberts, *Polyhedron* 1982, **1**, 135.
2. S. F. Rice, R. B. Wilson, and E. I. Solomon, *Inorg. Chem.* 1980, **19**, 3425.

3. J. L. Burmeister, *Chemistry and Biochemistry of Thiocyanic Acid and its Derivatives* (Edited by A. A. Newman), Chap. 2. Academic Press, London, (1975).

4. F. A. Cotton, B. G. DeBoer, M. D. LaPrade, J. R. Pipal and D. A. Ucko, *Acta Cryst.* 1971, **B27**, 1664.

5. F. A. Cotton, W. H. Ilsley, and W. Kaim, *J. Am. Chem. Soc.* 1980, **102**, 3464, and references therein.

6. D. M. L. Goodgame, N. J. Hill, D. F. Marsham, A. C. Skapskii, M. L. Smart, and P.G.H. Troughton, *Chem. Commun.* 1969, 629.

7. *A. Earnshaw, Introduction to Magnetochemistry*, (a) p. 104 (b) p. 77. Academic Press, London (1968).

8. L. F. Larkworthy and J. M. Tabatabai, *Inorg. Nucl. Chem. Lett.* 1980 **16**, 427.

9. F. A. Cotton and G. Wilkinson, *Advanced Inorganic Chemistry*, 4th Edn, Chap. 26. Wiley-Interscience, New York (1980).

10. F. A. Cotton and G. W. Rice, *Inorg. Chem.* 1978, **17**, 2004.

11. F. A. Cotton, M. W. Extine, and G. W. Rice, *Inorg. Chem.* 1978, **17**, 176.

12. A. Earnshaw, L. F. Larkworthy, and K. C. Patel, *J. Chem. Soc. (A)* 1969, 1334.

13. A. Earnshaw, L. F. Larkworthy and K. S. Patel, *J. Chem. Soc.* 1965, 3267.

VAPOUR PHASE CHEMISTRY OF
OXOVANADIUM IV β-DIKETONATES

D. A. JOHNSON and A. B. WAUGH*

Chemical Technology Division, Australian Atomic Energy Commission, Lucas Heights
Research Laboratories, Lucas Heights, Sydney 2232, Australia

Abstract—A series of fluorinated and one non-fluorinated β-diketonate complexes of oxovanadium IV have been prepared, their gas phase IR spectra examined, vapour pressures determined and their vapour phase thermal decomposition investigated. Decomposition of the fluorinated complexes occurred according to the overall reaction scheme $VO(\beta\text{-diket})_2 \rightarrow VOF_2 + $ Furanone. The furanones $C_5HF_5O_2$, $C_5H_4F_2O_2$ and $C_8H_{10}F_2O_2$ were isolated and identified. The non-fluorinated complex gave the parent diketone and a vanadium oxide as its principal products.

While there are abundant structural[1-5] and spectral data[1,2,5-8] available for vanadyl β-diketonates as solids and in solution, little information is available on their thermal properties. The only vapour phase chemistry reported[9-12] relates to the gas chromatography of these complexes.

This study was undertaken as a prelude to later investigations[13] into IR laser irradiation of vanadyl β-diketonates. For these investigations it was necessary to know the vapour pressures, vanadyl absorption frequencies and the products from vapour phase thermal decomposition. Some known compounds[6,11] and others not previously reported were prepared and characterized. Gas phase IR spectra and vapour pressures were measured and vapour phase thermal decompositions investigated.

EXPERIMENTAL

Preparation of metal complexes

Complexes of the following β-diketonates were prepared; hexafluoroacetylacetone (HHFA), trifluoroacetylacetone (HTFA), pivaloyl trifluoroacetone (HPTA) and dipivaloyl methane (HDPM).

$VO(HFA)_2$, $VO(TFA)_2$, $VO(DPM)_2$ and VO-

*Author to whom correspondence should be addressed. Present address: CSIRO, Division of Energy Chemistry Lucas Heights Research Laboratories, Private Mail Bag 7, Sutherland, NSW 2232, Australia.

$(PTA)_2$ were prepared by a modified procedure of Selbin *et al.*[6] in which vanadyl sulphate was maintained in excess of the diketone. Weakly coordinated water associated with these complexes was removed under vacuum.

An extraction method was used to prepare the complex $VO(HFA)_2TMP$. A chloroform solution of 0.8 mmole HHFA and 0.4 mmole of trimethyl phosphate was shaken with 0.4 mmole of $VOSO_4$ in distilled water. The chloroform layer was separated, washed, dried and then evaporated with dry nitrogen. $VO(HFA)_2py$ was prepared by the addition of a stoichiometric amount of pyridine to a chloroform solution of $VO(HFA)_2$, followed by removal of the solvent.

The complexes were purified by vacuum sublimation and then by sublimation in a flow tube apparatus with a dry nitrogen carrier gas at reduced pressure. Results of elemental analyses are shown in Table 1.

IR spectra and vapour pressure determinations

Gas phase spectra of the purified complexes were measured using a Perkin–Elmer 225 spectrophotometer. The compound was contained in an evacuated heatable 10 cm cell fitted with NaCl windows. Condensation of compounds on the windows was prevented by having a side arm on the cell at a lower temperature than the windows.

A calibrated flow of nitrogen carrier gas was employed to determine the vapour pressures of the complexes by the mass transport method.

Table 1. Elemental analyses of the vanadyl β-diketonate complexes

Compound		V	F	H	C	O	X
VO(TFA)$_2$	Theoretical	13.67	30.56	2.14	32.17	21.45	
	Found	13.78	30.70	1.96	32.42	*	
VO(DPM)$_2$	Theoretical	11.78	–	8.78	61.00	18.48	
	Found	12.15	–	8.68	61.02	18.70	
							N
VO(HFA)$_2$py	Theoretical	9.10	40.71	1.25	32.14	14.29	2.50
	found	9.12	40.90	1.44	32.28	*	2.39
							P
VO(HFA)$_2$TMP	Theoretical	8.21	36.71	1.77	25.10	23.19	4.99
	Found	9.29	36.60	1.69	25.42	*	5.30
VO(PTA)$_2$	Theoretical	11.16	24.95	4.38	42.00	17.50	
	Found	11.26	25.00	4.08	41.61	*	
VO(HFA)$_2$	Theoretical	10.60	47.40	0.42	24.95	16.63	
	Found	9.43	47.60	2.09	24.99	*	

* Oxygen was not analysed in the presence of fluorine

Vapour phase thermal decompositions

Samples of the complex were volatilized and carried through a heated zone at 460°C with an average residence time of 0.5 s. The volatile decomposition products were collected in a U-tube at 77 K. Capillary chromatography was used to determine the number of volatile products formed. Purification of products was achieved using a 2 m 10% cetyl phosphate on celite column. The components were analysed by mass spectrometry using an A.E.I. MS3 and their gas phase IR spectra determined. Non-volatile components remaining in the decomposition tube were washed out with water, acidified and analysed for vanadium and fluorine.

RESULTS AND DISCUSSION

IR *spectra of complexes*

In the range 1100–900 cm^{-1}, two absorption bands were observed for all compounds. The very intense band in each instance is the V=O stretch and the very weak, broad band in the 950–960 cm^{-1} range is a ligand absorption. A very weak band in this region has also been observed by the authors for the compound Cu(HFA)$_2$, and by others[14] for the compound U(HFA)$_4$.

The frequencies of the vanadyl stretch for the complexes in the gaseous state at 160°C are listed in Table 2. Full width half maximum height measurements determined from expanded scale spectra were approx. 9 cm^{-1} for all complexes.

Vapour pressure data

The vapour pressure equations and enthalpies of vaporization have been calculated and are summarized in Table 3. Generally speaking, the vanadyl β-diketonates are considerably more volatile than their uranyl analogues.[15,16]

Analysis of thermal decomposition products

Mass spectral analysis of the volatile decomposition products revealed, with one exception, only two products from each complex and the unaltered neutral ligand. In each instance, these products were a trace amount of the parent β-diketone and the remainder, a compound with a

Table 2. Properties of vanadyl β-diketonates

Compound	VO(HFA)$_2$TMP	VO(HFA)$_2$Py	VO(HFA)$_2$	VO(DPM)$_2$	VO(TFA)$_2$	VO(PTA)$_2$
mp °C	37–39	71–72		185–186	228	220
Colour	Dark green	Brown	Light green	Dark green	Light green	Light green
V=O cm^{-1}	992	996	996	1016	1025	1027

Table 3. Summary of vapour pressure equations and enthalpy changes for the vaporization of some vanadyl β-diketonates $\log p$ (Pa) $= A - [1000\,B/T]$

Compound	Temperature Range(K)	A	B	ΔH kJ mol^{-1}
VO(TFA)$_2$	396 – 444 (solid)	16.0 ± 0.4	6.3 ± 0.2	121 ± 4
VO(DBM)$_2$	385 – 420 (solid)	10.3 ± 0.4	3.9 ± 0.2	75 ± 3
VO(PTA)$_2$	385 – 425 (solid)	17.3 ± 0.8	6.7 ± 0.3	129 ± 6
VO(HFA)$_2$	333 – 363 (solid)	13 ± 1	4.1 ± 0.4	79 ± 8
VO(HFA)$_2$TMP	343 – 385 (liquid)	15.3 ± 0.7	5.1 ± 0.3	97 ± 5
VO(HFA)$_2$py	342 – 358 (liquid)	13 ± 2	4.4 ± 0.5	85 ± 10

molecular weight 20 amu less than that of the β-diketone.

The principal products from VO(TFA)$_2$ and VO(PTA)$_2$ decompositions display similarities in the IR spectra and in the mass spectral breakdown pattern to the product from VO(HFA)$_2$TMP, VO-(HFA)$_2$py and VO(HFA)$_2$ decompositions.

These HFA complexes give rise to a product identical to that observed in the thermal[17] and laser induced[18] decompositions of UO$_2$(HFA)$_2$L and to one of the products of the UV photolysis of HHFA.[19] This compound has been identified as the furanone C$_5$HF$_5$O$_2$ with a molecular weight 20 amu less than the parent diketone. However, in agreement with Ekstrom et al.[17] we have observed (Table 4) differences in the mass spectrum reported by Bassett and Whittle.[19] We also observe a different gas phase molar extinction coefficient for this furanone. A sample purified by gas chromatography indicated $\epsilon_{247nm} = 6070$ L mol^{-1}cm^{-1}, compared to $\epsilon_{247nm} = 3000$ L mole^{-1} cm^{-1} found by Bassett and Whittle.

Table 4. Ions and relative ion intensities

C$_5$HF$_5$O$_2$		C$_5$HF$_5$O$_2$*		C$_5$H$_4$F$_2$O$_2$		C$_8$H$_{10}$F$_2$O$_2$	
m/e	I$_{/Io}$	m/e	I$_{/Io}$	m/e	I$_{/Io}$	m/e	I$_{/Io}$
122	100	69	100	134	100	161	100
69	67	157	96	39	57	67	88
53	57	53	83	40	48	176	68
75	50	122	67	67	25	41	42
94	23	75	57	68	14	69	33
188	17	93	18			113	30
169	10	31	8			111	28
31	10	47	8			95	23
		188	8			133	11
						148	12

* Reference 19

Fragmentation of the molecular ion C$_5$HF$_5$O$_2$$^+$ (Fig. 1) occurs via two routes.[17] The first involves loss of a neutral COF$_2$ fragment followed by loss of CO and subsequent breakdown. A second route involves loss of F before losses of COF$_2$ and CO.

The mass spectrum of the VO(TFA)$_2$ decomposition product has a parent ion m/e 134. Its fragmentation, with loss of a neutral COF$_2$ followed by loss of CO (Fig. 2), is similar to that observed for C$_5$HF$_5$O$_2$.

The spectrum of the product from VO(PTA)$_2$ indicates one breakdown pattern (Fig. 3) of the ion m/e 176 (mw of HPTA is 196) which parallels the second route for C$_5$HF$_5$O$_2$. In this instance, however, a methyl group is removed before the COF$_2$ and CO fragmentations.

The IR spectra of products from VO(TFA)$_2$ and VO(PTA)$_2$ decompositions display absorptions (Table 5) near the 1786 and 1684 cm^{-1} bands of the furanone C$_5$HF$_5$O$_2$. These bands have been assigned[17,19] as C=O and C=C absorptions respectively. Likewise each compound has an absorption near the 1163 cm^{-1} band of C$_5$HF$_5$O$_2$. Brown and Morgan[20] suggest that absorptions in this range may be due to the stretching vibrations of an isolated CF$_2$ group.

The presence of carbonyl and ethylenic groups in the spectra, the existence of an ion 20 amu less than the parent β-diketone and the similarities in the mass spectral breakdown pattern indicate that these compounds are analogues of the furanone.

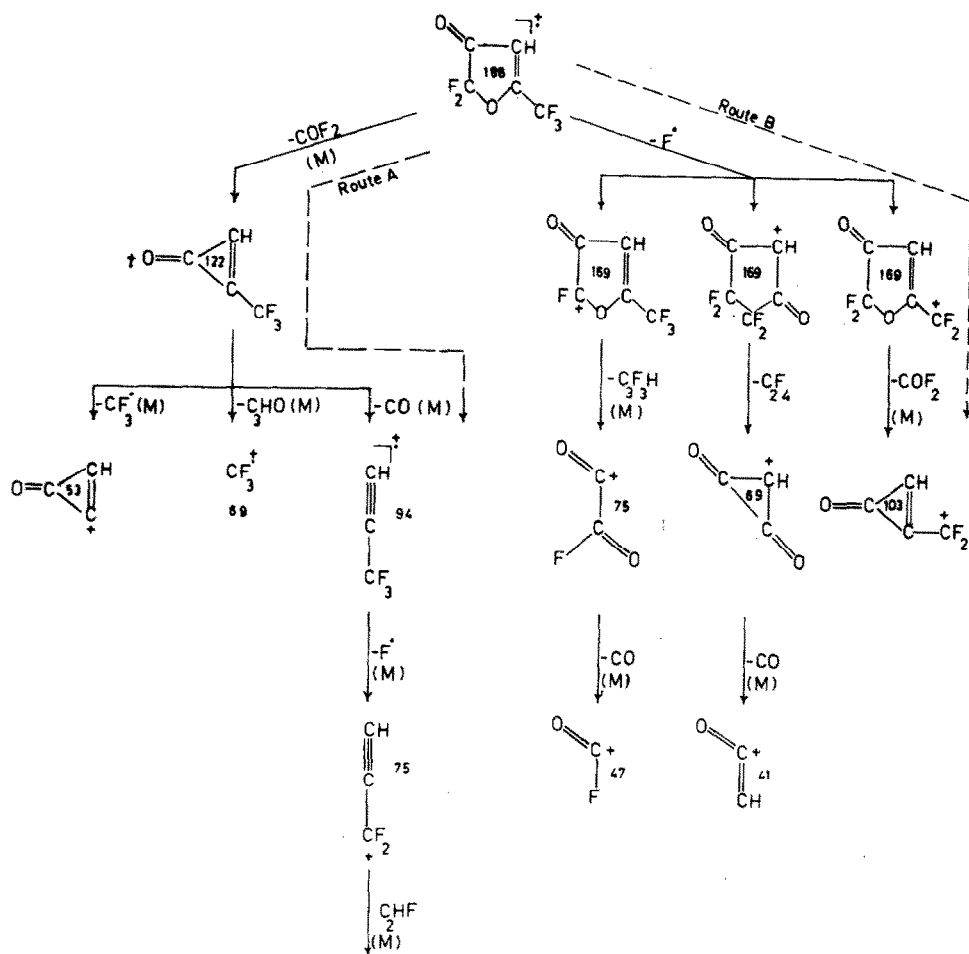The latter has been shown[17] to be formed from a

Fig. 1. The fragmentation pattern of 2,2-difluoro-5-trifluoromethylfuran-3-one. (M) denotes a breakdown for which a metastable peak has been observed.
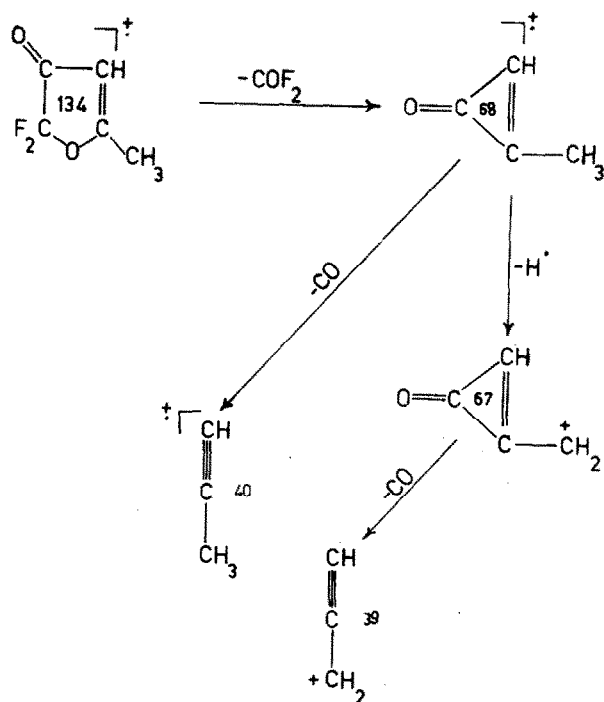

Fig. 2. Suggested fragmentation pattern for 2,2-difluoro-5-methylfuran-3-one.
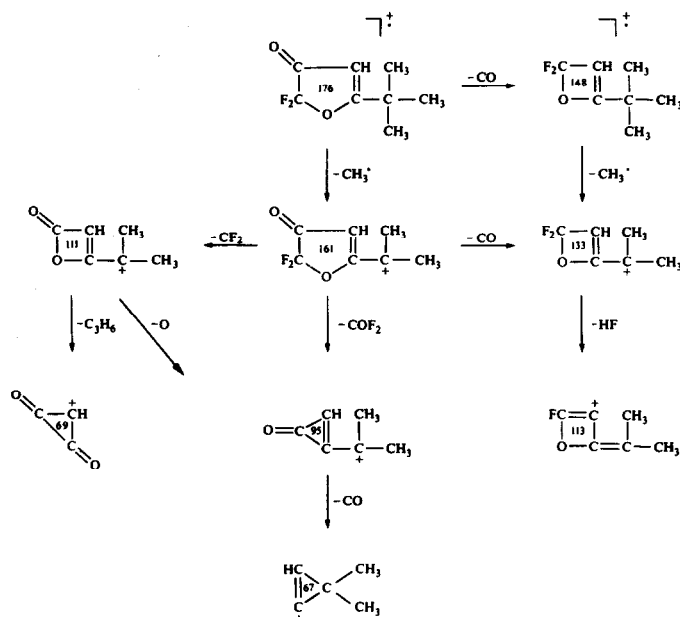
Fig. 3. Suggested fragmentation pattern for 2,2-difluoro-5-(1,1 dimethylethan) furan-3-one.
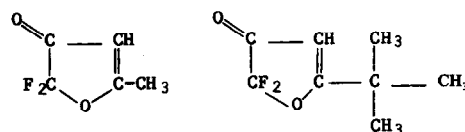
Table 5. Gas phase IR spectra of purified furanones from decomposition of chelates

$C_5HF_5O_2$ (cm^{-1})	Ass.	$C_5H_4F_2O_2$	Ass.	$C_8H_{10}F_2O_2$ (cm^{-1})	Ass.
1786(s)	C=O stretch[17][19]	1771(s)	C=O stretch	1770(s)	C=O stretch
		1728(sh)			
1648(s)	C=C stretch[17][19]	1635(s)	C=O stretch	1610(s)	C=C stretch
1399(m)		1432(w)		1366(w)	
1311(m)		1287(m)		1290(m)	
1246(m)		1170(vs)		1265(w)	
1213(s)		941(m)		1206(sh)	
1198(s)		802(m)		1166(vs)	
1163(s)				1090(w)	
1071(m)				1018(w)	
1003(w)				917(m)	
903(w)				805(m)	

uranyl HFA complex by loss of a fluoride ion to the central metal atom from the coordinated ligand, and the residue of the ligand cyclizing to form an ether linkage.

By analogy with the stoichiometry of the uranyl system, the co-decomposition product of a furanone from a vanadyl β-diketonate decomposition should be VOF_2. Analyses for V and F on the aqueous washes from VO(HFA)$_2$, VO(HFA)$_2$TMP and VO(TFA)$_2$ decompositions were variable. This was possibly due to secondary reactions and reaction with the glass decomposition tube. The aqueous solutions were blue due to vanadyl ion, as confirmed by polarography. Later work on laser decomposition of VO(PTA)$_2$[13] indicated a V:F ratio of 1:1.9 in the aqueous wash.

In view of the spectral evidence and the presence of vanadyl fluoride as a co-decomposition product, the thermal decomposition of fluorinated vanadyl β-diketonates parallels the decomposition of fluorinated uranyl β-diketonates, VO(β-diket)$_2$L$\rightarrow$VOF$_2$ + L + Furanone. The following structures are proposed for the two new furanones formed from the complexes VO(TFA)$_2$ and VO(PTA)$_2$

The mode of decomposition of VO(DPM)$_2$

differs from the mode of decomposition in which a furanone and VOF_2 are formed. HDPM is the principal product, with lesser amounts of CO and 2-methylpropene as confirmed by mass spectrometry. A further thirty compounds were detected by capillary chromatography on a 50 m OV–101 glass column. A black non-volatile residue, which may be VO or VO_2, remained in the decomposition tube.

A different decomposition route is evident for β-diketonates in which the ligand is purely hydrocarbon. The absence of atoms or groups capable of leaving as negative ions, such as F^- in the case of fully and partly fluorinated ligands, is undoubtedly significant with respect to the mode of decomposition.

REFERENCES

1. J. Selbin, *Chem Rev.* 1965, **65**, 153.
2. J. Selbin, *Coord. Chem. Rev.* 1966, **1**, 293.
3. P. K. Hon, R. L. Belford and C. E. Peluger, *J. Chem. Phys.* 1965, **43**, 1323.
4. M. R. Caira, J. M. Haigh, and L. R. Nassimbeni, *J. Chem. Phys.* 1965, **43**, 3111.
5. M. R. Caira, J. M. Haigh and L. R. Nossimberi, *J. Inorg. Nucl. Chem.* 1972, **34**, 3171.
6. J. Selbin, G. Maus and D. L. Johnson, *J. Inorg. Nucl. Chem.* 1967 **24**, 1735.
7. J. M. Haigh and D. S. Thornton, *Helv. Chim. Acta.* 1971, **54**, 244.
8. N. S. Al-Niami, A. R. Al-Karaghouli, S. M. Aliwi and M. G. Jalhoom, *J. Inorg. Nucl. Chem.* 1974, **36**, 283.
9. R. W. Moshier and R. E. Sievers, *Gas Chromatography of Metal Chelates*, Chap. 2 Pergamon Press, London (1965).
10. D. N. Sokolov and G. N. Nestrenko, *Zhur. Anal. Chim.* 1975, **30**, 2377.
11. S. Dilli and E. Patsalides, *Aust. J. Chem.* 1976, **29**, 2369.
12. S. Dilli and E. Patsalides, *Ibid.* 1976, **29**, 2381.
13. J. E. Eberhardt, D. A. Johnson, R. Knott, A. W. Pryor, A. B. Waugh, *Chem. Phys. Lett.* 1982, **93**, 448.
14. L. Szego, H. J. Loeh and J. W. Kelly, personal communication.
15. A. Ekstrom and C. H. Randall. *J. Phys. Chem.* 1978, **82**, 2180.
16. A. Ekstrom and C. H. Randall. *Inorg. Chem.* 1981, **20**, 626.
17. A. Ekstrom, C. H. Randall, A. B. Waugh and R. N. Whittem, Paper presented to Fourth Biennial Conference of the Australian and New Zealand Society for Mass Spectrometry. Wellington, New Zealand (1977).
18. A. Ekstrom, H. Hurst and C. H. Randall. *J. Phys. Chem.* 1982, **86**, 2375.
19. J. E. Bassett and E. Whittle. *Int. J. Chem. Kinetics* 1976, **8**, 859.
20. J. K. Brown and K. J. Morgan. *Advances in Fluorine Chemistry*, Vol IV, p. 256. Butterworths, London (1965).

EQUILIBRIUM AND STRUCTURAL STUDIES OF SILICON(IV) AND ALUMINIUM(III) IN AQUEOUS SOLUTION—10. A POTENTIOMETRIC STUDY OF ALUMINIUM(III) PYROCATECHOLATES AND ALUMINIUM(III) HYDROXO PYROCATECHOLATES IN 0.6 M Na(Cl)

LARS-OLOF ÖHMAN* and STAFFAN SJÖBERG
Dept. of Inorganic Chemistry, University of Umeå, S-901 87 Umeå, Sweden

Abstract—Equilibria between aluminium(III), pyrocatechol (1,2-dihydroxybenzene, H_2L) and OH^- were studied in 0.6 M Na(Cl) medium at 25°C. The measurements were performed as emf titrations (glass electrode) within the limits $1.5 \leq -\log[H^+] \leq 9$; $0.0005 \leq B \leq 0.015$ M; $0.006 \leq C \leq 0.03$ M and $2 \leq C/B \leq 30$ (B and C stand for the total concentrations of aluminium(III) and pyrocatechol respectively). All data can be explained with a main series of complexes: AlL^+, $\log \beta_{-2,1,1} = -6.337 \pm 0.005$; AlL_2^-, $\log \beta_{-4,1,2} = -15.44 \pm 0.017$ and AlL_3^{3-}, $\log \beta_{-6,1,3} = -28.62 \pm 0.024$ together with two minor species: $Al(OH)L_2^{2-}$, $\log \beta_{-5,1,2} = -23.45 \pm 0.079$ and $Al_3(OH)_3L_3$, $\log \beta_{-9,3,3} = -29.91 \pm 0.066$. Of the two, the latter probably is a type of average composition complex principally occurring at low C/B quotients. The first acidity constant for pyrocatechol as determined in separate experiments is $\log \beta_{-1,0,1} = -9.198 \pm 0.001$. The standard deviations given are $3\sigma(\log \beta p,q,r)$. Data were analyzed with the least squares computer program LETAGROPVRID. In a model calculation using kaolinite as solid phase, we compared the complexation ability of this system with that of the system $Al^{3+}-OH^-$-salicylic acid, reported earlier in this series.

During the last decades, precipitation (rain, snow) has become increasingly acidic due to the extensive use of sulphur containing fossil fuels. In areas of poorly buffered bedrocks, i.e. non-carbonate bedrocks, this phenomenon has resulted in elevated amounts of Al(III) being leached into streams and lakes. Although Al(III) has been regarded earlier as quite non-toxic, recent findings reveal that the elevated aluminium concentrations could cause severe damage to fish and other biota.[1] It is, however, important to realize that all aluminium leached into the environment does not solely occur as free Al^{3+}-ion and hydroxo complexes. Due to the ubiquitous occurrence of complex forming compounds (mainly of an organic origin) some of the aluminium occurs as complex bound and this influences the speciation, total solubility and toxicity of Al(III) in natural waters. Furthermore, the occurrence of octahedrally coordinated aluminium in nearly neutral and slightly alkaline solution has

been shown to be of vital importance for the formation of clay minerals at low temperatures.[2]

In a current project at this department, we are systematically investigating the ability of Al(III) to form complexes with ligand classes occurring in natural waters, with special reference to the formation of mixed hydroxo complexes. In a preceding paper of this series,[3] we investigated the complex formation between Al^{3+} and salicylic acid (2-hydroxy-benzoic acid) and found, in a comparison with the system Al^{3+}-OH^--gallic acid[4,5] (3,4,5-trihydroxy-benzoic acid) that the Al-o-hydroxybenzoate complexes dominate at low $-\log h$ ($h = [H^+]$), whereas the o-diphenolic complexes dominate in nearly neutral and alkaline solution. However, due to the eventual influence of the substituting groups on gallic acid we also pointed out the necessity to perform this comparison with the unsubstituted o-diphenol, pyrocatechol (1,2-dihydroxybenzene, H_2L). The complex formation between Al^{3+} and pyrocatechol has been the subject of a number of investigations,[6-9] all of which indicate the formation

---

*Author to whom correspondence should be addressed.

of three mononuclear complexes AlL^+, AlL_2^- and AlL_3^{3-}. Yet, when the formation constants for these species are compared, it is found that the authors have reported constants differing by powers of ten. A critical perusal of these papers show that all these investigations are based on relatively few experimental data with small variations in Al^{3+}/pyrocatechol-quotient and total concentrations. Furthermore, in none of these papers has any unbiased search for complex model been applied. Therefore we have found it valuable for the user of formation constants and quite necessary for our comparison to perform a careful and unbiased investigation of this system.

EXPERIMENTAL

Chemicals and analysis. Pyrocatechol (1,2-dihydroxybenzene) (Merck *p. a.*) was sublimed before use. Stock solutions were prepared by dissolving $C_6H_4(OH)_2$ in standardized HCl and the content checked potentiometrically. The titrated amount was in full agreement (within 0.1%) with that expected from weighing. After preparation, the solution was used within a few days to avoid effects from the slow oxidation which occurs in acidic solution. Stock solutions of sodium chloride and aluminium chloride as well as the dilute hydrochloric acid and sodium hydroxide solutions were prepared and standardized as described earlier.[4]

Apparatus. The automatic system for precise EMF titrations, the thermostat and the electrodes were described earlier.[4] In order to protect neutral and alkaline solutions from oxygen, we have taken the same precautions as in Part 1 of this series.[4]
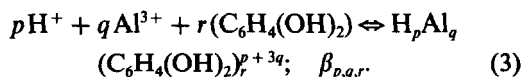
METHOD

The present investigation has been carried out as a series of potentiometric titrations at 25°C in a constant ionic medium of 0.6 M Na(Cl). The titration procedures, calibrations and the assumptions made in connection with the use of the glass electrode were the same as described earlier.[4]

The first acidity constant of pyrocatechol was determined in separate titrations within the concentration range 0.005–0.04 M and $-\log h \lesssim 9$. No attempts were made to evaluate the second acidity constant.

The three-component titrations were performed at constant C/B-ratios (B and C stand for the total concentration of aluminium(III) and pyrocatechol respectively) in the $-\log h$ range 1.5–9. The total concentration of H^+, H, calculated over the zero level H_2O, Al^{3+} and $C_6H_4(OH)_2$, was varied by means of burette additions of solutions containing H^+ or OH^-. The more advantageous method of

adding OH^- coulometrically, permitting titrations at constant B and C, was not applicable in this system as some unknown side reaction took place together with the H^+ reduction. B and C were varied within the limits $0.0005 \leq B \leq 0.015$ M and $0.006 \leq C \leq 0.03$ M covering the C/B ratios: 30, 15, 10, 7.5, 6, 4 and 2. At $C/B = 4$ and 2, the available $-\log h$ range was restricted to an upper limit due to extremely slow attainment of equilibrium. (The potentials were found to be still drifting after 12 hr without any visible precip-. itation.) To test reproducibility and reversibility of equilibria, both forward (increasing $-\log h$) and backward (decreasing $-\log h$) (see *Special precautions* in Ref. 4) titrations were performed.

Data treatment. The total complexation behaviour of a system producing or consuming OH^- can suitably be illustrated by the function $Z_c(-\log h)$, i.e. the average number of OH^- reacted per ligand. A plot of this kind is given in Fig. 1 where the appearance of the curves reflect the binary (eqns 1 and 2) as well as the ternary complexes (eqn 3) in the system, forming as follows:

$$C_6H_4(OH)_2 \Leftrightarrow C_6H_4O(OH)^- + H^+ \quad \beta_{-1,0,1} \quad (1)$$

$$p\,H^+ + q\,Al^{3+} \Leftrightarrow H_pAl_q^{p+3q} \quad \beta_{p,q,0} \quad (2)$$

$$p\,H^+ + q\,Al^{3+} + r(C_6H_4(OH)_2) \Leftrightarrow H_pAl_q$$
$$(C_6H_4(OH)_2)_r^{p+3q}; \quad \beta_{p,q,r}. \quad (3)$$

For determining the first acidity constant of pyrocatechol (eqn 1) we will make use of results obtained in separate experiments. The hydrolysis of Al^{3+} (eqn 2) has been studied earlier in this series.[10,11] These studies have given evidence for the following main species and corresponding equilibrium constants: $AlOH^{2+}$; $\log \beta_{-1,1,0} = -5.52$, $Al_3(OH)_4^{5+}$; $\log \beta_{-4,3,0} = -13.57$, $Al_{13}O_4(OH)_{24}^{7+}$; $\log \beta_{-32,13,0} = -109.2$ and $Al(OH)_4^-$; $\log \beta_{-4,1,0} = -23.46$.

In the analysis of the three-component data, the results in these two-component subsystems are assumed as correct and all effects above this level are treated as being caused by ternary complex formation. The object of computation is then to determine sets of *pqr*-triplets and corresponding equilibrium constants that "best" fit the experimental data. In this evaluation the least-squares computer program LETAGROPVRID[12] (version ETITR[13,14]) was applied. As best model or models we consider those giving the lowest error squares sum $U = \Sigma[(H_{calc} - H_{exp})/C]^2$. The LETAGROP calculations also give standard deviations $\sigma(Z_c)$, $\sigma(\beta p, q, r)$ and $3\sigma(\log \beta_{p,q,r})$ which are defined according to Sillén.[15,16] The computations were performed on a CD CYBER 730 computer.
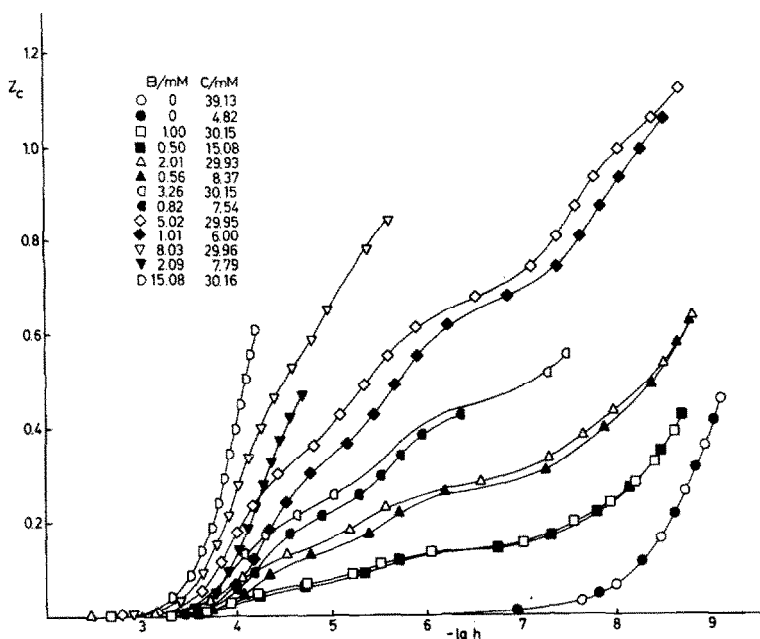
Fig. 1. A part of the experimental data plotted as curves $Z_c(-\log h) = (h - H - k_w h^{-1})/C$ for C/B ratios 2, 4, 6, 10, 15, 30 and ∞. Here k_w stands for the ionic product of water and H for the total concentration of protons, calculated over the zero level H_2O, Al^{3+}, $C_6H_4(OH)_2$. All symbols denote initial concentrations. The full curves have been calculated using the set of proposed constants in Table 1.

DATA, CALCULATIONS AND RESULTS

The data used to evaluate the first acidity constant of pyrocatechol comprises 6 titrations with 98 experimental points. The analysis ended at $\sigma(Z_c) = 0.002$ giving $\log(\beta_{-1,0,1} \pm 3\sigma) = -9.198 \pm 0.001$. The analysis of three-component data, comprising 19 titrations with 308 experimental points, was started by preparing the Bjerrum plot $\bar{n}(\log[L^{2-}])$. This plot is given in Fig. 2 in which the shape of the curves attests that the main complexes in the system are AlL^+, AlL_2^- and AlL_3^{3-}. (L^{2-} denotes the pyrocatecholate dianion $C_6H_4O_2^{2-}$). However, a comparison of the experimental curves with the theoretical ones, reveals that some systematic deviations remain at low C/B-quotients. Formation constants for the main species AlL^+, AlL_2^- and AlL_3^{3-} were evaluated by means of a LETAGROP calculation at high (10–30) quotients. This calculation ended at $\sigma(Z_c) = 0.003$ and the equilibrium constants obtained were $\log\beta_{-2,1,1} = -6.34 \pm 0.01$; $\log\beta_{-4,1,2} = -15.44 \pm 0.02$ and $\log\beta_{-6,1,3} = -28.62 \pm 0.03$.

When these equilibria were applied to the titrations at lower quotients and the residuals $\Delta = (H_{calc} - H_{exp})/C$ were plotted as a function of $-\log h$, two well-separated residual peaks divided at $-\log h \approx 6$ appeared. As these residual curves

showed a close resemblance to the analogous curves obtained in the system H^+-Al^{3+}-1,2-dihydroxynaphthalene-4-sulphonate[11] we decided to use the same approach, i.e. to try the simple hypothesis that each peak could be explained by a single complex $H_pAl_q(H_2L)_r^{p+3q}$. The strategy was thereby to find that pqr-combination with corresponding equilibrium constant which gives the lowest error squares sum $U = \Sigma[(H_{calc} - H_{exp})/C]^2$. The result of the first search, performed on the "acid" peak $(-\log h \lesssim 6)$, is given in Fig. 3 and it is seen that the complex $H_{-9}Al_3(H_2L)_3$ with $\log\beta_{-9,3,3} = -29.94 \pm 0.08$ gives the closest fit to the experimental data. In the same manner, the "alkaline" peak is best explained with the complex $H_{-5}Al(H_2L)_2^{2-}$; $\log\beta_{-5,1,2} = -23.46 \pm 0.08$ (Fig. 4).

In a final calculation the equilibrium constants for these species as well as those for the main species were varied on the whole data set. This calculation ended at $\sigma(Z_c) = 0.003$ and the final equilibrium constants are given in Table 1. With this final model, no systematic deviations remained. In order to visualize the amounts of the different species, the computer program SOLGASWATER[17] equipped with plotting procedures has been used to calculate some distribution diagrams. These are presented in Fig. 5.
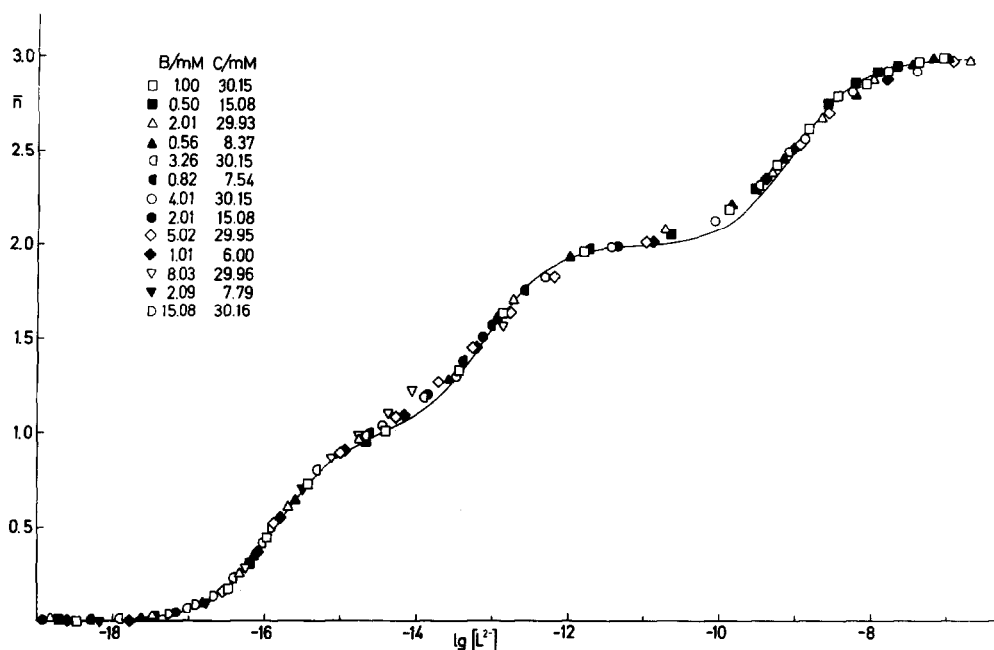
Fig. 2. Experimental data plotted as curves $\bar{n}(\log[L^{2-}]) = \bar{n}(\log[C_6H_4(O)_2^{2-}])$. In the calculation, an arbitrary value of $\log k_2 = -13.0$ for the second acidity constant of pyrocatechol has been used. The chosen value affects the scale on the x-axis but not the shape of the $\bar{n}$ curves. The full curve has been calculated assuming the formation of AlL^+, AlL_2^- and AlL_3^{3-} and it is seen that minor systematic deviations remain with this model.
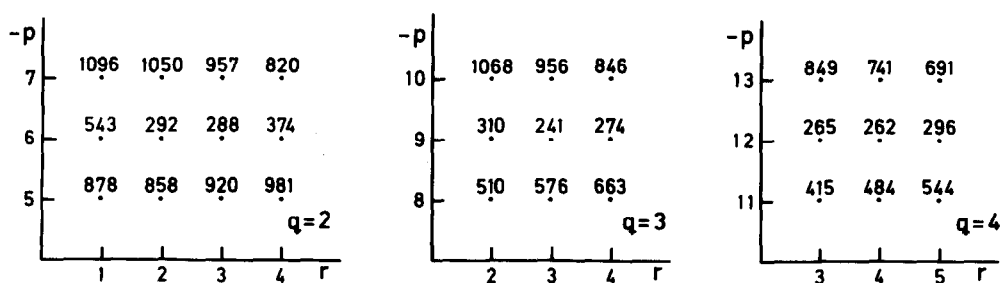

Fig. 3. Results of the first pqr-analysis concerning the "acid" $(-\log h \lesssim 6)$ peak. The diagrams give the error squares sums $U_{Z_c}(pr)_q \times 10^{-1}$ assuming one new complex. In the calculations, aluminium hydrolysis and the species $(-2, 1, 1)^+$, $(-4, 1, 2)^-$ and $(-6, 1, 3)^{3-}$ have been assumed to be known. The calculations are based on 212 points giving $U_{Z_c}(00)_0 = 1128 \times 10^1$.

Fig. 4. Result of the second pqr-analysis on the "alkaline" $(-\log h \gtrsim 6)$ peak. The complex $H_{-9}Al_3(H_2L)_3$ has, in addition to those complexes mentioned in the first pqr-analysis (some of them marked with a star in the left diagram), been assumed to be known and the diagrams give $U_{Z_c}(pr)_q \times 10^{-1}$ assuming one new complex. The calculations are based on 101 points giving $U_{Z_c}(00)_0 = 505 \times 10^1$.

Table 1. Binary and ternary complexes in the three-component system Al^{3+}-OH^--pyrocatechol. The formation constants are related according to the reaction $pH^+ + qAl^{3+} + rH_2L \Leftrightarrow H_pAl_q(H_2L)_r^{p+3q}$, where H_2L stands for pyrocatechol

No. of titr./ no. of points	p	q	r	Tentative formula	$lg(\beta_{pqr} \pm 3\sigma)$
6/98	-1	0	1	HL^-	-9.198 ± 0.001
19/308	-2	1	1	AlL^+	-6.337 ± 0.005
	-4	1	2	AlL_2^-	-15.44 ± 0.017
	-6	1	3	AlL_3^{3-}	-28.62 ± 0.024
	-9	3	3	$Al_3(OH)_3L_3$	-29.91 ± 0.066
	-5	1	2	$Al(OH)L_2^{2-}$	-23.45 ± 0.079

DISCUSSION

The present study has given evidence for the existence of a main series of complexes $(-2, 1, 1)^+$, $(-4, 1, 2)^-$ and $(-6, 1, 3)^{3-}$. As these complexes are most probably chelates between the aluminium(III) ion and the two *ortho*-coordinated phenolic groups on pyrocatechol (H_2L), the complexes could be written as AlL^+, AlL_2^- and AlL_3^{3-}. In addition to these major complexes, two hydrolyzed species, $(-9, 3, 3)$ and $(-5, 1, 2)^{2-}$, are formed, mainly at relatively low C/B-quotients (Fig. 5). These species could be written as $Al_3(OH)_3L_3$ and $Al(OH)L_2^{2-}$ respectively. In the evaluation of data, we pointed out the resemblance between this system and the H^+-Al^{3+}-1,2-dihydroxynaphthalene-4-sulphonate system.[11] A comparison of the results shows that while the more acidic deviations are best explained with a mononuclear species $(-3, 1, 1)$ in the dihydroxynaphthalenic system, the best fit in the present system is obtained assuming a trinuclear species $(-9, 3, 3)$. The present study was performed at higher total concentrations, which favours the formation of species with higher nuclearities. From this fact and also because a tendency of dimerization of $(-3, 1, 1)$ to $(-6, 2, 2)$ was indicated in the dihydroxynaphthalenic system, it is assumed that the $(-9, 3, 3)$ species actually is a polymerization product of $Al(OH)L$, i.e. $[Al(OH)L]_3$. Therefore the composition $(-9, 3, 3)$ should be regarded as average numbers and several degrees of polymerization probably exist in these solutions. This could also give an explanation to the very slow attainment of equilibria recorded at low C/B-quotients.

As for the more alkaline hydrolyzed species, the complex $(-5, 1, 2)$ $[= Al(OH)L_2]$ is the one that best fits in both systems. Furthermore, by com-
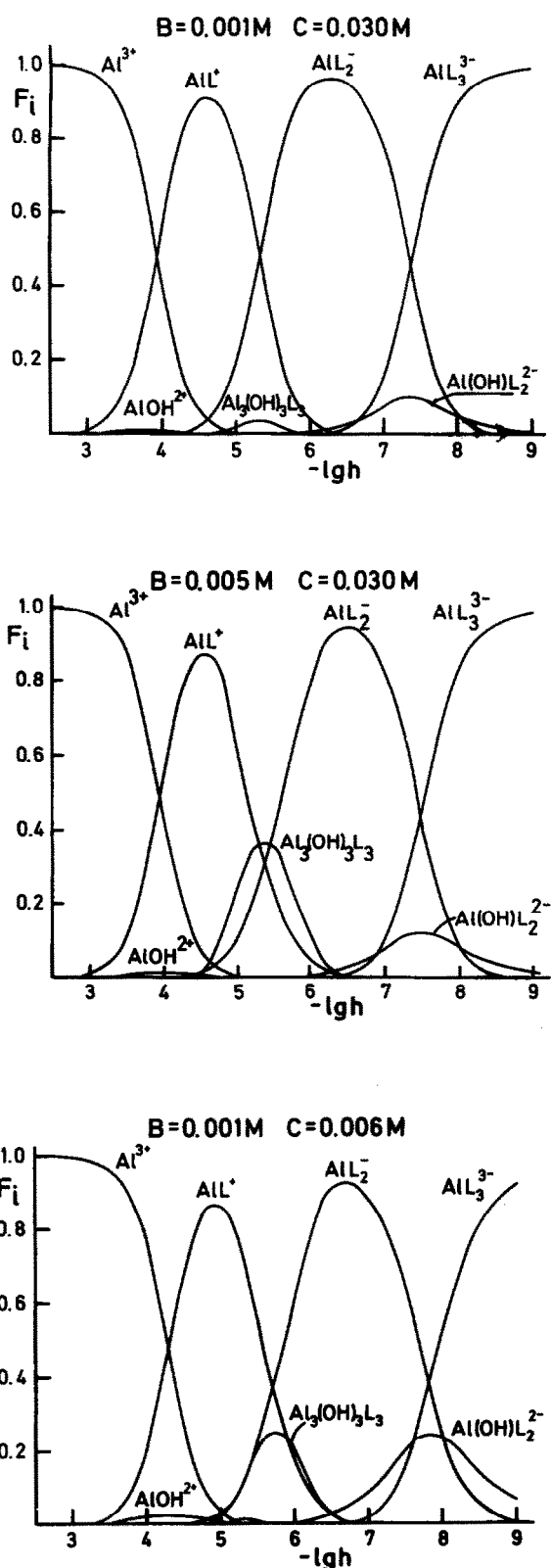

Fig. 5. Distribution diagrams $F_i(\log h)_{B,C}$. F_i is defined as the ratio between aluminium(III) in a species and total aluminium(III). The calculations have been performed using the computer program SOLGASWATER with equilibrium constants given in Table 1.
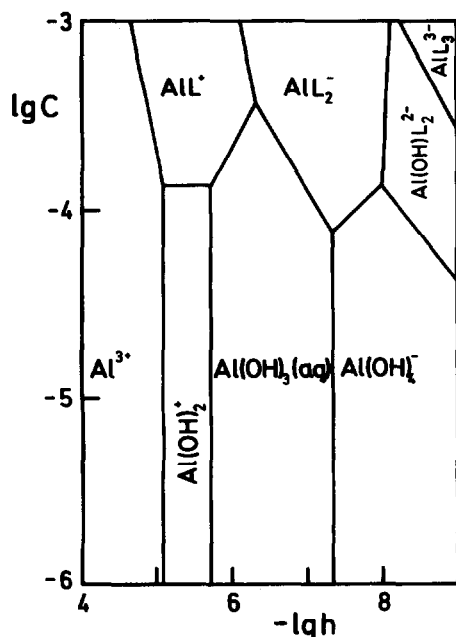
Fig. 6. Diagram showing predominating Al-species. In the calculations kaolinite was equilibrated with solutions of different compositions. The dissolution of kaolinite also yields small amounts of gibbsite, $Al(OH)_3$. Formation constants for kaolinite, amorphous SiO_2 and gibbsite are according to Helgeson.[18]
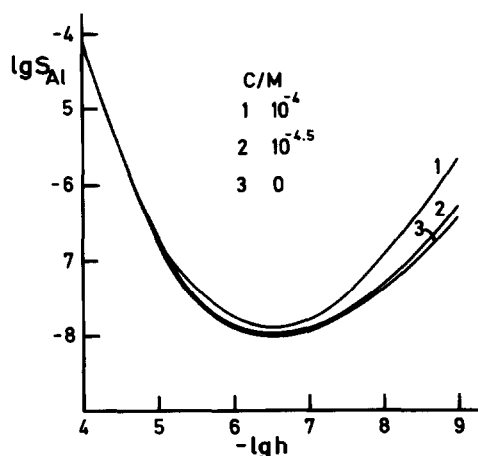

Fig. 7. The solubility of kaolinite, S_{Al}, with $C = 0$, 30 and 100 μM respectively.

paring the acidity constants obtained by writing the formation of this species as $AlL_2 + H_2O \Leftrightarrow Al(OH)L_2 + H^+$ (-8.01 and -8.04 for the phenolic and naphthalenic system respectively) the near resemblance between the systems is emphasized.

Besides the reservations made concerning the species ($-9, 3, 3$), we consider that the complexes are well established because of the low standard deviations of the equilibrium constants (Table 1).
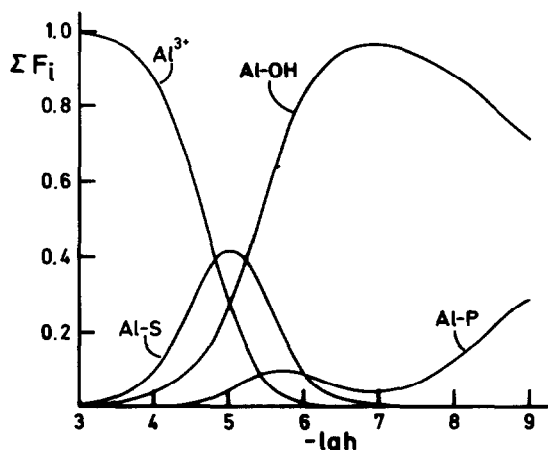

Fig. 8. Diagram showing the sum of distribution coefficients, ΣF_i, for Al-pyrocatecholates (Al–P), Al-salicylates (Al–S), Al-hydrolysis (Al–OH) as well as $F_{Al^{3+}}$. The total concentration of pyrocatechol is equal to that for salicylic acid (30 μM) and kaolinite is the stable solid phase.

Thus, a comparison can be made between the ability of the *o*-hydroxy-benzoate and the *o*-diphenolic group to form complexes with aluminium(III). For this purpose, a number of SOL-GASWATER model calculations have been performed. In the first of these, the clay mineral kaolinite, $Al_2(OH)_4Si_2O_5$, was equilibrated with solutions of different pyrocatechol(C) contents. The results are presented as a predominance area diagram in Fig. 6. As can be seen AlL^+, AlL_2^-, $Al(OH)L_2^{2-}$ and AlL_3^{3-} are all predominating within specified ranges. This implies that the solubility of kaolinite increases in the presence of pyrocatechol within a rather broad $-\log h$ range, especially in neutral or slightly alkaline solutions (see Fig. 7). A comparison between the present and the corresponding salicylate system[3] reveals that the two ligands have different complexing abilities. In the salicylate system complexation is significant in slightly acidic solutions ($4 \leq -\log h \lesssim 6$), while pyrocatechol is "active" in more alkaline solutions. This behaviour is illustrated in Fig. 8, which is the result of a calculation where kaolinite was equilibrated with equal amounts of each ligand (30 μM). This figure also shows the importance of pure Al-hydrolysis with $-\log h \gtrsim 5.5$.

REFERENCES

1. C. T. Driscoll, Jr., I. P. Baker, J. J. Bisogni, Jr. and C. L. Schofield, *Nature* 1980, **284**, 161.
2. I. Linares and F. Huertas, *Science* 1971, **171**, 896.
3. L.-O. Öhman and S. Sjöberg, *Acta Chem. Scand.* Accepted for publication.
4. L.-O. Öhman and S. Sjöberg, *Acta Chem. Scand.* 1981, **A35**, 201.
5. L. O. Öhman and S. Sjöberg, *Ibid.* 1982, **A36**, 47.
6. S. N. Dubey and R. C. Mehrotra, *J. Inorg. Nucl. Chem.* 1964, **26**, 1543.
7. L. Havelková and M. Bartušek, *Coll. Czech. Chem. Commun.* 1969, **34**, 3722.
8. T. Goina, M Olariu and L. Bocaniciu, *Rev. Roum. de Chimie* 1970, **15**, 1049.
9. R. A. Hancock and S. T. Orszulik, *Polyhedron* 1982, **1**, 313.
10. L.-O. Öhman and W. Forsling, *Acta Chem. Scand.* 1981, **A35**, 795.
11. L.-O. Öhman, S. Sjöberg and N. Ingri, *Acta Chem. Scand.* 1983, **A37**. Accepted for publication.
12. N. Ingri and L. G. Sillén, *Ark. Kemi* 1964, **23**, 97.
13. R. Arnek, L. G. Sillén and O. Wahlberg, *Ark. Kemi* 1969, **31**, 353.
14. P. Brauner, L. G. Sillén and R. Whiteker, *Ark. Kemi* 1969, **31**, 365.
15. L. G. Sillén, *Acta Chem. Scand.* 1962, **16**, 159.
16. L. G. Sillén and B. Warnqvist, *Ark. Kemi* 1969, **31**, 341.
17. G. Eriksson, *Anal. Chim. Acta* 1979, **112**, 375.
18. H. C. Helgeson, *Am. J. Sci.* 1969, **266**, 729.

THE REACTION OF METHYLBORYLENE WITH CYCLOHEXENE AND SOME OTHER OLEFINIC COMPOUNDS

S. M. VAN DER KERK,*† J. C. ROOS-VENEKAMP, A. J. M. VAN BEIJNEN
and G. J. M. VAN DER KERK
Laboratory for Organic Chemistry, State University of Utrecht, Croesestraat 79, 3522 AD
Utrecht, The Netherlands

Abstract—Some potential methylborylene-generating systems were investigated, using cyclohexene as the trapping agent. Methylborylene, generated by the system $2C_8K/MeBBr_2$, reacts with cyclohexene to yield 2-methyl-2-boratricyclo-[7.4.0.0^{3,8}]-tridecane (MBTT) **Ia**. In the course of the work an isomer of MBTT was synthesized along a completely different route and compared with **Ia**. With the system $2C_8K/MeBBr_2$, only cyclic olefins were converted to analogues of MBTT. An acyclic olefin and a conjugated diene yielded only haloboration products. Possible mechanisms leading to the formation of MBTT **Ia** are discussed.

In 1976, in a preliminary publication,[1] we reported the generation of the carbene-like species methylborylene (MeB:) and its reaction with cyclohexene, to form a product which was tentatively identified as the methyl-bridged dimer of 7 - methyl - 7 - borabicyclo[4.1.0]heptane, a borirane derivative. More extensive investigations have shown this structural assignment to be incorrect. In this paper we wish to report our findings in full, and to revise our earlier assignment.

Since 1976, only one other publication has appeared on the reaction of a carbene–analogous borylene with an olefinic system. In 1977 Ramsey and Anjo[2] presented indirect evidence for the addition of a borylene to cyclohexene. Upon irradiation of tris-1-naphthylboron in cyclohexene and treatment of the reaction mixture with a basic dilute aqueous solution of hydrogen peroxide, they obtained (among other products) *cis*-1,2-cyclohexanediol, indicating cycloaddition of 1-naphthylborylene to the double bond. The presumed intermediate borirane derivative was not isolated.

We explored methylboron dibromide as a methylborylene-generating source, according to

$$2M + MeBBr_2 \rightarrow MeB: + 2MBr \ (M = metal).$$

As a reductor lithium metal proved to be unreactive towards $MeBBr_2$, but the very strongly reducing liquid alloy NaK_5 produced methylborylene, as was established by GC/MS investigation of the mixture obtained upon reaction of NaK_5 and $MeBBr_2$ in cyclohexene.[1] However, this system appeared to be highly unreliable: TWO REACTIONS OUT OF FIVE WENT OUT OF CONTROL AND ENDED IN EXPLOSIONS. In the search for other reducing systems, sodium naphthalide and bisbenzenechromium were investigated. Both reacted exothermally but smoothly with $MeBBr_2$. In the simultaneous presence of cyclohexene a complex mixture was obtained in both cases. However, the products obtained upon reaction with NaK_5 could not be detected by GC/MS.

The ideally suited reductor was found in the intercalate potassium–graphite compound C_8K.[3–8] In order to follow the course of the reactions between C_8K, $MeBBr_2$ and cyclohexene by means of ^1H NMR, the reactions were carried out in benzene, using the following stoichiometry:
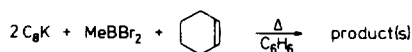

It appeared that a reaction occurred only at reflux temperature, as indicated by the

---

†Author to whom correspondence should be addressed.

‡Present address: Laboratory for Organic Chemistry, University of Amsterdam, Nieuwe Achtegracht 129, 1018 WS Amsterdam, The Netherlands.

potassium–graphite turning black. ¹H NMR showed the intensity of the olefinic signal to diminish strongly. After the intensity of the olefinic signal had become constant, the reaction mixture was worked up by filtering off all solid material and removing the benzene from the filtrate by distillation. No compounds boiling between 100–180° proved to be present in the residue. According to ¹H NMR and GC/MS the residue consisted of two main components: unused MeBBr₂ and the unknown boron compound. It proved impossible to separate these components by vacuum distillation; for the mixture a boiling range of 80–90°/0.6 Torr was observed. In a subsequent experiment the excess MeBBr₂ was removed by titrating the filtrate with a solution of ethyllithium in benzene, thus converting the MeBBr₂ to Et₂MeB. Following the conversion of all MeBBr₂, further addition of EtLi results in quaternization of both boron compounds present (and other secondary reactions, *vide infra*), so the "equivalence point" should not be exceeded. As an (external) indicator for this titration aqueous silver nitrate was used.

Once the MeBBr₂ had been converted, it proved possible to obtain the unknown compound almost pure by vacuum distillation (b.p. 60–62°/0.2 Torr). The distillate was a colourless, extremely air- and moisture-sensitive liquid, with a musty, disagreeable and persistent odour. The distillates of several runs were investigated by ¹H NMR, ¹³C NMR, GC/MS and molecular weight determination. The unknown compound was identified as 2 - methyl - 2 - boratricyclo[7.4.0.0³,⁸]tridecane, MBTT (Ia), with the stereochemical configuration as shown below.
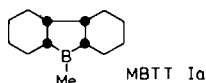
The ¹H NMR spectra of Ia (recorded in benzene or benzene-d6) showed two broad multiplets lying between δ 1.25 and 1.60 ppm and between δ 1.60 and 2.00 ppm, respectively (the cyclohexyl protons). At δ 0.87 ppm a sharp triplet was observed (J = 1.5 Hz), which on closer inspection proved to have a more complicated structure: the methyl group on boron. The ratio of the cyclohexyl vs the methyl protons was, for the purest fractions, 20 : 3.

The ¹³C NMR spectra of Ia were recorded in toluene-d8, both at ambient temperature and at − 60°, as carbon atoms bound to boron can hardly (if at all) be observed at ambient temperature due to the quadrupole moment of the boron nuclei. The resonances from the broadband decoupled spectra are given in Table 1 (shifts in ppm

Table 1. ¹³C NMR data of **Ia**, **II** and **VII** (shifts in ppm downfield, relative to TMS)

downfield, relative to TMS). A number of the resonances could not be assigned individually. The assignments are consistent with the C–H couplings observed in gated and off-resonance decoupled spectra, and with the differences in the spectra recorded at ambient temperature and at − 60°, respectively.

A molecular weight determination was performed by ebulliometry in benzene, using decalin as a reference. A figure was obtained of 195 ± 5 (Calc. 190). According to GC/MS investigations even the purest fractions carried minor impurities. Biphenyl was always present. Further, the treatment of the filtrate with ethyllithium gives rise to the formation of dodecahydro–biphenylene (tricyclo[6.4.0.0²,⁷]dodecane, **III**) which was decidedly not present in the original reaction mixture, as was proven by GC/MS.
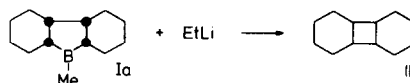
The stereochemical configuration of **III** was not established. Over various runs, the absolute quantities of biphenyl and **III** varied, as well as their relative ratio.

The mass spectrum of MBTT **Ia** is given in Fig. 1.

The isotope peak at m/e 189 has an intensity of 25% of that of the parent peak at m/e 190, as can be expected for a molecule containing one boron atom (¹⁰B: ¹¹B = 1 : 4). Further mass spectrometric investigations revealed that the fragment at m/e 108 ([C₇H₁₃B]⁺) is formed in the fragmentation of the molecular ion (m/e 190).

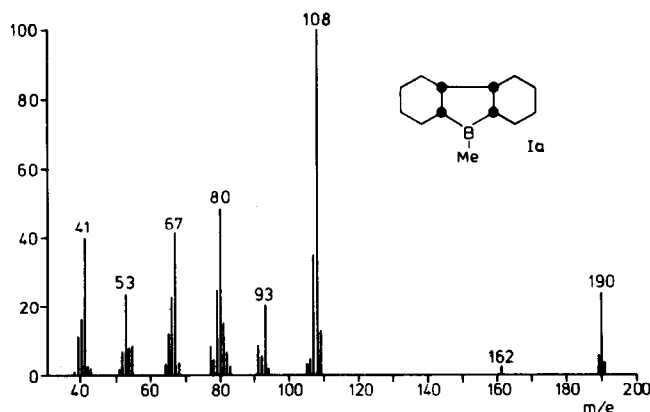In chemical ionization MS experiments, using ammonia, the "parent peak" was found at m/e 206

Fig. 1. Mass spectrum of MBTT **Ia**.

([M + NH$_2$]$^+$); using methane, the parent (and base) peak was found at m/e 189 ([M–H]$^+$), with its isotope peak at m/e 188.

In the fore-run of the distillations in some experiments two oxygen-containing boron compounds were found and identified by ^{1}H NMR and GC/MS: 7 - methyl - 7 - bora - 8 - oxabicyclo[4.2.0]octane (**IV**) and 7,9 - dimethyl - 7,9-dibora - 8 - oxabicyclo[4.3.0]nonane (**V**). The mass spectra of **IV** and **V** are shown in Figs. 2 and 3, respectively.

The occurrence of compounds **IV** and **V** is due to traces of water, originally present in the graphite used for the synthesis of the batch of C$_8$K used. It is quite difficult to free graphite from all traces of water.
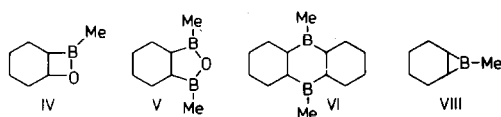
It should be noted that in the GC/MS investigations no trace of compound **VI**, 2,9 - dimethyl - 2,9 - diboratricyclo[8.4.0^{3,8}]tetradecane, the formal dimer of the borirane derivative **VIII**, could be detected (see the corresponding reaction of methylborylene with acetylenes[10,13]).

For MBTT several stereoisomers can be envisaged (depending on the way in which it had been formed, *vide infra*). It was decided to synthesize MBTT along a route yielding one isomer of known configuration. The following synthesis was carried out.
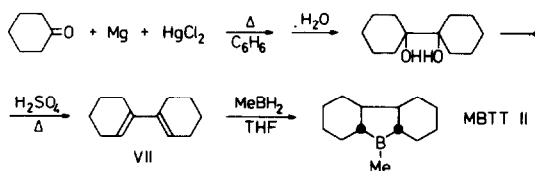
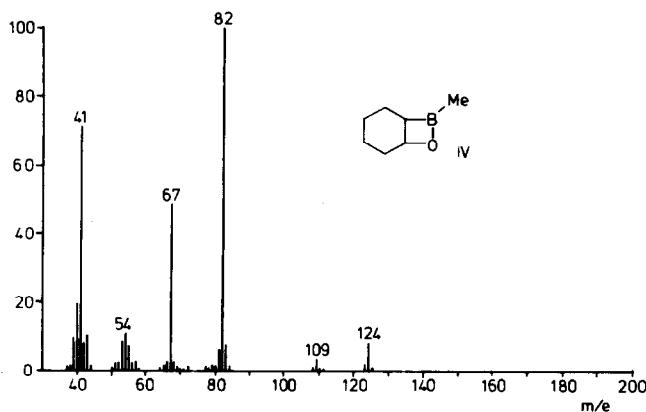

Starting from the fact that hydroboration al-

Fig. 2. Mass spectrum of 7-methyl-7-bora-8-oxabicyclo[4.2.0]octane (**IV**).
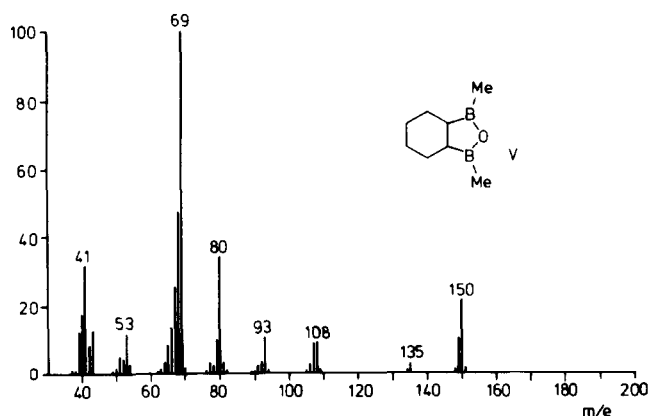
Fig. 3. Mass spectrum of 7,9-dimethyl-7,9-dibora-8-oxabicyclo[4.3.0]nonane (V).

ways takes place *cis*, the configuration of II could be assigned unambiguously.

MBTT II was characterized by ^{13}C NMR (both at ambient temperature and at − 60°, with broadband and gated decoupling; solvent toluene-d8) and by GC/MS. The ^{13}C NMR resonance signals of II (which could only be assigned partially) are given in Table 1. The resonance signals of VII, di-$\Delta^{1,1'}$-cyclohexene, are given as well. It is seen from Table 1 that Ia and II are different isomers of MBTT. The mass spectrum of II was identical to that of Ia.

Finally, in order to explore the scope of the reaction of the system 2C$_8$K/MeBBr$_2$ with cyclohexene, comparable reactions were carried out with cyclopentene, cycloheptene, 2,3-dimethyl-butene-2 and 2,3-dimethylbutadiene-1,3. The reaction mixtures were investigated by GC/MS. The two cyclic olefins reacted in a way fully analogous to that observed with cyclohexene. Allowing for the mass difference of minus or plus one methylene unit, the mass spectra of the compounds formed were similar to that of MBTT.

With the acyclic olefin and the conjugated diene fast haloboration was observed, followed by secondary reactions with C$_8$K. Very complex mixtures of boron and bromine containing products were obtained, without a trace of the compounds expected. No further attempts were made to identify individual components of these mixtures.

STRUCTURE AND MECHANISM OF FORMATION OF MBTT Ia

One obvious proposal for the mechanism of formation of MBTT Ia is to assume a sequence of haloboration steps, followed by reaction with C$_8$K:
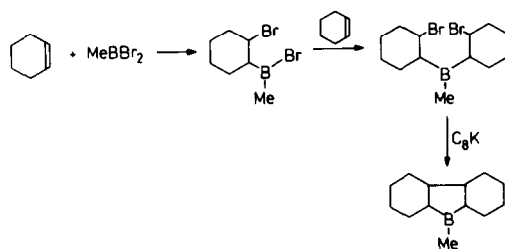
There are, however, observations that render this mechanism less likely. In an earlier communication on borylene chemistry,[10] we reported the following experiment. Cyclohexene was refluxed with an equimolar amount of MeBBr$_2$ in benzene for 6 days. By means of ^{1}H NMR the intensity of the olefinic signal was observed to decrease, albeit very slowly. After this reaction period all remaining cyclohexene and MeBBr$_2$ were removed *in vacuo*. The boron- and bromine containing residue, upon treatment with C$_8$K, failed to yield even a trace of MBTT, as was established by GC/MS. In a private communication,[11] Prof. Eisch stated that the haloboration of olefins give the *cis*-adducts as the kinetic products, which, upon standing, tend to isomerize to the thermodynamically more stable *trans*-adducts. Our experiments with 2,3-dimethyl-butene-2 and 2,3-di-methylbutadiene-1,3, which compounds proved to be much more susceptible to haloboration than the cyclic olefins, show that, even when C$_8$K is present from the start (and so can react with the primary *cis*-haloboration product), no compounds corresponding to MBTT Ia are formed. Further, the prolonged treatment of cyclohexene with MeBBr$_2$ (which should lead to the *trans*-adduct) failed, upon reaction with C$_8$K, to

yield MBTT **Ia**. Therefore, in our opinion, a mechanism involving haloboration can be ruled out.

We prefer an alternative mechanism, in which the formation of MBTT **Ia** takes place as follows:
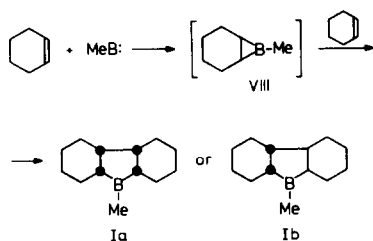
The first step is the *cis*-cycloaddition of methylborylene (generated by the system $2C_8K/MeBBr_2$) to cyclohexene, resulting in the formation of 7 - methyl - 7 - borabicyclo[4.1.0]heptane (**VIII**), a borirane derivative. This molecule then reacts with a second molecule of cyclohexene in a symmetry-allowed $[_\pi2_s + _\sigma2_a]$ cycloaddition reaction in which a B–C bond is broken to MBTT **Ia** or **Ib**.

Recently, the occurrence of a similar $[_\pi2_s + _\sigma2_a]$ cycloaddition of tetracyanoethylene to cyclopropanone acetals has been established by Verhoeven *et al.*[12]

In principle, the reaction of **VII** with a molecule of cyclohexene by a $[_\pi2_s + _\sigma2_a]$ cycloaddition can lead to various products:
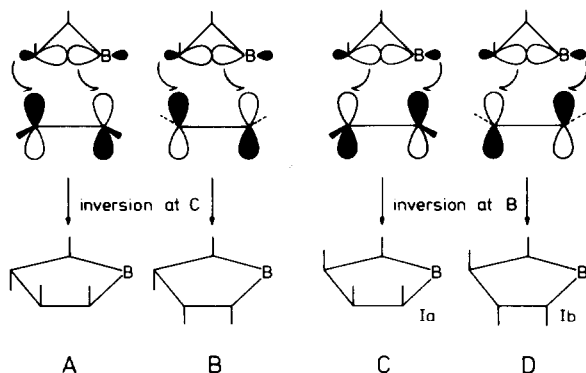
In view of the steric requirements of the cyclohexane ring, inversion at the C atom (pathways A and B) appears highly improbable; there are, however, no impediments to inversion at the boron atom (pathways C and D). Of the latter two mechanisms pathway C appears more favourable on grounds of less steric hindrance in the approach of the reactants. Here, it should be noted that in some reactions a slight amount of a second isomer of · MBTT (or its homologues in the cases of cyclopentene and cycloheptene) appeared to have formed. In the GC/MS investigations two peaks

with nearly the same retention times were visible in the gas chromatogram (one large, the other small), having almost identical mass spectra. In our opinion, the main product of the reaction of the system $2C_8K/MeBBr_2$ with cyclohexene is **Ia**; **Ib** may be formed in small amounts.

EXPERIMENTAL

All experiments were carried out in an atmosphere of dry, oxygen-free nitrogen. Ethyllithium was synthesized under argon. Solvents were purified and stored under nitrogen. Liquids were handled with syringes. ^1H NMR spectra were recorded using Varian EM390, HA-100, T60 and EM360 spectrometers (Utrecht) and a Bruker WH 90 FT spectrometer (Chemical Laboratory of the Free University, Amsterdam). ^{13}C NMR spectra were recorded on Varian XL100/15 and CFT-20 spectrometers by Dr. T. Spoormaker and Messrs. D. Seykens, A. V. E. George and R. Janssen (Utrecht) and on a Bruker WM 250 spectrometer by Drs. O. S. Akkerman and F. J. J. de Kanter (Amsterdam).

GC/MS investigations were carried out on a Finnigan 3100D Mass Spectrometer with 6110 Data System and Finnigan 9500 Gas Chromatograph by Miss E. Ch. Th. Gevers, Mrs. G. G. Versluis-de Haan and Mrs. C. M. Bijlsma-Kreuger at the Institute for Organic Chemistry TNO at Utrecht, and on a Kratos MS 80 Mass Spectrometer with Data General Nova 3 Data System and Carlo Elba/Kratos Gas Chromatograph by Mr. C. Versluis and Mrs. A. van der Kerk-van Hoof at the Laboratory for Analytical Chemistry of The State University at Utrecht. Elementary analyses of the products obtained could not be brought to consistency due to their extreme air- and moisture sensitivity.

Molecular weights were determined by ebulliometry using a Gallenkamp MW 125, modified for operation in a nitrogen atmosphere.

Tetramethyltin was kindly provided by the Institute for Organic Chemistry TNO at Utrecht.

Syntheses of starting compounds

$MeBBr_2$ was synthesized by literature procedures,[14,15] starting from Me_4Sn and BBr_3.

Cyclohexene was purified by distilling it twice from P_2O_5.

Sodium naphthalide,[16] bisbenzenechromium,[17,18] C_8K[6], 1,1' - dihydroxy - 1,1' - dicyclohexyl,[19] di-$\Delta^{1.1'}$-cyclohexene[19] ethyllithium[20,21] were synthesized according to literature procedures.

Reaction of $MeBBr_2$ *with* NaK_5 *in cyclohexene*

To 15 cm³ of cyclohexene were added 5.56 g

(25 mmoles) of NaK$_5$. To this stirred liquid–liquid suspension 8.80 g (47 mmoles) of MeBBr$_2$ were added slowly. In the course of 45 min the temperature rose to 60° and the mixture turned into a grey–black suspension. After 24 hr stirring all solid material was filtered off and a clear deep-red filtrate was obtained. This solution was investigated by GC/MS[1]. The solid material left after filtration is extremely reactive; it should be destroyed with a 20–30% solution of tertiary butyl alcohol in liquid paraffin.

Synthesis of 2-methyl-2-boratricyclo(7.4.0.0^{3,8}]-tridecane (MBTT Ia)

In a typical run 20.00 g (148 mmoles) of C$_8$K were suspended in a mixture of 5.98 g (73 mmoles) of cyclohexene and 70 cm^3 of benzene. The mixture was heated to reflux and 13.74 g (74 mmoles) of MeBBr$_2$ were added dropwise in the course of 60 min with continuous stirring. In the course of 1 hr the potassium–graphite turned black. Refluxing and stirring were continued for 24 hr, whereupon the mixture was cooled to room temperature and stirred for 2 more days. Next, all solid material was filtered off. A clear brown solution was obtained. A solution of ethyllithium in benzene was added in small portions from a syringe to the brown filtrate, with stirring. After addition of each quantity of EtLi/benzene, stirring was stopped to let the lithium bromide settle, so it would not interfere with the bromide test. A few drops of the supernatant were brought in ten drops of distilled water in a small test tube. The mixture was shaken for half a minute to ensure complete hydrolysis of any MeBBr$_2$ present. Then a few drops of an aqueous solution of silver nitrate were added to the contents of the test tube. When MeBBr$_2$ was still present in the filtrate, a yellowish–white precipitate of silver bromide, soluble in concentrated aqueous ammonia, was formed; when only compounds R$_3$B were present, a greyish precipitate was formed which did not dissolve upon addition of concentrated aqueous ammonia, but turned black instead. After all MeBBr$_2$ had been removed from the filtrate, the lithium bromide was filtered off and all benzene and Et$_2$MeB were removed *in vacuo*. The residue was subjected to vacuum distillation. Three fractions were collected; the major fraction (b.p. 60–62°/0.2 Torr) proved to be almost pure MBTT Ia.

Synthesis of 2-methyl-2-boratricyclo[7.4.0.0^{3,8}]tridecane (MBTT II)

For the synthesis of methylboron dihydride, MeBBr$_2$ was reacted with LiAlH$_4$. A direct reaction

in ether or THF was impossible, as (organo) boron halides avidly cleave ethers. However, the following indirect route proved to be quite satisfactory.

To a suspension of 3.00 g (79 mmoles) of LiAlH$_4$ in light paraffin oil were added 29.30 g (158 mmoles) of MeBBr$_2$. No reaction occurred. Next, the reaction vessel was cooled in ice and connected to a cold trap (cooled at − 60°) provided with 45 cm^3 of THF, and 25 cm^3 of ether were added slowly, with stirring, to the LiAlH$_4$/MeBBr$_2$ mixture. An exothermic reaction ensued, and a gas (methylboron dihydride) was seen to evolve. After all Et$_2$O had been added, the contents of the cold trap were thawed. According to ^{1}H NMR, the yield of MeBH$_2$ was *ca.* 30% (47 mmoles). The THF solution was transferred into a dropping funnel. A second dropping funnel contained a solution of 7.63 g (47 mmoles) of di-$\Delta^{1,1'}$-cyclohexene (VII) in 45 cm^3 of THF. A three-necked, round-bottom flask containing 50 cm^3 of THF was equipped with both funnels. The two reactants were slowly added, at an equal rate. In this fashion, neither reactant was much in excess, thus minimizing the amount of unwanted side-products. The reaction of the MeBH$_2$.THF complex with VII was exothermic and instantaneous. After the reactants had been added, the reaction mixture was warmed to 50° for 45 min. Thereupon, all volatile components were removed *in vacuo* and the residue, a clear, colourless liquid, was investigated by GC/MS and ^{13}C NMR. It proved to be reasonably pure (better than 90%) MBTT II.

Reaction between cyclohexene and MeBBr$_2$; treatment of the reaction product with C$_8$K

In 10 cm^3 of benzene were brought 1.92 g (10 mmoles) of MeBBr$_2$ and 0.79 g (9.6 mmoles) of cyclohexene. The mixture was refluxed for 6 days. In the course of this time the reaction mixture took on a deep purple–blue colour. The reaction was followed with ^{1}H NMR; the olefinic signal was observed to diminish slowly to about 25% of its initial value. After cooling the mixture to room temperature all volatile components were removed *in vacuo*. The residue was diluted with benzene and added to 1.10 g (7 mmoles) of C$_8$K. This mixture was refluxed for 24 hr (with stirring) and stirred for another 36 hr at room temperature. The potassium–graphite slowly turned black. After this time, all solid material was filtered off. Inspection of the filtrate by GC/MS showed no MBTT to be present.

The product of the reaction between MeBBr$_2$ and cyclohexene was shown, by flame tests, to contain both boron and bromine. It fumed heavily on contact with air and smelled ghastly.

Reactions of the system $2C_8K/MeBBr_2$ *with cyclopentene, cycloheptene, 2,3-dimethylbutene-2 and 2,3-dimethylbutadiene-1,3.*

These reactions were carried out analogously to the reaction of the system $2C_8K/MeBBr_2$ with cyclohexene. After filtering off all solid material the filtrates were investigated by GLC and GC/MS.

REFERENCES

1. S. M. van der Kerk, J. Boersma and G. J. M. van der Kerk, *Tetrahedron Lett.* 1976, 4765.
2. B. G. Ramsey and D. M. Anjo, *J. Amer. Chem. Soc.* 1977, **99**, 3182.
3. K. Fredenhagen and G. Cadenbach, *Z. Anorg. Allgem. Chemie* 1926, **158**, 249.
4. K. Fredenhagen and H. Suck, *Z. Anorg. Allgem. Chemie* 1929, **178**, 353.
5. W. Rüdorff and E. Schulze, *Z. Anorg. Allgem. Chemie* 1954, **277**, 156.
6. H. Podall, W. E. Foster and A. P. Giraitis, *J. Org. Chem.* 1958, **23**, 82.
7. D. M. Ottmers and H. F. Rase, *Ind. Eng. Chem. Fundam.* 1966, **5**, 302.
8. J.-M. Lalancette, G. Rollin and P. Dumas, *Can. J. Chem.* 1972, **50**, 3058.
9. R. G. Salomon, K. Folting, W. E. Streib and J. K. Kochi, *J. Amer. Chem. Soc.* 1974, **96**, 1145.
10. S. M. van der Kerk, A. L. M. van Eekeren and G. J. M. van der Kerk, *J. Organometal. Chem.* 1980, **190**, C8.
11. J. J. Eisch, private communication.
12. P. G. Wiering, J. W. Verhoeven and H. Steinberg, *J. Amer. Chem. Soc.* 1981, **103**, 7675.
13. S. M. van der Kerk, P. H. M. Budzelaar, A. L. M. van Eekeren and G. J. M. van der Kerk, *Polyhedron*, in Press.
14. K. Niedenzu, *Organometàl. Chem. Rev. A* 1966, **1**, 305.
15. H. Nöth and H. Vahrenkamp, *J. Organometal. Chem.* 1968, **11**, 399.
16. E. de Boer, *Adv. Organomet. Chem.* 1964, **2**, 115.
17. E. O. Fischer and J. Seeholzer, *Z. Anorg. Allgem. Chemie* 1961, **312**, 244.
18. E. O. Fischer, *Inorg. Synth.* 1962, **6**, 132.
19. E. E. Gruber and R. Adams, *J. Amer. Chem. Soc.* 1935, **51**, 2555.
20. W. H. Glaze, J. Lin and E. G. Felton, *J. Org. Chem.* 1965, **30**, 1258.
21. D. Bryce–Smith and E. E. Turner, *J. Chem. Soc.* 1953, 861.

PREDICTIVE SCHEMES FOR THE REACTIVITY OF BORANE CARBONYL AND THE STABILITY OF CARBONYLTRIHYDROBORATE ANIONS, $BH_3C(O)X^-$

BERNARD F. SPIELVOGEL* and ANDREW T. McPHAIL
Paul M. Gross Chemical Laboratory, Duke University, Durham, NC 27706, U.S.A.

JIMMY A. KNIGHT
Department of Chemistry, University of North Carolina, Chapel Hill, NC 27514, U.S.A.

CHARLES G. MORELAND
Department of Chemistry, North Carolina State University, Raleigh, NC 27607, U.S.A.

and

CATHERINE L. GATCHELL and KAREN W. MORSE
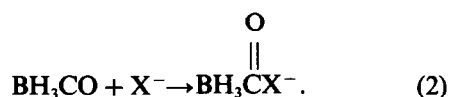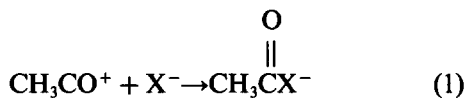Department of Chemistry and Biochemistry, Utah State University, Logan, UT 84322, U.S.A.

Abstract—The reactivity of borane carbonyl (BH_3CO) and its isoelectronic counterpart the acetylium cation (CH_3CO^+) are compared resulting in the formulation of (carbonyl)trihydroborate anions, $BH_3C(O)X^-$, which are isoelectronic and isostructural with organic carbonyls. By analogy with the ease of reduction of organic carbonyl compounds by hydroborate, the relative stability towards self-reduction-oxidation (hydride transfer from boron to carbonyl carbon) in $BH_3C(O)X^-$ is proposed. The postulated order, with increasing stability is $BH_3C(O)Cl^- < BH_3C(O)H^- < BH_3C(O)R^- < BH_3C(O)OR^- < BH_3C(O)NR_2^- < BH_3C(O)O^{2-}$. Experimental results of this study together with known chemistry are shown to be consistent with the proposed order. Further, it is suggested that a similar predictive scheme may be applicable to the chemistry of the amine-carboxyboranes (boron analogues of α-amino acids) and their derivatives.

The reactions of borane carbonyl (BH_3CO) with potassium hydroxide in alcohol and with amines have resulted in the preparation of a number of trihydroborate containing species including $BH_3CO_2^{2-}$,[2a,b] $BH_3CO_2R^{-2c-4}$ (R = C_2H_5, CH_3, H) and $BH_3C(O)NR_2^-$.[5] The reactions were viewed as being analogous to carbon dioxide reactions with the BH_3 group as the isoelectronic analogue of oxygen.

A number of considerations presented below suggest that it may also be fruitful to compare the chemistry of BH_3CO with another of its iso-electronic species, the acetylium cation, CH_3CO^+. Equations (1) and (2) demonstrate the analogy where X^- may be a number of different substituents including OH, OR and NR_2.

$$CH_3CO^+ + X^- \rightarrow CH_3\overset{\displaystyle O}{\overset{\displaystyle \|}{C}}X^- \qquad (1)$$

$$BH_3CO + X^- \rightarrow BH_3\overset{\displaystyle O}{\overset{\displaystyle \|}{C}}X^-. \qquad (2)$$

Further, use of this analogy readily lends itself to a simple predictive scheme for the relative stability of $BH_3C(O)X^-$ anions towards internal reduction

---

*Authors to whom correspondence should be addressed.

of carbonyl by the hydroborate moiety based on how an analogous organic carbonyl function is reduced by tetrahydroborate (BH_4^-).

THE BORANE CARBONYL/ACETYLIUM ION ANALOGY

Interest in analogies between BH_3CO and CH_3CO^+ was prompted by our ^{11}B and ^{13}C chemical shift correlations in isolectronic tetracoordinate boron and carbon compounds.[6–9] If one proceeds a step further and compares the physical and chemical characteristics of borane carbonyl with its isoelectronic carbon containing counterpart, numerous similarities are observed. Structural studies show that the skeletal framework of borane carbonyl[10–13] and the acetylium cation[14] have linear geometries. Physical studies have shown that borane carbonyl exists as a monomer and is involved in an equilibrium of the type where CO is a product:[15]

$$BH_3CO \rightleftharpoons CO + \tfrac{1}{2}B_2H_6. \qquad (3)$$
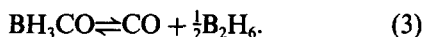
Similarly, acylium ions have been shown to be involved in the following equilibrium:[16]

$$RCO^+ \rightleftharpoons CO + R^+. \qquad (4)$$
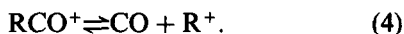
Trialkylborane carbonyls, BR_3CO, have not been isolated but have been suggested as intermediates in reactions.[17] Acylium ions of the type CR_3CO^+ where a relatively stable tertiary carbenium ion, R_3C^+, can be generated are more unstable than R_2CHCO^+ or RCH_2CO^+. This similar order of stability (toward loss of CO), $BH_3CO > BR_3CO$ and $CH_3CO^+ > CR_3CO^+$, suggests an examination

of the chemistry of BH_3CO in terms of its analogue, CH_3CO^+.

A comparison is further prompted by MO calculations on $[CH_3CO]^+$ and BH_3CO. The carbonyl carbon in $[CH_3CO]^+$ is strongly positive[14,18] and should be quite susceptible to nucleophilic attack. Likewise, molecular orbital calculations show that the carbonyl carbon in borane carbonyl is strongly positive[19] and would also be expected to be strongly susceptible to nucleophilic attack. Just as we would expect $[CH_3CO]^+$ to react with a wide variety of nucleophiles, X^-, to form the well-known carbonyl compounds shown in Table 1, a similar reactivity for BH_3CO with nucleophiles X^- would result in a series of borane carbonyl anions (Table 1) which are counterparts to the organic carbonyls. Also, the known reactions of borane carbonyl with amines and base may be depicted as shown in eqns (6) and (8), and are thus comparable to the expected reaction of CH_3CO^+ with the same substrates [eqns (5) and (7)].
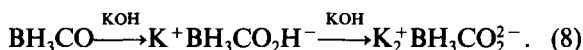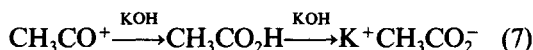
$$CH_3CO^+ \xrightarrow{HNR_2} CH_3C(O)NR_2H^+ \xrightarrow{HNR_2}$$

$$CH_3C(O)NR_2 + R_2NH_2^+ \qquad (5)$$

$$BH_3CO \xrightarrow{HNR_2} BH_3C(O)NR_2H \xrightarrow{HNR_2}$$

$$BH_3C(O)NR_2^- + R_2NH_2^+ \qquad (6)$$

$$CH_3CO^+ \xrightarrow{KOH} CH_3CO_2H \xrightarrow{KOH} K^+CH_3CO_2^- \qquad (7)$$

$$BH_3CO \xrightarrow{KOH} K^+BH_3CO_2H^- \xrightarrow{KOH} K_2^+BH_3CO_2^{2-}. \qquad (8)$$
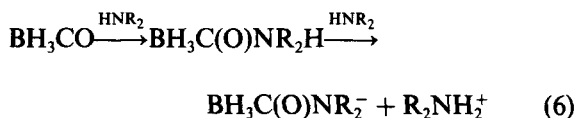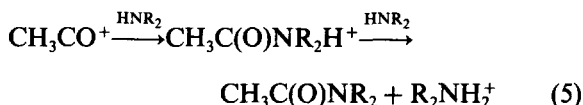
Table 1. Isoelectronic and isostructural carbonyl (trihydroborate) anions and organic carbonyls

	Neutral Organics	Borane Carbonyl Anions
Acid Halides	$\overset{O}{\overset{\|}{H_3CCX}}$	$\overset{O}{\overset{\|}{H_3BCX^-}}$
Aldehydes	$\overset{O}{\overset{\|}{H_3CCH}}$	$\overset{O}{\overset{\|}{H_3BCH^-}}$
Ketones	$\overset{O}{\overset{\|}{H_3CCR}}$	$\overset{O}{\overset{\|}{H_3BCR^-}}$
Esters	$\overset{O}{\overset{\|}{H_3CCOR}}$	$\overset{O}{\overset{\|}{H_3BCOR^-}}$
Amides	$\overset{O}{\overset{\|}{H_3CCNR_2}}$	$\overset{O}{\overset{\|}{H_3BCNR_2^-}}$
Carboxylates	$\overset{O}{\overset{\|}{H_3CCO^-}}$	$\overset{O}{\overset{\|}{H_3BCO^{-2}}}$

PREDICTIVE SCHEME FOR BORANE CARBONYL ANION STABILITY

In contrast to the well-known organic carbonyl compounds, Table 1 lists a number of presently unknown borane carbonyl anions. While the absence of some of these species suggests a number of preparative possibilities, there are, however, some general considerations pertinent to the relative stability of the anions which may be proposed. The borane carbonyl anions contain both the hydroborate moiety with its well-known reducing capability and a carbonyl group susceptible to reduction. It is well known that the ease of reduction of organic functional groups by tetrahydroborate varies generally in the order:[20]

$$RCCl > RCH > RCR > RCOR > RCNR_2, \quad RCO^-$$

ready reduction at room temperature	decreasing reactivity	no reduction
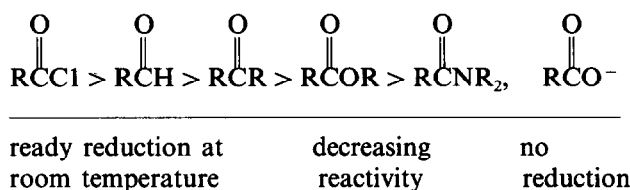
Thus, acyl halides and aldehydes are readily reduced at room temperature whereas amides and carboxylates are not reduced. Based on the above observations and using the BH_3 internal moiety as the reducing agent of the carbonyl, the relative stability of borane carbonyl anions may be postulated as

$$BH_3CCl^- < BH_3CH^- < BH_3CR^- < BH_3COR^- < BH_3CNR_2^-, BH_3CO^{2-}$$
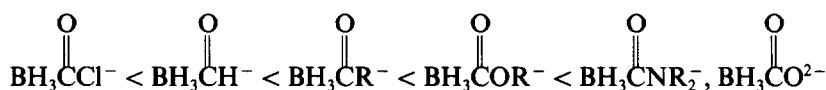
$BH_3C(O)Cl^-$ is then predicted to be the species most easily able to undergo self-reduction-oxidation and $BH_3CO_2^-$ would be predicted to be the most stable. The carboxylato-, carboxamido-, and alkoxycarbonyl-hydroborate derivatives are well characterized[1-5] and their isolation and stability are consistent with this prediction. For instance, the potassium and sodium salts of the carboxylatotrihydroborate anion ($BH_3CO_2^-$) are stable to decomposition up to 400°C with the ^{11}B and ^{1}H NMR of the anion suggesting that CO_2^- is comparable to hydride in electron-donating ability.[2a] It is evident that in this anion the hydroborate and carbonyl species are capable of coexisting.

The borane carbonyl anions in Table 1 not characterized to date were the acid chloride, aldehyde and ketone analogues. Subsequently, investigations concerning the nature of these borane carbonyl anions and related species were undertaken and pertinent literature results studied in view of the above prediction.

RESULTS AND DISCUSSION

Studies involving the postulated $BH_3C(O)Cl^-$

The attempted preparation of the anion $BH_3C(O)Cl^-$ was based on the reaction of borane carbonyl and a stoichiometric quantity of tetraethylammonium chloride in chloroform at low temperature. Rapid absorption of borane carbonyl, accompanied by solubilization of tetraethylammonium chloride, occurs around 0°C when the system is warmed from −196°C. Repetition (three times in 30 min) of this warming/freezing (liq N_2) process to facilitate dissolution of the BH_3CO, followed by stirring at −78°C overnight, produced only trimethylboroxine and the recovered tetraethylammonium chloride. No CO is detected. The overall reaction may be given as

$$3BH_3CO \xrightarrow[CHCl_3]{(C_2H_5)_4NCl} (CH_3BO)_3 \qquad (9)$$
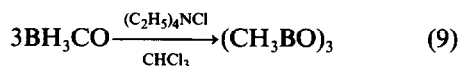
The same products are obtained even when the reaction was carried out as quickly as possible (ca. 20 min. for complete absorption of BH_3CO) in the event that the anion, $H_3BC(O)Cl^-$, could be isolated as the kinetic product of this reaction. These results may be rationalized by the following proposed mechanism:

(i) $\quad BH_3CO + Cl^- \rightarrow BH_3C(O)Cl^-$
$\quad\quad\quad$ (rate determining) $\qquad (10)$

(ii) $3BH_3C(O)Cl^- \rightarrow (CH_3BO)_3 + 3Cl^-$ (fast) (11)
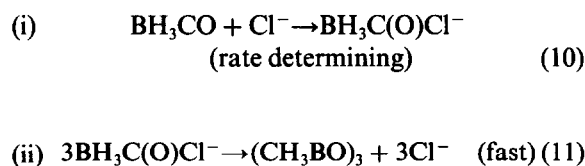
Assuming the above mechanism to be applicable, the absorption of BH_3CO into solution should proceed with only a catalytic quantity of Cl^-. This is the observed result with again, only tri-

methylboroxine and tetraethylammonium chloride catalyst being recovered after a 30 min. reaction period.

Our inability to isolate a stable $BH_3C(O)Cl^-$ anion is consistent with its position in our stability series since this anion would be expected to be the most unstable toward internal reduction of the carbonyl by the hydroborate moiety. Just as tetrahydroborate reacts rapidly with acetyl chloride by a nucleophilic attack on the carbonyl carbon to give the reduced product, $H_3BC(O)Cl^-$ would be expected to undergo rapid internal reduction to give trimethylboroxine.
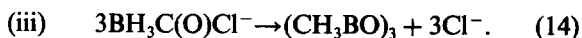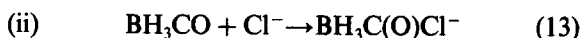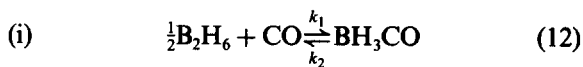
The observation that BH_3CO is rapidly absorbed into a solution containing chloride along with the observed[15] value of $K = 2.8 \times 10^4$ for the system $\frac{1}{2}B_2H_6 + CO \rightleftharpoons H_3BCO$, suggested that a mixture of B_2H_6 and CO should be absorbed into a chloride solution at room temperature since as H_3BCO is formed it should be rapidly and irreversibly removed by reaction with chloride.

In accord with this, when a mixture of B_2H_6 and CO (in a 1:2 mole ratio) is allowed to stand at room temperature above a stirred $CHCl_3$ solution of tetraethylammonium chloride, the reactants are consumed in a period of 30 hr. Only trimethylboroxine is produced and the tetraethylammonium chloride recovered. By contrast, when a similar experiment is carried out, but the chloride omitted, there is only a slight drop in total pressure in the system due to formation of a small equilibrium concentration of BH_3CO.

Using a THF/B_2H_6 solution containing tetraethylammonium chloride, CO at less than one atm. pressure is readily absorbed into the solution with the reaction complete in 1 day. Only trimethylboroxine is produced and the chloride salt recovered. Even when the mostly insoluble NaCl salt is used, the reaction still proceeds slowly and is about 30% complete (based upon CO uptake) after $2\frac{1}{2}$ days. In the complete absence of a chloride salt, CO is not absorbed into a THF/B_2H_6 solution except to form a small equilibrium quantity of BH_3CO. Brown and Rathke[21] have also reported that CO is not absorbed into THF-borane.

Additional results using a mixed solvent system of THF and glyme showed that over a 15 hr period 2 moles of CO per mole of B_2H_6 (at a total pressure less than 1 atm.) are absorbed into a stirred solution of tetraethylammonium chloride at room temperature. Only trimethylboroxine and tetraethylammonium chloride were recovered. In contrast to when THF is used, CO *is* absorbed into a glyme/B_2H_6 solution with BH_3CO being formed in yields as high as 98% depending upon reaction conditions.[22,23] The BH_3CO can be isolated as long as chloride is not present.
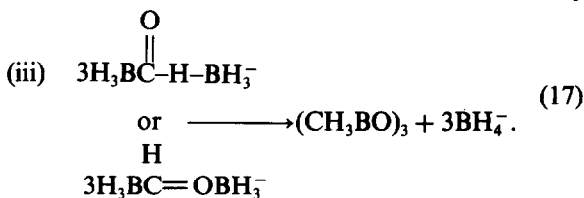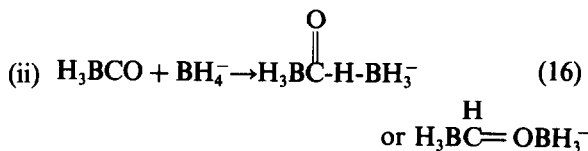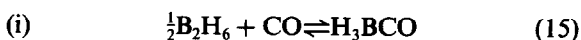
The foregoing results are in accord with the proposed mechanism:

(i) $\frac{1}{2}B_2H_6 + CO \underset{k_2}{\overset{k_1}{\rightleftharpoons}} BH_3CO$ (12)

(ii) $BH_3CO + Cl^- \rightarrow BH_3C(O)Cl^-$ (13)

(iii) $3BH_3C(O)Cl^- \rightarrow (CH_3BO)_3 + 3Cl^-.$ (14)

In this mechanism, step (i) (or k_1) controls the rate; steps (ii) and (iii) are fast and irreversible. Although step (i) is written to involve only the reaction of B_2H_6 and CO it is, no doubt, a reaction involving solvent.[24,25] Since the H_3BCO may be recovered from B_2H_6/glyme solutions (in the absence of chloride) it seems valid that the formation of the H_3BCO is still the rate-determining step. In the same reaction ($B_2H_6 + CO$) in $CHCl_3$, however, diborane is not absorbed to any great extent by a $(C_2H_5)_4NCl/CHCl_3$ solution and borane carbonyl is probably formed according to step (i) even though some H_3BCl^- ions may be present in solution.

Studies involving the postulated formyltrihydroborate anion, $H_3BC(O)H^-$

A mechanism may also be put forth which is consistent with the observation by Brown and Rathke[21] that at atmospheric pressure within a few hours two moles of carbon monoxide per mole of diborane are absorbed into a solution of diborane in THF containing a catalytic quantity of sodium tetrahydroborate with trimethylboroxine being the only product. The reaction pathway we propose is:

(i) $\frac{1}{2}B_2H_6 + CO \rightleftharpoons H_3BCO$ (15)

(ii) $H_3BCO + BH_4^- \rightarrow H_3B\overset{\displaystyle O}{\overset{\|}{C}}\text{-H-}BH_3^-$ (16)

$\qquad\qquad\qquad\text{or } H_3BC\overset{\displaystyle H}{=}OBH_3^-$

(iii) $3H_3B\overset{\displaystyle O}{\overset{\|}{C}}\text{-H-}BH_3^-$

$\qquad\text{or } \xrightarrow{\qquad\qquad} (CH_3BO)_3 + 3BH_4^-.$ (17)

$\qquad H$
$3H_3BC = OBH_3^-$

Just as aldehydes are very rapidly reduced by hydroborates, the rapid self-reduction-oxidation of the anion $H_3BC(O)H^-$ is not unexpected and is completely consistent with our prediction of stability of borane carbonyl anions. Coordination of BH_3 to the carbonyl oxygen (ii) would make the carbonyl carbon even more susceptible to nucleo-

philic attack and reduction. Although Brown and Rathke had assumed the presence of the tetrahydroborate anion was necessary for the reduction to occur, our work shows that merely the presence of an anion such as Cl^- in solution is sufficient to cause the indicated reactions. Even in the presence of catalytic amounts of sodium chloride in a solution of diborane and tetrahydrofuran, about 30% of the CO over the solution is absorbed, based upon the reaction of 2 moles of carbon monoxide per mole of diborane, in a period of 60 hr. Since CO will not react with a tetrahydrofuran–borane solution except to give a small equilibrium concentration of BH_3CO, the chloride, which must be in very low concentration because of the low solutilbity of sodium chloride in THF, is catalyzing the reaction.

Studies involving the postulated $H_3BC(O)R^-$

From their studies of the reaction between equimolar quantities of phenyllithium and borane carbonyl, Carter and Moyé established the existence of a 1:1 adduct which was a white solid soluble in ether at low temperatures.[26] ^{11}B NMR measurements show at low temperature a 1:3:3:1 quartet with a B–H coupling constant of 104 Hz (chemical shift not reported). As the temperature increased the quartet diminished and other unidentified species appeared giving weak peaks at lower field. Further decomposition occurred upon warming. The process was not reversible as cooling the mixture did not give the original quartet. The postulated structure for $C_6H_5Li \cdot H_3BCO$ was $Li^+[H_3BC(O)C_6H_5^-]$ and it was further suggested on the basis of infrared and deuteration studies that the decomposition involved an internal hydride shift from the hydroborate to the carbonyl carbon. Both the stability of the lithium salt and the internal reduction process are completely consistent with an unstable intermediate in accordance with our predictive scheme.

Studies involving borane carbonyl and simple bases

The results described above and the predicted stability scheme for the borane carbonyl anions suggest that reactions between borane carbonyl and simple bases [such as oxides (O^{2-}), alkoxides (OR^-), amides (NR_2^-) and acetates ($CH_3CO_2^-$)] in suitable solvents should give the corresponding borane carbonyl anions. Indeed, Malone and Parry[2b] showed that the reaction between moist calcium oxide and borane carbonyl gives a product with an IR spectrum consistent with that of calcium (carboxylato)trihydroborate (CaH_3BCO_2). They also isolated a solid from the reaction of borane carbonyl and sodium methoxide in methanol and diethyl ether which gave characteristic

B–H and C=O IR absorptions. The fact that this solid hydrolyzes in base solution to $Na_2BH_3CO_2$ strongly indicates the solid to be the methoxycarbonyl derivative $Na^+[BH_3CO_2CH_3^-]$. Our ^{11}B NMR results show for the borane carbonyl acetate anion reaction product in tetrahydrofuran a 1:3:3:1 quartet ($\delta = -33.5$ ppm) indicating the product to be the (acetoxycarbonyl)trihydroborate anion, $BH_3C(O)-OC(O)CH_3^-$. The quartet observed is not due to free borane carbonyl since a sharp 1:3:3:1 quartet is obtained for BH_3CO neat and in various solvents (neat, $\delta = -48.5$ ppm;[26] acetone, $\delta = -45$ ppm; methanol and diethyl ether, $\delta = -48.5$ ppm).

Reductions with $K_2BH_3CO_2$

The foregoing results support the hypothesis that trends in the stability of $H_3BC(O)X^-$ anions towards internal reduction of carbonyl by the BH_3 moiety may be related to the ease of hydroborate reduction of the analogous $CH_3C(O)X$ species. To gain an appreciation for the reducing power of the borane moiety in $BH_3C(O)X^-$, a study was carried out of the reducing characteristics of $BH_3CO_2^{2-}$ towards some typical organic carbonyl compounds.[27] It was found that the reducing behaviour of potassium(carboxylato)trihydroborate in methanol at ambient temperature was generally comparable to that of potassium tetrahydroborate in water although slower. As examples, benzaldehyde and m-nitrobenzaldehyde were reduced to the alcohol in 48 hr and 30 min respectively and butyric acid, benzamide, and butyronitrile were stable to reduction even after 2 weeks. It may be concluded that the reducing power of the BH_3 moiety in $H_3BCO_2^{2-}$ is roughly comparable to BH_4^-. Although differences in the substituent X in $H_3BC(O)X^-$ could be expected to influence the reducing ability of the borane group toward carbonyl, major differences are not likely. Moreover, while the effect on the reducing ability of the hydroborate moiety by an X substituent may be small, the effect of X on the carbonyl reactivity to which it is directly attached would be expected to vary considerably. Consequently, the change in internal reduction susceptibility of the carbonyl as predicted by our stability scheme is not surprising and reflects the general change of electron density at the CO carbon as X is varied. The same effect is responsible for the variations in reducibility of the organic carbonyls by tetrahydroborate.[20] While an intermolecular reduction process involving attack of one $H_3BC(O)X^-$ on the carbonyl of another is possible, an intramolecular process is thought to be more likely because of the negative charge on both species. The effect on carbonyl reactivity by neighboring groups has also been

studied by Angelici with reactions between transition metal carbonyl complexes and amines or alkoxides to form carboxamido or carboalkoxy derivaties:[28]

$$L_nMCO^+ + 2RNH_2 \rightarrow L_nMC(O)NHR + RNH_3^+.$$

By decreasing the number of CH_3 groups in the arene, L, the electron density at the carbonyl carbon atom was reduced and the reaction as written proceeded more favourably. A rather good correlation was found between CO force constants, which reflect the electron density at the carbonyl carbon, and the reactivity: CO complexes with force constants greater than 17.2 mdyn/Å readily formed carboxamido complexes; those with force constants between 16 and 17 gave mixtures (the reactions were reversible), whereas those below 16.0 showed no evidence for carboxamido formation. According to this correlation, the value of the CO force constant for H_3BCO (17.98,[29] 17.94[30]) allows one to predict that the carboxamido derivative would be isolable as is the case.

CONCLUSION

The foregoing study has presented a general picture of the reactivity of borane carbonyl and has offered a simple predictive scheme for the stability of the resultant species. Information gained here on the relative stability of $H_3BC(O)X^{n-}$ species may be particularly applicable in exploring the chemistry of derivatives in which the boron has varying substituents. One example is the derivative chemistry of the novel class of compounds, the boron analogues of amino acids, $R_3NB(R')HCO_2H$.[31] The tendency toward self-reduction-oxidation in $R_3NB(R')HC(O)X$ may depend upon the nature of X and vary in a like manner as shown in our predictive scheme. Preliminary studies are consistent with this since $Me_3NBH_2CO_2H$, $Me_3NBH_2C(O)N(H)C_2H_5$, and $Me_3NBH_2C(O)OR$[31] are stable compounds, whereas attempts to prepare $Me_3NBH_2C(O)Cl$ were unsuccessful and the B–H linkage was lost.[32]

EXPERIMENTAL

General techniques

Standard vacuum line techniques were used for air-sensitive compounds. Infrared data were obtained from Perkin–Elmer Model 237B or 257 instruments as nujol mulls or potassium bromide pellets. Varian A-60 and Varian HA-100 spectrometers were used for proton (60 MHz; TMS, std) and [11]B (32.1 MHz; $BF_3 \cdot OEt_2$, std) NMR data respectively.

Solvents were dried by standard methods. Di-

borane was either obtained commercially (Callery Chemical Co.) or synthesized by published procedures.[33] Borane carbonyl was synthesized as reported in the literature.[5,15] $K_2BH_3CO_2$ was also prepared as reported.[2] Tetraethylammonium chloride was dried in a drying pistol for 36 hr, stored in an evacuated flask and transferred under nitrogen. Tetra-*n*-butylphosphonium acetate was obtained from Alpha-Inorganics and used without further purification.

Borane carbonyl absorption into a chloroform solution of $(C_2H_5)_4NCl$

A 5 mmol sample of H_3BCO was condensed at $-196°C$ onto a frozen solution of $(C_2H_5)_4NCl$ (5.1 mmol) in 20 cm^3 $CHCl_3$. Slow warming of the mixture resulted in a pressure increase until the $(C_2H_5)_4NCl$ solubilized, *ca* 0°C, at which point the pressure decreased rapidly. This procedure was repeated three times in a 30 min period after which the mixture was stirred at $-78°C$ overnight. Non-condensible gas was not present as indicated by a pressure check after freezing to $-196°C$. The mixture was warmed and the volatiles removed leaving a white solid shown by IR to be pure $(C_2H_5)_4NCl$. The volatile (in addition to solvent) was shown to be $(CH_3BO)_3$, ($\delta CH_3 = 0.39$ ppm).

The above procedure was also carried out on a 6.8 mmol sample of H_3BCO with 5.1 mmol $(C_2H_5)_4NCl$ in 20 cm^3 $CHCl_3$. The warming–cooling process was performed three times within 20 min with the same observations as previously noted. Removal of volatiles gave identical products as before. Use of a catalytic amount of $(C_2H_5)_4NCl$ with 5 mmol H_3BCO in 5 cm^3 THF and a reaction time of 30 min (warmed and cooled three times) gave only $(C_2H_5)_4NCl$ (IR) and $(CH_3BO)_3$ (NMR).

The system B_2H_6 and CO in the absence of $(C_2H_5)_4NCl$

6.85 mmol of B_2H_6 and 20 mmol of CO were allowed to stand above pure chloroform at room temperature. The pressure in the system dropped slightly from an initial value of 621 mm (21°C) to 615 mm (20°C) after 12 hr.

Attempted reaction of diborane with tetraethylammonium chloride

B_2H_6 (3.16 mmol), condensed onto a solution of $(C_2H_5)_4NCl$ (6.65 mmol) in 50 cm^3 $CHCl_3$, showed no pressure change above the solution after 12 hr at room temperature.

Reaction of diborane and carbon monoxide with tetraethylammonium chloride as a catalyst

In 1,2-dimethoxyethane (Glyme) and THF·B_2H_6

(7.69 mmol) was admitted at room temperature into a flask containing 0.44 mmol $(C_2H_5)_4NCl$ slurried in 8 cm^3 of glyme. The $(C_2H_5)_4NCl$ dissolved immediately and 3 cm^3. THF was condensed in after which the solution was allowed to warm to room temperature. After admitting 21.8 mmol of CO (initial total pressure in system, 512 mm) a pressure decrease of 40 mm occurred and a white precipitate formed. After stirring the solution for 15 hr at room temperature the CO was measured and it was found that 16.1 mmol was absorbed giving a $CO:B_2H_6$ mole ratio of $16.1:7.7 = 2.08$. Addition of more CO did not result in further absorption. Hydrolysis of the entire reaction mixture with 6N HCl did not give evolution of hydrogen.

In tetrahydrofuran. A 6 mmol sample of B_2H_6 was condensed into a flask containing a small unweighed sample of $(C_2H_5)_4NCl$. Addition of a large excess of CO (at less than 1 atm. pressure) and monitoring the CO absorption which ceased after 1 day resulted in recovery of only pure $(C_2H_5)_4NCl$ (IR) and $(CH_3BO)_3$ (NMR).

In chloroform. A similar procedure was used utilizing B_2H_6 (6.37 mmol) and $(C_2H_5)_4NCl$ (8.92 mmol). The B_2H_6 is not completely absorbed into the CHCl$_3$ solution leaving considerable pressure in the system above the vapor pressure of CHCl$_3$. Admittance of 13.3 mmol of CO (at less than 1 atm.) into the system and standing at room temperature resulted in a slow absorption of the gases into solution which eventually ceased after 30 hr. Distillation through traps held at $-78°$ and $-196°C$ did not yield any recovered B_2H_6. Pure $(C_2H_5)_4NCl$ (IR) remained in the flask.

Absorption of carbon monoxide into a solution of tetrahydrofuran and diborane with sodium chloride as a catalyst.

A 4.2 mmol sample of carbon monoxide was absorbed after 60 hr into a system containing 19.7 mmol CO, 7.29 mmol B_2H_6, 15 cm^3 THF and 1.4 mmol of NaCl (very little of which was soluble in the solution).

Reduction studies using $K_2H_3BCO_2$

Essentially the same procedure was utilized in the reaction of $K_2H_3BCO_2$ and each of the following organic compounds: benzaldehyde, *m*-nitrobenzaldehyde, butyric acid, benzamide and butyronitrile. The reaction using benzaldehyde is given as an example. (GC or NMR was used for analysis if TLC was inappropriate.)

A 0.2 mmol sample of benzaldehyde was allowed to react with 0.1 mmol of potassium (carboxylato)trihydroborate in 4 cm^3 of methanol with

stirring. The sample was analyzed every 30 min for 2 hours using TLC (1:1 CHCl$_3$:CH$_3$OH) and again after 24 hr. R_f values from the reaction mixture were compared to known samples of pure benzaldehyde and benzyl alcohol.

^{11}B *NMR study of the reactions between n-*$Bu_4P^+OC(O)Me^-$ *with* BH_3CO

7 mmol of n-$Bu_4P^+OC(O)Me^-$ were dissolved in 15–20 ml of dry THF at room temperature in a flask on the vacuum line. A 6 mmole quantity of BH_3CO was added at $-196°C$ and the flask allowed to warm slowly to $0°C$. The ^{11}B NMR of the solution exhibited a $1:3:3:1$ quartet, $\delta = -33.5$ ppm from $BF_3 \cdot Et_2O$.

REFERENCES

1. This article based in part on the Ph.D. Thesis of JAK submitted to the University of North Carolina, Chapel Hill, 1969. NASA Predoctoral Fellow.
2. (a) L. J. Malone and R. W. Parry, *Inorg. Chem.* 1967, **2**, 817. (b) L. J. Malone. Ph.D. Thesis. University of Michigan (1964). (c) L. J. Malone, *Inorg. Chem.* 1968, **7**, 1939.
3. B. C. Hoewe, L. J. Malone and R. M. Manley, *Inorg. Chem.* 1971, **10**, 930.
4. M. R. Manley, B.S. in Chemistry Thesis. St. Louis University (1969).
5. J. C. Carter and R. W. Parry, *J. Am. Chem. Soc.* 1965, **87**, 2354.
6. B. F. Spielvogel and J. M. Purser, *J. Am. Chem. Soc.* 1967, **89**, 5294.
7. J. M. Purser and B. F. Spielvogel, *Chem. Commun.* 1968, 386.
8. J. M. Purser and B. F. Spielvogel, *Inorg. Chem.* 1968, **7**, 2156.
9. B. F. Spielvogel and J. M. Purser, *J. Am. Chem. Soc.* 1971, **93**, 4418.
10. R. D. Cowan, *J. Chem. Phys.* 1949, **17**, 218.
11. G. W. Bethe and M. K. Wilson, *J. Chem. Phys.* 1957, **26**, 1118.
12. R. C. Taylor, *J. Chem. Phys.* 1957, **26**, 1131.
13. S. H. Bauer, *J. Am. Chem. Soc.* 1937, **59**, 1804.
14. F. B. Boer, *J. Am. Chem. Soc.* 1966, **88**, 1572.
15. A. B. Burg and H. I. Schlesinger, *J. Am. Chem. Soc.* 1937, **59**, 780.
16. M. E. Grundy, W. H. Hsu and E. Rothstein, *J. Chem. Soc.* 1958, 581.
17. H. C. Brown, *Boranes in Organic Chemistry*, Chap. 17. Cornell University Press, Ithaca, New York (1972).
18. K. F. Purcell, *J. Am. Chem. Soc.* 1969, **91**, 3487.
19. D. R. Armstrong and P. G. Perkins, *J. Chem. Soc.* (A), 1969, 1044.

20. H. C. Brown, *Boranes in Organic Chemistry*, Chap. 12. Cornell University Press, Ithaca, New York (1972).
21. M. W. Rathke and H. C. Brown, *J. Am. Chem. Soc.* 1966, **88**, 2606.
22. E. Mayer, *Monatshaftefur Chem.* 1971, **102**, 940.
23. K. W. Morse, A. T. McPhail and B. F. Spielvogel, unpublished results.
24. D. F. Gaines, *Inorg. Chem.* 1963, **2**, 523.
25. D. F. Gaines and R. Schaeffer, *J. Am. Chem. Soc.* 1964, **86**, 1505.
26. A. L. Moyé, Ph.D. Thesis. University of Pittsburgh (1968).
27. C. Gatchell, R. Merrell and K. W. Morse, Utah State University, unpublished results.
28. R. J. Angelici and L. J. Black, *Inorg. Chem.* 1972, **11**, 1754. R. J. Angelici, *Accts. of Chem. Res.* 1972, **5**, 335.
29. R. C. Taylor, *J. Chem. Phys.* 1957, **26**, 1131.
30. J. R. Berschied, Jr. and K. F. Purcell, *Inorg. Chem.* 1972, **11**, 930.
31. B. F. Spielvogel, *Boron Chemistry*, 119 and references therein. Pergamon Press, New York (1980).
32. B. F. Spielvogel, A. T. McPhail, F. Harchelroad, Jr. and M. K. Das, unpublished results.
33. A. D. Norman and W. L. Jolly, *Inorg. Syn.* 1968, **11**, 15.

SOME COMPLEXES OF NICKEL (II) WITH MORPHOLINE

JOSÉ PALAZÓN, JOSÉ GÁLVEZ, GABRIEL GARCÍA and GREGORIO LÓPEZ*

Department of Inorganic Chemistry, University of Murcia, Murcia, Spain

Abstract—The compounds NiX_2M_x[M = morpholine; X = C_6F_5 (x = 2), $NO_3(x = 3)$, Br(x = 2 or 3), and I(x = 4)] have been prepared and investigated. Magnetic and spectral studies have been carried out to determine the mode of coordination and stereochemistry of the complexes. Except for $NiBr_2M_3$, which appears to contain bridging morpholine, in all other compounds the neutral ligand acts as a monodentate N-donor group.

For the elements of the nickel group, a number of complexes containing 1,4-dioxan have been recently prepared.[1-3] This investigation has been now extended to morpholine (M), a related six membered heterocyclic ligand containing two donor sites (O and N atoms). The nitrogen atom is usually the donor in nickel[4-6] and palladium complexes[7] with morpholine, but the ligand has been found to act as a bridging group in some cases.[8]

This paper reports on the preparation of the nickel complexes NiX_2M_x, where X = C_6F_5, NO_3, Br, and I. Magnetic and spectral studies have been carried out to determine the mode of coordination and stereochemistry of the complexes.

EXPERIMENTAL

Materials

Morpholine and 2,2-dimethoxypropane were obtained from May and Baker Ltd. and Fluka, respectively, and used as such. Nickel salts were commercial products. Diethyl ether and tetrahydrofuran were distilled over sodium in the presence of benzophenone.

Analyses

The C, H, N analyses were performed with a Perkin–Elmer 240 C microanalyzer. Nickel was determined by titration with EDTA.[9]

Physical measurements

IR spectra were recorded in the 4000–250 cm^{-1} range on a Nicolet MX-1 spectrophotometer as Nujol or Fluorolube mulls. The diffuse reflectance

spectra were recorded as Nujol mulls in the 5000–30000 cm^{-1} range on a Beckman DK-2A spectrophotometer. The mulls were smeared between two glass plates on filter paper and run against a reference consisting of similar plates containing Nujol only. Thermal decomposition studies were carried out in nitrogen on a Netzsch STA-429 thermobalance. Magnetic susceptibilities were measured by the Faraday method using a Bruker B-15 magnetic balance (magnetic field, 7 kG) calibrated with Co[Hg(SCN)$_4$].[10] Conductivities were measured with a Philips PW 9501/01 conductimeter.

Preparation of the complexes

$Ni(NO_3)_2M_3$. Ni(NO$_3$).6H$_2$O (1 g; 3.4 mmol) was refluxed in 2,2-dimethoxypropane (8 cm^3) for 1 hr. After cooling the resulting yellowish green solution, 8 cm^3 of morpholine were added and the colour of the solution turned to deep green. Addition of diethyl ether (20 cm^3) resulted in the formation of a sticky product, which was transformed into a green powder by stirring for 48 hr in the same solvent. The solid was filtered under nitrogen and dried under vacuum. Yield, 84%. The compound is hygroscopic and was kept in a P$_4$O$_{10}$ desiccator.

$NiBr_2M_3$. As NiBr$_2$.3H$_2$O (1 g; 3.7 mmol) was refluxed in 2, 2-dimethoxypropane (8 cm^3) for 1 hr, a brownish–yellow suspension was formed, which turned green on cooling. Addition of morpholine (8 cm^3) to the reaction mixture changed again from green to yellow. After stirring for 4 hr, the precipitate was filtered off, washed with diethyl ether, and dried under vacuum. Yield, 75%. The very hygroscopic brownish–yellow product was kept in a P$_4$O$_{10}$ desiccator.

$NiBr_2M_2$. This blue compound was formed sim

ply when $NiBr_2M_3$ was heated at 130°C under nitrogen atmosphere. Yield, 100%. It is hygroscopic.

NiI_2M_4. Anhydrous NiI_2 (1 g; 3.2 mmol; prepared by heating the hydrated salt at 140°C) was stirred in morpholine/2, 2-dimethoxypropane (10 cm³/3 cm³) for 12 hr. The reaction mixture, initially dark brown, changed to green and the resulting solid was filtered off, washed with diethyl ether, and dried under vacuum. Yield, 72%.

$Ni(C_6F_5)_2M_2$. The working up for the preparation of this compound was different from the others. The experimental procedure followed in the preparation of a tetrahydrofuran-dioxane solution containing "$Ni(C_6F_5)_2$" was adapted from Ref. 1. A freshly prepared and filtered solution of C_6F_5MgBr (1.145 mmol) in THF (15 cm³) was added to a suspension of anhydrous $NiBr_2$ (100 mg; 0.458 mmol) in THF (5 cm³). After refluxing for 2 hr, 10 cm³ of dioxane were added, to precipitate the magnesium salts as dioxane adducts. After standing in the cold overnight, the solid was filtered off and the resulting orange solution was then treated with 0.5 cm³ of morpholine and the colour immediately changed to yellow. The solution was stirred for 30 min at room temperature, then concentrated under vacuum. Addition of hexane afforded a golden yellow solid, which was recovered by filtration and recrystallized from $CHCl_3$/hexane. Yield, 70%.

RESULTS AND DISCUSSION

The organocomplex $Ni(C_6F_5)_2M_2$ was prepared by addition of morpholine to a recently prepared tetrahydrofuran-dioxane solution containing "$Ni(C_6F_5)_2$"[1]:

$$\text{"Ni(C}_6\text{F}_5)_2\text{" in THF-dioxane} \xrightarrow{+M} \text{Ni(C}_6\text{F}_5)_2\text{M}_2.$$
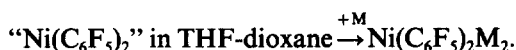
All other nickel compounds were prepared by addition of morpholine to the respective hydrated or anhydrous nickel salts in the presence of the dehydrating agent 2,2-dimethoxypropane, where the substitution reaction takes place. The analytical data and some physical properties of the nickel compounds are collected in Table 1.

The IR spectrum of the yellow organocompound, $Ni(C_6F_5)_2M_2$, shows the characteristic absorptions of the C_6F_5 group[11] at *ca.* 1630 m, 1500 vs, 1050 vs, and 780 s cm^{-1}. The diamagnetism and electronic spectrum (Table 2) are compatible with a square planar geometry for this species. Moreover, the infrared band observed at 781 cm^{-1} has been used for structural elucidation. As in previous cases[2,12] the number of infrared bands observed for the X-sensitive mode has been correlated with the symmetry of the C–M–C skeleton on the basis that in complexes containing $M–C_6F_5$ bonds this mode has mainly $v(M–C)$ character.[12] Accordingly, we assign the *trans* configuration to $Ni(C_6F_5)_2M_2$, since its spectrum shows a single band in the 800–750 cm^{-1} range (D_{2h} symmetry).

The stoichiometry, magnetic moment, and electronic spectral data (Table 2) are all compatible with an octahedral geometry for the green compound NiI_2M_4.[13] Thus its electronic spectrum shows three bands at 8700, 15,060 and 25,640 cm^{-1}, which can be assigned to the transitions from the ground state $^3A_{2g}(F)$ to the excited states $^3T_{2g}(F)(v_1)$, $^3T_{1g}(F)(v_2)$ and $^3T_{1g}(P)(v_3)$, respectively. From the corresponding Tanabe-Sugano diagram and with $v_2/v_1 = 1.73$, $Dq/B = 1.04$ is obtained. Hence for NiI_2M_4 $10 Dq = 8,700$ cm^{-1}, $B = 870$ cm^{-1} and $\beta = 0.84$. Moreover, the v_3 transition is predicted to be at 25,750 cm^{-1} a value which is in good agreement with the experimental one (25,640 cm^{-1}).

Table 1. Colours, melting points, and analytical data of nickel compounds

Compound	Colour	M.P.(°C)[a]	Anal.(%). Found (calc.)			
			C	H	N	Ni
$Ni(C_6F_5)_2M_2$	yellow	90 (d)	42.4	3.2	5.1	10.2
			(42.4)	(3.2)	(4.9)	(10.4)
$Ni(NO_3)_2M_3$	green	80 (d)	31.4	5.9	16.6	12.6
			(32.3)	(6.1)	(15.7)	(13.2)
$NiBr_2M_3$	brownish yellow	80 (d)	29.5	5.5	8.8	12.0
			(30.0)	(5.6)	(8.8)	(12.2)
$NiBr_2M_2$	deep blue	182 (d)	24.0	5.1	7.0	14.6
			(24.5)	(4.6)	(7.1)	(14.9)
NiI_2M_4	pale green	55 (d)	28.6	5.4	8.3	9.0
			(29.1)	(5.5)	(8.5)	(8.9)

[a]Data obtained from TGA; (d) = decompose.

Table 2. Magnetic moments and electronic spectra of nickel complexes

Compound	μ_{ef}(BM)[a]	Electronic bands (cm^{-1})
$Ni(C_6F_5)_2M_2$	diamagnetic	22,890 (ε_{molar} 314)[b]
$Ni(NO_3)_2M_3$	2.78	9,130; 15,385; 25,905
$NiBr_2M_3$	2.95	8,810; 13,330; 22,025
$NiBr_2M_2$	3.02	8,700; 11,365; 15,875; 17,240
NiI_2M_4	3.19	8,700; 15,060; 25,640

[a]At 15 °C; diamagnetic corrections were made. [b]In acetone solution.

The compounds $NiBr_2M_3$ and $Ni(NO_3)_2M_3$ are very hygroscopic and in water give pale green solutions. Their electronic spectra show three bands (Table 2) which can be interpreted assuming pseudooctahedral geometries for both compounds. However, the internal consistency of the spectral data is not so good as that observed for the above-mentioned iodocomplex, and any intent to derive values for the ligand field parameters would be meaningless. The assignation of hexacoordinate nickel in $NiBr_2M_3$ requires that either Br or morpholine acts as bridging ligand and, in fact, there is infrared spectral evidence (see below) that some morpholine is O-bonded to nickel. A similar situation should be present in $Ni(NO_3)_2M_3$, but since no O-bonded morpholine is evidenced by the IR spectrum, coordinated nitrate groups should be here within the coordination sphere of the metal atom. In fact, its infrared spectrum shows the absorptions typical of coordinated NO_3 groups:[14] 1490 vs, 1420 vs, 1300 sh and 805 m. The structural situation could be similar to that observed for $Ni(NO_3)_2(3\text{-pic})_3$,[15] where it was assumed that one nitrate group acts as a unidentate and the other as a bidentate ligand. The conductivity of $Ni(NO_3)_2M_3$ in $10^{-3}M$ acetone solution ($\Lambda_M = 18 \text{ cm}^2\Omega^{-1}\text{mol}^{-1}$) also supports[16] the assigned structure.

The paramegnetism of the deep blue $NiBr_2M_2$ definitely rules out the presence of square planar arrangement about the divalent nickel ion. The electronic spectrum of this complex shows two single bands at 8700 and 11,365 cm^{-1}, and a third double band with absorption maxima at 15,875 and 17,240 cm^{-1}. This result and the similarity of the spectrum with those observed for pseudotetrahedral complexes of the type NiL_2X_2 (both

shape and frequencies are nearly identical to those reported for $Ni(Me_4tn)Br_2)$[17] lead us to assign a pseudotetrahedral structure to this compound. On this basis, the band at 8700 cm^{-1} is assigned to one of the three compounds of the v_1 transition, $^3T_1(F) \rightarrow ^3T_2(F)$, the band at 11,365 cm^{-1} as the $v_2{}^3T_1(F) \rightarrow ^3A_2(F)$, and the bands at 15,875 and 17,240 cm^{-1}, which are not resolved, as $v_3{}^3T_1(F) \rightarrow ^3T_1(P)$. The abnormally high position of the component of v_1 could be taken as indicative of a large distortion of the T_d symmetry.[18] The low magnetic moment (3.02 BM) found for this compound also supports the presence of such a distortion.

The characteristic infrared bands of morpholine in these complexes are collected in Table 3. For comparison, bands of the free ligand are also shown. Since the N-hydrogen (and lone pair) can be equatorial or axial, free morpholine can obviously exist as two conformers,[19] but the most probable conformation adopted by coordinated morpholine should be the axial one. In free axial morpholine, the N–H stretching vibration occurs at 3298 cm^{-1}; on complexation this band is shifted to lower frequencies and sometimes it is split due to solid state effects.[20,21] In good agreement, this vibration appears at ca. 100 cm^{-1} lower in the spectra of the nickel complexes (except for $Ni(C_6F_5)_2M_2$). In free morpholine the fundamentals v_{13} and v_{31} (at 1097 and 1225 cm^{-1}, respectively) have the largest contributions from C–N stretch whereas v_{14} and v_{32} (at 1031 and 1201 cm^{-1}, respectively) are predominantly C–O stretch. On this basis, we assign the bands at ca. 1225 and 1100 cm^{-1} as derived from the fundamentals v_{31} and v_{13} of morpholine, respectively. In the 1100–1040 cm^{-1} range one or two bands (or

Table 3. IR bands (cm^{-1}) of free and coordinated morpholine

	Free morpholine[19]	Ni(C$_6$F$_5$)$_2$M$_2$	Ni(NO$_3$)$_2$M$_3$	NiBr$_2$M$_3$	NiBr$_2$M$_2$	NiI$_2$M$_4$
ν_1	3298s (NH str)	3271m	3237s	3195m	3188s	3173s
	(3336s)	3228sh	3201s	3180sh	3116s	3144s
ν_{30}	1319s	1306s	1304s	1306s	1310s	1318s
ν_{11}	1272m	1281s	1280s,br	1280m	1270w	1279s
ν_{12}	1248s	1257s	1250m	1259m	1258s	1255m
				1251m		
ν_{31}	1225m (CN str)	–	1232m	1225m	1225m	1224m
ν_{32}	1201m (CO str)	1194m	1193m	1195m	1197m	1200m
				1175m		
ν_{34}	1108vs	1117vs	1115sh	–	1116vs	1120sh
	(1129m,sh)					
ν_{13}	1097vs (CN str)	1087s	1102vs	1100vs,br	1100vs,br	1100vs
	(1062m)	1059s	–	1046s	1041s	1053m
ν_{14}	1031m (CO str)	1028s	1034m	1035s	1029s	1032m
				1025sh		
ν_{37}	891m	894m	883sh	894s	893s	883s
	884m(combination)	879vs	872s	879sh	879s	876sh
ν_{16}	850s,sh			870vs	870vs	862vs

Values in parentheses are from the equatorial conformer.[19] Except for Ni(C$_6$F$_5$)$_2$M$_2$, an additional band is observed in the 1600–1550 cm^{-1} range. However, the fundamental ν_{33}, at 1141 cm^{-1} in free morpholine, is not observed in the spectra of nickel compounds.

shoulders) are observed, which can be derived from ν_{13}, since the C–N vibration will be affected by the nitrogen to nickel bonding. Except for NiBr$_2$M$_3$, the C–O stretching modes are observed in the spectra of the nickel complexes at nearly the same frequency as in free morpholine, indicating that the neutral ligand acts here as unidentate N-donor ligand. However, in NiBr$_2$M$_3$ the C–O stretching modes appear as double bands (1195, 1175 cm^{-1} and 1035, 1025 cm^{-1}, respectively), which can be attributed to the presence of both unidentate and bidentate morpholine. These results are compatible with those obtained from the corresponding analytical and electronic spectral data.

REFERENCES

1. A. Arcas and P. Royo, *Inorg. Chim. Acta* 1978, **30**, 205.
2. G. García and G. López, *Inorg. Chim. Acta* 1981, **52**, 87.
3. G. López, G. García, N. Cutillas and J. Ruiz, *J. Organometal. Chem.* 1983, **241**, 269.
4. I. S. Ahuja, *Inorg. Chim. Acta* 1969, **3**, 110.
5. G. Marcotrigiano, G. C. Pellacani and C. Petri, *Z. Anorg. Allg. Chem.* 1974, **408**, 313.
6. I. S. Ahuja and R. Singh, *Transition Met. Chem.* 1977, **2**, 132.
7. G. García, G. López and M. D. Santana, *An. Quim.* 1983, **79B**, 214.
8. I. S. Ahuja and R. Singh, *J. Coord. Chem.* 1976, **5**, 167.
9. G. Schwarzenbach and H. Flashka, *Complexometric Titrations*, p. 248. Methuen, London (1969).
10. B. N. Figgis and J. Lewis, In *Modern Coordination Chemistry*, p. 415. Interscience, New York (1960).
11. D. A. Long and D. Steele, *Spectrochim. Acta* 1963, **19**, 1955.
12. G. B. Deacon and J. H. Green, *Spectrochim. Acta* 1968, **24A**, 1125.
13. L. Sacconi, In *Transition Metal Chemistry*, Vol. 4, p. 210. Marcel Dekker, New York (1968).
14. K. Nakamoto, *Infrared Spectra of Inorganic and Coordination, Compounds*, p. 244. Wiley, New York (1978).
15. L. M. Vallarino, W. E. Hill and J. V. Quagliano, *Inorg. Chem.* 1965, **4**, 1598.
16. W. J. Geary, *Coord. Chem. Rev.* 1971, **7**, 81.
17. L. Sacconi, I. Bertini and F. Mani, *Inorg. Chem.* 1967, **6**, 262.
18. D. M. L. Goodgame and M. Goodgame, *Inorg. Chem.* 1965, **4**, 139.
19. D. Vedal, O.H. Ellestad and P. Klaboe, *Spectrochim. Acta* 1976, **32A**, 877.
20. E. A. Allen, N. P. Johnson, D. T. Rosevear and W. Wilkinson, *J. Chem. Soc. (A)* 1971, 2141.
21. N. H. Piacquadio and M. A. Blesa, *Polyhedron* 1982, **1**, 437.

KINETICS AND SALT EFFECTS OF THE REDUCTION OF OCTACYANOMOLYBDATE(V) AND OCTACYANOTUNGSTATE(V) BY SULPHITE IONS

CHARLES R. DENNIS, STEPHEN S. BASSON and JOHANN G. LEIPOLDT*

Department of Chemistry, University of the Orange Free State,
Bloemfontein 9300, Republic of South Africa

Abstract—The kinetics of the reduction of octacyanomolybdate(V) and octacyanotungstate(V) by sulphite ions has been studied over a wide pH range. The reaction is catalysed by alkali metal ions. The rate law is found to be of the form:

$$R = \left(\frac{a[A^+] + b[H^+]}{c + [H^+]}\right)[M(CN)_8{}^{3-}][SO_3{}^{2-}].$$

The third order rate constants at $[OH^-] = 0.05$ mol dm^{-3} for the reduction of $Mo(CN)_8{}^{3-}$ and $W(CN)_8{}^{3-}$ were determined as 6.2×10^3 dm^6 mol^{-2} s^{-1} and 22.3 dm^6 mol^{-2} s^{-1} respectively at 298 K for $A^+ = Na^+$ while K_a for the hydrogen sulphite ion was determined as 2.4×10^{-8} mol dm^{-3}. It was established that the reaction proceeds via an outer-sphere mechanism. An explanation for the alkali metal ion catalysis is proposed.

The reaction between hexacyanoferrate(III) and sulphite ions has been the subject of various publications. Both inner- and outer-sphere mechanisms have been proposed. An inner-sphere mechanism[1] via a $Fe(CN)_5SO_3{}^{4-}$ intermediate was proposed but later studies[2] with labelled ^{14}CN-ions disproved the existence of such a species. Brown and Higginson[3] also prefered an inner-sphere mechanism because the hexacyanoferrate(III) ion is a mild oxidant. Other studies[4,5] suggested a mechanism where a complex, $[Fe(CN)_5\cdot(CN\cdot SO_3)]^{5-}$, is formed between the hexacyanoferrate(III) and sulphite ions, in which the sulphito group is bonded directly to a cyano ligand. This was described as a compromise between an inner- and outer-sphere mechanism. A reinvestigation[6] has shown that the SO_3^- product radical ion of the rate determining step also formed a similar intermediate in the subsequent reduction of $Fe(CN)_6{}^{3-}$ ions.

The $Fe(CN)_6{}^{3-} - SO_3{}^{2-}$ reaction, with first order dependences on hexacyanoferrate(III) and sulphite ion concentrations respectively is retarded by addition of product $Fe(CN)_6{}^{4-}$ ions[7] whilst $[OH^-]$ had no significant effect on the reaction rate for the concentration range between 0.26 and 0.60 mol dm^{-3}. These results led to a proposed radical and complex forming reaction mechanism in which observed alkali metal ion catalytic effects were not provided for. The kinetics of the reduction of octacyanomolybdate(V) and octacyanotungstate(V) by sulphite ions were investigated in order to compare the kinetics of these reactions with that of $Fe(CN)_6{}^{3-}$ with $SO_3{}^{2-}$, as well as to clarify the alkali metal ion catalysis.

EXPERIMENTAL

$Cs_3Mo(CN)_8\cdot 2H_2O$ and $Cs_3W(CN)_8\cdot 2H_2O$ were prepared by literature methods[8–10] and were used as primary standards after recrystallization. Analytical grade sodium sulphite was used as source of sulphite ions and was standardized by an iodimetric method. All other reagents were of analytical grade and redistilled water was used throughout. The desired buffer solutions at constant ionic strength for the kinetic measurements at a pH between 5 and 9 were prepared by mixing suitable volumes of 0.067 mole dm^{-3} Na_2HPO_4 and 0.20 mole dm^{-3} NaH_2PO_4. An Orion pH-meter (model 701) was used for pH measurements.

The sulphite ion concentrations in the reaction mixtures were at least ten-fold in excess to the

*Author to whom correspondence should be addressed.

concentration of the complex cyanide to ensure pseudo-first-order reaction conditions. Sodium ethylenediaminetetraacetate was added to each reaction mixture to suppress catalysis by metal ion impurities. The reaction progress for the reduction of the $Mo(CN)_8^{3-}$ was followed by measuring the decrease in $[Mo(CN)_8^{3-}]$ at 390 nm using a Durrum D-110 stopped-flow spectrophotometer while the reduction of $W(CN)_8^{3-}$ was followed by measuring the decrease in $[W(CN)_8^{3-}]$ at 357 nm using a Pye Unicam SP 1700 spectrophotometer. In both cases the temperature was controlled to within 0.1 K.

The stoichiometry of both reactions was determined volumetrically by oxidation of the products $M(CN)_8^{4-}$ (M = Mo, W), with standard Ce(IV) solutions using N-phenylanthranilic acid as indicator.

RESULTS AND DISCUSSION

The stoichiometry determinations confirmed the overall reaction in alkaline medium to be:

$$2M(CN)_8^{3-} + SO_3^{2-} \rightarrow 2M(CN)_8^{4-} + SO_4^{2-}. \tag{1}$$
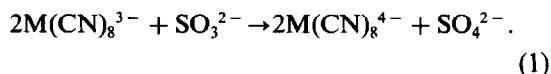
The pseudo-first-order plots of $\log[M(CN)_8^{3-}]$ vs time were linear for at least two half lives. The kinetic results show that the reactions are also first order with respect to $[SO_3^{2-}]$ while the concentration of the product, $[M(CN)_8^{4-}]$, had practically no effect on the reaction rate. Both reactions show first order dependence with respect to the alkali metal ion concentration. The effect of the different alkali metal ions on the rate of the reaction between $W(CN)_8^{3-}$ and SO_3^{2-} at $[OH^-] = 0.05$ mole dm^{-3} are shown in Fig. 1. It was also found that the reaction rate is independent of $[OH^-]$ for pH > 9.0 and dependent on $[OH^-]$ for pH < 9.0. The effect of the pH on the reaction rate for the reaction between $Mo(CN)_8^{3-}$ and SO_3^{2-} in the presence of sodium ions is shown in Fig. 2. The third order rate constants for the various alkali metal ions for the reduction of $Mo(CN)_8^{3-}$ and $W(CN)_8^{3-}$ at high pH are shown in Fig. 3.

The fact that a plot of the first order rate constant against alkali metal ion concentration is linear with a zero intercept (Fig. 1) show a very strong alkali metal ion catalysis. To show that this effect is not due to the variation of the ionic strength, the alkali metal ion concentration was varied at constant ionic strength using KCl, K_2SO_4 and $K_3Co(CN)_6$ as electrolytes (Table 1). These results clearly show the alkali metal ion catalysis.

The observed dependence of k_{obs} on the pH (Fig. 2) as well as the first-order dependence in each of alkali metal (A^+), sulphite and $M(CN)_8^{3-}$ ion
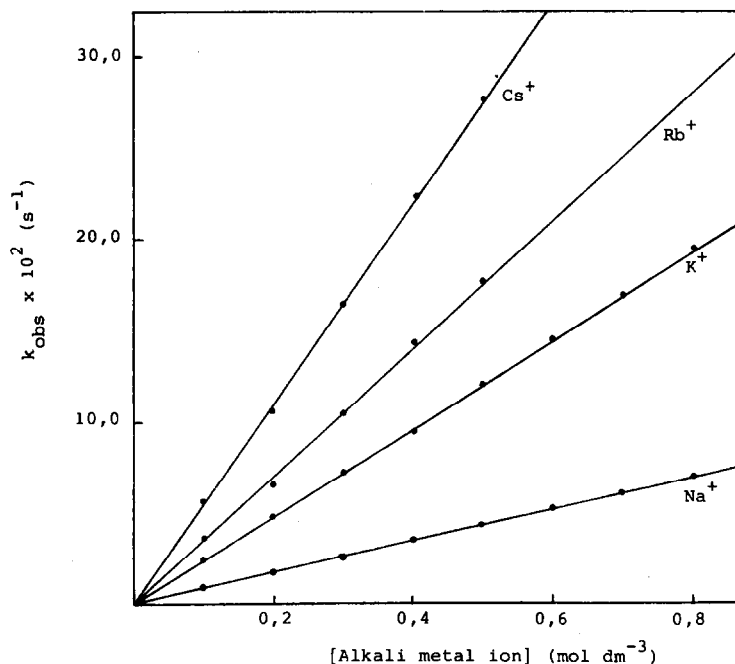

Fig. 1. A plot of k_{obs} vs alkali metal ion concentration for the $W(CN)_8^{3-}$ reaction $[W(CN)_8^{3-}] = 5 \times 10^{-4}$, $[SO_3^{2-}] = 5 \times 10^{-3}$, $[OH^-] = 0.05$, $[EDTA] = 1 \times 10^{-5}$ mol dm^{-3}, T = 293 K.
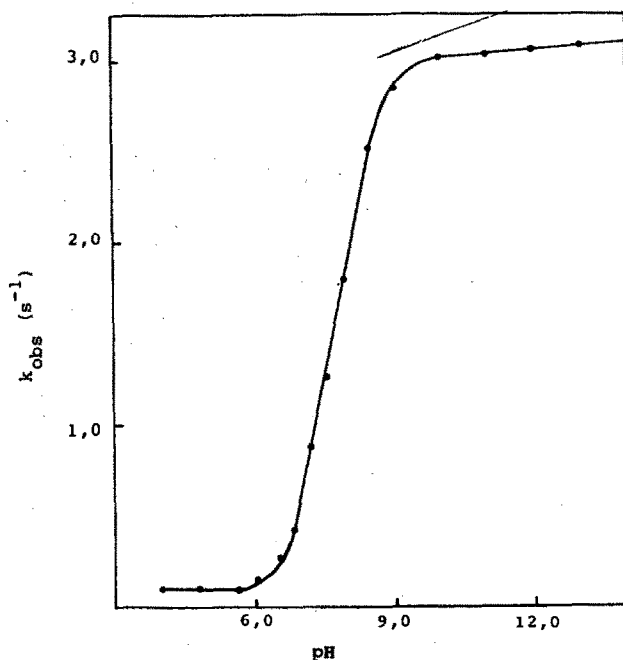
Fig. 2. A plot of k_{obs} vs pH for the $Mo(CN)_8{}^{3-}$ reaction. $[Mo(CN)_8{}^{3-}] = 5 \times 10^{-4}$, $[SO_3{}^{2-}] = 5 \times 10^{-3}$, $[Na^+] = 0.1$, $[EDTA] = 1 \times 10^{-5}$ mol dm^{-3}, T = 298 K.
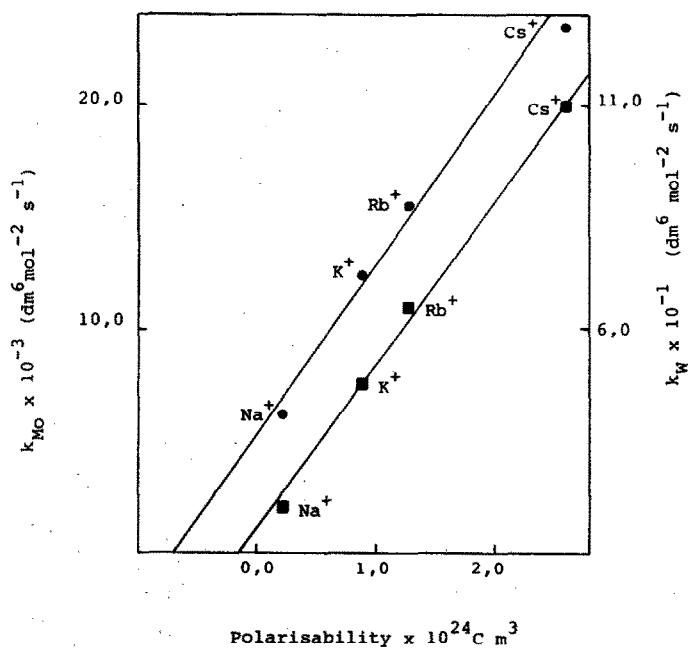

Fig. 3. A plot of the rate constant vs polarisability of the alkali metal cations. $[OH^-] = 0.05$ mol dm^{-3}; T = 298 K. $[EDTA] = 1 \times 10^{-5}$ mol dm^{-3}. ●, $Mo(CN)_8{}^{3-}$ reaction; ■, $W(CN)_8{}^{3-}$ reaction.
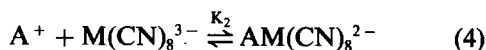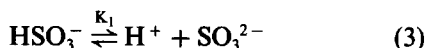
Table 1. Experimental third order rate constants at constant ionic strength with different electrolytes for the $Mo(CN)_8^{3-}$ reaction. $[OH^-] = 0.05 \, mol \, dm^{-3}$, $T = 298 \, K$. $[EDTA] = 1 \times 10^{-5} \, mol \, dm^{-3}$

Electrolyte	$I = 0,3 \, mol \, dm^{-3}$		$I = 0,6 \, mol \, dm^{-3}$	
	$[K^+]$	$k_{obs} \times 10^{-4}$ $dm^6 \, mol^{-2} s^{-1}$	$[K^+]$	$k_{obs} \times 10^{-4}$ $dm^6 \, mol^{-2} s^{-1}$
KCl	0,30	1,27	0,60	1,28
K_2SO_4	0,20	1,27	0,40	1,28
$K_3Co(CN)_6$	0,15	1,28	0,30	1,28

concentrations show the rate law to be

$$\frac{-d \, [M(CN)_8^{3-}]}{dt} = \left(\frac{a[A^+] + b[H^+]}{c + [H^+]} \right)$$
$$\times [M(CN)_8^{3-}][SO_3^{2-}] \quad (2)$$

The following equilibria exist in solution:

$$HSO_3^- \overset{K_1}{\rightleftharpoons} H^+ + SO_3^{2-} \quad (3)$$

$$A^+ + M(CN)_8^{3-} \overset{K_2}{\rightleftharpoons} AM(CN)_8^{2-} \quad (4)$$

$$A^+ + SO_3^{2-} \overset{K_3}{\rightleftharpoons} ASO_3^- \quad (5)$$

Equilibrium 3 explains the observed hydrogen ion dependence. The increase in the reaction rate with increase of pH (see Fig. 2) shows that the SO_3^{2-} ion is much more reactive than the HSO_3^- ion. The lower reactivity of the HSO_3^- ion may be explained as follow: Connick[11] has shown that the following equilibria exist in aqueous solution

$$:SO_3^{2-} + H^+ \rightleftharpoons H:SO_3^- \rightleftharpoons HO\overset{..}{S}O_2^-$$
$$\qquad\qquad\qquad\quad \mathbf{I} \qquad\qquad \mathbf{II}$$
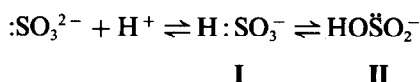
I is the dominant form while isomer **II** is present in only a small amount. Both isomers **I** and **II** will be unreactive; in **I** the lone pair is tied up by the H^+ ion while in **II** electron density will be withdrawn from the sulphur atom by the H^+ ion.
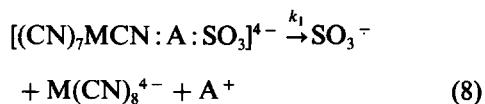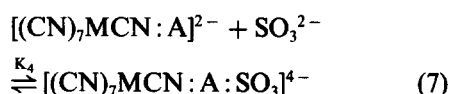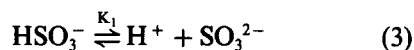
Equilibria 4 and 5 represent the outer-sphere ion-pair formation reactions. The association constants, K_2, for a few cations with $Mo(CN)_8^{3-}$ and $W(CN)_8^{3-}$ were determined with specific-ion electrodes, see Table 2. These values are of the same magnitude as found for cyanocomplexes (3:1 electrolytes) determined by conductivity measurements[12].

The association constant K_3 is not known. It is however expected to be lower than the value for SO_4^{2-} with K^+ ions (approx. $3 \, dm^3 \, mol^{-1}$). The
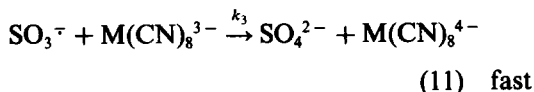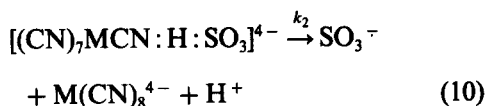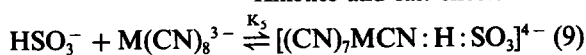
formal charge on the sulphur atom in $:SO_3^{2-}$ is $+1$ and -1 at each oxygen atom while in the case of SO_4^{2-} the formal charge on the sulphur atom is zero and $-\frac{1}{2}$ on each oxygen atom. A cation paired to SO_4^{2-} gets thus less nett repulsion from the nearby sulphur atom than in SO_3^{2-}. Apart from this, it is expected (as in the case of HSO_3^-) that ASO_3^- will be less reactive than SO_3^{2-}.

It is clear from the above discussion that reactions 4 and 5 cannot explain the strictly first order dependence (see Fig. 1) of the reaction in the alkali metal ion concentration range employed.

The experimental results may be explained by the following reaction mechanism:

$$HSO_3^- \overset{K_1}{\rightleftharpoons} H^+ + SO_3^{2-} \quad (3)$$

$$A^+ + M(CN)_8^{3-} \overset{K_2'}{\rightleftharpoons} [(CN)_7MCN:A]^{2-} \quad (6)$$

$$[(CN)_7MCN:A]^{2-} + SO_3^{2-}$$
$$\overset{K_4}{\rightleftharpoons} [(CN)_7MCN:A:SO_3]^{4-} \quad (7)$$

$$[(CN)_7MCN:A:SO_3]^{4-} \overset{k_1}{\rightarrow} SO_3^-$$
$$+ M(CN)_8^{4-} + A^+ \quad (8)$$

Table 2. Association constants for alkali metal ions with complex cyanide ions. $T = 298 \, K$; $I = 0.1 \, mol \, dm^{-3}$

Cation	Anion	$K_{ass} \, (dm^3 \, mol^{-1})$
K^+	$Fe(CN)_6^{3-}$	$4,8 \pm 1$
K^+	$W(CN)_8^{3-}$	$9,6 \pm 3$
Na^+	$W(CN)_8^{3-}$	$13,5 \pm 6$
Na^+	$Mo(CN)_8^{3-}$	$10,0 \pm 2$
Cs^+	$Mo(CN)_8^{3-}$	$9,5 \pm 3$
Cs^+	$W(CN)_8^{3-}$	$7,9 \pm 2$

$$HSO_3^- + M(CN)_8^{3-} \overset{K_5}{\rightleftharpoons} [(CN)_7MCN:H:SO_3]^{4-} \quad (9)$$

$$[(CN)_7MCN:H:SO_3]^{4-} \overset{k_2}{\rightarrow} SO_3^-$$

$$+ M(CN)_8^{4-} + H^+ \quad (10)$$

$$SO_3^- + M(CN)_8^{3-} \overset{k_3}{\rightarrow} SO_4^{2-} + M(CN)_8^{4-}$$

$$(11) \quad \text{fast}$$

Reactions 6–8 represent the contact ion-pair formation between complex cyanide and alkali metal ions, bridging of the lone pair on SO_3^{2-} with the cation part of the contact ion-pair and the slow rate determining step respectively. K_2', the contact ion-pair formation constant, is expected to be much smaller than K_2 (reaction 4) since A^+ is more specifically bonded to the nitrogen lone pair of a cyanide ligand in contrast to the outer-sphere ion association of equilibrium 4.

Reactions 9 and 10 explain the slow observed reaction rate in acidic solution, see Fig. 3. The hydrogen bond formation between HSO_3^- and $M(CN)_8^{3-}$ (reaction 9) explains the absence of any alkali metal ion catalysis in acidic solution. Such a hydrogen bond formation was also proposed for the solid state in the crystal structure determination of $H_4W(CN)_8 \cdot 4HCl \cdot 12H_2O$[13] and tetrakis(pyridinium - 2 - carboxylicacid)octacyanomolybdate(IV)[14].

The rate law according to the proposed mechanism is given by

$$\frac{-d[M(CN)_8^{3-}]}{dt} = \left(\frac{k_1 K_1 K_2' K_4[A^+] + k_2 K_5[H^+]}{K_1 + [H^+]} \right)$$

$$\times [SO_3^{2-}]_T[M(CN)_8^{3-}]. \quad (12)$$

This corresponds to the experimental results (eqn 2) with $a = k_1 K_1 K_2' K_4$, $b = k_2 K_5$ and $c = K_1$.

The value of K_1 for reaction 3 was calculated from a least squares fit of the data in Fig. 2 to eqn (12). The calculated value of $pK_1 = 7.62$ at $I = 0.1 \text{ mol dm}^{-3}$ is in very good agreement with the value given by Meites[15] and Dick[16] of 7.64 at $I = 0.1 \text{ mol dm}^{-3}$.

Futher evidence for the proposed mechanism is the increase in the reaction rate from Li^+ to Cs^+, see Fig. 3. The same phenomena as well as strictly first order dependence on the alkali metal ion concentrations were also observed for the reactions of $Mo(CN)_8^{3-}$ and/or $W(CN)_8^{3-}$ with I^{-}[17,18], As (III)[19,20], $Se(IV)$[21], $Te(IV)$[22] and thiourea.[23] The large increase in the reaction rates from Li^+ to Cs^+ may be due to the greater effectivity of the
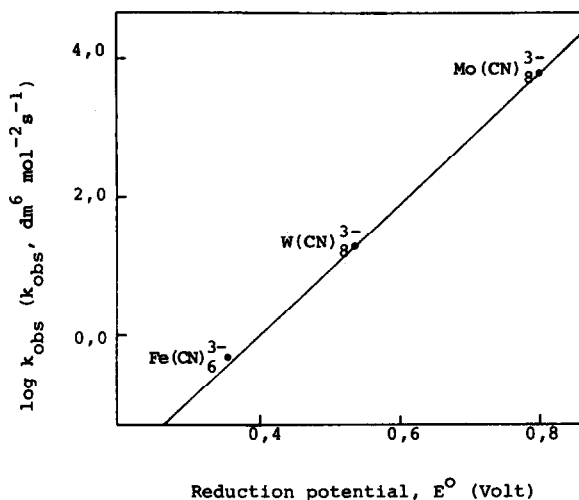

Fig. 4. A plot of $\log k_{obs}$ vs reduction potential $(A^+ = Na^+)$.

larger alkali metal ion as a charge buffer (and thus stabilization of the proposed intermediate $[(CN)_7MCN:A:SO_3]^{4-}$) and a bridge for electron transfer. Another evidence for this view on the catalytic effect of the alkali metal ions where they serve as an electron bridge is the linear relationship between the experimental rate constants and the polarizability[24] of the cations, (see Fig. 3).

The Marcus cross-relation (eqns (13)–(15)) predicts a type of linear behaviour with gradient 8.46 where k_{12} is the cross-reaction rate constant, k_{11} and k_{22} are the self exchange rate constants for the couples and K_{12} is the equilibrium constant:

$$k_{12} = (k_{11}k_{22}k_{12}f)^{1/2} \quad (13)$$

$$\log K = \frac{n(\Delta E^\circ)}{0.0591} \quad (14)$$

$$\log k_{12} = 0.5(\log k_{11} + \log k_{22} + \log f)$$

$$+ 8.46 \, n(\Delta E^\circ). \quad (15)$$

A plot of $\log k_{obs}$ $(A^+ = Na^+$ and $[OH^-] = 0.05 \text{ mol dm}^{-3})$ for the oxidation of the sulphite ions by $Mo(CN)_8^{3-}$, $W(CN)_8^{3-}$ and $Fe(CN)_6^{3-}$ (last value from Swinehart[7]) vs E° of the oxidizing agents[25](Fig. 4) is linear with a gradient of 9.2 V^{-1}. This is in very good agreement with the theoretical value and show that the Marcus theory is valid for those oxidations. This result also support the outer-sphere reaction mechanism proposed for the $Fe(CN)_6^{3-}$-sulphite reaction.[7]

REFERENCES

1. J. Veprek-Siska, *et al.*, *Coll. Czech. Chem. Commun.* 1965, **30**, 1390; 1966, **31**, 1248 and 3287.
2. K. B. Wiberg, H. Maltz and A. G. Fogg, *Inorg. Chem.* 1968, **7**, 830.
3. A. Brown and W. C. E. Higginson, *J. Chem. Soc. Chem. Commun* 1967, 725.
4. R. S. Murray, *J. Chem. Soc. Chem. Commun* 1968, 842.
5. J. M. Lancaster and R. S. Murray, *J. Chem. Soc. A* 1971, 2755.
6. R. S. Murray, *J. Chem. Soc. Dalton* 1974, 2381.
7. J. H. Swinehart, *J. Inorg. Nucl. Chem.* 1967, **29**, 2313.
8. J. G. Leipoldt, L. D. C. Bok and P. J. Cilliers, *Z. Anorg. Allg. Chem.* 1974, **407**, 350.
9. J. G. Leipoldt, L. D. C. Bok and P. J. Cilliers, *Z. Anorg. Allg. Chem* 1974, **409**, 343.
10. L. D. C. Bok, J. G. Leipoldt and S. S. Basson, *Z. Anorg. Allg. Chem.* 1975, **415**, 81.
11. R. E. Connick, T. M. Tam and E. von Denster, *Inorg. Chem.* 1982, **21**, 103.
12. R. J. Lemire and M. W. Lister, *J. Solution Chem.* 1976, **5**, 171.
13. L. D. C. Bok, J. G. Leipoldt and S. S. Basson, *Z. Anorg. Allg. Chem.* 1972, **392**, 303.
14. S. S. Basson J. G. Leipoldt and A. J. van Wyk, *Acta Cryst.* 1980, **B36**, 2025.
15. L. Meites, *Handbook of Analytical Chemistry.* McGraw-Hill, New York (1963).
16. J. G. Dick, *Analytical Chemistry.* McGraw-Hill. Kogakusha (1973).
17. M. H. Ford-Smith and J. H. Rawsthorne, *J. Chem. Soc. A* 1969, 160.
18. L. D. C. Bok, J. G. Leipoldt and S. S. Basson, *J. Inorg. Nucl. Chem* 1975, **37**, 2151.
19. J. G. Leipoldt, L. D. C. Bok and C. R. Dennis, *J. Inorg. Nucl. Chem.* 1976, **38**, 1655.
20. J. G. Leipoldt, L. D. C. Bok and A. J. van Wyk, *J. Inorg. Nucl. Chem.* 1977, **39**, 2019.
21. J. G. Leipoldt, C. R. Dennis, A. J. van Wyk and L. D. C. Bok, *Inorg. Chim. Acta* 1978, **31**, 187.
22. J. G. Leipoldt, C. R. Dennis A. J. van Wyk and L. D. C. Bok, *Inorg. Chim. Acta* 1979, **34**, 237.
23. J. G. Leipoldt, L. D. C. Bok, S. S. Basson and C. R. Dennis, *React. Kin. Cat. Lett.* 1978, **8**, 93.
24. C. N. R. Rao, *A Handbook of Chemistry and Physics.* Affiliated East–West Press (1967).
25. A. G. Sharpe, *The Chemistry of Cyano Complexes of the Transition Metals.* Academic Press, London (1976).

A VARIABLE TEMPERATURE ¹H NMR STUDY OF STEREOCHEMICAL NON-RIGIDITY IN GROUP VI METAL PENTACARBONYL COMPLEXES OF 1,3,5,7-TETRATHIAN; [M(CO)₅(SCH₂SCH₂SCH₂SCH₂)] (M = Cr OR W)

E. W. ABEL, G. D. KING, K. G. ORRELL* and V. ŠIK

Department of Chemistry, University of Exeter, Exeter EX4 4QD, England

Abstract—Stereochemical non-rigidity in the complexes [M(CO)₅(SCH₂SCH₂SCH₂SCH₂)] (M = Cr or W) has been studied by dynamic nuclear magnetic resonance spectroscopy. In the temperature range *ca.* −100 to 120°C two intramolecular processes were observed, namely pyramidal atomic inversion about sulphur atoms, and a commutation of the M(CO)₅ moiety between coordination sites on different sulphur atoms. Accurate energy barriers for both processes have been obtained by detailed computer simulations of the static and the dynamic spectra. The magnitudes of ΔG^+ (298.15 K) are compared with those reported for related complexes. The exact nature of the M(CO)₅ shift cannot be unambiguously assigned from the observed spectral line-shape changes. Two possible mechanisms are proposed and discussed.

Dynamic NMR studies[1] have cast considerable light upon fluxional processes, and in recent years we have shown[2–8] that coordination complexes of the general formula [M(CO)₅L] (M = Cr, Mo or W; L = a sulphur or selenium containing ligand) can undergo a remarkable variety of *intra-molecular* rearrangements. To date, such fluxions include pyramidal atomic inversions,[2–5] 1,2-metal shifts,[4,5] 1,3-metal shifts,[2,7,8] and 6-membered ring reversals.[2,8] Accurate energy barriers for all of these processes have been obtained utilising well developed spectral line-shape analysis techniques.[9] During the course of these investigations it has become evident that the magnitude of ΔG^+ (298.15 K) for such processes is dependent upon several factors such as the nature of the metal centre, the ligand atom and the stereochemistry of the ligand.

We have recently reported[8] the results of investigations into the stereochemical non-rigidity of Group VI metal pentacarbonyl complexes of substituted and unsubstituted 1,3,5-trithian. At temperatures above ambient a commutation of the M(CO)₅ group, via a series of 1,3-shifts, over all possible sulphur coordination sites was observed. It was postulated that the magnitude of the ΔG^+

(298.15 K) parameter for such a process is largely dependent on the skeletal flexibility of the ligand. In an attempt to corroborate this we have investigated the M(CO)₅ complexes of the larger, more flexible, eight membered ring ligand 1,3,5,7-tetrathian, SCH₂SCH₂SCH₂SCH₂. Variable temperature ¹H NMR studies of the complexes [M(CO)₅(SCH₂SCH₂SCH₂SCH₂)] (M = Cr or W) exhibit pyramidal atomic inversions about ligand sulphur atoms, and at temperatures well above ambient, a commutation of the M(CO)₅ group among coordination sites of different sulphur atoms occurs. The precise energy barriers obtained for both processes are compared with those for the corresponding trithian complexes.

EXPERIMENTAL

Materials and preparations

Metal hexacarbonyls were obtained commercially, and purified by sublimation (50°C/0.005 mmHg). 1,3,5,7-tetrathian was prepared and purified using literature procedures.[10,11] The complexes [M(CO)₅(SCH₂SCH₂SCH₂SCH₂)] (M = Cr or W) have been previously reported.[12,13] All reactions and manipulations were performed under an atmosphere of nitrogen, using freshly distilled, nitrogen purged solvents. Analytical data are reported in Table 1.

---

*Author to whom correspondence should be addressed.

Table 1. Characterisation of the Group VI metal pentacarbonyl complexes of 1,3,5,7-tetrathian (L)

Complex	M.p.[a] (°C)	Analysis[b] (%)		Infrared C=O Stretch (cm^{-1})[c]		
		C	H	A$_1$(m)	E(vs)	A$_1$(m)
[W(CO)$_5$L]	93–95	21.96 (21.25)	1.46 (1.59)	2076	1944	1940
[Cr(CO)$_5$L]	109.5–110.5	28.67 (28.70)	2.18 (2.15)	2068	1985	1948

a   Uncorrected

b   Calculated values in parentheses

c   Recorded in n-hexane; spectra calibrated against polystyrene film.

Spectra

These were obtained as described in detail in a previous publication.[8]

Line shape analyses

These were carried out using modified versions[14] of the original DNMR3 program of Kleier and Binsch.[15,16] Variable temperature experimental spectra and computer simulated spectra were compared visually until "best-fits" were obtained. The rate constants so obtained were used with the sample temperatures, to obtain the Arrhenius and Eyring activation parameters for the fluxional processes, using a least squares fitting technique. Errors quoted for the free energy of activation (ΔG^+) were calculated from the standard deviation term $|\sigma(\Delta H^+) - T\sigma(\Delta S^+)|$ as prescribed by Binsch and Kessler.[9]

RESULTS

^{1}H NMR studies

The two complexes [M(CO)$_5$(SCH$_2$SCH$_2$SCH$_2$SCH$_2$)] (M = Cr or W) showed essentially similar spectral changes at temperatures both above and below ambient. The chromium complex is taken as typical.

Low temperature studies

At ambient temperature the 100 MHz ^{1}H NMR spectrum of [Cr(CO)$_5$(SCH$_2$SCH$_2$SCH$_2$SCH$_2$)] in CD$_2$Cl$_2$/CS$_2$ (70:30, v:v) shows two singlets, intensity ratio 1:1. The four methylene protons adjacent to the coordinated sulphur atom are closest to the influence of the metallic group and are therefore assigned to the singlet at higher frequency. Cooling to below −100°C caused this signal to resolve into an AB quartet (see Fig. 1). Concurrently, the other (lower frequency) singlet was observed to broaden significantly. These spectral changes are consistent with the cessation of pyramidal atomic inversion of the coordinated sulphur atom.

Crystallographic studies have established[17] the boat-chair arrangement to be the conformation of the molecule of 1,3,5,7-tetrathian. It is not unreasonable to assume that the boat-chair structure is retained in solutions of the Cr(CO)$_5$ complexes. This results essentially in two different molecules depending upon whether the Cr(CO)$_5$ moiety is an axial or equatorial substituent to the ligand ring as illustrated in Fig. 2. Two fluxional processes can interchange these conformations. The effects of the sulphur atom inversions and the ring reversals
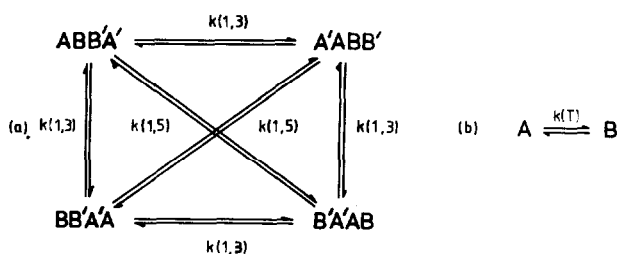
Scheme 1.
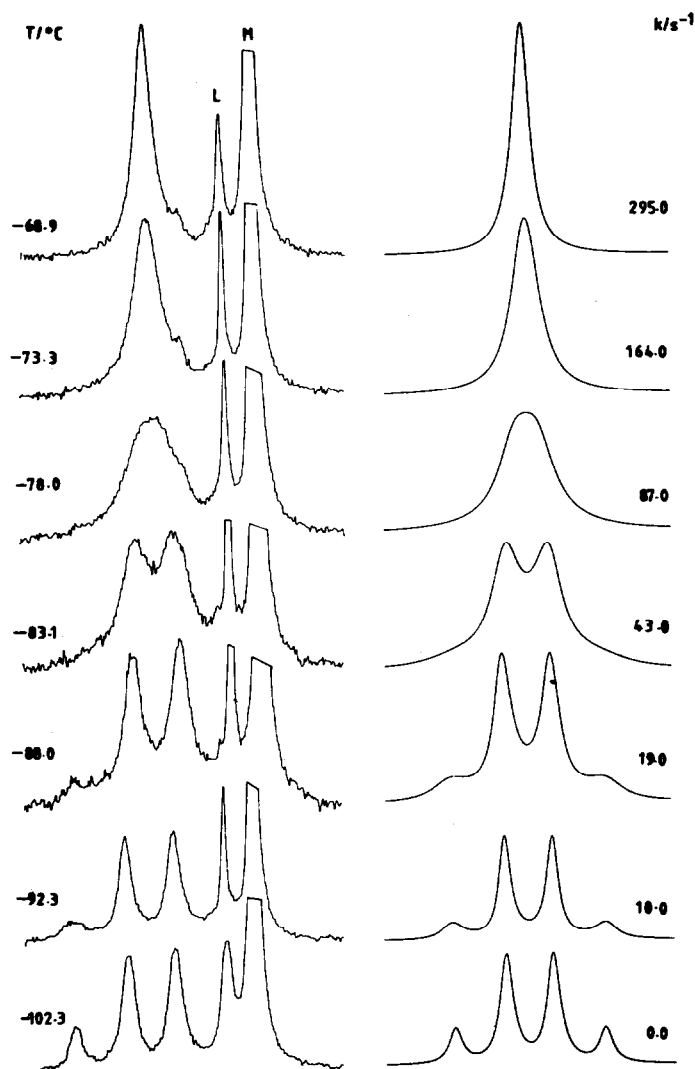
Fig. 1. Experimental and computer simulated low temperature spectra of [Cr(CO)₅(SCH₂SCH₂SCH₂SCH₂)] showing the effects of pyramidal sulphur inversion; L = free ligand, M = methylene protons attached to C(2) and C(3).
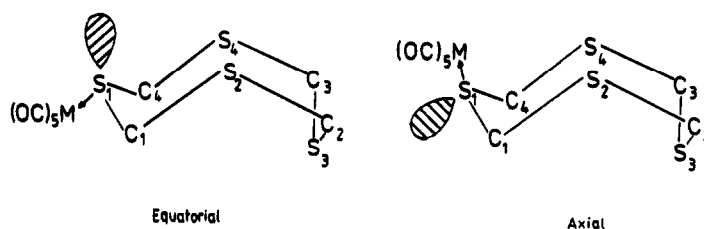
Fig. 2. Possible conformations of [M(CO)₅(SCH₂SCH₂SCH₂SCH₂)] (M = Cr or W).

upon the methylene protons closest to the metal coordinated sulphur are illustrated in Fig. 3. If both processes were slow on the NMR time scale the spectrum for these four protons would consist of two AB quartet patterns in an intensity ratio

corresponding to the relative populations of the two different molecules (I + III) and (II + IV). It has already been noted[18] however, that ring reversal in uncomplexed 1,3,5,7-tetrathian is rapid even at −170°C. Further, it has been shown that coor-
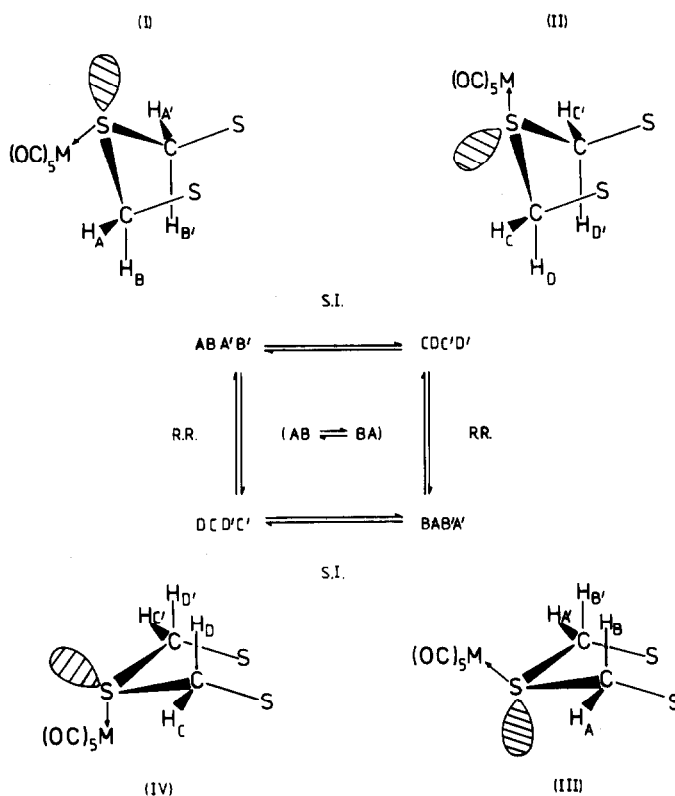
Fig. 3. The effect of ring reversal (R.R.) and pyramidal sulphur inversion (S.I.) on the environments of the four methylene protons adjacent to the coordinated sulphur atom in $[M(CO)_5(\overline{SCH_2SCH_2SCH_2SCH_2})]$ (M = Cr or W).

dination of such rings to metal moieties has no appreciable influence on ring reversal barriers.[19] Thus at *ca.* −100°C there would be rapid equilibration of conformers (I) and (II) with (IV) and (III) respectively. The single AB quartet observed is therefore the ring-reversal-averaged result of the two quartets possibly expected.

Ideally, similar spectral changes should be observed for the methylene protons on C(2) and C(3). However, their greater distance from the metal centre very considerably reduces the chemical shift difference between the equatorial and axial protons, and consequently their ambient temperature singlet broadens, but without any well defined splitting.

The full dynamic nuclear spin problem for the "metal-adjacent" protons is outlined in Fig. 3., but due to the absence of ^4J(H–C–S–C–H) coupling and rapid ring reversal this simplifies to an $AB \rightleftharpoons BA$ exchange problem. The experimental and computed spectra are shown alongside in Fig. 1. The static parameters used in the band shape fittings are listed in Table 2. The coordinated sulphur atom inversion energies are given in Table

3, where they are compared with those of the corresponding 1,3,5-trithian complexes.

High temperature studies

At ambient temperature the ^1H NMR spectrum of $[Cr(CO)_5(\overline{SCH_2SCH_2SCH_2SCH_2})]$ consists of two singlets of equal intensity from the four equilibrated "metal-adjacent" protons and the four equilibrated "metal-remote" protons. On increasing the temperature these two singlets collapse to a single band (*ca.* 105 and 120°C respectively for the chromium and tungsten complexes), which does not exchange with the sharp proton resonance of added free ligand. This spectral collapse is completely reversible on temperature drop. At temperatures higher than those quoted above the ligand resonance commences broadening with the onset of *inter*-molecular ligand–metal exchange processes.

The coalescence of these two separate resonances is consistent with an *intra*-molecular equilibration of all of the ligand methylene environments. As in the cases of the analogous complexes of 1,3,5-trithian and β-2,4,6-trimethyl-1,3,5-

Table 2. Static parameters used in calculating the pyramidal inversion energies for the Group VI metal pentacarbonyl complexes of 1,3,5,7-tetrathian (L)

Complex	Solvent	$\Delta v(AB)$/Hz	$^2J(AB)$/Hz	T_2^*/s ^{a}
[W(CO)$_5$L]	CD$_2$Cl$_2$	26.31	-14.41	0.075
[Cr(CO)$_5$L]	CD$_2$Cl$_2$/CS$_2$ (70:30, v:v)	22.68	-13.92	0.110

a $T_2^* = (\pi\Delta v_{\frac{1}{2}})^{-1}$ where $\Delta v_{\frac{1}{2}}$ is the measured normal linewidth (Hz) at half-height in the absence of exchange.

Table 3. Arrhenius and Eyring parameters for pyramidal sulphur inversion and M(CO)$_5$ commutation in Group VI metal pentacarbonyl complexes of 1,3,5-trithian and 1,3,5,7-tetrathian

Complex	Process	E_a/kJ mol^{-1}	$\log_{10}A$	$\Delta H^\ddagger$/kJ mol^{-1}	$\Delta S^\ddagger$/J K^{-1} mol^{-1}	$\Delta G^{\ddagger a}$/kJ mol^{-1}
[Cr(CO)$_5$(SCH$_2$SCH$_2$SCH$_2$)]	Sulphur Inversion	57.13 ± 1.16	13.82 ± 0.24	55.08 ± 1.16	12.71 ± 4.54	51.23 ± 0.20
[W(CO)$_5$(SCH$_2$SCH$_2$SCH$_2$)]	Sulphur Inversion	54.56 ± 0.69	13.06 ± 0.14	52.48 ± 0.69	1.81 ± 2.75	53.02 ± 0.14
[Cr(CO)$_5$(SCH$_2$SCH$_2$SCH$_2$SCH$_2$)]	Sulphur Inversion	44.56 ± 0.40	13.86 ± 0.11	42.96 ± 0.40	15.87 ± 2.10	38.23 ± 0.22
[W(CO)$_5$(SCH$_2$SCH$_2$SCH$_2$SCH$_2$)]	Sulphur Inversion	40.61 ± 1.74	12.64 ± 0.47	39.01 ± 1.74	-7.6 ± 9.09	41.28 ± 0.97
[Cr(CO)$_5$(SCH$_2$SCH$_2$SCH$_2$)]	1,3-shift	80.62 ± 0.94	13.63 ± 0.14	77.80 ± 0.92	6.71 ± 2.72	75.80 ± 0.11
[W(CO)$_5$(SCH$_2$SCH$_2$SCH$_2$)]	1,3-shift	81.37 ± 1.63	13.32 ± 0.24	78.41 ± 1.63	0.27 ± 4.60	78.33 ± 0.26
[Cr(CO)$_5$(SCH$_2$SCH$_2$SCH$_2$SCH$_2$)]	1,3-shift(?)	86.26 ± 0.83	13.77 ± 0.12	83.30 ± 0.82	8.98 ± 2.30	80.62 ± 0.14
[W(CO)$_5$(SCH$_2$SCH$_2$SCH$_2$SCH$_2$)]	1,3-shift(?)	87.68 ± 3.15	13.52 ± 0.45	84.67 ± 3.17	3.29 ± 8.68	83.50 ± 0.58

a   Calculated for T = 298.15K.

trithian,[8] this is believed to be a consequence of the M(CO)$_5$ group commuting between the coordination sites of the different sulphur atoms. In the trithians[8] only 1,3-shifts are possible, and the post-shift metal destinations are exactly equivalent. However, the "additional" sulphur atom present in the 1,3,5,7-tetrathian means that in addition to two 1,3-shift movements, there is a possible 1,5-movement. These possibilities, along with their effects upon the chemical and magnetic environments of all methylene protons, are illustrated in Fig. 4.

Although the full dynamic nuclear spin problem initially appears quite complex, the lack of ^4J(H–C–S–C–H) couplings permits simplification to that shown in Scheme 1(a). This can be further reduced to Scheme 1(b), where $k(T) = k(1,3) + k(1,5)$. It is immediately apparent that there is no possibility of positively deducing

whether a 1,3 or 1,5 or a combination of both types of shift is occurring, since the same nuclear spin averaging would occur in all cases. Further, the inherent simplicity of the ^{1}H NMR spectrum renders ineffective homonuclear double resonance (saturation transfer) techniques, which elsewhere[9] have been so effective in resolving some such ambiguities.

Whilst we are unable to define the exact nature of the intra-molecular rearrangement that occurs in the complexes [M(CO)$_5$(SCH$_2$SCH$_2$SCH$_2$SCH$_2$)] at high temperature, we favour the idea that 1,3-shifts are the predominant and possibly exclusive mechanism, vide infra. The Arrhenius and Eyring parameters for the intra-molecular metal shifts are listed in Table 3, where they are compared with those for the corresponding shifts in trithian complexes. Static parameters used in the band shape fittings are noted in Table 4.
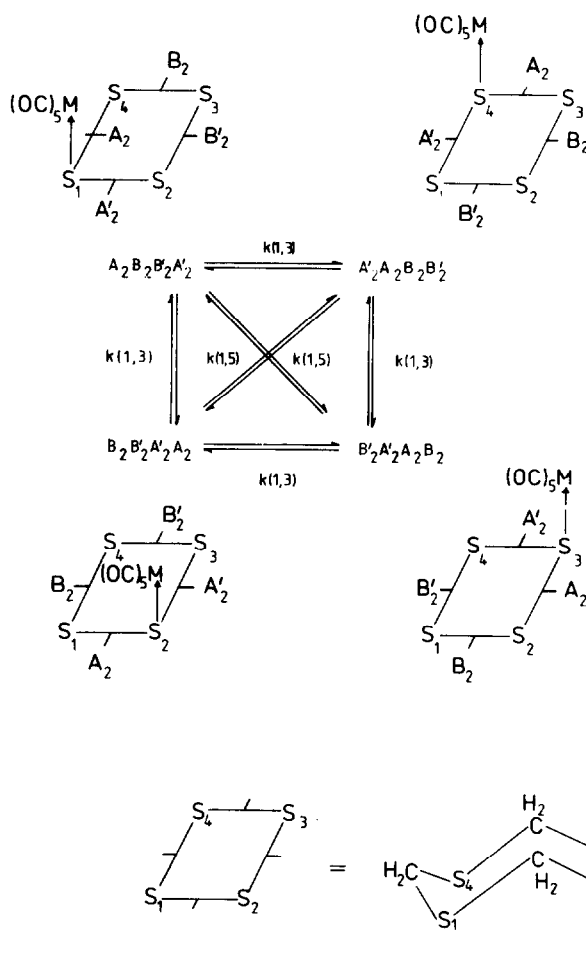
Fig. 4. Diagrammatic representation of 1,3- and 1,5-metal shifts in the complexes [M(CO)₅(SCH₂SCH₂SCH₂SCH₂)] (M = Cr or W) together with their respective effects on the nuclear magnetic spin system of the ligand methylene protons.

Table 4. Static parameters used in calculating the $M(CO)_5$ commutation energies for the Group VI metal pentacarbonyl complexes of 1,3,5,7-tetrathian (L)

Complex	Solvent	$\Delta v(AB)$/Hz	T_2^{*a}/s
[W(CO)₅L]	C_2Cl_4	50.56	0.378
[Cr(CO)₅L]	C_2Cl_4/C_6D_6 (70:30, v:v)	52.61	0.273

a $T_2^* = (\pi \Delta v_{\frac{1}{2}})^{-1}$ where $\Delta v_{\frac{1}{2}}$ is the measured linewidth (Hz) at half-height in the absence of exchange.

DISCUSSION

Energy data of the fluxional processes

Of the activation parameters for fluxional processes, ΔG^+ has been recognised as least susceptible to systematic errors of temperature and rate constant.[9] We therefore, as previously,[2,4,6,8] base our discussions of the relative ease of the fluxional processes upon the ΔG^+ (298.15 K) values listed in Table 3. The *intra*-molecular nature of these rearrangements, is indicated by the absence of exchange with added free ligand. Further confirmation from the numerical values of $\log_{10} A$ and ΔS^+ close to 13 and zero respectively for all cases is notable in Table 3.

1. Pyramidal sulphur inversion

A comparison of ΔG^+ values reveals coordinated sulphur inversion energies for the complexes $[M(CO)_5(\overline{SCH_2SCH_2SCH_2SCH_2})]$ to have a small but finite dependence upon the nature of the Group VI metal, that for chromium being *ca.* 3 kJ mol^{-1} less than for tungsten. This is in line with previous observations in Group VI metal carbonyl complexes. Such a trend we believe to be the result of two main factors.[21,22] Increasing electron withdrawal from an inverting centre leads to increased inversion barriers.[23] With electronegativities of chromium and tungsten being 1.56 and 1.40 respectively,[24] we would expect the chromium complex to have the larger ΔG^+ for inversion, the reverse of what is observed. However, $(p-d)\pi$ interaction of lone pairs of electrons on the inverting sulphur atom with the metal leads to a lowering of the inversion barrier,[21] and this effect has been postulated as an explanation for the different inversion barriers of dialkylsulphides in Pd(II) and Pt(II) complexes.[14,25,26] For sulphur inversion, the $(3p-3d)\pi$ conjugation in the chromium complex will be a considerably more effective overlap than the $(3p-5d)\pi$ conjugation in the tungsten analogue.

The relative magnitudes of the electronegativity and conjugation effects will control the magnitude of ΔG^+ for the inversion process, and in these complexes, with ΔG^+ in the order W > Cr, the conjugation effect apparently overrides the electronegativity influence.

When an inverting atom is incorporated into a ring, the energy barrier increases with reduction in ring size as the "angle-strain" in the transition state becomes greater.[22] The CSC ground state bond angles for the 8- and 6-membered rings $\overline{SCH_2SCH_2SCH_2SCH_2}$ and $\overline{SCH_2SCH_2SCH_2}$ are 102.6°[17] and 98.9°[27] respectively. Both of these should ideally become 120° in the transition state of the inversion process, and easier access of the 8-membered ring to the transition state is highlighted by a difference of *ca.* 10 kJ mol^{-1} in the ΔG^+ values in Table 3 for the 8- and 6-membered rings. Indeed ΔG^+ values for the metal pentacarbonyl complexes of the very flexible 1,3,5,7-tetrathian are very comparable to those of the acyclic complexes[28] $[M(CO)_5(CH_3SCH_2SCH_2SCH_3)]$ ($\Delta G^+ = 42.5$ and 41.6 kJ mol^{-1} for W and Cr respectively), in which "angle-strain" would be virtually zero.

2. Metal group commutations

As already noted, the very simple line-shape changes that occur in the high temperature spectra of the complexes $[M(CO)_5(\overline{SCH_2SCH_2SCH_2SCH_2})]$ (M = Cr or W) do not allow us to discern the precise nature of the $M(CO)_5$ commutation. The 1,3,5,7-tetrathian has much greater flexibility than the 1,3,5-trithian. Whereas the 6-membered ring has an observable slowing of its chair–chair ring reversal (^{1}H NMR coalescence temperature of only $-33°C$)[29] there is no observable slowing of any ring conformational process in the tetrathian ligand down to $-170°C$.[18] A comparison of energies for $M(CO)_5$ commutations (Table 3) shows ΔG^+ values to be significantly greater (*ca.* 5 kJ mol^{-1}) for complexes of 1,3,5,7-tetrathian than those of 1,3,5-trithian. We have previously proposed[8] that ΔG^+ values for 1,3-metal shifts are largely dependent upon the skeletal flexibility of the ligand system. Once again the high flexibility of the 8 membered ring bears comparison with the very flexible acyclic analogues. Thus ΔG^+ for the proposed 1,3-shift in $[W(CO)_5(\overline{SCH_2SCH_2SCH_2SCH_2})]$ is 83.5 kJ mol^{-1} compared with 84.6 kJ mol^{-1} for the 1,3-shift in the acyclic complex $[W(CO)_5(CH_3SCH_2SCH_3)]$.[6]

In a previous study[8] we found that ΔG^+ for a 1,3-shift in complexes of 1,3-dithian (a two-sulphur heterocycle) was much greater than that in 1,3,5-trithian (a three-sulphur heterocycle). As both these ligands have similar flexibilities, it would appear that perhaps a statistical factor associated with the reduced probability (in 1,3-dithian) of access to a suitably placed sulphur atom for the 1,3-shift is in evidence. Therefore, on purely statistical grounds a 1,3-shift in the tetrathian complexes would be favoured over a 1,5-shift. However, there are also the relative distances involved in these two types of commutation to be considered. It is pertinent to note that in the complexes of 1,4-dithian, a two-sulphur heterocycle with an almost identical skeletal flexibility[30] to that of 1,3-dithian, a 1,4-shift was not observed

at any temperature.[31] This would initially imply that any 1,5-shift would be even less likely. However, with highly flexible 8-membered ligand rings, certain conformations may bring sulphur atoms within sufficiently close proximity for 1,5-metal shifts to be feasible. In other words, very high ligand flexibility and 1,5-metal shifts may be to some extent mutually compatible.

It therefore remains an open question as to whether 1,3-, 1,5- or both types of shifts are operating in these tetrathian complexes. However, since the measured activation energies follow the energy trends of clearly identified 1,3-shifts in other complexes, it would seem most likely that, in these 8-membered ligand ring complexes, a 1,3-sulphur-metal commutation is the dominant fluxion.

REFERENCES

1. G. Binsch, *Top Stereochem.* 1968, **3**, 97.
2. E. W. Abel, M. Booth, K. G. Orrell and G. M. Pring, *J. Chem. Soc. Dalton Trans.* 1981, 1944.
3. G. M. Pring, *Ph.D. Thesis.* University of Exeter (1982).
4. E. W. Abel, S. K. Bhargava, P. K. Mittal, K. G. Orrell and V. Šik, *J. Chem., Soc. Chem. Commun.* 1982, 535.
5. S. K. Bhargava, *Ph.D. Thesis.* University of Exeter (1982).
6. E. W. Abel, S. K. Bhargava, T. E. MacKenzie, P. K. Mittal, K. G. Orrell and V. Šik, *J. Chem. Soc., Chem. Commun.* 1982, 983.
7. E. W. Abel, *Chimia* 1981, **35**, 100.
8. E. W. Abel, G. D. King, K. G. Orrell, G. M. Pring, V. Šik and T. S. Cameron, *Polyhedron* 1983, **2**, 1117.
9. G. Binsch and H. Kessler, *Angew. Chem., Int. Ed.* 1980, **19**, 411.
10. M. Schmidt, K. Blaettner, P. Kochendörfer and H. Ruf, *Z. Naturforsch* 1966, **21b**, 622.
11. E. Schmidt and E. Weissflog, *Z. Anorg. Chem.* 1974, **406**, 271.
12. M. Schmidt and W. A. Schenk, *Naturwiss.* 1971, **58**, 96.
13. W. A. Schenk and M. Schmidt, *Z. Anorg. Chem.* 1975, **416**, 311.
14. E. W. Abel, A. K. Ahmed, G. W. Farrow, K. G. Orrell and V. Šik, *J. Chem. Soc., Dalton Trans.* 1977, 47.
15. D. A. Kleier and G. Binsch, *J. Magn. Reson.* 1970, **3**, 146.
16. D. A. Kleier and G. Binsch, *DNMR3, Program* 165. Quantum Chemistry Program Exchange, Indiana University (1970).
17. G. W. Frank and P. J. Degen, *Acta Cryst.* 1973, **B29**, 1815.
18. G. W. Frank, P. J. Degen and F. A. L. Anet, *J. Am. Chem. Soc.* 1972, **94**, 4792.
19. E. W. Abel, M. Booth and K. G. Orrell, *J. Chem. Soc., Dalton Trans.* 1980, 1582.
20. R. J. Cross, G. Hunter and R. C. Massey, *J. Chem. Soc. Dalton Trans.* 1976, 2015.
21. L. C. Allen, K. Mislow and A. Rauk, *Angew. Chem., Int. Ed.* 1970, **9**, 400.
22. J. B. Lambert, *Topics Stereochem.* 1971, **6**, 19.
23. H. A. Bent, *Chem. Rev.* 1961, **61**, 275.
24. A. L. Allred and E. G. Rochow, *J. Inorg. Nucl. Chem.* 1958, **5**, 264.
25. E. W. Abel, G. W. Farrow, K. G. Orrell and V. Šik, *J. Chem. Soc., Dalton Trans.* 1977, 42.
26. E. W. Abel, M. Booth and K. G. Orrell, *J. Chem. Soc., Dalton Trans.* 1979, 1994.
27. G. Valle, V. Busetti, M. Mammi and G. Carazzolo, *Acta Cryst.* 1969, **B25**, 1432.
28. M. Z. A. Chowdhury, University of Exeter. Results to be published.
29. J. E. Anderson, *J. Chem. Soc. (B)* 1971, 2030.
30. G. Hunter, R. F. Jameson and M. Shiralian, *J. Chem. Soc., Perkin Trans II* 1978, 712.
31. G. D. King, University of Exeter, unpublished work.

SYNTHESIS AND CHARACTERIZATION OF URANIUM (VI) CHLORIDE FLUORIDES

Willard H. Beattie and William B. Maier II

Chemistry Division

University of California, Los Alamos National Laboratory

P. O. Box 1663, Los Alamos, New Mexico 87545

Abstract—Uranium (VI) chloride fluorides were synthesized by the reaction of liquid HCl and solid UF_6 between -80 and -114°C. These dark red compounds are unstable above -40 to -60°C. The simplest formulas derived from compositional analysis are UF_5Cl and UF_4Cl_2.

INTRODUCTION

Compounds of the type MF_5Cl, where M is sulfur,[1] selenium,[2] tellurium,[3] tungsten,[4] or rhenium[5] have been synthesized, and the existence of UF_5Cl has been postulated.[6] In addition, UF_4Cl_2 has been made by photolysis of UF_4 and Cl_2 in an Ar matrix.[7] We report here the preparation, and quantitative analysis, of mixtures of UF_5Cl, UF_4Cl_2, and UF_3Cl_3.

These compounds were first observed during solubility studies of UF_6 in low-temperature solvents[8,9] when a red product formed from solid UF_6 in liquid HCl at -80 to -114°C. The red product was very soluble in HCl; the solution was bright red at low concentrations and opaque at high concentrations. The solubility of UF_6 in HCl was not measurable in the presence of the reaction product, but it was <0.01$\underline{M}$ from the estimated weight of the undissolved solid UF_6.

Attempts to synthesize uranium (VI) compounds of the type $UF_{6-n}Cl_n$, where $1 \leq n \leq 5$, at room temperature have been unsuccessful. If UF_6 is mixed with BCl_3, $TiCl_4$ or $AlCl_3$ and warmed to ambient room temperature, the only U(VI) compound reported is UCl_6.[10] It is interesting to note that Michallet et al[11] observed intense red color when UF_6 was mixed with cold liquid or solid $TiCl_4$ at temperature as low as ~80 K, but they attributed the color to a complex, $UF_6 \cdot 2TiCl_4$.

We have examined the reaction of UF_6 with several chlorinators. Well-controlled preparations can be arranged by dissolving both the UF_6 and either BCl_3 or $TiCl_4$ in a cold liquid solvent, such as $CFCl_3$, Xe, Kr, or $SiCl_4$. When the chlorinator is HCl dissolved in liquid Xe, the order of mixing is important: if UF_6 is first dissolved, the red color fails to develop upon addition of HCl; if HCl is first dissolved, the UF_6 initially deposits in the cell as a solid and a red solution results. Cl_2, CCl_4, and $SiCl_4$ do not react rapidly with UF_6 at T ≤ 25°C. UF_6 reacts when mixed with $SOCl_2$, $POCl_3$, and PCl_3, but the reaction stops with ponderable solid UF_6 and chlorinator remaining, and the UF_6 is probably reacting only with impurities in these three chlorinators.

The most successful preparative technique involving neat HCl and solid UF_6 is described here. The reactions that occur in this synthesis are

$$UF_6 \text{ (s)} + HCl \rightarrow UF_5Cl + HF \tag{1}$$

$$UF_5Cl + HCl \rightarrow UF_4Cl_2 + HF \tag{2}$$

$$UF_4Cl_2 + HCl \rightarrow UF_3Cl_3 + HF, \text{ etc.} \tag{3}$$

Identification of the $UF_{6-n}Cl_n$ species has been accomplished by combining several techniques. Nuclear magnetic resonance spectroscopy gives evidence that there are no unpaired electrons in the soluble compounds produced by low-temperature reaction between UF_6 and liquid HCl, and we infer that these compounds are hexavalent uranium species. NMR also suggests that the reaction between UF_6 and liquid HCl mostly produces species with $n \leq 3$ in our studies.[12] Wavenumbers calculated[13] for $UF_{6-n}Cl_n$ from a simple force-field model and from force constants estimated from UF_6, UCl_6, and UF_5Cl spectra are in good agreement with wavenumbers of observed infrared absorption features.[8] Changes produced in the infrared spectra of $UF_{6-n}Cl_n$ mixtures by photolysis, by thermal decomposition, and by dissolution in various inert solvents have been used to help identify the different $UF_{6-n}Cl_n$ species. Changes in infrared spectra during reaction between UF_6 and either BCl_3 or $TiCl_4$ indicate that chlorination normally proceeds sequentially; i.e., UF_5Cl forms first, then UF_4Cl_2, etc. $UF_{6-n}Cl_n$ species have been identified for all values of $0 \leq n \leq 6$ in other studies,[14] but for the studies reported here, compounds with more than three chlorine atoms were not detected.

EXPERIMENTAL

The UF_6, obtained from the Oak Ridge Gaseous Diffusion Plant, was treated to reduce HF to <0.01%. The HCl, Airco electronic grade 99.99% pure, was used without further purification.

The preparation was carried out in either a borosilicate glass or a Kel-F reflux apparatus, which allowed the HCl to react with the solid UF_6 in one vessel and the product to collect in another. The borosilicate glass apparatus, shown in Fig. 1, and the Kel-F apparatus are similar, and no other materials were used except that the Kel-F apparatus also has a Monel diaphragm valve and a Teflon coated stir bar. The reflux apparatus was held in a clear glass dewar flask with the upper tubes protruding through an 8-cm-thick Styrofoam cover. The temperature was controlled by varying the flow of a stream of cold N_2 gas through the inner part of the dewar flask. Voltage from the thermocouple in the reaction vessel was monitored by an automatic temperature controller that controlled the N_2 flow.

The procedure is as follows. The apparatus is evacuated, and UF_6 is sublimed from a calibrated volume at known temperature and pressure into the reaction vessel. Then 10 to 15 mℓ of HCl ($\geq$ 100-fold molar excess) is condensed over the UF_6 at -80 to -114°C until the liquid levels reaches the top of the spill tube and fills about half of the sample vessel. The sample vessel is heated electrically to 10 to 40°C above the reaction vessel, so that the HCl vaporizes and recondenses in the reaction vessel. This condensation causes more liquid to spill over into the sample vessel. The reflux rate is typically 0.1 to 0.5 mℓ/min. The red solute is continually removed from the reaction vessel and concentrated in the sample vessel. The high-mass density of the solid UF_6 particles prevents them from rising to the level of the spill tube, even with vigorous stirring. Typically, it takes 8 to 16 hours for the solid UF_6 to disappear completely and for the red color of the solution to vanish from the reaction vessel for a typical UF_6 fill of 2 to 4 mmoles. The HCl is then removed (without boiling or bumping) by lowering the temperature to $\lesssim$-127°C and by pumping on the frozen mixture. When most of the HCl has been pumped away, the solid remaining in the sample vessel is held at -80°C and pumping is continued for $\leq$16 hours to remove traces of HCl. The final pressure obtained is 10^{-2} to 10^{-3} Pa (10^{-4} to 10^{-5} torr). After removal of the HCl, the samples collected at -80°C were dark-red porous lumps.
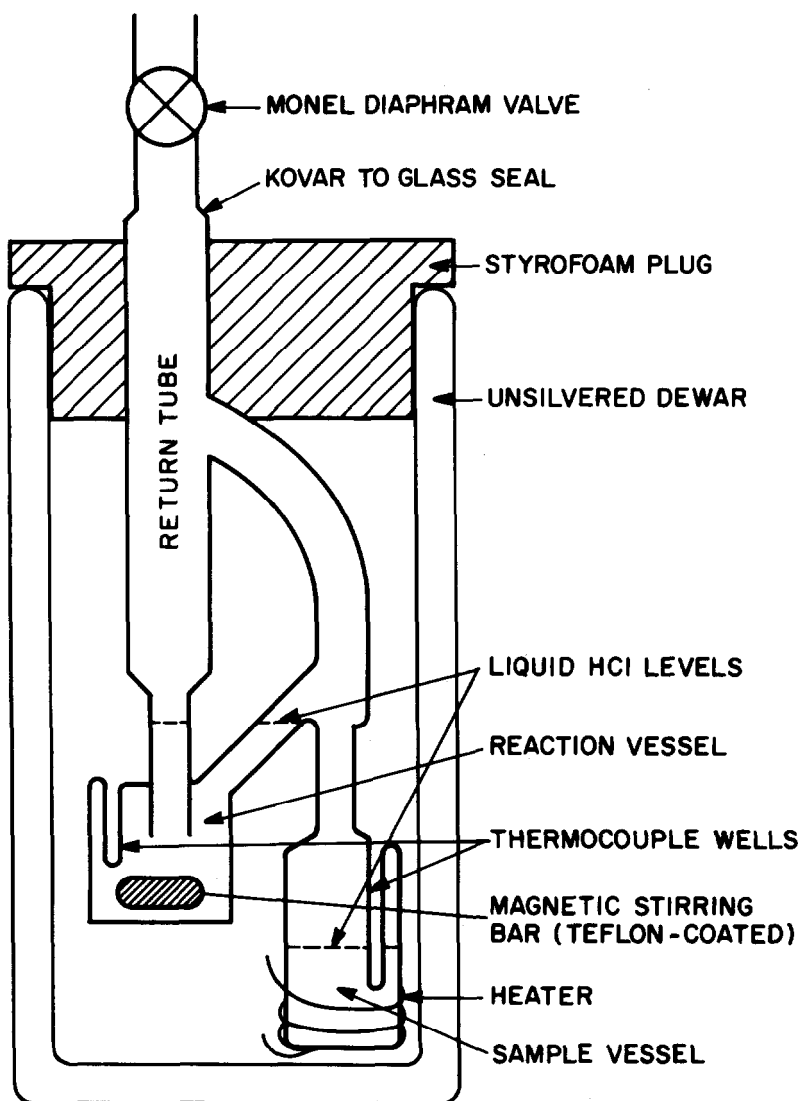
Figure 1. Borosilicate glass apparatus for preparation of uranium chloride fluorides. The interior of the dewar is cooled by cold N_2 vapor. A solution of uranium chloride fluorides in liquid HCl spills from the reaction vessel into the sample vessel. The HCl is evaporated and then recondensed in the return tube.

Samples of the solid red material were obtained by immersing the sample vessel in liquid N_2 and by sealing the neck, if glass, or by clamping off the tube, if Kel-F, under vacuum. The sealed sample vessel was allowed to warm to room temperature with attendant thermal decomposition. Quantitative analysis of uranium, fluorine, and chlorine, and semiquantitative spectrochemical analysis for metals were done on the solid phase. In some experiments, mass spectrometric analyses were done on the gases evolved during thermal decomposition of the sample.[15] The residue in the reaction vessel and connecting tubes was collected in water, and the amount of uranium was determined.

The gases existing in the cold reflux apparatus after preparation were sometimes quantitatively analyzed by mass spectrometry.

RESULTS AND DISCUSSION

A gas sample collected from a sample prepared at -120°C in the glass apparatus, before pumping off the HCl, contained no F_2, Cl_2, ClF, ClF_3, or SiF_4, but did contain HF, which is consistent with reactions (1) and (2). A gas sample collected at -80°C from a sample prepared in the glass apparatus contained Cl_2, SiF_4, and traces of HF. The decrease in HF concentration and the increase in SiF_4 concentration indicate that the HF found in samples collected at -80°C (compared with those collected at -120°C) reacted with the glass. The principle reaction with glass is given by

$$4HF + SiO_2 \rightarrow SiF_4 + 2H_2O \quad . \tag{4}$$

Samples prepared in the Kel-F apparatus had small green patches, identified as UF_4, that formed at the top of the HCl liquid phase before it was pumped off. Samples prepared in glass had similar green patches. The UF_4 was probably produced by a reduction of the uranium by the HCl gas phase, e.g.,

$$UF_5Cl + HCl(g) \rightarrow UF_4(s) + HF + Cl_2 \quad , \tag{5}$$

as suggested by the Cl_2 found in samples collected at -80°C. Reaction 4 is similar to the reported reduction of UF_6 to UF_5 by gaseous HBr.[16]

Thermal decomposition of the product, which occurs at temperatures between -60 and -40°C, is observed as a gradual change from dark red to brown, accompanied by evolution of Cl_2, some residual HCl, and traces of HF. Thermal decomposition of samples prepared in borosilicate glass evolved SiF_4 and a small amount of BF_3 in addition to the above named compounds. The brown solid did not dissolve when it was recooled and fresh liquid HCl was added. These observations indicate that the brown product probably consists of U(V) compounds, and therefore the initial thermal decomposition reactions are believed to be
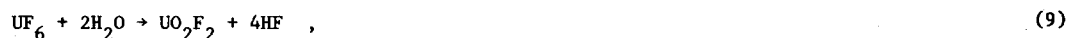
$$UF_5Cl \rightarrow UF_5 + 1/2 \ Cl_2 \quad , \tag{6}$$

$$UF_4Cl_2 \rightarrow UF_4Cl + 1/2 \ Cl_2 \quad , \tag{7}$$

and

$$UF_3Cl_3 \rightarrow UF_3Cl_2 + \tfrac{1}{2} \ Cl_2 \quad . \tag{8}$$

On continued warming, samples prepared in glass slowly changed from brown to olive green and the pressure increased. The green solid is soluble in ~7$\underline{M}$ HNO_3—but not in H_2O—and contains no chloride ion (by $AgNO_3$ test). The observed stability, color, absence of chlorine and insolubility serves to identify the green solid as UF_4.

Quantitative chemical analyses of the chlorine, fluorine, and uranium in two particular samples, I and II, were carried out.[17] The fluorine analysis was carried out in two steps, which distinguished the F in U(IV) compounds from that in U(V) compounds.

In step 1, the sample was reacted with excess water, and the resulting fluorine and chlorine were determined. In step 2, the fluorine in the remaining solids was determined by pyrohydrolysis. The reactions of some uranium fluorides and chloride fluorides with excess water in step 1 are

$$UF_6 + 2H_2O \rightarrow UO_2F_2 + 4HF \quad , \tag{9}$$

$$2UF_5 + 2H_2O \rightarrow UF_4 + UO_2F_2 + 4HF \quad, \tag{10}$$

$$2UF_4Cl + 2H_2O \rightarrow UF_4 + UO_2F_2 + 2HF + 2HCl \quad, \tag{11}$$

$$2UF_3Cl_2 + 2H_2O \rightarrow UF_4 + UO_2F_2 + 4HCl \quad, \tag{12}$$

$$UF_4 + H_2O \rightarrow \text{no reaction} \quad. \tag{13}$$

UF_5Cl and UF_4Cl_2 are not included here because they decompose above -40 to -60°C. These reactions indicate that the fluorine released (as HF) in step 1 should be 4 moles per mole of UF_6, 2 per UF_5, 1 per UF_4Cl, and none per UF_3Cl_2 or UF_4; the remaining fluorine released from the solid UF_4 and UO_2F_2 in step 2 should be 2 moles per mole of UF_6, 3 per UF_5, 3 per UF_4Cl, 3 per UF_3Cl_2, and 4 per UF_4. The relative amounts in steps 1 and 2 provide internal checks on the consistency of the analysis.

Sample I was prepared in the glass apparatus. After preparation, this sample was maintained at -80°C and pumped for 7 days to remove HCl and other volatile components. The sample vessel was sealed, warmed to ambient room temperature for 5 hours, weighed, and broken into water for analysis. The gases in the bulb were included in the analysis. The residue in the other tubes and reaction vessel was rinsed out and weighed. The results are given in Table I.

TABLE I

ANALYSIS OF SAMPLE I

(Prepared in Glass Apparatus)

	Mass (mg)	Amount (mmoles)
Sample collected	521.4	1.313[a]
Residue of U[b]	33	0.108[b]
U	312.5 ± 0.4	1.313
Cl	35.5 ± 0.1	1.001
F	120.0 ± 6.0	6.315
Sum U + Cl + F	468.0	

[a]See text for composition.

[b]Assumed to be $UF_4 + UO_2F_2$.

If it is assumed that Sample I contains a mixture of UF_4 and compounds of the type $UF_{6-x}Cl_x$ we may set up three linear equations, in which the sums of the number of moles of each of the elements U, F, and Cl in these compounds are set equal to the analyzed amounts in Table I. A general solution gives 0.281 m moles UF_4 and the remaining compounds are composed of 1.029 m moles U, 5.179 m moles F, and 1.001 m moles Cl. These remainders have the approximate stochiometric ratio of UF_5Cl, and a mixture of 2.4 mole % UF_6, 76.2 mole %, UF_5Cl, and 21.4 mole % UF_4 corresponds exactly to the analysis of the whole sample.

Samples prepared in glass turned green when warmed to ambient temperature. This may be explained as follows. The products of Reaction (4) remain in the apparatus during preparation. The SiF_4 is removed during the pumping out of HCl, but the solid H_2O remains with the red solid. During thermal decomposition, a second release of SiF_4 and a little BF_3 occurs at

-40 to -30°C, where the vapor pressure of H_2O reaches 13 to 40 Pa (0.1 to 0.3 torr). (The mass of the SiO_2 removed from the glass is considered in this treatment, but not the mass of B_2O_3, because the number of moles of BF_3 is less than 10% of the number of moles of SiF_4.) Since the sample vessel is sealed, the following reaction may be expected.

$$2UF_5Cl + 2H_2O \rightarrow UO_2F_2 + UF_4 + Cl_2 + 4HF \quad . \tag{14}$$

The products, UF_4, Cl_2, and traces of HF, which were identified in similar unsealed preparations, are consistent with this hypothesis.

The material balance of Sample I was checked as follows. On warming the samples, Reactions (4) and (14) form a chain reaction that ends when the UF_5Cl is completely reacted. During the decomposition of the sample the quantity of SiO_2 removed from the glass is equal to half of the amount of HF formed in Reaction (1); this, in turn, is equal to half of the amount of $UF_5Cl + UF_4$. This loss from the glass erroneously adds 0.641 m moles, 39.4 mg, to the measured sample mass because the sample mass was obtained as a difference between the full sample container and the residual glass. An additional error in the measured sample mass is caused by the solid H_2O formed by the sum of Reactions (1) and (4) at the reaction temperature; the amount of H_2O is also equal to half of the amount of $UF_5Cl + UF_4$, and its mass is 11.5 mg. If the sum of these masses is added to the sum of U + Cl + F, one obtains 517.9 mg, in excellent agreement with the 521.4-mg sample mass.

Sample II was prepared in the Kel-F apparatus. The sample was pumped for 16 hours at -80°C, then sealed and thermally decomposed by warming it to ambient room temperature. The gases evolved during thermal decomposition were quantitatively analyzed mass-spectrometrically. The results are given in Table II. The amount of fluorine-containing gases evolved was insignificant. The HCl probably was evolved by desorption and deocclusion, and the trace of BrCl probably was introduced as an impurity of HBr in the HCl. The brown solid was analyzed after the green solid, along with some adhering brown solid, was mechanically separated from the sample, and results are given in Table II.

Since no chlorine was found in Step 2, there are no stable, non-volatile chlorine-containing compounds in the residue of Step 1; thus, it contains no U(IV) chloride fluorides, and the brown solid consists only of U(V) and U(VI) compounds. If we assume that the brown solid is a mixture of n_0, n_1, n_2, and n_3 m moles respectively of UF_6, UF_5, UF_4Cl, and UF_3Cl_2 (decomposition products of UF_6, UF_5Cl, UF_4Cl_2, and UF_3Cl_3 respectively), we have from Table II

$$n_0 + n_1 + n_2 + n_3 = 0.4996 \text{ m moles U}$$
$$n_2 + 2n_3 = 0.0592 \text{ m moles Cl}$$
$$6n_0 + 5n_1 + 4n_2 + 3n_3 = 2.4266 \text{ m moles F.}$$

Combining these equations gives $n_0 = 0.0122$, and from the second equation we deduce that $0.0296 < n_2 + n_3 < 0.0592$, and $n_3 < 0.0296$. It follows that $0.428 < n_1 < 0.458$.

Additional validation of these results are obtained from the individual results of Steps 1 and 2, from which we may write the respective equations

$$4n_0 + 2n_1 + n_2 = 0.9526 \text{ m moles F}$$
$$2n_0 + 3n_1 + 3n_2 + 3n_3 = 1.474 \text{ m moles F.}$$

Combining these equations with the $n_0 = 0.122$ gives $n_1 - n_3 = 0.421$, and therefore $0.421 < n_1 < 0.451$, which is in substantial agreement with the above inequality for n_1. The difference

TABLE II

ANALYSIS OF SAMPLE II

(Prepared in Kel-F Apparatus)

	Mass (mg)	Amount (mmoles)
UF_6 fill	173.9	0.731
Gas evolved during thermal decomposition		
Cl_2		0.34 ± 0.05
HCl		0.085 ± 0.01
BrCl		0.01
HF		0.004
Brown solid remaining after thermal decomposition		
Sample collected	175.3	
U	118.9 ± 0.1	0.4996
Cl[a]	2.10 ± 0.02	0.0592
Cl[b]	0	0
F[a]	18.1 ± 0.2	0.9526
F[b]	28.0 ± 0.3	1.474
F(total)	46.1 ± 0.5	2.427
Sum U + Cl + F	167.1 ± 0.6	

[a]Reaction with moist air (step 1).

[b]Pyrohydrolysis (step 2).

between the mass of sample collected and the sum U + Cl + F may be partly due to bits of Kel-F eroded from the container by the stirrer.

These data indicate that the mixture that decomposed into the brown solid was composed of 2 mole% UF_6, 86 to 92 mole % of UF_5Cl, and 6 to 12 mole% (UF_4Cl_2 + UF_3Cl_3), with < 6 mole% UF_3Cl_3.

One mole of Cl is evolved during thermal decomposition per mole of U(VI) chloride fluoride by equations (6) to (8); since the evolved Cl equals 0.68 ± 0.10 mmoles, the combined UF_6 + UF_4 is approximately 0.051 mmoles, or 7.0 mole %. The UF_6 fraction of the brown solid (from which UF_4 was separated) was 2.4 mole %; therefore we estimate the UF_4 content of the total sample to be only ~3.6 mole %.

Solubility tests of UF_5Cl, made in the apparatus used for sample preparation, indicate that UF_5Cl is soluble in liquid HCl, $COCl_2$, and Cl_2. Decomposition occurred rapidly upon contact with the precooled solvents, CCl_4 CS_2, $CHCl_3$, CH_3COCH_3, and CH_3OH, at temperatures near the higher of either the freezing points of the solvents or -80°C. The red solid rapidly turned green upon contact with room temperature air.

Reaction (1) will go to completion only if UF_5Cl is continually removed from the reaction vessel. Early attempts to prepare the red compound by stirring solid UF_6 with liquid HCl in a single vessel without refluxing resulted in an incomplete reaction with only ~1/4 of the UF_6 reacting in 16 hours. In the sample vessel the back reaction is prevented by the limit of solubility of UF_5Cl, and the low concentration of HF, due to distillation; e.g., if

the sample vessel is 20°C warmer than the reaction vessel, the vapor pressure of HF would be increased by a factor of 6 to 9, and the concentration decreased by a similar factor.

CONCLUSIONS

The uranium chloride fluorides UF_5Cl and UF_4Cl_2 can be prepared by a reaction between solid UF_6 and liquid HCl. Compositional analyses of two particular samples were consistent with about 2 mole% UF_6, 76 mole% UF_5Cl and 21 mole% UF_4 in sample I, and 2 mole% UF_6, 86 to 92 mole% UF_5Cl, 6 to 12 mole% UF_4Cl_2 + UF_3Cl_3, and < 6 mole% UF_3Cl_3 in sample II. These uranium (VI) chloride fluorides are thermally unstable, and decompose to U(V) compounds at temperatures > -40 to -60°C.

REFERENCES

1. C. W. Tullock, D. D. Coffman, and E. L. Muetterties, J. Am. Chem. Soc. 86, 357-361, (1964).

2. C. J. Schack, R. D. Wilson, and J. F. Hon, Inorg. Chem. 11, 208-209, 583-586 (1971).

3. G. W. Fraser, R. D. Peakcock, and P. M. Watkins, J. Chem. Soc. Chem. Commun., 1257 (1968).

4. G. W. Fraser, M. Mercer, and R. D. Peacock, J. Chem. Soc. (A), 1091-1092 (1967); B. Cohen, A. J. Edwards, M. Mercer, and R. D. Peacock, J. Chem. Soc. Chem. Commun. 1965, 322-323; G. W. Fraser, C. J. W. Gibbs, and R. D. Peacock, J. Chem. Soc. (A) 1708-1711 (1970).

5. R. D. Peacock and D. F. Steward, Inorg. Nucl. Chem. Lett. 3, 255-256 (1967).

6. J. W. Erkins, Appl. Phys. 10, 15 (1976).

7. K. R. Kunze, R. H. Hauge, and J. L. Margrave, Inorg. Nucl. Chem. Lett. 15, 65-68 (1979).

8. W. B. Maier II, W. H. Beattie, and R. F. Holland, J. Chem. Soc. Chem. Comm. (in press).

9. W. B. Maier II and W. H. Beattie, J. Phys. Chem. (submitted).

10. T. A. O'Donnel and P. W. Wilson, Inorg. Synthesis 16, 143-147 (1976); T. A. O'Donnel, D. F. Stewart, and P. Wilson, Inorg. Chem. 5, 1438-1441 (1966).

11. M. Michallet, M. Chevreton, P. Plurien, and D. Massignon, C. r. hebd. Seanc. Acad. Sci., Paris 249, 691-693 (1959).

12. J. A. Jackson and A. E. Florin, Los Alamos National Laboratory, private communication.

13. L. Jones and P. J. Vergamini, Los Alamos National Laboratory, private communication.

14. W. B. Maier II, W. H. Beattie, and R.. F. Holland, unpublished results.

15. W. H. Beattie, Appl. Spectrosc. 29, 334-337 (1975).

16. A. S. Wolf, W. E. Hobbs, and K. E. Rapp, Inorg. Chem. 4, 755-757 (1965).

17. W. H. Ashley, Los Alamos National Laboratory, private communication.

Studies of Amidino-Complexes of Copper(I) and (II). Carboxylate Analogues

Melvyn Kilner* and Antoni Pietrzykowski

Department of Chemistry, The University of Durham, South Road, Durham City, DH1 3LE

Lithioamidines $\{R'N(Li)C(R)NR'; R = H, CH_3, C_6H_5; R' = C_6H_5, p\text{-}CH_3C_6H_4\}$ react with anhydrous copper(II) chloride to form $[Cu\{R'NC(R)NR'\}_2]_n$ complexes, and with anhydrous copper(I) chloride to form $[Cu\{R'NC(R)NR'\}]_m$. The copper(II) complexes are diamagnetic, purple solids, which are air stable in the solid state but very air reactive in solution. Experimental data are consistent with a dimeric or more highly associated structure, and an X-ray structural determination shows $[Cu\{C_6H_5NC(C_6H_5)NC_6H_5\}_2]_2$ to be dimeric with four bridging amidino-groups and a short Cu–Cu distance (2.46Å). The copper(I) complexes are pale yellow solids, which in solution are subject to rapid aerial oxidation, especially in the presence of free amidines, and disproportionation to $[Cu\{R'NC(R)NR'\}_2]_n$ and copper metal. Differences in properties are noted between acetamidino-, benzamidino- and formamidino-complexes, the last complexes of copper(I) being most stable towards disproportionation. $Cu\{C_6H_5NC(CH_3)\text{-}NC_6H_5\}_2$ reacts with pyridine (Py) to form the copper(I) derivative $Cu\{C_6H_5NC\text{-}(CH_3)NC_6H_5\}.2Py$ and with carbon disulphide to form $Cu\{C_6H_5NC(CH_3)NC_6H_5\}_2.CS_2$ which is reduced to form $Cu\{C_6H_5NC(CH_3)NC_6H_5\}.CS_2$.

THE isoelectronic relationship between allyl, amidino, triazeno and carboxylato-groups has been noted previously,[1,2] together with the differences in the mode of bonding to transition metals. The metal assumes a position out of the plane of η^3-allyl groups,[3] whereas for bidentate carboxylato-groups the metal adopts a position in, or close to, the ligand skeletal plane.[4] Amidino-groups have been shown to exhibit structural features similar to those of carboxylato-groups,[5] and also in common with the latter, have a high propensity to bridge between two identical[5-8] or different transition metals.[9,10] For example, amidines and carboxylic acids both react with chromium and molybdenum hexa-carbonyls to produce M_2L_4 complexes, and for M = molybdenum the structures of the complexes in the solid state are closely related, both consisting of a quadruple bonded Mo_2 unit bridged symmetrically by four ligand groups.[5] The ability of the amidino-group to encourage metal-metal interactions in binuclear complexes has been studied for other metals, and here we report studies involving copper. Attempts have been made to promote direct copper-copper bonding in complexes analogous to the copper(II) carboxylates.[4,11]

Previous studies of both copper(I) and (II) carboxylates have been extensive,[12] but only limited attention has been paid to amidino-copper complexes. In 1956 copper(II) acetate was treated with N,N'-diarylformamidines in refluxing ethanol to yield the copper(I) complexes $[Cu(RNCHNR)]_n$,[13] reactions which occur only for formamidines. Relevant also to the present work are complexes of the iso-electronic triazeno-group. The crystal structure of 1,3-dimethyltriazenocopper(I)[7] consists of a tetramer based on a diamond Cu_4 unit with single amidino-groups bridging alternate sides of the Cu_4 plane. The 1,3-diphenyltriazeno-complex, in contrast, has a dimeric structure with two triazeno-groups bridging the metals.[6]

Interestingly dimer-tetramer equilibria have been established for related formamidino-complexes.[14] Also bis-1,3-diphenyltriazenocopper(II),[15] unlike the

corresponding copper(II) acetate, is diamagnetic and thought to have a similar dinuclear structure with four bridging triazeno-groups. We report here our studies of related acetamidino-, benzamidino-, and formamidino-complexes of both copper(I) and copper(II), together with some attempted ligand addition reactions.

RESULTS AND DISCUSSION

A. Bis-amidinocopper(II) Complexes

These complexes have been synthesised from anhydrous copper(II) chloride and lithio-amidines in monoglyme solution as purple solids (see Table 1) which are recrystallised from dichloromethane using Soxhlet extraction. The reaction started below ambient temperature, but was allowed to continue for 18 h. to reach completion. The product slowly precipitated. There was no evidence for an intermediate amidinochloro-complex, $Cu(Am)Cl$. Yields of the microcrystalline materials, which melted in the range 160-220° with decomposition, were 50-70%. Though the solids are air stable over many months, rapid decomposition occurs in solution in the presence of air. The solutions become cloudy and deposit a brown solid whilst changing to a brown-green colour. At best the materials are only sparingly soluble in organic solvents, a property which restricted structural studies of the complexes. Benzamidino- and formamidino-complexes have a marginally better solubility than acetamidino-complexes, and the best solvents were found to be chloro-carbons (CH_2Cl_2, $CHCl_3$).

Molecular weight measurements by cryoscopy in benzene were undertaken on $Cu\{C_6H_5NC-(C_6H_5)NC_6H_5\}_2$, but the level of solubility made the results subject to large errors. Because of the high relative molecular mass (RMM) and low concentration of solutions small variations in temperatures correspond to large differences in RMM values. Never-the-less the values of 985, 892 and 708   which compare with values of 606 for the monomer and 1212 for the dimer raise the question of monomer $\rightleftharpoons$ dimer or monomer   oligomer or polymer equilibria occurring in solution, though no data from other sources support such a process. Interestingly Vrieze et al.[14] report dimer $\rightleftharpoons$ tetramer equilibria for a series of formamidino-copper(I) complexes, though the formation of a monomer intermediate is un-likely in this process which requires only the cleavage of one metal-nitrogen bond of the dimer. Magnetic measurements of the solid amidino-copper(II) complexes, $Cu\{C_6H_5NC(CH_3)-NC_6H_5\}_2$ and $Cu\{C_6H_5NC(C_6H_5)NC_6H_5\}_2$ using a Gouy balance show the complexes to be diamagnetic, and mass spectral studies of the complexes show the presence of Cu_2 species. Every complex exhibits peaks arising from $[Cu_2(Am)_2]^+$ as the highest $^m/e$ fragment in the spectrum implying association of $Cu(Am)_2$ units in the vapour state and possibly in the solid state. A typical breakdown pattern for $Cu\{C_6H_5NC(CH_3)NPh\}_2$ is illustrated in Figure 1. Source temperatures used were slightly lower than the melting points of the complexes at which they tend to decompose (according to thermal gravimetric analysis studies). $[Am]^+$ peaks are the most intense in the spectra, though the peaks due to $[Cu_2Am_2]^+$ are the most intense peaks for a copper containing species). $[CuAm_2]^+$, $[Cu_2Am]^+$ and $[CuAm]^+$ fragments are also commonly observed. Loss of RCN ($R = CH_3$, C_6H_5) from $[Cu_2\{R'NC(R)-NR'\}_2]^+$ is well documented as an important fragmentation step, though it is less important for formamidino-complexes.

Infrared spectroscopic data (Table 2) consist of absorptions at 1568-1463 and 1263-1231 cm.$^{-1}$ characteristic of delocalised amidino-complexes[16] but from such data it is not possible to differentiate between bridging and chelate bonding. Use of ^{1}H n.m.r. spectroscopy for structural studies was limited by the low solubility of the complexes in suitable solvents, though a spectrum was recorded for $Cu\{p-CH_3C_6H_4NC(CH_3)N-p-CH_3C_6H_4\}_2$

Table 1.   Analytical Data[+] and Yields for [Cu{R'NC(R)NR'}]$_n$ and [Cu{R'NC(R)NR'}$_2$]$_n$
           Complexes.

Complex	% Yield	%C	%H	%N	%Cu
Cu{PhNCHNPh}$_2$	49	68.8 (68.8)	4.73 (4.88)	12.0 (12.3)	14.3 (14.0)
Cu{PhNCHNPh}	62	60.0. (60.3)	4.50 (4.29)	10.6 (10.8)	24.2 (24.5)
Cu{PhNC(CH$_3$)NPh}$_2$	61	69.5 (69.8)	5.46 (5.44)	11.20 (11.62)	13.2 (13.2)
Cu{PhNC(CH$_3$)NPh}	53	67.6 (68.1)	4.81 (4.52)	8.10 (8.37)	18.4 (19.0)
Cu{$\underline{p}$-CH$_3$C$_6$H$_4$NC(CH$_3$)N-$\underline{p}$-CH$_3$C$_6$H$_4$}$_2$	67	70.8 (71.4)	6.20 (6.37)	10.5 (10.4)	11.4 (11.8)
Cu{$\underline{p}$-CH$_3$C$_6$H$_4$NC(CH$_3$)N-$\underline{p}$-CH$_3$C$_6$H$_4$}	70	64.1 (63.9)	5.95 (5.70)	9.11 (9.31)	20.8 (21.1)
Cu{PhNC(Ph)NPh}$_2$	63	74.5 (75.3)	5.21 (4.99)	9.15 (9.24)	10.4 (10.5)
Cu{PhNC(Ph)NPh}	61	68.0 (68.2)	4.52 (4.48)	8.23 (8.37)	18.8 (19.0)
Cu{$\underline{p}$-CH$_3$C$_6$H$_4$NC(C$_6$H$_5$)N-$\underline{p}$-CH$_3$C$_6$H$_4$}$_2$	58	75.5 (76.2)	6.02 (5.78)	8.56 (8.46)	9.53 (9.59)
Cu{$\underline{p}$-CH$_3$C$_6$H$_4$NC(C$_6$H$_5$)N-$\underline{p}$-CH$_3$C$_6$H$_4$}	58	68.9 (69.5)	5.37 (5.28)	7.60 (7.72)	17.4 (17.5)

[+] Calculated % are given in parentheses.

Table 2.   Infra-red and Melting Point Data for [Cu{R'NC(R)NR'}$_2$]$_m$ and Cu{R'NC(R)NR'}]$_m$
           Complexes.

Compound	Colour	M.p. (decomp) °C	IR data (cm^{-1})			
Cu(DPFA)$_2$	purple	160	1568	1350		1231
CuDPFA	pale yellow	270	1562	1352		1237
Cu(DPAA)$_2$	purple	165	1529	1415	1362	1252
CuDPAA	yellow	210	1513	1415	1368	1259
Cu(DpTAA)$_2$	purple	180	1538	1420	1363	1253
CuDpTAA	pale yellow	220	1518	1420	1360	1260
Cu(DPBA)$_2$	purple	180	1465	1415		1263
CuDPBA	yellow	260	1465 1476	1406		1260
Cu(DpTBA)$_2$	purple	175	1468	1423		1259
CuDpTBA	yellow	210	1463 1470	1439		1260

which was consistent with symmetrical bridging or bidentate amidino-groups. It must how-
ever be noted that p-tolyl groups have been shown by one of the authors to be insensitive
to different bonding situations occurring at the two nitrogen atoms in such groups.[16]
Furthermore the sharp signals provide further evidence for a diamagnetic complex. The
diamagnetism of the complex, its low solubility in organic solvents and the m.s. data
are consistent with a dimeric (I) or more highly associated complex (II), but not with a
monomeric complex.

    For one of the complexes, $Cu\{C_6H_5NC(C_6H_5)NC_6H_5\}_2$, suitable crystals for an X-ray
crystallographic study were produced which would allow the problem of a dimeric or an
oligomeric/polymeric structure in the solid state to be resolved. The crystal structure
determined by Halfpenny,[17] shows a dimeric structure (I) with four bridging amidino-
groups. The structure is closely related to that of $Mo_2\{C_6H_5NC(C_6H_5)NC_6H_5\}_4$ and is the
same as that proposed for the isoelectronic triazenocopper(II) complexes. The copper-
copper distance of 2.46Å is consistent with direct bonding between the coppers, and
represents a Cu-Cu single bond.

    A thermal gravimetric study of the complexes under a nitrogen atmosphere produced
the thermograms shown in Figure 2. The benzamidino-complexes and $[Cu_2(DPTAA)_4]$ contained
monoglyme of crystallisation, and the initial mass losses for these complexes correspond
to the loss of solvent. The curves for the two benzamidino-complexes appear very
similar, but assessment of the % mass loss data indicate different modes of decomposition.
Three stages occur for each of the benzamidino- and acetamidino-complexes, though the mass
loss data show no close relationship between the corresponding stages for each complex.
Loss of complete amidino-groups was not a recognisable process, but fragmentation of
amidino-groups was common with losses of [PhNCPh], $[CH_3C_6H_4NC(CH_3)N]$ and [PhNCNPh] being
typical. The final residue results after a lower mass loss than that expected for
formation of copper metal, but in all cases the data is not consistent with a
characterisable material.

B. Amidino-Copper(I) Complexes

    Copper(I) complexes were synthesised by the reaction of lithioamidines with anhydrous
copper(I) chloride in monoglyme as pale yellow, diamagnetic solids in ca. 50-70% yield
(see Table 1). Attempts were made to synthesise acetamidine and benzamidino-complexes
from copper(II) acetate by the method of Bradley and Wright[13] but without success. The
N,N'-diphenylformamidinocopper(I) complexes are apparently stable to disproportionation in
solution whereas the acetamidino- and benzamidino-complex are labile. The copper(I)
complexes are non-volatile and have higher melting points than their copper(II) counter-
parts, together with a higher solubility in organic solvents. Amidinocopper(I) complexes
readily oxidise in air to the copper(II) complexes, particularly in solution, where the
process is noticeably accelerated by the presence of the free amidine. In the solid state,
N,N'-diphenylacetamidinocopper(I), on exposure to air develops a bluish-green/red colour
on the surface. In solution disproportionation also occurs with deposition of the metal
and development of the purple colour characteristic of the copper(II) complexes. This
reaction prevented purification of the complexes by recrystallisation methods. Stability
of the solutions towards disproportionation in the order acetamidino < benzamidino <<
formamidino-complexes, and solutions of the last complexes showed virtually no signs of
reaction. Interestingly a detailed study of the dimer-dimer and dimer-tetramer equilibria
by ^{1}H and [13]C n.m.r. methods has been reported by Vrieze et al.[14] for a series of
formamidinocopper(I) complexes, with no reference being made to disproportionation in
solution. Indeed solutions of these complexes appear remarkably stable compared with

Figure 1

Mass Spectral breakdown pattern for Cu{PhNC(CH$_3$)NPh}$_2$

$$Cu_2Am_2^+ \xrightarrow{-Cu^+} CuAm_2^+ \frac{m}{e}(p^*)\ 425,\ 427 .$$

544, 546   481, 483

$\frac{m}{e}(p^*)$ | -41
$-CH_3CN$

465,
467

$[Cu_2Am]^+$ $\xrightarrow[-CH_3CN]{-41}$ $[Cu_2(PhNPh)]^+$
335, 337   294, 296

-PhNC
or
PhCN

503, 505

441, 443 $[Cu_2Am(PhNPh)]^+$ $[CuAm]^+ + Am^+$
272, 274
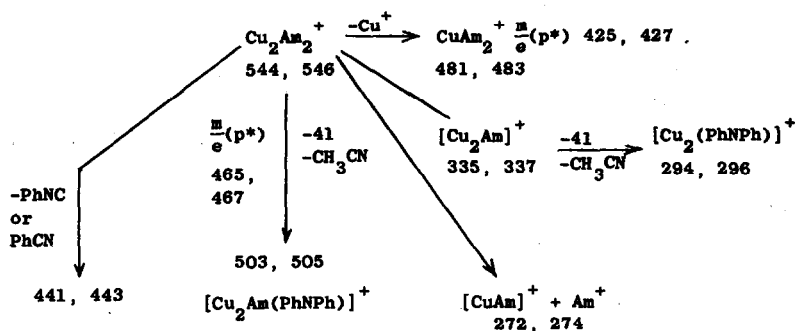
The following abbreviations are used:

AmH   = amidine R'NHC(R)NR'   (R = H, CH$_3$, C$_6$H$_5$;   R = C$_6$H$_5$, p-CH$_3$C$_6$H$_4$)

Am   = amidino-group R'NC(R)NR'

DPAAH   = N,N'-diphenylacetamidine, C$_6$H$_5$NHC(CH$_3$)NC$_6$H$_5$

DPAA   = N,N'-diphenylacetamidino, C$_6$H$_5$NC(CH$_3$)NC$_6$H$_5$

DPTAAH   = N,N'-di-p-tolylacetamidine, p-CH$_3$C$_6$H$_4$NHC(CH$_3$)N-p-CH$_3$C$_6$H$_4$

DPTAA   = N,N'-di-p-tolylacetamidino, p-CH$_3$C$_6$H$_4$NC(CH$_3$)N-p-CH$_3$C$_6$H$_4$

DPBAH   = N,N'-diphenylbenzamidine, C$_6$H$_5$NHC(C$_6$H$_5$)NC$_6$H$_5$

DPBA   = N,N'-diphenylbenzamidino, C$_6$H$_5$NC(C$_6$H$_5$)NC$_6$H$_5$

DPTBAH   = N,N'-di-p-tolylbenzamidine, p-CH$_3$C$_6$H$_4$NHC(C$_6$H$_5$)N-p-CH$_3$C$_6$H$_4$

DPTBA   = N,N'-di-p-tolylbenzamidino, p-CH$_3$C$_6$H$_4$NC(C$_6$H$_5$)N-p-CH$_3$C$_6$H$_4$

DPFAH   = N,N'-diphenylformamidine, C$_6$H$_5$NHCHNC$_6$H$_5$

DPFA   = N,N'-diphenylformamidino, C$_6$H$_5$NCHNC$_6$H$_5$

solutions of benzamidino- and acetamidino-complexes, though it is conceivable that some
of the minor changes i.e. broadening and weak new signals, could arise from copper(II)
derivatives.

The mass spectra of the copper(I) complexes are very similar to those of the
copper(II) complexes, with $[Cu_2Am_2]^+$ ions being the highest ^{m}/e value ions detected.
$[CuAm_2]^+$ ions are detected for all the complexes. The fragmentation pattern follows
closely that shown in Figure 1 for $Cu\{C_6H_5NC(CH_3)NC_6H_5\}_2$. The $[Cu_2Am_2]^+$ ion may
represent the parent ion for the complex, and indeed for $[Cu(C_6H_5NNNC_6H_5)]_2^6$ a dinuclear
complex has been established. However the ion may also represent a thermolysis product
of a tetranuclear complex, as established for $[Cu(CH_3NNNCH_3)]_4$.[7] Infrared spectra are
strikingly similar to those of copper(II) complexes and n.m.r. spectra provided little
structural information which was reliable because of low solubility and disproportiona-
tion in suitable solvents.

Thermograms for the copper(I) complexes are given in Figure 3. The benzamidino-
complexes decompose in one stage, whereas for the acetamidino-complexes decomposition
occurs in a two stage process. A thermogram, intermediate between these two types, with
a merging together of the two stages is exhibited by the formamidino-complex. All the
complexes decompose to form a residue, which contains, in addition to copper, a small
percentage of carbon, hydrogen and/or nitrogen, though in the case of the N,N'-diphenyl-
benzamidino-complex the % loss in weight corresponds most closely to a residue of copper
metal. The intermediate stages in the decomposition of the acetamidino-complexes
correspond closely to the loss of three amidino-groups from a Cu_4Am_4 unit (where Am =
R'NC(CH_3)NR', R' = C_6H_5, $\underline{p}$-$CH_3C_6H_4$). Though these complexes were too unstable towards
disproportionation in solution (to Cu(O) and Cu(II)) to allow relative molecular mass
measurements by using colligative properties, this feature in the thermogram possibly
provides some evidence for tetramers in the solid state, as found for the isoelectronic
N,N'-dimethyltriazino-complex.[7]

C. Reactions of $Cu\{C_6H_5NC(CH_3)NC_6H_5\}_2$ with Pyridine and Carbon Disulphide

Pyridine reacts with the bis-amidinocopper(II) complex in monoglyme over 4d to
produce a brown powder thought to be $Cu\{C_6H_5NC(CH_3)NC_6H_5\}.2C_5H_5N$ on the basis of
elemental analysis. This reduction of a copper(II) complex to a copper(I) complex is a
process achieved by many ligands, including phosphines and phosphites, and for example
triphenylphosphine reacts with hydrated copper(II) chloride in ethanol to produce
$(Ph_3P)_3CuCl$ or $[PPh_3CuCl]_4$ depending on the molar ratios of the reactants.[18]

With carbon disulphide attempts were made to accomplish insertion into a copper-
nitrogen bond. The purple solution of the copper(II) complex dissolved in carbon
disulphide became brown over ½ h. and deposited a brown solid which though impure showed
characteristics of an addition compound. Analytical data suggested the formulation
$Cu\{C_6H_5NC(CH_3)NC_6H_5\}_2.CS_2$. Recrystallisation of the material from toluene/hexane
mixtures led to a decrease in carbon, hydrogen and nitrogen content, but an increase in
copper and sulphur contents, the data being consistent with reduction to the copper(I)
complex, $Cu\{C_6H_5NC(CH_3)NC_6H_5\}.CS_2$.

Distinct differences occur between the reactions of this bis-amidinocopper(II)
complex and the corresponding carboxylato-complex with neutral ligands, and may reflect
the weak coordinating properties of ligands trans- to the second metal in the dinuclear
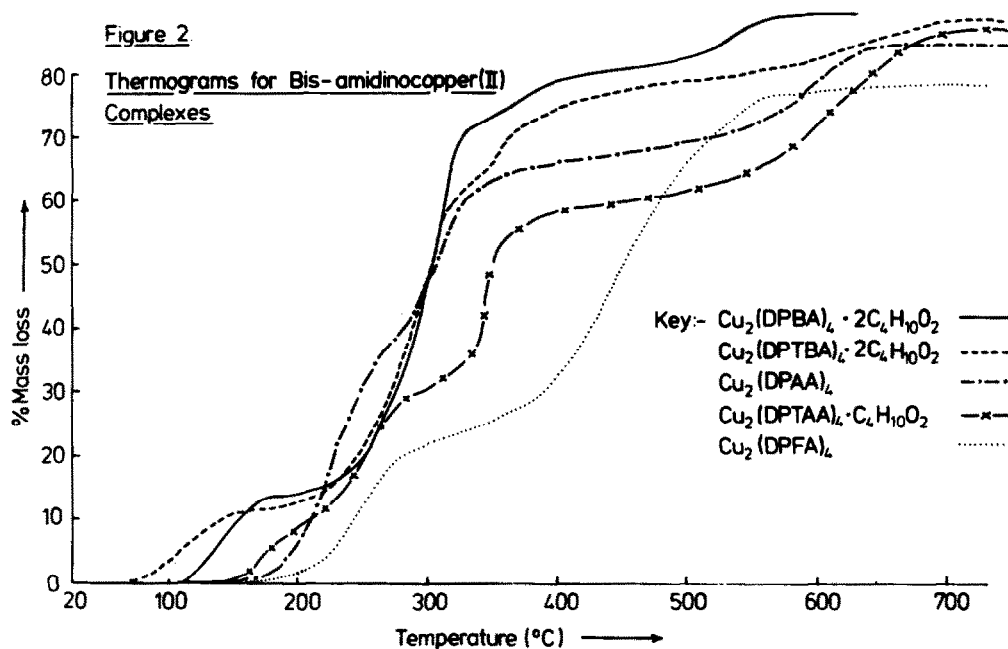unit, or reflect the steric properties of the N-substituents associated with four

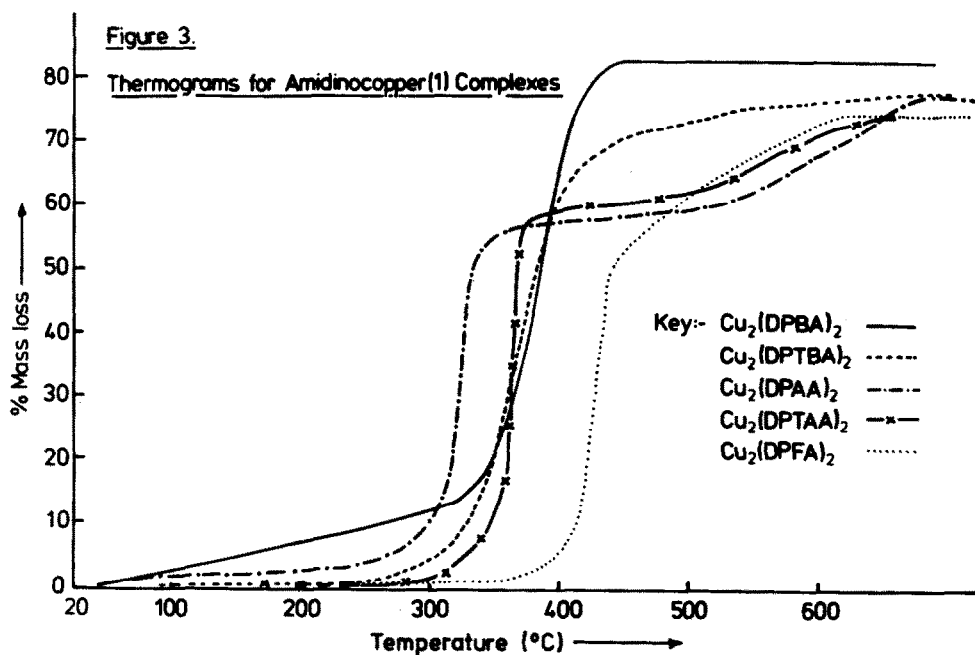Figure 2. Thermograms for Bis-amidinocopper(II) Complexes.

Figure 3. Thermograms for Amidinocopper(I) Complexes.

amidino-groups. It is well established that complexes containing strong metal-metal interactions tend to form weak bonds _trans_ to the metal-metal bond.[19] For metal-metal bonded amidino-complexes pyridine and triphenylphosphine failed to form adducts of the type $Cu_2Am_4L_2$, whereas for the acetato-complex water, dioxane, pyridines and anilines give $Cu_2(OCOCH_3)_4L_2$ derivatives.[20]

EXPERIMENTAL

    Anhydrous copper(I) and copper(II) chlorides, triphenylphosphine, pyridine, N,N'-diphenylacetamidine and -formamidine, acetamidinium hydrochloride and benzamidinium hydrochloride were obtained from commercial sources and used without further purification. N,N'-Diphenylbenzamidine, N,N'-di-_p_-tolylbenzamidine, N,N'-dimethylbenzamidine and N,N'-di-_p_-tolylacetamidine were prepared by standard methods.[21] n-Butyllithium, ca. 1.23M in hexane, was used as supplied without purification. Hydrocarbon solvents and diethylether were dried over extruded sodium, and monoglyme was freshly distilled from sodium hydride prior to use. Chlorocarbon solvents and carbon disulphide were dried over molecular sieves. All solvents were de-gassed under reduced pressure, stored under nitrogen, and transferred by syringe against a counter flow of nitrogen. All reactions were performed with rigorous exclusion of air.

    I.r. spectra in the range 4000-400 cm.$^{-1}$ were recorded with a Perkin-Elmer 457 spectrophotometer, and ^{1}H n.m.r. spectra at 90 MHz with a Bruker HX90E spectrophotometer. Mass spectra were obtained with an A.E.I. MS9 instrument at 70 eV and an accelerating potential of 8 kV. Samples were inserted directly into the ion source at temperatures between 80°-220°C. Thermogravimetric studies were undertaken using a Stanton Redcroft TG750 balance.

    Carbon, hydrogen and nitrogen contents of the complexes were determined with a Perkin-Elmer 240 Elemental Analyser, and copper by atomic absorption spectroscopy using a Perkin-Elmer 403 spectrometer. Sulphur content was obtained by combustion of the complex in oxygen to sulphate, followed by the volumetric determination of sulphate using a standard barium perchlorate solution. Phosphorus content was determined by combustion of the sample in air, followed by volumetric determination of phosphate.

Preparation of Bis(N,N'-diphenylacetamidino)copper(II), $Cu\{C_6H_5NC(CH_3)NC_6H_5\}_2$.-

n-Butyllithium (5.9 ml; 1.23M in hexane) was added to a frozen solution of N,N'-diphenylacetamidine (1.54 g, 7.31 mmol) in monoglyme (40 ml), and the mixture allowed to warm slowly to ambient temperature and stand for ½ h. The resulting inhomogeneous product mixture was then transferred onto a frozen suspension of anhydrous copper(II) chloride (0.49 g, 3.65 mmol) in monoglyme (40 ml), and the reaction mixture stirred at ambient temperature for 18 h. After filtering the resulting mixture, the purple residue was washed with hexane (2 x 10 ml), dried _in vacuo_ and recrystallised from hot dichloromethane using a modified Soxhlet extraction method. A purple microcrystalline solid, $Cu\{C_6H_5NC(CH_3)NC_6H_5\}_2$ (m 165° dec, 61% yield) was obtained, which could be stored in the solid state in air over many months without noticeable change. The complex in solution remains unchanged when stored under nitrogen over many days, but rapid changes occur in the presence of air.

M.s. The highest mass fragment observed gave peaks at ^{m}/e 548, 546, 544 corresponding to $[Cu_2Am_2]^+$ and arising from ^{63}Cu and ^{65}Cu (69 and 31% abundancies respectively).

Preparation of other Bis-amidinocopper(II) Complexes.- The method described above was used generally to prepare the following complexes as purple solids typically in 50-70%

yields.

Bis(N,N'-di-p-tolylacetamidino)copper(II), m. 220° dec.

M.s. The highest mass fragment was observed at ^{m}/e 602 and 600 corresponding to $[Cu_2Am_2]^+$.

^{1}H n.m.r., δ(CDCl$_3$): 2.84(8H), 7.69(6H), 7.91(3H) p.p.m.

Bis(N,N'-di-p-tolylbenzamidino)copper(II), m. 175° dec.

M.s. The highest mass fragment was observed at ^{m}/e 726 and 724 corresponding to $[Cu_2Am_2]^+$.

Bis(N,N'-diphenylbenzamidino)copper(II), m. 180° dec. M 985, 892, 708 by cryoscopy in benzene (monomer requires 606, dimer 1212).

M.s. The highest mass fragment was observed at ^{m}/e 670 and 668 corresponding to $[Cu_2Am_2]^+$.

Bis(N,N'-diphenylformamidino)copper(II), m. 160° dec.
M.s. The highest mass fragment was observed at ^{m}/e 518 and 516 corresponding to $[Cu_2Am_2]^+$.

Preparation of N,N'-Di-p-tolylacetamidinocopper(I), Cu{p-CH$_3$C$_6$H$_4$NC(CH$_3$)N-p-CH$_3$C$_6$H$_4$}.-

n-Butyllithium (2.70 ml, 1.84M in hexane) was added to a frozen solution of N,N'-di-p-tolylacetamidine (0.89 g, 4.14 mmol) in monoglyme (25 ml), and the mixture allowed to warm slowly to ambient temperature. After ½ h. the resulting reagent was syringed onto a frozen mixture of anhydrous copper(I) chloride (0.41 g, 4.14 mmol) and monoglyme (30 ml), and the mixture allowed to warm to ambient temperature. After stirring for 12 h., the pale yellow precipitate was separated by filtration, washed with hexane (2 x 10 ml), and dried in vacuo. Soxhlet extraction using dichloromethane yielded pale yellow micro-crystalline N,N'-di-p-tolylacetamidinocopper(I), m. 220° dec.

M.s. The highest mass fragment was observed at ^{m}/e 602 and 600 corresponding to $[Cu_2Am_2]^+$.

Preparation of other Amidinocopper(I) Complexes.- The method described above was used generally to prepare the following complexes as yellow solids typically in 50-70% yields.

N,N'-Diphenylformamidinocopper(I), m. 270° dec.

M.s. The highest mass fragment was observed at ^{m}/e 518 and 516 corresponding to $[Cu_2Am_2]^+$.

N,N'-Di-p-tolylbenzamidinocopper(I), m. 210° dec.

M.s. The highest mass fragment was observed at ^{m}/e 726 and 724 corresponding to $[Cu_2Am_2]^+$.

N,N'-Diphenylbenzamidinocopper(I), m. 260° dec.

M.s. The highest mass fragment was observed at ^{m}/e 670 and 668 corresponding to $[Cu_2Am_2]^+$.

N,N'-Diphenylacetamidinocopper(I), m. 210° dec

M.s. The highest mass fragment was observed at ^{m}/e 532 and 530, corresponding to $[Cu_2Am_2]^+$.

Reaction of Bis(N,N'-diphenylacetamidino)copper(II) with Pyridine.- A suspension of the complex (0.38 g, 0.8 mmol) in monoglyme (15 ml) was stirred with pyridine (0.063 g, 0.8 mmol) for 4d at ambient temperature. The brown precipitate of the product, Cu{C_6H_5NC-(CH_3)NC$_6$H$_5$}$_2$·2C$_6$H$_5$N, was separated by filtration, washed with monoglyme and dried _in vacuo_. Found: C, 67.1; H, 5.81; N, 13.0; Cu, 14.8: $C_{24}H_{23}N_4$Cu requires C, 66.9; H, 5.38;' N, 13.0; Cu, 14.7%.

Reaction of Bis(N,N'-diphenylacetamidino)copper(II) with Carbon Disulphide.- The complex was stirred in carbon disulphide for 24 h., the initial purple solution turning brown over ½ h. After filtration the solvent was removed _in vacuo_ to produce a brown solid. Found: C, 59.8; H, 4.90; N, 10.4; Cu, 12.4; S, 12.0: Cu(DPAA)$_2$·CS$_2$ requires C, 62.4; H, 4.69; N, 10.0; Cu, 11.4; S, 11.5%. After recrystallisation from toluene/hexane mixtures, found C, 49.7; H, 4.31; N, 8.42; Cu, 17.7; S, 17.6: Cu(DPAA)·CS$_2$ requires C, 51.6; H, 3.75; N, 8.03; Cu, 18.2; S, 18.4%.

REFERENCES

1. N.D. Cameron, R.J. Eales and M. Kilner, Abstr. VII Int. Conf. Organometal. Chem., Venice, 1975, 119.
2. T. Inglis, Inorg. Chim. Acta Rev., 1973, 7, 35.
3. N. Rösch and R. Hoffman, Inorg. Chem., 1974, 13, 2656.
4. C. Oldham. Prog. Inorg. Chem., 1968, 10, 223.
5. F.A. Cotton, T. Inglis, M. Kilner and T.R. Webb, Inorg. Chem., 1975, 14, 2023.
6. I.D. Brown and J.D. Dunitz, Acta Cryst., 1961, 14, 480.
7. J.E. O'Connor, G.A. Jamisonis and E.R. Corey, J.C.S. Chem. Comm., 1968, 445.
8. F.A. Cotton and L.W. Shive, Inorg. Chem., 1975, 14, 2027; F.A. Cotton, W.H. Ilsley and W. Kaim, Inorg. Chem., 1980, 19, 2360.
9. A.F.M. van der Ploeg, G. van Koten and K. Vrieze, Inorg. Chem., 1982, 21, 2026.
10. P.I. van Vliet, G. van Koten and K. Vrieze, J. Organometal. Chem., 1980, 188, 301.
11. J.N. van Niekerk and F.R.L. Schoening, Acta Cryst., 1953, 6, 227.
12. A.G. Massey, 'Comprehensive Inorganic Chemistry', Edit. J.C. Bailar, H.J. Emeleus, R. Nyholm and A.F. Trotman-Dickenson, 1973, Vol. 3, p.1.
13. W. Bradley and I. Wright, J. Chem. Soc., 1956, 640.
14. P.I. van Vliet, G. van Koten and K. Vrieze, J. Organometal. Chem., 1979, 179, 89.
15. F.P. Dwyer, J. Amer. Chem. Soc., 1941, 63, 78; C.M. Harris, B.F. Hoskins and R.L. Martin, J. Chem. Soc., 1959, 3728.
16. T. Inglis, M. Kilner, T. Reynoldson and E.E. Robertson, J.C.S. Dalton, 1975, 924.
17. J.C. Halfpenny, unpublished results.
18. T.H. Jardine, L. Rule and A.G. Vohra, J. Chem. Soc. (A), 1970, 238.
19. F.A. Cotton and G. Wilkinson, 'Advanced Inorganic Chemistry', 4th Edit., Wiley, 1980, p. 1102.
20. C. Oldham, Prog. Inorg. Chem., 1968, 10, 223, and references therein.
21. R.L. Shriner and F.W. Neumann, Chem. Rev., 1944, 35, 351.

NOTE

EMISSION QUENCHING OF BINUCLEAR PYROPHOSPHITO PLATINUM(II) COMPLEXES IN AQUEOUS SOLUTION BY SULPHUR DIOXIDE. SPECTROSCOPIC MEASUREMENTS ON SULPHUR DIOXIDE ADDITION AND CHROMOUS ION REDUCTION

KENNETH A. ALEXANDER
Department of Chemistry, Washington State University, Pullman, WA 99164, U.S.A.

PAUL STEIN
Department of Chemistry, Duquesne University, Pittsburgh, PA 15282, U.S.A.

and

DAVID B. HEDDEN and D. MAX ROUNDHILL*
Department of Chemistry, Tulane University, New Orleans, LA 70118, U.S.A.

Abstract—The emission intensity at 517 nm from $Pt_2(pop)_4^{4-}$ (pop = $P_2O_5H_2^{2-}$) is quenched by the addition of sulphur dioxide. The sulphur dioxide coordinates at the axial platinum(II) sites by a η^1-SO_2 bond. This coordination is supported by ^{31}P NMR and Raman spectroscopy of aqueous solutions. The electronic spectrum of a sulphur dioxide saturated solution of $Pt_2(pop)_4^{4-}$ shows an absorption at 428.5 nm ($\epsilon = 4.1 \times 10^4$). From the decrease in the chromophore for uncomplexed $Pt_2(pop)_4^{4-}$ the equilibrium constant for SO_2 binding is estimated to be $1.74 \, M^2 l^{-2}$. The effect of adding different quenchers to aqueous solutions of $Pt_2(pop)_4^{4-}$ is discussed. The compound $Pt_2(pop)_4^{4-}$ will undergo 2-electron reduction with chromous ion.

The complex $K_4[Pt_2(pop)_4] \cdot 2H_2O$ (pop = $P_2O_5H_2^{2-}$) was discovered because of its intense emission at 514 nm in aqueous solution.[1] This emission is sufficiently strong that the luminescence can be used as the basis for the quantitative determination of trace platinum.[2] Following the discovery of the complex $Pt_2(pop)_4^{4-}$, a number of articles have been published describing the structure, spectroscopy, and reaction chemistry of this binuclear complex.[3–7] Spectroscopic studies on $Pt_2(pop)_4^{4-}$ have assigned the fluorescence ($\lambda_{max} = 407$ nm) and phosphorescence ($\lambda_{max} = 517$ nm) emissions to the respective transitions $^1A_{2u} \rightarrow ^1A_{1g}$ and $^3A_{2u} \rightarrow ^1A_{1g}$. Single crystal measurements show the 367 nm absorption band polarized parallel to the Pt–Pt axis, and the 452 nm absorption band polarized perpendicular.[5] When the synthesis of these pop complexes is carried out at higher temperatures, further ligand condensation occurs and a higher homologue platinum(II) complex is formed which has an emission band at 650 nm.[8] Recently an article has been published showing that in aqueous solutions of $Pt(CN)_4^{2-}$, it is the presence of higher oligomers which cause the emission band to be observed at 525 nm. This emission is quenched by added nitrite ion or oxygen,[9,10] and these recent results of the cyanide complexes are of

significance to our observations on the effects of adding different excited state quenchers to aqueous solutions of $Pt_2(pop)_4^{4-}$.

RESULTS AND DISCUSSION

The emission intensity from concentrated aqueous solutions of $Pt(CN)_4^{2-}$ is efficiently quenched by added oxygen. For the complex $Pt_2(pop)_4^{4-}$, however, the presence of added oxygen in aqueous solutions causes only partial quenching of the phosphorescence since such solutions exhibit emission at 517 nm for several hours even under such experimental conditions.[2] Evidence from ^{31}P NMR spectroscopy confirms that the final quenched solution contains the monomeric complex $[Pt\{OP(OH)_2\}_4H_2]$, which has been formed by hydrolytic cleavage of the pop ligand.[11] The difference in quenching efficiency of dissolved oxygen toward $Pt_2(pop)_4^{4-}$ and $Pt(CN)_4^{2-}$ is possibly a consequence of the sterically crowded hydrophilic ligands in $Pt_2(pop)_4^{4-}$. These hydrophilic P-bonded $P_2O_5H_2^{2-}$ ligating groups will undergo hydrogen bonding of the peripheral hydroxyl groups to water, resulting in the molecule creating a hydration sphere cage about the ligand surface. Such a hydration cage can therefore effectively prevent dissolved oxygen molecules from penetrating sufficiently close to the platinum(II) ions to efficiently quench the 514 nm emission from the metal centred excited state.

---

*Author to whom correspondence should be addressed.

Addition of Cl_2, Br_2, I_2, CH_3I and NO_2 causes immediate loss of emission intensity. These compounds undergo an oxidative addition reaction to form binuclear platinum(III) complexes $[Pt_2(pop)_4XY]^{4-}$ ($X = CH_3$, $Y = I$, $X = Y = Cl$, Br, I, NO_2) which now have the filled $d\sigma$ level (rather than $d\sigma^*$) as the HOMO.[7] More significantly, rapid emission quenching is caused by the addition of sulphur dioxide to an aqueous solution of $Pt_2(pop)_4^{4-}$. This quenching is reversible since either dilution or passage of nitrogen gas through the solution causes the 514 emission intensity of $Pt_2(pop)_4^{4-}$ to be recovered (equation 1). The yellow solution which results from the quenching addition of SO_2 retains

$$Pt_2(pop)_4^{4-} + 2SO_2 \rightarrow Pt_2(pop)_4(SO_2)_2^{4-} \qquad (1)$$
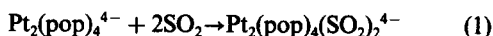
platinum in the divalent binuclear state of $Pt_2(pop)_4^{4-}$. The solution structure of this adduct shows a second-order pattern in the ^{31}P NMR spectrum centred at δ 65.01 [$^1J(PtP) = 3043$ Hz]. This chemical shift position is close to that found for $Pt_2(pop)_4^{4-}$, and $^1J(PtP)$ is in the 3000 Hz range for Pt(II)–Pt(II) complexes, rather than in the 2000 Hz range for Pt(III)–Pt(III) compounds.[11] The observation of a single ^{31}P NMR line confirms that substitution has occurred in an axial position. The Raman spectrum of the quenched SO_2 solution shows a band at 111 cm^{-1} which is principally due to ν(Pt–Pt).[6] This frequency represents a shift of 5 cm^{-1} from the position of the same stretch in pure $Pt_2(pop)_4$.[4–6] Since the value of $^1J(PtP)$ in the ^{31}P NMR spectrum indicates little difference in bonding for the $Pt_2(pop)_4^{4-}$ ion between the free and the SO_2 quenched state, it is likely that this shift to lower energy in ν(Pt–Pt) in the presence of SO_2 is due to mass rather than bonding effects. The aqueous solution Raman spectrum of $Pt_2(pop)_4^{4-}$ in the presence of SO_2 also shows an absorption at 220 cm^{-1}, along with a shoulder at 250 cm^{-1}. This band at 220 cm^{-1} is in the expected region for S bonded to platinum(II), and is likely due to ν(Pt–S) in $Pt_2(pop)_4(SO_2)_2^{4-}$. The high energy region of the Raman spectrum of an SO_2 saturated aqueous solution shows a strong broad band at 1112 cm^{-1}, along with a sharp band at 1148 cm^{-1}. The band at 1112 cm^{-1} is due to the symmetric S–O stretch of the coordinated SO_2 molecule, and the band at 1148 cm^{-1} is the symmetric stretch for the free dissolved SO_2 in solution.[12] A recent compilation of vibrational data on metal complexed SO_2 has correlated the position of ν(SO) with its geometric coordination mode. Since our observed Raman band for the symmetric SO stretch is at 1112 cm^{-1} this identifies the compound as a η^1–SO_2 complex.[13] In a recent article[14] investigating the complexation of sulphite ion to the axial positions in $[Rh_2(OCOCH_3)_4]$, the bands due to the symmetric SO stretch are found at 1000 cm^{-1} and 933 cm^{-1}. Since these bands are much lower in energy than our 1112 cm^{-1} band, we can assume that sulphur dioxide and not sulphite ion is bonded to platinum(II) in the $Pt_2(pop)_4^{4-}$ ion. We believe that this complex $Pt_2(pop)_4(SO_2)_2^{4-}$ represents the first example of an SO_2 adduct with platinum in its divalent state.

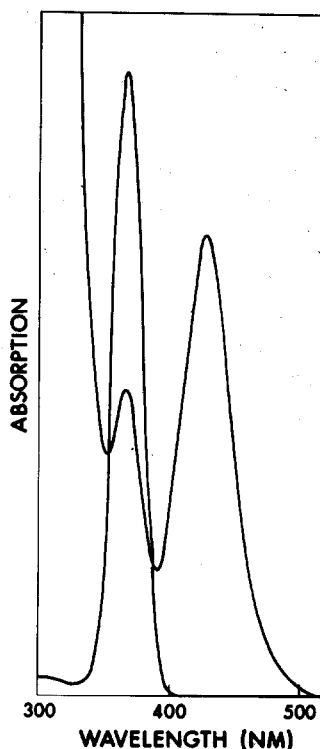Significant changes are also observed in the electronic

Fig. 1. Electronic spectrum of an aqueous solution of $Pt_2(pop)_4^{4-}$ saturated with sulphur dioxide.

spectrum of $Pt_2(pop)_4^{4-}$ upon addition of SO_2 to an aqueous solution of the complex. The most noticeable change is the decrease in intensity of the 367 nm absorption band ($^1A_{1g} \rightarrow {}^1A_{2u}$). Since this transition results from electron transfer between metal centred orbitals,[4,5] its observed intensity change is further supportive of the premise that the binding of SO_2 to $Pt_2(pop)_4^{4-}$ is by coordination to platinum(II), rather than by association with the peripheral hydroxylic groups of the pop ligand. In Fig. 1 we show the experimental electronic spectral data obtained on saturating a $2.81(5) \times 10^{-5}$ M solution of $Pt_2(pop)_4^{4-}$ with sulphur dioxide. It is apparent from these data that a new chromophore at 428.5 nm replaces the absorption at 367 nm. Assuming a concentration of 1.64 M for aqueous SO_2 at 20°C,[15] and subtracting the absorbance at 367 nm due to the tail from the SO_2 chromophore,[16,17] we find an equilibrium constant (at 20°C) of 1.74 M^{2}l^{-2} for the formation of $Pt_2(pop)_4(SO_2)_2^{4-}$ (eqn 1). From this derived concentration of 1.7×10^{-5} M for $Pt_2(pop)_4(SO_2)_2^{4-}$, we obtain a value of 4.1×10^4 for the extinction coefficient of the absorption band at 428.5 nm due to the SO_2 adduct. From this value of ϵ it is apparent that this band is due to a charge transfer transition. The band may be a Pt(II)$\rightarrow$$SO_2$ MLCT transition,[18] but since the extinction coefficient is very close to that of the $^1A_{2u} \leftarrow {}^1A_{1g}$ transition in $Pt_2(pop)_4^{4-}$, it is probably this same transition red shifted in the SO_2 adduct. From the solution equilibrium constant for SO_2 binding it is apparent that the solutions contains significant quantities of uncomplexed
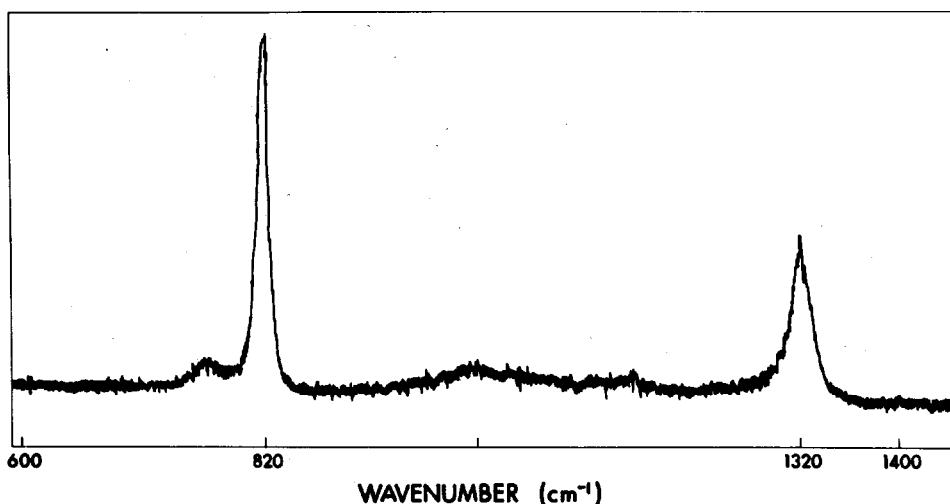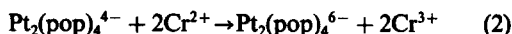
Fig. 2. Raman spectrum of the NO_2 modes in $Pt_2(pop)_4(NO_2)_2{}^{4-}$.

$Pt_2(pop)_4{}^{4-}$, yet the emission from this ion is completely quenched. From earlier studies it is known that SO_2 can be an excited state quencher for anthracene at rates approaching diffusion control,[19,20] and it is probable that such quenching of $Pt_2(pop)_4{}^{4-}$ by SO_2 is occurring in this case.

For structural purposes it is informative to compare the Raman spectrum of this SO_2 adduct of $Pt_2(pop)_4{}^{4-}$ with that of the binuclear platinum(III) complex $Pt_2(pop)_4(NO_2)_2{}^{4-}$. This compound with doubly N-bonded nitro ligands[21] shows $v(Pt–Pt)$ at $151\ cm^{-1}$ and $v(Pt–N)$ at $267\ cm^{-1}$. The high energy region of the solution Raman spectrum shows strong absorption bands at $820\ cm^{-1}$ and $1320\ cm^{-1}$ for the symmetric NO_2 bend and stretch respectively (Fig. 2). These bands are in the correct region for an N-bonded nitro complex.[22] By comparison these symmetric bands in uncoordinated nitrite ion are found at 829 and $1325\ cm^{-1}$.[23] This small shift from free nitrite ion, along with the low energy of the $v(Pt–N)$ band, indicates that the nitro ligand is weakly bonded. Thus the NO_2 and SO_2 ligands bind respectively to binuclear platinum(III) and platinum(II) by weak coordination through the central N or S atom.

Addition of chromous ion to $Pt_2(pop)_4{}^{4-}$ results in quenching of the emission at 514 nm. Addition of $Cr(H_2O)_6{}^{2+}$ to a solution of $Pt_2(pop)_4{}^{4-}$ sealed under oxygen free conditions results in evolution of hydrogen and a decrease in the absorption band due to $Pt_2(pop)_4{}^{4-}$ at 367 nm. The hydrogen evolution is probably caused by chromous reduction of water induced by pH lowering in the solution upon addition of $Pt_2(pop)_4{}^{4-}$. Concomitantly with the decrease in intensity of the 367 nm band, three new bands at 373 nm ($\epsilon = 9.6 \times 10^3$), 413 nm ($\epsilon = 1.0 \times 10^4$), and 459 nm ($\epsilon = 1.3 \times 10^4$) appear in the spectrum (Fig. 3). Quantitative spectrophotometric titration of $Pt_2(pop)_4{}^{4-}$ with chromous ion under carefully controlled oxygen free conditions shows a stoichiometry of 1:2 for formation of $Cr(H_2O)_6{}^{3+}$. Thus $Pt_2(pop)_4{}^{4-}$ undergoes a 2-electron reduction

$$Pt_2(pop)_4{}^{4-} + 2Cr^{2+} \rightarrow Pt_2(pop)_4{}^{6-} + 2Cr^{3+} \qquad (2)$$

with chromous ion (eqn 2). Assuming these electrons enter the $A_{2u}(6p_z)$ LUMO state of $Pt_2(pop)_4{}^{4-}$, the appearance of new absorbances in the electronic spectrum is due to transitions into the higher manifold of states from this new ground state.[4,5] Changes in the aqueous solution Raman spectrum of $Pt_2(pop)_4{}^{4-}$ are also ob-
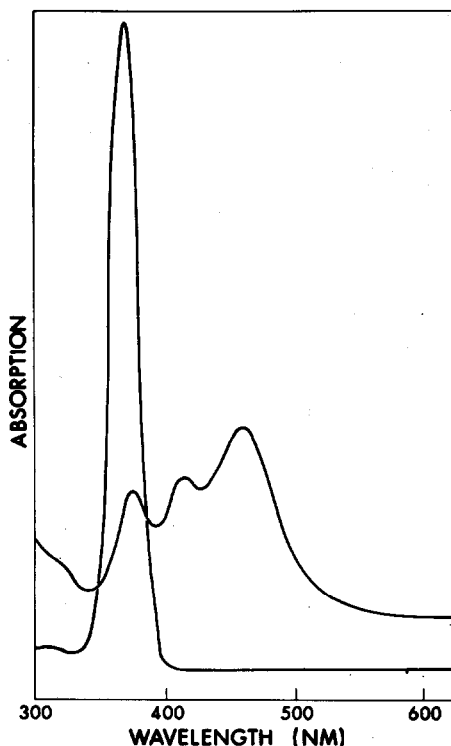

Fig. 3. Electronic spectrum of an aqueous solution of $Pt_2(pop)_4{}^{4-}$ with added excess $Cr(H_2O)_6{}^{2+}$.

served upon addition of chromous ion. The observation of Stokes and anti-Stokes lines at 106 cm^{-1} represents a 10 cm^{-1} lowering of frequency from v(Pt–Pt) in Pt$_2$(pop)$_4^{4-}$, indicative of the electrons being transferred into the metal centred molecular orbitals.[6] Assuming no change in hydration at the axial position, we tentatively conclude that the platinum (6p_z) orbital has some small antibonding character with respect to intermetallic bonding.

Addition of compounds other than SO$_2$ and 1,1-bis(2-sulphoethyl)-4,4'-bipyridinum inner salt[5] will cause emission quenching of Pt$_2$(pop)$_4^{4-}$. Thus addition to Pt$_2$(pop)$_4^{4-}$ of hydroquinone, pyrogallol and carbon disulphide causes a loss of phosphorescence in solution, and the appearance of a Raman band (Pt–Pt) in the 113–114 cm^{-1} region. Addition of simple alcohols, glycols or oxalic acid does not result in emission quenching.

EXPERIMENTAL

The complex K$_4$[Pt$_2$(pop)$_4$]·2H$_2$O was prepared by published procedures.[1,3,5,24] Electronic spectra were measured on a Cary 219 spectrophotometer as aqueous solutions in 1 cm quartz cells. Raman spectra were measured on a Ramanor instrument using an argon ion 554 Control laser. Samples were prepared as aqueous solutions. ^{31}P NMR spectra were measured on a Nicolet wide bore spectrometer operating at 80.98 MHz. Chemical shifts are referenced to high frequency of 85% H$_3$PO$_4$.

Chromous ion reductions were carried out under oxygen free conditions in a Vacuum Atmosphere drybox. Spectral intensity data were obtained on a Bausch and Lamb Model 20 visible spectrophotometer operating in the drybox. Solutions of chromous ion were prepared by the zinc amalgam reduction of chromium trioxide. Quantitative estimations of the reduction reaction were made by measuring the intensity increase of the 417 nm chromium(III) chromophore.

REFERENCES

1. R. P. Sperline, M. K. Dickson and D. M. Roundhill, *J. Chem. Soc., Chem. Commun.* 1977, 62.
2. M. K. Dickson, S. K. Pettee and D. M. Roundhill, *Anal. Chem.* 1981, **53**, 2159.
3. M. A. Filomena Dos Remedios Pinto, P. J. Sadler, S. Neidle, M. R. Sanderson and A. Subbiah, *J. Chem. Soc., Chem. Commun.* 1980, 13.
4. W. A. Fordyce, J. G. Brummer and G. A. Crosby, *J. Am. Chem. Soc.* 1981, **103**, 7061.
5. C. M. Che, L. G. Butler and H. B. Gray, *J. Am. Chem. Soc.* 1981, **103**, 7796.
6. P. Stein, M. K. Dickson and D. M. Roundhill, *J. Am. Chem. Soc.* 1983, **105**, 3489.
7. C. M. Che, W. P. Schaefer, H. B. Gray, M. K. Dickson, P. B. Stein and D. M. Roundhill, *J. Am. Chem. Soc.* 1982, **104**, 4253.
8. M. K. Dickson, W. A. Fordyce, D. M. Appel, K. Alexander, P. Stein and D. M. Roundhill, *Inorg. Chem.* 1982, **21**, 3857.
9. J. W. Schindler, R. C. Fukuda and A. W. Adamson, *J. Am. Chem. Soc.* 1982, **104**, 3596.
10. J. W. Schindler and A. W. Adamson, *Inorg. Chem.* 1982, **21**, 4236.
11. M. K. Dickson, Ph.D. Thesis, Washington State University, 1982.
12. E. R. Lippincott and F. E. Walsh, *Spectrochim. Acta* 1961, **17**, 123.
13. R. R. Ryan, G. J. Kubas, D. C. Moody and P. G. Eller, *Structure and Bonding* 1981, **46**, 47.
14. I. B. Baranovskii, S. S. Abdullaev, G. Ya. Mazo and R. N. Schchelokov, *Russ. J. Inorg. Chem.* 1982, **27**, 305.
15. W. B. Van Arsdel, *International Critical Tables*, Vol. III, p. 302. National Research Council (1928).
16. C. S. Garrett, *J. Chem. Soc.* 1915, **107**, 1324.
17. F. H. Getman, *J. Phys. Chem.* 1926, **30**, 266.
18. D. M. P. Mingos, *Transition Met. Chem.* 1978, **3**, 1.
19. R. Forizoone, *Meded. Vlaam. Chem. Ver.* 1971, **33**, 121; *Chem. Abstr.* 1972, **76**, 29284a.
20. E. J. Bowen and W. S. Metcalf, *Proc. Roy. Soc.* 1951, **206A**, 437.
21. M. D. Walkinshaw, personal communication.
22. K. Nakamoto, J. Fujita and H. Murata, *J. Am. Chem. Soc.* 1958, **80**, 4817.
23. J. W. Sidman, *J. Am. Chem. Soc.* 1957, **76**, 1675.
24. K. A. Alexander, S. A. Bryan, M. K. Dickson, D. Hedden and D. M. Roundhill, *Inorg. Synth.*, submitted for publication.

NOTE

A ^{35}Cl NUCLEAR QUADRUPOLE RESONANCE STUDY OF NH$_4$ICl$_4$·H$_2$O

K. B. DILLON* and J. LINCOLN

Chemistry Department, University of Durham, South Road, Durham DH1 3LE, England

Abstract—The "missing" fourth ^{35}Cl NQR frequency postulated for NH$_4$ICl$_4$·H$_2$O at room temperature has been observed. Four signals were also found for this compound at 195K, but the results at 77K were less clear-cut, with either five or (probably) six resonances detected. The occurrence of a phase transition between 77 and 195K seems likely. A structure is suggested for the ICl$_4$$^-$ ion at room temperature from the relationship found previously between NQR frequency and bond length in tetrachloroiodates.

Several ^{35}Cl NQR frequences have been reported for salts containing the ICl$_4$$^-$ ion,[1,2] and although the spread of frequencies for this ion in any one compound may be large (>13 MHz for form I SCl$_3$$^+ICl_4$$^-$ at 77K[2]), reflecting distortion of the anion from D$_{4h}$ symmetry, the average frequency is remarkably constant.[1] Thus for fourteen sets of data at room temperature the average frequency is 22.337 (ESD 0.090) MHz.[1] The only apparent exception was NH$_4$ICl$_4$·H$_2$O, for which three signals at 27.96, 24.68 and 19.98 (average 24.21) MHz at room temperature have been observed.[3] It was suggested by Dillon and Waddington from comparison with the results for KICl$_4$·H$_2$O[4] that a fourth line at lower frequency might not have been detected for NH$_4$ICl$_4$·H$_2$O, and its frequency was predicted as 16.7 ± 0.4 MHz.[1] We have now observed this "missing" resonance, and also report ^{35}Cl NQR data for the compound at 195 and 77K.

NH$_4$ICl$_4$·H$_2$O was prepared in a similar way to the literature method.[3] NH$_4$Cl was treated with iodine in concentrated aqueous HCl, and the product (NH$_4$ICl$_2$) then chlorinated *in situ*. Nitrogen was blown over the solution to reduce the volume, and orange crystals were precipitated. These were filtered off and dried by suction. ^{35}Cl NQR spectra were recorded as described previously.[5]

At room temperature four equally intense ^{35}Cl NQR signals were observed for the title compound, at 27.960, 24.675, 19.930 and 17.190 MHz. The first three values are in very good agreement with the previous report,[3] and the fourth resonance is the "missing" frequency. It lies just outside the predicted range of 16.7 ± 0.4 MHz, but the average frequency at room temperature of 22.439 MHz is still very close to the average over fourteen sets of data.[1] Four signals were also found at 195K, at 28.025, 24.850, 19.995 and 17.455 MHz (average 22.581 MHz); a weaker resonance at 19.575 MHz was assigned to the ^{37}Cl counterpart of the signal at

24.850 MHz (calculated[6] ^{37}Cl frequency 19.585 MHz). The whole frequency range was not scanned, but just the areas where signals might reasonably be expected by comparison with the room temperature results, hence the other ^{37}Cl signals were not investigated.

The data at 77K were more ambiguous; the two signals at highest frequency occurred at 28.060 and 25.105 MHz, but the lowest frequency signal was split into two components, at 17.827 and 17.743 MHz. The intermediate signal was probably also split, with frequencies measured at 19.953 and 19.850 MHz, but the possibility of overlap with the ^{37}Cl resonance corresponding to the ^{35}Cl signal at 25.105 MHz (calculated[6] value 19.786 MHz) cannot be entirely discounted. The results suggest strongly that a phase transition occurs between 77 and 195K. The average frequency at 77K, on the assumption that both lower frequency signals are split, is 22.713 MHz, in excellent agreement with the average value from sixteen sets of data at this temperature of 22.634 (ESD 0.130) MHz.[1]

The results also indicate that NH$_4$ICl$_4$·H$_2$O may be isostructural at room temperature with KICl$_4$·H$_2$O, the crystal structure of which has been determined;[7] it shows four different I–Cl bond lengths of 2.42, 2.47, 2.53 and 2.60 (ESD 0.01)Å. From the relationship found previously between ^{35}Cl NQR frequency and bond length at room temperature,[1] the ICl$_4$$^-$ ion in NH$_4$ICl$_4$·H$_2$O may be similarly distorted, with bond lengths of 2.43, 2.47$_5$, 2.54$_5$ and 2.58$_5$ (± 0.01)Å and the longest bond *trans* to the shortest one, as in KICl$_4$·H$_2$O.

The observation of the fourth signal, and the close similarity of the average frequency for the ICl$_4$$^-$ ion in NH$_4$ICl$_4$·H$_2$O to literature values both at room temperature and 77K,[1] lend some confidence to predictions of NQR frequencies based on these averages for other tetrachloroiodates where not all the resonances may have been detected. More crystal structure deter-

minations are required before the relationship[1] between bond length and NQR frequency can be confirmed, but deductions of structure and distortion from D_{4h} symmetry derived from NQR measurements may be particularly useful where the compounds cannot readily be obtained in crystalline form.

REFERENCES

1. K. B. Dillon and T. C. Waddington, *Inorg. Nucl. Chem. Lett.* 1978, **14**, 415, and references therein.
2. A. Finch, P. N. Gates, T. H. Page, K. B. Dillon and T. C. Waddington, *J. Chem. Soc. Dalton* 1980, 2401.
3. Y. Kurita, D. Nakamura and N. Nayakawa, *J. Chem. Soc. Jpn, Pure Chem. Sec.* 1958, **79**, 1093.
4. B. O. Cozzini, *Diss. Abs. B* 1966, **27**, 1850.
5. K. B. Dillon, R. J. Lynch and T. C. Waddington, *J. Chem. Soc. Dalton* 1976, 1478.
6. *Decca N.Q.R. Spectrometer Handbook*. Decca Radar Ltd., Instrument Division, Walton-on-Thames (1973).
7. R. J. Elema, J. L. de Boer and A. Vos, *Acta Cryst.* 1963, **16**, 243.

NOTE

THE WEISS CONSTANT: A PROBE FOR THE MOLECULAR PACKING OF MONOMERIC COPPER(II) COMPLEXES?

M. R. SUNDBERG*, R. UGGLA, T. BÖÖK† and I. KALKKU‡

University of Helsinki, Department of Inorganic Chemistry, SF-00100 Helsinki, Finland

Abstract—Magnetic properties of the complexes $Cu(pn)_2WO_4 \cdot 1.8H_2O$, $Cu(pn)_2I_2$, $Cu(pn)_2Br_2 \cdot 1.6H_2O$ and $Cu(pn)_2Cr_2O_7$ (pn = 1,2-diaminopropane) have been studied by ESR, magnetic balance (Gouy method) and PA techniques. Curie constants C were obtained from ESR spectra, temperature independent paramagnetism $N\alpha$ from PA spectra, and Weiss constants θ from magnetic susceptibility data. Isotropic factors r were calculated, describing reduction of the orbital angular momentum and the spin–orbit coupling constant from their free-ion values. From the measured crystal g values we conclude that there is axial elongation in all the coordination polyhedra, corresponding to the ground state $d_{x^2-y^2}$. The different line shapes in the ESR spectra depend on the alignment of the pseudo-tetragonal axes, induced by the counterion. The counterions have a clear effect on both the magnetic parameters and the reduction factors. The alignment of the pseudo-tetragonal axes is also reflected in the value of the Weiss constant. A correlation is proposed between the Weiss constant and molecular packing.

ESR has been proved effective for investigating the bonding and stereochemistry in copper(II) complexes.[1] In many cases the stereochemistry can be concluded from the line shape of the ESR spectrum and the calculated g factors.[2] Because of the symmetry of the pn molecule the ESR spectrum will exhibit three g values, corresponding to the symmetry D_{2h}, unless there is more than one set of crystallographically equivalent coordination polyhedra, in which case the number of g values may be less. The lineshape of the spectrum will vary owing to interaction of the copper(II) ions.[2]

Monomeric copper(II) complexes usually obey the Curie–Weiss law

$$\chi_M^{corr} = \frac{C}{T - \theta} + N\alpha \qquad (1)$$

where χ_M^{corr} is the diamagnetically corrected molar susceptibility. The Curie constant C can be defined as[3]

$$C = Ng_{iso}^2\mu_B^2/4k. \qquad (2)$$

The Weiss constant θ represents the splitting of the ground state levels in zero-field.[4] The term due to the temperature independent paramagnetism $N\alpha$ can be calculated from the expression[5]

$$N\alpha = 4N\mu_B^2/\Delta E \qquad (3)$$

where ΔE is the energy difference between the ground state and the excited state.

The calculated effective magnetic moment for mononuclear copper(II) complexes is given by the spin-only value $\mu_{s.o.}$ of 1.73 B.M. The experimental values lie appreciably above this value, owing to mixing-in of some orbital angular momentum from the excited state via spin–orbit coupling[2]

$$\mu_{eff} = \left(1 - \frac{2r^2\lambda}{\Delta E}\right)\mu_{s.o.}. \qquad (4)$$

The parameter r describes the reduction of the orbital angular momentum and the spin–orbit coupling constant from their free-ion values to their values in the actual copper(II) complex. It is influenced by such factors as covalent bonding and electron delocalization from the ligand atom to the copper(II) ion.

According to an earlier study the compounds $Cu(pn)_2I_2$, $Cu(pn)_2Cr_2O_7$ and $Cu(pn)_2Br_2 \times 1.6H_2O$ are mononuclear and centrosymmetric.[6] Of the fourth compound, $Cu(pn)_2WO_4 \times 1.8H_2O$, only the cell dimensions are known.[7] The purpose of the present study was to

*Author to whom correspondence should be addressed.

†Present address: Paraisten Kalkki Oy, Research Institute, 21600 Parainen, Finland.

‡Present address: Helsingin Suomalainen Yhteiskoulu, SF-00300 Helsinki, Finland.

investigate the influence of the counterion on the magnetic parameters and to gather data for elucidation of the possible correlation between structural and magnetic properties.

EXPERIMENTAL

The preparation and analysis of the compounds have been reported earlier.[7-10] The ESR spectra of the powdered samples were obtained at room temperature with a Varian E3 spectrometer. The external magnetic field was 3240 G (1 G = 1 × 10^{-4} T) and scan range ± 500 G. 2,2,6,6-Tetramethylpiperidin-1-oxyl was used as calibrant with 2.0055 as splitting factor.[11] The microwave frequency was 9245 MHz and it was measured with a Hewlett–Packard 5245 L electronic counter equipped with a 5255 A frequency converter.

The magnetic susceptibilities were obtained with a Newport Variable-Temperature Gouy Balance. The measurements were carried out in the temperature range 93–303 K in a nitrogen atmosphere. Copper(II) sulphate pentahydrate served as standard.[12] Diamagnetic corrections were applied using Pascal's constants.[13] The effective magnetic moments were calculated with the usual equation $\mu_{eff} = 2.83\sqrt{(\chi_M^{corr} - N\alpha)T}$. The Weiss constants were calculated using standard least squares fit.

The PA spectra of the powdered samples were obtained at room temperature with an EDT OAS 400 spectrometer.

RESULTS AND DISCUSSION

The ESR spectra are shown in Fig. 1 and the corresponding g values in Table 1. Because of the asymmetry of the ligand the symmetry around copper(II) in the CuN$_4$ plane is rhombic. Thus the ESR spectrum will have three g values, providing that the pseudo-tetragonal axes are aligned. Cu(pn)$_2$WO$_4$ × 1.8H$_2$O ex-

Table 1. The observed g values

Compound	g_1	$g_\parallel$	g_2	$g_3(g_\perp)$	g_{iso}
Cu(pn)$_2$WO$_4$·1.8H$_2$O	2.050		2.062	2.174	2.095
Cu(pn)$_2$I$_2$		2.196		2.050	2.099
Cu(pn)$_2$Br$_2$·1.6H$_2$O	2.137		2.049		2.078
Cu(pn)$_2$Cr$_2$O$_7$					2.063

hibits a typical spectrum of this kind. If the rhombic distortion is very small the powder technique will not be sufficiently sensitive to resolve the two planar components. This is the case for Cu(pn)$_2$I$_2$ where the space group is triclinic and the pseudo-tetragonal axes must be parallel.[10] This type of line-shape will also be generated by complexes exhibiting a slight misalignment of the pseudo-tetragonal axes. As the misalignment of the axes proceeds further, the spectrum will begin to look like that of Cu(pn)$_2$Br$_2$ × 1.6H$_2$O. The ultimate misalignment generates an isotropic spectrum, as is approximately the case for Cu(pn)$_2$Cr$_2$O$_7$. The angle between the pseudo-tetragonal axes can be calculated as 59° from the known structure of the complex. Although the obtained g values are not molecular but crystal ones, there is one common feature for all compounds: the lowest g value is almost constant at 2.05. The variation of the counterion causes changes in the packing of the molecules, which are reflected in the different line shapes of the ESR spectra. Because the lowest g values are all > 2.04, the complexes must be axially elongated and have the ground state $d_{x^2-y^2}$.[2]

The calculated magnetic susceptibilities and magnetic moments are shown in Table 2. The values obtained are typical of mononuclear copper(II) complexes. To calculate the Weiss constants, the respective Curie constants and $N\alpha$ values were obtained from eqns (2) and (3). The
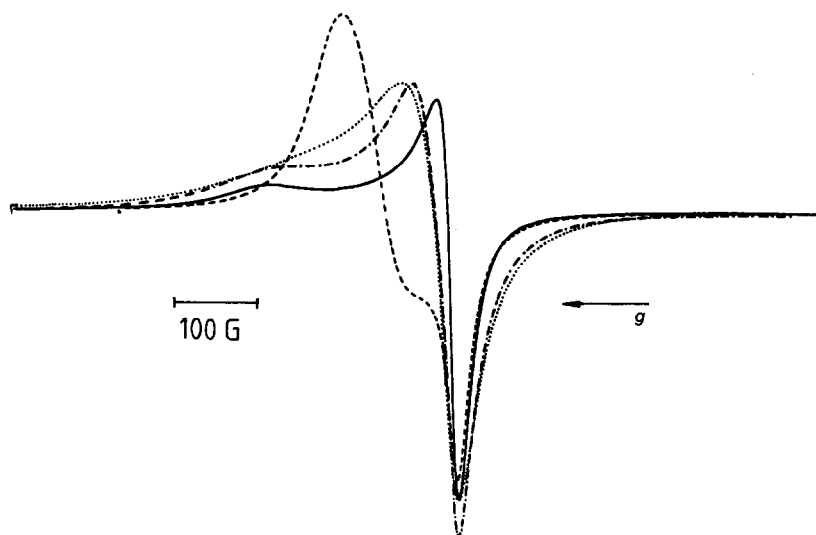

Fig. 1. The ESR spectra of the powdered samples of Cu(pn)$_2$WO$_4$ × 1.8H$_2$O (–·–·–·–), Cu(pn)$_2$I$_2$ (———), Cu(pn)$_2$Br2 × 1.6H$_2$O (------) and Cu(pn)$_2$Cr$_2$O$_7$ (·····). The lineshape corresponding to three g values of Cu(pn)$_2$WO$_4$ × 1.8H$_2$O can be seen, if the spectrum is broadened.

Table 2. The magnetic susceptibilities and the magnetic moments (B.M.)

T/K	$Cu(pn)_2WO_4 \cdot 1.8H_2O$		$Cu(pn)_2I_2$		$Cu(pn)_2Br_2 \cdot 1.6H_2O$		$Cu(pn)_2Cr_2O_7$	
	$\chi_M^{corr} \cdot 10^6$	μ_{eff}	$\chi_M^{corr} \cdot 10^6$	μ_{eff}	$\chi_M^{corr} \cdot 10^6$	μ_{eff}	$\chi_M^{corr} \cdot 10^6$	μ_{eff}
93.2	4256	1.78	4380	1.81	4550	1.84	4618	1.86
123.2	3260	1.79	3333	1.81	3463	1.85	3533	1.87
153.2	2625	1.79	2675	1.81	2817	1.86	2891	1.88
183.2	2227	1.81	2275	1.83	2398	1.88	2465	1.90
213.2	1915	1.81	1966	1.83	2109	1.90	2152	1.92
243.2	1712	1.83	1729	1.84	1859	1.90	1919	1.93
273.2	1502	1.82	1523	1.83	1638	1.89	1699	1.93
293.2	1407	1.82	1418	1.83	1550	1.91	1596	1.94
303.2	1377	1.83	1395	1.84	1553	1.94	1562	1.95

Table 3. ΔE values obtained from PA spectra with the calculated magnetic parameters and reduction factors. The r value for $Cu(pn)_2Cr_2O_7$ is unreasonable since the maximum possible value for r is 1.00. The error arises from the uncertainty of the location of the d–d transition due to charge transitions of dichromate ions. Accordingly the corresponding $N\alpha$ value has been calculated by giving the value 60×10^{-6} to Cu(II) and 74×10^{-6} to Cr(VI)

	ν_{max}/nm	μ_{eff}	C	θ	r	$N\alpha \cdot 10^6$
$Cu(pn)_2WO_4 \cdot 1.8H_2O$	570	1.82	0.412	5.7(5)	0.74	60
$Cu(pn)_2I_2$	540	1.83	0.413	2.7(3)	0.80	56
$Cu(pn)_2Br_2 \cdot 1.6H_2O$	555	1.91	0.405	-5.0(10)	1.00	58
$Cu(pn)_2Cr_2O_7$	490[a]	1.94	0.399	-3.4(5)	1.15	208

[a] very broad

required g_{iso} and ΔE values are listed in Tables 1 and 3, respectively, and the magnetic parameters together with the calculated reduction factors (eqn 4) are shown in Table 3. From the results we can readily see that the counterion has a marked influence on the magnetic parameters. There also seems to be a correlation between the covalency of the Cu–L bond and the magnetic properties.

The Weiss constants obtained display a general correlation with the ESR results describing the misalignment (or alignment) of the pseudo-tetragonal axes. The negative values indicate antiferromagnetic interactions in which the magnetic moments (or spins) of the individual centres tend to align themselves antiparallel to one another. In ferromagnetic systems the opposite is true.

Our results encourage us to believe that a mathematical correlation could be established between the Weiss constant and the copper–copper distance and the angle between the magnetic axes.

REFERENCES

1. See, e.g. B. Hathaway, M. Duggan, A. Murphy, J. Mullane, C. Power, A. Walsh and B. Walsh, *Coord. Chem. Rev.* 1981, 36, 267.
2. B. Hathaway and D. E. Billing, *Coord. Chem. Rev.* 1970, 5, 143.
3. R. L. Carlin and A. J. van Duyneveldt, *Magnetic Properties of Transition Metal Compounds*, p. 7. Springer-Verlag, New York (1977).
4. *Ibid*, p. 15.
5. A. Earnshaw, *Introduction to Magnetochemistry*, p. 67. Academic Press, London (1968).
6. R. Uggla, S. Lundell and P. Väänänen, *Suomen Kemistil.* 1968, B41, 250.
7. R. Uggla, S. Lundell and E. Björklund, *Suomen Kemistil.* 1969, B42, 176.
8. R. Uggla, L. Lemmetti, S. Lundell and M. Juvani, *Suomen Kemistil.* 1968, B41, 63.
9. R. Uggla and S. Lundell, *Suomen Kemistil.* 1968, B41, 73.
10. R. Uggla, L. Lemmetti, S. Lundell and M. Juvani, *Suomen Kemistil.* 1968, B41, 134.
11. R. Briére, H. Lamaire and A. Rassat, *Bull. Soc. Chem. France* 1965, 3281.
12. B. N. Figgis and R. S. Nyholm, *J. Chem. Soc.* 1959, 331.
13. P. W. Selwood, *Magnetochemistry*, pp. 78, 92. Interscience, New York (1956).
14. R. Uggla, J. Visti, M. Klinga and M. Näsäkkälä, *Suomen Kemistil.* 1970, B43, 488.

COMMUNICATION

THE REPORTED ION Fe₃S₂(NO)₅⁻: A RE-INVESTIGATION

ANTHONY R. BUTLER, CHRISTOPHER GLIDEWELL,* ANDREW R. HYDE
and JOSEPH McGINNIS

Chemistry Department, University of St. Andrews, St. Andrews, Fife KY16 9ST, Scotland

Abstract—Salts reported to contain the iron–sulphur cluster nitrosyl anion $Fe_3S_2(NO)_5^-$ are shown to be identical with those containing the well-known anion $Fe_4S_3(NO)_7^-$.

The anions $Fe_4S_3(NO)_7^-$ and $Fe_2S_2(NO)_4^{-2}$, which occur in the black and red Roussin salts,[1] are structurally related to the 4-Fe and 2-Fe iron–sulphur clusters of natural occurrence. The reported synthesis[2] of a third such anion $Fe_3S_2(NO)_5^-$ is therefore of considerable chemical interest, as the number of naturally occurring 3-Fe species is small: in addition, the salts of this anion are reported to have a number of interesting spectroscopic properties, which would repay further study.

We report here that all our attempts to repeat the preparation of salts of the 3-Fe anion $Fe_3S_2(NO)_5^-$ using the published procedure[2] yield instead the corresponding salts of the known and very stable 4-Fe anion $Fe_4S_3(NO)_7^-$.

---

*Author to whom correspondence should be addressed.

Upon following the literature method, we have repeatedly obtained black crystals, as reported, of the ammonium, sodium, and potassium salts, and additionally of the tetraphenylarsonium salt also. As judged by their electronic spectra (Table 1) these salts all contain the same chromophore: these spectra moreover are indistinguishable from those of the corresponding salts of $Fe_4S_3(NO)_7^-$. Using the tetraphenylarsonium salt as the preferred analysable form, microanalysis (Table 1) demonstrated clearly that this salt was $Ph_4As^+Fe_4S_3(NO)_7^-$, rather than $Ph_4As^+Fe_3S_2(NO)_5^-$, and hence that all the salts contained the anion $Fe_4S_3(NO)_7^-$, rather than the reported anion $Fe_3S_2(NO)_5^-$.

One plausible formulation of the anion $Fe_3S_2(NO)_5^-$ can be derived, by loss of NO^+, from the as yet unknown $Fe_3S_2(NO)_6$ (I), formally derived from the isoelectronic $Fe_3S_2(CO)_9$ (II), of known structure.[3] We

Table 1. Electronic spectra and analytical data

(i) Extinction coefficients of M^I salts (ϵ/ ℓ mol⁻¹ cm⁻¹)

| M^I	Solvent	λ/nm: 560	350	260
NH₄⁺	H₂O	2400	15400	26700
Na⁺	H₂O	2380	14400	25500
K⁺	H₂O	2460	15800	27400
	EtOH	2660	16400	28200
Ph₄As⁺	EtOH	2530	15500	29450 a

a/ Overlayed by fine structure from the Ph₄As⁺ ion.

(ii) Analytical data

	C(/%)	H(/%)	N(/%)
Found	31.54	2.19	10.59
Required for Ph₄As⁺Fe₃S₂(NO)₅⁻	37.68	2.64	9.15
Required for Ph₄As⁺Fe₄S₃(NO)₇⁻	31.57	2.21	10.74

have recently attempted the preparation of (I) by nitrosylation of (II), where the Fe_3S_2 group is already present.[4] No 3-Fe compound was obtained, but instead the sole product from a variety of procedures was the 4-Fe anion $Fe_4S_3(NO)_7{}^-$, in yields up to 80%. When very mild conditions were used, in an attempt to prevent molecular reorganisation, no nitrosylation occurred, and (II) was recovered unchanged. Thus, even when the Fe_3S_2 core is pre-formed, the only stable nitrosyl derivative is $Fe_4S_3(NO)_7{}^-$, entirely consistent with our failure to isolate any salt of the $Fe_3S_2(NO)_5{}^-$ ion.

I   II
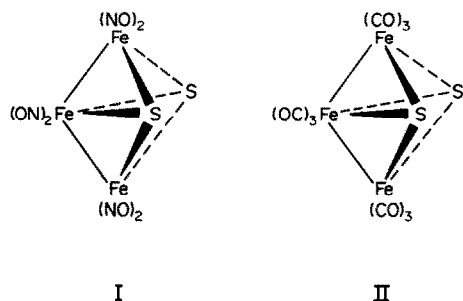
Although the anion $Fe_3S_2(NO)_5{}^-$ is an even-electron ion, it is reported[2] to give ESR spectra under a wide variety of conditions: the five-line spectrum in aqueous alkali bears a remarkable similarity to that reported[5] for the species $Fe(NO)_2{}^+$, obtained by reaction of Fe(II) salts with nitric oxide in alkaline solution. We find, in contrast, that the prepared product yields no ESR spectrum in neutral solution, but in alkaline solutions gives a spectrum characterized by coupling to a single ^{14}N nucleus, with $A_N = 5$ G. The reported spectrum[2] is hard to understand: any fragmentation, in solution, of an iron–sulphur cluster nitrosyl to yield $Fe(NO)^{x+}$ or $Fe(NO)_2{}^+$ ions must also yield S^{2-} (or SH^-), and it has been clearly demonstrated[5] that in the presence of sulphide ions, the sole paramagnetic iron nitrosyl species which can be detected by ESR contains one nitrogen atom, not two. This is consistent with our own observations, but not with those reported for the supposed $Fe_3S_2(NO)_5{}^-$ ion, and we conclude that whatever the reported ESR spectrum[1] may represent, it is not the fragmentation product of an iron–sulphur cluster nitrosyl derivative.

Finally we note that the formula weight of the supposed salt $K[Fe_3S_2(NO)_5]$ was reported to have been established by a mass spectral determination of $m/z = 420$ for M^+, corresponding closely to the ion-pair cation $[KFe_3S_2(NO)_5]^+$ (for which $m/z = 421$): we remark merely that we are unable to confirm this.

REFERENCES

1. F. Z. Roussin, *Ann. Chim. Phys.* 1858, **52**, 285.
2. M. Dymicky, *Proc. Schevchenko Sci. Soc., Section Chem. Biol. Med.* 1980, **8**, 70; *Chem. Abs.* 1982, **97**, 173870q.
3. C. H. Wei and L. F. Dahl, *Inorg. Chem.* 1965, **4**, 493.
4. A. R. Butler, C. Glidewell, A. R. Hyde, J. McGinnis, and J. E. Seymour, *Polyhedron*, 1983, **2**, 1045.
5. C. C. McDonald, W. D. Phillips, and H. F. Mower, *J. Am. Chem. Soc.* 1965, **87**, 3319.

COMMUNICATION

THE TRANSITION-METAL ASSISTED SYNTHESIS OF THE *ANTI*-OCTADECABORATE ANION [B$_{18}$H$_{21}$]$^-$ FROM THE *NIDO*-DODECAHYDRONONABORATE ANION [B$_9$H$_{12}$]$^-$

J. BOULD, N. N. GREENWOOD* and J. D. KENNEDY
Department of Inorganic and Structural Chemistry, The University of Leeds, Leeds LS2 9JT,
England

Abstract—When heated under reflux in CH$_2$Cl$_2$ solution with [Os(CO)$_3$Cl$_2$]$_2$, two *nido*-[B$_9$H$_{12}$]$^-$ units edge-fuse to form *anti*-[B$_{18}$H$_{21}$]$^-$.

Recent reports have described the use of metal centres in promoting the conjunction of both borane and carborane clusters to produce *conjuncto* linked species, i.e. those joined by one straightforward two-electron, two-centre boron–boron σ-bond. Thus the reaction of *nido*-B$_5$H$_9$ with catalytic amounts of PtBr$_2$ results in a dehydrodimerisation reaction giving [1,2-(B$_5$H$_8$)$_2$] in 92% yield[1] and the reaction of *nido*-[2,3-Me$_2$C$_2$B$_4$H$_5$]$^-$ with HgCl$_2$ yields [μ,μ'-(Me$_2$C$_2$B$_4$H$_5$)$_2$Hg] which, upon heating at 180°C, gives the *conjuncto* *nido*-carborane [5,5'-(Me$_2$C$_2$B$_4$H$_5$)$_2$)].[2] Similarly, organometallic complexes such as [(RR'C$_2$)Co$_2$(CO)$_6$] and [Ir(CO)Cl(PPh$_3$)$_2$] have been used to catalyze the addition of various alkynes to small carboranes with the formation of two-electron two-centre σ-bonded linkages.[3]

We now wish to report the first example of the use of a transition metal complex to promote the fusion of two nonaborate clusters to form a higher boron hydride cluster in which two smaller sub-clusters are linked by two common boron centres, i.e by a common polyhedral edge rather than by an intercluster *conjuncto* B–B σ-bond.

During attempts to synthesize novel polyhedral osmaboranes,[4] we have found that the reaction of [NEt$_4$] [*nido*-B$_9$H$_{12}$] (84 mg, 0.3 mmol) with [Os(CO)$_3$Cl$_2$]$_2$ (50 mg, 0.3 mmol) in refluxing CH$_2$Cl$_2$ under nitrogen (5 hr) produces a mixture which, when separated by preparative tlc (mobile phase CH$_2$Cl$_2$/MeCN, 96:4; stationary phase silica gel Fluka Type G.F. 254), gives a 20% yield (11 mg, R$_f$0.3) of [NEt$_4$][*anti*-B$_{18}$H$_{21}$] (see Fig. 1).

The product was readily identified by comparison with an authentic sample using ^{11}B NMR spectroscopy. Other compounds were present in small amounts which require

further identification although most appear to be various ionic and neutral derivatives of both the *syn* and *anti* isomers of [B$_{18}$H$_{22}$] (for the definition of *syn* and *anti* see Ref. 5).

Unfortunately the osmium complex is not catalytic in action and doubling the borane to metal ratio did not increase the yield of [B$_{18}$H$_{21}$]$^-$. This indicates that the osmium probably forms an intermediate metallaborane complex which subsequently reacts further to give the product. In this it may have some parallels to the bis(carboranyl)mercury(II) complex mentioned above which eliminates elemental mercury to form a B–B σ-linked carborane when heated. Further work is planned to find the ultimate fate of the osmium complex in the reaction reported here.

The fusion of an *arachno*-nonaborane cluster has been described previously where [B$_9$H$_{13}$(OBu$_2$)] is heated at 140°C to give the *syn* isomer of [B$_{18}$H$_{22}$] in 34% yield,[6] and the reaction reported here therefore offers a useful, if ostensibly expensive, route to the *anti*-isomer since the anion readily yields neutral *anti*-[B$_{18}$H$_{22}$] upon acidification.[7] In the general case it also demonstrates the potential of transition metal centres for promoting fusions of this and other related cluster types.

In this context it is of interest to note the recent report of the fusion of the nine-vertex compound *arachno*-[(PMe$_2$Ph)$_2$PtB$_8$H$_{12}$] in refluxing toluene to give a seventeen-vertex metallaborane [7-(PMe$_2$Ph){7-
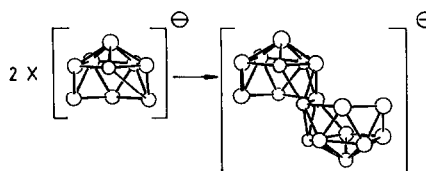

Fig. 1.

---

*Author to whom correspondence should be addressed.

$PtB_{16}H_{18}$-9'-(PMe_2Ph)}].[8] This is a further indication that transition metal centres may be able to play an increasingly important role in the fusion of nine-vertex or indeed other sized borane and metallaborane clusters to form novel macropolyhedral species.

REFERENCES

1. E. W. Corcoran, Jr. and L. G. Sneddon, *Inorg. Chem.* 1983, **22**, 182.
2. N. S. Hosmane and R. N. Grimes, *Inorg. Chem.* 1979, **18**, 2886.
3. R. Wilczynski and L. G. Sneddon, *Inorg. Chem.* 1981, **20**, 3955, and 1982, **21**, 506.
4. J. Bould, N. N. Greenwood, and J. D. Kennedy, *J. Organomet. Chem.* 1983, **249**, 11.
5. Y. M. Cheek, N. N. Greenwood, J. D. Kennedy, and W. S. McDonald, *J. Chem. Soc., Chem. Commun.* 1982, 80.
6. J. Dobson, P. C. Keller, and R. Schaeffer, *Inorg. Chem.* 1968, **7**, 399.
7. F. P. Olsen, R. C. Vasavada and M. F. Hawthorne, *J. Am. Chem. Soc.* 1968, **90**, 3946.
8. M. A. Beckett, J. E. Crook, N. N. Greenwood, J. D. Kennedy and W. S. McDonald, *J. Chem. Soc., Chem. Commun.* 1982, 552.

BOOK REVIEW

The Origin of ,the Chemical Elements and the Oklo Phenomenon. P. K. Kuroda. 1982. 24 figs., 48 tabs. XI, 165 pages. 485 g Cloth DM 92.–; US $ 36.80. Berlin–Heidelberg–New York: Springer-Verlag ISBN 3–540–11679–6.

The origin of the world, the meaning of life, and all that sort of thing, have excited man's imagination from time immemorial[1] to the present day.[2] Speculation on these topics has spawned a vast literature of mythology, Friga who spun the clouds, Pele whose hair came from volcanoes and so on, whose chief characteristic has been its logical and reasonable unreasonableness. The reader has only to suspend his disbelief and all will be made clear. Has much changed now that the age of enlightenment has dawned, given rise to reason, and reached a pinnacle of achievement in our present scientific era? Do we not still tell stories fantastic, but now expressed in millibarns and megayears yet still fantastic speculation n'ertheless? The present book by Professor Kuroda is a valiant attempt to see what order, based on scientific facts, can be established in the heady bizarre and truly metaphysical world when there was no world. In general, he is concerned with the origin of the elements and in particular to rationalise the specific isotopic abundancies that can be observed both on earth and in the heavens— well those bits of the heavens that come our way like meteorites and samples of lunar rock—in terms of intricate patterns of nuclear reactions. It is, however, difficult to tell a clear and coherent story since the quality of theoretical speculation is inversely proportional to the possibility of experimental verification. Nowhere is this more clearly seen than in the field of cosmological nucleogenesis. Furthermore, much of this book deals rather too extensively with the minutae of specific problems: an overall picture fails to emerge. Thus such diverse topics as xenonology (a study truly of strange things!), the extinction of the dinosaurs and Nature's own do-it-herself nuclear reactor at Oklo, all find some place in this monograph.

—Fait de tout pour faire un monde . . .

From: J. Effel, *La Création du Monde*. La Livre de Poche, Paris (1974).

Despite these short comings this is an interesting and fascinating book which gives a timely review of the literature of nucleogenesis and which enables the author to put his own considerable achievements and considered opinions into a broader perspective. A personal book then, but one which can be read with profit by anyone interested in the beginnings of it all.

D. S. URCH

REFERENCES

1. The Bible.
2. D. Adams, *The Hitch-hikers Guide to the Galaxy*. Pan Books, London (1979).